nature

Vol 262 No 5563 July 1 1976 55p

E 5 NOV 1976

Banerjee
5/11/76

Pure Chemistry Library
SCIENCE COLLEGE
[illegible] Upper Circular Road
CALCUTTA

(83)

(Vol. 262)
(No. 5563-5571)
(1-826p)
(July-August)
(1976)

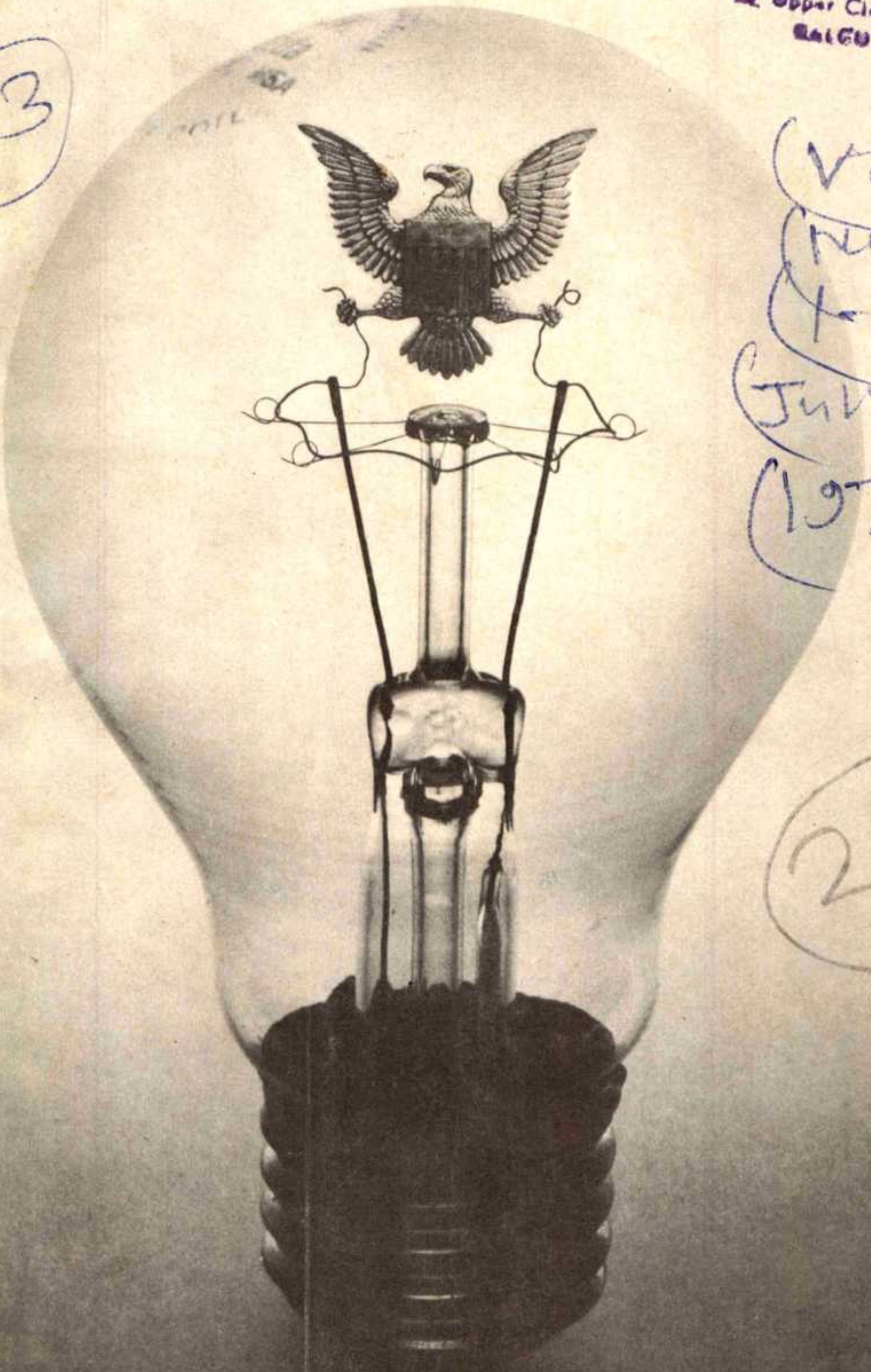

(258)

This manual contains a collection of experiments in

- **SPECTROPHOTOMETRY** • **FLUORIMETRY**
- **pH MEASUREMENT** • **DISSOLVED OXYGEN MEASUREMENT** carried out with a single instrument –

SPECTRO-PLUS

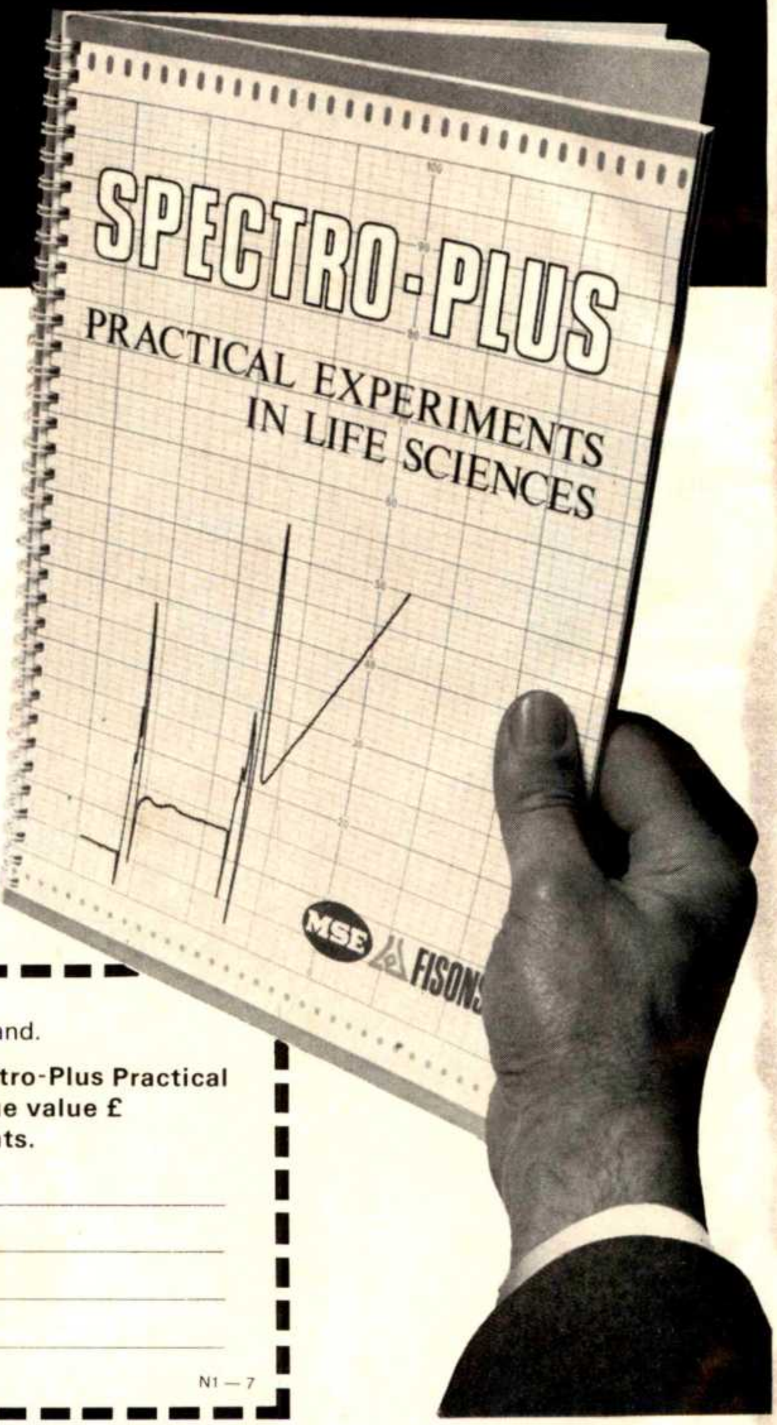

Spectro-Plus is a versatile multifunctional instrument with applications chiefly in life science related laboratories. As a tool for teaching in practical courses at universities and technical colleges its cost effectiveness is unmatched by any other device. As a UV spectrophotometer it is competitively priced; hence fluorescence, pH and oxygen measurements are gratuitous extras. Use the coupon below, send for the Spectro-Plus manual and see for yourself what is possible with this unique instrument.

The book contains an accurate record of experimental data from 25 experiments covering the four modes of Spectro-Plus.

It is of substantial general interest and although designed to assist every Spectro-Plus user it can stand on its own merits as a textbook of practical biochemistry.

Copies are available direct from MSE, price £3 each, post free.

To **MSE Scientific Instruments,**
Manor Royal, Crawley, West Sussex, England.

Please send me ☐ copies of the Spectro-Plus Practical Experiments Manual. I enclose cheque value £ made out to MSE Scientific Instruments.

Name ____________________

Position ____________________

Organisation ____________________

Address ____________________

N1 — 7

MSE **MSE Scientific Instruments**
Manor Royal, Crawley, West Sussex, England Telephone: Crawley 31100 Telex: 87119
FISONS

Circle No. 01 on Reader Enquiry Form.

© Macmillan Journals Ltd 1976
Published weekly
ISSN 0028-0836
Registered as a newspaper at the
British Post Office

London
4 Little Essex Street, WC2R 3LF
Telephone: (01) 836 6633 Telex: 262024
Telegrams: Phusis London WC2R 3LF

Washington
711 National Press Building, DC 20045
Telephone: (202) 737 2355
Telex: 64280

Editor
David Davies

Deputy Editor
Roger Woodham

Editorial Staff
Martin Goldman Allan Piper
*Sandy Grimwade Miranda Robertson
Eleanor Lawrence Fiona Selkirk
Mary Lindley Chris Sherwell
Peter Milford Hilary Taphouse
Peter Newmark Robert Vickers
Colin Norman Mary Wade
*Washington office

Publishing Director
Jenny Hughes

Display advertisement enquiries to:
Richard Webb in the London Office
or to
Mary Wade in the Washington Office
Telex: 64280

Classified advertisement enquiries to:
Advertising Department,
Nature,
4 Little Essex St,
London WC2R 3LF
Telephone (01) 836 6633
Telex 262024

Subscription enquiries to:
Macmillan Journals Ltd, Brunel Road,
Basingstoke, Hants. RG21 2XS
Telephone: Basingstoke 29242

Price

	UK	£35
Surface mail	Australia	A$58
	Europe	£35
	Japan	Y24.500
	USA (air/surface)	US$95
	Rest of world	£35
Airmail	Europe	£40
	Rest of world	US$118

US Postmaster, please send form 3579 to Nature. 711 National Press Building, Washington DC 20045

Second-class postage paid at New York, NY. US mailing agent is:

Expediters of the Printed Word Ltd,
527 Madison Avenue,
New York, NY 10022

Cover picture
The United States puts it all together.

Picture by Michael Freeman.

American science past and present: pages 9–27.

Vol. 262 No. 5563 July 1, 1976

nature
Volume 262 July 1, 1976

258

Too narrow-minded about energy? 1
Genetic manipulation: guidelines issued 2

NEWS AND VIEWS

Volcanoes and climate/Activation analysis/Grazing/Purines and pyrimidines/Magnetic dating 5

200 years of American science

Reflections on 200 years of science in the USA *N. Reingold* 9
The rise of 'prostituted' physics *S. R. Weart* 13
Population studies and the Old Order Amish *H. E. Cross* 17
Scientific networks in the age of the American Revolution *A. Thackray* 20
The Viking Mission search for life on Mars *H. P. Klein, J Lederberg, A. Rich, N. H. Horowitz, V. I. Oyama and G. V. Levin* 24

ARTICLES

Xenon record of the early solar system *D D. Sabu and O. K Manuel* 28
Translation *in vitro* of vesicular stomatitis virus mRNA lacking 5′-terminal 7-methylguanosine *J. K. Rose and H F Lodish* 32

LETTERS TO NATURE

X-ray pulses from globular clusters *J N. Bahcall and J. P. Ostriker* 37
Frequency variation of equatorial ionospheric scintillations *B. V. Krishna Murthy, K Krishna Murthy, C Raghava Reddi and S. Vaidyanathan* 38
Ocean temperatures and large-scale atmospheric variations *R. E. Newell and B. C. Weare* 40
Long term variations in western tropical Pacific cyclogenesis associated with the Southern Oscillation *J. M. Harding* 41
Three late-Devensian sites in West-central Scotland *J. H. Dickson, W. G. Jardine and R. J. Price* 43
Changes in net surface charge of hydrous alumina with phosphate adsorption *S. S. S. Rajan* 45
Conformational effects in drag reduction by polymers *P. S. Virk* 46
Effect of drag-reducing polymers on pulsation noise of small air bubbles *W. D. McComb and S. Ayyash* 47
Plasma treatment of coal *T. W. Scott and M Venugopalan* 48
pH-dependent heterosis of heavy metal-tolerant hybrid of the monkey flower *Mimulus guttatus* *M. Hani Soliman* 49
Increased lead ingestion in calcium-deficient monkeys *J. L. Jacobson and C. T. Snowdon* 51
Microvilli and cell swelling *S. Knutton, D. Jackson, J. M. Graham, K. J. Micklem and C. A. Pasternak* 52
Ionic mechanism of the H^+ pump in a snail neurone *R. C Thomas* 54
Role of axoplasmic transport in neurotrophic regulation of muscle end-plate acetylcholinesterase *H. L. Fernandez and N. C. Inestrosa* 55
Three-step yielding of load-clamped mammalian cardiac muscle *Ph. R. Housmans and D. L. Brutsaert* 56
New elastic protein from muscle *K. Maruyama, R. Natori and Y. Nonomura* 58

Pure Chemistry Library
SCIENCE COLLEGE

Guide to authors

- Articles are up to 3,000 words in length with at most six displayed items (figures and tables) and may either be reports of major research developments in a subject or broader reviews of progress.
- Letters are brief reports of research of unusual and wide interest, not in general longer than 1,000 words; at most they have three or four displayed items (figures and tables).
- 'Matters Arising' permits occasional short discussion of papers that have previously appeared in *Nature*. There is a limit of 300 words

Manuscripts may be submitted either to London or Washington Three typed copies should be submitted, each including lettered copies of figures. Typing (including references) should be double spaced. The title should be brief and informative. Pages should be numbered. References, tables and figure legends should start on separate pages. Experimental detail vital to the paper yet which would interrupt the narrative is best placed in the figure legends. Units should conform to the Système International. Greek characters should be identified in the margin on their first appearance. Equations should occupy single lines if possible, exp (a) is preferred to e^a if 'a' is more than one character. Articles should be accompanied by an abstract of not more than fifty words listing the main conclusions.

References are indicated by superscripts in the text. See any contemporary *Nature* for style, but note:

(i) To refer to several references by the same author at once, only one reference number need be given.

(ii) Cite first and last pages.

Abbreviations should follow the *World List of Scientific Periodicals*, fourth ed. (Butterworth, 1963-65). Symposia are often difficult to refer to and only published or soon-to-be-published volumes should be mentioned in references. Their publisher and place of publication should be clearly indicated. 'Personal communication' and 'unpublished work' should be incorporated in the text.

Artwork should be sent with the manuscript and clearly marked with author's name and the figure number Line drawings to be in Indian ink on heavy cartridge paper, tracing paper or similar materials: thin, shiny, torn or folded material should be avoided. Scales for graphs should be chosen such that simple figures will not occupy an inordinate amount of space Most figures are reduced to one column width so originals should be about as wide as a page of *Nature*. To enable figures, particularly maps, to be edited in the same style as the text they should contain only essential material. Ideally, an unlabelled original and a labelled copy should be provided: labelling on photographs should, if possible, be avoided entirely. Records, charts etc. which will not reproduce well should be redrawn or simply described in the text. We are always glad to see artwork for possible use on the cover, but cannot guarantee its return.

In order to save on postal expenses we return only the top copy and artwork of manuscripts that we cannot publish.

A fuller guide appeared in *Nature* (**246**, 238; 1973).

Down's syndrome and related abnormalities in an area of high background radiation in coastal Kerala — *N. Kochupillai, I. C. Verma, M. S. Grewal and V. Ramalingaswami* 60
Modulation of the synthesis *in vitro* of a hormone-induced protein by transfer RNA — *O. K. Sharma, D. N Beezley and E. Borek* 62
Human-mouse cell hybrid with human multiple Y chromosomes — *R Tantravahi, V G. Dev, D. A. Miller and O J. Miller* 63
Chromosomal proteins regulate steroid binding to chromatin — *T C. Spelsberg, R A Webster and G. M. Pikler* 65
Effect of maternal age on intercellular adhesion of embryonic chick liver cells — *J. Umbreit and S. Roseman* 67
Limited proliferation of stem cells surviving alkylating agents — *L. E. Botnick, E. C. Hannon and S. Hellman* 68
Transformation of the β_2 adrenoreceptor in normal rat liver into a β_1 type in Zajdela hepatoma — *M-L. Lacombe, E. Rene, G. Guellaen and J. Hanoune* 70
Effect of restriction endonucleases on infectivity of Rous sarcoma virus DNA — *H. Kopecka, J Hillova and M. Hill* 72
Spontaneous transformation of human skin fibroblasts derived from neoplastic patients — *B. Azzarone, D. Pedulla and C. A. Romanzi* 74
Enumeration of specific cytotoxic T cells — *R. M. Thorn and C. S. Henney* 75
Enhancement of delayed hypersensitivity by depletion of suppressor T cells with cyclophosphamide in mice — *A. Mitsuoka, M Baba and S. Morikawa* 77

BOOK REVIEWS

The Economic Superpowers and the Environment: the United States, the Soviet Union and Japan (Donald R Kelley, Kenneth R. Stunkel and Richard R. Wescott)—*Eric Ashby* 81
The Biology of Population Growth (Robert L. Snyder)—*M E. Solomon* 81
Donor–Acceptor Bond (E. N. Guryanova, I. P. Goldstein and I. P Romm)—*S. P. McGlynn* 82
Lysosomes: A survey (E. Holtzman)—*A. C. Allison* 82
Psycholinguistics: Introductory Perspectives (Joseph F Kess)—*P N. Johnson-Laird* 83
Receptor-Specific Proteins (Edwin R. Gold and Peter Balding)—*Irwin J. Goldstein* 83
Spectral and Chemical Characterisation of Organic Compounds: A Laboratory Handbook (W J. Criddle and G P. Ellis)—*Peter Sykes* 84
Mosquito Ecology: Field Sampling Methods (M. W Service)—*W. W Macdonald* 84
The Brown Rat (Graham Twigg)—*S. A. Barnett* 84
Membranes: A Series of Advances Vol 3 (George Eisenman, editor)—*P. F. Baker* 84
Laser Doppler Measurements (M. Watrasiewicz and M J. Rudd)—*H Eisenberg* 84

Newly on the market: calculators xiii

Reader enquiry service xxx

nature SUBSCRIPTION ORDER FORM

Subscription Department, Macmillan Journals Ltd, Brunel Road, Basingstoke, Hampshire, RG21 2XS England

Please enter me for a year's subscription to **Nature** starting with the issue dated ....

Please note that subscriptions may take up to 4 weeks to process.

Surface Rates	U K	Australia	Europe	Japan	USA & Canada	Rest of the World
	£35	A$58	£35	Y24,500	US $95	£35
Airmail Rates	Europe		Rest of the World		Personal Reduced Rate	
	£40		US$118		US$103	

Please note if applying for a Personal Airmail Reduced Rate subscription you must enclose a **personal cheque** and the address to which the journal is to be posted must be **your own address**

(Prices applicable only to orders started before July 1st 1976)
Orders must be accompanied by remittance Cheques should be made payable to Macmillan Journals Ltd

I enclose ....

NAME ....

ADDRESS ....

....

.... POSTAL/ZIP CODE ....

Registered No 785998 England Registered Office 4 Little Essex Street, London WC2R 3LF 22·1·76

© Macmillan Journals Ltd 1976

Published weekly
ISSN 0028-0836
Registered as a newspaper at the
British Post Office

London
4 Little Essex Street, WC2R 3LF
Telephone: (01) 836 6633 Telex: 262024
Telegrams: Phusis London WC2R 3LF

Washington
711 National Press Building, DC 20045
Telephone: (202) 737 2355
Telex: 64280

Editor
David Davies

Deputy Editor
Roger Woodham

Editorial Staff
Martin Goldman Allan Piper
*Sandy Grimwade Miranda Robertson
Eleanor Lawrence Fiona Selkirk
Mary Lindley Chris Sherwell
Peter Milford Hilary Taphouse
Peter Newmark Robert Vickers
Colin Norman Mary Wade
*Washington office

Publishing Director
Jenny Hughes

Display advertisement enquiries to:
Richard Webb in the London Office
or to
Mary Wade in the Washington Office
Telex: 64280

Classified advertisement enquiries to:
Advertising Department,
Nature,
4 Little Essex St,
London WC2R 3LF
Telephone (01) 836 6633
Telex 262024

Subscription enquiries to:
Macmillan Journals Ltd, Brunel Road,
Basingstoke, Hants. RG21 2XS
Telephone: Basingstoke 29242

Price

	UK	£35
Surface mail	Australia	A$58
	Europe	£35
	Japan	Y24.500
	USA (air/surface)	US$95
	Rest of world	£35
Airmail	Europe	£40
	Rest of world	US$118

US Postmaster, please send form 3579 to Nature
711 National Press Building, Washington DC 20045

Second-class postage paid at New York, NY.
US mailing agent is:

Expediters of the Printed Word Ltd.,
527 Madison Avenue,
New York, NY 10022

Cover picture

Anti-malaria campaign in Iran: spraying in the old caravanserai near Kamaradi. Alex Dorozynski writes on page 85.

WHO photograph by Philip Boncas

Vol. 262 No. 5564 **July 8, 1976**

nature

Volume 262 July 8, 1976

Is the world getting naughtier? 83
Towards an environmental ethic 84
The attack on tropical disease 85
USA/EEC 88

NEWS AND VIEWS

Factor VIII/Brain and intestinal peptides/Cathodoluminescence/Plate tectonics/Space science/Tropical trees 91

REVIEW ARTICLE

Quasars and the cosmological distance scale *M Rowan-Robinson* 97

ARTICLES

The Karari Industry: Early Pleistocene archaeological evidence from the terrain east of Lake Turkana, Kenya *J. W. K. Harris and G. Isaac* 102
Relationship between receptor and mammary tumour virus production after stimulation by glucocorticoid *G. Shyamala and C. Dickson* 107
4S *oop* RNA is a leader sequence for the immunity-establishment transcription in coliphage λ *A. Honigman, S.-L. Hu, R. Chase and W. Szybalski* 112

LETTERS TO NATURE

Sigma Orionis E as a mass-transfer binary system *J. E. Hesser, N. R. Walborn and P. Ugarte P.* 116
Evidence for a radioactive decay hypothesis for supernova luminosity *B. W. Rust, M. Leventhal and S. L. McCall* 118
Orientation of pulsar magnetic dipole moments *P. B. Jones* 120
Ocean bottom seismic measurements on the East Pacific Rise and Rivera Fracture Zone *W. A. Prothero, I. Reid, M. S. Reichle and J. N. Brune* 121
Further rubidium–strontium age and isotope evidence for the nature of the late Archaean plutonic event in West Greenland *S. Moorbath and R. J. Pankhurst* 124
Characterisation of monounsaturated fatty acids from an estuarine sediment *E. S. Van Vleet and J. G. Quinn* 126
Evidence for short term atmospheric ^{14}C variations about 4,000 yr BP *R. Burleigh and A. Hewson* 128
Lead isotope studies of metal sources for ancient Nigerian 'bronzes' *C. L. Goucher, J. H. Teilhet, K R. Wilson and T. J. Chow* 130
Parental investment, mate desertion and a fallacy *R. Dawkins and T. R. Carlisle* 131
Nitrate reductase as a possible predictive test of crop yield *C. B. Johnson, W. J. Whittington and G. C. Blackwood* 133
Possible origin for insoluble organic (kerogen) debris in sediments from insoluble cell-wall materials of algae and bacteria *R. P. Philp and M. Calvin* 134
Prepupal larval mosaics in *Drosophila melanogaster* *I. Kiss, G. Bencze, A. Fodor, J. Szabad and J. W. Fristrom* 136
Determination of cell shape by a cell surface protein component *L. Mallucci and V. Wells* 138
Precipitating antibodies in von Willebrand's disease *P. M. Mannucci, D. Meyer, Z. M. Ruggeri, J. Koutts, N. Ciavarella and J.-M. Lavergne* 141
Control of brain tryptophan concentration in rats on a high fat diet *P. H. Hutson, P. J. Knott and G. Curzon* 142

Guide to authors

- Articles are up to 3,000 words in length with at most six displayed items (figures and tables) and may either be reports of major research developments in a subject or broader reviews of progress.
- Letters are brief reports of research of unusual and wide interest, not in general longer than 1,000 words; at most they have three or four displayed items (figures and tables).
- 'Matters Arising' permits occasional short discussion of papers that have previously appeared in *Nature*. There is a limit of 300 words.

Manuscripts may be submitted either to London or Washington. Three typed copies should be submitted, each including lettered copies of figures Typing (including references) should be double spaced. The title should be brief and informative. Pages should be numbered. References, tables and figure legends should start on separate pages. Experimental detail vital to the paper yet which would interrupt the narrative is best placed in the figure legends Units should conform to the Système International. Greek characters should be identified in the margin on their first appearance. Equations should occupy single lines if possible, exp (*a*) is preferred to e^a if '*a*' is more than one character. Articles should be accompanied by an abstract of not more than fifty words listing the main conclusions.

References are indicated by superscripts in the text. See any contemporary *Nature* for style, but note:

(i) To refer to several references by the same author at once, only one reference number need be given.

(ii) Cite first and last pages.

Abbreviations should follow the *World List of Scientific Periodicals*, fourth ed. (Butterworth, 1963-65). Symposia are often difficult to refer to and only published or soon-to-be-published volumes should be mentioned in references. Their publisher and place of publication should be clearly indicated. 'Personal communication' and 'unpublished work' should be incorporated in the text.

Artwork should be sent with the manuscript and clearly marked with author's name and the figure number. Line drawings to be in Indian ink on heavy cartridge paper, tracing paper or similar materials: thin, shiny, torn or folded material should be avoided. Scales for graphs should be chosen such that simple figures will not occupy an inordinate amount of space. Most figures are reduced to one column width so originals should be about as wide as a page of *Nature* To enable figures, particularly maps, to be edited in the same style as the text they should contain only essential material. Ideally, an unlabelled original and a labelled copy should be provided: labelling on photographs should, if possible, be avoided entirely. Records, charts etc which will not reproduce well should be redrawn or simply described in the text. We are always glad to see artwork for possible use on the cover, but cannot guarantee its return.

In order to save on postal expenses we return only the top copy and artwork of manuscripts that we cannot publish

A fuller guide appeared in *Nature* (**246,** 238; 1973).

Inhibition by albumin of tryptophan uptake by rat brain — *P. Etienne, S N Young and T L Sourkes* 144
Monitoring of transmitter metabolites by voltammetry in cerebrospinal fluid following neural pathway stimulation — *R. M. Wightman, E. Strope, P. M Plotsky and R. N. Adams* 145
Periodate-induced increase in cyclic GMP in mouse and guinea pig splenic cells in association with mitogenesis — *M K. Haddox, L. T Furcht, S R Gentry, M E Moser, J. H Stephenson and N. D. Goldberg* 146
Evidence for non-deoxynucleotide linkers in Ehrlich ascites tumour cell DNA — *H. V Hershey and D Werner* 148
Intact 3′end of 16S rRNA is not required for specific mRNA binding — *J. V. Ravetch and K S. Jakes* 150
Occurrence of *trans*-ribosylzeatin in *Agrobacterium tumefaciens* tRNA — *R. W Chapman, R O. Morris and J. B. Zaerr* 153

Matters arising

Scrotal asymmetry: an appendix — *A. F. Stewart* 155
Specificity of transfer factor — *M P Arala-Chaves and H. H. Fudenberg* 155
Permeability of blood-cerebrospinal fluid barrier during foetal and perinatal life — *N. R. Saunders, K M. Dziegielewska, D. H Malinowska, M. L. Reynolds, J M Reynolds and K. Møllgard* 156
Reply — *M. Adinolfi, S. E. Beck, S A Haddad and M. J. Seller* 156

BOOK REVIEWS

The Naturalist in Britain: A Social History (D. E Allen)—*R Desmond* 157
Nature in Trust: The History of Nature Conservation in Britain (John Sheail)—*P Conder* 158
Resistance of *Pseudomonas aeruginosa* (M R. W. Brown, editor)—*E. S Anderson* 158
The Red Colobus Monkey (T. T Struhsaker)—*T. H. Clutton-Brock* 159
Meiotic Configurations: A Source of Information for Estimating Genetic Parameters (J. Sybenga)—*H Rees* 159
The Survival of Vegetative Microbes (T. R G. Gray and J R Postgate, editors)—*D C. Ellwood* 159
An Introduction to Electromagnetic Fields (R L Ferrari)—*P Silvester* 160
Methods of Optimisation (G. R Walsh)—*P Whittle* 160
Animal Migration and Navigation (Philip Street)—*John Krebs* 160
Introduction to Liquid Crystals (E B Priestley, Peter J Wojtowicz and Ping Sheng, editors)—*G. W. Gray* 160
The Seismics of Heterogeneous and Turbid Media (A. N. Nikolaev)—*J. A Hudson* 160
Reader enquiry service xvii

© Macmillan Journals Ltd 1976
Published weekly
ISSN 0028-0836
Registered as a newspaper at the
British Post Office

London
4 Little Essex Street, WC2R 3LF
Telephone: (01) 836 6633 Telex: 262024
Telegrams: Phusis London WC2R 3LF

Washington
711 National Press Building, DC 20045
Telephone: (202) 737 2355
Telex: 64280

Editor
David Davies

Deputy Editor
Roger Woodham

Editorial Staff
Martin Goldman Allan Piper
*Sandy Grimwade Miranda Robertson
Eleanor Lawrence Fiona Selkirk
Mary Lindley Chris Sherwell
Peter Milford Hilary Taphouse
Peter Newmark Robert Vickers
Colin Norman Mary Wade
*Washington office

Publishing Director
Jenny Hughes

Display advertisement enquiries to:
Richard Webb in the London Office
or to
Mary Wade in the Washington Office
Telex: 64280

Classified advertisement enquiries to:
Advertising Department,
Nature,
4 Little Essex St,
London WC2R 3LF
Telephone (01) 240 1011
Telex 262024

Subscription enquiries to:
Macmillan Journals Ltd, Brunel Road,
Basingstoke, Hants. RG21 2XS
Telephone: Basingstoke 29242

Price

	UK	£35
Surface mail	Australia	A$58
	Europe	£35
	Japan	Y24 500
	USA (air/surface)	US$95
	Rest of world	£35
Airmail	Europe	£40
	Rest of world	US$118

US Postmaster, please send form 3579 to Nature
711 National Press Building, Washington DC 20045

Second-class postage paid at New York, NY.
US mailing agent is

Expediters of the Printed Word Ltd.,
527 Madison Avenue,
New York, NY 10022

Cover picture

Windpower 1884-style, from *La Nature*, February 23, 1884. For more about the energy economics of windpower (and wave power) see page 206.
Mary Evans Picture Library

Vol. 262 No. 5565 **July 15, 1976**

nature

Volume 262 July 15, 1976

Nuclear industry goes public 161
The weather a week ahead 162
USA/EEC/Brazil/Sweden/Israel/In brief/Mellanby on nature conservation 163

Correspondence and competition 171

NEWS AND VIEWS

Electron density map/Nitrogen fixation/Transfer RNA/ Regulatory gene/Meteoroids and the Moon/Metalloproteins/Nuclear fission/Cytonet protein/Behaviour/ Haemopoiesis 172

ARTICLES

Giant radio galaxy NGC315 *A. H. Bridle, M. M. Davis, D. A. Meloy, E. B. Fomalont, R. G. Strom and A. G. Willis* 179
Repeated sequence specific to human males *H. Cooke* 182
Initiation sites of Rous sarcoma virus RNA-directed DNA synthesis *in vitro* *L. M. Cashion, R. H. Joho, M. A. Planitz, M. A. Billeter and C. Weissmann* 186
Proviral sequences of baboon endogenous type C RNA virus in DNA of human leukaemic tissues *F. Wong-Staal, D Gillespie and R C. Gallo* 190

LETTERS TO NATURE

Identification of Abell Cluster 754 with the X-ray source 3U0901–09 by Ariel V *J. P. Pye, B. A. Cooke and M. Elvis* 195
Inverse Compton spectra and the spectrum of Cygnus X-1 *D. M. Eardley and A. P. Lightman* 196
Neutron-capture cross sections for ^{186}Os and ^{187}Os and the age of the Universe *J. C. Browne and B. L. Berman* 197
Gravity signature of fossil plate boundaries in the Canadian Shield *R. A. Gibb and M. D. Thomas* 199
Dating of historical earthquakes by mud profiles of lake-bottom sediments *A. Ben-Menahem* 200
Ordered powder mixing *C. W. Yip and J A. Hersey* 202
Aluminium-26 in a manganese nodule *J.-L. Reyss and Y. Yokoyama* 203
Reactions of $O(2^1D_2)$ with chlorofluoromethanes and CCl_4 *R. J Donovan, K. Kaufmann and J. Wolfrum* 204
Energy analysis of wave-power and wind-power systems *P J. Musgrove* 206
Dinosaurs, endothermy and blood pressure *R. S. Seymour* 207
Acetylene reduction by legume root nodule protoplasts *W. J. Broughton, K. C. Wooi and C. H Hoh* 208
Inhibition by acetylene of conventional hydrogenase in nitrogen-fixing bacteria *L. A. Smith, S. Hill and M. G Yates* 209
Linear relationship between phytochrome photoequilibrium and growth in plants under simulated natural radiation *D. C. Morgan and H. Smith* 210
Hydromechanical adaptation in the solitary free-living coral *Fungia scutaria* *P. L. Jokiel and H. P. Cowdin* 212
Reshedding of *Toxoplasma* oocysts by chronically infected cats *J P. Dubey* 213
Inheritance of susceptibility to *Trypanosoma cruzi* infection in *Rhodnius prolixus* *I. Maudlin* 214
Functional inactivation of suppressor T cells by heat-killed macrophages *R. K. Gershon, D. D. Eardley and W. Ptak* 216

[illegible] SCIENCE COLLEGE [illegible]

Guide to authors

- Articles are up to 3,000 words in length with at most six displayed items (figures and tables) and may either be reports of major research developments in a subject or broader reviews of progress.
- Letters are brief reports of research of unusual and wide interest, not in general longer than 1,000 words; at most they have three or four displayed items (figures and tables).
- 'Matters Arising' permits occasional short discussion of papers that have previously appeared in *Nature*. There is a limit of 300 words.

Manuscripts may be submitted either to London or Washington. Three typed copies should be submitted, each including lettered copies of figures. Typing (including references) should be double spaced. The title should be brief and informative. Pages should be numbered. References, tables and figure legends should start on separate pages. Experimental detail vital to the paper yet which would interrupt the narrative is best placed in the figure legends. Units should conform to the Système International. Greek characters should be identified in the margin on their first appearance. Equations should occupy single lines if possible, exp (a) is preferred to e^a if 'a' is more than one character. Articles should be accompanied by an abstract of not more than fifty words listing the main conclusions.

References are indicated by superscripts in the text. See any contemporary *Nature* for style, but note:

(i) To refer to several references by the same author at once, only one reference number need be given.

(ii) Cite first and last pages.

Abbreviations should follow the *World List of Scientific Periodicals*, fourth ed. (Butterworth, 1963-65). Symposia are often difficult to refer to and only published or soon-to-be-published volumes should be mentioned in references. Their publisher and place of publication should be clearly indicated. 'Personal communication' and 'unpublished work' should be incorporated in the text.

Artwork should be sent with the manuscript and clearly marked with author's name and the figure number. Line drawings to be in Indian ink on heavy cartridge paper, tracing paper or similar materials: thin, shiny, torn or folded material should be avoided. Scales for graphs should be chosen such that simple figures will not occupy an inordinate amount of space. Most figures are reduced to one column width so originals should be about as wide as a page of *Nature*. To enable figures, particularly maps, to be edited in the same style as the text they should contain only essential material. Ideally, an unlabelled original and a labelled copy should be provided: labelling on photographs should, if possible, be avoided entirely. Records, charts etc. which will not reproduce well should be redrawn or simply described in the text. We are always glad to see artwork for possible use on the cover, but cannot guarantee its return.

In order to save on postal expenses we return only the top copy and artwork of manuscripts that we cannot publish.

A fuller guide appeared in *Nature* (**246**, 238; 1973).

Onset of acetylcholine sensitivity and endplate activity in developing myotome muscles of *Xenopus* — *S. Blackshaw and A. Warner* 217
Differential circadian rhythms in pineal and hypothalamic 5-HT induced by artificial photoperiods or melatonin — *C. A. Yates and J. Herbert* 219
Muscarinic agonists provide a new class of acaricide — *D C H Bigg and S. R. Purvis* 220
Transmission without spikes between locust interneurones and motoneurones — *M. Burrows and M. V. S. Siegler* 222
Microelectrode measurement of the intracellular *p*H of mammalian heart cells — *D. Ellis and R. C. Thomas* 224
Origin of plasma α_2HS-glycoprotein and its accumulation in bone — *J. T. Triffitt, U. Gebauer, B. A. Ashton, M. E. Owen and J. J. Reynolds* 226
Hybrid molecules and the superiority of the heterozygote — *E. Zouros* 227
Genetic transformation in *Drosophila* by microinjection of DNA — *S. Germeraad* 229
Integrator gene in *Aspergillus nidulans* — *H. N. Arst, Jr* 231
X-ray study of the rubidium salt of ADP — *M. A. Viswamitra, M. V. Hosur, Z. Shakked and O. Kennard* 234

Corrigendum 236

Errata 236

BOOK REVIEWS

Nuclear Power (Walter C. Patterson)—*Lord Hinton of Bankside* 237
Immunobiology of the Macrophage (David S. Nelson, editor)—*A. J. S. Davies* 237
Laser Spectroscopy (S. Haroche, J. C. Pebay-Peyroula, T. W. Hänsch and S. E. Harris, editors)—*Peter Knight* 238
Plant Virology: The Principles (Adrian Gibbs and Bryan Harrison)—*A. F. Posnette* 238
Islamic Science: An Illustrated Study (Seyyed Hossein Nasr)—*G. L. Lewis* 239
Canada's Continental Margins and Offshore Petroleum Exploration (C. J. Yorath, E. R. Parker and D. J. Glass, editors)—*R. C. Selley* 239

Obituary 240

Announcements 240

Person to person 242

Author index to Volume 261 iii

Reader enquiry service xxix

© Macmillan Journals Ltd 1976
Published weekly
ISSN 0028-0836
Registered as a newspaper at the
British Post Office

London
4 Little Essex Street, WC2R 3LF
Telephone: (01) 836 6633 Telex: 262024
Telegrams: Phusis London WC2R 3LF

Washington
711 National Press Building, DC 20045
Telephone: (202) 737 2355
Telex: 64280

Editor
David Davies

Deputy Editor
Roger Woodham

Editorial Staff
Martin Goldman Allan Piper
*Sandy Grimwade Miranda Robertson
Eleanor Lawrence Fiona Selkirk
Mary Lindley Chris Sherwell
Peter Milford Hilary Taphouse
Peter Newmark Robert Vickers
Colin Norman Mary Wade
*Washington office

Publishing Director
Jenny Hughes

Display advertisement enquiries to:
Richard Webb in the London Office
or to
Mary Wade in the Washington Office
Telex: 64280

Classified advertisement enquiries to:
Advertising Department,
Nature,
4 Little Essex St,
London WC2R 3LF
Telephone (01) 240 1011
Telex 262024

Subscription enquiries to:
Macmillan Journals Ltd, Brunel Road,
Basingstoke, Hants. RG21 2XS
Telephone: Basingstoke 29242

Price

	UK	£35
Surface mail	Australia	A$58
	Europe	£35
	Japan	Y24.500
	USA (air/surface)	US$95
	Rest of world	£35
Airmail	Europe	£40
	Rest of world	US$118

US Postmaster, please send form 3579 to Nature.
711 National Press Building, Washington DC 20045

Second-class postage paid at New York, NY.
US mailing agent is:

Expediters of the Printed Word Ltd.,
527 Madison Avenue,
New York, NY 10022

Cover picture

The Namib Desert beetle, in its head-down stance, collecting drinking water from fog. See page 284.

Vol. 262 No. 5566 **July 22, 1976**

Volume 262 July 22, 1976

Out of work in Argentina 243
Why are we waiting? 244
Solar energy breeders 244
Modelling the world, again 246
Britain/Canada/Third World/USSR/In brief/Jukes on sassafras tea 248

Correspondence 253

NEWS AND VIEWS

Chandler wobble/Palindromic DNA/Genetic engineering/Manganese/Q$_\beta$ replicase/Enzymes 254

ARTICLES

Excitation of the Chandler wobble by large earthquakes — *R. J. O'Connell and A. M. Dziewonski* 259
Possible evidence for penetration of interstellar dust into the Solar System — *J. L. Bertaux and J. E. Blamont* 263
Neutron diffraction studies of retinal rod outer segment membranes — *H. Saibil, M. Chabre and D. Worcester* 266

LETTERS TO NATURE

On being close to a black hole without falling in — *R. Znajek* 270
Outbursts of the recurrent nova T Coronae Borealis — *R. F. Webbink* 271
A plum-pudding model for interstellar grains — *S. Simons and I. P. Williams* 273
A comparison of acoustic Doppler vertical velocities with direct measurements in the atmospheric boundary layer — *S. J. Caughey, B. A. Crease, D. N. Asimakopoulos and R. S. Cole* 274
Hercynian high pressure/low temperature metamorphism in the Ile de Groix Blueschists — *M. S. N. Carpenter and L. Civetta* 276
'Space' charging of insulators — *D. K. Davies* 277
Charges and vacuum flashover — *D. K. Davies* 279
Aspartic acid racemisation in dentine as a measure of ageing — *P. M. Helfman and J. L. Bada* 279
Sun and shade differences in productivity of reef corals — *D. S. Wethey and J. W. Porter* 281
Frost sensitivity of *Zea mays* increased by application of *Pseudomonas syringae* — *D. C. Arny, S. E. Lindow and C. D. Upper* 282
Fog basking by the Namib Desert beetle, *Onymacris unguicularis* — *W. J. Hamilton, III and M. K. Seely* 284
Nucleating agents in the haemolymph of insects tolerant to freezing — *K. E. Zachariassen and H. T. Hammel* 285
Induction of male recombination in *Drosophila melanogaster* by injection of extracts of flies showing male recombination — *J. H. M. Sochacka and R. C. Woodruff* 287
Initiation of meiotic maturation in *Xenopus laevis* oocytes by lanthanum — *S. Schorderet-Slatkine, M. Schorderet and E.-E. Baulieu* 289
Benzpyrene induces sister chromatid exchanges in cultured human lymphocytes — *H. W. Rüdiger, F. Kohl, W. Mangels, P. von Wichert, C. R. Bartram, W. Wöhler and E. Passarge* 290
Expression of maternal and paternal antigens on trophoblast — *J. Carter* 292
Successful induction of specific tolerance to transplantation antigens using autoimmunisation against the recipient's own natural antibodies — *H. Binz and H. Wigzell* 294
Induction of transplantation tolerance using serum as antigen source — *M. Hašek, J. Chutná, V. Holáň and M. Sládeček* 295
Antibody response induced *in vitro* to the cell-surface alloantigen Thy-1 — *P. Lake* 297
Transition probability and the hormonal and density-dependent regulation of cell proliferation — *J. H. Robinson, J. A. Smith, N. F. Totty and P. N. Riddle* 298
Identification of the cell multiplication inhibitory factors in interferon preparations as interferons — *W. E. Stewart, II, I. Gresser, M. G. Tovey, M.-T. Bandu and S. Le Goff* 300

Guide to authors

- Articles are up to 3,000 words in length with at most six displayed items (figures and tables) and may either be reports of major research developments in a subject or broader reviews of progress.
- Letters are brief reports of research of unusual and wide interest, not in general longer than 1,000 words; at most they have three or four displayed items (figures and tables).
- 'Matters Arising' permits occasional short discussion of papers that have previously appeared in *Nature*. There is a limit of 300 words.

Manuscripts may be submitted either to London or Washington. Three typed copies should be submitted, each including lettered copies of figures. Typing (including references) should be double spaced. The title should be brief and informative. Pages should be numbered. References, tables and figure legends should start on separate pages. Experimental detail vital to the paper yet which would interrupt the narrative is best placed in the figure legends. Units should conform to the Système International. Greek characters should be identified in the margin on their first appearance. Equations should occupy single lines if possible, exp (a) is preferred to e^a if 'a' is more than one character. Articles should be accompanied by an abstract of not more than fifty words listing the main conclusions.

References are indicated by superscripts in the text. See any contemporary *Nature* for style, but note:

(i) To refer to several references by the same author at once, only one reference number need be given.

(ii) Cite first and last pages.

Abbreviations should follow the *World List of Scientific Periodicals*, fourth ed. (Butterworth, 1963-65). Symposia are often difficult to refer to and only published or soon-to-be-published volumes should be mentioned in references. Their publisher and place of publication should be clearly indicated. 'Personal communication' and 'unpublished work' should be incorporated in the text.

Artwork should be sent with the manuscript and clearly marked with author's name and the figure number. Line drawings to be in Indian ink on heavy cartridge paper, tracing paper or similar materials: thin, shiny, torn or folded material should be avoided. Scales for graphs should be chosen such that simple figures will not occupy an inordinate amount of space. Most figures are reduced to one column width so originals should be about as wide as a page of *Nature*. To enable figures, particularly maps, to be edited in the same style as the text they should contain only essential material. Ideally, an unlabelled original and a labelled copy should be provided: labelling on photographs should, if possible, be avoided entirely. Records, charts etc. which will not reproduce well should be redrawn or simply described in the text. We are always glad to see artwork for possible use on the cover, but cannot guarantee its return.

In order to save on postal expenses we return only the top copy and artwork of manuscripts that we cannot publish.

A fuller guide appeared in *Nature* (**246**, 238; 1973).

Antiviral and cell growth inhibitory activities reside in the same glycoprotein of human fibroblast interferon — *E. Knight, Jr* 302
Direct measurement of membrane motion and fluidity by electron microscopy — *S. W. Hui* 303
Potentiation of central reward by localised perfusion of acetylocholine and 5-hydroxytryptamine — *P. Redgrave and R. I. Horrell* 305
Stimulation of cerebral histamine H_2 receptors by clonidine — *Y. Audigier, A Virion and J.-C. Schwartz* 307
Synaptic vesicle cytochemistry changes when cultured sympathetic neurones develop cholinergic interactions — *M. Johnson, D. Ross, M. Meyers, R. Rees, R. Bunge, E. Wakshull and H. Burton* 308
Enkephalin regulates the levels of cyclic nucleotides in neuroblastoma × glioma hybrid cells — *M. Brandt, R. J. Gullis, K. Fischer, C. Buchen, B. Hamprecht, L. Moroder and E. Wunsch* 311
Enkephalin and opiate narcotics increase cyclic GMP accumulation in slices of rat neostriatum — *K. P. Minneman and L. L. Iversen* 313
A sequential *in vivo–in vitro* study of carcinogenesis induced in the rat brain by ethylnitrosourea — *J. P. Roscoe and P. J. Claisse* 314
Native collagen formation by liver parenchymal cells in culture — *K. Sakakibara, M. Saito, M. Umeda, K. Enaka and Y. Tsukada* 316
Identification of medicarpin as a phytoalexin in the broad bean plant (*Vicia faba* L.) — *J. A. Hargreaves, J. W. Mansfield and D. T. Coxon* 318
Initiation inhibition and reinitiation of the synthesis of heterogeneous nuclear RNA in living cells — *E. Egyházi* 319
Inactivation of parathyroid hormone mRNA by treatment with periodate and aniline — *B. Kemper* 321
Aqueous glasses as matrices in freeze-fracture electron microscopy — *F. Franks and H. le B. Skaer* 323
The hinge-bending mode in lysozyme — *J. A. McCammon, B. R. Gelin, M. Karplus and P. G. Wolynes* 325
Structure of bilirubin — *R. Bonnett, J. E. Davies and M. B. Hursthouse* 326
Erratum 328

Matters arising

Deposit-forming by zinc dithiophosphates in base oils during oxidation — *H. B. Silver* 329
Haemoglobin type and superovulation in ewes — *A. O. Trounson, S. M. Willadsen, R. M. Moor and E. M. Tucker* 329
Volcanic triggering of glaciation — *P. W. Francis* 329
Reply — *J. R. Bray* 330
Acoustic Bragg diffraction from human tissues — *R. C. Chivers* 330
Reply — *D. Nicholas and C. R. Hill* 330

BOOK REVIEWS

After the Australopithecines: Stratigraphy, Ecology and Culture Change in the Middle Pleistocene (Karl W. Butzer and Glynn Ll. Isaac, editors)—*W. W. Bishop* 331
Uniqueness and Diversity in Human Evolution: Morphometric Studies of Australopithecines (Charles E. Oxnard)—*Bernard Wood* 331
Space Structures: Their Harmony and Counterpoint (Arthur L. Loeb)—*A. L. Mackay* 332
Atlas of an Insect Brain (Nicholas J. Strausfeld)—*John A. Patterson* 332
Moulds of Understanding: a Pattern of Natural Philosophy (Joseph Needham)—*Frank Greenaway* 333
Starfish, Jellyfish and the Order of Life: Issues in Nineteenth-Century Sciences (Mary P. Winsor)—*Sydney Smith* 333
Spectrophotometric Determination of Elements (Zygmunt Marczenko)—*G. Davidson* 334
Migration and Homing in Animals (Klaus Schmidt-Koenig)—*John R. Krebs* 334
The Papers of Joseph Henry (Nathan Reingold, editor)—*David M. Knight* 334
The Food in Your Future: Steps to Abundance (Keith C. Barrons)—*John Rivers* 334
Obituary 335
Announcements 335
Person to Person 336
Reader enquiry service xviii

© Macmillan Journals Ltd 1976

Published weekly
ISSN 0028-0836
Registered as a newspaper at the
British Post Office

London
4 Little Essex Street, WC2R 3LF
Telephone: (01) 836 6633 Telex: 262024
Telegrams: Phusis London WC2R 3LF

Washington
711 National Press Building, DC 20045
Telephone: (202) 737 2355
Telex: 64280

Editor
David Davies

Deputy Editor
Roger Woodham

Editorial Staff
Martin Goldman Allan Piper
*Sandy Grimwade Miranda Robertson
Eleanor Lawrence Fiona Selkirk
Mary Lindley Chris Sherwell
Peter Milford Hilary Taphouse
Peter Newmark Robert Vickers
Colin Norman Mary Wade
*Washington office

Publishing Director
Jenny Hughes

Display advertisement enquiries to:
Richard Webb in the London Office
or to
Mary Wade in the Washington Office
Telex: 64280

Classified advertisement enquiries to:
Advertising Department,
Nature,
4 Little Essex St,
London WC2R 3LF
Telephone (01) 240 1011
Telex 262024

Subscription enquiries to:
Macmillan Journals Ltd, Brunel Road,
Basingstoke, Hants. RG21 2XS
Telephone: Basingstoke 29242

Price

	UK	£35
Surface mail	Australia	A$58
	Europe	£35
	Japan	Y24.500
	USA (air/surface)	US$95
	Rest of world	£35
Airmail	Europe	£40
	Rest of world	US$118

US Postmaster, please send form 3579 to Nature
711 National Press Building, Washington DC 20045

Second-class postage paid at New York, NY.
US mailing agent is·

Expediters of the Printed Word Ltd.,
527 Madison Avenue,
New York, NY 10022

Cover picture

Leaves of the carnivorous purple pitcher-plant (*Sarracenia purpurea*), wherein are found the immature stages of the pitcher-plant mosquito (Wyeomyia smithii). See page 384.

Vol. 262 No. 5567 **July 29, 1976**

nature

Volume 262 July 29, 1976

Making it in the Civil Service 337
Tracking nuclear decisions (1) JET: will it ever get started? 338
Tracking nuclear decisions (2) FBR: will it ever be stopped? 342
Tracking nuclear decisions (3) Exports: time for a stand? 345
In brief 346

NEWS AND VIEWS

Ionosphere/Transformation and tumours/Mars/Exploding stars/HLA and disease/Plant evolution/Aggression/Geochemistry 347

REVIEW ARTICLE

Analysis of erythropoeisis at the molecular level — *P. R. Harrison* 353

ARTICLES

Accretion flows in the magnetospheres of Vela X-1, A0535+26 and Her X-1 — *R. F. Elsner and F. K. Lamb* 356
Membrane action of DMSO and other chemical inducers of Friend leukaemic cell differentiation — *G. H. Lyman, H. D. Priesler and D. Papahadjopoulos* 360
Similarity of the crystal and solution structure of yeast tRNA$^{\mathrm{Phe}}$ — *G. T. Robillard, C. E. Tarr, F. Vosman and H. J. C. Berendsen* 363

LETTERS TO NATURE

The 21-cm absorption line in NGC1275 — *R. D. Ekers, J. M. van der Hulst and G. K. Miley* 369
New limit on the size distribution of γ-ray bursts — *J. Carter, A. J. Dean, R. K. Manchada and D. Ramsden* 370
Palynomorphs indicating Permian rocks in Ethiopia — *A. Davidson and D. C. McGregor* 371
Radiocarbon dates of Santorini volcanics — *H. Pichler and W. Friedrich* 373
Formation of Hercynian subplates, possible causes and consequences — *V. Lorenz* 374
Age relationships along the Hermitage Bay–Dover Fault system, Newfoundland — *J. Blenkinsop, P. F. Cucman and K. Bell* 377
Upper limit to earthquake size — *A. McGarr* 378
Ball lightning in Smethwick — *E. R. Wooding* 379
Non-crystallinity of ion-irradiated metals — *R. Andrew, W. A. Grant, P. J. Grundy, J. S. Williams and L. T. Chadderton* 380
Effect of roughness on rubber friction when waves of detachment are present — *G. A. D. Briggs and B. J. Briscoe* 381
Learning-like phenomena in stereopsis — *V. S. Ramachandran* 382
Counter-intuitive property of effective population size — *R. H. Crozier* 384
Geography of photoperiodic response in diapausing mosquito — *W. E. Bradshaw* 384
The dispersal of young post-larval bivalve molluscs by byssus threads — *J. B. Sigurdsson, C. W. Titman and P. A. Davies* 386
Nematocyst discharge and the effects of antibodies on feeding in hydra — *O. K. Wilby* 387
Excitability of nerve-free hydra — *R. D. Campbell, R. K. Josephson, W. E. Schwab and N. B. Rushforth* 388
Directional hearing in crickets — *K. G. Hill and G. S. Boyan* 390
Effect of phloridzin and phloroglucinol on apple shoots — *O. P. Jones* 392
Malate-switch hypothesis to explain the action of stomata — *D. J. F. Bowling* 393
Plant uptake and leaching of dimethylnitrosamine — *D. Dean-Raymond and M. Alexander* 394
Non-enzymatic photochemical reduction of nitrate in rice seedlings — *M. S. Naik, K. V. Sardhumbal and S. Prakash* 396

Pure Chemistry Library
SCIENCE COLLEGE

Guide to authors

- Articles are up to 3,000 words in length with at most six displayed items (figures and tables) and may either be reports of major research developments in a subject or broader reviews of progress.
- Letters are brief reports of research of unusual and wide interest, not in general longer than 1,000 words; at most they have three or four displayed items (figures and tables).
- 'Matters Arising' permits occasional short discussion of papers that have previously appeared in *Nature*. There is a limit of 300 words.

Manuscripts may be submitted either to London or Washington. Three typed copies should be submitted, each including lettered copies of figures. Typing (including references) should be double spaced. The title should be brief and informative. Pages should be numbered. References, tables and figure legends should start on separate pages. Experimental detail vital to the paper yet which would interrupt the narrative is best placed in the figure legends. Units should conform to the Système International. Greek characters should be identified in the margin on their first appearance. Equations should occupy single lines if possible, exp (a) is preferred to e^a if 'a' is more than one character. Articles should be accompanied by an abstract of not more than fifty words listing the main conclusions.

References are indicated by superscripts in the text. See any contemporary *Nature* for style, but note:

(i) To refer to several references by the same author at once, only one reference number need be given.

(ii) Cite first and last pages.

Abbreviations should follow the *World List of Scientific Periodicals*, fourth ed. (Butterworth, 1963-65). Symposia are often difficult to refer to and only published or soon-to-be-published volumes should be mentioned in references. Their publisher and place of publication should be clearly indicated. 'Personal communication' and 'unpublished work' should be incorporated in the text.

Artwork should be sent with the manuscript and clearly marked with author's name and the figure number. Line drawings to be in Indian ink on heavy cartridge paper, tracing paper or similar materials: thin, shiny, torn or folded material should be avoided. Scales for graphs should be chosen such that simple figures will not occupy an inordinate amount of space. Most figures are reduced to one column width so originals should be about as wide as a page of *Nature*. To enable figures, particularly maps, to be edited in the same style as the text they should contain only essential material. Ideally, an unlabelled original and a labelled copy should be provided: labelling on photographs should, if possible, be avoided entirely. Records, charts etc. which will not reproduce well should be redrawn or simply described in the text. We are always glad to see artwork for possible use on the cover, but cannot guarantee its return.

In order to save on postal expenses we return only the top copy and artwork of manuscripts that we cannot publish.

A fuller guide appeared in *Nature* (**246**, 238; 1973).

Immunopathology of schistosomiasis in athymic mice	*C-K. Hsu, S H Hsu, R. A. Whitney, Jr and C. T. Hansen*	397
Growth of *Mycobacterium leprae* and *M. marinum* in congenitally athymic (nude) mice	*M. J. Colston and G. R F. Hilson*	399
Control of lymphokine secretion by prostaglandins	*D. Gordon, M. A. Bray and J Morley*	401
Phorbol esters stimulate DNA synthesis and ornithine decarboxylase activity in mouse epidermal cell cultures	*S. H. Yuspa, U. Lichti, T. Ben, E. Patterson, H. Hennings, T. J. Slaga, N. Colburn and W. Kelsey*	402
Intracellular messenger role of cyclic GMP in exocrine pancreas	*J. Albano, K D. Bhoola and R. F. Harvey*	404
Role of oestrogen receptor in androgen-induced sexual differentiation of the brain	*B. R. Westley and D. F Salaman*	407
2-Amino-4-phosphonobutyric acid as a glutamate antagonist on locust muscle	*S. G. Cull-Candy, J. F. Donnellan, R. W. James and G. G. Lunt*	408
Susceptibility of teratocarcinoma cells to adenovirus type 2	*F. Kelly and M. Boccara*	409
Is the scrapie agent a virus?	*H. J. Cho*	411
Rifampicin-resistant RNA polymerase and NAD transferase activities in coliphage N4 virions	*A. Pesce, C. Casoli and G. C. Schito*	412
Human cytomegalovirus infection of WI-38 cells stimulates mitochondrial DNA synthesis	*T. Furukawa, S. Sakuma and S. A. Plotkin*	414
Rhodopsin analogues from highly hindered 7-*cis* isomers of retinal	*W. J. DeGrip, R S. H. Liu, V. Ramamurthy and A. Asato*	416
Oxygen and toxicity inhibition of amino acid biosynthesis	*D E. Boehme, K. Vincent and O. R. Brown*	418
Reactions involving singlet oxygen and the superoxide anion	*W. H. Koppenol*	418
The lipid bilayer as a 'solvent' for small hydrophobic molecules	*S. H. White*	421
Matters arising		
Quantification of secondary and tertiary structure base pairs in *E. coli* $tRNA_1^{Val}$	*P. H. Bolton and and D. R. Kearns*	423
Reply	*B. R. Reid*	424
BOOK REVIEW		
The Nile: Biology of an Ancient River (Julian Rzóska, editor)—*Malcolm Coe*		425
Pesticides: Boon or Bane (M. B. Green)—*F Moriarty*		426
Eukaryotes at the Subcellular Level: Development and Differentiation (Jerold Last, editor)—*H. J. Gould*		426
Beyond Aesthetics: Investigations into the Nature of Visual Art (Don Brothwell, editor)—*N. W. Pirie*		427
Uptake of Ions by Plant Roots (D. J. F. Bowling)—*D. A. Barber*		427
The Observation and Analysis of Stellar Photospheres (David F. Gray)—*Bernard Pagel*		428
Mammalian Cell Membranes (G. A. Jamieson and D. N. Robinson, editors)—*R. Colin Hughes*		428
Obituary		429
Announcements		430
Reader enquiry service		xviii

M

© Macmillan Journals Ltd 1976
Published weekly
ISSN 0028-0836
Registered as a newspaper at the
British Post Office

London
4 Little Essex Street, WC2R 3LF
Telephone: (01) 836 6633 Telex: 262024
Telegrams: Phusis London WC2R 3LF

Washington
711 National Press Building, DC 20045
Telephone: (202) 737 2355
Telex: 64280

Editor
David Davies

Deputy Editor
Roger Woodham

Editorial Staff
Martin Goldman Allan Piper
*Sandy Grimwade Miranda Robertson
Eleanor Lawrence Fiona Selkirk
Mary Lindley Chris Sherwell
Peter Milford Hilary Taphouse
Peter Newmark Robert Vickers
Colin Norman Mary Wade
*Washington office

Publishing Director
Jenny Hughes

Display advertisement enquiries to:
Richard Webb in the London Office
or to
Mary Wade in the Washington Office
Telex: 64280

Classified advertisement enquiries to:
Advertising Department,
Nature,
4 Little Essex St,
London WC2R 3LF
Telephone (01) 240 1011
Telex 262024

Subscription enquiries to:
Macmillan Journals Ltd, Brunel Road,
Basingstoke, Hants. RG21 2XS
Telephone: Basingstoke 29242

Price

	UK	£35
Surface mail	USA and Canada (air/surface)	US$98
	Rest of world	US$82 50
Airmail	Europe	US$94
	Rest of world	US$130

US Postmaster, please send form 3579 to Nature
711 National Press Building, Washington DC 20045

Second-class postage paid at New York, NY
US mailing agent is.

Expediters of the Printed Word Ltd.,
527 Madison Avenue,
New York, NY 10022

Cover picture

River meanders at Glendaruel,
Scotland.
See page 482.
(Aerofilms)

Vol. 262 No. 5568 August 5, 1976

nature

Volume 262 August 5, 1976

Still a lot to learn from the Chinese 431
The ecology of ecology 432
Science policy in Poland 434
Artificial intelligence in education 435
Britain/France/West Germany/Sweden/Canada In brief/Mellanby on forecasting 437
Correspondence 442

NEWS AND VIEWS

Anti-idiotypic antibodies/Charmed particles/Nuclear physics/Muscle disease/Protein folding/γ-Ray astronomy 443

REVIEW ARTICLE

Fundamental research in molecular biology: relevance to medicine *M. F. Perutz* 449

ARTICLES

Seeing order in 'amorphous' materials *O. L. Krivanek, P. H. Gaskell and A. Howie* 454
Isotropic cosmic expansion and the Rubin–Ford effect *S. M. Fall and B. J. T. Jones* 457
Fossil hominids from the Laetolil Beds *M. D. Leakey, R. L. Hay, G. H. Curtis, R. E. Drake, M K. Jackes and T. D. White* 460
Non-genetic individuality: chance in the single cell *J. L. Spudich and D E. Koshland, Jr* 467

LETTERS TO NATURE

Observations of X-ray and γ bursts *J. J. Quenby, M. J Coe, A R. Engel and J. S. Mills* 471
Positions and evidence for a steady component for X-ray burst sources *G. F Carpenter, G. K Skinner, A. M. Wilson and A. P. Willmore* 473
Observations of X-ray bursts from the vicinity of 3U1727—33 *K. O. Mason, S. J. Bell-Burnell and N. E. White* 474
The radio tail galaxies in Abell 1314 *G. D. Coleman, P. Hintzen, J S. Scott and M Tarenghi* 476
White dwarfs, the Galaxy and Dirac's cosmology *R. Stothers* 477
Extraction of metals from basalt by humic acids *A Singer and J. Navrot* 479
Climatic information from $^{18}O/^{16}O$ ratios of cellulose in tree rings *J. Gray and P. Thompson* 481
Geometry of river meanders *R. D. Hey* 482
New hominid from Lake Ndutu, Tanzania *A. A. Mturi* 484
New cranium of *Homo erectus* from Lake Ndutu, Tanzania *R. J. Clark* 485
Antennal receptor response to sex pheromone mimics in the American cockroach *H. Washio, C Nishino and W S. Bowers* 487
Ecdysone and oocyte morphogenesis in *Bombyx mori* *J.-M. Legay, B. Calvez, M. Hirn and M. L. De Reggi* 489
Covering response in sea urchins *J. M. Lawrence* 490
Testing the neutral mutation hypothesis by distribution of single locus heterozygosity *M. Nei, P. A. Fuerst and R. Chakraborty* 491
Y chromosome visibility in quinacrine-stained human spermatozoa *A. M Roberts and H Goodall* 493
Absence of axonemal arms in nasal mucosa cilia in Kartagener's syndrome *H. Pedersen and N. Mygind* 494
Separation of suppressor and killer T cells by surface phenotype *P. C. L. Beverley, J. Woody, M. Dunkley, M. Feldmann and I McKenzie* 495
Plasma membrane glycoprotein which mediates adhesion of fibroblasts to collagen *E. Pearlstein* 497
Temporary intestinal hypoxia induced by degradable microspheres *K. E. Arfors, J. O Forsberg, B. Larsson, D. H. Lewis, B. Rosengren and S. Odman* 500

[illegible]

Guide to authors

- Articles are up to 3,000 words in length with at most six displayed items (figures and tables) and may either be reports of major research developments in a subject or broader reviews of progress.
- Letters are brief reports of research of unusual and wide interest, not in general longer than 1,000 words; at most they have three or four displayed items (figures and tables).
- 'Matters Arising' permits occasional short discussion of papers that have previously appeared in *Nature*. There is a limit of 300 words.

Manuscripts may be submitted either to London or Washington. Three typed copies should be submitted, each including lettered copies of figures. Typing (including references) should be double spaced. The title should be brief and informative. Pages should be numbered. References, tables and figure legends should start on separate pages. Experimental detail vital to the paper yet which would interrupt the narrative is best placed in the figure legends. Units should conform to the Système International. Greek characters should be identified in the margin on their first appearance. Equations should occupy single lines if possible, exp (a) is preferred to e^a if 'a' is more than one character. Articles should be accompanied by an abstract of not more than fifty words listing the main conclusions.

References are indicated by superscripts in the text. See any contemporary *Nature* for style, but note:

(i) To refer to several references by the same author at once, only one reference number need be given

(ii) Cite first and last pages

Abbreviations should follow the *World List of Scientific Periodicals*, fourth ed. (Butterworth, 1963-65) Symposia are often difficult to refer to and only published or soon-to-be-published volumes should be mentioned in references. Their publisher and place of publication should be clearly indicated 'Personal communication' and 'unpublished work' should be incorporated in the text.

Artwork should be sent with the manuscript and clearly marked with author's name and the figure number. Line drawings to be in Indian ink on heavy cartridge paper, tracing paper or similar materials: thin, shiny, torn or folded material should be avoided. Scales for graphs should be chosen such that simple figures will not occupy an inordinate amount of space. Most figures are reduced to one column width so originals should be about as wide as a page of *Nature*. To enable figures, particularly maps, to be edited in the same style as the text they should contain only essential material. Ideally, an unlabelled original and a labelled copy should be provided: labelling on photographs should, if possible, be avoided entirely. Records, charts etc. which will not reproduce well should be redrawn or simply described in the text. We are always glad to see artwork for possible use on the cover, but cannot guarantee its return.

In order to save on postal expenses we return only the top copy and artwork of manuscripts that we cannot publish.

A fuller guide appeared in *Nature* (**246**, 238; 1973).

Metabolic adaptation to pregnancy shown by increased biosynthesis of insulin in islets of Langerhans isolated from pregnant rats — *A. J. Bone and K. W. Taylor* 501
Electrophysiological evidence for coupling between β cells of pancreatic islets — *H. P. Meissner* 502
Decrease of Na^+ conductance during desensitisation of the frog endplate — *K. Kuba and K. Koketsu* 504
Elevated levels of enkephalin in morphine-dependent rats — *R. Simantov and S. H. Snyder* 505
Prolactin suppresses releases of luteinising hormone during lactation in the monkey — *R. Maneckjee, B. R. Srinath and N. R. Moudgal* 507
Bacteria necessary to produce experimental autoimmune myasthenia gravis in acetylcholine receptor-immunised rabbits? — *E. Heilbronn, C. Mattsson and E. Stålberg* 509
Cyclic AMP and cyclic GMP may play opposing roles in influencing force of contraction in mammalian myocardium — *H. Nawrath* 509
Opposing effects of cyclic AMP and cyclic GMP on protein phosphorylation in tubulin preparations — *I. V. Sandoval and P. Cuatrecasas* 511
Structural properties of rat serum proteins which correlate with their degradative rates *in vivo* — *J. F. Dice and A. L. Goldberg* 514
Accessibility of DNA in condensed chromatin to nuclease digestion — *C. J. Bostock, S. Christie and F. T. Hatch* 516
Amphipathic enzyme–polymer conjugates — *R. A. G. Smith* 519

BOOK REVIEWS

Malnutrition and Brain Development (Myron Winick)—*John Dobbing* 521
Nutrition and the Developing Nervous System (Philip R. Dodge, Arthur L. Prensky and Ralph D. Feigin)—*John Dobbing* 521
Polymeric Carbons: Carbon Fibre, Glass and Char (G. M. Jenkins and K. Kawamura)—*Paul Calvert* 521
Landmark Experiments in Twentieth Century Physics (George L. Trigg)—*R. Latham* 522
The Nucleon-Nucleon Interaction (G. E. Brown and A. D. Jackson)—*Leonardo Castillejo* 522
Pioneers in Neuroendocrinology (Joseph Meites, Bernard T. Donovan and Samuel M. McCann, editors)—*Barend ter Haar* 523
Climate and Environment: The Atmospheric Impact on Man (John F. Griffiths)—*John Gribbin* 523

Obituary 524

Announcements 524

Newly on the market iii

Reader enquiry service xv

© Macmillan Journals Ltd 1976

Published weekly
ISSN 0028-0836
Registered as a newspaper at the
British Post Office

London
4 Little Essex Street, WC2R 3LF
Telephone: (01) 836 6633 Telex: 262024
Telegrams: Phusis London WC2R 3LF

Washington
711 National Press Building, DC 20045
Telephone: (202) 737 2355
Telex: 64280

Editor
David Davies

Deputy Editor
Roger Woodham

Editorial Staff
Martin Goldman
*Sandy Grimwade
Eleanor Lawrence
Mary Lindley
Peter Milford
Peter Newmark
*Colin Norman
Allan Piper
Miranda Robertson
Fiona Selkirk
Chris Sherwell
Hilary Taphouse
Robert Vickers
Mary Wade*

*Washington office

Publishing Director
Jenny Hughes

Display advertisement enquiries to:
Richard Webb in the London Office
or to
Mary Wade in the Washington Office
Telex: 64280

Classified advertisement enquiries to:
Advertising Department,
Nature,
4 Little Essex St,
London WC2R 3LF
Telephone (01) 240 1011
Telex 262024

Subscription enquiries to:
Macmillan Journals Ltd, Brunel Road,
Basingstoke, Hants. RG21 2XS
Telephone: Basingstoke 29242

Price

	UK	£35
Surface mail	USA and Canada (air/surface)	US$98
	Rest of world	US$82 50
Airmail	Europe	US$94
	Rest of world	US$130

US Postmaster, please send form 3579 to Nature.
711 National Press Building, Washington DC 20045

Second-class postage paid at New York, NY.
US mailing agent is

Expediters of the Printed Word Ltd ,
527 Madison Avenue,
New York, NY 10022

Cover picture

Vibratory cavitation erosion damage to a copper specimen exposed to a dilute polymer solution.
[D. Hulse, UMIST]

See page 572.

Vol. 262 No. 5569 August 12, 1976

Volume 262 August 12 1976

Aftermath of the Mark VA 525
Energy from warm rocks 526
Adjust, amend and heal 528
USA/Britain/UK energy/In brief/Jukes on mountains 530

NEWS AND VIEWS

Chromatin/Anaesthetics/Radiotelescope/Plasmids/High energy physics/Space/Pheromones/Geophysics 533

ARTICLES

Small-angle scattering experiments on biological materials using synchrotron radiation — *J. Bordas, I. H. Munro and A. M. Glazer* 541
Model for action of local anaesthetics — *A. G Lee* 545
Dietary practices and growth responses as predictors of longevity — *M. H. Ross, E. Lustbader and G. Bras* 548
gag Gene of mammalian type-C RNA tumour viruses — *M. Barbacid, J. R. Stephenson and S. A. Aaronson* 554

LETTERS TO NATURE

Solar neutrinos and solar accretion of interstellar matter — *M. J. Newman and R. J. Talbot, Jr.* 559
Solar neutrinos and galactic contamination of the Sun — *J R. Auman and W. H. McCrea* 560
Climatic effects during passage of the Solar System through interstellar clouds — *R. J. Talbot, Jr, D. M. Butler and M. J Newman* 561
Hard X-ray observations of Circinus X-1 during an outburst — *M. J. Coe, A. R. Engel and J. J. Quenby* 563
New H_2O maser near NGC7538 — *R. Genzel and D Downes* 564
The identity of lunar hydrolysable carbon — *A J. T Jull, G. Eglinton, C. T. Pillinger, G. M. Biggar and B. D. Batts* 566
Implications of metal dispersion from submarine hydrothermal systems for mineral exploration on mid-ocean ridges and in island arcs — *D. S. Cronan* 567
Observation of the interference of neutrons reflected from thin films — *J. B. Hayter, J. Penfold and W. G Williams* 569
Optical methods to select diamonds of very high lattice perfection — *E. M. Wilks* 570
Ordered states in systems of macroscopic particles — *W. van Megen and I. Snook* 571
Polymer effects on microjet impact and cavitation erosion — *R. Y Ting* 572
Leaf cultivar influences composition and ripening of apples — *G. D. Blanpied, L. L. Creasy, V. A. Blak and L. W. Lewis* 574
Watering converts a CAM plant to daytime CO_2 uptake — *T. L. Hartsock and P. S. Nobel* 574
Memory phases in *Drosophila* — *W. G. Quinn and Y. Dudai* 576
Maintenance of fluid volume in the starfish water vascular system — *R. D. Prusch and F Whoriskey* 577
Evolution of responses to relative homozygosity — *J. Seger* 578
Non-random inactivation of X chromosome in the rat yolk sac — *N. Wake, N. Takagi and M. Sasaki* 580
Parallel distribution of sister chromatid exchanges and chromosome aberrations — *N. Ueda, H. Uenaka, T. Akematsu and T. Sugiyama* 581
Communication through fimbriae during conjugation in a fungus — *A. W Day* 583
Induction of "natural killer" cells by BCG — *S. A. Wolfe, D E. Tracey and C. S. Henney* 584
Spleen cells from *Schistosoma mansoni*-infected mice produce diffusible stimulator of eosinophilopoiesis *in vivo* — *A. M. Miller, D. G. Colley and M. P. McGarry* 586

Guide to authors

- Articles are up to 3,000 words in length with at most six displayed items (figures and tables) and may either be reports of major research developments in a subject or broader reviews of progress.
- Letters are brief reports of research of unusual and wide interest, not in general longer than 1,000 words; at most they have three or four displayed items (figures and tables).
- 'Matters Arising' permits occasional short discussion of papers that have previously appeared in *Nature*. There is a limit of 300 words.

Manuscripts may be submitted either to London or Washington. Three typed copies should be submitted, each including lettered copies of figures. Typing (including references) should be double spaced The title should be brief and informative. Pages should be numbered. References, tables and figure legends should start on separate pages. Experimental detail vital to the paper yet which would interrupt the narrative is best placed in the figure legends. Units should conform to the Système International. Greek characters should be identified in the margin on their first appearance. Equations should occupy single lines if possible, exp (a) is preferred to e^a if 'a' is more than one character. Articles should be accompanied by an abstract of not more than fifty words listing the main conclusions.

References are indicated by superscripts in the text. See any contemporary *Nature* for style, but note:

(i) To refer to several references by the same author at once, only one reference number need be given.

(ii) Cite first and last pages.

Abbreviations should follow the *World List of Scientific Periodicals*, fourth ed. (Butterworth, 1963-65). Symposia are often difficult to refer to and only published or soon-to-be-published volumes should be mentioned in references. Their publisher and place of publication should be clearly indicated. 'Personal communication' and 'unpublished work' should be incorporated in the text.

Artwork should be sent with the manuscript and clearly marked with author's name and the figure number. Line drawings to be in Indian ink on heavy cartridge paper, tracing paper or similar materials: thin, shiny, torn or folded material should be avoided. Scales for graphs should be chosen such that simple figures will not occupy an inordinate amount of space. Most figures are reduced to one column width so originals should be about as wide as a page of *Nature*. To enable figures, particularly maps, to be edited in the same style as the text they should contain only essential material. Ideally, an unlabelled original and a labelled copy should be provided: labelling on photographs should, if possible, be avoided entirely. Records, charts etc. which will not reproduce well should be redrawn or simply described in the text. We are always glad to see artwork for possible use on the cover, but cannot guarantee its return.

In order to save on postal expenses we return only the top copy and artwork of manuscripts that we cannot publish.

A fuller guide appeared in *Nature* (**246**, 238; 1973).

Novel approach to the treatment of hydatid disease	*A. I. Kassis and C E. Tanner*	588
Identification of breast cancer transcortin and its inhibitory role in cell-mediated immunity	*L. Amaral and S. Werthamer*	589
Cyclic nucleotide-dependent phosphorylation of intestinal epithelium proteins	*H. R. de Jonge*	590
In vitro inhibition of cyclic AMP phosphodiesterase by cortisol	*J. Schmidtke, Th Wienker, M. Flugel and W. Engel*	593
(—)-Propranolol inhibits the behavioural responses of rats to increased 5-hydroxytryptamine in the central nervous system	*A. R Green and D. G. Grahame-Smith*	594
Decreased uptake of 5-hydroxytryptamine in blood platelets from depressed patients	*J Tuomisto and E Tukiainen*	596
Reduction of quantum contents of synaptic potentials after postsynaptic axotomy	*H. R. Brenner*	598
Re-examination of avian cochlear potentials	*M. Pierson and P. Dallos*	599
Rod–cone mechanism underlying the Purkinje shift	*D. A. Palmer*	601
Effects of enkephalin and morphine on Renshaw cells in feline spinal cord	*J. Davies and A. Dray*	603
Depression of nociceptive and other neurones in the brain by iontophoretically applied met-enkephalin	*R. G. Hill, C M. Pepper and J. F. Mitchell*	604
Changes in amino acid sensitivity during polypeptide 'desensitisation'	*J. Davies and A. Dray*	606
Hypothermia and intolerance to cold induced by intracisternal administration of the hypothalamic peptide neurotensin	*G. Bissette, C B. Nemeroff, P. T. Loosen, A J. Prange, Jr and M. A. Lipton*	607
Pancreatic gastrin in foetal and neonatal rats	*L.-I. Larsson, J. F. Rehfeld, F Sundler and R. Håkanson*	609
Kinetics of reaction in calcium-activated skinned muscle fibres	*D. G. Moisescu*	610
X-ray titration of binding of β, γ-imido-ATP to myosin in insect flight muscle	*R. S. Goody, J. B. Leigh, H G. Mannherz, R T. Tregear and G. Rosenbaum*	613
Phosphorylation of troponin I and the inotropic effect of adrenaline in the perfused rabbit heart	*R. J. Solaro, A. J. G Moir and S. V. Perry*	615
Increase in human skeletal muscle lactate produced by fenfluramine	*M. J. Kirby and P. Turner*	617
Ribosome slowed by mutation to streptomycin resistance	*D. J. Galas and E. W Branscomb*	617
Regulation of ribosomal RNA methylation in a temperature-sensitive mutant of BHK cells	*A J. Ouellette, E. Bandman and A Kumar*	619
Restriction of template capacity of rat liver chromatin by a non-histone peptide from calf thymus	*G. L. Gianfranceschi, D Amici and L. Guglielmi*	622
Independence of plasmid incompatibility and replication control functions in *Staphylococcus aureus*	*R. P. Novick and M Schwesinger*	623
Low angle X-ray diffraction patterns of squid retina	*C R. Worthington, S. K. Wang and C. M Folzer*	626
Corrigendum and Errata		628

Matters arising

Ionic clustering and collagen specificity	*B. B. Doyle, D. W. L. Hukins, D. J. S. Hulmes, A. Miller, C. J. Rattew and J Woodhead-Galloway*	629
Reply	*K. A. Piez and D Torchia*	629
Retinal sensitivity to short wavelength light	*J. Marshall and R. A. Weale*	629
Reply	*W. T. Ham*	629
Exudate-eating and tree-gouging in marmosets	*A. F. Coimbra-Filho and R. A. Mittermeier*	630

BOOK REVIEWS

Black Holes, Quasars and the Universe (H. L. Shipman)—*Paul Davies*	631
Galaxy Formation: A Personal View (John Gribbin)—*John E. Beckman*	631
Principles of Mossbauer Spectroscopy (T C. Gibb)—*G. Longworth*	632
Behavioural Pharmacology (Susan D. Iversen and Leslie L. Iversen)—*Steven Matthysse*	632
The Earlier Stone Age Settlement of Scandinavia (Grahame Clark)—*C. D. Morris*	633
Primary Productivity of the Biosphere (Helmut Lieth and Robert H. Whittaker, editors)—*Peter D. Moore*	633
Obituary	634
Announcements	634
Reader enquiry form	xviii

© Macmillan Journals Ltd 1976

Published weekly
ISSN 0028-0836
Registered as a newspaper at the
British Post Office

London
4 Little Essex Street, WC2R 3LF
Telephone: (01) 836 6633 Telex: 262024
Telegrams: Phusis London WC2R 3LF

Washington
711 National Press Building, DC 20045
Telephone: (202) 737 2355
Telex: 64280

Editor
David Davies

Deputy Editor
Roger Woodham

Editorial Staff

Martin Goldman	Allan Piper
*Sandy Grimwade	Miranda Robertson
Eleanor Lawrence	Fiona Selkirk
Mary Lindley	Chris Sherwell
Peter Milford	Hilary Taphouse
Peter Newmark	Robert Vickers
*Colin Norman	Mary Wade*

*Washington office

Publishing Director
Jenny Hughes

Display advertisement enquiries to:
Richard Webb in the London Office
or to
Mary Wade in the Washington Office
Telex: 64280

Classified advertisement enquiries to:
Advertising Department,
Nature,
4 Little Essex St,
London WC2R 3LF
Telephone (01) 240 1101
Telex 262024

Subscription enquiries to:
Macmillan Journals Ltd, Brunel Road,
Basingstoke, Hants. RG21 2XS
Telephone: Basingstoke 29242

Price

	UK	£35
Surface mail	USA and Canada (air/surface)	US$98
	Rest of world	US$82 50
Airmail	Europe	US$94
	Rest of world	US$130

US Postmaster, please send form 3579 to Nature. 711 National Press Building, Washington DC 20045

Second-class postage paid at New York, NY. US mailing agent is.

Expediters of the Printed Word Ltd.,
527 Madison Avenue,
New York, NY 10022

Cover picture

Frederic and Irene Joliot-Curie making measurements with the Hoffman electrometer in 1935.
[Courtesy Association Joliot-Curie, Institut du Radium, 11 rue Pierre Curie, Paris]

See page 727.

Vol. 262 No. 5570 **August 19, 1976**

nature

Volume 262 August 19 1976

Shadowy threshold		635
Toxic cloud over Seveso		636
Europe's ageing research staffs		638
Chemical weapons/Comecon/In brief/Mellanby on censorship		639
Correspondence		642

NEWS AND VIEWS

Dipolar geomagnetic field/Predation/Plate tectonics/ Ecological model/Trypanosomiasis/Galaxy		643

ARTICLES

Dynamo model of double radio sources	*R. V. E. Lovelace*	649
Actual and anticipated petrographic effects of carbonate undersaturation in shallow seawater	*E. T. Alexandersson*	653
Cellular basis for the T wave of the electrocardiogram	*I. Cohen, W. Giles and D. Noble*	657
Intracellular *p*H and activation of sea urchin eggs after fertilisation	*J. D. Johnson, D. Epel and M. Paul*	661
λ repressor regulates the switch between P_R and P_{rm} promoters	*A. Walz, V. Pirrotta and K. Ineichen*	665

LETTERS TO NATURE

The second highly polarised radio outburst in Cygnus X-3	*J. E. Ledden, P. E. Hodge and H. D. Aller*	669
Competition of neutrino and gravitational radiation in neutron star formation	*D. Kazanas and D. N. Schramm*	671
Detection of interstellar $HN^{13}C$	*R. D. Brown, P. D. Godfrey, J. W. V. Storey and F. O Clark*	672
The second *Z*-propagation window	*D. Jones*	674
Is the Earth expanding?	*J. van Diggelen*	675
Test of the dipolar nature of the geomagnetic field throughout Phanerozoic time	*M. E. Evans*	676
Frequency of foreshocks	*L. Jones and P. Molnar*	677
Semiconductor liquid junction solar cells based on anodic sulphide films	*B. Miller and A Heller*	680
Opto-acoustic spectroscopy of products of continuous photolysis of nitromethane	*M. J. Colles, A. M. Angus and E. E. Marinero*	681
New light on the skull anatomy and systematic position of *Oviraptor*	*H. Osmolska*	683
Hallucial tarsometatarsal joint in an Oligocene anthropoid *Aegyptopithecus zeuxis*	*G. C Conroy*	684
Control of intragroup aggression by male pigtail monkeys (*Macaca nemestrina*)	*M. Oswald and J Erwin*	686
Social and reproductive correlates of parasite ova emissions by baboons	*G. Hausfater and D. F. Watson*	688
Inhibition of *Leishmania donovani* transformation by hamster spleen homogenates and active human lymphocytes	*R. Brun, R. L. Berens and S. M. Krassner*	689
Generation of cytotoxic lymphocytes *in vitro* against autologous human leukaemia cells	*J. M. Zarling, P. C. Raich, M. McKeough and F. H Bach*	691
Sensitivity of H-2-less target cells and role of H-2 in T-cell-mediated cytolysis	*P. Golstein, F. Kelly, P. Avner and G. Gachelin*	693
Immune destruction of virus-infected cells early in the infectious cycle	*S. L. Shore, T. L. Cromeans and T J. Romano*	695
Increased ornithine decarboxylase activity in murine sarcoma virus infected cells	*A F. Gazdar, H B. Stull, L. J. Kilton and U. Bachrach*	696
Single ionic channels induced in lipid bilayers by polyene antibiotics amphotericin B and nystatine	*L. N. Ermishkin, Kh. M. Kasumov and V. M. Potzeluyev*	698

Guide to authors

- Articles are up to 3,000 words in length with at most six displayed items (figures and tables) and may either be reports of major research developments in a subject or broader reviews of progress.
- Letters are brief reports of research of unusual and wide interest, not in general longer than 1,000 words; at most they have three or four displayed items (figures and tables).
- 'Matters Arising' permits occasional short discussion of papers that have previously appeared in *Nature*. There is a limit of 300 words.

Manuscripts may be submitted either to London or Washington. Three typed copies should be submitted, each including lettered copies of figures. Typing (including references) should be double spaced. The title should be brief and informative. Pages should be numbered. References, tables and figure legends should start on separate pages. Experimental detail vital to the paper yet which would interrupt the narrative is best placed in the figure legends. Units should conform to the Système International. Greek characters should be identified in the margin on their first appearance. Equations should occupy single lines if possible, exp (a) is preferred to e^a if 'a' is more than one character. Articles should be accompanied by an abstract of not more than fifty words listing the main conclusions.

References are indicated by superscripts in the text. See any contemporary *Nature* for style, but note:

(i) To refer to several references by the same author at once, only one reference number need be given.

(ii) Cite first and last pages.

Abbreviations should follow the *World List of Scientific Periodicals*, fourth ed. (Butterworth, 1963-65). Symposia are often difficult to refer to and only published or soon-to-be-published volumes should be mentioned in references. Their publisher and place of publication should be clearly indicated. 'Personal communication' and 'unpublished work' should be incorporated in the text.

Artwork should be sent with the manuscript and clearly marked with author's name and the figure number. Line drawings to be in Indian ink on heavy cartridge paper, tracing paper or similar materials: thin, shiny, torn or folded material should be avoided. Scales for graphs should be chosen such that simple figures will not occupy an inordinate amount of space. Most figures are reduced to one column width so originals should be about as wide as a page of *Nature*. To enable figures, particularly maps, to be edited in the same style as the text they should contain only essential material. Ideally, an unlabelled original and a labelled copy should be provided: labelling on photographs should, if possible, be avoided entirely. Records, charts etc. which will not reproduce well should be redrawn or simply described in the text. We are always glad to see artwork for possible use on the cover, but cannot guarantee its return.

In order to save on postal expenses we return only the top copy and artwork of manuscripts that we cannot publish.

A fuller guide appeared in *Nature* (**246**, 238; 1973).

Release of novel prostaglandins and thromboxanes after immunological challenge of guinea pig lung — *W. Dawson, J. R. Boot, A. F. Cockerill, D. N. B. Mallen and D. J. Osborne* 699

ABO blood group determinants with branched cores — *K. Yamashita, Y. Tachibana, S. Takasaki and A. Kobata* 702

Lead competitively inhibits calcium-dependent synaptic transmission in the bullfrog sympathetic ganglion — *T. E. Kober and G. P. Cooper* 704

Type of sensory nerve fibre sprouting to form a neuroma — *M. Devor and P. D. Wall* 705

Swimming in the sea anemone *Stomphia coccinea* triggered by a slow conduction system — *I. D. Lawn* 708

Polarised light-sensitive interneurones in a swimming crab — *L. M. W. Leggett* 709

Aerial gas exchange in Australian arid-zone crab, *Parathelphusa transversa* Von Martens — *P. Greenaway and H. H. Taylor* 711

Calcium couples flagellar reversal to photostimulation in *Chlamydomonas reinhardtii* — *J. A. Schmidt and R. Eckert* 713

Bioconversion of light energy into chemical energy through reduction with water of nitrate to ammonia — *P. Candau, C. Manzano and M. Losada* 715

Cell differentiation without morphogenesis in *Dictyostelium discoideum* — *C. D. Town, J. D. Gross and R. R. Kay* 717

Somatic hybridisation of *Penicillium roquefortii* with *P. chrysogenum* after protoplast fusion — *J. Anné, H. Eyssen and P. De Somer* 719

Molecular imaging of dislocations in 16 chlorocopper phthalocyanine — *Y. Murata, T. Baird and J. R. Fryer* 721

Models for the bacterial iron-transport chelate enterochelin — *B. F. Anderson, D. A. Buckingham, G. B. Robertson, J. Webb, K. S. Murray and P. E. Clark* 722

Erratum 724

Matters arising

B-emission stars and X-ray sources — *P. Harmanec* 725

Environmental effects on alcohol selection by mice — *J. M. Joffe, J. Najman and N. Nettleton* 725

Reply — *C. L. Randall and D. Lester* 726

Molecular structure of NAD — *M. G. Rossmann* 726

Reply — *M. A. Viswamitra* 726

BOOK REVIEWS

Frederic Joliot-Curie: A Biography (Maurice Goldsmith)—*E. H. S. Burhop* 727

Marine Mussels: Their Ecology and Physiology (B. L. Bayne, editor)—*R. D. Purchon* 728

Primitive Sensory and Communication Systems: The Taxes and Tropisms of Micro-Organisms and Cells (M. J. Carlile, editor)—*J. T. Bonner* 729

The Dynamics of Spectroscopic Transitions: Illustrated by Magnetic Resonance and Laser Effects (James D. Macomber)—*R. E. Richards* 729

Trace Element Analysis (V. Valkovic)—*T. S. West* 729

Obituary 730

Announcements 730

Reader enquiry service xv

© Macmillan Journals Ltd 1976

Published weekly
ISSN 0028-0836
Registered as a newspaper at the
British Post Office

London
4 Little Essex Street, WC2R 3LF
Telephone: (01) 836 6633 Telex: 262024
Telegrams: Phusis London WC2R 3LF

Washington
711 National Press Building, DC 20045
Telephone: (202) 737 2355
Telex: 64280

Editor
David Davies

Deputy Editor
Roger Woodham

Editorial Staff
Martin Goldman Allan Piper
*Sandy Grimwade Miranda Robertson
Eleanor Lawrence Fiona Selkirk
Mary Lindley Chris Sherwell
Peter Milford Hilary Taphouse
Peter Newmark Robert Vickers
Colin Norman Mary Wade
*Washington office

Publishing Director
Jenny Hughes

Display advertisement enquiries to:
Richard Webb in the London Office
or to
Mary Wade in the Washington Office
Telex: 64280

Classified advertisement enquiries to:
Advertising Department,
Nature,
4 Little Essex St,
London WC2R 3LF
Telephone (01) 240 1101
Telex 262024

Subscription enquiries to:
Macmillan Journals Ltd, Brunel Road,
Basingstoke, Hants RG21 2XS
Telephone: Basingstoke 29242

Price

	UK	£35
Surface mail	USA and Canada (air/surface)	US$98
	Rest of world	US$82.50
Airmail	Europe	US$94
	Rest of world	US$130

US Postmaster, please send form 3579 to Nature.
711 National Press Building, Washington DC 20045

Second-class postage paid at New York, NY.
US mailing agent is

Expediters of the Printed Word Ltd ,
527 Madison Avenue,
New York, NY 10022

Cover picture

Part of a trumpet. A way of correcting for the acoustical inadequacies of a wind instrument is discussed on page 761.

Vol. 262 No. 5571 **August 26, 1976**

nature

Volume 262 August 26 1976

Which way now for journals? 731
Tennessee valley energy 732
US space/USSR space/In brief/Jukes on recombinant DNA 734

NEWS AND VIEWS

Plutonium/Enkephalin/Meteorite/Ribosome/Mercury/Familial dysautonomia 737

ARTICLES

The distribution of stars around a massive black hole *S. L. Shapiro and A. P. Lightman* 743
Plutonium levels in Kwajelein Lagoon *V. E. Noshkin, R. J. Eagle and K. M. Wong* 745
Identification of phage SP01 proteins coded by regulatory genes *33* and *34* *T. D. Fox* 748
Bacteriophage SP01 regulatory proteins directing late gene transcription *in vitro* *R. Tjian and J. Pero* 753
Nonsense suppressors of *Saccharomyces cerevisiae* can be generated by mutation of the tyrosine tRNA anticodon *P. W. Piper, M. Wasserstein, F. Engbaek, K. Kaltoft, J. E. Celis, J. Zeuthen, S. Liebman and F. Sherman* 757
Systematic approach to the correction of intonation in wind instruments *R. A. Smith and G. J. Daniell* 761

LETTERS TO NATURE

Does Mercury have a molten core? *S. J. Peale* 765
Structure of the extended solar magnetic field and the sunspot cycle variation in cosmic ray intensity *L. Svalgaard and J. M. Wilcox* 766
Glass-rich basaltic sand and gravel within the oceanic crust at 22°N *Scientific Party of the Deep Sea Drilling Project, Leg 46* 768
The post-spinel phase of forsterite *L.-G. Liu* 770
Liquid nitrogen enhancement of partially annealed fission tracks in glass *L. J. Pilione and D. P. Gold* 773
Direct measurement of long range forces between two mica surfaces in aqueous KNO_3 solutions *J. N. Israelachvili and G. E. Adams* 774
Axial, magnetron, cyclotron and spin-cyclotron-beat frequencies measured on a single electron almost at rest in free space (geonium) *R. Van Dyck, Jr, P. Ekstrom and H. Dehmelt* 776
Entropy reduction by motional sideband excitation *H. G. Dehmelt* 777
The low frequency dielectric constant of supercooled water *J. B. Hasted and M. Shahidi* 777
Conformation of Met^5-enkephalin determined by high field PMR spectroscopy *B. P. Roques, C. Garbay-Jaureguiberry, R. Oberlin, M. Anteunis and A. K. Lala* 778
Proton magnetic resonance studies of conformation and flexibility of enkephalin peptides *C. R. Jones, W. A. Gibbons and V. Garsky* 779
Mode of deactivation of the enkephalins by rat and human plasma and rat brain homogenates *J. M. Hambrook, B. A. Morgan, M. J. Rance and C. F. C. Smith* 782
Substance P and analgesia *J. M. Stewart, C. J. Getto, K. Neldner, E. B. Reeve, W. A. Krivoy and E. Zimmermann* 784
Colchicine inhibits mitogenesis in C1300 neuroblastoma cells that have been arrested in G_0 *M. E. Baker* 785
Inhibitory action of glutamic acid on cerebellar interneurones *C. Yamamoto, H. Yamashita and T. Chujo* 786
Growth of transplanted monoaminergic neurones into the adult hippocampus along the perforant path *A. Björklund, U. Stenevi and N.-A. Svendgaard* 787
Progesterone may act at hypothalamus and pituitary by way of enhancement of oestrogen retention *L. A. Reuter and R. D. Lisk* 790

Guide to authors

- Articles are up to 3,000 words in length with at most six displayed items (figures and tables) and may either be reports of major research developments in a subject or broader reviews of progress.
- Letters are brief reports of research of unusual and wide interest, not in general longer than 1,000 words; at most they have three or four displayed items (figures and tables).
- 'Matters Arising' permits occasional short discussion of papers that have previously appeared in *Nature*. There is a limit of 300 words.

Manuscripts may be submitted either to London or Washington. Three typed copies should be submitted, each including lettered copies of figures. Typing (including references) should be double spaced. The title should be brief and informative. Pages should be numbered. References, tables and figure legends should start on separate pages. Experimental detail vital to the paper yet which would interrupt the narrative is best placed in the figure legends. Units should conform to the Système International. Greek characters should be identified in the margin on their first appearance. Equations should occupy single lines if possible, exp (a) is preferred to e^a if 'a' is more than one character. Articles should be accompanied by an abstract of not more than fifty words listing the main conclusions.

References are indicated by superscripts in the text. See any contemporary *Nature* for style, but note:

(i) To refer to several references by the same author at once, only one reference number need be given.

(ii) Cite first and last pages.

Abbreviations should follow the *World List of Scientific Periodicals*, fourth ed. (Butterworth, 1963-65). Symposia are often difficult to refer to and only published or soon-to-be-published volumes should be mentioned in references. Their publisher and place of publication should be clearly indicated. 'Personal communication' and 'unpublished work' should be incorporated in the text.

Artwork should be sent with the manuscript and clearly marked with author's name and the figure number. Line drawings to be in Indian ink on heavy cartridge paper, tracing paper or similar materials: thin, shiny, torn or folded material should be avoided. Scales for graphs should be chosen such that simple figures will not occupy an inordinate amount of space. Most figures are reduced to one column width so originals should be about as wide as a page of *Nature*. To enable figures, particularly maps, to be edited in the same style as the text they should contain only essential material. Ideally, an unlabelled original and a labelled copy should be provided: labelling on photographs should, if possible, be avoided entirely. Records, charts etc. which will not reproduce well should be redrawn or simply described in the text. We are always glad to see artwork for possible use on the cover, but cannot guarantee its return.

In order to save on postal expenses we return only the top copy and artwork of manuscripts that we cannot publish.

A fuller guide appeared in *Nature* (**246**, 238; 1973).

Combination of insulin chains on an anti-insulin antibody–Sepharose column	*M. Klotz and B. Gutte*	791
Increase of glucagon receptors in hyperthyroidism	*S. N. Madsen and O. Sonne*	793
Simultaneous detection of two cell populations by two-colour fluorescence and application to the recognition of B-cell determinants	*J. J. van Rood, A. van Leeuwen and J. S. Ploem*	795
Helper T cells recognise antigen and macrophage surface components simultaneously	*J. W. Kappler and P. C. Marrack*	797
Distribution of β_2 microglobulin and HLA in chorionic villi of human placentae	*W. P Faulk and A. Temple*	799
Human milk samples from different ethnic groups contain RNase that inhibits, and plasma membrane that stimulates, reverse transcription	*M. R. Das, L. C. Padhy, R. Koshy, S. M. Sirsat and M. A. Rich*	802
Role of plasma membranes in stimulation of RNA-directed DNA synthesis	*L. C. Padhy, S. K. Kar, K. K. Rao and M. R. Das*	805
Ion effects on macromolecules in aqueous solution	*M. J. Hey, J. M. Clough and D. J. Taylor*	807
Structural order in chromatophore membranes of *Rhodospirillum rubrum*	*T. Ueki, M. Kataoka and T. Mitsui*	809
Bacterial utilisation of organic matter in the deep sea	*P. M. Williams and A. F. Carlucci*	810
Circadian rhythm of anaerobiosis in a polychaete annelid	*D. M. Scott*	811
Plutonium isotope ratios in polychaete worms	*T. M. Beasley and S. W. Fowler*	813
Occurrence of plutonium and americium in plaice from the north-eastern Irish Sea	*R. J. Pentreath and M. B. Lovett*	814
Presence of a buried mammalian carcass indicated by fungal fruiting bodies	*N. Sagara*	816
Appetitive learning, patterned alternation, and extinction in 10-d-old rats with non-lactating suckling as reward	*A. Amsel, D. R. Burdette and R. Letz*	816
Models and statistics for species diversity	*R. A. Kempton and L. R. Taylor*	818

Errata 820

Matters arising

Nuclear composition of cosmic rays	*L. W. Wilson*	821
The cosmic X-ray background	*G. Steigman*	821
Reply	*P. Carlqvist and B. Laurent*	822

BOOK REVIEWS

Das Spiel: Naturgesetze Steuern den Zufall (Manfred Eigen and Ruthild Winkler)—*I. Prigogine* 823

Invisible Allies: Microbes and Man's Future (Bernard Dixon)—*D. E. Hughes* 824

Ultrastructure and the Biology of Plant Cells (Brian E. S. Gunning and Martin W. Steer)—*Harry Smith* 825

Optics of Thin Films (Zdenek Knittel)—*O. S. Heavens* 825

Obituary 826

Announcements 826

Reader enquiry service xvi

nature

July 1, 1976

Too narrow-minded about energy?

THE gilt text inscribed around the ceiling of Church House, Westminster, speaks of "true light", "lending radiance" and "enduring in the heat" (admittedly "of the conflict"). A highly appropriate setting for Mr Anthony Wedgwood Benn's National Energy Conference last week, to which 470 were invited and at which 56 spoke.

Let it first be said that all those reasonable doubts that such an event could take place without degenerating into a shambles turned out to be unjustified, for which great credit to Mr Benn's chairmanship (and not least his restraint in not intervening in the debate at all himself) and to the speakers who never once exceeded their time limit But there is a world of difference between a well-ordered debate and open government; has Mr Benn done anything beyond ensure that all interested parties had a six-minute airing of the views?

There is no doubt the meeting was valuable in mutual education terms; almost all attenders had at least the courtesy to sit and listen to all contributions rather than break up into factions in the corridor to discuss heaven knows what. But what can Mr Benn and his staff do as a result of it all that he couldn't have done the day before?—for it can reasonably be assumed that he, as an exponent of open government, will have been familiar with all the points raised—even Sir Brian Flowers warning that the Royal Commission on Environmental Pollution will raise serious questions about living with plutonium, and even Mr Enoch Powell's brilliant oratory against any form of energy policy-making as ill-conceived and pernicious.

That Mr Benn and his department will have learnt little new from his conference is really the result of attempting to get too many things in focus in one day. The most incongruous of them was the question of disconnections of electricity and gas for non-payment. This was a bandwagon tailor-made for union leaders to jump on to, and although it provided some stirring talk, it managed to confuse a conference convened to talk about energy policy by diverting attention to matters of social policy, which should not be within Mr Benn's terms of reference.

Another structural weakness of the day was the lack of a challenging position paper. Before the conference everyone had been flooded with documents representing the positions of every conceivable interest, but the Department of Energy had, it seemed, decided to maintain a low profile. Its agenda and discussion paper was little more than a list of subject headings—and even that was largely ignored by speakers.

In hindsight, this was probably unfortunate. What was really needed was a major presentation, perhaps an hour in length and certainly well illustrated (not a slide was shown all day!), skilfully aimed at raising the more provocative issues and setting a more definite tone for the day. Perhaps Mr Benn will try this, as he undoubtedly has plans for future, smaller gatherings.

But whatever the next move is that Mr Benn has up his sleeve, his eventual plans for the gas industry are likely to provide the most sensitive litmus of true commitment to "open government". When Lord Ryder stood up to dismiss as economically senselesss the calls for a competitive restrictive tariff on North Sea gas, he was not only supporting the gas industry itself, but also voicing the majority opinion among institutionally disinterested energy experts. Lord Ryder's reference to a 1976 version of the mad hatter's tea party, and his warning of the dangers of a "wretched cartel with coal and electricity" will ensure one thing at least. If Mr Benn, often accused of a fondness for dogmatism, eventually opts for the recommendations of his political advisers and thus weighs down the nation's only economically sound energy industry, he will need a convincing case to defend himself against allegations of blind adherence to doctrine. While some sympathy must be felt for the coal and electricity chiefs, struggling through a difficult period, on current analyses a gas tax provides a poor solution to their own dilemma, and a poorer answer to the nation's broader, long-term energy problems.

The difficulties of the gas industry perhaps underline a disturbing thread running through the day (and conceivably the result of no strong position paper) the narrow-mindedness of most participants. An unspoken assumption seemed to be that self-sufficiency in Britain was the aim and if we talked about energy in any international forum at all (and almost all didn't) it was to be from a position of independence This was the much more explicit objective, two years ago, of Project Independence in the United States. It assumes that in the long run no foreigners are trustworthy. There is much danger in such chauvinism, which may go down well in some political circles but which could lead to some ridiculously expensive decisions being made in pursuit of xenophobia.

Britain in general depends heavily on importing and exporting and is inevitably vulnerable to the capriciousness of suppliers of raw materials and food. But foreign policy, recognising no alternative to large-scale importing, is aimed at maintaining the appropriate good relations Should energy be an exception to be protected by vast expenditures in research, development and implementation? This is one issue we would like to hear Mr Benn speak more of. □

Genetic manipulation: guidelines issued

The NIH ground rules for genetic manipulation experiments may not mark the end of an unprecedented debate within the scientific community. **Colin Norman** reports from Washington

AFTER two years of controversy and uncertainty, the National Institutes of Health (NIH) last week issued a complex set of guidelines governing the use of a powerful new technique for manipulating genes in living organisms. The guidelines establish safety rules for experiments which may revolutionize biology, but which also provide man with unprecedented ability to alter the characteristics of living things. They are, however, far from being the final word on whether, and under what circumstances, such research should be allowed to go ahead, for they are already being overtaken by events in some places.

On July 7, for example, the City Council in Cambridge, Mass., will vote on a resolution, proposed by the Mayor, which would ban for two years all such experiments at Harvard and MIT. And months of bitter debate at the University of Michigan have resulted in the adoption of regulations there which are more strict than those issued by NIH last week. The focus of the debate is clearly shifting from Washington into the university communities where the research will take place.

Nevertheless, the NIH guidelines will provide important ground rules for genetic manipulation experiments in many institutions, and their impact will extend far beyond the borders of the United States, for they are likely to influence the establishment of guidelines in many other countries. They have been developed by an extraordinary process of self-regulation by the scientific community.

The process began in 1973, when scientists familiar with the nascent technique began to worry about potential hazards associated with its use Their concerns led a committee of the National Academy of Sciences to issue a public statement in July 1974, urging scientists around the world to defer two types of experiments until the hazards have been defined The moratorium lasted until last February, when it was partly replaced by general guidelines recommended by an international group of geneticists which met at Asilomar, California Then an NIH advisory committee, consisting of scientists, took centre stage It laboured hard during most of last year trying to cast the Asilomar guidelines into more specific rules, completing its task by hammering out a set of complex proposals last December The proposals went to NIH Director Donald S. Fredrickson, who called a public meeting to discuss them, solicited the views of numerous scientists and non-scientists, and asked the advisory committee to reconsider some of its suggestions. The guidelines issued last week represent Fredrickson's distillation of the conflicting advice presented to him

They differ a little in detail, but not in philosophy, from the recommendations of the advisory committee. They will allow most planned experiments to go ahead, albeit under strict safety controls, outlawing only a handful of the more hazardous types of experiments They are, however, stricter than the Asilomar guidelines, a fact which Fredrickson suggested means that "the research will go forward in a manner responsive and appropriate to hazards that may be realised in the future". And Dr DeWitt Stetten, Deputy NIH Director for Science and chairman of the advisory committee, argued last week that "the issuance of the guidelines is in no sense an opening of the floodgates, rather it is a closing of the leaks (in the Asilomar guidelines)".

Be that as it may, the guidelines are not even NIH's final say on the matter. Their publication falls under the terms of the National Environmental Policy Act, which means that NIH must prepare an assessment of the potential impact of the research on the environment A draft assessment should be ready by September, and since it will be opened up for public comments before being cast in final form, another round of discussion of the risks and benefits of the research is in store. In the meantime, the guidelines will take effect, governing NIH's support of the research.

New dimension

Why have the guidelines taken so long to produce, and caused so much strife? The answer is that the research offers a spectacular mix of potential benefits and possible hazards, and it opens up an entirely new dimension in biology. The experiments consist, in short, of snipping genes from the DNA of any organism and splicing them into the DNA of another, perhaps entirely unrelated, organism. The resulting molecule—a recombinant DNA molecule—is copied (cloned) each time the new host reproduces, producing large quantities of the transplanted genes. The technique offers a powerful tool for probing the working of genes and their arrangement in complex organisms and, more distantly, it may offer a means of constructing special micro-organisms for a variety of medical, commercial and industrial uses.

But the worry is that the technique allows biologists to breach genetic barriers between species which have evolved over thousands of years. In short, it allows biologists to by-pass the processes of evolution. More specifically, foreign genes inserted into an organism may cause that organism to behave in a dangerous, and perhaps unpredictable, manner. The guidelines thus seek to ensure that micro-organisms bearing transplanted genes are contained in the laboratory.

They spell out our levels of physical containment to be used in such experiments, designated P1 to P4, ranging from use of standard microbiological techniques (P1) to the use of specially equipped facilities akin to biological warfare laboratories (P4). And, as a second line of defence, they spell out three levels of biological containment, EK1 to EK3, which must be used for experiments involving the insertion of genes into a strain of the common gut bacterium *E. coli*—the organism which will be used for most experiments. The levels are as follows:

- EK1—use of standard *E. coli* K12, a laboratory strain of *E. coli* which has been used for genetic experiments for decades Foreign genes are inserted into the bacterium by splicing them into a plasmid (a ring of bacterial DNA which reproduces independently from the bacterium's chromosomes) and reintroducing the recombinant into the bacterium, or by splicing them into the DNA of a bacteriophage which then infects *E. coli* K12.

- EK2—the use of specially mutated strains of *E. coli* or bacteriophage which, according to laboratory tests, are virtually incapable of surviving outside the laboratory so that the recombinant DNA will have less than 1 in 10^{-8} chances of surviving in the natural environment.

- EK3—the same as EK2 except that the survivability has been tested in animals, plants and other environments.

The guidelines assign specific physical and biological safety levels to various types of experiments on the basis of their potential hazards (see box) They also spell out safety rules for experiments involving recombinants formed by splicing genes into the DNA of animal viruses, which are then grown in cell cultures to provide multiple copies of the foreign genes. The final guidelines alter some of the containment levels proposed by the advisory committee, but no substantial alterations have been made.

Cautious approach

How did Fredrickson arrive at his final decision when confronted with such a wealth of conflicting advice? His first, and most fundamental, consideration was simply whether the research should be allowed to go ahead at all, in view of the potential hazards The majority of the commentators on the guidelines recommended that it should, but he was advised to take an extremely cautious approach by two of the most eminent of the commentators, neither of whom intends to conduct experiments with recombinant DNA.

Dr Robert Sinsheimer, chairman of the Department of Biology at California Institute of Technology, argued in a letter to Fredrickson that the experiments present a serious hazard if they breach the genetic barrier between higher organisms (eukaryotes) and lower organisms (prokaryotes). "One need not continue to spin out potential horror stories", he wrote, "the point is that we will be perturbing, in a major way, an extremely intricate ecological interaction which we understand only dimly". As for the guidelines themselves, Sinsheimer stated: "I cannot believe that under these proposed guidelines the organism can be contained. If the work is going on in a hundred laboratories about the United States, performed by technicians, graduate students, etc.; the organism will inevitably escape—and will enter into the various ecological niches known to be inhabited by *E. coli.*" He therefore proposed that all work with recombinant DNA should be performed under maximum containment conditions at a single institution in the United States, and that there should be an intensive effort to seek a microorganism more suitable than *E. coli* for the work.

The other eminent, though more flamboyant, critic of the guidelines, Erwin Chargaff of Columbia University, recommended that all work on recombinant DNA should be halted for at least two years to allow time for the hazards to be assessed Chargaff asked, in a letter published in *Science*, "Have we the right to counteract, irreversibly, the evolutionary wisdom of millions of years, in order to satisfy the ambition and the curiosity of a few scientists?"

The advisory committee did not consider Sinsheimer's or Chargaff's pro-

Guidelines in detail

The guidelines define four levels of physical containment, designated, in order of increasing stringency, P1 to P4, and three levels of biological containment, EK1 to EK3, and assign experiments to them on the basis of potential risk. The following is a summary of containment levels specified for various sources of DNA.

a. Shotgun experiments using *E. coli* as the host

Non-embryonic primate tissue	P3+EK3 or P4+EK2
Embryonic primate tissue or germ line cells	P3+EK2
Other mammals	P3+EK2
Birds	P3+EK2
Cold blooded vertebrates, non-embryonic	P2+EK2
embryonic or germ line	P2+EK1
If vertebrate produces a toxin	P3+EK2
Other cold blooded animals and lower eukaryotes	P2+EK1
If Class 2 pathogen*, produces a toxin, or carries a pathogen	P3+EK2
Plants	P2+EK1
Prokaryotes that exchange genes with *E. coli*	
Class 1 agents (non-pathogens)	P1+EK1
Low risk pathogens (for example, enterobacteria)	P2+EK1
Moderate risk pathogens (for example, *S. typhi*)	P2+EK2
Higher risk pathogens	banned
Prokaryotes that do not exchange genes with *E. coli*	
Class 1 agents	P2+EK2 or P3+EK1
Class 2 agents (moderate risk pathogens)	P3+EK2
Higher pathogens	banned

In all above cases, if DNA is at least 99% pure before cloning and contains no harmful genes, either physical or biological containment levels can be reduced one step.

b. Cloning plasmid, bacteriophage and other virus genes in *E. coli*

Animal viruses	P4+EK2 or P3+EK3
If clones free from harmful regions	P3+EK2
Plant viruses	P3+EK1 or P2+EK2
99% pure organelle DNA, Primates	P3+EK1 or P2+EK2
other eukaryotes	P2+EK1
Impure organelle DNA: shotgun conditions apply.	
Plasmid or phage DNA from hosts that exchange genes with *E. coli*	
If plasmid or phage genome does not contain harmful genes or if DNA segment 99% pure and characterised	P1+EK1
Otherwise, shotgun conditions apply.	
Plasmids and phage from hosts which do not exchange genes with *E. coli*	
Shotgun conditions apply, unless minimal risk that recombinant will increase pathogenicity or ecological potential of the host, then	P2+EK2 or P3+EK1

NB. cDNAs synthesised *in vitro* from cellular or viral RNAs are included in above categories.

c. Animal virus vectors

Defective polyoma virus+DNA from non-pathogen	P3
Defective polyoma virus+DNA from Class 2 agent	P4
If cloned recombinant contains no harmful genes and host range of polyoma unaltered, reduce to	P3
Defective SV40+DNA from non-pathogens	P4
If inserted DNA is 99% pure segment of prokaryotic DNA lacking toxigenic genes, or a segment of eukaryotic DNA whose function has been established and which has previously been cloned in a prokaryotic host-vector system, and if infectivity of SV40 in human cells unaltered	P3
Defective SV40 lacking substantial section of the late region+DNA from non-pathogens, if no helper used and no virus particles produced	P3
Defective SV40+DNA from non-pathogen can be used to transform established lines of non-permissive cells under P3 provided no infectious particles produced. Rescue of SV40 from such cells requires	P4

d. Plant host-vector systems

P2 conditions can be approximated by insect-free greenhouses, sterilization of plant, pots, soil and runoff water, and use of standard microbiological practice.

P3 conditions require use of growth chambers under negative pressure and routine fumigation for insect control.

Otherwise, similar conditions to those prescribed for animal systems apply.

*Classes for pathogenic agents as defined by the Center for Disease Control.

posals during its public meetings, but Fredrickson alluded to them in a lengthy statement published along with the guidelines. Recognising that the breaching of genetic barriers might pose a hazard, Fredrickson nevertheless argued that the research can be controlled so that it is carried out safely. Noting that "the international scientific community . . . has indicated a desire to proceed with research in a conservative manner", and that "most of the considerable public commentary on the subject, while urging caution, has also favoured proceeding", Fredrickson pointed out that there is, in any case, no way to prohibit the research throughout the world. "There is," he added, "no reason to attempt it."

Having decided that there should be no flat proscription on the research, Fredrickson turned to some of the chief concerns raised by the critics of the guidelines. The most prominent concern arises from the fact that most work with recombinant DNA will take place with the *E. coli* K12 bacterium. Since *E. coli* is a common inhabitant of the human gut, many observers have considered it a dangerous choice for the research. In particular, a group of scientists from the Boston area urged that a different host for transplanted genes be developed, and that the use of *E. coli* be phased out as swiftly as possible.

Fredrickson argues, however, that since the bacterium has been used for decades as the geneticists' workhorse, there is extensive knowledge of its behaviour and, moreover, there is good evidence that it is unlikely to survive for long in the environment in competition with wild strains of *E. coli*. In other words, *E. coli* K12 itself provides a level of biological containment. "I believe that because of this experience, *E. coli* K12 will provide a host-vector system that is safer than other systems", Fredrickson argued, and he declined to set a limit on when it should be phased out of the research.

Another area of concern with the proposed guidelines centred on how they should be implemented, and that section has been extensively revised. The guidelines strictly apply only to research supported by NIH, and investigators must comply with them before they can receive a grant. Some commentators suggested that principal investigators be required to obtain informed consent from all laboratory personnel before proceeding with recombinant DNA experiments, but Fredrickson opted instead for a requirement that the investigators simply inform all laboratory workers of the real and potential hazards associated with the experiments.

The guidelines also require that each institution where recombinant DNA experiments will be conducted should establish a biohazards committee, to ensure that facilities meet specified requirements, training is adequate and so on. The advisory committee had firmly recommended that such committees should not be responsible for determining the containment conditions for specific experiments, but Fredrickson deleted that prohibition, leaving the matter up to individual institutions.

A final point concerning implementation which is clearly worrying many people is that the guidelines do not apply to industry. Early last month, however, Fredrickson briefed officials from various industries on the guidelines and received from them expressions of support for their intent and their general provisions. Some officials expressed reservations about specific items, however, such as the provision prohibiting large-scale experiments with recombinant DNA, and the Pharmaceutical Manufacturers' Association has decided to convene a committee to review whether the guidelines are applicable to the drug industry.

Effect of guidelines

Now that these guidelines have been issued, how do they affect academic scientists conducting, or hoping to conduct, recombinant DNA experiments? First, they specify that many experiments should use EK2 or EK3 biological containment, and until crippled micro-organisms which meet those criteria are available, such experiments should not be conducted. The advisory committee which drafted the guidelines is responsible for certifying whether crippled strains meet the criteria.

A strain of *E. coli* produced by Roy Curtiss of the University of Alabama (called χ1776) has been proposed as an EK2 system with two specific plasmids (pSC101 and Col El-*kan*). Curtiss, who has built many crippling mutations into the bacteria in an effort which took the best part of a year, has provided the committee with reams of data on its survivability. Last month, a subcommittee voted unanimously that the strain meets the EK2 specifications, and the full committee is expected to approve it in the next few weeks. That would pave the way for many experiments.

But a confusing situation has developed with respect to two other candidate EK2 strains. At its last meeting in April, the committee approved a strain of bacteriophage lambda, developed by Philip Leder of NIH as an EK2 strain. But a subcommittee which met last month to consider a second candidate strain, developed by Fred Blattner at the University of Wisconsin, was divided on a matter which affects both strains. In short, two subcommittee members refused to endorse the use of either phage as an EK2 system unless they are used in conjunction with crippled bacteria. The full committee will take up that thorny issue when it next meets in September. Curtiss's *E. coli* strain, incidentally, is resistant to infection by phage λ

Many of the objections and reservations which critics have levelled at the guidelines are now beginning to crop up in local debates in and around the universities where the research will be conducted. In that regard, the situation brewing in Cambridge, Mass., may be an indication of things to come It began quietly a few months ago, when some researchers at Harvard proposed that a laboratory, meeting P3 requirements, be established in the Harvard Biology Labs. The facility, which would cost some $350,000, would have involved converting some existing laboratory space, and the intent was to undertake a variety of work in it, including some recombinant DNA experiments.

The proposal met with opposition within Harvard, however, largely because the biology labs are old, infested with cockroaches and with a species of ant which has so far evaded attempts at eradication. In short, critics suggested that the building is unsuitable for a P3 facility. Their criticisms broadened into an assault on the proposal to conduct recombinant DNA experiments at Harvard, however, and the dispute spilled over into the city when the matter was reported at length in Boston's weekly newspaper.

Approval of the laboratory by the Harvard authorities was all but assured, since the concept had been endorsed by a biohazards committee, Harvard's Committee on Research Policy, and the Dean of Arts and Sciences. But, when he read about the dispute in the newspapers, Cambridge city Mayor Alfred Velucci stepped in. He called a council meeting on June 23—ironically the day the NIH guidelines were issued—to discuss the matter, and a string of scientists testified about the potential hazards and benefits of recombinant DNA research By all accounts, the atmosphere was highly charged, and there was considerable heated discussion.

The matter has now gone well beyond the issue of whether the laboratory should be built, however, for Velucci has introduced a resolution which would prohibit all recombinant DNA experiments in Cambridge—even those deemed to have minimal risk—for two years. The council will vote on the resolution on July 7, and the outcome will be closely watched around the country. ☐

news and views

Prediction of volcanic activity and climate

from P. M Kelly and H. H. Lamb

CURRENT interest in climatic change has stemmed from the growing awareness that man's activities are everywhere circumscribed by his environment, and in particular, by the vagaries of climate. The fluctuations of weather and climate in most parts of the world have been increasingly troublesome in the past 20–25 yr. This has happened partly because of an apparently real increase in the variability from year to year, or from one group of about 5 yr to the next, which has affected the Indian monsoons and temperatures and rainfalls in middle latitudes of both hemispheres, and partly because the growth of population and the rationalisation of agriculture towards specialisation in one-crop economies in various regions has increased vulnerability to weather. Climatic change has provided a control on human affairs in certain regions in the past and now, with the ever increasing economic interdependence of nations, its effects must be considered in future planning in all spheres—industrial, social and economic. Unfortunately this need for climatic forecasts cannot yet be adequately catered for by meteorologists or climatologists, who are still trying to determine the causes of climatic change by study of the limited climatic record.

In recent years much evidence, both theoretical and observational, has been put forward suggesting that the amount of volcanic dust in the upper atmosphere may be the major control of climatic change during the postglacial. Stratospheric dust effectively reduces the amount of solar energy reaching the Earth's surface where this energy is made available to the atmospheric circulation and variations in the amount of this pollutant, caused by the varying frequency and magnitude of explosive volcanic eruptions, may produce corresponding fluctuations in the nature of the atmospheric circulation and climate. If this hypothesis is correct, prediction of climate will first necessitate prediction of volcanic activity. Although great steps are being taken in the forecasting of volcanic activity on time scales of days, prediction of volcanic activity on time scales of years and decades has been considered a remote possibility (and perhaps considered by many a distinct impossibility).

In last week's issue of *Nature*, Roosen *et al.* (**261**, 680; 1976) attempted to determine one cause of fluctuations in volcanic activity on time scales of centuries and provided a possible tool for the forecasting of tectonic activity and climate. They postulate that changes in the degree of tectonic activity may arise from variations in the rate of change of lunar tidal stress effects on the Earth's core and crust. Calculation of the long term variation of the tidal stress reveals a cycle of about 179 yr due to resonance effects arising from shorter period variations in the lunar orbit. There are many references to a cycle of about this length in the literature concerning climatic change, although in most cases the length of record analysed has been too short to evaluate the statistical significance and precise period of this fluctuation; its existence is not well-established Spectral analysis of the Camp Century, Greenland ice core δO^{18} record reveals a cycle of about 180 yr and Roosen *et al.* claim that 13% of the variance of the δO^{18} record can be explained by the derivative of the tidal stress curve during the period AD1200 to AD1970. The correlation breaks down during the periods AD1420 to AD1530 and AD1650 to AD1700, an effect which the authors tentatively attribute to dominance of the effect of the exceptionally low degree of solar disturbance during those spans of years.

Roosen *et al.* note that a cycle of about 180 yr has been observed in variations in solar activity, thereby providing an alternative explanation for this variation in climate. Therefore, before the climatic cycle of 180 yr can be used for forecasting purposes, it is essential that its existence be confirmed by analysis of other long climatic records and that its cause, solar and/or tectonic, be defined.

Research related to the past record of climate and the apparent causes, and rapidity, of climatic fluctuations and changes is being undertaken by scientists in many fields other than climatology. This is providing a great stimulus with many opportunities of increasing knowledge and verifying diagnoses as new data and new techniques of measurement and analysis are put forward. It is important that collaboration between workers in all the fields involved in the study of climatic change be initiated and fostered. A multidisciplinary approach is needed, both to compile the evidence of the facts of the past climatic record and to solve the problems of the causes of climatic change, which seem to extend from the Earth's core to the Sun (and, on the longest time scales, to the Galaxy beyond). Only from the work of organisations, ranging from the powerfully equipped mathematical laboratories of the atmospheric, oceanographic and Earth sciences to academic institutes and meetings where diverse specialists can be brought together, will the knowledge and understanding needed to develop sound advice on probable future climatic development be attained The specialists will include agriculturists and forestry research workers, palaeobotanists, geologists and, in some cases, archaeologists and interpreters of ancient texts and inscriptions. ☐

Activation analysis *in vivo*

from Keith Boddy

The Second East Kilbride Conference on Progress and Problems of *In vivo* Activation Analysis, organised by the Scottish Universities Research and Reactor Centre, was held on April 6–9, 1976.

DELIBERATE induction of radioactivity in animal tissues was reported in *Nature* almost 27 yr ago and some 12 yr have passed since the feasibility of *in vivo* neutron activation analysis in man was demonstrated. The technique involves exposure of the total body or the relevant region of the body, such as the thyroid, liver, spine or limb, to a low dose of neutrons and measurement of either the induced radioactivity or the prompt gamma rays emitted during irradiation. Total body *in vivo* neutron activation analysis (TBIVNAA) is a unique method providing direct and simultaneous measurements of the total body content of calcium, phosphorus, nitrogen, sodium and chlorine. Similarly, there are partial body methods (PBIVNAA) for determining the total thyroid content of iodine, calcium and phosphorus in sections of bone or cadmium and copper in the liver. The reproducibility of measurements is generally 2–4%, permitting the detection of relatively small changes in body composition due to disease or treatment, the patient being examined on an outpatient basis.

It was clear from the increasing number of centres using, or proposing to use, *in vivo* activation analysis and from the wide range of clinical applications described at the conference that the potential of the technique in medicine is being realised. Several groups are using TBIVNAA in examinations of osteoporosis, osteomalacia, renal failure, hyperparathyroidism and endocrine dysfunctions. Regional measurements of calcium in bone are being made in some of these disorders and of thyroid iodine in hyperthyroidism

The facilities at Brookhaven National Laboratory, New York, comprising 14 sources each of 50 Ci Pu–Be distributed along the anterior and posterior body surfaces for irradiation and the sophisticated whole-body counter using 54 sodium iodide detectors, were described by S. H. Cohn A wide variety of clinical studies are in progress: in thalassaemia, for example, gross depletion of skeletal calcium (50%) has been measured.

J. H. Fremlin (University of Birmingham) and his colleagues use a cyclotron for clinical measurements involving delayed gamma-ray emission and also for prompt gamma-ray analysis of total body nitrogen using hydrogen as an internal standard, as well as for the detection of cadium in liver. In regional analyses, spinal calcium is measured. The feasibility of determining copper and ion in liver in pathological situations has been demonstrated using PBIVNAA, and preliminary studies of their measurement by nuclear resonance fluorescence were described.

W. B. Nelp (University of Washington) and H. E. Palmer (Battelle Northwest Laboratories, Washington) and coworkers also use a cyclotron in a wide range of clinical studies. The technique of measuring total body calcium using the reaction ^{40}Ca (n,α) ^{37}Ar, first demonstrated by Palmer, in which the exhaled gas is collected, purified and counted in proportional counters, is now in clinical use. To measure calcium alone, smaller radiation doses can be used and whole-body counting is not required. This technique has also been adopted at Birmingham and at the Memorial Sloan Kettering Cancer Center, New York (J. S. Laughlin). The rate and completeness of exhalation of ^{37}Ar has been examined in detail by several groups. Although the exhalation pattern found was obviously complex, there was preliminary evidence that the technique was reproducible and could estimate total body calcium quantitatively in man.

The Medical Research Council cyclotron at Hammersmith Hospital is used by T. Spinks and colleagues for similar studies, and in some cases they measure calcium in the hand and the rate of removal of induced ^{24}Na.

In the system used at the University of Toronto by K. G. McNeil and J. E. Harrison, 12 sources each of 5 Ci of Pu–Be are distributed only about the thorax and lumbar region of the patient, precluding absolute measurements of total body content. But calcium and sodium indices have been derived, relating the expected counting-rates of these elements to body habitus, and the measured counting rate in the patient is compared with that expected as an indicator of normality. This approach has been used in various clinical disorders. Measurement of nitrogen *in vivo* is also being attempted by the prompt gamma-ray method.

At East Kilbride, K Boddy's group uses scanning irradiation with two sealed-tube 14-MeV neutron generators and a scanning shadow-shield whole-body counter for TBIVNAA. Changes of body composition in rheumatoid arthritis during treatment with non-steroid analgesics and with corticosteroids have been studied. The nuclear reactor is used to measure the thyroidal content of iodine in hyperthyroid patients, as M. J. Hooper (Western Infirmary, Glasgow) reported. A technique of "compound irradiation" with mixed neutron beams has been developed to improve the uniformity of activation in partial body calcium measurements.

A facility using two californium-252 neutron sources each of 200 μg for partial body *in vivo* neutron activation analysis, developed by the East Kilbride group, is being used for clinical studies by M. A. Smith and colleagues at the Western General Hospital, Edinburgh. A much larger californium-252 source of 3 mg is used by A. D. LeBlanc and colleagues at Baylor College and the NASA/Johnson Space Centre, Houston, in a facility for measuring regional changes in skeletal calcium in man and whole-body measurements of small animals. A facility described by B. Mazière (CEA, Orsay), uses two sources each of 200 μg of ^{252}Cf together with four sources each of 10 Ci of ^{238}Pu–Be for the simultaneous measurement of calcium and phosphorus in the hand.

Many participants felt it was desirable to be able to compare directly the results from different centres. A proposal by Palmer to establish an international intercomparison, based on anthropomorphic phantoms containing human skeletons, to be measured "blind" by the various groups and subsequently analysed chemically, was received enthusiastically. Palmer and Boddy were appointed co-chairmen with the task of establishing the interlaboratory comparison. ☐

Influence of grazing

from Peter D Moore

SOME controversy surrounds the degree of influence exerted by man's grazing animals on the vegetation of the arid parts of the world. There is much room for argument and speculation simply because there is a paucity of factual information, particularly regarding the history of vegetation development. The processes at work have taken considerable periods of time—many millennia in the case of the Middle East—and the separation of climatic and anthropogenic influences often proves impossible in attempts to assess the underlying factors which have determined the structure and composition of extant vegetation Some effort has recently been made to approach the problem from the point of view of excluding grazing animals and observing the development of plant communities within exclosures. But at best, such experiments will take many decades before any important conclusions can be drawn, and it is possible that some species will no longer be in a position to reinvade such experimental plots.

The problems faced in such places as North America and Australia are rather different from those of the Old World in that the history of man's pastoral activity is much shorter and is generally well documented. In such conditions there is a better chance of elucidating any changes in vegetation which have occurred during this time One approach which has recently been used is the analysis of population age structure in selected arid shrubs. If grazing pressures have severely influenced seedling survival, it should be possible to demonstrate that the younger shrubs are present at lower densities than would be expected for the maintenance of overall population levels. Crisp and Lange (*Oikos* **27**, 86; 1976) describe just such a study which they have undertaken on the shrub *Acacia burkittii* at Koonamore Station, a sheep-grazing area of southern Australia

Sheep grazing began at Koonamore in the 1860s at a density of 0.4 sheep ha^{-1}, and it is recorded that within 50 yr the vegetation had become badly degraded. In 1925 an area of this range (400 ha) was fenced to exclude rabbit and sheep grazing and studies of consequent vegetation change have been carried out. Some permanent plots were marked out and within these the *Acacia burkittii* has become established. As a result precise ages are known for several of these shrubs. On the basis of this knowledge, Crisp and Lange have produced a linear regression of a bush size index (height plus diameter) against age. Even in the absence of annual growth rings this permits the estimation of shrub age on the evidence of its size, though data are available only for shrubs less than 42 yr old. Similar calculations were made for a stem girth/age relationship and it was assumed that a linear extrapolation could be made from this to estimate the ages of the older shrubs (maximum calculated age was about 250 yr).

These figures can be used for the examination of the age structure of *Acacia* populations, and this has been done both in regions with almost a century of sheep grazing in their history and also in those which have experienced no sheep grazing, but only that of rabbits. Population histograms from all sites examined show high frequencies of shrubs of a century in age, but lower frequencies of younger shrubs. In a stable situation we would expect younger individuals to be at least as frequent as older ones up to the development of senescence. Reduced frequency of juveniles can often be correlated with the commencement of sheep grazing in the latter part of the nineteenth century, though rabbit grazing presents a complicating factor. In one site where there has been no sheep grazing, but only rabbit grazing, there is still a reduced frequency of shrubs in the 25–50 yr age group. Where grazing has been maintained to the present, the occurrence of *Acacia* shrubs less than 50 yr old is very low, or such juveniles are absent. Where sheep grazing was curtailed in 1925, there is a high frequency of young individuals, in spite of continued rabbit grazing.

There are several possible explanations for the form of these histograms apart from the sheep grazing effect. It is possible that a change in a climatic factor about 100 yr ago reduced the survival potential of *Acacia burkittii.* Crisp and Lange claim that reproduction in this shrub is not significantly affected by rainfall, but it is possible that the population of a natural predator of the seeds or seedlings, vertebrate or invertebrate, may be so influenced. There is also a possibility that *Acacia burkittii* is not a climax adapted species, but occupies a temporal niche in a successional development. There are many instances on record of species which invade and may even dominate a habitat for several decades during the course of succession but which fail to maintain viable populations in competitive conditions. For example, birch (*Betula pendula*) in temperate European forests invades areas after catastrophes and produces even aged populations. Twenty or 30 yr after invasion, the age structure of the population would look very similar in its basic shape to that of *Acacia,* for seedling establishment under a birch canopy is very poor in this species. Some successional dominants, such as *Typha latifolia* (McNaughton, *Ecology,* **49,** 367; 1968) secrete compounds which directly inhibit seedling germination which has the advantage of reducing self-competition.

Such alternative explanations, however, do not explain how the removal of sheep grazing can so profoundly increase the recruitment of new seedlings into the *Acacia* populations By far the simplest explanation is the one propounded by Crisp and Lange, that the introduction of sheep grazing in addition to natural predation and increasing rabbit predation, has placed an unacceptable demand on the regeneration potential of *Acacia burkittii.* The forecast from this data is that as time proceeds and older shrubs senesce and die, there will be little or no replacement and *Acacia* will become scarce. The implications of this for the general ecology, hydrology and pedology of these areas are of course unknown. ☐

Purine and pyrimidine metabolism

from A. C. Allison

A symposium on Purine and Pyrimidine Metabolism was held at the Ciba Foundation on June 9–11. The proceedings will be published early in 1977 by Elsevier/Excerpta Medica/North Holland.

So far most effort has gone into mapping metabolic pathways and their genetic control, and detailed information about purine synthesis in bacteria and fungi is now available. Much less is known about control in mammalian cells, but inherited deficiencies of enzymes of purine metabolism continue to yield interesting information. It has been known for some years that deficiency of hypoxaxthine-guanine phosphoribosyl transferase leads to excessive uric acid excretion and abnormal function of the central nervous system, including compulsive self-mutilation. This enzyme catalyses one of the salvage pathways of purine synthesis: the other depends on adenine phosphoribosyltransferase, and the clinical manifestations of deficiency of this enzyme in three patients, belonging to two families, were described by A. Simmonds (Guy's Hospital, London), working in collaboration with K. J. van Acker (Antwerp) and P. Cartier (Paris). In these patients adenine cannot be reutilised and is metabolised to 2,8-dihydroxyadenine which, being very insoluble, crystallises in the urine. The resulting stones can be confused with uric acid stones. The children have no neurological defect and respond well to allopurinol treatment.

Other inherited defects of purine metabolism are associated with immunodeficiency Purine nucleoside phosphorylase deficiency affects mainly thymus-dependent lymphocytes, whereas adenosine deaminase deficiency affects bone marrow-derived lymphocytes as well. W. N. Kelley (University of Michigan, Ann Arbor) reported that adenosine deaminase is present in a highly active small form (molecular weight 36,000), an intermediate form (114,000) and a large form (298,000). In human lymphocytes stimulated by mitogens T. Hovi (University of Helsinki) has found an early and sustained increase in *de novo* purine synthesis, and immunosuppressive drugs such as azathioprine and methotrexate inhibit this pathway.

These and other observations raise the possibility that purines can control not only purine synthesis (already well established) but also pyrimidine synthesis and even nucleic acid and protein synthesis. For example, when purine nucleotide levels in mammalian cells fall, nucleolar polymerase A activity declines and precursor ribosomal RNA is no longer synthesised. ADP-ribosylation of proteins may represent a major controlling system.

Another new idea that was discussed was the role of purines, especially ATP and adenosine, as neurotransmitters. This was enthusiastically expounded by G Burnstock (University College, London) and could have important implications in neurological diseases related to purine metabolism. ☐

Magnetic dating

from a Correspondent

For more than two decades, palaeomagnetists have been studying the magnetisation of rocks in order to construct polar wandering curves and to define the nature of recent secular variations of the geomagnetic field. Although this work is far from complete, the interest within the subject is turning increasingly towards using such observations in reverse, that is to use the magnetic properties of sediments, archaeological artefacts and so forth, as means of dating the different processes which have affected these materials by comparison with the increasingly well established magnetic chronology. This changing emphasis has been indicated by two recent meetings in the Department of Geophysics and Planetary Physics at the University of Newcastle upon Tyne. One was concerned with the possible application of palaeomagnetic techniques to sedimentological problems (held on May 14) and the other (held on January 8–9) with the status and development of the application of the same techniques within archaeology.

The meeting of geological interest was concerned chiefly with the formation of haematite within sandstones. It is well known that it takes some 5 to 10 Myr for rock debris in modern desert environments to change in colour to the reds associated with ancient desert sediments. B. Waugh (University of Hull) reported evidence on the different reactions involved in this breakdown, which has obvious implications for the time at which the haematite is formed and therefore the actual date of the magnetisation compared with the rock itself. Many red sediments seem to carry a magnetisation which is unrelated to this coloration as the pigment is too fine grained, but D W. Collinson (University of Newcastle upon Tyne) presented convincing evidence that in some red beds, the stable magnetisation is associated with the red pigment rather than detrital particles. Studies of Devonian sediments from Scotland, described by F. Turner (University of Aston) and R. Archer (University of Newcastle upon Tyne) showed that haematite formation in such desert sediments can be delayed for as much as 100 Myr, the diagenetic changes presumably being inhibited by a high initial organic content. If this is so, then magnetic dating of the formation of the haematite may also provide the age at which the release of liquid hydrocarbons from these lacustrine sediments finally ceased.

M. Noel (University of Newcastle upon Tyne) discussed the way in which the magnetic remanence and fabric change during deposition, thus leading to an improved understanding of the sedimentological processes and determining the original fabric of a rock before it is compacted and subjected to tectonic stresses. There was also some discussion of the way in which palaeomagnetic techniques could assist in the dating of dolomite formation (M. Tamar-Agha, University of Newcastle upon Tyne) and the identification of past environments, such as the determination of current flow when more standard markers are absent

The archaeological meeting was initially concerned with instrumental developments, reported by participants from the University of Newcastle upon Tyne, that now make possible much faster measurement of the remanence (L. Molyneux) and other magnetic properties of materials (A. de Sa), but also mean that a wide range of materials (D. H. Tarling) previously regarded as virtually non-magnetic, can be examined for their potential use in archaeomagnetic studies. Results from Bulgaria (M. Kovacheva) and Japan (K. Hirooka) were particularly interesting as they seem to indicate a synchroneity of behaviour in both areas. If this is confirmed, it suggests that a significant part of the secular variation of the geomagnetic field is attributable to 500 and 1,500-year wobbles of the main dipole. R. Thompson and N. Abrahamsen (Universities of Edinburgh and Aarhus, respectively) described studies of sediments, particularly in present-day lakes, which suggest that other components of secular variations are very localised and not attributable to the westward drift of the non-dipole field.

The meeting, however, was not so concerned with the implications of these studies for the origin of the Earth's magnetic field, but mainly with the ways in which sediments, although not ideal recorders, can be used to monitor geomagnetic changes and thus can be used for archaeomagnetic dating. One surprising feature was that sand-sized sediments seem to be better recorders than fine clays over achaeological time, as A J. Clark (Ancient Monuments Laboratory) reported, although the opposite seems to be true of geological deposits. There was discussion of the implications of geomagnetic changes on the climate (N.-A. Mörner, University of Stockholm) and production of ^{14}C (J Klein and H. Tauber, Universities of Pennsylvania and Copenhagen, respectively). Some correlations seem to exist, but it is difficult to determine how these processes interact with each other. Changes in the total magnetic moment of the Earth should only have minor affects on the ^{14}C inventory and it seems possible that any climatic response to changes in the height of the ionosphere may be the main agent in varying the interchange of carbon between its different reservoirs.

Both meetings tended to concentrate on the significance of the increased use of sediments in palaeomagnetic studies. There are obviously major problems in understanding the complex processes involved during deposition and it will be increasingly possible to study such behaviours magnetically, but it is also obvious that extreme care has to be taken in the use of sedimentary magnetisation for precise determination of previous geomagnetic properties. ☐

A hundred years ago

We publish below a correspondence which we cannot but regard with the greatest satisfaction; Government has at last seen it to be its duty to act upon the recommendation of the Duke of Devonshire's Commission, and make a substantial contribution towards the endowment of pure scientific research. We need scarcely remind our readers that from the first we have maintained that such endowment is the duty and interest of civilised states.

from *Nature*, 14, 185, June 29, 1876

200 years of American science

Reflections on 200 years of science in the United States

Nathan Reingold

Smithsonian Institution, Washington, DC 20560

In spite of its obvious importance today, the history of the sciences in the USA is usually neither the subject for research nor part of courses taught by non-American historians. Nor is this history known and understood, particularly in Europe. This is in marked contrast to an avid interest in current US science policies and developments, which cannot be wholly explicable without an understanding of their historic origins. Broadly speaking, these origins are US variants of certain western European traditions resulting, as it were, in cults of knowledge, nation, and people. Science and scientists have flourished, but uneasily, in the resulting environment.

EARLIER this year a British historian of science wrote to me to say he was giving a few lectures on the institutional history of American science before 1914 in his course. I was astonished. Hardly any non-American historians do research or display interest in science in the USA; presumably their courses reflect this. An East German has a few pieces dealing with astronomy; a Dutch historian this year published an article on a nineteenth century American physicist; a few years ago, British geologists did a multi-volume history of geomorphology, a field they defined as overwhelmingly derived from US geologists.

In contrast, there is no shortage of writings and courses outside the USA on science policy or sociology of science with strong emphasis on recent events in America. Nobel Prizes are counted, statistics marshalled, and very current trends analysed. In this dispensation, science in the USA starts with a contemporary occurrence—the Mansfield Amendment, Sputnik overhead, the atom bomb, or the arrival of refugees from Hitlerism. But research and development in the USA is important on a global scale. It did not spring up overnight but was the result of a complex, fascinating historical metamorphosis. In 1776 the British North Americans, south of former French Canada, had one great investigator, Benjamin Franklin, and a handful of others we can denote as scientists. By 1900 the new nation had essentially evolved a vigorous scientific community with many of the basic structural and functional characteristics so evident today. This included strong commitments to fundamental research in various fields. In the present century these characteristics produced what is now so visible. It is a meaningful historical movement, not simply a banal success story, and deserves critical scrutiny by scholars. Rather than give a recital of great names and notable contributions, or genealogies of institutions, let us consider the sciences in America as a set of historiographic problems particularly worth studying in comparative prospect.

Influence of De Tocqueville

Americans and Europeans are still influenced by De Tocqueville's *Democracy in America* (1835). The work is best described as a hortatory essay to the French in the form of an account of a mythical country perversely given the name of a real republic on the continent of North America. Noting the absence of the usual landmarks of European history—kings, churches, nobles, castles, dynastic squabbles and sectarian wars—De Tocqueville concluded that the mechanism of American history was different, a vast arena for the smooth workings of impersonal dynamic laws. He approved this lack of romance, drama, and great trends because of the desire to avoid the disruption of revolutions. This view recurs in the influential writings of Henry Adams, the descendant of Presidents who cast a jaundiced eye both on his society and on the consequences of science. That he thought America and China were alike in this sense says much about his insight into both histories. Like the immigrant myth of gold in American streets to explain prosperity, this Newtonian line of reasoning aborted analysis; change simply occurred, obviating any need for study of the prior actions of men and institutions.

De Tocqueville noted the presence of energetic go-getters intent on acquiring wealth, and he met no savants, devotees of abstract thought who required a niche immune from daily pressures in a hierarchical aristocratic society. A democratic society was technologically oriented and indifferent to basic research. In fact there were scientists in *ante-bellum* America. Someone like Nathaniel Bowditch, the translator of Laplace, or Joseph Henry at Princeton, might have dented his certitude. Or going forward in time to a school chum of Henry Adams, the mathematical physicist turned idealist philosopher, Charles Sanders Peirce, was every bit a grand savant. And there were others.

De Tocqueville did not say there would be no science nor great pure scientists in the United States. Applied science would yield bits of basic science—that is, he was of an older view that did not see basic science as logically and chronologically anterior to technology. And by chance a great pure scientist might arise in the American republic. De Tocqueville believed that pure science ideally required the individualism, the drama of an aristrocratic order. Although he was wrong in predicting a steady-state country (and Henry Adams in seeing the heat death of entropy), De Tocqueville had grasped an important truth. The western European ideal of a value-free science independent of society would take different forms in the USA. One can argue the extent to which this ideal was realised in Europe; the structured society of its nations, at the very least, permitted the illusion of realisation. Great men, ideas, great events existed, at least figuratively, in isolation. In the USA, their analogues were often bathed, if not immersed, in social, political, economic, and ideological realities.

To this day, many American scientists incline to the view that their society is indifferent, if not hostile, to basic science, in spite of ample evidence of the growth over time of support for research, even of the most abstruse nature. A proper perspective on this peculiar attitude is a comparison with literature, music and art. Once they too were presumed blighted by the American environment. A democratic society could support popular or vernacular cultures but not high cultures. No one makes this accusation any more in art, literature, or music. They flourish in symbiosis with the popular culture. Only in science is there uneasiness and sensitivity, obviously a phenomenon of great importance.

'Old West' influence

Early in the 1850s the aged Alexander von Humboldt wrote approvingly of American efforts in a wide range of physical and biological topics related to geography. Because he wanted Americans to receive greater international visibility, Joseph Henry of the Smithsonian Institution suggested preparing what eventually became the Royal Society's catalogue of scientific literature of the last century. As Henry originally limited the work to the exact sciences, he clearly had more than scientific geography in mind. Although the first series of the catalogue to 1863 disclosed that roughly 5% of the authors were from the USA, Europeans were not impressed. By the end of the century American activity in the earth sciences loomed large. Although an extension of Humboldt's view, geology reeked of the romance of the Old West, so attractive to generations of man-boys on both sides of the Atlantic. It did not hurt that the leader of the geological community in American was John Wesley Powell, whose hand was lost at Shiloh in the Civil War and who had first explored the untamed Colorado. Powell's other role as a pioneer ethnologist only heightened the effect. Although very creditable, the scientific exploration of the West was like the rumoured gold in the streets, something waiting there. It did not impress those interested in mathematical and experimental fields. But only by 1951–52, did a French geologist, Emanuel de Margerie, produce his two volume *Etudes américaines*. A few works noted that astronomy had become a very active discipline in the USA by 1900.

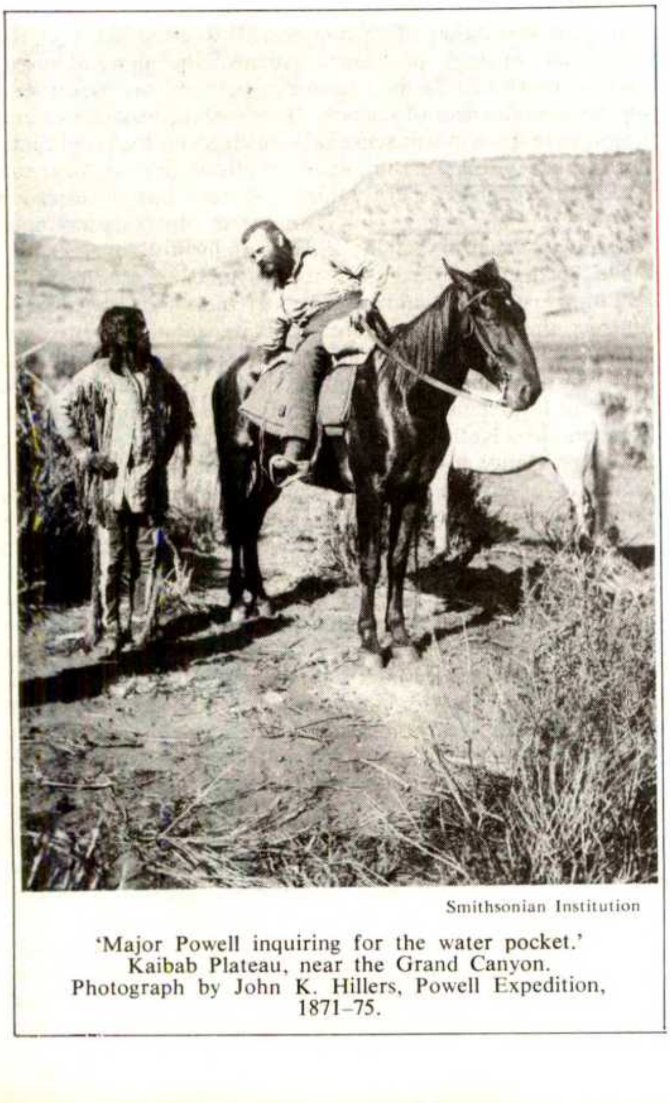

Smithsonian Institution

'Major Powell inquiring for the water pocket.'
Kaibab Plateau, near the Grand Canyon.
Photograph by John K. Hillers, Powell Expedition, 1871–75.

Shortly after that date, a significant act of recognition occurred. Reacting to the founding of the Carnegie Institution of Washington and the Rockefeller Institute, the Germans founded the Kaiser Wilhelm Gesellschaft. In the years before the First World War, a number of German observers commented favourably on the quality and scale of the sciences in the USA, warning against the threat to German hegemony in research. Apparently, the familiar competition of Britiain and France was less worrisome. One of the Carnegie beneficiaries, the astrophysicist George Ellery Hale, added Rockefeller funds and built the great 200-inch telescope at Mount Palomar. That great instrument and E. O. Lawrence's pre-Second World War cyclotron symbolised science in the USA to many on both sides of the Atlantic. Large scale reflected the natural endowment; great instrumentation reflected the supposed American propensity for 'practical' devices, not for the abstruse theorising of true savants. Attributes of Hale and Lawrence reinforced these stereotypes. Hale was a fabulous promoter and organiser, a veritable Morgan or Rockefeller of science; Lawrence, also a manipulator, went on to invent a television system. Usually overlooked were scientists of a different mould. A contemporary of Hale's, the great geneticist Thomas Hunt Morgan used the fruit fly in a series of austere, rigorous experiments. With a passion for scientific exactitude, he shunned empire building and applications. When Hale and Robert A. Millikan invited Morgan to the California Institute of Technology, they initially envisaged a programme of science applied to medicine; Morgan insisted on pure research. Although the USA was a world power in the sciences when Morgan went to Pasadena, a generation passed before a sustained serious historical research began and then largely because of the events of the Second World War and their consequences.

The emergence of American science

This 200 years of history is not explicable by any assumptions of American singularity. Like the nation, the sciences in the USA are part of western civilisation. The thirteen rebellious colonies were a provincial outpost of this civilisation. It is not wholly accidential that the first college in this country was founded in 1636 in Massachusetts Bay Colony in a village named Cambridge. Modern science originated in western Europe and developed an eastern wing in Russia and a western one in the USA. In spite of the obvious influence of British (and French) science, the most interesting comparisons and relations of the research scene in these former colonies of the UK are with Germany and the Soviet Union, a point to which I will return.

Because of its origins as a provincial outpost of western Europe, the USA was never properly described as a young country, that is, a country lacking the kind of history associated with the cultures of the European nations. More precisely, the USA had never experienced a youth consisting of dynastic and sectarian violence, a rigid class structure, and an all-powerful established church. It was born to adulthood in the sense of having many of the trappings of modernity. To conservatives, the lack of the usual traditions and their detritus was a basic flaw; to liberals and radicals their absence was a glorious opportunity. With some exceptions, both were sceptical about developing a high culture of science in a democratic environment.

In 1776, the USA was not a blank slate. Selectively, patterns of life and thought of seventeenth- and eighteenth-century

Europe flourished and persisted; in time they became Americanised, diverging from a western Europe undergoing its own reactions to intellectual and economic changes. At the same time, a kind of feedback from these European developments prevented any gross cultural split between the populations on both sides of the Atlantic. In the USA there was an avid pursuit of the European printed word. Even modest cities of the Mississippi valley in the *ante-bellum* era possessed a good number of books and journals. Young scientists visited Europe, and many went on to study at overseas universities. A Louis Agassiz came in 1846, as did many others in the last century. The German emigrés of the 1930s were simply an instance in a two-century-old process. In 1973 about 6,000 scientists and engineers emigrated to the USA. At all times in its history a minority of the scientists were foreign born.

Scientific heritage

The colonists in revolt insisted they were only asking for their just rights as Britons, even though most in the UK probably did not see the rights in that way. Facing western Europe, American investigators regarded science as part of their heritage; ruthlessly and cynically they brought over the ocean whatever they wanted of this scientific heritage, disregarding any plaints about the European nature of the best of science. Being provincials in the eyes of western Europe, they were often infuriated by patronising treatment. In fact, American scientists were still vexed by patronising Europeans as late as the years between the two world wars. Yet, from the very beginning, American investigators wanted nothing as much as the good opinions of their peers in Europe; at the same time many strongly desired to present their results as a symbolic return to Europe for the great gift of science.

Because of this ambiguous relationship with European science, the American scientific community developed a differing pattern of nationalism and internationalism than their overseas counterparts. Let us disregard the fatuous cliché that "The sciences were never at war". It is a meaningless truism applicable to sets of concepts and data, not communities of humans. Real, live scientists usually rise and salute when the flag is raised, especially during wartime. Even in peace, national differences and rivalries influence the behaviour of scientists. Being outside the rivalry between the French and Germans after Sedan and not sharing the British anguish that Perkin discovered the dye but Germany garnered the industry, American scientists could work very comfortably in an international setting. At the same time, national interests were never totally absent.

Another differing pattern arising from colonial roots is the development of a cult of the people, substituting for king, nobility and gentry. In a post-First World War movie about a hack senator trying for the presidency, William Powell in the title role makes a campaign promise to give a Harvard degree to every American at birth. Mass culture, like dreams, sometimes disclose suppressed beliefs. Just as scientists (and conservative critics) were uneasy about the lack of a proper hierarchy and widely agreed on norms, the American public had qualms about status based on education. Contrary to popular belief, the nation inherited a class system from Europe and still displays a social stratification based on wealth. Contrary to De Tocqueville, quite a number of families retained high status over many generations, in some instances even constituting a patriciate. This is in spite of a significant degree of upward mobility in the past for all groups with the notable exception of those of African descent. Yet classlessness is widely assumed in the form of crowding to a middle position.

Education

Education can provide a status countering classlessness. Traditionally, expertise is highly valued here. At the same time, it is one of the glories of American history that the learned have much power and honour but lack the certainty of an assured niche. When historians turned to the history of the sciences in America, they noted that scientists wanted an elite, meritocratic basis for their group, often rejecting the validity of public intrusion into their affairs. Filled with such historiographic problems, I spent a year in Britain in 1964–65 studying British analogues of my favourite nineteenth-century American scientists. An acquaintance in the Civil Service, now deceased, invited me to lunch at the Athenaeum Club. As I looked around, he said, "This is like your Cosmos Club in Washington". But I knew differently. Just a few days before I had read in manuscript a letter from an officer of the Royal Society to a council member, then little known. Charles Darwin was invited to the Athenaeum for lunch to discuss a matter before the Society. From my readings of many manuscripts, I had already concluded that in comparison to these British scientists, my American 'elitists' were raving egalitarians. Even if they had not been infected with republican or democratic principles, a continuing establishment control was not feasible given the size and complexity of the USA.

Smithsonian Institution

Charles Sanders Peirce (1839–1914).

Just as wealth conferred status over generations, so did education and intellectual attainments. Family groupings of scientists appeared in the last century. For example, modern geodesy was brought to the USA by the Swiss–American Ferdinand Rudolph Hassler. A generation later the Nova Scotia born mathematical astronomer Simon Newcomb married a Hassler. Their daughter became the wife of W. J. McGee, the geologist and anthropologist who was one of John Wesley Powell's lieutenants. Charles Sanders Peirce's father and brother were professors of mathematics at Harvard. J. Willard Gibbs' father (of the same name) was a professor of languages at Yale. William James' father was a Swedenborgian philosopher, undoubtedly a surprise to his teacher, the physicist Joseph Henry. A present foreign Fellow of the Royal Society is a third generation scientist.

These family groupings have never constituted an intellectual aristocracy because of the rapid growth of the scientific community over the past two centuries. A founder of the Institute for Advanced Study, the mathematician Oswald Veblen's father studied physics at John Hopkins during its golden age; he later taught at a midwestern university. Oswald's uncle Thorstein became a great social theorist. They were a family of Norwegian immigrant intellectuals. A small town in South Dakota produced two notable physicists, E. O. Lawrence and Merle Tuve. The so-called new immigration from eastern and southern Europe by now has yielded scientists of Jewish, Italian, Slavic and other ancestries. In spite of the persistence and importance of a few families as sources for recruits, the scientific community has never been a closed group. The newest immigrants from Asia are entering the various disciplines. By now about 5% of science and engineering doctorates are of Asiatic origin. Fifteen years of consciousness raising may very well result in an inflow of Blacks, women, Chicanos—even some more American Indians.

In the USA, scientists are overwhelmingly a middle class group. In spite of individuals from the upper class and some from the lower, becoming a scientist until recently was a means of going from the lower to the upper middle class. At present such social mobility seems on the wane. If true, it is all the more important to study that portion of the middle class producing the bulk of the professional classes which provides an essential element of stability in the USA. Relatively little is known about such families in contrast to concern for the genteel culture of the patriciate or the pains and traumas of the poor and the outcast. As scientists are less numerous, they are more accessible to research than other professional groups. Where family influences are lacking, we still do not know why a small minority of middle class youngsters in the past opted for scientific careers, until very recently a choice of limited remuneration and power.

Perhaps the youngsters acted because they, like most Americans, adhered to a cult of knowledge. Here the comparisons between the USA, Germany, and the Soviet Union are important. For more than half of its history, the USA was unknowingly in a race with Germany. Early in the eighteenth century, nearly 150 years before the UK, the Prussian state made elementary schooling compulsory and universal for males. With the later expansion of German universities, the British were fated to be overtaken. The Germans trained large numbers for particular niches in their society, each niche with a specific place in an elaborate hierarchy. The professoriate were an elite of elites, having gone beyond the doctorate in their habilitation, a point the Americans did not quite grasp when graduate schools arose under the influence of German higher education. What American scientists did note was the high status of the German professoriate. In Prussia each chair holder was a higher civil servant. American scientists often hungered for the same kind of assured high place in their own nation.

Throughout the nineteenth century Americans expanded all levels of their education system; in retrospect, they were trying to match Germany. The statistics are not very clear but, apparently, around 1900, the time Germans became conscious of an American threat, the USA had surpassed Germany in numbers, at least. Quality was another question. American universities were largely viewed as an extension of the democratic thrust to provide a responsible electorate. Some institutions viewed themselves in a patrician sense, as training cultured gentlemen for service to the society. Typically, even the mass schools regarded themselves as engaged in both cultural uplift and in a service role. The sciences served both purposes. Mass plus quality tended to become the ideal.

A number of examples. In the middle of the large state University of Illinois at Urbana before a library with nearly four million books is a plot of corn planted to remind all of the university's origin as a land grant school for agriculture and mechanic arts. When the University of Chicago opened its doors in 1891, it was a great university. This oft repeated judgment refers to its scholarly research strength. But its President, W. R. Harper, at the same time launched an extension programme of correspondence and evening courses. The Professor of Mathematics at Chicago, Eliakim H. Moore, the first pure mathematician elected to the National Academy of Sciences, received an honorary doctorate from Göttingen early in this century. He conceived his authority to extend from research in pure mathematics to supervising the training of elementary school teachers of arithmetic. Moore, Chicago, Illinois—like many other American institutions and individuals —wanted theory and practice, culture and service, elite and mass somehow combined or in juxtaposition.

The Soviet Union and the USA are probably the only remaining countries still believing in some form of the idea of progress, a Marxist version in one, and Enlightenment variant in the other. The two countries have curiously parallel histories in the sciences. Both were Humboldtian because of the need to manage their large land masses. Both turned engineering into mass professions of high status. The Russians have won the numbers race in that category, a more serious fact than mere heft of armed might. The USA lagged behind Russia in pure mathematics, and may still. Russian universities have a much different role in the sciences. Centralisation is greater in the Soviet Union, whereas egalitarian instincts limit centralisation in the USA. Our society has a primal urge to replicate anything deemed desirable. In addition, strong anachronistic sentiment for rusticity ultimately works against the big. Rusticity is something the Russians shun.

Besides the idea of progress, the cult of knowledge in the USA has other traces of the seventeenth and eighteenth centuries now largely absent from western Europe. By establishing much of the broad form and content of what now designated science, the Scientific Revolution defined some concerns as non-knowledge and started segregating the high culture of the sciences from the vernacular culture. But the useful arts partially escaped this exclusion until the nineteenth century. At the same time the casual amateur and the modest practitioner were increasingly displaced by the savant. (Significant scientific amateurism probably survived longer in the UK and the US than in Europe.) The scientific revolution gave form to a previously rather loose, amorphous conglomeration; and the Industrial Revolution hardened the new pattern.

Much of this process had by-passed the British North American colonies. The vernacular, the non-science, the amateur and the applied, survived and flourished after independence when the high culture of science began a slow steady growth. Europeans established a scheme of things in which there was a congruence between social, intellectual, and institutional hierarchies. Not a perfect congruence, but enough to avoid many of the problems of the Americans. On the western side of the Atlantic, the heritage of the past and the thrust of historical development did not neatly separate grand savant and practitioner; theoretician and earnest mechanic; the abstruse and the vernacular. They were scrambled together. A persisting tension developed between the scientific elite and their perception of fundamental research and the mass community and their thrust for diffusion of knowledge (often older and sometimes applied). As a result, the cult of knowledge in the US encompassed a research ideal, but not a basic research ideal in spite of all the exertions of many generations of scientists.

In this research ideal was a blurred boundary between theory and practice. Originally, religion provided a basis for pure research. The idea of design presupposing the existence of a Designer readily yielded a drive for research untrammelled by sordid motives. Secularisation purged the theological mission, leaving a pure research ideal. At the same time the old, general notion of the utility of knowledge was elevated by this association with a designing deity. All research carried out His purpose and disclosed His will. Only overly rationalistic, sensitive scientists worried about the problems of defining discrete forms of research styles and goals.

Although a happy compromise, even before the Civil War, American scientists launched a counter strategy, to fractionate off basic research by establishing enclaves largely immune to the national tendency to conflate theory and practice.

Higher education often served as the site of these enclaves. A notable recent example is the Institute for Advanced Study. As it were, the scientists were levying an overhead charge for theoretical science against the gross national product. Many were uneasy about the more common mode of supporting theoretical science, which also appeared before the Civil War. This is to define applied missions so as to necessarily include a basic research component. In the 1920s Harvard's E. H. Hall (of the Hall Effect) corresponded with C. J. Davisson (a future Nobel Laureate) of Bell Telephone Laboratories. Impressed by Davisson's work, Hall sent the head of the Laboratory, H. D. Arnold, a letter praising the company's enlightened support of basic research. Nothing of the sort was intended, Arnold replied; we are simply interested in ways of increasing the supply of electrons. Sweeping mandates like this are widely present in so-called mission-related research. Believing sincerely in their approach, the scientists still argue in favour of broad definitions of applied missions. But many also favour protected enclaves for basic research not subject to the vagaries of economics, international affairs, public health policies and the like. Yet, it is naive to hope for and expect immunity from the ebb and flow of history.

In spite of $32 billion for research and development in 1974, in spite of over a half million engaged in research and development, in spite of $4 billion for basic research, US scientists are still uneasy about their place in society. There is an overwhelming cult of the nation with dominating symbols—George Washington, the flag, the national anthem, Abraham Lincoln, the Statue of Liberty. Science is not represented among the symbols of the cult of the nation; even technology once had the iron horse and Thomas Edison. And our country has just gone through ten terrible years raising nagging doubts about progress. Largely because of the anti-science quirks of Lyndon Johnson and Richard Nixon, inflation has eroded the real strength of the national research budget.

From the vantage point of my ivory tower, I find prospects encouraging, starting with President Ford's increase in the budget to make up some of the slippage from the Johnson and Nixon years. American scientists have always functioned well while loudly complaining. Even before the Civil War, they demonstrated great talents as entrepreneurs, improvisers and artful dodgers. Nor am I nonplussed by the predicted numbers of surplus PhDs. Except for about fifteen post-Second World War years and perhaps a few years before the Great Depression, there has always been a surplus of scientists on paper. A surplus can act as a stimulus, both on the nation and on individuals.

Whatever happens, the course of the sciences in the USA will remain an arena of tensions and ambiguities, a historical movement in which prosaic reality turns out to be a symbol, often exhilarating, sometimes grotesque, occasionally a black comedy. It has been a history of trying to have one's cake and eat it. But perhaps that is true of all of the past 200 years of our national life.

I thank the US National Endowment for the Humanities for support.

The rise of 'prostituted' physics

Spencer R. Weart

Director, Center for History of Physics, American Institute of Physics, 335 East 45th Street, New York, New York 10017

"From its origins to the present day, American academic science has been permeated by the influence of American business". The reciprocal influence, of science on business and industry, has grown dramatically in the twentieth century. The rise of industrial research and its sustained vigour during this period is charted.

"WE are tired of seeing our professors degrading their chairs," physicist Henry Rowland told the American Association for the Advancement of Science in 1883, "by the pursuit of applied science instead of pure science . . . lingering by the wayside while the problem of the Universe remains unsolved"[1]*.

Like other leaders of science he was struggling to create in the universities a spirit of pure research, free from the dangerous temptations of commerce. The task proved hopeless: from its origins to the present day American academic science has been permeated by the influence of American business. The reciprocal influence of the colleges and universities on business was for a long time not as important—nor could it be, given the small size of the scientific community. For example, in 1900 there were slightly over 200 academic physicists in the USA[2]. They were already more numerous there than in any other single country, but were still too few to have much effect; the great advances academic physics made in the nineteenth century were usually put to practical use by semi-educated inventors and entrepreneurs. The number of physicists was, however, doubling every ten or twelve years. Over the next four decades academic physics, and science in general, entered into a new relationship with American industry. It was a relationship that became essential to the strength of both partners (for a general treatment and bibliography of US industrial research see ref. 3).

It was true, as Rowland complained, that during the nineteenth century some American professors were almost too familiar with the requirements of industry. Sometimes they would give free advice, as Joseph Henry and others gave Samuel F. B. Morse during his efforts to develop the telegraph. At other times they would take a fee. American colleges and universities were chronically poor, and their typical professor could neither enjoy a comfortable salary nor look forward to any pension whatsoever; nor did he have a particularly high status in his commercially-oriented society. Small wonder if he was more likely than his colleagues in Europe to pick up some income on the side. Even Rowland, when he discovered that he had diabetes and would soon be leaving his family on their own resources, took to inventing and consulting for industry. Yet the scientists remained first and last professors, working as consultants only occasionally. This was, as W. David Lewis has said, the "putting out" stage of American industrial research[4].

Around the end of the nineteenth century the universities grew greatly, becoming powerful, independent suppliers of

---

*Fuller documentation and much more detail will be found in Spencer Weart, *The Physics Business in America, 1919–1940. A Statistical Reconnaissance*," available from myself in preprint; to be published in a collection of essays on the sciences in America, edited by Nathan Reingold[10]. For unpublished sources this study has relied chiefly upon the manuscript, microfilm, and oral history archives of the Niels Bohr Library, American Institute of Physics, New York (AIP).

research. Industrial companies worked to encourage this development, although their contributions were small compared with the funds supplied by the governments of the various states, by tuition-paying students, and by affluent philanthropists. Nevertheless American business had a key role in this process; for example, it was from modern industrial ventures that most of the philanthropists derived their wealth.

But the universities, however strong they became, could not meet all the needs of the science-based industries which were growing rapidly around the turn of the century. C. E. Kenneth Mees, called by George Eastman to create a laboratory within the Eastman Kodak company, later explained why it was difficult for a company to have all its research done in universities. Industrial research requires persistence along particular lines of inquiry, he said, with specialised apparatus and training; this was difficult to obtain in a university and conflicted with the needs of teaching. Moreover, "the universities do not understand the requirements of the manufacturer and the manufacturer distrusts, because he does not understand, the language of the professor"[5].

The idea of solving these problems by transplanting academic scientists into business organisations seems to have originated with scientifically-trained men already working for the manufacturers. Industrial laboratories of a sort had existed for years, originally for quality control and testing, a little later for engineering and development work to improve existing products. But in 1900 General Electric established a new sort of industrial laboratory in which research was no longer tied to the day-to-day requirements of production (Fig. 1). The GE laboratories were followed within a dozen years by a number of others, notably those of Du Pont, the American Telephone and Telegraph company, and Kodak.

The professors, following Rowland's tradition, were less than enthusiastic about this development. Frank Jewett, who eventually became president of the Bell Telephone laboratories, recalled that his university mentor Albert A. Michelson "thought that when I entered industrial life . . . I was prostituting my training and my ideals"[6]. Such attitudes made it more difficult for industries to hire good staff. When GE tried to bring Willis R. Whitney from the Massachusetts Institute of Technology to head their new laboratory, they had to promise him that he could split his time between GE and MIT. After a period of commuting back and forth Whitney became so absorbed in the challenges of industrial research that he gave up his professorship[7]. This turned out to be a common experience: young scientists who moved reluctantly into industrial work soon found that it caught all their interest. Mees even warned that a lab director should take steps to keep his workers involved with the progress of pure science, lest they become too narrow[8].

Fig. 1 The first research laboratory of the General Electric company—a barn behind C. P. Steinmetz's house, about 1900.

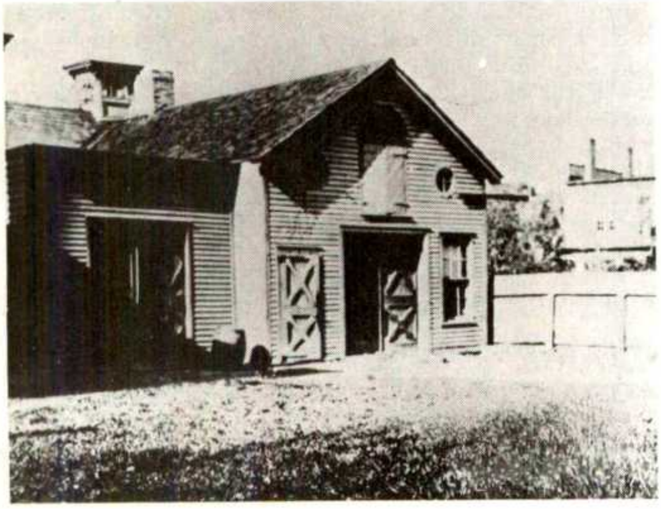

If industrial research was clearly established in the USA in 1910, it still could not be called a major movement. But by the 1920s broad changes were becoming apparent. There was, as one physicist noted with some distaste, an enormous advance of applied physics—in industry, in government laboratories, even in the universities themselves—a "fever of commercialised science"[9]. In 1913 physicists who were located in industrial labs made up only about a tenth of the membership of the American Physical Society. In 1920 they made up a quarter of the membership and this advance took place while the total membership of the society was doubling (my calculations, taken from *Bulletin of the American Physical Society*). The proportion of papers published in the leading American journal, *Physical Review*, which originated in industrial laboratories showed a similar fundamental increase (2% in 1910, 14% in 1915 and 22% in 1920) (my calculations and ref. 10). These facts substantiate what many men were claiming at the time: the relationships between physics and industry in America were revolutionised around the time of the First World War.

The trend was already evident before America entered the war, but the war itself was widely believed to have had a central role in accelerating the transformation. Around 1917 many physicists left their campuses, but not for the Front; for them, as for most Americans, the great event of the war was a fierce intensification of industrial organisation and production. Industrialists and scientists were thrust into closer contact with one another, both at the production level and at higher levels in Washington. The result was that industrialists and physicists alike become more aware of what could be done with physics. As one industrial physicist put it after the war, "Bankers have become science-minded. They are familiar in general with the influence of scientific research on the trend of security prices." They had come to esteem science, for in "commercial warfare . . . research supplies the ammunition"[11].

Research no longer meant simply development work aimed at cutting costs and improving an existing product. In some industries it had become essential to do the sort of research, sometimes verging on basic research, which could produce an entirely new product or could keep a company supplied with information and patents for defence against new products developed elsewhere. For example, both General Electric and the American Telephone and Telegraph company were able, thanks chiefly to the trained physicists in their laboratories, to maintain a strong position when the new field of radio communication emerged around the time of the First World War. It was such large companies that had the main role in industrial research; GE and ATT alone employed some 40% of all the American Physical Society members in industry between the two World Wars (my calculations, the mean of the fractions at 5-yr intervals over the period 1920–39).

The presence of trained scientists also brought a company various indirect benefits. Publicity and prestige were perhaps chief among these. As one knowledgeable observer bluntly stated, "The use of real or imaginary research laboratories to back up merchandise . . . has an importance to company prestige that cannot be exaggerated"[12]. This was only true, of course, because the 1920s were a golden age of scientific faith, not only among scientists and industrialists but also for the public at large. The *Nation* complained in 1928 that "A sentence which begins 'Science says' will generally be found to settle any argument in a social gathering, or sell any article from toothpaste to a refrigerator" (quoted in ref. 13).

For all these reasons a good market for trained physicists developed in industry. One straw in the wind was Ernest Fox Nichols, a prominent professor of physics who had worked for the Navy during the war and who in 1920 resigned from Yale to join GE. "The position," he informed the university as he departed, "offers complete freedom in the choice of research problems, and places at my unhampered disposal such human and material resources as no university I know of can at present offer"[14]. He might have added that industrial salaries left the universities far behind. Fears were expressed that the ranks of academic science would be decimated by the movement into industry.

Some academic scientists responded by defending the old ideals of pure, non-commercial research. The physicist in a college or university had his own rewards. "Financially his lot is not a wealthy one," as one of them admitted "nor socially is he high . . . [But] Close to nature and by it closer and closer every day to the Almighty God who made him, what matters it to the physicist if the days be dull or neighbouring man uncouth? His soul is more or less aloof from mortal strife"[15]. In short, it was all very well to go into industry if money was your object, but there was still something morally superior about the life of academic research.

In the end the schools were not drained but strengthened by the growth of industrial physics. For it was far less the established physicist who was snatched up than the new graduate. This meant that industry was supporting an increase in student enrolments which must have had much to do with the overall rise of academic physics departments between the two World Wars. Many physics teachers felt that their departments would be strengthened by attracting students destined for industry. Applied physics courses or programmes, sometimes labelled "engineering physics", were set up by physicists at a number of schools in the early and mid-1920s.

Industry took not only undergraduates trained in physics but also PhDs. Around 1900 only a tenth of the few PhDs graduating each year in the USA wound up in industry; in the 1920s about a fifth of the ever increasing number of new PhDs were going into industry (my calculations: the sample of new PhDs was drawn from ref. 16. For convenience I used Marckworth's original file cards, at AIP. Locations from *Bull. Am. Phys. Soc.*, and Cattell, J. M., *American Men of Science* (Science Press, New York, 1906–1944)). For research—where the quality of the personnel is everything—the leaders of industrial laboratories had concluded that the best workers were those with graduate training. To select and attract these recruits they had to have close contacts with the professors who were training students. This made for strong ties between industry and the campuses[17].

This also gave industry a new motive for supporting research in the universities. Through such support a company could keep its eye on promising young men while at the same time keeping abreast of scientific developments. For example, Corning Glass sponsored fellowships and research at Cornell, Illinois, MIT and Purdue on problems of chemical physics directly related to glass making. Such arrangements were probably rather common. In the absence of outright fellowship or grant support, a company could still contribute in smaller ways and keep up close relations; among the acknowledgments in papers published in the *Physical Review* in the 1920s one finds frequent thanks given to companies for the loan or construction of pieces of apparatus or the use of their laboratories.

All this led some to feel that the universities were "beginning to be led by the industries, instead of vice versa" (Pupin[18] apparently regarded this trend favourably). But in so far as the point was to train researchers, the exact nature of the research was secondary. Freedom of inquiry in universities was not seriously infringed on by the support industry gave; rather the possibilities for inquiry were broadened all around.

So it seemed that all was going well, and that aside from minor jealousies American physicists, industrial and academic, were advancing hand in hand in uninterruptible progress. Then came the Great Depression. When a system is struck by a heavy shock, we may hope to learn something; by listening to the seismic echoes we may study hidden internal structures. The Great Depression gives us an opportunity to do this for American physics.

The first thing to note is that academic physics did not suffer greatly. Often the professors had to accept some cut in pay, but since deflation was raising the value of the dollar, academic salaries did not drop in real terms. The research budgets of many university physics departments showed a pronounced increase in real terms through the 1930s. It is true that there were hiring freezes, and this meant that for two or three years during the worst of the Depression, few of the new PhDs could find academic jobs. But most of them simply stayed on at their schools, doing research, and found positions after the situation eased. Total US academic employment in 1938 was about 30% higher than in 1928.

The industrial physicists had a different experience, as Fig. 2 suggests. The graphs show swift growth during the

Fig. 2 *a*, Total non-farm employment in the USA, 1920–40, millions of people[19]. *b*, Research workers in a sample of US industrial laboratories. The figure for 1921 is raised by 23% as recommended by Perazich and Field[20]. Solid line is for all research personnel, thousands of people; dotted line is for physicists only (× 15). To the Perazich and Field sample I add the physicists in Bell, GE and Westinghouse laboratories; for Bell I use my counts from the APS *Bulletin*, and for the other two I use National Research Council, *Industrial Research Laboratories of the United States* (compiled by Hull, C.) (National Academy of Sciences, Washington, 1921–38).

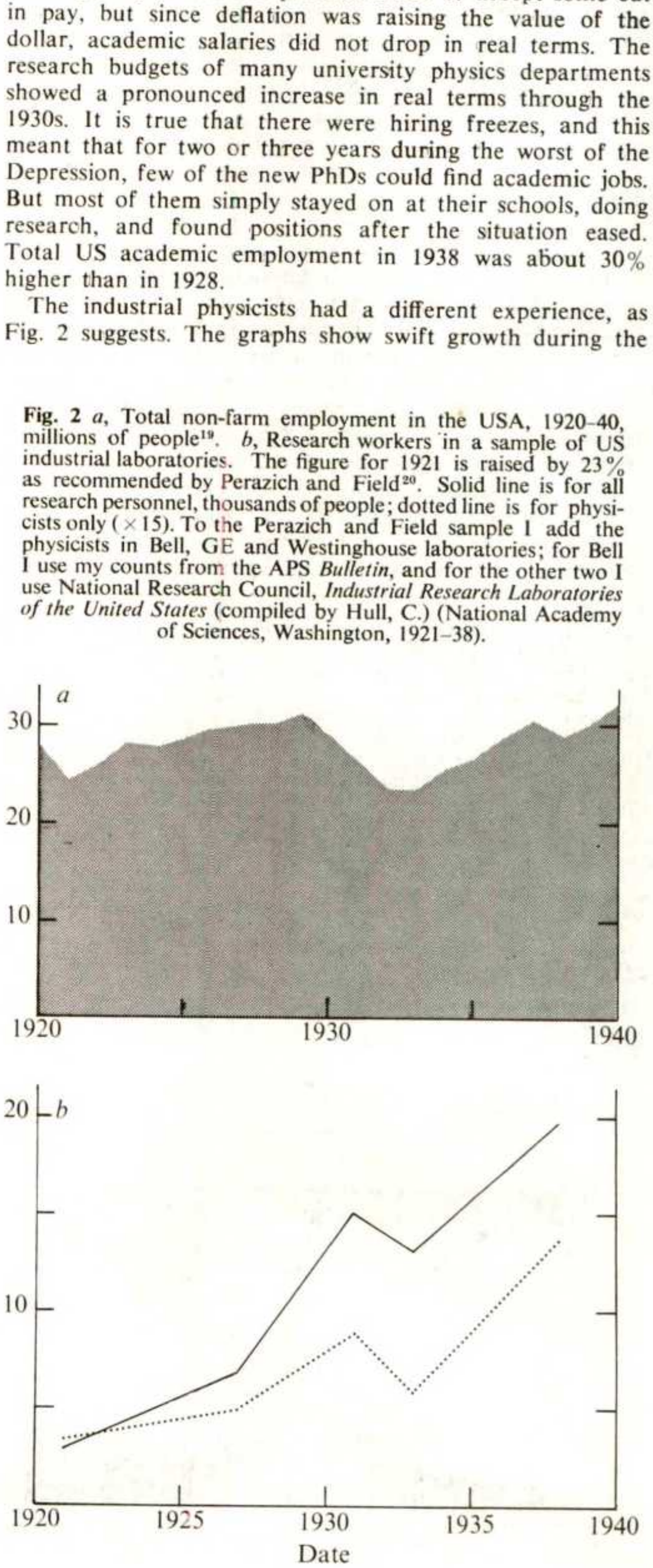

1920s, a terrifying plunge during the Depression—as bad as the general collapse of employment in the USA—and then recovery. Data on budgets are harder to come by than data on personnel, but they apparently followed a similar curve. In particular, the most important single employer of physicists in the USA, ATT, cut its research and development budget by over 25% in constant dollars from 1930 to 1933, but by 1939 this had recovered and was more than 10% higher than the 1930 figure (figures for 1916–35 are from ref. 21 and for 1939 from ref. 22).

Suffering from direct and indirect pay cuts, watching friends being laid off, for a few years the applied physicists had a hard time. The director of the General Electric laboratories suffered a nervous breakdown which the Depression was said to have helped bring on[23]. For the moment it seemed, as one industrial physicist declared in 1935, that "the era, or rather wave of industrial physics [had] subsided"[24].

But physicists in industry were spared the worst. In many laboratories research, including basic research, continued without interruption. The recovery shown in Fig. 2, so much stronger than the recovery of employment generally, also indicates a special position for industrial research. The net rise in the employment of physicists in industry from 1930 to 1938, ignoring what happened in between, was proportionally comparable to the rise in academic employment over the same interval. A large part of this swift recovery—perhaps as much as a third of it—was due to the exploitation of a new application for phyics: the use of geophysics in the oil industry. Gravimeters and seismographs greatly aided geological prospecting; thus physics research helped enlarge its own field of employment.

In the 1930s as in the 1920s, the employment of new physics PhDs provided an important connection between the campus and industry. The job problems of new PhD physicists were in large part due to hiring freezes in the academic world, but the collapse of industrial employment exacerbated their difficulties. Of 110 physicists who got their PhDs in 1928 and 1929 and whose location can be determined from the 1930 membership list of the American Physical Society, 24 were in industry and four more in government; but of 63 who got PhDs in 1934 and who are found in the 1935 list, only four were in industry and none in government. The rest were virtually all in academic institutions (my calculations from ref. 16). This decline did not escape the attention of the professors who sent the students forth.

Fig. 3 *a*, Membership of the American Physical Society, 1905–40. *b*, Location of employment of American Physical Society members, as percentage of those whose employment can be inferred from their addresses and was in the USA. From top to bottom the areas refer to the twenty universities with strongest physics departments; all other "education" including non-profit institutions; government; and 'industry' including business, medicine, and miscellaneous.

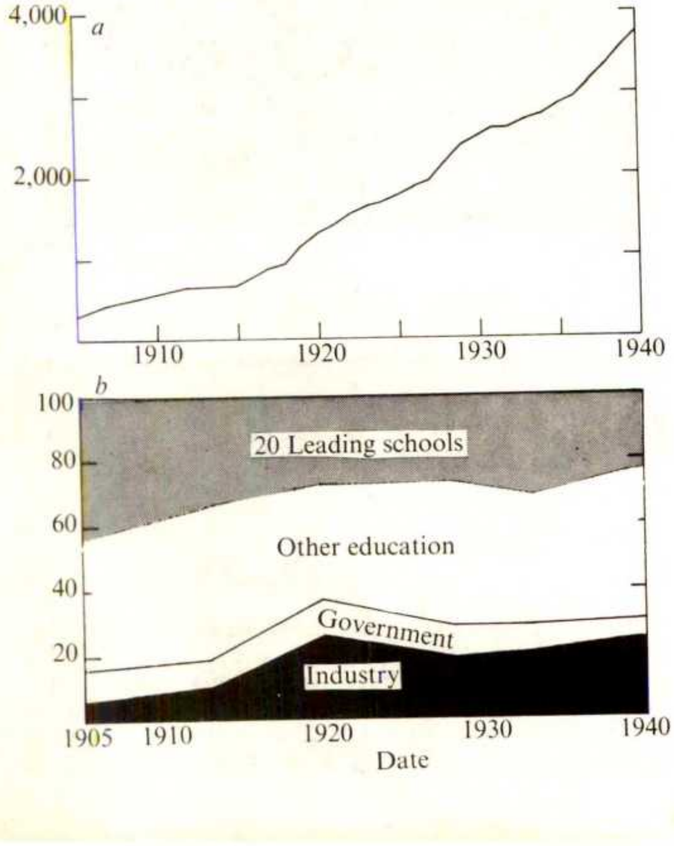

Academic physicists noted that there were applied fields to which physics could contribute but in which industry did not seem to be using the opportunity. Professors began working to persuade industrialists to employ physicists, and to train physics students so that the industrialists would want them. "A going concern must find a market for its product," one academic pointed out, "and this is true of the profession of physics"[25]. A leader of the physics community was equally blunt: "The number of teaching jobs available for physicists will always depend on the number of students taking physics. We know that the number of these students will increase if it becomes clear that there are industrial opportunities for them"[26].

Critics, industrialists and professors alike, charged that teaching was directed too much towards producing a new generation of teachers. The introduction of modern theoretical work into American university physics, which had been a prominent trend in the 1920s, did not impress these critics; what the physics graduate needed, they said, was less work with quantum mechanics and more with classical physics and a slide rule. Physicists feared that this sort of training was being usurped by the engineering faculties, whose graduates more and more resembled the product of the physics departments. To see how the universities were meeting these problems, physicist Henry Barton wrote letters to a number of physics departments at the end of 1935. He found that about half of them had taken, or were seriously planning to take, steps to increase the attractiveness of their students to industry[27]. Not all schools joined this movement, and at any rate the majority of students continued to end up with academic jobs. But at certain schools a majority of the physics PhDs who graduated in the 1930s found their homes in industry.

We have noted that the movement to teach applied physics in the universities included some elements of a reaction against pure and theoretical physics. The conflict also came to the fore in another theatre, the physics societies. Figure 3 analyses the chief of these, the American Physical Society. Figure 3*a* shows the growth of society membership from 1905 to 1940. The effects of the Depression, or even the First World War, on this curve would be difficult to prove. The breakdown of the membership (Fig. 3*b*) shows what percentages were in various locations. The shaded areas at the top, education (including private non-profit research institutes) dominate throughout. But there is a significant change in the proportions employed by industry (the black area) and by government (the white). Their combined total grows strongly into the 1920s and then drops off. Note that because of the rapid growth of the American Physical Society as a whole, the absolute number of applied physicists in it was higher in 1940 than in 1920; but they were never again so large a proportion of the total as they were in the 1920s, the golden age of applied physics research.

People noticed that not all those who might be called physicists were members of the American Physical Society. Many belonged to the engineering societies and called themselves engineers, even though their work was in direct application of physics research. In fact, of the 1,500 or 2,000 so-called physicists in industry in 1938 only about half were in the American Physical Society. The reason was that applied physicists were coming to feel themselves set apart from those in pure physics. "We did not feel at home in the Physical Society meetings," one of them recalled. "I once read a paper before the Physical Society, and I am sure the Physical Society was not interested in the paper"[28]. These feelings had gained strength through the 1920s as the numbers of applied physicists grew and as they noticed that the society was becoming more concerned with quantum mechanics and atomic spectra than with physics in the broadest sense. Already in 1916 the Optical Society of America was founded by a group at Eastman Kodak; in 1929 the Acoustical Society of America was founded at Bell Laboratories and the Society of Rheology was founded by people interested in the study of plastic materials. In 1930 there were rumours that a Society of Applied Physics would be created[29]. The trend seemed to be towards a complete schism in the physics community.

This was avoided by the founding in 1931 of the American Institute of Physics, which undertook operations such as publishing and public relations which were most efficiently done jointly. Throughout the mid-1930s this organisation had a leading role in bringing industrial and academic leaders together, in trying to explain the value of physicists to industry and the value of industry to physicists, and in working to persuade applied physicists to stay within the fold. Several conferences were held with joint academic–industrial participation[30–32]. "To those of us who have been engaged in industrial research," one physicist wrote in 1937, "... there appears to have been a social upheaval in the realm of the physical sciences in which the researcher in practical or applied fields has been lifted from the gutter of so-called 'prostituted' science and at least his better qualities held up as ideals for aspiring young physicists to emulate"[33].

The actions of academic physicists during the Depression period, through new curricula and new organisations, shows great sensitivity in the area of applied physics. If the professors were not all wrong, then this sensitivity is evidence that any weakening of applied physics or of its ties to the academic world would have been a heavy blow to all physics.

Fortunately, as we have seen, industrial physics recovered. Towards the end of the 1930s there were even hints that the most abstract physics of the universities might have some value for industry after all. General Electric advertised for a quantum theorist to look into the fundamental quantum processes involved in fluorescence, as in fluorescent lights; people at the Bell Telephone laboratories studied the quantum theory of solids, setting out on the path that would lead to the transistor; Westinghouse went into nuclear physics, a subject which later became one of its major fields of industrial interest.

In conclusion, the experience of the Depression indicates that the greatest strength of American physics still lay in the academic sector. But the anxious reaction of academics to the situation in industry suggests that a strong industrial research establishment had become as necessary, in the long run, to the universities as the universities had become to industry.

Finally, the situation has not changed greatly from the 1930s to the present day. For example, in 1973 some 53% of American PhD physicists worked in the universities, 24% in industry, 11% in government and 12% in federally funded research and development centres[34,35]. Except for the growth of federally funded centres at the expense of the universities, this is about the same as the situation before the Second World War. The relationship between academic and industrial physics research in America, established during the first four decades of the century, has proved as stable as it has been fruitful.

I thank Tessie Liu for research assistance.

[1] Rowland, H., *Physical Papers*, 596 (Johns Hopkins Univ. Press, Baltimore, 1902).

[2] Forman, P., Heilbron, J. L., and Weart, S., *Historical Studies in the Physical Sciences*, **5**, Table 1, 6 (Princeton University Press, Princeton, 1975).

[3] Birr, K. A., in *Science and Society in the United States* (edit. by Tassel, D. D., and Hall, M. G.), 35–80 (Dorsey, Homewood, Illinois, 1966).

[4] *Ibid.*, 67 and 289.

[5] Mees, C. H. K., *Science*, **43**, 763–73 (1916).

[6] United States, Temporary National Economic Committee, *Investigation of Concentration of Economic Power, Hearings . . . Part 3. Patents*, 949 (US Government Printing Office, Washington, DC, 1939).

[7] Birr, K., *Pioneering in Industrial Research: The Story of the General Electric Research Laboratory* (Public Affairs Press, Washington, DC, 1957).

[8] Mees, C. H. K., *Science*, **43**, 771 (1916).

[9] W. F. Meggers to Fred Hartman, Jan. 28, 1924, Meggers Collection/NBS, 1924, AIP.

[10] Weart, S., *The Physics Business in America, 1919–1940*. A Statistical Reconnaissance (edit. by Reingold, N.) (in preparation).

[11] Weidlin, E. R., and Hamor, W. A., *Science in Action. A Sketch of the Value of Scientific Research in American Industries*, 241 (McGraw-Hill, New York, 1931).

[12] Bichowsky, F. R., *Industrial Research*, 121–22 (Chemical Publishing Co., Brooklyn, 1942).

[13] Carter, P. A., *The American Scholar*, **45**, 785 (1975–76).

[14] *Science*, **51**, 458 (1920).

[15] Hamer, R., *Science*, **61**, 109–10 (1925).

[16] Marckworth, M. L., *Dissertations in Physics. An Indexed Bibliography of All Doctoral Theses Accepted by American Universities, 1861–1959* (Stanford University Press, Stanford, 1961).

[17] Sanderson, M., *The Universities and British Industry, 1850–1970* (Routledge and Kegan Paul, London, 1972).

[18] Pupin, M. I., *Science*, **61**, 26–30 (1925).

[19] United States, Bureau of the Census, *Historical Statistics of the United States. Colonial Times to 1957*, 73 (US Government Printing Office, Washington, DC, 1960).

[20] Perazich, G., and Field, R. M., *Industrial Research and Changing Technology*, Works Projects Administration, National Research Project, Report No. M–4, 78 (WPA, Philadelphia, 1940).

[21] United States, Federal Communications Commission, *Proposed Report, Telephone Investigation* (edit. by Walker, P. A.), 221 (US Government Printing Office, Washington, DC, 1938).

[22] United States, Temporary National Economic Committee, *Investigation of Concentration of Economic Power, Hearings . . . Part 3, Patents*, 974–975 (US Government Printing Office, Washington, DC, 1939).

[23] Birr, K., *Pioneering in Industrial Research, The Story of the General Electric Research Laboratory*, 120 (Public Affairs Press, Washington, DC, 1957).

[24] Hull, A. W., *Rev. Scient. Instr.*, **6**, 377–380, (1935).

[25] Elliott, D. S., *Am. Phys. Teacher*, **6**, 197–200 (1938).

[26] Barton, H. A., "Annual Report of the Director" (of the American Institute of Physics), Feb. 23, 1940, Barton Collection, AIP.

[27] Barton Collection/1, Committee on Training.

[28] Jones, L. A., *Rev. Scient. Instr.*, **7**, 113–123 (1936).

[29] Proceedings of The American Physical Society, Minutes of the Council, Nov. 28–29, 1930, APS Archives/Box 6, AIP.

[30] Compton, K. T., *Physics Today*, **5**, 4–7 (February 1952)

[31] Barton, H., *Physics Today*, **9**, 55–66 (January 1956).

[32] Weiner, C., *Physics Today*, **23**, 31–37 (October 1970).

[33] Olpin, A. R., *Am. Phys. Teacher*, **5**, 14–21 (1937).

[34] Porter, B. F., Barisch, S. F., and Sears, R. W., *Physics Today*, **27**, 23–32 (April 1974).

[35] United States, National Science Foundation, *Science Indicators 1974. Report of the National Science Board, 1975* (US Government Printing Office, Washington, DC, 1976).

Population studies and the Old Order Amish

Harold E. Cross

Section of Ophthalmology, University of Arizona, College of Medicine, Tucson, Arizona 85724

Populations of Old Order Amish, living in Pennsylvania, Ohio and Indiana, and isolated by their strict religious views, have provided human geneticists with a rich source of data.

LIFESTYLES in the United States, as in many other countries, have changed remarkably during the past 200 yr. Technological advances, with improved transportation and nearly instantaneous communication, have probably had the most significant impact on our social structure and cultural evolution. With progressive industrialisation and the need for highly specialised skills, these factors have contributed to the decline of relatively self-sufficient, isolated agrarian communities in which the nuclear family comprised the basic living unit. These have, of course, been replaced by large conglomerations of interdependent, amalgamated, and highly mobile masses to which the "melting pot" metaphor is perhaps more aptly applied than during the early days of settlement.

Nevertheless, certain segments of the US population have remained relatively unaffected. In some circumstances, the trend has been at least partially countered by cultural ties or economic restrictions as in the case of the ethnic and ghetto neighbourhoods of major metropolitan areas. In others, geographic barriers such as the Appalachian mountains of the eastern USA and the marshy bayous of the deep south, have effectively excluded these socioeconomic influences. Among the triracial isolates scattered throughout the eastern coastal states, racial barriers have prevented assimilation by restricting matings to individuals with a mixture of Indian, Caucasian and Negro ancestry.

The value of insular populations has long been recognised by human geneticists. Lacking the luxury of a highly proliferative species such as *Drosophila*, or the benefits of controlled breeding experiments available to a mouse geneticist, they are instead dependent on nature to provide the appropriate human population model. Human isolates, separated as they are from the prevailing cultural mores, often have at least some of the desirable characteristics of the biologist's experimental model. Many have large families, thus making available larger numbers of progeny for study. Social or religious taboos frequently limit dilution of the gene pool by restricting matings to members of the group. Such populations are often geographically concentrated due to their limited mobility and identification is facilitated by peculiarities of custom or dress.

Genetic aspects of isolates in industrialised countries have, however, received relatively little attention. Clinical investigations in Europe[1] and Scandinavia[2], as well as North America[3] have contributed significantly to the understanding of selected heritable diseases, and, in some instances, revealed "new" disorders. Other isolates in North America have been the object of demographic[4] and immunological[5] studies. In 1963, Hostetler[6] published the first major sociological study of the Old Order Amish whose unique features were immediately recognised by McKusick[7] as useful for genetic studies. Through their collaboration and that of others during the next decade, the Amish have become the most extensively studied isolate group in the USA.

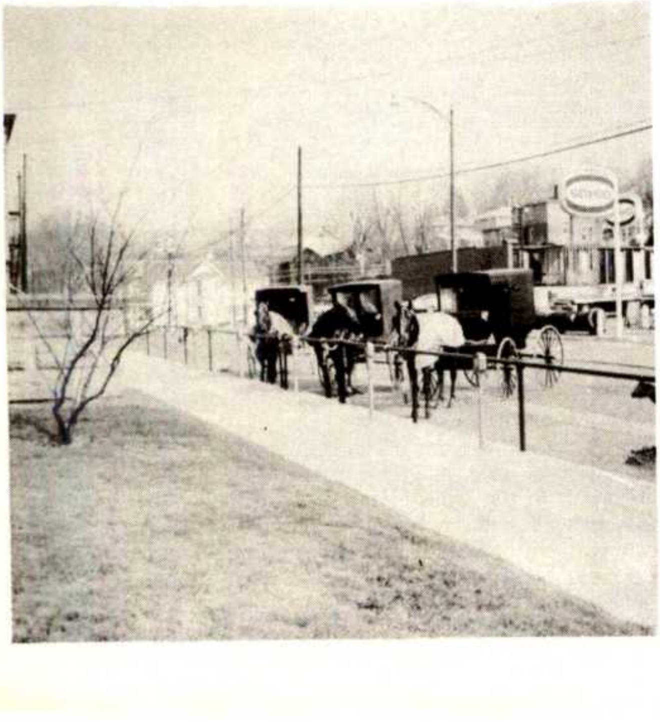

Fig. 1 North-east view from Millersburg, Ohio courthouse showing Amish horse-and-buggies tied to rails at parking meters. This blend of tradition and modern technology illustrates the accommodative attitude of non-Amish toward their unusual, isolationist Amish neighbours who, in turn, patronise "worldly" businesses without becoming assimilated.

The Amish constitute one of several religious factions classified as Anabaptists because of their opposition to infant baptism. Unlike all other Anabaptist sects, such as the Mennonites, Dunkards, Amish-Mennonites, and Beachy Amish, the Old Order Amish hold religious services in their homes rather than in churches or meeting houses. Although this unique feature absolutely distinguishes them, other characteristics make tentative indentification possible. Perhaps none is more conspicuous than their eschewal of technological innovations. Electricity and telephones are not allowed in their homes although in communities where Ma Bell has enterprisingly placed payphones in strategic locations, at least some Amish freely take advantage of the opportunity. The use of petrol engines is likewise forbidden, but curiously, steam is an acceptable, albeit rarely used, form of energy. This limitation, plus the interdiction of pneumatic tyres, has restricted transportation to the horse-and-buggy so familiar in their communities (Fig. 1).

All Amish are rural living and nearly all are farmers. They are highly clannish and have a strong interest in their ancestry and genealogical relationships. This has stimulated the publication of numerous genealogy volumes by which the ancestry of most members can be traced to the original immigrants. Perhaps most importantly, this simple folk society has somehow managed to resist assimilation and annihilation through strong internal disciplinary measures, including the practice of "shunning" or *Meidung*, by which transgressors are totally ostracised.

To the casual observer, however, personal appearance is the most striking peculiarity of these "plain-clothes people". Any form of personal adornment, including brightly coloured clothes, is strictly forbidden. All external clothing is handmade by the women from plain brown, blue or black fabrics. "Barndoor" trousers held up by suspenders and jackets with hook-and-eye fasteners are worn by the men; women's dresses are fastened with straight pins. Hair style for males is a uniformly cut, medium length, 'upside-down bowl' style (embellished with a beard without moustache after marriage), whereas females are forbidden to cut their hair. Instead, they wear it rolled up into a bun, covered with a prayer veil during all waking hours.

The Amish originated in the Canton of Berne, Switzerland, when followers of Jakob Ammann split from the parent Swiss Anabaptist sect between 1693 and 1697. Other converts came from eastern France, the Palatinate and Alsace–Lorraine. Never fully accepted in Europe, and viewed by their fellow citizens as rather peculiar, many Amish were strongly tempted by the religious freedoms promised in America. Immigration began perhaps as early as 1714 and continued for nearly 125 years. The first immigrants, mainly Swiss and numbering approximately 200, settled in eastern Pennsylvania as founders of the present group known as the Lancaster Amish. After about 1770, however, new immigrants, primarily from Alsace–Lorraine and nearby areas, found Pennsylvania too crowded and moved further west, chiefly to Ohio. The Holmes and Geauga County, Ohio Amish in the mid-nineteenth century became, in turn, the primary source of founders for the third major concentration of present-day Amish which is centered in Lagrange County, Indiana. Although Amish populations are now located in approximately 20 states, and a few recent attempts have been made to establish populations in the Honduras and South America, about 80% of the nearly 50,000 practising Amish live in the three states mentioned above. Migration and religious persecution eliminated all Amish from Europe.

The Amish are strictly endogamous, do not proselytise, and "outside" marriages with non-Amish are strictly forbidden. These restrictions, together with the limited number of founders, has led to a relatively high mean coefficient of consanguinity ($F = 0.00769$ in the Holmes County group), equivalent to second cousins once removed. In addition, however, their limited means of transportation, subtle differences in religious practices, and, in the case of the eastern Pennsylvania and Holmes County, Ohio groups, separate origins have effectively produced subisolates. For example, eight surnames account for 81% of the Lancaster Amish population whereas 77% of the Ohio Amish have a different set of eight surnames. The continued isolation of these two communities is illustrated by data from an analysis of 2,013 Holmes County couples living in 1966: only two partners came from Lancaster County. Such isolationism is evident even among Indiana and Ohio Amish with much closer ancestral and religious ties: only 116 marital partners left Indiana to join their mates in Holmes County, evidence of separation which no doubt portends even greater genetic dissimilarities in the future.

Interestingly, in spite of their usual pacifism and strong belief in non-violence, there is considerable internal strife. New religious factions are constantly being formed and dissolved. In Holmes County, for example, two groups known as the Stutzman and Stolzfus Amish split from the parent body in the early 1960s and marriages between any of the three groups is actively discouraged. If this practice persists, new genetic isolates may be formed.

The Amish community is primarily a spiritual one without distinct geographical boundaries. Amish farms are scattered throughout the rural communities, often sharing borders with non-Amish farms. Their religious charter, however, effectively prohibits social and cultural interaction with the non-Amish community with the result that their demographic characteristics[8] are quite distinct. As a result of their high crude birth rate (33.3 compared with 21.2 for the entire USA in 1964), the population pyramid[8] has a relatively broad base; 51.8% are less than 20 yr old and 28.7% are less than 10 yr old. The pyramid tapers more smoothly than that for non-Amish populations since their self-sufficient agrarian lifestyle renders them relatively independent of the cyclic effects of political, economic and social stimuli. Most men (69.8%) are farmers, at least in Holmes County where the most complete data have been collected. A further 13% are self-employed in supporting trades such as carpentry, blacksmithing, harness repairing and construction.

The Amish marry at a considerably later age than their rural counterparts (22.57 yr for a female, and 23.61 yr for males). Because of the obvious economic advantages of large families in a rural setting, and their strict interpretation of the biblical admonition to "be fruitful and multiply", children are considered highly desirable. Contraception, although not prohibited, is viewed as undesirable with the result that the female reproductive span is longer and birth intervals shorter than among other US rural populations. Among 792 completed Holmes County Amish families (in which the wife was at least 45 yr old), the mean number of pregnancies was 7.19 and more than, one-third (34.8%) reported 10 or more pregnancies. The net result is an intrinsic rate of natural increase (r) of 3.019 or a potential doubling of population size every 23 yr. Among modern North American isolates, only the Hutterites were found to have a higher rate ($r = 4.1265$). This increase is not achieved for the Amish, however, because there is a substantial attrition rate among young people who are lured away by the 'outside world'. Still, it is obvious that the Amish could lose four or five times the 10–15 % estimated to leave each generation, and still maintain their population size at the present reproductive rate.

Curiously, Holmes County Amish men tend to outlive their wives. The sex ratio in this population for those over the age of 55 yr is 1.216. Similar trends have been noted in other high fertility groups such as the Hutterites and northern Indiana Amish, giving rise to speculation that the emotional and psychological stresses of childbearing may have an adverse effect on longevity.

It is apparent that the Old Order Amish have several attributes that make them useful to human geneticists. Members are easily identified by their distinctive dress and customs. Their communities were founded by a limited number of ancestors, with identifiable origins. They maintain a closed population with virtually no dilution of the original gene pool. Families are large, illegitimacy rates are low, and the membership constitutes a relatively immobile society concentrated in specific geographical areas. Several additional features are of particular value to the medical geneticist: relatively stable socioeconomic values, uniform environment, high standards of living and medical care, a great interest in medicine, and strong resistance to institutionalisation of the chronically ill.

Table 1 Distribution of some rare recessive genes in the Old Order Amish

Isolate	Recessive disorder
Mifflin County, Pennsylvania	Pyruvate kinase-deficient haemolytic anaemia[9]
Lagrange County, Indiana	Phenylketonuria[10,11]
Lancaster County, Pennsylvania	Ellis–van Creveld syndrome[12]
Adams and Allen Counties, Indiana	Limb-girdle muscular dystrophy[13]
Holmes County, Ohio	Mast syndrome[14]
	Troyer syndrome[15]

Populations founded by a small number of ancestors may exhibit an unusually large number of otherwise rare hereditable traits if the founders carried a frequency of mutants that differed widely from the parent population. If the population further remains 'closed' by excluding matings with outsiders, the purity of the original gene pool is maintained, and the restricted number of available mates results in a high rate of consanguinity. Since consanguineous couples share ancestors, they are likely to inherit at least some identical genes, and chances are good that their offspring will inherit the "double dose" of mutants necessary for the expression of recessive disorders. These conditions were apparently satisfied in the case of Amish settlements since all of those studied have at least one recessive disorder occurring with relatively high frequency (Table 1).

The limited distribution of these genetic diseases is another indication of genetic isolation. Only one recessive disorder, a "new" type of dwarfism (cartilage-hair hypoplasia), seems to occur throughout most Amish communities including Holmes, Lancaster and Lagrange counties as well as among smaller settlements in Iowa, Oregon, Kansas, Illinois and Michigan[16]. Either the origin of this gene was more ancient, antedating the origin of the sect, and was introduced by multiple immigrants, or the descendants of the person or persons who introduced it were unusually nomadic.

The peculiar social and cultural restrictions of Amish life also make them useful for epidemiological and population studies. Certain aspects of the distribution of cervical cancer, for example, raises the suspicion that it might be a venereally transmitted disease. Women with increased risk are those with marital instability, early coitus or early marriage, multiple coital partners and other venereal infections. Under this hypothesis, groups with low risk for cancer of the cervix would practice (1) strictly endogamous matings (to avoid introduction of the responsible agent), (2) monogamous sexual behaviour (restricting the agent), and (3) strong group boundaries over many generations. These are, of course, characteristics of the Amish, maintained and enforced by their religious taboos. Divorce is forbidden and separation is extremely rare. In either case, marital infidelity is virtually unknown, although premarital conceptions probably occur with a frequency similar to other US populations. In most cases, however, the biological parents do become married with the result that the overall illegitimacy rate is low. Among 1,098 Amish offspring of 155 couples in northern Indiana, no paternal exclusions were found by ABO, Rh and MN blood group determinations[5]. Furthermore, their strict moral standards regarding marital fidelity and their condemnation of divorce limit the transmission of other venereal diseases, according to local physicians.

Table 2 ABO blood group frequencies in three Amish isolates

Blood group	Holmes County isolate*	Lancaster County isolate†	Adams County isolate‡	Random AngloSaxon population[19]
O	0.34	0.11	0.16	0.45
A	0.54	0.74	0.65	0.41
B	0.06	0.05	0.11	0.10
AB	0.06	0.11	0.08	0.04

*n = 1,027; ref. 18.
†n = 215; ref. 18.
‡n = 892; ref. 17.

Use of the Amish to test the possibility of venereal transmission of cervical cancer is especially valuable because its frequency among them can be compared with that found in non-Amish living in the same area where medical care practices are similar and the effect of economic and environmental factors is largely cancelled out.

A retrospective study in Holmes County, Ohio, based on 10,314 Papanicolaou vaginal smears obtained between 1950 and 1966, revealed a significantly lower frequency of cervical cancer in Amish women. Among 3,606 non-Amish women, three died of cervical cancer (a frequency similar to other rural populations) whereas none of the 2,068 Amish women examined died of this disease. These data are even more interesting because the Amish have several characteristics associated with high risk groups, such as a high rate of reproductivity, absence of contraception, and a low rate of circumcision (at least among older males). In view of the similarities of economic standards and medical care practices between the two groups, it seems plausible to attribute the difference in frequencies to some aspect of social or cultural behaviour. Social isolation and reduced sexual contacts between Amish and non-Amish might, therefore, account for the reduced rate of cervical cancer if it is caused by a venereally transmitted agent.

Blood group data are widely used by population geneticists in the study of evolution and genetic similarities of various groups. To further document subisolate formation among the Amish, ABO frequencies for three communities were determined. Blood was collected systematically from the Amish isolates located in Adams County, Indiana[17] and Lancaster County, Pennsylvania[18]. For the Holmes County community, however, extensive data already available were used by taking advantage of the fact that Amish do not have telephones. Due to their interest in medical illness and the relatively high frequency of haemophilia B (Christmas disease), Amish in this area give blood freely. Red Cross donor cards were compiled on all citizens of the area and Amish individuals identified by characteristic surname on cards without a telephone number. ABO frequencies among the three populations, as well as a random Anglo-Saxon sample, are compared in Table 2. It is apparent that the Amish not only differ from non-Amish in ABO frequencies but they evidently maintained significant isolation from each other.

In spite of their apparently effective isolation from the external world, and evident internal stability, the Amish exhibit signs of stress that may indicate their eventual acculturation, at least to some degree, with the larger rural community. Demands for higher education and restlessness among young people seem to be increasing. Pressure for relaxation of rules against the use of mechanical devices such as tractors and automobiles by older individuals is responsible for considerable internal strife and fragmentation. At the same time, rising costs and, in some areas, decreasing availability of good farm land is forcing many to resort to marginal, non-farming vocations, bringing them into closer contact with worldly temptations. Nevertheless, their reproductivity and strong internal sanctions make it unlikely that this unique society will disappear in the near future. In the meantime, these peculiar people have provided us with an unusual opportunity to study the genetic and epidemiological aspects of human disease to a degree that will be increasingly difficult to achieve among the modern population.

[1] Klein, D., *Birth Defects: Original Article Series*, **7**, 52–82 (Williams and Wilkins, Baltimore, 1971).
[2] Forsius, H., Eriksson, A., Nuutila, A., Vainio-Mattila, B., and Krause,, U., *Birth Defects: Original Article Series*, **7**, 83–98 (Williams and Wilkins Baltimore, 1971).
[3] Witkop, C. J., Jr. *et el.*, *Alabama J. med. Sci.*, **3**, 382–403 (1966).
[4] Eaton, J. W., and Mayer, A. J., *Hum. Biol.*, **25**, 206–264 (1953).
[5] Juberg, R. C., thesis, Univ. Michigan (1966).
[6] Hostetler, J. A., *Amish Society* (Johns Hopkins, Baltimore, 1963).
[7] McKusick, V. A., Hostetler, J. A., and Egeland, J. A., *Bull. Johns Hopkins Hosp.*, **115**, 203–222 (1964).
[8] Cross, H. E., and McKusick, V. A., *Soc. Biol.*, **17**, 83–101 (1970).
[9] Bowman, H. S., McKusick, V. A., and Dronamraju, K. R., *Am. J. hum. Genet.*, **17**, 1–8 (1965).
[10] Martin, P. H., Davis, L., and Askew, D., *J. Ind. State med. Ass.*, **56**, 997–999 (1963).
[11] Martin, P H., *J. Ind. State med. Ass.*, **61**, 1107–1108 (1968).
[12] McKusick, V. A., Egeland, J. A., Eldridge, R., and Krusen, D. E., *Bull. Johns Hopkins Hosp.*, **115**, 306–336 (1964).
[13] Jackson, C. E., and Carey, J. N., *Pediatrics*, **28**, 77–84 (1961).
[14] Cross, H. E., and McKusick, V. A., *Archs Neurol.*, **16**, 1–13 (1967).
[15] Cross, H. E., and McKusick, V. A., *Archs Neurol.*, **16**, 473–485 (1967).
[16] McKusick, V. A., Eldridge, R., Hostetler, J. A., Ruangit, V., and Egeland, H. A., *Bull. Johns Hopkins Hosp.*, **116**, 285–326 (1965).
[17] Jackson, C. E., Symon, W. E., Pruden, E. L., Kaehr, I. M., and Mann, J. D., *Am. J. hum. Genet.*, **20**, 522–527 (1968).
[18] McKusick, V. A., Bias, W. B., Norum, R. A., and Cross, H. E., *Humangenetik*, **5**, 36–41 (1967).
[19] Race, R. R., and Sanger, R., *Blood Groups in Man*, fourth ed. (Davis, Philadelphia, 1962).

Scientific networks in the age of the American Revolution

Arnold Thackray

Department of History and Sociology of Science, University of Pennsylvania, Philadelphia 19174

The channels of communication between scientists in the UK and USA during the late eighteenth and early nineteenth centuries, the growth in importance of the provincial centres and the relative position of London, are reviewed in the light of the social, cultural and political moods of the time.

"THE rights and liberties of our countrymen in America are much less dear to us than they ought to be." The words were those of a rising Manchester physician, in a June 1774 letter to a well known Philadelphia printer. The physician's concern encompassed more than remote, colonial affairs. The situation at home also gave cause for alarm. "The principles of despotism in our Governors and of passive obedience in the people seem to be advancing by an equal and alarming progression." These opinions were shared by other influential Mancunians, including a manufacturer who wrote some nine months later to Philadelphia's foremost physician, saying "I sincerely regret, from more general considerations than my own interest, the unhappy divisions that prevail between the mother country and her colonies. Soon may they again be united, and may their quarrels like those of lovers, tend to confirm and strengthen the mutual affection which ought to subsist between them."

The exchange of such sentiments was halted abruptly by the onset of the War of American Independence. It was almost ten years before the manufacturer wrote again, marvelling "how strange and unexpected have been the events . . . (causing) so long and unfortunate an interruption to our correspondence." He went on to say that "tho' separated and become subjects of different states, I trust that every spark of affection is not extinguished, or at least that individuals will renew and maintain their pristine attachments." The hope was expressed in the formal language and cast in the individualistic terms of the period. As events were to show, the hope was also eminently realisable, and a clue as to why may be found in a third letter. It was in September 1786 that the then premier physician of Manchester confided to his counterpart in the City of Brotherly Love: "I shall be happy in every opportunity of promoting a friendly and philosophical intercourse between my countrymen and the literati of America. The arts and sciences are the offspring of freedom; and I cordially rejoice that your noble exertions have secured to you these invaluable offspring."

The scientific network

The series of letters from which these quotations come provide us with a glimpse of an important scientific network of the late eighteenth century. The correspondents—Benjamin Franklin, Thomas Henry, Thomas Percival and Benjamin Rush—were all major figures in their day, as was Joseph Priestley. Franklin's work in electricity is well known, as is Priestley's discovery of oxygen. Thomas Henry was also influential in the chemistry of the period, publishing translations of the work of Antoine Lavoisier in 1776 and 1783. Percival in his turn was active in chemistry and meteorology, and was a pioneer of mortality statistics. He composed a standard work on *Medical Ethics*. Finally, Rush was not only a chemist and physician of note, but also a leading medical and psychiatric theorist. Each of the five participated actively in one particular link in the network of provincial, rationalistic dissent.

Other scientific networks, each encompassing its own appropriate linkages, were also significant in this era. Two come to mind as especially important. Most immediately and most obviously, the affairs of the Royal Society of London, and of much else besides, were quite unselfconsciously controlled by the members of a network that linked together the metropolitan elite, the English universities and certain interested and influential country gentry. One reason that Sir Joseph Banks was able to entrench himself as President of the Royal Society and thus to serve for the record span of almost forty-two years (November 1778–June 1820) was because he exemplified in himself the three elements of this central network of the late eighteenth century. The third network, connecting with but quite distinct from the previous two, was the one that centred on the scientific interests of the Scottish nation. Its members came from the ranks of Scotland's 'improving' landlords, from among the professors at her several universities and from those native-born students who emigrated to England and her dependencies in search of wider opportunity.

Analytically, we normally separate the science, the politics, the philosophy and the religion embraced by such men and involved in such networks, and treat each by itself. If, instead, we view the cultural values, social functions and intellectual commitments involved in more holistic fashion, we may understand better not only the ways in which images of science, progress and freedom were woven into the fabric of the American Revolution, but also the functions of scientific networks in the preindustrial age. The particular case of provincial, rationalistic dissent, as seen in the microcosm of the Philadelphia–Manchester link, may illuminate the macrocosm of social structure, political change and the growth of knowledge. Equally, our understanding of the macrocosm may help us comprehend what we see revealed in the microcosm.

London as a focal point

By the mid-eighteenth century, London was Europe's largest, richest, most complex and most cosmopolitan city. In population it was soon to outrank its nearest rival, Paris, by a factor of more than two. Within the English-speaking, as opposed to European, world, London's pre-eminence was even more pronounced. No other English-speaking city was one tenth of its size. Advantages of scale were reinforced by the city's commercial, financial, intellectual, legal, political and social significance as the centre of a newly united Britain and of a dawning empire. The Royal Society of London for Improving Natural Knowledge was thus in an enviable situation. A metropolitan elite of peers, gentlemen of independent means and successful physicians, clergy and lawyers gave tone and direction to its activities. Foreign ambassadors and visiting princes attended its sessions. Lowlier but more earnest visitors from the colonies, the provinces and the lesser metropolises of Dublin and Edinburgh brought information, specimens and favourite but unwinnowed ideas. On returning home they took not only tested knowledge and new theories, but heightened aspirations and fresh models of behaviour. Benjamin Franklin was one of 53 American colonists who became an FRS. Thomas Percival, Thomas Henry and Joseph Priestley were among the larger, but uncounted, group of English provincials who succesfully sought the heightened social standing and envied cosmopolitan connections implicit in the Fellowship. The subsequent ostracism of Priestley provides a vivid example of how member-

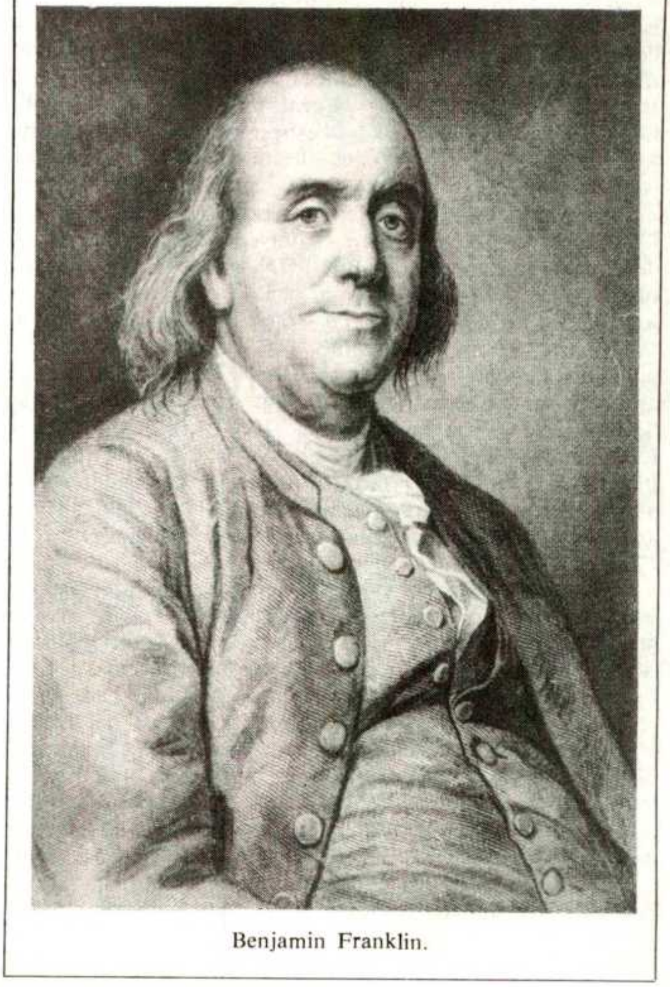

Benjamin Franklin.

R 388

ship still left one a likelier candidate for neglect than for office within what was correctly called the Royal Society of London.

Importance of provincial centres

Those on the provincial and colonial peripheries of the eighteenth century social world naturally sought approval from the centre and conformity with its values. Dissent was an alternative which was, however, sometimes as attractive as assimilation. Ambivalence between the two marked the growing mercantile communities of provincial cities from Birmingham to Boston. This ambivalence ensured good connections between provincial, rationalistic dissent and the central scientific network on the one hand, while also encouraging connection with Scottish science on the other. Those who literally dissented in central, religious values were of course, barred from graduation at either English university. Edinburgh provided a favourite locus for such dissenters. Its different devotional traditions and its own particular ambivalencies about English norms gave promise of congenial context. The varied clubs and institutions of the town and most especially its rapidly-growing university served as centres of socialisation into alternative values. Within the university itself, the medical school offered not only appropriate direction but also coveted certification for a burgeoning line of service and opportunity. Thomas Percival and Benjamin Rush both studied there. Percival later went so far as to secure an Edinburgh doctorate (of law) for his friend and mentor, Joseph Priestley (Priestley in his turn had sponsored the youthful Percival before the Royal Society).

Edinburgh-trained physicians were drawn to the new medical opportunities apparent in the 1750s and 1760s in such rising provincial towns as Philadelphia, Manchester, Liverpool, Bristol, Boston and Birmingham. Most dramatic is the case of Philadelphia. The city was beginning to develop its own intellectual life and to serve as centre for the scattered seaboard communities of British North America. It was thus the natural site for the continent's first medical school. Like Rush and its founder John Morgan, its earliest professors all enjoyed Edinburgh MDs. Custom and the reach of law as institutionalised in the monopoly power of Oxford, Cambridge and the (London) College of Physicians were sufficient to preclude such developments in England. But MDs with Scottish training played influential, if less formal, roles in provincial English towns, serving as nuclei round which social forms oriented to natural knowledge, polite behaviour and advanced political thought might crystallise. Their influence is apparent in the development of, among others, the Lunar Society of Birmingham (about 1765), the Manchester Literary and Philosophical Society (1781) and the Derby Philosophical Society (1783), as well as in the cognate cases of the American Philosophical Society (Philadelphia, 1769) and the American Academy of Arts and Sciences (Boston, 1780).

Medical men of all kinds, including apprentice-trained surgeons and apothecaries, were a key element in the growing eighteenth-century network of rationalistic, 'scientific' dissent in both its provincial and colonial forms. Family connection and religious conviction also had major roles. If Edinburgh-trained physicians were the shock troops of the movement, dissenting ministers of a Socinian turn of mind served as its theorists; the most notable of these was Joseph Priestley. Between his electrical investigations and his brilliant discoveries of ever more curious sorts of "air", he produced endless polemical broadsides on theology and served as a 'culture hero' to a generation. Priestley was directly associated not only with the Lunar Society and the Manchester Literary and Philosophical Society but also, eventually, with the American Philosophical Society. Less spectacular but more typical was the Turner family. William Turner was a Unitarian minister and an early member of the Manchester Literary and Philosophical Society. Using this as a model, he founded the Literary and Philosophical Society of Newcastle upon Tyne (1793), which he served as secretary for over forty years. His son later fashioned a similar 'Lit and Phil' in the burgeoning industrial town of Halifax.

Other examples of the connections between medicine, rationalistic dissent, merchant activity, manufacturing concerns and family lineage spring readily to mind. The Lunar Society provided a nexus for Darwins, Wedgwoods and Witherings to enjoy polite conversation, pursue natural knowledge and forge marriage alliances. Erasmus Darwin founded another Philosophical Society when he moved away to Derby in the early 1780s, and was promptly rewarded by election as an honorary member of the Manchester Society. As late as 1817–18 his grandson, Charles Darwin, attended a Unitarian school before arrangements were made for him to follow family tradition by reading medicine in Edinburgh. Finally, we note how a group associated with the Manchester Literary and Philosophical Society even went so far as to plan a pantisocracy in Pennsylvania when, following not only the American but the French Revolution, the political climate in England turned decisively against progressive, rational dissent. The movement to Philadelphia in 1794 of Thomas Cooper, Thomas Henry, Jr and the Joseph Priestleys, both senior and junior, may be seen as a last efflorescence within these eighteenth-century forms. (The first of the foursome obtained, the second unsuccessfully sought, and the third declined, a scientific chair within the University of Pennsylvania.)

The network and the revolution

The American Revolution symbolised the coming end of the symbiosis between provincial and colonial values. The path

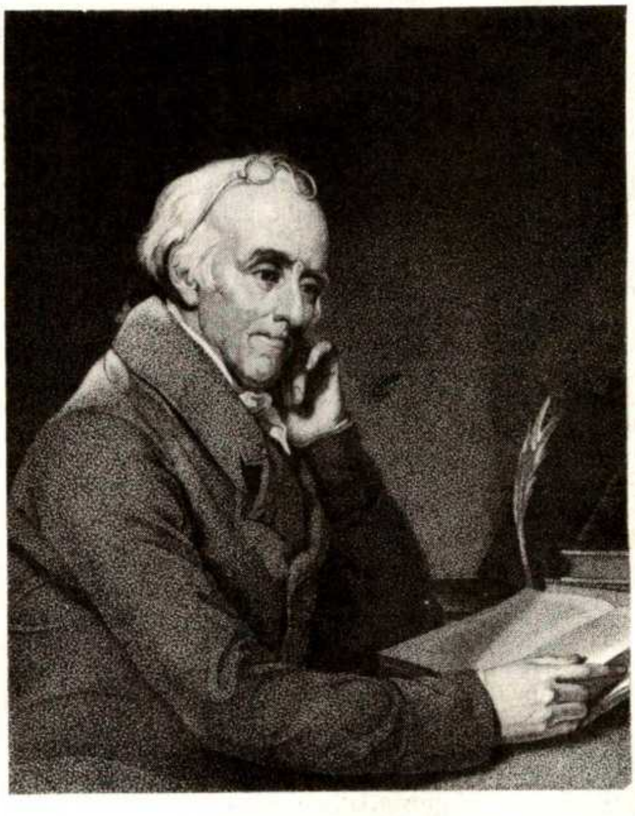

Benjamin Rush.

of development in the USA was to be one in which Americans painstakingly, precariously and long unsuccessfully sought to redefine "their" centre from London to somewhere—no one could agree where—in the new nation. Not until 1863 was an enduring National Academy of Sciences founded; not until the first World War did that Academy become a main voice in American science. The modes of federalism and pluralism developed in the USA contrasted strongly with the trend to centralism in British life. In the course of the nineteenth century the UK became a tightly integrated whole. The nature of that integration was neatly echoed in the new forms of science. The British Association for the Advancement of Science, founded in 1831, depended heavily for its sustenance on scientific societies spawned from the network of provincial, rationalistic dissent. Reflecting its origins, it never met in London although in its infant days it was captured, and has since been controlled, by the central elite. To say this, however, is to progress ahead of the story and we must rather return to the later eighteenth century, when an Anglo-American network of provincial, rationalistic dissent was a significant element in the world of science and culture. The letters which follow indicate the modes, styles and concerns of that network as seen in the particular linkage from Manchester to Philadelphia.

The earliest surviving communication from this link in the network is a letter from Thomas Percival to Benjamin Franklin of 1771. Characteristically, Percival encloses an offprint of a scientific publication, seeks critical commentary and concludes by saying "My friend Dr Priestley flattered me last summer with the prospect of seeing you at Manchester, and obligingly promised to introduce me to your acquaintance." It is not known how Franklin responded or when the two eventually met. The sustaining network of shared friends, values and commitments however, was such as lead to a ripening correspondence. Two years later Franklin wrote with commentary on census attempts, and remarks on climate and health. The following year Percival in his turn acknowledged receipt of "a packet of papers on the American affairs."' He was quick to point out that he had "distributed the pamphlets amongst persons of the first consequence in this town and neighbourhood. They have already circulated through a considerable number of hands and cannot fail of making some useful impressions." Percival was equally quick to "inclose a little paper" of his own "extracted from a long memoir which I shall soon send to . . . the Royal Society". The easy turn from political affairs to scientific enquiry highlights how, for Franklin, Percival and other members of the network, similar values underlay the two pursuits.

By this time Thomas Henry and Benjamin Rush were also active within the Manchester–Philadelphia strand of the network. In 1774 Henry sent Rush his book on the properties of magnesia. Rush returned the favour, conveying the first volume of the *Transactions* of the American Philosophical Society and announcing that he had proposed Henry as a member of that fledgling body. The parallelism of developments in the two cities, and the way in which the network was underpinned by common concerns with trade and with medicine may be seen in Henry's response. After dilating on the "very pleasing proofs of the progress science is making on your side of the Atlantic," he continued that "happy as I am at Manchester in the society of several men of real genius, and most diligent investigators of nature, yet I must think that an inhabitant of Philadelphia has ample reason to congratulate himself on being situated in a city where the literati so much abound. One of your Society, Dr Williamson, was at Manchester in January and seems to be a man of very extensive knowledge." (Hugh Williamson was just that and, as befitted a Pennsylvania-born, but Edinburgh-trained, physician, he was later to be a founder of the New York Literary and Philosophical Society.) Henry went on to mention "Dr Franklin, who . . . will carry you all the philosophical news," a new publication of Dr Percival which "he purposes to send by the first opportunity to you and Dr Morgan" and "Dr Priestley (who) is proceeding in his experiments and intends in about two months to publish . . . (details of how) he procures air six times more salubrious than common air (that is, the landmark discovery of oxygen)." Finally, it was reported that—in accord with best network practice—"Dr Priestley has kindly put up my name at the Royal Society; he and some other of my friends had recommended me to Dr Franklin who had promised me all his interest".

This letter, which also contains the remarks about "the unhappy divisions that prevail between the mother country and her colonies" shows this one strand of the network at the height of its power, at the moment when war was about to disrupt its activities and transform its contexts. Even so, the next letter from Henry to Rush (dated May 10, 1784) remarks that "the progress of literature and philosophy have not been wholly interrupted. As a proof of this a Society for the promotion of these objects has been established in this place, and has obtained some degree of celebrity . . . You were once so obliging to offer to get me elected into your respectable Society; and with your permission I will propose your name to be enrolled among our Honorary Associates." Henry's letter was conveyed by "Mr Joseph Hadfield" (who) belongs to a respectable commercial house here . . . and is going to settle in America." Symbolically covering the distance between both Manchester and Philadelphia philosophers and the Royal Society of London, the letter also reports how "a most excellent mathematician and philosopher and a very worthy man from Manchester had been "black balled", Sir Joseph (Banks) making a party against him". In like manner, Percival wrote to Franklin how "the loss of Sir John Pringle has almost ruined the Royal Society. But you are no stranger, I presume, to the disgraceful contentions of that learned body, and to the conduct of the President." Once again distance from London was but the obverse of the coin of network linkages. Percival also wrote to Franklin saying the Manchester Society was publishing one of his scientific papers and that "I am commissioned to return the thanks of the Society to you for this communication; to request your future correspondence; and to acquaint you that we have honoured our institution by electing you an extraordinary member." Once more, the message was conveyed by a commercial traveller between the two cities. That same envoy also carried Rush's diploma and another letter containing news of Priestley's work and greetings to Mancunians settled in Philadelphia.

Not altogether surprisingly, the American Philosophical Society returned the honour done two of its members by Percival and Henry. The ties of sentiment and interest were further strengthened by the formal exchange of publications. As president of the Manchester Society Percival wrote to Franklin, President of the American Philosophical Society, acknowledging receipt of "the Vol. of American Phil. Transactions" and sending the "present of our Memoirs". His letter referred to a visit of Dr and Mrs Priestley—the doctor "at this time gallantly engaged in attempts to convert the Jews to Christianity"—and touched extensively on the need to find means to purify the air of manufacturing towns, seeking Franklin's advice. We cannot pursue the means by which two other members of the Manchester group were elected to the American Philosophical Society in 1789. Nor can we fully share the surprise with which Percival reported to Rush the following year that "The Academy of Arts and Sciences at Cambridge in New England have lately conferred on me the unsolicited honour of election into their very respectable Society." Nor is it possible to follow the sequence from the French Revolution to the War of 1812 which brought this particular Anglo-American link to an end. Instead, I shall point to two passages which so perfectly express the common hopes of the members of the Manchester–Philadelphia strand in the network of provincial dissent, that it seems appropriate to conclude by quoting them in full. In October 1786 Percival wrote to Franklin that:

> "The diffusion of the arts and sciences through so many extensive regions of the globe must afford a subject of contemplation peculiarly satisfactory to your mind . . . And I hope that Sun which has so long blessed the nations (namely, Franklin himself) will not set till the interests of truth and knowledge, of civil and religious liberty, are truly established in the Western Hemisphere, which it now enlightens".

In March 1790 he put it this way, to Benjamin Rush:

> "I honour your enterprising genius, which is continually exerting itself in some liberal scientific and public spirited undertaking. Mental energy seems now to be the characteristic of America; and great are the expectations which may reasonably be formed concerning your rising republic".

I thank the John Simon Guggenheim Memorial Foundation and the National Science Foundation for partial support of the research reported here. I am also indebted to the Trustees of the British Museum, to the Birmingham Public Library, to the Library of the American Philosophical Society and to the Historical Society of Pennsylvania for permission to quote from letters in their possession. Robert Bud, David Miller and other students and colleagues at the University of Pennsylvania provided thoughtful criticism and generous assistance.

The Viking Mission search for life on Mars

Harold P. Klein
NASA-Ames Research Center, Mountain View, California
Joshua Lederberg
Stanford University, Stanford, California
Alexander Rich
Massachusetts Institute of Technology, Cambridge, Massachusetts
Norman H. Horowitz
California Institute of Technology, Pasadena, California
Vance I. Oyama & Gilbert V. Levin
Biospherics, Incorporated, Rockville, Maryland

On each of two unmanned Viking spacecraft, a number of investigations are planned to be conducted on the surface of Mars this summer. Included in the science payload are instruments designed to determine the state of chemical evolution, including the possible presence of living organisms, on that planet.

ON July 4, 1976, the first of a pair of unmanned spacecraft is scheduled to touch down on the planet Mars in an area located at 19.5°N and 34°W, in a region of low elevation, which seems to be a drainage basin for a large portion of the equatorial region of Mars (Fig. 1). Two months later, the second Viking spacecraft should touch down further north (44.3°N and 10°W) in another region of low elevation, relatively close to the edge of the northern winter ice cap, and at a latitude where maximum quantities of water vapour have been measured in the Martian atmosphere[1].

Aboard both of these landers will be identical science 'payloads', including cameras, meteorological and seismic stations, and analytical equipment to conduct analyses of the surface material. These investigations are now planned to be conducted over a period of two months on each lander, but it is possible that the experiments will continue over considerably extended periods of time—approaching a full Martian year—if further funding can be made available for an extended Viking mission. The scientific objectives of this mission are manifold, but, among these, an assessment of the organic evolutionary state of the planet including a search for extraterrestrial life, is of paramount importance. For the first time, another planet is to be probed directly for evidence supportive of modern ideas on the origin of life[2]. Mars, although not a hospitable planet as judged by terrestrial standards[3], is the one planet, other than Earth, that most nearly satisfies our theoretical presumptions of the conditions for life to have evolved[4].

For many years, telescopic evidence of morphological features, and their temporal changes, inspired speculative controversies about the presence of life on Mars. These older controversies no longer bear discussion in the light of the Mariner Mars-orbiter and fly-by missions (1964–71) which gave us a complete photographic mapping at resolutions of 1 km or better. It is now clear that water in a form available to living organisms is a likely limiting factor. The polar caps seems to contain substantial quantities of ice, but at temperatures far below those that would support any active terrestrial life. The temperate latitudes have congenial daytime temperatures, but humidities far below those known for any earthly desert. A number of mechanisms have, however, been proposed for possible local anomalies that could furnish moisture at temperatures consistent with metabolism[5]. In addition, the Mariner photographs show many surface features that are most easily explained by assuming that episodes of weather, precipitation and the carving of river valleys have occurred in the geological history of Mars.

These considerations have been taken into account, together with the engineering constraints, in planning the selection of landing sites. However, until our first successful landing, we have no reliable empirical basis for predictions about the local habitats of Mars. We have then been obliged

VIKING LANDING SITES

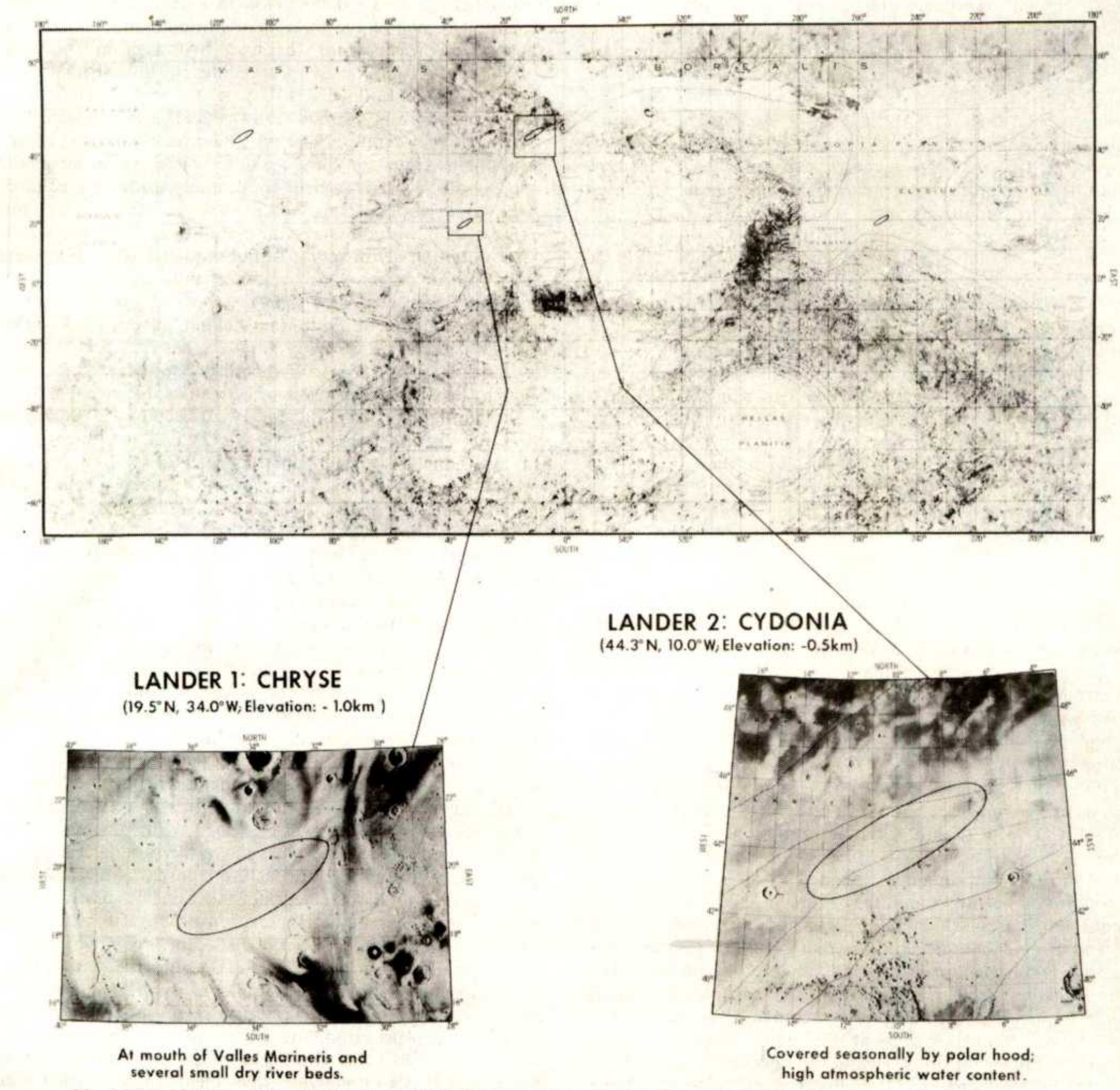
NORTH
VASTITAS
BOREALIS
HELLAS
PLANITIA
SOUTH
WEST
EAST
LANDER 2: CYDONIA
(44.3°N, 10.0°W, Elevation: -0.5km)
LANDER 1: CHRYSE
(19.5°N, 34.0°W, Elevation: - 1.0km)
At mouth of Valles Marineris and
several small dry river beds.
Covered seasonally by polar hood;
high atmospheric water content.

Fig. 1 Map of Mars, constructed from Mariner 9 photographs, showing the two prime landing sites for the Viking landers.

to try to outguess Nature over a range of possible realities in planning these experiments.

Scientific payloads of Viking mission

While all of the experiments are expected to contribute at least peripheral information pertaining to the local milieu of the landers (for example, local temperatures, wind speed and direction, atmospheric composition, elemental composition and magnetic properties of the surface material), three of the investigations hold the greatest promise for contributing directly to the question of organic chemical evolution on Mars.

The first of these is the imaging investigation, which will utilise two facsimile cameras, capable of stereoscopic imaging, on each lander. These cameras will scan the landing site area in black and white, colour and infrared, with a resolution of about 2 mm immediately below the landers. Examination of the surrounding terrain may reveal evidence of past or present living systems. Furthermore, frequent scans of this area may show signs (for example, colour changes) suggestive of living processes[6].

Also on board each Viking lander is an instrument that will perform organic analyses of the Martian surface material. This is essential not only for obtaining results which may be relevant to Martian life, but also may provide valuable information in assessing the state of molecular complexity if the planet is in a prebiotic state of evolution. The heart of this instrumentation is a mass spectrometer, chosen because of its high sensitivity, wide dynamic range, and broad applicability. For the analyses, samples will be heated in ovens at 200 °C and at 500 °C, and the evolved organic vapour (if any) will first pass through a chromatographic column for separation. A complete gas chromatogram takes 84 min and, during this period, the mass spectrometer will record a complete mass spectrum from mass 12 to mass 200 every 10.3 s (ref. 7).

The biological payload supports three separate experiments which are based on different assumptions about the nature of a possible Martian biology. In the face of our relative ignorance of the local environmental conditions on Mars—for example, up to the present, there is no positive indication that nitrogen is present on Mars[8]—there is ample reason to approach the question of life detection on Mars with a broad approach. The combination of biological experiments on Viking is thus designed to create a diverse set of environments within which to elicit evidence of metabolism. Three kinds of metabolic question will be asked. Is there evidence for building up of molecules containing carbon starting with ^{14}CO or $^{14}CO_2$? Can small radioactive organic molecules be broken down to $^{14}CO_2$? Are gases other than CO_2 produced or consumed? These broad experiments try to measure anabolic and catabolic reactions on Mars. The conditions vary from dry to wet; include the presence of simple and complex nutrient sources, as well as the absence of added nutrients; and include incubation in the light or dark.

For the biological experiments samples will be analysed several times during each mission. They will be obtained from the upper 4 cm of surface material and will be incubated for different periods of time in each experiment. Incubation temperatures are expected to run at 15 ± 10 °C. Furthermore, each of the experiments is provided with the capability to perform a control experiment with samples preheated to 160 °C for 3 h, in the event that any of the experiments gives a presumptive positive result.

Surface samples (approximately 6 cm^3) will be delivered into the biology instrument by an extendable boom at the end of which a jaw-like scoop digs into the surface to acquire samples (Fig. 2).

The biology instrument contains four modules, one for each of the three experiments, as well as a common service module, which contains a helium source used to rotate incubation cells, purge incubation chambers, and for other operations as well as a system of vents for gases and for liquid wastes. A detailed description[9] of the instrument is beyond the scope of this communication, but a brief account follows.

The pyrolytic release (or carbon assimilation) experiment is designed to measure either photosynthetic or dark fixation of CO_2 or CO into organic compounds[10,11]. Both of these gases are known to be present in the atmosphere of Mars, and the experiment is designed to simulate, as closely as conditions permit, the actual Martian environment. The experiment hardware includes a xenon arc lamp with a spectral range and distribution quite similar to the solar spectrum, and with an intensity of about 20% of the maximum Martian solar irradiation at the surface. The light source is provided with a filter to remove ultraviolet radiation below 340 nm to prevent the non-biological fixation of carbon monoxide into organic compounds, as has been reported by Hubbard *et al.*[12,13]. For this experiment, 20 μCi of a mixture of $^{14}CO_2$ and ^{14}CO (in a ratio of approximately 95 : 5) is injected into the headspace (containing Mars atmosphere) above a 0.25-cm^3 surface sample that has been sealed off in one of the three incubation chambers provided. Incubation proceeds for the next five days in the light. While the incubation is proceeding, a long background count is taken. Following this period, the original incubation atmosphere is automatically vented, and the sample is pyrolysed by heating to 625 °C. During this stage of the experiment sequence, any residual initial radioactive CO or CO_2 will be driven out of the sample, through a column, the organic vapour trap (OVT), and into a ^{14}C detector, while organic fragments will be adsorbed on the OVT. After counting at this point in the sequence, the radioactive gases in the detector are automatically vented, and the detector is then heated to remove adsorbed gases. Following this step, and several additional helium purges of the OVT and the detector, the organic matter that had been trapped on the OVT is now eluted by heating it to 650 °C for 3 min. During this heating, any trapped organics are released from the column and are simultaneously oxidised to CO_2 by copper oxide present in the packing of the OVT. The effluent from this procedure is purged into the detector and counted. A radioactive peak at this time would constitute presumptive evidence for biological activity, to be followed by a control experiment using heat-sterilised soil.

Fig. 2 Viking lander. Surface sampler is seen extended at left. Biology sample processor and distribution assembly is seen midway between the two cameras. Biology instrument is beneath this component and not visible in this figure.

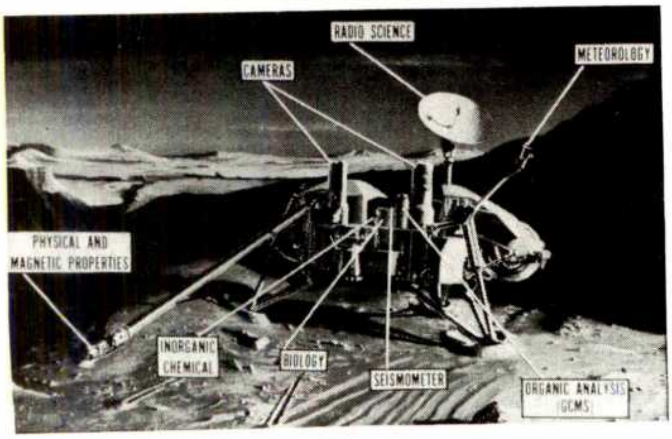

In addition to the sequence just described, the experiment can be modified by the introduction of water vapour into the incubation atmosphere by commands from Earth. Another commandable option in this experiment is to turn off the lamp to conduct a dark incubation.

The labelled release experiment[14] will test for metabolic activity during incubation of a surface sample that has been moistened with a solution of ^{14}C-labelled simple organic compounds, consisting of a mixture of one-, two-, and three-carbon compounds, all uniformly labelled and in dilute aqueous solution. For this experiment, one of the four incubation cells provided in this module will receive 0.5 cm^3 of surface material, and will be sealed with Martian atmosphere trapped in the headspace above the sample. Following this, a background count, lasting approximately 24 h, is taken, after which 0.115 cm^3 of nutrient is automatically injected onto the sample. Incubation proceeds for the ensuing 8 d. A second injection of labelled nutrient then occurs, and incubation continues for 2 d. During the entire time, the atmosphere above the sample is monitored by a ^{14}C detector to determine the kinetics of released labelled gas following each injection. Incubation is ended by a termination sequence to bring the background count down to pre-incubation levels. Following this 'clean-up' operation, the experiment is ready for another analysis cycle.

The gas exchange experiment[15] will be conducted in two different modes using the same equipment. In one mode (the 'humid' mode), Martian surface samples will be incubated in the presence of CO_2 and water vapour. This mode is based on the assumption that substrates may not be limiting on Mars, but that biological activity is dormant in these samples until enough water becomes available in the environment. The second mode (the 'heterotrophic' mode) assumes the presence of frankly heterotrophic organisms in the Martian surface.

For both of these experimental modes, it is further assumed that metabolism of active organisms in the samples will cause the disappearance or release of one or more gases known to be involved in terrestrial metabolic processes. For an analysis, 1 cm^3 of sample is delivered into the single incubation cell. A mixture of CO_2 and Kr (in He) is then added to serve as the incubation atmosphere. After this step, 0.5 cm^3 of nutrient is delivered to the bottom of the incubation cell. During incubation, the sample is retained in an inner-cup within the incubation cell so that the nutrient does not come into direct contact with the sample. The inner cup is porous and allows equilibration between the sample and the incubation atmosphere. Gas samples (100 ul) are taken from the headspace above the sample immediately after the nutrient has been injected and at specified times thereafter for the next 7 d. The gas samples are swept through a chromatographic column and the components detected by a thermal conductivity detector. If no command to the contrary is given after 7 d in the 'humid' mode, the instrument will automatically inject additional nutrient bringing the total aqueous volume now to 2.5 cm^3. With this amount of nutrient, the sample will be wet by the nutrient and incubation now will proceed in the 'heterotrophic' mode. (The nutrient solution contains both D- and L-amino acids as well as other organic substrates, growth factors and inorganic compounds.) Incubation continues in this mode with gas samplings at stipulated intervals for the next 9 d. At this point, options exist to proceed in various directions, depending on the data obtained. One is to drain the nutrient from the bottom of the cell and to introduce fresh atmosphere and fresh nutrient, and to incubate the original sample for an additional 19 d. Or, the initial incubation conditions can simply be extended for an additional 19-d period (that is, without draining the original nutrient or changing the gas atmosphere). If circumstances warrant it, the nutrient can be drained, the original sample dried, and a new sample introduced on top of the first one for a second analysis in the 'heterotrophic' mode.

In addition to the ^{14}C data from the two radioactivity detectors, and the gas chromatographic data, several other measurements will be telemetered periodically from the spacecraft during the course of these experiments. These include the status of the xenon lamp, the position of each incubation cell, temperature measurements of each incubation cell being used, and temperature measurements of both nuclear detectors, of the OVT and of the gas chromatographic column and detector. In addition, we will receive data on the pressure of the critical helium reservoir in the common services module.

Figure 3 shows one of the flight instruments in its final stages of assembly. It contains, in addition to the incubation cells and sample distribution system, four different gas supplies, two different nutrients, two ^{14}C detectors, a thermal conductivity detector and chromatographic system, 43 different heaters, 4 thermoelectric coolers, 39 miniature latching solenoid valves, a xenon arc lamp, 22,000 transitors, and 18,000 other electronic parts. All of this is packaged into a volume somewhat greater than 1 foot^3, and weighs 35 pounds.

The three biology experiments differ in their sensitivity, as measured by their responses to terrestrial organisms. Both the gas exchange and labelled release experiments have, by now, been tested against a wide variety of soils and they readily "detect" the presence of microbial flora in these samples when they are incubated in ambient terrestrial conditions. When these soil samples are incubated under the conditons in which the experiments will be operated on Mars, the responses are delayed by prolonged lag periods, but qualitatively similar responses are seen. In contrast, the pyrolytic release experiment does not respond to terrestrial soils at all when incubated in "Martian" conditions. Only when water is included in the incubation test cell is terrestrial biological activity demonstrable in this experiment. Accordingly, during the long test programme that preceded the manufacture of the flight instruments, several 'standard' soils were used to challenge the two 'wet' experiments. For the pyrolytic release experiment, soil was preincubated in the light in the presence of water to provide fixed radioactive carbon compounds, dried, and then used in this form to test the equipment. Since the final flight hardware is designed to work on Mars, and not on Earth, and because the design of the biology package precludes repetitive incubations (beyond four per experiment), and because of the rigid requirements to prevent terrestrial contamination, the flight instruments were not, and could not be, tested with terrestrial soils. Precursor instruments, built to flight specifications (with minor exceptions), did go through at least one prolonged test in simulated Martian conditions using one of our 'standard' soils, (containing 1×10^6 aerobic, and 5×10^4 anaerobic organisms per g; with a pH of 4.8 and an organic content of 0.8%). In addition, a flight-like instrument was installed on a lander and tested as part of a complete system, but these tests did not include analysis of any soils. Rather, known mixtures of gases were processed through the gas exchange hardware, and $^{14}CO_2$ was used to challenge the other two experiments. These tests[16], while not completely satisfying, in that only a part of the complete system was tested, gave results entirely consistent with extensive prior testing at the module level. Finally, at the component level (that is, detectors, chromatograph columns, and so on), many of the actual flight components were extensively tested for their scientific as well as their engineering characteristics. In these tests, no significant anomalies were uncovered. In summary, the testing programme was less than optimal, being limited by time and fiscal constraints, but met the minimum standards for confidence that the instruments will perform their nominal functions after landing on Mars.

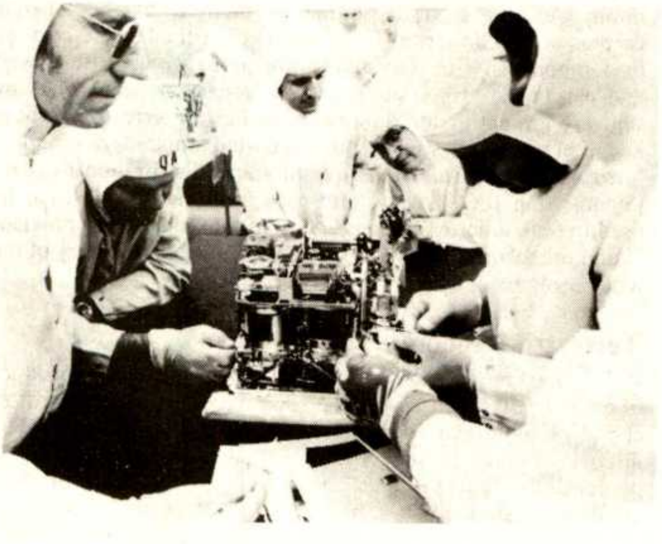

Fig. 3 Biology flight instrument in final stages of assembly.

The team of scientists selected by NASA, in 1969, to plan and conduct the biological investigation on the Viking spacecraft consisted of the authors and the late Dr Wolf Vishniac (University of Rochester, Rochester, New York). The following individuals are collaborators in these investigations: Bonnie Berdahl, Glenn Carle and Richard D. Johnson (NASA, Ames Research Center, Mountain View, California); George Hobby (California Institute of Technology, Pasadena, California); Jerry Hubbard (Georgia Institute of Technology, Atlanta, Georgia); and Patricia Straat (Biospherics, Incorporated, Rockville, Maryland).

[1] Farmer, C. B., and LaPorte, D. D., *Icarus*, **16**, 34 (1972).
[2] Horowitz, N. H., and Hubbard, J. S., *Ann. Rev. Genet.*, **8**, 393 (1974).
[3] Glasstone, S., *The Book of Mars*, NASA SP-179 (1968).
[4] Horowitz, N. H., *Acc. chem. Res.*, **9**, 1 (1976).
[5] Sagan, C., and Lederberg, J., *Icarus* (in the press).
[6] Mutch, T. A., *et al.*, *Icarus*, **16**, 92 (1972).
[7] Anderson, D. M., *et al.*, *Icarus*, **16**, 111 (1972).
[8] Barth, C. A., *Ann. Rev. Earth planet. Sci.*, **2**, 333 (1974).
[9] *Report No. 21020-6003-RU-00, August 1975* (TRW Systems Group, Redondo Beach, California 90278).
[10] Hubbard, J. S., Hobby, G. L., Horowitz, N. H., Geiger, P. J., and Morelli, F. A., *Appl. Microbiol.*, **19**, 32 (1970).
[11] Horowitz, N. H., Hubbard, J. S., and Hobby, G. L., *Icarus*, **16**, 147 (1972).
[12] Hubbard, J. S., Hardy, J. P., and Horowitz, N. H., *Proc. natn. Acad. Sci. U.S.A.*, **68**, 574 (1971).
[13] Hubbard, J. S., Hardy, J. P., Voecks, G. E., and Golub, E. E., *J. molec. Evol.*, **2**, 149 (1973).
[14] Levin, G. V., *Icarus*, **16**, 153 (1972).
[15] Oyama, V. I., *Icarus*, **16**, 167 (1972).
[16] *Reports Nos MMK 1124 and MMC 1141* (TRW Systems Group, Redondo Beach, California 90278).

articles

Xenon record of the early Solar System

D. D. Sabu
Department of Chemistry, Grambling State University, Grambling, Louisiana 71245

O. K. Manuel
Department of Chemistry, University of Missouri, Rolla, Missouri 65401

We suggest that xenon isotopes in meteorites and in outer regions of the Sun contain debris from a supernova which exploded in the vicinity of the present Solar System, and we conclude that xenon in the outer planets is enriched in this supernova debris.

IN 1960 Reynolds[1] noted that the isotopic composition of xenon trapped in the Richardton olivine–bronzite chondrite and in the Murray carbonaceous chondrite differed in a uniform manner from that of xenon in air. He concluded that the general isotopic anomaly pattern of xenon in meteorites was primordial in origin, that is, characteristic of xenon incorporated in the meteorites at the time of their formation. Subsequent analyses confirmed that xenon trapped in other stone meteorites exhibits a similar pattern of isotopic anomalies[2–4], now commonly designated as AVCC xenon.

In 1964 Reynolds and Turner[5] analysed the isotopic composition of xenon released by stepwise heating of the Renazzo chondrite and observed an unusual isotopic anomaly pattern in the xenon released at 700–900 °C. Relative to the two more abundant, β-shielded isotopes, ^{128}Xe and ^{130}Xe, there was an enrichment of the heavy isotopes, $^{131-136}$Xe, of the general form expected for a fission spectrum. It was noted that ^{124}Xe and ^{126}Xe also seemed to be enriched in the xenon released at these temperatures, and small amounts of these isotopes would have to be explained by some additional process. During the next eight years, analyses in several laboratories of xenon released by stepwise heating of other carbonaceous chondrites confirmed the presence of this strange xenon component[6–12]. Attempts to understand the origin of this component were, however, focused exclusively on the enrichment of the heavy isotopes, and the strange xenon came to be referred to as "fission-produced xenon"[9], "Renazzo fission"[8] and "CCF" as an abbreviation for carbonaceous chondrite fission[13].

Possible explanation

In discussing the anomalous xenon in Renazzo, Reynolds and Turner[5] had stated that there were relatively large errors in the measurements of the light isotopes, but by 1972 relatively large enrichments of this anomalous xenon had been observed in other carbonaceous chondrites. It was then noted[14] that all available data on xenon released from carbonaceous near 800 °C showed an excess of the light, proton-rich isotopes in addition to the enrichment of heavy, neutron-rich isotopes. This observation could not be explained by any of the mechanisms previously proposed to account for the excess heavy xenon isotopes—spontaneous fission[5] of ^{244}Pu, a carrier[8] of heavy xenon adsorbed on carbonaceous material, neutron-induced fission[9], isotopic mass-fractionation[10,11], or fission[15–17] of superheavy elements. We therefore suggested that the anomalous xenon represents an isotopically distinct component which had been trapped in carbonaceous chondrites and suggested two possible mechanisms for its production before being incorporated into the meteorite; either by a mixture of severely mass fractionated xenon with excess $^{131-136}$Xe from neutron-induced fission of transbismuth nuclides, or by a supernova explosion generating an excess of the proton-rich isotopes via the p process and an excess of the neutron-rich isotopes via the r process. At that time we noted that there was, however, no evidence among the other elements for distinct isotopic components from separate nucleosynthesis events. But isotopically distinct components of oxygen[18] and magnesium[19] were found in carbonaceous chondrites within the next two years, and others[20–22] expanded on the possible role of a supernova explosion in producing the anomalous xenon in carbonaceous chondrites.

Since the term CCF xenon had connotations of a mechanism which could only account for part of the isotopic pattern of anomalous xenon released from carbonaceous chondrites near 800 °C, we suggested component X as a more innocuous term for the xenon component enriched in the light and heavy isotopes[14]. In 1974 we[23] reported that component X contained at least seven of the nine stable xenon isotopes and noted that AVCC xenon itself contained component X, that is, before the incorporation of xenon in stone meteorites there were sufficient quantities of component X to produce an observable alteration in the isotopic composition of xenon in the region of accretion.

Very recently Lewis *et al.*[24] reported the results of a beautiful detailed study on the abundance and isotopic composition of noble gases in separated mineral fractions of the Allende carbonaceous chondrite. Their results offer the best description of component X. In the following sections we will use these[24] and earlier results of studies on carbonaceous chondrites by stepwise gas extraction data from studies on terrestrial xenon, and the results of studies on solar-wind implanted xenon in lunar soil to determine the quantity and distribution of component X in the solar system. This information will then be used to seek a better understanding of the origin of component X and the record it contains of events in the early history of the Solar System.

Terrestrial xenon

It is now known that radiogenic ^{129}Xe, the decay product of extinct ^{129}I which Reynolds[25] discovered in the Richardton chondrite, is a common component of meteoritic xenon. The discovery of radiogenic ^{129}Xe in mantle-derived CO_2 (refs 26–28) demonstrates that the Earth started to retain this decay product at about the same time as the meteorites. Because of uncertainties in correcting for this radiogenic component, we will not

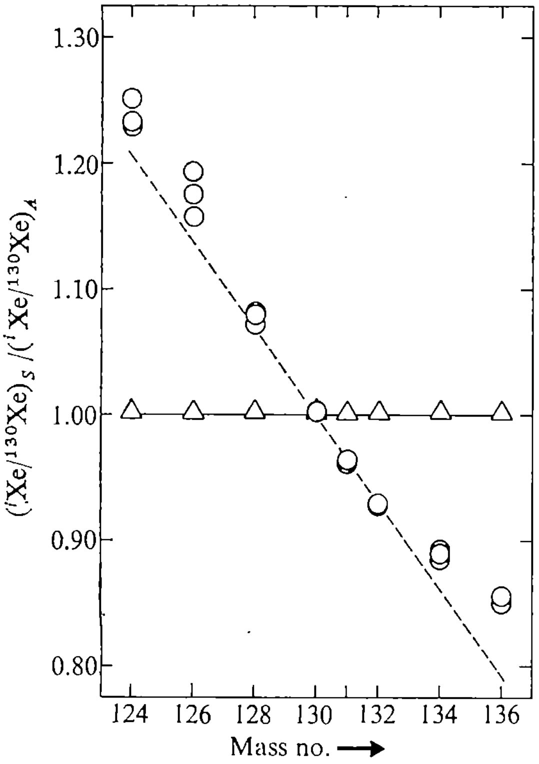

Fig. 1 A comparison of xenon isotope ratios in solar (S) and terrestrial xenon (A). The latter has been corrected for fission products from ^{244}Pu. Three separate estimates of solar xenon are in close agreement, and two of the estimates are coincident for xenon isotope ratios at masses 131 (refs 47, 48), 132 (refs 47, 48) and 136 (refs 43, 47).

consider the abundance of ^{129}Xe in comparing terrestrial and extraterrestrial xenon. Since excess $^{131-136}$Xe constitutes a major part of component X, however, it will be necessary to correct for fissiogenic $^{131-136}$Xe from another extinct radionuclide, ^{244}Pu. The latter was discovered in the Pasamonte achondrite by Rowe and Kuroda[29], and should have produced more than 15 times as much fissiogenic $^{131-136}$Xe as the spontaneous fission of ^{238}U over the history of the Earth.

The results of several analyses[30–32] of noble gases in shales and other carbonaceous minerals reveal extremely high concentrations of xenon, apparently from physical adsorption[33]. The suggestion that the atmosphere may contain only one-tenth[31] of the Earth's total inventory of xenon has been confirmed by analyses[28] of noble gases in a volcanic xenolith from the mantle. We will therefore consider the contribution from the fission of ^{244}Pu to the total concentrations of $^{131-136}$Xe in the 'crust–atmosphere' system, accepting the decay product of 17 Myr ^{129}I in the Earth's mantle[28] as evidence that ^{244}Pu in the mantle has made a negligible contribution to the isotopes, $^{131-136}$Xe, in this system. Since there are 8.2×10^{35} atoms of ^{136}Xe in the atmosphere[34], we estimate that the Earth contains a total of 8.2×10^{34} atoms of ^{136}Xe. Podosek[35] has shown that $^{244}\mathrm{Pu}/^{238}\mathrm{U} = 1.27 \times 10^{-2}$ when the St Severin meteorite started to retain ^{136}Xe from the decay of ^{244}Pu. Assuming that the Earth started retaining fissiogenic ^{136}Xe, ^{136f}Xe, at this time, an average uranium content of 1.3 p.p.m. for the Earth's crust[36], and a 6% fission yield at ^{136}Xe, then the decay parameters of ^{244}Pu (ref. 37) indicate that terrestrial xenon contains isotopes in the ratio $^{136f}\mathrm{Xe}/^{136}\mathrm{Xe} = 0.018$. From the fission yields of ^{244}Pu (ref. 38), and the isotopic composition of atmospheric xenon[39], we deduce the following isotopic composition of fission-free terrestrial xenon: $^{124}\mathrm{Xe}:{}^{126}\mathrm{Xe}:{}^{128}\mathrm{Xe}:{}^{130}\mathrm{Xe}:{}^{131}\mathrm{Xe}:{}^{132}\mathrm{Xe}:{}^{134}\mathrm{Xe}:{}^{136}\mathrm{Xe} = 2.353:2.206:47.03:\equiv 100:518.1:655.7:252.3:213.5$. We will use the symbol 'A' to designate fission-corrected atmospheric xenon of this composition in the following discussion on solar and meteoritic xenon. It should be stressed that we have purposely attempted to make a conservative estimate of the contribution of ^{244}Pu to $^{131-136}$Xe by selecting one of the higher estimates for the total xenon content of the Earth and by assuming that all of this xenon is in the 'crust–atmosphere' system. This was done so that we will not overestimate the amount of component X in other parts of the Solar System.

Solar xenon

Marti[40] first identified the presence of solar-wind implanted xenon in the Pesyanoe meteorite. Later studies of xenon in lunar fines and breccias confirmed the general isotope pattern which Marti reported in solar xenon. Several lunar scientists[41–44] interpreted the results of their xenon analyses as evidence that the isotopic compositions of atmospheric and solar xenon are related by mass fractionation and attempted to explain AVCC xenon as a mixture of solar xenon with CCF xenon. Although this interpretation of the three known reservoirs of xenon is not consistent with the experimental data[33,45], it was widely accepted as additional evidence for a large component of fission-produced xenon in carbonaceous chondrites.

Bogard *et al.*[46] and others[45] have noted that the 'true' isotopic composition of solar xenon is still not known because many variations observed in the isotopic composition of xenon in lunar soils arise from mass fractionation. To compare the isotopic composition of terrestrial and solar xenon, we have therefore selected similar estimates of the latter from analyses of xenon in lunar fines by three, well recognised laboratories: Pepin's laboratory at the University of Minnesota[43], Wasserburg's laboratory at the California Institute of Technology[47], and Geiss' laboratory at the University of Bern[48]. The authors identify this xenon as trapped lunar Xe (ref. 43), SUCOR Xe (ref. 47), and BEOC 12001 Xe (ref. 48). We normalise these xenon spectra to ^{130}Xe to facilitate identification of component X, which is enriched in both the light and the heavy isotopes relative to ^{130}Xe (refs 14 and 23).

The relationship between isotope ratios in solar xenon, $({}^{i}\mathrm{Xe}/^{130}\mathrm{Xe})_S$, and xenon isotope ratios in fission-free atmospheric xenon, $({}^{i}\mathrm{Xe}/^{130}\mathrm{Xe})_A$ is shown in Fig. 1. The dashed line corresponds to 3.45% per a.m.u. fractionation of the $({}^{i}\mathrm{Xe}/^{130}\mathrm{Xe})_A$ values. This fractionated terrestrial xenon is very similar to solar xenon at $^{128-132}$Xe, but the agreement is not very good at ^{124}Xe, ^{126}Xe, ^{134}Xe and ^{136}Xe. Since studies of xenon in carbonaceous chondrites show that component X is highly enriched in these four isotopes, we interpret Fig. 1 as evidence that solar-type xenon contains a larger fraction of component X than does terrestrial xenon. Deviations of the heavy isotopes from the fractionation line in Fig. 1 suggests that ~ 7% of ^{136}Xe in solar-wind xenon is from component X. This is a lower limit on the amount of component X in solar xenon; higher values would result if terrestrial xenon contains component X or a larger component of fissiogenic $^{131-136}$Xe than indicated by our purposely conservative estimate.

Meteoritic xenon

The isotopic compositions reported[24] for xenon in separated mineral fractions of Allende confirm the presence of an enrichment of both light and heavy xenon isotopes in component X. Figure 2 shows the correlation between the enrichment of the two lightest xenon isotopes and the heaviest xenon isotope in mineral separates of Allende[24] and in the gas released near 800 °C from earlier stepwise heating experiments on carbonaceous chondrites[5,8,10–12]. Our estimate of fission-free atmospheric xenon is also shown in Fig. 2, and changes in its composition which can be accounted for by mass fractionation are represented by dashed lines. We will discuss the intersections of the fractionation lines with the solid correlation lines later, after considering correlations of other constituents in the separated mineral fractions of Allende.

It has been suggested[24] that we were too hasty in concluding that the correlation shown in Fig. 2 is evidence that excesses of the light and heavy xenon isotopes were mixed before being

[illegible] Library
SCIENCE COLLEGE

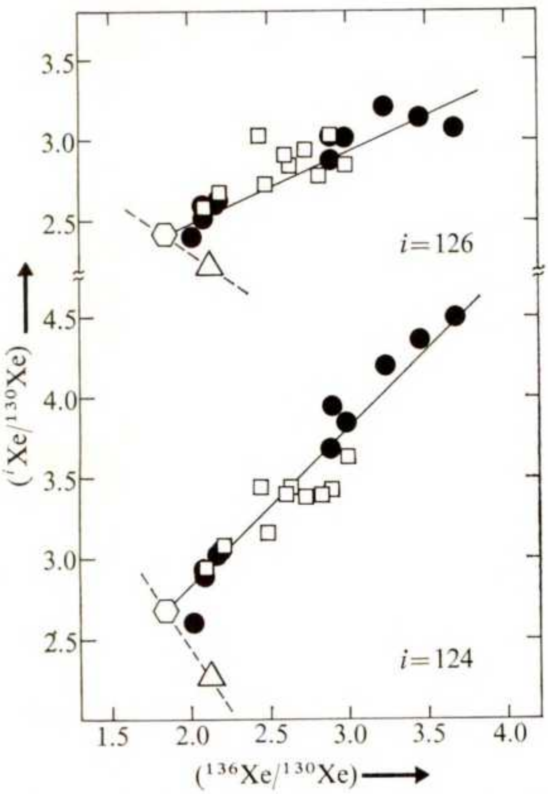

Fig. 2 The correlation of excess ^{124}Xe, ^{126}Xe and ^{136}Xe in mineral fractions of Allende[24] (●) and in xenon released by stepwise heating (☐) carbonaceous chondrites[5,8,10–12]. Isotope data from stepwise heating experiments are from a tabulation by Sabu *et al.*[23]. Fission of a volatile superheavy element cannot account for the correlations observed between light and heavy xenon isotopes.

trapped in meteorites. Anders *et al.*[49] suggest that the excess heavy xenon isotopes may be from *in situ* decay of a volatile superheavy element and the excess light xenon isotopes may be from an unknown isotopic fractionation mechanism which occurred during trapping. We will briefly examine the experimental evidence for this model.

First, we will examine the correlations of excess ^{136}Xe with volatile elements in mineral fractions at Allende, since the previously reported correlation[16] of excess ^{136}Xe with ^{132}Xe, In and Hg in bulk meteorite samples seems to form the basis for this model. The correlations which result from the recent analyses[24,49] on In and Xe are shown in Fig. 3; Hg values were not reported. In 3Cl the concentrations of excess ^{136}Xe is enriched 180-fold over its concentration in bulk Allende, but In concentrations are unchanged. The dashed line in Fig. 3 shows the 45° correlation of excess ^{136}Xe with ^{132}Xe in average carbonaceous chondrites[16]. The xenon in separated mineral fractions of Allende seem to define three sets of correlations between excess ^{136}Xe and ^{132}Xe, none of which agrees with the correlation found in bulk carbonaceous chondrites. As we have noted earlier[50], the 45° correlation reported[16] between excess ^{136}Xe and ^{132}Xe in various meteorites occurs because the bulk isotopic composition of xenon in these meteorites is constant. Fractions of xenon enriched in component X can, however, be isolated by stepwise heating experiments or by separating mineral fractions. As the degree of separation of component X increases, the correlation with ^{132}Xe decreases. The correlation is best for bulk meteorite samples because AVCC xenon itself contains component X. But we find little, if any, evidence in Fig. 3 to support the previously reported correlation[16] of excess ^{136} Xe with In or ^{132}Xe.

To seek evidence that the excess light xenon isotopes in component X result from an unknown fractionation process, we next look for the effects of this process in the isotopes of krypton. The isotope ratios of krypton and xenon in the separated mineral fractions of Allende[24] are shown in Fig. 4. These isotope ratios show an excellent correlation between the enrichment of the light xenon isotopes and the heavy krypton isotopes. Anders *et al.*[49] suggest that the heavy krypton isotopes were enriched by fractionation, but we know of no fractionation process which could enrich the heavy isotopes of krypton and the light isotopes of xenon to produce the correlations shown in Fig. 4. We have not considered the light krypton isotopes because of hydrocarbon background and large uncertainties[24] but conclude from Fig. 4 that isotopic mass fractionation is not a viable mechanism to account for the excess light xenon isotopes in component X.

We will therefore consider the possibility that component X indeed represents an isotopically distinct component of xenon which has been trapped, together with terrestrial type xenon, in meteorites. Figure 5 compares the isotopic composition of xenon in the Earth, in average carbonaceous chondrites[4] and in the mineral fraction of Allende showing the most anomalous xenon, 3CS4 (ref. 24). The dashed line defines the values of $(^{i}\mathrm{Xe}/^{130}\mathrm{Xe})_{\mathrm{A}}$ with 2.25% per a.m.u. fractionation. This fractionation is also shown by the hexagons in Fig. 2 at the intersections of the dashed fractionation lines and the solid correlations. AVCC xenon, the xenon in separated mineral fractions of Allende, and the xenon released by stepwise heating of carbonaceous chondrites can be understood in terms of various mixtures of mass fractionated terrestrial xenon and component X. Deviations from the fractionation line at ^{136}Xe suggest that ~ 7% of the ^{136}Xe in AVCC xenon, and 50% of the ^{136}Xe in the 3CS4 fraction of Allende, are from component X. We regard these values as lower limits for reasons stated earlier.

Before considering the implications of component X, we wish to stress that results of the recent analyses on xenon in mineral separates of Allende[24] are inconsistent with our earlier suggestion[14] that the excess light isotopes in component X might result from mass fractionation. In addition to the reasons cited earlier for rejecting this mechanism, Lewis *et al.*[24] point

Fig. 3 Correlations of the 'fission' product, $^{136\mathrm{f}}$Xe, with In (▲) and ^{132}Xe (●) in mineral fractions of Allende[24,49]. The dashed line represents the correlation of $^{136\mathrm{f}}$Xe with ^{132}Xe in bulk meteorites if the amount of $^{136\mathrm{f}}$Xe is calculated in the same manner used to calculate $^{136\mathrm{f}}$Xe in Allende minerals[24].

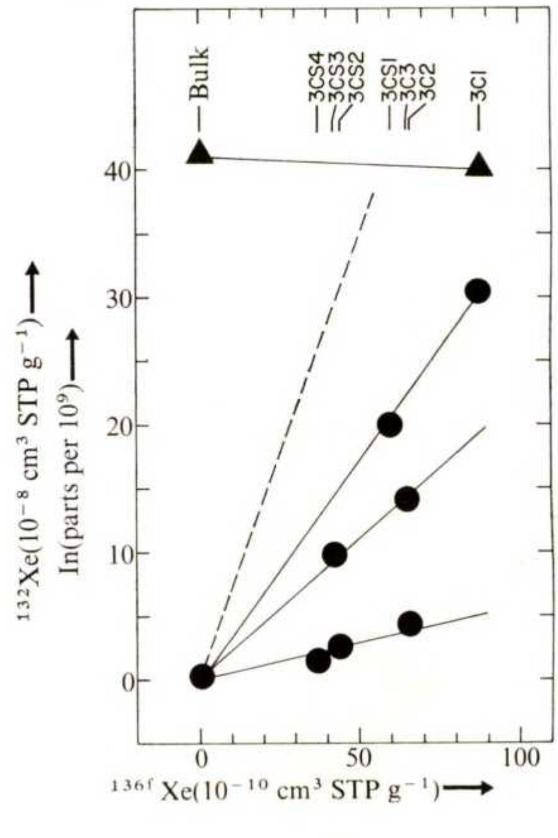

out that there is a definite excess of ^{124}Xe in the anomalous xenon above any plausible fractionation line through ^{126}Xe, ^{128}Xe and ^{130}Xe. This can be seen in Fig. 5 for the 3CS4 xenon. We therefore conclude that component X represents material from a supernova.

Implications of component X

We have shown that component X, an isotopically distinct type of xenon, is present in the Sun and in meteorites. The isotopic composition of xenon in the Earth, in meteorites and in the Sun can be understood in terms of mixtures of component X, fractionated terrestrial xenon, and radioactive decay processes. Terrestrial xenon seems to contain the least amount of component X, although recent analyses by Lightner and Marti[51] suggest that indigenous lunar xenon also contains little or no component X. We offer the following outline of a model to explain the abundance and distribution of component X, using the term Y when referring to the other xenon component.

Considering first the abundance of X and Y, it should be noted that both components made major contributions to xenon in our Solar System. The relatively small contribution of X to terrestrial and indigenous lunar xenon suggests that Y was dominant in the region where the inner planets accreted. Although X accounts for up to 50% of the ^{136}Xe in some mineral fractions of meteorites, such as the 3CS4 fraction from Allende, these minerals constitute such a small fraction of the total meteorite that they might be attributed to inclusions of small amounts of 'dust grains' which formed outside our Solar System. We have, however, shown that X is responsible for ~ 7% of the ^{136}Xe in both AVCC xenon and solar xenon. This observation requires relatively large amounts of X in the Solar System. In view of this, we regard the dominant role of X in certain meteorite minerals as evidence that X too was dominant in certain regions of our Solar System. We therefore conclude that the supernova was in the immediate vicinity of our Solar System.

Fig. 4 Correlations of excess heavy krypton isotopes with excess light xenon isotopes in mineral fractions of Allende[24] (●). The isotopic composition of atmospheric noble gases are represented by the open triangles (△).

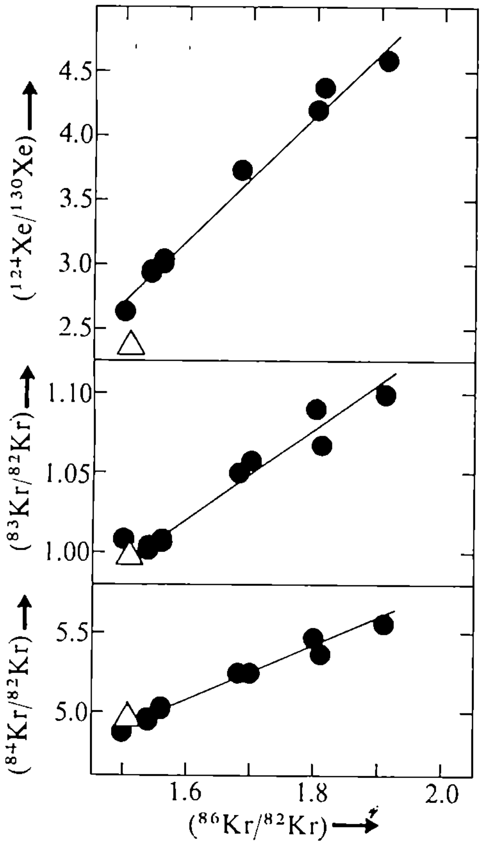

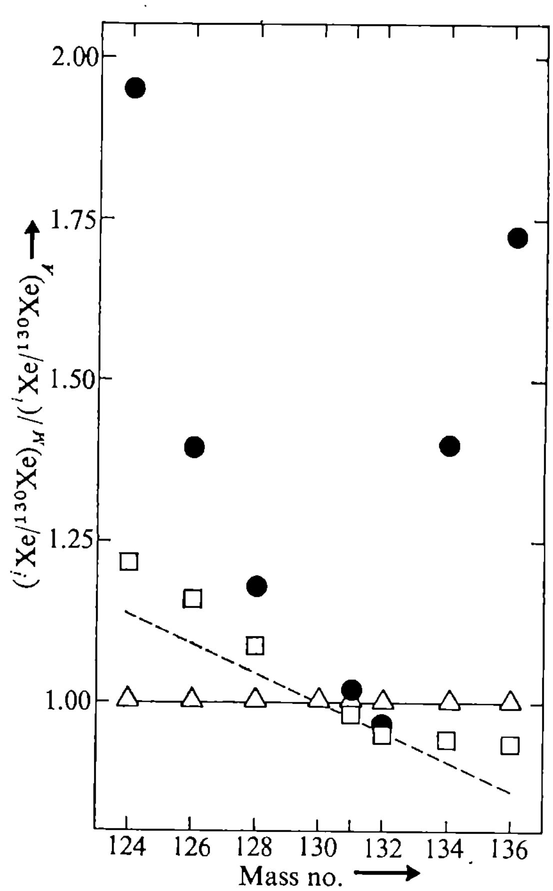

Fig. 5 A comparison of the xenon isotope ratios in AVCC[4] (□), in the 3CS4 fraction of Allende[24] (●) and in fission-free terrestrial xenon (△). Linear fraction of the latter, 2.5% per a.m.u., is represented by the dashed line. Deviations of meteorite xenon from this line arise from the presence of component X.

Considering next the distribution of X and Y, we suggest that these two isotopic components may correlate with other properties of our Solar System. As noted above, Y seems to have been dominant for the inner planets. In bulk meteorites X accounts for ~ 7% of the ^{136}Xe, but X is dominant in some meteorite minerals. The physical position of the parent meteorite material in the asteroid belt, and the occurrence of X-rich and Y-rich minerals in meteorites, suggests that this region may represent the boundary between regions where X and Y were dominant. There is an abrupt change in the character of planets in the region of the asteroid belt. The giant, less-dense planets lie beyond the asteroid belt and may contain relatively large contributions from X.

From the above considerations we conclude that our Sun was very likely once the smaller member of a binary star system. A supernova explosion of the other member produced debris rich in component X, in heavy krypton isotopes[24], in ^{244}Pu (ref. 52), ^{16}O (ref. 18) and ^{24}Mg (ref. 19), and perhaps rich in ^{26}Mg (ref. 19), helium and neon[24]. We expect that chemical elements of the outer planets will be enriched in these. Some of the debris also accumulated in the Sun, but the total solar abundance of X is not well defined, since material from the supernova may be enriched in the outer layers of the Sun. Hoyle[53] pointed out that initially low concentrations of helium, and high concentrations of metals in the iron group, in the Sun's core may account for the apparently low flux of solar neutrinos[54].

We thank Professor P. K. Kuroda for guidance in our graduate education.

Received February 4; accepted April 27, 1976.

[1] Reynolds, J. H., *Phys. Rev. Lett.*, **4**, 351 (1960).
[2] Krummenacher, D., Merrihue, C. M., Pepin, R. O., and Reynolds, J. H., *Geochim. cosmochim. Acta.*, **26**, 231 (1962)

[3] Marti, K., *Earth planet. Sci. Lett.*, **3**, 243 (1967).
[4] Eugster, O., Eberhardt, P., and Geiss, J., *Earth planet. Sci. Lett.*, **3**, 249 (1967).
[5] Reynolds, J. H., and Turner, G., *J. geophys. Res.*, **69**, 3263 (1964).
[6] Turner, G., *J. geophys. Res.*, **70**, 5433 (1965).
[7] Funk, H., Podosek, F., and Rowe, M. W., *Geochim. cosmochim. Acta*, **31**, 1721 (1967).
[8] Rowe, M. W., *Geochim. cosmochim. Acta*, **32**, 1317 (1968).
[9] Pepin, R. O., *Origin and Distribution of the Elements* (edit. by Ahrens, L. H.), 379 (Pergamon, Oxford and New York, 1968).
[10] Manuel, O. K., Wright, R. J., Miller, D. K., and Kuroda, P. K., *J. geophys. Res.*, **75**, 5693 (1970).
[11] Manuel, O. K., Wright, R. J., Miller, D. K., and Kuroda, P. K., *Geochim. cosmochim. Acta*, **36**, 961 (1972).
[12] Phinney, D. L., thesis, Univ. Minnesota (1971).
[13] Podosek, F. A., Huneke, J. C., Burnett, D. S., and Wasserburg, G. J., *Earth planet. Sci. Lett.*, **10**, 199 (1971).
[14] Manuel, O. K., Hennecke, E. W., and Sabu, D. D., *Nature*, **240**, 99 (1972).
[15] Srinivasan, B., Alexander, E. C., Jr, Manuel, O. K., and Troutner, D. E., *Phys. Rev.*, **179**, 1166 (1969).
[16] Anders, E., and Heymann, D., *Science*, **164**, 821 (1969)
[17] Dakowski, M., *Earth planet. Sci. Lett.*, **6**, 152 (1969).
[18] Clayton, R. N., Grossman, L., Mayeda, T. K., *Science*, **182**, 485 (1973).
[19] Lee, T., and Papanastassiou, D. A., *Geophys. Res. Lett.*, **1**, 225 (1974).
[20] Clayton, D. D., *Astrophys. J.*, **199**, 765 (1975).
[21] Black, D. C., *Nature*, **253**, 417 (1975).
[22] Clayton, D. D., *Geochim. cosmochim. Acta*, **40**, 563 (1976).
[23] Sabu, D. D., Hennecke, E. W., and Manuel, O. K., *Nature*, **251**, 21 (1974).
[24] Lewis, R. S., Srinivasan, B., and Anders, E., *Science*, **190**, 1251 (1975).
[25] Reynolds, J. H., *Phys. Rev. Lett.*, **4**, 8 (1960).
[26] Butler, W. A., Jeffrey, P. M., Reynolds, J. H., and Wasserburg, G. J., *J. geophys. Res.*, **68**, 3283 (1963).
[27] Boulos, M. S., and Manuel, O. K., *Science*, **174**, 1334 (1971).
[28] Hennecke, E. W., and Manuel, O. K., *Nature*, **257**, 778 (1975).
[29] Rowe, M. W., and Kuroda, P. K., *J. geophys. Res*, ,**70**, 709 (1965).
[30] Bogard, D. D., Rowe, M. W., Manuel, O. K., and Kuroda, P. K., *J. geophys. Res.*, **70**, 703 (1965).
[31] Canalas, R. A., Alexander, E. C., Jr. and Manuel, O. K., *J. geophys. Res.*, **73**, 3331 (1968).
[32] Phinney, D., *Earth planet, Sci. Lett.*, **16**, 413 (1972).
[33] Fanale, F. P., and Cannon, W. A., *Earth planet. Sci. Lett.*, **11**, 362 (1971).
[34] Verniani, F., *J. geophys. Res.*, **71**, 385 (1966).
[35] Podosek, F. A., *Earth planet. Sci. Lett.*, **8**, 183 (1970).
[36] Evans, R. D., and Goodman, C., *Bull. Geol. Soc. Am.*, **52**, 459 (1941).
[37] Fields, P. R., *et al.*, *Nature*, **212**, 131 (1966).
[38] Alexander, E. C., Jr, Lewis, R. S., and Reynolds, J. H., *Science*, **172**, 837 (1971).
[39] Nier, A. O., *Phys. Rev.*, **79**, 450 (1950).
[40] Marti, K., *Science*, **166**, 1263 (1969).
[41] Eberhardt, P., *et al.*, *Geochim. cosmochim. Acta*, Suppl. **1**, **2**, 1037 (1970).
[42] Hohenberg, C. M., Davis, P. K., Kaiser, W. A., Lewis, R. S., and Reynolds, J. H., *Geochim. cosmochim. Acta*, Suppl., **1**, **2**, 1283 (1970).
[43] Pepin, R. O., Nyquist, L. E., Phinney, D., and Black, D. C., *Geochim. cosmochim. Acta*, Suppl. **1**, **2**, 1435 (1970).
[44] Kaiser, W. A., *Earth planet. Sci. Lett.*, **13**, 387 (1972).
[45] Srinivasan, B., Hennecke, E. W., Sinclair, D. D., and Manuel, O. K., *Geochim. cosmochim. Acta*, Suppl. **3**, **2**, 1927 (1972).
[46] Bogard. D. D., Hirsch, W. C., and Nyquist, L. E., *Geochim. cosmochim. Acta*, Suppl., **5**, **2**, 1975 (1974).
[47] Podosek, F. A., Hueneke, J. C., Burnett, D. S., and Wasserburg, G. J., *Earth planet. Sci. Lett.*, **10**, 199 (1971).
[48] Eberhardt, P., *et al.*, *Geochim. cosmochim. Acta*, Suppl., **3**, **2**, **1821** (**1972**).
[49] Anders, E., Higuchi, H., Gros, J., Takahashi, H., and Morgan, J. W., *Science*, **190**, 1262 (1975).
[50] Sabu, D. D., and Manuel, O. K., *Trans. Mo. Acad. Sci.*, **5**, 16 (1971).
[51] Lightner, B. D., and Marti, K., *Geochim. cosmochim. Acta*, Suppl., **5**, **2**, **2023** (1974).
[52] Podosek, F. A., and Lewis, R. S., *Earth planet. Sci. Lett.*, **15**, **101** (**1972**).
[53] Hoyle, F., *Astrophys. J. Lett.*, **197**, L127 (1975).
[54] Baheall, J. N., and Davis, R., *Science*, **191**, 264 (1976).

Translation *in vitro* of vesicular stomatitis virus mRNA lacking 5′-terminal 7-methylguanosine

John K. Rose & Harvey F. Lodish

Department of Biology, Massachusetts Institute of Technology, Cambridge, Massachusetts 01239

The 5′-terminus 7-methylguanosine of vesicular stomatitis virus mRNA is not essential for translation of the mRNA. The 7-methylguanosine seems to have a mediating rather than an obligatory role in ribosome binding by the mRNA and in mRNA translation.

MESSENGER RNAs (mRNAs) from several animal viruses and animal cells contain the 5′-terminal structure $m^7G^{5'}ppp^{5'}NmpN(m)p$[1–10]. Vesicular stomatitis virus (VSV) and reovirus mRNAs synthesised by virion polymerases in the absence of S-adenosyl methionine contain the respective 5′-termini $G^{5'}ppp^{5'}ApAp$ and ppGp; these RNAs will not direct synthesis of virus proteins in cell-free extracts from wheat embryo unless the methylated 5′-terminus $m^7G^{5'}ppp^{5'}N(m)pNp$ has been formed[11,20]. Also, unmethylated reovirus mRNA will not bind to wheat germ ribosomes[12]. In the light of these experiments and others involving the chemical removal of the terminal 7-methylguanosine from globin mRNA[13], it has been suggested that the 7-methylguanosine is obligatory for translation of all mRNAs in eukaryotic cells[11–13].

We were led to question the requirement for 7-methylguanosine in translation by the finding that the 5′-terminus of poliovirus mRNA purified from the polyribosomes of infected HeLa cells has the 5′-terminus pUp[14]. We present here results which show, in contrast to previous work[11], that a terminal 7-methylguanosine is not obligatory for translation of VSV mRNAs. Oxidation or removal of the 7-methylguanosine reduces the rate of protein synthesis about threefold and has a similar effect on the rate of mRNA binding to ribosomes in a reticulocyte cell-free system. Furthermore, some of this inhibition may be due to non-specific effects of periodate oxidation.

Removal of 7-methylguanosine

Cells infected with VSV contain five monocistronic viral mRNAs which encode the five viral proteins[15–17], and these mRNAs are complementary to the single-stranded RNA genome of the virus[18]. VSV mRNAs purified from the polyribosomes of infected baby hamster kidney cells all possess a common 5′-terminal tetranucleotide structure, $m^7G^{5'}ppp^{5'}mAmpmAmpCp$. This has only partial base methylation of the first adenosine and partial base and ribose methylation of the second adenosine[5]. The 5′-terminal 7-methylguanosine, because it has free 2′,3′ (ribose) hydroxyl groups, is susceptible to oxidation with periodate, yielding a 2′,3′-dialdehyde. Further treatment with aniline results in loss of the 7-methylguanosine by β-elimination. We found that the procedure which previously gave quantitative removal of this nucleoside from the terminal tetranucleotide[5] was unsuitable for use on whole mRNA because it caused extensive degradation and aggregation of the mRNAs as well as some uncharacterised modifications of internal nucleotides. Therefore, we used the procedure detailed in Fig. 1 which involves use of less periodate and removal of periodate from the initial reaction by successive ethanol precipitations of the RNA before treatment with aniline. This procedure minimised but did not eliminate degradation, as is shown by polyacrylamide gel electrophoresis of the denatured mRNA (Fig. 1). The viral protein(s) encoded by the mRNA in each band have been described previously[16] and are indicated in the legend to Fig. 1. Both periodate oxidation and β-elimination resulted in detectable levels of degradation which are most obvious in the decreases in the peak heights of the larger RNA species. It is difficult to quantify the exact amount of degradation of each RNA species because of the presence of multiple RNA species on the gel; however, the results suggest a loss of about 50% of N protein

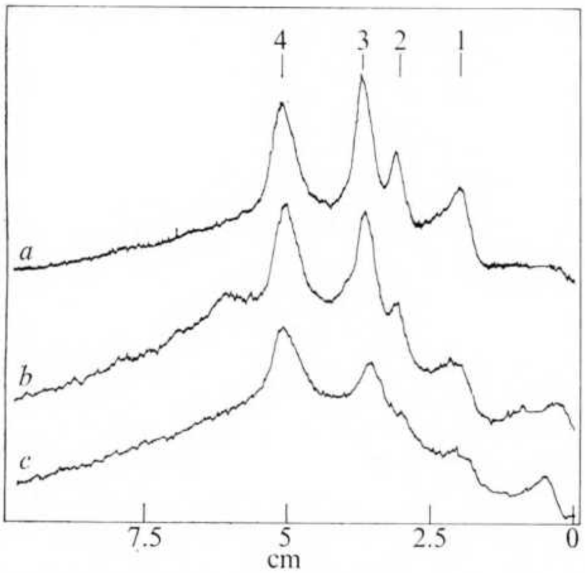

Fig. 1 Polyacrylamide gel electrophoresis of oxidised and β-eliminated VSV mRNAs. ^{32}P-labelled VSV mRNA was isolated by the following modification of a previous procedure[15]. A sample (2 l) of BHK-21 cells in spinner culture at 4×10^5 cells per ml were concentrated by centrifugation, washed twice with 100 ml of PO_4-free medium and then resuspended in 400 ml of PO_4-free medium. Actinomycin D (final concentration 5 µg ml^{-1}) and VSV (multiplicity of injection, 10) were then added, and incubation at 37 °C continued. One hour after addition of virus, 20 mCi of carrier-free $^{32}PO_4$ (New England Nuclear) was added, and incubation continued for 3 h. Infected cells were then isolated by centrifugation and resuspended in 10 ml of a solution containing 0.01 M $MgCl_2$, 0.01 M Tris–HCl (*p*H 7.4) and 25 µg ml^{-1} DNase I (Worthington, DPFF). Cells were lysed by addition of 0.1% sodium dodecyl sulphate (SDS) and incubated at 37 °C for 5 min. Then the extract lost detectable viscosity, and SDS and sodium acetate (*p*H 5 2) were added to final concentrations of 1% and 0.2 M, respectively, followed by extraction with an equal volume of a solution containing equal volumes of redistilled phenol and chloroform. After centrifugation, the aqueous layer was withdrawn and the phenol layer was re-extracted with 5 ml of 0.2 M sodium acetate (*p*H 5.2). The combined aqueous layers were then precipitated with 2 volumes of ethanol, followed by isolation of VSV mRNA by binding to and elution from 0.3 g of oligo(dT)-cellulose[15]. This procedure yielded from 3×10^8 to 10^9 c.p.m. in approximately 300 µg of mRNA. For periodate oxidation, 300 µg of lyophilised VSV mRNA (or 100 µg of VSV mRNA combined with 200 µg of unlabelled f2 phage RNA) was resuspended in 0.2 ml of 10 mM $NaIO_4$ (freshly dissolved) and incubated for 1 h at 23 °C in darkness. The RNA was then precipitated three times by addition of 0.4 ml of 0.1 M sodium acetate (*p*H 5.2) and 0.8 ml of ethanol. Half of the oxidised RNA was then resuspended in 0.1 ml of a solution containing equal volumes of 0.33 M aniline (*p*H 4.5, twice vacuum redistilled) and 0.15 M sodium acetate (*p*H 4.5) followed by incubation at 23 °C for 4 h. The RNA was then precipitated with ethanol three times as above.. Samples (approximately 10^5 c.p.m. each) of untreated (*a*), periodate-oxidised (*b*), and periodate-oxidised, β-eliminated RNA (*c*) were then denatured and subjected to electrophoresis on a 3.75% polyacrylamide slab gel containing 98% formamide, as described previously[15]. Microdensitometer scans of the autoradiogram of the wet gel are shown. Band 2 mRNA encodes the VSV G protein; band 3 encodes the N protein; and band 4 encodes the M and NS proteins[16].

mRNA (band 3) and 30% of M and NS mRNAs (band 4).

To quantify the removal of 7-methylguanosine from the mRNAs, samples were digested with penicillium nuclease (P1), an enzyme which degrades RNA to 5′ mononucleotides regardless of base or ribose modifications[19]. The 5′-terminal structures expected from P1 digestion of untreated and *β*-eliminated VSV mRNAs are $m^7G^{5'}ppp^{5'}(m)Am$ and ppp(m)Am, respectively[5]. To separate these termini from the 5′ mononucleotides, we subjected the digests to ionophoresis on DEAE paper at *p*H 3.5 (Fig. 2). Periodate oxidation and *β*-elimination resulted in the disappearance of radioactivity in $m^7G^{5'}ppp^{5'}(m)Am$ and its appearance in ppp(m)Am (lanes 1 and 2); the latter migrates much more slowly than the parent structure because of the loss of the positive charge on 7-methylguanosine and the gain of an additional negative charge from the unesterified phosphate. The structures of these nucleotides were demonstrated by their respective resistance and sensitivity to digestion with alkaline phosphatase digestion and by the identification of the products derived by venom phosphodiesterase digestion of each, as was done previously: $m^7G^{5'}ppp^{5'}(m)Am \xrightarrow{\text{venom}}$ pm^7G, Pi, p(m)Am; ppp(m)Am $\xrightarrow{\text{venom}}$ PPi, p(m)Am (ref. 5). The low levels of pppA and pppG in the mRNA preparations are derived from a fraction of the non-polysomal VSV RNAs which terminate in 5′ triphosphates[5].

No residual 5′-termini containing 7-methylguanosine were detected from *β*-eliminated mRNA (Table 1) since all residual radioactivity migrating at the position of $m^7G^{5'}ppp^{5'}(m)Am$ was sensitive to alkaline phosphatase. If 1% of the RNAs had contained the 5′-terminus $m^7G^{5'}ppp^{5'}(m)Am$), we would have detected it. Figure 2, lane 3, and Table 1 show that incubation of the *β*-eliminated RNA in the reticulocyte cell-free system in the conditions of protein synthesis does not result in the addition of 7-methylguanosine to the 5′ end; the end remains ppp(m)Am.

Translation without 7-methylguanosine

The products of translation of these mRNAs in the reticulocyte cell-free system were resolved by polyacrylamide

Fig. 2 DEAE paper iontophoresis at *p*H 3.5 of nuclease P1 digests of VSV mRNA. Samples containing 10 µg of RNA were incubated with 0.01 µg of P1 nuclease (Yamasa Shoyu Co., Tokyo) in 5 µl of 0.01 M MES (2-N morpholino-ethanesulphonic acid, *p*H 6.2) for 30 min at 37 °C. The limit digests of VSV mRNA were spotted on a sheet of Whatman DEAE (DE-81, 30×60 cm) paper and subjected to electrophoresis at 30 V cm^{-1} for 4 h in 5% acetic acid, 0.5% pyridine. Lane 1, untreated mRNA; lane 2, periodate-oxidised, β-eliminated mRNA; lane 3, periodate-oxidised, β-eliminated VSV mRNA purified after incubation in the reticulocyte cell-free system as described in Fig. 3.

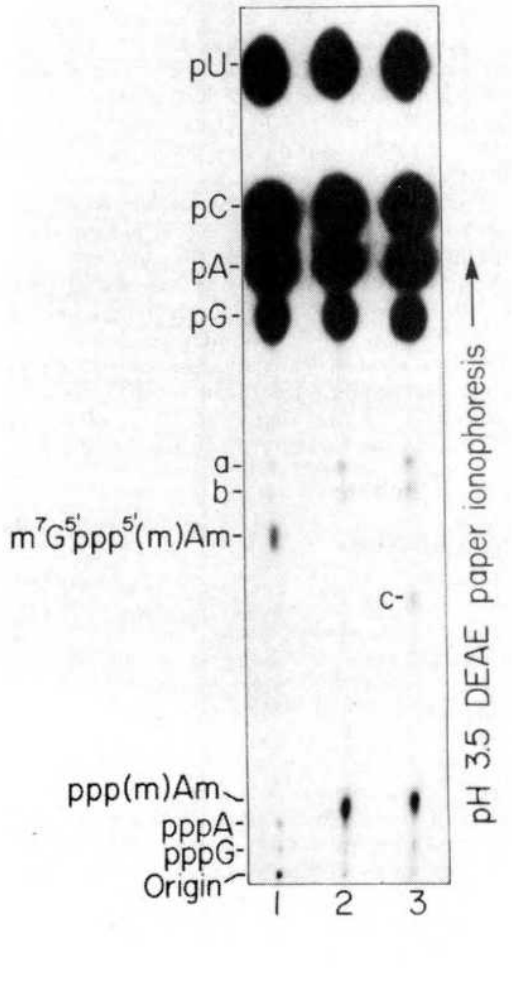

Table 1 Quantitification of 5′ termini

	% Total c.p.m. in each structure				
	${}_{\mathrm{HO}}{}^{\mathrm{m^7G5'ppp5'(m)Am}}{}_{\mathrm{OH}}$*	${}^{\mathrm{ppp(m)Am}}{}_{\mathrm{OH}}$	${}^{\mathrm{pppA}}{}_{\mathrm{OH}}$	${}^{\mathrm{pppG}}{}_{\mathrm{OH}}$	Total radioactivity (c.p.m.)
Untreated	0.17 (2141)	0.0006 (8)	0.019 (246)	0.018 (227)	1.26×10^6
Periodate-oxidised, β-eliminated	<0.0017 (<20)	0.17 (1874)	0.021 (241)	0.019 (208)	1.11×10^6
β-Eliminated (analysis after incubation in a protein synthesis reaction)	<0.0017 (<20)	0.16 (1788)	0.018 (212)	0.019 (210)	1.13×10^6

The 5′-terminal structures and 5′ monophosphates, separated as shown in Fig. 1, were cut out of the DEAE paper and radioactivity was determined in a scintillation spectrometer. For each structure c.p.m. are given in parentheses. Radioactivity in the spots labelled *a* and *b* (Fig. 2, lanes 1 and 2) was converted to P_i after alkaline phosphatase treatment and thus is either derived from modified nucleotides at internal positions in VSV mRNA or generated as an artefact of nuclease P1 digestion. The spot labelled (*c*) (Fig. 2, lane 3) appeared only in nuclease P1 digests of VSV mRNA which had been incubated in the reticulocyte cell-free system. Since half of the radioactivity in this compound was released as P_i after alkaline phosphatase digestion, it is presumably a P1-resistant modified dinucleotide of the form pNpN.

* We corrected for background due to trailing of mononucleotides into the region containing $m^7G^{5'}ppp^{5'}(m)Am$ as follows. Radioactivity in this region was eluted with 30% triethylammonium bicarbonate (*p*H 7.8), lyophilised, treated with alkaline phosphatase, and subjected to electrophoresis at *p*H 3.5 on Whatman No. 3MM paper, as described previously[5]. The radioactivity in ${}^{32}P_i$ relative to that in the phosphatase-insensitive structure $m^7G^{5'}ppp^{5'}(m)Am$ (16%) was taken as the fraction of contamination with mononucleotides, and the numbers in the table have been corrected for this contamination. All radioactivity in the region of $m^7G^{5'}ppp^{5'}(m)Am$ from β-eliminated RNA (285 and 260 c.p.m.) migrated as ${}^{32}P_i$ after phosphatase treatment, and the numbers given in the table have been corrected to the limits of detection of remaining $m^7G^{5'}ppp^{5'}(m)Am$.

gel electrophoresis. Figure 3*a* and *b* shows that synthesis of M, NS and N proteins is proportional to the concentration of added control RNA. Synthesis of the VSV G protein is presumably obscured by the large background peak of reticulocyte protein at 2 cm (compare Fig. 3*e*). Both periodate-treated and periodate-treated, β-eliminated mRNA direct the synthesis of authentic VSV M, NS and N proteins (Fig. 3*c* and *d*). Quantitation of these microdensitometer scans showed that periodate-treated RNA and periodate-treated, β-eliminated RNA directed the synthesis of 33% and 25%, respectively, of the amount of each of these proteins compared with the same amount of control RNA. The amount of protein synthesis directed by periodate-treated and periodate-treated, β-eliminated RNA was also directly proportional to added RNA concentrations (data not shown.

Because we were concerned that the reduced translation of the chemically treated VSV mRNA might in part be due to effects generated not by removal of the 7-methylguanosine but by internal oxidations of bases in the RNA as well as degradation, we performed control experiments on f2 phage RNA which had been mixed with the ^{32}P-labelled VSV mRNAs during the periodate-oxidation and β-elimination procedures. When translated in an *E. coli* cell-free system, periodate-oxidised, β-eliminated f2 RNA synthesised 80% of the amount of f2 coat protein (molecular weight 14,000) and only 50% the amount of RNA synthetase (molecular weight 50,000) as did untreated f2 RNA (data not shown). These experiments, as well as those showing degradation of VSV mRNAs described above, indicate that the level of translation in reticulocyte extracts after the periodate-aniline treatment must be regarded as a minimal estimate of the ability of VSV mRNA lacking 7-methylguanosine to function in protein synthesis.

Ribosome attachment

Two additional studies confirmed that VSV mRNA lacking 7-methylguanosine can participate in protein synthesis. After incubation in a reticulocyte extract in conditions of protein synthesis, 51% of control RNA is incorporated into polyribosomes; these contain, on average, 3.4 ribosomes per mRNA (Fig. 4*a*, Table 2). The same amount of periodate-treated, and slightly less periodate-treated, β-eliminated RNA is incorporated into polysomes. The decrease in the fraction of β-eliminated mRNA bound is due presumably to partial degradation of the RNA (Fig. 1). The average size of polysomes formed is reduced less than twofold compared with those from control RNA (Fig. 4*b* and *c*, Table 2). Assuming that the rate of polypeptide chain elongation and termination is the same for control and treated RNA, and that the average size of the VSV proteins produced is the same (compare Fig. 3), this experiment suggests that the rate of ribosome attachment to mRNAs lacking 7-methylguanosine is reduced less than twofold.

This conclusion is substantiated by the experiments in Figs 5 and 6 which measure directly the rate and extent of incorporation of mRNA into 80S initiation complexes. Incubation of control VSV mRNAs with reticulocyte extracts in the presence of anisomycin (1 mg ml^{-1}), a specific inhibitor of polypeptide chain elongation[25] results in incorporation of 54% of the RNA into an 80S complex (Fig. 5*a*). This complex remains stable in a solution of 0.5 M NaCl and 0.03 M magnesium acetate, but no initiation complexes are produced if the incubation mixture is of this ionic composition (data not shown). Hence, the rate of formation of an 80S complex can be determined accurately by diluting the incubation mixture into a solution of 0.5 M NaCl and 0.03 M magnesium acetate, followed by zone centrifugation to isolate the 80S complex. Figure 5 shows that 53% of periodate-treated RNA and 37% of periodate-treated, β-eliminated RNA is incorporated into a salt-stable initiation complex. Again, the reduction in the extent of binding is due, presumably, to degradation of RNA. The time required for half-maximum binding of control RNA to ribosomes is 12 s, while that for either periodate-treated RNA or periodate-treated β-eliminated RNA is about 35 s (Fig. 6). A threefold reduction in the rate of binding to ribosomes was also observed when untreated and periodate-treated, β-eliminated forms of a single VSV mRNA, that encoding N protein, were compared (control RNA, $t_{1/2}$=10.1 s; periodate-treated, β-eliminated RNA, 35.8 s; data not shown). This experiment rules out the possibility that the apparent reduction is due to preferential destruction of the larger VSV mRNAs by the chemical treatment.

The experiments reported here demonstrate that animal cell ribosomes can recognise the correct translation initiation sites on animal virus mRNAs from which the 5′-terminal 7-methylguanosine has been removed since such mRNAs direct the synthesis of authentic viral proteins. The changes which we observe in the ribosome binding of periodate-treated, and periodate-treated, β-eliminated mRNA are a threefold reduction in the rate of binding to ribosomes, a twofold reduction in average polysome size, and a 20–30% reduction in the total amount bound. The effect of the chemical treatments on the total amount of mRNA binding may be due only to mRNA degradation. Furthermore, we cannot rule out the possibility that the effect on the rate of binding may be due not to the removal of 7-methylguanosine but to nonspecific modifications introduced during periodate oxidation. Indeed, we have observed here that periodate oxidation on its own, which presumably leaves a dialdehyde

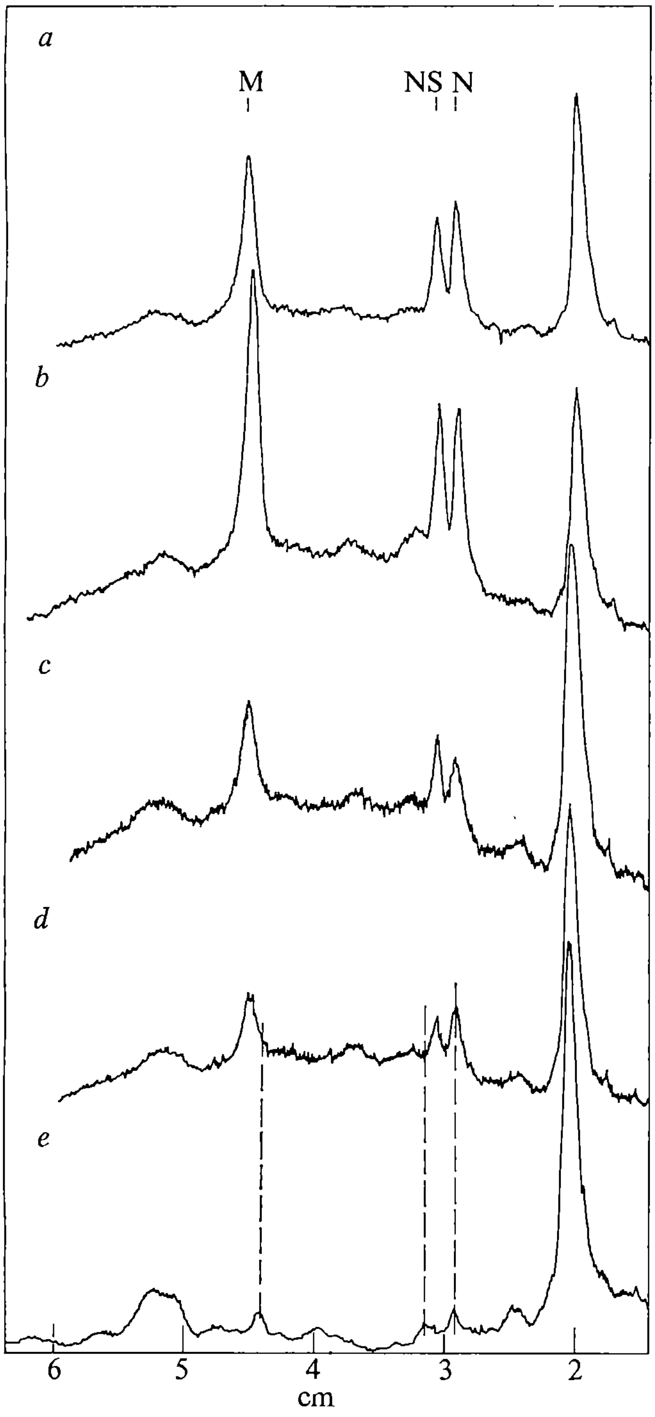

Fig. 3 Translation of VSV mRNAs Conditions for protein synthesis in cell-free extracts of rabbit reticulocytes have been described in detail[23]. Reactions (39 μl) containing 7 μCi ^{35}S-methionine (200,000 mCi mmol^{-1}, New England Nuclear), 10^{-4} M each of 19 non-radioactive amino acids, and the indicated amounts of ^{32}P-labelled VSV mRNA. S-Ado-Hcy (S-adenosylhomocysteine) was added to all reactions at a final concentration of 7.4×10^{-4} M to inhibit methylation. Incubation was at 30 °C for 60 min Pancreatic RNase (5 μg) was added, and incubation was continued for 5 min more. A sample (3 μl) of the reaction was analysed on a 13% polyacrylamide slab gel as detailed by Laemmli[24] Shown are scans of autoradiographs (10-d exposure) of the fixed, dried gel. The region of the gel containing the globin 7–9 cm) is not shown. *a*, 0.3 μg of control VSV mRNA (7.7 μg ml^{-1}), *b*, 0.6 μg of control VSV mRNA (15.4 μg ml^{-1}); *c*, 0.6 μg of periodate-treated VSV mRNA (15.4 μg ml^{-1}); *d*, 0.6 μg of periodate-treated and β-eliminated VSV mRNA (15.4 μg ml^{-1}), *e*, no added RNA.

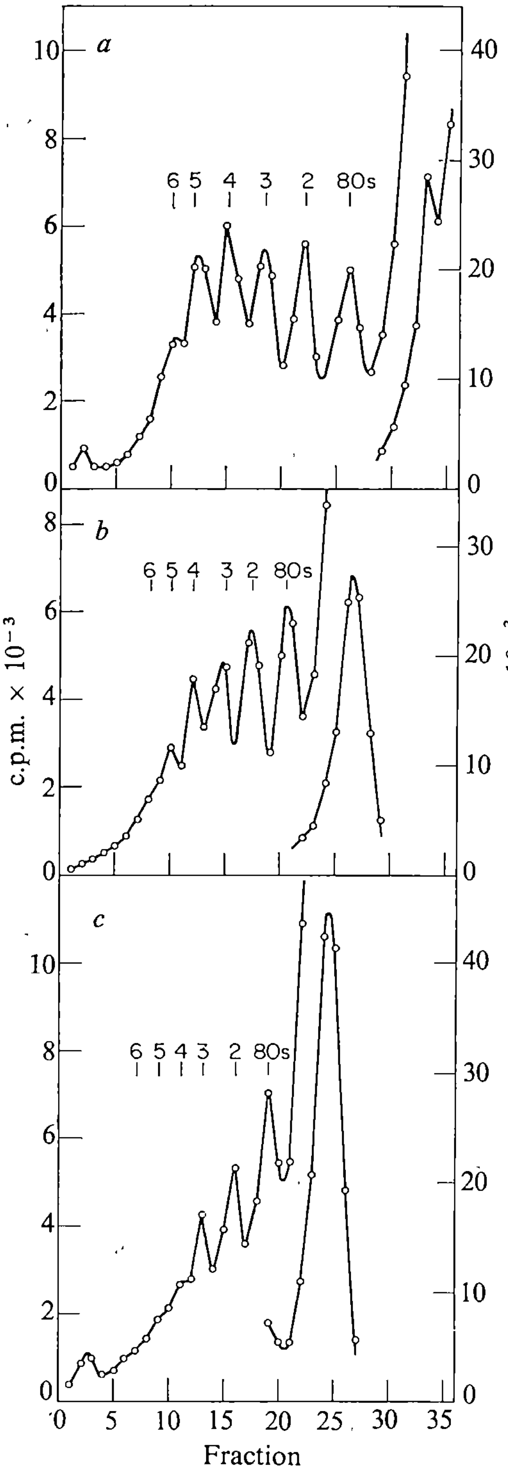

Fig. 4 Incorporation of labelled VSV mRNA into polysomes. Reticulocyte cell-free reactions (120 μl) contained 10^{-4} M each of 20 amino acids, 7×10^{-4} M S-Ado-Hcy, and 1.5×10^{5} c.p.m. (0.1 μg) of ^{32}P-labelled control VSV mRNA (*a*); periodate-treated RNA (*b*); or periodate-treated, β-eliminated RNA (*c*). Incubation was at 30 °C for 5 min. Reaction tubes were chilled on ice, and 1.2 ml of HSB (0.5 M NaCl, 0.03 M Mg (acetate)$_2$, 0.02 M HEPES, *p*H 7.5) was added. The samples were layered on a 36-ml 15–30% (w/v) linear sucrose gradient, made up in HSB, and centrifuged in a Beckman SW27 rotor at 4 °C at 26,500 r.p.m. for 4 h. Samples were collected through a flow cell in a Gilford recording spectrophotometer directly into scintillation vials. The arrows represent optical density peaks of the reticulocyte polysomes which are due, predominantly, to the endogenous globin mRNA. Each sample was bleached with alkaline hydrogen peroxide and counted using Aquasol (New England Nuclear) in a Beckman scintillation spectrometer. In control reactions (which were not incubated at 30 °C) only 2.3% of the radioactivity was found in the monosome or polysome regions of the gradient (data not shown). Analyses of data from this experiment are in Table 2.

Table 2 Incorporation of ^{32}P-labelled VSV mRNA into polysomes

	Control RNA	Periodate-treated RNA	Periodate-treated, β-eliminated RNA
c.p.m. in monosomes or polysomes $C = \sum_{i=1}^{7} C_i$	77,910	57,612	46,346
Proportionate number of ribosomes bound to VSV mRNA $R = \sum_{i=1}^{7} i\,C_i$	260,720	162,913	105,769
Ribosomes per bound mRNA $r = C/R$	3.35	2.83	2.28
Total c.p.m. recovered from gradient C_t	152,764	115,220	118,840
Fraction of mRNA bound to ribosomes $C_B = C/C_t$	0.51	0.50	0.39

In calculating the data given in line 2, the amount of radioactivity in any region of a polysome gradient was multiplied by the number of ribosomes per polysome (i), that is, by the number of ribosomes translating each mRNA in that peak. Hence, the total number of ribosomes translating the mRNAs is proportional to the sum of this product over all regions of the polysome gradient (line 2). Since the total radioactivity in polysomes (line 1) is proportional to the number of VSV mRNAs being translated, the average number of ribosomes per bound mRNA is given by line 3.

on the 7-methylguanosine as well as on the 3′-terminal adenosine of the mRNA, has virtually the same effect on reducing the rate of mRNA binding to ribosomes as does periodate-oxidation followed by β-elimination, which removes the oxidised nucleosides from the mRNA.

Conflicting data

Our conclusions conflict with those drawn in previous studies on translation of methylated and unmethylated VSV mRNAs synthesised *in vitro* by the virion-bound VSV polymerase. It was reported that VSV mRNAs synthesised *in vitro* terminate in $G^{5'}ppp^{5'}Ap$[20] and that translation of this RNA in the wheat embryo system will not occur unless methylation at the N^7-position of the guanosine has occurred before translation[11].

Attempting to reconcile these results with our own, we synthesised VSV RNA *in vitro* in the presence of S-adenosyl homocysteine and verified that the product RNA contains the 5′-terminus $G^{5'}ppp^{5'}Ap$. We found, however, that this product RNA does not contain any discrete VSV mRNA species comigrating with authentic VSV mRNA on formamide–polyacrylamide gels. Instead, 80% of the product RNA is larger than the N protein mRNA and heterogeneous in molecular weight, while the remaining 20% is present as bands running just faster than (approximately 100–200 nucleotides shorter than) the authentic VSV mRNAs (unpublished observations of M. Brock and J. Rose). In contrast, 80–90% of the *in vitro* product synthesised in the presence of S-adenosyl methiodine does comigrate with authentic VSV mRNAs. These results suggest that methylation is involved in synthesis or processing of VSV mRNAs into the correct poly(A)-containing mRNA species. The ability of these RNAs to function in *in vitro* protein synthesis is under study.

Extensive experiments carried out with reovirus mRNAs have also indicated a requirement for a 5′-terminal 7-methylguanosine in translation and ribosome binding[12]. If the methylated and unmethylated mRNAs compared in these experiments differ in no way other than the presence

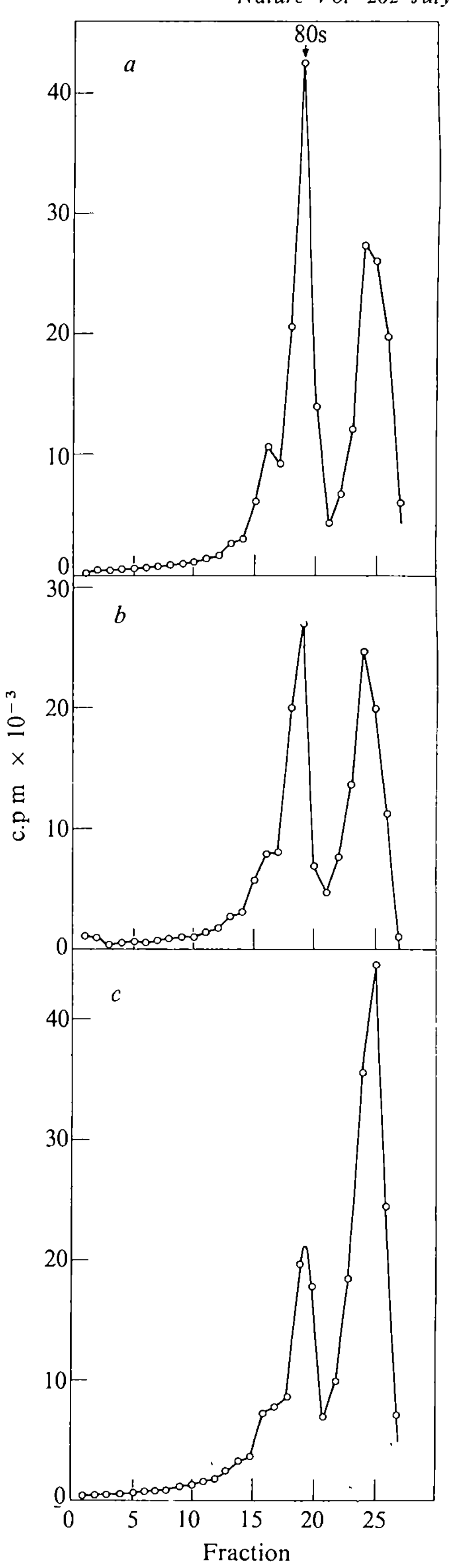

Fig. 5 Binding of ^{32}P-labelled VSV mRNAs to reticulocyte ribosomes. Reactions contained anisomycin (1 mg ml^{-1}), a specific inhibitor of polypeptide chain elongation[25] but were otherwise identical to those of Fig. 4. Gradient centrifugation and counting of the samples was as in Fig. 4. In reactions not incubated at 30 °C, 2.1–2.6% of the ^{32}P-labelled RNA was found to sediment faster than 40S (data not shown). The percentage of added ^{32}P-labelled mRNA bound to ribosomes after incubation was 54% (*a*); 53% (*b*), 37% (*c*). The concentration of VSV mRNA in each reaction was 1 μg ml^{-1}.

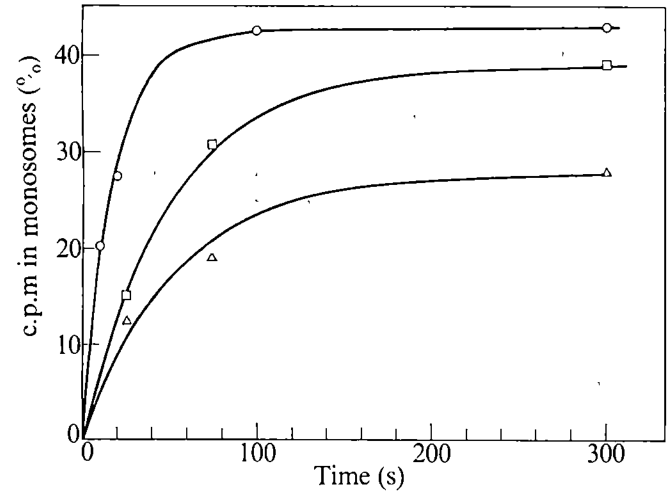

Fig. 6 Rate of binding of VSV mRNAs to reticulocyte ribosomes. Reactions (330 μl containing about 10^6 c.p m. of ^{32}P-labelled control VSV mRNA (○), periodate-treated RNA (□), or periodate-treated and β-eliminated RNA (△) were identical to those used in the study of Fig 5. Incubation was at 30 °C. At times indicated, 75 μl samples were added to 0.5 M HSB at 0 °C. Samples were layered on 13-ml linear 15–30% sucrose gradients in HSB and centrifuged for 3.4 h at 40,000 r.p.m. in the SW40 rotor at 4° C. Collection and counting was as in Fig. 5. The percentage of the radioactive RNA found in the 80S region of the gradient is plotted. A background of 2.1%, observed with unincubated samples, has been subtracted from each point. The solid curves are those of the first-order binding equation

$$C = C_\infty\left[1 - \left(\exp\frac{-t\ \ln 2}{t_{1/2}}\right)\right]$$

where C is the percentage of RNA bound to monosomes at time t, C_∞ is the maximum value of C, and $t_{1/2}$ is the time required for half-maximum binding of the RNA. For each RNA sample, C_∞ and $t_{1/2}$ were calculated by a least-squares program using the observed data points. These values are: control RNA, $C_\infty = 42\%$, $t_{1/2} = 11.7$ s, periodate-treated RNA, $C_\infty = 39\%$, $t_{1/2} = 34.6$ s; periodate-treated and β-eliminated RNA, $C_\infty = 28\%$, $t_{1/2} = 36.7$ s.

or absence of a 5′-terminal 7-methylguanosine as reported[12], then the results imply a more intimate involvement of 7-methylguanosine in translation of reovirus mRNAs than we observe for VSV mRNAs. This perhaps indicates a close proximity of the reovirus 5′ terminus to the translation initiation site, a situation already documented for the coat protein mRNA of brome grass mosaic virus[21].

We initially had great difficulty recovering translatable VSV mRNA after periodate-oxidation and β-elimination, and clearly did not completely overcome the problem of degradation. Thus, we suggest that similar studies indicating a requirement for 7-methylguanosine in translation of cellular mRNAs[11,22] should be more carefully controlled for possible nonspecific effects of the chemical procedure.

The model we favour is that in which the terminal 7-methylguanosine has different effects on translation of different mRNAs For some mRNAs, for example, poliovirus RNA and VSV mRNAs, it is clearly not essential, but it may facilitate ribosome attachment to VSV mRNA. For other mRNAs, a 5′-terminal 7-methylguanosine may be essential. It is also possible that wheat embryo ribosomes—used for much of the previous work—differ from animal ribosomes in their dependence on the 7-methylguanosine residue. Indeed, we have observed as much as a tenfold reduction in translation of periodate-treated, β-eliminated VSV mRNA in the wheat embryo system, perhaps indicating a more important role for 7-methylguanosine in this heterologous system. Thus, both the mRNA in question and the source of the translational components may be important factors in determining the effect of the 5′-terminal 7-methylguanosine.

We thank David Baltimore for suggestions on the manuscript, Barbara Small and Martin Brock for technical assistance, and Alan Weiner for suggesting control experiments with f2 phage RNA. This work was supported by grants from the American Cancer Society and the NIH. J.R. is recipient of a fellowship from the National Cystic Fibrosis Research Foundation, and H.F.L. was recipient of a research career development award from NIH.

Received March 15; accepted May 11, 1976.

[1] Wei, C. M , and Moss, B., *Proc natn Acad. Sci U S.A.*, 72, 318–322 (1975)
[2] Furuichi, Y , Morgan, M., Muthukrishnan, S., and Shatkin, A. J , *Proc natn. Acad. Sci. U.S A.*, 72, 362–366 (1975)
[3] Abraham, G , Rhodes, D. P., and Banerjee, A. K , *Cell*, 5, 51–58 (1975).
[4] Moyer, S. A., Abraham, G., Adler, R., and Banerjee, A. K , *Cell*, 5, 59–67 (1975).
[5] Rose, J K , *J biol. Chem* , 250, 8098–8104 (1975).
[6] Lavi, S., and Shatkin, A. J., *Proc natn. Acad. Sci. U.S A* , 72, 2012–2016 (1975).
[7] Adams, J M., and Cory, S , *Nature*, 255, 28–33 (1975)
[8] Wei, C M., Gershowitz, A., and Moss, B., *Cell*, 4, 379–386 (1975)
[9] Furuichi, Y , *et al.*, *Proc. natn Acad Sci U S A* , 72, 1904–1908 (1975)
[10] Perry, R P , Kelley, D E , Friderici, K., and Rottman, F , *Cell*, 4, 387–394 (1975)
[11] Both, G W , Banerjee, A K., and Shatkin, A J , *Proc. natn Acad. Sci U S.A* , 72, 1189–1193 (1975)
[12] Both, G. W., Furuichi, Y., Muthukrishnan, S , and Shatkin, A J., *Cell*, 6, 185–195 (1975)
[13] Muthukrishnan, S., Both, G. W , Furuichi, Y , and Shatkin, A J., *Nature*, 255, 33–37 (1975).
[14] Hewlett, M., Rose, J., and Baltimore, D , *Proc natn. Acad. Sci U S A* , 73, 327–330 (1976).
[15] Rose, J K., and Knipe, D., *J Virol* , 15, 994–1003 (1975).
[16] Knipe, D., Rose, J. K , and Lodish, H F , *J. Virol* , 15, 1004–1011 (1975)
[17] Both, G. W., Moyer, S A., and Banerjee, A. K , *J. Virol* , 15, 1012–1019 (1975)
[18] Huang, A , Baltimore, D , and Stampfer, M , *Virology*, 42, 946–957 (1970)
[19] Fugimoto, M , Kuniata, A , and Yoshino, H., *Agric. Biol. Chem* , 38, 1555–1561 (1974)
[20] Abraham, G., Rhodes, D P , and Banerjee, A K , *Nature*, 255, 37–40 (1975)
[21] Dasgupta, R , Shih, D. S., Saris, C , and Kaesberg, P , *Nature*, 256, 624–628 (1975).
[22] Rao, A , Wu, B C , Waxman, J., and Busch, H., *Biochem. biophys. Res Commun.*, 66, 1186–1193 (1975).
[23] Villa-Komaroff, L M , McDowell, M., Baltimore, D , and Lodish, H F.' *Methods in Enzymology*, 30, 709–721 (1974)
[24] Laemmli, U K , *Nature*, 227, 680–684 (1970).
[25] Lodish, H. F , *J biol Chem* , 246, 7131–7138 (1971).

letters to nature

X-ray pulses from globular clusters

GIANT X-ray pulses have been observed recently by several groups[1-7] from sources located in a number of celestial positions. Two of these sources may plausibly be identified with the globular cluster X-ray sources: NGC6624 and NGC1851. In several cases[2,7] the pulses seem to occur in approximately periodic sequences; in other sources the intervals are irregular, but in one case there is a relation between pulse strength and interpulse interval. The non-burst behaviour of globular cluster X-ray sources has been interpreted[8,9] in terms of massive ($\gtrsim 10^3 M_\odot$) black holes powered by accretion from a disk supplied by cluster gas. We suggest here that compact stars bound to the central massive black hole and orbiting through the accretion disk may produce, by several possible mechanisms, giant pulses. These pulses might be expected to exhibit a variety of types of X-ray behaviour corresponding to the uncertain characteristics (for example, density and spatial extent) of the individual accretion disks at the different points at which the orbits of the bound compact stars intersect the disks. We note that there may be more than one class of sources of giant X-ray bursts and that our speculation refers only to those sources in globular clusters.

We can easily estimate the expected orbital period of the star closest to the central black hole. The rate at which stars are captured has been computed by several authors[10-12]. It is to an order of magnitude, and neglecting dimensionless constants,

$$\dot{N} \lesssim \left(\frac{v_{\mathrm{r.m.s}}}{R}\right)_{\mathrm{core}} \left(\frac{M_{\mathrm{BH}}}{M_{\mathrm{core}}}\right)^{3} \simeq 10^{-7.0}(M_{\mathrm{BH}}/10^{3}M_{\odot})^{3}\ \mathrm{yr}^{-1} \qquad (1)$$

where 'core' refers to characteristics of the globular cluster core. (The rate at which the tightly-bound orbits relevant to the present discussion are populated may be less than this, but our results are, fortunately, insensitive to $\dot{N}$.) At small distances from the hole, gravitational radiation dominates the two-particle scattering and the drag caused by interaction with the disk. Stars with period, P, will spiral quickly towards the hole on a time scale

$$\tau_{\mathrm{rad}} \equiv \left(\frac{R}{\dot{R}}\right)_{\mathrm{GR}} = 10^{5.7}(M_{\mathrm{BH}}/10^{3}M_{\odot})^{-2/3} \times$$

$$\times (M_{*}/M_{\odot})^{-1}\left(\frac{P}{1\ \mathrm{h}}\right)^{8/3}\ \mathrm{yr} \qquad (2)$$

The time that a star spends at any given radius decreases rapidly with decreasing radius ($P \propto R^{3/2}$; $\tau_{\mathrm{rad}} \propto R^{4}$). Hence we find, by multiplying together equations (1) and (2), the period of the innermost stellar orbit that most likely contains one star

$$P \gtrsim 4(M_{\mathrm{BH}}/10^{3})^{-7/8}\ \mathrm{h} \qquad (3)$$

Thus a clock with a period of hours to one day is natural in this model, in agreement with observations[2,7]. (For main-sequence stars, tidal effects set a lower limit of this order to the orbital period.) Of course, the manifestation of this period requires various things about the accretion disk.

The duty cycle for 3U1820−30 is apparently very small ($\sim 10^{-3}$) so the interaction between the orbiting star and the disk would have to be relatively brief for this source, that is, a very thin disk ($\lesssim 10^{8.5}$ cm) would be required. At least two mechanisms for producing the pulses come to mind: (1) a small, hot, shocked area will be produced twice each orbit as the innermost star crashes through the disk. This might be seen directly: its properties will depend on whether it is caused by an ordinary star losing mass by tidal stripping and producing a bow shock (R. Silk, personal communication) or, more likely, a compact star producing an observable accretion wake; (2) ripples will proceed from the shocked zone towards the centre of the disk producing, when the wave train reaches the innermost stable orbit, extra accretion and luminosity. Depending on the orientation of the system with respect to our line of sight, and on whether or not the disk is optically thick to X rays, one would expect to see one or two pulses per orbital period. Irregularities and instabilities in the disk could produce the observed[2] r.m.s. phase jitter of $\lesssim 0.04$ per period.

There are certain additional observational consequences of this model: (1) globular clusters in our Galaxy can be far away ($\sim$10 kpc) so that one would not be surprised if some of the sources near the galactic centre or at low galactic latitude were associated with optically obscured globular clusters; (2) the galactic latitude dependence of the sources we consider should be similar to that of the known globular clusters except there may be a number of optically undiscovered X-ray globular clusters in the direction of the galactic centre (scale size $\sim$1 kpc by analogy with globular clusters in Andromeda); (3) more than one period per source might be found if there were more than one star orbiting near the hole. If this were discovered it would be difficult to explain on the usual binary hypotheses; (4) as noted previously[8], no eclipses should be seen according to this model and (5) a small odd–even effect caused by non-zero orbital eccentricity might be observable.

This work was supported in part by the NSF.

J. N. Bahcall
J. P. Ostriker

Institute of Advanced Studies,
Princeton, New Jersey 08540

Received March 25, accepted May 18, 1976

[1] Grindlay, J., and Heise, J., *IAU Circ.*, No. 2879 (1975).
[2] Clark, G., *IAU Circ.*, No. 2907 (1976).
[3] Lewin, W. H. G., *IAU Circ.*, Nos 2911, 2912, 2918 and 2922 (1976).
[4] Jones, C., and Forman, W., *IAU Circ.*, No. 2913 (1976).
[5] Clark, G., *IAU Circ.*, No. 2915 (1976).
[6] Grindlay, J. *et al.*, *Astrophys. J. Lett.* (in the press).
[7] Lewin, W. H. G., and Clark, G., *IAU Circ.*, No. 2922 (1976).
[8] Bahcall, J. N., and Ostriker, J. P., *Nature*, **256**, 23 (1975).
[9] Silk, J., and Arons, J., *Astrophys. J. Lett.*, **200**, L131 (1975).
[10] Bahcall, J. N., and Wolf, R. A., *Astrophys. J.* (in the press).
[11] Lightman, A., and Shapiro, S. L., *Astrophys. J.* (in the press).
[12] Frank, J., and Rees, M. J., *Mon. Not. R. astr. Soc.* (in the press).

Frequency variation of equatorial ionospheric scintillations

The fluctuations in the signal strength of v.h.f. and u.h.f. transmissions from satellites received at ground level contain valuable information about ionospheric irregularities. These fluctuations, usually called scintillations, depend on the frequency of transmission, characteristics of the irregularities and the angle of incidence. At equatorial latitudes, there have as yet been few such observations, and there are reasons to expect the scintillation characteristics at equatorial latitudes to be quite different from those at higher latitudes because the ionospheric irregularities (mainly spread F irregularities) responsible for scintillations differ widely in their characteristics with latitude. It is also well recognised that the equatorial region is a strong scintillation zone. At Trivandrum (dip 0°57′S, geographic longitude 76°57′E), a station close to the magnetic equator, amplitude and phase scintillations of the radio beacon transmissions on 40, 140 and 360 MHz as well as the amplitude scintillations of the 860-MHz television downlink from the geostationary satellite ATS-6 have been recorded since August 1975. Here we present preliminary results on the frequency variation of the scintillation index.

In Fig. 1 a typical record of scintillations on all the four frequencies is shown. The records at 40 and 140 MHz are synchronous whereas those on 360 and 860 MHz are not. It is a general observation that scintillations are faster at lower frequencies. The quasi-periods of fluctuations are in the range of few seconds to few tens of seconds, the quasi-periods being shorter at lower frequencies. Also, scintillations occur more frequently and earlier in the night at lower frequencies. We here consider only nocturnal scintillations which can be attributed to the phenomenon of spread F. For this study, data recorded during six nights in the month of October 1975 have been used. Of these, scintillations were observed on four nights at all four frequencies and on the other two nights scintillations were observed on 40, 140 and 360 MHz only.

Using the amplitude scintillation data on all the frequencies, the S_4 scintillation indices[1] have been evaluated. For this, the length of the data sample considered corresponds to $\sim$10 min, which is sufficiently long not to cause any error in the S_4 indices, considering the quasi-periods of the fluctuations.

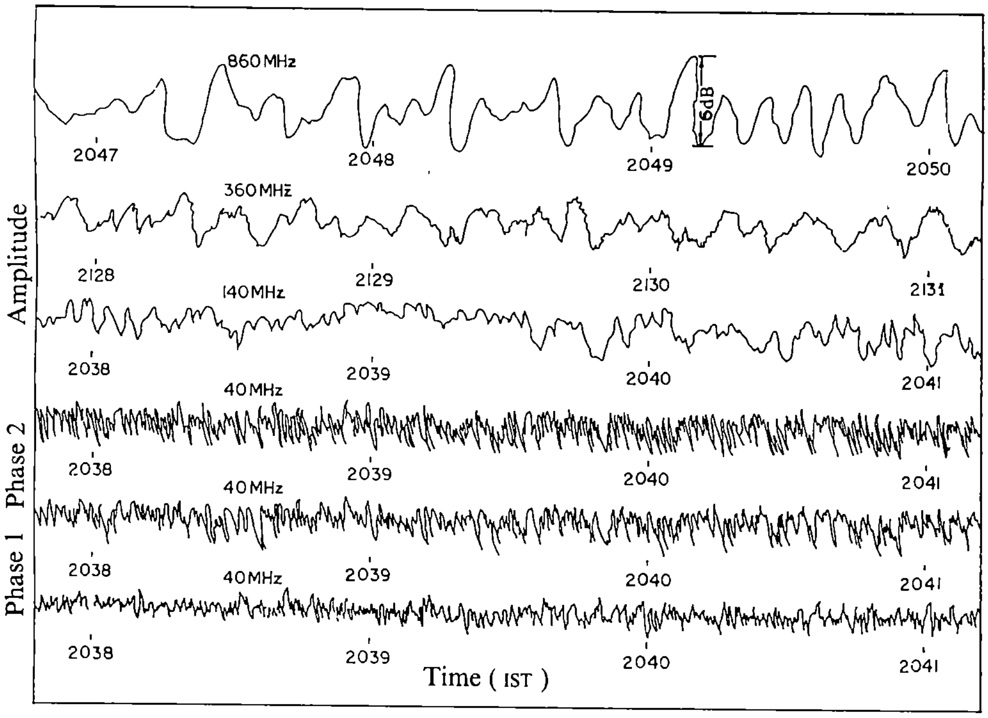

Fig. 1 Scintillations of ATS-6 transmissions recorded at Trivandrum. All traces taken on October 21, 1975 except the second (360 MHz), which was taken on October 24, 1975.

It is reasonable to assume that this interval is short enough for the scintillation characteristics not to vary within this interval except perhaps during onset and decay of scintillations. It may be noted that the onset and decay periods are not included in the present analysis.

The frequency variation of S_4 can be represented by

$$S_4 = \frac{K}{f^n}$$

where f is the exploration frequency, n is the frequency index and K is a constant depending on the scintillation conditions only. This equation can be rewritten as

$$\log_{10}\frac{(S_4)_1}{(S_4)_2} = n \log_{10}\frac{f_2}{f_1} \qquad (1)$$

where $(S_4)_1$ and $(S_4)_2$ are the scintillation indices corresponding to the frequencies f_1 and f_2. The quantities $\log_{10}[(S_4)_1/(S_4)_2]$ and $\log_{10}[(f_2)/(f_1)]$ are plotted in Fig. 2. It has been found that the points (circles and crosses in Fig. 2) fall around two straight lines having different slopes. The slope of line A is 1.2 and that of line B is 0.46. The line A corresponds to frequencies > 140 MHz whereas the line B includes data points at 40 but not 860 MHz. A careful examination of the data showed that the S_4 indices can be divided into two groups depending upon whether the S_4 index at 360 MHz is greater or less than ~0.5. The conditions corresponding to $S_4|_{360} > 0.5$ can be termed as strong scintillation conditions and those corresponding to $S_4|_{360} < 0.5$ as relatively weak scintillation conditions. The lines A and B (Fig. 2) represent weak and strong scintillation conditions respectively. It is also found that when the $S_4|_{140}$ is ~0.8, $S_4|_{40}$ is also about the same (the triangle point in Fig. 2) indicating no frequency variation of the S_4 index in the frequency range 40–140 MHz.

Fig. 2 Frequency variation of S_4 index.

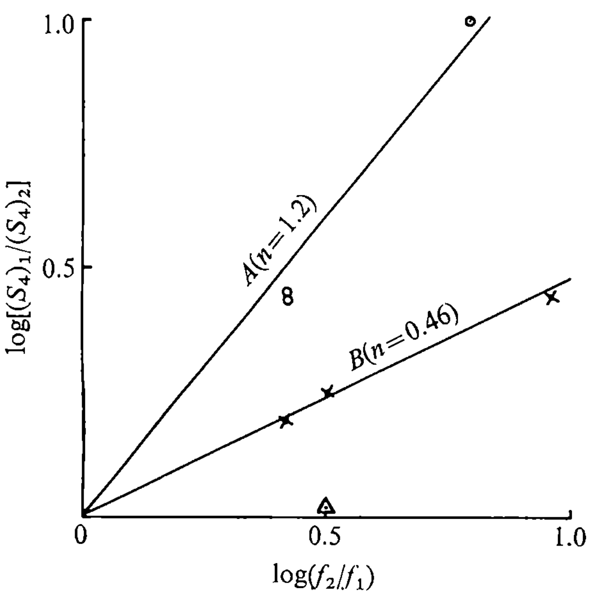

Recently Rufenach[2] has shown theoretically that, for the weak scattering case, n is between 1.4 and 1.6 depending on the exponent of the irregularity spectrum in the range 3.5–4.5. The multiple scattering case has been considered on theoretical grounds by Yeh *et al.*[3]. They had shown that n is $\leqslant 1$ for lower frequencies and it approaches a value of 1.5 at higher frequencies. The results presented here seem to agree with these theoretical considerations. The transition from the low to high frequency index appears to occur in the frequency range 140–360 MHz. The reason for the low value of n obtained here for the weak scattering case as compared to that given by Rufenach[2] and Yeh *et al.*[3] is perhaps that line A (Fig. 2) representing the weak scatter case is somewhat vitiated by $S_4|_{140} > 0.5$. A more detailed discussion on the theoretical interpretation of these results will be presented elsewhere.

B. V. KRISHNA MURTHY
K. KRISHNA MURTHY
C. RAGHAVA REDDI
S. VAIDYANATHAN

Space Physics Division,
Vikram Sarabhai Space Centre,
Trivandrum 695022, India

Received February 24, accepted May 5, 1976.

[1] Briggs, B. H., and Parkin, I. A., *J. atmos. terr. Phys.*, 25, 339 (1963).
[2] Rufenach, C. L., *J. geophys. Res.*, 791, 1562 (1974).
[3] Yeh, K. C., Liu, C. H., and Youakin, M. Y., *Radio Sci.*, 10, 97 (1975)

Ocean temperatures and large scale atmospheric variations

We here analyse some observations of sea surface temperatures to investigate several aspects of large scale ocean–atmosphere interactions, in particular El Nino and the Southern Oscillation

Monthly mean sea surface temperature observations for most of the Pacific Ocean between 50°N and 20°S for the period 1949–73 were given an empirical orthogonal function analysis based on values at 160 grid points, each centred in an area 10° longitude by 5° latitude[1]. This analysis produces orthogonal spatial functions and corresponding orthogonal time coefficients which are the best linear representations (predictors) of the data[2] The functions and coefficients may be thought of as analogues of the more familiar Fourier components and amplitudes, except that the empirical functions are determined from the interrelationships within the data itself.

Figure 1 illustrates the most important empirical function of the deviations of the sea surface temperatures from the 25-yr monthly means This function accounts for 23.1% of the total variance in the field. The temperature deviation explained (predicted) by this function for a given place and time is simply the product of the value of the function at that place and the value of the time coefficient for the month in question. The spatial pattern of this function reveals a large scale effect in which the equatorial and eastern Pacific vary in phase whereas the north-central and western Pacific are out of phase. The time series is a good measure of the occurrence and strength of the so-called El Nino (and its inverse), which is the name given to periods of warmer(cooler)-than-average water off Peru and along the equator.

The ultimate cause of the El Nino modulation is unknown, although it is believed to be closely linked to the equatorial wind-driven oceanic circulation. The pattern in Fig. 1 suggests an hypothesis for the termination of the equatorial warm-water periods. Higher equatorial sea-surface temperatures would tend to increase the rate of latent heat release in the tropical troposphere[3], and this may be associated with greater poleward atmospheric fluxes of heat and angular momentum[4]. These tendencies, coupled with an increased meridional subtropical atmospheric temperature gradient induced by the sea temperature anomalies, would result in strengthened mid-latitude westerlies and equatorial easterlies. The latter would act to increase cold upwelling along the equator and reduce the transport of warm water from the west towards Peru by the equatorial countercurrent[5]. The result would be the destruction of the El Nino conditions. A similar process was shown to be quite effective in increasing the easterlies in a numerical experiment by Rowntree[6]. This hypothesis is supported by the fact that, as indicated in Fig 1, El Nino generally ends in the Northern Hemisphere winter when the meridional fluxes in that hemisphere are a maximum[7]. Such a negative feedback would imply that any causal mechanism proposed for El Nino must incorporate a persistence sufficient to explain the 6–18 month existence of the warm conditions.

El Nino is closely related to or even a part of another phenomenon called the Southern Oscillation. The latter is a negative correlation of atmospheric pressure fluctuations in the south-eastern Pacific with those in the Indonesian region Lower pressures over the eastern Pacific tend to accompany warm water there and higher pressures over Indonesia. An empirical orthogonal analysis of tropical sea level pressure, temperatures, and rainfall by Kidson[8] shows the largest fraction of the longer term variability in these fields occurs in Southern Oscillation modes. Variations of the time coefficients of these modes are quite similar to those of Fig. 1 for the period of Kidson's study, 1951–60. We have also compared the entire record of sea temperature coefficients with the variations of sea level pressure at Darwin, Australia, which has been used as a simple index of the Southern Oscillation[9], for several lags and leads. The correlations at zero lag and when the sea temperatures lead the pressures by one month are both 0.55. The correlation when the pressure changes lead those of the sea temperatures by a month is 0.51, which is significantly different at the 95% confidence level.

Our sea temperature-time series also bears a remarkable resemblance to that of mean temperatures of the tropical troposphere recently reported by Angell and Korshover[10] for 1958–73, as shown in Fig 1 The only major discrepancy is for 1964–65 when the tropospheric temperatures remain below the mean whereas the sea temperatures are above In

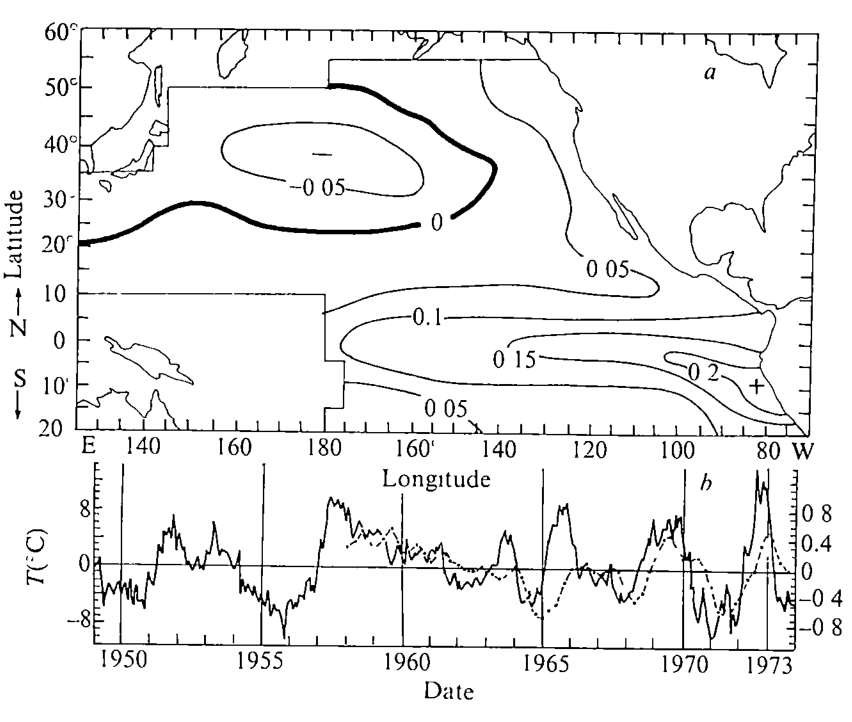

Fig. 1*a*, Empirical orthogonal function of sea-surface temperatures identifying the El Nino mode, and *b*, its corresponding time coefficients (solid line and left hand scale) and tropical troposphere mean temperatures (dotted line and right hand scale) The latter are derived from three-month means of 700–300 mbar thickness data for 14 stations situated near 20°N and 20°S, centred at January, April, July, and October[10]. Tics in the time series identify January of the respective year starting with January 1949 and ending with December 1973

fact, the correlation coefficient between the two variables is 0 74 for the whole period when the sea temperatures lead the air temperatures by 6 months This correlation increases to 0 80 when the years 1964–65 are excluded from the calculation Although there are several possible reasons for the breakdown in correlation in 1964–65, we discuss here only two. One hypothesis is that sea temperatures remain low during this period in other oceans thus holding tropospheric temperatures down. Preliminary results of an analysis of sea temperatures in the Atlantic indicate, however, a small warming rather than cooling during 1965. A second hypothesis is that the difference is associated with a surface cooling resulting from the large increase in stratospheric aerosol which followed the eruption of Mt Agung in March 1963 The additional aerosol was associated with a temperature increase in the tropical stratosphere of 2–6 °C which took several years to disappear[11] Direct solar radiation measured at the ground was concomitantly diminished[12] Since the middle tropical troposphere is mainly heated through latent heat liberation which is decreased during periods of reduced solar surface heating, part of the tropospheric cooling in 1964–65 could probably be ascribed to the effects of Mt Agung. The magnitude of that effect remains an open question

In addition to the six month phase lag which we have shown exists between tropical sea surface and tropospheric temperatures, Angell and Korshover report that tropospheric temperatures at high latitudes change six months later than those in the tropics. Although there are a number of possible factors that may introduce these lags, such as meridional oceanic transport processes and polar ice cap changes, separation of cause and effect is not possible at this time. Careful diagnostic studies and continuous monitoring of both ocean temperatures and volcanic eruptions, however, may enable us to use these phase lags to advantage in seasonal forecasting.

We thank the NSF and ERDA for support and John Kidson for a helpful review We also thank Alfredo Navato for his contribution.

REGINALD E NEWELL
BRYAN C WEARE

Department of Meteorology, 54–1520,
Massachusetts Institute of Technology,
Cambridge, Massachusetts 02139

Received February 16, accepted May 4, 1976

[1] Weare, B C, Navato, A R, and Newell, R E, *Proc WMO/IAMAP Symp Long-term Climatic Fluctuations, Norwich, August* 1975, WMO 421, 167–174 (World Meteorological Organization, Geneva, Switzerland, 1975)
[2] Lorenz, E N, *Empirical Orthogonal Functions and Statistical Weather Prediction*, Scientific Report, 1 (Statistical Forecasting Project Department of Meteorology, MIT, Cambridge Massachusetts, 1956)
[3] Bjerknes, J, *Mon Weath Rev*, 97, 163–172 (1969)
[4] Bjerknes J, *Tellus*, 18, 820–828 (1966)
[5] Wyrtki, K, *J phys Oceanogr*, 5, 572–582 (1975)
[6] Rowntree P R, *Q Jl R met Soc*, 98, 290–321 (1972)
Ramage, C S and Murakami, T., *Q Jl R met Soc*, 99, 393–394 (1974)
[7] Newell, R E, Vincent, D G, Dopplick, T G, Ferruzza, D, and Kidson, J. W, in *The Global Circulation of the Atmosphere* (edit by Corby, G A), 42–90 (Royal Meteorological Society, London, 1970)
[8] Kidson, J W, *Mon Weath Rev*, 103, 187–196 (1975)
[9] Quinn, W H, and Burt, W V, *J appl Meteorol*, 9, 20–28 (1970)
[10] Angell, J K, and Korshover, J, *Mon Weath Rev*, 103, 1007–1012 (1975)
[11] Newell, R E, *Nature*, 227, 697–699 (1970)
[12] Dyer, A J, and Hicks, B B, *Q Jl R met Soc*, 94, 545–554 (1968)

Long term variations in western tropical Pacific cyclogenesis associated with the Southern Oscillation

THE 'Southern Oscillation', as statistically defined by Sir Gilbert Walker, is the barometrically recorded exchange of air mass in tropical latitudes around the complete circumference of the globe[1,2]. Indices of Southern Oscillation based on the surface pressure differences between the Indonesian equatorial low (measured at Darwin, Australia) and the South Pacific subtropical high (considered the Southern Oscillation's eastern core and measured at Easter Island) have been used by Quinn[3–5], who relates fluctuations in these indices to anomalous equatorial rainfall and occurrences of 'El Niño', (the accumulation of anomalously warm water in the eastern tropical Pacific). In this paper, we use 12-month running means of monthly mean surface pressures over three areas across the northern tropical Pacific as an index of the Southern Oscillation index, and we find that pressure convergences in this index are associated with years of relatively low numbers of western Pacific tropical cyclones.

Bjerknes[2] describes a major mechanism in the operation of the Southern Oscillation in the zonal atmospheric circulation which occurs over the equatorial Pacific between the ascending branches of the Hadley cells of the North-east and South-east Trade Winds. The normal sea surface temperature condition of warm water in the western tropical Pacific and cooler water (caused by equatorial upwelling and South American coastal upwelling) in the eastern tropical Pacific drives a zonal convective circulation along the equator between these two regions The distinguishing feature of this particular east–west flow is the potential energy release involved in the dry descent of colder air over the eastern and central tropical Pacific combined with the ascent of warm moist air over the western tropical Pacific.

Anomalous warming of the eastern tropical Pacific sea surface has been related by Wyrtki[6] to increased transport of warm western tropical Pacific water into the eastern tropical Pacific by means of the equatorial countercurrent. These eastern tropical Pacific warmings, in the extreme being referred to as 'El Niño', seem to occur aperiodically from 2 to 7 yr apart The resultant decrease in equatorial sea surface temperature gradient across the Pacific reduces or halts the Walker Circulation, and is associated with the decrease of Southern Oscillation index, that is, a reduction of the difference between surface pressures at Darwin, Australia and Easter Island. What initiates a warming trend is not yet understood.

The situation of a well established Walker Circulation, with the ascent of warm moist air in the tropical western Pacific over a warm sea surface, enhances the first of the three conditions required for intense tropical cyclone formation As described by Palmen and Newton[7], the three conditions are "(1) Sufficiently large sea areas with a water temperature so high that moist air lifted from the lowest layers of the atmosphere (with almost the temperature of the sea surface), expanding pseudo-adiabatically, remains considerably warmer than the surrounding undisturbed atmosphere at least up to a level of ~ 12 km. (2) A Coriolis parameter larger than a certain minimum value, thus excluding a belt of ~ 5° to 8° latitude on either side of the equator. (3) Weak vertical wind shear and correspondingly, weak baroclinity in the basic current in a deep tropospheric layer"

Ramage[8] further notes that over the Pacific, near-equatorial troughs coincident with sea surface temperature maxima are the primary spawning grounds of almost all hurricanes The preconditions of Palmen and Newton[7] are then related to these troughs. Condition (1) is satisfied along the trough axis with the warmest sea surface temperature. Condition (2) is satisfied when the trough is > 5° from the equator where vortices can develop. Condition (3) is also satisfied, since weak vertical shear occurs above the sea surface temperature maximum associated with the trough axis.

It can be reasoned that a strong convective Walker Circulation, driven by the thermally derived pressure gradient between the warm western equatorial Pacific and

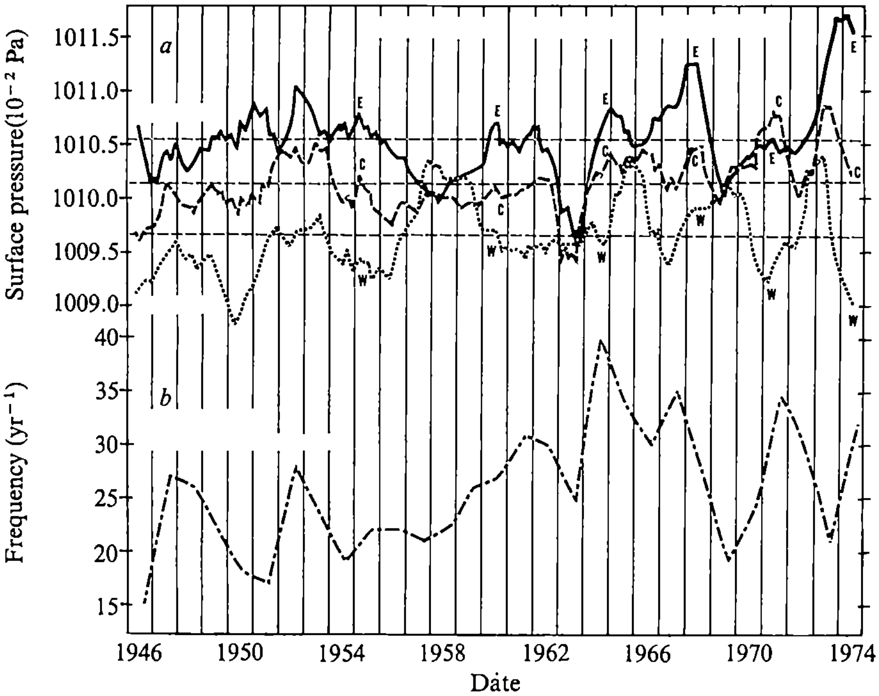

Fig. 1 Time series (1946–74) of 12-month running mean surface pressures (10^{-2} Pa, 1Pa = 10^{-5},bar) for EASTROPAC (E), CENTROPAC (C), and WESTROPAC (W) and *b*, frequencies of western Pacific tropical cyclones.

a cooler eastern equatorial Pacific, might reinforce the conditions of tropical cyclone development in the near-equatorial trough in the western Pacific.

The question thus arises whether an eastern tropical Pacific sea surface temperature warming with the resultant decline in Walker Circulation and decreased ascent of warm moist air in the tropical western Pacific can be associated with a decline in the total number of tropical cyclones in the western Pacific for the given 'warming' year.

Twice-daily surface pressure analyses from 1946 to 1974 were used in the present study. The data were digitised in a 63×63 polar stereographic grid (grid size at 60°N is 381 km). The manually analysed charts were digitised at the National Climatic Center (1946–55, 1960–62) and in the National Center for Atmospheric Research (1956–59). From January 1963 onwards, the numerically analysed surface pressure charts from Fleet Numerical Weather Centre were used. The properties of these digitised surface pressure data are further described by Larson[9].

Monthly means of surface pressure are computed for each grid point and each individual month, with emphasis mainly on three areas in the tropical Pacific in a latitudinal band, 0° to 15°N: The EASTROPAC area reaches from the Central American coast to 150°W; the CENTROPAC area lies between 150°W and 165°E; and the WESTROPAC area extends from 165°E to the Asian coast. The 0° to 15°N latitudinal band includes the main portion of the northeast tradewind zone, north equatorial current, and equatorial countercurrent The monthly means as well as 12-monthly running means of surface pressure are computed for these three different areas; the 12-month running means are computed to eliminate most of the seasonal cycle and depict the long term (> 1 yr) changes.

Plotted together (Fig 1*a*) the 12-month running mean surface pressures converge and diverge in good agreement with Quinn's[3–5] Southern Oscillation index and Wyrtki's[6] equatorial countercurrent index (Harding and Larson[10]). This indicates that the data represent a manifestation of the Southern Oscillation, north of the equator.

The total numbers of tropical storms plus typhoons in the western Pacific for each year, 1946–74, according to Hamilton[11], are plotted to give a measure of interannual variations in tropical cyclogenesis

More rigorous data treatment is not attempted because of the variety of available sources of pressure analyses and of the increased detectability of tropical cyclones with the advent of satellite meteorology in recent years.

Figures 1*a* and 1*b* present the 12-month running mean surface pressure plots for EASTROPAC, CENTROPAC and WESTROPAC as well as the yearly tropical cyclone numbers. The convergences of surface pressure between EASTROPAC and WESTROPAC (associated with EASTROPAC sea surface temperature warming (Wyrtki[6], Harding and Larson[10])) since 1956 are associated with the minima in the number of tropical cyclones in the corresponding years. This is as expected, in as much as these pressure convergences indicate decreases or stoppages of Walker Circulation, and the resulting decrease in the amount of warm moist air ascending in the tropical western Pacific. Also to be noted are the tropical cyclone maxima occurring with the greatest EASTROPAC–WESTROPAC pressure differential, which indicate strong Walker Circulation and well maintained ascension of warm moist air in WESTROPAC.

The results of this study indicate that fluctuations in the Southern Oscillation seem related to interannual variations of tropical cyclogenesis in the western Pacific. The mechanism which connects these phenomena is probably the large scale release of potential energy caused by the thermally driven equatorial Walker Circulation High pressure differential between the EASTROPAC and WESTROPAC represents good Walker Circulation and is associated with interannual maxima in western tropical Pacific cyclogenesis. Pressure convergence of EASTROPAC and WESTROPAC represents little or no Walker Circulation, and is associated with tropical cyclone minima

I thank Mr S. Larson, for providing the data on which Fig. 1*a* is based; Dr T. Laevastu, for advice; Ms W. Carlisle and Ms M. Dimock, for typing; Mr R. Clark, for drafting Fig. 1*a* and *b*, and Mr S. Bishop, for editorial assistance.

J. M. Harding

Naval Environmental Prediction Research Facility,
Monterey, California, 93940

Received December 8, 1975, accepted May 18, 1976.

[1] Walker, G T, *Mem India Meteorol. Dept*, 24, 275–332 (1924).
[2] Bjerknes, J, *Mon. Weath. Rev.*, 97, 163–172 (1969).
[3] Quinn, W. H., and Burt, W. V., *J. appl Meteorol.*, 9, 20–28 (1970).

[4] Quinn, W H., *J appl Meteorol*, 11, 616-628 (1972)
[5] Quinn, W. H., *J appl. Meteorol*, 13, 825-830 (1974).
[6] Wyrtki, K , *Science*, 180, 66-68 (1973)
[7] Palmen, E., and Newton, C., *Atmospheric Circulation Systems* (Academic Press, New York, 1969)
[8] Ramage, C. S , *Mon Weath Rev.*, 102, 745-753 (1974)
[9] Larson, S , thesis, Naval Postgraduate School (1974)
[10] Harding, J , and Larson, S , *EPRF Tech. Note* 22 (Naval Environmental Prediction Research Facility, Monterey, California 1975).
[11] Hamilton, G D , in *Annual Typhoon Report* (FWC/Joint Typhoon Warning Center, Guam, 1973)

Three late-Devensian sites in West-central Scotland

Preliminary investigations of late-Devensian sediments that include moss-sedge peat and moss detritus suitable for radiocarbon dating indicate movement of thick layers of till on the sides of drumlins in west-central Scotland since ~11,150 b.p. Two of the sites investigated are in inter-drumlin depressions on the north-eastern side of Glasgow: at Springburn (NS 609678) and Robroyston (NS 633676). The third site is between Paisley and Irvine on the floor of the Lochwinnoch Gap at North Kerse (NS 339556). The Quaternary sedimentary sequences at the three sites are shown in Fig. 1

At Robroyston the silt underlying the till contains sparse fruit stones of a pondweed, *Potamogeton* cf. *pectinatus* L., a submerged aquatic plant of base-rich water, but virtually no pollen Abundant remains of the algae *Botryococcus* and *Pediastrum* were found with a spore of the terrestrial, calcicolus moss genus *Encalypta* and numerous derived Carboniferous spores The peat, composed of the moss *Scorpidium scorpioides* (Hedw) Limpr. (another indicator of base-rich water) and a sedge (*Carex* sp), has a pollen flora overwhelmingly of Cyperaceae but wtih 13 other taxa of herbs and dwarf shrubs (Table 1). The radiocarbon-dated material was the *Scorpidium–Carex* peat which, on careful examination, showed no Carboniferous contamination.

The lower peat at Springburn, consisting of pure *Scorpidium scorpioides,* has a pollen flora fundamentally similar to that of Robroyston in its large proportion of Cyperaceae, its range of herbs and its very low proportion of trees (Table 1). The upper peat contains mixed oak forest pollen with high *Alnus, Corylus* and ferns. The lower radiocarbon-dated sample was the *Scorpidium* peat (no sign of Carboniferous contamination) and the upper was a highly decomposed peat.

Fig. 1 Late-Devensian sedimentary sequences at sites investigated at Robroyston, Springburn and North Kerse, based on borehole records (all three sites) and observations in excavation pits (Robroyston and Springburn) The locations of radiocarbon dated samples within the sequences are indicated by the relevant laboratory numbers Dates (in yr) are· SRR 696, 11,653 ± 190; BIRM 668, 11,210 ± 150; SRR 697, 11,265 ± 125, SRR 760, 5,994 ± 50; SRR 761, 11,140 ± 110 and SRR 756, 11,210 ± 190.

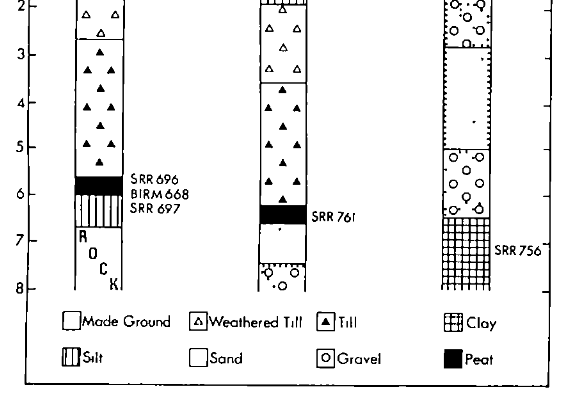

The two sub-till peats, from Robroyston and Springburn, indistinguishable in age and very similar in botanical content, point to identical, if perhaps very local, environments —wet tundra of a rich fen type in the inter-drumlin hollows, possibly with the adjacent grassy slopes bearing heliophilous herbs such as *Helianthemum* and *Artemisia.* Very little is known, as yet, of the late-Devensian vegetation of west-central Scotland, but it is now evident that rich fens with *Scorpidium* and *Carex* were widespread during the Allerød oscillation; there are previous records from Garscadden Mains (NS 524712), just West of Glasgow[1,2], and from Drymen (NS 490923) near Loch Lomond[3]

Table 2 lists the macroscopic plant assemblage sieved from ~ 500 ml of the clay at North Kerse. The assemblage is mainly, if not entirely, allochthonous. By far the most abundant fragments are of the moss *Rhacomitrium aruginosum*, an often abundant colonist of freshly exposed rock or mineral soil *Aulacomnium turgidum* is a common tundra moss, now rare in the Scottish mountains. This species and *Alchemilla vulgaris* agg. have few Quaternary records, the other taxa are well known from the British Quaternary[2,4] The material used for radiocarbon dating consisted of fragments of *Rhacomitrium* with a slight admixture of vascular plant debris Abundant small fragments of coal were separated by flotation and by manual removal under a dissecting microscope.

The evidence from the three sites may be synthesised as follows:

(1) At Robroyston and Springburn, glacial till on the flanks of drumlins overlies peat deposits dated ~ 11,650–11,150 b.p and containing flora indicative of tundra conditions The till in contact with the organic deposits is unweathered and resembles the typical grey till constituting the drumlins of central Glasgow[5], till that is commonly regarded as a product of the main Devensian glaciation, thought to have occurred in west-central Scotland broadly between 27,000 and 13,000 b p.

(2) At Springburn the till underlies peat dated 5,994± 50 b.p. and therefore must have been emplaced in its present position by natural processes rather than by the industrial activities of man. Inferentially, the till at Robroyston also was transported to its present position by natural processes.

(3) At North Kerse, the plant detritus dated 11,210± 190 b.p is indicative of tundra conditions The detritus is overlain by sands and gravels which, on initial investigation, are thought to have been deposited in an aqueous environment

Possible alternative interpretations of the evidence are these

(1) The till at Robroyston and Springburn was deposited directly by ice in its present positions in the course of a glaciation that occurred later than ~ 11,150 b.p The tundra conditions indicated by the peat deposit at Robroyston, the lower peat at Springburn and the dated organic detritus at North Kerse may represent the onset of colder, glacial conditions in west-central Scotland after a warm episode ~ 13,000–12,000 b p. (ref. 6) At North Kerse, the sands and gravels overlying the organic detritus may have been deposited penecontemporaneously with the till in a periglacial regime outside the area of glaciation at Robroyston and Springburn.

(2) After initial deposition by glacier ice, the till at Robroyston and Springburn was moved to its present positions by solifluction processes while contemporaneously the sands and gravels at North Kerse were deposited in a periglacial environment during a cold period that commenced ~ 11,200 b.p. (cf. the commonly recognised cold episode in Britain between 11,000 and 10,000 b.p.; with average July

Table 1 Taxa found in the peats at Robroyston and Springburn

Taxa	Sub-till peats Robroyston per cent P + S	 Springburn
Betula	2	4
Pinus	+	+
Salix	+	+
Gramineae	2	17
Cyperaceae	91	65
Ericales	1.5	—
Empetrum	—	+
Artemisia	—	+
Caryophyllaceae	—	+
Compositae	+	+
Cruciferae	+	—
Helianthemum	+	+
Myriophyllum alterniflorum	+	—
M verticillatum	+	—
Ranunculaceae	+	+
Rosaceae	+	7
Thalictrum	+	—
Umbelliferae	—	1 5
Valeriana	—	+
Filicales	+	—
Lycopodium selago	+	—
Selaginella selaginoides	+	—
Unidentified	+	+
$\Sigma P + S$	983	252

+, less than 1 per cent

temperatures below 11 °C suggested by the evidence of Coleoptera[6])

The first interpretation must be considered improbable on the grounds that first, in western Glasgow and its environs, grey till constituting drumlins, apparently of the same swarm as those at Robroyston and Springburn, is overlain at a number of locations by marine deposits containing mollusc shells dated 12,600–12,400 b p (ref. 7), and second, there is no known evidence to suggest that in west-central Scotland the ice margin of the Loch Lomond Readvance (maximum ~ 10,500 b p.) extended beyond the southern flank of the Loch Lomond Basin[8].

Table 2 North Kerse macroscopic plants

Taxa from dry ground habitats		Remains
Mosses	*Aulacomnium turgidum* (Wahl) Schwaegr	3 lf
	Encalypta sp.	1 cl
	Polytrichum alpinum Hedw.	4 st, 6 lf
	Rhacomitrium lanuginosum (Hedw.) Brid	> 100 st
Vascular Plants	*Alchemilla vulgaris* agg.	1 fr
	Salix sp.	1 tw
	Salix cf. herbacea L.	1 lf
Taxa from aquatic, wetland or streamside habitats		
Mosses	*Calliergon sarmentosum* (Wahl) Kindb.	11 st
	Philonotis sp	2 st
Vascular Plants	*Carex rostrata* Stokes	1 fr
	Menyanthes trifoliata L.	3 se
	Myriophyllum alterniflorum DC	2 fr
	Ranunculus subg. *Batrachium*	1 fr
	Selaginella selaginoides (L) Link	1 mg
Taxa unclassified by habitat		
Mosses	Amblystegiaceae	6 st
	Bryum sp.	3 st
	Pohlia sp.	3 st
	Polytrichum sect *Juniperifolia* Brid.	1 lf
Vascular Plants	cf. Cruciferae	2 se

lf, leaf; cl, calyptra; st, leafy stems;
fr, fruit; tw, twig; se, seed; mg, megaspore.

The second interpretation lends support to suggestions recently made regarding late-Devensian climatic conditions in Britain, and focuses attention on a number of interesting problems awaiting further investigation. According to Sissons[9], major periglacial features in Scotland seem to be restricted to the area outside the limit of the Loch Lomond Readvance, and such features are indicative of extremely severe climatic conditions that persisted down to sea level[10]. Published evidence of periglacial action in Scotland during the Loch Lomond Readvance consists mainly of solifluction and associated phenomena in the Highland region together with the record of fossil frost wedges in the Midland Valley and, to a lesser extent, in the Southern Uplands. The evidence from Robroyston and Springburn strongly suggests that large scale solifluction on the flanks of drumlins with a major feature of periglacial activity in west-central Scotland in the cold period that commenced ~ 11,000 b.p. and culminated in the Loch Lomond Readvance. Previously, minor solifluction on the slopes of drumlins has been considered probable, but the sites at Robroyston and Springburn provide the first evidence in west-central Scotland of mass movement of till several metres thick Clearly, because these examples of such movement exist, many more may be discovered in the future The presence of a datable peat layer below the soliflucted till at Robroyston and Springburn allowed the movement of the till to be deduced There may be many situations on the flanks of drumlins where adjacent peat layers did not accumulate before the Loch Lomond Readvance, but solifluction of large till masses occurred nevertheless. Such cases will be very difficult to detect. Till-fabric and till-fissure analyses[11] may prove effective in some situations At Robroyston and Springburn preliminary studies of these properties of the till proved inconclusive.

Future research arising from the preliminary study of the three sites may be directed to establishing the vegetational evidence for late-Devensian climatic conditions in west-central Scotland, to assessing the effectiveness of till-fabric and till-fissure analyses in determining mass movement of till on the sides of drumlins, and to considering the modifications of drumlin shapes that occur as the result of till solifluction.

The authors thank W. Bradford and E. McKinnon (Preconstruction Services), for providing borehole logs and peat samples from Springburn and Robroyston. The plant sample from North Kerse was collected by R Ward. Five radiocarbon dates were provided by the Scottish Universities Research and Reactor Centre and paid for by the University of Glasgow. One date was provided by Birmingham University Mrs C A. Dickson and Mr D. A. Stewart assisted with the botanical analyses.

J. H Dickson
Department of Botany,
W. G Jardine
Department of Geology,
R. J. Price
Department of Geography,
Glasgow University,
Glasgow, G12 8QQ, UK

Received April 1, accepted May 4, 1976

[1] Mitchell, G F , *New Phytol* , 50, 277–286 (1952)
[2] Dickson, J H , *Bryophytes of the Pleistocene* (Cambridge, 1973)
[3] Dickson, J H , in Vasari, Y., and Vasari, A , *Acta bot. Fenn* , 80, 62–65 (1968).
[4] Godwin, H., *History of the British Flora*, 2nd ed , (Cambridge, 1975)
[5] Jardine, W G , in *Excursion Guide to the Geology of the Glasgow District* (edit. by Bluck, B J) 156–169 (Glasgow, 1973)
[6] Coope, G R., in *Ice ages Ancient and Modern* (edit. by Wright, A. E and Moseley, F) 153–168 (Liverpool, 1975)
[7] Peacock, J D , *Nature phys Sci* , 230, 43–45 (1971)
[8] Price, R J , *Scott. geogr Mag* , 91, 134–145 (1975).
[9] Sissons, J B , *Scott J Geol.*, 10, 311–337 (1974)
[10] Sissons, J. B., *Boreas*, 3, 41–48 (1974)
[11] McGown, A., Saldivar-Sali, A , and Radwan, A. M., *Q Jl Engng Geol* , 7, 1–26 (1974).

Changes in net surface charge of hydrous alumina with phosphate adsorption

ADSORPTION of phosphate on hydrous metal oxides is of considerable importance in soil fertility and eutrophication studies. Phosphate is known to be adsorbed on the hydrous oxides displacing aquo (M–OH$_2$) and hydroxo (M–OH) ligands; its adsorption makes the oxide surface less positive[1–3]. I report here on a quantitative study in which phosphate was adsorbed on to hydrous oxides, displacing the ligands, and the simultaneous change in the net surface charge was measured.

The hydrous alumina used has been described elsewhere[3] and the pH value at the point of zero charge (PZC) was 9.3. The phosphate adsorbed and the hydroxyl ions released at different phosphate concentrations were measured at a constant pH (see ref. 3). The experimental conditions were: pH 5.0; 0.01 mol dm^{-3} NaCl medium; 3 h reaction time; 30 °C; nitrogen atmosphere. The pH was chosen so that phosphate existed in solution as the monovalent ion. The net surface charge (σ) was calculated from the counter ions retained by the oxide in the diffuse double layer (details will be published elsewhere).

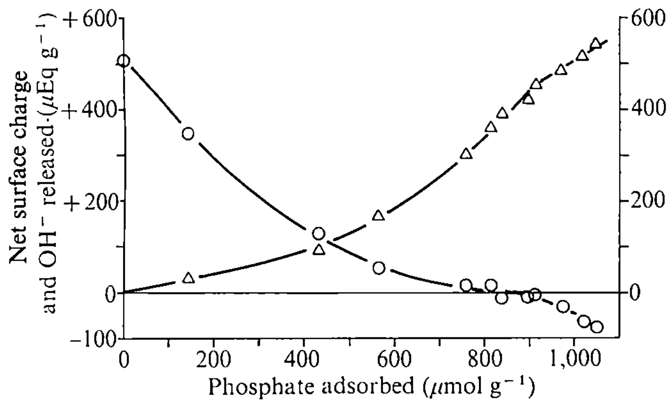

Fig. 1 Phosphate adsorption on hydrous alumina. Net surface charge (○) and OH$^-$ released (△) plotted against P adsorbed.

The hydroxyl ions released, and the σ values, are plotted against phosphate adsorbed in Fig. 1. Mathematical analysis of the hydroxyl ion curve shows that the differential (dOH$^-$/dP) increases with increasing phosphate adsorption from 0.11 to a maximum of 1.0 at about 900 μmol g^{-1} of phosphate adsorbed. At more than about 900 μmol g^{-1}, however, it abruptly decreases to 0.5 and remains constant.

The σ of the sample in the absence of phosphate (σ_0) was 507 μEq g^{-1} of positive charge. With increasing phosphate adsorption, σ decreased to zero, and with further adsorption it became negative.

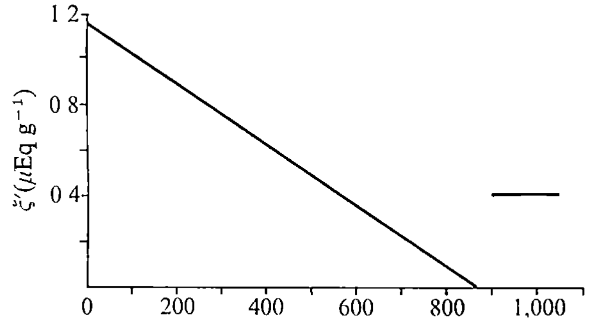

Fig. 2 Net charge acquired by the surface per unit μmol of phosphate adsorbed (ξ′) as a function of phosphate adsorbed.

At pH values more acid than the PZC pH, phosphate is probably adsorbed at the positive sites displacing OH$_2$, and at the neutral sites, effectively displacing OH$^-$ (refs 1–3).

$$\mathrm{Al\text{-}OH_2]^{1+} + H_2PO_4^- \rightleftharpoons Al\text{-}H_2PO_4]^0 + OH_2} \tag{1}$$

$$\mathrm{Al\text{-}OH]^0 + H_2PO_4^- \rightleftharpoons Al\text{-}H_2PO_4]^0 + OH^-} \tag{2}$$

Reaction (1) neutralises the positive charge, whereas reaction (2) leaves the surface charge unaltered.

Because of the greater lability of aquo groups, at low surface saturation more of these are displaced by phosphate, whereas with the increasing saturation the proportion of hydroxo groups released increases[3]. Therefore, the neutralisation of the positive charge would be initially rapid; this is seen from Fig. 1. There is little change in the σ within the phosphate adsorption range 800–900 μmol g^{-1}, and phosphate is adsorbed mostly by displacing hydroxyl ions, as is evidenced by the dOH/dP value of close to 1.

The net charge acquired by the surface per μmol of phosphate adsorbed (ξ′) at different adsorption values (Fig. 2) was calculated: the total net charge acquired by the surface, ξ ($\xi = \sigma_0 - \sigma_P$; σ_P = net charge on P added sample) was plotted as a function of phosphate adsorbed, and the equation that gave the best fit was differentiated. The differential curve (Fig. 2) shows that ξ′ varies with the type of ligand, OH$_2$ or OH$^-$, displaced by phosphate, which in turn varies with the surface saturation. These results suggest that earlier conclusions[4–6] that ξ′ is independent of surface saturation were based on observations of an experimental artefact. Other researchers have used either a titration method or have relied on separations of the phosphated sample from the matrix, followed by re-equilibration with another indifferent salt solution and extraction of the counter ions using yet another salt solution. It is likely that these methods would result in desorption and/or rearrangement of adsorbed phosphate.

The abrupt change in the slope of Fig. 1 at about 900 μmol g^{-1} phosphate adsorbed could signify[3,7] the disruption of hydrous alumina polymers. The fresh surface thus exposed would adsorb phosphate:

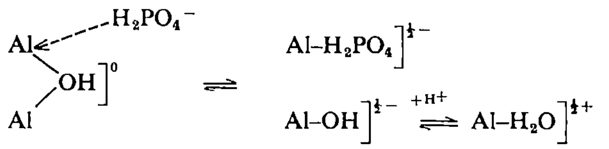

$$\mathrm{Al{\leftarrow}H_2PO_4^-,\ Al_2OH]^0 \rightleftharpoons Al\text{-}H_2PO_4]^{\frac{1}{2}-}\ \ Al\text{-}OH]^{\frac{1}{2}-} \overset{+H^+}{\rightleftharpoons} Al\text{-}H_2O]^{\frac{1}{2}+}}$$

$$\mathrm{Al\text{-}H_2O]^{\frac{1}{2}+} + H_2PO_4^- \rightleftharpoons Al\text{-}H_2PO_4]^{\frac{1}{2}-} + H_2O} \tag{3}$$

According to reaction (3) a net negative charge of 1 μEq is added for every 2 μmol of phosphate adsorbed. Thus, in the region of high phosphate adsorption (> 900 μmol g^{-1}) the expected ξ′ is 0.5, and the experimental value of 0.41 (Fig. 2) is in reasonable agreement.

Reactions (1) and (2) predict a 1:1 ratio between released OH$_2$ and ξ values. To test this, ξ values have been plotted against the number of μmol of OH$_2$ displaced (Fig. 3). The latter values were calculated from the difference between the amount of phosphate adsorbed and hydroxyl ions released. The four observations at > 900 μmol g^{-1} of phosphate adsorbed were not used because adsorption was on the new surface in that region, and different reaction paths are involved (3). The observed slope of 1.03±0.05 (r^2 = 0.989) agrees with the predicted value of 1.0.

The results presented add further evidence in support of the theory[3] on the nature of phosphate adsorption at different surface saturation values.

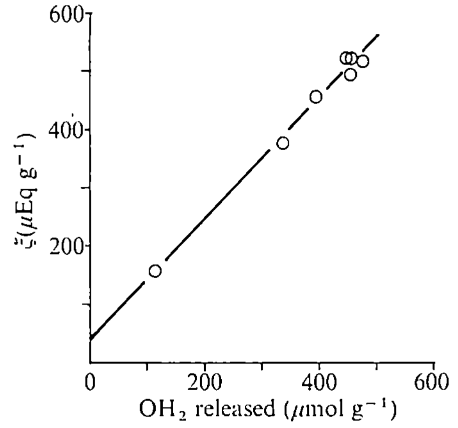

Fig. 3 Relationship between the net charge acquired (ξ) and aquo groups (OH_2) displaced by phosphate. $\xi = 40.46 + 1.03OH_2$; $r^2 = 0.989$.

I thank Dr J. H. Watkinson for correcting the manuscript, Mr D. M. Duganzich for statistical analysis, and the members of the Spectrolab for sodium determinations.

S. S. S. RĀJAN

Ruakura Agricultural Research Centre,
Private Bag,
Hamilton, New Zealand

Received February 9, accepted May 17, 1976.

[1] Hingston, F J., Atkinson, R J , Posner, A M , and Quirk, J. P , *Nature*, **215**, 1459–1461 (1967)
[2] Breeuwsma, A , and Lyklema, J , *J Colloid Interface Sci.*, 43, 437–448 (1973)
[3] Rajan, S S S., Perrott, K W , and Saunders, W M H , *J Soil Sci* , 25, 438–447 (1974).
[4] Hingston, F J , thesis, Univ Western Australia (1970)
[5] Mekaru, T , and Uehara, G., *Proc Soil Sci Soc. Am* , **36**, 296–300 (1972)
[6] Schalscha, E B., Pratt, P. F , and Soto, D , *Proc Soil Sci Soc Am* , **38**, 539–540 (1974)
[7] Rajan, S S S., *Nature*, 253, 434–436 (1975).

Conformational effects in drag reduction by polymers

An earlier study of drag reduction by polyelectrolyte solutions[1] revealed that the gross flow behaviour varied between extremes, termed types A and B, respectively characteristic of the collapsed and extended macromolecular conformations Here I show, from examination of all available experiments[1-5], that the crossover from type A to type B behaviour occurs at a characteristic conformation, which possibly reflects the role of macromolecular elasticity in the mechanism of drag reduction.

It should be recalled[6] that drag reduction by dilute polymer solutions in turbulent pipe flow is bounded between two universal asymptotes, that is, the Prandtl-Karman law and the maximum drag reduction aysmptote, that envelop a 'polymeric' regime in which the observed friction factor relations are approximately linear on coordinates of $f^{-1/2}$ against log $Ref^{1/2}$, where f is the friction factor and Re the Reynolds number. The behaviour exhibited by a family of polymer solutions is termed type A when the polymeric regime segments fan outwards from a common onset point on the Prandtl–Karman (Newtonian) line with slopes exceeding the Newtonian value and increasing with increasing polymer concentration, and type B when the polymeric regime segments lie roughly parallel to the Prandtl–Karman line but displaced upward from it, the more so with increasing additive concentration.

The dependence of a drag reduction modulus, κ, on a macromolecular excluded-volume parameter, E, is now sought from experimental data, these quantities being defined

$$\kappa = (\delta/c^{1/2})M^{1/2}N^{-3/2} \qquad (1)$$

$$E = \sigma\,([\eta]/[\eta]_\theta)^{1/3} \qquad (2)$$

κ is derived from friction factor measurements; δ is the observed Prandtl-Karman slope increment relative to solvent in the polymeric regime of drag reduction while c, M, and N, are respectively the macromolecular concentration, molecular weight, and skeletal links. E is formed from the polymer species chain conformation factor σ and the ratio of actual to theta point intrinsic viscosities, at zero shear, of the macromolecule; as long as the macromolecule remains random-coiling, E is evidently the ratio of actual to unhindered r.m.s. radii of gyration ($R_G/R_{G,of}$). The results are shown in Fig. 1, which shows κ against E on doubly logarithmic coordinates. An abrupt change in κ is observed at $E_x = 6 \pm 1$, defining a characteristic 'crossover' conformation. For $E < E_x$, in the region of type A gross flow behaviour, the drag reduction modulus is essentially independent of macromolecular conformation, and the examples in Fig. 1 all display magnitudes of $\kappa_A = 10^{-4}$, typical of random-coiling polymers with polymethylene types of skeleta[5]. For $E > E_x$, in the region of type B gross flow behaviour, the variation of κ with E cannot be ascertained for lack of data, but values of $\kappa_B = 10^{-5}$ are clearly an order of magnitude lower than κ_A. The behaviour described is well illustrated by results for two PAMH polymers in Fig. 1, one of which[1] yields $\kappa \times 10^6 = (61, 60, 61, 5, 5)$ for $E = (3.6, 3.7, 4.9, 6.8, 10.0)$ respectively while the other[2] (hollow squares) shows a very similar trend. The data[3,4] for random-coiling PEO and PIB polymers in good as well as in theta solvents both yield κ essentially independent of E over small ranges of $E < E_x$.

A possible physical interpretation of these results involves macromolecular rubber elasticity. E refers to the static (zero shear) conformation of a macromolecule in dilute solution. In

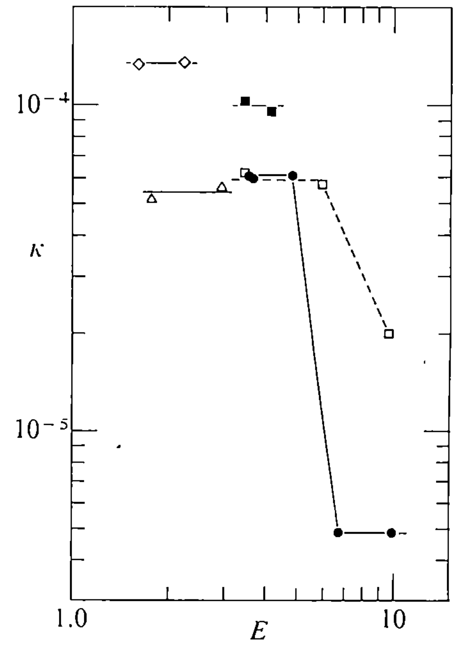

Fig. 1 The dependence of drag reduction slope modulus on macromolecular excluded volume

Symbol	Polymer	σ	Molecular weight ($\times 10^{-4}$)	Solvents	Pipe internal diameter (mm)	Reference
●	PAMH	2 30	15 2	Aq NaCl, 0–1 M	9 45	1
□	PAMH	2 30	9 2	Aq NaCl, 0–1 M	10 2	2
■	PAMH	2 30	7 8	Aq NaCl, 0 2–1 0 M	10 2	2
◇	PEO	1 60	0 76	Aq K_2SO_4, 0–0 6 M	4 57	3
△	PIB	1 82	0 89	Benzene, Cyclohexane	12 9	4

PAMH, Polyacrylamide, partially hydrolysed, PEO, polyethyleneoxide, PIB, polyisobutylene turbulent flow, a macromolecule suffers deformations about its mean conformation and the drag reduction modulus, κ, seems related to rubber elasticity[5] through a macromolecular chain deformation factor J, defined by

$$J = [(R_G'/R_G) - 1]/\beta^2 \qquad (3)$$

where R_G' and R_G respectively refer to deformed and mean conformations, whereas β is a non-dimensional strain rate. This suggests that the data of Fig. 1 arise because the elasticity of a macromolecular random coil is essentially independent of its excluded volume up to a certain conformation, E_x, and then decreases significantly for $E > E_x$. In this context, recent direct measurements of macromolecular extension in a Borda flow[6] are noteworthy. For two samples of PIB in decalin ($E \simeq 3$), it was found that at low strain rates the observed principal axis extension ratio (R_G'/R_G) yielded values of $J \simeq 10^{-1}$, of the order of magnitude theoretically predicted[7]. With increasing strain rate, however, the principle extension ratio tended to an asymptote with a maximum value $(R_G'/R_G) \simeq 3.5$, with corresponding lower values of $J \simeq 10^{-3}$. These experiments independently suggest that there is a characteristic macromolecular extension beyond which elastic deformation of the random-coil becomes difficult. Interestingly, the value of $R_{G,\mathrm{max}}'/R_{G,\mathrm{of}}(\sim 10)$ for PIB in a Borda flow is of the order of magnitude of our $E_x(\sim 6)$ obtained with PAMH during drag reduction, both of the polymers used possessing similar (but not identical) polymethylene skeleta.

P. S. VIRK

Department of Chemical Engineering,
Indian Institute of Technology,
Madras 600036, India

Received March 16; accepted May 12, 1976

1 Virk, P. S , *Nature*, **253**, 109 (1975).
2 Clarke, W B., thesis, MIT (1971).
3 Pruitt, G. T , Rosen B , and Crawford, H R , *Rept DTMB-2*, (*Western* Co , Dallas, Texas, 1966).
4 Hershey, H. C , and Zakin, J. L., *Chem. Engng Sci.*, **22**, 1847 (1967).
5 Virk, P S., *A. Inst. Ch E. JL*, **21**, 625 (1975).
6 Smith, K A , *et al* , *Proc CNRS Colloque Intnl Polymeres et Lubrification* (Brest, France, 1974)
7 Peterlin, A , *Pure Appl Chem* , **12**, 563 (1966).

Effect of drag-reducing polymers on pulsation noise of small air bubbles

PREVIOUSLY we have reported[1] that polyethyleneoxide (Polyox) in solution reduced the damping of free oscillations in a semi-circular manometer, whereas polyacrylamide (Separan: also an effective drag-reducer in turbulent flow) did not. Here we report the effect of these additives (Polyox grades WSR 301 and N3000; Separan grades AP 30, AP 273 and MG 200) on the pulsation noise radiated by small air bubbles in water.

The bubbles were produced by passing air through a submerged nozzle in a steel water-tank, 75 × 60 × 70 cm, which was mounted on an expanded polystyrene sheet (5 cm thick), on a concrete base. The compressed air supply consisted of a piston sliding in a cylinder. This was driven by an electric motor through a reduction gear which turned a threaded rod. The air outlet from the cylinder was connected by a flexible PVC tube to a brass nozzle, situated 23 cm below the water level, and mounted in a rubber bush to prevent resonance with the supporting rod. All the nozzles used were 7.5 cm long by 6.4-mm outside diameter, but the inside diameter varied between 2 and 5 mm to give a range of bubble sizes. This arrangement produced bubbles of uniform size at regular intervals. The average bubble size was determined from the volumetric displacement of the piston in the cylinder and the number of bubbles produced in a given time.

The bubble pulsation noise was detected by a hydrophone (Bruel and Kjaer type 8101: uniform frequency range up to 60 kHz), which was fixed at the same depth as the nozzle, but could be moved horizontally. The hydrophone was connected to a spectrum analyser (B and K model 2107). The output of the spectrum analyser was connected to a counter–timer (Bradley Electronics 234) used to determine bubble size and frequency of production, a storage oscilloscope (Tektronix 434) used for frequency spectrum and spatial attenuation measurements and an oscillograph (Bell and Howell model 5–137) used for measuring time-decay curves.

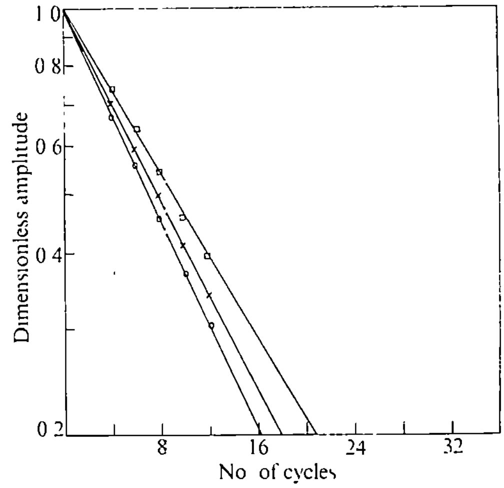

Fig. 1 Time decay of bubble pulsation noise. (Nozzle internal diameter 5 mm; bubble diameter 5.8 mm; f_0 (theoretical) 1,115 Hz; f_0 (experimental) 1,105 Hz). ×, water; □, 20 p.p.m. Separan AP 273; ○, 100 p.p.m. Separan AP 273.

Experiments were performed using nozzle diameters of 2, 3, 4 and 5 mm. In each case the additives affected bubble production. We found that at low concentrations, Polyox reduced bubble size (in agreement with previous results[2] on bubble growth in solutions of WSR 301) whereas Separan tended to increase the size of the bubbles. In both cases the effect was quite small, and the bubble radius quickly became independent of increasing additive concentration. Correspondingly the additives had only a small effect on the natural frequency of the bubble noise.

It was also noticed that all additives reduced the radiated sound intensity. This effect has previously been found with noise from turbulent boundary layers[3] and from the impact of small spheres[4] in polyox solutions.

The particular results we report here are concerned with the damping of the bubble noise. When a bubble leaves the nozzle, the emitted sound pulse takes the form[5]

$$P_s = P_0 \exp(-\pi\delta f_0 t) \cos(2\pi f_0 t)$$

where P_s is the instantaneous radiated sound pressure, P_0 is the sound pressure amplitude and f_0 is the natural frequency. The damping constant δ has been predicted theoretically[6], and

Fig. 2 Variation of reduction in damping with additive concentration. ×, Polyox WSR 301, □, Separan AP 273.

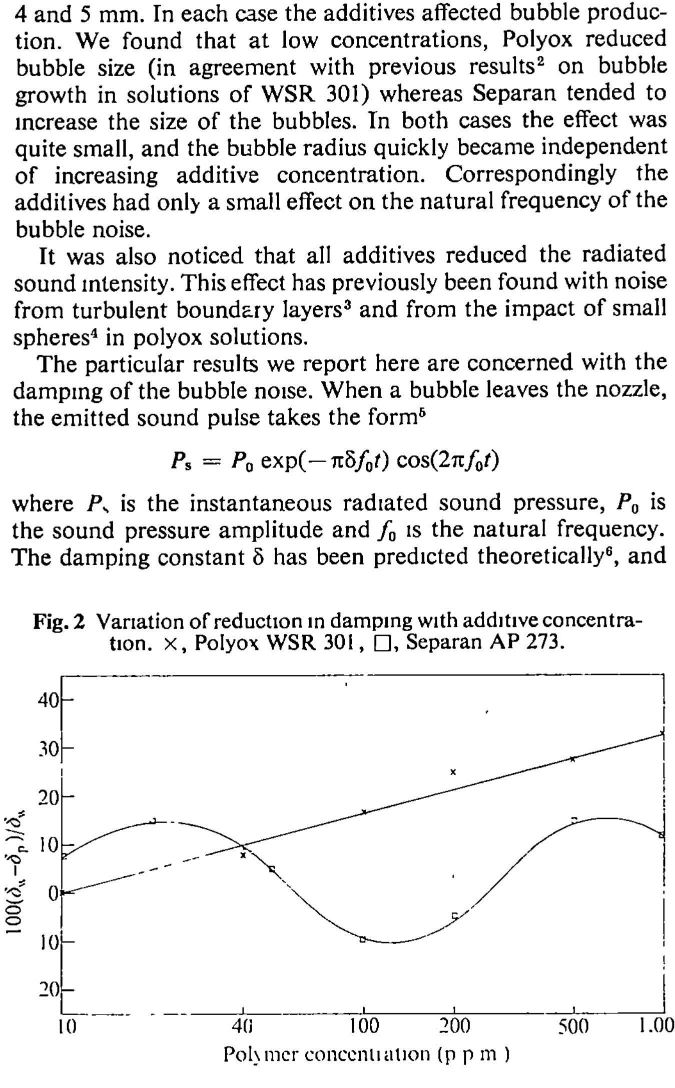

the predicted values confirmed experimentally for nitrogen bubbles in water[7].

To check our system, we first made a comparison with previous work on gas bubbles in water[6,7]. We found that our values for damping constant and natural frequency were as expected (within ±1%). Results for the 5-mm diameter nozzle are shown in Fig. 1. This nozzle size was found to be the most satisfactory in terms of producing a good quality signal with minimum nonlinear distortion and maximum reproducibility. Thus all results presented here were taken with the 5-mm nozzle.

We obtained the time-decay curve by running the oscillograph at a chart speed of 200 cm s^{-1}. The results were analysed by dividing the amplitude at any point by the peak amplitude, and plotting on semi-logarithmic graph paper against time (measured in number of cycles) It was found that all the polymer additives reduced the damping of the emitted sound pulse to some extent, but Separan AP 30 and AP 273 increased the damping at certain concentrations. Representative results for Separan AP 273 at concentrations of 20 and 100 p.p.m. (by weight) are presented in Fig. 1, where they may be compared with the decay curve for water.

These results may be put in a more quantitative form by defining the percentage change in damping constant $100(\delta_w-\delta_p)/\delta_w$, where δ_w is the damping constant in water and δ_p the damping constant with polymer additive. This is plotted against concentration for Polyox WSR 301 and Separan AP 273 in Fig. 2. At low concentrations WSR 301 had little effect. It was only at concentrations measured in hundreds of p.p.m. (which are large compared with amounts needed for turbulent drag reduction) that one noticed appreciable reductions, ~ 10%–40%. On the other hand, Separan AP 273 did reduce the damping of the bubble noise at low additive concentrations, but the subsequent dependence of the effect on increasing concentration was rather unusual (see Fig. 2). This oscillatory form of concentration dependence was also observed in the case of Separan AP 30. Possibly this may just reflect the complexity of the bubble noise decay, involving, as it does, energy losses by acoustic radiation, thermal conduction and viscous liquid friction.

W. D. McComb
S. Ayyash

School of Engineering Science,
Edinburgh University,
Edinburgh, UK

Received April 30, accepted May 17, 1976.

[1] McComb, W D, *Nature*, 251, 598 (1974)
[2] Ting, R. Y., Ellis, A T., *Phys Fluids*, 17, 1461 (1974).
[3] Barker, S J., *Phys Fluids*, 16, 1387 (1973).
[4] Sanders, J, Sendek, J., *J acoust Soc. Am.*, 45, 339 (1969).
[5] Strasberg, M., *J. acoust. Soc Am*, 28, 20 (1956).
[6] Devin, C., *J. acoust Soc Am.*, 31, 1654 (1959)
[7] Koger, H. G., Houghton, G, *J acoust. Soc Am*, 43, 1571 (1968).

Plasma treatment of coal

Coals of various ranks have been treated in electrical arcs or plasma jets generated from argon, hydrogen, and their mixtures. In most cases the plasmas contained enough energy to heat the coal to temperatures ⩾1,000 °C. In this range of temperatures, acetylene formation is thermodynamically favoured, and an argon–hydrogen plasma has been reported to yield a maximum acetylene yield of 74% by weight of coal[1-3]. Problems are encountered with the electrical arcs because of the instability induced in the arc column by appreciable forced convection[4]. From a practical point of view methane would be the preferred product from coal gasification, and we here report on efforts to find whether a low temperature plasma favoured methane formation

We applied 50-Hz electrical discharges through 15-cm long coaxial Pyrex tubes, the annular space (1 cm wide) of which was packed with a sample of bituminous coal (76 06% C, 5.48% H, 15.33% O, 1.05% N, and 2.09% S) and degassed at room temperature. The applied voltage was 26 kV and the current through the plasma was measured to be 2 6 mA, which means the power input was ~68 W. Gas chromatographic analysis using a 1.2-m long silica gel column at 0 °C revealed that the gaseous products pumping out of the plasma zone consisted mainly of hydrogen and carbon monoxide, with small amounts of methane. A 1 2-m long alumina column at 0 °C confirmed that acetylene was not present in the products.

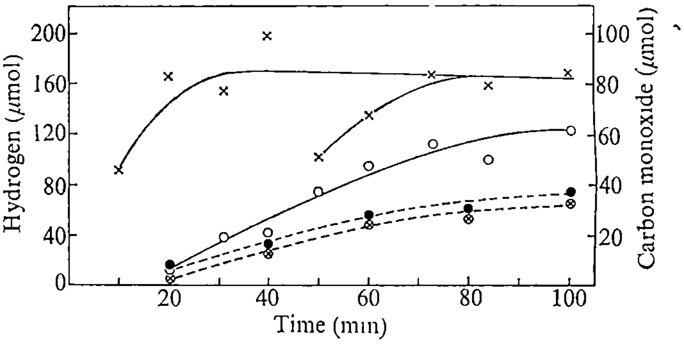

Fig 1 Hydrogen (×) and carbon monoxide (○) yields from a Siemens tube packed with bituminous coal and excited at 68 W. Solid symbols and dotted lines represent the yields from coal + 26 mmHg He.

Figure 1 shows the yields of hydrogen and carbon monoxide obtained at various time intervals from a sequential operation in which coal was excited, at first alone and then in the presence of 26 mmHg of helium. The influence of the added gas was to decrease the H_2 and CO production considerably. The relatively large amounts of H_2 obtained at the short time intervals appeared to arise from an initial desorption of gases from the coal as a result of the application of the high voltage.

Figure 2 shows the methane formation as a function of the discharge period. Here again the influence of the added helium was to decrease the methane production, except in the long runs ($t>1$ h) in which the addition of helium increased the conversion of coal into methane. On the other hand, in the short runs ($t<0.5$ h) more methane was produced in experiments in which hydrogen was added to coal which had not been previously treated in a plasma. Table 1 summarises data on the conversion of the carbon in coal

Fig 2 Methane production in a Siemens tube packed with bituminous coal and excited at 68 W. ×, ○, and ⊙ for yields from coal, coal + 26 mmHg He, and coal + 26 mmHg H_2, respectively. Dotted line and solid symbols represent the yields when coal was excited at first in the presence of H_2 and then in He.

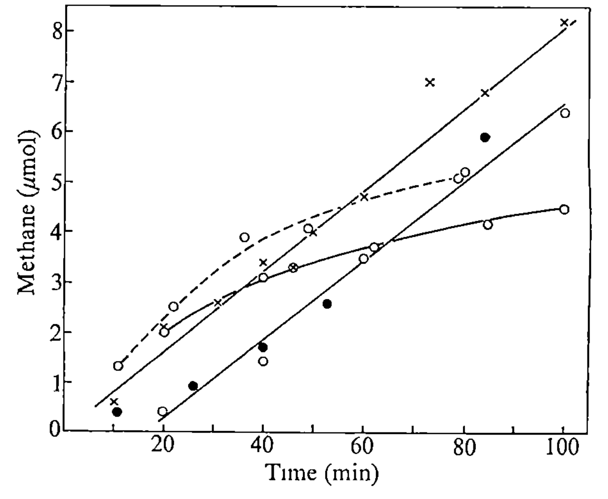

into methane The observed conversions are low for technical purposes, but this is to be expected because of the use of low frequency, low power discharges at low pressures and ordinary temperatures which allowed essentially non-pyrolytic reactions.

Table 1 Conversion of the carbon in bituminous coal into methane

Time (min)	Conversion into methane (mol per cent) Coal	Coal + He	Coal + H_2
10	12.2	—	17.6
20	12.2	5.2	21.5
40	13.9	8.0	16.2
60	9.1	11.1	11.7
80	12.0	14.8	12.3
100	11.8	14.7	10.8

The electron spin resonance spectrum of the coal subjected to plasma showed a 2.5-fold increase (~10^{18} spins per g) in the spin concentration over an untreated sample suggesting that a free radical mechanism may be involved in the gasification process

Further work using a flow-system with an argon–hydrogen mixture at atmospheric pressure is in progress.

T. W. Scott
M. Venugopalan

Department of Chemistry,
Western Illinois University,
Macomb, Illinois 61455

Received February 20; accepted May 14, 1976

[1] Nicholson, R., and Littlewood, K., *Nature*, **236**, 397 (1972)
[2] Littlewood, K., *Proc. Symp. Chem Oil Coal*, 1969, 517–25 (1972)
[3] Kawana, Y., *Chem Econ Eng Rev*, **4**, 13 (1972)
[4] Sheer, C., and Korman, S., *Adv. Chem Ser*, **131**, 42 (1974)

---

*p*H-dependent heterosis of heavy metal-tolerant and non-tolerant hybrid of the monkey flower *Mimulus guttatus*

ALTHOUGH the toxicity of heavy metals is known to be dependent on *p*H, no studies of heavy metal tolerance in plants[1,2] have included it as a variable. We have therefore investigated the direct effect of *p*H on root growth and root number of two strains of *Mimulus guttatus*, one tolerant and the other not tolerant to heavy metals[3]. We found that the tolerant strain is also tolerant to acidic *p*H, whereas the non-tolerant operates better in more neutral *p*H. The hybrid between the two strains showed *p*H-dependent heterosis.

The strains used were Napoleon (N) and Cerrig-y-drudion (C). N is tolerant to copper[3] and is an annual population collected from a copper mine tailing at a stream edge in the Napoleon locality, Calavaras country in central California. C is sensitive to copper[3], and was originally found at the edge of a stream, 2 miles south of the village of Cerrig-y-drudion in North Wales. Seeds were germinated in soil, and clones were established from a single seed and propagated by cuttings. In the following experiment N15 and C16 were used. Although there was much variation between clones (within each population) the range of metal tolerance for N did not overlap with that of C. The F_1 was obtained by crossing ♀♀N with ♂♂C. Only one plant was crossed and different plants were obtained from its seeds.

Cuttings (one node per cutting) of uniform size were obtained from different plants about 0.5 cm below the node. Each cutting was placed in an 11-ml plastic vial filled with a solution of calcium nitrate (0.5 g l^{-1}) with varied *p*H between 2 and 9. Acid *p*H was obtained with concentrated sulphuric acid, basic *p*H with sodium hydroxide. Normal calcium nitrate solution gave *p*H 5. Ten cuttings (replicates) from different plants were used at each *p*H.

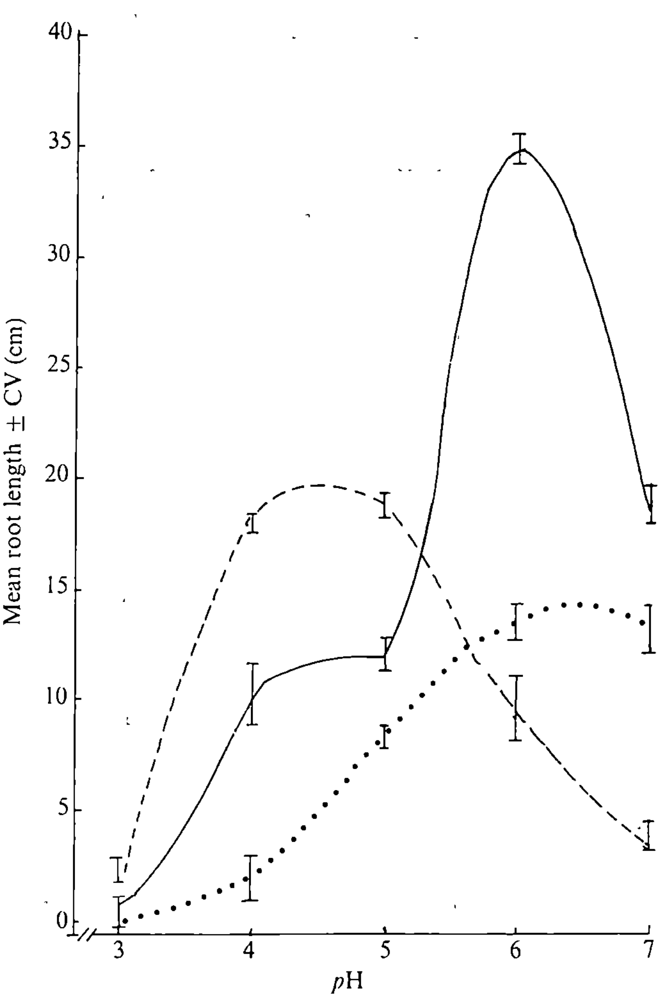

Fig. 1 Relationship between *p*H and mean root length (±coefficient of variation) – – –, N; . . , C; —, F_1.

Plastic vials were housed in wooden blocks so that light had no influence on root initiation. Each block was covered with a plastic bag to maintain humidity and placed in a growth chamber operating at a short light cycle (9 h with 25,833.6 lx), with a constant temperature of 20 °C and 55% relative humidity. The number and length of all roots from a given plant were measured. The mean of the 10 plants and coefficient of variation were calculated for each *p*H and genotype. The coefficient of variation was used to avoid any possible dependence of the variance on the mean.

The effects of different *p*H on root length are presented in Fig. 1 and Table 1. No cuttings developed any roots at *p*H 2, 8 and 9. The distribution of root growth between these levels was highly variable (Table 2). Analysis of variance using the actual data or their logarithms gave the same significant results. Using Duncan's multiple range test, it is possible to rank the effect of *p*H on root length as follows:

*p*H	3	4	7	5	6
Mean root length	0.60	10.18	12.05	13.05	19.47

where the means at *p*H 4, 7 and 5 are not significant from each other at $P = 0.05$.

The three genotypes were significantly different from each other in order C (7.52) > N (10 39) > F_1 (15.30). Analysis of variance (Table 2) and Fig. 1 indicate a significant effect of genotype on *p*H interaction. Strain N preferred the acidic

Table 1 Mean root length for each genotype at five levels of pH

Genotype	pH 3		4		5		6		7	
N	1.33*de*	(144)	18.11*a*	(37)	18.82*a*	(51)	9.74*abcde*	(136)	3.94*bcde*	(69)
C	0.00*e*	—	2.10*cde*	(98)	8.39*abcde*	(52)	13.67*ab*	(75)	13.43*abc*	(87)
F_1	0.46*e*	(172)	10.34*abcde*	(131)	11.94*abcd*	(86)	35.00	(74)	18.77*a*	(81)

Any two means with the same letter are not significantly different from each other at $P = 0.05$ by Duncan's Multiple Range test Values in parentheses are percentage of coefficients of variation.

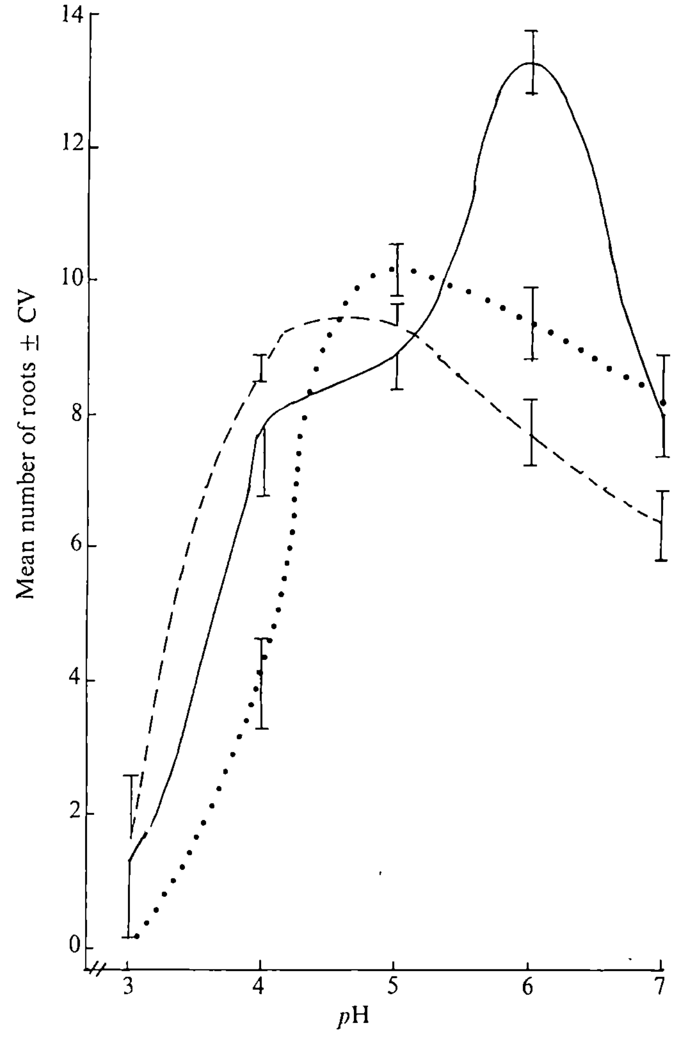

Fig. 2 Relationship between pH and mean number of roots per plant (±coefficient of variation) Symbols as in Fig 1.

solutions with a maximum peak between pH 4 and 5. Maximum root growth for strain C was in the more neutral solutions, between pH 6 and 7.

The F_1 grew better than either parent, with maximum growth at pH 6. Its performance at pH 6 and 7 indicated an overdominance in relation to its parents, whereas between pH 3 and 5 it was intermediate. This suggests two genes operating at different pH levels with different degrees of gene action. The presence of the shoulder at pH 4 substantiates this hypothesis.

Variation in pH was also found to affect number of roots per plant (Table 2). The average number of roots for the three genotypes could be ranked as follows:

pH	3	4	7	5	6
Mean number of roots	1.0	6.9	7.5	9.5	10.2

where any two adjacent numbers, excluding 1.0, are not significantly different from each other at $P = 0.05$ by Duncan's multiple range test.

These results indicate a gradual significant increase in number of roots from pH 3 to 5. The number of roots at pH 5 was not significantly different from those at pH 6, after which there was a significant decrease at pH 7. Although an analysis of variance did not reveal any effect of the genotype on the number of roots, t values for the difference between N and C at pH 4 $P = 0.01$) and N and F_1 at pH 6 ($P = 0.05$) were significant.

Phenotypic variation in length and number of roots were calculated within each genotype at each pH. These were expressed as the percentage of the coefficient of variation (Table 1). Analysis of variance on the square of such values indicated no statistical differences between genotypes or pH levels. When the genotypes were compared at each pH, however, the variability for total root growth of both F_1 and C was found to be larger than that of N at pH 4 ($F = 12.15$, $P < 0.01$ and 6.87, $P < 0.01$, respectively). Whereas at pH 6 the N strain had higher variability than both F_1 and C ($F = 3.43$, $P < 0.05$ and 3.28, $P < 0.05$, respectively).

The number of roots was less variable. The only significant differences for this trait are between F_1 or C and N at pH 4. F_1 and C variabilities are higher than that of N ($F = 23.97$, $P < 0.01$ and 11.74, $P < 0.01$ respectively) These results are similar to those obtained for root length at this pH.

It is obvious that N plants are more adapted to growing in lower pH soils than C plants. Whether this is due to direct effect of pH or due to adaptation to heavy metal ions is not known yet and needs to be investigated. (Dr Sheppard informed me that the Californian mines from which the material came are extremely acid compared with North Wales, and he has non-tolerant seeds from a very acid locality.) Undoubtedly, a study of the interaction between pH and heavy metal toxicity is of interest as indicated in Fig. 1, where for example, at pH 5 the N strain has better root growth than the C strain. This performance is reversed at pH 6 and 7 indicating pH-dependent (or conditional) toxicity for heavy metals.

Table 1 shows that pH tolerance of the F_1 is intermediate between that of its parents at pH 3–5 and is overdominant at pH 6–7. Changes in the degree of dominance due to changes in

Table 2 Analysis of variance for length of roots, number of roots, and the ratio between total growth and number of roots at different pH levels

Sources of variation	d.f.	Mean squares Length of roots	Number of roots	Length of roots/number of roots
Replicate(R)	9	101.14	34.73	0.62
pH level(L)	4	1,394.33†	395.86†	9.35†
Genotype(G)	2	774.79†	31.25	2.74*
RL	36	116.56	12.96	0.57
RG	18	135.51	20.76	0.43
LG	8	640.90†	35.42	4.65†
RLG	72	117.40	18.94	0.64

$^*P < 0.02$; $^†P < 0.01$

the concentrations of heavy metals were also observed[3]. Parsons[4] argued that the hybrid advantage is maximum in extreme environments; this is substantiated by the present results at the higher *p*H levels only. These results also support the theoretical study of environment—dependent heterosis[5].

I thank P. M. Sheppard for providing the seeds and both him and R. Knight for comments on the manuscript.

M. HANI SOLIMAN

Department of Microbiology and Genetics,
University of New England, Armidale,
New South Wales 2351, Australia

Received March 22, accepted May 11, 1976

[1] Bradshaw, A. D., *Nature*, 169, 1098 (1952).
[2] Antonovics, J., Bradshaw, A. D., and Turner, R. G., *Adv ecol Res.*, 7, 1-85 (1971).
[3] Allen, W. R., and Sheppard, P. M., *Proc. R. Soc*, B 177-196 (1971)
[4] Parsons, P. A., *Heredity*, 26, 479-482 (1971)
[5] Knight, R., *Theor appl Genet*, 43, 311-318 (1973)

Increased lead ingestion in calcium-deficient monkeys

VOLUNTARY ingestion of lead (lead pica) by children is a puzzling phenomenon. The resulting lead poisoning can lead to painful physical symptoms, mental retardation and brain damage[1-5]. Yet ingestion often persists after toxic symptoms appear if the child has access to lead[6]. We have shown that weanling rats made calcium deficient increased their voluntary ingestion of lead to levels much greater than those of control rats[7]. It was suggested that, because of the metabolic similarity of lead to calcium, ingestion of lead might relieve symptoms of calcium deficiency, attenuate the normal aversive effects of lead ingestion, and thus maintain continued ingestion. Rats, however, are not completely appropriate for an analogy to human lead ingestion because calcium metabolism differs considerably in the two organisms[8,9]. Rats seem to find lead acetate an aversive taste[7,10], whereas humans refer to it as "lead sugar" and report a sweet taste (paper presented at meeting of Midwestern Psychological Association, 1975 by R. W. Henderson and J. Dawley). Furthermore, the diet used with rats has been almost completely deficient in calcium (2 mg Ca per 100 g) producing severe symptoms of calcium deficiency, which have not been reported in humans with lead pica. If calcium deficiency leads to lead pica in humans, it must be a moderate or subclinical deficiency. We have therefore experimented with rhesus monkeys which were subjected to a moderately deficient diet providing 64% (108 mg Ca per 100 g) of their recommended daily calcium levels[11].

Four rhesus monkeys were separated from their mothers shortly after birth and maintained at the University of Wisconsin Primate Laboratory nursery. They were weaned from Similac formula to a Purina monkey chow from which the normally supplemented calcium carbonate and dicalcium phosphate had been removed, leaving 108 mg Ca per 100 g. The monkeys ingested approximately 100 g per day. Six lead ingestion tests were administered—three during deficiency and three during recovery from deficiency when the animals were feeding on normal monkey chow. Two control monkeys that had been weaned to normal chow were available for lead testing only during periods corresponding to the first two drinking tests of the deficient animals and the last drinking test during recovery. Each week the animals were weighed and blood samples were drawn to be analysed by atomic absorption spectrophotometry. Two months after calcium restoration to the deficient animals all animals were given whole body X rays.

Four concentrations of lead acetate (0.08, 0.16, 0.32, and 0.48% weight/volume) were paired with distilled water, and a pair of bottles each containing distilled water was also used. One pair of solutions was presented to an animal each day in a counterbalanced order. The relative positions of lead and distilled water bottles were alternated to control for side preferences, and each of the five pairs of solutions was presented twice. Solutions were presented at 1000 when the animals were being fed and removed at 1800. Distilled water was available overnight, but almost all fluid intake occurred during the hours of the test. For analyses the data were converted to lead acetate intake as a percentage of total intake and to the mg of lead ingested per kg of body weight.

A moderate level of calcium deficiency was produced. With calcium deficiency the body weights of the deficient

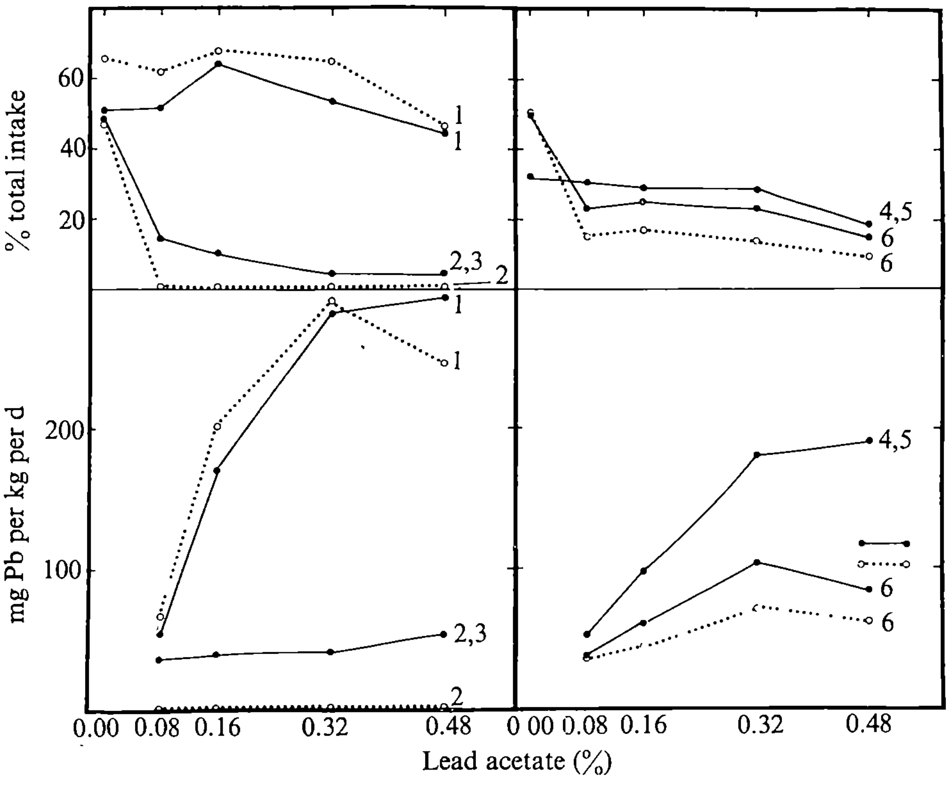

Fig. 1 Lead ingestion presented as percentage of total fluid intake (top) and mg of lead ingested per kg per day (bottom) during both calcium deficiency (left) and calcium restoration (right). Numbers at the side of each curve indicate the drinking test. Test 1 began 3 weeks after the deficient animals were weaned to calcium-deficient diet. Tests 2 and 3 began 8 weeks and 10 weeks respectively after the onset of deficiency. Tests 4 and 5 began 5 weeks and 7 weeks respectively after restoration of normal calcium, and test 6 began 24 weeks after calcium restoration. Results of tests 2 and 3 and, subsequently, tests 4 and 5 for the calcium-deficient animals did not differ so each of these pairs of tests is represented by a single mean curve. ○, Calcium deficient; ●, control.

animals decreased below those of the controls, but never went below 2 standard deviations of the mean body weights of normal monkeys at the same age at the Wisconsin Regional Primate Research Center The X rays revealed growth arrest lines in the long bones of the calcium-deficient animals presumably as a function of calcium deficiency. Because these lines were located 1.5–2.0 cm from the epiphyses, bone growth had resumed after restoration of full calcium levels and, thus, indicated that calcium deficiency had been reversed.

In the first lead drinking test both deficient and control animals ingested large amounts of lead solution at all concentrations, both in terms of percentage intake and in mg per kg of lead ingested Thus lead acetate seemed to be an initially "good-tasting" substance, in contrast to results from rats[7,10]. But after the seventh or eighth day of the first drinking test each of the control animals reduced their intake of lead solution from a mean of 273.3 ml d^{-1} to a mean of 1.4 ml d^{-1}. This low level of intake was maintained by control monkeys throughout the second lead ingestion test. Calcium-deficient animals showed some reduction in lead solution intake from the first to the second drinking test periods (mean 175.7 ml d^{-1} to 61 0 ml d^{-1}), but they maintained much higher intakes than did controls Even in a third drinking test the deficient animals maintained higher intake levels (mean 51.0 ml d^{-1}). These data are shown in the left-hand panel of Fig. 1. None of the intake measures on any of the calcium-deficient animals during either drinking tests 2 or 3 overlapped with the data of any control animal from drinking test 2 (Mann–Whitney U tests=0).

Blood lead levels were increased in both groups during lead ingestion tests (calcium-deficient mean±s.e.m.. baseline, 16.3±1.9 μg%; test 1, 228.4±25.2 μg%, test 2, 112 3±57.0 μg%; control: baseline, 20.5±1.5 μg%; test 1, 180 3±15.7 μg%; test 2, 96.2±6.2 μg%). Evaluation of the X rays of the calcium-deficient monkeys revealed radio-opaque lead deposits at the epiphyses of long bones. The animal evaluated as having the densest lead deposition was the one which had ingested the most lead; the one with the least lead deposition was the one ingesting the least lead. We did not, however, observe any overt symptoms of lead poisoning, possibly because of the temporal spacing of the lead drinking tests.

When normal monkey chow, containing five times the daily minimum recommended calcium levels for young rhesus monkeys, was given to the deficient monkeys, there was a slow, steady increase in body weight and X-ray evidence of renewed growth in long bones. But, the level of ingestion of lead acetate by the previously deficient monkeys remained high, as shown in the right hand panel of Fig. 1. Mean intakes of lead acetate were well above the intakes by control animals in both tests 2 and 6. Even 7 weeks of calcium restoration (test 5) did not eliminate these high levels of ingestion Six months after calcium restoration (test 6) the intakes of previously deficient and control animals did not differ. The increased lead ingestion of control animals relative to their test 2 levels probably reflects the several months that had passed without exposure to lead, after which the lead solutions again were the novel, "good-tasting" substances they appeared to be in test 1.

In spite of an initially positive taste valence, lead acetate was rejected quickly by normal monkeys. Calcium-deficient monkeys did not appear to recognise the presumed aversive effects of lead ingestion and continued to ingest lead at relatively high levels This increased ingestion continued until the restoration of normal calcium levels. It seems that the calcium-deficient animals were not sensitive to the negative aspects of lead ingestion, which caused complete cessation of lead ingestion in control animals This suggests that calcium-deficient animals would not be able to learn a taste aversion to a novel solution paired with the administration of lead acetate. We have shown that control rats reduced their ingestion of novel solutions paired with intragastric intubation of lead acetate, whereas calcium-deficient rats did not reduce lead-associated intake (C.T.S., unpublished) In pilot studies with rhesus monkeys we found reduced intake of lead-associated novel solution on 2 of 4 test days in control monkeys, but no reduction in monkeys that had been previously calcium deficient.

The reason why an organism should voluntarily ingest lead is partially explained. Primates seem to find lead initially "good-tasting" and ingest it in large quantities But, some post-ingestional, and presumably aversive, aspects of this continued lead ingestion eliminate subsequent lead ingestion in normal monkeys Calcium-deficient monkeys seem to be insensitive to the presumed aversive aspects of continued lead ingestion and thus do not stop ingesting lead. Given such insensitivity to aversive post-ingestional aspects of lead ingestion, calcium-deficient monkeys, even though recovered from calcium deficiency, might continue to respond to the positive taste valence of lead acetate, by continuing to ingest lead.

Since the calcium-deficient monkeys here suffered only a subclinical calcium deficiency but still ingested lead, children with lead pica may also experience only subclinical calcium deficiency. Almost all attention given to possible nutritional bases for lead pica has focused on iron deficiency, with repeated findings that iron supplementation does not reduce lead pica and that dietary iron seems to be at adequate levels[12–15]. It would be important to examine children with lead pica for evidence of subclinical calcium deficiency.

We thank Dr Mary Ann Peters for evaluating the X rays. This research was supported by grants from the USPHS and the University of Wisconsin Food Research Institute (C.T.S.).

JAMES L. JACOBSON
CHARLES T SNOWDON

Department of Psychology,
University of Wisconsin,
Madison, Wisconsin 53706

Received March 29, accepted May 4, 1976.

[1] Berg, J M , and Zapella, M , *J. ment Defic Res* , 8, 44 (1964)
[2] Mellins, R B , and Jenkins, C D , *J Am. med Ass* , 158, 15 (1955)
[3] Pentschew, A , *Acta Neuropath* , 5, 133 (1965).
[4] Perlstein, M. A., and Attala, R , *Clin Pediatr* , 5, 292 (1966)
[5] Thurston, D I , Middlekamp, J N , and Mason, E., *J. Pediatr* , 47, 413 (1955).
[6] Byers, R K , and Lord, E E , *Am J. Dis Child* , 66, 471 (1943).
[7] Snowdon, C T , and Sanderson, B A , *Science*, 183, 92 (1974)
[8] Nicolaysen, R , and Eeg-Larsen, N , *Vitamins and Hormones*, 11, 29 (1953).
[9] Nicolaysen, R , Eeg-Larsen, N , and Malm, O J , *Physiol Rev* , 33, 424 (1953)
[10] Mason, D J., and Stafford, H R , III, *J comp Physiol Psychol* , 59, 94 (1965).
[11] Greenberg, L D , in *Feeding and Nutrition of Non-Human Primates* (edit by Harris, R S), 136 (Academic, New York, 1970)
[12] Gutelius, M F , Millican, F K , Layman, E M , Cohen, G J , and Dublin, C C , *Pediatrics*, 29, 1012 (1962)
[13] Gutelius, M F , Millican, F. K , Layman, E M , Cohen, G. J., and Dublin, C C , *Pediatrics*, 29, 1018 (1962)
[14] Moody, J , Ferrand, C F., and Harris, P., *Pediatrics*, 55, 636 (1975)
[15] Watson, R J , Decker, E , and Lichtman, H C , *Pediatrics*, 21, 40 (1958).

Microvilli and cell swelling

MICROVILLI have various functions connected with an increase in surface area In the form of brush border of intestinal and renal epithelium, microvilli increase the absorptive capacity of cells. On tumour cells[1,2] they may have a role in invasiveness[3]. Their presence on cultured cells[4], which is apparently controlled by the intracellular concentration of cyclic AMP[5], increases the surface area so as to facilitate "spreading"[6] and cytokinesis[7,8] without concomitant membrane synthesis. In the latter two situations, cell volume remains constant, while the shape changes The most common situation in which the reverse occurs, that is an increase in surface area accompanying an increase in volume without a change in shape, is during cell swelling. Swelling due to entry of water is caused by (1)

Table 1 Binding of ^{131}I-con A by Lettree cells

Time of inc. (min)	Additions	Control cells	Swollen cells*
		^{131}I-bound (c.p.m.)†	
0	—	15,000	10,000
5	—	68,000	72,000
10	—	107,000	105,000
5	α-MM	8,000	9,500
0	Cold con A	8,800	7,200
5	Cold con A	54,000	67,000
10	Cold con A	63,000	61,000
5	Cold con A + α-MM	5,100	6,400

α-MM, α-methyl-D-mannoside (30 mM). Concentration of con A was 100 μg ml^{-1}.

* 1.2 M glycerol for 10 min at 4 °C, followed by 0.34% saline for 10 min at 4 °C.

† Cells at 4 °C incubated with ^{131}I-con A (375,000 c.p.m., 0.04 μg) in final volume of 0.1 ml; stopped by addition of 10 ml saline, spun and pellet assayed. Values are means of three experiments.

exposure of cells to a medium hypotonic relative to that of the cell content or (2) an increase in passive diffusion of cations[9], such that the Na/K pump cannot maintain an asymmetric intracellular/extracellular distribution. An example of (2) is afforded by the action of Sendai virus on cultured cells; passive permeability is increased[10–14] and cells swell (unpublished results of K.J.M. and C.A.P.). We show here that in both (1) and (2) the increase in surface area can be accounted for by an 'unfolding' of microvilli.

(1) Lettree cells (grown intraperitoneally in mice) were swollen by exposure to either hypotonic buffer (0.01 M sucrose, 1 mM bicarbonate, 2 mM Mg^{2+}, 2 mM Ca^{2+}) (Fig. 1*b*) or through uptake of glycerol[15] (1.2 M glycerol for 15 min at room temperature) followed by swelling in the presence of 0.25 M sucrose (Fig. 1*c*). In each case the fully swollen cells were virtually devoid of microvilli in contrast to the highly villated control cells (Fig. 1*a*). The increase in volume was from approximately 180 μm^3 to 420 μm^3 corresponding to an increase in surface area of approximately 120 μm^2. The number of microvilli on a Lettree cell (approximately 10^3 per cell; mean length 0.46 μm) increases the surface area by an average of approximately 110 μm^2. Swollen cells without microvilli bind as much ^{131}I-labelled concanavalin A (con A) as unswollen controls (Tables 1 and 2) in contrast to the effect of microvilli on agglutination by con A (Tables 1 and 2 and ref. 5). Because trypsin treatment causes rounding up of cells and a consequential increase in the number of microvilli it is possible that increased agglutinability (and perhaps stimulation of growth also[16]) of trypsin-treated cells[17,18] is partly due to an increase in the number of microvilli.

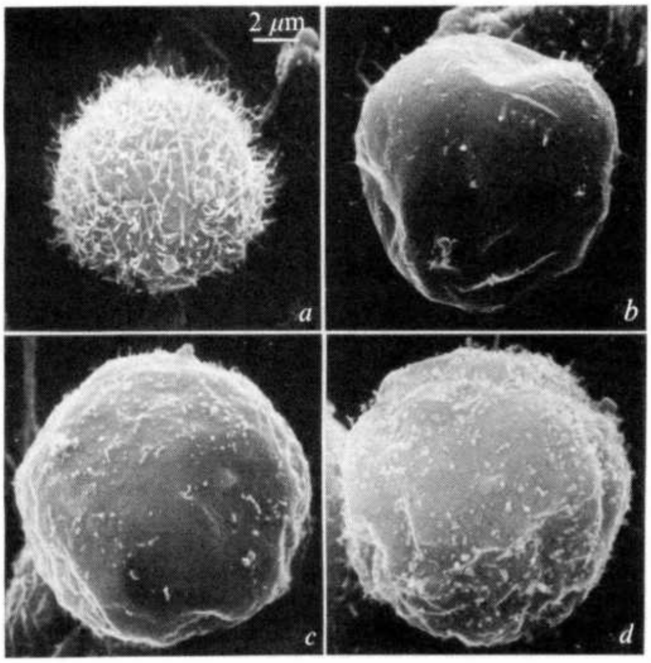

Fig. 1 Scanning electron micrographs of control Lettree cells (*a*), cells swollen in 0.01 M sucrose (*b*), glycerol-loaded cells swollen in 0.25 M sucrose (*c*) and cells after exposure to Sendai virus (*d*). Cells were fixed with glutaraldehyde at the same osmolarity as the swelling media and processed for scanning electron miscoscopy as described before[8].

(2) Lettree cells (2.6×10^4 per ml) were exposed to Sendai virus (80 haemagglutinating units per ml) at room temperature at a concentration insufficient to cause agglutination[13]. As cells increased in volume (from approximately 700 to 1,200 μm^3; Coulter size distribution mode value) most of the microvilli were lost again (Fig. 1*d*).

We conclude that the presence of microvilli enables cells rapidly to increase their volume, and hence to swell, without lysis. Mammalian erythrocytes, which are devoid of microvilli, are capable of a limited amount of swelling because in their normal shape (biconcave disk) the volume is not maximal; once a spherical shape has been adopted, lysis follows. Thus the same concentration of Sendai virus causes lysis of red cells but only swelling of villated cells. During cytolysis of cultured cells in the presence of antibody and complement, an increased cation permeability and cell swelling[19] also precedes lysis. This may explain why cells that are in the late S/G_2 phase of the cell cycle, and hence the most heavily villated[7,8], are the least sensitive to immune (or non-immune) cytolysis[20].

Table 2 Agglutination of Lettree cells by con A

Concentration of con A (μg ml^{-1})	Control cells	Swollen cells*
	Agglutination index†	
500	+++++	+
250	+++++	++
150	+++++	+++
100	++++	++
50	++++	++
0	+	+

* As in Table 1 but at room temperature.

†Cells at room temperature mixed with con A and agglutination assessed microscopically: +++++, <10% free cells; ++++, 10–30% free cells; +++, 30–50% free cells; ++, 50–70% free cells; +, >70% free cells.

Since swelling caused by treatment with hypotonic media or with Sendai virus is readily exploitable, the implication that the increase in volume results from an unfolding of microvilli should prove useful in elucidating the role of microvilli (and cyclic nucleotides) in more complex phenomena such as cytokinesis and other situations involving the cell surface.

We thank Sulochona Bose for assistance, Dr P. R. Robinson for ^{131}I-con A and the Cancer Research Campaign and the Wellcome Trust for financial support.

S. Knutton
D. Jackson
J. M. Graham
K. J. Micklem
C. A. Pasternak

Department of Biochemistry,
St George's Hospital Medical School,
Tooting, London SW17 0QT, UK

Received March 16; accepted May 20, 1976.

[1] O'Neill, C. H., and Follett, E. A. C., *J. Cell. Sci.*, **7**, 695–709 (1970).
[2] Porter, K., Prescott, D., and Frye, J., *J. Cell Biol.*, **57**, 815–836 (1973).
[3] Ambrose, E. J., in *Biology of Cancer*, 2nd ed. (edit. by Ambrose, E. J., and Roe, F. J. C.), 27–57 (Ellis Horwood, Chichester, 1975).
[4] Follett, E. A. C., and Goldman, R. D., *Expl Cell Res.*, **59**, 124–136 (1970).
[5] Willingham, M. C., and Pastan, I., *Proc. natn. Acad. Sci. U.S.A.*, **72**, 1263–1267 (1975).
[6] Trinkaus, J. P., and Ericson, C. A., *J. Cell. Biol.*, **63**, 351a (1974).
[7] Knutton, S., Sumner, M. C. B., and Pasternak, C. A., *Eighth Int. Cong. Electron Microscopy*, Canberra, **2**, 362–363 (Australian Academy of Science, Canberra, A.C.T., Australia, 1974).

[illegible]
SCIENCE COLLEGE
[illegible]

[8] Knutton, S., Sumner, M. C. B., and Pasternak, C. A., *J. Cell Biol.*, **66**, 568–576 (1975).
[9] Davson, H., and Ponder, E., *J. Cell comp. Physiol.*, **15**, 67–74 (1940).
[10] Klemperer, H. G., *Virology*, **12**, 540–552 (1960).
[11] Fuchs, P., and Giberman, E., *FEBS Lett.*, **31**, 127–130 (1973).
[12] Pasternak, C. A., and Micklem, K. J., *J. Membr. Biol.*, **14**, 293–303 (1973).
[13] Pasternak, C. A., and Micklem, K. J., *Biochem. J.*, **140**, 405–411 (1974).
[14] Pasternak, C. A., and Micklem, K. J., *Biochem. J.*, **144**, 593–595 (1974).
[15] Barber, A. J., and Jamieson, G. A., *J. biol. Chem.*, **245**, 6357–6365 (1970).
[16] Burger, M. M., *Fedn. Proc.*, **32**, 91–101 (1973).
[17] Burger, M. M., *Proc. natn. Acad. Sci. U.S.A.*, **62**, 994–1001 (1969).
[18] Inbar, M., and Sachs, L., *Proc. natn. Acad. Sci. U.S.A.*, **63**, 1418–1425 (1969).
[19] Green, H., Barrow, P., and Goldberg, B., *J. exp. Med.*, **110**, 699–713 (1959).
[20] Sumner, M. C. B., Collin, R. C. L. S., and Pasternak, C. A., *Tissue Antigens*, **3**, 477–484 (1973).

Ionic mechanism of the H^+ pump in a snail neurone

THE observed values of *p*H inside nerve and muscle cells are too high to be explained by a passive distribution of H^+ across the cell membrane[1–4]. Thus there is believed to be a system, provisionally named a H^+ or proton pump, which transports H^+ out of, or OH^- or HCO_3^- into the cell. In spite of its importance, little is known about this system, perhaps because it cannot easily be studied using radioisotopes, the use of which has yielded much information about the far better known Na pump. One way the H^+ pump can be investigated is by following intracellular *p*H (pH_i) with a *p*H-sensitive microelectrode: because a similar Na^+-sensitive microelectrode can be used to study the Na pump, it is also possible to compare the two pumps in the same preparation using essentially the same methods. Thus the recessed-tip type of *p*H-sensitive[3] or Na^+-sensitive[5] microelectrode can be used to record pH_i or intracellular Na^+ ($[Na^+]_i$) in cells, such as snail neurones, which are tough enough to permit intracellular iontophoretic injections of acid or Na salts. I report here experiments in which the mechanism of the H^+ pump has been investigated by comparing the response of pH_i to HCl injection with the response of $[Na^+]_i$ to NaCl injection.

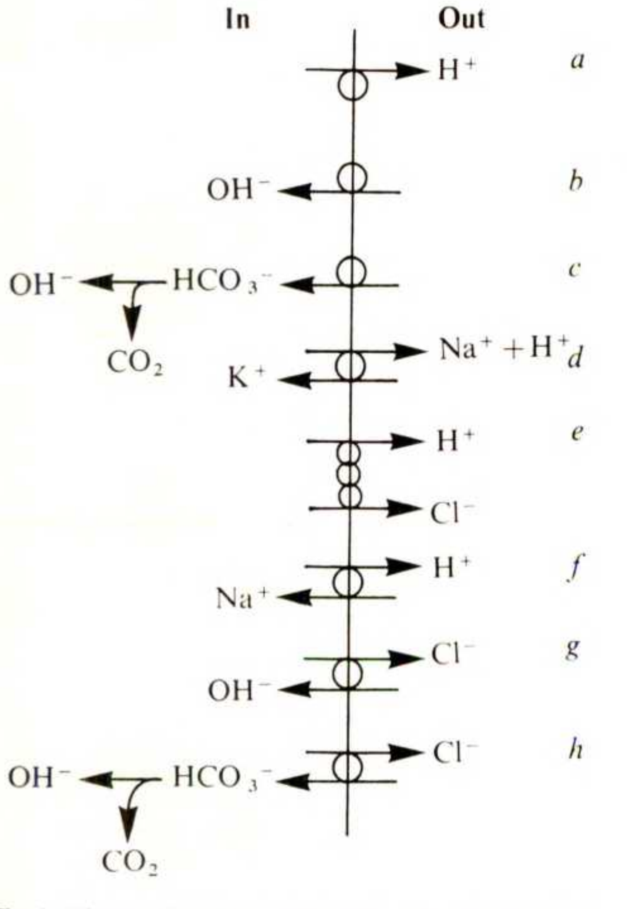

Fig. 1 Diagram showing possible mechanisms for the H^+ or proton pump in cell membranes, excluding any indication of the energy source. *a*, Simple uncoupled H^+ pump; *b*, hydroxyl ion pump; *c*, bicarbonate pump (inside the cell the bicarbonate would give rise to OH^- and CO_2, the latter being freely diffusible across the cell membrane); *d*, the Na or Na–K pump extruding H^+ as well as Na^+; *e*, a loosely coupled HCl pump; *f*, downhill Na^+ influx coupled to H^+ extrusion; *g*, chloride–hydroxyl ion exchange; *h*, chloride–bicarbonate ion exchange.

Various mechanisms have been proposed[6,7] to explain the mechanism of the H^+ pumps involved in both pH_i control and acid secretion by the stomach. Some of these mechanisms are outlined in Fig. 1. Schemes *a–d* involve the net transfer of charge across the cell membrane, and would thus be electrogenic[8], while *f–h* would be electrically neutral. The linked extrusion of H^+ and Cl^- shown in *e* could be electrogenic or neutral. Scheme *d* represents the well known Na pump (or more accurately, the Na–K pump) which might extrude H^+ rather than Na^+ (ref. 9). But evidence from experiments on the effects of ouabain, a specific inhibitor of the Na pump, on muscle pH_i does not support this idea[10]. For acid secretion by the stomach, most investigators apparently favour schemes *e* or *h*. The latter has been studied in great detail in red blood cells, where it is known as the "chloride shift", and is an important mechanism in CO_2 carriage by the blood. This anion-exchange in red blood cells is blocked by amino reactive agents[11] such as 4,4′-diisothiocyanostilbene-2,2′-disulphonic acid (DIDS). I have therefore tested the effects of both DIDS and ouabain on the Na and H^+ pumps in the snail.

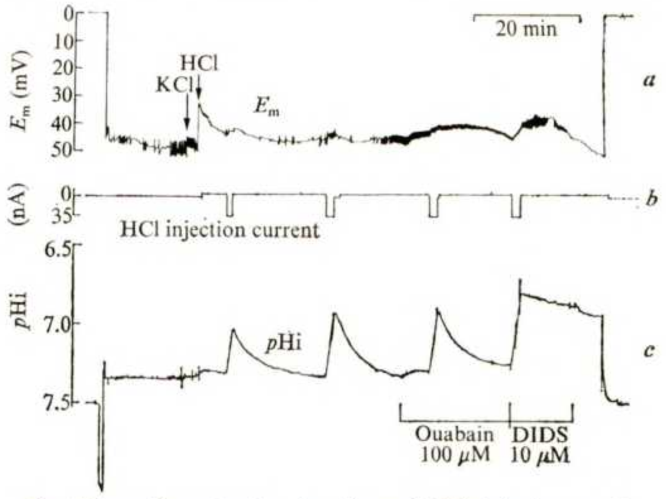

Fig. 2 Recordings showing the effects of HCl injection on E_m and intracellular *p*H (pH_i) of a snail neurone, and the response to external ouabain and DIDS. *a*, Potential between the E_m microelectrode and a reference electrode in the bath; *b*, iontophoretic injection current; *c*, potential between the E_m and *p*H microelectrodes. The voltage scale was the same for *a* and *c*. The *p*H microelectrode was inserted first, then the KCl-filled E_m microelectrode. After about 15 min, the two current-passing electrodes were inserted, and a 5-nA backing current was switched on between them to minimise H^+ leakage from the HCl microelectrodes. HCl injections were made by reversing the iontophoretic current and increasing it to 35 nA for 1 min (first injection) or 90 s (other injections). After the pH_i had recovered from the second injection, ouabain was applied in the superfusate, and after the third injection DIDS was applied, as indicated. Finally the electrodes were withdrawn from the cell.

The experiments were done on the largest neurone at the rear of the right pallial ganglion of the common snail, *Helix aspersa*, as described before[12]. The exposed suboesophageal ganglia were superfused with a continuously flowing snail Ringer (4 mM KCl, 80 mM NaCl, 7 mM $CaCl_2$, 5 mM $MgCl_2$, 22 mM $NaHCO_3$, 0.1 mM Na_2HPO_4/NaH_2PO_4 (*p*H 7.5), equilibrated with 2.5% CO_2 and 97.5%

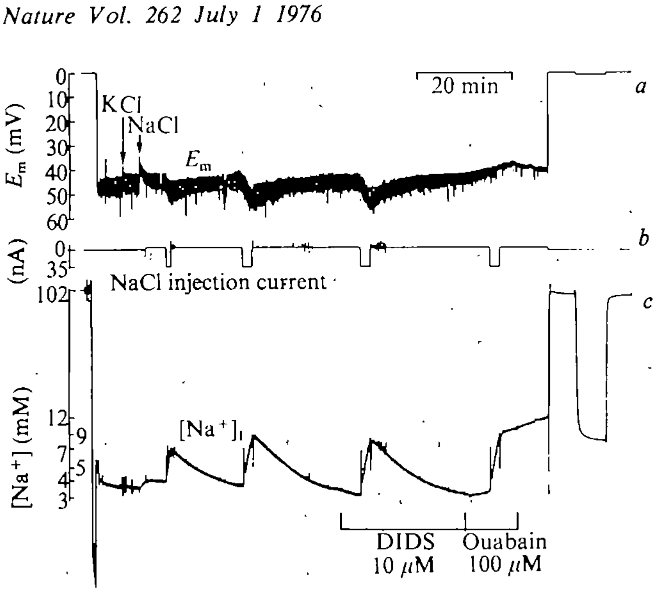

Fig. 3 The effects of NaCl injection on the E_m and $[Na^+]_i$ of a snail neurone, and the response to external DIDS and ouabain. Procedure was as in Fig. 2, except that the duration of the second, third and fourth injections was 2 min, the inhibitors were applied in reverse order and after withdrawal from the cell the electrodes were exposed to a Ringer with 9 mM Na.

O_2). The neurone was penetrated by four microelectrodes: one to measure membrane potential (E_m), one to measure Na^+_i or pH_i, and two for iontophoretic injection, of which one was filled with KCl and the other with NaCl or HCl.

The effects of ouabain and DIDS on the H^+ pump are shown in Fig. 2. During four injections of HCl the pH_i fell. After the first three injections it returned to the pre-injection level during 15 min. The application of the ouabain-containing Ringer caused a small fall in pH_i, presumably because of a slightly lower CO_2 level, but clearly did not block the pH_i recovery. But DIDS, applied at the beginning of the fourth injection, equally clearly did inhibit the pH_i recovery. Other experiments showed that the H^+ pump was very sensitive, 50% inhibition required only about 1 μm DIDS. Its analogue 4-acetamide-4′-isothiocyano-stilbene-2.2′-disulphonic acid (SITS) had the same effect.

Figure 2 also shows that the H^+ pump is not electrogenic: there were only small changes in E_m during pH_i recovery after the HCl injections. This rules out the mechanisms shown in Fig. 1*a–d*. In contrast, Fig. 3 shows the characteristic E_m increase associated with the electrogenic Na pump. The quantities of NaCl and HCl injected were similar; they were injected into the same cell (in different snail brains) and caused similar changes in the ion equilibrium potentials. Figure 3 also shows that DIDS had no effect on the Na pump while, as expected, ouabain blocked it completely.

In some ways the pH_i and $[Na^+]_i$ responses to HCl or NaCl injection were remarkably similar. The recovery of pH_i was faster, but both recoveries were exponential and repeatable. The effects of ouabain and DIDS were, however, completely different. This clearly rules out any direct connection between the Na and H^+ pumps, as in Fig. 1*d*.

Since DIDS and SITS are both well established inhibitors of anion exchange in red blood cells, and SITS also blocks the anion-dependent part of the short-circuit current across the turtle bladder[13], it is tempting to conclude that the H^+ pump in snail neurones is a Cl^-–HCO_3^- exchange system, as in Fig. 1*h*. The finding that the H^+ pump in both squid giant axons[14] and snail neurones[12] is stimulated by CO_2 and HCO_3^- certainly supports this mechanism.

The source of energy for what would be an 'uphill' movement of HCO_3^- into the cell is difficult to identify. The Cl^- equilibrium potential (E_{Cl}) in the neurone studied is normally close to or more negative than E_m, so Cl^- extrusion would also normally be uphill[15]. In my experiments E_{Cl} would have been greatly reduced by Cl^- injection, but in other experiments the speed of pH_i recovery was not affected by internal Cl^- levels. It is possible that the anion leaving the cell is not Cl^-, but it is hard to suggest an alternative. It is well established that the Na pump is driven by ATP, but preliminary experiments with metabolic inhibitors suggest that ATP may not be the energy source for the H^+ pump in snail neurones. For example, the uncoupling agent carbonyl cyanide *m*-chlorophenyl hydrazone (CC*m*P) blocks the Na pump at levels which have little effect on the H^+ pump. On the other hand, Boron and De Weer[14] found that 2 mM cyanide inhibited the H^+ pump in squid giant axons. Perhaps the H^+ pump can tolerate a much lower ATP : ADP ratio than the Na pump.

In conclusion, the results reported here show that there is no connection between the Na and H^+ pumps in snail neurones, and suggest that the H^+ pump is an electroneutral anion-exchange system in which the inward transport of HCO_3^- is coupled to the outward transport of other anions, presumably Cl^-.

I thank Professor H. Passow and Dr H. Fasold for DIDS, Dr Z. Kometiani for helpful discussions and Drs E. Mills and M. Purves for reading the manuscript.

Note added in proof: Recent experiments of mine on the snail neurone H^+ pump suggest that there may be some Na^+-H^+ exchange as well as the anion exchange described above. In mammalian cardiac and skeletal muscle SITS has no effect on the H^+ pump (D. Ellis and C. C. Aickin, personal communication), suggesting that the pump mechanism in muscle does not involve anion exchange.

R. C. THOMAS

Department of Physiology,
University of Bristol,
Bristol, BS8 1TD, UK

Received April 8; accepted May 4, 1976.

[1] Caldwell, P. C., *Int. Rev. Cytology*, **5**, 229–277 (1956); *J. Physiol., Lond.*, **142**, 22–62 (1958).
[2] Waddell, W. J., and Bates, R. G., *Physiol. Rev.*, **49**, 285–329 (1969).
[3] Thomas, R. C., *J. Physiol., Lond.*, **238**, 159–180 (1974).
[4] Boron, W. F., and De Weer, P., *J. gen. Physiol.*, **67**, 91–112 (1976).
[5] Thomas, R. C., *J. Physiol., Lond.*, **210**, 82–83P (1970).
[6] Woodbury, J. W., in *Physiology and Biophysics* (edit. by Ruch, T. C., and Patton, H. D.), 899–934 (Saunders, Philadelphia, London, 1968).
[7] Rehm, W. S. in *Metabolic Pathways*, **6** (edit. by Hokin, L. E.), 187–241 (Academic, New York, London, 1972).
[8] Thomas, R. C., *Physiol. Rev.*, **52**, 563–594 (1972).
[9] Fujita, M., *et al.*, *Biochem. J.*, **106**, 113–121 (1968).
[10] Roos, A., *J. Physiol., Lond.*, **249**, 1–25 (1975).
[11] Knauf, P. A., and Rothstein, A., *J. gen. Physiol.*, **58**, 190–210 (1971); Cabantchik, Z. I., and Rothstein, A., *J. Membr. Biol.*, **15**, 207–226 (1974).
[12] Thomas, R. C., *J. Physiol., Lond.*, **255**, 715–735 (1976).
[13] Ehrenspeck, G., and Brodsky, W. A., *Biochim. biophys. Acta*, **419**, 555–558 (1976).
[14] Boron, P. F., and De Weer, P., *Nature*, **259**, 240–241 (1976).
[15] Neild, T. O., and Thomas, R. C., *J. Physiol., Lond.*, **242**, 453–470 (1974).

Role of axoplasmic transport in neurotrophic regulation of muscle end plate acetylcholinesterase

THE mechanism underlying neural control of skeletal muscle acetylcholinesterase (AChE) is not fully understood[1]. The experimental evidence points to acetylcholine (ACh)[2] and nerve-evoked muscle activity[3] as the "trophic" mediators, but neither is sufficient to account for the entire effect of innervation on muscle[4]. It remains to be seen whether factors such as cell-to-cell contact, and/or some regulatory substance(s) released by motor nerves also contribute to the regulation of AChE activity. In turn, the regulatory substance(s) might be conveyed by axoplasmic transport, for blockage of this process causes denervation-like changes without disturbing neurotransmitter release or the consequent muscle contractile activity[5]. We report here a reversible change in the activity of endplate AChE that can be ascribed to a temporary interruption of axoplasmic transport.

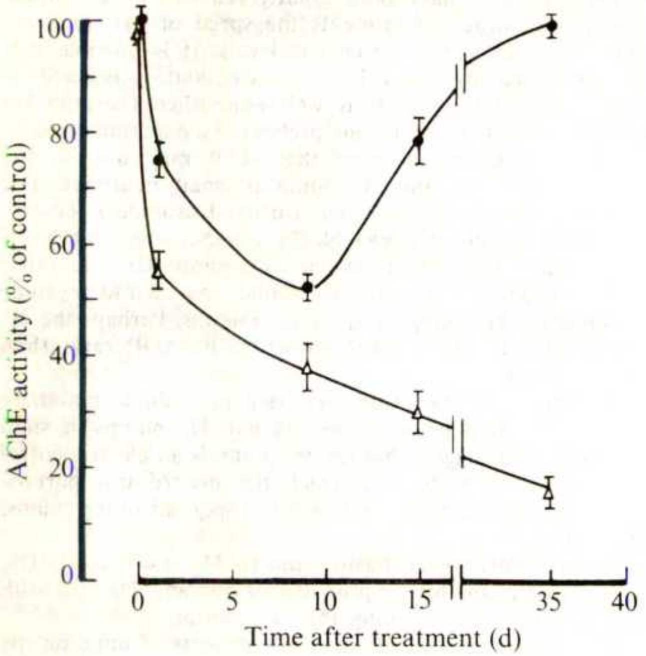

Fig. 1 Effect of axoplasmic transport blockage (●) and denervation (△) on AChE activity, in cat geniohyoid muscle. Muscle regions containing endplates were homogenised 1/50 (w/v) in ice-cold NaCl–Triton buffer, *p*H 7.3 (1 M NaCl, 0.1% Triton X-100, 0.05 M Tris–HCl, 0.2 mM EDTA). AChE activity as reported here is that portion of the homogenate-dependent ACh hydrolysis that is sensitive to 5 μM BW 284 C51 dibromide. Activity was measured by a radiochemical procedure in which release of ^{3}H-acetate from ^{3}H-ACh iodide (New England Nuclear, 50 mCi mmol^{-1}) was quantified by ion-exchange chromatography and scintillation spectrometry[8]. One unit of AChE activity is defined as 1 μmol ^{3}H-acetate formed per min. For each assay the final non-collagenous protein concentration[15] was 2–3 mg per ml of homogenate. At the concentrations used, Triton X-100 did not interfere with the AChE assay. Because of changes in the protein content of muscles undergoing atrophy and hypertrophy, the AChE activity could not be correlated with either the initial wet weight, or the particulate protein content of the individual muscle[16], therefore, the results are expressed by comparison of the treated side with the contralateral innervated muscle (control). Each sample was assayed at three concentrations and the activities obtained were proportional to the sample concentration. Each point represents the mean ± s.e. of three experiments.

Experiments were performed on adult cats, anaesthetised with sodium pentobarbital (36 mg kg^{-1}). Both hypoglossal nerves were injected under the epineurium (experimental: 5 μl of saline, 10 mM colchicine; control: 5 μl of saline), 5 mm distal to the emergence point of the lateral branch innervating the geniohyoid muscle. Thus surgical damage was avoided since the drug reached the nerve fibres under study only by diffusion[6]. In similar experiments, one of the nerves was transected while the contralateral was left intact. At various times after the operation, the geniohyoid muscles were exposed in order to record their electrical activity and contractile properties. Subsequently they were removed and regions containing most of the endplates (80% of the AChE released by collagenase treatment[7] came from these regions) were used to assay AChE[8]. Consistent with a previous report[6], 6–30 d after injection of colchicine, a drug known to interfere with axoplasmic transport[9], the muscles became hypersensitive to ACh and displayed fibrillation. Nerve conduction and the effective neuromuscular transmission were unaltered. These results were obtained through blockage of axoplasmic transport as induced by the direct action of colchicine on the motor nerve[6,10]. When applied locally under the epineurium, the drug does not reach the muscle cells. Further, when applied topically on to the muscle at concentrations that interrupt axoplasmic transport, the drug provoked none of the alterations observed when it was applied to the nerve. Thus colchicine may not necessarily cause denervation-like changes by acting on the muscle membrane[11].

Figure 1 illustrates that, after treatment with colchicine, the activity of endplate AChE gradually decreased (days 1–3), reached its lowest level (days 8–10) and returned to control values (days 25–30). In as much as colchicine blocks axoplasmic transport[10], the normal operation of this process seems to be essential for the neurotrophic regulation of endplate AChE activity. Our experiments are insufficient to elucidate the basic mechanism of this dependence. Nevertheless, we can assume that axoplasmic transport supplies some trophic factor to the postneural cell. This rationale is reinforced by findings which suggest the existence of a neurogenic diffusible substance affecting AChE activity of muscle in organ culture[12].

In contrast to the reversible effect of treatment with colchicine, denervation causes a greater enzymatic decay which persists for at least 35 d (Fig. 1). This quantitative difference can be ascribed to: (1) a partial blockage of axoplasmic transport, and/or (2) the regulatory action of other factors, such as muscle contractile activity or ACh itself. Muscle activity has been claimed to be the major factor involved in the control of chick muscle AChE[3], but in mammalian muscles it has no such influence[13]. In turn, the role of ACh in AChE regulation is supported by results obtained with botulinum toxin which—apart from inhibiting ACh release—may block the liberation of other neurogenic substances[2,14]. In view of our results, we conclude that axoplasmic transport is the most important mediator in the trans-synaptic regulation of skeletal muscle endplate AChE activity.

This research was supported by grants from PNUD/UNESCO and FIUC to H.L.F., and from NIH to Dr P. F. Davison, Boston Biomedical Research Institute. N.C.I. was supported by a CU predoctoral fellowship. We thank Dr J. V. Luco for valuable criticisms and Dr B. U. Ramírez for assistance and comments.

HUGO L. FERNANDEZ
NIBALDO C. INESTROSA

Laboratory of Neurophysiology,
Department of Cell Biology,
Catholic University,
Santiago, Chile

Received March 31; accepted May 5, 1976.

[1] Guth, L., *Physiol. Rev.*, **48**, 645–687 (1968).
[2] Drachman, D. B., *J. Physiol., Lond.*, **226**, 619–627 (1972).
[3] Walker, C. R., and Wilson, B. W., *Nature*, **256**, 215–216 (1975).
[4] Drachman, D. B., *Ann. N.Y. Acad. Sci.*, **228**, 160–176 (1974).
[5] Albuquerque, E. X., Warnick, J. E., Tasse, J. R., and Sansone, F. M., *Expl. Neurol.*, **37**, 607–634 (1972).
[6] Fernandez, H. L., and Ramirez, B. U., *Brain Res.*, **79**, 385–395 (1974).
[7] Hall, Z. W., and Kelly, R. B., *Nature new Biol.*, **232**, 62 (1971).
[8] Wilson, S. H., *et al J. biol. Chem.*, **247**, 3159–3169 (1972).
[9] Fernandez, H. L., Huneeus, F. C., and Davison, P. F., *J. Neurobiol.*, **1**, 395–409 (1970).
[10] Rodriguez-E, E., Ramirez, B. U., and Fernandez, H. L., *J. Neurocytol.*, **2**, 149–156 (1973).
[11] Lømo, T., *Nature*, **249**, 473–474 (1974).
[12] Lentz, T. L., *Expl. Neurol.*, **45**, 420–426 (1974).
[13] Guth, L., Brown, W. C., and Watson, P. K., *Expl. Neurol.*, **18**, 443–452 (1967).
[14] Jacobson, M., *Devl Neurobiol.* 275 (Holt, Rinehart and Winston, New York, 1970).
[15] Lowry, O. H., Rosebrough, N. J., Farr, A. L., and Randall, R. J., *J. biol. Chem.*, **193**, 265–275 (1951).
[16] Snyder, D. H., Rifenberick, D. H., and Max, S. R., *Expl. Neurol.*, **40**, 36–42 (1973).

Three-step yielding of load-clamped mammalian cardiac muscle

FROM mechanical transients of active skeletal muscle in response to length[1] or load[2,3] perturbations some aspects of the kinetics of crossbridge interactions between actin and myosin filaments have been studied. The analysis of tension transients following rapid length steps has indicated that crossbridges may be the major site of series compliance in active skeletal muscle[1,4,5]. The use of load steps[2,6] instead of length steps has the advantage that any series compliance does not change in length after the step. Yet, in the rapid skeletal muscle load steps cannot be applied sufficiently fast to distinguish the very early events in view of their possible relation to crossbridge interactions[5]. We have analysed length transients after small step increases of load, which did not exceed the isometric tension, during isotonic shortening of afterloaded twitch and tetanic contractions of slow mammalian cardiac muscle at a low temperature, that is cat papillary muscle at 19 °C. Our main conclusion was that motion of attached crossbridges is confined to near 0.80 (twitch) to 1.02 (tetanus) % of total muscle length.

Figure 1 illustrates the effects of a sudden increase of load during isotonic shortening of an afterloaded twitch. There were three distinct phases in the yielding of the muscle during the load clamp. An initial rapid lengthening (phase 1) accompanied the load step itself. The subsequent constant load resulted in a slower lengthening (phase 2) followed by a high velocity lengthening (phase 3). The amplitude of phase 1 varied with the magnitude of the load step (Fig. 1*d*), but was the same for a given load regardless of the time of the step (Fig. 1*c*). From the length changes during phase 1 for various loading and unloading steps at any given time, a single uninterrupted force–extension curve was obtained. The length change of phase 2 occurred at constant speed and varied with the magnitude of the imposed load. But analysis of load clamps at various instants before peak shortening (Fig. 1*c*), of various magnitudes (Fig. 1*d*) and at various isotonic loading conditions before length change, of phase 2 and the magnitude and speed of phase 2, measured as the length between the end of phase 1 and the length where phase 2 deviated from the tangent to phase 2, did not exceed a particular maximal value. That particular maximal value averaged 0.80±0.05 (s.e.m.; $n=14$ muscles) % of l_{max}. Moderate under- or overdamping of the load step made the transition from phase 1 to 2 respectively slightly more or less distinct than at critical damping but without altering the magnitude and speed of phase 2. The level of constant speed, but not the maximal length change, of phase 2 and the magnitude and speed of phase 3 seemed to be time dependent. To measure the contribution of changing activation in twitch contractions, we performed further experiments on muscles tetanised by trains of high-intensity electrical stimuli at [Ca^{2+}] 10 mM and caffeine 10 mM in the bathing solution[11].

Figure 2 (upper) shows two superimposed load clamps during steady shortening of an afterloaded tetanus. Again, three distinct lengthening phases were observed. Instantaneous phase 1 varied with the amplitude of the load step. The magnitude of the lengthening during phase 2 was respectively 0.99 and 0.96% for the load clamps *a* and *b*. The mean maximal value was 1.02±0.06 (s.e.m.; $n=10$ muscles) % of l_{max}. Transition to phase 3 occurred earlier in time and at a higher speed as the amplitude of the load step was increased. During a sustained tetanus, phase 3 was followed by a slow recovery (phase 4) without oscillations.

From force–extension analysis, phase 1 was shown to reflect instantaneous undamped series compliance accompanying the load step itself. The nature of series compliance in cardiac muscle is presumably more complex than in skeletal muscle[1,5,6], that is crossbridge links between actin and myosin filaments[1,4], branching[12], spiral arrangement of the fibres[13], shearing through Z-lines and intercalated disks[14], and damage of tissue adjacent to the clip[15]. We largely bypassed these problems by the conditions of isotonic loading at heavy afterloads, allowing for homogeneous temporal and spatial distribution of force and nearly maximal extension of all non-crossbridge sources of series elasticity before the clamp. Nevertheless, because of the unpredictable relative contribution of crossbridge and extra-crossbridge compliance, phase 1 was not analysed further.

Closer attention was focused on the delayed lengthening of the muscle during the steady-state phase of the load clamp when series elastic elements do not change in length. Analysis of length responses to load clamps in steady-state isotonic conditions also precluded the importance of an unpredictable relation that exists in isometric contractions between sarcomere length and the external length of the preparation and that results from the large amount of connective tissue with uneven distribution of forces[16]. Relating overall muscle length to sarcomere length was an assumption underlying the following discussion, and fluctuations of myofilaments about their mean positions within sarcomeres due to fluctuating forces along myofibrils[17] were omitted. Since sarcomere lengths at l_{max} obtained from living cardiac muscle[18] were reported to average 2.23 μm (ref. 19) and 2.30 μm (ref. 20) an assumed sarcomere length of 2.25 μm at l_{max} enables phase 2 to be expressed as an average length change of 9.0 nm per half sarcomere for twitch contractions. Accounting for internal shortening of about 5% of l_{max} resulting from extension of series elastic elements during the isometric phase of the afterloaded contraction[18], yielded a value of 8.6 nm per half sarcomere. Similar calculations for tetanised contractions provided a phase 2

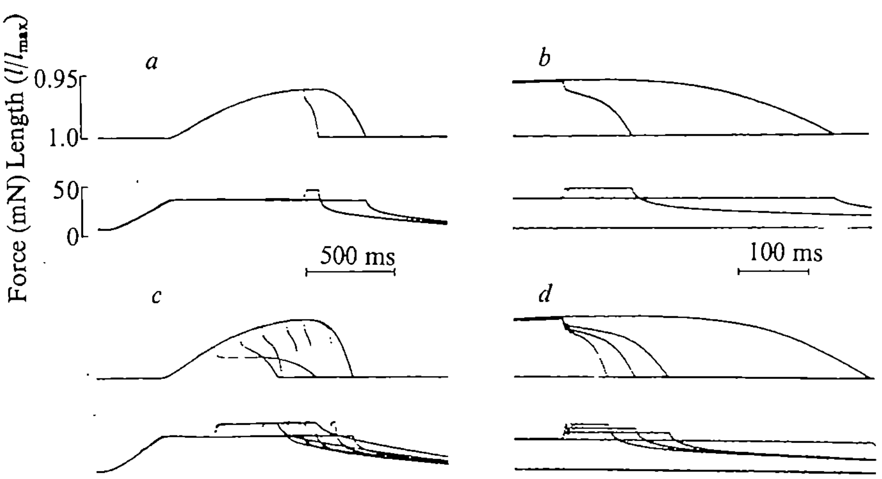

Fig. 1 Length responses of cardiac muscle to sudden increases in load in afterloaded twitch at 19 °C. Although 3-step yielding during load clamps was also observed at higher temperatures (29 °C), the time resolution of the phase 2 lengthening was less satisfactory for further analysis. Length and force gains were the same for all panels. *a*, Slow sweep length and force tracing of load clamp at a time near peak shortening of afterloaded isotonic twitch; control afterloaded contraction is also shown; preload was set at l_{max}, while afterload was augmented to near 70% of isometric conditions so that subsequent isotonic shortening had not proceeded below $0.95 l_{max}$ before the load clamp. *b*, Fast sweep tracings of contractions illustrated in *a*; fast sweep begins just before load clamp is applied; lengthening has three distinct phases. *c*, Slow sweep tracings of load clamps at various times during a twitch; fourth clamp from left is the same as in *a*. *d*, Fast sweep tracings of load clamps of various magnitudes at a given time during a twitch; middle clamp is the same as in *b*. All experiments were performed at the initial muscle length l_{max}, that is the length at which active force development of an isometric twitch was maximal. The experimental protocol has been extensively discussed previously[7-9]. Suitable muscles were selected on the basis of their ratio of resting to total force at l_{max} (refs. 7-9), the mean ratio being 0.11±0.01 (s.e.m.; n = 17 muscles) at 29 °C and 12 per min. To account for the long term memory of cardiac muscle for loading in preceding contractions[10], all test contractions were separated by a series of at least 6 equally loaded standardised contractions.

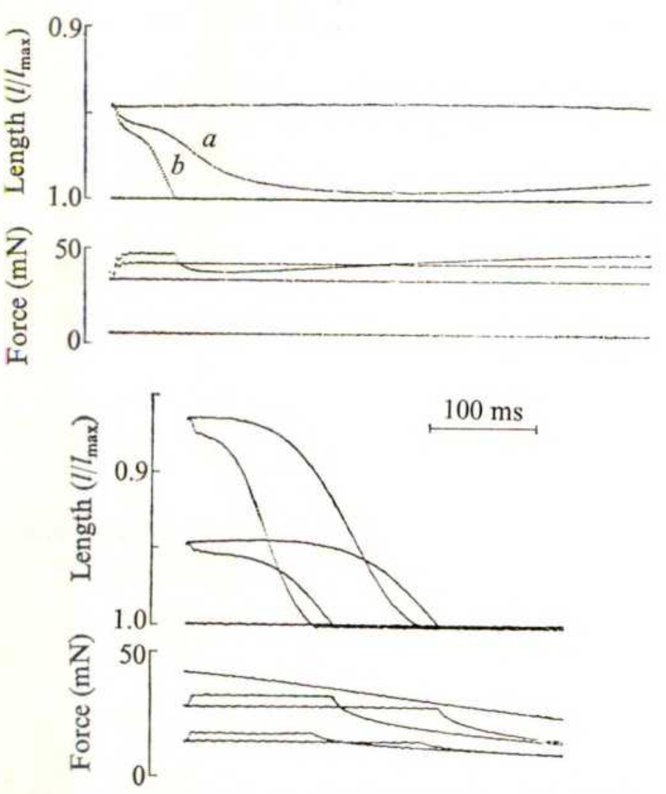

Fig. 2 Upper panel (tetanus): length responses of tetanised cardiac muscle to sudden increases in load (fast sweep); two clamps with different loads were applied during steady shortening of heavily afterloaded tetanus; isotonic shortening had proceeded to about 0.94 l_{max} before the clamps; control tetanic contraction is also shown. Tetanic stimulation train was sustained along the whole duration of the record. Lower panel (twitch): fast sweep record of load clamp before and after halving afterload and amplitude of load step during twitch at 19 °C. Part of the force tracing of an isometric twitch contraction is also shown.

length change of 10.9 nm per half sarcomere. These values are of the same order of magnitude as the extent of motion ascribed to crossbridges in skeletal muscle[1-5]. We therefore propose that during phase 2 attached crossbridges are forced to rotate back to their first point of attachment, as has been suggested for skeletal muscle[5,21]. To test the connection of the delayed phase 2 lengthening distance with the extent of a crossbridge stroke, both afterload and load-step magnitude were halved with respect to the control load clamp experiment (Fig. 2, lower). If it is assumed that the number of attached crossbridges is proportionally altered, the extent of phase 2 lengthening should nevertheless be the same in both conditions. The magnitude of phase 2 was not altered indeed ($n=11$ muscles; $P>0.5$) and thus reflects the full range of back rotation of attached crossbridges.

Rapid phase 3 lengthening might then result from forcible breakage of attached crossbridges. The fall of isometric force following completion of phase 3 in afterloaded tetanus was always clearly apparent, even in experiments where steady tetanic shortening at the time of the clamp had not proceeded to lengths below 0.98–0.99l_{max}. This suggested that the load step itself or the concomitant lengthening might have detached some load bearing crossbridges and that crossbridges in a less favourable position of attachment could have detached all along the clamp including during phases 1 and 2. Analysis of clamps, which after durations of 2–100 ms were reversed to the original load during phases 1 or 2 in twitch and tetanus, yielded the same conclusion in showing incomplete or delayed recovery to the original shortening tracing. Such crossbridge events could possibly account for the effect of deactivation caused by motion in heart muscle[22]. Although some crossbridge reattachment might have occurred from the onset of the load clamp[5], the far delayed recovery phase 4 during tetanus would predict reattaching during phases 1, 2 and 3 proceeding at a relatively much slower rate than detaching.

Another possible explanation is that of a lengthening pattern following the load step but not uniform with respect to time in all segments along the length of the preparation during a twitch, with lengthening in some portions of the fibre and actual shortening in others[1,6,23]. Phase 2 could then result from the delayed relaxation of those sarcomeres exhibiting the longest duration of mechanical activity. The three step yielding during tetanus under homogeneous temporal and spatial activation rules out the contribution of such longitudinal inhomogeneity of the duration of activity.

In conclusion, using the slow contraction mode of mammalian cardiac muscle at low temperature, we have analysed the delayed lengthening after load perturbations and we propose that in cardiac muscle, as in skeletal muscle[1], force is generated by the total number of bridges attached in parallel between myosin and actin, pivoting about their attachment with a turnover of 8.6–10.9 nm per half sarcomere, thus producing a force by extending the more compliant portion of the bridges by the same amount.

Ph. R. HOUSMANS
D. L. BRUTSAERT

Department of Physiology,
University of Antwerp,
Antwerp, Belgium

Received March 1; accepted May 6, 1976.

[1] Huxley, A. F., and Simmons, R. M., *Nature*, **233**, 533–538 (1971); *Cold Spring Harb. Symp. quant. Biol.*, **37**, 669–680 (1973).
[2] Podolsky, R. J., Nolan, A. C., and Zaveler, S. A., *Proc. natn. Acad. Sci. U.S.A.*, **64**, 504–511 (1969).
[3] Podolsky, R. J., and Nolan, A. C., *Cold Spring Harb. Symp. quant. Biol.*, **37**, 661–668 (1973).
[4] Bressler, B. H., and Clinch, N. F., *J. Physiol., Lond.*, **237**, 477–493 (1974); *Nature*, **256**, 221–222 (1975).
[5] Simmons, R. M., and Jewell, B. R., *Recent Adv. Physiol.*, **9**, 87–147 (1974).
[6] Katz, B., *J. Physiol., Lond.*, **96**, 45–64 (1939).
[7] Claes, V. A., and Brutsaert, D. L., *J. appl. Physiol.*, **31**, 497–498 (1971).
[8] Brutsaert, D. L., Claes, V. A., and Sonnenblick, E. H., *J. Physiol., Lond.*, **216**, 319–330 (1971).
[9] Brutsaert, D. L., and Claes, V. A., *Circulation Res.*, **35**, 345–357 (1974).
[10] Brutsaert, D. L., in *The Physiological Basis of Starling's Law of the Heart*, 155–175 (Ciba Foundation, London, 1974).
[11] Henderson, A. H., Forman, R., Brutsaert, D. L., and Sonnenblick, E. H., *Cardiovasc. Res. Suppl.*, **1**, 96–100 (1971).
[12] Muir, A. R., *J. Anat.*, **99**, 27–46 (1965).
[13] Rodbard, S., *Anat. Rec.*, **166**, 410 (1970).
[14] Abbott, B. C., and Gordon, D. G., *Circulation Res.*, **36**, 1–7 (1975).
[15] Krueger, J. W., and Pollack, G. H., *J. Physiol., Lond.*, **251**, 627–643 (1975).
[16] Winegrad, S., *J. gen. Physiol.*, **64**, 343–355 (1974).
[17] Carlson, F. D., *Biophys, J.*, **15**, 633–650 (1975).
[18] Page, S. G., in *The Physiological Basis of Starling's Law of the Heart*, 13–25 (Ciba Foundation, London, 1974).
[19] Julian, F. J., and Sollins, M. R., *Circulation Res.*, **37**, 299–308 (1975).
[20] Pollack, G. H., and Huntsman, L. L., *Am. J. Physiol.*, **227**, 383–389 (1974).
[21] Flitney, F. W., and Hirst, D. G., *J. Physiol., Lond.*, **246**, 68–69P (1975).
[22] Brady, A. J., *Physiol. Rev.*, **48**, 570–600 (1968).
[23] Taylor, S. R., in *The Physiological Basis of Starling's Law of the Heart*, 93–109 (Ciba Foundation, London, 1974).

New elastic protein from muscle

IT has long been assumed that an elastic component other than extracellular collagen fibres is present in muscle fibres to explain their elastic properties, especially during passive stretch[1,2] The presence of such an elastic component has been demonstrated in skinned fibres of frog skeletal muscle[3,4]. Furthermore, it has been observed that myofibrils after the removal of myosin are reversibly extended, indicating their structural continuity[5]. The chemical entity responsible for the intracellular elasticity of muscle has, however, remained obscure. When rabbit myofibrils were thoroughly extracted with salt solutions such as 0.6 M KI, it was noticed that remaining Z lines still maintained their continuity, although nothing could be seen between the adjacent Z lines under a phase microscope (compare ref. 6). Starting from this observation, we have been able to isolate an elastic protein from myofibrils which is clearly distinguishable from elastin or collagen.

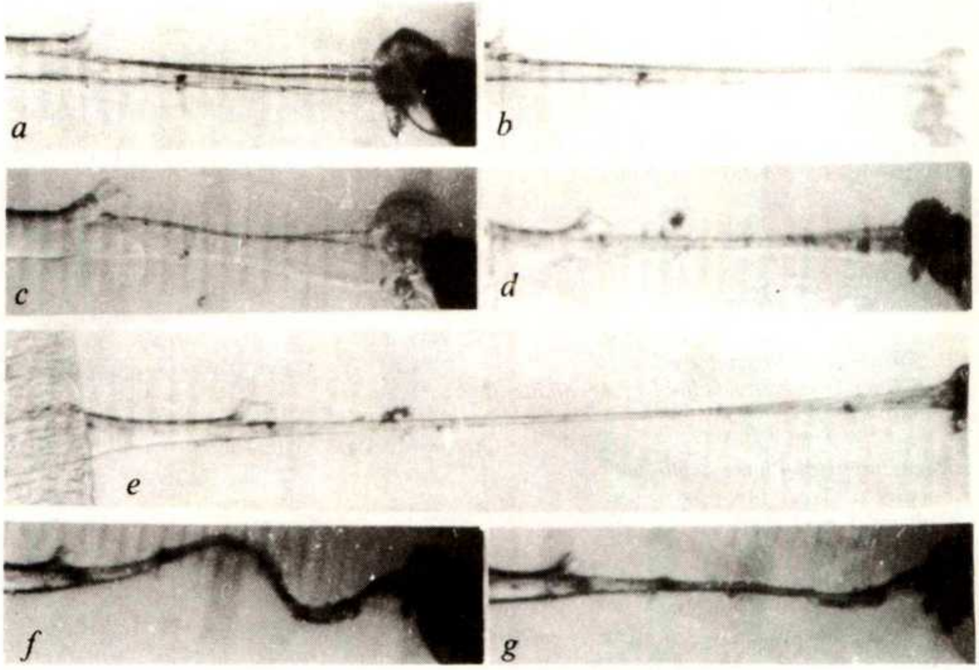

Fig. 1 Passive stretch of 'ghost' skinned fibres. *a*, Skinned fibres of sartorius muscle of the bullfrog in liquid paraffin, 20° C; *b*, stretched skinned fibres; *c*, skinned fibres treated with an alkaline solution (1 M KI, 0.1 M $Na_2S_2O_3$, *p*H 11.5); *d*, after 20 h in the alkaline solution, fibres were washed with Endo's solution (107 mM K-methanesulphonate, 4 mM $MgSO_4$, 4 mM ATP, 2 mM EGTA, 20 mM Tris-maleate, *p*H 6.8); *e*, the same, stretched; *f*, the same immediately after release; *g*, the same, 1 s after release.

Myofibrils were prepared from rabbit psoas muscle according to Perry and Grey[7]. It turned out, however, that the myofibrils contained broken muscle fibre fragments together with free myofibrils and it was necessary to separate them by sucrose density gradient centrifugation (see ref. 8). Light and electron microscopic examinations revealed that myofibrils were free of fibre fragments and connective tissues and fibre fragments were contaminated a little by free myofibrils. Both preparations were exhaustively extracted with Hasselbach–Schneider solution and water, and then with 0.6 M KI (ref. 9). After the residues were extracted with 1 N acetic acid overnight, they were washed with water and extracted in 0.1 N NaOH for several hours at room temperature. The suspension was centrifuged to remove a yellowish supernatant. After neutralisation the residue was treated with hot phenol to remove some glycoproteins. The phenol-insoluble material was washed with water. Approximately 50 mg of protein was obtained from pure myofibrils (1 g protein). A somewhat larger amount was present in fibre fragments (70 mg per 1 g protein). The final product was not soluble in 1% sodium dodecyl sulphate, and therefore, no protein band was detected in a gel electrophoresis.

As the phenol-treated residue was washed with water, the material became adhesive and finally formed a lump. It was possible to prepare a thread of the protein by cutting out the lump. Stretched to 130% of the initial length, the thread was at a tension of as much as 2 kg cm^{-2}. Examination of the tension–length relationship at different temperatures showed that the thread had rubber-like elasticity (compare ref. 4). The Young's elastic modulus was about 4×10^6 dyne cm^{-2}, a magnitude similar to that of unvulcanised rubber. The protein is therefore an elastic protein.

The amino acid composition of the muscle elastic protein is given in Table 1. The proteins from myofibrils and fibre fragments were similar to each other in amino acid composition. It is of some interest that the glycine content is much smaller than that of collagen, elastin[10] or resilin[11], which are well known as elastic proteins (see ref. 12). The muscle elastic protein contained a small amount of hydroxyproline, which is abundant in collagen or elastin (cf. ref. 12). The amino acid composition is similar to that of non-collagenous reticulin, an extracellular glycoprotein of the basement membranes[13], which is shown to be present in the endomysium of muscle[14]. There are distinct differences between the two proteins in hydroxyproline, cystine/2 and leucine content. The reticulin is soluble in 0.05 N NaOH[13]. Furthermore, the elastic protein from myofibrils and fibre fragments contained only 0.5–1.0% of neutral sugars in comparison with 4% of reticulin[13].

The localisation of the elastic protein in myofibrils is still obscure, but it seems that it is responsible for their continuity. After extraction of a skinned fibre of frog muscle with an alkaline solution of *p*H 11.5, the elastic structure seemed to remain intact, although other structures visible under the microscope disappeared. It developed tension when stretched and behaved as an elastic body (Fig. 1). Treatment with 0.1 N NaOH resulted in a considerable decrease in tension generation, suggesting that the elastic properties had been damaged.

The muscle elastic protein makes at least some contribution to the intracellular elasticity of muscle fibre. The relationship between the elastic protein and reticulin or collagen at the myotendinous junction is of much interest from the viewpoint of tension transmission.

Table 1 Amino acid composition of elastic protein from pure myofibrils and fibre fragments of rabbit psoas muscle*

	Pure myofibrils	Fibre fragments
Hypro	7	12
Asp	95	92
Thr	61	59
Ser	61	60
Glu	130	128
Pro	63	65
Gly	89	104
Ala	82	84
Cys/2	2	2
Val	62	60
Met	24	23
Ile	53	52
Leu	73	70
Tyr	30	28
Phe	29	29
Lys	66	61
His	16	15
Arg	57	56

*Number of residues per 1,000 residues

We thank Dr S. Matsubara, Dr S. Handa, Miss F. Murakami and Miss S. Kimura for assistance, and Professor Sir Andrew Huxley, FRS for his critical reading of the manuscript. We also thank a referee who drew our attention to work on non-collagenous reticulin. K.M. acknowledges a travelling fellowship to the Japan Society for Promotion of Science. This work was aided by a grant from the Muscular Dystrophy Associations of America, Inc.

K. MARUYAMA

Department of Biophysics,
Faculty of Science,
University of Kyoto,
Sakyo-ku, Kyoto 606

R. NATORI

Department of Physiology,
The Jikei University School of Medicine,
Minato-ku, Tokyo 105

Y. NONOMURA

Department of Pharmacology,
Faculty of Medicine,
University of Tokyo,
Bunkyo-ku, Tokyo 113

Received February 23; accepted May 18, 1976.

[1] Casella, C., *Acta physiol. scand.*, 21, 380–401 (1950).
[2] Buchtal, F., and Weis-Fogh, T., *Acta physiol. scand.*, 35, 345–364 (1956).
[3] Natori, R., *Jikeikai Med. J.*, 1, 18–28 (1954).
[4] Matsubara, S., *Jap. J. Physiol.*, 25, 227–240 (1975).
[5] Huxley, H. E., and Hanson, J., *Nature*, 173, 971–973 (1954).
[6] Huxley, H. E., and Hanson, J., *Biochim. biophys. Acta*, 23, 229–249 (1957).
[7] Perry, S. V., and Grey, T. C., *Biochem. J.*, 64, 184–192 (1956).
[8] Saide, J. D., and Ullrick, W. C., *J. molec. Biol.*, 87, 671–683 (1974).
[9] Maruyama, K., *J. Biochem. Tokyo*, 69, 369–386 (1971).
[10] Partridge, S. M., and Davis, H. F., *Biochem. J.*, 61, 21–30 (1955)
[11] Bailey, K., and Weis-Fogh, T., *Biochim. biophys. Acta*, 48, 452–459 (1961).
[12] Seifter, S., and Gallop, P. M., in *The Proteins*, 2nd ed., 4, (edit. by Neurath, H.), 153–458 (Academic, New York, 1966).
[13] Pras, M., and Glynn, L. E., *Br. J. exp. Path.*, 54, 449–456 (1973).
[14] Pras, M., Johnson, G..D., Holborow, E. J., and Glynn, L. E., *Immunology*, 27, 469–478 (1974).

Down's syndrome and related abnormalities in an area of high background radiation in coastal Kerala

BOTH point mutations and structural aberrations of chromosomes are induced by ionising radiations, causing genetic variation and abnormalities in man and other organisms. The mutagenic effects are dose dependent and in *Drosophila* a linear relationship between dose and mutation rate has been shown for doses up to 5 R (ref. 1). Although man accumulates approximately 5 R of radiation from the environment in 30 yr of reproductive life, it is not known whether this is of any radiobiological consequence[2]. Nor is it known whether in man there is a threshold phenomenon at low doses (several hundred or thousand mr. per year), although there is greater repair of mutational or pre-mutational damage after low-dose irradiation[3]. In a coastal area of Kerala, South India, the background radiation is 1,500–3,000 mr. yr^{-1} due to the presence of thorium-containing monazite mineral in the soil[4–7] (Fig. 1). A survey of the rat population in this area with respect to several measurable and non-measurable traits and of humans with regard to dermatoglyphics and demographic data such as fertility index, sex ratio and infant mortality rate revealed no mutational effects[4,7,8]. During an epidemiological study of nodular lesions of the thyroid in this area[9], we noticed an apparently high prevalence of Down's syndrome and other forms of severe mental retardation[10]. We therefore made a house-to-house survey of developmental abnormalities in this area and in a comparable control area without high background radiation[7] (Fig. 1). We also determined the frequency of chromosome aberrations in a sample of the normal population living in the study and control areas. The observations we report here support the view that radiation-induced genetic anomalies occur with above average frequency in the population living in the area with high background radiation. The area surveyed was the southernmost one-fifth of the Chavara-Neendakara strip (Fig. 1). In the thatched huts which constitute 75% of all households, the exposure risk is 1,500–3,000 mr. yr^{-1}, and personal exposure, as measured by calcium fluoride dosimeters, closely parallels the exposure risk in the households. The control area consisted of the Purakkade–Punnapura villages, with a background radiation of approximately 100 mr. yr^{-1} (ref. 7). Households were visited repeatedly to ensure examination of all members. Only gross abnormalities evident on clinical examination were recorded. Cytogenetic abnormalities were scored blind on slides prepared from 64-h micro-blood cultures[11].

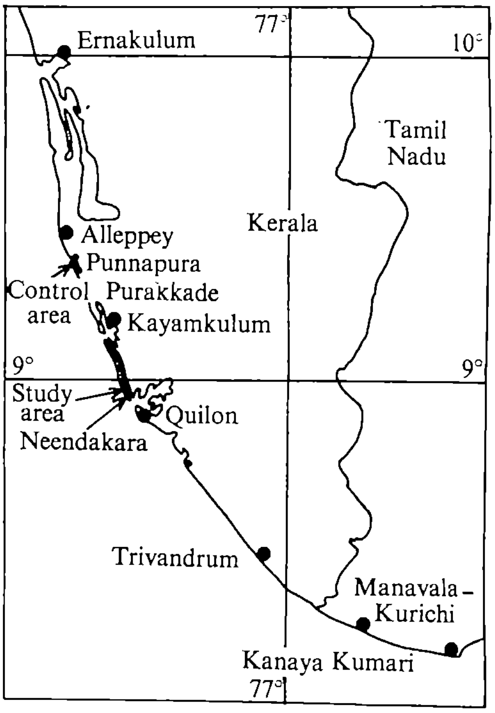

Fig. 1 Map showing the study and control areas.

Demographic and epidemiological details are reported elsewhere[9]. Briefly, the study and control populations were similar in age and sex structure, ethnic composition, living and diet habits, social customs, economic status and occupation. The mean age of all women was 30.3±7.09 yr and 30.12±7.04 yr in the study and control populations, respectively. The frequency distribution by age of women at the birth of the last child was similar in the two populations. The mean family size was 6.2 in the study and 6.4 in the control population. Rate of consanguinity was 12% in the study population and 15% in the control. Abortion rate per 1,000 pregnancies was 109 and 64.5, respectively, in study and control populations ($P > 0.05$), based on a random survey of 57 couples in the study area and 68 couples in the control area.

Table 1 Prevalence of severe mental retardation*

Type	Study population (12,918)		Control population (5,938)	
	Total	Per 1,000	Total	Per 1,000
Genetic				
Down's syndrome	12	0.93	0	0
SMR with physical abnormalities	12	0.93	1	0.17
Idiopathic	11	0.90	3	0.50
Acquired (Perinatal and postnatal)	6	0.46	3	0.50
TOTAL	41	3.1	7	1.16

The definition of severe mental retardation (SMR) is according to the WHO Classification of 1968. Figures in parentheses indicate the total number of persons surveyed.

Severe mental retardation was the commonest developmental abnormality encountered in the study area (Table 1). Clinically, 85% of the abnormalities detected in the study population were "genetic" in origin[10], compared with the 56% in the control population. The frequency of acquired retardation was comparable in the two populations. Prevalence of Down's syndrome was 0.93 per 1,000 in the study population, accounting for a third of the genetic retardations observed, whereas no cases were detected in the control population.

Chromatid and chromosome aberrations were scored in 1,705 metaphases from 46 subjects and in 1,547 metaphases from 39 individuals in the study and control areas, respectively. The mean frequency of aberrations was higher in the study area (chromatid, 3.0 ± 4.6 compared with 1.2 ± 1.9; chromosome, 1.9 ± 3.1 compared with 0.2 ± 0.6). Considering the high variance of mean aberration number, a χ^2 test was applied by grouping the data as shown in Table 2. This revealed no significant difference in chromatid aberrations between the two groups ($P > 0.05$), while the difference in the chromosome aberrations was significant ($P < 0.01$).

Table 2 Frequency of cytogenetic aberrations

% Aberrations	Chromatid		Chromosome	
	Study	Control	Study	Control
0	20	23	24	36
1–3	12	11	13	3
>3	14	5	9	0
	$P > 0.05$		$P < 0.01$	

Figures in columns 2–5 give numbers of individuals.
*These were mostly deletions (acentric fragments and minutiae), with few rings and dicentrics.

The observed frequency of Down's syndrome in the study population (1:1,076) was higher than in the control population ($P < 0.05$), and was significant for the following reasons. (1) Although no data are available on the population frequency of Down's syndrome in India, there are figures for the Eastern counties of England, 1:10,000; London, 1:3,000; Germany, 1:7,000; Denmark, 1:4,000; Australia, 1:2,083, and North-east Scotland, 1:2,000[12,13]. The frequency in Kerala is higher than in any of those (except the Shetland islands, for which the value is 1:714)[13] although infant mortality is four to five times greater than in these areas. (2) The frequency of Down's syndrome among births in India as a whole is 1:1,215 (ref. 14). In Madras, South India where the people are ethnically closer to those in Kerala, the incidence is lower (1:3,833). The frequency in the general population is expected to be lower than this because of the higher mortality among patients with Down's syndrome[15] while in Kerala the frequency is higher. (3) Most striking is the higher frequency of cases of Down's syndrome born to mothers aged 30–39 yr (Table 3). This figure of 1:81 can be compared with 1:880 and 1:290 for maternal ages of 30–34 yr and 35–39 yr, respectively, calculated by Penrose and Smith[12]. (4) The increase is also evident in a comparison of the proportion of cases of Down's syndrome born to mothers more than 30 yr old in the study area (91%) with that among 615 cases documented in India (51%)[16].

Table 3 Frequency of Down's syndrome distributed by maternal age at conception in study area

Maternal age (yr)	No. of females	% of all females	No. of cases	Frequency
20–29	862	13.6	1	1:862
30–39	729	11.5	9	1:81
40–49	532	8.4	2	1:266

Comparative figures for the distribution of females in the control population were: 20–29-yr group, 478 (16.5%); 30–39-yr group, 369 (12.7%); 40–49-yr group, 264 (9.1%). There was no case of Down's syndrome in this population.

Epidemiological and experimental evidence is accumulating which suggests an association between low dose irradiation of older mothers and non-disjunctional disorders in the offspring[17–19]. The maternal age-dependence suggests that the damaging event accelerates oocyte ageing and causes primary trisomy rather than translocation trisomy which is known to be independent of maternal age[17]. These observations agree remarkably well with our results. In 11 of 12 cases of Down's syndrome maternal age was greater than 30 yr and six of the cases who were successfully karyotyped had trisomy 21. The higher prevalence of chromosome aberrations in apparently normal subjects from the radiation area also supports the view that environmental radiation may be the cause of the genetic damage in the population. Similar cytogenetic findings have been reported from a Brazilian population living in an area of high natural radioactivity[20].

The prevalence of severe mental retardation of genetic origin was four times higher in the study than in the control population, whereas that due to acquired perinatal and postnatal causes is comparable. The nature of the genetic defect remains undetermined in most of these patients, except in the group with Down's syndrome, where trisomy 21 was demonstrated by karyotyping. Mental retardation was associated with different physical abnormalities in 12 patients in the study area. Although karyotyping was not done in these patients, chromosome imbalance is now recognised to be important in the genesis of such syndromes[21,22]. Kirman suggested that a grade of genetic defect intermediate between, on one hand, gross and visible chromosome errors, and, on the other hand, point mutations involving structural changes in the chromosomes, such as inversions and crossovers, may cause idiopathic mental retardation[23]. In view of these possibilities, radiation-induced genetic damage seems likely to be responsible for the high prevalence of mental retardation in the area we studied.

N. Kochupillai

I. C. Verma

M. S. Grewal

V. Ramalingaswami

Departments of Medicine, Pediatrics (Genetics),
Anatomy and Pathology,
All-India Institute of Medical Sciences, Ansari Nagar,
New Delhi—110016, India

Received November 24, 1975; accepted May 7, 1976.

[1] Glass, H. R., and Ritterhoff, R. K., *Science*, **133**, 1366 (1961).
[2] Grüneberg, H., *Nature*, **204**, 222–224 (1964).
[3] Russell, W. L., *Brookhaven Symp. Biol.*, **20**, 179–189 (1968).
[4] Grüneberg, H., *et al.*, *Med. Res. Council Spec. Rep. Ser., Lond.*, 307 (1966).
[5] *WHO Tech. Rep. Ser.*, **166**, 23 (1959).
[6] Ponnunni Kartha, K. I., *Hlth Phys.*, **15**, 368–369 (1968).
[7] Gopal Ayengar, A. R., *et al.*, in *Peaceful Uses of Atomic Energy*, **11**, 31–51 (International Atomic Energy Agency, Vienna, 1972).
[8] Ahuja, Y. R., Sharma, A., Nampoorthiri, U. K., Ahuja, M. R., and Dempster, E. R., *Hum. Biol.*, **45**, 167–179 (1973).
[9] Kochupillai, N., Thangavelu, M., and Ramalingaswami, V., *Indian J. med. Res.* (in the press).
[10] *WHO Tech. Rep. Ser.*, **392**, 8 (1968).
[11] Arakaki, D. T., and Sparkes, R. S., *Cytogenetics*, **2**, 57–60 (1963).
[12] Penrose, L. S., and Smith, G. F., in *Down's Anomaly* (Churchill, London, 1966).
[13] Ross, H. S., Innes, G., and Kidd, C., *Scot. med. J.*, **12**, 260–263 (1967).
[14] Verma, I. C., and Singh, M. B., *Lancet*, **i**, 1200 (1975).
[15] Hillard, L. T., and Kirman, B. H., *Mental Deficiency*, 310 (Churchill, London, 1957).
[16] Verma, I. C., Gupta, A. K., and Devanagondi, B. S., *Indian Pediat.*, **12**, 1239–1245 (1975).
[17] Alberman, E., *et al.*, *Ann. Hum. Genet.*, Lond., **36**, 195–208 (1972).
[18] Uchida, I. A., and Curtis, E. J., *Lancet*, ii, 848–850 (1961).
[19] Yamamoto, M., Shimada, M., Ende, A., and Watanabe, G., *Nature new Biol.*, **244**, 206–208 (1973).
[20] Barcinski, M. A., *et al.*, *Am. J. Hum. Genet.*, **27**, 802–806 (1975).
[21] Summitt, R. L., *J. Pediat.*, **74**, 58–66 (1969).
[22] *Report of the Advisory Committee on the Biological Effects of Ionizing Radiation*, **47** (National Academy of Sciences, Washington DC, 1972).
[23] Kirman, B. H., in *Mental Retardation and Developmental Disabilities*, **5**, *Clinical Aspects* (edit. by Wortis, J.), 1–24 (Butterworths, London, 1973).

Modulation of the synthesis *in vitro* of a hormone-induced protein by transfer RNA

WE have shown that transfer RNAs (tRNAs) and the enzymes which modify their structure at the macromolecular level (tRNA methyltransferases) are under hormonal control in the target tissue[1-3]. Oestrogen-induced, cell-specific protein synthesis in immature chick oviducts has been extensively studied[4-6]. Oestrogen induces cytodifferentiation of the primitive oviduct and the consequent synthesis by the tubular gland cells of ovalbumin, conalbumin, ovomucoid and lysozyme[7]. Continuous presence of oestrogen is required for the sustained synthesis of these proteins in immature chicks; withdrawal of oestrogen is accompanied by a gradual decline in cell-specific protein synthesis[6]. The tubular gland cells in the oviduct magnum, however, continue synthesising non-secretory proteins. Readministration of oestrogen to chicks after withdrawal (secondary stimulation) results in the restoration of the synthesis of cell-specific proteins without concomitant need for DNA synthesis. We report here that in an *in vitro* tRNA-dependent protein-synthesising system from Ehrlich ascites cells, stimulation of the translation of ovalbumin mRNA was significantly enhanced by tRNA extracted from the oviduct of oestrogen-stimulated immature chicks or from the oviduct of laying hens compared with tRNA from oviducts of withdrawn chicks. Therefore, the efficiency of synthesis *in vitro* of a hormone-induced protein can be regulated by tRNA.

We had found previously that oestrogen-induced synthesis of ovalbumin can be enhanced by tRNA isolated from the oviduct of the laying hen, when it is added to oviduct explants of immature chicks[8]. To study the mechanism of enhancement of ovalbumin synthesis by tRNA we developed an *in vitro* protein-synthesising system which is completely tRNA dependent[9]. Such a system was essential for studying the contribution of tRNAs from different sources to the efficiency and fidelity of translation of a specific messenger RNA (mRNA); otherwise the residual endogenous tRNA can mask any specific effect[10].

Figure 1 shows the effect of tRNA from three different sources on amino acid incorporation. It is evident that tRNA from the oviducts of oestrogen-stimulated chicks or from oviducts of laying hens produced an enhanced stimulation of amino acid incorporation in the presence of ovalbumin mRNA (*b*, upper curve). On the other hand, the tRNAs from the three sources were equally effective in stimulating amino acid incorporation with residual endogenous mRNA.

The efficiency of translation of oviduct mRNA was also assayed by the extent of synthesis of ovalbumin and the results are presented in Fig. 2. Ovalbumin, precipitable with specific antisera, was synthesised to a 70% greater extent in the presence of tRNA from oestrogen-stimulated chicks than in the presence of tRNA from chicks that had not received secondary oestrogen stimulation.

The identity of the polypeptides precipitated by antisera was confirmed by gel coelectrophoresis with authentic markers (Fig. 3). The faster moving components are probably nascent, incomplete ovalbumin precursors. The experiments were reproducibly repeated with three different preparations of tRNA, isolated from different batches of chicks, using separate preparations of the protein-synthesising system from Ehrlich ascites cells. There were some variations in the activity of the protein-synthesising systems. In different experiments, however, ovalbumin mRNA translation was 50–75% greater by oviduct tRNA from oestrogen-stimulated chicks than from withdrawn chicks. For reproducible results it is essential to use protein-synthesising systems which depend completely on the presence of exogenous tRNA.

To rule out the possibility that the relative inefficiency of oviduct tRNA from withdrawn chicks in the synthesis of ovalbumin stems from some unknown artefact of the isolation, its effectiveness in the translation of another mRNA was tested. In the efficiency of translation of rabbit

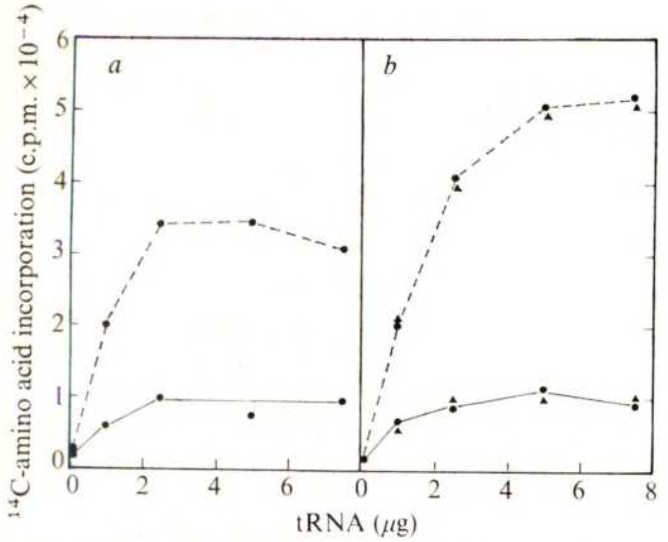

Fig. 1 Stimulation of protein synthesis by oviduct tRNA from immature chicks in a tRNA-dependent protein-synthesising system. The assay mixture contained in a volume of 100 μl: 20 mM Tris-HCl (*p*H 7.5), 1 mM ATP, 0.2 mM GTP, 6 mM creatine phosphate (all adjusted to *p*H 7.5), 20 μg creatine kinase, 0.5 μCi ^{14}C-amino acid mixture, 0.05 mM of each of the six freshly neutralised non-radioactive amino acids missing from the ^{14}C mixture, 6 mM mercaptoethanol, 50 mM KCl, 3 mM magnesium acetate, 3 μg oviduct mRNA, specified amounts of tRNA, 0.45 A_{260} units of DEAE–cellulose-passed ribosomes and 0.12 A_{280} units of ammonium sulphate fraction[9]. All incubations were carried out in duplicate at 37 °C for 90 min. The amino acid incorporation was linear up to 120 min. At the end of incubation to determine amino acid incorporation into polypeptides, 0.2 ml 0.2 N KOH was added and the tubes were further incubated for 20 min, 1 ml TCA was added and the samples were filtered through Whatman GF/C filters, washed 4–5 times with 5% TCA and once with ethanol. The filters were dried and counted in a liquid scintillation counter. *a*, Stimulation of protein synthesis with oviduct tRNA from withdrawn chicks with endogenous mRNA (●——●) and amino acid incorporation in the presence of oviduct mRNA (●- -●). *b*, Upper curve: stimulation of protein synthesis with oviduct mRNA by oviduct tRNA from oestrogen-stimulated chicks (●) or from laying hens (▲); lower curve: amino acid incorporation without oviduct mRNA. Four-day-old chicks were injected with oestradiol benzoate for 10 d followed by a withdrawal period of 3–4 weeks; the secondary oestrogen stimulation consisted of a single injection of 2 mg oestradiol[11]. Oviducts were removed aseptically, the magnum portion of the oviduct was freed of adjoining tissue and was immediately frozen in acetone-dry ice. Frozen tissue was homogenised in 5 volumes 50 mM Tris-HCl, *p*H 8.3, 5 mM EDTA, 75 mM NaCl, 0.5% SDS and an equal volume of buffer-saturated phenol in a Sorvall omnimixer at full speed for 1 min. The aqueous phase was re-extracted twice with phenol and the nucleic acids were precipitated with 0.1 volume 20% potassium acetate and 2 volumes ethanol. The tRNA was separated from the bulk nucleic acids by DEAE–cellulose chromatography and was treated with DNAse followed by Pronase[8] and extracted with phenol. The tRNA was deacylated[12] and further purified by gel filtration on Sephadex G-100 (ref. 8). Oviduct magnum tissue from 40 chicks (4–5 g) withdrawn from oestrogen for 3–4 weeks and from 5–6 chicks (5–6 g) which received secondary oestrogen stimulation, was used for the isolation of tRNA. The yield of purified tRNA from withdrawn chick oviducts was one-half (10 A_{260}) of the tRNA from secondary oestrogen-stimulated chicks. Oviduct mRNA was isolated by affinity chromatography on oligo (dT)-cellulose[13]. All glassware was dried overnight at 300 °C and the solutions were made in glass-distilled autoclaved water.

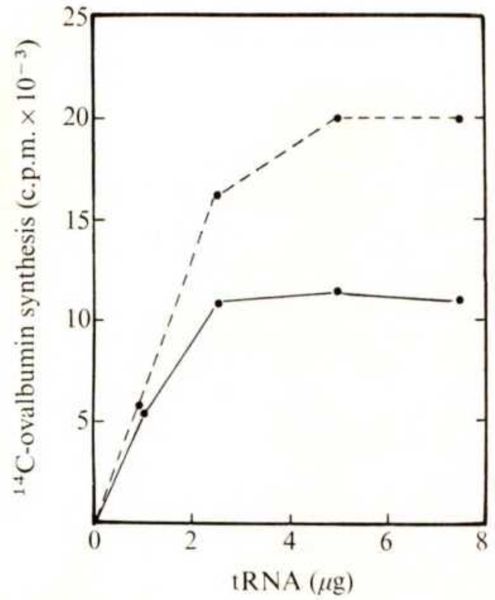

Fig. 2 Synthesis of ovalbumin in a tRNA-dependent protein-synthesising system. The details for protein synthesis were the same as described for Fig. 1. Ovalbumin synthesis was determined in aliquots of the assay mixture after incubation for 90 min at 37 °C by specific immunoprecipitation with antiserum against purified ovalbumin[14]. Aliquots (25 μl) of the reaction mixture were adjusted to 230 μl in plastic microfuge tubes (Beckman) by the addition of 15 mM NaCl in 10 mM sodium phosphate (*p*H 7.5); to this were added 10 μl ovalbumin (5 μg), 50 μl ovalbumin antiserum (antibody excess) and 20 μl 10% sodium deoxycholate. The contents of the tubes were mixed and incubated overnight at 37 °C. The precipitates were collected by centrifugation in Beckman microfuge (model 152), washed 3–4 times with 10 mM sodium phosphate (*p*H 7.5) containing 150 mM NaCl, 1% deoxycholate and 1% Triton X-100 (ref. 8). The pellet was dissolved in 0.1 ml NCS and counted[14]. Correction for nonspecific trapping of radioactivity by the immunoprecipitate was made by carrying out precipitation reactions in identical aliquots of the reaction mixture in the presence of 5 μg bovine serum albumin and 50 μl bovine albumin anti-serum. The immunoprecipitate from assay mixtures with oviduct mRNA usually contained 3,000–6,000 c.p.m. compared with 600–800 c.p.m. of nonspecific trapping. Ovalbumin synthesis was reproducibly quantified by this procedure. Ovalbumin-specific radioactivity was not precipitated from incubations in which rabbit globin mRNA or encephalomyocarditis viral RNA were translated. The specificity of the precipitation reaction was also checked by SDS–polyacrylamide gel electrophoresis of the antibody–antigen precipitate[14]. The radioactivity in the antibody–antigen precipitate from oestrogen-stimulated chick oviduct explants migrated as a single peak with the mobility of ovalbumin. Ovalbumin synthesis in the presence of oviduct tRNA from withdrawn chicks (●——●) and oestrogen-stimulated chicks (●- -●).

globin mRNA no differences were found in the tRNAs from the two sources (data not shown). The quality of the tRNAs from the two sources in the translation of mRNAs other than that of ovalbumin is also implied, albeit to a quantitatively lesser degree, by the equivalent translation of the endogenous mRNAs from the ascites cells (Fig. 1, lower curves).

Oestrogens are known to have multiple effects on target tissues. In the chick oviduct they can stimulate accumulation of specific mRNA[15–17], tRNA[18], tRNA methyltransferases[19], polysomes[11,20], endoplasmic reticulum[14,21] and factors essential for translation[22]. The findings presented here imply that the relative inefficiency of oviduct tRNA from withdrawn chicks in ovalbumin synthesis may be due to a deficiency in the population of tRNAs. The validity of such an assumption can be probed experimentally because the oviduct of the laying hen offers an abundant source of tRNAs which have a high efficiency of translation.

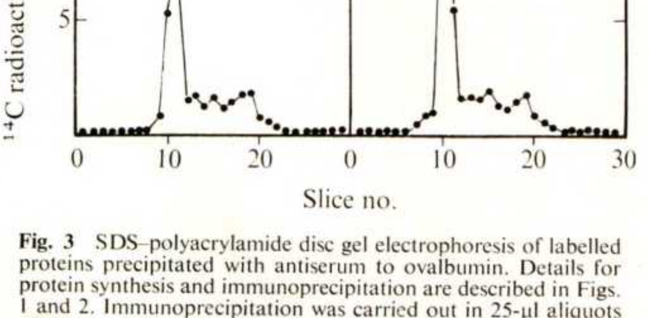

Fig. 3 SDS–polyacrylamide disc gel electrophoresis of labelled proteins precipitated with antiserum to ovalbumin. Details for protein synthesis and immunoprecipitation are described in Figs. 1 and 2. Immunoprecipitation was carried out in 25-μl aliquots of the reaction mixture of protein synthesis after 90 min incubation at 37 °C, washed antibody precipitates were mixed with ^{3}H-labelled ovalbumin and conalbumin synthesised in oestrogen-stimulated oviduct explants[14], as internal markers, and co-electrophoresed. The mobility of conalbumin (CON) and of ovalbumin (OV) is indicated. Oviduct mRNA was translated with 5 μg oviduct tRNA from withdrawn chicks (*a*) and oestrogen-stimulated chicks (*b*).

This work was supported by the NCI and the US ERDA.

Opendra K. Sharma
Dan N. Beezley
Ernest Borek

Department of Microbiology,
University of Colorado Medical Center,
Denver, Colorado 80220

Received March 8; accepted April 27, 1976.

[1] Sharma, O. K., and Borek, E., *Biochemistry*, **9**, 2507–2513 (1970).
[2] Sharma, O. K., Kerr, S. J., Wiesner, R. L., and Borek, E., *Fedn Proc.*, **30**, 16. (1971).
[3] Sharma, O. K., and Borek, E., *Adv. Enz. Reg.*, **12**, 85–102 (1974).
[4] O'Malley, B. W., McGuire, W. L., Kohler, P. O., and Korenman, S. G., *Recent Progr. Hormone Res.*, **25**, 105–160 (1969).
[5] Oka, T., and Schimke, R. T., *J. Cell Biol.*, **41**, 816–823 (1969).
[6] Oka, T., and Schimke, R. T., *J. Cell Biol.*, **43**, 123–137 (1969).
[7] Palmiter, R. D., *J. biol. Chem.*, **247**, 6450–6461 (1972).
[8] Sharma, O. K., Mays, L. L., and Borek, E., *J. biol. Chem.*, **248**, 7622–7624 (1973).
[9] Sharma, O. K., Roberts, W. K., Beezley, D. N., and Borek, E., *Biochim. biophys. Acta*, **390**, 327–331 (1975).
[10] Sharma, O. K., Beezley, D., and Roberts, W. K., *Fedn Proc.*, **35**, 1729 (1976).
[11] Palmiter, R. D., Christensen, A. K., and Schimke, R. T., *J. biol. Chem.*, **245**, 833–845 (1970).
[12] Sarin, P. S., and Zamecnik, P. G., *Biochim. biophys. Acta*, **91**, 653–655 (1964).
[13] Aviv, H., and Leder, P., *Proc. natn. Acad. Sci. U.S.A.*, **69**, 1408–1412 (1972).
[14] Palmiter, R. D., Oka, T., and Schimke, R. T., *J. biol. Chem.*, **246**, 724–737 (1971).
[15] Palmiter, R. D., *J. biol. Chem.*, **248**, 8260–8270 (1973).
[16] Roads, R. E., McKnight, G. S., and Schimke, R. T., *J. biol. Chem.*, **248**, 2031–2039 (1973).
[17] Chan, L., Means, A. R., and O'Malley, B. W., *Proc. natn. Acad. Sci. U.S.A.*, **70**, 1870–1874 (1973).
[18] O'Malley, B. W., Aranow, C. W., Peacock, A. C., and Dingman, C. W., *Science*, **162**, 567–568 (1968).
[19] Hacker, B., *Biochim. biophys. Acta*, **186**, 214–216 (1969).
[20] Means, A. R., Abrass, I. B., and O'Malley, B. W., *Biochemistry*, **10**, 1561–1570 (1971).
[21] Palmiter, R. D., and Wrenn, J. T., *J. Cell Biol.*, **50**, 598–615 (1971).
[22] Palmiter, R. D., *J. biol. Chem.*, **247**, 6770–6780 (1972).

Human–mouse cell hybrid with human multiple Y chromosomes

HUMAN–mouse cell hybrids usually exhibit preferential loss of human chromosomes[1,2]. After a time interval, which depends in part on the cell types used, most or sometimes all the human chromosomes segregate out from the hybrid cells[3]. In the course of investigation of the phenomenon of preferential loss of human chromosomes from hybrids between the mouse cell line RAG and human leukocytes, we isolated and analysed sixteen human–mouse (RH) hybrids. Seven of these hybrids had retained the human Y chromosome. Five of these had only one copy per cell of Y, one had two copies per cell and one, RH-28, had four copies of the Y in many cells. We decided to study more extensively this hybrid which seemed to have lost all the human chromosomes except number 17 and the Y.

Figure 1 shows a cell of RH-28 stained by the Q-banding technique which has four human Ys and a human chromosome 17. We determined the distribution of Y chromosomes in 95 cells of RH-28. The results presented in Fig. 2 show that the majority of the cells screened had three or four Y chromosomes. In a few cells the number of Y chromosomes was even higher. In one cell which had a much larger number of mouse chromosomes there were ten human Y chromosomes. The only other human chromosomes present in these hybrid cells was a single copy per cell of chromosome 17.

The presence of multiple copies of a specific human chromosome in human–mouse cell hybrids has been reported by Green *et al.*[4]. In their hybrids, the mouse parent was a thymidine kinase deficient (TK^-) mutant and Green *et al.* could, therefore, select for retention of human chromosome 17, which contains the *TK* gene. They tried to select lines with a high number of human chromosomes 17 by selecting subclones which grew in HAT medium containing low concentrations of thymidine. Three of ten subclones had higher mean numbers of chromosome 17.

We subcloned hybrid RH-28 to see whether we could select subclones in which all or most of the cells had the same number of Y chromosomes. The results (Fig. 3) indicate that in some of the subclones there was a stable number of Y chromosomes. Thus in subclone 8 all 25 cells scored had four Y chromosomes. In another subclone, 2, 30 of 34 cells scored had four Y chromosomes. In several other subclones the Y chromosomes seemed to have stabilised at a lower number per cell. In subclones 1, 3, 5

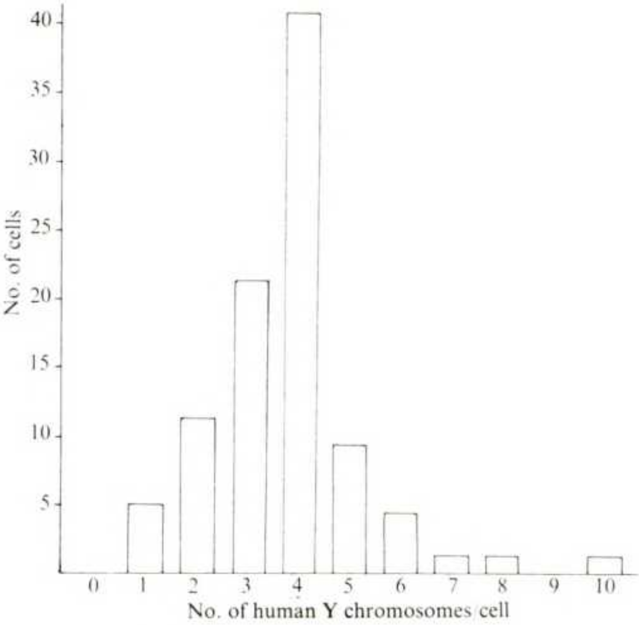

Fig. 2 Distribution of human Y chromosomes in cells of human–mouse hybrid RH-28.

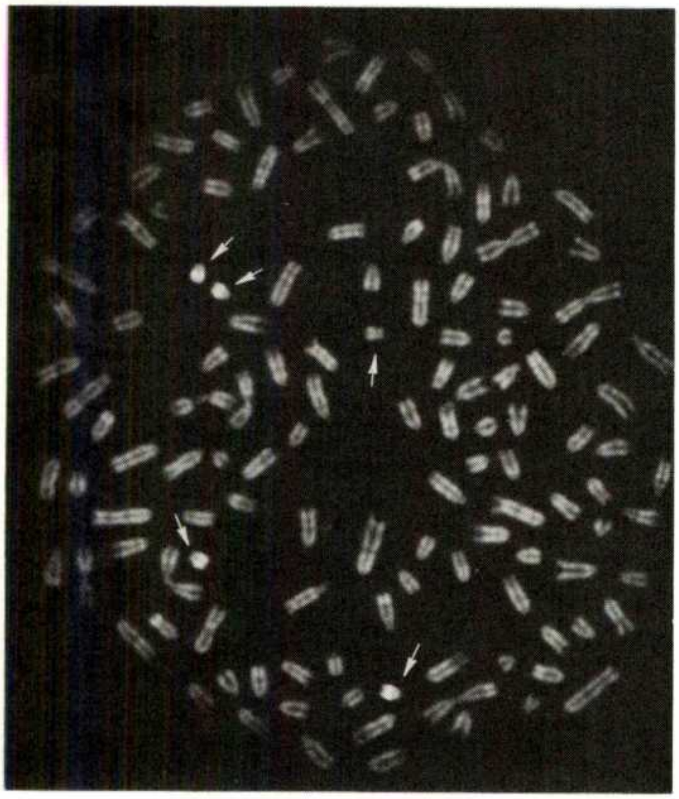

Fig. 1 A metaphase cell from RH-28 in which the human number 17 and four human Y chromosomes are indicated by arrows. The mouse parental line used in the hybridisation experiment was the hypoxanthine-guanine-phosphoribosyltransferase deficient (HPRT⁻) RAG cell line[8]. The other parental cells were unstimulated leukocytes from a human male. The cells were induced to fuse by β-propio-lactone inactivated Sendai virus[9,10]. Hybrids were selected in HAT medium[11]. The isolated hybrids were maintained in MEM medium. Four–six weeks after fusion, cells from 16 hybrids were collected, chromosome preparations made and the chromosomes identified by quinacrine banding patterns[12].

Fig. 3 Distribution of human Y chromosomes in cells from nine subclones of hybrid RH-28. The mean number per cell of human Y chromosomes and the mean number per cell of mouse chromosomes ( ) is included for each subclone.

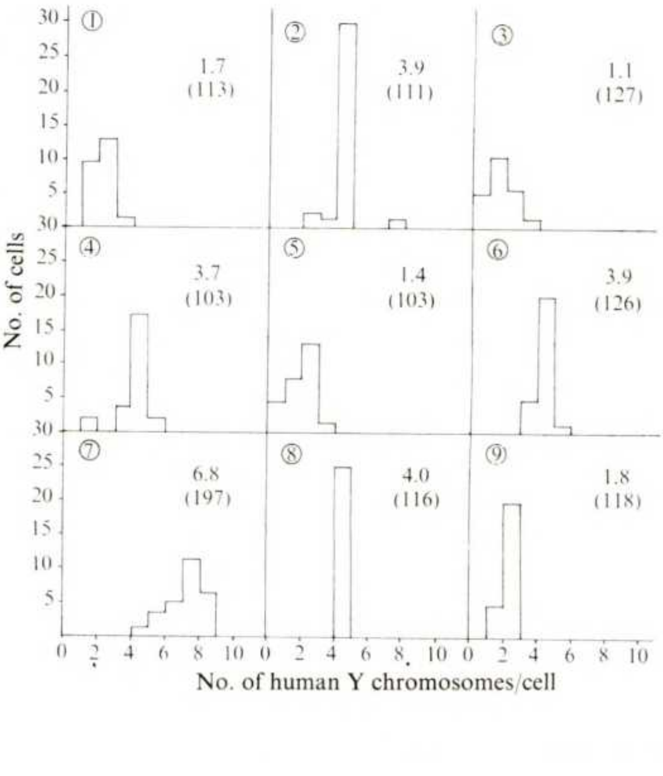

and 9, 85 of 97 cells scored had only one or two Y chromosomes. A different situation was found in subclone 7 in which the number of mouse chromosomes doubled and the number of Y chromosomes in the majority of cells scored was between six and eight per cell. This subclone was stable over a period of at least 100 generations with respect to the doubled number of mouse chromosomes and the number of human Ys. In most of the cells of the nine subclones one copy of human chromosome 17 was still present.

If the accumulation of the Y chromosomes in hybrid RH-28 resulted from non-disjunction and selection for multiple Y chromosomes per cell, then the stability of some subclones with four and others with only one or two Y chromosomes indicates that the frequency of non-disjunction and selection has decreased. This phenomenon of accumulation of the Y chromosome may be analogous to the accumulation of B chromosomes in a variety of species[5].

Mittwoch and Kirk[6] showed that in mammals, gonadal cells which contain a Y chromosome grow faster than cells which do not contain a Y. It is tempting to speculate that the selection for cell hybrids with multiple Y chromosomes is due to a faster rate of growth.

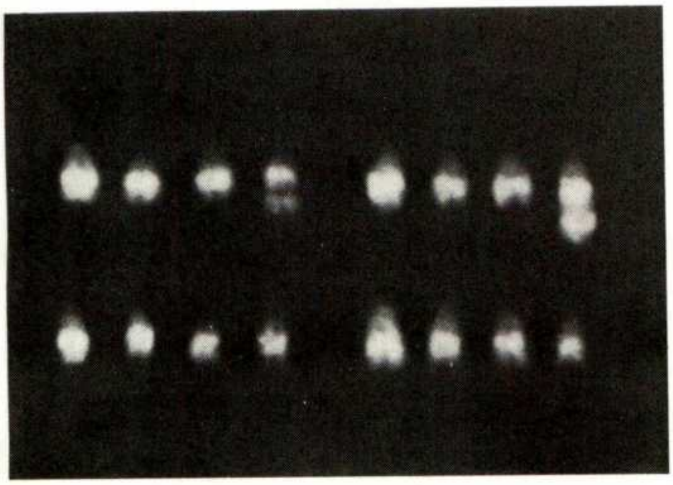

Fig. 4 Upper, human Y chromosomes from two cells of subclone 2. The Y chromosome on the right of each group is longer and has two quinacrine bright bands. Lower, human Y chromosomes from an RH-28 cell and a cell from subclone 6. Several of these Ys have a dull distal region.

In several subclones of the RH-28 hybrid the Y chromosome seemed to have undergone rearrangements which we are now investigating. Thus, in subclone 2 there were usually four Y chromosomes per cell. Three of these seemed to be normal whereas the fourth was almost twice as long and possessed two wide quinacrine bright bands instead of one (Fig. 4). In other cells, some of the Y chromosomes were altered in a different way, having a dull area distal to the bright band (Fig. 4).

The availability of human–mouse hybrid cell lines containing the human Y may enable us to isolate and characterise proteins which are produced by Y linked genes, for example the H–Y antigen[7]. To facilitate this we have already obtained subclones that have lost the only other human chromosome present, number 17, but have retained multiple copies of the Y chromosome.

This research was supported by grants from the National Foundation–March of Dimes and the NIH. M.M. was a visiting assistant professor on an Eleanor Roosevelt International Fellowship Award (American Cancer Society) during the time of this research. We thank Kuo Chueng for technical assistance.

MENASHE MARCUS

Department of Genetics,
Hebrew University of Jerusalem,
Jerusalem, Israel

RAMANA TANTRAVAHI
VAITHILINGAM G. DEV
DOROTHY A. MILLER
ORLANDO J. MILLER

Departments of Human Genetics and Development,
and Obstetrics and Gynecology,
College of Physicians and Surgeons,
Columbia University,
New York, New York 10032

Received April 1; accepted April 26, 1976.

[1] Weiss, M. C., and Green, H., *Proc. natn. Acad. Sci. U.S.A.*, **58**, 1104–1111 (1967).
[2] Ruddle, R. H., *Nature*, **242**, 165–169 (1973).
[3] Jami, J., and Grandchamp, S., *Proc. natn. Acad. Sci. U.S.A.*, **68**, 3097–3101 (1971).
[4] Green, H., Wang, R., Kehinde, O., and Meuth, M., *Nature new Biol.*, **234**, 138–140 (1971).
[5] Jones, R. N., *Int. Rev. Cytol.*, **40**, 1–100 (1975).
[6] Mittwoch, U., and Kirk, D., *Nature*, **257**, 791–792 (1975).
[7] Wachtel, S., *et al.*, *New Engl. J. Med.*, **293**, 1070–1072 (1975).
[8] Klebe, R. J., Chen, T., and Ruddle, F. H., *Proc. natn. Acad. Sci. U.S.A.*, **66**, 1220–1227 (1970).
[9] Neff, J. M., and Enders, J. F., *Proc. Soc. exp. Med.*, **127**, 260–267 (1970).
[10] Miggiano, V., Nabholz, M., and Bodmer, W., *Wistar Inst. Monogr.*, **9**, 61–76 (1967).
[11] Littlefield, J. W., *Science*, **145**, 709–710 (1964).
[12] Miller, D. A., *et al.*, *Cell*, **1**, 167–173 (1974).

Chromosomal proteins regulate steroid binding to chromatin

STEROID hormones accumulate in their respective target cells due to the presence of "receptor" proteins which bind the steroid with high affinity and specificity[1–4]. It seems that the steroid–receptor complexes then migrate and bind to nuclear chromatin[2–5]. Within about 15 min there is an alteration in transcription which is followed after 2 h by the appearance of specific messenger RNAs[6–9]. At present, the mechanism by which steroids alter gene expression is obscure. The group in our laboratory is attempting to identify the nuclear (or chromatin) component which binds the progesterone–receptor (P–R) complex because it is possible that the macromolecules involved are also involved in the steroid-induced modifications of gene expression. We have demonstrated recently more than one class of binding sites in chick oviduct nuclei *in vivo* and in hen oviduct nuclei and chromatin *in vitro*[10–12,13]. The highest affinity class of sites, representing 5,000–10,000 sites per cell nucleus, is suspected to be the biologically important class, because: (1) it is the only class which binds P–R *in vitro* in physiological ionic conditions (0.15–0.20 M KCl); (2) it is the only class bound *in vivo* when the steroid is at physiological levels in the serum; (3) binding to whole chromatin is tissue-specific, found only in oviduct chromatin, and (4) when these sites are saturated *in vivo* with the P–R, maximal responses of the RNA polymerase I and II activities are observed *in vitro*. Although additional nuclear binding to the sites of weaker affinity can be achieved *in vivo*, this causes no further alteration of polymerase activities[13]. We have also found that the low ionic conditions (0.01–0.05 M KCl), often used in binding assays, result in a pattern of nuclear binding which is non-saturable and shows no tissue specificity. When the ionic strength of the binding assays is increased to 0.15 M or 0.2 M KCl, there is a saturable, tissue-specific binding which measures selectively only the highest affinity class of binding sites[10–12]. We now present evidence which suggests that one fraction of the non-histone protein (NHP) (called AP_3) is involved in the high affinity binding of P–R to the chromatin of the progesterone target tissue—oviduct—while other fractions (AP_1 or AP_2) are involved in masking these binding sites. We also present data which indicate that the high affinity binding sites are present but completely masked in non-target tissues.

Figure 1 shows high affinity binding (that is, binding assayed in 0.15–0.2 M KCl) of P–R to hen oviduct nuclei and chromatin *in vitro*. The same high affinity binding to chick oviduct nuclei *in vivo* is shown for comparison. When the histones were removed, the *in vitro* binding was only slightly greater than that of whole chromatin. But when the acidic protein fractions AP_1 and AP_2 were also removed, the level of the high affinity binding to the oviduct material was enhanced four to fivefold. Finally, the removal of the remaining NHP (representing the AP_3 fraction) resulted in a loss of practically all high affinity binding. These results strongly support a role of NHP both in constituting part of the high affinity sites and in the masking of these sites in the oviduct (target tissue) nucleus. If the dissociated proteins were reconstituted back to the DNA, the high affinity sites were not only reinstated in the reconstituted hen oviduct chromatin but also at the same relative levels as the untreated hen oviduct chromatin, that is, the high affinity sites as well as the masking were restored. This ability to restore the native levels of binding to reconstituted chromatins was demonstrated previously with chick oviduct[14,15].

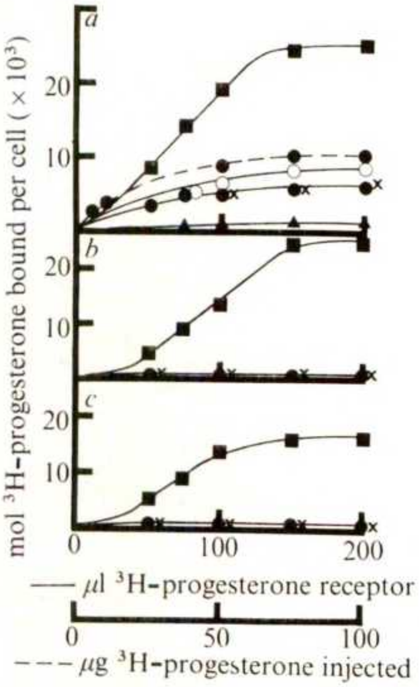

Fig. 1 Binding of ^{3}H-progesterone to high affinity sites in the nuclear material of oviduct (*a*), spleen (*b*) and erythrocytes (*c*) of the chicken. – – –, Binding to nuclei of the chick oviduct *in vivo* as described elsewhere[13]; ——, binding *in vitro* using isolated nuclear components and ^{3}H-progesterone–receptor complex as described elsewhere[11,12]. The *in vitro* binding to the soluble DNA–protein complexes was performed using streptomycin to precipitate the protein–DNA complexes, bound with the ^{3}H-progesterone–receptor complex, or using protein–DNA complexes attached to cellulose as described elsewhere[10]. High affinity binding *in vitro* was assayed under 0.15 M KCl using 0–200 μl of labelled receptor and 50 μg of DNA (as chromatin or protein–DNA complex). The removal of total histones as well as AP_1, AP_2 or total protein has been described elsewhere[2,12,14,15]. The efficiency of removing these fractions from chromatin DNA and the integrity of the nuclear components were assayed by polyacrylamide gel electrophoresis and quantitation of the protein: DNA using the Lowry[18] and diphenylamine[19] methods. The ^{3}H-progesterone–receptor complex was isolated, partially purified and assayed for its integrity as described elsewhere[11]. The symbols represent binding to: ●, isolated nuclei; ×, whole chromatin; ○, chromatin deficient in histone; ■, chromatin deficient in histone, AP_1, AP_2, and ▲, chromatin deficient in total protein (pure DNA). The number of molecules of ^{3}H-progesterone bound per cell was calculated using the specific activity of the steroid (47 Ci mmol^{-1} for the stock solution), 2.5×10^{-12} g DNA per diploid cell of the hen organs[20], and 26% counting efficiency. The 10,000 molecules bound per cell represents 180,000 c.p.m. per mg of DNA or 9,000 c.p.m. per assay (50 μg DNA).

Table 1 Extent of masking of high affinity sites

Source	Level of binding at saturation (molecules per cell)	% Total sites masked
Oviduct nuclei *in vivo*	10,600	58
Oviduct nuclei *in vitro*	5,951	76
Oviduct chromatin	7,441	71
Oviduct chromatin –histone	9,278	53
Oviduct chromatin –histone –AP_1, AP_2	25,290	0
DNA	2,055	—
Spleen nuclei	60	100
Spleen chromatin	48	100
Spleen chromatin –histone –AP_1, AP_2	24,106	0
Erythrocyte nuclei	357	98
Erythrocyte chromatin	416	97
Erythrocyte chromatin –histone –AP_1, AP_2	15,018	0

These data were taken from values in Fig. 1. The number of binding sites measured in each of the chromatin–histone AP_1, AP_2 preparations was assumed to represent the total sites in the respective chromatin and thus each of these preparations was assigned a 0% masking. The values at saturation for each preparation were taken at 100 μg of injected hormone for the *in vivo* binding and at 200 μl of labelled receptor preparation for the *in vitro* binding. The preparations of the nuclear components as well as the hormone binding assays were performed as described in the legend of Fig. 1.

It is interesting that the nuclei and chromatin of non-target tissues (hen spleen and erythrocyte) showed little high affinity binding (Fig. 1). The removal of histones and NHP fractions AP_1 and AP_2, however, resulted in a level of binding approximating that of the target tissue (hen oviduct). Thus, although the non-target tissues showed none or a few nuclear high affinity sites, these sites were present but completely masked by protein (Table 1). Assuming that all acceptor sites were unmasked in the chromatins devoid of histones, AP_1 and AP_2, the *in vivo* binding to chick oviduct nuclei showed 58% masking. The *in vitro* binding to hen oviduct nuclei/chromatin exhibited about a 60 to 80% masking while that to hen spleen or erythrocyte nuclei/chromatin showed essentially 100% masking.

The biological need for an apparent distribution of high affinity binding sites throughout the animal and the masking of them remains obscure. It would be interesting to assess whether or not the extent of masking varies under normal biological influences. Along these lines, Chatkoff and Julian[16] reported that progesterone treatment of ovariectomised rabbits caused an increase in the binding of oestrogen–receptor complex *in vitro* to uterine nuclei. Similarly, Spelsberg *et al.*[17] found that the levels of binding of the progesterone–receptor complex to oviduct nuclei *in vitro* varied during the oestrogen-induced development of the chick oviduct. Both these studies involved the high affinity sites described here because physiological ionic conditions were used in binding assays. The question arises whether or not transformed cells in culture or in mammary tumours which contain steroid receptors but which do not respond to the steroids, have masked nuclear "acceptor" sites. Thus, these cells may be unresponsive since the genome cannot bind the steroid–receptor complexes.

We thank Patti Midthun, Barbara Gosse, Brad Syverson and Paul Matthai for help and the NIH, the NCI and the Mayo Foundation for financial assistance.

THOMAS C. SPELSBERG*
ROBERT A. WEBSTER
GEORGE M. PIKLER

Department of Molecular Medicine,
Mayo Clinic and Graduate School of Medicine,
Rochester, Minnesota 55901

Received March 22; accepted May 4, 1976.

* To whom correspondence should be sent.

[1] Raspe, G. (ed.), *Advances in Biosciences*, 7 (Pergamon, New York, 1971).
[2] Spelsberg, T. C., in *Acidic Proteins of the Nucleus* (edit. by Cameron, I. L., and Jeter, P. R. Jr), 248–296 (Academic, New York, 1974).
[3] Jensen, E. V., and DeSombre, E. R., *A. Rev. Biochem.*, **41**, 203–230 (1972).
[4] O'Malley, B. W., and Means, A. R., *Science*, **183**, 610–620 (1974).
[5] Pasqualini, J. R. (ed.), *Receptors and Mechanisms of Action of Steroid Hormones* (Dekker, New York, 1976).
[6] Glasser, S. R., Chytil, F., and Spelsberg, T. C., *Biochem. J.*, **130**, 947–957 (1972).
[7] Chan, L., Means, A. R., and O'Malley, B. W., *Proc. natn. Acad. Sci. U.S.A.*, **70**, 1870–1874 (1973).
[8] Cox, R. F., Haines, M. E., and Emtage, J. S., *Eur. J. Biochem.*, **49**, 225–236 (1974).
[9] Schimke, R. T., McKnight, G. S., and Shapiro, D. J., in *Biochemical Actions of Hormones*, **3** (edit. by Litwack, G.), 245–269 (Academic, New York, 1975).
[10] Spelsberg, T. C., Webster, R. A., and Pikler, G. M., in *Chromosomal Proteins and Their Role in Gene Expression* (edit. by Stein, G., and Kleinsmith, L.), 153–186 (Academic, New York, 1975).
[11] Pikler, G. M., Webster, R. A., and Spelsberg, T. C., *Biochem. J.* (in the press).
[12] Webster, R. A., Pikler, G. M., and Spelsberg, T. C., *Biochem. J.* (in the press).
[13] Spelsberg, T. C., *Biochem. J.*, (in the press).
[14] Spelsberg, T. C., Steggles, A. W., and O'Malley, B. W., *J. biol. Chem.*, **246**, 4188–4197 (1974).
[15] Spelsberg, T. C., Steggles, A. W., Chytil, F., and O'Malley, B. W., *J. biol. Chem.*, **247**, 1369–1374 (1972).
[16] Chatkoff, M. L., and Julian, J. A., *Biochem. biophys. Res. Commun.*, **51**, 1015–1022 (1973).
[17] Spelsberg, T. C., Steggles, A. W., and O'Malley, B. W., *Biochim. biophys. Acta*, **254**, 129–134 (1971).
[18] Lowry, O. H., Rosebrough, N. J., Farr, A. L., and Randall, R. J., *J. biol. Chem.*, **193**, 265–275 (1951).
[19] Burton, K., *Biochem. J.*, **62**, 315–323 (1956).
[20] Sober, H. A., *Handbook of Biochemistry*, 11–111 (Chemical Rubber Co., Cleveland, 1970).

Effect of maternal age on intercellular adhesion of embryonic chick liver cells

In appropriate conditions single cells obtained by dissociation of embryonic tissues form organised cell masses resembling tissues. We wish to present results indicating that the adhesive properties of chick embryonic cells depend on maternal age. These unexpected observations were made in studies on the mechanism of intercellular adhesion. The formation of initial aggregates between chick embryonic liver cells is a two-step process[1]; cells rapidly and reversibly bind to each other to form aggregates in a step that is not inhibited by metabolic poisons. The reversibly bound cells are then converted into stably bound cells in a process requiring metabolic energy.

Current studies are concerned with the formation of stable bonds between chick embryonic liver cells. The formation of such bonds was stimulated by the addition of L-ascorbic acid and L-glutamine (or D-glucosamine); these compounds promoted the adhesion of more single cells, and the resulting aggregates were larger and appeared more compact. As shown here, however, this stimulation depended on the age of the hen from which the embryo was derived.

The addition of ascorbate and glutamine to single cells derived from the embryos of younger hens (about 20 weeks old) increased the number of cells in aggregates after 40 min by 30–50% (Fig. 1). In contrast, the aggregation of cells derived from older hens (about 40 weeks) was not altered significantly by ascorbate and glutamine. The mechanism of action of ascorbate and glutamine is being studied and the results will be presented elsewhere.

Eggs from White Leghorn chickens (Truslow Farms, Maryland) and suspensions of liver cells from 12-d-old embryos were prepared by a modified method of Howard *et al.*[2]. The cells, suspended in Earle's salt medium, were incubated on a rotary shaker (about 3×10^5 cells in 0.3 ml) and allowed to aggregate as described before[1]. The rate at which single cells formed aggregates was determined with a Coulter electronic particle counter[3]. Only single cells were counted, so that the number of single cells remaining in suspension decreased as aggregation proceeded. The decrease in single cells was an accurate measure of cell aggregation.

In a typical experiment with embryos from younger hens (27 weeks) 50% of the cells aggregated in 40 min. The addition of ascorbate and glutamine increased the extent of aggregation to about 75% (Fig. 1). When embryos from older hens (35 weeks) were used as a source of cells, however, no stimulation was obtained after addition of ascorbate and glutamine (Fig. 1).

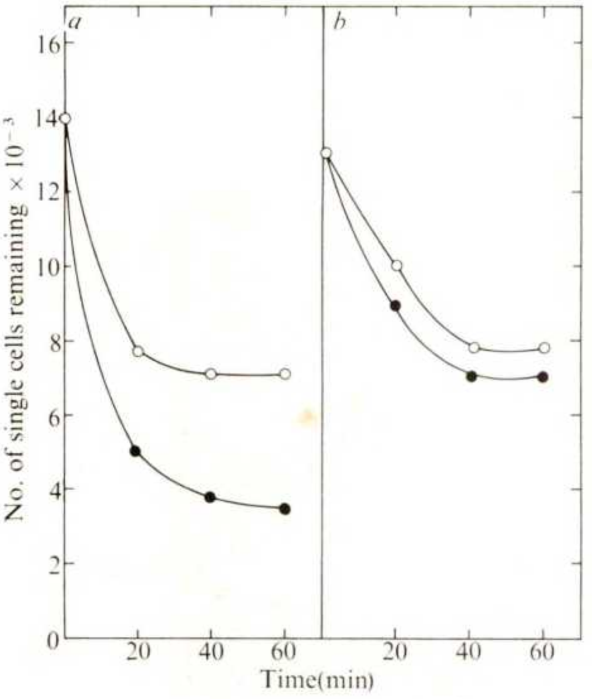

Fig. 1 Stimulation of liver cell aggregation by ascorbate and glutamine. Liver cells (2.9×10^5 cells, 0.3 ml) were allowed to aggregate at 37 °C in a rotary shaker in standard conditions[1] in the presence or absence of ascorbate (0.6 mg ml^{-1}) and glutamine (2.7 mM). After incubation, cells were diluted with 10 ml of cold balanced salts solution and the single cells remaining (after dissociation of the reversibly bound cells) were counted. The data presented are not multiplied by the constant dilution factor. *a*, Liver cells of embryos derived from younger hens (27 weeks) were incubated without additions (○) or with ascorbate and glutamine (●). *b*, Liver cells of embryos derived from older hens (35 weeks) were incubated without additions (○) or with ascorbate and glutamine (●).

The stimulation obtained by adding ascorbate and glutamine varied with the age of the laying hens (Fig. 2). This dependence on maternal age was observed with five different flocks of hens, and when 9- or 10-d-old embryos were used instead of 12-d-old hens. It was not influenced by the season of the year, indicating that the phenomenon was not affected by light–dark cycles nor moderate changes in temperature. The chickens were fed on an 18% protein breeder's mash without antibiotics, but with adequate vitamin C.

The livers of embryos from younger hens were also more readily dissociated into single cells than the livers of embryos from older hens. Not only was a higher yield of cells obtained after collagenase–hyaluronidase treatment of younger hens, but the preparations typically contained 50–80% single cells (the remaining cells were in aggregates of 2–20 cells) whereas livers from the embryos of older hens gave only 10–20% single cells.

Since the single cells were prepared with collagenase and it is well known that ascorbate is involved in the biosynthesis of collagen[4], it seemed possible that both cell yield and response to ascorbate might be related to collagen structure. One aspect of the structure that is important for mechanical stability of collagen fibres is the amount of covalent intermolecular cross linking. Furthermore, the amount of collagen cross linkage is increased with age in many animals[5]. But treatment *in vivo* with β-aminopropionitrile

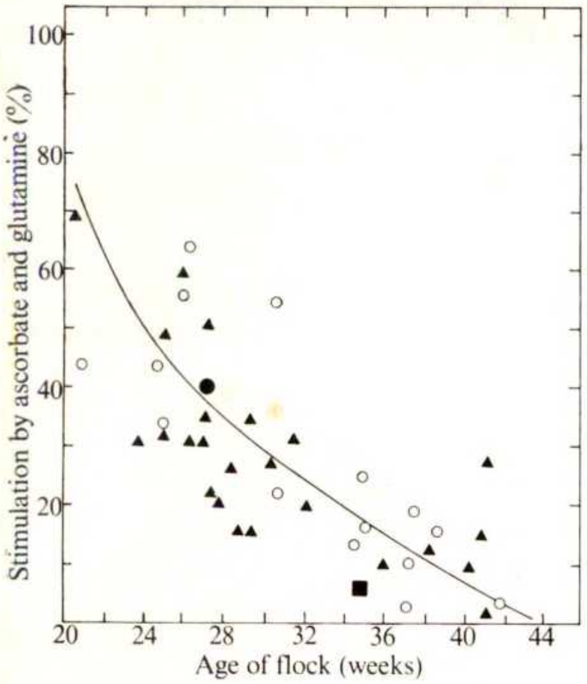

Fig. 2 Effect of maternal age on the stimulation of cell aggregation by ascorbate and glutamine. In each experiment about 3 × 10^6 liver cells were incubated in 0.3 ml of balanced salts solution on a rotary shaker at 37 °C. After 40 min, the samples were diluted with 10 ml of cold balanced salts solution and the number of single cells remaining was determined. To some of the vials L-ascorbate (0.7 mg ml^{-1}) and L-glutamine (27 mM) were added. The data presented here were obtained from two different flocks of chickens, one started in March (○) and one in August (▲). The abscissa indicated the age of the hens (note that efficient egg production began at 20 weeks), and the ordinate the percentage increase in the number of cells stably bound in aggregates caused by the addition of ascorbate and glutamine. The data in Fig. 1*a* were obtained in March and are indicated by ●; the data in Fig. 1*b* were obtained in May and are indicated by ■ in this figure.

(which inhibits cross linking[6,7]) had no effect on the response to ascorbate *in vitro*, suggesting that collagen cross linking was not involved in the age-dependent stimulation of aggregation by ascorbate.

Although the mechanism underlying the observations reported here is unknown, maternal age seems significantly to affect the adhesive properties of embryonic cells *in vitro*. If *in vitro* adhesiveness as measured in these studies reflects *in vivo* histogenesis, the elucidation of the mechanism by which maternal age affects cell adhesion may ultimately shed light on the relationship between birth defects and maternal age.

We thank Dr Björn Öbrink for helpful discussion. These studies were supported by grants and a contract from the NIH and a grant from the American Cancer Society. J. Umbreit was a postdoctoral fellow of the Jane Coffin Childs Memorial Fund for Medical Research and NICHHD.

JAY UMBREIT
SAUL ROSEMAN

Department of Biology and
McCollum-Pratt Institute,
John Hopkins University,
Baltimore, Maryland 21218

Received March 4; accepted May 11, 1976.

[1] Umbreit, J., and Roseman, S., *J. biol. Chem.*, **250**, 9360–9368 (1975).
[2] Howard, R. B., Lee, J. C., and Pesch, L. A., *J. Cell Biol.*, **57**, 642–658 (1973).
[3] Orr, C. W., and Roseman, S., *J. Membr. Biol.*, **1**, 109–124 (1969).
[4] Barnes, M. J., and Kodicek, E., *Vitamins and Hormones*, **30**, 1–43 (1972).
[5] Gross, J., in *Structural Aspects of Aging* (edit. by Bourne, G. H.), 177–195 (Pitman, London, 1961).
[6] Levene, C. I., *J. exp. Med.*, **113**, 795–810 (1961).
[7] Smith, D. J., and Shuster, R. C., *Archs biochem. Biophys.*, **98**, 498–501 (1962).

Limited proliferation of stem cells surviving alkylating agents

HAYFLICK observed that when human foetal tissue was cultivated *in vitro* the cells underwent 50±10 population doublings before death[1]. Whether this phenomenon is a property of all diploid cells in culture and is pertinent to cell renewal systems *in vivo* has been the subject of much discussion. Haematopoietic failure is rarely the cause of death in animal or man, presumably because this cell renewal system has a proliferative capacity which is either unlimited or, if limited, exceeds the life span of a normal animal. The proliferative capacity of the haematopoietic system, if restricted, might become exhausted when stressed by the prolonged use of cytotoxic agents. In these circumstances, significant stem cell division would be necessary to return to the steady state, thereby using much of the stem cell proliferative capacity. We have carried out experiments in mice attempting to simulate the clinical use of chemotherapeutic agents that might result in exhausting the proliferative capacity of haematopoietic stem cells. Two alkylating agents, Busulfan and L-phenylalanine (L-Pam) were investigated. Mice treated with Busulfan and to a lesser extent L-Pam demonstrate permanent damage to the proliferative capacity of surviving stem cells as measured by serial transplantation. Such data may have relevance to the use of these agents in the clinic where there is great interest in such agents to destroy presumed subclinical micrometastases in patients expected to have extended survival.

Using the haematopoietic system of mice, many investigators have attempted to demonstrate premature senescence *in vivo*. This system is useful because serial transplantation of bone marrow can be used as a measure of the proliferative capacity of haematopoietic cells. Further, the spleen colony-forming unit (CFU)[2] facilitates direct measurement of a stem cell population. Siminovitch *et al.*[3] demonstrated a decline in colony-forming ability of haematopoietic cells subjected to serial transplantation into lethally irradiated recipient mice. Metcalf and Moore[4] varied the interval between passages from 14 d to 187 d, and in spite of this increased interval observed progressive decline in CFUs per spleen. In a subsequent experiment, they used 10-d foetal liver and compared its transferability with that of marrow from both young and old mice. Foetal haematopoietic tissue sustained six passage generations, whereas young and old marrow cells survived only three such passages, suggesting that haematopoietic stem cells may have limited divisional capacity with most divisions taking place in the foetal period.

Others[5,6] feel that limited proliferative capacity is not a characteristic of stem cells. With prolonged intervals between passage, the transplanted marrow tends to regain normal CFU levels. No method has been used, however, to distinguish host from donor CFU. When such determinations were made, it was found that with increased number of passages and long intertransplant time, donor cells disappeared and host cells predominated[7].

We used C3H/HeJ male mice treated with Busulfan or L-Pam. The choice of Busulfan was based on the report by Morley and Blake[8] showing that high doses of Busulfan can cause aplastic anaemia in surviving mice. The choice of L-Pam was based on the current clinical use of this drug for two years to treat presumed subclinical micrometastases in patients with seemingly localised breast cancer[9]. We suggest that certain drugs given in low doses might cause enough stem cell depletion and subsequent division to limit the proliferative potential of the haematopoietic stem cell. We used serial transfers as a method of increasing the number of stem cell divisions and thus elicit defects in the

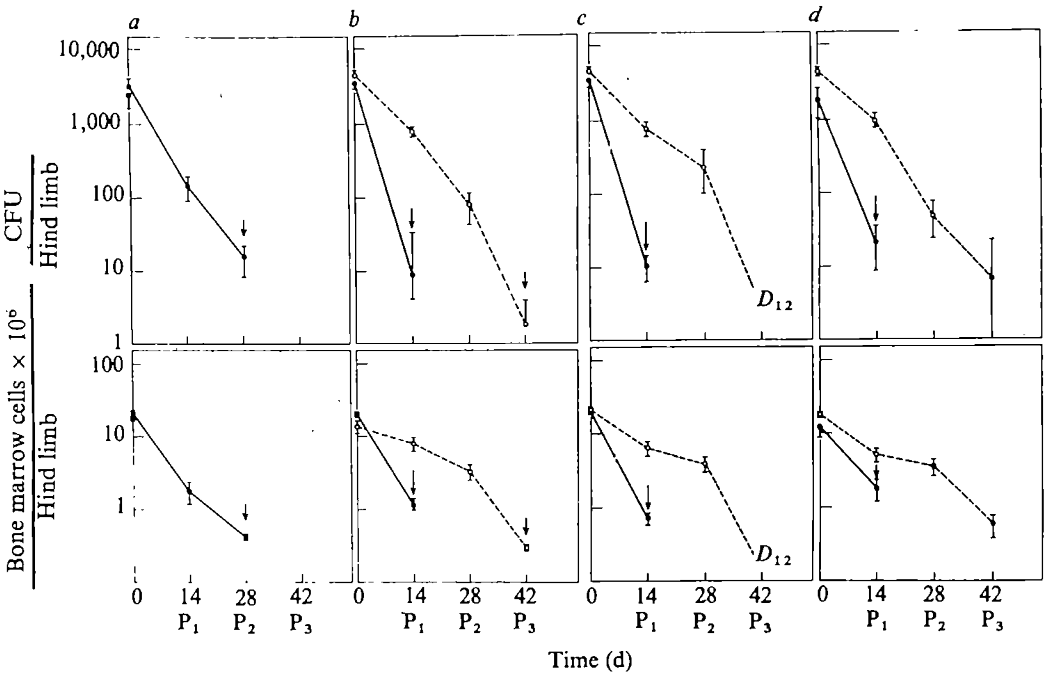

Fig. 1 Comparison of transferability of normal (○)compared with Busulfan-treated marrow (●). Arrow denotes inability to passage further due to insufficient cells. D_{time} denotes date of death of last passaged mouse. *a*, 5; *b*, 10; *c*, 15; *d*, 20 weeks post-drug.

proliferative capacity of the stem cell population that might not otherwise become apparent.

To avoid drug-induced death, drug doses were chosen to correspond to half the LD_{10} (ref. 10) (0.18 mg Busulfan and 0.068 mg L-Pam). These agents were given intraperitonally six times at weekly intervals. A control group was maintained in the same conditions as the experimental group and received weekly injections of the diluent. Peripheral blood counts were carried out weekly on tail vein blood samples of the experimental group during the period of drug administration and once every 2 weeks thereafter. No mouse was bled more than once every 16 weeks. Control mice were bled once every 4 weeks. Five weeks after drug completion, three mice from the control and experimental groups were killed for serial marrow passages into lethally irradiated recipients that received a whole body dose of 1,200 rad in divided doses of 700 and 500 rad separated by 3 h. The transfers were carried out every 5 weeks. One million cells were injected into ten lethally irradiated mice at each passage interval, and 14 d separated each passage. At the time of each passage, marrow cellularity was determined, and ten lethally irradiated mice were injected for spleen colony determinations as described previously[11].

The effect of Busulfan on the ability to passage marrow cells is illustrated in Fig. 1. At 5 weeks after drug administration, the Busulfan marrow could be passaged for 28 d. At 10 weeks, passage was only possible for 14 d, as compared with 42 d for controls. These same patterns continue at 15 and 20 weeks post-drug. Marrow CFU per hindlimb before transfer was normal at 10 weeks, whereas at 15 and 20 weeks it had dropped to less than normal levels. On the other hand, marrow cellularity in the non-passaged state does not fall below normal until 20 weeks post-drug. Peripheral blood counts at all these transfer times (5–20 weeks post-drug) were normal.

The effect of L-Pam on the CFU is not as marked (Fig.

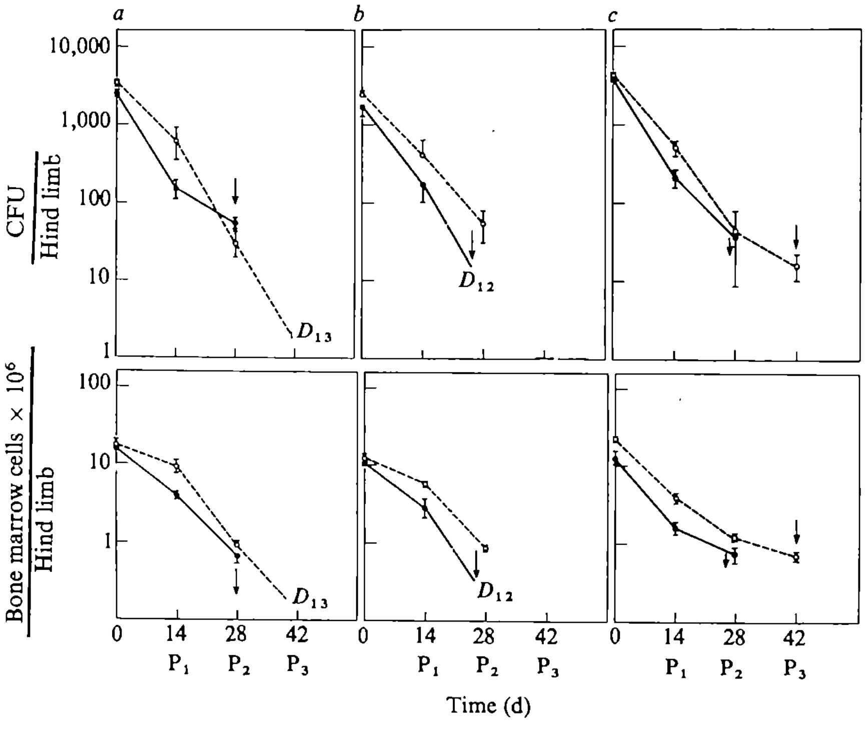

Fig. 2 Comparison of transferability of normal (○) compared with L-Pam-treated marrow (●). Arrow denotes inability to passage further due to insufficient cells. D_{time} denotes date of death of last passaged mouse. *a*, 5; *b*, 10; *c*, 15 weeks post-drug.

2). At all transfer times (5–15 weeks) L-Pam could not be passaged longer than 28 d, whereas control groups were kept in passage for 41 or 42 d. Marrow CFU and cellularity before transfer showed no difference compared with normal controls. The results are not as dramatic as those for Busulfan but are qualitatively similar as regards serial transplantation.

Considerations of seeding efficiency are complex and cannot easily explain the findings since with Busulfan the number of CFUs markedly decreased with each passage compared with control: whereas with L-Pam at 5 and 15 weeks the number of CFUs is similar to the control, but with both drugs there is a difference in serial transfer. There was no difference in spleen colony size between control and experimental groups at any stage of transfer. Detailed microscopic evaluation of the colonies, however, was not carried out.

Our results support the concept of there being limitations on the proliferative capacity of normal cells. Although limitation of proliferative capacity of the haematopoietic stem cell compartment is usually not an important constraint on life span, it may become critical when stressed by a prolonged application of, for example, Busulfan. An alternative but less likely explanation of these data is that the drugs cause the surviving cells to have a longer generation time and thus undergo less proliferation during each passage. This seems unlikely since the CFU number in the L-Pam groups after transfer was not decreased compared with control, although their ability to passage was decreased (28 compared with 42 d). Furthermore, Busulfan-treated mice showed a progressive decrease in passage ability (28 d at 5 weeks and 14 d thereafter), CFUs per hindlimb, and bone marrow cellularity per hindlimb.

Further work is necessary to determine whether marrow failure occurs as a result of these demonstrated defects in proliferative capacity. Although marrow failure may take many months to develop, its occurrence can be expected based on the results of Morley[12]. Experiments using other classes of cytotoxic agents[13] will be carried out to determine whether the stem cell can be spared by the use of such drugs. In the adult mouse and perhaps in man, the stem cells are proliferatively inactive; thus agents affecting only cells in cycle may be useful for destruction of micrometastases without causing significant stem-cell depletion.

We thank M. Ott and H. Grate for assistance. This work was supported by grants from the USPHS.

LESLIE E. BOTNICK

EILEEN C. HANNON

SAMUEL HELLMAN

Harvard Medical School,
Joint Center for Radiation Therapy,
50 Binney Street,
Boston, Massachussetts 02115

Received March 1; accepted May 4, 1976.

[1] Hayflick, L., *Expl Cell Res.*, **37**, 614–636 (1965).
[2] Till, J. E. and McCulloch, E. A., *Radiat. Res.*, **14**, 213–222 (1961).
[3] Siminovitch, L., *et al.*, *J. cell comp. Physiol.*, **64**, 23–31 (1964).
[4] Metcalf, D., and Moore, M. A. S., in *Frontiers of Biology—Haemopoietic Cells* (edit. by Neuberger, A. and Tatum, E. L.), 448–465 (North-Holland, Amsterdam, 1971).
[5] Lajtha, L. G., and Schofield, R., in *Advances in Gerontological Research* (edit. by Strehler, B. K.), 131–146 (Academic, New York, 1971).
[6] Vos, O., and Dolman, M. J. A. S., *Cell Tissue Kinet.*, **5**, 371–385 (1972).
[7] Micklem, H. S., *et al.*, in *Haemopoietic Stem Cells—Ciba Foundation Symposium*, 13, 285–301 (Elsevier, Amsterdam (1973).
[8] Morley, A., and Blake, J., *Blood*, **44**, 49–56 (1974).
[9] Fisher, B., *et al.*, *New Engl. J. Med.*, **292**, 117–122 (1975).
[10] Freirich, E. J., *et al.*, *Can. Chemother. Rep.*, **50**, 219–244 (1966).
[11] Hellman, S., and Grate, H., *J. exp. Med.*, **127**, 605–612 (1968).
[12] Morley, A., and Blake, J., *Blood*, **44**, 49–56 (1974).
[13] Bruce, W. R., *et al.*, *J. natn. Cancer Inst.*, **37**, 233–245 (1966).

Transformation of the β_2 adrenoceptor in normal rat liver into a β_1 type in Zajdela hepatoma

IN a large variety of tissues, malignant transformation is accompanied by changes in the cyclic AMP system[1]: adenylate cyclase may be functionally absent or modified, while various quantitative alterations of hormonal membrane receptors may also occur[2]. In liver, although the cyclase response to various activators may differ from one type of tumour to another[3] as well as during the process of carcinogenesis itself[4,5], an enhanced response to catecholamines is generally observed[4,6]. Here we describe gross modifications of the adenylate cyclase system in Zajdela ascites hepatoma cell line. Among these modifications is a hitherto undescribed qualitative alteration of the adrenoceptor.

Zajdela hepatoma, which was studied in the present work together with normal liver, was originally derived from parenchymal liver cells after chronic administration of dimethylaminoazobenzene[7]. It retains certain characteristics of the original cell[7] and, for example, it can resynthesise glycogen in certain culture conditions[8]; thus it can be justifiably compared with normal liver[9,10,11]. The animals used in this study were female, albino Wistar rats (~200 g body weight). A particulate fraction was prepared from normal liver by disruption with a Dounce homogeniser in 5 volumes (v/w) of 1 mM $NaHCO_3$. After two washing steps, which were performed by centrifugation at 2,000*g* for 10 min at 4 °C, the plasma membrane-enriched pellets were resuspended in the same $NaHCO_3$ solution (2 ml per g of liver). The corresponding fraction from Zajdela hepatoma was prepared from 20–50 ml of ascites fluid. Tumour cells were freed from contaminating erythrocytes by several washes in 0.2% NaCl. They were subsequently lysed in 1 mM $NaHCO_3$ for 10 min at 4 °C and the particulate fraction prepared as described for normal liver. As shown in Table 1, the cyclases from these two preparations had quite different activities in the absence as well as in the presence of stimulating agents. In the hepatoma, basal activity was ten times lower than in normal liver and hormonal responsiveness was altered in many ways. The effect of glucagon was detected only when its concentration was higher than 1 μM, which corresponded to a supramaximal concentration in

Table 1 Adenylate cyclase activity of Zajdela hepatoma and normal liver

		Adenylate cyclase activity (pmol per mg protein per 10 min) Normal liver	Zajdela hepatoma
Basal		95 ± 4	9.8 ± 0.5
+ adrenaline	(50 μM)	139 ± 6	170 ± 6
+ Glucagon	(1 μM)	1,300 ± 30	17.1 ± 0.6
+ NaF	(10 mM)	1,010 ± 16	196.4 ± 4.5
+ GTP	(0,1 mM)	198 ± 25	9.2 ± 0.4
+ GTP + Adrenaline		340 ± 30	162 ± 5

Adenylate cyclase activity was measured as described previously[12]. The assay medium contained 0.5 mM α-^{32}P-ATP (10^6 c.p.m.), 3 mM $MgCl_2$, 1 mM EDTA, 1 mM cyclic AMP, 50 mM Tris-HCl, *p*H 7.6, an ATP-regenerating system (consisting of 25 mM phosphocreatine and creatine phosphokinase (1 mg ml^{-1}) and the enzyme fraction (100–200 μg protein per assay) in a final volume of 60 μl. Incubation was initiated by the addition of the enzyme preparation and was performed for 10 min at 30 °C. Reactions were terminated according to White[13]. Protein was estimated by Lowry's procedure using bovine serum albumin as standard. Results are expressed in nmol of cyclic AMP formed in 10 min per mg of protein at 30 °C. Data represent the means ± s.e. of 3 experiments in which each point was assayed in triplicate. The mean responses differ from the basal activity with $P < 0.01$. It should be noted that the liver cyclase activated by catecholamines was completely inhibited by propranolol, a specific β antagonist. Addition of α-adrenergic blockers such as phentolamine or phenoxybenzamine did not alter the cyclase activity. α agonists such as oxymethazoline were completely ineffective (data not shown).

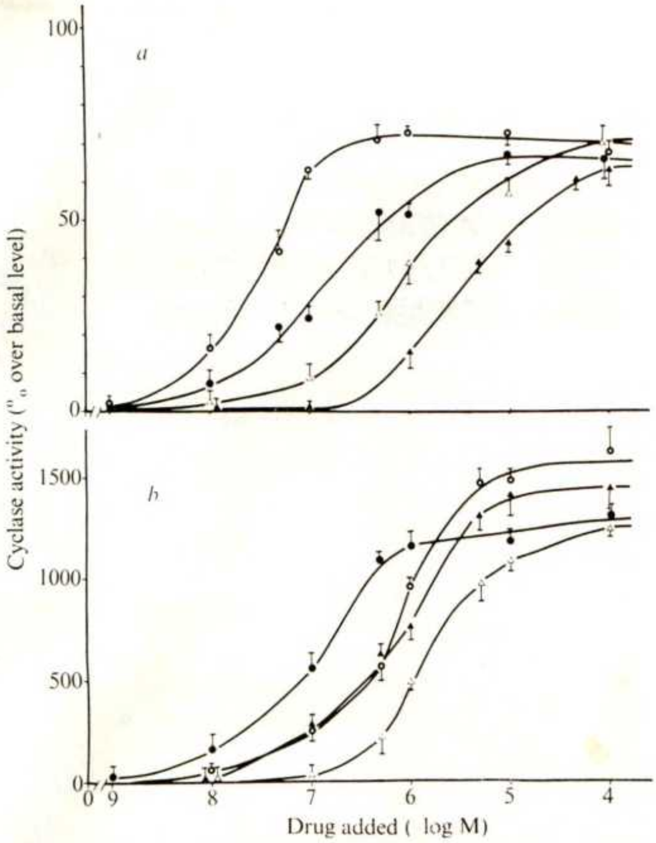

Fig. 1 Effect of various catecholamine agonists on cyclase activity. The enzyme preparations from normal liver (*a*) and from Zajdela hepatoma (*b*) were incubated as described in the legend to Table 1 and in the presence of varying concentrations of protokylol (○), isoproterenol (●), adrenaline (△) or noradrenaline (▲). The cyclase activity is expressed as percentage increase over the basal level (basal values are respectively 95 ± 4 and 9.8 ± 0.5 pmol cyclic AMP formed in 10 min per mg of protein in normal liver and in Zajdela hepatoma). Values represent the mean of three determinations; the standard errors are indicated by the bars. The apparent K_ms determined from this experiment and from two others are shown in Table 2.

normal liver[14]. In contrast, addition *in vitro* of 50 μM adrenaline effected a fifteenfold increase in the basal activity as compared to a twofold increase in normal liver. No synergistic effect of GTP could be observed in the present study (Table 1) although such an effect is a well known phenomenon in normal liver[12,15]. Guanylyl imidodiphosphate, an analogue of GTP which is not a substrate for nucleotidases, was also ineffective, even at high concentration (0.1 mM). The relative fluoride response was, however, present in Zajdela hepatoma and even enhanced as compared to normal liver. These phenomena (that is, low basal activity, and lack of effect of guanyl nucleotides), are probably indicative of marked changes in the catalytic component of the cyclase system. These changes are associated with a drastic alteration in the nature of glucagon binding or in its efficiency.

In view of the unusual character of cyclase stimulation by adrenaline in Zajdela hepatoma, its mechanism was further studied. The effects of various agonists were tested in a dose–response fashion and each experiment was repeated at least three times with different cyclase preparations from the normal liver and Zadjela hepatoma. In normal liver, the relative order of potency of the various agonists tested was the following: protokylol>isoproterenol>adrenaline>noradrenaline (Fig. 1*a*). This corresponds to a typical β_2 receptor[16,17,18]; we obtained similar results with a purified plasma membranes preparation (unpublished data). It should be noted that protokylol (an analogue of isoproterenol characterised by a more hydrophobic substitution on the amino nitrogen), had an apparent K_m of 30 nM, and is the best β_2 agonist available in terms of affinity for the receptor. Similar results with this compound were reported previously by Rosen *et al.*[19] for the β_2 receptor of frog erythrocytes. In Zajdela hepatoma cells (Fig. 1*b*), the order of relative potency of the various agonists was quite different: isoproterenol>protokylol>noradrenaline>adrenaline; while the affinity of isoproterenol was not modified, adrenaline became less potent than noradrenaline and protokylol less than isoproterenol. This corresponds to a β_1 receptor[16,17]. The apparent K_m values for the various agonists were calculated in three different experiments and are listed in Table 2. The relative potency ratio (apparent K_m noradrenaline/apparent K_m adrenaline) was 4.8 for normal liver and 0.56 for Zajdela hepatoma. These ratios are similar to those reported by Burges and Blackburn for rat lung (β_2 receptor) and rat heart (β_1 receptor), namely 6.2 and 0.6 respectively[17]. In addition, we tested the effect of (−)-nordefrine, a relatively specific β_1 agonist[16]. Its apparent K_m was 5 μM in normal liver and 1 μM in Zajdela hepatoma. These values are similar to those found with noradrenaline (4.3 μM and 1.3 μM respectively). To confirm this observation, further experiments were performed using specific antagonists. Their effect on adenylate cyclase was determined in the presence of a concentration of isoproterenol (1 μM) which resulted in a submaximal response. We used butoxamine as a β_2 inhibitor[20] and practolol as a β_1 inhibitor[21]. In normal liver, the isoproterenol-stimulated cyclase was blocked by 0.1 mM butoxamine, whereas practolol, at the same concentration, was completely ineffective. In contrast, in Zajdela hepatoma, 10 μM practolol inhibited cyclase activity by more than 75%, whereas butoxamine was only slightly active at the same concentration.

It would seem, therefore, that in our system, malignant transformation not only provokes quantitative changes in the adenylate cyclase system, but is accompanied by a unique and hitherto undescribed qualitative change, namely the switch of the adrenoceptor from the normal β_2 type to the β_1 type. It should be noted that in the ascites hepatoma, the cyclase did not respond to unusual or inappropriate stimulating agents (for example, ACTH, dopamine, adenosine, serotonine). It is possible that the two different types of receptors coexist in liver and that the shift from a β_2 to a β_1 type corresponds to a change in the β_1/β_2 ratio. However, we favour the hypothesis that the catecholamine β

Table 2 Action of catecholamines on adenylate cyclase activity in normal liver and in Zajdela hepatoma

Agonist	Normal liver	Zadjela hepatoma
	Apparent K_m	
Protokylol	0.02 (0.03; 0.015; 0.015)	1.6 (2.5; 1.0; 1.3)
Isoproterenol	0.18 (0.20; 0.15; 0.20)	0.20 (0.37; 0.13; 0.17)
Adrenaline	0.9 (0.9; 1.0; 0.8)	2.3 (3.0; 1.6; 2.5)
Noradrenaline	4.3 (5.0; 5.0; 3.0)	1.3 (1.8; 1.0; 1.2)
	Relative potency	
Protokylol/isoproterenol	0.11	8
Noradrenaline/adrenaline	4.8	0.56

The apparent K_m is the concentration of agonist required to produce half maximal stimulation of adenylate cyclase. Results are the means of values from three experiments which were performed in a manner similar to that shown in Fig. 1; individual values are given in parentheses. Relative potency refers to the ratio of the apparent K_m of protokylol to that of isoproterenol, and of noradrenaline to that of adrenaline.

receptor constitutes a single entity susceptible to secondary, and possibly to reversible modification towards either type. Our results are the first demonstration of such a shift and seem consistent with recent data indicating a transformation between α and β receptors in certain physiological conditions[22,23].

This work was supported by the Institut National de la Santé et de la Recherche Médicale, the Délégation Générale à la Recherche Scientifique et Technique, and by the Fondation pour la Recherche Médicale.

MARIE-LISE LACOMBE
EMMANUEL RENE
GEORGES GUELLAEN
JACQUES HANOUNE

Unité de Recherches INSERM U-99,
Hôpital Henri Mondor,
94010 Creteil, France

Received February 3; accepted May 6, 1976.

[1] Pastan, I. H., Johnson, G. S., and Anderson, W. B., *A. Rev. Biochem.*, **44**, 491–522 (1975).

[2] Chlapowski, F. J., Kelly, L. A., and Butcher, R. W., in *Advances in Cyclic Nucleotide Research*, **6** (edit. by Greengard, D. P., and Robison, G. A.), 245–338 (Raven, New York, 1975).

[3] Butcher, F. R., Scott, D. F., Potter, V. R., and Morris, H. P., *Cancer Res.*, **32**, 2135–2140 (1972).

[4] Boyd, H., Louis, C. J., and Martin, T. J., *Cancer Res.*, **34**, 1720–1725 (1974).

[5] Chayoth, R., Epstein, S. M., and Field, J. B., *Cancer Res.*, **33**, 1970–1974 (1973).

[6] Christoffersen, T., and Berg, T., *Biochim. biophys. Acta*, **381**, 72–77 (1975).

[7] Zajdela, F., in *Colloque Franco-Soviétique: "Quelques problémes posés par la cellule cancéreuse"*, (edit. by the D.G.R.S.T.), 47–76, (Gauthier-Villars, Paris, 1963).

[8] Beck, J. P., and Staedel, C., *10th FEBS Mtg, Paris*, Abstr. 310, (1975).

[9] Mandel, P., Wintzerith, M., Klein-Pete, N., and Mandel, L., *Nature*, **199**, 1000–1001 (1963).

[10] Bhargava, P. M., Szafarz, D., Bornecque, C. A., and Zajdela, F., *J. membr. Biol.*, **22**, 341–356 (1975).

[11] Dievard, J. C., and Bourrillon, R., *Biochim. biophys. Acta*, **345**, 198–212 (1974).

[12] Hanoune, J., Lacombe, M. L., and Pecker, F., *J. biol. Chem.*, **250**, 4569–4574 (1975).

[13] White, A. A. in *Methods in Enzymology*, **38C**, (edit. by Hardman, J. G. and O'Malley, B. W.), 41–46 (Academic, New York, 1974).

[14] Leray, F., Chambaut, A. M., Perrenoud, M. L., and Hanoune, J., *Eur. J. Biochem.*, **38**, 185–192 (1973).

[15] Rodbell, M., Birnbaumer, L., Pohl, S. L., and Krans, H. M. J., *J. biol. Chem.*, **246**, 1877–1882 (1971).

[16] Lands, A. M., Arnold, A., McAuliff, J. P., Luduena, F. P., and Brown, T. G. Jr, *Nature*, **214**, 597–598 (1967).

[17] Burges, R. A., and Blackburn, K. J., *Nature*, **235**, 249–250 (1972).

[18] Lefkowitz, R. J., *Biochem. Pharmac.*, **24**, 583–590 (1975).

[19] Rosen, O. M., Erlichman, J., and Rosen, S. M., *Molec. Pharmac.*, **6**, 524–531 (1970).

[20] Mayer, S. E., *J. Pharmac. exp. Ther.*, **181**, 116–125 (1972).

[21] Murad, F., *Biochim. biophys. Acta*, **304**, 181–187 (1973).

[22] Kunos, G., Vermes-Kunos, I., and Nickerson, M., *Nature*, **250**, 779–781 (1974).

[23] Amer, M. S., and Byrne, J. E., *Nature*, **256**, 421–424 (1975).

Effect of restriction endonucleases on infectivity of Rous sarcoma virus DNA

TRANSFECTION and molecular hybridisation assays show that animal cells infected with RNA tumour viruses carry DNA copies of the viral genome integrated into their chromosomes (for review see ref. 1). The transfection assay in particular enables the direct demonstration of the biological activity of the viral DNA[2–4]. Shearing of the DNA[5] and fractionation in sucrose gradients[6] provided evidence that the virus is specified by DNA pieces of about 6×10^6. Transfection kinetics[5] and transfection probabilities at the endpoint dilution of the DNA[1,7] show that one DNA piece of that size is sufficient to accomplish transfection.

Excision and extraction of the integrated viral DNA from cellular chromosomes requires an enzyme that will digest the cellular but not viral DNA. Such a selective digestion could be accomplished with restriction endonucleases for which there are no cleavage sites in the viral DNA. In this report we show that an enzyme from *Anabaena variabilis* (*Ava*I) satisfies these criteria, for it cleaves the DNA of cells transformed with Rous sarcoma virus (RSV) without abolishing the infectivity of this DNA.

DNA preparations from chicken cells transformed with RSV were used throughout the experiments because their high infectivity affords a reproducible transfection assay[1]. One of these DNAs was extracted from a clone (No. 52) of cells derived (with all probability) from a single chicken embryo fibroblast infected and transformed with a single particle of the Schmidt–Ruppin RSV, subgroup D (SR-D) The origin of the virus and the cells, the cloning procedure and the extraction of the DNA have been described elsewhere[8]. In transfection assays, virtually all of the chicken cell cultures which received 5 μg of this DNA gave rise to a non-defective (*nd*) sarcoma virus (ref. 1 and J.H., and M.H., submitted for publication). Thus the DNA is named *nd*SR-D DNA. The other DNA used was extracted from mass cultures of chicken fibroblasts transformed with the same SR-D virus as before. In contrast to the first DNA, this preparation gave rise, following transfection, to both *nd* and transformation-defective (*td*) viruses[8] and therefore is called *nd,td*SR-D DNA. The dose–response relationships in transfection assays with these two DNA preparations have been described elsewhere[1], where it was also shown that *td* viruses arise uniquely from *td*RSV DNA.

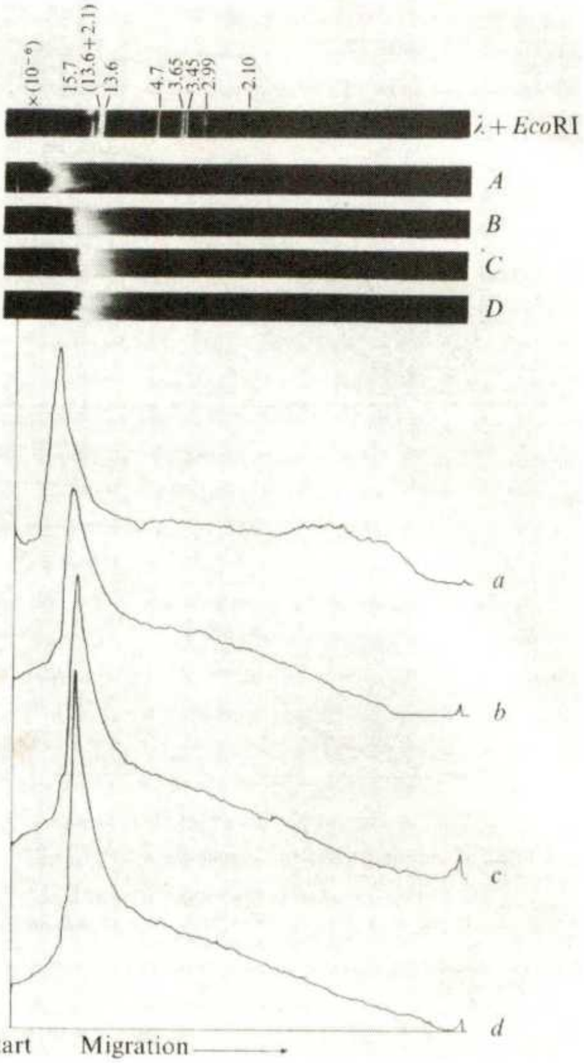

Fig. 1 Electrophoretic migration in 1% Agarose gels of phage λ DNA-*Eco*RI digest (λ+*Eco*RI), *nd,td*SR-D DNA (*A*), and *nd,td*SR-D DNA-*Ava*I digests (*B*, *C*, *D*). The *Eco*RI fragments of phage λ DNA were used as molecular weight markers. The *nd,td*SR-D DNA was either mock-digested for 9 h (*A*), or digested with *Ava*I endonuclease for 3 h (*B*), 6 h (*C*), and 9 h (*D*). The Joyce–Loebl densitometry tracings of *A*, *B*, *C*, and *D* are shown in *a*, *b*, *c*, and *d*, respectively.

The restriction endonucleases used in this study are listed in Table 1. Each enzyme was assayed by incubation with 1.5 μg of phage λ or SV40 DNA at 37 °C. Incubation times and references for the incubation conditions with different enzymes are given in Table 1. The DNA digests

Table 1 Transfection assays with undigested and restriction enzyme digested SR-D DNAs

Experiment	DNA	Restriction endonuclease, time of incubation (h) (ref.)	Transfection efficiency
1	*nd*SR-D DNA	none 16	3*nd*/3*
		*Hin*dII, 16 (14, 15)	0/3
		*Hin*dIII, 16 (15, 16)	0/3
		*Hin*dII+III, 16 (17)	0/3
		*Hae*III, 16 (18, 19)	0/3
		*Hpa*I, 16 (9)	0/3
		*Hpa*II, 16 (9)	0/3
2	*nd,td*SR-D DNA	none, 2.5	3*nd*/3
		*Eco*RI, 2.5 (20)	0/3
3	*nd*SR-D DNA	none, 2.5	2*nd*/3
		*Ava*I, 2.5†	1*nd*/3
		*Ava*II, 2.5†	0/3
4	*nd*SR-D DNA	*Ava*I, 3†	1*nd*/3
5	*nd*SR-D DNA	*Ava*I, 3†	2*nd*/3
	*nd,td*SR-D DNA	none, 3†	3*nd*/3
	*nd,td*SR-D DNA	*Ava*I, 3†	2*nd*+1*td*/3
6	*nd,td*SR-D DNA	none, 9†	3*nd*/3
		*Ava*I, 3†	2*nd*/3
		*Ava*I, 6†	1*nd*/3
		*Ava*I, 9†	1*nd*+1*td*/3

Transfection assays were carried out by means of DEAE–dextran (experiment 1) or calcium phosphate (experiments 2 to 6) in conditions described in refs 8 and 10. Each culture received 5 μg of undigested or digested DNA. The DNAs were extracted from SR-D-transformed chicken cells and consequently contained both the cellular and viral DNA as described in the text. *Eco*RI and *Ava* enzymes were provided by Drs A. Bernardi and G Roizès, respectively The *Haemophilus* enzymes were purified according to the procedure described in ref. 21. Incubation conditions of the DNA with the respective restriction enzymes are given by references in the table.

*Number of transfected (that is, virus producing) cultures per number of DNA-treated cultures The transfected cultures are designed with *nd* or *td* to indicate that the DNA gave rise to a transforming or non-transforming virus, respectively.

†K. Murray, S. G. Hughes, J. S Brown, and S. Bruce, submitted for publication.

vere analysed by electrophoresis in 1% Agarose gels and he resulting bands, were, located under ultraviolet light after staining with ethidium bromide[9].

The DNA (15 μg) extracted from chicken cells transformed with SR-D was mixed with appropriate amounts of the restriction enzymes and incubated in the conditions used for the enzyme assays (see also Table 1), and the reactions stopped by addition of 0.1 volume of 0.1 M EDTA. Then the volume of the mixture was adjusted with 0.14 M NaCl–0.05 M, Tris-HCl, *p*H 7.4, or HEPES-buffered saline solution (NaCl, 8 0 g l^{-1}; KCl, 0.37 g l^{-1}; $Na_2HPO_4.2H_2O$, 0.125 g l^{-1}; dextrose, 0.1 g l^{-1}; *N*-2-hydroxyethylpiperazine-*N*-2-ethane sulphonic acid, 5.0 g l^{-1}, *p*H 7.05) to make 6 ml, and the mixture was distributed into three secondary chicken cell cultures to assay its infectivity by means of the DEAE-dextran[8] or calcium phosphate[10] techniques, respectively. The cultures were kept growing for about 3 weeks (through four to five passages) and examined for the occurrence of transformed cells and, in non-transformed cultures, by reverse transcriptase assay[11] for type C particles in the culture medium.

The results are summarised in Table 1. Of the eight restriction endonucleases, seven rendered the DNA non-infectious. This suggests that RSV DNA contains cleavage sites for the enzymes *Hin*dII, *Hin*dIII, *Hae*III, *Hpa*I, *Hpa*II, *Eco*RI, and *Ava*II. The alternative view that loss of infectivity results from the cleavage of cellular rather than viral DNA sequences is improbable because mechanical shearing of the DNA preparations down to the average size of 6×10^6 daltons does not abolish their infectivity[5-7] and unintegrated viral DNA obtained from mouse cells early after infection with a murine leukaemia virus is infectious[12] though this DNA presumably lacks cellular sequences.

The case of the eighth enzyme, *Ava*I, was different. The electrophoretic analysis (Fig. 1) showed that digestion with *Ava*I gave a continuous distribution of fragments in which no sharp bands were visible, but with a maximum abundance of fragments larger than 20×10^6 daltons (as determined from comparison with migration patterns of phage λ DNA-*Eco*RI digest[13]). It is worth adding that the migration pattern of the 3-h digest was essentially the same as those of 6-h and 9-h digests (Fig. 1). This indicates that virtually all the *Ava*I sites of the DNA were cleaved within 3 h of incubation. In transfection assays (Table 1) the DNA cleaved with *Ava*I repeatedly gave rise to the virus though with a somewhat lower efficiency than that obtained with undigested DNA *A priori* such a difference in transfection efficiency could be attributed to a diminished uptake by recipient cells of DNA molecules of smaller size rather than to the cleavage of certain, but not all, molecules of viral DNA by the *Ava*I restriction enzyme. The possibility of incomplete digestion of the DNA by the enzyme was eliminated in experiment 6 (Table 1) showing that the DNA infectivity resists much longer incubation times than that (3 h) sufficient for exhaustive cleavage (Fig. 1).

Table 1 also shows that both *nd* and *td* viruses were recovered following transfection with *nd,td*SR-D DNA that had been treated with *Ava*I. This hardly surprising observation implies that no *Ava*I cleavage site is formed when a *td* virus DNA is generated from RNA (or less likely (ref. 1 and J.H., and M.H, submitted for publication) DNA) of the non-defective parent.

In conclusion the transfection assays show that cleavage sites for *Hin*dII, *Hin*dIII, *Hae*III, *Hpa*I, *Hpa*II, *Eco*RI, and *Ava*II restriction endonucleases occur within SR-D DNA In contrast, both *nd* and *td* SR-D DNAs lack cleavage sites for *Ava*I endonuclease This offers the means for isolation of fragments of cellular DNA containing the integrated viral DNA and the analysis of cellular DNA sequences adjacent to the integrated viral genome.

The authors thank Dr A. Bernardi for *Eco*RI, and Dr G Roizès for *Ava*I and *Ava*II restriction enzymes. The phage λ DNA was kindly provided by Drs A. Bernardi and P. Tiollais. This work was supported in part by the CNRS and by the University Paris-Sud.

H. KOPECKA

Laboratoire de Génétique Moléculaire,
Institut de Biologie Moléculaire,
Place Jussieu, Paris

J. HILLOVA
M. HILL

Département de Biologie Cellulaire et Moléculaire,
Equipe de Recherche No. 148 du CNRS,
Institut de Caneérologie et d' Immunogénétique,
Villejuif, France

Received March 24, accepted April 30, 1976.

[1] Hill, M., and Hillova, J , *Adv. Cancer Res* 23, 237–297 (1976)
[2] Hill, M., and Hillova, J , *C. r hebd. Séanc. Acad Sci., Paris*, **272**, 3094–3097 (1971)
[3] Hill, M , and Hillova, J., *Nature new Biol* , 237, 35–39 (1972).
[4] Hillova, J., Goubin, G , Coulaud, D., and Hill, M., *J. gen Virol.*, 23, 237–245 (1974).
[5] Cooper, G. M., and Temin, H. M., *J. Virol.*, **14**, 1132–1141 (1974)
[6] Goubin, G., thesis, Univ Paris VI (1976).
[7] Hill, M., Hillova, J., Dantchev, D., Mariage, R , and Goubin, G , *Cold Spring Harb. Symp. quant. Biol.*, 39, 1015–1025 (1974)
[8] Hillova, J , Dantchev, D., Mariage, R , Plichon, M -P., and Hill, M , *Virology*, 62, 197–208 (1974).
[9] Sharp, P A , Sugden, B., and Sambrook, J., *Biochemistry*, 12, 3055–3063 (1973).
[10] Hillova, J., Hill, M., Goubin, G , and Dantchev, D , *Intervirology* 5, 367–374 (1975).
[11] Aaronson, S A , Todaro, G. J., and Scolnick, E. M , *Science*, **174**, 157–159 (1971).
[12] Smotkin, D., Gianni, A M , Rozenblatt, S , and Weinberg, R A , *Proc natn Acad Sci. U.S.A.*, 72, 4910–4913 (1975).
[13] Allet, B., Jeppesen, P. G. N., Katagiri, K. J., and Delius, H , *Nature*, **241**, 120–123 (1973).
[14] Kelly, T. J , and Smith, H. O., *J. molec Biol.*, **51**, 393–409 (1970)
[15] Danna, K., and Nathans, D , *Proc natn. Acad Sci. U.S A.*, 68, 2913–2917 (1971).
[16] Old, R., Murray, K., and Roizès, G , *J. molec Biol* , **92**, 331–339 (1975)
[17] Smith, H , and Wilcox, K. W , *J molec Biol* , **51**, 379–391 (1970).
[18] Middleton, J. H., Edgell, M H., and Hutchison III, C A , *J. Virol.*, 10, 42–50 (1972).
[19] Lebowitz, P., Siegel, W , and Sklar, J , *J. molec Biol.*, **88**, 105–123 (1974).
[20] Yoshimori, R. N,, thesis, Univ. California, San Francisco (1971)
[21] Kopecka, H., *Biochim. biophys Acta*, **391**, 109–120 (1975)

Spontaneous transformation of human skin fibroblasts derived from neoplastic patients

IN the past 15 years a considerable amount of data has been published showing that normal human fibroblasts have a finite division potential when cultured *in vitro*[1,2]. We have described the spontaneous establishment *in vitro* of stromal fibroblasts derived from human lung cancers[3], but it was difficult to know whether the proliferating fibroblasts were normal stromal cells or tumour cells. Therefore we decided to culture the fibroblasts from the skin of patients with lung tumours to see whether they had the same fate *in vitro* Here we describe the spontaneous transformation of skin fibroblasts derived from four neoplastic patients.

Skin biopsies from four cancer patients were obtained from the edge of the marginal wounds at the beginning of the operation. Three of these patients had lung cancer and one had a solitary plasmocytoma of the mediastinum. At the time of the biopsy the patients had not been on chemo- or radiotherapy Tissue samples were cut into small pieces with fine forceps and four to five fragments were placed into 30-ml plastic flasks. Each fragment was covered with a drop of medium and incubated in 90% air : 10% CO_2 at 37 °C. After 24 h, 5 ml of medium was added to each flask. When the fibroblast outgrowth covered the surface of the culture vessels, the cells were detached with a trypsin-versene solution and transferred into two new flasks (1 : 2 split). Cultures were then subcultured routinely with 1 : 2 splits when the cells were confluent. The medium used throughout was Eagle's MEM supplemented with non-essential amino acids, 15% foetal calf serum, penicillin (100 U ml^{-1}) and streptomycin (100 $\mu g\ ml^{-1}$) Control cultures from thoracic skin biopsies of sex-matched but not age-matched normal donors were initiated and continued in the same conditions.

During the first five subcultures the cells from the cancer patients looked like normal fibroblasts disposed in orderly arrays. Between the sixth and the ninth passage, foci of epithelial-like cells began to appear. The latter progressively invaded the cultures, forming a criss-cross pattern with multilayering and random orientation. Cytogenetic analysis, performed at different passages (summarised in Table 1) showed that in all cultures derived from the skin of patients with lung tumours, an abnormal chromosome distribution appeared during the early phases of culture, contrasting with the near normal distribution found in the control skin fibroblasts and in WI-38 cells[4].

The colony-forming capacity in a semi-solid agar medium was also checked[5]. Fibroblasts from normal donors did not form colonies The cells from the patients, however, gave rise to more than 0.5% colonies. The cultures derived from donors with lung tumours were also found to form aggregates in the presence of concanavalin A[6] whereas the control cultures did not. From each culture derived from the patients it was possible to obtain cells which overcame phase III (ref. 1) and became established.

All cultures derived from normal donors went through the normal evolution previously reported[1,2] and died after serial subculture. Finally we should emphasise that when the fibroblasts were derived from skin explants and adapted to *in vitro* culture, and when transformation occurred, our laboratory contained no HeLa cells or other cell lines, which could have been sources of contamination.

Our results show that it is possible to obtain spontaneous transformation in cultures obtained from the skin biopsies

Table 1 Number of mitoses with different sets of chromosomes found in human fibroblasts cultivated from the skin of normal donors and from patients with lung tumours

Donor	Cell culture	Passage* mitoses scored	No. of chromosomes											
			<45	45	46	46–50	50/60	60–70	70–80	80–90	90–92	92–100	>100	>200
Normal Donors	SK-TOR	XIV/50		1	49									
	SK.1	IV/45			45									
	SK. 2	XII/50			50									
	WI 38	XVI/46	2	6	38									
Patients	Falla	I/50	18	14	16						2			
		†VII/50			1		27	5	1	2	2		12	1
	Nico	I/24	5	1	15						2		1	
		II/33	3	2	20		2				4		2	
		III/21	2	5	12		1				1			
		†X/50	4		3	3	31	6			1		1	1
	TAM	VI/50					16	23					11	
		†VI/50			1		9	24		1	1		12	2
	Ziani	Primary/30	5	4	16		2				2		1	
		I/37	8	4	11		7				4		3	
		II/50	14	3	25		2				6			
		†XII/50			1		40	7			1		1	

*Passages at which cytogenetic analysis was made A standard procedure using Colcemid and acetic acid orcein staining was used.
†Number of passages after transformation has occurred.

of patients with lung tumours. Transformation is characterised by an abnormal ploidy, a capacity to form colonies in a semi-solid agar medium, the formation of foci of piling up cells among the monolayers and the acquisition of an infinite life span. For the moment it is impossible to know if the transformed cells originated from skin fibroblasts or from tumour cells disseminated in the skin of the patients.

We thank Dr Alvaro Macieira-Coelho for critical revision of our manuscript.

B. AZZARONE
D. PEDULLÀ
C. A. ROMANZI

Institute of Medical Microbiology,
University of Genoa,
Genoa, Italy

Received August 14, 1975, accepted May 20, 1976

[1] Hayflick, L., *Expl Cell Res.*, 37, 614–624 (1965)
[2] Martin, G. M , Sprague, C A., and Epstein, C. J., *Lab. Invest* , 29, 86–92 (1910)
[3] Azzarone, B., and Pedulla, D , *Proc 6th int Symp Biol. Characterization of Human Tumors* (Excerpta Medica, Amsterdam, in the press)
[4] Chen, T H , and Ruddle, F M , *Proc Soc exp Biol Med* , 147, 533–535 (1974)
[5] McAllister, R. N , Reed, G , and Huebner, R J *J natn Cancer Inst* , 32, 43–53 (1967)
[6] Inbar, M , and Sachs, L., *Proc natn. Acad Sci. U S.A* , 63, 1418–1425 (1969)

Enumeration of specific cytotoxic T cells

EFFORTS directed towards the enumeration of effector cells involved in the cell-mediated immune response have so far met with little success. One of the principal reasons for this failure is the current ignorance of relationships between killer, lymphokine producer and suppressor T cells, all of which have effector functions. To date, attempts at quantification have focused principally on cytolytically active (killer) T cells largely because *in vitro* assays using target cells labelled with radioisotopes afford sensitive and reproducible measurement of their function[1].

Two factors have, however, hampered the enumeration of the killer cells in cytolytically-active lymphoid cell populations: (1) the effector T cell can kill more than one target cell[2,3] and (2) the number of effector cells cannot be distinguished from their intrinsic lytic efficiency. The latter factor is presumably a complex function comprising the mobility of effector cells, their avidity for target cells and their ability to lyse and disengage from targets. Standard assay conditions for *in vitro* cytotoxicity enable comparisons to be made between the lytic activities of different "immune" lymphoid cell populations, but these comparisons may bear little relation to the relative numbers of effector cells if there is wide variation in killing efficiency. We describe here an experimental approach in which efficiency is maximised and the number of cytolytically-active T cells within a lymphocyte population is determined by preventing killer cells from lysing more than one target.

The method was based on two findings: (1) Lymphocyte–target cell interactions take place in the presence of Mg^{2+}, but in the absence of Ca^{2+} these lessions do not lead to cytolysis[4]. (2) Cytochalasin A inhibits cytolysis (irreversibly) and does so by interfering with a stage in the lytic cycle which precedes the Ca^{2+}-dependent event(s). (It seems likely that cytochalasin A inhibits lymphocyte–target cell interactions, as does its congener cytochalasin B (ref. 5), although the validity of this assumption is unnecessary for the arguments which follow.)

Table 1 Maximising the interaction between effector and target cells

Target cells added (× 10^{-3})	Target cells killed (× 10^{-3})	
	3 h	5 h
25	2.8+0.1	2 8±0 2
50	3 6±0.3	3.8±0.3
100	3.7±0 5	3 6±0.4
200	3 6±0.7	4.0±0 5

Spleen cells (5 × 10^5) from sensitised animals were incubated with the indicated number of ^{51}Cr-labelled P815 target cells as described in Fig. 1. After 1 h at 37 °C, cytochalasin A was added and 10 min thereafter Ca^{2+}-containing medium The number of target cells specifically lysed (± s e m. for duplicates) was determined 3 and 5 h after the addition of Ca^{2+}—containing medium to show that maximum lysis had occurred.

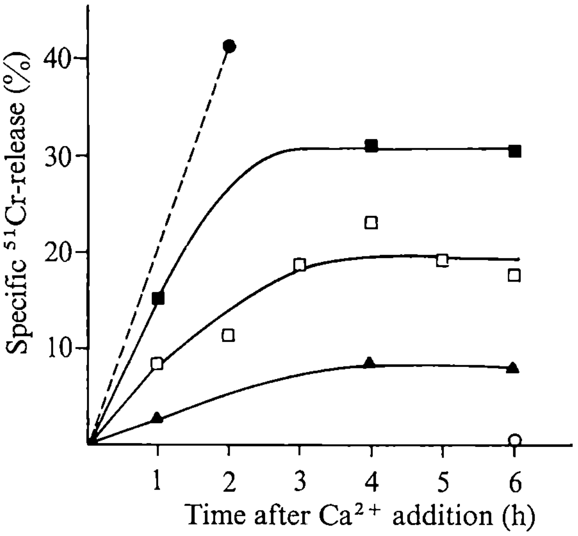

Fig. 1 Spleen and ^{51}Cr-labelled tumour cells were washed twice in Ca^{2+}-free medium (MEM-suspension, Microbiological Ass., containing 5 × 10^{-5} M EDTA to remove trace amounts of Ca^{2+}, and 5% dialysed foetal calf serum) just before use. Spleen (50 µl) and target cells (50 µl, 10 × 10^3) were added to conical-well microtitre plates which were centrifuged for 1 min (1,000 r p.m. No. 276 International Centrifuge rotor, 22 °C) and incubated for 1 h at 37 °C. Cytochalasin A (50 µl, 30 µg ml^{-1}, Aldrich; the stock solution, 10 mg ml^{-1} in dimethyl sulphoxide, was diluted with Ca^{2-}-free medium before use) was then added, followed 10 min later by 100 µl Ca^{2+}-containing medium (MEM–Earle's Salts, Microbiological Ass., containing 5% foetal calf serum). The specific release was calculated as follows:

$$\text{Specific release} = \frac{\text{Experimental c.p m.} - \text{control c p m.}}{(0.8) \times (\text{incorporated c.p.m.})}$$

where 0.8 is the fraction of the incorporated ^{51}Cr which is releasable by hypotonic lysis. The controls were spleen cells from uninjected C57BL/6 mice treated identically to the "immune" cells. The control release was 5% per h for all conditions. The following numbers of spleen cells were used: ▲, 2.5 × 10^5; □, 5 × 10^5; ■, 10 × 10^5; ●, 5 × 10^5 (no cytochalasin A was added); ○, 5 × 10^5 (no Ca^{2+}-containing medium was added).

Thus, by incubating lymphocytes with target cells in a medium containing Mg^{2+} but not Ca^{2+}, interactions occur which do not lead to lysis. If Ca^{2+} is added to such cultures together with cytochalasin A, those target cells which have functionally engaged with effector cells during the preincubation period will go on to lyse. The presence of cytochalasin A will, however, prevent any new interactions from proceeding to a Ca^{2+}-dependent stage, and thus new liaisons formed after the addition of Ca^{2+} will not lead to lysis. Assuming each effector cell becomes bound to one target cell during the preincubation period, the subsequent number of target cells which lyse when Ca^{2+} is added to the cultures is equivalent to the number of effector cells present.

Cytolytically active lymphoid cell populations were generated by immunising adult C57BL/6 mice (Jackson Laboratories) with a mouse mastocytoma (P815-X2) of the DBA/2 strain. Ten million P815 cells were given intraperitoneally and the lymphoid cell populations collected 10–12 d later in a manner previously described in detail[1,6]. The cell-mediated destruction of P815 cells in this system has been shown to be exclusively due to T cells[7].

Specific cytolysis was totally inhibited when lymphocytes

Table 2 Specific cytolysis as a function of interaction time in Ca^{2+}-free medium

Ca^{2+}-free incubation time before cytochalasin addition (minutes)	% Specific Lysis 3 h	5 h
0	0.0±0.1	0.0±0.1
30	20.5±0.1	21.0±0.2
60	23.0±0.2	23.5±0.1
120	22.5±0.1	25.0±0.1

Spleen cells (1×10^6) from sensitised animals and ^{51}Cr-labelled P815 target cells (2×10^4) were mixed in conical-well microtitre plates and centrifuged as described in Fig 1 After the incubation times indicated cytochalasin A was added and 10 min thereafter Ca^{2+}-containing medium. The percentage-specific lysis (± s e m for duplicates) was determined 3 and 5 h after the addition of Ca^{2+}-containing medium

and target cells were incubated in the presence of 3 $\mu g\ ml^{-1}$ (6×10^{-6} M) cytochalasin A Lymphoid cells preincubated for 10 min with cytochalasin A and then washed did not recover their lytic activity, but target cells treated in an identical manner were as susceptible to lysis as untreated cells (data not shown). The drug did not increase the rate of spontaneous release of ^{51}Cr from target cells (5, confirmed in experiments not shown).

The experimental protocol used to enumerate effector T cells is given in detail in Fig 1 (Cytochalasin A was added 10 min before Ca^{2+} to allow a finite time for the drug to exert its effect.) No cytolysis occurred when lymphocytes were incubated with target cells in a medium containing Mg^{2+} but not Ca^{2+} (Fig. 1). On the addition of Ca^{2+}, however, ^{51}Cr release readily occurred (Fig. 1). Two features of the target cell destruction following the addition of Ca^{2+} should be noted. (1) The number of target cells killed was proportional to the number of spleen cells present in the culture; (2) a period of about 3 h in medium containing Ca^{2+} was necessary to allow maximal ^{51}Cr release. To assure that the drug was effective and that the maximal ^{51}Cr release had occurred, lysis was determined 3 and 5 h after the addition of Ca^{2+} in the presence and absence of cytochalasin A.

If, as is our contention, the maximal amount of target cell destruction depicted in Fig. 1 is equivalent to the number of effector cells present in the lymphocyte population, several provisions must hold. First, for a given effector cell population, the maximum specific target cell destruction after the addition of Ca^{2+} to the cultures, should be directly proportional to the number of lymphocytes present. The data in Fig. 1 show this to be the case. Second, increasing the size of the target cell pool, above the minimum required to engage all effector cells, should not further increase the number of target cells killed. When 5×10^5 immune spleen cells were incubated with between 5×10^4 and 20×10^4 target cells, the number of target cells killed after the addition of Ca^{2+} was constant (Table 1) Third, the number of target cells killed should not be increased if the incubation period in Ca^{2+}-free medium is extended (that is, a maximal number of interactions had occurred in the preincubation time chosen). The number of functional engagements between lymphocyte and target cell did not significantly increase over the period 30 min to 2 h (Table 2), in keeping with previous studies[2,8].

Table 3 Frequency of specific cytolytic T cells in the spleens of alloimmunised mice

Experiment	Days after immunisation	Maximum number ($\times10^{-3}$) of target cells lysed per 5×10^5 viable cells	Frequency of effector cells (%)
1	10	11.0	2.2
2	10	9.0	1.8
3	10	7.0	1.4
4	10	5.0	1.0
5	10	3.5	0.7
6	11	8.0	1.6
7	11	6.0	1.2
8	11	4.5	0.9
9	12	4.0	0.8
10	12	4.0	0.8

The number of effector cells in each spleen cell suspension was determined using the experimental approach given in Table 2 Three spleens were pooled in each experiment

$$\text{Frequency} = \frac{\text{maximum number of target cells killed}}{5\times10^5\ \text{spleen cells}}$$

Since these criteria were fulfilled, the number of target cells maximally killed was equated with the number of effector cells. This approach was used on several occasions to enumerate effector cells in C57BL/6 spleen cell populations at the peak of the primary immune response (10–12 d) after immunisation with P815 cells. Table 3 shows that at this time between 0.7 and 2.2% of the total spleen cell population was specific anti-P815 T effector cells.

There are two principal assumptions necessary in order for our calculations to be valid. First, all effector cells must functionally interact with a target cell during the preincubation period (obviously if some effector cells do not engage a target cell the number of effector cells calculated will be an underestimate), and second, each effector cell must not functionally engage more than one target during incubation in the Ca^{2+}-free medium (or else the calculated value would be an overestimate of the effector cell incidence).

The first of the above assumptions seems warranted, for preincubation times between 30–120 min lead to the same amount of lysis following the addition of cytochalasin A and Ca^{2+} (Table 2). Indeed, in another experiment (not shown), there was no difference in the subsequent ^{51}Cr release whether cytochalasin A was added after 5 or 120 min. In all cases, however, cytochalasin A added at the same time as the target cells completely inhibited cytolysis. It would thus seem, in keeping with previous observations[8,9,11], that functional engagements between lymphocyte and target cell occur rapidly, and, in the conditions used in this study, are complete within 30 min.

The same arguments would seem to dictate that an effector cell does not functionally engage more than one target cell during the preincubation period. If that were the case, then extending the preincubation period would be expected to increase the number of such engagements. In fact, as earlier indicated (Table 2), preincubation periods between 30 and 120 min showed an identical number of functional interactions. It would seem unlikely that an effector cell undergoes multiple non-lytic interactions in the period 0–30 min but not thereafter, although admittedly this remains a faint possibility. It is also not likely that each effector engages several target cells simultaneously, for if this were the case, increasing the size of the target cell pool would increase the likelihood of such interactions. As Table 2 shows, however, lysis reaches a constant value not a constantly increasing one. Furthermore, extensive kinetic analysis of target cell death in ^{51}Cr-release killer assays provide evidence for "single hit" mechanisms of cytolysis[6].

Two methods of estimating effector cells have been used previously. One approach has been to equate the frequency of cytolytic T cells with the number of target cells specifically lysed in the presence of a great excess of target cells[6,10]. The possibility of the effector cells recycling (that is, that one lymphocyte kills more than one target cell) was largely ignored in those studies, and it is therefore likely that the calculated frequencies were overestimates Indeed, Henney[6] reported the incidence of effector cells in the system reevaluated here as approximately 4% of splenic lymphocytes, a number 2–3 times higher than the incidence estimated in the present study.

The frequency of cytolytically-active cells has also been measured by counting those lymphocytes which adhere to target cells[3,8,11]. The critical assumption in this approach is that each lymphocyte which binds to a target cell is a specific effector cell. This is almost certainly not the case; indeed, both precursor[12] and memory cells[13] have been shown to have affinity for homologous allogeneic cells, but neither of these T-cell populations are cytolytic[13,14]. The contribution of non-cytotoxic lymphocytes to the overall frequency of target-binding cells remains to be established.

We have thus described a novel method for calculating the incidence of specific cytolytically active T cells. The procedure used here measures only killer T cells and obviates the deficiencies of previous approaches to this problem by preventing the effector cell from 'recycling'. Obviously the enumeration of cytolytically-active T cells provides only a partial quantification of the overall cell-mediated immune response. The quantitative relationship between this T-cell compartment and those producing lymphokines, memory and regulator cells remains to be evaluated.

This work was supported by the NIAID and the NCI. R.M.T is the recipient of a research fellowship award from the US PHS and C.S.H. is the recipient of a research career development award from the NIAID.

RICHARD M. THORN
CHRISTOPHER S. HENNEY

Departments of Medicine and Microbiology,
Johns Hopkins University School of Medicine
and O'Neill Memorial Research Laboratories,
Good Samaritan Hospital,
Baltimore, Maryland

Received March 5; accepted May 4, 1976.

[1] Brunner, K. T., Mauel, J , Cerottini, J -C., and Chapuis, B , *Immunology*, 14, 181–196 (1968).
[2] Zagury, D., Bernard, J., Thierness, N , Feldman, M., and Berke, G., *Eur J. Immun.*, 5, 818–822 (1975).
[3] Martz, E., *Transplantation*, 21, 5–11 (1976)
[4] Plaut, M , Bubbers, J. E., and Henney, C S , *J. Immun* , 116, 150–155 (1976)
[5] Bubbers, J. E., and Henney, C S., *J. Immun* , 115, 145–149 (1975)
[6] Henney, C. S., *J. Immun.*, 107, 1558–1566 (1971).
[7] Cerottini, J.-C., Nordin, A A , and Brunner, K. T., *Nature*, 228, 1308–1309 (1970).
[8] Berke, G., Gabison, D., and Feldman, M., *Eur. J. Immun* , 5, 813–818 (1975).
[9] MacDonald, H. R., *Eur. J. Immun.*, 5, 251–254 (1975).
[10] Wilson, D., *J. exp Med.*, 122, 143–166 (1975)
[11] Martz, E., *J. Immun.*, 115, 261–267 (1975).
[12] Mage, M. G., and McHugh, L. L., *J. Immun* , 115, 911–913 (1975).
[13] Kamat, R., and Henney, C. S., *J. Immun.*, 115, 1592–1598 (1975).
[14] Cerottini, J.-C., Engers, H. D., MacDonald, H. R., and Brunner, K. T., *J. exp. Med.*, 140, 718–730 (1974).

Enhancement of delayed hypersensitivity by depletion of suppressor T cells with cyclophosphamide in mice

THE delayed hypersensitivity (DH) reaction seems to be enhanced by treatment with cyclophosphamide and this has been discussed in the context of depression of antibody production[1-4]. Askenase *et al*[5], however, reported that low doses of cyclophosphamide augmented the reaction to sheep erythrocytes without affecting antibody production. Polak and Turk[6] suggested that cyclophosphamide could break down immunological tolerance to the dinitrophenyl group, as measured by a skin reaction in guinea pigs after treatment with the drug to inhibit suppressor cells. The nature of the suppressing cells was not clear at the time. We report here that treatment of mice with cyclophosphamide also significantly affects DH reaction to methylated human serum albumin (MHSA)[7] which induces little antibody production, and that the enhanced DH reaction is caused by damage to T rather than B cells. Independent recovery, from the damage due to cyclophosphamide, by individual subpopulations of T cells accounts for the kinetics of this phenomenon.

Table 2 Suppressive effect of transferred lymphoid cells on enhanced DH to MHSA in mice treated with cyclophosphamide

Cyclophosphamide treatment	Cells transferred	No. of animals	DH on day 12
150 mg kg^{-1}	None	3	10.7±1.9
150 mg kg^{-1}	5×10^7 Spleen cells	4	9.3±1.5
150 mg kg^{-1}	2×10^7 Thymus cells	4	6.3±2.5
None	None	4	5.3±1.8

Male C57BL/6 mice (age 4 months) were given an intraperitoneal injection of cyclophosphamide (150 mg kg^{-1}) 4 d before sensitisation, and an intravenous transfer of spleen or thymus cells 2 d later.

Male C57BL/6 and (C57BL/6×CBA)F$_1$ mice aged 4 or 6 months were used : they seem to be high DH responders[8]. Animals were sensitised by an injection, into the left footpad, of an emulsion (0.05 ml) consisting of equal amounts of MHSA solution (5 mg ml^{-1} in saline) and Freund's complete adjuvant (3 mg of dead H$_{37}$R$_V$ tubercle bacilli per ml). A challenge injection of 0.02 ml of MHSA solution (1 mg ml^{-1}) was given into the right footpad on day 12 of sensitisation, as the optimal DH response was obtained by this method. Swelling of the right footpad was measured both immediately before and 24 h after the challenge, and the difference between two measurements in a thickness of 0.1 mm was used to describe the intensity of the DH response[9]. Mice received an intraperitoneal injection of cyclophosphamide (given by Shionogi Co., Osaka, 15 or 150 mg per kg body weight) at intervals before or after sensitisation, as indicated in Tables 1–3. Spleens and thymuses were removed from normal syngeneic male mice and the cells from them were suspended in and washed three times with RPMI-1640 medium. Appropriate numbers of these cells were transferred into the retro-ocular plexus of the cyclophosphamide-treated mice.

Table 1 shows the effects of cyclophosphamide on the DH response to MHSA when the drug was given 8 d or 1 d before sensitisation. There was marked enhancement of DH

Table 1 Effect of cyclophosphamide on DH to MHSA in mice

Cyclophosphamide treatment	Interval between treatment and sensitisation	No. of animals	DH on day 12*	Thymus weight (mg)
None	—	4	5.3±1.8	29±4
150 mg kg^{-1}	1	5	16.4±1.2	23±6 [14]†
	8	5	17.0±6.3	38±6 [21]†
15 mg kg^{-1}	1	5	7.5±1.5	35±9 [14]†
	8	5	9.0±4.2	35±4 [21]†

Male C57BL/6 mice (age 4 months) were given an intraperitoneal injection of cyclophosphamide (15 or 150 mg kg^{-1}) at various intervals before sensitisation.
*Each value represents mean ± s.e. (0.1 mm).
†Interval between treatment with cyclophosphamide and measurement.

Table 3 Effect of cyclophosphamide on effector cells in DH to MHSA in mice

Cyclophosphamide treatment	Interval between sensitisation and treatment	No. of animals	DH on day 12	Thymus weight (mg)
None	—	3	15.2±2.9	32±8
150 mg kg^{-1}	4	4	2.8±0.9	14±2 [9]*
	9	4	1.0±0.4	14±2 [4]*

Male (C57BL/6 × CBA)F$_1$ mice (age 6 months) were given an intraperitoneal injection of cyclophosphamide (150 mg kg^{-1}) 4 or 9 d after sensitisation.
*Interval between treatment with cyclophosphamide and measurement

response in animals treated with the large dose. Table 2 shows that transfer of 2×10^7 thymus cells from untreated mice almost eliminated the DH enhancing effect. Transplantation of 5×10^7 normal spleen cells did not influence the enhanced DH significantly. These observations suggest that the DH to MHSA in mice is enhanced because cyclophosphamide damages suppressive T cells in the immune regulatory systems.

Table 3 shows that administration of cyclophosphamide after sensitisation suppresses the DH response. A minimal response appeared only in the group treated with cyclophosphamide on day 4 after sensitisation. These results indicate that effector T cells which are responsible for DH are also sensitive to cyclophosphamide There have been several reports of the inhibitory effect of the drug on DH responses[10], and Kerckhaert *et al.*[11] demonstrated the sensitivity of effector T cells. In experiments not described in Tables 1–3 we observed that previous treatment of mice with cyclophosphamide was not necessary for DH enhancement, and that treatment after sensitisation (such as in Table 3) could enhance DH only if the interval between treatment and challenge injection was sufficiently long, for example 12 d. We further observed that when the interval was just 9 d, DH was neither suppressed nor enhanced. This result together with our previous finding[12] that significant DH to MHSA was obtained as early as 4 d after sensitisation, suggest that the effector T cells, once affected by cyclophosphamide, recover sufficiently to generate significant DH response after about 5 d. This seems to be consistent with previous observations[2,11]. The 13-d or 20-d interval between treatment with cyclophosphamide and challenge injection (Table 1) might be long enough for the effector cells recovering from the damage to be sensitised with the antigen retained at the site of injection This may explain the apparent resistance of effector T cells to cyclophosphamide in this and some previous experiments[6].

Thymus weight did not recover significantly until 9 d after treatment (Table 3), and then recovered considerably on day 14 and rebounded on day 21 (150 mg kg^{-1}, Table 1). Recovered lymphoid cells were histologically detectable in the cortex on day 9 after treatment, but were hardly detectable on day 4. This seems to be consistent with other observations[10,13], and probably supports the suggested recovery of effector T cells. But the sites recovering cells remain unknown.

The recovery of suppressor T cells is probably delayed more than that of effector cells, and seems to be within 4 weeks (unpublished observations). In previous experiments[14] concerned with suppressor T cells, we found that thymus cells transferred into old recipients, which showed a maximal DH response, suppressed the development of DH to MHSA When transfer was into young recipients who developed moderate DH to MHSA, suppression of DH was not observed. Studies on the influence of whole-body irradiation[8] or adult thymectomy[14] confirmed this, and suppressor T cells seemed to be in the category of short lived T cells Because of a greater delay in recovery of suppressor T cells than of effector T cells after cyclophosphamide-induced damage, the regulatory activity of the suppressors on the effectors could be minimised, resulting in an increased DH response.

Cyclophosphamide has generally been considered to have a selective suppressive effect on the B-cell functions in some circumstances. This is supported by various phenomena including suppression of antibody production[1], proportional decrease in non-θ-bearing lymphocytes[15] and cell depletion in the non-thymus-dependent areas of lymphoid tissue[13,16], and so on[10]. Suppression of antibody production is often accompanied by an increase in DH response. This may indicate regulation of DH by antibodies[2,3].

In contrast, we conclude that T cells as well as B cells are remarkably sensitive to cyclophosphamide and therefore both DH and antibody production are defective immediately after treatment. Time for recovery from the damage is different between T cell subpopulations, that is, long-lived effector cells and short-lived suppressor or regulatory cells The former seem to recover more promptly than the latter. We suggest that this causes enhanced DH to MHSA in mice treated with cyclophosphamide. But the possibility remains that the suppression of DH by cyclophosphamide after sensitisation is due, at least in part, to damage to bone marrow-derived monocytes rather than, or in addition to, that of sensitised effector T cells.

We thank Professors K. Yasuhira and T. Teramatsu for advice.

Akio Mitsuoka

Department of Thoracic Surgery,

Mitsuo Baba
Shigeru Morikawa

Department of Pathology,
Chest Disease Research Institute,
Kyoto University,
Kyoto 606, Japan

Received January 26; accepted May 18, 1976

[1] Turk, J L Parker, D , and Poulter, L. W., *Immunology*, 23, 493–501 (1972)
[2] Lagrange, P H., Mackaness, G B , and Miller, T E , *J. exp Med* , 139, 1529–1539 (1974)
[3] Mackaness, G B , Lagrange, P H , Miller, T E , and Ishibashi, T., in *Activation of Macrophages* (edit by Wagner, W -H., and Haln, H), 193–209 (Excerpta Medica and American Elsevier, 1974)
[4] Kerckhaert, J A M., *Ann. Immun* , 125, 559–568 (1974)
[5] Askenase, P W., Hayden, B J., and Gershon, R K , *J exp. Med* , 141, 697–702 (1975)
[6] Polak, L , and Turk, J L., *Nature*, 249, 654–656 (1974)
[7] Crowle, A J , Hu, C C , and Patrucco, A , *J. Allergy*, 42, 140–156 (1968).
[8] Baba, M , Harada, T , Morikawa, S , Yasuhira, K., and Mitsuoka, A., *Proc Jap. Soc Immun* , 5, 465–467 (1975).
[9] Morikawa, S , *Kekkaku* (Japanese), 48, 519–521 (1973)
[10] Bach, J.-F , *The Mode of Action of Immunosuppressive Agents*, 173–225 (North-Holland, and American Elsevier, 1975)
[11] Kerckhaert, J A M , van den Berg, G J , and Willers, J M. N , *Ann Immun* , 125, 415–426 (1974)
[12] Baba, M , Harada, T., and Morikawa, S , *Proc Jap Soc Immun* , 3, 177–179 (1973)
[13] Turk, J L , and Poulter, L W , *Clin exp Immun* , 10, 285–296 (1972)
[14] Morikawa, S., *Clin Immun* (Japanese), 7, 437–445 (1975)
[15] Poulter, L W , and Turk, J L , *Nature new Biol* , 238, 17–18 (1972)
[16] Stockman, G D., Heim, L. R , South, M A , and Trentin, J J , *J Immun* , **110**, 277–282 (1973)

nature

July 8, 1976

Is the world getting naughtier?

CONSIDER the following statements:

Military expenditure by Persian Gulf states has risen fivefold in real terms between 1971 and 1975

In the past 25 years more than 13,000 tanks have been delivered to Middle Eastern countries

By the year 1980 the world will be producing 80,000 kilograms of plutonium annually (8 kilograms is enough to make one nuclear weapon).

The People's Republic of China now seems to be launching satellites for military reconnaissance purposes.

About 125,000 scientists and engineers in the United States work on military research and development.

They are just a few of the pieces of information that make up the as-ever impressive compilation of military statistics put out by the Stockholm International Peace Research Institute (SIPRI) in its annual yearbook *World Armaments and Disarmament* (MIT Press and Almqvist & Wiksell; SKr 106). For nearly 10 years now the world has been in SIPRI's debt for providing an endless stream of hard and almost-hard facts on military matters all around the world. It is, of course, difficult to judge what impact this impartial reporting has had on public opinion and political thinking (particularly difficult in the United Kingdom where government is distinctly exclusive and as a consequence public opinion is poorly developed on all defence matters). But the global impact has not been negligible and we must hope that the Swedish government never loses its resolve to continue to support SIPRI.

That said, it must be noted that the character of SIPRI, at least as seen through its yearbook, continues to change (as we have reported on a couple of occasions previously). More and more are personal opinions being expressed in the commentaries. Words like "bonanza", "enormity", "seemingly endless", "frightening prospect" and so on crop up increasingly often. The world as seen by SIPRI seems to be getting continually more naughty and fractious. Of course, there are good grounds for showing concern, particularly at the way in which the Third World is picking up military momentum. But there are three reasons why we believe that SIPRI should steer clear of expressing views.

First, if it can't be detached and neutral, no-one else can. There are plenty of committed institutions around the world—committed to the environment, world government, disarmament and so on. SIPRI's strength has always been its detachment; others might use its figures in any way they choose but it would simply report. Although there is much populist appeal in the path it now seems to be treading, one suspects there is less respect from the hard-headed in the armament and disarmament community.

Second, although there is really no suggestion at all that SIPRI's figures are influenced by its views, there is a risk that the sort of things it will pay attention to could be so affected. Various forms of environmental warfare are discussed in the yearbook, for instance. For example, it is suggested that the ionosphere–Earth wave guide could be used to generate very low frequency electromagnetic fields to couple into people's alpha rhythms. "If methods could be devised to produce greater field strengths . . . either by natural (for example, lightning) or artificial means, then it may become hypothetically possible to impair the performance of a large group of people in selected regions over extended periods." Now this is the idlest of coffee-table musing with, at first sight, the severest of physical objections to be laid against it. Is it right that SIPRI, in its yearbook, should be mixing such vague ideas with its strong brew of hard facts?

Third, the news is not always as bad as SIPRI makes out. "The arms race between the two great powers continued unabated", says SIPRI. But in real terms, military expenditure in the Soviet Union has held roughly constant since 1968 and in the United States has declined in the same period by more than a quarter (aided, of course, by the withdrawal from Vietnam). The world total of annual military expenditures (which includes burgeoning Middle East figures) has remained on a plateau of 210,000 million US dollars (at 1970 prices) for seven years now, and as a percentage of gross domestic product has accordingly declined steadily. It goes without saying that this is a frightening sum of money, but with growing complexity and thus cost of armaments, constant expenditure means less commitment. SIPRI's own figures seem open to more optimistic interpretations □

Pure Chemistry Library

Towards an environmental ethic

How should decisions concerning the environment be made? Eric Ashby, examining recent work on the subject, offers his view

IN 1961 there was published in Washington a report under the modest title House Document 522. It ran to eleven volumes. It was prepared by the American Army Corps of Engineers. Its theme was a Comprehensive Survey of the Water Resources of the Delaware Basin. The report recommended that a dam should be built on the Delaware River at a place called Tocks Island in New Jersey. The dam would create a lake about 37 miles long. The estimated cost (when it was reviewed at 1975 prices) was about $400 millions.

House Document 522 includes a massive exercise in cost-benefit analysis. The recommendation to build a dam rested on four arguments: to diminish the danger of floods downstream; to provide a water reserve in case of drought; to run a hydro-electric power plant; and to create a recreation area of 72,000 acres which would attract (according to the first estimate) as many as 9 million visitors a year. These potential visitors were regarded as a substantial "benefit" in the cost-benefit analysis, on the assumption that they would be worth $1.35 per person per recreation day.

Of course the proposal generated massive opposition. Some of the quantified values were challenged, but the most powerful arguments against the proposal rested on unquantified values: desecration of the last free flowing river in the east of the USA; acres of wilderness alienated for roads and parking lots and motels; the plea that this beautiful part of the river should be treated as an endangered species. It is a debate familiar to us in Britain. We had something like it over the Cow Green reservoir in Upper Teesdale in the 1960s.

The dam is not yet built, nor at present is it likely to be built. But the fifteen-year-long controversy over it has produced one admirable and important second order consequence. It prompted the American Academy of Arts and Sciences to sponsor a study of the problems of decision-making about the environment. The prime problem is how to incorporate what the study calls "fragile" values into the "hard" values which can reasonably be quantified. For over four years a group including lawyers, scientists and philosophers have reflected on this issue. Their conclusions are now issued in a book[*] which is, I believe, the first serious and authoritative work on the philosophy of environmental protection. Its starting point is the Tocks Island controversy, which is going to be treated intensively in a second volume to be added to this study[†] But the reflections go far beyond that specific episode. In essays, all of which are careful and one or two of which are brilliant, the nine authors set out their attitudes to the conflict of values which is the inevitable dilemma facing those who have to make decisions about the exploitation of the environment by man.

The impressive feature of the book is that it does not reach a consensus; it does not offer formulae for decision-makers. Its authors have the courage to declare that there is no simple resolution to the question: how do you reconcile the protection of nature with the needs of industrial man? It eschews slick and glossy utopias. It was J. S. Mill who wrote that the test of good government is the degree to which it increases the sum of good qualities in the governed. All the authors agree that there are values about the environment which are "good" and values which are "bad". But, as Robert Dorfman writes in the last essay, "I do not believe that those questions can be answered definitely, now or ever; but neither can they be ignored. The progress that I see in our project is that it points the way to living honestly with these forever open questions".

In Britain those who make decisions about the environment are no longer philistines. The main difficulty about "soft" or "fragile" values is not that they are neglected in the decision-making process; it is, as Harvey Brooks writes, "bringing them into a common intellectual framework with the rest of the analysis" for the purpose of political decisions, where "hard" quantified data based on cost-benefit analysis is likely to be more easily accepted. One of the redeeming features of the consumer society which has to be put in the balance against its many ugly features is that "fragile" values do play an increasingly important part in political decisions about the environment. In the files of the Department of the Environment there are many examples of planning permissions being refused because unquantified values were deemed to carry greater weight than quantified ones

This is encouraging, but it does not dispose of the difficulties which arise when there is a conflict of values, a clash of "goods" and the necessity to make a choice between them. The American Academy has put us all in its debt by facing these difficulties head on, in the book the Academy has sponsored. Among the issues discussed in the book, two seem to me to be particularly important.

- Values can be compared more easily if they can all be expressed in the same units. Does this justify the attachment of a money-tag to all values, even though this means what economists call "shadow pricing" (for example, the "value" of a view of the South Downs is the extra cost of not defacing the view if a road or a line of electric pylons has to be built in the neighbourhood)? Or are the values themselves distorted as soon as you try to put a money-tag on them?
- Is it possible to declare certain clear ends or goals in environmental policy, and to accept these ends as "given"–"axiom values", as it were—so that all decisions about the environment become means toward unalterable values which are the ends?

In a closely argued and subtle essay, Laurence Tribe tackles both these issues He dismisses one common criticism of cost-benefit analysis of environmental problems: the criticism that to quantify "fragile" values (a view, a rare plant community, a river in its natural state) is *illogical.* All such concerns "can in theory be incorporated into a rigorous analysis . . ." The danger of incorporating them, of putting price tags on elusive externalities, is more subtle. It is twofold. First, it flattens any sense of obligation toward natural objects into an aspect of self interest ("What is its money value to *me*?"). Second, it exerts "an enormous reductionist pressure on all values that would otherwise seem incommensurable with a calculus of human wants." In other words, the very translation of the values into manageable units may deprive them of their significance. Tribe's essay, and others in the book, particularly the essay by Harvey Brooks, are a great encouragement to the decision-maker when he is presented with a tidy and misleadingly comprehensive assessment of some project which will have an impact on the environment, neatly distilled into cost-benefit equations The decisions he has to make, writes Harvey Brooks, "are fundamentally political in the sense that they ultimately involve competing or conflicting values, and therefore cannot be resolved by purely 'rational' (that is, empirical and logical-deductive) means."

---

[*] Tribe, L H , Schelling, C. S , and Voss, J (Eds) *When Values Conflict* (Ballinger, Cambridge, Mass., 1976) To be published in the UK by Wiley.

[†] Feiverson, H. A , Sinden, F. W., and Socolow, R H (Eds.) *Boundaries of Analysis* (Ballinger, Cambridge, Mass , 1976) To be published in the UK by Wiley.

If this view is accepted, there remains the problem of how values are to be incorporated into analysis if they cannot be quantified, or related to self interest. To the question "Does nature embody values apart from its usefulness in serving man's desires?", the answer seems to be, "Yes, but we are not clear, and cannot expect ever to be clear, what these values are." So Laurence Tribe proposes a fresh attitude to this issue. He concedes that most people are very vague about the values they hold on environmental matters and that "such inchoate values are crystallised into distinct preferences or criteria of choice only through the concrete process of seeking means to attain them and gradually discovering what such means entail." In other words, values evolve through the choices made in groping toward them, and it is an essential aspect of freedom that we can choose what we shall value.

The direction in which this argument leads is as follows. First, there are no sanctified principles upon which environmental decisions rest, no "axiom values"; but all decisions are rationalised in some provisionally held principles, and these provisionally held principles *evolve* in the light of the choices which are made and the observed consequences of these choices. (Consider, for instance, how our values about pesticides have evolved through experience of making decisions about the use of pesticides.) Second, the direction in which principles evolve in our attitude toward the environment is taking us beyond the crude criterion of self interest—witness the recent legislation in Britain to protect some species of wild animals and plants, so rare that not one in a hundred of the legislators is likely ever to have seen any of them! It is this sort of argument which leads Laurence Tribe to suggest that social values about environmental issues progress in a spiral (their direction depending upon their position in the spiral; a framework for choice, as he calls it, which "must incorporate procedures for its own evolution.") And as a starting point on the spiral, Tribe suggests that we "should avoid a premise of human domination—or indeed a premise of the total subservience of any form of being to any other."

A feeling of obligation toward organisms other than man and a responsibility for protecting natural objects—valleys, forests, wildernesses—is of course no novelty among individuals. It is the codification of this obligation or responsibility which is novel. Nearly ten years ago, for instance, there was a planning enquiry into the effect which a North Sea Gas terminal would have on an area of natural beauty on the Norfolk coast. It was the Minister of Housing and Local Government who had to decide whether the area of natural beauty would be damaged by the siting of the gas terminal. In a word, he had to act as the "guardian" of the area of natural beauty. This attitude to a natural object prompts one to ask whether natural objects, trees and woodlands, creatures other than man, should have "rights". At first sight this seems to be a sentimental and mystical attitude to nature. But that is not the view of some hard-headed practical lawyers. In 1972 an article by a professor of law in California, Christopher Stone, examined the singular thesis: Should Trees have Standing? The article has since been published as a book, together with judgement from the Supreme Court on the legal case which prompted Stone's article‡.

The circumstances which brought the action to the Supreme Court were these. The United States Forest Service had granted a permit to Walt Disney Enterprises Inc to "develop" Mineral King Valley in the Sierra Nevada mountains. The decision was challenged by the Sierra Club, which acts vigorously to defend natural objects in America. The Sierra Club lost its case for a reason which would apply to an analogous case if it were to be brought to the courts in Britain, namely because the Club had no sufficient "personal stake in the outcome of the controversy." But three members of the Supreme Court dissented from this decision, and one of the dissenting judgements, by Mr Justice Douglas, drew its inspiration from Stone's article in the California Law Review. He said: "The critical question of 'standing' would be simplified . . . if we fashioned a federal rule that allowed environmental issues to be litigated before federal agencies or federal courts in the name of the inanimate object about to be despoiled . . . Contemporary public concern for protecting nature's ecological equilibrium should lead to the conferral of standing upon environmental objects to sue for their own preservation."

In his lively essay, Stone examines the way rights in law have been conferred upon children (who have not always had rights in law), women, subject peoples formerly enslaved, and so on. He then reminds us that the "world of the lawyer is peopled with inanimate right-holders: trusts, corporations, joint ventures, municipalities . . ." So there is nothing unreasonable about putting natural objects, as the law puts other non-human things, into the category where their interests can be defended in courts by properly recognised guardians. Of course, before the principle could be adopted, many subsidiary questions (such as: Who should be the guardians?) would have to be settled. But the idea is worth serious reflection for it would be one more step in the evolution of an environmental ethic which does not rest on the assumption that nature is made for man. ☐

---

‡Stone, C. D., *Should Trees have Standing?* (Kaufmann, Los Altos, California, 1974).

The attack on tropical disease

Alex Dorozynski looks at the World Health Organisation's efforts to relieve man of one of his major burdens

IN spite of recent expressions of concern about the new economic order, interdependence of nations, and cooperation, there is one area of enormous importance to the developing world that has largely been ignored that of tropical diseases. They affect several hundred million people, represent a permanent human burden, and a major obstacle to development. Tropical disease research has hardly benefited from the explosion of knowledge in bio-medical sciences that has taken place in the developed world.

In fact, some of the tropical diseases are now recrudescent, because parasites have become resistant to drugs and vectors to insecticides, because agricultural development sometimes contributes to the creation of conditions required for a disease to become endemic, and because international aid toward the control of tropical diseases has shrunk in the face of increasing costs. In the past year, the World Health Organisation (WHO) has been mounting a new attack on these diseases. The approach is novel, and the outlook promising, although one major element of uncertainty still remains: will there be enough money to carry out this long term programme?

The global annual investment in tropical disease research is estimated by the WHO at about $30 million, which is a mere pittance of money in comparison to huge budgets devoted to other areas of bio-medical research. Advances in treatment and control of tropical diseases have been painstakingly slow, in spite of the fact that most of the causative agents are relatively simple parasites belonging to the lowest orders, protozoa or worms, that in most cases are completely incapable of independent life and rely for survival on the highly specialised environment provided by two or three or sometimes more successive hosts.

"According to the law that viability is inversely proportional to the stringency of ecological requirements," says Professor Christian de Duve, "the pathogenic parasites certainly occupy the bottom of the scale. They are puny enemies indeed." He is the director of the International Institute of Cellular and Molecular Pathology, Brussels, and a member of Rockefeller University, New York. A consultant of the WHO in the new "Programme of Research and Training in Tropical Diseases", he is one of the scientists who has suggested a new approach to tropical diseases research in which the basic biology of the parasite becomes the prime target.

The diseases

Six diseases have been selected as the initial targets of the WHO's Special Programme: malaria, schistosomiasis, trypanosomiasis, filariasis, leprosy, and leishmaniasis.

- Malaria is one of the most widespread diseases in the world, affecting some 200 million people. In Africa, about one-fourth of all adults suffer from malarial fever at one time or another, and at least one million children die of the diseases every year. In several areas of Asia and South America, *Plasmodium falciparum* (one of the four human malaria parasites, responsible for the severest forms of the diseases), has developed resistance to 4-aminoquinolines, major antimalarial drugs. In Asia resistant strains have progressed westward to reach the Indo-Pakistani subcontinent, and they represent a great threat to Africa, where *P. falciparum* is the main malaria parasite.

In addition, mosquitoes have developed resistance to some insecticides and, as a result of increased costs and reduced international assistance programmes, many countries cannot afford to carry out intensive anti-malarial campaigns.

India is an example. The number of cases there of malaria had been reduced to a low of 60,000 in 1962, but last year it exceeded four million (a 70-fold increase). In Africa, there appears to be no hope of malaria control in the near future. Dr Adetokunbo O. Lucas, former president of the Nigerian Medical Research Council, who in April become the director of the WHO Special Programme, points out that several intensive pilot projects have shown that infection is so deeply entrenched in the environment that spraying of insecticides and drug distribution are not sufficient to interrupt transmission.

In some parts of the world, malaria has inadvertently been promoted by irrigation. A typical example is that of the Gezira, the region between the White Nile and the Blue Nile south of Khartoum. Irrigation had turned the Gezira into the most densely populated and most prosperous agricultural region of Sudan, and the periodical drying out of peripheral irrigation ditches, possible when the area was almost exclusively planted to cotton, had to be abandoned when other crops (notably, rice) were introduced. In 1950, an outbreak of malaria affected more than half of the total labour force, and since then malaria has been endemic. A major effort is now under way to keep the diseases under control.

- Schistosomiasis, caused by trematodes (or fluke worms) also affects about 200 million people. Free-swimming larvae (or cercariae) penetrate through the skin of a person entering the water, migrate to the liver where they mature into adult worms that settle inside blood vessels and go on laying eggs for several years. Infected people may become emaciated, with an enlarged spleen and bloated abdomen, and many develop cancer. It is possible to treat individual cases with injections of antimonials and other compounds, but most of these can cause severe side effects. There is no adequate method for mass treatment.

Schistosomiasis is often associated with rural development. Thus the incidence of the disease has been increasing in Egypt and Sudan since the creation of Lake Nasser, and in Ghana since the construction of the Akosombo Dam on Lake Volta. In Northern Nigeria there has been a three-fold increase in three years around the lake created by the Kainji dam, and even in the semi-arid Arabian Peninsula irrigation has introduced schistosomiasis to regions where it did not previously exist.

- Filariasis affects about 300 million people. The two major filarial parasites, *Wucheria bancrofti* and *Brugia malayi*, transmitted by mosquitos, infect about 250 million people (mainly in Africa, the Indian subcontinent, South-East Asia, the Philippines, China, and the Pacific Islands). They cause elephantiasis of the legs, arms and genitals, by obstructing the flow of lymph.

One form of filariasis is onchocerciasis (or river blindness), caused by *Onchocerca volvulus*, transmitted by *Simulium damnosum*—the blackfly. In the upper basin of the Volta river, more than a million people are infected and thousands are blind. A costly control programme has been initiated in seven of the most affected countries; it involves the spraying from helicopters of the often inaccessible fast-flowing streams where the blackflies hatch, and the treatment of infected persons, but there is a need for better drugs, with less side effects and more effective against adult worms.

- Trypanosomiasis affects some 10 million people. The African form of the disease, sleeping sickness, is endemic over about 10 million square kilometres of land, much of it fertile but abandoned to the tsetse fly, vector of the disease. (It is estimated that this land could provide for a cattle population of 125 million.) The South American form of trypanosomiasis is Chagas' disease, incurable and fatal (it destroys the heart).
- Leprosy, one of the most perplexing infectious diseases, also affects at least 10 million people. Although Hansen's bacillus, or *Mycobacterium leprae*, was described more than a hundred years ago, it has not been grown *in vitro* (or, at least, no reported culture has yet been confirmed). Even the mode of transmission of the disease is not well understood, and although it is generally believed that infection is from man to man, Hansen's bacillus has also been identified in insects, and some researchers believe their bite may also be involved.
- Leishmaniasis, the sixth disease included as a target in the initial stages of the Special Programme, is caused by various protozoa of the genus *Leishmania*. Two of its forms are lethal: the South American *espundia*, which kills by destroying the face, and visceral leishmaniasis, or kala azar.

The programme

There are several reasons why the timing for a renewed effort to develop remedies against these diseases is propitious.

The means to control and treat them are limited, and there is relatively little research directed towards new remedies. A number of recent findings, however, both in parasitology and fundamental biology, can be used to explore new approaches. Several such approaches have been identified, and "task forces", or scientific working groups, have been formed by the WHO, consisting of top scientists in various disciplines, to pursue specific goals.

One group, for instance, is concerned with immunology of malaria, and its ultimate goal is to develop reliable, long-acting vaccines, which would undoubtedly revolutionise the control of malaria. Infection has long been known to produce a certain degree of immunity, and some experimental vaccines have already been produced Last year, it was shown that some people possess a genetic factor that prevents the invasion of red blood cells by malaria parasites. This genetic trait conferring resistance to malaria is called "Duffy negative", because red cells lack the Duffy antigen, named after the first person in whom it was discovered It appears that this antigen leads the parasites into the red blood cells, and that in Duffy negative people the absence of the antigen protects the blood cells against the parasites Some preliminary experiments indicate that certain enzymes can block the antigen, thus conferring anti-malarial protection to the cells.

An even more important finding was announced only last April by Professor William Trager of the Rockefeller University in New York, who is a member of the Special Programme's "task force" on immunity to malaria he has succeeded in maintaining a laboratory culture of *Plasmodium falciparum* for three months This is the first time that a continuous culture of any of the malaria parasites has been successfully established *in vitro* and gone through a large number of multiplication cycles Large amounts of pure *P falciparum* can now be available, and this is a significant step towards the development of a vaccine.

The harvest of a large number of *Mycobacteria leprae* is also possible since researchers in Louisiana found in 1971 that injection into nine-banded armadillos caused massive infection of the animals. (Previously, infection had been achieved only in mouse footpads, and it was very limited.)

The WHO's scientific working group on immunology of leprosy has already engaged in antigen preparation and purification, and three promising antigens have been isolated, one in Venezuela, one in the United Kingdom, and one in the USA. As with other task forces, the specialists from several countries meet periodically, either at the WHO headquarters in Geneva or elsewhere, to coordinate their efforts. There is good hope that a practical vaccine, providing long-term protection against *M. leprae* can be developed, and a tentative schedule has already been established if all goes well, field trials should start in four or five years

Less is known of the immunological aspects of schistosomiasis, filariasis, trypanosomiasis and leishmaniasis, but there is, nevertheless, hope that vaccines can also be developed against at least some of these diseases

Recent research has shown, for instance, that the *Schistosoma* parasite has a very sophisticated system to ensure its survival in spite of the immunological defences of the organism it invades When a free-swimming preadult cercaria penetrates through the skin of a person, it does trigger antibody production But within a few days, by the time the parasite reaches maturity. It appears to cover its antigens with proteins that mimic the host's own antigens Thus, if immunisation could increase the organism's reaction against the pre-adult cercaria, the schistosoma could be destroyed before it had time to protect itself.

High technology

At the same time, other participants in the Special Programme are exploring the possibility of entirely new approaches, relying on recent bio-medical knowledge Professor de Duve, for instance, is attempting to apply "lysosome therapy" to some of the tropical diseases "Lysosomes," he says,

> are essentially miniature little stomachs, which occur in all cells One of their principal functions is to serve in the digestion of food 'eaten' by the cells by a special capture process, called phagocytosis or pinocytosis, depending on the size of the food particles taken in As with humans, cells may be greedy or frugal, and they may exhibit a wide variety of tastes Our purpose is to take advantage of these differences to kill certain cells selectively by poisoning their favourite food .To do this, we bind the poison to a carrier molecule in such a way that it will be released when it gets in the lysosome, that is, in the stomach of the cells that have eaten this poisoned food.

Experiments in mice carried out at the International Institute of Cellular and Molecular Pathology in Brussels have shown that such "selective poisoning" can be effective against at least one *Trypanosoma* parasite A similar approach can be tried for the treatment of diseases such as schistosomiasis or onchocerciasis, caused by worms with very tough skins, whose weak points may be their "stomachs". Even the leprosy bacillus, which has no lysosomes of its own, may be susceptible to similar "poisoning" because it develops within membrane-bound vacuoles resembling lysosomes in the macrophages of its host.

Enzyme therapy is another possible approach. It is known, for instance, that fertilised eggs of the nematode worm, another parasite of man, manufacture chitin, a substance that protects the cell, since mammals do not produce chitin, interference with the enzymes needed to produce it could destroy nematode eggs without affecting the human host.

Interference with the parasites' nervous system could also be explored —notably by acting on chemotaxis, an important determinant of behaviour, or on neurotransmitters (experiments with *Caenorhabditis elegans,* a free-living soil nematode, have shown that tetramysole, an agonist of acetylcholine, a major neurotransmitter, effectively paralyses the worms, arresting feeding and mobility).

Vector control, likewise, can benefit from goal-oriented research, notably in the area of biological vector control. It is known that parasites can be infected by other parasites (for instance, mermithid worms can infect and kill the tsetse fly). But basic research into the biology of the insect and its predator, and into the ecological impact of such an approach, must first be carried out.

These are "high technology" approaches, that require the commitment of skilled manpower and adequate budgets. Their goal is the development of remedies on the basis of knowledge of parasite function and biology, rather than through often empirical, large-scale screening, such as has been widely used until now in anti-parasitic drug research.

The purpose of the Special Programme of Research and Training in Tropical Diseases is not, however, limited to such research, much of which must be carried out in institutes, universities, and pharmaceutical laboratories in the developed world. The very countries most affected by tropical diseases will be associated with the programme

At the beginning, the focus will be on Africa, which has the highest prevalence of the six diseases and where multiple infection is almost the rule. Several African countries have expressed their willingness to participate in and contribute to the programme, and Zambia has offered laboratories in the large Ndola hospital complex for the creation of a multidisciplinary research centre bringing under the same roof different aspects of laboratory research and clinical medicine. Strengthening of existing laboratories, creation of new ones if necessary, and training of additional indigenous personnel, are planned as part of the programme to promote self-reliance in the very parts of the world where tropical diseases are prevalent.

Several meetings devoted to the Special Programme, co-sponsored by the WHO and the United Nations Development Programme, have already been held, and scientific work has started with the help of initial funds contributed last year by several nations and organisations But a long-term commitment is needed, as the programme cannot be financed from the shrinking budgets of the WHO or UNDP This is why a meeting with potential donor nations and agencies will be held later this year. In view of the magnitude of the problem being tackled, and the results that can be expected, the initial annual budget of $15–$20 million (the price of a jet fighter or a few miles of superhighway) seems reasonable enough. ☐

Assessing the OTA

Congress's three-year-old Office Technology Assessment (OTA) has come under sharp, and potentially damaging, criticism from another Congressional committee and from the former chairman of its own advisory council. Both have argued that it has failed to live up to expectations and that there is still no clear understanding of its role and function. Colin Norman reports from Washington.

ESTABLISHED in 1972 by an Act of Congress, OTA is meant to furnish Congress with advice and analysis concerning scientific and technological issues. Its mission is frequently described as providing an early warning system on such matters. But its chief problem, which lies at the root of much of the criticism, is that on the one hand it is expected to study long-term issues, while on the other it is supposed to help Congress, which is more concerned with yearly budgets and two-yearly elections.

OTA studies and reports on matters referred to it by other committees of Congress, and it also generates some studies itself. Its operations are managed by a Director, Emilio Q. Daddario, a former Congressman who wrote the original legislation which led to OTA's establishment, and its policy is provided by a board consisting of six Senators and six Congressmen. In addition, an advisory council, whose members are drawn from industry and academia, provides advice on OTA's operations.

The first criticism of OTA's operations surfaced in the office's recently-published annual report, which contained a letter from Harold Brown, President of Caltech, resigning as chairman of OTA's advisory council, and a response from Representative Olin Teague, chairman of the office's governing board.

Written last December, the letter begins with some words of praise for a few OTA studies, but criticises the fact that the office has taken on too many trivial tasks and asserts that "few of us on the council, I believe, would say that we are satisfied with what has been accomplished, compared with what we hoped for and still believe possible". Brown suggests in particular that OTA has been concentrating too much on immediate problems. "inevitably there are strong pressures on the Congress as well as on the Executive Branch to concentrate on immediate problems. Certainly those problems must be faced as they arise. But there needs to be a balancing effort within the Congress to foresee problems of the medium and even the long term future".

Less gentle criticism has come from an obscure Congressional body, known as the House Commission on Information and Facilities, chaired by Representative Jack Brooks of Texas. On the basis of an 8-month study, the commission last week issued a report which concludes that "OTA remains substantially short of reaching levels of performance reasonably expected of an information resource of its size and cost and access to expertise". The report, in short, suggested that OTA has been beset by operational problems and by lack of a clear definition of its functions.

The report states that the Commission found confusion among OTA's staff, council and board, and between OTA and some Congressional committees, over the office's role and responsibilities. It suggests, therefore, that OTA's statutory authority should be reviewed, and a clear definition of technology assessment should be drawn up, presumably so that OTA's territory is staked out and so that there's no overlap of its functions with those of the Congressional Research Service or the General Accounting Office. The report goes on to state, however, that so far there has been no such overlap.

More specifically, the report expresses reservations about the fact that OTA has been performing a growing share of its studies itself, rather than having them done by outside contractors, and suggests that OTA should have a firmer policy on which kinds of studies should be performed in-house. That criticism conflicts, however, with a comment made by Brown in his letter. Listing some "substantial advances" made by OTA, Brown notes that "an initial tendency to think almost solely in terms of contracted studies has been succeeded by a more balanced procedure involving advisory panels, contracted studies, and some (as yet rather little) in-house assessment work".

But perhaps the Commission's most biting criticism concerns OTA's administrative structure. "Organisationally", it says, "OTA lacks the minimum of orderly structure", and it suggests that OTA should begin immediately, if necessary with the help of management consultants, to put itself in order.

Finally, both the Commission and Brown criticise the poor relations which have developed between OTA and its advisory council. "At one time or another", Brown states, "most Council members have expressed frustration about the relatively large amount of time, effort and persistence that they have invested in terms of the effect they feel they have had I believe that the important task of strengthening communications between the

NSF budget goes to conference

HOPES for at least a modest increase in funds for basic research in the United States have been unexpectedly revived by the Senate. After intensive lobbying from scientific and higher education organisations, the Senate last week restored most of the money which the House of Representatives had slashed from the budget of the National Science Foundation (NSF), and the matter must now be decided in a conference committee consisting of members from each body. It's a fair bet that NSF will end up with a small increase, though not as great as the 20% boost proposed by the Ford Administration.

President Ford's budget request for NSF for the fiscal year which begins on October 1 was designed to offset the effects of inflation, which has eaten deeply into support for basic research over the past few years But the House slashed nearly $60 million from NSF's budget, giving the agency less than a cost-of-living increase, largely on the grounds that basic research isn't too badly off in relation to other items in the federal budget.

The House's parsimony prompted a massive letter-writing campaign to key Senators, and a move to restore the funds, led by Senators Charles Mathias of Maryland and Edward Brooke of Massachusetts, proved successful. The senate agreed to Mr Ford's proposed 20% increase, in spite of opposition from Senator William Proxmire, Chairman of the Senate subcommittee which handles NSF's budget request. Proxmire said that he believes the increase is much too generous, but was outvoted in the committee.

The conference committee will probably settle on a figure about half way between the levels approved by the House and Senate, which would at least give basic research its first real increase in about five years.

Board and the Council needs to be faced during the coming year". And the House Commission on Information and Facilities, noting that there has been considerable confusion over the role of the council, suggests that "substantial revision of the Council's statutory function, or its abolition, be proposed on grounds that unless Council contributions are integrated more effectively in the policymaking process, its existence can only be a source of frustration and disharmony within the agency".

There is clearly going to be more debate before OTA is able to establish a comfortable role in which it acts as a long-term analyst and at the same time provides advice geared to Congress's short-term outlook. □

EEC

European science policy sought

The European Commission recently unveiled proposals for a Community science policy. Progress towards the aim of a common approach, reports Chris Sherwell, may prove to be more pedestrian than the enthusiasts are prepared to admit.

IF the expressions of satisfaction emanating from the vicinity of the Berlaymont Building in Brussels are anything to go by, Europe is now well on its way towards forging a science and technology policy for itself. The Commission of the EEC, which has its headquarters there, recently unveiled the results of a closed symposium which took place under its auspices in Milan towards the end of May.

The aim of the symposium was to gather suitable suggestions for guidelines regarding research and development which the Commission might present to the relevant Council of Ministers later this year. This it reckons to have achieved. Among the 100-odd participants were members of the European and the various national parliaments; members of the Commission and of the Economic and Social Committee (a consultative body serving the EEC and Euratom), and government officials; and the customary host of scientists, engineers, industrialists and trade unionists who help to make meetings like this more models of organisation than of representativeness.

The three-day symposium, at Milan's International Institute for Management of Technology, was organised by Directorate General XII (Research, Science and Education) of the Commission with the aid of CERD (the European Research and Development Committee), which is an independent 21-member body of scientists and engineers established by the Community in 1973 to advise the Commission on the formulation of a common science policy. It took place in the context of an effort finally launched two years ago to sow the first seeds of a revamped Community science and technology policy to replace the old sectoral approach of the previous sixteen years.

That effort in fact had its real beginnings many years ago, but it was only in January 1974 that the Council of Ministers found itself able to give expression to sentiments voiced at the Paris Heads of Government meeting in October 1972; the Council passed four resolutions which would provide a basis for a broad Community science and technology policy. The resolutions covered matters like coordination, participation in the European Science Foundation and programmes of action. The Commission was landed with the task of looking at the science policies of the nine member states with a view to producing Community-wide projects and a common approach externally.

The hope was that the terms of a full-blooded European science policy could be finalised by the end of 1976. The Council, when it met again in June 1975, urged that discussions on the objectives of such a policy be held "without delay", and the Milan symposium, being the major part of those discussions, heralded the end of this first phase in the new Community approach. The next phase begins if and when the Council approves the recommendations of the symposium's five working parties, each of which aimed to tackle separate areas of interest.

Recommendations

The Commission document sumarising the working parties' recommendations, taken as a whole, does not make exciting reading, being littered throughout with empty phrases characteristic of all ostensibly agonising searches for lowest-common-denominator agreements. Hidden in the interstices of the Commission's denatured language, however, is some sort of basis for the optimism now being expressed so expansively by the Director General at DGXII, Herr Gunter Schuster. Here, in essence, is the gist of the recommendations.

Working Party I: Long term objectives and priorities. The group recommends that a suitable instrument "such as proposed in 'Europe+30' " be established "at the earliest possible time", and that in the meantime a "small unit of specialists" be set up in or be linked to DGXII "without delay". Lord Kennet from Britain dissented on the latter point, arguing that such a staff should be actually in DGXII to avoid the danger of it becoming a substitute for Europe+30.

Among the many areas of high priority for research in the long term, the working party includes Europe's ecological system, climatic changes, water management and food shortages.

Working Party II: Medium term objectives and priorities. The main theme informing this group's recommendations emphasises the need to do more to bring innovations to potential customers. The group wants to "make operational, within the Communities (the EEC, the European Coal and Steel Community and Euratom), structures for securing and examining research and development proposals coming from any public or private European organisation". It also wants "to relaunch the Community development contract procedure" reserved for *European* [group's italics] groups of enterprises and multinationals, and "to establish structures for conveying the Commission's intentions". A consultative comittee for industry is suggested.

More specifically, the group hopes that certain subjects now neglected or insufficiently developed will receive "special consideration"—among them, hydrographical problems arising out of the existence of multinational basins, European epidemiological research, recycling and reclamation, basic biological research, and ethical problems in genetic matters.

Interestingly, there is a frank acknowledgment of the constraints within which such a policy can work. The human and financial resources the EEC has at its disposal, the group says, "are not considerable", and are so concentrated as to prevent the needs of a real European policy being met over a wider field—and in certain fields, the group declares, the EEC could not be satisfied with the role of a mere catalyst. The scientific and technical activity of the EEC, it stresses, is "an essential part of a true European economic community", and it expresses its hope for a separate budget that would allow further progress.

Working Party III: Coordination of national policies. After recognising that a common policy can only be built up "slowly and step by step out of the coordination of national policies and common sections", this group deals with coordination in four fields.

In basic science, it says, "the self-coordination of scientific groups, institutes, organisations and associations is the most important and useful instrument of coordination"—and here the group has in mind the cooperation already operating between Britain's SRC, France's CNRS, Germany's Max Planck Institutes, and so on. Where research is carried out almost totally by industry, coordination should be limited to the "harmonisation and coherent development of support activities in the member states".

Research and development for "public services and tasks", on the other hand, "is undoubtedly the central object for coordination in the Community", because in these spheres the national government have sufficient responsibilities. Finally, in the mixed sector ("the most difficult sector for coordination"), where it is noted that funds in all countries are heavily concentrated in a few areas (nuclear, space, electronics), the group states rather vacuously that projects performed by industry but financed by government "should not be excluded from coordination".

Working Party IV: Innovation policy. Industrial enterprise, says this group, is "the main actor in the innovation process", but it is governments which have to create a favourable climate—and promotion of innovation at the Community level "is at present hampered by the lack of a common industrial policy", which it calls "a serious obstacle to the development of comprehensive industrial R & D programmes".

The Community, it says, can make "an important contribution" towards creating the right climate: among other things, it could support cooperation in long term industrial research and development (fusion, aerospace, solar energy), finance demonstration projects, make more accessible those public markets where state agencies are large buyers of technology, and improve access for small and medium sized industries to technological innovation. The group, like the second working party, recommends that the Commission set up an industry consultative committee to give industrial viewpoints on the Community's R&D policy.

Herr Schuster, Director General at DGXII.

Far from judging the present economic plight of European countries a deterrent to innovation, the group rather believed this problem called for a special effort. Similarly, state participation in the field was less a constraint than a stimulus, although state encouragement of specific projects—not so much in fields of obvious community interest (energy supply, public transport) as in fields like cybernetics—demanded fundamental discussion. The general feeling was that there was insufficient coincidence between the long term projects of member states and those of the Community—and that the liaison now lacking could, unsurprisingly, only be promoted through greater coordination. Plainly, though, the overlap with Europe's much-sought-after industrial policy is regarded as vital to the success of any research policy relating to industry.

Working Party V: Dissemination and exploitation of results. The group recommended that "a readily and selectively accessible dissemination system for information about R&D" be set up within the Community, based on national information services and existing contacts between organisations. It further recommended that the Community's four-establishment Joint Research Centre (JRC) should have greater involvement in the exploitation of its own inventions, and that the Community should be able to provide companies with incentives where necessary (through exclusivity or lead times, for example). A small team of experts should also be available, with close links to scientists in the JRC and contractors, on the one hand, and to exploitation organisations in member states on the other.

Long way to go

All of which suggests that there is a long way to go before a real European policy is actually in operation. Although the recommendations reveal a rather limited number of specific institutional proposals, the general disposition in favour of a European approach, and one buttressed through additional budgetary support at that, shines through. The main emphasis, naturally enough, is on the key-word "coordination", perhaps the most crucial block in the fragile Community science edifice. But the question of how best this might be achieved, although begged throughout, does not receive a great deal in the way of answers.

Not that Europe's welter of institutions does not already include a goodly proportion of science-oriented bodies equipped to supply the answers. Apart from CERD, the most important is probably CREST, the Scientific and Technical Research Committee. It is the product of the January 1974 Council resolution on coordination, and is blessed with the task of "helping Community institutions to define objectives and securing the development of a common policy for science and technology." According to Working Party III, it is CREST which is to be regarded as the central committee where "coordination in all fields of R&D is focused", and Community officials looking to CREST to translate proposals into reality do point to its achievements—in the implementation of Community projects on new energy sources and scientific information, for example, and in planning cooperation with non-Community countries, which it does within the context of COST, the Committee of Senior Officials in Scientific and Technical Research.

But there is little question about how much has really been achieved so far. No one at the Commission doubts that progress has been and will continue to be slow, or that CREST has yet to come into its own. There are pilot projects in hand, in the fields of energy, medical research and the determination of research and development indicators, and these represent practical attempts at coordination and alignment. For the moment, however, they merely supplement existing instruments of coordination, which also include the Advisory Committees on Programme Management (ACPMs).

The perspective being adopted in Europe is thus distinctly medium to long term—CERD itself has proposed that a European Science Year be organised in 1978 or 1979, just before the United Nations World Science Year in 1980. In places the Commission's document makes a tilt towards the themes of humanising science and of Third World development, and there does seem to be an underlying view which argues that, if a European science policy is to have any chance of success at all, then somehow science itself will have to be brought closer to the proverbial man in the street, and be made to be seen as relevant to his needs. But if that laudable view is scuttled by the trials of actually identifying Europe's research requirements, and of formulating an acceptable policy (particularly regarding the distribution of its benefits and its burdens), there should be few surprised faces. □

news and views

Factor VIII

from D. E. G. Austen

FACTOR VIII activity is essential for normal blood clotting and haemostasis, and an inherited deficiency of this activity occurs in haemophiliacs and patients with von Willebrand's disease. In von Willebrand's disease there is also a deficiency of a closely related substance called factor VIII-related antigen (Zimmerman *et al.*, *J. clin. Invest.*, **50**, 244; 1972). The presence of this antigen is demonstrated by raising heterologous antibodies in animals to factor VIII preparations and using them in immunoelectrophoretic procedures. Precipitin lines reveal the presence of factor VIII-related antigen in the plasma or serum of both normal people and haemophiliacs, but not in the plasma or serum of patients with severe von Willebrand's disease.

Haemophilia is determined by an X-linked recessive mechanism of inheritance while von Willebrand's disease is inherited as an autosomal dominant condition. As far as is known, there is no inherited deficiency of antigen alone and the concentration of antigen in normal people and most patients with von Willebrand's disease is roughly proportional to their factor VIII activity. These various relationships between factor VIII and the antigen suggest that their production *in vivo* proceeds by a common route at some stage.

Subunits

Factor VIII is a glycoprotein and many workers have reported it to have a molecular weight of more than 10^6 as determined by gel filtration chromatography. It is relatively easy to bring about an apparent reduction in this molecular size using high or low ionic strength (Weiss *et al.*, *Thromb. Diath. haemorrh.*, **27**, 212; 1972; Owen and Wagner, *ibid*, **27**, 502; 1972) or reducing agents (Austen, *Br. J. Haemat.*, **27**, 89; 1974) and the factor VIII activity then appears by gel filtration to have a molecular weight of around 230,000. It has been suggested recently, however, that experimental conditions affect the speed at which low molecular weight factor VIII passes through the gel filtration column (Switzer and McKee, *J. clin. Invest.*, **57**, 925; 1976) and so the exact values of molecular weight should not be emphasised at this stage. Factor VIII-related antigen remains unchanged by variations in ionic strength or by very mild reducing conditions. As a result, gel filtration of the products of such reactions separates factor VIII activity from the antigen, although the extent of this separation is still a matter of discussion. Two different hypotheses have been suggested to explain these results. The first is that factor VIII is made up of several subunits which can be disaggregated, while at the same time, factor VIII-related antigen circulates as a completely separate molecule. The second possibility is that factor VIII consists of a small active molecule which is bound as a passenger to a large carrier molecule of factor VIII-related antigen and that disaggregation experiments simply separate the two.

Several workers have now also cleaved factor VIII-related antigen into subunits. Some have effected this in moderate reducing conditions and retained the antigenicity of the protein (Austen *et al.*, *Nature*, **253**, 55; 1975; Peake and Bloom, *Thromb. Haemostasis*, **35**, 191; 1976). Others have used severe conditions along with sodium dodecylsulphate (SDS) gel electrophoresis and report that they can detect the protein using staining techniques (Marchesi *et al.*, *J. clin. Invest.*, **51**, 2151; 1972; Legaz *et al.*, *J. biol. Chem.*, **248**, 3946; 1973; Switzer and McKee, *J. clin. Invest.*, **57**, 925; 1976). In both cases the molecular weight value obtained is close to that of the small active factor VIII fragment and this may suggest that the antigen and factor VIII are two proteins with a similar basic structure.

Antibodies

Another field of useful investigation has been concerned with the development of factor VIII antibodies. In patients suffering from haemophilia, antibodies can develop to infused therapeutic concentrates of the factor. Such antibodies will inactivate factor VIII both in its high molecular weight or its low molecular weight form. They are non-precipitating and are not believed to cross react with factor VIII-related antigen. But with severely affected von Willebrand's patients who have a minimal level of antigen the precipitating-type of antibody can develop, as Manucci *et al.* show (page 141 of this issue of *Nature*). These are directed against factor VIII-related antigen and have only a low level of cross reaction towards factor VIII activity.

More information can be obtained by studying antibodies produced in rabbits after infusion of factor VIII and the antigen. Here there is general agreement that antibodies can be separated which are directed against factor VIII-related antigen. On the other hand, antibodies which are directed against factor VIII-related antigen have been reported to have varying degrees of cross reaction with factor VIII activity, possibly depending on the experimental conditions. This work has been extended recently by a paper (Ratnoff *et al.*, *Blood*, **47**, 657; 1976) which reports that antibody directed against factor VIII-related antigen does not inactivate the low molecular weight fragment of factor VIII even though it does react with native factor VIII.

Interpretations

A reasonable solution to some of the apparent differences in reported results is suggested in a paper (Kernoff, *Nature new Biol.*, **244**, 148; 1973) which shows that the antibody against factor VIII-related antigen will precipitate factor VIII but that the complex retains factor VIII activity. As a result, an apparent inactivation could be obtained if the supernatant solution was assayed after centrifugation. An interesting confirmation of this was also seen in immunoelectrophoresis experiments (Bird and Rizza, *Br. J. Haemat.*, **31**, 5; 1975) where the actual precipitin lines formed by factor VIII-related antigen and its antibody were shown to possess factor VIII activity. (The sample subjected to the immunoelectrophoresis contained both active factor VIII and antigen.) Clearly factor VIII and factor VIII-related antigen have determinants in common, or alternatively the two are bound together.

The bonding of active factor VIII subunits must rely on electrostatic attraction since ionic strength changes are sufficient to sever them. Chemical reduction has also been shown to disaggregate factor VIII and this might be due to cleavage of intramolecular disulphide bridges between different parts of the same factor VIII subunit. When these are severed, different sections of the subunit could alter spatial configurations, and in that way geometrical changes would occur to a point where the electrostatic forces could no longer keep the subunits together. Bonds between the subunits of factor VIII-related antigen must be considerably stronger because more vigorous chemical reduction is required to disaggregate them. It would be anticipated that disulphide bonds are involved in some way but further conclusions are not possible at this stage.

Although there is considerable disagreement about the interpretation of the reported data on factor VIII, some useful conclusions can be drawn. Factor VIII-related antigen is shown to be a large molecule with a molecular weight of more than 10^6. Active factor VIII can be separated from factor VIII-related antigen and to that extent they must be considered as separate entities. But they have intriguing similarities. They are difficult to separate unless factor VIII is cleaved into subunits and they have some antigenic determinants in common. The size of their subunits seems to be similar. Exercise and fear in the human subject bring about a proportionate increase in both. It is also important that the infusion of haemophilic plasma into a patient with von Willebrand's disease produces factor VIII activity.

These results are fascinating and most of them could possibly be explained on the basis of several hypothesis. In my opinion, however, the most reasonable hypothesis is that factor VIII and factor VIII-related antigen are separate molecular species with a basic structural similarity. This does not exclude the possibility that other species with that same basic structure are also present. It is interesting to speculate that such a substance, or even factor VIII-related antigen itself, could be the precursor of factor VIII. If this were the case, then treatment of haemophilia in the future might be based on converting a precursor into its active form rather than direct factor VIII replacement. □

Peptides in brain and intestine

from A. G. E. Pearse

In 1931, while studying the distribution of acetylcholine, von Euler and Gaddum (*J. Physiol.*, **72,** 74) detected, in alcoholic extracts of equine brain and intestine, a smooth muscle stimulating and hypotensive agent which was later (Chang and Gaddum, *J. Physiol.*, **79,** 255; 1933) called substance P (for powder). Its identity as a peptide (protein) was soon established (von Euler, *Skand. Arch. Physiol.*, **73,** 142; 1936) but its isolation and characterisation had to wait for almost 40 years (Chang and Leeman, *J. biol. Chem.*, 245, 4784; 1970; Chang, Leeman and Niall, *Nature*, **232,** 86; 1971).

The story of substance P can now be seen to provide nearly all the clues required for an understanding of the recent spate of reports of peptides common to brain and intestine. The latter region can more accurately be described as 'gastrointestinal tract and pancreas' and the peptides are regarded on the one hand as presumptive or proven neurotransmitters and, on the other, as presumptive or actual hormones.

A current list of the common peptides, with their original and new locations, is given in Table 1. The first two peptides in the list are primarily of neural origin. Demonstrated in brain by radioimmunoassay, with highest concentrations in the substantia nigra and hypothalamus, substance P has now been localised, by immunocytochemical techniques, not only in the central nervous system (Hökfelt *et al.*, *Science*, **190,** 889; 1975), but also in some of the enterochromaffin (EC) cells of the gastrointestinal tract (Pearse and Polak, *Histochemistry*, **41,** 373; 1975) and bile ducts. This peptide (H–Arg–Pro–Lys–Pro–Gln–Gln–Phe–Phe–Gly–Leu–Met–NH_2) is probably widely distributed in primary sensory neurones and their processes, and in nerve terminals in many areas of the brain.

Somatostatin, named for its growth hormone release inhibiting properties, was isolated from ovine hypothalamus and characterised as a tetradecapeptide (H–Ala–Gly–Cys–Lys–Asn–Phe–Phe–Trp–Lys–Thr–Phe–Thr–Ser–Cys–OH) by Brazeau *et al.* (*Science*, **179,** 77; 1973). Later found to inhibit release of a much larger number of endocrine peptides, including insulin, glucagon and gastrin, somatostatin was detected by radioimmunoassay in the stomach and pancreas, in concentrations equal to those recorded in the hypothalamus (Arimura *et al.*, *Science*, **189,** 1007; 1975). It has been localised immunocytochemically in the neurones of the nucleus periventricularis of the hypothalamus, in nerve fibres in the neurohypophysis and in some nerve fibres in the wall of the intestine (Hökfelt *et al.*, *Acta endocr. Suppl.*, **80,** 200; 1975).

Using similar immunocytochemical techniques several groups, independently, have now demonstrated somatostatin-like immunoreactivity in the D cells of the pancreatic islets and upper gastrointestinal tract. Consideration of the physical associations of the D cells with cells producing insulin, glucagon and gastrin leads to the supposition that the actions of the peripheral variety of this hormone are paracrine, directed that is to neighbouring cells and tissues, rather than truly endocrine. The last two peptides in Table 1 are products of two types of gastrointestinal endocrine cell belonging to the APUD series (Pearse, *Proc. R. Soc. Lond.*, **B170,** 71; 1968; *J. Histochem. Cytochem.*, **17,** 303; 1969). The name is an acronym based on their amine-handling qualities (amine content and/or amine precursor uptake and decarboxylation), but it stands for a larger spectrum of common cytochemical and ultrastructural qualities.

Gastrins, of whatever molecular species, are almost completely restricted to the G cells of the pyloric antrum of the stomach. Contrary to recorded opinion (Greider and McGuigan, *Diabetes*, **20,** 389; 1971), there is no gastrin in the adult endocrine pancreas.

Last year a gastrin-like peptide was demonstrated by immunoassay in extracts of human and animal brain (Vanderhaegen *et al.*, *Nature*, **257,** 604; 1975), and levels in the cerebral grey matter were as high as 200 ng per g of dry tissue. Since it eluted later than gastrin-17 on gel filtration, the new peptide must be regarded as closely related to, rather than identical with, gastrin.

Vasoactive intestinal peptide (VIP) is a 28-residue peptide originally isolated from porcine duodenum and shown to be structurally and biologically related to secretin and glucagon (Mutt and Said, *Eur. J. Biochem.*, **42,** 281; 1974). Present in the gastrointestinal tract, from oesophagus to rectum (Bloom and Bryant, *Gut*, **14,** 823; 1973), it was there shown to be produced by an APUD cell now tentatively identified as the H cell (Polak *et al.*, *Gut*, **15,** 720; 1974).

Two contemporaneous papers have appeared recently both recording the presence of VIP in neural tissues. Said and Rosenberg (*Science*, **192,** 907; 1976) have measured VIP immunoreactivity in three neuroblastoma cell lines in culture, finding high levels in all three and in acid alcohol extracts of the central nervous system and sympathetic ganglia. Their values in p mol per g (wet weight) of tissue from dogs, are higher in frontal lobe cortex (19) and hypothalamus (20) than in duodenum, ileum and colon. Bryant *et al.* (*Lancet*, *i*, 991; 1976) likewise report high levels of VIP immunoreactivity in the cerebral cortex and hypothalamus of both man and pig, but in each case their average figures are lower than those recorded for the different regions of the gastrointestinal tract. In this second study a most important finding was that the bulk (94%) of VIP extractable from porcine and human brain elutes identically with, that is to say is virtually identical with, the pure intestinal peptide. Parallel immunocytochemical studies showed that in human and porcine intestine VIP is present not only in the endocrine VIP cells but also in some fine nerve fibres in the lamina propria, in the cell bodies of the myenteric plexus and in the adrenal medulla.

The two sides of the equation, neural and endocrine, are united by an essentially simple concept. First formulated some 10 years ago to explain the possession, by neurones and by endocrine cells producing polypeptide hormones, of a set of common cytochemical and ultrastructural characteristics, the APUD concept then postulated that the endocrine cells were derived from a common neuroectodermal ancestor. This was conceived as arising in the embryo from that transient but massive structure the neural crest, at one time considered as a fourth germ layer. Subsequent experimental work having shown that only seven of the 36 cells in the now amplified APUD series indeed arise from that structure, the concept has been extended to include, under the broad heading of neuroectoderm, not only the neural, tube, neural ridges and neural crest, but also the specialised ectoderm of the placodes (Pearse and Takor, *Clin. Endocr.*, Suppl. **5**, 291; 1976).

It is now postulated that all peptide-hormone-producing cells are derivatives of specialised ectoderm and therefore, effectively, of cell lines derived from the epiblast and programmed for ultimate neuroendocrine function. Thus regarded, the cells of the APUD series constitute a third division of the nervous system, functioning as third-line effectors with activities slower in onset and of longer duration than those of the second-line effectors of the autonomic division. These, in turn, are of slower onset and longer duration than those of the somatic division.

If the concept is simple and concise, its implications are diverse and far reaching. They depend, to a large extent, on the nature of the several disciplines involved and these range from neurobiology (physiology, pharmacology and biochemistry), endocrinology and peptide chemistry, through conventional and comparative embryology to, if it yet exists, the molecular variety of that science.

Table 1 Peptides common to intestine and brain

Peptide	"Original" location(s)	New location(s)
Substance P	Brain (cortex) Substantia nigra Dorsal root ganglia Peripheral nerves Substantia gelatinosa	Gastrointestinal EC cells
Somatostatin	Cerebral cortex N. periventricularis Neurohypophysis Pineal	Pancreatic islet D cells Gastrointestinal D cells
Gastrin	Gastric antrum (G cell) Duodenum	Cerebral cortex (grey matter)
VIP	Gastrointestinal tract especially duodenum, colon (H cell)	Cerebral cortex (grey matter) Hypothalamus

G, H and D, Wiesbaden classification of gastroenteropancreatic endocrine cells; EC, enterochromaffin; VIP, vasoactive intestinal peptide.

Table 2 Anuran and mammalian peptides with common amino acid sequences

Anuran peptide		Mammalian peptide	
		Nervous system	Endocrine system
Caerulein	(*Hyla* sp.) (*Xenopus laevis*)	Gastrin	Gastrin, CCK
Phyllocaerulein	(*Phyllomedusa* sp.)	Gastrin	Gastrin, CCK
Physalaemic	(*Physalaemus* sp.)	Substance P	Substance P
Uperolein	(*Uperoleia* sp.)	Substance P	Substance P
Bombesin	(*Bombina bombina*)	—	Bombesin

CCK, cholecystokinin–pancreozymin.

Neurotransmitter peptides, many probably identical with individual endocrine peptides of the gut, and others related to the peptide products of exocrine (but still APUD) cells in the cutaneous glands of anurans (Erspamer and Melchiorri, *Pure appl. Chem.*, **35**, 463; 1973), will certainly be found widely distributed in the central and peripheral nervous systems. Their precise role in these situations can be envisaged as a matter of some complexity and fuller investigations of peptidergic neurotransmission will surely make it necessary at least to augment the older cholinergic and adrenergic notation.

The list of frog skin peptides with amino acid sequences common either to neural or endocrine peptides makes interesting reading (Table 2). Anuran cutaneous glands arise from the specialised ectoderm of the region adjacent to the embryonic neural plate and neural crest. They thus have a common origin with cells producing the brain and intestinal peptides which we have been considering and presumably they have evolved, in parallel with the nervous system, as a response to the(hostile) external environment.

A similar problem is posed by the existence of peptide products which are common to the nervous system, pituitary gland, gastrointestinal tract and placenta. Notwithstanding the nomenclature by custom attached to its principal layers, the cells of the endocrine placenta can be seen to arise from the neuroectodermal epiblast of the yolk sac, a layer which is continuous with the epiblast of the neural plate (Takor and Pearse, in preparation). Thus the many peptide hormones produced by the placenta can be linked with their counterparts in other regions.

The work of Steiner *et al.* (*Rec. Prog. Horm. Res.*, **25**, 207; 1969), on proinsulin biosynthesis, provided protein chemists with a basis for several currently popular theories on the molecular evolution of peptide hormones. Steiner's own theory deriving insulin by way of a protoproinsulin from an ancestral intestinal protease, and Adelson's (*Nature*, **229**, 321; 1971) enterosecretory hypothesis deriving most peptide hormones from the entoderm of the primitive gut, seem to require reconsideration. Exact knowledge of structural correlations between brain and intestinal endocrine peptides is essential to proper understanding of their molecular evolution. Continued search for these peptides must be made in the earliest available vertebrates and in the invertebrate kingdom also.

For embryologists a clear challenge is posed by the close relationships now observed between neurotransmitter and endocrine peptides. In the hands of experimental embryologists the biological marker technique using avian chimaeras (Le Douarin, *Bull. biol. Franc. Belg.*, **103**, 435; 1969) has provided watertight evidence for the neural crest origin of a number of cells in the APUD series. Operative techniques of excision or exclusion (Andrew, *J. Embryol. exp. Morph.*, **31**, 589; 1974; Pictet *et al.*, *Science*, **191**, 191; 1976) have so far shown only that the gastrointestinal endocrine cells probably do not come from the definitive neural crest. Where they do come from is thus the problem that remains for the techniques of experimental embryology to answer.

Unquestionably the real future lies with the new science of molecular embryology.

This alone can provide an answer to the central question—how are individual cells in the embryonic epiblast programmed for neuroendocrine function and how, and at what stage, are the further series of instructions added which determine the ultimate endocrine function of each of the original cells? Already (Le Douarin, *Med. Biol.*, **52,** 281; 1974) we have learnt something of the timing and nature of the later stages of instruction but it is the problem of elucidating the earliest stages which provides the real challenge to experimental ingenuity. □

Cathodoluminescence of dislocations

from John Walker

DISLOCATIONS—misplaced planes of atoms which disturb the regular periodicity of otherwise perfect crystals—are important both theoretically and technically. They reduce a material's mechanical strength and affect its electrical properties; the quality and yield of electronic devices are inversely correlated with dislocation density. Hence dislocations have been extensively studied, and various techniques are used to observe them, including X-ray topography, electron microscopy and etch pit formation. A recent paper by Kiflawi and Lang (*Phil. Mag.*, **33,** 697–701; 1976) has demonstrated that a new weapon—cathodoluminescence—can be added to the technological armoury.

Cathodoluminescence is the release of light induced by electron bombardment, just as occurs in a television (cathode ray) tube. In earlier papers Lang and his colleagues showed that the growth history of a diamond crystal could be studied using cathodoluminescence, and reported the existence of defects, suspected of being dislocations, which emitted a linearly-polarised blue luminescence. The most recent report demonstrates in a diamond a one to one correspondence between dislocations (as revealed by X-ray topography) and the blue-emitting lines (see Fig. 1); this proves beyond doubt that they are dislocations.

Features that appear in Fig. 1*b* but not Fig. 1*a* are dislocations which are too deep in the crystal to be observed in cathodoluminescence. Features in Fig. 1*a* that do not appear in Fig. 1*b*, although linear, are not dislocations. Their emission is not polarised and does not saturate in intensity with increased electron beam current, unlike the dislocation lines.

One problem with cathodoluminescence in the topographical examination of crystals is that it is limited to a layer within 100 μm of the surface by the penetration depth of the electrons. Consequently crystals need to be cut according to the surface to be studied. Furthermore, the crystal must be transparent to the emitted radiation. Diamond is ideal in this respect, because it transmits well into the ultraviolet, and can therefore be examined visually.

A great advantage of cathodoluminescence is its power of discrimination. Different types of feature can be distinguished easily. The possible variables are colour (blues, greens, yellows and pinks have been observed so far), polarisation of the light, and variation of luminescent intensity with electron beam current (some features saturate, others do not). No doubt cathodoluminescence will be used a great deal in the future for the study of dislocations and growth features in crystals. □

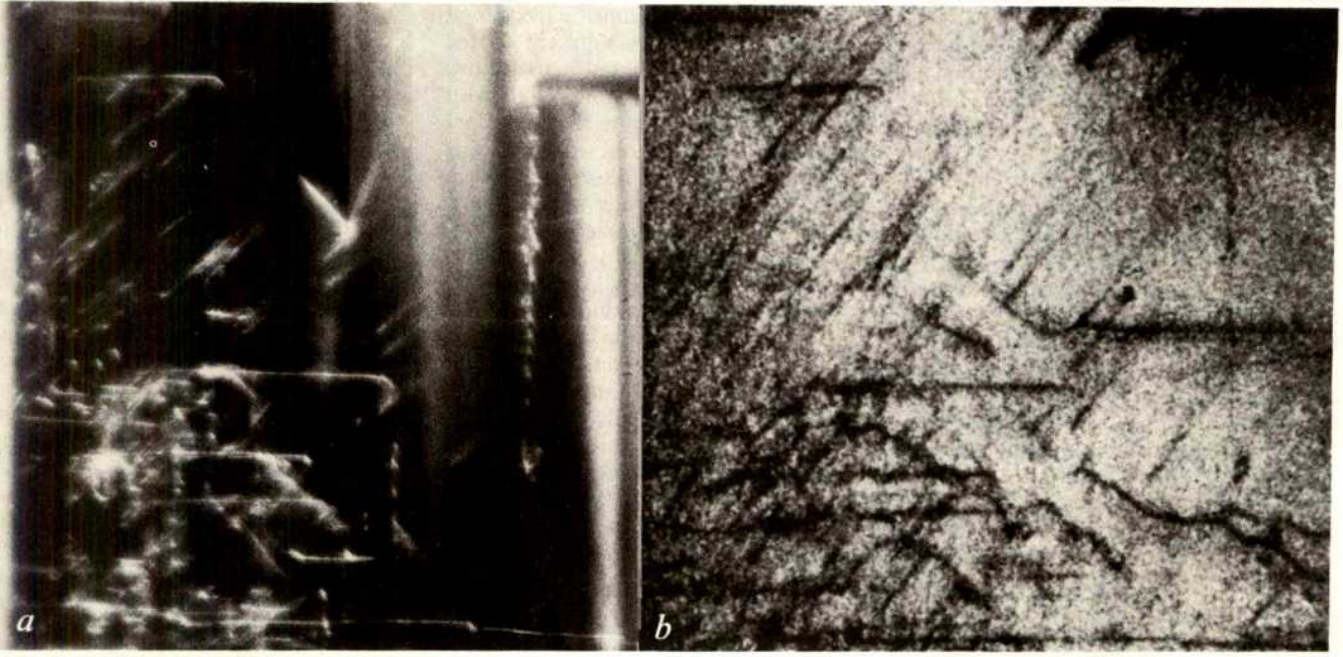

Fig. 1 Correspondence between cathodoluminescence images (*a*), and X-ray diffraction contrast images (*b*), of individual dislocations in a natural diamond.

How closely did the continents fit together?

from A. Hallam

A FUNDAMENTAL tenet of plate tectonics, that amount of crust created at oceanic ridges must equal the amount subducted elsewhere, has recently been challenged in a stimulating paper by Owen (*Phil. Trans. R. Soc.*, **A281,** 223; 1976). He has argued that the components of Wegener's supercontinent Pangaea moved apart as a consequence of 20% expansion of the Earth's diameter since the early Jurassic, less than 200 million years ago. This iconoclastic view is very radical in terms of physical theory and is no more likely to be widely accepted than the similar view put forward some years ago by the Australian geologist Warren Carey. Bearing in mind the unfavourable reaction to Wegener's continental drift hypothesis earlier this century, and its subsequent history, it behoves earth scientists to preserve an open mind on such matters, but they have the right to demand compelling evidence in favour of earth expansion and a clear demonstration of the inadequacy of current global tectonic theory.

It can hardly be said that Owen is especially convincing on either count, which is not to say that he makes no telling points. The gist of his argument is geometric, that the celebrated Bullard fit of the Atlantic continents, and its successors such as the Smith and Hallam fit of the Gondwana continents, pose awkward problems of continental overlap and misfit which have not been adequately explained away. For example, many geologists have been worried by the loss of much of Central America in the Bullard fit, despite the fact that extensive areas of old continental rocks occur there, and attempts to get round this problem by seemingly arbitrary *ad hoc* tectonic displacements and rotations, have lacked plausibility.

Likewise, if one adopts the Smith-Hallam fit, West Antarctica does not run naturally into its obvious geological continuation in Patagonia. More disturbing perhaps, a large gap is left west of Australia, which has led to the suggestion that the Wharton Basin in that region was ancient ocean, now disproved by the Deep Sea Drilling Project which has demonstrated that the basin is underlain by oceanic crust as young as elsewhere. On the other hand, fitting India against Australia, as others have done, leaves a corresponding gap in the western Indian Ocean.

Such problems can indeed be resolved, as Owen points out, by extremely rapid Earth expansion, but before leaping to such a drastic conclusion it is worth looking more closely at the original computer least squares fit pioneered by Bullard and his colleagues. This and subsequent fits were taken at the 500 fathoms (~1,000 m) contour for purely geometric reasons, because this gives the best fit and usually lies on the steepest part of the continental slope and is therefore well defined. It is only strictly valid if it coincides closely with the boundary of continental and oceanic crust, but geological and geophysical evidence has been accumulating that this is not the case.

Thus Talwani and Eldholm (*Bull. geol Soc. Am.*, **83**, 3575; 1972) argue persuasively that the extensive Voring Plateau off Norway, with an average depth of 2,000 m, is subsided and thinned continental crust. Similarly, Jansa *et al.* (*Geol. Surv. Canada Pap.* **74–30**, 51; 1975) make a convincing case for a wide zone off the Nova Scotia, eastern Newfoundland and north west African shelves as subsided continent, and suggest that the 3,500 m contour is a geologically more realistic estimate of the true continental edge. Very similar evidence and arguments have been put forward for the region offshore of Angola by Burollet and Byramjee (*Notes Mém. Comp. Fr. Pétroles*, no. 11, 71; 1974), leading to the same conclusion. An important implication is that a sector of subsided and attenuated continent well over 1,000 km wide in places must exist between Africa and America, and that the so-called Quiet Magnetic Zone is not entirely oceanic, as hitherto almost universally accepted by marine geophysicists.

A hundred years ago

VARIOUS sanitary measures (according to Dr Tholozoan) have recently been adopted by the Turkish and Persian Governments with reference to the outbreak of plague, which commenced in Mesopotamia in the early part of the year. Since the beginning of March a sanitary *cordon* has been established on the north of the invaded territory, on the most frequented route of Kurdistan and Syria, between Tecrit and Kilfri. On the south a quarantine of fifteen days is obligatory since April 1 on all vessels sailing on the Tigris and the Euphrates It is at Kourna, at the confluence of these rivers. The ports of the Persian Gulf are protected by a quarantine which vessels from affected localities have to undergo at the island of Kezzer, formed by junction of the Chotel Aral and Karoun. Since April 10 all communications by land between Persia and Mesopotamia are subject to a quarantine of fifteen days. For three years, it may be added, all pilgrimages into the infected country, by Persian subjects, have been interdicted.

from *Nature*, **14**, July 6, 218; 1876.

Burollet and Byramjee extend their zone of subsided continental crust round to the East African offshore zone and elsewhere, which has a significant bearing on the arguments recently put forward by Kent and Tarling (*Nature*, **261**, 304, 1976) against a fit of Madagascar snugly against Kenya and Tanzania. This they dismiss as implausible because of the known extent east of these mainland countries for hundreds of km of a thick sequence of late Palaeozoic and younger shallow marine and continental sediments. Kent and Tarling treat this as an argument for a more southerly former position of Madagascar, thereby dismissing without obvious justification palaeomagnetic evidence to the contrary, instead of appreciating that all that may be at fault is the geologically implausible tightness of fit if the 500 fathom contour is used. In this connection it is interesting to note that some new palaeomagnetic data just published supports the northerly fit for Madagascar (McElhinny and Embleton, *Earth planet. Sci. Lett*, **31**, 101; 1976).

Much more research on continental margins around the world will have to be undertaken before an accurate new continental fit can be reliably attempted, but already it seems likely that most if not all of the apparent geological inconsistencies of the older fits wil magically disappear, and the Tethys will not seem such an awkwardly eastward gaping ocean. ☐

Future of space science

from S. I. Rasool

A symposium on the Future of Science in Space was held as part of the 18th COSPAR meeting which took place in Philadelphia on June 7–18, 1976.

THE future of space science is becoming a matter of grave concern to the space scientist. The national space science budgets have considerably declined in their buying power and for the large pool of space experimenters in the Western world opportunities seem to be few. At the same time the exploratory phase in many disciplines is over. The days are long gone when a simple magnetometer, a geiger counter, or a TV camera flown anywhere in space or to a nearby planet would make an instant discovery Although the potential for major discoveries about the Universe is still great in some of the fields (such as infrared, ultraviolet and gamma ray astronomy) the emphasis in space science is going to be more towards "why" than "what". This immediately implies more sophisticated and correlative experiments in space, large space telescopes and observatories to study the remote regions of the Universe and more detailed study of the planets with orbiters, landers and probes rather than with flybys.

What are the chances that space science will progress at the same vigorous pace as it has done over the past two decades? What should be the major thrusts and priorities? What are the national policies towards space science? These were some of the questions discussed in a one and one-half day symposium and panel discussion convened by COSPAR (International Committee on Space Research) during its recent meeting.

If the objective of the organisers was to get a unified view of things, the meeting was a disappointment. Six individuals from six different countries not only gave a variety of views but made six different kinds of presentations. They ranged all the way from topical and systematic descriptions of future thrusts in space research to a philosophical discourse on the art of extrapolation and on the meaning of utopia. A few themes did recur and are noteworthy space research in the future will be more focused and will need more justification; with the advent of the Shuttle, the cost of doing science will, it is hoped, go down; space science cannot survive in isolation, it should be integrated with classical disciplines in science; high energy astrophysics has a great future in space and the Space Telescope is the next logical step in optical astronomy; the scientific aspect of remote sensing of the earth will be emphasised more, while considerable thought should be given to studying the planets from earth orbiting telescopes.

Representatives from the European Space Agency (ESA) and NASA who joined the speakers for the panel discussion sounded optimistic about the future of space science in the total programme. ESA has a new science advisory structure to optimise the science input in the programme planning. NASA views space exploration closely tied to the biological imperative—the challenge of the unknown—and therefore a vigorous programme of space science and exploration has been and will be supported by the American public. A large Space Telescope, high energy observatories, probes to planets and a possible sample return from Mars may be the highlights of the US space science programme in the next decade. It appeared from the statements of the Soviet representatives that the Soviet emphasis on Venus will continue. In space astronomy, radio interferometry may be emphasised and in magnetospheric physics, active experiments to understand plasma interactions. An earth surface mineral resources survey was also mentioned by the Soviet scientists.

What was really accomplished at this Symposium is not clear and apparently not many people expected much to happen either: of the 600 or so participants at this year's COSPAR, the audience for this Symposium probably never reached the 100 mark. ☐

Trees in the tropics

from P B. Tomlinson

> The Fourth Cabot Symposium held at Harvard Forest, Harvard University, April 26–30 had as its subject Tropical Trees as Living Systems.

An appreciation of the need for an understanding of tropical forests in terms of the individual diversity of tree species was the theme of the Symposium The enormity of this task is indicated by the floristic diversity of woody plants in the tropics In Malaysia, for example, M. E. D. Poore (*J Ecol.*, **56**, 143–196; 1968) found in a survey of 23.0 ha, 2,773 tree-sized individuals with a trunk girth greater than 91 cm, representing 375 species, 139 genera and 52 families. To obtain an equivalent diversity in a temperate flora one would have to map an area equal to a quarter of the United States. The systematic assessment of tropical tree floras is still incomplete, while most aspects of structure, growth, function, reproduction, and ecology remain uninvestigated. Generalisations about the biology of woody plants are still determined with temperate trees in mind, the more balanced view which might be obtained if tropical species were better understood has yet to be established. Consequently the uniqueness of this symposium was its examination of the tree as an individual, with a focus on many functional processes, and its attempt to deal mainly with tropical examples. The programme was so arranged that a gradual progression from a detailed consideration of construction and physiology led naturally to an appreciation of the tropical forest as a complex of interacting and highly diverse units. The result was an overview of our current understanding of aspects of the biology of tropical trees and the proceedings which are to be published should stimulate research on woody plants in the tropics.

Early sessions dealt with evolution, genetic diversity, and especially morphological patterns of organisation. The broad perspectives sought were indicated by the opening discussion of palaeobotanical evidence for the evolutionary origin of tropical trees and forests by J. Doyle (University of Michigan) which made the point that a better understanding of functional morphological relationships of leaf architecture would permit more conclusive palaeontological evaluation of theories of vegetative evolution in angiosperms. It was, therefore, appropriate that there should be a subsequent discussion of the adaptive significance of compound leaves by T. Givnish (Harvard University). This kind of interaction occurred throughout the meeting.

Tree architecture provided a framework for ample discussion, with emphasis on different kinds of trunk-branch axis differentiation in producing optimum patterns of leaf arrangement. The way in which the tree can often be regarded as a modular composition of equivalent units was emphasised by M.-F. Prévost (ORSTOM, Apiodoumé, Ivory Coast). Of the many examples of crown construction presented, none was more distinctive than that of the genus *Araucaria*. In New Caledonia J M Veillon (ORSTOM, Noumea) showed that most species produced repeating crowns since the first generation of branches developed by the trunk is succeeded by two or more subsequent ones originating from late-developing branches, the successive crowns overlapping each other like a nest of coffee tables. The need for a better appreciation of the complex hormonal control of branch expression was emphasised by A. Longman (Unit of Tree Biology, Institute of Terrestrial Ecology, Edinburgh) and G. Browning (University of Wales, Aberystwyth) but no better indication of the resulting regularity which is possible was found than in the quantitative analysis of *Terminalia* by J. B. Fisher (Fairchild Tropical Garden, Miami). This represents the first such precise analysis of a crown form familiar to tropical travellers and further demonstrated another common theme of the symposium, that quite simple methods and approaches can generate important new ideas. At the same time modern technology has its place, as was shown by R. Borchert (University of Kansas) whose computer simulation of shoot extension, based on known examples, suggests the existence of endogenous control of rhythms of shoot extension. Tropical trees are not necessarily subject to marked seasonal variation in climate and why shoot growth is usually not continuous is intriguing.

In the area of reproductive biology F. Ng (Forest Research Institute, Kepong) showed a greater diversity of seedling morphology in the tropics than the terminology devised for temperate trees can accommodate, with the obvious ecological implication of successful tree establishment as the basis for his study. The strategies that tropical trees have evolved in the evasion of seed predators were discussed by D. H. Janzen (University of Michigan). Predator pressure can be enormous and it was reassuring that J. Sarukhán (Universidad Nacional Autónoma de Mexico) could find survivors enough to make demographic studies of continuing populations of forest trees.

The several speakers who attempted an analysis of the forest itself were unanimous in presenting it as a dynamic system. R. A. A Oldeman (Mission ORSTOM, Ecuador) provided a provocative view of the forest as a population of trees whose developing architecture was the result of their individual ability to adapt to available energy levels through repeated cycles of growth. A contribution in which the data had been collected by University students (P. A. Ashton, University of Aberdeen) was particularly welcome since the tropical rain forest is an ideal training ground for future ecologists.

In all, 28 speakers from 13 countries participated. Such an overview is timely in view of the current rapid destruction of tropical forests, which was commented on repeatedly. At present the rate of increase in our understanding of tropical ecosystems is far exceeded by the rate of their destruction. Any corrective influence is appropriate. ☐

review article

Quasars and the cosmological distance scale

M. Rowan-Robinson*

There has been continuing controversy about the distances of the quasars since their discovery 13 years ago. Here one of the proponents of the view that at least some quasars are "local" explains why he now believes quasar redshifts are cosmological.

Twice this century the cosmological distance scale has been the subject of famous debates. In 1920 Shapley and Curtis[1] debated whether the spiral nebulae formed part of the Milky Way system. Fifty-two years later, in December 1972, Arp and Bahcall[2] debated whether the redshifts of quasars are cosmological.

Both debates were inconclusive at the time. Shapley was correct in his estimate of the vast overall dimensions of our Galaxy: but on the question at issue he was wrong. In the second debate interesting and suggestive arguments (and not a few weak ones) were presented both for the "cosmological" and "local" interpretations of quasar redshifts, but neither proponent was persuaded to yield ground. A compromise solution, that two types of quasar exist, one type local, the other cosmological[3], was unacceptable to both. Has the balance of the evidence shifted in the past three years? I believe that it has, and in this review I will try to explain why. For a more complete bibliography, the reader should consult Field *et al.*[2] and the more recent article by Burbidge[4], whose conclusions are the opposite of those expressed here.

The 1972 Arp–Bahcall debate rested on 7 main kinds of argument; (1) the redshift–distance relationship for normal galaxies, (2) continuity between quasars and other types of active and compact galaxy, (3) quasars in the directions of galaxies and clusters of galaxies with the same redshift as the quasar, (4) quasars in the same direction as bright galaxies of much lower redshift, (5) luminous filaments connecting galaxies and quasars with very different redshifts, (6) the overall distribution of quasars on the sky, (7) non-velocity redshifts in normal galaxies.

While the anomalies (4)–(7) have been neither impressively augmented in the interim, nor decisively eliminated, the evidence under (1) and (2) has strengthened considerably.

The redshift–distance relationship for normal galaxies

In a classic series of papers Sandage and Tammann[5-11] have put the redshift–distance relationship discovered by Hubble and Lundmark on to a solid basis, and have removed the possibility of any strong deviation from this linear behaviour within 200 Mpc.

In the first two papers[5,6], galaxies of the Local Group and of the nearby M81 group (3.25 Mpc away), for which distances can be established from Cepheid variable stars (assuming the known distance of the Hyades cluster), are used to calibrate two methods that can be used for more distant galaxies: the optical size of the largest H II regions in galaxies and the luminosity of the brighest stars in a galaxy. In both cases the quantities to be used as distance indicators depend on the luminosity and type of galaxy concerned, and this dependence has to be obtained from these nearest galaxies. In the third paper[7] those two methods are used to determine the distance of the M101 group of galaxies (7.2 Mpc), important because it provides the nearest example of an Sc galaxy of luminosity class I. van den Bergh[12] found that the appearance (surface brightness, degree of development) of spirals arms is correlated with the luminosity of the galaxy, and may be used to provide a luminosity classification of spiral galaxies. In the fourth paper[8] the same two methods are used to get the distances of 39 Sc galaxies with distances in the range 3–20 Mpc, and hence to calibrate the van den Bergh luminosity classes. In the fifth paper[9] distances to groups of galaxies within 30 Mpc are determined both by the H II region method and by Sc luminosity classes. The latter method is also used for more distant galaxies (to 50 Mpc). A convincing redshift–distance relation is obtained, the constant of proportionality being $H_0=57\pm3$ km s^{-1} Mpc^{-1} (the Hubble constant) and this linear relationship is "not only as isotropic as it can presently be determined (3σ $[\Delta H/H]\simeq 30\%$), but the flow is also as *quiet* as we can measure it". In fact Sandage and Tammann allow only $\sigma(\Delta v)\lesssim 50$ km s^{-1} as "a generous limit for the mean random motion" (of galaxies about the Hubble flow). In the sixth paper[10] the authors use a sample of remote Sc I galaxies (out to 200 Mpc) to determine $H_0=55\pm6$. Finally Sandage[11] uses a further remote sample of galaxies, from the Southern Hemisphere, to check the isotropy of the Hubble flow.

Sandage[13] had earlier shown, continuing the programme of Humason, Mayall and Sandage[14], that the brightest galaxies in rich clusters show a good correlation between magnitude and redshift, consistent with the Hubble relation together with the assumption that the luminosity of the brightest galaxies in clusters are all the same. This pushes the frontier to which the Hubble law has been tested to almost 3,000 Mpc.

Sandage and Tammann have concentrated on the four distance methods: Cepheids, H II regions, bright stars and Sc luminosity classes. van den Bergh[15] reviews distance estimates to the nearby Magellanic clouds by 11 different methods and shows that the methods broadly agree with one another. He also reviews the results of 12 methods of determining H_0 and arrives at a weighted mean of 93 ± 7. Most of these methods have, however, large uncertainties and the Sandage and Tammann value of 55 is within $2.6\,\sigma$ of all of them. It is also not clear that most of these methods have been calibrated with the same care as the Sandage and Tammann programme, especially for correlations of the chosen indicator with galaxy type and luminosity. The most important alternative method is one based on the expansion rate of supernovae[16], which is completely independent of the whole elaborate distance ladder built up from the Hyades cluster. This yields $H_0=60\pm15$,

---

*Queen Mary College, Mile End Road, London E1 4NS, UK

an impressive and rather remarkable confirmation of the Sandage and Tammann distance scale.

Dissenting points of view

Three of the main dissenting points of view focus on the questions of calibration, the Local Supercluster, and the so-called Rubin–Ford anomaly. The sceptic might also ask a fourth question: will the Hubble constant be reduced further?

Two criticisms have been directed at Sandage and Tammann's calibration of their distance scale Madore[17] has argued that additional corrections need to be applied to the determination of distances using Cepheid variables, which would have the effect of increasing H_0, and Denmat *et al.*[18] claim that with the Sandage and Tammann Sc luminosity class calibration, H_0 is different when determined by galaxies in different classes. If van den Bergh's original calibration is used, however, this difference disappears: an embarrassing side effect is then that H_0 decreases with distance. A dependence of the Hubble constant on distance had earlier been claimed by de Vaucouleurs[19].

Because of the rather small number of galaxies available for the calibration of each luminosity class, it is rather difficult to decide between an incorrect calibration of the relative luminosity of the different classes, and a dependence of H_0 on distance. The linearity of the magnitude–redshift relationship for brightest cluster galaxies[13] shows that such a dependence can only occur for distances nearer than the Virgo cluster, which fits well on to the relation for other clusters. An important argument against a dependence of H_0 on distance is therefore that the value of H_0 determined from the Virgo cluster alone[8] agrees well with that determined from all nearby galaxies.

The second issue is the long standing one of the local supercluster. de Vaucouleurs[20] has argued that the prominent band of galaxies across the north Galactic pole and passing through the Virgo cluster constitutes a disk-like "supercluster" of galaxies with the centre at Virgo and ourselves at one edge. The Sandage and Tammann programme deals a severe blow to this hypothesis, since they find no deviation from the linear Hubble flow correlated with direction along the supergalactic plane, or towards and away from Virgo. Jones[21] has argued that the local galaxy distribution can be understood in terms of Virgo being a rich cluster of normal dimensions (diameter $\sim$ 4 Mpc, instead of $\sim$ 40 Mpc for the supercluster). de Vaucouleurs has, however, reiterated his case for the existence of the supercluster, using evidence from nearby galaxies[22], hydrogen clouds[23], groups of galaxies[24], and clouds of galaxies[25]. In each case the number of objects seems rather small for a significant determination of distribution on the sky. A further problem is the strong effect of galactic obscuration below galactic latitude b=40°, so that only about one third of the sky can be studied in a relatively unobscured direction.

Third, cosmologists have been perplexed by the Rubin-Ford anomaly. Rubin, Ford and Rubin[26] studied a sample of 50 Sc I galaxies with $14 \lesssim m_{pg} \lesssim 15$, and $4{,}000 \lesssim v \lesssim 7{,}500$ km s^{-1}. They found different mean velocities for two hemipheres of the sky corresponding to a velocity of 700 km s^{-1} for the Solar System relative to these galaxies. Since our velocity relative to the microwave background is $\lesssim$ 300 km s^{-1} (ref. 27), a paradox of Michelson–Morley proportions seemed to be emerging. Jaakola *et al.*[28] claim a difference in the redshift distribution for compact galaxies with absorption spectra, over the two Rubin–Ford hemispheres, but only at the 2σ level.

Sandage and Tammann[9] find no evidence for a difference in H_0 between the two hemispheres when velocity-limited samples are studied. They conclude that the effect is due to the bias introduced by a magnitude-limited sample of a population in which there is an appreciable spread in the luminosity. Hartwick[29] discusses the contribution of interstellar absorption to such an effect.

Finally, the value of H_0 first given by Hubble[30] was 500, since when the accepted value has been steadily reduced. Have we reached the end of the road, or will there be yet another downward revision in a decade's time? Tammann[31] explains why the corrections have always tended to be downwards: "one is basically reluctant to accept the existence of objects which are much brighter and much larger than those one has previously experienced in the immediate neighbourhood". The value $H_0 = 55$ leads to an expansion time for the Universe, if the redshift is interpreted as due to recession, of 1.9×10^{10} yr, compared with the age of our Galaxy of 1×10^{10}–1.5×10^{10} yr, fitting in well with the idea of a 'big bang' universe in which galaxies form early on.

(There is, unfortunately, no direct evidence for interpreting the redshift as due to recession. The success of the big bang picture in explaining the microwave background, the primordial abundances of He and D, and the age of our Galaxy, constitute powerful indirect evidence Most of the discussion of this article is independent of the interpretation of the redshift.)

At present it is hard to imagine H_0 lying outside the range 30–100, but there are two arguments which might eventually force a lower value If the local supercluster could be shown to be a real object 40 Mpc in size, then for it not to be the largest cluster in the Universe, H_0 might have to be as low as 10. But the recession velocities of local supercluster galaxies would then be anomalously large. Second, the revision of stellar evolution theory needed to explain the low solar neutrino flux could substantially increase the life of stars on the main sequence, and hence the age of the oldest stars in the galaxy.

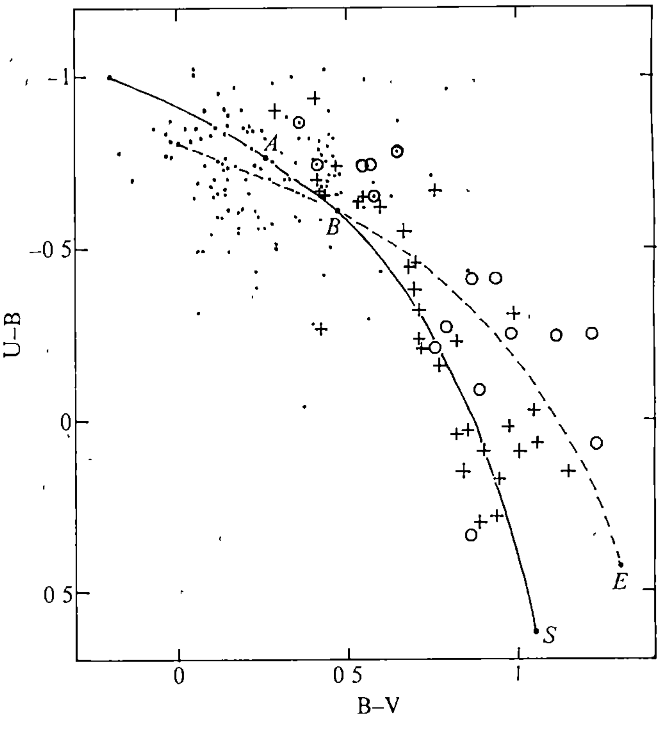

Fig. 1 Colour–colour (U–B against B–V) diagram for quasar (●, ref 40), N galaxies (○, ref 37) and Seyfert galaxies (+, refs 38, 39), together with mixture lines calculated by combining the light of a normal galaxy with that of a quasistellar nucleus, in different proportions (spiral at $z = 0$, B–V = 1.05, U–B = 0.62; solid curve (ref 38), elliptical at $z = 0.1$, B–V = 1.3, U–B = 0.53: broken curve (ref 37)) The circled dots at (0.36, –0.87), (0.58, –0.65), (0.41, –0.74), (0.64, –0.78) denote B46, B264, B340 and Ton 256, respectively, which have been classified as quasars, but which are fuzzy The points labelled *A* and *B* on the spiral and elliptical loci, respectively, denote the points at which the visual light from the quasistellar core equals that from the galaxy No Seyferts are found to the left of *A* and no N galaxies are found to the left of *B*

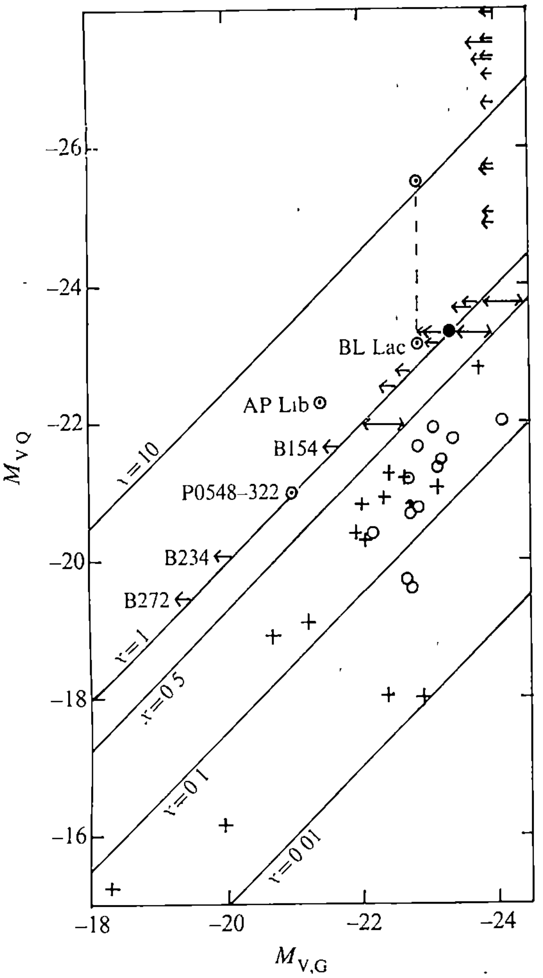

Fig. 2 Comparison of the absolute visual magnitudes of the quasistellar ($M_{V,Q}$) and galaxy ($M_{V,G}$) components in Seyferts (+, refs 38, 39, 42), N galaxies (○, ref. 37), BL Lac objects (⊙, refs 43–46) and optically selected QSOs (Ton 256 as filled dot, rest as arrows, refs 40, 47, 48). The redshifts of QSOs have been assumed to be cosmological, and H_0 has been taken as 50. Lines of constant $x = p_{oc}/p_{og}$, the ratio of the visual light from the core to that from the surrounding galaxy, are shown B46, B264, B340, which are fuzzy, are shown as having $0.5 \leqslant x \leqslant 1$, and the rest of the QSOs are shown with $x \geqslant 1$ or $M_{V,G} \geqslant -24$, the highest luminosity attained by galaxies.

Continuity between quasars and galaxies

The similarities between quasars and the nuclei of N galaxies and Seyferts have been commented on by many authors[32-36]. Sandage[37] showed that the colours of N galaxies as a function of aperture could be understood in terms of underluminous QSOs in the nuclei of normal giant elliptical galaxies. Weedman[38] and Penston *et al.*[39] have shown a similar relationship between Seyfert nuclei and spirals. Fig. 1 shows the colour–colour diagram for quasars, N galaxies and Seyferts, together with the loci obtained by adding quasars of different luminosity to normal elliptical and spiral galaxies.

Kristian[41] showed that amongst low redshift quasars, those with lower optical luminosity (assuming the redshift to be cosmological) tended to be fuzzy, while those of higher optical luminosity appeared stellar, which would be consistent with the idea of an underlying giant elliptical galaxy. Figure 2 compares the optical luminosities of the quasistellar (p_{oc}) and galactic (p_{og}) components in quasars, N galaxies and Seyferts. We suppose that quasars whcih have been described as fuzzy lie in the band $x = p_{oc}/p_{og} \sim 0.5$–$1$. If $x \gtrsim 1$ the object appears entirely stellar and is called a quasar. if $x \lesssim 0.5$ the object is sufficiently fuzzy to be called an N galaxy or Seyfert. In between there is a domain of uncertainty where objects are classified as quasars or N galaxies by different observers (for example, Ton 256, B264).

The BL Lac objects

The most interesting development of the past few years has been the discovery of the BL Lac objects. These are strong variable radio sources identified with QSOs of neutral colour, in which the spectra show no emission lines[49]. This seems to be due to a steep decline with increasing frequency of the optical continuum (also responsible for the neutral colours), with a consequent deficiency of ultraviolet photons to excite the lines[43] They are therefore simply quasars without an ultraviolet excess.

Table 1 lists the properties of the BL Lac objects identified to date. Oke and Gunn[43] succeeded in measuring the spectrum of the galaxy underlying BL Lac, with a redshift of $z = 0.07$. Baldwin *et al.*[50], however, failed to find any features in their spectrum of BL Lac. Thuan *et al.*[44] confirmed the redshift of $z = 0.070 \pm 0.005$, on the basis of several normal galaxy lines and bands. It would be clearly desirable to have this result confirmed by independent observers. Other BL Lac objects which have had redshifts determined are P0735+178[51], P0548−322[45], AP Lib[46] and B2 1101+38[52]. The separation into galactic and quasistellar components has been performed for BL Lac[43], P0548−322[45] and AP Lib[46], and they are included in Fig. 2. For AP Lib, $x \sim 3$, and for BL Lac, $x \sim 10$ when observed by Oke and Gunn[43], so these objects are firmly into the quasar band in Fig. 2. The identification of underlying galaxies in these objects is therefore one of the strongest pieces of evidence that quasars occur in galaxies. The high optical luminosity achieved by BL Lac at maximum removes any rationale for treating the quasars with flat spectrum, compact radio sources as a local population with properties similar to the low luminosity sources seen in Seyfert nuclei[3]. This type of activity is clear possible over a wide range of luminosity, up to the range seen in quasars, and no advantage is gained by the "local" hypothesis.

The strong variability of some quasars and BL Lac objects suggests that they may sometimes be found in a quiet phase, with $x \lesssim 1/2$, that is, becoming N galaxies. Spectra and photographs taken at these phases should show evidence of an underlying galaxy. Figure 2 shows, however, that the notion that QSOs are only to be found in giant ellipticals should be dropped. B154 and B234 show no fuzz even though they are respectively 1.6 and 3.2 magnitudes fainter than the mean for brightness cluster ellipticals. These QSOs can be occurring only in galaxies of modest optical luminosity.

Finally the case of 3C48 should be mentioned. Wampler *et al.*[74] succeeded in detecting emission lines from hot gas associated with the nebulosity surrounding this quasar. The lines are narrower, and have a slightly larger redshift, than those of the central quasar, thus ruling out the gravitational redshift. The high optical luminosity of 3C48 ($M_v = -25.5$) makes it unsurprising that an underlying galaxy was not detected.

Associations on the sky

Arp[2] has emphasised how apparent associations on the sky have an important role in establishing the conventional distance scale for galaxies. Groups and clusters of galaxies seen in a particular direction on the sky are normally assumed to be at the same distance.

Several quasars of low redshift have been found to be "near" galaxies and groups of galaxies of the same redshift (Table 2*a*), presumably establishing the cosmological nature of the redshift in these quasars (but this is disputed by Burbidge and O'Dell[89]). It is unfortunate that all the clearcut cases of this type are quasars with extended double radio sources, for which the continuity of the radio dimensions with those in radio galaxies and the fall off of angular size with redshift already support the cosmological interpretation

The best case involving a compact radio-source quasar is 4C11.50B = 1548+115a[90], but here two quasars are found near a group of galaxies[91,92], one with the same redshift as the group[80], one much larger, and it is unclear which is responsible

Table 1 Properties of BL Lac type objects

Name	Redshift	B	B–V	S(5GHz) (Jy)	α(5GHz) [$S(\nu)\alpha\nu^{\alpha}$]	Refs for data	$M_{V,Q}$	$M_{V,G}$	log P(5 GHz) (W Hz^{-1})
P0048−097 = OB−080		17.08	0.48	2 0	0.45	53, 54			
0219 + 42 = 3C66A		15.71	0.50	0.91	0.3	55, 56			
AO 0235+164		16.2−18.2	1.3	1.4−2.8		57			
0300+47 = 4C47.08 = OE400		18(pg)		2.4	0.0	58, 54			
P0537−441		12.6–16.9	0.5	5.0	0.7	59–61			
P0548–322	0.042	15.6	0.79	0.23	−0.52	45	−21.0	−21.0	24.2
P0735+178 = OI158 = VRO 17.07.02	0.424	14.5–16 7	0.52	2.1	−0.04	51, 60	−26.3		27.2
MA0829+04		15–16.9		0.95	0.15	62, 60			
0851+20 = OJ287 = VRO20.08 01		12.35–16.4	0.4	3.5	0.5±0.2	63, 49, 54			
B20912+29		15.1–17.0	0.34	0.24	−0.35	62, 53, 54			
UT0954+556 = OK 591 = 4C55.17				3.53 (1,415 MHz)	−0.28	64			
UT1020−103 = OL−133 = MSH 10−107		16(V)		0.7 (1,415 MHz)	−0.58	65, 66			
1057+10.0		17.60	0.38	0.19 (2,700 MHz)	−0.9	53, 67			
B2 1101+38	0.0308	13.1(pg)		0.54		52, 54	(−23.2)		24.3
B2 1147+24.5 = OM280		16.28–16.61	0.5	0.59	0.13	53, 68			
B2 1215+30 = ON325		13.9–16.0	0.5	0.33	−0 2±0.2	63, 49, 54			
B2 1219+28 = W Com = ON235		13.2–17.2	0 5	1.2	0.25	69, 49, 54			
1514−24 = AP Lib = OR−225	0.0486	14.0–16.4	0 6	2.2	0 0	46, 63, 49, 54	−22.3	−21.4	25.3
1538+149 = OR165 = 4C14.60		14.4–17.8	0.5	2.0	0.2	62, 60, 53			
B2 1652+39 = Mark 501	0.0337	14.60	0.72	2 0(408 MHz)	70		(−22.7)		(25.0)
1727+50 = I Zw187 = OT546		14 8–16 9	0.7	0.15	−0.4	63, 71, 54			
1749+09 = OT081 = LC 09.57		18(V)		1.83	0.1	72, 68			
2200+42 = BL Lac = OY401 = VRO 42.22.01	0.070	12.6–16.6	1.0	7.0	0.75	43, 44, 63, 54	−23.15 to −25.5	−22.86	26.2
2207+02		19(pg)				73			
2254+07 = OY091		15.7–17 3		1 0	0.15±0.1	62, 60			
P2335+03		18(pg)		0.61	0.64	73, 68			

The spectral indices are taken from ref. 62.

The luminosities given in the last 3 columns are calculated assuming $H_0 = 50$.

Note added in proof: Twelve further possible BL Lac objects are given by Kinman[125]. E M Burbidge *et al.*[126] have measured the absorption time redshift of AO 0235+164 as 0.5240, with a possible second system corresponding to $z = 0.85$.

for the associated extended double radio source. Argue *et al.*[90] propose that the double source, as well as the compact source, is associated with the smaller redshift quasar, but the centroids of the two emission regions are accurately aligned with the high redshift quasar. Clearly it is important to find unambiguous examples of low redshift, compact radio-source quasars in groups or clusters of galaxies.

Many examples have also been given of quasars "near" comparatively nearby galaxies, of much lower redshift than the quasar (Table 2*b*). Arp and G. R. Burbidge have been the strongest proponents of the arguments that these associations are real and that the redshifts of many or all quasars include a substantial intrinsic component. *Post hoc* calculations of the probability of these associations have been adduced as support for this interpretation[2,93], but all such calculations are fallacious from a philosophical point of view. Evidence that such associations are real must be of a statistical nature. A chosen large sample of bright (peculiar?) galaxies must be selected in advance, together with a comparable random set of positions on the sky as a control. Regions of the same size should be searched round each position in the two samples for quasars, and the redshifts determined. In this way clearcut evidence that quasars are to be found around bright galaxies can be obtained.

The number of close associations found to date is not especially remarkable. The number of quasars on the whole sky, N, brighter than magnitude B_Q and within 2′ of a galaxy brighter than m_G, is roughly

$$\log_{10}N \simeq 2.9+0.75(B_Q-20)+0.6(m_G-15.7)$$

using Sandage and Luyten's[94] $N-m$ relation for QSOs and the fact that there are on average about 1.6 galaxies per square degree in the Zwicky catalogue[95]. At present perhaps 1–2% of the sky has been searched for associations between quasar and Zwicky galaxies, giving a prediction of 8–16 such associations as compared with the 12 given in Table 2.

Two cases of pairs of quasars very close together (Ton 155, 156, 35″ apart[96]; 4C11.50a,b, 5″ apart[91,92]) have been given. It is interesting that Stockton[80] has found a galaxy near 4C11.50

Table 2 Associations of quasars with galaxies

Year	*a*, Associations with galaxies of the same redshift	*b*, Associations with galaxies of different redshift (within 2′ arc)
1969	B264 in cluster with $z = 0.095$ (75)*	1108+285 1.1′ from NGC3561 (81)
1970		Mark205 42″ from NGC4319 (82)
1971	P2251+11 in cluster with $z = 0$ 323 (76)	3C232 1.9′ from NGC3067 (83)
	Ton256 in cluster with $z = 0.131$ (76)	PHL226 0.8′ from ICI746 (83)
1972	3C323.1 in cluster with $z = 0.264$ (77)	3C455 23″ from NGC7413 (84)
		P1021−0.0 1.9′ from Zwicky galaxy (89)
		P2020−37 0 15″ from galaxy (86)
1973	RN8 (near 3C61.1) in cluster with $z = 0.184$	P0038−01.9 1 2′ from Zwicky galaxy (61)
	4C37 43 associated with galaxy $z = 0.370$ (79)	P0823+03 3 1.7′ from Zwicky galaxy (61)
1974	4C11 50a near galaxy with $z = 0.436$ (80)	
1975		Quasars 76″ from IC1417, 95″ from NGC5682 (87)
		QSO 58″ from IC2402 (88)

*Numbers in parentheses are ref. numbers.

with the same redshift as the low redshift quasar. Many more examples would have to be found (and again, in a well-defined search programme) to constitute evidence that these are real associations.

The situation on luminous filaments connecting galaxies with very different redshifts[2,97-101] remains inconclusive. Walker *et al.*[102] find no clear luminous connection between NGC4319 and Markaxian 205, or between the members of Seyfert's Sextet. They confirm the reality of the arm linking NGC7603 to its companion, but find no evidence of interaction.

Other evidence

Among the additional arguments cited in favour of the cosmological interpretation of quasar redshifts are (1) the decline with redshift of the maximum separation found in extended double radio sources in quasars[103-107] (2) H I absorption in quasars which may be due to an intervening gas cloud[108,109] (3) interpretation of some ultraviolet absorption lines as due to molecular hydrogen between us and large redshift quasars[110,111] (4) various claims of correlations of optical and radio brightness with redshift (of somewhat doubtful significance in view of the wide range of quasar radio and optical luminosities).

Supporting the "local" interpretation are (1) periodicities in the redshift distribution of quasars (and radio galaxies)[115-117] (2) excess redshifts in normal galaxies[118-122] (3) rapid radio variations requiring ultrarelativistic velocities[123] (such motions are anyway required in some radio galaxies and to understand multiple absorption redshift in quasar spectra).

None of these arguments seems really decisive either way.

Conclusion

The establishment of the redshift–distance relationship for galaxies on what seems to be an impregnable basis, to the extent that any "intrinsic" redshift effect cannot exceed 50 km s^{-1}, and the evidence that QSOs occur in galaxies and with luminosities at least ten times that of the galaxy, removes any doubt from the present author's mind that the redshifts of quasars are cosmological. Certainly there no longer seems to be any strong reason for maintaining that quasars with compact radio sources are local[3,124]. While efforts to detect galaxies believed to underline quasars, and to find associated groups of galaxies, should clearly continue, supporters of the "local" hypothesis have to meet the challenge of pursuing a well defined, unbiased, controlled programme to demonstrate statistically the association of quasars with relatively nearby galaxies. On the present evidence I believe that such a programme will fail.

[1] Shapley, H., and Curtis, H. D., *Bull. natn. Res. Council*, **2**, 171 (1921)
[2] Field, G. B., Arp, H., and Bahcall, J. N., *The Redshift Controversy* (W. A. Benjamin, Reading, Massachusetts, 1973).
[3] Rowan-Robinson, M., *Nature*, **236**, 112 (1972)
[4] Burbidge, G. R., *Nature phys. Sci.*, **246**, 17 (1973).
[5] Sandage, A., and Tammann, G. A., *Astrophys. J.*, **190**, 525 (1974).
[6] Sandage, A., and Tammann, G. A., *Astrophys. J.*, **191**, 603 (1974).
[7] Sandage, A., and Tammann, G. A., *Astrophys. J.*, **194**, 223 (1974).
[8] Sandage, A., and Tammann, G. A., *Astrophys. J.*, **194**, 559 (1974).
[9] Sandage, A., and Tammann, G. A., *Astrophys. J.*, **196**, 313 (1975)
[10] Sandage, A., and Tammann, G. A., *Astrophys. J.*, **197**, 265 (1975).
[11] Sandage, A., *Astrophys. J.*, **202**, 563 (1975).
[12] van den Bergh, S., *Astrophys. J.*, **131**, 215 and 558 (1960)
[13] Sandage, A., *Astrophys. J.*, **183**, 731 (1973)
[14] Humason, M. L., Mayall, N. U., and Sandage, A., *Astr. J.*, **61**, 97 (1956).
[15] van den Bergh, S., in *Structure and Evolution of Galaxies* (edit. by Setti G.), 247 (Reidel, Dordrecht, 1975)
[16] Kirshner, R. P., and Kwan, J., *Astrophys. J.*, **193**, 27 (1974).
[17] Madore, B. F., *Mon. Not. R. astr. Soc.* (in the press)
[18] le Denmat, G., Moles, M., Vigier, J. P., and Niete, J. L., *Nature*, **257**, 773 (1975)
[19] de Vaucouleurs, G., *IAU Symposium 44, External Galaxies and Quasistellar Objects* (edit. by Evans, D. S.), 353 (Reidel, Dordrecht, 1972).
[20] de Vaucouleurs, G., *Astr. J.*, **58**, 60 (1953), *Vistas in Astronomy*, **2** (edit. by Beer, A.), 1584 (Pergamon, Oxford, 1956), *Astr. J.*, **63**, 253 (1958), *Soviet Astr.*, **3**, 897 (1960)
[21] Jones, B. J. T., *Mon. Not. R. astr. Soc.*, **174**, 429 (1976)
[22] de Vaucouleurs, G., *Astrophys. J.*, **202**, 319 (1975)
[23] de Vaucouleurs, G., and Corwin, H. G., *Astrophys. J.*, **202**, 327 (1975).
[24] de Vaucouleurs, G., *Astrophys. J.*, **202**, 610 (1975).
[25] de Vaucouleurs, G., *Astrophys. J.*, **202**, 616 (1975).
[26] Rubin, V., Ford, W. K., and Rubin, J., *Astrophys. J. Lett.*, **183**, L111 (1973).
[27] Partridge, R. B., *IAU Symposium 63, Confrontation of Cosmological Models with Observation* (edit. by Longair, M. S.), 157 (Reidel, Dordrecht, 1974).
[28] Jaakola, T., Karoji, H., Moles, M., and Vigier, J. P., *Nature*, **256**, 24 (1975).
[29] Hartwick, F. D. A., *Astrophys. J. Lett.*, **195**, L7 (1975).
[30] Hubble, E., *Proc. natn. Acad. Sci. U.S.A.*, **15**, 168 (1929).
[31] Tammann, G. A., *IAU Symposium 63, Confrontation of Cosmological Models with Observation* (edit. by Longair, M. S.), 47 (Reidel, Dordrecht, 1974).
[32] Burbidge, G. R., Burbidge, E. M., and Sandage, A. R., *Rev. Mod. Phys.*, **35**, 947 (1963).
[33] Shklovskii, I. S., *Soviet Astr.*, **9**, 683 (1966).
[34] Zwicky, F., *Astrophys. J.*, **143**, 192 (1966).
[35] Burbridge, G. R., and Burbridge, E. M., *Quasistellar Objects* (Freeman, San Francisco, 1967)
[36] Sandage, A., *Highlights of Astronomy* (edit. by Perek, G.), 33 (Reidel, Dordrecht, 1967)
[37] Sandage, A., *Astrophys. J.*, **180**, 687 (1973)
[38] Weedman, D. W., *Astrophys. J.*, **183**, 29 (1973).
[39] Penston, M. V., Penston, M. J., Selmes, R. A., Becklin, E. E., and Neugebauer, G., *Mon. Not. R. astr. Soc.*, **169**, 357 (1974).
[40] Sandage, A., *Astrophys. J.*, **178**, 25 (1972)
[41] Kristian, J., *Astrophys. J. Lett.*, **179**, L61 (1973).
[42] Adams, T. F., and Weedman, D. W., *Astrophys., J.*, **199**, 19 (1975)
[43] Oke, J. B., and Gunn, J. E., *Astrophys. J. Lett.*, **189**, L5 (1974).
[44] Thuan, T. X., Oke, J. B., and Gunn, J. E., *Astrophys. J.*, **201**, 45 (1975)
[45] Disney, M. J., *Astrophys. J. Lett.*, **193**, L103 (1974).
[46] Disney, M. J., Peterson, B. A., and Rodgers, A. W., *Astrophys. J. Lett.*, **194**, L79 (1974).
[47] Silk, J., Smith, H. E., Spinrad, H., and Field, G. B., *Astrophys. J. Lett.*, **181**, L25 (1973).
[48] Braccesi, A., Formiggini, L., and Gandolfi, E., *Astr. Astrophys.*, **5**, 264 (1974).
[49] Strittmatter, P. A., Serkowski, K., Carswell, R. F., Merrill, K. M., and Burbidge, E. M., *Astrophys. J.*, **175**, L7 (1972)
[50] Baldwin, J. A., Burbidge, E. M., Robinson, L. B., and Wampler, E. J., *Astrophys. J. Lett.*, **195**, L55 (1975)
[51] Carswell, R. F., Strittmatter, P. A., Williams, R. E., Kinman, T. D., and Serkowski, K., *Astrophys. J. Lett.*, **190**, L101 (1975).
[52] Miller, H. R., *Astrophys. J. Lett.*, **201**, L109 (1975).
[53] Topia, S., Craine, E. R., and Johnson, K., *Astrophys. J.*, **203**, 291 (1976)
[54] Altschuler, D. R., and Wardle, J. F. C., *Nature*, **255**, 306 (1975).
[55] Wills, D., and Wills, B. J., *Astrophys. J. Lett.*, **190**, L97 (1974).
[56] Northover, K. J. E., *Mon. Not. R. astr. Soc.*, **165**, 369 (1973)
[57] Spinrad, H., and Smith, H. E., *Astrophys. J.*, **201**, 275 (1975).
[58] Porcas, R. W., Treverton, A. M., and Wilkinson, A., *Mon. Not. R. astr. Soc.*, **167**, 41p (1974)
[59] Liller, W., *Astrophys. J. Lett.*, **189**, L101 (1974)
[60] Usher, P. D., *Astrophys. J. Lett.*, **198**, L57 (1975).
[61] Browne, I. W. A., and McEwan, N. J., *Mon. Not. R. astr. Soc.*, **162**, 21p (1973).
[62] Pollock, J. T., *Astrophys. J. Lett.*, **198**, L57 (1975).
[63] Hall, D. A., and Usher, P. D., *Nature*, **241**, 31 (1973).
[64] Brundage, R. K., Dixon, R. S., Ehman, J. R., and Kraus, J. D., *Astr. J.*, **76**, 777 (1974)
[65] Wills, D., and Wills, B. J., *Astrophys. J.*, **190**, 271 (1974)
[66] Ehman, J. R., Dixon, R. S., and Kraus, J. D., *Astr. J.*, **75**, 351 (1970).
[67] Murdoch, H. S., and Hoskins, D. G., *Austr. J. Phys.*, **26**, 867 (1973)
[68] Condon, J. S., and Jauncey, D. L., *Astr. J.*, **79**, 1220 (1974).
[69] Pollock, J. T., Hall, D. L., Ambruster, C., and Usher, P. D., *Astr. Astrophys.*, **30**, 41 (1974).
[70] Khachikian, E. Ye., and Weedman, D. W., *Astrophys. J. Lett.*, **189**, L99 (1974).
[71] Sandage, A., *Astrophys. J. Lett.*, **150**, L171 (1967)
[72] Radivich, M. M., and Kraus, J. D., *Astr. J.*, **76**, 683 (1971).
[73] Strittmatter, P. A., Carswell, R. F., Gilbert, G., and Burbidge, E. M., *Astrophys. J.*, **190**, 509 (1974)
[74] Wampler, E. J., Robinson, L. B., Burbidge, E. M., and Baldwin, J. A. *Astrophys. J. Lett.*, **198**, L49 (1975).
[75] Bahcall, J. N., Schmidt, M., and Gunn, J. E., *Astrophys. J. Lett.*, **157**, L77 (1969).
[76] Gunn, J. E., *Astrophys. J. Lett.*, **164**, L113 (1971).
[77] Oemler, A., Gunn, J. E., and Oke, J. B., *Astrophys. J. Lett.*, **176**, L47 (1972).
[78] Miller, J. S., *et al.*, *Astrophys. J.*, **181**, 83 (1973).
[79] Stockton, A., *Nature phys. Sci.*, **246**, 251 (1973).
[80] Stockton, A., *Nature*, **250**, 308 (1974).
[81] Stockton, A. N., *Astrophys. J. Lett.*, **155**, L141 (1969)
[82] Weedman, D. W., *Astrophys. J. Lett.*, **161**, L113 (1970).
[83] Burbidge, E. M., Burbidge, G. R., Solomon, P. M., and Strittmatter, P. A., *Astrophys. J.*, **170**, 233 (1971)
[84] Arp, H. C., Burbidge, E. M., Mackay, C. D., and Strittmatter, P. A., *Astrophys. J. Lett.*, **171**, L41 (1971)
[85] Burbidge, G. R., Odell, S. L., and Strittmatter, P. A., *Astrophys. J.*, **175**, 601 (1972).
[86] Peterson, B. A., and Bolton, J. G., *Astrophys. Lett.*, **10**, 105 (1972)
[87] Arp, H., Baldwin, J. A., and Wampler, E. J., *Astrophys. J. Lett.*, **198**, L3 (1975)
[88] Colla, G., *et al.*, *Astr. Astrophys. Suppl.*, **20**, 1 (1975).
[89] Burbidge, G. R., and O'Dell, C. R., *Astrophys. J. Lett.*, **182**, L47 (1973)
[90] Argue, A. N., *et al.*, *Mon. Not. R. astr. Soc.*, **168**, 1p (1974)
[91] Wampler, E. J., Baldwin, J. A., Burke, W. L., Robinson, L. B., and Hazard, C., *Nature*, **246**, 203 (1973).
[92] Hazard, C., Sargent, W. L., Baldwin, J. A., and Wampler, E. J., *Nature*, **246**, 205 (1973).
[93] Burbidge, G. R., Burbidge, E. M., and O'Dell, C. R., *Nature*, **248**, 568 (1974).
[94] Sandage, A., and Luyten, W. I., *Astrophys. J.*, **155**, 913 (1969)
[95] Zwicky, F., Herzog, E., Wild, P., Karpowicz, M., and Kowal, C. T., *Catalogue of Galaxies and Clusters of Galaxies* (California Institute of Technology, Pasadena, 1961–68).
[96] Stockton, A. N., *Nature phys. Sci.*, **238**, 37 (1972)
[97] Arp, H., *Astrophys. Lett.*, **9**, 1 (1971).
[98] Lynds, R., and Millikan, A. G., *Astrophys. J. Lett.*, **176**, L5 (1972).
[99] Ford, H. C., and Epps, H. W., *Astrophys. Lett.*, **12**, 139 (1972)
[100] Adams, T. F., and Weymann, R. J., *Astrophys. Lett.*, **12**, 143 (1972)
[101] Arp, H., *Astrophys. Lett.*, **7**, 221 (1971).
[102] Walker, M. F., Pike, D., and McGee, J. D., *Astrophys. J. Lett.*, **194**, L125 (1974)
[103] Miley, G. R., *Mon. Not. R. astr. Soc.*, **152**, 477 (1971)
[104] Richter, G. M., *Astrophys. Lett.*, **13**, 63 (1973).
[105] van der Kruit, P. C., *Astrophys. Lett.*, **15**, 27 (1973).
[106] Strom, R. C., *Nature phys. Sci.*, **244**, 2 (1973).
[107] Wardle, J. F. C., and Miley, G. K., *Astr. Astrophys.*, **34**, 305 (1974)
[108] Brown, R. L., and Roberts, M. S., *Astrophys. J. Lett.*, **184**, L7 (1973).
[109] Haschick, A. D., and Burke, B. F., *Astrophys. J. Lett.*, **200**, L137 (1975)
[110] Carlson, R. W., *Astrophys. J. Lett.*, **190**, L99 (1974)
[111] Aaronson, M., Black, J. H., and McGee, C. F., *Astrophys. J. Lett.*, **191**, L53 (1974).
[112] Setti, G., and Woltjer, L., *Astrophys. J. Lett.*, **181**, L61 (1973)
[113] Bahcall, J. N., and Hills, R. E., *Astrophys. J.*, **179**, 699 (1973).
[114] Stannard, D., *Nature*, **246**, 295 (1973).
[115] Burbidge, G. R., and O'Dell, C. R., *Astrophys. J. Lett.*, **186**, L59 (1974).
[116] Karlsson, K. G., *Nature phys. Sci.*, **245**, 68 (1973).
[117] Teerikorpi, P., *Nature*, **252**, 110 (1974).
[118] Arp, H., *Nature*, **225**, 1033 (1970)
[119] Bottinelli, L., and Gougenheim, L., *Astr. Astrophys.*, **26**, 85 (1973)
[120] Jaakola, T., *Astr. Astrophys.*, **27**, 449 (1973)
[121] Collin-Souffrin, S., Pecker, J.-C., Tovmassian, H. M., *Astr. Astrophys.*, **30**, 351 (1974).
[122] Burke, J. A., and Hartwick. F. D. A., *Astr. Astrophys.*, **34**, 445 (1974).
[123] Jones, T. W., and Burbidge, G. R., *Astrophys. J.*, **186**, 791 (1974).
[124] Jaakola, T., Donner, K. J., and Teerikorpi, P., *Astrophys. Space. Sci.*, **37**, 301 (1975)
[125] Kinman, J. D., *Astrophys. J.*, **205**, 1 (1976)
[126] Burbidge, E. M., *et al.*, *Astrophys. J. Lett.*, **205**, L117 (1976).

articles

The Karari Industry: Early Pleistocene archaeological evidence from the terrain east of Lake Turkana, Kenya

John W. K. Harris & Glynn Isaac

Department of Anthropology, University of California, Berkeley, California 94720

Information concerning the technology, land-use patterns and activities of early hominids is being recovered from the Upper Member of the Koobi Fora Formation. The term Karari Industry is proposed for a distinctive local series of artefact assemblages that date to the period between 1.2 and 1.6 Myr BP.

THE area east of Lake Turkana (formerly Rudolf) is now well known for the large series of hominid and other fossils that Leakey *et al.* have recovered there[1-8] Researches in the area since 1970 have also yielded an abundance of archaeological traces that relate to the activities and behaviour of early hominids. Two series of archaeological occurrences can be recognised. An older series which occurs in the top of the Lower Member of the Koobi Fora Formation, chiefly in the KBS Tuff complex, has been the subject of preliminary reports[7-9]. The artefacts from these sites can be tentatively termed the KBS Industry A younger, contrasting series has subsequently been discovered in the Upper Member. This is described here for the first time, and we propose that it be designated the Karari Industry.

Provenance and stratigraphy

Sites pertaining to the newly discovered archaeological entity occur in great profusion along a low eroded ridge that has come to be known to our research group as the Karari Escarpment (Figs 1 and 2) and we have used the association with this topographic feature in naming the industry Samples of the industry, however, have also been recovered from the dip slope to the east of the Karari escarpment, and from the Ileret area. The locations of known sites are marked on Figs 1 and 2, but other areas remain to be explored and it is probable that the distribution will eventually prove wider than that shown.

All sites are designated in accordance with the standard African site enumeration system[10]. The letters identify a series of geographic rectangles bounded by lines of latitude and longitude at one quarter degree intervals. Thus FwJi denotes the square 4°15′–30′N and 36°0′–15′E while FxJj refers to the square 4°0′–15′N and 36°15′–30′E. The digits that follow are catalogue numbers that reflect the sequence of registration.

Table 1 summarises the stratigraphic relationships of the sites to each other and to the named units designated by Bowen and Vondra[11] Along the Karari escarpment and on the dip slope to the east, the sites are stratified in fluviatile deposits between the KBS Tuff complex and the Karari Tuff. They are particularly abundant in the strata associated with the Okote Tuff complex (formerly the BBS Tuff complex)[11]. They occur scattered through a cumulative thickness of some 50 m of sediments in the Karari area. In the Ileret area the sites occur in low energy river floodplain

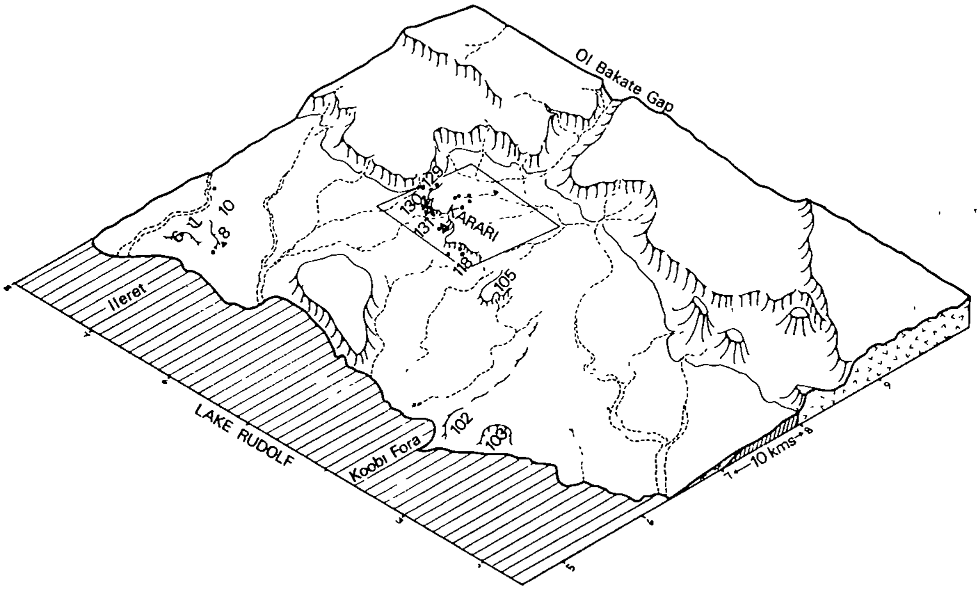

Fig. 1 Isometric block diagram showing the position of the Karari and Ileret sites in relation to present-day physiography. Numbers 1-131 refer to the expedition area numbers; rectangle designates the area shown in Fig. 2.

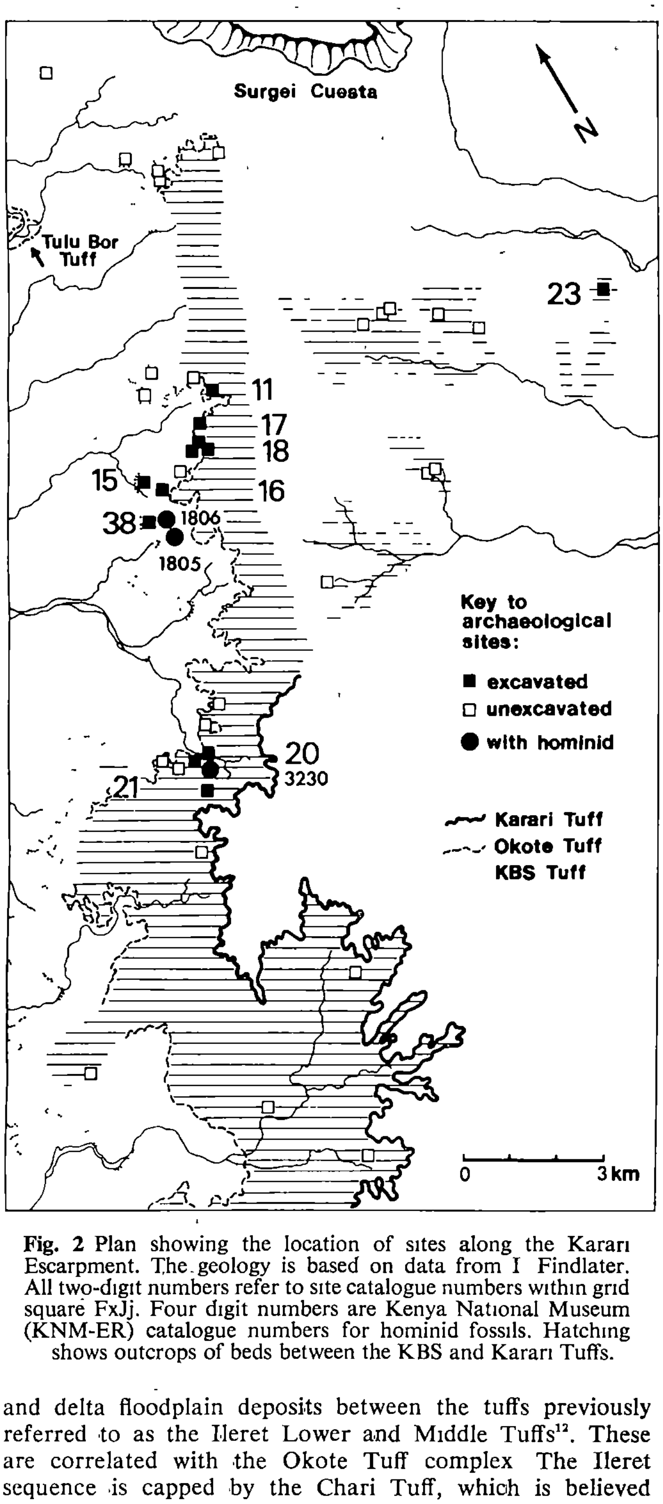

Fig. 2 Plan showing the location of sites along the Karari Escarpment. The geology is based on data from I Findlater. All two-digit numbers refer to site catalogue numbers within grid square FxJj. Four digit numbers are Kenya National Museum (KNM-ER) catalogue numbers for hominid fossils. Hatching shows outcrops of beds between the KBS and Karari Tuffs.

and delta floodplain deposits between the tuffs previously referred to as the Ileret Lower and Middle Tuffs[12]. These are correlated with the Okote Tuff complex The Ileret sequence is capped by the Chari Tuff, which is believed to correlate with the Karari Tuff, and thus the entire series of sites treated in this report can be said to derive from the stratigraphic interval between the KBS Tuff complex and the Chari-Karari Tuffs. Lake margin sediments that correlate with this interval also crop out in the vicinity of the Koobi Fora spit, but archaeological materials have not been recovered from these exposures.

In biostratigraphic terms, the interval from which the samples of the Karari Industry derives coincides largely with Maglio's *Loxodonta africana* zone[13].

Dating evidence

Table 2 shows the series of published potassium–argon determinations by Fitch and Miller that have a direct bearing on estimation of the age of the Karari archaeological occurrence[14]. An upper limit is set by dates of 1.32 ± 0.11 Myr and 1.22 ± 0.01 Myr for the Karari and Chari Tuffs, respectively. These dates are statistically indistinguishable and are believed to represent the same eruptive event. Technically, the lower age limit should be set by the age of the KBS Tuff, for which Fitch and Miller, using the $^{40}Ar/^{39}Ar$ step heating method, obtained a best estimate of 2.61 ± 0.26 Myr (ref. 14). Subsequently, Curtis *et al.* reported that they have made six conventional K–Ar determinations on samples from the KBS Tuff at the foot of the Karari Escarpment in Area 131. These values cluster closely around a mean of 1.8 Myr (ref. 15). The reasons for the discrepancy between the two sets of results are still under review. But, although the KBS Tuff is the marker horizon that forms the lowermost boundary of the stratigraphic interval containing the Karari Industry, most of the sites are contained in the strata at or above the level of the Okote Tuff complex and its equivalent at Ileret. Dates of 1.57 and 1.48 Myr for these tuffs, respectively, clearly provide the best indicators of the lower limits of the time interval in question.

Further chronological evidence has been obtained from palaeomagnetic stratigraphy[16]. The beds yielding the industry show predominantly reversed magnetic polarities and the few apparent normal results which were obtained at Ileret seem very likely to result from remagnetisation during the Brunhes Epoch. Since the Earth's field was reversed in the interval 1.2–1.6 Myr BP, the palaeomagnetic determinations for the Upper Member Beds are consistent with the K–Ar dates.

Biostratigraphic data are also concordant with these age determinations. On the basis of comparisons among various dated East African faunal samples, Maglio gave a best estimate of 1.3 Myr for the *Loxodonta africana* zone at East Rudolf, with the limits of uncertainty set at 1.0–1.6 Myr (ref. 13). More detailed work is being undertaken by J. M. Harris of the Kenya National Museum and his recent work does not suggest any need for major revisions in the biostratigraphic correlation of this part of the sequence, though the nomenclature will be changed (personal communication).

Characteristics of artefact samples

The overall characteristics of the series of artefact samples we have recovered can best be represented by the application of the typological system devised by Leakey[17], though it has been necessary to add one or two categories. Table 2 presents a summary for each excavated assemblage of the percentage incidence of specimens in each artefact category.

Each assemblage comprises two fundamentally distinct classes of specimens. first, there are comparatively thick, massive boulders, cobbles and blocks of stone from which flakes have been removed by percussion, and second, there are relatively thin slivers of stone produced by conchoidal fracture. The first are termed 'cores', in the broadest sense of the term, and the second, 'flakes' and 'flake fragments'. Superimposed on this dichotomy is another important distinction: items which have been purposively shaped to particular patterns are set apart and referred to as 'tools', the word having a restricted technical sense. By contrast, the category 'debitage' contains 'flakes' and 'flake fragments' which have not been secondarily trimmed, plus those 'cores' that are regarded merely as by-products of flake production. This semantic distinction is not meant to imply that items of debitage were never used as implements. There are good reasons for believing that unretouched sharp flakes were functionally as important as the formally defined 'tool' category. Objects that are 'non-tools', in the above sense, but which show damage attributable to use are put in the third category often defined 'utilised', but we prefer the designation 'edge damaged' for this set.

Among early stone industries most of the cores (*sensu lato*) also seem to have been designed as 'tools' and at

Table 1 Excavated Karari Industry sites in relation to stratigraphic markers and selected hominid fossil finds

Koobi Fora Coast Areas 102, 103	KBS Ridge Areas 105, 118	Karari Escarpment Areas 129, 130, 131	Ileret Areas 1–12				
Erosion		Karari Tuff	Chari Tuff		Karari Industry	*Loxodonta africana* zone	Upper Member
For example KNM-ER *1807*			For example KNM-ER *731, 739, 992* *741, 805, 993*				
Koobi Fora Tuff Complex		Okote Tuff Complex KNM-ER *3230* **FxJj 20 M, E, AB** **FxJj 19** **FxJj 16, 18** **FxJj 11**	For example KNM-ER *807* **FwJj 1** *803, 818* *808, 1463* *729*	Lower/ Middle Tuff Complex			
For example KNM-ER *730, 736, 737, 1808*	Erosion						
	KNM-ER *405, 738, 1476* *1477, 1478, 1479*	**FxJj 38** KNM-ER *1805* *1806* FxJj 15	For example KNM-ER *406, 407* *732, 815, 1592*			*Metridiochoerus andrewsi* zone	
KBS Tuff Complex	FxJj 1, 3, 10	FxJj 14	KBS Tuff Complex		KBS Industry	*Mesochoerus limnetes* zone	Lower Member
	FxJj 13	For example KNM-ER *1470, 1472, 1473* *1481, 1482, 1483*	For example KNM-ER *1590, 1593*				

Karari Industry sites are shown in bold face and hominid fossil finds in italic. KBS Industry sites are shown thus: FxJj 1 and so on.

Olduvai Gorge, M. D. Leakey found varied evidences of their usage as implements. For this reason in Tables 2 and 3 choppers, discoids, polyhedra, core scrapers and so on are all included as tools, although they undoubtedly also had importance as the source of flakes that were themselves useful. As Table 3 shows, in these assemblages, as in most Pleistocene industries, debitage is numerically the preponderant category with percentage values ranging from 58 to 99%. For the purpose of archaeological taxonomy, however, tools are usually regarded as the most important class.

Most of the artefacts are made of volcanic lava, particularly basalt, but also of feldspathic ignimbrite, rhyolite and a glassy welded tuff. The commonest source seems to have been the cobbles and boulders being transported by the streams that traversed the Karari area. This material was readily available and had good flaking qualities Less than 5% of the artefacts were made of other materials such as chert and quartz.

The most distinctive and abundant tool forms present are core scrapers and light duty scrapers (Fig. 3). Typical core scrapers are made on cobbles or split cobbles with one flat surface used as a striking platform. Commonly, more than one generation of flakes were removed from the dorsal surface to form a steep edge. In many cases, much of the perimeter of the scraper has been trimmed so that the dorsal face developed a keeled or domed configuration.

In contrast, the light duty scrapers are made of flakes or flake and core fragments, and are thin in cross-section compared with core scrapers. In many cases the trimming is regular and well controlled, giving the pieces slightly denticulated or serrated edges.

Other tool forms, such as choppers, protobifaces, dis-

Table 2 Potassium–argon dates for the upper part of the Koobi Fora Formation

Ileret	Karari Escarpment	KBS (Area 105)	Koobi Fora
Chari Tuff 1.22 ± 0.01 Myr (FMA 280, ref 14)	Karari Tuff 1.32 ± 0.10 Myr (FMA 290, ref. 14)		
Lower/Middle Tuff Complex 1.48 ± 0.17 Myr (FMA 278, ref. 14)	Okote Tuff Complex 1 56 ± 0.02 Myr (FMA 266, ref 14)		Koobi Fora Tuff 1.57 ± 0 0 Myr (FMA 270, ref. 14)
KBS Tuff Complex 1.57 Myr (Curtis *et al.*[15])	KBS Tuff Complex 1.82 ± 0 04 Myr (Curtis *et al* [15])	KBS Tuff 2 61 ± 0.26 Myr (Fitch *et al.*[14]) 1.61 Myr (Curtis *et al.*[15])	

coids and polyhedra occur with less frequency. A few bifaces and cleavers have been recovered from surface localities in circumstances that demonstrate conclusively their derivation from Upper Member beds. These tool forms, however, seem to be very rare in the material that is concentrated in occupation sites and have not yet been recovered by excavation.

The unbroken flakes show distinctive morphological features: small restricted platforms and diffuse bulbs of percussion. In particular, at sites associated with stream channels, battered cobbles and large boulder cores are present from which large well struck flakes had been struck. The trimming of the core tools must have also yielded numbers of flakes.

Comparisons and taxonomy

Very few datable artefact assemblages are known from the time span between 1 and 1.5 Myr BP. By far the largest and most detailed body of comparative data is that which derives from Bed II at Olduvai Gorge[17]. M. D. Leakey, who excavated the Olduvai material, recognised two main varieties among the samples that occur above the Lemuta Member: The Acheulian Industry and the Developed Oldowan Industry with the latter being subdivisible into phases A and B. Tables 2 and 3 show percentage frequency data for selected examples of Olduvai assemblages. Comparison of the two sets of data shows that not all the samples from the Upper Member of the Koobi Fora Formation are distinguishable from the Olduvai series; for example, FxJj 38 is not unlike FLKN level 5. But most Karari samples differed markedly, by virtue of the large percentages of core scrapers and other scrapers.

There are other contrasts. Polyhedra and discoids are more numerous at Karari sites but inhibit less battering and blunting of edges than is commonly evident in the Olduvai samples. The Karari assemblages lack spheroids and subspheroids, while these forms are present in relatively large proportions at most of the Bed II sites. The Karari Industry also contains core and cobble fragments with retouch on the ventral face, which could not be accommodated in any of the typological categories proposed by M. D. Leakey. A separate class has been added to the type list to represent these.

Very few awls, burins or picks have been recovered from the Karari sites, whereas at Olduvai these forms occur more frequently, although in small quantities. A variable series of unstandardised trimmed pieces in both the Olduvai and Karari samples have been classified as 'sundry tools'.

Other assemblages from the age range in question should be mentioned briefly. The samples from the Humbu Formation at Peninj include large percentages of bifaces and are therefore unlike the Karari material[18,19]. The tool component of the sample from Sterkfontein Extension site is dominated by choppers, polyhedra and spheroids and is therefore much more like the Developed Oldowan than the Karari Industry[20]. Although the time relationships of the early material from North Africa are not known with certainty, sites such as Ain Hanech, or Sidi Abderhaman Ancien Exploitation level J may be of comparable age[21]. None of these assemblages includes significant numbers of core scrapers of Karari type.

In each comparison it is largely the morphology of the core scrapers that distinguishes the Karari series. The form range of other tool categories such as choppers, polyhedra and discoids, overlaps extensively with that of the equivalent sets in other assemblages. The rare bifaces that derive from the Upper Member are very like those of Olduvai Bed II, Peninj or the Lower Acheulian of North Africa.

It thus emerges that the morphological pattern shown by the assemblages from the Upper Member of the Koobi Fora Formation falls outside the known range of other described, contemporary classificatory sets. In accordance with the procedures proposed by the 1965 Burg Wartenstein Symposium[22], and endorsed by the Sixth Pan-African Congress on Prehistory and the Study of the Quaternary, we propose to designate this distinctive series the Karari Industry.

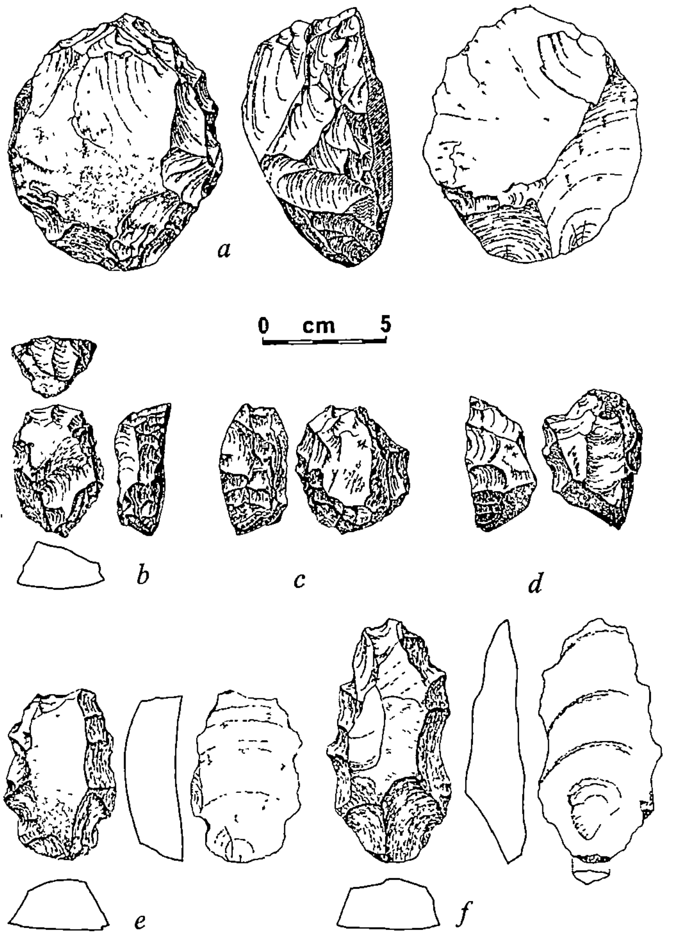

Fig. 3 *a*, Core scraper, FxJj 11; *b*, core scraper, FxJj 20 Main; *c* and *d*, core scrapers, FxJj 20 AB; *e*, core scraper, FxJj 20 IHS; *f*, light-duty scraper on flake, FxJj 18 NS. Made on lava. Drawings by Barbara Isaac.

As a formal definition we offer the following: the Karari Industry is a set of early Pleistocene artefact assemblages that shares broad, generalised features with other near-contemporary industries such as the Developed Oldowan Industry from Bed II at Olduvai, but which also shows distinctive patterns of differences from them. Generalised features held in common include the preponderance of opportunistic flaking technology in which highly organised, fixed patterns of core preparation are rare or lacking. Choppers, polyhedra and discoids are important components of the Karari Industry as in many other generalised industries. Handaxes and cleavers seem to have been a rare but significant part of the total artefact repertoire, as in the case of the Developed Oldowan B. The Karari Industry, however, is distinguishable from all other near-contemporaneous industries by the tendency of its component assemblages to include a conspicuous series of core scrapers. The percentage incidence of these is variable. A few assemblages, that clearly formed part of the material culture system that we are designating as the Karari Industry, show a low or negligible incidence of the key forms, but in most, where the sample is large enough, they are present in proportions well outside the range observed in other contemporary industries. In the Karari Industry even the scrapers that are not specifically core scrapers are distinct from those of most Oldowan assemblages in their tendency to be more massive.

From the [illegible] Library
SCIENCE COLLEGE

Table 3 Composition of assemblages assigned to Karari Industry compared with selected assemblages from Olduvai Gorge Beds I and II

	Overall composition*				Percentages of tool categories among tools											
Sites	No. of artefacts	% Debitage	% Tools*	No. of tools	Core scrapers†	Flake scrapers†	Choppers	Protobifaces	Bifaces	Discoids	Polyhedrons	Sundry tools	Other tools	RCCF	spheroids	% All scrapers
Karari Scarp assemblages from flood plain silts																
FxJj 11	337	95.8	3.6	12			(33)			(8)	(17)		(25)	17		
17	247	98.8	0.4	1						(100)						
18 IHS	3267	96.2	3.5	114	21	17	2	3		25	21	6		5		38
20 M	2510	97.5	1.7	42	2	31	12	5		19	7		2	21		33
20 E	1211	96.3	3.0	36	8	25	31			22	8		3	3		33
20 AB	3462	98 7	0.7	25	20	20	16			4	8			32		40
Karari Scarp assemblages from channel sands and gravels																
FxJj 16	173	57.8	26.0	45	18	18	27	4		9	16			9		36
18 GSL	1556	87.1	10.9	169	20	17	19	2		15	19	3		5		37
18 GSU	214	86.9	10.7	23	22	30	17			4	17	9				52
18 NS	993	91.0	5.9	58	14	29	10	3		14	19		5	5		43
21 surface	54	85.2	11.1	6			(17)		(67)				(17)			
23	73	97.2	1.4	1			(100)									
38	115	58.2	34.8	40		2	(72)			5		2		(18)		2
Ileret assemblage from Lake Margin flood plain silts																
FwJj 1	318	99.4	0.3	1			(100)									
Olduvai, Oldowan																
FLK Zinj.	2470	92.1	2.4	60	15	30	28			5	15		7			45
FLKN 5	151	60.9	19.9	30	10		77			10					3	10
Olduvai, Developed Oldowan A																
FLKN SC	234	26.1	41.0	96		14	26			9	4	6	4		36	14
HWKE 3–5	1989	59.0	20.5	409	4	12	33	3		2	6	8	4		28	16
Olduvai, Developed Oldowan B																
BK II	6801	83.6	9.2	628	3	17	16		6	5	1		20		32	20
FC West	1955	76.7	10.5	206	11	9	30		4	4	3	4	2		34	20
TK	2150	90.1	4.9	106	6	24	6		14		1		21		29	29
Olduvai, Acheulian																
EFHR	522	77.6	17.4	91	3	3	15		54	9	6				10	7

The data for Olduvai Gorge are from ref. 18. Percentages for the tool types relative to the tool subset are rounded to the nearest whole number. Values for samples of less than 20 are shown in parentheses. RCCF, retouched core and cobble fragments.

* The other minor categories for which percentages are not shown are 'modified' and 'edge damaged' (= utilised).

† For the Olduvai analyses the distinction is between heavy duty and light duty scrapers.

If an associated set of excavated artefacts is needed as a type sample of the newly defined industry, we would nominate the archaeological material from the FxJj 18 Site Complex as suitable. (That completes the definition.)

The decision to name this material as a distinguishable industry is based solely on considerations of the morphology of the archaeological materials. We do not necessarily wish to infer the former existence of a 'cultural entity' or an ethnic entity that could be equated with the Industry. We also wish at present to avoid a definite judgement on the formal taxonomic relationships at any level of classification wider than that involved in grouping a set of related assemblages into an Industry. Clearly the material may be related in some way to the contemporaneous Developed Oldowan and Acheulian at Olduvai. It involves elements of both modes 1 and 2 in the schema of Clark[23].

Palaeoecological context and behavioural interpretations

An extensive archaeological survey has been carried out at Ileret and along exposures of the Karari Escarpment to gain some understanding of the early Pleistocene man–land relationships represented in the area. The distribution of sites in relation to the mosaic of former habitats is potentially informative of the ecological relationships of early hominids. We found that they used the riverine floodplains and the alluvial fan deposits near the basin margins. Probably their range also included the valleys and hills of the more elevated surrounding terrain. These data are consistent with the idea that early hominids were mobile, opportunistic hunters and gatherers who used a wide range of resources.

More than 50 sites have been located and of these only two are in deposits laid down near the lake margins at Ileret, while the remainder are in varied alluvial deposits that formed 15–25 km inland from the shoreline. Of the 17 excavated sites nine are in direct association with the deposits of former stream channels while six are contained in the silty deposits of the broad floodplains that lay in between the stream channels. In addition to the excavated sites, we have located a further 40 archaeological occurrences through their surface traces, and these are potential sites for further investigation.

Several features emerge from an analysis of the pattern of distribution of the archaeological sites. Traces of past activities are found close to water sources, such as stream or river channels. This association has been observed elsewhere and may tentatively be explained by the fact that tree- and bush-lined stream channels would have provided shade and shelter as well as sources of nuts and berries. Ready access to raw material may have been another factor; in some cases, sites were located on gravel bars in stream channels in close proximity to patches of basalt cobbles and boulders.

Fossil bone is rather rare and poorly preserved in the deposits containing the Karari Industry. But sealed 'living floors' that contain stone artefacts plus small quantities of bone fragments, generally in a highly comminuted state, do occur chiefly in floodplain contexts Detailed study of bone samples is in progress.

Hominid remains occur interstratified with archaeological sites of the Karari Industry A hominid mandible, KNM-ER 3230 (*Australopithecus* cf. *boisei*) was recovered by excavation 10–15 cm stratigraphically above the artefact-bearing horizon at FxJj 20 E[25] In area 130, KNM-ER 1805 (*Homo* sp. ?) and KNM-ER 1806 (*Australopithecus* cf *boisei*) were recovered 40 m from FxJj 38 on the same stratigraphic horizon within channel deposits[6] A wealth of hominid fossils, including specimens assigned to *Australopithecus* (cf. *boisei*) and *Homo* have been recovered in beds of the Ileret Member[1–6].

The discovery of the Karari sites has added significantly to knowledge of artefacts that are more than 1 Myr old. Well dated, excavated samples were previously available only from Olduvai[17], Peninj[18,19], the Shungura Formation (Omo)[24], the Lower Member of the Koobi Fora Formation[8,9] and perhaps Ain Hanech in Algeria[21] and Sterkfontein in the Transvaal[20]. Variety among this series is considerable and we suspect that as the sample is enlarged, an even greater range of differences will be discovered between sets of sites characteristic of the various regions in which evidence is preserved. Many factors could have interacted to cause variety; for example, differences in the characteristics of available stone; differences in particular, local needs for certain implements and perhaps fluctuating regional differentiation in habits. To distinguish the relative importance of these and other factors, we will need a far larger sample of assemblages that have been drawn from a varied spectrum of contexts, in each of several separate sedimentary basins. Our naming of the Karari Industry as an entity is not intended to prejudice the outcome of this kind of research; it simply reflects the fact that the material from the Upper Member of the Koobi Fora Formation is distinctive and a clear unambiguous label is needed for it.

We thank Richard Leakey, Kamoya Kimeu and the National Museums of Kenya for encouragement and support. The archaeological work was financed by grants from the NSF and the project also in part by grants from the National Geographic Society and the NERC. We are also grateful for help from P. Abel, A. K. Behrensmeyer, B. Bowen, R. Bainbridge, D. Burggraff, I. Findlater, F. Fitch, H. Frank, J. M Harris, M. G Leakey, C. Vondra, H. White, B. Wood, Ingrid Herbich, J Barthelme, D. Crader, D. Gifford, J. G Gowlett, M. Mehlman, J. Onyango-Abuje, O. Odak, S. Wandibba, J. Kimengech, K. Kimeu, M. Mangoka, Mutete Numee and E. Kroll. Barbara Isaac drew the figures.

Received January 27; accepted May 19, 1976.

[1] Leakey, R. E. F., *Nature*, **226**, 223–224 (1970).
[2] Leakey, R. E F , *Nature*, 231, 241–245 (1971).
[3] Leakey, R E F , *Nature*, 237, 264–269 (1972).
[4] Leakey, R. E F., *Nature*, 242, 170–173 (1973)
[5] Leakey, R. E F., *Nature*, 242, 447–450 (1973)
[6] Leakey, R E F , *Nature*, **248**, 653–656 (1974).
[7] Leakey, M D , *Nature*, **226**, 228–230 (1970)
[8] Isaac, G L , Leakey, R E F , and Behrensmeyer, A. K., *Science*, **173**, 1129–1134 (1971).
[9] Isaac, G L., Harris, J W K , and Crader, D., in *Earliest Man and Environment in the Lake Rudolf Basin* (edit. by Coppens, Y , Isaac, G L , Howell, F C , and Leakey, R E F), 533–551 (University of Chicago Press, Chicago, 1976)
[10] Nelson, C. M , in the *Fourth Bulletin of the Commission on Nomenclature of the Pan African Congress on Prehistory* (mimeographed) (1971).
[11] Bowen, B E., and Vondra, C. F , *Nature*, **242**, 391–393 (1973)
[12] Vondra, C F , Johnson, G D., Bowen, B E , and Behrensmeyer, A K., *Nature*, **231**, 245–248 (1971)
[13] Maglio, V J , *Nature*, **239**, 379–385 (1972)
[14] Fitch, F. J , Findlater, I C , Watkins, R T , and Miller, J. A , *Nature*, **251**, 213–215 (1974).
[15] Curtis, G., Drake, R , Cerling, T E , Cerling, B L. and Hampel, J H , *Nature*, **258**, 395–398 (1975).
[16] Brock, A , and Isaac, G. L., *Nature*, 247, 344–348 (1974)
[17] Leakey, M. D , *Olduvai Gorge*, 3 (Cambridge University Press, London, 1971).
[18] Isaac, G L , in *Background to Evolution in Africa* (edit by Bishop, W W , and Clark, J D) (University of Chicago Press, Chicago. 1967)
[19] Isaac, G. L , and Curtis, G H , *Nature*, 249, 624 (1974)
[20] Leakey, M D , *Nature*, **225**, 1222 (1970).
[21] Biberson, P , *Le Paleolithique Inferior du Maroc Atlantique*, Fasc. 17 (Pub Service des Antiquites du Maroc, 1961).
[22] Bishop, W. W., and Clark, J D. (ed.), *Background to Evolution in Africa* (University of Chicago Press, Chicago, 1967).
[23] Clark, J. G D , *World Prehistory* (Cambridge University Press, London, 1969)
[24] Chavaillon, J , and Merrick, H. V., and Merrick, J. S , in *Earliest Man and Environment in the Lake Rudolf Basin* (edit by Coppens, Y., Isaac, G. L., Howell, F C , and Leakey, R E. F.), 565–584 (University of Chicago Press, Chicago, 1976)
[25] Leakey, R E. F , *Nature*, 261, 574–576 (1976)

Relationship between receptor and mammary tumour virus production after stimulation by glucocorticoid

G. Shyamala* & C. Dickson†

Department of Zoology and Cancer Research Laboratory, University of California, Berkeley, California 94720

A short exposure of primary cultures of mouse mammary tumour cells to glucocorticoids results in at least a threefold stimulation of mammary tumour virus (MTV) production. Specific interaction of glucocorticoids with the cytoplasmic and nuclear receptors can also be demonstrated. The biological potency of various steroids to stimulate MTV is related directly to the retention of the steroid–receptor complex in the nuclei. Progesterone has a high affinity for the cytoplasmic receptor, is not retained by the nuclei and does not stimulate or block the basal level of MTV production. It is, however, quite effective in abolishing the glucocorticoid-mediated stimulation of MTV and thus behaves as an antagonist of glucocorticoid.

CULTURES of cells and cell lines derived from primary mouse mammary tumours can be stimulated by glucocorticoids to produce increased quantities of mammary tumour virus (MTV) particles[1–7]. The biological activity of glucocorticoid hormones is believed to be mediated through a specific interaction of the steroid with the steroid hormone receptors[8]. The presence of cytoplasmic and nuclear glucocorticoid hormone receptors in mouse mammary tumour cells have been demonstrated[9–11]. A positive correlation has been reported between the binding of a steroid to the cytoplasmic glucocorticoid receptor and its biological potency in inducing MTV (ref. 11). These studies, however, failed to explain the role of progesterone in MTV synthesis because, in spite of its high affinity to the cytoplasmic receptor, it failed to stimulate MTV synthesis. Based on the observations that progesterone is an effective competitor for the cytoplasmic glucocorticoid receptor but cannot compete effectively with the glucocorticoid receptor-binding sites in the nuclei, we have postulated that progesterone is an antagonist of glucocorticoid action in mouse mammary tumour cells[10]. We now report the presence of cytoplasmic and nuclear glucocorticoid hormone receptors in cultured primary mouse mammary tumour cells; the acceleration of MTV production mediated by a short exposure to glucocorticoids as opposed to the continuous exposure to steroids used in previous studies, and an antagonistic action of progesterone on glucocorticoid-mediated stimulation of MTV.

---

*Present Address: Lady Davis Institute for Medical Research, Jewish General Hospital, 3755 Cote Ste-Catherine Road, Montreal, Quebec, Canada H3T 1E2.

†Present Address. Imperial Cancer Research Fund, Lincoln's Inn Fields, London WC2A 3PX, UK.

Mouse mammary tumour cell cultures were prepared from spontaneous mammary tumours arising in BALB/cfC3HCrgl and C3H/Crgl mice as described by McGrath[1]. There was no significant difference between BALB/cfC3H and C3H cells with respect to either virus production or the effect of hormones on MTV synthesis. Dissociated cells were plated in 60-mm or 100-mm Petri dishes (Falcon) at a seeding density of 5×10^5 cells per cm^2 in Dulbecco's modified Eagle's medium containing 15% foetal calf serum (Gibco), penicillin ($100\ U\ ml^{-1}$), streptomycin sulphate ($100\ \mu g\ ml^{-1}$) and bovine insulin ($10\ \mu g\ ml^{-1}$, Sigma). Cell cultures to be pulsed with steroids were changed to serum-free medium 24 h before the pulse, washed twice after the pulse and incubated for a further 24 h in serum-free medium. The resulting culture fluids were assayed for DNA polymerase activity.

For glucocorticoid receptor assays, all preparative procedures were carried out at 0–4 °C. The cells were homogenised in known volumes of TESH buffer (0.01 M Tris, 0.0015 M EDTA, 0.012 M thioglycerol, *p*H 7.4). The homogenate was centrifuged at 800*g* for 10 min. The supernatant was designated the cytoplasmic extract. The nuclear pellet was resuspended and centrifuged once in phosphate-buffered saline and once in phosphate-buffered saline containing 0.25 M sucrose. The pellet was then extracted with TESH–KCl buffer (TESH buffer containing 0.4 M KCl, *p*H 7.4) and centrifuged and the supernatant extract was designated the nuclear extract. The binding reaction was performed at 0–4 °C by incubation of aliquots of cytoplasmic extracts with known concentrations of the radioactive steroid, either alone or in the presence of competing non-radioactive steroid. After incubation for 120 min. (unless otherwise stated), binding in the cytoplasmic extract was assayed using a Sephadex G-25 filtration technique previously described[9] or by the DEAE–filter assay of Santi *et al.*[12]. Binding capacity determined by the two procedures did not differ significantly. The total radioactivity present in washed nuclear pellets was extracted with 3 ml of ethanol and counted with 10 ml of scintillation fluid. Bound and unbound labelled steroid in nuclear extracts was separated by gel filtration on Sephadex G-25 columns using TESH–KCl buffer.

The DNA polymerase activity present in the tissue culture fluid from tumour cell cultures was processed as previously described[2,13]. Assays were performed in reaction mixtures containing 50 mM Tris-HCl buffer, *p*H 8.3, 40 mM KCl, 10 mM $MgCl_2$, 0.04 A_{260} units of poly(rC)·oligo$(dG)_{12-18}$ (P. L. Biochemicals) and 5 μCi of ^{3}H-deoxyguanine triphosphate ($9.3\ Ci\ mmol^{-1}$) at 37 °C for 40 min. Assays were also performed using reaction mixtures containing Tris-HCl buffer, *p*H 7.4 and Mn^{2+} (0.5 mM).

To estimate DNA content, cell cultures were washed twice with Hanks balanced salts solution, scraped from the dish and precipitated with an equal volume of 10% perchloric acid (PCA) at 4 °C. After 30 min the precipitates were collecetd by centrifugation at 1,600*g* for 10 min and washed twice with cold 5% PCA and twice with 70% ethyl alcohol : 30% diethyl ether, and the pellet was allowed to dry. The pellet was dissolved in 1 N NaOH and left at 20 °C overnight, neutralised with HCl and reprecipitated with an equal volume of 10% PCA at 4 °C. The precipitate was washed twice with 5% PCA and hydrolysed in 5% PCA at 85–90 °C for 30 min. After hydrolysis the samples were mixed, centrifuged at 1,600*g* for 10 min and aliquots were assayed for deoxyribose content using the method described by Burton[14]. Hydrolysed calf thymus DNA was used as a standard.

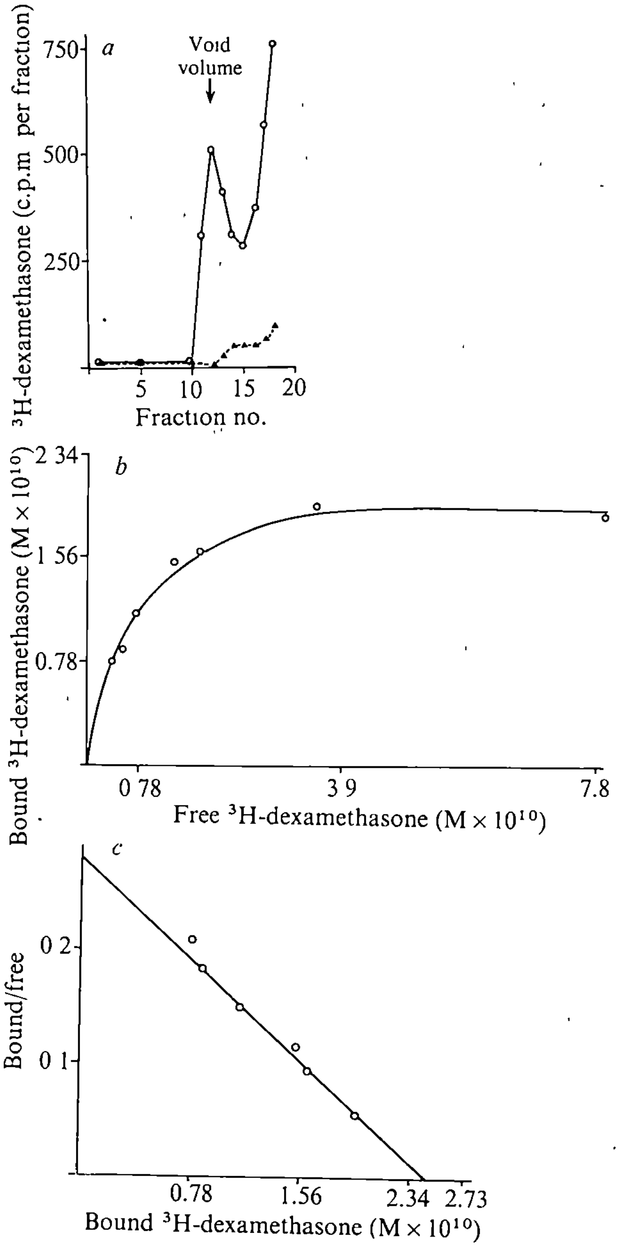

Fig. 1 (*a*), Binding of ^{3}H-dexamethasone in the cytoplasm of cultured mammary tumour cells. Samples (0.4 ml) of cytoplasm were incubated with 1.7×10^{-9} M of ^{3}H-dexamethasone (○) or with 1.7×10^{-9} M of ^{3}H-dexamethasone and 10^{-7} M unlabelled dexamethasone (▲) at 4 °C for 2 h. Bound radioactivity in each incubation was assayed on Sephadex G-25 columns (*b*), Kinetics of specific cytoplasmic binding of ^{3}H-dexamethasone. Samples of cytoplasmic extracts were incubated with various concentrations of ^{3}H-dexamethasone with or without 100-fold excess of unlabelled dexamethasone for 2 h at 0–4 °C. The data, represented as molar bound steroid in the total incubation, are plotted as a function of free-steroid concentration at equilibrium. The free steroid was determined by subtracting the bound steroid from the total steroid present in the incubation mixture. (*c*), Scatchard plot of the binding data from (*b*).

Strong interactions of ^{3}H-dexamethasone with the macromolecules of the cytoplasmic extract of mammary tumour cells in culture were revealed by gel filtration analyses (Fig. 1*a*). Specific binding was eliminated when the extract was incubated with labelled dexamethasone in the presence of an excess of unlabelled dexamethasone. This indicates that there was only a limited number of binding sites for dexamethasone. The amount of specifically bound ^{3}H-dexamethasone in the cytoplasmic extracts of cultured cells as a function of the free steroid concentration is shown in Fig. 1*b* Saturation of the binding sites was reached when the free steroid concentration was about 4×10^{-10} M. The specific binding data were also plotted by the Scatchard[15] technique (Fig. 1*c*) and yielded a single straight line, indicating that only a single class of binding site was present The equilibrium dissociation constant of the binding of the steroid to the receptor was estimated to be $8\,8\times10^{-10}$ M. The average dissociation constant as determined from four separate experiments using various concentrations of cytoplasmic extract was estimated to be 1.6×10^{-9} M. On the basis of the Scatchard plot, it can be assumed that 1 mol of steroid is bound to 1 mol of receptor. Thus, assuming 6.6×10^{-6} μg of DNA per cell nucleus, based on the average DNA content of the tumour cells in culture (0.015 μg DNA per 10^{7} cells), there are about 1,800 sites per cell. The average number of binding sites per cell as determined from four separate experiments was estimated to be approximately 1,400. Binding activity was destroyed by incubating cytoplasmic extracts with trypsin (500 μg ml^{-1}) or Pronase (100 μg ml^{-1}). Similar treatment, but with DNase (bovine pancreas 100 μg ml^{-1}) and RNase (100 μg ml^{-1}), had no effect on the binding. Therefore the cytoplasmic receptors seem to be proteins. Various non-radioactive steroids were tested for their ability to compete with ^{3}H-dexamethasone for the receptor binding (Fig. 2). The order of affinity of various steroids to the cytoplasmic receptor was dexamethasone > deoxycorticosterone > corticosterone > progesterone > hydrocortisone.

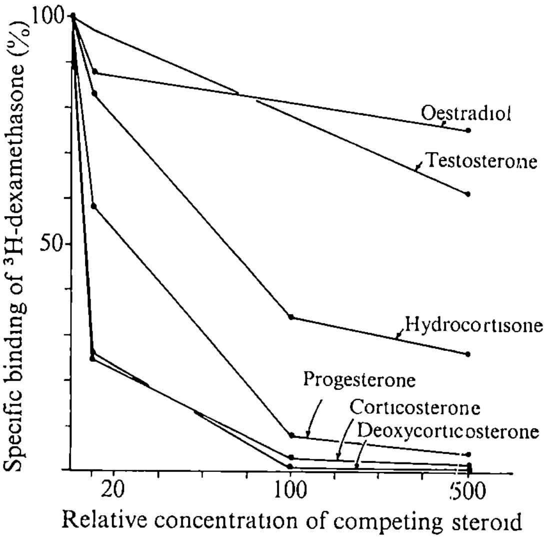

Fig. 2 Effect of various unlabelled steroids on binding of ^{3}H-dexamethasone to cytoplasmic extracts of mammary tumour cells in culture. Aliquots of cytoplasmic extracts were incubated with 10^{-9} M ^{3}H-dexamethasone alone or with various concentrations of non-radioactive steroids at 4 °C for 2 h Binding was measured by DEAE-filter assays as described in the text. Non-specific binding has been subtracted.

It has been proposed that the effect of glucocorticoids in target tissues results from steroid-mediated interaction of the receptor with the genome[16]. To examine this phenomenon in mammary tumour cell cultures, we made parallel studies on the nuclear localisation of dexamethasone and its stimulation of MTV. The data on the specific nuclear binding of steroids, and the subsequent stimulation of MTV in primary cultures of mammary tumour cells are shown in Fig. 3. The specific nuclear binding of dexamethasone was nearly complete by 30 min (Fig. 3*a*); as with other steroid receptor systems, nuclear binding was derived from the receptor in the cytoplasm because the total receptor binding in the cells remained constant throughout the experiment. The specific binding of ^{3}H-dexamethasone in the nuclei reached saturation with 10^{-8} M ^{3}H-dexamethasone in the incubation medium (Fig. 3*b*). As with fresh tumour slices[9,10], 10–20 times more than a saturating amount of steroid with respect to cytoplasmic receptor was required to achieve nuclear saturation. About 90% of the nuclear bound radioactivity could be solubilised and the radioactivity in the nuclear extract was bound to a macromolecule (Fig. 3*c*). Pulsing the cells with dexamethasone for 30 min was also sufficient to evoke a subsequent near maximal stimulation of MTV (Fig. 3*d*). The effect on MTV was most pronounced in the cultures assayed between 12 and 24 h after exposure to the steroid as opposed to earlier (0–12 h) or later (24–36 h) (data not shown). The dose–response curve for dexamethasone in stimulating MTV is presented in Fig. 3*e*, and Fig. 3*f* represents a plot of the relative potency of a given steroid to stimulate MTV and the amount of that steroid specifically bound in the nuclei.

Since mouse cells contain endogenous type C oncornaviruses which after induction may or may not be stimulated by glucocorticoids[7,17–19], the cultures were also monitored for the presence of type C virus, using the divalent cation preference of the DNA polymerase reaction. The MTV–DNA polymerase will utilise the template-primer poly(rC)·oligo(dG)$_{12-18}$ 70 times more efficiently with Mg^{2+} as the divalent cation than with Mn^{2+}, whereas murine type C viruses (Moloney MSV/MuLV) show a greater efficiency with manganese (our unpublished observations)[7,20,21,22]. Furthermore the DNA polymerase activity in the tissue culture fluid from mammary tumour cells was shown to be associated with the MTV virion by biophysical, morphological and immunological criteria[2]. In all the experiments described, parallel assays had been performed to determine the presence of type C viruses and no evidence was found for significant type C virus production. Furthermore, in some experiments, culture virus was also analysed for its viral polypeptide composition and in all cases only the MTV-specific polypeptide components were present (data not shown). Thus we are reasonably assured that the viral polymerase activities reported here represent the activity due to MTV and also reflect the virus production.

Previous studies from this laboratory[10] have demonstrated that the binding of progesterone to the glucocorticoid receptor of mouse mammary tumours does not lead to the translocation of the receptor to the nucleus and this was also true with tumour cells in culture (data not shown). As shown in Fig 3, the nuclear-bound steroid is closely related to the stimulation of MTV, and therefore as suggested previously[10], it is possible that progesterone acts as an antagonist to the glucocorticoid-mediated stimulation of MTV. The results of the following experiments demonstrate that this may indeed be true. Exposure of cell cultures to progesterone alone for 30 min did not stimulate MTV but neither did it block the basal level of MTV production (Table 1). This agrees with earlier observations made with progesterone on long term cultures of murine mammary tumour cells[2,7]. If cells were exposed to dexamethasone in the presence of an excess of progesterone, however, there was a reduction in the stimulation of MTV due to dexamethasone (Table 1). The average of three experiments on primary culture of tumour cells indicates that when a 100-fold excess of progesterone is added with dexamethasone, there is a 70% inhibition of the dexamethasone-mediated

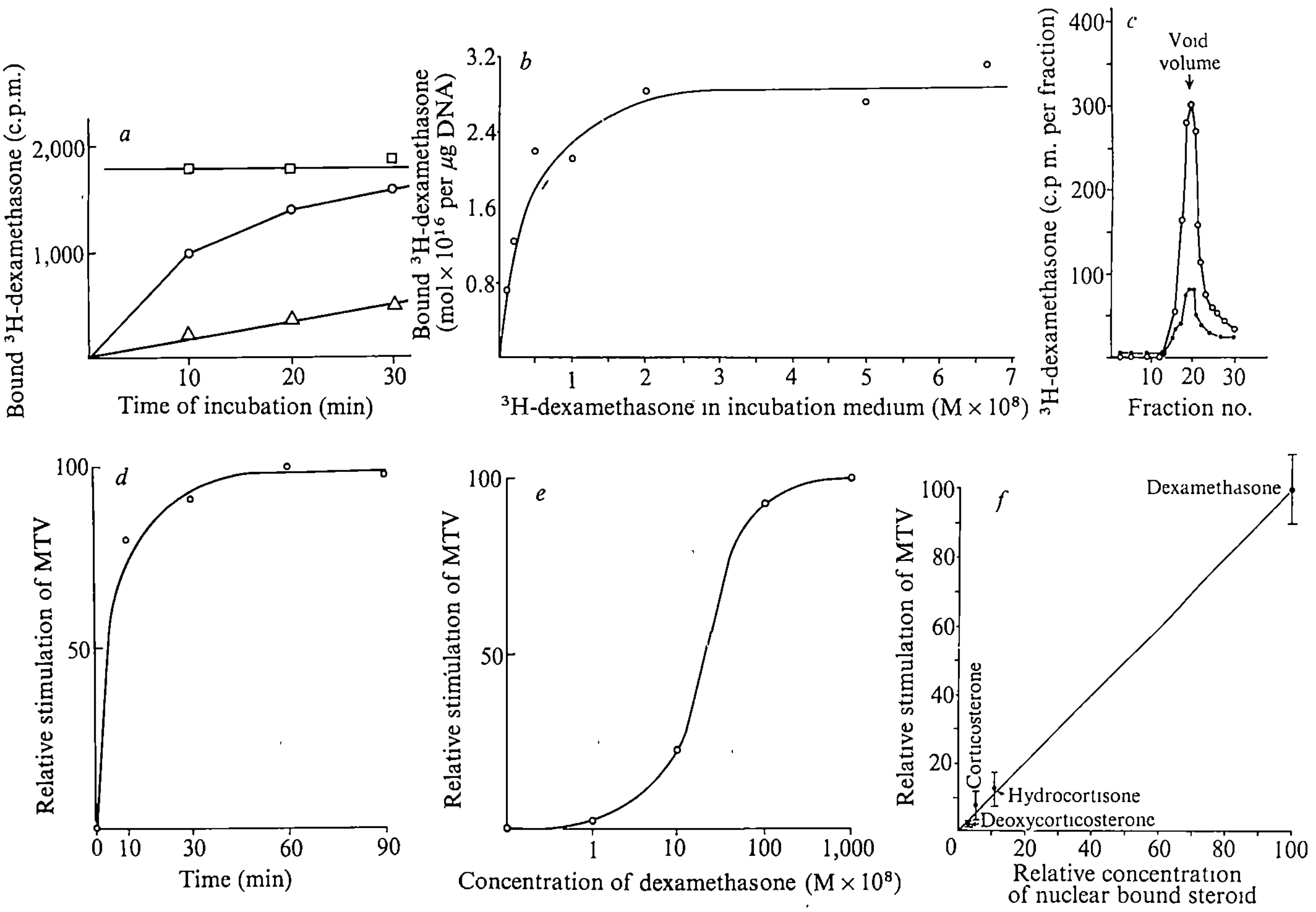

Fig. 3 Nuclear binding of ^{3}H-dexamethasone and its stimulation of MTV. In (*a*)–(*e*), to estimate binding to receptor, the cells were incubated at 37 °C with specific concentrations of ^{3}H-dexamethasone for specified times. Parallel sets of incubations were done with 100-fold excess of non-radioactive dexamethasone to determine nonspecific binding. At the end of the incubations, cell fractions were prepared and assayed for binding. The rate of MTV synthesis was estimated by assaying for DNA polymerase activity in the tissue culture fluid from duplicate cultures of tumour cells 24 h after exposure to steroid. (*a*), Cells were incubated with 10^{-8} M ^{3}H-dexamethasone with or without 100-fold excess of unlabelled dexamethasone. ○, Nuclear binding; □, specific nuclear and cytoplasmic binding; △, nonspecific nuclear binding. (*b*), Cells were incubated with various concentrations of ^{3}H-dexamethasone for 30 min. (*c*), Gel filtration on Sephadex G-25 columns of nuclear extracts of tumour cells in culture labelled with ^{3}H-dexamethasone only (○) or also with 100-fold excess of unlabelled dexamethasone (●). (*d*), Tumour cells were treated with dexamethasone for the times indicated, and culture fluid was assayed 24 h after exposure to steroid. (*e*), Cells were exposed to various concentrations of dexamethasone for 30 min and culture fluids were assayed after 24 h for DNA polymerase activity as indicated in the text. (*f*), Plot of the relative concentration of nuclear receptor-bound steroid and its relative stimulation of MTV. To estimate stimulation of MTV, cells were pulsed with 10^{-6} M of various steroids for 30 min and the tissue culture fluid was assayed 24 h later for viral DNA polymerase activity. To estimate nuclear receptor binding, the cells were treated with 10^{-8} M of various labelled steroids for 30 min, at the end of which binding assays were performed. Parallel cultures were treated also with 10^{-6} M unlabelled dexamethasone. Nonspecific binding was subtracted. The data are therefore due to the specific binding of the labelled steroid to sites specific for glucocorticoid receptor only. In each case the data were calculated as pmol nuclear-bound steroid per mg DNA. The data thus obtained for MTV and nuclear binding with each steroid is expressed as relative to that obtained with dexamethasone. The average stimulation of MTV due to dexamethasone was 2.5 times the basal level. The results are the average of six separate determinations ± s.d.

stimulation of MTV. This supports the notion that progesterone can antagonise the glucocorticoid-mediated stimulation of MTV. Table 1 also shows that to observe a significant antagonistic effect of progesterone on MTV stimulation, the levels of progesterone must be at least 100 times in excess of that of added dexamethasone. This is necessary since the affinity of progesterone to the glucocorticoid receptor is less than that of dexamethasone and hence binding of progesterone to receptor in levels equivalent to dexamethasone occurs only at higher concentrations of progesterone. Treatment of cells for short times with concentrations of progesterone as reported here do not result in any toxicity. This was ascertained by measuring the overall incorporation of labelled amino acids into total cell protein by the tumour cells at the time when the culture fluids were assayed for DNA polymerase activity (data not shown).

The ability of various steroids to stimulate MTV in cultured murine mammary tumour cells has been reported[1-7] and our studies confirm this for primary cultures of mammary tumour cells, and demonstrate that a 30-min exposure to steroids is sufficient to elicit the response at 24 h. Our studies show that cytoplasmic and nuclear glucocorticoid hormone receptors are present in tumour cells in primary culture and, as with other steroid hormone receptors, binding of the steroid to the cytoplasmic receptor is an initial event responsible for the subsequent steroid binding to the nuclei. Also, all steroids that bind to the cytoplasmic receptor of the mammary tumours are not retained by the nucleus, and progesterone falls into this category. This interaction of progesterone with the glucocorticoid receptor binding to nuclei has been described in detail[10]. In the studies reported here we have also demonstrated a direct relationship between the kinetics of the nuclear binding of a steroid and its subsequent stimulation of MTV. In addition, we have shown a quantitative correlation between the retention of the steroid–receptor complex in the nuclei as measured 30 min after exposure to steroid and its ability to stimulate MTV. Therefore, even though progesterone has a high affinity for the cytoplasmic receptor, its failure to remain bound to the receptor in the nucleus can lead to its inability to stimulate MTV. Similarly when used at appropriate concentrations with dexamethasone, it can block the stimulation of MTV by competing with dexamethasone for the cytoplasmic receptor sites and preventing its retention in the nucleus. Thus the data reported here are consistent with the role proposed for progesterone as an antagonist of glucocorticoid action in mammary tumours[10] and in hepatoma cells[23].

Table 1 Progesterone antagonism of dexamethasone-stimulated MTV production

Steroid treatment	Relative stimulation of MTV production ± s.d.
Dexamethasone (10^{-6}M)	$100 \pm 8.9\%$ $n = 6$
Dexamethasone (10^{-6}M) + progesterone (10^{-4}M)	$31.2 \pm 5.6\%$ $n = 6$
Dexamethasone (10^{-6}M) + progesterone (10^{-5}M)	$89.8 \pm 15\%$ $n = 4$
Progesterone (10^{-4}M)	$3.25 \pm 5.2\%$ $n = 4$
Progesterone (10^{-6}M)	$2.75 \pm 2.5\%$ $n = 4$

The results are expressed as % of the dexamethasone-stimulated DNA polymerase activity above the basal level. Cell cultures were pulsed for 30 min with the steroid combinations and the culture fluids were collected 24 h later and assayed for enzyme activity. The average incorporation of the Mg^{2+}-stimulated DNA polymerase activity at 100% was 25,400 c.p.m.

Based on the observed relationship between the retention of the steroid–receptor complex in the nuclei and the subsequent stimulation of MTV, some aspects of the steroid-mediated MTV synthesis can be explained. (1) Although a single, 30-min pulse with steroid is sufficient to translocate the receptor from the cytoplasm to the nucleus and to stimulate the subsequent MTV synthesis nearly threefold, when measured 24 h later, continuous exposure of the cells to the steroid is necessary to maintain the full level of MTV synthesis. This may be because it is necessary to retain in the nuclei optimal levels of steroid–receptor complexes for periods longer than 30 min. But when the steroid is removed from the medium at the end of the pulse, the equilibrium of the subcellular distribution of the steroid–receptor complex can be affected, causing some dissociation of the steroid from the complex in the nuclei. Since a quantitative relationship seems to exist between nuclear binding and MTV synthesis, this can lead to a decreased level of MTV synthesis. In this context it is important to mention that during the 24 h after the steroid pulse and washes, about 10^{-10} M steroid is released from the cells into the incubation medium. In separate experiments where the cells were exposed continuously to 10^{-10} M steroid, at the end of 24 h there was no detectable increase in the viral polymerase activity (data not shown). Thus the observed stimulation of MTV polymerase activity must result from the steroid–receptor complex formed during the pulse and not from the continuous presence of the low level of residual steroid in the medium. (2) Our dose–response curve for dexamethasone-mediated stimulation of MTV indicates that to obtain maximal stimulation, 10^{-6} M dexamethasone is needed while 10^{-8} M dexamethasone seems to be sufficient to saturate most of the receptor sites. It is important to remember, however, that the cells were pulsed with the steroid only for 30 min while the response was measured 24 h later. Thus, it is possible that with 10^{-6} M dexamethasone, there is a near maximal saturation of binding sites and a relatively smaller decrease in the dissociation of the steroid–receptor complex from the nuclei on withdrawal of the steroid at 30 min. This increase in the amount of steroid retained by the nuclei after withdrawal of 10^{-6} M dexamethasone as opposed to 10^{-8} M dexamethasone may be just enough to maintain maximal synthesis of MTV. This may be the reason why, with 10^{-5} M dexamethasone, there is no further increase in MTV synthesis. It is also likely, however, that the dose–response relationships of steroid binding and steroid-mediated MTV synthesis do not fit, and elucidation of this problem must await further studies. (3) Our data show that while deoxycorticosterone has at least as high an affinity as hydrocortisone for the cytoplasmic receptor, it is able to stimulate MTV only suboptimally. As reported earlier[10], even with saturation of all the receptor sites in the cytoplasm with deoxycorticosterone, there is only partial translocation, or retention, of the receptor to the nuclei and this may explain why this steroid is only suboptimally active, for even at high concentrations it cannot lead to maximal stimulation of MTV[2].

The mechanism by which steroids are believed to influence gene expression in target cells involves the binding of the steroid to the cytoplasmic receptor and its subsequent interaction with DNA and chromatin, the net result of which leads to the expression of the phenotypic effect. The data on the glucocorticoid receptor and MTV synthesis obtained with various steroids seem to fit this model. As reported here and elsewhere[10], specific binding of glucocorticoids to cytoplasmic and nuclear components occurs in mouse mammary tumours. As shown here, the interaction of the receptor with the nuclear components seems to be crucially related to MTV synthesis. The accumulation of MTV-specific RNA seems to be a primary response to the steroid[24] and reaches maximum at 6 h and finally as shown here, an effect on MTV synthesis can be demonstrated at 24 h. In this respect, the glucocorticoid-mediated stimulation of MTV is very similar to some of the most carefully studied examples of enzyme induction by steroids[25–27].

Finally, a comment is needed about the nature of glucocorticoid-mediated synthesis of MTV. All data reported so far indicate that the steroid-mediated phenomenon is an amplification of the MTV synthesising apparatus rather than a true induction. This argument is based on the fact that the cells in culture synthesise MTV even in the absence of added steroid and steroids are required only for maximal production. Furthermore, progesterone does not inhibit the basal level of MTV but only that which is mediated by the glucocorticoid. Our studies, however, cannot provide any information with respect to particular sequences involved in the cell–virus interaction which are amplified by the hormonal control. Further investigations are also necessary to see if the primary site of hormone action lies in the host cell or the integrated virus in the host cell.

We thank Dr S. Nandi for support, E. Reid for illustrations and J. Underhill for photography. This investigation was supported by a grant from the NCI.

Received December 4, 1975, accepted May 18, 1976.

[1] McGrath, C. M, *J natn Cancer Inst*, **47**, 455–467 (1971)
[2] Dickson, C, Haslam, S., and Nandi, S., *Virology*, **62**, 242–252 (1974).
[3] Parks, W. P, Scolnick, E. M, and Kozikowski, E. H, *Science*, **184**, 158–160 (1974).
[4] Fine, D L, Plowman, J K., Kelley, S. P, Arthur, L O, and Hillman, E A., *J natn Cancer Inst*, **52**, 1881–1886 (1974)
[5] Ringold, G., Lasfargues, E. Y, Bishop, J. M, and Varmus, H E, *Virology*, **65**, 135–147 (1975)
[6] Young, L. J. T, Cardiff, R. D, and Ashley, R, *J natn. Cancer Inst*, **54**, 1215–1221 (1975)
[7] Parks, W. P, Ransom, J C. Young, H A., and Scolnick, E M, *J. biol Chem*, **250**, 3330–3336 (1975)
[8] Thompson, E B., and Lippman, M E, *Prog Endocr Metabolism*, **23**, 159–201 (1974)
[9] Shyamala, G, *J biol. Chem.*, **249**, 2160–2163 (1974).
[10] Shyamala, G., *Biochemistry*, **14**, 437–444 (1975)
[11] Young, H. A, Scolnick, E M, and Parks, W. P, *J biol Chem*, **250**, 3337–3343 (1975).
[12] Santi, D. V., Sibley, C H, Perriard, E R, Tomkins, G M, and Baxter, J D., *Biochemistry*, **12**, 2412–2416 (1973).
[13] Dickson, C, *J. gen Virol*, **20**, 243–247 (1973)
[14] Burton, K., *Biochem J.*, **62**, 315–323 (1956)
[15] Scatchard, G, *Ann N Y Acad. Sci*, **51**, 660–672 (1949)
[16] Gemmeltoft, S, and Schaumburg, B, *Exerpta Med Found Int Congr*, Ser No. 256, 147 (1972).

[17] Paran, M, Gallo, R C, Richardson, L. S., and Wu, A. M., *Proc. natn Acad. Sci U.S A*, 70, 2391–2395 (1973)
[18] Wu, A M., Reitz, M S, Paran, M., and Gallo, R C., *J Virol*, 14, 802–812 (1974)
[19] Ihle, J. N., Lane, S E., Kenney, F. T., and Farrell, J C, *Cancer Res*, 35, 442–446 (1975).
[20] Dion, A. S., Vaidya, A. B., Sarkar, N H., and Moore, D. H., *Eighth Meeting on Mammary Cancer in Experimental Animals and Man*, 74, (1973)
[21] Howk, R S., Rye, L A., Killeen, L. A, Scolnick, E. M, and Parks, W. P., *Proc natn. Acad Sci. U S A.*, 70, 2117–2121 (1973)
[22] Michailides, R., Schlom, J., Dahlberg, J, and Perk, K, *J. Virol*, 16, 1039–1050, (1975)
[23] Rousseau, G G., Baxter, J. D, Higgins, S J., and Tomkins, G. M., *J molec. Biol*, 79, 539–554 (1973).
[24] Ringold, G. M., Yamamoto, K. R., Tomkins, G. M, Bishop, J. M, and Varmus, H E., *Cell*, 6, 299–305 (1975)
[25] Griffin, M J., and Cox, R. P., *J Cell Biol*, 29, 1–9 (1964).
[26] Granner, D. K, Thompson, E. B., and Tomkins, G. M., *J biol Chem*, 245, 1472–1478 (1970)
[27] Chader, G J., *Biochem biophys. Res. Commun.*, 43, 1102–1105 (1971).

4S *oop* RNA is a leader sequence for the immunity-establishment transcription in coliphage λ

A. Honigman, S.-L. Hu, R. Chase & W. Szybalski

McArdle Laboratory for Cancer Research, University of Wisconsin, Madison, Wisconsin 53706

oop *RNA, which is initiated at the* p_o *promoter and is 81 nucleotides long, can function as a leader sequence for the λ immunity establishment transcription, previously believed to originate at a special promoter* p_{re} *located in the* y *region. Thus,* oop *RNA seems to have a dual role, either favouring the lytic cycle as a primer for the initiation of λ DNA replication, or leading to the establishment of lysogeny when elongated into the* imm *transcript, which directs synthesis of the repressor.*

To establish and maintain the prophage state, phage λ directs synthesis of the repressor protein, the product of gene *c*I (ref. 1). There are two known modes of repressor synthesis: (1) In the establishment mode, observed early after λ infection, the *c*I transcription is believed to originate at the p_{re} promoter, hypothetically defined by the *c*Y mutations located in segment *y* just to the right of gene *cro* (Fig. 1), and is positively regulated by genes *c*II and *c*III (refs 2–5). (2) In the maintenance mode, characteristic of the established prophage, the *c*I transcription originates at the p_{rm} promoter (originally designated p_c promoter[6]) just to the left of gene *cro* (Fig. 1) and is both positively and negatively controlled by the *c*I product[2,3,7]. Both the maintenance and establishment modes of the *c*I transcription are under the negative control of gene *cro* (refs 1–6).

A small RNA species designated *oop* RNA (ref. 8) is synthesised a short distance upstream from the hypothetical location of the p_{re} promoter. Synthesis of *oop* RNA, which is believed to serve as primer for the initiation of λ DNA synthesis, depends on several phage and host replication functions[9]. Since establishment of lysogeny also depends on some replication functions[2,3,10] and because of the close proximity between the hypothetical location of p_{re} and the site of *oop* RNA synthesis, we sought to establish some relationship between these two entities. Moreover, the isolation and mapping of the *sar* mutations, which affect λ DNA replication but stimulate repressor synthesis overcoming the *c*Y defects, suggested that the establishment mode of repressor transcription might originate at the promoter, designated *pro*, between genes *c*II and *O* (ref. 10).

Specifically, we postulated that *oop* RNA, in addition to serving as the primer for DNA replication, can also have the role of a leader sequence that can be extended into the *imm* region by some anti-termination function, most likely depending on the *c*II and *c*III products. This would imply that the p_{re} promoter, as defined by the *c*Y mutations[2], either does not exist or has only a minor role, whereas the Pre function—that is, promotion of the establishment mode of *c*I transcription, is really carried out by the p_o promoter of the *oop* RNA (ref. 8). As will be discussed later, the *c*42 and similar *cis*-dominant mutations in the *y* segment, which were thought to define th

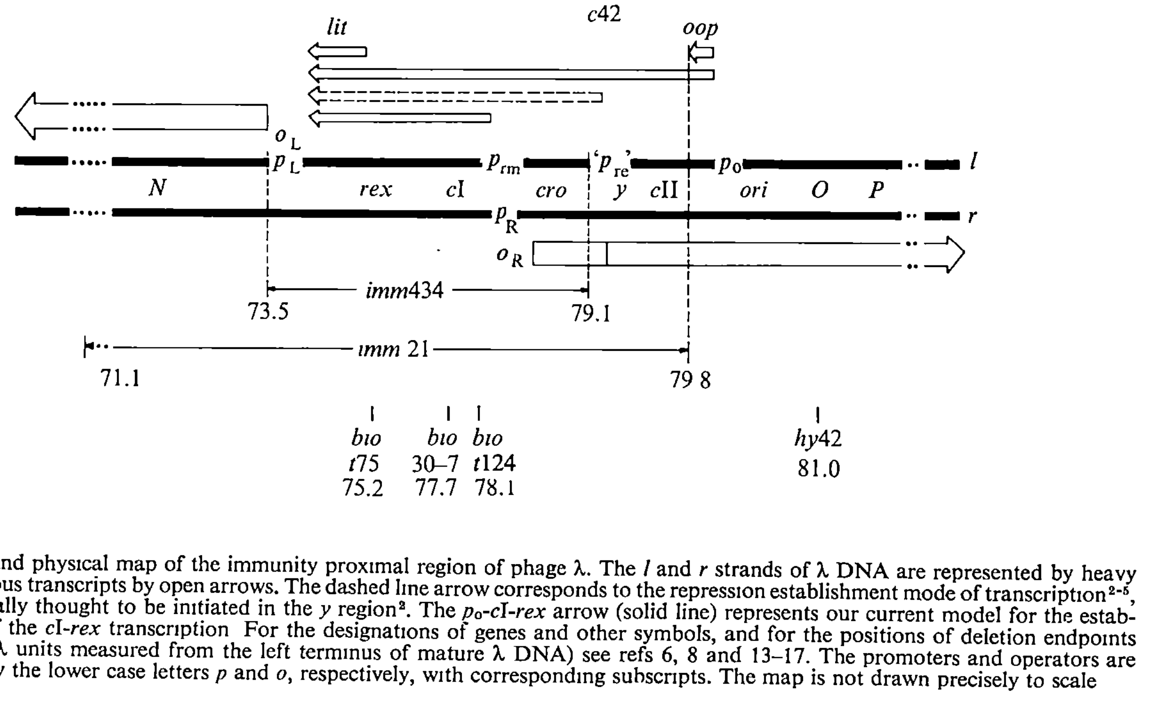

Fig. 1 Genetic and physical map of the immunity proximal region of phage λ. The *l* and *r* strands of λ DNA are represented by heavy lines and the various transcripts by open arrows. The dashed line arrow corresponds to the repression establishment mode of transcription[2-5], which was originally thought to be initiated in the *y* region[2]. The p_o-*c*I-*rex* arrow (solid line) represents our current model for the establishment mode of the *c*I-*rex* transcription. For the designations of genes and other symbols, and for the positions of deletion endpoints (expressed in % λ units measured from the left terminus of mature λ DNA) see refs 6, 8 and 13–17. The promoters and operators are represented by the lower case letters *p* and *o*, respectively, with corresponding subscripts. The map is not drawn precisely to scale

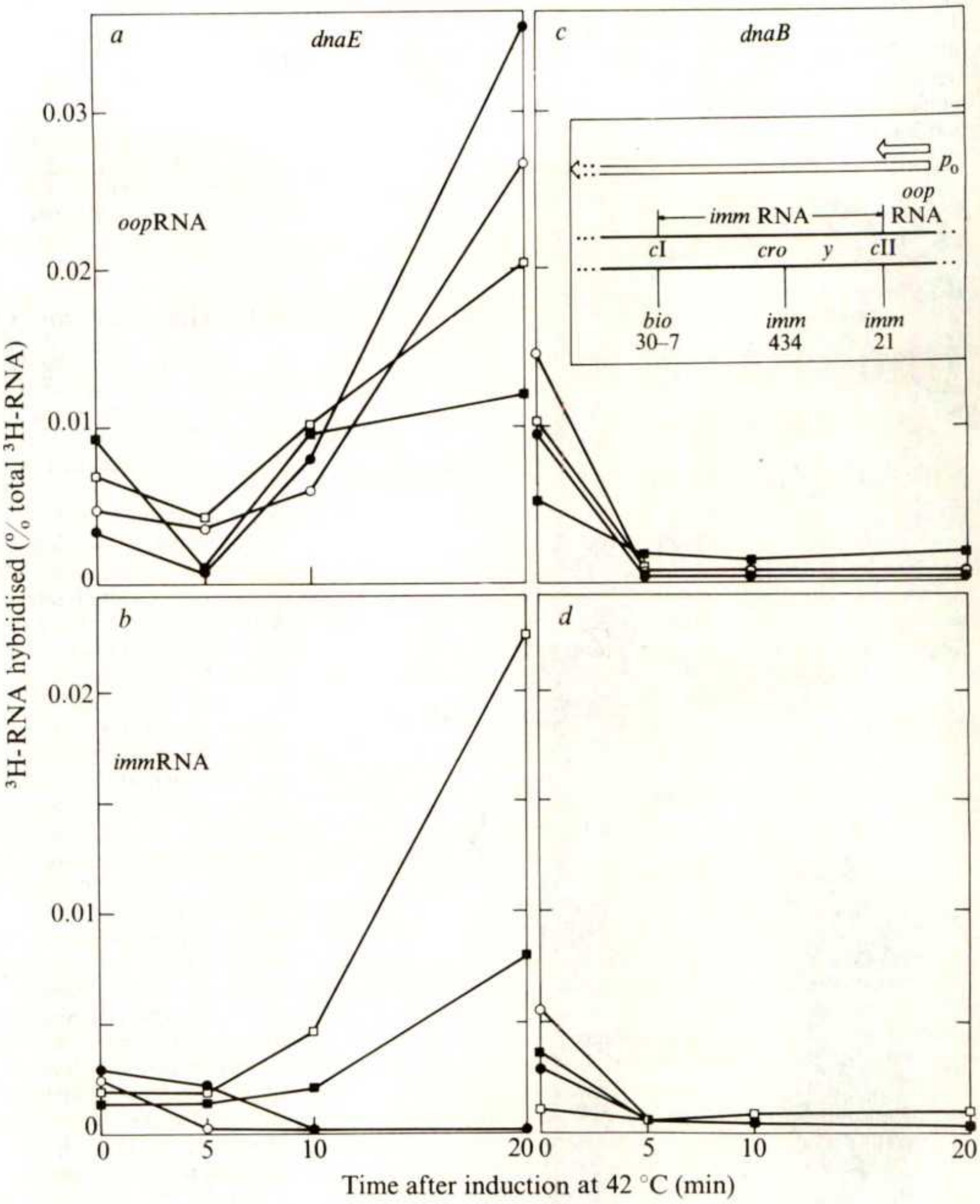

Fig. 2 Leftward transcription of the immunity and *oop* regions after prophage induction. The RNA was labelled for 1 min with ^{3}H-uridine either at 30 °C (zero time) or at the indicated times after induction at 42 °C. The extracted ^{3}H-RNA was first prehybridised to *l* strands of λ*bio*30-7 DNA (see Fig. 1 and inset in *c*), eluted, and then analytically hybridised with *l* strands of φ80λimmλ (hy5)[18] and its derivatives[8], φ80λimm434 and φ80λ*imm*21 (for methods see refs 8, 11). The *oop* transcription (panels *a* and *c*) is calculated as percentage total ^{3}H-RNA input that hybridises to Φ80λ*imm*21. The *imm* transcription (*b* and *d*) is similarly calculated as that ^{3}H-RNA which hybridises to φ80λ*imm*λ minus that to φ80λ *imm*21. Data for the *dnaE*ts (JG55 = E486) and *dnaB*ts (JG28 = Hfr H165/70) lysogens[9,19] are shown in *a*,*b* and *c*,*d*, respectively. The prophages were λ*c*I857 (○), λ*c*I857*cro*27, (□), λ*c*I857 *c*II68 (●) and λ*c*I857*cro*27*c*II68 (■), (see refs 2–4).

p_{re} promoter[1-3], might actually correspond to either transcriptional blocks or one of the sites of the anti-terminating effects of the products of genes *c*II and *c*III.

To prove that the p_o promoter can carry out the Pre function, two experimental approaches were used: one to explore the correlation between the *oop* and *c*I transcriptions, and the other to isolate and characterise the elongated *oop*-*c*I transcript.

Correlation between the establishment mode of *c*I transcription and synthesis of *oop* RNA

The ^{3}H-labelled, leftward-transcribed RNA was assayed by two-step analytical hybridisation[11] within the interval *c*I-*cro*-*y*-*c*II (establishment mode with exclusion of the complications due to the *lit* RNA; ref. 8) and in the *oop* region (see Figs 1 and 2). The experimental design included blockage of λ DNA replication so as to keep the gene dosage constant, inactivation of λ gene *cro* so as to eliminate the shifting expression of its various repressing functions, and thermal inactivation of the *c*Its product to induce prophage, and to minimise the maintenance mode of *c*I transcription and both the positive and negative effects of the repressor[2,3,7]. Because synthesis of *oop* RNA is known to depend on the λ replication functions *ori*, *O* and *P* and the host replication genes *dnaB* and *dnaG*, but not on *dnaE* (ref. 9), the *dnaE*$^-$ host mutation was used to block λ DNA synthesis (Fig. 2*a* and *b*). As controls, *dnaB*$^-$ hosts (Fig. 2*c* and *d*) and P^- λ mutants were included. In other words, the kinetics of the leftward *imm* and *oop* transcriptions were studied after induction of λ*c*Its857 prophage at 42 °C, in the absence of DNA replication and in *cro*$^-$ compared with *cro*$^+$ conditions.

In the *dnaB*$^-$ condition (Fig. 2*c* and *d*) or for P^- prophage in *dna*$^+$ host (to be published elsewhere) there is a perfect correlation between the *imm* transcription and *oop* RNA synthesis, since both are blocked after induction. This is not a general effect on transcription because the major leftward p_L transcription remains high (refs 11–12 and present data).

In *dnaE*$^-$ lysogens the perfect correlation between the *imm* and *oop* transcriptions was only observed in *cro*$^-$*c*II$^+$ conditions (Fig. 2*a* and *b*). In *cro*$^+$*c*II$^+$ and *cro*$^+$*c*II$^-$ lysogens the *imm* transcription, but not *oop* RNA synthesis, is eliminated. A somewhat intermediate situation is observed for the *cro*$^-$*c*II$^-$ prophage.

These data enable the following conclusions to be made. Synthesis of the *c*I RNA after induction depends in the same manner as that of the *oop* RNA on host and phage replication functions, such as *dnaB* and *P*, respectively. The *cro* product, an immunity-specific negative regulator, blocks selectively the *c*I transcription, thus decoupling it from the *oop* RNA synthesis. Not only does the *c*I transcription depend on the same factors as the *oop* RNA synthesis, but its full expression also requires the *c*II function. In *cro*$^-$ conditions, some *c*I transcription is observed even in the absence of the *c*II function.

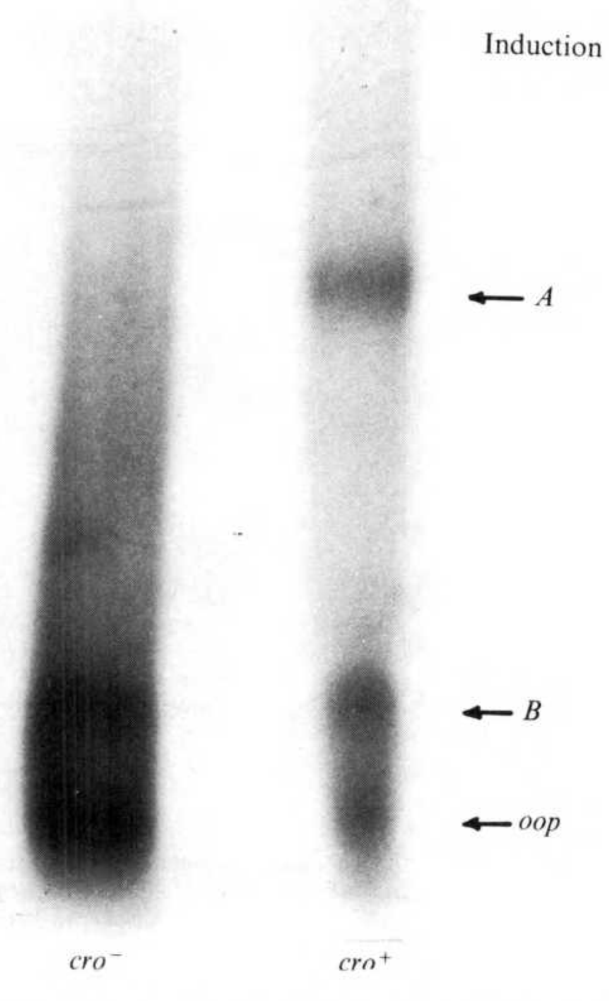

Fig. 3 Autoradiograms of λ RNA fractionated by polyacrylamide gel electrophoresis. The *dnaE*ts(λ*c*I857*cro*$^+$) and *dnaE*ts-(λ*c*I857*cro*27) lysogens were grown to $A_{575} = 0.35$ in MCGB medium[11] enriched with 0.4% yeast extract and 20 μg thymidine ml^{-1}. The cells were spun down, washed twice, resuspended in 10 mM $MgSO_4$ at 5×10^9 cells ml^{-1}, shaken 60 min at 30 °C and transferred to 20 ml labelling medium containing 25 mCi ^{32}P and prewarmed to 42 °C (see ref. 21). The RNA labelled from 0 to 20 min at 42 °C was extracted, heated to 80 °C for 4 min to dissociate any double-stranded RNA, hybridised to *l* strands of λ*bio*30-7 DNA (4 h at 40 °C in 50% formamide), collected on B6 nitrocellulose filters (Schleicher & Schuell), and eluted as described in ref. 21. The eluted ^{32}P-RNA was ethanol precipitated (3 volumes, overnight at −20 °C) and then dissolved in 30 μl buffer E (90 mM Tris, 8.9 mM H_3BO_3, 2 mM Na-EDTA, *p*H 8.3) containing 6 M urea, 0.1% bromphenol blue, and 20% (v/v) glycerol. The samples were layered on to a 3.5% polyacrylamide slab gel[22], and electrophoresed for 8–10 h at 25 mA in buffer E. X-ray film (Kodak NS54T) was exposed for 45 min to slabs contained in polyvinyl chloride wrap.

These results show that the establishment mode of *imm* RNA synthesis after prophage induction could be an extension of the *oop* transcription. At least two-thirds of this *imm* transcription seems to depend on the *c*II product and is completely blocked by the *cro* product. To distinguish between two alternatives—that of a single extended *oop*-*c*I transcript against the possibility that the *oop* and p_{re}–*c*I RNAs represent two separate but jointly regulated transcripts—it was necessary to isolate and characterise the RNA synthesised in the *oop*–*c*I region.

Isolation and characterisation of the elongated *oop*–*c*I RNA

The leftward RNA transcribed in the *c*I–*oop* region was isolated in two steps. RNA labelled with ^{32}P for 0–20 min after thermal induction of *dnaE*ts(λ*c*I857*cro*27) was first prehybridised in 50% formamide 40 °C to *l* strands of λ*bio*30-7 (Fig. 1), eluted, and then fractionated on a 3.5% polyacrylamide gel. The three major bands seen in Fig. 3*a* are: band *A* (about 9S), a plausible candidate for the *imm* RNA, band *B* (about 5S) probably originating in the *b*2 region and not further characterised, and band *C* (about 4S) identified as *oop* RNA. Only RNA bands *B* and *C* are produced by the induced *dnaE*ts(λ*c*I857*cro*$^+$) lysogen (Fig. 3*b*). The startpoint of RNA corresponding to the band *A* was determined by transcriptional mapping[8], and found to be located at about 80.1% λ units on the mature λ map, just to the right of the *imm*21 boundary (Fig. 4). Since this site is also the startpoint of *oop* RNA (ref. 8), we conclude that band *A* is the elongated *oop* transcript corresponding to the establishment immunity transcript.

This conclusion was corroborated by several additional experiments.

By prehybridisation to λ*bio*30-7 *l* strands followed by RNase treatment, the *oop*-*c*I-*rex* establishment immunity RNA was deliberately truncated to about 1,070 bases (2.3% λ units from the startpoint of *oop* to the *bio*30-7 endpoint; (see Fig. 1) which enabled it to enter the 3.5% polyacrylamide gel. The behaviour of this *oop*–*imm* transcript could be changed by either shortening it to about 900 bases or lengthening it to about 2,150 bases by prehybridisation to λ*bio*t124 or λ*bio*t75 *l* strands, respectively (Fig. 1). As expected, prehybridisation to λ*bio*t124 increases slightly the mobility of band *A* (gel not shown). The shortened transcript has the same startpoint at about 80% λ (Fig. 4). On prehybridisation to λ*bio*t75, the resulting RNA does not enter the 3.5% gels, but forms a band in the 2% polyacrylamide gel reinforced with 0.5% Agarose (gel not shown).

The complete absence of band *A* in the 3.5% gel and the presence of only one band *A* in the 2% gel after prehybridisation to the *l* strand of λ*bio*t75 DNA proves that band *A* (Fig. 3) corresponds to a single *oop*–*c*I RNA species, and not to two separate *oop*–*c*II and p_{re}–*c*I transcripts, fortuitously of roughly equal length.

As an alternative to the gel fractionation step, the *imm* RNA was also isolated as material excluded from the Sephadex G-75 column. As shown in Fig. 4, the startpoint of this RNA is also at about 80% λ.

Although we did not observe any *imm* RNA after induction of λ*cro*$^+$ lysogens, it is known that the immunity establishment pathway is observed early after infection with λ*cro*$^+$ phages[2, 3]. We therefore looked for band *A* after infection of *Escherichia coli dnaE*$^-$ with λ*c*I857*cro*$^+$. Band *A* (gel not shown), which corresponds to the joint *oop*–*c*I transcript as determined by transcriptional mapping (Fig. 4), is produced early after infection with either λ*cro*$^+$ or λ*cro*$^-$ but not with λ*cro*$^+$*c*II$^-$ or λ*cro*$^-$*c*II$^-$. The appearance of the *oop*–*imm* RNA early after infection but not after induction (Figs 3 and 4) might reflect the presence of some prophage products, possibly *rex* or traces of *cro*, at the time of induction, whereas after infection they might reach the critical concentration only after some delay.

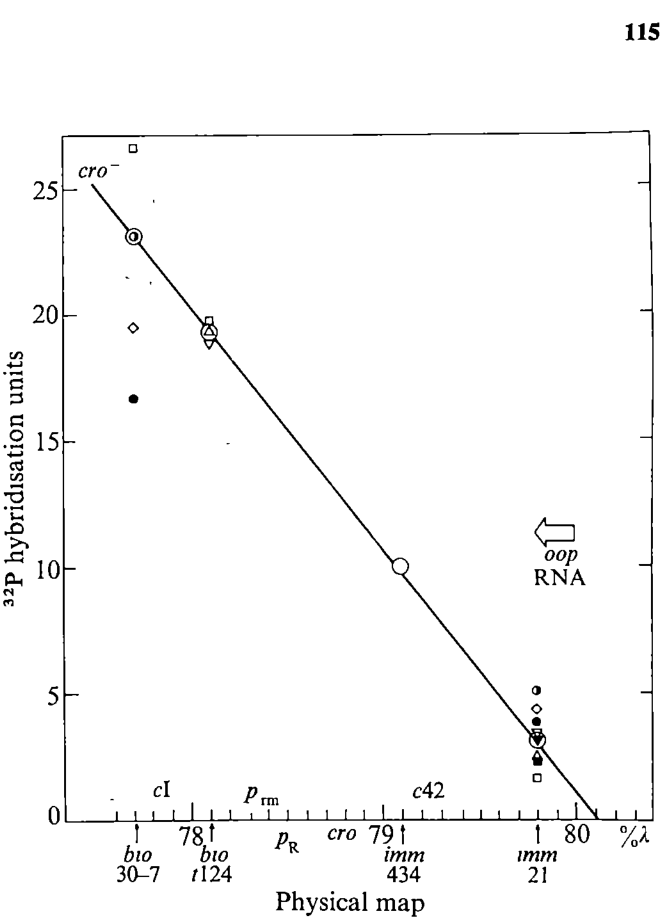

Fig. 4 The transcriptional mapping of the startpoint for the physically isolated immunity establishment RNA. ^{32}P-RNA corresponding to band *A* (see Fig. 3*a*) was isolated from the corresponding slice of the polyacrylamide gel by extraction with NTE buffer (0.3 M NaCl, 10 mM Tris-HCl, *p*H 8.1, and 1 mM Na.EDTA) for about 10 h at 4 °C, followed by ethanol precipitation of the RNA and redissolving in 1 ml NTE buffer. This RNA was hybridised to 10 µg *l* strand DNA of φ80λ*imm*λ (φ80*att*80*imm*λ; hy5) and its *imm*434 and *imm*21 derivatives specified in Fig. 2, as well as of φ80, φ80*hy*42, λ*rep*P22 and P22*rep*λ, in 0.4 ml NTE buffer containing 50% (v/v) formamide, at 40 °C for 4 h. After addition of 10 µg tRNA carrier, the nucleic acids were precipitated with 3 volumes ethanol (−20 °C, overnight), spun down, and redissolved in 0.4 ml NTE buffer. After addition of 0.4 µg pancreatic RNase, the solution was incubated for 15 min at 37 °C, supplemented with 10 ml 2×SSC, slowly filtered through B6 filters (see Fig. 3), and the radioactivity of the ^{32}P-RNA–DNA hybrids bound to the filters counted. Similar hybridisations were carried out with bands *A* obtained in other experiments and with the analogous *imm* RNA isolated as the fraction excluded from the G-75 Sephadex column. ^{32}P-RNA counts hybridising to φ80λ*imm*λ were plotted at the *bio*30-7 or *bio*t124 endpoint position on the abscissa, depending on which of these two λ*bio l*-strand DNAs was used for the prehybridisation of the extracted RNA before its fractionation. The *imm*434 and *imm*21 endpoint positions refer to the hybridisation values obtained with φ80λ*imm*434 and φ80λ*imm*21, respectively. After subtracting the φ80 or φ80*hy*42 background values, all hybridisation values were normalised to the φ80λ*imm*434 value taken as 10 units (see ordinate). □,◇, Induction of the E486(λ*c*I857*cro*⁻) lysogen;RNA prehybridised to λ*bio*30-7 (band *A*, Fig 3, in duplicate). ▽,▼,△, Induction of the E486(λ*c*I857*cro*⁻) lysogen; RNA prehybridised to λ*bio*t124 (band *A*, not shown, in triplicate). ◑,●, Infection of the E486 host with *cro*⁻ and *cro*⁺ λ*c*I857 phage multiplicity of infection 8) respectively;RNA labelled for 0–5 min after infection at 42 °C and prehybridised to λ*bio*30-7 (band *A*, not shown) ■, Induction of the E486(λ*c*I857*cro*⁻) lysogen;RNA prehybridised to λ*bio*t124 (fraction excluded from G-75 Sephadex column with 0.1 M ammonium acetate, *p*H 4.5 as solvent). ○, Average of all results with λ*cro*⁻(λ*c*I857*cro*27). Abscissa corresponds to the physical map of phage λ (see Fig. 1 and ref. 16).

Preliminary fingerprints of that portion of band *A* RNA which hybridises to φ80λ*imm*21 DNA indicate that this 5′-proximal sequence is identical to that of *oop* RNA (refs 20 and 21), (to be published elsewhere).

oop leader sequence and its dual role: p_0 compared with p_{re} promoter

The present study indicates that *oop* RNA can serve as a leader sequence and can be extended into the immunity transcript. This concept of termination–anti-termination (or attenuation) was known in λ transcription (see, for example, ref. 6) and later found in other operons[23,24]. Such a mechanism was postulated as one of the alternatives when *oop* RNA was first characterised[6,13,14]. Our results now make it unnecessary to invoke the presence of a p_{re} promoter to explain the *cis*-dominant effect of the *c*42 and other *c*Y mutations in the *y* region[2,3,25,26] (Fig. 1). The *c*Y mutations might represent either some polar blocks or inactivation of one of the sites at which the *c*II and *c*III products act as anti-terminators and enable the extension of *oop* RNA into the *imm* transcript. The latter explanation seems less likely, since the *c*II product is still required for suppression of the *c*Y defect by the *sar* mutation[10]. This subject is now being studied. Note that the p_0 promoter region and the *c*III product are in common for phages λ and λ*imm*21(hyl)[27], but the *c*II products differ. If the anti-terminating action of the *c*II protein depends on DNA sequence specificity, the first divergence in the sequence between λ and λ*imm*21 is at about 60 nucleotide pairs from the 5′ end of *oop* (M. Rosenberg, personal communication). It might be relevant that recognition for the N product, as defined by the *nut*L mutations, is over 30 nucleotide pairs downstream from the p_L promoter of λ (J. S. Salstrom and W. Szybalski, cited in ref. 17).

The simplest model consistent with the present and previous data is that *oop* RNA may serve a dual role, both as a primer for λ DNA replication[15] and as a primer or leader for the immunity establishment transcription. In conditions which presumably favour early *cro* expression, only short species of *oop* RNA would be synthesised, and this abundance of a primer for the initiation of DNA synthesis would channel the phage into the lytic cycle, which requires extensive λ DNA replication. Alternatively, probably when *cro* gene expression is slightly delayed or depressed, the availability of the *c*II and *c*III products would favour the elongation of the *oop* RNA into the *imm* transcript. This would lead to a burst of repressor synthesis and consequently channel the phage into the lysogenic pathway and establishment of the prophage state. It is interesting that the recently described *sar* mutation, which maps in the *oop* region, seems in certain conditions to favour the lysogenic pathway while depressing DNA synthesis[10].

Although this study has demonstrated new important features of the establishment mode of the immunity transcription, future work is needed to elucidate the function of the *y* region and the specific mechanisms by which the *cro*, *c*II and *c*III products regulate the elongation of the *oop* RNA into the *imm* transcript.

This work was supported by the NCI, We thank John S. Salstrom and Eric C. Rosenvold for discussions, and Lois Wilson for assistance with the preparation of DNA strands and Annelie James with the RNA fractionation. We also thank Drs G. Gussin, A. Oppenheim, A. B. Oppenheim and H. Echols for critical reading of the manuscript and comments.

Received March 29, accepted May 11, 1976

1 Eisen, H, and Ptashne, M, in *The Bacteriophage Lambda* (edit by Hershey, A H), 239-245. (Cold Spring Harbor Laboratory, Cold Spring Harbor, New York, 1971)
2 Reichardt, L, and Kaiser, A. D, *Proc natn Acad Sci. U S A*, **68**, 2185-2189 (1971).
3 Reichardt, L. F., *J. molec. Biol*, **93**, 267-309 (1975).
4 Echols, H., Green, L., Oppenheim, A. B., Oppenheim, A., and Honigman, A, *J. molec Biol.*, **80**, 203-216 (1973).
5 Spiegelman, W G., et al., *Proc natn Acad Sci. U S.A*, **69**, 3156-3160 (1972)

[6] Szybalski, W., *et al.*, *Cold Spring Harb. Symp. quant Biol*, **35**, 341-353 (1970).
[7] Meyer, R., Kleid, D., and Ptashne, M., *Proc. natn. Acad. Sci. U.S.A.*, **72**, 4785-4789 (1975).
[8] Hayes, S., and Szybalski, W., *Molec. gen. Genet.*, **126**, 275-290 (1973)
[9] Hayes, S., and Szybalski, W., in *Molecular Cytogenetics*, (edit. by Hamkalo, B. A., and Papaconstantinou, J.), 227-283 (Plenum, New York, 1973).
[10] Honigman, A., Oppenheim, A., Oppenheim, A. B., and Stevens, W F., *Molec. gen. Genet.*, **138**, 85-111 (1975).
[11] Bøvre, K., Lozeron, H. A., and Szybalski, W., in *Methods in Virology*, **5** (edit. by Maramorosch, K., and Koprowski, H.)., 271-292 (Academic, New York, 1971).
[12] Nijkamp, H. J. J., Bøvre, K., and Szybalski, W., *Molec. gen. Genet*, **111**, 23-24 (1971).
[13] Blattner, F. R., and Dahlberg, J. D., *Nature new Biol*, **237**, 227-232 (1972).
[14] Szybalski, W., in *Uptake of Informative Molecules by Living Cells* (edit. by Ledoux, L.), 59-82 (North-Holland, Amsterdam, 1972).
[15] Hayes, S., and Szybalski, W., in *DNA Synthesis and its Regulation* (edit by Goulian, M., Hanawalt, P., and Fox, C. F.), 486-512 (Benjamin, Menlo Park, 1975).
[16] Blattner, F. R., Fiandt, M., Hass, K. K., Twose, P. A., and Szybalski, W., *Virology*, **62**, 458-471 (1974).
[17] Szybalski, W, in *Handbook of Biochemistry and Molecular Biology*, third ed., *Nucleic Acids*, II (edit. by Fasman, G D.), 677-685 (CRC, Cleveland, 1976).
[18] Fiandt, M., Hradecna, Z., Lozeron, H. A, and Szybalski, W., in *The Bacteriophage Lambda* (edit by Hershey, A. D), 329-354 (Cold Spring Harbor Laboratory, Cold Spring Harbor, 1971)
[19] Wechsler, J. A. ,and Gross, J D, *Molec. gen Genet*, **113**, 273-284, (1971).
[20] Dahlberg, J. E., and Blattner, F. R, in *Virus Research* (edit. by Fox, C. F., and Robinson, W. S), 533-543 (Academic, New York, 1973).
[21] Smith, G. R, and Hedgpeth, J, *J biol Chem*, **250**, 4818-4821 (1975).
[22] Rosenberg, M., Weissman, S., and deCrombrugghe, B., *J biol. Chem*, **250**, 4755-4764 (1975).
[23] Kasai, T., *Nature*, **249**, 523-527 (1974).
[24] Bertrand, K., *et al.*, *Science*, **189**, 22-26 (1975).
[25] Kaiser, A. D, *Virology*, **3**, 42-61 (1957).
[26] Eisen, H., Pereira da Silva, L., and Jacob, F, *C.r hebd Séanc. Acad. Sci., Paris*, **266**, 1176-1178 (1968)
[27] Westmoreland, B C, Szybalski. W. and Ris, H., *Science* **163**, 1343-1348 (1969).

---

letters to nature

Sigma Orionis E as a mass-transfer binary system

SIGMA Orionis E, the first He-rich B star discovered[1,2], was recently found[3,4] to have an extremely broad (~ 1,800 km s^{-1}), rapidly varying Hα-emission feature. From independent spectroscopic, spectrophotometric, and photometric observations on 4 consecutive nights in December 1974, we have shown[4] that it is a variable, with $P \simeq 1.19$ d; however, incomplete phase coverage in those data, as well as uncertainty about the nature of the periodicity, has hampered the development of a model to account for the wealth of observed phenomena. Here we briefly communicate results of new continuous *uvby*β photometry carried out during the 11 consecutive nights December 28, 1975–January 7, 1976 (UT), together with some possible interpretations.

The observations were made with a single-channel, refrigerated, pulse-counting, 1P21 photometer on the number 1 0.4-m telescope of the Cerro Tololo Inter-American Observatory. As in the December 1974 observations, CTIO filter set number 3 was used throughout; however, for the new data differential photometric techniques were employed. The comparison star was HR1861, a *uvby*β standard star[5,6] with colours nearly identical to those of σ Ori E and ~ 1° away. Ten-second integrations were used. An observation, requiring ~ 5 min for completion, consisted of the measures: *y*,*b*,*v*,*u*,βW,2βN, recentre, and repeat in reverse order, where W and N refer to the wide and narrow Hβ filter, respectively. The nights were essentially moonless and sky readings were taken regularly throughout. Errors from photon counting statistical effects were < 0.007 mag in all observations. Differential extinction corrections were applied to the *uvby*β data with coefficients determined each night, except for 2 nights, greatly shortened by clouds, for which the means of the immediately adjacent nights were adopted. The Hβ data were reduced using the well known mean slope coefficients for the filters and a nightly determination of the zero point correction based on HR1861.

The resultant light and colour curves, of which those for *y*, *u*, and $u-b$ are given in Figs 1*a–c*, show two distinct minima. By comparison of the depths, particularly in *u*, we conclude that the minimum near phase $\varphi \simeq 0.63$ (hereafter called primary minimum) is the same as that observed[4] in December 1974. A primary minimum occurred in the new observations[7] at JD 2442778.819, which combines with the December 1974 data to yield an improved estimate of the period: 1.19080±0.00005 d. This value is in excellent agreement with one possible period, 1.19086 d, found from a comparison of the December 1973–January 1974 spectroscopic[3] and the December 1974 spectrophotometric[4] Hα-emission data; this agreement suggests that the period may be reasonably stable over a 2–3 yr interval.

Among the characteristics of the rather peculiar light curves, we point out the following: (1) The secondary minimum follows the primary by $0.43P$ (12.4 h), and the widths of both are ~ 3.0 h at half-depth. (2) The amplitudes of the minima are considerably greater in the ultraviolet, and the depths in *y*, *b*, *v*, and *u* of the primary (0.07, 0.06, 0.05, and 0.15 mag) and secondary (0.04, 0.04, 0.03, and 0.12 mag) minima vary non-monotonically with wavelength. The amplitudes of the $u-b$ colour minima are, however, similar. (3) The minima are asymmetrical, with the ingress into secondary minimum more gradual (by a factor of ~ 2) than the other transitions. (4) The light level outside the minima is not constant but seems to decline continuously between successive secondary minima, although the *v* light level is more irregular. With respect to December 1974 the mean magnitude levels at $0.8P$ have remained nearly constant in *y* and *b*, but the *u* level is brighter by ~ 0.04 mag in 1975–76; this observation suggests that secular changes with a colour dependence similar to that of the periodic ones may occur. (5) The Hβ phase diagram shows behaviour strongly reminiscent of that of W_{abs} (Hα) in Fig. 4 of Walborn and Hesser[4], which suggests that weak, variable emission is present at Hβ. Comparably detailed observations of more cycles are required to ascertain the permanence of the foregoing features in the light and colour curves, but correspondences between the December 1974 and 1975–76 data indicate that some of them are reasonably stable.

The general appearance of the light curves of σ Ori E, and that of the Hα profile when the emission is strong, are strikingly similar to observed properties of the dwarf nova system U Geminorum[8,9]. These properties are interpreted in terms of a mass-transfer binary in which a collapsed (white dwarf) component is surrounded by a rapidly rotating accretion disk containing an ultraviolet-bright spot with energy provided by the impinging stream of gas from the other star[10,11]. It is evident that a similar model could account for most of the principal characteristics of the light, colour and spectrum variations in σ Ori E. Particular reference is made to the illustration and discussion by Lin[12]. The primary minimum occurs when the hot spot is occulted by the B star, whereas the secondary minimum is caused by occultation of the spot by the optically thick disk itself. Since the spot is located on the following side of the disk, the secondary minimum will follow the primary by < $0.5P$, as observed. Moreover, since the line-emitting region is downstream from the hot spot in the disk, the principal Hα-emission maximum should follow inferior conjunction of the disk and have $V > R$, again as observed[4]. We note, however, that this model requires synchronous

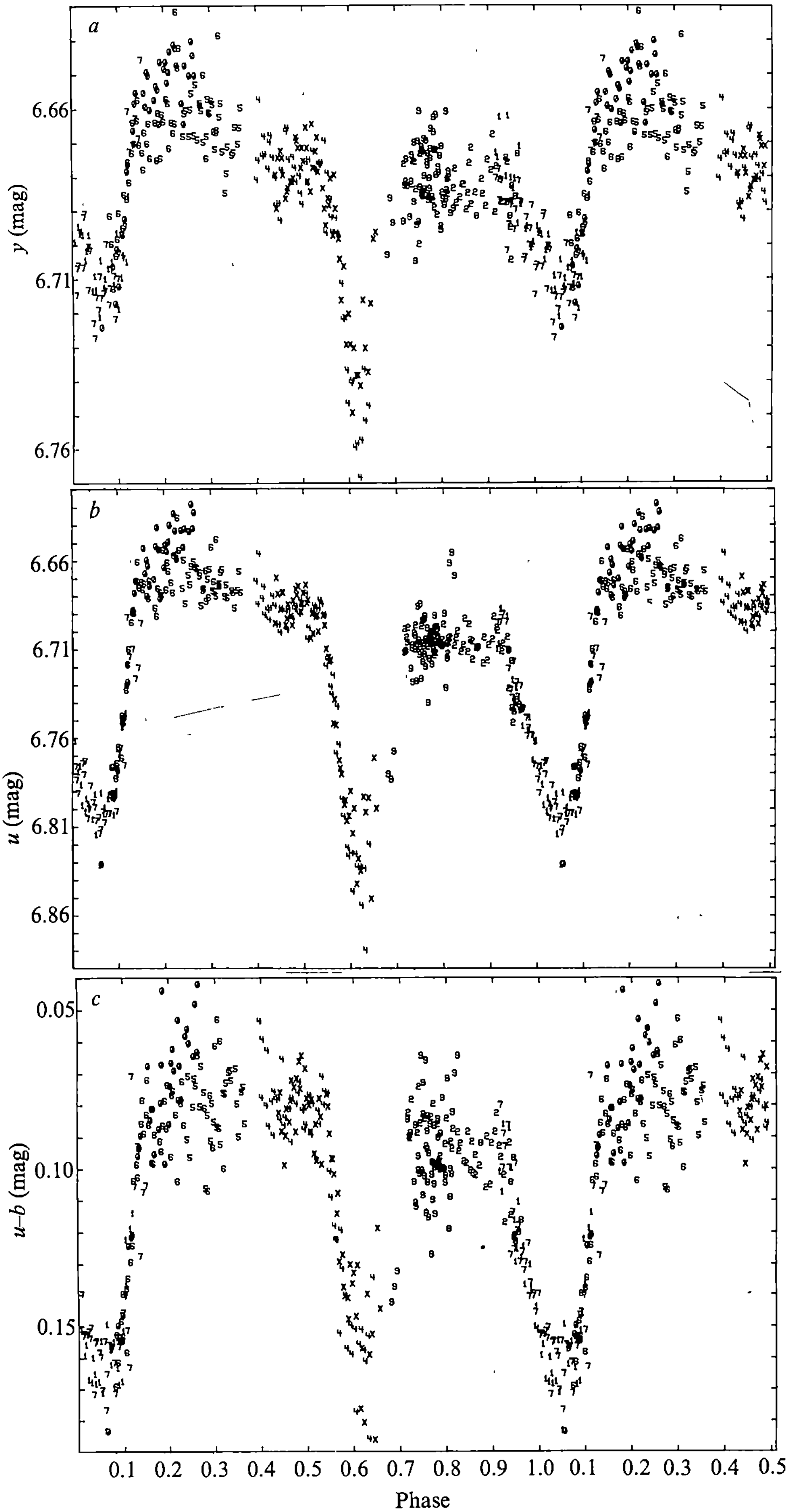

Fig. 1 *a–c*: *y*, *u*, and *u*–*b* light and colour curves for σ Ori E from the 1975–76 data, with 1975 December 28.0 = JD 2442774.5 as zero phase and a period, 1.19082 d, that differs insignificantly from the finally adopted value, 1.19080 d. The symbols serve to distinguish data from different nights: 0–9 correspond to December 28–January 6 and × to January 7. Because of occasional high humidity during the observations, it is uncertain if some fine details of the light curves (for example, the tendency for night 0 (28 December) to lie somewhat brighter than those of nights 5 or 6 at φ ≃ 0.2) arise from stellar variations or to slightly inaccurate differential extinction corrections The *u*–*b* colour is (normally) a reliable temperature indicator for B stars

rotation and a stable, inhomogeneous surface composition for the B star to explain the behaviour of the He line[4,13].

Bolton's[14] upper limit to the radial velocity variation of σ Ori E implies that any companion must have a mass $\lesssim 0.1 M_\odot$ for inclinations > 45°. Thus the secondary would be an M dwarf or a collapsed object. The latter alternative would be in agreement with the above model, as well as providing a ready explanation for the helium enhancement (or hydrogen deficiency) at the surface of σ Ori E in terms of a prior episode of mass transfer from an originally more massive companion. Since σ Ori E is located in a Trapezium-like system containing a 09.5-V component[2], the mass of the original primary in the mass-transfer binary picture would have been $\gtrsim 20 M_\odot$.

If this model is correct, high-frequency optical monitoring of σ Ori E might provide additional information; only one such study has been made at CTIO, before the development of the present working picture, and hence at a rather low sampling frequency. Beginning at 1974 December 6.084 UT, σ Ori E was monitored at Hα for 6 h with the 3-channel photometer at the 0.9-m telescope. A 20/80% neutral beamsplitter, 2 FW 130 (S20) photocells, and KPNO filters 210 ($\Delta\lambda = 159$ Å) and 71 ($\Delta\lambda = 54$ Å) were used for 2-s integrations. A total of 8,192 integrations was processed with power spectral techniques[15]; no peak > 0.0013 mag was found in the period range $4.0 < P <$ 1,640 s for the sampled phases.

While this paper was in preparation, an alternative but related interpretation of the light curves of σ Ori E occurred to one of us (N.R.W.) after reading the new results on Algol[16]. The alternative model follows from interpreting the two minima in σ Ori E as components of a single 'W-shaped' eclipse; indeed, the resulting ingress–egress symmetries strongly support the correctness of such an interpretation. In this case one is led to consider two ultraviolet-bright spots, most probably located at the equilateral Lagrangian points of the binary system, with the leading spot somewhat the brighter. 'Mid-eclipse' occurs at $\varphi \simeq 0.83$, with both Lagrangian points visible. The mass ratio condition for the existence of stable, equilateral Lagrangian points implies an upper limit to the secondary mass of the same order as that resulting from the radial velocity observations. If a plausible model with $\mathcal{M}_1 = 8 M_\odot$, $\mathcal{M}_2 = 0.1 M_\odot$, and centre-to-centre separation of two primary radii is assumed, the resulting geometry is strikingly simple, and many features of the light and colour curves are explained in a straightforward manner.

The implications of this model of σ Ori E for current theories of stellar evolution in massive binaries are sufficiently significant to justify extensive further observations. Most critically needed are high-accuracy radial velocities throughout the full 1.19 d cycle, preferably with simultaneous photoelectric monitoring. In addition, polarimetric, X-ray and radio observations of both moderate- and high-time resolution may provide key information for the evaluation of the proposed working model.

J.E.H. thanks Dr John Irwin for relinquishing a crucial night of telescope time; Sr. Guido Garay for programming assistance and the Yale University Observatory for their hospitality while this paper was being written. The Cerro Tololo Observatory is operated by the Association of Universities for Research in Astronomy, Inc., under contract with the NSF.

JAMES E. HESSER
NOLAN R. WALBORN
PATRICIO UGARTE P.

Cerro Tololo Inter-American Observatory,
La Serena, Chile

Received February 19; accepted May 7, 1976

1 Berger, J., *C. r. hebd. Séanc. Acad. Sci. Paris*, A217 (1956).
2 Greenstein, J. L., and Wallerstein, G., *Astrophys. J.*, 127, 237 (1958).
3 Walborn, N. R., *Astrophys. J. Lett.*, 191, L95 (1974).
4 Walborn N. R., and Hesser, J. E., *Astrophys. J. Lett.*, 205, L87 (1976).
5 Crawford, D. L., and Barnes, J. V., *Astr. J.*, 75, 978 (1970).
6 Crawford, D. L., and Mander, J. V., *Astr. J.*, 71, 114 (1966).
7 Hesser, J. E., and Ugarte P., *IAU Circ.*, No. 2911 (1976)
8 Kraft, R. P., *Astrophys. J.*, 135, 408 (1962).
9 Krzeminski, W., *Astrophys. J.*, 142, 1051 (1965)
10 Smak, J., *Acta Astr.*, 19, 287 (1969).
11 Warner B., and Nather, E., *Mon. Not. R. astr. Soc.*, 152, 219 (1971).
12 Lin, D. N. C., *Mon. Not. R. astr. Soc.*, 170, 379 (1975)
13 Thomsen, B., *Astr. Astrophys.*, 35, 479, (1974).
14 Bolton, C. T., *Astrophys. J. Lett.*, 192, L7 (1974)
15 Hesser, J. E., and Lasker, B. M., in *Proc. of IAU Colloq.*, 15; *Veroff. der Remeis-Sternwarte Bamberg*, 9, 1960 (1971)
16 Guinan, E. F., McCook, G. P., Bachmann, P. J., and Bistline, W. G., *Astr. J.*, 81, 57 (1976)

Evidence for a radioactive decay hypothesis for supernova luminosity

VAN HISE[1] has observed that the light curve for the Type I supernova 1937c is well represented by a sum of two exponentials with half lives which are ~0.75 the half lives of ^{56}Ni and ^{56}Co in the β-decay chain $^{56}\mathrm{Ni} \rightarrow {}^{56}\mathrm{Co} \rightarrow {}^{56}\mathrm{Fe}$. Colgate and McKee[2] had previously suggested this chain as a source of supernova luminosity, but the hypothesis was not widely accepted because of the variability of the decay rates of supernova light curves and because the interstellar medium would be overabundant in heavy elements. This letter presents observational evidence supporting a model of Leventhal and McCall[3] which overcomes these difficulties.

According to this model, a Type I supernova produces a white dwarf containing $\sim 0.2 M_\odot$ of ^{56}Ni. At terrestrial densities the decays of ^{56}Ni and ^{56}Co occur by capture of an inner shell electron 100 and 80% of the time, respectively, but in the interior of a white dwarf, the bare nuclei move through a Fermi sea of electrons, and the higher electron densities thus encountered would produce an enhancement of the decay rates. The supernova luminosity is given by

$$L(t) = A_1 \exp(-t/T_1) + A_2 \exp(-t/T_2) \qquad (1)$$

where T_1 and T_2 are the half lives of the steep, earlier and the flat, later portions of the light curve, and A_1 and A_2 are parameters whose values depend on the initial amount of ^{56}Ni, the energy releases per decay of ^{56}Ni and ^{56}Co, and the values of T_1 and T_2. If the model is correct, T_1 should not exceed the terrestrial half life of ^{56}Ni (8.8 d), T_2 should not exceed that of ^{56}Co (112 d), and the two should be related approximately by

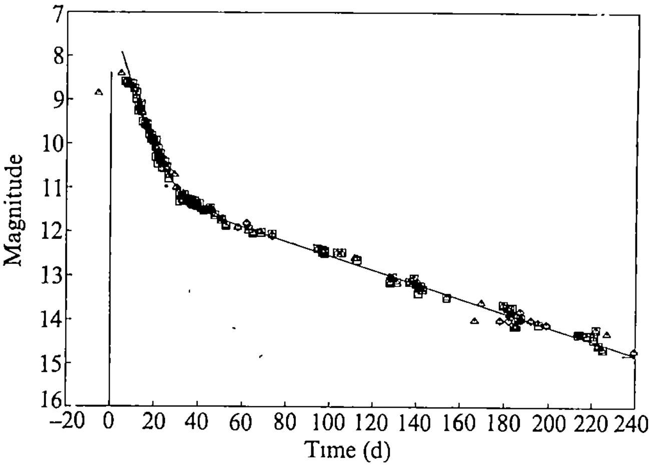

Fig. 1 Sum of exponentials fit to the light curve of SN1937c. The vertical line at $t = 0$ represents the estimate m_0 of peak apparent magnitude. □, Baade and Zwicky[9]; △, Parenago[10]; ◇, Deutsch[11]. For the values of the parameters of the fit see Table 1.

$$\frac{T_1}{8.8} = \frac{T_2}{112};\ T_2 = 12.7\,T_1 \qquad (2)$$

More precisely, according to Leventhal and McCall[3], at

Table 1 Results of the sum of exponentials fits

Supernova	Galaxy	$\frac{A_1}{L_0} \pm \sigma \frac{A_1}{L_0}$	$T_1 \pm \sigma(T_1)$	$\frac{A_2}{L_0} \pm \sigma \frac{A_2}{L_0}$	$T_2 \pm \sigma(T_2)$
1937c	IC4182	3.18±0.13	6.47±0.16	0.0980±0.0088	67.2±6.8
1937d	NGC1003	1.36±0.11	9.26±1.09	0.0708±0.0471	102.1±92.4
1939a	NGC4636	3.07±1.45	4.12±1.34	0.159±0.073	59.3±33.7
1954a	NGC4214	1.52±0.14	4.14±0.32	0.142±0.014	55.6±5.4
1954b	NGC5668	2.19±0.56	5.70±1.16	0.0964±0.0513	75.9±54.9
1956a	NGC3992	11.9±6.5	4.59±0.70	0.0896±0.0302	87.7±38.4
1957a	NGC2841	1.82±0.25	4.55±0.43	0.130±0.021	47.4±8.4
1961p	Anon.	1.64±0.07	10.3±0.7	0.0979±0.0259	112.3±40.5
1962j	NGC6835	3.14±1.12	7.48±1.34	0.111±0.048	114.8±81.4
1962l	NGC1073	3.39±0.78	5.21±0.77	0.181±0.064	68.1±34.6
1963p	NGC1084	5.44±1.19	4.96±0.44	0.0684±0.0217	61.2±20.5
1964l	NGC3938	2.65±0.49	5.96±0.46	0.0671±0.0081	120.4±22.9
1966j	NGC3198	4.44±2.18	7.11±1.01	0.0766±0.0108	112.3±22.4
1966n	Anon.	1.34±0.10	8.38±1.36	0.0917±0.0384	85.4±44.7
1967c	NGC3389	2.17±0.19	8.17±1.00	0.129±0.101	47.9±30.4

high matter densities the ^{56}Ni and ^{56}Co decay rates (d^{-1}) are given by

$$R_{Ni}=\frac{1}{8.8}\left(\frac{\bar{\rho}_{av}}{9.7\times10^{28}}\right)(1+0.61\times10^{10}\,\bar{\rho}_{av}^{-1/3})$$

$$R_{Co}=\frac{1}{558}+\frac{1}{139.4}\left(\frac{\bar{\rho}_{av}}{8.6\times10^{28}}\right)(1+0.60\times10^{10}\,\bar{\rho}_{av}^{-1/3})$$

where $\bar{\rho}_{av}$ is the electron density (cm^{-3}), 8.8 and 112 d are the terrestrial 1/e lives of ^{56}Ni and ^{56}Co, 9.7×10^{28} and 8.6×10^{28} cm^{-3} are the electron densities at Ni and Co nuclei in the terrestrial environment, and 1/558 d^{-1} represents the fraction (20% on Earth) of Co decays which involve positron emission. It is assumed here that the positron emission rate is unaffected by high densities. At low densities, electron binding occurs, so the effective decay rates can be calculated by the interpolation equations

$$T_1=\left[\left(\frac{1}{8.8}\right)^2+R_{Ni}{}^2\right]^{-1/2}$$

$$T_2=\left[\left(\frac{1}{112}\right)^2+R_{Co}{}^2\right]^{-1/2}$$

which define a curve well approximated by the straight line, equation (2).

Rust[4] has recently collected 37 Type I light curves from the literature and used techniques developed by Pskovskii[5,6] to reduce them to a common photometric system (the m_{pg} system). Fifteen of the curves were complete enough to give reasonable fits using a sum of two exponentials. The others did not extend far enough to define the more slowly decaying exponential.

The light curves consisted of measurements of apparent magnitude $m(t)$ versus time. Apparent magnitude is related to luminosity by

$$\frac{L(t)}{L_0}=10^{-0.4[m(t)-m_0]} \qquad (3)$$

where L_0 and m_0 are the luminosity and apparent magnitude at maximum brightness. Taking the moment of peak brightness as the zero-point of time and combining equations (1) and (3) gives

$$10^{-0.4[m(t)-m_0]}=\frac{A_1}{L_0}\exp(-t/T_1)+\frac{A_2}{L_0}\exp(-t/T_2) \qquad (4)$$

The values of T_1, T_2, (A_1/L_0) and (A_2/L_0) were determined for each light curve by nonlinear least squares fitting of this equation beginning a few days after peak brightness to assure that only the decay portion contributed to the fits. The method used was a damped Gauss–Newton iteration.

The results of the fits are given in Table 1. The standard deviations were estimated from the covariance matrix but should be regarded only as approximations (see ch. 7, ref. 7). The values were checked by repeating the fits using the separable parameter algorithm of Golub and Pereyra[8].

For all light curves in the sample the fitted curves represented the data points well and gave low values for the sum of squares of residuals, but only if the data were very complete did the fits specify the parameters with high certainty. This is illustrated in Figs 1 and 2 which represent one of the best and one of the worst fits. In both cases the curves accurately represent the data, but for SN1962j, $\sigma(T_2)$ is very large relative to T_2. The condition that the s.d. of both 1/e lives be less than the parameter values themselves provided a criterion for rejecting incomplete light curves from the sample.

Figure 3 is a plot of T_2 against T_1 with the error bars representing 1 s.d. The vertical and horizontal dashed lines represent the upper limits imposed by the terrestrial values. Only one point lies >1 s.d. beyond these limits, that point being ~ 2 s.d. out. Furthermore, there is a definite tendency for the points to lie along the predicted line $T_2 = 12.7\ T_1$ which is shown as a diagonal. Although the scatter is large, the correlation coefficient is $r = 0.529$, implying, at the 97.5% level of significance, that the data follow a non-random relationship. The average values of $\sigma(T_1)/T_1$ and $\sigma(T_2)/T_2$ are 0.13 and 0.43, a fact which invalidates both a standard regression of T_2 on T_1, which would

Fig. 2 Sum of exponentials fit to the light curve of SN1962j. Data points are taken from Bertola[12].

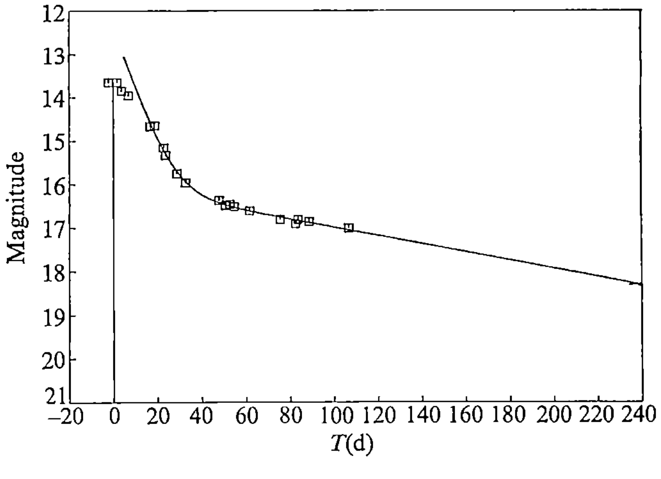

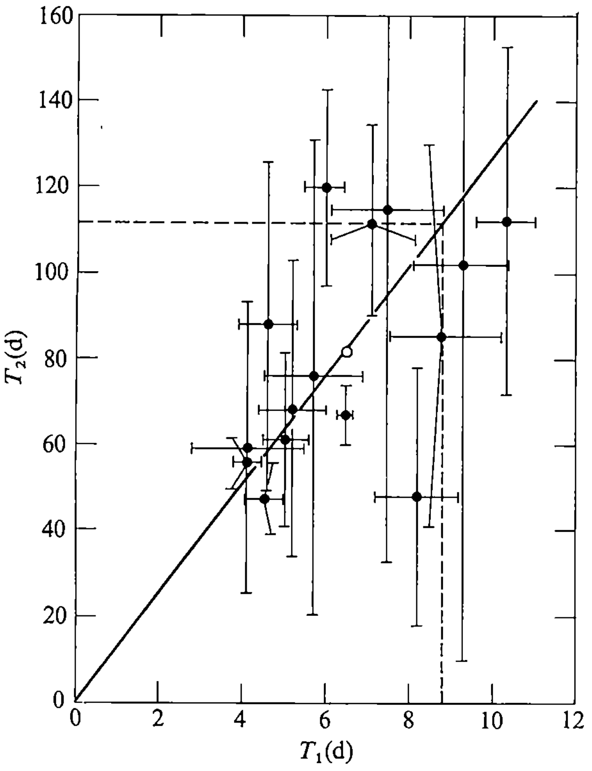

Fig. 3 Plot of the fitting parameters T_2 against T_1. The error bars represent the estimated s.d. but should not be interpreted as the major axes of error ellipsoids because the errors in T_1 and T_2 are correlated in each case.

assume the errors in T_1 are insignificant, and a major-axis regression, which would assume approximately equal errors in T_1 and T_2. It is, however, possible to use the computer generated T_1,T_2 variance matrices to obtain a maximum likelihood estimate of the best linear representation of the data (see ch. 4, ref. 7). The likelihood function can also be used to construct confidence regions in the space of the two parameters, that is, slope and intercept (ch. 7, ref. 7). When this procedure was applied to the data the point defined by equation (2), that is, slope = 12.7, intercept = 0, was found to lie well inside the 50% contour. This shows that the data are consistent with the predicted relation. A more dramatic measure of this consistency is furnished by the average values of T_1 and T_2 which are

$$\overline{T_1} = 6.46 \pm 1.98$$
$$\overline{T_2} = 81.2 \pm 25.7$$

where the indicated errors are the s.d. The point represented by these values is shown in Fig. 3 as an open circle lying almost exactly on the predicted line. These results constitute significant evidence supporting the $^{56}Ni \rightarrow {}^{56}Co \rightarrow {}^{56}Fe$ decay hypothesis. Furthermore, if the cold white dwarf model is correct, the fact that no T_2 is < 47 d implies an upper mass limit of $\sim 0.4 M_\odot$ for white dwarfs produced.

The authors would like to thank Ms Barbara J. Handley for assistance with the statistics and Professor Gene H. Golub for his nonlinear least squares program.

BERT W. RUST

Computer Sciences Division,
Oak Ridge National Laboratory,
Union Carbide Corporation, Nuclear Division,
Oak Ridge, Tennessee 37830

M. LEVENTHAL
S. L. MCCALL

Bell Laboratories,
Murray Hill, New Jersey 07974

Received November 24, 1975, accepted May 12, 1976.

[1] Van Hise, J. R , *Astrophys. J* , 192, 657–659 (1974)
[2] Colgate, S. A., and McKee, C , *Astrophys. J.*, 157, 623–643 (1969)
[3] Leventhal, M., and McCall, S L , *Nature*, 255, 690–692 (1975)
[4] Rust, B W., thesis, Univ Illinois (1974)
[5] Pskovskii, Yu. P , *Soviet Astr.* 11, 570–575 (1968).
[6] Pskovskii, Yu. P , *Soviet Astr* , 14, 798–805 (1971)
[7] Bard, Y , *Nonlinear Parameter Estimation* (Academic, New York, 1974)
[8] Golub, G H , and Pereyra, V., *SIAM J numer Anal* , 10, 413–432 (1973)
[9] Baade, W., and Zwicky, F., *Astrophys J* , 88, 411–421 (1938)
[10] Parenago, P., *Peremennye zvezdy*, 7, 109–123 (1949)
[11] Deutsch, A , *Poulkovo Observatory Circ* , No. 28, 73–75 (1939).
[12] Bertola, F , *Mem. Della Soc Astr. Ital* , 36, 299–307 (1965).

Orientation of pulsar magnetic dipole moments

THE angle between the magnetic dipole moment and the spin of a pulsar is an important parameter in studies of the pulse emission. In this letter, arguments based on the properties of the weak interaction between elementary particles and on the superfluidity of the core show that the torque associated with the rotating dipole moment is free to cause alignment with the spin only in pulsars older than the Crab, and possibly the Vela pulsar. On the basis that the sine of the angle follows an exponential law with a time constant of $\sim 10^6$ yr, the observed distribution of radio pulse widths can be explained by the group of models in which emission occurs from regions near the polar caps rather than the light cylinder.

The high electrical conductivity[1] of the interior matter implies that the magnetic field of a pulsar should be fixed with respect to the body axes of the star. The principal moments, and the torque acting on the star, determine the orientation, as a function of time, of the magnetic dipole moment relative to the spin. The torque can be expressed as the sum of three components

$$\mathbf{N} = \mathbf{N}_1 + \mathbf{N}_2 + \mathbf{N}_3$$

where $\mathbf{N}_1$ and $\mathbf{N}_2$ represent the electromagnetic torque and are, respectively, perpendicular and parallel to the magnetic dipole moment **p**. The component $\mathbf{N}_1$ can be approximated by the vacuum torque for the rotating external dipole field, and $\mathbf{N}_2$ represents the torque resulting from current flow between the corotating magnetosphere and the polar caps of the star. The component $\mathbf{N}_3$ represents the dissipative torque, which causes the axis of greatest principal moment to align with the spin. Owing to the temperature- and therefore time-dependence of $\mathbf{N}_3$, the angle ψ between spin and dipole moment is predicted for pulsars with the properties: (1) a mass such that there is no solid core; (2) an internal toroidal magnetic field with symmetry axis approximately colinear with **p**, to have the following time variation. At a time $t_1 \lesssim 10^3$ yr, ψ becomes approximately equal to $\pi/2$ and remains constant until $t_2 \gtrsim 10^4$ yr. For $t > t_2$, $\psi \rightarrow 0$ with a time constant determined by $\mathbf{N}_1$, $\mathbf{N}_2$ and by the values of ψ and of the period P at $t = t_2$. This form of $\psi(t)$ is consistent with the existence of a strong interpulse in the Crab pulsar and, if the slowing of the pulsar rotation is determined mainly by $\mathbf{N}_1$, provides a simple explanation of the secular variation of magnetic dipole moment postulated by Lyne, Ritchings and Smith[2].

This prediction of $\psi(t)$ depends only on general features of superfluidity and of the non-leptonic weak interaction Accurate knowledge of energy gaps or of the equation of state is not required.

At certain radii in the interior, neutrons, protons and Σ^- hyperons are expected to be in equilibrium. The protons[3] form an isotropic BCS superfluid with energy gap Δ. For such densities, the neutrons[4] may have a small anisotropic energy gap. If the proton energy gap alone is considered, the relaxation time for the non-leptonic weak interaction $n+n \rightleftharpoons p+\Sigma^-$ is proportional[5] to $(\beta\Delta)^{-5/2} \exp(\beta\Delta)$ in the limit $\beta\Delta \gg 1$, where $\beta^{-1} = k_B T$. If the spin is not parallel with the axis of greatest principal moment, the matter in the interior is subject to periodic pressure fluctuations having the period of the precession which must occur. As the pulsar cools, the relaxation time must increase until of the order of the precession period so

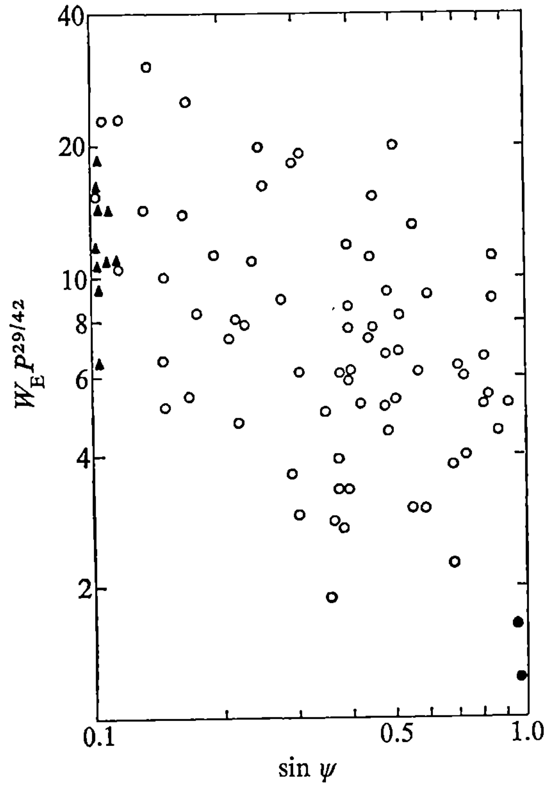

Fig. 1 The distribution of $W_E P^{29/42}$ and sinψ is shown for 82 pulsars, for $\tau_D = 10^6$ yr. The integrated pulse widths W_E, expressed in degrees, are those at 408 MHz listed by Lyne *et al.*[2]. The 10 pulsars with sinψ < 0.1 are shown separately as solid triangles on the left-hand side of the diagram. The Crab and Vela pulsars are likely to have $t < t_2$ and are represented by the two solid circles at the lower right-hand side.

that the coefficient of bulk or second viscosity is extremely large. In the Euler equations, the effect of the viscosity is expressed as a large torque $\mathbf{N}_3$ which causes the axis of greatest principal moment to become parallel with the spin at a time $t_1 \lesssim 10^3$ yr. The effect of a small neutron energy gap would be merely to reduce the value of t_1. Further cooling of the pulsar interior causes the viscosity and therefore $\mathbf{N}_3$ to become negligibly small at times $\sim 10^4$ yr. A more detailed discussion is given elsewhere (P. B. Jones, unpublished).

The distortion caused by the elasticity of the solid outer shell has an axis of symmetry which moves with respect to fixed body axes in such a way as to be approximately parallel to the spin direction. This motion is the result of plastic deformation which occurs for $t \lesssim t_1$ because the temperature is then of the order of 10^8 K and because the rotational surface oblateness greatly exceeds the likely critical strain. Thus the axis of greatest principal moment is determined by the toroidal internal magnetic field and is approximately perpendicular to **p**.

For $t > t_2$, and $\mathbf{N}_1 \gg \mathbf{N}_2$ and $\mathbf{N}_3$, $P \sec\psi$ is a constant of motion and sinψ decreases according to an exponential law with a mean time $\tau_D = P^2 \sec^2\psi(P\dot{P})^{-1}{}_{t=t_2}$. Owing to this alignment of the dipole moment, its component perpendicular to the spin has the time dependence postulated by Lyne *et al.*[2]. Plausible values of P, the period derivative $\dot{P}$, and ψ at $t_2 \simeq 10^4$ yr are quite consistent with $\tau_D \simeq 10^6$ yr given by Lyne *et al.*, whereas if the dissipative torque were neglected, $t_2 = 0$ and the predicted values of τ_D would be too small[6,7] to be consistent with the observed pulsar population.

In one group of pulse emission models[8–10], the microwave radiation is produced tangentially to their velocity by charged particles moving along field lines leaving the polar caps of the star and penetrating the light cylinder. The integrated pulse width is a function of the angle ψ and of the angular size of the emission cone, which is dependent on the period. For the most recent model[10] in this group, $W_E P^{29/42}$ should be proportional to $(\sin\psi)^{-1}$, apart from variations in the intersection of the emission cone by the line of sight. The expression for W_E given by a second group of models[11], those involving relativistic beaming, is very dependent on the velocity of the emitting region and no simple prediction seems possible.

Values of sinψ have been determined from the $\dot{P}$ measurements of Lyne *et al.*[2] for a universal $\tau_D = 10^6$ yr. The distribution of $W_E P^{29/42}$ and sinω shown in Fig. 1, a band of gradient −1, supports the polar cap group of models and the hypothesis that most pulsar magnetic dipole moments are aligning with the spins in a mean time $\sim 10^6$ yr. If the points shown as open circles were normally distributed about a straight line, the gradient of the line would be -0.99 ± 0.15.

P. B. JONES

Department of Nuclear Physics,
University of Oxford,
Oxford, UK

Received February 13; accepted May 24, 1976.

[1] Chanmugam, G., and Gabriel, M., *Astr. Astrophys.*, **11**, 268 (1971).
[2] Lyne, A. G., Ritchings, R. T., and Smith, F. G., *Mon. Not. R. astr. Soc.*, **171**, 579 (1975).
[3] Chao, N.-C., Clark, J. W., and Yang, C.-H., *Nucl. Phys. A*, **179**, 320 (1972).
[4] Hoffberg, M., Glassgold, A. E., Richardson, R. W., and Ruderman, M., *Phys. Rev. Lett.*, **24**, 775 (1970).
[5] Jones, P. B., *Proc. Roy. Soc.*, **A323**, 111 (1971).
[6] Davis, L., and Goldstein, M., *Astrophys. J. Lett.*, **159**, L81 (1970).
[7] Michel, F. C., and Goldwire, H. C., *Astrophys. Lett.*, **5**, 21 (1970).
[8] Gunn, J. E., and Ostriker, J. P., *Astrophys. J.*, **160**, 979 (1970).
[9] Roberts, D. H., and Sturrock, P. A., *Astrophys. J.*, **173**, L33 (1972).
[10] Ruderman, M. A., and Sutherland, P. G., *Astrophys. J.*, **196**, 51 (1975).
[11] Ginzburg, V. L., and Zheleznyakov, V. V., *A. Rev. Astr. Astrophys.*, **13**, 511–535 (1975).

Ocean bottom seismic measurements on the East Pacific Rise and Rivera Fracture Zone

WE describe preliminary results of a seismic experiment using ocean bottom seismometer capsules (OBS) in three separate tripartite arrays. The arrays were located on the central topographic high of the East Pacific Rise between the Rivera and Tamayo Fracture Zones (8 d in position), at the junction of the ridgecrest and the Rivera fracture zone (12 d), and on the Rivera fracture zone well away from the ridgecrest (9 d). Accurate locations and depths could be computed for events sufficiently close to each array, and showed that the main transform fault lay within the central trough. OBS capsules have been successfully used for refraction work[1,2] (also B. Lewis and C. Lister, unpublished) and microseismicity studies[3], but we report here the first use of arrays on a spreading centre–transform fault system for event locations. Other questions of importance to seismology can also be answered from these data.

The capsules[4] contain a 1-Hz vertical seismometer and triggered digital recording system. The capsule itself falls freely to the ocean bottom. When triggered acoustically or after a predetermined time, it is released and floats to the surface. An acoustic system facilitates accurate location of the capsule to within several metres relative to a surface ship.

Figure 1 shows sites and epicentre locations for a number of events recorded at arrays 2 and 3. Array 1 (the ridge array) is not shown. Figure 2 shows a sample of seismograms from array 3. At array 2, 105, 680, and 155 events were recorded on the 3 capsules, respectively. Of these, 67, 57, and 37 were recorded simultaneously by each of the three pair combinations of capsules. Thirty-one earthquakes were recorded simultaneously by all three capsules. Some of the events recorded (particularly those on LY), are spurious triggers caused by ground noise. Many, however, are earthquakes too small to trigger all capsules. All events recorded simultaneously on two or more capsules are believed to be earthquakes. At array

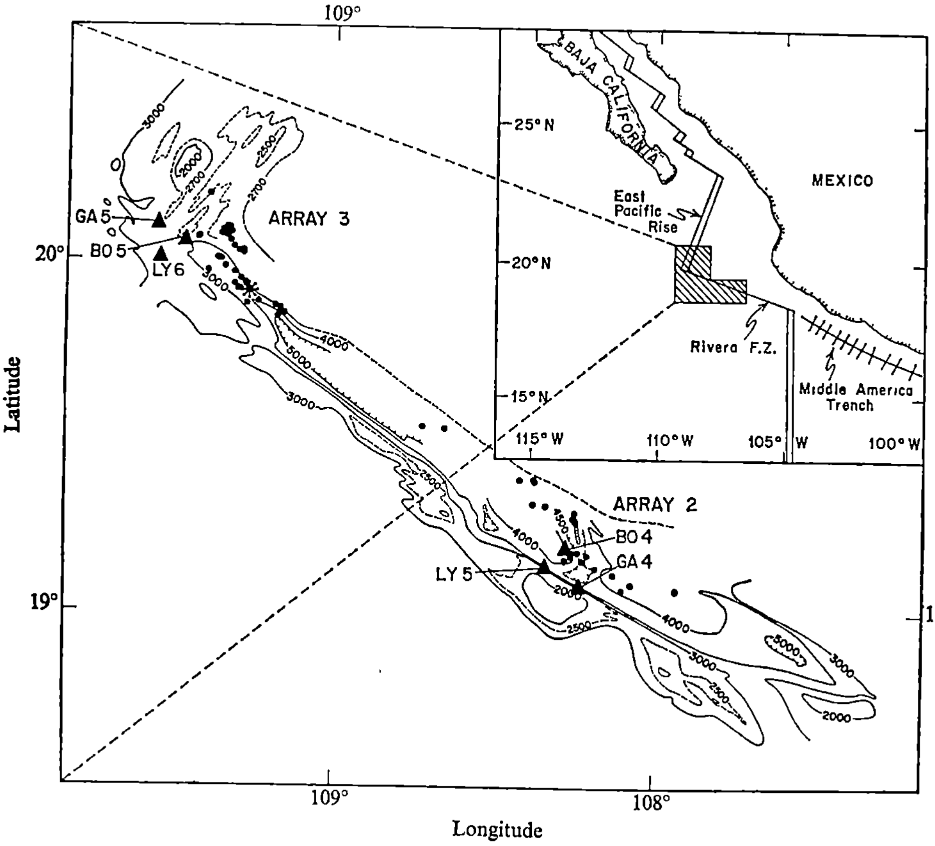

Fig. 1 Capsule sites and bathymetry (m). All of the well determined epicentres recorded at array 2 are shown. A representative sample of events recorded at array 3 are plotted. The asterisk shows the location of the swarm sequence.

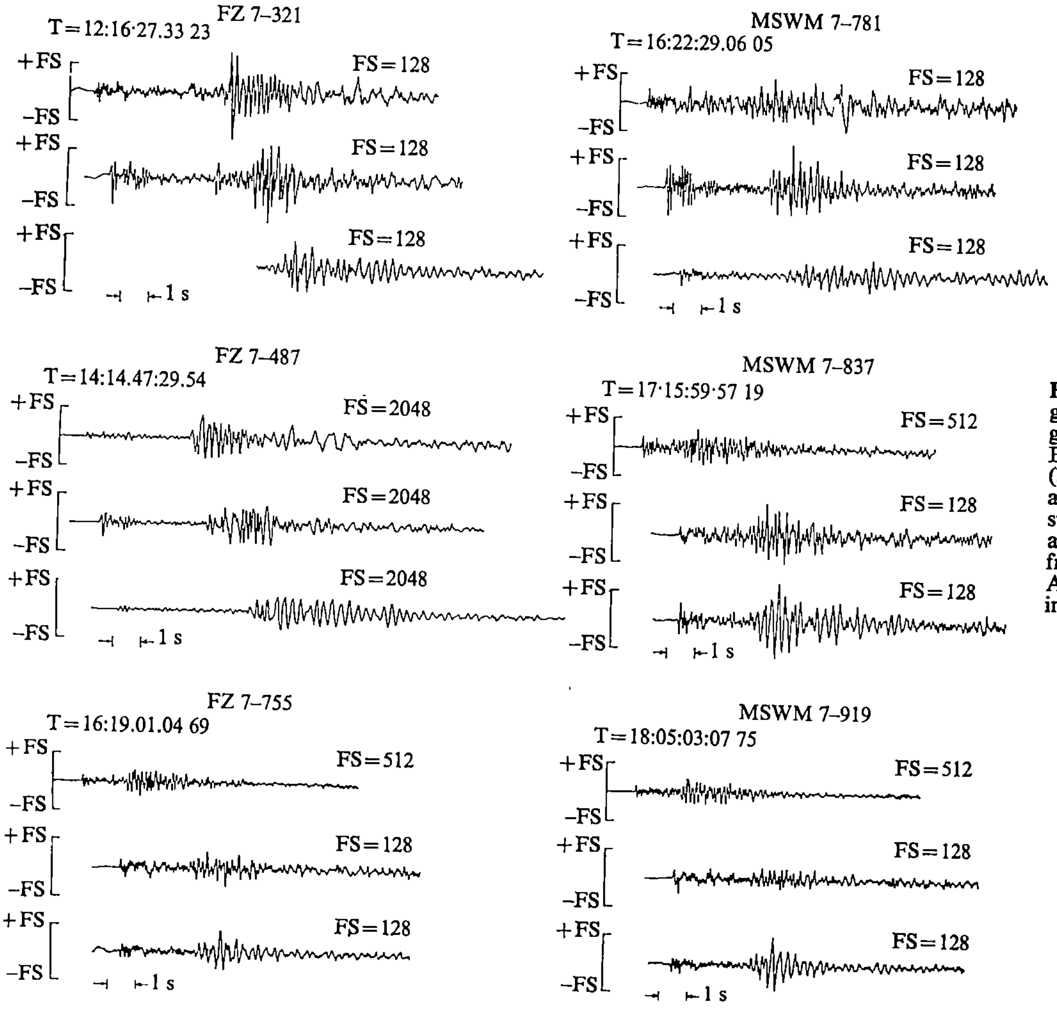

Fig. 2 This shows several seismograms recorded at array 3. Each group of 3 was recorded at BO5(top), LY6(middle), and GA5 (bottom). Events 7–755, 7–783, and 7–919 are from the small swarm sequence due east of the array. The others are down the fracture zone towards the asterisk. At 5 Hz, the seismometer response in counts μm^{-1} is 2.4×10^3. FS on the plot is in counts.

number 3, 254, 304, and 409 events, respectively, were recorded by the capsules. The pair combinations of capsules recorded 196, 213, and 309 events simultaneously. Of these, 183 were recorded on all three capsules. During this period, a swarm of earthquakes with a $M=4.3$, $M=4.3$, and $M=4.8$ sequence, and numerous smaller events, was recorded. The three larger events were recorded on World-Wide Network stations.

The locations of capsules BO and LY were determined by acoustic ranging, and triangulation from the ship, in conjunction with satellite fixes and/or fixes to a moored radar buoy. We estimate the accuracy of these locations to be within 100 m. Capsule GA's transponder failed, so we obtained the best possible estimate of ship position and drift before, during and after the drop. We estimate the location accuracy of GA to be within 400 m.

Epicentre locations and depths were calculated using a half-space location programme written by Ray Buland at IGPP. The locations shown in Fig. 1 were calculated with $V_P=6.5$ and $V_P/V_S=\sqrt{3}$. Seismic refraction results from the East Pacific Rise[5] indicate that this velocity is reached within the top 2 km of crust. For sources a few km deep, as these are believed to be, the half-space model is probably a good approximation as long as the events are near or within the array. Locations of events close to the array were found to be relatively insensitive to changes in velocity. All reasonable values for V_P gave epicentres and source depths which varied by at most 1 or 2 km. The locations of the more distant events varied by several km, but our basic conclusions are not affected by the uncertainty of velocity structure.

The tectonics of the area are shown schematically in the inset to Fig. 1 along with the bathymetry of the northern part of the Rivera Fracture Zone. A deep, steep-sided trough is flanked by ridges on both sides. The topography is generally extremely rugged. To the south-east, beyond the area shown, the trough disappears and the fracture zone continues as a single ridge. This change in character coincides with a change in strike, the topography trending more in an east–west direction.

Three immediate conclusions may be drawn from the pattern of seismicity near array 2:

(1) The general trend of epicentres is along the central trough. This suggests that transform faulting is taking place mainly inside this feature, rather than along the valley walls.

(2) There is a definite offset in the line of epicentres near the array. It is unlikely that this offset is an artefact of location errors. Location uncertainties make it impossible to draw any similar conclusions about the more distant events.

(3) A few of the events have epicentres very close to one of the capsules. This allows well-constrained source depths to be calculated. All reliable source depths were shallower than 10 km below the sea floor, suggesting 10 km as a lower limit for the thickness of the brittle zone on this area.

With array 3, we tried to cover the junction of the rise and fracture zone. There seem to be no epicentres located within the array. The epicentres shown in Fig. 1 for this array are some of the more reliable locations (that is, with the smallest travel-time residuals). We have not yet located all the events in this area, but the epicentres shown are probably a fairly good sample.

As in the central part of the fracture zone, the main trend of epicentres is along the rift. A few km from the ridge there is a second line of activity, parallel to the first. This might indicate an offset of the main transform fault, or possibly a subsidiary fault reflecting greater complexity of the faulting as the junction is approached.

The exact location of the spreading centre is uncertain, but presumably coincides with the topographic high of the rise. It seems that, as would be expected, the seismicity does not extend beyond this. We also note that there is a swarm-like cluster of events near the junction, east of the array. These results are similar to those of Reid and Macdonald[6] on the Mid-Atlantic Ridge. Since all the events located lie outside the array, little reliance can be placed on source depth determinations. It appears, however, that the depths of the nearest events are shallow, probably <5 km.

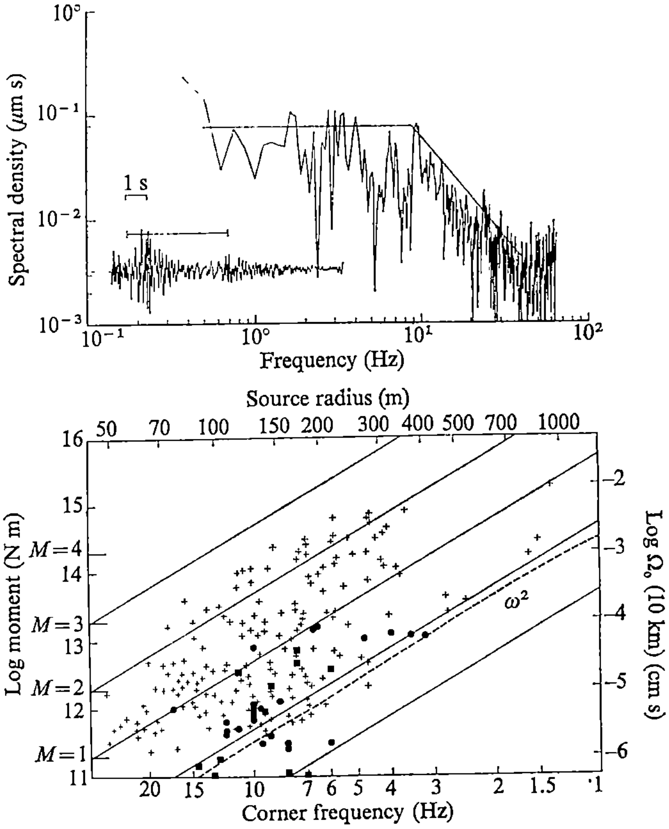

Fig. 3 Source parameters of 35 events recorded at Arrays 2 and 3. The upper portion of the figure is a ground motion spectrum of the S-wave of one of the events (Event 22). The line over the seismogram indicates the portion of the signal analysed. The source parameters from the aftershocks of the San Fernando earthquake of February 9, 1971 are shown (+) as a comparison to the oceanic data (■, Array 2; ●, Array 1). The diagonal lines give a logarithmic pressure scale, the top line gives the 10^8-Pa region (1 Pa$=10^{-5}$ bar), and each subsequent line gives a factor of 10 smaller a pressure, down to 10^4 Pa at the bottom.

S-wave spectra of 35 events of various sizes from arrays 2 and 3 have been computed. The spectra have been corrected for instrument response and an assumed Q of 250. This is a reasonable value of Q for S-waves on continental crust[7]. The moments and corner frequencies of nearby events are also relatively insensitive to the value of Q chosen. The instrument response was computed using measured seismometer and amplifier parameters. Figure 3 shows the spectrum of event 22 measured at capsule position BO 4 (Fig. 1). The rise at high frequencies is caused by the Q correction, which has the effect of dividing the background noise by a very small number. Also in Fig. 3 is a plot of the seismic moments against the corner frequencies of the 35 events studied. Although the results must be considered preliminary until more analysis is carried out, the stress drops estimated using the theory of Brune[8,9] do not reach values as high as those for aftershocks of the San Fernando earthquake of February 9, 1971, also plotted in Fig. 3 (ref. 7).

We conclude that epicentres of micro-earthquakes on the Rivera Fracture Zone indicate that the main transform fault lies inside the central trough. There is evidence that at least one offset occurs in this fault. One interpretation of this would be that this offset represents a minor spreading centre similar to, but on a smaller scale than, those in the Gulf of California. A small component of spreading on this section of the fracture zone would be consistent with the interpretation of the central trough as a rift feature. Source depths suggest a brittle zone ~10 km thick. S-wave spectra of 35 events suggest a lower upper-bound for stress drop than found for the San Fernando earthquake of February 9, 1971.

We thank the NSF for supporting this research effort. Numerous persons contributed in an important way to this project, including Dave Willoughby, Georgeanne Ray, John Orcutt, Paul Spudich, Dorothy Darling, and Captain Newbegin and the crew of the Ellen B. Scripps.

WILLIAM A. PROTHERO
IAN REID
MICHAEL S. REICHLE
JAMES N. BRUNE

Institute of Geophysics and Planetary Physics,
Scripps Institution of Oceanography,
University of California, San Diego,
La Jolla, California 92037

Received January 16; accepted May 17, 1976.

[1] Whitmarsh, P., *Nature*, 246, 297–299 (1973).
[2] Rowlett, H., McCamy, K., and Carpenter, G., *Trans Am. geophys. Un.*, 55, 294 (1974).
[3] Francis, T., and Porter, I., *Nature*, 240, 547–549 (1972).
[4] Prothero, W. A., *Bull. seis. Soc. Am.*, 64, 1251–1262 (1974).
[5] Orcutt, J., Kennett, B., Dorman, L., and Prothero, W., *Nature*, 256, 475–476 (1975).
[6] Reid, I., and Macdonald, K., *Nature*, 246, 88–90 (1973).
[7] Tucker, B. E., and Brune, J. N., *Seismograms, S-wave Spectra and Source Parameters for Aftershocks of the San Fernando Earthquake of February 9, 1971*, 69-122 (US Department of Commerce, NOAA, 1975).
[8] Brune, J. N., *J. geophys. Res.*, 75, 4997–5009 (1970).
[9] Brune, J. N., *J. geophys. Res.*, 76, 5002 (1971).

Further rubidium–strontium age and isotope evidence for the nature of the late Archaean plutonic event in West Greenland

THE gneisses of the Godthaabsfjord region of southern West Greenland have been grouped by McGregor[1] into an older and a younger set, respectively termed the Amîtsoq and Nûk gneisses. They are separated by dykes (the Ameralik dykes), metavolcanic and metasedimentary rocks (the Malene supracrustals) and stratiform meta-anorthosites. The Amîtsoq gneisses have been dated at ~3,700–3,800 Myr (refs 2–4). Pankhurst *et al.*[5] reported a Rb–Sr whole rock isochron age of 3,040±50 Myr and an initial $^{87}Sr/^{86}Sr$ ratio of 0.7026±0.0004 on a suite of Nûk gneisses from Björneöen, some 25-km northeast of Godthaab (Fig. 1). The isochron age was interpreted as the age of emplacement of the precursors of the Nûk gneisses, while the low initial ratio suggested that these precursors could not have been derived by partial or complete melting of the older Amîtsoq gneisses. Several geologists have expressed disagreement with this interpretation[6,7]. In particular, Chadwick *et al.*[7] disagreed with our conclusion that the Nûk gneisses represent essentially juvenile sialic crust formed in West Greenland ~2,800–3,000 Myr ago. We here present further evidence to support our interpretation.

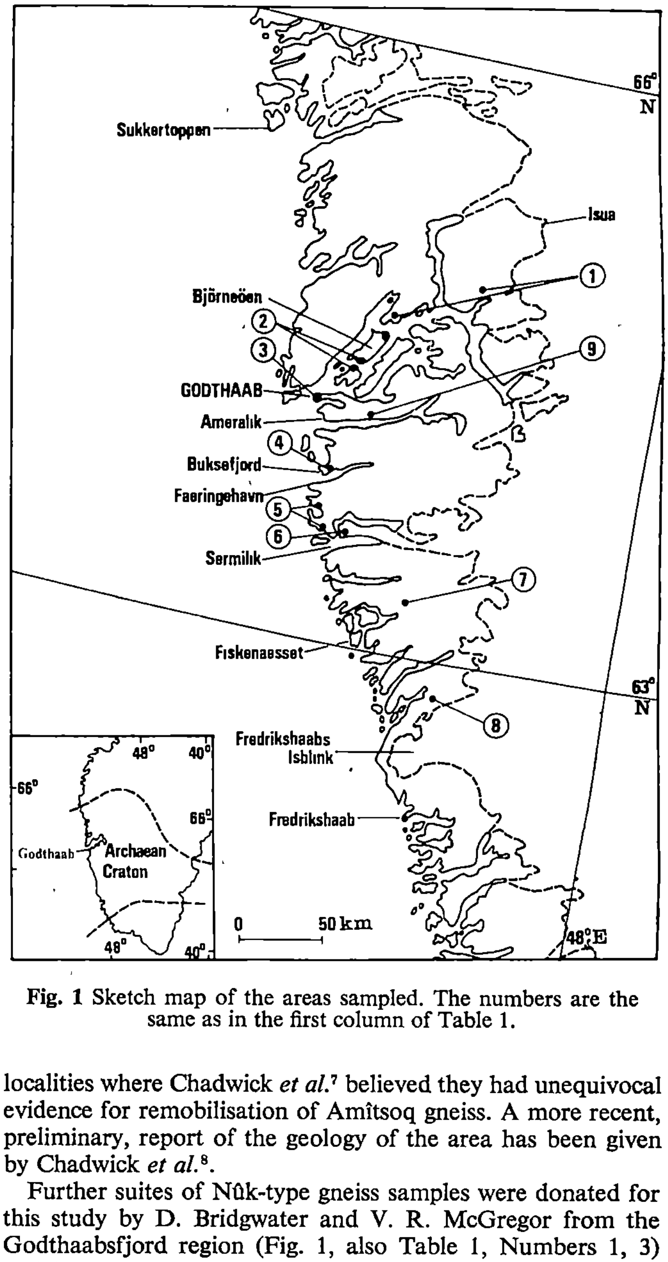

Fig. 1 Sketch map of the areas sampled. The numbers are the same as in the first column of Table 1.

A large collection of Nûk gneisses was made by us in 1973 from the area between Buksefjord and Sermilik (Fig. 1, also Table 1, Numbers 4, 5, 6). Some of these samples are from localities where Chadwick *et al.*[7] believed they had unequivocal evidence for remobilisation of Amîtsoq gneiss. A more recent, preliminary, report of the geology of the area has been given by Chadwick *et al.*[8].

Further suites of Nûk-type gneiss samples were donated for this study by D. Bridgwater and V. R. McGregor from the Godthaabsfjord region (Fig. 1, also Table 1, Numbers 1, 3) and by J. S. Myers from Fiskenaesset (Fig. 1, also Table 1, Number 7).

We summarise in Table 1 Rb–Sr whole rock isochron ages and initial $^{87}Sr/^{86}Sr$ ratios obtained on a total of 96 samples of Nûk-type gneisses grouped into different areas (Fig. 1). We also present whole rock data for the post-tectonic Qôrqut Granite (Fig. 1, also Table 1, Number 9), the last major rock-forming

Table 1 Summary of Rb–Sr age and isotope results for Nûk-type gneisses and Qôrqut granite

Area (see Fig. 1)	No. of Samples	Mean Rb (p.p.m.)	Mean Sr (p.p.m.)	R*	Age (Myr)†	Initial $^{87}Sr/^{86}Sr$	F‡
1. Head of Godthaabsfjord	11	82	494	0.48	2,850±60	0.7017±0.0002	1.5
2. Björneöen§	14	64	415	0.45	2,930±70	0.7023±0.0003	2.5
3. Godthaab	11	44	584	0.22	2,780±150	0.7026±0.0005	3.0
4. Buksefjorden	21	60	278	0.63	2,870±60	0.7015±0.0003	3.0
5. Faeringehavn	8	74	248	0.86	2,790±60	0.7031±0.0005	2.0
6. Sermilik	20	72	270	0.77	2,780±30	0.7020±0.0002	1.5
7. Fiskenaesset (Majorqap qâva)	11	86	488	0.51	2,880±50	0.7016±0.0003	2.5
8. Fredrikshaabs Isblink††	13	47	276	0.50	2,660±120	0.7032±0.0010	<1
9. Qôrqut Granite, Ameralik	7	215	133	4.8	2,520±90	0.709±0.007	1.0

*$R = {}^{87}Rb/^{86}Sr$ calculated from mean Rb and Sr.
†Decay constant for ^{87}Rb is 1.39×10^{-11} yr^{-1}.
‡F = Error factor required to achieve least squares fit (that is M.S.W.D. $\leqslant 2$). Errors are quoted at 2σ, after taking F into account.
§From Pankhurst *et al.*[5], reanalysed.
††From Pidgeon and Hopgood[18].

event in the Godthaabsfjord region[1]. (Individual analytical data for these 103 samples are not reported here, but may be obtained on request from the authors.) Full details of chemical and mass-spectrometric techniques have been described elsewhere[9]. Rb/Sr ratios were determined by a precise X-ray fluorescence (XRF) technique described by Pankhurst and O'Nions[10].

New analyses on the 14 samples from Björneöen reported by Pankhurst *et al.*[5] (Table 1, Number 3) yield slightly revised age and initial $^{87}Sr/^{86}Sr$ values of 2,930±70 Myr and 0.7023±0.0003, mainly from recalibration of the XRF method using USGS standard rocks[10]. These are, however, still within the error of the published values, quoted earlier. The ages reported in Table 1 for groups 1 to 7 range from 2,780 to 2,930 Myr, whilst the initial $^{87}Sr/^{86}Sr$ ratios range from 0.7015 to 0.7031. The errors within each range do not completely overlap, so that small, significant differences appear to exist, as discussed later. Nevertheless, our principal observation is that the grouping is remarkable for its overall coherence in age and initial ratio over the huge area sampled (Fig. 1).

Figure 2 is a composite Rb–Sr whole rock plot for all samples from groups 1–7 reported in Table 1. For comparison, the published values for the Amîtsoq gneisses are also plotted[2,4]. The plot demonstrates the lack of overlap between the Nûk and Amîtsoq linear arrays and also shows that both gneiss groups exhibit a similar range of Rb/Sr ratios. This is not surprising, considering the close overall petrological and geochemical similarity between the comparable variety of rock types (for example, granites, granodiorites, tonalites and diorites) which make up both the Nûk and Amîtsoq gneisses. This in itself argues against formation of the Nûk gneisses by reworking of Amîtsoq gneisses, since this would be expected to result in a general increase of Rb relative to Sr in the remobilised material.

Several samples from the Sermilik area (Table 1, Number 6) are at granulite grade, whereas all other samples in the present study are presumed to be at amphibolite grade. Clearly, metamorphic grade has had no effect on the Rb–Sr age or initial $^{87}Sr/^{86}Sr$ of the rocks. This accords with the view that the parent magmas of the Nûk gneisses were emplaced during an igneous event which was broadly contemporaneous with high-grade metamorphism and gneissification. This conclusion has been advanced specifically for the Ilivertalik granite on the south side of Sermilik, to which some of the present samples, which were all collected on the north side of Sermilik, may indeed belong, and which has yielded a U–Pb zircon age of 2,835±10 Myr (ref. 11). Moreover, the mean Rb–Sr age of ~2,850 Myr reported here for Nûk gneisses agrees within analytical error with the mean $^{207}Pb/^{206}Pb$ whole rock age of granulite facies gneisses and associated anorthosites from the Nordland–Sukkertoppen and Fiskenaesset areas, respectively north and south of Godthaab (Fig. 1)[12]. The Pb/Pb age was interpreted as the probable age of the granulite facies metamorphism, whilst the actual Pb isotope ratios suggested that the gneisses were not reworked Amîtsoq gneisses but represented an addition of crustal material from the upper mantle source regions within the period ~2,800–3,000 Myr ago.

Figure 3 shows averaged Rb–Sr growth lines for the major rock units so far analysed from West Greenland, plotted in relation to a hypothetically linear upper mantle growth line. Two groups of much younger gneisses from South Greenland ~1,700–1,800 Myr old[13], are also plotted for comparison.

Consideration of Fig. 3 supports our earlier conclusion that the Nûk gneiss precursors were not derived by partial melting and mobilisation of Amîtsoq gneisses, since the average growth lines of the latter are far too steep. By 2,850 Myr ago, the average $^{87}Sr/^{86}Sr$ ratios of Amîtsoq gneisses would have been ~0.705–0.715. This argument is strongly reinforced by the similarity in range of Rb/Sr ratios between the Nûk and Amîtsoq gneisses already noted above (Fig. 2).

We conclude that the "irrefutable" identification of Amîtsoq gneisses by Chadwick *et al.*[7,8] in the Buksefjorden–Sermilik area is contradicted by the dissimilarity of the present data with the established Rb–Sr chronology in the Godthaab region. In this connection, four whole-rock samples from just north of Sermilik, cut by amphibolite fragments considered as correlative with the Ameralik dykes, are included in Table 1, Number 6. They cannot be distinguished from the main body of data and separately yield an isochron age of 2,760±80 Myr and an initial $^{87}Sr/^{86}Sr$ ratio of 0.7020±0.0004.

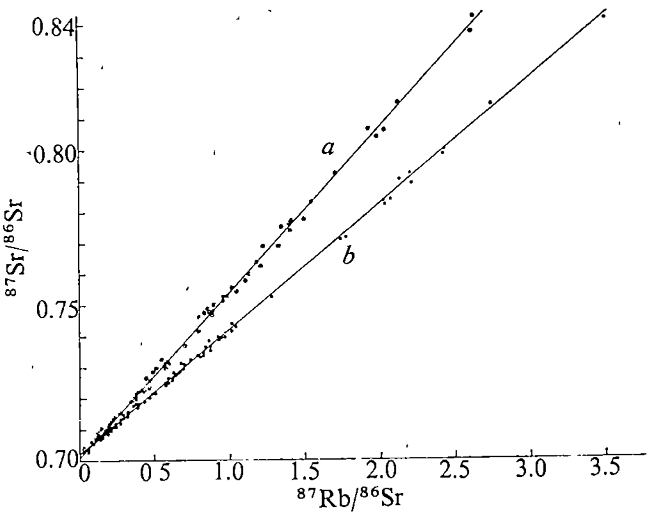

Fig. 2 Rb–Sr whole rock isochron plot for *a*, Amîtsoq gneisses[2,4], with 3,700-Myr reference line; *b*, Nûk-type gneisses, Groups 1 to 7, Table 1, with 2,850-Myr reference line. Three very high Rb/Sr points have been omitted from each line.

At the present time there is very little evidence for Archaean rocks with high $^{87}Sr/^{86}Sr$ ratios. Hurst *et al.*[14] report an age and initial $^{87}Sr/^{86}Sr$ ratio of 3,120±60 Myr and 0.7064±0.0012 for a group of late "Undifferentiated gneisses" from Saglek, Labrador, whilst Barton[15] has quoted a value of 0.7044±0.00010 for gneiss from Hebron, Labrador dated at ~3,600 Myr, although in the latter case we believe there has been a serious underestimation of the error. Barton quotes errors calculated by two different methods but, for no stated reason, uses the lowest error value. Little is known of the chemistry of the Saglek "Undifferentiated gneisses" and the possibility that there has been redistribution of ^{87}Sr in these rocks on the scale of sampling

Fig. 3 Average $^{87}Sr/^{86}Sr$ growth lines for: *A*, Amîtsoq gneisses[2,4] from *a*, Narssaq; *b*, Qilangarssuit; *c*, Praestefjord; *d*, Isua; *B*, Nûk-type gneisses (Table 1) from *e*, head of Godthaabsfjord; *f*, Björneoen; *g*, Godthaab; *h*, Buksefjorden; *i*, Faeringehavn; *j*, Sermilik; *k*, Majorqap qâva, Fiskenaesset; *C*, *l*, Fredrikshaab Isblink[16]; D, E, Ketilidian gneisses, South Greenland[13]; *m*, Group 1; *n*, Group 2; F, Qôrqut Granite, Ameralik. The line *p* represents a hypothetically linear upper mantle growth line. The inset is a magnification of points *B* and *C* for the Nûk-type gneisses listed in Table 1.

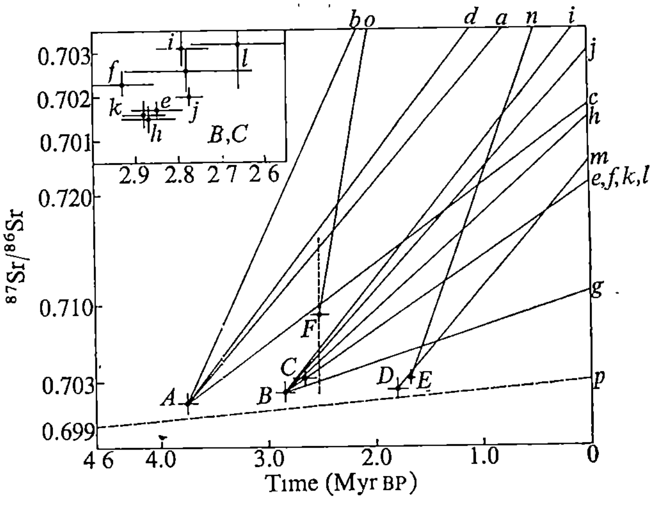

following a previous crustal history cannot be discounted. Such a process would mean that partial melting and intrusion of magma need not necessarily have occurred at 3,120±60 Myr ago. The only unequivocal case known to the authors in which Rb–Sr systems demonstrate "isotopic reworking" of Archaean crust is a Rb–Sr whole-rock isochron of 2,300±150 Myr with an initial $^{87}\mathrm{Sr}/^{86}\mathrm{Sr}$ ratio of 0.7126±0.0011 for gneiss from Vesterålen, Norway[16]. Pb isotopes in the same rocks preserve an age of ~3,500 Myr, however, so that in this case it is unlikely that "isotopic reworking" involved segregation of a partial melt.

The Qôrqut granite of West Greenland (Table 1, Number 9) gives a whole-rock isochron age of 2,520±90 Myr and initial $^{87}\mathrm{Sr}/^{86}\mathrm{Sr}$ of 0.709±0.007, in good agreement with a previously published mineral isochron for a related pagmatite[17]. The high Rb/Sr ratios of the analysed samples have so far precluded more precise determination of the initial $^{87}\mathrm{Sr}/^{86}\mathrm{Sr}$ ratio and this therefore remains ambiguous in terms of its petrogenetic implications. In view of the more extreme granitic aspect of the Qôrqut granite (predominantly quartz and K-feldspar with few mafic minerals) compared to the earlier gneisses it might well be derived by remobilisation of old crustal material.

The small but statistically significant range of age and initial $^{87}\mathrm{Sr}/^{86}\mathrm{Sr}$ ratios of the Nûk type gneisses in West Greenland (see Table 1 and inset, Fig. 3) may genuinely reflect small differences in the age of emplacement and pre-history of the parent magmas. We believe that a plutonic episode of such magnitude comprises complex, multistage processes lasting for perhaps 100–200 Myr. It is, however, also possible that the gneisses have variously suffered partial redistribution of radiogenic ^{87}Sr during the course of this episode, so that it is not possible to be absolutely sure that each of the isochrons in Table 1 records the specific age of emplacement of any one suite of cogenetic igneous rocks. The fact that none of the best fit lines are perfect isochrons (for which $F \leqslant 1$ in Table 1), and that there is a faint suggestion of inverse correlation between isochron age and initial $^{87}\mathrm{Sr}/^{86}\mathrm{Sr}$ ratio within the 2,900–2,650-Myr interval, emphasises this doubt, although the latter observation is rather heavily biased by the results of Pidgeon and Hopgood[18] from much further south at Frederikshaabs Isblink (Fig. 1, also Table 1, Number 8).

Our major conclusion remains that the igneous precursors of the Nûk gneisses throughout the area sampled represent a massive addition of new calc-alkaline material to the Archaean continental crust of West Greenland. These magmas separated from a low Rb/Sr source region, such as upper mantle, not more than 200 or 300 Myr at the most before the measured isochron ages of Table 1. Geochemical differentiation, magmatism and metamorphism all occurred during the same major plutonic episode[19,20]. There is as yet no isotopic evidence for the involvement of Amîtsoq gneisses in the formation of the Nûk gneiss precursors.

We thank D. Bridgwater, V. R. McGregor, J. S. Myers for providing samples; B. Chadwick, K. Coe, A. D. Gibbs, M. R. Sharpe, P. R. A. Wells for help in the field; all the above for stimulating discussion; R. Goodwin and M. Humm for skilled technical assistance; the NERC and the Geological Survey of Greenland for support.

S. MOORBATH
R. J. PANKHURST

*Department of Geology and Mineralogy,
University of Oxford,
Oxford, UK*

Received April 5; accepted May 17, 1976.

[1] McGregor, V R., *Phil. Trans. R. Soc.*, A273, 343 (1973).
[2] Moorbath, S., O'Nions, R. K., Pankhurst, R J., Gale, N. H , and McGregor, V. R., *Nature phys. Sci.*, 240, 78 (1972).
[3] Baadsgaard, H., *Earth planet. Sci Lett* , 19, 22 (1973)
[4] Moorbath, S., O'Nions, R. K , and Pankhurst, R J., *Earth planet Sci. Lett.*, 27, 229 (1975).
[5] Pankhurst, R. J , Moorbath, S., and McGregor, V R., *Nature phys. Sci* , 243, 24 (1973).
[6] Bridgwater, D., McGregor, V R., and Myers, J S , *Precamb Res* , 1, 179 (1974)
[7] Chadwick, B., Coe, K., Gibbs, A D., Sharpe, M. R , and Wells, P. R A , *Nature*, 249, 136 (1974).
[8] Chadwick, B., Coe, K , Stainforth, J. G., Vines, K. J., and Wells, P. R. A., *Geol. Surv. Greenland*, Rep. no. 75 (for 1974), 65 (1975).
[9] O'Nions, R. K , and Pankhurst, R. J., *Earth planet. Sci. Lett.*, 21, 13 (1973).
[10] Pankhurst, R J., and O'Nions, R. K., *Chem. Geol* , 12, 127 (1973).
[11] Pidgeon, R. T., Aftalion, M., and Kalsbeek, F., *Geol Surv of Greenland*, Rep. No. 73, 31 (1976).
[12] Black, L P., Moorbath, S., Pankhurst, R. J., and Windley, B. F., *Nature phys. Sci.*, 244, 50 (1973).
[13] Van Breemen, O , Aftalion, M., and Allaart, J. H., *Geol. Soc. Am Bull.*, 85, 403 (1974).
[14] Hurst, R. W., Bridgwater, D , Collerson, K. D , and Wetherill, G W., *Earth planet. Sci Lett.*, 27, 393 (1975).
[15] Barton, J. M., Jr, *Earth planet. Sci. Lett.*, 27, 427 (1975)
[16] Taylor, P. N., *Earth planet. Sci Lett* , 27, 35 (1975)
[17] Pankhurst, R J , Moorbath, S., Rex, D. C., and Turner, G., *Earth planet. Sci. Lett.*, 20, 157 (1973).
[18] Pidgeon, R. T., and Hopgood, A M., *Geochim. cosmochim. Acta*, 39, 1333 (1975).
[19] Moorbath, S., *Nature*, 254, 395 (1975).
[20] Moorbath, S., *Nature*, 255, 391 (1975).

Characterisation of monounsaturated fatty acids from an estuarine sediment

PREVIOUS investigations of fatty acids in marine sediments hav primarily been concerned with the concentrations of the individual acids rather than their chemical configuration[1–4]. Brown and Swidler[5] have demonstrated the ability of clay to catalyse the conversion of oleic acid (18:1Δ^9 *cis*) to elaidic acid (18:1Δ^9 *trans*) accompanied by extensive rearrangement of the double bond position. (18:1 = normal carbon chain length: number of double bonds). As most biologically produced olefinic acids are believed to be in the *cis* configuration, diagenetic changes in the sediment may alter the *cis* isomers to the more stable *trans* isomers, as well as cause migration of the double bond. Consequently, investigations of the monounsaturated fatty acid *cis*/*trans* ratio and position of the double bonds, with depth in the sediment, may yield significant information on diagenetic pathways of these acids. We have determined the presence of small amounts of palmitelaidic acid (16:1Δ^9 *trans*) and elaidic acid (18:1Δ^9 *trans*), as well as other positional isomers of these trans acids, in a Recent estuarine sediment. In addition, we have also confirmed that the major monounsaturated fatty acids are palmitoleic acid (16:1Δ^9 *cis*) and oleic acid (18:1Δ^9 *cis*). We give here the methods for isolating these acids and confirming their structures, and their geochemical significance is discussed.

The general collection and analytical procedures have previously been reported in detail[1–3]. Surface sediment (upper 8–10 cm) was collected from station D in Narragansett Bay, Rhode Island[2]. The sediment was saponified (under reflux) for 2 h using 2:1 (*v*/*v*) 0.5 *N* KOH in 90% methanol–benzene, filtered through a Whatman No. 1 filter, and the filtrate transferred to a separatory funnel. After addition of distilled water to give two phases, the non-saponifiable fraction was removed and backwashed with *p*H 10 distilled water. The resulting aqueous phase and the initial saponifiable fraction were then both acidified to *p*H 2 and extracted three times with petroleum ether. The combined ether phases were evaporated to near dryness at room temperature under reduced pressure using a rotary evaporator. Subsamples were then taken for each analysis.

To subsamples I and II were added 17:1Δ^{10} *cis* or 17:1Δ^{10} *trans* fatty acid internal standards. Each subsample was then methylated using BF_3–methanol and the methyl esters isolated by thin-layer chromatography (TLC)[1]. The methyl esters were further separated on $AgNO_3$–TLC to isolate both *cis* and *trans* monounsaturated esters[6,7].

The *cis* and *trans* fractions were individually analysed by flame ionisation gas–liquid chromatography (GLC) using a Hewlett-Packard model 5750 gas chromatograph. The resulting chromatogram for the *trans* methyl esters is shown in Fig. 1. The proper configurational assignments were made on the basis of relative retention times and coinjection with authentic standards on a stainless steel column (6m × 2.2mm inside diameter) containing GP-15% SP-2340 on 100/120 Chromosorb P, AW-DMCS (Supelco), resolution[8] = 0.83 for 16:1Δ^9 *cis*

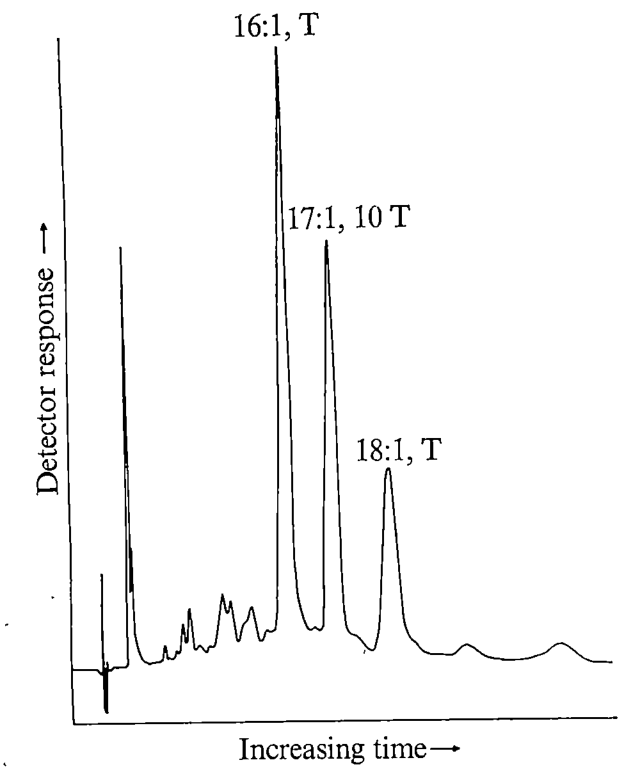

Fig. 1 Gas chromatogram of 16:1 and 18:1 *trans* methyl esters, in presence of 17:1Δ^{10} *trans* methyl ester internal standard, recovered from station D surface sediment.

and *trans*. Each sample was also hydrogenated and co-injected with standard saturated esters

To determine the quantitative amount of each acid, the areas of the peaks of the naturally occurring acids (before and after hydrogenation) were compared with the areas of the internal standard. (No natural 17:1 *cis* or *trans* was detected in the sediments.) The GLC analysis of I and II indicated the quantities of fatty acids in the sediment to be as follows (μg acid per g dry weight of sediment): for 16:1 *cis*, 17.1$\mu g\ g^{-1}$, for 16:1 *trans*, 1.7 $\mu g\ g^{-1}$, for 18:1 *cis*, 9.6 $\mu g\ g^{-1}$, and for 18:1 *trans*, 0.8 $\mu g\ g^{-1}$. Analytical uncertainty was found to be ± 10% or less. Thus in both cases, the *cis* isomer accounted for ~ 92% and the trans isomer ~ 8% of the total 16:1 and 18:1 acids.

To investigate the possibility of the *trans* isomer being generated from the *cis* isomer during the saponification, methylation, or TLC procedures, a series of blanks was carried through the entire analysis. Each blank consisted of a pre-extracted sediment plus various combinations of 16:1, 17:1 and 18:1 *cis* standard acids. No *trans* acids were generated during this procedure

The configurational assignments were verified by infrared spectroscopy and combined gas chromatography–mass spectrometry (GC–MS) analyses. Two separate subsamples, III and IV, were processed by the above methods without internal standards. Portions of the purified *cis* and *trans* methyl esters were each analysed by GC–MS (Finnigan 1015C). The resulting GC–MS spectra for these esters were compared with spectra for authentic standards and agreed well in all cases. The GC–MS spectrum for the *trans* methyl ester of the eighteen carbon fatty acid is shown in Fig. 2. This spectrum shows the molecular ion peak at *m/e* 296 (M^+). Some characteristic fragmentation peaks are *m/e* 265 (M^+ −31), *m/e* 264 (M^+ −32), *m/e* 222 (M^+ −74), and *m/e* 74 (McLafferty rearrangement)[9,10].

Separate portions of III and IV were analysed by infrared spectroscopy (Perkin Elmer model 521) and compared with authentic standard infrared spectra. The infrared spectrum of the *trans* methyl esters is presented in Fig. 3 and shows the characteristic *trans* absorption at 965 cm^{-1} (10.3 μm). The infrared spectrum of the *cis* methyl esters showed both the absence of the *trans* band at 965 cm^{-1} and the presence of a stronger absorption in the region of 3,015 cm^{-1} (3.32 μm). The infrared and GC–MS spectra together with the GLC analyses confirm the presence of both 16:1 and 18.1 *cis* and *trans* acids.

Portions of III and IV were oxidised using $KMnO_4$ in a modification of Downing and Greene's[11] procedure to determine the position of the double bond. The sixteen and eighteen carbon *cis* oxidation products yielded primarily the C_7 and C_9 methyl esters and the C_9 dimethyl ester, indicating the double bond to be predominantly in the 9–10 position for both fatty acids. The ratios of the dimethyl esters recovered indicate that ~ 62% of the double bonds in the *cis* isomers are in the 9–10 position, 19% are in the 11–12 position, and 19% are in other possible positions from C_5 to C_8, and C_{10}.

Analysis of the sixteen and eighteen carbon *trans* oxidation products again yielded primarily the C_9 dimethyl ester and the C_7 and C_9 methyl esters, indicating the double bonds in both *trans* isomers to be predominantly in the 9–10 position. The ratios of the dimethyl esters recovered from the oxidation of the *trans* isomers indicate that ~ 70% of the double bonds are in the 9–10 position, 23% are in the 11–12 position, and 7% are in other positions as above. Within the accuracy of the method, there is no significant difference between the positions of the double bonds in the *cis* and *trans* isomers.

The three most common monounsaturated fatty acids found in organisms are oleic acid, palmitoleic acid, and vaccenic acid (18:1Δ^{11} *cis*)[12]. It appears that the major monounsaturated acids present in the examined surface sediment are the 16:1Δ^9, 18:1Δ^9 and 18:1Δ^{11}. These are present as ~ 92% in the *cis* configuration and 8% in the *trans* configuration. Since the double bonds are primarily in two positions, the 9–10 and 11–12 positions, this would seem to indicate that the *cis* isomers present in this surface sediment result from a direct biological input. The *trans* isomers result from either a direct input or from microbial modification of the *cis* isomers in the sediments. The *trans* isomers apparently do not result from the clay catalysed isomerisation of the *cis* isomer. According to Brown and Swidler[5] the clay catalysed isomerisation of the *cis* octadecenoic acid yields a mixture of the *trans* isomers with the double bond ranging from the 2–17 positions, and the 9–10 *trans* isomer making up only 23% of the total.

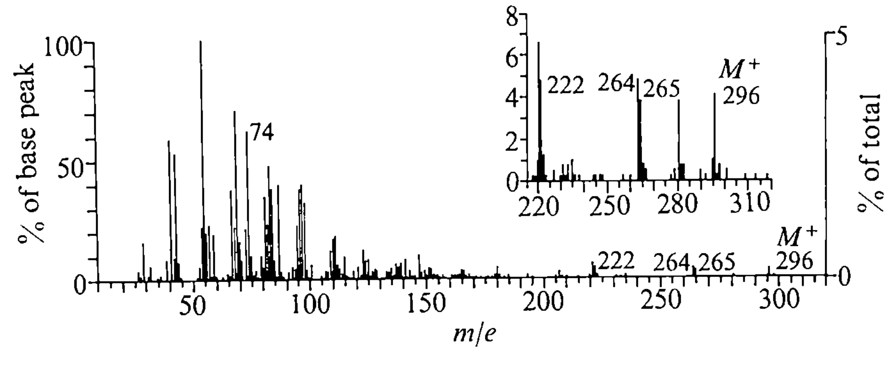

Fig. 2 GC–MS spectrum of 18:1 *trans* methyl ester recovered from station D surface sediment, no internal standard added (*m/e* 220–310 expanded in upper right).

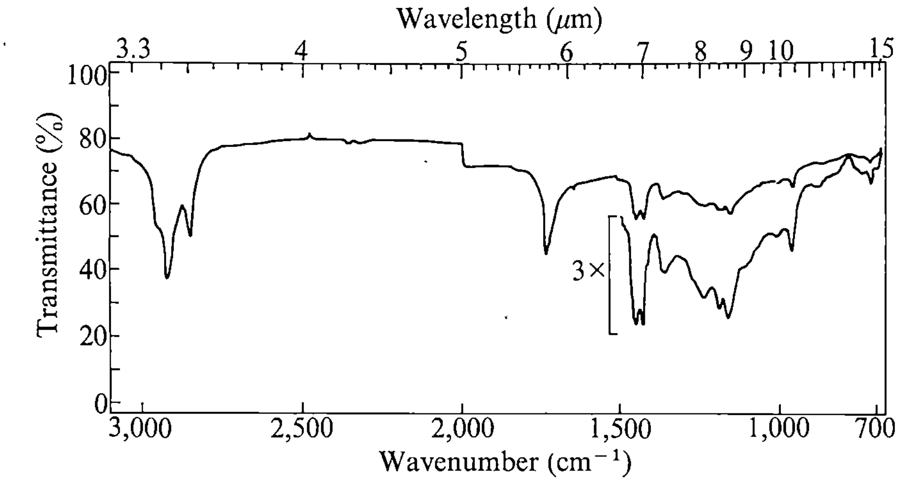

Fig. 3 Infrared spectrum of 16:1 and 18:1 *trans* methyl esters recovered from station D surface sediment; no internal standard added.

Although the absolute quantities of the monounsaturated fatty acids normally decrease with depth in the sediment[2], secondary effects may result from clay catalysis. As depth increases, the clay catalysed conversion of the *cis* to *trans* isomers may occur until an equilibrium mixture of *cis* and *trans* results (for the 18:1 acid, the equilibrium mixture is ~ 33% *cis*, 67% *trans*[5,13]). As the *cis* isomer is isomerised to the *trans* isomer, it may also result in a migration of the double bond throughout the molecule. Thus with increasing depth in the sediments, there exist two potential biogeochemical markers based on monounsaturated fatty acids, the ratio of *cis*/*trans* and the position of the double bond.

This work was supported by the National Sea Grant Program. We thank Dr Chris Brown for the infrared analyses and Dr Peter Rogerson and Curt Norwood for the GC–MS analyses.

EDWARD S. VAN VLEET
JAMES G. QUINN

Graduate School of Oceanography,
University of Rhode Island,
Kingston, Rhode Island 02881

Received February 5, accepted May 18, 1976.

1 Farrington, J. W., and Quinn, J. G , *Geochim cosmochim Acta*, 35, 735–741 (1971).
2 Farrington, J. W , and Quinn, J. G , *Nature*, 230, 67–69 (1971).
3 Farrington, J. W., and Quinn, J. G., *Geochim. cosmochim. Acta*, 37, 259–268 (1973).
4 Johnson, R. W., and Calder, J. A., *Geochim cosmochim Acta*, 37, 1943–1955 (1973).
5 Brown, L. H , and Swidler, R , *US Pat.* 2,065,248, *Nov.* 20, 1962; *Chem. Abstr.* 58, 11221F (1963).
6 Morris, L J., in *Metabolism and Physiological Significance of Lipids* (edit. by Dawson, M. C , and Rhodes, D. N.) (Wiley, New York, 1963).
7 Cubero, J. M , and Mangold, H. K., *Microchem J.*, 9, 227–236 (1965).
8 McNair, H M., and Bonelli, E. J., *Basic Gas Chromatography* (Varian Aerograph, Walnut Creek, 1968).
9 McCloskey, J. A., in *Topics in Lipid Chemistry* (edit. by Gunstone, F.D.) (Wiley, New York, 1970).
10 Silverstein, R. M , Bassler, G. C , and Morrill, T. C , *Spectrometric Identification of Organic Compounds* (Wiley, New York, 1974)
11 Downing, D. T., and Greene, R. S , *Lipids*, 3, 96–100 (1968).
12 White, A., Handler, P., and Smith, E L., *Principles of Biochemistry* (McGraw-Hill, New York, 1968)
13 Swern, D., and Scanlan, J. T., *Biochem. Prep.*, 3, 119–120 (1953)

Evidence for short term atmospheric ^{14}C variations about 4,000 yr BP

IT is well established from radiocarbon measurement of tree rings of known age that the natural ^{14}C level in the Earth's atmosphere has undergone a gradual change of more than 10% over the past 7,000 yr (see, for example, ref. 1). During this time there have probably also been periods of irregular fluctuation spanning a few hundred years (the so-called Suess 'wiggles'[2]). The existence, in addition to these effects, of substantial shorter term (~ 10–20 yr) variations possibly correlated with solar activity is less certain. Farmer and Baxter (ref. 3) found ^{14}C variations of up to 3% in 10 yr (equivalent to an age error of ±120 yr) over a consecutive sequence of 37 single tree rings taken from mid-nineteenth century wood grown in the Forest of Dean, England; but comparative measurements they made of twentieth century New Zealand wood were inconclusive. Twentieth century wood from Trondheim, Norway, showed a possible 0.6% variation[4], and twentieth century North American wood showed about 0.3% (ref. 5).

We present here the results of radiocarbon measurements of Red Deer antlers obtained from recent excavations of Neolithic flint mines at Grime's Graves, Norfolk. When taken with the archaeological evidence these results indicate that short term variations similar to those found in wood from the Forest of Dean may also have occurred at an earlier period.

During the later Neolithic in Britain (~2,000 yr b.c. on the basis of radiocarbon dating) flint was mined on a large scale at Grime's Graves. Shafts, typically about 13 m deep and 3–5 m in diameter, were sunk through superficial deposits into the Upper Cretaceous Middle Chalk to reach a more or less continuous 20-cm layer of tabular flint. At the base of the shafts 4–7 horizontal galleries ~ 75 cm–1.5 m high, 3–5 m wide and 5–10 m in length were cut. The antlers that were used for the radiocarbon measurements were used by the miners as levers or 'picks' (Fig. 1) and were found in large numbers amongst the chalk rubble filling the galleries (chalk waste from new galleries

Table 1 Radiocarbon dates for antlers from pit 15

Age estimate (date ±s.d.)*	Δ‰†	Standard deviation of Δ	δ^{13}C(‰)	Lab. No.
1,786±58	−12.7	4.6	−24 80	(BM-980)
1,870±46	− 6.2	3.6	−24.99	(BM-979)
1,877±45	− 5 6	3.5	−24.16	(BM-973)
1,899±44	− 3.9	3.4	−23.03	(BM-976)
1,915±44	− 2.7	3.4	−25.00	(BM-978)
1,918±56	− 2 5	4.3	−23.32	(BM-1001)
1,932±45	− 1.4	3.5	−21.16	(BM-1002)
1,937±47	− 1.0	3.6	−24 13	(BM-974)
1,940±42	− 0.8	3.2	−23.65	(BM-996)
1,990±41	+ 3.1	3.1	−24.10	(BM-975)
1,999±42	+ 3.7	3.2	−22.46	(BM-1003)
2,010±56	+ 4.6	4 3	−24.87	(BM-997)
2,042±45	+ 7.0	3.4	−23 00	(BM-998)
2,065±61	+ 8.7	4 6	−24.53	(BM-977)
2,072±57	+ 9.3	4 3	−23.25	(BM-1000)

*Dates, expressed in yr b c. (5,570-yr half life), have been corrected for isotopic fractionation (δ^{13}C) relative to the PDB standard. The s.d. was derived from about 15 replicate measurements of each sample (totalling > 10^4 counts).

†Δ values[10] have been calculated from a mean age of 1,950 yr b.c. See Fig. 2 for the general distribution of these samples within the galleries of pit 15.

was back filled into those from which flint had already been extracted, sealing discarded antlers in position). The antlers were preserved in an environment entirely free from contamination by more recent organic material. To eliminate the possibility of exchange with more ancient carbon only the protein matrix remaining after complete demineralisation with dilute hydrochloric acid was used for the radiocarbon measurements.

Table 1 lists the results of radiocarbon measurements (using the liquid scintillation counting method[6]) on antlers from one of the excavated pit groups (pit 15) originally made to obtain a series of archaeological dates for the mining activity. The measured ages are distributed over a range of some 300 radiocarbon years, with a mean value of 1,950 yr b.c. and a standard deviation for the distribution as a whole of 79 yr. This value is considerably larger than the average standard deviation for the individual age estimates (47 yr). Thus, it is very unlikely (at the 99% confidence level) that each of the samples measured has the same ^{14}C concentration. The data also show a tendency to cluster into an early group (older than 1,990 yr b.c.) and a late group (younger than 1,940 yr b.c.; with one possible outlier at 1,786 yr b.c.) which is related to the find positions of the antlers in the galleries (see Fig. 2). If that were because pit 15 was worked at separate periods the time spread needed to satisfy the data would be of the order of 120 yr, whereas all the available evidence indicates that this pit was actually worked for a single short period which probably did not exceed 10 yr, and may have been much less. One estimate[7] has suggested that one pit could have been fully exploited in six months. On this basis a reasonable estimate for the exploitation of the entire deep mining area at Grime's Graves (some 400 pits) would be less than 200 yr as groups of adjacent shafts were most probably open contemporaneously.

In support of the idea of rapid exploitation, excavated shafts show little trace of weathering implying that they were open for a short time and were then rapidly infilled artificially with the massive quantities of spoil resulting from the digging of new shafts nearby. Comparison with weathering evidence obtained from studies of artificial earthworks[8,9] suggests a maximum of 5–10 yr as a cautious overestimate of the length of time for which a shaft was open. Taken altogether this means that the galleries of any one excavated pit complex, whether they radiated from the central pit or from the shafts surrounding it, would most probably all have been cut within a decade at most and the abandoned antlers sealed in place within that time.

Therefore, we must assume that the variation found is attributable to an effect other than real age differences, and is inherent either in the measurement procedures used in our laboratory or in the samples themselves. Taking the first alternative, the samples were measured in small groups interspersed with measurements of other totally unrelated samples, over a period during which our well tried monitoring procedures revealed no abnormalities in the behaviour of the counting system, and we can see no reason to doubt the reliability of the results.

We therefore propose that the variations are most probably attributable to an effect inherent in the samples. Antlers grow and are shed each season, and since they would not be suitable for use as tools unless collected when freshly shed, those accumulated in any one pit complex must form a physical assemblage of short-lived material of a restricted age range. From the number of antlers found (over 70 in pit 15) it is evident also that they were regarded as expendable and were casually discarded when blunted or broken. It is reasonable to assume, therefore, that the ^{14}C activity of the antlers found in a particular gallery closely reflects the atmospheric activity in the summer before that gallery was mined. It is worth noting here that the antlers in the lower left hand corner of Fig. 2 all had a similar activity. The range of ^{14}C activity observed in the antlers from pit 15 as a whole is much larger than can be accounted for unless there were marked year-to-year changes in atmospheric ^{14}C activity. Our results would require a minimum atmospheric ^{14}C variation of the order of 2% over a period of 10 yr or less. In the light of previous findings (refs 3–5) that is not implausible, although the exact cause of the variations remains obscure.

Fig. 1 Deer antler pick.

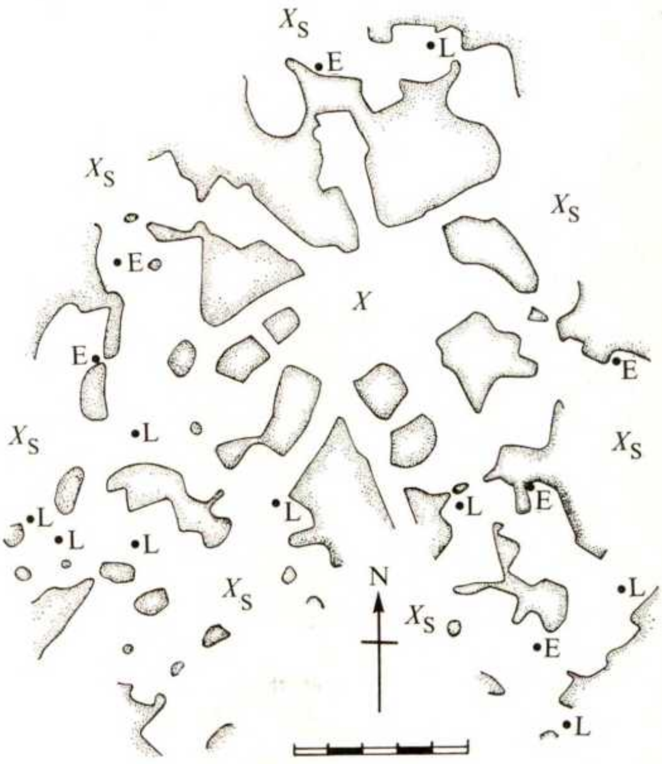

Fig. 2 Diagrammatic plan of the galleries of pit 15 at Grime's Graves, showing original position of each sample. E, L, indicate whether the radiocarbon age estimate obtained falls early or late in the sequence (see text and Table 1). ×, Shaft of pit 15; x_S, approximate positions of surrounding shafts. Scale in metres.

We recognise that our interpretation of these measurements must remain an hypothesis at present but the alternative explanation that the pit was in use over a 120-yr period is contrary to the archaeological evidence. Finally, the stable isotope values (δ^{13}C, Table 1) do not support the possibility that the observed ^{14}C variations are attributable to dietary factors affecting the deer. Clearly, more work is necessary, and we hope to substantiate our findings by excavating further material from a different pit at Grime's Graves during the coming season.

Our preliminary conclusion is that, although differing fundamentally from tree rings (where either the absolute or relative age is known initially) the special circumstances of the physical association of the antlers provides direct corroborative evidence for the kind of short term ^{14}C variation previously observed in recent tree rings.

More generally, we suggest that although knowledge of the ultimate resolution that radiocarbon dating can achieve is still

Pure Chemistry Library
SCIENCE COLLEGE
92 Upper Circular Road
CALCUTTA

inexact, all such assemblages of ancient short-lived material should be regarded as archival stores of geochemical data of great potential value.

RICHARD BURLEIGH
ANDREW HEWSON

Research Laboratory,
The British Museum,
London WC1B 3DG, UK

Received December 18, 1975; accepted May 27, 1976.

[1] Rafter, T. A., and Grant-Taylor, T. (eds), *Proc. 8th int. Radiocarbon Dating Conf., New Zealand*, (Royal Society of New Zealand, Wellington, 1972).
[2] Suess, H. E., in *Radiocarbon Variations and Absolute Chronology* (*Nobel Symposium* 12), (edit. by Olsson, I. U.), 303–311 (Wiley, New York, 1970).
[3] Farmer, J. G., and Baxter, M. S., in *Proc. 8th int. Radiocarbon Dating Conf.* (edit. by Rafter, T. A., and Grant-Taylor, T.), 75–85 (Royal Society of New Zealand, Wellington, 1972).
[4] Lerman, J. C., in *Radiocarbon Variations and Absolute Chronology* (*Nobel Symposium* 12), (edit. by Olsson, I. U.), 609–610 (Wiley, New York, 1970).
[5] Damon, P. E., Long, A., and Wallick, E. I., *Earth planet. Sci. Lett.*, **20**, 300–306 (1973).
[6] Burleigh, R., in *Liquid Scintillation Counting*, **2** (edit. by Crook, M. A., Johnson, P., and Scales, B.), 139–146 (Heyden and Son, London, 1972).
[7] Clark, J. G. D., *Prehistoric Europe; the Economic Basis*, 179–180 (Methuen, London, 1952).
[8] Jewell, P. A., and Dimbleby, G. W. (eds), *Proc. prehist. Soc.*, **32**, 313–342 (1966).
[9] Evans, J. G., and Limbrey, S. (eds), *Proc. prehist. Soc.*, **40**, 170–202 (1974).
[10] Broecker, W. S., and Olson, E. A., *Radiocarbon*, **3**, 176 (1961).

Lead isotope studies of metal sources for ancient Nigerian 'bronzes'

INTEREST in the composition of Nigerian 'bronzes' began in 1897, the year of the British punitive expedition to the city of Benin, when Nigerian metal art was brought to the attention of the western world as a spoil of war. In spite of the dissemination of much of this art to museums, and the subsequent focus of research, important questions concerning the chronological ordering of the pieces and relationships among forms and iconographies remain unanswered.

Elemental analyses of a number of these 'bronzes' (see refs 1–7) reveal that they are actually copper alloys with varying amounts of zinc, lead, tin and other metals. Though patterns of elemental composition can be discerned, statistically well defined measurements are not easily accomplished[8] and interpretation of the patterns is difficult.

Since the lead content of most pieces is appreciable ($\geq 1\%$–12%; see Table 1), enough, in fact, to suggest that its addition may have been intentional, we have conducted lead isotope analyses. As each lead ore deposit has a set of characteristic ratios among the isotopes, source distinctions can often be clearly drawn. Small samples in the tens of milligram range have been collected by scraping from approximately 180 'bronzes' from various museums in Nigeria, Europe and the United States. Analyses (see ref. 9) to determine lead isotope ratios have been made of samples from 17 of the more important 'bronzes' (Table 1 and Fig. 1). Only two of the three independent ratios are illustrated in Fig. 1, but all three ratios have been examined with interactive, three-dimensional computer graphics, and compared with isotopic ratios from known lead sources.

The lower panel of Fig. 1 shows a surprisingly strong clustering of the isotopic ratios. All of the Benin pieces have virtually the same isotopic ratios, in spite of a speculated range of production dates spanning approximately from the fifteenth to the nineteenth century. In this same cluster, which we identify as Benin +, pieces identified as 'Owo' (Table 1, *B*), 'Udo' (*J*) and 'Lower Niger' (*A*, *G*, *H* and *M*) are also found. In contrast, the two pieces excavated at Igbo–Ukwu (*P* and *Q*), for which there is evidence of a ninth century date[2] (which has, however, been contested[10]), show quite different values for the isotopic ratios. The single piece studied from Ife(*O*), considered by some[11] to be a cultural forerunner of Benin (and identified in Benin oral tradition as the source of Benin metal working knowledge[12]) has intermediate values for the two isotopic ratios shown in Fig. 1. One piece, the 'Lower Niger' ram's head pectoral (*H*), has two ratios falling in the Benin + cluster and one ratio resembling the Igbo–Ukwu pieces.

Three major conclusions can be drawn. First, the similarity of the isotopic ratios for the Benin + group provides evidence for a single source of lead for the entire time span and variety of locations represented by that group. (The 'Lower Niger' pectoral is a possible exception.) It is unlikely that lead from the Benin + group is a mixture from isotopically different sources since the mixing ratio would have to be nearly constant for all the pieces.

Second, support is lent to the hypothesis that Igbo–Ukwu, Ife and Benin were indeed separate traditions.

Third, the great majority of lead deposits in use today are ruled out as sources, as will be discussed elsewhere.

Several questions are raised, however:

- Why is there such a constancy of lead source throughout the Benin + group in the light of shifting trade patterns within Africa and with Europe.
- What is the nature of the apparent link between the makers of the Benin, 'Udo', 'Owo' and the 'Lower Niger' pieces?

Table 1 Lead isotope ratios in Nigerian 'bronzes'

		$\frac{^{206}\text{Pb}}{^{204}\text{Pb}}$	$\frac{^{206}\text{Pb}}{^{207}\text{Pb}}$	$\frac{^{206}\text{Pb}}{^{208}\text{Pb}}$
A	'Lower Niger' (NML 72.16.26)* Igala bell-head	18.41	1.1705	0.4774
B	'Owo' (Benin?) (I 65.4.1)† Stool	18.41	1.1726	0.4774
C	'Jebba' (NML exhibit) (0.80% Pb; ref. 11) Bowman	18.42	1.1740	0.4785
D	Benin (BM 1903.10-22.3)‡ Late Period head	18.47	1.1739	0.4786
E	Benin (BM 1963.Af9.1) Early Period head	18.49	1.1757	0.4780
F	Benin (BM 97.10-11.1) Early Period head of Queen Mother	18.49	1.1756	0.4780
G	'Lower Niger' (BM 1952.Af11.1) Huntsman	18.50	1.1758	0.4788
H	'Lower Niger' (BM 1930.4-23.1) Ram's head pectoral	18.47	1.1770	0.4839
I	Benin (BM 1949.Af46.156) Musician	18.48	1.1763	0.4772
J	'Udo-style' (Benin) (BM 1948.Af9.1) Head	18.43	1.1759	0.4797
K	Benin (BM 98.1-15.32) Plaque	18.43	1.1778	0.4789
L	Benin (BM 98.1-15.34) Plaque by Master of the Circled Cross	18.43	1.1771	0.4792
M	'Lower Niger' (BM 1956.Af27.224) Head	18.41	1.1771	0.4799
N	Benin (BM 97.10-11.1) Early Period head of Queen Mother	18.39	1.1773	0.4788
O	Ife (BM 1939. Af34.1) (11.4% Pb; ref. 3) Head	18.51	1.1881	0.4789
P	Igbo–Ukwu (NML 39.1.13) (6.4% Pb; ref. 2) Ritual vessel in shape of shell	18.75	1.1912	0.4822
Q	Igbo–Ukwu (NML 39.1.2) (4.5%, 9.8% Pb; ref. 2) Bowl	18.90	1.1986	0.4838
	Probable errors	±0.06	±0.001	±0.001

*Nigerian National Museum Lagos.
†University of Ife, Institute of African Studies.
‡British Museum, London.

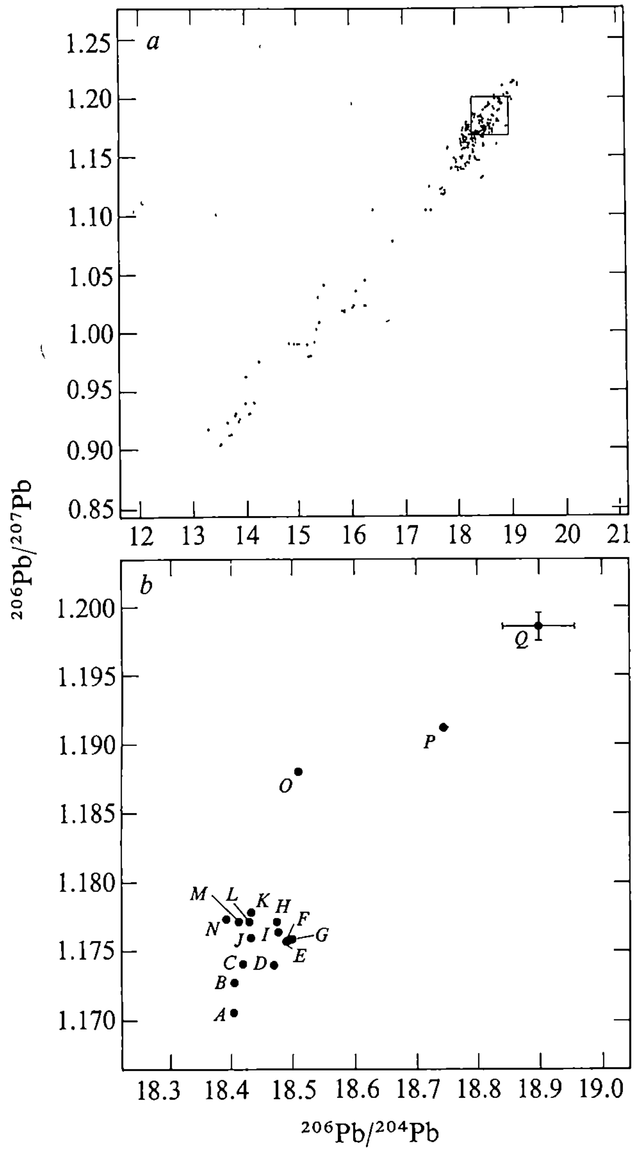

Fig. 1 *a*, Isotopic ratio distribution for geological lead samples from Africa and Europe from the Tables of refs 13–15 (small box corresponds to range shown in *b*), *b*, lead isotope ratios for Nigerian 'bronze' objects listed in Table 1 (probable errors for all measurements are as shown for object *Q*). *A–Q*, Objects listed in Table 1.

- Could the Ife piece be a mixture of the sources used by the Igbo–Ukwu culture which may have preceded it, and the Benin culture which may have followed it?
- What were the actual sources of the lead and the patterns of its trade? Were the sources local (Nigerian) or were the raw materials brought from elsewhere in Africa (perhaps on trans-Saharan trade routes) or did they arrive from Europe?

Work is continuing to attempt to answer some of these questions.

Support by the Chancellor's Club, the UCSD Foundation, the Project for Art/Science Studies, the Samuel H. Kress Foundation, the receipt of a University of California President's Undergraduate Fellowship, the help of the museums cited in Table 1, the use of computer systems supported by the NSF and the NIH, programming by Nathan Meyers, and helpful discussions with W. Fagg, D. Fraser, T. Shaw and F. Willett are acknowledged.

CANDICE L. GOUCHER
Departments of Chemistry and Visual Arts,
JEHANNE H. TEILHET
Department of Visual Arts,
KENT R. WILSON
Department of Chemistry,
TSAIHWA J. CHOW
Scripps Institution of Oceanography,
University of California, San Diego
La Jolla, California 92093

Received February 26, accepted May 28, 1976.

[1] Shaw, T., *W. Afr. J. Archaeol.*, 3, 233 (1973)
[2] Shaw, T., *J Afr. Hist.*, 16, 503–517 (1975).
[3] Barker, H., *Man*, 65, 23–24 (1965)
[4] Giauque, R., in *Black Gods and Kings Yoruba Art at UCLA* (by Thompson, R F), appendix (University of California, Los Angeles, Museum and Laboratories of Ethnic Arts and Technologies, 1971).
[5] Werner, O., and Willett, F., *Archaeometry*, 17, 141–156 (1975).
[6] Werner, O , *Baessler-Archiv*, N. F. 18, 51–153 (1970)
[7] Fraser, D , *Afr. Arts*, 8, 30–35 (1975).
[8] Chase, W T , in *Archaeol Chem.* (edited by Beck, C. W.), 148–185 (Am Chem. Soc , Washington, DC, 1974).
[9] Chow, T., *Nature*, 225, 295–296 (1970)
[10] Lawal, B., *J Afr Hist* , 14, 1–8 (1973).
[11] Willett, F., *Afr. Forum*, 3, 28–34 (1968).
[12] Egharevba, J., *A Short History of Benin* (Ibadan University Press, Ibadan, 1960)
[13] Russell, R. D., and Farquar, R. M., *Lead Isotopes in Geology* (Interscience, New York, 1960).
[14] Rankama, K., *Progress in Lead Isotope Geology* (Interscience, New York, 1963).
[15] Doe, B. R., *Lead Isotopes* (Springer, Berlin, 1970).

Parental investment, mate desertion and a fallacy

TRIVERS[1] defines parental investment as "any investment by the parent in an individual offspring that increases the offspring's chance of surviving . . . at the cost of the parent's ability to invest in other offspring". He has cleverly used this definition to elucidate many outstanding problems in social ethology[1–3]. But one of his most appealing usages of it is fallacious.

He states[1]: "At any point in time the individual whose cumulative investment is exceeded by his partner's is theoretically tempted to desert". The context is that of a mated pair of birds, cooperating in the rearing of young. At various times during incubation the female has invested more in the offspring than the male, and the male is said to be tempted to desert. At other times the male's cumulative investment is higher, and the female is then said to be tempted to desert.

If true, this idea would have interesting consequences. A female, in danger of being deserted after copulation, might force a male to invest heavily in her offspring before they are conceived. The price of copulation might be a well built nest and plenty of courtship feeding. Even useless 'labours of love' might be imposed as a means of increasing the male's investment before copulation, and therefore of reducing his temptation to desert afterwards. The theory also neatly uses the difference in gamete size to explain why females make better parents than males. As Trivers says[1]: ". . . her initial very great investment commits her to additional investment more than the male's initial slight investment commits him".

The idea has been influential[4], and it appeals to economic intuition. A government which has invested heavily in, for example, a supersonic airliner, is understandably reluctant to abandon it, even when sober judgment of future prospects suggests that it should do so. Similarly, a popular argument against American withdrawal from the Vietnam war was a retrospective one: "We cannot allow those boys to have died in vain". Intuition says that previous investment commits one to future investment.

The fallacy can be demonstrated by analogy. Suppose a female has an orphaned baby brother, the same age as her own son. She has only enough food to keep one of the two infants alive. Which should she prefer? Intuition points to the son, but this is not necessarily correct. There are no genetic grounds for preferring either infant: the mother's relatedness[5] to both is the same, 0.5. A naive application of parental investment theory predicts that the female should prefer the son on the grounds that she has already invested heavily in him: she should not let all her earlier investment go to waste by preferring the brother, in whom she has invested nothing.

This argument is wrong for it misunderstands why quantity of previous investment is important. A child in whom more has already been invested should be preferred only because he is going to need less investment in the future. This means he can be fledged (or weaned) sooner, and the parent will therefore be free to invest in new children sooner. Our hypothetical female should prefer whichever of the two children has already had most invested in him, regardless of who did the investing, because his future life can be bought more cheaply.

We now return to the original quotation from Trivers. The father and mother have an equal genetic stake in each offspring. Either parent's reluctance to desert at any moment should be related to the quantity of investment still needed to bring the offspring to maturity. This quantity will be negatively related to the amount that has already been invested: it does not matter who did that investing. Trivers almost acknowledges this in another part of the same paper[1], when he suggests that it may pay either partner, even the one who has so far invested most, to desert. This forcible closure of options puts the deserted partner in "a cruel bind". But Trivers's characterisation of the cruel bind is misleading: ". . . the deserted partner . . . has invested so much that he loses considerably if he also deserts the young, even though, which should make no difference to him, the partner would lose even more". The true nature of the cruel bind is this. Regardless of who did the previous investing, the young have had so much poured into them that either partner alone has a good chance of rearing them. To desert after one's partner has deserted is to condemn the young to death; to desert first merely condemns one's partner to make the difficult decision. Genes for deserting first are favoured by natural selection, precisely because genes for deserting second are not. But in either case, the important quantity influencing the decision is quantity of future investment which will be required.

It is of course true that previous investment by a particular parent is relevant to how much he or she can invest in the future: this is the basis of Trivers's definition. But for each particular parent this is a lifetime's calculation: the amount invested in the current offspring is only a small part. There is thus no justification, other than sheer coincidence, for Trivers[1] to draw the cumulative investment curves of his male and female with the same starting baseline. A parent should value the life of a particular child as a function of the proportion that this child represents of his total future reproductive prospects. These future prospects will be negatively correlated with the total amount he has invested in his lifetime, but only negligibly with the amount he has invested in the current particular child.

Does the theory that female coyness might evolve as a means of forcing males to invest early, thereby reducing their temptation to desert later, survive our objection to its parent assumption? This depends on how the majority of females in the population behave. If the majority play the same coy game, desertion tactics will not pay a male: he commits himself to a period of prolonged and costly courtship with a new female before she will let him copulate. If conditions are such that it would pay females to renounce coy tactics, however, the optimal strategy for a male could well be different. This is one of those cases of conflict of interest where the best strategy depends on what others are doing. We therefore suggest that the appropriate conceptual tool is Maynard Smith's[6–8] "evolutionarily stable strategy" (ESS). The contest is "asymmetric"[8], the basis of the asymmetry being sex. We seek a stable combination of male and female strategies, for example, a ratio of 'coy' to 'fast' females which is stable against an equally stable ratio of 'faithful' to 'philanderer' males. Preliminary analysis[9] suggests that there are conditions in which a stable equilibrium, consisting largely of coy females and faithful males, could evolve. More work is required (J. Maynard Smith, unpublished), but the point we make is that these are the lines along which the thinking must be. We must not simply assume that the partner who has invested least in the current offspring is the one most tempted to desert.

The other suggested consequence of Trivers's theory which we have already mentioned was that the female's high initial investment commits her to continued high investment: thus viviparity, milk-secretion, highly developed maternal care, and so on. Once again, the idea is wrongly expressed. A female is 'committed' to future investment in a child, not because of how much she has already invested in that child, but because of the cost of finishing the task, in relation to how much she would have to invest in order to bring a new child up to the same age.

In any case, the idea of past commitments leading to future commitments had difficulties in explaining the high incidence of paternal care among teleost fish[10]. Instances among birds and mammals where the father plays the main parental role are extremely rare; in the teleosts they are commonplace. Why the difference? The following theory makes use of Trivers's "cruel bind" idea, referred to earlier.

Gametes dry up in air, so this has forced terrestrial animals to copulate rather than practise external fertilisation as many fish do. After copulation, the female is left physically in possession of the zygote and while it is still in her body she cannot desert it, but the male can. However fast she lays it, the male is still offered the first opportunity to desert, thereby closing the female's options and forcing her into Trivers's cruel bind. For the reasons already discussed, this tends to lead to the evolution of maternal care.

Fish are not similarly obliged to copulate since there is no danger of their gametes drying up. In such externally fertilising species there is no automatic sense in which the female is left in possession, allowing the male to make his escape. Either sex might thus use the quick-desertion strategy. But there is a possible reason why the male might be more vulnerable to being left 'holding the baby'. Whichever partner spawns first is likely to be one jump ahead, but there is danger in spawning too early; the partner may not be ready. Sperm being lighter than eggs, tend to diffuse faster and so males have more to lose from premature spawning than females. Females can therefore afford to spawn earlier than males, putting them in a strong position to leave the male in possession of the newly conceived zygotes, forcing him into Trivers's cruel bind. This explains the widespread evolution of paternal care in fish. A comparative analysis of the incidence among teleosts[10] of external fertilisation against intromission, in relation to paternal against maternal care, might be rewarding.

In conclusion, a parent 'deciding' whether to desert a child should ask the following questions. How closely related[5] is this child to me? How likely is it to survive if I do, and if I do not, desert it? What proportion of my total future reproductive potential does this child represent? How much would it cost me to make a new child equivalent to this one? The parent should ignore its own previous investment in the particular child, except in so far as it affects the answers to these questions. Trivers is largely right, but partly for the wrong reasons.

We thank Dr. Robert L. Trivers for accepting our criticism and encouraging us to publish it.

R. DAWKINS
T. R. CARLISLE

Department of Zoology,
University of Oxford,
South Parks Road,
Oxford OX1 3PS, UK

Received May 12; accepted May 24, 1976

[1] Trivers, R. L., in *Sexual Selection and the Descent of Man* (edit. by B. Campbell) (Aldine, Chicago, 1972).
[2] Trivers, R L , *Am Zool.*, 14, 249–264 (1974).
[3] Trivers, R. L., and Hare, H., *Science*, 191, 249–263 (1976)
[4] Wilson, E O., *Sociobiology the New Synthesis* (Harvard, 1975).

[5] Hamilton, W. D., *J. theor. Biol.*, 7, 1–52 (1964)
[6] Maynard Smith, J , *On Evolution* (Edinburgh University Press, Edinburgh, 1972).
[7] Maynard Smith, J., and Price, G R , *Nature*, 246, 15–18 (1973).
[8] Maynard Smith, J., and Parker, G A., *Anim. Behav.*, 24, 159–175 (1976)
[9] Dawkins, R., *The Selfish Gene* (Oxford University Press, in the press).
[10] Breder, C. M , and Rosen, D E., *Modes of Reproduction in Fishes* (Natural History Press, New York, 1966)

Nitrate reductase as a possible predictive test of crop yield

NITROGEN supply is one of the key factors affecting the quality and quantity of crops. The amount of nitrogen fertiliser used is increasing year by year; on a worldwide basis we now use seven times the total fertiliser used in 1939 (ref. 1). In many developed countries the use of excess nitrogenous fertiliser is already causing environmental disturbance, especially in inland rivers and lakes, and represents a potential danger to drinking water supplies. By contrast, in much of the world crops are grown in conditions of nitrogen deficiency. Lacking in each situation is the availability of a reliable method for determining the amount of nitrogenous fertiliser, if any, which should be applied for optimal yield with minimum cost and environmental side effect, or for maximum use of limited resources. We have found that early season assays of nitrate reductase provide such a method.

Usually, whatever the source of nitrogen fertiliser, soil conditions ensure that nitrogen enters the plant predominantly as nitrate. The first and rate limiting step in nitrate utilisation is catalysed by the inducible enzyme, nitrate reductase[2] and Hageman's group in Illinois have demonstrated a correlation between nitrogen supply, nitrate reductase activity integrated throughout the year and grain yield in wheat[3] and maize[4] In these experiments, which were conducted in suboptimal nitrogen conditions, addition of further nitrogen, especially during the early part of the growing season, led to increases in nitrate reductase activity and in final grain yield.

We have examined the possibility of using nitrate reductase assays, early in the development of the crop, as a predictor of ultimate grain yield. In the first series of experiments wheat plants (Hope/Chinese Spring substitution line 7B) were grown in sand culture in controlled conditions in growth rooms, at a number of defined nitrate levels. Nitrate reductase activity in the uppermost fully expanded leaf (which was found to have the highest nitrate reductase activity (R. Hallam and G. C. Blackwood, unpublished results)) was measured weekly *in vitro* and the effect of nitrate concentration on nitrate reductase activity was compared with the effect on the final yield. The data are shown in Fig. 1. There is a good correlation between nitrate reductase and yield ($r = +0.90$, $n = 7$) at the earliest date of measurement, except at high (50 mM) nitrate concentrations. Similarly, there was a good correlation between grain yield and grain protein ($r = +0.969$, $n = 8$) indicating that increasing nitrogen supply had no effect on the protein content of the grain. Furthermore, there were no significant changes in amino acid composition. Thus early nitrate reductase activity provides a good estimate of ultimate grain yield.

The critical test of a predictive assay is its successful use on crops growing in the field To be sure of nitrogen deficient conditions for such a test, experiments were carried out (in collaboration with Dr. A. E. M. Hood of ICI's Jealott's Hill Research Station) on long standing nitrogen deficient plots at West Isley, Berkshire. Plots were treated with 0, 75, 112 or 150 kg ha^{-1} of nitrogen and measurements of nitrate reductase made early, in the middle and late in the growing season. The crop was spring barley var. Julia As before, samples for assay consisted of the uppermost fully expanded leaves and these were collected in the morning and stored at ambient temperature for several hours before nitrate reductase was determined by an *in vivo* assay in the laboratory, later in the day. Storage of intact leaves in this way did not significantly alter the enzyme activity. This is important if the test is to be of any practical use.

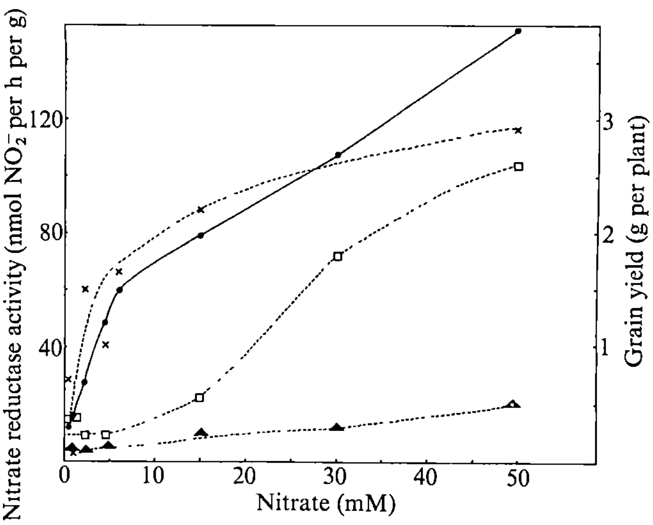

Fig. 1 Nitrate reductase activity as related to nitrate concentration in wheat (*Triticum aestivum* Hope/Chinese Spring, substitution line 7B). The enzyme was extracted from the first fully expanded leaf and assayed according to Filner[7] (×, 2 weeks; □, 3 weeks; ▲, 4 weeks after sowing). For comparison the final grain weight per plant is shown (●). Plants were grown in sand culture on Long Ashton growth medium[9] adjusted to give the desired NO_3^- concentration while maintaining constant ionic strength. Day length was 16 h; temperature 25/17 °C and light intensity 35 W m^{-2}.

The activities of nitrate reductase at the three times of measurements are compared with the final yield in Fig. 2. The data show that, on the earliest date of estimation (3–4 leaf stage), less than maximal nitrate reductase activity is a reliable predictor of suboptimal yield. This is in agreement with the data obtained in the growth room. Amino acid composition was unaffected by the treatments. Once again, there is an increase in yield obtainable at nitrogen levels in excess of those required for maximal nitrate reductase induction. As with the growth room experiments, however, the increase in yield at these high nitrogen levels is far less in relation to added nitrogen than that obtained at lower levels where yield is correlated with nitrate reductase activity.

Although the measurements reported here were carried out in the laboratory, the *in vivo* assay can easily be used in the field An alternative method which we also investigated,

Fig. 2 Nitrate reductase assayed on three dates (open columns) and final grain yield (hatched) in barley (*Hordeum vulgare*, var. Julia) plants. Enzyme activity was assayed *in vivo* by the method of Stewart *et al.*[8]. Standard errors: enzyme activity, ±0.155 µmol NO_3^- reduced per h per g; yield, ±238 kg ha^{-1}.

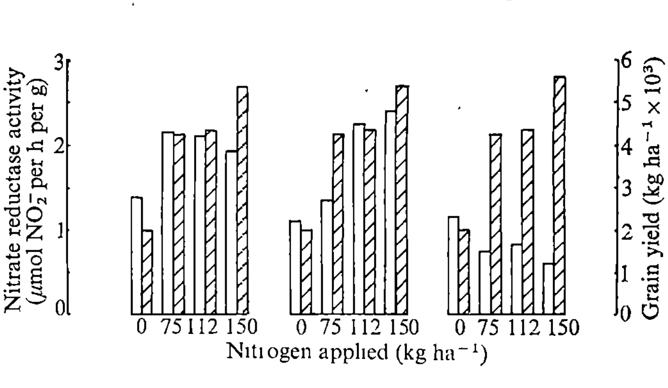

measurement of tissue nitrate, is far more complex and less reliable, and although it yielded similar results in our conditions, it is known that NO_3^- accumulation without related nitrate reduction can occur[5,6]. Although the nitrate reductase measurements do not correlate perfectly with final yield they provide a useful test for future yield except at the highest nitrogen levels and there is at present no remotely reliable alternative. Furthermore preliminary results of Hallam and Blackwood (unpublished) suggest that by careful selection of tissue for assay a correlation which is less time dependent can be obtained. The increasing cost and scarcity of natural resources, the important need to conserve our environment and a continuously increasing worldwide requirement for protein may well make such a test less than a luxury in the near future.

C. B. JOHNSON
W. J. WHITTINGTON
G. C. BLACKWOOD

University of Nottingham,
School of Agriculture,
Sutton Bonington,
Loughborough LE12 5RD, UK

Received March 16; accepted May 18, 1976.

[1] Cooke, G. W., *Fertilising for Maximum Yield* (Crosby Lockwood Staples, London, 1975).
[2] Schrader, L. E., Ritenour, G. L., Eilrich, G. L , and Hageman, R. H., *Pl Physiol., Lancaster*, 43, 930–940 (1968).
[3] Eilrich, G. L., and Hageman, R. H., *Crop Sci.*, 13, 59–66 (1973).
[4] Deckard, E. L., Lambert, R. J., and Hageman, R. H., *Crop Sci* , 13, 343–350 (1973).
[5] Heimer, Y. M., and Filner, P., *Biochim. biophys. Acta*, 215, 152–165 (1970).
[6] Heimer, Y. M., and Filner, P., *Biochim. biophys. Acta*, 230, 362–372 (1971)
[7] Filner, P., *Biochim. biophys. Acta.*, 118, 299–310 (1966).
[8] Stewart, G. R., Lee, J. A., and Orebamjo, T. O., *New Phytol.*, 72, 539–546 (1973).
[9] Hewitt, E. J., *Sand and Water Culture Methods used in the Study of Plant Nutrition* (Commonwealth Agricultural Bureaux, Farnham Royal, England, 1952).

Possible origin for insoluble organic (kerogen) debris in sediments from insoluble cell-wall materials of algae and bacteria

KEROGEN is an inert amorphous organic material insoluble in organic solvents, mineral acids, and bases[1]. In spite of its abundance, the precise molecular structure of this insoluble organic material has long remained an enigma. Structural determinations are complicated by the fact that the structure of any kerogen from different samples varies depending on the types of organic material originally responsible for its formation, and variations in the environmental conditions experienced during and after its formation. We have shown that kerogen-like material can be isolated from recently deposited algal mats. On oxidative degradation this material gives rise to products similar in nature to those obtained by degradation of ancient kerogens known to be of algal origin[2,3]. These results imply that kerogen-like precursors or proto-kerogens, are formed very rapidly on a geological time scale and are found in certain types of recent sediments rich in organic matter.

We have now carried out similar degradation studies on some pure cultures of blue-green and green algae and bacteria, to determine whether the types of degradation products produced would be comparable to those previously obtained from the degradation of ancient kerogens known to be of an algal origin. Microscopic examination of ancient shales, such as the Green River oil shale[4] or Tasmanian tasmanite[5], clearly shows that the bulk of the organic material in these shales is derived from blue-green or green algae, bacteria, fungi and other microorganisms. It is the organic material from the residues of these organisms which represents the starting point in the formation of algal kerogens, although major changes can occur in the structure of the residues after deposition in the sediments and the formation of kerogens. A study of the insoluble organic material from contemporary blue-green and green algae, and bacteria, however, should provide valuable comparative information on the origin and possible method of formation of algal kerogens.

The inertness of kerogen is testified to by the fact that it is the residue which remains after acid treatment of a rock or shale sample to remove minerals, such as carbonates and

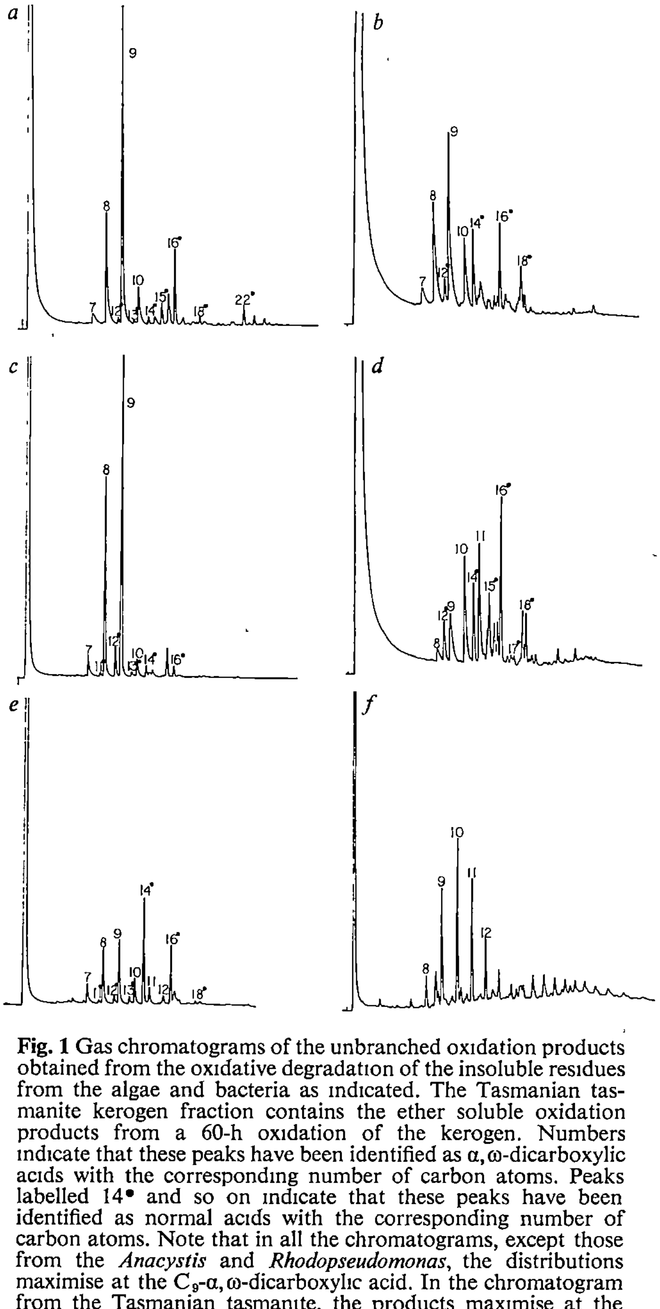

Fig. 1 Gas chromatograms of the unbranched oxidation products obtained from the oxidative degradation of the insoluble residues from the algae and bacteria as indicated. The Tasmanian tasmanite kerogen fraction contains the ether soluble oxidation products from a 60-h oxidation of the kerogen. Numbers indicate that these peaks have been identified as α,ω-dicarboxylic acids with the corresponding number of carbon atoms. Peaks labelled 14• and so on indicate that these peaks have been identified as normal acids with the corresponding number of carbon atoms. Note that in all the chromatograms, except those from the *Anacystis* and *Rhodopseudomonas*, the distributions maximise at the C_9-α,ω-dicarboxylic acid. In the chromatogram from the Tasmanian tasmanite, the products maximise at the C_{10}-α,ω-dicarboxylic acid. Note that the Tasmanian tasmanite chromatogram represents only the ether soluble degradation products; the normal acids, normally extracted with heptane, are not present in this chromatogram. Note, however, that the major degradation products from these organisms are basically the same as those from certain ancient kerogens although there are minor differences in the distributions. These chromatograms were obtained using a Varian 2700 gas chromatogram equipped with a FID detector. A 15-foot × 1/16-inch stainless steel column packed with Dexsil 300 on Gas Chrom Q was used for analysis in the following conditions: oven temperature 100–280 °C, 6° min^{-1}; injector temperature 280 °C; detector temperature 250 °C, and a helium flow rate of 15 ml min^{-1}. Computerised gas chromatography–mass spectroscopy analyses were carried out on a DuPont 491-2 mass spectrometer coupled with a Varian 204 GC Mass spectral data were acquired using a DuPont 21-904 data system. *a*, *Chlorella pyrenoidosa*; *b*, *Chlorobium*; *c*, *Phormidium luridium*; *d*, *Rhodopseudomonas spheroides*; *e*, *Anacystis nidulans*; *f*, Tasmanian tasmanite kerogen.

Table 1 Elemental analyses, yields and ratios of branched–unbranched products obtained from the insoluble organic residues of the organisms indicated

Organisms	Elemental analyses of residues						A*	B†	Ratio of branched–unbranched products
	%C	%H	%N	%O	%S	%Ash			
Algae									
Nostoc muscorum (blue-green)	45.4	6.1	14.0	28.6	0.7	5.2	2	16	13:1
Anacystis nidulans (blue-green)	48.9	7.1	13.2	29.6	0.5	0.7	2	45	5:1
Phormidium luridium (blue-green)	49.7	6.7	13.0	29.0	0.7	0.9	2	8	4:1
Chlorella pyrenoidosa (green)	51.4	6.8	13.2	27.7	0.7	0.2	2	7	5:2
Bacteria									
Rhodopseudomonas spheroides (photosynthetic)	52.5	6.9	11.3	28.4	0.8	0.1	1	6	2:1
Chlorobium (sulphur bacteria)	50.5	6.9	11.0	30.7	0.6	0.3	1	6	4:1

*Amount (g) of insoluble residues used in the oxidation reaction.

†Yields (mg) of products obtained on extraction of the oxidation reaction mixture with heptane and ethyl acetate

silicates, and exhaustive extraction of the remaining residue with organic solvents to remove any soluble lipid material[1]. Any humic material can also be removed from this residue by treatment with potassium hydroxide. Kerogen is the most abundant reservoir of organic carbon on the Earth, and as an example of its abundance it has been estimated that there are 3×10^{15} tons of kerogen, compared with 5×10^{12} tons of coal, in the Earth's crust[6].

Tissot *et al.* have characterised kerogens as originating either from algal debris, humic or plant debris, or from a mixture of both types of material. Of the two extremes, algal kerogens are generally considered to have an aliphatic-type structure and humic kerogens an aromatic structure[7]. Many chemical and physical degradation studies carried out on kerogens from ancient shales and sediments have yielded valuable, although limited, structural information. The reagents used in chemical degradation studies have included oxidative reagents such as potassium permanganate[8], chromic acid[9], and ozone[10], and reductive reagents such as lithium aluminium hydride[11]. Pyrolysis is another technique which has been used to degrade kerogens[12]. The majority of this work has been carried out on kerogens isolated from such ancient shales as the Green River oil shale[9] (Eocene, 50×10^6 yr) or Tasmanian tasmanite[5] (Permian, $220\text{–}275\times10^6$ yr), (see ref. 8 for additional examples of kerogens examined).

We have carried out degradation studies on the insoluble organic residues obtained from cultures of the algae and bacteria shown in Table 1. The conditions in which these cultures were prepared and the results of the soluble lipid analyses have been described previously[13,14]. Freeze-dried samples of algae and bacteria (Table 1) were treated as for the isolation of kerogen from an oil-shale sample. Each sample was exhaustively extracted with a mixture of toluene–methanol (1:1, using ultrasonication) and after 16 successive extractions the organic extracts were colourless, indicating removal of all readily soluble pigments and lipid material. (It was assumed that ultrasonication was sufficient to rupture the cells; however, the residues were not examined under the microscope either at this stage or after the HCl treatment. The possibility of some intracellular lipids remaining after extraction and hydrolysis cannot be completely excluded.) The residues were subsequently hydrolysed with 6 N HCl and, after centrifugation and removal of the aqueous layer, exhaustively extracted again with organic solvent. In the case of an oil shale, the kerogen is further concentrated by treatment with 48% HF and HNO_3 to remove silicates and pyrites, respectively[1]. This was unnecessary, however, in the case of these pure cultures for obvious reasons.

The resulting residues, after drying, were subjected to alkaline permanganate oxidation described previously[15]. The organic oxidation products were extracted from the reaction mixture with heptane and then ethyl acetate, and these extracts subsequently combined. After methylation of the extracts by BF_3/MeOH, they were fractionated into branched and unbranched fractions by urea adduction. These fractions were subsequently analysed by gas chromatography, and computerised–gas chromatography–mass spectrometry. Components in the various fractions were identified from their relative retention times, coinjection with standards where possible, interpretation of individual mass spectra, and comparison of mass spectra with authentic spectra wherever possible.

Table 1 shows the elemental analyses of the organic residues from the cultures, the yields and relative amounts of un-

Fig. 2 Gas chromatograms obtained of the branched oxidation products from *Phormidium luridium* (*a*) and *Chlorella pyrenoidosa* (*b*). Conditions as in Fig. 1. These two chromatograms illustrate the major features seen in the branched component fractions from all the samples. The C_{18}-ketone was the dominant product in all cases and the second major product was benzoic acid (as the methyl ester derivative used for gas chromatographic analysis). *Chlorella pyrenoidosa* was the exception, in that it was the only sample on degradation to give the isoprenoid acids (the label b-C_{16} indicates the peak corresponding to the C_{16}-isoprenoid acid) shown in this chromatogram.

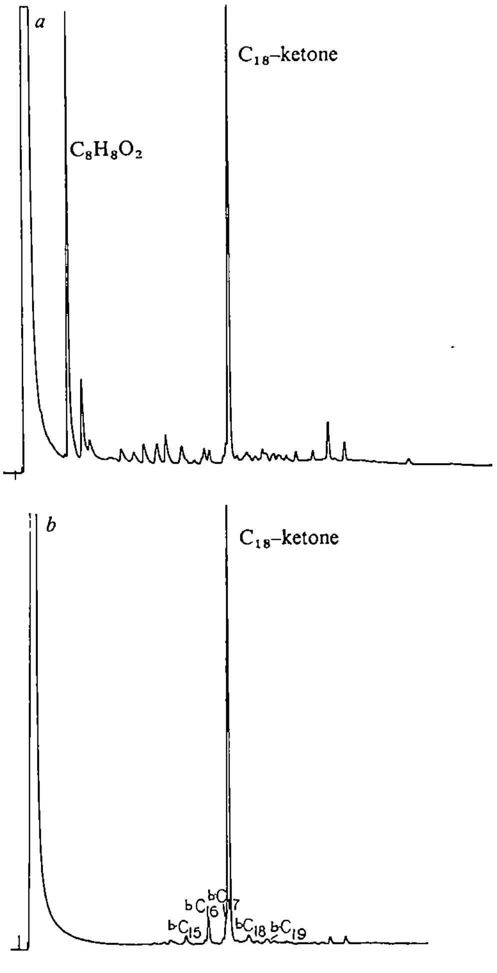

branched and branched components after oxidation and fractionation. The yields of oxidation products are noticeably low. This is not surprising and was indeed anticipated since it is known that the cell-wall material of blue-green algae consists mainly of protein and polysaccharides[16]. On oxidation this will give rise to water-soluble amino acids and carbohydrates which are removed in the aqueous layer during the extraction of oxidation products. These products were not examined.

Figures 1 and 2 show the chromatograms obtained from the analyses of the oxidation products of the insoluble residues and indicate the components which have been identified. The unbranched fractions were dominated by α,ω-dicarboxylic acids in the range C_6–C_{12} with maximum at C_9 and *n*-acids in the range C_{11}–C_{18} with a maximum at either C_{14}, C_{16} or C_{18} (Fig. 1). These acids were not found in the soluble lipid extracts (except for certain of the *n*-acids[13,14]) of the algae or bacteria and therefore do indeed represent degradation products of this insoluble cell debris. The branched fractions were less complex than the above mentioned fractions and in the majority of cases consisted of benzoic acid, a C_{18}-isoprenoidal ketone (6,10,14-trimethylpentadecan-2-one), and in one example, *Chlorella pyrenoidosa*, of C_{15}, C_{16}, C_{17}, C_{18} and C_{19} isoprenoidal acids in relatively small amounts. These degradation products in turn bear a remarkable resemblance to those obtained from the oxidative degradation of ancient kerogens known to be of algal origin—for example, kerogen from the Green River oil shale[9] or Tasmanian tasmanite[5]. The individual mixtures of products in this study are not anywhere near as complex as those from ancient kerogens. This is not surprising, however, when one realises the differences in age, thermal history, and environmental conditions that have been experienced by the ancient kerogens at the other end of the geological time scale.

There are several possible origins for these degradation products. First, they could be derived from intracellular chlorophyll, which is not removed during the extraction process. This would tend to support the theory of Oehler *et al.*[17] that intracellular chlorophyll becomes grafted on to cellular macromolecules, and with increasing maturation finally gives rise to kerogen. It would also support the theory of Burlingame and Simoneit[18], who proposed that the presence of the C_{18}-isoprenoid ketone in the degradation products of Green River shale kerogen indicated cross linking at the allyl rearrangement centre of phytol (derived from the phytyl side-chain of chlorophyll) during its incorporation into the kerogen moiety.

Second, it is possible that the degradation products are derived from cellular macromolecules which on oxidation give rise to the above mentioned products plus other water-soluble products not examined here. This would support the theory that it is this residual polymeric debris which is the source of the major building blocks of kerogen. With increasing time additional soluble lipid material can become condensed to this basic framework by irreversible chemical reactions, possibly catalysed by clay minerals in the local sedimentary environment. This mechanism plus condensation between the polymeric debris itself would give rise to the kerogen matrix as found in many sedimentary environments.

To extend our theory that the insoluble residues from algae and bacteria are the basic building blocks for kerogen, maturation experiments attempting to incorporate ^{14}C-labelled biolipids into these residues are underway It is anticipated that in simulated geological conditions, the degree of cross linking within the insoluble residues will increase and incorporation of the ^{14}C-biolipids will also occur.

This work was supported by NASA, the A. L. Day Fund, and in part by the US ERDA. We thank Mr S. Brown for assistance; and Dr B. R. Simoneit for a sample of the oxidative products of the Tasmanian tasmanite kerogen.

R. P. PHILP

Department of Chemistry,
University of California,
Berkeley, California 94720

M. CALVIN

Laboratory of Chemical Biodynamics,
University of California,
Berkeley, California 94720.

Received March 25; accepted May 11, 1976

[1] Robinson, W E., in *Organic Geochemistry Methods and Results* (edit by Eglinton, G., and Murphy, M.), 181–193 (Springer, Berlin, 1968)
[2] Philp, R. P., and Calvin, M., in *Proc second Int. Symp. environ. Biogeochem.* (edit. by Nriagu, J.), 131–148 (Ann Arbor, Michigan, 1976)
[3] Philp, R P , and Calvin, M., in *Advances in Organic Geochemistry, 1975* (in the press).
[4] Bradley, W. H , *Geol. Soc. Am. Bull.*, 84, 1121–1124 (1973)
[5] Simoneit, B R., and Burlingame, A L., *Geochim. cosmochim Acta*, 37, 595–610 (1973).
[6] Forsman, J P., in *Organic Geochemistry* (edit. by Breger, I. A.), 148–162 (Pergamon, Oxford, 1963).
[7] Tissot, B , Durand, B , Espitalie, J., and Combaz, A , *Am. Assoc. Petrol. Geol Bull.*, 58, 499–506 (1974).
[8] Djuricic, M. V., *et al* , in *Advances in Organic Geochemistry, 1971* (edit by von Gaertner, H R , and Wehner, H.), 305–321 (Pergamon, Oxford, 1972)
[9] Burlingame, A. L., and Simoneit, B. R., *Nature*, 222, 741–747 (1969).
[10] Van der Berg, M L J , de Leeuw, J W , and Schenck, P A , in *Advances in Organic Geochemistry, 1973* (edit by Tissot, B , and Bienner, F), 180–189 (Editions Technip, Paris, 1974).
[11] Lawlor, D. L., Fester, J I , and Robinson, W. E., *Fuel*, 42, 239–244 (1963).
[12] Gallegos, E. J , *Analyt Chem.*, 47, 1524–1528 (1975)
[13] Han, J , McCarthy, E. D , Van Hoeven, W., Calvin, M., and Bradley, W. H., *Proc. natn Acad Sci. U S.A.*, 59, 29–33 (1968)
[14] Han, J , McCarthy, E D., Calvin, M., and Benn, M. H , *J chem. Soc* , C, 2785–2791 (1968)
[15] Ogner, G., *Acta chem. scand.*, 27, 1601–1612 (1973).
[16] Dunn, J H., and Wolk, P. C., *J. Bact.*, 103, 153–158 (1970)
[17] Oehler, J. H , Aizenshtat, Z., and Schopf, J. W., *Am. Ass. petrol. Geol Bull.*, 58, 124–132 (1974)
[18] Burlingame, A. L , and Simoneit, B. R., in *Advances in Organic Geochemistry, 1973* (edit by Tissot, B., and Bienner, F.), 191–201 (Editions Technip, Paris, 1974).

Prepupal larval mosaics in *Drosophila melanogaster*

THE metamorphosis of insects provides a model system for the study of hormone action. In *Drosophila*, metamorphosis is initiated by the formation of a puparium with a rigid cuticle that becomes tanned early in the prepupal period. Subsequently many larval tissues degenerate and the imaginal tissues develop to produce the adult insect. These processes are initiated in *Drosophila* by the steroid moulting hormone, β-ecdysone[1]. We are interested in the mechanisms by which β-ecdysone elicits adult development. The recovery of mutants which cannot respond to the hormone would facilitate investigation into the nature of the action of β-ecdysone. We have isolated systematically a series of late larval and prepupal X-linked lethals (ref. 2 and unpublished results of I.K. *et al.*), about 15% of which are non-pupariating (*npr*) lethals in which metamorphosis is not initiated. We have investigated whether the *npr* condition is a result of the autonomous inability of the mutant target tissues to respond normally to β-ecdysone or rather is a stage-specific failure in the production of the hormone. Our results indicate that in most *npr* lethals the tissue cannot respond to the hormone. Futhermore, we estimate that there are 100–200 such lethals in the genome of *D. melanogaster*.

One way to investigate whether there is a failure in response to β-ecdysone or a loss of its synthesis for X-linked recessive lethals is to produce gynanders containing patches of male (X/O) tissue in which the recessive lethal is hemizygous (hence potentially expressed) and female (X/X) tissue in which the recessive gene is heterozygous (hence, phenotypically unexpressed). Production of such gynanders in *D melanogaster* is accomplished routinely by crossing ring-X males with females heterozygous for the lethal. In the progeny two types of females are produced; one type carrying the ring X and a lethal-bearing X chromosome, and a second type carrying the ring X and a non-lethal-bearing X (usually a balancer chromosome). During early nuclear divisions in the embryo the ring X chromosome is occasionally lost from some cells with the resultant production of an organism containing both male (X/O) and female (X/X) tissue. For progeny carrying the lethal one would predict that if the *npr* condition were autonomous there

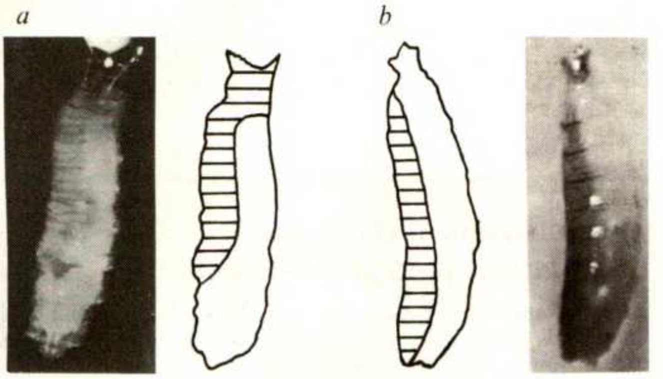

Fig. 1 Photographs and schematic diagrams of larval–prepupal mosaics; *l(1)d. norm.*–1*l*^{a}/*ring* (*l*)*2* (*b*) and *l*(*l*): *d. norm.*–*12*/*ring l*(*2*) (*a*). See ref. 3 and the legend to Fig. 2 for a description of genetic nomenclature and stocks. In the schematic diagrams the cross hatched regions represent tanned puparial tissue.

should be no adult gynanders produced, but instead developmentally arrested mosaics composed of prepupal (X/X) and larval (X/O) tissue. The latter condition would be identifiable readily by the presence of tanned puparial tissue sharply separated by distinct boundaries from white larval tissue.

Such larval-prepupal mosaics were obtained in all of six *npr* mutants investigated. Examples are shown (Fig. 1) involving two independently recovered *npr* lethals. There were sharp boundaries between the larval and the pupariated tissue. For three of the six mutants investigated there was good evidence that some of the mosaics resulted from gyander production. In one case, involving *l(1) d. norm.12*, the maroon-like marker had been added by recombination to the chromosome carrying the lethal. Since *ma-1* lacks aldehyde oxidase activity, male (X/O) tissue will be deficient in the enzyme activity and hemizygous for the lethal, but female (X/X) tissue will have aldehyde oxidase activity and be heterozygous for the lethal. Histochemical identification of the tissue distribution of the enzyme activity using Janning's method[4] revealed perfect correspondence between aldehyde oxidase negative and non-pupariating tissue as expected for male (X/O) tissue in a gynander. (Details of experiments using *ma-1* will be published elsewhere.) In a mosaic involving *l(1) d. norm.-1*^{a}, the anterior of the mosaic was larval, had yellow mouth hooks and thus could be identified as male (X/O) tissue because of the presence of the recessive *yellow* marker on the lethal-bearing X chromosome. The posterior, which had pupariated, contained ovaries, and thus was composed of female (X/X) tissue. In another case, involving *l(1) discless-1*, the larval region of the mosaic contained no imaginal disks while the pupariated region had normal imaginal disks. As a control, females carrying the ring X and a recessive X-linked lethal which causes death after puparium formation, *l(1) d. norm.-6*, failed to produce any larval-prepupal mosaics in contrast to the *npr* lethal *l(1) d. norm.-1*^{a} (Table 1). Adult gyanders of female sibs carrying a non-lethal X chromosome were found easily in both cases. Adult gynanders have not been found for any of the six *npr* mutants investigated. Nevertheless, because of the absence of appropriate markers, we lack evidence that some larval–prepupal mosaics are the result of gynander production for three of the six mutants investigated. Caution in interpretation is necessary because larval–prepupal intermediates can be produced by mistreating larvae (for example, by prolonged immersion in water). The results indicate, however, that 50% or more of X chromosome *npr* mutants involve autonomous defects in the target tissue.

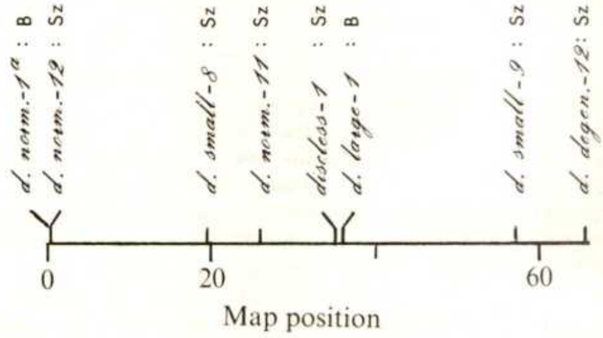

Fig. 2 Map positions of X chromosome *npr* mutants. The methods used for determining map positions are presented elsewhere (ref. 2 and unpublished results of I.K. *et al.*). Mutants isolated in Szeged are indicated by Sz; those isolated in Berkeley by B. The lethals are phenotypically described in terms of the condition of the imaginal disks. Mutant nomenclature: *l(1)*: lethal, first chromosome, has been omitted; *d.*: disk: *norm*: normal; *degen.*: degenerate.

Eight *npr* mutants have been mapped and assigned approximate map positions (Fig. 2). There are at least six (probably seven) loci involved. Based on map position and phenotypic similarity we conclude that two mutants, *l(1) d. norm.-12* and *l(1) d. norm.-1*^{a} are allelic and located slightly to the right of *yellow* (ref. 2 and unpublished results of I.K. *et al.*). Although *l(1) discless-1* and *l(1) d. large-1* map close to each other they are phenotypically very different and probably not allelic. From the above information, assuming that the induction of mutants follows a Poisson distribution, it is possible[5] to estimate the total number of *npr* genes. We calculate that the X chromosome contains about 20 npr genes and the whole genome of *D. melano-*

Table 1 Gynander recovery using two late-acting lethals

	Offspring						
	Males		Females				
			Binsn/ring X		Lethal/ring X		
Cross	Adult *Bin sn*	Adult lethal	Adult non-gynanders	Adult gynanders	Adult non-gynanders	Adult gynanders	Larval prepupal mosaics
npr–lethal; *ring* (*l*)*2*/ *Yy*$^{+}$♂♂ × *l*(*l*) *d. norm.*–*l*^{a}/*Binsn*♀♀	458	0	16	25	9	0	12
	% gynanders:		58% (25/41)			57% (12/21)	
Prepupal–lethal; *ing* (*l*)*2*/ *Yy*$^{+}$♂♂ × *l*(*l*) *d. norm.*–*6*/*Binsn* ♀♀	503	0	22	20	19	1	0
	% gynanders:		47% (20/42)			5%(1/20)	

For a description of genetic nomenclature and stocks see ref. 3 and the legend to Fig. 2. About 10 aged, virgin females were mated in vials with five males. Flies were transferred to fresh vials every 2 d for 2 weeks. Vials were examined twice daily from the emergence of the first offspring until no progeny or live larvae were found over 48 h. Stocks were maintained on standard *Drosophila* medium at 25 °C.

gaster about 100. A similar estimate can be obtained from the percentage of late acting lethals that are *npr* mutants. Of the late acting lethals on the X chromosome 17% (9/53) have the *npr* phenotype (ref. 2 and unpublished results of I.K. *et al.*). Shearn[5] estimates from studies on third chromosome lethals that there are about 900 genes in the *Drosophila* genome which cause late lethality. From this number we estimate that there are about 150 *npr* genes (17% of 900). Kiss and coworkers (unpublished) based on results involving late acting X chromosome lethals, estimate that there are about 750 late acting lethals in the *D. melanogaster* genome, about 125 of which will be *npr* lethals. Although these estimates are approximations, they all suggest that the total number of *npr* genes is small, that is 100–150. Thus, it should be possible to recover mutants of all such X-linked genes and probably of all those on the autosomes as well.

In cases where larval and prepupal mosaicism occurs, the presence of the two types of tissue together in the gynander indicates that the β-ecdysone titre has reached sufficient levels to initiate metamorphosis. Thus, in these cases the mutant tissue cannot respond normally to the hormonal stimulus. We estimate the total number of *npr* genes preventing a specific response of a target tissue to the hormonal stimulus to be 75 or more. But the bases of action of the mutants may be separable into at least three different classes, and all may not be involved in the response to β-ecdysone *per se*. In addition to the category of mutants in which functions necessary to produce a puparium are lost, one can imagine a category of mutants affecting the competence of the epidermal tissue to become programmed to respond to the hormone by puparium formation and a third category in which premature degeneration of the tissue precludes puparium formation. As *in vitro* test systems are available, involving larval target tissues (salivary glands[6], imaginal disks[7] and larval cuticle[8]), it should be possible to investigate the effects of the autonomous *npr* mutants at the cellular and molecular level and distinguish between the above possibilities.

The production of gynanders with both larval and prepupal tissues has implications for studies involving the recovery of adult gynanders. The inability to respond to β-ecdysone implicit in the autonomous *npr* condition is apparently not limited to the larval epidermis, but involves other larval tissues[2]. The maintenance of a substantial fraction of tissue in the juvenile form while another fraction proceeds into and through metamorphosis in all likelihood will result in the failure of eclosion of the adult fly. Thus, even if the effects of the lethal gene are limited to larval tissues, the recovery of adult gynanders might be rendered highly unlikely. Such a case is provided by *l(1) d. norm.-1*^{a} (Table 1) and also by *l(1) d. norm.-12* in which no gynander tissue has been found in carrier adult females (ring/lethal-bearing X) but in which mutant disks develop (albeit poorly) along with the host after transplantation into the haemocoel of a wild type larva[2].

This research was supported in part by a research grant from NIGMS and through the auspices of UNESCO.

ISTVAN KISS
GABOR BENCZE
ANDRAS FODOR
JANOS SZABAD

Institute of Genetics,
Biological Research Center,
Hungarian Academy of Science
Szeged, Hungary

JAMES W. FRISTROM

Department of Genetics,
University of California,
Berkeley, California 94720

Received January 30; accepted April 20, 1976.

[1] Borst, D., Bollenbacher, W., O'Connor, J., King, D., and Fristrom, J. *Devl Biol.*, **39**, 308–316 (1974).
[2] Stewart, M., Murphy, C., and Fristrom, J., *Devl Biol.*, **27**, 71–83 (1972).
[3] Lindsley, D. L., and Grell, E. H., *Carnegie Institute of Washington Publication* No. 627 (1968).
[4] Janning, W., *Wilhelm Roux Arch. Entw. Mech. Org.*, **174**, 313–332 (1974).
[5] Shearn, A., *Genetics*, **77**, 115–125 (1974).
[6] Ashburner, M., *Chromosoma*, **38**, 255–281 (1972).
[7] Fristrom, J., Logan, W., and Murphy, C., *Devl Biol.*, **39**, 308–316 (1974).
[8] Fain, M. J., and Riddiford, L. M., *Am. Zool.*, **13**, 1272 (1973).

Determination of cell shape by a cell surface protein component

CONSIDERABLE evidence derived from the study of animal cells cultured *in vitro* implicates the cell surface in the regulation of cell division and in the expression of the phenotypic state of the cell. Cell surface is a broad term used to indicate the lipid bilayer of the cytoplasmic membrane containing intrinsic (stably integrated) and peripheral (easily removable) protein constituents plus carbohydrate complexes[1–3]. There are indications that some of the intrinsic constituents are of fundamental importance in certain physiological processes such as ion transport and transport of metabolic precursors[4–8]. On the other hand, it is not known whether components that are more loosely bound to the cell surface play any specific role in cell physiology because no cellular function has so far been examined in relation to such components. We report here that determination of cell shape is affected by a cell surface protein component easily detachable from the cell exterior.

Secondary or tertiary mouse embryo fibroblasts (MEF) derived from the C57BL/6 strain were grown in Eagle's BHK medium supplemented with 5% foetal calf serum. A medium of the same composition and osmolarity as that of the culture medium, but containing no serum (serum-free medium, SFM), was used for washing and incubation during the experiments. Our first aim was to investigate whether any material could be removed from the cell surface without the aid of proteolytic enzymes or chelating agents. Cultures that had been washed

Fig. 1 *a*, Cells labelled with ^{14}C-amino acid mixture. *b*, Cells labelled with ^{3}H-D-glucosamine. Histograms on the left represent radioactivity associated with non-dialysable material from cultures 20 h after seeding; histograms on the right from cultures 72 h after seeding.

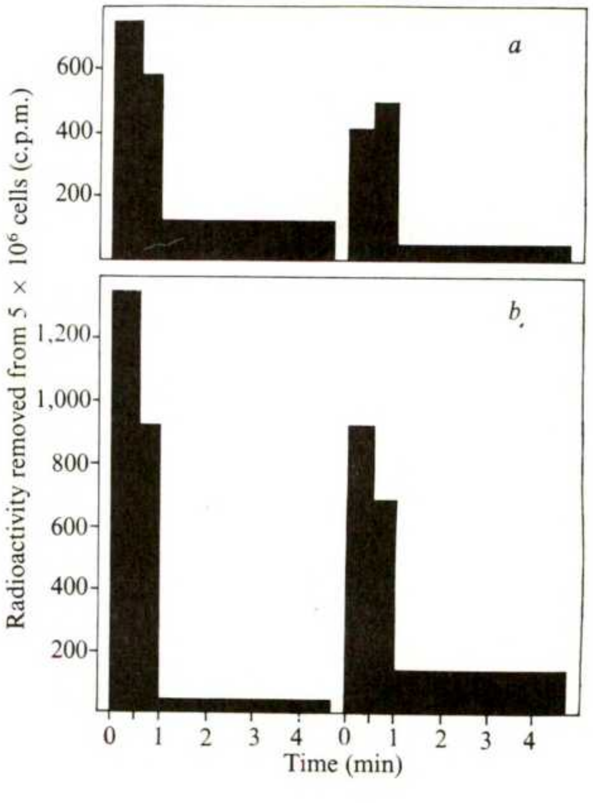

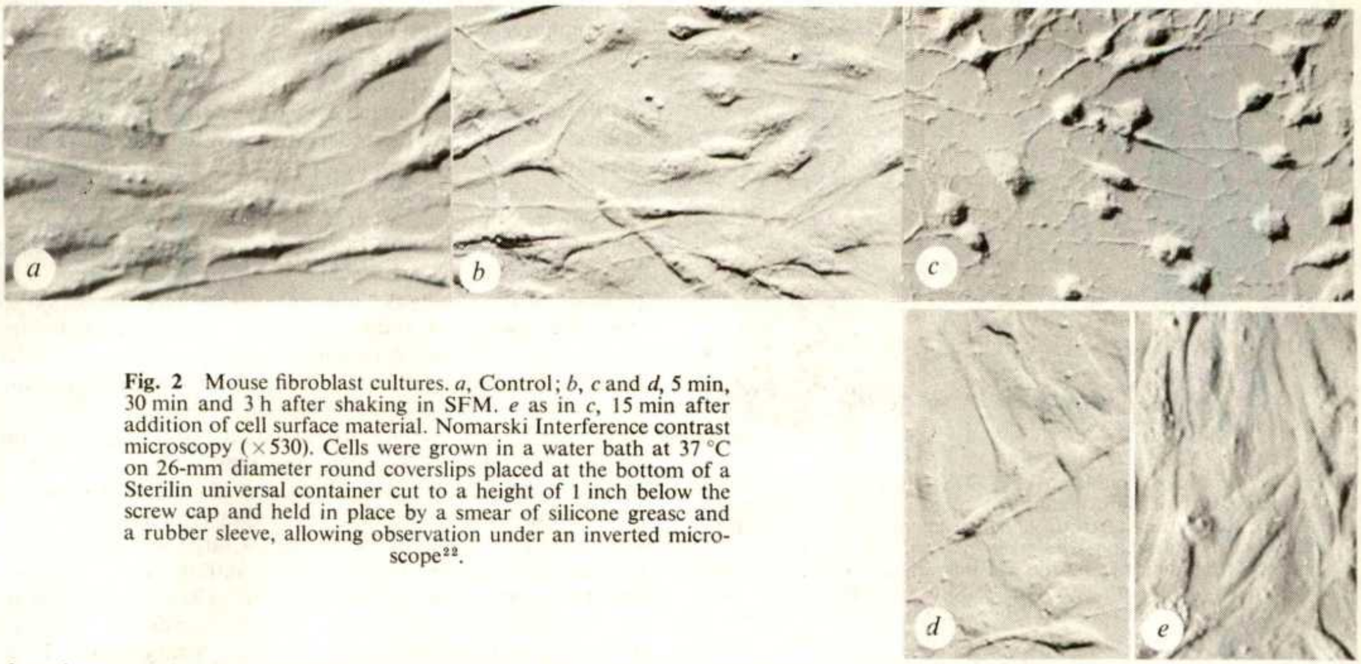

Fig. 2 Mouse fibroblast cultures. *a*, Control; *b*, *c* and *d*, 5 min, 30 min and 3 h after shaking in SFM. *e* as in *c*, 15 min after addition of cell surface material. Nomarski Interference contrast microscopy (×530). Cells were grown in a water bath at 37 °C on 26-mm diameter round coverslips placed at the bottom of a Sterilin universal container cut to a height of 1 inch below the screw cap and held in place by a smear of silicone grease and a rubber sleeve, allowing observation under an inverted microscope[22].

four times were incubated in SFM containing either ^{14}C-protein hydrolysate (50 mCi per matom C, 1 μCi ml^{-1}) or ^{3}H-D-glucosamine-HCl (3 Ci mmol^{-1}, 2.5 μCi ml^{-1}). After about 20 h the radioactive medium was removed, the cells were washed and fresh SFM, a quarter the original volume, was added. The cultures were then placed on a flat surface and submitted to horizontal shaking at 20 °C using a frequency of three excursions per second and an amplitude of 5 inches. The medium from each culture was collected at 30-s intervals, centrifuged at 2,000*g* for 10 min, dialysed in SFM and assessed for radioactivity. Figure 1 shows that both protein and carbohydrate containing macromolecules were freed easily, and that most of the radioactivity was removed with the pattern of a distinct entity within the first minute. A 3-h ^{51}Cr release assay[9] showed no difference between shaken and unshaken cultures, indicating that cell integrity had not been affected by the mechanical perturbation. In fact, the ease with which cellular material could be removed was demonstrated by gentler procedures. Simple SFM washings yielded variable but sizeable amounts of labelled components.

The most obvious and immediate parameter investigated in studies of cell behaviour is form. When returned to an incubator at 37 °C, cells that had been washed or shaken showed a degree of transient rounding. This could be reproduced with uniformity of response and with a consistent kinetic pattern if synchronised tertiary S phase fibroblasts were used and if the shaking procedure described above lasted for a standard period of 1 min. A reduction of the cell projected area and an increase of thickness was noticeable soon after incubation, and was followed by a progressively increasing rounding. At 20 min cells were markedly round with elongated cytoplasmic processes extending in thin ramifications. The rounded state was maintained for a short time, then, gradually, within about 3 h, the cells reverted to their original appearance. Figure 2 *a–d* shows some of the stages in the described sequence of events. Rounding did not occur nor could reflattening take place if the cells were left at or transferred to room temperature.

Among the factors that contribute to determination and maintenance of form are the architectural structures of the cell surface. It seems unlikely, however, when the phenomenon we describe is seen in the light of a cause–effect relationship, that constituents that are stably integrated in the surface membrane could have a primary (first in time) role in the initiation and modulation of the morphological changes as the principle of variation is implicit to the concept of modulation. Thus the induction of rounding that follows shaking in SFM is more likely to be a consequence of the removal of extrinsic factors required for the maintenance of cell shape and reversion to the flattened state to be due to the cell's ability to replace the removed components. To test this possibility we investigated whether the shaken material had any effect on cell morphology. The fraction removed from the cells after 1 min of shaking (Fig. 1) was concentrated by ultrafiltration through Amicon PM-10 membranes (10,000 molecular weight cutoff) to a protein content of 0.5 mg ml^{-1}. Dilutions of this preparation in SFM down to about 50 μg protein per ml prevented the induction of cell rounding when added immediately after shaking and caused rapid reflattening when added to rounded cells (Fig. 2*e*).

We used chromotographic separation to investigate whether this effect was due to the macromolecular complex as a whole or to any components in particular. Concentrated material (2 mg) was loaded on a column of Sephadex G-75 pre-equilibrated and eluted with SFM at 4 °C. Examination of the fractions

Fig. 3 Coomassie blue staining of 5% SDS–polyacrylamide gel electropherograms. *b*, Active fraction from Sephadex column; *a* and *c*, neighbouring fractions; *d*, unfractionated shaken material; *e*, immunoglobulin heavy and light chain (25,000 molecular weight bottom band); *f*, foetal calf serum. Arrow indicates band unique to active preparations. *a* to *c*, high contrast photography.

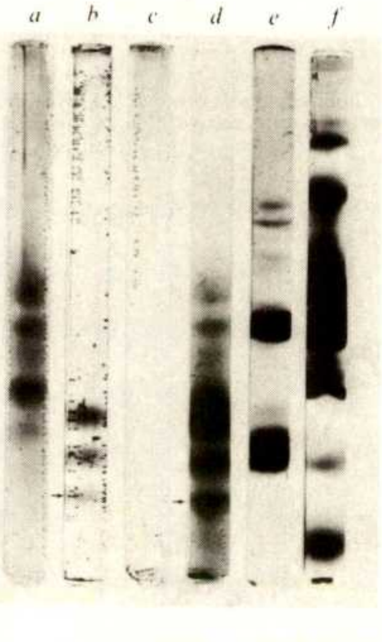

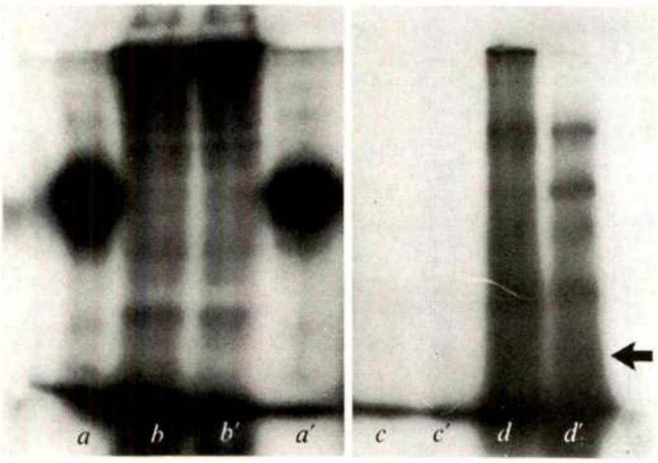

Fig. 4 Autoradiographs from 7.5% SDS polyacrylamide gel electropherograms of iodinated preparations run in duplicate. *c* and *c'*,; Active fraction from Sephadex column; *b* and *b'*, whole cell; *d* and *d'*, unfractionated shaken material; *a* and *a'*, foetal calf serum. Arrow indicates position of migration of corresponding band in the various preparations. No corresponding band was present in the serum.

showed that only one (no. 13; 20–25,000 expected molecular weight) had the protective activity detectable in the original material. The protein content of this fraction was about 10 μg ml^{-1} but a 1:2 dilution still retained activity. This fraction (no. 13) and the two neighbouring fractions (nos 12 and 14) were concentrated and examined by sodium dodecyl sulphate–polyacrylamide gel electrophoresis[10] in parallel with the original unfractioned material and with a sample of the foetal calf serum used for cultivating the cells. Comparison of the pattern of migration of the banded components after staining of proteins showed that only one band (< 25,000 molecular weight) was unique to those preparations able to maintain or reinduce the flattened state (Fig. 3). The cellular origin of this component was endorsed by the absence of a corresponding band in the serum. Staining of the gels by the periodic acid–Schiff method for carbohydrate[11] did not permit detection of the active component, indicating the possible absence of sugar residues in the protein molecule.

Although the procedure used clearly indicates that several cellular components were loosely attached to the cell exterior and could easily be removed, final identification of the active factor on the cell surface was sought by lactoperoxidase-catalysed iodination (^{125}I) of the intact cells, a technique used to label selectively membrane proteins exposed at the cell surface[12,13]. Parallel ^{125}I labelling of unfractionated material, of Sephadex fractions and of serum proteins was carried out by the chloramine-T method[14]. Lactoperoxidase iodination was done in monolayer cultures that had been washed three times in phosphate-buffered saline (PBS, containing Ca^{2+} and Mg^{2+}) to remove serum. After iodination the cells were washed twice in PBI (sodium iodide instead of chloride as in PBS) containing a protease inhibitor and then collected by scraping. Comparison of the autoradiograms after polyacrylamide slab gel electrophoresis showed a corresponding band in the active Sephadex fraction, the whole cell preparation and the concentrated material removed by shaking in SFM (Fig. 4). No correspondence was found with protein constituents of the iodinated serum. The presence of the common band and its relevance in relation to the effect exerted on morphology was corroborated by the results obtained from densitometric analysis (courtesy of Dr P. Gray, Imperial College, London) of autoradiographs from iodinated active and inactive preparations (Fig. 5).

This report describes an immediate relationship between the physiological state of the cell as expressed by shape and a protein component that originates from the cell surface where sizeable amounts can be removed without the aid of enzymes or chelating agents, as in the case of the large molecular weight surface glycoprotein found in untransformed mouse, hamster and chick cells[13,15–18]. We have evidence that the mechanism by which this component affects cell shape involves a transmembrane effect on the arrangement of the cell's cytokinetic structures, microfilaments in particular. Figure 6 shows that in the flattened state microfilaments close to the surface membrane have an orderly distribution which is modified to condensed patches near the surface when the rounded state is induced. We have found (unpublished work) that the constituent which affects cell shape is spontaneously released in the cell environment and that the extent and rate of this process is greater in quiescent cells. This indicates that the presence of this component within the surface and its con-

Table 1 Protection of cell rounding by shaken material from normal fibroblasts and from transformed cells

Cell type from which material derived	Cell type on which material tested MEF	3T3
Nil (SFM)	+	+
MEF	−	−
PVTT2	+	±
PVTT3	+	±
L57	+	+
CEF	+	+

PVTT2 and PVTT3, polyoma virus-transformed lines from C57BL/6; L57, spontaneously transformed line of C57BL/6 fibroblasts; CEF, chick embryo fibroblasts. +, rounding; −, protection. All shaken material preparations were derived from the same number of cells.

Fig. 5 Densitometric tracings of 7.5% SDS–polyacrylamide gel autoradiograms. *a* Unfractionated shaken material; *b*, active Sephadex fraction; *c*, neighbouring inactive fraction. Arrow indicates peak common to active preparations. Films scanned from right (top of gel) to left. Joyce-Loebl autodensitometer MK III, 0.096 density units per cm.

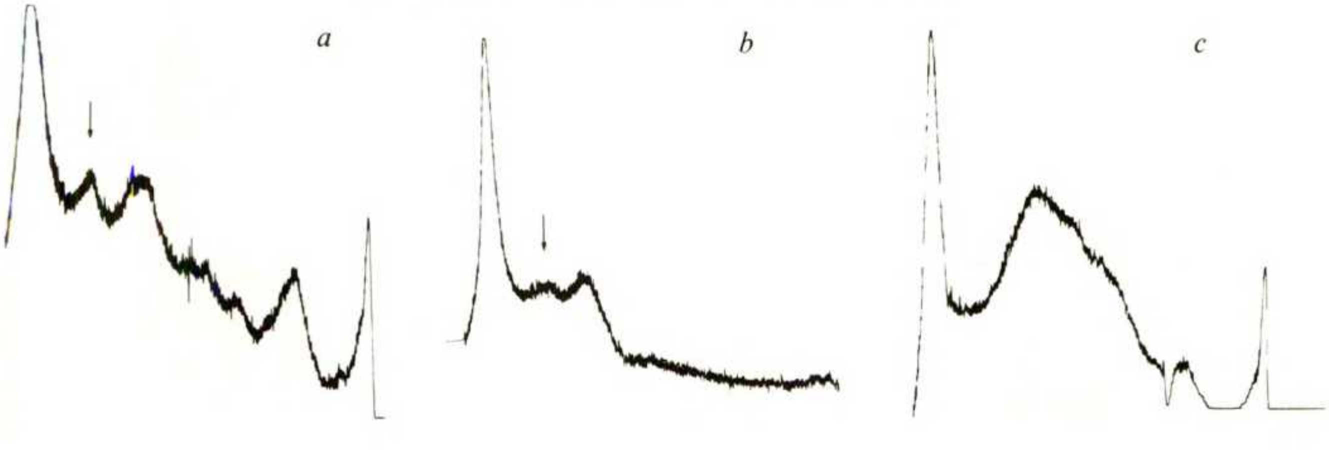

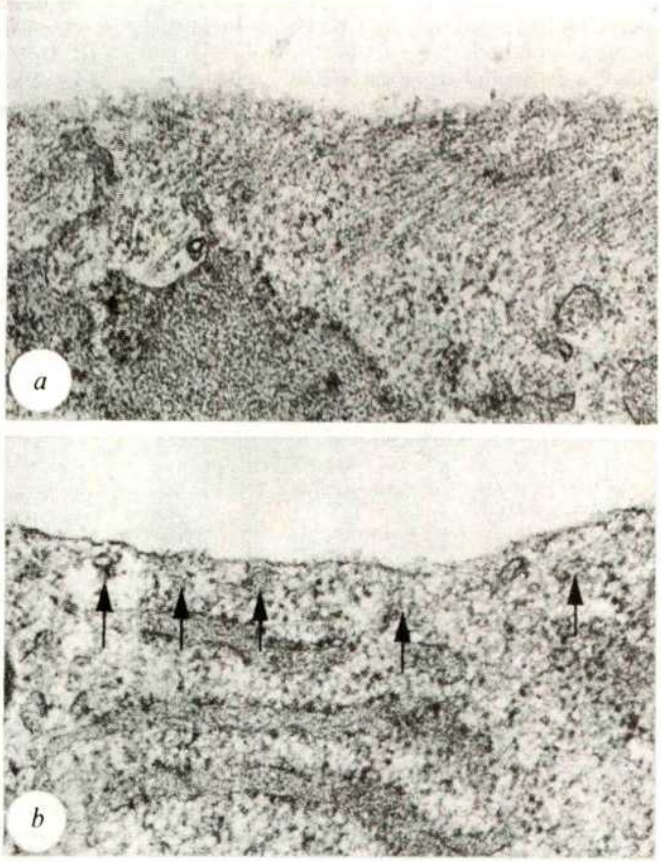

Fig. 6 Electronmicrographs of vertical sections through the upper surface of comparable regions of mouse fibroblasts (× 50,000). *a*, Control cell showing a regular array of microfilaments forming a layer close to the plasma membrane. *b*, Cell 15 min after induction of rounding, showing absence of microfilament layer and appearance of dense aggregations near the plasma membrane (arrows).

centration both at the surface and in the surrounding environment could be an important factor for the determination and modulation of shape during the cell cycle. In a separate report we shall describe its relationship with cytokinetic structures. We have also investigated whether the entire fraction removed by shaking transformed C57BL/6 cell lines[19] in SFM had any effect on the morphology of the normal C57 or 3T3 Swiss fibroblasts, as detectable by prevention or reversion of cell rounding. Table 1 shows that none of these tested materials exerted the marked protective effect shown by the preparation derived from normal fibroblasts. The significance of these results in relation to the presence of a surface factor that affects morphology and its relevance to the phenotypic state and altered growth properties of the cell during transformation will have to be investigated. In view of reports relating cell morphology to concentration of 3′, 5′-cyclic AMP[20,21], endogenous levels of this nucleotide were assessed in the various experimental conditions described above (courtesy of Dr E. Rozengurt, Imperial Cancer Research Fund Laboratories). The results showed that no detectable differences existed and that the changes of shape were not the consequence of variations in the intracellular concentration of cyclic AMP.

We thank the Cancer Research Campaign for support. We also thank Mr J. Crolla for assistance with the interference microscopy, and Dr L. Bannister for electron micrographs.

LIVIO MALLUCCI
VALERIE WELLS

Department of Microbiology,
Guy's Hospital Medical School,
London Bridge, London SE1, UK

Received March 5; accepted May 20, 1976.

1 Singer, S. J. ,and Nicolson, G. L., *Science*, **175**, 720–731 (1972).
2 Nicolson, G. L., *Int. Rev. Cytol.*, 39, 89–190 (1974).
3 Bretscher, M. S., and Raff, M. C., *Nature*, **285**, 43–49 (1975).
4 Inbar, M., Ben Bassat, H., and Sachs, L., *J. Membr. Biol.*, **6**, 195–209 (1971).
5 Isselbacher, K. J., *Proc. natn. Acad. Sci. U.S.A.*, **69**, 585–589 (1972).
6 Avruch, J., and Fairbanks, G., *Proc. natn. Acad. Sci. U.S.A.*, **69**, 1216–1220 (1972).
7 Cabantchik, Z. I., and Rothstein, A., *J. Membr. Biol.*, **10**, 311–330 (1972).
8 Pinto da Silva, P., *Proc. natn. Acad. Sci. U.S.A.*, **70**, 1339–1343 (1973).
9 Raff, M. C., *Nature*, **224**, 378–379 (1969).
10 Laemmli, U. K., *Nature*, **227**, 680–685 (1970).
11 McGuckin, W. F., and McKenzie, B. F., *Clin. Chem.*, **4**, 476–483 (1958).
12 Hubbard, A. L., and Cohn, Z. A., *J. Cell Biol.*, **55**, 390–405 (1972).
13 Hynes, R. O., *Proc. natn. Acad. Sci. U.S.A.*, **70**, 31703–174 (1973).
14 Hunter, W. M., and Greenwood, F. C., *Nature*, **194**, 495–496 (1962).
15 Hynes, R. O., *Cell*, **1**, 147–156 (1974).
16 Hogg, N. M., *Proc. natn. Acad. Sci. U.S.A.*, **71**, 489–492 (1974).
17 Vaheri, A., and Ruoslahti, E., *Int. J. Cancer*, **13**, 579–586 (1974).
18 Blumberg, P. M., and Robbins, P. W., *Cell*, **6**, 137–147 (1975).
19 Mallucci, L., and Skehel, J. J., *Nature new Biol.*, **232**, 197–181 (1971).
20 Hsie, A. W., and Puck, T. T., *Proc. natn. Acad. Sci. U.S.A.*, **68**, 358–361 (1971).
21 Johnson, G. S., Friedman, R. M., and Pastan, I., *Proc. natn. Acad. Sci. U.S.A.*, **68**, 425–429 (1971).
22 Mallucci, L., in *Concanavalin A as a Tool* (edit. by Bittiger, H., and Schnebli, H. P.), Ch. 5, 69–78 (Wiley, New York, 1976).

Precipitating antibodies in von Willebrand's disease

WE report the presence of precipitating antibodies in three patients with von Willebrand's disease (VWD), an inherited deficiency of factor VIII (anti-haemophilic factor, AHF). To our knowledge this is the first description of patients with complete biological and immunological deficiency of a plasma-clotting protein responding to replacement therapy by the production of antibodies with properties indistinguishable from those elicited in animals. AHF is a high molecular weight ($> 10^6$) glycoprotein complex[1] associated with two biological activities; one necessary for normal clotting (VIII: C) and the other for normal platelet function (Willebrand factor, VIIIR: WF). Specific antigenic determinants (VIIIR: AG) can be reliably quantified using heterologous antisera[2,3]. Any concept of the structure or the molecular genetics of AHF needs to incorporate the clinical and immunological findings in the two congenital disorders associated with AHF deficiency: haemophilia A and VWD. The former is a sex-linked deficiency of VIII: C alone whereas the latter represents a deficiency of all three parameters of the AHF complex and is inherited as an autosomal trait. Non-precipitating antibodies to AHF, acquired after replacement therapy, are common in haemophilia A (ref. 4) but only one case has been reported in VWD[5,6].

Purified IgG was prepared by precipitation with 40% ammonium sulphate and *n*-octanoic acid[7] from the plasma

Fig. 1 Double diffusion in agarose of purified human AHF complex (Vo) showing a line of identity between homologous antibodies in VWD (H.Ab) and heterologous (rabbit) antibodies (R. Ab).

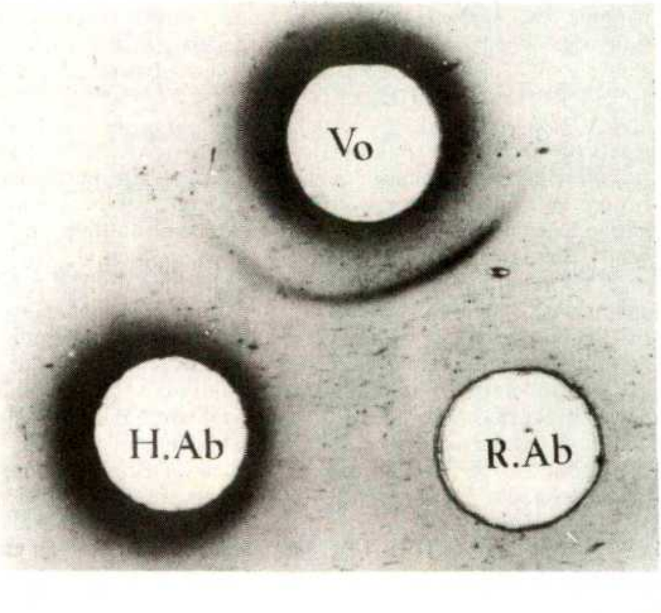

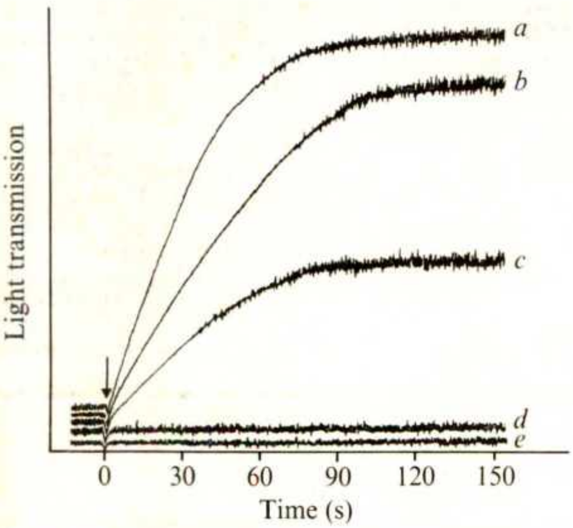

Fig. 2 Inhibition of ristocetin-induced platelet aggregation by plasma from VWD with inhibitor. 50 µl of patient plasma (serially diluted from 1:1 to 1:8) was mixed with 150 µl of normal platelet-rich plasma, followed by the addition of ristocetin (1.5 mg ml^{-1}). The control used was 50 µl of plasma from severe VWD patients with no inhibitor. Similar results were observed with purified IgG from the patients tested using either platelet-rich plasma or normal washed platelets plus normal platelet-poor plasma. *a*, Control; *b*, 1:8; *c*, 1:4; *d*, 1:2; *e*, 1:1.

of three patients with VWD who showed evidence for inhibitor (of 67 tested). The purified IgG in each case gave a line of precipitation with normal and haemophilia A plasma, but not with that of VWD. Precipitation between antibodies and VIIIR : AG from normal plasma was also demonstrated using the Laurell technique[8] and by radioimmunoassay[9]. These homologous antibodies therefore have similar properties to those raised in animals against purified human AHF, which is confirmed by the finding of a line of identity between both types of antibodies (Fig. 1). The purified IgG had a low titre ($<$ U ml^{-1}) of anti-VIII : C, whereas they strongly inhibited VIIIR: WF as measured with ristocetin (Fig. 2). This effect on platelet function was specific for VIIIR: WF, since there was no inhibition of ADP, collagen or adrenalin-induced platelet aggregation. These IgG partially inhibited bovine and porcine AHF-induced platelet aggregation, however, indicating that the effect was not species specific.

Our findings support the contention that VWD is the result of decreased synthesis of normal AHF (ref. 2). Only those rare patients who are completely deficient would have no immunological tolerance to the protein. Our three patients, two of them brothers, had been transfused on multiple occasions because of an unusual severity of the disease. The absence of measurable plasma levels of VIII: C (ref. 10; $<$0.01 U ml^{-1}), VIIIR : AG (ref. 9; $< 2.5\times10^{-4}$ U ml^{-1}) and VIIIR : WF (ref. 11; $<$0.03 U ml^{-1}) and the reduced levels of VIIIR: AG and VIIIR: WF in the parents is consistent with the homozygous state[12,13]. Challenge by transfusion in such patients would be expected to induce an antibody response which, as a result of the multiple antigenic stimulation from a totally foreign protein, could elicit polyvalent antibodies to AHF capable of binding and precipitation. Haemophiliacs seem to synthesise a non-functioning glycoprotein which may have very few antigenic determinants different from normal. Consequently antibodies are more common but precipitation is unlikely to occur because of the paucity of determinants and the difficulty in lattice formation between antigen and antibody.

In conclusion, precipitating antibodies have been found in three polytransfused patients with severe homozygous VWD. Such antibodies seem to be mainly directed towards VIIIR: WF and VIIIR: AG rather than towards VIII: C. Since VIII: C may reside on a separate molecule linked by non-covalent bonds to VIIIR: AG, it remains to be demonstrated whether the partial neutralisation of VIII: C is specific or secondary to steric hindrance.

P. M. Mannucci
Dominique Meyer
Z. M. Ruggeri
J. Koutts
N. Ciavarella
J.-M. Lavergne

Institut de Pathologie Cellulaire
(INSERM U143), Hôpital de Bicêtre,
94270 Le Kremlin-Bicêtre, France,
and Haemophilia and Thrombosis Centre,
University of Milano, Milano, Italy

Received February 16; accepted May 17, 1976.

1 Legaz, M. E., Schmer, G., Counts, R. B., and Davie, E. W., *J. biol. Chem.*, **248**, 3946–3955 (1973).
2 Zimmerman, T. S., Ratnoff, O. D., and Powell, A. E., *J. clin. Invest.*, **50**, 244–254 (1971).
3 Meyer, D., Lavergne, J. M., Larrieu, M. J., and Josso, F., *Thromb. Res.*, **1**, 183–196 (1972).
4 Shapiro, S. S., *Ann. N.Y. Acad. Sci.*, **240**, 350–361 (1975).
5 Sarji, K. E., Stratton, R. D., Wagner, R. H., and Brinkhous, K. M., *Proc. natn. Acad. Sci. U.S.A.*, **71**, 2937–2941 (1974).
6 Stratton, R. D., Wagner, R. H., Webster, W. P., and Brinkhous, K. M., *Proc. natn. Acad. Sci. U.S.A.*, **72**, 4167–4171 (1975).
7 Fine, J. M., and Streinbuch, M., *Rev. Eur. Etud. clin. Biol.*, **15**, 1115–1121 (1970).
8 Laurell, C. B., *Analyt. Biochem.*, **15**, 45–52 (1966).
9 Ruggeri, Z. M., Mannucci, P. M., Jeffcoate, S. L., and Ingram, G. I. C., *Br. J. Haemat.* (in the press).
10 Langdell, R. D., Wagner, R. H., and Brinkhous, K. M., *J. Lab. clin. Med.*, **41**, 637–642 (1953).
11 Weiss, H. J., Hoyer, L. W., Rickles, F. R., Varna, A., and Rogers, J., *J. clin. Invest.*, **52**, 2708–2716 (1973).
12 Veltkamp, J. J., and Van Tilburg, N. H., *New Engl. J. Med.*, **289**, 882–885 (1973).
13 Sultan, Y., Simeon, J., and Caen, J. P., *J. clin. Path.*, **28**, 309–316 (1975).

Control of brain tryptophan concentration in rats on a high fat diet

SYNTHESIS in the brain of the neurotransmitter 5-hydroxytryptamine (5-HT) is influenced by the concentration of its precursor tryptophan[1,2]. Much attention has therefore been paid to the determinants of brain tryptophan concentration. Evidence suggests that plasma free tryptophan is an important influence on brain tryptophan[3,4] and that both concentrations increase when plasma unesterified fatty acids (UFA) rise[3,5,6] and release plasma tryptophan from albumin[7,8]. Other results, however, disagree. Thus feeding rats for 2 h with high fat diets apparently led to large increases in serum UFA and free tryptophan but not brain tryptophan[9,10,11]. We now present evidence suggesting that the latter findings may have been due to *in vitro* lipolysis during either the preparation of serum or its dialysis at 37 °C for 3.5 h to separate free tryptophan[9]. Here we describe work in which precautions were taken to avoid *in vitro* changes and which is consistent with a relationship between plasma free tryptophan and brain tryptophan concentrations.

Male Sprague–Dawley rats (200–220 g) (Anglia Laboratory Animals) housed three per cage were maintained on ALGH standard rodent diet (Grain Harvesters) and tap water *ad libitum* and subjected to a 6 h: 18 h light: dark cycle. After a 5-d adaptation period, food but not water was withdrawn at 1600 and on the following day at 0800 the animals were given access to either their normal diet or to a high fat diet (fatty bacon and bread both fried in corn oil). After 2 h they were decapitated and blood was collected into both heparinised and plain tubes cooled in an ice bath, for the preparation of plasma and serum respectively. Total time between blood collection and separation of plasma and serum (by 5 min centrifugation at 2–4 °C) was 10 and 40 min, respectively. Samples of 0.5 ml of plasma were ultrafiltered for free tryptophan determination as before[3], but at 2–4 °C instead of room temperature. Plasma and serum samples (0.1 ml) were also frozen using solid CO_2 immediately after separation for subsequent determination of UFA[12]. Plasma and serum residues were then incubated in a water bath at 37 °C for 4 h, cooled to 2–4 °C and separate plasma samples were ultrafiltered for free tryptophan determination and frozen for determination of UFA as described above. Brains were stored at −20 °C for determination of tryptophan[3].

Plasma or serum samples from rats fed on the high fat diet were all lipaemic while those from control fed rats were all clear. UFA concentrations of unincubated plasmas were significantly greater in the former group and the percentage of free tryptophan increased. But as plasma total tryptophan was proportionately lower in the high fat fed rats (see legend to Fig. 1) free tryptophan concentrations of unincubated plasmas were similar in rats on either diet. As Fig. 1*a* shows, brain tryptophan concentrations were also similar and thus are consistent with the previously found relationship between plasma free tryptophan and brain tryptophan[3–6].

When, however, the plasma of rats given the high fat diet was incubated at 37 °C for 4 h, UFA and free tryptophan concentrations increased five- and sevenfold, respectively. (Plasma UFA had already increased more than fourfold in samples withdrawn after 2 h.) In a separate experiment incubation for 4 h did not alter the *p*H of plasma collected from rats given the high fat diet (before incubation, $p\mathrm{H}=7.75\pm0.05$, $n=3$; after incubation, $p\mathrm{H}=7.78\pm0.06$, $n=3$; values shown ± 1 s.d.). Incubation of plasma from control fed rats led to a relatively small increase in UFA and a negligible change of free tryptophan. The plasma *p*H of a separate group of control fed rats rose significantly ($P<0.001$) during incubation from 7.78 ± 0.03 ($n=3$) to 8.03 ± 0.03 ($n=3$). Comparison with a standard curve obtained by determining free tryptophan in plasma brought to various *p*H values with CO_2 showed that this increase of *p*H would have decreased free tryptophan by about 27%. Even if this is allowed for, it is apparent from Fig. 1 that UFA and free tryptophan both increased massively on incubation of plasmas of fat fed but not control fed animals.

Fig. 1 Plasma and serum UFA, plasma free tryptophan and brain tryptophan in rats fed control and high fat diets. *a*, Relationships between plasma UFA, plasma free tryptophan and brain tryptophan and the effect of incubation *in vitro* on the plasma values. Brain tryptophan of rats killed 2 h after exposure to each diet and plasma UFA and free tryptophan were determined before and after incubation of the same plasma at 37 °C for 4 h (see text for details). Control diet group, $n=6$, high fat group, $n=5$. Differences from values for same but unincubated plasma: $^*P<0.001$. Difference from value for plasma of rats fed control diet: † $P<0.01$. Plasma total tryptophan was 29.15 ± 3.87 μg ml^{-1} and 22.13 ± 3.69 μg ml^{-1} in the control and fat-fed groups (difference: $P<0.01$). *b*, UFA in plasma or serum of rats fed either diet before and after incubation as above (see text for details). $n=10$ per group. Differences from values for same but unincubated plasma or serum: * $P<0.01$; † $P<0.001$ Difference from value for plasma: ‡$P<0.05$

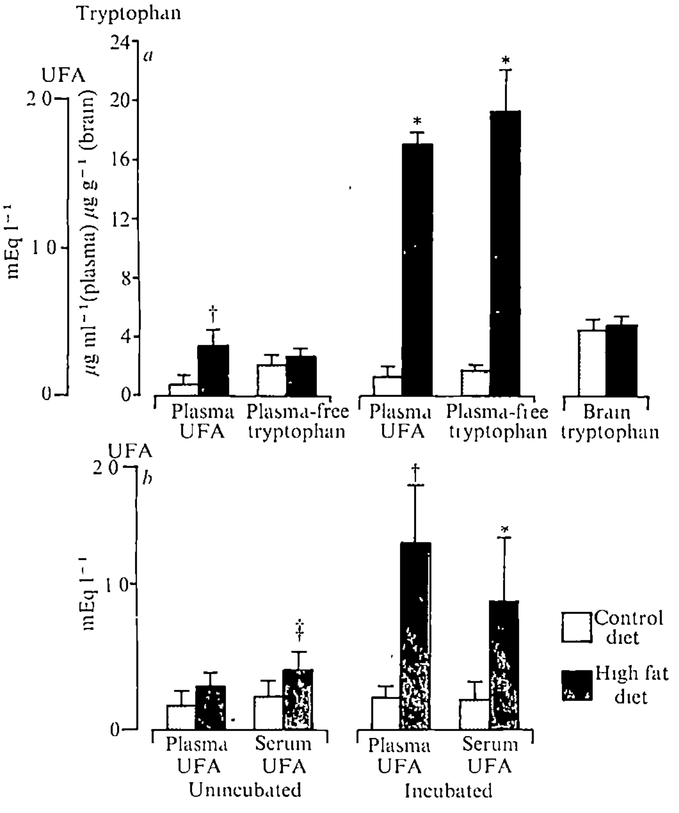

The work of Wurtman's group on free tryptophan and brain tryptophan was carried out not with plasma but with serum[9–11]. Results in Fig. 1*b* show that (in agreement with work on human blood[13]) UFA tended to be higher in serum than in plasma prepared from the same blood specimen. The increase was significant in serum from rats given the high fat diet. UFA (and therefore presumably also free tryptophan) continued to increase when the latter serum was incubated at 37 °C.

These results are consistent with many reports indicating *in vitro* lipolysis in plasma[13–16] especially after intake of fatty food[15], and suggest a reinterpretation of findings previously taken to show lack of effect of large *in vivo* increases of free tryptophan on brain tryptophan in rats fed on fat[9–11]. Considerable *in vitro* increases could have occurred in this work either during the preparation of serum or subsequently (although in one experiment[9] major changes were not found after serum incubation).

Our results therefore strengthen previous evidence that plasma free tryptophan is an important determinant of brain tryptophan concentration[3–6,17]. They do not imply that it is the only physiological influence involved. Insulin secretion, for example, can increase the uptake of tryptophan by the brain, possibly because it decreases plasma concentrations of competing amino acids[9,18,19]. Recent experiments in which plasma and brain tryptophan were determined after giving either insulin or the diabetogenic drug streptozotocin[17] indicate that plasma free tryptophan and insulin changes may influence brain tryptophan concentration concurrently.

We thank the MRC for a programme grant.

P. H. HUTSON
P. J. KNOTT
G. CURZON

Department of Neurochemistry,
Institute of Neurology,
Queen Square, London WC1N 3BG, UK

Received April 4, accepted May 18, 1976

[1] Eccleston, D., Ashcroft, G. W., and Crawford, T B. B , *J Neurochem.*, **12**, 493–503 (1965).
[2] Friedman, P A , Kappelman, A. H., and Kaufman, S , *J. biol. Chem* , **247**, 4165–4173 (1972)
[3] Knott, P. J., and Curzon, G., *Nature*, **239**, 452–453 (1972).
[4] Tagliamonte, A., Biggio, A , Vargiu, L , and Gessa, G. L , *Life Sci.*, **12**, 277–287 (1973)
[5] Curzon, G., and Knott, P J., in *Aromatic Amino Acids in The Brain* (edit. by Wurtman, R. J), Ciba Foundation Symp., 218–229 (Elsevier–North-Holland, Amsterdam, 1974).
[6] Knott, P J , and Curzon, G , *Biochem Pharmac* , **24**, 963–966 (1975).
[7] McMenamy, R H., *J biol Chem.*, **240**, 4235–4243 (1965).
[8] Curzon, G., Friedel, J , and Knott, P J , *Nature*, **242**, 198–200 (1973).
[9] Madras, B. K , Cohen, E L , Messing, R., Munro, H N , and Wurtman, R J , *Metabolism*, **23**, 1107–1116 (1974).
[10] Madras, B K., *et al* , *Nature*, **244**, 34–35 (1973)
[11] Madras, B K., Cohen, E L., Munro, H. N., and Wurtman, R. J., *Adv Biochem. Psychopharmac* , **11**, 143–151 (1974).
[12] Laurell, S , and Tibbling, G., *Clin. chim. Acta*, **16**, 57–62 (1967)
[13] Fairweather, D V I., and Layton, R , *J. clin. Path.*, **20**, 665–667 (1967)
[14] Anfinsen, C B., Boyle, E., and Brown, R. K , *Science*, **115**, 583–586 (1952).
[15] Jeffries, G. H , *Q Jl exp Physiol* , **39**, 77–81 (1954)
[16] Robinson, D. S , and French, J E., *Pharmac. Rev* , **12**, 241–263 (1960)
[17] Fernando, J C. R , Knott P. J., and Curzon, G , *J Neurochem* (in the press).
[18] Fernstrom, J D., and Wurtman, R. J , *Science*, **174**, 1023–1025 (1971).
[19] Fernstrom, J. D., and Wurtman, R. J , *Metabolism*, **21**, 337–342 (1972)

Inhibition by albumin of tryptophan uptake by rat brain

CHANGES in the tryptophan content of the brain influence the rate of synthesis of brain 5-hydroxytryptamine (5-HT). Therefore, factors that affect the delivery of tryptophan to the brain may affect its 5-HT content. Tryptophan in plasma can be displaced from its binding site on albumin by non-esterified fatty acids (NEFA)[1] and by certain drugs[2]. Although in some circumstances changes in non-albumin bound (NAB) plasma tryptophan, brought about by drugs and changes in plasma NEFA, parallel those of brain tryptophan[2,3], this relationship does not apply in all conditions. For example, after administration of glucose plasma NEFA decline, as does NAB tryptophan, but the brain tryptophan content increases[4]. Thus, it is uncertain whether binding of tryptophan to albumin is important in controlling brain tryptophan and hence brain 5-HT. To resolve this controversy we looked at the influence of albumin on the uptake of tryptophan by brain *in vivo*. We found that albumin inhibits tryptophan uptake, and that diffusion, a process that will depend only on the NAB plasma tryptophan concentration, has a small but significant role in the uptake of tryptophan by brain.

Tryptophan uptake by the brain was measured by the technique of Oldendorf[5]. Solutions containing ^{14}C-tryptophan and ^3H_2O (as a freely diffusible standard) were injected into the common carotid artery. After 15 s, when excess solution had been washed out of the microcirculation, the rat was decapitated. The $^{14}C{:}^3H$ ratio was determined in the brain and in the injected solution. The ratio for brain, expressed as a percentage of the ratio for the injected solution, is the brain uptake index (BUI).

In agreement with Pardridge and Oldendorf[6] we found that, as the concentration of tryptophan increased, the BUI decreased. BUI is a measure of the uptake of radioactive tryptophan. As the radioactivity in the solution was constant, the product BUI × (tryptophan concentration) is a measure of the total uptake of tryptophan from the injected solution. Figure 1 is a plot of BUI × (tryptophan concentration) against concentration. The uptake was analysed for conformity to one of two models: (1) active transport combined with non-saturable uptake by diffusion, equation (1); and (2) two active uptake systems with differing affinities, equation (2). The method used to discriminate between these models involves initial evaluation of the constants graphically, based on the double reciprocal plot of uptake against tryptophan concentration in the injected solution, followed by an iterative calculation designed to give the best fit of the line to the observed points[7].

$$v = \frac{V_s}{K+S} + K_d S \qquad (1)$$

$$v = \frac{V_1 S}{K_1+S} + \frac{V_2 S}{K_2+S} \qquad (2)$$

The fit to equation (1) was judged the more satisfactory on the basis of the low error mean square (0.0221) as compared with equation (2) (3.83). The fit of equation (1) to the experimental points is shown in line (*a*) of Fig. 1. The values obtained for the constants were $K = 160$ µM, $K_d = 4.51$ and $V = 5{,}920$ µM. By substituting these values in the two parts of equation (1), lines (*b*) and (*c*) were obtained. Note that at 100 µM tryptophan, in the physiological range for that amino acid, diffusion accounts for about 17% of the total uptake. At the concentration of NAB tryptophan found in the normal adult rat—25 µM—the non-saturable mechanism for uptake of the amino acid into the brain accounts for about 12% of the uptake. These data indicate that diffusion of tryptophan across the blood–brain barrier has a small but significant role in regulating the brain tryptophan and, consequently, the content of 5HT in the brain, especially after the administration of a tryptophan load.

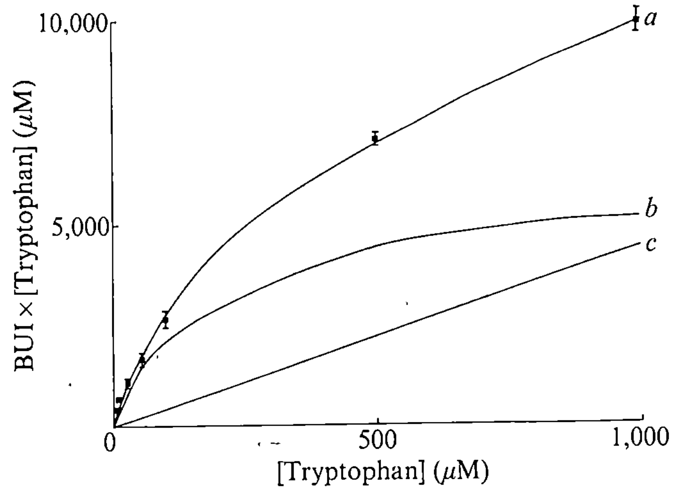

Fig. 1 The variation in tryptophan uptake by brain with various concentrations of tryptophan. A solution containing L-tryptophan, 3 ^{14}C-side chain (40 mCi mmol^{-1}, New England Nuclear) and ^3H_2O (as freely diffusible standard) was injected in the common carotid artery. BUI was measured at the following concentrations of injected tryptophan (TRP) (number of determinations given in parentheses): 6.25 µM (5), 12.5 (13), 25 (20), 50 (13), 100 (13), 500 (3), 1000 (3). The abscissa includes these concentrations The ordinate represents the amount of tryptophan taken up into the brain during the 15-s perfusion (see text). The points represent means ± standard error. Line *a* is drawn as the best fit to the experimental points obtained by methods described in the text. Lines *b* and *c* represent the components of line *a*, corresponding to the saturable and non-saturable processes, respectively.

If the tryptophan is injected in a bolus that contains plasma albumin, the BUI is reduced (Table 1). The addition of albumin to the solution reduced the concentration of tryptophan in free solution from 25 to 6 µM. The BUI for a solution of 6 µM should be, according to the graph in Fig. 1, 70%. But the albumin also reduces the ^{14}C tryptophan in free solution to the same extent, that is to 24% of its original value. Therefore, the BUI that might be expected if the uptake system acts only on tryptophan in free solution is 24% of 70, or 17. This is close, but not identical, to the actual value found, 22 ± 2 (Table 1). Thus, binding of tryptophan to albumin does inhibit its uptake by the brain, and must have some role in regulating the brain tryptophan content.

The uptake of tyrosine, an amino acid that does not bind to albumin, is unaffected by the presence of that protein in the injected solution (Table 1).

Albumin is not the only component of plasma that affects tryptophan uptake. Some amino acids inhibit the process by competing for the same transport system[5]. But this inhibition has been studied so far only with amino acid concentrations beyond the physiological range. Table 2 shows that when the

Table 1 Effect of albumin on tryptophan and tyrosine uptake by brain

Compound	Albumin	% Amino acid in free solution	BUI*
Tryptophan	−	100	40±3 (8)
	+	24	22±2 (9)
Tyrosine	−	100	30±3 (6)
	+	100	26±2 (6)

*BUI was determined as described in Fig. 1 using a tryptophan solution of 25 µM and L-tyrosine (^{14}C-U, 400 mCi mmol^{-1}, New England Nuclear) at 100 µM Rat albumin (Sigma) was used at a concentration of 60 mg ml^{-1} The fraction of tryptophan in free solution was determined by ultrafiltration using an Amicon propellant-pressurised ultrafiltration cell with UM 10 membranes (nominal molecular weight cutoff 10,000).

Table 2 The effect of amino acids on tryptophan uptake by brain

Amino acid	Control	Concentration of amino acids*(μM) Competing Low	Mean	High	Non-competing
Histidine		55	63	70	
Isoleucine		73	101	128	
Leucine		167	203	238	
Methionine		58	73	64	
Phenylalanine		70	83	96	
Tyrosine		96	123	151	
Valine		194	228	262	
Alanine					659
Glycine					302
Lysine					397
Proline					374
Threonine					370
BUI†	41±2 (7)	26±5 (6)	21±2 (6)	13±1 (6)	37±4 (5)

*Concentrations used for competing amino acids: the upper and lower limits of the physiological range as well as the mean[8], for non-competing amino acids: the mean of the physiological range for the rat.

†For a concentration of 25 μM tryptophan in the injected solution.

concentrations of a group of competing amino acids are raised from the lower to the upper limit of their physiological range there is considerable inhibition of tryptophan uptake. Thus, competition between amino acids for uptake by the brain is a physiological phenomenon, and it is possible that the increased brain tryptophan that is noted after glucose administration[4] occurs because of a decline in the plasma concentration of the competing amino acids. Alternatively, there might be a change in the activity of the actual uptake system. This factor is neglected when measurements are made on plasma and brain tryptophan alone, but it can be studied conveniently by the method of Oldendorf[5]. Studies in which uptake is measured as well as brain and plasma tryptophan content should elucidate fully the influences the components of plasma on brain tryptophan and 5-HT.

This work was supported by the MRC of Canada and the Conseil de la Recherche en Santé du Québec. P. E. held a fellowship of the CRSQ during this work.

P. ETIENNE
S. N. YOUNG
T. L. SOURKES

*Department of Psychiatry,
McGill University,
1033 Pine Avenue West
Montreal, Quebec,
Canada H3A 1A1*

Received March 4; accepted May 7, 1976.

1 McMenamy, R H., *J. biol. Chem.*, 239, 2835–2841 (1964).
2 Gessa, G. L , and Tagliamonte, A., *Adv. Biochem. Psychopharma.*, 11, 119–131 (1974).
3 Knott, P J., and Curzon, G , *Nature*, 239, 452–453 (1972).
4 Madras, B K., *et al.*, *Nature*, 244, 34–35 (1973).
5 Oldendorf, W. H., *Am. J. Physiol*, 221, 1629–1639 (1971).
6 Pardridge, W. M., and Oldendorf, W. H., *Biochim. biophys Acta*, 401, 128–136 (1975).
7 Denizeau, F., Wyse, J. R., and Sourkes, T. L., *J theor. Biol.* (in the press)
8 Altman, P. L., in *Blood and Other Body Fluids* (edit. by Dittmer, D. S.), 77 (Federation of American Societies for Experimental Biology, Washington, DC, 1975).

Monitoring of transmitter metabolites by voltammetry in cerebrospinal fluid following neural pathway stimulation

AN *in vivo* voltammetry technique has been developed which enables direct and continuous measurement to be made of the release of neurotransmitter metabolites in cerebrospinal fluid (CSF) after electrical stimulation or pharmacological manipulations of neural pathways. The measurement is very simple in principle. A potential is applied to a micro carbon electrode stereotaxically placed in a lateral ventricle. One then measures the minute current which results from the oxidation or reduction of small molecular weight constituents near the sensor electrode. The potential at which the electrolysis occurs serves as a qualitative indication of the constituent being monitored and the current itself is directly proportional to the concentration of this component in CSF.

The catecholamines and all their metabolites, as well as 5-hydroxytryptamine and its metabolites, are readily oxidised. Thus, the technique is applicable to catecholaminergic and serotoninergic neurotransmitter systems. Acetylcholine, GABA and various other aliphatic amines and acids which have suspected neurotransmitter roles are not electroactive and are not sensed by the electrode in the conditions used. We have previously described the *in vivo* voltammetry method especially for examining drugs injected directly into brain tissue[1,2]. We believe the present application is particularly significant because it provides continuous readout of CSF metabolites following stimulation of neural pathways without the necessity for perfusion or radioactive labelling.

In one test of the technique, we examined the metabolites transferred to the CSF following electrical stimulation of a well-established neural substrate, the dopaminergic nigrostriatal pathway. Rats were implanted with conventional bipolar stimulating electrodes in the pars compacta of the substantia nigra. At the same time, one or both lateral ventricles were implanted with a small guide cannula. Following several days of surgical recovery, the rat was anaesthetised and placed in the head holder of a stereotaxic apparatus. A micro carbon electrode was inserted in the cannula to a depth which ensured contact with the CSF of the lateral ventricle. It is well known that electrical stimulation of the substantia nigra causes a release into the CSF of the dopamine metabolite homovanillic acid (HVA)[3,4]. The latter was the sought-after electroactive component in these experiments.

Figure 1 illustrates the qualitative aspects of the electrochemical experiment. The cyclic current–voltage curves (voltammograms) of Figs 1*a* and *b* were initiated by a triangular wave potential sweep from 0.0 to 1.4 V and then returned to −0.2 V. (All potentials are measured against a micro saturated calomel electrode (SCE) normally placed in contact with brain tissue over the frontal sinus area.) Figure 1*a* shows the baseline level of com-

Fig. 1 Electrochemical signals in CSF at micro carbon electrode. *a*, Before stimulation; *b*, after stimulation.

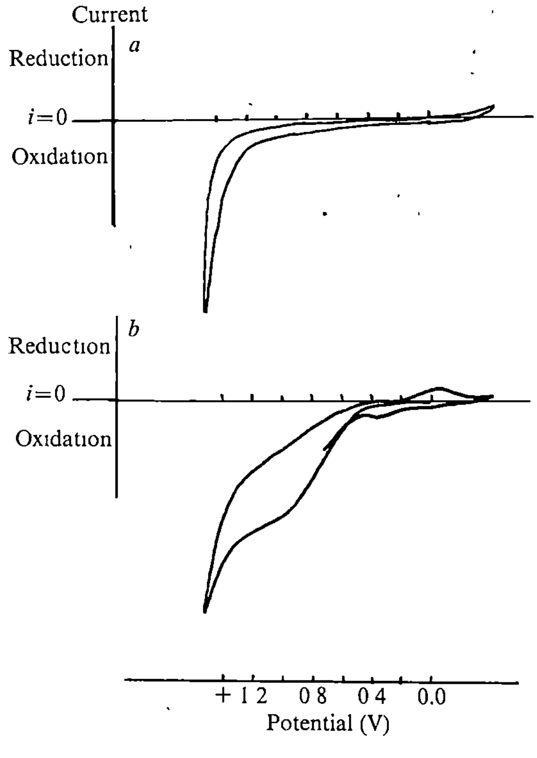

ponents in the CSF which can be oxidised within this potential range (primarily ascorbate and micromolar levels of HVA). At the current sensitivity used, very little oxidation current is seen in Fig. 1*a* in these "resting" conditions. Following stimulation of the substantia nigra, Fig. 1*b* shows a large current with a plateau at around +0.8 V which is a result of HVA oxidation. (Although this is a large increase, all electrochemical currents referred to herein are at most several hundred nA.) The small peaks around +0.1 V in Fig. 1*b* come from oxidation and reduction of dihydroxyphenylacetic acid (DOPAC) and its *o*-quinone. It is well established that DOPAC is formed during the electrolysis of HVA[5,6], and the small peaks serve as an additional electrochemical "marker" for the presence of HVA.

The quantitative measurements are carried out by fixing the potential at +0.8 V and monitoring the current due to HVA oxidation as a function of time. Before stimulation only the low baseline signal illustrated in Fig. 1*a* is monitored at +0.8 V. The substantia nigra was then stimulated for 20 0.5-s intervals using simple 60-Hz sine waves. In typical experiments, the baseline remained relatively constant for some 15–20 min after stimulation. There then was a sharp rise in HVA signal, followed by a more gradual disappearance. Often such stimulations could be repeated several times and Fig. 2 shows a typical result of two successive stimulations. Successful experiments were carried out with 12 of 22 rats stimulated. Because of difficulties with cannula placement in rat ventricles (our electrodes at present require cannulae of around 1 mm external diameter), we have recently repeated this type of experiment in rabbits. To date, four successful substantia nigra stimulations have been carried out with rabbits. It should be emphasised that no optimisation of stimulation parameters, anaesthetics, electrode size and so on has yet been investigated. A full report of the experimental details is in preparation.

Similar electrical stimulation was carried out in the region of the midline raphe nuclei with rabbits. As expected, an efflux of 5-hydroxyindole acetic acid (5-HIAA) into the CSF was observed by the voltammetric monitoring, but little or no change in HVA.

Pharmacological manipulations of neural substrates can also be monitored by this technique. For example, a large increase in HVA signal in ventricular CSF was observed some 30 min after an intraperitoneal injection of L-dopa in the rabbit.

Fig. 2 HVA current response in CSF following substantia nigra stimulation. Current-time product for 200-ms electrolysis was converted to mM concentrations of HVA by external calibrations.

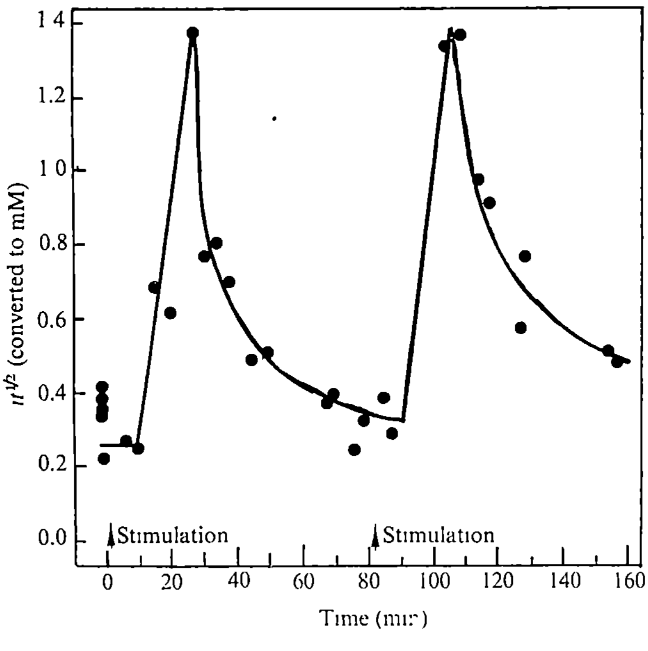

Since this type of electrochemical measurement is unfamiliar in electrophysiological studies, we expected its authenticity to be quite properly open to question. Thus, electrochemical measurements were routinely backed up by independent and unequivocal chemical identification of HVA, DOPAC or 5-HIAA by high performance liquid chromatography. When a successful stimulation or drug manipulation was obtained—as evidenced by a current rise at the sensing electrode—we lifted out the electrode and removed 2–5 ml of CSF with a Hamilton syringe. The CSF sample was injected directly into the injection port of a liquid chromatograph. The metabolites were directly analysed by high performance liquid chromatography on a DuPont SAX anion exchange column with a sensitive electrochemical detection system[7]. The CSF metabolites were identical with authentic samples injected into the column and quantitative correlations were possible.

We believe that the present technique will offer distinct advantages over existing methods for examining metabolite changes in CSF following neural pathway manipulation. It is the only technique we know making use of an on-line sensor that provides instantaneous and continuous monitoring of CSF metabolite levels (electrochemical response times are variable, but routinely are 10–20 ms). It involves minimal disturbance of the physiological milieu; electrical currents are always in the nA range and natural CSF and its flow patterns are used rather than perfusion. It is, of course, limited in its scope to the oxidisable neurotransmitter systems and their metabolites, as mentioned earlier. Although the present results are very promising, improvements in electrode miniaturisation, sensitivity and selectivity are desirable. We are now examining modifications to extend the technique to direct tissue measurements with neuronal pathway manipulation.

We thank the NSF and the NIH for support.

R. MARK WIGHTMAN
ELAINE STROPE
PAUL M. PLOTSKY
RALPH N. ADAMS

Department of Chemistry,
University of Kansas,
Lawrence, Kansas 66045

Received March 6; accepted May 4, 1976.

[1] McCreery, R., Dreiling, R., and Adams, R. N., *Brain Res.*, 73, 15–21 (1974).
[2] McCreery, R., Dreiling, R., and Adams, R. N., *Brain Res.*, 73, 23–33 (1974).
[3] Portig, P. J., and Vogt, M., *J. Physiol., Lond.*, 204, 687–715 (1969).
[4] Von Voightlander, P. F., and Moore, K. E., *Neuropharmacology*, 10, 733–741 (1971).
[5] Sternson, A. W., McCreery, R., Feinberg, B., and Adams, R. N., *J. Electroanalyt. Chem.*, 46, 313–321 (1973).
[6] Petek, M., Bruckenstein, S., Feinberg, B., and Adams, R. N., *J. Electroanalyt. Chem.*, 42, 397–401 (1973).
[7] Kissinger, P. T., Refshauge, C., Dreiling, R., and Adams, R. N., *Analyt. Lett.*, 6, 465–477 (1973).

Periodate-induced increase in cyclic GMP in mouse and guinea pig splenic cells in association with mitogenesis

INTERACTION of the lectins phytohaemagglutinin (PHA) and concanavalin A (con A) with the lymphocyte plasma membrane initiates a sequence of metabolic events leading to cell proliferation. The numerous alterations in cellular components and processes that occur early after mitogenic stimulation include enhanced uptake of nucleotides[2], amino acids[3,4], sugars[5], Ca^{2+} (ref. 6), and K^{+} (ref. 7), enhanced activity of several membrane enzymes[8,9], accelerated turnover of phospholipids[10,11], increased membrane fluidity[12] and an increased accumulation of cellular cyclic 3′,5′-guanosine monophosphate (cyclic GMP)[13–15]. Demonstrations that exogenous cyclic GMP can stimulate definable functions in lymphocytes[16,17], including proliferation[18], and

Fig. 1 Cyclic GMP and cyclic AMP levels and ^{3}H-thymidine incorporation after exposure of mouse splenic cells to IO_4. Spleens, removed from cervically dislocated 6–8-week-old BALB/c mice, were homogenised gently in PBS After sedimentation of connective tissue the suspended cells were removed, washed with PBS, and suspended at 20 × 10^6 cells per ml PBS. The IO_4, freshly dissolved in PBS, was introduced to achieve a final concentration of 5 mM while the cell suspension was maintained at 4 °C. Samples were collected for determination of cyclic nucleotides by adding perchloric acid to a final concentration of 1N. Acid extracts were purified by alumina and AG1X8 column chromatography, and assayed by radioimmuoassay[28] after conversion to the 2′-*O*-acetyl derivative[29] Cells in which the proliferative response was monitored were exposed to the IO_4 for 30 min, washed twice with PBS, and suspended at 2 × 10^6 cell per ml in RPMI 1640 containing foetal calf serum (5%), penicillin (110 μg ml^{-1}) and streptomycin (100 μg ml^{-1}). The cells were incubated in 5% CO_2 at 37 °C for 48 h before a terminal pulse with 1 μCi ^{3}H thymidine for 3 h Cultures were collected by a multiple automatic sample harvester and thymidine incorporation was determined by liquid scintillation spectrometry. The broken lines represent controls.

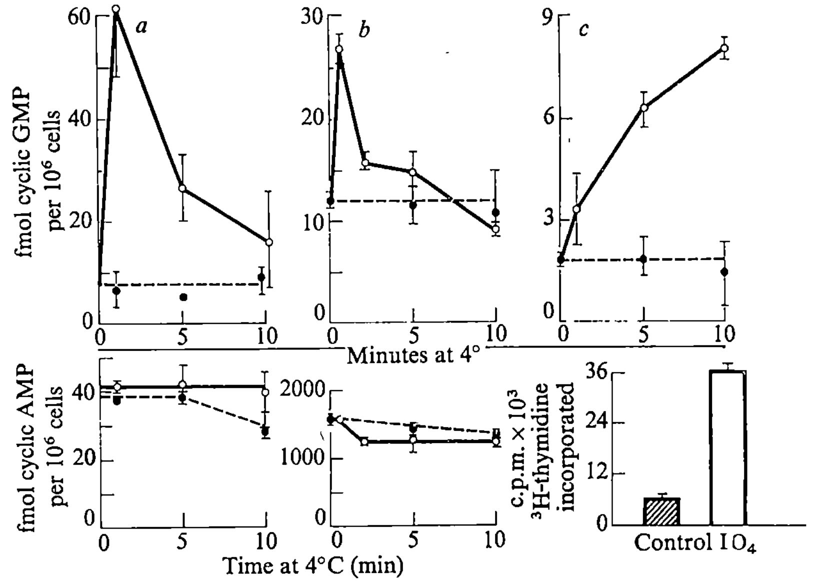

that there is an association between phytomitogen action and cyclic GMP accumulation suggest that this nucleotide is a positive effector of proliferation. To investigate further how cyclic GMP may be involved in this sequence of events, we have studied the effects that the oxidant periodate (IO_4) and the reducing agent cysteine have on the cyclic nucleotide levels of rodent splenic cells[1]. IO_4 stimulates lymphocyte proliferation[19] and because the oxidant produces definable chemical alterations in membrane components, which can be prevented by reducing agents[20], studies with these agents may provide insights into the regulation of cyclic GMP metabolism in relation to mitogenic stimulation.

Figure 1 shows the effect of IO_4 on the concentrations of the cyclic nucleotide in suspensions of mouse splenic cells, maintained at 4 °C, in three experiments The concentrations of cyclic GMP in the cells not exposed to the mitogen varied from animal to animal, ranging from 2.5 to 12.5 fmol per 10^6 cells. In spite of the variation, treatment with IO_4 consistently caused an enhanced accumulation of cyclic GMP but did not alter the concentration of cyclic 3′,5′-adenosine monophosphate (cyclic AMP). The increase in cyclic GMP concentration ranged from two- to tenfold and the temporal characteristics of the enhanced accumulation differed in each experiment shown. The IO_4-induced increases in cyclic GMP were accompanied by a stimulation of lymphocyte proliferation as illustrated by the increased amount of ^{3}H-thymidine incorporated into cells cultured after exposure to IO_4 (Fig. 1*c*).

The cyclic nucleotides in guinea pig splenic cells responded similarly when exposed to IO_4; cellular levels of cyclic GMP increased but cyclic AMP was unaffected (Fig. 2). The addition of $CaCl_2$ (0.2 mM) to the cation-free phosphate-buffered saline media (PBS) did not enhance the ability of IO_4 to promote accumulation of cyclic GMP.

The reducing agent cysteine prevented the IO_4-promoted increase in cyclic GMP. Cysteine alone or together with IO_4 significantly lowered (50%) the concentration of the cyclic nucleotide (Fig. 3). The increase in ^{3}H-thymidine incorporation seen after exposure to IO_4 alone was prevented in the cells exposed to IO_4 in combination with cysteine. There was no change in the cyclic AMP content after the addition of either the oxidising or the reducing agent.

Thirteen experiments were conducted to examine the effects of IO_4 on cyclic GMP levels. In the nine experiments in which an increase in cyclic GMP was detectable (70–1,000%) there was a concomitant increase in the rate of ^{3}H-thymidine incorporation. But in the other four experiments there was no measurable increase in either cyclic GMP or in ^{3}H-thymidine incorporation, indicating that IO_4 had no oxidative influence in these experiments.

The increases in cyclic GMP detectable after exposure to IO_4 were smaller than those reported after stimulation of human or rodent peripheral blood lymphocytes with PHA or con A[13,14]. This may reflect the difference between the cell populations studied or a difference in the nature of the mitogenic stimulus. In the conditions of mitogenic stimulation in our experiments, however, the changes occurred at 4 °C, which may have minimised the increases. Furthermore, splenic cell suspensions, although consisting primarily of lymphocytes, contain other cells such as polymorphonuclear leukocytes and macrophages. It is not possible to determine from the experiments reported here

Fig. 2 Effect of IO_4 on cyclic GMP of guinea pig splenic cells in the presence and absence of Ca^{2+}. Cell suspensions were prepared from guinea pigs (250–350 g) as described for Fig. 1. $CaCl_2$ (0.2 mM) was added to the cells suspended in PBS at 4 °C 10 min before addition of IO_4 (5 mM). ●, Plus Ca^{2+}; ○, without Ca^{2+}; ■, control plus Ca^{2+}; □, control without Ca^{2+}.

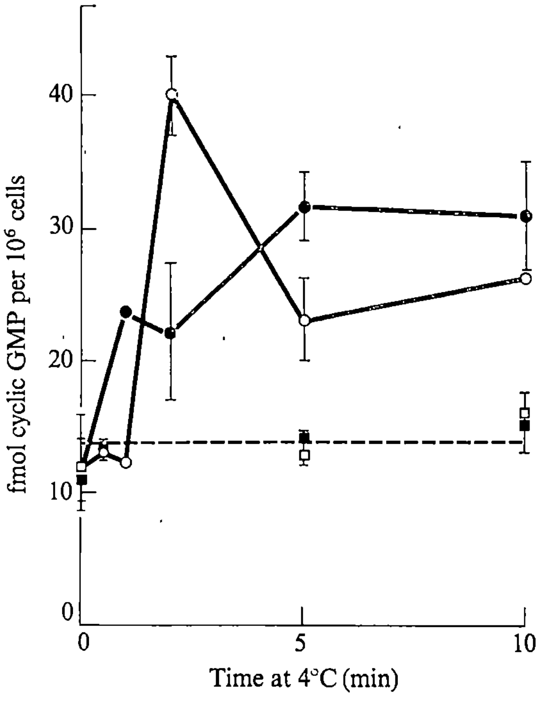

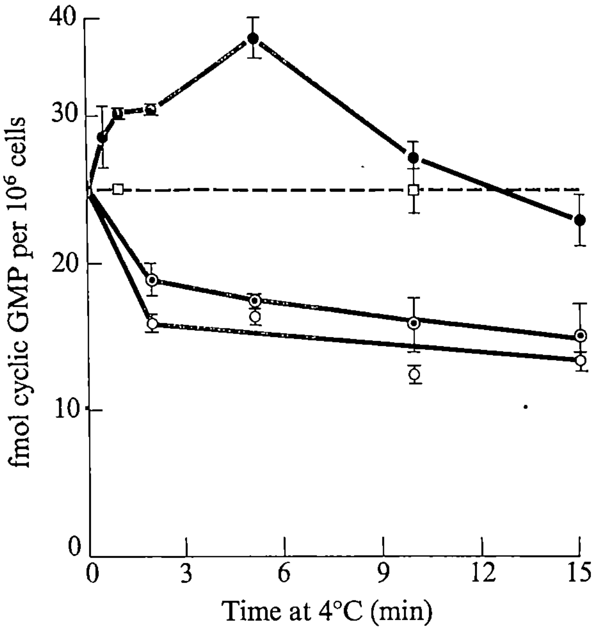

Fig. 3 Effect of cysteine on basal (○) and IO_4-stimulated (⊙) cyclic GMP of mouse splenic cells. All methods were as described in Fig. 1. Cysteine (1 mM) was added to the cells just before addition of the IO_4 (1 mM). ●, Plus IO_4 alone; □, control.

whether the increases in cyclic GMP derived from an alteration induced in lymphocytes directly or secondarily, or whether they reflect an influence on another cell type. The importance of this question increases in the light of demonstrations of a requirement for macrophages for IO_4 stimulation of lymphocytes[21] and of an involvement of cyclic GMP in the release of lymphocyte-stimulating factors by macrophages[22].

The ability of IO_4 to stimulate an increase in cyclic GMP suggests that an alteration of the cell membrane involving oxidation of a specific constituent, such as the sialic acid moiety indicated by the work of Novogrodsky[20], is coupled to a system involved in regulating guanylate cyclase. The reciprocal effects of IO_4 and cysteine on cyclic GMP suggest a mechanism for regulating guanylate cyclase activity through cellular events involving oxidation and reduction. This concept is supported by observations that soluble fractions of guanylate cyclase from platelets[23], and lung[24], as well as from lymphocytes (M. K. H., J. H. S. and N. D. G., unpublished observation), undergo a time dependent, O_2-requiring "autoactivation" which is inhibitable by the reducing agent dithiothreitol. Such a mechanism may be allied to that by which oxidation and reduction have been suggested to underlie the modulation of cell proliferation[27].

It is not known whether all the metabolic changes occurring early after mitogenic stimulation of lymphocytes are necessary for DNA synthesis; whether some, although not absolutely required, serve to modulate the rate of proliferation, or whether some are merely related to the generalised changes in the membrane. The number and variety of early events suggest that no single event signals commitment to proliferation.

Agents such as acetylcholine and imidazole can increase cyclic GMP in lymphocytes without promoting proliferation although they potentiate the action of phytomitogens[25,26]. Therefore, the increased cellular accumulation of this cyclic nucleotide is probably not the sole initiator of proliferation, but rather, acts in parallel or in sequence with the other metabolic changes resulting from mitogenic action.

This research was supported by grants from the NIH, the American Cancer Society and the Minnesota Leukemia Foundation.

M. K. HADDOX
L. T. FURCHT
S. R. GENTRY
M. E. MOSER
J. H. STEPHENSON
N. D. GOLDBERG

Departments of Pharmacology, and
Laboratory Medicine and Pathology,
University of Minnesota,
Minneapolis, Minnesota 55455

Received March 1; accepted April 13, 1976,

[1] Haddox, M. K., Furcht, L. T., Stephenson, J. H., Moser, M E , and Goldberg, N.D., *Fedn Proc.*, 35, 295 (1976)
[2] Peters, J. H., and Hansen, P., *Eur. J. Biochem.*, 19, 502–508 (1971)
[3] Mendelsohn, J , Skinner, S. A., and Kornfeld, S , *J. clin Invest.*, 50, 818–826 (1971).
[4] van den Berg, K. J., and Betel, I., *Expl Cell Res* , 76, 63–72 (1973).
[5] Peters, J. H., and Hausen, P , *Eur. J. Biochem.*, 19, 509–513 (1971).
[6] Whitney, R. B., and Sutherland, R. M., *Cell Immun* , 5, 137–147 (1972).
[7] Quastel, M R., and Kaplan, J. G., *Expl Cell Res* , 63, 230–233 (1971)
[8] Averdunk, R., *Z. Physiol. Chem* , 353, 79–87 (1972).
[9] Resch, K., Ferber, E , Odenthal , J., and Fischer, H., *Eur. J Immun* , 1, 162–165 (1971).
[10] Ferber, E., and Resch, K., *Biochim. biophys Acta*, 296, 335–349 (1973).
[11] Fisher, D. B , and Mueller, G. D., *Biochim. biophys. Acta*, 248, 434–448 (1971).
[12] Barnett, R. E., Scott, R. E., Furcht, L. T., and Kersey, J H , *Nature*, 249, 465–466 (1974).
[13] Hadden, J W., Hadden, E. M., Haddox, M. K., and Goldberg, N. D , *Proc. natn. Acad. Sci. U S.A.*, 69, 3024–3027 (1972).
[14] Schumm, D. E., Morris, H. P., and Webb, T. E., *Eur. J. Cancer*, 10, 107–113 (1974).
[15] Whitfield, J. F , MacManus, J. P., Boynton, A L , Gillan, D. J., and Isaacs, R. J., *J cell. Physiol* , 84, 445–458 (1974).
[16] Freedman, M. H., Raff, M. D., and Gomperts, B., *Nature*, 255, 378–382 (1975)
[17] Johnson, L. D , and Hadden, J W., *Biochem biophys. Res. Commun.*, 66, 1498–1505 (1975).
[18] Weinstein, Y., Chambers, D. A , Bourne, H. R., and Melmon, K. L., *Nature*, 251, 352–353 (1974)
[19] Novogrodsky, A., and Katchalski, E., *FEBS Lett.*, 12, 297–300 (1971)
[20] Novogrodsky, A., in *Immune Recognition* (edit. by Rosenthal, S.), 43–61 (Academic, New York, 1975).
[21] Greineder, D. K., and Rosenthal, A. S , *J. Immun.*, 115, 932–938 (1975).
[22] Diamantstein, T., and Ulmer, A., *Nature*, 256, 418–419 (1975).
[23] Bohme, E., Jung, R , and Mechler, I., in *Methods in Enzymology*, 38, C (edit. by Hardman, J. G., and O'Malley, B. W.), 199–202 (Academic, New York, 1974).
[24] White, A. A., and Lad, P. J., *Fedn Proc* , 34, 232 (1975).
[25] Goldberg, N. D., Haddox, M K., Hartle, D , and Hadden, J W., in *Proc. fifth int. Cong. Pharmac* , 146–169 (Karger, Basel, 1973).
[26] Hadden, J W., Coffey, R. G., Hadden, E. M., Lopez-Corrales, E., and Sunshine, G W , *Cell. Immun* , 20, 98–103 (1975).
[27] Furcht, L. T., and Gentry, S. *Cell. Immun.* (in the press)
[28] Steiner, A L., Pagliara, A. S., Chase, L. R , and Kipnis, D. M , *J. biol. Chem.*, 247, 114–1124 (1972).
[29] Glass, D. B., *et al.*, *Proc. natn. Acad. Sci. U.S.A* (in the press).

Evidence for non-deoxynucleotide linkers in Ehrlich ascites tumour cell DNA

ALTHOUGH many authors have used lysis of eukaryotic cells on alkaline sucrose gradients to measure the size of single-stranded DNA subunits, these studies cannot distinguish a true DNA subunit from a subunit containing non-DNA, alkali-stable linkers. We report here that when Ehrlich ascites tumour (EAT) cell DNA is treated with Pronase before alkali denaturation the size of the released subunit changes from $>$70S to 26S. T7 DNA present throughout remains unchanged in size, indicating that the change is not due to a soluble nonspecific nuclease.

Kavenoff and Zimm[1] have shown that the double-stranded DNA from *Drosophila* cells seems to be continuous throughout the length of the chromosome. These results do not, however, rule out the possibility of single-stranded nicks or non-deoxynucleotide linkers[2]. When eukaryotic DNA is lysed in alkali and measured either in alkaline sucrose gradients[3–6] or by viscoelastic techniques[7–8], it seems to have a molecular weight of 1×10^8–2×10^8 or larger. Although there is some disagreement, most authors consider this material to represent single-stranded DNA, particularly if the DNA is allowed to stand in alkaline detergent solutions for 3–6 h[4,5,7].

We also observe that nearly all the DNA of EAT cells (Gφ strain)[9] sediments faster than T4 (not shown) or T7 marker DNAs in alkaline sucrose gradients (Fig. 1*a*). This DNA has a molecular weight of 0.9×10^8–1.2×10^8 (not

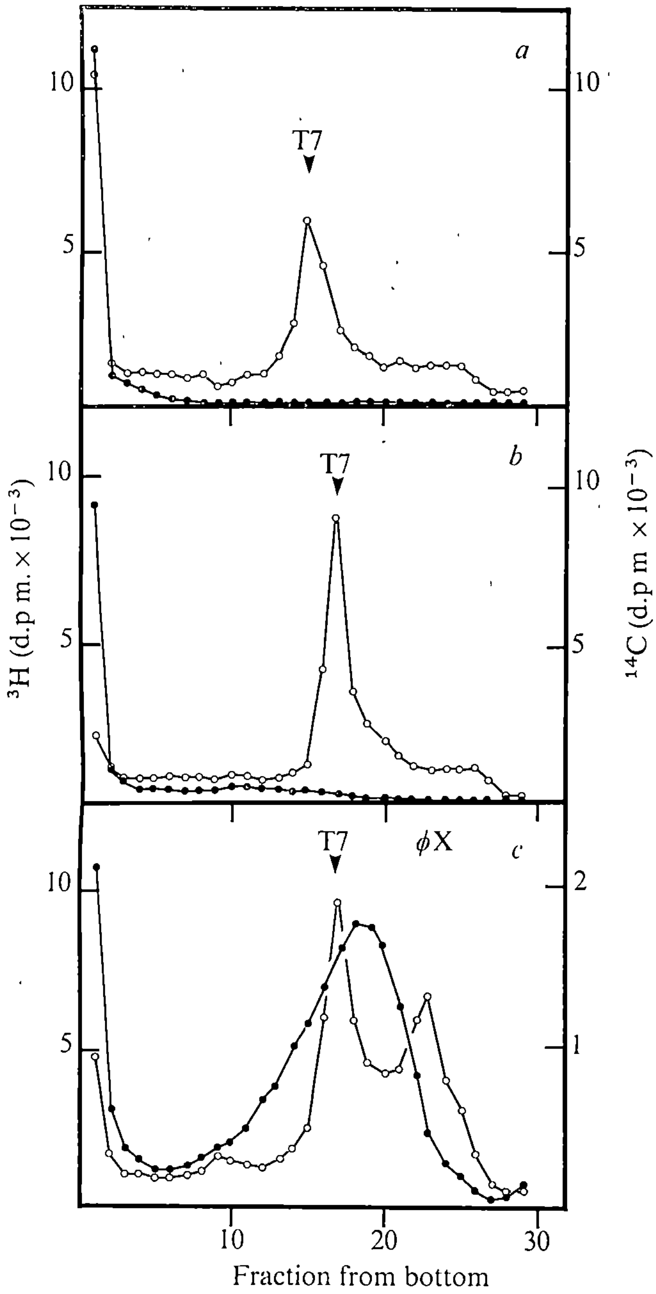

Fig. 1 Ehrlich ascites tumour cells were labelled by intraperitoneal injection of 5 μCi ^{14}C-thymidine (Amersham-Searle). The next day the cells were collected, washed twice by centrifugation in Hanks balanced salt solution, and suspended in 0.01 M EDTA, *p*H 7.5, at 10^{7} cells per ml. A cell suspension (0.5 ml) was added to 0.5 ml of lysis buffer at 50 °C in polyallomer SW 27 centrifuge tubes. The final concentrations in the lysate were 0.5 M NaCl, 0.05 M EDTA, *p*H 7.5, 0 3% sarkosyl detergent. ^{3}H-labelled T7 and ΦX phage markers and pretreated (10 min at 80 °C, 1 h autodigestion at 37 °C) Pronase P (3 mg ml^{-1}, Serva), when included, were present before addition of the cell suspension. Lysis was instantaneous. *a*, NaOH (0.1 ml of 1N) was added before cell lysis. After this alkaline lysis (*p*H 12), the lysate was at 20 °C for 9 h before gradient formation. ^{3}H-T7 was present throughout. *b*, Cells lysed at 50 °C in buffer without Pronase and incubated at 50 °C for 5 h, followed by addition of 0.1 ml 1 N NaOH for 4 h. ^{3}H-T7 was present throughout. *c*, Cells lysed at 50 °C in buffer with Pronase and incubated at 50 °C for 5 h, followed by addition of 0.1 ml 1N NaOH. ^{3}H-T7 and φX were present throughout 5–20% alkaline sucrose gradients containing 0 2 M NaCl, 0.3 N NaOH, 0.05 M EDTA, and 0 3% sarkosyl were formed beneath the lysate. Centrifugation was at 25,000 r.p m., 4 °C, for 12 h. Gradients were pumped from the bottom, fractions precipitated on Millipore filters with 10% trichloroacetic acid, washed with TCA and ethanol, and counted. ●, ^{14}C-labelled cell DNA; ○, ^{3}H-labelled phage DNA.

shown) after alkaline lysis for 3–6 h at a *p*H which is sufficient to denature DNA completely[4,7] and to dissociate all but the most tightly bound material. In agreement with previous research[8], very little cell protein cosediments with the rapidly sedimenting material. Indeed, only three protein bands are observed electrophoretically after protein specific iodination of this material (U. Plagens and D. Werner, unpublished). Shear was minimised by lysis of the cells and markers in polyallomer centrifuge tubes with subsequent formation of the sucrose gradient beneath the sample. If the cells were lysed initially in a neutral lysing solution and only made alkaline after 3–6 h at 50 °C, the DNA still sediments faster than 70S (Fig. 1*b*). Similar results are obtained at lower temperature, lower salt, less EDTA and sodium dodecyl sulphate (SDS) instead of sarkosyl. But if Pronase (3 mg ml^{-1}, heated to 80 °C for 10 min, autodigested at 37 °C for 60 min and exhibiting no nuclease activity on phage DNA) is present in the neutral lysing conditions, more than 80% of the single-stranded DNA released by alkali now sediments at 26–35S (6×10^{6}–12×10^{6} daltons) (Fig. 1*c*). This is more than an order of magnitude smaller than the smallest subunits observed after lysis of cells directly on alkaline sucrose gradients[3–6]. After exhaustive digestion with Pronase, the peak reaches a limit at 26S. With less extensive digestion, the peak is broader and closer to 35S. In each case, T7 marker DNA was present throughout the lysis and incubation of the cells. The marker remained apparently unchanged, giving an initial indication of the absence of substantial soluble DNase activity, either in the presence or absence of Pronase. Moreover, only in the case of immediate lysis in alkali is there any evidence of substantial entrapment of T7-sized DNA with the cellular DNA sedimenting to the bottom. Thus, there is no evidence that the rapidly sedimenting DNA observed in the absence of Pronase is a nonspecific aggregate of 26S subunits.

To more explicitly detect any DNase activity in, or activated by, the addition of Pronase, the experiment described in Fig. 2 was performed. ^{3}H-T7 was present during the neutral lysis of cells in the presence of Pronase and subsequent alkaline denaturation and ^{32}P-T7 was then added to the alkaline lysate (Fig. 2*a*). The label present throughout lysis and the label added only after alkaline denaturation cosediment. Alkaline lysis of the phage in the absence of cells and Pronase gives similar patterns (Fig. 2*b*) as does digestion of phage DNA with Pronase in the absence of cell DNA. The small excess of more slowly sedimenting material in the ^{3}H-labelled phage is also observed if the order of addition of phage is reversed. Similar lack of nuclease activity is observed for φX and λ DNA markers. It is thus unlikely that the change observed in the size of alkaline denatured EAT DNA after digestion with Pronase is due to a soluble DNase, since such a DNase activity must be able efficiently to recognise a site present in EAT DNA but not in any of the phage DNAs tested and to show this specificity in high salt, the absence of divalent ions, and detergent at 50 °C.

There are two general explanations for these results. EAT chromatin may contain a tightly-bound nuclease which is activated by the Pronase treatment. Such a tightly-bound nuclease activated by Pronase, SDS or heat has been described associated with colE1 plasmid DNA[10]. Alternatively, EAT DNA may contain a non-deoxynucleotide linker which is cleaved (or made alkali labile) by the Pronase treatment. Possible candidates for such a linker might include: (1) a modified, alkali-resistant ribonucleotide, such as a 2′-*O*-Me ribonucleotide, which is susceptible to an RNase activity present in, or activated by, the Pronase; (2) an RNA linker protected from alkaline degradation by a protein, either covalently linked or tightly-bound, and thus made susceptible to alkaline lysis after Pronase digestion, and (3) a protein or peptide linker in the DNA.

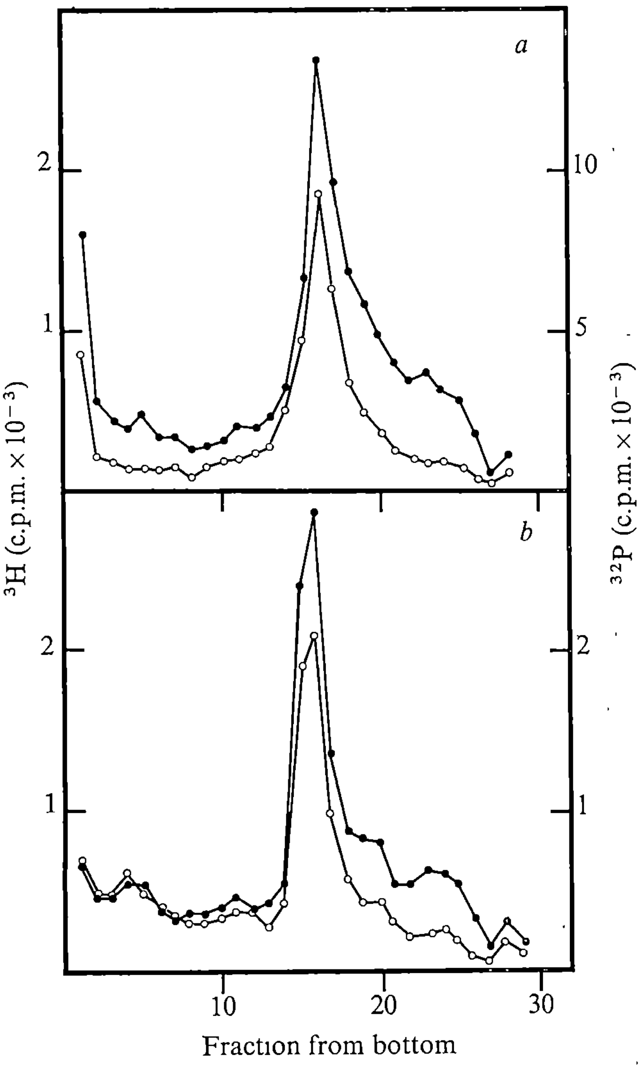

Fig. 2 *a*, 5 × 10^6 unlabelled Ehrlich ascites tumour cells were lysed in 1 ml of lysis buffer containing Pronase (3 mg ml^{-1}) and ^{3}H-T7 phage marker The lysate was incubated for 5 h at 50 °C, followed by addition of 0.1 ml of 1N NaOH. After addition of alkali, ^{32}P-T7 phage was added. *b*, ^{3}H and ^{32}P-labelled phage were lysed in 1 ml of lysis buffer made alkaline by addition of 0.1 ml of 1N NaOH. Alkaline sucrose gradients were formed, centrifuged, fractionated and counted as described in the legend to Fig. 1. ●, ^{3}H-T7; ○, ^{32}P-T7.

A preliminary experiment indicates that a chromatin-bound nuclease activated by Pronase is unlikely, since DNA lysed in alkali for 60 min, subsequently neutralised by dialysis, and treated with Pronase also exhibits primarily 26S DNA after a second alkaline lysis. Similarly treated DNA not digested with Pronase is rapidly sedimenting. It is unlikely that a chromatin-bound nuclease would survive the initial alkaline lysis.

RNA linkers have been observed in mitochondrial DNA[11], and we cannot, at present, exclude the possibility of a modified alkali-resistant RNA linker or an RNA linker protected from alkali by protein.

A protein or peptide linker should be affected by Pronase digestion. The possibility of protein linkers in eukaryotic chromatin has been indicated by the presence of associated, cosedimenting peptide sequences in purified DNA[12]. But the early discussions of protein linkers in DNA often assumed such linkers were "in register" on the anti-parallel strands[13]. Such "in register" linkers are unlikely since double-stranded DNA is insensitive to proteolysis[1]. Pronase-treated EAT cell DNA sedimented in neutral conditions is also extremely large if precautions are taken to avoid shear and denaturing conditions. It should be noted, however, that a protein linker has been observed in adenovirus DNA[14] and is apparently related to its replication.

Since stationary phase cells have been reported to have fragmented DNA of the size observed here[15], it is important to note that the EAT cells had a labelling index of 28±1%. Results similar to those described here have also been obtained with the Karzel strain[16] of EAT cells in exponential growth in tissue culture, using a lower cell density in the lysate.

Using similar lysing conditions with CHO (ref. 3) or mouse L cells[17], others have observed a single-strand subunit of 60×10^6 or 45×10^6 daltons, which is larger than the pieces observed here but smaller than subunits observed by simple alkaline lysis[3–8]. Moreover, Taylor *et al.*[18,19] have observed the double-strand equivalent of the single-stranded 26S DNA in CHO cells. These double-stranded fragments seemed to be enriched in newly-replicated DNA.

Many authors[3–8] have used lysis of eukaryotic cells in alkali to measure the size of long single-stranded DNA. The data presented here indicate that the single-stranded 'DNA' may be composed of smaller subunits linked by alkali stabile linkers which can be removed or made alkali labile by treatment with Pronase. The 26S subunits produced do not seem to be a result of soluble nuclease activity during digestion with Pronase.

We thank K. Geider and H. Kaerner for their assistance in preparing phage markers. This work was supported by the German Cancer Research Centre while H.V.H. was a visiting scientist at the Institute for Cell Research.

HOWARD V. HERSHEY

Department of Zoology,
Indiana University,
Bloomington, Indiana 47401

DIETER WERNER

Institut für Zellforschung,
Deutsches Krebsforschungszentrum,
D-69 Heidelberg, FRG

Received November 17, 1975; accepted May 18, 1976.

[1] Kavenoff, R., and Zimm, B. H , *Chromosoma*, **41**, 1–27 (1973).
[2] Hays, J B , and Zimm, B. H., *J. molec. Biol* , 48, 297–317 (1970).
[3] Hozier, J. C., and Taylor, J H , *J molec Biol* , 93, 181–201 (1975).
[4] Parodi, S., *et al* , *Biochim. biophys Acta*, 407, 174–190 (1975).
[5] Cleaver, J E., *Biochem biophys. Res Commun.*, 59, 92–99 (1974).
[6] Simpson, J , Nagle, W., Bick, M , and Belli, J., *Proc natn. Acad Sci U.S.A* , 70, 3660–3664 (1973).
[7] Linn, J. D., and Wheeler, K T , *Biochem. biophys. Res. Commun.*, 65, 712–716 (1975).
[8] Uhlenhopp, E. L., *Biophys. J.*, 15, 233–237 (1975)
[9] Lettre, R , Paweletz, N , Werner, D., and Granzow, C., *Naturwissenschaften*, **59**, 59–63 (1972)
[10] Clewell, D. B., and Helinski, D. R., *Proc. natn. Acad. Sci. U.S.A.*, 62, 1159–1166 (1969).
[11] Grossman, L. I., Watson, R , and Vinograd, J., *Proc. natn. Acad. Sci. U S.A.*, **70**, 3339–3343 (1973)
[12] Bendich, A., and Rosenkranz, H. S , *Prog Nucleic Acids Res.*, **1**, 219–230 (1963).
[13] Taylor, J. H., *Int. Rev Cytol* , 13, 39–73 (1962).
[14] Robinson, A J , Youngblood, H. B., and Bellet, A. J , *Virology*, 56, 54–69 (1973).
[15] Mego, W A , thesis, Florida State Univ (1970)
[16] Karzel, K , and Schmid, O J , *Arzneimittel-Forsch.*, **18**, 1500–1504 (1968).
[17] Fujiwara, Y , *Cancer Res* , 35, 2780–2789 (1975).
[18] Taylor, J. H , *Proc. natn. Acad Sci. U S A* , 70, 1083–1087 (1973).
[19] Taylor, J H , Adams, A. G., and Kurek, M. P., *Chromosoma* 41, 861–384 (1973).

Intact 3′ end of 16S rRNA is not required for specific mRNA binding

INITIATION of protein synthesis in bacteria requires that ribosomes bind to specific regions of messenger RNA (mRNA) in a complex which also contains fMet-tRNA, GTP, initiation factors[1] and involves the ribosomal proteins S1 and S12 (refs 2–5). Shine and Dalgarno proposed a mechanism for initiation of protein synthesis in which certain purine-rich nucleotide sequences near the initiator codon of prokaryotic messages were postulated to form base pairs with the nucleotide sequence (5′) ACCUCCUUA(3′) near the 3′ end of the 16S ribosomal RNA[6,7]. The formation, *in vitro*, of a complex between the 3′ end of the 16S rRNA from *Escherichia coli* ribosomes and the initiator

Fig. 1 Sucrose density gradient analysis of initiation complexes after RNase digestion. Binding reactions were carried out in conditions described by Steitz[9], at 37 °C in 0.1 ml of a solution containing 0.1 M Tris-HCl (*p*H 7.4), 0.05 M NH$_4$Cl; 0.005 M magnesium acetate (RBS buffer); 0.001 M GTP; 3–5 μg of purified *N*-formylmethionyl tRNA from *E. coli*; (α-^{32}P-UTP)-labelled f1 or φX174 mRNA synthesised *in vitro*, as described by Pieczenik, *et al.*[10], specific activity $\sim 2\times10^8$ counts μg^{-1}; 4.5 A_{260} of *E. coli* ribosomes, and 37.5 μg phage f2 RNA. The binding reactions were done in conditions of limiting ribosomes. This was determined by a set of binding reactions (not shown) with constant amounts of ribosomes and increasing amounts of unlabelled f2 RNA, as competitor for a constant amount of radioactively labelled mRNA. The ribosomes were isolated from S-30 extracts prepared as described by Webster, *et al.*[26] 0.225 ml of S-30 was incubated at 37 °C with TM buffer (50 mM Tris-HCl, *p*H 7.6; 30 mM NH$_3$Cl; 10 mM Mg acetate) (control) or with 0.06 ml of a solution of colicin E3, 2.2 mg ml^{-1}. At the end of 20 min, 18 μg of colicin E3 immunity protein[17] in TM buffer were added to terminate the action of the colicin. Aliquots were then removed to measure the capacity of the treated ribosomes to carry out f2 RNA-directed protein synthesis *in vitro*[17]. Debris was removed from the samples by centrifugation at 12,500 r.p.m. for 15 min and then the ribosomes were pelleted by centrifugation for 3.5 h at 35,000 r.p.m. in the SW50.1 rotor. The supernatants were discarded and the ribosomal pellets suspended in TM buffer to give a final concentration of approximately 1,000 A_{223} ml^{-1} for the binding reactions. Binding reactions were carried out for 12 min at 37 °C, cooled, and then pancreatic ribonuclease (Worthington) was added to give a final concentration of 5.5 μg ml^{-1}. Reactions were warmed at 37 °C for 30 s, incubated at room temperature for 20 min, cooled on ice, layered on to 5 ml 5–20% sucrose gradients in RBS buffer, centrifuged for 2.25 h at 37,000 r.p.m. in the SW50.1 rotor of the Beckman Model L2-65B ultracentrifuge, at 5 °C. Fractions of 2 drops each were collected through a needle at the bottom of the gradients and their Cerenkov radiation monitored. *a*, Binding of ribosomes to ^{32}P-f1 mRNA. ●, control ribosomes: ○, colicin E3-treated ribosomes; ×, binding reaction done in the absence of fMet-tRNA. *b*, Binding of ribosomes to ^{32}P-αX174 mRNA. ●, control ribosomes; ○, colicin E3-treated ribosomes.

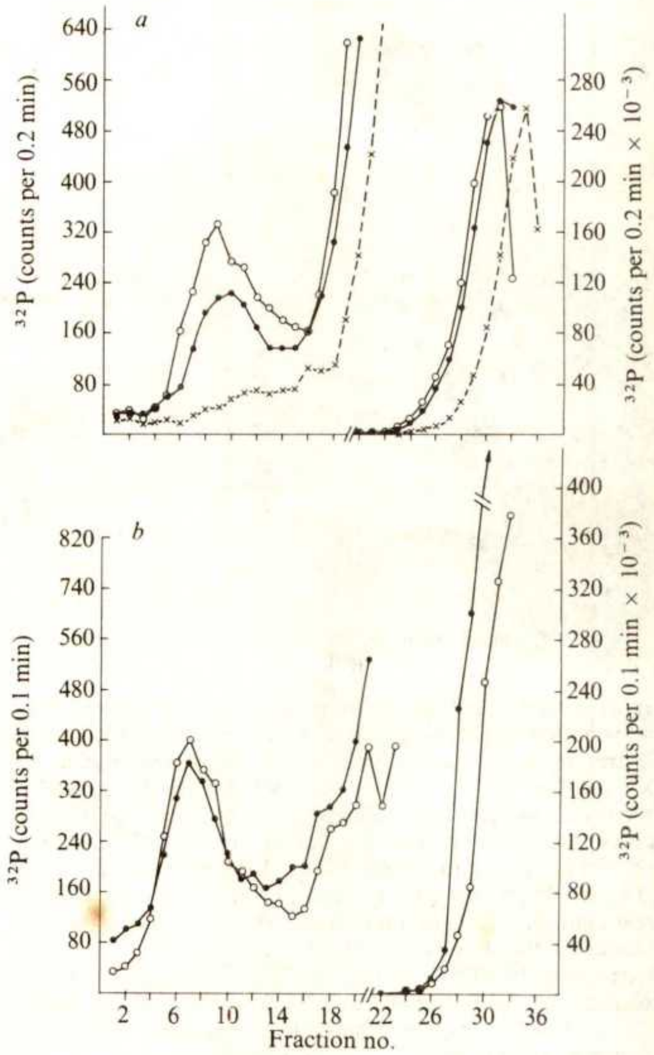

region of phage R17 A-protein mRNA has been demonstrated[8]. This binding supports the involvement of such base pairing in the binding of mRNA to ribosomes, at least for this message.

The ability of ribosomes to protect regions of mRNA of specific sequence from nuclease digestion is considered to be a general measure of specific binding between ribosomes and mRNA[9], and depends on the presence of fMet-tRNA[9] and yields specific sequences on fingerprint analysis[9].

Colicin E3 induces a specific break 49 nucleotides from the 3′ end of the 16S rRNA in the 30S ribosomal subunit, but does not lead to the loss of the cleavage product from the ribosome[11–15]. The question arose, given the Shine and Dalgarno hypothesis[6], as to whether colicin treatment of ribosomes would affect the mRNA binding reaction. We report here that treatment of *E. coli* ribosomes with colicin E3 had no significant effect on their ability to protect phage f1 or φX174 mRNA initiation sequences from RNase digestion (Fig. 1). Furthermore, fingerprinting analysis of the protected RNA suggests that the complexity and specificity of the protected RNA remain largely unchanged following colicin treatment (Fig. 2). The amount of radioactively labelled mRNA protected from RNase digestion was, in fact, consistently higher when colicin-treated ribosomes were used than when untreated ribosomes were used in the protection assay (Fig. 1).

As shown in Fig. 1, the colicin treatment had lowered the ability of the treated ribosomes to carry out f2 RNA-directed protein synthesis by 75%. Even when colicin treatment was carried out in the presence of f2 mRNA and supernatant factors, a procedure which inactivates ribosomes to greater than 90% (ref. 16), little or no decrease in their ability to protect initiation sequences was observed (data not shown).

Ribosomes treated in the presence of colicin E3 immunity protein, which prevents the action of colicin E3 *in vitro*[17], behaved like untreated, control ribosomes (data not shown).

To determine whether there were any differences in the sequences protected by treated ribosomes, the peaks of ribosome-bound mRNA from the reactions shown in Fig. 1 were collected, separated from the ribosomes, and subjected to two-dimensional T$_1$ fingerprint analysis, as described by Pieczenik, *et al.*[10]. The results for the f1 mRNA are shown in Fig. 2. The f1 mRNA protected by untreated and E3-treated ribosomes give similar fingerprints. There may be some minor differences in the amounts of some of the sequences protected, as measured by the intensity of the spots. No sequences were, however, completely eliminated, nor did any new spots appear as a result of the colicin treatment. The ribosome-protected fragments from φX174 mRNA (Fig. 1) were also subjected to two-dimensional T$_1$ fingerprint analysis, and here again the sequences protected by colicin-treated ribosomes did not differ appreciably from those protected by the untreated ribosomes (Ravetch, Robertson and Model, unpublished). Thus we infer that there was no change in the specific mRNA sequences protected by those ribosomes.

The three ribosome binding sites of phage f1 mRNA have been sequenced[10]. Their sequences have the potential to form base-pair interactions with the polypyrimidine stretch near the 3′ end of the 16S rRNA. These potential structures are shown in Fig. 3. Although the number of base pairs differ, the free energies estimated by using the method of Tinoco, *et al.*[18] are comparable. These potential structures can be expected to have similar stabilities.

Although Tai and Davis[19], Tai[20], and Konisky[21] have

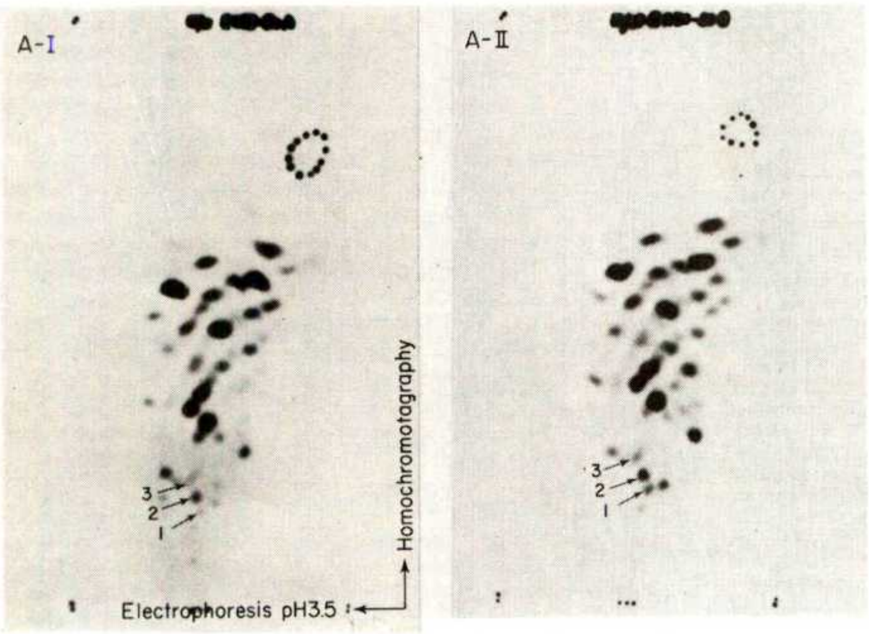

Fig. 2 T_1 fingerprint analysis of ribosome-protected fragments from ^{32}P-labelled f1 mRNA for untreated (*A*-I) and colicine E3-treated (*A*-II) ribosomes. Two-dimensional fingerprint analysis was carried out as described previously[27]. Arrows indicate the major T_1 oligonucleotides of the three ribosome binding sites of f1 mRNA[10]. The origins of chromatography were uniformly at the position marked in Fig. *A*-I.

reported that colicin E3 inhibits initiation of protein synthesis on natural messages, others have reported that colicin E3 treatment does not inhibit (AUG)-dependent binding of fMet-tRNA[22] or poly(U) or MS2 RNA[23] to 30S subunits. Our results indicate that colicin E3-induced cleavage of ribosomes does not prevent the formation of 70S initiation complexes on natural messages, so that block which colicin E3 causes in protein synthesis must be at a later step. Colicin treatment in the conditions used here does not result in release of the 3′ terminal RNA fragments from the 30S ribosomal subunit[13,15], so that while an intact 16S RNA is not required for initiation complex formation, the presence of the cleavage fragment may still be needed for proper alignment of the message on the ribosome.

Baan *et al.*[24] have found that cloacin DF13, which has a mode of action virtually identical to colicin E3 (ref. 25), does not appreciably inhibit the formation of an initiation complex between ribosomes and MS2 mRNA in the absence of IF-1. They find that cleavage by the cloacin causes a reduction in the rate, but not the final amount of initiation complex formed, and they postulate improper functioning of IF-1. The initiation complexes formed were fully reactive with puromycin. They also observed a reduced ability of the second aminoacyl tRNA (alanyl-tRNA for the case of MS2 RNA) to bind, but such alanyl-tRNA as did bind was able to participate in dipeptide formation. Their observations are in accord with our results. Our data and those described above[24], therefore, bear on the question as to whether colicin E3 treatment of ribosomes inhibits the initiation or elongation steps of protein synthesis. Since the peptidyl transferase has previously been shown to be undamaged by colicin E3 treatment[22], and dipeptide formation is not blocked[24], the lesion induced by colicin E3 is most likely in the translocation step of protein synthesis.

Fig. 3 Potential base-pair interactions between f1 mRNA ribosome binding sites and the 3′ end of 16S ribosomal RNA. Sequence determination was described by Pieczenik *et al.*[10]. Free energy estimates were made using the method of Tinoco *et al.*[18].

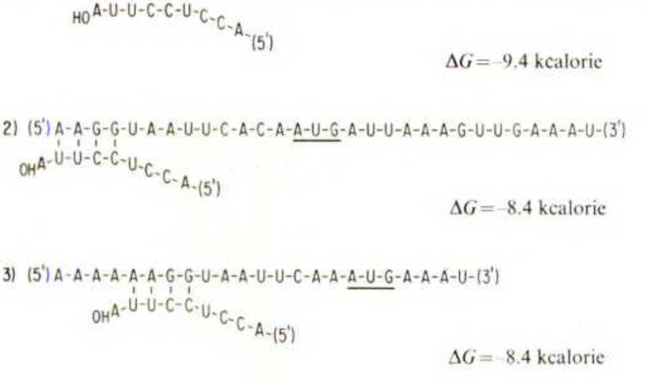
1) (5′) U-U-U-A-A G-G-A-A-A-C-U-U-C-C-U-C-A-U-G-A-A-A-A-A-G-U-C-U-U-U-(3′)
U
HO A-U-U-C-C-U-C-C-A-(5′)
ΔG = −9.4 kcalorie
2) (5′) A-A-G-G-U-A-A-U-U-C-A-C-A-A-U-G-A-U-U-A-A-A-G-U-U-G-A-A-A-U-(3′)
OH A-U-U-C-C-U-C-C-A-(5′)
ΔG = −8.4 kcalorie
3) (5′) A-A-A-A-A-A-G-G-U-A-A-U-U-C-A-A-A-U-G-A-A-A-U-(3′)
OH A-U-U-C-C-U-C-C-A-(5′)
ΔG = −8.4 kcalorie

Our results suggest that cleavage of the 3′ end of the 16S ribosomal RNA does not affect the specificity of the binding of ribosomes to f1 or φX174 mRA. An intact 3′ end of the 16S rRNA is apparently not essential to confer stability and specificity on mRNA binding. In fact, perhaps the greater flexibility of the 16S rRNA allowed by its cleavage by colicin E3 may be responsible for the enhanced level of binding observed after colicin E3 treatment (Fig. 1). The failure of colicin E3-treated ribosomes to function in f2 mRNA-directed protein synthesis implies, however, that an intact 16S rRNA is required for translocation to occur on the ribosomes.

We thank Peter Model for his encouragement and helpful advice and for providing us with radioactively labelled mRNA. We also thank Norton Zinder, Hugh Robertson and Joan Steitz for helpful discussions. This research was supported in part by grants from the NSF to N. D. Zinder and H. D. Robertson.

JEFFREY V. RAVETCH
KAREN S. JAKES

The Rockefeller University,
New York, New York 10021

Received March 15; accepted April 27, 1976.

[1] Lengyel, P., in *Ribosomes* (edit. by Nomura, M., Tissieres, A., and Lengyel, P.), 13–52 (Cold Spring Harbor Laboratory, New New York, 1974).
[2] Szer, W., and Leffler, S., *Proc. natn. Acad. Sci. U.S.A.*, **71**, 3611–3615 (1974).
[3] Szer, W., Hermoso, J., and Leffler, S., *Proc. natn. Acad. Sci. U.S.A.*, **72**, 2325–2329 (1975).
[4] Held, W. A., Gette, W. R., and Nomura, M., *Biochemistry*, **13**, 2115–2122 (1974).
[5] Goldberg, M. L., and Steitz, J. A., *Biochemistry*, **13**, 2123–2129 (1974).
[6] Shine, J., and Dalgarno, L., *Proc. natn. Acad. Sci. U.S.A.*, **71**, 1342–1346 (1974).
[7] Shine, J., and Dalgarno, L., *Nature*, **254**, 34–38 (1975).
[8] Steitz, J. A., and Jakes, K., *Proc. natn. Acad. Sci. U.S.A.*, **72**, 4734–4738 (1975).
[9] Steitz, J. A., *Nature*, **224**, 957–964 (1969).
[10] Pieczenik, G., Model, P., and Robertson, H. D., *J. molec. Biol.*, **90**, 191–214 (1974).
[11] Bowman, C. M., Dahlberg, J. E., Ikemura, T., Konisky, J., and Nomura, M., *Proc. natn. Acad. Sci. U.S.A.*, **68**, 964–968 (1971).
[12] Senior, B. W., and Holland, I. B., *Proc. natn. Acad. Sci. U.S.A.*, **68**, 959–963 (1971).

[13] Boon, T., *Proc. natn. Acad Sci U.S.A.*, 68, 2421–2425 (1971)
[14] Bowman, C. M., Sidikaro, J., and Nomura, M., *Nature new Biol.*, 234, 133–137 (1971).
[15] Dahlberg, A. E., and Dahlberg, J. E., *Proc natn Acad. Sci. U.S.A.*, 72, 2940–2944 (1975).
[16] Jakes, K., and Zinder, N. D , *J. biol. Chem.*, 249, 5507–5512 (1974).
[17] Jakes, K , Zinder, N. D., and Boon, T., *J. biol Chem.*, 249, 438–444 (1974).
[18] Tinoco, I., Jr, *et al.*, *Nature new Biol* , 246, 40–41 (1973).
[19] Tai, P.-C., and Davis, B. D., *Proc. natn. Acad Sci. U.S.A* , 71, 1021–1025 (1974).
[20] Tai, P.-C., *Biochem. biophys. Res. Commun.*, 67, 1466–1472 (1975)
[21] Konisky, J , *thesis*, Univ. Wisconsin, Madison (1968).
[22] Turnowsky, F., and Hogenauer, G., *Biochem biophys. Res. Commun.*, 55, 1246–1254 (1973).
[23] Konisky, J., and Nomura, M., *J. molec. Biol.*, 26, 181–195 (1967)
[24] Baan, R. A., Duijfjes, J. J., van Leerdam, E., van Knippenberg, P. H., and Bosch, L., *Proc. natn. Acad Sci. U.S.A.*, 73, 702–706 (1976)
[25] de Graaf, F. K., Niekus, H G. D., and Klootwijk, J., *FEBS Lett* , 35, 161–165 (1973).
[26] Webster, R. E., Engelhardt, D. L., Konigsberg, W., and Zinder, N. D., *J. molec. Biol.*, 29, 27–43 (1967)
[27] Barrell, B. G., in *Procedures in Nucleic Acid Research*, II (edit. by Cantoni, G L., and Davies, D. R.), 751–779 (Harper and Row, New York, 1971).

Occurrence of *trans*-ribosylzeatin in *Agrobacterium tumefaciens* tRNA

THE cytokinin-active N-6-isoprenoid-substituted purine nucleosides have wide distribution as minor components of the tRNA of animals, bacteria and plants. Skoog, Hall and others (refs in ref, 1) have shown that there are three classes of cytokinin nucleosides, and that one member of each predominates in the tRNA of organisms from each kingdom. Thus, animal tRNA contains 6-(3-methylbut-2-enylamino)-9-β-D-ribofuranosyl purine[2] (iPA); whereas in bacterial tRNA, the purine ring is thiomethylated and the predominant cytokinin-active nucleoside is 6-(3-methylbut-2-enylamino)-2-methylthio-9-β-D-ribofuranosyl purine[3] (ms-iPA). In plants, the isoprenoid side chain is hydroxylated and the predominant cytokinin-active nucleoside is 6-(4-hydroxy-3-methylbut-2-enylamino)-9-β-D-ribofuranosyl purine[4] (zeatin riboside, ZR). Minor amounts of 2-methylthio zeatin riboside (ms-ZR) are also present[5]. But the distribution of these nucleosides may not be quite so clearcut. The plant pathogenic prokaryote *Corynebacterium fascians* has been shown[6] to release *cis*-zeatin into the culture medium. Other evidence[7] suggests that *Pseudomonas aeruginosa* tRNA contains ms-ZR. It may be that some prokaryotes have acquired the ability to hydroxylate the isoprenoid side chain and that zeatin and its derivatives are not restricted to plants. We have now examined the cytokinin-active nucleosides from the tRNA of *Agrobacterium tumefaciens*, the causative organism of plant crown gall disease. Besides the expected ms-iPA and small amount of iPA, *trans*-ZR was present in significant amounts.

Four strains of *A. tumefaciens* were examined. Two strains, IIBV7 and C-58, are virulent and have been shown to harbour a large plasmid which is associated in some way with virulence[8]. The other two strains IIBNV6 and NT1, are avirulent and do not contain the plasmid. Strains C-58 and NT1 are very closely related in that NT1 is derived from C-58 by heat treatment which causes elimination of the plasmid with concurrent loss of virulence.

Cells were grown to late log phase on rich medium[9]. The tRNA was isolated by Kirby's procedure, purified by extraction with sodium acetate, and freed from traces of DNA by treatment with *m*-cresol-sodium benzoate[10]. Cytokinin-active nucleosides were isolated by alkaline hydrolysis and dephosphorylation with *E. coli* alkaline phosphatase and were extracted into 1-butanol. The butanol-soluble fraction was subjected to high pressure reversed-phase chromatography (HPLC) on octadecyl-substituted silica and cytokinin activity was detected in the column eluate by means of the cucumber cotyledon bioassay of Fletcher and McCullagh[11]. Figure 1 shows an HPLC profile obtained for IIBNV6 tRNA hydrolysate.

Standard cytokinins eluted from the column in decreasing order of polarity. The most polar, zeatin riboside, eluted before zeatin which in turn eluted before iPA, iP and ms-iPA. The hydrolysate contained five regions where cytokinin activity was significantly above baseline. The first two peaks of activity eluted at 16–24 ml and 32–36 ml and contained substances more polar than zeatin riboside. They have not been characterised further. The three major peaks (eluting at 40–48 ml, 56–64 ml and 68–76 ml) coeluted with authentic ZR, iPA and ms-iPA. To establish their identity, the appropriate fractions were pooled and the nucleosides were converted into their permethyl[12] or trimethylsilyl (TMS) ethers[13] which were then examined by gas chromatography–mass spectroscopy (GC–MS).

The fraction with mobility identical to iPA gave, when permethylated, a derivative which exhibited a single peak on gas chromatography identical in retention time to permethylated iPA. Examination of the mass spectrum of this peak showed it to possess a molecular ion $M^{+\bullet} = 391$ and major fragment ions at 376 (loss of $CH_3^{\bullet}$), 348 (loss of $C_3H_7^{\bullet}$ with ring closure of the isoprenoid side chain onto the purine N-1 position), 217 (fission of the base and ribose with transfer of a hydrogen atom to give $BH^{+\bullet}$), 202 (loss of $CH_3^{\bullet}$ from $BH)^{+\bullet}$, and 174 (loss of C_3H_7 from $BH^{+\bullet}$). The ion at $m/e = 45$ was characteristic of the fragment ion $CH_3OCH_2^{+}$ arising from the 6 position of ribose[12]. Studies with deuterated methyl iodide confirmed the fragmentation assignments and the presence of four methyl groups within the molecule. Its spectrum was identical with an authentic sample of tetramethyl iPA. Von Minden and McCloskey[15] have reported an identical spectrum and peak assignments for tetramethyl iPA.

Similarly, the HPLC fraction corresponding in mobility to ms-iPA gave on permethylation a product whose GC retention

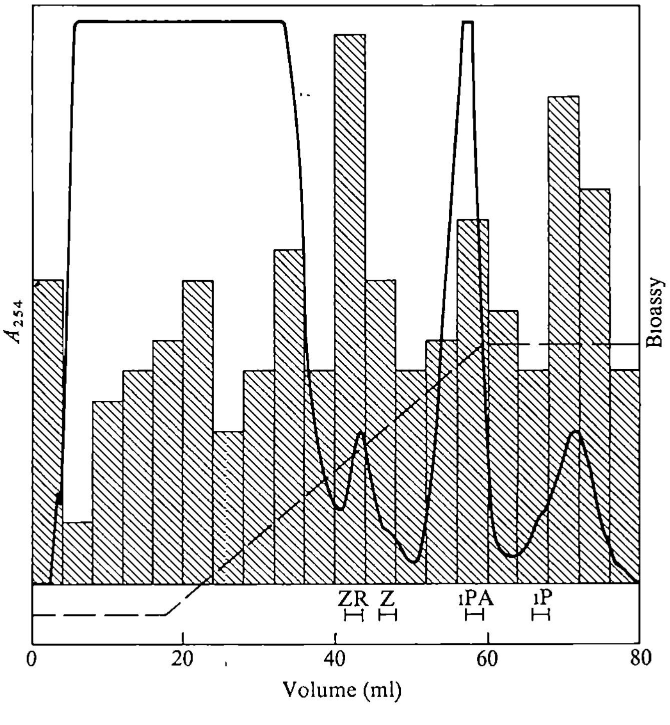

Fig. 1 High pressure liquid chromatography of *A. tumefaciens* (strain IIBNV6) tRNA hydrolysate. Purified tRNA (~2,000 A_{260} U from organisms grown in rich medium to late log phase was hydrolysed with 0.3 M KOH under nitrogen at 37 °C for 24 h, treated with bacterial alkaline phosphatase (Sigma, 150 U ml^{-1}) at *p*H 8.8 in the presence of 10 mM $MgCl_2$ at 37 °C for 16 h and extracted with 1-butanol. The extract was evaporated, taken up in a minimum volume of 5% ethanol, *p*H 3.5, and applied to a 0.3 × 60-cm column of octadecyl-substituted silica (C_{18}/Porasil B, 37-75 μm, Waters Associates) previously equilibrated with 0.02 M ammonium acetate buffer, *p*H 3.5, containing 5% ethanol. The column was eluted with a linearly increasing gradient of ethanol (5–50%) over 40 ml at a flow rate of 4 ml min^{-1}. Fractions (4 ml) were collected, lyophilised and assayed for the presence of cytokinin-active nucleosides by the procedure of Fletcher and McCullagh[11]. - - - -, Ethanol gradient; ——, A_{254}. Hatching shows cytokinin activity (arbitrary units). Cytokinin standards eluted at the positions indicated.

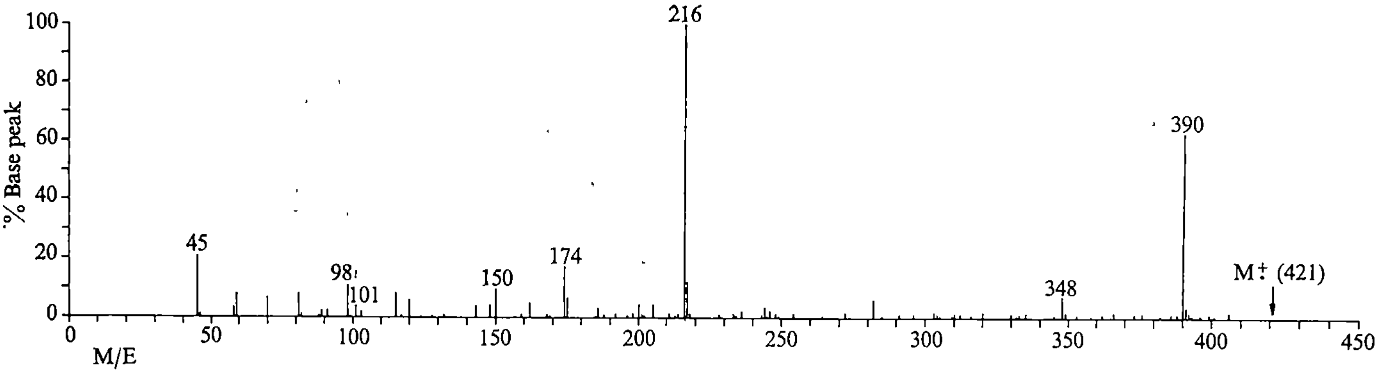

Fig. 2 Mass spectrum of permethylated nucleoside from *A. tumefaciens* tRNA HPLC fractions containing cytokinin-active material with the same mobility as ZR (Fig. 1 fractions 40–48 ml) were evaporated and the residue was permethylated by reaction with methyl iodide in the presence of a fivefold excess of dimethyl-sulphinyl anion in dimethylsulphoxide[12]. The reaction mixture was diluted with water, the permethyl ethers were extracted into chloroform and analysed by GC–MS GC conditions were: glass column; 3% Dexsil on Anachrom A, 28 cm; He carrier, flow 15 ml min^{-1}; 150 °C for 3 min, then 8 °C min^{-1} to 350 °C. The column effluent was admitted to the source of a Varian CH7 magnetic sector spectrometer through a single stage glass jet separator at 240 °C. Spectra were recorded continuously (at 70 eV) during the chromatographic run and processed, stored, and analysed on an accompanying data system (System Industries; System 150).

time and mass spectrum were identical with those of authentic tetramethyl ms-IPA. $\mathrm{M}^{+}_{\bullet} = 437$, fragment ions at *m/e* 423 ($-\mathrm{CH}_3^\bullet$), 394 ($-\mathrm{C_3H_7^\bullet}$ and side chain cyclisation), 263 ($\mathrm{BH}^{+}_{\bullet}$), 248 ($\mathrm{BH}^{+}_{\bullet}-\mathrm{CH}^\bullet$), and 220 ($-\mathrm{C_3H_7^\bullet}$ from $\mathrm{BH}^{+}_{\bullet}$). As expected, all major fragments derived from the adenine nucleus were shifted +46 mass units from the corresponding iPA fragments due to the presence of the thiomethyl group at the 2 position of the purine ring.

The HPLC fraction with mobility equal to that of ZR gave on permethylation a product which GC revealed to have two major components. The first gave a mass spectrum identical to authentic permethylated dimethyl adenosine and was not examined further. The second, whose spectrum is shown in Fig. 2 had major fragment ions present at 390 and 216, and a small molecular ion at 421. Its spectrum was identical to that of authentic pentamethyl ZR. Probable peak assignments (confirmed by deuteromethylation) are $\mathrm{M}^{+}_{\bullet} = 421$; 390, loss of $\mathrm{OCH}_3^\bullet$; 216, loss of $\mathrm{OCH}_3^\bullet$ from $\mathrm{BH}^{+}_{\bullet}$; 174, loss of $\mathrm{C_3H_7^\bullet}$ from $\mathrm{BH}^{+}_{\bullet}$ (cyclisation). Loss of the allylic methyl ether fragment ($\mathrm{OCH}_3^\bullet$) was favoured over the loss of $\mathrm{C_3H_7^\bullet}$ and subsequent ring closure found in iPA and ms-iPA. Details of these spectra will be published elsewhere.

Examination of the trimethylsilyl ethers derived from this HPLC fraction confirmed the presence of ZR. Gas liquid chromatography on Dexsil 300 can resolve *cis*-(TMS)$_4$ZR from *trans*-(TMS)$_4$ZR (ref. 13). The sample of (TMS)$_4$ZR from IIBNV6 hydrolysate had a retention time of 18.2 min, identical to that of authentic *trans*-(TMS)$_4$ZR. The *cis*-isomer in identical conditions had $R_t = 17.8$ min.

We conclude, therefore, that *A. tumefaciens* strain IIBNV6 tRNA contains, besides the iPA and ms-iPA expected for prokaryotes, the hydroxylated cytokinin nucleoside *trans*-ZR, the *cis*-isomer of which is normally found in plant tRNA. Other strains of *A. tumefaciens* also contained *trans*-ZR although at lower levels than IIBNV6. Visual estimates (from HPLC and GC traces) suggested that *trans*-ZR made up about 30% of the total cytokinin-active nucleosides in IIBNV6 tRNA. In the related virulent strain IIBV7 the level was comparable. In C-58 and NT1, however, the level was much lower (5–10% of the total) and a fourth active component was present. It had a mobility on HPLC intermediate between ZR and iPA, and has yet to be identified. Differences in cytokinin content between strains did not appear to correlate with virulence and may reflect the nutritional and growth status of the culture, as is the case for the modified nucleoside "Q" in BALB/3T3 tRNA (ref. 16).

The unequivocal demonstration of zeatin riboside in the tRNA of *A. tumefaciens* confirms evidence developed by others that some prokaryotes may be able to hydroxylate the isoprenoid sidechain of cytokinins. Cheryayil[7] used ^{35}S to demonstrate the probable presence of methylthiozeatinriboside in *Pseudomonas aeruginosa* tRNA while Torrey[17] has isolated a cytokinin from *Rhizobium* tRNA which, although not identified conclusively, has the chromatographic properties expected for zeatin riboside. In contrast, no evidence has been published for the presence of zeatin riboside in *E. coli*[3] or *Staphylococcus epidermidis*[18] tRNA. The common factor which unites those prokaryotes which can hydroxylate the isoprenoid side chain is their association with plants, either as pathogens or symbionts. It remains to be seen whether this factor has a necessary role in their association with the host plant or if it is merely fortuitous.

R. W. CHAPMAN
R. O. MORRIS

Department of Agricultural Chemistry,

J. B. ZAERR

Forest Research Laboratory,
Oregon State University,
Corvallis, Oregon 97331

Received March 24, accepted May 6, 1976.

[1] Skoog, F., and Armstrong, D. J., *A Rev. Pl. Physiol.*, 21, 359–384 (1970).
[2] Robins, M. J., Hall, R. H., and Thedford, R., *Biochemistry*, 6, 1837–1848 (1967).
[3] Burrows, W. J., *et al*, *Biochemistry*, 7, 3071–3076 (1969).
[4] Hall, R. H, Csonka, L., David, H, and McLennan, B., *Science*, 156, 69–71 (1967)
[5] Hecht, S. M., *et al.*, *Science*, 166, 1272–1274 (1969).
[6] Scarbrough, E., Armstrong, D J., Skoog, F., Frihart, C R, and Leonard, N J., *Proc natn. Acad Sci U.S A.*, 70, 3825–3829 (1973)
[7] Thimmappaya, B., and Cherayil, J. D, *Biochem biophys Res Commun*, 60, 665–672 (1974).
[8] Watson, B., Currier, T. C, Gordon, M. P, Chilton, M D, and Nester, E. W., *J. Bact*, 123, 255–264 (1975).
[9] Kado, C I., and Heskett, M G, *Phytopathology*, 60, 969–976 (1970).
[10] Hastings, J. R. B., and Kirby, K. S, *Biochem. J*, 100, 532–539 (1966).
[11] Fletcher, R A., and McCullagh, D., *Can. J Bot*, 49, 2197–2201 (1971)
[12] Hakomori, S, *Biochem. J., Tokyo*, 55, 205–208 (1964).
[13] Babcock, D F., and Morris, R O, *Biochemistry*, 9, 370ff–3705 (1970)
[14] Dolhun, J J, and Wiebers, J. L., *Org Mass Spectrom*, 3, 669–681 (1970).
[15] von Minden, D. L, and McCloskey, J. A, *J. Am. chem Soc*, 95, 7480–7490 (1973).
[16] Katze, J R, *Biochim. biophys. Acta*, 383, 131–139 (1975).
[17] Phillips, D A, and Torrey, J G., *Pl. Physiol, Lancaster.*, 49, 11–15 (1972)
[18] Armstrong, D J, *et al*, *J biol Chem*, 245, 2922–2926 (1970).

Nature **Index and Binders**

The **Index** for 1975 is now available, price £2.25. Copies of the 1974 index are still on sale, price £3.00. **Binders** for the journal are also available at £7.00 for four (a year of *Nature* fits into four binders).

Postage is included in the above prices. Orders should be sent, accompanied by remittance to Macmillan Journals Ltd, Brunel Road, Basingstoke, Hampshire, England.

matters arising

Scrotal asymmetry: an appendix

TESTICULAR asymmetry, as McManus has shown[1], was a not uncommon feature of Greek and Roman sculpture, the ancient artist, always attentive to nature, seems to have noticed that the right-hand testis is usually the higher, and inferred (apparently incorrectly) that the other ought therefore to be the larger.

For the historian, however, two questions still remain to be answered. when did the Greeks first discover this peculiarity, and how consistently did they observe it in the early stages of their art? McManus's data, coming as it does from museums in Italy, must of necessity be confined almost entirely to sculpture of the classical period onward (that is, from the fifth century BC to Roman times). Since the preceding century, from the birth of monumental sculpture in Greece around 600 BC, was an era of rapid development in both style and understanding of the the anatomy of the human body, it may be worthwhile to supplement his survey with a look at the 80 kouroi, or standing archaic youths, where this feature is preserved intact. I use Richter's typology[2], based on minute anatomical analyses and generally accepted today, and Harrison's revised chronology[3], which puts the beginning of the series at around 600 BC and its end just before 480 BC, the data of the Persian invasion and sack of Athens. The results (Tables 1–3) can be summarised as follows.

As might be expected, the early groups (Sounion and Orchomenos–Thera Table 1) show a propensity to equalise the testes in both height and size (or, occasionally, to model them as one; this is particularly the case with statuettes, and continues, though to a diminishing extent, down to the end of the Archaic period· see ref. 2, nos 13, 22, 26, and so on· in such cases I record the two as "equal") though even at this early date the right is already higher than the left in about two-fifths of the statues sampled In these and the six statues in which the opposite case obtains, the distribution of size seems to be more-or-less random.

By the middle of the century (Tenea–Volomandra and Melos groups: Table 2), the right testis is the higher in a majority of cases, though in only half of these is the other the larger: the tendency to equalise the testes in size is still dominant.

In the final period (Anavyssos–Ptoon 12 and Ptoon 20 groups: Table 3) the classical scheme is already established. Again, the right testis is usually the higher (though about a quarter of all sculptors, intent on symmetry, still persist in making the two equal in height and size—a practice that is, apparently, to continue), (see ref. 1, Table 1), and the left is now regularly the larger. Significantly, in no case now is the higher testis the larger: Greek sculptors seem to have bowed to the dictates of common sense, as opposed to science, even in the adolescence of their art.

A. F. STEWART

Department of Classics,
University of Otago,
Dunedin, New Zealand

Table 1 Analysis of the scrotal asymmetry of 26 statues from Richter's Sounion and Orchomenos–Thera groups (c 600–c.570 BC)

		Side of higher testicle			
		Left	Equal	Right	Total
Side of larger testicle	Left	3		6	9
	Equal		10	1	11
	Right	2		4	6
	Total	5	10	11	26

Table 2 Analysis of the scrotal asymmetry of 29 statues from Richter's Tenea–Volomandra and Melos groups (c 570–c 540 BC)

		Side of higher testicle			
		Left	Equal	Right	Total
Side of larger testicle	Left			9	9
	Equal	1	8	7	16
	Right	2		2	4
	Total	3	8	18	29

Table 3 Analysis of the scrotala symmetry of 25 statues from Richter's Anavyssos–Ptoon 12 and Ptoon 20 groups (c 540–c 480 BC)

		Side of higher testicle			
		Left	Equal	Right	Total
Side of larger testicle	Left			13	13
	Equal	1	6		7
	Right	5			5
	Total	6	6	13	25

Received April 20; accepted April 26, 1976

[1] McManus, I C., *Nature*, 259, 426 (1976)
[2] Richter, G M A , *Kouroi. Archaic Greek Youths. A study of the development of the kouros type in Greek sculpture*, 3rd ed (Phaidon, London, 1970).
[3] Harrison, E., *The Athenian Agora* 11, *Archaic and Archaistic Sculpture*, 3–13. (American School of Classical Studies, Princeton, New Jersey, 1965).

Specificity of transfer factor

THE letter by Salaman and Valdimarsson[1] is an important step forward in the understanding of the problem of whether the activities of dialysable transfer factor (TFd) are specific or not. They admit that two substances may be involved in the effects of dialysable leukocyte extracts (DLE)—one adjuvant-like material and another specific substance (that is, TFd). In fact, until recently, reports on the effects of TFd dealt with the effects of crude preparations of DLE or roughly purified fractions thereof.

There remains, however, one important point which, although suggested by Salaman and Valdimarsson when they reported that nonspecific effects are more evident in tuberculin-positive than tuberculin-negative individuals, is generally overlooked and which contributes to the confusion in this area of research. It was formerly claimed by medical practitioners that there were no "diseases", only "patients". In other words, a given disease may have a different clinical course, before and/or during treatment, in different patients. This raises the question of recipient peculiarity or, in the case of DLE, "recipient specificity" The effects of DLE are also surely dependent on the specific characteristics of the recipient; for example, it can often be observed that, no matter how strongly positive a leukocyte donor is to a given set of antigens by skin testing, the DLE preparation obtained induces positive skin-test reactivity only to one of the antigens in some recipients and only to another in other recipients, and some show increased lymphocyte DNA synthesis in the presence of antigens *in vitro* whereas others do not[2-4]. Therefore, investigators who intend to study the effects of DLE should consider (at least until it is clearly demonstrated to the contrary) that they are probably dealing not only with an adjuvant-like material and a donor-specific substance (TFd) but also, in both cases, with recipient specificity, which can mask the effects of these substances—if indeed they exist.

M. P. ARALA-CHAVES
H. HUGH FUDENBERG

Department of Basic and Clinical Immunology and Microbiology,
Medical University of South Carolina,
Charleston, South Carolina 29401

[1] Salaman, M. R , and Valdimarsson, H., *Nature*, 259, 250 (1976).
[2] Arala-Chaves, M. P , Proenca, R , and Sousa, M., *Cell. Immunl* , 10, 371 (1974).
[3] Arala-Chaves, M P., Ramos, M T F., and Rosado, R., *Cell Immunl* , 12, 160 (1974).
[4] Levin, A. S , Spitler, L. E , Stites, D P., and Fudenberg, H. H., *Proc. natn. Acad Sci U S A.*, 67, 821 (1970).

Permeability of blood–cerebrospinal fluid barrier during foetal and perinatal life

THE HIGH level of protein in early foetal cerebrospinal fluid (CSF) from human abortion material reported by Adinolfi *et al.*[1] is important confirmation of results obtained from earlier work on human[2] and animal foetal CSF[3,4]. Part of the high concentration of protein, however, may have been due to hypercapnia, since foetuses obtained from abortions are likely to be asphyxiated by the time CSF samples are taken. Hypercapnia increases the penetration of albumin[5] and other lipid insoluble molecules[6] from blood into CSF. This is suggested by the very high concentration of CSF protein in the 40-week foetus, compared with normal term newborn infant[7,8]. Adinolfi *et al.* suggest that their findings confirm the proposition suggested previously by several authors[9] that the blood–brain and blood–CSF barriers to protein are poorly developed in foetal and perinatal life. An alternative explanation for the high level of protein in foetal CSF, however, is that certain plasma proteins may be transported into foetal CSF at an early stage in brain development[4,10]. This was based on electron microscopical evidence that the tight junctions (which form the barrier to protein in adult brain[11]) of cerebral endothelial and choroid plexus epithelial cells are already well developed at a stage when the CSF protein level is very high. There is also evidence[4] from studies of isotopically-labelled protein that certain plasma proteins (for example, transferrin) may be transported into the CSF of early foetal brain, but not later in development. This finding has recently been supported by studies using human serum proteins detected by immunoassay[10] which showed that both transferrin (molecular weight 74,000) and α foetoprotein (molecular weight 64,000) penetrated from blood into CSF to a much greater extent than albumin (molecular weight 69,000) in 60-d-old foetal sheep—a stage when the CSF contained about 350 mg per 100 ml total protein (term is 147 d).

N. R. SAUNDERS
K. M. DZIEGIELEWSKA
D. H. MALINOWSKA
M. L. REYNOLDS

Department of Physiology,
University College London,
Gower Street, London WC1, UK

J. M. REYNOLDS

Department of Physiology,
Royal Dental Hospital
School of Dental Surgery,
Leicester Square, London WC2, UK

K. MØLLGARD

Department of Medical Anatomy A,
University of Copenhagen,
Denmark

[1] Adinolfi, M., Beck, S. E , Haddad, S. A , and Seller, M J., *Nature*, 259, 140–141 (1976).
[2] Klosowski, B N , *The Development of the Brain and its Disturbances—Harmful Factors* (translated by Haugh, B.), 8 (Pergamon, Oxford, 1963)
[3] Amtorp, O , and Sorenson, S. G , *J Physiol.*, 243, 387–400 (1974).
[4] Durbin, G. M , *et al* , *J Physiol* , *Lond.*, 250, 25–26P (1975).
[5] Hochwald, G. M , Malhan, C , and Brown, J., *Archs Neurol. Psychiat* , *Chicago*, 28, 150–155 (1973)
[6] Cameron, I R., Davson, H , and Segal, M B., *Yale J biol Med* , 42, 241–247 (1969).
[7] Piliero, S J., and Lending, M , *Am J. Dis. Childh* , 97, 788–789 (1959)
[8] Naidoo, B T , *S Afr Med J.*, 42, 933–935 (1968).
[9] Davson, H , *Physiology of the Cerebrospinal Fluid* (Churchill, London, 1967)
[10] Dziegielewska, K M , *et al.*, *J Physiol.*, *Lond* (in the press).
[11] Brightman, M W., in *The Choroid Plexus in Health and Disease* (edit. by Netsky, M G., and Shuangshoti, S), 86–112 (Wright, Bristol, 1975)

ADINOLFI ET AL. REPLY—We thank Saunders *et al.*[1] for calling our attention to their work[2], and as yet unpublished results[3]. Regarding the effect of hypercapnia, we do not discount it as a possible factor influencing the levels of plasma proteins in CSF. Saunders *et al.* must be aware of the difficulties of working with human foetal material; it is after all post-mortem material. We stated in our paper[4] that the results were based on a very selected group of foetuses. Many samples of foetal CSF were discarded because of contamination with blood and almost all foetuses obtained by termination with prostaglandin could not be used.

We acknowledge that the levels of some proteins were higher than expected in the 40-week-old foetus; whether this was due to hypercapnia or other factors we are unable to say. This does not, however, alter our conclusion that the permeability of the blood–CSF barrier is incomplete during foetal life.

Recent evidence, based on the estimations of the levels of specific plasma proteins such as albumin, α-foetoprotein, IgG and prealbumin in serum and CSF from the same foetus, suggests that the mechanisms of transfer vary among different proteins. Thus, for example, whereas the percentage of prealbumin in CSF, as compared with blood, varied between 40 and 70, the levels of other proteins varied from ~ 5 to 20%. These variations were found to be related to the ages of the foetuses.

In our paper[4] we merely presented our observations; at this stage of our work it seemed to be premature to advance any hypothesis on the mechanisms of transfer of plasma proteins from blood into CSF in human foetuses.

Paediatric Research Unit,
Prince Philip Research Laboratories,
Guy's Hospital Medical School,
London, UK

[1] Saunders, N. R , *et al.*, *Nature*, 262, 156 (1976)
[2] Durbin, G. M., *et al* , *J Physiol.*, *Lond.*, 250, 25–26P (1975).
[3] Dziegielewska, K M , *et al* , *J Physiol* , *Lond.* (in the press).
[4] Adinolfi, M., Beck, S E , Haddad, S. A , and Seller, M. J , *Nature*, 259, 140–141 (1976).

reviews

Spirit of Nature

R. Desmond

The Naturalist in Britain: A Social History By David Elliston Allen. Pp. xii+292. (Allen Lane: London, 1976.) £9.

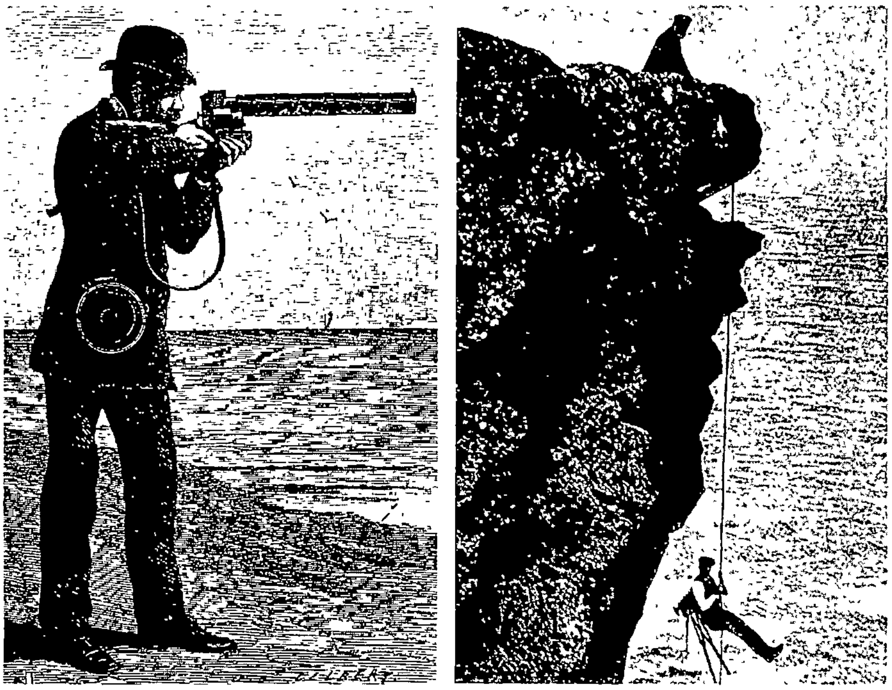

Left, *Photographic gun, taken from* Le Nature (*1882*); right, *bird photography under difficulties, taken from* Wild Life at Home *by R. Kearton (1899).*

Mr D. Allen, taking as his text Emerson's comment that once the facts of natural history are married to human history they become full of life, has attempted the first social account of British natural history. His survey begins with the early seventeenth century when naturalists began exchanging observations and discoveries, occasionally coming together on field excursions such as the 'herborisings' organised by the Society of Apothecaries. Mr Allen has not been able to add much to the little already known about the development of natural history studies in the seventeenth and early eighteenth centuries. By the middle of the eighteenth century the study of natural history was beginning to be accepted as an essential part of a liberal education and this is where Mr Allen's narrative really gets under way. As he points out, natural history attained respectability largely through the researches and teaching of the great Swedish naturalist, Carl Linnaeus. Botany in particular was caught up in the romantic movement which swept Europe. Jean-Jacques Rousseau, a seminal figure in this movement and no mean botanist himself, urged the study of botany as a way of communicating with the essential spirit of Nature.

A great deal of the book is devoted to an examination of the Victorian period when nature study became a popular pastime and was responsible for the many shell pictures and albums of pressed flowers which still survive It was with evident satisfaction that Charles Kingsley noted that "books of Natural History are finding their way more and more into drawing rooms and school-rooms, and exciting greater thirst for a knowledge which even 20 years ago, was considered superfluous for all but the professional student."

Serious research was fostered by the formation of societies such as the Aurelian Society in 1762, the Linnean Society in 1788, the Horticultural Society of London in 1804 and the Zoological Society of London in 1826. But as Mr Allen convincingly demonstrates, nowhere was enthusiasm and dedication more evident than in the humble gatherings of workingmen naturalists. Such was James Bolton of Halifax who not only taught himself botany but also mastered drawing and engraving to illustrate his books. Stamina and single-mindedness were the sterling qualities so many of these naturalists had in abundance. As a young man William MacGillivray walked 800 miles from Scotland just to see the fine bird collection in the British Museum

Philip Henry Gosse was so absorbed in his studies that his diary recorded his son's birth almost as a casual afterthought: "Received green swallow from Jamaica E[liza] delivered of a son" Country parsons stagnating in a cultural desert frequently sought refuge in the world of Nature One thinks of Gilbert White's meticulous observations at Selborne, M. J. Berkeley's important contributions to mycology, S R. Hole's delight in roses and the popularisation of natural history in the spate of books by F. O. Morris and J. G. Wood.

Entomology and botany have always been considered an appropriate female occupation, while the collecting of shells was once recommended because they "are so brightly clean, so ornamental to a boudoir " But women's involvement was not always through a gentle pursuit of culture In the nineteenth century Mrs Gatty and Mrs Griffiths made systematic collections of algae and Mary Anning discovered the first nearly complete skeleton of a Plesiosaurus in the Liassic cliffs near Lyme Regis.

Children were introduced to the marvels and mysteries of Nature in books such as E. and S. M. Fitton's *Conversations on Botany* (1817), set out in the familiar form of a catechism between child and parent Mr Allen only briefly touches on the passion for disseminating knowledge common to all Victorian reformers for whom education was a means to moral improvement. Religious bodies such as the Society for Promoting Christian Knowledge and the Religious Tract Society sponsored a number of primers of botany and zoology. Probably the limitations of space prevented Mr Allen from giving due weight to the important role of some commercial publishers, notably Richard Groombridge and Lovell Reeve, in promoting the production of inexpensive natural history books.

With the advancement of serious research in the universities and the emergence of new disciplines such as ecology, the gap between the professional and the amateur has inevitably widened. Nevertheless, the appeal of natural history has always been the scope it affords the amateur. Mr Allen is particularly good in explaining its increasing popularity during the present century, due in part, he maintains, to the rediscovery of the countryside by bicycle and motor-car. It is now no longer a matter for surprise when books like the Rev. W Keble Martin's *Concise British Flora in Colour* (1965) become instant bestsellers.

Mr Allen is a keen field botanist and it is therefore understandable that he gives a fuller treatment to botany than to zoology. Nonetheless he has unearthed much new or forgotten material from a vast assortment of printed and manuscript sources to compile this fascinating story of the discovery of Nature, and of the men and women who devoted their lives to its study. ☐

Mr Desmond is President of the UK Society for the Bibliography of Natural History.

Changing attitudes to wildlife

Nature in Trust· The History of Nature Conservation in Britain. By John Sheail. Pp. xiv+270. (Blackie· Glasgow and London, May 1976.) £5.95.

BEGINNING with a short survey of man's attitudes to nature preservation in the sixteenth century, Dr Sheail has traced, during the years for which he has the most complete documentation, the changing attitudes to the protection of wildlife. When naturalists first thought about protection they concentrated on preserving rare and distinctive plants and animals by means of legislation. Later, as the science of ecology developed, the concept of habitat protection prevailed. But having come to this conclusion land purchase was still not straightforward. The Society for the Promotion of Nature Reserves (SPNR) came into existence to promote the purchase of land by others, particularly the National Trust, and did not in those early days have money itself.

This book is a recital of facts gathered from the archives and files of voluntary bodies, particularly the SPNR and the Royal Society for the Protection of Birds (RSPB), and from governmental organisations. The bulk of the material relates to the first half of this century and chiefly between 1920 and 1950. It records the activities of the various committees which were set up, or which set themselves up, to examine the types of land which required protection, the different ways of acquiring it, the setting up of scientific authorities to manage the reserves, to undertake research, to advise governments and others on scientific problems.

At one point in the 1930s no one had clear ideas of what they wanted—what, for instance, the relationship should be between national parks and nature reserves, and the Government gave up trying to solve the problem. Although thought was given to environmental conservation in post-World War I reconstruction planning it fell to the voluntary bodies once again to persuade the Government to take action. Ultimately it was the committee headed by Sir Julian Huxley and the Nature Reserves Investigation Committee which began to produce the kind of recommendation that brought nature conservation out of the national park sphere of influence and that led to the establishment of the Nature Conservancy with its original triple function of reserve acquisition, research and scientific advice. Dr Sheail finally records briefly what has been happening since the 1950s.

I was enormously impressed by the facts that Dr Sheail has collected together and incorporated in his book. I wondered whether it would not have been possible to have digested them further or discussed their implication. He writes in an easy manner but at times I found it difficult to follow all the threads. The other point which rather worried me was that the book is described as *The History of Nature Conservation in Britain.* It is, however, more of a history of the development of the organisation side of nature conservation. There is no real discussion on the effect of writers, broadcasters and others who influenced the public to take a deeper interest in nature conservation, and various other activities.

I feel that the full history of nature conservation has still to be written. In saying this I am not denigrating what has been done in this volume. It is an enormous work of scholarship on one major aspect of the growth of conservation It is readable and will be of great value and interest. As a history it has lessons for the present.

Peter Conder

Peter Conder has recently retired as Director of the UK Royal Society for the Protection of Birds

---

Resistance in *Pseudomonas*

Resistance of Pseudomonas aeruginosa Edited by M R. W Brown. Pp. ix+335 (Wiley-Interscience: London and New York, September 1975.) £14.

THIS book is intended to define the problems associated with drug-resistant *Pseudomonas aeruginosa* from a number of different angles, in chapters written by different authors It suffers from the inevitable unevenness and repetition that result from diverse authorship in discussing a narrow field. The repetition is tiresome and it is clear that the editor did not exercise sufficient control over his team For example, chapters 4 and 5 present four electron micrographs in common, one of which is inverted in one chapter in relation to the other. The action of EDTA on *Pseudomonas* is mentioned too frequently. The chapter on antibiotic inactivation and its genetic basis carries some curious statements. For example, there is confusion between the spread of resistance plasmids and that of pathogenic bacterial clones carrying them. Intestinal bacteria other than *Pseudomonas* are very loosely referred to as "enterics" in this chapter. It also uses the term "evolution" imprecisely, and presents the puzzling statement that "there is good evidence that two clones of Gram-negative bacteria specifying resistance to gentamicin, including Pseudomonads, have become widespread in France". If there is more than one Pseudomonad there is no room in two clones for other genera And if there are one or more genera of bacteria other than Pseudomonads there is no room for a plurality of Pseudomonads.

The chapter on epidemiological typing presents details of a phage-typing scheme for *Pseudomonas* in such a way that no-one would realise that the principles and techniques it enunciates owe their origin and even terminology to the phage-typing schemes for *Salmonella typhi* and other salmonellae, none of which is mentioned It seems rather late in the day to publish a photograph of a surface spot titration of phage (Fig 1, p196), and Fig 2 on the same page is a poor illustration of a phage-typing result

Although valuable data are presented, there are faults, overstatements and omissions in all eight chapters of this book. All things considered it is of doubtful value at a price of £14.

E. S. Anderson

Red colobus

The Red Colobus Monkey. (Wildlife Behavior and Ecology.) By Thomas T. Struhsaker Pp xiv+311+37 plates (University of Chicago: Chicago and London, 1975.) £15.

ADEQUATE descriptions of the behaviour and ecology of rain forest mammals are rare, largely because difficult observations conditions impose severe restrictions on the scope and accuracy of the data which can be collected. Struhsaker's study of the red colobus is one of the few cases in which an observer has succeeded in producing a comprehensive survey both of social behaviour and feeding ecology, and represents a major achievement in this field

The four main chapters cover population dispersion, social behaviour (agonistic behaviour, grooming, sexual behaviour, mother–infant relationships and intragroup dispersion) and feeding ecology (food selection, ranging behaviour and interspecific relations). On each topic the author has been at pains to include both detailed qualitative descriptions of the behaviour patterns and, where relevant, quantitative material concerning their frequency.

The book is of particular interest because of the comparisons which it draws between the red colobus and the partially sympatric black-and-white colobus. The two species differ markedy in grouping patterns, red colobus living in large, multi-male troops which occupy extensive home-ranges—black-and-white in smaller and more cohesive single-male troops in defended territories The study shows that these differences are associated with variation in dietetic diversity and in the proportion of mature leaves in the diet at particular times of year.

Unlike its three precursors in the same series, this monograph is clearly aimed at specialists and is not easy to read, partly because the text relies heavily on 76 pages of tables published at the end of the volume.

T. H. Clutton-Brock

Chromosome configurations at meiosis

Meiotic Configurations. A Source of Information for Estimating Genetic Parameters. (Monographs on Theoretical and Applied Genetics, Vol. 1.) By J. Sybenga. Pp. x+251. (Springer: Berlin and New York, 1975.) DM68; $27.90.

DR SYBENGA gives an account of the different kinds of chromosome configurations encountered at meiosis; how they vary in response to change in genotype and environment, and to change in chromosome structure and number. He presents a critical survey of statistical methods by which the frequencies and distributions of the various kinds of configurations within and among individuals may be efficiently described and analysed. Many of the methods concern variation in configurations dependent on chiasma frequencies and distribution. Dr Sybenga is evidently sceptical of the ability of cytologists to score chiasmata with accuracy even in organisms, such as rye, with large chromosomes. The sceptisism, or modesty, embraces Dr Sybenga himself who, by way of caution, prefers to score the number of chromosome arms bound per bivalent rather than the number of chiasmata per arm I think Dr Sybenga is over modest. I know many who claim to score chiasmata with a very high degree of accuracy and thereby acquire more detailed information about the consequences of variation in chiasma formation!

To date, the emphasis in this field of investigation is of course on the *consequences* of variation in chiasma formation. We are still a long way from understanding the *mechanics* of chiasma formation or of other events at meiosis such as chromosome pairing. Many of the facts presented in this book provide clues as to why experiments seeking to elucidate the mechanisms are, to an unusual degree, difficult and inconclusive. Consider, for example, the question of establishing to what extent a structural change within a chromosome affects its ability to pair and form chiasmata with its homologous partner. We may introduce an alien chromosome segment, by transposition, and observe its effects. The trouble arises in interpreting these effects because the structural change is inevitably accompanied by a change in the chromosome genotype–that is in the content and arrangement of genes whose expression in itself affects pairing and chiasma formation independently of structural homology The effects of genotype and of structure are here, typically, confounded. Were we able to distinguish between them we would make some progress

Dr Sybenga, who has specialised in the study of meiosis, has produced a useful book, bursting with facts and figures which are presented with clarity and authority.

H. Rees

Life and death of microbes

The Survival of Vegetative Microbes. (Twenty-sixth Symposium of the Society for General Microbiology, April 1976.) Edited by T. R. G. Gray and J. R. Postgate. Pp. x+432. (Cambridge University: Cambridge and London, April 1976.) £12.

THIS year's Society of General Microbiology Symposium dealt with the subject of Survival of Vegetative Microbes and this book arises from it.

Death of microbes is a subject which impinges on many areas of microbiology but relatively little interest has been shown in such a 'vital' theme. This book brings together a number of chapters on this topic in an attempt to stimulate interest in this important area.

Professor Postgate introduces the subject in an admirably well written first chapter. Several of his comments on the problems of working in this field should be taken to heart by microbiologists, not least by some of the later contributors to the book. The next chapter by Professor Dawes is a classic review on the role of endogenous metabolism on survival of microbes.

The effect of other physiological stresses on survival are dealt with in a series of chapters on cold-shock and freezing, drying and aerosol stress, osmotic stress, ultraviolet and ionising radiation, light and heat. The next group of chapters deal with the survival of microbes in natural environments. Professor Morita's chapter deals with survival (in the sea, particularly) in conditions of extreme pressure. There then follows chapters on survival *in vivo* and in the soil. The last two contributions deal with the specific role of thymidine starvation, and the effect of chemicals on survival

Any book which is a collection of papers from different authors would be expected to vary in standard. This is indeed the case but the best are of a very high standard indeed. The two editors are to be congratulated in producing such a readable and informative book, and it is to be hoped that it will stimulate interest in this neglected area.

I strongly recommend that this book be general reading for all microbiologists so that they may appreciate the role that death as well as life may play in their areas of interest.

D. C. Ellwood

Books brief

An Introduction to Electromagnetic Fields. By R L. Ferrari Pp. xi+202 (Van Nostrand Reinhold· New York and London, September 1975) Cloth £7; Paperback £3.95

THIS is a slim volume which forms a welcome addition to the stock of available texts on electromagnetic fields Intended for an undergraduate audience, it uses extensively familiar examples of electric and magnetic phenomena to arrive at a clear physical understanding of field theory Comprehension is also considerably assisted by the liberal use of line drawings and illustrations Although the mathematical level of this book is comparable to others intended for the same audience, Ferrari's distinguishes itself by not forcing the mathematical pace, but rather by making full use of mathematics as a manipulative tool to assist in physical reasoning It is well written and eminently readable As a basis for a course of lectures, it would be desirable to supplement it by a well-chosen reading list of other books and articles, enabling the student to delve more deeply into areas of interest to him, and to pursue in some depths individual topics If its brevity can persuade a growing circle of engineering students to reach beyond a single volume to study a subject, rather than merely a book, it will have rendered great service.

P. Silvester

Methods of Optimisation By G R Walsh Pp x+200 (Wiley-Interscience: London, September 1975) Cloth £7.50; Paper £3.75.

THIS text essentially reviews a number of optimisation techniques, more from the algorithmic point of view than that of attempting a unified theoretical picture, but with enough theory given that the reader can establish a certain perspective In this spirit it runs through Lagrangian methods, non-linear programming (Kuhn–Tucker conditions, quadratic programming), search and gradient methods of optimisation (these sections quite thorough), some special techniques of constrained numerical optimisation, and a study of some special problems in dynamic programming In treating Lagrangian, Kuhn–Tucker and duality theory, the author regrettably never gets away from local versions of the results, and also misses their geometrical significance, which is so simplifying and illuminating As a medium-level no-nonsense introduction, however, the book is quite attractive.

P. Whittle

Animal Migration and Navigation By Philip Street Pp. 144. (David and Charles: Newton Abbot, London and Vancouver, March 1976) £4 95.

A POPULAR book such as this should ideally present a reasonably accurate account of the current state of knowledge in a readable and interesting style. Philip Street's book is certainly readable, but it is sadly inadequate as an account of modern work on migration and navigation. The author often digresses from the advertised subject matter—for example, to discuss infrared eyes in snakes, echolocation of prey in bats and communication in honeybees Much of the rest of the book consists of a catalogue of examples of long distance migrations in fish, marine mammals, amphibians, insects and birds. Although in his introduction, the author asserts that long distance navigation is one of the most fascinating aspects of animal behaviour, the book says very little about navigation (the term itself is never explained) and most of the work described is now out of date. For example, the chapter on bird migration and navigation discusses pigeon homing without mentioning any work more recent than about 1955, and the account of stellar orientation refers only to the early work of Sauer. One does not expect a popular book to be right up to date, but any such book should not be as outdated as this one.

John Krebs

Introduction to Liquid Crystals. Edited by E B. Priestley, Peter J Wojtowicz and Ping Sheng. Pp xi+356. (Plenum: New York and London, 1975.) $27.

THIS book derives from seminars given at RCA Laboratories in Princeton in 1973 and it is strongly polarised, theoretically and practically, towards the technology of using liquid crystals in electro-optical devices. The preface states this, but the book title is potentially misleading to those expecting an introduction to liquid crystals as a whole The book is also mainly concerned with the physics of the relevant liquid crystals (nematic, cholesteric, smectic A); the chemical input is small, and, disappointingly, no analysis of the relative chemical merits of available liquid crystal materials emerges. The book is, however, a valuable and timely text on the physics of liquid crystals in relation to their use in displays and one which will benefit all concerned with this technology.

Being multi-authored, the 18 chapters vary in quality; those on nematic order, continuum theory, electrohydrodynamic instabilities, Landau–de Gennes theory of phase transitions, and the packaging and addressing techniques for liquid crystal displays are very good. The end chapter on lyotropic liquid crystal systems and membranes points to a growing awareness of the possible technological scope for these types of system.

References to the 1974 literature are quite numerous. The presentation of the text, diagrams and equations is clear, and the index provided is adequate.

G. W. Gray

The Seismics of Heterogeneous and Turbid Media. By A. N. Nikolaev. Translated from Russian. Pp. iv+140. (Israel Program for Scientific Translations· Jerusalem; Wiley: Chichester, February 1976) £8.25; $16.50.

THIS is a study of the theory and observations of small-scale variations in the elastic parameters (the turbidity) of the Earth. Fundamental questions arising from the definition of "small-scale", and from the treatment of such variations as random, are unfortunately left largely unresolved; the underlying theory is based on the scalar wave equation and the reader is merely referred to the literature on the question of validity. Ultimately the author defines a "turbidity factor" which is to be integrated along a seismic ray to get the mean square variation in log amplitude—a formula quaintly described as "usually invalid" but "nevertheless . . . useful" Regrettably it is noted later on that its validity is not yet verified by experiment. Some model experiments, however, are described and the design of field experiments and analysis of certain observations are given in some detail. The net results are contained in plots of turbidity against depth for sections of one continental and three oceanic crusts, leaving the reader somewhat in the dark as to the related physical properties of the medium The book is very hard to read as the result of a rather ham-fisted translation

J. A. Hudson

nature

July 15, 1976

Nuclear industry goes public

RECENT years have demonstrated that, in Britain at least, if any of the components of the unholy government–industry–trades union triumvirate start making signs that they are taking a view on a matter, that matter is fast becoming an important issue. So when the *Financial Times* organises a conference on nuclear power—or, more precisely, "Nuclear Power and the Public Interest: the Implication for Business"—it's a fair bet that energy, and specifically nuclear energy, is an item on the UK public agenda.

Evidence for this, of course, was around before last week's conference. Mr Benn, the UK Energy Minister, saw to that (if the world's energy problems hadn't already done so) with his recent energy talk-in and his public debate six months ago on the reprocessing of nuclear fuel. But with evidence a-plenty offered at the conference to show that the future use of nuclear power in industrialised countries could not be escaped, short of a return to an agragrian economy or a drastic fall in living standards, the nuclear issue seemed more confined than usual.

Still, the problem of the long lead-times attaching to nuclear operations helps to make nuclear power the live issue it now is. The likelihood of a UK "energy gap" in the 1990s is disputed in some quarters and subject to uncertainties, but if it is to appear, and sooner rather than later, it means decisions on nuclear programmes are needed now, with a correspondingly bigger margin of doubt on all fronts. And where there are decisions to be made, there too will the issues be created.

Hardly surprising, then, that people in the nuclear industry should be talking, a little over-dramatically, of its very survival over the period of energy surplus. Hardly surprising, either, that the Department of Energy, which doesn't yet doubt that the nuclear option must at least be retained, should become the object of attention for those seeking to influence the decisions which the "public" character of the nuclear issue now foreshadows.

The critical decision, on whether to go ahead with a demonstration fast breeder reactor (FBR), is expected sometime in the autumn. Unexpected, if heavily qualified, support for a demonstration FBR came at the conference from the Chairman of the Royal Commission on Environmental Pollution, Sir Brian Flowers (now looking at the effect of nuclear power), and from Leslie Grainger of the National Coal Board. Great uncertainty was again expressed, however, about the fate of the Steam Generating Heavy Water Reactor (SGHWR).

On less specific though no less important aspects of nuclear power, grave doubts were expressed, and brave responses offered: about the disposal of radioactive wastes after reprocessing (confidence was expressed about glassification techniques, and about burial in deep holes or under the ocean bed); about health and safety in the nuclear industry (favourable comparisons were drawn with other industries, and especially coal); about proliferation through international nuclear trade (to stop this, claimed one businessman, would be to encourage countries to develop their own technology over a longer period); about the chances of a nuclear accident (all necessary precautions were taken) and nuclear terrorism (the chances of a successful action were minimal); and about the economic facts of nuclear power (which, like all economic "facts", it became apparent, translate only as interpretations). To emerge with the right questions seemed more important in the end than having pat answers.

This was less true of other controversial questions which were broached about the nuclear issue. What should the role of the state be in the nuclear industry, if not in encouraging private enterprise in its task? How was a stream of steady orders to be secured to tide the UK industry over the coming years, if not by breaking into the export business with a marketable reactor? How was any progress to be made without international cooperation, specifically with Britain's European partners? Disappointingly, these questions, for most delegates, contained their own answers.

Not that the unique long term aspects of nuclear power ("making decisions for future generations") weren't acknowledged. But views on nuclear power for the most part revealed differences of detail rather than principle. Although the differences weren't insubstantial for that, there was unfortunately no real voice posing the obvious question—namely, who or what is the anti-nuclear lobby in Britain? (Everyone knows the answer to the analogous American question.)

This latest conference on the subject indicated that the British nuclear industry is finding it necessary to change its public position by actually adopting one. But if nuclear power is really on the public agenda, there are still more fundamental issues to be discussed, if only to be confirmed as resolved. □

The weather a week ahead

Ernest Knighting describes the establishment of the European Centre for Medium Range Weather Forecasts

RELIABLE weather forecasts for a week or so ahead would be of great economic value; almost every industry, including agriculture, transport, building, shipping, fuel and power, would benefit in the planning of operations and, of course, the general public would be better able to plan outdoor activities. And if, as has been estimated, the benefit to Europe would be more than £100 million a year at 1970 values, it is well worth setting up an organisation to conduct research into problems associated with medium range forecasting, and eventually to provide operational forecasts.

The resources of skilled manpower and equipment required for such a task, however, exceed those normally available at national level. This makes an international co-operative effort necessary, and in October 1973 sixteen European nations signed a Convention establishing the European Centre for Medium Range Weather Forecasts. By November of last year a sufficient number of nations had ratified the Convention for the Centre to come into being. Belgium, Denmark, West Germany, Spain, France, Ireland, Yugoslavia, the Netherlands, Austria, Portugal, Switzerland, Finland, Sweden, Turkey and the UK have ratified, while both Greece and Italy are expected to ratify shortly.

The Centre's headquarters (to be erected by the UK Government) will be at Shinfield Park, Reading, England; temporary accommodation has meanwhile been provided at Bracknell. The Centre will have a staff of about 140, including about 70 graduates, mostly in the research and operations department. The present staff, numbering about 40, reflects the international character of the Centre, with nine member nations being represented. In addition there will be opportunities for visiting scientists to work at the Centre.

The Director, the well-known Danish meteorologist, Professor Aksel Wiin-Nielsen, was formerly Head of the Department of Atmospheric and Oceanic Sciences at the University of Michigan; he, together with a small planning staff, laid the foundations of the Centre's development so that at its official birth it was already well-advanced in its scientific and operational planning. When the Centre is fully operational it is expected to have a yearly budget of about £6 million; the cost will be met by the member nations, contributions being scaled according to the gross national product of each nation.

The central premise of the development of these operational forecasts is that the atmosphere may be regarded as a compressible fluid, its behaviour being described by the Navier–Stokes equation and the thermodynamic equations concerned with sources, sinks and the transfers of energy. Considerable progress has been made in the last two decades in using these equations for two distinct objectives. The first is for short-range weather forecasts for a day or two ahead, and it is now common for national services, especially those in extra-tropical latitudes, to base their short-range forecasts on the numerical integration of the equations. The problem is the prediction with considerable accuracy of the motion and development of weather-bearing systems, which have a lifetime of a week or so; it requires a fairly precise knowledge of the state of the atmosphere at the instant from which the forecast proceeds, while some slow acting physical processes may be neglected.

The second objective is to determine why the atmosphere has its general climatic structure and to throw light on climatic change. In this research the equations are integrated for perhaps a hundred days or more rather than for the one or two days of the short-range forecast. During this period many generations of weather-bearing systems undergo their life history and the emphasis is no longer on the initial detail but on the careful representation of the physical processes that are thought to be important for the atmospheric development over a long time, such as incoming and outgoing radiation, the transfer of energy at the earth's surface and so on.

Forecasting for up to ten days ahead presents a more difficult problem because both the initial details and the careful accounting for the physics have to be taken into consideration. The detail must be considered because the evolution of the atmospheric systems in existence initially has a considerable effect over the period; indeed, some of the systems may persist, although modified in form and position, for most or the whole of it. The changes caused by the slow acting physical processes can also be profound during the period; the effect of a change in sea surface temperature, for example, due perhaps to up-welling, can be remarkable. Over a few days the development of the weather bearing systems over Europe and the Atlantic can be affected by what is happening very far away, and forecasts for ten days ahead need to be global, taking into account the developments in the Southern Hemisphere, which are less well defined, as well as in the Northern Hemisphere.

Professor Wiin-Nielsen, ECMRWF Director

The equations describing the evolution of atmospheric motions are highly non-linear and whether any useful analytic solutions will ever be obtained seems doubtful. Certainly the only known methods of solution are numerical, and the arithmetic burden is enormous: operational numerical forecasts for a couple of days ahead require the use of large-scale computing facilities with speeds of operation of about 10 million instructions per second; computations associated with operational forecasting up to ten days ahead call for facilities about five times as fast.

If the Centre is to achieve the difficult, perhaps impossible, target it has set itself—namely to be in a position to provide daily operational forecasts before the end of 1980—there must be scientific research and development on three fronts. The first concerns the acquisition of the right daily data, its verification and reduction to a suitable form. This problem has become very complicated because a great number of meteorological data, especially those from satellites, are observed continuously and require special methods of assimilation if they are to be used in the forecasting process. The second concerns the important physical processes which often cannot be represented directly in the computations because the arithmetic has to be carried out for discrete grid points about 100 km apart. Atmospheric processes smaller in size than this can only be represented statistically in the computations. Many of the important energy transfers—those due to vertical instability and the development of cumulonimbus clouds, for example—are subgrid scale in size and their important contribution to the working of the atmosphere needs investigating. The third concerns the selection of the mathematical methods of integration, where there will be a delicate balance between accuracy and economy.

An additional complication is the problem of predictability which is currently exercising meteorologists. It is the problem of determining for how long ahead useful forecasts can be made. It is generally agreed that the limit is less than one month and more than five or six days, using current mathematical models and the meteorological observations presently available. Experimental determination of the limit by integration of the model equation is very difficult because a few integrations cannot give results representative of so variable a fluid as the atmosphere, while each integration predicting for, say, 14–20 days, is extremely costly. Experiments carried out up to date show that there is value in the forecasts up to ten days and this is confirmed by the few integrations carried out at the Centre. The Centre will cooperate as fully as it can in the First GARP Global Experiment, which is designed, among other objectives, to determine the limit of predictability.

With the aid of computer programmes for atmospheric models provided by the Geophysical Fluid Dynamics Laboratory of Princeton, the Department of Meteorology, UCLA, and the UK Meteorological Office, this research has already started. Ten days forecasts have already been made with these models, using both a CDC 6600 computer installed for the Centre's use by CDL in Bracknell and the UK Meteorological Office computer complex; their production is regarded as a familiarisation exercise.

A considerable effort must also be devoted to the selection and installation of suitable computing facilities; speeds of 50 million instructions per second are only just being developed and the selection of an integrated system capable of carrying out the data processing and the number-crunching on an operational basis will certainly present difficulties. Of course, the system must be available before 1980 since the Centre will need to develop its operational programmes on it.

Europe, through the member nations, has created the first scientific centre for the study and preparation of medium range weather forecasts. The international meteorological community has expressed great interest in this new venture with offers of help and cooperation. Already a cooperative agreement has been signed with the World Meteorological Organisation and the provision of computer programmes is one example of the help that has been made available. Nevertheless the Director and his staff face a difficult task in attempting to build up a new international scientific centre in a time of recession. □

USA

Science vs. the public

Colin Norman reports from Cambridge, Massachusetts, where attempts are being made to restrict recombinant DNA research.

In a move which establishes a virtually unprecedented degree of community control over an area of scientific research, the city council of Cambridge, Massachusetts, last week passed a resolution calling for a three-month moratorium on certain types of recombinant DNA research at Harvard and Massachusetts Institute of Technology. Though the moratorium will have little immediate impact, since experiments of the types outlawed by the council are not yet being conducted at either university, the council's actions could have broad and lasting implications.

While the moratorium is in effect, a special review board, also established by the council last week, will draw up recommendations to control recombinant DNA research in Cambridge. In addition the board has been given the astonishing task of reviewing all laboratory experiments in the city, to ensure that none of them poses a threat to public health.

The council's actions are the result of a bitter clash between groups of scientists, city officials and Cambridge residents over plans to conduct recombinant DNA research at Harvard and MIT. The dispute, which centres on the question of whether or not such experiments can be carried out safely, has been a bloody battle which has provided ample evidence of public distrust of scientists and which has further damaged the already abysmal relationships between the city and its two famous universities.

In a sense, the clash has also provided the first real test of public acceptability of federal safety guidelines governing recombinant DNA research issued last month by the National Institutes of Health (NIH) (see *Nature*, July 1). The guidelines were developed mostly by scientists, and have not previously been subjected to the intense public scrutiny now being lavished on them in Cambridge. Those who support the guidelines—and they include the vast majority of the scientific community—can take little comfort from the public debate in Cambridge. Moreover, many scientists are worried that similar clashes could break out elsewhere, a development which the Mayor of Cambridge has been doing his best to promote by trying to interest his fellow mayors in the issue.

The hostilities stem originally from a proposal, put forward two years ago by a group of scientists headed by Mark Ptashne, to convert some rooms on the fourth floor of the Harvard Biological Laboratories into a special safety facility. Designed primarily for experiments with the animal virus SV40—experiments which are frequently carried out in other institutions under much less stringent safety conditions—the facility became a major focus of controversy when the plans were modified to include space for some recombinant DNA work.

At present, Harvard researchers are restricted to experiments, judged by those who wrote the guidelines to entail little risk, which do not require special safety facilities. According to Matthew Meselson, Chairman of the Department of Biochemistry and Molecular Biology, about 30 people at Harvard are now working, at various levels, on such experiments. Construction of the safety laboratory—a moderate containment, or P3, facility under the NIH guidelines—would allow many other types of experiments to be undertaken at Harvard.

Opposition to the facility came first from scientists at Harvard. It took two forms. Some argued that although recombinant DNA research is an exciting and potentially revolutionary area of research which should be conducted at a major research institute like Harvard, the building housing the biological laboratories is unsuitable for a safety facility. It is old, infested with ants and cockroaches, and situated in a densely populated area. The second, more fundamental objection came from scientists who argued that recombinant DNA research is inherently so risky that virtually all such experiments should be confined initially to one or two specially equipped national facilities, or be outlawed entirely, until the hazards are better defined.

In spite of the intensity of the opposition construction of the facility has been approved in principle by a special biohazards committee, by Harvard's top-level committee on research policy, and by the Dean of Arts and Sciences. Final plans for the lab are now being drafted.

The internal dispute at the university spilled over into the city and mushroomed into a major political issue early last month when the matter was reported at length in the *Boston Phoenix*, a weekly area newspaper. At that point, Cambridge city Mayor Alfred E. Vellucci stepped in. An irascible, colourful, shrewd politician with 26 years' service on the council, Vellucci is no friend of Harvard or MIT. In fact, the strained relationships between town and gown in the city provide an important backdrop to the clash over recombinant DNA research in the city.

A major source of irritation is the fact that the two large, wealthy universities are situated in a predominantly industrial community and are exempt from paying many city taxes. There have also been problems over pressure on city housing—"If it gets any worse", Vellucci said in an interview last week, "we'll have to knock down some buildings for somewhere for people to live". A good example of town-gown friction came a few years ago when the city council passed a resolution, introduced by Vellucci, to pave over Harvard Yard and turn it into a parking lot. (The resolution, according to Vellucci, successfully spurred the universities into building more student parking facilities.)

Vellucci's dignity was pricked when he read in the *Phoenix* that Harvard scientists were planning to conduct reportedly dangerous experiments without first consulting city officials. And his belief in the dangers of the experiments was heightened by a visit from George Wald, a Nobel prizewinner and a vigorous opponent of the plans for the laboratory. Vellucci called a council meeting for June 23—ironically the day on which NIH issued its guidelines—to discuss the matter. The meeting provided a forum for a bitter clash between mostly radical scientists and their more establishment colleagues, with council members often bewildered and Mayor Vellucci enjoying the publicity, and especially enjoying the opportunity to haul Harvard intellectuals over the coals.

At one point in the proceedings, Vellucci particularly chastised Daniel Branton, chairman of the biohazards committee, for making little attempt to bring city officials into the discussions of plans for the safety laboratory. Branton protested that he had, but Vellucci scored a major debating point.

During the meeting, Vellucci proposed a resolution calling for a two-year moratorium on *all* recombinant DNA research in the city—even those experiments already under way which are judged to entail little risk. No vote was taken at that meeting, however, and it was adjourned after some five hours of bitter exchanges.

The next day, Vellucci issued a public statement declaring that the meeting "has made it clear to me that a 'cooling off' period is necessary in order for the mayor and the council to deal with this matter in a calm and rational way". He then softened his proposal for a two-year moratorium, calling instead for a three-month 'good faith' halt to the research "so that all concerned can properly review relevant testimony. He later offered another proposal to establish a review board to look into the issue and to examine other research programs at Harvard and MIT to see whether any pose a potential public health risk. A second council meeting was called on July 7 to resume testimony and to discuss the resolutions.

In the fortnight between the meetings, some councillors and the mayor spent a good deal of time contacting, and being contacted by, scientists. As a result, Vellucci announced to the meeting last week that he had "learned enough about recombinant DNA molecules in the last two weeks to take on all the Nobel prizewinners in the city of Cambridge". He has certainly taken on most of them.

The meeting began with a demonstration of techniques used in microbiology, for the councillors' edification. Meselson then described the formulation of the NIH guidelines, noting that in each new draft they were made more strict. And William Gartland, Director of the newly created NIH Recombinant DNA Activity Unit, described the guidelines themselves, pointing out in particular the contrast with the situation in the United Kingdom, where the whole business of setting regulations on the research is taking place behind closed doors.

At that stage, Councillor David Clem, a young, articulate council member who has obviously done his homework on the issue, proposed a number of amendments to Vellucci's resoultions. The most important change was an amendment to limit the moratorium to research requiring P3 and P4 facilities, according to the NIH guidelines. That amendment was accepted without debate, even though it meant the difference between stopping several experiments and stopping nothing.

Harvard has no P3 or P4 facility, so no such experiments are going on there. MIT, however, has a P3 facility in the Center for Cancer Research, but no P3 level experiments have yet been initiated. One experiment is being planned at the facility by Dr Philip Sharp, however. He said last week that he has been holding off on the research—which would involve inserting mammalian genes into *E. coli*—until the NIH guidelines had been published, and that it would take at least three months to get the experiment approved and under way.

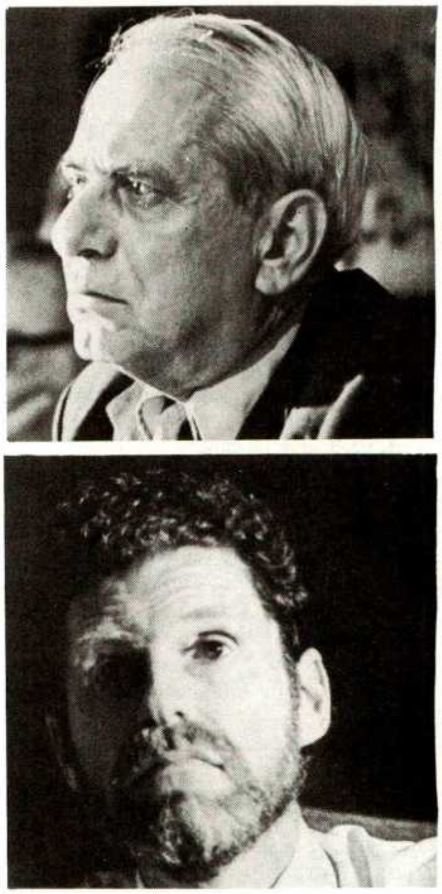

Mayor Alfred Vellucci (top) and (below) Daniel Branton

Photos: Noëleen Chedd

Another council member, Sandra Graham, then proposed that the moratorium should be extended from three months to six. After some debate, the amendment was defeated by six votes to two. Vellucci then proposed that the moratorium should be extended to two years if no agreement has been reached at the end of three months. That was also defeated by six votes to two. At that point, the resolution with Clem's amendment was approved by five votes to four.

The second resolution, establishing a Cambridge Laboratory Experimentation Review Board, was then voted on, and similarly approved by five votes to four.

With the amended resolutions approved further testimony on them became superfluous but it was taken anyway—until 12.45 am—with the council chamber packed with scientists and with people from both sides heatedly stating their views.

A number of interviews with scientists the day after the meeting demonstrated that both sides are relatively pleased with the outcome so far. Proponents of the research are happy that the moratorium will do no damage to current research and that it is much less restrictive than the original resolutions. And opponents of the research are pleased that the vote has established the principle of community control over scientific research.

There is, however, considerable unease within the scientific community, and with good reason. The council meeting secured a precarious ceasefire, which could easily erupt into renewed hostilities. An important factor in what happens next will be the work of the experimentation review board. Its terms of reference are broad and hazy, and its members are yet to be appointed. One potential member is George Wald, who was asked by Vellucci last week whether he would serve if asked and replied that he would be "happy and honoured to do so". Vellucci said after the meeting that the board would contain both supporters and opponents of the research and that some city residents would also be included. If necessary, he said, he would lock them all into a room and not let them out until they have come to an agreement.

Creation of the board has at least taken the council out of its uncomfortable position in the middle of the dispute. But if the board has not reached agreement at the end of three months, the council will be thrown right back in and there would then be a possibility that the moratorium would be lengthened and, perhaps, broadened. Alternatively, if the board vigorously pursues its mandate to look into all laboratory work in Cambridge, there is a danger that it could turn into a public witch hunt. "We will be keeping our fingers crossed in the next three months," says Richard Leahy, a dean in the Faculty of Arts and Sciences.

On the other hand, creation of the review board at least establishes a long-needed channel of communication between the university scientists and the city. It could provide an important vehicle for informing and educating the people of Cambridge about recombinant DNA research and about the process which led to adoption of the NIH guidelines. It is conceivable that it could even help smooth some of the causes of town–gown friction.

Another possibility which is clearly worrying people far removed from Cambridge is that similar clashes could erupt in other cities. In that respect, Vellucci has been active. Last month he attended a meeting of the United States Conference of Mayors armed with a resolution stating that "no university or institution may begin recombinant DNA experiments without first notifying the mayor of the city or town in which the experimentation will take place. Thereupon, the mayor and legislative body shall call a public hearing so that the public may be an active participant in the decision-making process". The resolution was referred to a committee for consideration, and Vellucci said last week that he intends to press the matter at future meetings.

It is possible that the dispute in Cambridge will now quietly die away. But with so many articulate and politically motivated scientists opposed to the research there, the prospects at this stage are far from certain. The next few months will be critical. ☐

EEC

JRC programme awaits approval

The Commission of the EEC has circulated final proposals for the next multiannual research programme of the Joint Research Centre. These now await ratification from the Council of Ministers. Chris Sherwell reports

THE multiannual research programme of the European Community's Joint Research Centre (JRC) for the four years beginning in January 1977, the final detailed proposals for which were submitted by the Commission to the Council of Ministers some two weeks ahead of the Council's May 24 meeting, may not be approved before September, even though preliminary discussions of the overall framework for the Community's 1977 budget are due to start later this month.

The Council decided at the May meeting to consult both the European Parliament and the Economic and Social Committee, even though there is a clear need for the JRC's budgetary requirements for 1977 to be entered into the budget for the coming financial year. The European Parliament is being urged to deliver its opinion no later than its part-session in September, which is about the time when the Finance Ministers are expected to be reaching more concrete budgetary decisions.

The Commission's proposed programme represents the outcome of many months of behind-the-scenes deliberation, including broad consultation with research and administrative staff. Last October the Commission sent to the Council its "Overall Concept" for the programme, setting out guidelines for the JRC's future role, and this the Council discussed at an inconclusive December meeting along with a document on a joint research and development policy. Other discussions took place in February, and the General Advisory Committee considered the draft programme in March and the Scientific and Technical Committee considered it in April.

The Commission has already stated that in framing the new programme it took into account "criticism made in the European Parliament and elsewhere" that the JRC "had engaged in too many 'half-baked' projects which it had not the resources to complete"—criticism which arose, it said, "in part from the failure of the member states to provide the Centre with effective guidelines".

Details of the final proposals now under consideration are shown in the accompanying table, but do not include the installation of the JET fusion project, which the Commission wants at Ispra, since a decision on the matter is still awaited.

In its final proposals the Commission points out, some would say rather obviously, that among the guiding principles of the programme, primary consideration was given to the Community's interests in science and technology. From its discussion of these principles and of the JRC's role, however, a few important points emerge, namely, the priority being accorded to energy and environment questions, the stress on a Community public service role for the JRC (that is, making equipment, know-how, products and services available), and the concentration of activities and research potential on a small number of projects. There is also emphasis on the "rolling plan" character of the proposed programme, and on management and staff aspects.

The three-year rolling system, proposed in order to allow a greater degree of adaptability, is quite simple. The four-year programme would be submitted during the third year, when the Council would adopt a new four-year programme in which the last year of the initial programme would become the first year of the new programme. The new programme would itself be submitted for revision during its third year, when a decision would be taken on the following programme. In the absence of decisions, current programmes would be continued according to the Council's original decisions.

Regarding the financial requirement over the forthcoming four-year period of 374.4 million units of account (£156 million), the Commission says the pattern of investment expenditure envisaged means in practice that it will not be divided into equal annual parts; rather, it is expected that the annual budgets will actually show a decrease over the four years.

The impact of proposals regarding researchers attached to the JRC has statistical consequences to which the Commission draws attention. Its concern over their mobility is reflected in the proposal, approved broadly by the European Parliament and still under examination by the Council (the Commission urges that it be adopted as soon as possible), for a different manner of payment; a new "research staff" concept is also adopted which stretches beyond existing "first line staff" to include associated technical support staff.

Thus, as the document goes on to point out, if the "research staff" number and programme expenditure are taken together as a measure of the distribution of effort within the JRC, programmes I, II and III (which can be broadly classed as "nuclear safety") take up 48% of the total, future

The Multiannual Research Programme of the JRC proposed by the European Commission

	Programme	Projects in programme	Personnel			Specific Programme Expenditures (muc)	Staff Costs research[2] (muc)	Global Supporting Costs (muc)	Total Costs (muc)
			Total	Research Staff	Others[1]				
I	Reactor Safety	Reliability and risk assessment; Light water reactors loss of coolant accidents; Liquid metal fast breeder subassembly thermohydraulics; Fuel coolant interactions and core melt-down; Dynamic structure loading and response; Structural failure prevention	440	239	201	16.52	38.38	37.23	92.13
II	Plutonium fuels and actinide research	Utilisation limits on plutonium fuels; Plutonium and actinide aspects of the safety of the nuclear fuel cycle; Actinide research	209	121	88	6.6	15.3	19.58	41.48
III	Management of nuclear materials and radioactive waste	Evaluation of long term hazards of radioactive waste disposal; Chemical separation and nuclear transmutation of actinides; Fuel materials management; Reactor component decontamination studies	161	97	64	4.36	15.78	14.24	34.38
IV	Solar energy	Thermal conversion in housing; construction of European installation to simulate solar irradiation; orientative research on advanced applications of solar energy	57	35	22	4.86	5.67	6.74	17.27
V	Hydrogen	Thermochemical processes for water decomposition; heat source coupling	78	50	28	2.4	8.14	5.92	16.46
VI	Conceptual studies on thermonuclear fusion	Participation in conceptual study of an experimental power reactor in connection with Euratom-CNEN association at Frascati (blanket neutronics, heat transfer and energy conversion systems etc)	14	8	6	0.28	1.28	0.99	2.55
VII	High temperature materials	Industrial needs; effect of operational environment on mechanical properties; failure modes in applications; relationship of structure and properties	51	36	15	2.21	4.44	2.54	9.19
VIII	Environment and resources	Atmosphere; water; chemicals, renewable (agricultural) resources	188	115	73	5.01	18.73	17.59	41.33
IX	Measurements, standards and reference techniques	Measurement of nuclear data; nuclear and non-nuclear reference methods and techniques; scientific support to the services of the Commission and Secretariat of Community Bureau of Reference	286	181	105	8.185	25.51	25.995	59.69
X	Services and support activities	Exploitation of high flux reactor; informatics; education and training; safeguards; technical evaluations in support to the Commission	221	116	105	26.505	14.94	18.465	59.91
	Totals		1,705[3]	998	707	76.93	148.17	149.29	374.39

Units of account based on value at 1 January 1977

[1] Does not include 471 local agents not presently classed as personnel because they are paid from funds allocated yearly from the appropriate section of the budget

[2] Includes laboratory equipment costs

[3] To this total must be added 183 people relating to the ESSOR reactor.

energies (programmes IV, V, VI and VII) take up 12%, environment and resources 10%, reference work 17% and support 13%

This as the Commission says, means that effectively 70% of the JRC's effort will be devoted to "energy and the environment", with much of the effort in energy concerned with nuclear safety. The Commission points out elsewhere that the proposals also achieve a better (60 · 40) balance in the ratio of payroll costs (214.6 muc) to operating expenses (159.8 muc).

The new programme, provided it is adopted in time, will follow on the existing multiannual programme, adopted in 1973, being carried out in the four JRC establishments at Geel (Belgium), Ispra (Italy), Karlsruhe (West Germany), and Petten (Holland) The large body of the work will be at Ispra. Karlsruhe will take the lead in plutonium fuels and actinide research, Petten will work on high temperature materials, and Geel will coordinate the work on reference methods. ☐

BRAZIL

● Brazilian engineers have now succeeded in modifying an automobile engine to run on pure alcohol. This could be significant in solving energy problems here, in view of the fact that Brazil imports more than 80% of the crude oil it uses for making petrol. The experimental engine, installed in a Brazilian-made Dodge sedan and demonstrated to government officials in Brasilia, achieved 23 miles per gallon—roughly the same as that model gets with a gasoline engine—and had no trouble keeping up a steady 55 miles per hour in a highway test. The alcohol engine also released far fewer pollutants in its exhaust than a standard engine. Brazil's commerce and industry minister, Severo Gomes, was impressed by the demonstration. He said that if an alcohol engine is produced in volume here, it will be put first in buses and taxis in big cities.

Brazil has the potential to be self-sufficient in alcohol fuel. It is the world's biggest cane sugar grower (sugar is the country's current prime source of alcohol), and it has unmeasured quantities of cassava, a plant whose root provides a basic food for millions of poor farmers and which local scientists say can also be made to yield commercially usable alcohol.

The government's oil refining monopoly, Petrobras, currently dilutes its gasoline by 20% with alcohol, to make imported crude oil stretch further.

● Sao Paulo, Brazil's biggest metropolis (city population: 7 million; including the suburbs: 10 million), also has South America's biggest air pollution problem A combination of thermal inversion, industrial smoke and automobile exhaust gives Sao Paulo the look of London in the days before anti-pollution measures went into effect in Britain. The air quality in Sao Paulo is often so bad that department stores take out newspaper advertisements for filter masks.

But now local health officials have persuaded the mayor's office and the police to cooperate in a plan called "Operation Winter", which will be put into effect on badly polluted days during the South American winter (June–September), when pollution-trapping temperature inversion is at its worst in Sao Paulo. The operation has three stages· a warning level, an alert level, and an emergency level when local authorities will prohibit the use of petrol and diesel-powered vehicles, shut down all factories and prohibit all burning.

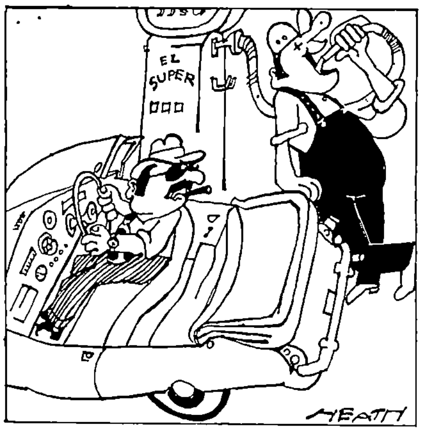

This type of action has never before been contemplated in Brazil, where the official line has been that pollution is the price a developing country must pay if it wishes to progress since time spent on its control is time wasted.

● Brazil has been complimented for its progressive laws protecting wildlife and, at the same time, criticised for its inability to enforce them. This is especially true in the vast, underpopulated Amazon region, where it is virtually impossible to control illegal trafficking of protected species of birds and animals.

Occasionally, though, the authorities get results. Police in Rio followed up a recent tip that dogs and cats in a residential neighbourhood had been mysteriously disappearing, and this led them to what apparently is a large-scale contraband ring for exporting Brazilian Amazon creatures such as monkeys, parrots, parakeets, tucans and canaries.

Four persons were arrested on suspicion of running an illegal animal trade to Europe, North America and Japan. The police found hundreds of caged birds and monkeys awaiting shipment out of the country. They also found many dead animals which did not survive flights from the Amazon city of Belem to Rio. The operators of the smuggling ring apparently had been using local dogs and cats to make food for the captured Amazon animals.

In similar actions, police in Sao Paulo and Fortaleza recently broke up illegal trafficking in songbirds which are protected by wildlife laws. There is a big local demand for many varieties of these popular birds in Brazil, and breeders and sellers seem willing to run the risks to make a profit.

● In another instance of Brazil's finally applying a law that had seemingly existed only on paper before, naval authorities in the north-eastern city of Salvador slapped a fine equivalent to $25,000 on a local titanium company after a pipe broke at its factory and sent sulphuric acid and ferrous sulphate spilling on to Atlantic Ocean beaches, leaving a brownish stain several miles long in the water. Among the beaches hit was Arembepe, which often is played up in tourist brochures as a Brazilian "unpolluted paradise".

● Brazil's biggest lagoon, Lagoa dos Patos, which is near the country's far southern tip, is becoming so polluted that fish and shrimp are dying *en masse*, and even some farm animals have died of poisoning after drinking water from it Scientists at the Rio Grande do Sul State Center for Toxicological Studies are not sure, but they think the cause is a sharp increase in the use of DDT and other insecticides on nearby farms Soybean and wheat production in Rio Grande do Sul have gone up dramatically in recent years, and farmers there traditionally have used large amounts of pesticides.

Fishermen around Lagoa dos Patos say their annual catch in the 3,800-square-mile lagoon is going down steadily. And bird watchers in the region have noticed that the once-common marsh cardinal no longer is seen and that the Patagonian duck does not stop at the lagoon any more on its winter flight north from Argentina.

Bruce Handler
Rio de Janeiro

SWEDEN

Nuclear fuel report out

After three and a half years of study, the Swedish Commission on Spent Nuclear Fuel and Radioactive Waste recently produced its final report. Wendy Barnaby sent this view from Stockholm.

"Even today's techniques offer satisfactory possibilities for the handling and storage of spent nuclear fuel and radioactive waste." Such is the assessment of the Swedish Commission on Spent Nuclear Fuel and Radioactive Waste, whose task was to study the management of low-, medium- and high-level radioactive wastes—that is, not only those from nuclear power plants, but also those from research institutions, hospitals and industry.

The timing of the report was no doubt planned to support the government's pro-nuclear power stance in the current general election campaign, in which the ruling Social Democrats are under heavy pressure from the opposition—part of which is adamantly opposed to nuclear power. Thus the report's claim—that its "central demand" was that all steps in the handling of radioactive waste had to be formulated with regard to the protection of people and their environment now and in the future—sounds suspiciously like an attempt to pull the carpet out from underneath the opposition, whose criticism of the safety and environmental aspects of nuclear power has mobilised an unusually large following. The latest opinion polls show that both government and opposition parties have lost support for their nuclear energy platforms since last January and that, while the opposition's policy is still more popular than the government's, more people are doubting the wisdom of either. This result will obviously stimulate each camp to even greater propaganda efforts than before, and the Commission's report will undoubtedly be one of the government's main weapons.

The report has not definitely pronounced on the fate of Sweden's spent fuel. "We recommend that this decision should be taken in 1981 or 1982", says the Commission's Secretary, Mr Philip Moding. The options are to continue sending spent fuel abroad for reprocessing, or to deal with it in Sweden reprocessed or not. In the long term, sending it abroad is no satisfactory solution. Under an agreement that will last until 1980, spent fuel from the Oskarshamn plant is being sent for reprocessing to Windscale in England. Negotiations are presently going on between the Swedish Nuclear Fuel Supply Company (SKBF) and United Reprocessors, jointly owned by British, French and German interests, for the spent fuel that will be taken from plants already in operation at Ringhals, Forsmark and Barsebäck. A preliminary understanding has been reached but nothing has been signed, and the hoped-for agreement would probably only last until 1980 anyway. "It will be necessary for us to build an intermediate storage capacity for spent fuel in any case", says the Director of SKBF and an expert adviser to the Commission, Dr Erik Svenke, "because even if we continue to send spent fuel abroad, the reprocessor will have the right to return the waste to Sweden and we would then have to store it here."

The report urges the acceleration of research into ways of handling spent fuel domestically without reprocessing. How seriously this proposition is meant is hard to say. A domestic solution will in the long term certainly be preferred to the difficulties and uncertainties of sending it abroad, especially as Sweden's neutrality makes the country seek as much independence as possible in questions related to its national security; and it seems almost certain that a reprocessing plant, with its attendant business opportunities and relative simplification of storage of remaining waste, will then seem the best solution. Dr Svenke is convinced that Sweden will have to build a reprocessing plant at some time. "A country with a civil nuclear programme has a responsibility to take care of its waste", he says

According to the report, any decision to build such a plant should go hand in hand with one to construct a fuel fabrication plant, to ensure that both plutonium and uranium are re-used as fuel. It estimates that a reprocessing plant with a capacity of 800 tons of uranium a year (and offering employment for 1,000 people) would take about 13 years to build. The Social Democrats' plans for Sweden's nuclear future envisage 13 reactors in operation by 1985 So far, five are running and five others are under construction. When all are operating, the country's total net nuclear power capacity will be about 10 GWe and, it is estimated, the reactors will produce about 300 tons of spent fuel a year. The reprocessing plant's excess capacity would be intended for other countries' waste. The Nordic countries would be obvious participants, although neither Denmark nor Norway has yet decided to build nuclear power plants. Finland, however, had three under construction at the beginning of this year, and it is expected that they will produce about 2.2 GWe by 1985.

The method of disposal recommended by the Commission is to melt the highly radioactive waste in glass and deposit the medium- and low-level waste in concrete, then store it all in vertical tunnels drilled out of bedrock at a depth of 300–400 metres. Studies made by the Geological Survey of Sweden have pronounced bedrock conditions stable and suitable for such storage. "It is very important that the Commission has demonstrated that the terminal storage problem can be solved in Swedish bedrock", says Dr Svenke. "It signifies that the fuel cycle can in fact be closed."

The President of Sweden's Friends of the Earth group, Lennart Daléus, however, is not so optimistic. "What the Commission is telling us", he maintains, "is that with current techniques and those they hope will be developed in the future, the problems of high-level radioactive waste disposal can be solved. But in fact this is more a hope than a technical certainty." He also raises broader issues which he says the report should have considered. What are the social and moral implications of undertaking to secure radioactivity for hundreds of years? How can we possibly be sure that future political regimes will be willing or able to take care of our waste? Dr Svenke does not think these issues are relevant. "The terminal storage of radioactive waste", he says, "is surely a technical problem. It does not have the same dimensions as other aspects of the question: the relationship between the spread of nuclear energy and the proliferation of nuclear weapons, for example"—although he is apparently prepared to take the risk of proliferation.

The report gives only a brief mention to the problems of terrorism and theft of plutonium, and it is noteworthy that one of the parliamentary members of the Commission, John Takman, felt obliged to publish an addendum to the report expressing his regret that the Commission had not taken more account of the relationship between nuclear energy and nuclear weapons. If the more pessimistic experts are proved right, and the spread of civil nuclear energy programmes does result in nuclear-weapon proliferation which does in turn produce global nuclear catastrophe, all the present arguments will be shown to be ironically irrelevant.

Such predictions, however, are not the stuff electoral victories are made of Sweden's nuclear future will have to wait for clarification until September, when the results are known. ☐

ISRAEL

● Some unfashionable opinions on science and defence were expressed in Israel by Sir John Kendrew, now Director-General of the European Molecular Biology Laboratory in Heidelberg, when he spoke at a symposium marking the 60th birthday of Israel's scientist-President, Professor Ephraim Katzir. Sir John pointed out that Israeli scientists, living in a nation which had fought several wars of national survival, faced little moral conflict when it came to doing defence research. British scientists, in contrast, found such research "boring and disreputable."

"We now tacitly assume, in my opinion contrary to the evidence, that defence research is no longer necessary, that the Western countries will probably never again be at war Our younger scientists don't want to get involved, and as a result our defence committees are manned by greybeards". Given the imperfections of the world we live in, Kendrew added, "I think that defence research is necessary still, even though it might not be as obvious as it was during the Second World War when I was masquerading as an Air Force officer and Crick as a Naval officer".

Kendrew expressed scepticism as to whether international agreements for arms control could be enforced, a scepticism which was not shared by Professor Carl Goran Heden of Stockholm's Karolinska Institute, who also participated in the symposium. As he stated in his multi-volume report on biological warfare that was prepared for the Stockholm International Peace Institute (SIPRI), Heden thinks that the major powers will make and keep agreements. He admits, however, that small groups of fanatics might take the law into their own hands, which emphasises the need for an international criminal code to deal with such groups.

● If Israeli lives are to be saved, military research may be less important than research on traffic accidents, which claim far more victims than do the fields of battle Israeli motorists kill off one another, as well as pedestrians, at a rate practically unequalled elsewhere In 1970, the last year for which figures are available, the accident rate per million kilometres travelled was 0 7 in the US, 1 3 in the UK and France and 2 3 in Israel. Only the drivers of Japan and Belgium were more lethal

In an attempt to cut down on the carnage, the Israeli police have decided to adopt a plan proposed by plasma physicist turned traffic expert Gerry Ben-David, who aims at re-educating the entire population of Israeli drivers. It is based on putting drivers under close observation and swiftly making them aware of their mistakes. First tried out on a very limited basis, it will now encompass 10% of Israeli highways.

Placed at strategic points along these roads will be specially trained teams, each member of which will concentrate on certain traffic violations. Every violation will be recorded, as will the licence number of the car concerned (though no attempt will be made to stop the vehicle). The violation data will be transferred for computer processing using standard techniques, and the computer programme will be then control all subsequent communication with the driver. Computerisation makes it possible to ensure that within a matter of days the person (or company) in whose name the car is registered will receive a letter from the traffic police giving full details of the offence and pointing out the dangers involved in such behaviour If the owner himself was not driving his vehicle at the time, he will be asked to identify the actual driver so that he can be contacted

During the initial, small-scale trial of the Ben-David scheme, observers witnessed an extraordinary number of traffic violations. One four-man team, for example, reported 6,086 offences in one month along just one section of the road, the most common violations being close driving, unnecessary driving in the lane reserved for passing, and speeding. Motorists "caught" up to three times were sent letters, while those guilty of more traffic violations were asked to come for a talk with the police or perhaps even forced to undergo a new driving test before being allowed to continue on the road.

While Dr Ben-David cannot yet prove that his scheme actually prevents traffic accidents, he notes that a follow-up carried out during the preliminary trial of his system showed that the observed violation rate dropped more than 50% for drivers who received a single letter and 80% for those who received three letters. When observation teams are operating over large stretches of Israeli highways, he feels certain that there will be a significant drop in the countrywide accident rate

Accident prevention in Israel involves special problems, notably the fact that 75% of the drivers have been on the road for less than 10 years. At the same time, drunkenness, a major cause of accidents in other Western countries, is practically unknown. In spite of the differences, if Dr Ben-David's system works in Israel it may also work elsewhere.

● After a hard day of driving, exhausted Israelis slump into their armchairs and turn on the TV, anxious for entertainment rather than education. It may be for this reason that Israeli TV allocates so little time for science, particularly locally produced programmes.

This month, however, viewers were introduced to an excellent new TV series on archaeology which gives them both science and entertainment, the latter stemming from the fact that the man who explains the archaeology is a master entertainer. Hebrew University Professor Yigael Yadin is no ordinary archaeologist: his descriptions of an excavation have the artistry of a well-crafted murder mystery, and an audience of laymen is kept breathlessly alert awaiting the discovery of an artifact which will reveal the true identity of an ancient civilisation or the cataclysmic event which brought about its destruction.

Yadin's archaeology programme features a "Find of the Month" and other recent discoveries as well as new interpretations of previously unearthed objects. One of the latter, which Yadin showed viewers on his last telecast, was a 6,000-year-old vessel with "beaks" which, until recently, had been called a "bird-like utensil" for want of a better term. Now, he explained, archaeologists have discovered its real purpose by taking a close look at the "food technology" of contemporary bedouin. As a film sequence convincingly demonstrated, the bedouin use a very similar container to make cheese and other processed milk products, which means, almost certainly, that the "bird-like utensil" was an ancient churn.

Another regular feature of the series, "Archaeology Around the Corner", highlights the fact that almost every Israeli town and village has one or more sites of interest. Yadin recently zeroed in on a site in West Jerusalem, where a partially exposed column, lying flat, is clearly visible A camera team was stationed near the object and then passers-by were asked what it was. Only after several rather comical replies did an interviewee correctly state that it was a column intended for use in the construction of the Second (Herodian) Temple which for some reason had been left lying several miles from the Temple site.

Nechemia Meyers
Rehovot

NUCLEAR BRIEF

US export moratorium ?

Proliferation of the international trade in nuclear technology is "very rapidly becoming a major political issue in the United States", Mr Llewellyn King, Editor of *Weekly Energy Report,* told the *Financial Times* conference on nuclear power last week. Hearings set for July 20 on the subject would bring it into the front line, and if proliferation became an issue in the coming elections, he predicted, there would be a "de facto moratorium on the export of nuclear technology", a change which would affect the world nuclear market. The issue was a "lively" one in Congress, and the President was "very concerned".

Reprocessing prospects

The prospects for the nuclear fuel reprocessing deal that British Nuclear Fuels Ltd (BNFL) is negotiating with Japan look "very good indeed", and there has been "very good progress" in negotiations with European countries for similar business, according to Mr Con Allday, managing director of the company. The deal, which involves BNFL's reprocessing facility at Windscale, attracted a good deal of publicity earlier this year, since when the French firm Cogema has been introduced on one side and changes have occurred in the team on the Japanese side. An Anglo-French mission recently visited Japan for talks.

Uranium fix

Canada is resisting the efforts of the US Justice Department, which has served subpoenas on two of the country's three major uranium producers, to investigate alleged attempts at price fixing. The chairman of one of the companies is also president of the Uranium Institute, the trade association representing the industry's producers and consumers which recently held its first annual general meeting in London. It has not been served with a subpoena, and stresses that its activity does not and would not include price fixing. Several companies in the United States have also been served with subpoenas.

Nature conservation

KENNETH MELLANBY

THE pressures on Britain's countryside increase, and so do the efforts of those concerned with wildlife conservation. Since the 1939–45 War, 146 National Nature Reserves covering nearly 120 thousand hectares have been designated, and voluntary organisations such as the Royal Society for the Protection of Birds, the National Trust, and the County Naturalists Trusts have obtained control of only slightly less ground. In these days of world shortages, and the need to produce more food in Britain to reduce imports and the balance of payments deficit, there is concern as to whether it is right to set aside so much land for the benefit of the minority of the population interested in our native animals and plants.

At a meeting recently organised by the Royal Society on the scientific aspects of nature conservation in Britain, two main topics were discussed. The first was the value of conservation as such; the second concerned the contribution of science, particularly ecology, to conservation and the management of nature reserves and other protected areas.

The conservation of the land, of water and of natural resources is clearly desirable, and wildlife may be looked upon as just another "resource". The difficulty is to give this a value, particularly a cash value. Many of the arguments about the economic importance of wildlife are unconvincing to the layman, and may prove counterproductive. It is true that several wild birds and plants may act as inexpensive and delicate indicators of pollution, but the important species are not confined to nature reserves. Wild plants have proved valuable in work in producing new crops, but it is difficult to argue convincingly that the gene pool of the Spring Gentian in upper Teesdale has a contribution to make to food production.

It is safer to base one's support for wildlife conservation on scientific, educational, cultural, aesthetic, recreational or even sentimental grounds. The scientific argument would perhaps appear to be the strongest, but even here the conservationist must not appear to claim too much. Nature reserves provide essential facilities for ecological research, and so make an important contribution to that science However, we may become involved in a circular argument: reserves are provided for research, which yield results which enable us to maintain those reserves so that they continue to provide facilities for more research. To the sceptic this may sound too much like "jobs for the boys". I believe that we conservationists should be honest, and admit that our motivation is not, mainly, economic. We should not be ashamed to admit that our interests are, at least partly, aesthetic and sentimental, and that we believe that conservation contributes to civilised living.

But if we do not claim that conservation is of economic importance, what do we say to those who complain that we are harming agriculture? Could not the quarter of a million hectares in different types of reserves be better used by our farmers? First, it should be noted that only a tiny fraction of these reserves is grade 1 or grade 2 farm land, suitable for arable cultivation. Secondly, we lose vastly greater areas, often of the best land, to housing, factories, motorways and airports. This loss now amounts to 30 thousand hectares a year; in four years the loss in area exceeds that of the 146 National Nature Reserves. The first priority should be to reduce, and eventually stop, this continuing erosion of our farmland.

In the meantime, conservationists are surely right in trying to acquire as many sites as possible. Modern farming, to be profitable, cannot afford to support wildlife except in marginal areas. We need reserves where wildlife has priority, and some areas should be on good farmland, which supports larger numbers of more species than the barren moors generally left to the conservationist. We certainly need to produce more food, but first let us cut out waste. Nearly a quarter of the food bought in our supermarkets ends up in our dustbins, and intensive livestock rearing wastes over ninety per cent of the rations fed. So long as these processes continue, conservationists need have few qualms when they designate new reserves, particularly as this land, unlike that used by industry, could easily be brought into fruitful cultivation in an emergency.

correspondence

Electrostatic energy storage

SIR,—With shortages of oil and petrol clearly facing us, it is time to consider all other ways of storing energy effectively Although leading possibilities for automotive use include advanced electric batteries and specially designed flywheels, the search for materials (particularly polymers) with high dielectric strength and static dielectric constant must not be overlooked; it might lead to economically attractive electrostatic storage systems.

The efficiency in converting the stored electric energy to mechanical energy to turn wheels can confidently be expected to be very high—close to 90%. This means that substantially less energy (about 1/7) need be stored in a vehicle for range, speed and acceleration on a par with a petrol-burning system. There is no exhaust to pollute the air and even thermal pollution by wasted heat is reduced by a factor of 9 or so at the vehicle. Recharging can be done more rapidly and efficiently than conventional battery charging: a few minutes should suffice at a service station equipped with suitable rectifying equipment and electricity supply lines of industrial capacity. Alternatively, the domestic electricity supply is generally adequate for overnight charging. With programmed parallel–series switching the variation in operating voltage can be kept modest and the extraction of stored energy can be made nearly complete.

The stored energy density in a sheet of dielectric can be expressed as

$$D = 0.4427\times 10^{6}\, Ka^{2}$$

with D in kJ m^{-3} and a in V Å^{-1}; K is the low frequency dielectric constant. Many commonly used capacitor dielectrics have dielectric constants below 10, corresponding to strong ionic or more often to non-polar interatomic bonds. A class of metal titanate ceramics, however, has dielectric constants up to 12,000. But the dielectric strength is the more critical parameter and is sharply reduced by various impurities. In paper-thin sheets, appropriate to capacitor construction, high purity can be achieved in mica ($a\simeq 0.022$) and organic polymers ($a\lesssim 0.028$).

Applying the energy storage formula for mica with a dielectric constant of ~5 to 7, we might expect a storage capacity of 1,000–1,500 kJ per m^3 of mica. Commercial energy storage capacitors are listed up to 600 kJ m^{-3}, based on a waxed paper dielectric, so this level of energy density is close to commercial practice. Recognising that there will be some additional volume required for the thin electrodes and an outer casing, a comparable organic polymer capacitor should have approximately the density of water, and thus an energy density of 1–2 kJ kg^{-1}.

If we take the lead-acid storage battery, at 44 kJ kg^{-1}, as an aiming point, we would need to develop a material with the dielectric strength of the best plastic, incorporating enough polarisable sites to raise the dielectric constant above 130. This is a reasonable aim in economic terms as the lead-acid battery is already marginally adequate for electric cars and trucks.

A further discussion of promising materials and ideas for study has been prepared (ORNL Report TM-29, June 1976).

Yours faithfully,

R. L. MACKLIN

Physics Division,
Oak Ridge National Laboratory,
Oak Ridge,
Tennessee 37830

Electrostatic energy discharge from humans

SIR,—The amount of electrostatic energy which can be stored in the capacitance represented by the human body does not appear to have been measured and reported in the literature. Besides being of phenomenological interest, this measurement could be important when considering the explosion hazard represented by anaesthetics and antiseptics when used in close proximity to electrostatically charged humans, such as in operating theatres and intensive care areas. In this regard, it has been suggested that ether vapour will explode when subjected to an electrostatic energy as small as 200 μjoules in magnitude.

An appreciation for the magnitude of the electrostatic voltage which the human body can be charged to; the capacitance represented by the human form; and the electrostatic energy stored by humans, can be obtained by discharging the body through a known resistance, and displaying the discharge curve on a storage oscilloscope.

The results obtained indicate that the electrostatic energy which the human body can store, and consequently dissipate, is in the order of 6.46±3.26 millijoules. The capacitance of the body is 65.9±12.1 pf, and the electrostatic voltages which the body can be charged to is 13,802±4,443 volts These measurements could be valuable when considering the role that the human body plays in the causing of explosions of volatile chemicals in hospital and industrial environments.

Yours faithfully,

A. E. MARBLE
D. MACVICAR
A. ROBERTS

Halifax, Nova Scotia, Canada

Competition 8

Du Pont's notepaper has "There's a world of things we're doing something about" imprinted on it, and the slogan for Rockwell International is "Where science gets down to business".

A prize of £10 is offered for the best one-sentence slogan (preferably tongue in cheek) for your (or anyone else's) laboratory, business or university The closing date for entries is August 31.

Competition 7 requested a modern headline for a scientific achievement, and there was a large entry, on fairly predictable themes. A. L. Mackay (London) receives honourable mention for "Prominent philosopher in public bath scandal". The £10 prize is shared equally between P. J. Fallon (London), for "Role of Earth probed by Pole", and C. F. Hammer (Wilmington, Delaware), whose "Bell discovers new use for wooden poles—wires to carry conversation over distances" seemed just right for the *New York Times.*

news and views

Interpreting protein electron density maps

from C. C. F. Blake

EVER since the subject began, protein crystallographers have been complaining that they work for a long time on a project without obtaining any significant information and then, literally overnight, they are overwhelmed with information The source of this surfeit of data is the electron density map of the protein which is calculated in the form of a three dimensional figure-field of electron density values that contains between 50,000 and 500,000 points, depending on the size of the protein and the resolution of the study. Although the figure-field will encompass one protein molecule, much of the data is redundant because it will inevitably include some volumes of liquid containing more or less-ordered water molecules, and parts of other (identical) protein molecules related by symmetry or simple translation to the central molecule.

In view of the vast amount of information present in the figure-field, total interpretation is not normally attempted, attention being naturally concentrated on the folding of the polypeptide chain and the location of side chains. This operation has always been carried out in the past by converting the figure-field into a stack of transparent sheets contoured in levels of equal electron density, and interpreted in terms of a physical molecular model This is, however, by no means straightforward, especially if an accurate model is required, because the ideal of building the model inside the electron density is a physical impossibility. After various laborious *ad hoc* methods had been used on the first proteins, a standard piece of apparatus—the optical comparator—was proposed by Richards (*J. molec. Biol*, **37**, 255, 1968), using the ingenious principle of optical superposition of the model and the contoured electron density map Although it is relatively easy to use, the comparator has certain disadvantages it is large and uses up valuable laboratory space; with larger proteins it becomes physically difficult to build the model, and some users have had difficulty with depth perception. Another problem associated with all physical models, however they are built, is the need to measure the spatial coordinates of all non-hydrogen atoms, a laborious process requiring some thousands to tens of thousands of accurate measurements. These coordinates are then returned to the computer, either for drawings to illustrate the structure, or for some kind of refinement process for improving their accuracy.

Since the current system requires very hard work to obtain a somewhat inaccurate model it seems desirable to seek an improved system, which clearly has to be computer based The most obvious improvement is to use a computer display system as an electronic Richards' comparator, as proposed by Katz and Levinthal (*A. Rev. Biophys. Bioengng*, **1**, 465–504; 1972). This requires expensive hardware and allows only a limited section of the map to be displayed for fitting at any one time. An alternative is to use the basic computer to attempt the appropriate pattern recognition on the figure-field in an automated or semi-automated procedure. This approach, whose development has been reported by Greer in a series of papers (Greer, *J molec. Biol.*, **82**, 279; 1974; **98**, 649; 1975; **100**, 427; 1976) has now reached the point where it has been used successfully to trace the main chain and produce a preliminary set of atomic coordinates of a Bence-Jones protein (Greer, *J. molec. Biol.*, **104**, 371; 1976)

The basic aim of Greer's approach is to reduce the electron density to a series of thin connected lines that trace the path of the polypeptide chain. Although the path of the polypeptide chain will be marked by a continuous string of above average density, in any real protein map it is by no means uniquely defined. Variation in thermal vibrations and possibly even of order will cause the level of the string of density to be quite variable, while disulphide bridges and strong intramolecular or intermolecular hydrogen-bond contacts will result in strong continuous features that do not represent the path of the main chain. These factors result in formidable problems in attempting to recognise and isolate the true main-chain density from these other similar, but spurious features, and Greer has had to develop a procedure that has a number of stages in each of which criteria have been evolved that successively eliminate density points which do not represent the main chain

The starting material is the electron density figure-field in a Cartesian coordinate system with a grid spacing of about 1 Å, that completely encloses a single molecule. The first operation is the elimination of all electron density points below a minimum value and "contouring" the remainder at equal intervals. The appropriate values are arrived at by inspection to give maximum main-chain continuity and a minimum of spurious cross connections. Starting with the lowest contour level, the remaining points are successively removed to leave a skeleton of lines that defines the basic connectivity in the map, using a three-dimensional generalisation of a method developed for processing micrographs of chromosome smears. This skeleton is then simplified by pruning easily distinguishable side chains down to the main chain, leaving a flag to mark the position of the α-carbon atoms At this point the description of the skeleton is transformed into a tree-like structure in which segments are defined as lines that lie between the tips or branch points in the skeleton; such a description restricts ambiguities to the points where segments meet. After this, all segments that represent parts of neighbouring molecules that obtrude into the Cartesian frame are removed to isolate a single molecule Simple loops in the skeleton are removed next by using simple rules to identify the true main-chain branch. The skeleton that remains represents primarily the main-chain and inter-main-chain bridges, possibly lacking one or two main-chain connections that were removed earlier. The final stage involves putting the skeleton through a process that selects the main chain on the basis of length and the presence of side chains, starting with the longest segment and attempting to add other segments to each end. This is an iterative procedure that includes examining skeletons calculated at lower electron density to locate weak main-chain connections eliminated from the main skeleton. Wisely, manual intervention is allowed for when the programme reaches an ambiguity that cannot be resolved easily.

Using the procedure on a 3-Å resolution map of the Bence-Jones protein Rhe, Greer has shown that it defined a main-chain line some 433 Å long, produced provisional coordinates for 113 α-carbon atoms, defined the basic β-sheet structure characteristic of Bence-Jones proteins and also found a short segment of α-helix. Even at this stage it is clear that the technique could be valuable and it seems probable that it can be developed further. Although some crystallographers will see this as a further encroachment of the computer into what they consider to be their proper province, most will note its real value in giving more time (and possibly a better start), for the important task of getting an accurate description of the molecule through which the biological problems can be solved. □

Hydrogenases and efficiency of nitrogen fixation in aerobes

from R. O. D. Dixon

WITH the high energy, and thus financial, cost of nitrogen fertilisers it is now important to rely, where possible, on microbial nitrogen fixation. The fixation of nitrogen by microorganisms occurs with varying efficiency in terms of substrate consumed for each nitrogen fixed. To use microorganisms to the best advantage it is well that we be able to identify factors which lead to greater efficiency of nitrogen fixation and thus to select the most efficient organisms.

It is known that metabolic energy in the form of ATP and reducing power is wasted, by the enzyme nitrogenase reducing protons rather than nitrogen. Evolution of hydrogen occurs with nitrogenase from all nitrogen-fixing microorganisms tested so far *in vitro*, although it has not been possible to test the extent to which this wastage occurs *in vivo* in most organisms because of the complicating presence of hydrogenases. In anaerobic organisms there is a hydrogenase which evolves hydrogen simultaneously with the nitrogenase whereas in aerobes, such as *Azotobacter*, hydrogen is taken up by a hydrogenase.

In experiments in which it was thought that the hydrogenase had been inhibited by carbon monoxide, no hydrogen evolution was detected from *Azotobacter*. It was thus suggested that, in this organism, the nitrogenase, atypically, did not reduce protons (Postgate, in *The Chemistry and Biochemistry of Nitrogen Fixation*, 161–190, Plenum, New York, 1971). This view, which was not universally accepted, has now been shown to be erroneous by Smith, Hill and Yates (page 209 of this issue of *Nature*) who report that the *Azotobacter* nitrogenase does not in fact differ *in vivo*, from that of the other nitrogen fixers. They confirm that the lack of hydrogen evolution from intact bacteria is due to hydrogen uptake by a hydrogenase.

That the hydrogen, taken up by the hydrogenase, may be put to some use was shown some time ago by Hyndman *et al.* (*J. Bact.*, **65**, 522–531; 1953). They showed that the hydrogen taken up by *Azotobacter* was oxidised with consequent synthesis of ATP. Similar observations were made more recently with hydrogenase in *Rhizobium* bacteroids (Dixon, *Arch. Mikrobiol.*, **85**, 193–201; 1972). Possession of this hydrogenase enables these aerobic organisms to recoup some of the ATP expended on wasteful evolution of hydrogen by nitrogenase. The suggestion was made earlier (Dixon, in *Nitrogen Fixation by Free-living Microorganisms* (edit. by Stewart, W.D.P.), Cambridge University Press, 1975), and is now reiterated by Smith *et al.*, that this reutilisation of hydrogen with ATP formation is the reason for the greater efficiency which has been found for *Azotobacter* nitrogen fixation over that of anaerobes such as *Clostridium* (Hill, Drozd, and Postgate, *J. appl Chem. Biotechnol.*, **22**, 541–558; 1972).

Although the presence of hydrogenases in free living organisms has precluded the investigation of the level of wastage by the evolution of hydrogen, the lack of hydrogenase in some root nodule associations has enabled Schubert and Evans (*Proc. natn. Acad. Sci. U.S.A.*, **73**, 1207–1211; 1976) to estimate the degree of efficiency of the fixation of nitrogen in a number of such associations. The more efficient associations, which included all the non-legume root nodules in the study, showed evidence of a hydrogenase which takes up the hydrogen evolved. The wastage of ATP and reducing power by evolution of hydrogen is estimated to vary between 40 and 60% of the total used by nitrogenase in those associations in which hydrogenase was not a complicating factor.

Schubert and Evans calculate that with a wastage of 50%, reutilisation of hydrogen could double the amount of nitrogen fixed in cases where the energy supply is limiting. It has indeed been demonstrated in a number of cases that the supply of photosynthate from the plant limits nitrogen fixation by root nodules. Although this calculation would seem to be optimistic, if one bears in mind that the estimate of molecules of ATP utilised, per pair of electrons transferred through nitrogenase for hydrogen evolution, is three to four and the P/O ratio obtained from hydrogen uptake is not likely to be better than two, substantial savings can be made. This would be reflected, as Schubert and Evans point out, either in an increase in dry matter yield, where photosynthate is not limiting, or in an increase in nitrogen fixed. Thus selection of a strain of *Rhizobium* which possesses this hydrogenase may pay dividends in the yields of some legume crops.

Much work has been done and is being pursued on the legume–root nodule association in order to understand the infection process and nodule development, with the long term aim of transferring nodulating capability to other agricultural crops, whereas little attention has been paid to non-legume associations. But the greater efficiency of nitrogen fixation of non-legume associations shown in the data of Schubert and Evans suggests that it may be well to give them more attention than in the past. □

Irregular associations

from E. G. Richards

FOR nearly a decade it has been known that complementary trinucleotides do not associate detectably. So, we may ask, how does the anticodon on the tRNA bind with such specificity to messenger triplets on the ribosome? Part, at least, of the answer must lie in the tRNA, for trinucleotides complementary to anticodons of tRNA associate with the latter and, more dramatically, as Eisinger showed some years ago, pairs of tRNA molecules with complementary anticodons bind together with an association constant as high as 10^6 M^{-1}.

The purist may wonder what relevance the participation of tRNA molecules in these unnatural acts may have to tRNA–messenger interaction but Grosjean, Söll and Crothers have come up with some interesting suggestions (*J. molec. Biol*, **102**, 499; 1976).

When such pairs of tRNA molecules interact, they do so with a small (0.1% of the total) absorbance change which

Regulatory genes in fungi

from a Correspondent

THE paper by Arst in this issue of *Nature* (page 231) marks another step in our understanding of regulation of gene action in the mould *Aspergillus nidulans.* In 1970, Hynes and Pateman (*Molec. gen Genet*, **108**, 97–106, 107–116) reported mutants which identified a gene whose product seemed to act as a positive regulator of the structural gene for amidase (*amdS*). Now Arst reports that this regulatory gene—now called *intA* for integrator—also regulates expression of two genes concerned with ω-amino acid metabolism. These latter two genes, *gatA* and *gabA*, code, respectively, for an inducible transaminase acting on β-alanine, γ-aminobutyrate or δ-aminovalerate and a permease for the same ω-amino acids. The three genes under control are all unlinked to *intA* and to each other. It seems that various mutations in *intA* can affect the control of *amdS, gatA* and *gabA* differentially, and can also be associated with changes in the relative responses to γ-aminobutyrate and β-alanine as effectors. The conclusion is that the *intA* product interacts with each of the three genes (or with controlling regions associated with them) and also with various small molecular effectors, and that these specificities can be altered by mutation. Arst draws attention to the similarity between *intA* and the type of integrator gene proposed by Britten and Davidson in 1969 (*Science,* **165**, 349–357) as part of an influential general model for regulation of gene action in eukaryotes.

Arst's report, together with earlier work, shows that sets of unlinked genes can be simultaneously subject to more than one system of integrative regulation. Arst and Cove and their colleages (for example, *Molec. gen. Genet.*, **126,** 111–141; 1973) had already described in *Aspergillus* a regulator gene, called *areA*, which is concerned with nitrogen catabolite repression, and which regulates the action of several other genes with functions in the generation of ammonium ion. A type of mutant allele, called *areA*^{r}, represses these other genes (including the amidase gene) even in the absence of ammonia. "Constitutive" alleles of *intA* can nullify the repressing effect of *areA*^{r}, the positive integrative control in this case over-riding the negative. In addition, one can have positive gene-specific regulation, acting in parallel with the "integrator" regulation. Thus, another regulatory gene, *amdA,* is found by Arst to act positively on *amdS* (more or less additively with *intA*) with no effect on *gabA* and *gatA*

The regulation of nitrogen metabolism in *Aspergillus,* thanks mainly to the work of J. A. Pateman in Glasgow, Arst (with D. J. Cove and C. Scazzocchio) in Cambridge, M. J. Hynes in Australia and P. Weglenski in Warsaw, is becoming an extremely complex story—excessively so, perhaps, in the opinion of some. But the complexity is there in the eukaryotic cell. Attempts to unravel the network of gene interactions are bound to produce something of a tangle at the outset, but perhaps some general features are beginning to emerge which will eventually fall into place in a higher-order pattern.

Grosjean *et al.* were able to monitor in temperature jump relaxation experiments. This absorbance change shows the right spectral distribution to be expected from the base pairs presumed to be formed, and is not manifest when the two anticodons are not complementary Moreover, the three complementary bases must be centred in the middle of each seven-membered anticodon loop for the reaction to be appreciably manifest. Thus, for interaction, the anticodons *per se* must be complementary, and complementarity between other bits of the anticodon loops does not help.

Returning to the temperature jump results, the authors found that the rate constant for the association reaction was close to that expected for the association of complementary trinucleotides, and, furthermore, virtually temperature independent. The surprise comes in the rate constant for the back dissociation reaction which was six orders of magnitude slower than expected. It follows that the equilibrium constant is 10^6 times higher than expected.

More detailed analysis showed that the entropy of interaction was not very different from that expected for trinucleotide interaction, but the enthalpy change was about −25 kcalories, which is about 10 kcalories larger than expected. This difference of 10 kcalories is sufficient to account for the factor at 10^6 and is at the kernel of the enhanced anticodon–anticodon interaction. This in itself suggested that stacking interactions were involved.

Pushing the investigation further, Grosjean *et al.* studied the interaction of *Escherichia coli* tRNA$^{\text{Glu}}$ with yeast tRNA$^{\text{Phe}}$ in the presence of EDTA, in which conditions the former species is in the denatured conformational state. The association was still observed, suggesting that the structural features which distinguish the two conformer states are not important to the association. Similarly the removal by specific cleavage of the first 16 nucleotides from the 5′ end of the tRNA$^{\text{Phe}}$ did not alter the interaction. On the other hand, fragments obtained from both these species such that anticodon helical arms could not form, still associated but with a constant reduced by about two orders of magnitude—leaving an enhancement of four orders still to be accounted for.

The remaining factors were deemed to reside in the "dangling ends" or the residual four bases in the anticodon loop that are not involved in the anticodon itself Grosjean *et al.* point out that the sixth base in the anticodon loop (that is the one at the 3′ end of the anticodon) is frequently modified. They go on to show that the association constant varies for species with similar anticodons but differs in the nature of the sixth base, and, in particular, that excision of the Y base from this position in tRNA$^{\text{Phe}}$ leads to a substantial reduction in the enthalpy of association.

Grosjean *et al.* tie all these observations together by postulating that the enhanced association constant and the increased enthalpy of association originates from the stacking of the two anticodon arm helices on either side of the helical region formed by the anticodon–anticodon interaction, with the 3′ dangling ends stacked up as jam in this three layer cake. I choose this analogy carefully since jam is well known to be sticky.

We are finally left with the thought that something similar happens in the codon–anticodon interaction. Maybe the ribosome holds the relevant portion of the messenger in a configuration similar to that in the tRNA and allows the interaction to be similarly stabilised by stacking.

These results also imply that the anticodon helical arm exists in both the native and denatured forms of *E. coli* tRNA$^{\text{Glu}}$. Further evidence of the similarities and differences between these two forms of tRNA comes from a paper by Jones, Kearns and Muench (*J. molec Biol.*, **103**, 747; 1976) who worked with *E. coli* tRNA$^{\text{Trp}}$. They measured the low field nuclear magnetic resonance (NMR) spectrum of the native form of this species and assigned to their satisfaction all parts of the 11 5–14.5 p.p.m. region to one or other structural feature expected of the clover leaf model in its surmised tertiary structure. There were thus 19 base pairs, a protected U or G and two tertiary base pairs including A_{14}–s^4U_8. The agreement between their experimental spectrum and that computed from these assignments was very reasonable. They then repeated the process for the denatured form and considered in detail the difference NMR spectrum between the two. They succeeded again in demonstrating a reasonable agreement between calculated and experimental spectra. The final result is a model for the denatured form in which stem, TUC arm and anticodon arm remain intact but the DiHU arm is undone and the anticodon arm extended by some of the original DiHU arm bases pairing with bases in the extra arm. This extension of four base-pairs involves one bulged out G. This model they argue is also consistent with the pattern of kethoxylation of both the native and denatured forms. In an argument too complex to repeat here they also consider and reject other possible pairing schemes for the denatured form.

Besides being consistent with their own data the model for the denatured form has several attractions. The small number of base pairs that needs to be undone for either form to revert to the other is consistent with the ease of this interconversion. Furthermore, if it is assumed that *E. coli* tRNA^{Trp} has a tertiary structure similar to that of yeast tRNA^{Phe} as vouchsafed by X-ray diffraction analysis, then this interconversion can be readily envisaged to occur with but minimal disruption of the tertiary structure.

If all this is accepted we can begin to point at those parts of the structure that are involved in the biological activities that are knocked out when the molecule is denatured. □

Meteoroid swarms colliding with the Moon

from David W. Hughes

METEORIC dust particles are continually striking the Moon with velocities between 2.4 and 74 km s^{-1}. On impact they lose their considerable kinetic energy and excavate a crater thus producing a large quantity of hot ejector most of which subsequently falls back to the lunar surface but some of which exceeds the escape velocity and moves off into space. A lunar seismic disturbance is also produced. The latter can be detected by the passive seismic network deployed by the Apollo astronauts. This consists of four stations arranged around an approximately equilateral triangle with sides about 1,100 km long. The Apollo 15 seismometer makes the northern apex at Hadley-Appenines, Apollo 16 is in the east in the crater Descartes, and the west apex has Apollo 12 in Oceanus Procellarum and, 180 km away, Apollo 14 at Fra Mauro. Each station has three long period (>1 s) seismometers, sensitive to motion along three orthogonal directions, and a fourth short period (<1 s) seismometer sensitive to vertical motion. Each can detect a ground movement of about 0.05 nm.

Fortunately lunar scientists think that the seismic signals produced by meteoroid impacts can be distinguished from those caused by moonquakes. Impact events have sharper first signal rise times, indistinct shear wave arrivals and lower frequencies in the wave train. This is due to the fact that the impact waves must traverse the surface scattering zone twice between the impact point and the seismometer. Moonquakes, caused by tectonic strains within the lunar interior cross the zone only once so the energy in their seismic wave is less diffuse.

During the 924 days between January 1, 1973 and July 13, 1975 the seismic network detected 815 signals interpreted as being caused by meteoroid impacts. These have been statistically analysed by Duennebier, Nakamura, Latham and Dorman (Geophysics Laboratory, University of Texas) in their recent paper in *Science* (**192**, 1000; 1976). If an event is detected at only one seismometer it is regarded as "small". The signal amplitude is probably proportional to $E^{1/2}/r$ where E is the energy of the meteoroid and r is the distance between the sensor and the impact point, so most of the small events are caused by impacting particles with masses between 50 and 10^3 g, the larger events, detected at two or more stations, being caused by 5×10^3 to 5×10^4 g meteoroids. The authors find that a plot of impact rate as a function of time shows several sharp peaks in activity. Also, the frequency of intervals where there are no impacts is significantly more than expected—expected, that is, if the meteoroids are scattered randomly in space and the resultant impact rates follow a binomial distribution. Duennebier *et al.* conclude that some of the objects in the 50 to 50,000 g size range are not distributed randomly in space but occur in swarms. One of the more impressive swarms detected by the network was estimated to be about 2×10^7 km across and have a total mass between 10^{13} and 10^{14} g.

Could these peaks in the rate curve be caused by the Moon passing through a stream of particles produced by a decaying or decayed comet? Meteor showers caused by just such a process are common on Earth. The problem is that only about 10% of the mass in a meteor stream is made up of particles with individual masses over 50 g (according to Hughes, *Space Res* XV, 565; 1975). A considerably smaller percentage of the sporadic Solar System dust cloud is made up of these large particles, however, so the meteor streams should stand out prominently above the background Now 50 and 50,000 g particles impacting with the Earth's upper atmosphere at around 40 km s^{-1} produce visual meteors of magnitude about −4 and −12 respectively and an increase in flux of these very bright meteors and fireballs has been noticed during meteor showers. Meteor streams are always detected from Earth at the same solar longitude (about the same time each year) and Duennebier *et al.* note that the lunar events show no yearly pattern. The fact that the Moon oscillates by 3.8×10^5 km about the Earth's orbit does not help to get over this problem as meteor streams such as the Perseids and Geminids are 2.0×10^6 and 1.0×10^6 km wide. Both these streams are rich in fireballs.

It was also noticed that the mass distribution of the incident particles changed during the high rate events, the percentage of smaller objects being larger in the swarms than during the normal sporadic influx. Unfortunately this is exactly the opposite to what is observed with visual meteor showers, where the percentage of large particles increases.

Two of the maxima occurred on consecutive months, near new Moon, whereas the June, 1975 maxima occurred at full Moon. This contrasts with the timing of the moonquakes observed at the Apollo 17 site (Cooper and Kovach, *Proc. Lunar Sci. Conf 6th*, 2863; 1975) which appear to be closely correlated with the 29-d lunar month and the 300 K temperature variation of the lunar surface layer that occurs between mid-day and midnight.

So these data reveal something of a mystery. Large moonquake rates result, according to the authors, from the impact with the Moon of swarms of particles with masses greater than 50 g. Should similar swarms be seen on Earth? The answer is no, because even the peak lunar activity only corresponds to an infall of one large meteoroid every 3 days over an area 100 km in radius. The converse though is puzzling. The annual meteor streams seen on Earth contain a significant flux of particles in the mass range supposedly detected on the Moon. This flux also exceeds the sporadic (non-shower) flux by nearly an order of magnitude. So why haven't these been observed in lunar seismic data? Using the influx rates for the large meteoroids which produce fireballs in the Earth's atmosphere, obtained from the American Prairie Network of all-sky cameras (McCrosky and Ceplecha in *Meteorite Res*, 600 (edit. by Milman, P.,) D. Reidel, Dordrecht, 1969), about

250 particles with masses greater than 50 g should hit the Moon each day. Even going to the upper limit (50,000 g), of Duennebier *et al.*'s mass range the rate is about 10 per day. This compares with the maximum rate of 12 events per day observed by the seismic network. If meteoroid impacts are being detected the major meteor showers should stand out clearly above the sporadic background. The fact that Duennebier *et al.* are not seeing these showers introduces the possibility that they are seeing something else. ☐

Metals in proteins

from S. D. Dover

THE environment of metals in metalloproteins is of growing interest with the advent of synchrotron radiation. As distinct from crystallographic studies, which reveal the whole molecule, X-ray absorption measurements in the neighbourhood of the absorption edge of a metal are indicative of the local environment.

The use of synchrotron radiation as a tool for studying that environment is probably at the beginning of its exponential growth phase. In this application a tunable source of X radiation is required so that the spectrum can be observed. Coventional tubes are designed to emit most of their X-ray energy in the characteristic radiation line. The white radiation background, for a similar wavelength spread, has a much lower intensity. This means that the power available from the synchrotron over a whole range of wavelengths is several orders of magnitude greater than from laboratory sources.

This factor makes it possible to measure in an acceptable time the X-ray absorption spectra of systems where the absorber is relatively dilute (as in metalloproteins). Results from the Stanford Synchrotron Radiation Project (SPEAR) have been reported (*Proc natn. Acad. Sci. U.S.A.*, **72,** 2340; 1975) where gains in speed of 10^4–10^5 over X-ray tubes have been obtained. For example, the spectrum for haemoglobin over a 400 eV range was measured at 1 eV steps in only 20 h. This gave an acceptably low noise compared with the modulation of the X-ray absorption.

It is the modulation of the absorption spectrum that is of interest. The spectrum of a free metal consists of a low absorption region below the absorption edge where the incident photon is insufficiently energetic to excite the K electron. With increasing energy of X rays, the absorption edge is reached as the K electron can be excited to empty bound states. Beyond the edge itself the photon energy is sufficient to cause the emission of a photoelectron. The absorption tends to decrease monotonically from the absorption edge.

In contrast the spectrum of a bound metal in this region (the region of the extended X-ray absorption fine structure, EXAFS) is affected by the photoelectron being scattered back to the metal emitter by neighbouring atoms, inhibiting absorption. Instead of decreasing monotonically, the spectrum is modulated as the wavelength of the photoelectron varies with the wavelength of the X-ray photon. It is as if the photoelectron is acting as a diffraction probe for the environment of the metal. The back-scattering from surrounding atoms will have the appearance of interference fringes according to their distances from the metal and the photoelectron wavelength. Theoretical analysis of the fine structure of the spectrum has been successful in terms of the atomic environment for metals themselves (*Adv. X-ray Anal*, **13,** 248; 1970) and the iron-sulphur system in rubredoxin (*Proc. natn. Acad. Sci. U S.A.*, **72,** 4003; 1975). Work is continuing on haemoglobin and metalloporphyrins (*Proc. natn. Acad. Sci. U.S.A.*, **72,** 2340; 1975) where the results from the porphyrins can be used in the interpretation of the environment of the haem iron.

The absorption edge itself is being studied in model compounds (*Proc. natn Acad. Sci. U.S.A.*, **73,** 1384; 1976) where the fine structure and position is affected by the available bound electronic states. These and other model compound studies together with those of metalloproteins provide the possibility of examining the electronic situation of metals in proteins, and the two regions of the X-ray absorption spectrum together hold the promise of revealing the whole local environment. ☐

Fission of medium weight nuclei

from P E. Hodgson

THE fission of heavy nuclei such as uranium and plutonium is a well known phenomenon of practical importance. In special circumstances lighter nuclei can also undergo fission, and evidence for the fission of nuclei of mass around 80 has recently been found by Braun-Munzinger and colleagues (*Phys. Rev. Lett.*, **36,** 849; 1976).

The experiment giving evidence of such fission is the interaction of 140 MeV ^{32}S ions with ^{50}Ti. This type of interaction has been studied for many years in order to determine the characteristics of heavy ion reactions, but the particular feature of the new experiment is an array of electronic counters that facilitates determination of the masses and energies of two of the products of the reaction. For

The cytonet protein

IN his report on the recent EMBO symposium, Bretscher (*Nature*, **261,** 336; 1976) refers to the protein which Pearse (*J. molec. Biol.*, **97,** 93; 1975; *Proc. natn. Acad. Sci. U.S.A.*, **73,** 1255; 1976) has shown to be associated with vesicle "coats". In separate publications on this same material in the biochemical and neuroanatomical literature, an important correlation appears to have gone unnoticed. Gray (*J. Neurocytol.*, **1,** 363; 1972; *Brain Res.*, **62,** 329; 1973) examined coated vesicles in presynaptic terminals in the central nervous system and concluded that the coat material is structurally indistinguishable from a fibrous network filling the intervesicular cytoplasm. He also noticed that coated vesicles are surrounded by a clear space which he interprets as a retraction zone caused by fracture of an extensive cytoplasmic network, part of which has artefactually collapsed onto the vesicle forming the coat. The coat then appears to be a distorted fragment of a diffuse yet discrete cytoplasmic organelle composed of a fibrous reticulum which Gray called the 'cytonet'.

Gray (*J. Neurocytol.*, **4,** 315; 1975) later repudiated not only vesicular coats but the entire cytonet structure as artefactual, thinking it to be composed of denatured protein complexes. However, Pearse's discovery that vesicular coats contain essentially one protein supports an interpretation of the cytonet as a distinct supramolecular structure. Since it pervades the cytoplasm of many cell types it seems likely to play some role in the spatial organisation of cytoplasmic components, particularly of organelles such as synaptic vesicles. It thus seems important that the protein which coats isolated vesicles should be considered in its broader association with the cytonet, rather than in the limited context of "coated vesicles" which subcellular fraction studies imply Pearse's proposed name for this protein (clathrin or "coat substance") is a misnomer. If the molecule must have a name 'cytonexin' would be better.

A. J. MATUS

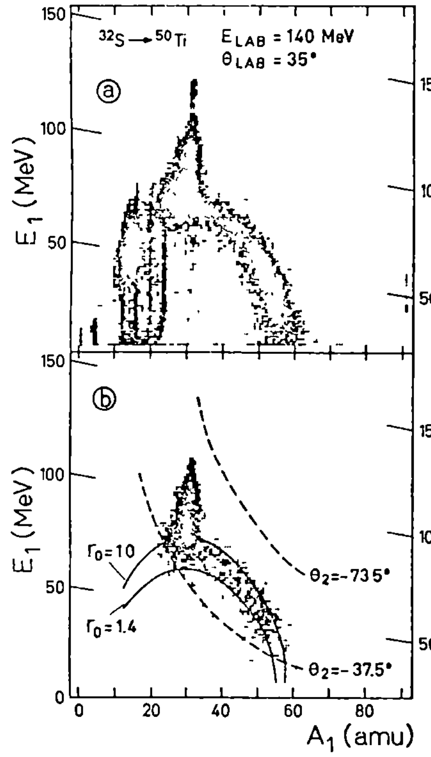

Fig. 1 Plot of the energy and mass number of particles emitted from the interaction of 140 MeV ^{32}S with ^{50}Ti. The top diagram shows all particles and the lower one only those emitted in coincidence with a second particle entering an ionisation chamber. The solid lines are calculated for the electrostatic repulsion of two spheres and the dashed lines are the kinematic constraints due to the detector geometry.

each interaction it is possible to measure the energy (E_1) and mass (A_1) of one of the reaction products by a time-of-flight telescope set at 35° to the incident beam and then the energy and energy loss in an ionisation chamber of a second particle emitted on the opposite side of the beam at the same time as the first, together with its angles of emission in and normal to the scattering plane.

Some of the results are shown in the figure in which each point represents a particle of energy E_1 and mass A_1 detected by the time-of-flight telescope. The top part shows all particles and the lower part only those emitted in coincidence with a second particle entering the ionisation chamber.

In these plots, the vertical lines around $A = 32$ correspond to the incident ^{32}S ions that have undergone peripheral elastic or quasielastic interactions with the loss or gain of a few nucleons. These interactions have been extensively studied and are now quite well understood. The broad band of points extending from $A \approx 32$ to $A \approx 50$ corresponds mostly to particles coming from the fission of the compound nucleus with $A \lesssim 82$ into two fragments of similar mass.

This identification is made by calculating the kinetic energies for the electrostatic repulsion of two charged spheres separated by $\{r_0(A_1^{1/3}+A_2^{1/3})+2\}$ fm for $r_0 = 1.0$ and 1.4; with the lighter fragments following the stability valley. The results of this calculation are shown by the solid lines in the figure, and they follow the experimental distribution very well.

Confirmation of this comes from the identification and kinematic correlations of the coincident particles. The ionisation chamber measurements of the second particle give its charge Z_2, and assuming its mass is $A_2 = 2Z_2+1$, the total mass of the fissioning nucleus is A_1+A_2. For all values of Z_2 between 12 and 16 the average value of A_1+A_2 is between 78.2 and 79.2 compared with the known total $A = 82$. This indicates that on the average about three nucleons are lost in the reaction. The mass distribution of the fission products is uniform from $A \approx 35$ to $A \approx 55$.

Additional studies of the energy distributions of the secondary particles also confirmed that fission had taken place. The correlation between A_1 and the angle of emission of the second particle showed that several nucleons are evaporated during the reaction, but it was not possible to distinguish between nucleons emitted before or after the fission process.

This experiment gives the first definite evidence for fission in this mass region and provides a way of studying the fission dynamics of highly excited nuclei with large angular momenta. ☐

Suspicious husbands

by John Krebs

On evolutionary grounds we would expect husbands to be suspicious. If a male is about to spend considerable time and effort in helping his mate to rear young he ought (in evolutionary terms) to check carefully that the young carry his genes. Male lions and langurs may even go to the extreme of killing off all the extant babies when they first take over a new harem: this ensures that the females will only rear children of the new group leader. The female herself, being equally related to her offspring regardless of the father, is not necessarily averse to infidelity.

While one can easily amuse oneself by developing such arguments as the logical outcome of the rules of natural selection (and perhaps even speculate on human analogies) it is not often that one comes across an experimental test. However, Erickson and Zenone (*Science*, **192**, 1353–54; 1976) have recently shown that male ring doves behave exactly as predicted by the theory.

The male ring dove shares with his mate the parental duties of nest building, incubation, and feeding the young, and so should be suspicious of a female which might have been inseminated by another male. The basis of Erickson and Zenone's experiment was the well established observation that male courtship displays have an important effect in stimulating ovarian activity. After a certain amount of courtship from a male, the female ring dove secretes ovarian steroids which cause her to start the so-called nest soliciting display, indicating her readiness to build a nest. Erickson and Zenone tested the reaction of 35 males to two groups of females: one that had been pre-exposed to courting males and brought into nesting condition, and one that had been kept in isolation. The first group of females immediately started nest soliciting when brought into contact with the test males, while the others did not. The reaction of the males was clear: they showed more aggression and less courtship towards the 'sexed up' females. Thus, as the theory predicts, males were suspicious of females that gave away the fact that they had been consorting with other males, and could have been fertilised by them. ☐

Haemopoiesis discussed

from J. J. T Owen

A symposium on Haemopoiesis in Vertebrate Embryos was held at the Institut d'Embryologie, Nogent-sur-Marne, France, on June 14–16. It was sponsored by the Delegation Generale à la Recherche Scientifique et Technique, Centre National de la Recherche Scientifique and the International Society of Developmental Biologists.

Many meetings these days seem to concentrate on highly specialist topics; perhaps it may be said that we learn more and more about less and less. This meeting was different and the organising committee should be congratulated on getting together scientists from various disciplines including embryology, immunology and haematology.

E. Cooper (Los Angeles) opened the meeting with an account of the evolution of blood cells and pointed out that the most primitive blood cell, a protohaemocyte, was involved in phagocytosis and nutrition. A lively debate followed about the origins of haemopoietic stem cells during ontogeny—an important topic that has generated a good deal of heat since the days o Maximow In particular, the origins thymus lymphocytes attracted spe interest—do they arise from the thymic rudiment itself or from blood-borne stem cells? E. P. Volpe (Tulane University) and N. Cohen (Basel) argued that experiments in which tissue primordia were transplanted between frog embryos of different ploidy states, proved that thymus lymphocytes are derived by differentiation of cells intrinsic to the thymic rudiment itself. Furthermore, Volpe suggested that a similar situation may exist in birds and mammals. But the elegant transplantation experiments of N. Le Douarin and her colleagues (Nogent-sur-Marne), using the structural differences between quail and chick nuclei as markers, demonstrate clearly that lymphocytes of the thymus and the bursa of Fabricius are derived from blood-borne stem cells. In addition, P. Deparis and A. Jaylet (Toulouse) and J. Charlemagne (Paris) presented evidence that thymus lymphocytes of newts and salamanders are of blood-borne origin. Hence, either there are fundamental differences in the pattern of lymphopoiesis among amphibia or, perhaps more likely, there is a common phylogenetic pattern involving migration of blood-borne stem cells to organs such as thymus. Volpe's results are compatible with the latter notion if stem cell migration occurs early in ontogeny and is restricted in time, as demonstrated by Le Douarin.

The source of blood-borne stem cells was also debated. It has been suggested that all haemopoietic stem cells are derived from yolk sac (Moore and Metcalfe, *Br. J. Haematol.* **18,** 279; 1970). F. Dieterlen-Lievre (Nogent-sur-Marne), however, demonstrated convincingly for the first time that definitive erythropoietic stem cells are derived from other sources. Yolk sac cells can populate the thymus, but they probably require a previous sojourn in the bone marrow (O. Stutman, New York).

The remarkable sequence of cellular and biochemical events which occurs during embryonic erythropoiesis—changing erythroid cell populations, changing haemoglobins and changing sites of erythropoiesis—was examined by several workers. J. Samarut *et al.* (Lyon) demonstrated the existence of separate erythroid stem cells specific for foetal and adult erythropoiesis respectively. Thus the situation contrasts with the synthesis of various immunoglobulin classes in B lymphocytes, which probably occurs in a single cell line (see Cooper below). J. Godet *et al.* (Lyon) identified membrane antigens specific for embryo and adult erythryocytes and A. Fantoni (Rome) showed that erythroid cells undergoing terminal differentiation in the 10–14-d mouse embryo synthesise haemoglobin by translating preformed long-lived messengers and that ageing leads to messengers which are unsuitable for terminating translation, thus resulting in reduced haemoglobin synthesis. The role of long-lived messengers in erythropoiesis leads one to wonder whether they may not operate in lymphopoiesis—perhaps explaining how a single lymphocyte can express two immunoglobulin classes at the same time. R. A. Rifkind (New York) discussed the regulation of foetal erythropoiesis. While erythropoietin serves as a cell-specific growth regulator (? at a proerythroblast stage), the rate of terminal differentiation is controlled at a more distal step along the erythroid pathway. In addition, changes in the composition of erythroid chromatin proteins probably have an important regulatory role (V. M. Ingram, Massachussetts Institute of Technology). R. Jacquot (Reims) and O. Gallien-Lartigue (Orsay) described new observations on the effects of glucocorticoids on foetal erythropoiesis.

The ontogeny of the immune response with its important implications for the generation of diversity of responsiveness was discussed next. L. Du Pasquier (Basel) pointed out that a broad range of antibody diversity appears early in amphibian development when the animals possess a small number of lymphocytes. This interesting observation is somewhat surprising in view of the restricted responsiveness of individual lymphocytes to antigen as envisaged by clonal selection and established by experiment. M. Cooper (University of Alabama, Birmingham) and P. Kincade (New York) showed that heterogeneity of responsiveness in terms of specificity and class of antibody is generated in the avian bursa of Fabricius from day 12 of incubation. Evidence that various immunoglobulin classes are generated within a single cell line by a preprogrammed switch mechanism in the bursa is convincing. On the basis of antigen binding studies, Cooper also suggested that specific clones of antigen-binding cells develop in a fixed sequential pattern which is not influenced by exogenous antigen. He interpreted this data as favouring a model in which individual stem cells give rise to multiple clones of B lymphocytes by a predetermined pattern of sequential expression of V-region genes. P. Toivanen (Turku, Finland) also pointed to the importance of the bursa which he showed was an important source of cells able to reconstitute immunodeficient chicks.

The importance of a circulating thymic factor (TF) in T-cell differentiation was discussed by J. F. Bach (Paris). This factor has been shown to possess several biological activities including restoration of suppressor and cytotoxic T-function in thymus-deprived mice. Its effect may be mediated by prostaglandins as well as cyclic AMP (M. A. Bach, Paris). TF seems to be one of the most functionally active factors of the various putative thymic hormones that have been described and so its further study is of considerable interest; however, the target cell for the action of these factors is as yet unclear and F. Loor (Basel) described studies with nude mice which suggested that T-cell differentiation begins at a prethymic level. Le Douarin *et al.*, however, presented evidence that stem cells which have already settled in the bursa can migrate to and differentiate in the thymus. Does this mean that stem cells which would have become B lymphocytes can instead become T cells if they are in the thymic microenvironment? Whatever the answer to these problems it is likely that various differentiation pathways are involved in the generation of T-cell subsets which were described in the thymus by M. Papiernik (Paris) and in the periphery by P. Häyry (Helsinki). Moreover, to obtain full functional maturation as described by R. Auerbach (University of Wisconsin, Madison), it seems likely that cell proliferation will be a crucial step as has been found in erythroid maturation by Rifkind.

In summary, the meeting was important in defining somewhat neglected areas for future study. In particular, most participants found the interdisciplinary approach of considerable value. □

A hundred years ago

Mr. Cross on Monday received a very numerous deputation from the British Medical Association, who laid before him their views with regard to the Vivisection Bill now before Parliament. These opinions were conveyed by Mr. Ernest Hart, Mr John Simon, Dr Wilks, senior physician of Guy's Hospital, and Sir W. Jenner, who raised his voice against a measure which would place men of science under police supervision, and would lay a ban upon them for inflicting cruelties on the lower animals when ten thousand times greater cruelties were inflicted by those who were going to pass this Bill. Such conduct would make those who passed it objects of scorn to all the scientific men in Europe. The Home Secretary, in reply, pointed out that the Bill was framed practically in accordance with the views of the Royal Commission, and that whether the Bill passed now depended entirely upon the line of conduct pursued by the medical profession.

from *Nature*, **14**, July 13, 241; 1876.

articles

Giant radio galaxy NGC315

A. H. Bridle
Queen's University at Kingston, Ontario, Canada

M. M. Davis & D. A. Meloy
Arecibo Observatory

E. B. Fomalont
National Radio Astronomy Observatory, Green Bank, West Virginia

R. G. Strom
Radiosterrenwacht, Dwingeloo, Netherlands

A. G. Willis
Sterrewacht, Leiden, Netherlands

A giant radio source with an unusual Z-shaped structure extending over nearly one degree on the sky has been detected around the nearby elliptical galaxy NGC315. The source has structure aligned with the minor axis of the optical galaxy on linear scales ranging from a few tens of kpc to ~ 1.7 Mpc. There is also a bright compact (<48 pc) source with an opaque radio spectrum located in the galactic nucleus. The physical properties of the extended emission are compared with those of the other three well studied giant radio galaxies—DA240, 3C236 and Centaurus A. The configurations of the giant systems with respect to their parent galaxies suggest that they are not produced by a gravitational slingshot process. The unusual morphology of the source is readily explained in terms of the rotating-beam model of Henriksen and Bridle.

WE report new radio observations of the bright (m_{pg}= 12.5 mag) elliptical galaxy NGC315 which reveal emission close to the minor axis of the galaxy over nearly 1° on the sky. This evidence suggests that it is a giant radio source some 1.7 Mpc in extent, at a distance of 100 Mpc. Only 3C236 has a linear size substantially larger than this.

Radio emission from NGC315 was first detected by Davis[1] in a 1.4-GHz survey where it was catalogued as DW0055+30. In the BDFL catalogue[2] of intense sources at 1.4 GHz it was included in the set of "confused fields", which have high probabilities of being multiple sources of large angular extent. Recently, Fanti *et al*[3] have presented a detailed study of the central radio source. We have mapped approximately one square degree around NGC315 at high sensitivity using the resurfaced Arecibo reflector at 2.38, 1.41 and 0.43 GHz and the Westerbork synthesis telescope at 0.61 GHz. The results confirm that NGC315 is associated with emission features at least 30′ and probably 1° in extent. High resolution maps of the central region have also been made with the NRAO 4-element interferometer at 2.7 and 8.1 GHz.

Radio structure of the source

Figure 1 shows contours of the emission around NGC315 observed at Arecibo with the system parameters listed in Table 1. The central source coincides with the visible galaxy and is joined by a bridge of emission to the peak of an extended feature ~16′ to the north-west in position angle −48°. The central source, the bridge and this north-preceding extended feature comprise the confused region

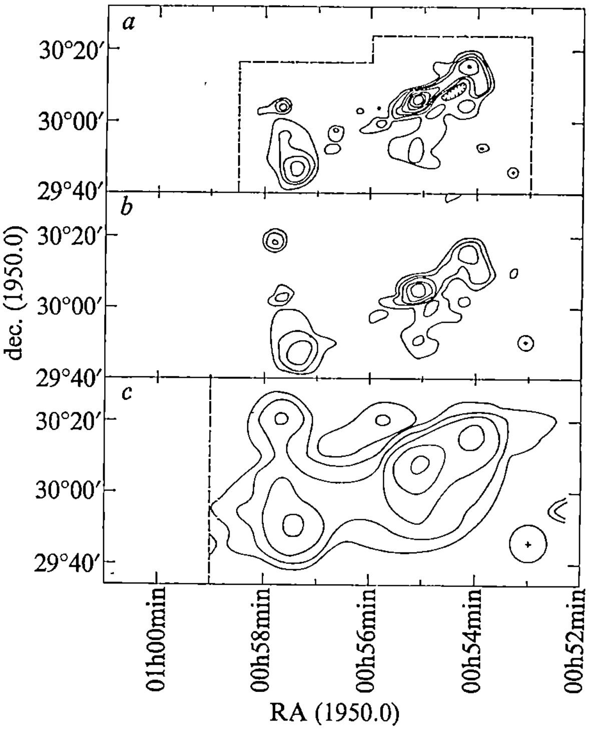

Fig. 1 Contours of the emission around NGC315 observed at Arecibo at three frequencies. *a*, 2.38 GHz, contours at 12.5, 25, 50, 100, 200, 400 and 800 mJy per beam. *b*, 1.41 GHz, contours at 50, 100, 200, 400, 800 mJy per beam. *c*, 0.43 GHz, contours at 125, 250, 500, 1,000, 2,000 mJy per beam. The dashed lines delimit the mapped regions and the half-power beamwidths are shown as the circles in the lower right corner of each map.

Table 1 Arecibo system parameters

Frequency (GHz)	Beamwidth (arc min)	System temperature (K)	Bandwidth (MHz)
2.38	3.0	42	20
1.41	4.0	120	10
0.43	10.0	120	2

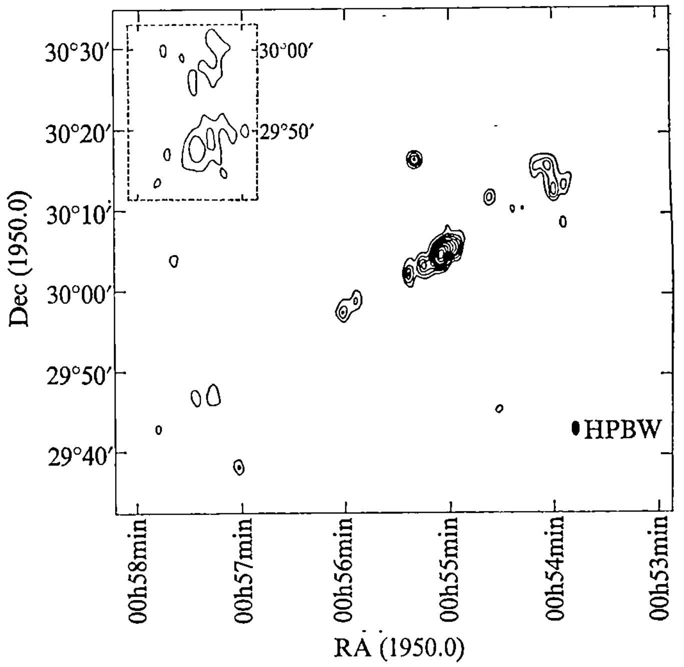

Fig. 2 Contours of the 0.61-GHz emission around NGC315 observed at Westerbork with 1′ (α) × 2′ (δ) resolution. Contours at 25, 50, 75, 100, 150, 200, 300, 400, 500, 750 and 1,000 mJy per beam. The insert, displaced in declination only and with the same contour values, shows the south-eastern lobe when convolved to a resolution of 2′ (α) × 4′ (δ). The maps have not been corrected for attenuation by the 1.4° primary beam.

noted by BDFL. The continuity of the radio emission from the galaxy to the extended feature leaves little doubt that all of this emission is related to NGC315. The 2.38-GHz map also clearly shows a spur of emission extending for >15′ SE of NGC315 towards the peak of a second emission feature located at 35′ from the galaxy in position angle 122°. This 'spur' is also visible, though less well defined, on the 1.4-GHz map; its alignment with the south-following feature suggests that the entire emission complex is associated with NGC315.

It is unlikely that the region is confused by foreground galactic features since the galactic latitude of the source is −32°. The probability of finding two unrelated extended features of this intensity aligned with 'bridge' and 'spur' protruding in nearly opposite directions from NGC315 is also very small. Inspection of the Palomar sky survey prints of the field shows that no other galaxies of brightness comparable to NGC315 are located within the extended radio features. The 14.1-mag galaxy NGC311 at 00 h 54 min 49.6 s, +30° 00′ 35″ (L. L. Dressel and J. J. Condon, unpublished) lies near the weak emission ~6′ from NGC315 in position angle ~220°, so this emission may not be related to NGC315. With this exception it is very probable that the entire extended structure shown in Fig. 1 is a single radio galaxy of exceptional angular extent.

The Westerbork telescope works at a frequency of 0.61 GHz, a synthesised beamwidth of 1′×2′, a system temperature of 350 K, a bandwidth of 4 MHz, a shortest baseline of 54 m, with increments of 72 m up to 1,422 m and an average HA of cuts of −76°, −35°, −1°, +37° and +77°. Observations consist of 12-min measurements made at five different hour angles. The resulting synthesised beam has radial grating responses which have been removed from the map by the usual CLEAN[4] procedure. The map in Fig. 2 shows a strong unresolved central component with a near-in extension of 2′ directed north-west and a longer but less intense counter component pointing south-east. Further to the south-east (near 00 h 56 min, +29° 58′) a small feature appears which is also well aligned with the major axis of the extended central emission. A ridge in the north-preceding component running nearly transverse to the source major axis is apparent. The south-following component, though heavily resolved, becomes clearly visible when the data are convolved to a 2′×4′ beam. Considering their different resolution and sensitivity, the Westerbork and Arecibo maps are in excellent agreement.

Figure 3 shows structure on a scale of ~90″ detected at 2.7 GHz near the unresolved nuclear source, which has been subtracted from this map for clarity. This structure is elongated along the position angle 133±3°, and is ten times brighter north-preceding the nucleus of NGC315 than on the south-following side at this resolution. In spite of the change in frequency, the structure seems similar to that shown in the 1.4-GHz map[3]. The emission, whose linear scale is ~50 kpc, comparable with that of some ordinary radio galaxies, comprises the most intense parts of the bridge and spur detected in the measurements at Arecibo and Westerbork. It also lies within NGC315, which has a diameter of 65 kpc and whose projected minor axis of 132±4° is close to that of the radio axis from ~50 kpc to 1.7 Mpc.

Comparison with other giant radio galaxies

Table 2 summarises the physical parameters of NGC315 using $z=0.0167$ (ref. 5) with the Hubble constant taken as 50 km s^{-1} Mpc^{-1}. The separation of the components places this radio source in the class of giant radio galaxies such as DA240, 3C236 and Centaurus A. Physical parameters[6] for these other sources are also given in Table 2.

As in the other giant sources, NGC315 contains a compact radio component located within the visible galaxy. An unresolved (<0.1″) source with an opaque spectrum

Table 2 Parameters of extended components of giant sources

	NGC315		DA240	3C236	Cen A
	North-preceding	South-following	Average	Average	Average
α(1950.0)	00 h 54 min 11±1 s	00 h 57 min 21±1 s	—	—	—
δ(1950.0)	30° 15′30″±1′	29° 46′ 10″±1′	—	—	—
Flux density (2.38 GHz)	0.55	0.45			
Projected distance from galaxy (kpc)	450	980	600	2,700	400
Volume (kpc^3)	1.3×10^6	2.2×10^6	2.7×10^8	1.3×10^9	9.9×10^7
Spectral index α	−0.52	−0.53	−0.77	−0.60	−0.6
Luminosity (W) 10 MHz–10 GHz	6.4×10^{33}	5.2×10^{33}	1.3×10^{35}	4×10^{35}	8×10^{34}
Minimum internal energy (J)*	6.0×10^{50}	6.7×10^{50}	1.4×10^{52}	5.4×10^{52}	9×10^{51}
Equipartition magnetic field* (gauss)	1.3×10^{-6}	1.1×10^{-6}	1.5×10^{-6}	1.2×10^{-6}	1.0×10^{-6}

*Assuming equal energies in protons and electrons, and that the source volume is uniformly filled.

coincides with the nucleus of NGC315 to within the ~3″ uncertainty in the optical position (ref. 3, and L. L. Dressel and J. J. Condon, unpublished).

The physical parameters of this nuclear source are given in Table 3. We can compare the 2.7-GHz and 8.1-GHz flux densities of the nuclear source with the values tabulated in ref. 3. This shows that the spectrum flattens out between 5 GHz and 8.1 GHz, if the source has not varied.

As in the other giant radio galaxies, the outer components of NGC315 are substantially extended transverse to their axis of separation from the optical galaxy. The NRAO interferometer observations show that neither peak in the outer components contains structure <5″ in extent stronger than 20 mJy at 2.7 GHz, and the Westerbork observations show there are no features <1′ stronger than 60 mJy at 0.61 GHz in the south-following component. The faint extensions of the outer components show an unusual symmetry with respect to the galaxy. The more distant, south-following component subtends the same angle (~40°) at the galaxy as does the closer, north-preceding component. The outer isophotes of both components are extended almost at right angles to the line joining their peaks, but in opposite directions. As the emission bridge and spur point towards these peaks, the overall form of the structure is best described as a Z shape whose extremities are equal arcs centred on the galaxy.

The extended features of the source seem to have a spectral index $\alpha=-0.5\pm0.2$ with little variation across the entire source except for the nuclear component. There is some indication from the 0.43-GHz map that the northwards extension of the south-following component may have a steeper spectrum than the rest of the source, but the present data do not allow us to place firm constraints on spectral index variations with size scales $\lesssim 5'$.

Discussion

As in the giant system 3C236 (refs 6, 7 and 8) the radio emission is elongated along the projected minor axis of the optical galaxy both far from NGC315 and near its nucleus. This is at variance with the gravitational 'slingshot' model of source formation[9] unless we make the unconventional assumption that NGC315 and 3C236 are both prolate rotators, so that their minor axis lies in their rotational equators Even then the observed alignments of their inner and outer radio structure would be statistically implausible. As the rotation axis of the giant source Cen A is known to lie near the overall elongation of both its large and small scale radio structure[10], the orientations of giant radio sources relative to their galaxies seem generally to conflict with a slingshot model for their origin. This contrasts with the orientations of double radio galaxies of 'normal' dimensions, which show no strong preference for galactic minor axes[11,12].

Fig. 3 Contours of the 2.7-GHz emission near the nucleus of NGC315 observed with the NRAO interferometer, after subtraction of the bright nuclear component (see Table 3) at the position marked by the cross The contour interval is 12 mJy/beam. The ellipse in the lower right corner indicates the half-power beamwidths, which are 11.4″ × 4.9″ with the major axis along position angle 138°. The dotted ellipse indicates the extent of the visible galaxy on the E print of the Palomar Sky Survey

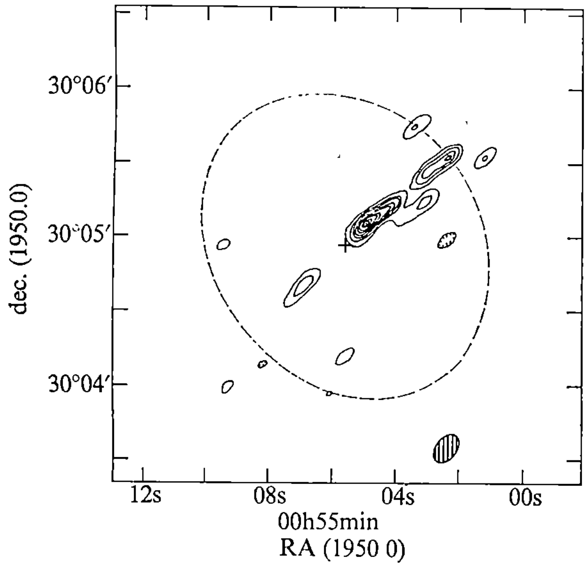

Table 3 NGC315—parameters of nuclear source

α(1950.0)	00 h 55 min 05.64±0.02 s
δ(1950.0)	30°04′56.8±0.2″
$S_{2.7}$	0.51±0.01 Jy
$S_{8.1}$	0.64±0.02 Jy
Diameter	<48 pc
Luminosity 10 MHz–10 GHz	7×10^{33} W
Minimum internal energy*	1.5×10^{46} J
Equipartition magnetic field*	$>10^{-3}$ gauss

*With assumptions as in Table 2.

The unusual Z-like configuration and rotational symmetry of the outer components with respect to NGC315 suggest that the development of a classical 'double' structure has been modified either by a mechanism acting on the components outside the galaxy or by a perturbation of the primary collimation mechanism producing the double structure. The source morphology could, for example, be produced by diffusion of particles and fields governed by asymmetries in the environments of the components such that material near the peak of the northern component can diffuse more readily towards the south, and vice versa. The fact that both components subtend the same angle at NGC315 would, however, require a specially contrived slab-like symmetry in the environment, extending over nearly 2 Mpc near the galaxy. Unless we regard the symmetrical appearance of the source as fortuitous, it is more attractive to consider an interpretation in which the primary source-collimating mechanism appears to have rotated on the sky during the lifetime of the radiating particles.

Such a rotation is implicit in the model of extended sources recently advanced by Henriksen and Bridle (to be published), in which relativistic particles are beamed from radio galaxies into double-source components along magnetic flux ropes which are rigidly coupled to the rotation of the central regions of the galaxies. In their model, the outer source components are produced where the rigidity of the rotating beams fails because their rotational velocity approaches that of light. The Z-shaped morphology of the NGC315 source can be understood on the Henriksen–Bridle model if the relativistic beams make an angle of ~20° with the rotation axis of the central region of NGC315, and the rotation rate of this region and thus of the beams is $\sim10^{-14}$ s^{-1}. The outer extensions of the source components would then be explained as trails of particles and magnetic field left behind around the orbits of the beam ends over $\sim10^{7}$ yr. As ejection of the beams near the galactic rotation axes favours the formation of giant sources, the orientational correlation observed for radio galaxies of different linear sizes is also consistent with this model. A detailed discussion of NGC315 in relation to the rotating-beam model will be given elsewhere (Henriksen and Bridle, in preparation).

It should be noted that this giant source has been recognised by the same observational procedure as were DA240 and 3C236, namely sensitive mapping of a confused field from the BDFL catalogue at resolutions of the order of a few arc min. As the BDFL confused fields are an essentially complete sample of such regions at 1.4 GHz, it is unlikely that radio galaxies of large angular size comprise $>5\%$ of extragalactic sources stronger than 2 Jy at 1.4 GHz, and possibly comprise substantially less than this. Although they are valuable testing grounds for theories of radio galaxies, the giant systems probably do not represent a numerically important source population that is absent from catalogues such as that of BDFL.

We thank Dr G. W. Brandie for assistance with the NRAO observations. This work was partially supported by the NRC of Canada The NRAO is operated by Associated Universities, Inc. under contract with the NSF The Westerbork Synthesis Radio Telescope is operated by the Netherlands Foundation for Radio Astronomy with financial support from the Netherlands Organisation for the Advancement of Pure Research.

Received April 11, accepted May 19, 1976.

[1] Davis, M M , *Bull astr. Insts Neth.*, 19, 201 (1967)
[2] Bridle, A H., Davis, M. M., Fomalont, E B , and Lequeux, J , *Astr J* , 77, 405 (1972)
[3] Fanti, R., Lari, C., Spencer, R. E , and Warwick, R S , *Mon. Not R astr Soc* , 174, 5P (1976).
[4] Hogbom, J. A , *Astr Astrophys* , *Suppl* , 15, 417 (1974).
[5] Colla, G., *et al* , *Astr Astrophys Suppl.*, 20, 1 (1974)
[6] Willis, A G , Strom, R G , and Wilson, A S., *Nature*, 250, 625 (1974).
[7] Wilkinson, P N , *Mon. Not R. astr Soc* , 160, 305 (1972).
[8] Fomalont, E. B , and Miley, G K., *Nature*, 257, 99 (1975)
[9] Saslaw, W C , Valtonen, M J , and Aarseth, S. J., *Astrophys J* , 190, 253 (1974).
[10] Burbidge, E. M , and Burbidge, G. R., *Astrophys J* , 129, 271 (1959)
[11] Bridle, A H , and Brandie, G W , *Astrophys Lett* , 15, 21 (1973)
[12] Gibson, D M., *Astr Astrophys* , 39, 377 (1975).

Repeated sequence specific to human males

Howard Cooke

MRC Mammalian Genome Unit, University of Edinburgh, West Mains Road, Edinburgh EH9 3JT, UK

Restriction enzyme analysis and nucleic acid hybridisation show that there is a repeated sequence in human male DNA which is not present in human female DNA. This sequence is shown to constitute about 50% of the DNA in the Y chromosome and is a simple tandemly repeated DNA.

THE contribution of DNA sequence organisation to chromosome structure and function has been the subject of much speculation[1-3], but there is still very little concrete evidence to relate to the theories As a starting point, it is useful to know the location of specific sequences within the chromosomes. The technique of *in situ* or cytological hybridisation has been applied successfully to repetitive sequences such as satellite DNA, ribosomal DNA, 5S DNA and other sequences of this type[4-6]. The method is especially powerful when applied to polytene chromosomes where even single copy genes can be located One limitation of the method is that it is designed to locate sequences which can be purified as either RNA or DNA. Different methods are needed if the aim is to analyse the composition of a particular chromosome. For this it would seem necessary to isolate the chromosome It is difficult to purify individual chromosomes at present, but they can in many cases be separated from the rest of the complement by the formation of heterokaryons[7]. Comparative methods can then be used to analyse the sequences on the odd chromosome.

A comparable situation exists when one sex has a heterogametic sex chromosome In principle this chromosome can be studied by comparison of male and female. The experiments reported here use this approach to study the DNA of the human Y chromosome

Repeated sequence specific to the Y chromosome

When human DNA is digested with a number of restriction enzymes and the products analysed by electrophoresis on Agarose gels, two enzymes, *Eco*RI and *Hae*III[8,9], produce prominent bands. The sizes of the *Eco*RI bands are 320 and 640 base pairs[10] The band pattern with *Hae*III is more complicated, with at least fifteen bands between 100 and 2,000 base pairs (Fig. 1). A comparison of male and female human DNAs after digestion with *Hae*III showed that there are two bands which are found only in DNA from males. As a check DNAs from 12 individual placentae were sexed by restriction in a blind test. The correct sex was predicted from electrophoresis of *Hae*III digests of the DNA in all 12 cases.

The fraction of the total DNA in the male specific bands was estimated by adding known amounts of linear SV40 DNA to total human DNA which had been digested with *Hae*III (*Eco*RI digestion of SV40 closed circular DNA was used to produce linear SV40 DNA molecules[11]). The areas in the male specific bands and in the SV40 bands were compared by microdensitometry of photographs of ethidium bromide fluorescence[12]. The peak area of the SV40 band was proportional to the amount of this DNA added to the total human DNA. By this method the larger male specific band was estimated to be 0 4±0.1% (ten measurements) of the total DNA in both a placental male DNA and DNA from a male derived neuroblastoma cell line. In an identical experiment DNA from a lymphoid XYY line was found to have a large male specific band which was 0.75±0.1% (five measurements) of the total DNA.

The smaller of the male specific bands is more difficult to quantify because of the higher background of other DNA sequences at this molecular weight, it constitutes about 0.2% and 0.4% of the total DNA respectively. The lymphoid XYY cell line used here has a karyotype which is near normal apart from the presence of two large chromosomes which fluoresce brightly when stained with quinacrine Doubling the number of Y chromosomes doubles the proportion of the total DNA present in both the large and the small male specific bands, and this strongly implies that the sequence is present on the Y chromosome itself.

Differences have been found in the amount of Y chromosome fluorescence but no significant differences in the amount of the male specific bands could be detected between male DNA samples from six different placentae and four cell lines The method is, however, not sensitive enough to detect small differences.

Fragment lengths were measured by gel electrophoresis on slab gels with marker DNAs in adjacent slots λ.cDNA restricted with *Eco*RI was used as a standard for the larger bands[13] and *Eco*RII digested mouse satellite DNA for the smaller bands[14] Band sizes are given in Fig. 1. The larger of the male specific bands is not separable from the smallest λ.*Eco*RI band when the two DNAs are analysed on the same gel slot Its molecular weight is 2.24×10^6, the smaller of the male specific bands has a molecular weight of 1.6×10^6.

The human diploid nucleus contains 3.5×10^{12} daltons of DNA[15]. From these values, from the fraction of the DNA present in each of the two male specific bands and from

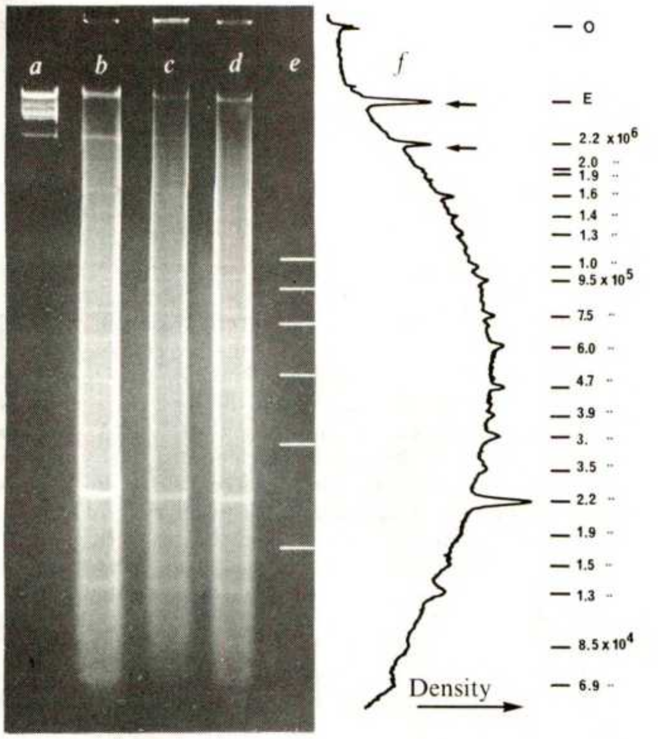

Fig. 1 DNAs restricted with different restriction enzymes after electrophoresis on a 2.5% Agarose slab gel. The gel was made up and run in 15 mM Tris, 18 mM NaH_2PO_4, 0.5 mM EDTA (*p*H 7.8) with a voltage gradient of 7 V cm^{-1} for 4 h. *a*, 0.2 microgrammes of λ.cDNA digested to completion with *Eco*RI in 10 mM NaCl, 10 mM MgCl, 10 mM 2-mercaptoethanol; the DNA was heated to 70 °C for 10 min after digestion to melt the sticky ends of the phage DNA. *b*, 10 µg of DNA from GIL cultured cells (this is a lymphoid cell line with two Y chromosomes—a gift from M. Steel). This DNA was digested to completion with *Hae*III in the buffer as in *a*. *c*, 10 µg of DNA from a male placenta digested with *Hae*III as in *b*. *d*, 10 µg of DNA from a female placenta digested as in *b* and *c*. *e*, 0.01 µg of mouse satellite DNA partially digested with *Endo*R *Eco*RII; the mouse satellite bands in this track were too faint to reproduce and so their positions were blocked in for this photograph. *f*, a trace of the pattern shown in slot *b* and reproduced at the same scale; the male specific bands are indicated by arrows and sizes in daltons of the principal bands given in the right hand column. O, origin of electrophoresis; E unresolved DNA.

their repeat length the number of copies of the sequences can be calculated as 6.2×10^3 for the large band, and 4.4×10^3 for the smaller band.

Restriction of fractions from a Ag–Cs_2SO_4 gradient followed by gel electrophoresis showed a considerable enrichment for the larger of the male specific bands on the light side of the main band DNA (Fig. 2). The smaller of the bands was not enriched in these fractions showing that the two bands arise from different repeated sequences. This is the region of the gradients which would be expected to contain human satellites III and IV[16].

Other restriction enzymes

Fractions from Ag–Cs_2SO_4 gradients which were enriched for the large male specific band were recycled on identical gradients to give further purification. This DNA was digested with a number of restriction endonucleases to attempt to map restriction sites within the *Hae*III repeat length. Seven other restriction enzymes were available, *Eco*RI, *Eco*RII, *Hae*I, *Hae*II, *Hin*dIII, *Hpa*II and *Bam*I[17]; of these only *Eco*RI gave a distinct band. This had the same mobility as the larger *Hae*III band, but had about one third the intensity. Double digestions with *Hae*III and the enzymes listed above confirmed that the *Hae*III repeat did not contain any of these restriction sites at a frequency high enough to give visible bands. The result with *Eco*RI suggests, however, that a subset of the repeated sequence contains *Eco*RI sites at the same spacing as the *Hae*III sites. At present it is not possible to say whether the two sites are on the same or separate molecules.

The resistance of this DNA fraction to such a wide range of restriction enzymes is to be expected since it is shown by sequence analysis described below to consist of a short repeat.

Isolation

As the 2.24×10^6-dalton fragment is not cleaved by a large number of restriction endonucleases, restriction with these enzymes can be used to remove most other sequences from the fragment partially purified by sizing. Human male DNA digested by *Hae*III was fractionated on a preparative gel electrophoresis apparatus (E. M. Southern, unpublished) and the DNA in the size class from 2 to 2.5×10^6 daltons taken, purified by CsCl centrifugation and concentrated. This DNA was then digested with *Hin*dIII, *Bam*I and *Eco*RII and fractionated on an Agarose slab gel. The male specific band was 70 to 80% pure as judged by microdensitometry of the gel photographs. The band was cut from the gel and the DNA recovered on to hydroxyapatite[12]. Male specific DNA was isolated in this way rather than by Ag–Cs_2SO_4 centrifugation because larger quantities of DNA could be used; the method is also faster and less expensive than centrifugation in Cs_2SO_4.

Homology with other sequences in male and female human DNA

It is clearly of interest to see whether the large male specific band has any sequence homology with other fractions both

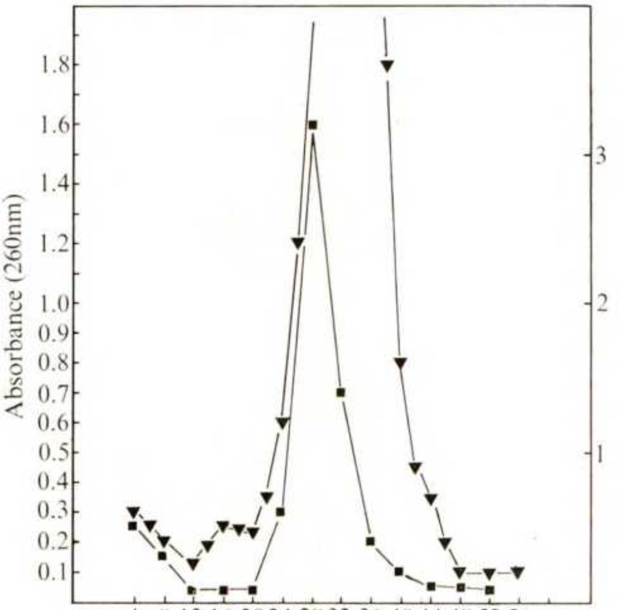

Fig. 2 Preparative Ag^{2+}–$CsSO_4$ centrifugation of human male DNA from placenta was carried out essentially as in ref. 21. Human male DNA was dialysed exhaustively against 0.1 M Na_2SO_4. Gradients were made up in 5 mM $Na_2B_4O_7$ (*p*H 9.3), 0.1 M Na_2SO_4, the silver to DNA phosphate ratio was adjusted to 0.2 and the final density of the solution to 1.48 g ml^{-1}. Centrifugation was carried out in a MSE 8 × 40 rotor at 32,000 r.p.m. for 4 d. The gradients were fractioned with a float from the top and groups of four fractions were pooled, dialysed against 4 M NaCl and the DNA concentrated by pelleting at 30,000 r.p.m. in a MSE 10 × 10 rotor overnight. Each set of pooled fractions was then restricted with *Hae*III and the products analysed by Agarose gel electrophoresis. The pattern in each slot was traced on a Joyce–Loebl recording microdensitometer and the percentage of the total area under the curve present in the male specific band calculated for each fraction: ▲, absorbance at 260 nm; ■, percentage of total DNA present in the male specific band.

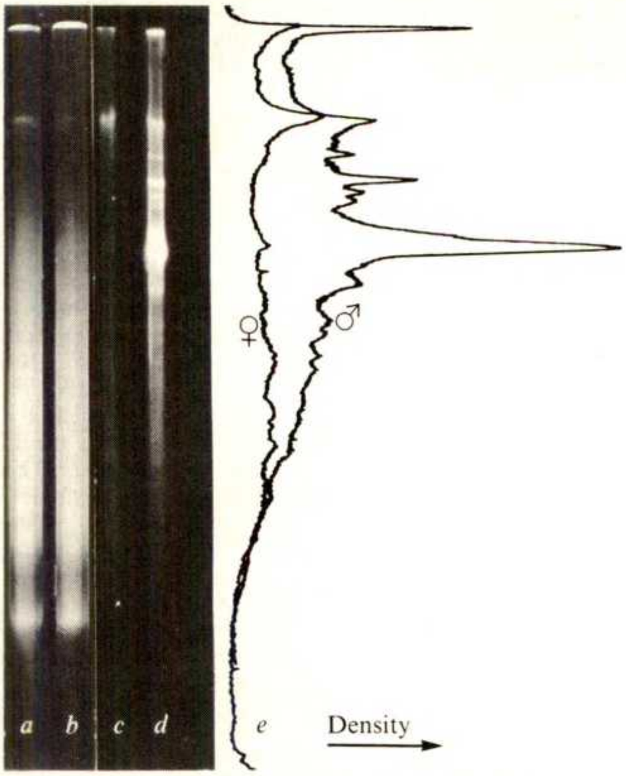

Fig. 3 Hybridisation of cRNA from the male specific band to male and female DNA. 80 μg of human male and female DNAs were digested to completion with *Hae*III then the fragments fractionated by electrophoresis on 0.8% Agarose tube gels, 1.0 cm diameter × 25 cm with a voltage gradient of 1 V cm^{-1} for 6 h. After electrophoresis the gel was photographed and the DNA fragments transferred to membrane filters as in ref. 20. Male and female DNAs were transferred simultaneously to one sheet of Millipore filter and this sheet of filter immersed for 18 h at 60 °C in a small volume (about 5–10 ml) of 2×SSC containing 0.01 microgrammes of ^{32}P-labelled cRNA with a specific activity of 2×10^8 d.p.m. μg^{-1}. After hybridisation and washing the filter was dried and autoradiographed. *a*, Gel containing female DNA before transfer to filter; *b*, gel containing male DNA before transfer to filter; *c*, negative of autoradiograph of hybridisation to female DNA; *d*, negative of autoradiograph of hybridisation to male DNA; *e*, microdensitometer trace of autoradiographs in *c* and *d*. *a*, *b*, *c*, *d*, and *e* are all reproduced on the same scale.

in male and female DNA. If, as has been suggested, tandemly-repeated sequences are involved in the meiotic pairing of chromosomes[18] it would seem unlikely that sequences related to the Y specific sequence will be found elsewhere.

Absence of an homologous band in the restriction pattern is not sufficient to rule out the possibility that female DNA contains a similar sequence. First, the method would not detect less than 1,000 copies and second, bearing in mind what is known about the evolution of repeated sequences[12,14,19], it is possible for related sequences to give completely different restriction patterns. A more sensitive and general test for sequence homology is given by molecular hybridisation and this method is especially convincing when applied to restriction fragments separated by gel electrophoresis[20].

An RNA copy of the 2.2×10^6-dalton fragment labelled with ^{32}P was synthesised using *E. coli* RNA polymerase. As judged by microdensitometry this fragment was 70% pure. *Hae*III fragments of male and female human DNA were separated on Agarose gels, denatured and transferred to strips of cellulose nitrate filter. The cRNA was then hybridised to the DNA bound to the cellulose and the strip was autoradiographed using X-ray film. The results of such an experiment are shown in Fig. 3.

As expected, male DNA gives a very intense band of hybrid at the position corresponding to 2.2×10^6 daltons, with weaker bands at positions corresponding to 4.5 and 6.7×10^6 daltons, the predicted sizes for dimer and trimer of the 2.2×10^6 dalton fragment. In addition, there are two bands between 2.2 and 4.5×10^6 daltons, and a number of indistinct bands smaller than 2.2×10^6 daltons. The male specific band which can be seen in *Hae*III restricted DNA at 1.6×10^6 daltons does not hybridise the cRNA probe used here and so is not closely related to the larger male specific sequence, in agreement with the behaviour in density gradients.

In contrast, female DNA gives a much weaker and different pattern. It shows one weak band at the position of DNA which is not cleaved by the restriction enzyme and a very faint band at the position of the larger male specific sequence. The latter is almost certainly due to sequences in the cRNA which originate from this size class of DNA and are not removed in purification of the Y specific sequence. The hybridisation to undegraded DNA occurs in both male and female and could be caused by a cross reaction to a related sequence present in both male and female DNA which does not contain the restriction site.

These results suggest that in human male DNA there is a complex family of repeated sequences related to the 2.2×10^6-dalton DNA fragment. This complexity most probably reflects the structure of the sequences on the Y chromosome since they are not present in female DNA. The presence of dimers and trimers of the 2.2×10^6-dalton sequence suggests that divergence is taking place in a tandemly-repeated sequence in a similar way to the *Mus musculus* and *Apodemus* satellites[12,14].

Fig. 4 Autoradiograph of RNase T_1 digest of ^{32}P labelled cRNA complementary to the male specific band. The cRNA was synthesised as in ref. 21 using ^{32}P-labelled GTP with a specific activity of 2 Ci mmol^{-1}. Electrophoresis and chromatography was carried out as in ref. 21, followed by chromatography on polyethylene-imine cellulose thin layers.

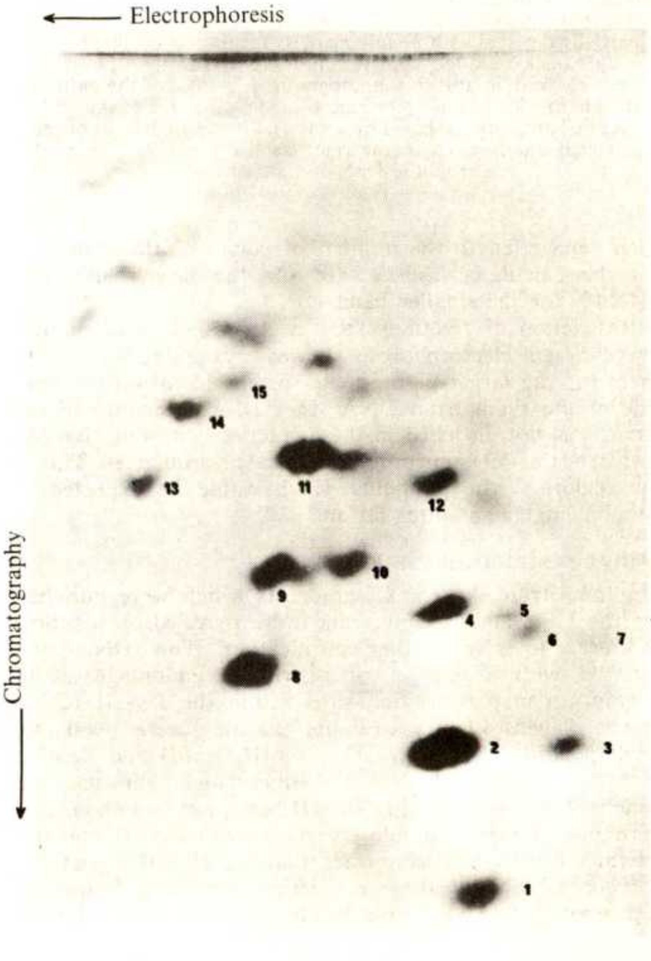

Fingerprint analysis

Figure 4 shows a ribonuclease T_1 fingerprint of cRNA transcribed from the large male specific band using ^{32}P-labelled GTP[21]. There are a number of intense spots which fall mostly in the short sequence region of the fingerprint with very small amounts of radioactive oligonucleotides present in the position of the longer sequences. The more intense spots (numbered in Fig. 4) were cut from the fingerprint and subjected to sequence analysis by pancreatic ribonuclease digestion. Table 1 gives the sequences of the spots from the ribonuclease T_1 fingerprint and the percentage of total counts in the excised spots for each sequence. Sixty-seven per cent of the total activity counted was in three sequences, AG, UG, and A_2 UGG; many of the sequences present in smaller amount could be accounted for by base substitution into these sequences. Although it is not possible to derive a definitive sequence from this data it is clear that the sequence is a simple one which has diverged from a repeating oligonucleotide such as $(AGUGG)_n$. This is the pattern of divergence which has been found in a number of satellite DNAs[22,23].

Table 1 Sequences of spots from ribonuclease T_1 fingerprints

Spot no.	% Counts	Composition	Sequence
1	5.5	G	G
2	33.6	AG	AG
3	2.3	CG	CG
4	5.8	A_2G	AAG
5	0.58	ACG	ACG
6	1.32	ACG	CAG
7	0.25	C_2G	CCG
8	16.9	UG	UG
9	5.5	AUG	AUG
10	3.0	CUG	CUG
11	16.9	A_2UG	A_2UG
12	2.66	C_2UG or A_3G	A_3G
13	1.9	U_2G	U_2G
14	2.5	U_2AG	U_2AG
15	0.87	—	—

Spots on the fingerprint in Fig. 4 were located by autoradiography, cut from the thin layer and counted in toluene base scintillator. After counting, the oligonucleotides were eluted, digested with ribonuclease A and analysed by electrophoresis as in ref. 21.

Discussion

The human Y chromosome is about the same size as chromosomes 21 and 22, each of which contains about 0.82% of the absorbence of the diploid karyotype at 257 nm[24]. On the assumption that the Y chromosome contains a similar proportion of the total DNA the two male specific bands described here would account for 70% of the DNA in the Y chromosome. The mammalian Y chromosome has been considered to be largely genetically inactive on the basis of its heterochromatic appearance[25]. It must, however, have genetic activity since genes on the Y chromosome must switch development of the embryonic gonad towards production of a testis[26]. In addition there seems likely to be a gene, or a function of the testis-determining gene, responsible for production of the H–Y antigen in mammals[27,28]. These loci must either be pericentric or on the short arm of the Y chromosome in man since an isochromosome of the long arm of the Y chromosome does not cause testis formation[29].

At least some of the repeated sequences described above are likely to be on the long arms because of the correlation between repeated sequences and heterochromatin[30] or more simply because it is unlikely that the short arms could contain 70% of the Y chromosome DNA.

Four human satellite DNAs have been reported present on the Y chromosome but they are also found on a fairly large group of other chromosomes[31]. Clearly this is not the case for the sequence described here but neither the satellite DNAs nor this sequence have been sufficiently well characterised to rule out the possibility that this sequence is related to one or more of the human satellites. The lack of hybridisation to female DNA suggests that this sequence is not simply one of the satellite DNAs but the behaviour in Ag–Cs_2SO_4 density gradients suggests that it is possible that satellite I, III and IV could be contaminated with this sequence. This might explain some of the *in situ* hybridisation of these satellites to the Y chromosome.

The conclusion which is inescapable from the *in situ* hybridisation and the experiments reported here is that the human Y chromosome must contain very little apart from simple sequence DNA.

The functions of repeated and satellite DNAs remain unknown in spite of much work on the structure and organisation of this class of DNA sequences. There are two questions raised by the data reported here which have obvious significance in terms of repeated sequence function; why is there so much repeated sequence DNA on the Y chromosome and why is the sequence described here found only on the Y chromosome? One answer to the first question could be that since the male-determining genes must segregate during spermatogenesis they must be present on a chromosome. If these genes are coded by small amounts of DNA then perhaps it is necessary to add other DNA to produce a chromosome. The repetitive sequences may be such genetically neutral DNA.

A further consequence of the need to ensure that genes on the Y chromosome segregate is that no crossing-over with other chromosomes can be tolerated[32]. This requirement could provide the answer to the second question above if the presence of a set of sequences unique to the Y chromosome prevented chiasmata formation with other chromosomes. The X and Y chromosomes in man have a terminal association during diakinesis and first meiotic metaphase[33] which involves the short arms of both chromosomes[34,35] but which does not have the normal form of synaptenemal complex and at meiosis they form a special structure as in most mammals[36]. The Y specific sequences could either be involved in this behaviour or could be a result of it.

The genetic isolation of the Y chromosome might allow a unique set of repeated sequences to be produced either by saltation[22] or by sister chromatid exchanges[37]. The formation must have been fairly recent since DNA from male chimpanzees shows no homologous band in the restriction pattern with *Hae*III (K. W. Jones, personal communication). It is of course possible that related sequences without the restriction site are present.

The availability of RNA complementary to a human Y specific sequence should allow further study of the evolution and distribution of these sequences. Clearly this type of study can be extended to repeated sequences of other chromosomes by the use of DNA from mouse/human somatic cell hybrids which contain only a single human chromosome.

I thank E. M. Southern and P. M. B. Walker for many discussions of this work and for criticisms of the manuscript, and C. Gosden for her help with the blind test and in providing placentae. This work was supported by the MRC

Note added in proof: A human Y specific sequence has been purified by extensive hybridisation of male and female DNA (ref. 38). The authors found that there is a repeated sequence DNA which constitutes between 2 and 11% of the human Y chromosome. This sequence is most likely to be one of the sequences described here. The major difference between the results reported in this paper and in ref. 38 is in the amount of the Y specific sequence. Calculations of the amount of sequences by Kunkel *et al.*, are rather indirect and assume that all Y specific repeated sequences are recovered at each step of purification. Cumulative losses in the purification procedure could thus account for

[illegible]
SCIENCE COLLEGE
[illegible]

an underestimate of the quality of Y specific repeated sequences present in the human genome.

Received March 10; accepted May 26, 1976.

[1] Britten, R. J., and Davidson, E. H., *Science*, **165**, 349–357 (1969).
[2] Laird, C. D., *et al.*, *Cold Spring Harb. Symp. quant Biol.*, **38**, 311–327 (1973).
[3] Sutton, W. D., *Nature new Biol.*, **237**, 70–71 (1972).
[4] Pardue, M. L., and Gall, J. G., *Science*, **168**, 1356–1368 (1970).
[5] Jones, K. W., *Nature*, **225**, 912–915 (1970).
[6] Pardue, M. L., and Birnstiel, M. L., *Symp. Medica Hoescht*, **6**, 75–85 (1972).
[7] Ruddle, F., *Nature*, **242**, 165–169 (1973)
[8] Yoshimuri, R. N., thesis, Univ. California (1971).
[9] Middleton, J. H., Edgell, M. H., and Hutchison, C. A., *J. Virol.*, **10**, 42–50 (1972).
[10] Philippsen, P., Streeck, R. F., and Zachau, H. G., *Eur. J. Biochem.*, **45**, 479–488 (1974).
[11] Danna, K. J., Sack. G. H., and Nathans, D., *J. molec. Biol.*, **78**, 363–376 (1973).
[12] Cooke, H. J., *J. molec. Biol.*, **94**, 87–99 (1975).
[13] Thomas, M., and Davis, R. W., *J. molec. Biol.*, **91**, 315–328 (1975).
[14] Southern, E. M., *J. molec. Biol.*, **94**, 51–69 (1975).
[15] Kimura, M., *Cold Spring Harb. Symp. quant. Biol.*, **38**, 515–524 (1973).
[16] Corneo, G., Ginelli, E., *Biochim. biophys. Acta*, **247**, 528–534 (1971).
[17] Murray, K., Murray, N. E., and Brammer, W. J., *Proc. 10th FEBS Meeting*, 193–207 (1975).
[18] Walker, P. M. B., *Prog. Biophys. Acta*, **247**, 528–534 (1971).
[19] Southern, E. M., *Symp. Medica Hoescht*, **6**, 19–27 (1972).
[20] Southern, E. M., *J. molec. Biol.*, **98**, 503–518 (1975).
[21] Biro, P. A., Carr-Brown, A., Southern, E. M., and Walker, P. M. B., *J. molec. Biol.*, **94**, 71–86 (1975).
[22] Southern, E. M., *Nature*, **227**, 794–798 (1970).
[23] Gall, J. G., and Atherton, D. D., *J. molec. Biol.*, **85**, 633–664 (1974).
[24] Mendelsohn, M. L., *et al.*, *Ann. N. Y. Acad. Sci.*, **157**, 376–383 (1969).
[25] Arrighi, F. E., and Hsu, T. C., *Cytogenetics*, **10**. 81–86 (1971).
[26] Ohno, S., *Nature*, **234**, 134–137 (1971).
[27] Wachtel, S. S., Ohno, S., Koo, G. C., and Boyse, E. A., *Nature*, **257**, 235–236 (1975).
[28] Bennett, D., Boyse, E. A., Lyon, M. F., Mathieson, B. J., Scheid, M., and Yanagisawa, K., *Nature*, **257**, 236–238 (1975).
[29] Jacobs, P. A., and Ross, A., *Nature*, **210**, 352–354 (1966).
[30] Yasmineh, W. G., and Yunis, J. J., *Biochem. biophys. Res. Commun.*, **35**, 779–781 (1969).
[31] Gosden, J. R., Mitchell, A. R., Buckland, R. A., Clayton, R. P., and Evans, H. J., *Expl Cell Res.*, **92**, 148–158 (1975).
[32] Ohno, S., *Sex Chromosomes and Sex Linked Genes* (Springer-Verlag, Berlin, 1967).
[33] Hulten, M., Lindsten, J., Pen-Ming, L. M., and Faraccaro, M , *Ann hum. Genet.*, **30**, 119–123 (1966).
[34] Pearson, P. L., and Bobrow, M., *Nature*, **226**, 959–961 (1970).
[35] Bobrow, M., Pearson, P. L., and Collacott, H. E. A. C., *Nature*, **232**, 555–557 (1971).
[36] Solari, A. J., *Int. Rev. Cytol.*, **38**, 273–317 (1974).
[37] Smith, G., *Cold Spring Harb. Symp. quant. Biol.*, **38**, 507–523 (1973).
[38] Kunkel, L. M., Smith, K. D., and Boyer, S. H., *Science*, **191**, 1189–1190 (1976).

Initiation sites of Rous sarcoma virus RNA-directed DNA synthesis *in vitro*

Linda M. Cashion, R. H. Joho, Margaret A. Planitz, M. A. Billeter & C. Weissmann

Institut für Molekularbiologie I, Universität Zürich, 8049 Zürich, Switzerland

Rous sarcoma virus DNA synthesis in disrupted virions is initiated mainly at a site about 200 nucleotides or less from the 5′ terminus, but other initiation sites throughout the RNA seem to be used as well. No AUG triplet occurs within a 5′ terminal segment of about 25 nucleotides.

THE RNA genome of avian oncornaviruses consists of two[1] identical RNA strands, each with a molecular weight of about 3×10^6 (about 10,000 nucleotides)[2-4]. During the early stages of the infective cycle the viral genome is transcribed into a complete double-stranded DNA copy of molecular weight 6×10^6 (ref. 5). When DNA is synthesised *in vitro*, however, in partially disrupted virus particles, the product is short, averaging only a few hundred nucleotides (see review by Green and Gerard[6]). Nonetheless, a small percentage of the DNA strands can reach a length of 1,500 to 4,500 nucleotides[7] or even the length of the viral RNA[8]. The short size of the bulk of the product is believed not to be due to nucleolytic scission of the DNA, since short DNA was also synthesised in reconstituted systems devoid of detectable nuclease activity[7,9]. A substantial fraction of the *in vitro* DNA product is complementary to a small region of the viral RNA[10,11], although sequences complementary to virtually all the viral RNA are present[10,12].

Several groups have reported that most or all DNA generated *in vitro* is attached to the 3′ end of a unique species of RNA primer[13,14] (tRNA^{Trp} in the case of Rous sarcoma virus RNA (ref. 15)) and that only one molecule of this primer is associated with each viral RNA subunit[16]. It therefore seemed reasonable to assume that DNA synthesis started close to the 3′ end of the RNA template and that premature chain termination gave rise to incomplete DNA strands with the properties described above. Recently, however, Taylor and Illmensee[16] reported that DNA transcription begins very close to the 5′ terminus of the RNA. This conclusion raised the question as to how sequences complementary to almost all the RNA are synthesised and how long DNA strands are generated.

We have examined the origin and the complexity of the DNA synthesised by disrupted Rous sarcoma virus, Prague B strain (Pr-B RSV), in the following way. The DNA was annealed with Pr-B RSV ^{32}P-RNA, and the hybridised RNA was characterised by digestion with RNase T_1 and identification of the resulting large oligonucleotides. The location on the viral RNA of the regions complementary to the cDNA could be determined from the physical map of large T_1 oligonucleotides of Pr-B RSV RNA established in our laboratory[17,18]. It was found that the most frequent DNA species corresponds to a region which is not more than 200 nucleotides in length and includes the 5′ terminus of the RNA. Several other non-contiguous regions of the viral RNA, notably one located in the middle of the molecule, were also represented in varying amounts. These findings suggest that the major initiation site is located near the 5′ terminus but that DNA synthesis may also originate at various other positions throughout the genome.

RSV ^{32}P-RNA complementary to RSV cDNA

DNA synthesised by partially disrupted Pr-B RSV particles in the presence of actinomycin D was purified and hybridised to Pr-B RSV ^{32}P-RNA. Hybridisations were carried out at two concentrations of DNA, the lower one to hybridise preferentially the more prevalent DNA species and the higher one to ascertain the overall complexity of the DNA. The preparations were treated with RNase T_1 and the RNase-resistant fractions were isolated by chromatography on Sephadex G-100. At the lower DNA concentration 4.7% of the RNA was hybridised and at the higher concentration 13.2%. A control which had been annealed to globin cDNA yielded 2.0% of the input radioactivity (mainly due to poly(A), see below) in the hybrid fraction. The same quantity of ^{3}H-labelled 70S Pr-B RSV RNA was then added to each sample as an internal standard to monitor the recovery of radioactivity throughout the subsequent analysis. The mixture was denatured and digested to completion with RNase T_1, and the products were separated by two-dimensional polyacrylamide gel electrophoresis.

A standard fingerprint pattern of 70S Pr-B RSV RNA is shown in Fig. 1*a*; the characteristic, large T_1 oligonucleotides which are numbered in the tracing (Fig. 1*a*′) have been characterised, and their relative order on the genome has been determined[17,18]. Figure 1*b* shows the oligonucleotides recovered after hybridisation at the lower DNA concentration: only two of the characteristic large T_1 oligonucleotides appeared as intense spots, namely T_{13} and to a lesser extent T_1. The identity of these oligonucleotides was ascertained from their pancreatic RNase digestion products (data not shown). Three further spots, T_{51}, T_{52} and T_{53}, were also prominent. These fragments

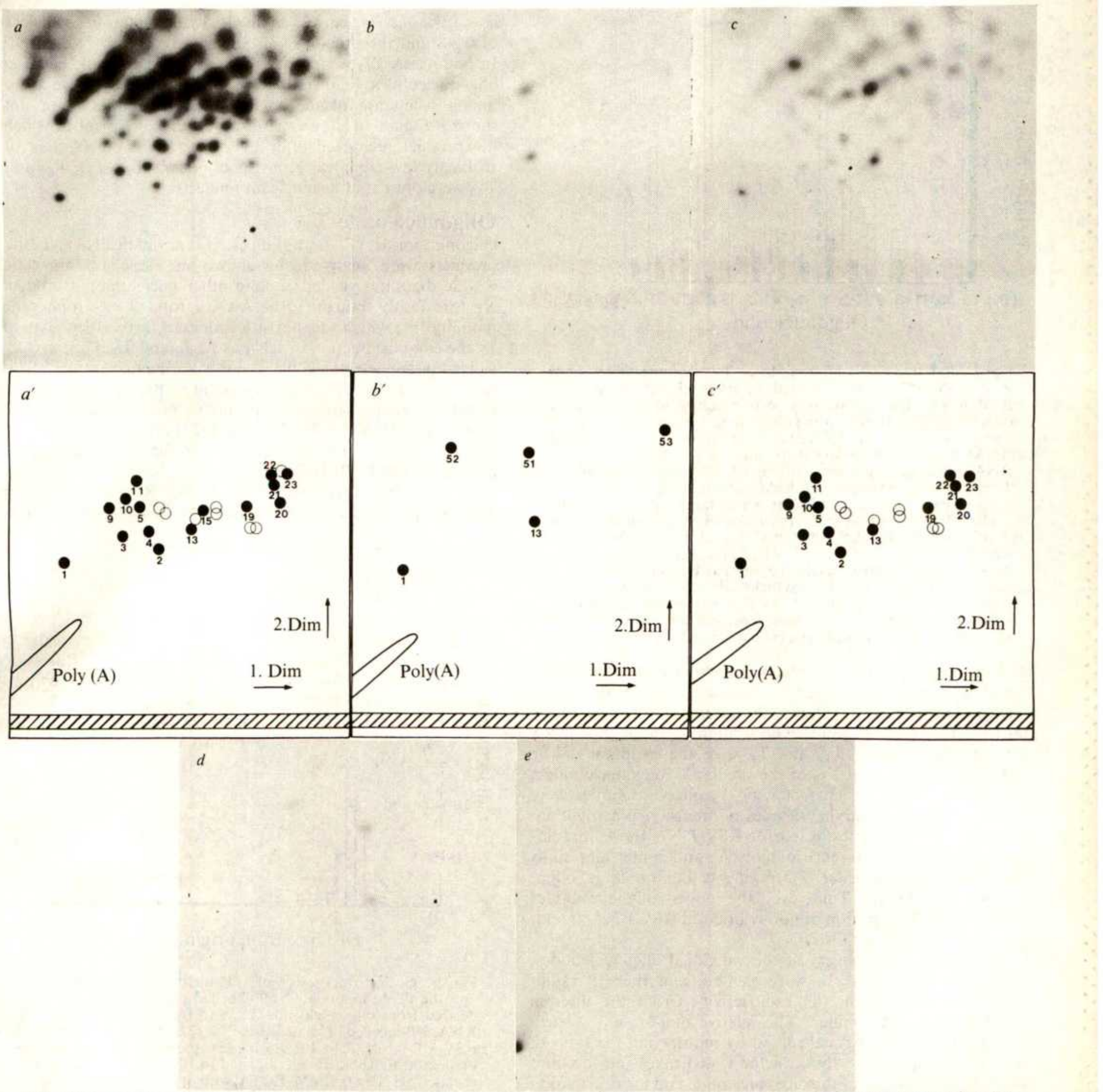

Fig. 1 Two-dimensional polyacrylamide gel electrophoresis of T_1 digests of Pr-B RSV ^{32}P-RNA recovered after hybridisation to different cDNA preparations. Rous sarcoma virus, Prague B strain (Pr-B RSV), was grown on chicken fibroblasts (Spafas, C/O, chf$^-$,obtained from R. Friis) as described[17], with the following modifications. Infected cells were passaged four or five times in Petri dishes and then seeded into Corning tissue culture roller flasks (490 cm^2, No. 25130) at a density of 3×10^7 cells per flask in 50–100 ml of Dulbecco's modified Eagle medium–10% Tryptone phosphate broth–5% calf serum. The virus was collected every 24 h and stored at −70 °C. Pr-B ^{32}P-RSV was prepared in roller bottles essentially as described[17]. Synthesis of Pr-B RSV DNA: Virus from 1 l of collected medium was concentrated by centrifugation for 60 min at 4 °C and 28,000 r.p.m. in the S30 Spinco rotor and suspended in 1 ml of 100 mM NaCl–50 mM Tris-HCl (*p*H 7.5)–1 mM EDTA. The concentrated virus suspension was incubated with 1 µl of β-mercaptoethanol and 0.3 ml of 1% NP 40 (w/v) for 5 min at 37 °C. The mixture was adjusted to 38 mM Tris-HCl (*p*H 8.0), 28 mM NaCl, 4.8 mM $MgCl_2$, 0.09 mM each dATP, dTTP, dCTP, and ^{32}P-dGTP (specific activity 3×10^3 c.p.m. nmol^{-1}), 24 µg ml^{-1} of actinomycin D (final volume, 2.1 ml) and incubated for 60 min at 37 °C. The preparation was then digested with 0.25 mg ml^{-1} of Pronase in the presence of 0.5% SDS for 15 min at 37 °C. After phenol extraction the combined aqueous phases were adjusted to 1% sodium acetate (*p*H 5) and precipitated with 2.5 vol of ethanol. After 2 h or longer at −20 °C, the precipitate was collected by centrifugation, redissolved in 250 µl of 50 mM NaCl–20 mM Tris-HCl (*p*H 8)–5 mM EDTA–0.1% sodium dodecylsulphate and chromatographed through a 0.6×8 cm column of Sephadex G-100 equilibrated with the same buffer. The excluded material was precipitated with ethanol, the precipitate dissolved in 100 µl of 0.2 M KOH, and digested for 16 h at 37 °C. The digest was neutralised and chromatographed through a 0.5×8 cm column of Sephadex G-100 in 20 mM Tris-HCl (*p*H 8)–0.1 M NaCl. The excluded material was precipitated with ethanol as above and dissolved in 20 mM Tris-HCl (*p*H 7.5)–5 mM EDTA. The yield in different preparations ranged from 0.3 to 1.5 nmol of incorporated dGMP. Analytical or preparative zonal centrifugation of the viral DNA was through a 4-ml 5–23% sucrose gradient in 50 mM Tris-HCl (*p*H 7.5)–0.2% SDS for 120 min at 55,000 r.p.m. and 15 °C in the SW60 Spinco rotor. A parallel tube was run with ^{125}I-labelled globin mRNA, Friend cell ribosomal ^{3}H-RNA and *E. coli* tRNA. Annealing reactions: 70S Pr-B RSV ^{32}P-RNA (specific activity > 10^6 c.p.m. µg^{-1}) was denatured in 20 mM Tris-HCl (*p*H 7.5)–5 mM EDTA for 1 min in a boiling water bath. Each annealing reaction mixture contained 2×10^6 c.p.m. of the denatured Pr-B RSV ^{32}P-RNA, DNA as indicated below, 0.5 M NaCl, 0.01 M Tris-HCl (*p*H 7.5) in 100 µl and was incubated for 4 h at 66 °C. The solution was diluted to 0.25 M NaCl (200 µl) and digestion carried out with 4 U of RNase T_1 (Calbiochem) for 30 min at 37 °C in the presence of 25 µg of yeast RNA (purified by phenol extraction). After phenol extraction the aqueous phase was chromatographed on a 1×16 cm column of Sephadex G-100 in 0.5 M NaCl–0.01 M Tris-HCl (*p*H 7.5). To the pooled excluded fractions were added Qβ RNA (100 µg) and 70S Pr-B RSV ^{3}H-RNA (2.5×10^5 c.p.m., specific activity > 10^6 c.p.m. µg^{-1}) as carrier and internal standard, respectively. The nucleic acids were precipitated twice with ethanol, taken up in 6 µl of 20 mM Tris-HCl (*p*H 7.5)–2 mM EDTA, sealed in a capillary, heated for 1 min in a boiling water bath and chilled. The RNA was digested with 16 U of RNase T_1 in 10 µl of the same Tris-EDTA buffer for 30 min at 39 °C. The products were subjected to two-dimensional polyacrylamide gel electrophoresis as described[17]. The autoradiograms are of the following samples: *a*, Total T_1 digest of untreated Pr-B RSV ^{32}P-RNA, directly subjected to two-dimensional polyacrylamide gel electrophoresis; *b–e*, were processed as described above; the DNA in the annealing mixtures was as follows: *b*, Pr-B RSV DNA, equivalent to 120 pmol of dGMP; recovery of ^{32}P radioactivity in hybrid, 4.2%; *c*, Pr-B RSV DNA equivalent to 500 pmol of dGMP; recovery in hybrid, 13.2%; *d*, Pr-B RSV DNA, equivalent to 80 pmol of dGMP; *e*, rabbit globin cDNA, $s_{20,w}$ about 9S (obtained from Dr Peter Curtis), 0.2 µg. *a′–c′* are tracings of *a–c*; *b′* also identifies the spots in *d*. The hatched bar in the tracing indicates the position of the gel strip from the first dimension.

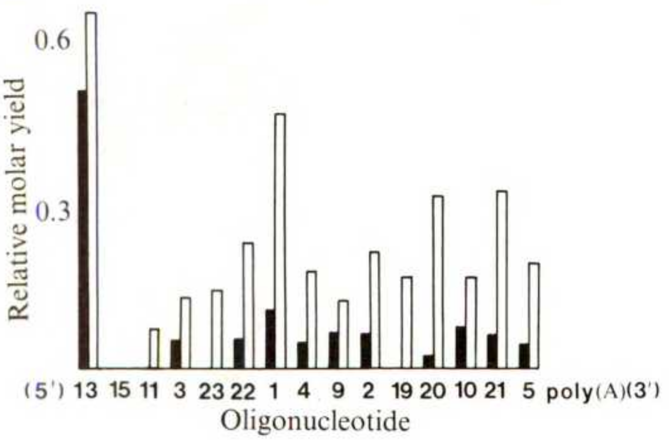

Fig. 2 Relative yields of some large T_1 oligonucleotides from Pr-B RSV ^{32}P-RNA recovered after hybridisation to Pr-B RSV RNA. The gel regions corresponding to the large T_1 oligonucleotides shown in the autoradiographs of Fig. 1*b* and *c* were excised, and the ^{32}P radioactivity (due to the hybridised RNA) and the ^{3}H radioactivity (due to the total Pr-B RSV RNA added as internal standard) were determined as described[17]. The relative recoveries were calculated by multiplying the $^{32}P/^3H$ ratio of each sample by a factor which takes into account the nucleotide composition of the particular oligonucleotide and the distribution of ^{3}H label between C and U, as described in the legend to Table 2 of ref. 17. The values (in arbitrary units; chosen to give approximately the estimated absolute yields) are plotted in the order of the oligonucleotide map as determined by Joho and Stoll (unpublished revision of the earlier map of Coffin and Billeter[17]). Solid bars represent the yields obtained after annealing at low, and open bars at high, DNA concentration.

had not been analysed or mapped previously since they are found in a gel region densely populated with smaller oligonucleotides. Figure 1*c* shows the fingerprint of T_1 oligonucleotides recovered after hybridisation at the higher DNA concentration. Again, T_{13} and T_1 were the strongest of the large and T_{51}, T_{52} and T_{53} of the smaller T_1 oligonucleotides; in addition almost all characteristic T_1 oligonucleotides were present, albeit with varying degrees of intensity. When globin-specific cDNA was substituted for RSV DNA the autoradiogram revealed the presence of poly(A) and some faint spots corresponding to smaller T_1 fragments but no large oligonucleotides (Fig. 1*e*). Thus, even the longest oligonucleotides generated by T_1 digestion of non-hybridised RSV RNA are not excluded by Sephadex G-100.

To measure the recovery of the individual oligonucleotides, the appropriate gel disks were excised, and the ^{32}P radioactivity as well as the ^{3}H radioactivity (from the internal standard) were determined. The relative molar yield of each ^{32}P-oligonucleotide was calculated by multiplying the ratio of its $^{32}P/^3H$ radioactivity by a factor which takes into account the base composition of the oligonucleotide and the distribution of ^{3}H label between UMP and CMP (see legend to Fig. 2 of ref. 17). The relative molar yields of selected large T_1 oligonucleotides which were well resolved on the autoradiogram and had been mapped earlier[17,18] (E. Stoll and R.H.J., unpublished results) are given in Fig. 2. Oligonucleotide T_{13}, which is recovered in highest molar yield (about 65% of the theoretical amount), had been mapped as the oligonucleotide closest to the 5′ end and, as shown below, in fact constitutes the 5′ terminus. Oligonucleotide T_1, which occurs in the next highest yield, is located in the middle of the map. After hybridisation at the lower DNA concentration the molar yield relative to T_{13} was 20% for oligonucleotide T_1 and 10% or less for all other nucleotides. At the higher DNA concentration the recovery of oligonucleotide T_1 was 70% compared with T_{13} while most other large oligonucleotides were present at 20 to 50%. Interestingly T_{15} and T_{11}, the two oligonucleotides closest to T_{13}, were barely detectable.

A similar protection experiment was performed with Pr-B RSV DNA fractionated on a neutral sucrose density gradient. Two fractions, one corresponding to a sedimentation coefficient of 0–4S and the other of 4–14S, were used for hybridisation. In both cases T_{13} was by far the most prominent of the large oligonucleotides, followed by T_1; T_{51}, T_{52} and T_{53} were again the most intense of the smaller oligonucleotides (data not shown). Figure 1*d* shows the result of an experiment in which the product recovered after hybridisation to cDNA was of strikingly low complexity; no spots besides T_{13}, T_{51}, T_{52} and T_{53} were present at a significant intensity.

Oligonucleotide T_{13}

Oligonucleotide T_{13} was digested enzymatically and the products were analysed. As shown in Table 1, pancreatic RNase digestion yielded, among other nucleotides, a product Xp (previously thought to be AAAC from its electrophoretic mobility[17,18]) which was not susceptible to further degradation by the combined action of RNases A, T_1 and T_2. This mixture yields mononucleotides from normal oligonucleotides. This resistance to digestion was reminiscent of the behaviour of the so-called capping group $m^7G^{5'}ppp^{5'}G^mpCp$ found at the 5′ terminus of RSV RNA by Keith and Fraenkel-Conrat[19] and Furuichi *et al.*[20]. To compare Xp with the authentic capping group, 30–40S Pr-B RSV ^{32}P-RNA was digested exhaustively with pancreatic RNase A, RNase T_1 and RNase T_2, and the digestion products were separated by two-dimensional electro-

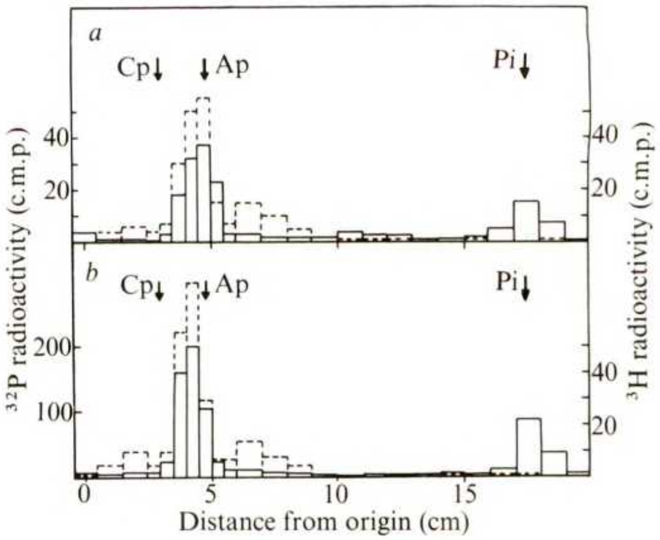

Fig. 3 Coelectrophoresis of ^{3}H-methyl-$m^7G^{5'}ppp^{5'}G^mpC_{OH}$ and the dephosphorylated ^{32}P-labelled putative capping group derived from oligonucleotide T_{13} and from 30–40S Pr-B RSV RNA. ^{32}P-labelled oligonucleotide T_{13} (7,000 c.p.m.) (*a*) and Pr-B RSV ^{32}P-RNA (3.4×10^6 c.p.m.) (*b*), prepared as described in the legend to Table 1 were digested in 10 µl of 7.5 mM sodium acetate (*p*H 4.5)–0.5 mM EDTA with RNase A (0.8 mg ml^{-1}) and a Takadiastase extract (containing RNase T_2 and T_1, about 80 U ml^{-1}, see ref. 32) for 2 h at 38 °C in the presence of 40–50 µg of yeast carrier RNA. The products were separated by two-dimensional electrophoresis as described by Adams and Cory[21]. In the case of (*a*) as well as of (*b*) a product (Xp and X′p respectively) with a mobility relative to Gp of 1.2 in the first, and 0.12 in the second, dimension was identified, in addition to the four standard nucleotides. X′p (990 c.p.m.) and Xp (225 c.p.m.) were eluted, mixed with 10 µg of yeast RNA and digested with 0.018 U of alkaline phosphatase from *E.coli* (Worthington) in 10 µl of 50 mM Tris-HCl (*p*H 8.8)–10 mM $MgCl_2$ for 60 min at 38 °C. The digests were mixed with about 1 A_{260} unit each of (3′)AMP and (3′)CMP, 0.1 µmol of unlabelled inorganic phosphate and ^{3}H-methyl-$m^7G^{5'}ppp^{5'}G^mpC_{OH}$ (about 2,000 c.p.m.; the preparation was a gift of Drs Furuichi and Shatkin) and subjected to electrophoresis on Whatman 3MM paper at *p*H 3.4 ^{32}P-phosphate was run in a parallel lane and located by autoradiography. The standard nucleotides were located in the ultraviolet light. Each lane, (*a*) and (*b*), was cut into strips which were placed in scintillation vials with 10 ml of toluene-based scintillator solution. ^{3}H radioactivity (— — — —) and ^{32}P radioactivity (————) were determined by scintillation counting. Background radioactivities (5 c.p.m. for ^{3}H, 9 c.p.m. for ^{32}P) were subtracted from each value.

Table 1 Digestion products of oligonucleotide T_{13}

RNases T_2+T_1+A	Pancreatic RNase A	RNAse U_2
0.82 Xp	0.8 Xp	0.8 X–C–Ap
5.4 Ap	3.0 A–Up	1.0 U–U–U–U–Ap
1.0 Gp	2.7 A–Cp	0.82 U–(C,U)–Ap
6.8 Cp	5.1 Cp	0.83 U–U–Gp
7.3 Up	5.1 Up	1.6 C–C–Ap
	1.0 Gp	1.0 C–Ap

Pr-B RSV ^{32}P-RNA (20×10^6 c.p.m.) was digested with RNase T_1, the products were separated by two-dimensional polyacrylamide gel electrophoresis and oligonucleotide 13 was extracted as described in ref. 17. Aliquots (1,000–3,000 c.p.m.) were digested with RNase U_2, pancreatic RNase A or with a mixture of RNases T_2, T_1 and A (for base analysis) as described[31]. The digestion products were separated at *p*H 3.5 on Whatman 3MM paper for base analysis and on DEAE paper in the other cases. The products of U_2 digestion were characterised by their mobilities and/or further digestion as for base analysis. The yields of all products were measured by scintillation counting. Molar compositions are relative to the underlined nucleotides; Xp, identified as the capping group (see text) contains five phosphate residues.

phoresis as described by Adams and Cory[21]. Oligonucleotide T_{13} was subjected to the same treatment in parallel. Pr-B RSV RNA yielded almost exclusively the four standard mononucleotides and about 0.042% of a product X′p with electrophoretic properties similar to those described for the capping group[21]. The mobility relative to Gp in the first dimension was 1.2, in the second 0.12; the corresponding values of Adams and Cory[21] were 1.1 and 0.092. Oligonucleotide T_{13} gave the four standard mononucleotides and 22.5% of a product Xp which had the same relative mobility as X′p. X′p and Xp were treated with phosphatase and subjected to one-dimensional electrophoresis. In both cases 22% of the radioactivity were released as inorganic phosphate (1.1 mol), and the residual oligonucleotides X'_{OH} and X_{OH} had the same electrophoretic mobility as authentic ^{3}H-CH$_3$-labelled.

$m^7G^{5'}ppp^{5'}G^mpC_{OH}$ was obtained from Dr A. Shatkin (Fig. 3). Digestion of X_{OH} and X'_{OH} with snake venom phosphodiesterase yielded inorganic phosphate and products with mobilities characteristic of 7mpG, pG and pC (data not shown). These experiments prove that oligonucleotide T_{13} contains the capping group and thus constitutes the 5′ terminus of Pr-B RSV RNA. From the data of Table 1 the partial sequence $m^7G^{5'}ppp^{5'}G^m$-C-C-A-(U_4A;U(C,U)A;2C_2A;CA)-U-U-Gp was deduced. Evidently the initiation codon A–U–G is not present within the first 25 nucleotides of Pr-B RSV RNA. It is of interest to note that in RAV-6 RNA the same capping group is associated with a large T_1 oligonucleotide of a somewhat different mobility which, with one exception, yields the same products as T_{13} on digestion with pancreatic and U_2 RNase and thus probably has a similar overall structure.

Initiation sites

We have demonstrated, by a new experimental approach, that a large proportion of the DNA synthesised *in vitro* by disrupted oncornavirus particles is complementary to a short segment of the viral RNA which contains the 5′ terminus, and a smaller proportion is complementary to almost all of the RNA sequences[10–12]. Our results confirm and extend the findings of Taylor and Illmensee[16]. These authors reported that the newly synthesised DNA, when isolated as a template–primer–product complex, is associated only with close to full-length, poly (A)-linked RNA and concluded that initiation occurs close to the 5′ end of the RNA. We found that a major fraction of *in vitro* cDNA with a sedimentation coefficient of 4S and less, that is, with chain lengths of certainly less than 200 nucleotides, hybridises to the 5′ terminal oligonucleotide (T_{13}) of Pr-B RSV RNA. The fact that the complexity of the RNA protected by the DNA is quite low, as judged by the appearance of only one large T_1 oligonucleotide in high yield and the virtual absence of the two T_1 oligonucleotides closest to the 5′ terminal fragment (T_{11} and T_{15}), argues against the possibility that the short size of our product was due to endonucleolytic cleavage (see also refs 7 and 9). Thus, the major initiation site must lie within 200 nucleotides from the 5′ terminus of the RNA, and the short size of the DNA could be explained if the 5′ end of the RNA constituted a termination point for a large part of the product transcribed *in vitro.*

DNA complementary to an RNA segment located in the middle of the genome was present at a level about 20% of the major DNA species, as judged by the relative amounts of oligonucleotides T_1 and T_{13} recovered after hybridisation at low DNA concentration. DNA sequences corresponding to other regions of the RNA, in particular close to the 3′ end, occurred each at less than 10% of the major species since in the hybridisation at high DNA concentration the characteristic large oligonucleotides were recovered with a yield half or less that of T_1. The occurrence of short cDNA species, corresponding to RNA segments located throughout the genome and present in significantly different amounts, suggests that DNA synthesis is initiated at not only one but more likely several additional sites throughout the RNA. Multiple initiation sites for cDNA synthesis have also been proposed by Rothenberg and Baltimore[22] for the murine leukaemia virus system. This proposal runs counter to the previous findings that all DNA synthesised *in vitro* initiates with the same nucleotide sequence at the 3′ end of a unique tRNA[13,14,15] associated with the 5′ end of 36S viral RNA[16]. The results were obtained, however, in the presence of only three deoxyribonucleoside triphosphates, that is, under conditions of limited synthesis, which might favour initiation at the main initiation site. Furthermore, in our experiments viral cDNA was synthesised in the presence of actinomycin D to suppress synthesis of double-stranded DNA[23,24]. cDNA synthesised in the presence of this drug (or of Mn^{2+}) has a higher complexity than that produced in its absence[12]; perhaps actinomycin favours the utilisation of minor initiation sites.

If DNA synthesis initiates at the 5′ terminal region by the addition of deoxynucleotides to $tRNA^{Trp}$, how does DNA synthesis originate at the other minor initiation sites? It has been assumed that the position defined by the 3′ terminus of the primer tRNA hydrogen-bonded[25–27] to viral RNA constitutes the attachment site for the RNA-dependent DNA polymerase. Panet *et al.*[28], however, have shown that the enzyme has a strong affinity for free $tRNA^{Trp}$; it is thus conceivable that a preformed polymerase–tRNA complex may initiate at many different sites, albeit with low efficiency. Alternatively (or in addition) a low level of initiation could occur at sites defined by the many other tRNAs[13,28,29] associated with 70S RNA, or possibly at the 3′ termini of accidental nicks in the 70S RNA, which could serve as primer template.

We do not know to what extent the *in vitro* findings with disrupted virus particles reflect the events which lead to the formation of a complete viral DNA transcript *in vivo.* If we assume, however, that the physiological initiation site is in fact located close to the 5′ terminus then one must postulate a transcription mechanism that allows polymerase molecules to continue elongation at the 3′ terminus, either of the same or a second molecule of the viral RNA. A model in which this feature is postulated was proposed by Cooper and Wyke[30]. Recently, it has been reported[7,8,22] that in appropriate reaction conditions the length of a small fraction of the cDNA synthesised by disrupted viral particles approaches that of the viral RNA. It will be of interest to ascertain whether DNA initiated at a site closer to the 3′ terminus is elongated extensively or whether DNA beginning close to the 5′ terminus is efficiently elongated across the (possibly ligated) gap between a 5′ and a 3′ terminus.

We thank Drs Furuichi and Shatkin for the gift of ^{3}H-methyl-$m^7G^{5'}ppp^{5'}G^mC_{OH}$ and Dr Curtis for rabbit globin cDNA. L.M.C. was supported by an NIH fellowship. This project was supported by the Schweizerische Nationalfonds.

Received March 18, accepted May 13, 1976.

[1] King, A. M. Q , *J biol Chem* , **251**, 141–149 (1976)
[2] Billeter, M. A , Parsons, J. T., and Coffin, J M , *Proc natn Acad Sci U.S A* , **71**, 3560–3564 (1974)
[3] Beemon, K , Duesberg, P., and Vogt, P., *Proc natn. Acad. Sci. U S A* , **71**, 4254–4258 (1974)
[4] Quade, K., Smith, R E., and Nichols, J L., *Virology*, **61**, 287–291 (1974)
[5] Varmus, H E , Guntaka, R V , Deng, C T , and Bishop, J M , *Cold Spring Harb. Symp. quant Biol* , **39**, 987–996 (1974)
[6] Green, M., and Gerard, G F., *Progr. Nucl Acid Res molec Biol.*, **14**, 187–334 (1974).
[7] Collett, M S , and Faras, A J , *J. Virol* , **16**, 1220–1228 (1975).
[8] Junghans, R P., Duesberg, P H , and Knight, C A , *Proc. natn. Acad Sci U.S A* , **72**, 4895–4899 (1975)
[9] Leis, J. P , and Hurwitz, J , *J Virol* , **9**, 130–142 (1972).
[10] Duesberg, P. H , and Canaani, E , *Virology*, **42**, 783–788 (1970).
[11] Varmus, H E , Levinson, W E , and Bishop, J M , *Nature new Biol* , **233**, 19–21 (1971).
[12] Garapin, A. C., Varmus, H. E., Faras, A J., Levinson, W E , and Bishop, J M , *Virology*, **52**, 264–274 (1973)
[13] Sawyer, R. C , and Dahlberg, J E., *J Virol* , **12**, 1226–1237 (1973).
[14] Taylor, J. M., Garfin, D. E , Levinson, W. E , Bishop, J. M., and Goodman, H M., *Biochemistry*, **13**, 3159–3163 (1974)
[15] Harada, F , Sawyer, R. C., and Dahlberg, J E., *J. biol Chem* , **250**, 3487–3497 (1975)
[16] Taylor, J M , and Illmensee, R , *J Virol* , **16**, 553–558 (1975)
[17] Coffin, J M , and Billeter, M A , *J molec Biol* , **100**, 293–318 (1976)
[18] Joho, R H , Billeter, M. A , and Weissmann, C , *Proc natn Acad Sci U S A* , **72**, 4772–4776 (1975)
[19] Keith, J., and Fraenkel-Conrat, H , *Proc natn. Acad Sci U S.A.*, **72**, 3347–3350 (1975).
[20] Furuichi, Y., Shatkin, A J , Stavnezer, E , and Bishop, J M , *Nature*, **257**, 618–620 (1975)
[21] Adams, J M , and Cory, S , *Nature*, **255**, 28–33 (1975)
[22] Rothenberg, E , and Baltimore, D , *J Virol* , **17**, 168–174 (1976)
[23] McDonnell, J P , *et al* , *Nature*, **228**, 433–435 (1970)
[24] Manly, K F , Smoler, D F , Bromfeld, E , and Baltimore, D , *J. Virol* , **7**, 106–111 (1971).
[25] Canaani, E., and Duesberg, P , *J Virol* , **10**, 23–31 (1972).
[26] Taylor, J M , Cordell-Stewart, B , Rohde, W , Goodman, H M , and Bishop, J M , *Virology*, **65**, 248–259 (1975)
[27] Dahlberg, J E , *et al* , *J. Virol* , **13**, 1126–1133 (1974)
[28] Panet, A , *et al* , *Proc natn. Acad. Sci U S A* , **72**, 2535–2539 (1975).
[29] Waters, L. C , Mullin, B. C., Ho, T., Yang, W -K , *Proc natn Acad Sci U.S.A.*, **72**, 2155–2159 (1975).
[30] Cooper, P D., and Wyke, J A , *Cold Spring Harb. Symp quant Biol* , **39**, 997–1004 (1974).
[31] Flavell, R. A , Sabo, D L , Bandle, E. F., and Weissmann, C , *J molec Biol* , **89**, 255–272 (1974)
[32] Hiramaru, M., Uchida, T., and Egami, F , *Analyt Biochem* , **17**, 135–142 (1966).

Proviral sequences of baboon endogenous type C RNA virus in DNA of human leukaemic tissues

Flossie Wong-Staal, David Gillespie & Robert C. Gallo

Laboratory of Tumor Cell Biology, National Cancer Institute, Bethesda, Maryland 20014

Hybridisation of RNA from a baboon endogenous type C RNA virus to DNA from tissues of leukaemic patients indicates that a virus of this type is horizontally transmitted among humans. DNA from several patients with leukaemia hybridised 70% of the hybridisable RNA from baboon endogenous type C RNA virus (BaEV) and yielded hybrids of high t_m*, whereas DNA from normal human tissues hybridised only 23% of the BaEV RNA, and the* t_m *of these hybrids was lower.*

SEVERAL studies link type C RNA viruses to human leukaemia. These include the detection of subviral components within blood leukocytes taken from leukaemic patients[1–11], the transient release of virus-like particles from these cells in short term culture[12,13] and the rare isolation of infectious virus from cultured human cells[14–19]. Nevertheless, evidence for the viral aetiology of human leukaemia or, in fact, for the presence of oncornaviruses in humans has been limited by the inability to detect in fresh human tissues one component expected of virus-infected cells, namely, a DNA provirus related to a major portion of the genome of a type C RNA virus[20].

The detection of a DNA provirus requires the availability of an appropriate viral nucleic acid for use as a detection probe. Early studies suggested that Rauscher mouse leukaemia virus ($MuLV_R$) might yield a useful probe[8–11], but subsequent work indicated that the $MuLV_R$-related RNA sequences detected in leukaemic blood leukocytes might also exist in the blood cells of normal people[4] and that these sequences might be more closely related to that of the primate RNA tumour virus, simian (woolly monkey) sarcoma-leukaemia virus (SiSV)[4,6,7]. So far, neither RNA probes from SiSV nor from $MuLV_R$ have been used successfully to detect DNA proviruses in human tumour cells[4].

The isolation of infectious virus from cultured human cells has provided a new impetus in the search for provirus in human cells. In one instance[14,15] the viruses obtained from cultured human leukaemic cells consisted of a mixture of two type C viruses; one closely related to SiSV and one closely related to viruses obtained from apparently normal baboons, the baboon endogenous virus, BaEV[21–24]. This result prompted us to examine various tissues from leukaemic patients for BaEV-related provirus. Evidence for BaEV-related provirus has very recently been reported in DNA from the spleen of the one particular patient, patient HL23, with acute myelogenous leukaemia (AML)[25] whose cells in culture had released virus, the HL23 virus (HL23V)[14]. We present here detailed hybridisation results that demonstrate the presence of BaEV-related provirus in seven of the leukaemic tissues studied and its absence from normal tissues. Specifically, these leukaemic tissues were chosen because of earlier evidence for the presence of other viral components in them. We also show that DNA sequences distantly related to BaEV were found in both normal and leukaemic humans.

BaEV sequences in human DNA

Figure 1 shows that more of the sequences in RNA from BaEV hybridised to DNA from spleens or peripheral blood leukocytes of some patients with myelogenous leukaemia than to DNA of tissues obtained from normal humans. DNA from some leukaemic patients (HL23, HL49) hybridised faster to BaEV RNA than did DNA from other patients but by a C_0t of 2×10^4 (200 h) DNA from all of the leukaemic patients presented in Fig. 1 hybridised significantly more BaEV RNA than did DNA from normal humans. It was not possible to extend the hybridisations longer than 200 h because of RNA degradation (dashed line, Fig. 1). DNA from human NC37 cells infected by BaEV should contain one provirus per haploid genome[23,24], and in this case BaEV sequences were readily detected (Fig. 1). Since the hybridisation conditions used detected DNA sequences present in one or more copies per haploid genome, the low hybridisation obtained with DNA from normal humans, relative to leukaemics, suggests that the sequences in the leukaemic DNA do not result from amplification of normal human chromosomal genes. In fact, the BaEV sequences in the DNA of some leukaemic patients (HL7, HL11) were probably present less than once per cell, as judged by the rate of hybridisation with BaEV RNA ($C_0t_{1/2}\sim10^4$) (Fig. 1).

The experiments shown in Fig. 1 used a DNA : ^{125}I-RNA ratio of about 2×10^7 : 1 To determine whether this ratio represented an excess of BaEV-related DNA sequences, hybridisations were carried out with varied DNA : RNA ratios ($C_0t = 2\times10^4$) (Fig. 2). The percentage ^{125}I-RNA hybridised to DNA against the DNA : RNA ratio is shown in Fig. 2*a*. The results indicate that even at the highest DNA : RNA ratio examined, the percentage of the RNA hybridised was still increasing. The data of Fig. 2*a* were therefore subjected to a double reciprocal analysis and the resulting curves were extrapolated to the *Y* axis (where RNA : DNA approaches 0, DNA : RNA approaches ∞) (Fig. 2*b*), to estimate the fraction of BaEV RNA that may hybridise at infinite DNA excess. The results (maximum percentage of the BaEV RNA hybridised at infinite DNA) shown in Table 1 demonstrate that DNA from some leukaemics hybridised 70% of the hybridisable BaEV RNA whereas DNA from normal human tissues hybridised only 23% of the RNA at DNA excess. Most extrapolated values were close to actual values obtained with large (1 mg for example) DNA inputs; where this was not the case, the actual values obtained were used (values in parentheses). BaEV sequences in the DNA of one patient (HL54) were detectable by DNA titration analyses and especially by the double reciprocal representation (Fig 2*b*), although they were not detected in kinetics experiments. The analysis of DNA from four tissues of normal persons (Table 1) establishes the lack of BaEV sequences in the normal human genome. The possible existence of some normal tissues with BaEV sequences or many normal tissues with very rare BaEV sequences (less than one copy per cell) is not evaluated here and would indicate infection of normal individuals.

Lack of detectable SiSV proviral sequences

As we have noted, some biochemical studies have indicated that leukaemic cells may sometimes contain molecules related to components of woolly monkey (simian) sarcoma–leukaemia virus, SiSV (refs 1–7, 13–19, 25, 28–30) and four laboratories have reported the release of infectious virus related or identical to SiSV from cultured human cells[14–19]. The case of patient HL23 (refs. 14–16, 25) involved release of an SiSV-related virus in addition to a virus closely related to BaEV.

In earlier work[4,5], however, it was not possible to detect proviral DNA related to the genome of SiSV in leukaemic patients. Since the DNA titration experiments detected BaEV sequences in DNA from leukaemic patients, this assay was applied to RNA from SiSV. Figure 2*c* nevertheless shows that no proviral sequences related to SiSV could be detected in tissues of patient HL23. DNA from normal humans hybridised very little of the SiSV RNA at finite DNA inputs, relative to the amount of BaEV RNA that was hybridised (Fig. 2*c*). Although sequences very distantly related to SiSV RNA may exist, inordinate amounts of DNA would be required for the formation of stable hybrid structures. It seems, therefore, that if the human leukaemic cells are infected by SiSV, the infection does not involve the classical mechanism of inserting one or more proviral DNA sequence per transformed cell. It remains possible, however, that provirus related to SiSV will be found in other patients.

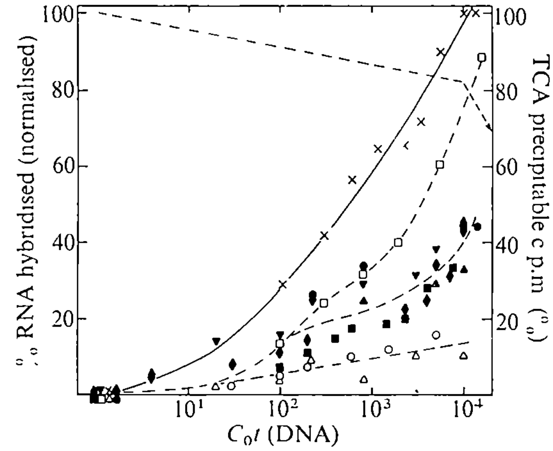

Fig. 1 Kinetics of hybridisation of BaEV RNA to cell DNA. Hybrids were formed between ^{125}I-RNA from BaEV (strain BAB8-K(FCf2TH)[9] (500–1,000 c p.m.; 10^8 c.p m μg^{-1}) and a 1×10^7- or 2×10^7-fold weight excess of cell DNA at 60 °C in 0.4 M phosphate buffer and monitored by resistance to RNase as detailed elsewhere[25]. Fifty-five percent of the RNA hybridised to DNA from normal baboons and all values have been normalised to this result. ×, Yellow baboon spleen (*Papio cynocephalus*); ○, NC37 human lymphoid cultured cells derived from a normal donor; □, NC37 cells infected by BaEV (NC37(BaEV)); ●, blood leukocytes of patient HL49, a 32-yr-old male Caucasian with CML (acute phase), a white blood cell (WBC) count of 1.4×10^5 μl^{-1}—treatment records were not available; ▼, blood leukocytes of patient HL50, a 62-yr-old male Caucasian with AML, a WBC count of 2.5×10^5 μl^{-1}—untreated; ▲, spleen taken at autopsy of patient HL23, a 51-yr-old female Caucasian with AML and under treatment with cytosine arabinonucleoside, vincristine, and prednisone; ◆, blood leukocytes from patient HL7, a 26-yr-old male Negro with CML (acute phase), WBC count of 6×10^5 μl^{-1}, and treated with prednisone and vincristine; ■, spleen taken at autopsy from patient HL11, a 59-yr-old male Caucasian with an unusual aggressive form of CMML and treated with hydroxyurea; △, liver taken from a normal human; — — — —, acid-precipitability of RNA. HL, human leukaemic; AML, acute myelogenous leukaemia; CML, chronic myelogenous leukaemia; CMML, chronic monomyelocytic leukaemic

Table 1 Maximum hybrid yield and t_m with BaEV RNA

Source of DNA	Disease	Maximum % RNA hybridised	t_m(°C)	Δt_m(°C)
HL23 spleen	AML	70	76	−1
HL50 leukocytes	AML	70	77	0
HL49 leukocytes	CML-A	70	78	+1
HL7 leukocytes	CML-A	(70)	79	+2
HL11 spleen	CMML	45	80	+3
HL54 leukocytes	AML	(40)	NT	—
HL51 spleen	AML	(30)	NT	—
HL55 leukocytes	ALL	(23)	NT	—
Normal human spleen	—	23	NT	—
Normal human liver	—	23	69	−8
Normal human blood leukocytes	—	23	NT	—
NC37 normal human lymphoid cell line	—	23	69	−8
NC37 (BaEV)	—	100	77	0
Normal baboon spleen	—	100	75–78*	—
Human leukocyte (× rRNA) (control)	—	—	82	—

The maximum percentage of the BaEV RNA that hybridised to DNA was estimated from Fig. 2*b*. t_m Values were measured as described in the text. Leukocytes, peripheral white blood cells; AML, acute myelogenous leukaemia; CML-A, acute phase of chronic myelogenous leukaemia; CMML, a case of aggressive chronic monomyelocytic leukaemia. The HL numbers correspond to those in earlier publications (refs 1–7, 14–16, 25, see also legends to Figs 1 and 2); NC37(BaEV), NC37 infected by BaEV. NT, not tested.

*Value varied with different species of baboon.

Thermal stability of hybrids formed with BaEV RNA and DNA from leukaemic patients

The thermal stability of hybrids formed at 60 °C was measured by exposure to a given temperature for 5 min in 0.15 M NaCl and then for 2 h at 37 °C in 0.45 M NaCl with RNase. Representative results are shown in Fig. 3 and are presented in entirety in Table 1. The thermal transitions of all BaEV RNA hybrids examined were broad. The t_m values of hybrids formed with DNA from positive leukaemic tissues were higher than that of hybrids formed with DNA from normal human tissues. They approached t_m values observed with hybrids formed between rRNA and cell DNA and, in fact, were higher in some instances than the t_m of hybrids formed with RNA of BaEV and DNA from normal baboons. Thus, whereas the BaEV-related sequences in DNA of normal baboons and human leukaemic tissues seem to be heterogeneous, they are equally closely related to RNA of BaEV. In contrast, the sequences in the DNA of normal human liver or NC37 cells differ more in nucleotide sequence from BaEV RNA and are therefore distinct from the more closely BaEV-related sequences in the spleens of leukaemic patients HL11 and HL23 and in the blood leukocytes of patients HL7, HL49, and HL50 (Table 1).

Phylogeny of BaEV RNA

Acceptance of the conclusion that the human leukaemic tissues contain BaEV DNA sequences is obviously contingent on the source of the ^{125}I-RNA and the DNA used. The genetic origin of the BaEV RNA could be tested by hybridising the RNA to DNA of selected primates. These experiments were not complicated by contamination with cell RNA since the BaEV used was obtained from canine thymus cells and therefore any contaminated cell RNA would be non-primate. On the basis of the data of Benveniste and Todaro[23,24] BaEV RNA would be expected to hybridise best to animals most phylogenetically related to baboons, and we found it to be so (Fig. 4). The data are presented as a double reciprocal analysis of DNA titration experiments using DNA from selected primates. The BaEV RNA was most closely related to DNA from baboons, of 18 Old World monkeys tested to date (Fig. 4 and L. Donehower, R. C. G., F. W.-S., and D. G., in preparation). The phylogenetic data and the hybridisation to proviral DNA in NC37 (BaEV) cells (Fig. 1) confirm that the ^{125}I-RNA was the labelled genome of BaEV.

Table 2 Hybridisation of type-specific ^{125}I-DNA to cell DNA

Source of unlabelled cell DNA	Source of ^{125}I type-specific DNA	
	Baboon (*P cynocephalus*)	Human
	% Hybridisation of subfamily-specific ^{125}I-DNA (±10)	
Human leukaemic tissues		
HL23 spleen	0	118
HL50 leukocytes	0	110
HL7 leukocytes	3	95
HL54 leukocytes	8	96
HL11 spleen	5	106
HL49 leukocytes	0	118
Human normal leukocytes	0	100
Normal primate tissues		
Yellow baboon spleen (*P. cynocephalus*)	100	0
Mandrill baboon brain (*P. sphinx*)	93	4
Macaque muscle (*Macaca mulatta*)	91	—
Sooty mangabey spleen (*Cercocebus atys*)	95	7
De Brazza guenon spleen (*Cercopithecus neglectus*)	0	—
Colobus (*Colobus abasinicus*)	0	0

DNA purified from tissues of a baboon (*P. cynocephalus*) and fragmented to a chain length of about 500 nucleotides was labelled with ^{125}I (3×10^7 c.p.m. μg^{-1}) by W. Prensky. It was self-annealed in 0.14 M PO_4 to a C_0t of 5 at 70 °C. Reannealed DNA was bound to hydroxyapatite (HAP) at 80 °C, unannealed DNA was washed from the HAP at 80 °C, and reannealed DNA was eluted at 100 °C. The ^{125}I-DNA eluting between 80 and 100 °C was mixed with a 10^5-fold weight excess of unlabelled genomic DNA from Old World primates, incubated at 100 °C to denature any double-stranded DNA, annealed at 80 °C for 15 min, and hybridised ^{125}I-DNA was purified on HAP as described above. ^{125}I eluting between 80 and 100 °C was scored as hybrid. Of the hybridisable ^{125}I-baboon DNA, two-thirds was specific for baboons, mangabeys, and macaques and one-third was less specific sequences which were conserved among all Old World primates tested, excluding prosimians. The more specific sequences were used for constructing Table 2 The units presented are percentages of "type-specific" hybridised relative to that hybridised to *P. cynocephalus* DNA and were reliable within ±10 units (±10% of the maximal value). The rationale for the experiment was that repeated sequences originating after man and baboon diverged from a common ancestor would be present in one of the animals and would be totally lacking in the repeated sequence fraction of the other. It has developed that these sequences are present in the fraction of genomic sequences that reanneal by a C_0t of 1–5 (repeated some 1,000 times) and that have a high thermal stability

Typing of DNA

This laboratory uses DNA from many non-human primates. Although obviously a very remote possibility, it was conceivable that the results described here were due to the selective, accidental contamination of the leukaemic tissues with primate tissues, with baboon tissue for example. An assay was devised therefore to ensure that the putative DNA preparations from human leukaemics were, in fact, human DNA. A specific ^{125}I-DNA probe was prepared from the repeated sequence populations of baboon and human DNA using the rationale of Rice[26] (Table 2). The baboon DNA probe had two useful properties: (1) in reconstruction experiments it detected very low amounts of baboon DNA (1%) in solutions of human DNA; and (2) it contained a very specific sequence component present in some members of the subfamily *Cercopithecinae* (baboons, macaques, and mangabeys) that was completely absent from other members of the same subfamily (guenons) as well as from other primates (other Old World monkeys, apes, prosimians, New World primates) (Table 3 and our unpublished data). Hybridisation experiments using the specific sequences from the DNA of baboons and humans and the unlabelled DNA preparations examined here showed that the human leukaemic DNA samples lacked baboon-specific sequences (Table 2), establishing that the hybridisation results obtained with BaEV RNA could not be explained by contamination of the human leukaemic DNA preparations with baboon DNA.

Interpretation of molecular hybridisation results

We conclude that five of the eight human leukaemic cases presented here had DNA sequences related to a major portion of the BaEV genome and that these sequences were absent from the normal human genome. In three of these cases, HL7, HL49, and HL50, DNA was prepared from fresh, unfrozen cells in 1974 and 1975. Aliquots of cells from these patients were stored frozen and DNA was again prepared from them in 1976. They were again positive and showed the same hybridisation kinetics as with DNA from the unfrozen cells. Therefore, the detection of BaEV proviral DNA in the positive patients was reproducible. Two other cases, patients HL51 and HL54, may also be positive (Table 1), but there was not enough DNA available for t_m analyses. The most plausible explanation of the molecular hybridisation findings is that the BaEV sequences were introduced from without by a viral agent and thus they merit the designation 'proviral' DNA sequences.

In summary, the supporting evidence is as follows. Kinetic, stoichiometric (DNA titration), and thermal stability measurements all indicated the presence of BaEV sequences in DNA from some human leukaemic tissues. Kinetic analyses showed that most of the BaEV proviral sequences in leukaemic DNA were infrequent ($C_0t_{1/2} > 10^4$), probably present at 0.1–1 copy per haploid genome. Stoichiometric studies showed that up to 70% of the hybridisable sequences in BaEV RNA were hybridised by DNA from spleens or blood leukocytes of leukaemic

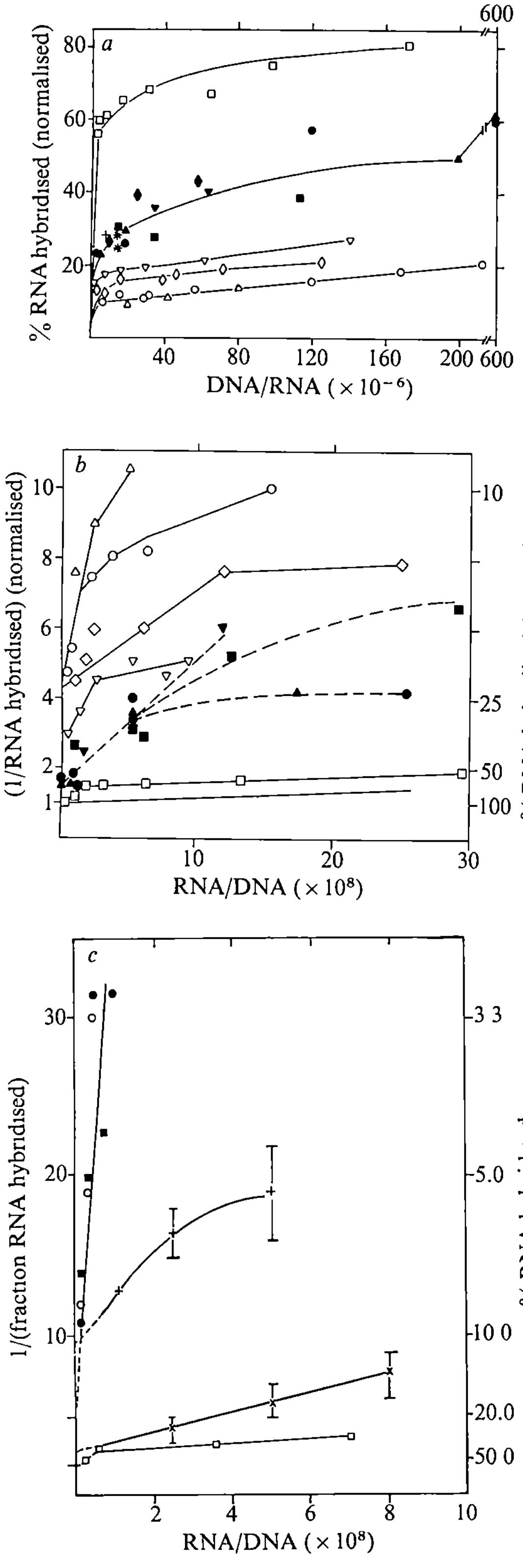

Fig. 2 Stoichiometry of hybridisation of BaEV RNA and SiSV RNA to cell DNA (DNA titration). Hybrids were formed between ^{125}I-RNA (10^8 c.p.m μg^{-1}) and cell DNA at 60 °C in 0 4 M phosphate buffer and a C_0t of 2×10^4 Hybrid formation was monitored by resistance to RNase *a* and *b*, Hybridisations with BaEV RNA. ○, NC37 human lymphoid cultured cell line derived from a normal donor, □, NC37 cells infected by BaEV; ●, blood leukocytes from patient HL49; ▼, blood leukocytes from patient HL50, ▲, spleen from patient HL23; ◆, blood leukocytes from patient HL7; ■, spleen from patient HL11; △, liver from a normal human; *, liver from patient HL51, a female Caucasian with AML and a white blood cell count of 5×10^5 μl^{-1}, other data not available; +, spleen from patient HL51; ◇, leukocytes from patient HL55, a 12-yr-old female Caucasian with ALL, other data not available; ▽, blood leukocytes from patient HL54, a 30-yr-old male Caucasian with AML. ——, *P. cynocephalus* spleen. ALL, acute lymphocytic leukaemia Results are normalised to the maximum hybridisation value obtained with DNA from *Papio cynocephalus* (55% of the RNA). *c*, Hybridisations with SiSV RNA. Hybrids were formed as described for *a* and *b*, but using ^{125}I-RNA from SiSV produced by NC37 cells. ■, NC37 normal human lymphoid cultured cell; □, NC37 cells infected by SiSV (NC37(SiSV)); ○, kidney from patient HL23; ●, spleen from patient HL23. For direct comparison, the results of *b* with BaEV RNA hybridised to normal (+) or leukaemic (×) human DNA are superimposed. Only the leukaemics described by solid symbols in *b* were used. The bars represent the high and low values obtained at each RNA:DNA ratio in *b* The results of *c* are not normalised. Note the differences in scales from *b*.

patients, compared with 23% hybridised by DNA from tissues of different normal humans, including liver, spleen, fresh blood leukocytes, and a cultured lymphoid cell line (NC37). The absence of the extra BaEV-related sequences in any one such tissue demonstrates that they are not Mendelian genes in normal humans and therefore do not arise in leukaemic DNA by amplification of normal human genes. Thermal stability measurements showed that among the BaEV-related sequences in the leukaemic tissues were some more closely related to BaEV RNA than any detected in normal human DNA. More specific conclusions, that is, the percentage mismatching, are premature because the DNA sequences involved seem to be heterogeneous, including the multiple BaEV sequences in normal baboons, and the t_m values obtained are an average of the stabilities of all of the RNA–DNA hybrids formed. Of the three measurements used, the DNA titration assay was the most sensitive for detecting BaEV proviral sequences.

Possible horizontal transmission of BaEV among humans

Though the sequences in human leukaemic DNA clearly qualify as BaEV sequences in the three molecular hybridisation assays described above, it was nonetheless initially surprising to find that a baboon type C virus, particularly a virus closely related to the one obtained from *Papio cynocephalus* (yellow baboon) had entered humans. In retrospect the concept is consistent with the following facts. (1) A BaEV-related P30 protein has been reported in human cells, including human leukaemic cells[28–30]. Although this was interpreted as expression of a human endogenous virus, which in theory may be related to BaEV, infection by exogenous BaEV itself is also consistent with the observed results. (2) Cross-species transmission of type C RNA viruses is now a well documented event[23,24,27]; in fact, one of the cases involved transmission of an ancestral BaEV to cats, probably in the Mediterranean basin[23,24]. (3) Although probably all Old World monkeys carry endogenous type C RNA viruses, only from baboons has the virus been isolated[21,22]. Thus, baboons seem to release BaEV with relative ease from many tissues. The virus is not completely controlled by its host and so is a candidate for infection between species. (4) BaEV grows readily in human cells. (5) *Papio cynocephalus* and its closely related kin, *Papio anubis* (dogface baboon), are found in Africa and could have had contact with primitive man. Once BaEV entered man it could then be transmitted with or without an intermediate vector among the human population (a phenomenon which we propose is occurring today). It seems that the transfer to man occurred recently since cases where cross-species transmission of type C RNA viruses apparently occurred more than 5 Myr ago resulted in more genetic change of the viruses isolated from the new host[23,24]. This is in contrast to the minimal differences between the BaEV RNA genome and the BaEV sequences in DNA of human leukaemics, or the sequences in the RNA of the BaEV component of HL23V.

The virus we call HL23V is similar and possibly identical in one of its two major components to BaEV[14,15]. It was repeatedly isolated from cultures of marrow and blood cells from patient HL23, with acute myelogenous leukaemia[16].

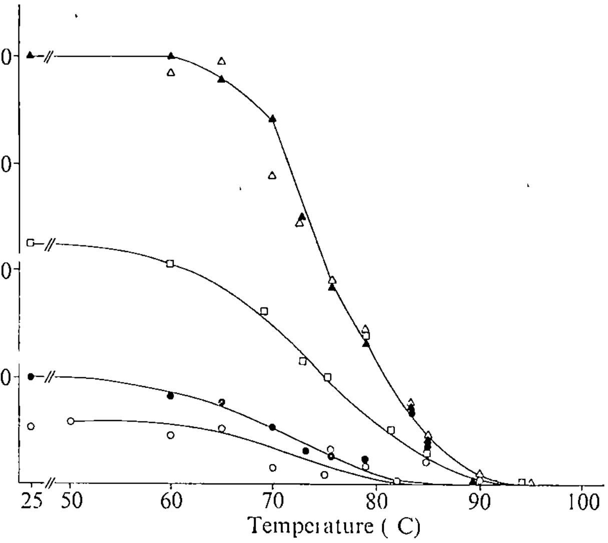

Fig. 3 Thermal stability of BaEV RNA-cell DNA hybrids Hybrids were formed between ^{125}I-BaEV RNA and a 5 × 10^6-fold weight excess of cell DNA at 60 °C in 0 4 M phosphate buffer and a C_0t of 2 × 10^1- The melting of the hybrid was accomplished as outlined in the text and in ref. 25 The t_m values for Table 2 reflect melting of half of the hybrids resistant to incubation at 60 °C. ●, NC37 normal human lymphoid culture cell line; ○, liver from a normal human, □, spleen of patient HL23; ▲, spleen of *P cynocephalus;* △, spleen of *P. anubis.*

The DNA purified from the spleen of this patient contains BaEV sequences (ref. 25 and this article) and the cytoplasm of the patient's fresh, uncultured, blood leukocytes contained virus-like particles with BaEV-related nucleic acids[25]. It will be of considerable interest now to see whether the RNA of this BaEV-related virus will detect more proviral sequences in the DNA of many human leukaemic tissues than did the RNA of the BaEV isolated from baboons.

It is also of interest that another patient with BaEV provirus (HL51) was a close contact of patient HL23, a woman who presented with AML slightly before HL23 and who ultimately died of the disease. That both leukaemic contacts had BaEV provirus could be significant. Though all the tissues examined in this study were from patients who were found earlier to possess other types of viral components[1-7,15,25], and most of them were positive for BaEV sequences, a more random survey of leukaemic patients is in progress and results obtained to date suggests that only about 20% of patients with myelogenous and lymphocytic leukaemia contain BaEV provirus in their blood leukocytes (N. Miller *et al.*, in preparation). We feel that BaEV may not be the only type C virus infecting the human population. Our results should be interpreted in the context of the detection of: (1) proviral sequences distantly related to Rauscher mouse leukaemia virus in DNA of some patients with leukaemia or lymphomas (G. Aulakh, D. G., and R. C. G., unpublished); (2) 'extra sequences', some related to RNA of Rauscher mouse leukaemia virus, in DNA of blood leukocytes of several patients with leukaemia but missing in DNA of blood leukocytes from normal persons[10,11,31]; (3) RNA related to Rauscher mouse leukaemia virus[8,9], Moloney mouse leukaemia virus[32], and simian sarcoma–leukaemia virus in blood leukocytes of some leukaemic patients (A. Tavitian, personal communication); (4) antibodies in humans directed against viruses of the HL23V-SiSV-gibbon ape leukaemia virus and BaEV families[33,34] and, less frequently, different antibodies directed against feline and mouse leukaemia viruses[34]; and (5) antigens in tissues of some humans related to those of baboon endogenous virus[28-30], simian sarcoma–leukaemia virus[29,30], and Friend mouse leukaemia virus[35]. Apart from such unlikely explanations as the discarding of particular DNA sequences during normal differentiation, and their selective retention in some leukaemic people, information storage in RNA of normal cells, or unstable episomal DNA sequences[36], the more likely possibility is that many RNA tumour viruses originating in animals are being horizontally transmitted among humans. Whether they are pathogenic in humans remains to be established, but the majority of reports suggesting the absence of type C RNA virus components in tissues of normal humans (but see ref. 4) suggests that their potential pathogenicity in humans should be considered. In any case, we feel the present results establish the presence of type C RNA virus information in humans.

Fig. 4 Stoichiometry of hybridisation of BaEV RNA to DNA from primates. See legend to Fig 2 for details ●, *P. cynocephalus* spleen, ○, sooty mangabey thymus; ▲, De Brazza guenon spleen, △, woolly monkey spleen, ————, liver from normal human. Values are not normalised.

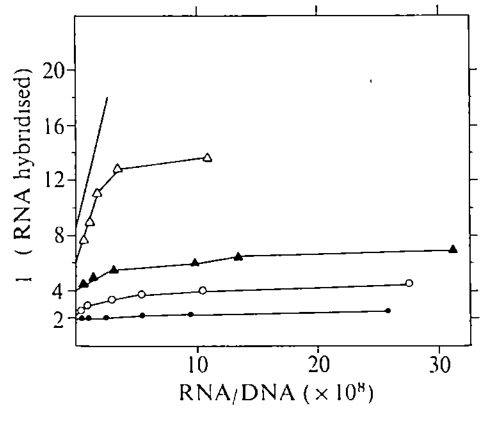

We thank Drs M. Reitz, R. Guy Smith, W. C. Saxinger, and N. Miller for helpful suggestions. We are also indebted to Drs K. McCredie, H. Braine, W. Blattner, Y. Hirshaut for supplying the tissues studied here. We thank L. Donehower and S. Josephs for technical assistance. We are grateful to D. Slater, R. Smith, E. Korwek, D. Strayer and P. Markham for assistance with the manuscript. This work was supported by the Virus Cancer Program and by the Division of Cancer Treatment, National Cancer Institute, Bethesda, Maryland.

Received February 27, accepted May 7, 1976

[1] Sarngadharan, M. G., Sarin, P S , Reitz, M S , and Gallo, R. C., *Nature new Biol.*, **244**, 206 (1973)
[2] Todaro, G J , and Gallo, R C., *Nature new Biol* , **244**, 206 (1973)
[3] Gallagher, R. E., Todaro, G J., Smith, R G , Livingston, D M., and Gallo, R. C., *Proc. natn Acad. Sci U S.A.*, **71**, 1209 (1974).
[4] Gallo, R C , *et al* , *Cold Spring Harb Symp quant Biol* , **39**, 933 (1974)
[5] Gillespie, D. H., Saxinger, W C., and Gallo, R C , *Prog. Nucl., Acid. Res molec. Biol* , **15**, 1 (1975).
[6] Gallo, R. C., Saxinger, W C , Miller, N R., and Gillespie, D. H., *Proc natn Acad Sci. U.S A* , **70**, 3219 (1973).
[7] Miller, N , *et al* , *Proc natn Acad Sci U S.A* , **71**, 3177 (1974).
[8] Baxt, W , Hehlman, R., and Spiegelman, S., *Nature new Biol.*, **240**, 72 (1972).
[9] Kufe, D , Hehlman, R , and Spiegelman, S , *Science*, **175**, 182 (1972)
[10] Baxt, W , and Spiegelman, S , *Proc. natn. Acad Sci U S.A* , **69**, 3737 (1972)
[11] Baxt, W , Yates, J W , Wallace, H J , Holland, J. F., and Spiegelman, S., *Proc natn. Acad. Sci U S A* , **70**, 2629 (1973).
[12] Kotler, M., Weinberg, E , Haspel, O , Olshevsky, U., and Becker, Y., *Nature new Biol* , **244**, 197 (1973).
[13] Mak, T. W., Kurtz, S., Manaster, J., and Housman, D , *Proc. natn Acad. Sci U.S A.*, **72**, 623 (1975).
[14] Gallagher, R. E., and Gallo, R. C , *Science*, **197**, 350 (1974)
[15] Teich, N. M., *et al.*, *Nature*, **256**, 551 (1975).
[16] Gallagher, R E , Salahuddin, S Z., Hall, W T., McCredie, K B , and Gallo, R. C., *Proc. natn Acad Sci U.S A* , **72**, 4137 (1975)
[17] Panem, S , Prochownik, E. V., Reale, F. R., and Kirsten, W. H , *Science*, **189**, 297 (1975).
[18] Nooter, K , Aarssen, A. M , Bentvelzen, P , and d'Groot, F. G , *Nature*, **256**, 595 (1975)
[19] Gabelman, N , Waxman, S , Smith, W , and Douglas, S. D , *Int. J Cancer*, **16**, 355 (1975).
[20] Temin, H., *Natn Cancer Inst. Monogr.*, **17**, 557 (1964).
[21] Todaro, G J , Sherr, C J , Benveniste, R E , and Lieber, M. M , *Cell*, **2**, 55 (1974).
[22] Benveniste, R E , Lieber, M. M , Livingston, D. M , Sherr, C. J., and Todaro, G. J , *Nature*, **248**, 17 (1974).
[23] Benveniste, R E., Sherr, C J , Lieber, M. M , Callahan, R , and Todaro, G. J., in *Fundamental Aspects of Neoplasia* (edit. by Gottleib, A),'29 (Springer, New York, 1975)
[24] Benveniste, R E , and Todaro, G. J , *Nature*, **252**, 170 (1974)
[25] Reitz, M S , *et al* , *Proc. natn. Acad. Sci U.S A.*, **73**, 2113 (1976).
[26] Rice, N in *Evolution of Genetic Systems* (edit. by H. H. Smith), 44 (Gordon and Breach, New York, 1972)
[27] Wong-Staal, F , Gallo, R C , and Gillespie, D , *Nature*, **256**, 670 (1975).

[28] Sherr, C. J., and Todaro, G. J., *Proc. natn. Acad Sci U S A.*, 71, 4703 (1974).
[29] Sherr, C. J., and Todaro, G. J , *Science* 197, 855 (1975).
[30] Strand, M , and August J. T., *J Virol* , 14, 1584 (1974)
[31] Baxt, W., *Proc. natn. Acad Sci. U.S A.*, 71, 2835 (1974).
[32] Larson, C. J , *et al* , *Proc. natn Acad. Sci. U.S.A.*, 72, 4900 (1975).
[33] Prochownik, E. V., and Kirsten, W. H., *Nature*, 260, 64 (1976).
[34] Aoki, T , Walling, M. J , Bushar, G. S., Liu, M., and Hsu, K. C., *Proc. natn. Acad. Sci. U S A* (in the press)
[35] Metzgar, R. S., Mohanakumar, T., and Bolognesi, D P , *J exp. Med.*, 143, 47–63 (1976).
[36] Gillespie, D., and Gallo, R. C., *VII Int. Symp. Comparative Research on Leukemia and Related Diseases* (S. Karger, New York, in the press).

letters to nature

Identification of Abell Cluster 754 with the X-ray source 3U0901 – 09 by Ariel V

THE faint, high galactic latitude X-ray source 3U0901−09 (ref. 1) has been previously associated[2], on positional grounds, with the rich cluster of galaxies, Abell 754 (distance class 3, richness class 2)[3]. Since the Uhuru 90%-confidence positional error box for 3U0901−09 is relatively large, having an area of 2.6 degree[2], it is worthwhile, in view of current theoretical interest in X-ray emission from clusters of galaxies (see, for example, ref. 8), to reduce the positional uncertainty and thus confirm or reject the proposed identification with A754.

The high energy (2–18 keV) detector system of the Ariel V X-ray sky survey instrument (SSI) has observed 3U0901-09 on a number of separate occasions over a period of a year (February 1975–February 1976) and the results are reported here. The SSI and data analysis are described elsewhere[4–6].

The SSI measured a statistically significant signal (> 3σ) from the vicinity of 3U0901-09 for nine sets of observations. The individual error boxes ('lines of position') from each set of SSI observations are combined to produce the Ariel V Sky survey 90%-confidence probability contour for the source location, shown in Fig. 1. This reduces, by over an order of magnitude, the uncertainty in the location of the X-ray source and supports the previous identification[2] of 3U0901–09 with A754. Our 90%-confidence error box has centroid (in celestial coordinates (degrees, 1950.0)) $\alpha=136.55$, $\delta=-9\ 56$, and area 0.11 degree[2]. We have paid particular attention to the possibility that A761 might also be a source of significant X-ray emission; careful examination of the individual observations, however, allows us to reject this possibility.

Fig. 1 90%-confidence positional error boxes for the X-ray source 3U0901-09 associated with A754, from Ariel V and Uhuru.

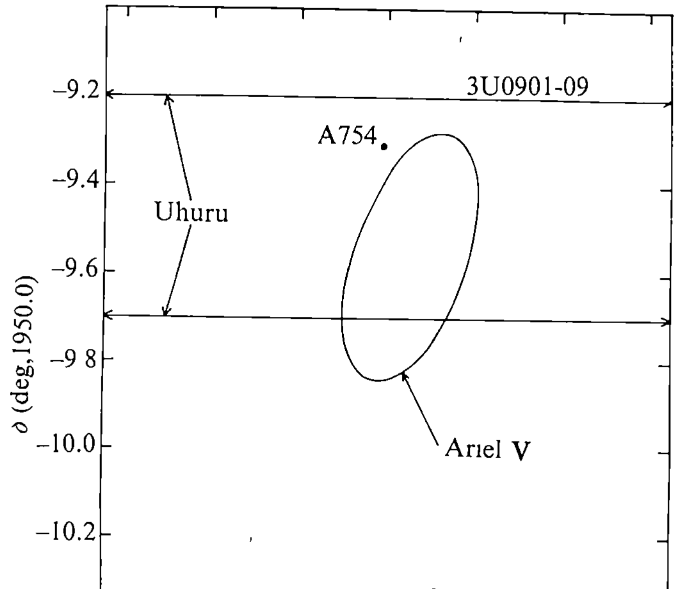

Each observation consisted of a summation of data over a period of 1–3 d. There is no significant intensity variation between the individual measurements (maximum deviation from the mean is ~1σ), and the mean intensity level is 1 9±0.2 Ariel V counts s^{-1} (2–18 keV), corresponding to ~ $(9.5\pm0.9)\times10^{-11}$ erg cm^2 s^{-1} (2–10 keV) or 5.5±0.5 Uhuru counts s^{-1} (2–6 keV), assuming a spectrum like that of the Coma cluster The uncertainties quoted are from Poisson errors on the count rates only. This is in close agreement with the Uhuru measurement[1,2] of 4.4±0.8 Uhuru counts s^{-1}. A redshift $z=0\ 0537$ for A754 (ref. 7) and a Hubble constant of 55 km s^{-1} Mpc^{-1} give a distance of 293 Mpc, implying, from the Ariel V intensity, an X-ray luminosity of $(9\ 8\pm0.9)\times10^{44}$ erg s^{-1} (2–10 keV).

It has been suggested that cluster X-ray luminosity can be positively correlated with: (1) cluster richness[8,10]; (2) cluster radio luminosity[9]; (3) the presence of one or more dominant central galaxies (usually optical type *cD* (ref. 11))[9,10]; possible explanations have been discussed in the literature[9,10,12]. Confirmation of A754 as an X-ray source strengthens these apparent correlations, A754 being both a *cD* type cluster[11] and a radio source[9]. Several theoretical studies of possible X-ray emission mechanisms in clusters of galaxies (see those reviewed in ref. 8), have suggested (differing) correlations between cluster X-ray luminosity and velocity dispersion Δv. It is therefore important to measure Δv for A754.

The Ariel V project is supported by the SRC.

J. P. PYE
B. A. COOKE
MARTIN ELVIS

X-ray Astronomy Group,
Department of Physics,
University of Leicester,
Leicester LE1 7RH, UK

Received May 6, accepted June 4, 1976.

[1] Giacconi, R , *et al* , *Astrophys J. Suppl.*, **27**, 37 (1974).
[2] Kellogg, E , Murray, S , Giacconi, R., Tananbaum, H , and Gursky,H , *Astrophys J Lett* , 185, L13 (1973).
[3] Abell, G O., *Astrophys. J Suppl.*, 3, 211 (1958)
[4] Ricketts, M. J., Cooke, B. A., and Pounds, K. A., *Nature*, 259, 546 (1976)
[5] Villa, G . *et al* , *Mon Not R. astr. Soc.* (in the press)
[6] Pye, J P , and Cooke, B. A , *Nature*, 260, 410 (1976)
[7] Noonan, T. A , *Astr J* , 78, 26 (1973)
[8] Kellogg, E. M , in *X-ray Astronomy* (edit. by Giacconi, R , and Gursky, H.), 321 (Reidel, Dordrecht, 1974).
[9] Owen, F N , *Astrophys. J. Lett.*, 189, L55 (1974)
[10] Bahcall, N A , *Astrophys J.*, 193, 529 (1974).
[11] Rood, H J , and Sastry, G. N , *Pub astr. Soc. Pacif* , 83, 313 (1971).
[12] Silk, J , Preprint (1976)

Inverse Compton spectra and the spectrum of Cygnus X-1

THE many X-ray observations of the black hole candidate Cyg X-1 show a variable power-law spectrum (see refs 1–8)

$$\frac{\mathrm{d}L}{\mathrm{d}E} \simeq (2\text{–}6)\times 10^{35}\,\mathrm{erg\,s^{-1}\,keV^{-1}}\left(\frac{E}{10\,\mathrm{keV}}\right)^{-p}\left(\frac{d}{2.5\,\mathrm{kpc}}\right)^{2} \qquad (1)$$

where d is the distance to the source. During the 'low state', in which the source spends ~90% of its time[7], $p \simeq 0.5$ and the power-law spectrum extends over 1 keV $\lesssim E \lesssim$ 100 keV, with a knee suggested at ~100 keV. During the transient 'high state', which persists for weeks to months, the total luminosity at $\gtrsim$ 1 keV increases by a factor 5–10 and the spectrum steepens to $2 \lesssim p \lesssim 4$ over the range 1 keV $\lesssim E \lesssim$ 10 keV. A hard excess above this steep slope is visible at > 10 keV, which contains ~10% of the total energy. In this paper we glean some information about the physics of the source by interpreting this spectrum as being caused by inverse Compton scattering by nonrelativistic electrons at a temperature $T_e \simeq 10^9$ K.

A power-law spectrum can arise from two familiar mechanisms when there exists a power-law distribution of ultrarelativistic electrons, namely inverse Compton scattering or synchrotron radiation. Recently, several workers[8–11] have pointed out a third mechanism that produces a power-law spectrum: repeated inverse Compton scattering of initially soft photons by a non-relativistic, thermal electron distribution in a finite cloud, optically thin for emission and absorption. If the soft photons are injected into the cloud with a characteristic photon energy E_s and spectrum $\mathrm{d}L_s/\mathrm{d}E$, then the emergent hard spectrum is

$$\mathrm{d}L/\mathrm{d}E \simeq \mathrm{d}L_s/\mathrm{d}E\,(E/E_s)^{-p};\; E_s \lesssim E \lesssim kT_e \qquad (2)$$

The electron distribution need not be precisely Maxwell-Boltzmann. The spectral index, p, is determined by the physical properties of the scattering cloud through the relation

$$p = -\frac{3}{2}+\left(\frac{9}{4}+\frac{4}{y}\right)^{1/2} \qquad (3)$$

where y is the "Comptonisation parameter", $y \equiv (4kT_e/m_ec^2)$. Max $(\tau_{es}, \tau_{es}{}^2)$ and τ_{es} is the electron scattering optical depth of the cloud. For $E \gtrsim kT_e$ (or, because of relativistic effects, $E \simeq$ 150 keV, whichever is less), the inverse Compton spectrum is no longer given by equation (2) and steepens roughly exponentially. The above spectrum applies as long as $y \lesssim 5$ (unsaturated "Comptonisation"), as long as the cloud acts as a single emitting region, and as long as inverse Compton scattering dominates other cooling mechanisms.

Fig. 1 X-ray energy spectrum $\mathrm{d}L/\mathrm{d}E$ of Cyg X-1. Observations show $\mathrm{d}L/\mathrm{d}E \propto E^{-p}$, $0.5 \lesssim p \lesssim 4$, for photon energy $E \gtrsim 0.5$ keV; these spectra we extrapolate down in E to their intersection with a Rayleigh–Jeans spectrum for $T = 10^9$ K. Also shown is a source spectrum for thermal cyclotron radiation.

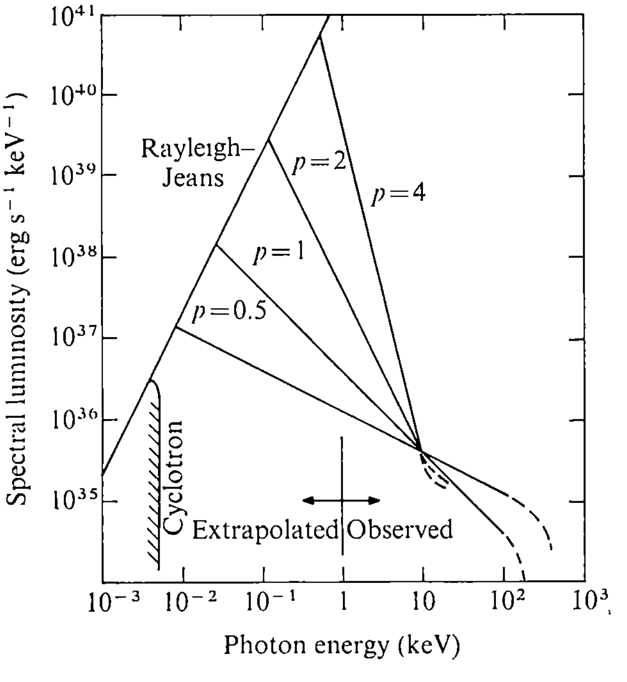

For any total luminosity L dictated, for example, by the rate of gravitational energy release which is powering the X-ray source, and for any luminosity L_s of the soft photon source, the cloud will adjust its y (and p) so that $\int(\mathrm{d}L/\mathrm{d}E)\mathrm{d}E = L$. If the cloud is not emitting enough energy because its spectrum is too soft, the electrons will heat up, y will increase, and the spectrum will get harder; see equations (2) and (3). Changes in either L or L_s can induce a change in y and hence in p.

To interpret the observed spectrum and its variations, let us first extrapolate the observed spectrum to < 1 keV and consider that energy E_{RJ} where it intersects the Rayleigh–Jeans portion of a black body spectrum

$$\mathrm{d}L_{RJ}/\mathrm{d}E \simeq 2\times 10^{43}\,\mathrm{erg\,s^{-1}\,keV^{-1}}(T_e/10^9\,\mathrm{K})(E/10\,\mathrm{keV})^2$$

(see Fig. 1). Here we have adopted a radius ~ $30(GM_{\text{black hole}}/c^2) \simeq 300GM_\odot/c^2 \simeq 5\times 10^7$ cm for the emitting region, typical of most models of Cyg X-1 (a factor of three greater or smaller would make little difference to our results). The intersection is given by

$$\left(\frac{E_{RJ}}{10\,\mathrm{keV}}\right)^{2+p} \simeq 10^{-8}\left(\frac{T_e}{10^9\,\mathrm{K}}\right)^{-1}\left(\frac{d}{2.5\,\mathrm{kpc}}\right)^{2} \qquad (4)$$

Now, any incoherent soft photon source cannot be more luminous than a black body; therefore we must have $E_s \gtrsim E_{RJ}$ as a strict lower limit on E_s; in fact, most possible sources (see following discussion) will be optically thick below some characteristic photon energy E_s, so that $E_s \simeq E_{RJ}$.

In the low state, $p \simeq 0.5$ and therefore $y \simeq 2$. If $T_e \simeq 10^9$ K, then we learn that $\tau_{es} \simeq 1$ and equation (4) yields $E_{RJ} \simeq 0.01$ keV. Thermal cyclotron radiation is likely to be the soft photon source here. The detailed models[9,12] of Cyg X-1 predict $B \simeq 10^7$ gauss in equipartition, giving $E_{\text{cyclotron}} \simeq 10^{-4}$ keV, and we calculate (using $\tau_{es} \simeq 1$) that self-absorption occurs up to about the 50th harmonic. Thus $E_s \simeq 0.005$ keV, in tolerable agreement with $E_{RJ} \simeq 0.01$ keV. Therefore, we suggest that the reason the spectrum of Cyg X-1 is never flatter than $p \simeq 0.5$ is that thermal cyclotron radiation is always present as a minimal soft photon source with $E_s \simeq E_{RJ} \simeq 0.01$ keV and $L_s \simeq 10^{34}$ erg s^{-1}. Examination of Fig. 1 clearly indicates that additional soft photon sources must lead to steeper spectral slopes.

In the high state, $p \simeq 4$, $y \simeq 0.2$ and almost all of the luminosity emerges near the soft photon input energy E_s. Apparently, a new soft photon source is operating which produces nearly the entire observed luminosity of the source $L_s \simeq L \simeq 10^{38}$ erg s^{-1} and which thus requires only a marginal boost (low y) from inverse Compton scattering to balance the rate of gravitational energy release, L. As striking as the observed transitions in state are, we infer an even more spectacular change in the nature of the soft photon source, amounting to a change by a factor of ~ 10^4 in L_s.

At $p = 4$, equation (4) gives $E_{RJ} \simeq 0.5$ keV for $T_e \simeq 10^9$ K and even higher E_{RJ} for lower T_e. A plausible candidate for the soft photon source in the high state is a cool, optically-thick accretion disk within the optically thin scattering cloud, since the temperature of a black body of our adopted radius and emitting the observed luminosity of Cyg X-1 would be about 5×10^6 K. At the steepest slope, $p \simeq 4$, one should almost certainly see a peak and turnover in the power-law spectrum not far below 1 keV, since a continuation of such a power law much lower than 1 keV would constitute an intensity exceeding the black-body intensity for any reasonable temperature. The excess hard flux seen at $E \gtrsim 10$ keV must originate in a different region of the source or by a different mechanism, according to this view.

DOUGLAS M. EARDLEY

Department of Physics,
Yale University,
New Haven, Connecticut 06520

ALAN P. LIGHTMAN

Center for Radiophysics and Space Research,
Cornell University,
Ithaca, New York 14850

Received March 23; accepted June 1, 1976.

[1] Agrawal, P. C , *et al* , *Astrophys. Space Sci.*, 18, 408–424 (1972)
[2] Tananbaum, H., Gursky, H., Kellogg, E., Giacconi, R , and Jones, C., *Astrophys. J. Lett.*, 177, L5–L10 (1972)
[3] Heise, J., *et al* , *Nature*, 256, 107–108 (1975).
[4] Sanford, P. W , Ives, J C , Bell Burnell, S J , Mason, K. O., and Murdin, P , *Nature*, 256, 109–111 (1975)
[5] Matteson, J L , Mushotzky, R. F., Paciesas, W S , and Laros, J. G , *Symposium on X-ray Binaries* (edit. by Kondo, Y., and Boldt, E) (Goddard Space Flight Center, Greenbelt, Maryland, in the press)
[6] Rothschild, R E , Boldt, E A., Holt, S S., and Serlemitsos, P J., *Symposium on X-ray Binaries* (edit. by Kondo, Y , and Boldt, E.) (Goddard Space Flight Center, Greenbelt, Maryland, in the press)
[7] Holt, S S , Boldt, E A , Serlemitsos, P J , and Kaluzienski, L J , *Astrophys J Lett* , 203, L63–L66 (1976)
[8] Coe, M. J., Engel, A. R , and Quenby, J. J , *Nature*, 259, 544–545 (1976).
[9] Shapiro, S. L., Lightman, A. P., and Eardley, D. M , *Astrophys J.*, 204, 187 (1976).
[10] Katz, J., *Astrophys. J.* (in the press).
[11] Eardley, D. M , *Symposium on X-Ray Binaries* (edit by Kondo, Y , and Boldt, E) (Goddard Space Flight Center, Greenbelt, Maryland, in the press).
[12] Mészáros, P., *Nature*, 258, 583–584 (1975)

Neutron-capture cross sections for ^{186}Os and ^{187}Os and the age of the Universe

WE have measured the neutron-capture cross sections for ^{186}Os and ^{187}Os in the energy range up to 150 keV, corresponding to stellar temperatures up to $\sim 18\times10^8$ K. The knowledge of these cross sections enables us to calibrate the $^{187}\text{Re}\rightarrow{}^{187}\text{Os}$ nuclear β-decay clock and thus to make a new radiogenic determination of the age of the Universe.

There are several techniques used by astrophysicists to determine the age of the Universe. These include the use of measurements of the expansion of the universe[1] (Hubble constant) and of observations of stars in globular clusters[2] as well as nucleosynthetic techniques. All of the techniques involving nucleosynthesis used to date, however, have been based on the theory of the *r*-process for the formation of the elements[3]. The *r*-process involves neutron capture on a rapid time scale in supernova events. It follows a path off the line of β stability and is responsible for the formation of all of the elements heavier than bismuth. By calculating the production ratios for various *r*-process nuclei such as ^{232}Th, ^{235}U and ^{238}U in supernova events and by measuring the current abundance ratios of the same nuclei, it is possible to arrive at a chronology of supernova events (and hence at the age of the Universe) This is the basis of the U–Th dating technique of Fowler and Hoyle[4].

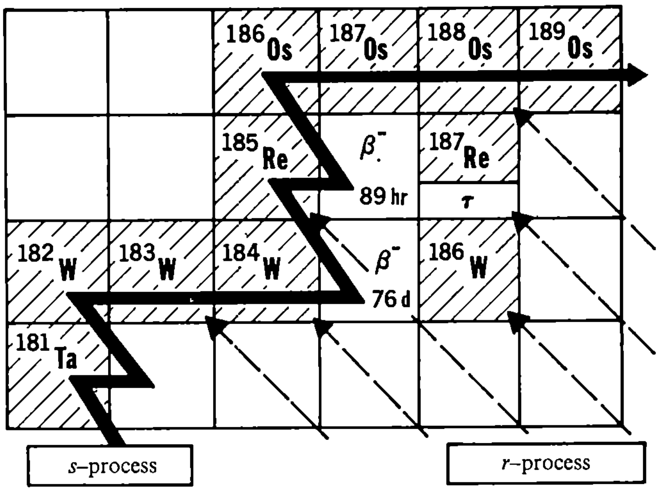

Fig. 1 The *s*-process (heavy line) and *r*-process (dashed line) paths in the vicinity of the Os isotopes. The shaded boxes represent stable nuclei except for ^{187}Re ($\tau_{1/2} = 44\times10^9$ yr). ^{186}Os and ^{187}Os are shielded from the *r*-process by ^{186}W and ^{187}Re, respectively.

In 1964, Clayton[5] suggested the use of a process which does not depend critically upon a knowledge of the *r*-process production rates. Rather it depends mainly upon the *s*-process, which rests upon a more firm theoretical footing. The *s*-process refers to neutron capture on a much slower time scale than the *r*-process, and it follows essentially the line of β stability. Clayton's suggestion involves the β decay of ^{187}Re to ^{187}Os, which has a half-life of $\sim 44\times10^9$ yr and which therefore is much longer than estimates of the age of the Universe obtained from the above mentioned dating techniques ((10–15) × 10^9 yr). Figure 1 shows a portion of the chart of the nuclides in the vicinity of the Re and Os isotopes. Both the *s*-process and the *r*-process paths are shown. It can be seen that ^{187}Re is an *r*-process nucleus, while both ^{186}Os and ^{187}Os are shielded from the *r*-process and hence their synthesis initially involves only the *s*-process. If we denote the *s*-process abundances of ^{186}Os and ^{187}Os as N_s^{186} and N_s^{187} and the radiogenic component of ^{187}Os

Fig. 2 The duration of nucleosynthesis Δ, before Solar System condensation as a function of the Maxwellian-averaged laboratory neutron-capture cross section ratio for ^{186}Os and ^{187}Os. The three (of the several possible) models for the supernova rate that are shown (*a*, uniform; *b*, exponential and *c*, sudden) are discussed in the text.

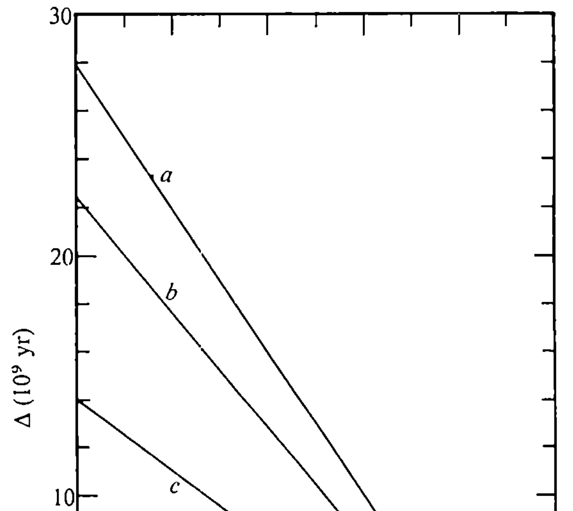

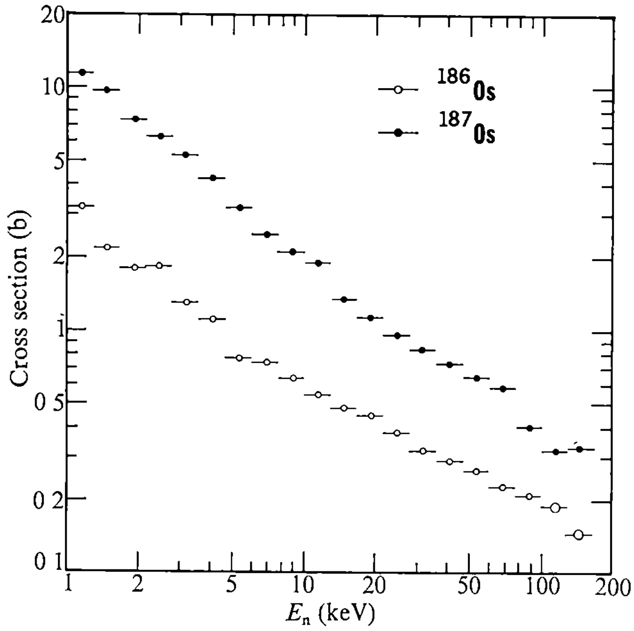

Fig. 3 The neutron-capture cross sections against laboratory neutron energy for ^{186}Os (○) and ^{187}Os (●). The horizontal bar represents the size of the energy bin into which the data have been averaged. (The energy resolution of the actual measurement was much better.) The uncertainty for each data point lies within the plotted symbol and typically is 5% at 30 keV.

resulting from the ^{187}Re β decay as N_{rad}^{187}, then the total abundances can be written as

$$N^{186} = N_s^{186}$$
$$N^{187} = N_s^{187} + N_{\text{rad}}^{187} \qquad (1)$$

One of the assumptions of the *s*-process is that $N\bar{\sigma}$ is constant for adjacent *s*-process nuclei, where $\bar{\sigma}$ refers to the Maxwellian-averaged neutron-capture cross section for a temperature appropriate to the site of the *s*-process ($kT \simeq 30$ keV). This assumption has been justified by Macklin *et al.*[6] for the tin, samarium, strontium, and zirconium isotopes. Using this result and equation (1), it is possible to write the ratio of the radiogenic component of ^{187}Os to its parent ^{187}Re abundance N_{Re}^{187} as

$$\frac{N_{\text{rad}}^{187}}{N_{\text{Re}}^{187}} = \frac{(N^{187}/N_{\text{Os}}) - f(\bar{\sigma}_{186}/\bar{\sigma}_{187})_{\text{LAB}}(N^{186}/N_{\text{Os}})}{N_{\text{Re}}^{187}/N_{\text{Re}}}\left(\frac{N_{\text{Os}}}{N_{\text{Re}}}\right) \qquad (2)$$

where N_{Os} and N_{Re} refer to the elemental abundances of Os and Re. The measured laboratory cross-section ratio $(\bar{\sigma}_{186}/\bar{\sigma}_{187})_{\text{LAB}}$ must be multiplied by the factor f since the Os nuclei in a stellar environment exist in excited states as well as the ground state. The most probable value for this factor has been calculated by Woosley and Fowler (personal communication) to be $f = 0.83$. The values used for the other parameters in equation (2) are listed in Table 1.

Table 1 Values used in equation (2) to compute $N_{\text{rad}}^{187}/N_{\text{Re}}^{187}$

N^{187}/N_{Os}	0.0123 ± 0.0006
N^{186}/N_{Os}	0.0159*
$N_{\text{Re}}^{187}/N_{\text{Re}}$	0.65*
$N_{\text{Os}}/N_{\text{Re}}$	12 ± 1.2

These values are averages of results obtained by geochemical methods, referred to the time of solar system condensation, using $\tau_{1/2} = 44 \times 10^9$ yr from ref. 7.
*The geochemical uncertainties for these quantities are negligible.

Clayton[5] used a simple model to determine the above ratio as a function of the time and duration of nucleosynthesis. He assumed that *r*-process nucleosyntheis (which formed ^{187}Re) began at a time Δ before the condensation of the Solar System and decreased exponentially at a rate λ_A. Therefore λ_A is a measure of the supernova rate in the Galaxy. If λ_B denotes the β-decay rate of ^{187}Re, one can express the ratio $N_{\text{rad}}^{187}/N_{\text{Re}}^{187}$ at the time of Solar System condensation, using the Bateman equations for radioactive growth and decay, as

$$\frac{N_{\text{rad}}^{187}}{N_{\text{Re}}^{187}} = \left\{\frac{\lambda_A - \lambda_B}{\lambda_A}\exp(\lambda_B\Delta)\frac{1-\exp(-\lambda_A\Delta)}{1-\exp[-(\lambda_A-\lambda_B)\Delta]}\right\} - 1 \qquad (3)$$

The two extreme cases of this model are (1) sudden synthesis (a single supernova event), for which $\lambda_A \to \infty$ and equation (3) becomes $N_{\text{rad}}^{187}/N_{\text{Re}}^{187} \simeq \lambda_B\Delta$, and (2) uniform synthesis (a constant rate of supernova events), for which $\lambda_A \to 0$ and equation (3) becomes

$$N_{\text{rad}}^{187}/N_{\text{Re}}^{187} \simeq \lambda_B\Delta/2$$

It should be noted that not only does case (1) result in the minimum value for Δ, but this value also is the average value for Δ, irrespective of the rate (or the rate of change) of supernova events, and hence independent of the model used for the time history of the stellar burning process.

If we now plot Δ as a function of $(\bar{\sigma}_{186}/\bar{\sigma}_{187})_{\text{LAB}}$ using equations (2) and (3) we obtain the curves shown in Fig. 2. The two extreme cases mentioned above are plotted along with an intermediate case where the supernova rate is assumed to be exponential in time, with its activity at Solar System condensation equal to $1/e$ of its initial value ($\lambda_A = 1/\Delta$). For the curves in Fig. 2, the β-decay half-life measurement of Herr *et al.*[7] ($\tau_{1/2} = 44 \times 10^9$ yr) was used for λ_B.

The purpose of our measurement therefore was to determine the ratio of the neutron-capture cross sections for ^{186}Os and ^{187}Os, Maxwellian averaged for $kT = 30$ keV, from which $N_{\text{rad}}^{187}/N_{\text{Re}}^{187}$ can be obtained using equation (2). From this ratio, the duration of nucleosynthesis (Δ), and hence the age of the Universe, can be obtained as discussed above. This measurement was performed using the neutron time-of-flight facility at the Livermore 100-MeV electron linac. Details of the experimental techniques used for these neutron-capture cross-section measurements are given in ref. 8. For the present experiment, the neutron-capture cross sections for ^{186}Os and ^{187}Os were measured over the neutron-energy interval from 2 eV to 150 keV, using a 3.278-g powdered-metal osmium sample enriched to 78% isotopic purity of ^{186}Os and a similar 2.959-g sample enriched to 71% isotopic purity of ^{187}Os. Since the impurities consisted of the other stable Os isotopes, the neutron-capture cross sections for all these isotopes were measured as well. The data were reduced to absolute cross sections by including a ^{165}Ho sample in the measurement and normalising to the measured ^{165}Ho(n,γ) cross section[9]. The resulting average neutron-capture cross sections obtained for ^{186}Os and ^{187}Os are shown in Fig. 3. These cross sections were Maxwellian averaged for $kT = 30$ keV, from which the value for $(\bar{\sigma}_{186}/\bar{\sigma}_{187})_{\text{LAB}} = 0.39 \pm 0.03$ was obtained. The uncertainty in this ratio includes systematic as well as statistical uncertainties in the measurement. Finally, the value obtained for $(\bar{\sigma}_{186}/\bar{\sigma}_{187})_{\text{LAB}}$ is only weakly dependent upon the choice of kT near 30 keV.

This measurement of $\bar{\sigma}_{186}/\bar{\sigma}_{187}$ therefore removes the major unknown in equations (2) and (3) that prevented, until now, the determination of the age of the Universe by the Re → Os clock. From Fig. 2, a value for $\Delta = (12.9 \pm 3) \times 10^9$ yr is obtained using the above value for the cross section ratio for the exponential case. (This 23% uncertainty results from the 8% uncertainty for the present measurement together with the uncertainties in the other quantities in equation (2).) This value can be compared directly with the U–Th dating method[4], which yielded $\Delta = (7 \pm 2) \times 10^9$ yr using the same exponential description.

Thus there is a substantial discrepancy between the results of the two dating techniques.

It should be pointed out that the Re → Os dating technique depends strongly on an accurate determination of λ_B ($= 1/\tau_B$). At the present time, the best two measurements[7,10] of this half life disagree by 50%. We have chosen to use the measurement of Herr *et al.*[7] in our determination of Δ. Since the value of τ_B from ref. 10 is much larger than that reported in ref. 7, the discrepancy between the present result for Δ and that obtained from the U–Th method would be increased considerably if the value for τ_B from ref. 10 were used. There are other uncertainties involved in the Re → Os method, some of which are discussed in detail by Clayton[5]. Another is the possibility that some of the ^{187}Re, and hence some of the radiogenic ^{187}Os, is produced by the *s*-process. These uncertainties involve, however, effects that are either not well understood or of a speculative nature; therefore they will not be discussed further here.

If, then, we assume that the time between the end of nucleosynthesis in the Galaxy and the present time is 4.7×10^9 yr, we obtain the age of the Galaxy to be $\Delta + 4.7 = 17.6$ (in units of 10^9 yr). The time between the beginning of the Universe and the formation of the Galaxy is not known, but current estimates[11] give $\sim 2 \times 10^9$ yr. Therefore the Re→Os dating method, based on the results reported here, indicates that the age of the Universe is $\sim 19.6 \times 10^9$ yr (and the uncertainty in this number probably is no greater than 4×10^9 yr). The present results thus yield an age which is greater than other recent estimates of this age, from the expansion of the Universe ($(16.6 \pm 1.7) \times 10^9$ yr, ref. 12), from globular clusters ($(13 \pm 3) \times 10^9$ yr), and from the U–Th method ($(14 \pm 3) \times 10^9$ yr).

This work was carried out under the auspices of the US ERDA.

J. C. Browne
B. L. Berman

Physics Department,
University of California,
Lawrence Livermore Laboratory,
Livermore, California 94550

Received March 25; accepted June 4, 1976

[1] Sandage, A., *Phys. Today*, 23, No. 2, 34–41 (1970); *Q Jl R astr. Soc*, 13, 282–296 (1972)
[2] Iben, I., Jr, *Science*, 155, 785–796 (1968).
[3] Burbidge, E. M., *et al.*, *Rev. mod. Phys.*, 29, 547–650 (1957).
[4] Fowler, W. A., and Hoyle, F., *Ann. Phys.*, 10, 280–302 (1960).
[5] Clayton, D. D., *Astrophys J*, 139, 637–663 (1964).
[6] Macklin, R. L, *et al.*, *Nature*, 194, 1272 (1972), *Nature*, 197, 369–370 (1963).
[7] Herr, W., *et al.*, *Z. Naturforsch.*, 16a, 1053–1058 (1961).
[8] Berman, B. L., and Browne, J. C., *Phys. Rev.*, C7, 2522–2531 (1973).
[9] Czirr, J. B., and Stelts, M. L, *Nucl Sci Engng*, 52, 299–309 (1973)
[10] Brodzinki, R. L., and Conway, D. C., *Phys. Rev*, 138, B1368–1371 (1965).
[11] Trimble, V, *Rev. mod. Phys.*, 47, 877–976 (1975).
[12] Sandage, A., and Tammann, G. A., *Astrophys. J.*, 197, 265–280 (1975).

Gravity signature of fossil plate boundaries in the Canadian Shield

The Canadian Shield is a mosaic of structural provinces, each with characteristic internal structural trends and styles of folding[1]. Boundaries between provinces have been delineated where trends are truncated along unconformities or along orogenic fronts. The validity of this subdivision of the shield has been supported by isotopic dating of orogenies[2]. Thus, the Superior province is the type region for the Kenoran Orogeny (2,560 Myr BP), and the Churchill and Grenville provinces are the type regions for the Hudsonian (1,800 Myr) and Grenvillian (1,000 Myr) orogenies, respectively.

Gravity signatures observed across structural province boundaries in five different areas are remarkably similar (Figs 1 and 2*a*). We suggest here that they originate from essentially identical crustal structures formed in response to fundamental processes operating during Precambrian episodes of cratonic convergence, collision and suturing. Three geosutures have so far been identified at or near structural province boundaries in the shield. The suture peripheral to the Superior Craton is the most easily recognised[3–5] because it is characterised by distinctive Aphebian (Lower Proterozoic) geosynclinal and oceanic sedimentary, volcanic, and ultramafic rocks, or their metamorphosed equivalents. The interpretation of these rocks as a suture therefore depends on the juxtaposition of pseudo-ophiolites typical of the plate accretion environment and geosynclinal sediments typical of zones of plate consumption[4]. The suture extends for some 3,200 km from the Manitoba nickel belt (Nelson Front) through the Split Lake–Fox River region of Manitoba and the Hudson Bay Lowlands of northern Ontario to eastern Hudson Bay and thence to the Cape Smith Belt and Labrador Trough of northern Quebec (Fig. 1). Reactivated basement of the Churchill Province is sharply separated by the suture rocks from the non-reactivated Superior Craton in Manitoba, Ungava and Quebec–Labrador[6,7]. Interpretations of large amplitude Bouguer anomalies associated with the Cape Smith Belt[8] and Labrador Trough[7,8] indicate that the cratons

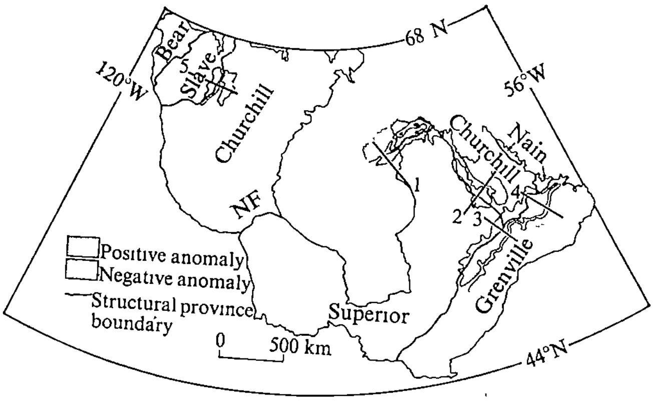

Fig. 1 Bouguer gravity anomalies at five structural province boundaries in the Canadian Shield. Gravity profiles (shown in Fig. 2*a*): 1, Superior–Churchill boundary (offshore extension of Cape Smith Belt); 2, Superior–Churchill boundary (Labrador Trough); 3, Superior–Grenville boundary (Grenville Front); 4, Churchill–Grenville boundary (Grenville Front); 5, Slave–Churchill boundary (Thelon Front). NF, Nelson Front.

Fig. 2 *a*, Bouguer gravity anomaly signatures along profiles 1–5 of Fig. 1 (vertical lines numbered 2–5 show positions of corresponding inter-province boundaries[22]); *b*, gravity signature (type anomaly) derived by averaging profiles 1–5. Unshaded envelope is described by standard deviation calculated at 5-km intervals along profiles; dotted curve, gravity effect of type model shown in *c*. *c*, Type crustal structure derived from type anomaly. Density contrasts in g cm^{-3}; depths in km

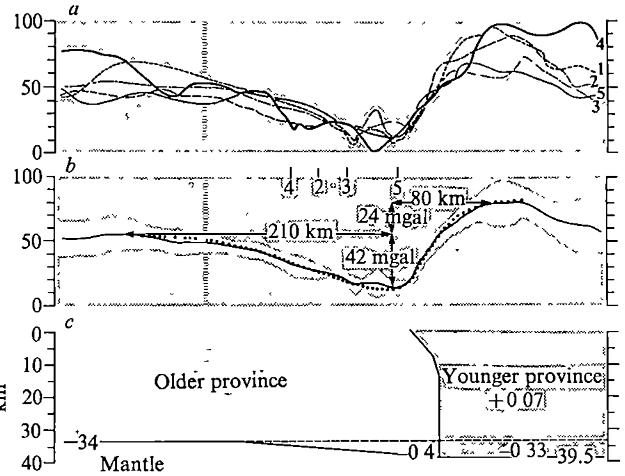

separated by the suture have different crustal densities and thicknesses.

Interpretations of palaeomagnetic data[9-11] suggest that part of the Grenville Province broke away from the remainder of the shield 1,250 Myr ago, and then rejoined it about 1,000 Myr ago. These events require that a suture also exists within the Grenville Province. Different locations have been suggested for such a suture[11-13]. Most recently, Thomas and Tanner[14] have suggested that the suture lies up to 100 km inside the Grenville Province, south of a zone believed to contain reworked rocks of the older adjacent provinces lying to the south of the Grenville Front[11]. This location is based on the interpretation of gravity anomalies along the front as an edge-effect between juxtaposed crustal blocks of different mean density and thickness[8,14,15]. The boundary between the blocks is the suture. It is cryptic in the sense that no clear surface indications of a suture have yet been recognised. Petrological investigations indicate, however, that rocks at present at the surface in this region were formed at temperatures of 700–750 °C, and at depths of about 20 km (ref. 12). At these crustal levels, ultramylonites and pseudotachylites are likely to be the only indicators of the line of suturing[6].

A third suture has been postulated at or near the metamorphic boundary between the Slave and Churchill provinces[16,17]; it is known as the Thelon Front[18]. Belts of cataclastic gneiss and mylonite occur roughly parallel with the front inside the Churchill Province[19]. The front is bounded on either side by coextensive negative (Slave) and positive (Churchill) acurate gravity anomalies (Fig. 1) which have also been interpreted as an edge-effect between juxtaposed crustal blocks of different mean density and thickness. According to this interpretation[17] the density discontinuity penetrates the crust and represents a cryptic suture between collided cratons. The gravity anomaly is almost identical to those found at the western extension of the Cape Smith Belt, the Labrador Trough, and the Grenville Front.

Bouguer anomaly profiles numbered 1–5 across these boundaries (Fig. 1) are shown on a common datum in Fig. 2*a*. Apart from short wavelength anomalies attributable to local geological features, all five profiles are remarkably similar. In each case the gravity profile decreases gradually from a background level over the older province to a minimum near the inter-province boundary zone, and then increases sharply to a broad maximum over the younger province, some 16 to 40 mgal higher than over the older province. The smoothed gravity signature, which we call the type anomaly, derived by averaging profiles 1 to 5, is shown in Fig. 2*b* within an envelope which varies according to the standard deviation calculated at intervals of 5 km along the profiles. If the anomaly over the older province is regarded as background, the amplitudes of the minimum and the maximum are −42 mgal and 24 mgal, respectively. The average gradients over the older and younger province margins are about 0.2 mgal km^{-1} and 0.8 mgal km^{-1}, respectively. Near the minimum, the gradient is much steeper (up to 1.8 mgal km^{-1}) over the younger province.

A type crustal model has been derived from the type anomaly; it is constrained in three ways. Seismic results[20,21] suggest that the crust underlying both the Superior and Slave provinces is about 34 km thick in the vicinity of the profiles. This thickness was assigned to the crust of the older province along with an assumed normal crustal density of 2.84 g cm^{-3}. The density of the upper mantle was assumed to be 3.24 g cm^{-3}. Keeping these parameters fixed the thickness and density of the younger crustal block were varied until the calculated anomaly matched the type anomaly. The crustal model is shown in Fig. 2*c*, and the computed anomaly in Fig. 2*b*. The crustal thickness of the younger province is 39.5 km, and the density is 2.91 g cm^{-3}. The density discontinuity dips towards the younger province from a point 13 km from the minimum, to a depth of 14 km at a distance of 35 km from the minimum, where it becomes vertical over the rest of its length. The base of the crust of the older province dips gently towards the contact over a distance of 160 km. This non-isostatic crust is required to fit the gravity minimum. The blocks are otherwise in approximate isostatic equilibrium.

The model indicates that the younger crustal block is consistently thicker and slightly denser than the older. This consistency is surprising, but all the more surprising because not only do the structures have a wide geographic distribution but they are also of vastly different ages. This suggests that similar processes have operated throughout much of Precambrian time. The density discontinuity of the type model penetrates the whole crust and separates cratons of different density, thickness, age and internal structure; it is interpreted as a vestigial suture between collided continental blocks. The model with slight modifications to crustal density and thickness can be applied to all five boundary zones and may apply to other examples in Canada and elsewhere wherever the gravity signature of the type model is recognised.

R. A. GIBB
M. D. THOMAS

Gravity and Geodynamics Division,
Earth Physics Branch,
Department of Energy, Mines and Resources,
Ottawa, Canada K1A 0Y3

Received April 27, accepted May 17, 1976.

[1] Stockwell, C H., *Geol Surv. Pap. Can*, 61-17, 108–118 (1961).
[2] Stockwell, C H, *Geol. Surv. Pap Can*, 72-52 (1973).
[3] Wilson, J. T., *Science, History and Hudson Bay* (edit by Beals, C S, and Shenstone, D. A), 1015–1033 (Department of Energy, Mines and Resources, Ottawa, 1968).
[4] Gibb, R A, and Walcott, R. I., *Earth planet. Sci Lett*, 10, 417–422 (1971).
[5] Burke, K, and Dewey, J F, *Implications of Continental Drift to the Earth Sciences*, 2 (edit by Tarling, D H., and Runcorn, S K.), 1035–1045 (Academic, New York, 1973)
[6] Dewey, J. F., and Burke, K. C A., *J. Geol*, 81, 683–692 (1973)
[7] Kearey, P., *Earth planet. Sci Lett*, 28, 371–378 (1976)
[8] Tanner, J G, thesis, Univ Durham (1969)
[9] Donaldson, J. A, and Irving, E., *Nature phys. Sci.*, **237**, 139–140 (1972)
[10] Irving, E., Emslie, R. F, and Ueno, H., *J. geophys Res.*, 79, 5491–5502 (1974)
[11] Irving, E, and McGlynn, J. C., *Phil Trans R. Soc*, A280, 433–468 (1976).
[12] Baer, A. J., Emslie, R F, Irving, E., and Tanner, J G, *Geoscience Can.*, 1, 54–61 (1974).
[13] Brown, R. L., Chappell, J. F., Moore, J. F., Jr, and Thompson, P. H., *Geoscience Can*, 2, 141–144 (1975).
[14] Thomas, M. D, and Tanner, J. G., *Nature*, 256, 392–394 (1975).
[15] Thomas, M. D, *Gravity Map Series*, 64–67 (Department of Energy, Mines and Resources, Ottawa, 1974).
[16] Gibb, R A, and Halliday, D. W., *Gravity Map Series*, 124–131 (Department of Energy, Mines and Resources, Ottawa, 1974).
[17] Gibb, R. A., and Thomas, M. D., *Tectonophysics* (in the press).
[18] Wright, G. M, *Mem. geol. Surv Can*, 350 (1967).
[19] Davidson, A., *Spec. Pap. geol Ass. Can*, 11, 381–433 (1972).
[20] Berry, M. J., and Fuchs, K., *Bull. seism. Soc. Am*, 63, 1393–1432 (1973).
[21] Barr, K. G., *J geophys Res.*, 76, 1929–1947 (1971)
[22] Stockwell, C. H, *Geol. Surv Can. Map 1251A* (1969)

Dating of historical earthquakes by mud profiles of lake-bottom sediments

RECENTLY, Ben-Menahem *et al.*[1] derived tectonic patterns and slip rates in the Jordan Rift Valley by combining a comprehensive study of seismological, historical, geological and morphological data. It was found that the principal seismic activity along the Jordan Valley is due to a left-lateral strike-slip fault, striking 11° east of north and extending for about 50 km from 32°N to 31°30′N along the 35°30′ meridian. Its most active part in the past four millenia has been near the monastery of John the Baptist which, according to tradition, is the place where the Israelites crossed the Jordan and where Jesus was baptised. The fault trace and its role in the historical seismicity of the area is shown in Fig. 1. It has an estimated mean rate of activity of 2–3 events per century at magnitudes from 5 to 7 (ref. 1) An aseismic slip rate of at least 3 mm yr^{-1} is taking place along this fault[1]. Here we show how this activity is reflected in an unusual limnological process which takes place at the bottom of the Dead Sea and which can serve as a 'geophysical clock' to date historical events.

The fault's seismicity has been reflected in many historical records, in particular the Bible, in which we find distant echoes of tectonic events as remote as 2000 BC. Lists of earthquakes have been compiled from many and diverse sources (see, for example, refs 2–5), and a new revised list,

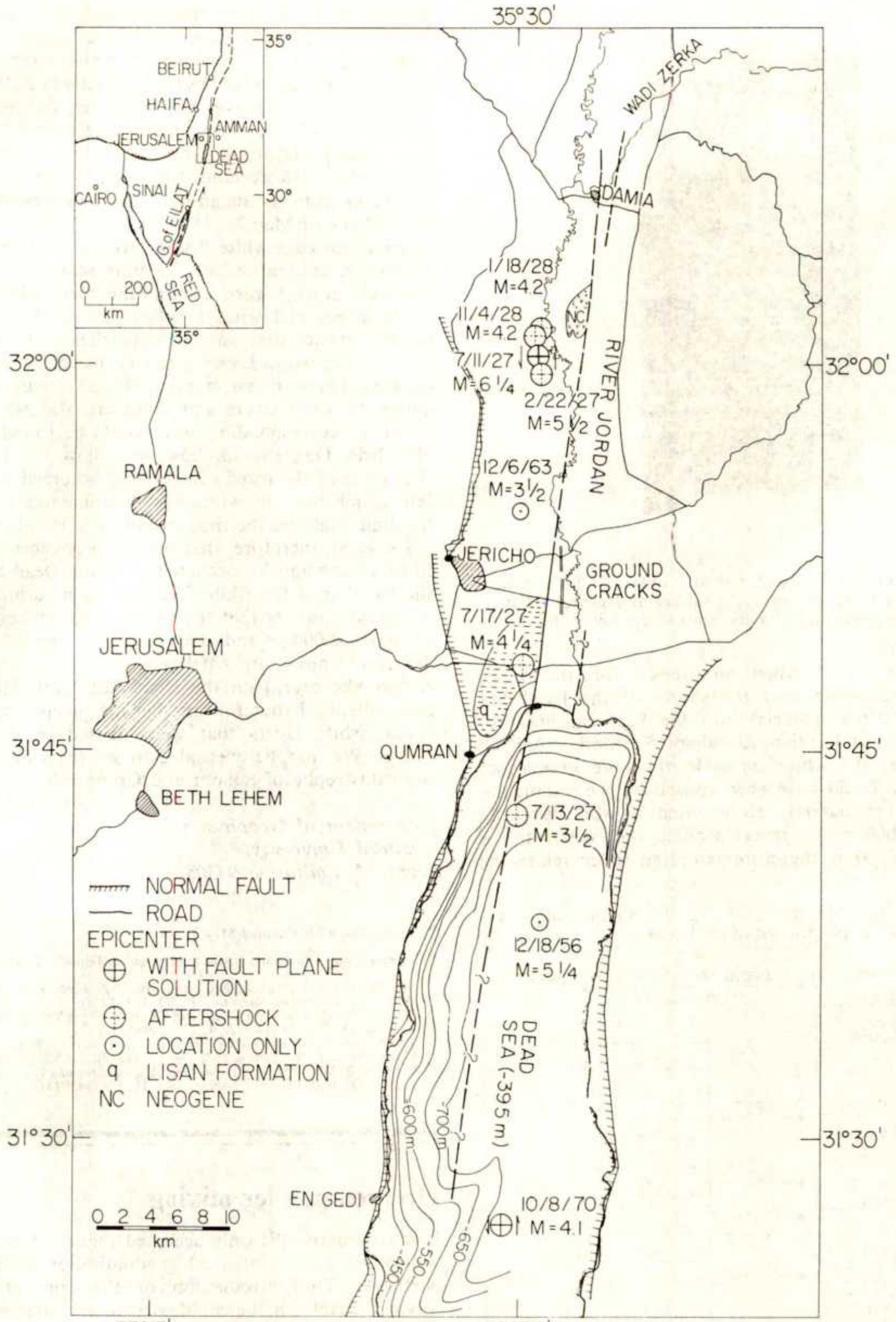

Fig. 1 Map of the Dead Sea fault (see ref. 1).

which is believed to include seismic events above a Richter magnitude 5, is given in ref. 1.

That list, although inaccurate and incomplete in detail, probably includes the major seismic events that have taken place around the Dead Sea fault during the past 4,000 yr. Although many of the epicentres are known with poor accuracy, the list suggests that the number of intermediate and major earthquakes in the area (M=5–7) was about 50 in the past 2,000 yr, yielding an average 'quiet' interval of 40 yr. We have used observations of Elazari-Volcani[6] who obtained a number of profiles of mud samples from depths of 70–330 m at different places in the Dead Sea during December 1941. At one place about 6 km south-west of the northern shore, a profile 170 cm long was obtained from a depth of 100 m. On dissecting the profile longitudinally, a 'spectrum of layers' of different colours—black, dark-blue, grey brown and white—was revealed (Fig. 2). The zones of sedimentation, distinctly seen, form no seasonal repeat pattern, as do, for example, the annual rings of trees. Similar observations were reported for many other lakes by Perfiliev[7].

On September 10, 1943, an earthquake was felt along the Jordan Valley. Macroseismic evidence placed the epicentre at the northern tip of the Dead Sea fault, with an estimated

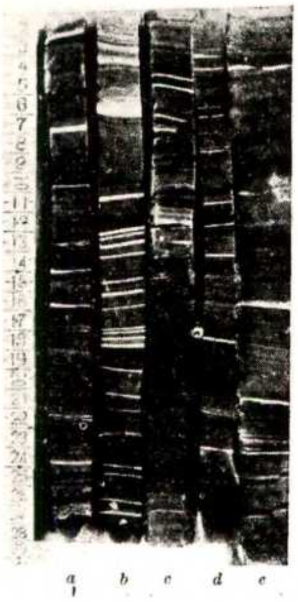

Fig. 2 'Spectrum' of layers of a mud profile of 170 cm long obtained from the bottom of the Dead Sea at depth of 100 m. Section starts at upper end of *a* and ends at the lower end of *e*.

Richter magnitude of 5. About one week before this event, new springs opened up near the shores of the Dead Sea and disgorged white material into the Sea, causing prolonged whitish discoloration for about 5 months. Ashbel[8] conjectured that the white layers in the core samples of Elazari-Volcani[6] could have been caused by the sedimentation of that white material. He counted 50 white layers in the total of 2,000 yearly layers seen in the 'spectrum' of Elazari-Volcani[6]. It is therefore tempting to correlate the time intervals of our chronological list with the length intervals of the white layers in Fig. 2.

Fig. 3 Dating of white layers of Fig. 2 with the aid of a chronological list of earthquakes.

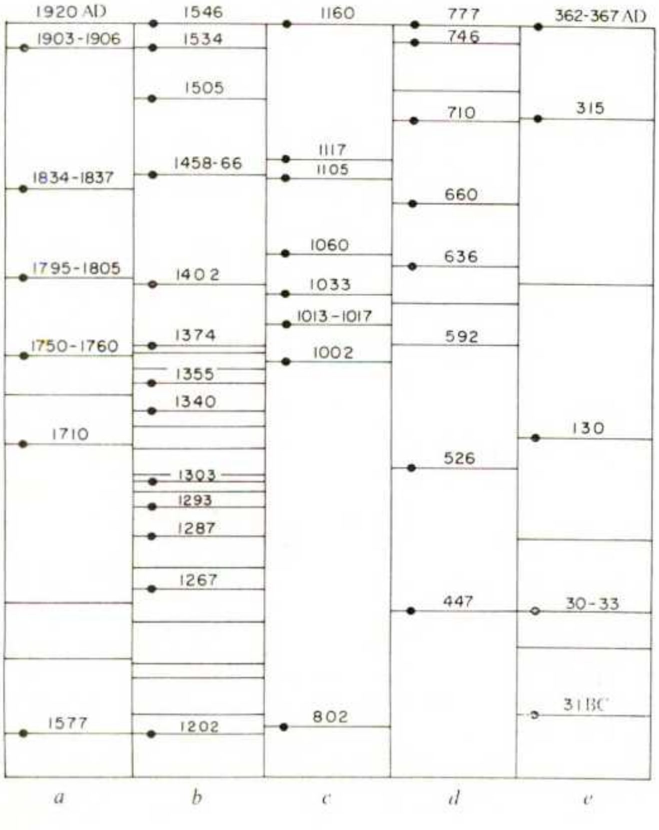

Starting with the conspicuous white layer in the upper part of a column *a* (opposite the numbers 2/3) we associate it with two earthquakes that occurred during this century on the Dead Sea fault (1903, 1906; see ref. 1). The next white layer is in the same column opposite the numbers 7/8. Assuming that the thickness of the layer is proportional to the magnitude, this could correspond to the great shock of May 23, 1834 ($M=6.25$) which is also known to have caused a white discoloration of the Dead Sea. This permits a 'calibration' of the time scale in Fig. 2 (18.5 yr per scale unit). Figure 3 shows the correlation between the white layers and what I believe to be the corresponding seismic events that gave rise to these layers. All in all, 65% of the white layers could be matched to listed earthquakes. There is an uncertainty of about 10 yr in the dating of some layers and there are also white layers for which no corresponding event could be found in the available lists. One should, however, allow for the possibility that some of the listed earthquakes occurred away from the fault, such that the white discoloration was faint, and that the time scale on the mud profile was not always linear.

I suggest, therefore, that there is a possible correlation of times of earthquake occurrence on the Dead Sea fault and the location of the white layers in the mud profile. There is no doubt however that the mud sample represents a period of about 2,000 yr and that the white layers *in toto* were definitely caused by earthquakes (or by accelerated pre-earthquake creep) on the Dead Sea fault during the past two millenia. I therefore predict that deeper mud cores will reveal white layers that were caused by earlier seismic events. We may be even able to see the white signature of the catastrophe of Sodom and Gomorrah.

Ari Ben-Menahem*

Department of Geophysics,
Stanford University,
Stanford, California 94305

Received March 23; accepted May 27, 1976.

* On leave from: Weizmann Institute of Science, Rehovot, Israel.

1. Ben-Menahem, A., Nur, A., and Vered, M., *Phys. Earth. planet. Int.* (in the press)
2. Willis, B., *Bull. seism. Soc. Am.*, **18**, 73–103 (1928).
3. Sieberg, A., *Handbuch der Geophysik IV* (Borntrager Verlag, Berlin, 1932).
4. Amiran, D., *Israel Explor. J.*, **1**, 223–239 (1951).
5. Ambraseys, N. N., *Bull. seism. Soc. Am.*, **52**, 895–913 (1962).
6. Elazari-Volcani, B., *Nature*, **152**, 274–275 (1943).
7. Perfiliev, B. W., *Ver. int. Verein. theor. angew. Limnol.*, **4**, 215–219 (1929).
8. Ashbel, D., *Bull. Palestine Explor. Soc.*, **11**, 57–58 (1943).

Ordered powder mixing

Until recently, the only accepted theory of powder mixing was based on a statistical randomisation of non-cohesive particles[1]. The introduction of the concept of ordered mixing[2] enables a logical theory to be established for the mixing of small cohesive particles to a considerable degree of homogeneity. The concept of ordered mixing has attracted considerable support[3–5]. A basic principle of ordered mixing is that fine particles will adhere, especially to larger particles. The adhesional forces involved may be electrostatic or surface tensional. For a homogeneous system to be formed, the weight of fine particles adhering to unit surface area of the larger particles should be constant. We report here such a condition in the mixing of a fluid energy milled closely sized fraction (2.6 μm) of salicylic acid with a multi-sized distribution of sucrose crystals, in the ratio 1 : 1,000 by weight.

The powders were mixed in a Revolvo-Cube rotating cube mixer for 6 h. The sucrose crystals were then classified by sieving. The collected fractions were each dissolved in 50%

Table 1 Ordered mixing of microfine salicylic acid with coarse sucrose crystals

Mean size fraction sucrose crystals (μm)	Weight of fraction (%)	Weight of salicylic acid/unit weight of sucrose ($\times 10^{-4}$)	Weight of salicylic acid/unit surface area of sucrose (10^{-7} g cm^{-2})	Surface area of sucrose coated (%)
462.5	3.34	4.58	5.61	2.04
		4.73	5.78	2.10
		4.52	5.52	2.01
390.0	20.10	7.10	7.31	2.67
		6.62	6.80	2.50
		6.41	6.59	2.41
302.5	52.43	9.05	7.22	2.63
		9.00	7.19	2.62
		8.74	6.98	2.54
215.0	21.02	13.1	7.46	2.72
		13.8	7.87	2.86
		12.9	7.32	2.67
168.0	2.34	17.0	7.39	2.69
		18.6	8.10	2.94
		16.9	7.35	2.67
137.5	0.78	19.3	7.10	2.56
		21.4	7.37	2.84
		19.8	7.20	2.63

ethanol and assayed for salicylic acid content. The results are given in Table 1.

Over the range of particle size, the weight of salicylic acid per unit surface area of sucrose crystals (assuming cubic crystals, as observed microscopically) is constant within the range of experimental error. From the projected area of the fine particles, it is possible to calculate that ~2.5% of the area of the larger sucrose particles is coated with fine particles at this level of mix dilution.

Segregation was not observed during the classification operation, as demonstrated by the lack of material passing through the finest sieve used.

These results demonstrate the possibility of ordered mixing processes for producing highly homogeneous mixtures of powdered materials. The application of this process to a wide number of different industrial uses is anticipated.

CHEE WAI YIP
JOHN A. HERSEY

School of Pharmaceutics,
Victorian College of Pharmacy,
381 Royal Parade Parkville,
Victoria 3052, Australia

Received May 3; accepted May 26, 1976.

[1] Lacey, P. M. C., *Trans. Inst. chem. Engrs, Lond.*, **21**, 53–59 (1943).
[2] Hersey, J. A., *Powder Technol.*, **11**, 41–44 (1975).
[3] Travers, D. N., *Powder Technol.*, **12**, 189–190 (1975).
[4] Kristensen, H. G., *Powder Technol.*, **13**, 103–121 (1976).
[5] Crooks, M. J., *Aust. J. pharm. Sci.*, **NS5**, 25–31 (1976).

Aluminium-26 in a manganese nodule

MANGANESE nodules are generally considered to have accumulated very slowly. Radiometric studies by ^{230}Th, ^{231}Pa, and ^{234}U/^{238}U suggest their growth rates to be a few mm per 10^6 yr (refs 1–3). This leads to an enigma: how do they escape from burial by associated marine sediments which are accumulating three orders of magnitude faster than the nodules? Though this problem remains open, the postulated slow growth rates might permit manganese nodules to accumulate in a small volume high concentrations of long lived cosmogenic radionuclides ^{10}Be ($\tau_{\frac{1}{2}} = 1.5$ Myr) and ^{26}Al ($\tau_{\frac{1}{2}} = 0.715$ Myr) which were formed through the bombardment of atmospheric constituents by galactic cosmic rays. Indeed, Somayajulu[4] and Krishnaswami *et al.*[5] have found that three manganese nodules from the Pacific basin concentrate considerable activities of ^{10}Be at their surface (9–68 d.p.m. kg^{-1}). These concentrations are several times higher than those found in pelagic sediments. We report here on a search for ^{26}Al in manganese nodules.

The TECHNO-1 manganese nodule, obtained by a dredge at a depth of 4,020 m at the north of Tuamotu archipelago has a crust ~ 1,000 cm^2 in area and ~ 3 cm thick. This crust covers a base of phillipsite. Half of the crust (425 cm^2) was provided for the present study. The crust was sliced horizontally into four sections: section I (0–2.3 mm), section II (2.3–8 mm), section III (8–14 mm), and section IV (14–23 mm).

For the analysis of ^{26}Al, the nodule material was leached twice in hot, 6 N HCl. After being isolated by centrifugation, the insoluble phases were completely dissolved in HF and the HCl-leached fraction and the HF-dissolved fraction were treated separately for further purification. Aluminium was precipitated with ammonium hydroxide, and iron, manganese and thorium were removed by the dissolution of aluminium hydroxide with NaOH. This purification process was repeated three more times, each time with the addition of a solution of Fe carrier which serves as scavenger for Th. The purified Al was finally converted to Al_2O_3 and counted. In our study, the HCl fraction and the HF fractions were counted together. The chemical yield of Al was 65 ± 5%. The Al content of the nodule was 2%.

^{26}Al decays mostly by the emission of a positron followed by a 1.83-MeV γ ray. The positron thermalises and produces two 0.511-MeV γ rays, enabling the concentration of ^{26}Al to be measured by the coincident detection of a 0.511-MeV γ ray in one counter, and the sum peak of the other two γ rays (total 2.34 MeV) in another. The measurements were carried out with a low-level $\gamma - \gamma$ coincidence spectrometer which consists of two semi-cylindrical NaI (Tl) scintillators 30×25 cm. The same spectrometer was previously used for our measurements of ^{26}Al in marine sediments[6]. The samples from the manganese nodule were counted for 30,000–60,000 min and the background, for 60,000 min. The background count rate was 0.0137 ± 0.0005 c.p.m. The counting efficiency for ^{26}Al was 5.3 ± 0.3%.

^{26}Al was detected in the first section, where its concentration of 0.29 ± 0.14 d.p.m. kg^{-1} (a net count rate of $15 \pm 7 \times 10^{-4}$ c.p.m.) was higher than that found in a Pacific sediment: by our measurement, 0.081 ± 0.046 d.p.m. kg^{-1} (ref. 6). Therefore the postulated concentration of long lived cosmonuclides in manganese nodule is also confirmed for ^{26}Al.

The enrichment of ^{26}Al in manganese nodule relative to that

Pure Chemistry Library.
SCIENCE COLLEGE

in sediment is more evident when the specific activities (d.p.m. ^{26}Al per kg Al) are compared: 15±7 d.p.m. per kg Al in the manganese nodule and 0.9±0.5 d.p.m. per kg Al in the sediment. This indicates that cosmogenic ^{26}Al precipitates from seawater for preference with oxides, hydroxides and/or authigenic aluminosilicates rather than with detrital silicate minerals.

Measurements of ^{26}Al and ^{10}Be in a Pacific sediment[6] showed that the ^{26}Al:^{10}Be ratio in the sediment, 0.109±0.012, is in good agreement with the theoretical production ratio of 0.013±0.006 as well as with that measured in Greenland ice by McCorkell *et al.*[7], 0.017±0.008. From this theoretical ratio and the measured ^{26}Al activity in the nodule, we estimated the ^{10}Be activity in the 0–2.3-mm section of TECHNO-1 to be 22±15 ^{10}Be d.p.m. kg^{-1}. This estimated activity is compatible to the ^{10}Be activities measured by Krishnaswami *et al.* in three manganese nodules: 17, 32, and 89 d.p.m. kg^{-1} (these values are calculated for the 0–2.3 section from their measurements of the extrapolated activity at the surface, N_0, and the depth L at which the activity becomes N_0/e, by using the equation

$$C_x = LN_0\,(1-\exp(-X/L))/X$$

where C_x is the concentration at O–X cm section). The agreement suggests that the ^{26}Al:^{10}Be ratio in manganese nodules is of the same order as that in sediments, which is expected from the similarity of the geochemical behaviours of the two nuclides in seawaters.

If we assume that the ^{26}Al content decreases exponentially as a function of depth in the TECHNO-1 manganese nodule and that the decrease of ^{26}Al arises from the postulated slow growth rate of nodule material (1–5 mm per 10^6 yr), then it is possible to estimate the ^{26}Al content in the 2.3–23-mm section from the measured content of ^{26}Al in the 0–2.3-mm section (0.29±0.14 d.p.m. kg^{-1}). Concentrations of 0.004±0.002, 0.06±0.03, and 0.11±0.05 d.p.m. kg^{-1} are calculated for growth rates of 1, 5 and 10 mm per 10^6 yr respectively. The observed net count rate of $1(\pm 9)\times 10^{-4}$ c.p.m. gives 0.003±0.024 d.p.m. kg^{-1}. The upper limit of the observations for the 2.3–23-mm section, 0.03 d.p.m. kg^{-1}, is therefore compatible with growth rates of 1–5 mm per 10^6 yr.

As a solution to the enigma of the non-burial of manganese nodules by sediments, Arrhenius[8] and Lalou and Brichet[9] hypothesised that the radionuclides of interest were not incorporated in the nodule matrix during its growth, but were adsorbed later. The present results for ^{26}Al are not necessarily incompatible with such a hypothesis, because most of the ^{26}Al is found only in the first few millimetres section, but the precision of the present measurements limits further discussions.

We thank Professor J. Labeyrie and Drs C. Lalou and Teh-Lung Ku for their helpful discussion and also Dr D'Ozouville of CNEXO for providing the sample of the manganese nodule.

J.-L. Reyss
Y. Yokoyama

Centre des Faibles Radioactivités,
Laboratoire mixte CNRS–CEA,
91190–Gif-sur-Yvette, France

Received February 24; accepted May 5, 1976.

[1] Bender, M. L., Ku, T. L., and Broecker, W. S., *Science*, **151**, 325–328 (1966).
[2] Barnes, S. S., and Dymond, J. R., *Nature*, **213**, 1218–1219 (1967).
[3] Ku, T. L., and Broecker, W. S., *Deep Sea Res.*, **16**, 625–637 (1969); *Earth planet. Sci. Lett.*, **2**, 317–320 (1967).
[4] Somayajulu, B. L. K., *Science*, **156**, 1219–1220 (1967).
[5] Krishnaswami, S., Somayajulu, B. L. K., and Moore, W. S., *Conference on Ferromanganese Deposits on the Ocean Floor* (edit. by Horn, D. R.), 117–121 (NSF, Washington DC, 1972).
[6] Reyss, J.-L., Yokoyama, Y., and Tanaka, S., *Science* (in the press).
[7] McCorkell, R., Fireman, E. L., and Langway, C. C., Jr, *Science*, **158**, 1690–1692 (1967).
[8] Arrhenius, G., *Trans. Am. Geophys. Un., US National Report* (1963–1967), 604 (1967).
[9] Lalou, C., and Brichet, E., *C. r. hebd. Séanc. Acad. Sci., Paris, Ser. D*, **275**, 815–818 (1972).

Reactions of $O(2^1D_2)$ with chlorofluoromethanes and CCl_4

UPPER atmosphere reactions involving chlorofluoromethanes are of considerable current interest[1-6]. It has been suggested that the diffusion of chlorofluoromethanes, from the troposphere into the stratosphere, where photochemical and reaction processes produce free chlorine atoms, could lead eventually to a depletion of ozone in the upper atmosphere[1,2], by way of the ClO_x cycle

$$Cl+O_3 \rightarrow ClO+O_2 \qquad (1)$$

$$ClO+O \rightarrow Cl+O_2 \qquad (2)$$

The work presented here was directed towards obtaining a more detailed understanding of the primary and secondary processes which take place in the photochemically initiated reaction between O_3 and the chlorofluoromethanes.

The reaction of $O(2^1D_2)$ with Freons 11–13 ($CFCl_3$, CF_2Cl_2 and CF_3Cl) is known to give rise to ClO radicals[6]

$$O(^1D)+CF_xCl_y \rightarrow ClO+CF_xCl_{y-1} \qquad (3)$$

and thus provides a means of direct entry into the ClO_x cycle. A number of other channels may, however, contribute to the overall rate of removal of $O(^1D)$, including quenching to the ground state, $O(^3P)$. Little is known about the importance of these other channels, or of the subsequent reactions of the CF_xCl_{y-1} radicals which can in some cases give rise to further release of Cl atoms. There is thus a clear need for laboratory based studies to establish the mechanism and kinetics of such reactions.

By using flash photolysis coupled to a fast-flow system with nozzle beam mass spectrometric sampling (Fig. 1), we have obtained direct evidence for a number of transient species which are produced in these photochemical systems. The formation of ClO by reaction (3) is confirmed and the first direct evidence for a competing channel leading to elimination of a halogen molecule (reaction (4) below) is presented. Secondary production of ClO following reaction between CCl_3 and O_3 is also reported.

$O(2^1D_2)$ atoms were produced by flash photolysing O_3 in the Hartley continuum (200–300 nm). The flash lamp was constructed of quartz and was operated with a continuous flow of argon at a pressure of ~100 N m^{-2}. Flash energies of 125–250 J (10 µF at 5–7 kV) were found to be adequate when signal averaging was used: the half life of the flash at 260 nm was ~1 ms. Reagents were mixed just before entry into the flow tube (typically, flow rates of 10 m s^{-1}, with total pressures in the range 300–400 N m^{-2} and O_3: halocarbon: He = 1 : 10 : 40 were used). He + O_3 mixtures were prepared by diverting part of the He flow through a trap containing O_3 adsorbed on silica gel at 195 K. Ozone was prepared by the method of Clough and Thrush[7] and the concentration in the flow system monitored optically by absorption at 260 nm; pressures in the range 1–40 N m^{-2} could be conveniently monitored with a path length of 10 cm.

Products of the primary and secondary radical reactions were monitored as a function of time with the mass spectrometer (Extranuclear quadrupole) set to sample a preselected mass number. The analogue output from the mass spectrometer was then digitised and stored in a 200-channel signal averager (Datalab, DL102A); in most cases it was necessary to average the results of sixteen experiments before adequate signal-to-noise ratios were obtained. Little electronic interference from the flash was observed, but some variation with mass number was found and was thus checked for all experimental runs.

Helium (99.9%) and Freons 11, 12 and 13 (Matheson) were taken directly from cylinders. Carbon tetrachloride vapour (laboratory grade) was obtained by pumping on the liquid, and

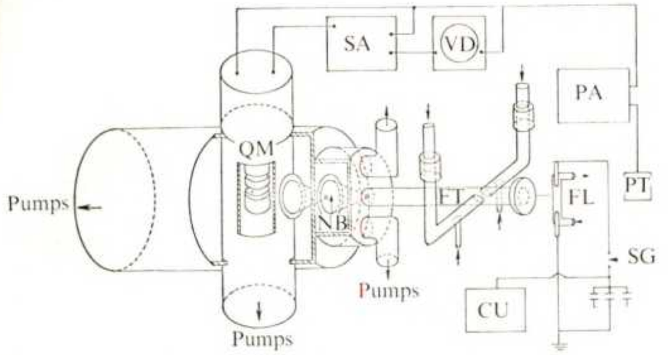

Fig. 1 Schematic representation of the flow tube flash unit and nozzle beam mass spectrometric sampling system: FT, flow tube; NB, nozzle beam sampling system; QM, quadrupole mass spectrometer; FL, flash lamp; CU, charging unit; SG, spark gap; PT, photo-trigger; PA, pulse amplifier; VD, visual display; SA, signal averager.

the flow regulated with a needle valve. The purity of all reagents was checked before an experimental run by direct sampling with the mass spectrometer.

The extent of photolysis for pure ozone was generally in the range 3–10% depending on the flash energies used. In the presence of the chlorofluoromethanes the extent of O_3 decomposition was seen to increase significantly as a result of secondary reactions. An increase by a factor of 3–8 was observed using Freon 11–13:ozone ratios around 5. The effect was less marked for CCl_4.

Formation of ClO was observed ($m/e = 51$) following the photolysis of O_3 in the presence of Freons 11–13 and CCl_4 (see Fig. 2), supporting previous observations using ultraviolet absorption spectroscopy[6]. No signal at $m/e = 51$ was observed when O_3 was excluded from the flow mixtures under otherwise identical conditions. The yield of ClO was found to increase with increasing partial pressure of O_3 (over the accessible range 5–13 N m^{-2}), as expected from the increase in $O(^1D)$ production. The yield of ClO also increased with the partial pressure of CF_3Cl, however in the presence of CF_2Cl_2, which is known to give the highest secondary yield of ClO under the conditions used (H. M. Gillespie and, R. J. D., unpublished results), the rate of decay of ClO increased with partial pressure of CF_2Cl_2 (over the range 40–80 N m^{-2}). As ClO is unreactive with closed shell species, this indicates that the concentration of free radicals or oxygen atoms increases as the partial pressure of CF_2Cl_2 is increased. This could be caused by a little photolysis of CF_2Cl_2 and will be examined in more detail in future work. The greatest yields of ClO were observed with CCl_4 (Fig. 2).

Fig. 2 Formation and decay of ClO following the photolysis of O_3 in the presence of CCl_4. *a*, Ozone, CCl_4 and He mixture: $P_{O_3} = 0.05$ mmHg, $P_{CCl_4} = 0.35$ mmHg, $P_{He} = 2.15$ mmHg. *b*, CCl_4 and He mixture: $P_{CCl_4} = 0.35$ mmHg, $P_{He} = 2.15$ mmHg. Mass spectrometer set to sample $m/e = 51(ClO^+)$, resolution set at 4.25; flow velocity = 10 m s^{-1}; traces are the result of averaging 16 experiments.

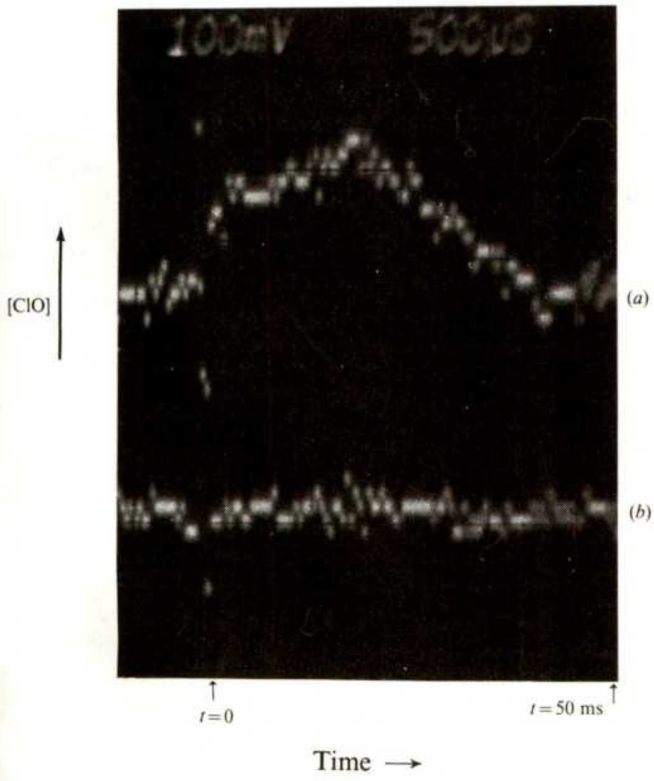

Other products observed immediately following photolysis of mixtures containing O_3, were FCl, CFClO (both from $CFCl_3$) and CF_2O from CF_2Cl_2. Small yields of CCl_2 and CFCl were also observed from direct photolysis of $CFCl_3$ and CF_2Cl_2 respectively. As these transient species have the same charge–mass ratio at CFClO and CF_2O, a small correction to yields of the latter species was made. A search was also made for the FO radical, however the large background signal at $m/e = 35$ (Cl^+) made measurements at this mass number very insensitive and no firm evidence for the presence of this radical was obtained.

The present work provides further direct evidence for reaction (3) and the first direct evidence for the channel

$$O(^1D) + CFCl_3 \rightarrow CCl_2O + FCl \qquad (4)$$

(secondary formation of FCl through atom recombination would be too slow to account for our observations). Pitts *et al.*[4] have observed CF_2O and CFClO as end products from Freons 12 and 11 respectively and have suggested that reactions similar to (4) were responsible, but secondary reactions can also lead to these end products. Further work to establish the absolute sensitivity of our system for species such as FCl will allow the importance of channel (4) to be assessed quantitatively.

The large yield of ClO from CCl_4 and the continued growth of this radical after the flash (Fig. 2) provides evidence that the CCl_3 radical, formed in the primary reaction between $O(^1D)$ and CCl_4, reacts further with O_3, yielding ClO. Little is known about the mechanism of the secondary reactions involving CCl_3 or CF_xCl_{y-1} radicals with O_3 or O_2, but our work indicates that the $CFCl_2$ radical gives rise to CFClO, possibly by the reactions

$$CFCl_2 + O_3 \rightarrow CFCl_2O^{\ddagger} + O_2 \qquad (5)$$

$$CFCl_2O^{\ddagger} \rightarrow CFClO + Cl \qquad (6)$$

where ‡ denotes vibration excitation, with the chlorine atom reacting further with O_3 to yield ClO.

R.J.D. thanks the Max-Planck-Gesellschaft for a Senior Scientist Fellowship.

R. J. DONOVAN*
K. KAUFMANN
J. WOLFRUM

Max-Planck-Institut für Strömungsforschung,
34 Göttingen, FRG

Received March 11; accepted June 1, 1976.

* Permanent address: Department of Chemistry, University of Edinburgh, West Mains Road, Edinburgh EH9 3JJ, UK.

[1] Molina, M. J., and Rowland, F. S., *Nature*, **249**, 810–812 (1974).
[2] Rowland, F. S., and Molina, M. J., *Rev. Geophys. Space Phys.*, **13**, 1–35 (1975).
[3] Stolarski, R. S., and Cicerone, R. J., *Can. J. Chem.*, **52**, 1610–1615 (1974).
[4] Pitts, J. N., Sandoval, H. L., and Atkinson, R., *Chem. Phys. Lett.*, **29**, 31–34 (1974).
[5] Lubkin, G. B., *Phys. Today*, October, 34–39 (1975).
[6] Gillespie, H. M., and Donovan, R. J., *Chem. Phys. Lett.*, **37**, 468–470 (1976).
[7] Clough, P. N., and Thrush, B. A., *Chemy Ind.*, November 19, 1971 (1966).

Energy analysis of wave-power and wind-power systems

THERE have been several recent suggestions that wave-power systems could provide a substantial part of Britain's energy requirements. The development of such systems presents, however, some formidable problems. One which has been largely overlooked concerns the energy investment required in their construction, compared with the predicted rate of energy return. The calculations which follow suggest that the energy recovery period may be many years. Similar calculations for wind-power systems, whose characteristics are known with greater precision, indicate a very much shorter energy recovery period. Moreover, though the wind is often regarded as a diffuse source of power, it is shown to offer a power density comparable with that assumed for wave-power systems.

Since no large scale wave-power system has yet been constructed, it is not possible to determine precise energy costs. There are, however, enough data available for one proposed system, the Salter rocking float[1–3], to provide a reasonable estimate. Salter[1] has shown in laboratory tests that his rocking float is a fairly efficient absorber of wave power and reports that at Station India in the North Atlantic the annual average power in the waves is 77 kW m^{-1}. He therefore suggests that "a few hundred kilometres of installation could meet the total present electrical requirements of the UK". Swift-Hook *et al.*[2] consider the efficiency of the rocking float for waves of various periods and state that a float 50 m in diameter tuned to a wave period of 10 s should theoretically absorb at least 50% of the incident wave power for wave periods in the range 7–17 s. Measured efficiencies are somewhat lower than theoretical predictions, but an overall average efficiency of 50% for a large scale rocking float may be feasible, and this would give a power output of 38.5 kW m^{-1} for a location comparable with Station India. A rocking float 50 m in diameter would have a displacement of ~ 2,000 tonnes (t) per metre length, but if one allows for the connecting structure between floats and the addition of a balancing float to counteract the torque produced by wave action, as suggested by Denton *et al.*[3], the displacement will be appreciably higher. Connected arrays of such rocking floats several hundred metres long have been proposed, giving a floating structure comparable in size to modern supertankers. The steel structure of such tankers accounts for about one quarter of their total displacement. If such a ratio can be maintained for wave-power systems, which are appreciably more complex mechanically, the power output of 38.5 kW m^{-1} would require 500 t per m of steel structure, that is the expected power output would be 77 W per t of steel. The energy required to produce 1 t of steel is 38.7 GJ (ref. 4) and it would therefore be 16 yr before the energy output from this wave-power system repaid the energy investment in its construction. Bearing in mind the severity of the working environment, this period is probably comparable with the lifetime of the structure.

The power output per unit displacement may be increased by reducing the diameter of the rocking float system. Smaller floats are, however, less efficient, and marine experience indicates that the ratio of structure weight to total displacement increases as the draught decreases. On balance it seems probable that reduced draught can give some reduction in the energy recovery period, but it is difficult at this time to quantify the improvement that is possible. Moreover, the energy recovery period of 16 yr calculated for the 50-m rocking float is based on assumptions which are somewhat optimistic. For example, Station India is 700 km offshore and well outside the continental shelf. As Denton *et al.*[3] point out, the cost of bringing electricity ashore by underground cable would be prohibitive if the wave-power systems were > 100 km offshore. Locations closer to the shore are therefore necessary and the power in the waves will be attenuated as the waves travel over relatively shallow water. The degree of attenuation will depend on the chosen location, but Salter[1] provides an example of the magnitude of this effect when he quotes the power in the waves at Seven Stones, off Lands End. Here the annual average wave power is 26 kW m^{-1}, one third that of Station India. There will, in any location, be a further loss of efficiency and power output because of the lack of alignment between the axis of the wave-power system and the incident waves. Allowing for all these factors it seems very doubtful whether the energy recovery period for a rocking float system can be reduced to much less than the estimated 16 yr. Other schemes for extracting power from the waves, such as the hinged float system[5], may possibly have a shorter energy recovery period, but there are insufficient data at present in the literature to provide a reasonable estimate of this.

How do wind-power systems compare with proposed wave-power systems? Over Great Britain as a whole the average power in the wind is at least an order of magnitude greater than the average electricity demand of 30 GW. The wind is usually considered to be a diffuse source of power but in good coastal locations the power flux is comparable with the range quoted for wave-power systems. Wind data[6] for Stornoway, measured at 12 m above ground level (37 m above mean sea level) indicates a year round average wind speed of 7.4 m s^{-1} and an average power flux of 606 W m^{-2}. Up to a height of 50 m, which is comparable with the draught of proposed wave-power systems, this gives an annual average power flux of 30.3 kW per metre length of wind-power installation. To the east of Britain at Bell Rock, which is 20 km offshore and near the Firth of Tay, the corresponding annual average power flux is 32.9 kW m^{-1}. Modern windmills have a peak efficiency of ~ 45% but at high wind speeds the efficiency decreases. Over the complete operating range of wind speeds an average efficiency of 30% can be expected. It has been suggested[7] that 10,000 windmills, each having a rated power output of 1 MW, could produce nearly 10% of our present electricity requirements and save 4.6×10^6 t oil per year. A 1-MW windmill of conventional design would have a diameter of ~ 50 m, and past experience[8] in the construction of windmills of this size and rating indicates that the average power output would be ~ 1,090 W per t of steel. This gives an energy recovery period of ~ 1.1 yr. Modern vertical axis windmills, such as that developed in recent years by Rangi, South and Templin[9,10], promise to give a significantly greater output per unit weight and should reduce the energy recovery period for windmills to a few months.

In conclusion, although wave-power systems apparently have the potential to provide a substantial proportion of Britain's energy, the energy investment in their construction seems large by comparison with their rate of energy return. Wind-power systems, however, have a known and very much shorter energy recovery period, and their use on a moderately large scale could make a real contribution towards meeting Britain's energy requirements.

P. J. MUSGROVE

Department of Engineering and Cybernetics,
Reading University,
Reading RG6 2AY, UK

Received February 25; accepted June 1, 1976.

[1] Salter, S. H., *Nature*, **249**, 720–724 (1974).
[2] Swift-Hook, D. T., Count, B. M., Glendenning, I., and Salter, S., *Nature*, **254**, 504–506 (1975).
[3] Denton, J. D., *et al.*, *CEGB Res.*, **2**, 28–40 (1975).
[4] *Energy Conservation in the UK* (HMSO, London, 1974).

[5] Woolley, M., and Platts, J., *New Scient.*, **66**, 241–243 (1975).
[6] *Tables of Surface Wind Speed and Direction over the United Kingdom*. Met. Office 792 (HMSO, London, 1968).
[7] *New Scient.*, **68**, 566 (1975).
[8] Putnam, P. C., *Power from the Wind* (Van Nostrand Reinhold, New York, 1948).
[9] Rangi, R. S., South, P., and Templin, R. J., *DME/NAE (Canada) Q. Bull.*, **2**, 1–14 (1974).
[10] *Proc. 2nd Workshop on Wind Energy Conversion Systems* (Washington, DC, 1975).

Dinosaurs, endothermy and blood pressure

THE recent resurgence of speculation about dinosaur physiology and behaviour has resulted in two notable and debatable interpretations. Bakker[1] summarises evidence of several investigators and concludes that dinosaurs were endothermic. Coombs[2], among others, suggests that the sauropod dinosaurs were mainly terrestrial, only occasionally entering shallow water. These hypotheses might well be viewed in the light of one line of evidence concerning the relationship between height of animals and hydrostatic pressures in the vascular system. Size alone can provide important insights into dinosaur cardiovascular performance which necessarily relates to the questions of endothermy and habitat. This report shows firstly, that high arterial blood pressures in large dinosaurs are consistent with the proposal that they were endothermic. Secondly, I suggest that if the long-necked sauropods were aquatic, they thereby avoided tremendous hydrostatic stresses on the cardiovascular system.

High tissue metabolism in endotherms demands high blood pressure and rapid flow in the systemic circuit to provide adequate exchange of metabolites. Blood flow must be equally rapid in the pulmonary circuit for efficient gas exchange, but the pulmonary blood pressure must be comparatively low to prevent either fluid filtration through the gas exchange surface[3] or energy waste inherent in excessive precapillary resistance. The evolutionary trend among vertebrates proceeds from the fishes which perfuse the gas exchanged at higher pressures than the other tissues, through amphibians and reptiles with roughly comparable pressures in two parallel circuits, to endotherms with high systemic and low pulmonary pressures[4]. A four-chambered heart and complete anatomical separation of the circuits seem to be required to maintain the large pressure difference between the circuits in endotherms.

Dinosaurs must have had systemic blood pressures high enough to move the blood from the heart to the head. The terrestrial bipedal ornithopods and theropods, for example, must have had central systemic blood pressures equal to at least the hydrostatic pressure of the blood column above the heart plus the head perfusion pressure. The vertical distances between the heart (centre of anterior body cavity) and the head in several large dinosaurs (Table 1) indicate that central blood pressures characteristic of living reptiles (about 20–70 mmHg)[5] could not even prevent collapse of the vessels in the head of the large dinosaurs much less provide adequate perfusion pressures. Because it is reasonable to assume that pulmonary blood pressure in dinosaurs was limited by the same constraints as in living air breathers, it is likely that at least these large dinosaurs had four-chambered hearts capable of producing large differences in pulmonary and systemic pressure.

Bakker[6] noted that, among all living vertebrates, only endotherms include animals with "fully erect gait" and he therefore suggested that dinosaurs were endothermic. By "erect", however, he meant somewhat more than simply a large heart–head distance and he was criticised for not showing the physiological basis for this correlation between gait and endothermy[7,8]. The relationship may be that both endothermy and high blood columns require high central systemic blood pressure. Thus, sustained high blood pressure inferred from the large vertical distance between the heart and the head in some dinosaurs supports (but does not prove) the proposition that dinosaurs were endotherms. Perhaps the advent of endothermy with its concurrent development of high systemic perfusion pressure enabled dinosaurs to become large and erect. The endotherms are the only living terrestrial vertebrates having heads more than about 50 cm above the heart. (Some snakes have long heart–head distances but they are subject to fainting if held in a vertical head-up position[9].) Consistently, short vertical heart–head distances characterise primitive reptiles which are thought to be ectothermic on the grounds of bone histology (see ref. 11 for literature) and predator–prey ratios in fossil bone deposits[10].

The sauropods present another interesting haemodynamic problem because of the extreme length of their necks. A specimen of *Brachiosaurus* in the Berlin Museum, for example, showed a vertical blood column of about 6.5 m above the heart; this would require a ventricular pressure of over 500 mmHg just to support the column[12]. The hearts of other large sauropods also must have had to develop high pressures if these dinosaurs held the head continuously erect and were terrestrial (Table 1). On the other hand, if the sauropods were aquatic, the blood pressure would be more or less equalised by the external hydrostatic pressure, thus placing less strain on the heart muscle.

It can be shown that vertebrate cardiac muscle operates within a limited range of ventricular wall stress. When the stress increases owing to pressure, the myocardium thickens, tending to normalise the stress. Not only does this adaptation occur within individual hearts, it also appears in phylogenetic comparisons. Both mean blood pressure and heart weight are generally 30–40% higher in birds than in mammals[5,13] for example. Giraffes, which have the highest blood pressure among mammals[14], are said to have hypertrophied hearts[15].

To estimate the degree of hypertrophy in sauropod hearts, I calculated the ventricular wall stresses in ten species of birds and mammals for which appropriate data are available (mouse, rat, dog, man, horse, cow, hen, turkey, and two ducks). The spherical model used is not precise but it is useful in a comparative way. According to the model, the mean stress averages about 1.0×10^5 dyne cm^{-2} ($\pm 0.3 \times 10^5$, the 99% confidence interval) in the species examined. If the heart of a 50-tonne sauropod was the same weight as that of a similarly sized whale (~ 200 kg)[16], it could have sustained pressures within the living vertebrate range. Under the assumptions that it operated within the range of stress indicated above, and it had to withstand pressures greater than 500 mmHg, it is evident that the heart would have been at least eight times heavier than the whale's heart but with the same internal ventricular volume. The spherical model increasingly underestimates stress in real hearts as the wall thickness: ventricular volume ratio increases with higher blood pressure[17]. Therefore the estimate of a 1.6-tonne heart is conservative. Such a thick-walled ventricle would be mechanically inefficient and its rate of oxygen consumption would be high. These potential disadvantages of extremely high blood pressure, as well as others listed by Hohnke[12], provide evidence favouring aquatic habits in sauropods.

Table 1 Estimated vertical distances between the head and heart in some large dinosaurs* and the associated hydrostatic pressure of the blood column

	Vertical distance (cm)	Hydrostatic pressure (mmHg)
Ornithopoda		
Hadrosaurus	100–150	77–116
Anatosaurus	200	155
Theropoda		
Ceratosaurus	90–150	70–116
Antrodemus	100	77
Tyrannosaurus	200–240	155–185
Sauropoda		
Apatosaurus	201	156
Brachiosaurus	655	508
Diplodocus	650	502
Camarasaurus	550	425

* Estimates from refs 12, 18 and 19.

Nevertheless, the possibilities remain that the sauropods achieved terrestrial life by possessing extremely hypertrophied hearts or an unusually strong myocardium. Alternatively, they simply might not have raised their heads high, or if they did, they endured a temporary cessation of blood flow to the brain.

I thank F. N. White and G. Sanson for stimulating discussion. This work was supported in part by a grant from the Australian Research Grants Committee.

ROGER S. SEYMOUR

Department of Zoology,
The University of Adelaide,
Adelaide, South Australia 5001

Received July 14, 1975; accepted May 18, 1976.

[1] Bakker, R. T., *Scient. Am.*, **232**, 58–78 (1975).
[2] Coombs, W. P., Jr, *Paleogeogr., Paleoclimatol., Paleoecol.*, **17**, 1–33 (1975).
[3] Rodbard, S., Brown, F., and Katz, L. N., *Am. Heart J.*, **38**, 863–871 (1949).
[4] Johansen, K., *Resp. Physiol.*, **14**, 193–210 (1972).
[5] Geddes, L. A., *The Direct and Indirect Measurement of Blood Pressure.* (Yearbook Medical Publishers, Chicago, 1970).
[6] Bakker, R. T., *Evolution*, **25**, 636–658 (1971).
[7] Bennett, A. F., and Dalzell, B., *Evolution*, **27**, 170–174 (1973).
[8] Feduccia, A., *Evolution*, **27**, 166–169 (1973).
[9] Prosser, C. L., and Brown, F. A., Jr, *Comparative Animal Physiology* (Saunders, London, 1961).
[10] Bakker, R. T., *Nature*, **238**, 81–85 (1972).
[11] Ricqlès, A. de., *C. r. hebd. Seanc. Acad. Sci. Paris*, **268**, 782–785 (1969).
[12] Hohnke, L. A., *Nature*, **244**, 309–310 (1973).
[13] Lasiewski, R. C., and Calder, W. A., Jr, *Resp. Physiol.*, **11**, 152–166 (1971).
[14] Van Citters, R. L., Kemper, W. S., and Franklin, D. L., *Science*, **152**, 384–386 (1966).
[15] Goss, R. J., in *Cardiac Hypertrophy* (edit. by Alpert, N. R.), 1–10 (Academic, New York, 1971).
[16] Clark, A. J., *Comparative Physiology of the Heart* (Cambridge University Press, London, 1927).
[17] Sandler, H., and Dodge, H. T., *Circulation Res.*, **13**, 91–104 (1963).
[18] Kurtén, B., *The Age of the Dinosaurs* (World University Library, London, 1968).
[19] Romer, A. S., *Vertebrate Paleontology* (University of Chicago Press, 1945).

Acetylene reduction by legume root nodule protoplasts

NITROGEN-FIXING protoplasts are of obvious importance in physiological studies of the assimilation of atmospheric nitrogen; in investigations of nodule development; in cloning trials for experimental and agricultural purposes[1]; and in somatic cell hybridisation[2–5]. Production of such protoplasts has proved elusive, however. Davey *et al.*[6] introduced a technique for the isolation of protoplasts from nodules. Protoplasts prepared by their procedure were incapable of nitrogenase (EC 1.7.99.2)-dependent acetylene reduction[7], presumably as a result of the extensive loss of leghaemoglobin during the isolation process[7]. By modifying the original procedure[6], we have obtained naked protoplasts which reduce acetylene after a lag period of about 2 d, and continue to do so for at least 11 d.

Protoplasts were isolated in a medium containing the following: 1% (w/v) Rhozyme HP 150 (Rohm and Haas); 0.5% (w/v) pectin lyase (EC 4.2.2.3 (ref. 8), Kikkoman Shoyu, Chiba-ken, Japan); 1% (w/v) cellulase (EC 3.2.1.4) (Onozuka R-10, Kinki Yakult Co., Tokyo); 1% (w/v) bovine serum albumin (Sigma) and a wash medium consisting of 0.6 M sorbitol; 0.05 M HEPES; 0.3% (w/v) potassium dextran sulphate (to inhibit protoplast fusion)[9]; 0.2 mM KH_2PO_4; 0.1 mM $MgSO_4$; 0.1 mM $CaCl_2$; 1.0 µM KI; 0.1 µM $CuSO_4$; with or without 1 mM KNO_3. The *p*H of the entire medium was adjusted to 5.8. Protoplasts were prepared from freshly harvested nodules of garden grown *Vigna unguiculata* (L.) Walp plants as previously described[7]. After collection, cells were separated from contaminating rhizobia by decantation in sterile wash medium. Settling of protoplasts was aided by gentle centrifugation (10*g* for 1 min), fresh wash medium was added and the process was repeated 10–15 times to give a final dilution of any extraneous rhizobia of 10^{10}–10^{15} times. The protoplasts (about 5×10^8 per ml) were incubated in 1.5 ml of wash medium at 25 °C, and acetylene reduction was assayed as described elsewhere[10].

Protoplasts obtained in this manner were intact as judged by light microscopy, possessed most of the original leghaemoglobin content[7], and began to reduce substantial amounts of acetylene after a lag period of between 24 and 48 h (Fig. 1*a*). Further evidence for the structural integrity of the protoplasts was deduced from the observation that when they were plated out on agar suitable for the growth of soyabean callus[11], rhizobial colonies were not formed, yet rhizobia from within the protoplasts (UMKL 76) were capable of good growth on this medium when cultured separately. The extent of the lag period could be reduced by removing NO_3^- from the wash medium used for incubation, but the presence of NO_3^- seemed to be essential during protoplast isolation. Represession of nitrogenase activity by NO_3^- is well known[12], and it is possible that NO_3^- levels must decrease to non-inhibitory concentrations before acetylene can be reduced.

Various substances were added to the incubation medium to test their effect on acetylene reduction. For example, 20 µmol of ATP stimulated it about sixfold (Fig. 1*b*). Other nucleotides had a similar effect. Similarly, phospho(enol)pyruvate and succinate enhanced acetylene-reduction activity, and the effect in the early stages of treatment was even greater than with ATP (Table 1). Addition of *V. unguiculata* leghaemoglobin to the medium (10–20 µmol) completely inhibited development of acetylene reduction activity. Most of these effects are similar to those seen in cell-free extracts of nitrogenase, and with nitrogenase in bacteroid preparations.

Holsten *et al.*[13] demonstrated that rhizobia could enter cultured soyabean callus cells. Under the microscope, the rhizobia could be seen within vesicles inside the host cells, and

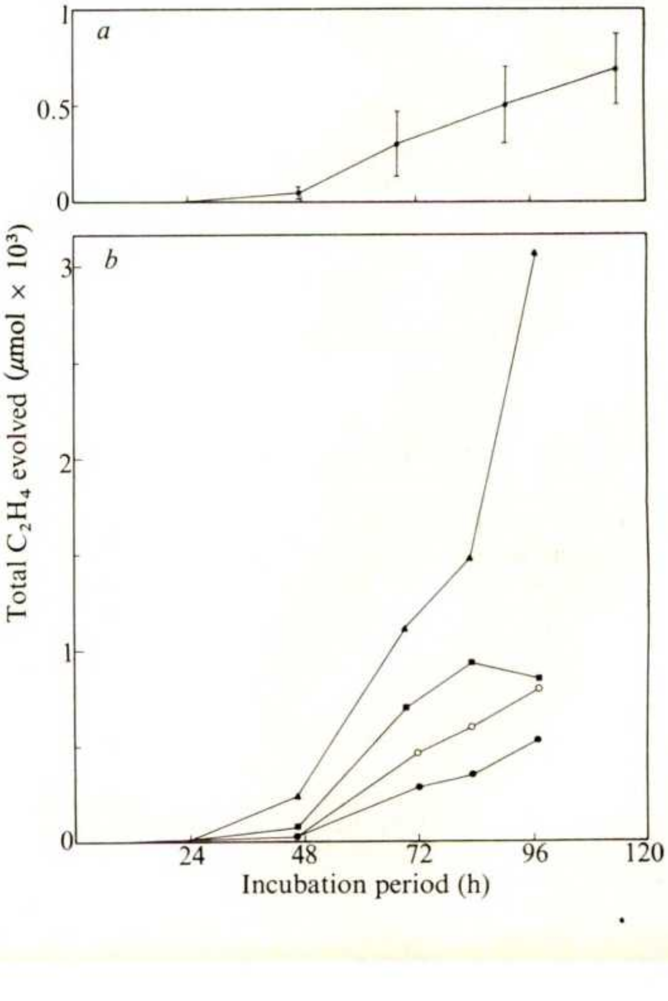

Fig. 1 *a*, Rate of acetylene reduction by protoplasts isolated from legume root nodules. Yields were within the range 30–50 mg dry weight of protoplasts extracted from 1 g fresh weight of nodules. Acetylene reduction was assayed in serum bottles of 29.5 ml capacity as described elsewhere[10]. Endogenous ethylene production was negligible (<0.01 nmol at the end of the experiment). Each point is the mean ± 1 s.d. of four replicates. *b*, Rate of acetylene reduction by protoplasts incubated with various amounts of ATP (amounts shown in µmol). Protoplasts were isolated from 1 g fresh weight of nodules and yielded 30–50 mg dry weight of material. ▲, + 20 µmol; ■, + 10 µmol; ○, + 5 µmol; ●, control.

Table 1 Effect of phospho (enol)pyruvate and succinate on acetylene reduction by root nodule protoplasts of *V. unguiculata*

Age of protoplasts (d)	Acetylene reduction (nmol C_2H_4/mg dry weight/h)		
	Protoplasts	Protoplasts + phospho (enol)pyruvate (40 μmol)	Protoplasts + succinate (40 μmol)
3	0.10 ± 0.01	0.52 ± 0.06	0.17 ± 0.01
4	0.11 ± 0.01	1.98 ± 0.20	1.44 ± 0.09
5	0.09 ± 0.03	3.28 ± 0.91	2.59 ± 0.62
6	1.08 ± 0.04	6.14 ± 0.80	6.20 ± 1.22
7	2.13 ± 0.15	9.42 ± 1.72	6.87 ± 1.70
8	2.04 ± 0.36	8.05 ± 2.04	7.21 ± 1.79
9	3.76 ± 0.32	11.06 ± 3.17	9.25 ± 1.80
11	3.45 ± 0.81	12.57 ± 2.73	13.09 ± 2.46

Each value is the mean (±1 s.d.) of three replicates. Protoplast dry weights were determined at the end of the experiment after oven drying at 80 °C until constant weight.

in this condition reduced acetylene to ethylene. Later work demonstrated acetylene reduction by rhizobia in the presence of plant callus cultures$^{14-16}$, although there was no direct contact between bacteria and plant. Then in late 1975 many authors showed that the rhizobia themselves could fix nitrogen in the absence of legumes$^{17-21}$. For these reasons it was imperative to show that the acetylene reduction reported above occurs within the plant membrane of the isolated protoplasts. As discussed, the protoplasts did not release rhizobia when cultured on an agar medium. Also, protoplasts which were actively reducing acetylene could be filtered on to nylon mesh (pore size 40 μm), washed extensively, and still retain the nitrogenase activity even in the semi-dry state. Furthermore, the wash-medium did not support acetylene reduction by the free-living UMKL 76, even with numbers as high as 4×10^{10} rhizobia per ml.

Thus the acetylene reduction observed in these experiments occurred within the cytoplasm of intact protoplasts. Maximum rates of reduction approximated 2–5% of that observed in fresh nodules (and this does not take into account the yield of protoplasts). In other experiments, rates of reduction of 12–13 nmol C_2H_4 produced per mg dry weight per hour were observed, which compares favourably with the reported values of about 46 nmol C_2H_4 produced per mg dry weight rhizobia per h (ref. 21).

We thank Mr R. Jesinger, Rohm and Haas Co, and Dr S. Ishii, Kikkoman Shoyu Co., for enzymes. Financial assistance was provided by the International Foundation for Science (Stockholm) and the University of Malaya.

W. J. BROUGHTON
K. C. WOOI
C. H. HOH

Department of Genetics and Cellular Biology,
University of Malaya,
Kuala Lumpur, Malaysia

Received March 23; accepted May 18, 1976.

[1] Nickell, L. G., and Torrey, J. G., *Science*, **166**, 1068–1069 (1969).
[2] Cocking, E. C., *A. Rev. Pl. Physiol.*, **23**, 29–50 (1972).
[3] Carlson, P. S., *Proc. natn. Acad. Sci. U.S.A.*, **701**, 598–602 (1973).
[4] Gamborg, O. L., and Miller, R. A., *Can. J. Bot.*, **51**, 1795–1799 (1973).
[5] Handmaker, S. D., *A. Rev. Microbiol.*, **27**, 189–204 (1973).
[6] Davey, M. R., Cocking, E. C., and Bush, E., *Nature*, **244**, 460–461 (1973).
[7] Hoh, C. H., and Broughton, W. J., in *Proc. natn. Tissue Culture Symp.* 1975, 42–50 (Rubber Research Institute of Malaysia, Kuala Lumpur, 1975).
[8] Ishii, S., and Yokotsuka, T., *Agric. biol. Chem.*, **39**, 313–321 (1975).
[9] Bremerskov, V., *Nature new Biol.*, **246**, 174 (1972).
[10] Williams, W. M., and Broughton, W. J., in *Soil Microbiology and Plant Nutrition* (University of Malaya Press, Kuala Lumpur, in the press).
[11] Constabel, F., in *Plant Tissue Culture Methods* 11–21 (National Research Council of Canada, Saskatoon, 1975).
[12] Sorger, G. J., *J. Bact.*, **98**, 56–61 (1969).
[13] Holsten, R. D., Burns, R. C., Hardy, R. W. F., and Hebert, R. R., *Nature*, **232**, 173–176 (1971).
[14] Child, J. J., *Nature*, **253**, 350–351 (1975).
[15] Scowroft, W. R., and Gibson, A. H., *Nature*, **253**, 351–352 (1975).
[16] Reporter, M., and Hermina, N., *Biochem. biophys. Res. Commun.*, **64**, 1126–1133, (1975).
[17] Pagan, J. D., Child, J. J., Scowcroft, W. R., and Gibson, A. H., *Nature*, **256** 406–407 (1975).
[18] Kurz, W. G., and La Rue, T. A., *Nature*, **256**, 407–408 (1975).
[19] McComb, J. A., Elliot, J., and Dilworth, M. J., *Nature*, **256**, 409–410 (1975).
[20] Keister, D. L., *J. Bact.*, **123**, 1265–1268 (1975).
[21] Tjepkema, J., and Evans, H. J., *Biochem. biophys. Res. Commun.*, **65**, 625–628 (1975).

Inhibition by acetylene of conventional hydrogenase in nitrogen-fixing bacteria

ONE of the earliest observations associated with nitrogen fixation was that all nitrogen-fixing organisms contained hydrogenase and nitrogenase[1]. We show here that acetylene, which is widely used as a substrate for nitrogenase, inhibits conventional hydrogenase activity and thus prevents the uptake of H_2 formed by nitrogenase in the presence of CO. Our evidence also suggests that azotobacter nitrogenase forms H_2 *in vivo* and that hydrogenase reoxidises this H_2 to provide reducing power for metabolism.

Hydrogenase can be classified into two major types: first, the ATP-dependent hydrogen-evolving capacity of nitrogenase, which accounts, in part, for the above correlation, and second, the hydrogenase which is not dependent on ATP. This second type can be subdivided into the reversible hydrogenases, common in anaerobic bacteria and presumably used as an electron sink to maintain a constant level of oxidised ferredoxin (or equivalent electron carrier), and the unidirectional, hydrogen-oxidising type found in azotobacter[2,4] and some nitrogen-fixing bacteroids[3]. Dixon[3] suggested three possible functions for this unidirectional hydrogenase: (1) as an oxygen scavenger to supplement respiratory protection of nitrogenase; (2) to prevent the H_2 evolved by nitrogenase from inhibiting the enzyme, and (3) enhancing the efficiency of nitrogenase by recycling the evolved H_2. There was little supportive evidence for these possibilities and the failure to observe H_2 evolution by nitrogen-fixing azotobacter under CO and argon, conditions favourable for any such evolution, led Postgate[5] to suggest that the nitrogenase site was anhydrous *in vivo* and that the hydrogen ion was unable to reach it. Brotonegoro[6], however, observed that nitrogen-fixing *A. chroococcum* evolved H_2 in the presence of CO if C_2H_2 was also present. We have investigated this observation.

The organisms used in this study were *Azotobacter chroococcum* (N.C.I.B. 8003) and *Klebsiella pneumoniae* M5A1. The growth, harvesting and preparation of crude supernatant extracts from these organisms have been described elsewhere[7,8]. Whole cells of *A. chroococcum* were obtained from batch cultures (100-ml volumes shaken in 250-ml conical flasks under air at 30 °C) and the *K. pneumoniae* cells were from a glucose-limited chemostat culture repressed for nitrogen fixation[9].

For the enzyme assays, the nitrogenase activity in crude supernatants[7] or whole cells[10] of *A. chroococcum* was measured by acetylene reduction or H_2 evolution[8]. Hydrogenase activity in both *A. chroococcum* and *K. pneumoniae* was determined manometrically[2,11].

Table 1 shows clearly that acetylene inhibited the ATP-independent H_2-evolving capacity of the reversible hydrogenase of *K. pneumoniae* and the H_2-oxidising capacity of the unidirectional hydrogenase of *A. chroococcum*, but that it did not inhibit the ATP-dependent H_2-evolving capacity of nitrogenase. C_2H_2 seemed to be a more effective inhibitor of hydrogenase than CO, particularly with whole cells of *A. chroococcum*.

Table 2 shows the effect of CO and C_2H_2 on hydrogen evolution by whole cells of *A. chroococcum*. The effect of the inhibitors varied with different batches of cells but 5% CO consistently inhibited acetylene reduction by > 95% and the rate of H_2 evolution was always greater in the presence of both CO and C_2H_2 than with either gas alone. NH_4-grown cells, repressed for nitrogenase activity, did not evolve H_2; this strongly suggests that the enzyme responsible in N_2-grown cells is nitrogenase.

We have confirmed the observation made by Brotonegoro[6] and extended it to show inhibition of conventional hydrogenase by acetylene. The evolution of H_2 which occurs

Table 1 Inhibition by acetylene and carbon monoxide of hydrogenase activity

Concentration of inhibitor (% C_2H_2 in gas phase)	Inhibition %				
	ATP-independent hydrogenase				ATP-dependent hydrogenase Crude preparation of nitrogenase from *A. chroococcum**
	Reversible hydrogenase from *K. pneumoniae*		Unidirectional (H_2 uptake) hydrogenase from *A. chroococcum*		
	Whole cells	Crude supernatant	Whole cells	Crude supernatant	
3.7	67				
6.5	82				
5.0		45	51(7)†	51(36)	0(0)
10.0		85	75	83	0
20.0			96	95	0

K. pneumoniae hydrogenase was measured in NH_4-grown cells and supernatants which contained no nitrogenase activity: H_2-evolving activity of whole cells (2.3 ml, 0.6 mg of protein) with added glucose (46 mM) was measured manometrically at 30 °C under argon. Crude supernatants (2.4 mg of protein) were also assayed manometrically under argon at 30 °C in 70-mM HEPES buffer, *p*H 7.2, $Na_2S_2O_4$ (20 mM) and methyl viologen (2 mM) in a final volume of 2.3 ml. The reactions were started by tipping either glucose or $Na_2S_2O_4$ from the side arm. *A. chroococcum* hydrogenase was measured manometrically at 30 °C by following H_2 uptake in 100-mM phosphate buffer *p*H 8.0, containing washed cells (0.5 mg (dry weight)) or crude supernatants (3.4 mg protein) with potassium ferricyanide (24 mM) as the electron acceptor. The atmosphere contained H_2 (80%), C_2H_2 as indicated with argon as the normalising gas.

Acetylene also failed to inhibit the H_2-evolving capacity of nitrogenase from *K. pneumoniae* in the presence of CO (Dr B. E. Smith, personal communication).

*The ATP-dependent H_2-evolving capacity of nitrogenase in crude supernatants of *A. chroococcum* was measured in the presence of 20% CO to prevent competition for electrons between the acetylene-reducing site and the H_2-evolving site. Otherwise, the assay conditions were as described by Yates and Planqué[7].

†The figures in parentheses show % inhibition by 5% CO.

when *A. chroococcum* is treated with both CO and C_2H_2 can now be interpreted simply; CO blocks all but the hydrogen-evolving function of nitrogenase[12] and CO plus C_2H_2, but mainly C_2H_2, blocks the conventional unidirectional hydrogenase which would otherwise reoxidise the hydrogen formed by nitrogenase. In experiments not reported here, the aerobe *Mycobacterium flavum* 301 shows a similar pattern of responses to CO and C_2H_2.

Table 2 H_2 evolution and acetylene reduction by N_2-fixing *A. chroococcum*

Amount of gas added to the atmosphere	C_2H_2 reduced (nmol h^{-1})	H_2 evolved (nmol h^{-1})
none	0	0
10% C_2H_2	780	20
5% CO	0	440
10% C_2H_2+5% CO	5	760

The nitrogenase activity of *A. chroococcum* was measured in 10 ml suspensions of whole cells (0.25 mg dry weight ml^{-1}) in 25-ml conical flasks at 30 °C under a PO_2 of 0.05 atm.

These results given a clear indication that H_2 is formed by azotobacter nitrogenase *in vivo* but, instead of being evolved, it is normally reoxidised by hydrogenase to provide additional reducing power for metabolism. This recycling of H_2 formed by ATP-dependent nitrogenase activity coupled with the ability of H_2 to support oxidative phosphorylation in azotobacter[2] may partly explain the apparently greater efficiency of nitrogenase in azotobacter compared with *C. pasteurianum*[13]; ATP-independent hydrogenase evolves H_2 during growth of *C. pasteurianum*. Thus, the evidence suggests that possessing hydrogenase improves the economy of N_2-fixing aerobes, so the correlation between hydrogenase and nitrogenase[1] now has a rational basis.

We wish to thank Professor J. R. Postgate and Dr Herman Bothe for useful discussions and Mrs Frances Campbell for technical assistance.

LINDA A. SMITH
SUSAN HILL
M. G. YATES

A. R. C. Unit of Nitrogen Fixation,
The University of Sussex,
Falmer, Brighton,
Sussex BN1 9QJ, UK

Received March 9; accepted May 27, 1976.

[1] Wilson, P. W., *Encyclopedia of Plant Physiology* (edit. by Ruthland, W.), 9–47 (Springer–Verlag, Berlin, 1958).
[2] Hyndman, L. A., Burris, R. H., and Wilson, P. W., *J. Bact.*, **65**, 522–531 (1953).
[3] Dixon, R. O. D., *Arch. Mikrobiol.*, **85**, 193–201 (1972).
[4] Mortenson, L. E., and Chen, J.-S., *Microbial Iron Metabolism* (edit. by Neilands, J. B.), 231–282 (Academic, New York, 1974).
[5] Postgate, J. R., *The Chemistry and Biochemistry of Nitrogen Fixation* (edit. by Postgate, J. R.), 161–190 (Plenum, London, 1971).
[6] Brotonegoro, S., thesis/meded, Landbouwhogeschool Wagenngen (1974).
[7] Yates, M. G., and Planqué, K., *Eur. J. Biochem.*, **60**, 467–476 (1975).
[8] Eady, R. R., Smith, B. E., Cook, K. A., and Postgate, J. R., *Biochem. J.*, **128**, 655–675 (1972).
[9] Hill, S., *J. gen. Microbiol.*, **93**, 335–345 (1976).
[10] Campbell, F. O., and Yates, M. G., *FEBS Lett.*, **37**, 203–206 (1973).
[11] Peck, H. D., and Gest, H., *J. Bact.*, **71**, 70–80 (1956).
[12] Bulen, W. A., LeComte, J. R., Burns, R. C., and Hinkson, J., *Non Heme Iron Proteins* (edit. by San Pietro, A.), 261–275 (Antioch Press, Yellow Springs, 1965).
[13] Hill, S., Drozd, J. W., and Postgate, J. R., *J. appl. Chem. Biotechnol.*, **22**, 541–558 (1972).

Linear relationship between phytochrome photoequilibrium and growth in plants under simulated natural radiation

DEVELOPMENT in higher plants is highly responsive to environmental factors, the most important, in natural conditions, being light. Perception of light quality involves at least two photoreceptors, of which phytochrome is the better understood[1]. Most work on its function, however, has been carried out with etiolated (that is dark grown) seedlings irradiated from relatively narrow wave band sources. There is no direct evidence on the function of phytochrome in the natural environment[2]. Using simulated natural radiation conditions, we have now found evidence to support the hypothesis that phytochrome acts to detect mutual shading through the changed quality of natural radiation, and to redirect development appropriately[3].

Phytochrome is a photochromic protein existing in two interconvertible forms; P_r, which absorbs maximally at 660 nm; and P_{fr}, absorbing maximally at 730 nm (ref. 1). Thus, in continuous irradiation with broad-band sources absorbed by both P_r and P_{fr}, a photodynamic equilibrium is achieved characterised by the steady-state proportions of P_r and P_{fr}. This photoequilibrium is usually determined as P_{fr}/P_{total} and is known as φ. We have recently shown that φ can be quantitatively related to the ratios of the quantum flux densities at 660 nm and 730 nm (known as ξ) using a range of natural and artificial radiation sources[3]. In addition, certain parameters of development were shown to be related, through φ, to ξ, in a predictable, although non-quantitative, manner[3]. We report here a direct linear relationship between a growth parameter (the logarithmic stem extension rate) and apparent phytochrome photoequilibrium (φ) as estimated from quantum flux density ratios (ξ).

In this work seeds of fat hen (*Chenopodium album* L.), a common weed of arable land, were collected from the field, germinated and grown to the third leaf stage in a controlled environment room (16 h, 20 °C day: 8 h, 15 °C night) under radiation from a bank of 80-W Warm White fluorescent tubes providing a quantum flux density of 180 μE m^{-2} s^{-1} of photosynthetically active radiation (PAR) as defined by McCree[4]. Seedlings selected for uniformity were then transferred to the light treatment chambers using the photo- and thermoperiod conditions described above.

The experimental light sources were designed to provide equivalent amounts of PAR using 6×2 foot 40-W Colour Matching 55 fluorescent tubes. To vary the phytochrome photoequilibrium while maintaining constant PAR, additional far red (>660 nm) radiation was provided from 60-W unfiltered tungsten bulbs, or from a bank of water-cooled 150-W clear tungsten filament lamps filtered through a red and a green sheet of Perspex. The PAR in all treatments was adjusted to 100 μE m^{-2} s^{-1}. The added far red radiation allowed a range of estimated phytochrome photoequilibria between $\varphi = 0.71$ and $\varphi = 0.29$. The spectral energy distribution of each radiation source was measured and the apparent phytochrome photoequilibria estimated from the ξ values as described previously[3].

Figure 1 shows the appearance of two originally identical seedlings after treatment with radiation of equal photosynthetic effectiveness but different ξ values for 21 d. The lower phytochrome photoequilibrium established in the plants given added far red radiation has led to extreme modification of developmental pattern. In particular, stem elongation, branching, flowering, and leaf pigmentation are modified.

Fig. 1 Photograph of *Chenopodium album* seedlings grown for 21 d under radiation sources providing equal quantum flux densities in the photosynthetically active regions (100 μE m^{-2} s^{-1}) but with different amounts of far red radiation establishing different phytochrome photoequilibria. The estimated photoequilibria under the two sources are *a*, 0.71; *b*, 0.38.

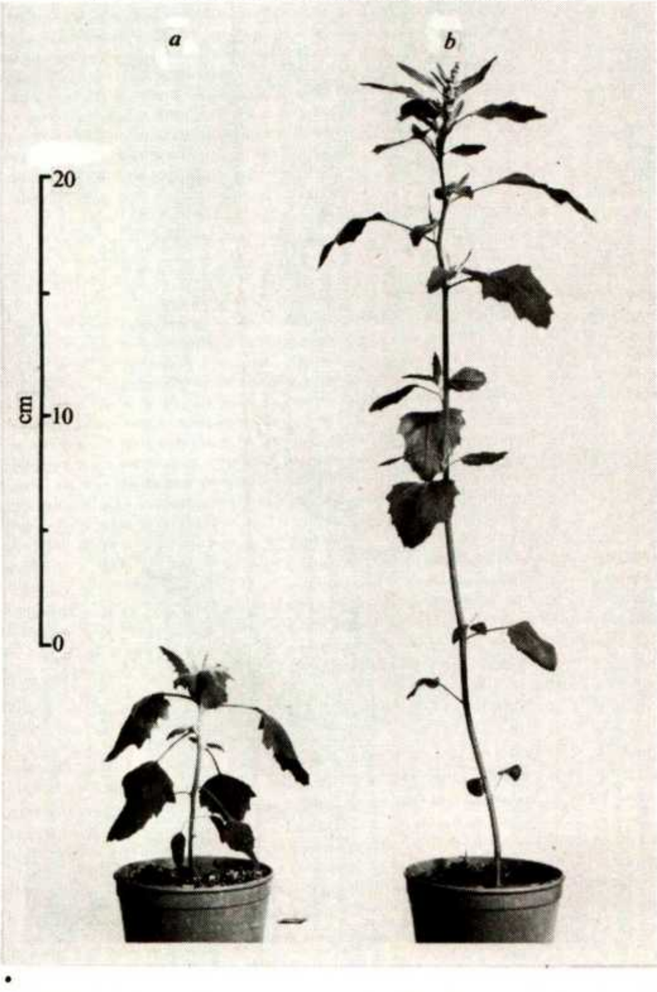

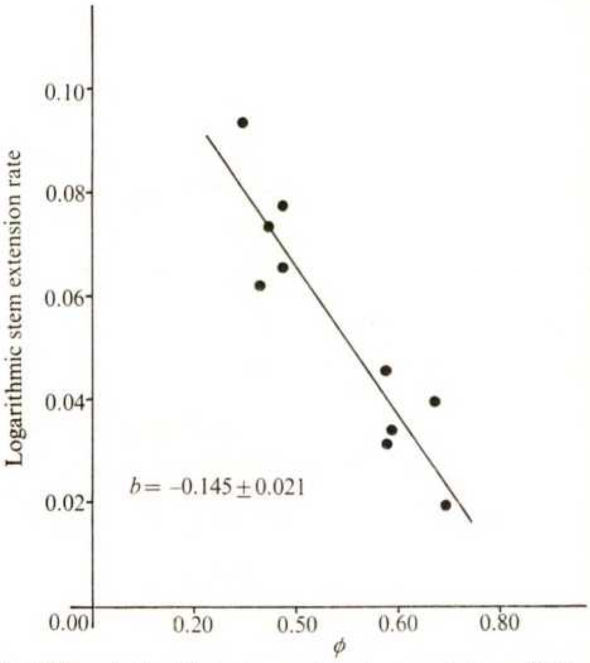

Fig. 2 The relationship between phytochrome photoequilibrium (φ) and the logarithmic rate constant of stem extension for *Chenopodium album* seedlings growing under equal amounts of PAR. The line has been fitted by regression analysis, and the correlation coefficient is −0.924.

During the early period of growth, *Chenopodium album* seedlings grow exponentially with respect to overall height. When plants were grown under radiation sources providing equivalent PAR but different phytochrome photoequilibria, the logarithmic rate constants of stem elongation were found to be directly, and linearly, related to the estimated phytochrome photoequilibria (Fig. 2). Other parameters of development are also related to φ, but the linear relationship with the logarithmic stem extension rate is the most clearcut response noted. Many workers have previously shown that a modification of φ at the end of the daily light period has substantial effects on growth[5-10]. In more detailed experiments to be published elsewhere, we have demonstrated that the phytochrome photoequilibrium established during the light period is responsible for at least 80% of the change observed in stem extension rate, and end-of-day effects, although important, are quantitatively much smaller, although again linearly related to φ, as first shown by Vince-Prue[8]. We have also shown that the linear relationship presented in Fig. 2 is not merely a quirk of *Chenopodium album*; it has been seen in other species including the stinging nettle (*Urtica dioica*) and rose-bay willow-herb (*Chamaenerion angustifolium*). A survey of sun- and shade-plants is being undertaken to search for systematic variation in responsivity to light quality.

These data strongly support the hypothesis we previously proposed that the principal function of phytochrome is to detect the quality of light in the red and far red wavelength regions, and thus to perceive mutual shading[2,3]. For plants adapted to an herbaceous (that is non-phanerophytic) habit, competition for light is extremely important, and a sensitive mechanism for response to mutual shading is clearly of great adaptive value.

The authors are grateful to the Natural Environment Research Council for financial support of this work.

DAVID C. MORGAN
HARRY SMITH

Department of Physiology and Environmental Studies,
University of Nottingham School of Agriculture,
Sutton Bonington,
Loughborough LE12 5RD, UK

Received April 20; accepted May 25, 1976.

[1] Smith, H., *Phytochrome and Photomorphogenesis* (McGraw-Hill, Maidenhead, 1975).
[2] Smith, H., in *Seed Ecology* (edit. by Heydecker, W.), 219–231 (Butterworths, London, 1973).
[3] Holmes, M. G., and Smith, H., *Nature*, **254**, 512–514 (1975).
[4] McCree, K. J., *Agric. Meteorol.*, **10**, 443–453 (1972).
[5] Downs, R. J., Hendricks, S. B., and Borthwick, H. A., *Bot. Gaz.*, **118**, 199–208 (1957).
[6] Kasperbauer, M. J., and Hiatt, A. J., *Tobacco Sci.*, **10**, 29–32 (1966).
[7] Tucker, D. J., and Mansfield, T. A., *Planta*, **102**, 140–151 (1972).
[8] Vince-Prue, D., *Annals. Acad. Brasil Ciencias*, **45** (Suplemento), 93–101 (1973).
[9] Lechnarny, A., and Jaques, R., *Physiol. Veg.*, **12**, 721–738 (1974).
[10] Sanchez, R. A., and Cogliatti, D., *Bot. Gaz.*, **136**, 281–285 (1975).

Hydromechanical adaptation in the solitary free-living coral *Fungia scutaria*

THE scleractinian coral *Fungia scutaria* produces a dense, diskoid skeleton that is adapted for stability and abrasion resistance in turbulent water. Water motion rights skeletons at velocities lower than needed to disturb upright corals. Flow of water over the coral is controlled largely by passive hydromechanical adaptations. Previous reports[1–3] suggest that muscular activity is the main mechanism enabling free-living solitary corals to follow their peculiar way of life. Our work indicates that passive hydromechanical adaptations can be a more important factor in shallow turbulent waters. Several species of free-living corals are known to migrate, avoid burial, and right themselves by action of their polyp[1,2] or by symbiotic activity of sipunculid worms[3]. Most other Indo-Pacific solitary corals such as *F. scutaria* are inactive, yet remain upright in turbulent waters. Dead skeletons of *F. scutaria* are generally found with the oral surface upward, and seem to resist erosion far better than other corals. We overturned dead skeletons in one area; they were righted during the next period of heavy waves, suggesting unique hydraulic and structural properties of the skeleton.

Fungia stability was tested on an intertidal bench subjected to wave-induced unidirectional flow of 30–50 cm s^{-1}. Occasional swells swept across the bench and accelerated flow. Between surges *Fungia* skeletons were set out, either upright or inverted. In the wake of the surge, the resting position of each skeleton was noted. Inverted skeletons were righted by single surges of 1–2 m s^{-1}. Overturned skeletons exposed to a single surge were righted 40 out of 50 times, whereas upright corals remained undisturbed in 49 out of 50 trials. The skeletons generally came to rest with their long axis parallel to the direction of current flow, reducing the cross-sectional area presented to the current and increasing stability.

About 70% of *Fungia* found on a reef flat in Kaneohe Bay, Hawaii, rested upright with their long axis aligned within 30° of the local set of storm waves. The hydraulic response of *Fungia* is similar to that of concavo-convex structures such as pelecypod valves in shallow marine environments[4,5]; in the case of *Fungia*, this response has adaptive significance.

Water flow over the coral surface was observed in a flume. Dye injected from a syringe was used to trace flow. In moving water, dye in contact with living or dead corals moves slowly towards the stomodaeum. The rough surface creates frictional drag and decreases water velocity at the boundary. For example, in a current of 30 cm s^{-1} (Fig. 1*d*) water moved at 0.3 cm s^{-1} on the downstream portion of the coral directly against the current and at 1 cm s^{-1} on the upstream portion of the disk. The radial exert septae have a major role in directing and reducing flow. Dead skeletons and living corals with contracted polyps direct flow into the stomodaeum (Fig. 1*d*); corals with expanded polyps or dead skeletons smoothed with cement (Fig. 1*e*) do not so direct the flow. In cross section *Fungia* resembles an airfoil, and a moving fluid induces a low pressure area over the stomodaeum. Reduction in current velocity at the coral surface permits flow into this area of low pressure and probably fascilitates ciliary control of the surface film[6] in all current conditions.

The ability of the living polyp to right the skeleton on various substrata and the role of burrowing crabs in the process were tested in continuous flow aquaria. Live corals and dead skeletons in a graded series of 10–100 g wet weight were placed upside down on the substrata (Table 1). Substrata used were sand, gravel and hard bottom. One experimental series included approximately 15 xanthid crabs (carapace width 3 cm). The other series excluded crabs. Although many of the live *Fungia* eventually righted themselves on the rubble substratum, the process took several days (compared with minutes for more active species[1,2]). Corals on sand and hard substratum did not right themselves. Crabs had a minor role in righting the corals, overturning two dead skeletons.

Ability to migrate to the surface was tested by burying ten living *Fungia* under 1 cm of sand. No coral reached the surface; all were dead at the end of 7 d. Strong currents and wave motion in the typical shallow water *F. scutaria* habitat causes erosion; the coral must avoid abrasion by moving rubble, overturning, and physical removal rather than *in situ* burial. Unlike its relatives which inhabit calm deep water (where sediments eventually come to rest), this species does not ordinarily encounter thick deposits of fine sediment.

Resistance to abrasion was tested for the four most abundant coral species in the area (Table 2). Live corals were tagged and the skeletal weight measured using the buoyant weighing technique[7]. The corals were placed in a cement mixer containing screened carbonate gravel of 2 cm diameter and flowing seawater. The drum of the mixer was then rotated 20 times in 1 min. The corals and abraded fragments were returned to a continuous flow aquarium and reweighed. The test fragmented the branched

Fig. 1 *F. scutaria* in unstable overturned position will begin rolling when subjected to strong current surge (*a*), presenting a larger cross section to water flow. This rights the coral (*b*, *c*) and leaves it in a stable position (*d*). Flow patterns over the surface of a living coral with a contracted polyp (*d*) are compared with that of the coral with an expanded polyp (*e*).

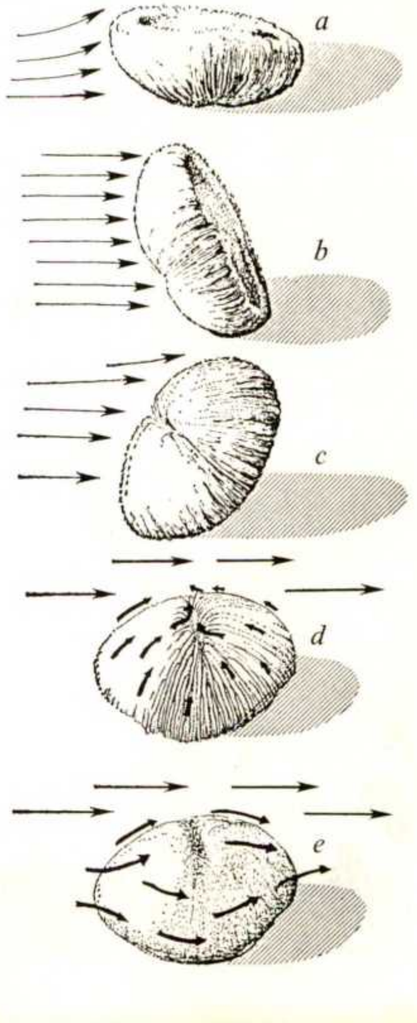

Table 1 Ability of *F. scutaria* to right themselves

	Position after 7 d			
	Live corals		Dead coral skeletons	
	Inverted	Upright	Inverted	Upright
Hard bottom with crabs	9	1	10	0
Hard bottom with crabs	9	1	10	0
Hard bottom without crabs	9	1	10	0
Hard bottom without crabs	10	0	10	0
Rubble with crabs	4	6	9	1
Rubble without crabs	3	7	10	0
Sand with crabs	10	0	9	1
Sand without crabs	10	0	10	0

colonial species and removed all tissue on exposed surfaces. *Fungia* remained intact and lost only a small amount of tissue and skeletal material on the septal margins and costal spines. The septocostal ornamentation fends off the abrasive rubble and protects exposed tissue.

Fungia lost only 1% of its skeleton compared with 40–80% loss for the other species (Table 2). Only the bases of the colonial species remained intact. Tissue regeneration in *Fungia* was complete in 5 d. Colonial corals and abraded fragments lost most of their tissues and died within a few days. *Porites* and *Montipora* eventually showed slight regeneration on the damaged bases, but approximately 90% of the original tissue area was killed.

Table 2 Abrasion resistance, density and cross sectional area/weight ratio of common Kaneohe Bay corals (five corals of each species)

Species	% Loss in abrasion test		Dry skeletal density (g cm^{-3})		Cross-sectional area/buoyant weight ratio (cm^2 g^{-1})	
	Mean	s.d	Mean	s.d.	Mean	s d.
F. scutaria	1.4	0.6	1.86	0.06	0.25	0.03
Montipora verrucosa	38.8	9.5	1.47	0.12	1.36	0.16
Porites compressa	47.4	17.1	1.53	0.06	0 59	0.12
Pocillopora damicornis	79.6	6.8	1.70	0 17	0.64	0.16

Fungia has the highest skeletal density of the species tested. It also shows a very low cross sectional area per unit buoyant weight, producing a stable low drag profile in moving water (Table 2). Specimens weighing as much as 3 kg have a centre of gravity within 2 cm of the substratum. Branched species of similar mass have a centre of gravity at least 5 cm above the substratum, leading to instability and a need for attachment. The high density of *Fungia* and its low surface-to-volume ratio[8] enhance abrasion resistance.

Thus, in addition to use of muscular activity, hydromechanical adaptation is a significant factor in many species of solitary free-living corals. *F. scutaria* is typical of solitary shallow water fungiids which have evolved hydrodynamically stable abrasion resistant skeletons. These corals passively use the surrounding energy field of moving water to their advantage, eliminating the need for a strong, muscular, active polyp.

This work was supported in part by the USNSF.

P. L. JOKIEL

Hawaii, 96744 Institute of Marine Biology,
Kaneohe, Hawaii

H. P. COWDIN

University of Santa Clara,
Santa Clara, California

Received March 23; accepted May 11, 1976

[1] Abe, N., *Palao. Trop. Biol. Stud*, 1, 671–694 (1939)
[2] Hubbard, J. A. E. B , *Nature*, 236, 457–459 (1972).
[3] Goreau, T. F., and Yonge, C M , *Nature*, 217, 421–423 (1968)
[4] Nagle, J. S., *J. Sediment Petrol.*, 37, 1124–1138 (1967)
[5] Menard, H. W., and Boucot, A. J , *Am. J. Sci*, 249, 131–151 (1951).
[6] Abe, N , *Palao. Trop. Biol. Sta Stud.*, 1, 469–521 (1938).
[7] Jokiel, P. L , Maragos, J. E., and Franzisket, L., *Handbook of Coral Reef Research Methods* (edit by Stoddart, D. R , and Johannes, R E) (UNESCO Monographs on Oceanographic Methodology, in the press).
[8] Driscoll, E. G , *J. Sedim. Petrol*, 37, 1117–1123 (1967).

Reshedding of *Toxoplasma* oocysts by chronically infected cats

INFECTION with *Toxoplasma gondii* is prevalent in man and animals. It can be acquired congenitally by the foetus from an infected mother[1], but also throughout life by eating undercooked meat[2] or by contact with contaminated faeces of cats[3]. All forms of *Toxoplasma* lose their infectivity quickly when exposed to the environment, with the exception of oocysts shed in feline faeces. These are remarkably resistant to ordinary environmental influences and can survive in most soil for several months[4]. In the acute phase of infection cats may shed several million oocysts in 1–2 weeks. It has been assumed that after the acute phase, chronically infected cats are safe as pets[5] since they have acquired immunity and oocysts seldom pass in the faeces[6–8]. I report here the reshedding of *T. gondii* oocysts by chronically infected cats in the absence of exogenous reinfection.

Twelve cats (four litters) were raised by their mothers from birth in my laboratory. Daily faecal examinations from birth did not reveal coccidian oocysts. Cats were weaned and bled for antibody determination at 83–106 d of age. Antibody to *Toxoplasma* was not detected in the sera of weaned cats by the Sabin–Feldman dye test. After weaning, all 12 cats were housed individually in stainless steel cages. Ten cats (nos 3–12) were fed 10[illegible] cysts of the M-7741 strain of *T. gondii* on day 0. Cats 1 and 2 were not fed *Toxoplasma* and served as controls. The faeces of all cats were examined daily for coccidian oocysts[9]. All 10 inoculated cats shed millions of *T. gondii* oocysts between 4 and 20 d after infection with *Toxoplasma* (Table 1). One cat (no. 7) reshed oocysts on day 28 after infection (Table 1). Three littermate cats (nos 9, 10, 12) spontaneously shed *Isospora felis* oocysts (Table 1). The remaining cats did not shed *I. felis* oocysts. The source of *I. felis* infection remained unknown.

To investigate interrelationships between *T. gondii* and other feline coccidia the animals were divided on day 30 after infection with *Toxoplasma* into two groups of six (*A* and *B*). Cats in group *A* (nos 1, 4, 6, 8, 10 and 11) were fed 10^4 sporulated oocysts of *I. rivolta* on day 30 after infection with *Toxoplasma* and 10^4 *I. felis* 13 d later. The effect of superinfection with *I. felis* and *I. rivolta* on established *Toxoplasma* infection seemed of particular significance in the light of Chessum's[10] report that a cat infected with *T. gondii* for 3 months started reshedding *Toxoplasma* oocysts 10 d after it was fed *I. felis* oocysts. *I. felis* and *I. rivolta* infections are asymptomatic in cats[11].

Both *I. rivolta* and *I. felis* caused patent infections in the inoculated cats. *I. rivolta* oocysts were shed between 6 and 12 d after *I. rivolta* was fed to the cats and *I. felis* were shed between 8 and 25 d after *I. felis* was fed to them. The cats in group *B* did not receive *I. felis* or *I. rivolta* and did not shed these organisms during this period. Four of five *Toxoplasma*-infected cats in group *A* reshed *T. gondii* oocysts beginning on day 10 after feeding with *I. felis* (or day 53 after infection with *Toxoplasma*); none reshed *I. rivolta*. Only one cat (no. 9) from group *B* reshed *T. gondii* oocysts during this period (Table 1).

On day 61 after infection with *Toxoplasma* cats in group *B* (nos 2, 3, 5, 7, 9 and 12) were fed 10^5 *I. felis* oocysts. All five *Toxoplasma*-infected cats (nos 3, 5, 7, 9 and 12) reshed *T. gondii* oocysts starting 9–14 d after feeding *I. felis* (Table 1). Cats 9 and 12 that were spontaneously infected with *I. felis* shed fewer *Toxoplasma* oocysts than did cats 3, 5 and 7 that were not previously infected with *I. felis*.

Overall, 9 of 10 cats reshed *Toxoplasma* oocysts. The reshed oocysts were identified as *T. gondii* by mouse to mouse passage.

Table 1 Shedding of *Toxoplasma* oocysts by cats with or without *I. rivolta* and *I felis* infection

Cat no.	Group	Primary Age of cats (d)	*Toxoplasma* infection Days oocysts shed	*Toxoplasma* infection No. of oocysts shed	*I. rivolta* fed PTID 30	*I. felis* fed PTID 43	Reshedding of *Toxoplasma* oocysts PTID oocysts shed	Reshedding of *Toxoplasma* oocysts No. of oocysts shed	*I. felis* fed PTID 61	Reshedding of *Toxoplasma* oocysts PTID oocysts shed	Reshedding of *Toxoplasma* oocysts oocysts shed
1*	A	89	None		Yes	Yes	None		No	None	
2*	B	89	None		No	No	None		Yes	None	
3	B	99	5–18	$10^{8\ 19}$	No	No	None		Yes	72–84	$10^{7\ 22}$
4	A	99	4–17	$10^{7\ 38}$	Yes	Yes	53–68	$10^{6.57}$	No	None	
5	B	99	5–18	$10^{7\ 27}$	No	No	None		Yes	70–85	$10^{7\ 17}$
6	A	106	4–15	$10^{7\ 50}$	Yes	Yes	53–63	$10^{6\ 24}$	No	None	
7	B	106	5–16	$10^{7.86}$	No	No	28	10^3‡	Yes	70–75	$10^{6\ 69}$
8	A	106	5–20	$10^{8.13}$	Yes	Yes	53–65	$10^{6.34}$	No	None	
9†	B	83	4–11	$10^{7\ 14}$	No	No	31-33,50	10^4‡	Yes	75–76	10^4‡
10†	A	83	5–16	$10^{8\ 13}$	Yes	Yes	None		No	None	
11	A	83	4–14	$10^{7.43}$	Yes	Yes	53–64	$10^{6\ 17}$	No	None	
12†	B	83	4–15	$10^{7\ 15}$	No	No	None		Yes	72–77	$10^{5\ 21}$

PTID, post-*Toxoplasma* infection day All cats except nos. 1 and 2 were fed 10^5 cysts of the M-7741 strain of *T. gondii* on day 0. Faeces of cats in group *A* were examined for 1–74 PTID and of group *B* for 1–85 PTID. Littermates are bracketed together.

*Cats 1 and 2 remained free of *Toxoplasma* infection throughout the experiment.

†Spontaneously infected with *I. felis* (cat 9 shed *I. felis* on days 2, 3; cat 10 shed 25–34, cat 12 shed 2–4, 9–20 PTID).

‡Estimated number of oocysts in daily sample. Only one or few oocysts seen in faecal-float preparation.

Reshedding of *T. gondii* oocysts by 9 of 10 cats within a short time (9–14 d) after feeding *I. felis* suggests a reactivation of latent *Toxoplasma* infection, probably by interfering with immunity to toxoplasmosis in the feline intestine.

Between 20 and 64% of cats in several surveys contained antibody to *T. gondii*[12], indicative of exposure to the organism. Many of these cats are presumably permanent carriers of *Toxoplasma*. As *I. felis* is also a common parasite of cats the present findings may have a public health significance, especially in homes with pregnant women. It is sound advice for pregnant women to handle cat faeces with care irrespective of the *Toxoplasma* infection status of the cat[5].

This work was supported by a research grant from Central Ohio Heart Chapter.

J. P. Dubey

Department of Veterinary Pathobiology,
College of Veterinary Medicine,
Ohio State University,
1925 Coffey Road, Columbus,
Ohio 43210

Received April 20; accepted May 20, 1976.

[1] Wolf, A., and Cowen, D., *Bull. neurol Inst. N.Y*, **6**, 306–335 (1937).
[2] Desmonts, G., *et al*, *Rev. F. Etudes clin Biol*, **10**, 952–958 (1965).
[3] Hutchison, W M, *Nature*, **206**, 961–962 (1965).
[4] Dubey, J P., Miller, N L., and Frenkel, J K., *J Parasitol*, **56**, 447–457 (1970).
[5] Frenkel, J. K., and Dubey, J P., *J infect Dis*, **126**, 664–673 (1972).
[6] Sheffield, H G, and Melton, M. L., *Proc. third int Cong Parasitol.*, **1**, 106–107 (1974).
[7] Overdulve, J. P., *Proc. third int Cong. Parasitol.*, **1**, 302–303 (1974)
[8] Dubey, J P, and Frenkel, J. K., *Vet Path.*, **11**, 350–379 (1974).
[9] Dubey, J. P., *J Am vet. med Ass.*, **162**, 873–877 (1973)
[10] Chessum, B. S., *Br. vet. J*, **128**, 33–36 (1972)
[11] Dubey, J P., and Streitel, R H., *Br. vet J*, **132** (in the press).
[12] Dubey, J. P., *Vet. Bull*, **38**, 495–499.

Inheritance of susceptibility to *Trypanosoma cruzi* infection in *Rhodnius prolixus*

MILLIONS of cases of Chagas' disease exist in Central and South America[1]. Apart from being virtually incurable, a major problem in this disease is symptomless carriers harbour trypanosomes all their lives but it is often difficult to demonstrate the parasite[2]. At present, the simplest and most sensitive method of diagnosis[3] is to feed uninfected triatomine bugs on the suspected case and subsequently to examine a faecal sample from the bug for the presence of trypanosomes There is, however, great variation both within and between species of Triatominae, in their susceptibility to infection with *Trypanosoma cruzi* (see, for example, refs 4 and 5), and though a genetic basis for this variation in susceptibility has been suggested[4], it has not been verified. Obviously, the production of a highly susceptible strain of triatomine bug that would provide a quick and accurate diagnosis of chronic Chagas' disease would be a distinct advantage. I report here on the selection of both susceptible and refractory lines of *Rhodnius prolixus*, and the results of this selection programme are related to the genetic control of susceptibility to infection with *T. cruzi*.

Two strains of *T.cruzi* were chosen for their differing characteristics. The Peru strain was originally isolated in 1963 and after passage in mice was stabilated by cryopreservation[6]. This highly virulent strain has a prepatent period of 8–14 d in mice, and is lethal at 25–30 d following inoculation of more than 100 organisms[7]. In contrast, strain 7, isolated in Brazil in 1965 and stabilated after passage in mice, is of low virulence. This strain also has a pre-patent period of 8 d, but, unlike the Peru strain, parasitaemia declines about 30 d after inoculation, and the mice generally recover.

To study the effect of selection on susceptibility in *R.prolixus* over successive generations, a standard system was used to infect the bugs and, later, to measure the infection. TO mice were first used to provide a non-infecting feed, given 28 d before the infecting blood meal. Six- to eight-week-old male mice of the same strain were then infected with one or other strain of *T.cruzi* and used to feed the bugs which had moulted to fifth instar larvae. Feeding took place either 14 d after infection of the mice with the virulent Peru strain or 21 d after infection with the less virulent *T.cruzi* strain 7. In both cases the mice were checked for patent parasitaemia before feeding commenced. Bugs were kept individually in glass tubes and maintained in incubators at 28 °C and 70% relative humidity. Thirty five days after infection, adult bugs were again fed on clean mice, and faeces produced by the bugs within 1 h of feeding were collected in 0.2 ml Hanks solution. Bugs which did not feed were removed from the experiment. The number of trypanosomes excreted in a 20 μl sample of the mixed faecal–Hanks suspension was counted by systematically scanning 100 fields (×450). In the absence of detectable parasites, the bug was given a further clean feed 14 d later, and the second faecal sample was examined. If this was again negative, the remaining faecal suspension was injected intraperitoneally into a non-infected mouse, and blood samples examined 14 and 21 d later.

Where trypanosomes were seen at the first examination of faeces, the score represented the number counted in 100 fields If a bug showed no evidence of infection on all tests it was scored as zero, whereas if positive at either the second (faecal) or third (blood) test it was assigned an

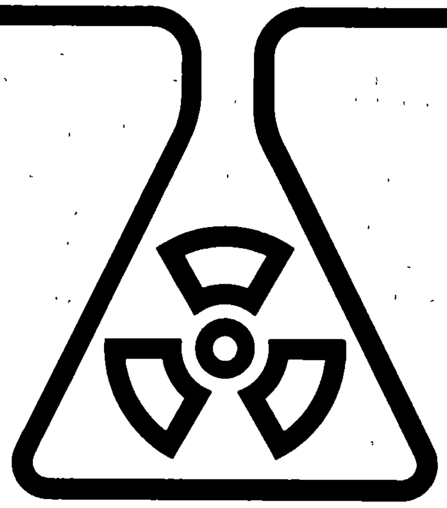

Of interest in neurochemical studies

L-2, 4-Diamino [4(n)-H^3] butyric acid 5-15Ci/mmol	TRK 504
[1-^{3}H]Taurine 5-15Ci/mmol	TRK 509
[^{35}S]Taurine 2-40mCi/mmol	SJ 42
ß-[3-^{14}C]Alanine 5-15mCi/mmol	CFA 568
ß-[3-^{3}H]Alanine 25-50Ci/mmol	TRK 512
4-Amino-*n*-[U-^{14}C]butyric acid (GABA) > 150mCi/mmol	CFB 151
4-Amino-*n*-[G-^{3}H]butyric acid (GABA) > 3Ci/mmol	TRK 468
2-Deoxy-D-[1-^{14}C]glucose > 50mCi/mmol	CFA 562
2-Deoxy-D-[1-H^3]glucose 5-25 Ci/mmol	TRK 383

Please enquire for further details

The Radiochemical Centre Amersham

The Radiochemical Centre Limited, Amersham, England.
Tel: Little Chalfont (024 04) 4444
In the Americas Amersham/Searle Corp, Illinois 60005
Tel 312-593-6300
In W Germany Amersham Buchler GmbH & Co, KG, Braunschweig
Tel 05307-4693-97

0795

Circle No. 06 on Reader Enquiry Form.

Galaxy Formation
John Gribbin

A personal view of galaxy formation – a subject which holds a central place in modern astrophysics. The book reflects the author's own interests in this field, and thus offers a new and different perspective to a fascinating topic. Formal mathematics is kept to a minimum and the general level of the text makes it suitable for the second year physics students at university.

Contents: Stars and Galaxies-Cosmology · The Expanding Universe – The Traditional Approach: Turbulence and Gravitational Instability – Layzer's Gravitational Clustering Hypothesis – Ambartsumian's Fragmentation Hypothesis – Continual Creation – Newtonian Cosmology and Jean's Criterion – The Retarded Core Hypothesis – The Growth of Irregularities in an Expanding Universe – The Evolution of Galaxies – Our Galaxy – The Present Balance and Future Prospects.

May 1976 h/c £5.95, p/b £2.95 96pp
h/c 333 19367 9, p/b 333 19512 4

For further details, please write to Anne Calcott (N), The Macmillan Press, Little Essex Street, London WC2R 3LF.

MACMILLAN PRESS

14 04 76

MEASURING SOLAR RADIATION ?

Then our range of instruments will interest you.

S.R.I.3	Solarimeter.
S.R.I.3A	Actinometer.
S.R.I.11	Pygeometer (long wave).
S.R.I.4	Nett Radiometer.
S.R.I.4U	Underwater Nett Radiometer.
S.R.I.5	Solari-Albedometer.
S.R.I.6	Reversing Albedometer.
S.R.I.7	Miniature Nett Radiometer.
S.R.I.12	Thermo Electric Flow Probe for low flows.
S.R.I.9	Soil Heat Flux Plate.

Pre-calibrated elements, and sensors available. Maintenance Service by air mail parts exchange.

We invite your enquiries.

SOLAR RADIATION INSTRUMENTS
21 ROSE STREET, ALTONA, VICTORIA
AUSTRALIA . . . 3018

Circle No. 07 on Reader Enquiry Form.

We're old hands at new labelled compounds

We make about 70 new labelled compounds a year—covering all aspects of research. It's a long-standing, but very essential, development programme. We rely on our customers, our technical representatives and our own scientists, to tell us which compounds are needed for new scientific investigations.

Our current catalogue lists our labelled compounds but goes to press before new products are in production. We try to let customers know what's new—by advertising, mailing and representative calls. But if you still haven't heard the news, please write or 'phone for our new catalogue supplement. You may want to discuss your own ideas on new labelled compounds, and we'll be very happy to consider them. Meanwhile, we'd like you to consider ours.

The Radiochemical Centre
Amersham

The Radiochemical Centre Limited, Amersham, England Tel. 024-04 444
In the Americas Amersham/Searle Corp Illinois 60005 Tel 312-593-6300
In W Germany Amersham Buchler GmbH & Co., KG, Braunschweig Tel 05307-4693-97.

Circle No. 05 on Reader Enquiry Form.

arbitrary score of 1. In all, 1,725 bugs were reared, given an infecting feed, and scored in this way.

Selection was subsequently made from the two parental populations of bugs on the basis of individual faecal trypanosome scores. A single-pair full-sib mating system was followed for both groups of bugs, resulting in 19 F_2 families in the Peru strain group, while in the strain 7 group selection was carried one generation further to produce 17 F_3 families.

Results showed that selection did not significantly increase the proportion of refractory (score zero) bugs in lines selected for refractoriness. This suggests that refractoriness to infection with *T.cruzi* is not controlled by alleles at a single locus in *R prolixus*. By contrast, a quantitative analysis of faecal scores (transformed to a log $(n+1)$ scale), revealed that the intensity of infection sustained by individual bugs is a heritable characteristic. First, significant difference ($P<0.001$) were found between bugs of the same generation infected with the two different strains of *T.cruzi* Bugs fed on strain 7 infected mice were found to have a mean faecal score almost twice as high as that of bugs infected with the more virulent Peru strain. Clearly, strain differences affect the intensity of infection of individual bugs as well as affecting susceptibility rates[4,8] (that is, proportions of infected bugs in a population).

Further analysis of F_1 and F_2 families of *R.prolixus* infected with different strains of trypanosome showed significant differences in faecal scores between sexes ($P<0$ 001), when tested against the considerable variation between families. The same was true of F_3 families infected with strain 7. Control weighing experiments to determine any possible effect of variation in the size of blood meal or faecal sample were negative. There was no significant difference in blood-meal size between male and female fifth instar larvae, although it was interesting to note that adult females took significantly larger blood meals than males and also excreted a significantly greater proportion of their meals within 1 h of feeding. Thus, it might be anticipated that adult females would have higher scores than males, but that is not the case In fact, male scores were significantly greater than female scores in all generations tested. Miles *et al.* failed to detect such a sex-difference, but their conclusion was based on tests with a small number of bugs. Significant differences in faecal scores were also found between families of all generations infected with either strain of trypanosome, reflecting a resemblance between the intensity of infection of related bugs—one of the basic characteristics of metric traits[9].

Fig. 1 Response to two-way selection for intensity of infection with *T. cruzi* strain 7 in *R prolixus*. Cumulated selection differentials for each generation (weighted according to the number of progeny scored) are plotted against the response to selection derived from faecal scores transformed to log $(n+1)$ scale, sexes averaged Regressions, calculated from 4 high and 5 low selection lines, show the realised heritability to be 3 6 ± 1.1% for increases in intensity of infection and, for reductions in intensity of infection, 7.3 ± 0.9%. This asymmetric response is a common feature of two-way selection programmes[14] ●, F_1 family means; ▲, F_2 family means; ■, F_3 family means. *A*, $b = 0.0368\pm0\ 0115$, *B*, $b = -0.0731\pm0.0091$.

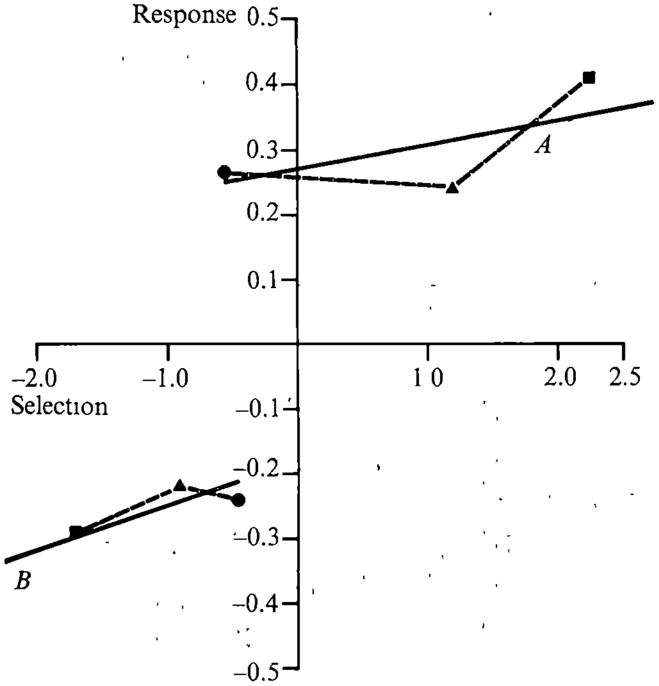

Figure 1 shows that selection for high and low levels of intensity of infection was successful. Analysis of F_3 family scores showed that differences between the selection lines were highly significant for both sexes ($P<0.001$) when tested against the variation between families within lines. The realised heritability of intensity of infection in *R.prolixus* was calculated from the regression of response (r) on selection differential (s)[10]. The regressions of both selection lines being highly significant ($P<0$ 001), the divergence of the two slopes provided an estimate of 5.5% for the heritability of this character. This low value relates to this laboratory colony and could differ for a natural population[9].

Knowledge of genetic mechanisms controlling the susceptibility of insect vectors to infection has so far been limited to mosquitoes and their malarial and filarial parasites, where to date only major gene control mechanisms have been demonstrated[11,12]. There have been attempts to quantify mosquito susceptibility to *Plasmodium gallinaceum* by counting oocysts[13], but significant parent–offspring regressions could not be shown. The present work has clearly shown that intensity of infection with *T.cruzi* in *R prolixus* is a metric character of low heritability, which is sex linked or at least sex limited. For the purposes of aiding the diagnosis of chronic Chagas' disease, it would be desirable to breed a colony of bugs that are highly susceptible to the multiplication of the few trypanosomes ingested from such patients. The present results indicate that using only male bugs of a susceptible stock for xenodiagnosis should enhance the sensitivity of this diagnostic test for chronic Chagas' disease.

I thank C. Constantinou for assistance, Dr D. S. Ketteridge for supply of trypanosomes and Professor D. S. Bertram for his encouragement. This work was financed by the Overseas Development Ministry.

I. Maudlin*

Department of Entomology,
London School of Hygiene and Tropical Medicine,
Keppel Street,
London WC1E 7HT, UK

Received April 14, accepted May 18, 1976

*Present address Clinical Research Centre, Watford Road, Harrow, Middlesex HA1 3UJ, UK.

[1] Handler, B , *Nature*, 259, 357 (1976)
[2] Marsden, P D , Mott, K. E , and Prata, A , *Gaz med Bahia* , 69, 65–69 (1969)
[3] *Bull Wld Hlth Org* , 50, 459–479 (1974).
[4] Phillips, N. R , and Bertram, D S , *J. Med Ent* , 4, 168–174 (1967)
[5] Miles, M. A , Patterson, J W , Marsden, P D , and Minter, D. M , *Trans R Soc. trop Med Hyg* , 69, 377–382 (1975)
[6] Lumsden, W H R , Herbert, W J , and McNeillage, G J C , *Techniques with Trypanosomes* (Churchill Livingstone, Edinburgh, 1973)
[7] Mshelbwala, A S , and Ormerod, W E , *J gen Microbiol* , 75, 339–350 (1973).
[8] Sherlock, I A , and Almeida, S P , *Revta Soc Bras. Med Trop.*, 7, 87–98 (1973)
[9] Falconer, D. S , *Introduction to Quantitative Genetics* (Oliver and Boyd, Edinburgh, 1967).
[10] Falconer, D S , *Cold Spring Harb Symp quant Biol* , 20, 178–196 (1955)
[11] Macdonald, W. W , in *Genetics of Insect Vectors of Disease* (edit by Wright, J. W , and Pal, R), (Elsevier, Amsterdam, 1967)
[12] McGreevy, P. B , McClelland, G. A M , and Lavoipierre, M. M J , *Ann. trop Med Parasit.*, 68, 97–109 (1974)
[13] Hovanitz, W , *Am J Hyg.*, 45, 67–81 (1947).
[14] Falconer, D. S , *Int Union biol. Sci . Naples*, B15, 16–41 (1954)

Functional inactivation of suppressor T cells by heat-killed macrophages

We have shown that peritoneal exudate macrophages, killed by heating at 56 °C for 30 min, can markedly suppress the antibody response to heterologous erythrocytes in primary Mishell–Dutton cultures[1]. This heat treatment does not destroy the ability of the macrophages to form rosettes with sheep red blood cells (SRBCs) in the presence of cytophilic antibody, suggesting that some membrane surfaces remain undamaged. The heat treatment, however, does prevent the macrophages from excluding Trypan blue dye, indicating that the cells are no longer viable. Treatment of the macrophages at higher temperatures or with 0.1% glutaraldehyde destroys both their ability to form rosettes and to suppress Mishell–Dutton cultures. Macrophage membranes, semi-purified by separation on sucrose gradients, can act similarly—that is, suppress primary Mishell–Dutton cultures and form rosettes with SRBCs in the presence of cytophilic antibody (W.P. and R.K.G., unpublished). The heat-killed macrophages do not diminish the viability of the cell cultures even when they are maximally suppressive We have interpreted these results to indicate that the dead macrophages suppress the immune response in culture by absorbing out, and thus rendering inoperative, some factors which are necessary for the cell interactions which result in the generation of plaque-forming cells. This contention is supported by the ability of the heat-killed macrophages to absorb out the helper activity found in the supernatants of mixed lymphocyte reactions (W.P. and R.K.G., unpublished). We reasoned that, if macrophages could absorb interaction factors, they might be able to absorb suppressive factors if they were added to a culture in which suppression was occurring and thus augment the response of suppressed but not normal cultures.

We used a newly described *in vitro* technique to generate educated spleen cells with the capacity to specifically suppress the *in vitro* response to SRBCs (ref. 2). The suppression is mediated by T cells and is antigen-specific when less than 10^6 educated cells are added to spleen cell cultures. We cultured 10^7 BDF_1 spleen cells with 2×10^6 SRBCs according to the Mishell–Dutton technique. Four days later we retrieved the educated cells from culture and added different doses of them to new primary Mishell–Dutton cultures along with 2×10^6 SRBCs. Varying numbers of heat-killed macrophages were included in the second cultures which were incubated for a further 4 d before assay for plaque-forming cells. The results of one such experiment are presented in Fig. 1. The horizontal line represents the response of normal cultures without educated cells or macrophages. Addition of 10^5 educated cells to 10^7 normal spleen cells markedly suppressed the anti-SRBC response, whereas addition of 10^4 educated cells had no effect and served as a control for the effect of adding educated cells. The addition of 10^4 or 3×10^4 heat-killed macrophages to the suppressed cultures produced a moderate augmentation of the response, whereas it had no effect on the non-suppressed culture The addition of 6×10^4 or 10^5 macrophages to the suppressed cultures brought their response back to approximately normal levels Again this number of heat-killed macrophages had no effect on the non-suppressed response. Adding 3×10^5, 6×10^5 or 10^6 heat-killed macrophages suppressed the response in all cultures. Interestingly, increasing the macrophage dose beyond 3×10^5 or 6×10^5 cells did not increase the amount of suppression. This plateau effect is commonly seen (ref. 1 and W.P. and R.K.G., unpublished) and indicates that there is a base level of the immune response which the heat-killed macrophages cannot suppress; on the other hand, live macrophages can suppress the response to a 0 level

Thus, there seems to be a differential susceptibility of suppression and help to the effect of heat-killed macrophages. Low numbers of macrophages can preferentially abrogate suppression but cannot bring the response significantly higher than the normal response level. When the number of macrophages is high enough to suppress the control cultures, they also suppress the cultures which contain the suppressor cells, probably acting in the latter situation by interfering with help rather than by augmenting suppression. Whether these differential effects are due to different sensitivities of suppressor and helper factors, differences in their affinities for macrophage receptors or different numbers or types of receptors and/or macrophages is at present under investigation.

Since heat-killed peritoneal exudate macrophages do not augment primary Mishell–Dutton cultures at any dose, and can reverse suppression when known suppressor cells are added to the culture, as we have shown here, our results suggest that some mediators of suppression may have affinity for macrophage surfaces Heat-killed macrophages may prevent their interacting with their target cells by absorbing them from the culture. Of course, the vast body work of Feldmann[3] documenting the importance of the macrophage membrane as a site for lymphocyte interaction supports this contention.

Independent of the exact explanation for the phenomenon we have described, the results we have presented have practical as well as theoretical significance. They indicate that one can use this *in vitro* technique to determine whether a poor response is due to a lack of stimulation or to suppression. One can titrate in heat-killed macrophages and if these cells result in an increase of the response, one can be reasonably certain that the response of the test cells is due to alleviation of suppression. The heat-killed macrophages have no inherent augmentory capacity of their own. Note also that the failure of macrophages to augment a response cannot be taken as evidence that suppression is not present. We do not know whether, in other systems, one would find the differential susceptibility of suppression and help that we found in this system. We have found, however, that heat-killed macrophages can augment the generation of cytotoxic killer cells to syngeneic tumour

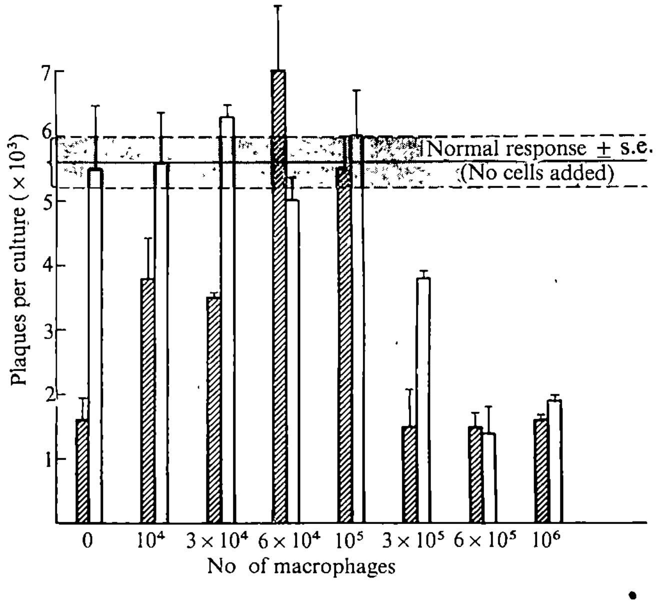

Fig. 1 Functional inactivation of suppressor cells by heat-killed macrophages. Educated cells were generated by culture of spleen cells *in vitro* with 2×10^6 SRBCs. The normal response to SRBCs of the assay cultures (horizontal line) was suppressed by 10^5 educated cells (hatched columns), whereas 10^4 educated cells (open columns) induced no suppression and served as the control. Increasing numbers of heat-killed macrophages were added to the suppressed or control cultures.

cells *in vitro* (C. Metzler, W.P. and R K.G., unpublished), suggesting that the generation of suppressor cells is one of the factors contributing to the difficulty in getting a good killer-cell response against tumour cells *in vitro*. In any case, the ability to use heat-killed macrophages in *in vitro* responses to document the presence of suppression in the cultures should be of help in dissecting out some of the complicated interactions between subpopulations of lymphocytes which control the immune response.

This work was supported by the NCI of the USPHS. D D.E. is a recipient of a postdoctoral fellowship from the NCI. W.P. was supported by a research grant from the WHO

RICHARD K. GERSHON
DIANE D. EARDLEY
WLODZIMIERZ PTAK*

Department of Pathology,
Yale University School of Medicine,
New Haven, Connecticut 06510

Received March 29, accepted April 27, 1976

* Present address · Department of Clinical and Experimental Immunology, School of Medicine, Cracow, Poland

[1] Ptak, W., and Gershon, R K, *J Immun*, 155, 1346–1350 (1975)
[2] Eardley, D D, and Gershon, R K, *J Immun* (in the press)
[3] Feldmann, M, *Transplant Rev*, 13, 3–34 (1972)

Onset of acetylcholine sensitivity and endplate activity in developing myotome muscles of *Xenopus*

THE distribution of acetylcholine receptors and the onset of functional innervation at the neuromuscular junction during development have been much investigated[1–3], as have the events during regeneration and reinnervation of muscle[4]. Although the first appearance of acetylcholine (ACh) sensitivity of the membrane has been charted in chick and mouse myoblasts differentiating in tissue culture[5], previous studies *in vivo* have either not tested for the initial appearance of ACh sensitivity[2], or found the muscle membrane to be already sensitive to externally applied ACh[1]. In the present study on *Xenopus* embryos we have followed the initial appearance of membrane depolarisation in response to applied ACh and the onset of functional innervation in differentiating myotome muscle *in vivo*.

Myotome formation from the presumptive mesoderm begins before the neural tube closes (stage 17)[6], and continues up to late swimming stages Figure 1 shows the arrangement of cells in the presumptive mesoderm and the fully formed myotomes described by Hamilton[7]; a new myotome is formed about every 20 min. The myotomes are innervated segmentally by cells in the ventrolateral part of the neural tube[7,8]. Innervation, like myotome formation, begins at the head end and proceeds tailwards. Flexions of the body first occurred between stages 21 (8 somites) and 24 (12–15 somites), the precise time varying between clutches of eggs.

Membrane potentials were recorded with microelectrodes filled with 0.8 M potassium citrate (resistance >100 M; tip potential < −8 mV). Embryos (stages 19 to 25) were pinned out in a small bath and superfused with Ringer solution (NaCl, 120 mM; KCl, 2.5 mM; $CaCl_2$, 2 mM; Tris, 2 mM; *p*H 7.4). The ectoderm was peeled away and the dermatome layer of the mesoderm left intact above the myotomes. The microelectrode was pushed through the dermatome into the muscle cells. Because cells in the myotome have membrane potentials 40 mV greater than those of the dermatome[10] and because the two cell layers are not electrically coupled to each other[10], the position of the microelectrode was never in doubt.

Figure 2 shows records taken in 1 of 37 experiments to test for acetylcholine sensitivity of the muscle membrane. The microelectrode was inserted while an embryo at stage 21 was superfused with Ringer solution. At 10-min intervals the bathing fluid was changed to Ringer containing 10^{-4} g ml^{-1} ACh, which should produce a maximal response; if no depolarisation had resulted after several minutes, Ringer solution was readmitted. Figure 2*a* illustrates the last test in which ACh was without effect, suggesting that the membrane did not yet contain functional ACh receptors. Figure 2*b* shows the prompt and rapid depolarisation of 44 mV produced by admission of ACh 9 min later. Subsequent tests gave depolarisations of similar time course and magnitude. The results of this and eight other experiments with test intervals of between 10 and 30 min suggest that ACh receptors become functional relatively quickly. On all occasions the first depolarisation produced by ACh was as great as that produced by subsequent tests, suggesting that the response is immediately established at its maximum level. In 23 other experiments ACh sensitivity was already present when testing began.

The depolarisation in response to bath-applied ACh was always relatively prompt and brought the membrane potential to between −12 and −5 mV, close to the value recorded in adult amphibian muscle, suggesting that the reversal potential, and therefore the underlying permeability changes, are the same as in adult muscle[11].

After the appearance of ACh receptors, random deflections of the membrane potential were recorded, indicating that spontaneous liberation of ACh from innervating motor nerves had begun. The interval between these two events was variable, ranging from 15 min to about 1 h; once endplate activity could be recorded, bath application of ACh always produced depolarisation. The initial potentials were small, possibly miniature endplate potentials produced by spontaneous release of ACh without electrical activity in the nerve. A period when extremely large spontaneous depolarisations (up to 60 mV) were recorded invariably followed. Figure 2*c* shows a pen record of such activity to-

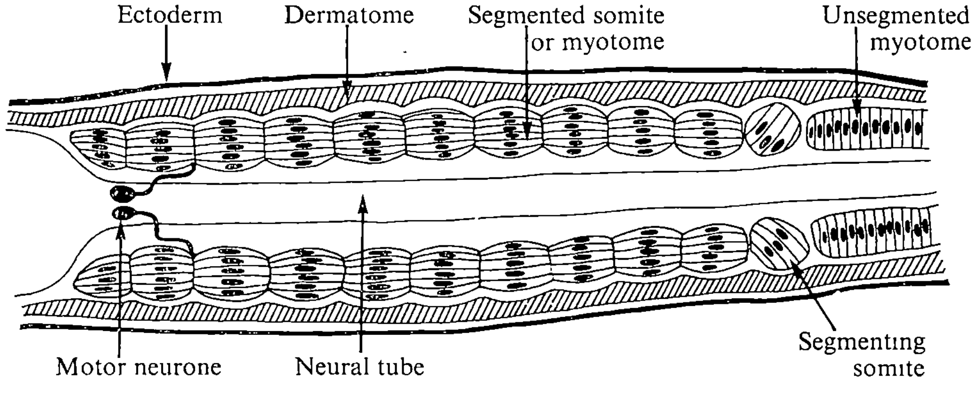

Fig. 1 Diagram of horizontal section through 10 somite *Xenopus* embryo to show arrangement of myotome cells

gether with the depolarisation produced by superfusion with ACh. A high gain oscilloscope record (Fig. 2*d*) shows these large depolarisations to take the form of summated endplate potentials. This activity seems most likely to be the consequence of action potentials in the motor nerve since very large miniature endplate potentials are not normally seen in developing neuromuscular junctions[1], and the input resistance of the electrically coupled muscle fibres is not particularly high. Both the spontaneous activity and the response to ACh were blocked by curare. Because electrical coupling between the muscle fibres is good[10], it was not possible to distinguish how many motor nerves contributed to the recorded spontaneous activity. Direct nerve stimulation is not possible in this preparation. Mn^{2+} abolished the endplate potentials, but not the response to perfusion with ACh. Figure 2*e* illustrates the ACh depolarisation in a preparation made silent by the addition of 2 mM Mn^{2+} to the bathing fluid.

Muscle action potentials were sometimes recorded before any visible endplate activity, although they usually appeared after spontaneous liberation of acetylcholine from the nerve had begun. In spite of high resting membrane potential, the earliest action potentials did not initiate muscle contraction, which was never seen before spontaneous endplate activity could be recorded. These findings make the suggestion that early flexions *Xenopus* embryos are myogenic in origin[9] extremely unlikely. It seems more probable that early movements are initiated by discharge from the motor nerves and achieved by transmission of the depolarisation from one myotome to the next along the low resistance intercellular pathway, as described by Blackshaw and Warner[10].

These experiments show that formation of the first functional neuromuscular junctions in *Xenopus* takes place between segmentation of the fourth and fifteenth myotome. The sequence of events is summarised in Fig. 3, where the appearance of functional ACh receptors has been put at stage 21½, with flexions beginning at stage 24 (about 2 h later). The onset of this sequence varied from clutch to clutch so that receptor appearance could occur as early as stage 19 with flexions following 2 h later at stage 21. On occasion however, the whole sequence from the appearance of ACh sensitivity was compressed into as little as 0.5 h. Thus both the timing of the initial insertion of ACh receptors and the length of time taken to establish functionally innervated, contracting muscle showed considerable variation from embryo to embryo. This implies that the development programme does not specify a precisely interrelated timing schedule for this sequence, suggesting that each event is to some extent independent.

Fig. 2 Membrane potential records taken during tests for acetylcholine sensitivity of myotome muscle membrane. *a*, Embryo stage 21 · 10^{-4} g ml^{-1} ACh has no effect on the resting potential of a myotome muscle cell. $E_m = -70$ mV *b*, Same embryo 9 min later: 10^{-4} g ml^{-1} ACh now produces large depolarisation. *c*, Embryo stage 24: spontaneous depolarising activity in muscle cell together with response to 10^{-4} g ml^{-1} ACh. $E_m = -75$ mV. *d*, Oscilloscope record to show spontaneous activity takes the form of summated endplate potentials. Note two miniature e p.p.s on rest of trace. Stage 23: *e*, Depolarisation produced by 10^{-4} g ml^{-1} ACh in preparation made silent by addition of 2 mM Mn^{2+} to the bathing fluid.

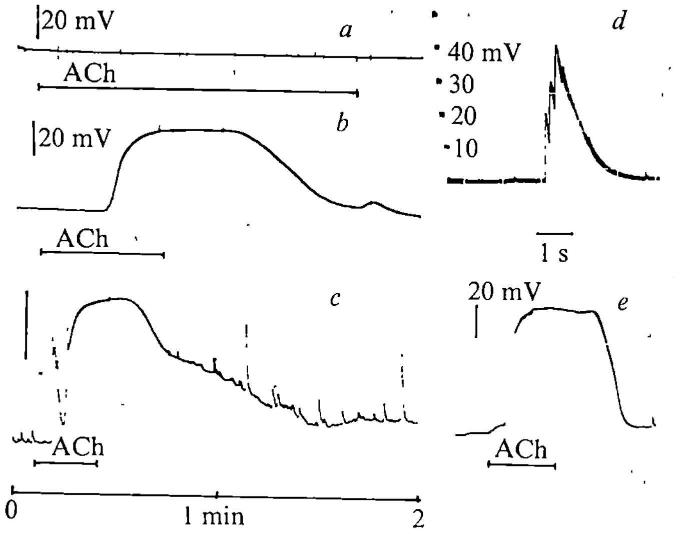

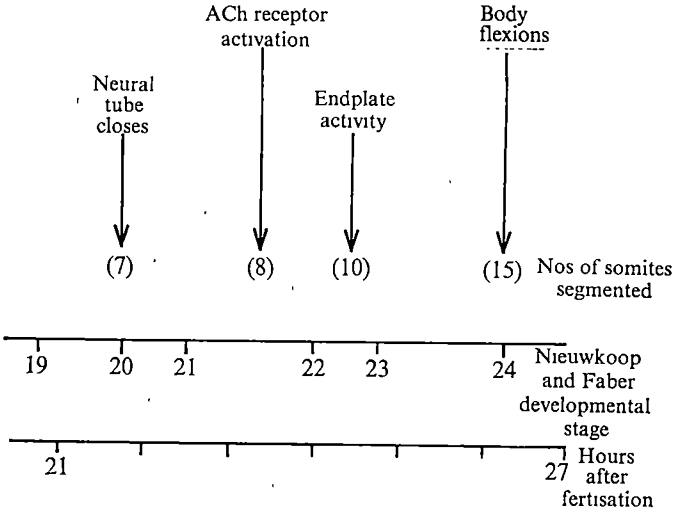

Fig. 3 Diagram to show sequence of events during differentiation of functional neuromuscular junctions in myotome muscle of *Xenopus*. Action potential generation in the muscle membrane may appear anywhere between stages 19 and 23.

The abrupt initial appearance of functional ACh receptors and the speed of subsequent events culminating in the establishment of the first neuromuscular junction, seems, at first sight, surprising. The overall speed of development of *Xenopus*, however, which moves from fertilised egg to flexing tadpole in only 27 h, makes a fast rate of this, and all other developmental sequences, inevitable.

The appearance of spontaneous endplate potentials could mark the time when the nerve ending first makes contact with the muscle. On that view acetylcholine sensitivity in the muscle membrane is established some time before the arrival of the nerve ending and could, therefore, serve in some way to guide the nerve to its final destination. The results are equally compatible with the view that the release of ACh does not begin until some time after the arrival of the nerve, functional connection being a relatively late event in the formation of the neuromuscular junction. Detailed anatomical studies, correlated with electrophysiological studies of the kind described here, might enable this point to be resolved.

We thank the MRC for support.

SUSANNA BLACKSHAW
ANNE WARNER

Department of Physiology,
Royal Free Hospital School of Medicine,
8 Hunter Street, London WC1N 1BP, UK

Received February 25; accepted May 26, 1976

[1] Bennett, M R., and Pettigrew, A G , *J Physiol*, *Lond*, 241, 515–546 (1974)
[2] Dennis, M. J , *J Physiol*, *Lond*, 244, 683–702 (1975).
[3] Diamond, J , and Miledi, R , *J Physiol*, *Lond*, 162, 393–408 (1962).
[4] Dennis, M. J , and Miledi, R., *J Physiol.*, *Lond*, 239, 571–594 (1974)
[5] Ritchie, A K , and Famborough, D. M , *J gen Physiol.*, 65, 327–356 (1975)
[6] Nieuwkoop, P D , and Faber, J , *Normal Table of* Xenopus laevis (North-Holland, Amsterdam, 1967)
[7] Hamilton, L , *J. Embryol exp Morph*, 22, 253–264 (1969).
[8] Coghill, G E., *J. comp. Neurol*, 41, 905–102 (1926).
[9] Muntz, L , *J Embryol exp. Morph*, 33, 757–774 (1975)
[10] Blackshaw, S E., and Warner, A E., *J Physiol*, *Lond*, 255, 191–209 (1976).
[11] Ginsborg, B L , *Pharmac. Rev*, 191, 289–325 (967)

Differential circadian rhythms in pineal and hypothalamic 5-HT induced by artificial photoperiods or melatonin

CHANGES in daylength are principally responsible for synchronising breeding with time of year in mammals and birds[1]: for example, ferrets begin to breed in spring and oestrus ends in autumn. Oestrus can be provoked by exposure to long photoperiods (such as 14 h light: 10 h dark, LD 14 : 10) during winter[2] and can be terminated prematurely if short photoperiods (LD 8 : 16) are given during summer[3]. The pineal is essential for both effects, which are prevented by removal of the gland[3,4] or its autonomic nerve supply[5] from the superior cervical ganglia (C.A.Y. unpublished results). The pineal contains large concentrations of the transmitter 5-hydroxytryptamine (5-HT), which has been implicated in the neural control of circadian rhythms, which themselves may be related to the genesis of annual rhythms[1]. In the pineal of the rat concentrations of 5-HT vary in phase with photoperiod, and this rhythm is prevented by ganglionectomy[6]. Inhibition of cerebral 5-HT synthesis prevents circadian rhythms in concentrations of both plasma adrenal corticosteroids[7] and luteinising hormone[8]. Lesions of the suprachiasmatic nuclei, which contain large concentrations of 5-HT[9,10], abolish circadian rhythms in eating and drinking[11], in running[12] and in concentrations of pineal *n*-acetyltransferase[13], which is the rate limiting enzyme in the synthesis of melatonin, a putative pineal hormone. The pineal must transmit information about photoperiod to neural structures regulating the pituitary, but the nature of the link is unknown. We report here that exposure of ferrets to either long or short photoperiods induces differential 5-HT rhythms in the pineal and hypothalamus, which are abolished by autonomic denervation, and that melatonin induces 5-HT rhythms characteristic of animals kept in short photoperiods.

Fig. 1 Circadian rhythms in 5-HT concentrations in various areas of brain, from ferrets kept for 8 weeks in either short (LD 8 : 16) (*a–d*), or long (LD 14 : 10) (*e–f*) days. *a*, *e*, Pineal gland; *b*, *f*, hypothalamus; *c*, *g*, midbrain; *d*, *h*, cerebral cortex. Levels in the hippocampus (not shown) were similar to those in the cerebral cortex. Five or six animals were killed by decapitation 30 min, 6, 11, 14 and 18 h after the lights came on 5-HT levels in the pineal, whole hypothalamus, midbrain and in samples from ventral hippocampus and dorsal cerebral cortex were measured fluorometrically[22]. Each point is the mean ±s.d in ng per mg wet tissue, except in the pineal (ng per gland) which weighs about 1 mg The hatched areas signify the dark part of the photoperiod. The figure in parentheses is the *F* ratio of the interaction (light treatment × time of day) derived from a two-way analysis of variance. $^*P<0.001$; †Not significant.

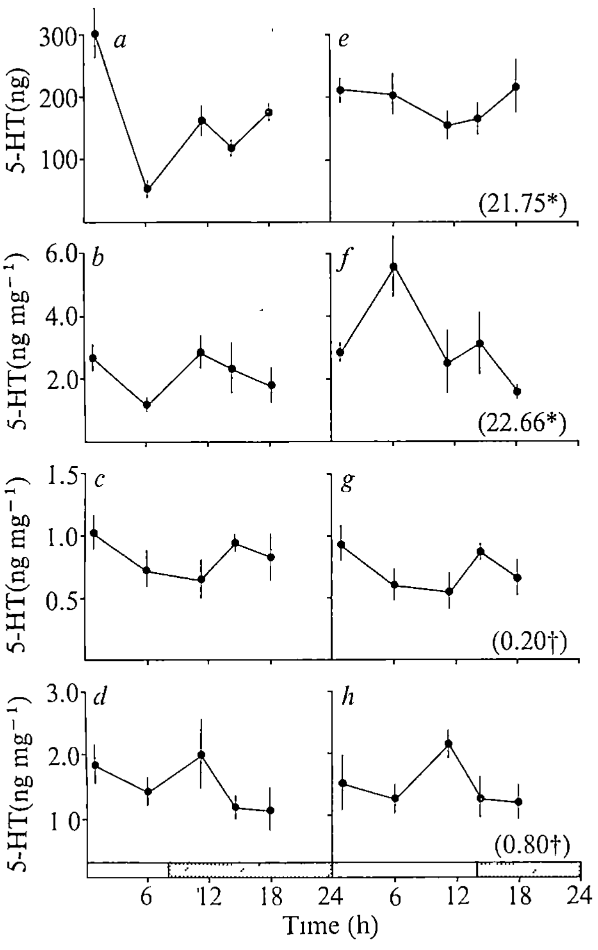

In the first experiment, mature female ferrets were exposed to either long (LD 14 : 10) or short (LD 8 : 16) photoperiods for 8 weeks, the interval required to activate or inhibit oestrus[3,4]. The ovaries were removed to prevent long days from selectively inducing oestrogen secretion. Illumination was from fluorescent tubes with a spectral output similar to that of daylight; feeding times and temperature fluctuations were similar under long and short photoperiods.

Figure 1 (*a–d*) shows that the circadian rhythm in 5-HT was similar in each brain area examined from animals kept in short photoperiods in spite of considerable differences between them in absolute values. Levels declined during the first 6 h of the photoperiod, rising again during the early part of the dark phase. In long photoperiods, however, the rhythm was different in the pineal and the hypothalamus (Fig. 1*e* and *f*). The rhythm in the pineal was attenuated, and this apparent difference was confirmed by a significant interaction between light treatment and time of day. There was also a striking difference in the 5-HT rhythms in the hypothalamus, levels rising during the first 6 h of the long photoperiod, the opposite of the situation observed during short days.

Circadian changes in 5-HT in midbrain, cerebral cortex and hippocampus appeared to be similar in long and short photoperiods (Fig. 1*g* and *h*) and there was no significant effect attributable to the interaction between the light regimes and time of day in these areas. Thus, two structures (pineal and hypothalamus) known to be concerned with the initiation of oestrus by long photoperiods show distinctive rhythms of 5-HT concentration in this condition, whereas the other areas examined do not.

In the second experiment, the preganglionic fibres to the superior cervical ganglia were severed (decentralised) 5–6 d before the animals were exposed to long or short photoperiods as in the first experiment. Figure 2 shows that circadian 5-HT levels were now similar in both photoperiods, and that those in either the pineal or the hypothalamus no longer exhibited a significant interaction between light treatment and time of day (Fig. 2*c* and *d*). The midbrain, cerebral cortex or hippocampus again showed no differential effects of light, as in the first experiment. The standard deviations of each point in Fig. 2 are conspicuously larger than those in Fig 1, suggesting that the 5-HT rhythms of decentralised animals might have been "free running", though this conclusion cannot be substantiated on the evidence presented here. Thus, a procedure which prevents the reproductive system of the ferret from responding to either long or short days also prevents the differential effects of the two photoperiods on 5-HT levels in the pineal and the hypothalamus.

Melatonin has been shown to affect cerebral 5-HT levels in rats. Injected 8 h after the onset of a photoperiod (LD 14 : 10), it abolished the circadian rhythm in pineal 5-HT, whereas treatment at 14 h was ineffective[14]. It may also increase hypothalamic and midbrain 5-HT levels[15]. Melatonin also replicates at least three of the effects of short photoperiods on the ferret's reproductive system, since it terminates the breeding season prematurely[3], antagonises the effects of long photoperiods on the initiation of oestrus[16] and restores photosensitivity to ferrets made photorefractory by prolonged exposure to long days[3]. In

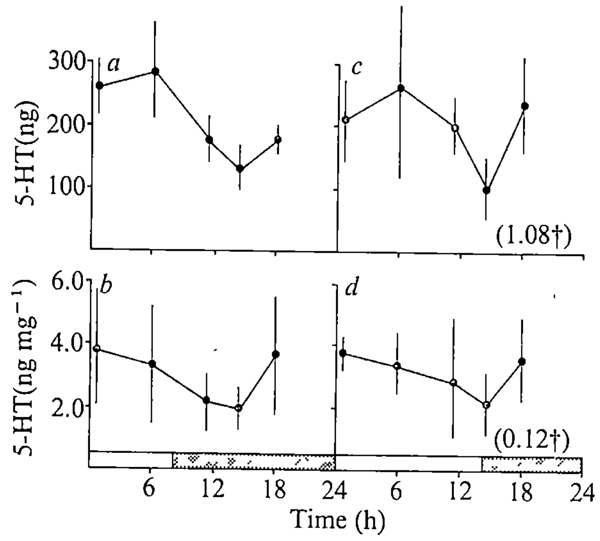

Fig. 2 Levels of 5-HT in the pineal (*a*, *c*) and hypothalamus (*b*, *d*) of ferrets kept in short (*a*, *b*) or long (*c*, *d*) photoperiods, after bilateral "decentralisation" of the superior cervical ganglia See Fig. 1 for further details.

the third experiment, therefore, two groups of ovariectomised ferrets were exposed to long photoperiods. The first received melatonin (1 mg d^{-1}) dissolved in arachis oil for 8 weeks, the second, control injections of oil. Injections were given 8 h after the onset of light, a time corresponding to the start of the dark phase in the short daylight regime used in the previous two experiments. Melatonin synthesis, in rats at least[17], seems to be accelerated during this dark phase. Figure 3*a* and *b* shows that melatonin given in this way to animals exposed to long photoperiods caused 5-HT rhythms in both pineal and hypothalamus characteristic of ferrets kept in short-days in the first experiment. Control injected animals (Fig. 3*c* and *d*) showed the rhythms expected for long-day conditions. Thus, a treatment which replicates some of the actions of short days on reproduction in ferrets also reconstitutes the short-day 5-HT rhythms in the pineal and the hypothalamus. The site at which melatonin acts to produce such effects in the ferret cannot be determined from these experiments.

We do not know whether the 5-HT rhythms reported here are directly concerned with reproduction, although 5-HT infused into the cerebral ventricles can alter gonadotropin secretion in rats[18] and sheep[19]. If they are, they might represent the neural basis for a variation on the Bunning hypothesis[20] which suggests that different photoperiods could shift the circadian photosensitive phase[21]. It seems equally possible that localised 5-HT rhythms may reflect part of the process which promotes or inhibits hypothalamic mechanisms concerned with gonadotropin secretion in appropriate environmental conditions. The latter interpretation receives some support from other (unpublished) experiments by us showing that oestrogen treatment, which presumably activates negative feedback mechanisms on the pituitary, attenuates 5-HT rhythms in both pineal and hypothalamus in either long or short day conditions. Whatever the interpretation, differential 5-HT rhythms in the pineal and hypothalamus could allow the animal's neuroendocrine system to discriminate between photoperiods which have the greatest significance for its reproductive function.

Fig. 3 Levels of 5-HT in the pineal gland (*a*, *c*) and hypothalamus (*b*, *d*) of ferrets kept in long photoperiods, given either 1 mg d^{-1} of melatonin (*a*, *b*) or arachis oil (*c*, *d*) 8 h after the start of the photoperiod (the time of injection is shown by arrows). See Fig. 1 for further details.

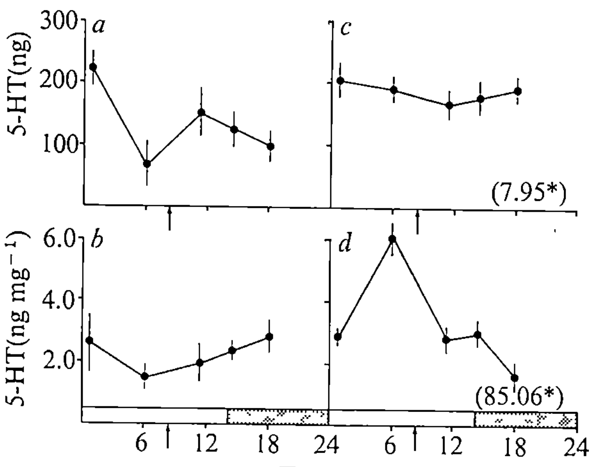

This work is supported by a grant from the ARC, and by an SRC Studentship to C.A.Y. We thank Mr D. Walters for statistical advice.

CAROL A. YATES
J. HERBERT

Department of Anatomy,
University of Cambridge,
Cambridge CB2 3DY, UK

Received April 12, accepted May 18, 1976.

[1] Sadlier, R. M. F. S , *The Ecology of Reproduction in Wild and Domestic Mammals* (Methuen, London, 1969).
[2] Bissonnette, J., *J. exp. Biol.*, 12, 315–320 (1935).
[3] Thorpe, P. A., and Herbert, J , *J. Endocr* (in the press).
[4] Herbert, J., *J. Endocr.*, 43, 625–636 (1969)
[5] Abrams, M. E., Marshall, W A., and Thomson, A. P D., *Nature*, 174, 311 (1954).
[6] Snyder, S H , Zweig, M., Axelrod, J., and Fischer, J E., *Proc natn. Acad Sci. U.S.A.*, 53, 301–305 (1965).
[7] Scapagnini, U., and Preziosi, P., *Prog. Brain Res* , 39, 181–183 (1973).
[8] Hery, M., Laplante, E., and Kordon, C , *J. Endocr.*, 67, 463–464 (1975).
[9] Saavedra, J. M., Palkovits, M., Brownstein, M. J., and Axelrod, J., *Brain Res* , 77, 157–165 (1974).
[10] Fuxe, K., *Z Zelforsch*, 65, 573–579 (1965)
[11] Stephan, F. R , and Zucker, I , *Proc. natn. Acad Sci. U.S.A.*, 69, 1583–1586 (1972).
[12] Stetson, M. H., and Watson-Whitmyre, M., *Science*, 191, 197–199 (1976).
[13] Moore, R. Y., in *The Neurosciences Third Study Program* (edit. by Schmitt, F. O., and Worden, F. G.), 537–542 (MIT Press, London, 1974).
[14] Fiske, V. M., and Huppert, L. C , *Science*, 162, 279 (1968).
[15] Anton-Tay, F., Chou, C , Anton, S , and Wurtman, R. J , *Science*, 162, 277–278 (1968).
[16] Herbert, J., in *The Pineal Gland, Ciba Foundation Symposium* (edit. by Wolstenhelme, G. E. W , and Knight, J.), 303–327 (Churchill Livingstone, London, 1970).
[17] Klein, D. C., in *The Neurosciences Third Study Program* (edit. by Schmitt, F. O., and Worden, F. G), 509–515 (MIT Press, London, 1974).
[18] Kordon, C., *Neuroendocrinology*, 4, 129 (1969)
[19] Domanski, E., Przekop, F., Skubiszewski, B., and Wolinska, E., *Neuroendocrinology*, 17, 265–273 (1975).
[20] Bunning, E., *Cold Spring Harb. Symp. quant. Biol.*, 25, 249 (1960).
[21] Lofts, B , and Lam, W. L , *J. Reprod. Fert., Suppl.*, 19 (1973).
[22] Ahtee, L., Sharman, D. F , and Vogt, M., *Br. J. Pharmac.*, 38, 72–85 (1970).

Muscarinic agonists provide a new class of acaricide

THE resistance of ticks to chemical methods of control is an increasingly serious problem[1–5], and new classes of compounds with high acaricidal activity and low mammalian toxicity are needed urgently. In the search for novel acaricides the nervous system is a prime target, and, in spite of evidence about the role of γ-aminobutyrate and glutamate in arthropod nervous transmission, acetylcholine is the only well established neurotransmitter[6–9]. So far only acetylcholinesterases have achieved an important role in the disruption of cholinergic neurotransmission. Anticholinergics, such as atropine, are ineffective, and cholinomimetics other than nicotine have been little investigated. We now report that certain muscarinic agonists are potent acaricides.

Known muscarinic agonists were tested for activity against the tick *Boophilus microplus*, using a strain resistant to organophosphorous insecticides (Biarra), and a susceptible strain (Yeerongpilly). Engorged females (2×6) were dipped in a solution of the test compound in methanol–acetone (1 : 1), dried on filter paper, and stored in vials for 4 weeks at 25 °C and 85% relative humidity. The concentration of compound required to prevent the production of viable eggs was taken to be the LC_{100}. The results are shown in Table 1, along with those for nicotine and the organophosphorous insecticide pyrimithate (Diothyl, ICI) as references. No significant differences were observed between results for Yeerongpilly and Biarra strains for the cholinomimetics, but pyrimithate was inactive against the latter.

The ixodicidal activity of the muscarinic agonists examined parallels to a large extent the activity observed in vertebrate systems. Thus arecoline and pilocarpine have a similar level of activity (on a weight basis) and are considerably less potent than oxotremorine[10]. Similarly compound 7, which has 10–20% of the activity of oxotremorine in vertebrate systems[11,12], is about 20% as active against ticks. Quaternisation of the nitrogen atom generally caused a marked decrease in ixodicidal activity, possibly due to poorer penetration, since compound 8, for example, is more active than the tertiary-amino compound (7) in vertebrates[11,13], although the methiodides of arecoline and oxotremorine are reported to be less active than the tertiary amines[10]. Tremorine, which is oxidised *in vivo* to oxotre-

Table 1 The toxicity of muscarinic agonists to *Boophilus microplus* (Yeerongpilly strain)

Compound no	Name	Structure	LC_{100} (% × 10^2)
1	Arecoline	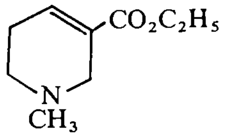	50
2	Arecoline methiodide	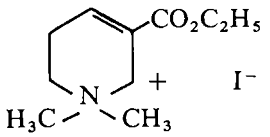	50
3	Pilocarpine	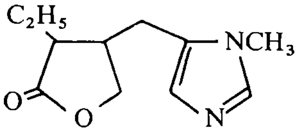	50
4	Oxotremorine	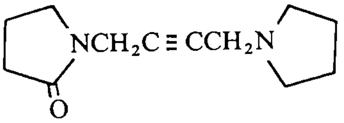	1
5	Oxotremorine methiodide	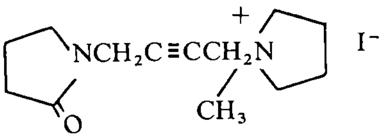	50
6	Tremorine	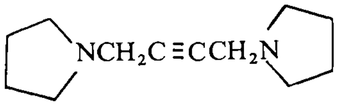	100
7	1-(4-Dimethylaminobut-2-ynyl) pyrrolid-2-one	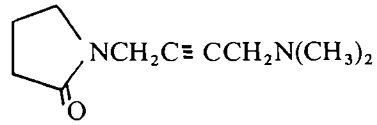	5
8	1-(4-Dimethylaminobut-2-ynyl) pyrrolid-2-one methiodide	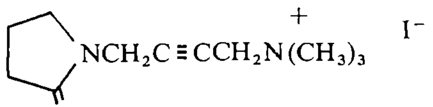	50
9	Pyrimithate	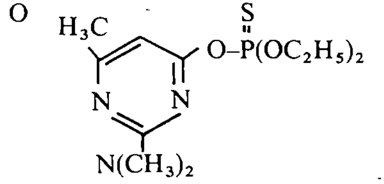	5–10
10	Nicotine	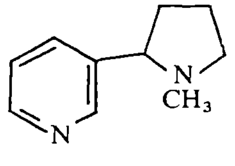	10–20

morine by mammals[14], showed only slight activity against ticks.

It is interesting that oxotremorine is considerably more potent than both nicotine and the reference organophosphorous compound. The cholinomimetics also showed activity against mites, but were completely inactive against *Musca domestica* (adults), *Aedes aegypti* (larvae), and *Lucilia pericata* (larvae). Further work is required to determine whether this difference between Insecta and Acarina is morphological or biochemical in origin.

In conclusion, the muscarinic agonists examined are acaricidal, and in some cases are highly potent. We suggest that this unexploited biochemical lesion may provide a useful starting point for the design of new acaricides.

We thank Dr F. S. Downing for the routine screening of compounds.

D. C. H. Bigg
S. R. Purvis

Imperial Chemical Industries Limited,
Pharmaceuticals Division,
Mereside, Alderley Park,
Macclesfield,
Cheshire SK10 4TG, UK

Received April 8; accepted May 18, 1976.

[1] Whitehead, G. B., *Adv. Acarol.*. 2, 53–70 (1965).
[2] Roulston, W. J., and Wharton, R. H., *Aust. Vet. J.*, 43, 129–134 (1967).
[3] Shaw, R. D., Cook, M., and Carson, R. E., *J. econ. Ent.*, 61, 1590–1594 (1968).
[4] Wharton, R. H., and Roulston, W. J., *A. Rev. Ent.*, 15, 381–404 (1970).
[5] Harrison, I. R., Palmer, B. H., and Wilmhurst, E. C., *Pesticide Sci.*, 4, 531–542 (1973).
[6] O'Connor, A. K., O'Brien, R. D., and Salpeter, M. M., *J. Insect. Physiol.*, 11, 1351–1358 (1965).
[7] Faeder, I. R., O'Brien, R. D., and Salpeter, M. M., *J. exp. Zool.*, 173, 187–202 (1970).
[8] Pitman, R. M., *Comp. gen. Pharmac.*, 2, 347–371 (1971).
[9] Gerschenfeld, H. M., *Physiol. Rev.*, 53, 1–119 (1973).
[10] Hanin, I., Jenden, D. J., and Cho, A. K., *Molec. Pharmac.*, 2, 352–359 (1966)
[11] Bebbington, A., Brimblecombe, R. W., and Shakeshaft, D., *Br. J Pharmac.*, 26, 56–67 (1966).
[12] Levy, J., and Michel-Ber, E., *C. r. Séanc. hebd. Acad. Sci , Paris*, 262, 2546–2549 (1966).
[13] Levy, J., and Michel-Ber, E., *Therapie*, 22, 671–688 (1967).
[14] Karlen, B., *Acta. pharm. suecica*, 7, 169–200 (1970).

Transmission without spikes between locust interneurones and motoneurones

MANY neurones, particularly in sensory systems of both vertebrates and invertebrates, do not produce action potentials[1–3]. In motor pathways within the central nervous system of arthropods there are interneurones whose slow changes in membrane potential can affect the frequency of action potentials in motoneurones[4–6]. Some of these interneurones normally produce spikes[6], but others apparently do not[4,5]. We have studied the properties of synaptic transmission between these non-spiking interneurones and motoneurones in the locust, *Schistocera gregaria*, in the course of investigating the integrative mechanisms underlying the generation of motor patterns[7].

Intracellular recordings were made in the metathoracic ganglion[8] from dorsally located somata of hindwing and hindleg motoneurones, identified physiologically by simultaneous extracellular recordings from appropriate muscles. Each motoneurone was individually identified so that intracellular recordings could be made from the same neurone in different locusts. Non-spiking neurones were penetrated intracellularly in the dorsal neuropile close to the neuropilar processes of the motoneurones. Most recordings were made with electrodes filled with potassium acetate but some were made with electrodes filled with cobaltous chloride[9] to allow the subsequent staining of the motoneurones and non-spiking neurones (Fig. 1). The non-spiking neurones have profuse arborisations within the metathoracic ganglion, but have no projections to other ganglia, nor any processes emerging in peripheral nerves; hence they are intraganglionic interneurones.

In a quiescent locust these interneurones are modulated

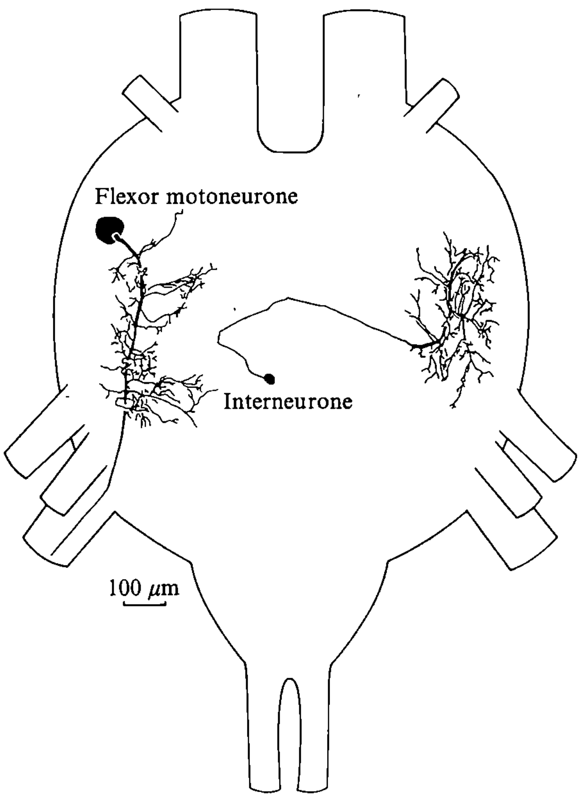

Fig. 1 Drawings of an interneurone and a motoneurone stained by intracellular injection of cobalt as viewed dorsally in a whole mount preparation of the metathoracic ganglion. The neurones were filled on the same side in different locusts but for clarity are drawn on opposite sides of the same ganglion. Left, the lateral fast flexor motoneurone of the left hind tibia whose soma is on the dorsal surface of the ganglion; right, an interneurone whose soma is ventral, which when depolarised resulted in a depolarisation of this flexor motoneurone. The extensive arborisations of the two neurones overlap in all three dimensions.

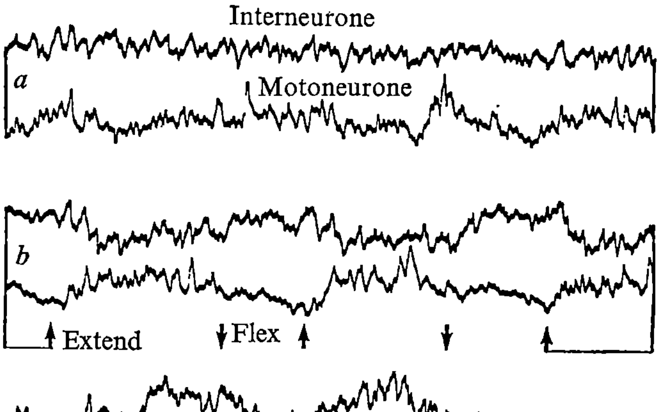

Fig. 2 Spontaneous and evoked sequences of synaptic potentials in a fast motoneurone innervating the flexor tibiae of the hind leg (lower traces) and in a presynaptic non-spiking interneurone (upper traces). *a*, In a quiescent locust both the interneurone and the motoneurone are modulated by a steady stream of synaptic potentials. *b*, Imposed extensions of the tibia of the hind leg, beginning at the upward arrows, result in a depolarisation of the motoneurone and a hyperpolarisation of the interneurone. *c*, Flexions of the tibia evoked by touching the head are accompanied by a depolarisation of the interneurone. Potentials of the flexor tibiae muscle are monitored extracellularly on the third trace.

by a steady stream of synaptic potentials, but do not spike (Fig. 2*a*). Imposed or evoked movements of the joint whose motor units they affect result in changes in the membrane potential of the interneurone (Fig. 2*b* and *c*). The interneurones do not spike, either as a result of synaptically driven depolarisations, or in response to an injected depolarising current as high as 50 nA. This current strength is at least ten times that needed to evoke spikes when injected into the neuropilar segment of a motoneurone. Currents as low as 2 nA injected into an interneurone result in a change in the membrane potential of motoneurones.

We have observed three effects on motoneurones of passing current into interneurones: first, an applied depolarisation of an interneurone results in the depolarisation of a motoneurone (Fig. 3*a*, i–iv); second, a depolarisation results in the hyperpolarisation of a motoneurone (Fig. 3*b*, i–iii); third, in some interneurones that produce the second effect, hyperpolarisation results in the depolarisation of the motoneurone (Fig. 3*b*, iv). Single interneurones have postsynaptic effects upon more than one motoneurone, as revealed by changes in the frequency of extracellularly recorded potentials in muscles innervated by other motoneurones (Fig. 3*b*).

The following analysis is concerned with the properties of transmission between interneurones and motoneurones when an interneurone is depolarised. Transmission is graded. A pulse of curent lasting a few hundred ms injected into an interneurone results in a slow change in the membrane potential of the motoneurone. There is no effect on the motoneurone if the same amount of current is passed when the electrode is just outside the interneurone. With intracellular stimulation of the interneurone, the amplitude of the slow change is linearly related to the magnitude of the depolarising current over the range tested (Fig. 3*c*). At higher current strengths the postsynaptic depolarisations can be large enough to evoke action potentials in the motoneurones. Brief pulses injected into an interneurone result in changes in the membrane potential of the motoneurone, which vary continuously with the strength of the applied current (Fig. 3*d*) At no time during brief stimulation of the interneurone does the membrane potential of the motoneurone change abruptly as would be expected if the interneurone itself, or an intervening interneurone, had spiked.

Fig. 3 Effects of non-spiking interneurones (first traces) upon a fast motoneurone (second traces) innervating a bifunctional muscle, the tergotrochanteral. This muscle elevates the hind wing in flight and depresses the trochanter of the hind leg in walking. *a*, *i–iv*, An interneurone which when depolarised results in a graded depolarisation of the motoneurone in a ganglion with all peripheral nerves cut. Current (third traces) was injected through the high resistance recording electrodes by means of a bridge circuit which was out of balance except at the lowest current strengths. *b*, A second interneurone in another locust affecting the same tergotrochanteral motoneurone: *i–iii*, depolarisation results in a graded hyperpolarisation of the motoneurone; *iv*, hyperpolarisation of the interneurone results in a slight depolarisation of the motoneurone which presumably indicates a decreased rate of release of transmitter. The third traces monitor the extracellular potentials of some coxal muscles of the hind leg whose motoneurones are also affected by this interneurone; the downward deflections are from the anterior adductor of the coxa, whose potentials are reduced in frequency when the interneurone is depolarised; the upward deflections are from another coxal muscle that is excited when the interneurone is hyperpolarised. The fourth traces monitor current. *c*, The graded nature of the transmission between the interneurones and the tergotrochanteral motoneurone is indicated by the relationship between presynaptic current and the change in postsynaptic voltage. Triangles are measurements taken from records of the interneurone–motoneurone pair shown in *a*; circles are from the pair shown in *b*. The voltage of the motoneurone was measured 300 ms after the onset of the stimulus. *d*, 1.5-ms current pulses of increasing strengths injected into the interneurone shown in *b* result in graded changes in voltage in the motoneurone. Calibration—Voltage: *a*, motoneurone 3.8 mV, interneurone 20 mV; *b*, motoneurone 7.7 mV, interneurone 20 mV; *d*, motoneurone 1.5 mV; interneurone 15 mV: current: *a*, 33 nA; *b*, 17 nA; *c*, 75 nA. Horizontal: *a*, *b*, 400 ms; *d*, 14.5 ms.

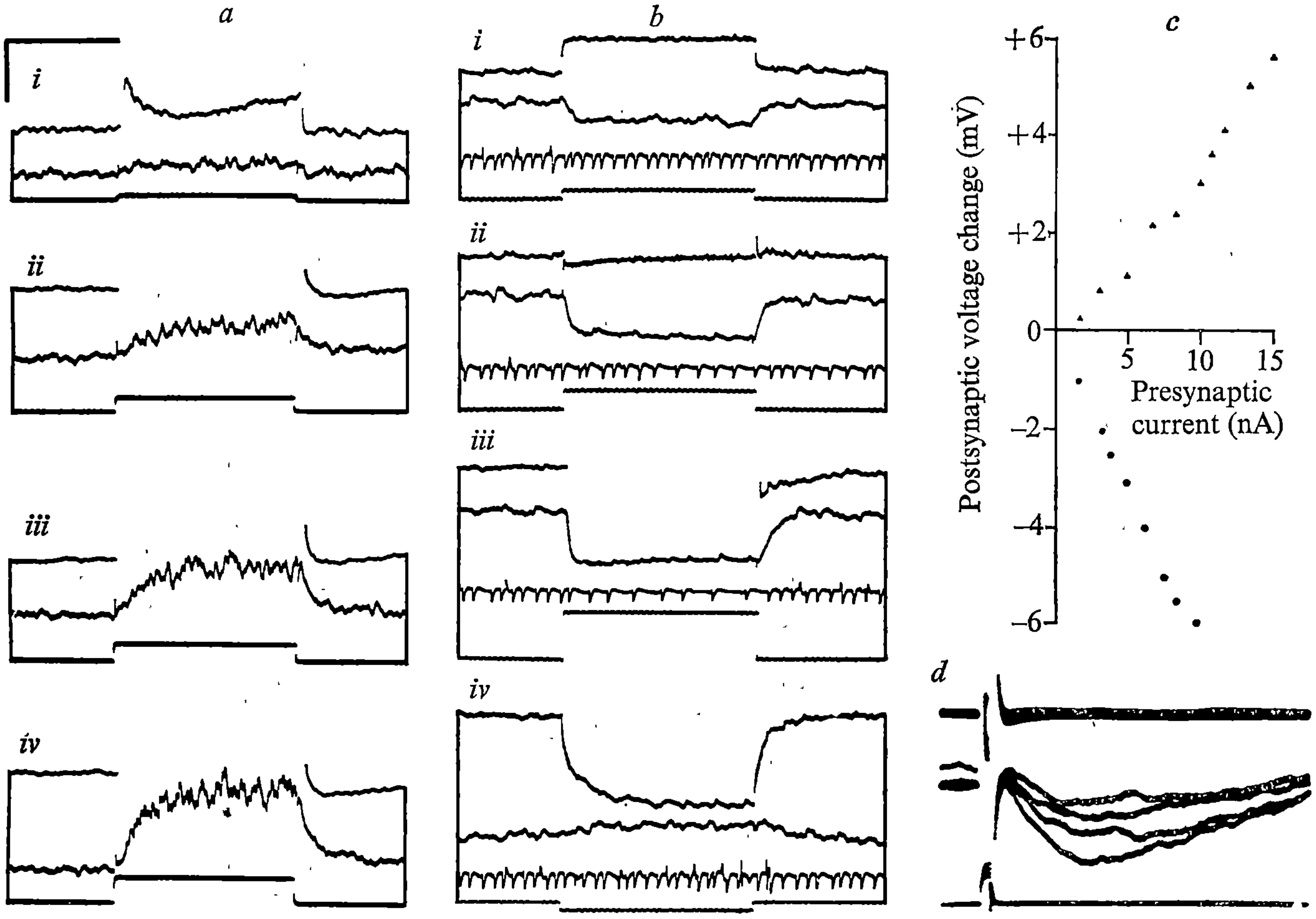

SCIENCE COLLEGE
Upper Circular Road

The most economical interpretation of the graded effect is that the interneurones synapse directly upon the motoneurones. The synaptic delay cannot be measured accurately because transmission is graded. Pulses (1 ms) of current injected into an interneurone are followed within 1 ms by a voltage change in the motoneurone, a delay similar to that observed between spiking interneurones and leg motoneurones of the locust. The gross anatomy is consistent with a monosynaptic connection because there is considerable spatial overlap in the neuropile of the fine branches of an interneurone and a motoneurone upon which it exerts an effect (Fig. 1).

The connections between the interneurones and motoneurones that we have encountered so far, seem to be chemically and not electrically mediated, for the following reasons. First, current of either polarity injected into a motoneurone has no effect upon the membrane potential of the presynaptic interneurone. Spikes in the motoneurone are not reflected in the interneurone. Second, a brief square wave depolarising pulse injected into an interneurone decays rapidly, but evokes a potential in the motoneurone that can persist for 45 ms (Fig. 3*d*). This prolonged effect is probably the result of transmitter release from the interneurone. It is not the result of passively charging the motoneurone through an electrical synapse, because the postsynaptic potential reaches its peak some 10 ms after the end of the stimulus, and is asymmetrical. Third, in those interneurones where depolarisation results in the hyperpolarisation of a motoneurone, the reversal of sign is most easily explained by supposing that the depolarisation increases the rate of release of a transmitter substance that has an inhibitory effect upon the motoneurone. Fourth, there is often a progressive increase in the transmembrane voltage fluctuations recorded in a motoneurone as it is depolarised by increasing amounts of current injected into an interneurone (Fig. 3*a*). Increased fluctuations of voltage have not been observed when a motoneurone is hyperpolarised by depolarisation of an interneurone. This is a consistent observation but we have no evidence which would favour one of many possible explanations. Current injected directly into the motoneurone, causing a similar shift of its membrane potential, does not give rise to an increase in the fluctuations of the transmembrane potential. The increased fluctuations in voltage on depolarisation can therefore be attributed to synaptic transmission. They are not caused by spikes in sensory feedback loops, as they are still recorded in a ganglion with all its peripheral nerves cut. There remain two possible explanations as to their origin. First, the interneurone has a direct connection with the motoneurone, but also excites spiking interneurones that in turn synapse on the motoneurone. This possibility of parallel pathways cannot yet be eliminated. Second, the voltage fluctuations could result from the release of transmitter from the interneurone directly on the motoneurone. This may be the only mechanism or it may operate in conjunction with the first mechanism. The effect is similar to that seen in a frog muscle fibre when the terminals of its motoneurone are depolarised by pulses of current which do not evoke action potentials[10]. At the frog neuromuscular junction the voltage fluctuations result from the random release of transmitter substance and a similar explanation may be appropriate for the non-spiking interneurones of the locust. We conclude that the non-spiking intraganglionic interneurones modulate the membrane potential of motoneurones by graded release of transmitter through monosynaptic pathways.

This work was supported by a grant from the Nuffield Foundation. M.B is the Balfour Student.

M. BURROWS
M. V. S. SIEGLER

Department of Zoology,
University of Cambridge,
Cambridge CB2 3EJ, UK

Received March 15; accepted May 26, 1976.

[1] Ripley, S. H., Bush, B. M. H , and Roberts, A , *Nature*, **218**, 1170–1171 (1968).
[2] Werblin, F. S , and Dowling, J. E., *J. Neurophysiol* , **32**, 339–355 (1969).
[3] Shaw, S R , *J Physiol., Lond* , 220, 145–175 (1972).
[4] Mendelson, M , *Science*, **171**, 1170–1173 (1971)
[5] Pearson, K G., and Fourtner, C. R , *J. Neurophysiol.*, **38**, 33–52 (1975).
[6] Maynard, D M., and Walton, K D , *J comp. Physiol.*, **97**, 215–243 (1975).
[7] Burrows, M., *J exp. Biol* , **63**, 713–733 (1975)
[8] Hoyle, G., and Burrows, M., *J. Neurobiol.*, **4**, 3–41 (1973).
[9] Pitman, R. M., Tweedle, C. D , and Cohen, M J., *Science*, **176**, 412–414 (1972).
[10] del Castillo, J., and Katz, B., *J. Physiol., Lond* , **124**, 586–604 (1954).

Microelectrode measurement of the intracellular *p*H of mammalian heart cells

RECESSED-TIP *p*H-sensitive microelectrodes[1] can be made sharp enough to be used on mammalian muscle cells. They permit not only the direct measurement of the intracellular *p*H (*p*H$_i$), but also the continuous recording of changes in *p*H$_i$ during experiments lasting for several hours. We report here the first measurements of the *p*H$_i$ of mammalian cardiac tissue made with this type of *p*H-sensitive microelectrode. Apart from one report of experiments with an open-tipped microelectrode[2], the only previous determinations of cardiac *p*H$_i$ have been made by the CO_2 or DMO methods[3], which are indirect and can detect only very slow changes. Earlier designs of *p*H-sensitive glass microelectrodes have been of little use because of their large size. The recessed-tip design (Fig. 1) lacks this drawback, as only its extreme tip, which can be as small as 0.5 μm in diameter, needs to be inside the cell. We have used these electrodes successfully in ventricular muscle preparations from several animals, but the results described here are confined to those obtained with sheep heart Purkinje fibres.

Our experimental arrangement is illustrated in Fig. 1. Free-running single Purkinje fibres were cut from sheep ventricles. A little side wall material was left attached to pin the fibre in the perfusion chamber where it was superfused at 35 °C. A recording from an experiment with this tissue is shown in Fig. 2. The *p*H-sensitive microelectrode recorded the membrane potential of a Purkinje fibre cell, minus an offset voltage proportional to *p*H$_i$, while a neighbouring cell was impaled with the KCl microelectrode. The KCl microelectrode output voltage was subtracted electronically from that of the *p*H electrode so that when both electrodes were intracellular, a *p*H$_i$ recording could

Fig. 1 Diagrammatic illustration of the preparation pinned into the experimental chamber. It was superfused continuously, and impaled with a conventional, KCl-filled microelectrode (left), and the *p*H-sensitive microelectrode (right). A diagram (not to scale) of ~ 0 2 mm of the tip of the latter is shown at the top.

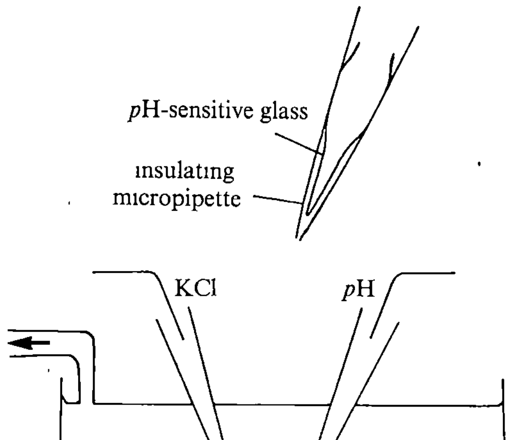

be obtained (Fig. 2, lower trace) which was independent of any changes in membrane potential. (Ideally both electrodes should be in the same cell. This is theoretically possible, but in practice it was found difficult to obtain good penetrations with both electrodes when the interelectrode distance was < 100 µm.) In this experiment, the preparation was perfused initially with saline equilibrated with 5% CO_2, 95% O_2. External CO_2 was then removed by changing the perfusion solution to one equilibrated with 100% O_2. This produced a transient increase in pH_i followed by a partial recovery to a level higher than in the absence of CO_2. On return to 5% CO_2 there was a transient pH_i decrease followed by a return to the control level. Essentially similar recoveries from changes in pH_i when CO_2 was changed have been observed in crab muscle[4], squid axon[5] and snail neurones[6].

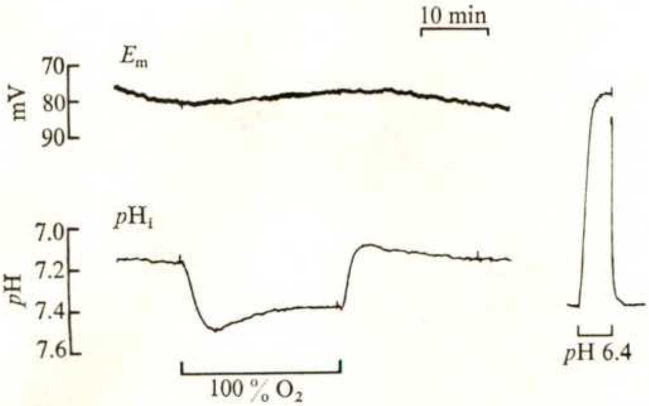

Fig. 2 Pen recording of an experiment to measure pH_i and the response to removal and replacement of external CO_2. The membrane potential was recorded by a conventional microelectrode (top trace) and the pH_i obtained when the pH-sensitive electrode is also intracellular (bottom trace). The pH-sensitivity of the electrode was tested (right) by a reduction of the solution pH to 6.40 (both electrodes extracellular). The preparations were perfused with a bicarbonate-buffered modified Tyrode solution composed of 140 mM Na^+, 4 mM K^+, 2mM Ca^{2+}, 1 mM Mg^{2+}, 2 mM pyruvate, 10 mM glucose, chloride and bicarbonate (reciprocally varied) to give a pH of 7.40 at 35 °C. The bicarbonate required was determined experimentally by titration. CO_2 levels were determined by a CO_2 gas analyser. These varied in nominally 95 % O_2: 5 % CO_2 gas cylinders from 4.25 to 4.79 % CO_2 (mean 4.61). Thus the bicarbonate concentration ranged from 17.5 to 22 mM. In the absence of CO_2 and bicarbonate, solutions contained 10 mM HEPES (*N*-2-hydroxyethyl piperazine-*N*-2-ethanesulphonic acid) buffer (also at pH 7.40). The changes in the pH_i when CO_2 was removed were not altered when Tris-maleate buffer was substituted for HEPES.

The results from a total of 14 experiments are summarised in Table 1. The mean pH_i in the absence of CO_2 is close to 7.2 and is significantly higher than when CO_2 is present. In general, our values for pH_i are somewhat higher than those obtained previously using the DMO technique in dog heart: 6.77 (ref. 7), 6.86 (ref. 8), and 7.01 (ref. 9) although Benson *et al.*[10] have reported similar values to those we have found. Lavellée[2] used open-tipped pH-selective microelectrodes and found a pH_i of 6.9 in rat atrial fibres (stimulated at a rate of 200 min^{-1}).

Table 1 Intracellular pH and membrane potential

Equilibration gas	pH_i	E_m (mV)
100 % O_2	7.20 ± 0.05	71.8 ± 3.7
95 % O_2: 5 % CO_2	7.02 ± 0.04	78.1 ± 2.5

Results are means ± s.e.m.; n = 14. Those from preparations with a membrane potential in 5 % CO_2 of < 60 mV were rejected.

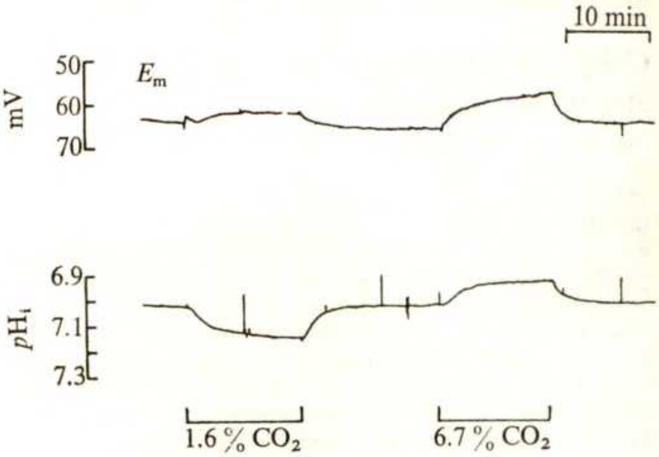

Fig. 3 Change in membrane potential (top) and pH_i (bottom) when the external CO_2 level was changed from 4.7 % to the levels indicated. The bicarbonate concentration (20.5 mM) was maintained constant so that the external pH varied from 7.40 in the control solution to 7.70 and 7.19 respectively in the two test solutions. The potassium concentration in this experiment was 8 mM.

From experiments of the type illustrated in Fig. 1 it is clear that pH_i is greatly influenced by CO_2 in the equilibration gas. We have used different CO_2:O_2 mixtures to see how pH_i varies with alteration of the external pH, and the results of an experiment of this type are illustrated in Fig. 3. All solutions contained the same bicarbonate concentration and were equilibrated with the CO_2 levels indicated. (The pH of these mixtures being measured for each experiment.) Alteration of the CO_2 content produced a change in pH_i to a new steady level within ~ 10 min, presumably by the reaction

$$CO_2 + H_2O = H_2CO_3 = H^+ + HCO_3^-$$

A linear relationship was found between pH_i and the external pH, but the pH_i change was only ~ 40 per cent of the change in external pH. This difference is caused by intracellular buffering.

These responses differ from those observed when the bicarbonate concentration is altered as well as the CO_2 content to maintain a constant external pH. In this case, the responses are similar to those shown in Fig. 1, that is, a large transient initial pH_i change followed by a partial recovery to a level nearer that of the control.

Direct measurement of pH_i with recessed-tip pH sensitive microelectrodes thus enables continuous recording of previously undetectable transient changes. The results show that alteration of CO_2 levels produces rapid changes in pH_i. The partial recovery of these changes when external pH is unchanged suggests the presence of some sort of H^+ pump in the cell membrane.

We are grateful to the MRC for support.

D. Ellis
R. C. Thomas

Department of Physiology,
University of Bristol,
Bristol BS8 1TD, UK

Received September 12, 1975; accepted May 14, 1976.

1 Thomas, R. C., *J. Physiol., Lond.*, **238**, 159–180 (1974).
2 Lavallée, M., *Circulation Res.*, **15**, 185–193 (1964).
3 Waddell, W. J., and Bates, R. C., *Physiol. Rev.*, **49**, 285–329 (1969).
4 Aickin, C. C., and Thomas R. C., *J. Physiol., Lond.*, **252**, 803–815 (1975).
5 Boron, W., and De Weer, P., *J. gen. Physiol.*, **67**, 91–112 (1976); *Nature*, **259**, 240–241 (1976).
6 Thomas, R. C., *J. Physiol., Lond.*, **255**, 715–735 (1976).
7 Schloerb, P. R., *Surg. Forum.*, **14**, 70–71 (1963).
8 Schloerb, P. R., and Grantham, J. J., *J. lab. clin. Med.*, **65**, 669–676 (1965).
9 Clancy, R. L., and Brown, E. B., *Am. J. Physiol.*, **211**, 1309–1312 (1966).
10 Benson, E. S., Freier, E. F., and Vijuns, R., *Am. J. Physiol.*, **209**, 941–944 (1965).

Origin of plasma α_2HS-glycoprotein and its accumulation in bone

WE have shown previously that a glycoprotein constituent of calcified cortical bone matrix is immunochemically identical to a component of blood plasma[1,2]. In bone and dentine this specific α-glycoprotein is concentrated in amounts relative to plasma albumin but is not present at greater concentrations than in plasma in various other tissues. This material, although mainly present in extravascular sites in bone, could originate from the plasma because it represents a substantial proportion of the radioactivity in bone tissue 12 d after injection of ^{14}C-total plasma glycoprotein[1]. Rabbit bone α-glycoprotein is analogous to human α_2HS-glycoprotein[3,4], which is located in mineralising areas in normal human bone matrix[5]. To our knowledge direct conclusive proof of the tissue origin of the plasma α_2HS-glycoprotein is lacking although most of the serum glycoproteins seem to be synthesised by the liver[6,7]. Nevertheless, its increased concentration in calcified tissues suggests that its presence in plasma could be a result of synthesis and release by bone tissue. We now report that the α_2HS-glycoprotein is synthesised by the liver and a proportion is subsequently accumulated in bone tissue.

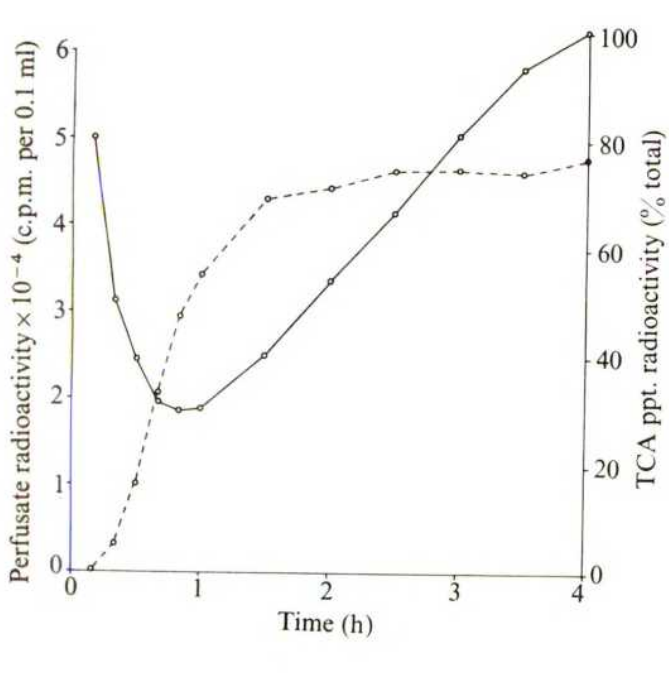

Fig. 1 Total radioactivity in liver perfusion medium (solid line), and the proportion precipitable by TCA (dashed line), with time after introduction of ^{14}C-glucosamine into the perfusate. The perfusion medium consisted of 2.6 g % (w/v) bovine plasma albumin in bicarbonate buffer[9] with bicarbonate added to 25 mM concentration and the addition of human erythrocytes to give 2.5% (w/v) haemoglobin. Blood contained in the liver was washed out with 30 ml perfusion medium before addition of 20 μCi D-1-^{14}C-glucosamine (The Radiochemical Centre, Amersham) to the perfusate. Perfusion was with a total of 50 ml of this medium at a flow rate of 27 ml min^{-1}. Samples (0.5–1 ml) of perfusate were taken at various time intervals up to 4 h after the addition of D-1-^{14}C-glucosamine and centrifuged at 2,000*g* for 30 min at 4 °C to remove erythrocytes. Portions (10 μl) of the supernatants were dissolved in 0.5 ml soluene (Packard) and 5 ml scintillation fluid[10] was added for assay of radioactivity by liquid scintillation. Samples (0.1 ml) of the supernatants were added to 1 ml 12% (w/v) aqueous TCA and allowed to stand overnight at 4 °C. The TCA precipitates were collected by centrifugation at 4 °C at 2,000*g* for 15 min and washed three times with 1 ml 12% (w/v) aqueous TCA containing 1 mg glucosamine ml^{-1}. The washed precipitates and individual supernatants were dissolved in soluene (1 ml) and their radioactive contents determined. All radioactivity determinations were corrected for quenching by internal standardisation.

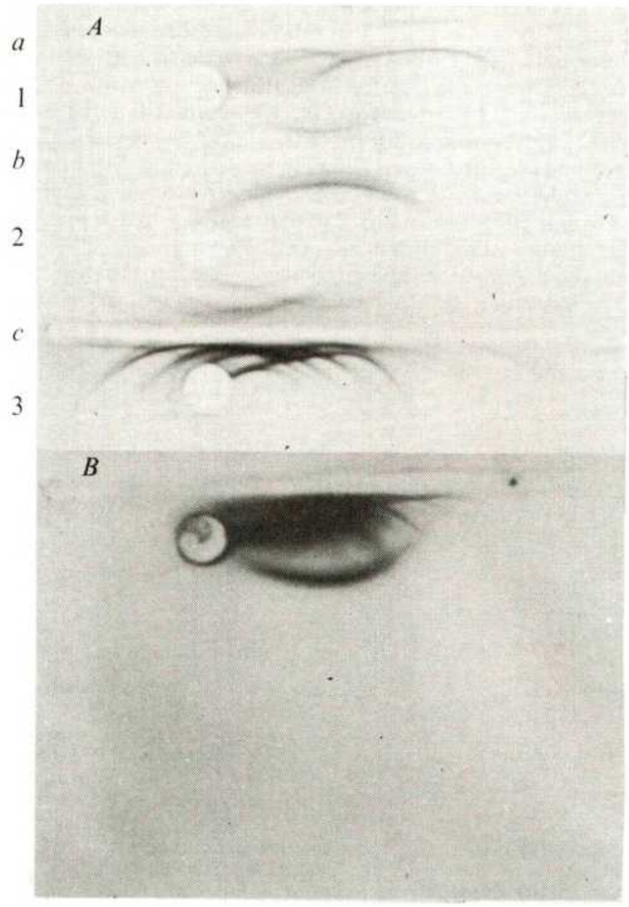

Fig. 2 Immunoelectrophoresis in 1% (w/v) agar gel in sodium barbitone buffer, *p*H 8.6, of rabbit liver perfusion medium and rabbit plasma against antiserum to rabbit plasma and antiserum to rabbit bone α-glycoprotein (*A*) and its autoradiograph (*B*). Electrophoresis was for 2 h at 100 V and autoradiography was by exposure to Kodirex X-ray plates (Kodak) for 10 d. Well (1), Perfusion medium 4 h after adding D-1-^{14}C-glucosamine. Well (2), Rabbit plasma to which an amount of D-1-^{14}C-glucosamine was added which was equivalent to the radioactivity present in well (1). Well (3), Rabbit plasma, non-radioactive. Troughs (*a*) and (*c*), Anti-rabbit plasma antiserum. Trough (*b*), Anti-rabbit bone α-glycoprotein antiserum.

Livers of 300–350 g Dutch rabbits were perfused *in situ* with medium containing D-1-^{14}C-glucosamine by a modification of the method of Hems *et al.*[8]. Total perfusion medium radioactivity fell rapidly to about the 1 h time point as the perfused liver removed radioactive precursor. This value then increased for the rest of the perfusion period (Fig. 1). With time of perfusion the radioactivity which was precipitable by trichloroacetic acid (TCA) increased from 5% at 20 min to 77% at 4 h. Column chromatography on BioGel P30 confirmed that TCA precipitability represented macromolecular radioactivity as similar results were obtained by both methods. Macromolecular radioactivity first appeared in the medium 10–20 min after addition of labelled precursor and this indicates the time required for uptake, synthesis and secretion of the glycoproteins by the liver[11]. 7% (w/v) polyacrylamide disk gel electrophoresis of the perfusion medium showed that a large proportion of the radioactively-labelled material had α-electrophoretic mobility (not shown).

Agar gel immunoelectrophoresis followed by autoradiography (Fig. 2) indicated that the liver perfusate contained numerous proteins reactive against polyvalent anti-rabbit plasma antiserum and their synthesis during perfusion is demonstrated by the autoradiogram. Antiserum against purified rabbit bone α-glycoprotein was produced as described previously[1] and Fig. 2 shows that liver synthesised a component showing immunological identity with this glycoprotein. No interaction between the immunoprecipitates and D-1-^{14}C-glucosamine during the washing and staining procedure was observed (Fig. 2). These results show that the liver is capable of synthesising the α-glycoprotein which has been found to make up approximately 4% of the rabbit cortical bone non-collagenous organic matrix[1].

To test whether bone tissue could also synthesise this component, eight rabbit half-calvaria (25 d gestation) were cultured, each in 1.5 ml medium for 48 h in the presence of 7.5 μCi 1-^{14}C-glucosamine, by the method of Reynolds[12]. After culture the embryonic bones were individually pooled and the non-collagenous proteins prepared by the method of Herring *et al.*[13].

The culture medium at 48 h contained very little radioactivity in macromolecular components (0.6% of total medium radioactivity) as assessed by chromatography on BioGel P30. DEAE-cellulose chromatography of macromolecular radioactivity from cultured bone collagenase digests showed that only 17% of the total radioactivity applied was eluted in the position of the particular α-glycoprotein under investigation[1,2]. This contrasts with the situation *in vivo* after D-1-^{14}C-glucosamine injection where a greater proportion is eluted in this less acidic fraction[1]. Immunoelectrophoresis of the less acidic fractions of cultured bone collagenase digests, which contained appreciable amounts of radioactivity, showed detectable amounts of α-glycoprotein (Fig. 3). But neither this immunoprecipitate nor any serum protein precipitated by polyvalent anti-rabbit plasma antiserum (Fig. 3) contained radioactivity as assessed by autoradiography on Kodirex X-ray plates for up to 60 d. Therefore embryonic bone tissue cannot synthesise this particular α-glycoprotein, even though it is present in foetal plasma (our unpublished observations).

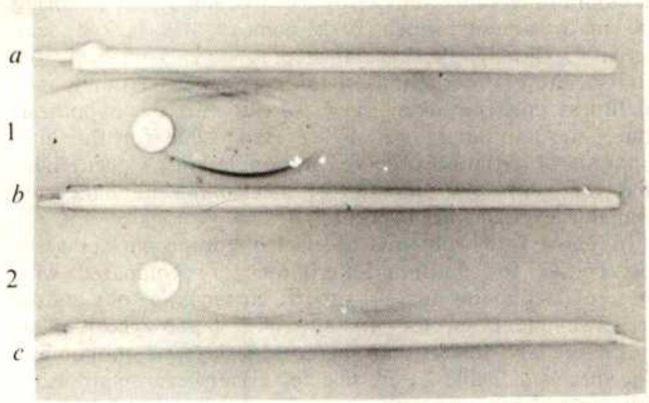

Fig. 3 Bone non-collagenous proteins prepared by the method of Herring *et al.*[13] were chromatographed on DEAE-cellulose as described previously[1,2]. The peak of radioactivity corresponding to the 0–0.2 M NaCl eluate was pooled, dialysed exhaustively against distilled water and freeze dried. The freeze-dried material was dissolved in 0.05 M Tris-HCl buffer *p*H 7.2 (0.2 ml) and samples (10 μl) of the solution used for immunoelectrophoresis in agar gel (1% w/v in sodium barbitone buffer *p*H 8.6). Stained with 1% amido black in 7% acetic acid. Well (1), 0–0.2 M NaCl eluate+normal rabbit plasma. Well (2), 0–0.2 M NaCl eluate. Troughs (*a*) and (*c*), Anti-rabbit plasma antiserum (40 μl). Trough (*b*), Anti-rabbit bone α-glycoprotein antiserum (40 μl).

The present results confirm our previous suggestion[1] that the rabbit α-glycoprotein analogous to human α_2HS-glycoprotein, which is concentrated in bone tissue relative to plasma albumin, is synthesised by the liver. These results are also the first direct demonstration that the α_2HS-glycoprotein is made by the liver, as implied by the work of Miller[6,7].

The accumulation of this α-glycoprotein in calcified matrix could be a result of its affinity for adsorption sites on bone mineral and our current work[3] confirms that this concentration effect occurs during the precipitation of calcium phosphates *in vitro*. This suggests a relatively high affinity of this plasma protein for calcium and the concentration in bone matrix could represent an aspect of a more basic involvement in calcium metabolism.

Certain serum fractions have been shown to delay the rate of transformation *in vitro* of an amorphous calcium phosphate to a more crystalline hydroxyapatite[14]. Whether the binding of the α-glycoprotein has any specific influence upon the rate of formation or on the nature of the bone mineral phase *in vivo* is not known. Whatever the physiological function of the particular affinity of the α_2HS-glycoprotein for bone matrix, our demonstration that this material is synthesised by the liver but not by bone tissue has interesting implications for bone physiology.

We thank Professor Sir Hans Krebs for helpful advice and Mr Philip Gregory of Professor Krebs' laboratory, Oxford for technical help with the liver perfusions. J.T.T. and M.E.O. are members of MRC External Scientific Staff.

J. T. TRIFFITT
U. GEBAUER
B. A. ASHTON
M. E. OWEN

Bone Research Laboratory,
Nuffield Department of Orthopaedic Surgery,
University of Oxford,
Nuffield Orthopaedic Centre,
Oxford OX3 7LD, UK

J. J. REYNOLDS

Tissue Physiology Laboratory,
Strangeways Research Laboratory,
Worts Causeway, Cambridge, UK

Received April 12; accepted May 18, 1976.

[1] Triffitt, J. T., and Owen, M. E., *Biochem. J.*, **136**, 125–134 (1975).
[2] Ashton, B. A., Triffitt, J. T., and Herring, G. M., *Eur. J. Biochem.*, **45**, 525–533 (1974).
[3] Ashton, B. A., Triffitt, J. T., and Höhling, H. J., *Calc. Tiss. Res.* (in the press).
[4] Schmid, K., and Burgi, W., *Biochim. biophys. Acta*, **47**, 440–450 (1961).
[5] Dickson, I. R., Poole, A. R., and Veis, A., *Nature*, **256**, 430–432 (1975).
[6] Miller, L. L., Hanavan, H. R., Titthasiri, N., and Chowdhury, A., *Adv. Chem. Ser.*, **44**, 17–40 (1964).
[7] Miller, L. L., and John, D. W., in *Plasma Protein Metabolism* (edit. by Rotschild, M. A., and Waldmann, T.), 207–222 (Academic Press, New York and London, 1970).
[8] Hems, R., Ross, B. D., Berry, M. N., and Krebs, H. A., *Biochem. J.*, **101**, 284–292 (1966).
[9] Krebs, H. A., and Henseleit, K., *Hoppe-Seyler's Z. physiol. Chem.*, **210**, 33 (1932).
[10] Bray, G. A., *Analyt. Biochem.*, **1**, 279–285 (1960).
[11] Anker, H. S., in *The Plasma Proteins* (edit. by Putman, F. W.), **II**, 267–307 (Academic Press, New York and London, 1960).
[12] Reynolds, J. J., in *The Biochemistry and Physiology of Bone*, **I**, 69–126 (Academic Press, New York and London, 1972).
[13] Herring, G. M., Ashton, B. A., and Chipperfield, A. R., *Prep. Biochem.*, **4**, 179–200 (1974).
[14] Blumenthal, N. C., Betts, F., and Posner, A. S., *Calc. Tiss. Res.*, **18**, 81–90 (1975).

Hybrid molecules and the superiority of the heterozygote

POPULATION geneticists have never agreed on the extent to which overdominance of fitness—that is, the situation in

Table 1 Comparisons of heterozygosities at monomeric and multimeric enzyme loci of four animal and two plant species*

Species	No. of monomeric enzymes	No. of multimeric enzymes	Normal deviate	*P*	Source
Homo sapiens	20	35	−1.369	0.085	Table 2
Peromyscus polionotus†	4	15	−2.160	0.015	21
Astyanax mexicanus‡	5	11	−2.553	0.005	22
Drosophila willistoni§	16	15	−1.622	0.052	23
Stephanomeria exiqua ssp. *carotifera*¶	3	5	−2.007	0.018	24
Lupinus texensis††	4	3	−1.591	0.056	25

*For *Homo sapiens* heterozygosities (H) were obtained directly from the source; for the other species they were calculated as $H = 1 - \Sigma p_i^2$ where p_i is the frequency of the electrophoretic allele weighted over populations. Heterozygosities at the two classes of enzymes were compared by applying the Wilcoxon two-sample rank test corrected for ties and discontinuity[6]. Symbolism of enzymes as in source.

†Monomers: Est-1 and 2, PGM-1 and 3; multimers: Est-3 and 4, PGI-1, LDH-1, LDH-2, LDH-3, MDH-1, MDH-2, MDH-3, α-GPDH-1, 6-PGDH-1, GOT-1, GOT-2, IDH-1, IDH-2. Amount of variation or degree of polymerisation unknown for the other enzyme loci listed in Selander *et al.*[21].

‡Monomers: Pep-1, PGM-1, Est-1, 2 and 3; multimers: αGPD-1, GPGD-1, PGI-1, PGI-2, GOT-1, GOT-2, MDH-1, MDH-2, IDH-2, LDH-1, LDH-2.

§Monomers: Lap-5, Est-2, 3, 4, 5 and 7, ALD-1 and 2, G6PDH, ME-2, PGM-1, ADK-1 and 2, HK-1, 2 and 3; multimers: ACPH-1, ADH, MDH-2, αGPDH, Fum, GOT, HBDH, IDH, ODH-1, ME-1, XDH, AO-1, AO-2, TO, TPI-2.

¶Monomers: Est-2 and 3, APH-1; multimers: GOT-1, 2 and 3, PGI, TO-1.

††Monomers: Est-1, Lap-1, PGM-1, ACPH-1; multimers: PGI-1, GOT-1 and 2.

Table 2 Heterozygosities (H) at 50 human enzyme loci*

Multimers	*H*	Source
Phosphohexose isomerase	0.0006	7
Lactate DH A	0.0020	7
Lactate DH B	0	7
NADH–isocitric DH† (soluble)	0.0056	7
NADH–isocitric DH (mitochondrial)	0	7
NAD–malate DH (soluble)	0.0019	7
Phosphogluconate DH	0.0372	7
Alcohol DH 1	0	7
Alcohol DH 2	0.0582	7
Alcohol DH 3	0.4824	7
Superoxide dismutase A	0.0006	7
Glutamate oxaloacetate transaminase (soluble)	0.0017	7
Glutamate oxaloacetate transaminase (mitochondrial)	0.0334	7
Glutamic–pyruvic transaminase (soluble)	0.4950	7
Nucleoside phosphorylase	0.0013	7
Acid phosphatase 2	0	7
Acid phosphatase 3	0.0011	7
Pyrophosphatase	0	7
Alkaline phosphatase (placental)	0.5020	7
Peptidase A	0.0009	7
Peptidase D	0.0140	7
Esterase D	0.1752	7
Glycerol-3-phosphate DH 2	0.0014	9
Malic enzyme (mitochondrial)	0.3000	8
Malic enzyme (soluble)	0	8
Glutathione peroxidase	0.0077	10
Phosphoglyceric acid mutase	0.0019	11
Glyoxalase I (red cells)	0.4771	12
NAD–malate DH (mitochondrial)	0.0004	13
2-3-Diphospho-glycerate mutase	0	8
Sorbitol DH	0	8
Cytidine deaminase	0.4545	14
Monomers	*H*	Source
Phosphoglucomutase 1	0.3664	7
Phosphoglucomutase 2	0.0007	7
Phosphoglucomutase 3	0.3828	7
NADH diaphorase	0.0101	7
Adenylate kinase	0.0768	7
Adenosine diaminase	0.1004	7
Acid phosphatase 1	0.5190	7
Peptidase B	0.0021	7
Peptidase C	0.0062	7
Fucosidase	0.3720	15
Hexokinase III	0.0303	16
Aconitase (soluble)	0.0159	17
Aconitase (mitochondrial)	0	17
Carbonic anydrase CA_{II}	0	18
Amylase (pancreatic)	0.0825	19
Amylase (salivary)	0.0141	20
Acetylesterase	0	8

*Data refer to caucasians only. No variants were detected at other enzyme loci listed in Harris *et al.*[7] and in Harris and Hopkinson[8], or there is no direct information as to whether they are monomers or multimers. In loci with very low heterozygosities observed differences in H may be of no significance. Loci with an H less than 0.01 may be characterised as monomorphic. Using this criterion 22 out of 33 multimers and 6 out of 17 monomers are monomorphic ($\chi^2 = 4.48$, d.f. = 1, $P = 0.034$). †DH, dehydrogenase.

which the fitness of the heterozygote exceeds the fitness of both homozygotes—is responsible for the maintenance of genetic variability in populations[1]. It has been proposed[2–4] that heteromultimers formed by random association of enzyme subunits coded by two different alleles provide a molecular basis for overdominance. This hypothesis stems from the observation that heteromultimers often differ from homomultimers in a number of aspects[5], sometimes restoring enzymatic activity when both homozygotes lacked such activity[2]. Clearly, the crucial step towards associating (or disassociating) observations of this type with overdominance of fitness must be taken if we were to test the hypothesis that heteromultimers *per se* are responsible for the high amounts of variation observed in populations. I argue here that the enormous amounts of electrophoretic data now available exclude this hypothesis.

In Table 1 the amounts of electrophoretic variability of loci coding for multimeric enzymes are compared with those of loci coding for monomeric enzymes in four animal and two plant species. In all cases heterozygosities at multimers are lower than heterozygosities at monomers. The species in Table 1 were selected either because a reasonably large number of both types of enzyme loci were studied and because the number of assayed individuals is quite high to allow one to ignore errors in gene frequency estimates, or because they represent broad taxonomic units embracing, practically, all diploid organisms. Data from other species of mammals, lizards, fish, fruit flies, and snails could be cited, the great majority of which seem to support this conclusion (for data on human enzyme loci see Table 2).

It has been argued that enzymes with multiple substrates[26] and enzymes regulating the flux through a pathway[27] are more variable than enzymes with single substrates or non-regulatory enzymes. The class of non-regulatory enzymes contains more multimers than monomers so it can be argued that the difference in amounts of variation is ultimately related to function rather than to presence or absence of hybrid bands. The validity of these hypotheses is in doubt as there is a growing list of enzymes with multiple substrate and with regulatory properties which, nevertheless, are exceptionally conservative[28]. But the argument that the difference in amount of polymorphism indicated here is ultimately related to function rather than to degree of polymerisation can be dealt with in a more direct way. In Table 3 I have listed amounts of electrophoretic variability of monomeric and multimeric enzymes of same *in vitro* biochemical function. Out of 27 pair-wise comparisons that

Table 3 Heterozygosities at monomeric and multimeric enzymes having the same *in vitro* function

Species	Monomer	Multimer	Source
D. subobscura	Est-3 0.448 Est-5 0.549	Est-7 0.168	29
D. mojavenis B	Est-2 0.081	Est-4 0.551 Est-5 0.565	30
D. arizonensis	Est-2 0.403	Est-4 0.573 Est-5 0.723	30
D. mulleri	Est-2 0.654	Est-4 0.505	30
D. aldrichi	Est-2 0.575	Est-4 0.781	30
D. virilis	Est-α 0.763	Est-β 0.402	31
D. willistoni	ME-2 0.300	ME-1 0.039	23
D. tropicalis	ME-2 0.169	ME-1 0.045	23
D. equinoxialis	ME-2 0.186	ME-1 0.033	23
D. paulistorum	ME-2 0 403	ME-1 0.010	23
Dacus oleae	Est-A 0.762	Est-B 0.583	32
Littorina obtusata	Est-1 0.510	Est-3 0.426	33
Peromyscus polionotus	Est-1 0.343 Est-2 0.313	Est-3 0.144 Est-4 0.047	21
Peromyscus floridanus	Est-1 0.488 Est-2 0.502	Est-4 0.252	34
H. sapiens	ACP_1 0.519	ACP_2 0 ACP_3 0.001	7
H. sapiens	Pep-B 0.002 Pep-C 0.006	Pep-A 0.001 Pep-D 0.014	7

are possible from Table 3, monomers have a higher amount of heterozygosity in 20. Evidently, within a given species or population monomeric enzymes are more polymorphic than multimeric enzymes of similar function.

After the demonstration[35-36] that populations do indeed contain alleles of same electrophoretic mobility one is not allowed to directly translate electrophoretic variability to actual variability. If polymerisation interferes with the electrophoretic expression of charge changes, then it is possible that amino acid substitutions result in changes in electrophoretic mobility more often in monomers than in multimers. There is evidence, however, that the number of different electrophoretic states that multimeric enzymes can assume is as high as, if not higher than, in monomeric enzymes. Some enzymes with the highest observed numbers of electrophoretic alleles are multimers: esterase B of *Dacus oleae*[32] (12 electrophoretic alleles), esterase 5 of *Drosophila pseudoobscura*[37] (12); acetaldehyde oxidase and xanthine dehydrogenase of *Drosophila willistoni*[23] (11 and 10, respectively); esterase E of *Colias eurytheme*[38] (13); esterase d of *Hemiagrus isola*[39] (18). In humans the enzyme with the highest observed number of electrophoretic alleles, 18 in all, is the dimeric placental alkaline phosphatase[40].

Lewontin (ref. 1, p. 71) has stressed the point that small amounts of unconditional overdominance will quickly lead to high degrees of heterozygosity. If heterozygotes for multimeric enzymes are endowed with high fitness and heterozygotes for monomeric enzymes are not, then we would expect multimeric enzymes to possess higher amounts of variation than monomeric enzymes. The opposite is true. Unless one assumes that the variation in multimers is maintained by overdominance, whereas the much higher variation in monomers is neutral or is maintained by some other form of balancing selection, it becomes difficult to adhere to the hypothesis that heteromolecules provide a basis for overdominance of fitness.

The evidence presented here renders the hypothesis of widespread unconditional overdominance less attractive, but it does not exclude the possibility that other forms of heterozygote superiority, such as marginal overdominance[41], are of importance in evolution Gillespie and Langley[26] have shown, however, that if selection coefficients fluctuate greatly as a result of change in the environment, then heterozygote intermediacy can often result in stable polymorphism. Their review of the literature shows that very rarely, if ever, do heterozygotes assume values above or below the range specified by the two homozygotes. Heterozygote intermediacy is also a concomitant of frequency dependent selection[42]. It seems very possible that, whatever fraction of the genetic variation is selectively maintained, the type of selection involved is one of fluctuations in selection coefficients with no intrinsic heterozygote superiority.

I thank Drs M. L. Tracey and G. R. Babbel for providing me with unpublished information. This work was supported by a grant from the NRC of Canada.

E. Zouros

Department of Biology,
Dalhousie University, Halifax,
Nova Scotia B3H 4J1, Canada

Received March 22; accepted May 11, 1976

1 Lewontin, R. C ,*The Genetic Basis of Evolutionary Change* (Columbia University, New York and London, 1974)
2 Fincham, J R S , *Gene Camplementation* (Benjamin, Amsterdam, 1966).
3 Fincham, J R S., *Heredity*, **28**, 387–391 (1972).
4 Schwartz, D., and Laughner, W J , *Science*, **166**, 626–627 (1969).
5 Singh, R S , Hubby, J L., and Lewontin, R. C , *Proc. natn. Acad. Sci U.S.A.*, **71**, 1808–1810 (1974).
6 Brownlee, K. A , *Statistical Theory and Methodology in Science and Engineering*, second ed (Wiley, New York, London and Sydney, 1965)
7 Harris, H , Hopkinson, D A , and Robson, E. B., *Ann Hum. Genet* , **37**, 237–253 (1974)
8 Harris, H , and Hopkinson, D A , *Ann Hum Genet* , **36**, 9–20 (1972)
9 Hopkinson, D. A , Peters, J., and Harris, H , *Ann Hum Genet* , **37**, 477–484 (1974).
10 Beutler, E., West, C , and Eeutler, B., *Ann. Hum Genet.*, **38**, 163–169 (1974).
11 Chen, S H , Anderson, J., Giblett, E R., and Lewis, M , *Am. J. Hum. Genet* , **26**, 73–77 (1974)
12 Kompf, J , Bissbort, S., Gussmann, S , and Ritter, H., *Humangenetik*, **27**, 141–143 (1975)
13 Beckman, G , and Christodoulou, C , *Hum. Hered* , **24**, 294–299 (1974)
14 Teng, Y S , Anderson, J. E , and Giblett, E. R , *Am J. Hum Genet* , **27**, 492–497 (1975)
15 Turner, M B , Turner., V. S., Beratis, N G., and Hirschhorn, *Am. J Hum Genet* , **27**, 651–661 (1975).
16 Povey, S., Corney, G , and Harris, H., *Ann Hum. Genet* , **38**, 407–415 (1975).
17 Slaughter, C. A , Hopkinson, D A., and Harris, H., *Ann. Hum Genet* , **39**, 193–202 (1975)
18 Hopkinson, D A , Coppock, J S , Munlemann, M F , and Edwards, Y. H , *Ann. Hum Genet* , **38**, 155–162 (1974).
19 Merritt, A. D , and Bixler, D., *Proc fourth Int Congr Hum. Genet.*, 120–121 (Excerpta Medica, Int Congr Ser No 233, Amsterdam, 1971)
20 Ward, J C., Merritt, A D , and Bixler, D , *Am J Hum Genet* , **23**, 403–409 (1971)
21 Selander, R K , Smith, M H., Yang, S Y., Johnson, W. E , and Gentry, J B., *Studies in Genetics* (Univ. Texas Publ No. 7103, 1971).
22 Avise, J. C., and Selander, R K., *Evolution*, **26**, 1–19 (1972)
23 Ayala, F. J., Tracey, M. L , Barr, L. G., McDonald, J. F., and Perez-Salas, S , *Genetics*, **77**, 343–384 (1974).
24 Gottlieb, L D , *Evolution*, **29**, 213–225 (1975)
25 Babbel, G. R , and Selander, R K , *Evolution*, **28**, 619–630 (1974)
26 Gillespie, J H., and Langley, C. H , *Genetics*, **76**, 837–848 (1974)
27 Johnson, G B , *Science*, **184**, 28–37 (1974)
28 Zouros, E , *Nature*, **254**, 446–448 (1975)
29 Zouros, E , Krimbas, C B., Tsakas, S., and Loukas, M , *Genetics*, **78**, 1233–1244 (1974)
30 Zouros, E , *Evolution*, **27**, 601–621 (1974)
31 Tsuno, K , *Genetics*, **80**, 585–594 (1975)
32 Zouros, E., and Krimbas, C B , *Genet. Res* , **14**, 249–258 (1969)
33 Berger, E. M , *Biol Bull* , **145**, 83–90 (1973).
34 Smith, M H., Selander, R. K., and Johnson, W E , *J Mamm. Genet.*, **54**, 1–13 (1973).
35 Bernstein, S C , Thockmorton, L H , and Hubby, J L , *Proc. natn. Acad. Sci U.S A* , **70**, 3928–3931 (1973)
36 Singh, R S., Hubby, J. L , and Thockmorton, L. H , *Genetics*, **80**, 637–650 (1975).
37 Prakash, S , Lewontin, R. C , and Hubby, J L , *Genetics*, **61**, 841–858 (1969).
38 Burns, M J , and Johnson F M , *Science*, **156**, 93–96 (1967)
39 Burns, M. J., and Johnson, F M , *Proc natn Acad Sci. U S A* , **68**, 34–37 (1971)
40 Donald, L J., and Robson, E B , *Ann Hum. Genet* , **37**, 303–313 (1968).
41 Wallace, K , and Yarbrough, K M , *Proc natn Acad Sci U.S A* , **57**, 645–649 (1967)
42 Kojima, K , and Yarbrough, K M , *Proc natn Acad Sci U.S A* , **57**, 645–649 (1967).

Genetic transformation in *Drosophila* by microinjection of DNA

THE experiments described here provide new evidence for DNA-induced gene-specific alterations in *Drosophila.* Host embryos homozygous for recessive alleles of several genes were treated with wild-type DNA by embryo microinjection. Several of the adults which developed from these injected embryos exhibited phenotypic alterations whereas none of the controls treated with host-type DNA showed any altered phenotype. In addition, the alterations were in two cases transmitted to the progeny of the injected flies, so that altered stocks could be established. If this represents genetic transformation and if it can be made to work routinely in eukaryotes, it promises to be equally or more useful than the corresponding process in prokaryotes, since it could be used to bioassay specific parts of the genome which are currently being isolated by various techniques.

Ten years ago Fox and Yoon[1] reported that *Drosophila* embryos soaked in solutions of DNA showed somatic changes in the emerging adults, and subsequently germinal changes[2], that were specific to the DNA used. In addition to *Drosophila*, the uptake, expression and transmission of exogenous DNA has been reported in both *Neurospora* and mammalian cells *in vitro*, as well as in a number of organisms less suited to further genetic analysis[3-7]. The fungal transformation phenomenon was observed after addition of wild-type DNA (or poly(A)-rich RNA) to the growth medium of a fragmented mutant culture[8-10]. The change observed in most studies was an alteration of the organism's dependence on inositol in the culture medium. The frequency of transformation was significantly greater than the observed reversion frequency, either spontaneous or induced, for the mutation. The treatment of cultured mammalian cells with metaphase chromosomes from different species and the subsequent detection of donor enzyme activity in clones derived from the treated cells[11-13] demonstrates further that higher eukaryotes can incorporate and utilise exogenous genetic material.

In *Drosophila*, somatic as well as germ-line alterations have been observed after soaking embryos in solutions of DNA extracted from genetically different animals. The process used to obtain eggs permeable to DNA is not, however, completely satisfactory. It involves inducing animals to lay premature eggs and has been found difficult as well as largely ineffective (less than 2% of the eggs were shown by autoradiography to take up the DNA)[14]. In an effort to streamline the transformation experiments (by eliminating the scoring of untreated animals) and to enable some quantification of the treatment, we have adapted an egg microinjection method[15] for this procedure. Although this process limits the number of embryos which can be treated, because of the low survival rate, it allows precision in the delivery of exogenous DNA and serves to increase the chance that a treated egg will be altered genetically.

The genetic outline of our experiment was basically the same as that used by Fox and Yoon[2]. Eggs collected from flies homozygous for the mutations *vermilion*, *v*, and *brown*, *bw*, were used as hosts for DNA extracted from wild-type adults. *Vermilion* and *brown* represent mutations in the ommochrome and pteridine biosynthetic pathways, respectively, and in combination result in the absence of pigment from the adult eyes. Furthermore, *vermilion* is non-autonomous in its expression so that a small patch of non-mutant tissue in the body of the animal can allow the eyes to develop the wild-type phenotype (brown pigmentation) in an otherwise mutant animal. This system, previously exploited by Fox, allows a "magnification" in the detection of first generation alterations, since transformation of tissues other than the eye can be detected by its effect on eye pigmentation. In addition, all hosts were homozygous for *yellow* (a cuticle marker) and most were homozygous for *forked* (a bristle mutation) and *maroon-like* (a mutation which can be detected by lack of staining for aldehyde oxidase in the internal organs). Embryos were injected during the nuclear multiplication stage. During this stage of embryogenesis the nuclei are dividing rapidly (13 divisions at 10-min intervals at 25 °C) and the embryo is a syncytium, that is, no cell membranes separate the nuclei. Injection at this stage should maximise the potential interaction between nuclei and exogenous DNA.

Table 1 Eye pigmentation in adults developing from embryos injected with DNA

Treatment	Adults emerged	Adults with pigmented eyes	Fertile adults*	Adults with pigmented progeny
v^+ DNA	138	8	100	2
v DNA	87	0†	61	0

DNA was extracted from whole adults by a procedure similar to that of Tartof[17]. A nuclear preparation was deproteinised using a mixture of chloroform–isoamyl alcohol (24:1) and phenol. The DNA was precipitated, resuspended and treated successively with RNase, Pronase, and phenol. The resulting preparation was dialysed extensively against SSC (0.15 M NaCl, 0.015 M sodium citrate) and then a modified insect Ringer's solution[18]. The DNA was then frozen in 100-µl aliquots at −70 °C. The concentration of DNA injected varied and the results above represent the animals surviving treatment with 44–100 µg ml^{-1}. Preblastoderm embryos 30–60 min old were injected with 10^{-4} µl DNA through glass needles 10–13 µm inner diameter. The injected embryos were maintained until hatching at 18–20 °C and the larvae were subsequently raised in yeast paste at 25 °C. The emerging adults were coded, scored, and then allowed to breed for at least 10 d with animals of the host stock. All F_1 progeny were scored for eye colour and 10 pairs of F_1 from each adult were maintained. F_2 and F_3 were similarly scored for deviations from expected eye colour.

*Adults whose progeny were scored at least three generations.

†$0.01 < P < 0.025$.

The results of these injections with respect to alterations of *vermilion* expression are summarised in Table 1. A significant number of adults developing from treated embryos had pigmented eyes. One of these flies also transmitted the pigmentation to one of his progeny forming a stable transformed line. Another stable line was established from the recovery of pigmented F_2 from an unpigmented injected animal. Genetic analysis of the two transformed lines demonstrated that the alterations were both linked to the X chromosome, which carries the *vermilion* locus. The alteration in one line is dominant and maps near *v* (1–33.2), whereas the other is semi-dominant and maps to the distal end of the chromosome (1–0.01). These results are similar to those of Fox *et al.*[16] and to the preliminary observations made by Limbourg-Bouchon using microinjection (B. Limbourg-Bouchon, personal communication). Neither of these lines showed any instability in the expression of the pigmentation after the first pigmented flies were isolated, nor has there been any reversion in the stocks. This contrasts with the behaviour of stocks produced by other workers where phenotypic instability (interpreted as somatic mosaicism of expression) and reversion are quite common[2,16], suggesting that there may be qualitatively different events induced by the DNA treatment. Adults were also examined for alterations in the expression of *y*, *bw*, *f*, and *mal*, but no alteration was observed (*y* and *bw*, 138 cases; *f* and *mal*, 88 cases). The detection of altered expression in these autonomous genes may be significantly less likely than for non-autonomous genes such as *vermilion*. It is also likely, however, that the transformation rate will be characteristic for each gene and that these other genes might simply transform at a lower frequency.

Our results indicate that the phenomenon observed by Fox and Yoon[2] can be duplicated using egg microinjection. In addition, the frequency of altered expression is significantly greater than that observed by soaking eggs (5% first generation transformants as opposed to 0.8%)[2]. Preliminary results from other laboratories using this technique indicate that an even higher rate may be attainable (B. Limbourg-Bouchon, personal communication; C.P. Liu, and A. S. Fox, personal communication). Microinjection allows precision in delivery, circumvents the uptake phenomenon which may be selective, and allows precise staging of each embryo. Experiments are now under way to transform loci whose genetic fine structure will allow an analysis of the mechanisms underlying this apparent genetic transformation.

I thank Drs Peter Bryant and Howard Schneiderman for their encouragement and support, and Mark Blake and Pat Venta for their technical assistance. This work was supported by a grant and a Predoctoral Traineeship from the NIH.

SUSAN GERMERAAD

Center for Pathobiology,
University of California,
Irvine, California 92717

Received March 22, accepted May 18, 1976.

[1] Fox, A. S., and Yoon, S. B., *Genetics*, 53, 897–911 (1966)

[2] Fox, A. S., and Yoon, S. B., *Proc. natn. Acad. Sci. U.S.A.*, 67, 1608–1615 (1970).

[3] Ottolenghi-Nightingale, E., *Proc. natn. Acad. Sci. U.S.A.*, 64, 184–189 (1969).

[4] Hess, D., *Z. Pfl.Physiol.*, 60, 348–358 (1969).

[5] Nawa, S., and Yamada, M.-A., *Genetics*, 58, 573–584 (1968).

[6] Ledoux, L., Huart, R., and Jacobs, M., *Nature*, 249, 17–21 (1974)

[7] Doy, C. H., Gresshoff, P. M., and Rolfe, B. G., *Proc. natn. Acad. Sci. U.S.A.*, 70, 723–726 (1973).

[8] Mishra, N. C., Szabo, G., and Tatum, E. L., in *The Role of RNA in Reproduction and Development* (edit. by Niu, N. C., and Segal, S. J.), 259–268 (North Holland Amsterdam, 1973)

[9] Mishra, N. C., and Tatum, E. L., *Proc. natn. Acad. Sci. U.S.A.*, 70, 3875–3879 (1973).

[10] Mishra, N. C., Niu, M. C., and Tatum, E. L., *Proc. natn. Acad. Sci. U.S.A.*, 72, 642–645 (1975).

[11] McBride, O. W., and Ozer, H. L., *Proc. natn. Acad. Sci. U.S.A.*, 70, 1258–1262 (1973)

[12] Willecke, K., and Ruddle, F. H., *Proc. natn. Acad. Sci. U.S.A.*, 72, 1792–1796 (1975).

[13] Burch, J. W., and McBride, O. W., *Proc. natn. Acad. Sci. U.S.A.*, 72, 1797–1801 (1975).

[14] Yoon, S. B., and Fox, A. S., *Nature*, 206, 910–913 (1965)

[15] Okada, M., Kleinman, I. A., and Schneiderman, H. A., *Devl Biol.*, 37, 43–54 (1974).

[16] Fox, A. S., Yoon, S. B., and Gelbart, W. M., *Proc. natn. Acad. Sci. U.S.A.*, 68, 342–346 (1971)

[17] Tartof, K. D., *Genetics*, 73, 57–71 (1973)

[18] Chan, L.-N., and Gehring, W., *Proc. natn. Acad. Sci. U.S.A.*, 68, 2217–2221 (1971).

Integrator gene in *Aspergillus nidulans*

ONE of the most intriguing problems in genetics is how the regulation of a particular structural gene can be programmed in such a way that its expression can be elicited in a variety of different contexts. Stated differently, how can the concomitant expression of two or more non-contiguous structural genes capable of independent expression be achieved? Britten and Davidson[1-3] have proposed a model for gene regulation which gives considerable insight into this problem. One feature of their model is the existence of positively acting regulatory genes, designated integrator genes, whose role is to achieve precisely this concomitant expression of non-contiguous structural genes. Although the model was developed to account for cell differentiation in higher eukaryotes, a similar, although possibly less elaborate, form of regulatory machinery might be applicable in lower eukaryotes. In the fungus *Aspergillus nidulans*, as in higher eukaryotes, functionally related genes are seldom clustered[4]. Given the considerable metabolic versatility of this organism, instances of inducible enzymes participating in more than one metabolic pathway should not be unduly rare. Evidence for the existence of integrator genes could come from the study of regulatory mutations affecting such enzymes. The model also requires the existence of receptor sites for integrator gene products, a not implausible requirement for *A. nidulans*, where several *cis*-acting regulatory mutations tightly linked to structural genes under their control have been identified (refs 5–8 and unpublished results of C. R. Bailey and H. N. A.). Here I report that the *int*A gene of *A. nidulans*, previously designated *amd*R and shown by Hynes and coworkers[9-11] to be a positive regulatory gene in linkage group II involved in acetamidase synthesis, is an integrator gene of the type described by Britten and Davidson. Moreover, *int*A is possibly especially interesting because one of the compounds whose metabolism it controls is γ-amino-*n*-butyric acid (GABA), whose metabolism has been extensively investigated in a wide variety of organisms because of its role in the regulation of neuronal activity.

Three probable structural genes are under *int*A control: *amd*S, the structural gene for acetamidase in linkage group III[9-11]; *gat*A in linkage group VII where recessive mutations eliminate GABA transaminase which also participates in the catabolism of β-alanine, δ-amino-*n*-valerate, and several other ω-amino acids (H. A. Penfold and H. N. A., unpublished); and *gab*A in linkage group VI where recessive mutations result in loss of a GABA-specific permease (H. A. Penfold and H. N. A., unpublished). *amd*A, another regulatory gene probably specifically controlling *amd*S, is located 5.3 ± 1.8 cM from *gat*A. But there is no interaction in double mutants and no reason to suppose that this linkage has any special significance.

*int*A mutations can affect expression of one or more of the structural genes. Partially dominant *int*A^c mutations can lead to high, constitutive levels of acetamidase[9,11] whereas recessive *int*A$^-$ mutations halve acetamidase levels[9]. *int*A mutations do not affect the structure of acetamidase[10]. *In vivo* effects of *int*A mutations are given in Tables 1 and 2. *int*A^c–2, –300, –302, and –304 enhance to varying extents utilisation of acrylamide and acetamide as nitrogen sources and acetamide as carbon source (Table 1). This enhancement is closely correlated with their abilities to suppress *are*A^r mutations for utilisation of acetamide as nitrogen source (Table 2). *are*A^r mutants lack a positively acting regulatory substance necessary for the synthesis of ammonium-repressible enzymes and consequently are unable to utilise nitrogen sources other than ammonium in glucose-minimal medium[7,12]. *int*A$^-$ mutations somewhat reduce utilisation of acetamide. *amd*A^d mutations enhance acetamide but not acrylamide utilisation and suppress *are*A^r mutations on acetamide. Expression of the *int*A^c and *amd*A^d phenotypes on acrylamide and acetamide media requires a functional allele of the *amd*S but not *gab*A and *gat*A genes. The strict additivity of *int*A$^-$–101 and the partially dominant *amd*A^d–301 in strains carrying both mutations (Tables 1 and 2) suggests that, as predicted by Britten and Davidson[2], *int*A and *amd*A might be regulating *amd*S in a parallel, positive fashion. As *int*A$^-$ mutations do not abolish amide inducibility of acetamidase[9], this form of regulation might involve *amd*A. Selection of *amd*A$^-$ alleles and a biochemical study of the effects of *amd*A mutations on acetamidase regulation are intended.

Effects of *int*A mutations on expression of the *gat*A gene are seen in Tables 1 and 3. *int*A$^-$ mutations prevent utilisation of GABA, β-alanine, and δ-amino-*n*-valerate as nitrogen sources and GABA as carbon source (Table 1). *int*A^c–2, –300, –302, –304, and –305 slightly enhance δ-amino-*n*-valerate utilisation. Mutants defective in the *orn*B gene in linkage group VIII are blocked before L-ornithine in the biosynthesis of L-arginine and require either ornithine or arginine[4,13]. GABA and β-alanine but not δ-amino-*n*-valerate can supplement *orn*B$^-$ strains (Table 3) but not the arginine/ornithine auxotrophies[4,13] of *orn*A–4, *orn*C–31, and *orn*D–10 strains or the arginine auxotrophies[4,13] of *arg*A–1, *arg*B–2, and *arg*C–3 strains. GABA and β-alanine, however, cannot supplement *orn*B$^-$ strains also carrying an *int*A$^-$ or *gat*A$^-$ mutation. *int*A^c–2, –300, –302, –304, and –305 exert, to varying degrees, locus-specific suppression of *orn*B$^-$ auxotrophies (Table 3) although not suppressing *orn*A–4, *orn*C–31, *orn*D–10, *arg*A–1, *arg*B–2, and *arg*C–3. This physiological suppression requires that the *gat*A gene but not the *amd*S and *gab*A genes be functional: *int*A^c *gat*A$^-$ *orn*B$^-$ triple mutants require arginine or ornithine and do not respond to GABA or β-alanine. *orn*B$^-$ mutations probably abolish the transaminase which normally converts *N*-acetyl-L-glutamic γ-semialdehyde to N^{α}-acetyl-L-ornithine. When induced by GABA or β-alanine or rendered constitutive by an *int*A^c mutation, the GABA transaminase can apparently catalyse this conversion.

Expression of the *gab*A permease in *int*A mutants can be followed in Tables 1 and 2. GABA is extremely toxic to *gat*A$^-$ mutants. *gab*A$^-$ and *int*A$^-$ mutations relieve this toxicity by reducing GABA uptake (H. A. Penfold and H. N. A., unpublished) so that *gab*A$^-$ *gat*A$^-$ and *int*A$^-$ *gat*A$^-$ double mutants but not *gat*A$^-$ single mutants can grow on GABA plus another nitrogen source such as nitrate (Table 1). Given their lack of *gat*A expression, the very growth of *int*A$^-$ mutants on GABA plus nitrate also illustrates lack of *gab*A expression. The

Table 1 Growth responses of wild-type and mutant strains

Relevant genotype	Acrylamide as N	Acetamide as N	Acetamide as C	Growth on media containing GABA as N	GABA+NO$_3$$^-$ as N	GABA as C	β-Alanine as N	δ-Amino-*n*-valerate as N
Wild type	—	3+	3+	5+	5+	5+	5+	4+
*int*A^{c}–2	4+	5+	5+	5+	5+	5+	5+	5+
*int*A^{c}–300	2+	5+	5+	5+	5+	5+	5+	5+
*int*A^{c}–302	3+	5+	5+	5+	5+	5+	5+	5+
*int*A^{c}–304	2+	5+	5+	5+	5+	5+	5+	5+
*int*A^{c}–305	—	3+	3+	5+	5+	5+	5+	5+
*amd*A^{d}–301, –303	—	5+	5+	5+	5+	5+	5+	4+
*int*A^{c}–2 *amd*A^{d}–301	4+	5+	5+	5+	5+	5+	5+	5+
*int*A^{c}–304 *amd*A^{d}–301	3+	5+	5+	5+	5+	5+	5+	5+
*int*A^{-}–44,–100,–101,–105,–106,–107	—	2+	+	—	5+	—	—	±
*int*A^{-}–500	—	2+	+	3+	5+	3+	—	4+
*amd*A^{d}–301 *int*A^{-}–101	—	3+	3+	—	5+	—	—	±
*amd*S–17	—	—	—	5+	5+	5+	5+	4+
*gab*A–2, –6	—	3+	3+	2+	5+	±	5+	4+
*gat*A–1, –2	+	4+	4+	—	—	—	—	—
*gab*A–2 *gat*A–1, –2	+	4+	4+	—	3+	—	—	—
*int*A^{-}–101 *gab*A–2	—	2+	+	—	5+	—	—	±
*int*A^{-}–101 *gat*–1, –2	—	2+	+	—	3+	—	—	—
*int*A^{-}–500 *gab*A–2	—	2+	+	2+	5+	±	—	4+
*int*A^{-}–500 *gat*A–1	—	2+	+	—	2+	—	—	—
*int*A^{c}–2 *amd*S–17	—	—	—	5+	5+	5+	5+	5+
*int*A^{c}–2 *gab*A–2	4+	5+	5+	2+	5+	±	5+	5+
*int*A^{c}–2 *gat*A–1, –2	4+	5+	5+	—	—	—	—	—
*amd*A^{d}–301 *amd*S–17	—	—	—	5+	5+	5+	5+	4+
*amd*A^{d}–301 *gat*A–1	+	5+	5+	—	—	—	—	—

—, No growth; ±, very slight growth; + up to 5+, increasing levels of growth. Growth scores on different media are not necessarily equivalent, but 5+ represents the maximum growth observed on any medium.

Growth tests were carried out at 37 °C on appropriately supplemented minimal medium[15] as described previously[16]. At least several different strains of each relevant genotype were tested. Nitrogen sources were added to 1% D-glucose-containing media at 10 mM (acrylamide, acetamide, sodium nitrate) or 5 mM (β-alanine, GABA, δ-amino-*n*-valerate). Carbon sources were added to a final concentration of 50 mM to glucose-free media. Growth scores on different media are not necessarily equivalent. All strains listed above utilise L-glutamate and L-aspartate normally as nitrogen or carbon sources.

*int*A^{c}–2 (formerly *amd*R^{c}–2), *int*A^{-}–44 (formerly *amd*R^{-}–44), and *amd*S–17 were provided by Dr M. J. Hynes, who has described their selection[9]. *int*A^{c}–300, *amd*A^{d}–301, and *int*A^{c}–302 (formerly designated *amd*^{d}–300, –301, and –302) were obtained as suppressors of *are*A^{r}–1 on acetamide as described previously[12]. *int*A^{c}–304, *amd*A^{d}–303, and *int*A^{c}–305 were obtained after *N*–methyl–*N′*–nitro–*N*–nitrosoguanidine (NTG) mutagenesis[17] of a strain of genotype *bi*A–1 *are*A^{r}–2 *fw*A–1 (biotin-requiring, unable to utilise nitrogen sources other than ammonium, fawn conidial colour) as suppressing *are*A^{r}–2 on acetamide, acetamide, and GABA as nitrogen sources, respectively. *int*A^{-}–100 and –101 were obtained as spontaneous mutations in strains of genotype *paba*A–1 *int*A^{c}–2 *mau*A–2 (*p*-aminobenzoate-requiring, *int*A^{c}–2 phenotype as described herein, lacking monoamine oxidase) and *pu*A–2 *int*A^{c}–300 (putrescine-requiring, *int*A^{c}–300 phenotype as described herein), respectively, resulting in resistance to 4 mg ml^{-1} 2-fluoroacetamide (Fluka, Buchs, Switzerland) on medium containing 72 mM acetate (*p*H 6.5) as sole carbon source and 5 mM urea as sole nitrogen source. *gab*A–2 and –6 were selected as unable to utilise 5 mM GABA as nitrogen source after NTG mutagenesis of a strain of genotype *bi*A–1 *pu*A–2 *fw*–A–1 using the putrescine starvation selection technique[18]. *int*A^{-}–105, –106, –107, and –500 and *gat*A–1 were selected after ultraviolet mutagenesis of a strain of genotype *paba*A–1, using replica plating[19], as able to utilise 5 mM L-proline but not 5 mM β-alanine as nitrogen source. *gat*A–2 was selected by Mr K. N. Rand. It was obtained after ultraviolet mutagenesis of a strain of genotype *paba*A–1 *are*A^{r}–120 as allowing utilisation of 10 mM acrylamide as nitrogen source in the presence of 1% (v/v) glycerol as sole carbon source. This weak suppression is presumably associated with the slight enhancement of acetamide and acrylamide utilisation by *gat*A^{-} mutations (which will nevertheless not suppress the more stringent *are*A^{r} alleles on acetamide or acrylamide) as seen above. A likely explanation is that *gat*A^{-} mutations enhance the accumulation of an endogenous inducer such as β-alanine which can activate the *int*A product, as no such enhancement occurs in strains also carrying an *int*A^{-} mutation.

Allelism has been demonstrated both by tight linkage (generally less than 0.5 cM) and, for recessive mutations resulting in loss of function, by a lack of complementation in diploids. The leakiest *int*A^{-} allele, *int*A^{-}–500, does not complement with *int*A^{-}–44, –100, –101, –105, –106, or –107. The *int*A^{-} mutations are recessive to *int*A^{+} on the media listed above whilst *int*A^{c}–2 is partially dominant to both *int*A^{+} and *int*A^{-}–101.

ability of the five *int*A^{c} mutations to suppress *are*A^{r} for utilisation of GABA as nitrogen source (Table 2) probably primarily reflects enhanced levels of the *gab*A permease because suppression of *are*A^{r} on GABA can also be achieved by a *cis*-dominant regulatory mutation tightly linked to *gab*A (unpublished results C. R. Bailey and H. N. A.). Suppression of *are*A^{r} on GABA requires functional alleles of both *gab*A and *gat*A but not *amd*S. The selection of mutations able to suppress *are*A^{r} mutations on two or more nitrogen sources metabolised by different pathways is probably a general method for obtaining derepressed alleles of integrator genes, provided synthesis of the necessary enzymes and permeases does not have an absolute requirement for a functional *are*A product (K. N. Rand and H. N. A., unpublished).

The probable route of GABA catabolism is shown in Fig. 1. Although *int*A controls both GABA uptake and transamination, it apparently does not regulate succinic semialdehyde dehydrogenase because *int*A^{-} strains utilise γ-hydroxy-*n*-butyrate as a carbon source. *ssu*A—1 strains can utilise neither GABA nor γ-hydroxy-*n*-butyrate as carbon sources (C. R. Bailey and H. N. A., unpublished).

As well as controlling three structural genes, the *int*A product must respond to at least two effectors, GABA and β-alanine or their derivatives, as shown by their ability to supplement *orn*B^{-} auxotrophies. If the *int*A product be directly involved in regulating *amd*S, *gat*A, and *gab*A, mutations affecting the specificity of the *int*A product might fall into one or both of two categories: (1) those having a differential effect on the expression of the three structural genes; and (2) those affecting response to one of the effectors more than the other. *int*A^{-}—500 is probably of the latter type since it affects responses to β-alanine much more drastically than responses to GABA or δ-amino-*n*-valerate (Tables 1 and 3). The lack of additivity of *int*A^{-}—500 and *gab*A—2 in double mutants and the relative resistance of *int*A^{-}—500 *gat*A—1 double mutants to GABA supports this conclusion. The fully *int*A^{-} phenotype of *int*A^{-}—500 on acetamide (Table 1) plus its resistance to acetamidase-catalysed, lethal hydrolysis of 2-fluoroacetamide[9] might indicate that *int*A^{-}—500 also falls into the first specificity category, stringently affecting *amd*S. It is more likely, however, that the mutant responses of *int*A^{-} strains to acetamide and its analogues are dependent on a small amount of endogenous effector

Table 2 Suppression of *are*A^{r} mutations

Relevant genotype	Nitrogen source δ-Amino-*n*-valerate or β-alanine or NO_3^-	Acetamide	GABA	NH_4^+
Wild type (*are*A^{+})	5+	5+	5+	5+
*are*A^{r}–1, –2, –19	–	–	–	5+
*int*A^{c}–2 *are*A^{r}–1,–2,–19	–	4+	3+	5+
*int*A^{c}–300 *are*A^{r}–1	–	3+	2+	5+
*int*A^{c}–302 *are*A^{r}–1	–	3+	+	5+
*int*A^{c}–304 *are*A^{r}–2	–	3+	±	5+
*int*A^{c}–305 *are*A^{r}–2	–	–	3+	5+
*amd*A^{d}–301 *are*A^{r}–1, –2, –19	–	3+	–	5+
*amd*A^{d}–303 *are*A^{r}–2	–	3+	–	5+
*int*A^{c}–304 *amd*A^{d}–301 *are*A^{r}–2	–	4+	±	5+
*int*A^{c}–2 *amd*S–17 *are*A^{r}–1	–	–	3+	5+
*int*A^{c}–2 *gab*A–2 *are*A^{r}–2	–	4+	–	5+
*int*A^{c}–2 *gat*A–2 *are*A^{r}–2	–	4+	–	5+
*amd*A^{d}–301 *amd*S–17 *are*A^{r}–1	–	–	–	5+
*amd*A^{d}–301 *int*A^{-}–101 *are*A^{r}–2	–	+	–	5+
*int*A^{-}–101 *are*A^{r}–1, –2	–	–	–	5+
*amd*S–17 *are*A^{r}–1	–	–	–	5+
*gab*A–2 *are*A^{r}–2	–	–	–	5+
*gat*A–2 *are*A^{r}–1, –2	–	–	–	5+

See legend to Table 1 for most details. Ammonium was added at 10 mM as the (+)-tartrate *are*A^{r}–1, –2, and –19 (formerly *amd*T–19) have been described previously[12] and lead to inability to utilise nitrogen sources other than ammonium. Growth scores on different media are not necessarily equivalent. When tested in diploids homozygous for *are*A^{r}–2, *int*A^{c}–2 and *amd*A^{d}–301 are partially dominant. None of the *int*A^{c} or *amd*A^{d} mutations suppress *are*A^{r} mutations on L-glutamate or L-aspartate as nitrogen sources

interacting with the *int*A product in *int*A^{+} strains. The behaviour of *int*A^{-}–500 might therefore suggest that β-alanine, an essential metabolite for synthesis of coenzyme A, is that effector. Its concentration must be sufficiently low for *orn*B^{-} mutations to result in complete auxotrophy. Low levels of β-alanine and GABA have been detected in *Neurospora crassa*[14].

*int*A^{c}–305 and –304 are probably specificity mutations of the first category. *int*A^{c}–305 strongly affects *gab*A expression but has little effect on expression of *amd*S and *gat*A. The opposite is true of *int*A^{c}–304. This indicates that the *gab*A receptor site for the *int*A product differs from those of the *amd*S and *gat*A genes. A diversity of receptor sites for the *are*A product has already been postulated[7]. The existence of such opposite phenotypes among *int*A alleles is only compatible with direct regulatory involvement of the *int*A product. Indirect involvement could only lead to a hierarchy of structural gene

Table 3 Supplementation and suppression of *orn*B^{-} mutations

Relevant genotype	Supplement L-Arginine or L-ornithine	β–Alanine	GABA	None
Wild type (*orn*B^{+})	5+	5+	5+	5+
*orn*B–7, –8, –9, –20, –300	5+	4+	3+	–
*int*A^{c}–2 *orn*B–7, –8, –9, –20, –300	5+	5+	5+	5+
*int*A^{c}–300 *orn*B–7	5+	5+	5+	2+
*int*A^{c}–302 *orn*B–7	5+	5+	5+	4+
*int*A^{c}–304 *orn*B–7	5+	5+	5+	3+
*int*A^{c}–305 *orn*B–7	5+	5+	5+	±
*amd*A^{d}–301 *orn*B–7	5+	4+	3+	–
*int*A^{c}–2 *amd*S–17 *orn*B–7	5+	5+	5+	4+
*int*A^{c}–2 *gab*A–2 *orn*B–7	5+	5+	5+	4+
*int*A^{c}–2 *gat*A–1, –2 *orn*B–7	5+	–	–	–
*amd*S–17 *orn*B–7	5+	4+	3+	–
*gab*A–2 *orn*B–7	5+	4+	3+	–
*gat*A–1, –2 *orn*B–7	5+	–	–	–
*int*A^{-}–101 *orn*B–7	5+	–	–	–
*int*A^{-}–500 *orn*B–7	5+	–	+	–

See legends to Tables 1 and 2 for most details. Supplementation by L-arginine and L-ornithine (as the monohydrochlorides) was tested at 5 mM with or without another nitrogen source. Unsupplemented medium contained 10 mM ammonium as nitrogen source. β-alanine and GABA were added with or without uric acid (100μg ml^{-1}) although they definitely supplement more efficiently in the absence of another nitrogen source. GABA supplementation of *orn*B^{-} strains is considerably improved by using strains also carrying a mutation relieving ammonium repression such as *mea*A–8[16,20] or *are*A^{d}–102 (formerly *amd*T–102)[12] or by using glucose-free medium with 50 mM GABA as sole carbon source. Presumably, self nitrogen metabolite repression[12] limits GABA supplementation of *orn*B^{-} single mutants growing on GABA as sole nitrogen source. Neither L-glutamate nor L-aspartate supplements *orn*B^{-} auxotrophies.

The arginine/ornithine auxotrophies *orn*B–7, –8, –9, and –20 are markers in standard use[4]. *orn*B–300 was selected after ultraviolet mutagenesis of a strain of genotype *y*A–2 *al*X–4 *panto*B–100 (yellow conidial colour, lacking allantoinase, requiring pantothenic acid), using replica plating, as able to grow on a medium containing 5 mM GABA but not 5 mM L-proline as nitrogen source. *orn*B–300 is temperature sensitive, resulting in auxotrophy at 37 °C but not at 25 °C It is tightly linked to *orn*B–7, and they do not complement in diploids.

When diploids homozygous for *orn*B–7 are tested on the above media, *int*A^{c}–2 is partially dominant whereas *int*A^{-}–101 is recessive.

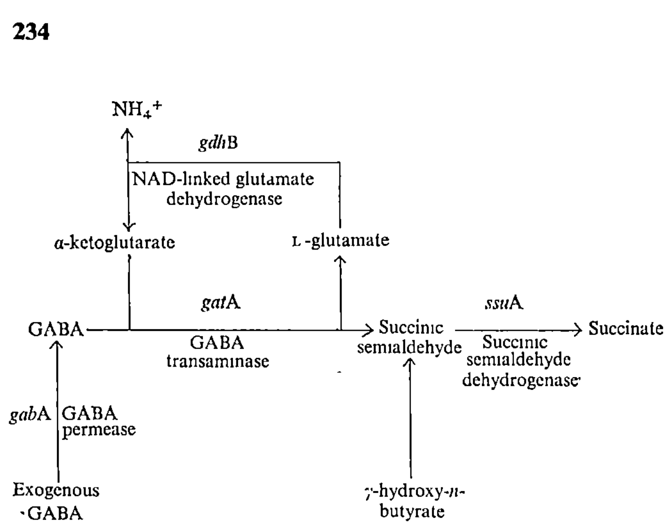

Fig. 1 The pathway of GABA catabolism in *A nidulans*, shown above, is probably very similar to that in *Escherichia coli*[21]. As expected[22–25] for compounds whose nitrogen is metabolised by way of L-glutamate before ammonium, GABA, β-alanine, and δ-amino-*n*-valerate supplement *gdh*A$^-$ mutants lacking the anabolic NADP-linked glutamate dehydrogenase, but are not utilised by *gdh*B$^-$ mutants lacking the catabolic NAD-linked glutamate dehydrogenase. GABA can also supplement *pyc*A$^-$ mutants[26] lacking pyruvate carboxylase and consequently requiring a source of a four-carbon dicarboxylic acid The utilisation of GABA is subject to both nitrogen metabolite[12] and carbon catabolite[27] repression (H. A. Penfold, C. R. Bailey, and H. N. A.).

expression. This type of evidence has also shown direct regulatory involvement of the *are*A gene product[7,12].

A full biochemical and genetical analysis of ω-amino acid catabolism and effects on acetamidase synthesis is in progress (H. A. Penfold, C. R. Bailey, and H. N. A., unpublished). We are particularly interested in seeing whether, as implied by results presented here, the binding of different effectors to the *int*A$^+$ product alters the relative efficiencies of expression of the three structural genes.

In conclusion, *int*A is a positive regulatory gene whose product directly affects the expression of three unlinked structural genes which can participate in different catabolic pathways. The structural genes code for an acetamidase, a GABA transaminase, and a GABA permease. At least the acetamidase is subject to an alternative, parallel mechanism of induction, involving the specific regulatory gene *amd*A, in addition to the induction mediated by the *int*A product. Therefore *int*A can be described as an integrator gene. The ability of (mostly point) mutations in *int*A to affect expression of any one or two or all three of the structural genes controlled by *int*A argues that *int*A is a single gene, not a battery of coordinately controlled contiguous genes. Of the alternative regulatory circuits offered by Britten and Davidson[1], *int*A therefore fits into the redundancy of receptor sites model rather than the redundancy of integrator genes model.

I thank Claudio Scazzocchio, Hugh Penfold, Keith Rand, Chris Bailey and especially Dick LePage for useful discussions and Bridget Pritchard and Mick Pierson for technical assistance, and the Royal Society for the Smithson Research Fellowship. This work was partially supported by a grant from the SRC to Professor J. M. Thoday.

Note added in proof: Confirming a crucial prediction, β-alanine and GABA induce acetamidase in wild-type but not in *inta*A$^-$-101 strains. β-alanine induces to a considerably higher level than acetamide, but simultaneous addition of β-alanine and acetamide results in only an intermediate, not an additive, level of induction. This probably indicates competition between the *int*A product (activated by β-alanine) and the *amd*A product (activated by acetamide) in the induction of acetamidase. Such competition could result from a partial or complete overlap of receptor sites.

HERBERT N. ARST, JR

Department of Genetics,
University of Cambridge,
Milton Road, Cambridge CB4 1XH, UK

Received April 15; accepted May 5, 1976.

[1] Britten, R. J., and Davidson, E. H., *Science*, 165, 349–357 (1969).
[2] Britten, R. J., and Davidson, E. H., *Q. Rev. Biol.*, 46, 111–138 (1971).
[3] Davidson, E. H., and Britten, R. J., *Q. Rev. Biol.*, 48, 565–613 (1973).
[4] Clutterbuck, A. J., in *Handbook of Genetics*, 1, (edit. by King, R. C.), 447–510 (Plenum, New York, 1974).
[5] Hynes, M. J., *Nature*, 253, 210–212 (1975)
[6] Arst, H. N., Jr, and MacDonald, D. W., *Nature*, 254, 26–31 (1975).
[7] Arst, H. N., Jr, and Scazzocchio, C., *Nature*, 254, 31–34 (1975).
[8] Lukaszkiewicz, Z., and Paszewski, A., *Nature*, 259, 337–338 (1976).
[9] Hynes, M. J., and Pateman, J. A. J., *Molec. gen. Genet.*, 108, 97–106; 107–116 (1970).
[10] Dunsmuir, P., and Hynes, M. J., *Molec. gen. Genet.*, 123, 333–346 (1973).
[11] Hynes, M. J., and Pateman, J. A., *J. gen. Microbiol.*, 63, 317–324 (1970).
[12] Arst, H. N., Jr, and Cove, D. J., *Molec. gen. Genet.*, 126, 111–141 (1973).
[13] Cybis, J., Piotrowska, M., and Weglenski, P., *Acta microbiol. Pol.*, A4, 163–169 (1972).
[14] Schmit, J. C., and Brody, S., *J. Bact.*, 124, 232–242 (1975).
[15] Cove, D. J., *Biochim. biophys. Acta*, 113, 51–56 (1966).
[16] Arst, H. N., Jr, and Cove, D. J., *J. Bact.*, 98, 1284–1293 (1969)
[17] Alderson, T., and Hartley, M. J., *Mutat. Res.*, 8, 255–264 (1969).
[18] Herman, C., and Clutterbuck, A. J., *Aspergillus News Lett.*, 7, 13–14 (1966).
[19] Mackintosh, M. E., and Pritchard, R. H., *Genet. Res.*, 4, 320–322 (1963).
[20] Arst, H. N., Jr, and Page, M. M., *Molec. gen. Genet.*, 121, 239–245 (1973).
[21] Dover, S., and Halpern, Y. S., *J. Bact.*, 109, 835–843 (1972).
[22] Arst, H. N., Jr, and MacDonald, D. W., *Molec. gen. Genet.*, 122, 261–265 (1973).
[23] Arst, H. N., Jr, Parbtani, A. A. M., and Cove, D. J., *Molec. gen. Genet.*, 138, 165–171 (1975).
[24] Kinghorn, J. R., and Pateman, J. A., *J. gen Microbiol.*, 78, 39–46 (1973).
[25] Kinghorn, J. R., and Pateman, J. A., *J. Bact.*, 125, 42–47 (1976).
[26] Skinner, V. M., and Armitt, S., *FEBS Lett.*, 20, 16–18 (1972).
[27] Bailey, C., and Arst, H. N., Jr, *Eur. J. Biochem.*, 51, 573–577 (1975).

X-ray study of the rubidium salt of ADP

ENZYMATIC reactions involving ATP and ADP require various metal ions as cofactors for catalytic activation. To understand the molecular mechanisms involved in these reactions it is important to know both the detailed geometry of these molecules and the way in which they bind to metal ions. Although numerous physical and chemical studies have been undertaken, particularly of divalent metal complexes in solution, the conformational and electronic aspects of these complexes are not fully understood. In the solid state, crystallographic studies have led to deductions on the conformations of ATP and ADP when bound to enzymes (refs 1–3 and H. C. Watson, personal communication) but the only crystal structures so far determined to atomic resolution are of the disodium salt of ATP[4] and the monorubidium salt of ADP[5]. The latter structure has so far only been published in part although some of its molecular features were reviewed recently[6].

The work reported here is on a different hydrate of monorubidium ADP containing one water molecule per nucleotide instead of three as in the earlier study. The Rb-ATP and ADP complexes are of biochemical importance as many enzyme systems associated with phosphate transfer require, in addition to divalent metal ions, univalent cations for activation (for example, K^+, Rb^+, NH_4^+)[7]. As part of our study of phosphate coenzymes we have attempted the preparation of single crystals of other mono- and divalent salts of ADP but so far without much success.

The monorubidium salt of ADP was crystallised as needles from water–alcohol solutions containing ADP free acid and RbBr (1:1). The solution was kept at 5 °C and *p*H 5.5 using Tris buffer. The space group ($P2_12_12$) and cell dimensions (a = 28.516(3) Å, b = 10.594(3) Å, c = 6.315(2) Å) agreed with those reported for the trihydrated rubidium salt by Muller and Deluke[5]. The measured density (D_m = 1.86 g cm^{-3}, D_x = 1.84 g cm^{-3}, Z = 4) indicated, however, the presence of only one water molecule per ADP molecule and this was later confirmed by the structure analysis.

A total of 1,440 unique reflections were collected on a

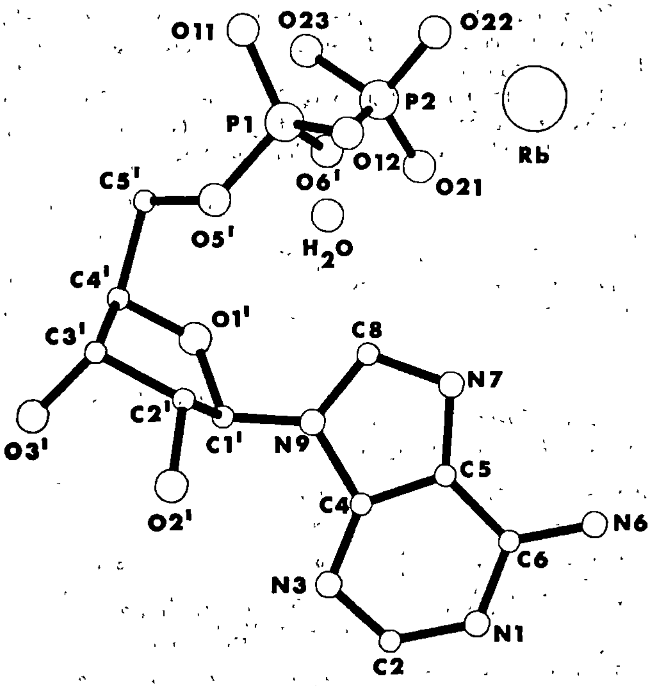

Fig. 1 View of the ADP molecule perpendicular to the base.

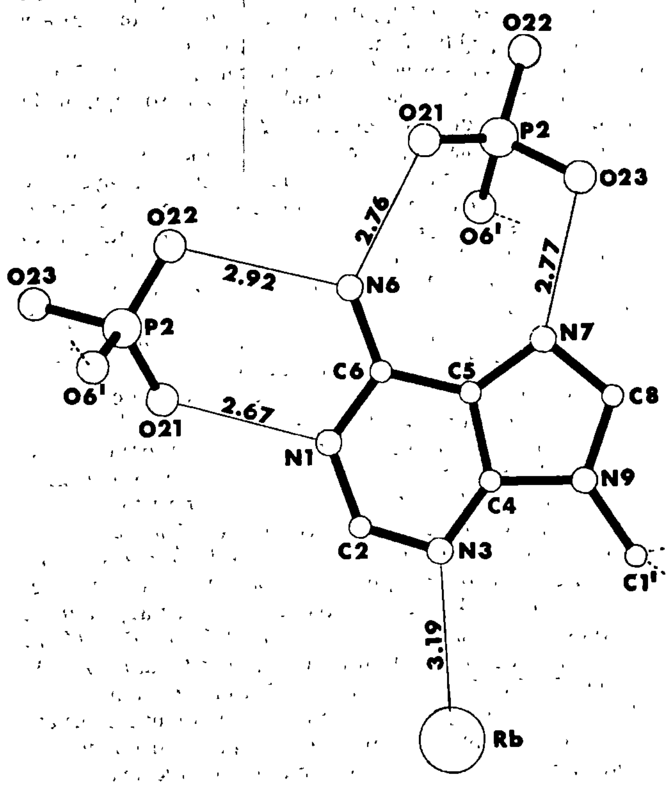

Fig. 2 Interactions involving the base atoms.

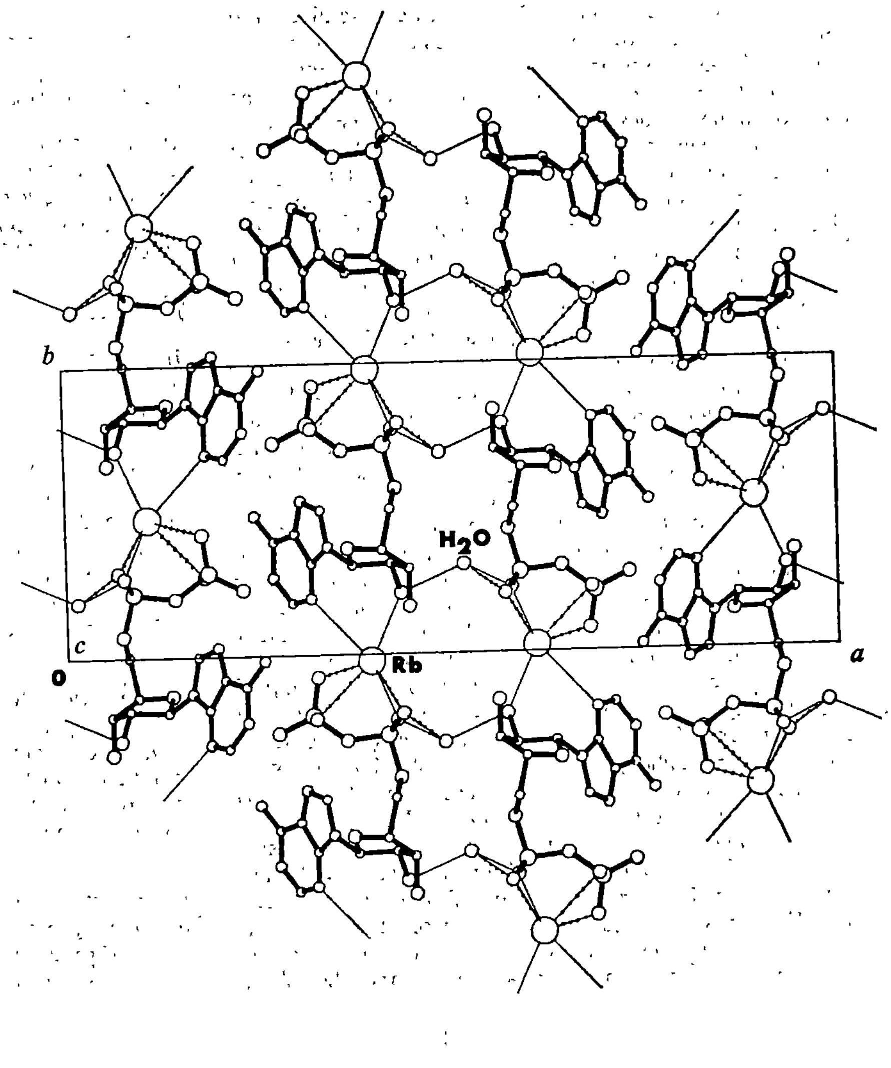

Fig. 3 Crystal packing viewed down the *c* axis showing the Rb$^+$ coordination and the hydrogen bonding with water molecules. (The dotted lines refer to contacts with molecules related by *c* translation.)

Syntex P2$_1$ diffractometer of which 1,200 were significant on the basis of $F > 3\sigma(F)$. The data were of moderate accuracy due to the poor quality of the crystal specimen.

The structure was solved by the application of MULTAN[8] and a difference Fourier synthesis and refined anisotropically in a full-matrix least squares program to $R = 11.9\%$.

A view of the molecule, perpendicular to the base, is shown in Fig. 1. The orientation of the base about the glycosidic C1′–N9 linkage is *anti*, the only conformation so far observed in the crystal structures of nucleotides. The dihedral angles O1′–C1′–N9–C8 and C2′–C1′–N9–C8 are 40.3° and −75.8°.

In the ribose ring, C2′ is displaced by 0.54 Å from the mean plane through C3′, C4′, O1′, C1′ corresponding to a typical C2′-*endo* puckering. The conformation about the C4′–C5′ bond is *gauche gauche* with torsion angles O5′–C5′–C4′–C3′ = 57.0° and O5′–C5′–C4′–O1′ = −63.3°. The conformation about C5′–O5′ is *trans* (P1–O5′–C5′–C4′ = 147.1°). A similar conformation has also been proposed as the predominant structure of ADP in solution, from a Fourier transform nuclear magnetic resonance (NMR) study[9]. The pyrophosphate moiety has a staggered conformation. A striking feature of the structure is the observed difference of 0.10 Å between the lengths of the two bridging bonds in the high energy linkage, which seems to be significant at the level of accuracy attained in the present analysis. The values for P1–O6′ and P2–O6′ are 1.54 and 1.64 Å respectively with an estimated s.d. of 0.02 Å. The angle P1–O6′–P2 is 135° (e.s.d. 1°). Corresponding values in other nucleoside diphosphates recently determined by us are 1.60 and 1.64 Å and 133° in cytidine diphosphocholine and 1.58 and 1.62 Å and 128° in cytidine diphosphoric acid[10].

In the crystal structure, the ADP molecule is folded but there is no Rb$^+$ bridge between the phosphate and adenine groups of the same molecule. Nor is there any evidence of other types of intramolecular interactions such as hydrogen bonding or metal binding between the pyrophosphate chain and the base or sugar moiety. In this respect, the ADP structure resembles the conformations found in the crystal structures of the dipotassium salt of uridine-5′-diphosphate (M.A.V., M. L. Post and O.K., unpublished) and the monosodium salt of cytidine diphosphocholine[10]. These coenzyme molecules, which are in very different crystalline environments, are also folded without any intramolecular metal ligation. They seem to take up the folded conformation preferentially and it is likely that any binding involving metal ions merely helps to stabilise the folded structure. A recent NMR study of ATP bound to lanthanide cations in aqueous solution[11] has been interpreted in terms of a folded conformation, with the lanthanide ion bound only to the β and γ phosphates but with no direct interaction with the purine ring.

It is interesting to note that in contrast to the folded conformation reported here, difference electron density maps suggest that ADP is in the extended form when bound to either lactate dehydrogenase[1] or phosphoglycerate kinase (refs 2, 3 and H. C. Watson, personal communication).

The extended crystal structure shows no self association between the bases through either hydrogen bonding, or base stacking. Instead there are two pairs of hydrogen bonds linking the adenine base to phosphate group of two neighbouring molecules (Fig. 2). One of these pairs has the Watson–Crick geometry, while the other involves the amino group and the imidazole nitrogen N7. These interactions and the binding of Rb$^+$ to N3 may be relevant to the recognition of the base by polar side groups of amino acids and metal ions in biological systems (to be published). The role of similar interaction in the sequence specific recognition of nucleic acids by proteins has recently been discussed by Seeman *et al.*[12].

Figure 3 shows the role of the Rb$^+$ ions and the water molecules. Each Rb$^+$ ion is bound to two ADP molecules through the negatively charged α and β phosphate oxygen atoms. The four Rb · · · O distances range from 2.85 to 3.33 Å. The sixfold coordination around Rb$^+$ is completed by N3 of the adenyl base of a third molecule at 3.19 Å and the ribose hydroxyl atom of the same molecule at 2.91 Å.

The water molecules lie in sheets perpendicular to the *a* axis interlinking layers of Rb–nucleotide complexes through hydrogen bonding.

The investigation was supported by the Indian Council for Medical Research, the MRC and the SRC (visiting fellowship to M.A.V. and provision of the diffractometer).

M. A. VISWAMITRA
M. V. HOSUR

*ICMR Unit on Genetics and Cell Biology
and Department of Physics,
Indian Institute of Science,
Bangalore–560012, India*

ZIPPORA SHAKKED
OLGA KENNARD*

*University Chemical Laboratory,
Lensfield Road, Cambridge CB2 1EW, UK*

Received January 30; accepted May 25, 1976

* External staff, Medical Research Council.

[1] Chandrasekhar, K., Mcpherson, A, Jr, Adams, M. J., and Rossman, M G., *J molec Biol.*, **76**, 503–517 (1973).
[2] Bryant, T. N, Watson, H C., Wendell, P L., *Nature*, **247**, 14–17 (1974).
[3] Blake, C. C. F., Evans, P R., *J. molec. Biol.*, **84**, 585–601 (1974).
[4] Kennard, O., *et al.*, *Proc. R. Soc.*, A325, 401–436 (1971).
[5] Muller, F. A, Deluke, A. B., *Am. cryst. Ass., Abstr. Papers* (Winter Meeting), 26 (1971)
[6] Sundaralingam, M, in *5th Jerusalem Symposium in Quantum Chemistry and Biochemistry* (edit by Bergmann, E. D, and Pullman, B), 417 (1973).
[7] Happold, F C., and Beechey, R B., in *15th Biochemical Society Symposium* (edit. by Crook, G M) (Cambridge University Press, London, 1958).
[8] Main, P., Woolfson, M. M, Lessinger, L, Germain, G., and Declerq, J P., *MULTAN, A System of Computer Programmes for the Automatic Solution of Crystal Structures from X-ray Diffraction Data* (1974).
[9] Sarma, R. H., Mynott, R. J., Hruska, F. E., and Wood, D J., *Can J. Chem.*, **51**, 1843–1851 (1973)
[10] Viswamitra, M. A, Seshadri, T. P., Post, M L., and Kennard, O., *Nature*, **258**, 497–501 (1975).
[11] Tanswell, P., Thornton, J. M, Korda, A. V., and Williams, R. J. P., *Eur. J. Biochem.*, **57**, 135–145 (1975).
[12] Seeman, N. C., Rosenberg, J. M., and Rich, A, *Proc natn. Acad. Sci. U.S A*, **73**, 804–808 (1976).

Corrigendum

In the article "Two short lived X-ray transients at high galactic latitude" by B. A. Cooke (*Nature*, **261**, 564; 1976) the scale and legend to Fig. 2*a* are in error. The scale should read 13 h not 3 h and the source designation in the legend should be A1353−40 not A0353−40.

Errata

In the article "Extinction-free measurements in crystallography" by A. McL Mathieson (*Nature*, **261**, 306; 1976), a sentence was omitted in the editing process. On line 12 of paragraph 1 mention of refs 5–7 should be deleted, and line 13 *et seq.* should read:

'. . . is applicable. The possibility exists of extrapolating to this condition, as a practical procedure, in relation to asymmetric reflection[5–7]. Starting with . . .'

In paragraph 4 line 7 of the right-hand column of page 307 'ref. 8' should be 'ref. 9', and in the caption to Fig. 2 the reference on the first line should be '5'.

In the article "Phosphorylation of yeast RNA polymerases" by G. Bell, P. Valenzuela and W. J. Rutter (*Nature*, **261**, 429; 1976) symbols were omitted from Fig. 1*a* which make it difficult to understand. The correct symbols are as follows. ^{32}P c.p.m. (○); RNA polymerase activity (●); Protein concentration (——).

In the article "Simple mathematical models with very complicated dynamics" by Robert May (*Nature*, **261**, 459–467; 1976) Figs 2 and 3 were transposed. The captions were in the correct position.

reviews

Introducing nuclear power

Lord Hinton of Bankside

Nuclear Power. (A Pelican Original) By Walter C. Patterson. Pp. 304. (Penguin: Harmondsworth, Middlesex, March 1976.) 80p.

WALTER PATTERSON'S book is written in two parts. The first, which he calls "The World of Nuclear Fission" is excellent, I have never read a better simple explanation of the theory and practice of nuclear reactors and their ancillary plants. I am less enthusiastic about the second part of the book, most of which deals with the hazards of nuclear power. It seems to me that, in his anxiety to make a case which is real, Patterson may be guilty of lack of balance. The impression which is given by the italic printing of some paragraphs is that they have been abstracted from official reports; my limited inside knowledge contradicts this impression. For instance, I have never heard the filters on the Windscale piles referred to as "Cockcroft's folly". The stacks had not been built (as stated in italic script) when information from America made it clear that filters were a necessary precaution.

These statements are, in themselves, of minor importance but they throw some doubt on italic accounts of other incidents. The italic paragraph about "the dramatic gesture of pouring away milk" after the Windscale incident seems to be romanticised; I had left the UK Atomic Energy Authority at the time of the incident and knew nothing of any discussions that took place but (although the milk could safely have been used in milk chocolate or as dried milk) it seems to me that it would have been a foolish firm which bought the milk and laid itself open to the unfounded accusation of selling a radioactive product. The italic paragraphs about the Enrico Fermi fast reactor and mention of the "China syndrome" are hardly a fair argument against the fast reactors which are being designed today and which use a ceramic and not a metallic fuel.

The book does not emphasise the world's real need for nuclear power. The rate of usage of exhaustable natural resources does not increase exponentially to a sharp peak and suddenly fall away to nothing; it conforms to a wave-shaped curve so that at some point in time growth becomes steadily slower until a peak is reached; and, thereafter, growth becomes negative (that is, the rate of usage diminishes).

There is good evidence to suggest that global resources of fossil fuels are such that we shall pass over the peak of such a curve at about the end of this century. It is highly improbable that renewable energy resources (wave power, solar energy and wind power) can make up the deficit; without nuclear power it is almost certain that standards of living will fall.

Nuclear power does give rise to some hazards but nothing in this world is absolutely safe. Nuclear power plants can be made as safe or safer than very many other industrial plants provided that engineers are not over-ambitious in extrapolating either the design parameters or the size of the construction programs With these reservations I would sooner accept the hazards of nuclear power than the risk of an energy famine.

The first part of Walter Patterson's book is an outstandingly good introduction to nuclear power for the intelligent layman. As a reminder of their responsibilities, Part 2 should be compulsory reading for those men who have responsibilities in the nuclear power industry; but its lack of balance may give a wrong impression to the lay-reader. ☐

Lord Hinton of Bankside is Deputy Chairman of the Electricity Supply Research Council and was formerly Managing Director (Industrial Group) of the UKAEA and Chairman of the UK Central Electricity Generating Board.

Macrophage house of fashion

Immunobiology of the Macrophage. Edited by David S. Nelson. Pp. xviii+633. (Academic· New York and London, April 1976.) $39, £21.45.

As the hemlines of Western ladies rise and fall and split and waver with each new season's modish rhythm so do the fads and fancies of immunologically orientated biologists Thus lymphocytes were 'discovered' in the sixties and are probably presently at their apogee of man-hour involvement. The macrophage was discovered at the turn of the century but, as Cohn puts it in the Introduction to this fascinating book, the doldrums soon descended on all but a few dedicated phagists. The book heralds the new golden age of the macrophage (compare Golden Age of Thymology; Miller, *Lancet*, **2**, 1299; 1967).

Some of the 24 chapters, each written by a different expert in the field, deal with macrophage involvement in various *in vitro* cell preparations; others with the heterogeneity of macrophages as determined by their site of origin and the complexities of their cell surfaces. The responses of macrophages to chemotactic factors and their capacities to produce and liberate factors which affect other cellular components of the immunological orchestra are described Many are the schemes of cell interaction. The papers by Volkman on monocytes, by Evans and Alexander on macrophage cytotoxicity, by Holtermann *et al.* on immunotherapy of skin tumours and that by Territo and Cline on macrophage disorders in man are all at the end of the book and all well worth reading.

The changes of tempo and topic make me long for the earlier one-man macrophage book of Nelson but he, although remaining an editor, has abandoned the role of a colossus in the field capable of comprehensive review. In spite of this dereliction of function it is Nelson's summarising chapter 9 and final short chapter which are most useful to the outsider. As he says "In the evolution of our complex mammalian system they (macrophages) seem almost ubiquitous, emerging from obscurity to make some lysozymes contribute to the complement system, help a T cell, present a stimulus to a B cell, or quell an unruly mutant."

Those with time and deep pockets (do all books cost £20 these days?) should buy this book. It is well produced, well edited and most informative. But perhaps more important its mastery will put you in on the ground floor of the current macrophage house of fashion.

A. J. S. Davies

Laser physics

Laser Spectroscopy: Proceedings of the Second International Conference, Megève, June 1975. (Lecture Notes in Physics, Vol. 43). Edited by S. Haroche, J. C. Pebay-Peyroula, T. W. Hänsch and S. E. Harris. Pp. x+468. (Springer: Berlin and New York, 1975.) DM 45; $18.50.

THE development of tunable laser systems has radically altered the nature of atomic and molecular physics. Used in conventional spectroscopy, the high intensity and monochromaticity of the tunable laser makes it an ideal probe of purely atomic properties such as excited state lifetimes, fine and hyperfine structure splittings and isotope shifts: the list of worthy results is endless. When the laser is used in a dynamic sense, new and exciting non-linear, intensity-dependent features emerge. Finally the extremely short duration of pulses generated by pulsed mode-locked lasers enables the photochemist to study ultrafast relaxation and transport mechanisms. This volume, demonstrates how laser spectroscopy has arrived at a semblance of maturity after a period of very rapid growth. The topics discussed here extend from the quantum electrodynamics of laser resonance fluorescence to laser isotope separation processes of economic importance. Invited papers presented at the conference are here printed directly from the authors' typescripts.

For me, some especially interesting papers were those of Cagnac on high resolution, two photon spectroscopy, Mollenauer on colour centre lasers, and Cohen-Tannoudji's review of the currently fashionable dynamic Stark effect in resonance fluorescence. Workers in laser physics or atomic physics will find much in this volume to entertain and to stimulate One fascinating feature is the large number of papers, some with carefully spelled-out background histories and dates, devoted to laser isotope separation. On this the editors make the curious comment: "Unfortunately, the free flow of information was here still severely hampered by secrecy and classification, and the wisdom of including such a 'political' topic in the program has since been seriously questioned".

No doubt some of the new results presented at the conference for the first time will either appear or already have appeared elsewhere in the literature. But as a review of the status of the field, this volume serves a very useful purpose and can be recommended to workers in atomic and laser physics.

Peter Knight

ATLA ABSTRACTS

is published twice yearly and contains news, reviews, and abstracts on "Alternatives To Laboratory Animals". Coverage includes a variety of disciplines in a wide selection of world scientific literature.

Have you a copy in your Library? If not, a free specimen will be sent on request.

FRAME,
312a Worple Road
London SW20 8QU
(Fund for the Replacement of Animals in Medical Experiments)

(Registered Charity No. 259464 England)
Tel: 01-946 1450

Circle No. 09 on Reader Enquiry Form.

Sound basis for plant virology course

Plant Virology: The Principles. By Adrian Gibbs and Bryan Harrison Pp. x+292. (Arnold: London, March 1976.) £16.

IN the Preface to this excellent book the authors describe its gestation period as 'lengthy', which is scarcely more informative than a piece of string; but as they state that they aimed to provide a text at the university teaching level, a need not filled by books which have since appeared, I suppose that this one grew from notes prepared for lectures given to students of the Imperial College, University of London, by Gibbs and Harrison some 10 years ago while they were both at Rothamsted. This speculation is relevant to an assessment, since a gestation period of several years would account for some characteristics which might otherwise puzzle or even irritate a reader I am not suggesting that the book is out of date; far from it; I am referring to differences between chapters in style and depth. Problems of selection would have grown erratically as reference lists lengthened because research papers proliferated on fashionable topics; as the cost of publication rose at an accelerating rate, hard choices would have to be made.

The layout of the book provides a sound basis for a lecture course for undergraduates. After the history and scope of plant virology, some groups of viruses and the cryptogram system are described, followed by accounts of virus effects on plants, and methods of experimental transmission. The next chapter deals with the composition and structure of plant viruses in considerable depth and seems over-elaborate compared with others Purification and properties are well covered in chapter 6, although the use of liquid nitrogen and of polyethylene glycol in extraction seem strange omissions. Assay methods are clearly described in three chapters separately considering infectivity, serology and physicochemical methods. After chapters on effects of inactivation and behaviour of viruses in plants, one on variation, strains and classification seems misplaced between them and those on means of transmission, ecology and ways of preventing crop losses. In my view, part of the penultimate and all of the final chapter should have been omitted and the space used to expand those chapters which seem unduly compressed—for example, 'Effect of Viruses on Plants'; the subjects in question are 'Viruses of Animals' and 'Plant Pathogens Confused With Viruses'.

The production is excellent (as befits its price), with clear type and illustrations and agreeably few typographical errors. I regret the absence of titles from the references, making it laborious to check that all are worth inclusion; one suspects that the authors' assurance that, in spite of their selection having been "somewhat arbitrary, most important papers are included," refers mainly to those by themselves and co-workers; otherwise the choice might best be described as whimsical.

The authors have disregarded their own warning in at least one instance. They rightly stress the hazards of identifying viruses on inadequate data, yet they apply the name "swollen shoot" to a virus of cacao trees in Trinidad. To the best of my knowledge, this and the West African swollen shoot virus have no established affinities besides a common vector.

Unquestionably this book is a valuable addition to the few on plant viruses and will be welcomed especially by the small band who teach the subject at English-speaking universities.

A. F. Posnette

Islamic science

Islamic Science: An Illustrated Study. By Seyyed Hossein Nasr. Pp. xiv+273. (World of Islam Festival: London, 1976.) £12.50.

A HANDSOME book, with 135 colour plates and 94 black-and-white pictures and diagrams, the photographs mostly by Roland Michaud. As for Seyyed Hossein Nasr's text, it may be recommended to those who already know enough about the subject to make allowances for the author's lack of objectivity and not to be led astray by his inaccuracies and his Humpty-Dumptyish way with words. Many of the author's convictions are shared by all reasonable people. But what the reader must bear in mind is that, although the implied contrast throughout is between the Islamic and non-Islamic worlds, what the author is really contrasting is the modern virtually world-wide technological civilisation on the one hand and an idealised Islamic Golden Age on the other. "In contrast to the modern situation, in traditional technology, of which many examples can still be seen in the Islamic world, the maximum possible recycling of all materials has always been the rule rather than the exception . . . The use of every part of the sheep for purposes as far apart as feeding the family to providing fertiliser for the land to making strings for musical instruments is a case in point" (p234). A case in point indeed; it was no less true in eleventh-century Birmingham than in eleventh-century Baghdad.

Photo: Roland Michaud

Contemporary Persian alchemist at work

The central thesis of the book seems to be summed up on p150: "Islamic civilisation had the means to make complicated machines and apply them to the problems of the daily life of the Islamic community. But like the Chinese, who made gunpowder but never made guns, the Muslims never took that step which would mean the creation of a technology out of harmony with the natural environment." The comparison with China, by the way, would be more acceptable if the previous page were not devoted to illustrations from Muslim works on the manufacture of cannon. Medieval Muslim men of science did not invent the steam-engine or the dynamo; nor did their Christian contemporaries, and no discredit to either party for that. But can one ascribe this failure to a conscious self-denying ordinance? It seems an affront to the genius of such men as al-Biruni and Ibn al-Haytham to suggest that they were less willing than any Western savant "To follow knowledge like a sinking star, Beyond the utmost bound of human thought."

As for the other faults alluded to above, one example of each must suffice. "In Islam animals are never 'slaughtered'; they are only allowed to be killed ritually (*dhibh*)" (p244; for *dhibh*, incidentally, read *dhabh*). This will be about as meaningful to most readers as saying "In France people never 'drive' cars; they only conduisent them".

"In Islamic sources the one Hermes of Alexandrian sources became three, hence the term Hermes Trismegistos (from the Arabic *al-muthallath bi'l-hikmah*) . . . " (p198). As the term was in use in the early third century, 400 yr before the coming of Islam, either Dr Nasr is wrong or someone in the Hellenistic world deserves credit for a remarkable piece of intelligent anticipation.

One feels a little mean at criticising so urbane a guide to Cloud-cuckoo-land; with caution on the part of the reader, this is a useful book. Even without, it is very beautiful.

G. L. Lewis

Petroleum geology of North American continental shelves

Canada's Continental Margins and Offshore Petroleum Exploration. (CSPG Memoir No. 4.) Edited by C. J. Yorath, E. R. Parker and D. J. Glass. Pp.898. (Canadian Society of Petroleum Geologists: Calgary, Alberta, 1975.) $19.

THIS excellent book is unfortunately misnamed, and may be ignored by European geologists (and especially petroleum geologists), for whom it may be very useful. Essentially this volume describes the geology of the continental shelves of North America, from Vancouver on the west coast to Florida on the east coast, of the Arctic Shelves adjacent to Canada, Greenland, Svalbard and Russia, and of the Eastern Atlantic shelves from North Cape to Morocco. These areas are described on the basis of geophysical maps, sea-bed sampling, sparse well control and adjacent onshore geology. These data are interpreted in the light of plate tectonics theory, and most papers review the petroleum prospects in the areas concerned.

The volume contains 50 papers which were presented at two symposia: the *Offshore Symposium* held at St John's, Newfoundland in May 1974, and in Calgary, Alberta in September of the same year. The editors took the view that it was more important to publish the book in haste, with minimal editing, rather than to delay publication for careful editing and preparation. This was probably the correct decision. A page of errata is included; there seem to be few misprints. Because of this haste there are maps without scales (for example, p301, 302, 304, 309), metres and feet get used for vertical depths on facing pages in the same paper (p570, 571), some microphotographs have no scale (p626), some ornaments are not explained in keys (p651), and some gravity maps lack contour values (p304). Although the editors claim to have checked references for ease of retrieval, I defy anyone to track down those listed on p852.

Much of the material is new, at least to this reviewer. Some of the North American east coast data have been published previously in the bulletins of the American Association of Petroleum Geologists, and even of the Canadian Society of Petroleum Geologists itself. Similarly the material presented on the continental shelves of north-western, Europe will be familiar to those who have read *Petroleum and the Continental Shelf of North-west Europe*, edited by A. W. Woodland (for review, see *Nature*, **259**, 607; 1976).

On balance, however, the editors are to be congratulated for having collated so much data on such a wide area from so many sources. This volume will provide a valuable source book for geologists, and especially petroleum geologists who are interested in the continental shelves of North America, the Arctic and Europe.

R. C. Selley

obituary

David M. Dennison died on April 3, 1976 at his home in Ann Arbor, Michigan. He was born on April 26, 1900 in Oberlin, Ohio, and, except for various leaves of absence, spent his whole academic career at the University of Michigan, where he joined the faculty in 1927. He was chairman of its Physics Department from 1955 to 1965 and retired in 1971. He was a member of the National Academy of Sciences, a Fellow of the American Physical Society and the recipient of various honours.

With his death, the world of Physics loses again one of that small number of pioneer theorists who made early basic contributions to quantum mechanics and to the understanding of the structure of matter, contributions which today are regarded as self-evident. Dennison obtained his Ph.D. in 1924 from the University of Michigan, where Harrison M. Randall and coworkers were using powerful new techniques for the observation of the infrared spectra of molecules. Dennison then spent three years visiting various physics centres in Europe. In 1926, when he was in Cambridge studying with R. H. Fowler, he proved that the hydrogen nucleus has a spin whose magnitude was half that of a quantum of rotation. That this nucleus might have a spin had been talked about widely, but no evidence had been presented. It is the more remarkable that Dennison's proof did not come from spectroscopic data, but from the study of a baffling anomaly in the variation with temperature of the specific heat of hydrogen. Dennison showed that the two configurations of the hydrogen molecule, one with parallel, the other with opposite nuclear spins, must be considered as two separate gases and that transitions from one into the other are very rare. This gave a complete quantitative explanation of the specific heat anomaly as well as a clarification of spectral data. That the volume ratio of the two gases had to be taken as three to one determined the value of the spin. The recognition of these two forms of hydrogen has today found an important use in the long-term storage of liquid hydrogen.

Another remarkable contribution made by Dennison in 1932 concerns the ammonium molecule NH_3. In this molecule the nitrogen atom is in the centre of the triangle, but just outside the plane, formed by the three hydrogen atoms. Dennison noted that a quantum mechanical effect makes it possible for the nitrogen to 'leak' through to the other side. The details were worked out in collaboration with G. E. Uhlenbeck, also at Michigan. It was shown that this non-classical effect caused the molecule to absorb radiation of ~1.5-cm wavelength, which might be produced by miniature magnetrons. Dennison inspired N. H. Williams and C. E. Cleeton at Michigan to attempt a unique experiment to detect this absorption. It was successful and represents the first experiment in microwave spectroscopy. During the second world war, Dennison collaborated with a group developing proximity fuses. Afterwards he spent some time together with T. H. Berlin computing orbits for the Michigan electron accelerator, though his primary interest remained the quantum theory of molecular structure and the interpretation of their spectra to which he contributed many important advances.

David Dennison was an excellent teacher with a genuine concern for students. He was a modest person, who never lost his temper and had many interests outside the field of physics. He was a fine scholar, a helpful friend with whom it was a great and beneficial pleasure to discuss all sorts of problems.

Samuel A. Goudsmit

Hans Thirring, Professor emeritus at Vienna University, died on March 22, 1976. He held the chair of Theoretical Physics from 1927 to 1958, except during the time of the Nazi regime when he was dismissed because of his pacifist convictions.

Thirring's scientific work dealt mainly with problems in general relativity. The prediction of the 'Thirring-Lense effect' is widely known. He also made important contributions to the quantum theory of specific heats. His 3-yr course on theoretical physics was an excellent example of how to present complicated material in a crystal clear way, and many generations of young physicists profited greatly from his outstanding teaching.

During World War 2 Thirring's thinking concentrated on the question how to achieve a peaceful world. The horrific prospects of nuclear warfare stimulated his activities. Thirring was the first to predict openly the feasibility of a hydrogen bomb, in his book *Die Geschichte der Atombombe* (1946). His further book, *Homo Sapiens,* outlined an educational and psychological way to a world without aggression, hatred and war. He was realist enough to expect not too much effect on mankind from the written word alone, and be put his convictions into practice. He was one of the pioneers of the Pugwash movement and he considered this free community of scientists of high reputation from all nations as one of the few hopeful developments towards peace in his time and for the future.

P. Weinzierl

announcements

Appointments

Professor **Frans E. Wickman** has been elected President of the Royal Swedish Academy of Sciences.

Dr A. Bull has been appointed to the second Chair in Applied Biology at the University of Wales, Cardiff.

Dr Ernest Ambler has been appointed the new Director of the National Bureau of Standards.

Professor Robert F. Whelan has been appointed Vice-Chancellor of the University of Liverpool.

Professor Francois Gros has been appointed as Director of the Institut Pasteur.

Dr Donald D. Brown will become the Director of the Carnegie Institution of Washington's Department of Embryology to succeed **Dr James D. Ebert** who is moving to the Marine Biological Laboratory in Woods Hole as the full-time President and Director.

Awards

The German Pharmacological Society has given the Schmiedeberg-Plakette to **Dr Hans Kosterlitz** of the University of Aberdeen for his work on opiate receptors.

Sir Karl Popper has been elected a Fellow of the Royal Society.

The IMO Prize has been awarded to **Academician Evgeny K. Fedorov** of the Institute of Applied Geophysics of the Academy of Sciences of the USSR

Sir James Lighthill and **Dr Max Perutz** have been elected associate members of the French Academy.

Meetings

August 18–21, **Convention of the Western Amateur Astronomers,** San Diego (PAA Reservations, PO Box 505, San Marcos, California 92069).

August 30–September 2, **The Physics of X-Ray Spectra,** Gaithersburg, Maryland (Dr W. G. Schweitzer, Physics Building, Room B164, NBS, Washington DC 20234).

August 30–September 3, **4th Symposium on Recent and Fossil Marine Diatoms,** Oslo (Dr G. R. Hasle, Department of Marine Biology and Limnology, University of Oslo, PO Box 1069 Blindern, Oslo 3, Norway).

September 5–10, **Cell Biology,** Boston (The Secretary, First International Congress on Cell Biology, PO Drawer ICCB, Boulder, Colorado 80302)

September 6–8, **5th European Drosophila Research Conference,** Louvain-La-Neuve (Professor F. A. Lints, Laboratoire de Génétique, Université de Louvain, Place Croix du Sud 2, B-1348 Louvain-La-Neuve, Belgium).

September 6–8, **Lipid Biochemistry,** Paris (J. Polonovski, Faculté de Médecine Saint-Antoine, 27 rue Chaligny, 75571 Paris Cedex 12, France).

September 6–10, **Soil Organic Matter,** Braunschweig, FRG9 (The IAEA, Kärtner Ring 11, PO Box 590, A-1011 Vienna, Austria).

September 13–24, **Oceanography,** Edinburgh (The Organising Committee, Joint Oceanographic Assembly 1976, c/o The Royal Society of Edinburgh, 22 George Street, Edinburgh EH2 2PQ, UK).

September 14–16, **Powder Coating,** Cincinnati (AFP/SME, 20501 Ford Road, PO Box 930, Dearborn, Michigan 48128).

September 14–17, **Nutrition,** Munich (Dr Angelika Janssen, Organisation Secretary, 2nd European Nutrition Conference, Medizinische Poliklinik der Universität München, Pettenkofterstrasse 8a, D 8000 München 2, FRG).

September 14–17, **3rd Symposium on Pharmacology of Thermoregulation,** Banff, Alberta, Canada (Prof. K. E. Cooper, Division of Medical Physiology, Faculty of Medicine, The University of Calgary, Calgary, Alberta, Canada T2N 1N4).

September 15, **DNA Repair and Late Effects,** Vienna (Institut für Biologie, Forschungszentrum Seibersdorf, A-244 Seibersdorf, Austria).

September 19–22, **Gallium Arsenide and Related Compounds,** Edinburgh (The Meetings Officer, The Institute of Physics, 47 Belgrave Square, London SW1X 8QX).

September 20–24, **Thermal Analysis,** Salford (Dr D. Dollimore, Department of Physical Chemistry, University of Salford, Salford M5 4WT, UK).

September 22–24, **Turbulence in Liquids,** Rolla, Missouri (Turbulence Symposium, Extension Division, University of Missouri-Rolla, Rolla, Missouri 65401).

September 23–24, **Symposium on Ecological Effects of Pesticides,** London (Institute of Biology, 41 Queen's Gate, London SW7 5HU).

September 24–26, **Instrumentation for Synchrotron Radiation,** Daresbury (Mrs S. A Lowndes, Daresbury Laboratory, Warrington WA4 4AD, UK).

September 27–29, **Wetting, Spreading and Adhesion,** Loughborough (Dr R. J. Akers, Department of Chemical Engineering, University of Technology, Loughborough, Leicestershire LE11 3TU, UK).

October 3–9, **Hill Land,** Morgantown (R L Reid, Hill Land Symposium Committee, College of Agriculture and Forestry, West Virginia University, Morgantown, West Virginia 26506).

December 2–9, **Pharmacology,** Buenos Aires (VI Congreso Latinoamericano de Farmacologia, Junin 956-5° piso, Buenos Aires, Argentina).

March 7–11, 1977, **Tropical Ecology,** Panama (Dr Reina T. de Araúz, President, Organising Committee, IV International Symposium of Tropical Ecology, PO Box 662, Panama 1, Rep. of Panama)

March 7–11, 1977, **Biologically Active Polypeptides,** Montbello, Quebec (CBS-CIC 1977 Joint Symposium, 151 Slater, Suite 906, Ottawa, Ontario K1P 5H3, Canada).

March 30–April 1, 1977, **Cybernetics of Movement and Classification,** Munich (Univ.-Doz. Dr G. Hauske, Lehrstuhl für Nachrichtentechnik der Technischen Universität München, Arcisstrasse 21, D-8000 München 2, FRG).

April 24–30, 1977, **Radiation Protection,** Paris (Mr Gilbert Bresson, General Secretary, IRPA IVth International Congress, B.P.33, 92260-Fontenay-aux-Roses, France).

May 2–5, 1977, **Cytology,** Tokyo (A. Meisels, MD, FIAC, General Secretary, 6th International Congress of Cytology, 1050 Chemin Ste-Foy, Quebec 6, P.Q., Canada).

June 19–25, 1977, **Inborn Errors of Metabolism in Man,** Tel Aviv (Scientific Secretariat, Dr O. Sperling, PO Box 16271, Tel Aviv, Israel).

June 27–July 1, 1977, **Amorphous and Liquid Semiconductors,** Edinburgh (Conference Secretariat, Centre for Industrial Consultancy and Liaison, University of Edinburgh, 14 George Square, Edinburgh EH8 9JZ).

July 3–8, 1977, **Immunology,** Sydney (The Secretary General, 3rd International Congress of Immunology, PO Box 391, Darlinghurst, N.S.W. 2010, Australia).

July 11–14, 1977, **Dendrochronology in Northern Europe,** London (The Organising Secretary, Symposium, National Maritime Museum, Greenwich, London SE10 9NF).

August 7–13, 1977, **General Relativity and Gravitation,** Waterloo, Ontario (GR8, Applied Mathematics Department, University of Waterloo, Waterloo, Ontario N2L 3G1, Canada).

September 5–8, 1977, **New Processes of Waste Water Treatment and Recovery,** London (Deadline for abstracts: December 31), (Dr D H. Sharp, General Secretary, Society of Chemical Industry, 14 Belgrave Square, London SW1X 8PS, UK).

September 5–9, 1977, **Hypoxic Cell Sensitisers in Radiobiology and Radiotherapy,** Cambridge (Dr G. E. Adams, CRC Gray Laboratory, Mount Vernon Hospital, Northwood, Middlesex HA6 2RN, UK).

September 6–11, 1977, **11th World Congress of Neurology,** Amsterdam (Secretariat, c/o Holland Organising Centre, 16 Lange Voorhout, The Hague, The Netherlands).

September 13–16, 1977, **Nuclear Quadrupole Resonance Spectroscopy,** Osaka, Japan (4th International NQR Symposium, Faculty of Science, Osaka University, Toyonaka 560, Japan).

Autumn, 1977, **Phosphate Compounds,** Rabat, Morocco (Mr M. Kabbaj, Director of Technical Research, Institut Mondial du Phosphate, 8 rue de Penthièvre, 75008 Paris, France).

Reports and Publications

Australia Commonwealth Scientific and Industrial Research Organization. Division of Food Research: Report of Research 1974/1975 Pp. 115 (Sydney: CSIRO, 1975.) [113

The United Republic of Tanzania Ministry of Commerce and Industries. Annual Report of the Mineral Resources Division, 1967 Pp. iii + 104 (Dodoma, Tanzania· Geology and Mines Division, 1974) Shs.8/- [123

CERN—European Organization for Nuclear Research. CERN 76–02 List of Publications Covering Bubble Chamber Experiments Carried Out at CERN During the Period 1960–1974 Compiled by E. W D. Steel. Pp vii + 110. (Geneva CERN, 1976) [123

Canada Department of Energy, Mines and Resources Geological Survey of Canada. Bulletin 233· Structural Style Influenced by Lithofacies, Rocky Mountain Main Ranges, Alberta—British Columbia By D. G. Cook Pp. 73 $4 Bulletin 245· The Geology and Petrology of the Ice River Alkaline Complex, British Columbia By K L. Currie. Pp 68. $6. Bulletin 252 Miospores and Microplankton from Aptian-Albian Rocks Along Horton River, District of Mackenzie By W. W. Brideaux and D J McIntyre Pp. 85 (14 plates). $6. Paper 74–37· Cambrian Sttatigraphy from Western Alberta to Northeastern British Columbia By D. C. Pugh Pp. vi + 31 (Ottawa Information Canada, 1975.) [123

CERN—European Organization for Nuclear Research. CERN 76–01 Copper-Beryllium Alloys for Technical Applications By W Heller. Pp. 39. (Geneva CERN, 1976) [163

United States Department of the Interior· Geological Survey Professional Paper 784 Early Paleozoic Brachiopods of the Moose River Synclinorium, Maine By Arthur J Boucot Pp iv + 81 + 23 plates $1.75. Professional Paper 865 Normapolles Pollen from the Mississippi Embayment By Robert H Tschuddy. Pp v + 42 + 20 plates (Washington, DC US Government Printing Office, 1973 and 1975) [163

United States Naval Observatory Circular No 152: Total Solar Eclipse of 23 October 1976 By Alan D Fiala and J. S. Duncombe Pp 23. (Washington, DC US Naval Observatory, 1975 [173

CERN—European Organization for Nuclear Research CERN 76–03: Systeme Tridimensionnel de Coordonnees Utilise au CERN Par J Gervaise, M Mayoud et E, Menant. pP 21 (Geneve· CERN, 1976.) [173

United States Department of the Interior Geological Survey. Bulletin 1401. Rapid Analysis of Silicate, Carbonate, and Phosphate Rocks—Revised Edition. By Leonard Shapiro. Pp v + 76 Bulletin 1417· Annotated Bibliography of Studies on the Density and other Volumetric Properties for Major Components in Geothermal Waters, 1928–74 By R W. Potter, II, D. R Shaw and J. L. Haas, Jr Pp iii + 78 Water-Supply Paper 1798–L: Effects of Land Use and Retention Practices on Sediment Yields in the Stony Brook Basin, New Jersey. By Lawrence J. Mansue and Peter W. Anderson. Pp. iii + 33 55 cents Water-Supply Paper 2039–A· Chemical Quality and Temperature of Water in Flaming Gorge Reservoir, Wyoming and Utah, and the Effect of the Reservoir on the Green River By E L. Bolke and K. M. Waddell Pp. iv + 26 + plate 1. (Washington, DC. US Government Printing Office, 1973, 1974 and 1975) [183

Planning and Organization of Services for Alcoholism and Drug Dependence—Report on a Symposium, Albi, 30 June—4 July 1975. Pp. 49. (Copenhagen Regional Office for Europe, WHO, 1976) [183

Smithsonian Contributions to Paleobiology, No 19 Permian Brachiopods of West Texas, III By G. Arthur Cooper and Richard E. Grant. Part 1 Text Pp x + 795–1298. Part 2· Plates viii + 1299–1921 (Washington, DC Smithsonian Institution Press, 1975 For sale by US Government Printing Office.) [183

United States Department of the Interior Geological Survey. Bulletin 1408: New and Refined Methods of Trace Analysis Useful in Geochemical Exploration. By F. N. Ward. Pp. iv + 105 (Washington, DC· US Government Printing Office, 1975) [193

National Research Council Canada. NRCC No. 14106 Arboviruses and Human Health in Canada. By D. M McLean. Pp. 35. (Associate Committee on Scientific Criteria for Environmental Quality) (Ottawa National Research Council Canada, 1975.) $1.25 [193

Norsk Polarinstitutt. Arbok 1974 Pp. 269. (Oslo Norsk Polarinstitutt, 1976.) [223

United States Department of the Interior Geological Survey. Bulletin 1405–B· A Summary of Tertiary Volcanic Stratigraphy of the Southwestern High Plateaus and Adjacent Great Basin, Utah By Peter D. Rowley, John J. Anderson and Paul L Williams. Pp. iv + 20. (Washington, DC US Government Printing Office, 1975.) [223

Smithsonian Contributions to Zoology, No 217 Cyclopoid Copepoda Associated with Asteroid Echinoderms in New Caledonia By Arthur G Humes Pp. iii + 19. (Washington, DC. Smithsonian Institution Press, 1976 For sale by US Government Printing Office.) [223

Royal Netherlands Meteorological Institute Publication No. 153 On Earthquake Risk for Nuclear Power Plants (Proceedings of the ESC Symposium in Luxembourg on 20–22 October 1975) Edited by A R Ritsema Pp. 192 (De Bilt, Netherlands Royal Netherlands Meteorological Institute, 1976) [223

Settlement in Israel (Israel National Report to Habitat, United Nations Conference on Human Settlements) Edited by Valerie Brachya and Paulette Mandelbaum. (Publication No 76–01) Pp 79. (Jerusalem· Ministry of the Interior, Environmental Protection Service, 1976) [253

The Buffaloes of China. By W. Ross Cockrill (Australian Freedom from Hunger Campaign.) Pp. x + 96. (Rome FAO; London HMSO, 1976) $8 [253

United States Department of the Interior. Geological Survey. Professional Paper 801 Jurassic Paleobiogeography of Alaska. By Ralph W Imlay and Robert L. Detterman Pp iii + 34 (Washington, DC US Government Printing Office, 1973) 65 cents. [253

Twenty-Two Dimensions of the Population Problem. By Lester R Brown, Patricia L. McGrath and Brice Stokes (Worldwatch Paper No 5) Pp 83 (Washington, DC· Worldwatch Institute, 1776 Massachusetts Avenue, NW., 1976) $2. [263

Journal of Membrane Science, Vol. 1, No. 1, March 1976. Edited by H. K Lonsdale Pp 1–114. Published Quarterly Subscription rate – US$56 95, Dfl. 142 (Amsterdam Elsevier Scientific Publishing Company, 1976.) [293

Academie Royale de Belgique Annuaire pour 1976. Pp 302. (Bruxelles. Academie Royale de Belgique, 1976) [293

Introducing WHO Pp 88. (Geneva. WHO, London HMSO, 1976.) Sw fr 10 [293

Service d'Etude des Sols et de la Carte Pedologique de France. Carte Pedologique de France a 1/1000,000. Angouleme, H–16. Notice Explicative par G. Callot Pp. 171 (Versailles Institut National de la Recherche Agronomique, 1975) F.53.50. [293

Académie Royale de Belgique. Mémoires de la Classe des Sciences. 2e Serie, T CLII, Fasc. 1 Structures Presque Complexes Généralisées Equations á Structure Presque Complexe. Par Jran-Claude Vansnick. Pp 46. (Bruxelles Academie Royal de Belgique, 1975.) [293

Argentino Direccion Nacional del Antartico. Contribucions. No 169· Caracteristicas Teratologicas en Coscinodiscus Bouvet Karst en Puerto Paraiso y Estrecho de Bismarck, Antartida. Por L J C. Mertinez Maccdiavello. Pp 9 No 171. Estrucura y Citologia Pineal en Pinguinos Antarticos Estudio Comparativo en dos Especies (Pygoscelis Papua y Adeliae) Por L. G A. Benelbaz y Dr. Ramon S. Piezzi. Pp. 15 No. 172 Rasgos Morfologicos de Isla Decepcion, Islas Shetland del sur Antartida Agentina Por Antonio P Igarzabal. Pp. 30. No. 173: Geologia del Extremo Occidental del Cabo Spring—Costa de Danco, Anartida Argentina Por R. A. Llorente, J E. Mendia y J. P. Spikermann. Pp. 19. No. 174 Estado Volcanico de la Isla Decepcion, Islas Shetland del Sur, Antartid a Argentino. Por J G Viramonte y Nestor H. Fourcade. Pp. 12 No 182· Caracterizacion de los Estados dy Vigilia y Sueno de *Phalacrocorax artriceps* (Aves, Phalacrocoracidae) Por A. P. Tomo, J S Panizza y J. M Affani. Pp 14. No. 183: El Sistema Inmunoglobulinico del Pygoscelis Papua Por O D Castrelos, M Romero Mercado, C Abatangelo y R A. Margni Pp 12 (Buenoa Sires Instituto Antartico Argentino, 1973 and 1974.) [303

Smithsonian Contributions to Zoology. No 216. Study of the Monotypic Fish Family Pholidichthyidae (Perciformes) By Victor G. Springer and Warren C Freihofer Pp. iii + 43. (Washington, DC· Smithsonian Institution Press, 1975. For sale by US Government Printing Office.) [303

Person to Person

Scientist going on sabbatical from Jerusalem would like to exchange flats with someone in London. Four-room flat (3 bedrooms), central heating and all conveniences with schools nearby near the Hebrew University (Beit Hakerem). Available mid-August 1976 for 12 months (Dr S. Moshkovitz, Geological Survey, 30 Malkhei Street, Jerusalem, Israel.)

NASA is seeking proposals for scientific investigations of Jupiter, to make *in situ* (by probe) and remote measurements (by orbiter) of the planet, its environment and its satellites. Primary emphasis is on direct entry measurements and the characterisation of the magnetosphere of the planet and its interaction with the satellites. Proposals for the Probe investigations by November 1, 1976, and for the Orbiter investigations, December 1, 1976 to Dr M. A Mitz, Chief, Advance Planning, Lunar and Planetary Programs Office, Code SL, NASA Headquarters, Washington, DC, 20546.

A seminar on Scientific and Technical Publishing in a Multilingual Society is being held in Luxembourg by the Commission of the European Communities on November 11–12, 1976. The chief aim is to generate proposals for measures which might be taken in the framework of the European Community. For further information contact Mr J. M. Gibb, D.G. XIII, European Centre, Kirchberg, Luxembourg.

The David Anderson-Berry prize will be awarded for recent work on the effects of X-rays and other forms of radiation on living tissues. Published work will be taken into consideration if submitted with the application In addition to direct application for the Prize, proposals may be made on behalf of others. Applications and proposals must be in the hands of the General Secretary, Royal Society of Edinburgh, 22/24 George Street, Edinburgh EH2 2PQ, Scotland, not later than September 30, 1976.

The Bigfoot Research Society is looking for organisations willing and able to analyse specimens hoped to be collected during field studies of this shy animal. Write to: James R. Spink, Bigfoot Research Society, PO Box 61-1564, North Miami, Florida 33161.

Sydney–Paris. Wanted, two- to three-bedroom furnished flat or house within commuting distance of Meudon-Bellevue (Paris) in exchange for a three-bedroom furnished house in Lindfield (13 km N of Sydney) for approximately 1 yr beginning during September 1976. Dr D. M. Eagles, National Measurement Laboratory, CSIRO, Chippendale, NSW 2008, Australia.

ACCOMMODATION: Scientist going on sabbatical leave to Orsay offers exchange of comfortable three-bedroom house in Peterborough, Ontario, Canada for a similar one in the southern or south-eastern suburbs of Paris from September 1, 1976 to August 31, 1977. Please contact Professor R. Alfred, Physics Department, Trent University, Peterborough, Ontario, Canada.

There will be no charge for this service. Send items (not more than 60 words) to Martin Goldman at the London office. The section will include exchanges of accommodation, personal announcements and scientific queries We reserve the right to decline material submitted. No commercial transactions

nature

July 22, 1976

Out of work in Argentina

THE letter (page 253) from more than 60 Italian scientists drawing the scientific community's attention to the situation in Argentina is a grim reminder of the difficulties surrounding university and government institutional work on a continent which for many of us in the Anglo-Saxon world is still remote and in some way unreal.

The intellectual in Argentina has never been as secure as his counterpart in West Europe and North America. Universities have been watched very closely by successive governments, and the appointments of rectors and deans have often been purely political affairs As a result there has been a steady trickle of emigrants to more secure territory—a trickle that has sometimes swelled to a flood (in 1966, for instance, 1,100 found themselves out of a job). The turnover in university staff has been accordingly immense; one academic in Britain, who has fairly strong ties with Argentina, remarked that almost every Argentinian scientist he had known had been forced, at some time, to leave. The quality of young people coming up through the major universities is, it is widely agreed, suffering as a result.

Argentina's problems in recent years have, of course, gone much deeper than instability in universities and there was genuine hope when General Videla came to power that he would be able to act against the terrorism which had led to so much indiscriminate killing. To a certain extent he has succeeded because terrorism by the left has been sat on very firmly; however, right-wing activities do not seem to have been significantly restrained. The bewildering variety of competing security organisations and the divisions within the armed forces add to the complexity of the situation. An exiled Argentinian commented that knowing how one stood in La Plata would not necessarily make one safe in Buenos Aires, and so on. It is small wonder that universities have become places of fear and that gun-carrying soldiers are in evidence.

If recent dismissals are, in general, politically directed against the left, they are not universally so; several well known right wingers have also been relieved of their posts. What seems to have happened is that the government, faced with a truly depressing economic situation requiring urgent international support, and forced to make major cuts in public expenditure, has used the opportunity to thin its ranks of those who have taken up certain political stances in the past. Those who have steered clear of politics or who openly support the Junta can survive, though in somewhat straitened circumstances.

It used to be that, with families widely spread over South America, people in trouble could move over to Chile, Uruguay or Paraguay. Indeed Uruguay was often called the Switzerland of South America. No longer; the Uruguayans in their zeal to stamp out the Tupamaro guerillas seem to have 'processed' an extraordinary large proportion of the population and to have allowed torture to become rampant. The fate of the mathematician Jose Massera who has been imprisoned since last October and has suffered some grievous injuries is likely to deter most academics from choosing to move over to Montevideo.

The pressure, then, is really on the wider community of scientists to continue to absorb where necessary or, even more, just to keep in touch—a plea made most simply and expressively by the writers of the letter. From the Europe–North American axis it is very easy conveniently to forget the difficulties of doing science elsewhere, to look down on scientists struggling with poor facilities and heavy teaching loads, and to ignore colleagues off the axis when passing round the gossip, the early warnings, the bits of advice. Even well endowed Australians, with regular jet flights to the Northern Hemisphere, know that. How much more so does the problem afflict Argentinians, and how much more must we simply not stand by uninterested. □

Why are we waiting?

ALTHOUGH Mr Mulley, UK Secretary for Education and Science, has had the report of the Williams Working Party on Genetic Manipulation of Micro-organisms on his desk for well over a month, it is due to remain there for at least a "few more weeks". Until then scientists will be in the dark over the details of the code of practice that will apply to recombinant DNA research in Britain. There are several possible excuses for Mr Mulley's tardiness. None of them is good enough.

The Williams Working Party had its origins in a statement published by Professor Paul Berg and his colleagues in July 1974 in which they expressed concern at some of the possible consequences of the research they themselves had pioneered. The improbable pathway to disaster that they foresaw involved the escape from laboratory containment of bacteria whose genes had been experimentally recombined with genetic material from another organism, the survival of those bacteria in the outside world, their colonisation of the human intestine and the expression of their foreign genetic component to the detriment of the human host.

That scenario was taken seriously enough on both sides of the Atlantic that most scientists have since held to a voluntary moratorium on suspect research. American concern, latterly under the auspices of the National Institutes of Health, culminated four weeks ago in the issue of a complex series of guidelines. The British wheels were set in motion in July 1974 with the Ashby Working Party, convened by the Advisory Board for the Research Councils, which reported in December of that year. Seven months later Mr Mulley set up the Williams Working Party to produce a code of practice and to consider the establishment of a central advisory service for laboratories carrying out the procedures in question.

The Williams Working Party report is unlikely to contain many surprises. It will not recommend the proscription of any particular experiments but will suggest the precautionary measures that are appropriate for various categories of research. Few specific experiments will be quoted and no attempt to quantify their dangers will be made. The report is expected to endorse Ashby's suggestion of a central advisory service and to recommend how it might operate.

The scientific community anxiously awaits the report and Mr Mulley's reactions to it. The longer they have to wait for a go-ahead on experiments which in some cases have been on ice for two years, the worse (whatever the precautions suggested) will become the atmosphere of frustration and suspicion that has gradually built up. Inevitably moratorium-breaking has already occurred, and the consequences for those involved have on occasion been unpleasant.

Why then is Mr Mulley keeping us waiting? One possibility is that he is reserving the right to modify his reactions in the light of the response at home and abroad to the American guidelines. If so the delay could well be lengthy in view of the recent clash between Cambridge (Massachusetts) City Council and Harvard University. The trouble arose when the Mayor of Cambridge attempted to block plans to build a high containment laboratory within the Harvard Biological Laboratories; at the moment there is a three-month moratorium during which the council will review the position before deciding on the future of Harvard's genetic engineers. Similar problems are expected in other American cities. Although there is a reasonable chance that such clashes will be avoided in Britain, the longer Mr Mulley delays, the more likely they are to occur.

A second reason for delay may simply be the need for extensive briefing and consultation between departments If so Mr Mulley must lavishly oil the cogs of bureaucracy. Most likely the delay is due to his consideration of the introduction of statutory controls of recombinant DNA research. Although the Working Party is thought to have been reluctant to recommend statutory controls, they may have made some suggestions in that direction because of forceful representation from the unions. The same pressures, which clearly must be respected since the unions represent those most likely to be directly carrying out the research, may now be holding Mr Mulley back.

The British code of practice, with or without statutory backing, could be very influential. In contrast to the American code, which applies only to NIH-supported research, the British code will apply to all academic institutes and probably also to industry via the Health and Safety Executive. If that breadth is matched by an authoritative depth and practical recommendations, the code could well be adopted by other European countries. That could happen through the European Molecular Biology Organisation which meets to consider the matter on August 12. It would be a great pity if the British code had not emerged by then. ☐

Solar energy breeders

Malcolm Slesser and Ian Hounam of the Energy Studies Unit at the University of Strathclyde, Glasgow, offer an opinion on a largely ignored aspect of solar energy

SOLAR energy has not been taken seriously as a solution to our energy supply problem and for good reason. It requires considerable land area and the sun has an unhappy knack of ducking behind clouds or withdrawing into a winter solstice. But there is one aspect of solar energy that is significantly in favour of its large scale development, an aspect which has so far received scant attention. This is the potential for solar energy devices to breed energy. No other device can do that. Yet, given the right technology, we calculate that with an initial investment by 1980 in 1 MW of solar power, it would be possible for solar energy to provide 90% of the world's energy needs within 40 years, without placing any burden upon existing energy resources.

The importance of this claim can hardly be exaggerated. If a solar breeder system was in operation, nearly all the energy from North Sea oil could be devoted to current needs and not, for example, to building alternative energy systems that will be needed when oil runs out. If we have a viable solar breeder system, worldwide, then once that system has grown large enough to satisfy the bulk of world demand the price of energy will fall to a trivial value, because after all the sun is a free good. Such a fact would utterly change the basis of a manufacturing or even a service orientated economy.

What, then, is an energy breeder? It is a device which "breeds" capacity to generate useful energy without consuming energy stocks. In this sense nuclear "breeders" are not breeders but extenders, increasing the potential energy of uranium by roughly 100/0.7, where the 0.7 is the proportion of Uranium 235 occurring in natural uranium. But when a solar capture device (SCD) (or any solar induced device such as a wind or wave generator) delivers in its lifetime more energy than needed to maintain and rebuild itself, then some of that surplus can build more SCDs, thus breeding energy.

Breeding success depends on the pay-back time of the initial energy of manufacture, and energy analysis provides us with a means of assessing it. Through a method known as dynamic net energy analysis, in which energy required to construct and service an energy production or transformation system is set against the system output as a function of time, one can test various breeding scenarios. Unfortunately the energy investment data so far produced on constructing solar energy devices (other than solar heat devices) is unconvincing, and tends to consider only optimal sunlight conditions. Moreover, all too often figures include only direct energy costs, and the more obvious ones like the energy requirements of structural steel and glass No comprehensive results have been published enabling one to estimate the gross energy requirement to build and operate an SCD in an average situation.

Our own tentative energy analysis of 1972 photo-voltaic technology has shown it would take about 40 years output to pay for the energy investment, and since its expected life may be about 30 years it is clearly a sink, not a breeder. However, the new technology of ribbon melting of silicon looked like reducing that to 10 years. In recent discussions with the Office of Technology Assessment in the USA we have learnt of systems which are said to require only a two-year pay-back time. This clearly provides tremendous breeding potential.

If a system could grow while also satisfying its own energy needs—that is to say the energy for construction and operation—it then places no burden on the existing fossil and nuclear energy infrastructure, and the only charge upon the building programme is the labour and management and the land needed for expansion of the system.

Choosing a datum of 1980 for the initiation of the programme of breeding, with an initial 1 MW output capacity SCD system, we examined a range of pay-back times varying from the pessimistic result at Strathclyde (10 years) to the optimistic views of the Office of Technology Assessment (2 years) for various investment policies, to show that energy breeding is a possibility even with as large a value of pay-back time as 10 years, though the rate of breeding is too low to be of real interest. Thus for a policy of 5% investment in new capacity, by 2030 the programme would only have developed an output capacity of 12.2 MW (as against the original 1 MW in 1980) and a net output power would be a mere 4.3 MW—reflecting a system doubling time of about 14.5 years. Yet even that is greater than the global rate of growth in energy demand.

On the other hand, if we accept the optimistic value of pay-back time of 2 years being claimed in some quarters, an SCD breeding programme could be spectacularly successful. For example, with an investment fraction of 40%, an initial output capacity of 1 MW in 1980 would have grown to an output capacity of 8.8×10^6 MW by 2020, giving a net power output to the non-solar energy sector of the economy of 1.7×10^6 MW. By this time the doubling time of the SCD system is only 3.2 years, a rate of growth of energy supply higher than the most horrific energy demand scenarios.

Of course by no means all problems are solved. Though the programme provides its own energy requirements, there are still the problems of land availability and manpower. Some will point out that there is also a need for steel, glass and so on. But of course, the energy analysis has taken that into account through the energy required for construction. Nevertheless, there remains the task of assessing whether the necessary industrial infrastructure to sustain the solar programme can be created, a question we do not attempt to answer here. We merely set out to show that, given the appropriate technology (low pay-back time), a solar capture system could breed itself, and hence in time solve the global energy supply problem. The devices with larger than two-year pay-back times are less satisfactory. Clearly, then, in view of the tremendous opportunities presented by a device with a two-year pay-back time, a massive research programme is justified.

The SCD system output capacity could match even the most ambitious forecasts of demand (4.5×10^6 MW) within 40 years of initiation. From an initial recycle fraction of 80% to new investment, the construction programme falls away to 7% in the 40th year. In net energy terms this is a lower figure than found in our present fossil and nuclear fuel industries. It would be consistent with a price, in current terms, of around £100 per kW for photo-voltaic collectors.

It is interesting to consider what happens to the cost of conventional fossil and nuclear fuels if such a programme took place. By the year 40 (2020), solar energy could so nearly supply all energy needs that oil, gas, coal and nuclear sources will have lost much of the scarcity value they now enjoy. True, oil and gas will remain valuable for their feedstock potential, but nuclear reactors could be rendered redundant and coal mining unnecessary, save as a source of carbon. In such a situation presumably the price of energy falls to a trivial value.

This is offset by the land requirement of SCDs. Taking the 40 year level of output of 4.2×10^6 MW, and assuming that the two-year pay-back time has been achieved, with collection of 20% efficiency, a huge land area is required, around 30,000 km^2 (equivalent to about 12% of the British Isles), but it is spread world wide. However, if the same period of two-year pay-back time applies to solar generated SCDs such as wave and wind power generation, then land requirement falls considerably.

In order to effect the programme, a cumulative energy investment of 1.7×10^6 MW years of energy would have been used—that is about 25×10^9 tons coal equivalent. This is a huge quantity of energy, and reflects a huge amount of material and man power. None of that energy, however, would have come from global energy resources, but from within the programme. Secondly, the basic problem facing all industrialised societies is the need to build a new energy infrastructure within the next 30–50 years. When we examined the task of doing this for the UK imagining an eventual replacement of fossil energy by nuclear and some solar, we found that the massive energy investment called for placed restrictions of UK export of North Sea oil, and a serious limitation on UK economic growth, for the energy investment had to come from existing energy resources and transformation devices. The SCD breeding system, however, permits a parallel economic development without this strain being placed on existing energy resources.

In reality an SCD breeding programme would differ considerably from the simple model presented here. For one thing much of this growth would be dispersed—some citizens for example, building wind generators in their back yards. Technology would change rapidly, and pay-back times would vary according to the sophistication and purpose and location of the device. Much solar energy could be turned directly to heat, through collectors. It is still too early to find whether the torrid dunes of the Sahara will pay a more or less important role than the ceaseless waves of the North Atlantic and South Pacific. But given a short pay-back time and an integrated breeding and development programme, prospects for a low cost energy, nuclear-free world do look good. □

SCIENCE COLLEGE

Modelling the world, again

David Spurgeon in Ottawa looks at two recently published studies of the world's future

WHEN it was published in 1972, *The Limits to Growth* was a kind of landmark, crystallising in a mathematical model the views of those who believed that the world had come to a turning-point in its profligate use of resources, its growing pollution of the environment, and its inexorable population growth. Its message was basically a simple one: that if current trends continued, disaster was certain, because resources which were finite would soon be exhausted, pollution which was increasing would soon become intolerable, and the press of population which was exponential would soon outrun living space.

For many the book was authoritative because it was backed by computer studies—and perhaps because it reinforced existing fears or prejudices. But given its assumptions, its conclusions seemed rather obvious, and it provoked a rash of criticisms, as well as a number of similar studies. Whatever else may be said of it, though, it succeeded in raising the public's consciousness of some of mankind's major problems and prospects.

Two recently published studies* deal directly with the kinds of problem examined by *The Limits to Growth*: one, *Catastrophe or New Society?*, arose as a specific response to it, while the other, *The Next 200 Years*, could be said to have been undertaken in response to its underlying philosophy. Both disagree totally with the assumptions and conclusions of *The Limits to Growth*, while at the same time proceed from assumptions totally at odds with each other. What they have in common is a basic conclusion that the limits to growth—if any—are not physical, as suggested in *The Limits to Growth*, but sociopolitical, and that mankind is not doomed either to a no-growth economy or to disaster but is capable of providing a worthwhile and satisfying future for all. Where they differ is in how such a future could be brought about.

The basic premise of *The Next 200 Years* is that what we need is not less growth, but more—and along pretty much the same lines as at present—at least until world-wide economic development has been completed. After that growth rates will slow and many economies will reach a more or less steady state. *Catastrophe or New Society?*, on the other hand, sees achievement of a good life for all, particularly those in developing countries, as impossible without certain fundamental changes in society. What is wrong with the arguments of Meadows and his ilk, in its view, is that they accept, "in a totally uncritical manner, the central values of society as it now is." Herrera and his colleagues maintain that the major problems facing society

> are based on the uneven distribution of power, both between nations and within nations The result is oppression and alienation, largely founded on exploitation. The deterioration of the physical environment is not an inevitable consequence of human progress, but the result of social organisations based largely on destructive values.

In its place must be constructed a new type of society—socialist, egalitarian, fully participatory, and non-consumerist.

Both books project the future from a very clear ideological base, though the base is made more explicit and acknowledged more directly by Herrera's group than by Kahn's. Both are essentially utopian (Herrera's admittedly so, Kahn's not) and suffer from the basic fault of all such modelling of enormously complex systems. oversimplification, and the necessary exclusion of all sorts of potentially important variables that either cannot be accurately quantified or cannot be foreseen.

Kahn and colleagues argue that "the current malaise", as they call it, is propelled by a combination of compassion and guilt for the plight of the world's poor and the coincidental occurrence of world-wide crises in the supply of food and energy. They believe that the movement toward this view "has gone too far", and argue that there is both need and opportunity for economic growth—that precisely because America and the rest of the developed world use resources so intensely, there will be stimulation, not depression, of the economies of developing nations Using what seems, as far as they reveal it, to be questionable data, the Kahn group suggests current population growth fears may be nothing much more than "an amusing episode in human history". Looking backward from 2176, as they pretend to be able to do, they say "the temporary nature of the current population phenomenon becomes very obvious".

Similarly, energy supplies are no problem. Examining current fossil fuel reserves (on the basis of a 1973 US Geological Survey that has since been withdrawn by that agency and drastically revised downwards) and the prospects for other energy sources, both conventional and non-conventional, developed or not, the authors conclude:

> Except for temporary fluctuations caused by bad luck or poor management, the world need not worry about energy shortages or costs in the future And energy abundance is probably the world's best insurance that the entire human population (even 15–20 billion) can be well cared for, at least physically, during many centuries to come.

The same goes for raw materials ". . . there is an abundance of raw materials for future generations as well as the present one, and . . . the more man develops economically and technologically, the more there will be for all of humanity."

And as for food, "the position we argue is that, except for the occasional regional fluctuations caused by natural disaster, inappropriate policies or the misapplication of resources, the long-term prospect is for adequate food supplies". Within 200 years, the authors say, it will be possible to increase world food consumption to the level of the United States today. What will happen if "inappropriate policies or the misapplication of resources" continues to be the rule, as it is today, is not dealt with. Yet that, as the authors of the Latin American world model recognise, is precisely where the real problem lies.

To give them their due, the Kahn group do recognise this. They go so far as to state that

> any limits to growth are more likely to arise from psychological, cultural or social limits to demand, or from incompetency, bad luck and/or monopolistic practices interfering with supply, rather than from fundamental physical limits on available resources

What seems odd is their faith in things as they are, and their acceptance that they will continue that way.

> . . . Large income gaps between nations could persist for centuries . . . there are few peasants, workers or even businessmen in developing nations who care much about gaps (whether arithmetic or geometric), no matter how much intellectuals, academics and some businessmen may profess to. The major objective of most people is to increase their own safety and improve their own standard of living and their own capabilities. When they make comparisons, it is

---

***Catastrophe or New Society? A Latin American World Model,* Amilcar O. Herrera, Hugo D. Scolnik, Graciela Chichilnisky, Gilberto C Gallopin, Jorge E. Hardoy, Diana Mosovich, Enrique Otieza, Gilda L. de Romero Brest, Carlos E. Suárez, and Luis Talavera (IDRC-064e; International Development Research Centre, Ottawa, Canada; 1976).

The Next 200 Years: A Scenario for America and the World, Herman Kahn, William Brown, and Leon Martel, with the assistance of the Hudson Institute (William Morrow and Company, Inc., New York; 1976).

> usually with others at their socioeconomic level or with those who have recently been at their own or a lower level.

By such a yardstick, much of the Third World should have nothing to worry about. The Kahn group sees communist Asians with a GNP per capita of about $1,000 by the year 2000, and about half of the Third World with about double that. A desperately poor group, mostly in India but also in parts of Latin America and Africa, could—even with "reasonable" policies—attain only an average of about $200 per capita by the year 2000. But in another hundred years almost all societies should have a GNP per capita of more than $2,000. The fact that others may have 10 to 20 times more is, in their view, of no consequence.

The Latin American world model is based on the premise that, in the new society proposed, the production system has the satisfaction of basic human needs as a main objective. These needs are nutrition, housing, education and health. The mathematical model was constructed around the satisfaction of these needs, differentiated into five sectors: nutrition, education, housing, capital goods, and finally, consumer goods and other services. It was built to test the physical viability of the proposed society. This involved determining the period of time needed and the conditions under which the different regions could satisfy the basic needs to given levels.

The level of food was taken as 3,000 calories and 100 grams of protein per day (3,200 calories in advanced countries); of education, 12 years of basic education between the ages of 7 and 18; and of housing, one house per family. In the developed countries, the minimum dwelling would have an area of 70 square metres for an average family of 3.5 people, costing $4,900 to build. For Africa and Asia, the standard house was more modest because of the current desperate housing situation: 7 square metres per person, at $23.40 per square metre in Africa and $11.20 in Asia. Housing conditions would reach developing country standards in 20 years.

The annual cost of education per student in underdeveloped countries reached a maximum of $150, and an aggregated yield of 4 tonnes per hectare per year was assumed in agriculture. In developed regions, economic growth would be restricted to 1–2% when GNP per capita exceeded $4,500 annually. And for underdeveloped regions, once basic needs were satisfied, growth in GNP per capita had to be at least 2%. This is to gradually reduce the gap between the developed and underdeveloped regions.

What did the model predict? For developed countries basic needs were shown to be satisfied in the first few years of the computer run (which ended in the year 2060). GNP per capita reached $9,470 in that year (slightly less than Kahn's projection). Latin America could fulfill its basic needs in the early 1990s, and its GNP per capita would rise from $372 in 1960 to $5,746 in 2060. Interestingly, the population growth rate, which was 2.8% in 1960, decreased as general well-being improved, and was only 0.43% by 2060, approaching stabilisation. The consequence for Latin America, then, is that it could satisfy its whole population's basic needs within a generation of the implementation of the proposed policies.

It would take Africa longer: that continent could satisfy its basic needs by 2008. GNP per capita, $137 in 1960, would reach only $559 in 2008, and $2,657 in the last year of the run. Thus if the policies proposed were applied, Africa could satisfy the basic needs of its population with 30 years after 1980, according to the model.

Asia's position is very different. According to the model, basic needs could not be satisfied by 2060. Food consumption of 2800 calories could be achieved by 1992; that level would be maintained until the mid-2020s, but would decline after that until levels reached were incompatible with survival. Nor were housing needs achieved, with only 0.82 house for every family in 2040. Education would be the only basic need totally satisfied by 2040.

"The problem in Asia arises in the food sector," says the report. "By 2010, all available land is being cultivated. Thereafter, economic effort in the sector is devoted to increasing livestock and fisheries. This, however, is not enough to feed the growing population adequately". If agricultural yields were increased from 4 to 6 tonnes per hectare, however, basic needs could be satisfied. GNP per inhabitant—$89.70 in 1960—reaches $1,516 in 2060. But food remains a problem, for in the mid-2030s the remaining land has been used, and "it is inevitable that some years after 2060 Asia will not be able to feed its inhabitants adequately."

Finally, a run was carried out to test the effect of cessation of technological progress in the evolution of the regions involved. It was supposed that there would be no more technological progress after the year 2000. This produced significant effects. In Latin America, it increased the time necessary to satisfy basic needs, increased the population growth rate, and reduced GNP per capita (from $5,746 in 2060 to $1,173). In Africa, as in Asia, minimum objectives could not even be achieved: the economic system collapsed. Only food reached the target level in Africa, and then only for a brief period. In Asia, none of the basic needs were met. Thus technological progress is seen as essential for liberation from underdevelopment and misery.

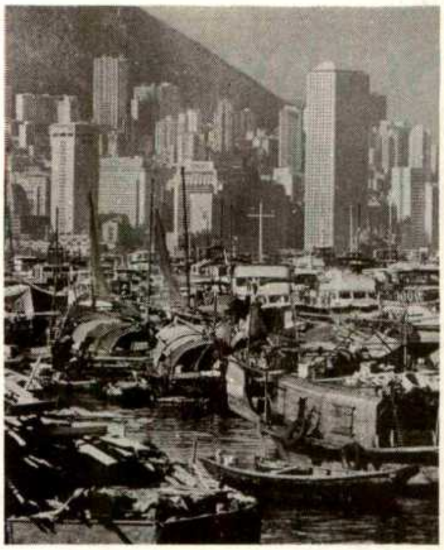

Two views of the limits to growth?

International aid is not seen by either the Kahn or the Herrera study to be a decisive factor in raising the level of well-being of Third World countries. Under conditions currently prevailing, even increased international aid would only contribute to increased spending by privileged sectors and have little or no effect on the living standards of the majority of the people. In direct contrast to the Kahn hypothesis, Herrera and his colleagues maintain that economic growth without concurrent drastic modification in income distribution would not achieve an adequate level of well-being for the entire populations of developing countries.

Many people tend to argue that studies like these are nothing more than a form of wish fulfillment; that they will increase the skepticism of laymen ignorant of the true nature of future studies and mathematical modelling because they seem to indicate that computer studies can be used to prove any thesis their authors wish; that their obvious political naiveté or ideological bias makes them trivial, if not dangerous. Others will see them as useful contributions to a continuing debate—a debate that must be kept going if solutions are to be found for the problems they deal with. Perhaps they will have done all they can if they succeed in showing, as both studies are intended to do, in the words of the Herrera group, "that the fate of man does not depend, in the last instance, on insurmountable physical barriers but on social and political factors that man must modify." □

BRITAIN

SGHWR: green to amber?

Allan Piper reports on uncertainties surrounding the next generation of British nuclear reactors.

GROWING doubts about the future of the British-designed Steam Generating Heavy Water Reactor (SGHWR) have led the House of Commons Select Committee on Science and Technology to call an inquiry into progress on the reactor system, now at the end of the design stage. The committee two years ago successfully urged the controversial adoption of the SGHWR for the next phase of Britain's nuclear energy programme. It has now expressed concern over "the widely reported intention of the Secretary of State for Energy [Mr Anthony Wedgwood Benn] to review the SGHWR project in the near future".

In fact Mr Benn is currently awaiting reports on technical and economic aspects of the SGHWR from the United Kingdom Atomic Energy Authority (UKAEA), which has recommended a "take-stock" review, and from the Central Electricity Generating Board (CEGB). Parliamentary questions and statements from key leaders of management and unions within the nuclear industry have fed speculation that the reactor may be abandoned as part of the government's present review of public expenditure.

Mr Benn is expected to appear as an early witness in the select committee inquiry, probably before the forthcoming Parliamentary recess. The heads of the nuclear industries and the CEGB will be invited to appear at a later date.

Disagreement over the choice of the SGHWR as the commercial successor to the Advanced Gas Cooled Reactor (AGR) has continued since the initial 4,000 MW ordering programme was announced by Mr Benn's predecessor in July 1974. The go-ahead came then in spite of opposition within the nuclear industry and the CEGB's preference for a much larger programme using mostly American Pressurised Water Reactors (PWRs). The SGHWR was eventually favoured on safety grounds even though estimated construction costs were around 10% higher.

Officially, the SGHWR still has the green light. But there are amber tinges. The PWR has been given a clean bill of health by the Chief Scientist at theDepartment of Energy (DEN), while technical difficulties have pushed design costs of the SGHWR above original expectations. Following a major design review in the middle of 1975, and a further revision earlier this year, the CEGB has calculated that the SGHWR could eventually prove more costly than equivalent coal-fired capacity.

This week Mr Benn spoke in Parliament of the new activity on the American reactor front. Last month he admitted that the UKAEA had recommended a careful look at progress on the SGHWR project, and hinted that once reports have been received the reactor's future will be considered in the light of recent changes on the energy scene. The CEGB, which currently has 15,000 MW of new generating capacity either under construction or ready for commissioning, will probably indicate that with the present slump in electricity demand the first commercial SGHWR planned for Sizewell in Essex is no longer urgently required.

Ditching the project would mean the loss of political face and perhaps more, but it would also avoid economic and technological complications. Development of the SGHWR is not regarded as a crucial step along the path towards fast breeder reactor (FBR) technology, while the export potential of the reactor remains limited; most other countries are expected to opt for the comparatively well proven PWR. Moreover, imported Canadian heavy water, needed to moderate the SGHWR, is likely to prove unexpectedly expensive.

Within the nuclear industry there is feeling that buoyancy can be maintained without the SGHWR if further commercial AGRs can be ordered. The first of the two AGR reactors at the 1,250 MW installation at Hinkley Point in Somerset is now running successfully up to full power, bringing confidence that the much-publicised developmental hitches can now be left behind. Additionally, there are hopes that with a go-ahead for the first commercial FBR this autumn, fast breeder technology could lag only three or four years behind SGHWR technology.

If the SGHWR is abandoned Britain could buy herself into PWR technology and establish an export base under licence. Japan and the USA, and several European countries, however, already have strong footholds in the market, which means that Britain would probably be restricted to the manufacture and export of component hardware. Mr Benn's junior, Alex Eadie, is meanwhile stressing that any reversal of SGHWR policy would not be at the expense of British technology.

Last week the DEN would only reaffirm that Mr Benn was awaiting reports from the UKAEA and CEGB. The UKAEA says simply that it is carrying out an appraisal which will be made available to Mr Benn in the near future. The CEGB is giving no outward sign that any imminent interruption to the SGHWR project is foreseen, and does not expect to have reliable cost figures ready for Mr Benn before next spring. An initial safety report is awaited from the Nuclear Power Company, responsible for design; this is not expected to arrive at the CEGB until next month, and is to be followed in turn by more detailed specifications in April 1977. ☐

CANADA

Towards a conserver society

Like other industrialised countries, Canada must look to conservation as an important element in its future energy stategy. This point has received considerable emphasis from an important quarter, as David Spurgeon reports from Ottawa

ENERGY conservation seems to be the major pre-occupation of the Science Council of Canada in its tenth anniversary year, judging by the statements and publications emanating from its members. The most recent came from the chairman, Josef Kates, who is president of a Toronto firm of systems analysts. "Energy conservation is not an option—it is a necessity," he says in the council's annual report. " . . .The *highest priority* in any comprehensive national energy policy should be *a wide-ranging, imaginative energy conservation effort.* Such an effort must involve every individual and every organisation, private or public."

Dr Kates reinforced his points at a press conference given when the report was published. The reason for his concern is that Canada is the "second most energy intensive country in the world, and energy shortages could threaten the very fabric of our way of life." He says that if Canada's energy requirements also double by 1990, as is currently forecast, the needed capital investment could be as high as $200 billion—or about 5 to 6% of GNP between then and now. This is some 50% higher than the 3.5% average between 1950 and 1975, and the interest rate on this capital is likely to be from 50 to 100% higher than in the 1960s.

This may mean that by the 1990s energy costs will be twice or three times what they are today, and if per capita consumption is also 50 to 100% higher, energy costs could require from two to four times today's proportion of personal income. Canada's historical advantage in such energy-intensive industries as forest products, mining, agriculture, metallurgical and chemical industries could therefore be seriously attenuated. And if primary industries weaken, Canadians could not look to the secondary sector for compensation.

Dr Kates proposes that a much higher priority be given immediately to a comprehensive energy conservation programme, and that Canada must now begin to develop the energy technologies that will permit her to achieve a stable energy use pattern in the long run. This means exploiting renewable energy forms such as solar, wind, geothermal, biomass and tidal power. A major programme of research and development, of the kind first proposed by the Science Council in 1968, must be undertaken "to demonstrate the feasibility of alternative energy technologies."

A recent investigation indicates that "if we were able to hold Canadian energy consumption at present levels and continue to use existing or moderately-expanded hydro-electric capacity to provide approximately 25% of our energy needs, the remaining 75% (now met almost totally by nonrenewable hydrocarbons, oil, gas and coal) could be provided within the next 50 years or so by renewable resources such as solar, biomass and wind energy."

At the press conference Dr Kates described the Conserver Society study the council's largest and most important project. The concepts behind this study, outlined in the "Statement of Concern" published in *Science Forum*, are summed up in the comment that "we face a transition from a 'consumer society' to a 'conserver society' "—that is, to a society which included among its features "doing more with less," "a greater appreciation of external or social costs," a return to the habits of thrift, saving and avoidance of waste for society as a whole, and so on.

"The transition to a Conserver Society," the Science Council paper says, "does not mean that we are going into a period of austerity and shortages. In fact, it is the reverse. Only by adopting a more rational and conserving approach to the common energy, resource, and environmental pool that sustains us all, can we ensure a continuing high standard of living for future generations." ☐

THIRD WORLD

Talking about technology transfer

The transfer of technology from developed to underdeveloped countries, a subject examined at UNCTAD IV at the end of May, was also discussed at the recent World Employment Conference. Robin Sharp reports

SCIENCE and technology, said the man on the rostrum, could increase production everywhere "on a scale that would make poverty unnecessary as a global phenomenon within the foreseeable future." The speaker was a senior official of the United Nations Development Programme, addressing last month's World Employment Conference in Geneva.

But for many people his otherwise heartening words raised questions. How is the scientific know-how and technology of the rich to be adapted and made relevant to the needs of the poor? How are the benefits of these high-cost, skill-intensive fields to be transferred to those possessing limited skills and no hard currency? And how, at the end of the day, can it be ensured that the transfer does not enrich 10 men at the expense of a thousand others? Among the many dilemmas of development these are some of the most intractable, and the debates in Geneva proved it once again.

Some of the figures can be frightening. In the industrialised countries, the average investment required to create one job is in the region of $5,000. The developing countries, with most of the world's poverty, need to create five times as many jobs per million population in order to meet the basic needs of their people, with only one-tenth of the per capita income available to do it. Hence, on a rough rule-of-thumb calculation, an average investment of $250 per job is what they can afford. There is little science and less technology to be had for that kind of money.

On this fundamental issue, delegates to the World Employment Conference found themselves deeply divided. At one end of the spectrum, speakers denounced the appropriate technology movement as a neo-colonialist strategem designed to perpetuate the supremacy of the rich countries. In more measured terms, the French Minister of Labour also questioned the international division of labour proposed to the conference by the International Labour Organisation (ILO), whereby developing countries would specialise in the production of everyday consumer goods, using less sophisticated technology and unskilled labour, while the industrialised countries would concentrate their economies even more in the high-technology sectors.

Put more favourably, however, what the ILO was proposing in its report to the conference was a Basic Needs Strategy in which much greater effort in the field of appropriate technology was seen as essential for maximising the use of labour in the Third World. Given the present level of 300 million unemployed or underemployed in the developing countries, and their estimated need for 1,000 million new jobs over the next 25 years, the ILO strategy is to many the more persuasive formulation. With it has to be swallowed a slower rate of national growth, but in most developing countries the alternative—in terms of human and social cost—would be even less palatable.

Among Third World delegations, the Latin Americans in particular were convinced that they should "continue to incorporate the most advanced technology into those activities where it was necessary in order to eliminate the technological gap." At their preparatory meeting, by contrast, the African group had strongly endorsed the need for more work on appropriate technology as a matter of priority.

In the end, it was the western industrialised countries which blocked the ILO's proposal for two new bodies to promote efforts in this field. A Consultative Group on Appropriate Technology was suggested as a mechanism for mobilising resources and determining research priorities, linked with an International Appropriate Technology Unit designed to identify and focus research in areas where technological innovation would have a significant impact.

Again lacking the support of the employers and western governments, the developing countries and the workers' group declared their support for an international code of conduct on technology transfer, as proposed by UNCTAD a month previously in Nairobi. As well as recommending a timetable for drafting and adoption of this code by the end of next year, the UNCTAD meeting also agreed on the immediate setting-up of regional technological centres under the aegis of either UNCTAD or the UN Industrial

Development Organisation.

Attention was also drawn in Geneva to the damaging restrictive practices contained in a dusty old piece of international law—the Paris Convention of 1883—which defined industrial property rights for a world very different from that of today. With its regulations tivity techniques which would condemn the developing countries to a permaon patents and like matters often working to the detriment of developing countries, they and the workers' group called for this Convention to be "drastically revised."

In its final report, the World Employment Conference endeavoured to strike a balance between the need for technologies which will generate the maximum possible growth of employment and the avoidance of low-producnently inferior role in the world economy. In practice, the technology choices of developing countries tend towards the capital-intensive end of the spectrum where work places will be few and far between for the one thousand million job-hunters in the year 2000. The danger is that what the report calls a "strategy of equilibrium" will be taken by most governments as an endorsement of whatever their policy now happens to be. ☐

USSR

Down Georgia way

Wendy Barnaby, recently in the Georgian SSR, describes some of the scientific work going on there

It takes two and a half hours to fly from Moscow to Tbilisi, the capital of the Georgian Soviet Socialist Republic. In this sunny space between the Black and Caspian Seas, the amount of human effort devoted to science depends on how successfully it—and everything else—competes with the five million Georgians' favourite occupation: the ceremonious consumption of their excellent local wines. And, as a few days spent with the Georgian Academy of Sciences shows, science is coming out of the competition extraordinarily well.

Astrophysical astronomy is concentrated in the southern republics of the Soviet Union, where the weather permits good observation. The air is especially clear on Mt Kanobili (1,700 m), 250 km from Tbilisi and only about 40 km from the Turkish border. Spread throughout the trees on the mountain top is the Academy's Abastumani Observatory, founded in 1937 as the first experimental mountain astro-physical observatory in the USSR. Work here is mainly concerned with galactic research. The resident scientists (including many women) study stars' spectra and classify them in order to examine the distribution of the stars according to their age and chemical composition. From such a distribution investigations are made of the structure of our galaxy. So far, about 100,000 stars have been classified, using a telescope whose diameter is the third largest in the world. During their last 20 years' research, the astronomers have discovered two of the 150 Supernova stars as well as about 100 emission stars.

The observatory's stellar telescope has a diameter of 125 cm and is the biggest fully automatic one in the USSR. The computer attached to it processes 1 million bits of information a second, and its memory stores 32,000 bits. Observations, which can be made on 160–170 nights a year, are mainly for determining the stars' chemical composition, physical properties and light variation. The solar telescope is used more frequently: generally on 260 days a year. Through studying the physical properties of solar flares and sun spots, the astronomers hope to be able to predict solar activity. They also do photometric and spectroscopic studies of optic radiation of the sun's atmosphere, and of radio emission at 220 MHz. The resulting data is shared under the Solar Service Programme.

Back at Tbilisi, the Underground Gravimetric Laboratory of the Academy's Institute of Geophysics is the centre of the Communist countries' cooperative efforts to study earth tides. Half burrowed into a hill overlooking the city, the laboratory is accumulating data which it is hoped will lead to the prediction of earthquakes. In tunnels leading off from basement passages, two double-component quartz extensometers composed of welded quartz tubes have been fixed so that their movements will reflect the tidal and secular deformations of the earth's crust, enabling these to be observed. Any movement is recorded photoelectrically, with a reading of 1 mm on the tape corresponding to a change of 0.1 micron on the ground. Between 1965 and 1972, the value of the recorded drift of one extensometer in the direction N 60°E was 11.9×10^{-6}. The value of deformation in the direction N 30°W between 1966 and 1972 was 14.7×10^{-6}.

Further down the passages, tiltmeters on basalt bases record changes in N–S and E–W directions. The instruments are housed in a chamber 60 m under the ground, where the diurnal temperature variation does not exceed 0.005 °C. From 1967 to 1972, the total drift in the N–S direction was 0.4 microns, and that in the E–W direction was 3.0 microns. The readings from both tiltmeters and extensometers are interpreted by the laboratory's staff as evidence of the existenc of secular movements of the earth's surface. So far there has been no success in using this knowledge to predict earthquakes: neither at this laboratory, nor at a new seismic station nearby, where equipment is being installed for the measurement of seismic waves from local and distant events. (Incidentally, the scientists at the station claimed that their research will enable them to locate and identify nuclear explosions in rock and in the Northern Hemisphere down to less than 10 kilotons. If the station were integrated into an international net, it could presumably contribute to the verification of any future comprehensive test ban treaty).

The Gravimetric Laboratory's methods are also being used to measure the earth's movements at a hydroelectric dam under construction about 50 km from Tbilisi. The plant, which will be completed in 1978, will have a capacity of 130 MW. Its artificial lake will hold 500 million cubic metres which will irrigate 45,000 hectares of land and supply drinking water to Tbilisi and its industrial area for 80–100 years.

Another of the laboratory's activities is the suppression of hail which threatens to destroy large parts of Georgia's grape crops every year. In 1974, 20,000 rockets containing silver iodide were launched from 34 automatically-synchronised firing points to save 360,000 hectares. Radar was used to detect clouds up to 15,000 metres, and results were good if the approaching front was narrow but not so good if it was broad. Because silver iodide is very toxic and expensive, research is being done into substitutes—ice with chemicals, for example.

In addition to coping with a heavy load of scientific work, a number of Academicians—including the Vice-President—represent Georgia in the Supreme Soviet of the USSR. This involves them in political activity to a degree extremely rare for active scientists in the West. Such involvement undoubtedly has its good and bad sides, but inasmuch as it contributes to the activism of science it seems a pity that Western scientists do not become more politically involved in their own societies. ☐

USSR

- The State Committee of Supply (Gossnab) of the Soviet Union is holding up scientific progress, a recent *Pravda* editorial has implied. Soviet policy is, of course, committed to the idea of the scientific and technical revolution as the panacea for social and economic ills, but according to *Pravda* Gossnab persists in supplying research institutes and experimental enterprises as if they were ordinary industrial concerns.

This criticism, from the official organ of the Party, reinforces the picture presented by individual scientists of a vast bureaucracy of order-forms, in which it is virtually impossible, once a project has started, to acquire some auxiliary equipment or reagents not envisaged in the original plan. The vivid description by such unofficial sources is of a standard procedure which includes over-ordering what is definitely needed and arranging to exchange surpluses with another laboratory to provide for unforeseen requirements. The success of a laboratory, it has even been claimed, depends not so much on the abilities of its top scientists, but on the wiliness of its "Fixer" in arranging such unofficial supplies.

Although *Pravda* makes no overt reference to this self-help system, this is clearly what lies behind the statement that "in the opinion of many scientists and specialists, what is needed is a system for the immediate supply of everything found to be necessary during the course of experiments and the development of experimental models." This "would permit the acceleration of scientific progress", presumably by making allowances for serendipity and eliminating the need for a marked degree of prescience. Gossnab, however, "is delaying with the creation of such a system".

The tendency to treat science as simply another branch of production is not, however, confined to Gossnab. The implementation of basic research in industry is one of the major themes of Soviet planning; considerable funds have accordingly been allocated to this end and a large number of research bases have been set up. Not all these facilities, however, are being used for their proper purpose. Thus, the Ministry of Gas Production has an excellent research establishment at Donetsk, but instead of using it for testing experimental models of new equipment, a large proportion of it has been handed over to routine production, while only a small fraction is used for the prime purpose of research and development. Examples of proper cooperation in this field, such as that developed by the Byelorussian Academy of Sciences and its subsidiary institutes on the one hand, and the industrial enterprises of the Byelorussian Republic on the other, to form what *Pravda* describes as "a truly powerful experimental base of science", are still, it would seem, sufficiently rare to evoke glowing press reports when they occur.

Another major problem facing Soviet research is the lack of sufficient scientific instruments. Here the problem is one of demand exceeding supply, so that in spite of considerable efforts by the relevant Ministries (Instrumentation, Automation and so on) and scientific bodies from the Academy of Sciences downwards, there are still considerable shortages. One recent development has been the establishment of rental centres, from which expensive and complex equipment may be borrowed for specific experimental projects. Such centres are already in operation in Moscow and Leningrad, and the Rental Department of the Siberian Metrology Institute, now in its fourth year of operation, supplies "hundreds of scientific and industrial organisations" of the developing regions of Siberia. The collective use of equipment, whether via rental centres or "on the principle of the comradely mutual aid and cooperation of Institutes" is especially recommended. The use of computers in planning scientific supply is urged, but with the cautious proviso that computers are to be employed thriftily.

For several years now, centralised and computerised planning has been a major aim of the logistics of Soviet science. This new emphasis on economy of computer use, and the suggestion that individual institutes might profitably make mutual equipment-sharing arrangements with other institutes, is a far cry from legalising the present system of unofficial exchanges of specially stockpiled surpluses. It does, however, indicate a growing recognition on the part of the authorities that running research and development on the same state-wide standardised pattern used for the production industries is at least problematical.

- The Soviet space programme, being based on Tsiolkovskii's concept of long-term orbital space stations as a prerequisite of any manned missions to the moon or planets, has always been greatly concerned with the medical problem of prolonged weightlessness. The death of the Soyuz 11 team upon re-entry, although finally proved to be due to a faulty hatch-seal, at first evoked considerable fears that the tragedy was due to some unsuspected side-effect of prolonged weightlessness. Accordingly, in addition to the usual programmes of astrophysical observations and the checking of equipment, the current Soyuz 21/Salyut 5 mission is paying special attention to the effects of weightlessness.

As usual, medical data—cardiovascular and respiratory action—is being telemetered to ground control; in addition, however, the cosmonauts have on board what the TASS agency describes as a special set of scales to enable loss of body mass to be monitored. What precise form these scales take, and how they can operate in conditions of zero gravity, is not specified. A similar question is posed by another on-board experiment—the presence of a tank of guppy fish which will be periodically filmed to record their adaptation (if any) to weightlessness—since submersion in water is a standard procedure for simulating weightlessness in pre-flight training missions.

Whatever the precise significance of these experiments, however, it seems clear that Soviet plans are moving towards longer and longer missions. Increasing attention is being paid to both physical and psychological well-being—an endless-belt "running track" and a colour-slide projector for light entertainment are carried on the latest mission. A new central control panel aboard Salyut 5 gives greater facility for the cosmonauts to operate scientific equipment during experiments, reducing their dependence on ground control and preparing the way for fully autonomous space missions whether in orbit or beyond.

Vera Rich

IN BRIEF

ESA scientific programme

The European Space Agency is in the process of selecting its future scientific satellite and shuttle payloads. Studies of 16 possible projects were presented to European scientists at the end of last month in Paris. The astronomy and solar system working groups subsequently made recommendations and the Science Advisory Committee then listed the next scientific projects to be undertaken: cooperation on the space telescope with NASA, an out-of-ecliptic and solar stereoscopy mission and a large infrared telescope on Spacelab. Final decisions will be taken in September, but UK scientists are meeting this week to identify their main areas of interest. They may also voice their objections about where the axe has fallen among the original projects.

Reprocessing debate continnes

The social, technological and environmental problems associated with the management of radioactive nuclear waste came under the spotlight last week during an international meeting of nuclear power experts in Denver, Colorado. Sir John Hill, Chairman of the UKAEA, pointing to national and international regulatory agencies, warned against premature adoption of inadequate short term safeguards on the one hand, and unnecessary delays to nuclear expansion pending the development of a "final [reprocessing] solution" on the other. Sir John foresaw no imminent changes in UK waste management policy, so that work on vitrification processes would continue, which need not ultimately preclude incineration. Even with widespread nuclear development, he said, radioactive waste arisings would be small compared with world mercury and arsenic stocks.

Meanwhile, amid reports that western Europe will have only about half of the reprocessing capacity it needs by 1980, work has begun on the site for British Nuclear Fuels Ltd's (BNFL) new reprocessing facility at Windscale. With construction costs estimated at £350 millions (the UK Government has just underwritten BNFL borrowing of £75 millions) the installation is expected to handle 1,000 tonnes of spent fuel a year by the mid-1980s.

A call for an outright ban on the sale of the technology for reprocessing will, however, be made at the annual conference of the British Labour Party in September. A motion urges the UK Government to consult with the group of nuclear exporting countries on the matter.

Mad about safrole

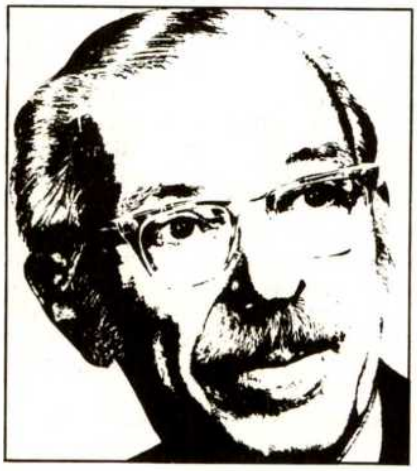

THOMAS H. JUKES

THE name of sassafras tea conjures up thoughts of early days in North America, of folk medicine, and of a tree whose leaves, charmingly enough, grow in three different shapes on the same branch—some are three-fingered, some are mitten-shaped, and some are just oval. The name is Spanish, but the Onondaga tribe in New York State called it Wah-eh-nak-kas—"smelling stick".

Pull up a sassafras seedling. You can peel the bark from the root, and sniff at the fragrance of the core. This spicy aroma led to its use as a flavour for root beer, which is a popular soft drink well-known to Americans and Canadians. But, alas, after many generations of people had enjoyed the natural flavour of sassafras, it turned out that safrole, the substance responsible for this, caused cancer in rats. Oil of sassafras, which contains about 80% safrole, was therefore banned as a food additive in 1960.

Manufacturers of flavoring extracts switched to methyl salicylate, present in wintergreen berries, as a substitute for oil of sassafras, and root beer continued to flow wherever soft drinks were sold in North America. The change made for a somewhat linimentous tang in the beverage, but the salicylates have a clean bill of health in the field of cancer. Also, wintergreen grows beneath sassafras trees in the Appalachian woodlands, so that there was an ecological link between the old flavour and the new.

But safrole still lurked in packages of dried sassafras root that are sold in "health food" stores to lovers of herb teas. These infusions are rumoured to be good, in a generalised way, for what ails you. By sipping them, you get all the benefits of hot water plus whatever happens to be in dandelion heads, camomile, dried parsley, peppermint leaves, comfrey, rosemary (that's for remembrance), verbena, yerba maté, and, of course, sassafras.

Since these ingredients contain hundreds of compounds that have never been biologically tested for anything, herb teas are apparently considered harmless, and in addition, their consumption is hallowed by ancient custom. Unhappily for tradition, the Commissioner of Food and Drugs sternly pointed the finger "to make it clear that the prohibition on the use of safrole in food includes safrole-containing sassafras sold to make sassafras tea; effective June 10, 1976."

Comments had come from private citizens and people in the herb tea business. Several felt it was unlikely that sassafras tea is injurious to health even if safrole is carcinogenic, in one case because the tea is consumed in the spring, and in another because it had "been used for centuries without reports of carcinogenic or other toxic effects." Others noted that safrole was present in other foods such as nutmeg and mace and that hence the ban should include "all food substances containing detectable amounts of safrole."

This, of course, would be in accordance with the rules laid down by the "Delaney Amendment" in the Food Additives Law. The Commissioner replied, in effect, that he couldn't ban everything, and he had to take care of the most concentrated source of safrole first. One correspondent stated that the fat of charcoal-broiled steak contains carcinogens and that "action on sassafras should be deferred until something is done about that." No one mentioned cigarettes.

Several comments expressed various forms of anguish that a natural food, or food constituent, or ingredient, or component should be regulated, saying that this treatment should be reserved for chemical additives. Gently, the Commissioner reminded them that all food ingredients, including natural food constituents, are chemicals, also that the definition of "food" includes food additives.

The ban showed that sauce for the Red Dye No. 2 goose is also sauce for the sassafras tea gander.

correspondence

Plea for Argentinians

SIR,—We are writing to call the attention of your readers to the harassment many of our colleagues in Argentina are undergoing at the present time.

The Junta Miltar headed by the general Jorge Videla has recently passed a law (ley de prescindibilidad, n.21.274) which allows to "release from duty" any employee of the public administration for unspecified "reasons of service", without further justification. This law has been the ground for expelling political dissenters from the universities and other scientific institutions, mainly in Buenos Aires and La Plata. The most affected institutions are, so far, the CONICET (Consejo Nacional de Investigaciones Cientificas y Technicas), the institutes depending on the Comision Nacional de Estudios Geoheliofisicos, and the Institudo Nacional de Tecnologia Agropecuaria. Not less than 550 persons have lost their jobs: biologists, physicists, chemists, medical doctors, architects, technicians and officers, some of them after 20 years, or more, of service.

On May 7 the newspaper *La Opinion* reported that the Representative on the Junta Militar in the Ministry of Education acting as State Secretary for Science and Technology had decided to "release" 90 employees. The newspaper quoted a few names of distinguished scientists. On May 12, in *La Opinion*, Horacio Encabo (vice-Director of the Centro de Investigaciones Neurologicas Torcuato Di Tella) expressed his worries in an article emphasising the risks for the development of Argentina of a scientific policy inspired by the criterion: "quien no es occidental y cristiano es subversivo" (who is not occidental and christian is subversive). Encabo was "released from duty" five days later.

Besides protesting against these vexations there are other ways of supporting this courageous political and moral stand of our colleagues: anyone can join us by writing to those he or she may know personally or by name: informing them of his or her work by sending reprints of preprints or reports in fields of common interest: doing anything else to let them know that they are not left alone or forgotten by the world community of scientists to which they belong.

Yours faithfully,

F. ACCASCINA, G. OLIVIERI, G. TECCE, G. TOSCHI (*Rome*);
G. G. ALOISI, G. MARINO, U. MAZZUCATO, G. REICHENBACH (*Perugia*);
R. ANDREOLI, L. ANTOLINI, P. BARALDI, I. BARALDI, M. C. BRUNI, L. BENEDETTI, P. G. DE-BENEDETTI, R. BATISTUZZI, S. BUFFAGNI, I. M. CRAMAROSSA, G. FABBRI, A. FABRETTI, G. FINI, G. GAVIOLI, A. GUISTI, G. GRANDI, L. MENABUE, P. MIRONE, F. MOMICCHIOLI, G. PELLACANI, A. RASTELLI, E. SORAGNI, G. TOSI (*Modena*);
G. BIGNAMI, A. CARPI, N. FRONTALI (*Istituto Superiore Sanità, Roma*);
L. BUSETTO, G. L. BENDANOLI, P. BISCARINI, M. CARLOTTI, G. DI LONARDO, G. GALLONI, G. NIVELLINI, P. PALMIERI, C. STREMMENOS, F. TULLINI, A. TROMBETTI, C. ZAULI (*Bologna*);
R. BARBIERI, M. CARAPEZZA, G. GIUDICE, G. LA GRUTTA, M. LEONE, F. ODDO, U. M PALMA, M. B PALMA-VITTORELLI, L. PAOLONI, G. SERRAVALLE (*Palermo*);
E. CLEMENTI, S. PIZZINI (*Istituto di Ricerche "G. Donegani" Novara*);
S. CALIFANO, E. FERRONI (*Firenze*);
G GIACOMETTI, E. VIANELLO (*Padova*);
G. ALBANESE, G. CASNATI, R. FIESCHI, M. FONTANA, C. GIORI, L. OLEARI, E. SCROCCO (*Parma*);
A MONROY (*Stazione Zoologica Napoli*).

Nuclear trade

SIR,—As one who objects to all nuclear explosions, I would like to comment on "Heavy Water Allegations" (June 17, page 537). While I can understand Senator Ribicoff's concern about India misusing US-supplied heavy water, I personally feel that most of those who object to India's nuclear tests are hypocritical. How else does one explain the deafening silence that greeted the revelation that Israel had at least twenty bombs in the 20–30 kiloton range? The critics of India's nuclear tests might well support Israel, using the well-worn argument that Israel is a perennially threatened state But does any state's territorial integrity warrant a nuclear holocaust? I do not know if the US has aided Israel's nuclear programme, but I think it is reasonable to suppose that it did. If so, why does not Senator Ribicoff condemn Israeli nuclear tests?

The only way to save the world from nuclear destruction is to ensure that no country has a nuclear bomb. The present NPT cannot achieve this end because it is iniquitous. It assumes that the top five nuclear powers are the only ones which can be expected to behave responsibly. No self-respecting nation can tolerate this super-power arrogance. Those that have signed the NPT have done so under pressure. What we need today is a total elimination of nuclear arms. If this sounds naive and unattainable then, I assert, we have to be naive and we have to attain the unattainable if we want to prevent a world-wide Hiroshima.

The cynicism which characterises all super-power pronouncements on nuclear arms must give way to an enlightened idealism. The USA and the USSR should really be talking of Strategic Arms Elimination and not of Limitation. The West has provided enlightened leadership on several issues. Is it too much to expect it to collectively lead the world back to peace and sanity? You have produced both Bertrand Russell and Ronald Reagan. Is it unrealistic to expect that you would follow the former and not the latter?

Yours faithfully,

C. S. G. PRASAD

Macmillan Company of India Ltd.,
New Delhi 110002

Genetic engineering

SIR,—If, as Mr Norman reports, (July 1, page 2), the NIH did indeed recommend that, for safer recombination experiments, the recombinant DNA have "less than 1 in 10^{-8} chances of surviving in the natural environment", then the critics of such experiments should have even more qualms one in 10^{-8} is equivalent to 100,000,000 to 1.

Yours faithfully,

JEROME G BUESCHER

Department of Microbiology,
Thomas Jefferson University,
Philadelphia, Pa.

Human anatomy

SIR,—We were interested to see Anthony Harris's measurements of asymmetry in young women (May 6, page 10) and the response of Connolly and Dangerfield (May 20, page 188), and have found our ratios right to left of ankle 1.006, calf 1 02, biceps 1.04, wrist 1.02.

We conclude, assuming we are average females, that Anthony Harris's conclusions are correct and asymmetry is commonplace

Yours faithfully,

JUDY WHALLEY, ENID THOMAS, HILARY LANE, MARY BROND, GAIL WESTON, SUE WILKINSON, SANDRA NIXON, PENNY ELSIP

Department of Food Sciences,
Polytechnic of North London,
London, UK

news and views

Are earthquakes a major cause of the Chandler wobble?

from Hiroo Kanamori

WHETHER or not earthquakes are a major cause of the Earth's free Eulerian nutation (period of 14 months), widely known as the Chandler wobble, has been a controversial issue. The present consensus seems to be that the crustal deformation associated with earthquakes is much too small to explain the amplitude of the Chandler wobble. O'Connell and Dziewonski (page 259 of this issue of *Nature*), however, suggest that earthquakes represent the major factor in the wobble excitation. Since their analysis is very direct and unambiguous, it is important to examine what makes their conclusion distinct from others'.

At one time, there were significant disagreements between theoretical results concerning the excitation of the Chandler wobble obtained by different investigators. This controversy, however, seems to have been completely settled, and the theory is now formulated in a rigorous framework. Observationally, the overall pattern of polar motion seems to be well established, although the data may not be good enough to allow correlation of the fine structure of the trajectory with individual earthquakes.

The physical size of great earthquakes has only recently been measured very accurately. Traditionally, the earthquake magnitude M_s (often called the Richter scale) is determined at periods of about 20 s, but it does not necessarily represent the total crustal deformation associated with earthquakes. In fact, the M_s scale is saturated at a magnitude of about 8 or when the fault length becomes about 100 km. Any earthquake whose fault length exceeds 100 km has M_s of 8.3 ± 0.3 regardless of whether the fault length is 100 or 1,000 km. This does not mean that other measures of earthquake "size" such as energy or seismic moment are similarly bounded. In order to measure accurately the physical size of great earthquakes, precise measurements of long-period seismic waves are necessary. The amount of the overall crustal deformation is best expressed by the seismic moment M_o which is proportional to the product of the fault area and the average displacement on the fault. With the recent progress in long-period seismology, the seismic moment has been determined for many great earthquakes. The fault geometry of great earthquakes is also important. With the advent of plate tectonics, it is reasonable to assume a fault geometry which is consistent with the contemporary plate motion.

In these circumstances, the paper by O'Connell and Dziewonski represents a very timely contribution. Most discussions in the past have dealt with either statistical correlations or correlations between an individual break in polar motion and a particular earthquake. The statistical arguments are somewhat indirect, and the arguments on individual events are hampered by the poor quality of the data. In order to circumvent these shortcomings, O'Connell and Dziewonski used geometries of great earthquakes predicted by plate tectonics, and computed the cumulative effects of earthquakes on polar motion rather than the effect of individual events.

Since the seismic moment M_o is not known for most old earthquakes, O'Connell and Dziewonski estimated it by using the relation $\log M_o = 8.8 + 2.5\,M_s$ which is obtained from the work of Chinnery and North (*Science*, **190**, 1197–1198; 1975). The M_s scale used in the above formula is based on Gutenberg and Richter (*Seismicity of the Earth*, Princeton University Press, 1954) and is very close to what is called the 20 s surface-wave magnitude. On the other hand, O'Connell and Dziewonski used the magnitude scale adopted in Duda's catalogue (*Tectonophysics*, **2**, 409–452; 1965) to estimate M_o. The magnitude scale used in Duda's catalogue is, however, different from Gutenberg–Richter's M_s; the former is systematically larger than the latter, a fact which is not widely recognised.

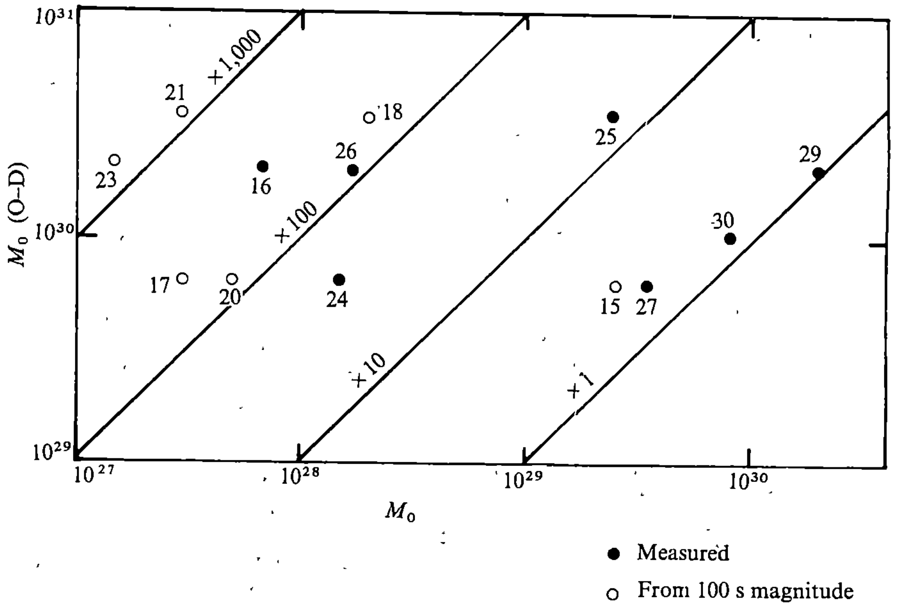

Fig. 1 Measured seismic moment M_o *versus* seismic moment M_o (O-D) assigned by O'Connell and Dziewonski for thirteen earthquakes. Closed circles indicate earthquakes for which M_o is directly determined (from Kanamori and Anderson, *Bull Seismol. Soc Am.*, **65**, 1073–1095; 1975; Ben-Menahem, Aboodi, and Schild, *Phys Earth planet. Int.*, **9**, 265–289; 1974), and open circles are for earthquakes for which M_o is estimated from the 100 s magnitude (Brune, and Engen, *Bull. Seismol. Soc. Am.*, **59**, 923–933; 1969). Numbers refer to those in Table 1 of O'Connell and Dziewonski.

For shallow ($H \leqslant 60$ km) earthquakes for the period from 1905 to 1952 listed in Table 1 by O'Connell and Dziewonski, the average difference between the two scales is 0.3. Thus, the use of Duda's values in the above M_0 *versus* M_s relation results in an over-estimate of M_0 by a factor of 5.6. Since the polar shift is linear with the seismic moment, this difference would mean that the effect on the Chandler wobble computed by O'Connell and Dziewonski is, on the average, 5.6 times too large. However, it is more important to note that because of the saturation of the M_s scale beyond 8, any M_0 *versus* M_s relation is useless for earthquakes of $M_s \geqslant 8$. For these large earthquakes direct determinations of M_0 are essential. Fortunately, for seven earthquakes listed in Table 1 of O'Connell and Dziewonski, a direct determination of M_0 has been made, and for six other earthquakes the 100 s magnitude (from which M_0 can be estimated fairly accurately) has been determined. In Fig. 1, these seismic moments are compared with those estimated by O'Connell and Dziewonski from Duda's catalogue through the M_0 *versus* M_s relation. For earthquakes with very large rupture dimensions such as the Chilean (No. 29), the Alaskan (No. 30) and the Kamchatka (No. 27) earthquakes, the agreement is very good, but for many earthquakes with smaller rupture dimensions, M_0 seems to be overestimated by more than two orders of magnitude. For most events before 1923 no direct determination of M_0 has been made, but it seems almost certain from the above comparison that M_0 is overestimated in a similar manner.

O'Connell and Dziewonski, in fact, considered most of these problems carefully in their article, but in view of the good accuracy of moment determinations even for relatively old earthquakes it appears that the direct effect of earthquakes is about one order of magnitude too small to explain the Chandler wobble. But as they suggest, it is possible that earthquakes accompany very large aseismic deformation which has not been detected by existing seismological instruments. Then the fact that O'Connell and Dziewonski could explain the temporal behaviour of the Chandler wobble amplitude by using the mechanisms of earthquakes derived from plate motion may suggest that accelerated, but aseismic, plate motions are associated with great earthquakes (Anderson, *Science*, **182**, 49–50; 1974). Although such aseismic deformation has been suggested from several independent observations (of tsunami earthquakes, slow pre- and post- seismic deformations, disparity between plate motion and seismic slip rate for example), the details are at present unknown. With world-wide deployment of high-quality ultra-long period instrumentation (see Agnew *et al.*, *EOS*, **57**, 180–188; 1976), it is hoped that the nature of such aseismic deformation will be revealed in the near future. ☐

Long palindromes in eukaryotic DNA

from T. Cavalier-Smith

ONE of the most fascinating differences in the organisation of DNA in eukaryote cells (those with a distinct nucleus) from that in prokaryotes (bacteria and blue-green algae) is the abundant occurrence—in higher eukaryotes at least—of long palindromes. When applied to nucleotide sequences in double-stranded DNA the word 'palindrome' usually means regions of DNA with an axis of two-fold rotational symmetry which would be read the same in both directions by the cell's transcription machinery:

$$\begin{array}{c}\longrightarrow\\ \mathrm{C\ A\ T\ A\ T\ G}\\ \mathrm{G\ T\ A\ T\ A\ C}\\ \longleftarrow\end{array}$$

would for example, be transcribed to give an RNA molecule with the sequence $\underrightarrow{\mathrm{C\,A\,U\,A\,U\,G}}$ whichever end the RNA polymerase started, because the polarity of the transcript (shown by the arrow) is always antiparallel to that of the template strand.

(A few authors call sequences like

$$\begin{array}{c}\longleftarrow\\ \mathrm{G\ T\ A\ A\ T\ G}\\ \mathrm{C\ A\ T\ T\ A\ C}\\ \longrightarrow\end{array}$$

"palindromes", but though when no account is taken of polarity each individual strand appears palindromic, the sequence does not show two-fold symmetry, and if it were read in both directions by RNA polymerase two quite different RNA sequences would be made—its biological meaning is quite different when read backwards. Here I use 'palindrome' only for sequences with two-fold symmetry.)

Since palindromes are inverted repeats they can be easily identified because the two strands are self complementary. If denatured to separate the strands and then returned to renaturing conditions each strand will rapidly fold back on itself to form a double-stranded hairpin loop:

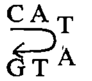

These can be separated from non-palindromic DNA because they bind strongly to hydroxylapatite. Wilson and Thomas (*J. molec. Biol.*, **84**, 115; 1974) found numerous almost perfect palindromes in *Drosophila*, *Xenopus* and human DNA. Usually 300–1,200 nucleotide pairs long, they form several percent of the total DNA and like non-inverted medium repetitive sequences, are widely dispersed in the DNA and not clustered in some special fraction. Such long palindromes are absent in prokaryotes and may be of profound significance for the organisation of eukaryote chromosomes. In searching for explanations one must bear in mind that not all eukaryote palindromes are perfect. Many are not or have impaired terminal loops (Schmid *et al.*, *Cell*, **5**, 159; 1975; Perlman *et al.*, *Cell*, **8**, 33; 1976).

Palindromes could have many functions. Short ones can serve as recognition sites on the DNA for proteins which themselves have two-fold rotational symmetry. Such short palindromes do exist in prokaryotes· the recognition sites for the *lac* repressor and several bacterial restriction nucleases are palindromes, but these are too short to be detected by hyroxylapatite which in conditions usually used only binds double strands of over 50 base pairs. Another suggestion is that palindromes form pairs of lateral hairpin loops in the DNA which could be important for recombination or other functions. (Sobell, *Prog. Nucl. Acid Res. molec. Biol.*, **13**, 153; 1973). Such paired loops have not been found in isolated DNA, though they can be generated *in vitro* (Karrer and Gall, *J. molec. Biol.*, **104**, 421; 1976). A looped secondary structure (like that of tRNA on a larger scale) would be expected in RNA transcripts of palindromic DNA and has been found in nuclear RNA, including both heterogeneous nuclear RNA and low molecular weight nuclear RNA, though not in cytoplasmic mRNA; however, the length of these loops (which could have an important role in regulation of transcription or RNA processing or transport) is generally shorter than the palindromes seen in the DNA.

Recent studies in *Xenopus* (Perlman *et al.*, *op cit.*) argue against a specific control function for long palindromes. It appears from renaturation kinetic studies that the unique DNA attached to isolated palindromic DNA can include all unique sequences in the genome, and not just a small specific subfraction as would be expected if the palindromes were always attached to the same adjacent sequences. Perlman *et al.*'s interpretation is that the 100,000 palindromes of *Xenopus* are inserted at different sites in different copies of the genome, and that at any one time one tenth or fewer of the palindromic insertion sites (which must occur at average intervals of 2,500 base pairs or less) are occupied. If correct, this implies a more fluid model for the eukaryote genome than is traditional. One would have to postulate either that palindromes are continually being generated or destroyed or are being swapped from one chromosome site to another, probably even during the lifetime of a single individual. Schmid and Deininger (*Cell*, **6**, 345; 1975) have shown that palindromes are randomly positioned with respect to unique and middle repetitive sequences in human DNA.

In 1974 I suggested a mechanism for the replication of the ends (telomeres) of linear chromosomes which requires terminal palindromes (not necessarily very long ones) and an endonuclease specific for the palindromic sequence (*Nature*, **250**, 467). There are indications that a number of viruses, notably adeno-associated virus (Strauss *et al.*, *Proc. natn. Acad. Sci. U.S.A.*, **73**, 742; 1976) may replicate in this way; moreover, as predicted, the ends of the gene-sized minichromosomes of hypotrich ciliate macronuclei are palindromic and probably generated by palindrome specific endonucleases (Wesley, *Proc. natn. Acad. Sci. U.S.A.*, **72**, 678; 1975). Now Karrer and Gall (*J. molec. Biol.*, **104**, 421; 1976) and Engberg *et al.* (*J. molec. Biol.*, **104**, 455; 1976) have both shown that in *Tetrahymena* macronuclei, where in contrast to hypotrich ciliates the bulk of the DNA is not cleaved into gene-sized pieces, the rDNA exists as numerous small linear DNA molecules each of which is a perfect palindrome over 20,000 nucleotide pairs long. This rDNA is amplified 20 times in total amount relative to the rest of the macronuclear DNA, but each molecule contains only two (inverted) copies of each of the two RNA genes.

If, as Karrer and Gall postulate, these long palindromes also have short identical inverted repeats at each end, they could replicate either according to my model or by way of a circular intermediate. Terminal 'minipalindromes' would make it very easy to explain their formation during amplification by failure of the sequence specific nuclease to nick just one end. The study of this process could have far reaching implications for the understanding of eukaryote chromosome organisation. It is in fact very tempting to suggest that all eukaryote chromosomes, and not merely those of hypotrich ciliates, consist of a linear array of potentially independent replicative units terminated by short palindromic sequences.

To end on an even more speculative note, Sparrow and Naumann (*Science*, **192**, 524; 1976) review evidence that the doubling of whole chromosomes may be a major cause of the evolutionary increase in genome size; they suggest this could occur in linear chromosomes by a slight modification of my palindromic telomere replication mechanism suggested by Bateman (*Nature* **253**, 379; 1975) so as to generate a double length chromosome that would (until the genes inevitably diverged during evolution) be a single palindrome like that of the *Tetrahymena* rDNA giant palindrome only far longer. □

Expression of a eukaryotic gene in *Escherichia coli*

from John Atkins

THE development of the technology of cloning DNA fragments from diverse sources in *E. coli* and potentially other organisms, by linking them to a plasmid or phage replicon has provoked much discussion. The possible expression of eukaryotic DNA to produce functional proteins when cloned in *E. coli* has been a key question. A positive answer would greatly facilitate the isolation of a substantial number of eukaryotic genes by enabling their protein products to be detected by complementation of well-studied prokaryotic mutants. Currently the chromosomal eukaryotic genes, which have been identified on cloned segments, are limited to those whose mRNA copies are a large proportion of the total mRNA, generally of some specialised cell type or after appropriate induction, and so can be isolated in relatively pure form. The ribosomal RNA genes also belong to this category (see *News and Views, Nature*, **259**, 173; 1976). Thus an assay based on complementation of auxotrophs would provide a significant extension of the range of genes which could be identified and so studied. Another main reason for the interest in whether eukaryotic genes can be expressed at the protein level, using the existing vectors, is industrial. Will the vectors which have been developed for *E. coli* hosts enable certain valuable eukaryotic proteins to be produced in organisms such as *E. coli* when grown in fermenters?

A number of different groups have started experiments to answer this question about the expression of eukaryotic genes in *E. coli*, but credit is due to Struhl, Cameron and Davis who describe a careful genetic analysis of the first successful experiments in the current issue of the *Proceedings of the National Academy of Sciences* (**73**, 1471–1475; 1976). As the cloning vector this Stanford-based group used bacteriophage lambda. One of the features of certain λ vectors is that transcription originating at one of the powerful λ promoters (P_L) continues into the heterologous cloned DNA and does not terminate at normal (that is rho) termination sites. The Stanford group did not have to utilise this feature of λ, however, as they found that transcription was initiated within the yeast fragment. Whether transcription originated at a sequence fortuitously recognised by *E coli* RNA polymerase (compare cloned mouse mitochondrial DNA, Chang, Larsman, Clayton and Cohen, *Cell*, **6**, 231; 1975) or at the correct yeast promoter, is unknown.

The two *E. coli* mutants used for the complementation tests were histidine auxotrophs both with non-revertible non-suppressible mutations in the *his*B gene such that imidazole glycerol phosphate (IGP) dehydratase activity was not present, although the other enzyme activity, histidinol phosphatase, coded by the same gene was retained (the complementation patterns in the *his*B gene and relationship to the subunit composition of the two enzyme activities are discussed by Loper *et al.*, *Brookhaven Symp*, **17**, 15; 1964). Struhl *et al.* isolated λ phages carrying yeast DNA which complemented both *his* mutants lacking IGP dehydratase although they did not complement single site mutants lacking histidinol phosphatase. This is reassuring as the yeast genes coding for the two enzyme activities are widely separated on the yeast genome. Davis and coworkers next made ^{32}P-labelled complementary RNA *in vitro* using *E. coli* RNA polymerase and DNA from the λ carrying the yeast histidine gene as a template. This RNA was then hybridised to separated fragments derived from an independently prepared yeast DNA sample, and the DNA fragment which gave positive hybridisation was the same size as the cloned yeast fragment from which the complementary RNA was synthesised. As the authors point out, this argues against any contaminant phage being responsible for the complementation. Struhl *et al.* have not yet characterised the enzyme produced, nor the DNA fragment in detail, and any real measure of the efficiency of translation also awaits study. This latter aspect is of interest as one of the very few reports from analogous cell-free translation studies gave a low efficiency of translation (Crawford and Gesteland, *J. molec. Biol.*, **74**, 627; 1973) and whether the efficiency is greater *in vivo* (in relation to other *in vivo* translation), or if it is very message dependent, is unknown. Consequently, any generalisations from the present study should await the results of complementation studies done with a considerable number of different auxotrophs.

The presentation at the recent Miles Symposium by J. Carbon and colleagues suggest that such reports will soon be forthcoming. ☐

More rapidly growing manganese

from Peter J. Smith

Two years ago Scott *et al.* (*Geophys. Res. Lett.*, **1**, 355; 1974) reported the discovery of an unusual manganese oxide crust about 5 km from the axis of the mid-Atlantic ridge at 26°N. The sample in question, a 4.2 cm thick deposit of birnessite with a trace of todorokite, had an abnormally low iron concentration (compared with typical ferromanganese nodules and crusts), was depleted in ^{230}Th and ^{231}Pa and contained unexpectedly small amounts of Cu, Ni and Co. Its most startling characteristic, however, was its rapid growth rate. Whereas ferromanganese nodules and crusts grow on the ocean floor at typical rates of 0.1–1.0 cm per million years, the new sample had apparently grown at a rate of 13.0–25.0 cm per million years.

On the basis of all the evidence Scott and his colleagues concluded that their newly-discovered crust was a product of hydrothermal activity along an active ridge crest and had not, as 'normal' ferromanganese crust, precipitated from seawater. At that time the importance of hydrothermal processes at ridges, though not unrecognised (for example, Lister, *Eos*, **55**, 740; 1974 and others had recently drawn attention to it), was not widely appreciated. Today, however, the situation is rather different Hydrothermal activity is increasingly commonly acknowledged to play a major part in heat transfer at oceanic ridges, probably explaining both the great variability of axial heat flow and the low average axial heat flow observed compared with that predicted from cooling lithosphere models. It is probably also closely involved with the formation of metal-rich sediments at ridge crests.

It is in this changing context that Moore and Vogt (*Earth planet. Sci. Lett.*, **29**, 349; 1976) now report the discovery of two more manganese oxide crusts (A and B), similar to that of Scott and his coworkers but from the vicinity of the Galapagos spreading axis. Sample A is a 2–4 cm thick deposit recovered from an almost sediment-free wall of an axial valley of the spreading centre where the basement age estimated from magnetic anomalies is 0.3 Myr. It consists of a grey banded zone comprising mixed todorokite and birnessite covering a darker friable zone of todorokite. Assuming this sample to have remained a chemically closed system, its maximum age obtained from the ^{230}Th/^{234}U ratio is 6,000 years at a depth of 9–13 mm within the crust and 9,000 years at 6–9 mm. On this basis the growth rate for the outer 1 cm was therefore 100–200 cm per million years, or 100–2,000 times greater than the rate for seawater-precipitated deposits.

Compared with typical ocean floor ferromanganese deposits, sample A has very low Fe/Mn and ^{232}Th/^{238}U ratios, a higher manganese concentration and lower transition metal concentrations. These properties, combined with the rapid growth rate, strongly support the idea of formation by ridge hydrothermal activity in an area where the supply of manganese is enhanced. Indeed, circumstances suggest that hydrothermal activity may be more vigorous here than is usual along spreading axes, for the recovery site is close to the position of the proposed Galapagos hot spot. Be that as it may, the chief competing explanation—that the extra manganese is remobilised from a sedimentary source—would seem to be ruled out by the obvious lack of sediment at the recovery site and a direct association of the crust with igneous rocks such as tholeiitic basalts and, unusually, soda rhyolite.

Sample B, a 4–6 cm thick crust recovered further from the ridge axis at a point where the basement age is 2.4 Myr, is more complex, less amenable to study but in some ways more interesting than sample A It has a 4–6 cm core of grey todorokite and birnessite which is chemically similar to sample A and thus believed likewise to be of hydrothermal origin. But, by contrast, the core is covered with a 3 mm thick layer of darker material indistinguishable from seawater-precipitated manganese deposits.

Chemical analysis shows that this sample could not have remained a closed system. No ages can therefore be calculated from the ^{230}Th/^{234}U ratio, although given the basement age the growth rate must have been at least 2.5 cm per million years. Assuming average precipitation growth rates, the 3 mm covering would then have taken about 1 million years to form around the core. The implication is that the core formed hydrothermally whilst the sample was close to the spreading axis, but acquired a seawater-precipitated coating more slowly as it was taken out of the hydrothermal zone by seafloor spreading.

Taken together, these two samples provide further support for the existence of hydrothermal processes at ridge crests. Why such activity should lead to extreme fractionation of iron and manganese, and thus to deposits abnormally rich in manganese, is another question, however. Moore and Vogt support the view that the iron was removed from the hydrothermal solutions before they debouched into the seawater. Bonatti *et al.* (*Econ. Geol.*, **67**, 717; 1972), following Krauskopf, noted, for example, that iron should precipitate from a hydrothermal fluid before manganese as sulphides or oxides, thereby gradually lowering the Fe/Mn ratio in the remaining fluid. Clearly this process could produce a solution depleted in iron so that at debouchment the manganese would be rapidly oxidised and precipitated. But this explanation is almost certainly incomplete— and there are other possibilities. The full details and significance of hydrothermal activity at ridge crests have yet to be worked out.

Borrowed polypeptides in Qβ replicase

from Pamela Hamlyn

THE enzyme which replicates the genetic material of the single-stranded RNA phage $Q\beta$ — $Q\beta$ replicase — has many interesting properties, not least its specificity. The enzyme recognises, and begins initiation, at the oligonucleotide CCCA found at the 3′ end of both the plus and minus strands (it is a two step replication). The first residue to be incorporated is a G; the A is not copied. *In vitro* the enzyme will replicate poly(C) and C-containing copolymers which suggests it is not too choosy, perhaps only requiring some Cs at the 3′ terminus. But it will not replicate the RNA of other similar phages which also end with CCCA. Weissman has proposed—and there is some supporting evidence—that as well as the terminal Cs the enzyme also recognises another region within the RNA molecule and it is the spatial relationship between these regions that acts as a signal for initiation (Weissman *et al.*, *A. Rev Biochem.*, **42**, 303; 1973)

Another notable feature of $Q\beta$ replicase is that three of the four subunits comprising the enzyme are polypeptides 'borrowed' from the host —*E. coli.* One is the ribosomal protein S1 which the host uses for the correct recognition and binding of mRNA. The other two requisitioned polypeptides are also involved in protein synthesis in the host; they are the polypeptide elongation factors (EF) Tu and Ts Their known function in protein synthesis could be very neatly fitted with possible functions in the Qβ replicase. EF-Tu is able to bind GTP which is the only nucleotide with which Qβ replicase can initiate replication. EF-Ts can remove GDP from EF-Tu in a catalytic exchange reaction. In addition, EF-Tu is able to bind aminoacyl-tRNA and, since Qβ RNA and tRNA both have CCA at their 3′ end, the suggestion was readily made that EF-Tu in the replicase was involved in enzyme—template binding.

The method used to test these hypotheses was to alter the EF-Tu and EF-Ts subunits so that they are no longer effective in supporting protein synthesis, and then to reconstitute Qβ replicase with these modified subunits and test for enzymatic activity with synthetic and natural templates. Brown and Blumenthal have performed these experiments with unexpected results. (Brown and Blumenthal, *J. biol Chem.*, **251**, 2749; 1976; and *Proc. natn. Acad. Sci. U.S.A.*, **73**, 1131; 1976). Using chemical modifiers, they have altered the aminoacyl tRNA binding site of the enzyme subunit which is EF-Tu and shown that, although it now no longer supports protein synthesis, Qβ replicase reconstituted with it is active —in fact its specific activity is very similar to the native enzyme. To investigate the GTP binding site on EF-Tu they used kirromycin, an antibiotic that inhibits protein synthesis by altering the GTP binding properties of EF-Tu but has no effect on the aminoacyl-tRNA binding site. Low levels of kirromycin which effectively inhibit protein synthesis do not affect the replicase activity, suggesting that in replicase EF-Tu does not function by binding GTP. Further careful experiments using reconstituted replicase revealed that kirromycin acted on the enzyme by preventing the formation of an EF-Tu·Ts complex. The authors think that it is as a complex that these two subunits function in native replicase. Support for this is provided by the experiments described in their paper in the *Proceedings of the National Academy of Sciences.* EF-Tu and EF-Ts have been chemically 'crosslinked' (joined covalently) and this complex used to reconstitute the enzyme. Although in this state the elongation factors cannot perform their function in protein synthesis, they do not at all inhibit the activity of the reconstituted enzyme.

Since the replicase is not utilising the known abilities of EF-Tu and EF-Ts perhaps they perform other functions in the host, as yet undiscovered by scientists but recognised by Qβ as useful. More likely the authors think, is that the two subunits have some structural role, perhaps holding subunit II, the one coded for by Qβ, in its active configuration. The enzyme has the ability to unfold its template RNA as it copies it and to keep the two complementary strands apart. Perhaps EF-Tu·Ts could be involved. □

Zinc in enzymes

from Peter J. Sadler

WHEN cultured in normal conditions, yeast uses a zinc metalloenzyme, alcohol dehydrogenase (YADH), during the final stage of the fermentation process, for the conversion of acetaldehyde to ethanol. The role of zinc in the enzyme is intriguing. If Co^{2+} is added to the culture medium it becomes incorporated into the enzyme, and green (but still active) enzyme crystals instead of colourless (Zn) ones (Curdel and Iwatsubo, *FEBS Lett.*, **1**, 133; 1968) can be isolated. Furthermore, if Zn^{2+} is excluded from the growth medium and Mn^{2+} is added, an active Mn^{2+} enzyme is isolated (Coleman and Weiner, *Biochemistry*, **12**, 3466; 1973).

The natural yeast enzyme has a molecular weight of 140,000 and contains four zinc ions. Their role is thought to be similar to the four zinc ions in the mammalian liver enzyme (molecular weight 80,000) which converts ingested alcohol to acetaldehyde. This enzyme (LADH) has recently been the subject of X-ray crystallographic analyses at 2.4 Å resolution (Eklund *et al.*, *J. molec. Biol.*, **102**, 27; 1976) and detailed metal exchange studies in solution (Stykowski and Vallee, *Proc. natn. Acad. Sci. U.S.A.*, **73**, 344; 1976). A close look at these results reveals the conditions in which metal ions can be swopped and activity retained.

Early attempts to remove zinc from LADH and to reconstitute it with other metal ions met with difficulty. Enzyme activity decreases as zinc is removed, but slow conformational changes occur through oxidation of formerly stable SH groups to S-S bonds (Oppenheimer, Green and McKay, *Archs Biochem. Biophys.*, **119**, 552; 1967).

But successful exchange reactions can be performed under an N_2 atmosphere. The zinc atoms behave in pairs: Zn_2 (Zn_2) representing non-catalytic (catalytic) ions. The pairs exchange at different rates. For example, Zn_2 (Zn_2) dialysed against radioactive $^{65}Zn_2$ (Zn_2) initially becomes $^{65}Zn_2$ (Zn_2) and finally $^{65}Zn_2$ ($^{65}Zn_2$). Similarly, $^{65}Zn_2$ (Zn_2) with Co^{2+} added becomes Co_2 (Zn_2) after 12 h (4 °C, *p*H 5.5), and Co_2 (Co_2) after 120 h. But Co_2 (Zn_2) has an identical activity to Zn_2 (Zn_2), whereas Co_2 (Co_2) is only 64% as active. Hence the term catalytic to describe the second pair of zinc ions.

The crystallographic analysis shows the enzyme to be a dimer of two identical subunits, each having two zinc binding sites and one coenzyme (NAD^+) site. As predicted by earlier spectroscopic studies (Foster, Hill and Williams, *Biochem. Soc. Symp.*, **31**, 187; 1970) on YADH, the zinc coordination sites are (distorted) tetrahedral and include cysteine (sulphur) ligands: four cysteines for the non-catalytic zinc, and two plus one histidine (N) and one water molecule for the catalytic zinc. The latter, which is the faster ion in exchange, is situated at the bottom of a 20 Å pocket, whereas the non-catalytic zinc is in a cleft on the enzyme's surface.

An alternative differentiation of the zinc atoms involves binding 1,10-phenanthroline (OP). OP inhibits reversibly Zn_2 (Zn_2) or Co_2 (Zn_2) by binding at catalytic zinc (H_2O displacement) without removing them. OP irreversibly inhibits Co_2 (Co_2) by removing the catalytic cobalt ions. A difference in behaviour of Co and Zn is notable here.

A near-tetrahedral zinc with a water ligand is now becoming familiar at zinc sites in metalloenzymes: carbonic anhydrase (3 His, H_2O), carboxypeptidase (2 His, Glu, H_2O), thermolysin (2 His, Glu, H_2O). Woolley (*Nature*, **258**, 677; 1975) has recently discussed the enhanced reactivity of such water ligands. This may vary with the fractional change placed on Zn by the other ligands, and may account for the exceptional catalytic efficiency of carbonic anhydrase which has one of the largest known turnover numbers, 600,000 s^{-1}.

The non-catalytic zinc or cobalt ions in LADH may simply have structural roles, but this coordination site is strikingly similar to the iron site in rubredoxin and bacterial ferredoxins, and a sequence spacing of coordinated cysteines, X, $X + 3$ is a regular occurrence. Substitution of the non-catalytic zinc with iron should not only produce an enzyme with interesting properties, but also perhaps with evolutionary significance! □

A hundred years ago

VIOLENT shocks of earthquake were felt again on the 5th inst. at Corinth and the surrounding district. The direction of the motion was east to west. Shortly after noon on Monday an earthquake occurred in Vienna Three violent shocks, lasting two seconds, were felt. A panic ensued. Several houses are damaged, and a portion of the old walls has been split.

from *Nature*, **14**, July 20, 260; 1876

articles

Excitation of the Chandler wobble by large earthquakes

Richard J. O'Connell
Department of Geological Sciences, Harvard University, Cambridge, Massachusetts 02138
Adam M. Dziewonski
Applied Seismology Group, Lincoln Laboratory, Massachusetts Institute of Technology, Cambridge, Massachusetts 02142

Superposition of the polar shifts computed for 234 large earthquakes ($M_s \geq 7.8$) that occurred between the years 1901 and 1970 yields a synthetic curve that closely resembles the observed pattern of variations of the Chandler wobble during the same period. We conclude that earthquakes represent the major factor in the wobble excitation.

SINCE its discovery in 1891, the Eulerian free nutation of the Earth, popularly called the Chandler wobble, has been of considerable interest to astronomers, meteorologists, oceanographers and solid earth geophysicists. Throughout this time the mechanisms exciting the wobble have remained elusive, and although atmospheric motions, core–mantle interactions and earthquakes have all been considered, none of these has been either clearly identified as the principal source of excitation or entirely rejected as a partial contributor.

The period of the wobble depends on the Earth's oblateness and its elastic properties, and the observed period is reasonably well accounted for by current Earth models, with the greatest uncertainty coming from lack of exact knowledge of the effect of the oceans[1]. The observed variation of amplitude of the wobble has not been satisfactorily explained, although several different mechanisms have been proposed. These variations must be caused by damping and the excitation of the wobble. These two mechanisms cannot be studied independently, of course, since the excitation needed to account for the observed wobble depends on the magnitude of damping.

None of the estimates of the frequency or damping of the wobble have explicity considered the mechanisms exciting the wobble, and it is conceivable that particular excitations could introduce considerable bias into estimates of the intrinsic frequency and damping of the wobble. For this reason it is advantageous to calculate the excitation from specific mechanisms to remove any such biases, before interpreting the results in terms of the intrinsic properties of the Earth.

In this study we consider the cumulative effect of major earthquakes that occurred between 1901 and 1970 as a source of excitation of the wobble. Previous investigations of the role of earthquakes in exciting the wobble have yielded no clear conclusions. Although Munk and MacDonald[2], among others, had concluded that displacements associated with earthquakes were too small to excite the wobble, Smylie and Mansinha[3] presented evidence for a correlation between times of occurrence of major earthquakes and changes in the direction of polar motion. This suggested that earthquakes could be responsible for a sizeable fraction of the excitation and revived interest in the subject which has become one of the more controversial topics in the geophysical literature.

Subsequent studies[4,5] concentrated on the correlation between individual earthquakes and short term changes in polar motion. Because of the considerable uncertainty in the exact location of the pole at any time, a definite correlation between polar motion and earthquakes could not be firmly established[6,7]. In addition, Dahlen[8] concluded that earthquakes could not account for the observed amplitude of the wobble; his result was based on the calculated pole shifts for the 1960 Chilean and 1964 Alaskan earthquakes and a Monte Carlo simulation of seismicity averaged over the whole Earth.

Nevertheless, there is still highly suggestive evidence of a correlation between global seismicity and changes in the amplitude of the wobble over the period of the past 70 yr (refs 9–11). This suggests that the cumulative effect of earthquakes may account for the long term variations in the amplitude of the wobble, even though the effect of any individual earthquake is too small to be detected above the noise in the data on polar motion. To investigate this possibility we calculated the polar motion expected from major earthquakes over the past 70 yr and compared it with actual polar motion data over the same period. This requires specification of the time, location and source parameters of the earthquakes, as well as the calculation of the change of the Earth's inertia tensor caused by an earthquake.

The synthetic Chandler wobble

The evaluation of the change in the Earth's inertia tensor involves calculation of the static displacement field resulting from an earthquake. Previous workers have solved this problem directly[8,12–14], but some of the numerical results differed by an order of magnitude. Here we make use of the representation of the static displacement field by a linear superposition of normal modes[15]; only the normal modes of degree 0 and 2 contribute to changes in the moment of inertia. The advantage of this approach is that it has been empirically tested; all the modes that significantly contribute to the change in the inertia tensor have been observed (modes ${}_0S_0$, ${}_0S_2$ and ${}_1S_2$ account for more than 95% of the effect) and their excitation and eigenfrequencies can be explained by realistic models of the Earth's structure and the seismic source mechanism. In addition, this independent calculation resolves the differences among the numerical results obtained by other workers.

The change in the inertia tensor C_{ij} caused by an earthquake with an equivalent source moment tensor M_{kl} can be written

$$\Delta C_{ij} = D_{ijkl} M_{kl}$$

where D_{ijkl} is a fourth rank tensor whose components depend on 6 canonical functions of the model of the Earth evaluated at the source depth, and the latitude and longitude of the epicentre. The components of D_{ijkl} and canonical functions for both a uniform Earth model and a realistic Earth model PEM-C (ref. 16) are given in Dziewonski and O'Connell[17]. The expression of the inertia change in terms of the complete moment tensor M_{kl} permits consideration of source mechanisms more general than a double couple[18,19].

The changes of the inertia tensor caused by the 1960 Chilean and 1964 Alaskan earthquakes calculated using the normal mode approach agree well with those calculated by Dahlen[8], so long as similar Earth models are used. Substantial differences can result from using Earth models that differ at the source depth, and a uniform Earth model gives noticeably different results from a realistic Earth model[17].

To specify the source moment tensor for an earthquake one needs to know the orientation of the fault plane and direction of the slip vector (for lack of better evidence, at this time, we shall use the traditional double couple model) as well as the scalar seismic moment. Most large earthquakes occur at plate boundaries and the source mechanisms that have been determined for several earthquakes are remarkably consistent with current plate tectonic models; for example refs 20–23. This suggests that one may reliably estimate the source parameters of large earthquakes on plate boundaries from knowledge of the type of a plate boundary and relative motion between the plates.

The earthquakes with magnitudes $M_s \geq 7.8$ used to calculate the excitation of the Chandler wobble are taken from the catalogue compiled by Duda[24], primarily based on the study of Gutenberg and Richter[25], and supplemented by information from the *Bulletin of the Seismological Society of America* for the years 1965–1970. Since it is the seismic moment M_0 that determines the static displacement, we have used an approximate empirical relation to determine the moments from the reported magnitudes. Figure 1, after Chinnery and North[26], shows the relation between M_0 and M_s for a number of earthquakes for which both have been independently determined.

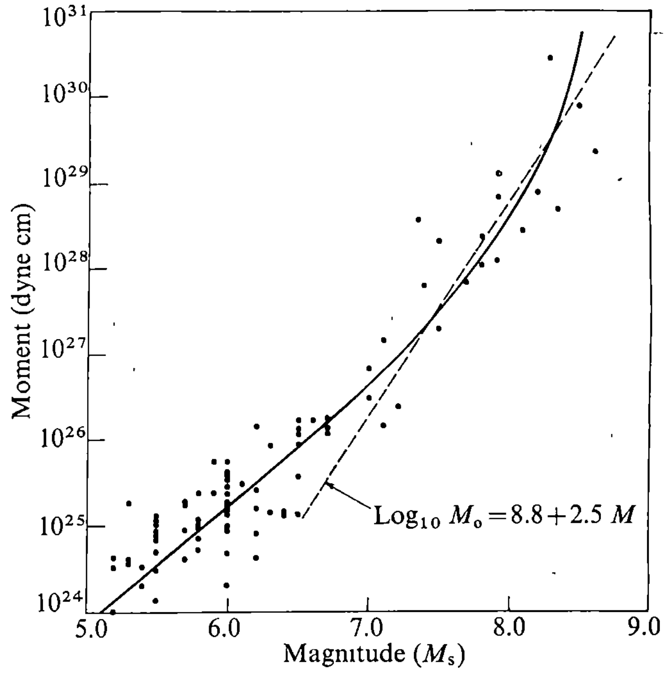

Fig. 1 Relation between seismic moment M_0 and magnitude M_s after Chinnery and North [26]. The dashed line gives the relation used to calculate the pole shifts from earthquakes.

The solid line is the relation between moment and magnitude proposed by Chinnery and North. The dashed line shows the relation we have used to determine the moments; it obviously is a reasonable approximation to the data for magnitudes greater than 7.5.

The paucity of data for the largest magnitudes makes it difficult to assess the reliability of the relation we use, which gives moments of 2×10^{28} dyne cm for $M_s = 7.8$ to $M_0 =$

Table 1 Times and locations of the thirty largest earthquakes contributing to the excitation of the Chandler wobble. The magnitude and direction of the pole shift as well as the change in length of day from each earthquake is shown. Depths designated s were assigned a standard value of 33 km. Earth model PEM-A (ref. 16) was used to calculate the pole shifts*

No.	Year	Month	Day	Lat.	Long.	Depth (km)	Mag	Shift (0.01″)	Dir (°E)	Change in length of day (μs)
1	1901	Aug	9	−22.0	170.0	s	8.4	0.60	336.2	−7.02
2	1902	Sep	23	16.0	−93.0	s	8.4	0.49	296.3	−5.83
3	1905	Apr	4	33.0	76.0	s	8.6	1.62	89.4	−2.60
4	1906	Jan	21	34.0	138.0	340	8.4	0.83	101.4	1.84
5	1906	Jan	31	1.0	−81.5	s	8.9	1.39	218.0	−160.17
6	1906	Aug	17	−33.0	−72.0	s	8.6	2.56	108.0	−16.09
7	1906	Sep	14	−7.0	149.0	s	8.4	0.79	239.0	−0.03
8	1910	Jun	16	−19.0	169.5	100	8.6	1.78	340.7	−26.53
9	1911	Jun	15	29.0	129.0	160	8.7	4.86	105.7	−17.96
10	1914	Nov	24	22.0	143.0	110	8.7	3.07	160.6	−43.10
11	1917	May	1	−29.0	−177.0	60	8.6	2.33	9.0	−18.26
12	1917	Jun	26	−15.5	−173.0	s	8.7	4.33	277.3	−0.69
13	1919	Apr	30	−19.0	−172.5	s	8.4	0.55	19.6	−8.13
14	1922	Nov	11	−28.5	−70.0	s	8.4	0.72	110.8	−6.15
15	1923	Feb	3	54.0	161.0	s	8.4	0.71	146.1	2.07
16	1929	Mar	7	51.0	−170.0	60	8.6	2.10	171.9	6.95
17	1934	Jan	15	26.5	86.5	s	8.4	0.53	95.3	−3.40
18	1938	Nov	10	55.5	−158.0	s	8.7	3.89	189.1	17.54
19	1939	Dec	21	0.0	123.0	150	8.6	0.84	106.7	−4.36
20	1940	May	24	−10.5	−77.0	60	8.4	0.33	73.9	−8.76
21	1941	Jun	26	12.5	92.5	60	8.7	4.30	178.4	−13.57
22	1941	Nov	25	37.5	−18.5	s	8.4	0.53	323.6	−0.27
23	1942	Aug	24	−15.0	−76.0	60	8.6	1.30	75.6	−22.71
24	1946	Dec	20	32.5	134.5	s	8.4	0.77	116.8	−3.20
25	1950	Aug	15	28.5	96.5	s	8.7	2.86	122.3	−11.83
26	1952	Mar	4	42.5	143.0	s	8.6	2.77	131.2	−5.00
27	1952	Nov	4	52.8	159.5	s	8.4	0.82	147.2	1.69
28	1958	Nov	6	44.5	148.5	75	8.7	4.50	130.4	−2.47
29	1960	May	22	−39.5	−74.5	s	8.6	2.56	109.2	−9.80
30	1964	Mar	28	61.1	−147.6	20	8.5	1.11	202.7	7.92

*The indicated pole shifts correspond to a change of the position of the principal axis of the moment of inertia about which the instantaneous rotation axis moves in a circular arc with a 14-month period.

3.5×10^{30} dyne cm for $M_s = 8.7$. Nevertheless, these values are grossly consistent with the data, and are all less than the largest moment measured, which was $\sim6\times10^{30}$ for the 1960 Chilean earthquake[23]. Furthermore, the slope of 2.5 in our equation is consistent with the value of 3 proposed by Kanamori and Anderson[27] for large earthquakes.

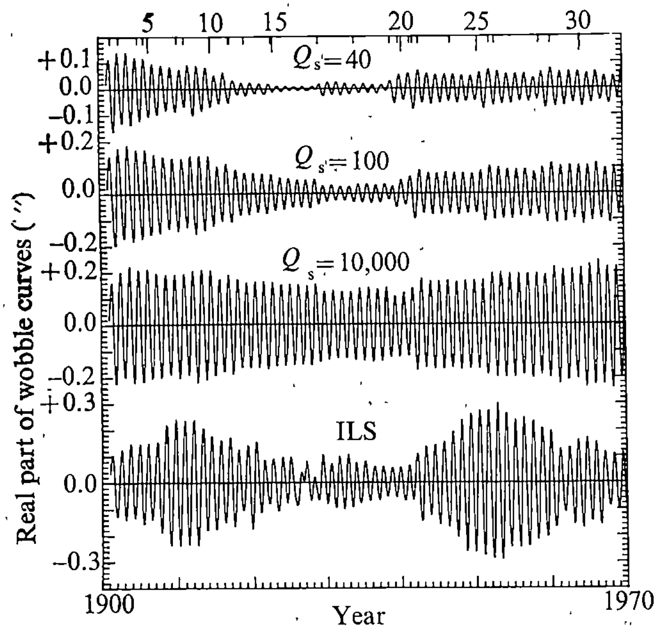

Fig. 2 Simulated polar motion curves resulting from excitation by large earthquakes; the damping for each is determined by Q_s. ILS is smoothed observed polar motion with annual term removed[30]. Only the component along the Greenwich meridian is shown.

The remaining source parameters were determined from plate tectonic models. Using the data of Solomon *et al.*[28] for the positions of the boundaries and relative motions of the plates, we assign fault plane parameters to earthquakes of three types: normal faulting at mid-ocean ridges (dip = 45°, perpendicular to the ridge axis), transform faulting on fracture zones (dip = 90°) and thrust faulting at converging plate boundaries (dip = 20°, perpendicular to plate boundary in the direction of the Benioff zone). Such an assignment was straightforward except for large earthquakes in Asia, and those at complex plate boundaries, which were omitted.

The calculated pole shift and direction are given in Table 1 for the 30 largest earthquakes of those considered. Also shown is the change in length of day resulting from the change in the polar moment of inertia of the Earth. For all cases the moments used were derived from the listed magnitudes by use of the relation in Fig. 1. Results for a different magnitude–moment relation can be obtained by appropriate scaling of the magnitude of the pole shift.

Conspicously absent in Table 1 is the great Sanriku earthquake of March 2, 1933. It occurred near the junction of the Philippine, Pacific and Eurasian plates and it was difficult to assign a particular source mechanism to it. Also, Kanamori[29] has shown that it was not typical of the large shallow earthquakes in the subduction zones; its moment[27] is estimated to be as low as 4.3×10^{28}.

From the calculated pole shifts for 234 earthquakes with magnitudes at least 7.8 between 1901 and 1970 we can compute a synthetic polar wobble curve that would result from this source of excitation alone. For this we also require the starting position $m(t_0)$ of the pole in January 1901 and the frequency ω_0 and damping, Q of the Chandler wobble.

The synthetic wobble $m(t)$ is computed from

$$m(t) = m(t_0)\exp[i\omega(t-t_0)] + \\ + \sum_k s_k H(t-t_k)\left\{1-\left(1+\frac{\omega_0}{\Omega}\right)\exp[i\omega(t-t_k)]\right\}$$

where ω is the complex circular frequency of the Chandler wobble: $\omega = \omega_0(1+i/2Q)$, s_k are the complex pole shifts caused by earthquakes at times t_k, Ω is the frequency of the diurnal rotation and H is the unit step function[12]. The complex function $m(t)$ is referred to the coordinate system in which the real axis corresponds to the Greenwich meridian and the imaginary axis points towards 90°E.

Figure 2 shows the real part (m_x) of three such synthetic wobble curves obtained using $\omega_0 = 5.287$ radians yr^{-1} after Wilson[30] and three different values of Q. Shown for comparison is a smoothed version of the ILS polar motion data, with the annual term removed, also from Wilson[30]. The initial pole location is the same for all curves, and each curve has been bandpass filtered from 0.3 to 0.98 cycles yr^{-1} to facilitate comparison. The ticks on the top of the figure mark the times of the earthquakes in Table 1.

The general trend of the amplitude of the wobble can be seen in the ILS data. The observed amplitude was large in 1910, decreased fairly uniformly from 1910 to 1920 and remained small until 1940 when it began to increase again to reach the maximum value by 1954. Since then there has been an irregular decline in amplitude. The synthetic wobble time series, particularly for $Q = 100$, reproduce the principal features of these amplitude changes. The decrease in the synthetic wobble is caused by the cumulative effect of several large earthquakes from 1914 to 1929. This occurs even for the case with $Q = 10,000$ and it is thus apparent that earthquakes can reduce the amplitude of the wobble and a rapid decay of amplitude need not be attributed to intrinsic dissipation. Similarly, the increase in the synthetic wobble amplitude arises from large earthquakes from 1938 through 1950 which gradually re-excite the wobble. We should note that the decline in amplitude observed since

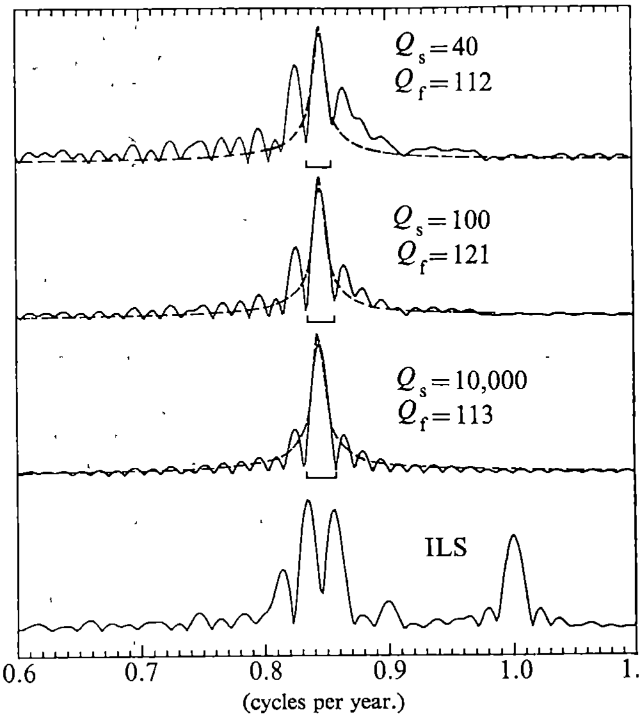

Fig. 3 Power spectra (—) of the simulated and observed (ILS) polar motion shown in Fig. 2. Resonance curves were fitted to the central peaks to determine Q_f (— — — —).

1954 is not reproduced in the synthetic wobble curves; this may be an effect of other sources of excitation or accumulation of the phase shift due to a difference between the actual ω_0 and the value of Wilson[30].

The power spectra of the three synthetic time functions $m(t)$ are compared in Fig. 3 with the power spectra of the ILS data. Although it is clear that we were not able to reproduce exactly the observed spectra, the synthetic curves for $Q_s = 40$ and $Q_s = 100$, each having three well developed maxima, exhibit a similar order of complexity. Also shown is a least squares fit of a resonance curve to the central peak of the synthetic series, which yields an estimate Q_f that is nearly independent of the intrinsic Q_s of the model. This illustrates the fact that a damping of an episodically excited harmonic oscillator cannot be estimated from its spectrum, unless specific assumptions about the nature of the excitation are made[31]. It is clear that reliable estimates of both the frequency and damping of the wobble may depend on the detailed nature of the excitation, especially if it is dominated by a relatively few large impulsive events. Thus an accurate evaluation of the excitation from earthquakes (or other sources) may permit determination of the effective elastic and anelastic properties of the earth at the Chandler wobble period sufficiently precise for comparison with those inferred from seismic observations.

Discussion

The fact that synthetic wobble calculations reproduce the principal variations of amplitude of the observed Chandler wobble substantiates the correlation between global seismicity and changes in the amplitude of the wobble noted by Myerson[9]. Since a given earthquake can either increase or decrease the amplitude of the wobble, the fact that the cumulative effect of several earthquakes is in accord with observations strongly suggests that the correlation is indeed real, and that earthquakes make a noticeable contribution to the excitation of the wobble. Comparison of amplitudes of the synthetic and observed wobble suggests that the earthquake series, with the specific moments assigned through our magnitude–moment relationship could account for $\sim \frac{1}{2}$ of the excitation; the remainder could come from other sources. For example, Wilson[30] has stated that the atmosphere can account for $\sim \frac{1}{2}$ of the observed wobble, and possibly more. If this is true, then the relative contributions to the excitation of the wobble by the atmosphere and earthquakes could be of comparable magnitude.

The magnitude of the seismic excitation exhibited by the synthetic wobble curves depends on the moments assigned to the individual earthquakes. These are quite uncertain, as can be seen by the scatter of points around the lines in Fig. 1. Furthermore, it must be noted that the moments calculated here for some of the earthquakes before 1960 are larger than have been previously reported for the same events (see Table 1 in ref. 27). The moments of earlier earthquakes may have been underestimated because of the lack of adequate long period instrumentation that would allow measurements of amplitudes of surface waves and free oscillations at periods of at least several hundred seconds, so that their wavelengths would be significantly greater than the source dimensions.

While seismic moments are usually estimated from the radiation of the seismic waves associated with the main shock, excitation of the wobble would be affected by the displacements that may take place over a relatively long period of time (several weeks) before and after an event. For example, Kanamori and Cipar[23] identified an 'aseismic' event several minutes before the main Chilean shock (1960); the moment of this event could be equal to, or perhaps even exceed, that of the main shock[32]. Dziewonski and Gilbert[18] reported release of isotropic stress preceding two deep earthquakes; the spectra indicated the aseismic character of these events. Such 'silent earthquakes', whether or not they are followed by major seismic events, may be more common than previously believed. In fact, such a conclusion is suggested by the work of Davies and Brune[33], who compared the cumulative seismic moment release with the average plate tectonic displacement rates at converging plate boundaries. Although they found a good correspondence between cumulative moment release and plate-tectonic slip rates, this only held for shallow earthquakes with an assumed depth of faulting < 60 km. They noted that differential motion at greater depths seems to be accomplished by aseismic deformation. Such deformation may well be associated with large earthquakes and would increase the total shift of the pole over that calculated from the observed amplitudes of seismic waves. In fact the static moments associated with great earthquakes, or aseismic events, are sufficiently uncertain that one cannot rule out the possibility that these account for most of the excitation of the wobble.

This conclusion is not in agreement with that earlier reached by Dahlen[8]. At that time no earthquake had been assigned a moment greater than 10^{30} dyne cm; which led him to restrict the maximum allowed moment to that value. Subsequent redeterminations of the seismic moment of the great Chilean earthquake[23,32] relaxes this restriction and makes plausible the implications of the moment–magnitude relationship used in this report. This, in turn, leads to the calculated excitation comparable to that observed. We note, however, that the 70-yr average of the polar shifts from earthquakes listed in Table 1 is only $0.008'' \text{ yr}^{-1}$; approximately equal to that computed by Dahlen[8] for the 1964 Alaskan earthquake.

The results of this study indicate that the cumulative effects of major earthquakes can account for at least a large part of the excitation of the Chandler wobble, and in particular for the long term variations of the amplitude of the wobble. This, together with recent estimates of the atmospheric excitation of the wobble[30], indicates that these two mechanisms may well account for the entire excitation. If this is verified by more detailed analysis, it should permit more accurate determination of the period and damping of the wobble, and of the effective elastic properties of the Earth at very long periods.

We thank Stephen N. Cohn for his assistance and Don L. Anderson for helpful conversations. This research was supported by the NSF and by the Advanced Research Projects Agency of the Department of Defense.

Received April 27; accepted May 26, 1976.

[1] Jeffreys, H , and Vicente, R. O., *Mon. Not. R. astr. Soc.*, 117, 142 (1957).
[2] Munk, W. H., and MacDonald, G. J F., *The Rotation of the Earth*, (Cambridge University Press, 1960).
[3] Smylie ,D. E., and Mansinha, L., *J. geophys. Res.*, 73, 7761 (1968).
[4] Smylie, D. E., Clarke, G. K. C , and Mansinha, L , in *Earthquake Displacement Fields and the Rotation of the Earth*, (edit by Mansinha, L , Smylie, D. E., and Beck, A. E·), 99 (D Reidel, Dordrecht, 1970).
[5] Masinha, L., and Smylie, D. E , in *Earthquake Displacement Fields and the Rotation of the Earth*, (edit. by Mansinha, L., Smylie, D. E., and Beck, A. E.), 122 (D. Reidel, Dordrecht, 1970).
[6] Haubrich, R. A., in *Earthquake Displacement Fields and the Rotation of the Earth*, (edit. by Masinha, L , Smylie, D. E , and Beck, A. E.), 149 (D Reidel, Dordrecht, 1970).
[7] Wells, F. J., thesis, Brown Univ. (1972).
[8] Dahlen, F. A , *Geophys J. R. astr. Soc.*, 32, 203 (1973).
[9] Myerson, R. J., in *Earthquake Displacement Fields and the Rotation of the Earth*, (edit by Mansinha, L., Smylie, D. E., and Beck, A. E), 159 (D Reidel, Dordrecht, 1970).
[10] Anderson, D. L., *Science*, 186, 49 (1974).
[11] Press, F , and Briggs, P., *Nature*, 256, 270 (1975).
[12] Dahlen, F. A., *Geophys. J. R. astr. Soc* , 25, 157 (1971).
[13] Smylie, D. E., and Mansinha, L., *Geophys. J. R. astr. Soc.*, 23, 329, (1971).
[14] Israel, M , Ben Menahem, A., and Singh, S. J., *Geophys. J. R. astr. Soc.*, 32, 219 (1973).
[15] Gilbert, F., *Geophys. J. R. astr. Soc.*, 22, 223 (1971).
[16] Dziewonski, A. M., Hales, A. L., and Lapwood, E. R., *Phys Earth planet. Int.*, 10, 12 (1975).
[17] Dziewonski, A. M., and O'Connell, R. J., in *Semiannual Technical Summary, Seismic Discrimination*, (MIT Lincoln Laboratory, December 1975).
[18] Dziewonski, A. M , and Gilbert, F., *Nature*, 247, 185 (1974)
[19] Gilbert, F , and Dziewonski A M. *Phil. Trans. R. Soc.*, A278, 187 (1975).
[20] Kanamori, H., *J geophys. Res* , 75, 5011 (1970).
[21] Kanamori, H., *J. geophys. Res* , 75, 5029 (1970).
[22] Wu, F T., and Kanamori, H., *J. geophys. Res* , 78, 6082 (1973).
[23] Kanamori, H , and Cipar, J. J., *Phys. Earth planet. Int.*, 9, 128 (1974).
[24] Duda, S. J , *Tectonophysics*, 2, 409 (1965).
[25] Gutenberg, B., and Richter, C. F., *Seismicity of the Earth and Associated Phenomena* (Princeton, 1954).
[26] Chinnery, M. A., and North, R. G., *Science*, 190, 1197 (1975)
[27] Kanamori, H., and Anderson, D. L., *Bull. seism. Soc Am* , 65, 1073 (1975).
[28] Solomon, S. C., Sleep, N. H., and Richardson, R. M., *Geophys. J. R. astr. Soc.*, 42, 769 (1975).
[29] Kanamori, H., *Phys. Earth planet Int* , 4, 289 (1971).
[30] Wilson, C. R., thesis, Univ. California, San Diego (1975).
[31] Jeffreys, H., in *Rotation of the Earth* (edit. by Melchior, P., and Yumi, S.), 39 (D. Reidel, Dordrecht, 1972).
[32] Kanamori, H., and Anderson, D L., *J. geophys Res.*, 80, 1075 (1975)
[33] Davies, G. F., and Brune, J. N., *Nature*, 229, 101 (1971).

Possible evidence for penetration of interstellar dust into the Solar System

J. L. Bertaux & J. E. Blamont

CNRS, Service d'Aéronomie, BP No 3-91370 Verrières Le Buisson, France

Because of the motion of the Sun through the surrounding interstellar medium, interstellar dust particles may penetrate deep into the Solar System. In this paper, we investigate the conditions for this penetration and find that the distribution of such particles should peak along the line of gravitational focusing. Two possible consequences are compared with experimental results: the rate at which particles should strike a micrometeoroid detector and the distribution of scattered solar light. We find that the number density of particles penetrating the solar system, derived from this comparison, is much smaller than predicted by a crude model of interstellar matter.

THE velocity of the Solar System relative to local interstellar matter has recently been determined by observation on the interplanetary emissions of hydrogen at 1,216 Å (refs 1 and 2) and of helium at 584 Å (ref. 3). These show that the Solar System is moving through the interstellar gas with a velocity[4] of ~20 km s^{-1} in the direction[3] $\alpha = 252°$, $\delta = -15°$ (equatorial coordinates), different from the apex direction by ~50°, lying in the galactic plane and near (7±3°) the ecliptic plane (Fig. 1).

The measured density of H (0.1 atoms cm^{-3}) and He (0.01 atoms cm^{-3}) and the high temperature of H found by Bertaux *et al.*[4] with the Soviet probe Mars-7 ($(6-13)\times10^3$ K) indicate that the Solar System is not now moving through an interstellar cloud, but through the so-called intercloud medium. These results indicate that the lack of hydrogen found around the Gum Nebula by the Copernicus measurements[5] does not hold for the immediate vicinity of the Solar System.

Matter penetrating into the heliosphere is subjected to two opposing inverse square forces, gravity and radiation pressure. The latter dominates for hydrogen atoms, which are deviated by and from the Sun along divergent hyperbolae, and the former dominates for all heavier atoms including helium atoms: gravitational focusing creates a zone of increased density in the downwind region of the Solar System, along the line $-V_W$ (Fig. 1). Both depletion of hydrogen and enhancement of helium have been observed in the Sun's wake.

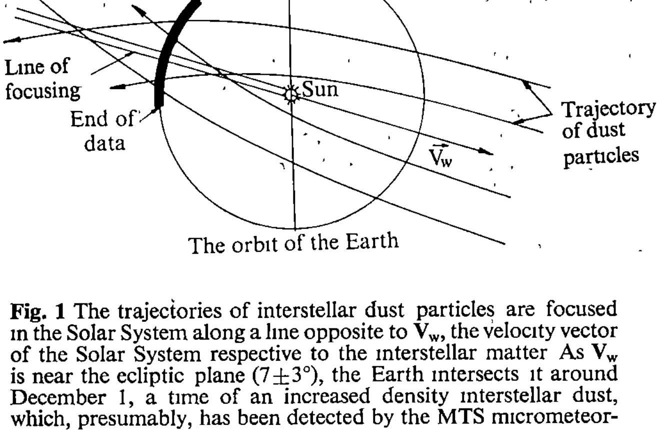

Fig. 1 The trajectories of interstellar dust particles are focused in the Solar System along a line opposite to V_w, the velocity vector of the Solar System respective to the interstellar matter As V_w is near the ecliptic plane (7±3°), the Earth intersects it around December 1, a time of an increased density interstellar dust, which, presumably, has been detected by the MTS micrometeoroids instrument.

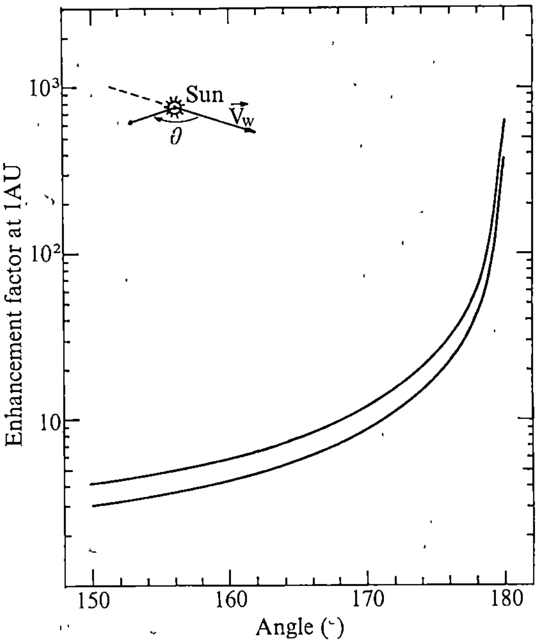

Fig. 2 The enhancement factor of dust particle density in the Solar System caused by gravitational focusing, is computed at 1 AU as a function of angle θ with V_w, for two values of p (the ratio of radiation pressure to gravitation) $p = 0$ (upper curve) and $p = 0.5$ (lower curve).

Since interstellar matter contains dust as well as gas, gravitational focusing will cause an increase in the number density of dust grains along the direction $-V_W$ ($\alpha = 72°, \delta = +15°$). Such an increase should be detectable when the Earth's orbit takes it across this region of space, that is, from November to January.

Distribution of dust grains

We have used a computer program, which we had developed originally to determine the density distribution of interstellar hydrogen and helium in the interplanetary medium, to compute the density distribution of dust grains in the Solar System as a function of the distance to the Sun and the angle θ, measured from the direction V_w of the incident beam (Fig. 2, inset). In this coordinate system, gravitational focusing occurs for $\theta \simeq 180°$. Figure 2 shows the density enhancement factor, E, at 1 AU as a function of θ from 150° to 180°. This factor is defined as the position-dependent number density of particles when solar forces are taken into account, relative to the density of particles in the nearby interstellar medium. The upper curve

Table 1 Parameters of the grains of interstellar dust used in this paper

	Graphite covered with ice	Graphite	Silicate
Relative number	1	10^2	10^3
Radius (μm)	0.5	0.02	0.02
Density of particles (g cm^{-3})	2	2	2.5
Mass of particle (g)	1.04×10^{-12}	6.7×10^{-17}	8.4×10^{-17}
Mass distribution (g cm^{-3})	1.6×10^{-27}	10^{-29}	1.3×10^{-28}
Mass distribution (%)	92	0.6	7
Number density of particles (cm^{-3})	1.5×10^{-15}	1.5×10^{-13}	1.5×10^{-12}
p = radiation pressure/gravity	>1	>1	<1

applies for negligible radiation pressure, the lower for a radiation pressure equal to half the gravitational force. These curves were calculated for dust grains with an isotropic velocity dispersion of 0.1 km s^{-1} added to their bulk velocity of 20 km s^{-1}; a dispersion of 1 km s^{-1} gives almost the same result.

Our model of the interstellar dust

To evaluate quantitatively the possible effects of such a density enhancement, we adopted a crude model of the interstellar dust. The mass ratio of dust to gas was taken as 10^{-2} and the dust was supposed to contain three types of particles: 1 graphite particle covered with ice (radius 0.5 μm) to 10^2 graphite particles (radius 0.02 μm) to 10^3 silicate particles (radius 0.02 μm). The resulting mass and number distribution of these particles in the interstellar medium in the vicinity of the Sun are shown in Table 1. Since the hydrogen number density is 0.1 atoms cm^{-3}, or 1.7×10^{-25} g cm^{-3}, the total dust density is $\simeq 1.7\times10^{-27}$ g cm^{-3} on our model.

The ratio of radiation pressure to gravity—the last figure in Table 1—depends on the size and type of particle and is a crucial parameter in our study. For the first two types of particles, this ratio is greater than one[6]; they do not penetrate deeply inside the Solar System and are not subjected to gravitational focusing. For non-metallic and non-absorbing material, like silicate particles, this ratio is, however, less than one. This is also true for quartz and obsidian particles[7]. Radiation pressure acts as a differentiation process for interstellar matter penetrating the Solar System. Only particles with $p < 1$ will be focused along the downwind axis.

Consequences: (1) micrometeoroids

We invoke this enhancement to explain the observations reported by Alvarez[8] using two micrometeoroid detectors of the MOS capacitor type in terrestrial orbit on board the MTS satellite. The number of impacts as a function of time is shown in Fig. 3. The count rate (slope of the curve) presents a sharp increase (by a factor of 5) around the beginning of November which corresponds to an ecliptic longitude $\lambda = 43°$ for the Earth (Fig. 1). The increase persists up to at least $\lambda = 93°$—just what is expected from the location of the line $-V_W$ (Fig. 1).

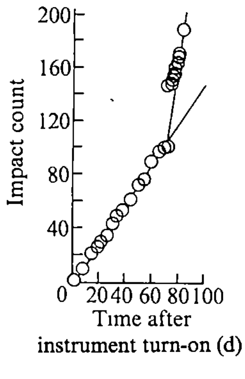

Fig. 3 The cumulative count for impacts detected by the MTS micrometeoroid instrument plotted as a function of time after the second instrument turn-on, which occured 2 yr. after launch. An initial penetration rate of 4.3×10^{-4} m^{-2} s^{-1} (slope of lower line) becomes 2.0×10^{-3} m^{-2} s^{-1}.

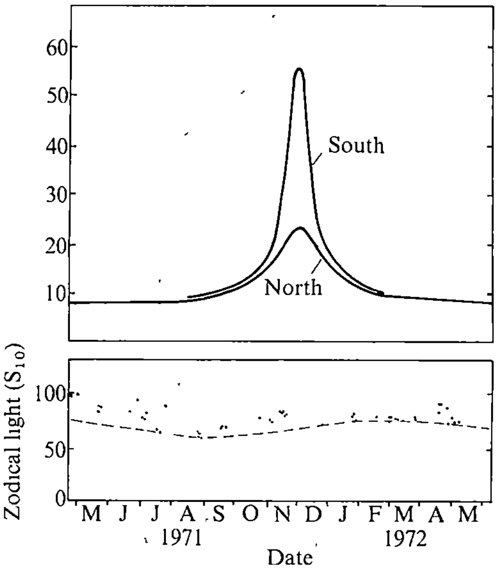

Fig. 4 D2–A observations of zodiacal light in the direction of North ecliptic pole (lower graph) show a bump in November and December, compared with the dashed line showing the expected value. According to the model computation shown in the upper graph, this bump might be produced by the penetration of interstellar dust into the Solar System, concentrated along the line of gravitational focusing, characterised by $n_d\sigma = 2\times10^{-23}$ cm^{-1}.

From the maximum count rate $P_{max} = 2\times10^{-3}$ m^{-2} s^{-1}, and our simple model of gravitational focusing, we may infer the fraction of dust in the near interstellar medium for which $p < 1$. Particles with a velocity V_W of 20 km s^{-1} at infinity have a velocity at 1 AU $V_1 \simeq 46$ km s^{-1} (from conservation of energy). For this velocity one of the two MTS detectors is sensitive to particles with mass $m > 3\times10^{-17}$ g, whereas the other is sensitive to $m > 3\times10^{-16}$ g. The second detector also showed an enhancement at the same time, but somewhat less pronounced. Thus we estimate that the enhancement detected by the MTS instruments comes mainly from particles of interstellar origin with a mass $m \simeq 2\times10^{-16}$ g; this corresponds to a particle radius of ~ 0.03 μm. If n_d is the number of particles in the incident beam (per cm^3) the flux, F, at 1 AU in the region of enhancement is

$$F = n_d E V_1$$

since $E = 10$, $V_1 = 46$ km s^{-1}, $F = 2\times10^{-7}$ cm^{-2} s^{-1} we find

$$n_d \simeq 4.3\times10^{-15} \text{ cm}^{-3}$$

and a dust density of $\sim 10^{-30}$ g cm^{-3}

Possible explanations

These numbers are very much lower than our crude model predicts, even if only silicate particles are considered. To explain this discrepancy, it may be that:

(1) MTS detectors are sensitive to only a small fraction of the interstellar dust particles which penetrate the Solar System;

(2) radiation pressure (or some other process) eliminates most of the particles that could have been detected by MTS; or

(3) the interstellar dust–gas ratio around the Sun is smaller than the galactic mean, which could be connected to the embedding of the Solar System in the 'intercloud' type of interstellar matter.

Consequences: (2) zodiacal light

We have also tried to compute the contribution to zodiacal light of solar light scattered by the interstellar particles inside the Solar System. Only spherical silicate particles were considered, on which the effect of radiation pressure was assumed to be negligible. For any point in the Solar System (r,θ) the emissivity $\varepsilon(r,\theta)$ is

$$\varepsilon(r,\theta) = n_d E(r,\theta)\,\sigma F_s\left(\frac{r_0}{r}\right)^2 \qquad (1)$$

where σ is the scattering cross section and F_s the solar flux at $r_0 = 1$ AU. If the scattering is assumed to be isotropic, the intensity is

$$I = \frac{1}{4\pi}\int \varepsilon(l)\,\mathrm{d}l \qquad (2)$$

If, therefore, all particles have the same σ, the zodiacal intensity caused by interstellar dust is proportional to $n_d\sigma$.

The intensity at 1 AU was computed in the direction of North and South ecliptic poles, as a function of Earth's position (or time of the year). It is shown in Fig. 4, together with observations[9] of zodiacal light collected by a photometer in the French satellite D2–A in the direction of North ecliptic pole during the year 1971–72. The solar flux in equation (1) was taken as $F_S = 6.2\times10^{13}$ photons cm^{-2} s^{-1} Å^{-1}, at the effective wavelength of the D2–A photometer (6,563 Å). The intensity is measured in S_{10} units (equivalent brightness of one tenth magnitude star per square degree; 1 S_{10} = 360 photons cm^{-2} s^{-1} Å^{-1} sr^{-1}).

The dashed line traced through the D2–A points represents the expected variation of zodiacal light, since the Earth's orbital plane does not coincide exactly with the symmetry plane of the zodiacal cloud[9]. The data points in November and December are ~ 15 S_{10} above this line. This 'bump' agrees with the maximum computed for light scattered by interstellar material. For the model computation, the value of $n_d\sigma$ was adjusted to 2×10^{-23} cm^{-1}, which also gives for the bumps computed for the North pole, a value of 15 S_{10}. The observations of zodiacal light in this direction therefore provide information about the product $n_d\sigma$. If the bump in the measurements is genuine, we have $n_d\sigma \simeq 2\times10^{-23}$ cm^{-1}. If the bump is accidental, this value for n_d becomes an upper limit.

Since the line of gravitational focusing lies ~ 7°S of the ecliptic plane, a stronger effect is expected in the direction of the South ecliptic pole, with an increase of ~ 50 S_{10} at the time of maximum (Fig. 4). Unfortunately, South ecliptic pole observations are hampered by the presence of the Magellanic clouds. For an observatory attached to the Earth, the strongest intensity of light by interstellar dust should be observed not far from the line of gravitational focusing. This would happen around December 1, when the Earth is at an ecliptic longitude $\gamma = 72°$, in the general anti-solar direction. For these conditions, the distribution of intensity scattered by interstellar material was computed with the use of equations (1) and (2) taking $n_d\sigma = 2\times10^{-23}$ cm^{-1}.

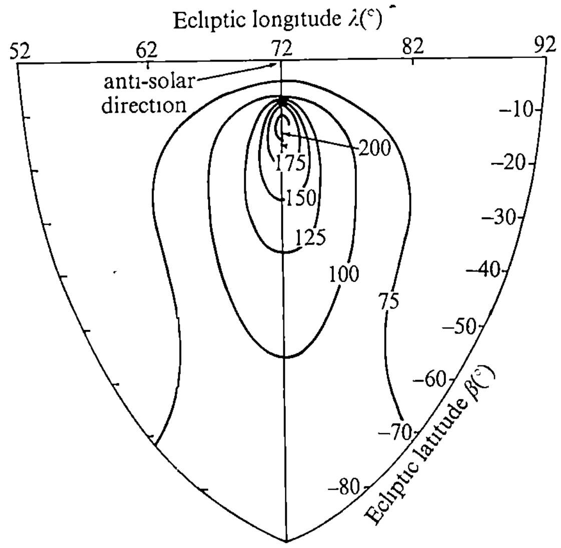

Fig. 5 Isophotes of the 'trail of light' (which would be superimposed on the zodiacal light pattern, when observed from Earth on December 1, south of the anti-solar direction) produced by the gravitational focusing of interstellar dust particles characterised by $n_d = 2\times10^{-23}$ cm^{-1}. Intensity levels are in units of S_{10} (see text).

The maximum intensity appears at the ecliptic longitude of $\gamma = 72°$, slightly south of the ecliptic latitude $\beta = -7°$ (which is the direction of gravitational focusing) because of the effect of perspective. As the longitude scale of Fig. 5 is five times larger than the latitude scale, the 'true' shape of such a conspicuous feature would be much narrower, like a pencil of light.

The maximum brightness of this feature, which would be superimposed on the usual zodiacal light pattern, is ~ 200 S_{10}, to be compared with a mean gegenschein brightness of 180 S_{10}. Unfortunately, gegenschein observations close to December 1 are scarce, because of a strong galactic background in the anti-solar direction at this time. From a long series of gegenschein observations obtained at Tenerife, however, Dumont (personal communication) estimated that if such a feature were brighter than 50 S_{10}, it would have been observed. Therefore, one can derive another upper limit for $n_d\sigma$, 5×10^{-24} cm^{-1}, which is more stringent than the one derived from the D2–A observations, and will serve as a basis for discussion in the following (if the November–December bump of D2–A observations was revealed to be connected with interstellar dust, one would have to explain this discrepancy with gegenschein observations).

Table 2 Parameters for the scattering of zodiacal light

Particle radius, a(10^{-8} m)	$x = \frac{2\pi a}{\gamma}$	Scattering cross section ρ (cm^{-2})	Particle mass (g)	Optical upper limit on n_d	$n_d m$ (g cm^{-3})
1.75	0.2	4.3×10^{-15}	5.6×10^{-17}	1.2×10^{-9}	6.7×10^{-26}
3.5	0.4	2.7×10^{-13}	4.5×10^{-16}	1.9×10^{-11}	8.5×10^{-27}
5.2	0.6	3.1×10^{-12}	1.5×10^{-15}	1.6×10^{-12}	2.4×10^{-27}
7	0.8	1.7×10^{-11}	3.6×10^{-15}	2.8×10^{-13}	1.0×10^{-27}
8.7	1.0	6.2×10^{-11}	7×10^{-15}	8.1×10^{-14}	5.7×10^{-28}

Discussion

As the scattering cross section σ is a strong function of the radius of particle a, the upper limit on $n_d\sigma$ gives an upper limit on n_d which is a function of a, or $x = 2\pi a/\lambda$ (Table 2). The optical characteristics of spherical silicate particles are taken from Wickramasinghe[10]: $n = 1.55, k = 0$, at $\lambda = 6{,}560$ Å.

Even with a particle radius approaching 0.1 μm (last line of Table 2), the optical upper limit on n_d, 8.1×10^{-14} cm^{-3}, is still ~ 20 times larger than that derived from the micrometeoroid rate as measured by MTS detectors. Optical observations do not therefore contradict, up to now, MTS observations.

Table 2 indicates that the penetration into the Solar System of interstellar silicate particles with an assumed number density of 1.5×10^{-12} cm^{-3} (as in our crude model) would have been observed optically only if these particles had a radius larger than 0.05 μm (which goes against our assumptions). This crude model is therefore consistent with the absense of a conspicuous 'trail of light' along the line of gravitational focusing. The best way to detect interstellar dust particles in the Solar System would probably be to launch a space probe equipped with micrometeoroid detectors on a trajectory intersecting the line of gravitational focusing.

We are indebted to Dr Alvarez for early communication of his results and to Dr Dumont, for discussions of his observations of zodiacal light.

Received May 11; accepted June 1, 1976.

1 Bertaux, J. L., and Blamont, J. E., *Astr. Astrophys.*, 11, 200 (1971).
2 Thomas, G. E., and Krassa, R. F., *Astr. Astrophys.*, 11, 218 (1971).
3 Weller, C. S., and Meier, R. R., *Astrophys. J.*, 193, 471 (1974).
4 Bertaux, J. L., *et al.*, *Astr. Astrophys*, 46, 19 (1976).
5 Bohlin, R. C., *Astrophys. J.*, 200, 402 (1975).
6 Biermann, L., NASA SP-150, 279 (1967).
7 Burns, J. A., Soter, S., and Lamy, P., *AGU Meeting*, (San Francisco, December 1975).
8 Alvarez, J. M., *IAU Colloquium*, (Heidelberg, 1975).
9 Levasseur, A. C., and Blamont, J. E., *Space Research*, XV (1975).
10 Wickramasinghe, N. C., *Light Scattering Functions for Small Particles*, (Adam Hilger, London, 1973).

Neutron diffraction studies of retinal rod outer segment membranes

Helen Saibil
Department of Biophysics, University of London King's College, 26–29 Drury Lane, London WC2, UK
Marc Chabre
Biophysique, Département de Recherche Fondamentale, CENG, BP85, 38041 Grenoble, France
David Worcester
Materials Physics Division, AERE, Harwell, Didcot, Oxfordshire, UK

Neutron diffraction measurements on isolated retinal rod outer segments show that most of the visual pigment protein, rhodopsin, is embedded in the hydrophobic core of the disk membrane. A very slight outward shift of protein at the cytoplasmic side of the membrane is associated with pigment bleaching.

STRUCTURAL analysis of retinal rod outer segment (ROS) membranes by X-ray diffraction has indicated that rhodopsin, which constitutes almost all the membrane protein, is partially or wholly immersed in the hydrophobic layer of the membrane, but details of its distribution are not unequivocally determined[1-7]. Differences in lamellar diffraction intensities between dark-adapted and bleached membranes[4,5] are interpreted as due to a small increase in electron density near the cytoplasmic (interdisk) side of the membrane. Movement of rhodopsin into the membrane on bleaching was deduced from measurements of diffraction in the plane of the membrane[8], but these measurements have been questioned[7]. Information from X-ray diffraction studies is limited by the imperfect stacking of the membranes, the low contrasts of electron densities among the components of the lipid–protein–water structure, and by the difficulty of placing electron density profiles on an absolute scale. Consequently, features in the electron density profile and changes on bleaching cannot be attributed with certainty to particular membrane components.

With the development of the high flux neutron beam facilities of the Institut Laue-Langevin, Grenoble, and the low angle scattering instrument D-11 (ref. 9), it has become possible to record neutron diffraction from small samples in times comparable with those of X-ray diffraction. A major advantage of neutron scattering studies is that the neutron scattering densities of biological membrane components are between those of H_2O and D_2O. Therefore, the range of contrast between the cytoplasm and the membrane can be varied from positive to negative by varying the H_2O/D_2O content of the Ringer's solution. The linear relationship between structure factors and D_2O percentage establishes the variation of phase of each order with contrast, using diffraction intensities from a single sample in at least three different H_2O/D_2O mixtures[10,11]. Furthermore, contrast variation data together with the existence of a clearly defined water layer provide an absolute scale of neutron scattering density. Using these neutron diffraction methods[12], we have obtained new, quantitative information on the distribution of proteins, lipids and water in the ROS disk membrane, and on structural changes associated with bleaching of the visual pigment.

Lamellar organisation in dark-adapted ROS membranes

Seven orders of lamellar neutron diffraction were measured in H_2O and 20%, 40% and 100% D_2O Ringer solutions from isolated frog rods prepared and oriented using a magnetic field, as described previously[7]. Figure 1 shows contour maps of neutron diffraction patterns: a D_2O pattern showing four lamellar diffraction orders (*a*); and an H_2O pattern with seven lamellar diffraction orders and diffuse scatter at right angles to the lamellar diffraction visible (*b*). Orders 1–4 are very intense in H_2O, 40% and 100% D_2O and are about 10 times larger than the higher orders. In 20% D_2O, which has a scattering density close to the average scattering density of the membrane, the pattern is very weak and orders 6 and 7 are prominent.

For phase assignment, the large range of contrast available

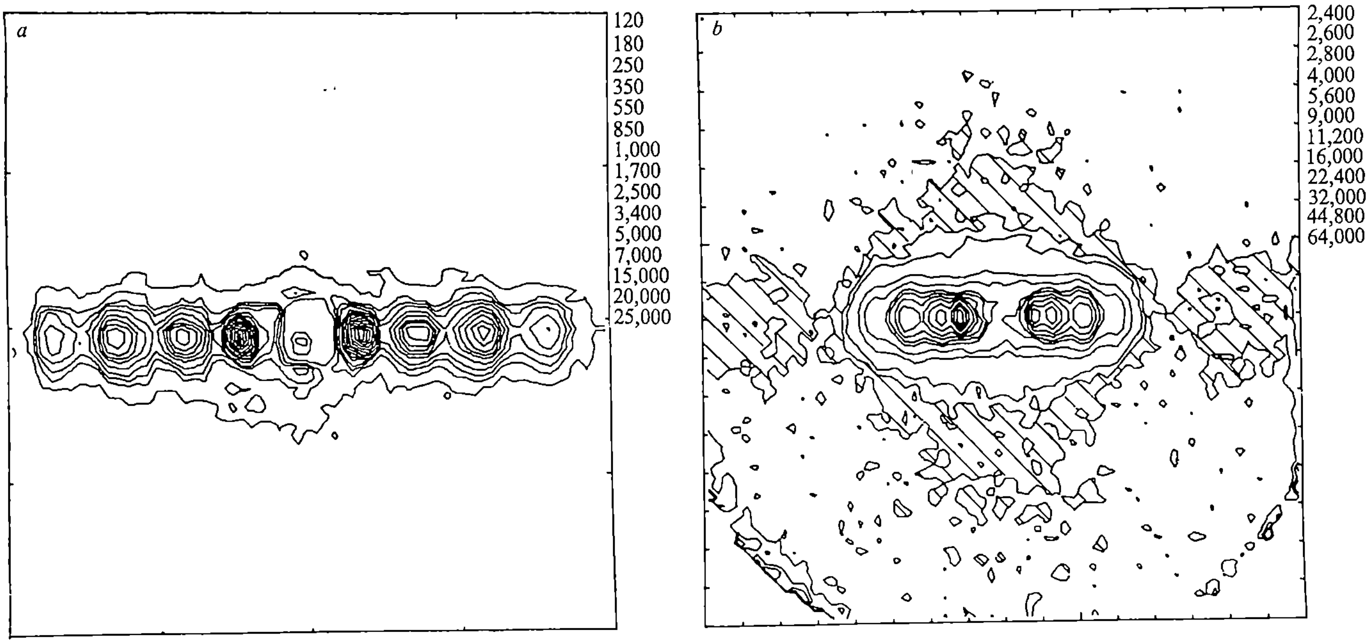

Fig. 1 Neutron diffraction patterns from freshly isolated frog ROS oriented using a magnetic field of 17 kgauss are shown in these contour maps of data obtained with the two-dimensional (64×64 cm) detector of the low angle scattering instrument D-11 at the Institut Laue–Langevin[9]. The contour lines connect points of equal diffraction intensity, and the numbers beside the maps refer to the number of counts in successive contour levels. The distribution of neutron wavelengths was triangular, with $\Delta\lambda/\lambda$ (FWHM)=8% Rods from 10–12 retinae were suspended in Ringer's solution, in a standard quartz spectrophotometer cell of 2 mm path length, and allowed to sediment in a horizontal magnetic field, forming an oriented pellet 1 mm thick. The long axes of the rods aligned along the field direction, and therefore the disk membranes were perpendicular to the field. The lamellar spacing was 295 Å, and the unit cell is centrosymmetric. *a*, Diffraction pattern in D_2O Ringer with a neutron wavelength of 9 Å. Four orders of lamellar diffraction are visible on each side of the central beam stop. The counting time was 10 min. The mosaic spread is less than 10° (FWHM). *b*, Diffraction pattern in H_2O Ringer, with a neutron wavelength of 4.4 Å Lamellar orders up to 7 and broad in-plane diffraction are visible. Order 1, is partly masked by the beam stop. The counting time was 1 h. Shading has been added to the region bounded by the lowest intensity contours to make order 7 and in-plane diffraction clearer.

enabled simple deductions: (1) In D_2O, every component of the membrane appears with negative contrast and orders 1–4 are prominent. Of all the possible phase factor combinations for those four orders, only one (−+++) gave a reasonable position in the unit cell, consistent with X-ray and electron microscopy results, for a negatively contrasting membrane. (2) In 20% D_2O, the relative neutron scattering densities of protein, phospholipid headgroups, hydrocarbon chains and Ringer's solution are close to their relative electron densities Therefore, the diffraction intensities and the phases should be the same for neutron scattering in 20% D_2O and X-ray scattering. In fact, the neutron diffraction pattern in 20% D_2O is very similar to the X-ray pattern. We conclude that the phases are also the same. The X-ray phases have been determined by osmotic swelling[3–5]. These phases for the neutron pattern in 20% D_2O and the linearity of structure factor with D_2O percentage (Fig 2) give the phase of each order at all contrasts The above two procedures gave consistent phase assignments for all orders except the very weak fifth order. An experiment with osmotic shrinking in D_2O indicated the presence of a zero in the

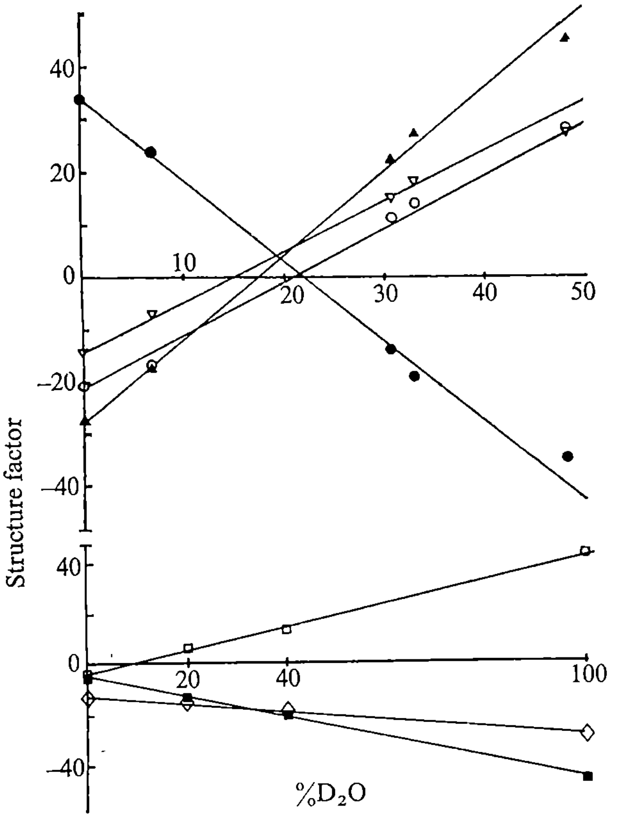

Fig. 2 Contrast variation. Structure factors 1–7 are plotted against the D_2O percentage of the Ringer's solution to establish phase changes between H_2O and D_2O. The data for orders 1–4 (●,1; ○,2; ▲,3; ▽,4) were measured with the same sample, to keep a fixed intensity scale. To change the contrast at the end of a measurement, a known amount of the supernatant solution was removed from the sample cell without losing or bleaching any rods, and replaced by a different solution. The rods were then resuspended in the new mixture, reoriented in the magnetic field and allowed to resediment. This process was completed in a few minutes. Orders 5–7 (□,5; ■,6; ◇,7) were scaled from longer measurements on other samples by normalising to order 3. Intensities (I_h) were obtained by integrating the lamellar diffraction peaks over their arcs of mosaic spread, and multiplying by a Lorentz factor of h, giving structure factors $F_h=\sqrt{(hI_h)}$ To obtain the intensities of the higher orders, the peak shapes along the lamellar axis were approximated by Gaussians of half-width calculated from the beam size, wavelength broadening and natural widths due to the lattice disorder (natural widths obtained from X-ray data). In 20% D_2O, both the intensity, which was very weak, and the phase of order 5, were uncertain

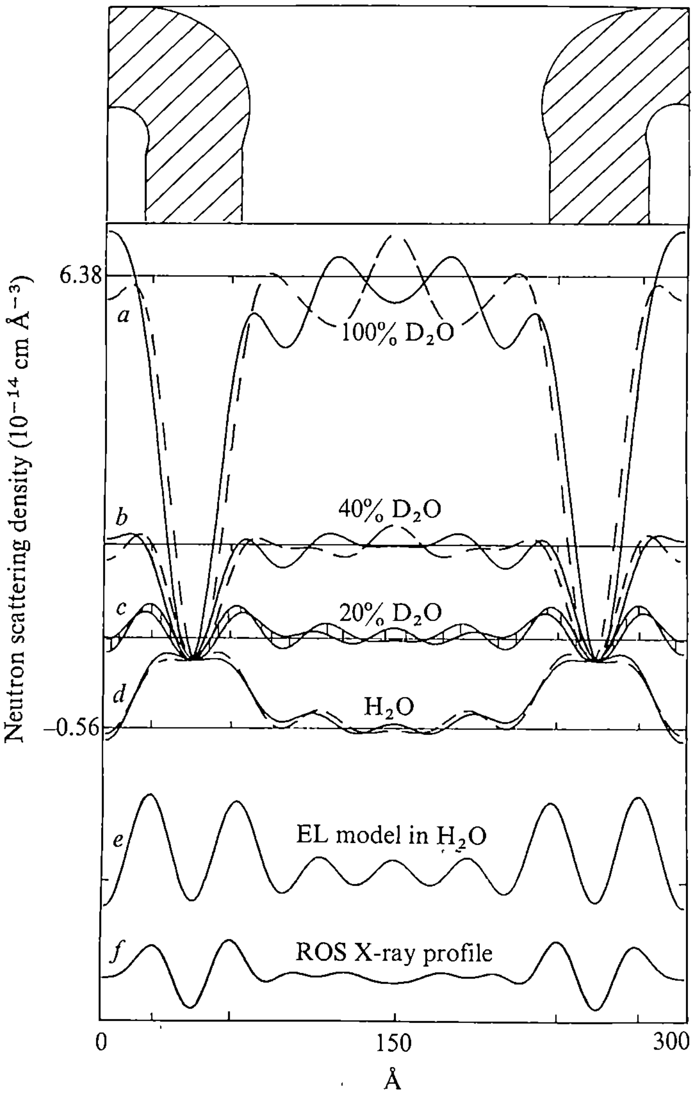

Fig. 3 *a–d*, Neutron scattering density profiles of ROS computed with seven orders of diffraction, in 100% D_2O, 40% D_2O, 20% D_2O and H_2O Ringer's solutions. Structure factors used are those shown in Fig. 2. – – – – –, Alternative phasing of order 5 Order 5 is taken as zero in the 20% D_2O profile (*c*), with upper and lower limiting profiles shown. Absolute density scaling: The structure factors were scaled as described in Fig. 2. Relative positions of the profiles were established by making the H_2O and 40% D_2O profiles coincide at the centre of the membrane, assuming no water penetration at that point. Up to 10% water penetration at the centre of the membrane changes the scale negligibly. The H_2O and 40% D_2O water levels were then used to define the absolute density scale. The other profiles were then set on this scale without further adjustment. The assumption of a carbohydrate content in the cytoplasm of 20 g 100 ml^{-1} (ref. 15) shifts the scale slightly. Protein and lipid headgroups have neutron scattering densities about equal to that of 40% D_2O, whereas lipid hydrocarbon chain scattering density is close to that of H_2O, increasing slightly with unsaturation. In 40% D_2O, the only component of the membrane contrasting with the Ringer's solution is the paraffin chain region. The small width observed (27.5 Å FWHM) of the density profile at this contrast confirms the presence of a lipid bilayer. This width is 60 Å in H_2O, and 32 Å in D_2O. *e*, Model density profile derived from egg lecithin bilayer neutron scattering data in H_2O (ref. 14), calculated for the same resolution and unit cell as the ROS data. The main difference between profiles *d* and *e* reflects the presence of rhodopsin in *d*, indicating that a considerable fraction of the protein must be inside the bilayer. *f*, Electron density profile of ROS (ref. 7), computed with ten orders, showing the polar headgroup positions. Computed with seven orders, it is identical to *c*. Density scales for *e* and *f* are arbitrary.

Fourier transform between orders 1 and 2, and tended to favour a positive sign for order 5 in D_2O. The phasing of orders 1–4 also agrees with that determined by Yeager in neutron diffraction experiments on intact retina[13].

Neutron scattering density profiles of ROS computed with 7 orders are shown in Fig 3, on an absolute density scale. The profile in H_2O (*d*) is markedly different from the neutron scattering density profile of phospholipid bilayers (*e*) and myelin[14] at the same resolution, in that it shows a fairly flat distribution of scattering density across the membrane instead of a pronounced dip at the centre. In the ROS, the scattering density at the centre of the membrane is matched by the fluid medium when the Ringer's solution contains 15% D_2O. This means that the non-exchangeable material in the hydrophobic region has the scattering density of 15% D_2O, or 18% D_2O if one allows for 20 g carbohydrate per 100 ml cytoplasm[15], independent of the amount of water penetration or proton exchange. Taking the average ROS fatty acid chain composition for frog ROS of 18 : 2 (calculated from ref 16), we find that about one-third of the volume in the hydrophobic region consists of protein. This could account for all of the protein. The water penetration in the membrane, assuming none at the centre, is given by the difference between the D_2O and H_2O profiles. From the variation in scattering density in the polar headgroup region (located by the electron density profile) we find that this region is about one-half water by volume.

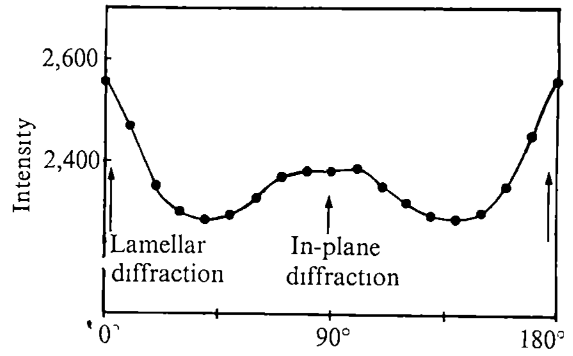

Fig. 4 The broad in-plane diffraction is shown by this azimuthal scan of the diffraction intensity at a reciprocal spacing at about (50 Å)$^{-1}$ from ROS in H_2O Ringer's solution The origin of the angular scan is in the lamellar direction.

Equatorial diffraction

Diffraction in the direction perpendicular to the lamellar diffraction arises from interference between neighbouring rhodopsin molecules in the plane of the membrane. Diffuse equatorial diffraction centred near (50 Å)$^{-1}$ has been observed in X-ray diffraction studies[1,3,7]. We measured in-plane diffraction in H_2O (Figs 1*b* and 4) It was much less clear in D_2O because of the very intense lamellar diffraction, and we could only estimate an upper limit for its intensity, which was about equal to the H_2O in-plane intensity. On an absolute scale, the equatorial intensity in 40% D_2O is within a factor of two of that in H_2O. These observations show that the in-plane intensity is insensitive to the scattering density of the fluid medium. Consequently it must primarily arise from protein–hydrocarbon chain contrast within the membrane. Allowing for uncertainties in these intensity measurements, we estimate that less than one-third of the protein volume is contrasting with the aqueous medium. The limit is mainly set by the measurement in 40% D_2O, where the protein–cytoplasm contrast is very small.

Structural changes on bleaching

To investigate structural changes associated with total bleaching of rhodopsin, we recorded continuous sequences of spectra within a few minutes from dark-adapted samples

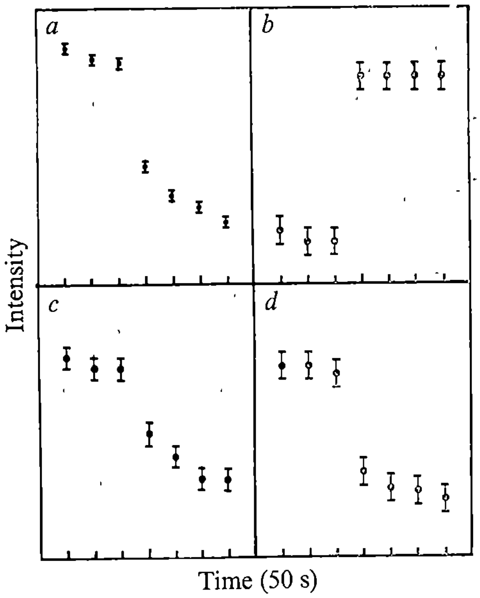

Fig. 5 Intensity changes on bleaching for the first 4 orders of diffraction in 100% D_2O. Orders: *a*, 1; *b*, 2; *c*, 3; *d*, 4. The sequence of 50-s measurements was carried out on the same sample, which was exposed to light after the third measurement. Intensity changes amounted to 10% in order 1, 15% in 2, 7% in 3, and 10% in 4. Changes of comparable magnitude were observed in H_2O Ringer's solution, but the changes were much smaller in 40% D_2O Ringer's solution.

which were bleached in the middle of the sequences. In H_2O and D_2O, small but significant intensity changes were observed in the first 4 orders. In the weaker orders 5–7 the changes were too small to be measured in a short time. Bleaching had very little effect on the pattern in 40% D_2O. The bleaching sequence in D_2O Ringer's solution is shown in Fig. 5.

Since orders 1–4 are very intense at the above three contrasts, the small intensity changes observed on bleaching are most unlikely to be accompanied by phase changes. This is not the case with X rays, where order 2 is close to zero before bleaching and increases after bleaching, so that the difference profile is not uniquely defined. Neutron scattering density profiles in H_2O and D_2O and their changes on bleaching are shown in Fig. 6.

Although the differences between the profiles are smaller than the Fourier cutoff ripples, the differences are significant because they come from significant changes in the structure factors (Fig. 5). The observed effects are not accounted for by changes in *d* spacing, since X-ray diffraction experiments have shown that such changes in isolated rods are small and transient, with no net change in the time scale of our experiments (Fig 2 of ref. 17). Furthermore, the minimal changes in 40% D_2O rule out a shift of the lipid bilayer within the unit cell. Protein, however, has the same scattering density as 40% D_2O and the observed changes on bleaching are consistent with an outward shift of protein at the cytoplasmic side of the membrane. Quantitatively, the observed change in the profile can be accounted for by a shift of the centre of gravity of the protein by about 1 Å.

Conclusions

Our essential finding is that the shape of the ROS neutron scattering density profile in H_2O is not dominated by the bilayer arrangement of the lipids, as for the X-ray profile, and the contribution of protein to the structure is clearly seen. From the density profiles we calculate that a lower limit of 20% of the volume of the hydrophobic region consists of protein, allowing for uncertainty in the scattering density level at the centre of the membrane due to Fourier cutoff effects and the possible presence of carbohydrate in the cytoplasm. This accounts for 50% of the total rhodopsin. Our upper limit locates all the rhodopsin in the hydrophobic region, which would then contain 35% protein by volume. The profiles also indicate a slight asymmetry in the membrane, with protein probably extending into the cytoplasmic space, but not into the intradisk space.

Since contrast variation was done without adding molecules which could be excluded from regions of hydrated protein, like sucrose, but merely by isotopic exchange of water, dry protein mass was observed. The part of the protein which extends outside the hydrocarbon chain region could be highly hydrated. There is definitely a large water penetration in the lipid headgroup region.

Insensitivity of equatorial diffraction to the scattering density of the Ringer's solution confirms that most of the protein is inside the membrane. These results on ROS membrane structure show that the electron density profile obtained from X-ray diffraction[1–7] should be interpreted as the electron density variation of the lipid bilayer, superimposed on a fairly uniform protein contribution

The changes observed on bleaching of rhodopsin in our experiments agree with the X-ray results[4,5,7]. Furthermore, the contrast variation results identify the observed change as an outward shift of protein at the cytoplasmic side of the membrane. It cannot be decided whether this is due to a very small shift of the entire protein molecule or to a larger displacement of a small part of the protein. It seems that the only other evidence for a structural change in the intact membrane comes from small birefringence changes on bleaching[15], and, more specifically, for the protein in the

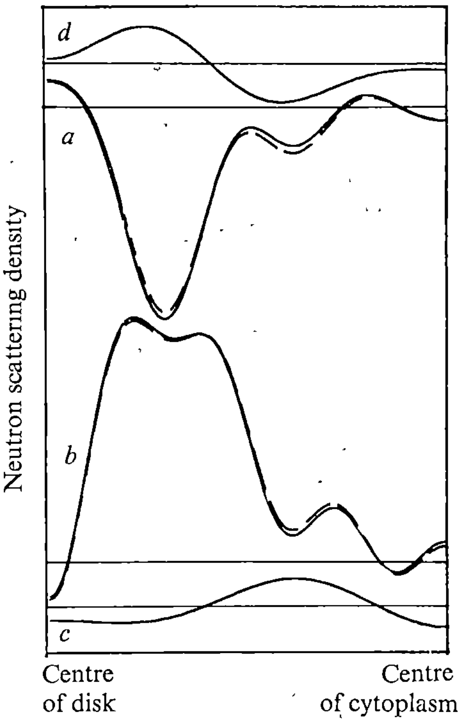

Fig. 6 Scattering density profiles of ROS disks before (——) and after (– – – –) bleaching, and their difference profiles (×5), (bleached – unbleached). Changes in orders 1–4 have been included in this computation. Changes in orders 5–7 are smaller and are not included in the difference profiles. The H_2O and D_2O data are on different density scales. *a*, In D_2O Ringer's solution. *b*, in H_2O Ringer's solution; *c*, H_2O difference profile (×5); *d*, D_2O difference profile (×5). The increase in density at the intradisk side in the D_2O profile may be accounted for by a shift of D_2O into that region, resulting from increased hydrogen–deuterium exchange on bleached rhodopsin[18].

membrane, from the observation of changes in the hydrogen exchange kinetics on bleaching[18].

We thank the Institut Laue-Langevin for providing access to neutron facilities; the staff on D-11 for assistance; Drs K. Ibel and B. Jacrot for discussions. M.C. is supported by the CNRS and by the DGRST (Comité des membranes biologiques). H. S. is supported by a postgraduate scholarship from the DGES, Ministère de l'Education Gouvernement du Québec, and thanks Dr A. E. Blaurock and Professor M. H. F. Wilkins for guidance and encouragement.

Received March 30, accepted June 3, 1976

[1] Blaurock, A. E., and Wilkins, M H. F., *Nature*, 223, 906–909 (1969).

[2] Gras, W. J. and Worthington, C R., *Proc natn. Acad. Sci U S A.*, 63, 233–238 (1969)

[3] Blaurock, A. E. and Wilkins, M. H. F., *Nature*, 236, 313–314 (1972).

[4] Corless, J. M., *Nature*, 237, 229–231 (1972)

[5] Chabre, M. and Cavaggioni, A., *Nature new Biol.*, 244, 118–120 (1973)

[6] Worthington, C. R., *A. Rev. Biophys. Bioengng*, 3, 53–80 (1974).

[7] Chabre, M., *Biochim. biophys. Acta*, 382, 322–335 (1975).

[8] Blasie, J. K., *Biophys. J.*, 12, 191–204 (1972)

[9] Ibel, K., *J. appl. Crystallogr.*, 9, 630–643 (1976).

[10] Worcester, D. L and Franks, N. P., *J molec. Biol.*, 100, 359–378 (1976).

[11] Worcester, D. L., in *Proc. 1975 Brookhaven biol. Symp* (Brookhaven National Laboratory, Long Island, in the press)

[12] Chabre M., Saibil, H. R., and Worcester, D L., *ibid*

[13] Yeager, M., *ibid.*

[14] Worcester, D. L., in *Biological Membranes*, 3 (edit. by Chapman, D. and Wallach, D. F. H.), (Academic, London, 1976).

[15] Liebman, P. A., Kaplan, M. W., Jagger, W. S , and Bargoot, F. G., *Nature*, 251, 31–36 (1974).

[16] Mason, W. T., Fager, R. S., and Abrahamson, E. W., *Biochemistry*, 12, 2147–2150 (1973).

[17] Chabre, M., and Cavaggioni, A., *Biochim. biophys. Acta*, 382, 336–343 (1975).

[18] Downer, N. W., and Englander, S. W., *Nature*, 254, 625–627 (1975).

---

letters to nature

On being close to a black hole without falling in

I SHOW here that for any $\varepsilon > 0$ it is possible for a magnetic field to hold plasma in equilibrium at a radius $r_0 = r_g(1+\varepsilon)$ relative to a Schwarzschild black hole of (radius r_g) and that this equilibrium need not be subject to the kind of relativistic instability that destroys circular orbits of radius $r < 3r_g$. (Putting $c = G = 1$, $r_g = 2M$ is the radius of the event horizon of a hole of mass M.) Astrophysical plausibility does not stop ε from being much smaller than unity.

Normal indices refer to Schwarzschild coordinates, whereas barred indices refer to the corresponding orthonormal tetrad and label physical quantities which can be measured by observers at rest relative to the hole. Suppose there is a thin disk of matter at rest in the $\theta = \pi/2$ plane with current density $J_{\bar{\varphi}}$ and energy density ρ as measured by an observer at rest in the disk. The current is to interact with a magnetic field $B_{\bar{\theta}}$ to produce a Lorentz force balancing gravity. I shall assume that both the matter and the field have negligible gravitational effect, so that the Schwarzschild metric is valid. Then

$$T^{r\beta}{}_{,\beta} = (\rho+p)M/r^2+\partial p/\partial r-2p\left(1-\frac{2M}{r}\right)/r$$

Here p is the gas pressure. I shall assume that the plasma is not highly relativistic, so that $p \ll \rho$ and $T^{r\beta}{}_{,\beta} = \rho M/r^2$. Taking the radial component of the equation of motion $T^{\alpha\beta}{}_{;\beta} = F^{\alpha\beta}J_\beta$ and integrating with $r\mathrm{d}\theta$, I obtain

$$\begin{aligned}\sigma M/r^2 = F^{r\beta}I_\beta &= (1-(2M/r))^{\frac{1}{2}}F^{\bar{r}\bar{\varphi}}I_{\bar{\varphi}}\\ &= (1-(2M/r))^{\frac{1}{2}}(-B_{\bar{\varphi}})I_{\bar{\varphi}} \qquad (1)\end{aligned}$$

where σ and $I_{\bar{\varphi}}$ are the energy and current surface densities.

Suppose for simplicity that the magnetic field is mainly generated far from the hole so that near the hole it seems to be uniform. Suppose this 'uniform' field has magnitude B_∞ and points in the $\theta = 0$ direction at infinity. Then $B_{\bar{\theta}} = -(1-(2M/r))^{1/2}B_\infty$ on $\theta = \pi/2$ (ref. 1). The field generated by the local current is of the order $(1-(2M/r))^{1/2}I_{\bar{\varphi}}$ except where $I_{\bar{\varphi}}(r)$ varies rapidly, for example at the edge of a current disk[2]. For consistency it should be assumed that $I_{\bar{\varphi}}(r) \ll B_\infty$ and varies smoothly. This is not an important restriction as boundary conditions at the event horizon require $B_{\bar{\theta}} \simeq B_\infty(1-(2M/r))^{1/2}$ close to the event horizon, B_∞ being a constant[2], and the only place one might expect $I_{\bar{\varphi}}$ to be discontinuous is at the inner edge of the disk, where the effect would be to make $B_{\bar{\theta}}$ more negative, and thus to oppose gravity. Substituting the assumed form for $B_{\bar{\theta}}$ into equation (1)

$$(\sigma/I_{\bar{\varphi}})M = (r^2-2Mr)B_\infty \qquad (2)$$

Let $\sigma/I_{\bar{\varphi}} = \alpha(m_p/ce)$, where m_p and e are the mass and charge of a proton. m_p/ce is the dimensionless number 8.99×10^{-19} when $c = G = 1$. Clearly $\alpha > 1$. If the electrons and protons are streaming relative to each other with a relativistic velocity, their kinetic energy contributes to σ, and if two-stream instability is to be avoided the plasma must be relativistically hot, which also increases σ. The relativistic current would cause a significant mechanical stress $T^{\varphi\varphi}$, which because of the curvature of the coordinate system would contribute to the radial balance equation as a force opposing gravity; this is just the centrifugal force from the circular motion of the particles. I shall assume that the current is nonrelativistic (so that $T^{\varphi\varphi}$ is not significant near the event horizon) and take $\alpha \gtrsim 10$. Fixing α at its lower limit in equation (2) and solving for r, I obtain r_0, the smallest radius at which matter can be stationary, given B_∞ and M

$$\begin{aligned}r_0/r_g &= (1+(1+4\varepsilon)^{1/2})/2,\\ \varepsilon &= 5.3\alpha(B_\infty/1\ \text{gauss})^{-1}(M/M_\odot)^{-1} \qquad (3)\end{aligned}$$

If $\varepsilon \ll 1$, $r_0/r_g \simeq 1+\varepsilon$. If the field is a significant gravitational source $B_\infty \gtrsim 10^{19}(M/M_\odot)^{-1}$ gauss. Hence B_∞ can be large enough for $\varepsilon \ll 1$ without being so large that the Schwarzschild metric is invalid.

This result does not contradict Gibbons' limit on how near to a black hole a rope can be lowered[3]. Gibbons' rope has constant energy density per unit length. By the weak energy condition this gives an upper limit on the tension the rope can take without breaking. Tension is greatest at the top end of the rope, but gravity exerts its greatest force on the energy present at the bottom of the rope. The rope breaks at the top. This can be avoided by strengthening the rope at the top and lightening it at the bottom, for example by lowering a tapered rope. This is effectively happening here. The magnetic field can be regarded as a medium with pressures and stresses. The energy in a spherical shell of radius r and unit thickness $\sim r^2B_\infty^2$. There is only a small amount of energy near the hole requiring support, and a lot of energy to take the strain far away from the hole. Hence equilibrium is possible.

It only remains to consider stability. Distant field sources can be expected to vary on time scales much longer than the free-fall time near the hole. I shall therefore take the uniform, externally imposed part of the field to be constant. Because of high

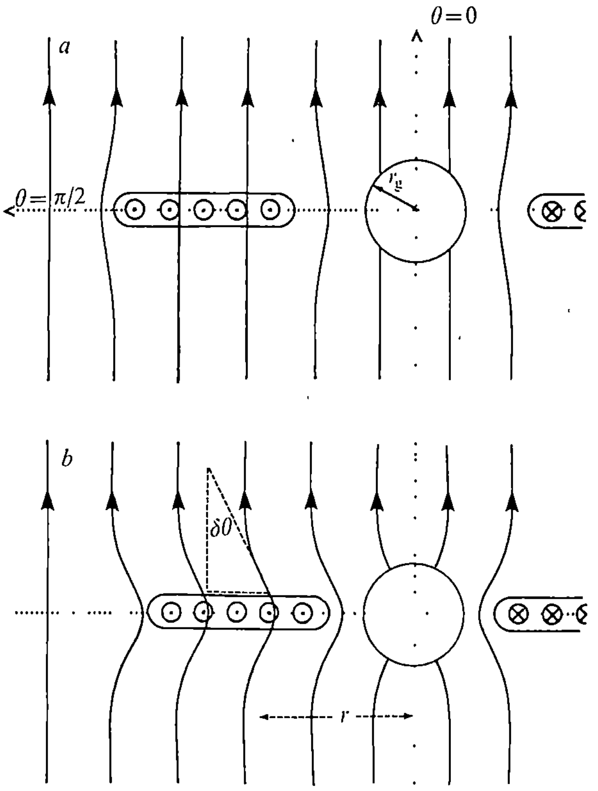

Fig. 1 *a*, Cross section of current disk and black hole in unperturbed state. Large circle is the event horizon of the hole. Small circles with dots denote current coming out of the paper etc. The magnetic field lines are lines of constant $A_\varphi \simeq (B_\infty/2)r^2 \sin^2\theta$ *b*, Perturbed state. Field lines are frozen into the disk and at infinity. A field line through an element of the disk displaced a radial distance δr will be similarly displaced. At the disk surface the line is rotated through an angle $\delta\theta$ as seen on this diagram—a local observer would see it rotated through an angle

$$\overline{\delta\theta} = \delta\theta(1-(r_g/r))^{-1/2}$$

conductivity, any perturbation of the plasma drags the field lines with it. The perturbed field consists of the original uniform field and a perturbation field generated by currents in the plasma. For a given perturbation, the electromagnetic energy increases by an amount proportional to ${B_\infty}^2$, while the decrease in gravitational potential energy is fixed. Thus the perturbation is stable if B_∞ is large enough. Equation (1) yields

$$\left(\frac{\sigma}{-B_{\bar{\theta}}}\right)M = r^2(1-(2M/r))^{1/2}I_{\bar{\varphi}} \qquad (4)$$

Consider a perturbation (not necessarily axisymmetric) that takes a fluid element from r to $r+\delta r$, and does not extend over a length scale$\gg r$. For that element the left-hand side of equation (4) stays constant, because surface energy and flux satisfy identical conservation laws. The perturbation is stable if, and only if, the right-hand side increases. When unperturbed the field lines (from a static observer's viewpoint lines of constant covariant vector potential $A_\varphi(r,\theta)$) are nearly straight (Fig. 1*a*). Because the perturbation field is approximately dipolar at heights$\gg r$ above the disk the field lines there will also be almost straight (Fig. 1*b*). This gives a lower limit on the angle $\delta\theta$ through which the field lines have been rotated near the disk: $\delta\theta \gtrsim (-\delta r)/r$, and implies $\delta I_{\bar{\varphi}} \gtrsim B_\infty(-\delta r)/r$. Close to the hole the disk would seem to be stable if $I_{\bar{\varphi}} \lesssim 2B_\infty(1-(2M/r))^{1/2}$.

For a stellar black hole $M \simeq 10M_\odot$, while for a black hole in a galactic nucleus or QSO $M \simeq (10^8\text{–}10^9)M_\odot$. Typical interstellar fields have magnitudes of only $\sim 10^{-5}$ gauss, but fields frozen into accreting plasma get amplified by many orders of magnitude[4], so that B_∞ is in fact much greater. Small scale fields dissipate faster than large scale fields. It is possible that plasma is in quasi-static equilibrium near to some black holes. This is a consequence of m_p/ce being a small number, that is, of the strength of electromagnetic forces compared with gravity.

I wish to thank Professor M. Rees and Drs R. Blandford and F. Lamb for many useful conversations. I acknowledge an SRC studentship.

ROMAN ZNAJEK

Institute of Astronomy,
Madingley Road,
Cambridge, UK

Received January 29; accepted May 10, 1976.

[1] Ginzburg, V. L., and Ozernoi, L. M., *Sov. Phys. JETP*, **20**, 689–695 (1965)
[2] Znajek, R. L., (in the press).
[3] Gibbons, G. W., *Nature phys. Sci.*, **240**, 77 (1972).
[4] Bisnovatyi-Kogan, G. S., and Ruzmaikin, A. A., *Astrophys. Space Sci.*, **28**, 45–59 (1974).

Outbursts of the recurrent nova T Coronae Borealis

THE recurrent nova T CrB has long been regarded as an anomaly among cataclysmic variables. It is a binary system consisting of an M3III giant and a blue companion[1]. From the radial velocity curves, Kraft[2] found component masses of $\geq 3.7M_\odot$ and $\geq 2.6M_\odot$, respectively, later revised downwards to $2.6M_\odot$ and $1.9M_\odot$ by Paczyński[3]. Nevertheless, the mass of the blue component is clearly greater than the Chandrasekhar limit, even though the blue components of common novae are widely believed to be white dwarfs. The binary period, 227.5 d, is > 300 times longer than that of GK Per[3], the longest period known among the remaining cataclysmic variables, and in stark contrast with the 0.0567-d period of WZ Sge, the only other recurrent nova of known binary period. Warner[4] has suggested, however, that T CrB is typical of the majority of recurrent novae. In this paper we interpret the behaviour of T CrB in terms of accretion in a binary system.

Two outbursts of T CrB have been observed, in 1866 (JD 2,402,734) and in 1946 (JD 2,431,861), these being apparently remarkably similar[5]. In neither case was the eruption detected before the nova was already declining in brightness, but evidence exists suggesting that the initial rise is extraordinarily rapid[6].

The brightness variations in this system in the interval immediately surrounding the 1946 outburst[7,8] are shown in Fig. 1. Three features are clearly visible in the light curve: (1) There is a sudden decrease in brightness by about one magnitude (visual) to a minimum, $m_v \simeq 10.8$, at JD 2,431,599. What scattered observations exist of this phenomenon suggest that superimposed on the recovery from minimum is a decaying oscillation with period ~ 41 d and initial amplitude, $\Delta m_v \simeq 0.15$; (2) 263 d later, the principal maximum, $m_v \simeq 3.4$, occurs. The system remains within one magnitude of maximum for approximately three days only, and the decline is exceptionally rapid (0.5 mag d^{-1}). The total energy output in visual light during this outburst amount to ~ 1,400 times the mean daily output of the giant component[5] ($m_v \simeq 10.2$) in a quiescent state; (3) 106 d following the principal maximum, the system again begins brightening, reaching a secondary maximum, $m_v \simeq 8.06$, near JD 2,432,020, with fluctuations at maximum of a few tenths of a magnitude. The system drops to $m_v \simeq 9.4$ within the next 80 d, followed by an extremely prolonged decline[9] ($\geq$ 25 yr) to its present light level, $m_v \simeq 10.15$ (personal communication from J. A. Mattei).

This outburst behaviour carries the distinct signature of an episodic accretion event. The minimum preceding outburst is associated with the dynamical ejection of a coherent mass of gas by the lobe-filling giant. Bath[10] has shown the existence of such an instability generally among lobe-filling giants, and

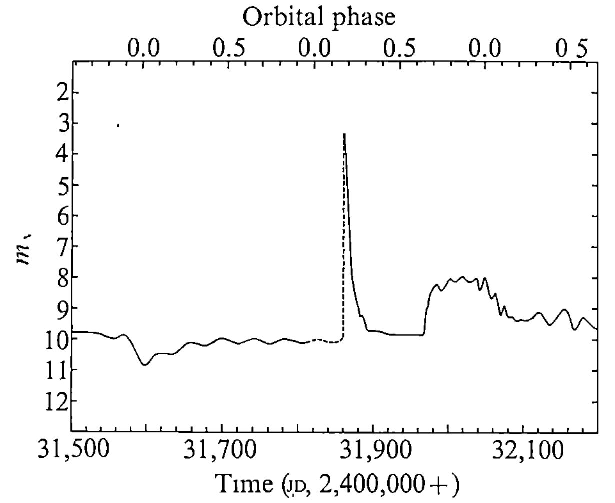

Fig. 1 The light curve of T CrB during the 1946 outburst, reconstructed from visual observations by members of the AAVSO (ref. 7). The dotted portion of the curve near JD 2,431,840 represents a gap in observational records while T CrB was unfavourably located with respect to the Sun. The observations shown before the outburst are those of a single observer, L. C. Peltier. The oscillations shown in this portion of the light curve are suggested by his observations, but the number of observations is relatively small. There is unusually large observational scatter after JD 2,432,070, suggesting an enhanced level of rapid photometric activity. The orbital phases indicated at the top of the figure are computed from an ephemeris by Paczyński[3].

time-dependent calculations of such events find the mass-losing star underluminous following the ejection[11]. The recovery from minimum is characterised by a timescale[11]

$$\tau_{th} \simeq \frac{RT\Delta M}{\Delta L}$$

where R is the ideal gas constant. A lobe-filling M3III giant[12], $T_e = 3{,}350$ K, has a luminosity $L_g = 1{,}250 L_\odot$. Taking $\Delta L \simeq L_g$, and assuming a mean temperature, $T \simeq 10^5$ K, for the ionisation zones, the observed timescale, $\tau_{th} \simeq 100$ d, indicates $\Delta M \simeq 10^{-3} M_\odot$ transferred. The possible 41-d periodicity superimposed on the recovery is consistent with a low order pulsational mode of the giant (P. R. Wood, personal communication), excited by the ejection episode.

The principal maximum is of such short duration that it must correspond to a dynamical phenomenon. The matter ejected by the giant initially takes up an extremely eccentric orbit around the secondary. This orbit is made circular dynamically, by supersonic collisions within the orbiting material. A simple estimate, following Lubow and Shu[13], indicates that 1.09×10^{14} erg g^{-1} is dissipated in this way for the adopted binary parameters. Allowing a bolometric correction of 1.81 mag for the giant[12], the visual energy output is found to be 1.12×10^{44} erg by comparison with the quiescent giant luminosity, giving $\Delta M = 5.2 \times 10^{-4} M_\odot$, in good agreement with the estimate obtained above. The resultant circular orbit has a radius $R_d = 19.9 R_\odot$, period 7.49 d.

Viscous dissipation within this accretion ring broadens it into a disk which gradually reaches down to the surface of the accreting star[14]. As it does so, its luminosity increases, reaching a maximum as its inner edge reaches the surface of the central star. The height of that maximum is a direct measure of the surface potential of the star, and the interval between the principal and secondary maxima reveals the viscous timescale of the disk.

The secondary maximum of T CrB clearly reveals the secondary as a main-sequence star (first suggested by Plavec[15,16] and Harmanec[17]). The mass and luminosity of the giant component indicate an age[18] of $\sim 4.7 \times 10^8$ yr for the system, placing the main-sequence companion in core hydrogen burning ($X_c \simeq 0.28$), with radius $R \simeq 1.81 R_\odot$. In the time-dependent, constant-viscosity disk model[14], the interval between the creation of an accretion ring (primary maximum) and the point at which the light level rises to within 1.5 mag of secondary maximum (an observationally well defined quantity) is $\Delta t = 0.118\ \tau_v$ where τ_v is the natural viscous timescale

$$\tau_v = \frac{R_d^2}{6\nu}$$

Thus, the viscous timescale of the accretion disk in T CrB is $\tau_v = 930$ d. The predicted height of secondary maximum for the assumed main-sequence companion is $m_v = 7.77$, in good agreement with the observed maximum (8.06 m), and far lower (by more than five magnitudes) than that expected for a massive white dwarf companion. The effective Reynolds number of the disk is

$$R_v \simeq 6 \left\{ \frac{GM_2}{R_d^3} \right\}^{1/2} \tau_v \simeq 4{,}700$$

indicating that the disk is turbulent.

Dwarf novae are widely believed to be accretion episodes of a very similar kind[19,20]. Bailey[21] has recently found an empirical relationship among dwarf novae between the rate of decline from maximum and the orbital period, P

$$\tau \simeq 9.2 P$$

where τ is the time required to decline one magnitude. For T CrB, the inferred timescale, $\tau = 2{,}090$ d, is in excellent agreement with the time required for a theoretical constant-viscosity disk with $\tau_v = 930$ d to decline from one magnitude below maximum to two magnitudes below maximum, $\Delta t = 2{,}320$ d.

Details of this model, and a reinterpretation of Kraft's observations[2] will be published separately. The author gratefully acknowledges invaluable discussions with J. W. Truran, R. P. Kraft, G. T. Bath, J. E. Pringle, and P. R. Wood. Special credit is due to the many amateur astronomers throughout the world, and the American Association of Variable Star Observers (AAVSO) and its Director, Janet Mattei, in particular. Without their patient observations this discovery would not have been possible. This research was supported by the NSF.

RONALD F. WEBBINK

Department of Astronomy,
University of Illinois,
Urbana, Illinois 61801

Received May 3, accepted June 8, 1976.

[1] Sanford, R. F., *Astrophys. J.*, **109**, 81–91 (1949)
[2] Kraft, R. P., *Astrophys. J.*, **127**, 625–641 (1958).
[3] Paczynski, B., *Acta Astr.*, **15**, 197–210 (1965).
[4] Warner, B., in *The Structure and Evolution of Close Binary Systems, IAU Symp* **73** (edit. by Mitton, S., and Whelan, J.), (D. Reidel, Dordrecht, in the press)
[5] Pettit, E., *Publs astr Soc. Pacif.*, **58**, 359–362 (1946).
[6] Pettit, E., *Publs astr. Soc. Pacif.*, **58**, 153–156 (1946).
[7] Campbell, L., *Ann Harv. Coll. Obs.*, **116**, 160 (1947); *Ann. Harv. Coll. Obs.*, **116**, 227, 255–256 (1948).
[8] Mayall, M. W., *Am. Ass. var. Star Obs., Q. Rep.*, **1**, 22–23, 25; **2**, 19–21, 49 (1950); **3**, 16–17, 34 (1951).
[9] Isles, J. E., *J. Br. astr. Ass.*, **84**, 203–208 (1974)
[10] Bath, G. T., *Astrophys J.*, **158**, 571–587 (1969); *Astrophys. J*, **173**, 121–134 (1972).
[11] Bath, G T., *Mon. Not. R. astr. Soc.*, **171**, 311–328 (1975).
[12] Lee, T. A., *Astrophys. J.*, **162**, 217–238 (1970).
[13] Lubow, S. H, and Shu, F. H., *Astrophys. J.*, **198**, 383–405 (1975).
[14] Lynden-Bell, D., and Pringle, J. E., *Mon. Not. R astr. Soc*, **168**, 603–637 (1974)
[15] Plavec, M., in *Extended Atmospheres and Circumstellar Matter in Spectroscopic Binary Systems, IAU Symp.*, **51** (edit. by Batten, A H.), 216–259 (D. Reidel, Dordrecht, 1973).
[16] Plavec, M., Ulrich, R. K., and Polidan, R. S., *Publs astr. Soc. Pacif.*, **85**, 769–805 (1973).
[17] Harmanec, P., in *Late Stages of Stellar Evolution, IAU Symp*, **66** (edit. by Tayler, R. J., and Hesser, J. E.), 195 (Reidel, Dordrecht, 1974)
[18] Iben, I., Jr, *Astrophys. J*, **142**, 1447–1467 (1965), *Astrophys. J*, **147**, 624–649, 650–663 (1967).
[19] Bath, G. T., *Nature phys. Sci.*, **246**, 84–87 (1973).
[20] Bath, G. T., Evans, W. D., Papaloizou, J., and Pringle, J. E., *Mon. Not. R astr. Soc.*, **169**, 447–470 (1974).
[21] Bailey, J., *J Br. astr. Ass.*, **86**, 30–32 (1975).

A plum-pudding model for interstellar grains

THERE seem to be two basic mechanisms by which interstellar grains can grow; the condensation of gaseous molecules (mostly of the CNO type) on to their surfaces and the coagulation on collision of individual grains. In general, as has been shown by Simons and Williams[1], condensation leads to a more rapid growth rate than coagulation resulting from the thermal motion of the grains. If, however, relative motions can be set up within the grain population, then this increases the collision rate and so also increases the rate of growth by coagulation. Now, for small grains, the force on them from radiation pressure depends on a different function of the grain radius, a, than does the viscous drag generated by the ambient gas. (For simple models these functions are respectively a^3 and a^2.) Consequently, grains of differing sizes will be caused to move with different velocities through the ambient gas by radiation, the larger ones moving faster. This causes these grains to capture further grains by coagulation which in turn enhances their relative velocity even further. The purpose of the present communication is to show that this growth caused by radiation pressure coagulation is probably of the same order as that from gas atom condensation, and to point out an important consequence of this.

Let us focus attention on a particular grain, G. Atoms will be incident on this grain both in the form of free atoms and in the form of those bound in other grains. In each case the number of atoms Z adhering to G per unit time will be given by

$$Z = vnA\sigma$$

where v is the velocity of the incident atoms relative to G, n is the number of these atoms per unit volume, A is the effective cross section of G and σ is the sticking coefficient. Thus the ratio of grain growth from condensation to that caused by radiation pressure coagulation is given by

$$X \simeq \frac{v_a n_a A_a \sigma_a}{v_g n_g A_g \sigma_g} \tag{1}$$

where the subscripts a and g refer, respectively, to free atoms and to those bound in grains.

To calculate v_g we note first that due to its charge, prolonged grain motion can only occur parallel to the magnetic field **H**. In this direction, the force on grains of radius a from radiation is given by

$$F_R = \pi a^2 Q(a) P \beta \tag{2}$$

where P is the radiation pressure and β the cosine of the angle between **H** and the direction of the radiation pressure. $Q(a)$ is the mean efficiency factor for radiation averaged over all frequencies. For blackbody radiation characterised by a temperature of $\sim 10^4$ K, such as may typically be found in the Galaxy, acting on a grain composed of material with a complex refractive index

$$Q(a) \simeq 5 \times 10^4 a \tag{3}$$

(see Simons and Williams[2], Greenberg[3]), for all values of a such that $Q(a) \leqslant 1$. Simons and Williams[2] have shown that for the general galactic radiation field

$$P \simeq 1.2 \times 10^{-13} \text{ (cgs units)}$$

and that the gravitational field of the interstellar cloud within which the grain is situated is unimportant as far as the motion of that grain is concerned. Also since the galactic field acts equally on grain and cloud, in any discussion of their relative motion it may be ignored. The relative velocity of the grain is thus determined by balancing the driving radiation pressure by the viscous drag of the ambient gas which has the form (Baines *et al.*[4])

$$F_{Res} = \pi a^2 \rho v W \gamma \tag{4}$$

v being the relative velocity, W the mean thermal velocity and ρ the gas density. γ is a factor, numerically of order unity, which depends on the way gas molecules are reflected from the surface of the grain. For typical interstellar clouds (see Lequeux[5]) we find that

$$F_{Res} \simeq 4.5 \times 10^{-18} \pi v a^2 \tag{5}$$

and from equations (2) and (5) we get

$$v \simeq 1.3 \times 10^4 Q(a) \tag{6}$$

taking $\beta = \frac{1}{2}$. Thus the relative velocity of two species of grain of radii a_1 and a_2 is given by

$$v = 7 \times 10^8 (a_1 - a_2) \tag{7}$$

the larger grains moving faster than the smaller ones. Since we are concerned with the growth of grains to their present size we take as representative values $a_1 \simeq 4 \times 10^{-6}$ cm and $a_2 \simeq a_1/2$. This yields

$$v_g \simeq 15 \text{ m s}^{-1} \tag{8}$$

As far as v_a is concerned, we suppose the atoms to be predominantly oxygen and the gas temperature to be ~ 100 K. This gives $v_a \simeq 300$ m s^{-1}, so that

$$v_a / v_g \simeq 20 \tag{9}$$

As far as n_a/n_g is concerned, it is generally assumed that the mass of heavy condensible atoms is roughly equally divided between free atoms and those bound in grains. In view of this we shall take

$$n_a / n_g \simeq 1 \tag{10}$$

It is generally supposed that atoms such as C and Si are precominantly bound in grains so that the ratio n_a/n_g may well be < 1, though values > 1 cannot be entirely ruled out.

A_a will be the geometric cross section πa^2 of the grain G with radius a. If the other grains incident on it have radius a', then

$$A_g \simeq \pi (a + a')^2$$

Now a' can be both greater or smaller than a, so that a reasonable estimate is presumably made by setting $a' = a$. This gives

$$A_a / A_g \simeq 1/4 \tag{11}$$

The value of σ_a has been estimated theoretically for O atoms (in ref. 6) to be $\sigma_a \simeq 0.3$. The best available evidence for σ_g would seem to be from experiments on the acoustic coagulation of terrestrial aerosols[7]. In these experiments coagulation proceeded efficiently for all relative grain velocities involved, which ranged up to several m s^{-1}. Since v_g (equation (8)) is greater than these velocities only by a factor ~ 3, we suggest taking

$$\sigma_g \simeq 1$$

in the absence of any evidence to the contrary. This gives

$$\sigma_a / \sigma_g \simeq 0.3 \tag{12}$$

Pure Chemistry Library
SCIENCE COLLEGE.
[illegible] Circular Road

It then follows from equations (1), (9), (10), (11), (12) that

$$X \simeq 2 \qquad (13)$$

In spite of the various uncertainties in the above estimation the result (equation (13)) would seem to substantiate our contention that growth from radiation pressure coagulation is probably of the same order as that from condensation. This has a very important consequence since it leads to the possibility of the formation of a grain possessing a novel type of internal structure; we call this a "plum-pudding" grain.

Initially a grain with a single silicate type nucleus will build up an ice mantle by condensation. Collision with a similar grain followed by coagulation will lead to a larger grain consisting of two separate silicate type cores surrounded by ice. As growth by both mechanisms proceeds, a multicored grain of silicates and similar material embedded in an ice matrix is formed, similar to plums in a pudding.

Such a grain would have rather novel optical characteristics, the main feature being that it would, at one and the same time, exhibit structure at two characteristic lengths, that of the nuclei and that of the whole assembly, including the ice. One might speculate that with such a grain it would be possible to explain the optical observations which according to Whittet *et al.*[8] have hitherto required the existence of three distinct grain models. Speculating further, the requirement of large grains, pointed out by Rowan-Robinson[9], might also be met by our type of grain structure.

The above treatment would seem to demonstrate the plausibility of the existence of plum-pudding grains. A quantitative treatment of their growth, structure, size and optical properties remains, however, to be performed. Work on this is currently in progress and will be published elsewhere.

S. Simons
I. P. Williams

Department of Applied Mathematics,
Queen Mary College,
Mile End Road, London E1 4NS, UK

Received December 4, 1975, accepted June 7, 1976.

[1] Simons, S., and Williams, I. P., *Astr. Space Sci.*, 32, 493 (1975)
[2] Simons, S., and Williams, I. P., *Astr. Space Sci* (in the press).
[3] Greenberg, M , *Nice Symposium on the Origin of the Solar System*, 135 (CNRS, 1972).
[4] Baines, M. J., Williams, I P., and Asebiomo, A. S , *Mon Not. R. astr. Soc.*, 130, 63 (1965).
[5] Lequeux, J., *Nice Symposium on the Origin of the Solar System*, 118 (CNRS, 1972).
[6] Wickramasinghe, N. C., and Nandy, K , *Rep Prog Phys.*, 35, 157 (1972).
[7] Mednikov, E. P., *Acoustic Coagulation and Precipitation of Aerosols* (Consultants Bureau, New York, 1965).
[8] Whittet, D. C. B , Daigawansa, I. J., Dickinson, P. M., Marsden, J. P., and Thomas, B., *Mon. Not. R astr. Soc.*, 175, 197 (1976).
[9] Rowan-Robinson, G M , *Mon. Not. R. astr Soc* , 172, 109 (1975).

A comparison of acoustic Doppler vertical velocities with direct measurements in the atmospheric boundary layer

THE quantitative evaluation of the intensity of acoustic echoes from the first few hundred metres of the atmospheric boundary layer (in both stable and convective situations) has been the subject of much recent experimental work[1-5]. The acoustic echo, however, contains Doppler information on the vertical air motion and this could prove of great use in the specification of further important boundary layer statistics such as σ_w^2, the variance of the vertical wind speed[6] and ε, the rate of dissipation of turbulent kinetic energy. Beran *et al.*[7] using a sounder in the monostatic mode (transmitter and receiver aerials located together) derived the profile of the vertical wind component using the acoustic Doppler technique. They did not, however, verify that the estimates of the winds were correct, nor did they record the magnitudes of the Doppler shifts in the weak echo regions between the periods of thermal activity. This paper presents a quantitative comparison between acoustic Doppler vertical winds and direct estimates measured at a fixed height in the atmosphere.

The acoustic sounder operates at a frequency of 1,730 Hz transmitting pulses of length 74 ms at a pulse repetition frequency of 0.44 Hz and up to 25 W of acoustic power. The aerial (which is used for both transmission and reception) is a 6 × 6 array of 16.5-cm diameter re-entrant horn loudspeakers. These figures correspond to a height range of 380 m and a range resolution of 12.25 m. The pulse length (and hence the resolution) and the transmitted power can be varied. The receiver gain can be varied up to 155 dB which includes a ramp gain to compensate for the spherical divergence of the acoustic echoes as they are received from the longer ranges[8]. The transmit pulse is used to synchronise a gating system which controls the selection of the signal received from any chosen height for Doppler shift determination. The gating system provides five gates of variable width hence allowing the signal to be analysed at five different heights. A Hewlett–Packard spectrum analyser with an 8553B r.f. section is used to produce the frequency spectrum of the received echo. The oscilloscope display is automatically photographed using a cine camera triggered by the same gating circuit. The photographed power spectra can be analysed subsequently to determine the frequency shift by use of an expression for the radial velocity v of a scattering eddy given by Beran *et al.*[7]

$$v=\frac{C}{2}\left(\frac{f_0}{f_d}-1\right)$$

for relatively low velocities of up to 2 m s^{-1}. Here f_0 is the transmitted carrier frequency and f_d is the frequency of the scattered signal.

Direct estimates of the vertical velocity were made using a 'reduced' version of the turbulence probe described by Readings and Butler[9]. Basically this instrument consists of a set of sensors mounted on a vane which keeps them facing into wind. The vane is attached to the tethering cable of a large kite balloon (~ 1,300 m^3 volume) and is free to move in the horizontal plane. In this particular application the sensors consisted of a hot wire (double 'V' shaped) inclinometer mounted on a damped pendulum at the front of the vane and a multislot photoelectric anemometer fitted with a 6-cup polystyrene rotor. These sensors record the inclination (ϕ) of the wind vector to the local horizontal (as seen by the sensor) and the total wind speed, V. Thus the instrumentation does not precisely measure the absolute magnitude of the vertical velocity but rather its variability about some chosen mean. The mean value is set by assuming that the average inclination of the flow is zero, $\bar{\bar{\phi}}=0$, where the double bar represents the complete period of a run (typically ~ 1 h). Average vertical velocities ($\bar{w}$) over time periods corresponding to fifty sounder pulses are then obtained from the relationship

$$\bar{w}=\overline{V\sin(\phi-\bar{\bar{\phi}})}$$

Several experiments have recently been carried out to determine the overall accuracy of the balloon-borne turbulence instrumentation including the sensitivity of the observations to sensor design, frequency response, data reduction techniques and the influence of probe motion as it sways with the balloon cable (see Readings and Butler[9], Haugen *et al.*[10]). The results show that the tolerance on the vertical velocity estimates is ~5% and that this wind component is negligibly affected by balloon cable movement.

The results described concern four experiments carried out in convective conditions and two in stable conditions. Figure 1*a* shows the facsimile recording for one of the runs in convective conditions on June 18, 1975. The sequence of thermal activity is clearly shown. During this run the turbulence probe, providing the direct measurements, was located at a height of 70 m. Figure 1*b* shows the comparison between vertical velocities as recorded by the sounder and the probe, the latter being averaged over a time interval corresponding to twenty sounder pulses that is, 46 s, which for the wind speed present during this run is equivalent to a spatial scale of ~ 200 m. This distance is much greater than the separation of probe and sounder scattering volume (80 m). Sufficient signal was still received during periods of weak echo to record a Doppler shift, provided the gain of the receiver was sufficiently high. For both convective and stable conditions the received signal was too weak to permit the recording of the Doppler spectrum on ~ 5% of the total number of occasions. Comparison of Fig. 1*a* and *b* shows that there is little apparent connection between the intensity of the echo (C_T^2) and the updraughts as seen by both sounder and turbulence probes. Beran *et al.*[7] have, however, observed that areas of maximum C_T^2 were associated with regions of maximum vertical wind shear. This is of importance in the qualitative interpretation of acoustic sounder facsimile records and merits further study.

Figure 2 shows a plot of vertical velocity estimates from the acoustic Doppler measurements averaged over fifty pulses against direct measurements over a corresponding time interval using data from all four runs in convective conditions. The data are seen to scatter fairly well about a line of unit slope. A best fit line through the data has slope 0.75 and intercept 0.2 m s^{-1} on the sounder axis. It is not clear to what extent the scatter in this plot is produced by real spatial differences in the vertical velocity field or by the inherent errors in the technique. It should be emphasised that the probe provides a continuous estimate of the vertical velocity at one point only whereas the sounder estimates refer to a discrete set of observations averaged in height (over a resolution depth) and in the horizontal (over the beam area). The values of the correlation coefficients for unstable conditions ranged between 0.7 and 0.9 and the standard deviations of the direct and indirect estimates of vertical velocity were between 0.43 and 0.53 m s^{-1} and 0.4 and 0.6 m s^{-1} respectively. Figure 3 shows the facsimile recording and the plot of vertical velocity against time obtained during stable conditions on June 26, 1975. For these conditions the correlation coefficients were 0.7 and 0.9 with direct and indirect standard deviations of 0.06 and 0.04 m s^{-1} and 0.1 and 0.06 m s^{-1} respectively. The variances recorded refer to the frequency band set by the run duration and the averaging period.

Fig. 1 *a*, Facsimile recording of convective conditions between 10.33 and 11.20 on June 18, 1975. *b*, Comparison between sounder estimates (○) and direct measurements (●) of vertical velocities averaged over twenty pulses.

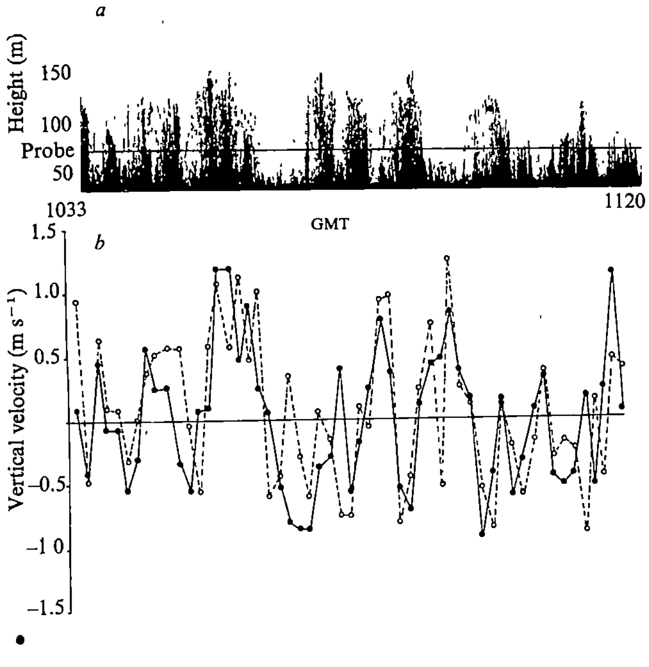

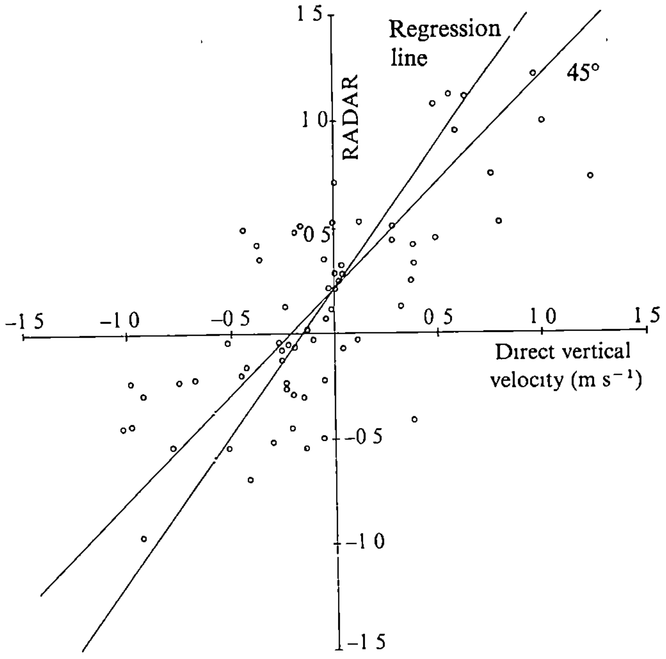

Fig. 2 Plot of vertical velocity estimates from the acoustic Doppler measurements against the direct measurements from all four experiments in convective conditions.

Three sources of error indicated by Spizzichino[11] have been considered in some detail. These are (1) instrumental error; (2) refraction effects and; (3) apparent vertical velocities introduced by horizontal wind components because of the finite beamwidth of the acoustic antenna. The relationship that describes the instrumental error is

$$\sigma_w^2 = \frac{\sqrt{(3)}\lambda^2 b_1^2}{4N\tau_G S_1}$$

where $S_1=((1/\tau_G^2)+b_1^2)^{\frac{1}{2}}$, N is the number of pulses, τ_G is the actual width of the sampling gate and b_1 is the bandwidth of the Doppler signal. For the present results b_1 is ~ 10 Hz, τ_G is 180 ms and N is 50, giving a value for σ_w of 0.12 m s^{-1}, which is reasonably small. For $N=5$, σ_w becomes 0.4 m s^{-1} and in accordance with this the scatter in a plot of direct against sounder estimates was much greater than that in Fig. 2 and such that no discernible trend could be identified. A further source of error is in the determination of the position of the peak of the power spectra, necessary for the measurement of the frequency shift. This error was estimated to be ~ 0.1 m s^{-1} for a single spectral photograph.

The error from refraction can be found if the integrated wind profile to the height of the observation is known. During these experiments this was obtained using the Cardington Balthum[12] and this error turned out to be ~ 0.2 m s^{-1}. This indicates a systematic overestimation of the vertical velocity by the sounder and may be responsible for the positive intercept of the regression line on the sounder axis (see Fig. 2).

The error from the finite antenna beamwidth (~ 10°) is more difficult to assess since it depends on whether the observation time is long enough for the reflectivity being considered to be statistically uniform in the scattering volume. If this is the case then it merely produces spectral broadening and is already included in the instrumental error which involves b_1. If, however, the reflectivity is not uniform and there are many reflectivity maxima within the scattering volume, then the echo spectrum will also exhibit subsidiary maxima. Such

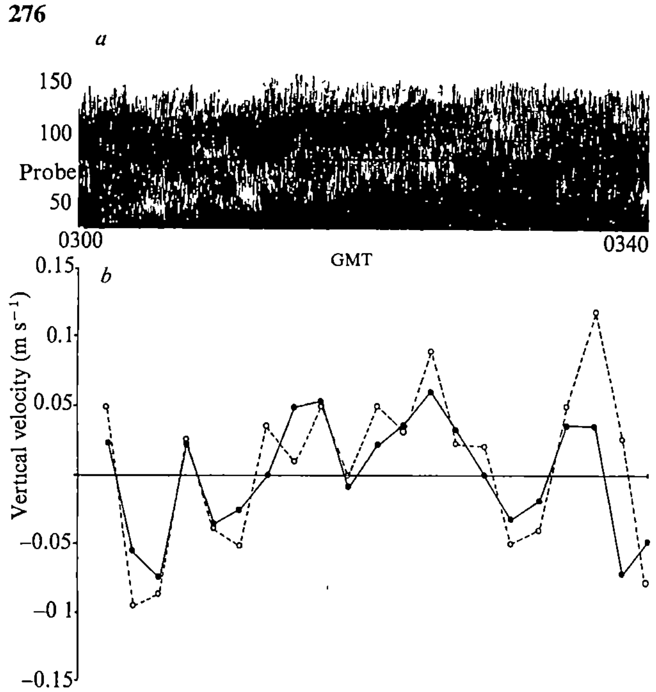

Fig. 3 *a*, Facsimile recording of an inversion between 03.00 and 03.40 on June 26, 1975. *b*, Comparison between sounder estimates (○) and direct measurements (●) of vertical velocities averaged over fifty pulses.

spectra were infrequently observed (~ 2% of the time) and hence for the data presented here this error can be neglected

The results presented above show that reasonable estimates of the vertical wind velocity can be obtained from the returns of a monostatic acoustic sounder operating in both stable and convective atmospheric conditions. The standard deviations of the velocity fluctuations agree well and correlation coefficients between sounder and direct estimates were found to be in the range 0.7–0.9. This technique may offer a quantitative remote method of assessing the mixing quality of the lower atmosphere and could prove of great use in studies of atmospheric diffusion and environmental pollution.

We thank the SRC for support, and staff of the Meteorological Research Unit, Cardington, for their assistance.

S. J. CAUGHEY
B. A. CREASE

Meteorological Research Unit,
RAF Cardington,
Bedford, Bedfordshire, UK

D. N. ASIMAKOPOULOS
R S. COLE

Department of Electronic and Electrical Engineering,
University College London,
Gower Street,
London WC1E 6BT, UK

Received March 17, accepted June 10, 1976

[1] Asimakopoulos, D N , Cole, R. S , Caughey, S J , Moss, S H and Readings, C J , *Atmos Environ* , 9, 775–776 (1975).
[2] Asimakopoulos, D N , Cole, R S , Caughey, S J , and Crease, B. A , *Boundary Layer Meteorol* (in the press)
[3] Neff, W. D., *NOAA Tech Rep*, ERL—322—WPL 38, Boulder, Colorado, (1975).
[4] Haugen D. A., Kaimal J C and Newman J. T *AFCRL Instrumentation Paper No 236*, Bedford, Mass, 59 pp (1975)
[5] MacAllister, L G., *J atm terr Phys* , 30, 1439–1440 (1968)
[6] Kelton, C , and Bricout, P., *Bull Am met Soc* , 45, 571–580 (1964)
[7] Beran, D W., Little, C. G , and Willmarth, B. C., *Nature*, 230, 160–162 (1971)
[8] Simmons, W R , Wescott, J. W., and Hall, F. F , Jr, *NOAA Tech Rep* ERL–216–WPL 17, Boulder, Colorado, (1971)
[9] Readings, C. J , and Butler, H E , *Met Mag , Lond* , 101, 286–298 (1972)
[10] Haugen, D. A , Kaimal, J C , Readings, C J and Rayment, R , *J appl Met* , 14, 540–545 (1975)
[11] Spizzichino, A , *J geophys Res*, 79, 5585–5591 (1974)
[12] Painter, H. E , *Met. Mag , Lond* , 99, 93–98 (1970)

Hercynian high pressure/low metamorphism temperature in the Ile de Groix Blueschists

WE present here an interpretation of K–Ar ages obtained on four glaucophanes, four phengites and one barroisite separated from aluminous, calcareous and basic schists cropping out on the Ile de Groix, off southern Brittany in France. The data include two glaucophane–phengite pairs (PM6 and PC10) and a composite separate specially enriched in barroisite. (Table 1).

Field relations and chemical mineralogy are best known for the glaucophanic eclogite PC10, which occurs in boudins having axes of elongation parallel with the dominant N–S mineral lineation in the south-east of the island. This metabasic boudin lies in a matrix of chloritoid micaschist, and is apparently not an exotic block (the encasing schist has an approximately cofacial paragenesis).

The pressure/temperature conditions during the metamorphism of the PC10 glaucophanic eclogite have been inferred from the Fe/Mg partitioning between adjacent garnet and clinopyroxene rims and from the jadeite content of omphacite in equilibrium with quartz and albite[3] (for analysis of all minerals and rocks except PC10 see refs 1 and 2). This gives an intersection of equilibria at 400 °C and 8K bar pressure, which is consistent with blueschist facies rocks from New Caledonia and Japan, and suggests that metamorphism took place in a region of low geothermal gradient (about 17 °C km^{-1} if average density = 2.9 g cm^{-3})—possibly in a subduction zone.

The concordance of K–Ar dates for two glaucophane–phengite pairs from widely separated aluminous and basic schist outcrops on Groix demands either a simple cooling age or mineral growth age interpretation; there is no evidence in either case for excess ^{40}Ar.

If we assume a maximum prograde growth temperature of 400 °C for the Groix phengites and glaucophanes in equilibrium, it is very likely that they grew at or beneath their blocking temperatures for Ar diffusion[4]. Thus, the age recorded would be the peak of high pressure/low temperature metamorphism rather than the cooling age. Even if mineral reactions ceased before the system became closed to Ar diffusion, it seems unlikely, in the context of a downgoing lithospheric slab, that high pressure/low temperature conditions could prevail for any significant interval of time after the peak of metamorphism was reached[5]. So, because of dynamic instability of the geo-

Table 1 Mineral assemblages of whole-rock specimens*

PM6:	Phengite + ferroglaucophane + chloritoid + quartz + sphene + chlorite. Aluminous schist, possibly metatuffaceous sediment, from Pen Men.
LM8:	Phengite + quartz + garnet + chlorite + glaucophane. Aluminous schist Common pelite lithology from Loc Maria.
LH11:	Epidote + glaucophane + quartz + garnet + phengite. 'Calcareous' schist, probably from margin of metabasic body, near Loc Maria.
LH13:	Epidote +, garnet + quartz + glaucophane + phengite. 'Calcareous' schist, probably basic metatuff from margin of metabasic body near Loc Maria.
PC10:	Garnet + glaucophane/barroisite + omphacite + epidote + phengite + albite + quartz + sphene. Basic schist from core of boudin, Pointe des Chats.

*Listed in order of decreasing modal abundance; dated mineral separates underlined.

Table 2 Data from minerals*

Sample no.	Mineral	^{40}Ar rad mol g^{-1} ($\times 10^{-8}$)	^{40}Ar rad (%)	K_2O (%)	^{40}Ar/^{36}Ar	^{40}K/^{36}Ar ($\times 10^3$)	Age (Myr)	
LM-8	Phengite	0.523	95.4	9.88(±0.04)	7,234	329	328.3(±9.0)	330.2
LM-8	Phengite	0.518	87.3	As above	2,470	105	326.0(±8.8)	
LM-8	Phengite	0.537	97.5	As above	11,863	544	336.3(±9.2)	
PM-6	Phengite	0.544	84.7	10.28(±0.16)	1,976	80.4	327.7(±10.3)	327.5
PM-6	Phengite	0.543	95.1	As above	6.815	311	327.2(±10.3)	
LH-13	Phengite	0.519	96.2	9.59(±0.19)	4,851	215	334.6(±11.4)	336.7
LH-13	Phengite	0.523	83.1	As above	1,859	71.9	338.9(±11.4)	
PC-10	Phengite (< 100 mesh)	0.577	86.3	10.64 (±0.09)	2,230	88.9	339.3(±9.7)	339.1
PC-10	Phengite (> 100 mesh)	0.527	86.8	9.49(±0.09)	2,311	92.3	342.7(±9.9)	
PC-10	Phengite (> 100 mesh)	0.515	95.3	As above	6,451	288	335.5(±9.6)	
PC-10	Glaucophane (80% pure)‡	0.00422	34.2	0.0837(±0.0010)	461	8.31	313.2(±10.0)	317.0
PC-10	Glaucophane (80% pure)	0.00437	58.3	As above	765	23.0	320.7(±10.2)	
PC-10	Glaucophane (70% pure)‡	0.00593	17.8	0.118(±0.002)	361	3.23	313.2(±12.7)	
PC-10	Omphacite + garnet + barroisite	0.00586	46.3	0.124(±0.001)	576	15.1	294.6(±8.2)	
PM-6	Ferro-glaucophane	0.000801	9.2	0.0151(±0.0005)	325	1.40	329 (±33)†	
LH-11	Glaucophane	0.000546	6.0	0.0107(±0.0005)	315	1.05	318 (±32)†	

*$\lambda_c = 0.585 \times 10^{-10}$ yr^{-1}; $\lambda_\beta = 4.72 \times 10^{-10}$ yr^{-1}; ^{40}K/K = 1.19×10^{-4} atom/atom.

†The 1σ precision of the age determinations for PM-6 glaucophane and LH-11 glaucophane (with ^{40}Ar rad < 10%) has been evaluated at 10%.

‡Barroisite rims are the main impurity. Microprobe gives barroisite rims K_2O = 0.24%, glaucophane core K_2O = 0.04%.

^{40}Ar was determined by isotope dilution mass spectrometry at the University of Naples, using a GD-150 Varian Mat mass spectrometer and the ^{38}Ar-enriched Zurich spike. The calibration was checked by LP-6 USGS standard, a muscovite internal standard (MCT) and Bern LP-6 biotite. K was determined in duplicate by flame atomic absorption with a Perkin Elmer 306 by the method of standard additions. Errors are maximum deviations from the mean. The errors (1σ) for K–Ar dates have been evaluated using the Cox and Dalrymple formula[9].

thermal gradient in an area of blueschist formation, the minerals grew quickly and were uplifted soon afterwards. Thus, the growth age of minerals from such an environment would be indistinguishable within error from the cooling age, given reasonable estimates of uplift rate (see Table 2).

A high pressure/low temperature metamorphic event 335±20 Myr ago on Groix would postdate the intrusion of anatectic granites on the mainland by about 40 Myr (ref. 6), but would coincide with the intrusion of early Variscan granites throughout Brittany 340 Myr BP (ref. 7). This juxtaposition of blueschist with a region of active plutonism from 380 to 340 Myr BP is similar to that observed in the Mesozoic and Tertiary paired metamorphic belts of Japan and California. In the case of Groix, however, no 'median' tectonic line or suture is exposed, the blueschist 'belt' is restricted to one island, and the level of erosion of the 'hot belt' is so deep that the volcanic arc has been stripped off, revealing the underlying batholiths and migmatites.

As soon as subduction of the blueschists had ended, uplift was probably brought about by isostatic response to rapid erosion of the volcanic arc and cordillera to the north. Thermal relaxation to a more normal geothermal gradient after subduction would have produced a rise in temperature during off-loading, and a consequent retrogression of the blueschist facies minerals. If the uplift rate were fast enough, however, the blueschists of Groix would have reached the Earth's surface before the thermal relaxation 'wave' could erase much of the blueschist assemblage.

The barroisites seem to have grown at the expense of glaucophane, omphacite and garnet during a late rise in temperature that did not exceed the Ar-blocking temperature of glaucophane—otherwise the glaucophane ages would all be reset at 294 Myr BP. This would account for the fact that the barroisite overgrowths on glaucophane are significantly younger by about 40 Myr than the high pressure/low temperature metamorphic assemblage. Furthermore, the apparent slight discordance between the ages of PC10 phengite and glaucophane can be explained by the influence of younger, K-rich barroisite rims in the impure PC10 glaucophane separates. The age of this late retrogression (294 Myr BP) corresponds well with uplift and cooling ages throughout the Hercynides, and is synchronous with the intrusion of younger Variscan granites[7], a major break in sedimentation and the main phase of Hercynian folding (Sudetic phase: Westphalian in age).

The Hercynian age proposed for the blueschist metamorphism on Groix is at variance with previous structural interpretations that have related early isoclinal fold phases to the Cadomian Orogeny (690–570 Myr BP)[8]. The basic glaucophane schist assemblages have been considered to have developed from pre-existing, possibly Cadomian, eclogites[1]. By contrast, we consider it very likely that both fold structures and metamorphic assemblages on Groix are Hercynian in age, and that the original lavas and sediments need be no older than 400–500 Myr (unpublished Sr isotope data, M. S. N. C. and P. N. Taylor).

We thank Pam Shreeve of the Oxford Geology Department for her K_2O determinations. Professor Howie of King's College, University of London allowed us to use Z. Makanjuola's mineral separates.

M. S. N. CARPENTER

Department of Geology and Mineralogy,
Parks Road,
Oxford, UK

L. CIVETTA

Istituto di Geologia e Geofisica,
dell'Universita degli Studi di Napoli,
Largo S. Marcellino, 10,
80138 Napoli, Italy

Received March 18; accepted June 6, 1976.

[1] Makanjuola, Z. A., and Howie, R. A., *Contr. Miner. Petrol.*, 35, 83–118 (1972).
[2] Makanjuola, Z. A., thesis, Univ. London (1967).
[3] Råheim, A., and Green, D. H., *Lithos*, **8**, 317–328 (1975).
[4] Jager, E., *Eclog. geol. Helv.*, **66**, 11–21 (1973).
[5] Oxburgh, E. R., and Turcotte, D. L., *Schweiz. miner. petrogr. Mitt.*, **54**, 641–662 (1974).
[6] Vidal, P., *Bull. Soc. geol. Fr.*, **7**, (15), 239–245 (1973).
[7] Adams, C. J., thesis, Univ. Oxford (1967).
[8] Cogné, J., Jeannette, D., and Ruhland, M., *Bull. Serv. Carte geol. Als. Lorr.*, **19**, 41–96 (1966).
[9] Cox, A., and Dalrymple, G. B., *J. geophys. Res.*, **72**, 2603–2614 (1967).

'Space' charging of insulators

THE charging of satellite surfaces by space radiation often results in electrical discharges. These can interfere seriously with electrical systems on board[1]. The surface potentials may vary according to the differing charging properties of dissimilar materials, local changes in capacitance or differences in the radiation environment. Investigations of radiation-induced electron emission have been directed predominantly at metallic or semiconducting materials, and there is a paucity of data on the charging of dielectrics. The work reported here considers

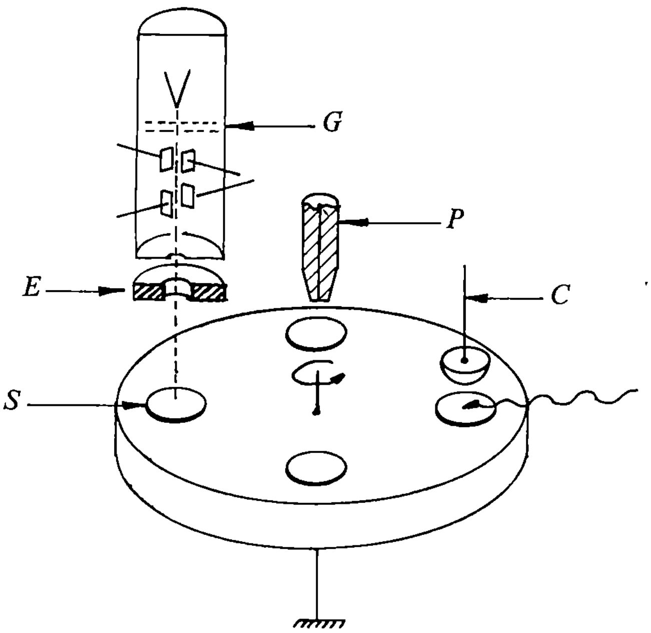

Fig. 1 Schematic diagram of experiment showing the specimen, *S*, mounted on the earthed, rotatable table; the counter electrode, *C*; an electron gun, *G*, with associated electrode; *E*; and the charge measuring probe, *P*.

photon-induced charging. Electron-induced charging is considered in ref. 2.

Photoelectric emission from fused silica on irradiation with ultraviolet light has been examined *in vacuo* ~ 10^{-5} mmHg. A schematic diagram of the experiment is shown in Fig. 1. Resonance radiation from, successively, a helium (21.2 eV), neon (16.85 eV) and argon (11.83 eV), discharge is directed, through a monochromator, obliquely on to dielectric specimens mounted on an earthed, rotatable table. The specimens are irradiated when positioned beneath the counter electrode, the charge being subsequently determined by scanning the specimens beneath a probe (see ref. 3).

The equilibrium charge densities produced on specimens of SiO_2, 300 μm thick, have been measured for several extracting (positive) counter electrode potentials. Figure 2 shows the charge densities determined for zero extracting potential plotted against the incident photon energy. The line shown indicates the geometric capacitance of the specimens. The saturation charge density would be expected to follow the photon energy linearly, the retarding surface potential at equilibrium being just sufficient to overcome the photoelectron emission energy, thus inhibiting emission. As evidenced, there is a tendency for the higher charge densities to be less than those predicted, and this may indicate a process of photoconductive loss.

Fig. 2 Equilibrium charge density measured on the SiO_2 specimens plotted against the incident photon energy. The line shows the specimen capacitance.

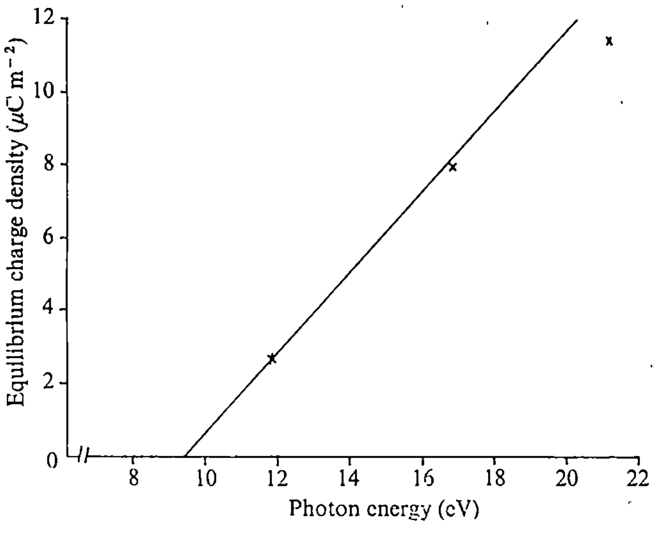

Positive potentials applied to the counter electrode increase the equilibrium charge density (Fig. 3). Data for all of the wavelengths used are presented, again with the line showing the specimen capacitance. Evidently, the equilibrium charge density is well described by

$$\sigma = \varepsilon\varepsilon_0(h\nu - \varphi_p + V_a)/d\,,\ \mathrm{C\ m^{-2}}$$

where, ε, d and φ_p, are the specimen permittivity, thickness and photoelectric threshold energy, respectively; $h\nu$ is the incident photon energy, and V_a is the counter electrode potential.

The temporal growth of charge has been examined, the emission current being found to decrease monotonically as the surface retarding potential increases. The mode of current decay with an applied extracting field seems different from that for zero potential, suggesting that penetration of the field into the dielectric may affect the excitation process as well as increase the probability of escape of the photoelectron. These investigations will be described more fully elsewhere.

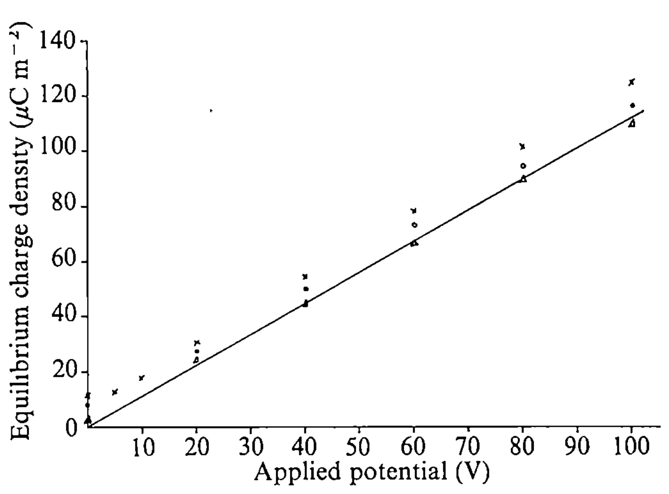

Fig. 3 Equilbrium charge density against applied counter electrode potential, for 21.2eV(×), 16.9eV(○) and 11.83eV(△) incident radiation. Specimen capacitance shown by solid line.

These experiments have shown that photocharging by solar radiation, which is often discounted[4], may not after all be insignificant, particularly in view of the extensive range of photon energies observed in the solar spectrum[5]. Also, it is evident that the equilibrium charges on insulators in space may be highly influenced by local electric fields.

D. Keith Davies

ERA Limited,
Cleeve Road,
Leatherhead,
Surrey KT22 7SA, UK

Received March 22; accepted June 1, 1976

[1] Nanevicz, J. E., Adamo, R. C., and Shaw, R. R., *Proc Conf. Lightning and Static Electricity*, Culham (1975).
[2] Davies, D. K., *Nature*, **262**, 279 (1976)
[3] Davies, D. K., *J. Phys D*, **6**, 1017–24 (1973).
[4] Grard, R. J. L., Knott, K., and Pedersen, A., *Photon and Particle Interactions with surfaces and Space* (edit. by Grard, R. J. L.), 163 (Reidel, Dordrecht, 1973).
[5] Walbridge, E., *High Altitude Observatory, Int. Rep. Ncar*, Boulder, Colorado (1971).

Charges and vacuum flashover

THE increasing importance of vacuum insulation in technology[1] and the recognition of the disruptive effects of surface discharges on satellites in space[2] both impart fresh impetus to the understanding of the flashover effect. Solid insulators are certainly a source of gas *in vacuo*, particularly under bombardment, and can also cause local enhancement of electric stress through the acquisition of surface charges.

de Tourreil and Srivastava[3], among others, have measured positive charges on insulators at stresses well below those necessary for flashover. They proposed a charging process based on secondary electron emission following bombardment of the dielectric by electrons initially field-emitted from the cathode. A secondary emission coefficient, δ, greater than unity (more out than in) obtains for most dielectrics[4] but strictly between well defined limits of input electron energies, that is, $\sim 1\,\text{eV} < E <$ a few keV, for instance. Outside these limits the insulator would charge negatively. Moreover, the emission energy of the secondary electrons is quite small, ~ few eV (ref. 5), and so very little positive charge on the insulator would preclude further emission. These effects are clearly illustrated by the simple experiment, shown schematically in Fig. 1 of ref. 6, in which electrons, with energies of up to 3 keV, are directed through a counter electrode on to insulator specimens, and the charges produced measured.

Specimens of fused silica (300 μm thick) and of two polymers—polycarbonate (55 μm) and polyimide (50 μm)—have been investigated. Figure 1 presents the measured charge densities for zero extracting field plotted as a function of the input beam energy. The upper secondary emission threshold energy (E_2) of the primary electrons is clearly displayed. For higher input energies, the insulator charges negatively, thereby slowing incoming electrons which thus arrive at the surface with precisely the threshold energy, so that equilibrium is attained ($\delta=1$). The full lines agree with the calculated geometric capacitance of the specimens to within 5%.

The occurrence of this dynamic process, rather than of complete repulsion of a high energy, primary beam (the other stable condition) is important since it indicates continued interaction even in the highly charged equilibrium state. Local discharges would probably dissipate larger areas of charge, for example, because of the increased surface conductivity.

Fig. 1 Charge densities measured on SiO_2 (*a*), polycarbonate, (*b*), and polyimide (*c*), specimens, plotted against input electron energy.

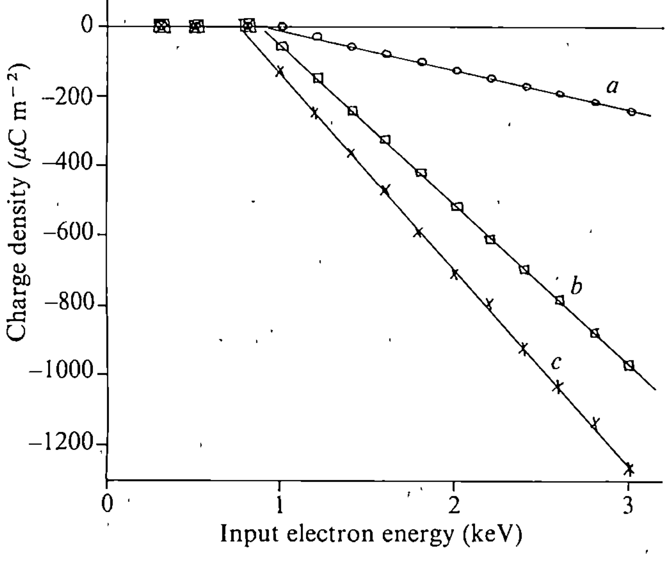

For input energies below the threshold (E_2) very little (virtually random) charge is detected on the dielectrics. If an extracting field is generated, however, by applying positive potentials to the counter electrode, positive charge densities are observed, these being independent of the primary beam energy but linearly dependent on the extracting potential. Above the threshold the extracting potential has no effect.

These observations suggest that the straightforward secondary emission theory of insulator charging, leading subsequently to breakdown, may be inadequate. The electric stress at flashover is usually greater than around 5 MV m^{-1}, so the maximum free path for primary electrons in this field, if they are to collide with the insulator surface with energy less than the upper threshold energy, ~ 1 keV, is less than 0.2 mm. Thus, for insulators of greater length, such primary electrons must originate from adjacent sites on the dielectric surface itself. That may be possible; but what happens to the electrons with greater than the threshold energy, that is, those originating further than 0.2 mm from the point of collision? They would charge the insulator negatively, irrespective of any apparent extracting field, except, perhaps, in three possible conditions:

- At low (near grazing) angles of incidence the considerably reduced normal depth of penetration of the primary beam may result in the emission of secondaries, even at high primary beam energies, that is, the secondary threshold energy may be greatly increased.
- The enhanced conductivity of the irradiated surface layers of the insulator may have an important role in establishing local potential gradients.
- The collision of particles originating from both the electrode and the dielectric surfaces may have an important independent role in charging the insulator surface.

To my knowledge these aspects have not been investigated.

D. KEITH DAVIES

ERA Limited,
Cleeve Road,
Leatherhead,
Surrey KT22 7SA, UK

Received March 22; accepted June 1, 1976

[1] Trump, J. G., *Proc. Vth int Symp. Discharge and Electrical Insulation in Vacuo*, 15–20 (Poznan, 1972)
[2] Rosen, A., *Astronautics and Aeronautics*, 13, 36–44 (1975)
[3] de Tourreil, C. H., and Srivastava, K. D, *Proc. Vth int. Symp. on Discharge and Electrical Insulation in Vacuo*, 295–299 (Poznan, 1972)
[4] Dekker, A. J., *Solid State Physics*, 418 (Macmillan, London, 1958).
[5] Hachenberg, O., and Brauer, N., *Adv. Elec. and Elec. Phys.*, XI, 425 (1959)
[6] Davies, D. K., *Nature*, 262, 277–278 (1976).

Aspartic acid racemisation in dentine as a measure of ageing

THE L-amino acids initially present in bone protein undergo slow racemisation over geological time at a rate which is proportional to temperature[1,2]. We have shown[3] that at the human body temperature of ~37 °C aspartyl residues in tooth enamel protein also undergo racemisation at a rate which corresponds to an enrichment in the D-aspartic acid content of ~0.1% per year. No D-aspartic acid increase was detected in haemoglobin, a protein with a more rapid turnover. We concluded that D-aspartyl residues accumulate in the metabolically stable protein in tooth enamel during the human lifetime as a result of *in situ* racemisation. We proposed that the irreversible first-order rate equation calculated from the enamel results could be used to deduce the age of any stable protein from a long lived mammal and thus the age of the organism itself. The error among samples from old individuals was large, however, probably because attrition and caries reduce the amount of uncontaminated enamel, and thus tend to limit the usefulness of tooth enamel for age determinations. In this report, we show that tooth dentine is a more suitable material, and the extent of aspartic acid racemisation in this fraction can be used as a reliable indicator of mammalian age.

Measurements of the D/L aspartic acid ratio were carried out on 20 samples of dentinal protein extracted from human teeth whose donors ranged in age from 11 to 75 yr. Teeth were obtained from dentists and cleaned of any soft tissue. The teeth were desiccated, the roots removed, and the crowns ground with a mortar and pestle. Dentine fragments were separated by hand under ultraviolet light, because they fluoresce and enamel does not. The dentine fragments were cleaned by ultrasonication in double-distilled water and dilute HCl. They were then dissolved in 6 N HCl, sealed in tubes, and hydrolysed at 100 °C. Hydrolysis was for 6 h rather than 24 h, in order to minimise the amount of acid-catalysed racemisation. Since aspartic acid is released preferentially[4] and the enantiomers should be equally labile, total hydrolysis of the dentine protein was not necessary. The hydrolysate was dried in a rotary evaporator and desalted on Dowex 50W-X8 cation exchange resin, and the fraction containing aspartic acid isolated and derivatised as described elsewhere[5].

A plot of the dentine data is shown in Fig. 1. The least squares fit of the points can be expressed by the equation

$$\ln[1 + (\textsc{d}/\textsc{l})] = 7.87(\pm 0.39) \times 10^{-4}\,\mathrm{yr}^{-1} t_{\mathrm{d}} + 0.014 \qquad (1)$$

where t_d is the age of the dentine in years. The correlation coefficient, $r = 0.979$, indicates that 96% of the variation in the D/L ratio is accounted for by the age of the tooth. The standard deviation for the dentine results is ±0.0034. The close agreement between the two 35-yr-old teeth, extracted from two different individuals, illustrates the reproducibility of the analyses.

The first-order rate constant k_{asp} for aspartic acid racemisation for dentine (the slope of the line in Fig. 1) falls within one standard deviation of the value for enamel. This indicates that the bulk of dentinal protein is not turned over, although the odontoblasts lining the pulp cavity remain viable throughout life and may deposit secondary dentine as a response to heavy wear[6]. The primary protein in enamel is non-collagenous, but 90% of the organic matrix in dentine is composed of collagen, and there is a phosphoprotein component which may account for 20% of the aspartic acid content of human dentine. Thus, we probably have three examples of metabolically inert polypeptides in which the aspartyl residues show increasing racemisation with increasing age. Moreover, collagen comprises 25–30% of the protein in the human body, and it is distributed as connective tissue throughout every organ system. This study shows that ~6% of the L-aspartyl residues in metabolically stable protein will have racemised to the D-enantiomers by 60 yr of age. It seems reasonable to assume that some of the physicochemical properties of the molecules will be altered as a result of this small amount of racemisation, and the effects should become more significant with increasing age. If a similar racemisation process occurs in all metabolically inactive proteins, then it may be part of the complex ageing changes which take place in mammals.

Fig. 1 Plot of ln[1+(D/L)] for aspartic acid against age of the dentine in years (solid line). Actual ages of tooth donors are corrected, depending on the type of tooth, by the values listed in ref 3. The slope (7 87×10⁻⁴ yr⁻¹) of the dentine line is equal to k_{asp} for tooth dentine at approximately 37 °C. The broken lines represent the k_{asp} values calculated for a ±0.7 °C difference in body temperature. ○, Individual of known age; △, exact ages unknown but estimated by dentists (these points were not used to calculate the least squares fit); ◇, albumin; □, bovine tendon collagen.

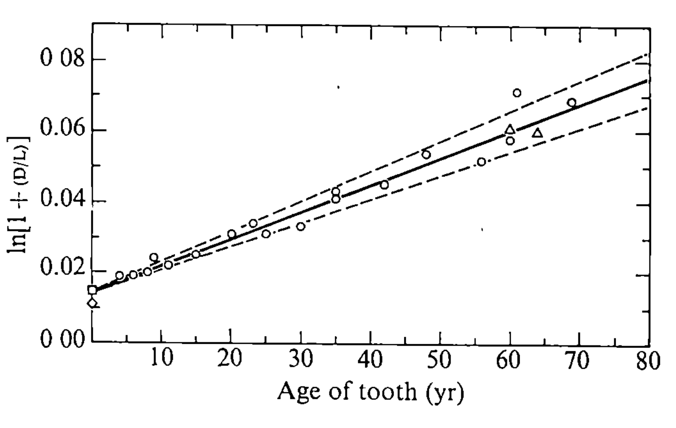

These results also indicate that dentine can be used, in the same manner as enamel, for estimating the age of a mammalian tooth. In many respects, racemisation analyses of dentine should be more reliable. First, dentine accounts for a much greater proportion by weight of a tooth than does enamel. In addition, the percentage composition of protein in dentine is 100 times that in enamel[8]. Thus, the chances of contaminating a sample are significantly reduced when dentine is analysed. Enamel is subject to surface alterations (attrition, bacteria, caries) which could affect its amino acid composition, whereas dentine is relatively sheltered by the enamel layer. Among people experiencing heavy tooth attrition, to the extent that very little of the crown remains after 40–50 yr, root dentine could be analysed.

The analytical advantages of dentine over enamel are reflected by the correlation coefficients. Since the total error is $(1-r^2)100$, all sources of error (experimental and contamination) amount to 4% in the dentine results, as compared with 15% for enamel. The standard deviation of the enamel values is more than twice that of the dentine values.

It is interesting that the enamel samples older than 50 yr had a standard deviation 2.4 times that of younger samples[3]. Although there are only four dentine samples of known age above 50 yr, a similar age-related increase in the scatter occurs with the dentine values. The standard deviation for dentine analyses of teeth greater than 50 yr old is 0.0060, compared with 0.0021 for teeth less than that age. Temperature is one factor which could cause small differences in the rate of racemisation between individuals. Human body temperature averages 36.9 °C and has a range of ±0.7 °C (ref. 9). This temperature variation would result in a change of about ±12% in the value of k_{asp} (an activation energy of 33 kcalorie mol⁻¹ was used in this calculation[10]). The broken lines in Fig. 1 represent the estimated k_{asp} values at 37.6 °C and at 36.2 °C. It can be seen that changes in the rate constant produce greater deviations among older tooth samples than among younger ones. Two standard deviations (±2σ) of the experimental k_{asp} for dentine fall within the range of the k_{asp} values calculated for a ±0.7 °C difference in body temperature. Thus, the 2–3 times increase in the standard deviation among dentine and enamel samples greater than 50 yr old could be due to differences in body temperature among the individuals.

The racemisation ageing method can now be used to test claims of unusual longevity among the populations of Georgia in the USSR, Hunza, and Vilcabamba, Ecuador. Given a tooth suitable for analysis, an age estimate will fall within ±10% of the individual's actual age (approximately ±2σ of the dentine distribution), and body temperature information will further reduce the error. We would appreciate the cooperation of gerontologists and dentists in obtaining tooth samples from these or other very old people.

We are grateful for the cooperation of Drs J. F. Jones, James E. Murphy, William N. Smith and Roy Galen Slack. This work was supported by a grant from the National Science Foundation. P.M.H. is a National Institutes of Health Predoctoral Trainee and J.L.B. is an Alfred P. Sloan fellow.

PATRICIA MASTERS HELFMAN

Department of Biology,
University of California, San Diego

JEFFREY L BADA

Scripps Institution of Oceanography and
Institute of Marine Resources,
University of California, San Diego,
La Jolla, California 92093

Received March 22, accepted May 25, 1976.

[1] Bada, J L., and Helfman, P M., *World Archaeol*, 7, 160–173 (1975).
[2] Schroeder, R A, and Bada, J L, *Science*, 182, 479–482 (1973).
[3] Helfman, P. M, and Bada, J L, *Proc natn. Acad Sci. U.S A*, 72, 2891–2894 (1975).
[4] Blackburn, S., and Lee, G R., *Biochem J*, 58, 227–231 (1954)
[5] Bada, J. L, and Protsch, R., *Proc natn Acad. Sci U.S A*, 70, 1331–1334 (1973).
[6] Philippas, G. G., and Applebaum, E, *J. dent Res*, 45, 778–789 (1966)
[7] Butler, W. T, in *The Comparative Molecular Biology of Extracellular Matrices* (edit. by Slavkin, H.C.), 255-260 (Academic, New York, 1972).
[8] Weatherell, J A., and Robinson, C, in *Biological Mineralization* (edit. by Zipkin, I.), 43–74 (Wiley, New York, 1973).
[9] Spector, W. S. (ed.), *Handbook of Biological Data*, 343 (Saunders, Philadelphia, 1956).
[10] Bada, J. L, Kvenvolden, K A, and Peterson, E, *Nature*, 245, 308–310 (1973).

Sun and shade differences in productivity of reef corals

REEF CORALS are mutualistic symbiotic associations between cnidarians and dinoflagellates. The algae photosynthesise and translocate photosynthate to the animal partner, although the animal is capable of heterotrophic nutrition[1–5]. Some reef corals have wide bathymetric ranges[6,7] and the growth and survival of individuals in the deeper regions of the euphotic zone could result from an increase in the energy efficiency of the symbiotic complex. A number of reports document the laboratory-determined photosynthesis–radiation responses of corals[8–12] and zooxanthellae[13], but because the details of the habitat or depth from which the animals were collected are rarely described, comparisons among results in the literature are difficult. Here we provide evidence for the existence of 'sun' (heliophytic) and 'shade' (sciophytic) differences in the net photosynthesis–radiant flux intensity response of individuals of one coral species from 10 and 25 m depth on the same reef in an atoll lagoon.

Individuals of the foliaceous coral *Pavona praetorta* Dana were collected underwater at the Marine Pier Pinnacle Reef 300 m west of Enewetak Island (site Fred), Enewetak Atoll, Marshall Islands. Immediately after collection, the specimens were placed at the same depth in 1.5-l Perspex containers in which net rates of photosynthesis were determined (Fig. 1). Oxygen production per unit chlorophyll *a* was measured for 5-min intervals as a function of radiant flux intensity, and the data were fitted to the Michaelis–Menten equation by an iterative maximum likelihood solution method, which improves on an initial Lineweaver–Burk estimate[14,15].

The best fit Michaelis–Menten curves for the *Pavona* specimens are plotted in Fig. 1 with 99% confidence limits (one-tailed Student's t test, $n-2$ d.f.) for P_{max} (maximum photosynthetic rate) and K_m (radiant flux intensity at half saturation). By analogy to enzyme kinetics, K_m is a measure of the affinity of the photosynthetic system for radiant energy. The lack of overlap of the confidence limits indicates that the K_m for the 25-m specimens are lower than the value for the 10-m specimen (Table 1). Therefore, relative to their maximum photosynthetic rates, the deep water individuals saturate their photosynthetic machinery at lower radiation intensities than the shallow water individual. This is analogous to the 'sun' and 'shade' differences documented for canopy and understory plants[16] and for phytoplankton acclimatised to high and low light intensities[17,18]. The saturation of deep water individuals at lower radiation intensities is consistent with Margalef's[19] observation of greater A_{450} of pigments from deep water corals compared with conspecifics from shallow water. The measured difference in photosynthetic response is not likely to be due to spectral quality changes in the light between 10 and 25 m, because the 640–670-nm light which affects the red action spectrum peak of photosynthesis[13] amounts to only 2% of the total light flux at 18 m and 0.03% at 25 m (ref. 20), a difference below the resolution range of our *in situ* light meter circuit. We found no difference in temperature between study sites, and von Arx[21] has estimated that atoll lagoons have complete water overturn every 150 h, indicating that temperature stratification is unlikely. Therefore we believe that the differences in photosynthetic response between the two study sites are not temperature related.

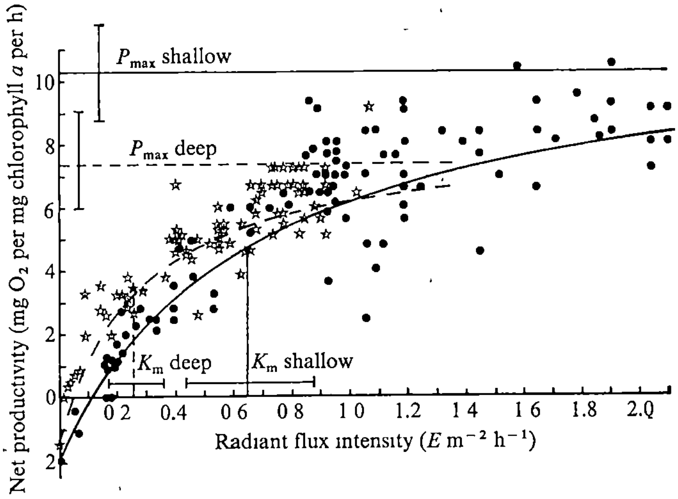

Fig. 1 · Photosynthesis–radiation intensity relationships for *Pavona* from 10 m (●) and 25 m (open star). E, einstein (= 6.02×10^{23} quanta). Ideal curves, maximum photosynthetic rates (P_{max}), radiant flux intensities at half saturation (K_m), and their 99% confidence limits are from maximum-likelihood regression analysis[14,15]. 25-m data are from one of the two replicates. Values at zero radiant flux are means: shallow specimen $x = -1.84$, s.d. = 0.29, $N = 71$; deep specimen $x = -1.41$, s d. = 0.27, $N = 117$ Experiments were run for 26 h *in situ* in Perspex chambers which were stirred continuously and flushed with ambient water at 35-min intervals The instrument design was modified from that of McCloskey[22]. Oxygen concentrations in the chambers were monitored with silver–platinum electrodes[23] and photosynthetically active radiation (400–700 nm) at the depth of the respirometers was measured with a quantum sensor (Lambda Instruments). These values were recorded continuously on strip chart recorders (Esterline Angus Minigraph). The electrodes were calibrated in air-saturated seawater and a yeast suspension in dilute sucrose solution, according to the tables of Green and Carritt[24], and checked with an independently calibrated commercial oxygen meter (Yellow Springs Model 57). The *in situ* light sensor was calibrated with a factory-calibrated quantum radiometer (Lambda Instruments). After termination of the experiments, the corals were frozen. Chlorophyll was extracted in 90% acetone (20 h, dark, 5 °C) Extinctions were measured in 10-mm cells (Beckman Model DU Spectrophotometer), and total chlorophyll *a* was estimated by the trichromatic equations of Richards[25].

Franzisket's[11] data from specimens collected at 3 m indicate K_m values higher than our 25-m specimens and within the range of our 10-m samples, corroborating our interpretation that 'sun' and 'shade' differences exist in the photosynthetic response of corals from high and low light regimes (Table 1). Evidence in support of the phenomenon comes from our *in situ* data for *Plerogyra*, *Porites* and *Acropora* from the Philippines and from Barnes and Taylor's[12] *in vitro* data on *Montastrea annularis* from the Caribbean (Table 1). The 18-m depth specimens have K_m values in the range of our 25-m *Pavona*, the *Montastrea* from 15-m is intermediate between our 25-m and 10-m *Pavona*, and the *Acropora* from 3 m exhibits a K_m in the range of Franzisket's[11] 3-m specimens and our 10-m *Pavona*. The overlap in K_m among the different coral species

Table 1 Half-saturation constants for photosynthesis as fit to the Michaelis–Menten* equation

Species	Depth (m)	K_m (E m^{-2} h^{-1}), Maximum likelihood estimate	One-tailed confidence limits Lower ($P < 0.01$)	Upper
P. praetorta Dana	25	0.26	0.18	0.37
P. praetorta Dana	25	0.14	0.00	0.38
P. praetorta Dana	10	0.63	0.43	0.88
Plerogyra sinuosa Dana	18	0.18	0.10	0.26
Porites lutea Milne Edwards and Haime	18	0.11	0.07	0.15
Acropora cf. *arbuscula* Dana	3	1.23	0.76	1.99
Kaneohe Bay corals, Hawaii† (ref. 11)	3	0.65	0.46	0.86
Montastrea annularis Ellis and Solander[12]	15	0.41	0.21	0.67

Each line represents a 24-h incubation of a single coral.

*Michaelis–Menten equation: $P = (P_{\max} \times I)/(K_m + I)$ or $P_{\text{relative}} = P_{\text{observed}}/P_{\max} = I/(K_m + I)$

†Pooled data from four species: (*Fungia scutaria* Lamarck, *Montipora verrucosa* Lamarck, *Porites compressa* Dana and *Pocillopora meandrina* Verrill); regressions run separately were not significantly different ($P > 0.05$).

suggests that, given a particular light regime, the algal photosynthetic efficiency relative to the maximum photosynthetic rate is independent of the coral species that the algae inhabit. In addition, Kawaguti[8] found the compensation light intensity was related to habitat: individuals from deeper or shaded places showed lower values.

The existence of acclimation to ambient light regime in corals suggests that extrapolation from measurements on individuals at one depth to the behaviour of the population over the whole depth range is not valid. Similarly, the efficiency of translocation of photosynthate from alga to animal partner may vary with depth. *In situ* 24-h measurements on individuals from a range of depths and species are needed to begin to resolve the question of the trophic plasticity of corals as a function of habitat.

D.S.W. is supported by a USNSF Graduate Fellowship. The work at Enewetak was supported by a USERDA grant through the University of Hawaii—Mid-Pacific Marine Laboratory Program to J.W.P. Philippine support came from a USNSF grant through the Scripps Institution of Oceanography RV Alpha Helix Program to J.W.P. R. Trench and K. Porter provided field assistance, and with C. Richardson, D. Titman, D. Heisey, C. S. Yocum, and S. Ohlhorst, aided in discussion of the project. R. Tyler, R. Reed, J. Mite, L. McCloskey, L. Somers and P. Blackburn aided in the design and testing of the instruments.

DAVID S. WETHEY

Division of Biological Sciences,

JAMES W. PORTER

School of Natural Resources,
The University of Michigan,
Ann Arbor, Michigan 48109

Received March 22, accepted May 18, 1976

[1] Muscatine, L., and Cernichiari, E., *Biol. Bull.*, **137**, 506–523 (1969).
[2] Smith, D. C., Muscatine, L., and Lewis, D., *Biol. Rev.*, **44**, 17–90 (1969).
[3] Trench, R. K., *Proc. R. Soc.*, **B177**, 225–235 (1971), *Helgol. wiss. Meeresunters.*, **26**, 174–216 (1974).
[4] Yonge, C. M., *Gt Bar. Reef Exped. 1928–29 Sci. Rep.*, **1**, 15–57 (1931)
[5] Porter, J. W., *Proc. second Int. Symp. Coral Reefs*, **1**, 111–125 (1974)
[6] Wells, J. W., *US Geol. Surv. Prof. Pap.*, **260**, 385–486 (1954).
[7] Goreau, T. F., and Wells, J. W., *Bull. Mar. Sci.*, **17**, 442–453 (1967)
[8] Kawaguti, S., *Palao. Trop. Biol. Sta. Stud.*, **1**, 187–198 (1937).
[9] Kanwisher, J. W., and Wainrwight, S. A., *Biol. Bull.*, **133**, 378–390 (1966).
[10] Roffman, B., *Comp. Biochem. Physiol.*, **27**, 405–418 (1968)
[11] Franzisket, L., *Forma et Functio*, **1**, 153–158 (1969).
[12] Barnes, D. J., and Taylor, D. L., *Helgol. wiss. Meeresunters.*, **24**, 284–291 (1973).
[13] Halldal, P., *Biol. Bull.*, **134**, 411–424 (1968).
[14] Bliss, C. I., and James, A. T., *Biometrics*, **22**, 573–602 (1966)
[15] Hanson, K. R., Ling, R., and Havir, E., *Biochem. biophys. Res. Commun.*, **29**, 194–197 (1967)
[16] Boysen Jensen, P., *Die Stoffproduktion der Pflanzen* (Fischer, Jena, 1932)
[17] Steeman Nielsen, E., and Jørgensen, E. J., *Physiol. Plant.*, **21**, 401–413 (1968).
[18] Steeman Nielsen, E., *Marine Photosynthesis* (Elsevier,Amsterdam, 1973).
[19] Margalef, R., *Invest. Pesq.*, **15**, 81–101 (1959).
[20] Jerlov, N. G., *Marine Ecology*, **1**(1), (edit. by Kinne, O.), 95–102 (Wiley-Interscience, New York, 1970)
[21] von Arx, W. S., *US Geol. Surv. Prof. Pap.*, **260**, 265–273 (1954).
[22] McCloskey, L. R., Kanwisher, J. W., and Lawton, K. D., *Abstr. third Int. Symp. Coelenterate Biol.* (in the press)
[23] Kanwisher, J. W., Lawton, K. D., and McCloskey, L. R., *Limnol. Oceanogr.*, **19**, 700–704 (1974).
[24] Green, E. G., and Carritt, D. E., *J. Mar. Res.*, **25**, 140–147 (1967).
[25] Strickland, J. D. H., and Parsons, T. R., *Bull. Fish. Res. Bd Can.*, **167**, 1–310 (1972).

Frost sensitivity of *Zea mays* increased by application of *Pseudomonas syringae*

DRIED, powdered corn leaves (*Zea mays* L.) dusted on to the leaves of corn seedlings, will increase frost damage to treated seedlings relative to untreated controls at ~ −4 °C (refs 1, 2). In a preliminary attempt to isolate the entity responsible for this activity, we found that water extracts of corn leaf powder from healthy field-grown plants caused as much increase in frost sensitivity when applied as a spray to seedling corn, as did application of the powder itself when tested as described below. Addition of either streptomycin or tetracycline (1,000 p.p.m.) to these water extracts eliminated their activity, suggesting the possible role of bacteria in this effect.

Corn seedlings for frost sensitivity measurements were grown in sterilised vermiculite in a plant growth chamber (day· 18 h, 30 °C; night· 6 h, 20 °C) to the 3-leaf stage. Plants were watered daily with nutrient solution. Ten or more pots (6 plants per 10-cm pot) were used for each treatment. Unless otherwise noted, treatment was given 24 h before freezing and the plants were held in a mist chamber until 20 min before freezing. Immediately before freezing, all pots were positioned randomly in a controlled temperature chamber at ~ 0 °C. The air temperature was lowered at ~ 0.1 °C min^{-1} to −3.0 °C and then at ~ 0.04 °C min^{-1} to −3.5—−4.0 °C. Maximal differences in frost damage between treated and untreated plants occurred in this temperature range. The air temperature in the chamber was then increased at ~ 1.0 °C min^{-1} to 30 °C. Frost damage was assessed by counting the number of leaves per plant with symptoms of frost injury.

Forty-two bacterial isolates of varying colony colour and morphology were obtained by dilution plating from water extracts of corn leaf powder. Each isolate was grown on nutrient agar, suspended in 0.1 M phosphate buffer, *p*H 7.0, sprayed on to corn seedlings and assayed for the ability to increase frost sensitivity of corn at −3.5 to −4.0 °C. Only one of the 42 isolates was active in increasing the frost sensitivity of corn seedlings. When leaves of corn seedlings were sprayed with suspensions of this isolate in buffer 24 h before freezing > 95% of the leaves were damaged at −3.5 to −4.0 °C, whereas < 8% of the leaves of plants sprayed with buffer alone were damaged at this temperature On the basis of its response to standard physiological tests[3,4], this isolate was identified as *Pseudomonas syringae* van Hall, a species that includes strains pathogenic to a large number of diverse host plants including corn[5]. We have not observed pathological symptoms even when corn plants were held without freezing for up to 10 d after inoculation.

For ~ 8 h after application of the bacteria, the frost sensitivity of corn plants did not increase. It increased steadily from ~ 8 h until ~ 24 h (Fig. 1), after which little change occurred for at least 5 d. The amount of frost damage observed in seedling corn plants increased with increased *P. syringae* populations applied[6]. At each time interval shown in Fig. 1, more leaves sprayed with 4×10^6 cells ml^{-1} were damaged than those sprayed with 4×10^5 cells ml^{-1}. As indicated in Fig. 2, suspensions as dilute as 1.5×10^4 cells ml^{-1} caused significant increases in frost sensitivity (75% damage for plants held under mist for 24 h before freezing). Application of higher *P. syringae* populations (~ 10^7 cells ml^{-1} with wet leaves or 10^8 cells ml^{-1} with dry leaves) resulted in frost damage to nearly all leaves; untreated control plants showed damage to fewer than one leaf in 12. Plants held in a mist chamber for 24 h between application of cells and freezing, sustained greater frost damage at all applied cell densities than plants left dry during this period. The increase in frost sensitivity both with moisture and with time suggest that either growth of the bacteria or movement to some favourable site(s) on or in the leaves, or both, are important in enhancing frost sensitivity.

Sixty-four of the 67 tested isolates of *P. syringae* increased the frost sensitivity of corn seedlings. Three of five isolates of the closely related species, *P. coronafaciens*[7] also were active, whereas one isolate each of *P. tabaci, P. glycinea, P. phaseolicola, P. marginalis,* four isolates of *Erwinia stewartii* and one of *Escherichia coli* were not active.

Even plants very sensitive to frost can withstand temperatures slightly below 0 °C (refs 8–11) because of the supercooling of intracellular water. Frost damage to such plants in the field has been reported to occur at ~ −2–−5 °C, presumably by explosive crystallisation of supercooled intracellular water[8]. Similarly, almost all our growth chamber-grown plants with *P. syringae* on their leaves were killed at −4 °C (Fig. 2). Plants lacking leaf surface populations of *P. syringae*, however, were not substantially damaged until the temperature reached was ~ −8.0 °C (Fig. 3). Thus, our *P. syringae*-treated plants seem to be almost equal in frost sensitivity to plants in the field. It is our growth charmber-grown controls, lacking leaf populations of *P. syringae*, that differ substantially from field-grown plants with regard to frost sensitivity.

Although the importance of ice nuclei in initiating ice crystallisation, and thus frost damage, has been recognised[11], the nature and source of these ice nuclei remain unknown. Maki *et al.*[12] have reported that *P. syringae* is active as an ice nucleus at temperatures as warm as −2 to −3 °C. We have found that all 64 isolates of *P. syringae* and all 3 of *P. coronafaciens* which increased frost sensitivity of corn were also active in ice nucleation at −5 °C or above as measured by a modification of the procedure of Vali[13]. All isolates which did not increase the frost sensitivity of corn (including the 41 inactive isolates from water extracts of corn leaf powder) were not active in ice nucleation at

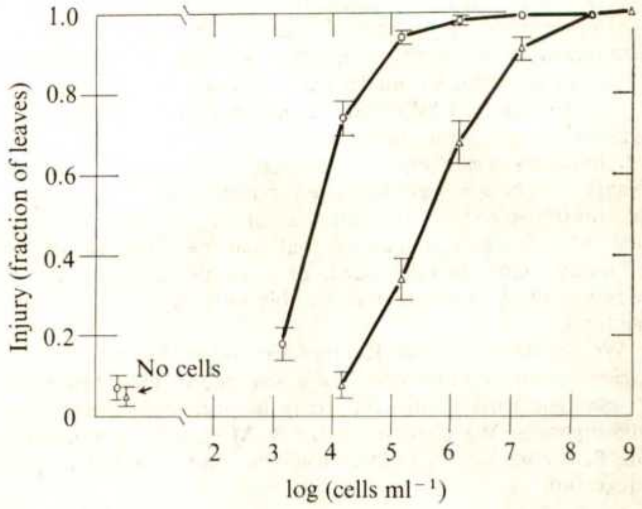

Fig. 2 Effect of applied *P. syringae* populations on frost injury to corn seedlings. Three-leaf-stage corn seedlings were sprayed with cell suspensions in 0.1 M phosphate buffer *p*H 7.0 (0.5 ml per plant) and held in a dark mist chamber at 24 °C (○) or left dry in the dark at 24 °C (△) for 24 h before freezing. The vertical bars represent the s.e.m.

Fig. 1 Effect of the duration of the time between application of *P. syringae* and freezing on frost injury. Three-leaf-stage corn seedlings were sprayed with cell suspensions of 4×10^5(△) or 4×10^6 (○) cells ml^{-1} in 0.1 M phosphate buffer *p*H 7.0 (0.5 ml per plant) and incubated in a mist chamber for the times shown on the abscissa before freezing. The vertical bars represent the s.e.m.

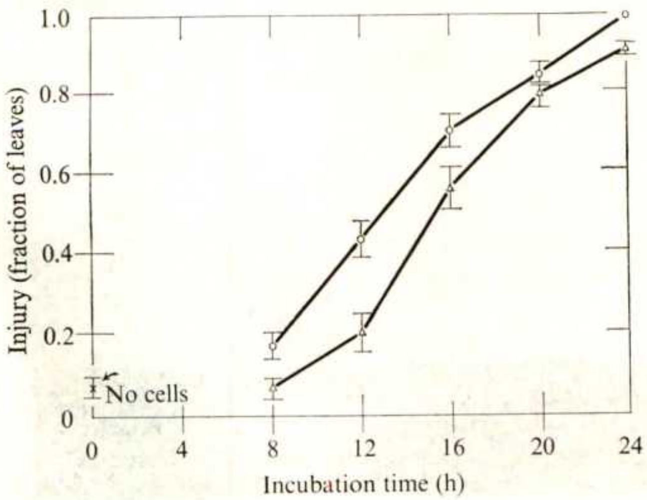

Fig. 3 Frost sensitivity of corn seedlings lacking leaf surface populations of *P. syringae*. Three-leaf-stage corn seedlings were placed in a controlled environmental chamber at 0 °C and were cooled at the rate of ~0.05 °C min^{-1}. Groups of plants were removed from the chamber at temperatures shown on the abscissa and placed in a growth chamber at 30 °C. The vertical bars represent the s.e.m.

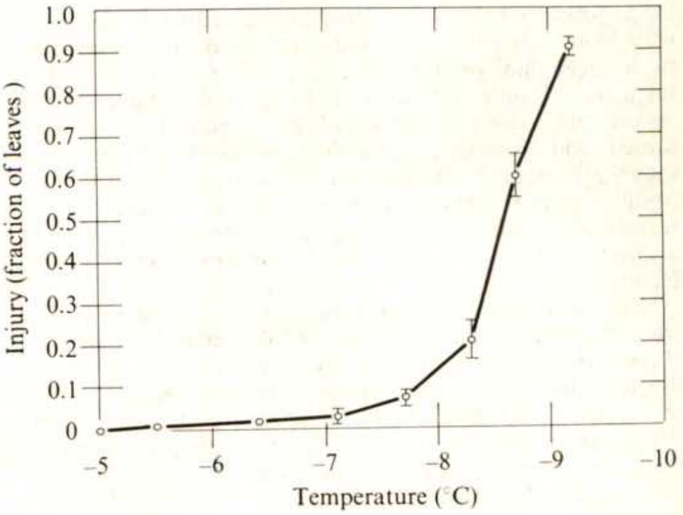

−5 °C. Thus, the decreased frost sensitivity of our untreated control plants may be caused by supercooling to temperatures below those that are possible in the presence of active bacterial ice nuclei (for example, *P. syringae*).

The part played by epiphytic bacteria in promoting frost sensitivity has not been recognised previously. Large epiphytic bacterial populations exist on the leaves of most plants[14–19]. *P. syringae* has been reported as a component of these epiphytic populations on host and non-host plants[16,17,19]. Thus, it may be that 'natural' frost sensitivity of many plants is influenced, or even determined, by the presence of *P. syringae* and possibly certain other epiphytic bacteria.

We thank Dr Arthur Kelman for use of his extensive *P. syringae* culture collection, for assistance in identifying our *P. syringae* isolate, and for many helpful ideas during this investigation. We also thank Dr B. M. Lund for providing the *P. coronafaciens* isolates used here and for her helpful suggestions.

D. C. ARNY

1630 Linden Drive,
Madison, Wisconsin 53706

S. E. LINDOW
C. D. UPPER

Plant Disease Research Unit,
Madison, Wisconsin 53706
Department of Plant Pathology,
University of Wisconsin,
Madison, Wisconsin 53706

Received February 23; accepted May 18, 1976.

[1] Hoppe, P. E., Arny, D. C., and Martens, J. W., *Pl. Dis. Reptr.*, **48**, 815–816 (1964).
[2] Upper, C. D., Arny, D. C., and Vojtik, F. C., *Phytopathology*, **62**, 794 (1972).
[3] Lelliott, R. A., Billings, F., and Hayward, A. C., *J. appl. Bact.*, **29**, 470–489 (1966).
[4] Klement, Z., *Nature*, **199**, 299–300 (1963).
[5] Kendrick, J. B., *Iowa Agric. exp. Sta. Bull.*, **100**, 303–334 (1926).
[6] Lindow, S., Arny, D. C., and Upper, C. D., *Am. Phytopath. Soc. Proc.*, **2**, 57 (1975).
[7] Dye, D. W., *Rev. Pl. Path.*, **53**, 953–962 (1974).
[8] Olien, C., *A. Rev. Pl. Physiol.*, **18**, 387–408 (1967).
[9] Shaw, R. H., *Pl. Physiol.*, **29**, 102–104 (1954).
[10] Suneson, C. A., *J. Am. Soc. Agron.*, **33**, 829–834 (1941).
[11] Chandler, W. H., *Proc. Am. Soc. hort. Sci.*, **64**, 552–572 (1954).
[12] Maki, L. R., Galyon, E. L., Chang-Chien, M., and Caldwell, D. R., *Appl. Microbiol.*, **28**, 456–459 (1974).
[13] Vali, G., *J. atmos. Sci.*, **28**, 402–409 (1971).
[14] Crosse, J. E., *Ann. appl. Biol.*, **47**, 306–317 (1959).
[15] Crosse, J. E., *Ann. appl. Biol.*, **52**, 97–104 (1963).
[16] Ercolani, G. L., Hagedorn, D. J., Kelman, A., and Rand, R. E., *Phytopathology*, **64**, 1330–1339 (1974).
[17] Leben, C., *A. Rev. Phytopath.*, **3**, 209–230 (1965).
[18] Leben, C., and Miller, T. D., *Phytopathology*, **63**, 1464–1467 (1973).
[19] Leben, C., Schroth, M. N., and Hildebrand, D. C., *Phytopathology*, **60**, 677–680 (1970).

Fog basking by the Namib Desert beetle, *Onymacris unguicularis*

THE Namib Desert along the south-western coast of Africa supports a sand dune fauna without counterpart elsewhere in the world[1]. The trophic base of the arthropod fauna is wind-blown detritus[2]. Aperiodic advective fog collection from vegetation[3] or detritus[4] is a possible source of water for diverse Namib animals. For the specialised fauna living in vegetation-less dunes, fog collection from detritus[4], disturbed sand projections[5], directly from humid air[6], or from water precipitated on the body[4,7], seem to be the only possible water uptake methods. Water uptake from saturated or subsaturated air, demonstrated for a few arthropod species[6], is not a physiological capability of Namib tenebrionids already investigated[4,6,7].

Here we report field observations of direct water uptake from fog precipitated on the body of the tenebrionid beetle, *Onymacris unguicularis*. In early October 1975 we established a study area on sand dunes south of the Kuiseb River at Gobabeb (23°34′S, 15°03′E, elevation 408 m), South West Africa, and continued observations through January 1976. On a series of small linear dunes all *O. unguicularis* were collected and marked with small (diameter 2.5 mm) numbered disks glued to the thorax. The study area, including 5 km of dune ridges, was traversed every afternoon, during the peak activity period of these beetles. We took all beetles collected to the laboratory, weighed them, and returned them to their dunes within 2 h of capture. The beetles either burrowed into dune slipfaces when returned or remained active, feeding on detritus for an hour or more before retiring to subsurface sands. Collections were repeated daily and numbering continued until over 90% of all beetles collected were numbered individuals. Recollection of marked individuals was facilitated in this environment because, in spite of the large spatial dimension of the study area there is no vegetation and these large (13–22 mm) black beetles stand out against the reddish sand substrate.

Ordinarily *O. unguicularis* are diurnal, preferring the warm part of day, and remaining buried in the sand of dune slipfaces overnight. But during nocturnal fogs they emerge and climb the slipface to the crest. There they take a characteristic head-down stance (Fig. 1), facing into the fog-laden wind. Dune slipfaces oriented into the wind also intercept fog. Beetles emerging there adopt the typical head-standing posture where they emerge.

As water collects on these beetles it trickles down the body to the mouth. Actual uptake of water was established by collecting beetles at the end of the head-standing performance, when they burrowed into subsurface sands. They were then taken to the laboratory and allowed to dry for 2 h. All adhering sand grains were removed with a brush and the beetles were weighed. Fog water uptake ranged from an

Fig. 1 *a*, Windward view of *Onymacris unguicularis* in a typical fog-collecting stance. *b*, Another individual at the usual fog-collecting site, the crest of a sand dune. Note the water collected under the head, which is being drunk.

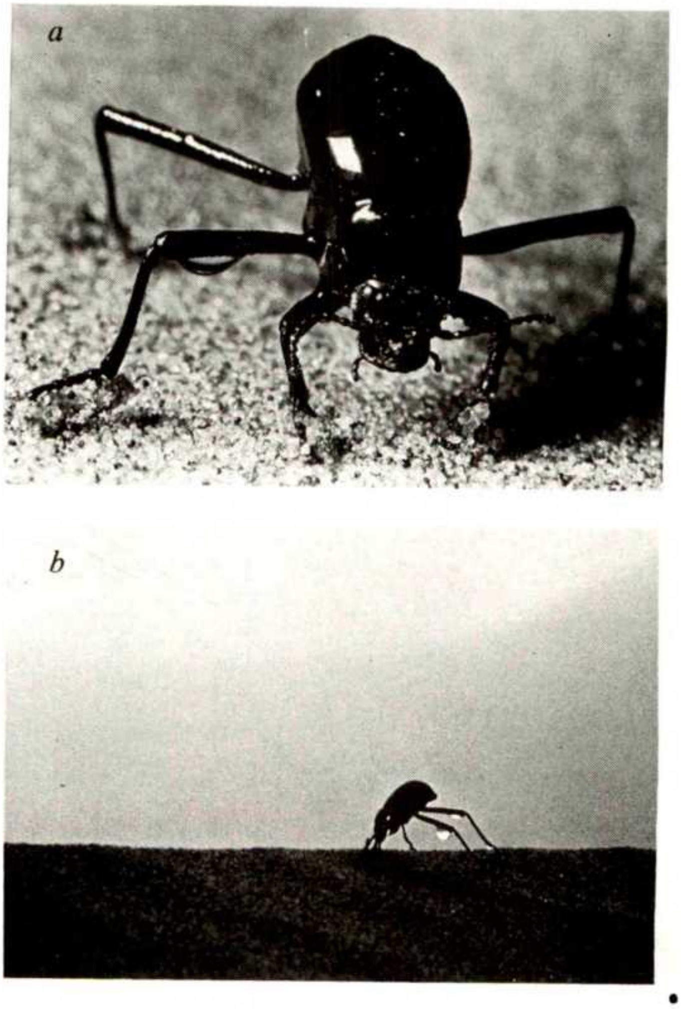

Table 1 Fog water gain expressed as percentage weight change of total body weight following fogs of various strengths on the Namib Desert

Date	Fog (mm)	Weight change (%) Mean	Corrected mean	Minimum	Maximum	*N*
October 14, 1975	0.50	+13.36	+14.50	+3.57	+34.01	24
November 5, 1975	0.35	+ 0.49	+ 1.63	−1.99	+10.48	32
November 25, 1975	0.10	+ 4.33	+ 5.47	−5.76	+16.31	52
November 29, 1975	0.65	+ 7.25	+ 8.39	−2.19	+20.79	33
December 1, 1975	0.10	+ 0.97	+ 2.11	−2.46	+ 4.91	16

The correction factor of 1.14% determined to be the mean overnight weight loss without fog has been added to the mean to provide a corrected mean weight change during fog more closely approximating the actual uptake of fog water but is not applied to the maximum and minimum weight changes.

average of 12% to no gain for various fogs (Table 1). The maximum weight gain by an individual in a single fog was 34% of total body weight before the fog. These values are for beetles captured and weighed the evening before a fog, and recaptured the morning immediately following the fog.

To determine the weight changes from evening weighing to morning weighing in the absence of an intervening fog, a control sample of beetles was weighed, marked and placed on a dune in the evening, then recaptured the following fog-less morning. Of 48 such recaptures all but three individuals lost weight ($\bar{x}$ change −1.14%, range −3.00% to +0.72%). Thus any mean weight increase by a population of beetles overnight during a fog can be assigned to uptake of fog water.

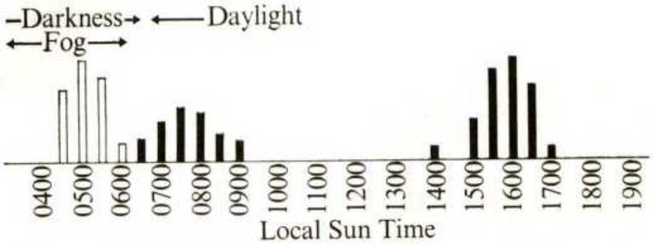

Fig. 2 The timing of activity by *O. unguicularis* on November 12, 1975. The open colums represent individuals holding the fog-collecting posture. The dark colums are individuals actively engaged in other activities. The maximum number of active individuals at any time was 45 on this date.

Fog basking by *O. unguicularis* occurs at times when they are not ordinarily active (Fig. 2). They may emerge any time during the night that wet fogs occur. Their usual foraging periods occur during the morning and late afternoon, coinciding in the afternoon with the strongest winds which transport the detritus on which they feed.

Onymacris unguicularis is active throughout the year and thus encounters variable intervals between fogs. Fogs as light as 0.1 mm on the Gobabeb fog screen elicited fog basking.

Another group of Namib dune tenebrionid beetles, genus *Lepidochora*, living near Gobabeb build ridges in the sand to catch water[5] and we have observed spiders, lepismids and other tenebrionids active on foggy mornings. Direct collection of fog water seems to be important in the water economy of some Namib Desert animals, and to involve in certain cases highly developed methods.

We thank Drs E. B. Edney and M. D. Robinson for valuable comments. This study was supported by the CSIR and Transvaal Museum (M.K.S.) and the National Science Foundation (W.J.H.). The permission to conduct this study from the Nature Conservation Department, South West Africa, is gratefully acknowledged.

William J. Hamilton, III

Institute of Ecology,
University of California,
Davis, California 95616

Mary K. Seely

Desert Ecological Research Unit,
PO Box 953,
Walvis Bay, 9190,
South West Africa

Recieved April 21; accepted May 11, 1976.

[1] Koch, C., *J. South West Afr. Sci. Soc.*, **15**, 8–32, 76–92 (1961); *Ann. Trans. Mus.*, **24**, 61–106 (1962).
[2] Brinck, P., *Hamstrom Zool. Pap., Lund*, 120–137 (1956).
[3] Louw, G. N., and Holm, E., *Madoqua II*, **1**, 67–85 (1972).
[4] Louw, G. N., *Symp. zool. Soc. Lond.*, **31**, 297–314 (1972).
[5] Seely, M. K., and Hamilton, W. J., III, *Science* (in the press).
[6] Edney, E. B., *Physiol. Zool.*, **44**, 61–76 (1971).
[7] Louw, G. N., and Hamilton, W. J., III, *Madoqua II*, **1**, 87–95 (1972).

Nucleating agents in the haemolymph of insects tolerant to freezing

MANY insects that survive the winter in cold, exposed habitats in arctic or temperate regions are sensitive to freezing. These insects usually have supercooling points below −15 °C, and their capacity for supercooling has been shown to increase considerably with increasing concentrations of glycerol in their body fluid[1]. On the other hand, adult insects that are tolerant to freezing ('freeze tolerant') seem to freeze invariably at high subzero temperatures (from −6 to −10 °C), without regard to the concentration of glycerol and other polyols in their body fluid[2–4]. We report here that haemolymph from freeze-tolerant adult beetles contains a substance, which induces freezing in the haemolymph at about −6.5 °C. Haemolymph from freeze-sensitive species seems to lack this substance. Such substances probably constitute the physical basis of the remarkably high supercooling points of freeze-tolerant adult insects.

During the winter of 1975 we found that several species of tenebrionid beetle, inhabiting the mountain areas of southern California, were tolerant to freezing. These beetles had supercooling points from −5.5 to − 7.0 °C, whereas freeze-sensitive beetles froze at temperatures from −12 to −20 °C. Preliminary experiments showed that 5-μl samples of isolated haemolymph from freeze-tolerant (*Eleodes blanchardi* Blaisd.) and freeze-sensitive (*Iphthimus laevissimus* Csy.) tenebrionids froze within the same temperature range as did the respective intact beetles. Mixtures of haemolymph from the two species, however, also froze within the range of the intact freeze-tolerant beetles, even when the haemolymph of this species constituted as little as 5% of the volume of the mixture. These observations indicate that haemolymph from freeze-tolerant *E. blanchardi* contains nucleating agents, which induce freezing at a few degrees below zero, and which probably cause the low supercooling capacity of these beetles. Similar nucleating agents might be the cause of the high supercooling points reported for other freeze-tolerant beetles.

If freezing at high subzero temperatures is physiologically important to freeze-tolerant insects, they would be expected to contain nucleating agents, except in cases where freezing, as described by Salt[5], is initiated by inoculation. To investigate the distribution of nucleating agents, we took

Table 1 Supercooling points of intact beetles and of samples of 0.9% solution of NaCl containing haemolymph from beetles of the same species

Species	Locality and season of collection	Freeze tolerance	Supercooling points (°C) Intact beetles*	 0.9% NaCl+ haemolymph†
Eleodes blanchardi Blaisd.	M, W	+	− 6.3±0.6 (n = 8)	− 5.7±0.3 (n = 4, m = 12)
Eleodes blanchardi Blaisd.	M, S	—	− 9.3 (n = 1)	−15.3±3.1 (n = 2, m = 7)
Eleodes omissa LeC. ssp. *pygmaea* Blaisd.	C, S	?	—	−18.0±2.6 (n = 1, m = 4)
Coelocnemis magna LeC.	M, W	+	− 6.4 (n = 1)	− 6.3±0.6 (n = 1, m = 3)
Coelocnemis magna LeC.	M, S	—	− 6.8 (n = 1)	− 6.4±0.0 (n = 1, m = 4)
Coelocnemis magna LeC.	C, S	?	—	−18.6±1.7 (n = 1, m = 4)
Coelocnemis californicus Mann.	M, W	+	− 6.8±0.4 (n = 2)	− 5.9±0.2 (n = 1, m = 3)
Coelocnemis californicus Mann.	M, S	—	− 8.8±1.1 (n = 2)	−14.4±2.5 (n = 2, m = 8)
Iphthimus laevissimus Csy.	M, W	—	−15.9±1.7 (n = 3)	−17.1±2.8 (n = 2, m = 6)
Rhagium inquisitor L.	N, W	—	−17.0±2.1 (n = 5)	−18.2±5.4 (n = 1, m = 4)

Beetles of the genus *Coelocnemis* are classified according to Doyen[6].

M and C, beetles collected in the mountains and on the coast in southern California, respectively; N, beetles collected in Norway; S and W, beetles collected in summer and winter, respectively.

*Mean ± s.d. of n beetles.

†Mean ± s.d. of m parallel 5-μl samples of NaCl solution, containing about 5% of haemolymph obtained from n beetles. Samples of NaCl solution were kept inside thin glass capillaries, and the haemolymph was added by means of a microsyringe. Supercooling points were determined by cooling at a rate of 20 °C h^{-1}, while the temperature was measured by means of a copper–constantan thermocouple. Supercooling points were indicated by a sudden increase in temperature, due to the release of heat of fusion of water.

samples of haemolymph from several species of beetles representing different kinds of water survival, and examined their effect on the supercooling points of samples of 0.9% solution of NaCl. The survey included both freeze-tolerant and freeze-sensitive species, which were collected in the mountains of southern California and around Oslo. We also included beetles collected on the coast near San Diego, where they are probably never exposed to subzero temperatures. Beetles were collected in summer and winter and kept in the laboratory at +4 °C and +20 °C, respectively, for up to 1 month. They were fed on dry oak leaves and pieces of apple, but starved for 1–2 d before being used, to prevent possible nucleators in the gut contents from influencing the supercooling points of the intact beetles. To judge whether beetles were freeze tolerant or not, we cooled them at a rate of about 20 °C h^{-1} until they froze spontaneously. When the temperature of a freezing beetle had returned to its supercooling point, it was thawed slowly. To be classified as freeze tolerant, the beetles had to behave in an apparently normal way during the following 2 d, while kept at room temperature. The beetles here classified as freeze sensitive all looked dead after thawing, and they did not recover during the period of observation.

The results in Table 1 show that haemolymph from all freeze-tolerant beetles induced freezing in the NaCl solutions at temperatures of −5.4–−6.9 °C. During summer these beetles became sensitive to freezing, and at this time the freezing-inducing effect of their haemolymph was usually lost too. One exception was a freeze-sensitive *Coelocnemis magna* LeC.[6], which was collected in the mountains in the summer, and which had nucleating agents in its haemolymph. No other beetles had haemolymph which altered the supercooling points of NaCl solutions significantly, indicating that the haemolymph of these species lacked nucleating agents. The coastal species were not examined with respect to freeze tolerance, but they were presumably freeze sensitive. These results suggest that only freeze-tolerant species have nucleating agents in their haemolymph, and that these agents are usually present in winter only.

Table 1 shows that summer beetles of the freeze-tolerant species, which lacked nucleating agents in their haemolymph, had supercooling points 1–3 °C lower than beetles collected in winter. This indicates the presence of other, possibly intracellular, nucleating agents, the effect of which would be masked by the nucleating agents in the haemolymph during winter.

When freeze-tolerant *E. blanchardi* were kept at +20 °C for 2 weeks (not shown in Table 1), they became sensitive to freezing. The nucleating effect of their haemolymph, however, was still present, and the supercooling points of the intact beetles did not change, indicating that freezing at high subzero temperatures in itself does not make the beetles freeze tolerant. Furthermore, it reveals that in these

Fig. 1 Supercooling points of solutions of NaCl (○) and glycerol (△), solutions of NaCl (●) and glycerol (▲) containing 5% of haemolymph from freeze-tolerant *Eleodes blanchardi*, and solutions of NaCl (⊗) containing 5% of the same haemolymph previously heated to +100 °C for 5 min, all plotted as a function of the osmolality of the solutions. Each point is the mean of 4–12 parallel 5-μl samples, and the bars represent the standard deviation. The regression line of points representing solutions containing native haemolymph is indicated by the solid line, and the theoretical melting points are indicated by the dashed line. The osmolality is calculated from the concentration of solute according to data from the *Handbook of Chemistry and Physics*[8]. The change in osmolality caused by the addition of haemolymph to the solutions is small and has not been adjusted for in the calculations.

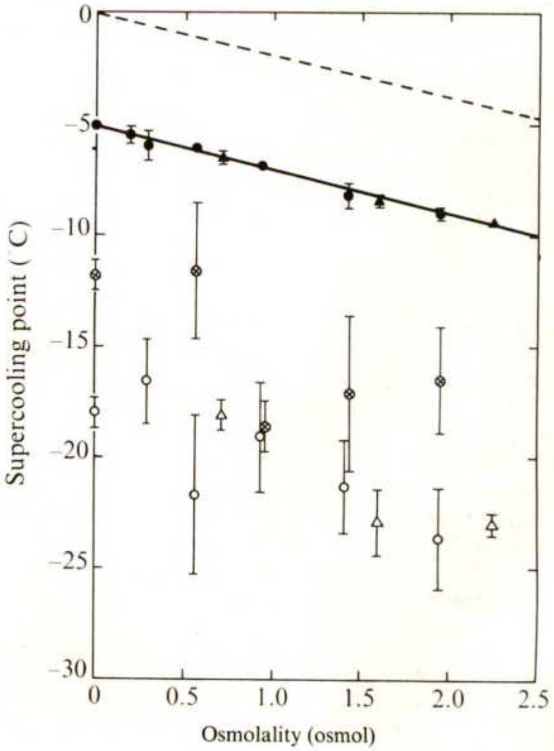

circumstances there is a time lag between the inactivation of the nucleating agents and that of other factors which cause freeze tolerance in the beetles. A similar time lag might explain the presence of nucleating agents in the haemolymph of the freeze-sensitive *C. magna* (Table 1).

To learn more about the properties of the ice nucleators in the haemolymph, we examined the effect of haemolymph from *E. blanchardi* on the supercooling points of solutions of NaCl and glycerol. Several concentrations of solutes were used, so that the osmolality varied from near 0 to about 2 osmol. Corresponding values of osmolality and supercooling points of both pure solutions and solutions containing haemolymph are shown in Fig. 1, which shows that haemolymph from *E. blanchardi* caused a considerable increase in the supercooling points of the solutions. The supercooling points of solutions containing haemolymph are linearly related to the osmolality, and the points representing NaCl and glycerol solutions lie on the same line, indicating that the effect of glycerol is due only to its osmotic activity. The calculated regression line for all points representing solutions containing haemolymph has the formula

$$y = -5.3 - 1.95x$$

The slope of this line (-1.95 °C per osmol) is approximately the same as the osmolal freezing point depression (-1.86 °C per osmol), which is indicated by the dashed line on Fig. 1. Thus the supercooling capacity of solutions containing haemolymph does not change significantly as the osmolality of the solution changes, indicating that the nucleating agents induce freezing at a certain degree of supercooling, regardless of the osmolality of the solutions. This degree of supercooling corresponds to the difference in ordinate values of the two lines, that is 5.3 °C. The dispersion of the points around the regression line is remarkably low, suggesting that when the solutions are supercooled by 5.3 °C, there is a large increase in the statistical probability that an ice nucleus will form.

By heating the haemolymph to +100 °C for 5 min before it was added to the solutions, the supercooling points were lowered markedly, indicating that the nucleating agents are temperature sensitive. Some nucleating effect was still present, however, since the new supercooling points were still above those of solutions without haemolymph.

Freeze tolerance in adult insects has been known only during the past few years, and little is known about the mechanisms involved. Data from different kinds of freeze-tolerant organisms, including beetles[2], indicate that ice formation is limited to the extracellular compartments, and that extracellular ice protects the organisms against intracellular freezing, which is believed to be injurious. According to this model, extracellular ice, which is considered to be unable to penetrate cell membranes, concentrates the extracellular solutes and causes an osmotic flux of water out of the cells. Thus, at sufficiently low freezing rates, allowing water to leave the cells as the freezing proceeds, the intracellular as well as the extracellular fluid would be kept at or near its melting point[7]. Consequently, the probability of an injurious intracellular freezing would become very small. The presence of nucleating agents in the haemolymph of freeze-tolerant beetles, ensuring extracellular freezing at high subzero temperatures, gives further support to this model.

K.E.Z. was supported by Thanks to Scandinavia, Inc., New York, and by the US Educational Foundation in Norway.

KARL ERIK ZACHARIASSEN*
HAROLD T. HAMMEL

Physiological Research Laboratory,
Scripps Institution of Oceanography,
University of California, San Diego,
California 92037

Received January 29; accepted May 19, 1976.

*Present address: Institute of Zoophysiology, University of Oslo, Blindern, Oslo, 3, Norway.

[1] Sømme, L., *Can. J. Zool.*, **42**, 87–101 (1964).
[2] Miller, L. K., *Science*, **166**, 105–106 (1969).
[3] Ohyama, Y., and Asahina, E., *J. Insect Physiol.*, **18**, 267–282 (1972).
[4] Miller, L. K., and Smith, J. S., *Nature*, **258**, 519–520 (1975).
[5] Salt, R. W., *Can. Ent.*, **95**, 1190–1202 (1963).
[6] Doyen, J. T., *Univ. Calif. Publ. Ent.*, **73**, 1–110 (1974).
[7] Mazur, P., *J. gen. Physiol.*, **47**, 347–369 (1963).
[8] Weast, R. C. (ed.), *Handbook of Chemistry and Physics*, fifty-third ed. (Chemical Rubber Co., Cleveland, 1972).

Induction of male recombination in *Drosophila melanogaster* by injection of extracts of flies showing male recombination

MORGAN[1,2] was the first to report that no spontaneous recombination occurs in males of *Drosophila melanogaster*. Since then recombination has been induced in *D.melanogaster* males by various treatments[3], for example, X rays. In an attempt to study the control of recombination in *D. melanogaster*, Reddi *et al.*[4] injected males with ovarian extracts and, surprisingly, induced recombination. Subsequent attempts to repeat this experiment failed[5,6]. It is known that some natural populations of *D. melanogaster* show spontaneous male recombination[7-10], and it has been suggested that this may be caused by episomes or viruses[8,9,11]. It is therefore possible that these male recombination-inducing factors could be transferred by injection, and that the failure to reproduce these results[4] might have been due to the use of strains lacking such factors. We have therefore tested whether or not male recombination could be induced by injecting extracts of flies from strains showing male recombination into flies lacking male recombination.

An extract of *OKI* flies, a strain from Oklahoma that shows male recombination[12], was prepared by homogenising together 10 each of newly emerged males and females in 4 ml of *Drosophila* Ringer solution, and centrifuging at 2,000 r.p.m. for 2 min. The supernatant was injected into virgin females which were homozygous for the recessive chromosome markers, *dp b cn bw; ve* (dumpy wings, 2–13.0, black body colour, 2–48.0, cinnabar eye colour, 2–57.5; brown eye colour, 2–104.5; veinlet wings, 3–0.2) until their abdomens were visibly distended. These females were mated individually to *Canton-S* (*CS*) males, a wild-type strain which when crossed to the marker strain gives F_1 males that produce no recombinants. The heterozygous male progeny were mated individually to *dp b cn bw; ve* females every 3–5 d for a total of four transfers. Their progeny were then scored for second chromosome male recombination. All presumptive recombinants were tested by backcrosses to *dp b cn bw; ve* flies. Control flies were injected with *CS* fly extract or *Drosophila* Ringer solution.

The results are summarised in Table 1. Male recombination occurred only in sons of females injected with *OKI* extract. The pattern of recombination along the second chromosome (Table 1) was similar to that found in *OKI/dp b cn bw* males[12], in that the events occurred mainly in the centromeric region (*b–cn*) and in the right arm (*cn–bw*). In addition, the distribution of recombination events does not fit a Poisson distribution (index of dispersion $x_{51}{}^2 = 163.5$, $P < 0.001$). Some of these induced recombination events therefore occurred as clusters, suggesting a premeiotic origin. A similar observation has been made with *OKI/dp b cn bw* flies (unpublished results of R. C. W. and J. N. Thompson). It should also be noted that the factor(s) causing male recombination could be transmitted over at least one generation.

In a second experiment 1–2-d-old *CS/dp b cn bw; CS/ve* males were injected with an *OKI* ovarian extract prepared by dissecting 100 fertilised *OKI* ovaries into 0.1 ml of a 0.4% saline solution, homogenising and centrifuging at 14,500 r.p.m. for 12 min. Control males were injected with a similarly prepared *CS* ovarian extract, or were left uninjected. After 1 or 2 d, injected

Table 1 Frequencies of male recombination induced by *OKI* extract

Experiment 1 (whole-fly homogenate) Treatment	Injection of *OKI* homogenate					Injection of *CS* homogenate					Injection of Ringer solution					
Injected ♀♀	*A*	*B*	*C*	*D*	*E*	*A*	*B*	*C*	*D*	*E*	*A*	*B*	*C*	*D*	*E*	*F*
No. of ♂♂ tested	5	9	5	16	17	15	15	15	15	2	15	12	15	10	9	9
No. of ♂♂ with recombination progeny	0	1	1	1	3	0	0	0	0	0	0	0	0	0	0	0
Mean ± s.d. of progeny size	328 ±87	347 ±77	355 ±175	275 ±66	249 ±56	191 ±63	209 ±56	208 ±56	196 ±61	240 ±29	193 ±54	221 ±54	212 ±67	229 ±40	197 ±31	214 ±44
No. of recombinations	0	4	2	5	6	0	0	0	0	0	0	0	0	0	0	0
Total no. of progeny	1,639	3,127	1,777	4,401	4,237	2,865	3,137	3,124	2,944	479	2,888	2,653	3,178	2,291	1,774	1,929
Frequency of recombination	0%	0.13%	0.11%	0.11%	0.14%	0	0	0	0	0	0	0	0	0	0	0
Region of second chromosome where recombination occurred					♂1 ♂2 ♂3											
dp–b	–	–	–	–	– 2+b cn bw –											
b–cn	–	4++cn bw	2++cn bw	1 dp b++	– – –											
cn–bw	–	–	–	{2 dp b cn+ 2+++bw	1+++bw – {2 dp b cn+ 1+++bw											
Overall frequency of recombination*	17/15,181 = 0.11%†					0/12,549 = 0%					0/14,713 = 0%					

Experiment 2 (ovarian extract) Treatment	Injection of *OKI* ovarian extract				Injection of *CS* ovarian extract	Uninjected
No. of ♂♂ tested	50				70	
No. of ♂♂ with recombination progeny	4				0	
Mean ± s.d. of progeny size	160±103				198±74	
Region of second chromosome where recombination occurred	♂1	♂2	♂3	♂4		
dp–b	–	–	–	2 dp+++		
b–cn	1++cn bw	3++cn bw	2 dp b++	–		
cn–bw	–	–	–	–		
Overall frequency ♂ recombination*	8/7,989 = 0.10%†				0/13,856 = 0%	0/26,792 = 0%

*The frequencies of male recombination among males that showed recombination in experiment 1 was 17/1845 = 0.92%, and in experiment 2, 8/1135 = 0.71%.
†These results are significantly different from the controls at the 0.1% level by Fisher's exact test.

males were mated individually to *dp b cn bw; ve* virgin females for 4 d and then were remated every 3 d to fresh *dp b cn bw*; *ve* virgin females for five broods. The progeny were scored for second chromosome male recombination.

The results (summarised in Table 1), support those of the first experiment, and suggest that the factor(s) can be transferred by ovarian extracts.

As a further statistical test on the combined data from this study, a Fisher's exact test was performed on the number of *OK1* extract-treated males that produced any recombinant progeny (10/102) compared with the corresponding number of control males (*CS* and Ringer-injected) (0/202). These results show that significantly more treated males showed recombination than did control males ($P = 0.000025$).

The results of the previous attempts[4-6] to induce male recombination by ovarian extract injections can be explained if Reddi *et al.*[4] injected an ovarian extract from flies showing male recombination, and the others[5,6] did not. Further experiments are planned to investigate the nature of the male recombination-inducing factor in the extracts of *OK1* flies.

We thank Professor J. M. Thoday and Drs M. Ashburner, J. Holden and G. P. Richards for discussions and suggestions, and Miss A. Forster for technical assistance.

Note added in proof: Slatko and Hiraizumi (personal communication), using a *D. melanogaster* line that contains the *Male recombination* element, have observed results similar to those in this article.

J. H. M. SOCHACKA
R. C. WOODRUFF

Department of Genetics,
University of Cambridge,
Cambridge CB4 1XH, UK

Received March 23; accepted May 20, 1976.

[1] Morgan, T. H., *Science*, **36**, 718–720 (1912).
[2] Morgan, T. H., *Biol. Bull.*, **26**, 195–204 (1914).
[3] Hannah-Alava, A., in *Adv. Genetics*, **13**, 157–226 (1965).
[4] Reddi, O. S., Reddy, G. M., and Rao, M. S., *Nature*, **208**, 203 (1965).
[5] Singer, K. M., Chovnick, A., Suzuki, D. T., Baillie, D., and Hoar, D., *Nature*, **214**, 503–504 (1967).
[6] Saraswathy, T., *Experientia*, **26**, 799 (1970).
[7] Hiraizumi, Y., *Proc. natn. Acad. Sci. U.S.A.*, **68**, 268–270 (1971).
[8] Waddle, F. R., and Oster, I. I., *J. Genet.*, **61**, 177–183 (1974).
[9] Voelker, R. A., *Mutat. Res.*, **22**, 265–276 (1974).
[10] Kidwell, M. G., and Kidwell, J. F., *Nature*, **253**, 755–756 (1975).
[11] Roberts, P., in *Genetics and Biology of Drosophila* (edit. by Ashburner, M., and Novitski, E.), (Academic, London, 1976).
[12] Woodruff, R. C., and Thompson, J. N., Jr, *Genetics*, **80**, 586 (1975).

Initiation of meiotic maturation in *Xenopus laevis* oocytes by lanthanum

PROGESTERONE can induce true maturation of isolated amphibian oocytes *in vitro*[1]. It has been found recently that the ionophore A23187, in the presence of high magnesium or calcium concentrations, can also promote meiosis *in vitro*[2], and it has been observed that 0.5–1 mM propranolol and some related compounds, are potent inducers of maturational events in *Xenopus laevis* oocytes[3]. This last result suggests that displacement of membrane calcium might be involved in maturation, because this is known to occur in other systems treated with high concentrations of propranolol[4]. We have therefore studied the action of La^{3+}, since this ion is expected to act specifically at the superficial plasma membrane calcium sites[5]. We report here that maturation is induced by La^{3+}, indicating strongly that calcium ion movements have a role in the initiation of oocyte maturation.

Ovarian tissues were removed from *Xenopus laevis* females through a small incision made on the lateral abdominal wall. To obtain fully grown oocytes free of follicle cells, the ovaries were treated with collagenase[6]. In each experiment, all oocytes were obtained from the same animal. The experiments were conducted at room temperature, in a modified Ringer solution to which La^{3+} was added as the chloride salt. La^{3+} at 5 or 10 mM promotes maturational events in *Xenopus laevis* oocytes (Table 1). The maturation is not abortive, since microscopic examination reveals the existence of the spindle moving to the cortex (Fig. 1). La^{3+}-induced maturation presents several other characteristics common to progesterone-induced maturation. The breakdown of the germinal vesicle takes place after about the same length of incubation, and maturational responses to both agents are inhibited by cycloheximide (Table 1; ref. 7); La^{3+}, like progesterone, is not able to induce maturation when injected into the oocytes (data not shown).

Table 1 Maturation of *Xenopus laevis* oocytes, as indicated by germinal vesicle breakdown, after continuous exposure to lanthanum or progesterone

Treatment		Female *A*	*B*	*C*
Modified Ringer		0	0	0
La^{3+}(mM)	0.01	—	—	0
	0.1	—	—	2
	0.5	—	—	3
	1	0	—	5
	2.5	50	—	
	5	60	55	72
	10	75	62	92
La^{3+} (mM) + cycloheximide (100 μg ml^{-1})	10	0	0	0
Progesterone (1 μg ml^{-1})		97	100	91

One hundred isolated oocytes were used for each set of conditions. The table shows the number of matured oocytes after 15 h incubation. La^{3+} was administered in solution as the chloride salt in Ringer solution containing no bicarbonate buffer.
—, Not tested.

Furthermore, a similar preferential protein synthesis is activated by progesterone and La^{3+}. It has been shown previously that during progesterone-induced maturation *in vitro*, several electrophoretically defined soluble proteins are increased selectively[8]. We studied this effect by double labelling of proteins, injecting ^{3}H-leucine into treated oocytes (maturing) and ^{14}C-leucine into control oocytes (resting)

Fig. 1 Meiotic metaphase of oocyte in which maturation was induced *in vitro* by La^{3+}, at 5 mM (chloride salt). Magnification × 800. The oocyte was fixed in Smith's solution. Sections (7 μm) were stained with Feulgen's reagent and counterstained with light-green.

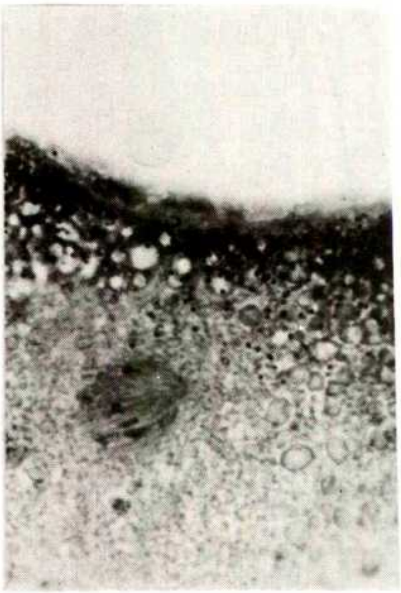

(Fig. 2). Control/control experiments with injection of ^{3}H- and ^{14}C-leucine into non-treated oocytes did not show any peaks, and the ^{3}H/^{14}C ratio of electrophoresed proteins was normalised to 1. The same pattern of induced proteins was observed when La^{3+} was substituted for progesterone (Fig. 2). In each case, two distinct peaks were found, with several smaller peaks in between. For both these agents, the increase above the control ^{3}H/^{14}C ratio was 150–200% for the small molecular weight peak and 130–150% for the large molecular weight peak.

Fig. 2 Normalised gel electrophoresis patterns of proteins during maturation induced by progesterone (▲) and La^{3+} (■). The curves show ^{3}H/^{14}C ratios, expressed as the percentage increase above the controls (●). Labelling was for 2 h beginning approximately 15 h after continuous exposure to progesterone or La^{3+}. Twenty-five matured oocytes were injected with 70 nl of ^{3}H-Leu and 25 non-treated oocytes were injected with 70 nl of ^{14}C-Leu. Control/control (●) was performed by injecting 25 non-treated oocytes with ^{3}H-Leu and 25 other non-treated oocytes with ^{14}C-Leu (^{3}H-Leu, 55 Ci mmol^{-1}; ^{14}C-Leu, 324 mCi mmol^{-1}, Amersham). Appropriate amounts of non-radioactive amino acids were added to obtain identical concentrations of ^{3}H- and ^{14}C-amino acids and a ^{3}H/^{14}C d.p.m. ratio of about 10. Treated and control oocytes were pooled and homogenised in 2 ml of saline solution. The 105,000*g* supernatant was obtained and dialysed as reported previously[8]. Sodium dodecyl sulphate (0.1%)–polyacrylamide gel (6%) electrophoresis was performed under 2 mA per tube for 20 min and then 5 mA per tube (migration towards anode on the left). Gels were re-electrophoresed in 7% acetic during 2 h and sliced immediately. Soluene (0.5 ml) was added and the supernatant left for 3 h at 50 °C. Radioactivity was then counted in an appropriate scintillation mixture. Left peak, histones migrate at this level; right peak (higher molecular weight), molecular weight greater than 100,000. Other details are in ref. 12.

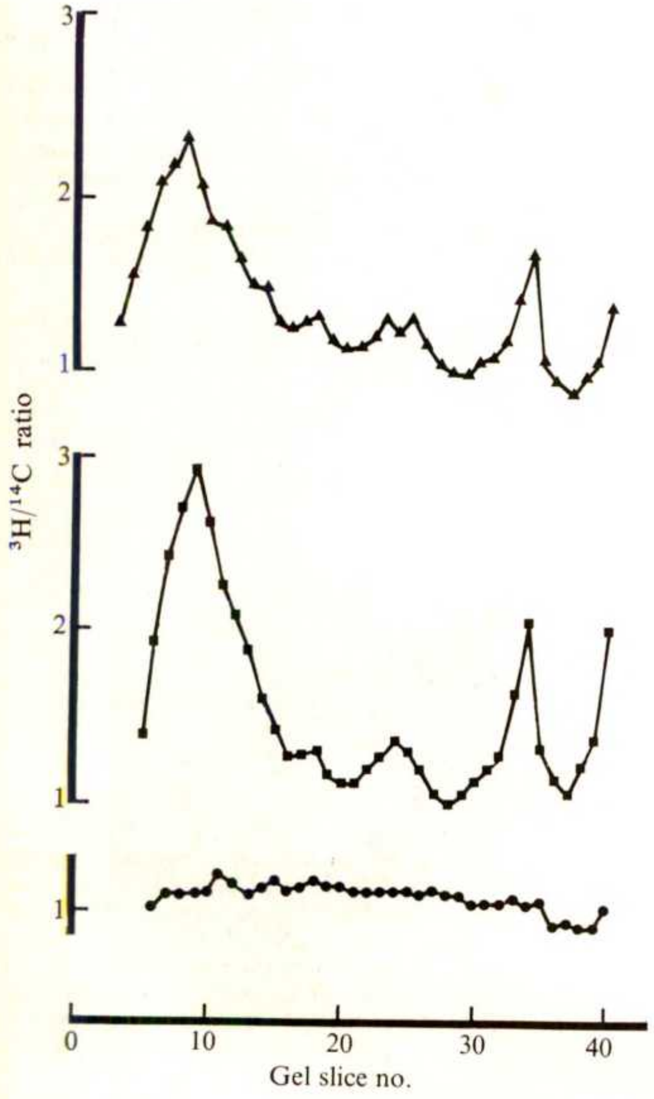

Incubation in Ca^{2+} alone in high concentration does not lead to maturation[2]. Although ionophore A23187 induces maturation in amphibian oocytes given certain conditions of divalent ionic concentration[2], La^{3+} seems to be a more appropriate agent to investigate the possible involvement of Ca^{2+} in this, and other systems[5,9]. High concentrations of extracellular La^{3+} displace external membrane calcium, and block both Ca^{2+} uptake and efflux, resulting in a release of internal sequestered Ca^{2+} (ref. 5). Our finding that La^{3+} induces maturation makes it likely that Ca^{2+} is involved in the initiation of maturation. Since injected Ca^{2+} is without effect[10], however, it must be that the Ca^{2+} movements involved are highly regulated, or need to be sustained during the period of maturation. Injected La^{3+} is without effect, probably because it is unable to react with the appropriate membrane sites.

The present results imply that progesterone, the likely physiological inducing agent[11], acts at specific membrane sites, leading to well defined movements of Ca^{2+} inside the cell. The altered Ca^{2+} distribution would in turn be the intermediary step for the series of further events promoting maturation.

This work was supported by grants from the SNSF and WHO. We thank Dr G. Jones for help with the preparation of the manuscript, Dr Y. Timowska for scientific assistance and Mrs M. Romios for technical help.

SABINE SCHORDERET-SLATKINE

Station de Zoologie expérimentale,
154 rte de Malagnou, CH Geneva

MICHEL SCHORDERET

Départment de Pharmacologie,
Ecole de Médecine,
CH Geneva, Switzerland

ETIENNE-EMILE BAULIEU

Unité de Recherches sur le Métabolisme Moléculaire et la Physio-Pathologie des Stéroides de l'Inserm,
Hôpital de Bicêtre,
Université Paris-Sud,
78 rue du Général Leclerc,
94270-Bicêtre, France

Received April 6; accepted June 3, 1976.

[1] Schuetz, A. W., *Proc. Soc. exp. Biol. Med.*, **124**, 1307–1310 (1967).
[2] Wasserman, W. J., and Masui, Y., *J. exp. Zool.*, **193**, 369–375 (1975).
[3] Schorderet-Slatkine, S., and Schorderet, M., *C. r. hebd. Séanc. Acad. Sci., Paris*, **282**, 1733–1736 (1976).
[4] Porzig, H., *J. Physiol., Lond.*, **249**, 27–49 (1975).
[5] Weiss, G. B., *A. Rev. Pharmac.*, **14**, 343–354 (1974).
[6] Schorderet-Slatkine, S., and Drury, K. C., *Cell Differentiation*, **2**, 247–254 (1973).
[7] Schorderet-Slatkine, S., *Cell Differentiation*, **1**, 179–189 (1972).
[8] Pennequin, P., Schorderet-Slatkine, S., Drury, K. C., and Baulieu, E. E., *FEBS Lett.*, **51**, 156–160 (1975).
[9] De Sousa, R. C., *J. Physiol., Paris*, **71**, 5A–71A (1975).
[10] Merriam, R. W., *Expl Cell Res.*, **69**, 75–80 (1971).
[11] Fortune, J. E., Concannon, P. W., and Hansel, W., *Biol. Reprod.*, **13**, 561–567 (1975).
[12] Schorderet-Slatkine, S., and Baulieu, E. E., *Ann. N.Y. Acad. Sci.* (in the press).

Benzpyrene induces sister chromatid exchanges in cultured human lymphocytes

A WIDE variety of chemical mutagen/carcinogens induce sister chromatid exchanges (SCE) in cultured Chinese hamster cells and can thus be studied at the chromosomal level[1,2]. Certain polycyclic hydrocarbons, such as benzo(*a*)-pyrene, 3-methylcholanthrene, dimethylbenzanthracene and others are important in the aetiology of human bronchial carcinoma[3]. The substances are not themselves carcinogenic, but are converted to carcinogenic epoxides by the enzyme arylhydrocarbonhydroxylase.[4] Epoxides bind non-enzymatically to DNA, unless they are converted enzymatically to inert water-soluble metabolites by epoxide hydratase[5] and glutathione-*S*-transferase[6]. The carcinogenic effect of polycyclic hydrocarbons is closely connected with the regulation of the enzyme activities and genetic variability can thus be expected. It has been observed at the population level by family studies[7] and at the cellular level by biochemical differences in the hydrocarbon-degrading enzyme system[8]. We have investigated the possible induction of sister chromatid exchanges by benzo(*a*)pyrene and show that the rate of SCE does not correlate with different rates of benzpyrene metabolism. We therefore suggest that genetic differences in benzpyrene metabolism are unrelated to genetic variation in the predisposition to bronchial carcinomas.

We tested the intracellular benzo(*a*)pyrene (BP) metabolism by measuring the formation of tritiated H_2O-soluble products from ^{3}H-BP in cultured lymphocytes isolated by a Ficoll–Hypaque gradient as described in Fig. 1. An inhibitor of the monooxygenase system[9], alpha-naphthylflavone (ANF, 5 μg ml^{-1}) was used as a control. We found wide individual differences in BP metabolism among 22 individuals. The one with the highest metabolic activity (WW) showed 3.8 ± 0.5 times the activity of the lowest (HR) in each of six independent determinations. ANF reduced the amount of water-soluble products to background levels in both.

To determine sister chromatid exchange rate (SCE), 10^8 isolated lymphocytes were incubated in 5 ml of chromosome medium Ia (Gibco) together with 5-bromodeoxyuridine (BUdR) (30 μg ml^{-1}) for 70 h at 37 °C in the dark. Parallel assays were made in duplicate with 10^{-6} M BP and 55 μg ml^{-1} ANF. Chromosomes were prepared by standard techniques and the slides were stained with acridine orange (125 μg ml^{-1}) in phosphate buffer at *p*H 6.0 and analysed by fluorescence microscopy.

The results are summarised in Fig. 1. The SCE rate nearly doubled after incubation with BP, but not in the presence of ANF (55 μg ml^{-1}). This concentration inhibits the formation of water-soluble products by more than 95%. Benzpyrene failed to induce SCEs when it was present for only 30 h of culture, instead of the usual 70 h, and it did not influence the total number of second generation metaphases found at 70 h. The fast (WW) and the slow (HR) BP-metabolising individuals did not differ in the rate of SCE induction.

This result, at first surprising, corresponds to differences in BP metabolism between different strains of mice which, nevertheless, do not differ in the rate of benzpyrene-induced tumours[10,11]. The inhibition of the first BP-oxidising step (AHH) by ANF prevents the carcinogenic effect of BP as indicated by the normal SCE induction. The similar SCE induction between the high (WW) and the low (HR) BP-metabolising individuals (Fig. 2) indicates, however, that BP metabolism and carcinogenesis are not related in a simple, proportional way[12]. A high rate of benzpyrene conversion cannot serve as an indication of the effective concentration of carcinogenic epoxides and their effects on DNA. The formation of water-soluble products from BP only indicates that BP is being degraded, but does not give any information about the current levels of ultimate carcinogens formed during this steady-state process. How much epoxide binds to DNA is also unknown. Finally, we do not know how much epoxide is removed by DNA repair and how much remains fixed in the DNA following the next replication.

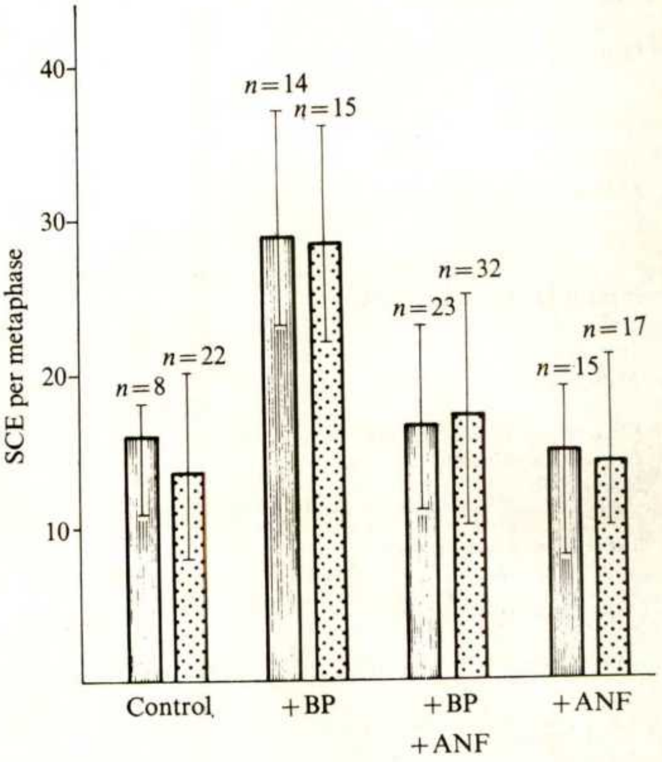

Fig. 1 Induction of sister chromatid exchanges (SCE) by benzypyrene (BP) and its inhibition by alpha-naphthylflavone in lymphocyte cultures with different rates of intracellular BP metabolism. Lymphocytes were isolated from 20 ml of heparinised blood by a Ficoll–Hypaque gradient[13] which yielded a 70–85% pure preparation of about 2×70^7 lymphocytes. The BP metabolism was determined by seeding 5×10^5 cells into each of 96 wells of a Cook's microtitre plate (Falcon, Oxnard, California) together with 200 µl of Ham's F-12 culture medium containing 16% foetal calf serum and 150 nM of ^{3}H-BP (specific activity 25 Ci mmol^{-1}, (Amersham-Buchler, Braunschweig, Germany). Water-soluble products were determined after 8 h of incubation by the method of Huberman and Sachs[14]. SCEs were scored in phytohaemagglutinin-stimulated lymphocytes after 70 h of incubation at 37 °C. The height of the columns (shaded, fast; dotted, slow, BP-metabolising individual) indicate the mean and the bars the range of SCE per metaphase. Benzo(*a*)pyrene (Sigma) was dissolved in chloroform : methanol (2:1), extracted twice by equal amounts of 1 N NaOH and recrystallised from the organic phase in the cold. A stock solution (10 mM) of BP in acetone was mixed with a 40-fold amount of foetal bovine serum and added to the series indicated to give a final BP concentration of 1 µM. The monooxygenase inhibitor ANF (Fluka) was also first dissolved in acetone mixed with foetal bovine serum and added where indicated at a final concentration of 55 µg ml^{-1}. The rate of SCE induction in the presence of the inhibitor does not differ from cultures without BP or controls. There is only a minimal SCE induction by BP, in the presence of ANF, probably as a result of incomplete inhibition of the monooxygenase system. At the concentration used, formation of water-soluble products was less than 5% of controls without ANF.

The induction of SCEs by benzpyrene reported here probably reflects the intracellular carcinogenic effect of benzpyrene, although it is not understood in molecular terms. The lack of correlation between the activity of intracellular benzpyrene metabolism and SCE rate suggests that genetic differences in BP metabolism are not related to genetic differences in the predisposition towards development of bronchial carcinoma as revealed by family studies[7]. How the rate of benzpyrene-induced sister chromatid exchanges differs between patients with bronchial carcinoma and control patients is being investigated.

We thank Professor F. Oesch, Mainz, for discussions. This work was supported in part by grants from the Deutsche Forschungsgemeinschaft.

H. W. Rüdiger
F. Kohl
W. Mangels
P. von Wichert

I. Medizinische Klinik,
Universität Hamburg,

C. R. Bartram
W. Wöhler

Institut für Humangenetik,
Universität Hamburg,
Martinistrasse 52,
2000 Hamburg 20, FRG

E. Passarge

Institut für Humangenetik,
Universitätsklinikum Essen,
Essen, FRG

Received April 20; accepted May 20, 1976.

[1] Perry, P., and Evans, H. J., *Nature*, **258**, 121 (1975).
[2] Latt, S. A., *Proc. natn. Acad. Sci. U.S.A.*, **70**, 3395–3399 (1973).
[3] Gray, N., and Hill, D., *Lancet*, i, 1252–1253 (1975).
[4] Grover, P. L., Sims, P., Mitschley, B. C. V., and Roe, F. J. C., *Br. J. Cancer*, **31**, 182 (1975).
[5] Oesch, F., and Glatt, H. R., *Experientia*, **31**, 720 (1975).
[6] Nemoto, N., Gelboin, H. V., Habig, H. W., Ketley, J. N., and Jakoby, W. B., *Nature*, **255**, 512 (1975).
[7] Tokuhata, G., and Lilienfeld, A. M., *J. natn. Cancer Inst.*, **30**, 289–312 (1963).
[8] Kellermann, G., Lutyen-Kellermann, M., and Shaw, C. R., *Am. J. Hum. Genet.*, **25**, 327–331 (1973).
[9] Diamond, C., and Gelboin, H. V., *Science*, **166**, 1023 (1969).
[10] Benedict, W. F., Considine, N., and Nebert, D. W., *Molec. Pharmac.*, **6**, 266–277 (1973).
[11] Nebert, D. W., Benedict, W. F., Gielen, J. E., Oesch, F., and Daly, J. W., *Molec. Pharmac.*, **8**, 374–379 (1972).
[12] Kellermann, G., Shaw, C. R., and Luyten-Kellermann, M., *New Engl. J. Med.*, **289**, 934–937 (1973).
[13] Böyum, A., *Scand. J. clin. Lab. Invest.*, **21**, Suppl., 97 (1968).
[14] Hubermann, E., and Sachs, L., *Int. J. Cancer*, **11**, 412–418 (1973).

Expression of maternal and paternal antigens on trophoblast

GENETICALLY different individuals will not usually accept tissue grafts from one another. The best known exception to this is the ability of the foetus to act as a homograft. Fertilised mouse eggs contain both paternally and maternally derived antigens[1,2], but it has not so far been demonstrated whether paternal antigens are expressed on mouse trophoblast, the embryo tissue which forms initial contact with the maternal circulation. If present, such antigens may be masked by a mucopolysaccharide[3]; this has been disputed by Simmons *et al.*[4]. Alternatively, it has been proposed that trophoblast lacks transplantation antigens[5] and Searle *et al.*[6] failed to immunise a recipient with mouse trophoblast when tested either by skin grafting or cell-mediated cytotoxicity. It has been suggested, however, that histocompatibility antigens on human trophoblast were responsible for cytotoxic antibody found in the sera of 12-week human pregnancies[7], and Nakakita showed antibody production in mice to human trophoblast, using immune adherence[8]. I now report the presence of both paternal and maternal antigens on trophoblast outgrowths of mouse blastocysts *in vitro*.

Blastocysts flushed from the uteri of either CBA/Fa or C57 BL/Mcl females 3.5 d after coitus were cultured on glass coverslips. On day 4 of culture, the mixed immune haemadsorption technique[10] (MHA) modified by Tachibana *et al.*[11] was used to detect antigens on the outgrowths. Trophoblast and indicator cells (sheep red blood cells) were coated with specific antisera raised in mice, and linked together by a rabbit anti-mouse IgG serum (Capell Laboratories). Photographs were taken as a cross check. Figure 1 shows a 3.0 reaction. The attachment of sensitised red cells to trophoblast outgrowths from crosses of (CBA × CBA), (C57BL × CBA) and (CBA × C57BL) incubated with anti-CBA serum (Fig. 2) shows that both maternal and paternal antigens are expressed on the trophoblast. For each pair of crosses the difference between the mean degree of red-cell attachment was significant ($P < 0.01$). This suggests that the amount of CBA antigen present is greater with a CBA mother than with a CBA father, and greater still when both parents are CBA. Control data for (CBA × CBA) trophoblast outgrowths are shown in Table 1. Normal CBA or C57BL sera and anti-C57BL serum gave scores of 0. After absorption

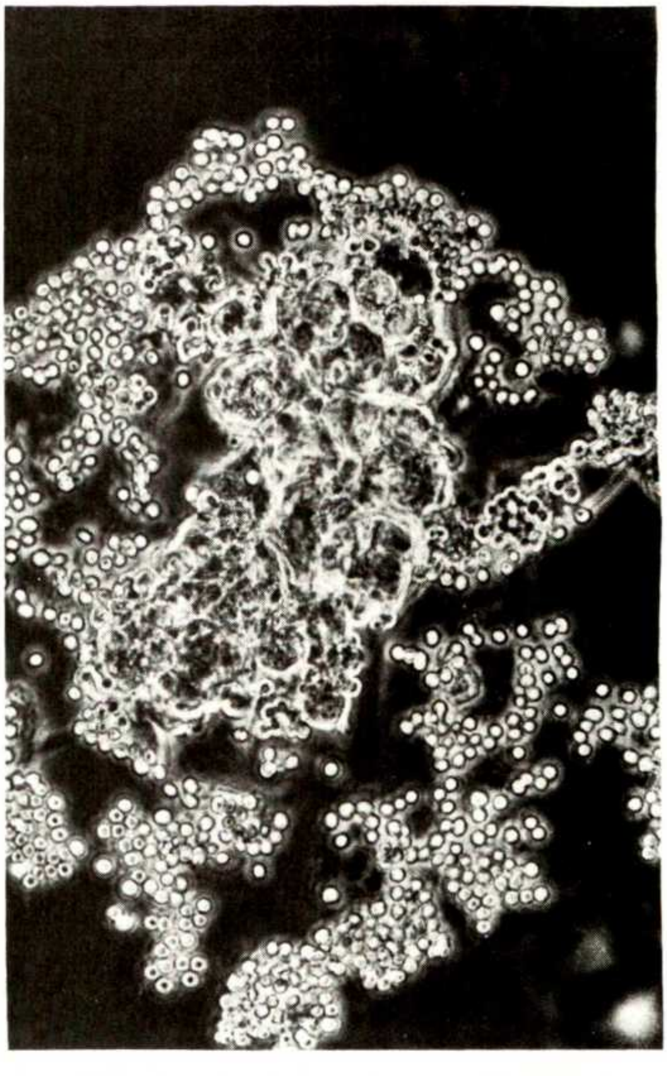

Fig. 1 A (C57BL × CBA) blastocyst cultured in Snow's medium[9] and 10% foetal calf serum under oil and incubated at 37 °C in an atmosphere of 10% CO_2 in air. Attachment of sensitised red cells to the resulting outgrowth after MHA is shown. Antiserum to a mixture of male and female CBA/Fa spleen cells was raised in C57BL/Mcl mice. Approximately half a donor spleen was given to each recipient weekly for between 7 and 10 weeks. Antiserum to the sheep erythrocytes was raised in A-strain mice. Recipients were given 0.2 ml of a 1% suspension of sheep red blood cells (SRBC) each week for between 7 and 10 weeks. Optimal conditions for the sensitisation of SRBCs were established. After washing three times in phosphate-buffered saline (PBS) they were incubated in a 1:1,000 dilution of anti-SRBC serum followed by a 1:100 dilution of anti-mouse IgG serum and finally diluted to 4% (v/v) and stored at 4 °C. There were three washes with PBS between each step in the procedure. On day 4, outgrowths on coverslips were rinsed in PBS and incubated for 1 h with selected antisera, rinsed and layered with sensitised SRBCs (1.0% v/v). After 1 h at room temperature, unattached erythrocytes were washed off and the strength of the reaction was estimated microscopically according to the percentage of target cells (that is, trophoblast of the outgrowth) to which sensitised SRBCs were attached, expressed on the following scale: 4.0 (100% attachment); 3.5 (90%); 3.0 (50–80%); 2.0 (<50%); 1.0 (<25%); 0.5 (<10%); 0 (0%). The above outgrowth was given a score of 3.0.

Table 1 Expression of CBA cell-surface antigens on trophoblast outgrowths of blastocysts from a CBA×CBA mating after incubation with control sera

Serum	Cell type used for absorption	Serum dilution	Mean score±s.e.m.	
Anti-CBA	—	1:160	3.80±0.06	(34)
Anti-CBA	CBA liver and spleen	1:160	2.00*	(3)
Anti-CBA	C57BL liver and spleen	1:160	3.75±0.25	(4)
Anti-CBA	CBA lymph node and spleen	1:160	0.52±0.07*	(24)
Anti-CBA	C57BL lymph node and spleen	1:160	3.84±0.05	(29)
Normal CBA	—	1:40	0	(13)
Normal C57BL	—	1:40	0	(10)
Anti-C57BL	—	1:40	0	(20)

Absorptions were carried out with a 50:50 mixture of washed liver and spleen cells or lymph node and spleen cells for 2×1 h at 37 °C. Results are expressed as mean score ± s.e.m. The number of outgrowths per group is in parentheses.
$^*P < 0.001$ for corresponding controls.

Table 2 Expression of C57BL cell-surface antigens on trophoblast outgrowths after incubation with normal sera, anti-C57BL serum, or absorbed anti-C57BL serum, diluted 1:40

Origin of blastocysts Mother Father	Anti-C57BL serum	Anti-C57BL serum absorbed with C57BL cells	Anti-C57BL serum absorbed with CBA cells	Normal C57BL serum	Normal CBA serum	Anti-CBA serum 1:160
C57BL×C57BL	3.86±0.14 (4)	1.00±0.14* (10)	3.38±0.34 (8)	0 (4)	0 (4)	0 (10)
CBA×C57BL	3.31±0.23 (13)	1.00 (2)	3.00 (2)	—	—	—
C57BL×CBA	3.00 (2)	0.89±0.07* (9)	3.00±0.37 (6)	—	—	—

Absorptions were carried out with a 50.50 mixture of washed spleen cells and lymph node cells for 2×1 h at 37 °C. Results are expressed as mean score ± s.e.m. The number of outgrowths per group is in parentheses.
$^*P < 0.001$ for corresponding controls

Fig. 2 The expression of CBA cell surface antigens on trophoblast outgrowths after incubation with serial dilutions of anti-CBA serum. Blastocysts were recovered from CBA females mated to CBA (×) or C57BL (●) males, and from C57BL females mated to CBA males (○) Data were accumulated from 14 experiments A least squares analysis of variance according to the method of fitting constants[12] gave a mean square value of 0.2623 with 152 residual degrees of freedom. Duncan's new multiple range test[13] was used to analyse the difference between the means of the three crosses ($P < 0.01$)

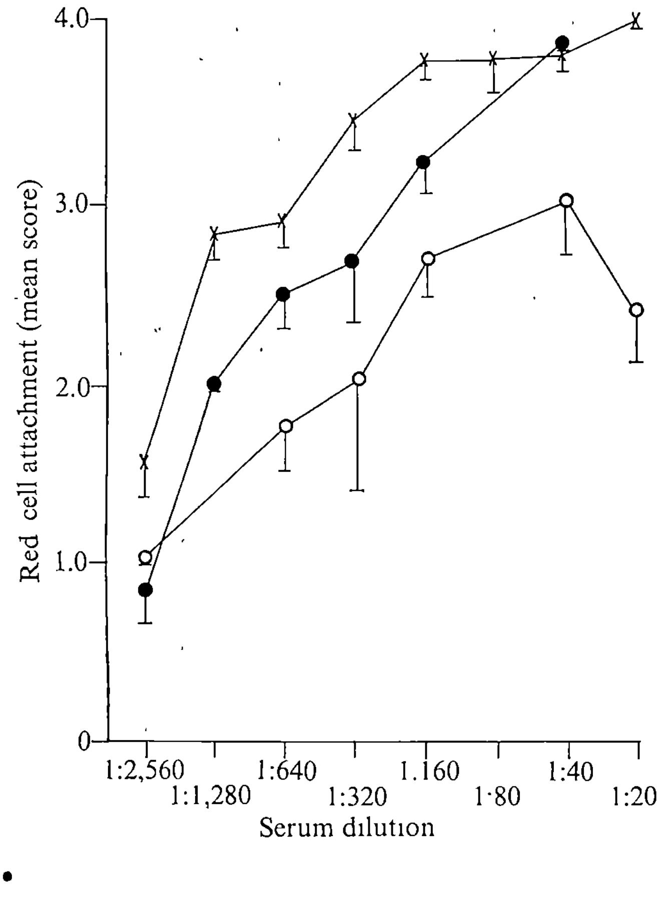

of the anti-CBA serum with a mixture of spleen and lymph node cells from CBA mice, red-cell attachment was reduced by 86%. Total absorption of the activity was not expected because the antiserum was made to both intracellular and cell membrane-bound antigens of spleen cells, whereas the absorption would only remove antibodies raised against the latter. A mixture of CBA liver and spleen cells only reduced the reaction by 50%. Absorption with C57BL cells had no effect.

Table 2 shows results obtained with blastocysts from (C57BL×C57BL), (CBA×C57BL) and (C57BL×CBA) matings incubated with anti-C57BL serum and control sera. Both maternal and paternal antigens are present but a comparison of their relative expression cannot be made because of the small number of outgrowths studied when the C57BL is the mother.

These experiments show that trophoblast *in vitro* exhibits antigenicity derived from both the maternal and paternal genome. The antigens expressed could be either major histocompatibility antigens of the H-2 type or minor antigens (for example, H-3, H-6), since both are present on spleen cells.

I thank Dr A. McLaren, Dr J. Ansell, Dr R. Hancock and G. Mahon for criticism and advice. This work was supported by the Ford Foundation.

JAN CARTER

Department of Biochemistry,
Trinity College,
Dublin, Ireland

Received January 19; accepted May 26, 1976

1 Hakansson, S , Heyner, S , Sundqvist, K G., and Bergstrom, S , *Int J. Fert.*, 20, 137–140 (1975)
2 Searle, R. F., Johnson, M H , Billington, W. D , Elson, J., and Clutterbuck-Jackson, S., *Transplantation*, 18, 136–141 (1974)
3 Currie, G A , van Dorrninck, W , and Bagshawe, K D , *Nature*, 219, 191–192 (1968).
4 Simmons, R. L , Lipschultz, M L , Rios, A , and Ray, P K , *Nature new Biol.*, 231, 111–112 (1971)
5 Simmons, R L , Cruse, V , and McKay, D. G , *Am J Obstet Gynec*, 97, 218–230 (1967)
6 Searle, R F , Jenkinson, E J , and Johnson, M H , *Nature*, 255, 719–720 (1975).
7 van der Werf, A J M , *Lancet*, i, 595 (1971).
8 Nakakita, T , *Nagoya Med J*, 17, 89–102 (1972)
9 Ansell, J. D , and Snow, M H L , *J Embryol exp. Morph*, 33, 43–56 (1975)
10 Fagraeus, A , Espmark, J A , and Jonsson, J , *Immunology*, 9, 161–175 (1965)
11 Tachibana, T., Worst. P , and Klein, E , *Immunology*, 19, 809–816 (1970)
12 Steel, R G D., and Torrie, J H., *Principles and Procedures of Statistics* (McGraw-Hill, New York, Toronto and London, 1960)
13 Nathenson, S G , and Cullen, S E , *Biochim biophys. Acta*, 344, 1–25 (1974)

Successful induction of specific tolerance to transplantation antigens using autoimmunisation against the recipient's own natural antibodies

ORGAN transplantation, especially of kidneys, is now an accepted method in medical care. In spite of careful matching to obtain the most suitable combination between donor and recipients as to blood group and HLA antigens, varying degrees of incompatibility have to be accepted. This makes prolonged use of immunosuppressive drugs necessary. Such therapy, however, may in itself cause serious and even lethal complications. Specific tolerance to the donor antigens with full reactivity against other antigens is the ideal. Classical induction of transplantation tolerance requires massive inoculation of foreign cells, may result in serious graft-*versus*-host reactions and is not considered feasible in human kidney grafts. We describe here a new method of inducing specific immune tolerance to a given set of alloantigens, which can be carried out in adults and which will leave reactivity against other antigens intact.

Every individual seems to have lymphocytes with predetermined receptors for various parts of the major histocompatibility complex antigens of the species. When tested against a given set of such MRC antigens, 3–10% of a normal mouse or rat T-lymphocyte population will express immune competence[1,2] or specific receptors for antigens of that particular MHC locus[3,4]. These receptors can be characterised according to two characteristics, their specific antigen-binding capacity and their unique antigenic or idiotypic markers[5,6]. Two other facts make these receptors useful for the induction of specific immune tolerance. They are found in detectable amounts in normal serum or urine of the individual[7]. It can be shown that the individual is able to produce specific anti-receptor antibodies against its own naturally occurring receptors, if the latter are presented to the individual in a concentrated, modified form. We describe results showing the validity of the latter statement.

Normal Lewis rats (MHC type Ag-B^1) have in their sera or urine idiotypic receptor molecules with specificity for other Ag-B alloantigens, e.g. against DA (Ag-B^4) and BN (Ag-B^3). Using anti-(Lewis-anti-DA) idiotypic antibodies linked to Sepharose it is possible to isolate the anti-DA receptors from normal Lewis serum[7]. Normal Lewis serum (300 ml) was thus passed over such an anti-idiotypic column and the bound material was acid eluted and cross linked with glutaraldehyde[8]. Cross-linked material (20 μg) in Freund's complete adjuvant was injected subcutaneously into each of four normal adult Lewis rats. The animals received a boost on day 21. On day 40 the animals were bled and their blood lymphocytes used as responder cells in MLC tests against DA or BN. Four days later the animals received DA skin grafts on the left back side and BN grafts on the right side.

Table 2 Delayed rejection of DA skin on immunised Lewis rats

Immunised Lewis rats No	Rejection of DA skin on day	Mean	Rejection of BN skin on day	Mean
1	21	30.3	12	11.8
2	35		11	
3	27		11	
4	38		13	

Three control normal Lewis rats rejected DA skin between day 9 and 10 and BN skin between day 10 and 12. Full thickness skin grafts were carried out as described elsewhere[10].

As shown in Table 1, these Lewis rats showed a specific lack of reactivity against DA alloantigens in the MLC and they accepted DA skin grafts for some 30 d (See Table 2). Reactivity against BN alloantigens was in both tests completely normal. In three similar experiments with skin grafts essentially the same results were obtained. The mean survival of DA or (Lewis ×DA)F$_1$ skin grafts on 20 adult Lewis rats treated in the above way was 24±1.7 (s.e.) days. BN or (Lewis×BN)F$_1$ grafts were all rejected within 11 d.

On day 91 the animals were bled again and their sera tested, after extensive absorption with (L×DA)F$_1$ lymphocytes in order to remove possible anti-DA alloantibodies produced after skin rejection, for the ability to bind to normal Lewis or DA T lymphocytes using as second layer ^{125}I-protein A as an indicator for surface-bound IgG antibodies[5]. All sera contained antibodies capable of reacting with normal Lewis lymphocytes but not with DA lymphocytes. To prove the auto-anti-idiotypic nature of these autoantibodies the sera were now tested for their ability to cause specific inhibition of MLC as had previously been done using "conventional" anti-idiotypic antibodies[5].

As shown in Table 3, treatment of normal Lewis T lymphocytes with the antisera in the presence of complement did result in a highly reduced activity against DA but not against BN alloantigens in the MLC test. Thus, the autoantisera did indeed contain the expected anti-idiotypic antibodies.

Finally, on day 91 after the bleeding, each of the animals was inoculated with 2.5×10^7 (Lewis ×DA)F$_1$ and (Lewis×BN)F$_1$ lymphocytes. Animals were killed 10 d later and their antisera were tested for alloantibodies using the protein A test. Then weak alloantibody titres against DA alloantigens could be detected in the autoimmunised animals, ranging from 1:32 to 1:256. Whether these alloantibodies contained the "normal" Lewis-anti-DA idiotypes was not tested. The control animals treated in exactly the same way as the experimental animals except for the immunisation with idiotypic receptors had anti-DA titres ranging from 1:4,096 to 1:16,384. Both groups of animals had similar titres against BN alloantigens (range 1:2,048 to 1:4,096). Thus, not only did the auto-anti-idiotypic

Table 1 Lack of reactivity in MLC of autoimmune Lewis rats against DA alloantigens

Responder cells from immunised Lewis rats No.	^{3}H-TdR incorporation in mixture against DA Mean c.p m. of duplicates ± s.e.	^{3}H-TdR incorporation in mixture against BN. Mean c.p.m. of duplicates ± s e.	^{3}H-TdR incorporation of responder cells alone. Mean c p.m. of duplicates ± s.e.
1	9,141±1,124	40,343±7,927	7,875±1,131
2	10,227±610	45,663±18,925	8,410±424
3	11,910±2,429	38,841±8,850	9,495±619
4	9,723±3,714	42,346±1,371	9,667±224
Responder cells from normal Lewis rat	139,464±15,855	39,271±5,808	5,336±455

The MLC was performed in flat-bottom microtitre plates in EHAA medium[9] complemented with the double amount of glutamine and 0 5% fresh normal BN rat serum using 0.25×10^6 responder cells and 0.5×10^6 spleen cells irradiated with 2,000 R as stimulator cells. Cultures were collected after 120 h after a 6-h pulse with 1 μCi of ^{3}H-TdR (ref. 5) Stimulator cells alone gave between 200 and 400 c.p.m.

Table 3 Serum from immunised Lewis animals specifically inhibits MLC

Lewis responder cells treated with serum and complement: Serum from immunised Lewis rats No	^{3}H-TdR incorporation* of mixture against DA. Mean c p.m. of triplicates ± s.e	^{3}H-TdR incorporation* of mixture against BN. Mean c.p.m. of triplicates ± s e.	^{3}H-TdR incorporation of responder cells alone. Mean c.p.m. of duplicates ± s.e.
1	32,344±6,801 (43%)	31,179±2,601 (89%)	3,684±567
2	32,151±3,139 (43%)	26,809±2,428 (77%)	3,740±563
3	20,837±5,501 (28%)	34,537±2,186 (99%)	3,996±226
4	35,512±3,851 ((47%)	38,172±2,703 (110%)	3,860±333
Normal Lewis serum pool	75,456±6,074 100%)	34,855±4,374 (100%)	3,457±1,454

Conditions for the MLC essentially the same as in Table 1. For further details for the treatment of the responder cells with antiserum and complement see ref. 5. Sera from another group of immunised Lewis animals inhibited MLC completely in a specific way.
*Values significantly different from values of normal Lewis serum and complement-treated groups are underlined

reaction significantly and specifically wipe out the T-cell mediated reactivity against the relevant alloantigens but there was also a drastic reduction in the alloantibody producing ability of these individuals. Using lymphocytes from auto-idiotype-immunised rats we have also been able to demonstrate that they largely lack the corresponding idiotypes, for example Lewis rats immunised with Lewis-anti-DA receptors lack lymphocytes with idiotypes signifying anti-DA reactivity but show normal distribution of anti-BN idiotype positive lymphocytes. Whether this reduction is particularly pronounced in the B-or the T-lymphocyte population is unknown.

We have thus presented data demonstrating that selective autoimmunity against a given group of antigen-binding receptors can lead to specific immune tolerance, probably due to the physical elimination of this group of immunocompetent cells. No side effects of this autoimmune procedure have so far been noted and the individuals express completely normal reactivity against other antigens. The skin-graft tolerance is highly significant; as in the rat many minor as well as the major Ag-B locus antigens do contribute to skin-graft rejection. In spite of this, grafts often survived for up to a month in the absence of any nonspecific immunosuppressive therapy. It thus seems clear that our techniques may allow the induction of long lasting immune tolerance through autoimmune reactions against the relevant idiotypic receptors. The specificity of this procedure would be as high as that of 'classical' immune tolerance and could in particular be carried out in adult, immunocompetent individuals. Improvements to make the approach more general by testing other species of animals and using alloantigenic immunosorbants instead of anti-idiotypic immunosorbants are required. Already at this early stage, however, it seems that autoimmune reactions can be used in a productive manner to manipulate the immune system in the transplantation immune system, in allergic disorders and perhaps even to regulate the course of certain autoimmune diseases.

This work was supported by an EMBO fellowship (H.B.), by the Swedish Cancer Society and by the US National Institutes of Health (H.W.).

H. Binz
H. Wigzell

Department of Immunology,
Uppsala University,
Biomedical Center,
Box 582 S-751 23 Uppsala, Sweden

Received April 26, accepted June 3, 1976

1 Wilson, D. B., Blyth, I. L., and Nowell, P C., *J. exp Med.*, **128**, 1157 (1968).
2 Ford, W. L., Simmonds, S I, and Atkins, R C, *J. exp Med.*, **141**, 681 (1975)
3 Binz, H, Bachi, T., Wigzell, H., Ramseier, H, and Lindenmann, J., *Proc natn Acad. Sci. U S.A.*, 72, 3210 (1975).
4 Binz, H., and Wigzell, H., *J exp. Med*, **142**, 1218 (1975).
5 Binz, H., and Wigzell, H., *J exp Med*, **142**, 197 (1975).
6 Binz, H., and Wigzell, H, *J exp Med.*, **142**, 1231 (1975)
7 Binz, H, and Wigzell, H., *Scand J Immun.*, **4**, 591 (1975)
8 Daugharty, H., Hopper, J. E, McDonald, A B, and Nisonoff, A, *J exp. Med*, **130**, 1047 (1969)
9 Click, R. E., Benck, L., and Alter, B J., *Cell Immun.*, **3**, 264 (1972).
10 Billingham, R. E, and Silvers, W K., *Transplantation of Tissues and Cells* (The Wistar Institute Press, Philadelphia, 1961).

Induction of transplantation tolerance using serum as antigen source

It has been shown that massive doses of allogeneic serum produce the prolongation of renal allograft survival in adult pigs[1]. Furthermore, alloantigenic activity was demonstrated in human serum by inhibiting certain reactions *in vitro*[2–6]; and in some strains of mice, the presence of histocompatibility (H) antigens in the serum could be demonstrated by inhibition of the cytotoxicity of specific alloantisera[7].

This study was designed to determine whether transplantation tolerance in rats can be induced by multiple massive doses of serum. Rats of the AVN strain were injected with allogeneic or syngeneic serum in increasing doses three times weekly from birth to the 6th week of age (1st week, 3×0.3 ml; 2nd week, 3×0.5 ml; 3rd week, 3×1 ml; 4th and 5th weeks, 3×1.5 ml; 6th week, 3×2 ml). The donors of allogeneic sera were rats of the congenic strains Lewis (Lew) or Lew.1A, differing from the AVN strain recipients in, respectively, both H–1 plus non-H–1 antigens and in the non-H–1 antigens only. Four weeks after birth, animals were skin grafted. The group treated with Lew serum, the control groups treated with AVN serum and the group of untreated animals simultaneously received the

Fig. 1 Survival of Lew.1A skin grafts after treatment with Lew.1A serum (●). AVN serum (○), untreated controls (△).

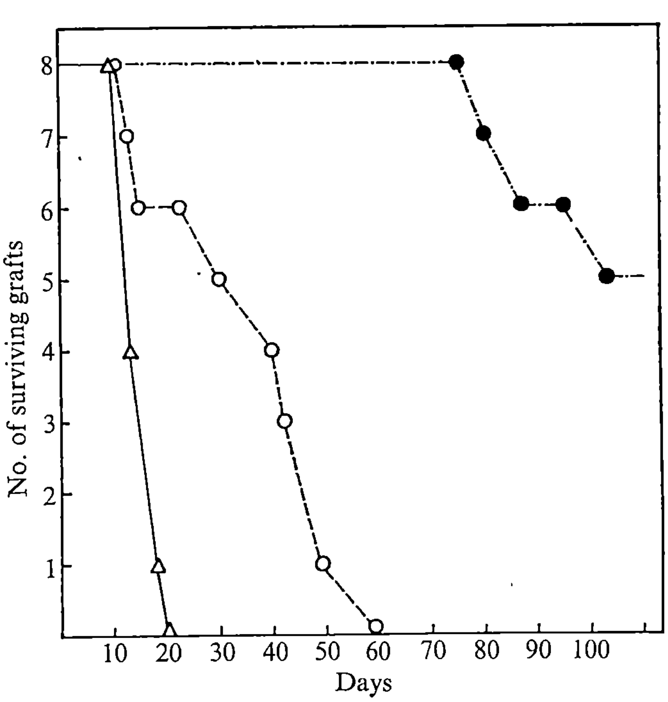

Table 1 Testing of AVN anti-Lew cytotoxic antibodies in AVN rats injected with Lew or AVN serum from birth

Group	Treatment	Serum titre*	Percentage ^{51}Cr release±s.e.†
1	—	1:8–1:64	28 8±4.7
2	AVN serum	1:8–1:128	37.0±12.6
3	Lew serum	–	15.5±1.9‡

*The cytotoxic activity of the serum was determined by the ^{51}Cr release from labelled lymphocytes of the strain Lew by the standard technique[8]. The cytotoxic titre was determined as the highest serum dilution showing significantly higher ^{51}Cr release than a similar dilution of normal serum.

†Percentage of released activity with a 1:1 dilution of serum.

‡Statistically significant ($P < 0.001$) inhibition of cytotoxic antibody production in comparison with group 1 or group 2 and non-significant difference from the value of ^{51}Cr release in the tests of serum from normal untransplanted rats (13.1±0.3%).

Lew and Lew.1A skin grafts. The group treated with Lew.1A serum and the corresponding control groups received only Lew.1A skin grafts.

A high degree of tolerance was obtained in the animals with the non-H–1 antigenic difference. Figure 1 shows the survival of skin grafts in animals treated with Lew.1A serum. All grafts survived 75 d and most of them more than 100 d. In addition to the specific antigenic activity of the serum, its nonspecific component(s) had some effect, as evident from the prolongation of skin graft survival in the control animals treated with syngeneic serum. Also, the Lew serum induced a high degree of tolerance of non-H–1 different Lew.1A grafts (Fig. 2). All these grafts survived 100 d and most of them persisted further. Again the nonspecific effect of the syngeneic serum was evident in the ability to prolong the Lew.1A skin-graft survival. With the H–1 plus non-H–1 antigenic difference (Fig. 3), skin grafts in two of eight animals had significantly prolonged survival times; the nonspecific effect of the serum was not at all apparent. In this group of animals, the possible presence of cytotoxic H–1 antibodies was also investigated. Serum samples were collected 17 d after skin grafting for the cytotoxicity test[8]. In comparison with the untreated controls (Table 1, Group 1) and Group 2 given syngeneic AVN serum, the Group 3 animals treated with Lew serum showed complete inhibition of anti-Lew antibody production.

Fig. 2 Survival of Lew.1A skin grafts after treatment with Lew serum (●), AVN serum (○), untreated controls (△)

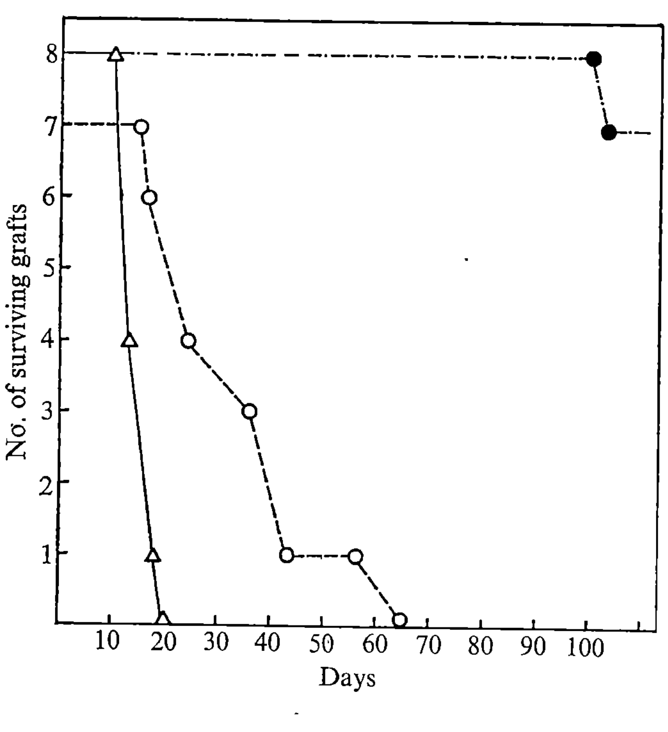

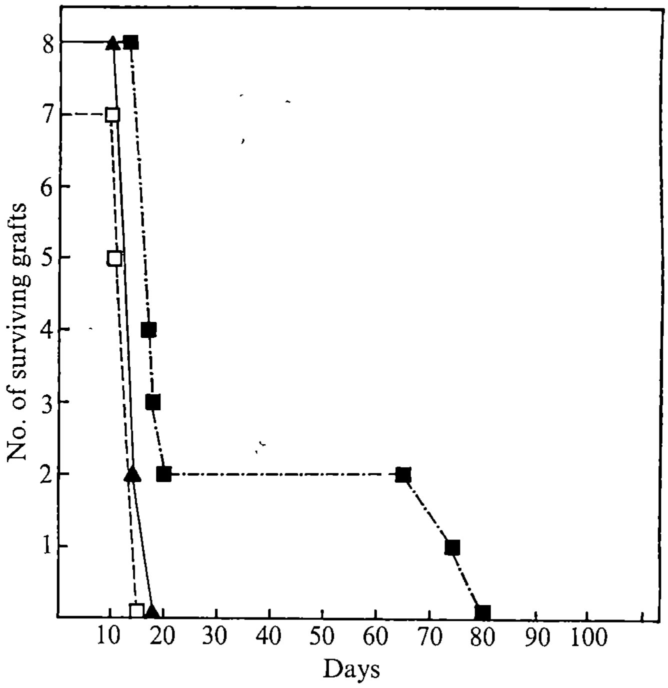

Fig. 3 Survival of Lew skin grafts after treatment with Lew serum (■), AVN serum (□), untreated controls (▲).

In spite of the presumably low content of antigens in the serum, permanent tolerance of skin grafts can be induced in rats, at least in the non-H–1 incompatible combination. The antigenic difference between the donor and recipient strains is relatively strong, as shown by the acute rejection of skin grafts in untreated controls. With the H–1 plus non-H–1 difference, the degree of tolerance achieved is considerably lower. This does not, however, exclude the possibility that it can be increased by concentrated antigen from the serum. The nonspecific immunosuppressive effect of normal serum on non-H–1 incompatible skin grafts is consistent with previous findings[9–14]. To summarise the present data, it seems that the serum may be a very good source of soluble H antigens useful for the induction of transplantation tolerance.

MILAN HAŠEK
JITKA CHUTNÁ
VLADIMÍR HOLÁŇ
MILOŠ SLÁDEČEK

Institute of Molecular Genetics,
Czechoslovak Academy of Sciences,
Prague 6, Czechoslovakia

Received April 22, accepted May 24, 1976.

[1] Calne, R Y , *et al.*, *Nature*, **227**, 903 (1970).
[2] Charlton, R. K , and Zmijewski, C. M., *Science*, **170**, 636 (1970).
[3] van Rood, J J , van Leeuwen, A., and van Santen, M C. T , *Nature*, **226**, 366 (1970)
[4] Schultz, J S., and Shreffler, D. C , *Transplantation*, **13**, 186 (1972).
[5] Aster, R H., Miskovich, B H , and Rodey, G E , *Transplantation*, **16**, 205 (1973).
[6] Oh, S. K , Pellegrino, M A , Ferrone, S , Sevier, E. D , and Reisfeld, R. A , *Eur. J Immun* , **5**, 161 (1975).
[7] Callahan, G N., Ferrone, S , Allison, J. P , and Reisfeld, R. A , *Transplantation*, **20**, 431 (1975).
[8] Sanderson, A. R., *Immunology*, **9**, 287 (1965).
[9] Kamrin, B B , *Proc. Soc exp Biol Med.*, **100**, 58 (1959).
[10] Mowbray, J F , *Transplantation*, **1**, 15 (1963).
[11] Pokorná, Z , and Vojtíšková, M , *Folia biol.*, *Prague*, **12**, 88, (1966).
[12] Mannick, J. A., and Schmid, K , *Transplantation*, **5**, 1231 (1967).
[13] Nelken, D , and Glaser, M , *Transplantation*, **14**, 268 (1972)
[14] Hanna, N , Kalderon, R , and Nelken, D., *Immunology*, **29**, 433 (1975).

●

Antibody response induced *in vitro* to the cell-surface alloantigen Thy–1

MANY important antibody responses are provoked by antigens on the surfaces of nucleated cells and, in spite of wide interest, little is known of the immunobiology of these responses. Alloantigens comprise an intriguing class of surface antigens because they may stimulate antibody production by B cells as well as target-cell killing by T cells and also because alloantigens are themselves intimately involved in the immunological recognition of other cellular antigens, such as viral antigens[1], autoantigens[2], surface-bound haptens[3], other alloantigens[4] and tumour-associated antigens[5]. Studies of antibody responses *in vitro*, involving potent xenoantigens, have contributed greatly to the understanding of cellular and molecular interactions in immunity[6]. This has suggested the potential of such systems for the study of responses to weaker antigens of nucleated cells. In this report I define such an experimental approach with the induction *in vitro* of primary and secondary responses to the murine alloantigen Thy–1 as measured with a modified plaque-forming cell (PFC) assay, developed from the method of Fuji *et al*[7].

Thy–1 is present as two allelic variants, Thy–1.1 (strain AKR) and Thy–1.2 (CBA)[8], and is expressed in high density at the surface of thymic lymphocytes which serve as target cells in the PFC assay. In initial experiments the induction of a response to Thy–1 was attempted by coculturing normal or primed AKR spleen cells with antigen in the form of viable CBA thymocytes. Very few PFC lytic to CBA thymus cells appeared although the duration of culture and cell ratios were varied. By contrast, the use of a cell-free supernatant of thymocyte cultures induced substantial PFC responses. A comparison of the ability of thymus cells and supernatant to induce a primary response is shown in Table 1. CBA but not AKR thymocyte supernatants (AKR-T-SN) induced the production of PFC from AKR spleen cells, at an optimal dilution of antigen of 1/15. Addition of CBA thymocytes to spleen cell cultures failed to generate PFC although they were present in numbers consonant on the concentrations of cells which yield immunogenic supernatants (2.5×10^6–5.0×10^6 ml^{-1}). In the absence of antigen, no PFC are detected in primary responses. Figure 1 illustrates the specificity of the primary response and also follows the response kinetics which show a maximum at 4 d. Later peak responses (5–6 d) have been found in other experiments. The AKR-T-SN, which fails to stimulate AKR spleen cells, can stimulate large anti-AKR PFC responses of CBA spleen cells (optimal dilution 1/10–1/25, data not shown). Reciprocity of the response, however, does not prove immunological specificity since it is possible that allogeneic supernatants simply induce polyclonal PFC responses. Further evidence for specificity was obtained through the use of third-party thymus supernatants derived from the congenic strains A/Thy–1.1 and A/Thy–1.2. Titrations of the immunogenicity of A/Thy–1.1-T-SN and A/Thy–1.2-T-SN paralleled precisely those of AKR-T-SN and CBA-T-SN, respectively (unpublished results). Since both A/Thy–1 strains have numerous alloantigens absent in AKR which excepting Thy–1.2, fail to induce PFC, it follows that the induction of PFC is antigen specific and attributable fully and exclusively to the Thy–1 antigen.

Secondary *in vitro* responses of AKR spleen cells from mice immunised *in vivo* with CBA thymocytes differ from primary responses in kinetics and in optimal antigen dose. The secondary response exhibits a sharp peak at 3 d and the optimal concentration of supernatant antigen is about 1/10 of that optimal for generating primary responses; an example of a secondary response is shown in Table 2. In this experiment the specificity of induction is evident, as AKR-T-SN produced only few PFC above a small background now detected in the absence of added antigen.

Although an antigenic difference at the Thy-1 locus induces the PFC response and other alloantigens fail to do so, it was possible that Thy–1 substance acted nonspecifically to augment immunity to another alloantigen or autoantigen and that the PFC response was not directed at Thy–1. This was examined by testing one pool of AKR anti-CBA PFC against a panel of thymus cells from strains AKR, A/Thy–1.1, CBA and A/Thy–1.2. Mean PFC per group on day 3 was 0, 0, 143, and 134, respectively, which rules out the possibility of autoantibody

Table 1 Comparison of the ability of thymus cells and thymus-cell culture supernatant to induce a primary antibody response to Thy–1 *in vitro*

Thymus cells as antigen	PFC per culture (±1 s.e.m.) (CBA target cells)	Culture medium as antigen (T-SN)	PFC per culture (±1 s.e.m.) (CBA target cells)
CBA 50.0×10^5	3±2.3	CBA 1:5	35±16.6
CBA 10.0×10^5	1±1.0	CBA 1:15	164±11.0
CBA 5.0×10^5	2±1.2	CBA 1:75	84±11.1
CBA 2.5×10^5	1±0.3	CBA 1:150	50±22.3
CBA 1.0×10^5	0±0		
CBA 0.5×10^5	1±0.7	Medium alone	0
AKR 50.0×10^5	0±0.3	AKR 1:5	4±3.3
AKR 5.0×10^5	4±2.3	AKR 1:15	10±2.0
AKR 1.0×10^5	1±1.0	AKR 1:75	2±0.3
		AKR 1:150	3±1.3

A modified Marbrook culture system was used[6] in which 15×10^6 spleen cells, in 1 ml of appropriate medium were placed into the inner dialysis compartment and 15 ml of Eagle's modified minimal essential medium (MEM) containing 5% newborn calf serum (MEM-CA_5) and 2-mercaptoethanol (5×10^{-5} M) were added to the outer flask. Thymocyte culture supernatant was prepared by cultivating thymocytes (62.5×10^6 ml^{-1}) in Dulbecco's modified MEM (E4) containing 10% foetal calf serum (E4-F_{10}) for 20 h at 37 °C in 10% CO_2 and air and collecting the supernatants by centrifugation at 250*g* and passage through a Millipore membrane (0.22 µm). PFC assays were based on the method of Fuji *et al.*[7], and modified to accommodate a Trypan blue staining routine[11]. Briefly, aspirated cultures were collected into pellets by centrifugation at 100*g* for 15 min and 0.05 ml of a 12% suspension of appropriate thymocytes (in MEM-CA_{10}) was added. The tubes were then warmed to 37 °C to receive 0.35 ml of 0.6% agar in E4-CA_{10}, the latter maintained at 45–50 °C. After mixing, the suspension was applied to the surface of a 50-mm Petri dish containing 1–2 ml of solid 1% Agarose (Induboise A37, L'Industrie Biologique Francaise, Gennevilliers) in phosphate-buffered saline (PBS). After gelation, 3.0 ml of E4-CA_{10} was added to each of the dishes which were then incubated at 37 °C for 3.5 to 4.5 h. Each dish then received 1.5 ml of complement (rabbit serum absorbed with mouse spleen cells) diluted 1:15 in E4-CA_{10}. After further incubation for 0.75 h the dishes were drained and stained with 1.5 ml of 0.2% Trypan blue for 20 min at 20 °C. The dishes were rinsed with PBS and the plaques were counted using a dissecting microscope (Baush and Lomb, ×10) adjusted for diffuse indirect illumination. In these experiments normal AKR spleen cells were suspended in 1 ml of various dilutions of thymocyte supernatant in E4-F_{10} or in E4-F_{10} containing various numbers of thymocytes, which were then added to the inner culture chamber. Triplicate or quadruplicate cultures were assayed for PFC after incubation for 4 d at 37 °C in a humid 10% CO_2–90% air atmosphere.

Table 2 Specificity of the induction of a secondary anti-Thy-1 response *in vitro* of AKR spleen cells by antigenic supernatants of thymocytes

AKR supernatant antigen (AKR-T-SN)	PFC per culture (±1 s.e.m.)	CBA supernatant antigen (CBA-T-SN)	PFC per culture (±1 s.e.m.)
1:25	33±19.7	1:50	198±9.5
1:125	(1) 21±7.0	1:125	(1) 340±60.0
1:500	17±9.6	1:500	166±61.9
		1:1,500	55±8.7
Medium alone	12±5.2	1:5,000	7±3.7

Cultures were assayed after 3 d for PFC. For priming, AKR mice received 4×10^7 CBA thymus cells intravenously 2–8 weeks before use The data were obtained with CBA target cells in the PFC assay; figures in parentheses are the mean autoantibody PFC per culture detected with AKR thymus cells as targets using portions of the same cultures

production and shows that virtually all the *in vitro* secondary alloantibody PFC produce anti-Thy-1 antibody. Primary response PFC, however, do contain an interesting subpopulation (10–20%) of autoantibody PFC.

These experiments demonstrate that alloantibody responses to a surface antigen of nucleated cells can be induced entirely *in vitro*. Both primary and secondary responses are produced, the latter with *in vivo* primed spleen cells, and are shown to differ in kinetics and in sensitivity to antigen. In contrast with *in vivo* PFC responses, which are induced on challenge with viable thymus cells (ref. 7 and my unpublished results), the *in vitro* responses are induced only with antigenic supernatants of cultured thymocytes. A rapid appearance of immunogen (⩽ 4 h) in culture supernatants was found in preliminary studies consistent with the release of Thy-1 antigen from thymocytes detected by Vitetta *et al.*[9]. Therefore, the failure of thymus cells to stimulate PFC cannot be ascribed to a late release of antigen and is the subject of a study in progress. Preliminary experiments involving gel filtration indicate that the cell-free immunogen is much larger than molecular Thy-1; it therefore probably comprises Thy-1 in association with other surface molecules. The contribution of the latter to the immunogenicity of Thy-1 remains to be determined.

This experimental system, more generally, permits access to some basic problems of cell-surface immunogenicity, such as interactions among distinct surface molecules, the handling and presentation of antigen, the role of T cells and the determinants they recognise, control mechanisms of the response and the possibility of a rational approach to the manipulation of the response[10]. In this respect, cell-surface antigens in autoimmunity, and those of viral and tumour origin are interesting candidates.

Fig. 1 Kinetics and specificity of a primary anti-Thy-1 PFC response to CBA target cells induced *in vitro* with AKR spleen cells stimulated by thymus cell culture supernatant. *a*, Response to CBA supernatant diluted 1:25; *b*, response to AKR supernatant diluted 1:25; *c*, response to medium alone. Vertical bars represent ±1 s.e.m.

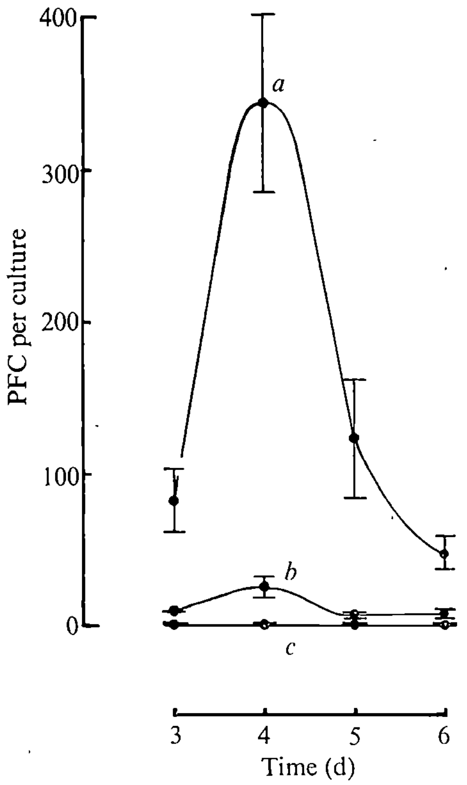

I thank Professor N. A. Mitchison for advice, Dr D. C. Parker for assistance and suggestions, Dr Elizabeth Simpson for congenic mice, and Juliet Strang for technical help. I thank the MRC of Canada for a postdoctoral fellowship.

PHIL LAKE

Imperial Cancer Research Fund,
Tumour Immunology Unit,
Department of Zoology,
University College London,
London WC1E 6BT, UK

Received April 12, accepted May 26, 1976

[1] Zinkernagel, R. M , and Doherty, P C., *Nature*, 248, 701–703 (1974)
[2] Iverson, G M , and Lindenmann, J , *Eur J. Immun* , 2, 195–201 (1972)
[3] Shearer, G. M., *Eur J Immun* , 4, 527–533 (1974)
[4] Bevan, M J , *Nature*, 256, 419–421 (1975).
[5] Wainberg, M. A , Markson, Y , Weiss, D W , and Dojanski, F , *Proc natn. Acad Sci. U S A.*, 71, 3565–3569 (1974)
[6] Feldman, M , in *Lymphocytes—Structure and Function* (edit. by Marchalonis, J J) (Dekker, New York, in the press)
[7] Fuji. H , Zaleski, M., and Milgrom, F., *Transplant Proc* , 3, 852–855 (1971)
[8] Snell, G. D., *Transplant Proc.*, 3, 1133–1139 (1971)
[9] Vitetta, E S , Uhr, J. W , and Boyse, E. A., *Eur J Immun* , 4, 276–282 (1974).
[10] Knight, R A , Leech, S , Mitchison, N. A , and Shellam, G , in *Seventh Miles Symp , Vienna*, 425–433 (Johns Hopkins University Press, Baltimore, 1974)
[11] Taylor, G M , and Bennett, J , *J. Immun Meth* , 2, 213–219 (1973).

Transition probability and the hormonal and density-dependent regulation of cell proliferation

WE have recently been studying cultured cells derived from the androgen-responsive mouse mammary tumour, Shionogi 115 (S115)[1,2]. Here we show, from time-lapse cinemicrographic analysis of these cells, that regulation of proliferation rates by both cell population density and physiological concentrations of testosterone is achieved by changes in 'transition probability'.

It is increasingly apparent that cell division depends on the occurrence of a random transition in G_1 (refs 3–5). On this basis, a model of the cell cycle has been proposed which also quantitatively accounts for the observed heterogeneity of cell cycle times within cell populations[3]. According to this model, the cell cycle is divided into two parts; one called the B phase where cells are proceeding towards division, and the other called the A state, where cells are not proceeding to division but are 'waiting' for a random triggering event to occur before proceeding. A cell may remain in this A state for any length of time and it has been shown that in steady-state conditions, the cell has a constant probability per unit time ('transition probability') of leaving the A state and entering the B phase[3]. It is thought that cells enter the A state in the G_1 phase of the cell cycle because the kinetics of entry of cells into the S phase are identical with the kinetics of entry into division[6]. The B phase then comprises part of G_1, and S, G_2 and M phases of the 'classical' cell cycle. The A state has much in common with the conventional G_0 in that cells in 'A' or 'G_0' are not proceeding towards division. Although G_0 is often regarded as a kind of refuge into which a fraction of cells can retreat when conditions are unfavourable for proliferation, all cells are supposed to enter the A state in every cell cycle, irrespective of their proliferation rate. Even optimally growing transformed fibroblasts enter the A state and then have a given transition probability of leaving and progressing to DNA synthesis and division.

According to the model, proliferation rates could be changed by altering either the duration of B phase (T_B) or the transition probability, or both. There is evidence that proliferation rates of animal cells are regulated in the main by changes in transition probability (P) rather than by changes in T_B (refs 4 and 5).

S115 cells are particularly interesting because physiological concentrations of testosterone have two distinct, reversible effects on the cells. First, at any density, testosterone stimulates the proliferation rate approximately twofold. Second, cells seeded in the presence of testosterone grow exponentially and fail to exhibit density-dependent regulation of proliferation rate until high densities (0.3×10^{6} cells cm^{-2}) are reached, whereas cells seeded in the absence of the hormone proliferate in a density-regulated manner; that is, proliferation rate decreases continuously over a wide range of increasing densities. Thus the phenomenon of density-dependent regulation of proliferation rate may be studied by comparing the behaviour of cells grown either in the presence or absence of a known, purified hormone.

Generation times of S115 cells growing in modified Eagle's medium have been analysed by time-lapse cinematography. The data is plotted as the logarithm of the percentage of undivided cells against age (Fig. 1). This type of curve is an α curve, (where α_t is the percentage of cells with intermitotic times $\geqslant t$)[3]. In an ideal population of cells having identical durations of B phases (T_B) and identical transition probability, α_t remains at 100% for ages up to T_B, then declines exponentially at a rate determined by the transition probability. It has been shown[3] that in steady-state cultures α curves exhibit initial curvature, produced by variability in the length of the B phase (T_B), followed by an exponential tail. The shortest intermitotic time gives the value of the minimum T_B, whereas the point at which the α curve becomes linear gives the maximum T_B. If a given treatment were to change T_B and not P, then the α curves for the treated and untreated populations would be parallel but laterally displaced from each other along the abscissa. Conversely, a change in P and not T_B would produce two lines with different slopes, but the same origin on the abscissa. It can be seen in Fig. 1 that the origins of the two curves for testosterone-treated and untreated cells are similar and the slopes of the exponential tails of the α curves are different, indicating that the minimum T_B is unchanged, but transition probability is different in each case.

Fig. 1 Semi-logarithmic plot of % cells undivided at age t (α) against t for S115 cells. S115 cells were cultured in Dulbecco's modified Eagle's medium containing 2% foetal calf serum and 30 mM HEPES as described previously[6]. Testosterone (T), when added, was present at 3×10^{-8} M. Exposures were made at 3-min intervals and individual intermitotic times measured by frame-by-frame analysis. The time of mitosis was taken when the cell rounded up before division. Number of observations = 93 for +T, 91 for −T. ○, + testosterone, ●, −testosterone. Inset, increase in cell number during the course of the filming.

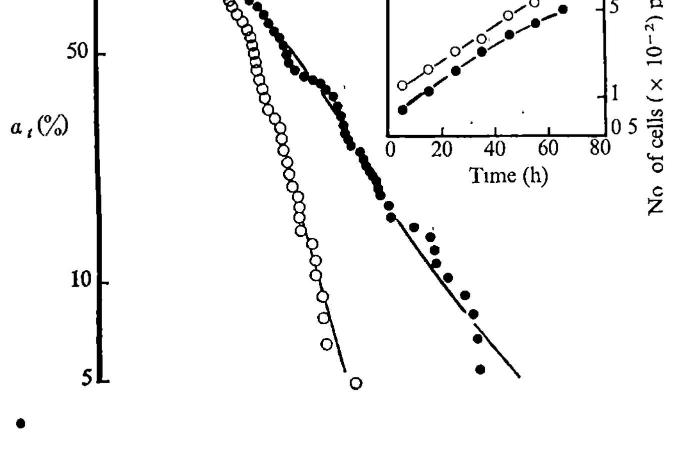

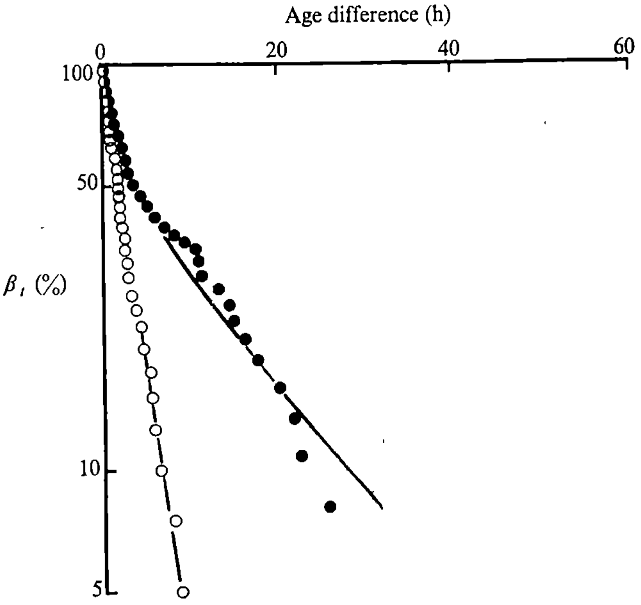

Fig. 2 Semi-logarithmic plot of % of sibling pairs with differences in intermitotic time > t (β) against t for S115 cells. Data were taken from the same film as Fig. 1. Number of sibling pairs = 40 for +T; 43 for −T. Symbols as Fig. 1.

Calculation of transition probability from the α curve is subject to some error since it is difficult to detect exactly when the initial curvature finishes. It has been shown that the differences in sibling intermitotic times can be used to give a better estimate of transition probability[4] because, in steady-state cultures, differences in intermitotic times of sibling cells are due entirely to differences in the times they spend in A state, their B phases being of identical duration[7]. The data in Fig. 2 are plotted on semi-logarithmic axes, giving a so-called β curve (where β_t is the percentage of sibling pairs with differences $\geqslant t$)[7]. Theoretically, β curves should yield a straight line plot if cells are growing exponentially, but not otherwise. Indeed this was found to be the case; the β curve for the exponentially growing, testosterone-treated cells gave a straight line, and that for the untreated cells curved upwards. The curvature indicates that transition probability is variable in the untreated cultures. To test whether this variability was a function of density, the data for sibling differences of the untreated cells were split into two groups on the basis of the time of division of the parent cell (Fig. 3). One group represents early divisions of the parent cell (less than 15 h after the beginning of the time-lapse film), whereas the other group represents later divisions (more than 15 h). The data in Fig. 3 show that the β curve of sibling cells dividing at later times is less steep than that of cells dividing at early times; that is, the mean transition pro-

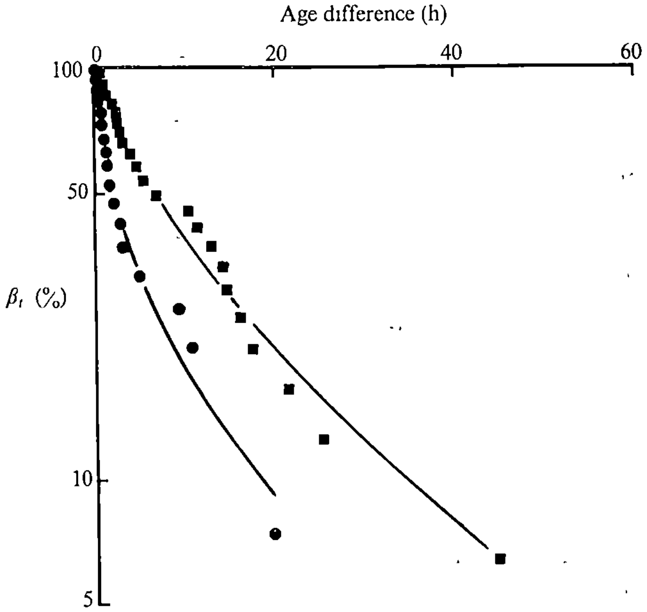

Fig. 3 Semi-logarithmic plot of β against t for two groups of the untreated cells ●, Analysis of siblings derived from parent cells which divided in the time interval 0–15 h from the beginning of the film. ■, Analysis of siblings derived from parent cells which divided at times > 15 h. Number of sibling pairs in the first group = 19; in the second group = 24

bability of later dividers is less than that of early dividers. Furthermore, both curves still display marked curvature, indicating that transition probability decreases continuously with density. In addition, α curves of the two groups demonstrated that there was little, if any, change in T_B with density (not shown).

In conclusion, both testosterone and cell population density affect proliferation rate by changing transition probability; both have little effect on the B phase of the cell cycle. The transition probability model may be successfully applied to non-steady-state cultures as well as to cultures growing exponentially.

JEFFERY H. ROBINSON
JAMES A. SMITH
NICHOLAS F. TOTTY

Department of Hormone Biochemistry

PETER N. RIDDLE

Cinemicroscopy Laboratory,
Imperial Cancer Research Fund,
Lincoln's Inn Fields,
London WC2A 3PX, UK

Received April 9, accepted May 26, 1976.

[1] Robinson, J H , *J. Cell Physiol* (in the press)
[2] Robinson, J H , and Smith, J A , *J Cell Physiol* (in the press)
[3] Smith, J. A , and Martin, L , *Proc natn Acad Sci. U S.A* , 70, 1263–1267 (1973)
[4] Smith, J A , and Martin, L , in *Cell Cycle Controls* (edit. by Cameron, I. L., and Zimmerman, A.), 43–59 (Academic, New York, 1974)
[5] Brooks, R F , *J. Cell Physiol* , 86, 369–378 (1973).
[6] Lnger, M D., Tobey, R A , and Saponara, A G , *J Cell Biol* , 36, 583–593 (1968)
[7] Minor, P D., and Smith, J. A , *Nature*, 248, 241–243 (1974)

Identification of the cell multiplication inhibitory factors in interferon preparations as interferons

THERE has been some controversy for the past few years concerning the inhibitory effect of interferon on cell multiplication We and others have presented evidence that interferon itself is the responsible factor[1-13]. Some investigators have, however, failed to observe any inhibition of cell multiplication with interferon preparations[14-17]; while others have observed inhibition but ascribed this effect to substances other than interferon in their preparations, either because no inhibition was observed when more purified preparations were used[18] or because of apparently inconstant ratios between antiviral and cell multiplication inhibitory (CMI) activities in a given preparation[19-21]. It has been claimed that the factor responsible for the CMI activity of human leukocyte interferon preparations could be physically separated from the factor responsible for the antiviral activity[22]. We provide strong evidence that the antiviral and CMI activities of interferon preparations are indeed intrinsic properties of the covalent structure of interferons.

Human[23] and mouse[24] interferon preparations can be reactivated after being unfolded under denaturing conditions in hot sodium dodecyl sulphate (SDS), a procedure which dissociates all non-covalently linked molecules[25] The finding that the antiviral activity of interferon can be recovered after such treatment has enabled the separation and identification of distinct molecular forms of both mouse[26,27] and human[28] interferons by electrophoresis in SDS–polyacrylamide gels. Accordingly, in our experiments human leukocyte and mouse C-243 cell culture interferon preparations were boiled in the presence of SDS, either in non-reducing or reducing conditions, were subjected to electrophoresis in SDS–polyacrylamide gels, and gel fractions tested for antiviral and CMI activities

The human leukocyte interferon preparation, electrophoresed after boiling in SDS in non-reducing conditions, contained two peaks of antiviral activity, one at about 21,000 daltons and one at approximately 15,000 daltons (ref 28 and Fig. 1*a*). The two peaks of antiviral activity coincide with the distribution of the CMI activity; there is a very good quantitative correlation between the antiviral activity and the CMI activity of each of the gel fractions.

When human leukocyte interferon was boiled in the presence of mercaptoethanol there was a loss of antiviral activity of the 15,000-dalton component, with only partial loss of the antiviral activity of the 21,000-dalton component (ref. 28 and Fig. 1*b*). Likewise, CMI activity was present in the 21,000-dalton component and markedly decreased or absent in the 15,000-dalton component (Fig. 1*b*).

Unreduced mouse C-243 cell interferon exhibited a major peak of antiviral activity at an apparent molecular weight of 38,000 and a minor peak at about 22,000 (Fig. 2*a*). Thus, these mouse interferon preparations are similar in molecular heterogeneities to mouse interferon preparations produced in L-929 cells induced with Newcastle disease virus[26] and in Lpa cells induced with MM virus[27]. There was a direct quantitative correlation between the antiviral and CMI activities in the regions of the two peaks (Fig 2*a*) Also when C-243 cell interferon was boiled in reducing conditions and electrophoresed in SDS–polyacrylamide gels, there was again a direct quantitative correlation between the two activities (Fig. 2*b*) and neither activity was present at 22,000 daltons.

In other experiments, gel eluates were assayed for both antiviral and CMI activities in cultures of $L_{\text{u-10}}$ cells, which were as sensitive as L-929 cells to the antiviral activity of mouse interferons and were approximately as sensitive as the L-1210 cells to the CMI activity of mouse interferon preparations. As in the experiments just described, the profiles of the two activities could be virtually superposed Also, it was found that about 1% of both the antiviral and CMI activities of human leukocyte interferon crossed on mouse $L_{\text{u-10}}$ cells. When these mouse cells were used to assay gel eluates of electrophoresed human leukocyte interferon preparations, activity profiles were obtained for both antiviral and CMI activities which correlated with those found in human cell assays, with each fraction being active in the mouse cells at about 1% of its activity in human cells.

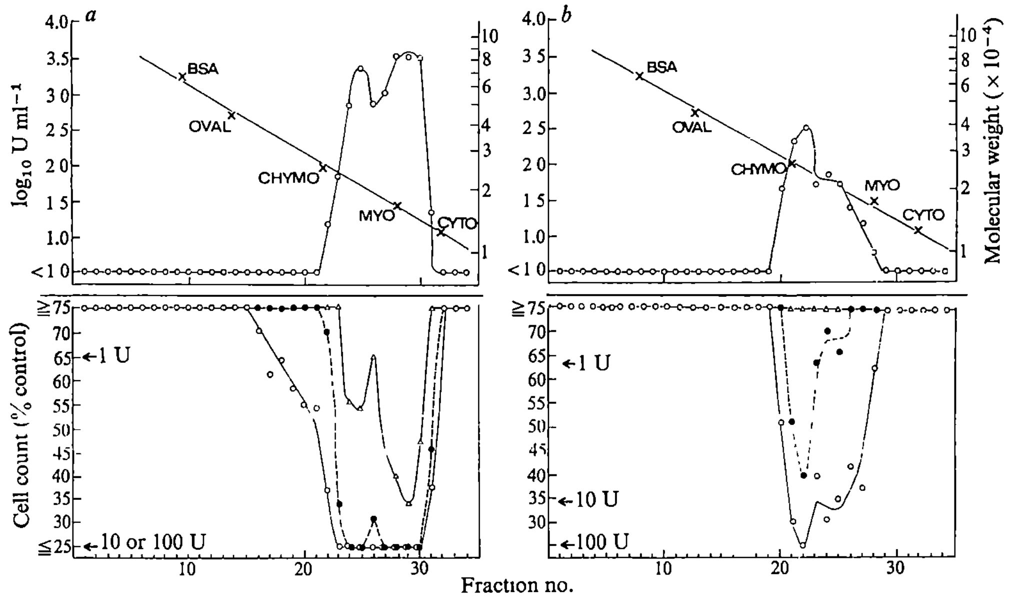

Fig. 1 SDS-polyacrylamide gel electrophoresis of human leukocyte interferon assayed for antiviral and CMI activities in non-reducing (*a*) and reducing (*b*) conditions. *a*, Human leukocyte interferon induced by Sendai virus[29] containing approximately 10^6 U (human standard reference 69/19) and 2.5 mg protein per ml in 0.01 M phosphate buffer, *p*H 7.2 was constituted to contain 1% SDS and 5 M urea and was boiled for 1 min. An aliquot of 0.1 ml was applied to the gel and, following electrophoresis, 5-mm gel fractions were eluted in 2 ml Eagle's MEM containing 10% calf serum. Conditions for electrophoresis were as described previously[26]. Upper panel: antiviral activity was assayed on human diploid skin fibroblasts challenged with vesicular stomatitis virus (VSV). BSA, bovine serum albumin; OVA, ovalbumin; CHYMO, chymotrypsinogen; MYO, myoglobin; CYTO, cytochrome *c*. Lower panel: CMI activity was assayed on Burkitt lymphoma cells (Daudi line)[30]. All gel eluates were incubated with 5×10^4 Daudi cells per ml in 2 ml RPMI medium containing 10% foetal calf serum, and cell multiplication was determined after 3 d incubation by counting viable cells in an haemocytometer using the Trypan blue exclusion test. Native human leukocyte interferon at 1, 10 and 100 U ml^{-1} was used as reference. All eluates were tested at a 1:10 dilution (○) and, where indicated, at a 1:100 (●) or a 1:1,000 dilution (△). All points are averages of duplicate determinations. *b*, The same human leukocyte interferon preparation was constituted to contain 1% SDS, 1% mercaptoethanol and 5 M urea and was boiled for 1 min before application to gel.

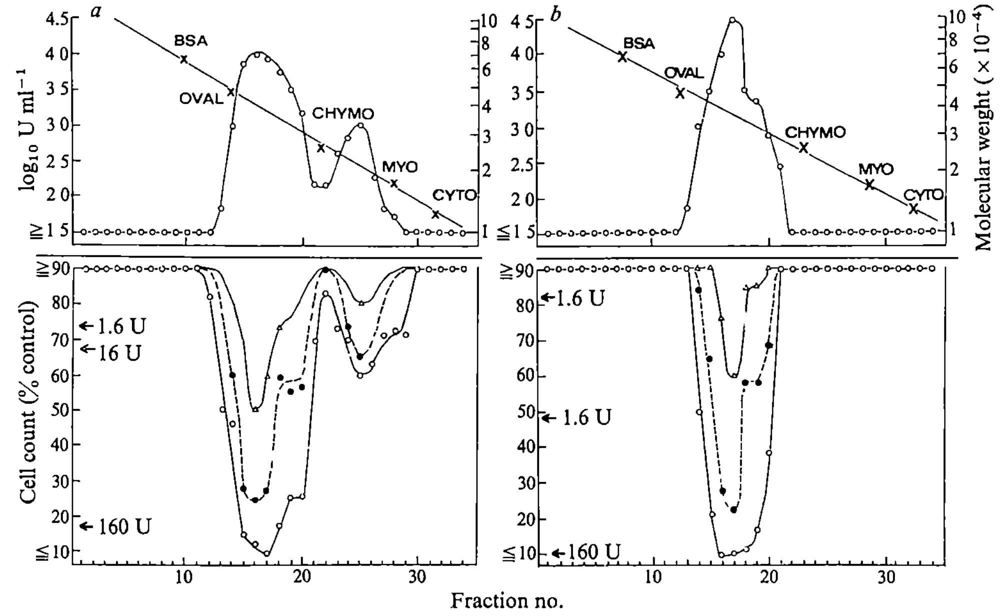

Fig. 2 SDS-polyacrylamide gel electrophoresis of mouse C-243 cell interferon assayed for antiviral and CMI activities in non-reducing (*a*) and reducing (*b*) conditions. *a*, Mouse C-243 cell interferon induced by Newcastle disease virus[31] containing approximately 3×10^6 U and 1 mg protein per ml in 0.01 M phosphate, *p*H 7.2, was constituted to contain 1% SDS and 5 M urea and was boiled for 1 min. An aliquot of 0.1 ml was applied to the gel and, following electrophoresis, fractions were eluted as in Fig. 1. Upper panel: antiviral activity as assayed on mouse L cells challenged with VSV[31]. Lower panel: CMI activity was assayed on mouse leukaemia L-1210 cells[2]. All gel eluates were incubated with 5×10^4 L 1210 cells ml^{-1} in 2 ml RPMI medium containing 5% horse serum, and cell multiplication was determined after 3 d incubation by counting viable cells in an haemocytometer using the Trypan blue exclusion test. Native mouse interferon at 1.6, 16, and 160 U ml^{-1} was used as reference. All eluates were tested at a 1:10 dilution (○) and, where indicated, at a 1:100 dilution (●) or at a 1:1,000 dilution (△). All points are averages of duplicate determinations. *b*, The same mouse C-243 cell interferon preparation was treated in the same reducing conditions as in Fig. 1*b*, before application to gel.

The direct quantitative correlation between the antiviral and CMI activities of both human leukocyte and mouse C-243 cell interferons—(after boiling these interferons in SDS and subjecting them to electrophoresis in SDS-polyacrylamide gels)—shows that the CMI activity is exerted by molecules with heterogeneities of the same size as those of the interferons in the preparations. Furthemore, as there were two peaks of activity for unreduced human leukocyte (21,000 and 15,000 daltons) and mouse interferon (38,000 and 22,000) the CMI factor is present in exactly the same proportion as the interferons of each of those sizes. Therefore, either both activities reside in the covalent structure of the same molecules (interferons), or there are two distinct populations of molecules that induce antiviral activity and two distinct populations of molecules, of the same two sizes and present in the same relative proportions as the two interferon populations, that induce CMI activity. Furthermore, in the case of human leukocyte interferon, each of these populations responsible for CMI activity, like the interferons, exert only ~ 1% of homologous activity in heterologous cells. The finding that the correlation between the two activities is unchanged when these interferons are boiled in reducing conditions and electrophoresed in SDS, indicates not only that the two activities reside in physically similar molecules (in terms of size heterogeneities) and are present in the same proportions, but that they are also due to chemically similar molecules (in terms of effects of reduction of disulphide bonds in detergent solution).

We thank Dr Kari Cantell for human leukocyte interferon and the Philippe Foundation for their help. W.E S., II was supported by EMBO. This work was aided in part by grants from the Del Duca Foundation and the Direction de Recherches et Moyens d'Essais.

WILLIAM E. STEWART, II
ION GRESSER
MICHAEL G. TOVEY
MARIE-THERESE BANDU
SYLVIA LE GOFF

Institut de Recherches
Scientifiques sur le Cancer,
94800 Villejuif, France

Received March 19, accepted May 20, 1976.

[1] Paucker, K , Cantell, K , and Henle, W., *Virology*, 17, 324–334 (1962)
[2] Gresser, I , Brouty-Boyé, D , Thomas, M. T and Macieira-Coelho, A , *Proc natn Acad Sci U S A* , 66, 1052–1058 (1970).
[3] Lindahl-Magnusson, P , Leary, P., and Gresser, I , *Proc Soc exp Biol Med* , 138, 1044–1050 (1971)
[4] Gresser, I., *et al* , *Proc Soc. exp. Biol Med* , 142, 7–10 (1973).
[5] Gresser, I , Bandu, M T , and Brouty-Boyé, D., *J. natn Cancer Inst* , 52, 553–559 (1974)
[6] Lee, S H S ; O'Shaughnessy, M V , and Rozee, K R , *Proc Soc exp Biol Med* , 139, 1438–1440 (1972)
[7] Ohwaki, M , and Kawade, Y , *Acta Virol* , 16, 477–486 (1972)
[8] McNeill, T A , and Gresser, I , *Nature new Biol* , 244, 173–174 (1973)
[9] Knight, E , Jr, *J Cell Biol* , 56, 846–849 (1973)
[10] Gaflney, E. V , Picciano, P. T , and Grant, C A., *J natn. Cancer Inst* , 50, 871–878 (1973).
[11] Hilfenhaus, J , and Karges, H E., *Z Naturforsch* , 29, 619–622 (1974)
[12] Strander, H , and Cantell, K , *In Vitro*, monograph 3, 49–56 (1974)
[13] Tan, Y H , *Nature*, 260, 141–143 (1976)
[14] Baron, S , and Isaacs, A *Br med J* , 1, 18–20 (1962)
[15] Levy, H B , and Merigan, T C , *Proc Soc exp Biol Med* , 121, 53–55 (1966).
[16] Moehring, J M , and Stinebring, W R , *Proc Soc exp. Biol Med* , 137, 191–193 (1971)
[17] Oxman, M N , Levin, M J , and Metz, D H , *Symp Antivirals with Clinical Potential, Stanford University, 1975, J infect Dis.* (in the press).
[18] Baron, S , Merigan, T C , and McKerlie, M L , *Proc Soc exp Biol Med* , 121, 50–52 (1966)
[19] Borecky, L., Fuchsberger, N , Hajnicka, V , Stancek, D , and Zemla, J , *Acta Virol.*, 16, 356–358 (1972)
[20] Borecky, L , Fuchsberger, N , Hajnicka, V , and Lackovic, V , *Biomedicine*, 19, 281–286 (1973)
[21] Matsuzawa, T , and Kawade, Y , *Acta Virol* , 18, 383–390 (1974)
[22] Dahl, H , and Degré, M , *Nature*, 257, 799–801 (1975)
[23] Stewart, W E , II, *et al* , *J gen Virol* , 26, 327–331 (1975)
[24] Stewart, W E , II, De Somer, P and De Clercq, E , *J gen Virol* , 24, 567–570 (1974)
[25] Maizel, J V , Jr, in *Methods in Virology*, 5 (edit by Maromorosch, K , and Koprowski, H), 179–246 (Academic, New York, 1971)
[26] Stewart, W E , II, *Virology*, 61, 80–86 (1974)
[27] Knight, E , Jr, *J biol Chem.*, 250, 4139–4144 (1975)
[28] Stewart, W. E , II, and Desmyter, J , *Virology*, 67, 68–73 (1975)
[29] Cantell, K , Hirvonen, S , Mogensen, K. E , and Pyhala, L , *In Vitro*, monograph 3, 35–38 (1974)
[30] Klein, E , Klein, G., Nadkarni, J J , Wigzell, H , and Clifford, P., *Cancer Res* , 28, 1300–1312 (1968)
[31] Tovey, M. G , Begon-Lours, J , and Gresser, I., *Proc Soc. exp. Biol. Med.*, **146**, 809–815 (1974).

Antiviral and cell growth inhibitory activities reside in the same glycoprotein of human fibroblast interferon

IT has been shown repeatedly that preparations of mouse interferon inhibit the growth of mouse cells *in vitro*[1–4]. In addition to inducing the antiviral state and inhibiting cell growth, preparations of mouse interferon stimulate interferon production by priming[5], enhance phagocytic activity[6], and potentiate in cells the toxic effect of double-stranded RNA[7]. All attempts with preparations of mouse interferon to separate the antiviral activity from the non-antiviral activities have been unsuccessful[3,5,8]. With human interferon few experiments have been reported, although the data available indicate inhibition of growth by preparations of human leukocyte interferon[9–11]. It has been claimed that the antiviral and cell growth inhibitory activities of human leukocyte interferon reside in different molecules and can be separated from each other by certain methods of fractionation[12]. In a more recent report[13], however, separation of the two activities could not be demonstrated even in drastic denaturing conditions. I have shown that both the antiviral and the cell growth inhibitory activity of human fibroblast interferon reside in the same glycoprotein.

Human fibroblast interferon was purified to homogeneity as described previously[14]. Before the final fractionate step on sodium dodecyl sulphate (SDS)-polyacrylamide gel the interferon was heated at 100 °C for 2 min in a buffer of 0.1 M Tris, *p*H 6.8, 0.1% SDS, 1% β-mercaptoethanol, and 5 M urea. The interferon was homogeneous and identical both biologically and chemically to the homogeneous interferon described in ref. 14. This homogeneous interferon was used in all experiments. Interferon was assayed on human fibroblast cells by a microassay technique[15] with vesicular stomatitis virus (VSV) as the challenge virus. All interferon units are expressed as international units (human standard reference 69/19). Human diploid fibroblasts between the twentieth and thirtieth doubling obtained from neonatal foreskin tissue were seeded into plastic flasks (25 cm^2) at 2×10^4–8×10^4 cells per flask. Cells were grown at 37 °C in 4 ml of Eagle's MEM supplemented with 10% foetal calf serum, 1.1 $g\,l^{-1}$ sodium bicarbonate 0.012 M HEPES buffer, 0.006 M Tricene buffer, and 50 $\mu g\,ml^{-1}$ gentomycin. The medium was changed every 5–7 d. In these conditions the cells grow with a doubling time of 35–40 h and to a final density between 1×10^6 and 2×16^6 cells per flask. The number of cells in each flask was counted in a haemocytometer after treatment of the cultures with a solution of 0.125% trypsin and 5×10^4 M versene in phosphate-buffered saline (PBS). Cell counts were performed every 24 or 48 h. Growth inhibition is defined as that inhibition which results in an increase of ⩾50% in the time for cell doubling.

The effect of homogeneous human fibroblast interferon on the growth of fibroblast cells in culture is shown in Fig 1. With either 200 U ml^{-1} (Fig. 1*a*) or 500 U ml^{-1} (Fig. 1*b*) the rate of cell growth is inhibited appreciably. The growth inhibition could be reversed by removal of the interferon-containing medium, washing the cells once with MEM then allowing the cells to grow in MEM only (Fig. 1*a*). Cells whose growth had been inhibited by the homogeneous interferon showed no toxic effects for the duration of the experiment (6–10 d, Fig. 1). Cells were routinely observed for 6–10 d after the addition of interferon. Caution

Another cultured cell, the Daudi cell line, derived from a
pure preparations of interferon, for in an earlier exploratory experiment with a preparation of impure fibroblast interferon (1×10^6 U mg^{-1}) a growth-inhibitory, but also toxic, effect was observed. In this case the cells rounded and detached from the surface 2–4 d after the addition of the interferon preparation (E. K., Jr, unpublished).

I conclude that the antiviral and growth inhibitory activity of human fibroblast interferon reside in the same glycoprotein. This may represent a difference between human fibroblast and leukocyte interferons since preparations of leukocyte interferon are reported to contain the two activities in separate molecules[12]. This separation of activities in preparations of leukocyte interferon has not been confirmed by electrophoresis of the interferon on polyacrylamide gel in conditions of drastic denaturation[13]. In the purification of the fibroblast interferon, growth inhibitory activity has not been found with the absence of the antiviral activity nor has a partial separation of the two activities been observed.

The very potent growth inhibitory activity of preparations of purified mouse interferon has been shown previously[3]. With the fibroblast cells, significant growth inhibition is observed at 200 U ml^{-1}. A molar concentration can therefore be calculated for growth inhibition as has been calculated for the antiviral activity of fibroblast interferon[14]. Thus, from an interferon concentration of 200 U ml^{-1}, a molecular weight of 20,000, (ref. 14) and a specific activity of 2×10^8 U mg^{-1}, a concentration for a significant growth inhibition of human fibroblasts of 4×10^{-11} M is calculated.

Fig. 1 Inhibition of the growth of human diploid fibroblast cells by homogeneous interferon. Cells were seeded at 2×10^4–8×10^4 cells per flask in 4 ml medium. After 24 h the medium was changed in all flasks with half of the flasks getting medium containing interferon. *a*, Interferon, 200 U ml^{-1}; *b*, interferon, 500 U ml^{-1}. ●, With interferon; ○, interferon removed; ■, control.

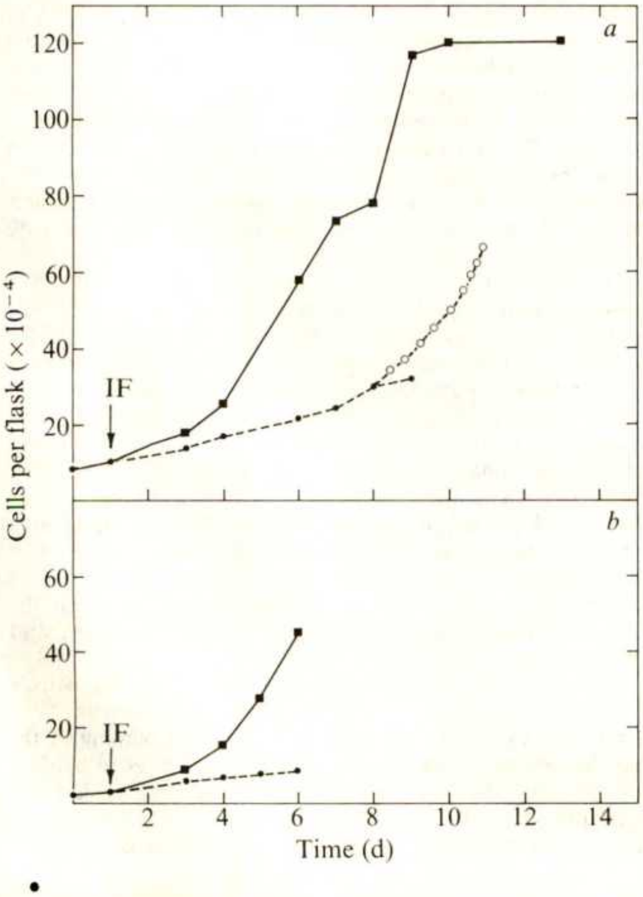

Another cultured cell, the Daudi cell line, derived from a Burkitt's lymphoma[16], has been shown to be particularly sensitive to preparations of leukocyte interferon for growth inhibition[17]. The growth of Daudi cells can be significantly inhibited at 1–5 interferon units per ml (refs 13 and 17).

There is an extensive list[18] of polypeptide hormones which regulate cell growth both *in vivo* and *in vitro* but unlike interferon most of the polypeptide hormones stimulate cell growth. For instance, insulin stimulates DNA synthesis in resting 3T3 cells at 3×10^{-9} M[19]. Fibroblast growth factor shows measurable stimulation of DNA synthesis in 3T3 cells at 4×10^{-11} M and maximum stimulation at 1×10^{-10} M (ref. 20). Cell growth inhibition has been reported for adrenocorticotropin (ACTH)[21] and factors such as 'chalones'[22].

I thank Dr R. Z. Lockart, Jr for discussions and suggestions, Miss Diana Fahey for technical assistance and Mr. N. Ferreira for preparing the interferon.

E. KNIGHT, JR

Central Research and Development Department,
E. I. du Pont de Nemours and Co.,
Wilmington, Delaware 19898

Received March 19; accepted June 1, 1976.

[1] Paucker, K., Cantell, K., and Henle, W., *Virology*, **17**, 324–338 (1962).
[2] Gresser, I., Fontaine-Brouty-Boye, D., Thomas, M. T., and Macieira-Coelho, A., *Proc. natn. Acad. Sci. U.S.A.*, **66**, 1052–1058 (1970).
[3] Ohwaki, M., and Kawade, Y., *Acta Virol.*, **16**, 477–486 (1972).
[4] McNeil, T. A., and Gresser, I., *Nature new Biol.*, **244**, 173–174 (1973).
[5] Stewart, W. E. II, Gosser, L. B., and Lockart, R. Z., Jr, *J. Virol.*, **7**, 792–801 (1971)
[6] Huang, K. Y., Donohoe, R. M., Gordon, F. B., and Dressler, H. R., *Infect. Immun.*, **4**, 581–588 (1971).
[7] Stewart, W. E., II, DeClercq, E., Billiau, A., Desmyter, J., and DeSomer, P., *Proc. natn. Acad. Sci. U.S.A.*, **69**, 1851–1854 (1972).
[8] Stewart, W. E., II, *et al.*, *Nature new Biol.*, **246**, 141–143 (1973).
[9] Cantell, K., *Ann. N.Y. Acad. Sci.*, **173**, 160–168 (1970).
[10] Lee, S. H. S., O'Shaughnessy, M. V., and Rozee, K. R., *Proc. Soc. exp. Biol. Med.*, **139**, 1438–1440 (1972).
[11] Gaffney, E. V., Picciano, P. T., and Grant, C. A., *J. natn. Cancer Inst.*, **50**, 871–878 (1973).
[12] Dahl, H., and Degre, M., *Nature*, **257**, 799–801 (1975).
[13] Stewart, W. E. II, Gresser, I., Tovey, M. G., Bandu, M., and LeGoff, S., *Nature*, **262**, 300–302 (1976).
[14] Knight, E., Jr, *Proc. natn. Acad. Sci. U.S.A.*, **73**, 520–523 (1976).
[15] Armstrong, J. A., *Appl. Microbiol.*, **21**, 723–725 (1971).
[16] Klein, E., *et al.*, *Cancer Res.*, **28**, 1300–1312 (1968).
[17] Adams, A., Strander, H., and Cantell, K., *J. gen. Virol.*, **28**, 207–217 (1975).
[18] Holley, R. W., *Nature*, **258**, 487–490 (1975).
[19] Holley, R. W., and Kiernan, J. A., *Proc. natn. Acad. Sci. U.S.A.*, **71**, 2908–2911 (1974).
[20] Gospodarowicz, D., *J. biol. Chem.*, **250**, 2515–2520 (1975).
[21] Masui, H., and Garren, L. D., *Proc. natn. Acad. Sci. U.S.A.*, **68**, 3206–3210 (1971)
[22] Bullough, W., and Laurence, E., *Expl Cell Res.*, **211** 394 (1960).

Direct measurement of membrane motion and fluidity by electron microscopy

THE mobility of cell membrane components[1] has been measured either in the light microscope scale (by visual labelling[2] and by the recovery of fluorescent bleaching[3,4]) or at the molecular level (by nuclear magnetic resonance (NMR)[5] and spin label EPR[6] methods). In this report, a new method, using electron microscopic techniques to measure membrane motion, is described. This method reduces the spatial and temporal averaging processes inherent in many other methods, and extends the resolution limit of observation to the nanometer scale. The main difficulty in applying electron optical techniques to kinetic measurement had been the requirement that the specimen be placed in a vacuum. The recent development of environmental stages[7] has partly overcome this problem. The direct observation of reaction kinetics in an electron microscope is now possible. The application of this technique to biological research enables biological reactions to be observed at high resolution in a physiological environment.

For model membrane studies, various molar mixtures of cholesterol, dipalmitoyl phosphatidylcholine and natural phosphatidylserine (extracted from bovine brain)[8] were used. The chloroform solution of the lipids were spread as monomolecular layers on the surface of the liquid subphase in a Langmuir trough. The subphase solution contained 5 mM Tris-HCl buffered to various *p*Hs. Polystyrene latex spheres (Dow) of sizes 0.237 μm or 0.088 μm were introduced into the subphase at a concentration of 0.005% solid. The charged latex spheres were electrostatically attached to the polar head group of the phospholipids at appropriate *p*H values. When bilayers were formed from the monolayers of the lipid mixtures as previously described[9], the latex spheres adhered to the hydrophilic surface of the bilayers. They served as membrane markers when the unsupported single bilayer was viewed in an electron microscope in a hydration stage[10]. The marked bilayers were kept fully hydrated at all experimental temperatures. The electron beam current was kept below 10^{-4} A cm^{-2} at the specimen level, the beam being deflected from the area of interest between photographing periods. Electron micrographs were recorded on Kodak No-Screen X-ray film. The images of the unsupported bilayer membranes were extremely dim at the low beam current. Focusing was made on an area adjacent to the area of interest. Time-lapse micrographs of several second intervals, as well as timed exposures of several seconds, were taken.

Two types of particle motion were observed. The fast, random motion of the particles was best described as a two-dimensional Brownian motion. The loci of the particles consisted of zig-zag tracks of random walk, as shown in Fig. 1. The mean square displacements $\overline{\Delta}^2$ were measured from the micrographs of exposure time τ, and the two-dimensional lateral diffusion coefficients D of the membranes were deduced from Einstein's equation: $\overline{\Delta}^2=4D\tau$. For a bilayer of an equimolar mixture of dipalmitoyl phosphatidylcholine and cholesterol at 15 °C, the r.m.s. displacement of 20 labels was 0.54 μm in 5 s. This value gave a diffusion coefficient D to be $(1.4\pm0.3)\times10^{-10}$ $\mathrm{cm}^2\ \mathrm{s}^{-1}$, the error being the standard deviation. This value is to be compared with those of bilayers of 4:1 molar mixtures of egg lecithin and cholesterol at 40 °C, that is 1.9×10^{-9} $\mathrm{cm}^2\ \mathrm{s}^{-1}$ and 1.5×10^{-7} $\mathrm{cm}^2\ \mathrm{s}^{-1}$ respectively from NMR[5] and spin label EPR[6] experiments. A recent measurement by fluorescent labelling method (W. W. Webb, personal communication) on egg lecithin and cholesterol bilayers also yielded a value of D in the range of 10^{-8} $\mathrm{cm}^2\ \mathrm{s}^{-1}$. Our low value was probably a result of the large size of the labelling spheres, which were expected to cover thousands of lipid molecules. The motion of the labels represented the collective motion of many lipid molecules attached to the labels, instead of the diffusion of a single molecule. The grouping of lipid molecules by the labels was expected to impede the fast diffusion motion of individual molecules. The higher cholesterol content, saturated hydrocarbon chains and the lower temperature of our specimens, may also have accounted for some of the discrepancies. Detailed measurements of D as functions of temperature and composition by this method will be published elsewhere.

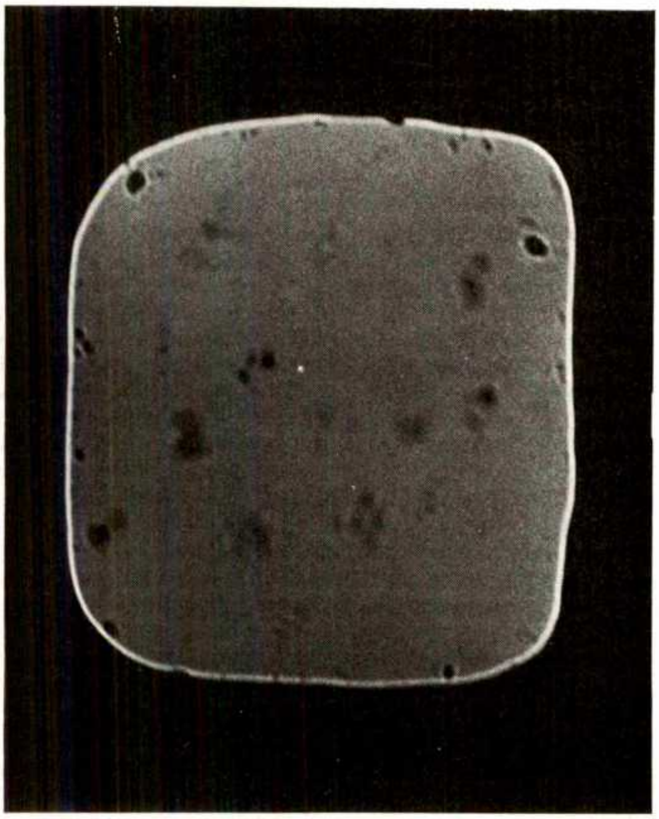

Fig. 1 Electron micrograph of the movement of 0.088-μm polystyrene latex microspheres attached to an unsupported bilayer of an equimolar mixture of dipalmitoyl phosphatidylcholine and cholesterol at 15 °C in saturated water vapour. The exposure time is 5 s. The loci of the movement of the micrographs appear as blurred patches, with darkened spots indicating points of changing direction of the path of random walk. Bright fringes are caused by defocusing of the objective lens for contrast enhancement (magnification ×7,480).

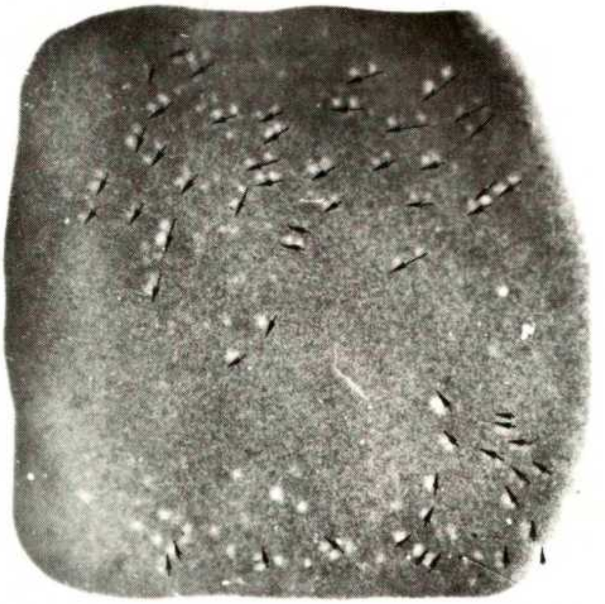

Fig. 2 The superposition of two negatives from consecutive electron micrographs of a microsphere-labelled bilayer of an equimolar mixture of dipalmitoyl phosphatidylcholine and cholesterol at 4 °C in saturated water vapour. The micrographs were taken 5 s apart. Arrows adjacent to the white sphere images indicate the relative positions of the microspheres from the first to the second micrograph (magnification ×6,528).

As the temperature of the specimen was lowered below the transition temperature of the bilayer membrane, the fast random motion was reduced. Time-lapse photographs of 10 s or more apart showed a convective movement of particles; the neighbouring particles often drifted along similar directions. Figure 2 shows the drift or marker particles. The mean drift velocity was 3×10^{-6} cm s^{-1}. If this is taken to be the "diffuse" velocity, the apparent value of D would be 10^{-11} $\mathrm{cm}^2\ \mathrm{s}^{-1}$, in rough agreement with NMR line shape measurement[11]. The coordinated drifting of particles indicated that the whole area moved as one patch. The boundaries between patches were discernible in the micrograph. The existence of patches or domains below the transition temperature agreed with the observations by electron microscopy[12,13] and diffraction[9], and with much indirect evidence[6].

Human erythrocyte membranes were prepared by the method of Jung[14]. The ghost membranes were labelled with latex microspheres of mean diameter 0.126 μm. The binding of the charged spheres to the ghost membranes was checked by dark field light microscopy. The ghost membrane suspension was either placed on the Formvar–carbon coated grids or directly on uncoated fine mesh (1,500 CPI) grids. Excess liquid on the grids was removed and the grids were viewed in the hydration stage. When uncoated grids were used, the labelled ghosts were seen to drift freely with the thin liquid film formed over the fine mesh holes. The movement of the marker particles in this case represented both the relative motion on the membrane, and the rotation and tumbling motions of the membranes as a whole. The latter type of motion was eliminated if the membrane sacs were deposited on Formvar–carbon substrates. An example of the marker movement on a ghost sac supported by Formvar–carbon substrate is shown in Fig. 3. The motion of the labels seemed to be more convective than diffusive even at 37 °C. (If the displacement of the labels was treated as diffusive, the apparent value of D would be in the order of 10^{-11} cm^2 s^{-1}.) A fluorimetric study[15] of the erythrocyte ghost membrane gave an upper limit of D to be 3×10^{-12} cm^2 s^{-1}. Both results suggested that the diffusive motion in human erythrocyte ghost membrane was damped. It should be interesting to note that the apparent D values in 3T3 cell membranes, measured by a similar collective labelling method using a light microscope[2], were the order of 10^{-11} cm^2 s^{-1}. A similar value was obtained from mouse L cell membranes by a fluorimetric study[4].

By using an electron microscope, the size of the marker particles can be reduced below the resolution limit of light microscopes (~0.5 μm), and the microscopic motion of the membrane can be followed in greater detail. Smaller labels are now being tested. The membrane motion observed in the submicrometre scale is the result of the collective behaviour of membrane molecules, rather than the motion of the individual molecules. The detailed movement of the membrane in this scale has vital biological significance[1]. By studying membrane motion in this scale, one can bridge the knowledge obtained from measurements in the single molecular level[5,6] and that from bulk viscosity measurement[2]. Observation of movements of microdomains as well as specific sites on the cell surface such as anionic sites, antigens and lectin receptors may now be possible with specific labelling techniques.

Fig. 3 Electron micrographs of microsphere-labelled human erythrocyte ghost membrane taken 4 s apart. The membranes are kept fully hydrated at 37 °C. The arrows on the first micrograph indicate the direction of movement of the labelling microspheres to the positions on the second micrograph. The spheres appear as dark on the hydrated membrane sac. Large, dark patches are liquid (magnification ×9,640).

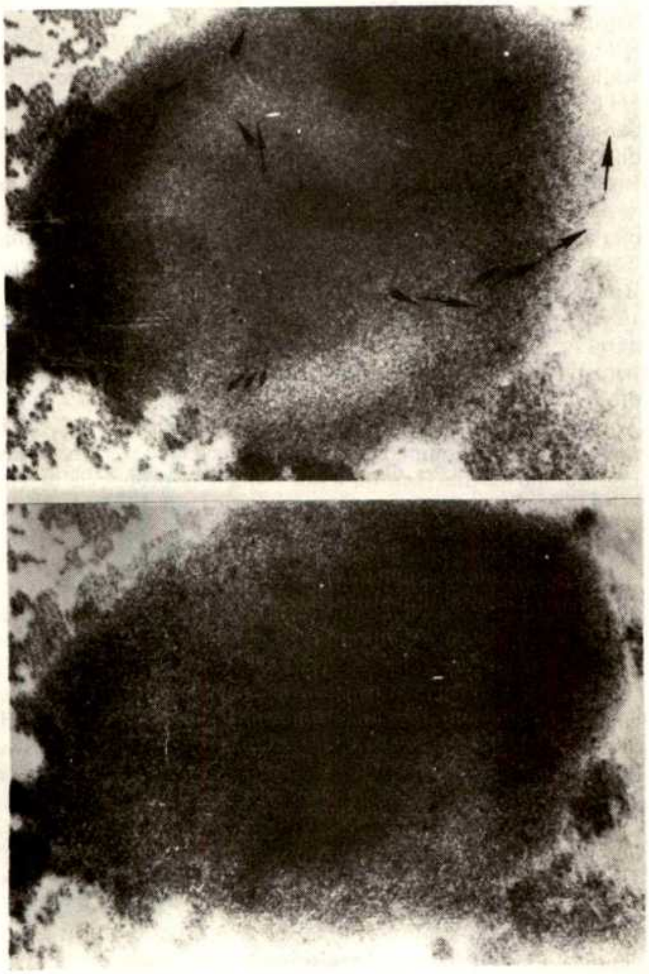

This work was supported by a US grant from the National Cancer Institute. I have appreciated discussions with Dr D. F. Parsons. Lipid specimens were provided by Dr D. Papahadjopoulos. I am the recipient of a career development award from the NCI.

S. W. HUI

Department of Biophysics,
Roswell Park Memorial Institute,
666 Elm Street,
Buffalo, New York 14263

Received February 9; accepted May 25, 1976.

[1] Edidin, M., *A. Rev. Biophys. Bioengng*, **3**, 179–201 (1974).
[2] Albrecht-Buhler, G., and Solomon, F., *Expl Cell Res.*, **85**, 225–233 (1974).
[3] Poo, M. M., and Cone, R. A., *Nature*, **247**, 438–440 (1974).
[4] Edidin, M., Zagyenski, Y., and Lardner, T. J., *Science*, **191**, 466–467 (1976).
[5] Lee, A. G., Birdsall, N. J. M., and Metcalfe, J. C., *Biochemistry*, **12**, 1650–1659 (1973).
[6] Shimshick, E. J., and McConnell, H. M., *Biochemistry*, **12**, 2351–2360 (1973).
[7] Parsons, D. F., *Science*, **186**, 407–414 (1974).
[8] Papahadjopoulos, D., and Miller, N., *Biochim. biophys. Acta*, **135**, 624–638 (1967).
[9] Hui, S. W., Parsons, D. F., and Cowden, M., *Proc. natn. Acad. Sci. U.S.A.*, **71**, 5068–5072 (1974).
[10] Hui, S. W., Hausner, G. G., and Parsons, D. F., *J. Phys. E.*, **9**, 69–72 (1976).
[11] Ulmius, J., Wennerstrom, H., Lindblom, G., and Arvidson, G., *Biochim. biophys. Acta*, **389**, 197–202 (1973).
[12] Hui, S. W., and Parsons, D. F., *Science*, **190**, 383–384 (1975).
[13] Ververgert, P. H. J., Verkleij, A. J., Elbers, P. F., and Van Deenen, L. L. M., *Biochim. biophys. Acta*, **311**, 320–329 (1973).
[14] Jung, C. Y., *Archs Biochem. Biophys.*, **147**, 215–226 (1971).
[15] Peters, R., Peters, J., Tews, K. H., and Bahr, W., *Biochim. biophys. Acta*, **367**, 282–294 (1974).

Potentiation of central reward by localised perfusion of acetylcholine and 5-hydroxytryptamine

THERE is considerable evidence that the ascending catecholaminergic systems of the brain[1] are involved with behaviour that is contingent on reward. Much of this evidence concerns the variables which influence intracranial self-stimulation behaviour[2]. Because the anatomical and neurochemical correlates of self-stimulation are specified, evaluation of the catecholamine hypothesis should ideally involve the manipulation or measurement of neurochemical activity within restricted regions of the brain. We have made a first step in determining the neurochemical code of the excitatory input to the dopaminergic systems which originate in the ventral mesencephalon (VM) and which are thought to play a part in intracranial self-stimulation[3]. A technique well suited for this purpose is push–pull perfusion with which exogenous putative neurotransmitters can be administered to discrete regions of the brain by way of the perfusion medium. Using this technique it was possible to establish dose–response relationships between self-stimulation of the medial forebrain bundle (MFB), through which fibres of the catecholaminergic systems pass, and perfusion of 5-hydroxytryptamine (5-HT) or acetylcholine (ACh) in the VM.

In each of eight male Norwegian hooded rats (250–350 g) a monopolar stimulating electrode (diameter 0.25 mm) and a stainless steel guide cannula (20 gauge thin wall) were stereotaxically implanted according to the coordinate system of De Groot[4]. The electrode was placed in the MFB (AP, 4.4; L, 1.7; HV, −9.0); and the guide cannula was positioned so that its tip rested 2–4 mm above the sites intended for perfusion (AP, 3.0–2.0; L, 1.0–1.5; HV, −5.0).

Five to seven days after surgery the rats were taught to depress a lever in a Skinner box in order to receive intracranial electrical stimulation. The stimulation parameters were individually adjusted for each rat so that a rate of lever pressing approximately 50% of maximum was obtained. Training continued until response rates were stable over a period of 90 min. Subsequently, that period was divided into three consecutive periods of 30 min which were designated pre-perfusion, perfusion and post-perfusion. The electrical stimulation parameters were identical for each of these three periods. The average frequency of lever pressing for the pre- and post-perfusion periods was determined. The frequency of lever pressing for the perfusion period was then expressed as a percentage deviation from this value.

Fig. 1 *a*, A histological section of rat brain showing a lesion made by the push–pull cannulae. The section was obtained from the brain of one of the animals used in this study. *b*, Representative frontal sections of rat brain modified from the stereotaxic atlas of Pelligrino and Cushman[3] indicating the confirmed placement of perfusion sites. cp, Posterior commissure; hp, fasciculus retroflexus; ip, interpeduncular nucleus; lm, medial lemniscus; nr, red nucleus; p, pons; pvg, central grey substance; sn, substantia nigra; vtn, Tsai's ventral tegmental nucleus.

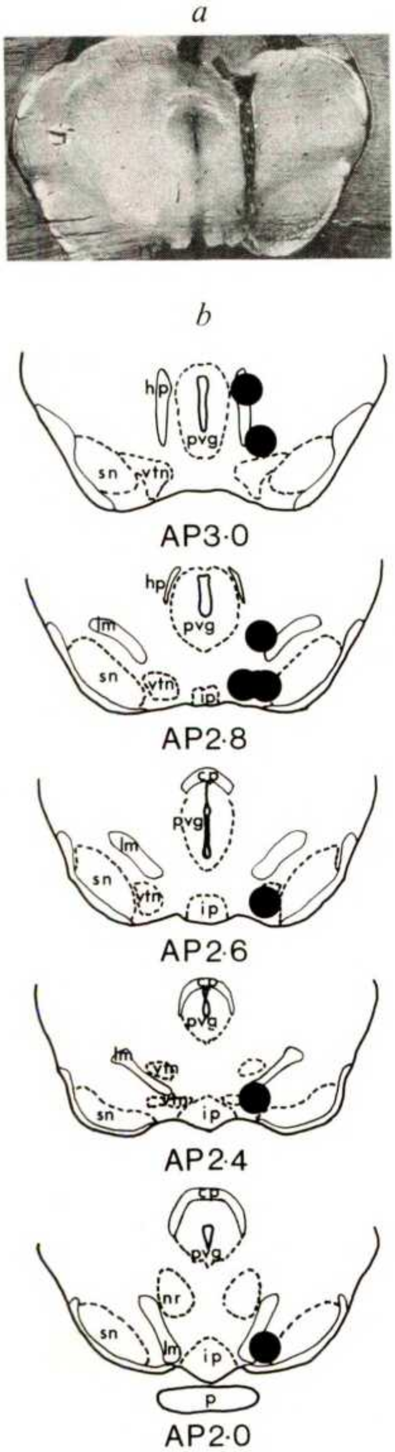

Because push–pull systems available at present often cause excessive traumatisation of brain tissues[5] a modified system was developed for use in the present study. Briefly, this system comprises the addition of a calibrated monitor tube to the pull side of the normally closed push–pull system. The level of fluid in this tube indicates the pressure in the pull line and gives immediate notice of any obstructions occurring within the brain. This facility prevents the inadvertent induction of expansion lesions and experimental hydrocephalus.

At the start of the "perfusion period" a concentric push–pull cannula assembly[6] was lowered through the guide cannula until its tip extended 2-4 mm beyond that of the guide. The rate of perfusion was between 0.6 and 1.7 μl min^{-1}. The perfusion was continued during the second experimental period and was continuously monitored for blockages occurring within the pull line. In the event of a blockage the cannulae were temporarily removed, flushed clear and replaced.

The perfusion medium was an artificial cerebrospinal fluid (CSF) consisting of: NaCl, 127.7 mM; KCl, 2.5 mM; $CaCl_2$, 1.3 mM; $MgCl_2$, 0.9 mM; $NaHCO_3$, 21.0 mM; Na_2HPO_4, 2.5 mM and glucose 3.4 mM. To this stock solution the required amounts of 5-hydroxytryptamine, creatine sulphate or acetylcholine chloride were added immediately before each experiment.

Each of six animals was tested with four doses of ACh, while each of four animals was tested with four doses of 5HT. The four dose levels, as well as a CSF vehicle control condition for both ACh and 5HT, were administered in a different random order for each animal. Successive perfusions with a given animal were separated by at least 24 h.

After completion of all behavioural testing, the position of the electrode tip and the site of perfusion in each animal were verified according to normal histological procedures. Brain tissue was fixed by an intracardial perfusion of a 10% formal saline solution after which it was embedded in paraffin wax. Serial sections of 8 μm were cut and stained with haematoxylin using the modified Weil–Weigert method of Wolf[7].

All electrodes were found to be located in the MFB region within 0.5 mm of the stated stereotaxic coordinates. Fig. 1*a* shows the type of lesion which is produced by the present push–pull perfusion technique, and Fig. 1*b* represents the loci of all perfusion sites.

The mean percentage changes (± s.e.) in MFB self-stimulation of four rats, when different doses of 5-HT were perfused in local areas of the VM, are shown in Fig. 2*a*. 5-HT increased self-stimulation in each of the four rats, an effect which was statistically significant ($P<0.02$, Kruskal–Wallis one-way analysis of variance[8]) for the group as a whole. In two of the animals the facilitatory effect of 5-HT disappeared at the two highest doses of 5-HT. Also in two animals, the effects of 5-HT on self-stimulation were accompanied by marked contraversive turning behaviour.

Figure 2*b* illustrates the mean percentage changes (± s.e.) in MFB self-stimulation of six rats when different doses of ACh were perfused in the VM. Following a significant increase in self-stimulation behaviour ($P<0.02$, Kruskal–Wallis one-way analysis of variance) response rates were depressed below baseline levels as the concentration of ACh in the perfusate was increased. Facilitation of self-stimula-

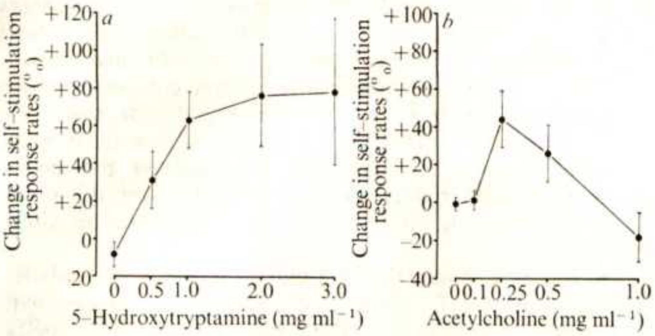

Fig. 2 *a*, Illustration of the mean percentage changes (± s.e.) in MFB self-stimulation of four rats when different doses of 5-HT were perfused in the ventral mesencephalon. *b*, Illustration of the mean percentage changes (± s.e.) in MFB self-stimulation of six rats when different doses of ACH were perfused in the ventral mesencephalon.

tion by ACh was observed in each of the six animals at the dose of 0.25 mg ml^{-1}.

The present results show that a given animal can be perfused repeatedly with the modified push–pull system without causing excessive physical trauma to the brain. The push–pull perfusion was used in preference to the intracranial microinjection technique for two reasons. First, the push–pull perfusion provides a degree of temporal control over chemical stimulation of the brain which is impossible to replicate with microinjections. Secondly, the continual replacement of fresh ACh from the push syringe obviates the need for substitute cholinergic agonists or cholinesterase inhibitors.

The finding that MFB self-stimulation was potentiated by localised perfusions of 5-HT in the VM is contrary to the inhibitory influence of 5-HT on self-stimulation suggested by Wise *et al.*[9] and by Poschel *et al.*[10]. The position adopted by these authors was based on experiments which involved the administration of pharmacological or neurotoxic agents either systemically or by way of the cerebral ventricles. These procedures will affect neurochemical activity in large areas of the brain. In contrast, the present results were obtained by perfusing 5-HT within restricted regions of the VM. The differences between the general and specific manipulation of 5-HT systems suggests an anatomical coding of brain function in which 5-HT may be used at different morphological locations in order to achieve opposite or competing behavioural or physiological effects.

The favoured explanation of the present results is that 5-HT and ACh may be exciting, directly or indirectly, the dopaminergic cell bodies known to be present in the VM. Supporting this view is, first, the fact that in some animals, marked contraversive rotation was observed in response to 5-HT. Dopaminergic systems in the VM have been strongly implicated in mediation of this behaviour[11]. Second, a pathway originating in the serotonergic cell group of the median raphe, from which self-stimulation can be obtained, terminates in the ventral mesencephalic tegmentum[12]. Third, self-stimulation of the serotonergic cell bodies of the median raphe can be modified by drugs which affect mainly catecholaminergic systems of the brain[13]. This implies that activity initiated in the median raphe might be relayed postsynaptically by way of catecholaminergic systems. The results of the present experiments suggest a possible anatomical substrate for the proposed interaction between serotonergic and catecholaminergic systems involved in central reward. Fourth, acetylcholinesterase has been localised within the dopamine-containing neurones of substantia nigra[14], presumably this is to inactivate ACh released from neurones afferent to the substantia nigra. Although the proposed explanation of the present results may be satisfactory for those perfusion sites located in or near areas containing the dopaminergic cell bodies[1], further investigation will be needed to clarify the role of 5-HT and ACh at the more dorsally located perfusion sites.

We acknowledge the expert assistance with the histology of Miss Gill Dolman. P. R. is supported by the Science Research Council.

Peter Redgrave
R. Ian Horrell

Department of Psychology,
The University,
Hull HU6 7RX, UK

Received April 13; accepted May 26, 1976.

[1] Ungerstedt, U., *Acta physiol. scand.*, **82**, suppl. 367, 1–48 (1971).
[2] German, D. C., and Bowden, D. M., *Brain Res.*, **73**, 381–419 (1974).
[3] Crow, T. J., *Brain Res.*, **36**, 265–273 (1972).
[4] Pelligrino, L. J., and Cushman, A. J., *A Stereotaxic Atlas of the Rat Brain* (Appleton-Century-Crofts, New York, 1967).
[5] Chase, T. N., and Kopin, I. J., *Nature*, **217**, 466–467 (1968).
[6] Myers, R. D., in *Methods in Psychobiology*, **2** (edit. by Myers, R. D.), 169–211 (Academic, London and New York, 1971).
[7] Wolf, G., in *Methods in Psychobiology*, **1** (edit. by Myers, R. D.), 281–300 (Academic, London and New York, 1971).
[8] Siegel, S., *Nonparametric Statistics for the Behavioural Sciences*, 184–193 (McGraw-Hill, New York, 1956).
[9] Wise, C. D., Berger, B. D., and Stein, L., *Biol. Psychiat.*, **6**, 3–21 (1973).
[10] Poschel, B. P. H., Ninteman, F. W., McLean, J. R., and Potoczak, D., *Life Sci.*, **15**, 1515–1522 (1974).
[11] Ungerstedt, U., and Arbuthnott, G., *Brain Res.*, **241**, 485–493 (1970).
[12] Simon, H., and Le Moal, M., *Expl Brain Res.*, **23** (suppl.) 190 (1975).
[13] Miliaressis, E., Bouchard, A., and Jacobowitz, D. M., *Brain Res.*, **98**, 144–201 (1975).
[14] Butcher, L. L., Talbot, K., and Bilezikjian, L., *Proc. West. pharmac. Soc.*, **18**, 256–259 (1975).

Stimulation of cerebral histamine H_2 receptors by clonidine

CLONIDINE (2-[(2,6-dichlorophenyl)amino]-2-imidazoline) is a potent antihypertensive agent whose site of action is believed to be in the central nervous system[1] but its mechanism of action is far from clear. Because of its effects on peripheral tissue, it has been generally accepted that the drug stimulates alpha-adrenergic receptors[1]. A recent report has, however, challenged this view: far from stimulating the receptors responsible for the accumulation of cyclic AMP in rat cortex, the drug seems to act as a potent alpha-adrenergic antagonist[2]. On the other hand, clonidine has been reported to stimulate gastric secretion by activation of histamine H_2 receptors[3]. It was therefore of interest to check whether clonidine could also act on H_2 receptors in brain tissues where they have been characterised[4–6]. We now report that clonidine strongly stimulates the accumulation of cyclic AMP in slices from guinea pig brain through activation of H_2 receptors.

Male Hartley guinea pigs (300 g; Janvier, Le Genest) were killed by decapitation and slices were prepared from the hippocampus and incubated according to Baudry *et al.*[4]. The hippocampus was selected because of the strong stimulation of adenylate cyclase elicited by histamine in this region[6]. Cyclic AMP was assayed at the end of 15-min incubations by the protein kinase binding method and proteins were determined by the method of Lowry *et al.* with bovine serum albumin as standard[4].

As shown in Fig. 1, clonidine induced a concentration-dependent accumulation of cyclic AMP. The half maximal stimulation was obtained with 50 μM and the maximal effect, representing a fivefold increase, was achieved by 500 μM.

The nature of the receptors involved in the effect of a supramaximal concentration of the drug was investigated with different kinds of antagonists.

Neither phentolamine, an alpha-adrenergic antagonist, nor timolol, a specific blocker of beta-receptors, nor mepyramine, a histamine H_1 antagonist, had any effect,

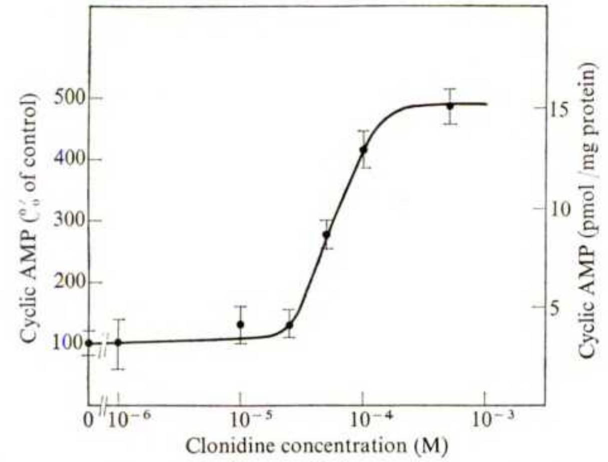

Fig. 1 Effect of increasing concentrations of clonidine on cyclic AMP accumulation in slices from guinea pig hippocampus. Each value represents the mean ± s.e.m. of three to four experiments.

even at 100 μM, on the clonidine-induced stimulation. On the other hand, the action of clonidine was partially inhibited by 1 μM of the H_2 antagonist, metiamide[7] and totally blocked at 100 μM of this agent. Furthermore, the stimulation elicited by 100 μM clonidine and 100 μM 4-methylhistamine, an agonist of H_2 receptors were not additive (Y.A., A.V., and J.S., to be published).

Taken together these results clearly indicate that clonidine stimulates histamine H_2 receptors in brain tissues, as already demonstrated in stomach[3] and heart[8]. In fact clonidine seems to be one of the most potent agonist of H_2 receptors available: both the EC_{50} and the maximal stimulation of cyclic AMP accumulation were of the same magnitude as for 4-methylhistamine (Y.A., A.V., and J.S., to be published).

It is not clear whether this action of clonidine on cerebral histamine receptors is related to its hypotensive properties. Since this drug exerts its cardiovascular effects at very low dosage (in the range of 100 μmol kg^{-1}), its strong efficacy *in vivo* hardly seems compatible with the EC_{50} determined in our *in vitro* system. In this respect, the blockade of adrenergic alpha-receptors in slices from rat brain occurs at a much lower concentration[2]. In addition, very little information is available concerning the possible involvement of histaminergic neurones in the central control of blood pressure. It has only been demonstrated[9] that the intraventricular administration of histamine elicits tachycardia and hypertension in several species; however this action seems to be mediated by way of H_1 receptors and the effects of a selective stimulation of cerebral H_2 receptors remain to be assessed.

Fig. 2 Effect of antagonists of H_1 or H_2 histaminergic and alpha- or beta-adrenergic receptors on the accumulation of cyclic AMP elicited by a supramaximal concentration of clonidine. None of the agents affected the basal level of cyclic AMP. Each value is the mean ± s.e.m. of four experiments. The width of the horizontal line represents the s.e.m. of unstimulated controls. Blank areas, 10^{-4} M; hatched areas, 10^{-6} M. $^*P < 0.005$. $^\dagger P < 0.0005$.

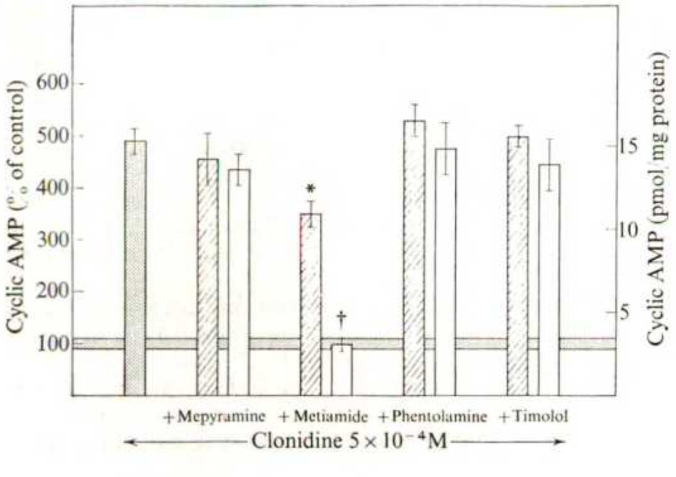

On the other hand, the high magnitude of the stimulation of the cyclic AMP system that we observe, together with the almost complete inhibition by intraventricular metiamide of the clonidine-induced hypotension which has been recently reported by Karppanen *et al.*[10] lend strong support to the idea that histamine H_2 receptors in brain could be involved in the action of clonidine.

We thank Professor H. Schmitt for helpful discussions.

YVES AUDIGIER
ALAIN VIRION
JEAN-CHARLES SCHWARTZ

Unité 109 de Neurobiologie,
2ter rue d'Alésia,
75014 Paris, France

Received March 22; accepted May 26, 1976.

1. Schmitt, H., *Actualités pharmacologiques*, **24**, 93–131 (1971).
2. Skolnick, P., and Daly, J. W., *Molec. Pharmac.*, **11**, 545–551 (1975).
3. Karppanen, H. O., and Westermann, E., *Naunyn Schmiedeberg's Archs. Pharmac.*, **279**, 83–87 (1973).
4. Baudry, M., Martres, M. P., and Schwartz, J. C., *Nature*, **253**, 362–363 (1975).
5. Haas, H. L., and Bucher, U. M., *Nature*, **255**, 634–635 (1975).
6. Hegstrand, L. R., Kanof, P. D., and Greengard, P., *Nature*, **260**, 163–165 (1976).
7. Black, J. W., Duncan, W. A. M., Emmet, J. C., Ganellin, C. R., Hesselbo, T., Parsons, M. E., and Wyllie, J. H., *Agents and Actions*, **3**, 133–137 (1973).
8. Csongraby, A., and Kobinger, W., *Naunyn-Schmiedeberg's Archs. Pharmac.*, **282**, 123–129 (1974).
9. Finch, L., and Hicks, P. E., *Br. J. Pharmac.*, 274P–275P (1975).
10. Karppanen, H. O., Paakkari, I., Paakkari, P., Huotari, R., and Orma, A. L., *Nature*, **259**, 587–588 (1976).

Synaptic vesicle cytochemistry changes when cultured sympathetic neurones develop cholinergic interactions

THE principal neurones of the rat superior cervical ganglion (SCG) can be established as dissociated cells in long term cultures[1] without the survival of the small intensely fluorescent "interneurone" normally found in the animal. These isolated sympathetic neurones (SCGN) exhibit certain expected adrenergic characteristics such as the synthesis and accumulation of catecholamines[2–4]. They also specifically take up exogenous noradrenaline and demonstrate Ca^{2+}-dependent release of this transmitter during induced depolarisation[5]. When these neurones are cocultured with thoracic spinal cord explants, they receive a typical cholinergic preganglionic input[6]. When cultured with the appropriate target of brown fat, the SCGN will provide characteristic noradrenergic contacts with the fat cells[7]. The interpretation of these generally expected results is confounded by the following observations: (1) cultures of dissociated sympathetic neurones form numerous synaptic contacts with each other[8–10]; (2) cytochemical studies of these synapses show that they contain predominantly dense-cored vesicles and thus appear to be noradrenergic[8–11]; and (3) physiological studies clearly indicate that synaptic signals between these cultured neurones are nicotinic–cholinergic[7,11]. In addition, dissociated SCGN will provide cholinergic innervation to striated muscle in culture[12]. Only one type of neurone, however, has been described in these cultures. We have investigated whether synaptic endings with the morphological characteristics of noradrenergic terminals were the only synaptic type to be found in cultures where cholinergic interactions between neurones were readily demonstrable. If, as previously reported, only synapses with noradrenergic cytochemical characteristics were found, it would strongly suggest that one synaptic type was handling both noradrenaline (NA) and acetylcholine (ACh). If two synaptic types were found it would suggest that two types of neurones were present in these cultured networks, thus providing a possible explanation for the paradoxical results discussed above.

We established sympathetic neuronal networks by dissociating the SCG from perinatal rats by a method previously described[9], but without antimitotic agents to suppress non-neuronal cell growth. In these conditions a substantial number of non-neuronal cells are present although these do not develop to the point of forming a confluent monolayer. We chose these conditions that foster cholinergic mechanisms (discussion in ref. 13) although we have observed cholinergic transmission in cultures entirely free of supporting cells[7]. All results presented here derive from one group of 60 cultures that was established simultaneously from one group of foetuses and maintained in an identical manner. After initial settling on to 24-mm Aclar dishes, each culture contained about 2,000 neurones, a number which remained essentially constant throughout the experiment. The use of a gridded culture dish assisted in counting the number of neurones per dish. Less extensive studies of previous culture series confirmed the results. The methods used for anatomical, biochemical and physiological analyses are given in the figure legends.

Choline acetyltransferase (ChAc) activity, which was very low in these cultures when first established, increased with age. ChAc activity in SCGN, expressed relative to number of neurones, increased more than 1,000-fold between one and 7.5 weeks (Fig. 1). The increase in ChAc activity during the development of SCGN *in vitro* probably reflects increased biosynthetic capacity for the production of ACh. The presence of this enzyme is considered a reliable indicator of the presence of cholinergic mechanisms[14–16]. During the same period acetylcholinesterase and dopa decarboxylase activities increased 30- and 20-fold, respectively, in this same culture series (our unpublished observations).

Physiological recordings indicated that nicotinic–cholinergic (hexamethonium-sensitive) synaptic interactions between the SCGN increased in potency and complexity with age in culture (Fig. 2*a* and *b*). In young cultures (20–33 d) only single responses (Fig. 2*a*), often with high failure rates, were observed. Reciprocal connections, frequent suprathreshold responses, and repetitive discharges (Fig. 2*b*) were first seen after 36 d in culture. The increased efficacy of synaptic transmission with age *in vitro* correlated with increased probability of finding interactions (Fig. 2*c*).

Fig. 1 Increase in ChAc activity with time in culture. ChAc activity was assayed radiometrically at 37 °C in homogenates of cultures by a modification[18] of existing methods[19,20]. Enzyme activity for each culture was expressed relative to the number of neurones in that culture. Values for time points between 7 and 53 d are means ± s.e.m. of activities in eight, eight, three, three, three, four and two cultures, respectively. The average number of neurones per culture was 2,160 ± 92 ($n = 31$). ChAc activities at 7 and 14 d were 0.83 ± 0.1 and 23.9 ± 3.7 pmol ACh produced per 100 neurones per h, respectively.

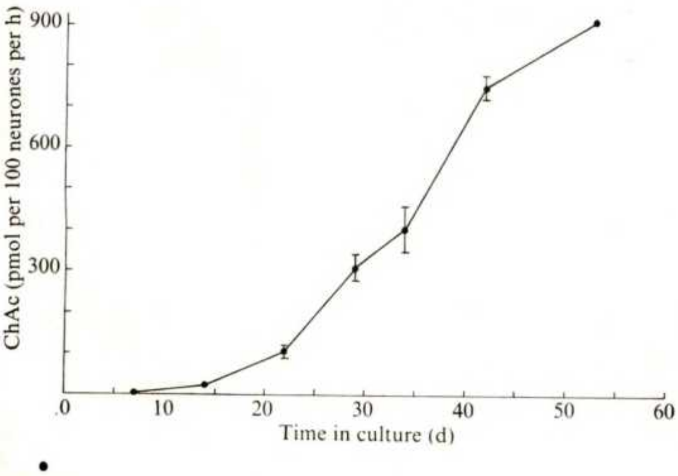

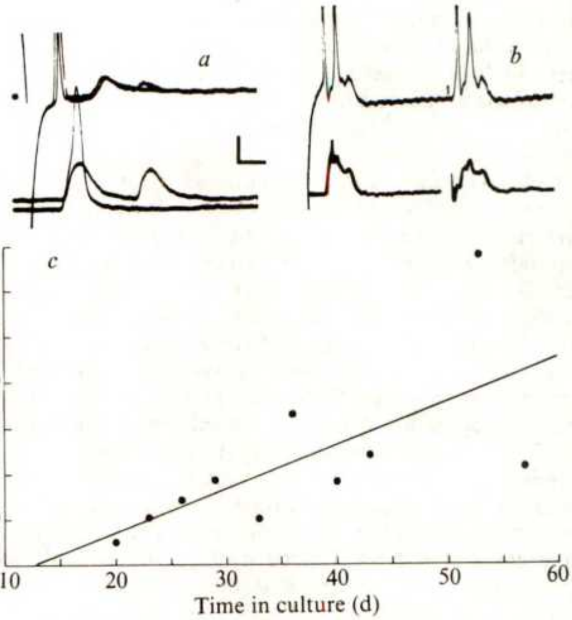

Fig. 2 Development of synaptic interactions as a function of days in culture. Intracellular recordings were obtained with 1M potassium citrate electrodes from SCGN that were maintained with a continuous perfusion of Eagle's MEM supplemented with antibiotics or with medium containing 10^{-4} M hexamethonium[6]. Evoked synaptic potentials were sought by sequentially stimulating, with anode break excitation, each of a pair of simultaneously impaled neurones. Examples of recordings taken from a 33- and 53-d culture are shown in *a* and *b*, respectively. *a*, Two superimposed stimulus trials of the cell shown in the upper trace (L9) evoked short latency subthreshold or suprathreshold responses in the cell shown in the lower trace (R6). Electrical stimulation of R6 did not reveal reciprocal connections to L9. The first subthreshold potentials in L9 (upper trace) were due to recurrent connections; late potentials occurring concurrently in both neurones were due to spontaneous activation from some unknown source. *b*, Direct stimulation of cell shown in upper trace (L3) from a 53-d culture evoked a short latency abortive action potential, followed by multiple subthreshold potentials, in cell shown in lower trace (R3) as well as recurrent suprathreshold plus multiple subthreshold responses in L3. Stimulation of R3 (shown as break in lower baseline) evoked a reciprocal suprathreshold response in L3 which, in turn, elicited the same complex sequence of responses seen when L3 was stimulated electrically. Only single responses were seen in young cultures (20–33 d) whereas repetitive and suprathreshold activation was frequently observed in older cultures (36–57 d). In more than 25 pairs of cells studied pharmacologically, hexamethonium reversibly blocked the synaptic activity. Calibration: *a*, 10 mV, 20 ms and *b*, 10 mV, 50 ms. *c*, Plot of the ratio of cells synaptically driven to number of cells stimulated as a function of age in culture. Each dot based on recordings from an average of 50 cells (range 40–60) from a single culture. Positive slope of linear regression line ($r = 0.66$ with $P < 0.05$) suggests that the probability of finding synaptically coupled neurones increases with age in culture.

Detailed morphological studies were carried out on these SCGN cultures at 1 and 8 weeks. Preloading with NA and $KMnO_4$ fixation techniques were used specifically to demonstrate catecholamine-containing dense-cored synaptic vesicles (see legend to Fig. 3). Figure 3 illustrates examples of synaptic profiles in contact with neuronal somata and proximal dendrites after 1 week (Fig. 3*a*) and 8 weeks (Fig. 3*b*). The vesicle population in the endings in the 1-week culture was predominantly dense-cored with few clear vesicles. In contrast, the synapse shown from the 8-week culture contained mainly clear vesicles. Less than 10% of the population of synaptic vesicles was clear in most terminals examined after 1 week, whereas by 8 weeks most terminals contained more than 80% clear vesicles (Fig. 4). But some profiles after 8 weeks retained a high percentage of dense-cored vesicles (as in Fig. 3*a*) with a low proportion of clear vesicles. On one neuronal soma from an 8-week culture, eight synaptic profiles contained principally clear vesicles and one profile showed a predominance of vesicles containing dense cores. Occasionally at 8 weeks, endings containing a large number of clear vesicles had several vesicles with striking dense cores. Some profiles consisted of two to three connected varicosities each of which contained the same predominant type of synaptic vesicle. Studies in progress indicate that the shift in type within the synaptic vesicle population may occur as early as 2 weeks *in vitro*.

These results indicate that acetylcholine synthesis, cholinergic transmission and synaptic terminals containing clear vesicles develop with time in culture, a critical change occurring around 2 weeks *in vitro*. This development is gradual and not total since profiles containing principally dense-cored vesicles are still present at 8 weeks. As the number of neurones per culture dish remains stable after 1 week, these results suggest that one neurone type maintains two distinct synaptic endings and neurotransmitter enzyme systems or, alternatively, that two different neuronal types are present after 2 weeks *in vitro*. The critical question now centres on the source of the large numbers of cholinergic neurones present in older cultures. The small number (about 5%) of cholinergic neurones which may be present in the normal rat SCG[17] could not explain the accumulation of the large number of cholinergic "driver" cells found in late cultures (Fig. 2). Are these cells gradually evolving in culture from one originally undetermined multi-potential precursor population or from a differentiated noradrenergic neurone whose properties are altered in the culture environment? We anticipate that an extensive characterisation of the types of synaptic profiles present during successive weeks *in vitro*, together with additional biochemical and physiological experiments, will resolve this issue.

Fig. 3 Electron micrographs of synaptic endings found on SCG neurones after 1 week (*a*) and 8 weeks (*b*) in culture. Dissociated neurones of the SCG dissected from perinatal rats were established in culture as described before[1]. Instead of a Leibovitz-based medium, a standard feed containing 65% Eagle's MEM with glutamine added, 25% human placental serum, 10% chick embryo extract, 3% 1.1 M glucose and nerve growth factor was used. At weekly intervals from 1 to 8 weeks the cultures were rinsed in Leibovitz medium (L-15) and incubated for 30 min in freshly prepared 10^{-5} M noradrenaline in Leibovitz to which ascorbic acid (0.2 mg ml^{-1}) was added. The *p*H was adjusted to 7.2–7.3 before incubation. A rinse in L-15 was followed by fixation with 3% $KMnO_4$ in Krebs' Ringer phosphate (*p*H 7.1, 4 °C) and by *en bloc* staining with 1% uranyl acetate in maleic acid buffer (*p*H 5.2, 4 °C). Embedding in Epon–Araldite followed dehydration. As expected with this fixation, postsynaptic densities are not demonstrated. Both (*a*) and (*b*) are at the same magnification.

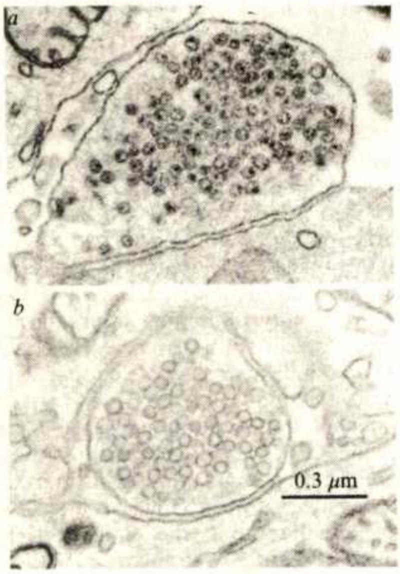

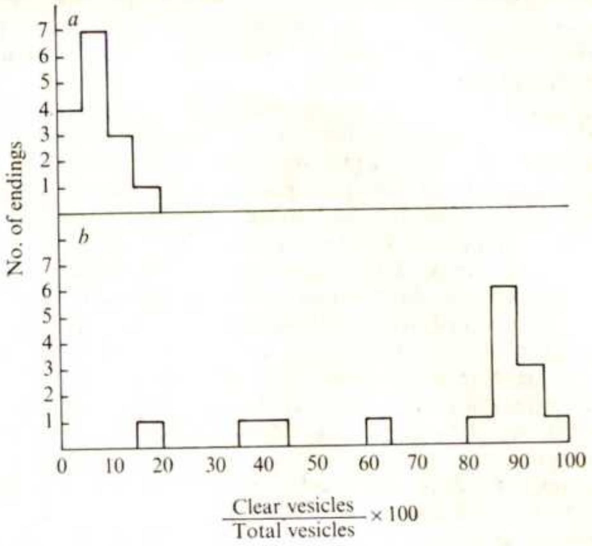

Fig. 4 Number of endings (ordinate) containing listed percentages of clear vesicles (abscissa) after 1(*a*) and 8(*b*) weeks *in vitro*. Consecutive endings found on the neuronal somata and proximal dendrites (as illustrated in Fig. 3) were photographed and printed at a standard magnification to count and classify vesicles measuring 40–70 nm as dense-cored or clear. Fifteen total endings at both 1 and 8 weeks are illustrated. Total vesicles ranged from 18 to 162 and 26 to 163, respectively.

This work was supported by grants from the NINCDS.

Mary Johnson
David Ross
Marta Meyers
Rosemary Rees*
Richard Bunge

Department of Anatomy and Neurobiology,

E. Wakshull
H. Burton

Department of Physiology and Biophysics,
Washington University School of Medicine,
660 South Euclid Avenue,
St Louis, Missouri 63110

Received March 22; accepted May 11, 1976.

*Present address: National Institutes of Health, Bethesda, Maryland 20014.

[1] Bray, D., *Proc. natn. Acad. Sci. USA.*, **65**, 905–910 (1970).
[2] Mains, R. E., and Patterson, P. H., *J. Cell Biol.*, **59**, 329–345 (1973).
[3] Mains, R. E., and Patterson, P. H., *J. Cell Biol.*, **59**, 346–360 (1973).
[4] Mains, R. E., and Patterson, P. H., *J. Cell Biol.*, **59**, 361–366 (1973).
[5] Burton, H., and Bunge, R. P., *Brain Res.*, **97**, 157–162 (1975).
[6] Ko, C-P., Burton, H., and Bunge, R. P., *Brain Res.* (in the press).
[7] Ko, C-P., Burton, H., Johnson, M. I., and Bunge, R. P., *Brain Res.* (in the press).
[8] Claude, P., *J. Cell Biol.*, **59**, 57a (1973).
[9] Bunge, R. P., Rees, R., Wood, P., Burton, H., and Ko, C-P., *Brain Res.*, **66**, 401–412 (1974).
[10] Rees, R., and Bunge, R. P., *J. comp. Neurol.*, **157**, 1–12 (1974).
[11] O'Lague, P. H., Obata, K., Claude, P., Furshpan, E. J., and Potter, D. D., *Proc. natn. Acad. Sci. U.S.A.*, **71**, 3602–3606 (1974).
[12] Nurse, C. A., and O'Lague, P. H., *Proc. natn. Acad. Sci. U.S.A.*, **72**, 1955–1959 (1975).
[13] Patterson, P. H., and Chun, L., *Proc. natn. Acad. Sci. U.S.A.*, **71**, 3607–3610 (1974).
[14] Feldberg, W., *Physiol. Rev.*, **25**, 596–642 (1945).
[15] Hebb, C. O., in *Cholinesterase and Anticholinesterase Agents, Handbook of Experimental Pharmacology* (edit. by Koelle, G. B.), **15**, XV, 56–88 (Springer, Berlin, 1963).
[16] Silver, A., *Int. Rev. Neurobiol.*, **10**, 57–109 (1967).
[17] Yamauchi, A., Lever, J. D., and Kemp, K. W., *J. Anat.*, **114**, 271–282 (1973).
[18] Ross, D., Cohen, A. I., and McDougal, D. B., Jr, *Invest. Ophthal.*, **14**, 756–761 (1975).
[19] McCaman, R. E., and Hunt, J. M., *J. Neurochem.*, **12**, 253–259 (1965).
[20] Fonnum, F., *Biochem. J.*, **113**, 291–298 (1969).

Enkephalin regulates the levels of cyclic nucleotides in neuroblastoma x glioma hybrid cells

NARCOTICS do not normally occur *in vivo*. "Opiate receptors" must therefore have evolved to recognise endogenous ligands, which are mimicked by the opiates[1]. Indeed such compounds have been isolated[2-5] and their structure elucidated as that of the two pentapeptides leucine- and methionine-enkephalin[6]. Neuroblastoma × glioma hybrid cells 108CC15 display many properties characteristic of neurones[7]. In these cells morphine and other narcotics[8-10] prevent the increase in the level of cyclic AMP that is caused by prostaglandin E_1 (PGE_1)[11]. The opiates also increase the level of cyclic GMP in the hybrid cells[12]. On long term incubation with morphine, the hybrid cells show phenomena which can be interpreted as biochemical correlates of morphine tolerance, dependence and withdrawal[9,13].

Fig. 1 Leu-enk (*a*) and levorphanol (*b*) inhibit the elevation by PGE_1 (0.3 μM) of the level of cyclic AMP in the neuroblastoma × glioma hybrid line 108CC15. 2.5 ± 10^5 viable cells were seeded on to replica plates (85 mm in diameter) containing 20 ml of growth medium[11]. The cells were grown for 4 d before the medium was removed. The cells were first washed and then incubated with 5 ml of incubation medium[14] and the various additions at 37 °C for 10 min. Leu-enk was added as a 100-fold concentrated solution in water. 1.9 million viable cells per plate, 90% viability (exclusion of nigrosin), passage number 17. After the incubation the cellular content of cyclic AMP was determined as described[14], with the exception that the columns for the purification of cyclic AMP were modified[12] and that the nucleotide was eluted with 5 ml of 0.05 M HCl. Each value is the mean ± s.d. of data obtained from three parallel incubations. Leu-enk was synthesised by conventional methods coupling Z–Tyr–(BZL)–Gly–Gly–OH[15] and H–Phe–Leu–OH[16] by the mixed anhydride procedure to yield Z–Tyr–(BZL)–Gly–Gly–Phe–Leu–OH (melting point 181–183 °C $(\alpha)^{20}_{546}$ −25.8 ° and $(\alpha)^{20}_{D}$ −21.7 °, c, 1.06 in dimethylformamide). Hydrogenolytic removal of the protecting groups led to chromatographically and sequentially homogeneous leu-enk (melting point 197–199 °C (dec.); $(\alpha)^{20}_{546}$ +35.3 ° and $(\alpha)^{20}_{D}$ +29.1 °, c, 1.15 in water; amino acid ratios in acid hydrolysate: Tyr 1.00 (1), Gly 1.95 (2), Phe 1.00 (1), Leu 1.00 (1); ultraviolet maximum (water) 274.5 nm, $\varepsilon = 1,350\ M^{-1}\ cm^{-1}$).

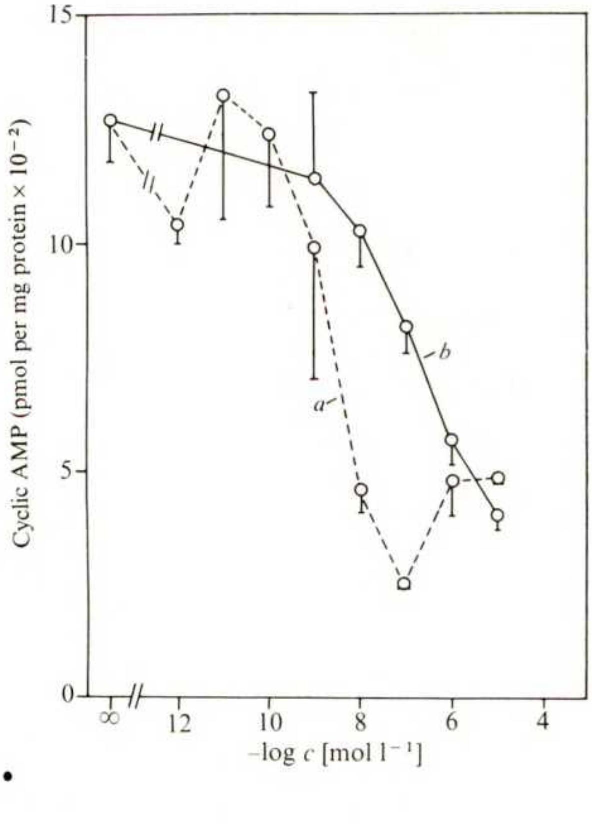

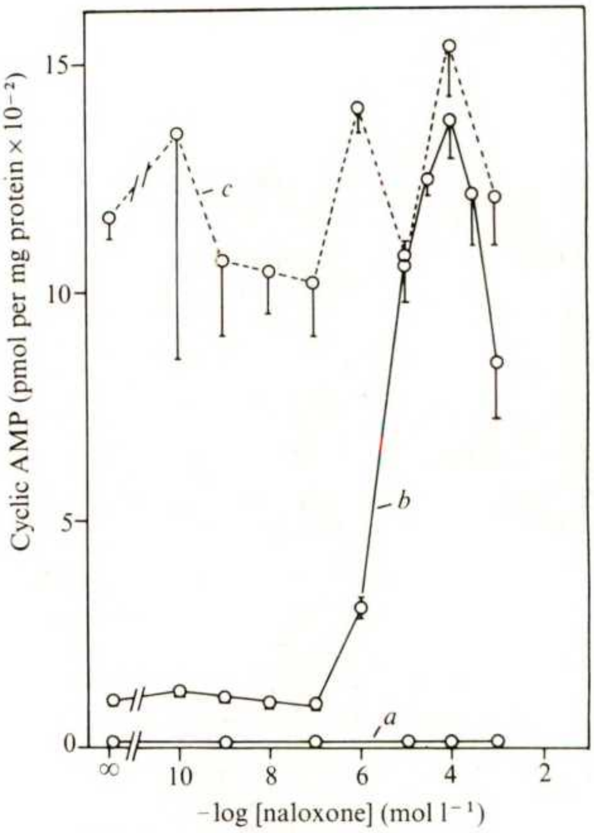

Fig. 2 Naloxone prevents the inhibition by leu-enk of the PGE_1-induced increase in the level of cyclic AMP. *a*, Absence of PGE_1 and leu-enk; *b*, Presence of 0.3 μM PGE_1 and 0.1 μM leu-enk; *c*, Presence of PGE_1. 2.3×10^6 viable 108CC15 cells per plate, viability 92%, passage number 16. Other details as in Fig. 1.

Here we report that leucine-enkephalin (leu-enk) has effects like those of opiates on the hybrid cells.

PGE_1 strongly elevates the level of cyclic AMP in the hybrid cells[11]. Increasing concentrations of leu-enk progressively prevent this increase (Fig. 1*a*) until maximal inhibition is observed at 0.1 μm (concentration at which 50% inhibition takes place, IC_{50}, 3 nM). In the range 0.1–1 μM leu-enk the curve rises again, but there is no further increase between 1 and 10 μM leu-enk (Fig. 1*a*). In several independent experiments the same results were obtained. Such an increase in the level of cyclic AMP was also observed at concentrations above 0.1 mM of morphine and its congeners[8]. Levorphanol (Fig. 1*b*) is a less potent inhibitor of the PGE_1 elevation of cyclic AMP than leu-enk. Its IC_{50} value (0.3 μM), which is identical to that reported[9], is approximately 2 orders of magnitude higher than that of leu-enk. In the absence of PGE_1 1 μM leu-enk maximally lowers the level of cyclic AMP from 19.8 ± 2.6 to 9.6 ± 1.4 pmol mg^{-1} protein. As is the case with morphine[10,17,18], the action of leu-enk is due to an inhibition of the formation of cyclic AMP and is not associated with an increase in cyclic AMP phosphodiesterase activity. The increase from 796 ± 176 in the presence of PGE_1 to $4,940 \pm 220$ seen in the presence of PGE_1 and the phosphodiesterase inhibitor isobutylmethylxanthine is partially suppressed to $2,590 \pm 60$ pmol cyclic AMP per mg protein if 0.1 μM leu-enk is included in the incubation medium.

Naloxone completely prevents the inhibition by leu-enk of the PGE_1-induced rise in the level of cyclic AMP (Fig. 2*b*). In the absence of leu-enk (Fig. 2*c*), or of PGE_1 and leu-enk (Fig. 2*a*), naloxone has no effect.

As is the case with morphine[12] (Fig. 3*a*), leu-enk (Fig. 3*b*) causes an elevation of the intracellular level of cyclic GMP. The half-maximal stimulating concentrations (EC_{50}) of morphine and leu-enk are around 0.1 μM (Fig. 3*a*) and 0.3 nM

(Fig. 3*b*), respectively. From one experiment to another these EC_{50} values vary considerably, but they seem to change in parallel with one another.

Naloxone prevents the increase in the level of cyclic GMP that is elicited by leu-enk (Fig. 4*a*). Its IC_{50} value is 20 pM. Up to a concentration of 10 nM, naloxone alone causes no effects of its own on the level of cyclic GMP. At more elevated concentrations it raises the level of cyclic GMP even in the absence of leu-enk (Fig. 4*b*).

The influence of leu-enk or opiates on the levels of cyclic nucleotides are strongly dependent on the presence of high concentrations (154 mM) of Na^+, as used in the present experiments. In the absence of Na^+, leu-enk at pM concentrations elevates the level of cyclic AMP (these authors, in preparation). This phenomenon may be related to the observation that opiate agonist binding is favoured at low, and antagonist binding at high concentrations of sodium ions[19,20].

Besides the short-term effects of leu-enk, long term effects similar to those reported for morphine[9,13], can be observed. If the hybrid cells are preincubated for 6 h with 1 μM leu-enk, the level of cyclic AMP that is reached during the subsequent main incubation (10 min) with 0.3 μM PGE_1 rises from 830±40 to 1,190±130 pmol cyclic AMP per mg protein. If 1 μM leu-enk is added at $t = 0$ and 3 h of the 6 h preincubation period, the subsequent stimulation by PGE_1 raises the level of cyclic AMP to 1,830±140 pmol per mg protein. Details of these experiments will be published elsewhere (our results, in preparation).

The data presented demonstrate an analogous influence on the hybrid cells of opiates and leu-enk. The opiates and leu-enk both depress the rate of formation of cyclic AMP and cause an increase in the level of cyclic GMP. The effects are all blocked by naloxone. Data almost identical to these for leu-enk were obtained with methionine-enkephalin. The similarity in the actions of opiates and leu-enk is paralleled by their structural similarity (J. R. Smythies, personal communication, and refs 21 and 22). The physiological meaning of the increased levels of cyclic GMP remains to be discovered. The short term action of opiates, that is, the depression of the formation of cyclic AMP, is probably correlated with its analgesic effect[23,24]. From analogy then, one may conclude that the enkephalins are neurohormones that, in the brain, suppress the sensation of pain. From studies on animals[25] and the neuroblastoma × glioma hybrid cells 108CC15 (refs 9 and 13) it could be deduced that the phenomena of tolerance, withdrawal and dependence seen after long term influence of morphine are connected with increased formation of cyclic AMP. The fact that one does not become addicted to one's endogenous enkephalins is probably due to the degradation of the material[3]. In contrast, with the cell culture system, long term effects do occur. This extends the analogy between opiates and the enkephalins to their long term effects. It leads to the prediction that an inhibitor of the degradation of enkephalin, if applied properly to an animal, may cause opiate tolerance and dependence. The long term effects on the hybrid cells also suggest that breakdown of leu-enk in the culture does occur, although at a moderate rate.

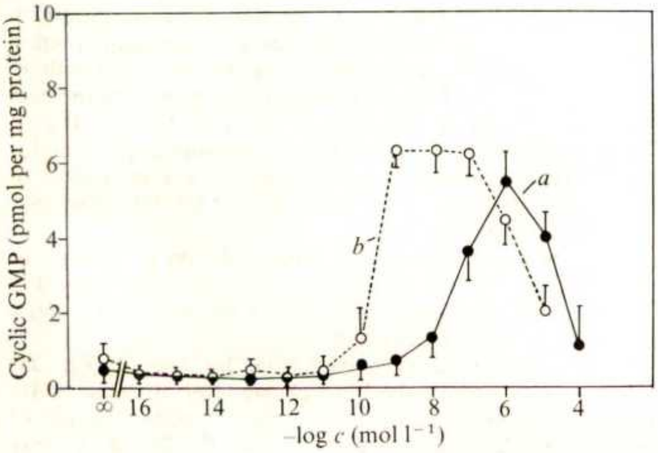

Fig. 3 Morphine (*a*) and leu-enk (*b*) elevate the levels of cyclic GMP in hybrid cells 108CC15. 1.0 × 10^6 viable cells per plate, viability 95%, passage number 17. The cells were incubated in incubation medium for 30 s and their content of cyclic GMP was determined as described[12].

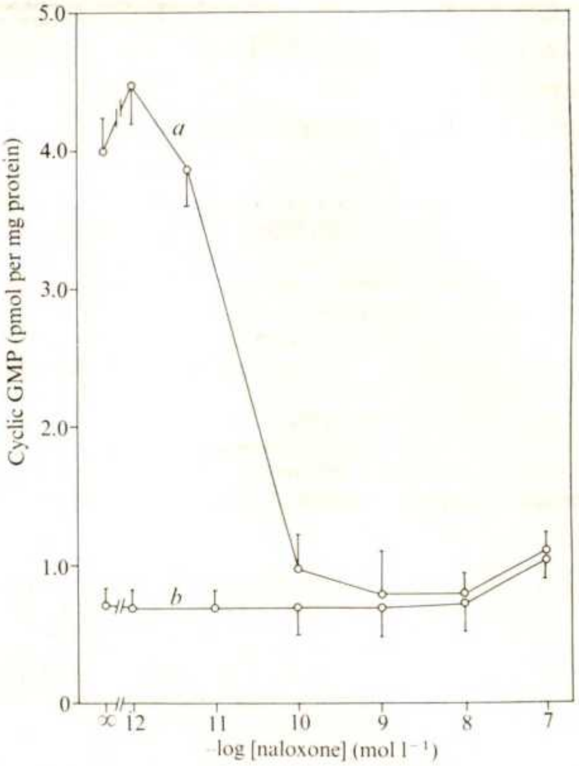

Fig. 4 Naloxone inhibits the increase in the level of cyclic GMP caused by leu-enk. *a*, Presence of 0.1 μM leu-enk; *b*, absence of leu-enk. 1.2 × 10^6 viable cells, viability 97%, passage number 14. Other details as in Fig. 3.

This work was supported by the Sonderforschungsbereich 51 of the Deutsche Forschungsgemeinschaft. We thank Dr J. Pike for PGE_1.

MICHAEL BRANDT
ROBERT J. GULLIS
KARIN FISCHER
CLAUDIA BUCHEN
BERND HAMPRECHT
Department of Enzyme Chemistry and Metabolism
LUIS MORODER
ERICH WÜNSCH

Department of Peptide Chemistry,
Max-Planck-Institut für Biochemie,
8033 Martinsried, FRG

Received March 25, accepted May 20, 1976.

[1] Collier, H. O. J., *Proc 5th Int. Cong. Pharmac.*, **1**, 65–76 (Karger, Basel, 1973).
[2] Terenius, L., and Wahlström, A., *Acta pharmac. toxi.*, **35**, (*Suppl.*), 55 (1974); *Acta physiol. scand.*, **94**, 74–81 (1975); *Life Sci.*, **16**, 1759–1764 (1975).
[3] Hughes, J., *Brain Res.*, **88**, 295–308 (1975).
[4] Pasternak, G. W., Goodman, R., and Snyder, S. H., *Life Sci.*, **16**, 1765–1769 (1975).
[5] Teschemacher, H., Opheim, K. E., Cox, B. M., and Goldstein, A., *Life Sci.*, **16**, 1771–1776 (1975).
[6] Hughes, J., *et al.*, *Nature*, **258**, 577–579 (1975).
[7] Hamprecht, B., in *25 Colloquium der Gesellschaft für Biologische Chemie* (edit. by Jaenicke, L.), 391–423 (Springer, Berlin 1974); *Angew. Chem.*, **88**, 211–223 (1976); *Angew. Chem. Int. ed.*, **15**, 194–206 (1976).
[8] Traber, J., Fischer, K., Latzin, S., and Hamprecht, B., *Nature*, **253**, 120–122 (1975).
[9] Traber, J., Gullis, R., and Hamprecht, B., *Proc. 10th FEBS Meeting*, **41**, 165–177 (1975); *Life Sci.*, **16**, 1863–1868 (1975).
[10] Sharma, S. K., Nirenberg, M., and Klee, W. A., *Proc. natn. Acad. Sci. U.S.A.*, **72**, 590–594 (1975).

[11] Hampprecht, B., and Schultz, J., *Hoppe-Seyler's Z. physiol. Chem.*, **354**, 1633–1641 (1973).
[12] Gullis, R., Traber, J., and Hamprecht, B., *Nature*, **256**, 57–59 (1975).
[13] Klee, W. A., Sharma, S. K., and Nirenberg, M., *Life Sci.*, **16**, 1869–1874 (1975).
[14] Traber, J., Fischer, K., Latzin, S., and Hamprecht, B., *Proc. 9th Int. cong. Collegium Internationale Neuropsychopharmacologicum*, 956–969 (1974).
[15] Konishi, M., Ioshida, N., and Izumiya, N., *Bull. chem. Soc. Japan*, **44**, 2801–2804 (1971).
[16] Pravda, Z., Poduska, K., and Blaha, K., *Coll. Czech. Chem. Comm.*, **29**, 2626–2631 (1964).
[17] Collier, H. O. J., and Roy, A. C., *Nature*, **248**, 24–27 (1974).
[18] Traber, J., thesis, Univ. Munich (1976).
[19] Simon, E. J., Hiller, J. M., and Edelman, I., *Proc. natn. Acad. Sci. U.S.A.*, **70**, 1947–1949 (1973).
[20] Pert, C. B., and Snyder, S. H., *Molec. Pharmac.*, **10**, 868–879 (1974).
[21] Bradbury, A. F., Smyth, D. G., and Snell, C. R., *Nature*, **260**, 165–166 (1976).
[22] Horn, A. S., and Rodgers, J. R., *Nature*, **260**, 795–797 (1976).
[23] Ho, I. K., Loh, H. H., and Way, E. L., *Nature*, **238**, 397–398 (1972); *J. Pharmac. exp. Ther.*, **185**, 336–346 (1973).
[24] Collier, H. O. J., and Roy, A. C., *Prostaglandins*, **7**, 361–376 (1974).
[25] Collier, H. O. J., and Francis, D. L., *Nature*, **255**, 159–162 (1975).

Enkephalin and opiate narcotics increase cyclic GMP accumulation in slices of rat neostriatum

SEVERAL recent studies suggest that cyclic nucleotides are involved in the cellular actions of the opiate narcotics[1-6]. Following the observation by Collier and Roy[1] that low concentrations of morphine inhibited prostaglandin E_1 (PGE_1)-stimulated adenylate cyclase activity in rat brain, Traber *et al.*[2] showed that morphine acted similarly to block the rise in intracellular 3′,5′-adenosine monophosphate (cyclic AMP) induced by PGE_1 in cultured neuroblastoma, or in a hybrid cell line of neuroblastoma × glioma with a high density of opiate receptor binding sites. Sharma *et al.*[3] found that morphine inhibited basal adenylate cyclase activity in this cell line and Gullis *et al.*[4] observed that morphine increased the 3′,5′-guanosine monophosphate (cyclic GMP) and reduced the cyclic AMP content of these cells. Racagni *et al.*[5] have also demonstrated that injection of analgesic doses of morphine *in vivo* to rats also increased cyclic GMP concentration in the neostriatum. These effects have generally been found to be stereospecific and blocked by the opiate receptor antagonist drug naloxone, suggesting that they are mediated through specific opiate receptors. We have extended these observations to *in vitro* studies on slices of rat neostriatum, an area with a very high density of opiate receptor binding sites[6], and have also examined the effects of enkephalin on this system.

Slices of rat neostriatum were incubated for 15 min at 37 °C in Krebs–Ringer bicarbonate buffer containing 1 mM isobutylmethylxanthine (IBMX) (a potent phosphodiesterase inhibitor) and added drugs, as previously described by Forn *et al.*[7] (see legend to Fig. 1). Cyclic AMP and cyclic GMP in boiled tissue extracts were determined by sensitive protein binding and radioimmunoassay techniques (see legend to Fig. 1).

Morphine (10^{-7}–10^{-5} M) increased the accumulation of cyclic GMP in rat striatal slices to a maximum of 200% of control values (Fig. 1). The tissue content of cyclic AMP was concomitantly decreased to about 80% of control, although this effect did not always attain statistical significance. Very similar control and morphine-stimulated values were obtained after isolation and separation of the two cyclic nucleotides by ion-exchange chromatography (Fig. 1 legend). The half-maximum response for both cyclic nucleotides occurred at a morphine concentration of about 3×10^{-8} M. The dose–response curve for morphine was bell-shaped and higher morphine concentrations (10^{-4}–10^{-3} M) caused no significant changes in the tissue content of either cyclic nucleotide. Naloxone (10^{-6} M) completely blocked the effects of morphine (10^{-6} M) on the accumulation of both cyclic nucleotides (Table 1). Indeed, although naloxone alone had no action, in the presence of morphine and naloxone the accumulation of cyclic GMP was significantly reduced below control values (Table 1), although the tissue content of cyclic AMP was unaffected. Levorphanol, an active congener of morphine at concentrations from 10^{-8} to 10^{-3} M mimicked the actions of morphine on cyclic nucleotide accumulation although the reduction in tissue cyclic AMP was not significant, whereas the inactive enantiomer dextrorphan tested at the same concentrations had no effect (Table 1). The latter observations suggest that the actions of morphine on cyclic nucleotide accumulation in rat striatal slices are due to an interaction with specific opiate receptors in this tissue.

The enkephalins are pentapeptides, isolated from porcine brain and characterised by Hughes *et al.*[8], which seem to be specific opiate receptor agonists. Two similar

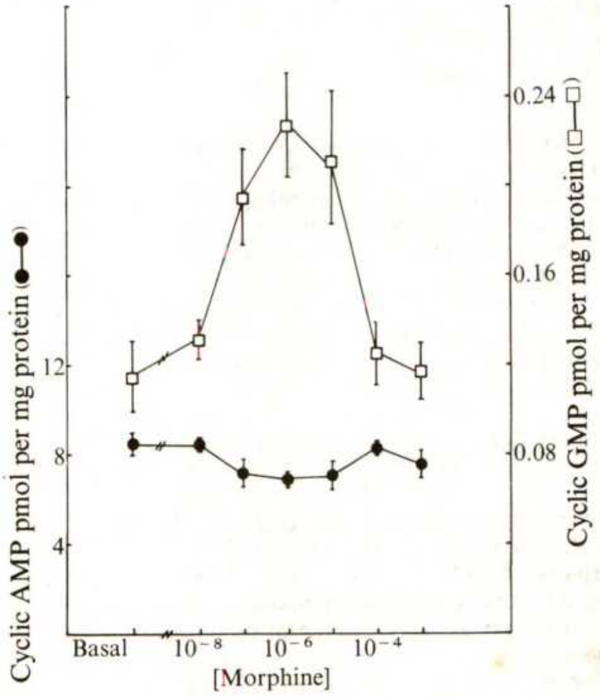

Fig. 1 Effect of morphine on cyclic nucleotide concentrations in slices of rat neostriatum. The tissue preparation, incubation and extraction procedues were as described by Forn *et al.*[7]. After preincubation for 60 min at 37 °C, samples of neostriatal slices (260 × 260 μm; total 10 mg wet weight) were incubated for a further 15 min in the presence of various concentrations of morphine hydrochloride. Tissue extracts were prepared by boiling and centrifugation, 50 μl was taken for cyclic AMP determination by the method of Brown *et al.*[11]; and 100 μl was taken for determination of cyclic GMP by radioimmunoassay. The remaining tissue was dissolved in 1 ml 1 N NaOH and protein was measured by the method of Lowry *et al.*[12]. The cyclic GMP radioimmunoassay antiserum and method were provided by Dr J. Albano and will be described in detail elsewhere. The radioimmunoassay procedure was briefly as follows: 100 μl supernatant was added to 100 μl ^{3}H-cyclic GMP (0.02 μCi, 1.0 pmol) in 50 mM Tris-HCl (*p*H 7.4) containing 2 mM theophylline and 6 mM β-mercaptoethanol. Antiserum (100 μl) diluted in the same buffer was added and the tubes left at 2–4 °C for 6–18 h. The antibody complex was separated by membrane filtration; filters were washed with 5 ml of buffer and dissolved in 4 ml ethoxyethanol; 10 ml of 0.4% butyl PBD in toluene added and radioactivity determined. A standard curve for displacement of bound ^{3}H-cyclic GMP was determined using non-radioactive cyclic GMP. The sensitivity of the assay was 0.02 pmol cyclic GMP in 100 μl. Known amounts of both cyclic AMP and cyclic GMP added either separately or together as internal standards were quantitatively recovered, and the amount of each cyclic nucleotide measured was linearly related to the volume of supernatant used for assay. Cyclic GMP did not interfere with cyclic AMP determinations when present in up to a tenfold excess; cyclic AMP did not interfere with cyclic GMP when present in up to a 500-fold excess. In some experiments incubations were terminated by the addition of 1 ml 5% trichloroacetic acid, the tissue was homogenised and the cyclic nucleotides were isolated and separated by the method of Matsuzawa and Nirenberg[13]. All incubations were performed in quadruplicate, and the data are expressed as means ± s.e.m.

Table 1 Effect of specific opiate narcotics and naloxone on cyclic nucleotide levels in slices of rat neostriatum

Drug	Cyclic AMP (pmol per mg protein)	Cyclic GMP (pmol per mg protein)
Control	9.1±0.84	0.15±0.014
10^{-6} M morphine	7.4±0.26*	0.28±0.037†
10^{-6} M naloxone	9.2±0.31	0.14±0.016
10^{-6} M morphine + 10^{-6} M naloxone	9.1±0.51	0.10±0.010*
10^{-6} M levorphanol	8.0±0.71	0.26±0.036*
10^{-7} M levorphanol	7.6±0.17	0.29±0.036†
10^{-6} M dextrorphan	9.2±0.87	0.16±0.016
10^{-7} M dextrorphan	9.1±0.28	0.17±0.019

All values are means ± s.e.m. for four separate incubations, see Fig. 1 legend for details.
*$P < 0.05$.
†$P < 0.01$ compared with control values.

peptides exist, one with leucine as the C-terminal amino acid (leu-enkephalin) and one with methionine as the C-terminal amino acid (met-enkephalin). The addition of either of these compounds at concentrations up to 10^{-4} M did not affect cyclic AMP or cyclic GMP accumulation in slices of rat neostriatum (Table 2). This result was, however, not unexpected, since both forms of enkephalin are rapidly inactivated in tissues at 37 °C (ref. 9). We also tested the effects of these substances in the presence of a peptidase inhibitor, bacitracin[10], (30 μg ml^{-1}) (Sigma Chemical Co.). At this concentration, bacitracin did not by itself significantly affect cyclic nucleotide levels nor did it interfere with the cyclic GMP response elicited by morphine (Table 2). In the presence of bacitracin, both leu- and met-enkephalin (10^{-4} M) increased cyclic GMP accumulation in rat striatal slices to an extent similar to that seen with morphine (Table 2), and this effect was blocked by naloxone. Cyclic AMP accumulation was also decreased to a level similar to that observed in the presence of morphine (Table 2).

The effects of morphine on cyclic nucleotide accumulation in rat striatal slices are strikingly similar to those observed previously in neuroblastoma × glioma hybrid cells[4], although the EC_{50} for morphine is approximately one order of magnitude lower in striatal slices than in cell cultures, and the effect on both nucleotides is relatively greater in the cultured cells. Morphine displays a bell-shaped dose–response curve in both systems and in each case the presence of morphine and naloxone significantly decreases cyclic GMP below control levels.

Table 2 Effect of leu- and met-enkephalin on cyclic nucleotide levels in slices of rat neostriatum

Drug(s)	Cyclic AMP (pmol per mg protein)	Cyclic GMP (pmol per mg protein)
Control	8.1±0.42	0.14±0.006
10^{-6} M morphine	6.7±0.91	0.23±0.014†
10^{-4} M leu-enkephalin	8.1±0.40	0.15±0.016
10^{-4} M met-enkephalin	8.2±0.43	0.14±0.011
30 μg ml^{-1} bacitracin	7.7±0.29	0.15±0.015
10^{-6} M morphine + 30 μg ml^{-1} bacitracin	6.8±0.32*	0.22±0.024*
10^{-4} M leu-enkephalin + 30 μg ml^{-1} bacitracin	6.7±0.81	0.22±0.028*
10^{-4} M met-enkephalin + 30 μg ml^{-1} bacitracin	6.6±0.12†	0.25±0.011†
10^{-4} M leu-enkephalin + 30 μg ml^{-1} bacitracin + 10^{-6} M naloxone	8.0±0.18	0.14±0.014
10^{-4} M met-enkephalin + 30 μg ml^{-1} bacitracin + 10^{-6} M naloxone	7.5±0.26	0.13±0.025

All values are means ± s.e.m. for four separate incubations, see Fig. 1 legend for details.
*$P < 0.05$.
†$P < 0.01$ compared with control values.

The potency of enkephalins (both leu- and met-) in displacing the specific binding of radiolabelled ligands from opiate receptors and on isolated test tissues is similar to that of morphine[8]. The fact that much higher concentrations of enkephalins are necessary to increase cyclic GMP levels in rat striatal slices probably reflects the instability of these substances in mammalian tissues and an incomplete inhibition of brain peptidases in our experiments. Higher concentrations of bacitracin were tested, but were found to interfere with the opiate response. It is, therefore, not yet possible to compare the true potencies of enkephalin and the opiate narcotics in this system. Nevertheless, the fact that the naturally occurring peptides, leu- and met-enkephalin increase cyclic GMP accumulation in rat striatal slices in the presence of a peptidase inhibitor raises the possibility that this response may also occur *in vivo*, and that it may represent a mechanism by which the actions of these substances, as well as those of morphine and other exogenously applied opiate narcotics are mediated at the cellular level.

We thank Dr J. Albano for the generous gift of cyclic GMP antiserum and Dr R. Miller for suggesting the use of bacitracin. Leu- and met-enkephalins were generously provided by Dr G. Metcalf, Reckitt and Colman Ltd, Hull, England; morphine, levorphanol and dextrorphan by Roche Products Ltd and naloxone by Endo Laboratories. K.P.M. is a graduate fellow of the US National Science Foundation.

KENNETH P. MINNEMAN
LESLIE L. IVERSEN

MRC Neurochemical Pharmacology Unit,
Department of Pharmacology,
Medical School, Hills Road,
Cambridge CB2 2QD, UK

Received April 12; accepted May 26, 1976.

[1] Collier, H. O. S., and Roy, A. C., *Nature*, **248**, 24–27 (1974).
[2] Traber, J., Fischer, K., Latzin, S., and Hamprecht, B., *Nature*, **253**, 120–122 (1975).
[3] Sharma, S. H., Klee, W. A., and Nirenberg, M., *Proc. natn. Acad. Sci. U.S.A.*, **72**, 3092–3096 (1975).
[4] Gullis, R., Traber, J., and Hamprecht, B., *Nature*, **256**, 57–59 (1975).
[5] Racagni, G., Zsilla, G., Guidotti, A., and Costa, E., *J. Pharm. Pharmac.*, **28**, 258–260 (1976).
[6] Pert, C. B., Kuhar, M. J., and Snyder, S. H., in *The Opiate Narcotics*, 97–101 (Pergamon, Oxford, 1975).
[7] Forn, J., Krueger, B., and Greengard, P., *Science*, **186**, 1118–1120 (1974).
[8] Hughes, J., *et al.*, *Nature*, **258**, 577–579 (1975).
[9] Hughes, J., *Brain Res.*, **88**, 295–308 (1975).
[10] Desbuquois, B., Krug, F., and Cuatrecasas, P., *Biochim. biophys. Acta*, **343**, 101–120 (1974).
[11] Brown, B. L., Albano, J. D. M., Ekins, R. P., and Sgherzi, A. M., *Adv. Cyclic Nucleotide Res.*, **2**, 25–40 (1972).
[12] Lowry, O. H., Rosebrough, N. J., Farr, A. L., and Randall, R. J., *J. biol. Chem.*, **193**, 265–275 (1951).
[13] Matsuzawa, H., and Nirenberg, M., *Proc. natn. Acad. Sci. U.S.A.*, **72**, 3472–3476 (1975).

A sequential *in vivo–in vitro* study of carcinogenesis induced in the rat brain by ethylnitrosourea

THE processes which occur between exposure to a chemical carcinogen and the appearance of a gross tumour, the latent period, are still largely unknown. One approach to investigating how the biological properties of cells are altered during this time is to monitor the behaviour of cells cultured from target organs at different times after carcinogen treatment. A system in which a single dose of a chemical results in a high yield of tumours is a good starting point for such experiments. When pregnant rats are injected with ethylnitrosourea (ENU) almost every one of the progeny develops tumours of the nervous system[1], of which macro- and microtumours of the brain constitute ~ 60% (predominantly cerebral gliomas[2]). To investigate the pro-

Table 1 Agar growth and tumorigenicity of cultures derived 138–145 d after exposure to ENU or buffer

Culture	Passage level	Average no. of colonies per 10^4 cells plated	Plating efficiency in agar (%)	Passage level	No. of animals with tumours/ No. injected	Average time before killed (d)
22E	10	10	0.1	11	7/7	57.7
22A	10	286	2.9	10	8/8	44.6
23A	13	0	0	13	0/6	>265
23C	10	0	0			(1)

To initiate cultures the brain tissue was sliced, chopped into small pieces (about 1 mm^3) and incubated in 10 ml of dissociating medium (0.05% collagenase and 5% foetal calf serum in phosphate-buffered saline without divalent cations) at 37 °C for 20 min with occasional agitation. The suspension was dispersed with 10 or more excursions in a 10-ml pipette, centrifuged and resuspended in Dulbecco's modification of Eagle's medium with 15% foetal calf serum. The medium was changed on the following day to remove debris and unattached cells. Subculturing took place at weekly intervals soon after the cultures became confluent. To test for growth in agar, cells were plated at up to 10^4 in 1 ml of 0.3% Bacto-agar in Dulbecco's medium and 15% foetal calf serum. The base layer was 0.6% agar made up in the same medium. Two to four plates were prepared for each culture. Colonies of 22E and 22A were counted 2–4 weeks after plating, by which time many were macroscopic. The control cultures were observed for up to 3 months with feeding and were negative throughout. To test for tumorigenicity, cells were injected subcutaneously at 1×10^6–2×10^6 per newborn animal (< 5 d old). Animals were examined three times each week and killed when the tumours were about 1 cm in diameter (1): 23C was injected a number of times but due to cannibalism only one animal survived from experiments at comparable passage levels. (It had no tumour at 104 d.) There was a large number of successful injections at later passages and these animals, together with those injected with 23A cells, are still under observation. Preliminary histological observation has indicated that the tumours formed by 22E and 22A are not fibrosarcomas, and have features of glial tumours. A more extensive examination is in progress and details will be published elsewhere.

cess of carcinogenesis during the latent period, cultures have been prepared from ENU-induced gliomas and from ENU-treated animals at different times before the appearance of such tumours.

Pregnant rats of the BD–IX inbred line were injected intraperitoneally with ENU at 40–50 mg per kg body weight on days 15 or 16 of pregnancy. The average latent period for brain tumours was 246 d. Cultures prepared from cerebral gliomas consisted mainly of cells resembling glia and cells with thin cytoplasm, indistinct boundaries and often what looked like incipient processes. We have called the latter type "basal layer cells"[3,4]. These are likely to be morphologically undifferentiated glia because they formed processes in response to dibutyryl adenosine cyclic monophosphate[3], and because clones with a similar morphology have many of the characteristics of astrocytes[4,5]. The tumour cultures grew in 0.3% agar and were tumorigenic[4].

For the initial set of experiments to investigate the latent period, cultures were prepared from a group of animals 138–145 d after transplacental exposure to either ENU or buffer. The cerebra of five ENU-treated and two buffer-treated animals were cultured. Two of the former cultures (22E, 22A) contained islands of cells resembling basal layer cells and associated glia characteristic of tumour cultures. There was no sign of a visible tumour during the slicing and chopping of brain tissue in either case. The two cultures were further investigated. The tumour-like cells which were initially in a minority, gradually became predominant on passaging. Both cultures contained cells which grew in agar and formed tumours in animals (Table 1). The cultures from buffer-exposed animals (23A, 23C) did not contain cells resembling cultured tumour cells, did not grow in agar and have not so far produced tumours (Table 1).

To investigate cells very early in the latent period, a culture was prepared from the pooled brains of an entire litter of foetuses 2 d after transplacental exposure to ENU or buffer. The primary cultures from ENU-treated (BE10) and control (BE11) foetuses were morphologically indistinguishable. Tests for growth in agar and in animals were negative after many passages. At the 40th passage level, however, the BE10 culture formed small colonies, several weeks after plating in agar.

At later transfers macroscopic colonies developed in 2–4 weeks; the result of one experiment is given in Table 2. Further, two clones of BE10, BE10-13 and BE10-7 grew in agar and were tumorigenic (Table 2).

The culturing of cells shortly after treatment of an animal with a chemical as we have done in one set of experiments has been suggested as a test for carcinogens[6]. The method has also been used to ensure that target cells are affected by the ultimate carcinogen[7,8], a situation not necessarily obtained by *in vitro* treatment of cultured cells. Kidney cells cultured 20 h to 7 d after the injection of rats with dimethylnitrosamine showed several transformed properties, but were not tumorigenic[7]. Laerum and Rajewsky[8] have reported that brain cultures made 20–90 h after transplacental exposure to ENU went through a series of changes. They describe the formation of piled-up foci of cells or 'nodules' which were washed off and cultured. These gave rise to cells which grew in 0.15% agar and became tumorigenic after a total of about 200 d in culture. Their control cultures died out before nodule formation so that no measure of spontaneous transformation could be made. The formation of foci which we have called 'clusters' has been observed in both ENU-treated and control cultures. These have been washed from the BE10 and BE11 cultures and maintained separately. There are some differences in the two cultures, for example, that from BE10 has a higher plating efficiency in agar (0.4–0.5 %) than that from BE11 (0.01–0.1 %) depending on passage level. Moreover, some of the animals injected several months before with the former have recently been found to have tumours. All four cultures

Table 2 Agar growth and tumorigenicity of cultures derived 48 h after treatment with ENU or buffer

Culture	Passage level	Average no. of colonies per 10^4 cells plated	Plating efficiency in agar (%)	Passage level	No. of animals with tumours/ No. injected	Average time before killed (d)
BE10	57	$354/10^4$	3.5	60		(1)
BE11	57	$<1/10^4$	<0.01	60		(1)
BE10-7	24	$360/10^3$	36	28	8/8	95.1
BE10-13	32	$54/10^4$	0.5	34	5/5	40

BE10-13 was derived at the 10th and BE10-7 at the 20th transfer of BE10. This was before the earliest time at which cluster formation was observed in BE10. Other experimental details as in Table 1. (1) These animals are still under observation. The tumours formed by BE10-7 and BE10-13 are not fibrosarcomas and have glial features. Further histological observations are in progress and the results will be published elsewhere.

are being maintained and tested to estimate the extent of spontaneous transformation.

It seems, therefore, that at a time equivalent to about 3/5 of the average latent period, ENU-treated animals, have cells which, in culture, behave in a manner indistinguishable from tumour cells. These are not readily detected in cultures taken very early in the latent period. The results so far, however, suggest that there are cells present at 48 h with the potential to become tumorigenic, and that this potential is revealed after prolonged culturing. Experiments are in progress to try to detect these cells without such extensive culturing and to define the time at which committed cancer cells can first be readily detected in culture. It has recently been found that histological changes were first observed about 9 weeks after exposure of the foetuses to ENU (P. L. Lantos, personal communication). The combined *in vivo–in vitro* method used at a series of times in the latent period thus seems to be a valuable approach to investigating the process of carcinogenesis.

We thank Professor P. N. Magee for gifts of ENU and for discussions, and Miss S. L. Davies for technical assistance. The work was supported by a grant from the Cancer Research Campaign.

J. P. ROSCOE
P. J. CLAISSE

School of Pathology,
Middlesex Hospital Medical School,
Riding House Street,
London W1P 7LD, UK

Received April 28; accepted May 20, 1976.

[1] Druckrey, H., Ivankovic, S., and Preussmann, R., *Nature*, **210**, 1378–1379 (1966).
[2] Wechsler, W., *et al.*, *Ann. N.Y. Acad. Sci.*, **159**, 360–408 (1969).
[3] Roscoe, J. P., and Gibbs, B. E., *J. natn. Cancer Inst.*, **53**, 581–583 (1974).
[4] Lantos, P. L., Roscoe, J. P., and Skidmore, C. J., *Br. J. exp. Path.*, **57**, 95–104 (1976).
[5] Claisse, P. J., and Roscoe, J. P., *Brain Res.* **109**, 423–425 (1976).
[6] DiPaolo, J. A., Nelson, R. L., Donovan, P. J., and Evans. C. H., *Archs Path.*, **95**, 380–385 (1973).
[7] Borland, R., and Hard, G. C., *Eur. J. Cancer*, **10**, 177–184 (1974).
[8] Laerum, O. D., and Rajewsky, M. F., *J. natn. Cancer Inst.*, **55**, 1177–1187 (1975).

Native collagen formation by liver parenchymal cells in culture

IN normal supporting tissue and repair tissue of animals collagen is usually considered to be produced by cells of mesenchymal origin. Little is known, however, about the type of cell which synthesises collagen in organs which undergo diffuse fibrosis without known physical trauma, such as in cirrhosis of the liver. Tissue culture has shown, however, that epithelial cells[1], including cancer cells[2] and smooth muscle cells[3], can synthesise collagen. We report here that an epithelial clone, originating from the liver cell line of rat forms a considerable amount of native collagen in culture.

An epithelial cell line from the liver of a JAR-2 suckling rat[4] was established as before[5]. The culture medium consisted of 0.5% lactalbumin hydrolysate medium (LE) supplemented with 10% calf serum (CS). After 200 d of culture the cells dispersed with 0.25% trypsin were seeded in 60-mm plastic Falcon plates for cloning. Inocula varied between a high of 1×10^3 and a low of 3×10 cells per plate, and the 1×10^3 plate yielded colonies derived from single cells. Two colonies which were cytologically distinguishable from each other were picked out and cultured continuously. One consisted of rather small roundish cells and the other of larger polygonal cells. They were designated clones BB and BC, respectively. Both clones have been maintained by serial passages for 4 yr and 3 months in culture flasks containing Ham's F 12 medium and 10% CS or foetal bovine serum (FBS). The cell replication cycle of these clones was 20–31 h after 21 generations. Plating efficiency was 35–55% after 19 generations. The cells were epithelioid, proliferated as monolayers, and achieved contact inhibition.

Table 1 Production of serum proteins by cloned liver cell lines

Culture generation	Al* (ng ml^{-1})	AFP† (ng ml^{-1})	Trans.‡
BB cells			
8	1,340	ND§	—
16	ND§	—	—
16	270	—	—
25	ND§	ND§	(+)
25	540	ND§	(−)
25	570	105	(−)
25	670	ND§	(+)
41	ND§	ND§	—
BC cells			
9	2,400	ND§	—
20	ND§	—	—
20	ND§	—	—
27	340	ND§	(+)
27	550	ND§	(−)
27	420	ND§	(+)
27	500	82	(+)
43	ND§	ND§	—

The supernatants of culture media were collected 3–4 d after plating of cells and used for analysis with or without concentration.

* Assays performed by Mancini's radial immunodiffusion technique[6] for 20-times concentrated samples. The sensitivity limit of this method is 300 ng ml^{-1}.

† Values determined by radioimmunoassay[7] without concentration. The sensitivity limit is 20 ng ml^{-1}.

‡ Qualitative assays by immunoautoradiography[8].

§ Non-detectable activity.

To detect liver-type metabolic activities of the cells, assays

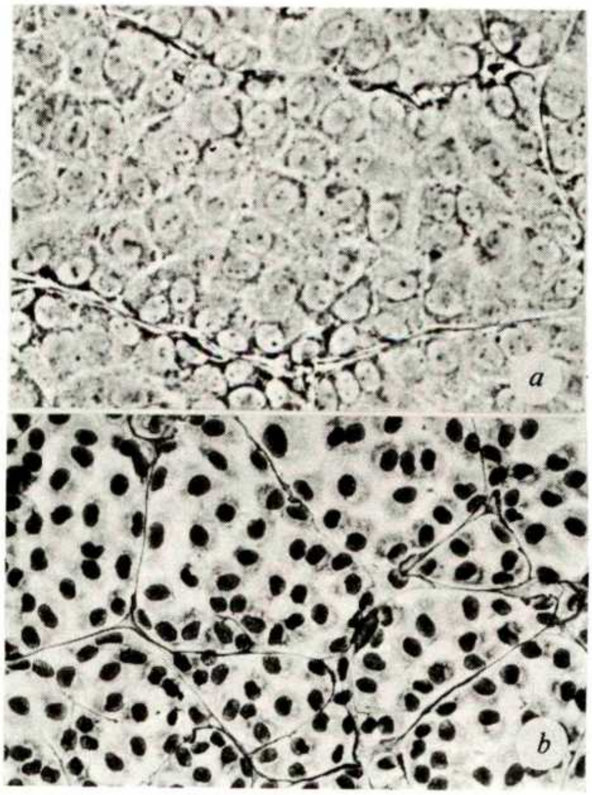

Fig. 1 Micrographs of a cloned liver cell line BC cultured on cover slip for 28 d without transfer. *a*, Unfixed, phase-contrast illumination(× 587); *b*, fixed with absolute methanol, stained by silver impregnation. Collagen fibres stained purple-brown situated between cells (× 293).

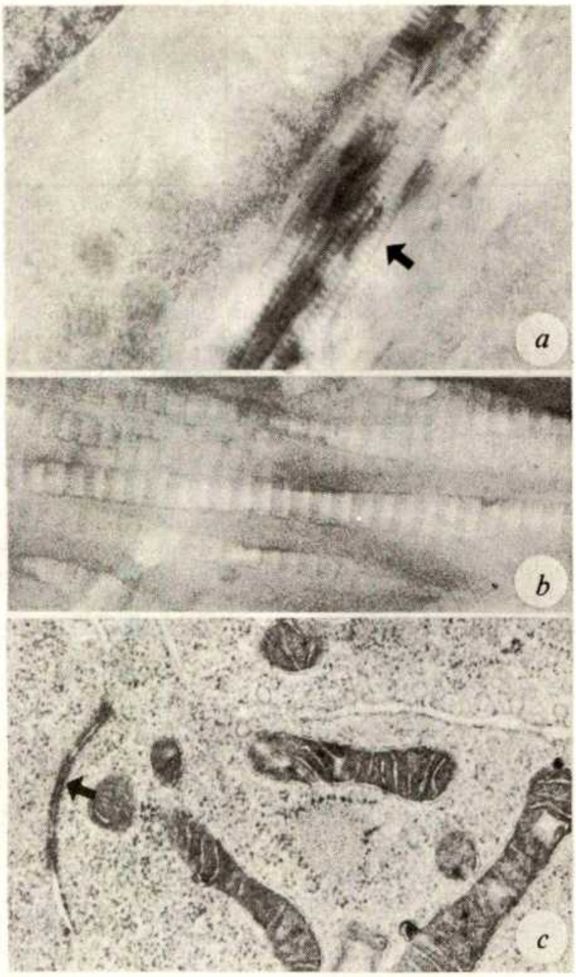

Fig. 2 Electron micrographs of BC cells grown in the same conditions as described for Fig. 1. *a*, Bundle of collagen fibrils in the extracellular space (arrow), negatively stained with 20% phosphotungstic acid by the method of Kushida *et al.*[10] (× 18,182); *b*, higher magnification of collagen fibrils shown in *a*, demonstrating the banding pattern and periodicity of 640 Å (× 45,455); *c*, the portion of two adjacent cells illustrating the desmosome (arrow) and typical small inpocketings of the plasma membrane, stained with uranyl acetate and lead citrate (× 20,545). Fixation, dehydration and embedding in Epon were as in the original plastic culture plates by the published procedure[9].

of rat serum albumin (Al), α-foetoprotein (AFP), and transferrin (trans.) in the culture fluid were performed after eight to 43 generations. Table 1 shows that these clones produced all three serum proteins, indicating that they were clones of rat liver parenchymal cells.

Although there was some difference in cytological appearances of the two clones, a particularly noticeable feature developed under the phase contrast microscope in BC cells left as a full sheet for more than 3 weeks without transfer. Thin fibre-like intercellular structures appeared, increased with time, began to enclose a portion of the culture, and finally divided the whole culture into multiple nodular areas (Fig. 1*a*). This process was usually complete within 6 weeks in our culture conditions.

To identify these structures we used silver impregnation, Mallory-Azan, resorcin-fuchsin, and periodic acid-Schiff. These staining methods, especially the former two, gave the characteristic colour reactions of collagen fibres (Fig. 1*b*). There was no collagen reaction in BB cells. Electron micrographs of BC cells revealed fibrils of characteristic collagen periodicity, deposited in broad intercellular spaces which separated the cells from each other (Fig. 2*a* and *b*). Where cell perimeters were in contact they were connected tightly to desmosomes, arranged in a direction in which collagen fibrils were rearely found (Fig. 2*c*).

To preclude the possibility of contamination of fibroblasts in the original BC clone, we recloned it. Three subclones, BC.S1, BC.S2, and BC.S3, were obtained from plates seeded with 1×10^2 cells by the same procedure as before. The subclones were morphologically similar to the parent clone. For quantitative proof of these findings a hydroxyproline assay of the cell layers maintained for 21 d without subculture was performed by the method of Prockop and Udenfriend[11]. Table 2 shows that values obtained from clone BC and its subclones were more than five times greater than that from the mouse fibroblast line 3T3 (Table 2), for which electron microscopy had shown evidence of production of collagen in extremely small amounts[9].

To see whether the cells had undergone spontaneous malignant transformation, we tested colony-forming capacity in soft agar, tumorigenicity in the cheek pouches of golden hamsters treated with antithymocyte serum, and chromosome number between 48 and 53 generations. No colony developed in soft agar, nor did the cheek pouches of the hamsters reveal any sign of tumours. The predominant mode of chromosome number was 59, indicating hypotriploidy.

Table 2 Hydroxyproline in cell layers after 21 d in culture without transfer

Cells	nmol per 10^7 cells
BC	152
BC.S1	123
BC.S2	139
BC.S3	98
Embryo*	184
3T3†	18
HeLa.S3‡	< 10

Cells growing in monolayer were scraped from the plates, washed twice with Hanks' solution by centrifugation at 1,500 r.p.m. for 5 min, hydrolysed at 110 °C for 24 h, and hydroxyproline was determined. For each determination trypsinised replicate cultures were used for cell counts.

* Primary culture of the whole embryo of JAR-2 strain rat as a positive control of collagen synthesis *in vitro*.

† A mouse fibroblast line[12].

‡ A cloned subline of HeLa, human uterine cancer cell line[13]. Assay for this cell line was exceptionally performed after 10 d in culture.

Our data demonstrate the production of native collagen by one of two clonal lines of rat liver cells. Both had synthesised *in vitro* three proteins which are regarded as the differential products of liver parenchyma in early culture generations.

The question arises whether collagen synthesis is a normal function of liver parenchymal cells. It is widely believed that collagen fibres in the liver are formed by the sinusoid lining cells and the fibroblasts of Glisson's capsule.

There are, however, data suggesting that liver parenchymal cells participate in collagen synthesis *in vivo*[14]: 100 times more protocollagen proline hydroxylase activity was reported in the parenchymal cell fraction than in the mesenchymal cell fraction, both of which were isolated from the same adult rat liver. Our results support these findings. They also enable us to speculate that liver parenchymal cells produce the collagen fibres found in the space of Disse, overproduction of which is normally controlled by a homoeostatic mechanism. We suggest that the marked increase of collagen fibres in liver cirrhosis represents a failure of this mechanism.

We thank Dr T. Tachikawa for assistance with electron micrography. This work was supported by a grant in aid

of cancer research from the Ministry of Education, Science and Culture, Japan.

KOOKO SAKAKIBARA
MAMORU SAITO

Department of Carcinogenesis and Cancer Susceptibility,
Institute of Medical Science,
University of Tokyo, Shirokanedai,
Minatoku, Tokyo 108

MAKOTO UMEDA
KUMIKO ENAKA

Tissue Culture Laboratory,
Yokohama City University,
School of Medicine, Yokohama

YUTAKA TSUKADA

Department of Biochemistry,
Hokkaido University School of Medicine,
Sapporo, Japan

Received March 26; accepted May 15, 1976.

[1] Hay, E. D., and Dodson, J. W., *J. Cell Biol.*, **57**, 190–213 (1973).
[2] Green, H., and Goldenberg, B., *Proc. natn. Acad. Sci. U.S.A.*, **53**, 1360–1365 (1965).
[3] Ross, R., *J. Cell Biol.*, **50**, 172–186 (1971).
[4] Katsuta, H., and Takaoka, T., *Jap. J. exp. Med.*, **33**, 265–275 (1963).
[5] Umeda, M., and Saito, M., *Jap. J. exp. Med.*, **39**, 601–613 (1969).
[6] Mancini, G., Carbonara, A. O., and Heremans, J. F., *Immunochemistry*, **2**, 235–254 (1965).
[7] Nishi, S., Kobayashi, K., and Hirai, H., *Proc. Jap. Cancer Ass., 33rd Annual Mtg*, 161 (1974).
[8] Tsukada, Y., and Hirai, H., *Ann. N. Y. Acad. Sci.*, **259**, 37–44 (1975).
[9] Goldenberg, B., Green, H., and Todaro, G. J., *Expl Cell Res.*, **31**, 444–447 (1963).
[10] Kushida, H., and Fujita, K., *J. Electron Microsc.*, **16**, 281 (1967).
[11] Prockop, D. J., and Udenfriend, S., *Analyt. Biochem.*, **1**, 228–239 (1960).
[12] Todaro, G., and Green, H., *J. Cell Biol.*, **17**, 299–313 (1963).
[13] Puck, T. T., Marcus, P., and Cieciura, S. J., *J. exp. Med.*, **103**, 273–284 (1956).
[14] Ohuchi, K., and Tsurufuji, S., *Biochim. biophys. Acta*, **258**, 731–740 (1972).

Identification of medicarpin as a phytoalexin in the broad bean plant (*Vicia faba* L.)

THE analysis of phytoalexin induction has been proposed as a dynamic approach to plant systematics[1]. It has also been pointed out that production of the furanoacetylene wyerone acid[2] by *Vicia faba* is an intriguing anomaly to the more general accumulation of isoflavanoid phytoalexins by members of the Leguminosae. In our studies on phytoalexin production by *V. faba*, three related furanoacetylenes (Fig. 1), wyerone acid (*a*), wyerone (*b*)[3] and wyerone epoxide (*c*)[4], have been identified as the major components of the multiple phytoalexin response of the broad bean plant to fungal infection[5]. In addition to these phytoalexins other minor inhibitors were detected in bioassays of thin layer chromatograms of methanol extracts of infected tissues[5]. Only one of these inhibitors reacted with *p*-nitroaniline[6] to give an orange coloration indicating phenolic character. No anti-fungal compounds were detected in extracts of healthy tissues. Here we report the identification of the phenolic inhibitor as medicarpin (3-hydroxy-9-methoxy pterocarpan) (Fig. 1*d*), a phytoalexin present in a wide range of leguminous species[1].

Fig. 1 *a*, Wyerone acid (R = H); *b*, wyerone (R = Me); *c*, wyerone epoxide; *d*, medicarpin

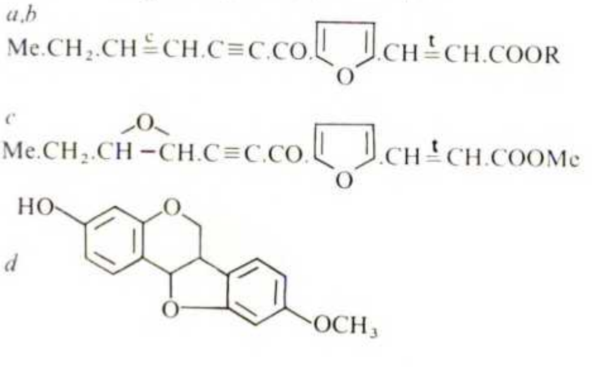
a,b
Me.CH₂.CH ═ CH.C≡C.CO. .CH ═ CH.COOR
c
t
O
c
Me.CH₂.CH — CH.C≡C.CO. .CH ═ CH.COOMe
O
t
O
HO
O
d
O
OCH₃

Table 1 Yields of phytoalexins from *V. faba* pod endocarp tissue bearing limited lesions caused by *B. cinerea* 4 d after fungal inoculation

Phytoalexin	Yield (μg per g fresh tissue)
Wyerone	217
Wyerone acid	219
Wyerone epoxide	30.7
Medicarpin	19.5

Yields are the mean of results from two experiments. Samples (about 4 g) of infected tissue were macerated in diethyl ether and the ether extract subjected to thin-layer chromatography (TLC) on precoated plates (Merck 5715). Wyerone acid was isolated after TLC in ether–methanol (6:1) and like other wyerone derivatives was recognised by its blue fluorescence under ultraviolet light (366 nm) at R_F 0.53. TLC of extracts in hexane–acetone (2:1) followed by chloroform–petrol (2:1) enabled purification of wyerone (R_F 0.6), wyerone epoxide (R_F 0.53) and medicarpin (R_F 0.31); the latter quenched the fluorescence of silica gel under ultraviolet light (254 nm). After elution in methanol concentrations of the phytoalexins were recorded by ultraviolet spectrophotometry[2,4].

Pod endocarp tissue (2.5 kg) bearing limited lesions caused by *Botrytis cinerea* was collected 5 d after fungal inoculation[7]. Diethyl ether extracts of the infected tissue[3] were subjected to preparative layer chromatography (PLC) on silica gel (Merck GF254 type 60) using hexane–acetone (2:1) followed after drying with chloroform–petroleum spirit 60–80 °C (2:1) as solvents. The band giving a positive *p*-nitroaniline test (R_F 0.34) was eluted and the phenolic compound repurified by PLC in chloroform (R_F 0.35) and finally chloroform–methanol (10:1).

After elution from R_F 0.6 the inhibitor (7 mg) was crystallised from ether–hexane. Proton magnetic resonance spectra of the crystalline product in deuteriochloroform were consistent with structure *d* in Fig. 1. Recorded optical activity ($[\alpha]_D^{20} - 214°$ $c = 0.19$, chloroform, melting point 129–130 °C); and ultraviolet absorption spectrum λ_{max} (ethanol) 287 (log $\varepsilon = 3.94$), 282 (3.88), 226 (4.14), 210 nm (4.53) were virtually identical to those published for medicarpin[8]. Identification was confirmed by comparison of the mass spectra obtained for our sample and authentic medicarpin.

To date *Vicia faba* seems to be unique in its *de novo* production of chemically unrelated compounds which act as phytoalexins. Much lower concentrations of medicarpin than of wyerone derivatives accumulated within infected tissue (Table 1). This suggests that medicarpin is probably not of great significance to the inhibition of growth of invading fungal hyphae. Medicarpin biosynthesis in *V. faba* may represent the expression of a primitive resistance response which has been largely superseded by the accumulation of the furanoacetylenes. Preliminary examination of the production of wyerone derivatives in pod tissues of different species of *Vicia* in response to infection by *B. cinerea* indicated that the more primitive[9] *V. cracca*, *V. sativa*, *V. sepium* and *V. sylvatica* do not produce wyerone or wyerone acid. These inhibitors, however, were induced in pods of *V. galilea* and *V. narbonensis*, two species closely related to *V. faba*.

Our results provide further support for the proposal that analysis of phytoalexin induction may become an invaluable approach to plant systematic and phylogenetic relationships. It should prove worthwhile to examine medicarpin and furanoacetylene induction within the genus *Vicia*. Note, however, that in our experience, investigation of phytoalexin accumulation within infection droplets[1] does not provide a complete picture of phytoalexin induction. It is only by thorough analysis of infected tissue that the more subtle relationships are likely to be discerned. For example, we have detected only trace amounts of medicarpin and wyerone within infection droplets containing conidia of *B. cinerea* incubated on leaves or pod seed cavities of *V. faba*.

We thank Dr V. J. Higgins (University of Toronto) for a sample of authentic medicarpin and Dr P. H. Davis (University

of Edinburgh) for seed of *V. galilea*. J.A.H. was supported by the ARC.

J. A. HARGREAVES
J. W. MANSFIELD

Biology Department,
The University,
Stirling FK9 4LA, UK

D. T. COXON

Chemistry Division,
Agricultural Research Council,
Food Research Institute,
Colney Lane,
Norwich NR4 7UA, UK

Received April 8; accepted April 13, 1976.

[1] Ingham, J. L., and Harborne, J. B., *Nature*, 260, 241–243 (1976).
[2] Letcher, R. M., Widdowson, D. A., Deverall, B. J., and Mansfield, J. W., *Phytochemistry*, 9, 249–252 (1970).
[3] Hargreaves, J. A., Mansfield, J. W., and Coxon, D. T., *Phytochemistry* 15, 651–653 (1976).
[4] Hargreaves, J. A., Mansfield, J. W., Coxon, D. T., and Price, K. R., *Phytochemistry* (in the press).
[5] Hargreaves, J. A., and Mansfield, J. W., *Ann. appl. Biol.*, **81**, 271–276 (1975).
[6] Ribereau-Gayon, P., *Plant Phenolics* (Oliver & Boyd; Edinburgh and London, 1972).
[7] Purkayastha, R. P., and Deverall, B. J., *Ann. appl. Biol.*, 56, 269–287 (1965).
[8] Smith, D. G., McInnes, A. G., Higgins, V. J., and Millar, R. L., *Physiol. Pl. Path.*, 1, 41–44 (1971).
[9] Kupicha, F. K., thesis, Univ. Edinburgh (1974).

Initiation inhibition and reinitiation of the synthesis of heterogeneous nuclear RNA in living cells

THE nucleoside analogue 5,6-dichloro-1-β-D-ribofuranosylbenzimidazole (DRB) inhibits the synthesis of heterogeneous nuclear RNA (hnRNA) at the initiation level in explanted salivary glands of *Chironomus tentans*, but does not interfere with the synthesis of ribosomal RNA and transfer RNA (refs 1–4). When the radioactive RNA precursors and the inhibitor are coincidently added to the glands the labelling of hnRNA transcripts produced by smaller transcriptional units is suppressed before that of the larger ones[2,3]. If, however, the glands are pretreated with DRB, and the time of preincubation is sufficiently long, labelling of small as well as large hnRNA transcripts is equally eliminated, and the DNA template becomes depleted of nascent hnRNA chains[2–4]. Important questions, arising from these findings, are whether DRB can be washed out from the cells, and whether a reinitiation of hnRNA synthesis can subsequently be achieved. This paper presents data which show that the initiation of the RNA synthesis resumes when glands pretreated with DRB are washed and replenished with inhibitor-free medium.

A reversal of transcription inhibition by DRB should result in a preferential labelling of hnRNA chains in the lower molecular weight ranges, if the incubation period after removal of DRB is brief enough (< 15–30 min). Labelled molecules in the 75–100S range could be expected only around 30 min (calculated synthesis time of the largest hnRNA molecules) after transferring inhibited glands to a DRB-free medium. A reversal of the effect of DRB on polyinosinicpolycytidylic acid-induced interferon production in a strain of diploid human fibroblast has been reported[5]. The superinducing action of DRB was promptly abolished by removing DRB from the cells. The reversibility of the transcription by DRB also increases its usefulness as a tool in studies of transcription mechanism and metabolism of hnRNA in living cells.

In an attempt to examine whether DRB is a reversible inhibitor of the synthesis of chromosomal hnRNA and to record the sequence of hnRNA events after a possible reinitiation of the transcription, explanted glands were preincubated with DRB in 50 μl of Cannon's modified insect medium for 30 min at 18 °C (refs 6 and 7). The glands were then washed and replenished with inhibitor-free medium supplied with ^{3}H-cytidine and ^{3}H-uridine and were incubated for different periods. Fixation of glands, microdissection of chromosomes, extraction and electrophoresis of RNA and the measurement of radioactivity were carried out as described elsewhere[2-4,8]. The RNA of chromosome IV, dominated by Balbiani ring 1 and 2 RNA, shows labelling kinetics different from those of chromosomes I to III (refs 2–4), and therefore the present analyses of chromosomal RNA do not include RNA from chromosome IV.

To demonstrate the effect of DRB on the initiation of hnRNA synthesis in chromosomes I to III, explanted glands were preincubated with DRB for 15 and 30 min before labelling for 20 min with tritiated cytidine and uridine in the continued presence of the analogue (Fig. 1). The control glands were labelled in similar conditions, but without inhibitor. The electrophoretic profile of labelled chromosomal hnRNA from control cells shows an heterogeneous distribution of molecules in the 16–100S range as described earlier[2,3,9]. When DRB was added to the incubation system 15 min before isotopic nucleosides, there was an almost complete disappearance of label in the 23–38S range of hnRNA, but incorporation into the 75–100S region was considerably less affected, as observed previously. If, however, the preincubation period with DRB, before administration of the tritiated RNA precursors, was prolonged from 15 to 30 min, the synthesis of short hnRNA molecules as well as of

Fig. 1 Electrophoretic analysis of chromosomal hnRNA labelled for 20 min in the absence and in the presence of DRB after preincubation in the presence of DRB. Salivary glands were incubated at 18 °C for 15 and 30 min in 50 μl of incubation medium containing DRB (65 μM). They were then transferred to another 50 μl of the same medium containing DRB, 100 μCi of ^{3}H-cytidine at 29 Ci mmol^{-1} and 200 μCi of ^{3}H-uridine at 44 Ci mmol^{-1} (Amersham) and incubated for 20 min. Labelling with tritiated nucleosides in the absence of DRB was carried out in parallel. For labelling with isotopic nucleosides after preincubation for 15 min (● and ▲) sister glands were used. Chromosomes I to III were microdissected from 20 cells (four glands). The labelled RNA from each sample was released by Pronase–sodium dodecyl sulphate treatment, and the electrophoresis was carried out in 1% Agarose gel. Before radioactivity measurement, the gel was sliced and the slices counted in a Packard liquid scintillation spectrometer (Model 3380). *E. coli* RNA was used as marker. The position of 75S and 38S were determined in parallel analyses of BR 2 RNA and nucleolar RNA, respectively. ●, Normal cells; ▲, 15 min of preincubation in DRB; ○, 30 min of preincubation in DRB.

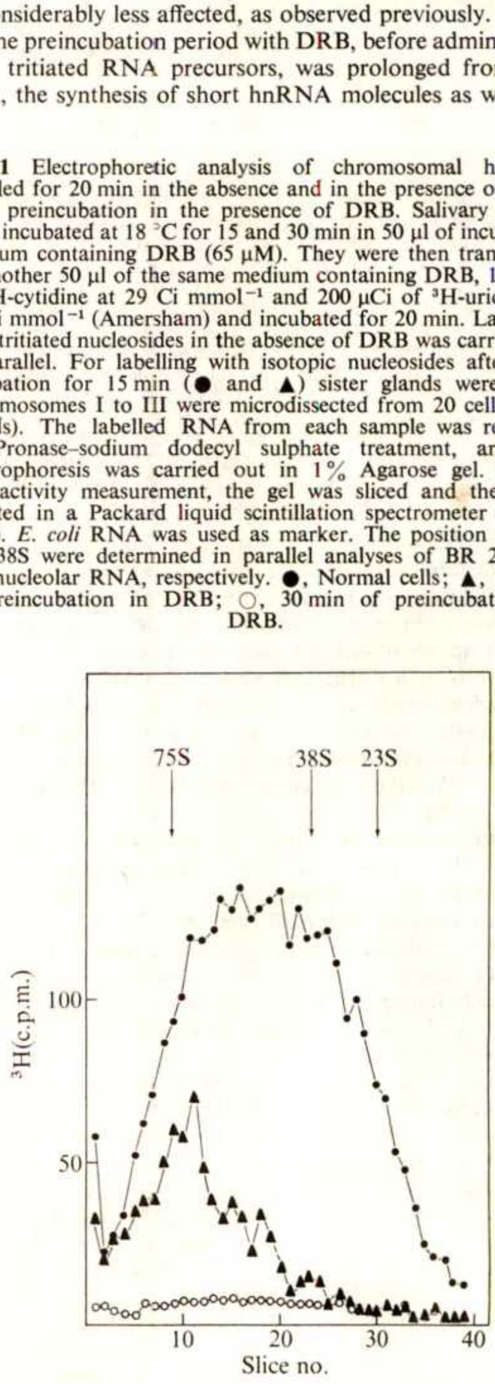

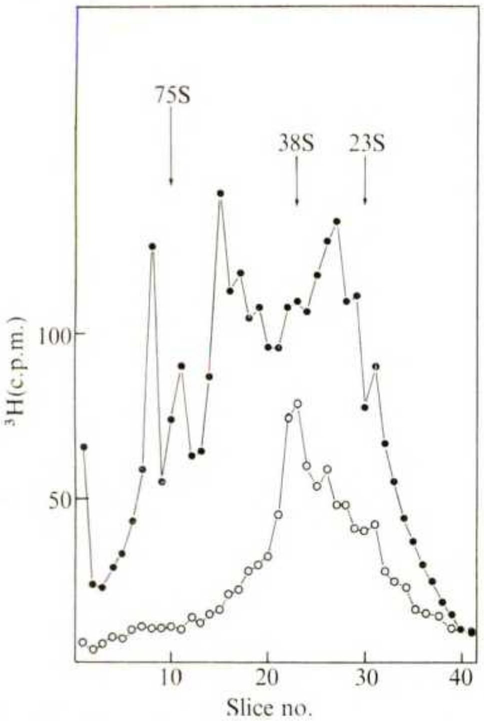

Fig. 2 Electrophoretic analyses of chromosomal hnRNA labelled for 15 min without preincubation in DRB, and after preincubation in DRB followed by removal of DRB from the cells before addition of isotopic nucleosides. Four glands were incubated at 18 °C for 30 min in 50 µl of incubation medium containing DRB (65 µM). The glands were then transferred to an inhibitor-free medium, and were rinsed 3 times each in a volume of 0.5 ml. They were then placed in 50 µl of DRB-free medium containing 100 µCi of ^{3}H-cytidine and 200 µCi of ^{3}H-uridine and incubated for 15 min. For labelling with tritiated nucleosides without preincubation with DRB (control glands), the sister glands were used in an otherwise parallel procedure. Chromosomes I to III were dissected from 20 cells (four glands). For other data see the legend to Fig. 1. ●, Normal cells; ○, DRB-treated cells.

long molecules was equally interrupted, though 5–10% of the labelled material, distributed evenly over the whole spectrum, survived the drug treatment. On the basis of these and previous observations[2-4], it seems likely that the DNA segments which serve as template for hnRNA synthesis are essentially cleared of nascent RNA chains 30 min after addition of DRB.

An efficient reinitiation of transcription after inhibition by DRB is conditional on first, that the intracellular DRB concentration is rapidly reducable to a level not being inhibitory; and second, that the interference of DRB or DRB metabolite (presumably a DRB triphosphate) with the initiation mechanism is reversible after removal of the compound from the cells. Experiments were designed to clear the DNA template of nascent hnRNA chains by blocking the initiation of new chains with DRB for 30 min, and then to reverse the inhibition of initiation simply by washing out DRB from the cells. After rinsing in excess volumes of incubation medium lacking the inhibitor (3×0.5 ml), the glands were incubated for 15 min in a drug-free medium supplemented with tritiated cytidine and uridine (Fig. 2). The control glands were incubated for the same period but without DRB throughout. Although the electrophoretic analysis of hnRNA derived from control cells shows heterogeneous distribution of label in the 16–100S range[2,3], the corresponding analysis of hnRNA from DRB-pretreated and washed glands shows essentially one broad and somewhat asymmetric peak in the 23–38S region. It has a rather steep slope on the high molecular weight side, but is less steep on the other side. Thus, 15 min after removal of DRB from pretreated glands, transcription inhibition seems to be reversed, and a reinitiation of hnRNA synthesis has been taking place. The maximum sizes of hnRNA chains initiated and elongated after removal of inhibitor are, however, significantly less than that of hnRNA produced by cells with an uninterrupted and continuous initiation of transcription. Most of the labelled chains have a molecular size not exceeding that of the 38S marker, although there is also some label in the 38–100S range. This latter material can probably be attributed to radioactivity associated with growing chains which were not eliminated during pretreatment with DRB (refs 1, 2 and Fig. 1). Such uninhibited RNA chains of the larger transcriptional units are then able to produce labelled hnRNA molecules in the 38–100S range immediately after administration of labelled RNA precursors irrespective of whether or not reinitiation is taking place.

To follow the sequence of hnRNA events after drug treatment and replenishment with drug-free medium, isotopic nucleosides were added to the glands 5 min (Fig. 3*a*) and 30 min (Fig. 3*b*) after removal of DRB, and the incorporation continued for 20 min. Control glands were incubated in a similar way but in the absence of inhibitor throughout incubation. The electrophoretic profile of chromosomal hnRNA, derived from glands to which tritiated nucleosides were introduced 5 min after removal of DRB, agrees reasonably well with that of hnRNA extracted from control cells in the range below the 38S marker (Fig. 3*a*). The amount of labelled material in the 38–100S range, however, is lower in treated cells, decreasing gradually from the 38S region towards the 100S range. In the 75–100S region, it comprises 30–40% of the radioactivity level found in the normal pattern. Considering that escape labelling of hnRNA during DRB treatment constitutes not more than 5–10% of the uninterrupted RNA labelling, it seems probable that reinitiated 75–100S RNA molecules have attained their maximum size (finished transcripts) 25 min after reversal of inhibitory action. It should be observed, however, that even though reinitiated hnRNA chains in the 75–100S range have been completed 25 min after removal of DRB, the amount of labelled

Fig. 3 Electrophoretic analyses of chromosomal hnRNA labelled for 20 min without preincubation in DRB, and after preincubation in DRB followed by removal of DRB from the cells before addition of isotopic nucleosides. In each experiment four glands from four different animals were incubated at 18 °C for 30 min in 50 µl of incubation medium containing DRB (65 µM). The glands were then transferred to an inhibitor-free medium and rinsed 3 times each in a volume of 0.5 ml and placed in 50 µl of fresh medium for *a*, 5 and *b*, 30 min. Next, 100 µCi of ^{3}H-cytidine and 200 µCi of ^{3}H-uridine were introduced to the medium and the glands were labelled for 20 min. For labelling with tritiated nucleosides without preincubation in DRB (control glands), the sister glands were used in an otherwise parallel procedure. Chromosomes I to III were dissected from 20 cells (four glands). For other details see the legend to Fig. 1. ●, Normal cells; ○, DRB-treated cells.

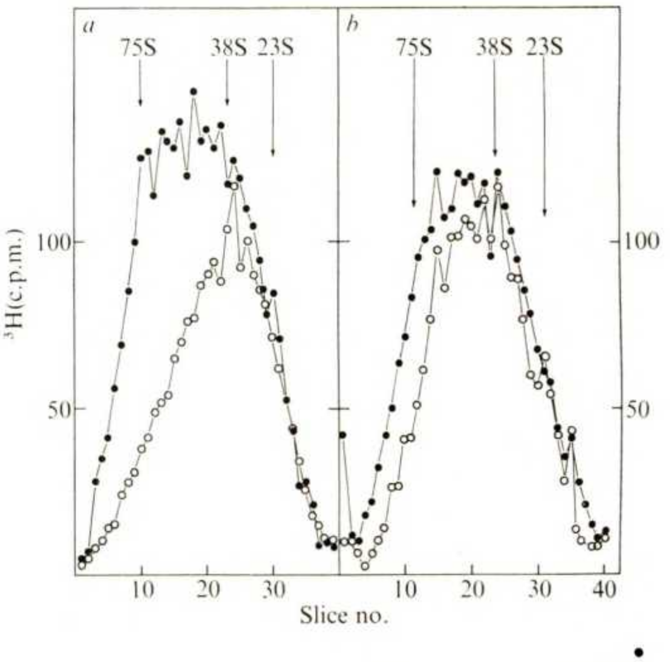

RNA in this part of the spectrum is, still 60–70% lower than that in untreated cells. This may be because: (1) transcription initiation is not restored to normal efficiency after replacement of medium containing DRB with inhibitor-free medium (partial reinitiation); and/or (2) finished hnRNA molecules accumulate after their completion on chromosomes I to III. The latter would imply that chromosomal RNA extracts from control cells contain a larger quantity of finished molecules than that from cells which were pretreated with DRB for 30 min and incubated in inhibitor-free medium for 25 min after removal of DRB (Fig. 3*a*).

The finding that hnRNA molecules migrating faster than 38S display a normal rate of labelling if isotopic nucleosides are added 5 min after transferring glands to drug-free medium (Fig. 3*a*) argues against inefficiency in transcription reinitiation. Previous observations that hnRNA on the chromosomes I to III attains maximum specific activity after 45–90 min of incorporation[2], whereas the labelling of Balbiani ring RNA of similar size reaches a plateau value after 20 min of labelling[10] are compatible with an accumulation of hnRNA molecules on the chromosomes I to III after their completion. Therefore, to restore the rate of labelling and accumulation of chromosomal 75–100S RNA to the normal condition after removal of DRB from inhibited cells, incubation for 20 min or longer would be required before the addition of radioactive RNA precursors. In the experiment shown in Fig. 3*b*, the interval between washing and replenishing DRB-treated glands with drug-free medium and administration of isotopic nucleosides was prolonged to about 30 min. As predicted, the electrophoretic patterns of chromosomal hnRNA derived from inhibited and washed cells and from untreated cells display a reasonably good agreement, although absolute equality cannot be claimed. The results in Fig. 3 strongly indicate that 25 min of incubation after washing out DRB from cells (5 min in the absence plus 20 min in the presence of radioactive nucleosides) pretreated with the drug for 30 min, is sufficiently long to reinitiate, elongate and complete hnRNA chains migrating as 75–100S RNA. To bring the rate of the synthesis (accumulation) of the largest hnRNA molecules on the chromosomes I to III to a level similar to that before exposure to transcription inhibition, however, incubation in inhibitor-free medium for at least 30 min is demanded after removal of DRB. The principal reason for that is probably the accumulation of newly made hnRNA on chromosomes I to III rather than, or in addition to, an inefficient reinitiation of the transcription.

I thank Agneta Askendal and Amina Ossoinak for skillful technical assistance. The investigation was supported by the Swedish Cancer Society and Karolinska Institutet (Reservationsanslaget).

ENDRE EGYHÁZI

Department of Histology,
Karolinska Institutet,
S-104 01 Stockholm, Sweden

Received March 19; accepted May 26, 1976.

1 Egyházi, E., Daneholt, B., Edström, J.-E., Lambert, B., and Ringborg, U., *J. Cell Biol.*, **47**, 416–420 (1970).
2 Egyházi, E., *J. molec. Biol.*, **84**, 173–183 (1974).
3 Egyházi, E., *Biochim. biophys. Acta*, **378**, 205–215 (1975).
4 Egyházi, E., *Proc. natn. Acad. Sci. U.S.A.*, **72**, 947–950 (1975).
5 Sehgal, P. B., Tamm, I., and Vilcek, J., *Science*, **190**, 282–284 (1975).
6 Cannon, G. B., *Science*, **146**, 1063 (1964).
7 Ringborg, U., and Rydlander, L., *J. Cell Biol.*, **51**, 355–368 (1971).
8 Edström, J.-E., in *Methods in Cell Physiology*, **1** (edit. by Prescott, D.), 417–447 (Academic, New York, 1964).
9 Daneholt, B., Edström, J.-E., Egyházi, E., Lambert, B., and Ringborg, U., *Chromosoma*, **28**, 399–417 (1969).
10 Egyházi, E., *Cell*, **7**, 507–515 (1976).

Inactivation of parathyroid hormone mRNA by treatment with periodate and aniline

TRANSLATION of parathyroid hormone (PTH) mRNA in extracts of wheat germ[1] or Krebs II ascites cells[2] produces a polypeptide which contains the structure of PTH but which is larger than either PTH or its biosynthetic precursor proparathyroid hormone[3,4] (proPTH). In the wheat germ system, this cell-free protein, designated pre-proparathyroid hormone (pre-proPTH) contains a methionine at the amino terminus[5] derived from initiator methionyl-tRNA[6]. Although this observation suggests that initiation of the synthesis of pre-proPTH is normal in the cell-free system, it is possible that *in vitro* initiation occurs at a codon that codes for an internal methionine *in vivo*. Such an artefact could be due to a degraded mRNA in which the *in vivo* initiator codon is lost or inactivated.

Recent studies on the structure of mRNA have suggested a method for demonstrating that an isolated mRNA is intact at the 5′ end and thus that the proper initiator codon is present. Many mRNAs of viruses and eukaryotic cells have been shown to be blocked at the 5′ end by a 7-methlyguanosine linked through its 5′ hydroxyl by way of a triphosphate or pyrophosphate to the 5′ hydroxyl of the penultimate nucleoside[7]. This 5′–5′ linked structure is necessary for the translation of mRNAs of vesicular stomatitis virus, reovirus, and haemoglobin[8,9] and mRNA from brine shrimp[10]. The 7-methylguanosine can be removed from the mRNAs by oxidation with periodate followed by a β elimination reaction catalysed by aniline[9]. I have compared the effects of periodate and aniline treatment on the activity of PTH mRNA with the effects on the activities of haemoglobin mRNA which has a blocked 5′ terminus and with satellite tobacco necrosis virus (STNV) mRNA which does not contain a methylated blocked 5′ terminus[11,12] and is actively translated in the wheat germ cell-free protein synthesising system without being methylated (J. M. Clark, Jr, personal communication).

Treatment with periodate followed by aniline inhibited the translation of PTH and haemoglobin mRNAs by 90% or more, compared with controls incubated in the same manner without periodate and aniline (Fig. 1*a* and *b*). In contrast, the activity of STNV mRNA was inhibited only about 15% by this treatment, an inhibition similar to that observed in the control incubated with aniline alone (Fig. 1*c*). Treatment with periodate alone substantially reduced the activity of haemoglobin and PTH mRNA but had no inhibitory effect on STNV RNA. The resistance of STNV RNA to this treatment minimises the possibility that the periodate inhibition is a nonspecific effect. The inhibition may be due to spontaneous β elimination of the oxidised mRNA, or the oxidation of the sugar moiety on methylguanosine may alter the 5′ end enough to decrease the efficiency of initiation. The present data do not allow us to distinguish between these two possibilities. Rao *et al.*[13], however, have shown that periodate treatment alone completely inhibits the activity of rat liver mRNA and have concluded that the unoxidised ribose is required for activity. It is not clear why they observed nearly 100% inhibition after periodate oxidation and I observed only a 50% inhibition.

The effect of aniline treatment alone on the activity of the mRNAs was somewhat variable. The activity of haemoglobin mRNA was not reduced by aniline treatment while PTH mRNA and STNV RNA were inhibited by about 50 and 15%, respectively. Steinschneider and Frankel-Conrat have reported that aniline treatment alone reduced the infectivity of tobacco mosaic virus RNA by 50% and that some aniline was tightly bound to the RNA and could not be removed by extensive washing[14]. Thus, different mRNA may be differentially sensitive to treatment by aniline.

Although treatment with either periodate or aniline alone reduced the activity of PTH mRNA, the inhibition after treatment with both chemicals was more than simply a summation of the two individual inhibitions. In the experiment shown in Fig. 1*a*, the sample treated with aniline and periodate should have been about 25% of control if the effects of aniline and periodate were additive instead of the observed 4% of control. In another experiment the

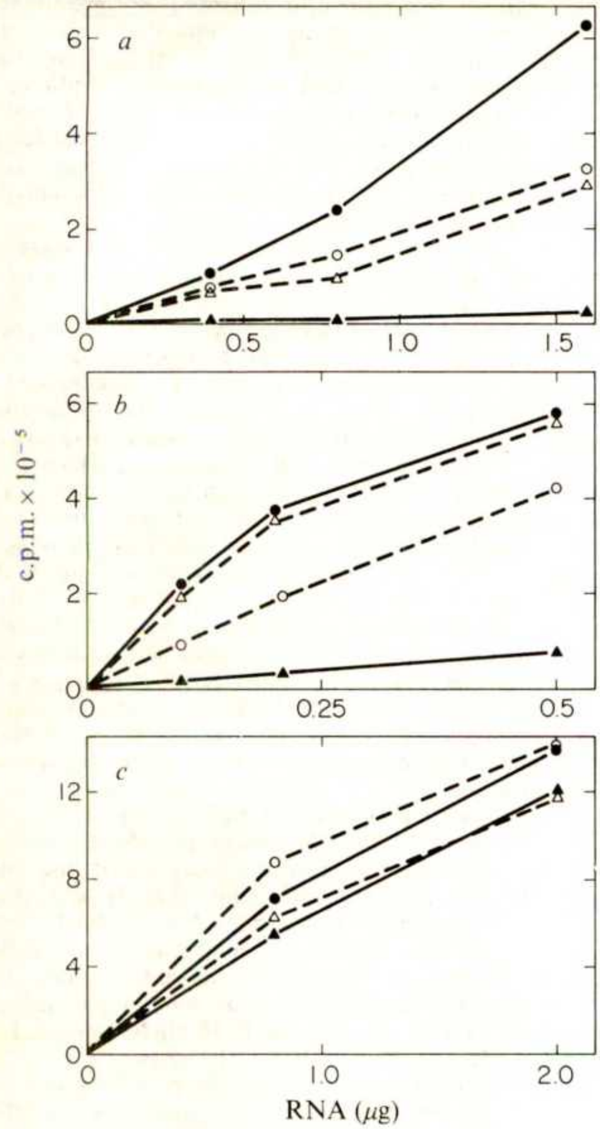

Fig. 1 Translation in wheat germ extracts of PTH (*a*), haemoglobin (*b*) and STNV (*c*) mRNAs after treatment with periodate and aniline. Haemoglobin mRNA was isolated as described by Labrie[15]. Parathyroid RNA sedimenting between 8S and 14S (designated PTH mRNA in this report) was isolated as described previously[1] with modifications. Bovine parathyroid glands were obtained at the time of slaughter and were stored in liquid nitrogen. About 1 g of glands was sliced and then homogenised for 1 min in a Waring blender in 5 ml of phenol, 5 ml of chloroform containing 4% isoamyl alcohol and 2 ml of 10% sodium dodecyl sulphate. 5 ml of buffer (0.01 M Tris-HCl, *p*H 7.4, 0.1 M NaCl, 0.001 M EDTA, 0.1% sodium dodecyl sulphate) was added and RNA was extracted by shaking with phenol–chloroform as described previously[1]. DNA and low molecular weight RNA were extracted from the sample with 3 M sodium acetate, *p*H 6.0, 7.5 mM EDTA[16] and the RNA sedimenting on a sucrose gradient from 8S to 14S was isolated from the high molecular weight RNA as before[1]. The mRNAs were incubated with periodate and aniline as described by Steinschneider and Fraenkel-Conrat[14] and modified by Mayer *et al.*[17]. 10 μg of haemoglobin or STNV mRNA or 4 μg of PTH mRNA were incubated in 50 μl of 0.1 M sodium acetate, *p*H 5.3, 1 mM EDTA containing 1 mM sodium periodate for 2 h at room temperature in the dark. Glucose was added to 10 mM, 150 μl ethanol were added and RNA was precipitated overnight at −20 °C. The RNA was centrifuged in a Brinkman microfuge, washed with ethanol, dried under vacuum and dissolved in 50 μl of 0.33 M aniline HCl. After incubation for 2 h at room temperature in the dark, NaCl was added to 0.3 M and 150 μl of ethanol were added. The samples were left overnight at −20 °C, and the RNA was centrifuged, washed twice with ethanol, dried under vacuum and dissolved in 25 μl of H_2O for translation in the wheat germ extracts. Controls were incubated in the same manner except that either aniline or periodate or both were not added. Conditions for the translation of the mRNA in the wheat germ cell-free system have been described[1]. 5–10 μCi of ^{35}S-methionine (300 Ci $mmol^{-1}$, Amersham Searle) were added to each reaction of 25 μl. Total trichloroacetic acid-insoluble radioactivity was determined in 1- or 2- μl aliquots of the reaction. The amounts of radioactivity and RNA indicated in the figure are the c.p.m. and μg, respectively, in a reaction of 25 μl. The amount of radioactivity (*a*, 0.43×10^5 c.p.m.; *b*, 0.26×10^5 c.p.m.; and *c*, 0.45×10^5) incorporated into protein if mRNA was not added to the reaction was subtracted from each of the plotted values. ●, Incubated without aniline or periodate; △, incubated with aniline and without periodate; ○, incubated with periodate and without aniline; ▲, incubated with periodate and aniline.

treatment with aniline and periodate was reversed. The samples treated with either periodate or aniline alone were 73% and 85% of control, respectively. The sample treated in reverse order with aniline and periodate was 54% of control, near the 62% expected as a result of simple additive effects, while the sample treated with periodate and then aniline was 19% of control. The inhibition was less in this experiment than that shown in Fig. 1, probably because 0.27 M aniline was used instead of 0.33 M aniline. This synergistic action suggests that the effect of the periodate/aniline treatment is the result of a β-elimination reaction which would be expected if PTH mRNA has a nucleoside in 5′–5′ linkage at the 5′ end.

Analysis of the products of the translation of the mRNAs in the wheat germ extracts by sodium dodecyl sulphate slab gel electrophoresis is shown in Fig. 2. Each of the mRNAs directs primarily the synthesis of the expected protein products. If STNV RNA is mixed with either PTH mRNA or haemoglobin mRNA, both the RNAs in the mixture direct the synthesis of their respective proteins (Fig. 2*b* and *g*) but after treatment of the mixture with periodate and aniline, essentially only STNV proteins are observed (Fig. 2*c* and *h*).

These experiments demonstrate that inactivation of mRNAs by treatment with periodate and aniline is an effective means of determining whether mRNAs contain a 5′–5′ linked nucleoside at the 5′ terminus, particularly with an impure preparation of mRNA such as that used in this report for PTH mRNA when direct chemical analysis is not possible. The inactivation of haemoglobin and PTH mRNAs by this treatment supports studies with other mRNAs indicating that the blocked 5′ end is required for maximal activity of mRNA[8-10]. Simply demonstrating that periodate–aniline treatment causes inhibition of mRNA activity is not sufficient to conclude that a particular mRNA contains such a 5′–5′ linked nucleoside since treatment with aniline or periodate alone can cause substantial inhibition. The controls of treatment with aniline or periodate alone are thus essential to interpreting the results. Furthermore, addition of a mRNA without a blocked 5′ terminus to the reaction as in the experiment in Fig. 2 can control other nonspecific factors such as RNase activity or physical loss of the mRNA during the procedure. For the many mRNAs that contain polyadenylic acid, the demonstration of a blocked 5′ end by this method, combined with the demonstration that polyadenylic acid is present at the 3′ end, will be useful criteria for establishing that a mRNA has not been partially degraded during isolation.

The data presented indicate that PTH mRNA contains a blocked 5′ terminus and thus is probably intact at the 5′ terminus. If this is true, then the normal initiator codon *in vivo* is present and it is unlikely that the translation of PTH mRNA *in vitro* is the result of false initiation at an internal codon. This further strengthens the contention that pre-proPTH represents all of the information present in PTH mRNA that is translated into protein.

I thank Dr John M. Clark, Jr for providing STNV RNA and for helpful discussions and Calihan and Co., Meats, Peoria, Illinois, for the bovine parathyroid glands. This

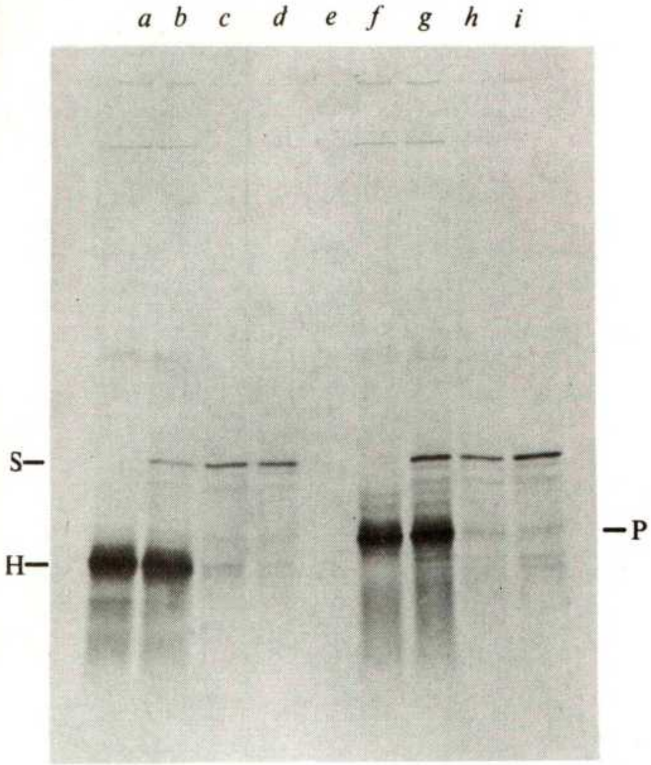

Fig. 2 Analysis by sodium dodecyl sulphate gel electrophoresis of the radioactive proteins synthesised in the wheat germ extracts. Translation of mRNA was as described in the legend to Fig. 1 and 5 µl of the reactions were analysed on 15% acrylamide slab gels according to Laemmli[18] as described previously[6]. The autoradiogram was prepared by exposing the dried gel to Kodak RP Royal X-ray film for 18 h. RNA added to each reaction of 25 µl was: *a*, 0.2 µg haemoglobin mRNA; *b*, 0.2 µg haemoglobin mRNA+0.4 µg STNV mRNA; *c*, same as *b* after treatment of the mixture with periodate and aniline; *d*, 0.4 µg STNV RNA; *e*, none; *f*, 1.6 µg PTH mRNA; *g*, 1.6 µg PTH mRNA+0.8 µg STNV mRNA; *h*, same as *g* after treatment of the mixture with periodate and aniline; *i*, 0.8 µg STNV mRNA. The positions of haemoglobin, STNV coat protein and pre-proPTH are indicated by H, S, and P, respectively.

work was supported in part by a USPHS general research support grant to the University of Illinois College of Medicine.

BYRON KEMPER

Department of Physiology and Biophysics and
School of Basic Medical Sciences,
University of Illinois,
Urbana, Illinois 61801

Received March 26; accepted May 25, 1976.

[1] Kemper, B. Habener, J. F., Mulligan, R. C., Potts, J. T., Jr, and Rich, A., *Proc. natn. Acad. Sci. U.S.A.*, **71**, 3731–3735 (1974).
[2] Habener, J. F., Kemper, B., Potts, J. T., Jr, and Rich, A., *Biochem. biophys. Res. Commun.*, **67**, 1114–1121 (1975).
[3] Kemper, B., Habener, J. F., Potts, J. T., Jr, and Rich, A. *Proc. natn. Acad. Sci. U.S.A.*, **69**, 643–647 (1972).
[4] Cohn, D. V., MacGregor, R. R., Chu, L. L. H., Kimmel, J. R., and Hamilton, J. W., *Proc. natn. Acad. Sci. U.S.A.*, **69**, 1521–1525 (1972).
[5] Kemper, B., Habener, J. F., Ernst, M. D., Potts, J. T., Jr, and Rich, A., *Biochemistry*, **15**, 15–20 (1976).
[6] Kemper, B., Habener, J. F., Potts, J. T., Jr, and Rich, A., *Biochemistry*, **15**, 20–25 (1976).
[7] Both, G. W., Furuichi, Y., Muthukrishnan, S., and Shatkin, A. J., *Cell*, **6**, 185–195 (1975).
[8] Both, G. W., Banerjee, A. K., and Shatkin, A. J., *Proc. natn. Acad. Sci. U.S.A.*, **72**, 1189–1193 (1975).
[9] Muthukrishnan, S., Both, G. W., Furuichi, Y., and Shatkin, A. J., *Nature*, **255**, 33–37 (1975).
[10] Muthukrishnan, S., *et al.*, *J. biol. Chem.*, **250**, 9336–9341 (1975).
[11] Wimmer, E., Chang, A. Y., Clark, J. M., Jr, and Reichmann, M. E., *J. molec. Biol.*, **38**, 59–73 (1968).
[12] Horst, J., Fraenkel-Conrat, H., and Mandeles, S., *Biochemistry*, **10**, 4748–4752 (1971).
[13] Rao, M. S., Wu, B. C., Waxman, J., and Busch, H., *Biochem. biophys. Res. Commun.*, **66**, 1186–1193 (1975).
[14] Steinschneider, A., and Fraenkel-Conrat, H., *Biochemistry*, **5**, 2735–2743 (1966).
[15] Labrie, F., *Nature*, **221**, 1217–1222 (1969).
[16] Palmiter, R. D., *J. biol. Chem.*, **248**, 2095–2106 (1973).
[17] Mayer, S. A., Abraham, G., Alder, R., and Banerjee, A. K., *Cell*, **5**, 59–67 (1975).
[18] Laemmli, U. K., *Nature*, **227**, 680–685 (1970).

Aqueous glasses as matrices in freeze-fracture electron microscopy

FREEZING is an important technique in the preservation of the morphology of biological materials for electron microscopic examination. Methods relying on freeze-fracturing, sometimes followed by etching, have been developed and have led to advances in the interpretation of biological ultrastructure[1]. Other, related applications of freezing are for the preservation of biological activity[2] and the preparation of biological specimens for microanalysis of low molecular weight components[3]. The freezing of cells and tissues can, like all other methods of fixation, give rise to artefacts, although probably to a lesser extent than the more traditional methods. The most important factors governing the quality of biological freezing include the size distribution of the ice crystals, the extent of supercooling and the possibility of osmotic dehydration and shrinkage of cells. Very high cooling rates are considered essential to minimise the deleterious effects of ice crystals, and to overcome excessive osmotic shrinkage of cells by extracellular ice formation, the use of cryoprotective agents is common. It is believed that an effective, penetrating cryoprotectant must diffuse into the cell without, at the same time, interfering with its morphology. Glycerol and dimethylsulphoxide fulfil these conditions and are widely used as cryoprotectants, although it is known that they can interfere with the physiological functions of some cells[4].

The available evidence suggests that, in the appropriate conditions, the cell contents are readily supercooled[5], and so it should be possible to protect cells from freeze damage by controlling the formation and growth of ice nuclei in the extracellular fluid, even in the absence of penetrating cryoprotectants. We have achieved this using water-soluble synthetic or modified natural polymers.

In favourable conditions, suitable polymers in aqueous solution can be made to yield vitreous states which are devoid of ice crystallites at low temperatures. The experimental requirements are a combination of high viscosity (that is,

Fig. 1 50% PVP solution quenched, freeze-fractured and subsequently etched for 5 min at 173 K. (× 19,440)

high molecular weight and adequately high concentration) and fast cooling. Even where, for practical reasons, complete vitrification is not possible and submicroscopic ice nuclei develop during quenching, these are prevented from growing at the temperatures normally used for freeze-fracturing (120–170 K) by the very low diffusion rates in the embedding polymer solution. One of the main advantages of polymeric cryoprotectants is their inability to penetrate the cell, so they are less likely to interfere with the physiological functions, or alter the morphology. Also, by virtue of their high molecular weights, they cause hardly any osmotic flow of water from the cell.

The polymers which are most effective for the achievement of vitreous states are those with a large water-binding capacity, for example, polyvinyl pyrrolidone (PVP), polyvinyl alcohol, dextran and polyethylene glycol. Several others, such as modified starches and celluloses, although interacting strongly with water, do not yield sufficiently concentrated solutions at the molecular weights normally obtainable. Most of our exploratory work has been with PVP of average molecular weights 44,000 and 700,000, used at concentrations of 25 and 50 weight %. The aqueous solution of the polymer was quenched in melting Freon 22 and then transferred to liquid nitrogen. It was freeze-fractured (Balzer BA 360 M Freeze Etching Unit) at 173 K, some specimens subsequently being etched at this temperature. Tungsten/tantalum replicas backed with carbon were prepared and examined by transmission electron microscopy.

Figure 1 shows an electron micrograph of a quenched 50% PVP of average molecular weight 44,000. At the magnification used there is no evidence of any ice crystals, and the largest structural units are ~ 10 nm in diameter. Figure 2 represents two differential scanning thermograms (Perkin Elmer DSC.2) obtained by cooling and heating the same solution. Although the fastest cooling rate which could be achieved in the calorimeter was only 80 K min^{-1}, the cooling trace shows the complete suppression of ice formation; instead a vitrification (T_g) is indicated at 200 K. The same T_g is seen in the warming trace (10 K min^{-1}), followed by a devitrification (T_d) at 220 K, and finally by melting (T_m). These transition temperatures are in reasonable agreement with those reported previously[6].

A 25% PVP solution, treated in the same way showed (Fig. 3) general structural features similar to those in Fig. 1, but ice nucleation sites which have given rise to spherulitic crystallites of micrometre dimensions are indicated. Raising the temperature and maintaining it at 200 K for 2 h did not, however, lead to a further crystal growth.

These processes in the 25% solution could not be monitored by scanning calorimetry, because even the fastest cooling rate which could be achieved in the calorimeter was too slow to prevent the total freezing of the solution. This confirms a

Fig. 2 Differential scanning thermogram obtained by heating a 50% PVP solution. T_g, Glass transition; T_d, devitrification; T_m, melting point.

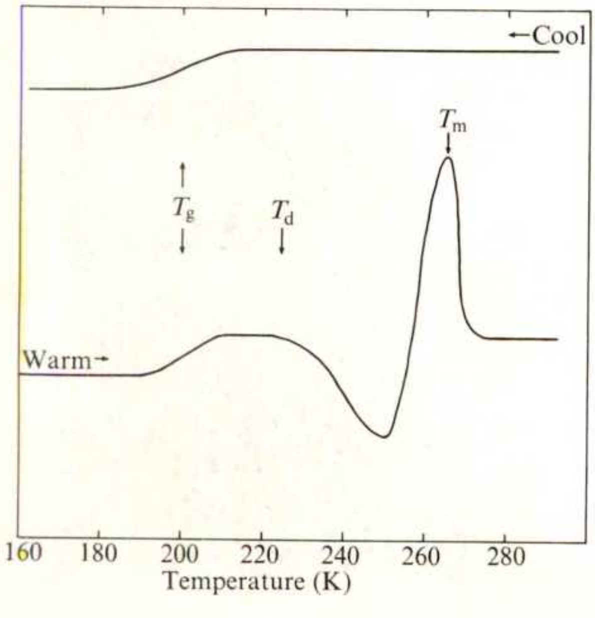

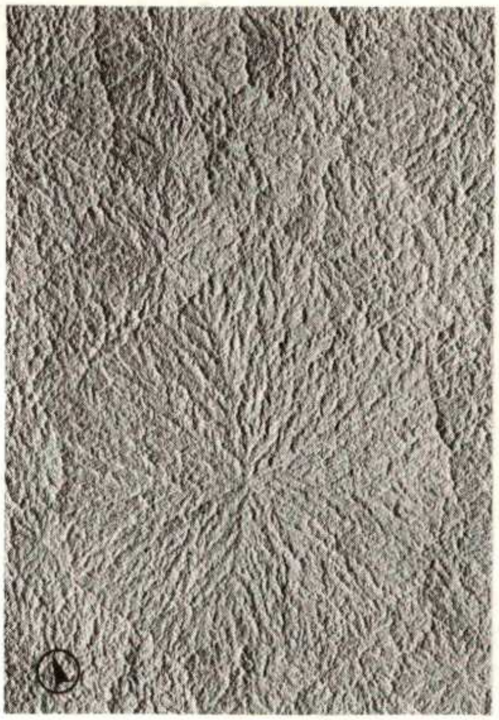

Fig. 3 25% PVP solution treated as for Fig. 1. (× 19,440)

Fig. 4 Nerve cell from the interganglionic connective from the cockroach (*Periplaneta americana*) central nervous system. Freshly dissected tissue was incubated in buffered 50% PVP for 30 min before quenching. Microtubules (arrows) can be distinguished clearly in the cytoplasmic background, showing the absence of ice damage. (× 18,000)

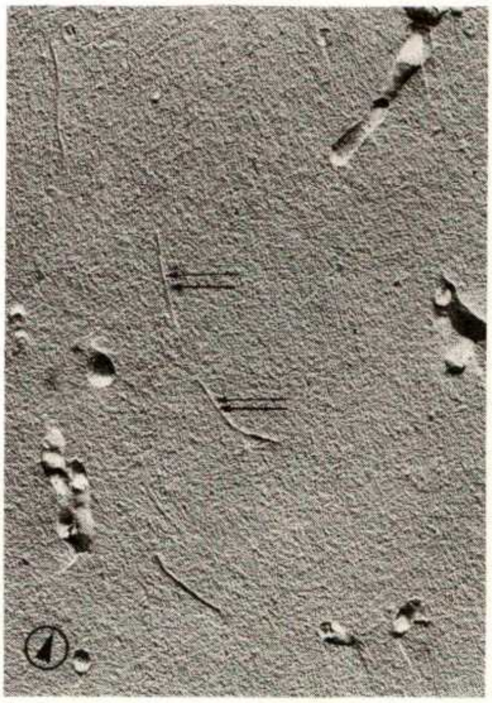

previous observation[6], made using a calorimeter especially designed for much faster cooling, where it was not possible to identify T_g, because ice developed during sample cooling.

Experiments were also carried out in which PVP solutions containing single cells and tissues of animal and plant origin were similarly quenched and fractured. In all cases, extracellular medium had the appearance shown in Fig. 1 and no ice crystals could be detected in the cytoplasm. Figure 4 shows an example taken from the central nervous system of the cockroach. The cell shown comes from the centre of the tissue which is ~ 1 mm thick and the absence of ice in the cytoplasm suggests that intracellular cryoprotection is afforded even when the cell is not in direct contact with the medium containing the polymer.

Further work is in progress to investigate the influence of different polymer systems and different experimental conditions on the morphological details of quenched cells and tissues. A more detailed report will be published elsewhere.

We thank Mr W. M. Lee for technical assistance with the freeze-fracturing and Mr R. Hemming for performing the scanning calorimetry.

FELIX FRANKS*

Department of Botany,

HELEN LE B. SKAER

ARC Unit of Invertebrate Chemistry and Physiology,
Department of Zoology,
University of Cambridge,
Cambridge, UK

Received February 4; accepted June 8, 1976

*Permanent address. Biosciences Division, Unilever Research Laboratory Colworth/Welwyn, Colworth House, Sharnbrook, Bedford MK44 1LQ, UK.

[1] *Freeze Etching Techniques and Applications* (edit. by Benedetti. E. L., and Favard, P),(Société Francaise de Microscopie Electronique, Paris, 1973).
[2] Farrant, J., *Proc. R. Soc* (in the press).
[3] Echlin, P., *J. Microscopie Biol. cell.*, 22, 215–226 (1975).
[4] Moor, H., *Phil. Trans. R Soc.*, B261, 121–131 (1971).
[5] Rasmussen, D. H , Macaulay, M N., and MacKenzie, A. P., *Cryobiology*, 12, 328–339 (1975).
[6] MacKenzie, A. P., and Rasmussen, D. H , in *Water Structure at the Water–Polymer Interface* (edit. by Jellinek, H. H. G.), 146–172 (Plenum, New York, 1972)

The hinge-bending mode in lysozyme

A COMPLETE description of an enzyme requires a knowledge of its structure and the dynamics of its function. From the crystal structures of enzymes and enzyme–inhibitor complexes and the known chemistry of model systems, it has been possible in some cases to draw reasonable inferences concerning the mechanisms of enzyme-catalysed reactions. Little has been done so far, however, to supplement such essentially static results by an investigation of the reaction dynamics. This requires an understanding of the internal motions of the enzyme, as well as those of the substrate, since both are likely to be essential to the function. Here we present a theoretical study of a low frequency vibration involving the two globular lobes of lysozyme between which the cleft containing the active site is located[1]. Any motion involving this cleft could play a part in the catalytic activity; in fact, atom displacements of up to 0.75 Å found in a comparison of the free enzyme and the enzyme–inhibitor complex indicate that the cleft has closed down in the latter[2]. The force constant for the low frequency bending vibration corresponding to the opening and closing of the cleft is obtained from empirical energy functions[3]. Because the protein surface moves appreciably during the vibration, damping effects resulting from the viscous dissipation in the solvent are included in the calculation[4,5].

To model the hinge-bending mode, the lysozyme molecule is assumed to be composed of two essentially rigid lobes (lobe 1: residues 5–36 and 98–129; lobe 2: residues 40–94), connected by a hinge region consisting of the amino-terminal end (residues 1–4) and two short polypeptide chain segments (residues 37–39, 95–97) running from one lobe to the other[1]. A natural axis parallel to the cleft is obtained for the bending motion by passing a line through $C_\alpha 38$ and $C_\alpha 97$, an excellent view of the cleft and the chosen axis can be obtained from diagram L4 of Dickerson and Geis[6].

The bending motion of lysozyme in the presence of solvent is determined by the Langevin equation for a damped harmonic oscillator[7], which has the form

$$I\frac{d^2\theta}{dt^2} + f\frac{d\theta}{dt} + k\theta = N_r(t) \qquad (1)$$

Here, θ is the angular displacement from the equilibrium position, I the effective moment of inertia, f the friction coefficient, and k the force constant associated with the relative motion of the lobes; $N_r(t)$ represents a randomly fluctuating torque characteristic of Brownian motion. The properties of a system governed by equation (1) are well known[7]. To apply the results to the present case, it is necessary only to determine the parameters I, f, and k.

The force constant k was estimated from an empirical energy function that expresses the total conformational energy as a function of the Cartesian coordinates of the heavy atoms[3]; it includes terms associated with bond lengths, bond angles, dihedral angles, hydrogen bonds and non-bonded interactions. To obtain an equilibrium starting structure, the real space refined coordinates of lysozyme[8] were subjected to 200 steps of steepest-descent energy refinement. The potential function for bending was then determined by rotating residues 39–96 rigidly about the chosen axis and computing the conformational energy of the distorted protein as a function of the bending angle. To obtain a more realistic potential function, the same rigid rotations were performed, but at each bending angle there followed a 100-cycle energy minimisation which allowed for adiabatic relaxation of the protein[3]. The bending angle was kept fixed during the relaxation by imposing constraints on residues distant from the hinge in the interior of each lobe (residues 44–51, 61 and 65–73 in lobe 2, residues 109–122 in lobe 1). The results of the two calculations are shown in Fig. 1; a parabolic fit to the points yields the force constants $k_r = 4.1 \times 10^{14}$ erg rad^{-2} mol^{-1} (rigid), and $k_a = 3.3 \times 10^{13}$ erg rad^{-2} mol^{-1} (adiabatic). Total moments of inertia about the bending axis were computed for residues 38–97 (I_2) and for the rest of the molecule (I_1); the values are $I_2 = 1.01 \times 10^{-10}$ g cm^2 mol^{-1} and $I_1 = 1.08 \times 10^{-10}$ g cm^2 mol^{-1}. Water molecules associated with the protein were ignored in this calculation. The friction coefficient was estimated by a modified Stokes law[9] appropriate for the hydrodynamic interaction of two spheres of radius 10 Å separated by a gap of 5 Å, undergoing small relative motions about an axis 20 Å from the sphere centres; the resulting value is $f = 5.7 \times 10^2$ g cm^2 s^{-1} mol^{-1}.

If hydrodynamic effects are neglected, equation (1) reduces to the equation for a simple harmonic oscillator. With the approximation $I = (I_1 I_2/I_1 + I_2)$, the resulting frequencies are $\omega_r = 15$ cm^{-1} and $\omega_a = 4.2$ cm^{-1}. These very low frequencies result from a balance between the large force constant and the large moment of inertia associated with the bending motion. The effective CCN bending force constant for an α carbon is 2×10^{12} erg rad^{-2} mol^{-1}, less than 1/10 of k_a. The additional contributions to k_a come from a large number of non-bonded contacts (20–50, depending on the bending angle), involving atoms in the hinge region and in the lobes (for example, for closing, Leu 56 O . . . Trp 108 N_{ε_1}, Trp 63 C_{η_2} . . . Asp 101 O_{δ_2} and for opening His 15 N_{ε_2} . . . Thr 89 O_{γ_1}, His 15 C_{δ_2} . . . Thr 89 O_{γ_1}). The large difference between k_r and k_a arises from small atomic displacements ($\leqslant 0.5$ Å) that alleviate the close non-bonded contacts produced by the rigid motion.

Introduction of the hydrodynamic terms in equation (1) demonstrates that for an aqueous medium the inequality

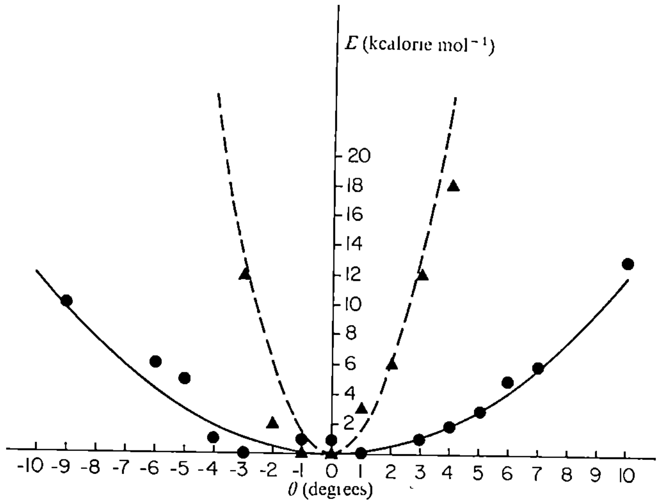

Fig. 1 Change in conformational energy produced by opening ($\theta<0$) or closing ($\theta>0$) the lysozyme cleft. Calculated values are for the rigid bending potential (▲), and for the adiabatic bending potential (●); the curves are parabolic fits to the points. The $\theta=0$ value corresponds to the minimum energy geometry for each of the potentials; the adiabatic minimum corresponds to an energy 34 kcalorie mol^{-1} below the rigid curve and is displaced toward a more open configuration by 5°.

($f^2 > 4Ik$) is satisfied so that the motion is 'overdamped'; that is, rather than vibrating periodically with the calculated frequency, the two lobes move relative to each other in a diffusive manner in accord with the Smoluchowski equation[7]. Quantitatively, the inertial effects decay rapidly, with a time constant $\tau_I = (I/f) \simeq 10^{-13}$ s, and the relaxation time for displacements from equilibrium is $\tau_\theta \simeq f/k_a \simeq 2\times10^{-11}$ s; this latter value is to be compared with the undamped vibration period, $\tau = 8\times10^{-12}$ s.

The time constant τ_θ for the diffusional displacement of the lobes is sufficiently large to justify the use of the adiabatic potential; that is, the local torsional and bending motions required to remove the repulsive contacts have vibrational periods that are much shorter than τ_θ.

It is possible that the cleft motion involving the active site cleft has a significant effect on the rate constants for substrate binding to lysozyme. The time required for a molecule the size of glucose to diffuse freely 5 Å is $> 5\times10^{-10}$ s at 300 K, and, thus, substantially $> \tau_\theta$. Since opening or closing fluctuations on the order of twice the root mean square value ($\langle\theta^2\rangle^{1/2} \simeq 1.6°$) correspond to displacements of over 1 Å in the outer part of the cleft region, the coupling between substrate binding and the cleft vibrational mode requires a more detailed study taking into account the enzyme–substrate interaction; for example, the motion could be significantly perturbed by the presence of the substrate.

It is important also to note that the lobe motion examined here is so rapid, compared with the transport phenomena usually considered for biopolymers (such as diffusion and sedimentation), that the traditional approximations of incompressible and quasi-steady flow used in determining f have to be questioned. In particular, the Reynolds number, which measures the deviation from quasi-steady flow[10], $=R^2/\eta\tau_\theta$, is 0.1–0.2 (R is the lysozyme radius and η is the kinematic viscosity) and the Mach number, which measures the deviation from incompressible flow[11], $=R/c\tau_\theta$, is 0.1 (c is the speed of sound in water). Thus, the present treatment is valid only as a first approximation. Moreover, a more detailed molecular approach to the solvent behaviour (for example, the water in the cleft) might be appropriate, although computer studies indicate that bulk water responds in a viscous manner to shearing forces on the molecular scale for times greater than 5×10^{-13} s (ref. 12).

The method used and the results obtained for the diffusive behaviour of the hinge-bending mode of lysozyme may be of wider interest in the theory of biopolymers. Active site clefts are found in many enzymes[13] and their opening and closing may be generally involved in the substrate-binding step. Also, the relative displacements of domains or subunits, which are linked by flexible hinges (as in the immunoglobulins[14–16]) or interact only by non-bonded forces (as in the haemoglobin tetramer[17]) are likely to require similar considerations, in which the balance between internal forces and hydrodynamic damping effects are essential. Finally, any experiments designed to observe such motions[18,19] will have to take account of the results obtained here (for example, preliminary calculations indicate that the Raman band associated with the lysozyme bending mode will be damped out in solution, although binding of an inhibitor could lead to underdamped motion and an observable Raman band).

We thank John Deutch for discussions and the NSF and NIH for support. The lysozyme coordinates were provided by R. Diamond.

J. ANDREW McCAMMON
BRUCE R. GELIN
MARTIN KARPLUS

Department of Chemistry,
Harvard University,
Cambridge, Massachusetts 02138

PETER G. WOLYNES

Department of Chemistry,
Massachusetts Institute of Technology,
Cambridge, Massachusetts 02139

Received March 19, accepted May 25,1976.

1 Blake, C C. F., Mair, G A., North, A. C T., Phillips, D C., and Sarma, V. R , *Proc R. Soc.*, B167, 365–377 (1967).
2 Imoto, T , Johnson, L N , North, A C T., and Rupley, J A , in *The Enzymes*, VII (edit. by Boyer, P D), (Academic, New York, 1972)
3 Gelin, B R., and Karplus, M., *Proc. natn Acad. Sci. U.S A* , 72, 2002–2006 (1975).
4 deGennes, P. G., and Papoular, M , in *Polarization, Materiere et Rayonnement* (Presses Universitaire de France, Paris, 1969).
5 Suezaki, Y , and Go, N , *Int. J. Peptide and Protein Res* , 7, 333–334 (1975)
6 Dickerson, R. E., and Geis, I., *The Structure and Action of Proteins* (Benjamin, Menlo Park, California, 1969)
7 Chandrasekhar, S., *Rev mod. Phys* , 15, 1–89 (1943).
8 Diamond, R., *J molec. Biol* , 82, 371–391 (1974).
9 Honig, E P., Roebersen, G. J., and Wiersema, P. H , *J. Colloid Interface Sci* , 36, 97–109 (1971)
10 Happel, J , and Brenner, H , *Low Reynolds Number Hydrodynamics*, 54 (Prentice-Hall, Englewood Cliffs, New Jersey, 1965)
11 Landau, L D., and Lifshitz, E. M , *Fluid Mechanics* (Pergamon, London, 1959)
12 Rahman, A , and Stillinger, F. H , *Phys Rev. A*, 10, 368–378 (1974)
13 Matthews, B. W., in *The Proteins*, 3 (edit by Neurath, H., and Mill, R L.), (Academic, New York, 1972)
14 Edmundson, A. B., Ely, K. R., Abola, E. E , Schiffer, M , and Panagiotopoulos, N , *Biochemistry*, 14, 3953–3961 (1975)
15 Colman, P. M , Deisenhofer, J , Huber, R , and Palm, W., *J molec. Biol.*, 100, 257–282 (1976).
16 Yguerabide, J., Epstein, H F , and Stryer, L., *J. molec Biol* , 51, 573–590 (1970)
17 Perutz, M , *Nature*, 228, 726–739 (1970).
18 Morgan, R S , and Peticolas, W. L , *Int J. Peptide Protein Res* , 7, 361–365 (1975).
19 Genzel, L , *et al* , *Biopolymers*, 15, 219–225 (1976)

Structure of bilirubin

THE biological breakdown of haem proceeds through a series of intermediates of which the orange-yellow bile pigment, bilirubin, the chromophore responsible for coloration in the various forms of jaundice, is a key member. In the adult human, for example, erythrocytes have a lifetime of about 3 months and their destruction produces about 300 mg bilirubin each day[1,2]. Although there were some early doubts (arising from the possibility of a cyclisation between the C18 vinyl group and the oxygen function at C19)[3], the gross chemical structure (Fig. 1) for bilirubin has been beyond reasonable dispute for

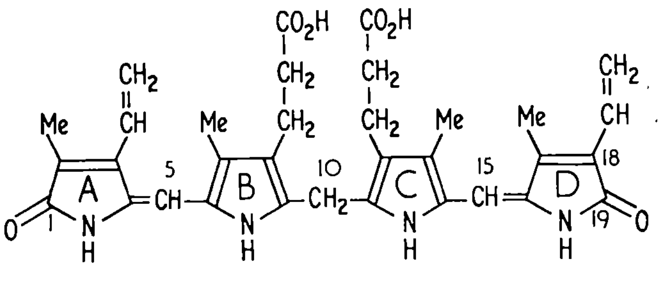

Fig. 1 Gross structure of bilirubin (also called bilirubin IXα).

many years[4]. There remain, however, considerable structural uncertainties with respect to (1) stereochemistry, the geometry around bridges 5 and 15 being unknown, and represented variously as *E* or *Z* in the current literature. (The two configurations, *E* and *Z*, have been recognised in a model pyrromethanone system, however, (see ref. 5 and Fig. 2)); (2) tautomerism, although spectroscopic evidence favours the lactam formula for rings A and D (shown in Fig. 1) over the lactim[6-9]; and (3)

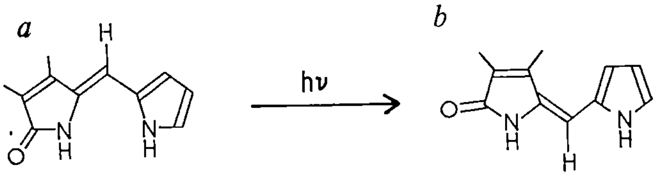

Fig. 2 *a*, *Z* configuration; *b*, *E* configuration.

conformation, although several speculations, supported by spectroscopic evidence and model making, are available[10-17]. We report the X-ray analysis of bilirubin—the first such analysis of a naturally occurring linear tetrapyrrole—which shows that bilirubin has the *Z* configuration at the C4–C5 and C15–C16 bonds, and possesses in the crystal a ridge tile conformation with considerable intramolecular hydrogen bonding.

Crystals of bilirubin were grown by allowing diethyl ether to diffuse slowly (isothermal distillation technique, room temperature, dark) into a solution of bilirubin in anhydrous pyridine containing a trace of anhydrous ammonia. Crystals were mounted in glass capillaries in the presence of mother liquor. Crystal data: $C_{33}H_{36}N_4O_6$, molecular weight 584; crystal class triclinic; space group $P\bar{1}$; $a = 19.439$, $b = 11.707$, $c = 15.500$ Å; $\alpha = 97.19°$, $\beta = 100.22°$, $\gamma = 118.20°$; $V = 2{,}969$ Å^3 $\rho_{calc} = 1.31$ g cm^{-3} for $Z = 4$.

Fig. 3 Structure of bilirubin. Hydrogen bonds are indicated by fine lines.

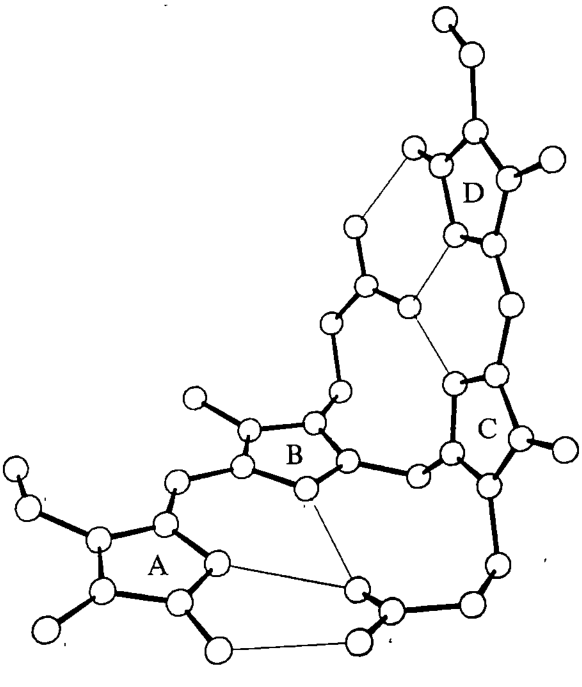

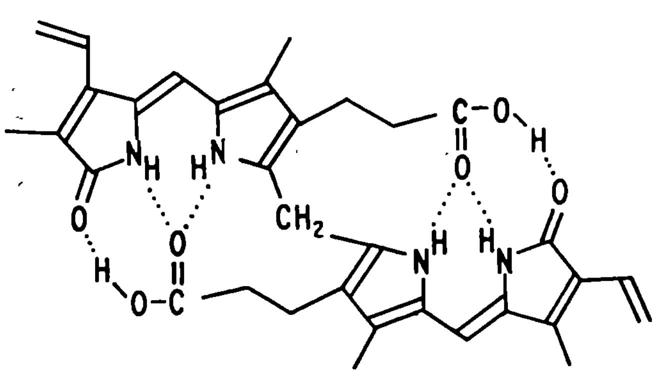

Fig. 4 Structure shown in Fig. 3 in simplified form.

X-ray diffraction patterns recorded from these crystals generally revealed that reflections with odd *h* indices were diffuse, indicating disorder in the *x* direction. (It seems likely that this disorder may have frustrated previous attempts to determine the structure.) The amount of this diffuse scatter varied from crystal to crystal: in some cases the *h*-odd reflections were so diffuse that the triclinic cell seemed to be halved ($a = 9.720$ Å, $Z = 2$). In the crystal selected for detailed examination, the *h*-odd reflections had initially been somewhat diffuse, but had gradually sharpened during maturation (5 weeks, room temperature, dark). The diffraction pattern then contained virtually no diffuse effects.

Two complete sets of data were collected from this crystal: a set of photographic Weissenberg data collected about two axes ([010] and [111]) and scanned using the SRC Microdensitometer Service at Harwell; and a set of counter-data collected using a Nonius CAD4 diffractometer. The photographic set contained 1,323 unique observed reflections (37% of the possible number of unique reflections to a limit of $2\theta(\mathrm{CuK}_\alpha) = 80°$); and, of the 6,095 reflections measured by the diffractometer, only 1,408 obeyed the condition $F_{obs} > 3\sigma F_{obs}$. This serious lack of data arose because the average intensity of the X-ray reflections rapidly decreased with increasing scattering angle: few reflections were found above $2\theta(\mathrm{CuK}_\alpha) = 70°$.

The structure was solved using the diffractometer data and a computer program written by Dr G. M. Sheldrick (Cambridge), which uses a multisolution procedure incorporating negative quartets. Details of this solution will be published elsewhere. Full matrix constrained-bond length refinement of the photographic data (which proved the better set for refinement purposes) with hydrogen atoms in geometrically calculated positions has given $R = 12.5\%$. Because of the small number of observed reflections the structure is not an accurately

Fig. 5 Model compound 3.

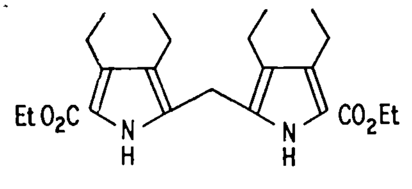

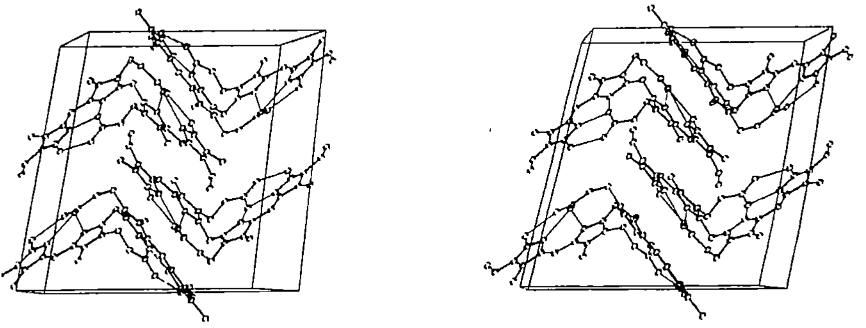

Fig. 6 Packing of bilirubin molecules in the unit cell. The *b* axis is approximately perpendicular to the page, and the *c* axis is horizontal.

determined one: estimated standard deviations of individual bond lengths were generally in the range 0.02–0.05 Å.

The two independent molecules of bilirubin in the asymmetric unit of the structure both have the conformation shown in Fig. 3 and represented in a simplified way in Fig. 4. The molecule takes the form of a ridge tile, the ridge being along the line $C8^1$–C10–$C12^1$. Thus rings A and B lie in one plane, and rings C and D in another, the interplanar angle being about 98°. Six intramolecular hydrogen bonds (two sets, each involving a carboxylic acid group, a pyrrole-imino hydrogen, and a terminal lactam system) stabilise this conformation. The average $N \cdots O$ and $O \cdots O$ distances in these hydrogen bonds are 2.70 and 2.53 Å, respectively. There is no evidence for intermolecular hydrogen bonds: the low solubility of bilirubin in water, which has important biological consequences, can readily be understood in terms of this pattern of hydrogen bonding. Although the hydrogen bonding, and therefore the conformation, may well be altered in very polar solvents (such as dimethylformamide and methanolic ammonia), it seems likely that in less polar solvents (such as chloroform) the conformation with six hydrogen bonds (Fig. 3) will be retained. Unfortunately, the X-ray data are neither sufficiently numerous nor sufficiently accurate to allow determination of the position of the hydrogen atoms in these hydrogen bonds and we are not able to make a clear cut assignment of either the lactam or the lactim formulations.

The X-ray result provides independent proof of the correctness of the gross chemical structure assigned to bilirubin by Fischer *et al.*[4] The stereochemistry about the double bonds at the *meso*-bridges (C5 and C15) is frequently, even in modern work[18,19], represented as *E*. The *Z* configuration (Fig. 4) is now shown to be correct. This type of structure seems to have been first portrayed by Blauer and King[14]; the first discussion in detail was by Kuenzle *et al.*[15].

The observed bond lengths suggest that delocalisation over an individual conjugated system of two pyrrole rings (that is, A+B or C+D) is rather limited since C4–C5 and C15–C16 seem to be essentially double bonds (average 1.30 Å) whereas C5–C6 and C14–C15 resemble single bonds (average 1.48 Å). This supports the view that bilirubin can be regarded as a 2,2′-dipyrrolylmethane (that is, rings B+C) with conjugating substituents at the α positions (compare with the model compound shown in Fig. 5)[18].

The packing of the four bilirubin molecules in the unit cell is shown in Fig. 6. Taking the original analogy further, we now have a stack of ridge tiles interleaved with a similar but inverted stack. Figure 6 suggests an explanation for the diffuse *h*-odd reflections observed in the diffraction patterns of most of our crystals: enantiomeric conformations of bilirubin (related by inversion centres) have very similar ridge tile shapes and the orientation of any ridge tile is virtually unaltered by a rotation of 180° about a direction approximately parallel to the a^* axis (vertical in Fig. 6). On the basis of Fig. 6, it is not difficult to imagine disordered structures which would give an apparent halving of the *a* axis. We have, indeed, collected a third set of data from a disordered crystal, and successfully refined it to $R = 19.7\%$ by assuming that either enantiomer may occupy any molecular site, the packing of the ridge tiles remaining constant.

We thank Dr S. Neidle and Dr J. C. M. Stewart for an earlier attempt on this problem; Dr G. M. Sheldrick (Cambridge) for assistance; Dr M. Elder and his staff at the SRC Microdensitometer Service for measuring the Weissenberg films; and the MRC for financial support.

RAYMOND BONNETT
JOHN E. DAVIES
MICHAEL B. HURSTHOUSE

Department of Chemistry,
Queen Mary College,
Mile End Road,
London E1 4NS, UK

Received March 8; accepted May 27, 1976

[1] Lathe, G H , *Essays in Biochemistry*, **8**, 107–148 (CRC, Cleveland, Ohio, 1972).
[2] Schmid, R., and McDonagh, A. F , *Ann N.Y. Acad Sci* , **244**, 533–552 (1975)
[3] Fischer, H , and Orth, H., *Die Chemie des Pyrrols*, **2.1**, 626 (Akademische. Verlagsgesellschaft, Leipzig, 1937).
[4] Fischer, H , Plieninger, H., and Weissbarth, O., *Hoppe-Seyler's Z Physiol. Chem.*, **268**, 231–260 (1941).
[5] Falk, H., Grubmayr, K., Herzig, U , and Hofer, O., *Tetrahedron Lett.*, 559–562 (1975).
[6] Gray, C H , Kulczycka, A., and Nicholson, D. C., *J chem Soc.*, 2276–2285 (1961)
[7] Kuenzle, C C , *Biochem J.*, **119**, 395–409 (1970).
[8] Hutchinson, D W , Johnson, B , and Knell, A. J., *Biochem. J.*, **123**, 483–484 (1971)
[9] Manitto, P , Ricca, G. S., and Monti, D., *Gazzetta Chim. Ital* , **104**, 633–637 (1974).
[10] Nichol, A. W , and Morell, D. B , *Biochim. biophys. Acta*, **177**, 599–609 (1969).
[11] Fog, J , and Jellum, E., *Nature*, **198**, 88–89 (1963)
[12] Fog, J., and Bugge-Asperheim, B , *Nature*, **203**, 756–757 (1964)
[13] Brodersen, R , Flodgaard, H., and Hansen, J K , *Acta scand. Chim* , **21**, 2284–2285 (1967).
[14] Blauer, G., and King, T E., *J. biol Chem* , **245**, 372–381 (1970).
[15] Kuenzle, C. C., Weibel, M H , Pelloni, R. R., and Hemmerich, P , *Biochem J.*, **133**, 364–368 (1973).
[16] Knell, A. J., Hancock, F , and Hutchinson, D. W., in *Metabolism and Chemistry of Bilirubin and Related Tetrapyrrols* (edit. by Bakkan, A F and Fog, J), 234–239 (Pediatric Research Institute, Oslo, 1975)
[17] Manitto, P , and Monti, D., *J. chem. Soc Chem. Comm* , 112–123 (1976).
[18] Bonnett, R., Hursthouse, M B , and Neidle, S , *J C.S. Perkin Trans.*, **II**, 902–906, 1335–1340 (1972)
[19] Rudiger, W., *Fortschr. Chem. Organ. Natur.*, **29**, 60–139 (1971).

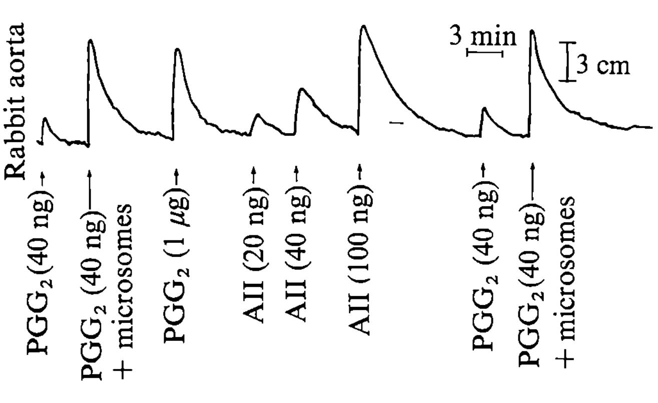

Erratum

In the article "Identification of an enzyme in platelet microsomes which generates thromboxane A_2 from prostaglandin endoperoxides" by P. Needleman, S. Moncada, S. Bunting, J. R. Vane, M. Hamberg and B. Samuelsson (*Nature*, **261**, 558; 1976) microsomes were added to the wrong dose in Fig. 5 and the vertical scale (3 cm) was too large. Both are correct in the version reprinted below.

matters arising

Deposit-forming by zinc dithiophosphates in base oils during oxidation

A RECENT report by Bird and Galvin[1] has described experiments in which specimens of En 31 steel were immersed in solutions of zinc dialkyldithiophosphates in white oil and either heated over a range of temperatures for 16 h or rubbed for 10 min against a disk of the same material. Electron spectroscopic investigations of the surface films formed at 140 °C showed a product having a zinc–phosphorus–sulphur ratio of 1 : 1 : 0.6, and this ratio was said to be constant over a range of conditions, and was thus assumed to be a decomposition product of the original additive. Zinc phosphate, sulphide and sulphite formations were not observed.

Work in our laboratories on the oxidation stabilities of mineral oil blends of zinc dithiophosphates has revealed similar decomposition residues. The formation of these was, however, found to depend on both the hydrocarbon group in the dithiophosphate and the nature of the base oil. Thus, when a solution of a zinc disecondary alkyl dithiophosphate in a high sulphur content base oil was heated at 120 °C for 164 h and subjected to a stream of dry oxygen, a residue was formed which had a zinc (24.6%)–phosphorus (12.6%)–sulphur (4.5%) ratio of 1.0 : 1.08 : 0.37, which was not too dissimilar from that found at the iron surface by Bird and Galvin[1]. Further, X-ray examination of this residue showed that it was a complex inorganic material in which zinc oxide, sulphide or phosphate was absent. When blends of this additive in low sulphur content mineral oil base fluids were similarly tested this residue was not produced.

Substitution of zinc diprimary alkyl or diaryl dithiophosphates in the above range of base oils failed to produce any residues. It was therefore concluded that the decomposition was a function both of the base oil and the hydrocarbon group in the dithiophosphate. Previous work has suggested[2] that the decomposition of zinc dialkyldithiophosphates is dependent on the number of β-hydrogen atoms attached to the alkyl constituent, and this is fully consistent with the results obtained in our present work.

H. B. SILVER

BP Research Centre,
Chertsey Road,
Sunbury-on-Thames, UK

[1] Bird, R. J., and Galvin, G. B., *Nature*, 254, 130 (1975).
[2] Dickert, J. J , and Rowe, C. N., *J. org. Chem.*, 32, 647 (1967).

Haemoglobin type and superovulation in ewes

PANT and Pandey[1] reported that haemoglobin (Hb) type in Binaneri ewes influences the ovulatory response to exogenous gonadotropin (pregnant mare's serum gonadotropin, PMSG). The practical and physiological implications of this finding prompt us to present the results of a study of the relationship between Hb type and ovulatory response to PMSG in parous, non-lactating Welsh Mountain ewes.

Eighty-six ewes were given 1,000, 1,100 or 1,250 IU PMSG (Folligon, Intervet) on day 12 (day 0 is the day of oestrus) of the oestrous cycle and ovulation rate assessed by counting the corpora lutea present at laparotomy on days 2–8 of the subsequent cycle. Hb type was determined by starch gel electrophoresis in a Tris-EDTA borate buffer system, *p*H 8.2 (ref. 2). An analysis of variance of ovulation rate, after transformation of the raw data to $(x + 1)^{\frac{1}{2}}$, showed no significant effect of either Hb type or dose of PMSG. Table 1 shows the mean ovulation rates for Hb type, the data being pooled for dose of PMSG.

A further 16 ewes were given 500 IU PMSG and ovulation rate examined as before. Mean ± s.e. (number of ewes) ovulation rate for AA, BB and AB Hb types were 1.3±0.21 ($n = 6$), 1.6±0.24 ($n = 5$) and 2.2±0.37 ($n = 5$), respectively.

These results argue strongly against a correlation between Hb type and ovulatory response to superovulation in Welsh Mountain ewes. Breed or environmental differences may, however, explain the discrepancy between our results and those of Pant and Pandey[1]. It is clear that Hb type in Welsh Mountain ewes is not a major determinant of the very substantial individual variation in ovulation rate observed after administration of PMSG.

A. O. TROUNSON
S. M. WILLADSEN
R. M. MOOR

ARC Unit of Reproductive Physiology and Biochemistry,
307 Huntingdon Road,
Cambridge CB3 0JQ, UK

ELIZABETH M. TUCKER

ARC Institute of Animal Physiology,
Babraham, Cambridge CB2 4AT, UK

[1] Pant H. C , and Pandey, M. D., *Nature*, 258, 738–739 (1975).
[2] Gahne, B., Rendel, J , and Venge, O., *Nature*, 186, 907–908 (1960)

Table 1 Hb type and ovulatory response to PMSG* in Welsh Mountain ewes

Hb type	AA	BB	AB	Total
Ovulation rate (mean±s.e.)	8.6±0.96	8.2±0.90	10.0±1.29	8 9±0.63
No. of ewes	20	35	31	86

*PMSG at 1,000–1,250 IU.

Volcanic triggering of glaciation

IN his latest contribution to the discussion of the links between volcanism and glaciation[1], Bray perpetuates a concept that he proposed in much stronger terms in his two earlier contributions on the same subject[2,3]; namely that there is evidence of "an apparent correlation between major phases of global ice advance and ash eruptions in New Zealand, Japan and southern South America over the past 42,000 yr". This represents a slight modification of his earlier view that there were worldwide 'waves' of volcanic activity that could be correlated with the same ice advances[3].

I am not in a position to comment on the evidence from Japan or New Zealand, but in my opinion the postulation of correlatable episodes of volcanic activity and ice advance in southern South America is extremely unwise, simply because there is so little factual evidence. All such postulations are based on the widely quoted but rarely read work of Auer[4–7]. It is clear from his descriptions that the ash horizons that Auer used in his work, were, in most cases, air-fall ashes from single volcanic eruptions, which may have been quite small. There is no evidence for any massive eruptions, nor for any waves of eruptions. The weakness of the evidence for such waves is compounded by the very small number of published radiocarbon dates; there are probably less than a dozen such dates for volcanic eruptions in the whole of South America.

It is quite correct, as Bray states, that "the possibility that large Pleistocene ice sheets were initially triggered by massive volcanic eruptions is not contradicted by the geological record". But until further data are available from Patagonia, and especially studies of the ash deposits by volcanologists, the evidence from southern South America should not be used either to support or contradict the argument.

P. W. FRANCIS

Department of Earth Sciences,
The Open University,
Walton Hall,
Milton Keynes MK 7 6AA, UK

[1] Bray, J. R., *Nature*, **260**, 414–415 (1976).
[2] Bray, J. R., *Nature*, **248**, 42–43 (1974)
[3] Bray, J. R., *Nature*, **252**, 679–670 (1974).
[4] Auer, V., *Suomal. Tiedeakat. Toim. Sarja A, III, Geologica-Geographica*, **45**, 226 (1956).
[5] Auer, V., *Suomal. Tiedeakat. Toim. Sarja A, III, Geologica-Geographica*, **50**, 239 (1958).
[6] Auer, V., *Suomal. Tiedeakat. Toim. Sarja A, III, Geologica-Geographica*, **60**, 247 (1959).
[7] Auer, V., *Suomal Tiedeakat. Toim. Sarja A, III, Geologica-Geographica*, **80**, 160 (1965)

BRAY REPLIES—The main point of Francis[1] is that the evidence of late Pleistocene and Holocene volcanism in southern South America[2] is based on a small number of published radiocarbon dates. The reason I originally included the southern South America volcanic data was that both the radiocarbon-dated ashes and the indirectly dated ashes all occurred at the same time as periods of volcanic activity in New Zealand and Japan. This occurrence seemed to be more than coincidental and I suggested that the apparent synchroneity of volcanic ash data from the three areas reinforced the hypothesis that there have been global waves of volcanic acitivity separated by periods of relative quiescence. Since then, South American volcanic ash dates of 9,000, 11,000, 21,000, 22,000–26,000 and 30,000 yr BP have been published[3] which are also coincident with the New Zealand and Japanese volcanic phases. In addition, I have made a preliminary compilation of North American and European volcanic ash dates which show the following distribution (in 1,000 ^{14}C yr b.p.): 0.2–0.4; 0.6–0.8; 1.2–1.3; 1.6–1.8; 2.0–2.6; 2.8; 3.3–3.5; 3.9; 4.4; 5.0; 6.6; 8.3–8.9; 11.3; 11.7–12.0; 13.1; 18.6; 19.7; 28.5; 31.0; 35.0; 39.5–40.5. A comparison of these dates with the New Zealand and Japanese data in Table 1 (ref. 2) shows that all but five dates are synchronous.

Francis' other point, that some of the southern South American eruptions were minor is correct, but not contradictory to the theme of global waves of volcanic eruptions in the late Pleistocene which have influenced climate and perhaps triggered glacial expansion. In any case, if the large mid-continental Northern Hemisphere ice sheets were triggered by massive eruptions[4], then it is likely that these eruptions occurred in the Northern Hemisphere or perhaps the tropical portion of the Southern Hemisphere. It is in these regions that many of the largest Pleistocene eruptions have occurred as shown by the land record and especially by the ash layers in the ocean[5].

PO Box 494,
Nelson, New Zealand

[1] Francis, P. W., *Nature*, **262**, 329–330 (1976).
[2] Bray, J. R., *Nature*, **252**, 679–680 (1974).
[3] Van Geel, B , and Van der Hammen, T., *Palaeogeogr., Palaeoclimatol , Palaeoecol.*, **14**, 9–92 (1973)
[4] Bray, J. R., *Nature*, **260**, 414–415 (1976).
[5] Kennett, J P., and Thunell, R. C., *Science*, **187**, 497–503 (1975).

Acoustic Bragg diffraction from human tissues

NICHOLAS AND HILL[1] claim to have presented "qualitative evidence that the method can provide objective characterisation of tissue structure", and that the "diffraction phenomenon . . . can be quantitatively related to the specific structure of the type of tissue".

They present their evidence for the objective characterisation in Fig. 4, where three sets of tissue specimens (of unspecified condition) have a statistical significant difference over a portion of the curve, the curve having been obtained by an arbitrary seven-point smoothing. Whereas the first claim of the authors may be true, the second, regarding the specific structure of the type of tissue, is surely not substantiated by the evidence presented. Differentiation between tissue types may have been demonstrated but there is no evidence presented for its relationship to specific structure. Indeed, it is known[2,3] that the Fourier transform of angular correlation is a spatial spectrum, so that the peaks in the spectrum of Nicholas and Hill's Fig. 3 indicate distances of significance in the tissue specimens, presumably related to structure, as the parallel with X-ray diffraction suggests. This potential source of helpful fundamental information has been removed by cavalier smoothing.

In a field characterised by complexity[4], bedevilled by incomplete reporting[5], and yearning for independent confirmation, the significance of the results reported[1] demands more careful and precise consideration.

R. C. CHIVERS

Department of Physics,
University of Surrey,
Guildford GU2 5XH, UK

[1] Nicholas, D , and Hill, C. R., *Nature*, **257**, 305–306 (1975).
[2] Welsby, V. G , *J. Sound Vib* , **8**, 64 (1968)
[3] Chivers, R. C., *Proc. 8th int. Cong. Acoustics, London*, 359 (1974).
[4] Chivers, R C., and Hill, C. R., *Phys. Med. Biol.*, **42**, 799–815 (1975).
[5] Chivers, R. C , and Hill, C. R , *Ultrasound Med. Biol* , **2**, 25–29 (1975).

NICHOLAS AND HILL REPLY—We accept the criticism[1] of our statement[2] that "this diffraction phenomenon . . . can be quantitatively related to the specific structure of the type of tissue". This statement is out of place in the article concerned and should have been omitted: its truth, however, has been confirmed in other publications[3,4]. The other points raised by Chivers are, in our view, unjustified and in some cases inaccurate.

In all of our investigations the tissues were freshly excised, pathologically normal specimens: although this was not stated explicitly it was thought that the implication of comparing pathologically abnormal tissues with the reported results, justified such an omission.

Chivers' criticism[1] of the curves depicted in our original Fig. 4 (ref. 2)—that the range of the seven-point average was not specified—is, we believe, taken in context, not valid. It was stated in our report[2] that the power spectra were calculated using a fast Fourier transform and, as such, they are both finite and discrete. We also stated that the data in each resulting spectrum was averaged over consecutive seven-points. Thus it is that the range of our averaging was over the whole spectrum, as should be obvious if Fig. 4 is compared with Fig. 3.

Finally, Chivers' comments on the validity of our smoothing procedure should be considered in the light of our objective. We clearly stated that "several possible analytical approaches could be taken towards establishing the significance of differences or similarities between such traces and we report here the results of one of these". Useful information has indeed been removed by smoothing, but the advantage gained is the relative ease with which different traces can thus be compared. It is apparent from our Fig. 3 that the peak separation is of the order of 0.01 cycles per degree, which corresponds to a separation in the angular traces of Fig. 2 of approximately 100°; hardly a significant contribution when considering the 50° of trace illustrated. Chivers' comments on this point, although strictly valid, are therefore of limited relevance to the results presented. We did not imply that the peaks in the power spectrum were artefacts, but merely indicated that the picket-fence effect must have led to some degradation of the resulting power spectra.

Our article was intended purely as an introduction to a new and exciting aspect of tissue characterisation and did not claim to be a complete report. It remains our belief, however, that the results we presented are both significant and precisely defined.

Institute of Cancer Research,
Royal Marsden Hospital

[1] Chivers, R C., *Nature*, **261**, 330 (1976).
[2] Nicholas, D., and Hill, C. R., *Nature*, **257**, 305–306 (1975).
[3] Nicholas, D., and Hill, C. R , in *Proc. Symp. Ultrasonics International* (Iliffe, London, 1975).
[4] Nicholas, D., thesis, Univ. London (1976).

Announcing a New Elsevier Journal

JOURNAL OF MECHANICAL WORKING TECHNOLOGY

Editor:
F. W. TRAVIS, Department of Mechanical Engineering, Sunderland Polytechnic, Chester Road, Sunderland SR1 3SD, U.K.

Advisory Board:
J. M. Alexander (London), B. Avitzur (Bethlehem, Pa.), B. N. Cole (Leeds), J. L. Duncan (Hamilton, Ont.), H. Kudo (Yokohama).

Editorial Board:
T. Altan (Columbus, Ohio), P. Avenas (Paris), I. S. Brammar (Clayton, Vict.), H. Conrad (Lexington, Ky.), B. Crossland (Belfast), L. F. Gillemot (Budapest), F. Jovane (Bari), S. P. Keeler (Ecorse, Mich.), K. Kormi (Abadan), P. E. Lagasse (Louvain), H. Lippmann (Munich), A. T. Male (Pittsburgh, Pa.), Z. Marciniak (Warsaw), K. Matsuno (Tokyo), A. H. Meleka (Bristol), T. Nakagawa (Tokyo), K. Osakada (Kobe), P. L. B. Oxley (Kensington, N.S.W.), R. Pearce (Cranfield), H. L. D. Pugh (East Kilbride), G. W. Rowe (Birmingham), M. W. Sagal (Princeton, N.J.), P. O. Strandell (Stockholm), K. Yoshida (Saitama).

Regional Editors:
For Japan - T. Jimma (Tokyo); for North America - J. A. Schey (Waterloo, Ont.).

Industrial relevance will be a prerequisite of papers accepted for publication and all papers will be required to contain a summary describing the industrial significance of the work and the industrial implications arising from the results of the work. There would appear to be great advantage in the mechanical working field, as in many others, in providing an area of common ground for the academics and the industrialists, to better allow the results of the work of the former to be put to the service of the latter, and so that current industrial problems can be clearly identified. The scope will encompass:

(i) Sheet metalforming in all its variations, including blanking and piercing, pressing and deep drawing, stretch forming, fluid and rubber forming and all other related processes, including high-rate forming and explosive welding.
(ii) Bulk forming processes, including hot and cold forging, rolling and extrusion, and developments in these areas such as injection upsetting, ring rolling, rotary forging, hydrostatic extrusion.
(iii) Powder and non-metal forming, including all aspects of the compaction, sintering, forging and extrusion of powder compacts and the forming of polymers.
(iv) In addition to papers arising from within the clearly defined areas described above, the journal will welcome papers concerned with the relevant areas of materials technology and metallurgy, e.g. thermomechanical treatments, annealing schedules, superplastic materials and with other related topics such as lubrication, process economics and "total system" concepts. Likewise, although the journal is primarily concerned with mechanical working (as opposed to cutting or fabrication), papers offering a comparison of production by the latter operations with production by mechanical working, will be eligible for publication.

The subscription price for Volume 1 (1977) is US $57.75/Dfl. 144.00 including postage.

JOURNAL OF MECHANICAL WORKING TECHNOLOGY will initially be published in quarterly issues; the first issue is expected to appear early in 1977. Free sample copies of this new journal will be available from the Publisher.

Journals are automatically sent by air to the USA and Canada at no extra cost and to Japan, Australia and New Zealand with a small additional postal charge.
Manuscripts should be submitted to the Editor. Instructions to Authors are available from the Publisher on request. Fifty reprints will be supplied free of charge. There will be no page charge.

ELSEVIER SCIENTIFIC PUBLISHING CO.
P.O. Box 211, Amsterdam, The Netherlands

The Dutch guilder price is definitive. US $ prices are subject to exchange rate fluctuations

0357

Circle No. 07 on Reader Enquiry Form.

WILEY
INTERSCIENCE

Dynamic Light Scattering: With Applications to Chemistry, Biology and Physics

By **B. J. Berne**, *Columbia University*, and **R. Pecora**, *Stanford University*

An introduction to the principles governing the application of light scattering to problems in chemistry, biology and physics. Stresses the use of light scattering to study the time dependence of thermal fluctuation in fluid systems.

384 pages	March 1976	£16.50 $27.70

Gluconeogenesis: Its Regulation in Mammalian Species

Edited by **R. W. Hanson**, *Temple University, Medical School*, and **M. A. Mehlman**, *National Institute of Health*

Concentrates on the current state of glucose studies in relation to such human problems as the metabolic regulation of a basic biochemical process which has extensive clinical implications.

620 pages	June 1976	£18.60 $35.40

Microbial Transformations of Non-Steroid Cyclic Compounds

By **K. Kieslich**

The book has two aims firstly it gives preparative organic chemists, microbiologists, biochemists, and biotechnologists an introduction to microbial transformations, and secondly it provides a previously non-existent reference work.

1284 pages	June 1976	£42.50 $85.00

Published by Georg Thieme Verlag Stuttgart, and distributed by John Wiley & Sons Ltd.

Elements of Physical Geology

By **J. H. Zumberge**, *University of Nebraska*, and **C. A. Nelson**, *University of Southern California*

A fundamental text that emphasises the tectonic development of oceans, continents, geological processes, resources from the earth, and environmental problems associated with the geologic sciences.

430 pages	March 1976	£7.20 $14.40

Sewage Treatment in Hot Climates

By **D. Mara**, *University of Dundee*

This book presents modern design procedures for those processes such as waste stabilisation ponds which are suitable for the treatment of sewage in hot climates, while at the same time providing a clear description of their physical and biological basis.

184 pages	June 1976	£7.00 $17.00

The Physics and Chemistry of Minerals and Rocks

Edited by **Dr. R. G. J. Strens**, *School of Physics, The University, Newcastle upon Tyne*

The papers in this volume have three main themes: transport properties, including electrical and thermal properties and convection; the dependence of the macroscopic properties of rocks and minerals on their microstructure; and the reactions, properties and structure of minerals, particularly those containing transition metal ions, at high pressure.

714 pages	May 1976	£19.50 $39.75

Radiopharmacy

Edited by **M. Tubis** and **W. Wolf**, both of *University of Southern California, Los Angeles*

An authoritative interdisciplinary text and reference covering the production, preparation, dispensing, and application of radioactive pharmaceuticals.

928 pages	June 1976	£27.65 $49.40

Artificial and Natural Radionuclides in Marine Life

By **V. G. Tsytsugina, N. S. Risik** and **G. E. Lazorenko**, *Academy of Sciences of the Ukranian SSR*

This book presents the results of research into the karyology and radiation cytogenetics of marine fish, the accumulation and distribution of uranium in marine organisms, and the mechanism by which radionuclides are taken up by algae.

122 pages	February 1976	£9.00 $16.65

Published by IPST Keter, and distributed by John Wiley and Sons Ltd.

Handbook of Environmental Education: With International Case Studies

Edited by **R. N. Saveland**, *University of Georgia*

A Handbook of Environmental Education is sponsored by the International Union for the Conservation of Nature (IUCN). It provides information on methods of environmental education and will promote exchange of details of new methods and materials. The book describes the present world position in environmental education and points the way for future developments.

278 pages	June 1976	£7.50 $14.75

Two important books which are now published in paper editions:—

Mycogenetics: An Introduction to the General Genetics of Fungi

By **J. H. Burnett**, *Sibthorpian Professor of Rural Economy and Fellow of St. John's College, Oxford*

This text puts the subject of fungal genetics in a broad context; it provides a genuine introduction starting from the basis of genetics, using familiar cytological and fungal types.

390 pages	May 1975	(cloth) £12.50	$25.60
390 pages	June 1976	(paper) £3.90	$8.60

Environment and Plant Ecology

By **J. R. Etherington**, *University College, Cardiff, Wales*, and **W. Armstrong**, *University of Hull*

This book discusses the relationship between environment and plant physiological function as the underlying explanation for plant ecological behaviour. It attempts to analyse the integrated function of the ecosystem in terms of the multiple interactions between environment and organisms.

390 pages	February 1975	(cloth) £7.75 $15.90
	In Press	(paper) approx. £3.95 $8.10

JOHN WILEY & SONS
NEW YORK CHICHESTER SYDNEY TORONTO
John Wiley & Sons Ltd Baffins Lane Chichester Sussex PO19 1UD England

Circle No. 05 on Reader Enquiry Form.

reviews

Sorting the muddle in the Middle

W. W. Bishop

After the Australopithecines: Stratigraphy, Ecology, and Culture Change in the Middle Pleistocene (World Anthropology.) Edited by Karl W. Butzer and Glynn Ll. Isaac. Pp. xv+911. (Mouton: The Hague and Paris, 1975.) (Distributed in US and Canada by Aldine: Chicago.) Dutch Guilders 127.50.

THIS is a most timely review of work on the span of the Quaternary, dubbed broadly Middle Pleistocene, younger than the australopithecine—bearing strata that have been calibrated by potassium–argon dating. The period is terminated by the advent of the Later Pleistocene which is followed by the lower limit of radiocarbon dating at ±50,000 yr b.p. The continental deposits in 'the middle' represent a period when reliable dates from sources independent of the fossil faunas or artefact assemblages for which an age is sought are extremely scarce. Lithological comparisons are rendered difficult by isolation of the sedimentary basins and the parochial nature of the deposits. Attempts have been made to use climatic change as the vehicle for correlation, but these are largely unsatisfactory until the Last Interglacial (Ipswichian—Eemian) denotes the onset of the Later Pleistocene.

Middle Pleistocene continental stratigraphy in the Old World is therefore a muddle which this volume does a great deal to clarify by isolating the problems and suggesting solutions. I must carp a little at the length, not to say verbosity, of several of the contributions. Thus 21 papers amount to 887 pages, including excellent black and white illustrations. This yields an average of 42 pages per contributor and is the reason that for most students of the Quaternary, from the undergraduate to professorial grade, this volume priced at £26 sterling per copy, sadly seems destined almost solely for library shelves.

With this caveat it must be noted that the papers have been carefully selected by the editors and the scope of the book is broad but balanced. The geological contributions include the record of deep sea cores (Shackleton), the Mediterranean littoral (Butzer), volcanics of the Massif Central (Bout), European Loess stratigraphy (Kukla) and sediments of East Anglia (Gladfelter). On this substratum, interglacial correlation is discussed by Turner, and various aspects of mammalian palaeontology by Kahlke, Janossy, Jaeger and Maglio, respectively.

The lithic industries of Africa, the Middle East and Europe are then placed into the stratigraphic framework by Mary Leakey, Isaac, Deacon, Bar-Yosef, Clark, Freeman and de Lumley. Finally, Pilbeam reviews the fossil evidence for Middle Pleistocene toolmaking hominids.

The volume is an essential reference book for all workers involved in the problems of the Middle Pleistocene. Space does not permit an analysis of the papers beyond noting that they provide the most up-to-date statement in this field. The papers were revised and submitted to the editors after a conference organised in July 1973 by the Wenner–Gren Foundation for Anthropological Research at Burg Wartenstein, Austria.

The meat of the conference and the conclusions arising from this meeting between workers in different disciplines are provided in two short concluding chapters by Butzer on the Geology and Ecology (18pp) and Isaac on the Archaeology and Anthropology (14pp), together with two Appendices containing correlation charts and the recommendations of the meeting.

The most potent wine is kept until the end of the book (pp901–903). It was recommended unanimously by the conference that the lower boundary of the Middle Pleistocene be defined as the junction between the Matuyama Reversed Epoch and the Brunhes Normal Epoch of the palaeomagnetic reversal chronology (that is at about 0.7 Myr). Magnetostratigraphy is still at an early stage of development but the reasons for choosing "this unique global criterion" include the difficulty experienced in trying to apply other methods; its application to both marine and continental sediments; the fact that it can be established in many existing litho-stratigraphic units; and in some areas there is a good fit with the existing local placement of the boundary. The fact that a major change from the current location of the boundary would be necessary in some other areas points the need to use some global parameter.

The proposed upper boundary is the beginning of the marine transgression associated with the onset of the Last Interglacial. Although the inadequacy of this boundary is recognised it seems to be the best available at present. It is to be hoped that those concerned with codes of stratigraphic nomenclature will recognise the value of the proposed palaeomagnetic reversal boundary for the lower limit and that stratigraphic connoisseurs will find this new wine acceptable to the international palate. ☐

W. W. Bishop is Professor and Head of the Department of Geology at Queen Mary College, University of London, UK. His research interests for the past 20 years have centred on the geological background to fossil man in East Africa.

Controversial morphometrics

Uniqueness and Diversity in Human Evolution: Morphometric Studies of Australopithecines. By Charles E. Oxnard. Pp. viii+133. (University of Chicago: Chicago and London, 1975.) £9.00.

IN spite of caveats about the tentative nature of the results in this volume Oxnard has thrown down the gauntlet firmly at the feet of hominid paleontologists Implicitly throughout much of the book, and explicitly in the final chapter, he claims that the Australopithecines (including *Homo habilis* and *'Homo africanus'*) should be formally excluded from any ancestral relationship to man. The basis for this view is that morphometric studies he cites show them not only to be unique but also, in several computer analyses their nearest analogues are orang-utans, specialised Asian apes. The test is whether Oxnard's book contains sufficiently cogent evidence for such a bold view.

The book is in three sections. The first two chapters consist of a theoretical discussion about how best structure and behaviour can be equated, a review of discriminant analysis and methods for displaying the results, and a review of locomotor classification.

The sine–cosine graphs, apart from inducing vertigo, do provide a convenient way of detecting specimens which although projected on the main canonical axes, in morphometric 'reality' lie some distance away. These chapters are heavy going and the writing style, with long and involved sentences, makes the reader's task more difficult.

The middle section is the longest and reviews multivariate morphometric studies on fossil hominid remains of the upper and lower limb girdles, several tali, humeral fragments, metacarpals and a toe bone. This is no place to take issue on technical details of the analyses and Oxnard fairly draws attention to the differences between the way he and other workers interpret the results of canonical analysis.

The last section is an attempt to synthesise the results followed by a discussion of their relevance, and it is here that the greatest controversy lies. It has recently become evident that locomotor assessments of early hominid fossils were bedevilled because modern human bipedalism was considered as the only bipedal arrangement possible: no close affinities to modern bones, no bipedalism Now it is widely recognised that other models may have existed either as precursors of the modern human system or as parallel models which were destined for extinction. Therefore the 'uniqueness' of some of the fossils comes as no surprise

Some of the analyses are claimed to show similarities between fossil hominid fragments and orang-utan bones, implying a close functional rather than a genetic relationship Whereas the statistical implications of these results are exhaustively examined their conversion back into any biological reality is naive. Most of the fossils are fragmentary, and some form only part of functional units of which other parts are preserved. There is no examination of which variables underly the association with the orang-utan, nor is there any attempt at a functional anatomical or biomechanical explanation of why bones that do not look alike behave similarly in the analyses.

Morphometrics is only one of the methods available to hominid paleontologists in their attempts to analyse the functional implications of hominid fossils and unravel the phylogeny of early man. Such studies were at one time properly criticised for eschewing numerical data, but such data taken in isolation do not guarantee relevant results. The evidence presented in this book, based as it is on only a fraction of the available fossil evidence, is too narrow and conceptually limited to play more than a subsidiary role in the very necessary re-evaluation of our ideas about early hominid structure, function and phylogeny.

Oxnard has nonetheless performed a useful service; the controversy produced by this book may well stimulate the necessary, more balanced, research.

Bernard Wood

Bernard Wood is a senior lecturer in the Department of Anatomy at the Middlesex Hospital Medical School, London, UK.

Crystallography

Space Structures: Their Harmony and Counterpoint. By Arthur L. Loeb Pp. xviii+169 (Addison-Wesley: Reading, Massachusetts and London, February 1976.) Cloth $19.50; paper $9.50.

THE structure of ordinary Euclidean space is not as simple as it seems. Just as the complexity of chemistry arises from the Pauli exclusion principle, forbidding two electrons to have the same set of quantum numbers, so much of the complex structure of space arises from what we might call the Democritean exclusion principle—no two atoms may have the same set of (x, y, z, t) space–time quantum numbers (otherwise knots would fall apart).

Arthur Loeb has produced a fascinating book, at about A-level standard, of interest to crystallographers and applied artists working in space. Indeed it is dedicated to all 'philomorphs'—a useful coinage for a spectrum recognisable as including the 'dome-folk' as well as the graph theorists, the cubists and the biomorphologists.

Much of the material is an exposition of the consequences of the Euler-Schläfli relationship (faces+vertices=edges+2), which is at the heart of the phase rule of chemistry and expresses surprisingly powerful constraints—seen at their best in Rhines' and Craig's analysis of grain growth in aluminium (*Metall. Trans.*, **5**, 413–425, 1974). Truncation, stellation and the division of space into Dirichelet domains are also discussed. It is all fairly familiar material, but well-presented without the obscurities with which graph theoreticians so often cloak their theorems, and is thus of wide popular interest.

A. L. Mackay

Dr Mackay is a reader in the Department of Crystallography at Birkbeck College, University of London, UK

Mapping the insect brain

Atlas of an Insect Brain. By Nicholas J. Strausfeld. Pp. xii+214. (71 plates.) (Springer: Berlin and New York, 1976.) $118.10.

THE combination of Nick Strausfeld's scientific knowledge and literary and artistic abilities with a large format and high production standards has resulted in an admirable monograph about the neuroanatomy of the fly's brain, the text of which merits much discussion and suggests many experiments. There is also an abundance of photomicrographs and drawings, of high quality, illustrating those exquisite ramifications of nerve cells which are so beloved by anatomists, but which can cause the physiologist to despair sometimes of ever fully comprehending the workings of the nervous system.

Divided into seven chapters and two appendices, the book begins with a historical survey and proceeds to a description of the major cell types found in the fly's brain together with a classification of neurones based on the shapes of the processes of the nerve cells. The third chapter describes the primary compartments of the brain and the fourth, the coordinate system which gives the *Atlas* a stereotaxic frame of reference. The *Atlas* itself, composed of serial sections of the brain stained by reduced silver methods, forms chapter 6 and this is preceeded by a chapter which considers some quantitative aspects of brain structure. The final chapter shows the forms and dispositions of various neurones as revealed by variations of the Golgi impregnation technique. One appendix gives a multi-author and multi-lingual dictionary of the terminology of the fly's brain, whereas the other provides valuable information about the various histological techniques which can be applied to the insect nervous system

The vast amount of anatomical information presented forms an excellent substratum on which to build future experiments and into which previous physiological and behavioural studies can be integrated. The neuroanatomy and possible function are related in a heuristically worthwhile manner. The book is marred only by the high incidence of uncorrected typographical errors.

John A. Patterson

John Patterson is at Hunter College of the City University of New York, New York.

Poetic self-portrait

Moulds of Understanding: a Pattern of Natural Philosophy. By Joseph Needham. Pp 320. (Allen and Unwin: London, April 1976.) £7.75.

JOSEPH NEEDHAM is so widely known personally that it must be almost impossible to find a detached reviewer for any of his works. I certainly cannot claim to be detached. This collection of essays confirms one's respect even though it may not convert one to his political convictions. It waves a wide arm over the extensive view he has of ethical imperatives, human love and the sense of what is holy. For this is what these essays are about, even though their titles and their content are scientific in origin and substance.

To call the essays *A Pattern of Natural Philosophy* is to stretch the phrase far beyond its traditional use. They have been selected by Gary Werskey, obviously with a bias towards one aspect of Needham's thought—the political—so that they coalesce into a self-portrait, an animated image of a man who has never forgotten his personal beginnings, but never lowers his sights from the destiny of human kind. Cambridge has been his immediate world, described in an essay of 1932 in poetic language which acknowledges his debt to those contemporaries who chose poetry itself as their way of life.

To those who know only his Chinese work or the earlier embryology, it will come as a surprise to find orthodox Christian religion playing a large part in the formation of his outlook both then and now. One might expect, of course, to find early evidence of his well-known socialist convictions, which he has exhibited ever since with both style and humility which others might do well to emulate, whatever their political convictions may be. But it is fascinating to find judgements of great weight being derived from an appreciation of the numinous elements in the traditional church liturgy (the exponents of so-called popularised versions of the long familiar liturgy in both Anglican and Roman churches might learn something to their advantage from what Needham has to say on this subject).

The other essays are grouped under the headings 'Understanding' (all three concerned in some way or other with science and religion), 'Process' (three studies of evolution considered in relation to the organisational interpretation of the Second Law of Thermodynamics), 'Process and Understanding' (three presentations of a view of man, and particularly scientific man, in a future society formed as much by religious enlightenment as by universal socialism) The final essay is a brief attempt to relate the current Chinese experience to what Needham believes are the World's needs.

One could wish to have more of his rebuttal of the fashionable anti-science of today. For, although a socialism we cannot all accept and a religion for which each of us must be free to seek an alternative, give shape to Needham's philosophy, the solid substance of it is universal science, a progressive science whose development in East and West has played a part in the evolution of the human species just as much as any more obviously biological factor.

Apart from anything else it is a most entertaining book to read, because it is full of good humour and courtesy. He treats his reader by the light of one of his favourite Confucian precepts: "Behave to every man as one receiving a great guest". **Frank Greenaway**

Frank Greenaway is Keeper of the Department of Chemistry at the Science Museum, London, UK.

Delight in animal form

Starfish, Jellyfish, and the Order of Life: Issues in Nineteenth-Century Sciences. (Yale Studies in the History of Science and Medicine, Vol. 10.) By Mary P. Winsor, Pp. x+228. (Yale University: New Haven and London, January 1976.) £10 50.

MARY PICKARD WINSOR'S *Starfish, Jellyfish and the Order of Life* is the tenth in a series of works developed from PhD theses. Her original study was of "Issues in the Classification of Radiates"—a history of the decline and fragmentation of a miscellany of lower Invertebrates so collected together by Cuvier as one of the four major divisions of the Animal Kingdom. Professor Winsor sees the need "to follow scientists into the farthest corners of their research, lest the historian should mirror uncritically their own self-portrait" and to "go beyond . . . textbooks, prefaces and essays intended for the general public". This book is successfully illustrated by half-tone offset lithos of the (mostly) lithographic plates. There is a lively interest in, and competent assessment of MacLeay's Quinorianism, the early study of Alternation of Generations by the student priest Michael Sars of Norway and the Dane Johan Japetus Smith Steenstrup. The young, somewhat erratic, but already the probing doubter T. H. Huxley's relationship with W. S. MacLeay is splendidly documented, and there are a whole sequence of discoveries made in the Agassiz Library at Harvard which houses Louis' and his son Alexander's collection of annotated offprints That radial starfish had bilateral larvae, as Johannes Müller observed on Heligoland, was a great trial to Louis. Moreover many illustrations of what varieties of meaning lay behind the description "Natural Classification" are presented with sufficient documentation. A rich and full book for historians of science, of marine biology and those zoologists who may still delight in animal form. Darwin was much more closely involved in this story than Dr Winsor realises. Her attempts in her glossary to explain the Animals to the historians range at times from the naive to the grotesque. The bibliographies are remarkably good The writing has wit and elegance.

Sydney Smith

Sydney Smith is a lecturer in the Department of Zoology at the University of Cambridge, UK.

BOOKS
ON PURE
AND APPLIED SCIENCE

Books reviewed or mentioned in this journal are available from stock.

Catalogues on application.
Please state interests.

SCIENTIFIC LIBRARY
ANNUAL SUBSCRIPTION from £5.00
Reduced rates for multiple subscriptions
Available in U.K. only
Prospectus free on request

H. K. LEWIS & Co. Ltd.
LONDON: 136 GOWER STREET,
WC1E 6BS
Telephone: 01-387 4282

Circle No. 06 on Reader Enquiry Form.

Books brief

Spectrophotometric Determination of Elements. By Zygmunt Marczenko. Pp. xi+643. (Ellis Horwood: Chichester, February 1976.) £19.50; $42.90.

THIS volume is one of a series on analytical chemistry being produced by Ellis Horwood Ltd It is based on original Polish (1968) and Russian (1971) editions, but it has been extensively revised and up-dated for the English version, and now includes nearly 7,000 references, up to the end of 1973.

Part I (100pp) deals with the general principles of spectrophotometric analysis, a survey of available spectrophotometric reagents, and a discussion of preconcentration and separation procedures for the elements. Part II (520pp) is a thorough and systematic practical guide to the separation and determination of the individual elements.

The theoretical background to analytical spectrophotometry is briefly but adequately described in Section I, but this is essentially a practical handbook. Descriptions of the determinations of individual elements are presented in a standardised format, and these descriptions are written in a clear and easy-to-follow style. Several possible analytical procedures are outlined in all cases, and the listing of useful colorimetric reagents is extremely thorough.

A useful feature of Marczenko's book for readers in Western Europe and the US is that it covers the Russian and East European literature comprehensively, and includes references to some journals not readily accessible.

The book is well produced, seems to be reasonably free from typographical errors, and although not cheap it should be a useful acquisition for analytical laboratories, or individual research workers needing to use spectrophotometry to analyse for a wide range of elements.

G. Davidson

Migration and Homing in Animals. (Zoophysiology and Ecology, Vol. 6.) By Klaus Schmidt-Koenig Pp xii+99 (Springer Berlin and New York, 1975) DM46; $18.90.

THIS book provides a short, useful summary of the literature, but its excessive price (the text is only 77 small pages) will prohibit its intended audience of laymen and students from buying it. In any case the style of the book makes it more suitable for a reader who is already familiar with some of the original work than for a complete novice The writing is on the whole clear, if uninspired; however, the text is often too terse and dogmatic for the uninitiated. For example, on p48, orientation experiments with turtles and lizards are dismissed as "methodologically . . . not convincing" with no further explanation. Similarly on p65, it is stated as fact that clock-shifting experiments with pigeons refute the sun-arc hypothesis, without explaining why. I would have thought that an introductory book should not only present results but also explain, where possible, the reasoning behind their interpretation.

The organisation of the book is taxonomic: the author works through various groups of arthropods and vertebrates, in each case summarising the field evidence on migration and homing before outlining the experimental work aimed at elucidating mechanisms of orientation or navigation The literature survey seems to be accurate and fairly up to date (especially the section on birds—the author's own interest), and the text is well illustrated. Inexplicably, the book ends with an appendix on statistical methods for the analysis of orientation data, which is rather esoteric for an introductory book

John R. Krebs

The Papers of Joseph Henry. Vol. 2: November 1832–December 1835—The Princeton Years. Edited by Nathan Reingold. Pp. xxxix+524. (Smithsonian Institution: Washington, DC, December 1975.) $30.

THIS second volume maintains the high standard and interest of the first (for review, see *Nature*, **242**, 481–482, 1973). It consists of letters from and to—and occasionally about—Joseph Henry during his early years as a professor at Princeton, interspersed with notebook entries describing his work on electromagnetic induction and other topics. At first there is little about his research; but once really settled in Princeton, and having established contacts with men of science in Philadelphia, Henry got down to work once more We see some of the frustrations of working in what was then a provincial situation, far from the great centres of science in Europe; for although Henry anticipated Faraday in some discoveries his work did not quickly become known outside the USA, and it is only as this volume ends that Henry can be seen making contact with physicists in Europe. These volumes, with their very full and helpful footnotes and indices, not only give us an excellent picture of Henry's social and intellectual life, but are particularly valuable also for casting much light on the gradual formation of a scientific community in the US. Historians will turn to these papers to learn not only about Henry, but about men of science and learning, scientific institutions, and technology in his day as well.

David M. Knight

The Food in Your Future: Steps to Abundance By Keith C. Barrons. Pp. 180. (Van Nostrand Reinhold: New York and London, November 1975.) £4.

I TOOK an immediate dislike to Dr Barrons' book, and with each chapter my dislike intensified. It is surely unreasonable of him to collect together as enemies of good nutrition everyone from conservationists to the Pope. He is also out of date. One might expect 'The Great Protein War' to be about the reappraisal by nutritionists of the status of protein in the dietary pantheon. To Dr Barrons it is the basis for future agricultural strategy, although he does not seem to be aware it was an obsolescent one a decade ago.

The final chapter, entitled 'You—A Part of the Solution?', crystallised his view. Future world food needs are to be met by technology, and somebody called Johnny Q. Citizen eating less, wasting less and lobbying congress. Decency, democracy and technology, these three—a strange recipe in an era when the Green Revolution has wilted and political cynicism become a way of life But overall, although Dr Barrons' book is a tedious, stylistic nightmare, his optimism about both the technological fix and the goodness of man is attractive. His claim that agricultural technology has delivered the goods is true. His belief that it would continue to do so is impressive

I don't like the book, but I admire it for the optimism that pervades it. I shall therefore read it again, and I recommend my colleagues to do the same

John Rivers

obituary

Leonard Ary Woodward died on June 5 at the age of 73. After starting at Oxford reading mathematics, he switched to chemistry for his final degree, and then went to Leipzig for his Ph.D. (1931), where he developed his lifelong interest in spectroscopy.

He came back to the UK, and, after working for a time at the DSIR, returned to Oxford in 1939, where he was to remain for the rest of his career. It was here that, during the war, he worked on the separation of uranium isotopes by diffusion, research which was to have such influential results. After the war, though, he resumed his work on Raman spectroscopy, a field to which he made major theoretical and experimental contributions. He was made the Aldrichian Praelector in Chemistry in 1966 and served for many years as Dean and then Vice-Principal of Jesus College.

Victor Ivor Little, reader in experimental physics at Royal Holloway College, University of London, died on May 30 at the age of 56.

On graduating, in 1941 from King's College, London, he was swept up in the war effort, working on radar and the countermeasures to the V1 and V2. This experience confirmed his feelings of the practical importance of physics, an enthusiastic belief he later expressed in some measure by his work, as Chairman of the Examination Board, in restructuring the London 'A' level exams. He was also a brilliant lecturer.

His major scientific work was done in the field of non-linear optics; he early realised the exciting research possibilities of the laser. He was the first to show that standing laser radiation in fluids could create a three-dimensional grating—like a Bragg crystal grating, but on a much larger scale—and, more recently, he contributed to the development of very intense liquid laser sources.

William Bernard Crow, FLS, FZS, FRSM, died on June 28 at the age of 80. In a varied career as biologist and anthropologist, he studied at the Universities of London and Wales, worked for the Ministry of Munitions in the First World War, returned to Cardiff as a lecturer, became head of the department of Biology at Huddersfield Technical College, senior lecturer at the South West Essex Technical College, a lecturer in adult education (Northern Command) during the Second World War, went to the Leicester College of Technology and finally became Head of the Department of Biology at the Davies, Laing and Dick Tutorial College.

His major scientific interest was in morphology. He published much research in this field as well as a textbook, *Contributions to the Principles of Morphology* (1929). His broad outside interests, however, are reflected in the titles of some of his other publications: *Voice and the Vocal Apparatus; The Science of Dreams, A Synopsis of Biology, A History of Magic, Witchcraft and Occultism* and *Occult Properties of Herbs.*

announcements

Appointments

Professor J. E. Enderby to the Chair of Physics at the University of Bristol.
Dr. H. K. Moffatt to the Chair of Applied Mathematics at the University of Bristol.
Professor D. L. Gardner to the Chair of Histopathology at the University of Manchester.
Dr T. B. Grimley and **Dr A. Ledwith** as Professors of Chemistry at the University of Liverpool.

Awards

The EPS Hewlett–Packard Europhysics Prize has been awarded to **Professor Wolfgang Helfrich** of the Freie Universitat, Berlin for work on the physics of Liquid Crystals.

The President of the USA has awarded the National Medal of Science to: **John W. Backus** of San Francisco; **Manson Benedict** of Weston, Massachusetts; **Hans A. Bethe** of Ithaca, New York; **Shiing-Shen Chern** of El Cerrito, California; **George B. Dantzig** of Stanford, California; **Hallowell Davis** of St Louis, Missouri; **Paul Gyorgy** (posthumous award); **Sterling Brown Hendricks** of Silver Spring, Maryland; **Joseph O. Hirschfelder** of Madison, Wisconsin; **William H. Pickering** of Pasadena, California; **Lewis H. Sarett** of Skillman, New Jersey; **Frederick E. Terman,** of Stanford, California, **Orville Alvin Vogel** of Pullman, Washington; **E. Bright Wilson, Jr** of Concord, Massachusetts and **Chien-Shiung Wu** of New York.
The Simon Memorial Prize of the Institute of Physics has been awarded to **Drs D. M. Lee, D. Osheroff** and **R. C. Richardson** for their work on the superfluid phase of ^{3}He.

Meetings

August 21–27, **Birth Defects,** Montreal (Deadline for abstracts: March 1, 1977) (International Birth Defects Congress Ltd, 1275 Mamoroneck Avenue, White Plains, New York 10605).

September 7–10, **Meeting of the European Geophysical Society,** Amsterdam (3rd EGS Meeting (Registration), c/o Vrije Universiteit, de Boelelaan 1105, Amsterdam).

September 13–15, **Solar Energy in Agriculture,** Reading (The Secretary, UK-ISES, The Royal Institution, 21 Albemarle Street, London W1X 4BS).

September 26–28, **Planning for Water and Waste in Hot Countries,** Loughborough (John Pickford, University of Technology, Loughborough, Leics. LE11 3TU, UK).
September 29–October 1, **Comparative Planetology,** College Park (Dr Cyril Ponnamperuma, Laboratory of Chemical Evolution, Department of Chemistry, University of Maryland, College Park, Maryland 20742).
September 30–October 1, **Pacific NW Regional Meeting of the AGU,** Victoria, British Columbia (Deadline for abstracts: August 27) (John T. Weaver, Dept of Physics, University of Victoria, Victoria, B.C., Canada V8W 2Y2).

October 18–20, **Protein Synthesis,**

Bethesda, Maryland (Dr William Merrick, Symposium Director, Building 10, Room 7D-18, NIH, Bethesda, Maryland 20014).

October 28, **Sources for Emission Spectroscopy,** Middlesbrough (The Analytical Division, Chemical Society, Burlington House, London W1V 0BN).

November 17–18, **Ozone/Chlorine Dioxide Oxidation Products of Organic Materials,** Cincinnati (Dr Rip G. Rice, International Ozone Institute, Syracuse University, New York 13210).

November 24, **Synthesis of Cyclic Compounds,** London (The Assistant Secretary, Society of Chemical Industry, 14 Belgrave Square, London SW1 8PS).

November 24, **Applications of Fluorimetry to Chromotography,** Guildford (Mr D. Irish, UV Group, c/o Pye Unicam Ltd, York Street, Cambridge).

December 10, **Observation of Surfaces and Surface Reactions by TEM,** London (Deadline for abstracts to Dr W. M. Stobbs, Cavendish Laboratory, Madingley Road, Cambridge CB3 0ME: November 1) (The Meetings Officer, The Institute of Physics, 47 Belgrave Square, London SW1 8QX).

December 13–15, **Optical Properties and Effects of Atmospheric Aerosols,** Williamsburg, Virgina (Deadline for papers: September 10) (Franklin S. Harris, Jr, MS475, NASA Langley Research Center, Hampton, Virginia 23665).

January 10–14, 1977, **Molecular Cloning of Recombinant DNA** and **Genetic Manipulation as it affects the Cancer Problem,** Miami (Miami Winter Symposia, PO Box 520906, Miami, Florida 33152).

March 29–31, 1977, **Luminescence Processes in Phosphors for Cathode-Ray Tubes and Lamps,** Weybridge, Surrey (Dr P. Greenough, General Electric Co Ltd, Hirst Research Centre, East Lane, Wembley, Middlesex HA9 7PP, UK).

April 25–29, 1977, **Mitosis: Facts and Questions** (Deadline for applications: September 30) (Organising Committee, Kennwort: Mitosis, Institut für Zellforschung, Deutsches Krebsforschungszentrum, PO Box 101949, D-6900 Heidelberg, FRG).

June 1–3, 1977, **Pathobiology of Environmental Pollutants,** University of Connecticut (Deadline for abstracts: January 1, 1977) (George Migaki, D.V.M., Registry of Comparative Pathology, Armed Forces Institute of Pathology, Washington, D.C. 20306).

July 6–8, 1977, **Hot Electrons in Semiconductors,** Denton, Texas (Deadline for abstracts· March 1, 1977) (Dr D. G. Seiler, Physics Dept, North Texas State University, Denton, Texas 76203.)

August 9–19, 1977, **IASPEI/IAVCEI Assembly,** Durham (Dr R. E. Long, IASPEI/IAVCEI Assembly Office, University of Durham, Dept of Geological Sciences, Science Laboratories, South Road, Durham DH1 3LE, UK).

Person to Person

The Superconducting Magnet Research Group at the SRC Rutherford Laboratory now provides superconductor testing facilities for users in industry, universities and other research establishments. Tests on the behaviour of the critical superconducting current will be performed with two superconducting magnets: One of 85-mm bore produces 9 T, while the second gives 10.5 T in a 50-mm bore solenoid. A 15-T magnet will be available later.

The Commission of the European Communities, advised by the Committee on Medical Research and Public Health (CRM/CREST), is sponsoring European Travelling Fellowships for physicians, medical researchers or public health officers who are actively engaged in public health or population studies. Applications to the Commission of the European Communities, Directorate-General Research, Science and Education, XII/C-1, 200, rue de la Loi 1049, Brussels.

There will be no charge for this service Send items (not more than 60 words) to Martin Goldman at the London office. The section will include exchanges of accommodation, personal announcements and scientific queries. We reserve the right to decline material submitted. No commercial transactions.

September 4–9, 1977, **4th International Congress of Photosynthesis,** Reading (Dr J. Coombs, c/o Tate and Lyle Ltd, Group Research and Development, PO Box 68, Reading RG6 2BX, Berks, UK).

September 6–9, 1977, **Plant Cell and Tissue Culture: Principles and Applications,** Columbus, Ohio (Fourth Annual Colloquium, College of Biological Sciences, 484 W. 12th Avenue, The Ohio State University, Columbus, Ohio 43210).

September 19–22, 1977, **Electron Diffraction,** London (The Meetings Officer, The Institute of Physics, 47 Belgrave Square, London SW1 8QX).

September 19–24, 1977, **Availability and Rational Uses of Energy Resources,** Istanbul (The Secretary General of the World Energy Conference, 5 Bury Street, St James's, London SW1Y 6AB, UK).

October 31–November 3, 1977, **Advancing Energy Technology,** Eastbourne, Sussex (Deadline for abstracts: January 3, 1977) (Prof A. Williams, The University of Leeds, Leeds LS2 9JT, UK).

Reports and Publications

Gt Britain

Bulletin of the British Museum (Natural History). Entomology Vol 33, No. 1 + The Classification of the Anomaloninae (Hymenoptera Ichneumonidae) By Ian David Gauld. Pp. 1–135. (London British Museum (Natural History), 1976.) £10 70. [233

Memoirs of the Royal Astronomical Society. Vol. 81, Part 2 Polarimetric Observations of the Zodiacal Light in Hawaii from 1969 to 1974. By L. W Bandermann and R. D. Wolstencroft. The Nebular Complexes of the Large and Small Magellanic Clouds. By R. D Davies, K H. Elliott and J. Meaburn. Pp. 37–128 + 21 plates (Oxford and London. Blackwell Scientific Publications, 1976. Published for the Royal Astronomical Society.) [233

Superstar Technologies (The problem of monitoring technologies in those instances where technical competance is monopolised by a small number of institutions committed to the same interest.) The Report of a Working Party Convener Geoffrey Chin Council Representative· Professor John Ziman, FRS. Pp. 66. (Chichester. Barry Rose (Publishers), Ltd, in association with The Council for Science and Society, London.) £2 [243

Imperial Cancer Research Fund Annual Report and Accounts, 1975. Pp. 41. Scientific Report. Pp 162. (London Imperial Cancer Research Fund, 1976) [243

University of Oxford Annual Reports, 1973/1974 Pp. 12. (Oxford The University, 1976.) 75p. [263

The Small Towns of Hampshire. The Archaeological and Historical Implications of Development. By Michael Hughes Pp iv + 148. (Southampton Hampshire Archaeological Committee, Department of Archaeology, The University, 1976.) £1.50 [263

Radio, Television and the Arts. By Howard Newby. (BBC Lunch-Time Lectures, Tenth Series, No 4) Pp. 16 (London· BBC, 1976.) [293

Bulletin of the British Museum (Natural History). Entomology. Vol. 33, No. 2. A Review of the Genus *Anotylus* C. G. Thomson (Coleoptera. Staphylinidae). By P. M. Hammond. Pp. 137–187 + 3 plates. (London· British Museum (Natural History), 1976.) £4.35. [293

Natural Environment Research Council. Institute of Geological Sciences. Geomagnetic Bulletin No. 5 Magnetic Results 1971—Eskdalemuir, Hartland and Lerwick Observatories. Pp. vi + 97 £4.50. Geomagnetic Bulletin No. 6· Annual Mean Values of Geomagnetic Elements since 1941. Pp. 170. £7. (London. HMSO, 1975 and 1976) [293

Proceedings of the Royal Irish Academy. Vol. 76, Section A. No. 1: On the Coefficients in the Recursion Formulae of Orthogonal Polynomials By G. Freud. Pp. 1–6. 45p. No. 2: A Note on Complementation in Lattices of Convergence Functions. By C. A. Boyd. Pp. 7–10 25p. No. 3. A Note on the Reflection Principle for Harmonic Functions. By D. H. Armitage. Pp. 11–14. 28p. No 4. The Ideal Centre of a Banach Lattice. By A. W. Wickstead. Pp. 15–24. 48p No 5. Haar Measures for Groupoids By A. K. Seda. Pp. 25–36 48p. No. 6· On the Construction of the Kerr Congruence. By P. A. Hogan Pp. 37–42. 45p. No. 7 Relaxation Effects in Rotational Brownian Motion. By J. T. Lewis, J. McConnell and B K. P. Scaife. Pp. 43–70. 92p. No. 8· Modified Kohn Variational Principle, The Virial Theorem and the Second Virial Coefficient. By W. D. Burns and B. L. Moiseiwitsch. Pp. 71–78. 50p Vol. 76, Section B. No. 4. Stratigraphy Sedimentology and Structure of the Bray Group in County Wicklow and South County Dublin. By P. M. Bruck and T. J. Reeves. Pp. 53–78 + plates 1–3 87p. No 5: Formation of Oxo-Compounds from Chlorobenzodiazines in Dimethylsulphoxide. By D. Twomey. Pp. 79–86. 25p. No. 6: A Preliminary List of the Fungus-Gnats (Diptera Mycetophilidae) of Ireland By P. J. Chandler. Pp. 87–110 66p No. 7 The Submarine Extensions of the Thorr and Fanad Plutons, County Donegal. By D. Evans and R J. Whittington. Pp. 111–120. 40p. (Dublin Royal Irish Academy, 1976.) [303

Other countries

US Department of the Interior. Geological Survey. Bulletin 1395–E: Changes in Nomenclature of Upper Precambrian to Lower Paleozoic(?) Formations in the Natick Quadrangle, Eastern Massachusetts, and Their Tentative Correlations with Rocks in Rhode Island and Connecticut. By A. E. Nelson. Pp iii + 15. (Washington, DCL US Government Printing Office, 1974.) 35 cents. [303

Toxicology Research Projects Directory, Vol. 1, No. 1, January 1976. (An Indexed Directory of Current Research Project Abstracts in Toxicology and Related Fields.) Pp 701. (Bethesda, Md. Toxicology Information Subcommittee of the DHEW Committee to Coordinate Toxicology and Related Programs, 1976. Orders to Toxicology Document and Data Depository, National Technical Information Service, Springfield, Virginia, 22161. Specify Publication No. NTISUB/B/021–76/001.) Single issue $20. Subscription (4 issues) $65. [313

Smithsonian Contributions to Zoology, No. 213· Communication Mechanisms and Social Integration in the Black Spider Monkey, *Ateles fusciceps robustus*, and Related Species. By John F. Eisenberg. Pp. vi + 108. (Washington, DC: Smithsonian Institution Press, 1976. For sale by US Government Printing Office) [313

nature

July 29, 1976

Making it in the Civil Service

IT is now eight years since the Fulton Report on the British Civil Service advocated fairly comprehensive reforms in many aspects of the service, ranging from recruitment policies and staff training to job categorisation. Eight years is not a long period for an organisation with such inbuilt momentum as the Civil Service, but the Select Committee on Expenditure of the House of Commons deems it time to have a look at the way reform has been progressing Last week was the turn of the Institution of Professional Civil Servants (IPCS), the body which represents professional, technical and scientific civil servants, to give its first evidence.

This past year hasn't been a particularly good one for the Civil Service. It has been the victim of a fairly regular stream of what the IPCS called "unfair attacks" and what others might call penetrating questioning of its role; the mutterings—and much more that hasn't surfaced—can be fairly clearly associated with the privileged position in which the civil servant finds him or herself at the moment. There has always, of course, been grumbling about job security and its dulling effect, the complaints have recently been about the way in which salaries and pension rights in the public sector seem to have become so much more favourable than those in the private sector, in which there is little job security.

It is, then, inevitable that what civil servants say about themselves and their situation is looked at in a rather hawk-eyed way; the IPCS at least didn't fall into the trap of telling the committee its members were underpaid. But they are, it was claimed, underprivileged —the words "second class" kept cropping up. In short, the IPCS believes there has not been a proper commitment by the Civil Service Department to implementing Fulton recommendations on removing vertical barriers between different classes or categories, notably the Administrative, Professional and Scientific categories At the very top this has been done, at least formally, though whether it means much is questionable. What the IPCS would like to see is the removal of category labels much further down the system, in the hopes that this would allow policy-making and management prospects to open up at all levels for those who are at present confined by being 'professionals' or scientific'.

For all the IPCS's professed admiration for the administrators, this move is a thinly disguised assault on the administrative citadel wherein, in the spirit of the genteel class warfare that is alleged to go on in the Civil Service, are housed the first-class characters who really have all the power and make all the decisions. Scientists, of course, run their own laboratories, so the call by the IPCS must be seen as an attempt to broaden the stage on which their members can operate.

There are problems The first is that the IPCS, in making the point elsewhere in their submission that the distinction between generalists (that is, administrators) and specialists is artificial, acknowledges that administration contains a range of specialisms such as finance, accounts, contracts, personnel and computers and indeed that "public administration itself is a specialism". If we are all specialists now, the administrators will prove as defensive about opening up their ranks as would scientists about having administrators join them in some scientific venture.

The second problem is the sort of person who might be helped by such schemes. Outstanding professionals find their way to the top and go where they want to go without the need for much outside help. There is, however, a much greater number of what might be called the solid and reliable, and a real and as yet unsolved difficulty inherent in Civil Service use of professionals is how to prevent the solid and reliable from becoming disheartened, maybe as early as their mid-thirties, at the lack of prospects. But are there large numbers of jobs going begging in the administration categories or are there posts that ought to be created to allow these people to spread their wings? There are, after all, many solid and reliable administrators who are also likely to be in pursuit of such posts. The challenge then, is to the IPCS to do some extensive research and provide the Select Committee with some formidable evidence, down to chapter and verse, that there really are, as Fulton asserted, a significant number of jobs in the service, requiring both technical and managerial ability, which could be filled by technical people and which at present are not.

We have in the past advocated more radical approaches to the problem, particularly the golden handshake and enhanced mobility into and out of the service, but we believe that a detailed case is worth making for a different sort of solution. ☐

Tracking nuclear decisions (1)

JET: will it ever get started?

Chris Sherwell traces the tortuous course of a decision the EEC cannot take

WHEN, on the last day of last month, Mr Gaston Thorn relinquished the presidency of the EEC's Council of Ministers, he was frustrated and dissatisfied. The inertia paralysing the Community, he indicated, could be relieved by a move in the Council away from unanimous voting. It was the echo of a view expressed in many quarters many times before, though not perhaps by so senior or so obviously political a personage as the Luxembourg Prime Minister.

The widely-praised Heads of Government meeting two weeks later provided a much-needed boost for the Community. But its upper echelons are plainly troubled. Herr Guido Brunner, European Commissioner for Research, gave vent to his feelings when he visited London earlier last month. He too spoke of majority voting. But he had a specific matter on his mind—the Joint European Torus, JET. JET represents the next stage in the Community's effort to harness the power of nuclear fusion (see box, page 341). It also offers a remarkably fine illustration of what torments men like Gaston Thorn and Guido Brunner, not to mention scores of Community officials and countless people in the nine member states.

The immediate problem is that the Nine cannot agree to go ahead with the project without deciding on where it should be sited. The latest effort, at last week's meeting of the Council of Foreign Ministers, produced a piece of diplomatic mystification: the European Commission had asked for a decision of principle, before the summer recess, on the building of JET. This, it was thought, would facilitate a decision on the site when the Council of Research Ministers meets in October, and thus help prevent a split in the JET design team.

But the delays which have brought matters to their sorry pass were not ended. The Foreign Ministers watered down the Commission proposal, deciding merely to "adopt a favourable opinion on the rapid undertaking of the enterprise", which they thought should be put before the next Council of Research Ministers meeting for a decision. In short, the ball was put right back where it had been before, in the Research Ministers' court, and without any further movement over the site. This means that when a decision on where to site JET comes in October—if it comes then—a full year will have been lost on a programme in which time is regarded as being of major importance.

What makes things worse, however, is that there must be some doubt attached to the prospect of an October decision, for the precedents are truly inauspicious.

Euratom infusion

The Community's Fusion Programme, under the overall directorship of Signor Donato Palumbo of Italy, has its origins in the 1950s with the formation of Euratom and the EEC itself. Two five-year programmes were implemented between 1958 and 1967; work continued on a year-to-year basis between 1968 and 1970, when a third five-year programme was agreed. Once it was appreciated that, with the progress being made in fusion research, plans to build a large Tokamak—JET—could only be realised through an EEC-wide effort, a European design team of more than 50 members was brought together. The overall EEC fusion effort was coordinated by Euratom through a complex bureaucratic web of steering committees; JET is its centrepiece.

The laboratories at Culham, near Oxford, were offered as a location for the JET team. They form the United Kingdom Atomic Energy Authority's fusion research centre and, in the words of a Culham man, were offered "without prejudice to the final decision on the site for JET", which it was expected would be made by the end of 1975, when the original two-year contracts for the team's members expired.

All the advice the European Commission received in its wide consultations on the project acknowledged the risk attached to it, but the response was positive and members of the European Parliament gave their backing. So, with progress on the conceptual design of JET—a design which received additional backing at international meetings—the new overall plan for fusion research for the next five-year period (1976–1980) was put forward.

The total fusion effort for the period was put at 246 million units of account (mua). The estimated cost of the JET project was 135 mua—£80 million; the Community as a collective accepted responsibility for 80% of this (108 mua); member states would contribute the balance in proportion to GNP. Of the £80 million, some 21½% would go on the JET device itself, 23½% on manpower, 17% on power supplies; the rest was for buildings (11½%), auxiliary systems (6¼%), the operating budget (6½%), instrumentation (5¼%) and contingencies.

As long as all these details were busily working their way up through committees towards the key arena of the Council of Research Ministers, and the customary problems involved in setting up a Council meeting persisted, a quick decision was not possible. With the putative deadline of 1976 looming closer, efforts were redoubled to secure a commitment on JET from the Council. But the Council of Finance Ministers, meeting first, would not decide on a financial allocation for a project on which a decision had yet to be taken. The Commission, facing the prospect of a sanctioned project not going ahead in the absence of a budget, obtained money to tide things over from the European Parliament under a special provision. It was a foretaste of the degree to which the Commission's ingenuity would be taxed. The Research Ministers finally met in December. And at that point the trouble really started.

See the sites

The meeting provided the first real indication that the Commission had completely underestimated the political problems involved. It emerged that Britain, with Culham, France, with Cadarache, West Germany, with Garching and Julich, and Belgium, with Mol, all thought their own sites were suitable for JET. Italy, pushing for the Italian establishment of the Community's Joint Research Centre (JRC) at Ispra, refused to approve the whole 1976–1980 research programme in thermonuclear fusion and plasma physics unless a decision on JET's site was taken at the same time. No decision was taken, the programme was not approved, and the meeting broke up. Ahead of the next meeting, set for February, the Council's Atomic Questions Group exchanged views, and the Committee of Permanent Representatives examined its report, without taking anything further.

The difficulties were quickly compounded. Italy, having sought bilateral talks on the matter, failed to persuade Britain to support Ispra, and the British goverment started disclosing its own pro-Culham position publicly in the House of Lords. West Germany reasserted its willingness to take on 15% of the project's overall costs if Jülich or Garching was chosen as the site. Researchers at Culham reportedly began writing to Brussels urging an early decision.

That was not all. In late January, the Commission released the results of its

Confusion profusion: the arguments about the site

"If JET goes to Ispra, it is better that it does not get done at all." **Senior official, Culham fusion research centre.**

"If JET does not go to Ispra, it is not worth doing." **Senior official, European Commission.**

Culham and Ispra are probably the two main contending sites for the JET project. France's involvement in the Superphénix fast breeder is thought to make its bid for Cadarache more an attempt to score political points than a determined effort to win the project. Garching's candidacy is regarded with more severe respect and remains a powerful contender, but it has not planned to take JET in the way that Culham, with the design team, has done.

Only Italy defends Ispra with vigour; apart from Britain, though, none of the Nine openly backs Culham. The arguments concerning all the sites are finely balanced. The technical assessment of the Commission's site committee looked at the alternatives in terms of power supplies, infrastructure, safety and social facilities. On each criterion each site was fair to excellent: no site was best on all aspects, but all sites were suitable for the construction of JET.

It was chiefly on the power supply and social aspects that the Commission originally chose Ispra. It is fed directly from a conveniently located power supply; it already has an adequate infrastructure and social facilities, including an international school; it has staff already available for the project; and it has the equipment and expertise needed for the heavy engineering involved in handling large-scale plant and materials.

But the arguments in favour of Ispra now, if they didn't do so before, traverse broader territory than this. Perhaps the most potent actually comes from its supporters in the Commission itself, representing the collective Community interest. It is in the best long term Community interests, the argument goes, that the project be pursued as a Community effort. The project, particularly as it is largely Community financed, should therefore preferably be sited at a Community centre. And the premier establishment of the Community's Joint Research Centre (JRC)—indeed the only one capable of handling the project—is at Ispra, in northern Italy.

The argument goes further, into psychology. Ispra, it says, has been dogged by uncertainty in recent years, and the latest programme of research is due to end this year. Although much of the multi-annual programme planned for 1977–80 will be conducted at Ispra, JET would insure its own future as the Community's leading research centre, which might in turn halt the fragmentation of research. Siting the project at Ispra would at the same time compensate Italy's loss by its exclusion from the UK–West Germany–Netherlands Gas Centrifuge Treaty for Uranium Enrichment.

The case against Ispra has come mainly from Britain, a point that has not gone unnoticed amongst senior Community officials. It turns most importantly on the project's chances of success. The chief scientist at the Energy Department, Dr Walter Marshall, not known as a fusion enthusiast, puts it this way: there is "an appreciable chance" that the project will fail, not because it is badly conceived but because it is so ambitious; it should not therefore go to any site which "lacks experience and know-how in solving the plasma physics problems that are bound to arise." Ispra's fusion experience (often described in Britain as "modest") is not great.

Marshall does think that the project should go ahead. But he judges that other sites, including Culham, satisfy his criterion in a way that Ispra does not. Moreover, he is "very much frightened" that if the counter-arguments about symbols of European collaboration win the day, then the project really will be a failure. If he could be persuaded of the scientific capability of a site, he has said, he would recommend it, but this he says has not been done; there had only been a "review of the characteristics" of the sites.

The implication is that a site (like Ispra) ought not to be chosen for an additional reason—to solve an administrative problem. Others allege in addition that Ispra's resources, and its capacity to get them, are not great. It has even been said that scientists would be reluctant to work at Ispra, especially as it has not managed a large project before. Past labour problems add to its reported reputation for mismanagement—a reputation also pinned on the Commission, whose allegedly closed mind over the matter has proved a sore point in Britain. That Ispra could prove to be the most expensive site, which is also suggested, is a point that Guido Brunner, European Research Commissioner, disputes. He says the differences in cost between the various sites is no more than 10%.

The arguments in favour of Culham are partly the arguments against Ispra reversed. Culham, it is said, is already a centre of excellence in fusion, commanding large experience and resources, possessing a good "track record" and making progress that is more than comparable with the USA and USSR. Furthermore, it not only fits the bill on such essential criteria as power supplies, it also has the land ready to take JET and, most importantly, a team already settled there to continue the work it has successfully begun. Such continuity, it is argued, ensures the maximum chances of success. Culham, says Alex Eadie, junior minister at the Energy Department, is the best site on technical, scientific and operational grounds. But another reason offered in support of Culham is more nakedly political: namely, that there is as yet no high technology Community project in Britain. This gives it some sort of advantage over Garching, for example, since West Germany has the Patent Office and the European Molecular Biology Organisation.

Arguments against Culham throw doubts on its back-up facilities, on the lack of a school and so on. Beyond these, though, it is said that expertise in fusion is not really relevant for much of the project's duration, since most of the time would be spent in JET's construction; moreover, any problems that arose would probably be too big for any one laboratory to solve alone. More subtle arguments point to the recent experience with the Dragon high temperature reactor project at Winfrith, Dorset, during which Britain attracted from many European countries criticism of its foot-dragging, if not obstructionist, tactics over the project's fate.

The site stand-off preventing JET's take-off is thus a complicated affair. It has tried the patience of the contending host countries, whose Community spirit is already under scrutiny. It has aggravated the frustrations of the smaller member states who these days have enough reason to feel left out in the cold. And it has threatened the role of the Commission, whose ambiguous position has rendered its influence and authority more tenuous than it might otherwise have been. The Community's worst enemies couldn't ask for more. ☐

independent siting committee. It had not previously pushed any one site; now it came down in favour of Ispra. Moreover, it delivered its view as a communication instead of as a "proposed decision" for the Council, as was customary; this it defended by saying that only the whole project, including the matter of the site, and not the site alone, involved a decision. The boundaries of the Commission's competence to decide on the matter thus became an issue as well.

The February 24 meeting of the Research Council began by avoiding an immediate break-up over the site. British, French and West German pressure wrought a reduction in the total fusion budget from 246 mua to 232 mua, thereby leaving less for the fusion research not directly related to JET. This, however, entailed the abandonment by Italy of the position under which she had linked a decision on the site with approval of other fusion research programmes; but she still insisted, successfully, that the meeting sanction just one year's expenditure—20.8 mua. But that at least meant the programme could go ahead.

When it came to discussions of the site, however, none of the contending countries withdrew their applications to host the project. After hours of debate, the Ministers failed even to agree on a method for deciding where JET should go. They rejected a proposal that the Commission, as the competent authority, should decide, and also the idea of an exhaustive ballot among themselves. Eventually, applying an old adage ("When in doubt, never commit yourself, committee yourself"), they agreed to call for a new report on the alternative sites. This was to come from a special committee established by the meeting, the Consultative Committee for the Fusion Programme, consisting of a representative from each of the Nine, a Commission representative and representatives from third countries involved in the fusion programme. It would report on comparative technical merits in May, in time for the next Council meeting, set for mid-June.

Some states openly regarded this as a waste of time; Italy hoped that the question of the site would not be reopened. For the Commission, Brunner still claimed the matter was within its competence: he couldn't see what new light would be thrown on the problem by more technical assessments; only something very dramatic could change the Commission's mind. For all its immobility though, the Commission did not apparently intend to try and impose its choice.

By now the threat of rising costs was starting to make speed vital; so too was the ground being lost against the USA and USSR; and the team's declining morale, with the increasing prospect of its break-up in spite of a renegotiation of contracts for a six-month extension. But the rest of the fusion programme was assured for a year; and the new committee had also been accorded a general role in respect of the whole programme, which would help its development. All the same, it looked as though the JET problem was so intractable that it would need resolution by the Council of Foreign Ministers or by the nine Heads of Govenrment—a suggestion which the Dutch had by now put forward.

Fight goes on

With the fighting now well developed, two sites were withdrawn—Mol in Belgium and Jülich in West Germany. Reports of job offers from the USA for members of the design team grew, and a few actually left the project. Britain made a climb-down more difficult when she put her view favouring Culham to the House of Commons in March. The "common front" of trade unions at Ispra called a press conference later that month to urge a decision in favour of Ispra and of a Europe independent in energy and science.

The Consultative Committee, at its first meeting in early April, received an independent report on JET's design details from the UK-based Risley group. This confirmed the team's plans, and the Committee recommended that a decision to build was needed forthwith. It recommended too the immediate creation of a management committee for JET together with a strengthened fusion directorate at the Commission. But the Committee also heard estimates that certain costs had drifted upwards, making overall costs some 23 mua greater than the original 135 mua. Another meeting was set for mid-May to discuss a final report following consultations with the JET team over the Risley report. Incredibly, the Committee did not discuss the matter of the site.

Neither was it discussed at the Council of Foreign Ministers meeting in early May, even though Luxembourg, backed by Belgium and Holland, was trying to put it on the agenda. In fact the agenda was already too full. The lack of movement encouraged some European parliamentarians to speak out volubly, questioning whether European collaboration was possible, and whether latest estimates of Europe's future energy requirements didn't tilt the balance one way or the other. In mid-May Brunner signed the draft agreement on Sweden's participation in the fusion programme; negotiations with Switzerland, something which with the Swedish precedent was not expected to take long, were almost

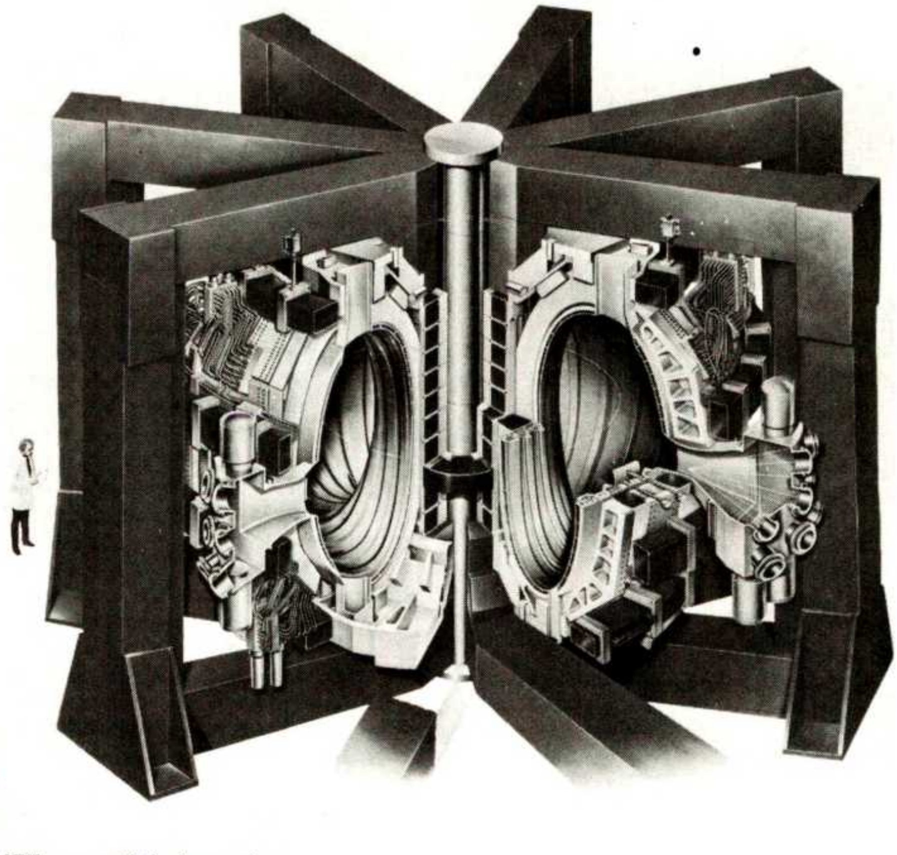
EEC picture

JET : an artist's impression

ready to commence and soon received the go-ahead. The pace was quickening again.

The Italian general election, set for June 20, just two days after the crucial Council of Research Ministers meeting, now intervened. With the prospect of an upset result producing an Italian government which might disagree with any decision taken by the Council, it began to seem pointless having the meeting at all. At Italy's request it was decided that the meeting would not take place. The Dutch proposed a meeting for mid-July; this was agreed in principle. As late as the first week of June, Brunner was expressing the hope that a decision on the site would be taken at such a meeting. Days later it was clear that no meeting was likely before the summer recesss. No early decision on the site would therefore be possible unless the idea of a determination by the nine Foreign Ministers was resuscitated.

The Commission had itself come round to this view. It had also been busy on the central problem of the site: by the end of May it had finished preparing additional information for the Council of Research Ministers in order to make the choice easier. This included, first of all, the news that consultations concerning the higher cost estimates had produced agreement that the extra amounts involved were in fact negligible, at about 5 mua. The Commission also contended that insufficient emphasis had been attached previously to the matter of the power supply: if JET was to be fed directly, Ispra, fed by a line from a thermal and a hydroelectric station, possessed another advantage over other sites. Finally, the Commission stressed the costs of delay. Increasingly frustrated, it therefore argued that no attempt to justify a further delay could be based on arguments of a scientific, technical, financial or adminstrative nature.

With no prospect of a meeting of the Council of Research Ministers before mid-October, and the need for decisions growing more desperate, it was now time to change tack. At the end of June, therefore, and at the request of the Dutch (who were about to take over the Council presidencies), the nine Foreign Ministers had a brief exchange on the siting of JET. The Commission was now looking for a decision of principle on the building of JET before the recess in order at least to supply more adhesive to the JET team than the second six-month extension to contracts just put together.

The matter was put on the agenda of the Heads of Government meeting on July 12. The boost they were busy giving to the Community did not extend as far as JET, however, and it was not discussed. Assurances were given that last week's Foreign Ministers meeting would deal with the matter in some detail though it was not on the official agenda. Nothing approaching progress which would satisfy the Commission resulted. The recess is now imminent. October is two more months away.

JET lag importance

The persistent procrastination, far from indicating that the EEC perceives the JET decision as having comparatively minor consequence, is precisely a reflection of the project's importance. JET is a major Community research project, perhaps the first of its type,

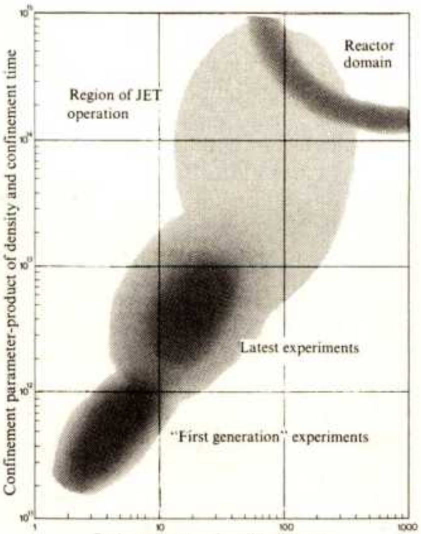

Fusion research: where it's at

FUSION research, which seeks to harness the energy released when nuclei of light elements are brought together to form heavier ones, aims ultimately to design a practical fusion reactor that produces electricity economically. The aim is thus to approach more closely the conditions at which the energy released from the deuterium–tritium reaction (the fusion reaction selected as the most promising of several possibilities) is greater than that expended both in heating the plasma in which the reaction occurs, and in losses.

The immediate goals are therefore to find ways of heating the plasma to the necessary temperature, and to confine that plasma for the necessary time. Apart from the passage of electric current, methods of heating currently being investigated include the use of intense laser beams and the use of beams of high-energy neutralised particles originally produced from an ion source. The method of confinement in a doughnut (torus) shape uses a helical magnetic field. This is made up of two components, a toroidal field produced by large external coils, and a poloidal field which, in the case of tokamaks like jet, is produced by a toroidal current in the plasma.

Tokamaks, however, represent only one of three classes of toroidal device now being examined for their confinement capabilities. These are in fact distinguished by the way the poloidal field is produced:

(a) **Tokamaks,** and **Reversed-field Pinches** (high beta systems). In tokamaks the toroidal field is greater than the poloidal field; in reversed-field pinches the two are about the same and the toroidal field is reversed in the outer regions of the plasma. In both, the plasma current which heats the plasma also creates the poloidal field.

(b) **Stellarators** (low beta systems). In this class of device, currents in helical conductors wrapped round the torus and outside the plasma produce the field which, with the toroidal field, confines the plasma.

(c) **Toroidal multipole.** Here the poloidal field is produced by a steady current flowing in a levitated superconducting ring located in the centre of the vacuum chamber with the plasma.

Magnetic confinement produces a plasma of modest density, so the confinement time necessary to boost the "confinement parameter" (density x confinement time) is longer compared to a plasma of very high density.

Obtaining a high-density plasma is the aim of inertial confinement, in which the necessary time of confinement is actually shorter than the period in which the particles will escape from the reacting zone. This confinement is achieved by irradiation with high-power laser beams. Extremely intense, short laser pulses bombard a solid deuterium–tritium fuel pellet, causing it to turn into a plasma so hot and so compressed that fusion reactions yield a surplus of energy before the pellet decays as a result of expansion. The method does not simply offer the possibility of avoiding the difficulties of using magnetic fields for confinement; it also offers the theoretical possibility of using a series of laser pulses to cause a succession of these explosions.

The selling of fusion power has turned largely on its ostensible advantages in respect of the fuel it uses and its safety. But the supply of lithium (used to produce tritium) is at least not certain, and neutron production in the reactor has the potential to make the reactor materials highly radioactive. There are other problems relating to possible lithium fires and tritium leakage. And since fusion is so patently a prospect for the distant future, guesses about its economics remain exactly that—all of which makes any choice between fusion and fast-breeder fission, if such a choice exists, correspondingly more difficult to make.

JET is effectively a "third generation" tokamak device. Its equivalent in the USSR is known as T–20, in the USA as TFTR, and in Japan as JT–60. "Second generation" tokamaks include DITE at Culham, T–10 in the USSR and PLT in the USA.

For the post-Jet period, the following sort of sequence is imagined:

1980–1985	Tritium burning experiment
1985–1990	Experimental reactor
1990–2000	Prototype
2000–2010	Demonstration

Other common facilities envisaged over this period include a material testing facility and a superconducting magnet assembly.

perhaps the first of many. Money is to be spent, and there are contracts to be had. That means large and powerful interests are involved, not just on both sides of various sectors of manufacturing industry, but within state administrations and institutions and within the EEC's own administrative structures.

With so much at stake, the decision on the site had to become the prime focus of interest. To win JET was (and is) to win fusion in Europe. There are some, notably the Italians, who have claimed that JET, being just one part of an even larger overall programme, would not by its location determine where the European centre of excellence would lie. The argument is that the other projects to come would be sited elsewhere. But no one seems to believe it. Whoever wins JET, most are saying, acquires the huge investment that goes with it, the location for future reactors and the investment that goes with them too; whatever the spreading of the contracts, and no matter what clauses are inserted as safeguards into the agreement, the host country is said to have the advantage. That country's cap acquires the fusion feather—and the reputation, the prestige and the national pride. It seems rather a lot to hang on a unanimous decision of a group of Research Ministers.

The Commission, in the form of Signor Palumbo, finds all this a trifle exaggerated. He claims that the press has "transformed a technical and limited problem into one of prestige", and points out that there is another aspect of the problem beyond the interest of a country in having JET. This is the interest in having JET at the best possible site. Suppose, he says, a super-intelligent, objective man could identify both the best and the worst sites among those competing for JET. The difference between the value of the best site and the value of the worst site, he argues, is hugely outweighed by the damage done by a one-year delay to the JET project and to the common fusion programme. Indeed, all sites could host JET. The choice of the site, while blocking everything, is thus irrelevant, he claims, and he goes on the repeat the growing view—that if the Commission's choice is not approved, the Council of Ministers must give up its jealously guarded unanimity rule to come to a definite choice.

He certainly seems to be right about the urgency. Existing programmes for medium scale devices at Jülich, Cadarache, Garching and Culham all depend technically and financially on a decision on the site for JET. Delay is discouraging the JET staff even further, making it difficult to maintain the team and impossible to expand it. It has been possible to farm out some small study contracts relating to the project, but money available for this is almost totally spent, and a Council decision is required for more. Plans for buildings cannot be finalised, of course, buildings cannot be built, and orders cannot be placed for equipment that might be unsuitable or superfluous if another site is chosen. As the Commission has itself put it, any decision concerning further work without the site being known would be unrealistic, perhaps dangerous and almost certainly expensive.

Just how expensive is perhaps not appreciated. The delay, apart from jeopardising the project itself and the whole fusion programme, may now be jeopardising the spirit of cooperation that exists in Europe. It may also be damaging the credibility of the Community's decision-making procedures among other international organisations and in other non-EEC countries. Most importantly, it may soon start affecting Europe's own public, whose tacit support for the expenditure of so much money is less likely if the persistent delays (and the corresponding progress of the Americans and Russians) make the project seem pointless.

Optimists point out that a decision in October would mean that a delay of only a year had been incurred. No decision in October might mean leaving the decision as late as the next Heads of Government meeting in The Hague in December. But the viability of the whole project may have been brought into question by that time: as Herr Schuster, Director General at DG XII in Brussels, puts it, if there is no decision by then, the project is dead in an EEC framework. Yet it is Schuster who freely acknowledges that the German elections later this year might intervene, Italian-style.

An alternative has already been mooted: that JET becomes a British–French–German operation. But a British minister has already said Britain is committed to European collaboration. And the Commission heaps derision on the idea. Alternative combinations, it is said, are "futurology": the three countries can't agree among themselves, and JET is anyway "owned 100%," by the Commission. But political facts could conceivably change things. The Community is being brought into disrepute. Fusion itself is being brought into disrepute. Unless something is done, a Community fusion project might therefore be a forlorn hope. □

Tracking nuclear decisions (2)

FBR: will it ever be stopped?

Allan Piper looks at the arguments concerning the fast breeder reactor

THE UK Energy Secretary, Anthony Wedgwood Benn, decides this autumn whether Britain will build a commercial scale fast breeder reactor. It is a measure of the task he faces that, from one viewpoint, the FBR is an elegant and timely solution to immediately foreseeable energy problems, while from another it looks like potentially the most disastrous technological development imaginable. The dichotomy is simply explained: the reactor's most attractive advantage—an ability to create its own fuel—is precisely its major disadvantage. For the fuel so created is plutonium, the stuff of nuclear weaponry.

Mr Benn is fully aware of the enormity of his decision's implications, whatever he chooses. Not much is known of how he will reach it, beyond the fact that a certain amount of public debate is involved. Some people believe the decision is being taken too quickly and ought to be delayed, saying the FBR is not yet needed; others contend that an early decision is vital for the industry and the country. The arguments are complicated, but what Mr Benn has to decide is, first, whether fast reactor technology is an essential element of the future energy scene; second, whether it can be developed to an acceptable level of safety; and, finally, whether it is socially desirable. He must make his decision against a backdrop of clear signs that the FBR will be developed elsewhere if not in Britain, and delay could spoil the chances of an early foothold in a potentially lucrative worldwide market.

The case for the FBR rests squarely on its fuel breeding capacity (see box, page 344). Unlike existing commercial thermal reactors, which use less than 1% of the energy available in uranium, the FBR extracts more than 60%. At the same time it contributes towards future energy supplies by "breeding" plutonium. These simple advantages mark it out as the potential saviour of an energy hungry world.

Consideration of Britain's nuclear fuel prospect highlights the possible benefits of the FBR. Since the middle 1950s the UK thermal reactor pro-

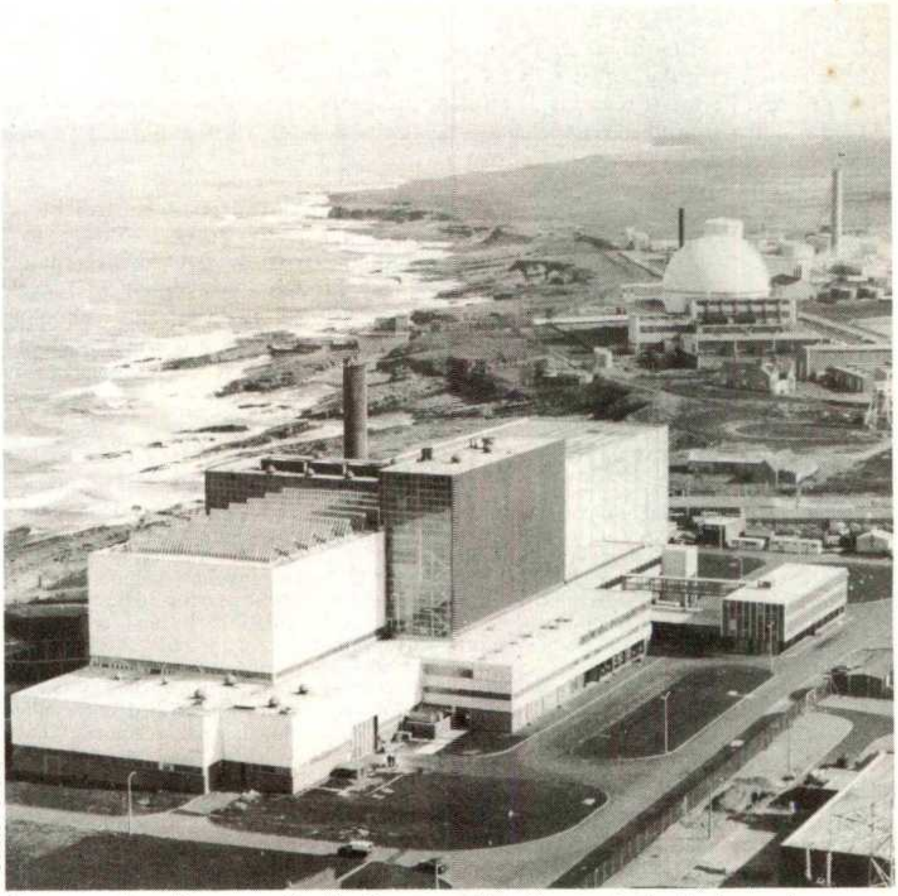

Prototype Fast Reactor with the Dounreay Fast Reactor in the background

Photo: UKAEA

gramme has produced 20,000 tons of depleted uranium. Ordinarily of little value, this stackpile, together with the 13 tons or so of plutonium that have also accumulated, could be used in fast breeders to provide as much energy as the nation's total known reserves of coal. For a country with a sizeable (5 GW) and expanding nuclear programme, this represents an indigenous energy source that could become ever more crucial as the domestic requirements of the uranium exporting nations themselves increase. British imports from Canada could be squeezed, as could possible future supplies from Australia. A large political question mark hangs over Namibian uranium, Britain's only other source of reactor fuel.

Worldwide nuclear expansion will also introduce economic pressures. Present assessments of world uranium reserves are as elastic as the market prices assumed in calculations, but at the existing price of around $15 a pound an estimated 3.4 million tons of high grade ore are available, though only half of that is so far proven. Whether this can last beyond 1990, even with today's worldwide nuclear capacity, is already a matter of debate.

There is less doubt, however, that by the turn of the century the continued use of thermal reactors alone could force the exploitation of lower grade ores. The consequent increase in prices, which might rise as high as $100–$200 a pound if forecasts from the US Energy Research and Development Administration prove correct, is likely to be matched only by the increased amount of environmental despoliation accompanying the extraction of ores with energy contents similar to that of coal. (Currently used ores provide around 25,000 times as much energy as coal in thermal reactors, or up to about 1.5 million times as much in fast breeders.)

What bearing this has on the case for a British FBR programme is rather a matter of viewpoint. On the one hand, energy demand forecasts from within the nuclear industry and the Department of Energy (DEN) identify the FBR as an indispensable cornerstone of the British energy scene until fusion power arrives. On the other, it is easy to query the accuracy of forecasts. The degree of uncertainty involved was underlined during the recent national energy conference when British Gas leaders refuted predictions of a UK energy gap before the end of the century.

Independent research units similarly believe that electrical energy demands may already be near to peaking, while pressure groups claim that demand can be regulated by conservation measures, ensuring that sufficient nuclear capacity is achieved economically using more efficient thermal reactors systems such as CANDU (see box). There are also calls for more research and development (R&D) effort on high temperature reactors, which open up the possibilities of the thorium cycle. But the UK Atomic Energy Authority (UKAEA) is less enthusiastic, wary of the huge initial uranium investments needed to launch such a programme.

UKAEA forecasts predict that by the turn of the century almost 75% of the national energy demand must be met by nuclear power. Of the 198 GW needed to do this job, almost 33 GW, nearly seven times the current total installed nuclear capacity, will come from fast breeders. Whether this target is treated entirely seriously by the DEN remains doubtful, particularly as the Central Electricity Generating Board (CEGB) could by then handle a maximum of only 20 GW from FBRs. Moreover, Walter Marshall, Chief Scientist at the DEN, has several times publicly voiced the conviction that the number of commercial fast breeders operating by the year 2000 is unlikely to exceed two or three.

Nonetheless, this only reinforces the UKAEA's case for early clearance for their planned 1,300 MW demonstrated FBR, CFR–1. It has built up a good head of steam for the off. Its R&D effort on FBR technology extends back over 25 years, with operational experience dating from the start-up of the 14 MW experimental FBR at Dounreay in Scotland (DFR) in 1959. The programme advanced a further major step two years ago with the introduction at low power of a 250 MW prototype (PFR), also at Dounreay.

Estimates of the total cost involved in coming thus far vary between £200 and £400 millions, but the UKAEA's present level of financial commitment speaks for itself. Though cuts of up to £4 millions are expected as part of current UK expenditure savings, R&D spending on FBR technology over the past three years has stood at around an annual £40 millions, almost a third of the total nuclear R&D cake, and by far the largest single slice. Moreover, about half of the overall nuclear R&D workforce is involved with the FBR.

The UKAEA therefore understandably feels that the next logical step is the design and construction of CFR–1, expected to take about 10 years. Confidence generated by almost two decades of reasonable progress with DFR, which has pumped more than 500 kWh into the national grid, extends beyond the reactor itself, into every area of the related fuel cycle.

At least one group does not share the UKAEA's confidence. Friends of the Earth (FOE) have vocally attacked the international record of fast reactor development with single minded conviction. During a recent House of

Commons Select Committee meeting FOE listed a series of developmental setbacks that provokes sober reflection. The Enrico-Fermi FBR in Detroit, Michigan, for example, was constantly beset by potentially dangerous disruptions during its sporadic, nine-year operational life, while more recently the Soviet BN–350 FBR on the Caspian coast has suffered several serious leaks in the steam generating plant. Welding has, indeed, proved a persistent problem, and has delayed the full-power operation of the Dounreay PFR. The molten sodium used in the cooling circuits is highly corrosive. Void formation—the occurrence of gas bubbles in the coolant—is another major problem common to all FBRs and has still to be overcome.

Remaining hitches in reactor technology can, it is argued, be straightened out during the 20-year run-up to a commercial FBR network. But doubts linger over the associated fuel cycle. They arise not only at the technological level, where experience already gained by British Nuclear Fuels Ltd has been encouraging, if somewhat controversial, but also at environmental and political levels.

In a submission last year to the Royal Commission on Environmental Pollution (RCEP), which is due to publish a report on radiological hazards before Mr Benn's autumn decision, the UKAEA covered the environmental issues. Its arguments that the hazards of long-lived, highly active wastes can be satisfactorily controlled are likely to tip the scales in favour of the FBR. Mr Benn has indicated that the RCEP report will influence his decision, and it is now clear that the Commission itself, for some time reportedly divided over nuclear issues, will back CFR–1. In a recent reference to commercial FBR development Sir Brian Flowers, Chairman of the RCEP, said that while the implications and alternatives had not been explored with the level of resources and dedication devoted to the nuclear programme itself, he would not oppose the building of CFR–1 alone.

But the social and political implications of FBR reprocessing most worry those who believe that one step forward to CFR–1 will carry too much momentum for subsequent withdrawal. Though FBRs produce plutonium at a slower net rate than thermal reactors their proliferation would introduce the need for widespread plutonium transport. On UKAEA reckoning there could be 250 tons at various stages of the fuel cycle in Britain by the year 2000.

FBR opponents fear that the security measures required would be not far short of Draconian. A Bill to introduce the arming of nuclear security police has already been passed by the UK Parliament, and a US Government official this month called for an armed international security force. Additional doubts have been expressed about the sort of political arrangements needed to ensure worldwide adherence to safeguards such as those already implemented on a more limited scale by the International Atomic Energy Agency.

In France, the political and technological fears have led to civil disturbances involving qualified and well-informed opponents of the 1,200 MW Superphénix project now beginning on on the Rhône. But in Britain there is little public awareness of the issues. Sir Brian Flowers recently charged that the UK Government apparently preferred to keep things in the dark. Similar concern has also led the Liberal Peer, Lord Avebury, to call for a Green Paper once the RCEP report is available, and to hint that a national referendum would not be inappropriate. Mr Benn has said only that a questionnaire will be produced for limited, and so far unspecified, circulation.

Though it is clear that the case for

How the FBR is different

NUCLEAR power installations harness the heat energy released during controlled nuclear fission, and convert it into usable electricity. Fast breeder reactors (FBRs) differ from existing commercial reactors (known as "thermal" reactors) because, along with energy, they produce more fissile material than they consume—a self-sustaining bonus which could considerably stretch world uranium resources.

Like fast breeders, thermal reactors produce some plutonium but only in minute amounts. This is because more than 97% of the uranium used in thermal reactors fuel is non-fissile uranium-238, which is partially converted into plutonium while fission of the small fraction of uranium-235 proceeds. But plutonium is itself fissile, and most of it rapidly breaks down again, adding to the overall energy output of the system. (The Canadian CANDU reactor is designed to take full benefit of this phenomenon, optimising fuel efficiency.) Thus only about 1% of spent fuel from thermal reactors remains as plutonium.

On the other hand, the FBR can breed plutonium, using fast neutrons rather than the slow neutrons used in thermal reactors. Although fast neutrons are less efficient in inducing fission, the chain reaction they set up produces the greater number of additional neutrons needed to convert uranium-238. Consequently, the moderators used to decelerate fast neutrons in thermal reactors are absent from fast breeders.

The problem of decreased fission efficiency is overcome by pushing the neutron density in FBR fuel elements above the level achieved in thermal reactors. This means that the core assembly must be extremely compact, while the concentration of fissile material must be boosted way above the maximum enrichment factor of 3% needed in thermal fuel.

The 14 MW experimental FBR at Dounreay (DFR), for instance, uses 75% enriched metallic uranium in a core of little more than 100 litres. At Dounreay, as in all FBRs, the uranium-238 needed for breeding is located in a "blanket" around the core, where the neutron density is no longer sufficient to break down the fissile plutonium formed.

In assessing the doubling time of an FBR—the period required for the reactor to reproduce the amount of fissile material originally in the reactor core—the entire fuel cycle is considered. At any one instant, for example, fissile material may be within the reactor itself, undergoing cooling, reprocessing or refabrication, or in transport.

It is thus possible to control the doubling time by retiming any of the operations involved in the cycle. Current UKAEA plans envisage a doubling time of about 28 years for Britain's first commercial FBRs early next century, a figure that neatly matches the expected expansion rate of the reactors themselves.

With the high neutron density in an FBR core, heat is generated more efficiently than in thermal reactors. Thus, while most thermal reactors operate at temperatures well below 300 °C, the 250 MW prototype FBR at Dounreay (PFR) has a design outlet temperature of almost 600 °C. Fast breeder fuel elements must be designed to withstand the extra heat.

It soon became apparent that the metallic uranium core used in the DFR would melt at operating temperatures above 350 °C. As a result, the PFR is fuelled by sintered pellets of uranium oxide and plutonium oxide. Uranium-235 is not an essential component, however, and fast breeders of the future could be fuelled with fissile plutonium-239 alone, though uranium-238 breeding material would, of course, have to be present. It is in by-passing the need for the scarce uranium-235 isotope that the FBR can stretch available uranium resources.

The fast breeders so far developed in Britain, France, Germany, Japan, the USA and the USSR are all designed to use liquid metal coolant circuits to carry the heat away from the core. They are therefore known as liquid metal fast breeder reactors. By using sodium, which is normally molten between 98 °C and 880 °C, the unnecessary hazards associated with pressurised operation procedures can be avoided.

To minimise the risk of radioactive contamination, sodium circulated around the core in the primary reactor chamber passes its collected heat onto a secondary, external sodium circuit shielded from radiation. This circuit in turn carries heat to the steam generators.

FBR development has not run altogether smoothly. After 17 years operational experience with the DFR and the PFR, the UK nuclear industry is still struggling with problems in the steam generating plant of the PFR. The CEGB, however, which is prepared to have 20 GW of FBR capacity plugged into the national grid by the year 2000, has also declared a watchful interest in the development of helium-cooled fast breeders, which could provide an even better alternative to the liquid metal FBRs.

the FBR is far from open and shut, Mr Benn's view of international developments may persuade him to nod CFR-1 through. France, Germany, and the USA are all aiming for commercial FBR capacity by the 1990s, with Japan and Russia not far behind. UKAEA collaboration agreements already exist in one form or another with all of these countries, while the CEGB, currently chasing a minor share of the Superphénix project, also holds an interest in the German SNR-30 FBR prototype.

UKAEA feeling is that delays with CFR-1 will not help strengthen collaboration, perhaps damaging Britain's relative position in a commercial development race that will be run anyway. One man who disagrees is John Surrey, who last month resigned as nuclear adviser to the Select Committee on Science and Technology. He has argued publicly that Britain can learn much from the sidelines, and that restraint at this stage will allow the channelling of larger funds into other areas of energy R&D, including conservation. The UKAEA must hope that Mr Benn is unimpressed by that reasoning: it has already placed a contract with the Nuclear Power Company for design and engineering work "related" to CFR-1. On the question of a possible site, there has been official silence. □

Tracking nuclear decisions (3)

Exports: time for a stand?

Colin Norman in Washington examines the NRC's problems concerning the export of uranium to India

EARLY next month, the Nuclear Regulatory Commission (NRC) will decide whether to allow 12,261 kg of slightly enriched uranium to be exported to India. Its decision, the toughest it has yet faced, will have major foreign policy implications, for it will represent a crucial milestone in the United States' efforts to prevent the proliferation of nuclear weapons. In fact, it is the kind of foreign policy decision that is usually made by the President.

NRC is thrust into the middle of the issue because it alone has the authority to grant or deny an application for a licence to export nuclear material from the United States. Its decisions can only be overturned by an Act of Congress. In this instance, it has under consideration an application to export fuel for the giant Tarapur Atomic Reactor Station near Bombay, an American-built reactor which has been operating since the early 1960s with fuel supplied by the United States.

Understandably, NRC is treating the matter with considerable caution. Last week, it held a public hearing to receive testimony on the licence application—the first public hearing ever called to discuss a nuclear export licence—and it was given a wealth of conflicting advice. On the one hand, the State Department and the Commission's own staff recommended that the application be approved, while on the other, a powerful coalition of arms control experts, Congressmen, environmentalists and nuclear critics argued that the licence should be denied.

Underlying the debate, of course, is the fact that on May 18, 1974, Indian scientists exploded a nuclear device constructed from plutonium produced in a Canadian-supplied reactor. It was the first time that any nation had used imported technology to join the nuclear club, and as a result Canada earlier this year decided to bar any further nuclear assistance to India. Opponents of the request to ship enriched uranium for the Tarapur reactor are urging that the United States should follow Canada's example.

Representative Clarence D. Long of Maryland for example, told NRC that "our response to India is the first test of whether the United States has a real policy of stemming the spread of nuclear weapons". Similar sentiments were also expressed by Dr Herbert Scoville, former deputy Director of the Central Intelligence Agency, and Adrian Fisher, former chief negotiator for the Nuclear Non-proliferation Treaty (NPT). Fisher argued, for example, that "the continued supply by the US of nuclear fuel for the Indian atomic program can only be looked on by other nations as tacit approval by the United States of the Indian nuclear explosive program".

The United States has been supplying enriched uranium for the Tarapur reactor for more than a decade under a unique agreement. In short, the agreement specifies that the reactor can only be operated with fuel supplied by the United States, and that such fuel cannot be used in any other facility in India. The United States also has an option to buy back spent fuel discharged from the reactor—nearly 200,000 tons have so far been accumulated—and no reprocessing of that fuel can take place in India without US permission. Moreover, operation of the Tarapur reactor is subject to monitoring by the International Atomic Energy Agency (IAEA).

But India has an extensive nuclear programme in addition to the Tarapur reactor which is not covered by the agreement and which is not subject to international safeguards. The explosive device detonated in 1974, for example, was made from plutonium produced in a Canadian-supplied research reactor and separated in a small reprocessing plant built by the Indians themselves. And a new factor has recently been introduced because India has recently completed construction of a large reprocessing facility adjacent to the Tarapur reactor. According to State Department spokesmen at last week's NRC hearing, the facility is now undergoing tests and it will soon have the capacity to reprocess much of the spent fuel from India's entire nuclear programme. The construction of the plant has given India at least the capacity of building large numbers of explosive devices.

Opponents of the proposal to ship more fuel for Tarapur, led by the Natural Resources Defense Council, the Union of Concerned Scientists and the Sierra Club, argued at last week's hearings that, at the very least, NRC should deny the application until India has agreed to several stringent conditions. First, the Indian government should pledge not to construct further explosive devices. Second, the United States should exercise its option to buy back spent fuel already produced by the Tarapur reactor. Third, India should agree to place all its nuclear facilities under international safeguards. And fourth, India should agree not to reprocess any spent fuel, at least for the time being.

Clearly, the Indian government would not readily accept such conditions. But the opponents of the licence application point out that India would be hard pressed to find an alternative fuel supplier. The only other exporter of enriched uranium is the Soviet Union, and potential European exporters are at least ten years away from having significant export capacity. Thus, they argue that "if India wishes to avoid a shut-down of the Tarapur reactors, it may well have to deal with the United States, and the Commission has leverage to obtain non-proliferation ends".

But those views are not shared by the State Department. In a long statement delivered to the NRC last week, for example, Assistant Secretary of State Myron Kratzer argued that "the credibility of the United States as a reliable supplier of nuclear materials, equipment, and services is an essential element in achievement of our non-proliferation objectives". Kratzer argued that the US–Indian agreement covering the Tarapur reactor is sufficient to prevent diversion of its plutonium to weapons production. And he warned that if the United States refuses to ship more fuel for the reactor, the Indian government could claim that the original agreement had been broken and that the spent fuel is therefore no longer under safeguards.

Kratzer announced, however, that the State Department is looking into the possibility of taking up the option to buy back the spent fuel which has already accumulated from the Tarapur reactor.

One key issue which surfaced during last week's hearings concerns the extent to which the United States provided aid for the production of India's first explosive device. The Cirus reactor, which provided plutonium for the device, was moderated by heavy water bought from the United States on condition that it be used only for peaceful purposes.

When Senator Abraham Ribicoff last month drew attention to the possibility that American material had helped India produce its first atomic blast, the State Department demurred. It argued that, by the time the Cirus reactor began producing plutonium for the device, the US-supplied heavy water had been replaced with heavy water manufactured in India. Kratzer confirmed last week, however, that some US-supplied heavy water was probably still in the reactors at the time India used it to manufacture plutonium for the explosive. Consequently, critics of the proposed fuel sale argued that India cannot be trusted to abide by its pledges not to develop nuclear weapons.

The nub of this whole dispute is really that the opponents of the application are arguing that the time has come for the United States to make a public demonstration that it is serious in its efforts to deter the spread of nuclear weapons, while the State Department is arguing that abrogation of the agreement to fuel Tarapur would jeopardise those US non-proliferation policies. The four NRC commissioners will be hard put to decide which side is correct.

At this stage, it's difficult to predict with certainty what the Commissioners will decide, but at least there is a clue. Earlier this year, there were two applications outstanding for exports of fuel for Tarapur—the 12,261 kg which was the subject of last week's hearings, and a separate shipment of 9,165 kg. Because at least one shipment was required urgently to avoid shutdown of the reactors, NRC approved the export of the smaller quantity on July 2. It did so by a vote of 3 to 1, but explicitly stated that the action would not prejudice its consideration of the second licence application. Its final decision will probably be made in the first week of August. □

IN BRIEF

Stever's appointment

After weeks of uncertainty and delay, President Ford last week nominated Dr H. Guyford Stever to be his science adviser and the first Director of the new White House Office of Science and Technology Policy (OSTP). Stever's nomination must be confirmed by the Senate, but swift approval is expected. The appointment was delayed because four right-wing Republican Senators last month criticised Stever's record as Director of the National Science Foundation and urged Ford not to nominate him for the White House post. The delay has ensured that OSTP will have little influence for several months. The Ford Administration's longevity is in considerable doubt, and with the election in full swing, few people will pay attention to the office. Nevertheless, President Ford can at least claim that he has restored science advice to the White House.

The axeman cometh

The £1,000 million public expenditure cuts announced by the UK Government last week, which are due to take effect in 1977–78, have not left science-related activities unscathed. With the axe falling on capital investment programmes of the nationalised industries, the energy sector (with the exception of the British National Oil Corporation) is particularly hard hit. Coal, gas and electricity will be seeking a total saving of about £70 million through deferred projects. Apart from the Selby coal scheme, this may involve a 12-month postponement on the Steam Generating Heavy Water Reactor and a cutback on research and development of the fast breeder reactor. A cut of £100 million is being sought from the Ministry of Defence: most of the cuts will be achieved by removing or rephasing existing programmes, and research work may not escape. At the Department of Education and Science the science budget will be cut in 1977–78 by £5 million. Details have yet to be made known, and it is thought that advice from the Advisory Board for the Research Councils will be sought before final decisions are made.

Geothermal energy research programme

A three-year programme of geothermal research in the UK is to be supported by the Department of Energy following the publication of a report, *Geothermal Energy: the case for research in the United Kingdom* (HMSO, £1.85). The report, by Dr J. D. Garnish of the Energy Technology Support Unit (ETSU), Harwell, reckons that likely returns warrant a modest research programme of collection and refinement of data.

Interest centres on two techniques—the extraction of hot water from aquifers in sedimentary basins or near springs, and the hydrofracturing of rocks, usually granite, with a higher than average temperature. Temperatures likely to be encountered with either technique are in the 100 to 200 °C range.

Much of the £840,000 involved in the research programme (which ETSU will supervise) will go to the Institute of Geological Sciences for data gathering, particularly in Cornwall, Durham, Bath, Bristol, the Hampshire Basin and the Midland Valley of Scotland. Imperial College and Oxford University are also likely to receive support.

Plea for prisoners

Two scientists, Sergei Kovalyov (Soviet Union) and Sandor Arancibia (Chile) were the subject of appeals by a group of distinguished biologists on the occasion of international congresses of endocrinology and biochemistry in Hamburg recently. Kovalyov, an electrophysiologist, was sentenced in December 1975 to seven years in prison and three years exile for anti-Soviet activities. Arancibia, a neuroendocrinologist, was given a life sentence—he had been a prefect in the Valdivian region before the 1973 change of regime. Signatories included A. Lwoff, F. Jacob, J.-P. Changeux, F. Gros, F. Morel, Y. Laporte, E. Baulieu, J. Nunez, C. Kordon, C. B. Anfinsen, C. deDuve, G. Wald, D. Baltimore, R. Dulbecco, S. Luria, A. Szent-Györgyi, J. D. Watson, H. Krebs, H. Temin, J. Axelrod, V. Ramirez, L. Martini and J.-P. Waller. They call on Mr Brezhnev and General Pinochet to free their colleagues strictly for humanitarian purposes since "their lives are in danger and those of their families are broken".

news and views

The history of the term 'ionosphere'

from C. S. Gillmor

FOR more than four decades the term "ionosphere" has been used to designate the ionised regions from about 60 kilometres to some thousands of kilometres above the Earth's surface. These regions were not always so named. In the first years after G. Marconi's demonstration in 1901 of trans-Atlantic radio communication, some pioneers of wireless, such as A. E. Kennelly, O. Heaviside and J. Erskine-Murray, designated the upper atmospheric region which supposedly played a part in long distance radio transmission as the "upper reflecting surface" or the "conducting layer". Many others, of course, believed no such ionised region existed. Discussion was stimulated by G. Marconi's lectures where he described the difference between day and night transmission (Marconi, *Proc. R. Soc. A.*, **70**, 344–347; 1902). Marconi termed the "day effect" (what would later be called the "night effect"), the phenomenon that radio transmission during the daytime seemed possible over a distance only two-fifths as great as that at night. Marconi's original explanation was that this was due to local effects of sunlight on the transmitting antennae. Others attributed the effect to increased ionisation of the upper atmosphere by the Sun.

The work of W. H. Eccles, L. de Forest, and L. F. Fuller just before World War I (Tuve, *J. atmos. terr. Phys.*, **36**, 2079–2083; 1974) stimulated a great debate on the nature and effective height of the upper region. Though Eccles suggested the name "Heaviside layer" in 1912 (Eccles, *Proc. R. Soc. A.*, **87**, 79–99, 1912), no single term emerged. L. W. Austin, O. Lodge, L. Cohen, G. W. O. Howe and others spoke of the "upper atmosphere", "upper conducting layer", "far upper regions", and "ionised upper atmosphere". Following World War I, Eccles' term was revived and "Heaviside layer" ("Kennelly-Heaviside layer" according to some), became the most frequently used term with "upper conducting layer" the next preferred.

By the early 1920s it was not so clear that "Heaviside layer" should be synonymous with the upper ionised regions of the atmosphere because various geophysical phenomena were known to occur at different heights in the upper atmosphere. A. Schuster called them the "upper conducting *layers*" (Schuster, *Electrician*, **89**, 325; Sept. 22, 1922). W. H. Eccles pointed out that the "night effect" was probably caused by the lower edge of the upper region of the atmosphere where free electrons "exist more or less permanently" (Eccles, *Electrician*, **94**, 208; Feb. 20, 1925). This lower edge is the Heaviside layer, he said, and it might be located higher or lower than the ionised region needed to explain the diurnal magnetic variations. Below this was the "middle atmosphere" where ions of molecular size are formed daily by sunlight. These ideas were not new, he said, but had been assumed long ago by students of wireless.

As a scientific specialty matures it concerns itself with standards of measurement, technique and nomenclature. This is evidenced by the actions of the British Radio Research Board (RRB), set up after World War I. In the autumn of 1921 the RRB Sub-Committee A, on Propagation of Wireless Waves, discussed (*RRB Sub-Committee A, Paper 27*; 1921) the recommendations of an international committee which had proposed standardising terms: "radio" in place of "wireless telegraphy"; "atmospherics" in place of "parasitics", "statics" or "X" (strays); "electronic tube" in place of "valve", "lamp" or "audion": and "antenna" in place of "aerial". In the spring of 1924 the Sub-Committee discussed (*RRB Sub-Committee A, Paper 68;* March 8, 1924) terms for the classification of radio emissions (Continuous Waves (CW) and modulated forms of CW, and Damped Waves). It was probably at some similar meeting in the autumn of 1926 that the question was raised of agreeing on a term to designate the entire atmospheric region or regions where ionised particles accounted for the major phenomena. In fact, R. A. Watson-Watt referred to recent discussions on nomenclature in a letter to the Secretary of the RRB. In this letter (Gardiner, *Nature*, **224**, 1096; 1969), dated November 8, 1926, Watson-Watt suggested the term "ionosphere" in place of what had been loosely termed the "upper conducting layer", and mentioned the analogy to stratosphere and troposphere.

Now it seems that E. V. Appleton was thinking similarly, for in a letter (*Edinburgh University Library, MS. Gen. 1985/21*) to J. A. Ratcliffe dated November 2, 1926 Appleton wrote:

> "For the ionised part of the upper atmosphere I think the terms ionosphere or electrosphere might be useful. Which do you prefer? Cf. Stratosphere & Troposphere".

Watson-Watt and Appleton had numerous opportunities in those days for conversation at the Radio Research Station at Slough, at meetings of the RRB, and at King's College, London. In spite of the RRB discussions, "ionosphere" seems at first to have fared little better than the terms designed to replace "wireless" or "valve". The first to use the term "ionosphere" in print was Watson-Watt in 1929 in the Symond Memorial Lecture to the Royal Meteorological Society (Watson-Watt, *Q. Jl R. met. Soc.*, **55**, 273–301; 1929). He noted:

> "It might be permissible to call it the Balfour-Stewart-Fitzgerald-Heaviside - Kennelly - Zenneck - Schuster -Eccles-Larmor- Appleton space, but something less direct is desirable. I have suggested the name ionosphere to make a systematic group troposphere, stratosphere, ionosphere but meanwhile the term 'upper conducting layers' seems to hold the field".

The term was next used, in its German form "ionosphäre", by H. Plendl who, independently, suggested it early in 1931 and used it in articles published later that year (Plendl, *Jb. dt. Vers Anst. Luftf.*, 665–671; 1931).

"Ionosphere" came into use widely beginning only in the period 1932-1934 when Watson-Watt, Appleton, Ratcliffe, W. Dieminger, I. Ranzi, D. F. Martyn, S. K. Mitra and others began to use the word in the *titles* of published papers and lectures. An example of its legitimisation was the prominent use of "Ionosphere" in the Kelvin Lecture delivered at the Institution of Electrical Engineers in April 1933 by Sir Frank Smith, Secretary of the Department of Scientific and Industrial Research (Smith, *Electrician*, **110**, 581–582; May 5, 1933). It was thus that the term began to appear in library indices and abstracting categories. It then began to be used in related forms; the pulsing vertical incidence radar became known as the ionosonde, and ionospheric workers were sometimes known as ionospherists. Use of the term was at its relative maximum during the early 1950s when about 35% of all published papers on ionospheric physics (Manning, *Bibliography of the Ionosphere*, Stanford University Press, Stanford, California, 1962) had the word ionosphere or a form of it in their titles. This trend has reversed as other specialties have developed out of ionospheric physics and terms such as "magnetosphere" and "STP" (solar–terrestrial–physics) have come into common use to designate many subjects which formerly were included primarily within the specialty of ionospheric physics. ☐

Transformation and tumorigenicity

from Robert Shields

SOME recent observations on the properties of cells transformed by mammalian tumour viruses and their ability to cause tumours when injected into the commonly used nude mouse, raise several questions on the validity of treating these experimental systems as a model for real cancers.

Ever since the first mammalian cell cultures were transformed by tumour viruses a great deal of effort has been expended in attempts to understand the process of oncogenic change *in vitro*. Studies using a few cell types and even fewer viruses have collected an enormous number of *in vitro* cellular properties that are often associated with tumorigenicity. These include changes in cellular morphology, increased cell autonomy, loss of density-dependent inhibition of growth, decreased dependence on high levels of serum in the culture fluid, increased agglutinability by plant lectins, changes in membrane composition, increased ability to grow in gel suspension (loss of anchorage dependence) and so on and so on. What is a pity is that much of the work on these properties has been performed on established lines of virally transformed cells so it has been impossible to unravel which changes are caused by the virus and which have arisen through selection in culture.

One way around this problem has been to select at random clones of 3T3 or primary rat embryo cells recently infected with SV40 and examine each clone for various parameters of transformation (Risser and Pollack, *Virology*, **59**, 477, 1974; Risser, Rifkin, and Pollack, *Cold Spring Harbor Symp. quant. Biol.*, **39**, 317; 1974). In this way it was hoped to find which parameters of transformed cells are related to the viral gene, which changes are related to each other, and which changes confer tumorigenicity.

The results from these experiments showed that the virus was able to elicit a whole spectrum of changes. The only alteration in some clones of 3T3 cells was that they could grow in low concentrations of serum, and that they could grow to higher cell densities. These cells were negative for the virus-specified T antigen, no virus could be rescued from them and the cells could be fully transformed by reinfection with SV40. All this suggests that these changes may be caused by a hit and run action of the virus rather than by the continued presence of the viral gene.

The only *in vitro* cellular property that correlated with the ability of the cells to cause tumours in nude mice (which lack cell-mediated immunity), was their ability to grow in methocel suspension (anchorage independence) (Shin *et al.*, *Proc. natn. Acad. Sci. U.S.A.*, **72**, 4435; 1975) and this property was in turn correlated with the ability of the cells to produce a protease that converts plasminogen in the serum to plasmin (Pollack *et al.*, *Proc. natn. Acad. Sci. U.S.A.*, **71**, 4792; 1974). These experiments were performed with only two cell types and one transforming agent but many other reports have suggested a correlation between anchorage-independent growth and tumorigenicity (Freedman and Shin, *Cell*, **3**, 355; 1974; Laug *et al.*, *J. natn. Cancer Inst.*, **54**, 173; 1975).

The correlation between growth in suspension and tumorigenicity is far from absolute, however. Examination of epithelial cell lines derived from a number of human carcinomas show that some cells grow in suspension and fail to form tumours in nude mice, some anchorage-dependent lines are tumorigenic and furthermore there is no correlation between the ability to activate plasmin and either growth in suspension or tumorigenicity (Marshall, Franks and Carbonell, personal communication; Pearlstein *et al.*, *Cancer Res.*, **36**, 1575; 1976; Jones *et al.*, *Int. J. Cancer*, **16**, 616; 1975).

These observations raise several questions not least of which is the suitability of the commonly used 'fibroblast' cells and their viral transformants as suitable models for real cancer, but also the use of the nude mouse as a means of detecting tumorigenicity.

There have been mutterings about established cell lines such as 3T3 for some time, especially because of their heteroploid karyotype. It is now clear, however, that the BALB/c3T3 cell line is frankly tumorigenic when attached to glass beads and innoculated into suitable hosts (Boone, *Science*, **188**, 68; 1975). Moreover, the tumours formed are 'vasoformative sarcomas' (Boone *et al.*, *Cancer Res.*, **36**, 1626; 1976) so it seems that these cells are not fibroblasts but arise from endothelial tissue. In fact, a great many cell lines established from a wide variety of tissues appear to be derived from the endothelial cells and pericytes of small blood vessels (Franks and Wilson, *Eur. J. Cancer*, **6**, 517; 1970), so many of the different established cell lines may represent a very restricted sample of the variety of cell types in the body.

Studies of the incidence with age of a great many naturally occurring cancers in man lend support to the hypothesis that cancer cells arise after a small number of heritable changes have occurred in a normal cell. Presumably the altered cell becomes a successful cancer if these changes result in it being better able to proliferate than the cell type it comes from. There is no reason to suppose that the changes which confer a selective advantage on one cell type in one environment will confer selective advantage on another, nor even that selective advantage within a given tissue need arise through a unique series of steps; other pathways could be equally effective. As a consequence tumour cells from widely different tissues might be expected to have widely different properties when studied *in vitro*. After all what is good for the endothelial cell may not be so good for the bladder.

Such generalisations that have been drawn about the nature of neoplastic change from the use of cultured cells may simply reflect the small number of cell types examined and the even smaller number of oncogenic agents.

•

Mars from Viking 1

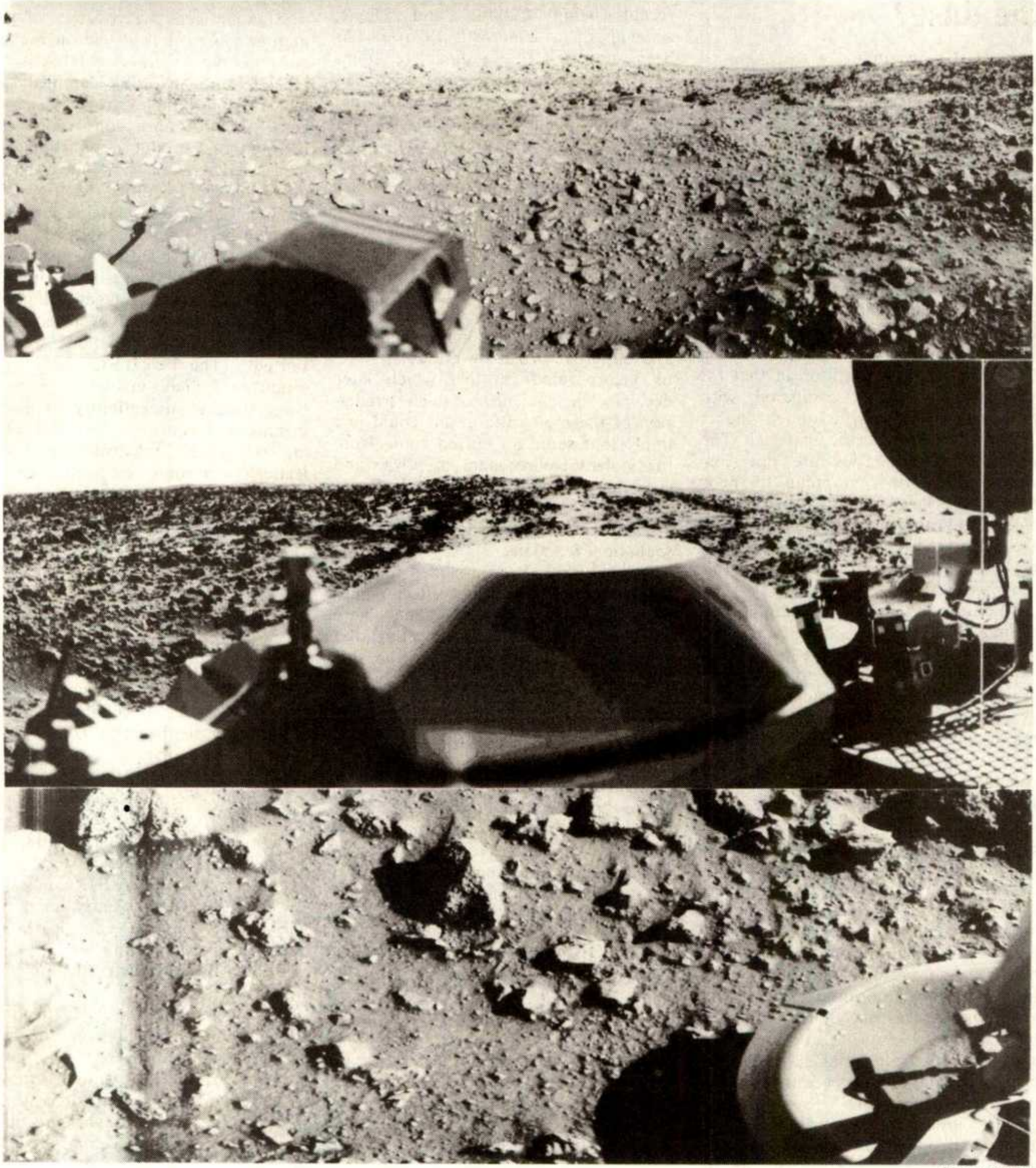

Photo: NASA

THE top two pictures provide the first panorama of the Martian landscape as seen from Viking 1, taken in the late Martian afternoon. A plateau can be seen on the horizon to the left of the top picture, approximately 3 kilometres (1.8 miles) away. The out-of-focus spacecraft component left of centre is the housing for the sample arm (which is now in full working order after becoming jammed when first tested). The centre photograph is the continuation to the right of the 300° panorama. At left is the low-gain antenna which receives commands from Earth. In the right foreground are colour charts for lander camera calibration, a mirror for the Viking magnetic properties experiment and part of a grid on the top of the lander body. At upper right is the high-gain dish antenna for direct communication between the landed spacecraft and Earth. Toward the right edge is an array of smooth fine-grained material which shows some hint of ripple structure and may be the beginning of a large dune field off to the right of the picture.

The bottom picture, the first ever of the surface of Mars, was taken minutes after the spacecraft landed.

Do exploding stars leave tracks in the dust?

from M. G. Edmunds

HAVE grains of dust, formed in the explosion of stars, managed to survive incorporation into Solar System meteorites? A most interesting observation, although unfortunately open to rather ambiguous theoretical interpretation, has recently been reported by J. Audouze and co-workers (*Astrophys. J. Lett.* **206,** L185; 1976).

They examined micron-sized grains extracted from a separated part of the Orgueil meteorite. The material from which these grains came shows an unusual chemical composition in that the abundance of ^{22}Ne, compared with other neon isotopes, is much higher than in most meteoritic material. The unusual isotope ratios are not consistent with either trapping of neon from the solar wind, or with creation of neon by nuclear reactions involving the impact of high-energy cosmic ray particles. The origin of the excess ^{22}Ne remains disputed.

Audouze *et al.* use a technique of chemically etching the radiation damage tracks left by the passage of energetic heavy ions through the grains. The etched tracks can be examined with a high voltage electron microscope. They found tracks in those grains which appeared amorphous and rounded, and the density of tracks implies that these grains have been strongly irradiated at some time. Andouze *et al.* take the view that the irradiating particles were probably heavy ions with masses comparable to iron nuclei. An experimental exposure to a beam of iron nuclei caused crystalline grains (which did not initially have tracks) to show tracks similar to those found in the amorphous grains. By assuming the currently observed ratio of heavy ions to protons in cosmic rays and particles from solar flares, a net proton irradiation can be estimated for the amorphous grains.

One interpretation of the ^{22}Ne anomaly is offered by production from spallation nuclear reaction of the irradiating protons on ^{25}Mg, but this requires that the energy spectrum of the protons has a rather peculiar "pulse" shape to avoid overproduction of the other neon isotopes. A high flux of particles might have occurred during the early history of the Solar System, but the observed irradiation would imply a very much higher flux of particles from the Sun at early times compared with that observed today.

A second interpretation is perhaps more interesting. It may be possible for grains to condense in the expanding envelope of gas generated by the supernova or nova explosion of a star. In a series of papers (the most recent being Clayton and Hoyle, *Astrophys. J.*, **203,** 490; 1976) it has been suggested that radioactive atoms from the explosive nucleosynthesis occurring in novae or supernovae could become trapped in the grains as they condense. If these grains could subsequently survive the physical conditions during the formation of the Solar System and be incorporated into meteorites, then the products of radiodecay of the nuclei trapped in the grains could show up as isotopic anomalies. The excess ^{22}Ne for example might come from the decay of ^{22}Na produced in explosive nucleosynthesis, and either absorbed by grains as ^{22}Ne, or incorporated as ^{22}Na which later decays. The evidence of high irradiation of the meteoritic grains could just imply that some do indeed come from the violent environment of novae and supernovae where high particle fluxes are expected. The particle flux could also provide some additional ^{22}Ne by spallation reactions.

It has usually been assumed that the meteoritic isotope ratios reflect conditions in the early Solar System. There exists a real difficulty in accepting that grains from novae or supernovae survive into meteorites. Such grains would bring other isotopic anomalies with them which would upset the elegant inferences about the timescales involved in the formation of the Solar System drawn from isotope ratios (so-called "nucleocosmochronology"). But there are plenty of isotopic anomalies, and a surprising lack of them for certain elements, to keep discussion alive before a revision of timescales is accepted. Audouze *et al.*'s paper at least indicates that violent irradiation of grains existing when the meteorites formed did occur somewhere, and has to be explained. □

HLA and disease

from G. Nicholas Rogentine Jr

> The First International Symposium on HLA and disease was held in Paris on June 23–25. It was organised by J. Dausset and A. Svejgaard. The proceedings will be published as a book.

BASIC and clinical scientists gathered in Paris to try to understand the meaning of the association of HLA antigens with disease. While the meeting did not fully achieve this goal, it did establish clearly that many highly significant HLA antigen frequency perturbations exist in a remarkable variety of human diseases.

HLA antigens are products of genes at four closely linked loci on the sixth chromosome. HLA-A, HLA-B and HLA-C antigens are identified serologically on lymphocytes. These antigens are found on most cell membranes. Products of the fourth locus, HLA-D, are defined by the mixed leukocyte culture reaction; these products or closely related ones also seem to be B-lymphocyte alloantigens.

Most of the exciting new data was presented in the workshops, organised according to disease classification. Well established associations were confirmed and many new correlations were reported. The clearest, all highly significant and involving increases (suggesting a susceptibility to disease) in antigen frequency, were the following: HLA-B27, ankylosing spondylitis, Reiter's syndrome and acute anterior uveitis; HLA-Dw4, rheumatoid arthritis; HLA-Dw2 and HLA-B7, multiple sclerosis; HLA-Dw3 and/or HLA-B8, gluten-sensitive enteropathy, dermatitis herpetiformis, myasthenia gravis (in young females without thyomas), juvenile diabetes, Graves' disease, chronic active hepatitis and Sjögren's syndrome; HLA-B5, Behcet's disease; HLA-A3, idiopathic haemochromatosis; HLA-A2, childhood acute lymphocytic leukaemia; HLA-A2 and SIN2, nasophanyngeal carcinoma in Chinese; HLA-A1, Hodgkin's disease; HLA-Bw40, oesophageal carcinoma in Northern Iranians. In Orientals, who as a race do not have HLA-B8, myasthenia gravis and Graves' disease were associated with HLA-B12 and HLA-Bw35, respectively. Nearly all patients with gluten-sensitive enteropathy and dermatitis herpetiformis are also positive for a B-lymphocyte alloantigen not linked to HLA.

A strong theme unrelated to disease susceptibility emerged from the workshop on malignant diseases: the possession of certain HLA antigens may be associated with long term survival. This has been seen in acute lymphocytic and acute myelocytic leukaemia, Hodgkin's disease, and bronchogenic carcinoma. These observations need confirmation by large scale prospective studies.

What do these associations mean pathophysiologically? As suggested by H. McDevitt (Palo Alto), many correlations could be explained by invoking a pathogenically active immune response gene in linkage disequilibrium with the disease-associated HLA gene, the latter being merely a marker. Linkage disequilibrium is known to occur all along the HLA region and, by analogy with mice, immune response genes probably reside in this area, too. But proof of a human immune response gene does not exist yet. R. Zinkernagel (La Jolla) and G. Shearer (Bethesda) suggested that HLA antigens are directly involved in the disease process by analogy with their findings with mice—the "altered self" hypothesis, in which histocompatibility antigens are modified by viruses or other substances rendering them susceptible to attack by autologous T lymphocytes. A. Svejgaard (Copenhagen) speculated that HLA antigens might competitively inhibit binding of various non-immune ligands, hormones, for example, and in this way provoke disease. F. Lilly's (New York) work with murine Friend virus leukaemogenesis suggests that some D-region H-2 antigens are receptors for leukaemia virus and thus participate directly in disease susceptibility. The mouse D region seems to be analogous with the human HLA-A locus. This locus is implicated in leukaemia, Hodgkin's disease and nasopharyngeal carcinoma.

Although no definite pathophysiological links between HLA and disease have been found, in at least two disorders—gluten-sensitive enteropathy and chronic active hepatitis—they may be discovered soon. Both these diseases have known causal agents and disordered immunity. Both are HLA-Dw3 or HLA-B8-associated.

J. Dausset (Paris) emphasised several areas where these associations might be clinically useful. One interesting area is preventative medicine and early diagnosis Any HLA–disease association necessarily implies a greater risk of developing the disease in a person who has that particular antigen. The relative risk for developing ankylosing spondylitis in HLA-B27 positive Caucasian males is about 90 times that of HLA-B27 negative males. Although most HLA-B27 positives do not develop this disease, nevertheless, they are more likely to do so than the B27 negatives. Knowing these risk factors can help focus awareness on the kinds of diseases most likely to affect each individual during his lifetime. It is not too far-fetched to expect that establishing HLA types will become an integral part of preventative medicine and health maintenance in the future. ☐

A hundred years ago

LIEUT. CHRISTIE, R. E., writing to us from Madras with regard to the use of selenium in telegraphy, says that if we could do away with the man (or woman) signaller, and substitute a commutator actuated by a current of electricity generated by the action of light upon a piece of selenium, we should (supposing the sensitiveness of the selenium to be adequate) have a combination capable of enormously increased rapidity. The message to be transmitted would be first set up (by mechanical means) in the Morse character, in long and short *slits* in an opaque screen; and this perforated screen being passed rapidly between the selenium and a source of light, the currents of electricity would be generated which are required for actuating the commutator. The possibility of such a combination depends on the sensitiveness of selenium to the influence of light. Assuming the combination to be possible, the rapidity of signalling would seem to be limited only by either the mechanical conditions of the commutator (or relay), or the power of the printing instrument at the receiving station.

THE Vienna earthquake, to which we referred last week, occurred on July 17 at 1.22 P.M. The principal seat of the commotion was Scheibbs, a small country place forty miles west of Vienna; almost every house in Scheibbs has been damaged. The area of the commotion was very large, equal to about two-thirds of England. It reached Austria proper, Moravia, part of Bohemia, and Hungary. The last earthquake in Vienna was on January 3, 1873. Fifteen instances of earthquake have been recorded in Vienna from the beginning of the thirteenth to the end of the eighteenth century. None of them produced any real damage, except those of September, 1590, and December 4, 1689.

from *Nature*, **14**, July 27, 279; 1876.

r, K and evolution

from Peter D. Moore

THERE is a taxonomic imperative in man which makes him delight in pigeon holes and simple labels. One of its most recent products in the ecological field has been the concept of *r* and *K* selection, whereby organisms can be classified along a continuum according to the proportion of their energy expended on reproduction. A high proportion results in a high initial rate of population increase (*r* in the logistic equation describing population growth). In unstable, unpredictable habitats, selective pressures operate in favour of this type of organism, whereas such taxa are at no advantage in stable environments.

Within many groups of organisms it is possible to recognise species which tend towards one end or other of the *r–K* continuum. For example, Southward *et al.* (*Am. Nat.*, **108**, 791; 1974) have considered its application to birds and Lepidoptera, and come to the conclusion that *r*-selected organisms are more likely sources of evolution and speciation than are *K*-selected organisms. Some rapidly evolving plant taxa even seem to have an *r–K* spectrum exhibited within a species or microspecies cluster, for example, in dandelions (Solbrig and Simpson, *J. Ecol.*, **62**, 473; 1974) and in sunflowers (Gaines *et al.*, *Am. Nat.*, **108**, 889; 1974).

Two further examples of this evolutionary process have now come to light, the kidney vetch (*Anthyllis vulneraria*) in Europe and the bigberry manzanita (*Arctostaphylos glauca*) in North America. Sterk (*Acta. bot. neerl.*, **24**, 315; 1975) has examined the population dynamics of coastal and inland populations of *Anthyllis* in the Netherlands. In the open, unstable, coastal sites the population density fluctuated from year to year. Mortality seemed to be related to stresses in the abiotic environment, such as drought, whereas mortality in the inland, stable sites was the outcome of competitive interplay. In the inland sites, fewer flowers were produced per plant than at the coast and flowering began when the plants were older. The data seem to conform with the idea of a relative *r* and *K* selection being operative respectively at the coast and inland sites.

Vasek and Clovis (*Am. J. Bot.*, **63**, 189; 1976) describe two ecotypes of *Arctostaphylos glauca*, one an upright shrub of the chaparral, and the other a low, spreading plant of desert pinyon woodland. Apart from these morphological differences, the two ecotypes differ in their flowering behaviour. The chaparral ecotype produces almost double the number of flowers, is more seasonally constrained in its flowering, and the total amount of fruit produced is about five times that of the desert ecotype. The morphological adaptations of these plants can be related to climatic conditions; fruiting potential may be a consequence of disturbance of the chaparral by frequent fires. In the more stable desert community, vegetative reproduction (by layering) becomes possible and seed production is therefore of lesser importance. Once again it can be argued that these ecotypes represent a genetic divergence in response to *r* and *K* selection in these habitats, but in this case the contribution of vegetative spread to the reproductive capacity of the "*K*-selected" ecotype complicates the issue. Seed production is easily measured so it is tempting to use this as an index of a plant's capacity to expand its population rapidly (high '*r*'). But in many plant species this represents only a portion of the total energy resource devoted to reproduction.

If the selective pressures of stable environments always favour a reduction in seed output, how does one explain the figures of Salisbury (*Proc. R. Soc., Lond.*, **B188**, 183; 1975, and **192**, 323; 1976) concerning seed production in plants? Within a single habitat, such as calcareous grassland, there is a considerable range of seed production per plant, for example, *Thesium humifusum*, produces 100 per plant, *Polygala calcarea*, 270; *Carlina vulgaris*, 680, *Anacamptis pyramidalis*, 35,000; *Senecio jacobaea*, 50,000; *Orchis maculata*, 56,000 and *Orobanche elatior*, 98,000 As Salisbury points out, these figures relate most closely to the relative risks experienced with different mechanisms of seed dispersal, wind being more risky (and therefore more wasteful) than animal dispersal.

Salisbury (1976) quotes *Juncus effusus* and *J. tenuis* as an example of contrasting seed production resulting from the use of different dispersal mechanisms *J effusus* produces between 1 5 and 3 million seeds per plant (wind dispersed) whereas *J. tenuis* produces 3,000–4,000 (adhesion to animals and vehicles). Thus two species of the same genus, both occupying unstable habitats, in the successional sense, differ in their seed production by three orders of magnitude.

Evidently there are several evolutionary answers to any environmental problem. In a given set of conditions, the output of seed from a taxon is influenced by such factors as the relative importance of vegetative reproduction and the seed dispersal mechanism used, as well as any response to the stabiltiy (*r*–*K*) gradient The simplest answers may be the most attractive, but they are not necessarily the most complete ones. □

Aggression in sticklebacks

from John Krebs

THE question of how different types of aggression in animals are related to one another has been a source of continual controversy. Aggressive behaviour in natural conditions is usually seen in competitive social encounters between members of the same species, for example in territorial defence and dominance disputes On the other hand many experimental laboratory studies have been concerned with attacks directed at inanimate objects or at members of another species (for example a rat attacking a mouse). There have been few attempts to examine whether or not aggression in these different contexts depends on a common internal mechanism.

In a recent study F. A. Huntingford (*Anim. Behav.*, **24**, 245–260; 1976) has examined this question. Using that traditional ethological beast, the three-spined stickleback, she carried out a series of experiments to test whether individual males which were highly aggressive in one context would also score high in other situations. It has long been known that a male stickleback will vigorously attack a 'rival' male which is presented to him near his nest in a glass tube. Huntingford used this technique to compare the aggressive response, measured by biting and lunging, to a rival male, a male of the closely related but quite distinct ten-spined stickleback, and a female smooth newt (a common inhabitant of the streams favoured by sticklebacks). Briefly, she found that the aggression scores for individual males to all three stimuli were well correlated. In two further experiments, Huntingford measured the reaction of the same group of males to a predator (a pike) and to being placed in an unfamiliar tank She analysed these results by Principle Components Analysis and was able to identify a group of behaviours which could be classified as indicating 'boldness'; these included approaching the pike and showing normal swimming movements. Individuals which had scored high on the aggression tests also tended to be bold in the face of a predator and in an unfamiliar tank, and this was not simply a result of higher overall activity.

These results suggest that territorial aggression and aggression against predators may depend in part on common internal factors. Huntingford points out that this makes evolutionary sense, because stickleback populations exposed to heavy predation should not only tend to become timid in the presence of a predator, but also make themselves inconspicuous by not engaging in vigorous territorial displays. •

Chemistry does not define environment

from Peter J. Smith

IN the past, many workers have placed great reliance on chemical characteristics as indicators of the geological, and especially crustal, environments in which Archean basalts were emplaced. Some, for example, have seen the lack of crustal contamination observed in low-potassium tholeiites in greenstone belts as an important argument against the presence of sialic crust beneath the successions. Others have regarded the calc-alkaline affinities of certain greenstone basalts as evidence of an original island arc environment. According to Gill and Bridgwater (*Earth planet. Sci. Lett.*, **29**, 276, 1976), however, the use of chemical comparisons between modern basalts and Archean basic rocks to identify ancient environments must now be regarded as a questionable procedure.

Gill and Bridgwater base their case on a study of the Ameralik dykes of West Greenland. This heterogeneous group of metamorphosed minor basic intrusions, emplaced in 3,700–3,600 Myr old gneisses forming part of the western edge of the North Atlantic craton, has been affected variably by subsequent magmatic and tectonic events which enable a lower limit of 3,040 Myr to be placed on the dykes' ages. The total area of older sialic crust cut by the dykes exceeds 12,000 km^2, although there is no *a priori* reason for supposing all the dykes to have been emplaced in a single episode nor any for supposing all the dykes to have been derived from the same parent magma.

And the chemistry of the dykes suggests that any such suppositions would indeed be wrong Although all the dykes studied were basaltic, their compositions ranged from that of primitive basalts reminiscent of modern oceanic basalts to more differentiated types akin to iron-rich tholeiites of modern continental flood basalt provinces. Some of this variation is undoubtedly due to subsequent metasomatism; but Gill and Bridgwater conclude from Rare Earth Element patterns, Ni, Sr, Ti and Zr contents and other chemical indicators that much of it reflects a range of primary compositions.

If this is so, the dilemma is clear. The ridge-like Ameralik basalts, for example, were evidently not intruded into early ocean floor, although had they not equally evidently been intruded into granite gneiss their chemistry could have been taken incorrectly to indicate an oceanic origin. Moreover, these same ridge-like basalts are comparable in composition to greenstone successions in South Africa and Australia and some greenstone belts in the Canadian Shield. It is most reasonable, claim Gill and Bridgwater, to assume that the primary compositional variations represent differences in the depth of melting in the mantle and/or the speed at which the magmas rose to the surface. In other words, the variations reflect changes in the melting régime and/or degree of differentiation rather than differences in crustal environment (oceanic, continental, island arc). Ergo, inferences about crustal environment drawn from chemistry alone must be suspect. □

review article

Analysis of erythropoiesis at the molecular level

P. R. Harrison*

Recent work has clarified how different erythroid functions may be regulated during normal erythropoiesis, and have helped to define the role of the hormone erythropoietin. Studies with cell lines (Friend cells) capable of undergoing erythroid differentiation in culture have made possible a comparison of normal and leukaemic erythropoiesis, by the combined approaches of cell biology, molecular biology and somatic cell genetics.

Normal erythroid systems

ERYTHROPOIESIS has been recognised for many years as a useful model system for investigating how functions characteristic of a specialised differentiated cell are regulated in a coordinate manner within a single cell lineage. It is well established that erythroid cells as well as other blood cell types (almost certainly also including the lymphocyte population) are derived from a common haematopoietic stem cell (CFU-S, Fig. 1), and that commitment of CFU-S cells to a particular haematopoietic lineage is influenced by the microenvironment of particular haematopoietic organs. An elegant demonstration of the importance of such microenvironmental factors in commitment is in the classical experiments by Trentin and coworkers[1] which show that the type of haematopoietic cells formed (granulocytic or erythroid) changes dramatically in colonies growing across the junction of a plug of marrow grafted into spleen tissue The existence of the Steel (*Sl*) mutant in mice also demonstrates how a specific genetic locus can govern microenvironmental function in haematopoietic stem cell proliferation and differentiation, particularly affecting the erythroid lineage[2,3].

After commitment to the erythroid lineage, erythroid stem cells seem to proliferate for a few generations before becoming sensitive to the hormone erythropoietin[4]. An age structure therefore exists within the committed erythroid stem cell population; this is further demonstrated by recent techniques in which erythroid precursor cells are cloned *in vitro*[5–7] In the presence of erythropoietin, two types of colony are produced· the first appears within 2 d of culture and consists of small differentiated erythroid colonies (about 60 cells) which are presumed to arise from late committed erythroid stem cells (CFU-E, Fig. 1) of limited proliferative potential[5,6]. The second type of colony appears later (after about 10 d of culture) but comprises very large numbers (about 10^4) of differentiated erythroid cells[7,8]. These colonies are thought to arise by extensive proliferation of stem cells isolated soon after commitment to the erythroid line (BFU-E, Fig. 1).

Various groups of workers have attempted to analyse the regulatory mechanisms governing how committed erythroid stem cells differentiate to mature red blood cells, using various normal erythropoietic systems, for example, foetal liver during the hepatic phase of erythropoiesis. Recent work now seems to have established beyond reasonable doubt that foetal erythropoiesis is initiated by haematopoietic stem cells migrating from the yolk sac[9], rather than by stem cells originating *in situ* by inductive effects within the foetal liver itself[10] CFU-S stem cells reach maximum numbers in foetal liver from day 14 of gestation[11], whereas stem cells committed to the erythroid line reach a peak at the days 15–16 of gestation (that is at the time of maximum production of red blood cells), after which they decline rapidly[2].

For many years, several groups have sought to analyse the process of erythroid differentiation in molecular terms, using *in vitro* cultures of erythroid cells. It is now generally accepted that erythropoietin acts primarily by increasing the proliferation of committed erythroid stem cells and proerythroblasts which then differentiate into mature erythroid cells containing haemoglobin[12–14]. More recent work by groups at the Beatson Institute and Columbia University (Marks, Rifkind and coworkers) has been concerned with identifying the stage at which the globin genes become active during erythroid development and whether erythropoietin has any effect on the timing of these events. At the Beatson Institute we have tried to elucidate this question by determining the earliest erythroid precursor cell in which globin messenger RNA accumulates, using a novel autoradiographic procedure[15] for detecting cytoplasmic globin messenger RNA in fixed preparations of cells by *in situ* hybridisation with globin cDNA (that is, a highly radioactive transcript of globin messenger RNA prepared using reverse transcriptase). These studies show that globin messenger RNAs accumulate at the basophilic erythroblast stage (Fig. 1), but are not present in significant amounts in proerythroblasts from early foetal livers[16]. This conclusion is also consistent with conventional hybridisation studies[16] with immature erythroid cells obtained from total foetal liver cells by removing mature cells by immune lysis using an antiserum raised against erythrocytes[17,18]. Subsequent studies by the Beatson group have shown that elevated levels of erythropoietin enhance the accumulation of globin messenger RNAs in proerythroblasts, both in developing foetal livers *in vivo* or in culture *in vitro*, and in spleens of anaemic adult mice[19]. As suggested by Clissold[20], this result may explain her finding that immature erythroblasts isolated from severely anaemic rabbits, but not normal rabbits, are able to differentiate in culture without erythropoietin. This effect of elevated erythropoietin levels can have the result that globin messenger RNA and subsequently haemoglobin accumulate earlier than normal relative to other morpho-

---

*Address: The Beatson Institute for Cancer Research, 132 Hill Street, Glasgow G3 6UD, UK.

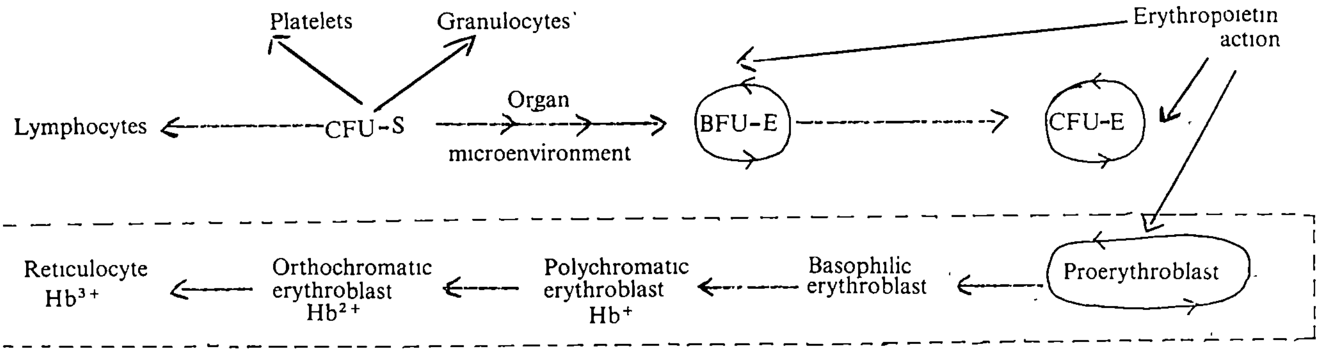

Fig. 1 Outline of formation of erythroid cells. Hb^{+}–Hb^{3+} cells containing increasing amounts of haemoglobin. The cell types in the dotted box represent the recognisable erythroid series.

logical criteria, so that an atypical series of macroerythroblasts may be formed[13,14] similar to that found in certain megaloblastic anaemias[21].

Independently, the Columbia group has arrived at basically similar conclusions. Immature erythroid precursor cells (80–90% proerythroblasts[22]) from foetal liver cells isolated by the immune-lysis procedure, contain negligible globin messenger RNAs as assayed either by translation in the Krebs ascites system[23] or by hybridisation with globin cDNA[24]. After culture of such cells for 10 or 22 h, however, the cellular level of globin messenger RNAs increases 5 or 100 times[24] during which time most of the cells differentiate to the basophilic erythroblast stage[22] and begin to synthesise globin chains[23], although haemoglobin is not detectable cytochemically until 44 h of culture[24]. These studies, therefore, also support the hypothesis that globin messenger RNA accumulation is enhanced between the proerythroblast and basophilic erythroblast stages of development; and further show that there is no pool of untranslatable globin messenger RNA in immature erythroid cells. However, the Columbia group find that treatment of cultures with erythropoietin does not increase the average cellular content of globin messenger RNA; although the number of globin messenger RNA-containing cells is greatly increased[24]. The explanation for this discrepancy may be in the doses of erythropoietin, or the degree of anaemia, involved in the two series of experiments.

The Friend cell system

Studies with normal erythropoietic systems are limited by the difficulties of obtaining large numbers of erythroid cells at specific stages of development, the short term nature of the *in vitro* culture systems, and the impossibility of performing genetic studies. The discovery by Dr Charlotte Friend of tissue culture cell lines which are capable of undergoing erythroid differentiation has therefore opened up new possibilities.

Friend cells were obtained by culturing fragments of spleens from mice infected with the Friend virus complex[25]. The nature and host control of Friend virus infection have already been reviewed in considerable detail[26,27] and will not be further considered here in spite of their importance and relevance. In interpreting any studies with Friend cells, it is, however, important to be clear about their relationship to normal erythroid precursor cells. Although this is still to some extent a subject of controversy[28], it seems most probable that the target cell for Friend virus is a late committed erythroid stem cell (CFU-E, Fig. 1). Two recent and compelling lines of evidence favour this hypothesis. First, the elimination of multipotential, but not erythroid committed stem cells, does not eliminate Friend virus-induced proliferation of erythroid cells in the spleens of polycythaemic mice; whereas no response to Friend virus is observed in mice in which the committed erythroid cell compartment has been depressed[29] Second, inoculation of lethally irradiated mice with normal spleen cells gives rise to erythroid, granulocytic and megakaryocytic colonies in the spleen; however, infection of such mice with Friend virus four days after grafting yields in addition hyperbasophilic (Friend cell) colonies solely within the differentiated erythroid colonies[10], although all types of haematopoietic colonies in the spleen are known to contain multi-potential stem cells[1]. Thus, although the number of non-erythroid cell types may also be affected[31], Friend virus seems to have specific effects on committed erythroid cells, rendering them capable of proliferation and differentiation independently of the hormone erythropoietin[32–34]. Friend cell lines established in culture seem to be transformed erythroid precursor cells selected by the culture conditions (or otherwise) which are arrested at the proerythroblast stage of development[25], and are not responsive to erythropoietin[35–37]. In this respect, Friend cells are therefore quite different from normal erythroid precursor cells. In fact, there is one report that Friend cells grown *in vivo* or in plasma clots *in vitro* do show manifestations of granulocytic differentiation[38], but this remains to be substantiated.

On treatment with dimethylsulphoxide (DMSO)[39] or a range of other chemical agents[40–43], Friend cells undergo a series of changes many of which are characteristics of normal erythroid cell differentiation; for example: chromatin condensation and other morphological changes resulting in a non-dividing cell[39]; accumulation of globin messenger RNAs[44–46] and strain-specific globins[47,48], increase in δ-aminolaevulinic acid synthetase activity[49] and haem synthesis[39]; erythrocyte-specific membrane changes[50,51] and an increase in the major erythrocyte-specific membrane protein (H. Eisen, personal communication); and an increase in carbonic anhydrase activity[52]. Changes in histone F2A2 subfractions also occur[53]. Thus, although Friend cells are abnormal in their dependence of the hormone erythropoietin, in certain conditions they do exhibit many characteristics of normal erythropoiesis.

Recently, Orkin *et al.*[54] have shown that during treatment of Friend cells with DMSO the ratio of α to β globin mRNAs decreases from about 3.5 to about 1.0, the value characteristic of the normal erythrocyte. Our own hybridisation studies performed with purified normal erythroid precursor cells[16], and also those of the Columbia University group[24], suggest, but do not prove definitively, that this differential timing of expression of the α and β globin genes is not a characteristic of normal erythroid cell development.

The mechanism whereby the various inducers of erythroid differentiation operate is not clear. Sieber[55] has made the interesting observation that DMSO enhances the sensitivity of normal CFU-Es, but not BFU-Es, to non-saturating doses of erythropoietin. This result may be related to the finding that Friend cells seem to be marginally sensitive to erythropoietin after DMSO treatment[35]. Certainly, membrane function seems to be involved since local anaesthetics prevent the action of all inducers of erythroid differentiation so far tested without affecting proliferation of Friend cells[56] *per se*.

Several circumstantial lines of evidence suggest that induction of differentiation in Friend cells requires some cell-cycle dependent process. McClintock and Papaconstantinou[57] have observed a correlation between the cell doubling time and the time of onset of haemoglobin synthesis. But Levy and his coworkers[18] made the surprising observation that treatment of Friend cells for 24–30 h is required before the intracellular space is equilibrated with respect to DMSO in the culture medium. Nevertheless, their results with synchronised Friend cells also suggest that the cells do require at least one period of DNA synthesis in the presence of DMSO for haemoglobin to be induced. In contrast, using a Friend cell line of independent origin (T3C12), Leder and Leder[19] have reported that the inhibition of DNA synthesis with hydroxyurea does not prevent the induction of haemoglobin by butyric acid.

We (P. R. H, D Conkie, A Wood, G. Yeoh and J. Paul, unpublished) have attempted to examine this problem at the single cell level, by cloning various Friend cell lines in methocel. In these conditions, most of the cells in clones grown in the presence of various inducers (DMSO, *N*-methylopyrrolidone, *N*-methylacetamide or butyric acid) produce haemoglobin within 3–4 d. Clones arrested at the single-cell stage by the action of hydroxyurea or cytosine arabinoside, or by omission of isoleucine from the culture medium, however, fail to produce haemoglobin; whereas many of the doublet colonies (or binucleate single cells) in the same cultures do produce haemoglobin. Moreover, single cells arrested for 3 d in inducer in the absence of isoleucine do proliferate and produce haemoglobin 4 d after addition of isoleucine. Thus, it seems quite clear that induction of haemoglobin synthesis in our Friend cell lines (which were obtained from Dr C. Friend as were those of McClintock and Papaconstantinou and Levy *et al.*) are dependent on some process within the cell cycle, but that this does not necessarily involve asymmetric division since in many of the doublet colonies both daughter cells contain haemoglobin. Our studies with the T3C12 cell line seem to suggest, in agreement with the findings of Leder and Leder[59], that a considerable proportion of butyric acid-treated cells arrested with hydroxyurea can produce haemoglobin. Interestingly, in our experiments many of these haemoglobin-containing single cells are in fact binucleate. Thus the discrepancies between the various groups of workers may be more apparent than real, if some process before, or associated with, nuclear division is required for differentiation. Alternatively, butyric acid may act differently from the other inducers; it is also possible that the T3C12 cell line may have been transformed by Friend virus at a later stage of development. Resolution of this question is clearly of importance in elucidating whether, and at what stage, a critical cell division is involved in erythroid cell differentiation.

Friend cell lines are also a useful system in which to attempt more sophisticated molecular and genetic studies of erythroid differentiation. In our own laboratory, a three-stage strategy has been adopted. The first is to obtain stable non-inducible variants, second, these variants are then screened to find out at what molecular level erythroid differentiation is affected; and third, variants are subjected to genetic analysis by cell fusion. By exploiting the fact that the inducible cells differentiate to a non-dividing stage in the presence of DMSO, we can isolate non-inducible variants by continuous growth or cloning in DMSO[60] Most of our DMSO-resistant lines are also non-inducible by other inducers, although one DMSO-resistant line does respond to *N*-methylpyrrolidone. One DMSO-resistant variant (FtI^{D-}) fails to accumulate globin-specifying sequences in the nucleus, either because of a defect in transcription of the globin genes or instability of the transcripts[61]. Moreover, this defect acts in a *trans*-dominant manner in preventing haemoglobin or globin RNA accumulation in cell hybrids constructed between the FtI^{D-} variant and the normal inducible parent. A second variant, FwI^{D-}, also fails to accumulate haemoglobin[60] or globin messenger RNAs[61] in response to DMSO or butyric acid, unless it is also treated with haemin[61]. This effect of haemin is specific for the FwI^{D-} variant, and cannot be replaced by a precursor to haem (δ-aminolaevulinic acid). Moreover, this defect in inducibility also operates in a *trans*-dominant manner, although loss of a few, as yet unidentified, chromosomes can lead to re-expression of haemoglobin synthesis[61,62]. Extinction of induction of globin messenger RNA has also been reported by Orkin *et al.*[63] in hybrids constructed between high and low inducible cell lines and by Deisseroth *et al.*[64] in cell hybrids between Friend cells and fibroblasts. Interestingly, however, hybrids between Friend cells and human bone marrow or Chinese hamster erythroid cells could be induced to synthesise globins of both parental types, although in these intraspecific hybrids, extensive segregation of human or Chinese hamster chromosomes had occurred[65]. Thus the general picture which emerges from these studies is that when a Friend cell is fused to a non-inducible, or non-erythroid, cell, extinction of induction of haemoglobin production occurs. This result is similar to that obtained with other differentiating systems (reviewed in refs 66 and 67). Often it has been assumed that extinction of differentiation is due to a negative control system analogous to the bacterial repression systems acting at transcription. In none of these cell fusion experiments cited, however, has it yet been proven that extinction acts at the transcriptional level. For example, although in our own studies we have demonstrated that extinction of haemoglobin synthesis in certain cell hybrids acts at the nuclear level, it has not yet proved possible to demonstrate that globin gene transcripts are not synthesised.

That regulation of differentiation can operate at different molecular levels is illustrated by our molecular analysis of a hybrid cell formed between the Friend cell and the lymphoma cell. This hybrid cell shows extinction of induction of haemoglobin and morphological differentiation, although globin messenger RNA is inducible[61]. Both functions are, however, expressed on treatment with haemin in addition to DMSO[61]. The precise role of haem in this process requires clarification, for example, by studies of factors in Friend cells analogous to the haemin-controlled repressor in reticulocytes[68]. Furthermore, it is not yet known whether this phenomenon is a property merely of this lymphoma cell line, of lymphoma cells in general or of normal lymphoid cells. But this interesting observation illustrates at the molecular level the diversity of control mechanisms which affect regulation or erythroid differentiation and shows how complex interactions may exist between independent erythroid functions.

Perspectives

The experiments described in this article give some indication of the possibilities of normal erythroid cells and particularly the Friend cell system as a model of a differentiating cell, in which to attempt to dissect the regulatory mechanisms by a combination of cellular, molecular and genetic approaches. It may, therefore, be useful to take a sober look at some of the limitations of the system. The Friend cell is a transformed cell and its relevance as a model for normal differentiation must, therefore, be evaluated critically· as mentioned above, Friend cells seem to be abnormal in that their proliferation is no longer regulated by erythropoietin as in the normal erythroid precursor cell; but differentiation, once it is induced, seems to be relatively normal. Second, the Friend cell is derived from cells transformed after commitment to the erythroid line and the events induced by DMSO may, therefore, be relevant only to the later processes of erythroid differentiation. The important question of the molecular nature of the events concerned with commitment of haematopoietic stem cells to the erythroid line probably cannot be answered with the Friend cell system. Hope that this may prove possible in the future stems from the work of Dexter and colleagues[69], who have been able to maintain multi-potential stem cells in culture using an appropriate feeder layer. Another promising approach for the future lies in differentiation of teratocarcinoma cells (reviewed in ref. 70) which various groups of workers have recently shown to behave like normal germ cells when transplanted into the environment of the normal embryo at the blastocyst stage of development[71,72]. It may prove possible to mimic commitment of stem cells to the erythroid line with normal haematopoietic stem cells or teratocarcinoma cells cultured in the appropriate environment. Application to these systems of the kind of molecular/genetic analysis developed for the Friend cell system could then increase enormously our understanding of the relationship between commitment to the erythroid line and subsequent differentiation.

1 Trentin, J. J., in *Regulation of Haematopoiesis*, 1 (edit. by Gordon, A S.), 161–186 (Appleton-Century-Crofts, New York, 1970).
2 Cole, R. J., in *Second Symp Br. Soc Developmental Biol* (edit by Balls, M , and Wild, A. E.), 335–358 (Cambridge University Press, London, 1975).
3 Wolf, W. S , *Cell Tissue Kinet* , 7, 89–98 (1974)
4 Lajtha, L. G., and Schofield, R , *Differentiation*, 2, 313–320 (1974).
5 Stephenson, J. A., Axelrad, A. A , McLeod, D. L., and Shreeve, M., *Proc. natn Acad Sci. U S A.*, 68, 1542–46 (1971)
6 Iscove, N. N., Sieber, F., and Winterhalter, K H., *J Cell Physiol* , 83, 309–320 (1974).
7 Axelrad, A. A , McLeod, D L., Shreeve, M. M., and Heath, D S , *Hemopoiesis in Culture* (edit. by Robinson, W A) 226–237 (DHEW Publication No. NIH 74–205, 1973).
8 Iscove, N N., and Sieber, F., *Expl Hemat.*, 3, 32 (1975
9 Johnson, G R., and Moore, M A. S., *Nature*, 258, 726–728 (1975)
10 Rifkind, R A., Chui, D., and Epler, H., *J. Cell Biol* , 40, 343–365 (1969).
11 Silini, G., Pozzi, L. V , and Pons, S., *J. Embryol exp. Morph* , 17, 303–318 (1967)
12 Chui, D. H K., Djaldetti, M., Marks, P A , and Rifkind, R. A., *J Cell Biol.*, 51, 585–595 (1971)
13 Paul, J., Conkie, D., and Burgos, H , *J Embryol. exp. Morph.*, 29, 453–472 (1973)
14 Harrison, P. R., Conkie, D , and Paul, J., in *The Cell Cycle in Development and Differentiation* (edit. by Balls, M , and Billett, F S), 341–364 (Cambridge University Press, London, 1973).
15 Harrison, P. R , Conkie, D., Paul, J , and Jones, K., *FEBS Lett* , 32, 109–112 (1973).
16 Harrison, P. R., Conkie, D., Affara, N., and Paul, J , *J. Cell Biol.*, 63, 402–413 (1974).
17 Borsook, H., Ratner, K , and Tattrie, B , *Nature*, 221, 1261 (1969).
18 Cantor, L. N , Morris, A J., Marks, P. A , and Rifkind, R. A , *Proc natn. Acad Sci. U S.A* , 69, 1337–1341 (1972).
19 Conkie, D., Kleiman, L., Harrison, P R., and Paul, J., *Expl Cell Res.*, 93, 315–324 (1975).
20 Clissold, P. M , *Expl Cell Res.*, 89, 389–398 (1974)
21 Killman, S.-A., *Cell Tissue Kinet.*, 3, 217–228 (1970).
22 Ramirez, F., *et al.*, *Trans. Ass. Am. Phys.* (in the press).
23 Terada, M., *et al.*, *Proc. natn Acad Sci U.S.A.*, 69, 3575–3579 (1972).
24 Ramirez, F., *et al.*, *J. biol Chem.*, 250, 6054–6058 (1975).
25 Friend, C , Patuleia, M. C., and de Harven, E., *Natn. Cancer Inst Monogr.*, 22, 505–514 (1966)
26 Lilly, F., *J natn. Cancer Inst.*, 49, 927–934 (1972):
27 Steeves, R A , *J. natn. Cancer Inst* , 54, 289–297 (1975)
28 Seidel, H J., in *Unifying Concepts of Leukemia*, 935–942 (S Karger, Basel, 1973)
29 Fredrickson, T , Tambourin, P , Wendling, F , Jasmin, C., and Smajda, F., *J. natn Cancer Inst* , 55, 443–446 (1975)
30 Tambourin, P. E., and Wendling, F., *Nature*, 256, 320–322 (1975)
31 Golde, D W., Faille, A , Sullivan, A., and Friend, C , *Cancer Res.*, 36, 115–119 (1976)
32 Mirand, E. A , *Science*, 156, 832–833 (1967)
33 Hawkins, W. D., and Krantz, S. B , *Nature*, 253, 731–732 (1975)
34 Liao, S K., and Axelrad, A A , *Int. J Cancer*, 15, 467–482 (1975).
35 Friend, C., Scher, W , and Rossi, G B , in *The Biology of Large RNA Viruses*, (edit. by Barry, R. D , and Mahy, B W. J.), 267 (Academic, New York, 1970)
36 Preisler, H. D , and Giladi, M., *Nature*, 251, 645–646 (1974)
37 Kluge, N , Gaedicke, G., Steinheider, G , Dube, S , and Ostertag, W , *Expl Cell Res.*, 88, 257–262 (1974)
38 Preisler, H. D., Bjornsson, S , Mori, M , and Barcos, M , *Cell Differentiation*, 4, 273–283 (1975)
39 Friend, C., Scher, W , Holland, J G , and Sato, T., *Proc natn Acad Sci U.S.A* , 68, 378–382 (1971)
40 Scher, W., Preisler, H. D , and Friend, C , *J. Cell Physiol.*, 81, 63–70 (1973)
41 Tanaka, M., *et al* , *Proc. natn Acad Sci. U S 4* , 72, 1003–1006 (1975).
42 Preisler, H. D , and Lyman, G , *Cell Differentiation*, 4, 179–185 (1975)
43 Leder, A , and Leder, P., *Cell*, 5, 319–322 (1975).
44 Ross, J., Ikawa, Y , and Leder, P , *Proc. natn. Acad Sci. U S A.*, 69, 3620–3623 (1972).
45 Gilmour, R S., Harrison, P R , Windass, J. W , Affara, N , and Paul, J , *Cell Differentiation*, 3l, 9–22 (1974).
46 Harrison, P. R., Gilmour, R. S , Affara, N , Conkie, D , and Paul, J., *Cell Differentiation*, 3, 23–30 (1974).
47 Ostertag, W., Melderis, H., Steinheider, G , Kluge, N , and Dube, S., *Nature new Biol* , 239, 231–234 (1972).
48 Boyer, S. H., Wuu, K D , Noyes, A N , Young, R., Scher, W., Friend, C. Preisler, H. D , and Bank, A , *Blood*, 40, 823–835 (1972)
49 Ebert, P. S., and Ikawa, Y., *Proc. Soc. exp. Biol. Med* , 106, 601–604 (1974)
50 Furusawa, M., Ikawa, Y., and Sugano, H., *Proc Japan. Acad.*, 47, 220–224 (1971)
51 Fujunami, N , Sugimoto, Y., and Hagiwara, A , *Development, Growth and Differentiation*, 15, 141–151 (1973)
52 Kabat, D., Sherton, C C., Evans, L. H , Bigley, R , and Koler, R. D., *Cell*, 5, 331–338 (1975)
53 Blankstein, L. A., and Levy, S. B , *Nature* (in the press).
54 Orkin, S H , Swan, D , and Leder, P., *J. biol Chem* , 250, 8753–8760 (1975).
55 Sieber, F , in *Progress in Differentiation Research* (edit. by Muller-Berat, H.), 521–528 (North-Holland, Amsterdam, 1976).
56 Bernstein, A., Boyd, A S , Crichley, V., and Lamb, V , in *Symposium on Biogenesis and Turnover of Membrane Molecules* (Society of General Physiologists, in the press).
57 McClintock, P. R , and Papaconstantinou, J., *Proc. natn. Acad Sci U.S A* , 71, 4551–4555 (1974).
58 Levy, J , Terada, M , Rifkind, R. A , and Marks, P. A., *Proc. natn Acad. Sci. U.S.A.*, 72, 28–32 (1975).
59 Leder, A., Orkin, S , and Leder, P., *Science*, 190, 893–894 (1975).
60 Conkie, D , Affara, N., Harrison, P. R , Paul, J , and Jones, K., *J Cell Biol.*, 63, 414–419 (1974).
61 Harrison, P. R., Affara, N., Conkie, D., Rutherford, T., Sommerville, J., and Paul, J in *Progress in Differentiation Research* (edit. by Muller-Berat, N), 135–146 (North-Holland, Amsterdam, 1976).
62 Paul, J., and Hickey, I , *Expl Cell Res.*, 87, 20–30 (1974).
63 Orkin, S. H., Harosi, R. I., and Leder, P., *Proc. natn. Acad Sci U.S.A.*, 72, 98–102 (1975).
64 Deisseroth, A., Burk, R., Picciano, D., Minna, J , Anderson, W. F , and Neinhuis, A., *Proc. natn. Acad. Sci U.S A* , 72, 1102–1106 (1975).
65 Deisseroth, A , Barker, J., Anderson, W F., and Nienhuis, A., *Proc. natn. Acad. Sci U.S.A.*, 72, 2682–2686 (1975)
66 Davis, F. M., and Adelberg, E A , *Bact. Rev.*, 37, 197–214 (1973).
67 Davidson, R. L., and de la Cruz, F. F (eds), *Somatic Cell Hybridisation* (Raven, New York, 1974).
68 Cimadevilla, J M., and Hardesty, B., *Biochem. biophys. Res. Commun.*, 63, 931–937 (1975).
69 Dexter, T. M., and Testa, M G , *Methods in Cell Biology* (edit. by Prescott, D. M); (Academic, New York, in the press)
70 Martin, G , *Cell*, 5, 229–243 (1975).
71 Mintz, B , and Illmensee, K., *Proc natn. Acad. Sci U.S A.*, 72, 3585–3589 (1975).
72 Papaioannou, V. E., McBurney, M W., Gardner, R. L , and Evans, M. J , *Nature*, 258, 70–73 (1975).

---

articles

Accretion flows in the magnetospheres of Vela X-1, AO535+26 and Her X-1

R. F. Elsner

Department of Physics, University of Illinois at Urbana-Champaign, Urbana, Illinois 61801

F. K. Lamb

Department of Physics, University of Illinois and Institute of Astronomy, University of Cambridge, Cambridge CB3 OHA, UK

We suggest a model for the complex pulse shapes of the long period, pulsating X-ray sources, Vela X-1 and AO535+26. We discuss the flow of accreting matter on to these slow rotators and contrast it with that expected in systems such as Her X-1 which contain a rapidly rotating neutron star.

THE recent discovery of the pulsating X-ray source AO535+26 (ref. 1) and unexpected detection of X-ray pulsations in the relatively well studied binary source Vela X-1 (ref. 2) have aroused considerable interest, in part because their pulse periods (104 s in AO535+26 and 283 s in Vela X-1) and very complex 1–10 keV pulse shapes (refs 2, 3) are strikingly different from those of the previously identified pulsating X-ray sources Her X-1 and Cen X-3, which are believed to be rotating neutron stars (see refs 4 and 5).

Several pieces of evidence indicate that in spite of these differences, Vela X-1 and AO535+26 may also be rotating neutron stars. Optical and X-ray observations yield a probable lower bound of $1.4M_\odot$ on the mass of Vela X-1 (ref. 6, and references therein), very close to the upper mass limit for slowly rotating white dwarfs. If Vela X-1 is at a distance $D \sim 1.3$ kpc (refs 6, 7), it has a typical X-ray luminosity $L_x \sim 0.2\text{–}2\times10^{36}$ erg s^{-1} (ref. 2). The distance to AO535+26 is as yet unknown, but its 1975 May high state intensity was comparable with that of the Crab Nebula[3], implying $L_x \gtrsim 3\times10^{36}$ erg s^{-1} if $D \gtrsim 1$ kpc. Such high luminosities are incompatible with current models of X-ray emission by degenerate dwarfs (see ref. 8). The long rotation periods of these sources may be the result of spin down by a combination of magnetic torques and interaction with surrounding plasma[9], or the result of spin down in the pre-supernova star, leading to formation of a few neutron stars with spin periods as long as $10\text{–}10^3$ s (ref. 10).

Our purpose is, first, to suggest that the complex pulse shapes of Vela X-1 and AO535+26 in the energy range 1–10 keV can be understood if both are slowly rotating neutron stars in which broad, smooth emission pulse shapes, like those seen at 15–30 keV, are modified as the result of cyclotron absorption by clumps of matter entrained in magnetic field irregularities near the stellar surface.

Second, we suggest that accretion flows in the magnetospheres of rapidly rotating neutron stars, such as Her X-1 and Cen X-3, are different from those in slow rotators, and that the observed properties of these sources reflect this difference. In slow rotators accreting plasma probably enters the magnetosphere as a consequence of the Rayleigh–Taylor instability of the magnetospheric boundary (ref. 11), and may plunge close to the surface of the star before being channelled towards polar emission regions by the stellar magnetic field. In fast rotators, on the other hand, the near cancellation of gravitational and centrifugal forces at the magnetospheric boundary may lead to accumulation of matter there, and to more effective channelling of plasma towards the polar caps while it is still far from the star.

We discuss the observational implications of this model of accretion flows, and draw attention to ways in which the differences between fast and slow rotators can be explored observationally.

Accretion by slow rotators

Consider first accretion by slowly rotating neutron stars. Let us assume for the moment that accreting matter approaches a star of mass M approximately radially; at a radius r_s from the star it is shock heated to a temperature $T_s \sim T_{ff}(r_s)$, where

$$T_{ff}(r) = GMm_p/k_Br = 1.6\times10^{10}(M/M_\odot)(r/10^8\text{ cm})^{-1}\text{ K} \quad (1)$$

in terms of the proton mass, m_p. The radius r_s at which shock heating occurs is determined by the radius, r_A, of the Alfvén surface, where the Alfvén velocity v_A in the stellar magnetic field equals the plasma inflow velocity, v, and the magnetic field of the star first dominates the flow[12]. Regardless of the complexity of the magnetic field near the surface of the star, at large distances the stellar field will be dominated by its dipole component; for spherically-symmetric, radial free-fall towards a star with dipole moment μ_{30}, in units of 10^{30} gauss cm^3, r_A has the characteristic value

$$r_A{}^0 = 2.9\times10^8\,\mu_{30}{}^{4/7}\,(M/M_\odot)^{1/7}\,L_{37}{}^{-2/7}\,R_6{}^{-2/7}\text{ cm} \quad (2)$$

Here L_{37} is the accretion luminosity in units of 10^{37} erg s^{-1} and R_6 is the stellar radius in units of 10^6 cm. The effect of the star's rotation on the accretion flow can, to a first approximation, be neglected if the angular velocity of the star, Ω_s, satisfies $\Omega_s \ll \Omega_k(r_A) = (GM/r_A{}^3)^{1/2}$ or, equivalently, $r_A \ll r_c \equiv (GM/\Omega_s{}^2)^{1/3}$ (ref. 12). This is the condition for 'slow rotation'.

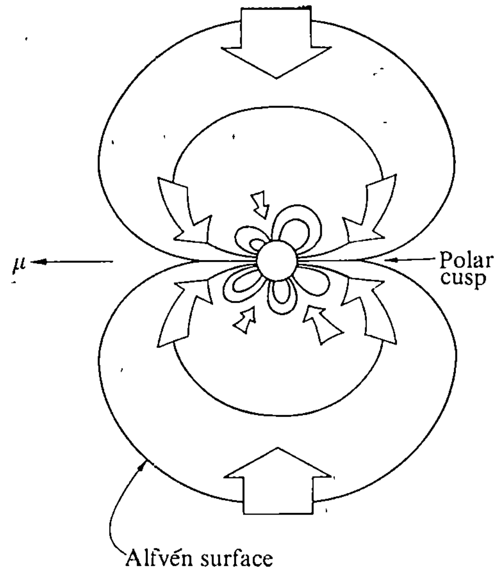

Fig. 1 Suggested plasma flow pattern in slow rotators with complex surface magnetic fields. Plasma enters the magnetosphere as the result of the Rayleigh–Taylor instability of the magnetospheric boundary and plunges close to the stellar surface before being channelled by the stellar magnetic field. Most of the plasma is channelled towards the polar caps, but some flows along field lines that lead to other parts of the stellar surface.

The flow of highly conducting plasma towards the star tends to close the magnetosphere (ref. 12). Since the magnetospheric boundary is convex towards the accreting plasma, the gradient of the field is such as to stabilise the boundary. Nevertheless, the weight of the plasma will drive the boundary locally Rayleigh–Taylor instable if

$$g_{eff} = \cos\theta GM/r_m{}^2 - \kappa B_m{}^2/4\pi\rho_m > 0 \quad (3)$$

Here θ is the angle between the radius vector and the outward normal to the boundary, r_m is the exact radius of the magnetospheric boundary ($\sim r_A$), B_m and ρ_m are the stellar magnetic field and plasma density at the boundary, $\kappa \sim 1/r_m$ is the curvature of the boundary, and we have neglected radiation pressure forces. If the boundary is in magnetohydrostatic equilibrium, one has $B_m{}^2/8\pi = n_mk_BT_m$, where n_m and T_m are the particle density and temperature in the plasma just outside the boundary. Thus, the condition for the onset of the Rayleigh–Taylor instability can be written

$$T_m < T_{crit} = \cos\theta T_{ff}(r_m)/(2\kappa r_m)$$

where B_m, r_m, and κ are roughly independent of T_m.

Detailed model calculations show that in the absence of cooling, the weight of the plasma is insufficient to drive the boundary unstable (Elsner and Lamb, to be published; see also ref. 13). These calculations show further that instability sets in when the plasma at the boundary has cooled to a temperature $T_{crit} \sim 0.3T_{ff}(r_m)$, and that $T_{crit}/T_{ff}(r_m)$ is largest at the magnetic equator. Once instability occurs, plasma may penetrate the magnetosphere over much of the magnetospheric boundary except at the axes of the polar cusps, where the boundary is stable. Unfortunately, there are at present no reliable calculations of the properties of the fully developed Rayleigh–Taylor instability in the nonlinear regime, and the precise boundary condition to be imposed on the flow at r_m is therefore unknown. Therefore we adopt the simplest boundary condition that gives a qualitatively correct flow solution: since the growth of the Rayleigh–Taylor instability is rapid and other modes of plasma entry are relatively ineffective, we shall assume that, in a steady state, the region of shock-heated plasma extends a distance Δ_s outside r_m such that T_m is less than but of order T_{crit}.

If the neutron star accretes plasma from a disk, the flow may still resemble in certain respects the flow just described. Thus if the disk thickens near r_A and the flow becomes roughly

Table 1 Characteristics of fast and slow rotators

Source property	Slow rotators ($r_A \ll r_c$)	Fast rotators ($r_A \simeq r_c$)
Period changes	Either spin up or spin down, but not both, unless disk flow reverses	Spin down as well as spin up, even if disk flow does not reverse
t_s	$\sim t_s^0$ for disk inflow	$\gg t_s^0$ even for disk inflow
Spectrum	Intense soft ($\sim$0.1 keV) component not expected	Intense soft ($\sim$0.1 keV) component possible
Pulse shapes	More complex at lower energies, simpler at higher energies	Simpler at all energies

spherically symmetric there, the flow outside the magnetosphere should resemble the post-shock flow described above. Even if the disk remains thin, the Rayleigh–Taylor instability may well play an important role in allowing the relatively cold disk plasma to penetrate the magnetosphere.

Of particular relevance for the present discussion, recent research on two-dimensional models of accretion disks around magnetic stars (ref. 14 and Ghosh, Lamb, and Pethick, in preparation) suggests that radial flow velocities $v_r \sim v_{ff}$ in the neighbourhood of r_A are a general feature of disk accretion by slow rotators (if shear stresses are large, v_r may become $\sim v_{ff}$ outside the magnetospheric boundary; in any case one expects $v_r \sim v_{ff}$ inside the magnetosphere). If this is the case, one expects $r_A \sim r_A^0$ even for disk inflow[12] and, for disks rotating in the same direction as the star, a spin up timescale, t_s, of order

$$t_s^0 = \frac{I\Omega_s}{(MGMr_A^0)^{\frac{1}{2}}} \tag{4}$$

where I is the star's moment of inertia and M is the mass accretion rate.

For sources with luminosities $L \gtrsim 10^{36}$ erg s^{-1}, the optical depth to Compton scattering of shock-heated plasma outside r_A is

$$\tau_c \simeq 0.03\left(\frac{r_A}{10^8\text{cm}}\right)^{-4/5}\left(\frac{M}{M_\odot}\right)^{1/5}\left(\frac{\ln\Lambda}{15}\right)^{-2/5} R_6^{3/5} \tag{5}$$

where $\ln\Lambda$ is the Coulomb logarithm, $\sim$ 15 at r_A. Thus, in slow rotators the rapid development of the Rayleigh–Taylor instability and the large inflow velocities at r_A imply that there is little plasma there to absorb and reradiate keV X rays produced at the stellar surface. An intense soft component ($\varepsilon \sim 0.1$ keV) is therefore not expected in the spectrum of slow rotators.

Pulse shapes

Although the Rayleigh–Taylor instability causes plasma to penetrate the magnetosphere 'between' stellar field lines, the plasma is unlikely to be effectively channelled along these field lines until it is threaded by them; this can occur either by diffusion of the infalling plasma on to stellar field lines or by reconnection of magnetic field lines embedded in the infalling plasma to stellar field lines. If cooling is rapid and threading occurs relatively slowly, the plasma may fall to within a few stellar radii of the star's surface before being funnelled towards the magnetic poles. If in addition the topology of the stellar surface field is complex, with numerous flux concentrations at points other than the poles of the dipolar component of the field, the flow pattern of plasma near the stellar surface may be similar to that shown schematically in Fig. 1.

How long can small scale magnetic flux concentrations be expected to survive in the crust of a neutron star? If the crustal conductivity is σ, such concentrations will decay away on a time scale

$$t_d \simeq 4\pi\sigma l_m^2/c^2 = 4\times10^6\,(l_m/10^5\,\text{cm})^2\,(\sigma/10^{24}\,\text{s}^{-1})\,\text{yr} \tag{6}$$

assuming they go to a depth $\sim l_m$. To be present now, they may have had to survive for an evolutionary timescale $t_{ev} \sim 10^6$ yr (ref. 15), which would require $\sigma \gtrsim 3\times10^{23}$ s^{-1} if $l_m \sim 10^5$ cm. Now the temperature of the stellar surface must be $\lesssim 10^6$ K, since otherwise it would be seen as an intense source of soft X rays, and the temperature in the crust itself may be similar. Recent calculations of crustal conductivities[16] show that at this temperature, field decay in the crust from electron–phonon interactions would be entirely negligible after 10^6 yr, while that from electron–charge disorder interactions would be negligible except in lighter stars ($M \lesssim 0.5\,M_\odot$) whose crusts are as impure as possible. Decay from scattering off dislocations can also be neglected unless the distance between dislocations is microscopic. Thus, it is entirely reasonable that a large proportion of neutron star X-ray sources may have complex surface magnetic fields.

Since the dipole component of the field is dominant except within a few stellar radii of the surface, most of the matter will still be channelled to the polar caps, as in purely dipolar models, and most of the keV X-ray emission will come from hot spots there, producing broad, smooth pulses at energies $\varepsilon \gg \hbar\omega_c \simeq 10B_{12}$ keV, where B_{12} is the surface field in units of 10^{12} gauss and $\omega_c = eB/m_ec$ is the electron cyclotron frequency. A small fraction of the accreting plasma is, however, likely to be channelled along field lines that lead to other parts of the stellar surface. Then, as the star turns, the broad emission pattern from the polar hot spots will be seen through varying amounts of cyclotron-absorbing plasma, producing complex waveforms at energies $\varepsilon \sim \hbar\omega_c$.

For surface field strengths $B \sim 10^{11}$–10^{12} gauss and temperatures $k_BT \sim 10^7$–10^8 K one has $\hbar\omega_c \sim k_BT$, and the quantum-mechanical expression[17] for the cyclotron cross section must be used. The optical depth through a clump of dimension size l_c at $\varepsilon = \hbar\omega_c$ is

$$\tau_{cyc} = \frac{l_c\omega_{pe}^2}{c\omega_c}\left(\frac{\pi m_ec^2}{2k_BT}\right)^{1/2}\frac{1}{1-\exp(-\hbar\omega_c/k_BT)} \tag{7}$$

where ω_{pe} is the electron plasma frequency. Thus one has $\tau_{cyc} \gtrsim 1$ for column densities $\rho l_c \gtrsim 2.9\times10^{-5}B_{12}T_8^{1/2}$ g cm^{-2}, where $T_8 = T/10^8$ K. For clumps of dimension $l_c \sim 10^5$ cm, this represents a density only $\sim 10^{-3}$ that above the polar caps.

In the absence of absorption processes, cyclotron scattering, in which an electron makes a transition from one Landau orbital to the next higher one and back again, is likely to dominate, and will create an anisotropic angular distribution of the radiation emitted by the polar caps without significantly altering its energy distribution. For example, if there are N clumps of size $l_c \sim 10^5$ cm at a distance $d \sim 10^6$ cm from a polar cap, then when a clump is in the line of sight, the X-ray flux at energy ε from that polar cap will be reduced to a fraction $f \sim N(l_c/d)^2 \sim 0.01\,N$ of its value when the line of sight lies between clumps, assuming $\exp(-\tau_{cyc}(\varepsilon)) \ll f \ll 1$. On the other hand, if the energy falling on the clumps were thermalised and then reradiated, the temperature T_c of the clumps would be a factor $\sim (l_p/d)^{1.2} \sim 0.3$ lower than that of polar caps of dimension l_p, and the energy distribution as well as the angular distribution would be altered. In either case the spectrum would appear heavily 'absorbed' at low points in the pulse waveform.

Vela X-1 and A0535+26

If A0535+26 and Vela X-1 are magnetic neutron stars with spin periods, P, of 104 and 283 s, respectively, then both are probably slow rotators. Using the estimate (2) for r_A^0, the condition $r_A^0 \ll r_c$ becomes $L \gg L_{crit}$, where

$$L_{crit} = 1.0\times10^{38}\,P^{-7/3}\,\mu_{30}^2\,(M/M_\odot)^{-2/3}\,R_6^{-1}\,\text{erg s}^{-1} \tag{8}$$

a condition which is easily satisfied by Vela X-1, and by

AO535+26 if it has an accretion luminosity $L \gtrsim 10^{35}$ erg s^{-1}, assuming $\mu_{30} \sim 1$. (Note, however, that $L_{\rm crit}$ depends sensitively on μ.)

Consider now some of the observational implications of the hypothesis that these sources are slowly rotating neutron stars:

(1) If there is a Keplerian accretion disk around the magnetosphere and the disk rotates in the same direction as the star, the star should spin up on a timescale $\sim t_s^0$, with $\dot{P}$ proportional to L. Changes from spin up to spin down should not occur as the result of accretion torques unless the flow departs from this pattern. In the absence of disk flow, t_s should be $\gg t_s^0$, while a reversed disk could lead to spin down on the timescale t_s^0. (Were these sources degenerate dwarfs, the timescale t_s^0 would be very much longer, since I would be $\sim 10^6$ times larger.)

(2) Because little plasma accumulates near r_A, intense soft X-ray emission is not expected.

(3) If the complex 1—10-keV pulse shapes arise from scattering or absorption by clumps of matter entrained in complex magnetic fields near the stellar surface, as we have suggested, the number and positions of the basic features in time-averaged pulse waveforms should remain fixed, since the field configuration is fixed, although the sizes of various features may change if the flow pattern of the plasma approaching r_A changes. (Were the features instead caused by random clumping of the infalling plasma, independent of the surface field geometry, they should average out on timescales of minutes. Such complicated pulse shapes also seem unlikely to be the result of complex variations in $\dot{M}$ controlled at the magnetospheric boundary[12] since it is there, at $r \gg R$, that the stellar field should be most symmetric; moreover, in slow rotators plasma is likely to enter the magnetosphere over a substantial fraction of its surface, at least in the absence of strong X-ray beaming effects.)

We note that the narrowness of some of the features (in AO535+26, for example, some have widths $\leqslant 0.05$ in pulse phase) favours an interpretation in terms of scattering or absorption rather than beaming, since such narrow features are unlikely to be produced by beaming in quasi-thermal sources such as these, but can easily be produced by absorption if the absorbing clumps are small, close to the stellar surface, and have sizes comparable with those of the polar cap emitting regions

(4) If the features at 1–10 keV are caused by cyclotron scattering in plasma clumps a distance $\sim d$ above the surface and d is $\sim 10^5$ cm, then the surface fields in both stars must be $\sim 10^{12}$–10^{13} gauss. Above 15 keV the polarisation should change smoothly across the pulses (see ref. 19); below 10 keV the polarisation should change smoothly across a given peak in the waveform, but could change abruptly from one peak to the next, since it is the result of absorption of smoothly varying polarised emission at the polar caps by clumps of matter whose absorption polarisations may differ significantly from one to another.

Comparison with fast rotators

We have seen that many of the properties of Vela X-1 and AO535+26 can be understood if they are slowly rotating neutron stars. For comparison, let us consider briefly how the properties of fast rotators, in which $r_A \simeq r_c$, might be expected to differ from those of slow rotators

If a fast rotator is fed by an accretion disk around its rotation equator, rotating in the same sense as the star, the force of gravity at the disk–magnetospheric boundary will be largely cancelled by centrigufal forces; as a result the growth rate of the Rayleigh–Taylor instability will be reduced and the plasma will fall inward between stellar magnetic field lines more slowly. Thus there will be more time for the accreting plasma to become threaded by stellar field lines far from the stellar surface, perhaps helped along by the Kelvin–Helmholtz instability (see also ref. 13), and channelling of the flow by the stellar field is therefore likely to occur at $r \gg R$. Finally, since the dipolar component of the field dominates at $r \gg R$, the flow is likely to be more effectively funnelled towards the two polar caps than in slow rotators.

If this difference in the accretion flow does occur, it will be reflected by the properties of such sources:

(1) If an extreme fast rotator is surrounded by a Keplerian accretion disk rotating in the same direction as the star, the accretion torque caused by material stresses at r_A can be largely cancelled or even reversed by magnetic and viscous stresses. Thus, even if such a source is disk fed, the average spin up timescale should be longer than t_s^0, and occasional episodes of spin down would be expected.

(2) If the infall of plasma is significantly slowed by near cancellation of gravity by centrifugal forces, a substantial quantity of matter may accumulate near r_A, producing a soft X-ray component in the spectrum by reprocessing keV X rays emitted at the stellar surface[5]. If sufficient matter accumulates, the pulsed fraction in the energy range 0.1–1 keV will be reduced, and the pulse phase in general shifted from that at 1–10 keV.

(3) If the slowly infalling plasma is effectively channelled along stellar field lines far from the star's surface, essentially all of the plasma may be funnelled towards the two polar caps, producing broad, smooth pulses throughout the keV energy range.

These expected properties of fast rotators surrounded by accretion disks are well illustrated by Her X-1, which has a spin period of 1.24 s. Assuming $M = 1.3 M_\odot$ (ref. 20), $R_6 = 1.5$ (ref. 21), and $L_{37} = 5.8$, appropriate to a distance of 6 kpc (ref. 7), equation (2) gives $r_A^0 \sim r_c$ for $\mu_{30} \sim 1$, indicating that Her X-1 is indeed a fast rotator. Even though Her X-1 is believed to be surrounded by a Keplerian accretion disk[6] it shows episodes of spin down as well as spin up[4]. Moreover, the observed average spin up time, 3×10^6 yr (ref. 22), is a factor ~ 40 longer than the slow-rotator estimate (4), if $I \simeq 2 \times 10^{45}$ g cm^2 (ref. 21). This factor is too large to be accounted for by uncertainties in I or in r_A (since $t_s^0 \propto r_A^{-1/2}$, r_A would have to be a factor $\sim 10^3$ smaller than our estimate), and is strong evidence that material stresses at r_A are closely cancelled by magnetic and viscous stresses. In addition, there is an intense soft X-ray component in the spectrum of Her X-1 (ref. 23) that has been interpreted in terms of a centrifugally-supported opaque shell of accumulated matter partially surrounding the neutron star magnetosphere (ref. 24; reprocessing by plasma at the magnetospheric boundary has also been mentioned in ref. 25). Such an accumulation of matter cannot be supported by magnetic forces or radiation pressure since it would be Rayleigh–Taylor instable on a dynamical timescale. Finally, the pulse waveforms seen in Her X-1 are comparatively simple throughout the energy range 1–30 keV, as would be expected if all the accreting plasma were funnelled towards the two polar caps. (Alternatively, these simple pulse shapes could arise simply from the absence of complex surface magnetic fields in Her X-1, but we believe this possibility is less likely.)

If a fast rotator is fed by more nearly radial inflow, or by a disk which is not aligned with the stellar rotation, the accretion flow is likely to be more complicated with a possibility of centrifugally-supported matter in the rotation equator and rapid inflow near the rotation axis.

Discussion

We have suggested that Vela X-1 and AO535+26 are slowly rotating neutron stars in which complex 1–10-keV pulse shapes are produced by cyclotron absorption near the stellar surface, and have indicated several ways in which this hypothesis can be checked.

We have also suggested that accretion flows in the magnetospheres of fast rotators are different from those in slow rotators, and that the properties of X-ray sources will reflect this difference. Some of these properties are summarised in Table 1. Further study of other pulsating X-ray sources will show whether this model of accretion flows is correct. Thus SMC X-1, with a recently discovered period of 0.71 s (ref. 26) and a luminosity $\sim 6\times10^{38}$ erg s^{-1} is a prime candidate for fast rotation, while 3U1728–24, with a period of 123 s (refs 27, 28) and a luminosity (if it lies near the galactic centre) $\sim 10^{38}$ erg s^{-1}, should be a slow rotator. It is also possible that 3U1813−14, 3U1223−62, and 3U0352+30, which have recently been reported to be pulsating[27], are slowly rotating neutron stars.

A further implication of this model of accretion flows is that a rapidly rotating neutron star located in a binary system where the mass transfer rate is very high might be completely surrounded by a centrifugally-supported opaque cloud. If such a cloud smears out periodic intensity variations without reprocessing too large a fraction of the keV X-ray emission into soft X rays, it could account for the observed properties of unpulsed sources like Sco X-1 and Cyg X-2 (ref. 5); such a possibility has also been recently suggested by Sunyaev (private communication through R. McCray).

We conclude by pointing out that a given source can change from fast rotation to slow rotation, or vice versa, if it is 'choked' or 'starved' of accreting matter. One source that might show such transitions is Cen X-3, which shows some characteristics of both types of accretion flows and apparently undergoes large changes in accretion rate[29]. Although Cen X-3 usually has a comparatively simple pulse shape and also shows occasional spin down episodes[30], both of which are characteristics of fast rotators, equation (2) gives r_A only $\sim 0.3\ r_c$ for $P = 4.84$ s, $\mu_{30} \sim 1$, and $L_{37} \sim 6$ (appropriate for an X-ray high state at a distance ~ 10 kpc), and the average spin up timescale is $\sim 3\times10^3$ yr, in rough agreement with the slow rotator result, equation (4). Cen X-3 has been observed to have a more pronounced double pulse structure during what is believed to have been a 'choke-out' (Fabbiano and Schreier, personal communication), but the observation appears inconclusive as a test of the accretion flow pattern. The enhanced pulse-to-pulse variations in pulse shape seen during one 'starve-out' are probably unrelated to the increased complexity in the time-averaged waveform expected were Cen X-3 to become a true slow rotator. Clearly, observation of a transition from fast to slow rotation would provide an important check on the model.

We thank Professors D. Q. Lamb, D. Pines, and M. J. Rees and Dr A. C. Fabian for helpful conversations. One of us (F.K.L.) thanks the Institute of Astronomy, Cambridge, for its warm hospitality. This research was supported in part by the NSF and by the Alfred P. Sloan Foundation.

Received February 20, accepted May 17, 1976

[1] Rosenberg, F. D., Eyles, C J, Skinner, G K, and Willmore, A. P., *Nature*, 256, 628 (1975)
[2] McClintock, J. E., *et al*, *Astrophys J Lett*, 206, L99 (1976)
[3] Bradt, H., *et al*, *Astrophys J Lett*, 204, L67 (1976).
[4] Giacconi, R, *Ann. N.Y. Acad Sci*, 262, 312 (1975)
[5] Lamb, F. K, *Ann. N.Y. Acad Sci*, 262, 331 (1975).
[6] Rappaport, S., Joss, P C, and McClintock, J. E, *Astrophys. J Lett.*, 206, L103 (1976)
[7] Bahcall, J N, *Proc Enrico Fermi Summer School on the Physics and Astrophysics of Neutron Stars and Black Holes* (Varenna, Italy, in the press)
[8] Fabian, A C., Pringle, J E, and Rees, M. J., *Mon. Not. R. astr. Soc*, 175, 43 (1976)
[9] Fabian, A. C, *Mon Not. R. astr. Soc*, 173, 161 (1975).
[10] Lamb, D. Q., Lamb, F K, and Arnett, W. D, *B A A S*, 7, 545 (1975)
[11] Elsner, R. F., and Lamb, F K, in Lamb, F K., *Proc. Int. Conf on X-rays in Space*, 613 (University of Calgary, August, 1974)
[12] Lamb, F K, Pethick, C J., and Pines, D, *Astrophys J*, 184, 271 (1973)
[13] Arons, J., and Lea, S., *Astrophys J.* (in the press)
[14] Lynden-Bell, D, and Pringle, J E, *Mon Not R astr Soc*, 168, 603 (1974)
[15] van den Heuvel, E P J, *Proc 16th Int Solvay Congress*, 131 (1974).
[16] Ewart, G. M., Guyer, R. A., and Greenstein, G., *Astrophys J.*, 202, 238 (1975).
[17] Lamb, F. K., and Sutherland, P G, *Proc. IAU Symp.*, 53, 265 (1974).
[18] Feigelson, E. D., *Nature*, 253, 250 (1975)
[19] Rees, M J., *Mon. Not R. astr Soc*, 171, 457 (1975)
[20] Middleditch, J, and Nelson, J, *Astrophys J* (in the press).
[21] Pandharipande, V. R., Pines, D., and Smith, R. A., *Astrophys J* (in the press).
[22] Lamb, F K., Pines, D., and Shaham, J., *Proc. Symp. on X-ray Binaries, Goddard Space Flight Center, October 1975* (in the press)
[23] Shulman, S, Friedman, H, Fritz, G., Henry, R C, and Yentis, D J, *Astrophys J. Lett.*, 199, L101 (1975).
[24] McCray, R, and Lamb, F K, *Astrophys. J. Lett.*, 204, 415 (1976)
[25] Basko, M M, and Sunyaev, R A, *Mon. Not R astr. Soc.* (in the press).
[26] Lucke, R, Yentis, D, Friedman, H, Fritz, G., and Shulman, S., *Astrophys J. Lett*, 208, L25 (1976).
[27] White, N. E, *et al.*, *B A A.S*, (in the press)
[28] Lewin, W H G, Hoffman, J, and Doty, J, *B A.A.S* (in the press)
[29] Schreier, E J, Swartz, K., Giacconi, R., Fabbiano, G., and Morin, J., *Astrophys. J.*, 204, 539 (1976).
[30] Fabbiano, G., and Schreier, E. J., *B.A.A S.*, (in the press).

Membrane action of DMSO and other chemical inducers of Friend leukaemic cell differentiation

Gary H. Lyman & Harvey D. Preisler
Department of Medicine

Demetrios Papahadjopoulos
Department of Experimental Pathology, Roswell Park Memorial Institute, 666 Elm Street, Buffalo, New York 14263

DMSO and other cryoprotective agents produce a pronounced increase on the phase transition temperature of phospholipid membranes, indicating an increased stability. The effects of DMSO and the other cryoprotective agents, divalent cations, and local anaesthetics on the transition temperature of phospholipid membranes seem to correlate with their effects on the differentiation of Friend leukaemic cells in vitro. *These studies suggest that the induction of differentiation by cryoprotective agents may be the result of the interaction of these agents with cell membranes.*

GROWTH of Friend leukaemic cells (FLC) in suspension culture in the presence of any one of a variety of cryoprotective agents results in the differentiation of these cells along the erythroid pathway[1,2]. Although evidence has been presented that DMSO must ultimately influence the control of differentiation at the level of transcription[3], the primary site of action of these agents remains unknown. The known properties of these agents as penetrant-carriers and cryoprotectants suggested to us that their initial and perhaps major effects might be on the cell membrane. Considerable speculation has recently been directed towards possible alteration of membrane properties during cell differentiation and malignant transformation[4]. We have used differential scanning calorimetry (DSC) to study the effects of these agents on membrane properties. This technique has been used extensively to obtain a direct measure of a temperature and enthalpy of the lipid phase transition from the solid to the liquid-crystalline state[5,6]. The temperature at which the phase transition occurs in a given system is related to the fluidity of the membranes, and lipid fluidity has been shown to be an important parameter in various functions of biological membranes[7–9].

The studies reported here demonstrate that DMSO and other compounds which induce cell differentiation, alter the properties of phospholipid membranes causing the appearance of a new transition at higher temperatures. This effect indicates stabilisation of the membranes and we interpret it as evidence for decreased membrane fluidity. Local anaesthetics, which increase membrane fluidity[10,11] inhibit the artificial membrane effects as well as the induction of benzidine positivity in FLC *in vitro* by these chemical agents. Divalent cations enhance the effects of the inducing agents and reverse the inhibitory effects of the local anaesthetics on the artificial membranes and on FLC growing in suspension culture. These studies suggest that interaction of chemical inducing agents with membrane phospholipids may be involved indirectly in the induction of FLC differentiation by the same agents.

Effects of DMSO on phospholipid membrane transition temperature

Our initial studies were with DMSO, the first inducer recognised and one of the most potent agents available. Figure 1 demonstrates the effect of increasing concentrations of DMSO on the thermotropic properties of DMPG. Increasing concentrations of DMSO produce a shift of the T_c of the normal transition towards higher temperatures (mid-point T_c from 33.0 to 36.8 °C), while apparently reducing its magnitude until it disappears (curve *e*). DMSO also causes the appearance of a previously unrecognised endothermic transition at much higher temperatures (60–70 °C) which also shifts towards higher temperatures with increasing concentrations (Fig. 1). The upper transition first appears at a DMSO concentration of 2% (v/v), it becomes predominant at about 20% (v/v/) and is the only transition present at 30% (v/v). It should be noted that the optimal concentration of DMSO for inducing FLC differentiation is 2% (v/v) which is in the range of observed effects on phospholipid membranes seen here. The appearance of the new transition at high temperature was associated with visible flocculation of the lipid preparation following dispersion of the sample.

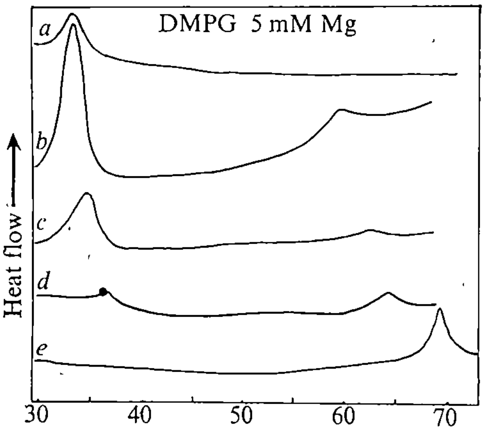

Fig. 1 The phospholipid used in these studies was dimyristoylphosphatidylglycerol (DMPG) synthesised as described previously[12]. It was stored under nitrogen in sealed ampoules at −50 °C at a concentration of approximately 10 µmol ml^{-1}. Multilamellar vesicles were prepared by the method of Bangham *et al.*[13]. The phospholipid was dispersed in phosphate-buffered saline (PBS) prepared in the presence of 5 mM magnesium chloride but free of calcium. Following dispersion at 37 °C, 2–3 µmol of lipid were distributed into individual sample tubes to which was added 5–10 ml of the solution to be studied The vesicles were then incubated in PBS in the presence of 5 mM magnesium chloride for 3 h at 37 °C in the following conditions: *a*, controls, no additions or in the presence of; *b*, DMSO 2% (v/v), 0.26 M; *c*, DMSO 10% (v/v), 1 3 M; *d*, DMSO 20% (v/v), 2.6 M; *e*, DMSO 30% (v/v) 3.9 M After incubation, the lipid suspension was centrifuged at 2,000 r p m for 30 min and the wet pellet transferred to a sample pan and covered Using a PBS standard, the phase transition temperature (T_c) of the phospholipid vesicle suspension was determined using a Differential Scanning Calorimeter (DSC-2, Perkin-Elmer, Norwalk, Connecticut). In all the studies a sensitivity scale of 1 mcalorie s^{-1}, a chart speed of 20 mm min^{-1} and a scanning rate of 50 °C min^{-1} were used The T_c, defined as the midpoint of the transition temperature, was found by heating the lipid samples at the indicated rate. The amount of lipid in each sample was not identical in each sample, so that the total heat of the transition which is represented by the area under the peak varies with different samples Consequently, comparisons between different samples were made only with respect to the T_c, and with the relative area under each peak when two peaks were present

Table 1 Effects of chemical inducers

Inducer	Benzidine-positive cells* (%) Experiment No. 1		Experiment No. 2	
Control§‡	0.3	0.3	0.6	0
DMSO 1% (0 13M)	8	14	4	9
DMSO+Mg†	24	19	37	—
DMSO+Ca†	17	17	18	19
DMSO+Dib.†	3	8	0	1
DMSO+Dib.+Ca†	11	13	9	5
TMU (4.3×10^{-3}M)	38	38	47	47
TMU+Proc.†	26	14	24	13
TMU+Proc.+Ca†	45	47	42	34

*Friend leukaemic cells (FLC), line 745A, were grown in suspension culture in Eagle's basal media with Earle's balanced salts (Gibco), made 15% with foetal calf serum (FCS) (Gibco). The cells were incubated at 37 °C in a humidified atmosphere consisting of 5% CO_2 and 95% room air. Cultures were seeded at 1×10^5 cells ml^{-1} and routinely passed at 3–4-d intervals. The chemical agents under study were added either alone or in combination at the time of seeding of the culture into 2-ml plates in duplicate. After 5 d of growth the cultures were collected, counted, and slides were made using a centrifuge, stained with benzidine Wright–Giemsa and the proportion of benzidine-positive cells was determined by one observer who counted 300 cells in a single blinded fashion. Cell viability was determined by Trypan blue exclusion

†Concentrations: Mg^{2+}, 8×10^{-3} M; Ca^{2+}, 14.3×10^{-3} M; Dibucaine, 5×10^{-6} M; Procaine, 7.3×10^{-4} M. Procaine hydrochloride was from McGraw Laboratories, Glendale, California and magnesium chloride, $6H_2O$ from Fischer Sci Co , Fairlawn, New Jersey.

‡Control cultures had no agents added. The benzidine-positive cell counts for Mg, Ca, Dibucaine, and Procaine control cultures were identical to the control counts noted above.

§Standard BME contains 8×10^{-4} M Mg^{2+} and 1.9×10^{-3} M Ca^{2+}. For the cases where additions were made the final concentrations were as indicated‡.

Effects of other inducers of differentiation on transition temperature

As shown earlier[1,2] DMSO, DMF, PNO, and TMU are all effective inducers of erythroid differentiation of FLC *in vitro* The results presented in Fig. 2 indicate that all these agents induced the appearance of a new transition at higher temperatures (upper T_c) which is similar to that produced by DMSO. The temperature of the upper transition did not always rise with increasing concentrations as observed with DMSO. The effects of the compounds on the lower peak varied somewhat with some compounds causing an increase (curve *b*) in the lower T_c with increasing concentration, while others caused little change (curves *c* and *d*) or a small decrease of the lower T_c (curve *e*). Butyric acid (data not shown) is unique among the effective inducers studied[14] in that at low concentrations (0 01 M) it raises the T_c while at higher concentrations (0.1 M) it lowers the T_c, and at even higher concentrations (1 0 M) it eliminates the transition in the temperature range tested It was not established whether butyric acid produced a new transition at much higher temperatures.

The urea family of compounds has been found to have varying effects on the induction of erythroid differentiation in FLC in the following order· TMU is an extremely potent inducer of differentiation, DMU is a moderate inducer and urea a very weak inducer[2] At concentrations of 30% (v/v) in the absence of Mg^{2+}, urea had no effect on the lower T_c and did not produce a new transition at higher temperatures.

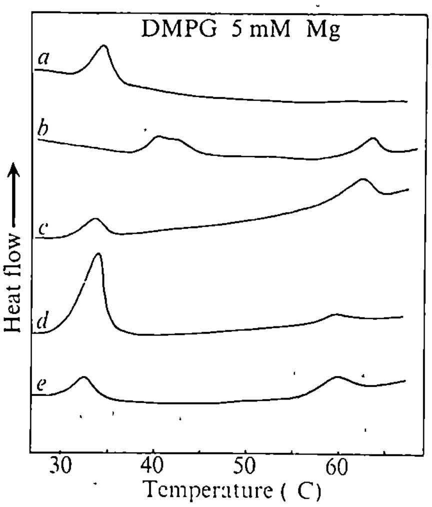

Fig. 2 Differential scanning calorimetry of DMPG vesicles in the presence of various inducers of erythroid differentiation. Vesicles were prepared in the presence of PBS with 5 mM magnesium chloride: *a*, Control. All further calorimetry thermograms were obtained in the same conditions except for the presence of: *b*, DMSO 15% (v/v), 1.95 M; *c*, DMF 15% (v/v), 1.95 M; *d*, PNO 10% stock solution (v/v), 0.81 M; *e*, TMU 10% (v/v), 0.86 M. PNO stock solution was 8.1 M, made by dissolving 100 g PNO in 130 ml of sterile water. The agents used in these studies were used as provided or dissolved in PBS (1 l contains: 900 ml 0.145 M NaCl; 80.40 ml 0.067 M Na_2HPO_4; 19.60 ml 0.067 M KH_2PO_4) and were obtained from the following companies: dimethylsulphoxide (DMSO), pyridine-*N*-oxide (PNO), tetramethylurea (TMU), dimethylurea (DMU), and butyric acid (BA), all from Eastman Kodak, Rochester, New York; dimethylformamide (DMF), urea, Fischer Sci. Co., Fairlawn, New Jersey.

On the other hand, both DMU and TMU were effective in abolishing the lower transition and producing one at much higher temperatures. TMU, which is the most potent inducer of differentiation in our system[2], in the presence of 5 mM Mg^{2+} caused the appearance of an upper transition at the lowest concentration tested (0.2% v/v), which is clearly within the range for inducing differentiation of FLC *in vitro* (0.1% v/v is optimal concentration).

Antagonistic effects of local anaesthetics and chemical inducers

It has previously been demonstrated that local anaesthetics increased the fluidity of acidic phospholipid membranes as indicated by a decrease of the T_c (ref. 11). Since the inducing agents were found to have the opposite effect on the T_c, we studied the interactions of these agents in the same system (Fig. 3).

As discussed above, the presence of DMSO results in an upward shift of the normal T_c and the appearance of a new transition of much higher T_c (Fig. 3, curve *c*). Dibucaine, on the other hand, lowers the normal T_c (curve *d*) When the vesicles were exposed simultaneously to dibucaine and DMSO, the upper T_c disappeared and the lower T_c was at midpoint between the peaks obtained when each agent was present alone (curve *e*) The disappearance of the upper T_c coincided with the disappearance of the DMSO-induced flocculation associated with the appearance of the upper T_c.

The addition of calcium to the mixture of DMSO and dibucaine not only restored the DMSO-induced upper peak, but also diminished the size of the lower transition compared with that shown by DMSO alone at that concentration (curve *f*). The exothermic (inverted) peak shown in curve *f* at 26 °C is usually obtained at higher concentrations of DMSO alone (30%). A more detailed study of the synergism of the effects of DMSO and divalent metals will be reported elsewhere[22].

Divalent cations and local anaesthetics on differentiation induction

The effects of inducing agents, divalent cations, and local anaesthetics on the properties of artificial phospholipid membranes led up to examine their effects on FLC growing in suspension culture. Friend leukaemic cells were grown in the presence of each of these agents alone or in combination (Table 1). DMSO 1% (v/v) induces a low degree of erythyroid differentiation. Increased concentration of calcium and, to a somewhat greater extent magnesium, seem to enhance the ability of DMSO to induce differentiation although they do not induce differentiation on their own at the concentrations used. Both dibucaine and procaine were found to inhibit to a large extent the development of benzidine positivity induced by DMSO and TMU in terms of both the proportion of benzidine-positive cells in the culture as well as the degree of positivity of the individual cells. Furthermore, calcium was able to restore and perhaps slightly enhance the DMSO-induced benzidine positivity previously inhibted by the local anaesthetics. None of these compounds alone or in combination, nor the addition of calcium, had any effect on the number or viability of cells present after 5 d of culture when compared with control cultures. Two additional observations are of interest. When FLC were grown in higher concentrations of DMSO or TMU (at 0.27 M or 8.6×10^{-3} M respectively) the topical anaesthetics produced little if any inhibition of benzidine positivity Additionally, although the addition of calcium had no effect on the rate of cell growth, the benzidine-positive cells in these cultures were vacuolated.

Membrane effects of cryoprotective agents

Cryoprotective agents which induce Friend leukaemic cell differentiation *in vitro* have variable effects on the normal T_c of phospholipid vesicles but consistently induce the appearance of a new endothermic peak at higher temperature. We interpret this as evidence for a stabilisation of the lipid bilayers indicating a decrease in membrane fluidity. Although high concentrations of inducing agents were frequently used, detectable effects on membrane fluidity were obtained with concentrations in the range used to induce differentiation in culture. Our previous studies with cryoprotective agents suggested that the ability of an agent to induce FLC differentiation paralleled the basicity of the agent[1]. Our current studies are in accord with these in that we have found that the effects of these agents in 'stabilising' phospholipid membranes are much more pronounced with acidic than with neutral phospholipids[22] it therefore seems that ionic charge interactions and perhaps hydrogen bonding[15] may be involved in the interaction of these compounds with phospholipid membranes.

The DSC studies demonstrated that agents, such as local anaesthetics[10,11,16] which increase membrane fluidity, inhibit the DMSO effect on membranes, whereas on the other hand, factors which decrease membrane fluidity such as Ca^{2+} and Mg^{2+} [17,18], enhance the DMSO effect An analogous relationship was found between the actions of divalent metals (enhancing) and a local anaesthetic (inhibiting) on cell differentiation induced by DMSO as judged by the development of benzidine positivity. But the inhibition of benzidine positivity by local anaesthetics[19] raises several questions in itself, since not only was the proportion of benzidine-positive cells decreased, but the degree of benzidine positivity of the differentiating cells was also reduced. This latter observation raises the possibility that the local anaesthetics may interfere only with the synthesis of haem and perhaps not inhibit at the same site where DMSO is involved directly in inducing FLC differentiation. For example, DMSO and other inducing agents have several different effects, whereas the local anaesthetics may merely inhibit mitochondrial synthesis of

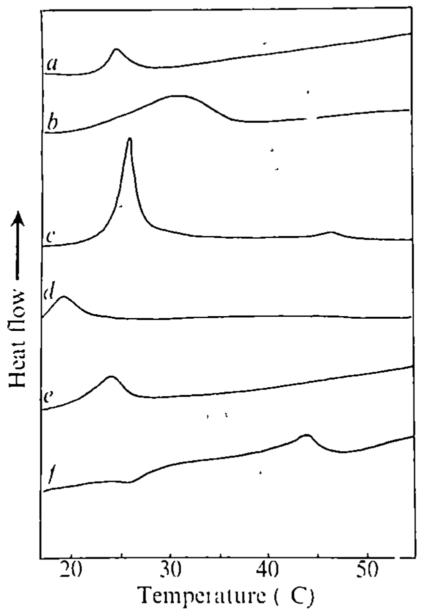

Fig. 3 Differential scanning calorimetry of DMPG vesicles in the presence of DMSO, dibucaine and calcium *a*, Thermogram obtained from vesicles prepared in the presence of PBS alone The remaining curves were obtained from vesicles to which were added: *b*, calcium chloride 5×10^{-4} M; *c*, DMSO 20% (v/v), 2.6 M; *d*, dibucaine hydrochloride 5×10^{-5} M; *e*, DMSO 20% (v/v), 2.6 M and dibucaine hydrochloride 5×10^{-5} M; *f*, DMSO 20% (v/v), 2.6 M, dibucaine hydrochloride 5×10^{-5} M, and calcium chloride 5×10^{-4} M Dibucaine hydrochloride was obtained from K and D Laboratories, Plainview, New York.; calcium chloride from Upjohn Co, Kalamazoo, Michigan.

haem. Other manifestations of differentiation may therefore not be inhibited by the local anaesthetics.

Our studies suggest that the cryoprotective ability of these compounds may also be related to their membrane effects. It is possible that a decrease in fluidity of the cell membrane could render the cell and its subcellular organelles more resistant to distortion during freezing. In fact, preliminary experiments in our laboratory suggest that local anaesthetics may inhibit DMSO cryoprotection of erythrocytes.

Although not ruling out a direct effect on transcription, the studies reported here suggest that in FLC line 745A interaction of the cryoprotective inducers with the cell membrane may play an important part in the induction of differentiation of murine erythroleukaemic cells. A decrease in membrane fluidity could alter the transport and permeability properties of the membrane or cause the 'release' of an intracellular messenger which would itself be responsible for initiating the transcription of those mRNAs necessary for erythroid differentiation. On the other hand, the same physical interactions which occur between the agents and the phospholipid membranes and the associated water molecules could also occur at other sites within the cell (including proteins, or nucleic acids). The conformational changes produced at such sites[20,21] could result in differentiation by directly effecting the transcription of mRNAs associated with differentiation. Although these lipid vesicle studies seem to be predictive of the effects of cryoprotective agents on FLC line 745A, they are not predictive of their effects on line 745D, a cell line which is refractory to DMSO and only minimally responsive to other cryoprotective agents[2]. It thus seems possible that the difference in responsiveness between lines 745A and 745D may be a result of differences in their cell membranes.

We thank G. Christoff, E. Taylor, T. Isac and R. Lazo for technical assistance. This work was supported by US Public Health Service grants from the National Institutes of Health.

Received October 20, 1975; accepted May 25, 1976

1 Preisler, H D., and Lyman, G H., *Cell Differentiation*, 4. 179–815 (1975).
2 Preisler, H D, Christoff, G, and Taylor, E, *Blood*, 47, 363–368 (1976)
3 Preisler, H. D, Houseman, D, Scher, W., and Friend, C, *Proc natn. Acad Sci U S A*, 70, 2956–2959 (1973)
4 Pollack, R E, and Hough, P V C, *A Rev Med*, 25, 431–446 (1974)
5 Ladbrooke, B D, and Chapman, D, *Chem phys Lipids*, 3, 304–356 (1969).
6 Hinz, H J, and Sturtevant, J M, *J biol. Chem*, 247, 6071–6075 (1972).
7 Linden, C D., Wright, K. L, McConnell, H M, and Fox, C F, *Proc. natn Acad Sci. U.S A.*, 70, 2271–2275 (1973).
8 Overath, P, and Trauble, H, *Biochemistry*, 12, 2625–2634 (1973).
9 Raison, J K, *J Bioenerg*, 4, 285–309 (1973)
10 Hubbell, W. L, Metcalfe, J C, Metcalfe, S M, and McConnell, H M, *Biochim biophys Acta*, 219, 415–427 (1970).
11 Papahadjopoulos, D' Jacobson, K, Poste, G., and Shepard, G., *Biochim. biophys. Acta*, 394, 504–519 (1975)
12 Papahadjopoulos, D., Jacobson, K., Nir, S, and Isac, T, *Biochim biophys Acta*, 311, 330–348 (1973)
13 Bangham, A. D, Standish, M. M, and Watkins, J C., *J molec Biol*, 13, 238–252 (1965)
14 Leder, A, and Leder, P, *Cell*, 5, 319–322 (1975)
15 Rammler, D H., and Zafferoni, A, *Ann. N Y Acad Sci*, 141, 13–23 (1967)
16 Colley, C. M., and Metcalfe, J C., *FEBS Lett*, 24, 241–246 (1972).
17 Jacobson, K, and Papahadjopoulos, D, *Biochemistry*, 14, 152–161 (1975)
18 Trauble, H., and Eibl, H, *Proc. natn Acad Sci U.S A*, 71, 214–219 (1974)
19 Bernstein, A., Boyd, A S., Brichley, V., and Lamb., V., in *Biogenesis and Turnover of Membrane Macromolecules* (edit by Cook, J. S), 145–159 (Raven, New York, 1976)
20 Henderson, T R., Henderson, R. F, and Johnson, G. E, *Arch. Biochem. Biophys.*, 132, 242–248 (1969)
21 Herskovits, T T., *Archs Biochem Biophys.*, 97, 474–484 (1962).
22 Lyman, G.H, Papahadjopoulos, D, and Preisler, H D, *Biochim biophys. Acta* (in the press).

Similarity of the crystal and solution structure of yeast tRNA$^{\rm Phe}$

G. T. Robillard, C. E. Tarr*, F. Vosman & H. J. C. Berendsen

Department of Physical Chemistry, University of Groningen, Zernikelaan, Groningen, The Netherlands

A comparison of the crystal and the solution structure of yeast tRNA$^{\rm Phe}$ has been carried out by calculating the low field NMR spectrum from refined X-ray structure coordinates. The similarity between the computed and observed spectra show that the crystal and solution structure are virtually identical.

NUCLEAR magnetic resonance (NMR), in theory, can provide information on the solution structure of a macromolecule at the same level of resolution as obtained with X rays in solids. In particular, the chemical shift and relaxation parameters contained in an NMR spectrum are sensitive functions of the local environments of individual nuclei. Nevertheless, the transition from the theoretical argument to the practical task of attempting to extract such information from NMR spectra poses significant problems since the magnitude of individual effects are not precisely known and difficult to calculate.

---

* Permanent address: Department of Physics, University of Maine, Orono, Maine 04473.

Table 1 Optimised ring current values

Nucleotide	Ring currents Giessner-Prettre and Pullman[6]	Optimised
Adenine		
Hexagonal ring	0.88	0.763
Pentagonal ring	0.67	0.580
Guanine		
Hexagonal ring	0.25	0.288
Pentagonal ring	0.63	0.725
Cytosine	0.27	0.210
Uracil	0.08	0.107

Calculation of magnetic ring currents, however, has reached a significantly high level of accuracy to be useful in predicting resonance positions if these positions, to a reasonable approximation, are determined only by ring current effects. In the case of NMR spectra of tRNA it is likely that ring currents are the dominant shift mechanism determining resonance positions.

Each ring NH · · · N hydrogen bonded proton in a Watson–Crick base pair generates a resonance in the low field region of the proton NMR spectrum of tRNA[1] The chemical shift of a proton in such an environment is a combination of three principal effects: (1) deshielding by polarisation of the NH bond due to the adjacent electronegative atoms of the hydrogen bond; (2) deshielding arising from the ring currents of the two aromatic rings between which this hydrogen bonded proton is located; and (3) shifts caused by the ring currents of bases stacked above and below the base pair containing the proton in question. The magnitude of these three effects may be as large as several parts per million. All other shift mechanisms generate shifts on the order of a few tenths of a part per million.

Fig. 1 360-MHz proton NMR spectra of yeast tRNA^{Phe} in H_2O solutions taken at 35 °C. The spectra represent 1-h accumulations in the continuous wave mode with a sweep rate of 12 s per 2,400 Hz. Solvent composition was: *A*, 1 mM tRNA, 1 mM EDTA and 10 mM sodium cacodylate *p*H 7; *B*, 1 mM tRNA, 1 mM EDTA, 10 mM sodium cacodylate *p*H 7, 15 mM $MgCl_2$, 0.1 M NaCl.

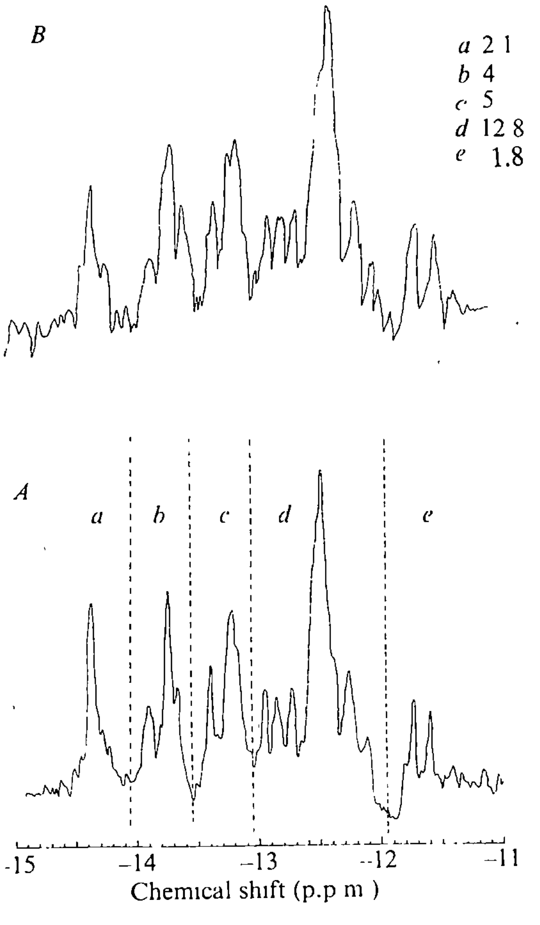

Since the X-ray structure of yeast tRNA^{Phe} has now been solved[2,3] and refined coordinates are available, we have calculated, directly from the coordinates, the ring current shift which each hydrogen bonded proton experiences from all other aromatic rings in the molecule. The results show that, on the basis of the resulting NMR spectrum, the X-ray crystal structure and the solution structure are virtually identical.

Ring current calculations

We have used the theory of Haigh and Mallion[4] to calculate the ring current shifts of the hydrogen bonded protons. In this theory, which is based on McWeeny's quantum mechanical treatment[5], all contributions to the ring current shifts are standard geometric terms that are calculated from the positions of ring atoms, multiplied by a factor proportional to the magnitude of the ring current. Haigh and Mallion used an empirical factor that is relevant only for in-plane protons attached to aromatic ring systems, but that should be scaled up by a factor of 2.6 for large distances. We have used this factor of 2.6 as appropriate for the distances occurring in tRNA. Our program for calculating the ring current shifts places a proton on a straight line between the donor and acceptor nitrogens at a distance of 1.02 Å from the donor It then sums the ring current contributions of every ring in the molecule excluding the donor and acceptor rings for the base pair of interest These rings are considered separately when determining starting positions for a hydrogen bonded proton in a given type of base pair.

Ring currents for the four isolated bases A, G, U and C have been calculated by Giessner-Prettre and Pullman[6] and are expressed relative to the ring currents in benzene (see Table 1). For several reasons calculated values of ring currents can be considered to be only approximately correct: (1) ring currents, derived from second-order perturbation theory, are sensitive to approximations used in the quantum mechanical treatment; (2) in hydrogen bonded base pairs the ring currents may deviate substantially from those in isolated bases; (3) the neglect of the effect of charges in heterocyclic rings; and (4) the inaccuracy of the geometric terms used in the calculation of shifts all may influence the apparent ring currents. Empirical adjustments for each of the ring currents should therefore be made to properly account for the observed shifts. We used the calculated ring currents[6] as starting values in an iterative procedure that successively refined each value. First, the A and G ring currents, and the difference between the AU and GC starting positions were varied and the computer was allowed to make a best fit between the nearest members of the calculated and the observed spectra. Then the C and U ring currents were refined keeping A and G fixed. These new values then provided the basis for a final slight refinement of A and G ring currents. In each case, the pentagonal and hexagonal ring currents of each purine were varied by the same factor, thus leaving only four ring currents to be refined. Because of the rapid convergence of this technique, no further iteration was required. A major advantage of this procedure is that one is not required to make detailed *a priori* assignments of given base pairs to specific resonances in the observed spectrum and thereby prejudice the outcome.

The values arrived at by this optimisation procedure are listed in Table 1. As can be seen, the optimum values for this calculation are only slightly different from the values calculated by Giessner-Prettre and Pullman[6]. Furthermore, the changes are consistent with those expected from hydrogen bonding between base pairs. During hydrogen bonding the electron density in the electron cloud, and hence the ring current, is expected to increase on the donor base and decrease on the acceptor base. This is precisely what occurs when the ring

Table 2 Base pair ring current shift

Helix	Base pair	Ring current shift (p.p.m)
Acceptor	GC 1	+1.2244
	CG 2	+1.0705
	GC 3	+1.4032
	AU 5	+0.6150
	UA 6	+0.6151
	UA 7	+1.0451
DHU	GC 10	+0.9852
	CG 11	+0.4379
	UA 12	+0.3418
	CG 13	+0 5539
Anticodon	CG 27	+1.1602
	CG 28	+1.9580
	AU 29	+1.1530
	GC 30	+0.9366
	AΨ 31	+0.2392
TUC	CG 49	+1.3464
	UA 50	+1.5445
	GC 51	+1 2773
	UA 52	+1.1299
	GC 53	+0.9840
Tertiary	U8–A14	+0.5369
	T54–A58	+0 4942
	G22–m^{7}G46	+1.7710
	G19–C56	+0.8615
	m$_2^2$G26–A44	+0 4052
	G15–C48	+0.4003

currents are optimised. We are confident, therefore, that the optimisation procedure has not led to incorrect answers.

Yeast tRNA^{Phe} NMR spectrum

For the purpose of making detailed comparisons between observed and calculated spectra, it was necessary to use the most highly resolved spectra of tRNA^{Phe} available. Figure 1 shows the low field NMR spectra of yeast tRNA^{Phe} taken at 360 MHz in the absence or presence of Mg^{2+} (B R. Reid, personal communication). Except for slight shifts in resonance positions and the narrowing of the resonances in the absence of Mg^{2+}, the two spectra are identical. Because of the higher magnetic fields and the special solvent conditions, however, the resolution in the no Mg^{2+} spectrum (Fig 1*A*) reveals a number of features not observed in previously published spectra of this molecule[7–10]. There are seven well resolved resonances below −11.5 p.p.m. all of which have approximately unit intensity. When the total integrated intensity in the spectrum is calculated relative to any one of these individual resonances we find 26 ± 1 protons between −15 and −11.5 p.p.m. as shown in the table on the side of spectrum in Fig 1*B* (B. R. Reid and G. T. R., in preparation). Similar spectral resolution plus an independent calibration on the high field methyl resonances has led us recently to the same conclusion in the case of *Escherichia coli* tRNA$_1^{Val}$ (refs 11 and 12). The intensity in the low field region of yeast tRNA^{Phe} must then be attributed to the 20 secondary structure Watson–Crick hyrodgen bonded base pair protons (Fig 2) plus hydrogen bonded protons from tertiary interactions. There are five tertiary interactions involving ring NH· · ·N type hydrogen bonds which should account for five of the resonances in this region. Only one proton resonance is left unaccounted for and its origin will be discussed in the following section

Table 3 Proton resonance positions

Base pair	Chemical shift (p.p.m) Calculated	 Observed
UA 12	−14.01	−13.91
AU 5	−13.74	−13 72
UA 6	−13.74	−13.72
UA 7	−13.31	−13.38
UA 52	−13.22	−13.25
AU 29	−13.20	−13.22
AU 31	−13.18	−13 18
CG 11	−13 10	−13.16
CG 13	−12.98	−12.93
UA 50	−12.81	−12.83
GC 30	−12.60	−12.57
GC 10	−12 55	−12.51
GC 53	−12.55	−12.49
CG 2	−12.47	−12 47
CG 27	−12.38	−12.42
GC 1	−12.31	−12 39
GC 51	−12 26	−12.27
CG 49	−12.19	−12.23
GC 3	−12.13	−12.09
CG 28	−11.58	−11.58
T54–A58	−14 38	−14 40
U8–A14	−14.42	−14.40
G19–C56	−12 68	−12.72
G22–m^{7}G46	−12.47	−12 47
G15–C48	−11 78	−11 72
m$_2^2$G26–A44	−13.81	−13 81

Base pair offsets: Watson–Crick AU, −14 35; Watson–Crick GC, −13.54; reversed Hoogstein AU, −14.90; AΨ ≃ −13 50.

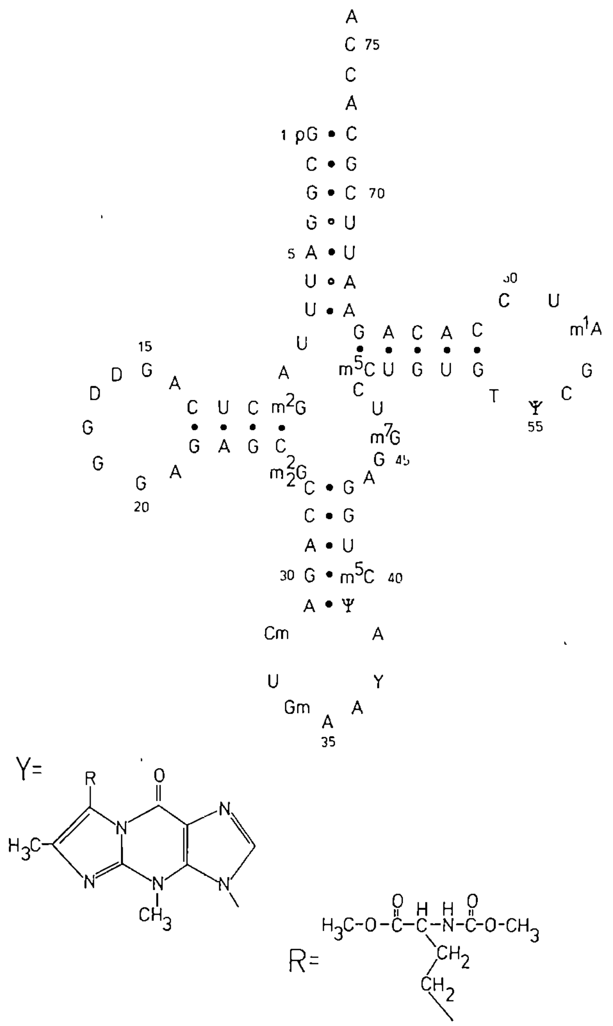

Fig. 2 Cloverleaf sequence of yeast tRNA^{Phe} (refs 14 and 15)

Figure 3*A* is a computer fit of the original spectrum in Fig. 1*A*. It was prepared by assigning a number of Lorentzian lines of equal intensity and linewidths to the positions where they occur in the original spectrum. Twenty-six lines were used to generate this spectrum and comparison with Fig. 1 demonstrates that the integration shown in this figure accurately reflects the number of protons in each peak of the original spectrum. The individual positions used in this fit were the same as those used in the ring current optimisation discussed above The optimised ring current values for the four bases obtained by this procedure (Table 1) have been used in the Haigh and Mallion ring current

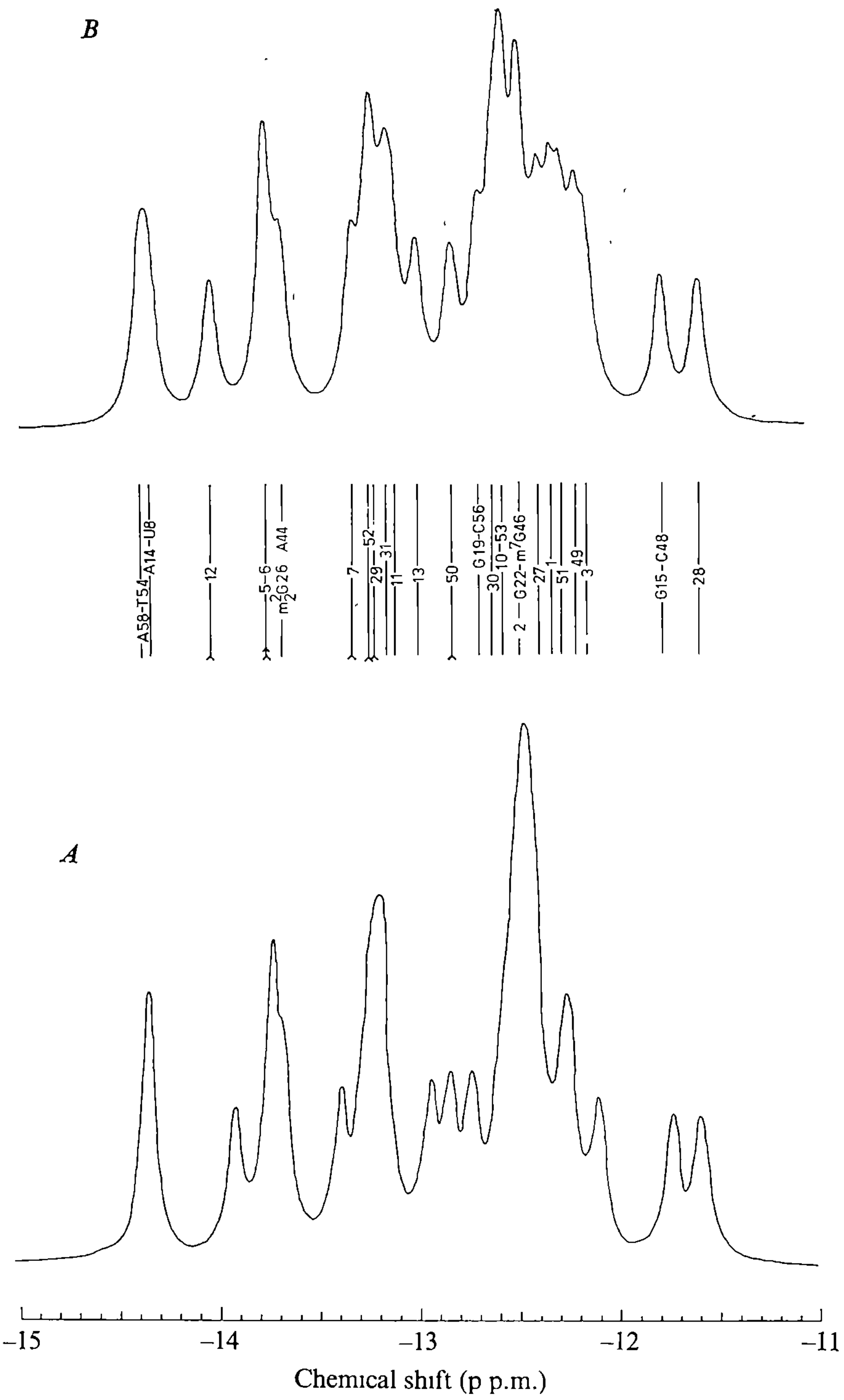

Fig. 3 *A*, Computer fit of the spectrum in Fig. 1*A* prepared as described in the text, *B*, spectrum calculated from the X-ray structure coordinate and optimised ring current values using the procedures and offsets described in the text and Tables 1–3. The indicated base pair positions are those assigned by the computer from the calculations. Secondary structure resonances are denoted by the normal conventions 1, 2 . . . . Secondary structure AU resonances are denoted by an ^ at the bottom of the line. Tertiary structure resonances are denoted by the full lettering and numbering of the base pair, that is, U8–A14 and so on.

calculation along with the X-ray crystal structure coordinates of yeast tRNA$^{\mathrm{Phe}}$ refined by Sussman and Kim (personal communication). The resulting spectrum (Fig. 3*B*) compares very closely with the original (Fig. 3*A*). Since the NMR spectrum of tRNA$^{\mathrm{Phe}}$ can be quite accurately calculated from the crystal structure coordinates simply by summation of the ring currents arising from each aromatic substituent in the molecule, there must be a very high degree of similarity between the solution and crystal structure

Resonances from secondary structure base pairs

A base pair hydrogen bonded proton will experience deshielding ring currents from the aromatic rings of the donor and acceptor bases. If the distance between the donor and acceptor bases varies slightly, as they do in the refined crystal structure coordinates (2.8–3.1 Å), there will be slight alterations in the ring current shift. Since it is not clear, however, that these differences are physically meaningful at the current level of resolution of the X-ray coordinates, they have been ignored in the present calculations Any error which results from this approximation will be small since the differences in degree of deshielding originating from these slight changes amount to only a few Hz. Deshielding also arises from the electronegative atoms of the hydrogen bond as stated previously. Since it is impossible to determine accurately the hydrogen bond strengths and correlate them with deshielding effects we have again assumed that the deshielding arising from the hydrogen bonded situation of the proton is the same for a given type of base pair. Thus the starting position for a proton in each type of isolated base pair is allowed to be a variable in the optimisation procedure discussed above. The parameters found were −14.35 and −13.54 p.p.m. for Watson–Crick AU and GC base-paired hydrogen bonded protons, respectively.

Resonance from AΨ base pair

The aromatic ring of the "Y" base is stacked in the anticodon loop, one ring removed from the Aψ base pair. In the present calculation the ring current shift arising from this base was calculated using the ring current value provided by B. Pullman (personal communication). The total ring current shift experienced by the Aψ hydrogen bonded proton is 0.24 p.p.m. In studies of the anticodon fragment of yeast tRNA^{Phe}, Lightfoot *et al.*[9] found the Aψ resonance occurring in region *c* of Fig. 2 and set the starting position at −13.5 p.p.m. We find that the Aψ could occur in either region *b* or *c* depending on the starting position and the magnitude of the ring current shift which the proton experiences. In the absence of other information, therefore, we prefer to rely tentatively on the fragment studies and assign the resonance to region *c* with the Aψ starting position in the region of −13.5 p.p.m.

Resonances from tertiary structure interactions

The calculated resonance positions marked in Fig. 3 show that the two protons in region *a*, and one each in regions *b*, *c*, *d* and *e* are not normal Watson–Crick AU or GC secondary structure resonances Having assigned AΨ 31 to region *c* in the previous section, the tertiary interactions must generate resonances in the remaining regions. The tertiary structure interactions involving U8–A14 and T54–A58 are of the reversed Hoogstein type (see Fig. 4*b*). These two tertiaries experience approximately the same ring currents as do the hydrogen bonded protons of AU5, 6 and 12 (see Table 2). If the AU offset is the same for both Watson–Crick and reversed Hoogstein base pairs, five protons fall into region *b* and none into region *a* of Fig. 1. It is probable, however, that protons in the reversed Hoogstein arrangement have a starting position to lower field than Watson–Crick AU protons. In the reversed Hoogstein arrangement (Fig. 4*b*), the hydrogen bond acceptor is N7 of the five-membered ring instead of N1 of the six-membered ring. It has been shown by calculations on the tautomeric forms of purines[13] that the ring currents in both the hexagonal and pentagonal rings are a factor of 2–3 higher if a proton is attached to the N7 compared with the N1. The change in ring currents on hydrogen bonding N7 in place of N1 is

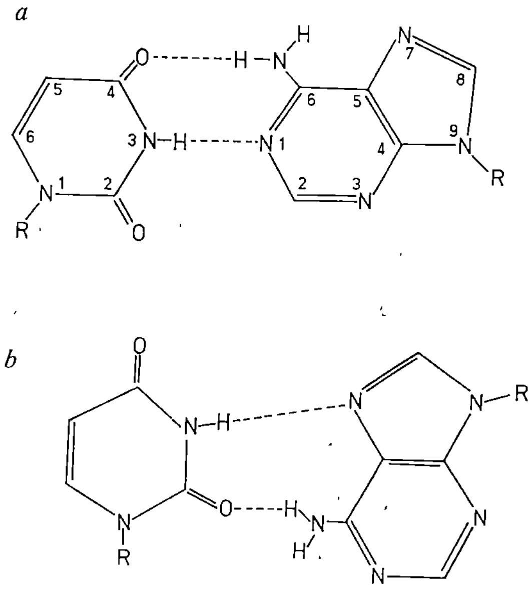

Fig. 4 Comparison of Watson–Crick AU base pairing (*a*) and reversed Hoogstein AU base pairing (*b*).

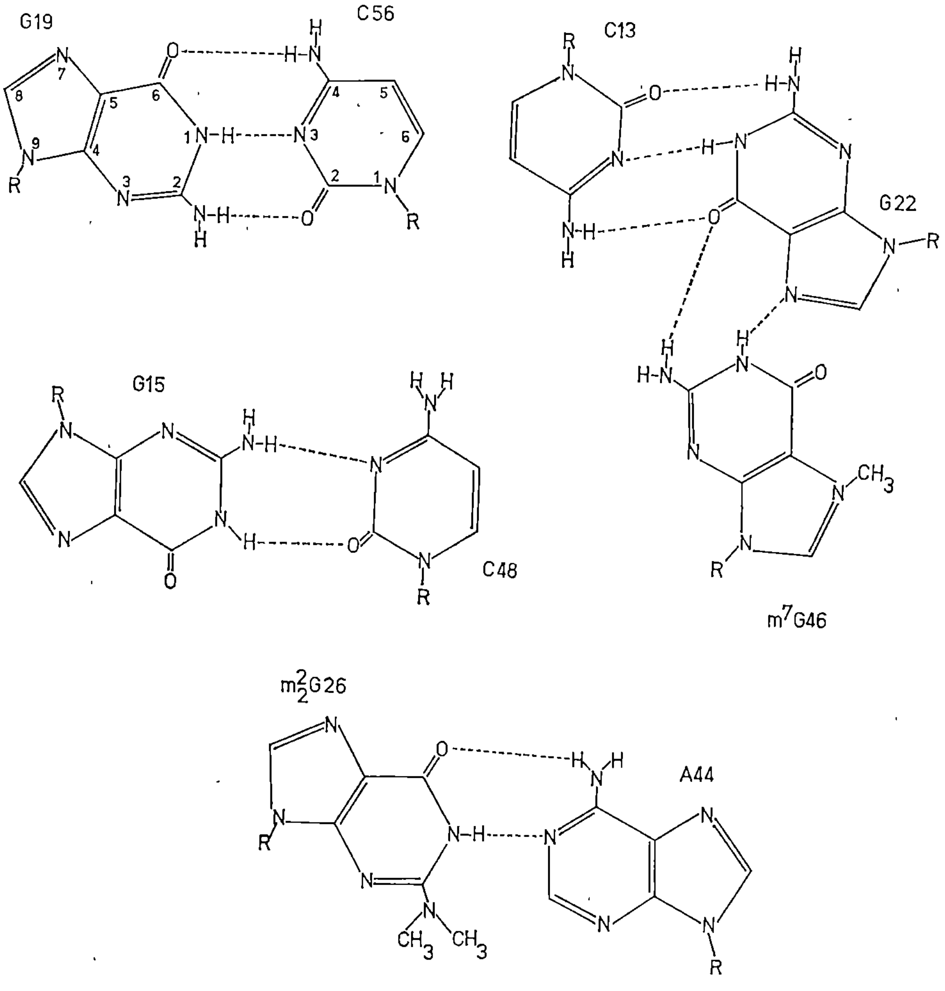

Fig. 5 Tertiary structure base pairing interactions, excluding the AU reversed Hoogstein, which are suggested to contribute resonances in the low field region of the NMR spectrum of yeast tRNA^{Phe} (refs 2 and 3).

expected to be in the same direction. Thus the deshielding experienced by the proton in the reversed Hoogstein pair is expected to be greater than in the Watson–Crick base pair and the starting position should occur at lower field. Setting the reversed Hoogstein AU offset at −14.9 p.p.m. places the two tertiaries U8–A14 and T54–A58 in peak *a* at −14.4 p.p.m. A lower field starting position for the reversed Hoogstein base pair may also arise from a localisation of positive charge on the five-membered ring when hydrogen bonding occurs at N7. In contrast, the positive charge which develops when hydrogen bonding occurs at N1 in a Watson–Crick arrangement may be withdrawn from the ring by resonance interaction with the NH_2 group. A higher degree of positive charge on the ring would result in greater deshielding and a lower field position for the reversed Hoogstein AU base pair proton.

Figure 5 shows the remaining tertiary structure interactions which are likely to give rise to resonances in the −15 to −11.5 p.p.m. region of the NMR spectrum. Since G19–C56 is a normal Watson–Crick base pair we have used the standard GC starting position of −13.54 p.p.m. which places the resonance from this base pair in region *d* (see Fig. 3). Only one proton each in regions *b*, *d* and *e* remain unaccounted for. Allowing for the strong deshielding ring currents which should arise from both rings in the tertiary base pair m^2_2G26–A44, the starting position for this resonance should certainly be lower than a normal Watson–Crick GC and may be more nearly the same as a Watson–Crick AU proton resonance. Therefore, we have tentatively placed m^2_2G26–A44 in peak *b* with a starting position of −14.2 p.p.m. The G22–m^7 G46 interaction (Fig. 5), is of the reversed Hoogstein type. By analogy with the arguments presented for the AU reversed Hoogstein resonance starting positions we expect this GG reversed Hoogstein offset to be to lower field than a Watson–Crick GC starting position. The difference between a Watson–Crick and a reversed Hoogstein AU offset is 0.55 p p.m. With the G22–m^7G46 resonance assigned to region *d* at −12.47 p.p.m. the GG reversed Hoogstein interaction has a starting position of −14.2 p.p.m. (0.65 p.p.m. to lower field than the Watson–Crick GC interaction). The ring NH of G15 hydrogen bonded to the exocyclic oxygen of C48 should be less deshielded than a normal Watson–Crick GC and we have tentatively assigned this proton to region *e* as indicated in Fig. 3 with a low field starting position of approximately −12.1 p.p.m.

Comparison with previous NMR data

The original analysis of the yeast $tRNA^{Phe}$ NMR spectrum was made with considerable help from NMR spectra of fragments of the individual helices[9]. Since the helical region structure was expected to be fairly stable in the presence or absence of the rest of the molecule, the spectra obtained were assumed to reflect the resonance positions of the base pairs for a given helix in the intact molecule. If one compares the fragment data with the assignments which have evolved from the present calculations of the secondary structure resonance positions, it is immediately evident that the present assignments are in very close agreement with the fragment data. The only noticeable deviation is the assignment of GC 13 in the DHU helix which was originally assigned to one of the two highest field resonances. Our calculations show, however, that GC 13 suffers very little upfield shift (see Fig. 3 and Table 2).

The major change which must be made as a result of these studies is that the Watson–Crick AU starting position is changed to −14.35 p.p.m. In the early studies, without knowledge of AU tertiary structure resonances it was necessary to set the offset to lower field to account for the resonances which occurred below −14 p.p.m. This, however, necessitated raising the A and G ring currents 20% above published values.

The results of removing the sulphur from thiouridine in *E. coli* $tRNA_1^{Val}$ (ref. 11) provide further support for assigning the resonances in region *a* of Fig. 1, to the tertiary AU resonances. When the sulphur was removed from s_4U8 by cyanogen bromide treatment the resonance which occurred at −14.9 p.p.m. in the NRM spectrum of *E. coli* $tRNA_1^{Val}$ disappeared and was replaced by a new resonance at −14.2 p.p m. This treatment should have changed a s_1U8–A14 tertiary base pair into a normal U8–A14 tertiary base pair as we have in yeast $tRNA^{Phe}$. The new resonance which appeared was located very close to that which we have assigned to the U8–A14 tertiary in the present spectra.

Kallenbach *et al.*[16] observed resonances at −13.8 and −13.2 p.p.m. when studying AMP interacting with oligo(U_{15}). Assuming the Watson–Crick AU offset of −14.6 p.p.m. originally used by Shulman *et al.*[8], the −13.8 p.p.m. resonance was assigned to ring NH · · · N Watson–Crick interactions while the −13.2 p.p.m. resonance was assigned to hydrogen bonded protons in the reversed Hoogstein interactions. The offsets proposed in this paper reverse the order of these assignments. Furthermore, when these offsets are used in conjunction with new ring current shift tables (Robillard *et al.*, in preparation) the position of the Watson–Crick and reversed Hoogstein resonance interactions for this polymer are predicted to occur exactly at the observed positions.

In their studies of ribosyl ApApGpCpUpUp double-stranded helix, Kan *et al.*[17] observed an AU resonance assigned to the internal AU base pair. At 0° the resonance occurred at −14.2 p.p.m. Since this base pair proton is expected to receive an upfield shift of approximately 0.5 p.p.m. from the neighbouring G, it would seem that the present starting position of −14.35 p.p.m. for a Watson–Crick AU base paired proton resonance is incorrect. It should be realised, however, that the temperature-dependent measurements of this fragment show a continuing shift as a function of decreasing temperature even after changes in the resonance line widths have ceased. As has been shown[17], this could arise from a structural change in the helix geometry (fraying effects). Thus it is likely that these fragments studies are not directly comparable with studies on larger polymers.

Conclusions

Table 3 contains the resonance positions of the protons in the observed spectrum and compares them with those which we have calculated using the offsets given at the bottom of the table and the ring current shifts in Table 2. The r.m.s. error between the resonances in the two columns is less than 0.05 p.p m. (18 Hz) when only the 20 secondary structure resonances are included. The agreement between the calculated and observed positions, which is even within the observed linewidth, can be considered as very satisfactory since in the optimisation procedure only five adjustable parameters were used to calculate 20 relative line positions. These parameters were the four ring currents and the difference between the AU and GC starting positions. The deviations which are still observed may well represent slight differences between crystal and solution structure. They may also arise from a slightly incorrectly refined structure in one part of the molecule. Further experiments are in progress to examine these possibilities as well as the accuracy of our optimised ring currents and starting positions for the individual base pair types.

We thank the ZWO (Netherlands Foundation for Pure Research) for support of the high resolution NMR facility at the University of Groningen, B. Pullman for providing the "Y" base ring current, R. Kaptein for assistance with the ring current calculation programmes, and R. G. Shulman and B. R. Reid for their stimulating ideas and suggestions. We would also like to thank S. H. Kim for providing refined coordinates as soon as they were available.

Received April 28, accepted June 2, 1976.

[1] Kearns, D R , Patel, D , Shulman, R G , and Yamane, T , *J molec. Biol.*, **61**, 265–270 (1970).
[2] Quigley, G. J , *et al.*, *Proc. natn. Acad Sci U.S A* , **72**, 4866–4870 (1975).
[3] Ladner, J. E , *et al* , *Proc. natn. Acad Sci. U.S.A.*, **72**, 4414–4418 (1975).
[4] Haigh, C W , and Mallion, R B., *Molec. Phys* , **22**, 955–970 (1971).
[5] McWeeny, R , *Molec. Phys.*, **1**, 311–321 (1958).

[6] Giessner-Prettre, C., and Pullman, B., *C r. hebd. Séanc Acad. Sci., Paris*, **261**, 2521–2523 (1965).
[7] Wong, Y. P., Kearns, D. R., Reid, B. R , and Shulman, R. G., *J. molec Biol.*, **72**, 725–740 (1972)
[8] Shulman, R. G., Hilbers, C. W., Kearns, D. R , Reid, B. R., and Wong, Y. P . *J. molec Biol* , **78**, 57–69 (1973)
[9] Lightfoot, D. R., Wong, K. L., Kearns, D R , Reid, B R , and Shulman, R G , *J molec. Biol.*, **78**, 71–89 (1973).
[10] Hilbers, C. W., Shulman, R G., and Kim, S. H., *Biochem biophys Res Commun* , **55**, 953–960 (1973)
[11] Reid, B. R., *et al.*, *Proc. natn. Acad. Sci U.S.A.*, **72**, 2049–2053 (1975).
[12] Reid, B. R., and Robillard, G. T., *Nature*, **257**, 287–291 (1975).
[13] Giessner-Prettre, C., and Pullman, B , *C. r. hebd Séanc Acad Sci., Paris*, **268**, 1115–1117 (1969).
[14] RajBhandary, U. U., *et al.*, *Proc natn. Acad. Sci U.S.A.*, **57**, 751 (1967).
[15] Nakanishi, K., Furutachi, N , Funamizu, M., Grunberger, D., and Weinstein, I. B., *J. Am. chem. Soc.*, **92**, 7617 (1970).
[16] Kallenbach, N. R., Daniel, W. E., and Kaminker, M. A., *Biochemistry*, **15**, 1218–1224 (1976)
[17] Kan, A. S., Borer, P. N., and Ts'o, P. O. P., *Biochemistry*, **14**, 4864–4869 (1975).

letters to nature

The 21-cm absorption line in NGC1275

De Young, Roberts and Saslaw[1] detected H I absorption in NGC1275 with a velocity of 8,120 km s^{-1}. This is ~ 3,000 km s^{-1} larger than the systemic velocity of NGC1275 and is the same as that of the enigmatic system of gas filaments extending 40″ from the nucleus[2,3]. The observations of De Young *et al.* were made with a single dish with insufficient angular resolution to determine which of the various radio continuum sources were being absorbed. They argue that the absorption is probably occurring in the components < 0.2″ rather than in the 5′ halo component, but they were unaware of an intermediate scale 30″ component[4]. Here we present observations made with sufficient angular resolution to decide unambiguously between these possibilities. Our data can also be used to place a limit on the H I mass of possible foreground objects which could be causing the absorption.

Table 1 Flux densities in each channel

$c\Delta\lambda/\lambda_0$* (km s^{-1})	Average flux densities† (Jy) 'short' (50″)	Average flux densities† (Jy) 'long' (20″)	Relative flux densities‡ (Jy) 'short' (50″)	Relative flux densities‡ (Jy) 'long' (20″)
8,085	10.86	9.37	−0.039	−0.053
8,126	10.62	9.14	−0.285	−0.291
8,167	10.89	9.41	−0.013	−0.017
8,209	10.91	9.42	−0.016	−0.008
8,250	10.91	9.42	−0.004	−0.006
8,291	10.91	9.43	0.005	0.001
8,332	10.92	9.43	0.011	0.004
8,373	10.90	9.43	−0.011	0.001

* Corrected to heliocentric.

† Calibrated with respect to 3C48 and 3C147 (assumed flux densities 15.91 and 21.90 respectively). The errors in these values are ±(0.007+1%).

‡ With respect to the channels with the highest four velocities.

The observations were obtained with the Westerbork Synthesis Radio Telescope and its 80-channel filter spectrometer[5]. The measurements with the ten shorter baselines (36–684 m in 72-m increments) were made on August 11, 1974, and those with the 10 longer baselines (756–1,404 m in 72-m increments) on November 15, 1974. The eight frequency channels have a half-power bandwidth of 129 kHz ($c\,\Delta\lambda/\lambda_0$ = 27 km s^{-1}) and cover the range in $c\Delta\lambda/\lambda_0$ from 8,085 to 8,373 km s^{-1}. Table 1 gives the amplitudes in each channel averaged at the position of the continuum source. For the shorter baselines this corresponds to the flux density from a region ~ 50″×75″ in diameter (EW×NS) centred on the nucleus of NGC1275. For the longer baselines this is the flux density from components < (20″×30″) at the position of the nucleus.

For each observation, the variations in amplitude for the highest four velocities are consistent with that expected from receiver noise, so we have taken the average of these four channels to represent the mean continuum amplitude and have also tabulated the amplitudes relative to this value. To compare our result with that of De Young *et al.*[1], we have convolved their profile with our broader bandpass, and we have used the more accurate gain calibration of the 300′ antenna[6]. This gives an absorption of 0.26±0.02 Jy, in agreement with our value of 0.287±0.006 Jy in the 8,085 km s^{-1} channel.

Table 2 lists the angular sizes and flux densities of the main components of NGC1275 at the epoch of these observations. The deepest absorption seen by De Young *et al.*[1] corresponds to 1.4 Jy, so it is possible that this could have occurred in any of the three continuum components. Figure 1*a* shows the fringe amplitude of continuum emission in position angles 0° and 90°. The three angular size scales as described by Miley and Perola[4] are clearly seen. In Fig. 1*b* we show the difference between the channel containing the strongest absorption and the channels containing the continuum. It is clear from this plot that the absorbed component is unresolved and we can place a limit of < 6″ EW and < 9″ NS on its angular size. Furthermore, from the interferometer phase we can see that the position of the absorbed component is within 1″ of the position of the small diameter continuum source.

From this we can exclude the possibility that the major part of the absorption is occurring in either the 3′×4′ halo component or the 30″ intermediate component but it is still possible

Fig. 1 *a*, The fringe amplitude of the continuum emission from NGC1275 in position angles 0° (×) and 90° (●) plotted against the interferometer baseline in wavelengths. Note that the amplitude scale is offset from zero. *b*, The difference between the channel containing the strongest absorption and the average of the channels containing the continuum emission.

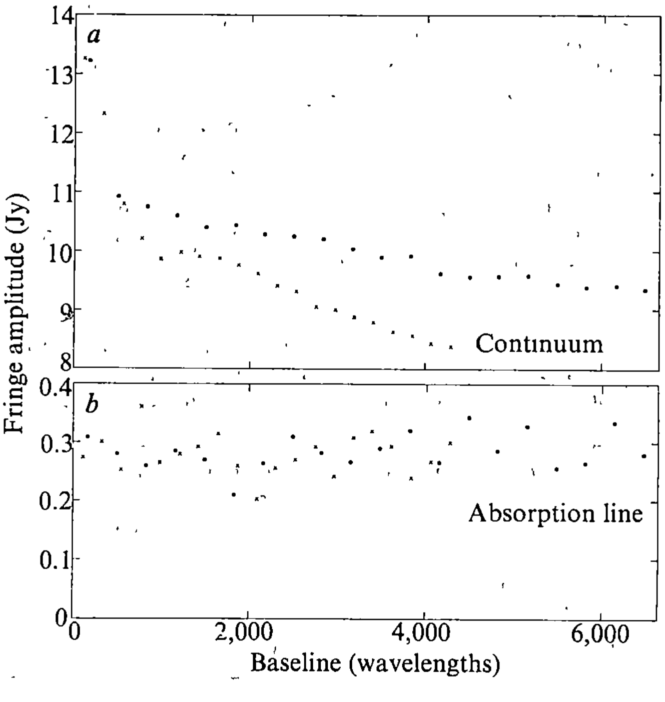

Table 2 Flux densities and absorption of the components

Component	Size*	Flux density (Jy)	Absorption (Jy)	Absorption %
Compact	<0.05″	8.6‡	0.29	3.4
Intermediate	35″×12″	2.2	<0.07	<3§
Halo	4′×3′	2.0¶	<0.05	<2

* Half intensity diameters of equivalent Gaussian distributions. Major axis position angle 170°.

† Average over our 27-km s^{-1} bandwidth.

‡ Variable—see text.

§ Upper limits are 3×r.m.s.

¶ The continuum fringe amplitudes in Fig. 1 also include a contribution from NGC1265 at the shorter spacings.

that a smaller fraction of the total absorption is occurring in these components. We can set limits on this fraction by fitting Gaussian components of the appropriate sizes to the absorption visibility in Fig. 1*b*. The resulting upper limits which correspond to 3×r.m.s. are also given in Table 2. Since the limits correspond to a fractional absorption in the larger scale components less than that seen in the compact component we can just exclude an absorbing cloud at 8,126 km s^{-1} uniformly covering the larger scale components, but we could not exclude a non-uniform cloud.

Table 3 summarises information from Westerbork on the variability of the continuum emission from the compact component at 1.4 GHz. The continuum emission has increased by 15% since 1971 and this is similar to the 10% increase between our present value of the absorption and that seen by De Young *et al.*[1]. The different calibration and velocity resolution of these two observations makes this result rather uncertain, however. Further accurate monitoring of the absorption line would indicate whether the continuum component responsible for the absorption is the variable component or some other part of the complex of small scale continuum structures known to be present[7].

One of the possible hypotheses to explain the absorption is that there is a foreground galaxy or H I cloud moving towards NGC1275 with a velocity of +3,000 km s^{-1}. Such a large positive velocity is not impossible if it is a member of the Perseus cluster, which has an r.m.s. velocity dispersion of 1,500 km s^{-1}. To detect such an object, we can either search for emission at velocities away from the absorption line velocity or search for emission from a larger region than that seen in absorption.

Since we do not see any feature in Table 1 exceeding the noise level we can set a 3σ limit of < 0.024 Jy in a 27-km s^{-1} channel on any emission feature in the velocity range 8,167 to 8,373 km s^{-1}. Comparison of the 50″ and 20″ data enables similar limits to be put on any emission at the absorption velocity coming from an area of ~ 50″ diameter centred on the galaxy. This corresponds to 18 kpc for an assumed distance of 75 Mpc for NGC1275.

For a foreground object smaller than or comparable with this size with a velocity dispersion ΔV in km s^{-1} our flux density limit gives a limit to the mass of neutral hydrogen, $M_{\rm H\,I}$, of

$$M_{\rm HI} < 3\times10^7\,(\Delta V)\,M_\odot$$

If ΔV is much greater than 200 km s^{-1} our limit is less well defined since the total profile would be wider than our velocity coverage. Thus a galaxy having the same distribution of H I velocities as the optical filaments ($\Delta V \simeq 250$ km s^{-1}) would have $M_{\rm HI} < 7.5\times10^9 M_\odot$. A late-type galaxy with this profile width would have $M_{\rm total} \lesssim 8\times10^{11} M_\odot$ and $M_{\rm HI} \simeq 6\times10^9 M_\odot$ (ref. 8), which is just below our present detection limit.

Table 3 Continuum variability of the compact component at 1.4 GHz

Date	Frequency (MHz)	Flux density (Jy)
June 5, 1971	1,415	7.3±0.1
August 11, 1974	1,383	8.6±0.1
October 10, 1974	1,415	8.7±0.1
November 15, 1974	1,383	8.6±0.1

We thank Professor J. H. Oort and Drs A. G. de Bruyn and G. S. Shostak for helpful comments on this paper.

R. D. EKERS
J. M. VAN DER HULST

Kapteyn Laboratory, Groningen

G. K. MILEY

Sterrewacht, Leiden, The Netherlands

Received May 10; accepted June 10, 1976.

[1] De Young, D. S., Roberts, M. S., and Saslaw, W. C., *Astrophys J*, 185, 809 (1973).
[2] Burbidge, E. M., and Burbidge, G. R., *Astrophys. J.*, 142, 1351 (1965)
[3] Lynds, R., *Astrophys. J. Lett.*, 159, L151 (1970).
[4] Miley, G. K., and Perola, G. C., *Astr. Astrophys*, 45, 223 (1976).
[5] Allen, R. J., Hamaker, J. P., and Wellington, K. J., *Astr. Astrophys*, 31, 71 (1974).
[6] Fisher, J. R., and Tully, R. B., *Astr. Astrophys*, 44, 151 (1975).
[7] Pauliny-Toth, I. I., *et al*, *Nature*, 259, 17 (1976).
[8] Roberts, M. S., in *External Galaxies and Quasi-Stellar Objects* (edit. by Evans, D. S.) (1972).

New limit on the size distribution of γ-ray bursts

SINCE the discovery of γ-ray bursts of non-solar origin in 1973 (ref. 1), about 42 events have been confirmed. All have been observed by X-ray and γ-ray detectors on various satellites, though a number of unconfirmed bursts have also been observed by balloon-borne instruments[2]. The lack of confirmation in the latter cases is not surprising, because of short exposure time and differing sensitivities. The detected flux ranges between about 3×10^{-6} erg cm^{-2} for the smallest burst to 5×10^{-4} erg cm^{-2} for the largest observed burst. The integral size distribution of these events above 10^{-4} erg cm^{-2} follows an $S^{-1.5}$ law, suggesting an isotropic distribution of the sources. For events with energy of less than 10^{-4} erg cm^{-2}, however, the observed distribution seems to flatten out, and the choice of number index ($\alpha=0.5$, 1.0 or 1.5) in this region is not strongly supported by experimental results.

We present here a new upper limit for the number of bursts which deposit more than about 2×10^{-7} erg cm^{-2} in the energy range 100–1,000 keV. The result indicates the direction in which future γ-ray burst experiments might go.

Our instrument comprised a 125-mm NaI(Tl) detector 10 mm thick, shielded from photons originating in the lower hemisphere by a graded shield. The pulses were analysed in four integral channels between 40 and 1,000 keV. The prescaling factor and the sampling rate for each channel was matched to the available telemetry capacity. The counting rate between 100 and 1,000 keV was sampled every 0.6 s, for 300–1,000 keV and 600–1,000 keV every 2 s, while counts between 40 and 1,000 keV were read out 6 times in 5 min. The instrument was flown as a piggy-back experiment on the first transatlantic balloon flight launched at 0505 UT on August 15, 1975 from Trapani, Sicily (38°N, 13°E). The balloon reached a ceiling altitude of about 3.0 g cm^{-2} at 0740 UT, and floated for 78 h before being cut down over Kentucky, USA[6]. The data were transmitted using a high-frequency radio link and were recorded at two ground stations, one in Sicily and the other in Chesapeake Beach, USA. The region of sky observed during this flight included a complete band across the celestial sphere defined by $\delta=+38\pm60°$.

The counting rates observed in each energy channel indicated the perfectly normal behaviour of the instrument. The changes in the detector counting rates from time to time were well understood in terms of variations in the residual atmospheric depth and other detector parameters. Since this transatlantic flight was the first of its kind, good scientific data were obtained for only about 70% of the time at float altitude. The loss of data arose mostly from the particular configuration of the high frequency communications system used on this proving flight. The criterion

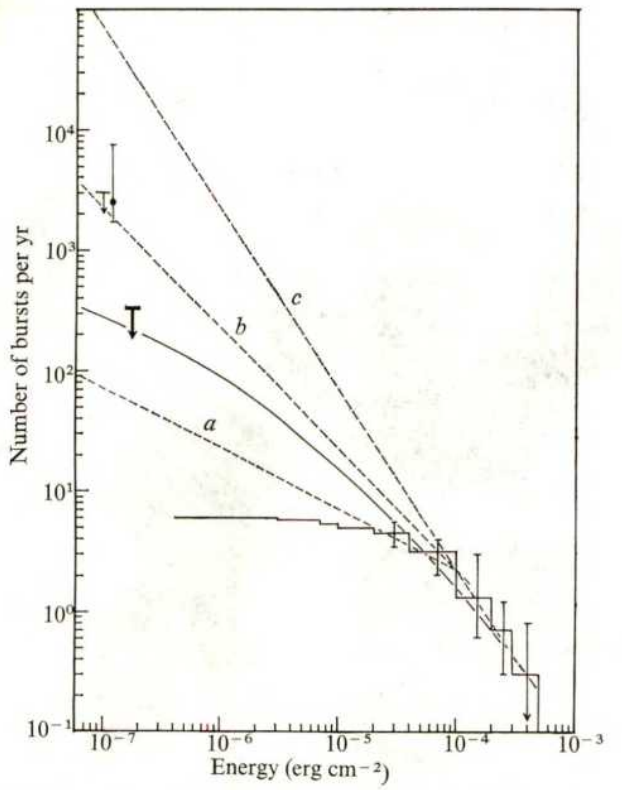

Fig. 1 Observed data of γ-ray bursts along with the results reported here. The limits defined by Cline *et al.* are those presented in ref. 5. Solid line, modified galactic distribution, $S^{-1.0}$ with a break point around 5×10^{-5} erg cm^{-2} and the dotted lines represent the form $N \propto S^{-\alpha}$ where $\alpha = 0.5$ (*a*), 1 (*b*) or 1.5 (*c*) for one-two- and three-dimensional distribution; stepped line, Vela events; ●, ref. 2; thin arrows, ref. 4; thick arrows, our results.

for the detection of a burst was that the counting rates per interval should each increase by more than 3σ above the background rate in at least three successive 0.6-s intervals. No candidate burst event could be found in the data. Such an excess would have corresponded to a signal strength of 0.36 photon cm^{-2} in the energy region 100–1,000 keV. This is equivalent to 0.1 photon cm^{-2} in terms of the Vela detector threshold, assuming an E^{-2} differential photon spectrum. Figure 1 shows the log*N*–log*S* distribution observed for Vela events along with the upper limit derived from this experiment. It can be seen that the limit is a factor of 5 lower than that expected from an S^{-1} distribution and about 100 times smaller than the value expected from an $S^{-1.5}$ number distribution. A 95% confidence upper limit would be higher than the plotted value by a factor of 3. That limit is still lower than that expected, even on the assumption of a two-dimensional distribution of burst sources. The present results favour the $S^{-0.5}$ spectrum for γ-ray bursts.

The results seem to demonstrate that the bursts are not of extragalactic origin, otherwise they would give an isotropic distribution. Similar conclusions have been suggested by Strong *et al.*[3] on the basis of the general features of observed γ-ray bursts. A galactic distribution of nearby sources would follow an $S^{-1.5}$ distribution for sources up to 300 pc, which is typical of the thickness of the galaxy. It would then change to an S^{-1} distribution for sources up to 3 kpc, which is the distance to the galactic anticentre, and then tend towards an $S^{-0.5}$ distribution beyond that point. If the break point at 10^{-4} erg cm^{-2} in the Vela data is genuine, and occurs because of the limited thickness of the galaxy, then one would also expect to find a less defined change of slope at about 10^{-6} erg cm^{-2}. On this basis, the expected number of bursts would be about 3 times greater than the upper limit obtained in our detector. But a pure disk population of burst sources with an S^{-1} distribution, and with a Gaussian distribution in its intrinsic source luminosities, would have a steeper slope on the log*N*–log*S* curve for energies greater than that expected from the mean luminosity. A log*N*–log*S* distribution has been calculated for such a disk population with a mean luminosity corresponding to a detected energy of 10^{-4} erg cm^{-2}. This also includes a further flattening between 10^{-5} and 10^{-6} erg cm^{-2} which arises when sources are at a distance of 3 kpc.

We believe that our results are consistent with a size distribution of $S^{-1.5}$ above 10^{-4} erg cm^{-2} and $S^{-0.5}$ below this energy, as determined for the Vela bursts. A distribution function obtained from a galactic population with a Gaussian spread in intrinsic luminosities having a break point at $\sim 5 \times 10^{-5}$ erg cm^{-2} would, however, also be compatible with our data. The break point at 10^{-4} erg cm^{-2} in the case of the Vela events may arise because of the characteristics of the Vela detection system, since it is optimised for events having a fast rise time. A slowly rising burst could escape detection. For example, the event of April 27, 1972 was seen by Apollo 16 but was not detected by the Vela satellites.

In view of the two competing spectra, $S^{-0.5}$ and S^{-1}, modified by a Gaussian distribution in luminosities, a reduction by a factor of about 10 in the limit obtained by this experiment is needed to establish the true nature of the source origin. Clearly, reducing the threshold sensitivity much below that of the present detector has little advantage, whereas the extension of the observation period reduces the limit in direct proportion to the flight length. Exposure times of up to 500 h could be obtained in relatively few flights using the techniques developed for the transatlantic balloon facility. It is important that some of the future long duration flights should be made in the Southern Hemisphere, where the galactic centre would pass within the field of view of the detectors. When quasi-omnidirectional detectors are used, it will be necessary to qualify any result on the size spectrum of γ-ray bursts with information on the sky coordinates of the region observed. The true form of the size spectrum is of extreme importance in the development of theories to explain γ-ray bursts. Some attempts at a theoretical explanation of this class of event have been made, but any quantitative picture will change drastically if the size spectrum follows either of these two distribution or, in the extreme case, if the distribution has a cutoff at lower energies.

We thank the SRC, Consiglio Nazionale delle Richerce and US National Scientific Balloon Facility for help with the first transatlantic balloon flight. We also thank the Naval Research Laboratories (Washington) for the use of their Chesapeake Beach radio receiving station.

J. Carter
A. J. Dean
R. K. Manchada*
D. Ramsden

Department of Physics,
University of Southampton,
Southampton SO6 5NH, UK

Received May 3; accepted June 14, 1976.

*Permanent address: TATA Institute of Fundamental Research, Bombay, India.

1 Klebesadel, R. W., Strong, I. B., and Olson, R. A., *Astrophys. J. Lett.*, **182**, L85 (1973).
2 Bewick, A., Coe, M. J., Mills, J. S., and Quenby, J. J., *Nature*, **258**, 686 (1975).
3 Strong, I. B., Klebesadel, R. W., and Evans, W. D., *Proc. 14th int. Conf. Cosmic Rays, Munchen*, **1**, 234 (1975).
4 Cline, T., and Desai, U. D., *Proc. 9th ESLAB Symp.*, **ESRO-SP106**, 37 (1974).
5 Cowsik, R., *Proc. 14th int. Conf. Cosmic Rays, Munchen*, *14*, 3758 (1975).
6 Ramsden, D., and Baker, R., *University of Southampton Report*.

Palynomorphs indicating Permian rocks in Ethiopia

Karroo (Carboniferous to Triassic) strata have been reported in Ethiopia[1,11,12], but without firm documentation. Other sediments lying on the crystalline basement but beneath the Jurassic Adigrat Sandstone[2] may also be of Karroo age[3–5]. To our knowledge, however, the occurrences reported here are the first palaeontologically substantiated records of Permian strata in Ethiopia. Localities are shown in Fig. 1.

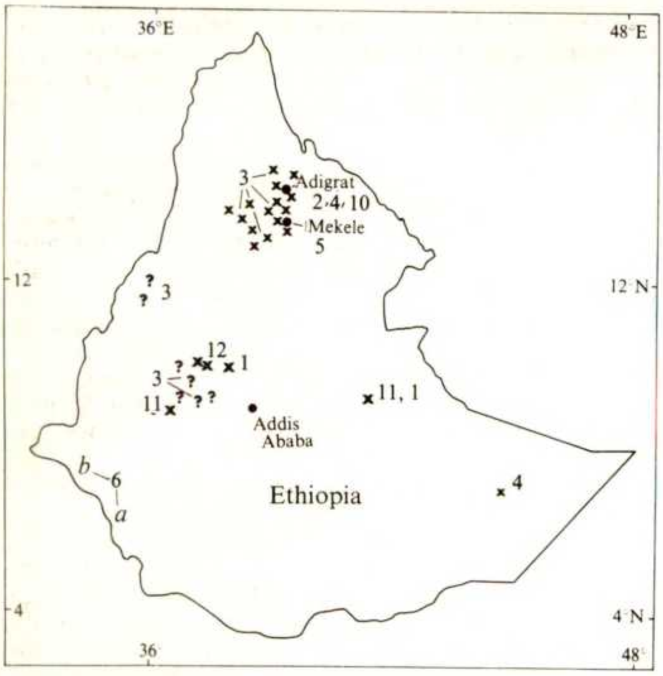

Fig. 1 Localities of post-Precambrian and pre-Jurassic (pre-Adigrat) strata in Ethiopia. *a*, Kari sandstone; *b*, Gilo sandstone; **x**, probable Karroo; x, pre-Adigrat; ?, Adigrat ?; numbers, references.

Several outcrop areas of apparently unfossiliferous fluviatile sandstones and conglomerates were discovered in western Kefa and Ilubabor Provines, south-western Ethiopia, in 1974 during reconnaissance mapping[6] The sediments are consolidated, tilted, and faulted; they lie unconformably on late Precambrian(?) crystalline basement and are overlain by mid to late Tertiary basalts with shallow angular unconformity. They differ distinctly in facies and thickness from the red, residual conglomeratic sandstone, generally less than 10 m thick and of unknown age, that marks the basement–basalt unconformity to the south-east[6,13,14]. Samples suitable for palynological analysis, taken from two localities 125 km apart (Fig. 1, *a* and *b*), yielded identifiable Permian miospores. At locality *a*, the Kari sandstone, comprising at least 30 m of fluviatile sandstones with minor conglomerate and siltstone, occurs in several small outcrop areas, in part fault bounded, in which the strata dip gently south-westwards. Miospores are common, but most are corroded, broken, and dark brown to black, indicating a relatively high degree of thermal metamorphism of the organic material, and some post-depositional oxidation. On prolonged laboratory oxidation they became sufficiently translucent to allow identification of the following: *Alisporites* sp.; *Granulatisporites micronodosus* Balme and Hennelly; (?)*Horriditriletes ramosus* (B. and H.) Bharadwaj and Salujha; *Klausipollenites schaubergeri* (P. and K.) Klaus (Fig. 2*c*); *Kraeuselisporites* sp.; *Parasaccites* sp. (Fig. 2*a*); *Protohaploxypinus* sp. (Fig. 2*b*); *Striatopodocarpites* sp.; *Vittatina* sp. (Fig. 2*d*); and *V.* (?) *costabilis* Wilson. As the fossils were difficult to identify because of rather poor preservation, no information on the quantitative composition of the assemblage was obtained. On broad comparisons, the assemblage is like those from the Lower and Upper Permian of Gondwanaland in its relatively high percentage of *Striatiti*. It also resembles those from the Upper Permian of Europe in the presence of *Klausipollenites schaubergeri*. Thus, like Upper Permian assemblages of Gabon[7], it seems to be somewhat transitional in composition between Gondwana and European assemblages.

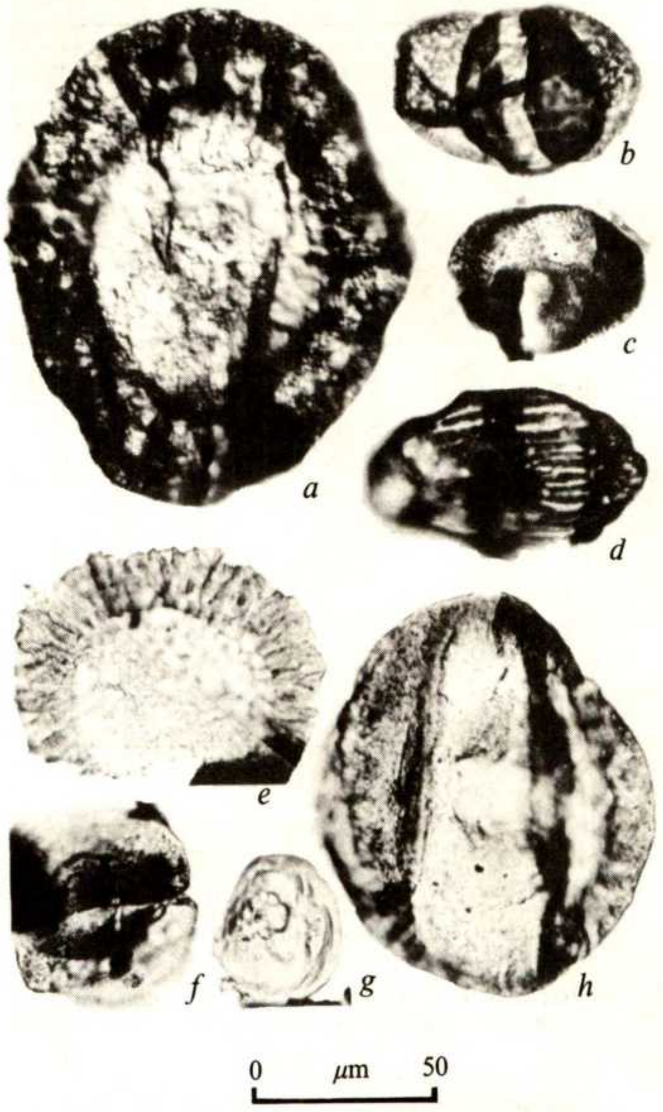

Fig. 2 *a–d*, Miospores from the Kari sandstone: *a*, *Parasaccites sp*. (GSC 45731); *b*, *Protohaploxypinus* sp. (GSC 45732); *c*, *Klausipollenites schaubergeri* (P. and K.) Klaus (GSC 45733); *d*, *Vittatina* sp. (GSC 45734). *e–h*, Miospores from the Gilo sandstone: *e*, (?)*Nuskoisporites gondwanensis* (B. and H.), (GSC 45735); *f*, (?) *Pallidosporites magnus* Schaar. (GSC 45736); *g*, (?) *Marsupipollenites* sp. (GSC 45737); *h*, (?)*Divarisaccus* sp. (GSC 45738). Numbers in brackets refer to specimens in the National Type Collection, Geological Survey of Canada, Ottawa.

At locality *b* (Fig. 1), the Gilo sandstone occurs in two basins separated by a north-westerly-trending basement arch. The poorly exposed south-western occurrence, 100 km^2 in area, is a homocline faulted against basement on its south-west side, and may contain as much as 1,500 m of strata, unless it is repeated by unrecognised faults. The north-eastern basin plunges gently north-westwards, and contains at least 300 m of strata, sparsely exposed within a 250 km^2 area. Calcite-cemented feldspathic quartz sandstones predominate, with interbedded arkosic conglomerate in the basal part. The transportation direction in both basins is mainly to the south-west. Miospores are relatively rare in the available sample from the north-eastern basin. In contrast to those from the Kari sandstone, they seem to have been little affected by thermal metamorphism, being brownish yellow without laboratory oxidation. The following were recognised: *Alisporites* sp.; *Cordaitina* sp.; (?)*Divarisaccus* sp. (Fig. 2*h*); *Kraeuselisporites* sp.; (?)*Marsupipollenites* sp. (Fig. 2*g*); (?)*Nuskoisporites gondwanensis* Balme and Hennelly (Fig. 2*e*); (?)*Pallidosporites magnus* Schaarschmidt (Fig. 2*f*); *Parasaccites* sp.; and *Protohaploxypinus* sp. Most specimens are corroded, and this, coupled with their relative rarity in the studied sample, makes precise age determination difficult. Therefore, as with the Kari sandstone sample, it is only possible to determine the age in broad terms from the palynological data. Striate pollen are rare, and large, radially symmetrical monosaccate forms comprise a greater proportion of the assemblage than in the Kari sandstone, suggesting a closer affinity with Lower rather than Upper Permian assemblages of the Gondwana region[8,15]. This suggestion is supported by the observation of a single specimen of (?)*Nuskoisporites gondwanensis* Balme and Hennelly (Fig. 2*e*; (?)=*Parasaccites* sp. of Segroves[9]).

The limited miospore assemblages we have studied from the Kari and Gilo sandstones, although evidently Permian and similar to those of the Gondwana Province, can be cautiously dated more precisely as late and early Permian, respectively. Considering that the samples reported here were not collected specifically for palynological studies, however, it seems reasonable to predict that samples collected primarily for that purpose would give a better yield of palynomorphs and enable a more precise determination of the age and geological history of Permian strata in this part of Ethiopia.

In western central Ethiopia, 300–400 km north-east of the Kari and Gilo sandstones, large tracts of clastic sediments have been mapped as Adigrat Sandstone[3], although pre-Adigrat sediments are known[1,12] or suspected to be present locally. The term Adigrat Sandstone was at first applied collectively to sandstones lying in the same stratigraphic position in northern Ethiopia[10], but later work[2,5] has shown that parts of the original unit, namely the Enticho Sandstone, the Edaga Arbi Tillite, and the Enguya Sandstone, are older than the basal clastic sediments of the Mesozoic marine transgression, to which the name Adigrat Sandstone has now been restricted[2]. The Adigrat Sandstone as redefined is Jurassic and is known to thin westwards beneath its cover of marine limestones[4], although its rapid thinning to the west where overlying limestones are absent may be attributable in part to later erosion. On the basis of the occurrence of Permian strata in south-western Ethiopia reported here, and the recognition of pre-Adigrat sediments to the north-east, it seems likely that much of the apparently thick sedimentary succession mapped as Adigrat Sandstone in western central Ethiopia may also be of Karroo age. If so, Karroo sediments are more widespread north of their formerly recognised northern limit than was previously suspected.

A. DAVIDSON
D. C. MCGREGOR

Geological Survey of Canada,
Ottawa, Canada

Received April 12; accepted June 1, 1976.

[1] Beauchamp, J., and Lemoigne, Y., *C. r hebd. Séanc. Acad. Sci., Paris*, D278, 29–32 (1974)
[2] Dow, D. B , Beyth, M , and Hailu, T., *Geol Mag.*, 108, 53–59 (1971).
[3] Kazmin, V., *Geological Map of Ethiopia* (Imperial Ethiopian Government, Addis Ababa, 1973).
[4] Beyth, M , in *Sedimentary Basins of the African Coasts*, Part 2 (edit. by Blant, G.), 179–191 (Ass. Afr. geol. Surv., Paris, 1973).
[5] Morton, W. H., *Bull. geophys. Obs Addis Ababa*, 15, 1–14 (1975).
[6] Davidson, A , *et al.*, *Preliminary Report on the Geology and Geochemistry of Parts of Gemu Gofa, Kefa, and Ilubabor Provinces, Ethiopia* (Ethiopian Government, Addis Ababa, 1976).
[7] Jardiné, S., *Rev. Palaeobot. Palynol.*, 17, 75–112 (1974)
[8] Balme, B E , and Playford, G., *Rev. Micropaléont.*, 10, 179–192 (1967)
[9] Segroves, K. L., *Grana Palynol.*, 9, 174–227 (1969)
[10] Blanford, W. T., *Observations on the Geology and Zoology of Abyssinia* (Macmillan, London, 1870).
[11] von zur Muhlen, L., *Z dt. geol. Ges* , 83, 625–634 (1931)
[12] Mohr, P. A., *Nature*, 199, 1086 (1963).
[13] Davidson, A., *et al* , *Prelim Rep Geology and Geochemistry of Parts of Sidamo, Gemu Gofa and Kefa Provinces, Ethiopia* (Imperial Ethiopian Government, 1973).
[14] Levitte, D , Columba, J., and Mohr, P., *Bull geol Soc. Am* , 85, 417–422 (1974).
[15] Balme, B. E., in *Ancient Pacific Floras; the Pollen Story* (edit. by Cranwell, L.M), 49–80 (University of Hawaii Press, Honolulu, 1964).

Radiocarbon dates of Santorini volcanics

THE caldera walls of the ring-islands Thera and Therasia, belonging to the Santorini Group (Fig. 1) in the southern Aegean, are built up of lavas and pyroclastics, among which pumice layers are particularly striking (Fig. 2). The top layer (Bo, abbreviated from the German term "oberer Bimsstein"[1]) comprises air-fall pumice and ashes, overlain by thick pyroclastic flows[2,3]. It was produced by the catastrophic outburst of the Thera volcano in late-Minoan time, which culminated in the collapse of the Santorini caldera[4]. The decline of the Minoan civilisation around 1500 BC has been attributed to these volcanic events[5]. The Upper Pumice Series buried late-Minoan settlements on Thera and Therasia, and an important settlement near Akrotiri in the southern part of Thera is still being excavated[6]. The Upper Pumice Series rests on an old soil horizon (black layer in Fig. 2) in which remnants of late-Minoan houses were found in 1869 (ref. 7). Wood from such houses found at the base of the pumice quarries south of the town of Fira has provided radiocarbon dates of 3,370±100 yr b.p. (ref. 8). This age coincides exactly with archaeological data for the destruction of late-Minoan settlements on Santorini[6].

The Bo palaeosol is spread all over Thera and Therasia. Its thickness locally reaches 3–4 m, for example, on Therasia, where carbonised plants have been found in its lower parts. ^{14}C dating of these plants has given an age of 12,950±756 yr b.p. The palaeosol horizon rests unconformably on a small sequence of welded tuffs and slightly welded pumice flow deposits. A maximum thickness of 12 m for these ignimbrites occurs in the southern part of Thera. The walls of the partly excavated late-Minoan town near Akrotiri are founded on these ignimbrites. ^{14}C ages of charred trees which sporadically occur in the pumice flow deposits forming the lower part of the ignimbrite series have provided ^{14}C dates of 18,050±340, 18,165±210 and

Fig. 1 The Santorini Group in the Aegean Sea, Greece. The old ring-islands Thera and Therasia surround the late-Minoan Santorini caldera and the post-Minoan Kameni islands. *P*, location of the schematic profile (Fig. 2).

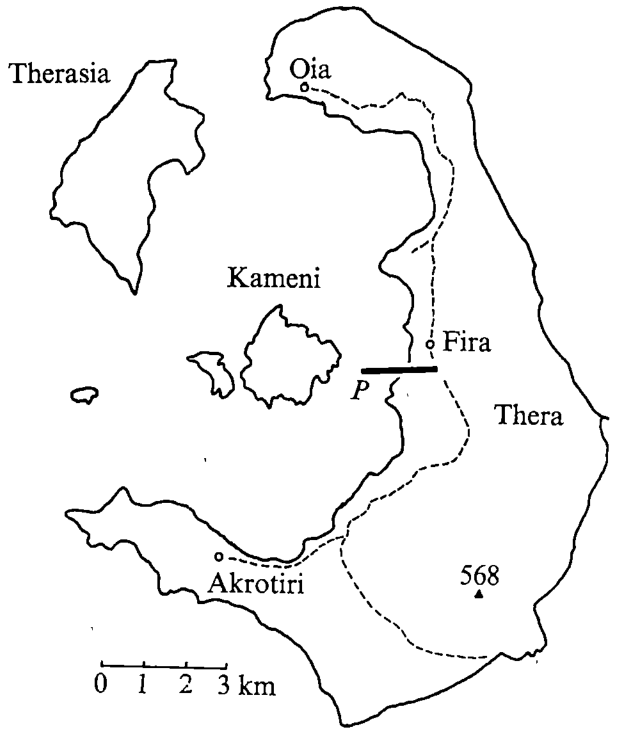

18,880±230 yr b.p. (ref. 3). The ages show that an exceptionally long interval of about 15,000 yr without any volcanic activity on Santorini preceded the late-Minoan outburst. During this interval the contemporaneous volcanic top layers were deeply decomposed and altered to a thick palaeosol.

The ignimbrite series is underlain by a stratigraphic sequence of at least 19 alternating pyroclastic strata comprising mostly dark ashes, cinders, scoriae, pumice, bombs, xenolithic lapilli, blocks, and so on. Many of these strata can be subdivided into numerous small beds and horizons. The total thickness of the complete sequence underlain by the Middle Pumice Series (Bm, "mittlerer Bimsstein") amounts to about 30 m. The sequence represents a long period of volcanic activity of the Thera and adjacent volcanoes with some overlap of their products. Intervals of quiescence are marked by some decomposed ash layers and fossil soil horizons, four of which are rich in plant fossils (*Chamerops, Olea, Pistacia, Phoenix,* and *Tamarix*). All of these genera still exist among Mediterranean flora. This means that during that time the Mediterranean climate was the same as at present.

Radiocarbon dating of a carbonised piece of tree found about 1.5 m under the lower plant horizon in the lower part of the pyroclastic sequence, has given an age of 36,700± 1,025–950 yr b.p. (determination by the Niedersächsisches Landesamt für Bodenforschung, Hannover). Another ^{14}C dating of the same sample (performed in the Geochron Laboratories, Cambridge, Massachusetts) has shown an age of more than 37,000 yr b.p. Therefore, the plant horizons of Santorini can be correlated with the Kalabaki I and II interstadial (between 37,000 and 35,000 yr b.p.) demonstrated by palynological studies near Thessaloniki in northern Greece[9].

Twenty distinctive tephra layers, derived from various sources[10], have been identified in Quaternary deep-sea cores of the eastern Mediterranean[11]. Mellis[12] has correlated the upper tephra layer in the cores collected on the Albatross with the Upper Pumice Series on Santorini.

His correlation has been confirmed by Ninkovich and Heezen[13], who have identified the Upper Tephra Layer in 14 cores collected on the Vema. The Middle Tephra Layer, which has been detected in Vema core 10–58, has been correlated with the Lower Pumice Series (Fig. 2, Bu, "unterer Bimsstein") on Santorini. Based on a ^{14}C age of 17,860 yr b.p., taken from carbonised pumice found on the neighbouring island of Anaphi, the Lower Pumice Series was deposited[14], probably 17,000–18,000 yr b.p. This is inconsistent, however, with the age of the Lower Pumice Series if the plant horizons (37,000 yr) and their stratigraphic position (Fig. 2) are taken into account. According to that evidence, that part of the volcanic sequence on Santorini which underlies the plant horizons, including the Middle (Bm) and the Lower Pumice Series (Bu), must be older than 37,000 yr.

Fig. 2 Schematic profile (*P* in Fig. 1) of the caldera walls of Thera, south of Fira. For explanation see text. *a*, Upper Pumice (Bo); *b*, palaeosol; *c*, ignimbrites; *d*, Middle Pumice (Bm); *e*, Lower Pumice; *f*, lavas. Figures denote radiocarbon ages (yr b.p.)

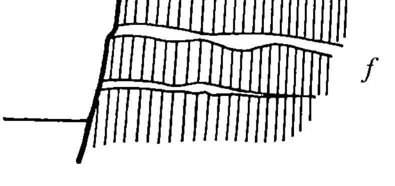

The Middle Tephra Layer of the Vema 10–58 core, however, can more appropriately be correlated with the ignimbrite series, for which an age of between 18,000 and 18,500 yr can be fixed. Mineralogical and petrochemical characteristics of the Middle Tephra Layer[14] correspond exactly to the pumice in the lower part of the ignimbrite series. The refractive index of the glass is 1.514 (ref. 15), about the same as in the Lower Pumice Series. Therefore, the refractive index cannot be used as a discriminative factor[14] between the two pumice series. It may also be noted that a layer in the Albatross core 189 has provided an age of 17,200±500 yr b.p. (ref. 16), which roughly fits with the age of the ignimbrite series.

Based on the fact that the Middle Tephra Layer is not to be correlated with the Lower Pumice Series but corresponds to the stratigraphically younger Ignimbrite Series, the position of the Lower Pumice Series in the deep sea cores is still unknown. In any case, the corresponding tephra layer must be situated below the "Ischia Tephra"[14] (or "Lower Tephra"[13]), which has an age of 24,000 yr b.p.

We thank the Deutsche Forschungusgemeinschaft and the Carlsberg Foundation for financial support, the Niedersächsisches Landesmat für Bodenforschung, Hannover and the Institut für Umweltphysik/University of Heidelberg for ^{14}C determinations. The help of the Greek authorities, of Peter Nomikos, Athens, M. A. Geyh, Hannover, K. O. Münnich, Heidelberg, and A. Boettcher, Aachen, is acknowledged.

HANS PICHLER

Mineralogisch-Petrographisches,
Institut der Universität,
Wilhemstrasse 56,
D-74 Tübingen, FRG

WALTER FRIEDRICH

Laboratoriet for Palaeontologi og Stratigrafi,
Geologisk Institut,
Aarhus Universitet,
DK-8000 Aarhus, Denmark

Received May 26, accepted June 26, 1976.

1 Reck, H., Santorin, *Der Werdegang eines Inselvulkans und sein Ausbruch* 1925–28 (Reimer, Berlin 1936).
2 Pichler, H., *Naturwissenschaften*, 60, 198 (1973).
3 Gunther, D., and Pichler, H , *N Jb Geol Palaont. Mh.*, 394–415 (1973).
4 Pichler, H., Gunther, D., and Kussmaul, S., *Naturwissenschaften*, 59, 188–197 (1972).
5 Marinatos, Sp., *Antiquity*, **13**, 425–439 (1939)
6 Marinatos, Sp., *Excavations at Thera I-V* (Athens, 1972)
7 Fouqué, F., *Rev Deux Mondes*, 39, 923–943 (1869).
8 Galanopoulos, A G., *Annls géol hell.*, 9, 184–185 (1958).
9 Wijmstra, T. A., *Acta Bot Neerlandia*, 18, 511–527 (1969).
10 Bond, A., *Nature*, **259**, 194–195 (1976).
11 Ryan, W B. F., in *The Mediterranean Sea*, 149–169 (Dowden, Hutchinson and Ross, Stroudsburg, 1972).
12 Mellis, O , *Deep Sea Res.*, 2, 89–92 (1954).
13 Ninkovich, D., and Heezen, B. C., *Colston Papers*, 17, 413–452 (Butterworths, London, 1965).
14 Keller, J., and Ninkovich, D., *Z. dt. geol Ges.*, 123, 579–587 (1972)
15 Gunther, D., thesis Univ. Tubingen (1972).
16 Rubin, M , and Suess, H. E., *Science*, **121**, 481–488 (1955).

Formation of Hercynian subplates, possible causes and consequences

WITH the exception of the microplate models of Badham and Halls[1] and Riding[2] models of Hercynian plate tectonics[3–7] have assumed the existence of only one plate, that is, South Europe, between Africa and the Tethys in the south and North America–Europe and the Mid-European Ocean in the north. The South European plate has generally been considered as a stable unit. Studies of the Alpine

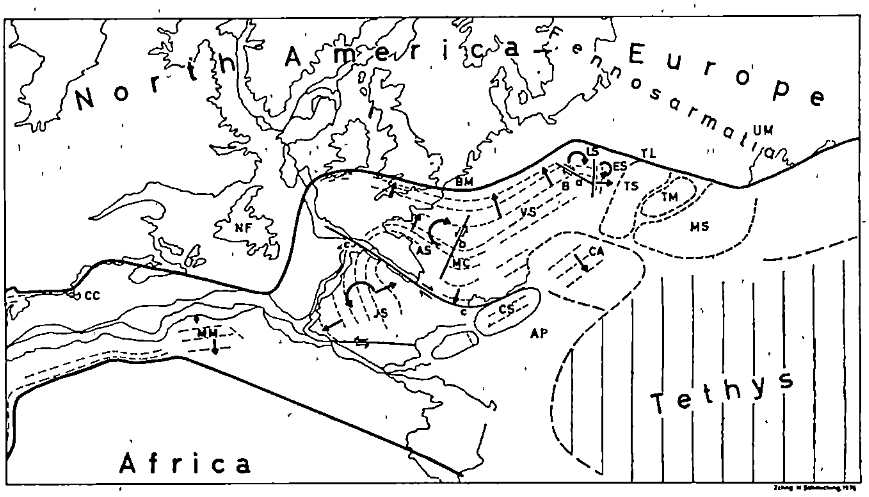

Fig. 1 Schematic map of the South Europe plate and neighbouring plates for the late Hercynian time showing subplates, major wrench faults, and general structural trends within South Europe. Base map after Bullard *et al.*[24] and Dewey *et al.*[8]. Thick lines = continental margins of bordering plates; thick arrows = direction of migrating fold-belts; thick curved arrows = direction of rotation of subplates in respect to Variscan subplate. Key to abbreviations: AP = Apulia; AS = Amorican subplate; B = Bohemia; BM = Massif of Brabant; CA = Carnics; CC = Cape Cod; CS = Corsica–Sardinia; ES = East Sudetan subplate; IS = Iberian subplate; LS = Lugian–Silesian subplate; MC = Massif Central; MM = Moroccan Meseta; MS = Moesian subplate?; NF = Newfoundland; TL = Tornquist Line; TM = Tirgu–Mures subplate?; TS = Tatride subplate?; UM = Ukrainian Massif; VS = Variscan subplate; a = Elbe wrench fault; b = Sillon Houiller wrench fault; c = Biscaya–Pyrenees wrench fault.

system[8], however, suggest that such an assumption may not be valid. I assume here that during the Carboniferous, South Europe was originally an elongated plate with nearly straight margins and internal structures. Collision with the irregular continental margins of the bounding plates North America–Europe and Africa induced subdivision of South Europe into semi-independent subunits, that is, into subplates, and formation of major arc-like structures and wrench faults.

Both North America–Europe and Africa were large plates. The postulated South Europe plate in contrast was characterised by great length and small but variable width compatible with an origin by accretion of new crust at an island arc system. In general, the oldest rocks of the plate occur within a central ridge that extends from Bohemia through the Massif Central, Brittany into Iberia and the Moroccan Meseta. Distribution of younger rocks to either side has been taken to indicate that two fold belts migrated away from the central ridge, one towards the north and the other towards the south[7,9–12] (Fig. 1). This process has been ascribed to the oceanward movement of two opposed subduction zones[3,13]. Metamorphism and emplacement of granites also began in the central ridge and became progressively younger towards the plate margins.

Dehydration and partial melting of former oceanic crust subducted beneath South Europe during the Carboniferous may have led to the formation of zones of hot partially molten upper mantle material above the opposed subduction zones. Diapiric uprise and lateral spreading of this material may have in turn caused widespread partial melting in the lower crust of South Europe and high temperature–low pressure metamorphism of upper crustal rocks[13]. As a consequence South Europe during the greater part of the Carboniferous was probably a rather thin and hot plate with a rigid crust ~ 20 km thick. In contrast the adjacent parts of both North America–Europe and Africa did not experience extensive granite emplacement and high temperature–low pressure metamorphism during the Carboniferous. It can therefore be assumed that the heatflow within both plates was lower than under South Europe and that both plates were cooler and consequently characterised by thicker lithosphere than South Europe. Applying this concept, which is of critical importance to the model given below, it is likely that the mechanical properties of the thin and hot South Europe plate were quite unusual and very different from those of the two major plates bordering it.

Uplift of the crust of South Europe, regional erosion of the central zone, formation of intermontane troughs and associated volcanism were also probably related directly to the uprise of hot upper mantle material. Spreading of this material caused migration in the onset of uplift, erosion, trough formation and volcanism[13]. This activity persisted into the Lower Permian in spite of the cessation of subduction in Upper Carboniferous time because of the collisions between the South Europe plate and the bounding North America–Europe and Africa plates.

According to McKerrow and Ziegler[14] and Dewey and Kidd[15] the pre-Hercynian margin of eastern North America and southern Britain was formed by rifting during the Devonian when northern South America and North America–Europe collided and then separated again soon after. Subsequently, South Europe and Africa were sutured to North America–Europe by continent–continent collisions[5,6,13], events which also apparently caused the ter-

Fig. 2 *a*, Sketch map of the pre-collision South Europe plate with its two subduction zones (thrust lines), the bordering oceans and the irregular continental margins of North America–Europe and Africa. Arrows indicate potential direction of drift. *b*, Sketch map of the South Europe plate near the end of the continent–continent collisions. The South Europe plate adjusted to the irregular continental margins of the neighbouring plates by distortion, that is, formation of subplates. Curved arrows indicate sense of rotation of subplates.

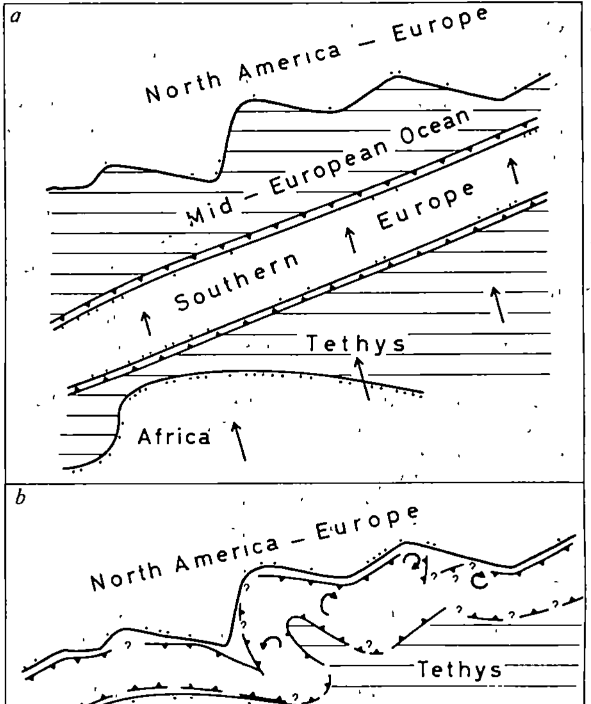

mination of subduction of oceanic crust of the Tethys further to the east. The suture line, represented by Hercynian fold belts, is not straight, but probably reflects the pre-existing form of the North America–Europe continental margin. Assuming that the southern continental margin of North America–Europe underwent little modification during suturing it is likely that its previous form was irregular and of a configuration typical of rifted margins. There are projections and embayments. Long relatively straight segments meet at rather sharp bends in the manner described by Dewey and Burke[16].

During its northward approach, South Europe eventually managed to fit into the irregularities of the southern continental margin of North America–Europe. South Europe is unlikely to have possessed the required configuration to fit the irregularities of the continental margin of the northern plate in the manner of a jig-saw puzzle. A more reasonable assumption is that the original configuration of South Europe was one of almost straight structural trends within the plate and also an originally straight northern plate margin (Fig 2) This form would be favoured by an origin of the plate as a series of island arcs. During collision South Europe would have needed to adjust until it eventually fitted all irregularities of the southern continental margin of the North America–Europe assuming these were relatively unmodified by the collision. Progressive subduction of the Mid-European ocean crust between North America–Europe and South Europe would have allowed the latter plate to collide first with the southernmost projections of the former, then through internal deformation and wedging aside of large slices to advance further northwards and finally fit into the embayments of the continental margin of North America–Europe.

During this process, South Europe probably collided first with the Ukrainian Massif of Fennosarmatia. Along newly forming wrench faults subplates were driven aside and rotated, and were left behind by the main part of South Europe, which was able to proceed further northwards, west of the Tornquist line. Such subplates are the Lugian–Silesian and East Sudetan subplates, probably also the Hercynian massifs in the realm of the Carpathians, that is, the Tatride, Tirgu–Mures, and Moesian subplates (Fig. 1). Palaeomagnetic studies of Upper Carboniferous rocks from the Bohemian Massif and the Inner Sudetic basin separated by the Elbe wrench fault indicate a late Hercynian rotation of 17° between these areas[17]. This relatively small rotation is believed to represent only part of the total rotation which is assumed to have commenced before the Westphalian. Evaluation of deep boreholes clearly shows that a postulated connection between the Rhenohercynian zone and Westphalian coal measures of the Ruhr district with equivalent zones of the Sudetic Mountains and the Upper Silesian coal basin[18] does not exist[19]. This is believed to be caused by the disruption of the originally continuous fold belt during its formation by collision with Fennosarmatia. In spite of this disruption, later development of both areas followed similar paths, for example in the deposition of the Upper Carboniferous coal measures.

Another important bend in the southern continental margin of North Europe existed at the south-eastern margin of the Massif of Brabant, Belguim. South of this, nappe structures, unique in the Rhenohercynian zone, were probably developed in response to a local concentration of compressional forces. To the west of this bend there extended a large embayment bounded to the west by Newfoundland. It is postulated that the South Europe plate reacted to contact with this embayment by formation of several subplates. West of the Variscan subplate, the Amorican and Iberian subplates formed, separated from each other by major wrench faults, that is, the Sillon Houiller and the Biscaya–Pyrenees wrench faults[20]. The Amorican subplate rotated clockwise relative to the Variscan subplate and Iberia in turn rotated anticlockwise relative to both the Variscan and Amorican subplates, these rotations, together with translations, finally resulted in the closure of the embayment. This process of rotation of both subplates in opposite directions would have caused intense shearing stresses and consequent intense internal deformation of both subplates. It is assumed that the partially molten and thus relatively soft lower crust could have reacted by plastic deformation recorded by the two large basement arcs in the Massif Central and in Brittany–NW Iberia whereas the more rigid upper crust could have reacted only through formation of many wrench faults within both subplates[20]. Further analysis of the wrench fault system should clarify the mechanism by which the two subplates moved into the embayment.

Another consequence of this major tectonic event was that the south-eastern continental margins of both subplates which were originally colinear, were rotated until they finally came into contact. In addition, the two fold belts situated north-east of the Iberian ridge and south of the Massif Central were probably also initially colinear, and only during the later part of their evolution, that is, during collision of South Europe with North America–Europe, did they rotate to face each other, migrate towards each other and eventually come into contact in the general region of the Pyrenees. It seems quite possible that some crustal slices from the southern margin of South Europe were driven aside during this subplate collision. Van der Voo[21] recently discussed palaeomagnetic data from some Palaeozoic Iberian rocks and concluded that Iberia rotated for at least 40°, that is the total value of the anticlockwise rotation of Iberia exceeds its Mesozoic value of 35°.

To the south-west of the large embayment, the Newfoundland projection and the bend in the continental margin near Cape Cod may have induced formation of major wrench faults, and thus the formation of several subplates, now located in Morocco, Algeria, and Southern Spain. In western Morocco, the general structural trend of the Hercynian fold belt is NE–SW to N–S. At the northern margin of the Moroccan Meseta, between Rabat and Tiflet, however, there is a sharp bend in the structures towards the east[22,23]. Varied structural trends in the Hercynian Massifs of NE Morocco and Algeria may in part be due to formation of Hercynian subplates. The Iberian and North African subplates must have been separated by major wrench faults across which large changes in the structural trends took place. Collision of the Moroccan, Algerian, and Iberian parts of South Europe with Africa probably also facilitated the squeezing of South Europe into the large Brabant–Newfoundland embayment.

During collision with elongated South Europe the irregular rifted continental margins of North America–Europe and Africa are believed, as argued above, to have induced formation of major arc-like basement structures and many wrench faults, some of which form the boundaries of subplates and thus to have produced the diversity in major structural trends of the Hercynian fold belt. The postulated mechanical properties of the South Europe plate, in contrast to those of the two large plates that flanked it, are believed to have enabled South Europe to react in the manner outlined. The force that drove South Europe against the flanking plates was apparently not as great as during collisions associated with the Alpine system. The scarcity of large nappes and lack of areas of strong post-collision uplift arising from one continental plate overriding another lend support to this model. A reason for this could have been a reduction in the velocities of the approach of the two large plates because of the spread of hot mantle material beneath the South Europe plate.

Late Hercynian formation of intermontane troughs, many of which are located on wrench faults, and associated volcanicity commenced in uppermost Viséan time. These late

Hercynian processes were very similar on the postulated subplates of South Europe, even in post-collision Lower Permian time. Thus crustal spreading of South Europe took place in a number of different directions simultaneously as the subplates in this respect behaved as individual units. This again seems to have been possible only if the force driving South Europe against the adjacent plates was not very great.

Two other possible consequences of the model are that the formation of the irregularly rifted continental margins of North America–Europe and north-western Africa might have influenced the pattern of subsequent opening in the relevant area of the North Atlantic, and ultimately may have played a part in the behaviour of South Europe during the Alpine cycle of plate tectonic processes. Some of the major wrench faults between the Hercynian subplates, being major zones of weakness may have been reactivated during the opening of the North Atlantic and during the Alpine cycle. Some of the subplates were probably blocked out and developed into microplates. Thus the heritage from the rifted continental margin of North America–Europe and the Hercynian plate tectonics may, in part, have caused some of the peculiarities of the Alpine orogenic belts, for example the numerous microplates described from the Mediterranean area[8] and some of the arc-like fold belts as in the Carpathians.

Revision of an earlier version of the manuscript by I. A. Nicholls is acknowledged.

VOLKER LORENZ

Geologisches Institut,
Universität,
65 Mainz, FRG

Received April 5; accepted June 1, 1976.

[1] Badham, J. P. N., and Halls, C., *Geology*, 3, 373–376 (1975).
[2] Riding, R., *Earth planet. Sci. Lett.*, 24, 125–135 (1974)
[3] Anderson, T. A., *Geol. Soc. Am. Bull.*, 86, 77–82 (1975).
[4] Burrett, C. F., *Nature*, 239, 155–157 (1972).
[5] Dewey, J F., and Burke, K. C. A., *J. Geol*, 81, 683–692 (1973).
[6] Johnson, G. A. L., in *Implications of Continental Drift to the Earth Sciences*, 2 (edit. by Tarling, D H., and Runcorn, K S.), 843–850 (Academic, London, 1973).
[7] Laurent, R., *24th Int. Geol. Congr.*, Sect 3, 363–370 (1972).
[8] Dewey, J. F., Pitman, W. C., III, Ryan, W. B. F., and Bonin, J, *Geol Soc. Am. Bull.*, 84, 3137–3180 (1973).
[9] Flugel, H. W., *Geol. Rdsch.*, 64, 1–62 (1975).
[10] Krebs, W., *Geotekt. Forsch.*, 28, 1–71 (1968).
[11] Lotze, F, *Geotekt. Forsch.*, 6, 78–97 (1945).
[12] Wunderlich, H. G., *Geol. Rdsch.*, 54, 861–882 (1965).
[13] Lorenz, V., and Nicholls, I. A., in *The Continental Permian in Central, West, and South Europe* (edit by Falke, H., NATO ASI Series), C 22, 313–342, (Reidel, Dordrecht, Holland, 1976).
[14] McKerrow, W S., and Ziegler, A M., *Nature phys Sci.*, 240, 92–94 (1972)
[15] Dewey, J. F., and Kidd, W. S F, *Geology*, 2, 543–546 (1974).
[16] Dewey, J. F., and Burke, K., *Geology*, 2, 57–60 (1974).
[17] Birkenmajer, K., Krs, M., and Nairn, A. E M., *Geol. Soc. Am Bull.*, 79, 589–608 (1968).
[18] Stille, H., *Beih geol. Jb.*, 2, 1–138 (1951).
[19] Dvorák, J, and Paproth, E., *Neues Jb. Geol Palaont Mh.*, 65–88 (1969)
[20] Arthaud, F., and Matte, P., *Tectonophysics*, 25, 137–171 (1975).
[21] Van der Voo, R, *Tectonophysics*, 7, 5–56 (1969).
[22] Krenkel, E., *Geologie Afrikas. Dritter Teil*, 1003–1918 (Borntrager, Berlin, 1934).
[23] Gigout, M., *19th Int. Geol. Congr*, Sect 2, 29–40 (1953).
[24] Bullard, E., Everett, J. E, and Smith, A G., *Phil Trans. R. Soc.*, A258, 41–51 (1965).

Age relationships along the Hermitage Bay–Dover Fault System, Newfoundland

WE present here geochronological evidence that parts of the Central Mobile Belt and the Avalon Zone of Newfoundland have been contiguous since the Ordovician or earlier, and that some time after about 4 Myr, significant movement took place along part of the boundary.

Wilson[1] has used fossil, lithological, and palaeoclimatic evidence to suggest the existence of a Lower Palaeozoic Proto-Atlantic Ocean close to, but not coincident with, the site of the present Atlantic. The fossil evidence he cited showed that the Avalon Zone (Fig. 1) of the island of Newfoundland was on the European side of the Proto-Atlantic ocean in Cambrian and Lower Ordovician times, whereas the Western Platform (Fig. 1) was on the North American side of the ocean. The same evidence also suggested that the Proto-Atlantic ocean became narrower later in the Ordovician, although to what extent is very much a matter of debate. Wilson proposed that closure of the ocean and the consequent collision of the opposing continental margins was the mechanism responsible for much of the orogenic activity in Europe and eastern North America during Palaeozoic time, and that the opening of the present Atlantic resulted in transposition of fragments of the continents, such as is found in Newfoundland. Others (see ref. 2) have extended Wilson's original idea.

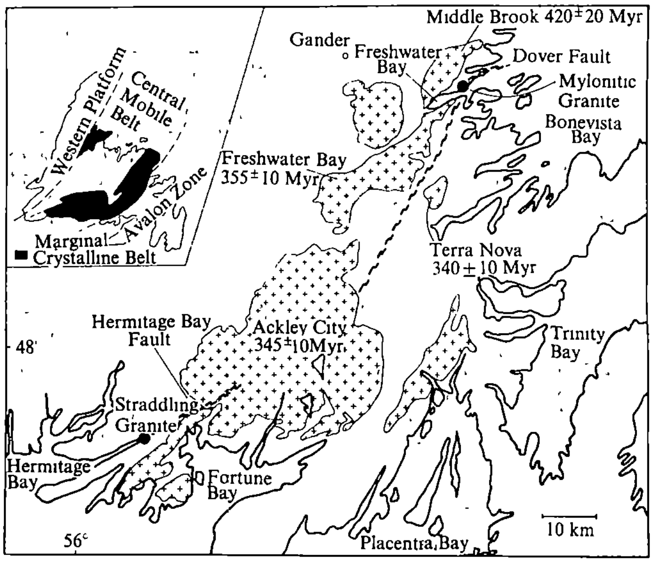

Fig. 1 Diagram showing the relationship of the Mylonitic and Straddling granites to the Hermitage Bay–Dover Fault System. The Rb–Sr age data are taken from ref. 8.

The site of closure of the Proto-Atlantic ocean may be marked in Newfoundland by the boundary between the Central Mobile Belt (Fig. 1) and the Avalon Zone[3,4], though alternative proposals have been made[5,6]. The boundary separates a long strip of gneissic rocks and metasedimentary sequences (the Gander Zone) from the much less deformed, late Precambrian volcanics and sediments of the Avalon Zone[4]. The proposal has been made that the Hermitage Bay–Dover Fault System, a supposedly continuous fault system with a length of over 200 km, marks the boundary[7]. Unfortunately, a large part of it is obscured by the Ackley City Granite (Fig. 1), which has been dated at 345±10 Myr (ref. 8).

Our geochronological evidence is provided by Rb–Sr, total-rock ages from two granites intimately associated with the Hermitage Bay–Dover Fault System. The "Straddling" Granite, at the head of Hermitage Bay, gives an isochron age of 490±10 Myr (Fig. 2*a*), and the "Mylonitic" Granite, adjacent to the Dover Fault, gives an age of 400±30 Myr (Fig. 2*b*). (Both intrusions have yet to receive formal names.) The analytical information is provided in Table 1.

The "Straddling" Granite, as its name implies, straddles the boundary between the Gander and Avalon Zones, and is cut by a breccia zone 50–100 m wide, which is the most southerly expression of the Hermitage Bay Fault. The pluton intrudes both the Garrison Hills Gneiss of the Gander Zone, and volcanics of the Connaigre Bay Group of the Avalon Zone. Although the granite is brecciated, (O'Driscoll, private communication) there is no sign of mylonitisation.

The "Mylonitic" Granite[7,9] occurs adjacent to the trace of the Dover Fault, which is marked by a zone of mylonitisation 300–500 m wide and at least 20 km long[7]. The fault separates the Bonavista Bay Gneiss Complex (Gander Zone)

Table 1 Analytical results

Sample	Petrographic notes	Rb (p.p.m.)*	Sr (p.p.m.)*	^{87}Rb/^{86}Sr (atomic)†	^{87}Sr/^{86}Sr (atomic)‡
Straddling Granite	Medium to fine-grained granite, alkali feldspar mainly microcline, some perthite. Euhedral to subhedral plagioclase (~An_{34}), altered to sericite and epidote. Anhedral quartz with some serrate boundaries, undulose extinction. Some polygonised grains Accessory minerals: epidote, sericite, carbonate, sphene, apatite, chlorite				
SG–1		130	214	1.75	0.7158
SG–2		119	19	18.0	0.8367
SG–3		73	20	10.5	0.7779
SG–4		23	92	0.72	0.7094
SG–5		20	92	0.62	0.7087
SG–6		29	132	0.63	0.7087
Mylonitic Granite	Medium to fine-grained granite, alkali feldspar mainly microcline, some perthite Granitic texture still evident in all but two of the samples. Plagioclase (An_{21}–An_{32}) altered and fractured, quartz usually anhedral, polygonised grains common, undulose extinction. Pronounced cataclastic deformation in MG–4 and MG–5; foliation defined by alternating bands of muscovite and fine-grained quartzofeldspathic material. Some feldspars augened, accessory minerals include sericite, epidote, chlorite and sphene				
MG–1		129	113	3.3	0.7255
MG–2		102	105	2.8	0.7234
MG–3		92	89	3.0	0.7245
MG–4		72	161	1.30	0.7146
MG–5		55	160	0.99	0.7117

*±2%
†±2%
‡±0.1%
} at 99% confidence level; $\lambda^{87}Rb = 1.47\times10^{-11}$ yr^{-1}

from volcanics of the Love Cove Group (Avalon Zone); the latter are considered to be unconformably overlain by sediments of the Musgravetown Group (Avalon Zone). The granite exhibits a mylonitic fabric close to the fault, and there is some evidence for later brecciation. The age of 400±30 Myr, we feel, represents the emplacement age of the granite and not the age of mylonitisation, since the samples dated were cataclastically deformed to markedly different degrees, yet still define an excellent isochron. Samples MG-4 and MG-5 (see Table 1) are the only true mylonites; the rest retain their granitic textures.

Fig. 2 *a*, Rb–Sr isochron for the Straddling Granite: $t = 490\pm10$ Myr; $R_i = 0.7039\pm0.0006$; MSWD, 2.7. *b*, Rb–Sr isochron for the Mylonitic Granite: $t = 400\pm30$ Myr; $R_i = 0.7064\pm0.0012$; MSWD, 1.4. (Uncertainties given at 95% confidence level). (MSWD, Mean square of weighted deviates)

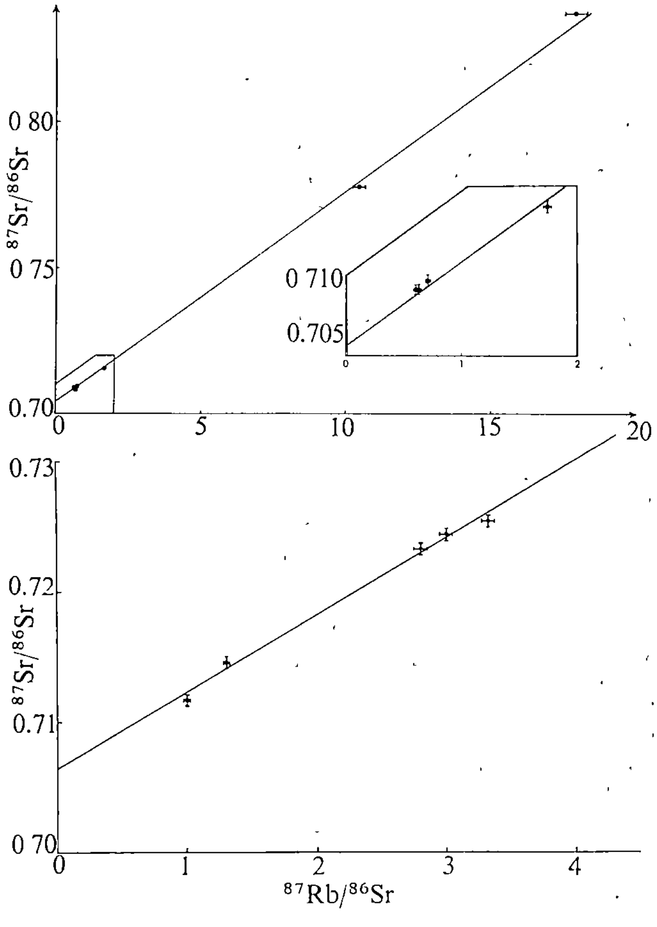

The isotopic data from the Straddling Granite are consistent with the geological evidence which suggests that the Garrison Hills Gneiss and the Connaigre Bay Group are both Precambrian[10,11]. The significant finding, however, is that the southern portions of the Avalon and Gander Zones were in contact by the Ordovician, and it therefore seems extremely unlikely that the boundary between the Avalon Zone and the Central Mobile Belt represents the suture of the Proto-Atlantic Ocean.

We thank R. F. Blackwood, C. F. O'Driscoll, and D. F. Strong for discussion and for samples, J. S. Stevenson for technical assistance, and T. J. S. Cole, D. P. Menagh for help with the mass spectrometry. The study was funded by the National Research Council of Canada.

John Blenkinsop
P. F. Cucman
Keith Bell

Department of Geology,
Carleton University,
Ottawa, Canada

Received May 22; accepted June 8, 1976.

[1] Wilson, J. T., *Nature*, **211**, 676–681 (1966).
[2] Dewey, J F., and Kidd, W S F., *Geology*, **2**, 543–546 (1974)
[3] Anderson, F D., *Geol Surv. Can.*, Map 8–1965 (1965)
[4] Williams, H, Kennedy, M. J, and Neale, E. R W., in *The Ocean Basins and Margins The North Atlantic*, 2 (edit. by Nairn, A. E. M., and Stehli, F. G.), 79–123 (Plenum, New York and London, 1974)
[5] Schenk, P E, *Can. J Earth Sci*, **8**, 1218–1251 (1971)
[6] Brown, P A., *Nature phys. Sci.*, **245**, 9–10 (1973).
[7] Blackwood, R. F., and Kennedy, M. J., *Can J Earth Sci*, **12**, 320–325 (1975).
[8] Bell, K., and Blenkinsop, J, *Nature*, **254**, 410–411 (1975)
[9] Jenness, S. E., *Mem. geol. Surv Can.*, **327** (1963)
[10] Widmer, K., thesis, Princeton Univ. (1950).
[11] Williams, H., *Pap. geol. Surv. Can.*, 70–65 (1971)

Upper limit to earthquake size

Chinnery and North[1] have used data relating surface wave magnitude to seismic moment, M_0, to convert magnitude–frequency statistics for the Earth into a seismic moment distribution. For M_0 values ranging from about 2×10^{25} to 2×10^{30} dyne cm they found that their data could be represented by

$$\log N = 17.47 - 0.61 \log M_0 \qquad (1)$$

where N is the number of shallow earthquakes (depth < 70 km) each year with seismic moment greater than or equal to M_0. On

Table 1 Data on relative plate motion (adapted from Kaula[6])

Boundary type	Length (km)	Assumed width (km)	Mean transverse velocity (cm yr^{-1})	μ (dyne cm^{-2})	Contribution to M_0(tot) (dyne cm)
Ocean subducted under ocean	13,100	200	4.07	6×10^{11}	0.64×10^{29}
Ocean subducted under shelf	22,400	200	5.37	6×10^{11}	1.44×10^{29}
Ocean subducted under cordillera	10,700	200	8.32	6×10^{11}	1.07×10^{29}
Continent–continent collision	9,100	200	2.66	6×10^{11}	0.29×10^{29}
Oceanic fracture zone	16,900	5	1.32	3×10^{11}	3.4×10^{26}
Continent or island fracture zone	9,600	20	0.35	3×10^{11}	2.0×10^{26}
				M_0(tot)	3.44×10^{29}

the basis of the remarkably good fit of equation (1) to their data, they argued that seismic moments considerably in excess of 2×10^{30} dyne cm were likely to occur as they did not consider it probable that the linear trend stopped immediately beyond the last data point. I have used recent results on the movement of lithospheric plates in conjunction with equation (1) to estimate an upper limit for M_0. It turns out that this upper limit is probably not much in excess of the moment of the Chile earthquake of 1960 ($\sim2\times10^{30}$ dyne cm) (ref. 2).

Nearly all of worldwide seismic deformation occurs at plate boundaries (see, for example, ref. 3). Most of the seismic deformation occurs in subduction zones and nearly all of the remainder in fracture zones. Brune[4] and Davies and Brune[5] have shown that seismic failure could account for essentially all of the relative motion at these plate boundaries. Accordingly, aseismic failure is assumed to be of little importance over the interplate boundaries defined by large shallow shocks.

According to Brune[4], the total seismic moment each year, M_0 (tot), that is consistent with the relative motion of all of the tectonic plates is

$$M_0\,(\text{tot}) = \Sigma\mu_i D_i L_i W_i \qquad (2)$$

where the summation is over all of the plate boundaries that are associated with large earthquakes. At each boundary, μ_i is the modulus of rigidity, D_i is the annual relative displacement, and L_i and W_i are the length and width, respectively, of the boundary. Because the material comprising the interplate boundaries has a finite strength, there can be no worldwide secular increase in elastic strain energy at these boundaries. Thus M_0 (tot) represents the average annual amount of seismic deformation that must occur to accommodate the observed interplate motion. Equating the total seismic moment to M_0 (tot) leads to

$$\int_0^{M_0(\text{max})} M_0\,[-(\mathrm{d}N/\mathrm{d}M_0)]\mathrm{d}M_0 = M_0\,(\text{tot}) \qquad (3)$$

where the integrand is calculated from equation (1), and M_0 (max) is the maximum possible seismic moment. From equation (3)

$$M_0(\text{max}) = [M_0(\text{tot})/4.62\times10^{17}]^{2.564} \qquad (4)$$

(Equation (4) is a statistical relationship in that equation (1) was based partly on worldwide magnitude–frequency statistics.)

To perform the integration of equation (3) it is necessary to assume that equation (1) is the correct distribution of M_0 up to M_0 (max). If M_0 (max) is not much in excess of 2×10^{30} dyne cm (the upper limit of the data presented by Chinnery and North[1]) then this assumption is reasonable. From equation (4), then, an upper bound to earthquake moments can be calculated if M_0 (tot) can be estimated from the results of studies of the motions of plates of lithosphere. The calculation of M_0 (max), (equation (4)) does not depend on the time interval of one year, which was chosen for convenience.

Kaula[6] presented data on relative plate motions in a convenient form for the calculation of M_0 (tot). Table 2 of his paper lists the total lengths and mean transverse velocities of various types of interplate boundaries. His data for boundaries associated with large shocks are relisted here (Table 1) along with assumed widths for the zones of contact between plates, rigidities and the corresponding moments calculated from equation (2). The last column of Table 1 shows that in calculations of M_0 (tot) the contributions from the fracture zones are negligible.

The most critical assumption in the estimation of M_0 (tot) is the width of the zones of contact for shallow underthrusting. An average width of 200 km (Table 1) was chosen here on the basis of evidence reviewed by Kelleher *et al.*[8]. It does not seem likely that the average width of contact is less than 150 km or greater than 250 km.

From equation (4) M_0 (max) $= 2.75\times10^{30}$ dyne cm, which is not much greater than the moment of the Chile earthquake of 1960. For average widths of shallow underthrusting as little as 150 km or as great as 250 km the corresponding maximum moments (equation (4)) are 1.3×10^{30} and 4.9×10^{30} dyne cm. Thus, earthquakes substantially larger than the Chile shock of 1960 do not seem possible in view of the bounds associated with the relative motion of tectonic plates if equation (1), based on about 40 yr of seismic data, is the correct distribution of M_0 for the past 30,000 yr or more; the time resolution of the boundary rates in Table 1 is probably no better than 30,000 yr (Kaula, private communication). There is a possibility that the worldwide seismic-slip rate has decreased over the past 70 yr (ref. 5). This possibility introduces some uncertainty into the use of equation (1) for periods of time much greater than 40 yr.

I thank L. O. Nicolaysen, S. M. Spottiswoode and D. O'Connor for helpful suggestions.

A. McGarr

Bernard Price Institute of Geophysical Research,
University of Witwatersrand,
Johannesburg, South Africa

Received February 9; accepted June 26, 1976.

[1] Chinnery, M. A., and North, R. G., *Science*, 190, 1197–1198 (1975).
[2] Kanamori, H., and Anderson, D. L., *Bull Am. seism. Soc.*, 65, 1073–1095 (1975).
[3] Isacks, B., Oliver, J , and Sykes, L. R., *J. geophys. Res* , 73, 5855–5899 (1968).
[4] Brune, J. N., *J. geophys. Res* , 73, 777–784 (1968)
[5] Davies, G. F., and Brune, J. N., *Nature phys Sci.*, 229, 101–107 (1971).
[6] Kaula, W. M., *J. geophys. Res.*, 80, 244–248 (1975).
[7] Kelleher, J., Savino, J., Rowlett, H , and McCann, W., *J. geophys. Res* , 79, 4889–4899 (1974).

Ball lightning in Smethwick

BALL lightning has been observed on many occasions, but there have been few events[1–5] which have provided evidence with which to test any of the available explanations of the phenomenon. Consequently considerable weight has been placed on the "tub of water" event[1]. The occurrence reported by Stenhoff[6] has presented unique evidence which enables us to carry out a number of simple calculations. The lady concerned describes the fireball appearing 39–40″ above the floor, then dropping 2 or 3″ when she tried to stop it with her hand. It was apparent for ~1 s and had a diameter of ~4″ but also had a halo.

The position of the hole in the dress is consistent with the fireball being ~700 mm above the floor when it struck. The hole is 100×70 mm, but the narrowest part indicates that the core of the fireball was ~20 mm in diameter. The surface of the fabric had melted over an area about 300 mm across.

The material seems to be a polyester which would melt at 250 °C and have a specific heat capacity of 1.2 J g^{-1} K^{-1}. To melt the material where there is now a hole would require 200 J and to melt the surface to a depth of 0.1 mm, 240 J. Even if this were only 10% of the total energy, it is $<10^{-2}$ of the values quoted previously. Very little charring had occurred.

An estimate may be made of the energy radiated by the fireball since the lady said that "she seemed to glow all over" as the fireball approached. Assuming this sensation to be equivalent to a 1-kW radiator at a distance of 0.5 m, the flux would be 0.6 kW m^{-1}. A body area of 0.6 m^2 would receive 400 J in 1 s. An equivalent power would be radiated by a spherical black body of 10 cm diameter at 950 °C or at 3,500 °C for a diameter of 1 cm. The thermal energy contained in the sphere would then be 2 kJ. In a dense plasma, radiation trapping reduces the rate of loss of energy and thus implies a higher temperature[10]. Since the ball did not convect rapidly, its mean density must have been close to that of the ambient air, indicating a confining force which if magnetic would require a field ~1.5 T. It is interesting to note that Brand[7] concluded that there was no heat effect with "the type of ball lightning that floats free in the air"[8].

It has been proposed that ^{15}O and ^{17}F are formed during a lightning discharge[9,10] but their half lives are 2.1 min and 66 s respectively, so there was no point in measuring β activity when the dress became available for examination 10 weeks after the event. A γ spectrum taken over a period of 1,000 min for energies from 0 to 3.6 Mev produced a total count over 400 channels of 1.1 c.p.m. above background, implying an activity of 1.6 pCi. No signs of chemical reaction were apparent.

The lady is alive and healthy, so we know that she has not been subjected to harmful ionising radiation. Taking a figure of 500 rad as the maximum exposure that may be suffered without apparent physiological effect, an upper limit of 250 J may be placed on the whole body radiation. This energy would be produced by the annihilation of 10^{-11} g of antimatter at a distance of 10 cm, a figure which is $<10^{-2}$ that discussed in an antimatter theory of ball lightning[5].

The burn suffered in the vicinity of the gold wedding ring permits another estimate of energy to be made. The burn was described as being lighter than a scald, so it is assumed that the skin temperature rose no more than 100 °C. About 3 kJ would heat the surface of the hand (10×10 cm^2) to a depth of 1 mm. To heat the ring up to 100 °C by an electromagnetic field[11] would require a current of 10^3 A and imply an electric component of the e.m. field of 10^4 V cm^{-1}. The resonant frequency would be 10^9 Hz, assuming an inductance of 10^{-9} H and capacitance of 10^{-11} F. Although large d.c. electric fields are present during thunderstorms, only small electromagnetic fields at GHz frequency have been measured[12].

These orders of magnitude 'guesstimates' suggest that the energy associated with this fireball is $\sim10^{-3}$ of that calculated previously[13]. Nothing can be found to support the theories based on radioactivity, antimatter or magnetic fields Furthermore, the low energies estimated are inconsistent with the assumptions on which some models of ball lightning are based.

I am grateful to Miss Stephanie Pearson for drawing my attention to this event, to the lady who suffered the alarming experience, to Dr Desmond MacMahon, Dr R. S. Higginbotham, Dr Colin Whitehead for advice and assistance with measurements, and to Mark Stenhoff for discussions.

E. R. Wooding

Physics Department,
Royal Holloway College,
University of London,
Egham, Surrey TW20 0EX, UK

Received April 20, accepted May 17, 1976.

1 Morris, W , *Daily Mail*, November 5 (1936).
2 Fleming, S J , and Aitken, M J., *Nature*, 252, 220–221 (1974)
3 Mills, A A , *Nature*, 233, 131–132 (1971).
4 Dmitriev, M. T., *Sov Phys tech. Phys.*, 14, 284 (1969).
5 Ashby, D. E. T. F., and Whitehead, C., *Nature*, 230, 180–182 (1971).
6 Stenhoff, M , *Nature*, 260, 596–597 (1976)
7 Brand, W , *Der Kugelblitz* (Henri Grand, Hamburg, 1923).
8 Singer, S., *The Nature of Ball Lightning* (Plenum, New York and London, 1971).
9 Kivel, B., and Mayer, H , *J quant Spectrosc. radiat Transfer*, 5, 13–38 (1965)
10 Altschuler, M D., House, L. L., and Hildner, E., *Nature*, 228, 545 (1970)
11 Kapitsa, P. L , *Dokl. Akad. Nauk SSSR*, 101, 245 (1955).
12 Kosarev, E. L., *et al* , *Sov Phys tech. Phys.*, 13, 1477–1479 (1969).
13 Goodlet, B. L., *J. Instn elect. Engrs*, 81, 1 (1937).

Non-crystallinity of ion-irradiated metals

The preparation of various metals and metallic alloys in a non-crystalline state using splat cooling, vapour quenching or electrochemical deposition techniques has been reported by many authors. A distinguishing characteristic of such amorphous films is a severe modification of the structure factor from that of the crystalline state. Although usually formed only at low temperatures the non-crystalline state may in some cases be metastable to above room temperature, this being particularly true for alloys near the eutectic. We examine here evidence for metastable non-crystalline alloys resulting from ion irradiation.

The structural modifcation of metals by ion irradiation has traditionally been treated in terms of replacement collision sequences or thermal spikes followed by a return to crystallinity with the freezing-in of point defects. At high ion doses the agglomeration of point defects may occur, but the final structure is considered to be that of a defected crystal. This is in contrast to the behaviour of ion-irradiated semiconductors, in which demorphisation occurs. Since, however, each collision cascade causes the temporary displacement of a large number of metal atoms and energy dissipation is rapid, the situation locally may well be compared with splat cooling, and the formation of a non-crystalline state in suitable cases might be anticipated. Stephens *et al.*[1] have reported that Rutherford backscattering and channelling analysis of Dy^+ implanted into single-crystal Ni produced a disorder peak structure which is uncharacteristic of metals, but which can usually be obtained with semiconductors rendered amorphous by ion bombardment. The Dy-implanted Ni system was consequently chosen for more detailed transmission electron microscopy examination, the results of which are reported here.

In our experiments, high purity Ni samples prepared for transmission electron microscopic examination were irradiated at room temperature with 20 keV Dy^+ ions to doses of 10^{16} ions cm^{-2}, thus giving a peak implant concentration of ~ 30 atom% as confirmed by Rutherford backscattering. Analysis using electron diffraction in the TEM shows, in addition to Ni matrix reflections attributable to the undamaged crystal lying beyond the ion range, a single diffuse scattering maximum with a peak intensity scattering parameter $s = 2.99 \pm 0.01$ Å^{-1}, and a half intensity width $\Delta s = 1.1 \pm 0.2$ Å^{-1}. This should be compared with the value $s = 3.085$ Å^{-1} for ⟨111⟩ Ni. Dark field images using the diffuse ring show a generally high background intensity with occasional resolved crystallites in the 30–100 Å range. The former should be expected since application of the Scherrer particle size broadening equation to the measurements quoted already indicated particle dimensions of <10 Å, which is below the resolution limit of the microscopy. On annealing above ~ 400 °C the diffuse ring sharpens and widens to a good Ni ⟨111⟩ fit concurrent with the appearance of additional sharp rings attributable to higher order Ni reflections. Dark-field microscopy confirms the presence of large numbers of Ni crystallites 50–200 Å in size.

Various models of amorphous solids based on the random packing of hard spheres with no appreciable order beyond first neighbours have been proposed; an alternative model for a quasi-amorphous solid is a microcrystalline arrangement in which isolated groups of atoms adopt the parent crystal structure but are separated by localised energy barriers to recrystallisation. In particular, Wang and Merz[2] have proposed a microcrystalline arrangement in which atomic groups may take up the crystal structure of any one of a number of polymorphic forms, and have correlated the occurrence of noncrystallinity with bonding anisotropy and polymorphicity. According to this classification, Ni, with three polymorphs, should be one of the least structurally stable metals. For very small crystals the difference between a microcrystalline solid and a true amorphous solid becomes increasingly indistinct, although it is interesting to note that the observed increase in nearest-neighbour distance in our experiments has also been observed by Davies and Grundy[3] in amorphous Ni films where a dense random packing model seemed justified.

Numerous authors have noted the enhanced stability of non-crystalline metals when alloyed with other metals or metalloids, and Nagel and Tauc[4], using a nearly free electron approach, have suggested that this stability is attributable to a shift in the effective valency, causing the Fermi level to lie at a dip in the density of states function. Thus, an alloy with concentration x of element valency z_2 in z_1 should be most stable against recrystallisation when

$$1.7 \approx z_1(1-x)+z_2x$$

Substitution of $z_1=1$ for Ni, which as a group VIII element may be treated as having only one free electron per atom in the liquid, and $z_2=3$ for Dy gives $x=35\%$, similar to the peak concentrations achieved in the implantations reported here.

Of interest here are the data of Cullis, Poate and Borders[5] who have observed a diffuse diffraction maximum following ion implantation of W^+ into Cu at concentrations in excess of 10 atom%. This figure may be compared with a most stable concentration of 14 atom% predicted by the equation given here.

Finally, we have noted the complete absence of a noncrystalline phase in Pb^+ irradiated Ni up to concentrations of ~ 35 atom%, where $z_2=2$ gives $x=70\%$.

Financial support from both NATO and the Science Research Council is gratefully acknowledged. The authors also acknowledge G. Carter for suggesting the study and possible interpretation, and discussions with C. E. Christodoulides and G. A. Stephens have been most helpful.

R. ANDREW
W. A. GRANT
P. J. GRUNDY
J. S. WILLIAMS

Department of Electrical Engineering,
University of Salford,
Salford M5 4WT, UK

L. T. CHADDERTON

H.C. Oersted Institute,
University of Copenhagen,
Copenhagen, Denmark

Received April 20; accepted June 14, 1976.

[1] Stephens, G. A., Robinson, E., and Williams, J. S., *Ion Implantation in Semiconductors and Other Materials*, 375 (Plenum, New York, 1975).
[2] Wang, R., and Merz, M. D., *Nature*, 260, 35–36 (1976)
[3] Davies. L. B., and Grundy, P. J., *Phys Stat Sol.*, 8(a), 189–197 (1971)
[4] Nagel, S. R., and Tauc, J., *Phys Rev Lett*, 35, 380–383 (1975).
[5] Cullis, A. G., Poate, J. M., and Borders, J. A., *Appl Phys Lett*, 28, 314–316 (1976).

Effect of roughness on rubber friction when waves of detachment are present

IN some circumstances, when rubber moves over a hard surface no true sliding occurs. Instead, the contact area is crossed by waves of detachment[1]; and it is only in these regions, where contact has temporarily been lost, that there is any relative motion of the two surfaces. The effect resembles the motion of a caterpillar on a leaf. It is now well established that when an elastometer slides over a smooth surface in these conditions, the frictional force may be accounted for in terms of the net work required to peel the rubber away from the counterface and readhere it[2,3]. We have now found that waves of detachment may be present when the counterface is rough, and that the same explanation of the friction force applies.

The adhesion of rubber depends markedly on the roughness of the surface with which it is in contact[4,5]. Slight roughness can increase the adhesion compared with an ideally smooth surface, while larger values of roughness can greatly reduce it[6]. When a cylinder rolls on clean rubber, the two surfaces are adhering together at the front of the contact and peeling apart at the rear. The net work for this process at a given velocity may be measured by rolling cylinders down an inclined plane.

For the friction experiments, silicone rubber was moulded to be optically smooth. The counterface was Perspex, which was roughened by blasting with fine particles. The two surfaces were brought together in a crossed cylinders configuration with a sliding speed of 1 mm s^{-1}. The frictional force was recorded, and the waves were filmed at 200 frames s^{-1}.

If Γ is the net work required to peel apart and readhere unit area, A the observed area of contact, and f the number of waves crossing the interface per s; then the energy required in 1 s may be equated to the work done by the frictional force F moving at the sliding speed V thus

$$FV=\Gamma fA$$

Thus, a value of Γ may be deduced and compared with Γ measured directly from rolling experiments for the same surface at the velocity of the waves. This is done in Table 1, and the agreement is fairly satisfactory for a friction experiment.

Table 1 Correlation between the adhesion energy required to account for the frictional force in terms of waves of detachment (Γ_1), and the adhesion energy deduced directly from rolling experiments (Γ_2)

Ra (μm)		*F* (N)	*f* (s^{-1})	*V* (mm s^{-1})	Γ_1 (J m^{-1})	Γ_2 (J m^{-2})
0.04	*	0.156	5.09	10.92	2.40	2 21
0.05	*	0 157	5.49	10 56	2.24	2.14
0.16	†	0 157	4.79	12.42	2.57	3.72
0.30	†	0.164	4.88	10.38	2.63	4.16
0.95	†	0.164	3.30	8.92	4.01	4.81
1.00	†	0 165	4.08	9.31	3.17	5.03
1.29	†	0.162	3.58	9.90	3.54	5 03
1.73	†	0.167	3 50	9.60	3.73	3.72
2.38	†	0.161	3.32	10.22	3.80	4.16
3.09	‡	0.168	4.72	8.56	2 79	2.84
3.14	†	0 162	4.24	9.74	2.99	3 94
6.46	‡	0.179	4.96	10.94	2.82	2.63
7.87	‡	0.186	6.15	10.71	2.37	1.74
8.79	§	0.187	7.05	10.54	2.08	1.93
9.20	‡	0.184	6.05	10.17	2 38	1.36

The normal load was 0 1 N and the imposed sliding speed 1 mm s^{-1}. The results are for a range of roughness measured in terms of the centre line average (*Ra*). *F* is the frictional force, *f* the number of waves crossing the interface per second, and *V* the mean wave velocity. The rubber was Dow Corning XF-13-523 dielectric gel. The surfaces were prepared by blasting with fine particles as follows: *, untreated; †, glass beads; ‡, metal particles; §, sand. The correlation coefficient for the last two columns is 0.79.

At the highest roughness it became difficult to see exactly where contact existed. Waves were clearly observed to propagate, but it may be that with the low true contact area here there is also some interfacial sliding.

It is interesting to note that the coefficient of friction does not vary markedly with roughness. This is because of two competing factors. A Burgers vector, b, may be defined for a wave as the interfacial displacment which results when it passes. The total displacment per s is

$$V=fb$$

When Γ increases, bigger waves form, and they have a larger Burgers vector. Therefore they do not form so often and f decreases, so that F does not change very much.

It has similarly been observed that F may be insensitive to change in V, even though Γ is markedly velocity dependent. This may represent a general result for rubber friction when waves of detachment are present, that although the frictional force is to be accounted for in terms of the net adhesion energy Γ, changes in Γ may have little effect on the coefficient of friction for a particular elastomer.

A theoretical account, which is in preparation, provides a more detailed explanation of these observations. We are grateful to Professor D. Tabor for help and encouragement, and also to the SRC for an Assist award to G.A.D.B.

G. A. D. BRIGGS
B. J. BRISCOE

Cavendish Laboratory,
Cambridge CB3 0HE, UK

Received May 6, accepted June 7, 1976.

[1] Schallmach, A., *Wear*, 17, 310–312 (1971).
[2] Roberts, A D., and Jackson, S. A., *Nature*, 257, 118–120 (1975).
[3] Briggs, G A D., and Briscoe, B. J , *Wear*, 35, 357–364 (1975).
[4] Johnson, K. L., in *The Mechanisms of the Contact between Deformable Bodies* (edit. by de Pato, A. D., and Kalker, J J), 26–40 (Delft University Press, Delft, 1975).
[5] Fuller, K. N. G., and Tabor, D., *Proc R. Soc.*, A345, 327–342 (1975).
[6] Briggs, G. A. D , and Briscoe, B J , *Nature*, 260, 313–315 (1976).

Learning-like phenomena in stereopsis

WHEN confronted with Julesz random-dot stereograms[1] for the first time, naive observers often need as long as a minute or more to see a global figure in depth. With repeated exposure to the stereograms this perception time is progressively reduced until they begin to see depth almost instantaneously[2]. This acceleration of the stereoscopic process over successive trials is a remarkable example of perceptual learning[2,3], and unlike many other kinds of perceptual learning it seems to be a purely visual effect. Further, stereopsis is a basic visual function for which much of the processing may occur as early as the prestriate cortex[4]. It is important to note that learning-like changes can affect such a process, and knowledge of elementary visual function may be helpful in determining just what is learned. Here I explore the position specificity of stereo-learning, and find that in most observers a significant proportion of the learning that is acquired in one retinal area does not transfer to neighbouring areas. One question raised by this finding is whether such position specificity necessarily implies localisation of the learning process to specific anatomical areas in the brain.

The stimulus used (Fig. 1) was a Xerox of Fig. 4.5–3 from Julesz's book[5]. The global figure portrayed (Fig. 3) was a 'saddle' with a 'doughnut' threaded through it (hyperbolic paraboloid with torus) and the pattern was composed of 1,000×1,000 disparity elements, of which 90% were white and 10% black. The maximum disparity was in the range of 30′.

The stereogram was displayed through a three-channel tachistoscope (Electronics Developments). The two half images were carefully aligned before the experiment so that the surround had zero disparity, and crossed polaroids were used to separate the two eye pictures. The whole stereogram subtended 9° at the viewing distance used.

A tiny yellow fixation rectangle was displayed (to both eyes) through the third channel of the tachistoscope. This ensured that the observer was converging on the plane of zero disparity in the stereogram. The stereogram was mounted in such a way that the fixation spot occupied a position between the 'saddle' and the 'doughnut' portions of the global figure as shown in Fig. 2. This will be explained below in greater detail. During the experiment the observer was asked to fixate this spot and never to move his eyes away from the spot. He was also encouraged to move his eyes very slightly within the spot to prevent the image from fading.

Each trial began with the exposure of the fixation rectangle. The subject initiated the exposure of the patterns by pressing a button on command which also started a timer. He was instructed to hold the button pressed until he could clearly see the curved three-dimensional surface of the saddle surrounded by the doughnut. A pencil sketch of the figure was shown to him. It was emphasised that he should use a constant criterion for reporting the emergence of the figure. His release of the button stopped the timer and recorded his perception time on that trial. The button release also switched off the stereogram. There was then a 10-s interval before he was required to initiate the next trial.

Trials were begun with the 'saddle' portion of the global figure occupying a position either to the right (seven observers) or to the left (seven observers) of the fixation point. They were continued until the perception time reached an asymptotic value. After the normal intertrial interval the whole stereogram was shifted by 2.5°, so that the saddle now came to lie on the opposite side of the fixation spot. To ensure that the observer knew exactly where to expect the global figure he was told that the stereogram had been shifted. The time course of his learning was then followed over a number of trials for this new position to the stereogram.

Fourteen subjects were used and all were naive as to the purpose of the experiment. Some of them had seen the 'standard' Julesz stereogram before, but not complex three-dimensional surfaces.

In Fig. 3 the perception time is plotted as a function of trial number for each subject. The line joining the points is broken where the stereogram was moved to a new position. The graphs clearly show the decrease of perception time over trials with the initial position of the stereogram.

Change in position produced an increase in perception time for 13 of the 14 subjects. In most of these 13 cases the time on the first trial for the new position was far outside the range of the preceding asymptotic trials. On subsequent trials there was a steady decline in perception time usually down to the original asymptotic value. In at least nine of the observers the magnitude of change was large (20–50 s change from the original asymptotic level) and a 'criterion' shift seems very unlikely. Most of them, on being questioned, reported unhesitatingly that they had not in fact seen anything during the long latent period on the first trial for the new position of the stereogram and that they had seen the figure emerge only just before button release. These results suggest that a significant proportion of the learning that is acquired in a particular retinal area, remains confined to that area.

When interpreting this lack of transfer, however, the possible role of nonspecific 'distraction' effects must be considered. The involvement of such effects seems unlikely for the following reasons. The same result was obtained on four additional subjects when a 'distributed practice'

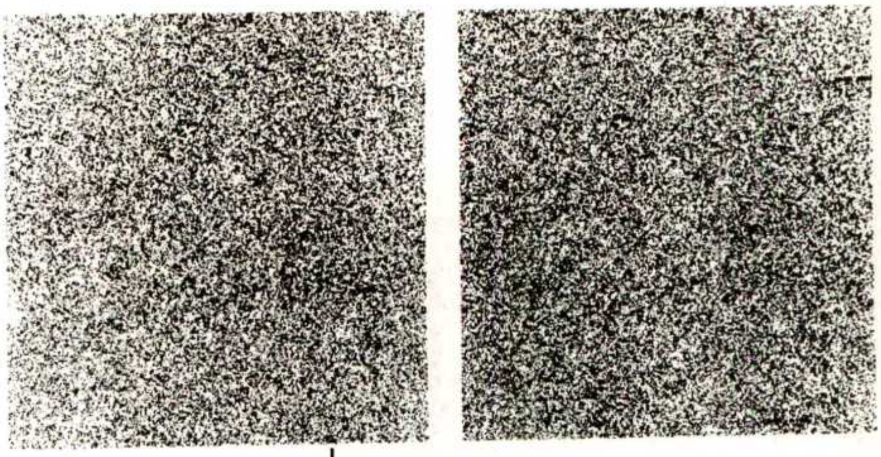

Fig. 1 Random-dot stereogram composed of 1,000 × 1,000 disparity elements portraying a cyclopean hyperbolic paraboloid with torus. If the reader has not seen random-dot stereograms before, he will notice the long latency before the stereoscopic figure emerges (about 1.5 min; average for 20 subjects). With six or seven exposures to the same pattern the perception time is progressively reduced to just 1–2 s. Once the figure has been seen, wide conjugate eye movements may be made without 'losing' the global percept. It would seem that although the learning *per se* is position specific, the solution to the global stereopsis 'problem' is invariant with respect to spatial location.

paradigm was used extending over several days. 'Long term' stereo learning was found to be position specific to the same degree as the short term effects reported above. The learning is not specific to the particular random sequence of dots used. Changing the random sequence without shifting the global figure resulted in complete transfer of learning.

The role of eye movements in stereo learning also remains to be elucidated. Testing an additional eight naive subjects, I found that as soon as they had become skilled, seven of them could see complex three-dimensional surfaces (for example, Fig. 1) in 150-ms flashes. When the stereogram was then shifted to a new position, these eight subjects showed the same basic relearning effect as the 13 subjects in Fig. 3. It seems likely, therefore, that at least some component of stereo learning occurs in the visual centres independent of eye movements. But this point needs to be confirmed using stabilised images.

Fig. 2 Sketch of the cyclopean figure which was shown to the observers, illustrates the way in which the figure is shifted in relation to the fixation spot.

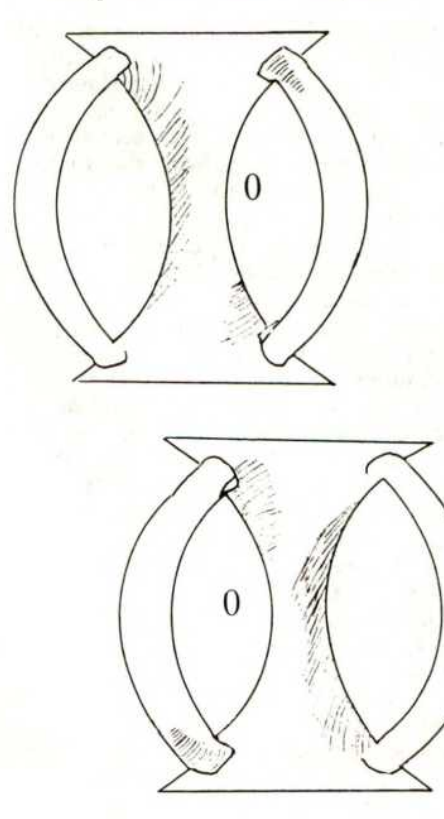

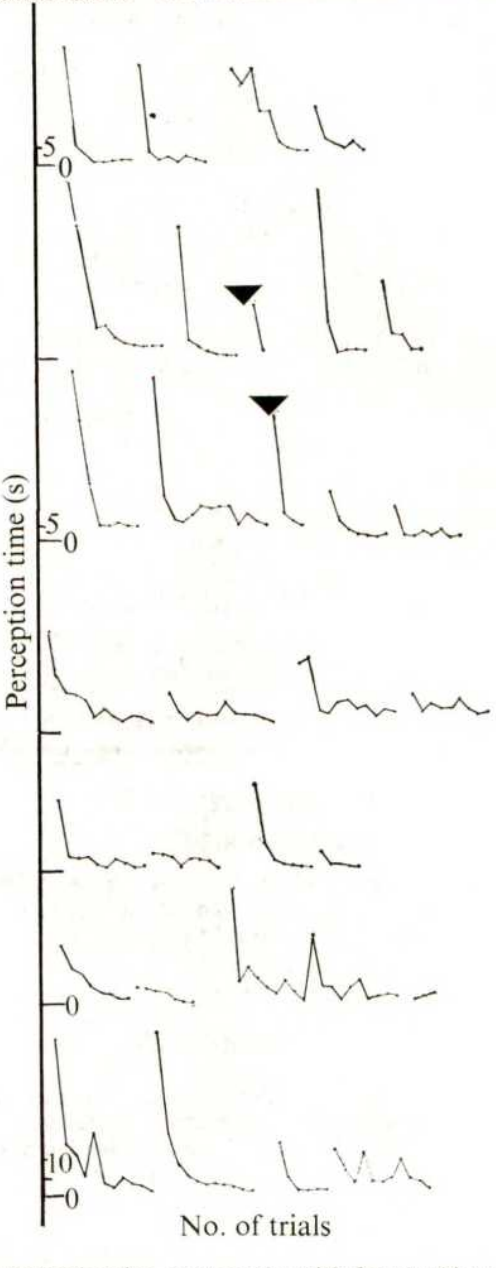

Fig. 3 Perception time on successive trials for 14 subjects. Each point refers to a single trial. On some trials the perception time was too long to be included in the graph; for these the line ending at the top of the plotting area points to the position of the data point. Data for each subject plotted to the same scale. The line connecting the dots is broken where the pattern was shifted between trials. Two of the subjects (*c* and *e*) were switched back again to the original position of the stereogram after they had reached an asymptote on the second position: ▼, point where this change was made. They apparently retained very little of the training they had acquired on the first position.

It is possible that what the observer initially learns is a strategy of vergence movements to bring disparate portions sequentially into register. As the observer becomes more skilled, overt eye movements are eliminated and the 'perception' of global stereopsis may simply involve a subliminal activation of the 'phase sequence' of sensory and motor elements that were originally driving the vergence system. This is equivalent to saying that vergence is replaced by 'cortical shifts' or that the Panum areas are permanently 'extended' by training. This line of reasoning is similar to that used by Hebb[6] to explain form perception.

Visual memory is generally invariant with respect to location in the visual field[7,8]; some authors have pointed out analogies between holograms and memory and suggested that the brain may store spatial Fourier transforms of visual inputs[9]. From my finding, however, that stereo learning is position specific, as well as from the observations of Wallach and Austin[10], it may not be too fanciful to suggest that at least some forms of visual memory are encoded and stored in specific brain areas in such a way as to become unavailable to neighbouring areas.

There is obviously considerable scope for further experiments in this field. Most conventional learning paradigms—such as massed compared with distributed practice, 'forgetting', relearning, and so on—could be fruitfully studied using Julesz patterns as stimuli. Such studies could provide novel insights into mechanisms underlying perceptual memory and learning.

I thank Dr O. J. Braddick, Dr C. Blakemore, Dr A. Baddeley, Professor B. Julesz and A. Adlard for help and discussions.

V. S. Ramachandran

*Psychological Laboratory,
Cambridge CB2 3EB, UK*

Received September 24, 1975; accepted May 17, 1976.

1 Julesz, B., *Bell. Syst. Tech.*, J39, 1125 (1960).
2 Ramachandran, V. S., and Braddick, O., *Perception*, 2, 371 (1973).
3 Sekuler, R., *A. Rev. Psychol.*, 25, 196 (1974).
4 Hubel, D. H., and Wiesel, T. N., *Nature*, 225, 41–2 (1970).
5 Julesz, B., *Foundations of Cyclopean Perception* (University of Chicago Press, 1971).
6 Hebb, D. O., *Organisation of Behaviour* (Wiley, New York, 1949).
7 Sutherland, N. S., *Proc. R. Soc.*, B171, 297–317 (1968).
8 Neisser, U., *Cognitive psychology* (Appleton-Century-Crofts, New York, 1967).
9 Pribram, K. H., *Languages of the Brain*, 140–166 (Prentice-Hall, Eaglewood Cliffs, New Jersey, 1971).
10 Wallach, H., and Austin, P., *Am. J. Psychol.*, 67, 338–340 (1954).

Counter-intuitive property of effective population size

CONSIDER an organism with both autosomal and X-linked loci. The effective population sizes for an autosomal (N_{ea}) and an X-linked (N_{es}) locus can be shown[1] to be

$$N_{ea} = 4MF/(F+M) \qquad (1)$$

$$N_{es} = 4.5MF/(F+2M) \qquad (2)$$

where M and F are, respectively, the numbers of reproducing males and females in a random-mating population.

The ratio of the X-linked effective population size to that for autosomal loci is, from equations (1) and (2)

$$N_{es}/N_{ea} = 9(F+M)/8(F+2M) \qquad (3)$$

From (3), X-linked loci have only 75% of the effective population size that autosomal loci have when males and females are equally abundant, and the discrepancy increases when males outnumber females, as seems intuitively obvious. When there are seven females for every male, however, the two types of loci have the same effective population size; when the proportion of females is increased further, X-linked loci have the greater effective population size. The asymptotic values approached by the ratio N_{es}/N_{ea} are 9/8, as the number of females per male increases, and 9/16, as the number of males per female becomes infinitely large.

The biological significance of the above observation is hard to evaluate, but two points can be made. First, many insects, particularly parasitoids, have extremely female-biased sex ratios, and these species are mostly male haploids[2]. Second, it is now possible to test the influence of effective population size on genic diversity, in that preliminary evidence[3] indicates that male haploid and X-linked loci have fewer polymorphisms than autosomal loci. If this difference is general and effective population size differences are the major cause for it, then it should be still greater in male-biased male diploids, but in highly female-biased such species' X-linked loci should be more polymorphic than autosomal ones.

I thank the referee for suggesting inclusion of the asymptotic values.

R. H. Crozier

*School of Zoology,
University of New South Wales,
Kensington, New South Wales 2033,
Australia*

Received March 15; accepted June 1, 1976.

1 Wright, S., *Evolution and the Genetics of Populations*, 2, 123 (University of Chicago, Chicago and London, 1969).
2 Hamilton, W. D., *Science*, 156, 477–488 (1967).
3 Crozier, R. H., *A. Rev. Ent.* (in the press).

Geography of photoperiodic response in diapausing mosquito

IN temperate latitudes, many arthropods rely on photoperiod to cue their seasonal development. Although the relationship between critical photoperiod and latitude is well illustrated, that between critical photoperiod and altitude remains obscure[1,2]. I wish to consider photoperiodic control of dormancy in the pitcher-plant mosquito, *Wyeomyia smithii*, and quantify the relative effects of altitude and latitude on the photoperiodic response of an organism.

W. smithii is found from the Gulf coast to Labrador and northern Manitoba[3–6] where it confines its breeding site to the water-filled leaves of a single species of plant, *Sarracenia purpurea*. The larvae overwinter in the pitchers in a state of developmental arrest. Short days evoke and maintain, while long days avert or terminate this diapause[7,8]. The photoperiod which promotes 50% development and initiates or maintains 50% diapause is known as the critical photoperiod[2,7,9,10]. In *W. smithii*, the critical photoperiod is the same for the initiation and termination of diapause among larvae reared in the laboratory and for the termination of diapause among larvae collected during early autumn[7]. I have collected larvae north of 38°N latitude only during the autumn (autumn larvae) and south of this latitude only during the winter (winter larvae). I packed the autumn larvae in ice on the day of capture and maintained them on ice until they reached the laboratory where I stored them in an ordinary refrigerator at 4±2 °C until the start of experiments. All experiments were begun within 45 d of capture. Since the winter larvae received unknown chilling in nature which might have affected the critical photoperiod[11,12], I reared them in the laboratory and determined the critical photoperiod for the initiation of diapause in the F_1 generation. Whether considering the maintenance of diapause among autumn larvae or the initiation of diapause among the F_1 of winter larvae, I exposed them to a range of LD 10 : 14 to LD 17 : 7 in 30-min increments at 25±1 °C. Rearing procedures and the criteria for diapause and development were the same as in previous studies[7,13].

I determined the critical photoperiod for 22 populations of *W. smithii* collected over a range of 19° latitude, 20° longitude and 1,200 m altitude. The critical photoperiods ranged from 12 to 16 h of light per day (Fig. 1) and were closely correlated with latitude ($t=14.26$; $P<0.001$) and altitude ($t=9.25$; $P<0.001$) but not longitude ($t=1.71$; $P>0.10$). Latitude accounted for 80.5% of the variation in critical photoperiod and altitude an additional 15.5%. Critical photoperiod may then be estimated from latitude and altitude by the least-squares regression equation

$$\text{critical photoperiod}=6.51+0.185 \text{ latitude}+0.00129 \text{ altitude}$$

To correlate critical photoperiod with climatic variables, I modelled the growing season (mean number of freeze-free days) for 26 cities in the United States north of latitude 30°N and east of longitude 90°W (ref. 14). Although city temperatures are not the same as in bogs, they are presumably correlated[15]. I found that growing season was closely correlated ($r=0.97$) with latitude ($t=15.39$; $P<0.001$) and altitude ($t=4.59$; $P<0.001$) but not longitude ($t=0.42$; $P>0.60$). I then calculated the growing season for each locality in Fig 1 using its latitude and altitude and the least-squares regression equation relating growing season to these parameters

$$\text{growing season}=585.93-9.33 \text{ latitude}-0.094 \text{ altitude}$$

I found that growing season calculated in this manner was an excellent predictor of critical photoperiod in *W. smithii* (Fig. 2). This degree of correlation between an ecogeographic character and a specific climatic variable is unprecedented. In many other studies[16-20], the ecogeographic characters being examined are affected by a wide range of environmental influences which may be changing independently of geography. The photoperiodic response of *W. smithii* tracks climate so closely for several reasons. First, photoperiodism is a physiological adaptation concerned mainly with the timing of seasonal development; second, the low variation in microhabitat offered by the leaves of *Sarracenia purpurea* over a wide geographic range permits a more direct expression of this adaptation. Third, critical photoperiod in *W. smithii* is a continuous variable over the range considered, rather than a discontinuous variable as in some other insects[21,22].

To account for geographic differences in the timing of phenological events, including seeding and harvest dates of winter wheat and insect emergence, Hopkins proposed a bioclimatic law[23] equating a 1° increase in latitude with a rise in altitude of 122 m, or somewhat less than my estimate of 142 m per °N. My results are not grounds for modifying Hopkins' law and its prediction of phenological events, but rather point to the departure from this law by the photoperiodic cues which mediate seasonal development. The disparity between Hopkins' law and critical photoperiod in *W. smithii* relates to the observation that, for a given date between the spring and autumnal equinox, daylengths are longer in the north than in the south[24]. Consequently, insects on a southern mountain should use a shorter daylength to enter diapause on a given calender date than will those in a population further north which enters diapause on the same date. One would then have to go higher up the mountain than predicted from the bioclimatic law to find a locality where the mosquitoes are using the same critical photoperiod as the northern population. Hopkins' bioclimatic law in temperate and north-temperate latitudes may thus be expected to underestimate the effect of altitude on photoperiodism.

Fig. 1 Relationship between critical photoperiod, altitude and latitude. Circles on the regression plane indicate where the projections of the data points cross that plane. $r \doteq 0.98$; $P < 0.001$.

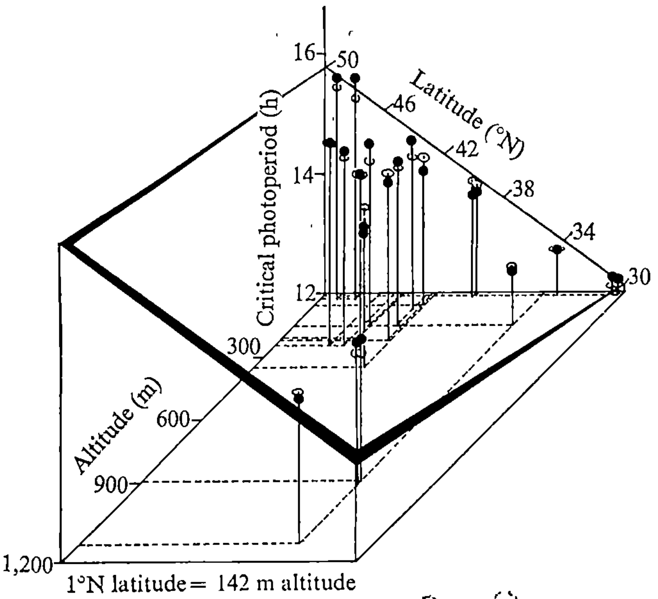

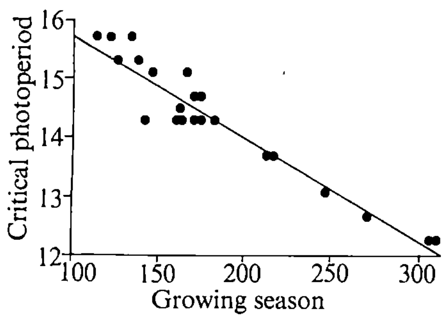

Fig. 2 Correlation of critical photoperiod with growing season. Freeze-free days for each locality were calculated from a least-squares regression equation relating number of freeze-free days of 26 cities in eastern North America to latitude and altitude. $r = 0.96$; $P < 0.001$.

I thank C. M. Holzapfel and L. P. Lounibos for discussion and critical review of this study, J. Shepherd for assistance in collections, B. R. Ingram and D. R. Strong for logistical support, R. W. Burrows and A. M. Simons for permission to work on their land, and F. C. Evans for permission to use the University of Michigan's E. S. George Reserve. Support was provided by grants from the NIH, NSF and the University of Oregon Office of Scientific and Scholarly Research.

WILLIAM E. BRADSHAW

Department of Biology,
University of Oregon,
Eugene, Oregon 97403

Received May 7, accepted June 22, 1976.

1 Danilevskii, A. S., *Photoperiodism and Seasonal Development of Insects* (Oliver and Boyd, Edinburgh, 1965).
2 Danilevskii, A. S, Goryshin, N. I., and Tyshchenko, V. P, *A. Rev. Ent.*, **15**, 201–244 (1970)
3 Burgess, I., and Rempel, J. G., *Can. Ent.*, **103**, 886–887 (1971).
4 Dodge, H. R., *Proc Entomol. Soc. Wash.*, **49**, 117–122 (1947).
5 Carpenter, S J., and LaCasse, W. J., *Mosquitoes of North America* (University of California Press, Berkeley, 1955).
6 Haufe, W O., *Can. Ent*, **84**, 254–263 (1952)
7 Bradshaw, W. E, and Lounibos, L. P., *Can J. Zool.*, **50**, 713–719 (1972)
8 Smith, S M, and Brust, R A., *Can. J Zool*, **49**, 1065–1073 (1971).
9 Beck, S D, *Insect Photoperiodism* (Academic, New York, 1968).
10 Lees, A D, *The Physiology of Diapause in Arthropods* (University Press, Cambridge, 1955)
11 Bradshaw, W. E, *Biol. Bull*, **146**, 11–19 (1974).
12 Tauber, M J, and Tauber, C. A, *Nature*, **258**, 711–712 (1975).
13 Lounibos, L. P., and Bradshaw, W E., *Can J Zool*, **53**, 215–221 (1975).
14 *Climatic Atlas of the United States* (US Department of Commerce, Washington DC, 1968)
15 Haufe, W. O., and Burgess, L., *Ecology*, **37**, 500–519.
16 Ruibal, R., *Copeia*, 212–221 (1957).
17 Johnston, R. F., *Condor*, **56**, 268–273 (1954).
18 Lord, R D., *Am. Midl. Nat.*, **64**, 488–499 (1960).
19 Hardwick, D. F., and Lefkovitch, L. P., *Can Ent.*, **103**, 1217–1235 (1971).

Pure Chemistry Library.
SCIENCE COLLEGE.

[20] Snyder, G. K., and Weathers, W. W., *Am. Nat.*, 109, 93–101 (1975).
[21] Masaki, S., *Evolution*, 26, 587–600 (1972)
[22] Petersen, B., *Zool. Bidr Uppsala*, 26, 329–531 (1947).
[23] Hopkins, A. D., *US Dept Agric. Misc. Publ.*, 280, 1–188 (1938).
[24] *Tables of Sunrise, Sunset, and Twilight* (Nautical Almanac Office, US Naval Observatory, Washington, DC, 1962).

The dispersal of young post-larval bivalve molluscs by byssus threads

New observations, both in the marine environment and in the laboratory, indicate that the byssus in young post-larval bivalves has a hitherto unsuspected function—that of dispersal. The method of transport is analogous to the gossamer flight of young spiders. In the laboratory, small scale currents will induce the secretion of what seems to be a single long thread which, by increasing the viscous drag exerted on the young bivalves, enables them to be carried along on relatively small currents. The threads, which stain readily in Alcian blue (a stain selective for acid mucopolysaccharides) are typically long compared with the length scale of the animal itself: for instance an *Abra* 1 mm long can produce a 2–4-μm diameter thread of length greater than 3 cm. This mechanism, which we term byssus drifting, is functional from the late pediveliger stage up to at least 2.5 mm size in some species, and it has been found to be present in the 20 species tested so far and listed in Table 1 (a functional byssus has not been reported previously[1] in post-larval bivalves of those genera marked with an asterisk).

The increase in drag produced by the byssus in the process of drifting was investigated experimentally in a simple apparatus which consisted essentially of a vertical glass tube enclosed at either end by fine-mesh netting and into which the animals could be introduced and confined. The upward flow of seawater through the tube was adjusted until a critical current speed, U, was obtained at which an animal could be suspended motionless relative to the tube. Where possible, three sets of readings of U were taken for each animal in each of the following states of activity: (1) live, inactive; that is immediately after the animal has been introduced into the tube and is still closed as a result of being handled, and therefore has not secreted threads into the water, (2) active; that is byssus drifting, and (3) dead (killed in 1% formalin in seawater).

While byssus drifting, an animal hangs from the thread with the ventral shell margins uppermost and held horizontally. The valves are generally only slightly open and the heel of the foot is brought close to the gape. Frequently an animal was observed to detach itself from its thread and fall freely through the tube. In some cases secretion of a new thread would check the descent or even produce upward motion. Sometimes the valves may be opened and shut rapidly several times in succession. At other times the foot is protruded and its anterior part may be wriggled about, or the animal may either swing from side to side (*Mytilus*) or perform what seemed to be digging movements (Tellinacea). The siphons are frequently protruded in the Tellinacea. Contrary to other observations[2], it was concluded from experimental observations on byssus drifting animals that the protrusion of the foot produces an insignificant increase in drag. Nelson[3] reported that post-larval *Mytilus* could remain pelagic by the secretion of gas into the mantle cavity. Gas bubbles have occasionally been seen in the mantle cavity of *Mytilus* during our experiments, but these are possibly caused by transferring the animals from seawater at a temperature of 9 °C to seawater of up to 20 °C in the apparatus.

It is usual[4] in hydrodynamics to express the effect of fluid drag on a moving body in terms of a dimensionless drag coefficient, C_D, defined as the ratio of the drag force per unit area to the quantity $\frac{1}{2}\rho U^2$, where ρ is the density of the fluid and U is its velocity relative to the body. By the nature of the terminal velocity measurements made in this study, the drag force on the body is simply equal to its weight in water. Assuming uniformity of shape within a given species, the drag coefficient for a body of volume, V, surface area, A, and density ρ_b can therefore be written as

$$C_D = (2g(\rho_b - \rho)V)/A\rho U^2 = kC_D^*$$

where k is a constant determined by the acceleration due to gravity, the relative density of the body, and some geometrical factor directly proportional to its ratio of volume to area. C_D^* is a modified drag parameter equal to a/U^2, where a is a typical linear dimension of the shell and the constant, k, takes a different value for each species.

Table 1 Species in which byssus drifting has been found to occur

Subclass Protobranchia	
Superfamily Nuculacea	*Nucula tenuis*
Subclass Lamellibranchia	
Superfamily Mytilacea	*Mytilus edulis, Modiolus* sp. *Musculus marmoratus*
Superfamily Anomiacea	*Heteranomia squamula*
Superfamily Cyamiacea	*Turtonia minuta*
Superfamily Erycinacea	*Montacuta ferruginosa, M. substriata*
Superfamily Cardiacea	*Cardium echinatum*
Superfamily Veneracea	*Venerupis pullastra*
Superfamily Mactracea	*Mactra corallina**, *Spisula** sp.
Superfamily Tellinacea	*Tellina tenuis**, *Gari fervensis**, *Abra alba**, *Donax vittatus**
Superfamily Solenacea	*Cultellus pellucidus, Ensis** sp.
Superfamily Saxicavacea	*Hiatella arctica, H. gallicana*
Superfamily Myacea	*Mya truncata, Corbula gibba*

Byssus drifting has been found to occur in all the 22 bivalve species tested so far.

*Those species or genera in which a functional byssus has not been reported previously.

Figure 1*a* and *b* shows values of the modified drag parameter C_D^*, plotted in the conventional manner as a function of the Reynolds number, Re ($=aU/\nu$, where ν is the kinematic viscosity of the fluid), for the species *Mytilus edulis* and *Abra alba*, respectively. Both graphs show that, in terms of the drag experienced by the bivalves, the dead and inactive samples behave in an almost identical manner, and the form of their behaviour is in excellent agreement with the classical experimental data[4,5] on the flow past a rigid body, in this Reynolds number range. Small individual departures from the classical curves can be ascribed to small amounts of debris attached to their shells.

Active animals, on the other hand, behave quite differently. This is illustrated by the large random departures from the

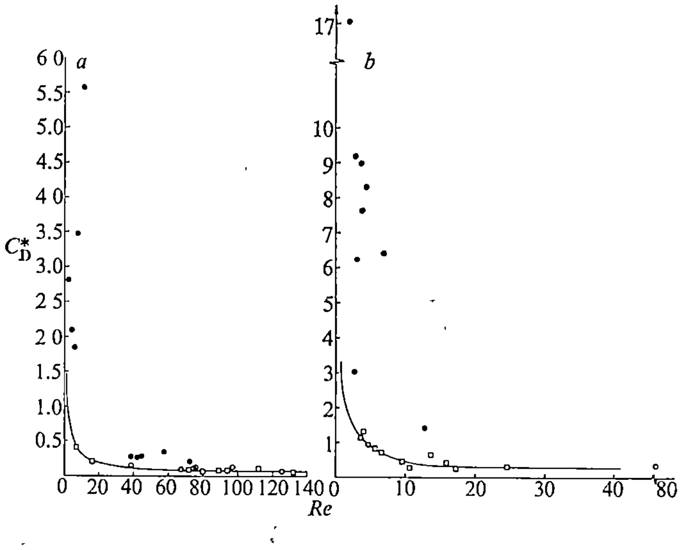

Fig. 1 Plot of modified drag coefficient, C_D^*, against Reynolds number, Re, for ●, live active; ○, live inactive; and □, dead samples of *Mytilus edulis* (*a*) and *Abra alba* (*b*). The solid curve represents a best fit to the data of the classical experimental results[4,5] on the flow past a sphere in this Reynolds number range.

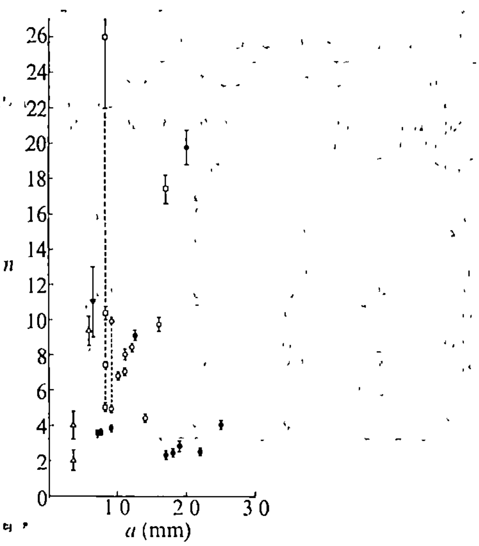

Fig. 2 Measured fractional increase in drag, *n*, plotted against shell length, *a*, for ●, *Mytilus edulis*; ○, *Abra alba*; □, *Gari*; △, *Montacuta*; and ▼, *Nucula*.

'dead' curves, indicating the presence of large drag forces which are not due to the shape of their shells alone but must be provided by some other mechanism. Figure 2 shows the relative increase in drag, *n*, defined as

$$n = (C_D^*)_{\text{active}}/(C_D^*)_{\text{dead}},$$

for active individuals of several species, plotted against shell length, *a*. It is seen that the drag increase is rarely less than a factor of three, while some adept 'drifters' acquire an increase of 20–30 times the value they experience when inactive. The large errors associated with some values of *n* are due to the relatively small number of observations in certain size ranges of these species. Hatched lines joining some points show the drag characteristics of the same animals can vary with time, corresponding to various stages of activity.

The experiments certainly indicate that byssus drifting constitutes an effective means of transport for young post-larval bivalves and that the upward components of ocean currents which are required to suspend active individuals are typically only 1 cm s^{-1}. The importance of this mechanism can hardly be doubted and the fact that it seems to be of widespread occurrence in bivalves supports that view. It is almost certainly the mechanism by which post-larval bivalves enter on a second pelagic or migratory phase reported for a few littoral bivalve species[2,6], the best documented case being that of *M. edulis*[2]. Preliminary field observations indicate that a prolongation of the larval pelagic phase by a post-larval "bysso-pelagic" phase may be a regular feature of the life history of several sublittoral bivalve species. *A. alba* up to 2 mm in length, and *Montacuta ferruginosa* and *M. substriata* up to 0.8 mm in length, together with post-larvae of several other species, have been taken in considerable numbers in plankton samples. At these sizes the ages of the above species may be from several months to over a year[7], indicating the possible duration of the "bysso-pelagic" phase. Further investigations into the occurrence and nature of byssus drifting are presently in progress.

Acknowledgements are due to the staff of the Dove Marine Laboratory for their advice and Dr D. J. Tritton is thanked for his helpful criticism of the drag data interpretation. Part of this work was carried out while one of the authors (J.B.S.) was in receipt of a British Council scholarship.

JON BALDUR SIGURDSSON

Department of Zoology,
Dove Marine Laboratory,

C. W. TITMAN
PETER A. DAVIES

Institute of Lunar and Planetary Science,
School of Physics,
University of Newcastle-upon-Tyne,
Newcastle-upon-Tyne NE1 7RU, UK.

Received May 11; accepted June 16, 1976.

1 Yonge, C. M., *J. Mar. biol. Ass. U.K.*, 42, 113–125 (1962).
2 Bayne, B. L., *J. Anim. Ecol.*, 33, 515–523 (1964).
3 Nelson, T., *Biol Bull. Woods Hole*, 55, 180–192 (1928).
4 Batchelor, G. K., *An Introduction to Fluid Dynamics* (Cambridge University Press, 1970).
5 Schlichting, H., *Boundary Layer Theory* (Pergamon, London, 1955).
6 Baggerman, B., *Archives Neerlandaises de Zoologie*, 10, 315–342 (1953).
7 Muus, K., *Ophelia*, 12, 79–116 (1973).

Nematocyst discharge and the effects of antibodies on feeding in hydra

WHILE attempting to isolate hydra morphogens by column chromatography of tissue homogenates, I decided that a bacteria-free culture would be advantageous. Having established that a final concentration of 100 μg ml^{-1} penicillin G plus 100 μg ml^{-1} streptomycin in the normal[1] culture medium M gave a 100-fold reduction in bacterial contamination in 24 h, I found that hydra could not feed in this solution; indeed, they seemed unaware of *Artemia* larvae bumping into them. On transferring the hydra to fresh medium without antibiotic they were immediately able to feed normally.

I then tested three aspects of normal feeding in hydra: the initial capture by discharge of nematocysts on contact; the subsequent contraction of the tentacles bringing the captured prey to the mouth and the opening of the mouth and engulfment of the prey. Nematocyst discharge can be stimulated by electric shock[2] mechanical plus chemical stimulation[3] or brief sonication. For example, a 0.1-s burst from a Dowe Soniprobe into 10 ml of medium M containing 100 hydra gives >80% discharge of nematocysts, as judged by counting stenotheles using a haemocytometer.

This mechanical discharge can be inhibited by first suspending the hydra in a medium of high osmotic pressure as indicated in Table 1. A 10-s sonication with the microtip at the no. 8 setting in 2 M sucrose gives only 5% discharge. Nuclei are also left intact in these conditions, in spite of rupture of all cell walls and homogenisation of cytoplasm[4]. These observations would seem to confirm the 'osmotic hypothesis' for the discharge of nematocysts[5] with one reservation: 2 M sucrose has an osmotic pressure equivalent to 1 M NaCl, yet even 2 M NaCl is not so efficient at inhibiting discharge. There is, therefore, the possibility of some additional influence in 2 M sucrose, possibly viscosity, aiding the osmotic effect.

Using a membrane filter with pore size 5 μm, it is possible to remove nematocysts from the homogenates that are produced and thus obtain a preparation that is relatively free from the nematocyst toxin that is a major component of many 'inhibitory' extracts[6]. The tentacle movement and mouth opening, collectively known as the "feeding response" can be stimulated by 5×10^{-4} M reduced glutathione in medium M (ref. 7). Table 2 shows the effects of various concentrations of the antibiotics on

Table 1 Percentage discharge of nemotocysts on sonication in a medium of high osmotic pressure

Solution	Sonication time and power setting	% Discharge
1 M Sucrose	5 s, no. 8	8.5
	10 s, no. 8	22.5
2 M Sucrose	5 s, no. 8	2.0
	10 s, no. 8	5.0
2 M NaCl	5 s, no. 4	>10
4 M NaCl	5 s, no. 4	2.5
5 M NaCl	5 s, no. 4	<1.0
40% Methanol	5 s, no. 4	2.0

Table 2 Effect of antibiotics on feeding response and prey capture

Antibiotic concentration (μg ml^{-1})		Feeding response (estimated means of 10 animals each in 5×10^{-6}M reduced glutathione)						Capture of *Artemia* (4 hydra+200 *Artemia* in 4 ml medium)		
		Degree of response		Time of response (min)				Total number caught		Initial capture rate *Artemia* per hydra per s
				Tentacles	Mouth open					
Penicillin G	Streptomycin	Tentacles	Mouth	waving for	From	To	For	in 5 s	in 5 min	
100	100	±	–	4 0	1.5	4.0	2.5	0	0	0.0
10	10	++	±	6.0	0.6	4.6	4.0	40	100+	2.0
1	1	++	+	6.0	0.5	5.0	4.5	40	100+	2.0
100	0	+	–	5.0	1.0	2.5	1.5	48	100+	2.4
10	0	++	±	6.0	0.3	4.3	4.0	50	100+	2.5
1	0	++	±	6.0	0.5	4.5	4.0	50	100+	2.5
0	100	±	–	4.0	2.0	4.0	2.0	0	0	0.0
0	10	+	+	5.0	0.5	5.0	4.5	41	100+	2.1
0	1	++	+	6.0	0.75	5.5	4.75	48	100+	2.4
Control 0	0	++	++	6.0	0.25	5.75	5.5	40	100+	2.0

++, Excellent; +, good; ±, fair; –, poor.

the components of normal feeding in *Hydra littoralis* starved for 24 h. The figures given for the timing of tentacle waving and mouth opening are estimates based on the simultaneous observations of 10 hydra. The lack of precise data for individual animals makes an accurate statistical analysis impossible; the trends, however, are clear.

Together, penicillin G and streptomycin at 100 μg ml^{-1} reduce both the length of time that tentacles wave and the time the mouth is open. Mouth opening is also delayed compared with the control but the most important effect is on initial capture, indicating a total inhibition of nematocyst discharge. These effects are totally lost or much reduced at lower antibiotic concentrations.

On its own, penicillin G at 100 μg ml^{-1} delays and reduces the mouth opening time but has little or no effect on tentacle waving and nematocyst discharge. Streptomycin, on the other hand, at 100 μg ml^{-1} affects all the functions tested, in particular totally inhibiting nematocyst discharge. Again the effects are lost or much reduced when the antibiotics are diluted.

It should be noted that 5×10^{-6} M glutathione is apparently a suboptimal concentration for this particular clone of hydra, since Lenhoff[7] found a mean mouth opening time of 36 min commencing 0.7 min after application of reduced glutathione.

Streptomycin at 100 μg ml^{-1} has, however, no inhibitory effect on artificial mechanical nematocyst discharge by sonication. A temporary paralysis of the cnidocil trigger[6] is therefore indicated, but the exact mode of action is unknown. The effects on the feeding response suggest that the antibiotics may also interfere with cell to cell communication in hydra, either through the 'nerve net' or the direct electrical contacts that exist between cells[8]. The true significance of this effect is, however, in doubt since a rough χ^2 'goodness of fit' comparison between the most extreme results and the controls gives a chance probability of 0.1. Known inhibitors of the feeding response are structurally similar to glutathione, having the same peptide backbone and apparently acting by competition for a receptor site[7]. No more definite hypothesis can be advanced for the effect of streptomycin, but a warning note should be sounded with respect to the routine use of antibiotics in any experimental situation; there may be unforeseen modifications in cell surface recognition sites, sensory structures or intercellular communication equivalent to those described here.

OWEN K. WILBY

Developmental Biology Building,
124 Observatory Road,
Glasgow G76 8LP, UK

Received March 8; accepted May 25, 1976.

[1] Webster, G , and Wolpert, L , *J Embryol. exp. Morph.*, 16, 91–104 (1966).
[2] Kline, E. S., in *The Biology of Hydra* (edit by Loomis, W. F., and Lenhoff, H. M.), 153–168 (University of Miami Press, Miami, 1961).
[3] Lentz, T. H , in *The Cell Biology of Hydra*, 119–123 (North Holland, Amsterdam, 1966).
[4] Webster, G., and Hamilton, S., *J. Embryol. exp. Morph* , 27, 301–316 (1972).
[5] Mariscal, R. N , in *Coelenterate Biology* (edit. by Muscatine, L . and Lenhoff, H. M), 129–166 (Academic, New York, 1974)
[6] Davis, L. V., *J exp. Zool*, 164, 187–194 (1967).
[7] Lenhoff, H. M., in *The Biology of Hydra* (edit. by Loomis, W. F., and Lehnoff, H. M), 203–232 (University of Miami Press, Miami, 1961).
[8] Josephson, R K , in *Coelenterate Biology* (edit. by Muscatine, L , and Lenoff, H M.), 245–273 (Academic, New York, 1974).

Excitability of nerve-free hydra

THE simplest nervous systems known are those of coelenterate polyps, of which hydra is one. Nerve cells of the common freshwater hydra occur in a diffuse, two-dimensional nerve net dispersed among the epithelial cells of the outer, ectodermal layer[1–4]. There are also a few nerve cells in the inner, endodermal layer but these are scattered and do not seem to form a continuous net[5]. Nowhere in a hydra are there nerve cell concentrations or clusters of sufficient complexity to warrant being called ganglia. There have been many behavioural and electrophysiological investigations of hydra[6–9], but the function of the nervous system in the control of behaviour is still unclear. In other coelenterates epithelial cells have been shown to be capable of propagating behavioural signals[10,11]. Several conducting systems coupled with spontaneously active pacemakers have been identified in hydra, but it is not known which of these conducting systems, if any, are neuronal and which result from activity in non-neuronal, epithelial cells. We have investigated the behaviour of *Hydra attenuata* in effectively nerve-free animals and show that such behaviour as remains, is controlled by non-neuronal cells.

It is now possible to create hydra which are virtually free of nerve cells, by treating the animals with colchicine[12]. Colchicine causes the endodermal digestive cells to send processes through the mesoglea and engulf ectodermal nerve cells, interstitial cells and nematoblasts, and draw them into the endoderm where they are digested. After two successive treatments, the hydra consist almost solely of epithelial cells and endodermal gland cells, with only a few cells of the other types remaining. Most of these animals are totally nerve free. Because colchicine treatment removes both the nerve cells and their progenitors, the interstitial cells, these hydra and their buds subsequently remain nerve free. The colchicine-treated animals are somewhat smaller than untreated animals and have altered proportions, but possess all body parts and reproduce by budding. Lacking nematocysts, the treated animals cannot capture prey and are fed by forcing newly hatched *Artemia* through the mouth directly into the gut.

Experimental animals were maintained and studied in 'M' solution[13] supplemented with 50 μg ml^{-1} of the antibiotic rifampicin. The hydra were subjected to two 8-h treatments with 0.4% colchicine spaced two weeks apart[12]. They were then fed three times weekly for 3 months before the experiments.

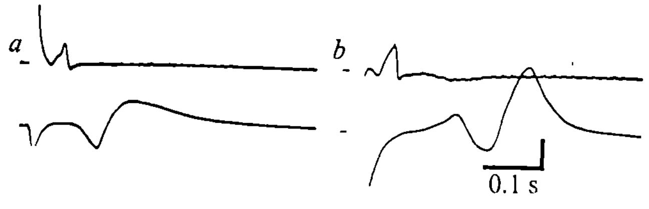

Fig. 1 CPs from a normal (*a*) and a nerve-free hydra (*b*). Positive potentials are upward deflections The animals were stimulated near the base; the upper traces were recorded from a basal disk electrode, the lower traces from an oral electrode. Latency values from the same two animals are plotted in Fig. 2. Vertical calibration: *a*, 5 mV; *b*, upper trace 2 mV, lower trace 5 mV.

Control hydra similar in size to the treated hydra were selected from a mass culture: some were kept in M solution and others in M solution containing rifampicin. All animals were starved for 48 h before the experiments.

Electrophysiological studies have previously identified three classes of spontaneous electrical potentials in normal hydra[9]: (1) contraction pulses (CPs), generated by the ectodermal cell layer and associated with symmetrical, longitudinal contraction of the body column; (2) rhythmic potentials (RPs), generated by the endodermal cell layer and associated with contraction of endodermal circular muscles leading to column elongation; and (3) tentacle contraction pulses (TCPs), produced by the tentacles and associated with tentacle contraction. In normal hydra, these potentials occur somewhat sporadically with a mean frequency of the order of 1 per several minutes. Colchicine-treated animals show virtually no spontaneous behaviour, and not a single spontaneous electrical response was recorded in a total of 10 h of recording[14] from five treated animals. The behavioural inertness of colchicine-treated animals is particularly apparent in a time-lapse film, exposed at one frame per 30 s, of a dish containing a normal and a treated animal. In the film (which compresses 33 h of activity into 5 min) the normal animal contracts, elongates and sways from side to side, continuously, whereas the treated animal is motionless except for slight rippling contractions and occasional discharging of gut fluid through the mouth. Passano[15] suggested that a major function of nerve cells in primitive organisms is to initiate spontaneous activity. The absence of spontaneity in colchicine-treated hydra is thus consistent with this view.

Colchicine-treated animals are relatively unresponsive to external stimuli. Bright light, mild mechanical agitation, and *Artemia* extract all fail to elicit the electrical potentials or behaviour they do in the normal animal[9] Strong mechanical stimulation, such as pinching with forceps, or electrical stimulation of the column, does however, initiate propagated CPs and column contraction. The CPs of colchicine-treated hydra are of somewhat longer duration than those of normal animals (Fig. 1). The conduction velocity of the CPs was determined by recording them from the basal and oral ends of a hydra while the animal was stimulated at various positions along the column. As a stimulating electrode is moved from the base towards the mouth of an animal, the delay between an applied shock and the appearance of the recorded CP peak increases at the basal electrode and decreases at the oral one. The ratio of change in distance to change in latency gives the conduction velocity[7] (Fig. 2). Conduction velocity determinations were made from four colchicine-treated hydra, four untreated animals which had been transferred to culture solution containing antibiotic, and four animals grown and tested in normal culture solution. The colchicine-treated animals were the same used to investigate spontaneous activity; one of the latter was too small for conduction velocity measurements. For each animal the column was stimulated sequentially at three points: near the base, near the middle of the column, and near the oral electrode. Usually 10 sets of stimuli were given to each animal. The measured conduction velocity was different in the basal and oral directions, but the direction of preferred conduction varied from animal to animal. Basal and oral conduction velocities were averaged to give a single value for each animal. The CP conduction velocities of normal animals (5.7 cm s^{-1}, s.e. = 0.4) and antibiotic-treated controls (5.2 cm s^{-1}, s.e. = 0.2) were not significantly different, indicating that the rifampicin did not affect this parameter. These conduction velocities are not significantly different from that earlier reported for *H. littoralis* (5.2 cm s^{-1}, s.e. = 0.3; ref. 7). The CP conduction velocity in colchicine-treated animals (1.8 cm s^{-1}, s.e. = 0.2) was significantly lower than that of untreated animals.

One possible explanation for the reduced conduction velocity in colchicine-treated animals would be that the treatment directly alters the excitability of epithelial cells. In preliminary experiments we have found that the conduction velocity in the column returns to near normal after nerve-free animals are repopulated with interstitial (and thus nerve) cells from a temporary implant of normal tissue[16]. This indicates that colchicine does not have long term effects on the epithelial cells and that the depressed conduction velocity is related directly to the absence of nerve cells.

The effectiveness of the colchicine treatment in rendering the animals nerve free was verified by counting cells in macerated preparations of these animals[17]. When present, nerve cells are readily detected by this method. In normal animals approximately 5% of the column cells are nerve cells. Samples, each containing ~ 1,000 cells, were selected from the top, middle and bottom of the column of each treated hydra. The three samples together constituted about half of all the cells in the hydra. No nerve cells were found in four of the five treated animals. In the remaining animal, three nerve cells

Fig. 2 The latency between a stimulus to the column and the appearance of the positive peak of the evoked CP at the basal (*c*) and oral (*b*) electrodes. ●, A nerve-free hydra (H_1); ○, a normal hydra (H_2) H_1 and H_2 indicate the total length of each animal. The sketch in *a* illustrates the electrode placement; B_e and H_e are the basal and hypostomal recording electrodes, and S_e is the moveable stimulating electrode.

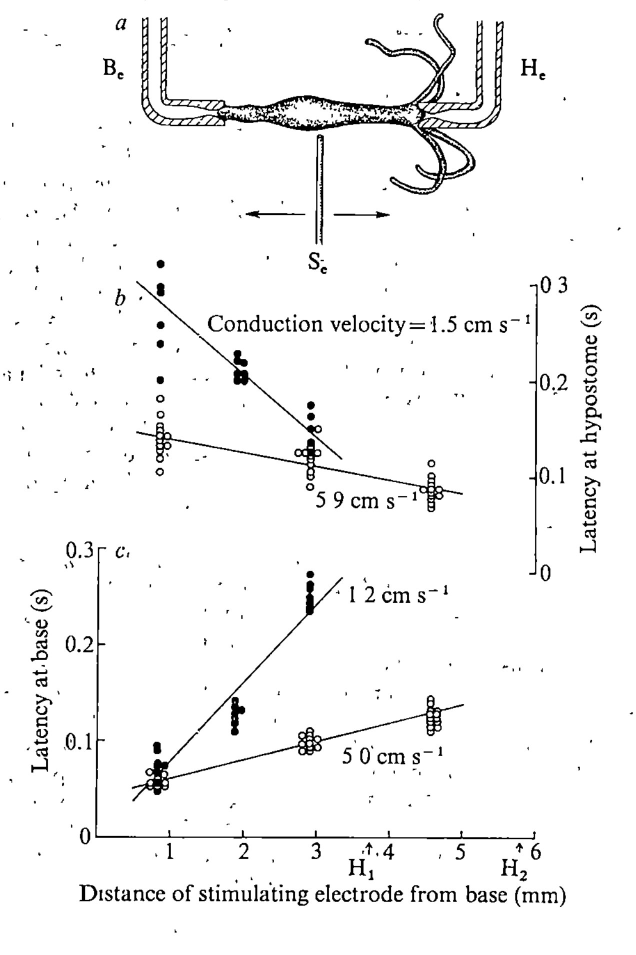

were found in samples containing a total of 2,749 non-neuronal cells. All the hydra had about five "big interstitial cells"[17] per 1,000 epithelial cells. Thus, four of the animals were apparently free of nerves and the fifth certainly contained too few nerve cells to form a continuous nerve net.

From these results, we conclude that: (1) nerve cells are necessary for normal spontaneous behaviour in hydra; (2) epithelial cells of hydra are excitable, and can conduct electrical signals which elicit column contraction; and (3) conduction velocity in the column is reduced in the absence of nerve cells. These experiments provide the first direct demonstration of non-neuronal conduction in hydra.

This work was supported by NIH grants to R. D. C., R. K. J. and N. B. R., and by an NSF grant to R. K. J.

R. D. CAMPBELL
R. K. JOSEPHSON
W. E. SCHWAB

School of Biological Sciences,
University of California, Irvine,
Irvine, California 92717

N. B. RUSHFORTH

Department of Biology,
Case Western Reserve University,
Cleveland, Ohio 44106

Received April 26; accepted June 1, 1976.

[1] Bullock, T. H., and Horridge, G. A , *Structure and Function in the Nervous Systems of Invertebrates* (W. H. Freeman, San Francisco, 1965).
[2] Davis, L E., Burnett, A L., and Haynes, J. F , *J. exp. Zool.*, 167, 295–311 (1968).
[3] Lentz, T L., *Primitive Nervous Systems* (Yale University Press, New Haven, 1968)
[4] Davis, L. E., *Z Zellforsch. mikrosk. Anat* , 123, 1–17 (1972)
[5] Semal-Van Gansen, P , *Bull Acad R Belg Cl Sci.*, 38, 718–735 (1952).
[6] Passano, L. M., and McCullough, C. B., *J exp Biol.*, 41, 643–664 (1964), 42, 205–231 (1965)
[7] Josephson, R. K , *J. exp. Biol.*, 47, 179–190 (1967)
[8] Kass-Simon, G., *Publ. Seto mar Biol Lab.*, 20, 583–594 (1973).
[9] Rushforth, N. B., in *Invertebrate Learning*, I, (edit. by Corning, W C , Dyal, J. A., and Willows, A O. D.), 123–169 (Plenum, New York, 1973)
[10] Mackie, G O , *Am Zool.*, 5, 439–453 (1965); *Q. Rev Biol.*, 45, 319–332 (1970).
[11] Mackie, G. O , and Passano, L M., *J. gen Physiol.*, 52, 600–621 (1968).
[12] Campbell, R. D., *J cell. Sci.*, 21, 1–13, (1976).
[13] Lenhoff, H M , and Brown, R. D., *Lab. Anim* , 4, 139–154 (1970).
[14] Rushforth, N. B., *Biol Bull.*, 140, 255–273 (1971)
[15] Passano, L. M., *Proc. natn Acad. Sci. U S A.*, 50, 306–313 (1963).
[16] Marcum, B. A., and Campbell, R. D., *Am. Zool* , 16, 186 (1976).
[17] David, C N., *Wilhelm Roux Arch. Entw Mech Org.*, 171, 259–268 (1973).

Directional hearing in crickets

CRICKETS have auditory organs at the proximal ends of the fore-tibiae; the binaural sensory input enables orientation to a sound source and in response to sound, crickets turn towards the more intensely stimulated of their two ears[1]. Airborne vibrations activate the auditory tympana of the ears, and are communicated to sensory scolopidia attached to the outer surface of the leg trachea, which forms an air space behind the tympanum[2,3]. For directionally-sensitive hearing, the responses of the two ears should differ when the direction of incident sound forms an angle with the insect's body axis. Directional hearing in crickets has previously been attributed to shielding of the contralateral ear by the insect's body[4]. We believe that shielding is insufficient to account for observed directionality, and propose an alternative theory which predicts the directional sensitivity of the cricket auditory system measured physiologically

We examined two species of cricket, *Teleogryllus commodus* and a smaller undescribed species we designate WB2 (specimens of which are lodged with the Australian National Insect Collection, Canberra). In anechoic conditions[5], we recorded auditory sensory thresholds to the sound frequency of the species song from primary fibres in the leg nerve, and from interneurones in the cervical connective. The directional sensitivity measured at each level in the sensory pathway is similar, and we found no influence of contralateral input on directionality. In normal preparations, crickets were mounted, ventral side up, on a thin vertical support which projected into a uniform sound field radiated horizontally. The prothoracic legs were held with the femora horizontal and perpendicular to the body axis, and the tibiae projecting vertically. Wings and other legs were removed. In other preparations, the cricket was mounted on its side with one foreleg extended vertically and the other held close to the body and covered with vaseline. In the latter preparations, sound was directed on to one ear only, and the orientation of this ear to the horizontal was near normal, although inverted.

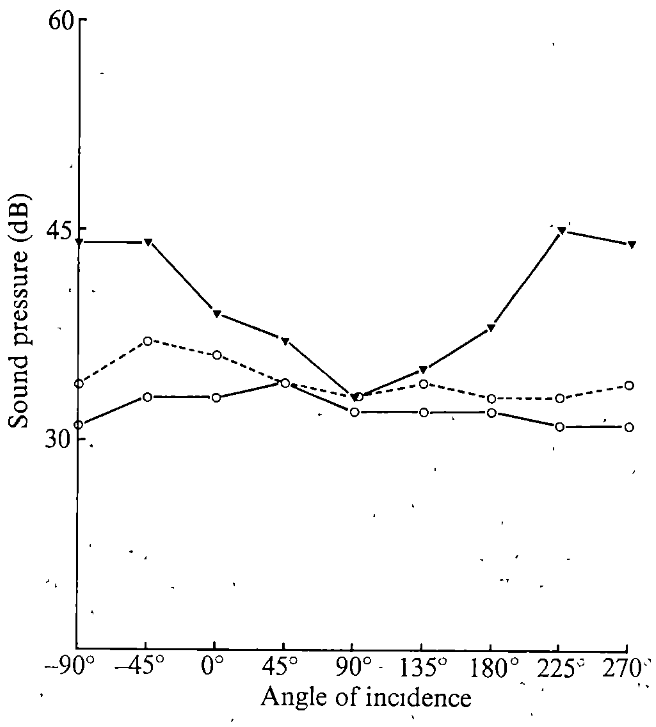

Fig. 1 Auditory thresholds obtained from the cervical connective in species WB2 in response to 4.5-kHz stimuli presented at different angles of incidence. ▼, Intact preparation, note the directional sensitivity; ○, single ear preparations; ——, individual ear in a free sound field; – –, individual ear asymmetrically shielded with a wax block. The single ear preparations have no directional sensitivity.

When rotated through 360° in the sound field, normal preparations showed auditory thresholds which differed by 10 to 25 dB for ipsilateral and contralateral incidence of sound. When one ear only was stimulated from different directions, no directional sensitivity was observed. Further, when a wax block approximating in size and shape to the head and prothorax of the cricket was placed next to the single ear, in the position normally occupied by the body, the preparation remained non-directional (Fig. 1). These results indicate that the auditory system is directional only when both ears are stimulated simultaneously, that the individual ear is non-directional; and that shielding of the contralateral ear by the insect's body does not account for the directional response.

In normal preparations, the directional sensitivity is abolished in two ways: (1) by blocking the trachea in either foreleg or in the prothorax and (2) by covering the tympanum of the opposite ear with vaseline. Independently, Zhantiev *et al.*[6] have demonstrated that directionality of hearing in *Gryllus bimaculatus* is decreased when the contralateral foreleg is removed and the leg trachea blocked. In crickets, therefore, the prothoracic leg tracheal system normally conducts sound from one ear to the other, and the directional response is the result of the interaction of the external and internal sound pressures at each tympanum. If sound is prevented from entering and traversing the internal tracheal pathway in any way, the auditory system is non-directional.

The elements of the prothoracic tracheal system on which directional hearing depends are illustrated in Fig. 2. Simple acoustical considerations explain the basis of the directional sensitivity. When a plane sound wave is incident at an angle to the body axis, a sound pressure of unit amplitude acting on the outside of the ipsilateral tympanum may be described by $\cos(\omega t)$. The net pressure acting at the ipsilateral tympanum is the difference between the external pressure and the internal pressure transmitted along the trachea from the opposite ear. The phase angle between the external and internal pressures results from the extra distance traversed by sound reaching the inside of the tympanum, namely, the effective distance between the ears, which is a function of the angle of incidence, and the length of the internal tracheal pathway. If it is assumed that there are no other phase changes or amplitude losses, then, at the tympanum

$$P_{(\text{net})} = \cos(\omega t) - \cos(\omega t + \frac{l}{\lambda} 2\pi \sin\theta + \frac{L}{\lambda} 2\pi) \qquad (1)$$

where l is the external distance between the ears, L is the length of the tracheal pathway, θ is the angle of incidence of sound and λ is the wavelength of sound. In the species we have studied, $l+L$ is nearly half the wavelength of the species' song. (In *T. commodus*, $l+L = 38$ mm, $\lambda/2 = 43$ mm; in species WB2, $l+L = 30$ mm, $\lambda/2 = 38$ mm.) Thus when $\sin\theta = 1$, the phase angle between the external and internal sound pressures at the tympanum approaches π, and the amplitude of $P_{(\text{net})}$ is a maximum. Conversely, when $\sin\theta = -1$, the phase angle between external and internal sound pressures approaches zero, and the amplitude of $P_{(\text{net})}$ is a minimum.

Using equation (1) with the appropriate anatomical and song frequency values, we have calculated the relative amplitude of the net sound pressure at the tympanum for values of θ and expressed it in dB. For each species, this calculated net sound pressure at the ear for different directions of sound corresponds to the experimental directional sensitivity (Fig. 3).

Fig. 2 Drawing of a cricket showing the apposed leg tracheae which form a sound pathway between the two tibial auditory organs. Sound reaches the exterior and interior of the tympanic membrane along paths of different length. When sound is incident at an angle θ to the body axis, the path to the interior of the ipsilateral tympanum through the tracheae exceeds that to the exterior of the tympanum by the extra distance of the contralateral ear from the source $l \sin\theta$, plus L (the length of the tracheal pathway). Therefore, the net sound pressure at the tympanum is the resultant of the exterior and interior sound pressures, which differ in phase by $2\pi/\lambda\ (l \sin\theta + L)$, where λ is the wavelength of incident sound.

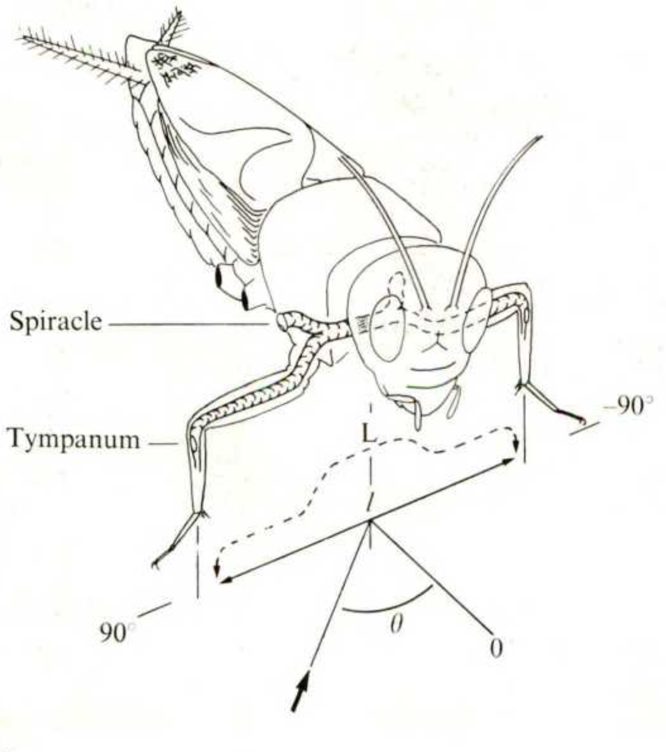

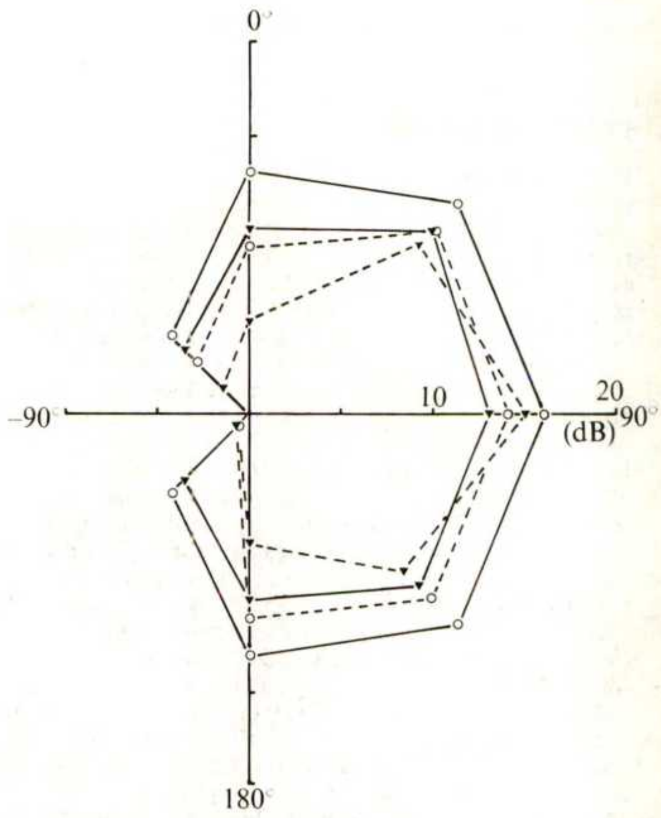

Fig. 3 Predicted net sound pressure at the auditory tympana (——) for values of θ compared with measured hearing sensitivity (– –) for *T. commodus* (▼) and species WB2 (○) on polar coordinates.

Transmission of sound along the tracheal pathway is limited with respect to frequency according to the resonance characteristics of the tube. The directional sensitivity of normal preparations applies only to a narrow frequency band near the tuned frequency of the ear, and which corresponds to the frequency of the species' song.

This account of the basis of directional hearing in crickets is consistent with the inability of unilaterally deafened crickets to locate a sound source in phonotaxis trials[1], and with the specificity shown by female crickets in their orientation to signals having different carrier frequencies[7]. The mechanism illustrates the importance of the leg trachea as an integral part of the auditory system. In tettigoniids also, the leg trachea has a crucial, but fundamentally different role in hearing[5,8]. The cricket derives the directional sensitivity of its ears from the fact that the tracheae of the forelegs are interconnected acoustically at the midline.

We thank Dr E. Ball, Dr C. E. Hill and Professor G. A. Horridge for their help in the preparation of the manuscript.

K. G. Hill
G. S. Boyan

Department of Neurobiology,
Research School of Biological Sciences,
Australian National University,
Canberra City 2601, Australia

Received February 25; accepted June 8, 1976.

1 Murphey, R. K., and Zaretsky, M. D., *J. exp. Biol.*, **56**, 335–352 (1972).
2 Schwabe, J., *Zoologica (Stuttgart)*, **20**, Heft 50, 1–154 (1906).
3 Young, D., and Ball, E., *Z. Zellforsch.*, **147**, 313–324 (1974).
4 Michelsen, A., and Nocke, H., *Adv. Insect Physiol.*, **10**, 247–296 (1974).
5 Nocke, H., *J. comp. Physiol.*, **100**, 25–57 (1975).
6 Zhantiev, R. D., Kalinkina, I. N., and Chukanov, V. S., *Entomol. Obozr.*, **54** (2), 249–257 (1975) (in Russian).
7 Hill, K. G., *J. comp. Physiol.*, **93**, 7–18 (1974).
8 Lewis, D. B., *J. exp. Biol.*, **60**, 821–869 (1974).

Effect of phloridzin and phloroglucinol on apple shoots

PHENOLIC compounds and their glycosides are widespread in plants. They have uncertain metabolic roles, although they are regarded as metabolic by-products conferring resistance to pathogens[1,2]. Phloridzin, the 2′-glucoside of phloretic acid, for example, is unique to species of *Malus* and is the major phenolic compound of commercial apple trees (*Malus pumila* Mill), representing 3–7% of the dry weight of leaves as well as occurring in bark and roots[3]. It is not involved in resistance to apple scab as formerly supposed[4], but affects the metabolism of many organisms. It inhibits growth of wheat coleoptiles[5] and tomato roots[6] but more than doubles photosynthetic rates in *Elodea*[7,8]. In animals it inhibits the utilisation of carbohydrates[9], and one of the degradation products[4,10] of phloridzin, phloroglucinol, acts synergistically with auxin to promote growth of oat mesocotyls[11]. There have been indications that phloridzin, and phloroglucinol, promote the expansion of apple leaves[12] and the rooting of apple shoots[13], respectively. This suggests that phloridzin may have important effects on *Malus*. I have now shown that phloridzin promotes the growth of cultured apple shoots. The effect is pronounced and has practical application.

Tips (1–2 cm) of shoots (2–5 cm) of M.7 or M.26 (virus-free) apple rootstocks were cultured as described previously[14] in sterile conditions in test tubes (15 × 2.5 cm), each containing 10 ml culture medium. Shoot tips were kept at 25 °C and received 16 h light daily from Crompton white tubes giving 14 W m^{-2} at the surface of each culture tube.

Phloridzin and phloroglucinol (10^{-3} M) were added to a basic medium (medium 1)—Quoirin's medium B (ref. 15) with the vitamins and glycine replaced by the vitamins used by Wetmore and Sorokin[16]. For one test with phloridzin, indol-3-yl acetic acid (IAA) was omitted and for others with phloroglucinol, medium 2 was used—as medium 1 but with only 0.5 mg l^{-1} benzyl amino purine (BA), thiamine hydrochloride (0.4 mg l^{-1}) and inositol (100 mg l^{-1}) in place of the vitamins, and with indol-3-yl butyric acid (1 mg l^{-1}) as ammonium salt (IBA) in place of IAA. All constituents of the media were sterilised by autoclaving at 103 kN m^{-2} for 5 min, except for phloridzin, phloroglucinol, and IBA which were passed through Millipore filters (0.45 μm diameter).

Table 1 and Fig. 1 summarise the results and show that the two phenolic compounds markedly stimulated shoot growth. With medium 1 minus IAA, each tip produced a single shoot, and phloridzin increased internode extension, leaf production and expansion. With medium 1 each tip produced between one and three shoots, and phloridzin and phloroglucinol promoted internode extension and increased the number of shoots per tip to between three and six. The shoots originated from terminal and lateral meristems and not *de novo* from callus at the base of cultures (Fig. 1).

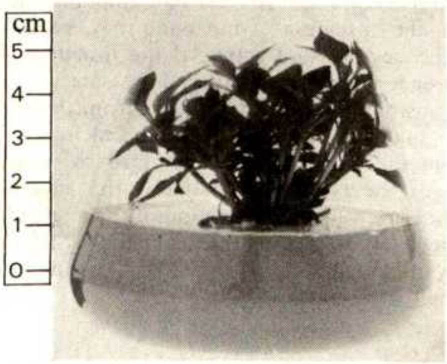

Fig. 1 Effect of phloridzin on M.7 shoots. *a*, Inoculum; *b*, after 5 weeks on medium 1; *c*, after 5 weeks on medium 1 plus 10^{-3} M phloridzin.

Fifteen cultures of M.26 that had produced two shoots each during 4 weeks on medium 1, were transferred singly to 35-ml volumes of medium 2 in 100-ml flasks. This procedure was repeated with medium 2 plus 10^{-3} M phloroglucinol, and in this case 15 cultures were also transferred to 125-ml volumes of medium in 250-ml flasks. After 5 weeks, each culture with 35 or 125-ml medium plus phloroglucinol had produced between 8 and 14 or 20 and 38 shoots, respectively, 2–5 cm long (Fig. 2). With unsupplemented medium 2, however, there were only 3–5 shoots per culture, all less than 2 cm long.

Fig. 2 Effect of phloroglucinol on M.26 shoots. M.26 shoot culture on medium 2 + 10^{-3} M phloroglucinol 5 weeks after initiation from a culture with two shoots.

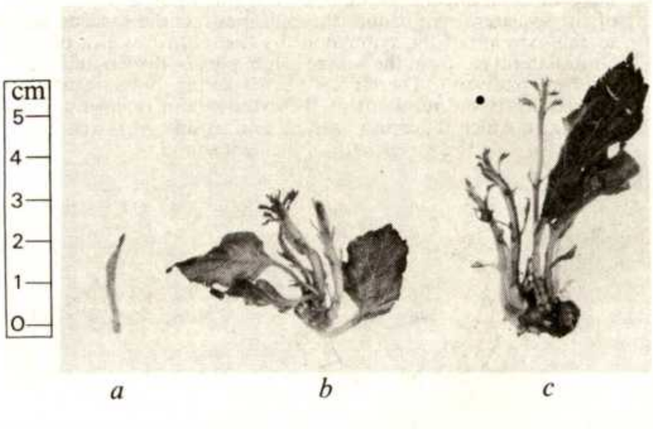

Table 1 Effect of 10^{-3} M phloridzin (PZ) and phloroglucinol (PG) on apple shoots

Shoots	Medium	No. of replicates	Mean growth values*				
			Fresh weight (mg)	No. of shoots per culture	Shoot length (mm)	No. of leaves + primordia	Leaf area† (cm^2)
M.7	1 −IAA	15	152	1.0	17	13	1.78
	1−IAA + PZ	13	257¶	1.0	24§	17‡	2.73¶
M.7	1 + PZ	20	755	2.4	21	14	—
		17	1108¶	3.7¶	29‡	14	—
M.26	1 + PZ	12	715	2.0	17	17	—
		12	1120¶	3.3‡	24‡	16	—
M.7	1 + PG	10	359	1.0	32	19	—
		6	783¶	3.0¶	44¶	20	—

*Culture period 5 weeks except with medium 1 −IAA, where it was 3 weeks.
† Of oldest leaf.
Significantly greater than without PZ or PG (P = ‡ 0.05; §0.01; ¶0.001).

No roots developed in any of the tests described so far, but 100 shoots excised from cultures grown with medium 2 plus phloroglucinol all rooted within 5 weeks when transferred to fresh medium of the same composition but without BA.

These results suggest that phloridzin, possibly through the production of phloroglucinol, is involved in the growth of apple trees. From a practical point of view, the effect on the development of apple shoots has potential for improved propagation of apple trees *in vitro*[18]. Methods described recently[17] gave much less shoot growth and rooting than described here with phenolic compounds.

I thank Mr D. O'Farrell for technical assistance.

O. P. JONES

East Malling Research Station,
Maidstone, Kent, UK

Received April 13; accepted June 1, 1976.

[1] Levine, D. A., *Am. Nat.*, 105, No. 942, 157–181 (1971).
[2] Towers, G. H. N., *Biochemistry of Phenolic Compounds* (edit. by Harborne, J. B.), 250 (Academic, London and New York, 1964)
[3] Williams, A. H., *Nature*, 202, 824 (1964).
[4] Hunter, L. D., *Phytochemistry*, 14, 1519 (1975).
[5] Hancock, C. R., Barlow, H. W. B., and Lacey, H J., *J. exp. Bot*, 12, 401 (1961).
[6] Street, H. E, and Lowe, J, *Ann. Bot, Lond. N.S.*, 14, 307 (1950).
[7] Marrè, E., *Boll. Soc. ital. Biol. sper*, 26, 1299 (1950).
[8] Marrè, E., and Servattaz, O., *Nuova G. bot. ital. N.S.*, 62, (1955).
[9] Shapiro, B., *Biochem. J*, XIi, 151 (1974).
[10] Grochowska, Maria, J., *Plant Physiol, Lancaster*, 41, No. 3, 432 (1966).
[11] Nitsch, J. P., and Nitsch, C., *Ann. Physiol. Vég.*, 4, 211 (1962).
[12] Jones, O. P., and Obrenović, Snezana, *Rep. E Malling Res. Stn 1975*, 67 (1976).
[13] Jones, O. P., and Hatfield, S. G. S., *J. hort. Sci.* (in the press).
[14] Jones, O. P, *J. hort. Sci.*, 48, 181 (1973).
[15] Quoirin, M., *Bull. Rech. Agron, Gembloux* 9(2), 189 (1974).
[16] Wetmore, R. H., and Sorokin, S., *J. Arnold Arbor.*, 36, 305 (1955).
[17] Abbott, A. J., and Whiteley, E, *Scientia Hort.*, 4, 183 (1976).
[18] Patent applied for, *Patent application no 29730/76.*

Malate-switch hypothesis to explain the action of stomata

DURING the past ten years major advances have been made in our understanding of the mechanics of stomata. A most important discovery has been that potassium enters the guard cells in sufficient quantities to account for the decreases in osmotic potential which occur on stomatal opening[1]. Association of potassium with stomatal movements has now been reported for at least 22 species[2]. There is doubt, however, about the nature of the anions which accompany K^+. Chloride has been found to balance about 40% of the K^+ in *Zea mays*[3] and considerably less in *Commelina communis*[4]. Malate could be the balancing anion as it has been found to accumulate in the guard cells on stomatal opening[5] although it is not clear whether it is synthesised in the guard cells or is transported there from the surrounding cells. Clearly an understanding of the mechanism of the ion transport in and out of the guard cells is necessary as a first step to the unravelling of the stomatal mechanism. An hypothesis is proposed here which attempts to explain the transport aspect of stomatal function. It is based mainly on data obtained from studies with the monocotyledon *C. communis* but should be applicable to other species.

Stomata of *C. communis* have a complex structure with a number of subsidiary cells (Fig. 1). K^+ and Cl^- concentrations in each type of cell have been determined for stomata in both the open and closed states[4,6]. There seemed to be considerable transport of K^+ and Cl^- between the cells during opening and closure but Cl^- never accounted for more than 27% of the K^+. Table 1 shows data for K, Cl and malate concentrations in the lower epidermis of *C. communis* leaves with open and closed stomata. They show that the total amounts of these ions do not change with stomatal aperture and assuming a valence of 1.5 for malate it approximately balances the K^+ not accounted for by Cl^-. It seems reasonable to assume, therefore, that as the malate concentration in the leaf epidermis does not change, malate is not synthesised or broken down to any marked extent but moves with potassium from cell to cell during stomatal activity.

Table 1 Levels of malic acid, K^+ and Cl^- (mol m^{-3}) obtained from water extracts of the lower epidermis of the leaf of *Commelina communis*

	Malic acid	K^+	Cl^-
Stomata open	64.0	147.3	49.2
Stomata closed	61.3	139.9	48.0

Figures are means of five determinations.

The vacuolar *p*H of each of the cells of the stomatal complex of *C. communis* changes with stomatal movements, The *p*H of the guard cell for example, rises from 5.1 to 5.7 when stomata open[7]. Knowing the concentrations of K^+ and Cl^- (refs 4 and 6) and the *p*H, it is possible to write down the approximate concentrations of mono- and divalent malate in each cell for open and closed stomata (Tables 2 and 3). The data in Tables 2 and 3 are rounded off to make the figures for open and closed stomata symmetrical. The most significant point is that the concentrations of monovalent malate varies little between the cells both when the stoma is open and when it is closed. On the other hand, there is a steep gradient in the concentrations of divalent malate across the stomatal complex. The gradient is reversed when the stomata open or close.

It is proposed that K^+ moves from cell to cell with the monovalent malate but that the divalent form of malate is unable to move and is locked in the cell. Cram[8] has evidence that malate is taken into barley root cells as the singly ionised form rather than as doubly ionised or unionised molecules. It is suggested that stomatal closure brought about by factors such as darkness, high ambient CO_2 and abscisic acid occurs because these factors cause the *p*H of the guard cells to drop from 5.8 to 5.1. The majority of the malate will switch from the divalent to the monovalent form and a gradient of monovalent malate will develop across the stomatal complex (Table 3). Monovalent malate will thus move across the stomatal complex and eventually reach the epidermal cell whose *p*H will rise, locking the malate in its vacuole as the divalent form. Equilibrium will be reached when the gradient of monovalent malate is zero and the situation of Table 2 will prevail with the stomata closed.

Stomatal opening would be brought about in the reverse manner. It is proposed that the factors which usually bring about opening such as light, low CO_2, high temperature and circadian rhythms all work by bringing about a rise in the *p*H of the guard cells. Malate would switch from being predominantly monovalent to being mainly divalent. A gradient in monovalent malate would be set up and K malate would flow into the guard cells (Table 2). On entering the guard cell the malate would be switched to the divalent form and locked in the cell. The osmotic potential of the guard cell would fall, the turgor pressure rise and the stoma would open. The gradient of monovalent malate would again become zero and a new equilibrium would be attained (Table 3).

It is proposed that the energy for stomatal opening and

Fig. 1 Diagram to show the arrangement of the cells in the stomatal complex of *Commelina communis.*

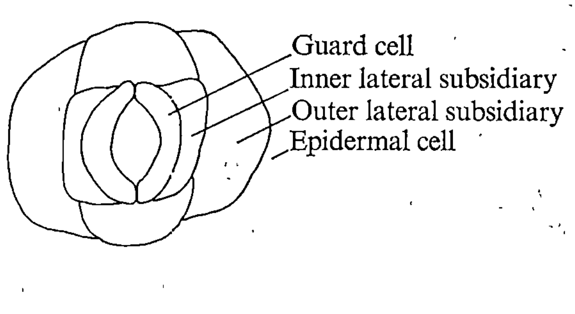

Table 2 *p*H and concentrations of di- and monovalent malate (mol m^{-3}) in the various cells of the stomatal complex of *C. communis* when the stomata are closed and also about to open

Stomata closed	GC	ILS	OLS	EPID
*p*H	5.1	5.5	5.7	5.8
Monovalent malate	32	50	45	60
Divalent malate	9	25	53	120
Pre-opening	(*p*H 5.8)			
Malate⁻	10	50	45	60
Malate²⁻	20	25	53	120

GC, Guard cell; ILS, inner lateral subsidiary; OLS, outer lateral subsidiary; EPID, epidermal cell.

closing would be expended in bringing about the change in *p*H of the guard cell from the *p*K value of malic acid of 5.1 to 5.8 and back again. It is assumed that all the environmental factors which cause stomatal opening and closure work by changing the *p*H of the guard cell and so operating the malate switch. This would explain why a number of factors can influence stomata by acting independently and also by seeming to act together. For example, before dawn endogenous rhythm could cause a partial rise in guard-cell *p*H which would be completed by a reduction in ambient CO_2 at the onset of photosynthesis at dawn. This would explain how stomata anticipate dawn by partially opening before the light period. It is not the purpose of this paper to suggest how environmental factors cause the change in guard cell *p*H.

Table 3 *p*H and concentrations of di- and monovalent malate (mol m^{-3}) in the various cells of the stomatal complex of *C. communis* with the stomata open and also about to close

Stomata open	GC	ILS	OLS	EPID
*p*H	5.8	5.7	5.5	5.1
Malate⁻	60	60	50	32
Malate²⁻	120	70	25	9
Pre-closing	(*p*H 5 1)			
Malate⁻	192	60	50	32
Malate²⁻	53	73	25	9

It follows from this hypothesis that: (1) Opening and closing of stomata should always be preceded by a *p*H change in the guard cells. (2) The important ion is not K^+ but malate and this would explain why other monovalent cations are effective in bringing about stomatal opening[9,10].

Although malate is considered to be the important ion in *C. communis* because of its ability to switch its valence, it is possible that other organic acids may provide the switch anion in some other species. There are, however, few organic acids which have *p*K values at the *p*H normally found in plant cells.

The mechanism of transport of the ions between the cells of the stomatal complex is not crucial to the validity of the hypothesis but the gradients envisaged suggest that diffusion could be the most important factor. In this case the active transport found between the cells[4,6] would be secondarily active. Primary active transport between the cells cannot, however, be ruled out at the present time.

D. J. F. BOWLING

Department of Botany,
University of Aberdeen,
St Machar Drive,
Aberdeen AB9 2UD, UK

Received May 10, accepted May 23, 1976.

[1] Meidner, H., and Willmer, C, *Curr. Adv Pl Sci.*, **17**, 1–15 (1975).
[2] Dayanandan, P., and Kaufman, P. B., *Am. J. Bot.*, **62**, 221–231 (1975)
[3] Raschke, K., and Fellows, M. P., *Planta*, **101**, 296–316 (1971).
[4] Penny, M G., Kelday, L. S., and Bowling, D. J F., *Planta* (in the press)
[5] Allaway, W. G., *Planta*, **110**, 63–70 (1973).
[6] Penny, M. G., and Bowling, D J. F., *Planta*, **119**, 17–25 (1974).
[7] Penny, M G., and Bowling, D. J. F., *Planta*, **122**, 209–212 (1975).
[8] Cram, W. J., *J exp. Bot*, **25**, 253–268 (1974).
[9] Humble, G D., and Hsiao, T C, *Pl. Physiol., Lancaster*, **44**, 230–234 (1969)
[10] Willmer, C M, and Mansfield, T. A., *New Phytol.*, **68**, 363–375 (1969).

Plant uptake and leaching of dimethylnitrosamine

THE occurrence of carcinogenic nitrosamines is of considerable interest because they have been found in foods consumed by humans[1] and they can be produced, at least *in vitro*, from agricultural chemicals[2,3]. Furthermore, the widespread occurrence of potential precursors of nitrosamines—secondary or tertiary amines and inorganic nitrogen compounds that are readily converted to nitrite by microorganisms—led to studies demonstrating that the carcinogens can be formed in soil samples and aquatic environments[4,5]. A hazardous chemical in soil is not of toxicological significance, however, unless it is volatilised or enters the human food chain by being assimilated by food crops or leached through soil into ground waters ultimately used for drinking. We report here that dimethylnitrosamine (DMNA) can be assimilated by the roots of lettuce and spinach, is translocated to the tops and that it also moves readily through soil.

Lettuce was grown from seed in quartz sand or Williamson silt loam contained in clay pots and incubated at 16 °C in a growth chamber in which the daylength was 16 h. The plants were watered daily with Hoagland's inorganic nutrient solution[6] at one-quarter strength; the leaves were not wetted during the watering. Spinach was grown from seed in the same nutrient solution, the liquid being aerated constantly and replaced weekly. The spinach plants were maintained at 20 °C under Growlux fluorescent lights timed to provide a 16-h day. After two months, the various pots received either 0.57 µCi of ^{14}C-DMNA plus the unlabelled nitroso compound to a final concentration of 100 µg ml^{-1}, or 0 057 µCi of ^{14}C-DMNA plus unlabelled nitrosamine to a final concentration of 10 µg ml^{-1}. The total amounts of DMNA added were 2.50 and 0.25 mg for the high and low levels of exposure, respectively. After 2 d, the aerial portions of these plants, as well as of plants not exposed to the nitrosamine, were harvested and washed, and 100-g portions homogenised in 150 ml of 6.0 N NaOH. The homogenised slurry was refluxed for 30 min, filtered through glasswool, and steam-distilled, half of the volume being collected as distillate. The distillate was extracted three times with volumes of methylene chloride one-third that of the distillate, and the extract was dried with Na_2SO_4 and concentrated to 2 ml by evaporation in a Kuderma–Danish evaporative concentrator operating at 60 °C. Half of the extract was added to 10 ml of a scintillation cocktail containing 5 g PPO, 0.1 g POPOP, and 1 l of toluene, and the radioactivity was counted on a Beckman model LC-100C liquid scintillation system. A second experiment with lettuce growing in sand was conducted similarly, but the plants were harvested at 4, 9 and 15 d.

The results show that both spinach and lettuce can absorb radioactivity from the growth medium (Table 1), the amount assimilated being proportional to the amount of ^{14}C-DMNA added to the pots. The absorbed ^{14}C disappeared with time, in agreement with results on nitrosamine uptake by *Lepidium sativum*[7]. The percentage of radioactivity taken up by lettuce grown in soil was slightly higher than that of plants grown in sand. The quantity of DMNA taken up per unit weight of plant material was, however, severalfold greater for the soil-grown plants, possibly because of the lower yield obtained when the lettuce was grown in the silt loam. It has been reported that cereals can absorb nitrosamines[8], and the present findings not only extend previous observations, but pertain to two major vegetable crops.

To confirm the identity of the labelled product, 2-month-old lettuce plants were exposed for 2 d to 5.7 µCi of ^{14}C-DMNA in 25 ml of nutrient solution made to 500 µg ml^{-1}

Table 1 Uptake of dimethylnitrosamine by spinach and lettuce

Plant	Growth medium	^{14}C-DMNA supplied (μCi)	Length of exposure (d)	DMNA taken up* (μg per g dry wt)	DMNA taken up by plant* (%)
Lettuce	Sand	0.057	2	1.38	3.20
		0.57	2	14.38	3.25
Lettuce	Soil	0.57	2	106.0	5.06
Spinach	Water	0.057	2	0.54	0.38
		0.57	2	5.60	0.27
Lettuce	Sand	0.57	4	7.04	1.56
			9	1.40	0.21
			15	0.07	0.02

*Each figure represents the average of four replicates.

with the unlabelled nitrosamine. Compounds containing the radioactivity were extracted and concentrated, and then 0.5 ml of the methylene chloride extract was placed on each of two silica gel thin-layer plates (Eastman chromatogram sheets), only one of which was exposed to ultraviolet radiation (240 nm) for 15 min before development. After development in hexane–diethyl ether–methylene chloride (4 : 3 : 2), the chromatograms were counted on a strip chart recorder (Actigraph III, Nuclear Chicago), and the location of the radioactivity was compared with that on chromatograms of authentic ^{14}C-DMNA. The radioactivity on the non-irradiated chromatogram had the same R_f value (0.34) as ^{14}C-DMNA, and the radioactivity on the ultraviolet-irradiated chromatogram had the same R_f value (0.03) as ^{14}C-dimethylamine, which is formed by the photolytic cleavage of DMNA. The yield of dimethylamine was essentially stoichiometric. As a further confirmation of identity, the extract was analysed by gas chromatography using a Varian Aerograph series 1700 gas chromatograph equipped with a flame ionisation detector and a 1.84 m×3.2 mm stainless steel column packed with 10% Carbowax 20M on Chromosorb W-HMDS. The column was maintained at 80 °C for 5 min and then programmed to 110 °C at a rate of 2 °C min^{-1}. The retention times of the unknown and authentic DMNA (512 s) were identical.

Fig. 1 Leaching of chloride (●) and dimethylnitrosamine (○) through columns of four soils. *a*, Deerfield; *b*, Scarboro; *c*, Lima; *d*, Williamson.

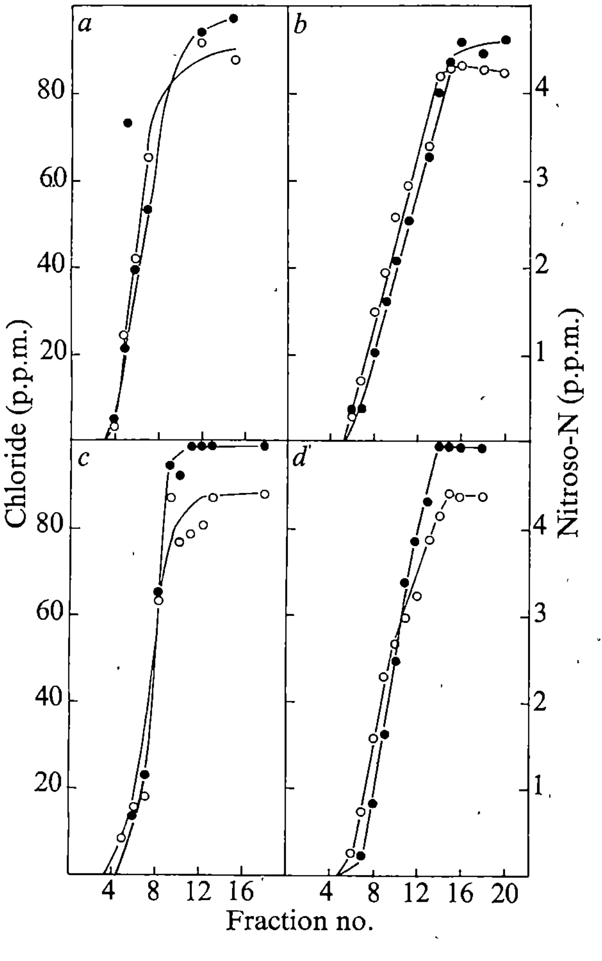

To determine whether DMNA can leach through soil, columns of Williamson silt loam (*p*H 5.8, 1.9% organic matter), Lima loam (*p*H 7.8, 3.8% organic matter), Deerfield sand (*p*H 5.1, 2.5% organic matter), and Scarboro sand (*p*H 5.6, 14.8% organic matter) were prepared using 100–200 g of air-dry soil that had been passed through a 2-mm sieve. The columns were moistened with distilled water to bring the soil to field capacity, and a solution containing 100 μg ml^{-1} of chloride and DMNA (5 μg nitroso nitrogen ml^{-1}) was allowed to pass through the column. Equal fractions (10 ml) were collected, and the fractions analysed for chloride and DMNA content using the methods of Bergmann and Sanik[9] and Daiber and Preussmann[10], respectively. Nitrite, which gives a positive reaction in the method of DMNA analysis, was determined in all samples by the procedure of Montgomery and Dymock[11], and corrections were made for the small amounts present in the first few fractions. The results in Fig. 1 demonstrate that DMNA is not retained by the soils but moves as readily as chloride. Because the soils were open to the atmosphere, some of the added DMNA may have been lost through volatilisation.

The earlier findings that nitrosamines can be formed and are persistent in samples of soil[4,5,12] and our observation that DMNA can potentially move from soil into food crops and downwards into groundwater suggest that a hazard may exist from a previously unrecognised source of exposure. Investigations on nitrosamine uptake by edible crops and movement through soil are also important in light of the report that the *N*-nitroso derivative of at least one pesticide has been found in a municipal water supply (D. H. Fine, personal communication). Further research is required to determine whether such a possible hazard is in fact a reality.

This investigation was supported in part by a NIH Fellowship from the NIEHS.

DEBORAH DEAN-RAYMOND
M. ALEXANDER

Laboratory of Soil Microbiology,
Department of Agronomy,
Cornell University,
Ithaca, New York 14853

Received April 9; accepted June 1, 1976.

[1] Scanlan, R. A., *CRC Crit. Rev. Food Technol.*, 5, 357–402 (1975).
[2] Elespuru, R. K., and Lijinsky, W., *Food Cosmet. Toxicol.*, 11, 807–817 (1973)
[3] Ungerer, O., Eisenbrand, G , and Preussmann, R., *Z. Krebsforsch.*, 81, 217–224 (1974).

[4] Ayanaba, A., and Alexander, M., *J Environ. Qual.*, 3, 83–89 (1974)
[5] Ayanaba, A., Verstraete, W., and Alexander, M, *Proc. Soil Sci. Soc. Am.*, 37, 565–568 (1973).
[6] Hoagland, D. R, and Arnon, D. I., *Calif. Agric Exp Sta. Circ*, 347 (Berkeley, California, 1938).
[7] Sander, J., Ladenstein, M., LaBar, J, and Schweinsberg, F, in *N-Nitroso Compounds in the Environment* (edit. by Bogovski, P., and Walker, E. A.), 205–210 (International Agency for Research on Cancer, Lyon, 1975)
[8] Dressel, J., *Landw. Forsch., Sonderh.*, 28, 273–279 (1973).
[9] Bergmann, J. G., and Sanik, J., Jr, *Analyt. Chem.*, 29, 241–243 (1957).
[10] Daiber, D., and Preussmann, R, *Z analyt Chem*, 206, 344–352 (1964).
[11] Montgomery, H. A. C., and Dymock, J. F., *Analyst*, 86, 414–416 (1968).
[12] Tate, R. L., and Alexander, M., *J. natn. Cancer Inst.*, 54, 327–330 (1975).

Non-enzymatic photochemical reduction of nitrate in rice seedlings

LIGHT plays an important role in nitrate assimilation in leaves by providing the reductants and by stimulating the synthesis of nitrate and nitrite reductases[1-3]. Activity of nitrate reductase is considered to be the rate-limiting step in nitrate assimilation and in the production of grains and grain proteins in crop plants[4,5]. It has been known for some time, however, that the ultraviolet radiation in sunlight photochemically reduces nitrate in aqueous solution to nitrite[6,7]. Stoy[8,9] reported that ultraviolet light had a much stronger effect on nitrate assimilation in wheat leaves than light of longer wavelengths. We have observed, in experimental conditions, significant accumulation of nitrite in rice leaves exposed to sunlight, even when nitrate reductase activity was negligible, so we have investigated non-enzymatic photochemical reduction of nitrate in leaves.

The absorption spectrum of 0.2 M KNO_3 measured in a Gilford spectrophotometer showed a trough at 260 nm ($E = 0.3$) and a sharp peak at 302 nm ($E = 1.04$). Negligible absorption was observed at wavelengths 340 nm and above. On the other hand, 0.2 M $NaNO_2$ revealed a broad absorption band ($E = 1.25$–1.75) in the whole range of wavelengths from 260 to 325 nm, after which it showed a decline, with negligible absorption at 400 nm and above.

When 10 mM KNO_3 solution was exposed to bright sunlight of intensity from 7,000 to 10,000 foot candles (70–108 klx), about 10 to 20 nmol NO_2^- ml^{-1} h^{-1} was produced. This could be compared with the amount of nitrite produced *in vitro* by an active preparation of nitrate reductase from rice leaves, incubated with 0.34 mM NADH and 10 mM KNO_3, which was found to be 20–30 nmol NO_2^- ml^{-1} h^{-1}. When 10 mM $NaNO_2$ was irradiated with sunlight, negligible loss of nitrite was observed.

That the ultraviolet component of solar radiation was responsible for the reduction of nitrate was easily confirmed by using filters, which absorbed that part. Negligible quantities of nitrite were formed when nitrate solution was treated with such filtered sunlight. Exposure of nitrate to ultraviolet light from a mercury lamp was as effective for reduction as direct sunlight.

To detect non-enzymatic accumulation of nitrite in leaves exposed to sunlight, it was necessary to eliminate, or diminish considerably, the activities of both nitrate and nitrite reductases. In order to achieve this, rice seedlings were grown in complete darkness. It is known that synthesis of the two enzymes is retarded in etiolated plants[2,3]. When these leaves are exposed to sunlight, however, the enzymes are likely to be synthesised as the chloroplasts develop and to prevent this, nitrate was added in the presence of sodium tungstate and chloramphenicol. Tungstate blocks the *in vivo* synthesis of an active nitrate reductase, by forming the enzymatically inactive tungsten analogue by replacement of molybdenum in the enzyme molecule[10]. Chloramphenicol, an inhibitor of protein synthesis on 70S ribosomes, inhibits the formation of nitrite reductase, which requires protein synthesis on chloroplastic ribosomes, without affecting the synthesis of nitrate reductase, which takes place on 80S ribosomes in the cytoplasm[3,11]. Thus, by a combination of tungstate and chloramphenicol treatments, we hoped to diminish the activities of nitrate reductase and nitrite reductase considerably.

Results show that in normal seedlings grown in sunlight with nitrate (Table 1; treatment 1), the activities of the two enzymes were quite high. Free nitrite was not detected in the leaves because of its rapid reduction to ammonia in healthy seedlings. The seedlings in which the activities of the two enzymes were blocked (treatment 3) progressively accumulated nitrite for up to 4 h in leaves exposed to sunlight. The same result was brought about by ultraviolet light from a mercury lamp; but detached leaves kept in the dark did not accumulate nitrite. When the seedlings were treated with chloramphenicol (treat-

Table 1 Effect of sunlight on the accumulation of nitrite in leaves of rice seedlings

Conditions of growth of seedlings: Treatment number	Light regime	Additions to nutrient solution	Period of exposure of detached leaves to sunlight (h)	Nitrate reductase (μmol NO_2^- per 20 min per g tissue) *In vitro*	*In vivo*	Nitrite reductase (μmol NO_2^- reduced per 20 min per g tissue)	Nitrate (μmol per g tissue)	Nitrite (μmol per g tissue)
1	Sunlight	KNO_3	4	1.92	0.182	13.4	12.1	Nil
2	Sunlight	KNO_3 + chloramphenicol	4	1.08	0.096	1.2	11.4	0.220
3	Dark	KNO_3 + tungstate + chloramphenicol	0					0.012
			1					0.027
			2					0.044
			3					0.062
			4	0.04	Nil	1.0	12.2	0.083
		(Detached leaves kept in the dark)	4					0 012
		(Detached leaves exposed to ultraviolet light from a mercury lamp)	1					0.041

Seedlings of rice (*Oryza sativa*), variety Taichung Native-1 were raised in well washed quartz sand with Hoagland solution lacking nitrate as described earlier[3]. Seedlings grown in sunlight in treatments 1 and 2 were exposed during the day (10 h) and kept in dark during the night. In treatment 1, 15 mM KNO_3 was added on the 14th day In treatment 2, 15 mM KNO_3 and 3 mg ml^{-1} chloramphenicol were added on day 14 and seedlings kept in the dark for 2 d In treatment 3, on day 14, 15 mM KNO_3 with 5 mM sodium tungstate and 3 mg ml^{-1} chloramphenicol were added to the nutrient solution and also sprayed on the etiolated plants and seedlings kept in the dark for 2 more days. Leaves from 15-d-old seedlings from the three treatments were detached from plants and immersed in 15 mM KNO_3 solution so that the bottom 1 cm dipped into the solution and the remaining portion was exposed to sunlight. The nitrate solution was kept in flasks covered with a black paper, so it was not exposed to sunlight and photochemical reduction of nitrate in the flasks was avoided The protruding leaves alone were exposed to light for different intervals as indicated in the table. At the end of this period, leaf extracts were prepared and *in vitro* activities of nitrate reductase and nitrite reductase were assayed as described previously, using NADH and reduced methyl viologen as electron donors, respectively[3]. *In vivo* nitrate reductase activity in the leaf disks was assayed by the method of Jaworski[12]. Nitrite content in the leaf extracts as well as in the enzyme assays, was determined by the standard Greiss–Ilosvay colorimetric method Nitrate content in suitably diluted leaf extracts was determined after its quantitative enzymic reduction to nitrite by an active dialysed nitrate reductase obtained from rice leaves.

ment 2), the activity of nitrite reductase was negligible, whereas nitrate reductase was synthesised during a 4-h exposure of green detached leaves to sunlight. In these conditions, large quantities of nitrite accumulated. The amount of nitrite accumulated *in situ* was about three times that formed by the assumed photochemical reduction observed in treatment 3.

Activity *in vivo* of nitrate reductase in leaf disks was less than 10% of the *in vitro* activity in leaf extracts, assayed in the presence of excess NADH. Similar results indicating a comparatively low *in vivo* activity of nitrate reductase have been reported[13,14]. Moreover, it is uncertain whether either the *in vivo* or *in vitro* assay is a true reflection of the *in situ* nitrate assimilation. The estimated input of reduced nitrogen based on *in vivo* enzyme assay is known to exceed substantially the actual accumulation of reduced nitrogen by the plant *in situ*[5]. Our results show that photochemical reduction of nitrate could be as large as 30% of the *in situ* reduction.

In plants exposed to very bright sunlight, as in tropical countries, photochemical reduction of nitrate could thus be significant. Activity of nitrate reductase alone may not, therefore, be a factor limiting the rate of nitrate assimilation.

K.V.S. thanks the Indian Council of Agricultural Research for a Senior Research Fellowship.

M. S. NAIK
K. V. SARDHAMBAL
SHIV PRAKASH

Biochemistry Division,
Indian Agricultural Research Institute,
New Delhi 110012, India

Received December 11, 1975; accepted June 1, 1976

[1] Beevers, L., and Hageman, R H., *A Rev. Pl. Physiol.*, **20**, 495–522 (1969).
[2] Beevers, L., and Hageman, R. H., in *Photophysiology*, 7, 85–113 (Academic, New York and London, 1972)
[3] Sawhney, S. K., and Naik, M. S., *Biochem. J*, **130**, 475–486 (1972).
[4] Eilrich, G. L., and Hageman, R. H, *Crop Sci*, **13**, 59–66 (1973).
[5] Beckard, E. L., Lambert, R. J., and Hageman, R. H., *Crop Sci.*, **13**, 343–350 (1973).
[6] Baudisch, O., and Meyer, E., *Z. phys.-chem.*, **89**, 175 (1914).
[7] Moore, B, *Proc R. Soc.*, **B40**, 158–166 (1919).
[8] Stoy, V, *Physiologia Pl.*, **8**, 963–986 (1955)
[9] Stoy, V., *Biochim. biophys. Acta*, **21**, 395–396 (1956).
[10] Notton, B. A., and Hewitt, E. J., *Biochem biophys. Res. Commun.*, **44**, 702–710 (1971).
[11] Sawhney, S. K., and Naik, M. S., *Biochem. biophys. Res. Commun.*, **51**, 67–73 (1973).
[12] Jaworski, E. G., *Biochem. biophys Res. Commun.*, **43**, 1274–1279 (1971).
[13] Klepper, L., Flesher, D., and Hageman, R H., *Pl. Physiol.*, **48**, 580–590 (1971).
[14] Brunetti, N., and Hageman, R. H, *Pl. Physiol.* (*Suppl.*), P180 (1973).

Immunopathology of schistosomiasis in athymic mice

EOSINOPHILIA—tissue eosinophil infiltrates—granuloma and IgE formation are associated with helminth infections. Eosinophils phagocytose antigen–antibody complexes, neutralise histamine and serotonin, mediate inflammatory reactions and modify delayed hypersensitivity[1]. The tissue-invasive stage of some parasitic infections provides suitable antigen and stimulates the production of IgE, which in turn induce eosinophilotaxis. We have investigated the need of T-cell participation in the eosinophil response, IgE formation and granuloma formation in schistosomiasis in congenitally athymic mice which have profound deficiency in T-cell dependent immune response. We looked in particular at eggs as they are important in the pathogenesis of schistosomiasis. They are trapped in tissues and induce chronic granulomatous inflammation with numerous eosinophils. Warren *et al.*[2–6] reported that egg granuloma is a cell-mediated hypersensitivity reaction and it is significantly altered in immunosuppressed mice.

Sixteen homozygous athymic nude (*nu*/*nu* mice with an outbred Swiss mouse background and 16 normal heterozygous (*nu*/+) littermates 9 weeks old were housed in specific pathogen-free conditions (mouse hepatitis virus). They were infected through tail immersion with 35–40 *Schistosoma mansoni* (Puerto Rico strain) cercariae freshly released from the intermediate snail host, *Biomphalaria glabrata*. This level of infection results in a chronic murine hepatosplenic disease which closely resembles, pathophysiologically, human chronic schistosomiasis[7]. Animals were killed 52, 58 and 66 d after infection. Although *nu*/+ mice had ruffled hair coat and hunched back, *nu*/*nu* mice showed no remarkable signs of illness. The hepatosplenomegaly and enlargement of mesentery lymph node associated with schistosomiasis was significantly more severe in *nu*/+ mice. Microscopic examination of the liver showed that *S. mansoni* eggs were trapped in the small intrahepatic blood vessels and granuloma was formed around them. In the immune-intact normal mice, the egg granuloma was a circumscribed lesion consisting of predominately eosinophils, macrophages, lymphocytes, epithelioid cells, granulation tissue and sometimes giant cells. Reparative fibrosis was distinct. The white necrotic hepatic lesions in athymic mice were smaller than those in control mice. The sizes of egg granulomas, determined by measuring two diameters at right angles to each other with an ocular micrometer 52, 58 and 66 d after infection, are presented in Table 1. The mean sizes of granulomas in athymic mice were significantly smaller than those in heterozygous mice at $P<0.001$ as calculated by Student's *t* test. Granulomas decreased in size during the course of infection. No tissue eosinophils were found in the egg granuloma in the athymic mice, whereas neutrophils, macrophages, lymphocytes, epithelioid cells and pigments were usually present. We did not see giant cells in granulomas. Occasionally only a few or no inflammatory cells were found around the eggs. Granulation tissue or collagen formation was observed in some egg granuloma lesions, although they were not as well established as those

Fig. 1 The lymphocyte transformation of splenic cells of athymic (*nu*/*nu*) and heterozygous (*nu*/+) mice 52 d after infection with 35–40 *S. mansoni* cercariae. The blastogenic activities stimulated with 20 μg of PHA, 40 μg of LPS and 12 μg of adult *S. mansoni* antigen, are expressed as the stimulation index by comparing the thymidine uptake by infected splenic cells with the thymidine uptake by control (unsensitised) splenic cells. The spleen cell suspension (2×10^6) was added to each well of microtrays and cultured in triplicate The soluble adult antigen was prepared by homogenised lyophilised worms in RPMI 1640 medium, centrifuged at 2,500 r p.m. for 30 min. The supernatant was sterilised by passing through a 0.45-μm filter and used as antigen. After 72 h of incubation at 37 °C, 2 μCi of ^{3}H-thymidine were introduced to each well; incubated for another 16 h, cells were collected, extracted and counted in a scintillation counter.

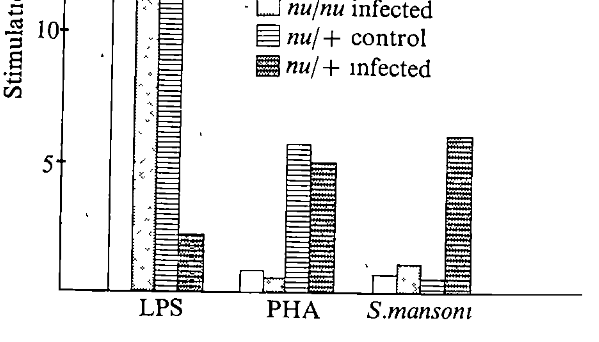

Table 1 Comparison of egg granulomas in athymic and heterozygous mice infected with 35–40 *S. mansoni* cercariae

Time	Day 52		Day 58		Day 66	
Genotype	*nu*/*nu*	*nu*/+	*nu*/*nu*	*nu*/+	*nu*/*nu*	*nu*/+
No. mice studied	4	4	6	6	6	6
No. granulomas measured	52	41	70	53	64	46
Granuloma size (μm)						
range ($L \times W$)*	57–660 ×47–340	76–780 ×48–540	57–456 ×48–342	114–576 ×113–475	49–313 ×47–247	161–523 ×85–486
mean ($L \times W$)†	254×192	479×341	214×141	379×291	161×104	381×293
s.d. ($L \times W$)	111×83	143×115	97×67	112×91	57×38	90×80
P	<0.001		<0.001		<0.001	
% Eggs without cell response‡	9	2	6	0	6	0

*$L \times W$, range of length (L) by range of width (W).
†Mean of length by mean of width.
‡Measurement included in granuloma size.

in normal mice. Small granulomas with few eosinophils were observed occasionally in the intestinal wall of the athymic mice.

Blood eosinophilia was studied in seven athymic and 10 normal mice before and after infection at weekly intervals. Tail blood smears were made at about 1400 and were stained by the Jenner–Giemsa method. A total of 300 leukocytes was examined per slide. Circulating eosinophils were observed in infected athymic mice (2–4%) although their levels were significantly lower ($P<0.001$) than those in infected heterozygotes (10–12%) after 7 weeks infection. Evidently the eosinophilpoeisis in athymic mice was not impaired. The role and specific function of eosinophils in the granuloma has not been established. According to Walls *et al.*[8] the destruction of liver tissue by eggs should stimulate the local eosinophil response. This apparently is not true in infected nude mice. The migration of tissue eosinophils to the affected sites seems to be dependent on T cells or other thymus factors which are absent in athymic mice. Eosinophils are known to ingest antibody–antigen complex. The complex may not be formed in nude mice because of the lack of the functional T cell required to produce anti-parasitic antibodies.

The lymphocyte responsiveness of athymic mice and heterozygotes to specific adult *S. mansoni* antigens and to nonspecific mitogens, phytohaemagglutinin (PHA) and *Salmonella typhimurium* lipopolysaccharide (LPS) was determined by measuring the incorporation of ^{3}H-thymidine into DNA. The blastogenesis of spleen cells of infected and non-infected athymic mice and heterozygotes is shown in Fig. 1. The B cells of both non-infected and infected nude mice, as well as the non-infected heterozygotes responded strongly to LPS, while the B-cell function of infected *nu*/+ mice was greatly depressed. T cells of non-infected and infected *nu*/+ mice reacted vigorously to PHA stimulation in contrast to those of nude mice. In the response to adult *S mansoni* antigen, infected *nu*/+ mice reacted strongly, whereas the nude mice (infected and non-infected) and control *nu*/+ mice spleen cells were not stimulated by the specific antigen. This evidence indicates that the lymphocyte responsiveness to *S. mansoni* is dependent on T cells or thymus factor.

Table 2 Titre of reaginic antibodies in sera of *nu*/*nu* and *nu*/+ mice infected with 100 *S. mansoni* cercariae determined by the PCA reactivity in rats or nude mice

	Time after infection							
	Day 49		Day 53		Day 58		Day 72	
Genotype	IgE	IgG$_1$	IgE	IgG$_1$	IgE	IgG$_1$	IgE	IgG$_1$
nu/+	40	40	10	20	40	30	10	40
nu/*nu*	0	0	0	0	0	0	0	0

The presence of IgE in pooled sera was measured by the PCA test in rats (adult male Sprague–Dawley) with a latent period of 24 h and in female nude mice with 72 h of sensitisation. The IgG$_1$ antibody was determined by PCA reactions in nude mice with a latency of 3 h. A sample of 0.05 ml of diluted sera was injected intradermally into each skin site. The antigens for intravenous challenge were soluble crude extracts from adult *S. mansoni* worms or eggs and were adjusted to 0.8 mg of protein per ml of solution. The volume was 1 ml per rat and 0.2 ml per mouse in mixing with equal amounts of 1% potamine sky blue dye solution. The size and bluing intensity of PCA reactions on the underside of skin were read 20–30 min after antigen challenge through the tail vein. The highest dilution of sera giving a reaction, 5 mm greater than normal serum control in at least half of PCA recipients, was regarded as the titre.

The relationship between functional T cells and reaginic antibodies (IgE and IgG$_1$) was studied in nude and *nu*/+ mice infected with 100 *S mansoni* cercariae. We found that T-cell deficient nude mice were unable to produce detectable levels of IgE and IgG$_1$ antibodies whereas the *nu*/+ mice produce both long term skin-sensitising IgE antibody and short term skin-sensitising IgG$_1$ antibody as early as 49 d after infection (Table 2). Both IgE and IgG$_1$ persisted in the blood for more than 10 weeks after infection. Evidently, the IgE and IgG$_1$ formation in response to *S. mansoni* antigens may require the participation of T cells. We have not observed significant quantitative differences in levels of both IgE and IgG$_1$ antibodies in *nu*/+ mice responding to soluble adult or egg antigen. Mota *et al.*[9] were unable to detect reaginic antibody in ICR mice infected with 150 *S mansoni* cercariae by passive cutaneous anaphylaxis (PCA) in mice. Our finding, however, confirms the recent report[10] that both IgE and IgG$_1$ were produced in CBA/J mice with chronic schistosomiasis. The lack of reaginic antibodies in nude mice may contribute to the absence of the local tissue eosinophil reaction[1].

Buchanan *et al.*[11] failed to induce egg granulomas in the liver and intestines of experimentally T-cell-depleted mice. Our study, however, has demonstrated that congenitally athymic mice can form granulomas around *S. mansoni* eggs. The lymphocytes in granulomas of athymic mice might be B-lymphocyte-related cells that respond to certain T-cell independent antigens. Therefore the egg granulomas may be mediated partly by B cells, if not solely by T cells This remains to be studied. We did not see giant cells in the granulomas of athymic mice, although it is not uncommon in normal mice The observation suggests the association of giant cell formation with thymus factor[12].

This work was supported in part by a grant from the NIH.

CHAO-KUANG HSU

Division of Laboratory Animal Medicine,
School of Medicine and
Department of Pathhobiology, School of Hygiene and Public Health

SUSAN H. HSU

Department of Medicine,
School of Medicine,
Johns Hopkins University,
Baltimore, Maryland 21205

ROBERT A. WHITNEY, JR
CARL T. HANSEN

*Veterinary Resources Branch,
Division of Resources Services,
National Intitutes of Health,
Bethesda, Maryland 20014*

Received January 28, accepted May 25, 1976.

[1] Honsinger, R. W, Jr, Silverstein, D, and Van Arsdel, P. O., *J. Allergy clin. Immun.*, 49, 142–155 (1972).
[2] Warren, K. S., Domingo, E. O., and Cowan, R. B. T, *Am. J. Path.*, 51, 735–756 (1967).
[3] Hang, L. M., Warren, K. S., and Boros, D. L., *Expl Parasit*, 35, 288–298 (1974).
[4] Domingo, E O., Cowan, R. B. T, and Warren, K. S., *Am. J trop. Med. Hyg*, 16, 284–292 (1967).
[5] Domingo, E. O., and Warren, K. S, *Am. J. Path.*, 51, 757–767 (1967).
[6] Domingo, E. O., and Warren, K. S., *Am. J. Path*, 52, 613–631 (1968)
[7] Warren, K. S, *Trans R. Soc. trop Med. Hyg.*, 66, 417–434 (1972).
[8] Walls, R. S, and Beeson, P. B, *Clin exp Immun.*, 12, 111–119 (1972)
[9] Mota, I., Sadun, E H, and Gore, R W., *Expl Parasit.*, 24, 251–258 (1969).
[10] Colley, D. G., *J Immun.*, 115, 150–156 (1975).
[11] Buchanan, R D., Fine, D. P., and Colley, D. C., *Am. J. Path.*, 71, 207–208 (1973).
[12] Unanue, E. R, and Benaceraff, B, *Am. J. Path.*, 71, 349–364 (1973)

Growth of *Mycobacterium leprae* and *M. marinum* in congenitally athymic (nude) mice

THE failure to grow the leprosy bacillus, *Mycobacterium leprae*, *in vitro* means that there is a requirement for a highly susceptible experimental animal model. The only animal confirmed so far as naturally highly susceptible is the nine-banded armadillo, of which at least some specimens develop, after inoculation, a disseminated disease which resembles human lepromatous leprosy[1]. The inoculation of *M. leprae* into the footpads of mice results in a localised, self-limiting infection, with a maximum bacillary yield of about $10^{6\cdot5}$ organisms per footpad[2]. Suppression of the immune response of the mouse, by thymectomy and irradiation, results in enhancement of the footpad infection, and dissemination of *M. leprae* bacilli to internal organs and peripheral tissue such as ears, nose and tail[3]. This ability to enhance infection by nonspecific depression of T-cell function suggests that the congenitally athymic, or nude, mouse might provide a suitable, naturally susceptible host for *M. leprae*. In spite of the severe impairment of the cellular immune response of nude mice[4–7], the only report of the growth of *M. leprae* in such mice concluded that there was no significant increase in bacillary proliferation, and no tendency to promote a generalised infection[8]. This conclusion was based, however, on observations made only 6 months after inoculation—an interval that is almost certainly too short for detection of significant enhancement or dissemination.

To investigate further the growth of *M. leprae* in nude mice, we established a small breeding colony based on the mating of a closed, but not inbred group of mice. Heterozygous females (nu/+) were mated with homozygous males (nu/nu) to give a progeny half homozygous and half heterozygous. The homozygous mice were used as experimental (nude) mice, and the heterozygous, phenotypically normal littermates were used as controls.

In a preliminary experiment, *Mycobacterium marinum* was used as the infecting agent. Infection of mice with *M. marinum* and *M. leprae* is analogous[9]; growth of both organisms reaches a maximum of 10^6–10^7 bacilli per footpad, followed by killing of the organisms. But, the fact that *M. marinum* grows much more rapidly than *M. leprae* and is cultivable *in vitro* makes it a convenient model for the study of the *M. leprae* infection.

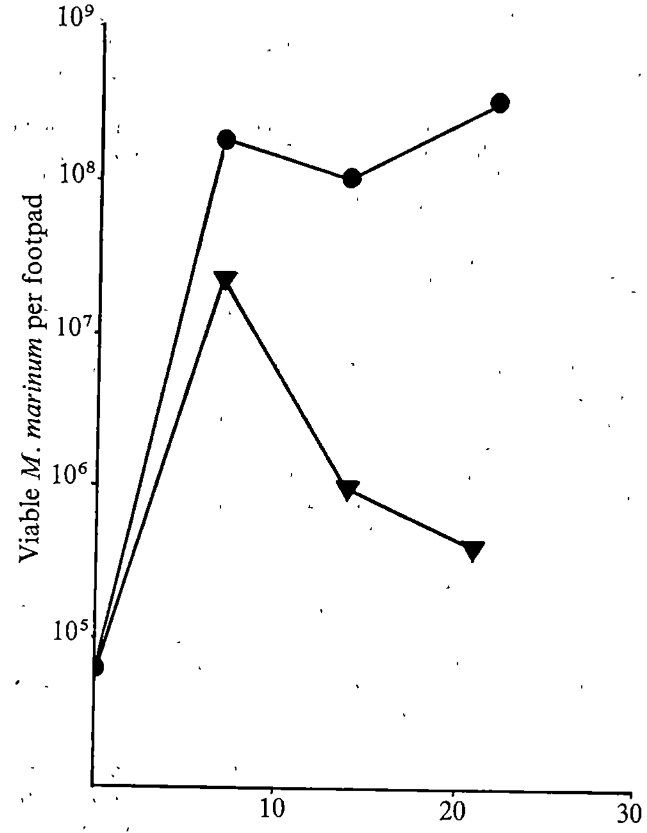

Fig. 1 Growth of *M. marinum* in the footpads of nude mice (●) and control mice (▼). Each sample represents the viable count of bacilli from the pooled tissue of three mice. Footpads were removed and homogenised in Middlebrook–Dubos medium, and viable counts made by the method of Miles and Misra[13].

Mice were inoculated with *M. marinum* in the left hind footpad and bacillary growth was monitored as shown in Fig. 1. *M. marinum* grew to a peak of $10^{7\cdot2}$ viable bacilli per footpad by 7 d in control mice, and this was followed by a rapid decline in viable numbers, falling to $10^{5\cdot4}$ at 21 d. In the nude mouse group, the number of organisms had reached $10^{8\cdot2}$ per footpad by 7 d, and although this was followed by a plateau, there was no decline in viable numbers.

At the same time that footpads were collected, liver, lungs, spleen and the contralateral footpads were also removed and examined for the presence of viable bacilli (Table 1). Viable organisms were detectable in the internal organs of nude mice at all collections, whereas at no stage of the infection were viable organisms recoverable from the internal organs of control mice.

To study the growth of *M. leprae* in nude mice, 30 nude and

Table 1 Recovery of viable *M. marinum* from mouse tissue after inoculation in the left hind footpad

Time after infection (d)	Right footpad	Left footpad	Liver	Spleen	Lung
		Nude mice (viable *M. marinum* per organ)			
7	1.9×10^8	—	1.3×10^4	1.5×10^4	2.4×10^3
14	1.1×10^8	—	4.4×10^3	6.4×10^5	1.6×10^3
21	3.6×10^8	—	7.2×10^5	8.6×10^6	1.4×10^6
		Control mice (viable *M. marinum* per organ)			
7	2.4×10^7	—	—	—	—
14	9.6×10^5	—	—	—	—
21	4.0×10^5	—	—	—	—

Each sample represents the viable count of bacilli from the pooled tissue of three mice. Tissue was removed and homogenised in Middlebrook–Dubos medium, and viable counts were made by the method of Miles and Misra[13]. — Represents $< 10^3$ viable *M. marinum* per organ.

60 control mice were inoculated into both hind footpads, with bacilli from a biopsy specimen from an untreated lepromatous leprosy patient. The results are shown in Fig. 2. Because of the poor survival of nude mice, they were not killed for collection, but footpads were removed and bacillary counts were made at their natural death. Collection of *M. leprae* from mouse tissue, and counting of acid-fast bacilli were carried out as described before[10]. There was no evidence of an increase in bacillary numbers in any of the mice during the first 4 months after inoculation, but while growth in the control group reached a maximum at about 10^6 bacilli per footpad, counts in nude mice continued to rise. Enhancement of bacillary growth in the two longest surviving nude mice, collected at 266 and 322 d, was highly significant ($P \ll 0.01$), and was accompanied by clearly visible swelling of the footpads.

The longest surviving nude mouse was examined for the presence of acid-fast bacilli in ears, nose, testes, tail, forepaws, liver and spleen (Fig. 3). A few bacilli were detectable in the testes, nose, tail and forepaws, though in the testes, tail and forepaws, the numbers were only just above the level of detection and represent only one or two bacilli observed by the counting technique. Significant levels of bacilli were present in liver and spleen, however, with $10^{5.6}$ and $10^{5.3}$, respectively. The liver and spleen are also heavily infected with leprosy bacilli in the highly susceptible nine-banded armadillo[11]. No acid-fast bacilli were recoverable from the internal organs or peripheral tissue, other than the inoculation site, in control mice.

Confirmation of the identity of the *M. leprae* bacilli collected from nude mice was made by removal of acid fastness by pretreatment with pyridine[12], and by subinoculation into the footpads of normal mice—bacillary growth reached a maximum of 10^6 120 d after inoculation, conforming to the classical growth pattern of *M. leprae*.

Thus, in contrast to the findings of Prabhakaran *et al.*, whose observations were made over only 6 months, we found that inoculation of *M. leprae* into the footpads of nude mice resulted in a very significantly enhanced infection compared with immunologically normal mice; and the recovery of significant numbers of bacilli from the spleen and liver of the longest surviving nude mouse certainly suggests a tendency to promote a systemic *M. leprae* infection. If the problems of survival can be overcome, the nude mouse could prove to be of considerable value as a model for the study of lepromatous leprosy and as a means of detecting a small number of viable organisms against a large background of dead bacilli in the tissues of patients undergoing therapy.

Fig. 2 Growth of *M. leprae* in the footpads of nude mice. Each point on the control curve (⊙) represents the mean value of twelve mouse footpad counts, and the shaded area is the 95% upper confidence limit of the control group during the plateau phase. Nude mouse values (●) are the bacillary counts of individual footpads removed at autopsy.

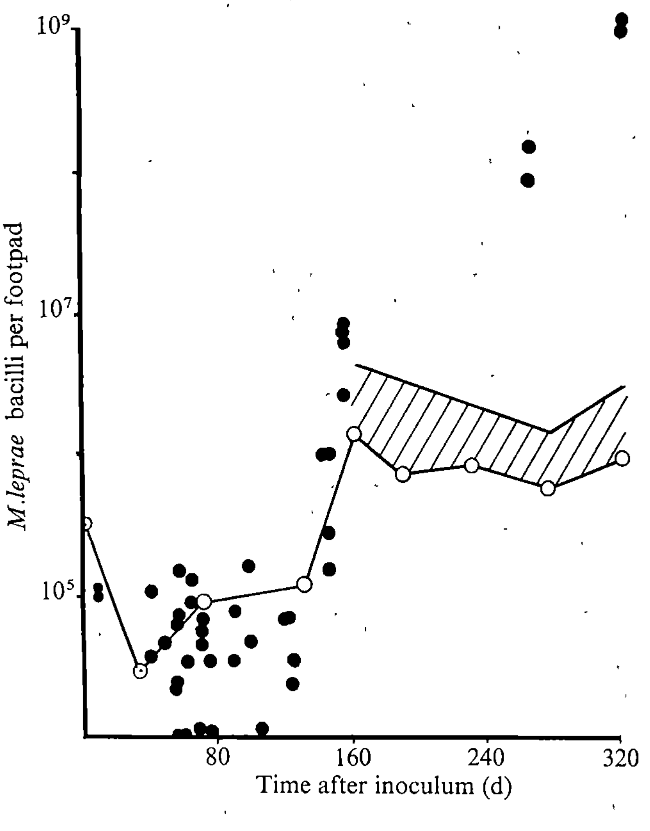

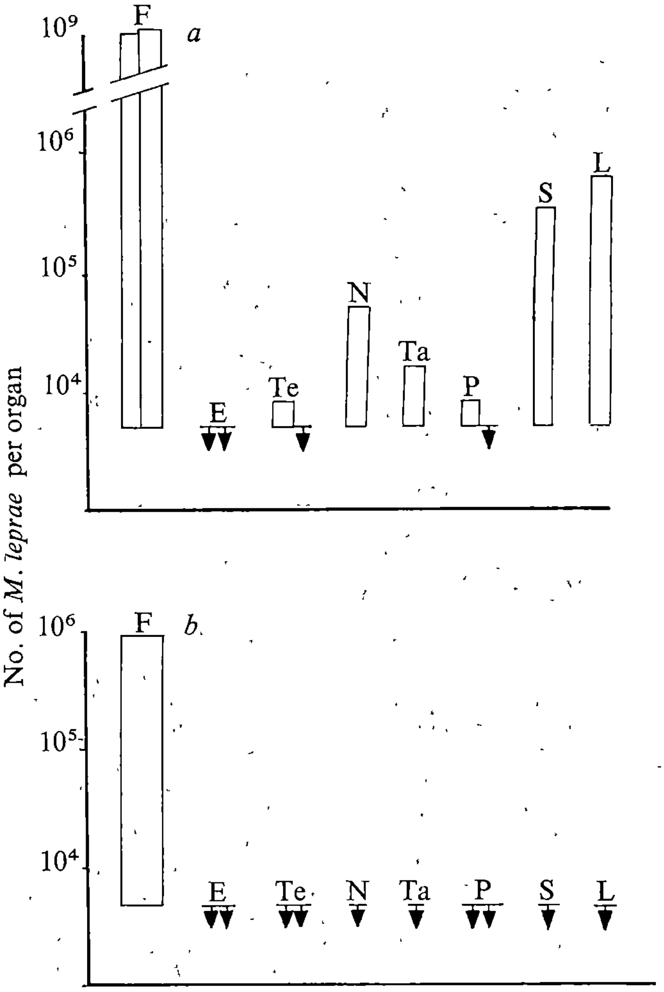

Fig. 3 The recovery of *M. leprae* from the internal organs and peripheral tissue of the longest surviving nude mouse, and from control mice (mean value of six mice), following footpad inoculation. All mice were sampled 322 days after inoculation. F: footpads; E: ears; Te: testes; N: nose; Ta: tail; P: forepaws; S: spleen; L: liver.

This work was supported by a grant from the Overseas Development Administration, London.

M. J. Colston
G. R. F. Hilson

Department of Medical Microbiology,
St George's Hospital Medical School,
London SW17 0QT, UK

Received May 7; accepted May 28, 1976.

1 Kirchheimer, W. F., and Storrs, E. E., *Int. J. Lepr.* 39, 693–702 (1971).
2 Shepard, C. C., *Int. J. Lepr*, 30, 291–306 (1962)
3 Rees, R J. W., Waters, M. F. R., Weddel, A. G. M, and Palmer, E, *Nature*, 215, 599–602 (1967).
4 Manning, D M, Reed, N. D., and Schaffer, C. F., *J. exp. Med.*, **138**, 488–494 (1973).
5 Wortis, H. H., *Clin. exp Immun*, **8**, 305–317 (1971)
6 Pennycuick, P. R., *Transplantation*, 11, 417–418 (1971)
7 Rouse, B. T., Rollinghoff, M., and Warner, N. L., *Eur. J. Immun.*, 3, 218–224 (1973).
8 Prabhakaran, K., Harris, E. B., and Kirchheimer, W. F., *Experientia*, 31, 784 (1975).

[9] Clark, H. F., and Shepard, C. C., *J Bact.*, **86**, 1057–1069 (1963).
[10] Holmes, I. B., and Hilson, G. R. F., *J med. Microbiol.*, **5**, 251–261 (1972).
[11] Kirchheimer, W. F , Storrs, E. E., and Binford, C. H., *Int. J. Lepr.*, **40**, 229–242 (1972).
[12] Convit, J., and Pinardi, M. E., *Int. J. Lepr.*, **40**, 130–132 (1972).
[13] Miles, A. A., and Misra, S. S., *J. Hyg.*, **38**, 732 (1938).

Control of lymphokine secretion by prostaglandins

SEVERAL lines of evidence exist implicating prostaglandins (PGs) as mediators in inflammation[1]. In type IV hypersensitivity (delayed hypersensitivity, cellular immunity) reactions, although there is evidence of PG involvement[2,3] lymphokines, the products of antigen-activated thymus-dependent lymphocytes, have received greater attention as potential mediators[4,5]. It has been reported that PGE$_1$ is a potent inhibitor of lymphocyte activation *in vitro*[6] and we have observed that guinea pig peritoneal exudate macrophages produce substantial amounts of E-type PG (ref. 7). It is well established that macrophages are capable of modifying lymphocyte activation[8,9], and that there is close association between these two cell types in reactions of cellular immunity *in vitro*[10] and *in vivo*[11]. We have now shown that production of E-type PGs by macrophages modifies the secretion of lymphokines by lymphocytes in response to antigen and that this may serve to provide a negative feedback mechanism for regulating the extent and duration of reactions of cellular immunity.

The *in vitro* test that shows the best quantitative correlation with delayed hypersensitivity reactions in the guinea pig is macrophage migration inhibition[4] and so we have used this test both for measurement of the reactivity of sensitised lymphocytes to antigen and for the direct measurement of lymphokine activity. Antigen-induced cell migration inhibition of sensitised cells was reduced by PGE$_1$ (0.1–1.0 μg ml^{-1}), although the inhibition of cell migration by preformed lymphokine was not affected by PGs of the E series (Table 1), suggesting that lymphokine formation rather than lymphokine action on target cells was inhibited by PGE compounds. Neither PGF$_{2\alpha}$ nor PGA$_1$, at these concentrations, influenced antigen-induced cell migration inhibition (Table 1). On the other hand, indomethacin (0.1 μg ml^{-1}), a potent prostaglandin synthase inhibitor[1], enhanced antigen-induced inhibition, but had no effect on lymphokine-induced inhibition (Table 1), implying that there is sufficient endogenous PG biosynthesis in these cultures to modify the response to antigen. These observations support the proposition that endogenous E-type PGs act by reducing the lymphokine secretion by antigen-activated lymphocytes, rather than by modifying the action of lymphokines on target cells.

Accordingly, we have measured lymphokine production by lymph node lymphocytes in response to specific antigen, in the presence and absence of E-type PGs and indomethacin. PGE$_1$ (0.1–1.0 μg ml^{-1}) and PGE$_2$ (0.1–1.0 μg ml^{-1}) produced dose-related inhibition of antigen-induced lymphokine secretion, measured in terms of migration inhibitory activity (Table 2). These results are in agreement with the direct effects of PGE compounds on antigen-induced migration inhibition. We have obtained similar results to those shown in Tables 1 and 2 for mitogenic lymphokine, in that antigen-induced stimulation of DNA synthesis in lymph node lymphocytes was inhibited by PGE$_1$ and PGE$_2$ (0.1 and 1.0 μg ml^{-1}) and that this action of E-type PGs was accompanied by reduced production of mitogenic lymphokine.

Table 2 Effect of prostaglandins E$_1$ and E$_2$ and indomethacin on lymphokine formation measured by guinea pig cell migration inhibition

Treatment (μg ml^{-1}) Inducing antigen	Drug	Response (% ± s.e.m.) PGE$_1$	PGE$_2$	Indomethacin
–	–	100±2.2	100±2.2	100±2.3
1,000	–	52.3±1.5	57.8±1.5	71.9±2.3
1,000	0.1	64.7±3.0	71.7±1.6	65.9±2.2
1,000	1.0	81.7±4.9	81.6±4.3	ND

Lymphocytes were obtained from the teased lymph nodes of BGG-sensitised animals. They were placed in culture tubes at 1×10^7 cells ml^{-1} in Eagle's MEM supplemented with 5% pooled normal guinea pig serum. BGG (1 mg ml^{-1}) with or without E-type PGs were added to test cultures and after 24 h incubation at 37 °C, culture supernatants were partially purified and tested for migration inhibitory activity. Results were expressed as percentage response of control ± s.e.m. Supernatants without added antigen or drugs were taken as controls.

Table 1 Effects of prostaglandins and indomethacin on antigen- or lymphokine-induced guinea pig cell migration inhibition

Treatment (μg ml^{-1}) Ag	LK	Drug	Response (%±s.e.m.) PGE$_1$	PGE$_2$	PGF$_{2\alpha}$	PGA$_1$	Indomethacin
–	–	–	100±3.0	100±3.8	100±6.0	100±4.7	100±4.4
–	–	0.1	99.9±4.9	103.1±4.4	102.6±4.6	102.5±2.6	96.0±4.6
–	–	1.0	97.7±1.9	94.5±3.4	93.5±4.9	95.8±6.2	ND
5.0	–	–	67.3±3.0	44.4±0.4	41.8±0.4	48.6±3.8	69.4±2.2
5.0	–	0.1	76.2±3.9	55.1±2.2	46.2±4.3	46.7±5.3	57.5±3.9
5.0	–	1.0	88.9±4.4	61.1±2.5	43.3±2.9	50.3±4.6	ND
–	100	–	74.7±2.9	71.5±2.6	ND	ND	56.7±1.6
–	100	0.1	73.6±0.1	74.2±4.9	ND	ND	58.1±3.3
–	100	1.0	76.5±4.1	73.1±2.8	ND	ND	ND

Cell migration inhibition was carried out as described previously[17]. Guinea pig peritoneal exudate cells in Eagle's MEM with 10% foetal calf serum were cultured at 4×10^6 cells per capillary tube in chambers with or without antigen, lymphokine or drugs. Cell migration was recorded after 40 h as area (mm^2) and then expressed as percentage inhibition of control (that is, with no addition) ± s.e.m. Purified protein derivative of tuberculin (PPD) was used as antigen (Ag) with tuberculin-sensitised animals (0.1 ml BCG intraperitoneally 4 weeks before use) and preformed lymphokine (LK) was generated from bovine gamma globulin (BGG) sensitive lymph node lymphocytes in culture with 1.0 mg ml^{-1} BGG. Lymphokine preparations were partially purified by ammonium sulphate precipitation as described previously[17].

Indomethacin (0.1 μg ml^{-1}) had only a slight enhancing effect on lymphokine secretion by lymph node lymphocytes (Table 2), whereas it clearly augmented antigen-induced inhibition of cell migration—a system which utilises mixed cell populations (that is, macrophages and polymorphonuclear (PMN) leukocytes, in addition to lymphocytes) (Table 1). These observations confirmed that the action of PGE was at the level of lymphokine secretion by lymphocytes, but implied that the source of endogenous E-type PGs was unlikely to be the lymphocytes themselves.

As a result of these findings, we have examined PG production by inflammatory cell populations (lymphocytes, macrophages and PMN leukocytes) during short term culture. Macrophage-rich cell populations (60–80% macrophages, 10–30% PMN leukocytes, 10% lymphocytes) produced substantial amounts of PGE-like activity (mean±s.e. = 11.6±2.1 ng PGE$_2$ per 10^6 cells per 24 h) whereas PMN leukocytes (80–90% leukocytes, 10–20% monocytes) and lymph node lymphocytes (>90% lymphocytes) were much less active in this respect (0.45±0.03 ng and 1.7±0.11 ng PGE$_2$ per 10^6

Table 3 *In vitro* prostaglandin production by guinea pig inflammatory cell populations stimulated by lymphokine or specific antigen

Antigen ($\mu g\ ml^{-1}$)	PGE_2 (ng per 10^6 cells per 24 h)	Lymphokine ($\mu g\ ml^{-1}$)	PGE_2 (ng per 10^6 cells per 24 h)
0	7.60±0.86*	0	6.87±0.73*
0.01	6.22±0.92	4.0	5.13±0.16
0.1	9.24±0.56	20.0	7.89±0.48
1.0	11.58±0.83	100.0	11.58±1.43
10.0	20.38±1.41	500.0	23.87±1.89
100.0	26.00±0.98		

*Mean ± s.e.m.

Sterile Falcon culture tubes containing 5×10^5 washed, macrophage-rich peritoneal exudate cells and increasing doses of specific antigen (PPD) or lymphokine were incubated at 37 °C for 24 h and the supernatants removed and stored at −20 °C before assay for PG activity by radioimmunoassay using sheep anti-PGE_2-BSA. Anti-PGE_2 antiserum cross reacted with PGE_2 (100%); PGE_1 (55%); $PGF_{2\alpha}$ (1.5%); 15-keto PGE_2 (1.2%); PGA_2 (0.6%); PGB_2 (0.2%).

cells per 24 h, respectively). Macrophage populations (>90% macrophages) enriched by selection of glass-adherent cells show a similar PG-synthesising capacity to that of unseparated exudate cell populations, further implying that the macrophage is the major cell type responsible for PG production.

Prostaglandin-like activity was mainly E-type, as detected by radioimmunoassay, had the properties of an acidic lipid on extraction into ethyl acetate and cochromatographed with authentic PGE_2 on thin-layer chromatography. The biological activity of the material on rat stomach strip, human Fallopian tube and ADP-induced platelet aggregation suggested that the bulk of the activity resembled PGE_2 rather than PGE_1, a conclusion consistent with the high proportion of arachidonic acid (the PG_2 precursor) in macrophage membrane phospholipids[12]. A dose-related increase in PGE production was induced by specific antigen using sensitised cells and by preformed lymphokine using non-sensitised cells (Table 3), thus satisfying an obligatory requirement of the negative feedback hypothesis. Furthermore, indomethacin at a concentration which completely inhibited PGE production (0.1 $\mu g\ ml^{-1}$) increased the formation of macrophage migration inhibitory lymphokine by antigen-stimulated peritoneal exudate cells from 19.7±2.1% inhibition (untreated cells) to 29.53±2.6% inhibition (treated cells), confirming that the level of PGE production is sufficient to modify lymphokine generation *in vitro*.

We have established here that E-type PGs inhibit lymphocyte activation and the secretion of lymphokines and that such preparations stimulate E-type PG production by macrophages. This is consistent with the proposition that E-type PG production in response to lymphokine stimulation provides a negative feedback mechanism for regulation of the cellular immune response. Inhibition of mediator secretion by PGs in allergic reactions is not restricted to type IV hypersensitivity reactions. Thus, PGE_1 and PGE_2 are both effective inhibitors of histamine secretion by human basophils in type I hypersensitivity[13] and antigen-induced SRS-A production by lung fragments[14]. Consistent with this phenomenon is the observation that low doses of indomethacin enhance SRS-A release from passively sensitised human lung[15]. In these situations, in contrast to the type IV response, the cellular origin of PG production has not been clearly established. In type III allergic reactions, although PGE_1 can inhibit the release of lysosomal enzymes from PMN leukocytes[16], the capacity of such cells to produce PGE seems to be insufficient for this effect to be of physiological relevance. The inability of therapeutic doses of non-steroidal anti-inflammatory drugs to affect markedly types I, III and IV hypersensitivity reactions *in vivo* implies that other control systems also operate in physiological, as opposed to pathological, circumstances.

The self-limiting mechanism that we propose for type IV reactions has the virtue of relating lymphokine, lysosomal enzyme and PG release to a common basis. This relationship may have interesting consequences, both for aetiology and pathogenesis in chronic inflammatory diseases[16], and in the design of anti-inflammatory drugs, by highlighting potential loci of action that have hitherto received little attention.

D. GORDON
M. A. BRAY
J. MORLEY

Department of Clinical Pharmacology,
(Asthma Research Council),
Cardiothoracic Institute,
Fulham Road,
London SW3 6HP, UK

Received November 6, 1975, accepted June 1, 1976

1 Vane, J. R., in *Inflammation Mechanisms and Control* (edit. by Lepow, I. H., and Ward, P. A.), 261–279 (Academic, New York and London, 1972)
2 Greaves, M W., Sondergaard, J., and McDonald-Gibson, W , *Br med. J* , 2, 258–260 (1971).
3 Goldyne, M E., Winkelmann, R K., and Ryan, R J., *Prostaglandins*, 4, 737–749 (1973).
4 David, J R., and David, R. R., *Progr Allergy*, 16, 300–449 (1972).
5 Yamamoto, K , and Takahashi, Y., *Nature new Biol* , 233, 261–263 (1971).
6 Smith, J. W , Steiner, A L , and Parker, C. W , *J clin Invest* , 50, 442–448 (1971).
7 Bray, M. A , Gordon, D., and Morley, J , *Br J Pharmac* , 52, 453P (1974)
8 Waldman, S R., and Gottlieb, A. A., *Cell Immun* , 9, 142–156 (1973)
9 Calderon, J , and Unanue, E R , *Nature*, 253, 359–361 (1975).
10 Nielsen, M. H., Jensen, H , Braendstrup, O., and Werdelin, O , *J exp. Med* , 140, 1260–1272 (1974).
11 Webb, F. W. S , Baker, M., Weisbart, R. T. R., Bluestone, R., and Goldberg, L , *Ann Rheum. Dis* , 34, 38–42 (1975)
12 Mason, R. J., Stossel, T. P , and Vaughan, M., *J clin Invest.*, 54, 378–386 (1974).
13 Lichtenstein, L M , Gillespie, E., Bourne, H. R , and Henney, C S , *Prostaglandins*, 2, 519–528 (1972)
14 Orange, R P., Austen, W. G , and Austen, K. F , *J exp. Med.*, 134, Suppl. 136S (1971).
15 Walker, J. L., in *Advances in Biosciences*, 9 (edit. by Bergstrom, S., and Bernhard, S.), 235–240 (Pergamon Vieweg, Braunschweig, 1973)
16 Morley, J., *Prostaglandins*, 8, 315–326 (1974).
17 Morley, J., Wolstencroft, R. A , and Dumonde, D C , in *Handbook of Experimental Immunology* (edit. by Weir, D M), ch. 28 (Blackwell, Oxford 1973).

Phorbol esters stimulate DNA synthesis and ornithine decarboxylase activity in mouse epidermal cell cultures

TUMOUR-PROMOTING agents have been defined by their ability to promote tumour formation on carcinogen-initiated mouse skin. The most potent of these agents are the diesters of phorbol which are the active components of croton oil, the classic promoting substance. Phorbol esters can be chemically modified in a number of positions to form molecules with a wide range of promoter potency[1]. Such modifications have been useful in determining structure–function relationships[2]. A good correlation exists between the ability of phorbol esters to promote epidermal tumours and their ability to stimulate epidermal macromolecular synthesis *in vivo*[3,4]. In particular, all tumour promoters stimulate synthesis of epidermal DNA, although not all chemicals which induce hyperplasia are promoters[1]. Recently O'Brien *et al.*[5] suggested that the degree of induction of ornithine decarboxylase (ODC) activity in mouse skin after application of promoting and non-promoting compounds correlates well with their promoting potency. Evidence from our laboratory indicates that brief exposure to the potent phorbol ester 12-*O*-tetradecanoyl-phorbol-13-acetate (TPA), stimulates DNA synthesis and

ODC activity in mouse epidermal cell cultures (S.H.Y., T.B., E.P., D. Michael, K. Elgjo and H.H., to be published, and U.L. and S.H.Y., to be published). Using such a culture system, we have examined a series of phorbol esters to test the correlation of promoter potency *in vivo* with the stimulation of DNA synthesis and ODC activity *in vitro*.

Mouse epidermal cells were isolated and cultured as previously reported[6,7]. Phorbol esters were dissolved in DMSO as stock solutions of 1 mg ml^{-1} or 0.1 mg ml^{-1} and stored at −70 °C. Experimental media were prepared immediately before use In most experiments cells were exposed to the promoter for 1 h (except for phorbol which was kept continuously in medium), starting 20–24 h after plating. After removal of the promoter, cells were washed with phosphate-buffered saline and reincubated in complete medium (CM)[7], which was changed daily for the assay of DNA synthesis.

The dose–response curve for stimulation of DNA synthesis in cells treated with the relatively strong promoter 12-*O*-hexadecanoylphorbol-13-acetate (HPA) is shown in Fig. 1*a*. At all doses tested there was an initial inhibition of DNA synthesis at 24 h after the 1-h pulse treatment, followed by a return to near-normal or elevated levels by 2 d. The highest dose (1 μg ml^{-1}) tested gave the largest initial inhibition. By day 3 after treatment, effective doses produced a dose-dependent stimulation with a maximum usually occurring on day 4. Cells responded to doses as low as 0.05 μg ml^{-1} (8×10^{-8} M). Exposure to more than 0.5 μg ml^{-1} seemed to reduce the ultimate stimulation, perhaps because of increased initial toxicity. These results, however, were collected from experiments carried out on separate cell isolates (solid lines and dashed lines), making absolute dose–response comparisons across experiments difficult to interpret accurately. Similar studies using TPA as promoter[14] demonstrated a dose-dependent stimulation of DNA synthesis at doses between 10^{-5} and 10^{-9} M.

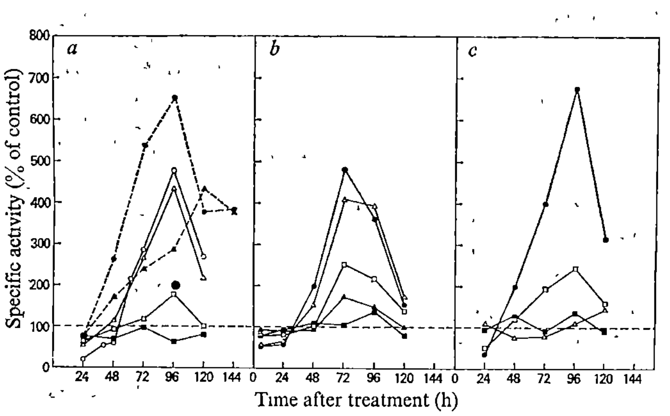

Fig. 1 Promoter-stimulated DNA synthesis. Epidermal cells were seeded at 7.5×10^6 cells per dish into 100-mm culture dishes. Twenty-four hours after plating, cultures were exposed to medium containing phorbol esters or vehicle (DMSO 0.1%) for 1 h, washed, reset with growth medium and changed daily. Concentration of the phorbol esters are given in μg per ml of culture medium. In the case of phorbol treatment (*c*), the experimental medium remained continuously, with a fresh solution prepared daily. At indicated intervals after treatment, dishes were pulsed with 1 μCi ml^{-1} methyl-^{3}H-thymidine (6 Ci mmol^{-1}, Schwarz–Mann, Orangeburg, New York) for 1 h. Labelled cells were washed three times with cold phosphate-buffered saline containing 0.1% unlabelled thymidine, scraped from the dishes, centrifuged and the pellets frozen. Pellets were washed three times with 0.2 N PCA and hydrolysed in 0.5 N PCA at 90 °C for 20 min. The DNA content of each hydrolysate was determined by the diphenylamine reaction[10] and radioactivity by counting an aliquot in Hydromix (Yorktown Research, New Hyde Park, New York) in a Beckman LS 250 scintillation counter. Results are expressed as the specific activity (c.p.m. per μg DNA) of the treated groups relative to the DMSO control. All data represent the average of at least duplicate dishes. The variation in control values for each point within experiments was less than 20%. *a*, Data collected on different primary cell isolates represented by – – –, HPA 0.5 (●) and 0.05 (▲) μg ml^{-1}; ——, HPA 1.0 (○), 0.1 (△), 0.01 (□) and 0.001 (■) μg ml^{-1}. The time course and maximum stimulation of DNA synthesis varies somewhat for different primary cell populations. *b*: ●, TPA 0.1 μg ml^{-1}; △, PDBe 1.0; ▲, PDBe 0.1; □, PDBu 1.0; ■, PDBu 0.1. *c*: ●, TPA 0.1 μg ml^{-1}; □, MeTPA 1.0; ■, MeTPA 0.1; △, phorbol 1.0.

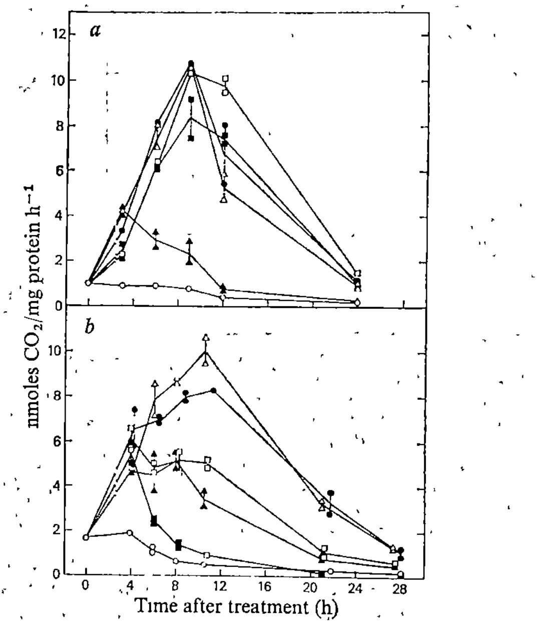

Fig. 2 Epidermal ornithine decarboxylase activity after 1-h treatment with phorbol esters. Cells were plated at 3×10^6 cells per 60-mm culture dish and treated at 21 h (*a*) and 23 h (*b*). *a*: ●, TPA 0 1 μg ml^{-1}; □, HPA 1.0; ■, HPA 0.1; △, PDBu 1.0; ▲, PDBu 0.1, ○, DMSO. *b*: ●, TPA 0.1 μg ml^{-1}; □, MeTPA 1.0; ■, MeTPA 0.1; △, PDBe 1.0; ▲, PDBe 0.1; ○, phorbol 1.0. At indicated times after the start of the treatment, duplicate dishes were washed with PBS and stored frozen until assayed. Cells were scraped from dishes and suspended in 300 μl PBS. ODC was measured on 50-μl aliquots of the cell lysate in a final volume of 100 μl containing 0.25 μmol dithiothreitol, 0.1 μmol EDTA, 0.01 μmol pyridoxal phosphate, 5.0 μmol sodium phosphate, *p*H 7.2 and 0.1 μCi L-1-^{14}C-ornithine (2.3 mCi mmol^{-1}, diluted from DL-1-^{14}C-ornithine HCl, New England Nuclear, Boston, Massachusetts, 54 mCi mmol^{-1}, with non-radioactive L-ornithine). The incubation was carried our for 1 h at 37 °C in 17 × 100-mm Falcon culture tubes capped with serum stoppers equipped with polypropylene centre wells (Kontes Glass Co., Vineland, New Jersey) containing a filter paper wick. The reaction was stopped with 0.2 ml 2 N perchloric acid and $^{14}CO_2$ was trapped by 0.2 ml NCS (Amersham/Searle Corp., Arlington Heights, Illinois) in the centre well during an additional 1-h incubation. The centre well and its content was counted in 10 ml Spectrafluor (Amersham/Searle) in toluene. Counts were corrected for blanks that contained all components except the cell lysate. Protein was measured on 50-μl aliquots of the cell lysate by the method of Lowry as detailed by Layne[11]. Each point on the graph represents the average of duplicate determinations of specific enzyme activity on cells from a single culture dish (variation <10%). In *b* the DMSO control and phorbol-treated culture values are superimposed.

When the less potent tumour-promoting phorbol esters, phorbol dibenzoate (PDBe) and phorbol dibutyrate (PDBu), are compared with TPA for ability to stimulate DNA synthesis (Fig. 1*b*), one finds that at approximately equimolar doses, PDBe and PDBu are much less effective than TPA At 0.1 μg ml^{-1} PDBu induces no stimulation, whereas PDBe stimulates only slightly. At doses 10 times higher than TPA, the stimulation with PDBe is equivalent to TPA, whereas that with PDBu is less than half of that found with TPA. Phorbol itself, a non-promoter for mouse skin, failed to stimuate even at a dose of 1 μg ml^{-1} (Fig. 1*c*). But 4-*O*-tetradecanoylphorbol-13-acetate (MeTPA), also reported to be a non-promoter for skin carcinogenesis[8], induced an initial inhibition followed by a twofold stimulation of DNA

Table 1 Correlation between potency of phorbol esters for promoting skin tumours and their ability to stimulate DNA synthesis and induce ODC activity in epidermal cells *in vitro*

Phorbol ester	Molecular weight	Tumour-promoting potency (1/TD$_{50}$)*	Maximum stimulation of DNA synthesis *in vitro*† 0.1 μg ml^{-1}	1 μg ml^{-1}	Maximum induction of ODC *in vitro*† 0.1 μg ml^{-1}	1.0 μg ml^{-1}
TPA	616.8	15.4	1.00	—	1.00	—
HPA‡	644.8	5.4	—‡	—	0.76	0.97
PDBe	572.7	<1.5§	0.19	0.82	0.55	1.3
PDBu	504.6	0.1	0.11	0.40	0.34	0.95
MeTPA	630.8	Non-promoter	0.07	0.26	0.44	0.51
PDA¶	448.5	Non-promoter	0	0	0	0
Phorbol	364.4	Non-promoter	—	0	0	0

*TD$_{50}$ = total dose (μmol) of promoter required to produce papillomas on 50% of CD-1 mice previously initiated with 51 μg 7,12-dimethylbenz(*a*)anthracene. Data for TPA, HPA, PDBe, PDA and phorbol derived from ref. 12; data for PDBu derived from ref. 13; data for MeTPA from ref. 8 and mouse strain was not identified.

†Maximum stimulation did not always occur at same time after treatment.

‡DNA synthesis after HPA and TPA was not studied simultaneously in the same cell prepartions. Since variations in absolute responses occur in different cell preparations (see Fig. 1*b* and *c*), direct comparisons between HPA and TPA cannot confidently be made. Based on experience with a number of separate experiments, TPA induces 20–30% more stimulation than HPA at approximately equimolar doses.

§Data available only for 20% tumour incidence in CD-1 mice (see ref. 9).

¶Phorbol-13,20-diacetate calculated from data reported in ref. 14 and unpublished work of S.H.Y., T.B., E.P., D. Michael, K. Elgjo and H.H.

Tumour-promoting potency was assigned as indicated from appropriate literature citation. Capacity to stimulate DNA synthesis and induce ODC activity was measured using data in Figs 1 and 2, or as otherwise noted. Comparisons were made only with data from experiments performed on the same primary cell isolate. For both indices the maximum level of stimulation induced by TPA after subtraction of vehicle control levels, was assigned a value of 1.00. Other compounds are presented as the ratio of their net values (maximum stimulation minus vehicle control) to that of TPA. Repeated experiments indicate that the absolute ratios presented would vary from experiment to experiment, but the relative rankings would be constant.

synthesis at a dose of 1 μg ml^{-1} (Fig. 1*c*). At 0.1 μg ml^{-1} it was ineffective. This compound has also been reported to inhibit replicative and repair DNA synthesis in human fibroblast cultures at doses greater than 1 μg ml^{-1} (ref. 8).

Induction of ornithine decarboxylase activity has been proposed as a marker for promoter activity *in vivo*[5] and *in vitro* (our unpublished work). The results in Fig. 2 demonstrate the relative effectiveness with which a series of phorbol esters induce ODC in epidermal cells *in vitro*. At a dose of 0.1 μg ml^{-1}, TPA induces a 5–10-fold rise in activity within 6–12 h of exposure, with a return to near-normal values by 24–28 h. The time course and maximum level of stimulated enzyme activity varies somewhat for different primary cell populations. As seen for stimulation of DNA synthesis, HPA (1 μg ml^{-1} and 0.1 μg ml^{-1}), PDBu (1 μg ml^{-1}) and PDBe (1 μg ml^{-1}) induced a similar rise in ODC activity, whereas PDBu (0.1 μg ml^{-1}), PDBe (0.1 μg ml^{-1}) and MeTPA (1 μg ml^{-1}) were less effective as inducers. Phorbol (1 μg ml^{-1}), phorbol-13,20-diacetate (1 μg ml^{-1}, not shown) and the DMSO vehicle were completely ineffective in inducing ODC. The lower dose of MeTPA (0.1 μg ml^{-1}) caused a transient early rise in activity which returned to control values by 8 h. The accelerated kinetics of induction and decay seen with 0.1 μg ml^{-1} MeTPA and PDBu were at doses which failed to stimulate DNA synthesis; the significance of this observation remains to be determined.

These results indicate that there is a good correlation between the potency of phorbol esters for promoting skin tumours *in vivo* and their ability to stimulate DNA synthesis and induce ODC activity in epidermal cells *in vitro* (Table 1). The molecular weights of all compounds other than HPA and MeTPA are lower than that of TPA. Therefore the molar concentrations at which they were tested exceeded the TPA concentration. Only HPA seems to approach the effectiveness of TPA in stimulating both DNA synthesis and ODC activity at the same molar concentration. For MeTPA, results *in vitro* suggest that it has biological activity and should be retested as a promoter *in vivo*, preferably on mice sensitive to formation of skin tumours[9], before it is accepted as a negative control for TPA. Although promoter and non-promoter compounds outside the phorbol family must be tested before more general conclusions are reached, mouse epidermal cell cultures seem to be a useful system for identifying and appraising potential promoting agents. Additionally, the similarity between *in vivo* and *in vitro* results indicates that this model should be useful for investigating the cellular mechanisms of promoter action and for studying two-stage carcinogenesis *in vitro*.

STUART H. YUSPA
ULRIKE LICHTI
THERESA BEN
ELROY PATTERSON
HENRY HENNINGS

Experimental Pathology Branch,
Division Cancer Cause and Prevention,
National Cancer Institute,
Bethesda, Maryland 20014

THOMAS J. SLAGA

Oak Ridge National Laboratory,
Oak Ridge, Tennessee

NANCY COLBURN
WILLIAM KELSEY

University of Michigan,
Ann Arbor, Michigan

Received April 19, accepted May 25, 1976

1 Boutwell, R. K., *CRC Crit. Rev. in Toxicol*, 419–443 (1974).
2 Hecker, E., and Schmidt, R., *Fortschr Chem. org. NatStoffe*, 31, 377–467 (1974).
3 Baird, W. M., Sedgwick, J. A., and Boutwell, R. K., *Cancer Res.*, 31, 1434–1439 (1971).
4 Baird, W. M., Melera, P. W., and Boutwell, R. K., *Cancer Res.*, 32, 781–788 (1972).
5 O'Brien, T. G., Simsiman, R. C., and Boutwell, R. K., *Cancer Res.*, 35, 2426–2433 (1975).
6 Yuspa, S. H., and Harris, C. C., *Expl Cell Res.*, 86, 95–105 (1974).
7 Yuspa, S. H., Hennings, H., Dermer, P., and Michael, D., *Cancer Res.*, 36, 947–951 (1976).
8 Langenbach, R., and Kuszynski, C., *J natn. Cancer Inst.*, 55, 801–802 (1975).
9 Baird, W. M., and Boutwell, R. K., *Cancer Res.*, 31, 1074–1079 (1971).
10 Burton, K., *Biochem. J*, 62, 315–333 (1956).
11 Layne, E., in *Methods in Enzymology*, III (edit. by Colowick, S. P., and Kaplan, N. O.), 448–450 (Academic, New York, 1957).
12 Slaga, T. J., Scribner, J. D., Thompson, S., and Viaje, A., *J. natn. Cancer Inst* (in the press).
13 Scribner, J. D., and Boutwell, R. K., *Eur. J. Cancer*, 8, 617–621 (1972).
14 Lichti, U., and Yuspa, S. H., *Proc Am. Ass. Cancer Res, Abstr.*, 17, 138 (1976).

Intracellular messenger role of cyclic GMP in exocrine pancreas

THE response of cells to hormones and neurotransmitters is mediated by chemical regulators, of which calcium, adenosine cyclic 3′,5′-monophosphate (cyclic AMP) and guanosine cyclic 3′,5′-monophosphate (cyclic GMP) are considered to be of primary importance. The endogenous occurrence of

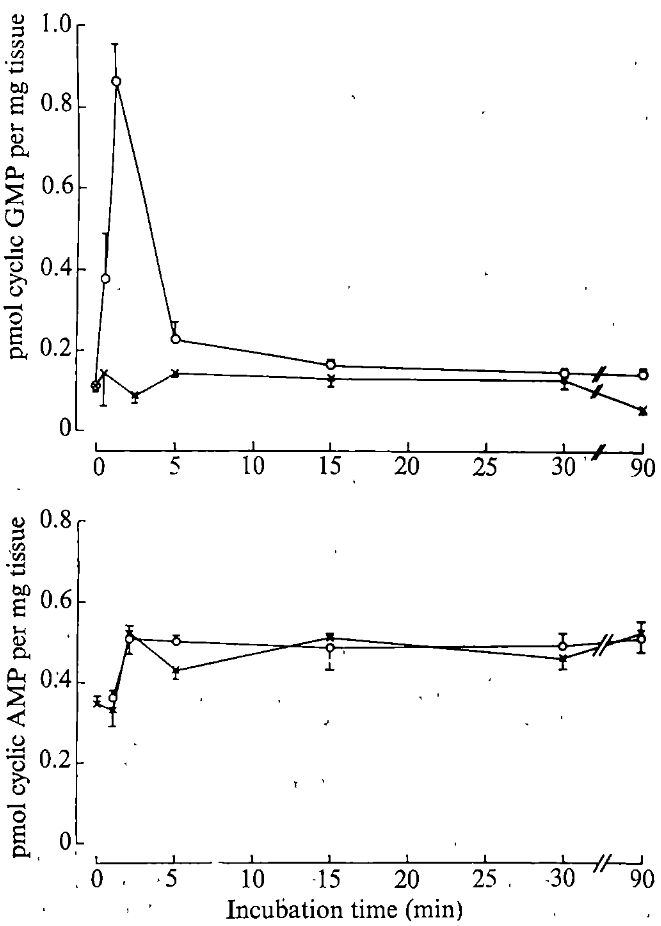

Fig. 1 Time course of cyclic GMP and cyclic AMP levels in isolated guinea pig pancreatic slices produced by CCK (1 U ml^{-1}; GIH preparation). Pooled pancreatic slices were initially incubated for 15 min. Three or four slices of total weight between 80–110 mg were then incubated in individual Erhlenmeyer flasks containing 2 ml of Krebs–Ringer bicarbonate buffer with 0.5% bovine serum albumin. Each flask was gassed with 95% O_2–5% CO_2. After preincubation for 15 min, CCK was added to the flask. On completion of incubation the slices were removed and frozen in an aluminium clamp precooled in liquid nitrogen. The frozen tissue was dropped into 0.5 ml of 6 mM theophylline at 100 °C and boiled for 10 min. The denatured tissue slices were homogenised fully. The homogenate was stored overnight at −20 °C, after addition of 0.5 ml of acid ethanol (1% HCl in absolute ethanol). The samples were centrifuged at 1,500g for 5 min and the supernatants were decanted. Each precipitate was washed with 0.5 ml of acid alcohol and, after respinning, the corresponding supernatants were pooled. The extracts were taken to dryness at 50 °C and the dried residue was resuspended in 0.5 ml of 50 mM Tris-HCl buffer, pH 7.4. Samples of 50 µl were used for measuring cyclic GMP and cyclic AMP. Cyclic AMP was measured by a binding protein method[6,7]. Cyclic GMP values were determined using a rabbit antiserum (HO/2/75) raised to succinylated cyclic GMP conjugated to human serum albumin[8]. A sample of 100 µl of antiserum diluted 1:1,000 in Tris buffer (50 mM, pH 7.4), 50 µl of tritiated cyclic GMP, specific activity 21 Ci mmol^{-1}, containing 3 nCi of ^{3}H-cyclic GMP, and 50 µl of cyclic GMP standards (0–3 pmol), or unknown samples, were incubated at 4 °C for 12 h. Free and antibody-bound ^{3}H-cyclic GMP were separated by filtration through a 0.45-µm Millipore filter. Filters were then extracted in a toluene–methoxyethanol-based scintillant, and the antibody-bound ^{3}H-cyclic GMP was measured in a liquid scintillation spectrometer. Cyclic AMP in a concentration of 1 pmol ml^{-1} showed a cross reaction in the assay of less than 0.2%, and other cyclic nucleotides less than 0.01%. Nucleotides, and nucleotide monophosphates, diphosphates and triphosphates, showed virtually no cross reaction up to a concentration of 10^4 pmol ml^{-1}. Dilutions of pancreatic cyclic GMP showed parallelism with dilutions of standard cyclic GMP. As a further check that the immunoreactive material was identical with cyclic GMP, control pancreatic slices and slices stimulated with acetylcholine were extracted using the standard trichloroacetic acid procedure. The extracts were then divided and one portion of each was treated with 50 µl of beef heart cyclic nucleotide phosphodiesterase (Sigma), at a concentration of 1 mg ml^{-1}, for 60 min at 37 °C and then boiled for 4 min. Standard cyclic GMP was treated similarly. The immunoreactive cyclic GMP in the control and stimulated samples were destroyed to the same extent as the standard cyclic GMP. Each experimental point represents the mean of three incubations. The tissue cyclic nucleotide content of each incubation sample was measured in triplicate The cyclic nucleotide values are calculated as pmol of cyclic nucleotide per mg wet weight pancreatic tissue. The vertical bars indicate 1 s.e.m. a, Cyclic GMP levels; b, cyclic GMP levels; × control; ○, CCK (1 U ml^{-1}).

cyclic GMP was discovered more than 10 yr ago, but until recently its formation has been reported chiefly in association with the activation of cholinergic muscarinic receptors[1,2]. The description in the pancreas of a cyclic GMP-dependent protein kinase[3], a cyclic GMP phosphodiesterase[4], and the ability *in vivo* of cholecystokinin to increase cyclic GMP levels[5], suggested a physiological role for cyclic GMP in the mediation of hormone action. We report here experiments on isolated guinea pig pancreatic slices, in which the hormone cholecystokinin (CCK) and the neurotransmitter acetylcholine (ACh) both produced a marked, transient increase in the tissue level of cyclic GMP, which preceded the release of secretory enzymes. Exposure of the isolated pancreatic slices to the hormone secretin evoked a more prolonged increase in cyclic AMP, without any significant effect on cyclic GMP.

CCK (GIH Research Unit, Karolinska Institute), highly purified CCK (given by Professor Viktor Mutt), and the synthetic C-terminal octapeptide of CCK (given by Dr Miguel Ondetti, Squibb Institute), all produced within seconds a rapid increase in cyclic GMP that reached peak values at 2 min and fell rapidly to near the control level by 5 min (Fig. 1). The increase in cyclic GMP preceded any significant acceleration in the release of zymogens (Fig. 2). ACh evoked a pattern of increase in cyclic GMP that was similar to that obtained with CCK with regard to time course and relationship to onset of enzyme release. The increase in cyclic GMP triggered by ACh (10^{-7}–10^{-3} M) and CCK (5×10^{-8}–1×10^{-7} M) was dose related. Atropine abolished the ACh-mediated zymogen release and increase

Fig. 2 Stimulation of enzyme secretion from isolated guinea pig pancreatic slices by CCK. Tissue was incubated as described for Fig. 1. The esterase activity of the kallikrein-trypsin-like proteases released into the medium was determined by hydrolysis of the synthetic substrate, benzoyl-l-arginine-ethyl ester (BAEE), after activation of the proenzymes by enterokinase. A sample 0.5 ml of enzyme solution was incubated with 0.1 ml enterokinase (50 µg) for 10 min at 37 °C before assay. The accumulated proenzyme activity is expressed as BAEE ΔE_{386} U per mg wet weight tissue, with 1 U equivalent to an absorbance change recorded as absorbance units per min per ml of enzyme solution × 10^6. Vertical bars indicate 1 s.e.m. ×, Control; ○, CCK (GIH, 1 U ml^{-1}); ▲, secretin (GIH, 1 U ml^{-1}).

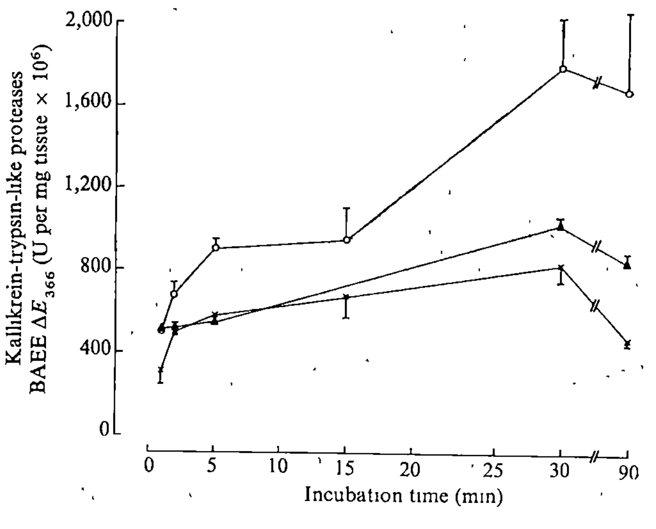

in the tissue level of cyclic GMP (Fig. 3), but did not affect the CCK response. Both ACh and CCK failed to alter significantly the basal cyclic AMP values in actively secreting pancreatic slices. In the presence of the phosphodiesterase inhibitors, theophylline (3 mM) and 3-isobutyl-1-methylxanthine (IBMX, 0.5 mM), basal levels of cyclic AMP were increased about fivefold, but no further increase was observed with CCK. In contrast, the basal levels of cyclic GMP were increased to a lesser extent (about twofold) by theophylline and IBMX and the increase in cyclic GMP caused by CCK was potentiated. In three separate experiments, the synthetic analogue 8-bromo cyclic GMP (1 mM) increased enzyme secretion over control values by 27.5% ($P<0.025$) in pancreatic slices incubated for 30 min.

Secretin, in the presence of trasylol (260 U ml^{-1}), produced a rapid increase in cyclic AMP that reached a maximum at 1 min but remained elevated for at least 30 min and returned to basal values at 90 min (Fig. 4). Secretin did not significantly alter cyclic GMP levels, even in the presence of theophylline (3 mM) and trasylol (260 U ml^{-1}).

Enzyme secretion from pancreatic exocrine acinar cells is stimulated by CCK and the vagus nerve (ACh). Activation by CCK and ACh of specific receptors on the plasma membrane of acinar cells results in a rapid, marked, but transient increase in cyclic GMP. This may trigger the intracellular mobilisation of ionised calcium, which is considered to initiate the release of zymogens from acinar cells. Alternatively, it is possible that the increase in cyclic GMP results from, rather than precedes, the changes in intracellular calcium. The difference in the time courses of cyclic GMP and the accumulated enzyme secretion may be explained by the fact that the transient increase in cyclic GMP, through activation of a cyclic GMP-dependent protein kinase[3], may trigger intracellular release of ionised calcium which then stimulates the enzyme secretion; this response once initiated may be maintained by regenerative release of calcium or by some other molecular mechanism. The secretion of electrolytes and water that accompanies enzyme release is primarily controlled by the hormone secretin. The interaction of secretin with cell receptors activates adenylate cyclase[10], resulting in increased formation of cyclic AMP. The sequential molecular events through which cyclic nucleotides stimulate enzyme and electrolyte secretion are still obscure. Our results strongly suggest that in the exocrine pancreas each of the two major physiological functions is modulated by a specific cyclic nucleotide, enzyme secretion by cyclic GMP, and fluid and ion secretion by cyclic AMP. Dysfunction of the molecular mechanisms involved in the turnover of the two messengers may be of considerable importance in the aetiology of pancreatic disease.

Fig. 3 Histogram of the effect of atropine on the increase in cyclic GMP and enzyme secretion evoked by acetylcholine. Isolated pancreatic slices were incubated in Ehrlenmeyer flasks as described in Fig. 1. Atropine (10^{-6} M) was added to the appropriate Krebs–Ringer buffer solution at the beginning of the 15 min of preincubation. Open columns, control; diagonally hatched columns, acetylcholine (10^{-6} M); vertically hatched columns, atropine (10^{-6} M); closed columns, atropine (10^{-6} M) + acetylcholine (10^{-6} M). The vertical bars represent 1 s.e.m. *a*, Cyclic GMP content of pancreatic slices after 1 min of incubation with drug, expressed as pmol per mg wet weight tissue. *b*, Accumulated release of kallikrein-trypsin zymogens after 30 min into the incubation medium, expressed as BAEE ΔE_{366} units per mg wet weight of tissue, 1 U being equivalent to an absorbance change recorded as absorbance units per min per ml of enzyme solution × 10^6.

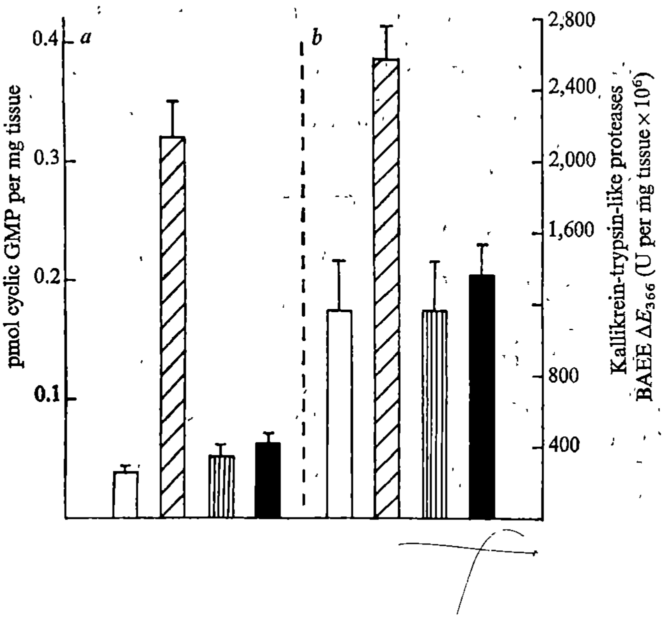

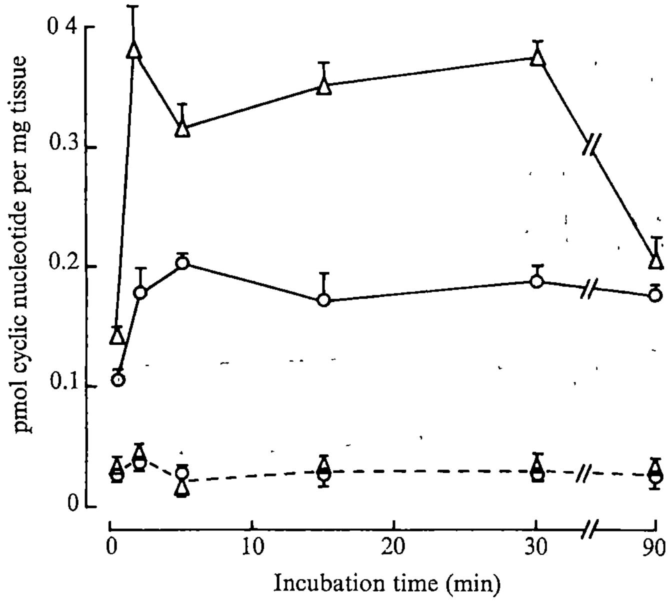

Fig. 4 Time course of cyclic AMP and cyclic GMP formation in guinea pig pancreatic slices after addition of secretin. Tissue incubation and cyclic nucleotide measurement were as described in Fig. 1, except that the Krebs–Ringer buffer solution contained trasylol (260 U ml^{-1}). Levels of cyclic nucleotides are expressed as pmol per mg wet weight. The vertical bars represent 1 s.e.m. ○, Control; △, secretin (1 U ml^{-1}); ——, cyclic AMP; - - -, cyclic GMP.

This research was supported by grants from the Wellcome Trust and the MRC.

JANET ALBANO
Departments of Pharmacology and Medicine,

K. D. BHOOLA
Department of Pharmacology,

R. F. HARVEY

Department of Medicine,
The Medical School,
University of Bristol,
University Walk,
Bristol BS8 1TD, UK

Received January 17, accepted June 1, 1976.

[1] George, W. J., Polson, J B., O'Toole, A G., and Goldberg, N. D., *Proc. natn. Acad. Sci. U.S.A*, **66**, 398–403 (1970).
[2] Schultz, G., and Hardman, J. G., *Adv Cyclic Nucleotide Res.*, **5**, 339–352 (1975).
[3] Van-Leemput-Coutrez, N., Camus, J, and Christophe, J, *Biochem. biophys. Res. Commun.*, **54**, 182–190 (1973).
[4] Robberecht, P., Deschodt-Lanckman, M., De Neef, P., and Christophe, J., *Eur J. Biochem.*, **41**, 585–591 (1974).
[5] Robberecht, P., Deschodt-Lanckman, M., De Neef, P., Borgeat, P., and Christope, J, *FEBS Lett.*, **43**, 129–142 (1974).
[6] Brown, B L, Albano, J D. M., Ekins, R. P, Sgherzi, A. M., and Tampion, W., *Biochem J.*, **121**, 561–562 (1971).
[7] Albano, J. D. M, Barnes, G. D., Maudsley, D V., Brown, B. L, and Ekins, R P, *Analyt Biochem.*, **60**, 130–141 (1974).
[8] Steiner, A L., Parker, C. W., and Kipnis, D M., *J. biol. Chem*, **247**, 1106–1113 (1972)
[9] Bhoola, K. D., Dorey, G, and Jones, C. W., *J. Physiol., Lond*, **235**, 503–522 (1973).
[10] Lemon, M. J. C., and Bhoola, K. D., *Biochim. biophys. Acta*, **385**, 101–113 (1975).

Role of oestrogen receptor in androgen-induced sexual differentiation of the brain

THE sexual differentiation of gonadotropin secretion[1] and female sexual behaviour[2] occurs in the rat hypothalamus[5] during the early postnatal period and is produced by testicular androgen in the male, although it may be mimicked in the female by administration of oestrogen or androgen[3]. The mechanism of this neural differentiation probably involves the aromatisation of testicular androgen to oestrogen in the hypothalamus[4], followed by a complex series of biochemical events contingent on the binding of this oestrogen to a receptor and the translocation of the steroid–receptor complex to the nucleus. Cytosol oestrogen receptors[6–8] and aromatising enzymes[4] have been demonstrated in the neonatal brain; aromatising enzymes are localised to the differentiating areas[4] whereas oestrogen receptors are found throughout the forebrain[6,7]. In the study reported here, we have measured the nuclear oestrogen receptor in the neonatal brain using a nuclear exchange assay[9] and have found that its distribution is consistent with the postulated role of the oestrogen receptor in the sexual differentiation of the brain.

Two regions of the 4-d-old brain were used, one containing the ventral half (HYP) and the other the dorsal half (CORT) of all brain between two coronal cuts, one immediately rostral to the optic chiasma and the other immediately caudal to the mammillary bodies.

Figure 1 shows the exchange of ^{3}H-oestradiol in purified nuclei prepared from the HYP region of neonatal males. Saturable, diethylstilboestrol (DES)-suppressible, exchanged ^{3}H-oestradiol was found in nuclei from the neonatal male HYP region with a K_d of 3.4×10^{-10} M, a value typical of oestrogen receptors[13] and close to the K_d for oestradiol of the cytosol oestrogen receptor from neonatal rat brain[6].

Table 1 shows that 2.4×10^9 sites per mg of DNA were found in the neonatal HYP region, but none in the male CORT region or either region of the female brain. To test the hypothesis that the steroid responsible for the nuclear translocation of the oestrogen receptor in the male hypothalamus was secreted by the testis, nuclear sites were assayed in male rats 24 h after castration on day 3. No sites were detectable in either brain region of these animals. We then measured nuclear oestrogen receptor in females injected systemically with 50 μg of testosterone. This gave an identical distribution of nuclear receptor to that seen in the neonatal male but with about three times the number of sites found in the male HYP region (Table 1).

Thus nuclear oestrogen receptor sites appear solely in the HYP region under the influence of the testis or exogenous testosterone and this is consistent with their organising effect on the neonatal hypothalamus being exerted through the oestrogen receptor. These findings substantiate our previous study in which nuclear binding was measured after injection of radioactive steroid[14]. The low affinity of testosterone for the neonatal brain oestrogen receptor[6] and various studies on aromatisation in the neonatal brain[4,15] suggest that obligatory aromatisation precedes the binding of testosterone to the oestrogen receptor.

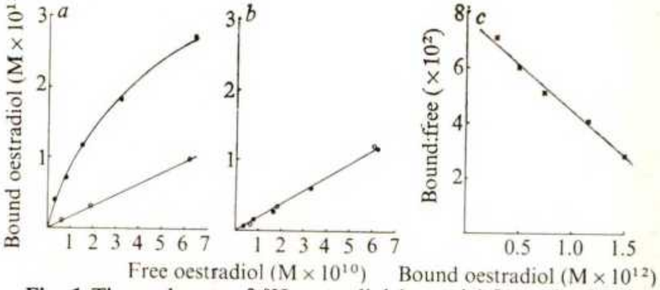

Fig. 1 The exchange of ^{3}H-oestradiol in nuclei from the HYP region (*a*) and CORT region (*b*) of 4-d-old male rats. Purified nuclei were prepared by the method of Plapinger and McEwen[12] and samples (about 200 μg of DNA), suspended in 0.4 ml buffer (1 mM phosphate, 0.32 M sucrose, 3 mM $MgCl_2$, *p*H 6.5) were incubated with various concentrations of ^{3}H-oestradiol (95 Ci mmol^{-1}) for 1 h at 37 °C as described by Anderson *et al.*[9]. A separate series of tubes was incubated in the presence of a 200-fold molar excess of DES for the determination of nonspecifically bound ^{3}H-oestradiol. After incubation, the nuclei were washed four times by sedimentation (800*g* for 10 min) and resuspension for 25 min at 0°–2 °C in 1 ml of fresh buffer. Radioactivity in the washed nuclei was measured, with an efficiency of 50%, after overnight extraction into 10 ml of scintillant (PPO 4 g l^{-1}; POPOP, 0.1 g l^{-1} in toluene). Specific binding was determined by subtraction of nonspecifically bound ^{3}H-oestradiol (○) from total bound ^{3}H-oestradiol (●) and plotted according to Scatchard[10] (*c*, male HYP region only), to give the dissociation constant (K_d) and number of specific binding sites (N_s). Samples of nuclei were analysed for DNA by the method of Burton[11].

After intracerebral injection of 0.27 μg of DES, nuclear oestrogen receptor was found in similar amounts in the HYP and CORT regions of both male and female brain (Table 1). The number of sites was four to five times that in the male HYP region and we find this is the maximum number of sites obtainable by intracerebral injection of DES. The distribution of nuclear oestrogen receptor after intracerebral injection of DES is identical to that of the cytosol receptor in the untreated animal, that is, it is found throughout the forebrain[6,7]. This is in marked contrast to the distribution of nuclear receptor after testosterone injection which mirrors the localisation of the aromatase enzymes, that is, nuclear receptor is found only in the HYP region. Thus there seems to be no inherent difference between the HYP and CORT receptors except in their proximity to aromatising enzymes. Cortical receptors are translocated to the nucleus when exposed to oestrogen and so may be important in some undefined aspect of brain development occurring when oestrogen levels are high, for example, prenatally or around day 10 of life in the female[16].

It is probable, from the lack of nuclear oestrogen receptor in the CORT region of the untreated male and both regions of

Table 1 Distribution and dissociation constant of nuclear-bound oestrogen receptor in purified nuclei from brain of untreated and steroid-injected 4-d-old rats

	HYP		CORT	
	N_s per mg DNA($\times 10^{-9}$)	$K_d \times 10^{10}$(M)	N_s per mg DNA($\times 10^{-9}$)	$K_d \times 10^{10}$(M)
4-d-old male	2.40±0.15	3.41±0.30	*	*
4-d-old male, castrated day 3	*	*	*	*
4-d-old female	*	*	*	*
4-d-old female 3 h after 50 μg testosterone subcutaneously in oil (50 μl)	7.20±0.46	2.01±0.37	*	*
4-d-old female 1 h after 0.27 μg DES intracerebrally in saline (10 μl)	8.78±0.90	3.52±0.37	8.95±0.38	4.27±0.95
4-d-old male 1 h after 0.27 μg DES intracerebrally in saline (10 μl)	12.05±2.66	4.66±0.53	11.94±2.25	4.57±0.53

Number of sites (N_s) and dissociation constant (K_d) were obtained as described in Fig. 1.
*Undetectable.

the untreated female and castrate male, that no receptor has been translocated by circulating oestrogen. This is consistent with there being very little oestrogen circulating in the 4-d animal[16], and any oestrogen present being sequestered by low affinity binding proteins of the blood and brain[17]. We believe that measurement of the nuclear receptor is likely to show where a steroid is acting, in contrast to the measurement of the cytosol receptor which merely shows where a steroid has the potential to act. In addition, we show that target tissue metabolism of a steroid may restrict nuclear translocation to a subset within a population of receptors, thereby restricting the action of the steroid to a few cells of a target organ though many may contain the receptor; this may be of relevance to other steroid sensitive tissues.

In conclusion, the distribution of the nuclear oestrogen receptor contrasts markedly with that of the cytosol receptor in the neonatal brain and is entirely consistent with the postulated roles of the oestrogen receptor and aromatisation in the androgen-induced sexual differentiation of the brain.

B. R. Westley
D. F. Salaman

Department of Anatomy,
Medical School,
University of Bristol,
Bristol BS8 1TD, UK

Received May 3; accepted June 16, 1976.

[1] Harris, G. W., *Endocrinology*, **75**, 627–648 (1964).
[2] Beach, F. A., in *Biopsychology of Development* (edit. by Tobach, E., Aronson, L. R., and Shaw, E.), 249–296 (Academic, New York, 1971).
[3] Gorski, R. A., in *Frontiers in Neuroendocrinology* (edit. by Martini, L., and Ganong, W. F.), 237–290 (Oxford University Press, New York, 1971).
[4] Reddy, V. V. R., Naftolin, F., and Ryan, K. J., *Endocrinology*, **94**, 117–121 (1974).
[5] Barraclough, C. A., and Gorski, R. A., *Endocrinology*, **68**, 68–79 (1961).
[6] Barley, J., Ginsburg, M., Greenstein, B. D., McLusky, N. J., and Thomas, P. J., *Nature*, **252**, 259–260 (1974).
[7] Salaman, D. F., Thomas, P. J., and Westley, B. R., *Ann. Biol. biochem. biophys.* (in the press).
[8] Fox, T. O., *Nature*, **258**, 441–444 (1975).
[9] Anderson, J., Clark, J. H., and Peck, E. J., Jr, *Biochem. J.*, **126**, 561–567 (1972).
[10] Scatchard, G., *Ann. N.Y. Acad. Sci.*, **51**, 660–672 (1949).
[11] Burton, K., *Biochem. J.*, **62**, 315–323 (1956).
[12] Plapinger, L., and McEwen, B. S., *Endocrinology*, **93**, 1119–1128 (1973).
[13] Jensen, E. V., and Desombre, E. R., *A. Rev. Biochem.*, **41**, 203–230 (1972).
[14] Westley, B. R., and Salaman, D. F., *Brain Res.* (in the press).
[15] Lieberburg, I., and McEwen, B. S., *Brain Res.*, **85**, 165–170 (1975).
[16] Meijs-Roelofs, H. M. A., Uilenbroek, J. T. J., De Jong, F. H., and Welschen, R., *J. Endocr.*, **59**, 295–304 (1973).
[17] McEwen, B. S., Plapinger, L., Chaptal, C., Gerlach, J., and Wallach, G., *Brain Res.*, **96**, 400–406 (1975).

2-Amino-4-phosphonobutyric acid as a glutamate antagonist on locust muscle

THE characterisation of glutamate receptors in nerve and muscle membranes requires compounds which interact specifically with these receptors. In the vertebrate central nervous system various substances are reported to act as agonists or antagonists of glutamate (reviewed in refs 1 and 2). At the locust and crustacean nerve–muscle junctions, where the receptors are readily accessible for biochemical and pharmacological characterisation, comparatively few compounds activate the glutamate-sensitive receptors or antagonise the excitatory action of glutamate[3–9] and so such substances are needed. We report here that the glutamate analogue, DL-2-amino-4-phosphonobuytyric acid (DL-APB) (Fig. 1), inhibits the binding of glutamate to 'receptor-like' hydrophobic proteolipids isolated from locust muscle[10,11] and antagonises the excitatory action of glutamate applied iontophoretically to receptors present in the locust muscle membrane. The shape and charge distribution of DL-APB are appropriate for interaction with glutamate receptors[2,7,12].

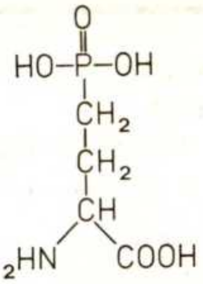

Fig. 1 2-Amino-4-phosphonobutyric acid.

Proteolipids were extracted from approximately 2 g of the total intrathoracic muscle of locusts (*Schistocerca gregaria*)[10]. U-^{14}C-L-glutamate (Amersham) was added to the proteolipid preparations which were then incubated at room temperature for 20 min before chromatography on a column (20×2 cm) of Sephadex LH 20 equilibrated with chloroform[10]. The effect of DL-APB (Calbiochem) on the binding of glutamate was measured by preincubating the proteolipid with DL-APB for 1 h before addition of U-^{14}C-glutamate[11]. Electrophysiological experiments were made on the extensor tibiae muscle, where junctional glutamate receptors are accessible to drugs applied iontophoretically[13]. Double and multi-barrel micropipettes of high resistance (200–300 MΩ)[13,14], with braking currents of 4×10^{8}–6×10^{-9} A were used to apply L-glutamate (Na salt, 0.1 M, *p*H 8) and DL-APB (Na salt, 0.1 M, *p*H 7) to glutamate receptors in the muscle membrane. In some experiments drugs were applied from two separate micropipettes, to exclude the possibility that interaction between barrels of the micropipette was affecting the observations.

Experiments on isolated proteolipids were made over a range of glutamate concentrations from 3.7×10^{-6} M to 1.0×10^{-4} M. Glutamate binding to the proteolipid was obtained by measuring the amount of glutamate associated with the peak of proteolipid eluted with chloroform[10,11]. Saturation of binding occurred between 6.6×10^{-5} and 1.0×10^{-4} M when 7.25 nmol glutamate per mg proteolipid were bound. The dissociation constant, K_d, of the binding site was 8×10^{-6} M. The effect of DL-APB on the binding of glutamate to the proteolipid was measured over a range of glutamate concentrations (3.7×10^{-6}–3.8×10^{-5} M) and over a range of DL-APB concentrations (1.0×10^{-5}–5.1×10^{-5} M). Lineweaver–Burke and Dixon plots revealed that DL-APB behaves as a competitive inhibitor of glutamate binding with an apparent dissociation constant, K_d, of 6.6×10^{-5} M.

The iontophoretic application of glutamate to junctional glutamate receptors resulted in a rapid and transient depolarisation with a slower time course than the excitatory junction potential produced by nerve stimulation. The iontophoretic application of DL-APB from the adjacent barrel to junctional glutamate receptors produced no detect-

Fig. 2 Time course of the inhibitory action of DL-APB on the junctional response to glutamate. The drugs are applied iontophoretically to junctional glutamate receptors from adjacent barrels of a twin-barrelled micropipette. Five superimposed traces are shown and on each, a single pulse of DL-APB precedes a smaller pulse of glutamate. As the interval between the DL-APB pulse and the glutamate pulse is increased, the junctional response to glutamate increases, that is, the inhibitory action of DL-APB decreases. The current passing through each barrel of the micropipette is monitored on the lower trace. 15 nC calibration refers to DL-APB which is the first pulse on the lower trace.

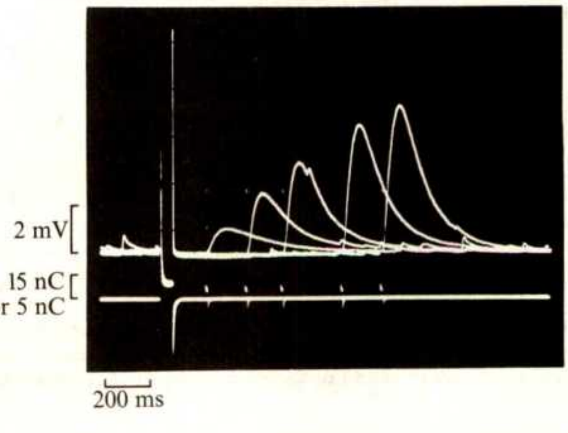

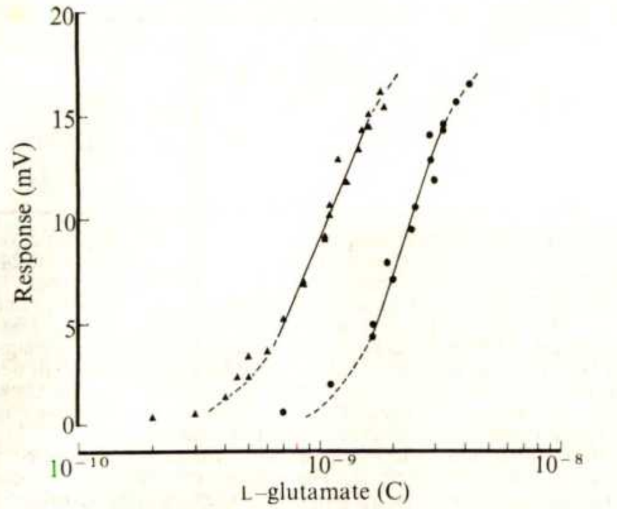

Fig. 3 Log dose–response curves illustrating the effect of locally applied glutamate alone (▲) and in the presence of DL-APB (●). The drugs were applied iontophoretically to junctional glutamate receptors from adjacent barrels of a twin-barrelled micropipette. In the right-hand curve, pulses of glutamate were applied in the presence of a constant pulse of DL-APB. Ordinate, amplitude of the junctional depolarising response to glutamate; abscissa, logarithmic scale of current (in C) passing through the glutamate barrel of the micropipette.

able response. When a pulse of DL-APB was applied to the junction during a steady glutamate application, however, the glutamate depolarisation was rapidly reduced and then recovered to the original depolarised level.

In most experiments a single pulse (40 ms) of DL-APB was followed by a single pulse (10 ms) of glutamate. Sufficient time was then allowed for complete recovery of receptors before again applying a single pulse of each drug. This precaution eliminated possible desensitisation effects. When glutamate application followed DL-APB application by a sufficiently short interval, the response to glutamate was absent or greatly diminished (Fig. 2). To study the time course of action of DL-APB the interval between single pulses of the two drugs was varied. The time constant of decay of DL-APB action (~400–500 ms) is approximately one third that of (+)-tubocurarine action at the frog endplate[16]. The difference in time constants may represent a difference in the dissociation rate of the drug receptor complexes or in the speed of diffusion of the drugs away from the receptors.

The degree of interaction between glutamate and DL-APB varied depending on the dose of the two drugs (measured in nC), so for a constant dose of DL-APB the inhibition of the response to glutamate became less as the glutamate dose was increased. This may not necessarily represent competition between the agonist and the antagonist, because the time constant of dissociation of DL-APB from receptors is much longer than the rapid rise of the glutamate depolarisation, during which time dissociation would need to occur. In addition, larger doses of glutamate can be expected to reach more distant receptors[15,17,18] which may be less affected by DL-APB.

To determine whether these two drugs were interacting in a competitive or non-competitive manner, dose–response curves were obtained for glutamate both in the presence and absence of a constant DL-APB pulse (Fig. 3). Problems arose from rapid decay of DL-APB action and the need to have a constant amount of inhibitor present over a larger area than was reached by glutamate. These were overcome by applying a short glutamate pulse (10 ms) at a fixed time during a much longer DL-APB pulse (500 ms). The dose–response curves for glutamate in the presence of DL-APB showed a parallel shift to the right, consistent with the concept of a competitive antagonism between the DL-APB and glutamate molecules, for the glutamate receptor, although the possibility of a postsynaptic action of the DL-APB molecule at a level other than the glutamate receptor, cannot be discounted.

The junctional response to iontophoretically applied glutamate was not markedly inhibited by the application of DL-APB (5×10^{-4} M) in the bathing medium. Similarly miniature excitatory junctional potentials, which result from spontaneous release of transmitter packets, were unaltered. The apparent difference in effectiveness when DL-APB is applied iontophoretically may well reflect a difference in the concentration of drug reaching the receptors. Previous studies, however, have also shown that relatively high concentrations of substances, which specifically block the postsynaptic action of glutamate, may be required to produce antagonism of glutamate[3,4].

Both the biochemical and electrophysiological findings support the suggestion that DL-APB acts as a glutamate antagonist at the insect myoneural junction. It is hoped that the drug will prove to be a useful tool in the investigation of the nature and mode of action of the postsynaptic glutamate receptor.

S.G.C.-C. held a Royal Society European Science Exchange Programme Fellowship and thanks Professor S. Thesleff for his hospitality and encouragement. R.W.J. is in receipt of an SRC/CAPS award in conjunction with Shell Research Limited.

S. G. CULL-CANDY*

Institute of Pharmacology,
University of Lund,
Lund, Sweden

J. F. DONNELLAN

Shell Biosciences Laboratory,
Shell Research Limited,
Sittingbourne, Kent ME9 8AG, UK

R. W. JAMES
G. G. LUNT

Department of Biochemistry,
Bath University,
Bath BA2 7AY, UK

Received October 27, 1975; accepted June 16, 1976.

*Present address: Department of Biophysics, University College London, Gower Street, London WC1E 6BT, UK.

1 Krnjević, K., *Physiol. Rev.*, **54**, 418–540 (1974).
2 Buu, N. T., Puil, E., and van Gelder, N. M., *Gen. Pharmac.*, 7, 5–14 (1976).
3 Lowagie, C., and Gerschenfeld, H. M., *Nature*, **248**, 533–535 (1974).
4 Clements, A. N., and May, T. E., *J. exp. Biol.*, **61**, 421–442 (1974).
5 Shinozaki, H., and Shibuya, J., *Neuropharmacology*, **13**, 665–672 (1974).
6 Lunt, G. G., in *Insect Biochemistry and Function* (edit. by Candy, D. J., and Kilby, B. A.), 283–305 (Chapman and Hall, London, 1975).
7 Usherwood, P. N. R., and Cull-Candy, S. G., in *Insect Muscle* (edit. by Usherwood, P. N. R.), 207–208 (Academic, New York and London, 1975).
8 Crawford, A. C., and McBurney, R. N., *Proc. R. Soc.*, **B192**, 481–489 (1976).
9 Anderson, C. R., Cull-Candy, S. G., and Miledi, R., *Nature*, **261**, 151–153 (1976).
10 Lunt, G. G., *Comp. gen. Pharmac.*, **4**, 75–79 (1973).
11 James, R. W., Lunt, G. G., and Donnellan, J. F., *Proc. 9th FEBS Mtg.*, 258 (Hung. Biochem. Soc., Budapest, 1974).
12 Curtis, D. R., and Watkins, J. C., *J. Neurochem*, **6**, 117–141 (1960).
13 Cull-Candy, S. G., *J. Physiol., Lond.*, **255**, 449–464 (1976).
14 Dreyer, F., and Peper, K., *Pflugers Arch.*, **348**, 263–272 (1974).
15 Cull-Candy, S. G., and Usherwood, P. N. R., *Nature new Biol.*, **246**, 62–64 (1973).
16 Castillo, J. del, and Katz, B., *Proc. R. Soc.*, **B146**, 339–356 (1957).
17 Katz, B., and Miledi, R., *J. Physiol., Lond.*, **170**, 379–388 (1964).
18 Feltz, A., and Mallart, A., *J. Physiol., Lond.*, **218**, 85–100 (1971).

Susceptibility of teratocarcinoma cells to adenovirus type 2

As mouse embryos develop they become susceptible to infection by the small DNA oncogenic viruses, simian virus 40 and polyoma[1,2]. Recently, the mouse teratocarcinoma, an alternative model system for the study of early development[3,4], was used in an approach to understanding how differentiation affects host–virus interaction (ref. 5 and M.B. and F.K., unpublished). Several differential teratocarcinoma lines were shown to be fully permissive to polyoma virus and could be transformed by SV40, therefore reacting to viral infection like most commonly used mouse cells. In contrast, the multipotential embryonal carcinoma cells were resistant to both viruses and the block seems to lie early in the lytic cycle, after penetration of the virus, but before synthesis of the viral T antigen. Adenoviruses have much in common with the papovaviruses but are larger and more complex. We therefore examined the susceptibility of teratocarcinoma cells to these viruses. Here we report that both embryonal carcinoma cells and cells from a differentiated teratocarcinoma line are susceptible to adenovirus type 2.

The two teratocarcinoma cell lines used in this study have been derived from the transplantable mouse teratocarcinoma OTT 60-50-970 isolated by Stevens[6]. PCC3 (clone A/1) is a primitive embryonal carcinoma line which undergoes differentiation when injected into mice as well as *in vitro*[7,8]. PCD3 was derived from embryoid bodies which were allowed to differentiate *in vitro*: it has a stable fibroblast morphology in culture and is non-tumorigenic (H. Jakob, personal communication). HeLa cells were used as a susceptible control. Following infection of PCC3 and PCD3 cells by adenovirus type 2, we screened the cells for production of viral antigens and infectious viral particles, as described in Table 1.

In brief, adenovirus antigens were detected by indirect immunofluorescence on cells seeded on glass coverslips, 20 h and 36 h after infection. The specific reagents were hamster anti-T antigen antiserum and rabbit multivalent capsid antiserum. Normal non-immune sera were used as controls. The indicator was fluorescein-conjugated anti-γ globulins (Institut Pasteur).

Virus titres were determined by the formation of foci on layers of HeLa cells[9]. These foci were stained by indirect immunofluorescence, with the use of anti-capsid serum as the specific reagent.

The results are summarised in Table 1. Synthesis of adenovirus-specific T antigen and of late capsid proteins was found to occur in both the primitive PCC3 and the differentiated PCD3 cells. The fluorescence pattern of the T antigen is characteristic of adenovirus, as shown in Fig. 1. Both types of cell produced infectious virus, although at a titre 50–100 times lower than HeLa cells.

Fig. 1 T-antigen immunofluorescence (indirect test) in Ad2-infected (*a*) multipotential PCC3/A/1 cells, and (*b*) differentiated PCD3 cells (see legend Table 1).

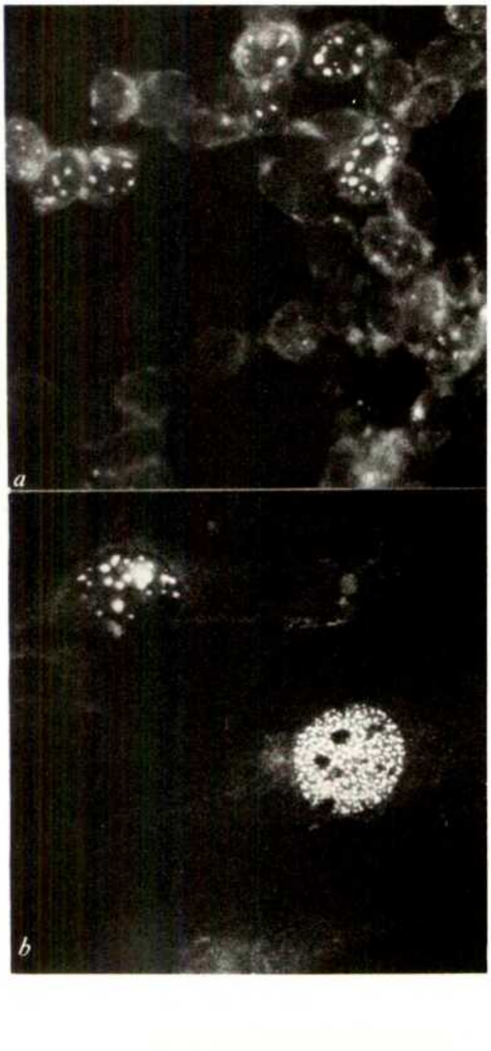

Table 1 Ad 2 antigens and virus production in HeLa cells and in two teratocarcinoma cell lines

Cells	T antigen*	Capsid antigen‡	FFU ml^{-1}†
HeLa	50	100	1.0 10^8
PCC3/A/1	40	16	1.7 10^6
PCD3	38	53	0.9 10^6

For detection of viral antigens, cells were seeded on glass coverslips (2×10^5 cells per 35-mm plastic Petri dish) and grown for 24 h at 37 °C in Dulbecco's modified Eagle's medium containing 10% foetal calf serum and in an atmosphere containing 12% CO_2. Cells were infected with adenovirus type 2 (a gift from Pierre Boulanger, INSERM, Lille) at an input multiplicity of 10 plaque-forming units per cell. Virus was adsorbed for 1 h at 37 °C. Cells were then covered with medium containing 2% foetal calf serum. Coverslips were removed 20 h and 36 h after infection, washed three times in phosphate-buffered saline and fixed in methanol–acetone (3 : 7) at −20 °C for 5 min. Adenovirus-specific proteins were detected by indirect immunofluorescence. The specific reagents were hamster anti-T-antigen antiserum (a gift from Pierre Boulanger, originally from Dr R. V. Gilden) and rabbit multivalent capsid antiserum (Pierre Boulanger). The indicator was fluorescein-conjugated anti-γ globulins (Institut Pasteur). *% cells positive 20 h after infection; †% cells positive 36 h after infection. Virus production was determined by fluorescent focus assay on HeLa cells[9]. Cells were grown and infected in the conditions described above on 60-mm dishes. Cells and overlying medium were collected 48 h after infection and frozen and thawed 3 times. HeLa cells grown on coverslips were infected with convenient dilutions of the cell extracts. They were fixed 48 h after infection and stained by indirect immuno-fluorescence using rabbit multivalent capsid antiserum, as the specific reagent. ‡Virus yield expressed as fluorescent focus units (FFU).

These results show clearly that adenovirus type 2 can infect the primitive teratocarcinoma cells as efficiently as it can the differentiated cells. In contrast, the primitive cells are resistant to both polyoma virus and SV40: less than 1 in 10^4 cells was T-antigen and V-antigen positive after polyoma infection and no T-antigen positive cell could be detected after SV40 infection (M. Boccara and F. Kelly, unpublished). The diversity in response to the viruses is interesting in view of both similarities and differences exhibited by papovaviruses and adenoviruses. All three viruses replicate exclusively in the nuclei of the permissive cells and the viral genome is integrated into the host chromosome during the lytic cycle[10]. Adenoviruses, however, contain seven times as much DNA and are also more complex. In particular, at least two early genes of adenovirus are necessary for replication of the viral DNA[11], whereas early mutants of SV40 and polyoma fall into only one complementation group. It is also interesting to note that adenovirus recombines far more efficiently than does SV40 or polyoma.

Because very little is known about the early events which take place in the nucleus before initiation of viral transcription and the appearance of the T antigen, one can only speculate on the basis for the different response of the primitive stem cells to papovaviruses and adenoviruses. The hypothesis we favour is that one or several cellular functions required early in the lytic cycle of SV40 and polyoma, possibly recombination between host and viral genomes, is missing in these cells. A function, carried or coded by the more complex adenoviruses could obviate this deficiency. Experiments are in progress to test whether coinfection by adenovirus will help SV40 or polyoma to infect primitive teratocarcinoma cells. We are also attempting to obtain clones of primitive cells containing a fragment of the adenoviral genome, which may be useful as a marker during their differentiation.

This work was supported by grants from the NIH, the

André Meyer Foundation, the CNRS, the Délégation Générale à la Recherche Scientifique et Technique and the Fondation Del Duca.

FRANÇOISE KELLY
MARTINE BOCCARA

Département de Biologie moléculaire,
Institut Pasteur,
25 rue du Dr Roux,
75015 Paris, France

Received February 23; accepted June 8, 1976.

[1] Solter, D., Biczysko, W., and Koprowski, H., in *Viruses, Evolution and Cancer* (edit. by Kurstak, E., and Maramorosch, K.), 3–30 (Academic, New York, 1974).
[2] Dawe, C. J., in *Tissue Interaction in Carcinogenesis* (edit. by Tarin, D.), 305–358 (Academic, New York, 1972).
[3] Jacob, F., in *The Early Development of Mammals* (edit. by Balls and Wild), 233–241 (Cambridge University Press, Cambridge, 1975).
[4] Gail, R. M., *Cell*, **5**, 229–243 (1975).
[5] Swartzendruber, D. E., and Lehman, J. M., *J. cell. Physiol.*, **85**, 179–187 (1975).
[6] Stevens, L. C., *Devl Biol.*, **21**, 364–382 (1970).
[7] Jakob, H., Boon, T., Gaillard, J., Nicolas, J. F., and Jacob, F., *Ann. Microbiol.* (*Inst. Pasteur*), **124B**, 269–282 (1973).
[8] Nicolas, J. F., Dubois, P., Jakob, H., Gaillard, J., and Jacob, F., *Ann. Microbiol.* (*Inst. Pasteur*), **126A**, 3–22 (1975).
[9] Philipson, L., *Virology*, **15**, 263–268 (1961).
[10] Tooze, J., in *The Molecular Biology of Tumor Virus* (edit. by Cold Spring Harbor Laboratory), 420–469 (Cold Spring Harbor, New York, 1973).
[11] Ginsberg, H. S., Ensinger, M. J., Kauffman, R. S., Mayer, A. J., and Lundholm, U., *Cold Spring Harb. Symp. quant. Biol.*, **39**, 419–426 (1974).

Is the scrapie agent a virus ?

THE nature of the scrapie agent has been obscure for many years. It is not known whether it is a virus in a strict sense, some replicating agent which is devoid of nucleic acid[1,2], or a transmissible self-replicating cellular membrane[3,4]. In previous experiments with the Chandler strain of the scrapie agent, numerous 14-nm virus-like particles were isolated[5] from infected mouse brains using repeated fluorocarbon extraction procedures which have been used for the isolation of Aleutian disease virus from infected mink tissues[6,7]. The present experiments were designed; first, to determine if similar 14-nm virus-like particles could be isolated from hamster brains infected with scrapie agent; and second, to determine if the 14-nm virus-like particles induce scrapie in mice and hamsters.

Hamster brains (39 g) infected with the scrapie agent were obtained from Dr R. F. Marsh[8] of the University of Wisconsin. The hamster brain suspensions were extracted repeatedly with fluorocarbon as described previously[5]. The final scrapie extracts from the 39 g of hamster scrapie brains were resuspended in 1.5 ml of 0.05 M Tris-HCl, *p*H 7.4. A CsCl density gradient ultracentrifugation was performed with these hamster scrapie extracts at 25 °C at 243,000*g* for 72 h. In the same run, three other preparations (mouse scrapie brain extracts, normal mouse brain extracts and normal hamster brain extracts) were also ultracentrifuged. Mouse scrapie brain extracts and normal mouse brain extracts were used as prepared previously[5]. Normal hamster brain extracts were prepared from the same strain of 10-week-old hamsters (LVG: LAK strain) (purchased from Lakeview Farms, Newfield, New Jersey). From 68 g of normal hamster brains, 1.7 ml of normal hamster brain extract was prepared. After the CsCl gradient ultracentrifugation, only one band was visible with the normal mouse brain and normal hamster brain extracts. This band was located in the region of buoyant density of 1.29–1.30 g cm^{-3} in the CsCl (fraction 5). With the mouse and hamster scrapie extracts, however, one band was observed at the same place and another in the region of buoyant density of 1.33–1.34 g cm^{-3} (fraction 6). Numerous virus-like particles, measuring about 14–15 nm in diameter as seen previously[5] were observed in the second band of both hamster and mouse scrapie extracts. The structure and size of these particles from these two scrapie extracts from mice and hamsters are identical. No virus-like particles were observed in the first band (density 1.29–1.30 g cm^{-3}) of any of the four different preparations, nor in the regions of buoyant density of 1.33–1.34 g cm^{-3} of normal hamster or mouse brain extracts. The CsCl gradient was collected in 10 fractions from the top of the tube using Pasteur pipettes. Particles with the structure of membranes were not detected in the fractions from the four different extracts.

Comparative titres of infectivity of the different stages of fluorocarbon extractions and the CsCl gradient fractions of mouse scrapie extracts were determined in mice. Groups of six to ten Swiss albino mice were inoculated intracerebrally with 0.03 ml in serial tenfold dilutions of the various scrapie preparations. Each experiment of mouse scrapie infectivity was terminated 47 weeks after inoculation and brains and spinal cords removed from those mice which developed scrapie symptoms. Scrapie was diagnosed by the astrocyte response in these tissues using the Cajal's gold sublimate method as described by Hadlow[9]. The infective dose (ID_{50}) defined as that dilution of material which induced scrapie in 50% of the inoculated animals, was calculated by the method of Reed and Muench[10].

The results of titration of mouse scrapie preparations are shown in Table 1. Scrapie infectivity was markedly reduced by the repeated fluorocarbon extraction procedures and CsCl gradient ultracentrifugation. In the CsCl gradient of mouse scrapie extracts, maximum infectivity was detected in the pooled fractions 6–8 which yielded 14-nm virus-like particles. In this group of mice, scrapie symptoms were first observed 23 weeks after inoculation, whereas in those mice inoculated with mouse scrapie brain suspension, scrapie symptoms were first observed at 17–18 weeks after infection. The astrocyte response was always detected in mice which developed scrapie symptoms.

Infectivity of hamster scrapie brain (195 ml), final hamster scrapie extracts (1.5 ml) and of the pool of fractions 6–7 (1.5 ml) of the CsCl gradient of hamster scrapie extracts which yielded the 14-nm virus-like particles, was titrated in hamsters by inoculation with 0.05 ml intracerebrally. The infectivity titres of these three inocula were ID_{50} $10^{8.7}$, $10^{5.5}$ and $10^{3.5}$ per 0.05 ml respectively during the observation period of 39 weeks. The diagnosis of scrapie in hamsters was also confirmed by astrocyte response. In hamsters, scrapie symptoms were first observed 10 weeks after infection with hamster scrapie brain suspension and after 12 weeks with the other two preparations. The infectivity titre of hamster scrapie extracts is being determined more precisely using fractions 1–5 collected from the top of the CsCl gradient, and fractions 6–10 through a hole in the bottom of the tube.

Previous studies[5] showed that the final mouse scrapie extract from 132 g of brain contained 8.8 mg of protein in a total volume of 10 ml. Therefore, the fluorocarbon stage in the purification of virus-like particles leads to the removal of about 99.99% or "4 logs" of brain tissues. In the present experiments 5.8 $\log_{10}ID_{50}$ units of mouse infectivity and 5.2 $\log_{10}ID_{50}$ units of hamster infectivity were lost during fluorocarbon treatment, and exposure to CsCl caused further decreases in the infective titre. This marked reduction of scrapie infectivity is consistent with the observations of others[11] that the scrapie agent is inactivated by various lypophilic solvents and by CsCl. The density of the 14-nm particles and the maximum infectivity found in fractions 6–8, is however, consistent with the report of Gibbs[12] in which maximum scrapie infectivity was observed at densities between 1.32 and 1.37 g cm^{-3} in a CsCl gradient.

In view of the findings that identical 14-nm virus-like particles were isolated from the brains of two different animal species (mouse and hamster) obtained from two different laboratories, scrapie infectivity was detected in the fractions yielding these 14-nm particles, and as these virus-like particles form a homogenous band is a CsCl gradient, I suggest that the 14-nm particles are likely to be the causative agent of scrapie.

I thank W. J. Hadlow for providing mouse scrapie brains

Table 1 Infectivity of mouse scrapie brain extracts

Preparations		Amount (ml)	Titres of scrapie infectivity $\log_{10}ID_{50}$ per 0.03 ml	Total titres ($\log_{10}ID_{50}$)
Scrapie mouse brains suspension		790	7.0	11.4
↓				
Freon 113 extraction				
↓				
10,000*g* 30 min supernatant		660	4.9	9.2
↓				
100,000*g* 5 h supernatant		660	2.0	6.3
↓				
100,000*g* 5 h pellets		100	Not done	—
↓				
Freon 113 extraction				
↓				
10,000*g* 30 min supernatant		100	3.8	7.3
↓				
100,000*g* 10 h supernatant		100	1.4	4.9
↓				
100,000*g* 10 h pellets (mouse scrapie extracts)		10	3.1	5.6
CsCl fractions*	Electron microscopy	Total amount		
1–4 pool	No virus	10†	$\leqslant 0.5$	$\leqslant 3.0$
5	No virus	10	$\leqslant 0.58$‡	$\leqslant 3.08$
6–8 pool	Numerous 14-nm virus-like particles and some ferritins	10	2.5	5.0
9–10 pool	Ferritins	10	$\leqslant 0.5$	$\leqslant 3.0$

* Fractions were collected from top of the table. Two bands were visible: in fraction 5 (density 1.29–1.30 g cm^{-3}) and in fraction 6 (density 1.33–1.34 g cm^{-3}).

† Only 1 ml of the total amount of 10 ml mouse scrapie extract was centrifuged on CsCl. The CsCl fractions were diluted with 0.85% saline, concentrated by centrifugation at 300,000*g* for 5 h and the pellets were suspended in 1 ml of saline.

‡ Scrapie was diagnosed in one of 7 inoculated at 10^{-1} dilution at 35 weeks. No mice showed scrapie symptoms at 10^{-1} or higher dilutions in the fractions 1–4 and 9–10 pools.

and technical advice on Cajal's gold sublimate method, and R. F. Marsh for hamster scrapie brains.

HYUN J. CHO

Animal Pathology Division,
Health of Animals Branch,
Agriculture Canada,
Animal Diseases Research Institute (W),
PO Box 640, Lethbridge,
Alberta, Canada T1J 3Z4

Received January 16; accepted May 25, 1976.

[1] Alper, T., Haig, D. A., and Clarke, M. C., *Biochem. biophys. Res. Commun.*, **22**, 278–284 (1966).
[2] Alper, T., Cramp, W. A., Haig, D. A., and Clarke, M. C., *Nature*, **214**, 764–766 (1967).
[3] Gibbons, R. A., and Hunter, G. D., *Nature*, **215**, 1041–1043 (1967).
[4] Millson, G. C., Hunter, G. D., and Kimberlin, R. H., *J. comp. Path.*, **81**, 255–265 (1971).
[5] Cho, H. J., and Greig, A. S., *Nature*, **257**, 685–686 (1975).
[6] Cho, H. J., and Ingram, D. G., *Nature new Biol.*, **243**, 174–176 (1973).
[7] Cho, H. J., in *Slow Virus Diseases of Animals and Man* (edit. by Kimberlin, R. H.), ch. 8, 159–174 (Elsevier, Amsterdam, 1976).
[8] Marsh, R. F., and Kimberlin, R. H., *J. Infect. Dis.*, **131**, 104–110 (1975).
[9] Hadlow, W. J., *Res. Vet. Sci.*, **2**, 289–341 (1961).
[10] Reed, L. J., and Muench, M., *Am. J. Hyg.*, **27**, 493–497 (1938).
[11] Mould, D. L., Dawson, A. M., and Smith, W., *Res. Vet. Sci.*, **6**, 151–154 (1965).
[12] Gibbs, C. J., Jr, *Curr. Top. Microbiol.*, **40**, 44–58 (1967).

Rifampicin-resistant RNA polymerase and NAD transferase activities in coliphage N4 virions

SEVERAL animal viruses carry within the infectious particle a number of enzymatic activities[1,2]. Prominent among these are the RNA synthetases of orthomixo, paramixo, rhabdo- and diplornaviruses[3–6], the DNA-dependent RNA polymerase of poxviruses[7] and the reverse transcriptases of oncornaviruses[8,9], all of which play important roles in the virus life cycle. Exclusion of vital enzymes from the virion of all complex bacterial viruses seems, on the other hand, to have been the result of the evolutionary trend followed by these agents. A notable exception to this rule seems to be represented by coliphage N4 (ref. 10). It has been reported that transcription of N4 early genes[11,12] and incorporation of ^{32}P-orthophosphate into several host proteins[13] occur in *Escherichia coli* cells treated before infection with rifampicin and chloramphenicol. A possible explanation for these findings was that N4 injects into the cell the relevant enzymes along with its DNA. We report here the detection of a rifampicin-resistant RNA polymerase and a nicotinamide adenine dinucleotide (NAD) transferase in purified N4 particles.

To demonstrate the existence of virion-associated enzymes several procedures were successfully developed for the rupture of the virus protein coat[14] since preliminary experiments failed to show any activity in intact phage preparations. Disruption of isopycnically purified N4 (ref. 10) by three cycles of freezing in liquid nitrogen and thawing at 37 °C was finally adopted for the sake of simplicity. These NA cryolysates were briefly sonicated and the DNA precipitated with streptomycin. Residual intact virions, ghosts and DNA were removed by centrifugation, and the clear extracts, after dialysis, served as the source of enzyme.

Table 1 shows that incorporation of ^{3}H-UTP into RNA was mediated by these N4 preparations in a modified RNA polymerase assay[15]. Like the RNA polymerase of *E. coli*, N4 enzyme requires all four ribonucleotide triphosphates, Mg^{2+} and a DNA template for optimal activity. The acid-insoluble product is totally susceptible to RNase digestion, and it is not synthesised in the presence of actinomycin D. On the other hand, N4 enzyme is inhibited by low concentrations of monovalent ions and by phosphates, and shows a stringent template specificity in that only homologous phage DNA acts as an efficient primer. Furthermore, the functioning of N4 polymerase is highly resistant to the antibiotic rifampicin at concentrations that inhibit *E. coli* RNA polymerase[16,17].

As an indication of the fidelity of transcription by the phage enzyme, RNA synthesised *in vitro* from N4 DNA hybridised with high efficiency (43%) to denatured N4 DNA

Table 1 Characteristics of N4 virion-associated RNA polymerase activity

	Activity (%)
Complete system	100
Omit ATP, or CTP, or GTP	1
Omit Mg^{2+}	8
Omit N4 DNA	2
Add calf thymus DNA (50 μg ml^{-1})	18
Add *E.coli* DNA (200 μg ml^{-1})	7
Add 0.15 M KCl	21
Add 0.05 M K phosphate, *p*H 7.0	19
Add RNase (10 μg ml^{-1})	1
Add actinomycin D (10 μg ml^{-1})	1
Add rifampicin (5 μg ml^{-1})	96

Isopycnically purified N4 preparations were obtained as described previously[30]. After three cycles of freezing in liquid nitrogen and thawing at 37 °C the viscous lysates were sonicated for 30 s in a Branson apparatus at an output of 50 W. Removal of DNA was effected by adding streptomycin to a final concentration of 6%. After 15 min at 4 °C, precipitated DNA, ghosts and residual intact phage particles were sedimented by spinning at 40,000 r.p.m. for 90 min in the 50 rotor of an L3-50 Spinco ultracentrifuge. After thorough dialysis against 0.01 M Tris-HCl buffer, *p*H 7.2, containing 0.001 M $MgCl_2$, the clear extract was used as the source of enzyme.

Complete system for the assay of N4 polymerase activity contained 10 μmol Tris-HCl (*p*H 7.9), 2.5 μmol $MgCl_2$, 25 nmol dithiothreitol, 25 nmol EDTA, 125 μg bovine serum albumin, 2 pmol N4 DNA, 37.5 nmol each of the four ribonucleoside triphosphates of which UTP was labelled with ^3H (Amersham, England; specific activity 5×10^3–2×10^4 c.p.m. $nmol^{-1}$) and 30 μl N4 cryolysate in a final volume of 250 μl. After incubation at 37 °C for 15 min, the reaction was terminated by the addition of 3 ml ice-cold 5% TCA containing 10^{-2} M sodium pyrophosphate. The acid-insoluble RNA product was collected on Whatman GF/C filters, washed and counted as reported previously[30]. For the complete system 100% activity was 5,200 c.p.m.

(Table 2). In addition, unlabelled RNA synthesised by N4-infected Hfr 3300 cells either untreated or pretreated with rifampicin and chloramphenicol[11,12] competed (greater than 90% inhibition) with labelled RNA produced *in vitro*. These data indicate that the RNA species synthesised *in vitro* by N4 virion polymerase are not qualitatively different from those produced during *in vivo* infection.

Phosphorylation of proteins is catalysed by phage-coded products through at least two mechanisms involving either protein kinases that transfer phosphate from ATP to seryl groups of acceptor molecules[18], or NAD transferases that modify target polypeptides by the simultaneous addition of adenosine and phosphorus[19–21]. None of these enzymes has been shown to be virion associated.

N4 particles do not carry a protein kinase since ^{32}P was not transferred to proteins in reaction mixtures containing γ-^{32}P-ATP (not shown). On the other hand, N4 cryolysates were active in transferring radioactivity from ^{14}C-NAD into acid-precipitable linkage with various acceptor proteins (Table 3). Among those proteins tested, lysozyme was the best acceptor. Dithiothreitol markedly stimulated ^{14}C-NAD incorporation possibly implying an activation of the enzyme by thiol compounds[21].

The label bound to the reaction product resisted heat treatment in mild acidic and alkaline conditions, and digestion with DNase. After treatment with Pronase and snake venom phosphodiesterase ^{14}C-radioactivity was converted to an acid-soluble form (not shown). These results suggest that N4 enzyme may be similar to the ADP–ribosyl transferase activities that have been established for diphtheria toxin[21,22], *Pseudomonas aeruginosa* PA toxin[23] and T4 'alteration' factor[20].

In a preliminary effort to characterise the molecular nature of N4 enzymes, $^{35}SO_4$-labelled isopycnically purified virions were disrupted, treated with DNase, and clarified from ghosts and residual intact particles by centrifugation; the supernatant containing both enzymatic activities was electrophoresed in sodium dodecyl sulphate (SDS)–polyacrylamide slab gels[24]. In the autoradiogram shown in Fig. 1 two radioactive bands with approximate molecular weight of 65,000 are visible. Whether these polypeptides can be considered dissociated subunits of one or both N4 enzymes or merely represent internal proteins, remains to be established.

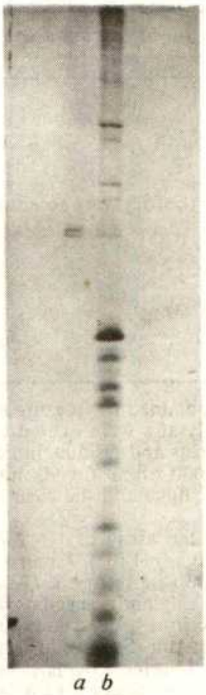

Fig. 1 Identification of polypeptides present in N4 virion cryolysates. Isopycnically purified $^{35}SO_4$-labelled N4 particles[30], disrupted by three cycles of freezing and thawing, were treated with DNase (5 μg ml^{-1}) for 15 min at 37 °C. Ghosts and residual intact virions were removed by spinning as specified in Table 1. Samples of intact radioactive particles (25 μl, 50,000 c.p.m.) and enzymatically active cryolysates (25 μl, 1,100 c.p.m.) were prepared for SDS–polyacrylamide electrophoresis in 10% slab gels using the procedures and apparatus described previously[24,34]. In the autoradiogram shown the origin of electrophoresis is at the top. *a*, Migration pattern of N4 cryolysates; *b*, migration pattern of intact N4 virion polypeptides.

Although rifampicin-resistant phage-coded RNA polymerases are known to be synthesised in infected cells during the life cycle of T7 (ref. 25), T3 (ref. 26), PBS2 (ref. 27) and gh-1 (ref. 28) bacteriophages, N4 enzyme provides the first example of a virion-associated transcription apparatus in bacterial viruses.

The occurrence of this enzyme as an integral part of N4 may be of evolutionary significance for a virus which replicates exclusively in the polar regions of its host[29]. Besides,

Table 2 Hybridisation–competition of N4 RNA polymerase product by various RNA preparations

Type of non-radioactive competing RNA	Amount of *in vitro* RNA (c.p.m.)	c.p.m. in hybrid	% RNA hybridised
None	3.1×10^3	1.3×10^3	43
Uninfected *E.coli* RNA (200 μg ml^{-1})	3.1×10^3	1.3×10^3	43
RNA isolated from *E.coli* cells 4 min after N4 infection (50 μg ml^{-1})	3.1×10^3	1.2×10^2	3.9
RNA isolated from *E.coli* cells pretreated with rifampicin and chloramphenicol, and infected for 4 min with N4 (50 μg ml^{-1})	3.1×10^3	1.1×10^2	3.5

Labelled RNA synthesised by N4 virion-associated RNA polymerase in the conditions reported in Table 1, was purified from the reaction mixture by phenol extraction[11]. Competitor RNA molecules were prepared from uninfected or N4-infected *E.coli* Hfr 3300 cells as specified previously[11]. Conditions of N4 infection in the presence of chloramphenicol and rifampicin have been described[12]. RNA–DNA hybridisation was carried out as already reported[11] using N4 DNA (2 μg) bound to nitrocellulose filters.

Table 3 Characteristics of N4 virion-associated NAD transferase activity

	Activity (%)
Complete system	100
Omit dithiothreitol	7
Omit Mg^{2+}	52
Substitute lysozyme with the following acceptor proteins:	
Histones	63
E.coli cell-free extract	56
RNase	30
Protamine	9
Bovine serum albumin	7
N4 ghosts	6
Casein	5

N4 cryolysates were obtained by freezing and thawing as specified in Table 1. The viscous lysates were treated with DNase (3 μg ml^{-1}) at 37 °C for 15 min. Ghosts and residual intact virions were removed by centrifugation at 40,000 r.p.m. for 90 min in the 50 rotor of an L3-50 Spinco Ultracentrifuge and the clear extract was used as the source of enzyme.

Complete system for the assay of N4 NAD transferase activity contained 4 μmol Tris-HCl (*p*H 8.2), 7.5 nmol EDTA, 3 μmol dithiothreitol, 4 μmol $MgCl_2$, 30 μg lysozyme (Koch and Light), 50 pmol ^{14}C-NAD (Amersham, England; specific activity 280 Ci mol^{-1}) and 15 μl N4 cryolysate in a total volume of 65 μl. RNase (Boehringer) bovine serum albumin (Sigma), histones (Sigma, fraction II), Protamine (Sigma) and Caseine (Sigma), when used as acceptors, were present in the reaction mixture at a concentration of 30 μg. Hfr 3300 cells grown in 50 ml M9S medium[29] at a concentration of 5×10^8 ml^{-1} were collected by centrifugation, washed in distilled water, resuspended in 1 ml 0.001 M Tris-HCl buffer (*p*H 8.2) and sonicated at 0 °C for 2 min in a Branson sonifier at an output of 70 W. After centrifugation at 10,000 r.p.m. for 10 min, 10 μl of the clear cell-free extract were added to the NAD transferase reaction. Purified N4 ghosts prepared as reported previously[14] were added at a final concentration of 20 μg. After incubation at 25 °C for 60 min the reaction was terminated by addition of 65 μl 10% TCA. The acid-insoluble radioactivity was collected on Whatman GF/C filters, washed with 5% TCA and counted as detailed previously[30]. For the complete system 100% activity was 1,850 c.p.m.

the identification of a rifampicin-resistant RNA polymerase in N4 particles provides a likely explanation for the drug resistance of phage transcription during the early stages of replication[11,12]. This enzyme is injected along with the phage genome at infection. Once in the cell the injected polymerase will immediately direct the synthesis of additional drug-resistant RNA polymerase molecules by transcribing N4 cistrons 3 and 4 (ref. 30) which probably code for this activity. Expression of the early genes then takes place at a suitable rate and the phage DNA is replicated[11,12]. Late genes are next transcribed with the mandatory participation of an N4-modified form of *E. coli* polymerase[31]. During morphogenesis N4-coded RNA polymerase or a catalytically active subassembly of this enzyme is finally packaged into the infectious virions. Mero complex models of N4 gene expression can also be constructed on the basis of present and previous evidence.

When injected into the host, N4-associated NAD transferase catalyses the phosphorylation of about 30 bacterial proteins, which do not include any of the host RNA polymerase subunits[13]. A NAD transferase which 'alters' the α subunit of *E. coli* RNA polymerase[19,32] has been tentatively located by Horvitz[33] in T4 particles. T4 mutants deficient in 'alteration' have been shown to be perfectly viable[33]. It has been suggested that the main role of 'alteration' may reside in the ability to confer a broad host range on T4 phage[33]. Since N4 replicates productively only in the K12 strains of *E. coli*[30], amplification of the host range by possession of the virion-associated NAD transferase seems improbable. Considering the scarcity of receptors for N4 on the surface of sensitive cells[29], we favour the hypothesis that during evolution N4 NAD transferase was retained in the virion because of some positive role it may have in initiating the infectious process. Detailed physicochemical and biochemical characterisation of N4 virion-associated enzymes will be reported elsewhere.

This work was supported by a grant from the Italian Consiglio Nazionale delle Ricerche.

ADELAIDE PESCE*
CLAUDIO CASOLI
GIAN CARLO SCHITO

Institute of Microbiology,
University of Parma Medical School,
43100 Parma, Italy

Received March 1; accepted May 26, 1976.

*Permanent address: Chair of Parasitology, University of Parma Medical School, Parma, Italy.

[1] Dales, S., *Bact. Rev.*, **37**, 103–135 (1973).
[2] Shatkin, A. J., *A. Rev. Biochem.*, **43**, 643–664 (1974).
[3] Chow, N. L., and Simpson, R. W., *Proc. natn. Acad. Sci. U.S.A.*, **68**, 752–756 (1971).
[4] Huang, A. S., Baltimore, D., and Bratt, M. A., *J. Virol.*, **7**, 389–394 (1971).
[5] Baltimore, D., Huang, A. S., and Stampfer, M., *Proc. natn. Acad. Sci. U.S.A.*, **66**, 572–576 (1970).
[6] Shatkin, A. J., and Sipe, J. D., *Proc. natn. Acad. Sci. U.S.A.*, **61**, 1462–1469 (1968).
[7] Kates, J. R., and McAuslan, B. R., *Proc. natn. Acad. Sci. U.S.A.*, **58**, 134–141 (1967).
[8] Baltimore, D., *Nature*, **226**, 1209–1211 (1970).
[9] Temin, H. M., and Mizutani, S., *Nature*, **226**, 1211–1213 (1970).
[10] Schito, G. C., Rialdi, G., and Pesce, A., *Biochim. biophys. Acta*, **129**, 482–490 (1966).
[11] Rothman-Denes, L. B., and Schito, G. C., *Virology*, **60**, 65–72 (1974)
[12] Schito, G. C., Giraldi, M., and Toni, M., *Nature*, **251**, 340–342 (1974).
[13] Casoli, C., and Pesce, A., *17th natn. Congr. Microbiol.*, **2**, 551–555 (1975).
[14] Pesce, A. and Schito, G. C., *Biochim. biophys. Acta*, **236**, 450–457 (1971).
[15] Burgess, R. R., *J. biol. Chem.*, **244**, 6160–6167 (1969).
[16] Riva, S., and Silvestri, L. G., *A. Rev. Microbiol.*, **26**, 199–224 (1972).
[17] Zillig, W., *et al.*, *Cold Spring Harb. Symp. quant. Biol.*, **35**, 47–58 (1970).
[18] Rahmsdorf, H. J., *et al.*, *Proc. natn. Acad. Sci. U.S.A.*, **71**, 586–589 (1974).
[19] Goff, C. G., and Weber, K., *Cold Spring Harb. Symp. quant. Biol.*, **35**, 101–108 (1970).
[20] Goff, C. G., *J. biol. Chem.*, **249**, 6181–6190 (1974).
[21] Pappenheimer, A. M., and Gill, M. D., *Science*, **182**, 353–358 (1973).
[22] Honjo, T., Nishizuka, Y., Kato, I., and Hayaishi, O., *J. biol. Chem.*, **246**, 4251–4260 (1971).
[23] Iglewski, B. H., and Kabat, D., *Proc. natn. Acad. Sci. U.S.A.*, **72**, 2284–2288 (1975).
[24] Giraldi, M., Toni, M., and Schito, G. C., *Virology*, **55**, 476–482 (1973).
[25] Chamberlin, M., McGrath, J., and Waskell, L., *Nature*, **228**, 227–231 (1970).
[26] Maitra, U., *Biochem. biophys. Res. Commun.*, **43**, 443–450 (1971).
[27] Clark, S., Losick, R., and Pero. J., *Nature*, **252**, 21–24 (1974).
[28] Towle, H. C., Jolly, J. F., and Boezi, J. A., *J. biol. Chem.*, **250**, 1723–1733 (1975).
[29] Schito, G. C., *J. Virol.*, **13**, 186–196 (1974).
[30] Schito, G. C., *Virology*, **55**, 254–265 (1973).
[31] Pesce, A., Casoli, C., and Schito, G. C., *Third Int. Congr. Virol., Abstract of Papers*, 267 (Madrid, 1975).
[32] Seifert, W., Rabussay, D., and Zillig, W., *FEBS Lett.*, **16**, 175–179 (1971).
[33] Horvitz, H. R., *J. molec. Biol.*, **90**, 739–750 (1974).
[34] Toni, M., Conti, G., and Schito, G. C., *Biochem. biophys. Res. Commun.*, **68**, 545–550 (1976).

Human cytomegalovirus infection of WI-38 cells stimulates mitochondrial DNA synthesis

HUMAN cytomegalovirus (HCMV) infection has been shown to lead to the stimulation of host cell DNA and RNA synthesis in both permissive and non-permissive cells[1-3]. This effect on DNA synthesis occurred at about 12–16 h after infection, and preceded synthesis of viral DNA by 36 h. The host cell DNA species which are stimulated have not been characterised. We show here that much of the stimulation of DNA synthesis was due to an increased rate of mitochondrial DNA synthesis and that ethidium bromide inhibited HMCV replication.

Confluent cultures of WI-38 cells were infected with HCMV at a multiplicity of infection of 1 plaque-forming unit (PFU) per cell. In all the experiments (unless otherwise noted) WI-38 cells were infected at least 5 d after reaching confluency in minimum essential medium (MEM) plus 10% foetal bovine serum. After infection the cultures were refed with MEM containing 0.4% foetal bovine serum, to minimise the stimulatory effect of serum on cellular DNA, and incubated at 37 °C. In these conditions, typical nuclear inclusion bodies for HCMV were demonstrated in virtually all of the cells 3 d after infection. Total DNA synthesis was measured by labelling the cells for 60 min with ^{3}H-thymidine (^{3}H-dT) at various times after infection. Mock-infected cultures were used as controls.

The incorporation of ^{3}H-dT into cellular DNA and the HCMV infectivity of WI-38 cells at various intervals are shown in Fig. 1. Infectivity was not seen until 48 h after infection, when a small amount of virus was detected; this amount subsequently increased.

Apparently the incorporation of ^{3}H-dT occurred in two phases· the first reaching a maximum at 16 h after infection, then decreasing until 36 h, when the second phase begins. Previous DNA analysis by equilibrium CsCl centrifugation showed viral DNA only in specimens obtained 36 h after infection (ref. 1) and reached a peak at 96 h.

Mitochondrial DNA was isolated from cytoplasmic extracts by zonal centrifugation in sucrose density gradients and then analysed in equilibrium CsCl–ethidium bromide gradients. Figure 2 presents the incorporation of 3H-dT into the mitochondrial DNA of WI-38 cells labelled for 1 h at 16 h after infection. Most of the radioactive precursor was incorporated into mitochondrial DNA. The rate of ^{3}H-dT incorporation into mitochondrial DNA in infected cells was approximately five times that in control cells. As expected[4], the greater part of the incorporated radioactivity was found in the same fraction as the closed circular SV40 DNA added to the gradient as a marker.

Analysis of mitochondrial DNA at various times after infection revealed that the rate of incorporation of ^{3}H-dT into mitochondrial DNA of infected cells was always 1.5 to 5 times higher than in the control cells and the greatest increase occurred between 12 and 18 h after infection. Mitochondrial DNA labelled with ^{14}C-dT and prepared from mock-infected cells by the same type of CsCl gradient procedure was then mixed with SV40 DNA as marker, and the mixture sedimented through a 5–20% sucrose gradient at neutral *p*H. The peaks of ^{3}H-dT label from infected cells coincided with the peaks of the ^{14}C label from mock-infected cell DNA (Fig. 3).

Greater incorporation of a DNA precursor into mitochondrial DNA is insufficient as evidence of an increase in the rate of synthesis of mitochondrial DNA in the infected cells, because the pool size of thymidine, the kinase levels and the rate of turnover may differ from those in uninfected cells. For these reasons, additional experiments were carried out at 12 and 24 h past infection. Cultures prelabelled with ^{32}P were used to measure specificity of the acid-soluble pool of dT triphosphate. Inorganic $^{32}PO_4$ (5 μCi ml^{-1}) was added to the culture and the cells were continuously labelled for 48 h before infection. ^{3}H-dT (10 μCi ml^{-1}) was added to infected and non-infected cells for 1 h at 12 h and 24 h after infection. The ratio of ^{32}P to ^{3}H in dT triphosphate was measured using the methods for acid-soluble extracts and polyethyleneimine thin-layer chromatography as described by Neuhard *et al.*[5]. The specific activities of the acid-soluble pools of dT triphosphate were unaffected in both infected and uninfected cultures.

Fig. 1 Monolayers of WI-38 cells in 3-cm Petri dishes containing 3×10^5 cells were infected at an input multiplicity of 1. At various times after infection, ^{3}H-dT was added at a concentration of 1 µCi ml^{-1} and the cells incubated at 37 °C for 60 min After incubation the cells were lysed with 0.1% sodium dodecylsulphate and precipitated with 5% trichloroacetic acid. Precipitates were filtered and radioactivity counted. Infectivity of cell-associated virus was assayed after disrupting the cells by sonication[13]. ○, Infectivity; incorporation of ^{3}H-dT, ●, mock-infected cells; ■, infected cells

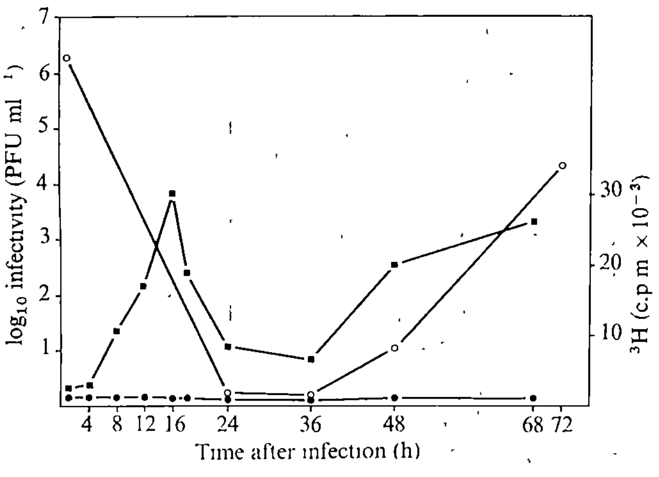

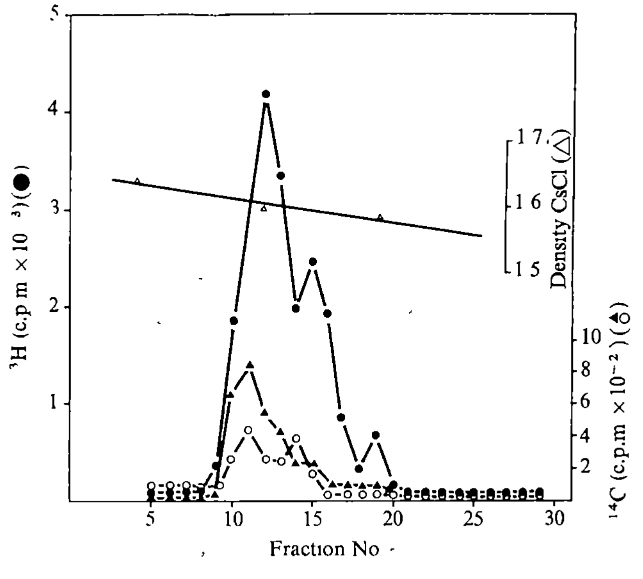

Fig. 2 WI-38 cells (3×10^6) were infected, 5 d after reaching confluent monolayers, with HCMV at a multiplicity of 1 PFU per cell. At 16 h after infection, cells were labelled for 1 h with 5 µCi ml^{-1} of ^{3}H-dT (specific activity 6.7 Ci mmol^{-1}). Mock-infected cells were treated identically. At the end of the incubation cytoplasmic extracts were prepared according to a method previously described[14], and were layered on to 15–30% sucrose–sodium dodecylsulphate gradients and centrifuged at 25,000 r.p.m. in an SW27 rotor for 16 h at 25 °C. Fractions were collected from the gradient. The fractions corresponding to the lower half of the gradient were pooled and precipitated with alcohol. Nucleic acids were resuspended in 10 mM Tris (*p*H 7.6) and 1 mM EDTA made 2 M in CsCl, and left overnight. After centrifugation at 15,000*g* for 10 min, the solution received CsCl to a density of 1.530 g cm^{-1} and ethidium bromide to a concentration of 250 µg ml^{-1}. Centrifugation was carried out in the SW50 Spinco rotor for 36 h at 44,000 r.p.m. at 20 °C. The position of supercoiled DNA molecules was checked using SV40 circular DNA labelled with ^{14}C as a marker. ●, Infected; ○, mock-infected; ▲, SV40 circular DNA.

Because HCMV has a long eclipse period (48–72 h)[6–8], the stimulation of mitochondrial DNA occurs before viral replication. It was interesting, therefore, to determine the effect of ethidium bromide on both mitochondrial DNA and viral production. Confluent monolayers of WI-38 cells were infected with HCMV and after allowing 1 h for virus adsorption, medium containing various concentrations of ethidium bromide was added. At intervals after infection, the total incorporation of ^{3}H-dT into DNA was measured as in the experiment presented in Fig. 1. Infectivity of cell-associated virus was assayed 3 d after infection. At concentrations of 5 and 1 μg ml^{-1}, ethidium bromide completely abolished the HCMV-induced DNA stimulation and decreased infectivity by more than three orders of magnitude. At a concentration of 0.1 μg ml^{-1} of ethidium bromide, incorporation of ^{3}H into DNA was only slightly decreased whereas infectivity was about ten times lower than in the untreated culture (Fig. 4).

The data presented here indicate that HCMV stimulated mitochondrial DNA in cells where DNA synthesis was repressed by contact inhibition or by depletion of serum[9]. The stimulation of mitochondrial DNA preceded viral DNA replication and was thus an expression of an early function of the viral genome. These results are not analogous to those observed in cells infected with simian virus 40 (SV40), polyoma or herpes simplex virus. SV40 and polyoma stimulate mitochondrial DNA synthesis concomitantly with virus-directed induction of nuclear DNA

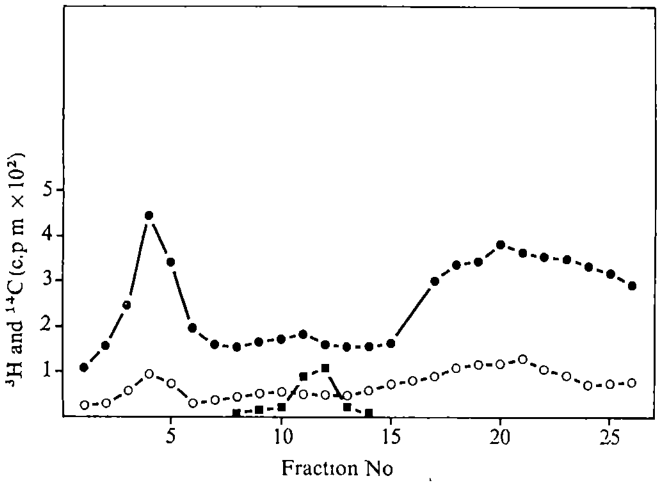

Fig. 3 DNAs from infected or mock-infected cells were first purified by centrifugation in CsCl–ethidium bromide gradients as described in Fig. 2. The two peaks from these gradients (fractions 12 and 15) were then dialysed and sedimented through a neutral 5–20% sucrose gradient for 10 h at 25,000 r.p.m. in an SW27 rotor. Fractions were collected as shown in the figure, and radioactivity measured. A sample of SV40 circular DNA was added to a gradient containing mock-infected cell DNA ●, ^{3}H-DNA from infected cells; ○, ^{14}C-DNA from mock-infected cells; ■, SV40 DNA.

synthesis[4,10,11]. In herpes simplex infection, nucleus-directed macromolecular synthesis is progressively inhibited, and mitochondrial stimulation may reflect the elimination of the nuclear repressor system for mitochondrial DNA replication[11].

That stimulation of mitochondrial DNA synthesis by HCMV is not mediated through a stimulation of nuclear DNA is indicated by the fact that the latter was demonstrated only late in the growth cycle of the virus. Further work is necessary to clarify the relationship between the stimulation of mitochondrial and nuclear DNA.

Although the biological significance of the inhibitory effect of ethidium bromide on the growth of HCMV must remain speculative, two possibilities can be considered. HCMV may require more energy from mitochondria for replication than do other viruses. Alternatively, since, at low concentrations, more ethidium bromide is bound to supercoiled DNAs than to normal double helices[12], the DNA of HCMV may form circular DNA at a certain stage of the replication cycle. In any case it is clear from the data that HCMV acts as a trigger for the stimulation of mitochondrial DNA synthesis and this stimulation may be a necessary factor for subsequent HCMV replication.

Fig. 4 Confluent monolayers of WI-38 cells in Petri dishes (diameter 3 cm) were infected with HCMV. After 1 h absorption, the cells were incubated in media containing various concentrations of ethidium bromide. At the indicated times after infection, ^{3}H-dT was added at a concentration of 1 µCi ml^{-1} for 30 min. Samples to measure radioactivity incorporated into the cells were processed in the same manner as that described in Fig. 1. Infectivity of cell-associated virus was assayed at 4 d after infection. ○, Without drug; □, 0.1 µg ethidium bromide; △, 1 µg ethidium bromide; ●, 5 µg ethidium bromide.

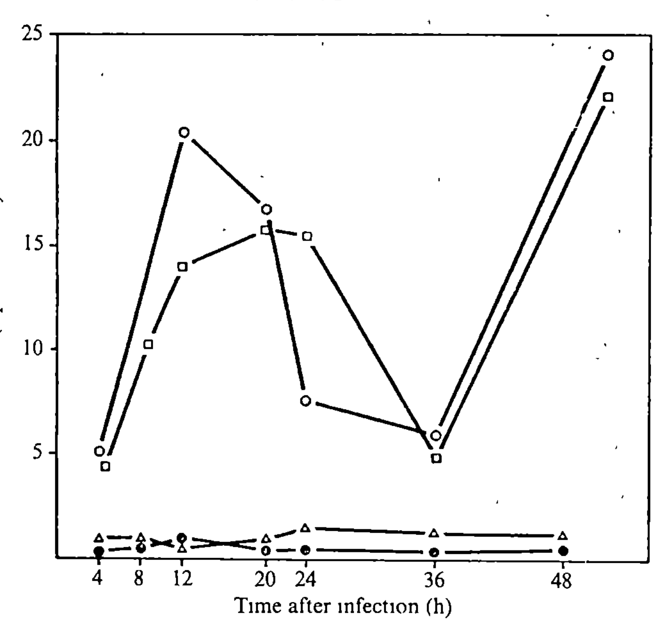

This work was supported in part by a USPHS research grant from the National Institute of Allergy and Infectious Diseases.

TORU FURUKAWA
SADATOSHI SAKUMA
STANLEY A. PLOTKIN

The Wistar Institute of Anatomy and Biology,
36th Street at Spruce,
Philadelphia, Pennsylvania 19104

Received December 15, 1975, accepted June 1, 1976

[1] St Jeor, S , Albrecht, T B , Funk, F D , and Rapp, F , *J Virol.*, 13, 353 (1974)
[2] Tanaka, S , Furukawa, T., and Plotkin, S A , *J Virol* , 15, 297 (1975)
[3] Furukawa, T., Tanaka, S , and Plotkin, S. A , *Proc Soc exp Biol Med.*, 148, 211 (1975)
[4] Levine, A. J , *Proc. natn. Acad Sci U S.A.*, 68, 717 (1971)
[5] Neuhard, J , Randerath, E , and Randerath, K , *Analyt Biochem* , 13, 211 (1965)
[6] Plummer, G , Goodheart, C. R., Henson, D , and Bowling, C. P., *Virology*, 39, 134 (1969).
[7] Iwasaki, Y., Furukawa, T., Plotkin, S A., and Koprowski, H., *Arch. Gesamte Virusforsch* , 40, 311 (1973).
[8] Smith, J. D , and Harven, E de, *J. Virol* , 14, 945 (1974)
[9] Wiebel, F., and Baserga, R., *J. Cell Physiol.*, 74, 191 (1974)
[10] Vesco, C., and Basilico, C , *Nature*, 229, 336 (1971).
[11] Radsak, K , and Albring, M , *J gen. Virol* , 25, 457 (1974).
[12] Neuberger, A., and Tatum, E L., *Frontiers of Biology*, II (North Holland, 1969).
[13] Furukawa, T., Fioretti, A , and Plotkin, S. A., *J Virol.*, 11, 991 (1973).
[14] Vesco, C , and Penman, S , *Biochem biophys. Res. Commun.*, 35, 249 (1969)

Rhodopsin analogues from highly hindered 7-*cis* isomers of retinal

ALL known visual pigments have as chromophore the sterically hindered 11-*cis* isomer of retinal. Shortly after this was established, an unsuccessful attempt was made to prepare the much more hindered 7-*cis*-retinal by partial reduction of the corresponding 7,8-acetylene[1]. But, four new geometric isomers of retinal, all apparently 7-*cis*, have been synthesised by a six-step non-stereospecific sequence[2]. Structural assignments of the isomers were originally based on spectral data of two fractions of partially separated mixtures of isomers (7-*cis* and 7,9-di*cis*; 7,13-di*cis* and 7,9,13-tri*cis*). Their configurations were, therefore, not completely firm. Since then two of the four isomers (7-*cis* and 7,9-di*cis*) have been isolated by high pressure liquid chromatography (HPLC). Their nuclear magnetic resonance (NMR) spectra unambiguously confirmed the tentative assignments made earlier. That of 7-*cis*-retinal is shown in Fig. 1 as a representative example. The remaining two 13-*cis* isomers remain unseparated in various HPLC conditions. Their structures, however, have since been confirmed through a sterоselective synthesis of 7,9,13-tri*cis*-retinal[3]. We report here preliminary results of the interaction of these 7-*cis*-retinal isomers with cattle opsin.

The ultraviolet absorption spectra of 7-*cis*-, 7,9-di*cis*- and 7,9,13-tri*cis*-retinal are shown in Fig. 2 together with that of all-*trans*-retinal. The relatively small hyposochromic shift of the α-band of the 7-*cis* isomers is consistent with the view of increased non-planarity only near the terminal positions of the polyene chain (that is, about the 6,7-bond) in 7-*cis* isomers[4-7]. Thus, the 7,9,13-tri*cis* isomer has a higher molar absorbance than 11-*cis* (36,600 compared with 26,400 (ref. 8)).

All three isomers were tested with cattle opsin as to their possible formation of 7-*cis* analogues of rhodopsin. Cattle rod outer segment (ROS) membranes were isolated from frozen Hormel retina and stored in buffered solution according to the reported procedures[9,10]. When incubated with opsin in suspen-

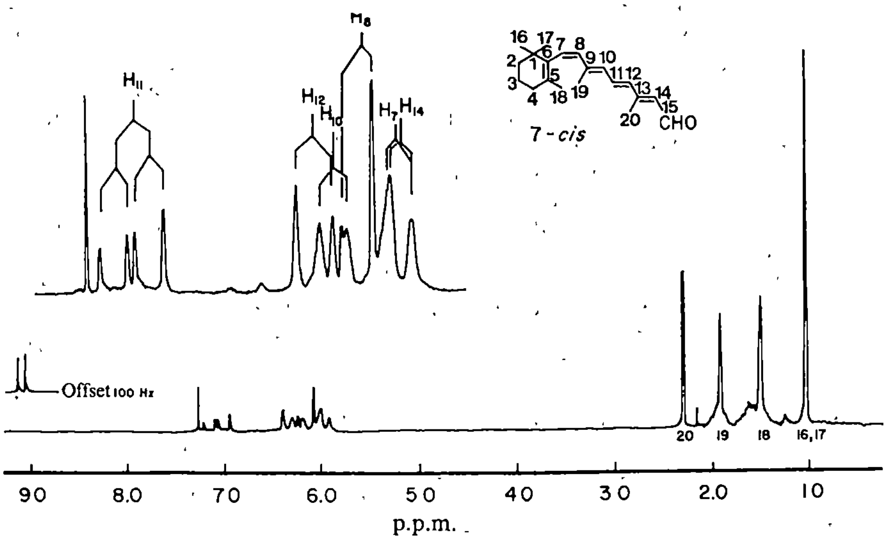

Fig. 1 Fourier-transform NMR spectrum of 7-*cis*-retinal in $CDCl_3$ recorded on a Varian XL-100 spectrometer The inset shows an expansion of the region between δ6 and 7 p.p.m. The 7-*cis* isomers were purified and isolated by HPLC on Corasil II or μ-Porasil columns The major differences between the 7-*trans* and 7-*cis* isomers are the shift of H_{18} and and H_7 from about δ1.7 p.p.m. resp. 6.3 p.p.m. (7-*trans*) to about δ1.5 p.p.m resp. 6.0 p.p.m. (7-*cis*) and the decrease of the coupling constant $J_{7,8}$ from 16 Hz (7-*trans*) to about 12 Hz (7-*cis*)

sion or in digitonin solution, the 7-*cis*-retinals as well as the all-*trans* slowly gave new absorption bands near 450 nm. The all-*trans* species, however, is due to random protonated Schiff bases between retinal and the various amoni groups present. With 0.1 M-hydroxylamine these are converted within seconds into retinal oxime (λ_{max} 367 nm), with $NaBH_4$ to retinylamines (λ_{max} 325 nm)[8], while addition of 11-*cis*-retinal immediately generates rhodopsin. On the other hand, the new species formed by all the 7-*cis* isomers are stable in darkness to these reagents. Illumination destroys the 7-*cis* pigments, forming all-*trans*-retinal and opsin. The opsin can again recombine with 11-*cis*-retinal forming rhodopsin.

These data exclude the possibility that the new pigments are due to nonspecific interactions with opsin. The difference spectra before and after illumination in the presence of hydroxylamine show maxima at 450±2 nm (7-*cis*), 460±2 nm (7,9-di*cis*) and 455±3 nm (7,9,13-tri*cis*) (Fig. 3). The rate of pigment formation with the 7-*cis* retinals is only about 1/150 as rapid as with 11-*cis*-retinal.

The 7-*cis* photopigments are clearly less stable than rhodopsin. They are bleached in the dark in 1% Triton X-100 or CTAB at room temperature, and seem to have a narrower *p*H-stability profile than rhodopsin. Attempts to purify the new pigments chromatographically have been hampered by this low thermal stability. Preliminary results indicate, however, that the difference spectrum maxima correspond with true absorption maxima. Furthermore, the molar absorbances are not far different from that of rhodopsin.

Fig. 2 Absorbance spectra of all-*trans*-(. . . .), 7-*cis*-(——), 7,9-di*cis*-(- - -) and 7,9,13- tri*cis*-retinal (- · - · -)in *n*-heptane. λ_{max}, in parentheses, and molar absorbance coefficients (last two from ref. 6): all-*trans*, (368) 48,000; 7-*cis*, (359) 44,100; 7,9-di*cis*, (351) 42,500; 7,9,13-tri*cis*, (346) 36,600, 11-*cis*, (365) 26,400, 9-*cis*, (363) 37,700.

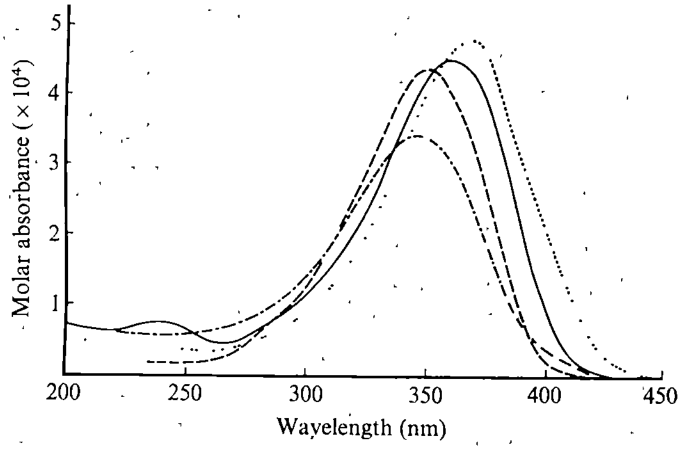

Our observations indicate that the active site of opsin is much less exclusive than originally thought. It seems to accept most of the known geometrical isomers of retinal (*cis* at 7-, 9-, 11-, 7,9-, 7,9,13- and 9,13 (ref. 11). Only 13-*cis*- and all-*trans*-retinals do

Fig. 3 Difference spectra of digitonin solutions of the pigments formed from opsin and various 7-*cis* isomers, obtained by subtracting the spectra of the bleached from those of the unbleached pigments in the presence of 0.1 M hydroxylamine. Illumination by a GE 150-W reflector flood light bulb at 35 cm through a 3-cm 6% $CuSO_4$ solution as a heat filter and a Balzers 482-nm interference filter. A mixture of 7,9,13-tri*cis*- and 7,13-di*cis*-retinal (about 1:3) also gives a pigment with a λ_{max} at about 457 nm, indicating that 7,13-di*cis*-retinal also reacts with opsin Although the properties of the new pigments clearly indicate that they are different from each other and from known pigments (rhodopsin, isorhodopsin I, II), we have not yet established rigorously the geometry of the retinals in the new pigments Indirect evidence is our observation that the λ_{max} of the oximes liberated during thermal denaturation in 1% CTAB+0 1 M hydroxylamine corresponds with that obtained with the original retinal isomer (λ_{max} oximes: 7-*cis*, 353 nm; 7,9-di*cis*, 345 nm; 7,9,13-tri*cis*, 344 nm, all-*trans*, 359 nm). ——, 7-*cis*; - - -, 7,9-di*cis*; · - · - · -, 7,9,13,-tri*cis*.

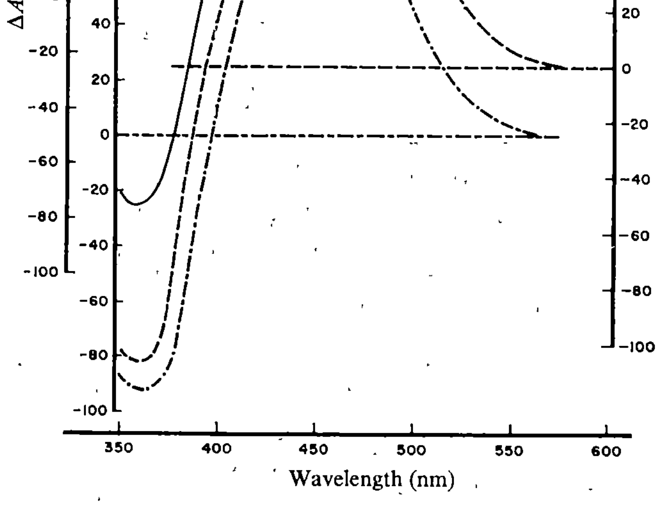

not give rise to special pigments. But the rate of pigment formation and λ_{max} of the resulting pigments differ considerably for the various accepted isomers, 11-*cis* showing by far the highest rate and the largest redshift. As for the 7-*cis* analogues, the low reaction rate, low thermal stability and the smallest redshift observed suggest that conformational changes in the protein and/or the retinals take place in the formation of 7-*cis* pigments and that the final fit involves less interaction between the sidechain of the 7-*cis*-retinals and opsin than in the case of 11-*cis*-retinal. Apparently in the 7-*cis* analogues the protein is in a thermodynamically less stable state and contributes less to the absorbance characteristics of the pigment. The 7,8-*cis* bond introduces a large twist between ring and sidechain and therefore affects the shape of the retinal molecule to a much greater extent than the 9-, 11- or 13-*cis* bonds. This might explain why in the case of 7-*cis* isomers the geometry of the rest of the chain appears to be much less important than in the case of 7-*trans* isomers and has little influence on the reactivity with opsin. As compared with protonated Schiff bases of 7-*cis*-retinals with *n*-butylamine (λ_{max} 410–425 nm in Triton X-100 solution) the 7-*cis* pigments show a smaller redshift (20–25 nm for 7-*cis* and 35–40 nm for the 7,9-di*cis* and 7,9,13-tri*cis*) than those in isorhodopsin and rhodopsin (50–60 nm). Similar to 11-*cis*, we suggest the shifts of the 7-*cis* isomers result from some secondary interaction (but to a lesser extent) between opsin and retinal, which is enhanced by the 9-*cis* geomtetry.

We thank Professor George Wald and Mr Paul Brown for their interest and for facilities. R.S.H.L. expresses appreciation for their hospitality during his stay there. This work was supported by the USPHS and the NSF. Fellowships from the Dutch Organization for the Advancement of Basic Research (W.D.G.) and the John Simon Guggenheim Foundation (R.S.H.L.) are acknowledged.

W. J. DeGRIP

Biological Laboratories,
Harvard University,
16 Divinity Avenue,
Cambridge, Massachusetts 02138

R. S. H. LIU
V. RAMAMURTHY
A. ASATO

Department of Chemistry,
University of Hawaii,
2545 The Mall,
Honolulu, Hawaii 96822

Received April 7, accepted May 10, 1976

[1] Oroshnik, W., Brown, P. K., Hubbard, R., and Wald, G., *Proc. natn. Acad. Sci. U.S.A.*, 42, 578–580 (1956).
[2] Ramamurthy, V., and Liu, R. S. H., *Tetrahedron*, 31, 201–206 (1975).
[3] Asato, A. E., and Liu, R. S. H., *J. Am. chem. Soc.*, 97, 4128–4130 (1975).
[4] Ramamurthy, V., Bopp, T. T., and Liu, R. S. H., *Tetrahedron Lett.*, 3915–3916 (1972).
[5] Ramamurthy, V., thesis, Univ. Hawaii (1974).
[6] Honig, B., Hudson, B., Sykes, B. D., and Karplus, M., *Proc. natn. Acad. Sci. U.S.A.*, 68, 1289–1293 (1971).
[7] Honig, B., Warshel, A., and Karplus, M., *Acc. chem. Res.*, 8, 92–100 (1975).
[8] Hubbard, R., Brown, P. K., and Bownds, D., *Meth. Enzym.*, 18, 615–653 (1971).
[9] DeGrip, W. J., Daemen, F. J. M., and Bonting, S. L., *Vision Res.*, 12, 1697–1707 (1972).
[10] DeGrip, W. J., thesis, Univ. Nijmegen (1974).
[11] Crouch, R., Parvin, V., Nakanishi, and Ebrey, T., *Proc. natn. Acad. Sci. U.S.A.*, 72, 1538–1592 (1975).

Oxygen and toxicity inhibition of amino acid biosynthesis

ALTHOUGH oxygen is of therapeutic benefit for various human diseases, its usefulness is limited by its toxicity[1,2]. In spite of progress, the cause of the convulsions observed in humans and other animals exposed to hyperbaric oxygen remains unknown[3,4], and the biochemical basis of the lung damage resulting from chronic exposure to increased oxygen tensions is poorly understood[5]. Oxygen toxicity, although necessarily expressed in different ways, affects various life forms from bacteria to man[3,4]. There is considerable theoretical basis and experimental evidence for mechanisms of toxicity shared at the cellular and subcellular levels, and research on basic sites of toxicity has often involved tissue cultures or bacteria[2]. The growth and respiration of *Escherichia coli* is rapidly, but reversibly, inhibited by hyperbaric oxygen in minimal salts medium[6]. Significant protection for some microbes against the growth-inhibitory effects of hyperbaric oxygen has been obtained with nutritional supplements, including yeast extract[7]. We have now found that *E. coli* E-26, the source of which has been identified previously[6], is protected from oxygen toxicity by yeast extract because of its amino acid content: a mixture of 20 amino acids gave similar protection.

Table 1 Contributions of individual amino acids to protection from oxygen-induced growth inhibition

Amino acid deleted	Generation time in a gas phase of 1 atm air	Generation time in a gas phase of 4.2 atm O_2	Normalised* ratio
None	27.6±1.2	49.5±0.9	1.00±0.05
All	41.5±1.1	978±102	12.98±1.27†
Alanine	29.8±2.1	52.7±1.3	0.99±0.07
Arginine	31.4±2.0	48.3±1.2	0.87±0.05
Asparagine	29.2±1.4	75.4±4.5	1.45±0.12†
Aspartic acid	29.6±2.0	49.5±0.7	0.95±0.06
Cysteine	30.1±1.4	92.5±8.7	1.77±0.24†
Glutamine	32.7±1.6	54.9±1.2	0.94±0.06
Glutamic acid	27.9±1.0	51.0±0.8	1.02±0.04
Glycine	26.6±1.4	51.1±1.7	1.09±0.09
Histidine	35.4±1.8	55.9±2.3	0.89±0.07
Isoleucine	32.4±1.1	243±50	3.39±0.60†
Leucine	31.2±1.3	144±8.7	2.58±0.22†
Lysine	30.2±0.9	67.2±5.9	1.26±0.14
Methionine	31.9±0.8	88.4±8.4	1.55±0.17†
Phenylalanine	30.7±1.0	93.8±3.6	1.70±0.10†
Proline	28.3±0.8	52.5±1.9	1.03±0.05
Serine	34.5±2.0	52.5±2.5	0.84±0.02
Threonine	30.1±1.4	71.4±5.1	1.36±0.13†
Tryptophane	29.5±1.3	178±14	3.33±0.23†
Tyrosine	31.1±1.9	287±63	5.40±1.29†
Valine	35.6±1.7	901±181	13.95±2.80†
10 Non-protective‡ amino acids	29.0±0.9	72.5±1.8	1.38±0.03†
10 Non-protective§ amino acids plus threonine	40.1±3.9	106±2.5	1.50±0.11†
None; vitamins added¶	31.0±0.9	58.2±0.8	1.04±0.03

A defined basal salts medium containing glucose as the sole carbon source[6] was supplemented with mixtures of the 20 amino acids listed (each 0.65 mM) minus the indicated amino acids. Cultures were adapted to growth in the individual test media with air as the gas phase and grown in small vials with stirring in a vessel which could be pressurised. The vessel was incubated in a constant temperature bath at 37 °C. During exponential growth at an absorbance of 0.1 to 0.2 at 500 nm, the cultures were subjected to a gas phase of 1 atm of air plus 4 atm of oxygen by pressurisation with pure oxygen. After 1 h, the vessel was decompressed. All samples for absorbance measurements were collected in tubes chilled in ice and measured immediately with a Gilford spectrophotometer (the relationship between absorbance and plate colony counts was linear up to 0.8 *A*, all measurements were made below 0.8). Generation times with a gas phase of 1 atm of air were calculated from the slope of best fit relating four determinations of the logarithm of absorbance at 500 nm to minutes of incubation; generation times in hyperbaric oxygen were extrapolated from changes in the logarithm of absorbance during 1 h in hyperbaric oxygen. Values are averages ± s.e. with $n = 8$, except $n = 12$ for methionine and threonine; $n = 4$ for omission of all 20 amino acids, $n = 4$ for omission of 10 amino acids plus threonine, and $n = 4$ for 20 amino acids plus vitamins.

*The quotient obtained by dividing the ratio of the hyperbaric oxygen to air generation times by the value of this ratio with none of the amino acids omitted. This ratio compensates for the differences in growth rates in the various media and is normalised with respect to the protection with all amino acids included. The values of normalised ratios increase as protection of growth in hyperbaric oxygen is reduced.

†Significantly different at $P < 0.05$ from the value obtained with none of the amino acids omitted using Student's *t* test.

‡The amino acids included were: asparagine, cysteine, isoleucine, leucine, methionine, phenylalanine, threonine, tryptophan, tyrosine and valine.

§The amino acids included were the same as indicated in the previous footnote, except that threonine was not included.

¶*p*-Aminobenzoic acid, niacin, and pantothenic acid, each 0.65 mM.

Single deletions of amino acids from the mixture (Table 1) revealed that 10 amino acids were not required for protection against growth inhibition in hyperbaric oxygen, but that deletion of valine, tyrosine, isoleucine, tryptophan, leucine, phenylalanine, cysteine, methionine, asparagine or threonine (listed in order of decreasing effect) caused significant ($P \leqslant 0.05$) loss of the protection afforded by the mixture of 20 amino acids.

The simplest interpretation of these data is that hyperbaric oxygen significantly reduced synthesis of certain amino acids (those which provided protection when included). Presumably, oxygen inhibits specific enzymes involved in synthesis of these amino acids, although proof awaits direct enzyme assay.

To reduce the number of enzymes that might be involved, intermediates of biosynthetic pathways for several amino acids were substituted for the appropriate amino acids to test their ability to protect cells from hyperbaric oxygen (Table 2). α-Ketoisovalerate substituted for leucine (Table 2), suggesting that the pathway, containing four enzymes, from α-ketoisovalerate to leucine, is functional in oxygen-poisoned cells. In the parallel pathway for synthesis of leucine, valine and isoleucine, there is apparently a block (or blocks) in oxygen-poisoned cells of acetohydroxy acid synthetase, acetoxy acid reductoisomerase or dihydroxy acid dehydratase, for α-ketobutyrate did not substitute for isoleucine. Valine transaminase was not sensitive because α-ketoisovalerate substituted for valine. Leucine seemed to be the least critical of the branched-chain amino acids, perhaps because valine transamination is reversible and valine in the medium could provide a source of α-ketoisovalerate for the non-blocked series of reactions leading to leucine synthesis. Valine was among the most critical of the amino acids for protection from oxygen toxicity (Table 1). With valine biosynthesis blocked before α-ketoisovalerate, and no valine in the medium, the cells not only would lack valine for protein synthesis, but could make neither pantothenate nor products (such as coenzyme A) from pantothenate.

The synthesis of cysteine from serine was apparently impaired in hyperbaric oxygen (Table 1). Homocysteine substituted for methionine (Table 2), indicating that inhibition occurred before homocysteine, and that the methyl transferase was relatively insensitive to hyperbaric oxygen. The sensitive site in methionine synthesis probably also accounts for the requirement for threonine during exposure to hyperbaric oxygen (Table 1). Asparagine was apparently required during exposure to hyperbaric oxygen because of inhibition of asparagine synthetase.

The vitamins and vitamin precursor tested (Table 2) revealed no additional protection even though their synthesis was impaired in hyperbaric oxygen (Tables 1 and 2). But failure to synthesise these vitamins probably would not have become growth limiting during the 1 h of exposure.

Explanation of the results obtained with precursors of aromatic amino acids requires consideration of the presence of three isozymes for the production of deoxyheptulosonic acid 2-phosphate and two isozymes for production of prephenic acid, and separate feedback and repression by phenylalanine, tyrosine and tryptophan of the isozymes and the enzyme involved in conversion of chorismate to anthranilate. The permeability of the cell to the intermediates is also a factor. To minimise these problems, cells were preadapted to each different medium before exposure to hyperbaric oxygen.

Shikimate did not substitute for all three aromatic amino acids when absent simultaneously during hyperbaric intoxication, whereas chorismate partially substituted for them (Table 2). This indicated that hyperbaric oxygen significantly impaired the conversion of shikimate to chorismate, but that there was also impairment before chorismate. Deletions of individual aromatic amino acids, with inclusions of each of four intermediates (Table 2), suggested several conclusions. Deletion of phenylalanine decreased protection less than deletion of either tryptophan or tyrosine (Table 2), suggesting that the enzymes in the part of the pathway common to the biosynthesis of all three aromatic amino acids (shikimate kinase, pyruvylshikimate-phosphate synthase or chorismate synthase) were less sensitive than one or more enzymes in the branch pathways from chorismate to tryptophan and tyrosine. There was no significant inhibition of the series of enzymes required for converting anthranilate to tryptophan.

The inconsistency in the failure of prephenate to substitute for phenylalanine (Table 2) could be explained by the known lack of permeability of cells to prephenate. But prephenate apparently penetrated these cells since it reduced the growth inhibition due to hyperbaric oxygen in tyrosine-deprived cells (Table 2). It is conceivable, however, that cells might adapt to prephenate transport when deprived of tyrosine, but not when deprived of phenylalanine.

The inclusion of only the 10 amino acids which, when individually omitted, caused a significant ($P \geqslant 0.05$) decrease in growth in hyperbaric oxygen (Table 1), gave almost as much protection as the 20 amino acids (normalised ratio of 1.38 ± 0.03 compared with 1.00 ± 0.05). The difference between these ratios, however, was significant ($P \geqslant 0.05$), indicating that other

Table 2 Inhibition of amino acid biosynthesis

Amino acid deleted	Precursor added	Generation time in a gas phase* Of 1atm air	4.2 atm O_2	Normalised ratio
None	None	27.6±1.2	49.5±0.9	1.00±0.05
Isoleucine	α-Ketobutyrate	32.2±1.4	240±12.6	4.14±0.21†
Leucine	α-Ketoisovalerate	29.9±0.4	64.4±6.5	1.20±0.12
Valine	α-Ketoisovalerate	27.3±0.2	63.2±2.0	1.28±0.04
Methionine	Homocysteine	28.9±0.6	60.7±1.0	1.16±0.17
Aromatics	Shikimate	32.5±2.0	982±325	17.32±6.43†
Aromatics	Chorismate	34.8±1.2	185±40	2.99±0.77†
Phenylalanine	Shikimate	29.6±3.0	97.5±6.1	1.87±0.09†
Phenylalanine	Chorismate	42.5±2.1	81.0±1.2	1.06±0.05
Phenylalanine	Prephenate	28.4±0.6	92.5±2.9	1.80±0.08†
Phenylalanine	β-Phenylpyruvate	26.8±0.7	63.8±2.4	1.32±0.08
Tyrosine	Shikimate	25.8±0.2	295±7.4	6.30±0.13†
Tyrosine	Chorismate	30.4±0.8	191±19	3.53±0.39†
Tyrosine	Prephenate	34.0±2.0	157±9.7	2.56±0.19†
Tyrosine	*p*-Hydroxyphenylpyruvate	28.0±0.6	69.6±1.9	1.37±0.04†
Tryptophan	Shikimate	30.6±1.3	218±12	3.94±0.25†
Tryptophan	Chorismate	27.7±0.6	186±12	3.70±0.26†
Tryptophan	Anthranilate	29.9±1.2	72.8±2.3	1.35±0.06

Normalised ratio was obtained as described in Table 1

Media and test conditions were as described for Table 1. Precursor concentrations were 0.65 mM except anthranilate (0.5 mM) and shikimate and chorismate (1.3 mM) when substituted for all three aromatic amino acids.

*As for Table 1, except $n = 4$ for all except $n = 8$ for shikimate with phenylalanine omitted, and $n = 11$ for chorismate with tyrosine omitted. Where more than one precursor for a given amino acid was tested, the precursors are listed in the table in the order of their biosynthesis

†As for Table 1.

amino acids, which when omitted singly did not produce significant decrease in protection, may have small protective effects in concert.

The significance of the inhibition of amino acid biosynthesis (which also leads to inability to synthesise nicotinic acid, NAD, NADP, folic acid, pantothenic acid and coenzyme A) is immediately apparent with respect to the growth-inhibitory effects of hyperbaric oxygen for *E. coli* incubated in minimal salts medium, where all its amino acids and the indicated growth factors must be synthesised. The potential significance of these biosynthetic inhibitions for the functioning of mammalian systems is speculative. All the amino acids, except cysteine and asparagine whose biosyntheses were inhibited, are essential for man and rat. The inhibition of synthesis of essential amino acids is obviously irrelevant in higher mammals in terms of protein synthesis and growth. But because of the significant roles of amino acids as precursors for neurotransmitter synthesis, and as neurotransmitters in the central nervous system[8], work is in progress to identify the specific oxygen-sensitive enzymes, and to investigate their potential roles in oxygen toxicity in higher systems.

This research was supported by the Office of Naval Research.

Daniel E. Boehme
Kim Vincent
Olen R. Brown

John M. Dalton Research Center,
University of Missouri,
Columbia, Missouri 65201

Received March 25; accepted May 18, 1976.

[1] Wolfe, W. G , and DeVries, C., *A Rev. Med.*, 26, 203–217 (1975)
[2] Barach, A. L., and Segal, M. S , *Ann Allergy*, 30, 113–121 (1972).
[3] Haugaard, N., *Physiol. Rev.*, 48, 311–373 (1968)
[4] Haugaard, N., in *Underwater Physiology* (edit by Lambertsen, C J), (Academic, New York, 1971).
[5] Gacad, G , and Massaro, D., *J. clin Invest.*, 52, 559–565 (1973).
[6] Brown, O. R., *Microbios*, 5, 7–16 (1972).
[7] Gottlieb, S. F., *A. Rev. Microbiol* , 25, 111–152 (1971).
[8] Curtis, D. R., *Med J. Aust.*, 2, 723–731 (1974).

Reactions involving singlet oxygen and the superoxide anion

In discussing reactions involving the superoxide anion O_2^-, it is generally considered that the radical itself or singlet oxygen generated from O_2^- is harmful to molecules of biological importance[1,2]. Since the demonstration that singlet oxygen participates in reactions is technically difficult, conclusions about its effects are rather speculative. I show here, on thermodynamic grounds, in which reactions singlet oxygen can be formed from O_2^- and in which reactions this is improbable.

By way of illustration I shall use an oxidation state diagram for oxygen at *p*H 7, adapted from Phillips and Williams[3] (see Fig. 1). In this diagram, the free energy per oxygen atom at *p*H 7 ($\Delta G_O'$) is plotted against the formal charge per oxygen atom (n). The ordinate at the left-hand side is related to the one at the right by $\Delta G_O' = nF\Delta E_O'$, in which F is the Faraday. By plotting the values this way, the slope of the line joining the species A and B represents the reduction potential E_O' of the couple A/B. All of the species above the line joining O_2 to H_2O are thermodynamically unstable.

To explain the diagram, I have chosen as examples: the disproportionation of O_2, the Haber–Weiss cycle, the reaction of O_2^- with superoxide dismutase and the reduction of ferricytochrome *c* by O_2^-. First the disproportionation of O_2. O_2^- is not stable; it reacts with itself and forms oxygen and hydrogen peroxide

$$2O_2^- + 2H^+ \rightarrow H_2O_2 + O_2 \qquad (1)$$

where $k = 4.5 \times 10^5\ M^{-1}\ s^{-1}$ at *p*H 7, 22 °C (ref. 7).
Depending on the energy state of the oxygen molecule, the above reaction can have a $\Delta G_O'$ of -29.0 kcalorie ($^3\Sigma_g^- O_2$), -6.4 kcalorie ($^1\Delta_g O_2$) or $+7.6$ kcalorie ($^1\Sigma_g^+ O_2$). Therefore, as the reaction involving $^1\Sigma_g^+ O_2$ has a positive $\Delta G_O'$, O_2^- can be a source of $^1\Delta_g O_2$ but not of $^1\Sigma_g^+ O_2$.

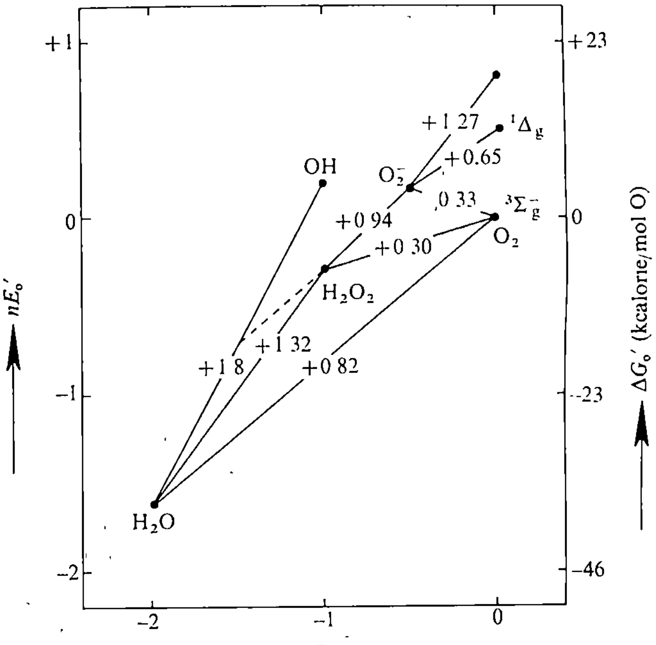

Fig. 1 Oxidation state diagram of oxygen ($P_{O_2} = 1$ atm; $T = 25$ °C) at *p*H 7. Abscissa: formal charge, n, per O atom; ordinate, left: n times reduction potential E_O; right: free energy per oxygen atom at *p*H 7, $\Delta G_O'$. The numbers refer to the slopes of the line E_O' (A/B) denotes the reduction potential of the couple A/B at *p*H 7 under otherwise standard conditions relative to the potential of the normal hydrogen electrode. For this diagram the following data were used: The triangle H_2O_2, O_2 (triplet), O_2^- was constructed using the E_O' values given by Muir Wood[4]. The differences in energy between the $^3\Sigma_g^-$ and $^1\Delta_g$, and between the $^3\Sigma_g^-$ and $^1\Sigma_g^+$ level of oxygen have been given as 22.6 and 37 kcalorie mol^{-1}, respectively[5]. The differences in entropy between the several forms of oxygen can be neglected with respect to the uncertainties in the values of the energy differences. The reduction potentials of the couples H_2O_2/H_2O, OH/H_2O and O_2/H_2O were computed from standard reduction potentials[6].

In 1934 Haber and Weiss[8] proposed a mechanism for the disproportionation of hydrogen peroxide initiated by iron ions. The 'chain' reactions are

$$O_2^- + H_2O_2 + H^+ \rightarrow OH\cdot + H_2O + O_2 \qquad (2)$$

$$OH\cdot + H_2O_2 \rightarrow O_2^- + H_2O + H^+ \qquad (3)$$

Kellog and Fridovich[9] recently postulated that reaction (2) "liberates electronically excited singlet oxygen". Figure 1 shows that this is possible. The reaction can be split up

$$H_2O_2 + H^+ + e^- \rightarrow OH\cdot + H_2O;\ E_O' = +0.8\ V$$

(see dotted line in figure) and

$$O_2^- \rightarrow {}^1\Delta_g O_2 + e^-;\ E_O' = +0.65\ V$$

Since E_O' ($H_2O_2/OH\cdot$, H_2O) is larger than E_O' ($^1\Delta_g O_2/O_2^-$), the formation of $^1\Delta_g O_2$ is possible with $\Delta G_O' = -3.5$ kcalorie. Reaction (3) is also thermodynamically favourable

$$OH\cdot + H^+ + e^- \rightarrow H_2O;\ E_O' = +1.8\ V$$
$$\Delta G_O' = -19.8\ \text{kcalorie}$$

and

$$H_2O_2 \rightarrow O_2^- + 2H^+ + e^-;\ E_O' = +0.94\ V$$

Arneson[10] assumed that singlet oxygen was formed as a product of the chain-terminating reaction

$$OH\cdot + O_2^- + H^+ \rightarrow O_2 + H_2O \qquad (4)$$

It can be shown in the same way that the formation of triplet and both forms of singlet oxygen is possible.

The sum of reactions (2) and (3) is

$$2H_2O_2 \rightarrow O_2+2H_2O \qquad (5)$$

From Fig. 1 it can be seen that hydrogen peroxide is unstable even with respect to $^1\Sigma_g{}^+O_2$ and H_2O: $\Delta G_0' = -5.0$ kcalorie per mol H_2O_2. In the Haber–Weiss cycle, however, $^1\Sigma_g{}^+O_2$ cannot be formed. This may be because the energy released in reaction (3) is not available for the excitation of oxygen.

Superoxide dismutase (SOD) reacts with $O_2{}^-$ at an almost diffusion-controlled rate ($k = (2.37\pm0.18)\times10^9$ M^{-1} s^{-1})[11]. The proposed mechanism is

$$\text{SOD–Cu}^{2+}+O_2{}^- \rightarrow \text{SOD–Cu}^{+}+O_2 \qquad (6)$$

$$\text{SOD–Cu}^{+}+O_2{}^-+2H^+ \rightarrow \text{SOD–Cu}^{2+}+H_2O_2 \qquad (7)$$

The reduction potential of the couple SOD–Cu^{2+}/SOD–Cu$^+$ (+0.42 V (ref. 12)) is too low to oxidise $O_2{}^-$ to $^1\Delta_gO_2$. The energy liberated by reaction (6) is 17.1 kcalorie and that from reaction (7) is 11.9 kcalorie. It has been argued[13] that superoxide dismutase also catalyses the conversion of $^1\Delta_gO_2$ to $^3\Sigma_g{}^-O_2$: $\Delta G_0' = -22.6$ kcalorie per mol O_2. It is not yet known whether this energy is dissipated over the protein molecule and finally transduced to water molecules, or whether is it used for a thermodynamically unfavourable reaction. Apparently the superoxide dismutase molecule can receive energies up to 22.6 kcalorie per mol SOD in single-step reactions without damaging itself. This is probably the reason why only one copper ion at a time is active, as the simultaneous reduction of both copper ions by $O_2{}^-$ would liberate 34.2 kcalorie per mol SOD.

Under suitable conditions ferricytochrome *c* reacts[14] with $O_2{}^-$ (Koppenol and Van Buuren, unpublished). The couple ferri-/ferrocytochrome *c* has a reduction potential of +0.26 V at *p*H 7 (ref. 15). This value is not high enough to cause $^1\Delta O_2$ to be formed. Measurements of the enzymatic activity after reaction with $O_2{}^-$ indicate that the protein is still in its native form (Koppenol and Van Buuren, unpublished).

It is clear that when $O_2{}^-$ reacts with a molecule it can act both as an oxidising or a reducing agent. It is possible that a protein can be damaged by such a reaction, but there is not much evidence for this in the literature[1].

It is unlikely that either of the forms of singlet oxygen will be produced if $O_2{}^-$ reduces the protein molecule, as there are hardly any proteins with redox potentials as high as +0.65 V. Poupko and Rosenthal[16] have reached the same conclusion, but their arguments have to be reconsidered, as they assumed that the ground state of $O_2{}^-$ lies below that of oxygen. This assumption was based on a measurement in the gas phase[17] and is not applicable to reactions in solution.

If $O_2{}^-$ does not react with the protein it is possible that $^1\Delta_gO_2$ and H_2O_2 will be formed by reaction (1). This form of oxygen can react with various groups, for instance unsaturated bonds, and therefore has a destructive effect on the protein. It may be therefore that the main function of superoxide dismutase is to prevent the production of $^1\Delta_gO_2$ by reacting with $O_2{}^-$.

I thank K. J. H. van Buuren, G. H. J. Broers and J. Butler for discussion and comments during the preparation of this paper.

W. H. KOPPENOL

Department of Molecular Biophysics,
University of Utrecht,
Sorbonnelaan 4, Utrecht,
The Netherlands

Received April 7, accepted May 19, 1976.

[1] Bors, W, Saran, M., Lengfelder, E, Spottl, R., and Michel, C., *Curr. Top. Rad Res. Quart.*, 9, 247–309 (1974).

[2] Politzer, I. R., Griffin, G. W., and Laseter, J. L., *Chem.-Biol. Interact.*, 3, 73–93 (1971).

[3] Phillips, C. S. G, and Williams, R J P., in *Inorganic Chemistry*, 314, 509 (Pergamon, Oxford, 1965).

[4] Muir Wood, P., *FEBS Lett.*, 44, 22–24 (1974).

[5] Ebsworth, E. A. V., Connor, J. A., and Turner, J. J.; *Comprehensive inorg Chem*, 2, 714, 715 (1973).

[6] *Handbook of Chemistry and Physics*, fifty-first ed. (edit. by Weast, R. C.), D112 (Chemical Rubber Co., Cleveland, 1970/71).

[7] Behar, D., Czapski, G., Rabani, J., Dorfman, L. M, and Schwarz, H. A., *J. phys. Chem*, 74, 3209–3213 (1970).

[8] Haber, F., and Weiss, J., *Proc. R. Soc.*, A147, 332–351 (1934).

[9] Kellog, E. W., and Fridovich, I., *J. biol. Chem.*, 250, 8812–8817 (1975).

[10] Arneson, R. M., *Archs Biochem. Biophys.*, 136, 352–360 (1970).

[11] Fielden, E M., *et al.*, *Biochem. J.*, 139, 49–60 (1974).

[12] Fee, J. A., and Dicorletto, P. E., *Biochemistry*, 12, 4893–4899 (1973).

[13] Weser, U., Paschen, W., and Younes, M., *Biochem. biophys. Res Commun.*, 66, 769–778 (1975).

[14] Butler, J., Jayson, G. G., and Swallow, A. J., *Biochim biophys. Acta*, 408, 215–222 (1975).

[15] Margalit, R., and Schejter, A., *Eur. J. Biochem.*, 32, 492–499 (1973).

[16] Poupko, R., and Rosenthal, I., *J. phys. Chem.*, 77, 1722–1724 (1973).

[17] Nalley, S. J, and Compton, R. N., *Chem. Phys. Lett.*, 9, 529–533 (1971).

The lipid bilayer as a 'solvent' for small hydrophobic molecules

THE cell membrane is viewed at present as a two-dimensional solution in which the lipid bilayer acts as a viscous 'solvent' for oriented integral proteins[1]. Accepting this model as a working hypothesis, questions arise as to the nature of the hydrophobic interior of the bilayer and what rules proteins, lipoproteins, or polypeptides obey in interacting with it. The simplest hypothesis for the interior is that it is equivalent to a bulk alkyl solvent (albeit a very thin one). If this hypothesis is correct, the enthalpy of transfer (ΔH) of a solute molecule (for example, an alkane) from a bulk alkyl solvent to the bilayer interior should be small. That is, the solute–solvent interaction energy should be about the same in the bilayer as in the bulk alkyl. I have examined this hypothesis experimentally by measuring the solubility of *n*-hexadecane in planar bilayer membranes formed from glycerol-1-monooleate (1-GMO). The acyl chain of 1-GMO is approximately equivalent to 1-heptadecene. The enthalpy of transfer of *n*-hexadecane from pure liquid into 1-heptadecene can be estimated from solubility parameter theory[2] to be only a few calories per mol. Thus, the mixing of *n*-hexadecane in the bilayer interior should be nearly athermal: I have found, however, that ΔH is orders of magnitude larger than expected. This result has important implications for understanding the bilayer as a two-dimensional solution.

The thickness, and therefore the specific electrical capaci-

Fig. 1 Temperature dependence of the specific geometric capacitance (C_g) of planar bilayers formed from glycerol-1-monooleate (1-GMO). Aqueous phase: unbuffered 0.1 M NaCl. The curve through the points is a least squares fit to $C_g = a+bT$ where $a = 0.7005\pm0.0026$ (s.d.) μF cm^{-2} and $b = -0.00471\pm0.00097$ (s.d.) μF cm^{-2} °C^{-1}. Each point is the mean of measurements on three membranes (error bars or point diameter, s.e.m.). C_g of each membrane was determined in triplicate. Desorption measurements at the air–water interface using a Langmuir balance indicate that the 1-GMO is slightly soluble in the aqueous phase and that the solubility increases as temperature decreases (S. H. W. and N. L. Gershfeld, unpublished). The aqueous phase was therefore equilibrated at 20 °C with the bulk lipid solution (10 mg GMO per ml). Each membrane was allowed to 'age' for 10–20 min to ensure equilibration between microlenses and bilayer. In these conditions, C_g was invariant in time within the limit of ±0.3%, and I believe the membranes were in physicochemical equilibrium.

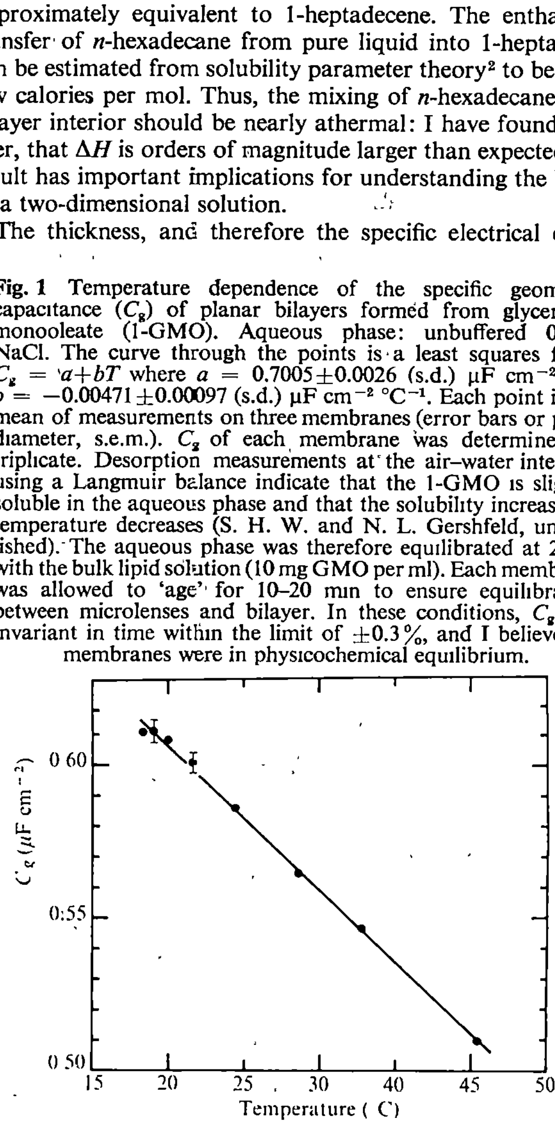

tance, of planar bilayer membranes[3] depends strongly on temperature[4,5], because the bilayer concentration of alkane solvent (used to form the bilayer) is temperature dependent. The bilayer is believed to be in physicochemical equilibrium with the bulk Plateau–Gibbs border (annulus) surrounding it and numerous microlenses[6,7] of excess solvent trapped within it. Consequently, the planar bilayer may be viewed as a bilayer solution at saturation equilibrium with bulk alkane. Therefore, if the composition of the bilayer is measured as a function of temperature, the thermodynamics of transfer of alkane from the bulk state (microlenses and annulus) to the bilayer interior can be estimated using standard equations for saturated solutions[2]. In this way, the interior of the bilayer can be compared directly with the interior of the bulk alkane solvent.

I estimated bilayer composition at various temperatures from measurements of specific geometric capacitance (C_g) using methods described in detail elsewhere[5,8–10] (see Fig. 2 for summary), and the results at equilibrium conditions are shown in Fig. 1. The points can accurately be fitted with a straight line ($r = -0.9987$). The mole fraction (X_S) of *n*-hexadecane was calculated for each point and $\ln X_S$ plotted against $1/T$ and $\ln T$ (Fig. 2*a* and *b*). The enthalpy (ΔH) and entropy (ΔS) of transfer of hexadecane from bulk to bilayer were calculated from these plots and found to be $+3.79 \pm 0.10$ kcalorie mol^{-1} and $+12.6 \pm 0.3$ entropy units (EU) respectively.

These large values of ΔH and ΔS indicate that the *n*-hexadecane molecules are not bound as tightly in the bilayer as in bulk and that they have more motional freedom. One explanation is that, in general, the cohesive forces in the bilayer are not as large as in bulk. The work of Gershfeld and Pagano[12] and Katz[13] however, indicates that the cohesive forces between acyl chains in monolayers and bilayers are the same as in bulk. An alternative explanation is that the hexadecane molecules are located largely in the deep interior[5,7] of the bilayer between the monolayers. Numerous X-ray diffraction studies of bilayers reveal a zone of low electron density in the bilayer mid-plane due to the methyl ($-CH_3$) groups (see, for example, ref. 18). There is thus little interdigitation between the apposed monolayers and a well defined interface must exist between the monolayers. Because the methyl groups have a lower polarisability than methylene ($-CH_2-$) groups, molecules located chiefly in the mid-plane should be subjected to smaller van der Waals' cohesive forces than if they are located parallel to methylene-rich acyl chains within the monolayers. Some hexadecanes must, of course be situated within the monolayers, but simple calculations show that these probably account for $\leqslant 20\%$ of the total

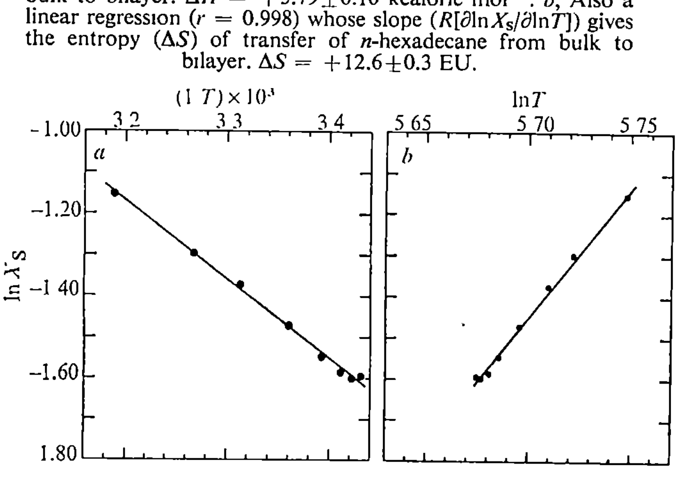

Fig. 2 Temperature dependence of the composition of GMO–hexadecane membranes in a plot of *a*, $\ln X_S$ against $(1/T)$ and *b*, $\ln X_S$ against $\ln T$, where X_S is the mole fraction of *n*-hexadecane in the bilayer. X_S was estimated from the values of C_g using standard techniques[5,10]. Briefly, bilayer thickness δ_B was calculated from $C_g = \varepsilon_0 \varepsilon_B / \delta_B$ where $\varepsilon_0 = 8.85 \times 10^{-14}$ F cm^{-1} and ε_B is the dielectric coefficient of the hydrophobic core. X_S can be calculated straightforwardly using the bulk densities and dielectric coefficients of the acyl chains (AC) (ref. 17) and hexadecane solvent (S), the number n_{AC} of acyl chains per unit area of bilayer, and the equations $\delta_B = v_{AC} n_{AC} + v_S n_S$, $X_S = n_S/(n_S + n_{AC})$; v represents molecular volume. Fettiplace *et al.*[10] and Pagano *et al.*[11] have reported values for n_{AC} at single temperatures; I estimated values at other temperatures using correction procedures similar to those described elsewhere[5]. The corrections are slight and the errors incurred without them are small. At 20 °C, $n_{AC} = 5.26 \times 10^{14}$ cm^{-2} (ref 10) and $X_S = 0\ 205$. *a*, The curve is a linear regression ($r = -0.998$) whose slope ($-R[\partial \ln X_S / \partial (1/T)]$) gives the enthalpy ($\Delta H$) of transfer of *n*-hexadecane from bulk to bilayer. $\Delta H = +3.79 \pm 0.10$ kcalorie mol^{-1}. *b*, Also a linear regression ($r = 0.998$) whose slope ($R[\partial \ln X_S / \partial \ln T]$) gives the entropy ($\Delta S$) of transfer of *n*-hexadecane from bulk to bilayer. $\Delta S = +12.6 \pm 0.3$ EU.

I therefore propose that the mid-plane of the bilayer is a special region because of the high concentration of methyl groups with smaller cohesive forces than found between the methylenes of the acyl chains. Support for this hypothesis is given by Dean and Hayes[15] who measured the heat of sorption of hexane vapour on close-packed stearic acid monolayers at the vapour–water interface. At low partial pressures of hexane (that is, low surface coverage by adsorbed hexanes), the heat of sorption is 4.5 kcalorie mol^{-1}. At high partial pressures (high surface coverage approaching closest packing of hexanes on the stearic acid surface) the heat of sorption becomes identical to the heat of vaporisation of liquid hexane (7.5 kcalorie mol^{-1}). This indicates that the exposed $-CH_3$ surface of the stearic acid does not attract the hexanes as strongly as the fully covered hexane surface or bulk liquid.

Experiments are in progress to examine the thermodynamics of transfer of other alkanes into bilayers containing various acyl chains. Preliminary data for tetradecane–GMO bilayers give values of $\Delta H \simeq 1.2$ kcalorie mol^{-1} and $\Delta S \simeq 4$ EU at 25 °C. The trend of the data suggests that shorter alkane molecules experience cohesive forces closer to bulk values. One reason for this is the larger volume fraction of the bilayer occupied by the smaller alkanes[5,10] which means more nearest-neighbours will be alkanes rather than acyl methyl groups. Results[14] on the solubility of hexane in various phospholipids indicates that significant differences can be expected among different types of acyl chains, and also that the interior of phospholipid bilayer dispersions is different from bulk alkyl solvents.

Finally, I should add that the results reported here for hexadecane depend on the assumptions made about how much the area per molecule of GMO varies with temperature. If the changes are large compared with those used to calculate X_S, then ΔH and ΔS could be much larger. Using a *de novo* method of calculating bilayer composition which predicts relatively large changes in area per molecule[16], I have calculated $\Delta H \simeq +9$ kcalorie mol^{-1} and $\Delta S \simeq 30$ EU. Thus, the values reported here probably represent lower limits.

I thank Dr Sidney Simon for useful and enjoyable discussions and my family for their patience. The research was supported by grants from the NIH and the NSF. The generous support of the Guggenheim Multiple Sclerosis Foundation is also appreciated.

STEPHEN H. WHITE

Department of Physiology,
University of California Irvine,
Irvine, California 92717

Received April 29, accepted June 8, 1976.

[1] Singer, S. J., and Nicolson, G L., *Science*, **175**, 720–731 (1972).
[2] Hildebrand, J. H , Prausnitz, J. M , and Scott, R. L , *Regular and Related Solutions*, (Van Nostrand Reinhold, New York, 1970).
[3] Mueller, P., Rudin, D O., Tien, H. T , and Westcott, W. C , *Circulation*, **26**, 1167–1170 (1962).
[4] White, S. H , *Biochim biophys. Acta*, **196**, 354–357 (1970), *Biophys. J.*, **10**, 1127–1148 (1970).
[5] White, S H., *Biochim. biophys. Acta*, **356**, 8–16 (1974), *Biophys. J.*, **15**, 95–117 (1975).
[6] Henn, F. A., and Thompson, T. E., *J. molec Biol.*, **31**, 227–235 (1968).
[7] Andrews, D M , and Haydon, D. A., *J. molec. Biol.*, **32**, 149–150 (1968).
[8] White, S H , and Thompson, T. E , *Biochim. biophys. Acta*, **323**, 7–22 (1973)
[9] White, S. H., and Blessum, D. N., *Rev Sci Instrum.*, **46**, 1462–1466 (1975)
[10] Fettiplace, R., Andrews, D. M., and Haydon, D. A., *J. Membr. Biol.*, **5**, 277–296 (1971).
[11] Pagano, R E , Ruysschaert, J M., and Miller, I. R , *J. Membr. Biol.*, **10**, 11–30 (1972).
[12] Gershfeld, N. L., and Pagano, R. E., *J. phys. Chem.*, **76**, 1231–1237 (1972).
[13] Katz, Y., *Biophys. J.*, **16**, 52a (1976).
[14] Simon, S A , Stone, W L., and Busto-Latorre, P., *Biophys J.*, **16**, 137a (1976).
[15] Dean, R. B., and Hayes, K. E., *J. Am. chem. Soc.*, **74**, 5982–5984, (1952).
[16] White, S. H., *Biophys. J.*, **16**, 193a (1976).
[17] Requena, J., and Haydon, D. A , *Proc. R. Soc* , **A347**, 161–177 (1975)
[18] Lesslauer, W., and Blasie, J. K., *Biophys. J* , **12**, 175–190 (1972)

matters arising

Quantification of secondary and tertiary structure base pairs in *E. coli* tRNA$_1^{Val}$

NUCLEAR magnetic resonance (NMR) is useful in the investigation of the base-pairing structure of tRNAs in solution because each Watson–Crick base pair and some tertiary structure base pairs give rise to resonances in the low field (11–15 p.p.m.) region of the spectrum[1,2] To determine the total number of base pairs present in tRNA it is necessary to integrate the low field NMR spectrum We have not been satisfied with previous methods[3-6] used to integrate tRNA spectra and present here a new method, based on using resonances in the aromatic region of the NMR spectrum. More accurate integration became necessary after X-ray diffraction results indicated that there are several tertiary structure base pairs[7,8] in tRNA and after we found evidence for four common resonances in the low field region where are due to tertiary structure interactions[2].

In Fig. 1 the low field NMR spectrum of *Escherichia coli* tRNA$_1^{Val}$ is compared with the resonances in the aromatic region of the spectrum in identical experimental conditions. The intensity in the aromatic region (8.5–6.5 p.p.m.) should correspond to 89 protons (one from each C,G,U and two from each A) and a comparison of the integrated intensity in the two regions indicates there are 23 ± 1 resonances (base pairs) in the low field spectrum. To check the method, we compared relative intensities in the aromatic (8.5–6.5 p p.m.) and ribose regions (6 0–5.0) and found they agreed (± 5%) with the value computed on the basis of sequence. Before commenting on these results, we will first discuss other methods which have been used and state why we believe that the use of the aromatic resonances is superior.

One method previously used by us and others to integrate tRNA spectra was to assume that one (or more) partially resolved resonance in the low field region of the spectrum has a known intensity, and then to use this resonance to calibrate the intensity of the rest of the spectrum[3-6]. One problem is that it is not possible to prove that the reference resonance corresponds to the assumed intensity. Another major problem arises from the Lorentzian line shape of the resonances. For example, for a resonance with a full half width ($\Delta\nu_{1/2}$) of 20 Hz, it is necessary to integrate over $6\Delta\nu_{1/2}=$ 120 Hz to include 90% of its intensity To include >95% of the intensity, the integration must be over $12\Delta\nu_{1/2}$, or 240 Hz If neighbouring resonances are located within 2–4$\Delta\nu_{1/2}$, there are additional problems with the allocation of intensity in the overlap region. Because of contributions from the Lorentzian tails, resolved resonances seem to have less intensity than do resonances which are bunched together. Therefore, if a resolved resonance is used as the intensity standard, the total intensity in the rest of the spectrum will seem to be larger by about 10%. When the collection of aromatic resonances are used as the intensity standard, however, the integration includes a relatively wide spectral range (10–20$\Delta\nu_{1/2}$) and tails of various resonances add together to give a reliable value for the total intensity. It is possible that the line shapes of the resonances observed in tRNA are not Lorentzian (as a result of incomplete motional narrowing, exchange or magnetic field inhomogeneity). A number of tRNA spectra have been simulated through the use of Lorentzian lines and, to within the limitations of experimental signal-to-noise ratio, the lines seem to be Lorentzian. Magnetic field inhomogeneity does not contribute to the line shape with the spectrophotometer we used.

Methyl resonances have also been used as internal standards to calibrate the intensity in the low field spectra[5], but, in addition to the problems already mentioned, there are complications caused by impurities[9] and undermethylation[10]. Impurities in the methyl region can be difficult to detect and the presence of a small amount of contamination can lead to larger percentage errors when this region is used as the integration standard rather than the aromatic region.

We have eliminated these problems by using the aromatic resonances as

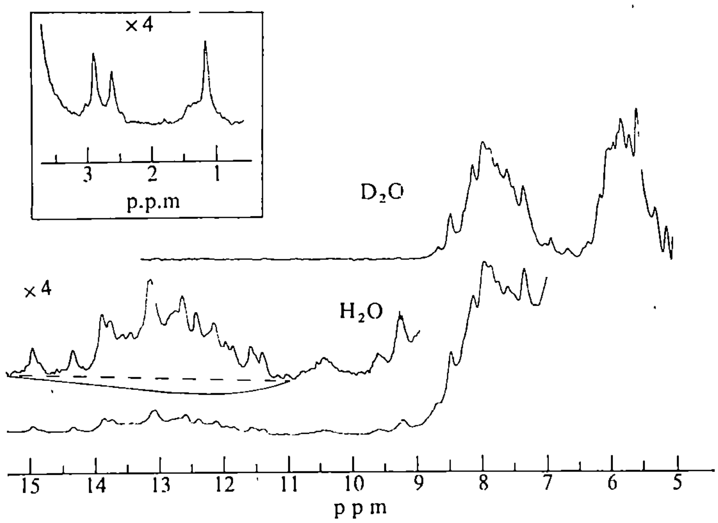

Fig. 1 300-MHz spectrum of tRNA$_1^{Val}$ in various experimental conditions. The spectrum at the bottom is that of tRNA^{Val} in normal NMR conditions, that is, dialysed against 0.1 M NaCl, 10 mM $MgCl_2$ and 10 mM $K_2H_2PO_4$ *p*H 7.0. These spectrum of the methyl region was also obtained in those conditions. The sample was then dried to $\frac{1}{3}$–$\frac{1}{4}$ of its original volume and then returned to its original volume with D_2O. This procedure was repeated several times until the sample was 95–98% D_2O. The spectrum of the aromatic region was obtained with the D_2O sample in experimental conditions identical to those for the H_2O sample. The methyl region of the spectrum was also investigated for the D_2O sample and the intensity compared with that of the H_2O sample. It was found to be within 5% indicating that there was no loss of the sample during the solvent change The aromatic region contains 89 protons. Using the dashed baseline the low field region contains 23 protons, whereas use of the solid baseline gives an intensity of 26 protons for the low field region.

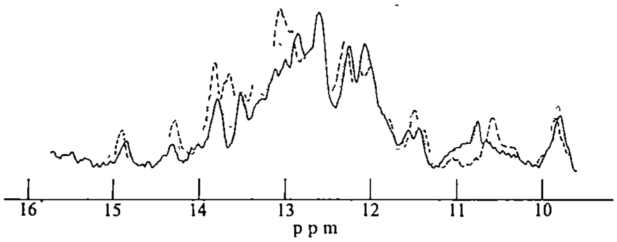

Fig. 2 300-MHz NMR spectrum of *E. coli* tRNA$_1^{\mathrm{Val}}$ in the presence of various amounts of magnesium at 35 °C. The sample was prepared by dissolving desalted tRNA in 0.1 M NaCl, 10 mM K_2H_4PO *p*H 7.0. The intensities of the spectra correspond to 20 ± 1 (no Mg, ——), 21.5 ± 1 (5 mM Mg, · ·) and 23 ± 1 (15 mM Mg, - - -) protons per molecule.

the intensity standard. the signal-to-noise ratio is excellent, there are no problems from impurities, and a large collection of resonances covering some 600 Hz are used to integrate a low field spectrum spanning 900 Hz.

The results with tRNA$_1^{\mathrm{Val}}$ corroborate our earlier suggestion that, in the presence of adequate levels of magnesium (or at sufficiently low temperatures), most *E. coli* tRNA contain 3–4 additional low field resonances due to tertiary structure base pairs[2]. Our result for tRNA$_1^{\mathrm{Val}}$ (23 ± 1) is slightly lower than that (26 ± 1) recently obtained by Reid and Robillard[5] using methyl and low field resonances as integration standards.

The results with *E. coli* tRNA$_1^{\mathrm{Val}}$ indicating the presence of 3–4 extra resonances in addition to those expected from the cloverleaf secondary structure, disagree with our earlier integrations on other tRNA which indicated that the total number of base pairs is somewhat lower (typically around 20)[1,3,4]. The spectra in Fig. 2 illustrate the effect of magnesium on the low field spectrum of tRNA$_1^{\mathrm{Val}}$. As the magnesium level is increased, the intensity in the low field region increases and most of this increase is at positions previously assigned to resonances from common tertiary interactions[2]. By comparing spectra obtained with low and high levels of magnesium present, we estimate that half of the error in our previous integrations was a result of the low level of magnesium we used. The other half of the error can be attributed to the less accurate integration methods used.

Since this paper was submitted, we have re-examined a number of the tRNAs which we originally studied, and find that with higher magnesium levels and our new method of integration, most of the tRNAs contain 3–4 resonances in the low field region (11.5–15 p.p.m.) in addition to those expected from the cloverleaf secondary structure. Details of this work will be presented elsewhere.

The support of the US Public Health Service is gratefully acknowledged.

PHILIP H. BOLTON
DAVID R. KEARNS

Department of Chemistry,
University of California, San Diego,
La Jolla, California 92093

[1] Kearns, D R, and Shulman, R. G, *Accts Chem. Res.*, 7, 33–39 (1974).
[2] Bolton, P H., and Kearns, D R, *Nature*, 255, 347–349 (1975).
[3] Lightfoot, D. R., Wong, K. L., Kearns, D R., Reid, B. R, and Shulman, R. G, *J. molec. Biol.*, 78, 71–89 (1973).
[4] Shulman, R. G., Hilbers, C. W, Kearns, D. R., Reid, B. R., and Wong, Y P, *J. molec. Biol.*, 78, 57–69 (1973).
[5] Reid, B. R., and Robillard, G T., *Nature*, 257, 287–291 (1975).
[6] Daniel, W. E, Jr, and Cohn, M, *Proc. natn. Acad. Sci U.S.A.*, 72, 2582 (1975).
[7] Robertus, J. D., *et al.*, *Nature*, 250, 546–551 (1974).
[8] Kim, S. H., *et al*, *Science*, 185, 435–440 (1974).
[9] Kastrup, R. V, and Schmidt, P. G., *Biochemistry*, 14, 3612–3617 (1975).
[10] Singhal, R P, and Best, A. N., *Biochim biophys Acta*, 331, 357–368 (1974)

REID REPLIES—Bolton and Kearns[1] take exception to our interpretation[2] of the NMR spectrum of tRNA$_1^{\mathrm{Val}}$. Part of their problem arises from the poor resolution in their spectra which is due to either magnetic inhomogeneity or sample impurity, or both. The bumps and shoulders in their spectrum are clearly recognisable as the individually resolved resonances in our spectra[2], but unfortunately cannot be integrated separately in the Bolton and Kearns spectrum[1]. They also object to our use of several resolved single resonances as unit intensities, but we have already pointed out why these resonances cannot contain two protons[2]. More serious objections can be raised concerning the Bolton and Kearns method of integration, which they presumably adopted as a result of their poor spectral resolution. First, the statement that the 8.5–6.5-p.p.m. region should contain 89 protons (the G aromatic proton, both A aromatic protons and one of the two aromatic protons of C and U) has not been verified experimentally and makes the dangerous assumption that no aromatic protons are shifted upfield or downfield out of this region by local ring current effects and that no ribose protons are shifted downfield into this region from the adjacent 'ribose region'. Second, their method of calculating the low field intensity suffers from the inaccuracies inherent in comparing two large numbers. In spite of these problems they have established an intensity that is within 4 protons of the correct value

The fact that Kastrup and Schmidt's samples are contaminated with quaternary ammonium salts from RPC5 (ref. 3), and that careful chromatography resolves (and removes) undermethylated tRNA species[4], is not relevant to either our spectra or our samples.

As Bolton and Kearns admit, the presence of several tertiary base pair resonances in tRNA spectra is in disagreement with their earlier integrations; it is also in disagreement with recently published integrations from that laboratory[4–6] of spectra obtained in the presence of excess magnesium. Since these studies did not acknowledge the presence of tertiary resonances, one can seriously doubt the interpretations made from the observed changes in the NMR spectra.

Finally, I would also add that we are well aware of the Lorentzian nature and line shape of NMR resonances.

University of California,
Riverside

[1] Bolton, P. H., and Kearns, D R., *Nature*, 262, 423–424 (1976)
[2] Reid, B. R., and Robillard, G T., *Nature*, 257, 287–291 (1975)
[3] Kastrup, R V, and Schmidt, P. G., *Biochemistry*, 14, 3612–3617 (1975)
[4] Jones, C R, and Kearns, D. R, *Biochemistry*, 14, 2660–2665 (1975).
[4] Wong, K L., Kearns, D R., Wintermeyer, W., and Zachau, H. G., *Biochim. biophys Acta*, 395, 1–4 (1975)
[6] Rordorf, B. F., Kearns, D. R., Hawkins, E., and Chang, S. H., *Biopolymers*, 15, 325–336 (1976).

Matters arising

Matters Arising is meant as a vehicle for comment and discussion about papers that appear in *Nature*. The originator of a Matters Arising contribution should initially send his manuscript to the author of the original paper and both parties should, wherever possible, agree on what is to be submitted. Neither contribution nor reply (if one is necessary) should be longer than 300 words and the briefest of replies, to the effect that a point is taken, should be considered.

reviews

Waters of the Nile

Malcolm Coe

The Nile: Biology of an Ancient River. (Monographiae Biologicae, Vol. 29.) Edited by Julian Rzóska. Pp. 417. (Junk: The Hague, 1976.) Dutch Guilders 120.

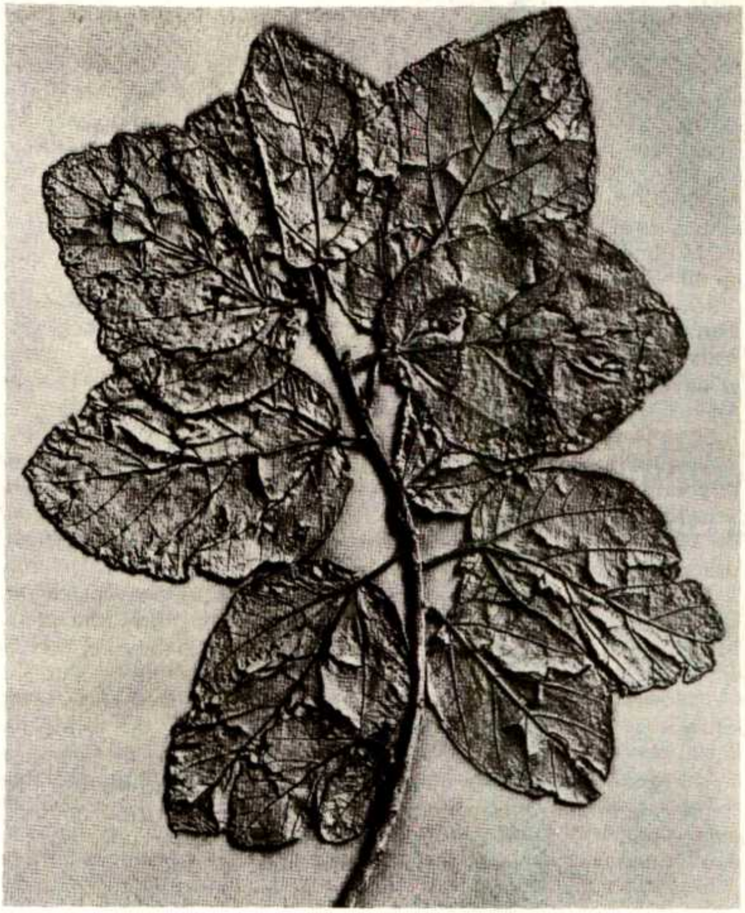

Branch of sacred sycomore or mulberry fig (*Ficus sycomorus*) from a 20th dynasty Egyptian tomb. The tree is "not indigenous but (has been) cultivated in Egypt since times immemorial. It originates from Arabia and Somaliland. Its ancient name was Nehet-entep, and its fruits have been found in tombs of all ages, the earliest from the first dynasty. It was dedicated to Hathor, the Goddess of love and marriage. Even today a vestige of this belief can be seen in the custom of women visiting the sycamore when troubled by matrimonial cares".

No other river in the world can be as closely woven into the history of mankind as the Nile, sweeping for 32 degrees of latitude from the Equator to the Mediterranean. Such prehistoric and historic associations have been largely due to the fact that the "fluviatile" civilisations that have come and gone along its banks have been dependent not only on its life-giving waters but also on the huge and fertile silt burdens that it has carried from the interior of this vast continent.

For us today the memory of Baker, Burton, and Speke who sought to find the source of the Nile are still comparatively fresh, yet the Nile's origins in snow-covered mountains (the Mountains of the Moon) are almost as old as human written history itself.

The history of the Nile valley begins with the regression of the Mediterranean in the Upper Miocene when about 5.5 Myr ago the sea dried up completely and as a consequence of this low sea bed level the resulting intense erosion led to the formation of the Nile valley. Later the great tectonic and climatic events of the Pleistocene resulted in great changes in the southern water sources, leading eventually to the formation of the Neonile about 30,000 yr ago. In spite of the long history of a 'Nile System', however, the river as we know it today is probably no older than 12,500 yr and possibly even as young as 10,000 yr.

Since this vast artery passes for about two-thirds of its length over arid (water-limited) country, the flora and fauna of much of its surroundings stands in stark contrast to the largely detritus-based biota of the river itself.

The fish fauna of the Nile has for so long formed an important item of diet for the civilisations that have waxed and waned along its banks. In all, the river and lakes located at its origins comprises some 320 species of fish of which 62% of them are endemic.

The problems related to development in the desert environment concern not only the problems of huge silt burdens but also concomitant biological effects such as the invasion of the water hyacinth *Eichhornia crassipes* and the spread of the mollusc vectors of schistosomiasis.

Julian Rzóska has brought together a team of distinguished authors who have described the history, geomorphology, hydrology and biology of this great river and its environs in great detail.

The first four chapters deal largely with the history and prehistory of the Nile system, and later sections describe in detail the biotic and abiotic components of the system and its constituent parts.

Although most of this book is concerned with describing the main biotic and abiotic components of this important system, it is inevitable that a vital part must deal with the effects of human interaction, particularly with regard to the Aswan High Dam.

Considering the huge problems that have faced the editor in attempting to condense such a vast assemblage of data this book will be a valuable source for all students of tropical limnology. If the presentation has a failing it is that the fragmentation under such a large number of chapter headings makes it difficult to view the Nile system as a whole rather than its constituent parts. ☐

Malcolm Coe is a member of the Animal Ecology Research Group in the Department of Zoology at the University of Oxford, UK.

Cost–benefit analysis for pesticides

Pesticides: Boon or Bane (Environmental Studies.) By M. B. Green. Pp. x+111. (Elek: London, May 1976.) £2.95.

THIS short book is intended primarily for use in university courses of environmental studies, and by those who are professionally involved with pesticides —farmers, industrialists and legislators. The author is involved in the development of new crop protection products by Imperial Chemical Industries.

The subject of gains and losses from the use of pesticides is developed round the theme of cost–benefit analysis, which is clearly distinguished from investment appraisal. Some of the difficulties are rather glossed-over. How does one optimise costs and benefits for the community as a whole? Those individuals and groups who bear the external losses often gain no compensation except the altruistic satisfaction that their loss is sombody else's gain. Nor is a detailed example given, so that the subject lacks a feel of reality. Does, for example, control of red spider mite count as a credit or debit? Doubtless orchards sprayed to control red spider mite show a profit over those not so sprayed, but this mite only became a pest after insecticides were used.

The quantitative evidence presented for the agricultural benefits of pesticides is disappointing. Figures are given for both Great Briatin and the USA of increases in crop yield, during recent decades, but this will depend on many things besides pesticides—for example, fertilisers, new plant varieties, and irrigation. Estimates are given, mostly for the USA, which has more severe pest problems than we do in Great Britain, for the financial gain from use of pesticides, albeit with no standard error or other indication of these estimates' reliability. The only example for Great Britain (chapter 4) quotes work by Wheatley and Coaker to show that, for at least 30% of the Brussels sprouts grown in 1968/69, increased use of pesticides would have increased the financial loss.

Discussion of biological effects is very limited: virtually no discussion of pest resurgence, development of resistance to pesticides, or of the creation of new pests. The chapter on effects on wildlife is distinctly misleading.

Most of us are probably agreed that pesticides have an important role. This book shows how this role is seen by a scientist whose job it is to produce them. **F. Moriarty**

Dr F. Moriarty has worked at Monks Wood Experimental Station since 1964. His research has been concerned principally with the biological effects of pollutants, especially organochlorine insecticides, on wildlife.

Developments in differentiation

Eukaryotes at the Subcellular Level: Development and Differentiation. (Methods in Molecular Biology.) Edited by Jerold Last. Pp. x+460. (Dekker: New York and Basel, January 1976.) $32.50.

MESSENGER RNA (mRNA) metabolism is one of the important control points in the information flow from DNA to protein. In studies of development and differentiation therefore it is often desirable to measure the concentration or turnover of specific mRNAs. Until recently this could not be done because the concentrations were below the threshold of detection using the available methods. Two developments have altered the situation: first, the purification of specific eukaryotic mRNAs; second, the copying of mRNA by reverse transcriptase. As P. J. Williamson puts it in his chapter on nucleic acid hybridisation methods: "Mother Nature, working in collaboration with Temin and Baltimore, provided the key to an assay in an enzyme from RNA tumor viruses that copies RNA into DNA". By following the instructions in this manual, other research workers should likewise be able to make pure mRNA templates and complementary DNA, sensitive to as little as 1 pg of specific RNA or DNA, which is sufficient for many purposes.

This book strikes a good balance between highly specialised information, peculiar to the differentiating systems at the focus of individual chapters, and more general methods. The latter include the isolation, separation characterisation and transcription of mRNA, and the use of nucleic hybridisation kinetics. The authors place due emphasis on various ways which have been found to avoid common pitfalls, for example, the synthesis of incomplete chains *in vitro*, polypeptides in the case of the popular wheat germ translation system (used to assay messenger activity), or DNA copies of mRNA in the case of reverse transcriptase. Mother Nature does not always collaborate with molecular biologists in her distribution of enzymes. Consequently, readers will appreciate the tips for eliminating or suppressing unwanted nucleases in various preparations. A high degree of specificity is required for many of the bioassays. Nonspecific precipitation can invalidate the results obtained using antibodies to characterise the products of *in vitro* translation, and several authors describe how they keep this to a minimum. A certain overlap between chapters concerning these tricky areas of experimentation is if anything helpful.

The mass of detail on gel electrophoresis of RNA and protein, repeated for a number of systems, is perhaps excessive, especially in view of the abundance of earlier reviews. On the other hand, there is too little space devoted to the manipulative aspects of hybridisation, particularly when the use of small (2 μl) reaction mixtures in capillaries is recommended. The editor rightly celebrates the use of immunoprecipitation to isolate specific polysomes for purification of the less abundant messengers. It was disappointing, however, not to find this method represented anywhere in the text, not even for the isolation of ovalbumin mRNA, which nicely demonstrates its potential. It was refreshing to read about biological systems as diverse as the insect chorion, slime moulds, red blood cells, lung, muscle and oviduct, in successive chapters. One important system is conspicuous by its absence; much progress has been made with immunoglobulin mRNA, and methods used in this work are sufficiently specialised to merit description.

The book is valuable as a timely source of information about *new* methods in molecular biology which are not collected together elsewhere. Like sucrose gradient centrifugation, the new methods will be of enduring value to future molecular biologists. The material in this book is well organised and thoroughly cross-referenced. My only complaint about this, the eighth in the series, is the grouping of the Figures at the ends of the chapters. To use this manual effectively, the reader must be dextrous in using his fingers to mark the appropriate parts of the text, the Figures, and the references, while turning the pages with his right hand. I am glad to possess this book: there should soon be many well-stained copies on laboratory benches everywhere. **H. J. Gould**

Dr Gould is a lecturer in the Department of Biophysics at King's College, University of London, UK.

Scientific approach to art

Beyond Aesthetics: Investigations Into the Nature of Visual Art. Edited by Don Brothwell. Pp. 212+80 photographs. (Thames and Hudson: London, May 1976.) £9.50.

THE writers of the 12 essays collected here have tried to be objective about the visual arts. The task was fairly easy for two of them. Creedy describes the British system of art education, and says it is the best in the world. There is a light-hearted piece on the demography of artists by Cox. Statistics are hard to come by, and classification is capricious, but their pay, hours of work, and expectation of life seem about average. The apparent hazards of being an artist in France become comprehensible when one discovers that the category includes acrobats. Research has unexpected hazards. A chimpanzee bit her keeper for the first time when a drawing was incautiously interfered with. Whiten uses this as evidence for the intensity of the artistic impulse once it is aroused. It is odd that apes, unlike some birds, show little artistry when wild. This latency is perhaps similar to that shown by Eskimos. Decorating clothing and tools was traditional, but Brothwell says that the strikingly vigorous statuettes, now so much admired, were not made before European contact.

Defects in colour vision are as common among students at several art schools as in the general population. Pickford comments that nearly half of the group was unaware of the defect until tested in early adulthood. He comments also on the greater than average incidence of myopia and astigmatism among artists. He questions the idea that artistic differences between races have a physiological basis, although he comments on the curious absence of precise words for *blue* in many languages. It was this that led to the suggestion that colour perception varied. In a second article Pickford tries to make sense of aesthetic preferences in spite of their fluidity. Fluidity is the theme of Rookmaaker's article on art and morals. Using the depiction of nakedness as an example, he argues that anything can become acceptable if it is introduced in sufficiently small steps.

It is a pity Weale was not given more space to discuss the geometry and physics of art. Compression and too few illustrations make it difficult to understand all the interesting things he has to say on such subjects as deliberate distortion and the *pointilliste* technique. Writing of the use artists make of scientific illustrations he comments ". . . if a pattern appears in a book it is part of science, but if it is brushed on to a canvas it becomes art."

There are two unsurprising articles on children's drawings and paintings, and an article on cross-cultural psychology that is surprising only because of the number of platitudes and tautologies crammed into it.

N. W. Pirie

N. W. Pirie has recently retired as head of the department of biochemistry at Rothamsted Experimental Station, Harpenden, UK.

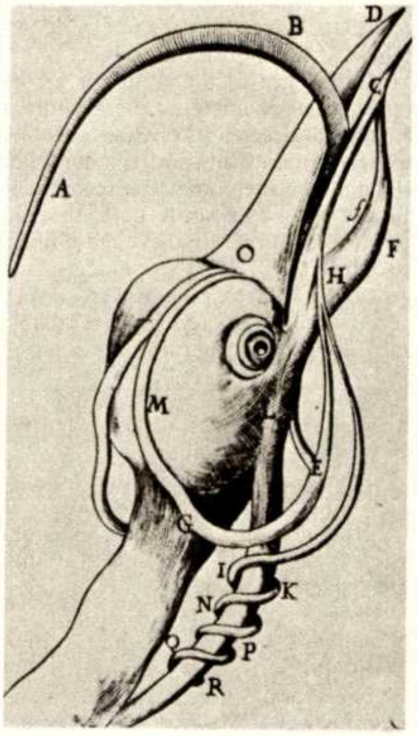

Tongue and hyobranchial apparatus of a woodpecker. By G. A. Borelli, published in Rome in 1681. Taken from *A History of Comparative Anatomy: From Aristotle to the Eighteenth Century.* By F. J. Cole. Pp. 520. (Dover: New York; Constable: London, March 1976.) £3.90 paper.

Ion transport in plants

Uptake of Ions by Plant Roots. By D. J. F. Bowling. Pp. xi+212. (Chapman and Hall: London, Halsted: New York, March 1976). £6.50.

THE uptake of ions by plant roots is a subject which over the years has probably had more man-hours devoted to it than any other single aspect of plant physiology. In consequence an extensive, very diverse and often contradictory literature has accumulated. From time to time courageous individuals attempt to digest this material and produce a coherent exposition of the process. The would-be author is presumably initially inspired to his task by a conviction that he can see order where others cannot and inevitably therefore there will be; as Dr Bowling states in his preface, "some undue bias and personal foibles". His bias is towards the electrophysiology of roots, a topic which is well described. Realisation of this bias, however, seems to have caused the author to over-compensate to the extent that in a short book (185 pages of text) covering a vast subject he seems to have devoted a disproportionate amount of space to discussion of already well documented topics.

Although covering not merely the uptake of ions by roots, as the book's title implies, but also their transfer to shoots together with related information on leaves and algae has led to some superficiality in presentation, Dr Bowling has, however, produced an interesting and logically presented book. He looks on the overall process as being divisible into four sections or links in a chain: movement of salts in the soil to the root surface; uptake into the root; transport across the root and movement in the xylem to the shoot. Separate chapters deal with what Dr Bowling describes as "the more theoretical aspects of salt uptake".

Finally, there is a chapter which although headed 'Some conclusions and a look into the future' attempts firstly, to analyse results from his laboratory on the absorption of potassium and water by a sunflower plant grown in potting compost in controlled conditions in the light of the previous chapters; and secondly, describes briefly some recent experiments on the existence of specific ion binding proteins in the plasma membrane and the action of ionophores or ion-carrying agents. It is a pity that more space could not have been devoted to the relevance of these latter two aspects to the electrophysiological and kinetic approaches described earlier.

Because of its breadth of coverage the book is a good source of reference to the literature up to 1974 and it should prove useful to students and others specialising in the subject. I hope, however, that before the next printing is set, it will be re-proofed to remove some omissions in the references and misprints in the text.

D. A. Barber

Dr Barber is a Principal Scientific Officer at the Agricultural Research Council's Letcombe Laboratory, Wantage, UK.

Stellar photospheres

The Observation and Analysis of Stellar Photospheres. By David F. Gray. Pp. xv+471. (Wiley-Interscience: New York and London, January 1976.) $27.70; £14.

THE study of stellar atmospheres (or even of just their photospheres, which are the layers emitting the bulk of the radiation) has become too vast a subject to be comprehensively covered in depth in a single book, and so it is natural (and indeed desirable) to find authors concentrating on their own particular fields of research interest while summarising other aspects more briefly. The distinctive and very valuable feature of the present book is that it provides a detailed elementary introduction to the experimental measurement and analysis of stellar spectral characteristics using predominantly Fourier techniques—a subject in which the author has himself done some very useful work and which is coming to be an essential tool in all spectral analysis with the advent of high speed multichannel detectors and digital microdensitometers.

In other respects, the book is a clear, well written and exceptionally well illustrated introduction from the practical point of view with enough of the theory of stellar atmospheres given (accompanied by many numerical formulae and tables) to show the application to the determination of effective temperature, pressure, gravity, radius, chemical composition and velocity fields. Difficult theoretical issues, like the intricacies of iteration to flux constancy and the effect of departures from local thermodynamic equilibrium, are mentioned and summarised as accurately as is possible within a few words supplemented by references, which is quite suitable for a text of finite size. It is always a weakness in this kind of treatment, however, that the reader does not quite get a physical feeling for the subject.

The presence of a few minor errors in places (for example, in the treatment of inward-directed radiation in the theory of radiative transfer) does not help and on these matters the reader will do well to consult both the old classical texts of Woolley and Stibbs, Unsöld and Aller and the modern one by Mihalas. There is, however, a very fine discussion (not otherwise available in textbooks or perhaps anywhere else) of the use of line profiles to sort out rotation and different sorts of 'turbulence'—a field in which the author's Fourier methods offer an enticing vista of new research.

In the spirit of the generally practical approach of this book, there are extensive sections on spectrometers and detectors. These are generally very good, although it is a matter for some regret that the roles of grating blaze angle and camera speed in the efficiency of spectrographs have not been explicitly brought out. The treatment of instrumental profile and scattered light corrections is excellent.

Particularly in its treatment of the practical aspects of stellar spectrum analysis, this is a valuable book that is strongly recommended for all astronomical libraries and could be a worthwhile investment for research workers and graduate students; the price is not too unreasonable in present-day conditions. **Bernard Pagel**

Bernard Pagel is Deputy Chief Scientific Officer at the Royal Greenwich Observatory and Visiting Professor at the Astronomy Centre, University of Sussex, UK.

Membrane research

Mammalian Cell Membranes. Vol. 1: General Concepts. Edited by G. A. Jamieson and D. N. Robinson. Pp. 276. (Butterworth: London and Boston, Massachusetts, 1976.) £18.

IT has been said that a week is a long time in politics and things are becoming almost as fluid in membrane research. Since 1973, for instance, when much of the material in this book was prepared, the complete sequence of a transmembrane protein has been established by Marchesi and his colleagues. The molecular basis of ion conductance across membranes has become clearer at least conceptually in artist's impressions if not in hard fact, and the proteins involved are being characterised. Similarly the importance of microfilaments and microtubules in membrane function in non-muscle cells has been realised.

Some of the treatment understandably has a slightly old-fashioned look. For example, in Rose's short chapter on the anatomy of the mammalian cell discussion of the various forms of junctional complexes in cells must be inadequate in view of the considerable advances made on their structure and function. Two other examples concern surface labelling procedures particularly with lactoperoxidase-catalysed iodination and SDS–polyacrylamide gel electrophoresis. The description is very scanty considering the recent extensive use of these techniques.

The book is the first in a five-volume series, and according to the Editors is an introduction to "the most essential aspects of physical and chemical studies which have contributed to present knowledge of membrane structure." This volume, however, is sharply divided on the basis of these criteria. On the one hand there are clear and straightforward descriptions, respectively, of the cultivation of cells by Robinson and a brief account by Glick of selected methods of plasma membrane preparation largely from cultured cells. Physical methods are covered by Levine and Chapman, and enzyme markers are summarised in a useful chapter by Hinton and Reid. The remainder of the book consists of four short speculative chapters on specialised, even esoteric, topics. Gingell argues for the electrostatic control of diffusion of proteins in membranes. The basic point is that proteins carry high negative charges (mainly due to sialic acid groups) that must be overcome by ligand binding before condensation can occur. Condensation of transmembrane proteins, equated by Gingell with intramembranous particles, is considered to be obligatory for formation of ion channels through the membrane. Well, maybe; but hardly the basic facts required for an introduction to membrane science. One difficulty too is the as yet inconclusive evidence, except in erythrocytes, that intramembranous particles can be clustered by ligand interaction with surface membrane proteins.

The infant science of the mechanical properties of cellular membranes is interestingly reviewed by Canham, and Lenard and Landsberger discuss some models of membrane structure. The biogenesis of mammalian membranes is summarised by Malhotra. I enjoyed reading these four chapters and, for my money, they recommend the book for this year's bookshelf.

On the whole each chapter is well written and free of serious factual or typographical errors. The book should be useful to research workers and to final year undergraduates. The person who discovers on p32 that trypsin "catalyses the hydrolysis of peptide bonds between the carboxy group of arginine or lysine and the amino group of an adjacent amino acid" is likely to have difficulty in following many of the complex arguments that follow elsewhere in the book. The editors are to be congratulated on setting a good standard for the first volume and I look forward to the arrival of the remaining volumes. **R. Colin Hughes**

R. Colin Hughes is a member of the scientific staff of the Medical Research Council at the National Institute for Medical Research, Mill Hill, London, UK.

obituary

ROBIN LAURANCE

Jacques Lucien Monod died at his family home in Cannes on May 31, 1976 at the age of 66. He was one of the foremost leaders of the revolution in molecular biology, helping to lay the framework of our understanding of gene action and protein synthesis. Monod was a scientist of the first rank, both in his experimental work and in his ideas. By his scientific research and by his Essay on the Natural Philosophy of Modern Biology (translated into English as *Chance and Necessity*) he has left an indelible mark on the intellectual history of the 20th century.

Monod was born in Paris in 1910. When he was seven his family moved to Cannes where he lived and studied till he was eighteen, so that he thought of himself more a man of the Midi than a Parisian. His father was a painter, an unusual vocation at that time for one of Huguenot stock, coming from a family which had produced many doctors, pastors, civil servants and academics. His mother was American, a native of Milwaukee, the daughter of a New England mother and a Scottish immigrant father. Early influences were his father, who in addition to his artistic sensibilities had a strong interest in science and in Darwin in particular; also his Greek master, a scholar whom he admired for his civilised attitude to life. Scientifically, he acknowledged among his immediate elders the impact of George Teissier, André Lwoff, Boris Ephrussi and Louis Rapkine. Perhaps most important of all was his year's stay, in 1936, with Morgan's group at Caltech. Their full, free and critical discussions, together with the easy personal relationships between people of different ages, were a revelation to him and strongly influenced his style of organising research.

In his scientific career Monod, though never seriously impeded, did not get off to a flying start as many young men do nowadays. It was at the beginning of the war, after a famous reply to André Lwoff ("L'adaptation enzymatique? Connais pas! ") that he first became aware of the nature of the phenomenon he was studying. Only after the war, when he had joined the Pasteur under Lwoff, did he fully recognise the depth of the problem which was to become his life's work. By then he was 37. But once having recognised it, he pursued it with tenacity, versatility and imagination. His logic was relentless; his intuition variable but profound. No wonder that many of his younger colleagues came to feel that to work with him was a scientific education in itself.

The results are now in every textbook. There is no space here to follow the story in all its details, nor to show how the commonplaces of today grew out of the confusions of yesterday. The concentration on β-galatosidase; the arrival of Mel Cohn ("acquisition précieuse") who knew about proteins and also how to use the Tiselius apparatus; the proof that the appearance of enzyme activity represented *de novo* synthesis (a big surprise at the time); the skilful use of lactose analogues to separate the inductive from the substrate activity and the discovery of the permease and the transacetylase. Finally the grand collaboration with François Jacob (from the other end of the corridor) leading to their immensely skilful dissection of the inductive process by genetics; the realisation, from certain mutants, that the synthesis of all three proteins could be turned on and off together (the operon); the postulate that the *i* gene product was a protein—the inhibitor—and the famous PaJaMo experiment of Pardee, Jacob and Monod which suggested that the message was unstable. It is difficult now to recall that at that time the ribosomal RNA was assumed to be the message. The realisation that the ribosome was a reading head, which could read any message, came as a great flash of understanding. After that the road to the genetic code was wide open.

Meanwhile Monod, with Jacob and Changeux, had recognised that the properties required for the inhibitor were, at first sight, unusual for a protein. On reflection, however, they realised that such properties were in fact common—their existence had simply not been appreciated. Thus was born the theory of allosterie. Various earlier workers (including those studying haemoglobin) had glimpsed the idea but had not recognised its generality and its profound importance. For now one could see how any metabolic pathway could be linked, control-wise, to any other. Without this type of mechanism even the simplest organisms could not regulate themselves and higher organisms could not exist.

In 1969 Monod gave the Robbins Lectures at Pomona College in California. He used the occasion to develop and make precise his general ideas about biology, man and society. The lectures became a book, originally written in English, rewritten by him in French under the title *Le Hasard et la Nécessité*. Its publication made a strong impact and it became a best-seller. It aroused the almost united opposition of the French intellectual establishment which has always preferred Marx, Freud and Teilhard de Chardin to Darwin and Mendel. Written with force and clarity, in an unmistakable personal style, it presented a view of the universe that to many lay readers appeared strange, sombre, arid and austere. This is all the more surprising since the central vision of life that it projected is shared by the great majority of working scientists of any distinction. It would be difficult to find a better example to display the deep rift between science and the rest of our culture.

Monod was not aloof from public affairs. He was a persistent critic of the French University system and of the way in which French science was supported. Thus it was not entirely surprising that in 1971 he accepted the invitation to become Director-General of the Pasteur Institute. This decision came partly from his strong sense of duty; he was naturally reluctant to have to give up his research and his writing, but the Institute was in a bad way, having become desperately short of money. Monod threw himself wholeheartedly into his new job. He tried many things: appeals for funds, both public and private; the setting up of a production subsidiary with the aim to exploit useful ideas from the research side of the Institute; various economies and a limited reduction of staff. Finally he toyed with a scheme, strongly opposed by many of his colleagues, to move the laboratory outside Paris. But the opposition to such a move was too strong and the sums of money required too great; only the government could supply them, a source he somewhat distrusted, as he feared for the Institute's independence. Looking back one can see that the Pasteur had to change and to change radically. It needed a scientist of Monod's stature to make the changes possible and reasonably palatable.

Science was the dominant activity in Monod's life but it was not the only one. During the war he worked for the French underground, receiving recognition for this perilous work from both the French and the American governments. He became a keen mountaineer only to give it up for sailing; the characteristic mixture of discipline and freedom appealed strongly to his temperament. He would sail his 37′ boat single-handed or with the assistance of a mere amateur. Having a wide intellectual curiosity, he was remarkably well read, both in classical and modern authors—Camus was a personal friend. But his main passion outside science was music. He both played the cello and conducted. In his twenties he even wondered whether to give up science for music, and all through his life he tried to find time to make music with his friends.

Monod was a man of great personal charm. His English was perfect, though simpler than his French. Thanks to his good ear and his American mother, he spoke it without any trace of the heavy accent which most Frenchmen find difficult to discard. Good-looking, though small of stature, he commanded attention by his intelligence, his clarity, his incisiveness and by the obvious breadth and depth of his interests. Never lacking in courage, he combined a debonair manner and an impish sense of humour with a deep moral commitment to any issue he regarded as fundamental. He had great warmth for his friends and treated his students with affection and candour, as if they were members of his family. To others he could be charming but somewhat more remote. Though his creative powers flowered most abundantly in his scientific work he combined within himself, in a natural harmony, the scientist, the philosopher, the man of action and the musician. He might well have made a world reputation by concentrating on any one of these roles. Such a range of gifts is rare. It is fortunate for us that he chose science, otherwise the development of molecular biology would have been very different.

The formal outlines of Monod's career will be recorded here only briefly. He obtained his first degree in 1931 and his doctorate in 1941, both from Paris. He joined the Pasteur Institute in 1945 as Chef de Laboratoire, becoming Chef de Service in 1953, head of the department of Cellular Biochemistry in 1954 and Director-General in 1971.

His stay at Caltech in 1936 was supported by the Rockefeller Foundation. While at the Pasteur he held a chair at the University of Paris from 1959 to 1967, followed by a chair in Molecular Biology at the Collège de France from 1967 to 1972. From 1962 onwards he was a non-resident fellow of the Salk Institute.

Monod received many honours, including Foreign Membership of the Royal Society and the US National Academy, among others, and several prizes, culminating in the award of the Nobel Prize for Physiology and Medicine in 1965 which he shared with Lwoff and Jacob.

His wife, the former Odette Bruhl, whom he married in 1938, died in 1972. They had two sons, twins, who survive him. Both are scientists. **F.H.C.C.**

announcements

Meetings

August 30–31, **L'Anthropologie et la Biologie des Populations Andines,** Toulouse, France (Prof Georges Lambert, Centre d'Hemotypologie du CNRS, Colloque d'Anthropologie et Biologie des Populations Andines, Hôpital de Purpan, Avenue de Grande-Bretagne, 31052 Toulouse Cedex, France).

September 2–3, **564th Meeting of the Biochemical Society,** Dublin (The Meetings Officer, The Biochemical Society, 7 Warwick Court, Holborn, London WC1R 5DP).

September 6–8, **Biochemistry of Lipids,** Paris (J. Polonovski, Faculté de Médecine Saint-Antoine, 27, rue Chaligny, F 75571 Paris Cedex 12, France).

September 21–23, **Science and Technology of Water Soluble Polymers,** Cardiff (The Short Courses Secretary, Planning Section, UWIST, King Edward VII Avenue, Cardiff CF1 3NU, UK).

September 24–25, **Joint Radiological Meeting of the RCR and the BIR,** Leeds (The General Secretary, BIR, 32 Welbeck Street, London W1M 7PG).

October 7–8, **Meeting of the South-eastern Cancer Research Association on Membrane Receptors, Regulation of Gene Expression and Chemical Carcinogens,** Atlanta, Georgia (Dr Edward Bresnick, Chairman of the Dept of Cellular and Molecular Biology, Medical College of Georgia, Augusta, Georgia 30902).

nature

August 5, 1976

Still a lot to learn from the Chinese

TEN thousand, a hundred thousand, a million dead in the latest earthquake at Tangshan in China? It seems as if the Chinese authorities are not at present going to talk about the scale of the disaster, maybe believing that details of fatalities will produce some sort of ghoulish exultation in other countries and result in an indefinable loss of face. Certainly some silly people who, a year ago, would have dubbed the prediction which saved tens of thousands of lives on the Liaoning Peninsula a "spectacular success" have been talking about the present catastrophe as a "spectacular failure" of prediction. Such views can no doubt be discounted as shallow, but they do perhaps show why China will be sensitive to worldwide comment, and they do make it all the more necessary that the Chinese should understand the serious and compelling reasons why earthquake scientists, engineers and social scientists the world over want to learn as many lessons as quickly as possible from China, now an acknowledged leader in the field of prediction.

Even though there do not seem to have been any open alerts about the most recent quake, those who have recently returned from China report that there had been concern over magnetic field changes and that there was a feeling that seismic activity was migrating in the general direction of Tangshan. More remarkably, travellers continue to bring back accounts of unusual phenomena preceding and accompanying earthquakes, which seem to indicate that there is still a lot to learn about the art of prediction.

Animal behaviour as a predictor has now, of course, become an object of popular fascination the world over. For one thing, the jumpiness of cats, dogs and snakes can be understood by a much wider public than can fluctuations in the velocity of elastic waves; for another, it does bring science down to a folksy level at which the good amateur observer is just as valued as the professional. There are few branches of science where this is true today, and it is excellent news that amateur involvement has been given such a good name by the Chinese. Even the most sceptical Western observer will be impressed by the sheer crescendo of reportings of unusual phenomena last year in the weeks before the Liaoning earthquake. The latest addition to the collection is 'earthquake lights'. Like anomalous animal behaviour, this has been a subject attracting practically no attention at all from seismologists, yet there is now a report from a respected Chinese seismologist of a glow in the air at the same time as a quake—something that had previously only been the subject of discounted hearsay.

What the Chinese have succeeded in doing, and what this most recent calamity will certainly not dissuade them from continuing, is to raise the consciousness of people to unusual phenomena, even to the extent of encouraging them to file reports. This is a lesson that should not be lost in California, the Soviet Union, Japan, the Middle East or other places scourged by earthquakes. There are encouraging signs that at least the inhabitants of San Francisco and Los Angeles are prepared to learn from the Chinese experience that the experts need all the help they can get. That is why it is important that the momentum of interest which has been developing should not be stifled by suppression of news and of the interchange of scientists.

There is a lesson in all this for the international organisations, too. Countries which have developed technologies for their home market invariably start to turn their thoughts to export potential before long. And if the technology is one like railways, air-traffic control or defence systems, the inevitable interchange of personnel, training of technicians and stationing of advisers creates a dependency which is a modern form of imperialism. Just because China is at present reeling under a disaster and no other country can yet do any better does not mean that in ten years time there will not be an exportable commodity—and that certain countries, already with tribulations enough of their own, will not be asked to buy an expensive system and absorb a thousand advisers. UNESCO, rather well equipped in this field, should take this matter seriously while it is still a cloud on the horizon. □

The ecology of ecology

"Ecology has become a social movement as well as a branch of biology". Philip Lowe of University College, London, and Michael Worboys of Sheffield City Polytechnic give their view on the role of science in the environmental movement

ENVIRONMENTAL concern, and with it the apparent immediacy of the ecological crisis, has of late receded. A downturn in the business cycle has sets its own limits to growth, and apocryphal warnings of the decline of Western capitalist democracies have superseded the environmentalists' warnings of natural decay. But many environmental problems remain, and one enduring feature of many of these is their implication of modern science, both as cause and as solution.

From the anxiety over radioactive fall-out and pesticides, through to current worries about fluorocarbons, nuclear power and hazards of the workplace, science has often been cast as the villain of the piece. Yet scientists have also been in the forefront in alerting society about these problems and in campaigning for action. Moreover, a leading role for science has been proposed in evaluating risks from pollution, in developing new resources and in the general formulation of solutions and strategies in response to environmental problems.

This ambivalence with regard to science—which is, incidentally, very common where science impinges upon social issues—creates many difficulties. For example, different scientists may regard the same "problem" very differently. Whose assessment or warning do we believe? To solve environmental problems, do we need more science, less science or different science? To which group of scientists, if any, do we turn for solutions? One common response to questions of this sort has been to look to ecology and ecologists as sources of "wisdom" and "healing". The received notion that ecology is about wholeness and the natural has left it seemingly untainted by the reductionist and industrial associations of most modern science.

Indeed, its marginality to mainstream science, of which ecologists have long complained, now proves to be an asset in a period when science generally is being questioned and attacked. Most environmentalists and environmental pressure groups have fallen in behind the banner of Ecology. They have used ecological information vicariously and promoted the adoption of ecological values, giving rise to a whole new genre of social polemic best described as popular ecology. In short, ecology has become a social movement as well as a branch of biology, and it is the connection between these two aspects of ecology that needs to be explored.

Is politics redundant?

The literature of the contemporary environmental movement and popular ecology is characterised by a general rejection of conflict, especially political conflict: the lesson of ecology in its broadest sense is supposedly harmony, balance and symbiosis. As in technocracy, where traditional politics is deemed redundant through the overriding and deterministic effects of man's technological situation, so in popular ecology politics is declared equally redundant because of the imperatives of man's ecological predicament. Compelling physical and natural constraints supersede and replace moral, social and political considerations.

In Britain, the establishment of an Ecology Party indicates the presumption that environmental issues transcend orthodox political alignments. Formed in 1973 as a direct consequence of the appeal in the *Blueprint for Survival* for "a national movement to act at national level, and if need be to assume political status and contest the next general election", it was known initially as the People Party—its subsequent change of name illustrating nicely how ecology has come to be seen as bigger than all of us. The electoral ambitions of the Ecology Party, its commitment to come to power by democratic means and work within the framework of a mixed capitalist economy and a parliamentary democracy, are somewhat at odds with its very radical manifesto proposals for de-growth, decentralisation and population control "to provide a working basis for ecological government". However, recent correspondence in their broadsheet, *Alliance*, has argued that it may in fact be essential for government, composed of an aware elite—the writer used the Spaceship Captain analogy—"to introduce ecology without taking the people into its confidence".

But most environmentalists would not completely abolish politics. Some view politics as the refined tool of environmental management, enabling fine and delicate control of human well-being within the greater and larger purposes of the biosphere. The implication is that, as well as transcending political differences, environmental problems are also non-political in the sense that their solutions are management or technical issues. Hence, politics should no longer be about power, its use and distribution, but, instead, about the forms or techniques of government most appropriate to cope with urgent environmental problems.

Conventional response

The conventional response of the scientific establishment to environmental problems was expressed by the Council for Scientific Policy in 1972, when it urged that "more science will be needed, not less, to provide remedies and to enable society to take precautions against pollution", and called for the "closer integration of science into social policies". Thus, more "scientific" planning, monitoring and management are advocated, in such forms as technology assessment, environmental impact analysis, quantitative environmental forecasting and ecological evaluation—activities viewed by their practitioners as so many exercises in applied rationality, but criticised by others for clothing implicit political assumptions and implications in a pseudo-scientific mystique of "objective" knowledge and "rational" techniques. What is clear is that their practice seems to be based on the assumption of the availability of consensually defined social goals which, if absent, can be summonsed by the persuasive presentation of the facts of the matter.

●

Ecological coalition

Conservation, when treated in these terms, appears to be an unadulterated good thing; equated with applied ecology and with its own quantitative techniques, it seems beyond the realm of politics. The supposed political consensus surrounding the practice of conservation in Britain, however, can also be seen to be the operation of a coalition of powerful rural vested interests, whose use of ecological rhetoric has enjoyed the active support or acquiescence of professional ecologists. In fact, popular ecology has long been very closely linked with the interests and ambitions of professional ecologists.

The institutionalisation of a scientific discipline such as ecology is generally accompanied by the competitive development of a disciplinary ideology which publicises the putative social utility and world-view of the discipline and plays an essential role in the establishment of cohesion and a sense of collective identity amongst its practitioners. In Britain, the emergence of ecology as a distinct discipline dates from the turn of the century. Government recognition of its potential utility came in 1949 with the establishment of the Nature Conservancy as both a research council for ecology and an agency for the formation and management of nature reserves.

Initially, the Nature Conservancy commanded a very much smaller share of resources than the other research councils, and ecology, with its amateur connotations of natural history, had a low status in the scientific community. But the Conservancy proved very successful in lobbying government and popularising ecology, and took the leading role in forging various groups into an effective and dynamic environmental lobby. In the late 1960s members of the Conservancy played a crucial part in popularising the existence of an environmental crisis and figured prominently in the institutional developments that were the outcome of the resulting public and governmental concern. Hence a strong element in ecological propaganda is a direct product of competition within science.

Whose preserve?

The further suggestion that the environmental crisis reflected the pre-eminence of the physical sciences over the environmental sciences has also had considerable currency. It is indeed true that many science-related activities associated with both the generation and control of environmental problems, have been the preserve of chemists and engineers, largely to the exclusion of biologists. Thus, much pollution, such as that due to pesticides, detergents and nuclear radiation, has been seen to be consequent upon faulty and diminutive knowledge of environmental biology as compared with, say, physics and chemistry—indicating to some the need for a greater share of resources to be devoted to research and training in the environmental sciences.

To many others, however, this analysis, in confining itself to relative deficiencies within science, does not go far enough and fails to recognise the economic and social basis of the organisation of science. The preponderance of the chemical control of pests over their biological control, for example, and the resultant pollution and development of pest resistance, may be less a function of the power of chemists over biologists than of the power of the chemical industry within society. Professional competition and interfactional disputes within science often need to be understood in terms of the relationship between scientific disciplines and elites and powerful interests external to science.

Beyond tactical responses

The plausibility of ecologists has been of crucial importance, and was directly involved in their popularisation of the environmental crisis, just as their professional interests are deeply enmeshed in "technical" solutions to environmental problems. In some instances, however, the appeal to ecology has gone beyond the search for tactical responses to particular problems, towards the claim that ecology can contribute to a radical re-ordering of human purposes and a re-orienting of society away from environmental disaster. The findings, concepts and approach of ecology have proved a rich source of ideas and analogies in the construction of environmentally sound social programmes—niche theory, the ecosystem concept, energy flow, materials recycling, limits of tolerance and succession have been deployed in many and varied contexts.

Beyond this have come calls for ecological ideals, an ecological ethic, an ecological morality, ecological values and ecological determinism. Certainly, the synthetic nature of ecology and its claims to transcend the narrowness of other disciplines have always been a source of its popular support. But, in this case, science appears to be adopting a leading role in society as a value-affirming, goal-setting and consensus-generating institution. At a time of change and dissent from established values, when it is generally accepted that traditional institutions have lost much of their authority, science, albeit reunified and chastened by the example of ecology, is turned to by those who value order and stability as the one authoritative voice.

Science assailed

Such appeals to science, however, come at a time when its own moral influence has also been assailed, by the attacks of what many identify as an anti-science movement. The response of critics like Roszak to the social problems of modern science has been to reject science—the objective, rational and calculating consciousness—in favour of a more subjective, intuitive and feeling type of knowledge. For Roszak, the discipline of ecology, and not high energy physics, should be the model science—a view shared by influential and respected proponents of ecology such as Max Nicholson and Barry Commoner.

The separate debate over social responsibility in science has raised other questions about the direction and control of science. The self-doubt that has been generated has prompted some leading scientists to demand greater solidarity and less dissent within the scientific community so as to render it less vulnerable to external attack and to preserve its authority in society. Indeed, internal fragmentation has been identified as one cause of the inability of science to respond effectively to environmental problems, and calls for a "unified science", based on ecology and the related general systems theory, predict the consequent restoration of the weakened position of science in society. The holistic image of ecology, its promise of making whole that which was fragmented, and its widespread popular support, might help revive the moral influence of science, and regenerate consensus both within and outside of science.

Crisis highlighted

The environmental crisus thus highlights a crisis of confidence within science and a crisis of science's authority in society. Mary Douglas, in her essay "Environments at Risk" (*Times Literary Supplement*, October 30, 1970), has supported this view by drawing attention to the problems of credibility that scientists face in warning society of possible environmental dangers. Indeed, the environmental movement has been interpreted by Michael King (*Technology and Society*, **8**, 1; 1973) as a bid by certain scientists to relocate and extend the basis of scientific authority. Science as a mere source of useful knowledge confers upon scientists the very limited and fragile power of technicians, but the ecologists' claim to appreciate the wisdom of Nature, as well as the orthodox scientists' knowledge of natural laws, might legitimate a continuous and central involvement in the formulation of political purposes and values. ☐

Science policy in Poland

Science has not escaped recent developments in Poland. **Below,** a Special Correspondent describes the trends.

AFTER four relatively fat years science in Poland seems to be entering a less happy period. Following the dismissal of Mr Gomulka during the stormy days of December 1969, his successors initiated a more dynamic economic policy and science was declared an essential factor of economic growth. The new leaders were keen to present themselves as scientifically oriented people. A honeymoon for science began with the setting up of a special committee, headed by the well-known sociologist Professor Jan Szczepanski, to develop long term policy in education at all levels. The state pocket was enriched by loans from abroad and was opened wider for science.

As a result of this, research and development expenditure rose from 1.4–1.6% of GNP in 1969 to about 2.5% in 1975. GNP itself rose by about 60% during this period and so the funds available for science were almost doubled—a dramatic increase, especially in comparison with stagnating funds for science in Western countries. These official figures perhaps exaggerate the increase to some extent because the definition of what is meant by science for budgeting purposes is vague and some expenditures not included previously are now under the heading of science. A sharp rise in the money available is, however, an indisputable feature of this period and witnessed by a number of new buildings, better endowment of institutes and laboratories, improvement of the level of scientific work in many fields and wider contacts between Polish and foreign scientists.

The rise of money was not accompanied by a proportional rise of scientific staff or number of students. In the 1950s the relative number of students in Poland was greater than in most Western countries. But since the further rise of the number of students was slow (especially after the student riots in 1968) Poland has been overtaken by most European countries. The accompanying table of numbers from the official Statistical Yearbook, 1975, shows the recent trends.

It has never been easy in Poland to spend all the money allocated for science, and it may be even more difficult in the future. Budgets of Universities and Institutes are being tightened by a large number of regulations more relevant to industry than to science. This is a feature of the five-year plan for the 1976–1980 period for the development of different aspects of technology. Plans of this kind—strange as it sounds—have also been compiled for basic science. A low opinion of the value of the whole time-consuming and inelastic planning system is common in the scientific community.

In spite of the earlier generous flow of money the housing conditions of many scientific institutions remain poor. Many courses in the University of Warsaw are given in buildings belonging to different secondary schools dispersed over the city of Warsaw. The salaries of academic staff are very small in relation both to academic salaries in other countries of the communist block and salaries of other professional groups in Poland. The salary of a senior member of the staff (*adiunkt*) of a research institute is equal to the average salary of those working in the state sector (about 3500 zlotys per month, that is, $120 on the official tourist exchange rate—a figure which gives an accurate impression of the buying power of the earnings). From September 1976 the salaries will rise by about 15%. The rise of salaries previously given to all other professional groups is now reaching the last group of government employees, namely, those working in the scientific institutes.

The honeymoon of the Polish scientific intelligentia was over in 1973, close to the time of the much advertised Second Congress of Polish Sciences. It seems that the reason for this change of the official attitude was related to the disillusion of the government that Polish science will contribute significantly to the immediate improvement of the economy. Unfortunately these idle hopes have been repeatedly supported by a large number of short-sighted Polish scientists eager to satisfy their personal goals.

In Poland as in most eastern-block countries the intermediate link between scientific research and technology, the link responsible for implementation of new products and processes, is very weak. Its functions are frequently performed with doubtful results by purely academic institutions, for example in the institutions of the Polish Academy of Sciences (PAS). Thus the sharp rise of the level of Polish industry in 1970–75 was only marginally based on the achievements of Polish scientists and engineers, and was due mainly to the purchase of know-how from abroad; noting this, the leaders of the country have begun to treat science not as a producer of goods but as a consumer.

The social sciences in Poland depend on official doctrine to a lesser extent than in other countries of the communist block. However, in spite of the official statements made in 1970 interest in their work has declined steadily. The report of the education committee under Szczepanski has been shelved, and the education policy actually introduced bears little relation to its conclusions. Poland was fortunate to have after the war three economists of international distinction, Oscar Lange, Michael Kalecki and Edward Lipinski, but their economic advice has been used in several other countries and never in Poland. Of these three only Professor Lipinski, member of PAS, is alive, but his views expressed in a number of letters having a wide hand-to-hand circulation are not taken into account by the authorities.

In contrast to other groups of Polish intellectuals the scientists are relatively meek. Not many scientists or scholars signed the letters of protest against the recent revision of the Polish constitution legalizing the leading role of the party and friendship to the USSR. Those who did are being punished: younger people are not having their contracts renewed, and others, as for example Professor Stefan Amsterdamski, philosopher, are prohibited from going abroad even to attend conferences.

According to official statements the government is not planning to increase the quota of places for students in universities. This means that the situation of an applicant will be about the same as during the last few years due to the fact that the post-war demographical bulge is now close to its end. The announced quota based on the evaluation of future demands is very conservative and recently it became clear that for example the number of

Student trends in Poland

Year	No. of students per 10,000 of population	No. of resident students per 10,000 of population	No. of students per 1,000 of population in the age group 19–24	No. of resident students per 1,000 of population in the age group 19–24
1970–71	101	64	136	87
1974–75	126	76	139	84

The official number of students per 10,000 of population given in the international part of the Yearbook is 144, but this includes also students in higher schools under the Ministry of Defence and the Ministry of Internal Affairs. In these schools there are about 80,000 students, and the total number of students in other institutions of higher education is 427,000.

physicians needed exceeds the number of accepted medical students.

During the academic year 1975–76 there was a considerable rise of political activity among students. They raised their voices in protest against the changes in the constitution. More recently they protested against the expulsion of their colleague Mr Jacek Smykala from the Medical Academy in Szczecin (during a tutorial class in economics he asked what part of the national budget is allocated to the police force), and against the imprisonment of their colleague Mr Stanislaw Kruszynski from the Catholic University in Lublin (the only private university in Poland), who was sentenced to six months in prison for writing unfavourable opinions about the social system in Poland in private letters to his relatives and friends. From Warsaw University alone about 800 people signed this protest.

At the beginning of 1976 a reduction of staff (up to 10%) took place in many research institutes, including those connected directly with industry. These reductions touched universities and industries of PAS to a lesser extent but it was decided to freeze the number of their staff for the next three years.

The Polish economy, as is commonly accepted, is now entering a very difficult period. One of the signs of this was the government's proposals to increase the food prices in June (meat by about 70%, sugar 100% and so on) which would have caused a fall in the spending power of wages by about 20 to 30%. The wave of strikes (70 to 80% of big factories according to unofficial figures) and unrest in a few places forced the government to rescind this proposal. Science seems to be near the top of the list for economies. According to some sources it has already been decided to halve the rate of investment in science. Considerable political tension in the whole country has not by-passed the scientists. Speculations about personal changes have wide circulation. Meanwhile the repressions against those involved in strikes and protests have already begun.

As in all countries of the communist block, scientists in Poland have no real representation to defend their own interests and those of science. The Polish Academy of Sciences is the agent of the government and provides no more than formal representation. For example, recently, in June 1976, after the abortive attempt to increase prices, the Praesidium of PAS at its meeting in the metallurgical factory in Silesia wrote a letter of adulation to Mr Gierek, the Secretary of the Party. A few months previously, his son, Professor Adam Gierek, was elected to the PAS; perhaps those who voted in his favour had in mind the dire fate of the Romanian Academy, which, as it is said, was a consequence of its refusal to elect Mrs Ceaucescu (wife of the Secretary of the Party in Romania) to the Academy.

Photo: AP

Polish leader Edward Gierek

These and similar steps do not contribute to the authority of PAS and do not reflect the views of the Polish scientific community. An interesting new development in this community and in the whole group of intellectuals is the collaboration of differently minded people, rightists and leftists, catholics and even members of the party. This collaboration is an outcome of the common feeling that the present policy endangers not only the further development of science, but also the very existence of independent Poland, and that the most important task confronting the intelligentsia is the defence of the national identity. □

Artificial intelligence in education

Miranda Robertson discusses research aimed at exploiting computers in human communication and teaching

If the principal goal of research in artificial intelligence (AI) has been the development of intelligent machines, an increasingly conspicuous sideline is the promotion of intelligence in human beings. This social orientation has been stimulated partly by Newell and Simon at Carnegie Mellon, and the ideas of Papert and Minsky, at the Massachusetts Institute of Technology, (MIT), who see in artificial intelligence a new way of looking at the nature and development of natural intelligence.

Papert has for some years been an advocate of the use of sophisticated computer programming languages to help children learn how to think. Writing a program in a high-level language involves the expression of thought processes which would not usually be formulated. When there is a mistake ("bug") in the program, the child can retrace his thoughts in the program and understand his own mistake. The result, Papert believes, is to increase the child's intellectual effectiveness in general and make him more articulate.

LOGO learning for children

That is the idea behind experiments which have been going on in the LOGO laboratory at MIT for about three years. LOGO is a high level language which children can use to program various devices, the best known of which is a mechanical "turtle" with a retractable pen.

Usually, the child begins by learning how to draw geometric designs by programming the turtle; later, as the system becomes more familiar, the turtle can be replaced by a somewhat nimbler oscilloscope trace. One important advantage of a LOGO system over more conventional curricula is that children enjoy working with it and it can be used to overcome the resistance that many children develop to learning mathematics.

So far, the experiments at MIT have not been sufficiently systematic to produce clear evidence for Papert's persuasive arguments. Up to now, the children have been drawn largely from the families of MIT research workers and from a local school, neither (probably) very representative; and the classes have been supervised by research staff, in particular Dr Jeanne Bamberger, rather than by professional teachers.

There has for some time been talk of an entire school geared to the LOGO system, and where about half the school curriculum would be undertaken at a computer terminal. But this ambitious project is not expected to start in earnest for another two years, during which a small group of teachers will be trained in LOGO, a pilot LOGO educational project will be run with the cooperation of one of the Cambridge or Boston schools, and some thought will be given to how the children's intellectual development should be evaluated.

Evaluation presents a special problem because it is not clear that the intellectual abilities LOGO is supposed to foster would necessarily be revealed by conventional psychometric tests. Papert and his colleague Marvin Minsky, who specialises in theories of intelligence, maintain not only that conventional tests are inappropriate, but that the qualitative difference they would expect to see in the children would be great enough to make statistical tests unnecessary. On the other hand they do not expect to be able to show those differences with anything short of a total "LOGO environment" and that is two or three years off.

In the meantime, however, their ideas have inspired a number of schools and universities elsewhere to set up their own experiments with LOGO or other similar systems. Of those, a small research project and the Artificial Intelligence Department at the University of Edinburgh is the furthest advanced with a scheme for providing more rigorous experimental evidence. Jim Howe, Tim O'Shea and Ben du Boulay have enlisted the cooperation both of a local school and of a teacher training college with the aim of finding out how learning may not only help pupils to learn, but teachers to teach. Eleven-year-old children from George Herriots, a direct grant Edinburgh boys' school, have now been taking part for a year in LOGO classes in the course of which a LOGO curriculum has been designed, and practical experience has led to various improvements both in the language itself and to the development of new devices.

Children with problems

Although the Edinburgh group do not entirely share Minsky's and Papert's contempt for all psychological testing (indeed part of the research project is to design suitable tests), the most striking effects they have seen so far have been precisely of a kind that psychometric tests would miss. Some of the most interesting evidence so far is anecdotal, and the example of one particular child with a problem suggests that a particular advantage of LOGO learning may be in bridging the communications gap between teacher and pupil, especially where for one reason or another that is particularly difficult.

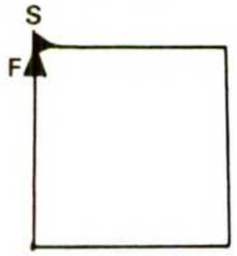

```
w: TO SQUARE
d:1 FORWARD 100
d:2 RIGHT 90
d:3 FORWARD 100
d:4 RIGHT 90
d:5 FORWARD 100
d:6 RIGHT 90
d:7 FORWARD 100
square defined
w:  SQUARE
```

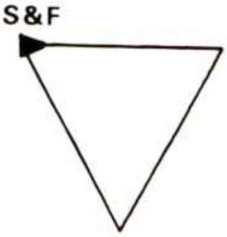

```
w: TO TRIANGLE
d:1 FORWARD 100
d:2 RIGHT 120
d:3 FORWARD 100
d:4 RIGHT 120
d:5 FORWARD 100
d:6 RIGHT 120
d:  END
triangle defined
w:  TRIANGLE
```

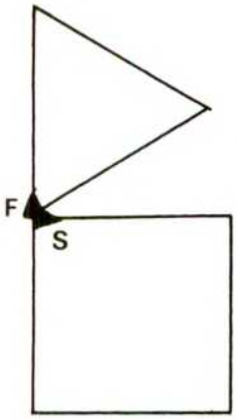

```
w:  TO HOUSE
d:1 SQUARE
d:2 TRIANGLE
END
house defined
w:  HOUSE
```

This is an example of a "bug" which is commonly encountered when, having learned to write procedures to draw a square and a triangle, the child puts the two programs together to make a "house". In this particular case, the bug arises because the turtle's change in orientation (indicated by arrows: S=starting position, F=finishing position) in the course of drawing the two shapes has not been correctly predicted.

w : prompt typed when the computer is ready to take a command; d: prompt typed when computer is in the definition mode.

The anecdotal evidence concerns a "dyslexic" boy who was included by chance in the first group of 18 children to be taught LOGO. In spite of remedial lessons from sympathetic and enthusiastic specialists for two years, neither his reading and writing nor his classroom performance had improved, and he was well established in the role of class clown and dunce. LOGO programming, unlike the rest of his school work, however, came relatively easily to him and he rapidly reached a point where he was able to teach other boys. That brought about a change in his classmates' attitude to him and a conspicuous increase in his own self-confidence. O'Shea illustrates the point with an account of an argument between the boy and his teacher during a classroom lesson on sets. Asked to name the set of even numbers divisible by two and the set of odd numbers divisible by two, he responded with, "the set that never finishes and the set that never starts". The textbook answers are the infinite set and the empty set, and the teacher marked him wrong.

In a way that would have been uncharacteristic before he started learning LOGO, the boy argued with his teacher and as a result was awarded half marks. Part of the significance of that story, for Howe and O'Shea, lies in the phrasing of the boy's "wrong" response, which, like the definition of a LOGO program, is expressed in terms of procedures. The implication is that learning LOGO supplied not only the confidence to argue, but the language in which to do so (incidentally, a school inspector spontaneously remarked of other boys in the group that they were exceptionally mathematically argumentative).

LOGO learning for teachers

One of Papert's most important claims has been that learning LOGO provides a descriptive system within which to think and communicate; and this is relevant not only to the private intellectual development of individual children, but to the interaction between pupil and teacher: it can also help the teacher to understand and express what he has to teach. Papert maintains that what makes so many common skills (such as riding a bicycle) so hard to teach is the lack of an adequate way of describing them. Because learning with LOGO is learning within a descriptive system, it makes everything explicit and thus automatically more communicable.

That is the rationale for an experimental LOGO course which Ben du Boulay has been running at a local college for trainee primary school teachers. Primary school mathematics teaching is often a special problem partly because the teachers' own grip on the subject is none too firm. The aim of du Boulay's part of the Edinburgh project is to see whether LOGO learning has a function in helping primary teachers both to understand and to explain mathematics. That research is still at a preliminary stage.

But LOGO learning as a "catalyst" to communication is an important theme of the Edinburgh research. The particular term catalyst has been adopted by Sylvia Weir to describe the effect of LOGO learning on communications between an autistic child and the normal adults who work with him. Weir, working with Ricky Emmanuel, has found that allowing an autistic child to control the turtle from an array of buttons on a box stimulated him to communicate with them in a spontaneous way they had rarely seen in any other context.

She attributes this "humanising" effect to what she calls "shared relevance": the transparent connections between the pressing of the buttons and the movements of the turtle, and between the turtle's actions and the child's own movements in space provide, in her view, a basis of shared relevance, or a common framework, within which the child and the adults can communicate. Building on a framework of shared knowledge is the basis for any intelligent and effective teaching, and educationists acknowledge that good teaching must depend on the teacher's being able to reach out to the child's position and lead him from there. LOGO learning may be a special help where the subnormality of the child makes the gap unusually large and the teacher's task unusually difficult.

Future of LOGO

But the commitment of the Edinburgh group is to find hard evidence for the possible benefits of computer-based teaching systems like LOGO. Most of the known methods of educational assessment will be used for that purpose, and Howe and O'Shea have added one new test specially designed to reflect some of the skills that LOGO is supposed to promote. O'Shea calls it the "articulation test", and it tests the ability of a child sitting on one side of an opaque screen to instruct his partner on the other side on how to construct a particular pattern from coloured blocks. That apparently simple problem has been known to reduce an untutored child to tears of inarticulate frustration, so the results should be interesting; but so far, they are only suggestive.

On what evidence there already is, what part are computer-based systems really likely to play in future education? Papert purports to believe that the future of education and computer-based systems are one and the same, and the next few decades will see the day when each child sits at home at his own computer terminal, without going to school at all. Expense he shrugs off on the grounds that electronics, unlike anything else, are getting exponentially cheaper (consider the cost of the pocket calculator five years ago and now). Nonetheless, equipment of any kind is expensive and computers and their peripherals will remain more expensive than books. And although the Edinburgh research team has been impressed by the way that Papert's educational insights have been borne out, from the practical point of view their attitude is both more conservative and more pragmatic than his.

First, they do not see in LOGO a means of disposing of the teacher: the idea is that such systems may make conventional teaching methods more effective, not that they should replace them. Second, experience is beginning to suggest that the most effective use of computer systems may turn out to be in the education of subnormal children or those with other special problems. If the Edinburgh group can be accused of having a vision, then it is of machines which foster human interactions, rather than making them obsolete. □

BRITAIN •

Benn spells it out

Developments on the British energy front are fast and furious, with nuclear power capturing most attention. Chris Sherwell reports.

FAST moving sectors of the British economy are not in great abundance these days, but there is one that is beginning to behave in a manner representative of a seething hive of activity. Hardly surprising, for it is none other than the energy sector itself. And not a little of this is due to the increasingly voluble debate over nuclear power.

The arguments over whether Britain should have nuclear power already having been settled, the manner in which it is to be deployed and utilised is now at issue. That includes the question of timing, so there are tactical as well as strategic policy decisions to be taken. The latest involves the Steam Generating Heavy Water Reactor (SGHWR), expenditure on which was deferred for a year in the latest round of government spending cuts.

The cut means a saving for 1977–78 of £40 million, and a reduction of £5 million on research for the project. That in turn has made the broadening debate on the future of the SGHWR either more pointless or more controversial, depending on your perspective. But it hasn't prevented a start to the hearings of the House of Commons Select Committee on Science and Technology on the subject. They began this week, Mr Anthony Wedgwood Benn, Secretary of State for Energy, answering questions.

Mr Benn was fresh from his discussions at the end of last week with Sir Arthur Hawkins, chairman of the Central Electricity Generating Board (CEGB), who supported the pressurised water reactor when a choice was being made in Britain in 1974 but has since, on Mr Benn's testimony, given every assistance regarding the SGHWR. Sir Arthur was, however, expected to deploy cost estimates and electricity demand forecasts to advise against an immediate go-ahead, on the SGHWR or anything else. Mr Benn also had before him a report submitted within the past week from Sir John Hill, chairman of the UK Atomic Energy Authority (UKAEA), assessing the progress made so far on the SGHWR.

It was soon apparent that Mr Benn was concerned to make only four main points. One, as he pointed out at the beginning, the middle and the end of his evidence, the British Government has not yet reached a decision to cancel the SGHWR, nor even a preliminary view on the matter. Two, the decision through spending cuts to postpone for a year its commissioning, while possibly having consequences for the nuclear industry outside the SGHWR programme, was the product of deferment presenting itself as an option. This was in turn a result of "natural slippage" on the SGHWR's reference design and safety standards working in the same direction as the effect of falling demand for power stations on energy forecasts.

Third, the initiative which resulted in the circumstances under which the SGHWR was now under scrutiny lay not with the government but with the UKAEA. Sir John Hill had approached Mr Benn and given his view on the SGHWR; Mr Benn had asked him to put this before the UKAEA board for its considered judgment, and that had been done.

It was this, in fact, which made the hearing the more revealing, for the report itself was actually supplied to the committee by Mr Benn before the hearings and was used as a basis for questioning Mr Benn. Inevitably, some of its details came tumbling out.

The UKAEA's view, it emerges, is that, because of lower electricity demand and public expenditure stringency, the SGHWR is less attractive than it was two years ago. The "consensus view" of the board is, with the exception of the historically enthusiastic South of Scotland Electricity Board, that the SGHWR be replaced for the remaining thermal reactor programme by Pressurised Water Reactors (PWRs) or Advanced Gas Cooled Reactors (AGRs)—and that the AGR is the more promising, although operational experience is needed.

The UKAEA went further than this. Subject to a satisfactory outcome of the Nuclear Inspectorate's review of the PWR, there was a "strong argument" that the future needs of the nuclear industry could be met by the construction of PWRs under licence. This, Mr Benn freely acknowledged, would, if acted upon, constitute a reversal of the government's decision taken two years ago when his predecessor, Mr Varley, was at the Department of Energy. And, he said later, in the field of high technology one shouldn't "chop and change" once a decision was taken; he added reassuringly that he himself was "reluctant to be driven off".

The precise extent of his reluctance was twice made quite plain when he made his fourth point. This outlined his response thus far to the UKAEA, and it amounts to a warning. If the SGHWR programme is dropped, says Mr Benn, it could be a setback to the country's whole reactor programme. A decision to go for the PWR would mean re-commencing the whole effort to produce a reference design to meet UK conditions, and thus more delays, and even then it would not certainly provide a solution. It would also set aside the past two years' work, and previous work carried out at Winfrith in Dorset.

Moreover, this would amount to a statement from the UKAEA that it had lost confidence in its own system. That would in turn rebound and damage the credibility not just of the UKAEA, but of the systems it sponsors, including the fast breeder, and of the whole nuclear idea. The nuclear issue, in short, might be thrown right back into the public arena, "where it may belong". ☐

FRANCE

Staying nuclear

France's nuclear programme has come in for some domestic criticism recently, but looks like pressing ahead. A Correspondent reports

It is August, France is on holiday, and that has brought a degree of quiescence to town and country. There is even time for some sort of break from politics, or at least from certain political issues. But it remains uncertain whether, come September, one issue in particular will have been allowed completely to die away. The issue is energy —specifically nuclear energy. Specifically the fast breeder reactor. For, despite all the impressions conveyed abroad, the priority France gives to her nuclear programme in her overall energy strategy does not go totally unchallenged. And the priority given within that to the breeder reactor has not escaped attention.

The whole issue finally blew up early last month, at a place called Creys-Malville, which is near Lyons and on the Rhône. Under construction there is perhaps the most advanced reactor of its type in the world. Superphénix, it is called, and it is expected to be on stream in the early 1980s—all 1,200 MW of it. Like Britain, France already has a prototype breeder reactor, a 250 MW plant known as Phénix situated on the Rhône at Marcoule. But while Britain agonises about whether to go ahead with a demonstration commercial-scale breeder, France is on her way—or looked to be until last month, when there was a new development.

It was Europe's anti-nuclear lobby which stepped in. Superphénix, already the object of trade union protests, became the butt of criticism from ecologists and environmentalists as well. They came in hundreds and camped outside the site where workmen toiled. The jamboree lasted several days. The way it was brought to an end, however, aroused even more indignation than perhaps the construction itself: riot police moved in with tear gas and truncheons to evict the demonstrators, and some of the protesters were hurt.

The criticism in France, as in other industrialised countries contemplating the use of the fast breeder reactor, is emotive inasmuch as it rides on the back of fear, particularly about the implications of the large-scale production of plutonium. It is not less rational, or less important, for that. But its form is characteristic. So, too, is the response from Electricité de France (EDF) and other interests within the French nuclear industry, and from the government too. Just look at France's energy position, they say.

Imports account for something like 75% of the country's energy requirements, a dependence which France must seek to reduce, if only for strategic reasons. What is more, the argument runs, unlike Britain, the country has no oil, and its coal reserves don't compare with those of Britain or Germany. That means nuclear power is likely to make economic sense as well. And the alternative threat of an energy shortage embodies implications as alarming as nuclear power for people's lives.

Of course France, like other industrialised countries, has been forced to revise its energy demand forecasts in light of general economic developments. Energy use last year, for example, dropped by over 5%, more than the fall in national product, and there is increasing emphasis on energy conservation. A fair amount of encouragement is also given to research and development on new sources of energy.

But no one seriously doubts that France needs nuclear power now and will need it even more in the future. Even a special commission examining energy policy in France, formed partly in response to concern expressed last year by 400 academics at the increasing use of nuclear power, has not recommended any slowdown. Following a review of the nuclear programme earlier this year plans for power capacity over the next few years includes construction of 6,000 MW of nuclear power this year and next, and 5,000 MW in 1978. The change this represents on the original programme is marginal, and, despite the protests, the talk is still of 40,000–45,000 MW of nuclear power 1985. By that time most of the country's electricity will be nuclear generated and a substantial proportion of its total energy will be coming from nuclear plants.

●

All of this, moreover, will be taking place within the context of a thoroughly reorganised nuclear industry. Plans for conventional plant will continue to focus on the pressurised water reactors. Looking ahead, France expects that the new generation of fast breeders will be needed in the 1980s. That is why Superphénix received the go-ahead earlier this year. And the fact that France has secured the cooperation on the project of both Italy and Germany while retaining a 51% interest for EDF is of perhaps greater consequence to many of those awaiting a British decision on the fast breeder than the debate on its implications which is now growing in all the industrial countries.

- The final contract for the controversial Franco–South African deal involving the sale by a French consortium of two nuclear power plants to the South African Electricity Supply Commission (Escom) were not signed by the deadline of July 31 last week following the development of a complication, apparently over safeguards attaching to the deal. A South African delegation left Paris after 24 hours of talks without having signed anything, and although French spokesmen sounded confident this raised doubts about whether the deal would go through. It now appears that an agreement concerning safeguards was later initialled in Paris and will be submitted to the International Atomic Energy Agency and Euratom. It is thought that once this is accepted, it will pave the way for the signing of the main contracts.

WEST GERMANY

Exporting for survival

West Germany's nuclear industry is not becoming any less involved in the politically sensitive area of exports. A Correspondent reports.

FURTHER developments in the field of nuclear exports have come with news of additional moves from West Germany exploiting this increasingly lucrative market. Reports quoting West German Economics Ministry officials and spokesmen for the country's leading power station constructor, Kraftwerk Union, indicate that West Germany has been clearing the way with Nigeria for negotiations to begin on the first sale of a 500–600 MW German nuclear plant to a black African country.

The news coincides with the visit to West Germany of the Nigerian Prime Minister, General Yardua. It also comes just a week after Brazil had signed delivery contracts with Kraftwerk Union for the construction of two nuclear reactors as part of last year's government-to-government agreement, and less than a month after the signing in Tehran of the contract between Kraftwerk Union and the Atomic Energy Authority of Iran for the turnkey supply of two 1,200 MW pressurised water reactors.

With the signing of the latter contract, West Germany has become the first western enterprise actually to conclude a nuclear contract with Iran. The reactors, which are to be built near the city of Bushehr on the shore of the Persian Gulf, were begun this time last year after a letter of intent was issued to Kraftwerk Union in November 1974. Of the 3,800 employees presently on site, about 600 are German expatriates.

Kraftwerk Union describes the plants it exports as the most reliable reactor systems, and generally cites the Biblis plant in Germany in support. In fact, as Rheinisch-Westfaelische Elektrizitaeswerk (RWE) confirmed last week, that station has now revealed technical problems in the course of a planned shutdown, and the length of the closure is now likely to be doubled to four months.

What this means in terms of costs for Kraftwerk Union is uncertain, but it does not expect to operate at break-even point until the 1980s anyway. The star of Germany's nuclear industry, the company is crucially dependent on exports to supplement the home market and so render possible the economies of scale necessary to compete favourably with the USA. But some overseas contracts were lost in the first half of 1975. These included the plan for a nuclear power station at Kaliningrad on the Soviet–Polish border, which fell through because of East German objections concerning the supply of electricity, and deals with South Africa, Sweden and Switzerland.

The company also appears to be finding that permits are now taking much longer to obtain, and greater safety measures, among other things, are extending the construction time for the average plant. Germany has its own protectors of the environment too, keen to prevent (or at least delay) construction of plants beyond the ten or so already in operation. ☐

SWEDEN

Suffering without support

Wendy Barnaby reports from Stockholm on the state of basic technical research in Sweden

To live in Sweden is to be impressed by the sophistication of the country's technology: a level of accomplishment which thrives on extensive research and development. There is, however, one part of this body of excellence which is ailing. Basic technical research is, in fact, close to death.

Nobody seems to know exactly what basic technical research is, but everyone agrees that it is conducted for the extension of knowledge, without any specific application in view—although it may of course be used if the necessary techniques are developed. It is also differentiated from pure fundamental research, which has no possible or likely practical application and which is supported in Sweden by the Natural Science Research Council. Opinion is unanimous, too, on the extent to which basic technical research is presently being supported. In the words of a spokesman at the Academy of Engineering Sciences, it is being given "no money at all".

This is hardly an exaggeration. Its needs used to be met by the State Technical Research Council. This body was disbanded in 1968 and replaced by the Swedish Board for Technical Development (STU) whose emphasis has been on supporting applied research, specifically of the sort that will further innovation and technical expertise in Swedish industry. Including governmental and industrial outlays, Sweden spends about Sk4,000 million (about $900 million) annually on research and development. For the 1975–76 financial year, STU's budget amounted to about $56 million, of which—according to a spokesman there—about $10 million was devoted to basic technical research.

Or, rather, to some types of that research. For there has been a reorientation of grant-giving to favour certain areas of "big" science—space and elementary particle research, for example. This has resulted in fewer numbers of bigger grants being given in these areas, rather than a multitude of smaller grants covering a broader range. Dr Gösta Lagermalm, STU's senior policy adviser, agrees that because of this change of emphasis, the complaints of physicists, chemists and biologists trying to pursue "small" basic technical research are justified.

Part of the work of a governmental commission set up in 1972 to survey Swedish research councils and make suggestions for changes in their organisation was to consider this particular problem. During the commission's investigations, STU was asked to indicate those projects supported by its 1971–72 budget which had had their support reduced or cut off entirely in succeeding budgets because they were too much oriented towards basic technical research. STU replied that in 1971–72, it had given about $1.2 million to 49 such projects. This fell in 1972–73 to just over $650,000 for 31 projects, only four of which would be kept on for 1973–74—all for the last time.

But approaching the problem through statistics does not really give the feel of it. Neither can it be gauged by comparing the number of applications for basic technical research grants received with those approved. As one professor at the Institute of Technology explained, colleagues of his who have been refused grants no longer apply for them, even though they still want to pursue their work and believe that it is more important for the country's technical development than the short term projects they are forced to switch to. Another said that some colleagues he knew had tried to get funds by dressing their basic technical research applications to make them look like projects which would yield practicable results quickly.

Various propositions have been put forward to find a new home for basic technical research. Some have suggested that the Natural Science Research Council should take on the job, others that STU should be given more funds in order to bring the research under its umbrella. Another suggestion was that this sort of research should have its own dispensing body. The governmental commission recommended last year that STU assume full responsibility for "support for technical research of a basic nature". This would mean setting up another grant-giving body within the framework of STU, a task which seems hardly likely to be undertaken in view of the fact that yet another commission is presently studying the aims and structure of STU itself, and is not due to report for another 18 months or so.

Thus, while the planners plan, part of the activity they are meant to be stimulating is simply being strangled, with the limiting of scientific enquiry and the lowering of morale of those academics concerned as the result. □

CANADA

Council rift over report

The Science Council of Canada received a little more public attention over a recent incident than it wanted. David Spurgeon reports from Ottawa

THE well-known French-Canadian science broadcaster Fernand Seguin resigned from the Science Council recently when it would not publish his dissenting views on a council report on population, technology and resources. The report calls for a sharp reduction in immigration to slow Canada's population growth and maintain its high standard of living. It also proposes that Canada should use high technology to increase its food production and exports of food and raw materials.

Mr Seguin contended that the large increases in food exports proposed would help create a small club of privileged countries and would support the US stategy which seeks to use food as a political weapon in a way that the OPEC countries have used their oil. He maintained that the high technology called for in the report would require massive participation by multinational companies, a large-scale influx of foreign capital, and construction of more than 100 nuclear power plants in Canada. The upshot would be that Canada would align itself with US "food imperialism", and "hunger-stricken countries would have to come and eat from our hand".

Another council member, Dr Ursula Franklin, professor of metallurgy and materials science at the University of Toronto, also disagreed with the council report. She re-assessed her position on the council as a result of the refusal to issue a minority report, but later decided not to resign, saying she would continue her participation in the council's project on the Conserver Society, of which she is head. (The Conserver Society is one of the three themes around which the council has recently structured its programme. The other two themes are technological independence and industrial strategy, and the health of the Canadian scientific community.)

In a newspaper interview ahead of the council study's publication, the study's chairman (and a former council chairman), Dr Omond Solandt, proposed cutting immigration to Canada from last year's 143,000 to an annual net figure of 50,0000 to produce a population of 28 to 30 million by the end of the century (present population is about 22 million). He argued that Canada can only export food if it does not import people. Furthermore, he said that Canada could feed four or five times as many people by exporting grain as it could if they lived in this country, since people in developing nations consume only about 400 pounds of grain a year compared to 2,000 pounds consumed by North Americans.

Energy would also be a problem, said Dr Solandt, because Canadians consume more energy than do people in developing nations. "If we brought in another 20 million, it would completely disrupt the economy," he said. "We probably wouldn't be able to feed the people brought in, and we certainly wouldn't be able to keep them warm." Dr Franklin has contended that it is not possible for a country with Canada's small population to increase food and raw material production greatly without high technology, and says this will mean that Canada will increasingly have to sell out to foreign capital. It would also require highly centralised planning.

In Dr Franklin's mind, the problem with the Science Council report is not so much with its population targets as with these problems of technology. Immigration levels can be adjusted up and down, but high technology is irreversible, she maintains. It also involves environmental and social costs, and she says council members have demonstrated an unwillingness to come to terms with the inevitable social problems.

The council chairman, Josef Kates, said the minority report was refused because it had nothing constructive to offer. French-Canadian reporters raised the issue at a press conference held to release the council's annual report only a day or two after the controversy surfaced and vice-chairman Claude Fortier, director of the department of physiology at Laval University, acknowledged that the council has published minority reports in the past.

The council accepts the right of members to differ with a majority report, but the council reserves the right to decide the mode of transmission of the minority report, he said. Sometimes this is simply a note, sometimes it is done in the letter of transmissal of the report to the Minister of State for Science and Technology (the method to be followed in this case). Dr Fortier said no report of council had had more discussion than this one (a remark that echoed Dr Solandt's comment that the study was the most difficult ever undertaken by the council). Both Dr Fortier and executive director J. J. Shepherd said they regretted Mr Seguin's departure. □

IN BRIEF

Sea Law, round four

The Law of the Sea Conference convened in New York for another seven-week session this week surrounded by a major new uncertainty, the Presidential campaign in the United States, but with some other problems effectively sidestepped by the sprinkling (not to say, flood) of unilateral declarations of 200-mile fishing limits made in the past few months. The EEC countries have now declared their joint intent to introduce a community fishing limit, even if the conference does not come up with a proper agreement. It is, however, the wider question of how to deal with mineral resources on other parts of the sea bed that is likely to exercise the New York session most. How are these resources to be exploited "for the benefit of mankind as a whole" (to coin a conference phrase)? And would the proposed International Seabed Authority actually wrap up every manganese nodule so inextricably in red tape as to make a good principle impossible to work out in practice? Any real decisions are likely to have to await a fifth round of conference—and the result of the US election in November.

What's happening on Mars?

Two of the three experiments carried on the Viking lander and designed to detect reactions in the soil characteristic of living organisms have so far yielded data. One, measuring the conversion of radioactively-labelled nutrients to labelled carbon dioxide, showed an initial rapid burst of activity which has since died down to almost nothing. In another, the soil released large amounts of oxygen when initially dampened with water, even before the experiment proper (of adding a concentrated 'chicken soup' of nutrients) had begun, but nothing has happened since.

The best guess at the moment is that the Martian soil contains large amounts of bound oxygen, a not improbable speculation as the soil is rich in iron minerals which in some circumstances can readily bind oxygen under the influence of ultaviolet light. This would accord with earlier speculation that oxygen and hydrogen originating from water might be trapped in the iron minerals on Mars. So far it looks as though Mars may be the Mecca of the soil chemist (since no known soil on Earth has ever produced similar reactions, although the search is now on amongst desert soils) but that the question of life there remains as much of an enigma as ever.

Forecasting error

KENNETH MELLANBY

PLANNING must be based on the best possible forecasts of future developments. Unfortunately the best is generally not very good. Dr Walter Marshall told a conference on Renewable Sources of Energy organised recently by the Royal Society of Arts that the only certain thing about forecasts of energy use was that they would always prove to be wrong. Thus the Central Electricity Generating Board's projections made in the early 1960s overestimated the peak load for current used in 1975 by some 40%, which makes one suspicious of their figure foretelling a doubling or even trebling of the use of electricity in the period up to the year 2,000.

Population projections are even more difficult. Thus one report published shortly before the 1939–45 war, when England and Wales had a population of 41 million, suggested that this might fall to 31 million by 1975, and that the chances of a population increase were remote. In fact numbers increased by 8 million. The most recent figures issued by the Office of Population Censuses and Surveys suggest that the present trend to ZPG (zero population growth) will suffer a modest reverse after 1981, and that numbers in England and Wales will grow by about 1½ million by 1991. It will be interesting for those who survive to see what really happens.

Forecasting traffic densities, on which future road programmes are based, is an equally chancy business. Until recently the Department of the Environment decreed that their figures produced by the Road Research Laboratory must not be questioned. This arrogant attitude has at length been somewhat relaxed, but an enormous increase in the number of private cars and of their use is still postulated. Yet there is little reason to believe that traffic projections are any more accurate than those for power or population.

Unfortunately many people seem to think that forecasting is becoming increasingly scientific, and that the use of computers is making the results more reliable. It is true that a great deal of mathematical skill has gone into the study of population trends, energy use and traffic census, and that the calculations arising therefrom have sometimes been speeded up by suitable computer programs, but unfortunately there has been no improvement in obtaining the data used. The whole process has too often been one of "garbage in, garbage out". There are so many unknown and uncontrolled variables that it might be better to rely on crude sums done on the back of envelopes, than to use elegant calculations and expensive machinery which give a spurious illusion of scientific accuracy.

Some errors cannot be eliminated. We could foretell the birthrate accurately for about eight months from any date, and, provided there is no war or major epidemic, estimates of death rates and total population are foreseeable for a similar period. Forecasts for longer periods are simply guesses, affected by social factors which, so far, have defied accurate quantification. Only some form of rigid totalitarianism could improve the statistics.

Unfortunately some projections have a built-in source of error. Our government is committed to the idea of economic growth. Scientists in public employment appear to be expected to assume that this growth will take place, and that there will be increased energy consumption, more consumer goods, more travel and a growing "environmental impact". It is assumed that government policy will stimulate this growth in the economy. Some believe this to be likely, others describe schemes intended to produce growth as "pouring out public funds like water, to create lakes in which lame ducks will sink". It may be impossible to keep politics out of forecasting, but political factors should be identified and not concealed.

correspondence

Lithium supplies

SIR,—We fully support the contention of Walton and Spooner (June 17, pages 533–5) that there is a pressing need to identify further resources of lithium, but would take issue with them on a few points.

In Table 2 some 50% of their total resources derives from North American brine deposits. However, J. D. Vine (*Journ. Research U.S. Geol. Surv.*, **3**, 4, 479–85; 1975) recently emphasised that the amount of *recoverable* lithium at Silver Peak is, in fact, lower than the published reserves by a factor of 10. Should a similar factor apply to other brine deposits the shortfall between Western world reserves and projected consumption becomes critically magnified.

Our present, limited, understanding of the geochemistry of lithium suggests that more small brine and pegmatite sources may be discovered in the developed countries. Even so, the best prospects for large reserves lie in Africa and South America, sources which for various reasons may not automatically be available to the technologically advanced Western nations. We may be obliged to rely, therefore, on known smaller domestic deposits and on exploration and development of new types of lithium deposit.

Walton and Spooner state that the European countries "possess no presently identified significant lithium resources": though true of reserves it is not so of resources. Small lithium pegmatites and lithia brine flows are known in several European countries, including Great Britain, but none is exploited at present. Given suitable financial inducement to development, they could make a valuable though comparatively small contribution to our requirements.

Of more significance are the lithium-rich portions of the Variscan granites, in which lithium occurs largely in "lithionite" mica. In Cornwall, for example, parts of just such a major lithium resource have been affected by kaolinisation and some of the lithionite could be extracted during the working of china clay. As yet the distribution of lithionite-granite in the Cornubian batholith is imperfectly known and we have only sparse information on the variations in lithium content and none on isotopic composition. Nevertheless, exploitation of zinnwaldite mica from granites of the Czechoslovakian Erzgebirge, albeit under a different economic philosophy, indicates that this type of deposit may have an important role to play in the supply of future lithium requirements and argues for a direct programme of geological and chemical engineering research ino the lithium potentialities in the Western European Variscides.

Yours faithfully,

K. E. BEER

Institute of Geological Sciences,
Hoopern House,
Exeter

J. R. HAWKES

Exhibition Road,
London, UK

Bran and sawdust

SIR,—It was suggested by Dr Jukes (May 13, page 92) that bran and sawdust constitute a safe diet. This is not so. There is evidence (Mackarness, *Not All in the Mind* (Pan; 1976)) that, on an evolutionary time scale, cereal is a recent addition to our diet, one to which we have not yet become adapted, and a Stone Age pre-cereal diet was recommended.

As for sawdust, it is highly likely that timber is carcinogenic: wood workers have a high incidence of nasal adenocarcinoma (Acheson *et al.*, *Brit. J. industr. Med.*, **29**, 21; 1972), while mice bedded on wood shavings show an increase in so-called "spontaneous" tumors (Sabine *et al.*, *J. Natl Cancer Inst.*, **50**, 1237; 1973).

It is high time to accept the fact that nothing whatever is completely safe.

Yours faithfully,

VALDA M. CRADDOCK

MRC Toxicology Unit,
Carshalton, Surrey

Canned crab

SIR,—In 1959 Ecuador declared the unoccupied lands of the Galapagos Archipelago a national park; by 1968 a department of national parks and wildlife was created to administer the park. The national park service service started collecting an entrance fee in 1972 that, in part, is used to finance conservation programs in the islands. Although conservation efforts have grown, tourism has grown more spectacularly. For instance, since 1969 the number of tourist boats have more than doubled.

There is currently an effort to extend the national park to protect the marine life near the Galapagos shores. It will be difficult to regulate the fishing but this may become necessary. Packing boats started to visit the islands regularly in 1972, allowing fishermen to go farther and stay out longer. Many of the endemic species such as the Galapagos penguin are dependent on small fish which could become commercially valuable. The Galapagos penguin is subject to total nesting failures suggesting that competing pressure from humans could, over a period of time, reduce their population.

Dramatic decreases in species number or composition will probably be detected but subtle changes could go unremarked. In 1972 when no more than 80 tourists were visiting Pta. Espinosa, Fernandina weekly, a hermit crab with a discarded film can marched through my camp in July and August. Our camp site was a mile from the tourist landing and we had no similar film canisters. The hermit crab's aluminium home should have heated up rapidly in the hot equatorial sun, which may be why the crab stayed in the shade of the mangroves. Pesticides have been found in almost every remote corner of the world; the film canister may be next.

Yours faithfully,

DEE BOERSMA

Institute for Environmental Studies,
University of Washington,
Seattle, Washington

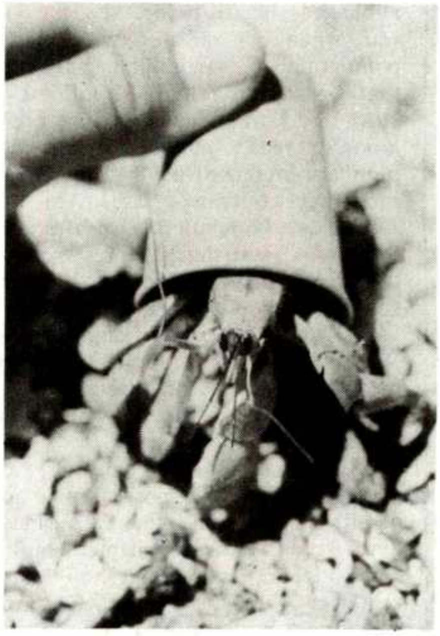

news and views

Anti-idiotypic antibodies: a clinical future?

from L. Brent and P. J. Kilshaw

ONE of the most recent concepts emerging from the witches brew of present-day immunology is the exciting possibility that antibodies directed against the receptor sites of other antibodies may have a role in regulating the immune response.

It is more than a decade ago that Oudin and Michel (*C.r. hebd. Acad Sci Paris*, **257**, 805, 1963) observed that antibody receptor sites (which bind antigens in a highly specific manner) themselves bear antigenic determinants and that these 'idiotypic' determinants (or idiotypes) can evoke antibody production in animals belonging to the same species. Idiotypes owe their existence to the unique configuration of the variable region of specific antibody molecules, and they should not be confused with 'allotypes'—again first described by Oudin—which are antigenic specificities present in the immunoglobulins and other proteins of different groups of individuals of the same species and determined by different alleles of the same gene The vast repertoire of antibody receptor sites within a single individual is associated with a great heterogeneity of idiotypic determinants, and so the production of antibodies with combining sites for the stimulating antigen is matched by the appearance of a limited range of idiotypes. The observation that antibodies can combine with the receptor sites of other antibodies led Jerne (*Ann Immun Inst. Pasteur*, **125C**, 373; 1974) to suggest that the production of anti-idiotypic antibodies might be a normal event that modulates the degree and duration of the response. This could theoretically be the case provided that lymphocytes carry receptor sites on their surface identical to those on immunoglobulin molecules· by combining with these receptors, anti-idiotypic antibodies could prevent contact between lymphocytes and their specific antigens or even cause cell death, thus limiting the immune response. Such a mechanism would presumably depend on the replication of specific idiotypes up to or beyond the threshold at which antibody production against them ensues; that is, by an increase in the antibody titre in the case of B cell responses, and for T cell responses, an increase in the number of cells with specific receptors. At present there is little direct experimental evidence to support this fascinating theory, but over the past few years there have been a number of successful attempts to suppress both humoral and cellular responses by passively administering anti-idiotypic antibodies or by actively stimulating their production.

The urgent need for a specific form of immunosuppression in clinical transplantation has provided an additional incentive for the study of anti-idiotypic antibodies, using T cell receptors or alloantibodies directed against specific transplantation antigens. Ramseier and Lindenmann (*Path. Microbiol.*, **34**, 379; 1969) were the first in the field· they reasoned that if an F_1 hybrid mouse resulting from the mating of animals of two inbred strains (say A and B) is injected with lymphocytes from one of the parental strains (say A), the only antigenic determinants present on the injected cells recognised as foreign by the F_1 recipient would be receptors for antigens of strain B. (A mouse which possesses both A and B antigens on its cells will not have receptors for either). In these circumstances the production of anti-(anti-B) antibodies could be expected. Using a rather indirect and cumbersome test, the PAR (Product of Antigenic Recognition) asay, Ramseier and Lindenmann (see *Transplant. Rev*, **10**, 57; 1972) showed that sera taken from animals sensitised in this manner were capable of suppressing the *in vitro* reactivity of strain A lymphocytes against alloantigens of the B strain. The immunosuppressive moiety responsible for this effect was not, however, fully characterised.

More recently, Binz, Wigzell and their colleagues (see Binz, Kimura and Wigzell, *Scand. J Immun*; **4**, 413; 1975) have adopted a similar approach using the inbred rat strains Lewis and DA They found that anti-receptor site antibodies could be prepared optimally by injecting purified T (thymus-dependent) lymphocytes from one of the parental strains (Lewis say) into F_1 hybrid recipients. In this case then, sera taken from the hybrids would specifically abolish the response of Lewis lymphocytes against DA antigens, and this has been shown with the aid of graft-*versus*-host and mixed lymphocyte culture reactions These assays test the ability of lymphocytes to recognise and respond to specific alloantigens Furthermore the F_1 hybrid antisera formed a precipitate with alloantibodies of the appropriate specificity and they agglutinated alloantibody-coated red cells.

Anti-idiotypic antibodies might be expected to provide a useful tool for characterising the elusive T cell receptors for antigens of various kinds. By absorbing putative anti-receptor site antibodies with purified T cells or with alloantibodies, Binz and Wigzell (*J. exp. Med.*, **142**, 197; 1975) were able to show that the idiotypes on the T cell receptors were closely similar to, or identical with, those present within the combining sites of immunoglobulin molecules Further, they succeeded in identifying receptors from both T and B cells in the body fluids of normal Lewis rats.

In a paper published in *Nature* recently Binz and Wigzell (*Nature*, **262**, 294; 1976) describe the effects of an anti-idiotypic response on the survival of allogeneic rat skin grafts. To evoke the anti-idiotypic response they sensitised Lewis rats with Lewis receptors specific for antigens of the DA strain The receptors were isolated from the serum of normal Lewis rats with the aid of an immunosorbent consisting of antibodies specific for Lewis anti-DA idiotypes coupled to sepharose particles, dissociated from the immunosorbent, treated with gluteraldehyde (this causes cross-linking and increases immunogenicity) and injected in Freund's adjuvant into four Lewis rats. This procedure was repeated three weeks later. DA skin grafts transplanted to these animals 19 days later had a mean survival time of 30 days, one of them surviving for 38 days, compared with 10 days in the untreated controls. (This observation was confirmed in a larger group of recipients, in which the mean survival time proved to be somewhat less, 24 days.) The partial unresponsiveness was specific in that grafts from a third strain (BN) transplanted at the same time were rejected with a mean survival time of 12 days. The lymphocytes of the four immunised Lewis rats were tested for MLC reactivity before skin transplantation and found to be nonreactive to DA but fully responsive to BN antigens. Some time after they had rejected their skin grafts the sera from these rats were subjected to rigorous tests which established without doubt that anti-idiotypic antibodies were still present in significant amounts—a finding that received support from the observation that these animals suffered from an impairment of alloantibody production when they were challenged with (DA×Lewis)F_1 hybrid lymphocytes.

Binz and Wigzell propose that anti-idiotypic antibodies caused the physical elimination of cell clones which were specifically reactive to DA antigens. Whilst the results are impressive and the authors' interpretation entirely plausible a note of caution must nevertheless be sounded, especially in relation to the clinical application suggested by Binz and Wigzell. First, the complexity of the manipulations involved is considerable Second, investigations involving the immunoregulatory powers of anti-idiotypic antibodies in transplantation have been largely dominated by the Lewis and DA rat strains, and it is now vital to show that the phenomenon extends to other strains and to other species. Third, the prolongation of graft survival achieved in these experiments, though considerable, is strictly limited: in view of the apparent presence of anti-idiotypic antibodies long after the grafts had been rejected one may well wonder why survival was not more prolonged or even permanent. It would seem that anti-idiotypic antibodies alone are not sufficient to guarantee complete unresponsiveness. Finally, the active production of these antibodies depends on pretreatment of graft recipients; even if it were possible to apply the rat methodology to human graft recipients (and there must be considerable doubt about that) pretreatment would not be practicable in the transplantation of cadaveric grafts, that is, in a situation in which the intercession of a specific form of immunosuppression is most needed. Perhaps the most likely application to man will be in the control of autoimmune diseases.

Despite these reservations the data of Binz and Wigzell are clearly of the greatest importance, if only because of their impact on theories of antibody formation and control. Anti-idiotypic antibodies with specific immunoregulatory properties have been described in other systems, and these have so far always involved antigens that evoke antibodies of very narrow clonality (that is with a narrow range of idiotypic determinants), such as phosphoryl choline (Cosenza, *Eur. J. Immun.*, **6**, 114; 1976) and group A streptococcal carbohydrate (Eichmann, *Eur. J. Immun*, **5**, 511; 1975). Time alone will tell whether this special feature is a prerequisite for the production and immunoregulatory properties of anti-idiotypic antibodies. ☐

Associated production of charm

from W. T. Toner

A NEW heavy particle with two properties characteristic of the charm scheme (see *News and Views*, **259**, 622; 1976) has been discovered by the Stanford-Berkeley collaboration working on the SPEAR storage ring at Stanford in California (Goldhaber *et al.*, *Phys. Rev. Lett.*, August 2, 1976). It was observed in decay modes containing K mesons and seems always to be produced in association with one or other of two heavier particles whose presence is inferred from indirect evidence.

When the same group discovered the ψ family and showed that the unexpectedly large rate for the annihilation of high energy electrons and positrons began suddenly at the point where the ψ series changed from having uniquely narrow widths to a more normal shape, most particle physicists confidently assumed that the excess was due to the copious production of charmed particles into which the heavier ψ's could decay rapidly· it should be as easy to create two oppositely charmed particles out of the annihilation energy as two charged particles. There should be no difficulty in finding them since theorists predicted frequent decays involving K mesons.

Months later when the only reports from Stanford were of fruitless searches, people began to find excuses. Easily identified decay modes containing K mesons and no neutral particles might be rarer than one had thought. It now seems that everyone had underestimated the amount of careful work needed to find even the most obvious decays. In fact, with hindsight, one can find some evidence for the new particle in the previous negative report (Boyarski *et al*, *Phys. Rev. Lett.*, **35**, 196; 1975).

In the experiment every electron–positron annihilation event which results in two or more charged particles being detected is recorded. After cases with electrons or mu-mesons are eliminated, each event is analysed to test the hypothesis that a particle was produced which decayed into a π and a K meson. Charmed lives, though unusually long, should still be much too short for the charmed particles themselves to leave tracks; only π and K mesons or protons (anti-protons if negatively charged) can be recorded.

From a rough determination of the velocity of each particle and a precise measure of its momentum, the analysis programme first computes the relative probability that the particle was a π meson, a K meson or a proton so that a precise mass can be assigned When the decision is ambiguous between K and π, both possibilities are included and the event is analysed as if it were two (or more) different events each with an appropriate fractional statistical weight. The energy of each particle can now be calculated accurately from Einstein's relation between mass (m) energy (E), momentum (p) and the velocity of light (c)· $E^2-p^2c^2=m^2c^4$.

If an event contains a π and a K meson of opposite charge their energies and momenta are added and the "effective mass" of the pair is calculated. The event is next treated as if no other measurements were available (very few events are complete) and the energy and momentum of the "missing" system containing all other particles produced is found by subtraction from the values given by the storage ring parameters for the annihilation as a whole The mass of the system recoiling against the pair, known loosely as the "missing mass", is now calculated from the mass–energy relation. The analysis is repeated for any other possible ($\pi^{\pm}$ $K^{\mp}$) pairing.

"Effective" and "missing" mass histograms are built up with results from many thousands of individual annihilations. In most cases there is no relationship between the paired particles. Such random pairings give the histograms a smooth shape on which are superimposed peaks at distinct masses corresponding to correct pairings of the decay products of real particles.

The SPEAR effective mass histogram shows an unmistakable peak at a mass of $1.86\,\mathrm{GeV}/c^2$. If the missing mass histogram is restricted to events with a π–K effective mass of this value, a strong signal is seen which more recent data show to be two peaks with "missing masses" of 2.02 and 2.15 GeV/c^2. No decay modes have as yet been reported for these heavy recoils. The widths of the peaks are unusually small for particles with such large masses but the experimental resolution is not fine enough to class them apart on the grounds of width alone. The data strongly suggest but do not yet prove that all non-random π–K pairs with a mass of $1.86\,\mathrm{GeV}/c^2$ are produced in association with recoils in the high mass peaks. Similar features are found in the analysis of $(K^\pm\, \pi^\pm\, \pi^\mp\, \pi^\mp)$ systems.

It is very hard indeed to explain these observations in terms of "just" three more ordinary particles. Besides, were they so they should have been seen in many experiments at proton accelerators The associated production of charmed particles is the only natural explanation.

Progress in the spectroscopy of charmed particles should be rapid now that three masses and two decay modes have been identified. They can be used as tracers to help identify the cascade decays of heavier charmed particles which should contain them. If these particles are the same as those seen decaying with the emission of positrons in the neutrino experiments (*News and Views, loc. cit.*), events not containing positrons should have ($K\pi$) pairs and ($K\pi\pi\pi$) systems at this mass in relative amounts predictable from the SPEAR data. And so on.

The large and extraordinarily productive group working at SPEAR will continue their experiments. If they go on at the present rate the new particles will soon outnumber the experimenters. Further results from the SPEAR group were presented at the recent Tbilisi conference a report of which will be appearing in a forthcoming issue.

Quasi-superheavy nuclei

from P E. Hodgson

THE recent discovery of superheavy nuclei in monazite, a mineral from Madagascar (*News and Views*, **261**, 627; 1976; *Phys. Rev Lett.*, **37**, 11; 1976) will stimulate further interest in the transient quasi-superheavy nuclei that are formed briefly during collisions of heavy ions.

In such collisions, the heavy ions remain near each other for a short time that depends on their relative velocity. Two lead nuclei, for example, one stationary and the other moving with 10 MeV per nucleon remain within two nuclear diameters of each other for about 3×10^{-22} s. Since this separation is far smaller than the radius of the innermost electron orbit there is no difference, from the point of view of the electrons, between two colliding lead nuclei and the single nucleus that would be formed by their fusion.

The electrons in the colliding ions are in the orbits appropriate to lead, and when the two nuclei collide the two electron clouds are in violent interaction. If now the nuclear interaction time is long enough these electron clouds can rearrange themselves in the configuration corresponding to the electron orbits of the combined superheavy nucleus. This system of two colliding nuclei and the electron cloud of the combined nucleus is called a quasi-superheavy nucleus.

The likelihood of formation of such nuclei depends on a delicate balance of interaction and rearrangement times, so that they can only exist, if at all, for a limited range of relative velocity of the colliding ions. If this velocity is too low, the nuclei will not be able sufficiently to overcome their mutual electrostatic repulsion to appear to their electrons as a single entity. If on the other hand the velocity is too high, they will not remain in close contact long enough for the electrons to rearrange themselves into the electronic configuration of the combined system.

Calculations have been made of these limiting velocities, and it is found that the ratio of the upper to the lower velocity is about 0.13, independent of the atomic number or the electron shell. Thus for all electron shells there is a range of velocities for which the system can be considered a quasi-atom The optimum distance of closest approach which corresponds to the greatest lifetime of the quasi-atom gives $T_{\max}=(n^3/Z^2)\times10^{-15}$ seconds where n is the principal quantum number of the electron orbit and Z the nuclear charge.

One way of showing that a quasi-atom has been formed is to detect one or more of the characteristic X rays due to inner shell transitions and to verify that they have the required frequencies This is the classical method due to Moseley for measuring the nuclear charge. For such transitions to take place it is first necessary to form a vacancy by removing an electron from an inner shell.

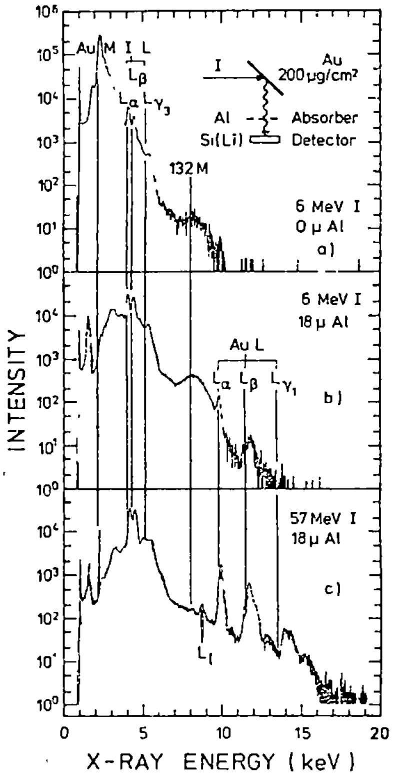

X-ray spectra from a gold target bombarded with iodine. The broad peak around 8 keV is attributed to X rays from the combined system with $Z=132$.

This can be done by forming a vacancy in the projectile and then transferring it to the combined system. Such vacancies can be produced in heavy ion collisions mainly by electron promotion, in which some of the energy of the interaction is changed to excitation energy. The vacancy then has to live long enough for the X-ray transition to take place and since it can be destroyed by a collision with a nearby atom there is a competition between the transition time and the collision time. The probability of X-ray emission thus depends strongly on the density of the gas.

The first experimental evidence for quasi-molecular X rays was obtained by Saris *et al.* (*Phys. Rev. Lett.*, **28**, 717; 1972) who bombarded argon-saturated silicon targets with 70–600 keV argon ions. This gave a continuous X-ray distribution between the characteristic L and K X-ray lines of argon. These X rays are attributed to transitions to the $2p\pi$ level of the molecular system. In a later experiment they confirmed the density dependence of the X rays and compared the results from various targets. This work has since been extended and confirmed by several other groups.

The X rays from the quasi-superheavy nucleus with $Z=132$ have been found by Mokler *et al.* (*Phys. Rev. Lett.*, **29**, 827; 1972). They bombarded a gold target with iodine and some of their X-ray spectra are shown in the figure. The broad peak at about 8 keV is attributed to transitions in the quasi-superheavy nucleus. This occurs at the expected energy and detailed calculations of other possible processes showed that none of them could account for this peak. Similar results were obtained with other targets.

It is now possible to make relativistic many-electron calculations of the energies of the states during the collision process and hence to find the energies and intensities of the expected X rays for different interacting ions as a function of energy. The detailed experimental confirmation of these results shows that the phenomenon is essentially understood. There still remain many questions that require further study, in particular the possibility of other mechanisms contributing to the X-ray emission and the angular distribution of the emitted radiation. A review of the present status of this work has recently been published by Armbruster (*Enrico Fermi Summer Course*, LXii; 1976). □

Muscle disease at Durango

from Jeremy Brockes

The Fifth International Scientific Conference sponsored by the Muscular Dystrophy Association of America, entitled Pathogenesis of the Human Muscular Dystrophies, was held at Tamarron, Durango, Colorado from June 21 to 25, 1976. The program Coordinator was Dr Lewis P. Rowland of the Columbia-Presbyterian Medical Center, New York.

THE human muscular dystrophies are a complex of hereditary disorders whose underlying mechanisms are completely unknown. It was thus appropriate that the seventy contributors to the Fifth MDA conference considered many aspects of normal and abnormal muscle biology. In this report, I have concentrated on new information that may be of direct relevance for understanding or diagnosing these diseases.

In terms of understanding the mechanism of a muscle disease, the most exciting presentations came on the first day when recent work on the autoimmune basis of myasthenia gravis was presented by J. Lindstrom (Salk Institute) and D. B. Drachman (Johns Hopkins University). It has recently been shown in a number of laboratories that the serum of myasthenia patients contains antibodies that react with acetylcholine receptor. Drachman showed that certain features of the disease can be passively transferred to a mouse with purified gamma globulin from a patient. The mouse exhibits decremental responses to nerve stimulation together with a decrease in endplate acetylcholine receptors and other characteristic features of the myasthenia syndrome. These effects are in part dependent on the third component of complement, as evidenced by the ability of cobra venom factor (which depletes C3) to abrogate the transferred disease, but independent of later components as shown by transfer into the C5 deficient strain. The effects of antibody were further considered by Lindstrom in an animal model. When purified electric eel receptor is injected into rats, the animals mount an immune response which leads to the syndrome of Experimental Autoimmune Myasthenia Gravis (EAMG). In the acute phase of this disease, approximately 10–15 days after injection, cross-reacting antibodies attach to junctional receptors in the synaptic cleft and attract phagocytic cells, mainly macrophages. This leads to a partial disjunction of nerve and muscle, and further morphological abnormalities in the post-synaptic membrane which were described by A. G. Engel (The Mayo Clinic). The acute phase is succeeded about two weeks later by a chronic reaction in which antibody-induced modulation of junctional receptors leads to failure of junctional transmission, progressive weakness and (usually) death. The reason for the apparent breakdown of tolerance to nicotinic acetylcholine receptors in the human disease, and the source of antigen that drives the response, are not known. In view of the close connections between myasthenia and the thymus, one candidate for the responsible antigen is the thymic myoid cell. Drachman reported that cultured rodent myoid cells possess acetylcholine receptors on their surface as evidenced by α-bungarotoxin autoradiography and acetylcholine iontophoresis.

In contrast to myasthenia, the human muscular dystrophies present a confusing picture. Presentations by T. Munsat (University of Southern California) and P Becker (University of Gottingen) attested to the heterogeneity of these disorders, and the problems of classifying them. Most of the investigations on human muscular dystrophy were on the Duchenne type, and several investigators spoke of the problems of obtaining adequate biopsy material. A variety of biochemical, physiological and anatomical abnormalities were described. While there was some talk of an underlying membrane defect, the evidence for this is not yet compelling. Controversies about the neurogenic or myogenic origin of dystrophy continue unabated, with disagreements about counting motor units and interpreting physiological recordings. The interpretation of transplantation or culture experiments in experimental animals with muscular dystrophy is complicated by possibilities of early inductive abnormalities between ectoderm and mesoderm (suggested by A. McComas (McMaster University)), and the failure of dystrophic muscle to retain some of its characteristics in culture.

One approach to muscular dystrophy is to regard it as resulting from a basic defect expressed in all cells, but of particular consequence for muscle. A. D. Roses and S. Appel (Duke University), reported their studies of abnormal phosphorylation of components in or under the erythrocyte membrane. When incubated with labelled ATP, erythrocytes from patients with Duchenne dystrophy show a significant increase in spectrin phosphorylation over controls. If the phosphorylated spectrin is analysed by isoelectric focusing, a subset revealed by this method shows a clear difference from controls. While the molecular basis of this difference is not yet clear, it is not shown by the mothers of dystrophics, and therefore presents an exciting possibility for prenatal diagnosis. In the case of patients with myotonic dystrophy, Appel reported a decrease in the phosphorylation of erythrocyte band 3, a major transmembrane glycoprotein in human erythrocytes thought to be responsible for ion transport. Such erythrocytes also show a defect of Ca^{2+}-dependent K efflux in certain circumstances, and the defect in phosphorylation could be related to decreased Ca^{2+} entry or a failure to activate the K^+ conductance. The relationship of the erythrocyte abnormalities to those in the muscle cell is unclear. In a lucid presentation, R. Layzer (University of California, San Francisco) pointed out that the same hereditary defect, for example in phosphofructokinase isozymes, can have quite different consequences in the two cell types Nonetheless, the erythrocyte work is an encouraging new direction, particularly for diagnosis.

Meanwhile it is possible that less direct approaches to therapy may prove useful. The importance of the balance between rates of protein synthesis and degradation was stressed for general metabolism by A. L. Goldberg (Harvard Medical School), and for the regulation of acetylcholine receptor levels by D. M. Fambrough (Carnegie

Institute). A. Stracher (State University of New York) discussed the properties of low molecular weight, non-toxic, protease inhibitors such as pepstatin and presented interesting preliminary evidence of their effects in retarding degeneration of dystrophic chick muscle explants and monolayers The presence of segmental necrosis in Duchenne muscle fibres was stressed by several speakers, and J. Desmedt (University of Brussels) presented physiological evidence for collateral reinnervation of the resulting aneural segments. It might be possible to promote controlled regeneration in dystrophic muscle, with recovery of function after reinnervation.

While there are new diagnostic possibilities, the basic defects in dystrophic muscle remain as elusive as those in cancer cells. Nonetheless, the progress in myasthenia illustrates how advances in basic research can quickly be important in a clinical context. Thus the breadth of the MDA's support, and their personal involvement as exemplified in an address by Jerry Lewis, the National Chairman, offer cause for hope. □

Protein folding experiments: do proteins cheat?

from Barry Robson

THOSE fundamental components of biological machinery, the proteins, are synthesised by the ribosomes of living cells as linear polymers of twenty different kinds of amino acid. Investigators who seek to explain, and even predict, the functional three-dimensional structures of protein molecules on the basis of their amino acid sequences alone are often criticised for neglecting the presence of the ribosome and other biological structures when the protein folds up. Their defence has been that proteins can be unfolded by certain solvents so that a fully unfolded, flexible and random structure is attained, and then refolded without the aid of the ribosome or anything more complex than water, salts, and a healthy temperature and *p*H. Proving experimentally that the amino acid sequence carries all the information for the three-dimensional biological structure is rather like examining a student, however, for in order to prove that the student knows his stuff it is important to ensure that he can think out the problem set to him without taking any written record into the examination room. The experiments of Garel, Nall, and Baldwin (*Proc. natn. Acad. Sci. U.S.A.*, **73**, 1853; 1976) raise the possibility that some protein molecules at least may cheat because they cannot be fully unfolded but retain some elements of their original three-dimensional structure before refolding.

Baldwin's group unfolded the protein ribonuclease A in aqueous solutions of guanidine hydrochloride or urea, and carefully analysed the kinetics of refolding when the guanidine hydrochloride or urea was diluted out. They conclude that the unfolded protein is an equilibrium mixture of two species, one which slowly refolds to the biologically functional, compact state and one which refolds to the same state but 450 times more rapidly. The protein was described as fully unfolded on the basis of difference spectroscopy techniques, which measure the exposure of aromatic amino acid residues to the solvent. Although there is another instance of complete unfolding in terms of solvent exposure, but not in terms of other criteria (Robson and Pain, *Biochem. J.*, **155**, 331–334; 1976) the fraction of rapidly refolding form (about one fifth) is remarkably constant over a variety of conditions. The report of Baldwin's group is thus a cautionary tale: proteins may sometimes cheat because of the invigilance, perhaps unavoidable, of the investigators. Although four-fifths of the unfolded ribonuclease A molecules presumably do not cheat and eventually also reach the correctly folded state, apparently by initial conversion to the rapidly re-folding form (Hagerman and Baldwin, *Biochemistry*, **15**, 1462–1473; 1976), it is possible that there are many proteins with an even more stable rapid refolding form which constitutes a very much larger fraction of the unfolded population. Such proteins would have no option but to cheat, unless some more thorough method or combination of methods of denaturation were used.

Experiments on other apparently completely unfolded proteins have frequently demonstrated complex refolding kinetics, but have not necessarily implied the presence of a stable unfolded and fast refolding form. The relatively unstable intermediates detected in this way are generally believed to represent partly ordered structures initiating a direct and readily traversable route to the folded state, and so guide the folding process. Such guidance or "nucleation" is in fact theoretically necessary in order to account for the rapidity of folding processes which are many orders of magnitude faster than would be predicted from a purely random search of all possible polymer configurations. The question therefore arises as to whether the fast folding species of ribonuclease A is a partly ordered nucleating structure in the usual sense, which just happens to have a high degree of stability.

The authors note, however, that there is an alternative hypothesis based on the proposal of Brandts, Halvorson, and Brennan (*Biochemistry*, **14**, 4953–4963; 1975) that the amino acid residue proline may undergo *cis-trans* interconversion in the unfolded form of a protein. The fast refolding species could therefore represent forms in which all proline residues are in the correct configuration as found in the correctly folded protein. Although purists might argue that such a form would be a "nucleating structure" in the most general sense, the term usually refers to rapidly formed chain structures in which at least several amino acid residues have a fairly specific position in space relative to one another. It would therefore be rather unfair to accuse the protein molecule of cheating if the only structure it retained were the correct configuration of the proline groups.

Even the most detailed test-tube experiments on the configurational statistics of unfolded proteins may not be able to rule out the possibility of small elements of local structure important to the refolding process. Perhaps the real proof that proteins carry all the information for their own folding resides in computer simulations in which the investigator has full control over the initial conformation of the protein molecule. □

NASA Goddard gamma-ray symposium

from F. W. Stecker and C. E. Fichtel

An international symposium on The Structure and Content of the Galaxy and Galactic Gamma Rays was held at NASA Goddard Space Flight Center in Greenbelt, Maryland on June 2–4, 1976.

THE emphasis of the conference was placed on the relationship of γ-ray astrophysics to other fields of galactic astronomy.

D. Thompson and R. Hartman (Goddard Space Flight Center) presented the results from the Second Small Astronomy Satellite, SAS-2. Evidence for pulsed γ radiation from four radio pulsars, PSR 0531+21, PSR 0833-45, PSR 1818-04 and PSR 1747-46 was reported. Only one radio pulsar has been seen at optical and X-ray wavelengths. In addition, several general features in the γ-ray data were correlated with galactic structural features. The γ rays seen by SAS-2 from the direction of Cygnus were determined to have a periodicity of 4.8 h, matching the frequency and phase of the X-ray source Cygnus X-3.

A description of the COS-B satellite γ-ray detector was given by B. Swanenburg (Huygens Laboratorium). Preliminary results were presented by J. Paul (Saclay), H. Mayer-Hasselwander (Max-Planck Institute, Garching) and R. Buccheri (University of Palermo). These results included confirmation of a strong γ-ray source near galactic coordinates 195°, + 5°, and an indication of a change in the intensity of the Vela source since the time of the SAS-2 observations. The temporal analysis of PSR 0833-45 indicated that the γ-ray pulses were quite narrow.

G. Share (US Naval Research Laboratory) noted that the galactic γ-ray energy spectrum below 30 MeV showed the predicted steep shape characteristic of bremsstrahlung radiation. J. Grindlay (Center for Astrophysics, Cambridge, Massachusetts) noted that there are now two known sources emitting γ rays at energies $\geq 10^{12}$ eV.

P. Sturrock (Stanford University) suggested that a cascade process resulting from electron–positron pair creation in the pulsar magnetic field may be the cause of the pulsed γ radiation. H. Ogelman (Middle East University, Ankara) pointed out that pulsars radiate predominantly in the 1–1,000 MeV range. W. B. Burton (National Radio Astronomy Observatory) and N. Scoville (University of Massachusetts), both presented new observations of the 2 6 mm CO emission line which indicated that molecular clouds in the Galaxy (mostly H_2) are concentrated between galactic radii of 4 and 8 kpc in contrast to the atomic hydrogen, which is relatively uniform in distribution at radii from 4 to 14 kpc. The measurements also show that H_2 clouds are more tightly confined to the galactic plane than atomic hydrogen gas. E Jenkins (Princeton University) noted that ultraviolet measurements of the molecular hydrogen in the local region of the galaxy give a value of the density a factor of four lower than that implied from the CO observations for a galactic radius of 10 kpc, although the results are not necessarily in conflict owing to selection effects.

W. Roberts (University of Virginia) discused the spiral density wave theory of galactic structure and stated that the apparently striking separation of atomic and molecular hydrogen could be the result of stronger compression of gas in the inner galaxy, and an increase of the frequency at which the interstellar gas is periodically compressed.

J Baldwin (Cavendish Laboratory, Cambridge) noted that the non-thermal galactic radiation implies a much broader distribution of the cosmic ray electrons than of matter in the glalaxy. This has been found also to be the case in other spiral galaxies. J. Seiradakis (Max-Planck-Institut, Bonn) showed that, within the present limited statistics, the radial distribution of pulsars is generally correlated with that of other young (Population I) galactic objects. Both G. Fazio (Center for Astrophysics) and J. L. Puget (Observatory Meudon) discussed the significance of the local molecular hydrogen clouds in terms of infrared and γ-ray emissions. Puget concluded that the γ-ray observations indicate that the cosmic ray densities inside and outside clouds are similar.

R. Lingenfelter (University of California, Los Angeles) discussed the γ-ray lines emitted by the excited nuclei produced by interactions of cosmic rays with interstellar matter. He predicted that the 4.4 MeV carbon line would be the most intense. D. Arnett (University of Illinois) described the possibility of studying the results of nucleosynthesis in supernovae by examining the γ-ray lines emitted by the end products, and noted that the time interval after the explosion before the supernova envelope becomes transparent to γ rays was much longer than had been estimated earlier.

E. Parker (University of Chicago) gave a comprehensive lecture on cosmic ray propagation and galactic containment, in which he noted that the cosmic rays, the magnetic field, and the interstellar gas strongly affect each other dynamically. He concluded that if cosmic rays leave the galaxy, it must be as a consequence of collective cosmic-ray pressure.

The part that γ-ray astronomy can play in determining the large-scale galactic structure was then discussed. D Kniffen (Goddard) emphasised that the cosmic ray electrons and protons can be studied independently by looking at different portions of the γ-ray spectrum, and that γ-ray observations should be particularly valuable in searching for spiral structure. F. Stecker (Goddard) showed that galactic γ-ray emission is correlated with the molecular cloud distribution in the galaxy and that the deduced cosmic ray distribution appears to follow the supernova remnant and pulsar distributions in the galaxy, favouring a galactic supernova origin for most cosmic rays. He also discussed γ-ray implications for cosmic ray propagation and the galactic contribution to the high latitude γ-ray background.

After almost two decades of strenuous effort developing instruments of sufficient sophistication and sensitivity, there have been significant advancements in γ-ray astronomy in the past few years Not only has the general level of the galactic radiation been established, but also its broad features. With improved angular resolution and much greater sensitivity, γ-ray astronomy together with astronomy at other wavelengths hold great promise for the study of our Galaxy, other galaxies and high energy processess in astronomical objects. □

A hundred years ago

A FALL of meteorites, we learn from *Aftonblad*, took place on June 28, between 11 and 12 a.m., near Stalldalen, a station on the Swedish Central Railway, in the northernmost part of Örebrolän. Several fell, some on the ground and others in a lake. Two were found, one about the size of the fist and weighing 4½ lbs., the other smaller. Eye-witnesses stated that a loud whistling was first heard in the air from west to east, and a light was plainly distinguishable; although the sky was clear and cloudless, thereafter two very sharp reports were heard, the second succeeding the first after a momentary interval, followed by several others less sharp, resembling thunder, after which the falling stones were observed by eight or ten persons; and finally, there was seen in the air a whirling smoke, not very high up. A meteor was observed simultaneously at Stockholm and at other places. At thirteen English miles south-west of Linkoping it was seen first in a north-westerly direction pretty high up in the sky, and it then sank down in about ten seconds towards the horizon in the west. It had the appearance of a large pear a foot long, which, notwithstanding the bright sunshine, left behind a clear shining streak of six or eight feet in apparent length, which finally broke up into a multitude of starlike sparks. Here no noise was heard. According to a communication from the Stockholm Meteorological Bureau, there is reason to believe that the phenomena arose from the "kulblixt" (*foudre globulaire*), which generally appears as a luminous round object, and often, on approaching the ground, assumes a lengthened form and a blinding white colour, and bursts asunder, commonly with a loud report.
from *Nature*, **14**, August 3, 300; 1876.

review article

Fundamental research in molecular biology: relevance to medicine[*]

M. F. Perutz[†]

Molecular biology has given us new insights into many phenomena of clinical importance; it has suggested new therapeutic approaches to several diseases and has provided sensitive new methods for detecting chemical carcinogens. None of these applications had been foreseen.

MOLECULAR biology is sometimes said to be of little medical significance because it has not cured anyone yet. A hundred years ago the same might have been said of histology. At that time cellular anatomy and pathology began to improve our understanding of many diseases, today molecular anatomy and pathology give us much deeper insights. I shall illustrate this theme by examples taken from four different fields of research. The first two are from the fields with which I am most familiar, the structure and function of proteins; the second two are from molecular genetics. I shall show first how research on the structure of protein-digesting enzymes has led to an understanding of blood clotting and other important functions whose relationship to digestion no one had suspected. I shall then relate how my own work on the structure of haemoglobin has improved our understanding of genetic diseases and how basic research on autoxidation of haemoglobin has suggested a way of treating certain inherited anaemias. My next two themes are concerned with the effects of ultraviolet light and chemical carcinogens on nucleic acids and their relationship to human cancer. Finally, I shall ask whether any of this research could have been planned from the outset with a view to its medical applications.

Proteolytic enzymes and their inhibitors

In the 1950s the structure and catalytic mechanism of enzymes still ranked as one of the great unsolved problems in biochemistry. At that time two of my colleagues, B. S. Hartley and D. M. Blow, became interested in the proteolytic enzyme chymotrypsin, simply because they regarded it as the most hopeful and interesting one to attack. This enzyme is closely related to two other pancreatic proteolytic enzymes, trypsin and elastase. Chymotrypsin splits fastest those peptide bonds that follow amino acids with aromatic side chains, while trypsin goes for peptide bonds that follow basic side chains, and elastase for those with very short side chains. All three enzymes are secreted into the jejunum in the form of inactive precursors, known as chymotrypsinogen, trypsinogen and proelastase, all three precursors are activated by trypsin.

The pancreas also makes a small protein which scavenges and inhibits any traces of free activated trypsin. This is the pancreatic trypsin inhibitor.

Hartley and his colleagues determined the amino acid sequence of chymotrypsin and chymotrypsinogen[1] while Blow and others solved the three-dimensional structure of chymotrypsin by X-ray analysis[2]. Other workers followed with the structure of chymotrypsinogen, of trypsin, of elastase, of the trypsin inhibitor and of the trypsin–trypsin inhibitor complex. Together, Blow, Hartley and their colleagues worked out the mechanism of activation and catalysis[3], and R. Huber and Blow that of inhibition[4].

Chymotrypsin consists of 242 amino acid residues in three separate chains, which are linked by disulphide bonds. Its active site contains a serine, a histidine and an aspartate juxtaposed so that protons can shuttle backwards and forwards between them, forming what Hartley and Blow called a charge relay system.

The substrate is recognised by a pocket that lies next to the active site and is so tailored that it attracts the side chain of the amino acid preceding the peptide bond to be split. In the inactive precursor that specificity pocket is closed. Trypsin activates the precursors by splitting their chains in a way that allows the pocket to open. The pancreatic trypsin inhibitor mimics a substrate by presenting to the enzyme a side chain which its specificity pocket recognises, but the peptide bond following that side chain is so shielded from water that the enzyme cannot split it. Instead, the inhibitor remains firmly attached to the enzyme in a position resembling the one fleetingly occupied by a substrate at the first intermediate stage of catalysis[3].

The mechanisms of activation, recognition and catalysis of chymotrypsin first became known in outline in 1969, and the way in which the pancreatic trypsin inhibitor blocks trypsin in 1972; some further important details have been added since. Whenever nature has invented an effective and versatile device, it tends to exploit it over and over again for different functions. The same mechanisms of activation, recognition, catalysis and inhibition have now been found in at least four other functions: the clotting of blood, the dissolution of blood clots, the disposal of complexes of antigen and antibody by complement, and the lowering of blood pressure by the release of kinins. The raising of blood pressure by the release of angiotensins is also due to a proteolytic enzyme known as renin, but this is an acid proteinase related to pepsin, and its structure is still unknown. The interplay of protein digesting enzymes and their inhibitors seems to be important also in degenerative diseases such as pulmonary emphysema and rheumatoid arthritis.

---

[*] This paper is an abbreviated version of a paper presented at Ciba Foundation Symposium 44, *Research and Medical Practice*, held in January 1976 under the chairmanship of Sir Douglas Black and to be published by Elsevier/Excerpta Medica/North-Holland, Amsterdam, in summer 1976.

[†] MRC Laboratory of Molecular Biology, Hills Road, Cambridge CB2 2QH.

Suitable stimuli to blood platelets set off a chain reaction which causes blood to clot with very high velocity. This is due to a cascade of proteolytic enzymes and auxiliary proteins whose purpose it is to activate thrombin and liberate it from the platelets into the plasma (Fig. 1). It is now certain that part of the thrombin molecule has a structure which is almost identical to that of trypsin; in the clotting factors XIa, IXa and Xa, the parts of the sequences that have so far been analysed, are also like those of trypsin. The precursor of each of these enzymes is activated by the preceding enzyme in the clotting cascade by the same kind of mechanism by which trypsin opens the specificity pocket in trypsinogen or chymotrypsinogen, and each possesses the same charge relay system for the hydrolysis of peptide bonds. The functioning of the cascade depends on the presence of calcium ions and on nutrition with adequate amounts of vitamin K.

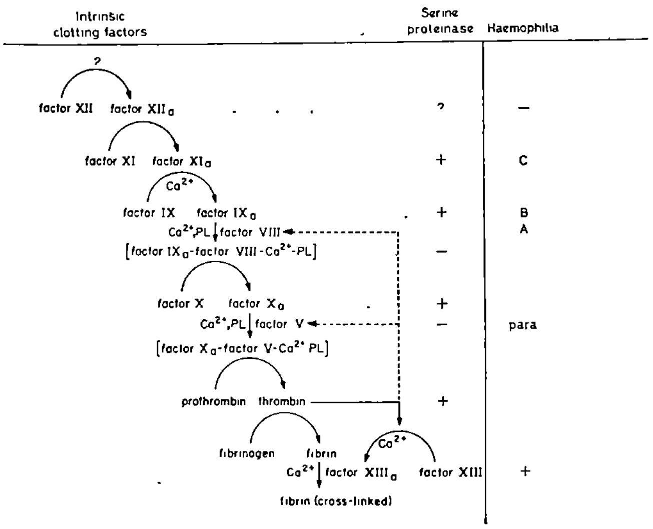

Fig. 1 Cascade of intrinsic clotting factors. Those marked + are enzymes similar to trypsin (reproduced, with permission, from the article by Davie and Kirby[6]).

The clotting factors possess several refinements which the pancreatic enzymes lack. Their specificities are probably greater and they are activated not in free solution, where they would be too widely dispersed, but on the surface of phospholipid membranes of blood platelets where they are crowded together. Prothrombin, the precursor of thrombin, has an extra 274 amino acids which are not found in trypsinogen, forming an attachment which binds it to the membrane, but only in the presence of calcium ions. On activation by factor Xa this attachment is split off and thrombin is released into the plasma. A great advance has recently been made in our understanding of the role of calcium and its dependence on vitamin K. It has been found that calcium ions are bound to prothrombin by 10 residues of a new amino acid, γ-carboxyglutamate; the residues lie near the amino terminus of the chain The new amino acid is made after the polypeptide chain of prothrombin has been assembled in the liver, by an enzyme system that adds a second carboxyl group to each of the first ten glutamates; and this subsidiary enzyme system that adds carboxyl groups requires vitamin K as a cofactor. In the clotting cascade, the other three trypsin-like factors or enzymes also require calcium in order to be activated, which implies that they are subject to the same vitamin K dependent modifications as prothrombin These discoveries explain how vitamin K antagonists interfere with blood clotting: by reducing the calcium affinity of prothrombin and of three other clotting factors they prevent their binding to the phospholipid membrane and thereby inhibit their activation[7].

The therapeutic uses of vitamin K antagonists were discovered long before its mode of action was understood, but the new discoveries will allow the antagonists to be applied more rationally and with greater knowledge of their possible side effects. For example, the presence of the new amino acid γ-carboxyglutamate in prothrombin suggested that it might be worth while to search for it in other calcium binding proteins. This search has led to the isolation of the amino acid from a protein in the bones of 14-week-old chicken, which suggests that it may be needed for the deposition of calcium in developing bones[8], and explains why treatment of women during the first 3 months of pregnancy with anticoagulants of the dicoumarol type has led to bone anomalies in the foetus Quite recently, γ-carboxyglutamate has also been found in a small protein isolated from adult bones of several species, including humans. The amino acid forms part of a peptide whose sequence bears no resemblance to that of the *N*-terminal peptide of prothrombin, showing that it is part of a quite different protein specific to bone, and indicating that vitamin K is essential for the formation and maintenance of bone structure[37].

There are at least two natural anticoagulants which prevent clotting getting out of hand. An excess of free thrombin in the plasma stops activation of more prothrombin by splitting off its first 156 residues, thus detaching it from the phospholipid membrane before it can be activated A plasma inhibitor, AIII antithrombin, inhibits thrombin and other clotting factors by a mechanism apparently similar to that by which the pancreatic inhibitor blocks trypsin, except that by itself AIII antithrombin acts much more slowly. It has recently been found that heparin exerts its instant anticlotting effect by accelerating the reaction of AIII antithrombin with thrombin and with other factors. Patients with a congenital deficiency of AIII antithrombin have an increased tendency to thrombosis[9], which shows that this inhibitor is an essential part of the checks and balances in the clotting system.

AIII antithrombin is one of six different antiproteinases so far discovered in human plasma. Another of the six that has recently assumed medical importance is α_1-antitrypsin, because people with an inherited deficiency of this inhibitor are predisposed to pulmonary emphysema. The mechanism of lung destruction in these patients is still unclear but is believed to be due to digesting enzymes from granulocytes and macrophages. These may cause emphysema even in people with normal levels of α_1-antitrypsin if they are released in excess by chronic lung irritation. It now looks as if pulmonary emphysema may be only one example of a degenerative disease where protein-digesting enzymes have a decisive role. For example, one such enzyme, though of a type different from trypsin, has been found in the joints of rheumatoid arthritis patients. Knowledge of the three-dimensional structure of these enzymes may open the way to the synthesis of tailor-made inhibitors for the treatment of such diseases.

Haemoglobin diseases

In 1949 Pauling, Itano, Singer and Wells published a paper entitled "Sickle Cell Anaemia, a Molecular Disease"[10]. They showed that homozygotes suffering from this autosomal recessive disease had a haemoglobin which differed from the normal by the absence of two negative charges. Ingram later discovered that this was due to the replacement of a single amino acid residue among the 287 in the half molecule of haemoglobin; one glutamate was replaced by a valine. (Recently the same replacement of a single glutamic acid by a valine has been found in a variant human α_1-antitrypsin(S). The replacement is harmless in heterozygotes (SM) carrying both the normal (M) and the variant (S) gene, but it may predispose SS homozygotes to pulmonary emphysema[11].) This was the first time that a genetic mutation was shown to cause the replacement of an amino acid in a protein. A search for other haemoglobin diseases soon followed, and now more than 200 different abnormal haemoglobins are known, which give rise to a variety of haematological disorders whose cause had been unrecognised before, these may affect both the synthesis and life span of red blood cells.

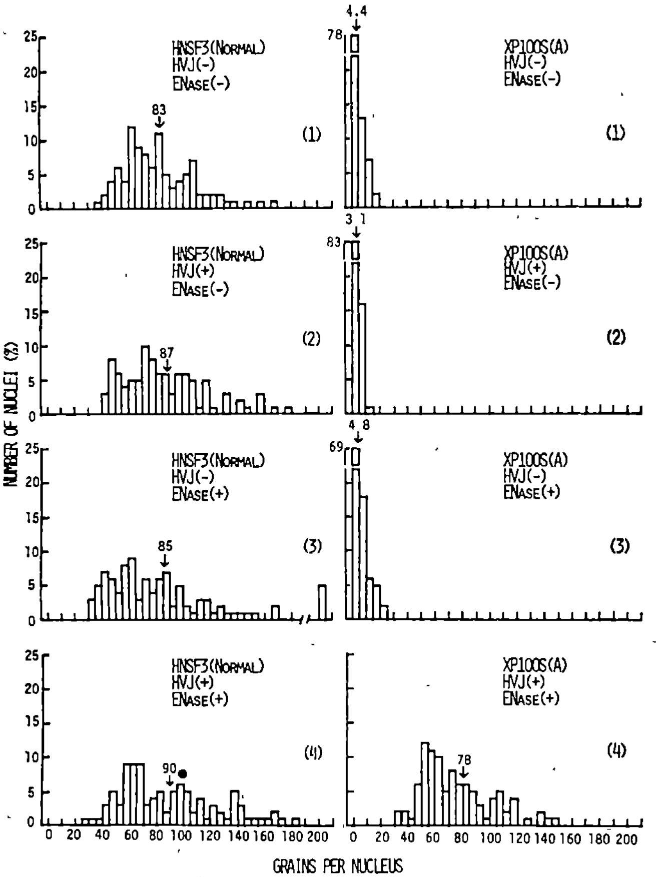

Fig. 2 Histograms showing numbers of silver grains produced by the disintegration of ^3H labels after ultraviolet irradiation in nuclei of normal skin fibroblasts (left) and fibroblasts from a xeroderma pigmentosum patient (right) HNSF3: normal skin fibroblasts. XP100S(A): xeroderma pigmentosa cells group A. HVJ: ultraviolet inactivated Sendai virus. ENase: endonuclease from T4 infected *E. coli*. (Reproduced, with permission, from Tanaka *et al.*[21].)

The dual respiratory function of haemoglobin depends on a reversible change of structure. The venous form of haemoglobin has a low affinity for oxygen and a high one for hydrogen ions, CO_2 and 2,3-diphosphoglycerate; in the arterial form these relative affinities are reversed Efficient respiratory transport depends on correct regulation of the equilibrium between the two forms. My colleagues and I have determined their three-dimensional structure in atomic detail[12,13]. H. Lehmann and I then attempted to interpret the clinical symptoms of the haemoglobin diseases in stereochemical terms[14]. In most of them the abnormality consists of the replacement of a single amino acid residue, as it does in sickle cell anaemia, but the position of that residue is crucial in deciding the nature of the symptoms. If the residue lies on the surface, as often happens, there may not be any symptoms, at least in heterozygotes, because the haemoglobin molecule hardly "feels" the wrong residue.

In homozygotes, on the other hand, superficial replacements may reduce the solubility of the haemoglobin in the red cell This happens in sickle cell anaemia where the venous form of haemoglobin actually crystallises out. Prevention of this crystallisation would relieve the disease, but has proved very difficult The structure of the areas of contact between neighbouring molecules of sickle cell haemoglobin is now being worked out in atomic detail and may form the basis for a synthetic approach to the inhibition of crystallisation

The surface of the haemoglobin molecule is studded with electrically charged amino acid side chains which ensure its high solubility in water. Its interior structure, on the other hand, is stabilised by hydrocarbon side chains which make it impenetrable to water. In several abnormal haemoglobins this water-repellent armour is breached, so that they become unstable and form amorphous precipitates in the red cell known as Heinz bodies. Similar denatured precipitates are seen in thalassaemia where the red cells contain unequal numbers of α and β chains. The precipitates make the red cells more rigid and therefore more fragile, and this was believed to be the main cause of the associated haemolytic anaemias Denaturation of haemoglobin is also accompanied by oxidation of the haem iron from its normal ferrous to the ferric state. It has now been found that it is this oxidation rather than the presence of denatured haemoglobin precipitates which mainly causes haemolysis. The mechanism is this. In the first step of the reaction the iron-bound oxygen molecule is reduced to superoxide ion which may then dissociate from the haem and produce hydrogen peroxide ion, hydroxyl radicals and singlet oxygen in the surrounding water[15]. These are all oxidising agents, hydroxyl radical being the most powerful among them, and they attack the lipids of the cell membrane with resulting haemolysis. The obvious remedy is the administration of drugs designed to trap free radicals such as vitamin E or 2,3-dihydrobenzoic acid. These are now under trial[16,17]. In the long term practical results of much wider importance should result from the study of the abnormal haemoglobins. In the first place they have shown that the genetic code in humans is the same as in *E. coli*, which is a prerequisite for relieving congenital diseases by any kind of genetic engineering. They have proved that human genes are subject to a fairly high rate of mutation (the frequency of abnormal haemoglobins in the human population may be greater than 1 in 500), but that these mutations may be harmless if they merely replace residues at the surface of enzymes away from their active sites Interior replacements on the other hand, may affect the function and stability of enzymes. In favourable circumstances knowledge of their three-dimensional structure may allow us to mitigate such effects.

I started to study haemoglobin by X-ray crystallography in 1937 because at that time the structure of proteins seemed the most important unsolved problem in biochemistry, but I never dreamt that its solution would one day throw light on the nature of inherited diseases.

Xeroderma pigmentosum

The mutations which give rise to the abnormal haemoglobins occur spontaneously, perhaps by random errors inherent in the genetic process. It had long been known that the rate of mutation can be enhanced by external factors such as radiation and certain chemicals. It had also been suspected that some of the same factors which produce mutations give rise to cancer, but no exact correlation had been shown.

Ultraviolet light damages DNA by causing two pyrimidine bases, usually, but not always, on the same strand, to become covalently linked. In ultraviolet-sensitive bacteria this linkage inhibits DNA replication and thereby stops further growth. But there are strains of the same bacteria which are resistant to ultraviolet and it turns out that these possess an enzyme system which excises the dimers and repairs the gap, thus allowing growth to start again[18]. Now it appears that normal human skin cells have an enzyme system for the repair of ultraviolet damage similar to that of ultraviolet resistant bacteria. There is a rare autosomal recessive human disease in which the skin is extremely sensitive to ultraviolet light; it is called xeroderma pigmentosum. Sufferers from this disease—the homozygotes—are also very liable to skin cancer. In 1969 J. E. Cleaver discovered that fibroblasts from such patients lack an enzyme necessary for the repair of ultraviolet-damaged DNA[19]. Investigators later found that there are six geneticaly distinct types of enzymatic deficiency, that is six complementation groups, five of which are deficient in DNA repair and the sixth in another as yet unknown function[20]; Japanese workers have now shown that ultraviolet resistance can be restored to all those five types of fibroblasts that are deficient in DNA repair by an enzyme which is an endonuclease from T4 phage infected *E coli*[21] (Fig. 2). Their results are exciting because they suggest that it may become possible to treat patients with this kind of enzyme, even if it is not yet clear how it could be applied. Quite recently, an altered endonuclease concerned with the repair of depurinated sites has been found in fibroblasts from two of the complementation groups that were known to be deficient in DNA repair[38].

Table 1 Correlation between carcinogenic and mutagenic activity of chemicals

	car + mut +	car 0 mut 0	car + mut 0	car 0 mut +	?	correlation (%)
Aromatic amines and so on	21	9	2	—	12	94
Fungal toxins and antibiotics	8	2	—	2	2	83
Esters, epoxides, carbamates and so on	14	6	4	2	2	77
Nitro aromatics and heterocycles	26	1	—	3	2	90
Miscellaneous heterocycles	1	7	3	—	—	73
Miscellaneous nitrogen compounds	7	2	2	2	—	69
Nitrosamines and so on	20	2	1	—	—	96
Polycyclic aromatics	27	7	—	3	1	92
Miscellaneous aliphatics and aromatics	1	10	4	—	5	73
Alkyl halides	16	1	3	2	2	77
Azo dyes and diazo compounds	12	2	—	1	2	93
Cigarette smoke condensate	1	—	—	—	—	100
Common biochemicals	—	42	—	—	—	100
Totals	154	91	19	15	28	88

106 non-carcinogens 14% positive, but 86% negative

173 carcinogens 89% positive, but 11% negative

Detection of chemical carcinogens

Discovery of the cause of xeroderma pigmentosum was important because it linked the occurrence of a cancer with a mutagenic event whose nature and repair could be explained in the same molecular terms as in bacteria. Evidence in favour of a causal link between the frequency of somatic mutation and the incidence of cancer has long been accumulating, yet many of the most potent chemical carcinogens seemed to have no mutagenic effect in microorganisms. This paradox was finally resolved by Bruce Ames Ames had devoted nearly 20 years to the study of the control of protein synthesis in *Salmonella typhimurium*. His work, like that of Hartley and Blow on chymotrypsin and mine on haemoglobin, was undertaken without any foreknowledge of possible applications.

The chromosome of *Salmonella* contains an operon that codes for histidine biosynthesis. Transcription of the enzymatic genes of this operon into messenger RNA is controlled by an operator gene which responds to the level of histidine in the cell, switching transcription on when histidine is scarce and switching it off when it is plentiful. Certain mutant strains of *Salmonella* cannot grow unless histidine is supplied in the medium; this has turned out to be due to mutations in the histidine genes Ames selected four such strains. In one of them the DNA differs from that of the wild type by the replacement of a GC by an AT pair, or vice versa. In the remaining three strains the DNA carried mutations of a kind first correctly interpreted by Crick, Barnett, Brenner and Watts-Tobin when they established the nature of the genetic code[22,23] Decoding of the sequence of nucleotide bases makes sense only if the reading frame is positioned correctly with respect to the succession of coding triplets. Certain mutagens such as proflavine intercalate between the base pairs of DNA and thereby interfere with its replication so that base pairs are either added or deleted, and the reading frame is thus shifted.

Three of the four strains of *Salmonella* used by Ames carry mutations of this type in the histidine genes[24,25]. Ames plated these histidine-requiring strains of *Salmonella* on a histidine-free nutrient, applied chemical carcinogens and waited for the growth of colonies in which a reversion of the original mutation had allowed the resumption of histidine biosynthesis. The presence of 10^9 organisms on each plate allowed rare genetic events to be detected. The smallness of the bacterial chromosomes increased the likelihood of reversions of the original mutation to other mutations which might be lethal. The time needed for one experiment was only 2 d.

Initially only some of the known chemical carcinogens caused growth of revertant colonies but Ames and his colleagues improved the sensitivity of his system step by step until he was able to prove a strong correlation between carcinogenicity and reversion. He introduced two additional mutations: one raises the sensitivity by eliminating the repair mechanism already mentioned, that repairs ultraviolet and other damage, and the other strips the bacterial surface of part of its protective lipopolysaccharide layer which makes it more permeable to large molecules. He also increased mutagenesis in his tester strains by incorporating a plasmid[26] which appears to channel DNA damage down an error-prone repair pathway (SOS repair)[27–30].

Ames made one more improvement in the system which proved decisive. It had been discovered that in mammals many compounds are non-carcinogenic as such, but are converted into carcinogens by hydroxylating enzymes in the liver. Ames decided to mimic this conversion by adding rat or human liver homogenate together with a system for generating nicotinamide adenine nucleotide diphosphate to his cultures[31–33]. The results show a strong correlation between carcinogenesis in mammals and mutagenesis in *Salmonella*[34,35]. Ninety per cent (157/175) of the carcinogens were mutagenic in the test including almost all of the known human carcinogens that were tested. Despite the severe limitations inherent in defining non-carcinogenicity, few "non-carcinogens" showed any degree of mutagenicity (Table 1). The mutagens include tar from cigarette smoke and oxidative hair dyes (Fig. 3)[36]. Another mutagen is chloracetaldehyde, a possible metabolite of dichloroethane and of vinylchloride, two chemicals of which several million tons are produced in the USA each year. In the first instance, all these mutagens probably act by stopping DNA replication and thereby inducing the error prone SOS repair mechanism. Mutagens which do not do this, such as EMS, base analogs and deaminating agents, appear to be weakly or not carcinogenic (M. Radman, private communication). Study of the SOS repair mechanism would therefore seem a promising approach to the understanding of radiation and chemically induced carcinogenesis.

Ames' method offers a cheap, quick and sensitive way of screening chemicals for mutagenicity. For instance, 1 ng of 2-aminoanthracene doubled the spontaneous reversion rate of about 20 colonies, and 500 ng gave 11,000 revertant colonies compared with about 30 in the controls. In view of the correlation between mutagens and carcinogens any compound which is a potent mutagen is now suspected also of being carcinogenic. Other screening tests in bacteria and mammalian cells have been reviewed by Bridges[39].

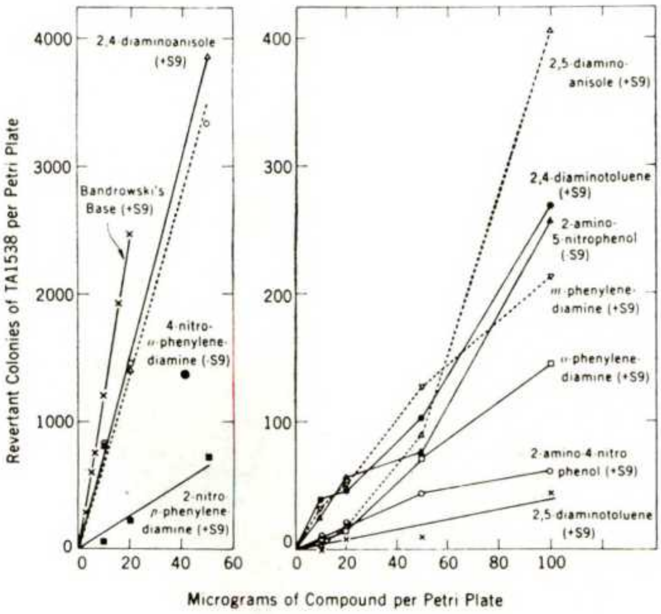

Fig. 3 Dose–response curves of the mutagenicity of chemicals extracted from hair dyes. Revertant colonies were counted after incubating the Petri plates for 48 ha t 37 °C with the chemical mutagen and the microsomal activation system (S9) where indicated. (Reproduced, with permission, from Ames *et al.*[36].)

The first impact of Ames' work should be to eliminate known carcinogens from our food and daily habits so as to reduce the number of carcinogenic events to which we are being exposed—and, incidentally, to let us stop worrying about many other commonly used chemicals which turn out to be harmless. In the long run this research and the work on xeroderma pigmentosum may help us to unravel the exact molecular mechanism by which ultraviolet irradiation and chemicals that revert frame shift and other mutations cause cancer.

What has molecular biology contributed to this work? It has supplied the basic concepts of microbial genetics, mutagenesis, repair and feed-back control; it has supplied the techniques of transferring genetic material from one strain of bacteria to another which Ames used to build up the sensitivity of his system. These concepts and techniques were developed by scientists who set out to interpret fundamental biological processes in physical and chemical terms. Generally the problems were so complex that it took very many years to solve them. At the outset our ignorance was too profound for us to foresee the relationship of our work to human disease, and it became apparent only afterwards. Although we know more now than when we started, molecular biology is still too young a science for it to be clear exactly where it will pay off, whence we may do best if we spread our efforts over a wide field. Since research is the art of the soluble, it is often more profitable to study a basic problem in microorganisms where it can be solved, rather than in mammalian cells which are so much more complex. One of my examples has shown how such an indirect approach has helped to unravel pathogenic events in man. It would be a mistake if all molecular biologists switched to mammalian cells as has recently become the fashion, or as they are being forced to do by policy decisions of supporting agencies. There is a unity of life at the molecular level which implies that anything found to be true in *E. coli* may also hold in man.

In the future, the most important contribution of molecular biology to medical practice may well be genetic engineering, but early hopes that eukaryotic genes could be transcribed and translated in prokaryotes have not yet materialised. Instead, workers may try to see if cultures of animal viruses carrying human genes could be used for the manufacture of therapeutically important human proteins.

[1] Hartley, B. S., *Phil. Trans. R. Soc.*, **B257**, 77–86 (1973).
[2] Birktoft, J. J., Blow, D. M., Henderson, R., and Steitz, T. A., *Phil. Trans. R. Soc.*, **B257**, 67–76 (1973).
[3] Stroud, R. M., *Scient. Am.*, **231**, 74–89 (1974).
[4] Blow, D. M., and Smith, J. M., *Phil. Trans. R. Soc.*, **B272**, 87–98 (1975).
[5] Huber, R., Kukla, D., Steigemann, W., Deisenhofer, J., and Jones, A., in *Bayer Symposium: Proteinase Inhibitors*, (edit. by Fritz, H., *et al.*) 497–512 (Springer Verlag, Berlin, 1974).
[6] Davie, E. W., and Kirby, E. P., in *Current Topics in Cellular Regulation*, **7**, 51–86 (Academic, New York and London, 1973).
[7] Magnusson, S., *Boerhaave Series for Postgraduate Medical Education No. 10*, 25–46 (Leiden University Press, Leiden, 1975).
[8] Hauschka, P. V., Lian, J. B., and Gallop, P. M., *Proc. natn. Acad. Sci. U.S.A.*, **72**, 3925–3929 (1975).
[9] Marcinac, E., Farley, C. H., and DeSimone, P. A., *Blood*, **43**, 219–231 (1974).
[10] Pauling, L., Itano, M. A., Singer, S. J., and Wells, I. C., *Science*, **110**, 543 (1949).
[11] Owen, M. C., and Carrell, R. W., *Br. med. J.*, **1**, 130–131 (1976).
[12] Perutz, M. F., *Proc. R. Soc.*, **B173**, 113–140 (1969).
[13] Fermi, G., *J. molec. Biol.*, **97**, 237–256 (1975).
[14] Perutz, M. F., and Lehmann, H., *Nature*, **219**, 902–909 (1968).
[15] Misra, H. P., and Fridovich, I., *J. biol. Chem.*, **247**, 6960–6962 (1972).
[16] Carrell, R. W., Winterbourn, C. C., and Rachmilewitz, E. A., *Br. J.Haemat.*, **30**, 259–264 (1975).
[17] Graziano, J. H., Grady, R. W., and Cerami, A., *J. Pharmac. exp. Ther.*, **190**, 570–575 (1975).
[18] Setlow, R. B., and Carrier, W. L., *Proc. natn. Acad. Sci. U.S.A.*, **51**, 226–231 (1964).
[19] Cleaver, J. E., *Proc. natn. Acad. Sci. U.S.A.*, **63**, 428–435 (1969).
[20] Kraemer, K. H., *et al.*, *Proc. natn. Acad. Sci. U.S.A.*, **72**, 59–63 (1975).
[21] Tanaka, K., Sekiguchi, M., and Okada, Y., *Proc. natn. Acad. Sci. U.S.A.*, **72**, 4071–4075 (1975).
[22] Crick, F. H. C., Barnett, L., Brenner, S., and Watts-Tobin, R. J., *Nature*, **192**, 1227–1232 (1961).
[23] Crick, F. H. C., *Scient. Am.*, **207**, 66–73 (1962).
[24] Ames, B. N., in *Chemical Mutagens: Principles and Methods for their Detection*, **1** (edit. by Hollaender, A.), 267–282 (Plenum, New York, 1971).
[25] Ames, B. N., Gurney, E. G., Miller, J. A., and Bartsch, H., *Proc. natn. Acad. Sci. U.S.A.*, **69**, 3128–3132 (1972).
[26] McPhee, D. G., *Appl. Microbiol.*, **26**, 1004–1005 (1973).
[27] Defais, M., Fauqet, P., Radman, M., and Errera, M., *Virology*, **43**, 495–503 (1971).
[28] Witkin, E. M., and George, D. L., *Genetics (suppl.)*, **73**, 91–108 (1973).
[29] Radman, M., *Molecular Mechanisms for Repair of DNA, Part A: Basic Life Sciences*, **5A**, Hollaender, A., general ed. (edit. by Hanawalt, P. C., and Setlow, R. B.), 355–367 (Plenum, New York, 1975).
[30] Witkin, E. M., *ibid.*, 347–353 and 369–378.
[31] Malling, H. V., *Mutation Res.*, **13**, 425–429 (1971).
[32] Slater, E. E., Anderson, M. D., and Rosenkranz, H. S., *Cancer Res.*, **31**, 970–973 (1971).
[33] Garner, R. C., Miller, E. C., and Miller, J. A., *Cancer Res.*, **32**, 2058–2066 (1972).
[34] McCann, J., Choi, E., Yamasaki, E., and Ames, B. N., *Proc. natn. Acad. Sci. U.S.A.*, **72**, 5135–5139 (1975).
[35] McCann, J., and Ames, B. N , *Proc. natn. Acad. Sci. U.S.A.*, **73**, 950–954 (1976).
[36] Ames, B. N., Kammen, H. O., and Yamasaki, E., *Proc. natn. Acad. Sci. U.S.A.*, **72**, 2423–2427 (1975).
[37] Price, P. A., Otsuka, A. S., Poser, J. W. and Raman, N., *Proc. natn. Acad. Sci. U.S.A.*, **73**, 1447–1451 (1975).
[38] Kuhnlein, U., Penhoet, E. E. and Lynn, S., *Proc. natn. Acad. Sci. U.S.A.*, **73**, 1169–1173 (1976).
[39] Bridges, B. A., *Nature*, **261**, 195–200 (1976).

SCIENCE COLLEGE

articles

Seeing order in 'amorphous' materials

O. L. Krivanek, P. H. Gaskell* & A. Howie

Cavendish Laboratory, Cambridge, UK

Careful analysis of high resolution electron micrographs of amorphous materials, making use of a simple optical simulation technique, provides a means for discriminating between 'meaningful' and 'meaningless' images, and for detecting ordered regions as small as 15 Å in the 'meaningful' ones. Such regions, comprising only about 100 atoms, have been directly observed in 'amorphous' carbon, and it is possible that they exist in a range of other 'amorphous' materials.

THE past decade has witnessed a dramatic improvement in the resolving power of high resolution electron microscopes. Atomic planes spaced less than 1 Å apart have been imaged[1], and heavy single atoms have not only been directly observed[2,3] but their movement between successive exposures followed as well[4]. Routinely attainable point-to-point resolution has come down to around 5 Å and less.

The typical nearest-neighbour distances in most solids are about 2 Å, and many important crystallographic planes have a separation of 3 Å and more. The resolving power of electron microscopes therefore makes it natural to inquire about the possibilities of an atom-by-atom determination of the specimen structure. Such an approach should be particularly fruitful in the case of amorphous (non-crystalline) materials, since in these the conventional structure research based on X-ray, electron or neutron diffraction yields only statistical data averaged over the whole specimen. It describes the probability that an atom A will have a neighbour B a distance r away, but tells us very little about the local deviations from the average structure.

The first step in the direction of structure determination by direct imaging is a search for small ordered domains within the non-crystalline sample. Such investigations have already yielded much useful information, such as the 'wavy onion' structure of the carbon black particles[5,6], and a detailed description of the carbon graphitisation process[6]. In materials other than amorphous carbon the results have been less clear. In amorphous Ge the early dark field (image formed with scattered electrons only) observations of small bright spots about 14 Å in diameter[7,8], interpreted in terms of small wurtzite crystallites[7], have been overtaken by observations of much smaller dark field spots[9,10] and interpretations denying the presence of any crystallites[8,10]. Similarly, bright field observations of small patches of fringes[9–12], interpreted as direct imaging of the crystallite lattice planes[9,11,12], have also given rise to interpretations[10] in terms of relatively ordered regions within the continuous random network model[13,14], or have simply been discarded as statistical peaking in order within an essentially random image[15].

Meaningful images or just random noise?

The diversity of opinions about the images of amorphous materials is the result of two fundamental difficulties, best illustrated by an analogy. An individual telephone conversation may remain identifiable even when received over a line with poor frequency response, but once several conversations are superimposed, the total loses all its information content and becomes just noise, in spite of being made up of individually meaningful signals. Similarly, an atom imaged by an electron microscope with a necessarily limited spatial frequency response may remain individually identifiable, but when the images of several such atoms are superimposed, the total may just become a random, unintelligible noise.

Computing the images of various existing structural models for amorphous materials has shown that, for specimens of sufficient thickness, images of completely different models become qualitatively indistinguishable, and image features corresponding to particular structural configurations within the specimen may become completely washed out[16,17]. This suggests that many experimental images (for which the thickness of the amorphous specimen is usually quite considerable) may indeed be nothing but random, frequency-filtered noise.

Random noise has been the subject of many mathematical studies, mainly in the context of communication engineering.

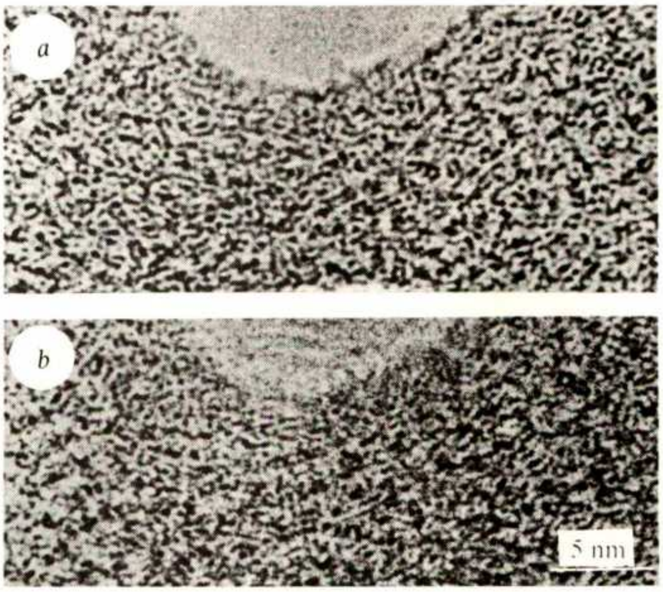

Fig. 1 *a*, Direct reconstruction of an axial bright field micrograph of vapour-deposited amorphous Ge. *b*, Phase-randomised reconstruction of the same image. A Perspex plate, sprayed with transparent lacquer until the droplets (about 0.1 mm in size) just started merging, served as the random phase screen for this and all the other phase-randomised images shown in this article. The resulting surface roughness was enough to ensure that each original patch of fringes was spread over a large area in the reconstruction, rather than merely shifted sideways.

By virtue of the Central Limit Theorem[18], many different mathematical representations of the noise are possible. The one most commonly used is

$$I(\mathbf{r}) = 1 + \sum_{n} c_n \cos(2\pi \mathbf{q}_n.\mathbf{r} + \varphi_n) \qquad (1)$$

$I(\mathbf{r})$ is the intensity at a point $\mathbf{r}$ in the image plane, the c_ns are the coefficients defining the image spatial frequency power spectrum, $\mathbf{q}$ is the spatial frequency variable and φ_n represents the phase. The summation is taken over all the points of the spatial frequency plane needed to define the image area being considered, and the phases φ_n are taken to be distributed randomly in the interval $(0,2\pi)$. The representation (1) then describes the bright field image of a weak random object (with an unscattered beam of intensity 1). It leads to the prediction of many interesting properties of the random function[19,20], some of which are directly applicable to the electron images. For instance, the probability of finding the image intensity I, at an image point selected at random, lying between I and $I + \mathrm{d}I$, follows a Gaussian distribution in I. Dark field images are describable by an expression similar to equation (1), although for these the intensity distribution is a negative exponential[21] rather than a Gaussian one. These distributions can be used to test the randomness of actual electron images[17], but since they treat each image point independently and are therefore incapable of evaluating any patterns within the image, such tests are not particularly sensitive to non-random features. A better test of image randomness that concentrates on groups of image fringes is described here.

An optical simulation technique

It is clear that equation (1), being nothing but a Fourier summation, can be used to represent any image. The random bright field image description only follows upon taking the phases to be random. When the phase information is deliberately removed (by randomising the phases), we obtain an image which has lost all the information on the exact specimen structure the original may have contained. This random image will obviously differ from the original in detail, but it is possible that qualitatively the two images will be identical: every patch of fringes in the original micrograph may be matched by a similar patch of fringes produced in the random image by purely statistical effects. Should this be the case, it is clear that the fringe patches in the original image should not be taken as structurally meaningful. Should the two images display marked differences in the number and regularity of fringe patches present, however, some interesting conclusions about the nature of the specimen should follow from the original.

The randomisation of the phases φ_n can be carried out either computationally or in an optical bench[17]. The second approach enjoys the advantage of greater simplicity and an ability to handle large image areas. It produces the phase-randomised image in three stages: a diffraction pattern (the spatial frequency power spectrum) of the original micrograph is formed, the phases are randomised by inserting a random phase screen into the diffraction plane, and finally a reverse optical transform leads to the phase-randomised reconstruction. To avoid undesirable interference between the main (unscattered) beam and the inserted phase screen, the main beam is allowed to pass through a hole in the screen. The resulting reconstruction is a simulated 'random' micrograph: although its spatial frequency power spectrum is unchanged from the original, it has become just random noise.

Ordered regions in amorphous Ge, SiO_2 and C

Figures 1, 2 and 3 show how the phase-randomisation technique works in practice. In each figure, image *a* is a direct reconstruction of the original micrograph (recorded with the random phase screen removed) and image *b* is its phase-randomised counterpart. The three examples are arranged by the amount of ordered structures visible in the original images. In Fig. 1*a* the 4-Å structures are quite irregular and in Fig. 2*a* some fringes running in the vertical direction appear: even more fringes can be seen in Fig. 3*a*. Such differences may be obvious to the eye, but it is clearly impossible to differentiate between meaningful and fortuitous image features on the basis of such qualitative remarks alone. One can, of course, define objective criteria of fringe regularity such as the signal-to-noise ratio of a group of fringes[17], and then evaluate the significance of the fringes by comparing the experimental values of their signal-to-noise ratio with the theoretical prediction for fringes produced by random effects. Such treatment, however, works with the absolute values of fringe regularity and demands that all the parameters influencing the image formation (such as the amount of inelastic scattering present, astigmatism of the objective lens, specimen drift and so on) be known accurately, which is usually not the case.

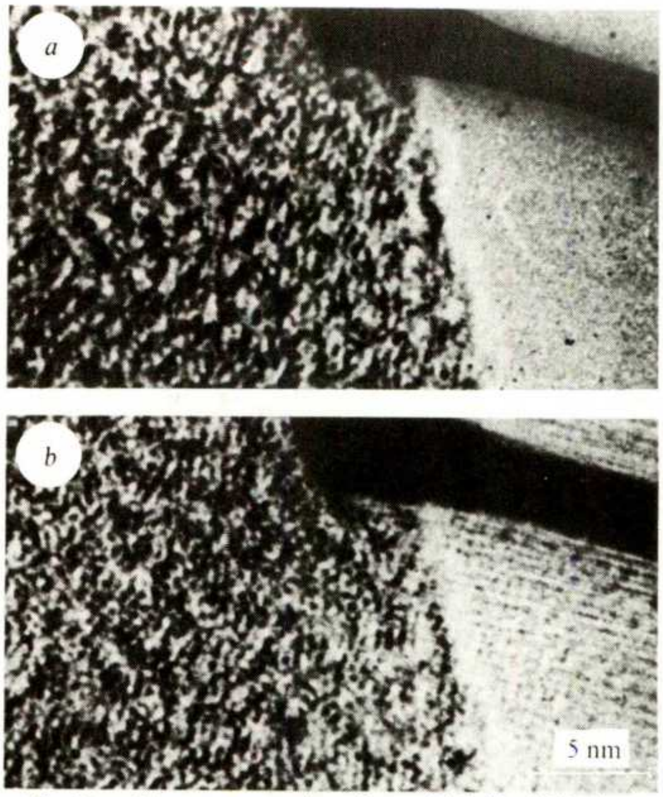

Fig. 2 *a*, Direct reconstruction of an axial bright field micrograph of amphorous SiO_2 prepared by fragmentation of a "Spectrosil" disk. *b*, Phase-randomised reconstruction of the same image.

By creating an individual reference standard with which the original image can be compared, the phase-randomisation technique altogether avoids the need for such considerations. In the case of amorphous germanium (Fig. 1), for example, the phase-randomised reconstruction is completely different from the original in detail, but it is not difficult to see that qualitatively the two images have remained indistinguishable, with the extent of ordering of the 4-Å structures being about the same in either image. The phase-randomised reconstruction for amorphous carbon (Fig. 3*b*), on the other hand, does not show any ordered image structures comparable to those visible in the original image. Specifically, the patches of relatively straight and parallel fringes spaced about 4 Å apart identifiable at several places in Fig. 3*a* (particularly near the edge of the specimen) find no equivalent in the randomised reconstruction.

Optical diffractograms showing the spatial frequency power spectrum of the direct and phase-randomised images of amorphous carbon are shown in Fig. 4. It can be seen that the phase-randomisation procedure has hardly changed the power spectrum at all, so that the different appearance of Fig. 3*a* and *b* is entirely due to the modification of the phases. It is also worth noting that because the lowest spatial frequencies have passed, together with the main beam, through the hole in the random-phase screen, the coarse image detail has not been altered by the phase randomisation, while the fine image structure has been completely changed by it. As a result of the phase randomisation, the fine structures in all the phase-randomised reconstructions extended well over the specimen edge (see Fig. 3*b*), and the marker shown in Fig. 2*a* reappears in Fig. 2*b* decomposed into its individual spatial frequency components, no longer fitting together as before.

By comparison with the amorphous germanium and amorphous carbon examples, the amorphous silica image (Fig. 2) constitutes an intermediate case. Analysis of the spatial frequencies of the original image by optical diffraction indicates that, due to astigmatism, some directional filtering has taken place. Such filtering will lead to a micrograph with fringes running predominantly in one direction, and directional effects will remain even in the phase-randomised image, showing that the original fringes had no structural meaning whatever. Vertical fringes qualitatively similar to the ones in the direct reconstruction do indeed appear in Fig. 2*b*, but since they are somewhat more broken up than those visible in Fig. 2*a*, it is difficult to pronounce judgment on the original image with any certainty.

It should perhaps be emphasised that the intention of this article is to describe a technique for discriminating between meaningful and fortuitous features in high resolution bright field electron micrographs; the three examples used are merely intended to serve as an illustration. It would not be correct to reach any definite conclusion regarding the structure of amorphous materials on the basis of small parts of three electron micrographs, particularly since the structure of these materials is known to depend strongly on the preparation conditions (evaporation rate, substrate temperatures and so on). The possibility of providing a detailed quantitative description of order in such materials in fact constitutes one of the most attractive applications of this technique. Nevertheless, the results obtained with amorphous Ge and C may perhaps be taken as indicative of the results to be expected in these materials. The micrograph of evaporated amorphous Ge (Fig. 1*a*) contained no image features attributable to well defined ordered regions within the specimen. The fringes seen in the image of evaporated amorphous C were, however, shown definitely not to arise from any fortuitous superposition of the images of distant individual atoms, and must therefore be taken as evidence for small (about 10 to 15 Å) ordered regions within the material. These regions most probably consist of a few parallel graphite-like planes lying along the direction of the illuminating electron beam.

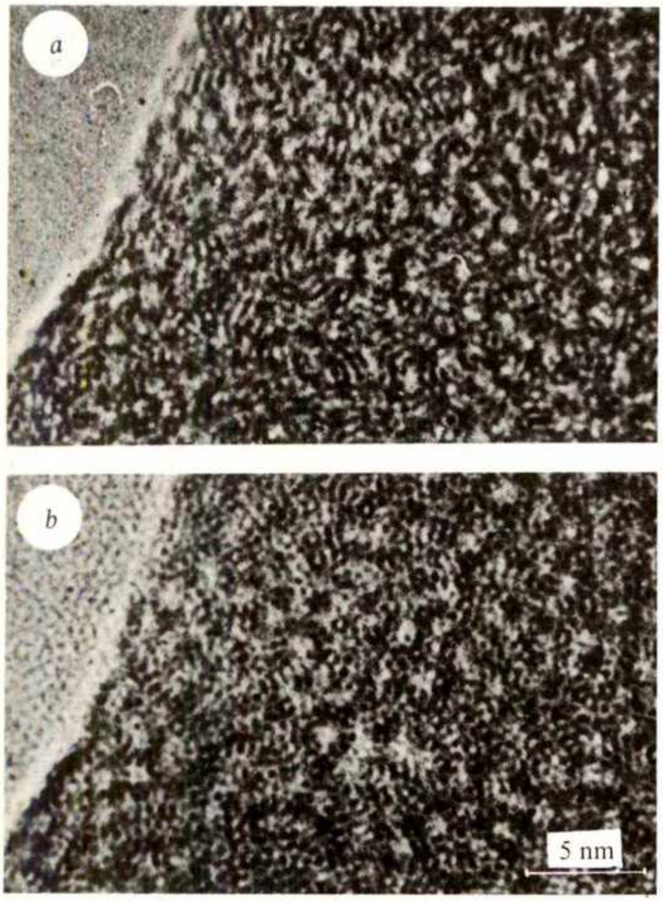

Fig. 3 *a*, Direct reconstruction of an axial bright field micrograph of vapour-deposited amorphous C. *b*, Phase-randomised reconstruction of the same image.

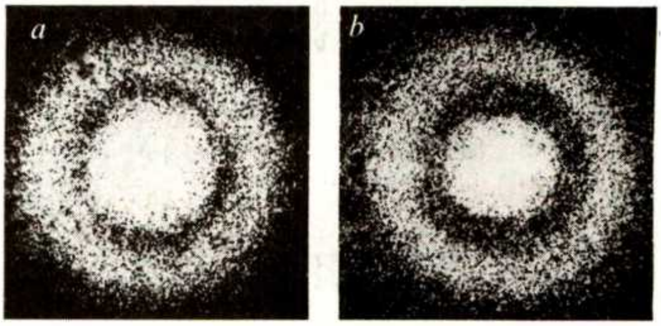

Fig. 4 *a*, Diffractogram of Fig. 3*a*. *b*, Diffractogram of Fig. 3*b*. They show that the micrograph of Fig. 3*a* was recorded at the broad second transfer interval underfocus ($z_0 \simeq -1{,}400$ Å) with negligible astigmatism ($c_a < 20$ Å). The disappearance of the outer part of the first transfer interval in *b* is due to the opaque edge of the hole in the random-phase screen.

The absence of any fringes in the Ge micrograph that could be safely attributed to non-random causes does not, however, mean that the specimen contained no ordered regions at all. It can be shown that in a Ge specimen 100 Å thick the image of a fully diffracting 15-Å crystallite would be obscured by the images of the atoms in the remaining 85 Å. Only crystallites larger than about 18 Å would remain directly visible[17]. A similar result also applies for amorphous silica: in a SiO_2 film 100 Å thick, only ordered regions larger than about 18 Å will remain directly visible, and 15-Å ones will be obscured in films thicker than about 50 Å. In amorphous C this limitation is much less severe, owing mainly to the perfect alignment of the atoms into the graphite planes, which consequently stand out clearly from the amorphous background; 15-Å graphite crystallites should remain visible even when embedded in films up to 150 Å thick.

The average thickness of the Ge specimen (as determined by monitoring its deposition by a quartz crystal oscillator) was about 100 Å. It therefore follows that ordered regions smaller than 18 Å will not be identifiable. Near the specimen edge (top half of Fig. 1*a*) the thickness is, however, likely to be smaller, so that the lack of non-random features there places an upper limit of about 15 Å on the size of ordered regions possibly present. The amorphous C film was also about 100 Å thick, which means that the actual direct observation of the 15-Å ordered domains raises no contradiction. In regions much thicker than 100 Å the fringes attributable to these domains will be obscured.

To summarise, high resolution electron microscopy has given rise to an approach to the study of the structure of amorphous materials that is radically different from the conventional methods based on the analysis of diffraction patterns. The first task confronting a researcher using the new approach is the differentiation between structurally meaningful images and those in which too many overlapping atoms obscure the underlying structure. This problem has been solved by the simple technique of optical simulation of random noise with power spectrum identical to the original image. In the image of amorphous Ge examined here the technique shows no evidence of crystallites, and thus places an upper limit of about 15 Å on the size of ordered regions possibly present. In amorphous C, however, small (~15 Å) ordered regions have been detected with the technique. It seems quite possible that similar ordering will be discovered in many other types of non-crystalline materials.

This research was supported by the SRC.

Received March 29, accepted May 12, 1976

*Pilkington Brothers Ltd., Ormskirk, Lancashire, UK

[1] Sieber, P., and Tonar, K , *Optik*; **42**, 375–380 (1975)
[2] Crewe, A. V., *Science*, **168**, 1338–1340 (1970)
[3] Hashimoto, H., Kumao. A., Hino, K., Yotsumo, H , and Ono, A., *Jap. J appl Phys.*, **10**, 1115–1116 (1971).
[4] Crewe, A. V , Langmore, J , Isaacson, M., and Retsky, M., *Proc 8th Int. EM Congr.* (*Canberra*), **1**, 260–261 (1974)
[5] Ban, L. L., and Hess, W. M , *Proc. 26th EMSA Meeting*, 256–257 (1968).
[6] Ban, L' L., *Surface and Defect Properties of Solids*, **1**, 54–94 (The Chemical Society, London, 1972).
[7] Rudee, M. L., *Phys stat solidi* (*b*), **46**, K1–K3 (1971).
[8] Chaudhari, P., Graczyk, J. F., and Herd, S R., *Phys stat solidi* (*b*), **51**, 801–820 (1972).
[9] Howie, A., Krivanek, O. L , and Rudee, M L , *Phil Mag.*, **27**, 235–255 (1973).
[10] Herd, S. R , and Chaudhari, P , *Phys stat. solidi* (*a*), **26**, 627–642 (1974)
[11] Rudee, M L., and Howie, A., *Phil. Mag* , **25**, 1001–1007 (1972).
[12] Gaskell, P. H , and Howie, A , *Proc. 12th Int. Semicond Conf.* (*Stuttgart*), 1076–1080 (1974).
[13] Polk, D. E., *J Non-Cryst. Sol.*, **5**, 365–376 (1971)
[14] Polk, D E., and Boudreaux, D. S., *Phys. Rev. Lett* , **31**, 92–95 (1973)
[15] Berry, M. V., and Doyle, P. A , *J. Phys. C* , **6**, L6–L9 (1973).
[16] Krivanek, O. L , and Howie, A., *J. appl. Crystallogr.*, **8**, 213–219 (1975)
[17] Krivanek, O. L., thesis, Univ. Cambridge (1975).
[18] Fry, T. C., *Probability and its Engineering Uses* (Van Nostrand, Princeton, 1965).
[19] Rice, S O., *Bell Syst tech. J* , **23**, 282–332 (1944); *ibid.*, **24**, 46–156 (1945).
[20] Longuet-Higgins, M. S., *Phil. Trans. R. Soc.*, **A249**, 321–387 (1956), *ibid* , **A250** 157–174 (1957).
[21] Dainty, J. C., *Opt. Acta*, **17**, 761–772 (1970).

Isotropic cosmic expansion and the Rubin–Ford effect

S. Michael Fall & Bernard J. T. Jones

nstitute of Astronomy, Madingley Road, Cambridge CB3 0HA, UK

We show that the Rubin–Ford (RFR) data, often taken as evidence for large scale anisotropic cosmic expansion, probably only reflect the inhomogeneous distribution of galaxies in the region of the Rubin–Ford sample. The data RFR have presented are consistent with isotropic expansion, an unperturbed galaxy velocity field and hence a low density Universe.

RUBIN, Ford and Rubin[1] have reported on 'a curious distribution of radial velocities of Sc I galaxies' which has sometimes been taken as evidence for large scale anisotropic cosmic expansion. The Rubin–Ford sample consists of 74 galaxies with measured radial velocities (corrected for galactic rotation) and apparent magnitudes (as determined by Zwicky) in the 'window' $14.0 \leqslant m_{\mathrm{Zw}} \leqslant 15.0$. These galaxies were chosen from a larger sample of 200 galaxies, selected from Palomar Sky Survey plates and classified as being of type Sc I according to the David Dunlap Observatory system[2].

RFR note in ref. 1 that the apparent velocity distribution of their sample is distinctly anisotropic. In one region of the sky (called region I), most of the sample galaxies have radial velocities $v_{\mathrm{I}} \simeq 4{,}950$ km s^{-1}, while in the opposite region (called region II) most of the sample galaxies have radial velocities $v_{\mathrm{II}} \simeq 6{,}400$ km s^{-1}. The mean apparent magnitudes of sample galaxies in the two regions differ by only 0.1 mag and the mean apparent diameters differ by only 14%. Since Sc I galaxies are thought to be good 'standard candles', RFR make the suggestion that their data may be evidence for anisotropic cosmic expansion. If true, this would have important cosmological implications, especially in view of the apparent isotropy of the microwave background radiation. Our purpose in this article is to point out that the Rubin–Ford data are consistent with isotropic expansion and indeed, the effect might have been expected on the hypothesis that the expansion is isotropic.

Inhomogeneities

The idea underlying our argument is illustrated in Fig. 1 where we have plotted the positions of Sc I galaxies in the Rubin–Ford sample with declinations in the range $20° < \delta < 42°$. We have also plotted all galaxy clusters in this declination band with radial velocities $< 10{,}000$ km s^{-1} and tabulated in Noonan's list of clusters with published redshifts[3]. Those clusters classified by Abell[4] as being 'rich' are represented by a circle of radius 10 h^{-1} Mpc (where h is the Hubble constant measured in units of 100 km s^{-1} Mpc^{-1}). From Peebles' Abell cluster–galaxy correlation function[5], this radius corresponds to a rich cluster density contour at some 3 times the background density. The other clusters were plotted with radii of 7 h^{-1} Mpc unless they seemed, from an inspection of Zwicky's catalogue[6] to be particularly small or poor. In that case they were plotted with radii of 4 h^{-1} Mpc. The sizes are only meant to give a rough indication of the distribution of galaxies in the vicinity of clusters. To estimate the completeness of Noonan's list in this region, we have checked the Zwicky catalogue and find only one (or possibly two) additional clusters which are comparable with those of known radial velocities.

The correlation between the positions of Rubin–Ford Sc I galaxies and clusters in Fig. 1 is quite striking. Only one of the Sc I galaxies is significantly isolated from any cluster. RFR point out that some 60% of their sample galaxies life outside the cores of known clusters. Nonetheless, it is apparent from Fig. 1 that they are associated with the Perseus–Pisces complex and Abell's[7] supercluster no. 6 (including Coma and A1367). This would be expected on the 'cloud picture' of the galaxy distribution[8–10]. Figure 1 suggests to us that the apparent anisotropy in the radial velocities of Sc I galaxies may reflect only the inhomogeneities in the distribution of galaxies in the region of the Rubin–Ford sample.

Of course, we have picked the declination band where the effect is most dramatic to illustrate the basic idea underlying our hypothesis. To show that the correlation of Sc I galaxies with clusters is a general phenomenon, we present in Table 1 the number of Rubin–Ford sample galaxies and Noonan clusters in the high and low velocity bands of regions I and II for the whole sky north of $\delta = -3°$. We note that the ratio of the number of clusters to Sc I galaxies in the low velocity band of region I is nearly the same as this ratio for the high velocity band of region II, as expected on our hypothesis. We also note that there is an apparent deficit of high velocity Sc I galaxies in

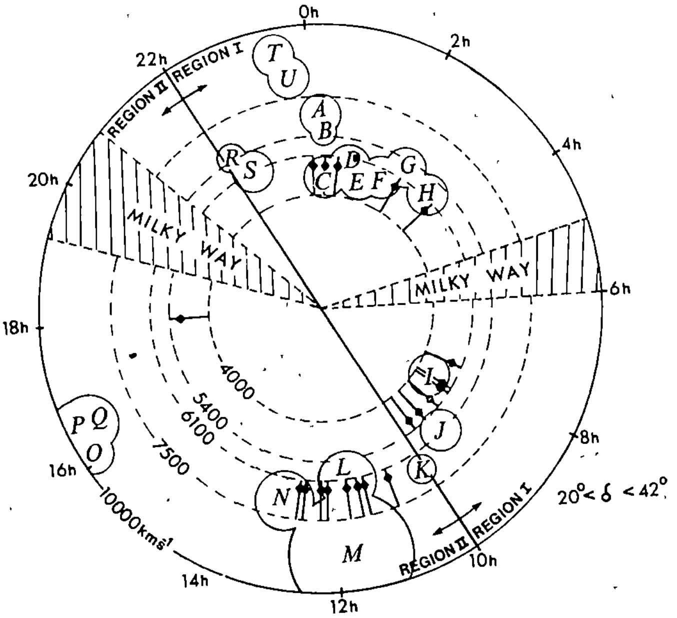

Fig. 1 Clusters (○) and Rubin–Ford Sc I galaxies (-◆-) with $20° < \delta < 42°$. Clusters: *A*, *B*, Anonymous; *C*, Perseus C_2; *D*, Z501–5; *E*, Z501–5; *F*, Z522–9; *G*, A347; *H*, A426, Z540–1 (Perseus); *I*, Z119–1 (Cancer); J, A779, Z181–17; *K*, Z211–58; *L*, A1367, Z127–2; *M*, Abell Supercluster no. 6; *N*, A1656, Z160–1 (Coma); *O*, A2162, Z167–8; *P*, A2199, Z224–12; *Q*, A2197, Z224–12; *R*, Z513–2; *S*, Z514–3; *T*, A2634, Z476–5; *U*, A2666, Z476–5. Numbers preceded by A are entries in Abell's catalogue[4] and numbers preceded by Z are entries in Zwicky's catalogue[6]. All radial velocities are from Noonan[3] except *C* which is from Zwicky[9] and *M* which is from Abell[7]. The circular scale gives RA (h), the radial scale gives velocity (km s^{-1}).

region I. As the high velocity clusters in region I are among the poorest in the sample, however, this fact should not be given equal weight.

The two-cloud model

Figure 1, together with the Rubin–Ford comment that most of their sample galaxies in region I have velocities near 4,950 km s^{-1} and those in region II have velocities near 6,400 km s^{-1}, suggests that we idealise to a model in which galaxies lie in two 'clouds' with those velocities. We shall refer to this model as the 'two-cloud model' and denote the low velocity cloud I and the high velocity cloud II. Of course, the applicability of the model results from the particular magnitude window chosen by RFR and the distribution of clusters within it (compare Fig. 1). In what follows, we shall assume (1) that the Sc I galaxies in both clouds are drawn from a universal urn, that is from the same luminosity function and size distribution, and (2) that there is no anisotropy in the cosmic expansion, that is, distances are given by Hubble's law with a direction independent Hubble constant. We shall then endeavour to show that this model is consistent with the data presented in ref. 1 by RFR; we shall 'predict' (1) the 0.1 apparent magnitude difference between low and high velocity sample galaxies and (2) the 14% difference in mean angular diameters.

First, we compute the mean apparent magnitudes of high and low velocity galaxies expected on the two-cloud model in a manner suggested by Sandage and Tammann's discussion of the Rubin–Ford effect[11]. We adopt the luminosity function for Sc I galaxies suggested by van den Bergh[2] and Sandage and Tammann[11]; a Gaussian with mean absolute (photographic) magnitude

$$\bar{M} = -20.0 + 5\log h \qquad (1)$$

and dispersion

$$\sigma(M) = 0.50 \text{ mag} \qquad (2)$$

With this luminosity function we compute mean apparent magnitudes

$$\bar{m}_{\rm I} = 14.17, \quad \bar{m}_{\rm II} = 14.30 \quad \text{(model)} \qquad (3)$$

for the low and high velocity clouds respectively. The calculation is illustrated in Fig. 2 and is of course independent of *h* and the numbers of galaxies in the clouds. We have adopted a photometric correction of −0.1 mag to Zwicky magnitudes as suggested by Sandage and Tammann[11]. The predicted mean apparent magnitudes (3) are to be compared with the mean apparent magnitudes of the Rubin–Ford sample, corrected for galactic obscuration

$$\bar{m}_{\rm I}^{c} = 14.20 \pm 0.07, \quad \bar{m}_{\rm II}^{c} = 14.30 \pm 0.06 \quad \text{(Rubin–Ford data)} \qquad (4)$$

The agreement is remarkably good. We note that the predicted magnitudes are somewhat sensitive to the adopted magnitude window, but that their near equality is not. This near equality is mainly a consequence of the fact that the one-magnitude window chosen by RFR is comparable with the dispersion in the absolute magnitudes of Sc I galaxies.

Next we estimate the ratio of the mean angular diameters of the low and high velocity galaxies expected on the two-cloud model. We shall assume that galaxy diameters *d* and luminosities *L* are related by

$$d \propto L^{(1-\varepsilon)/2} \qquad (5)$$

where ε is a parameter to be discussed presently. From (5) and the relationship between distances, luminosities and apparent and absolute magnitudes, it follows that the ratio of the mean angular diameters for galaxies in clouds I and II is

$$\bar{\theta}_{\rm I}/\bar{\theta}_{\rm II} = (v_{\rm II}/v_{\rm I})^{\varepsilon}\,[1 + \tfrac{1}{5}(1-\varepsilon)(\bar{m}_{\rm II} - \bar{m}_{\rm I})\ln(10) + \ldots] \qquad (6)$$

to first order in $(\bar{m}_{\rm II} - \bar{m}_{\rm I})$. For the two-cloud model appropriate to the Rubin–Ford data this becomes

$$\bar{\theta}_{\rm I}/\bar{\theta}_{\rm II} \simeq (1.29)^{\varepsilon}\,(1.06 - 0.06\varepsilon) \quad \text{(model)} \qquad (7)$$

with the mean apparent magnitude difference calculated above (equation (3)). The case $\varepsilon = 0$ corresponds to luminosities uncorrelated with mean surface brightness as Hubble[12] found to be appropriate for elliptical galaxies, and the extreme case $\varepsilon = 1$ corresponds to luminosities uncorrelated with diameters.

Unfortunately, it is rather difficult to determine the luminosity–diameter relation for Sc I galaxies because one requires a large sample of galaxies, all at the same distance. It would be surprising if the value of ε appropriate to Sc I galaxies did not lie in the range (0,1) bracketed by the extreme cases mentioned above. We expect it to lie nearer the value $\varepsilon = 0.23$ found by Heidman *et al.*[13] to fit the data on spiral galaxies in the Virgo cluster best. This is similar to the value $\varepsilon = 0.17$ found by Holmberg[14] to fit the data on galaxies of all morphological types. In any case, the dependence of equation (7) on ε is rather weak in this neighbourhood. With $\varepsilon = 0.23$, equation (7) gives the ratio

$$\bar{\theta}_{\rm I}/\bar{\theta}_{\rm II} \simeq 1.11 \quad \text{(model)} \qquad (8)$$

Table 1 Numbers of Rubin–Ford ScI galaxies and Noonan clusters north of $\delta = -3°$

	Low velocity (4,000–5,400 km s^{-1})		High velocity (6,100–7,500 km s^{-1})	
Region	Galaxies	Clusters	Galaxies	Clusters
I	20	5	2	5
II	1	0	12	3

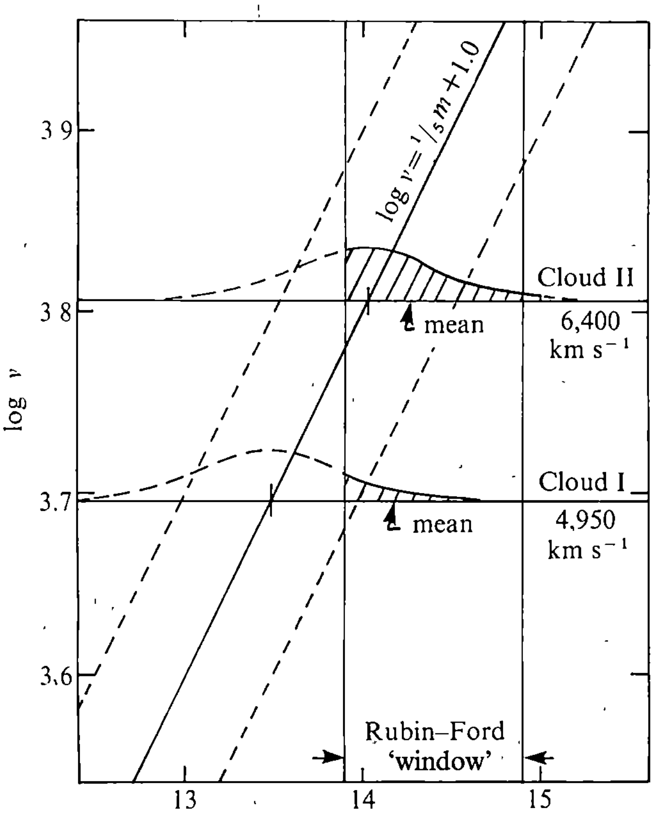

Fig. 2 Graph illustrating the calculation of mean apparent magnitudes for low and high velocity galaxies on the two-cloud model. The dashed diagonal lines are $\sigma = 0.50$ mag away from the mean velocity–magnitude line. All velocities are in km s^{-1}.

which is to be compared with the ratio

$$\bar{\theta}_{I}/\bar{\theta}_{II} = 1.14 \pm 0.10 \quad \text{(Rubin–Ford data)} \qquad (9)$$

quoted by RFR for their sample. In view of the large scatter in the angular diameters of Rubin–Ford galaxies, the agreement between equations (8) and (9) is entirely satisfactory.

The local velocity field

RFR have also pointed out that there is an apparent anisotropy in the radial velocities of the bright Sc I and Sc I–II galaxies studied by van den Bergh[2] and that the effect is similar in magnitude and in direction to that in the Rubin–Ford sample. That is, the van den Bergh galaxies in the Rubin–Ford region I seem to yield a Hubble constant similar to that of Rubin–Ford galaxies in region I but significantly smaller than that of both van den Bergh and Rubin–Ford galaxies in region II. RFR argue from this that inhomogeneity scales of at least 70 h^{-1} Mpc are required by the hypothesis of isotropic expansion. How can this be reconciled with our assumption of isotropic expansion and inhomogeneities on the more reasonable scale of 15 h^{-1} Mpc? We have re-examined the data on van den Bergh's sample of Sc I and Sc I–II galaxies and find that the anomaly arises mainly from those galaxies lying within ~20° of the centre of the Ursa Major complex. This is a small part of Rubin–Ford region I which we shall refer to as subregion U. Most of the van den Bergh galaxies in Rubin–Ford region II lie within ~20° of the Virgo cluster, a subregion which we shall denote by V.

Because of the unknown distribution of galaxies behind the Ursa Major and Virgo complexes, a detailed calculation is out of the question. The following remarks, however, strongly suggest that the anomaly may indeed be caused by inhomogeneities on the smaller scales: (1) the mean velocities of van den Bergh Sc I and Sc I–II galaxies lying in subregion U is very close to the mean velocity of both de Vaucouleurs[15] groups and Turner–Gott[16] groups lying in that subregion; (2) the mean velocity of van den Bergh Sc I and Sc I–II galaxies lying in subregion V is ~2,000 km s^{-1}, almost 1,000 km s^{-1} larger than the mean recessional velocity of the Virgo cluster. The apparent discrepancy could therefore be reconciled with isotropic expansion and moderate inhomogeneities on a theme similar to the two-cloud model if the Virgo complex in fact extends for 15 h^{-1} Mpc or so in the radial direction. Another possibility is simply that the velocities of some of the Sc I and Sc I–II galaxies in subregion V are dominated by the core of the Virgo cluster and are therefore not indicators of their distance. Indeed, according to Tammann[17] the van den Bergh galaxies having NGC numbers 4254, 4303, 4321 and 4535 lie in the core of the Virgo cluster. If these galaxies are put at the distance of the Virgo cluster, the anomaly between subregions U and V nearly disappears, and the remaining difference might be accounted for along the lines mentioned above.

Discussion

The agreement between the 'predictions' of the two-cloud model and the data reported by RFR in ref. 1 is encouraging. We emphasise again that the applicability of the model results from the particular, narrow magnitude window chosen by RFR and the distribution of galaxies (as suggested by the distribution of clusters) within that window. Unfortunately, the radial galaxy distribution at these distances is not yet accurately known over large parts of the sky and that is, of course, the reason for our choosing clusters of galaxies as a reflection of the distribution of galaxies. Recently, Chincarini and Rood have studied the radial velocity distribution of individual galaxies in the direction of the Coma cluster and its surroundings[18] and the Perseus–Pisces complex (G. Chincarini, personal communication) and find distributions quite consistent the cloud picture depicted in Fig. 1. We note that the density enhancements required to produce the Rubin–Ford effect on the hypothesis of isotropic expansion are of ~1 on radial scales ~15 h^{-1} Mpc (corresponding to the Rubin–Ford magnitude window). Studies of the distribution of galaxies within the Local Supercluster[19] indicate that the required matter gradients are not atypical. On the hypotheses of uniform expansion and a uniform matter distribution on the very largest scales, the Rubin–Ford effect should of course vanish. Support for this comes from Evans and Hart[20] who report no anisotropy in the angular diameter–redshift relationship for elliptical galaxies with radial velocities in the range 1,200 km s^{-1} to 25,000 km s^{-1}.

The Rubin–Ford effect should appear, on our hypothesis, in the distribution of any 'standard candles' in a one-magnitude window scaled to the RFR window (that is scaled by the difference in the mean absolute magnitudes of Sc I galaxies and that of the other standard candle). Le Denmat and Vigier[21] have suggested that type I supernovae may be appropriate standard candles and have discovered an effect similar to the RFR effect in their distribution. Considering, however, the methods used in searching for supernovae, their apparent distribution is almost guaranteed to coincide with the distribution of galaxy clusters, and would have been expected to exhibit an anisotropic velocity distribution on our hypothesis. We have re-examined the data on type I and possible type I supernovae[22,23] in the magnitude windows $15.3 \leqslant m \leqslant 16.3$ and $15.7 \leqslant m \leqslant 16.7$. These correspond respectively to supernovae mean absolute magnitudes 1.4 mag (ref. 24) and 1.8 mag (ref. 25) fainter than Sc I galaxies (see equation (1)). We do indeed find that most of these supernovae have occurred in galaxies which are members of the Coma, Cancer and Perseus–Pisces clusters (see Fig. 1). Jaakola *et al.*[26] have also noted an effect similar to the Rubin–Ford effect in the distribution of compact galaxies with absorption spectra. It is not clear, however, that these objects represent standard candles in the sense required to evaluate our hypothesis.

In summary, we have shown that the Rubin–Ford data are consistent with the hypothesis of isotropic cosmic expansion. In view of the similarity of Sandage and Tammann's[11] velocity–magnitude relationship (see their Fig. 4) in the supergalactic centre and anticentre directions, a peculiar anisotropy in the absolute magnitudes of Sc I galaxies which just compensates any anisotropy in the velocities is required if the cosmic expansion is not to be isotropic. We consider such a conspiracy to be less plausible than the hypothesis of isotropic expansion. The issue cannot be finally decided, however, until radial velocities and radial distribution of other kinds of matter at these distances are more accurately known. This will require velocity and magnitude data for several kinds of standard candles ('standard candle' meaning, in this context, a class of objects with an absolute magnitude dispersion $\lesssim 0.50$ mag, corresponding to the inhomogeneity scale $15\,h^{-1}$ Mpc at these distances).

Of course, we do not expect the cosmic expansion to be perfectly isotropic in the direction of clusters and clouds of galaxies because these matter inhomogeneities will have perturbed the expansion to some extent. Since the perturbed galaxy velocities near an inhomogeneity are determined by the absolute amount of matter in the inhomogeneity, its mass and hence the mean matter density of the Universe can, in principle, be determined once the galaxy distribution and velocity field near the inhomogeneity are mapped out[18,27–29]. As we have shown, the Rubin–Ford data are consistent with an unperturbed galaxy velocity field and hence a low density Universe. Paradoxically, the apparent anisotropy of the radial velocities reported by RFR in ref. 1 may impose a rather strong upper limit to the mean matter density of the Universe. To see this, refer back to Fig. 1. Suppose now that matter is decelerated towards the centre of the supercluster at RA 12 h. Then the matter on this side of the supercluster centre will be closer to us than the distance assigned on the two-cloud model from Hubble's law. The galaxies in this cloud would then appear too bright to be consistent with the Rubin–Ford data. At this stage, we refrain from carrying out a calculation of the mean matter density on this basis because of the uncertainties inherent in the limited data at hand. In view of the importance of this parameter and the hypothesis of isotropic expansion to cosmology, it would be very desirable to have more velocity and magnitude data for galaxies at these distances.

We thank Barry Madore, Martin Rees and Simon White for interesting discussions and helpful comments. S.M.F. acknowledges support from the Cambridge Philosophical Society.

Received May 11, accepted June 1, 1976

1 Rubin, V. C , Ford, W K , Jr, and Rubin, J S . *Astrophys J Lett.*, **183**, L111 (1973).
2 van den Bergh, S , *Astrophys J* , **131**, 215 (1960)
3 Noonan, T W., *Astr J* , **78**, 26 (1973)
4 Abell, G O , *Astrophys J Suppl* , **3**, 211 (1958)
5 Peebles, P. J E , *Astrophys J Suppl* , **28**, 37 (1974)
6 Zwicky, F , Herzog, E., Wild, P , Karpowicz, M , and Kowal, C. T , *Catalogue of Galaxies and Clusters of Galaxies* (California Institute of Technology Press, Pasadena, 1961–1968)
7 Abell, G O., *Astr J* , **66**, 607 (1961).
8 Shapley, H., *Galaxies* (Harvard University Press, Cambridge, Massachusetts, 1972).
9 Zwicky, F , *Handbuch der Physik*, Vol LIII, 390 (Springer, Heidelberg, 1959)
10 Hauser, M , and Peebles, P J. E., *Astrophys J.*, **185**, 757 (1974)
11 Sandage, A , and Tammann, G A , *Astrophys J* , **197**, 265 (1975).
12 Hubble, E *Astrophys J.*, **71**, 231 (1930)
13 Heidman, J , Heidman, N., and de Vaucouleurs, G., *Mem R astr Soc* , **76**, 121 (1972)
14 Holmberg, E., *Ark Astr* , **5**, 305 (1969)
15 de Vaucouleurs, G , in *Stars and Stellar Systems*, Vol IX (Chicago, 1965).
16 Turner, E. L , and Gott, J. R., III, *Astrophys J* (in the press)
17 Tammann, G A , *Astr Astrophys* , **21**, 355 (1972)
18 Chincarini, G., and Rood, H J , *Astrophys. J.*, **206**, 30 (1976)
19 Jones, B J T , *Mon Not. R. astr. Soc* , **174**, 429 (1976)
20 Evans, A., and Hart, D , *Nature*, **259**, 468 (1976)
21 Le Denmat, G., and Vigier, J -P , *C r hebd Séanc Acad Sci , Paris*, **280B**, 459 (1975).
22 Kowal, C. T , and Sargent, W L. W , *Astr. J* , **76**, 756 (1971).
23 Kukarkin, *et al* , *General Catalogue of Variable Stars*, **III** (Sternberg State Astronomical Institute, Moscow, 1971)
24 Kowal, C. T , *Astr J* , **73**, 1021 (1968).
25 Barbon, R , Capaccioli, M., and Ciatti, F , *Astr Astrophys* , **44**, 267 (1975)
26 Jaakkola, T , Karoji, H., Moles, M., and Vigier, J -P , *Nature*, **256**, 24 (1975).
27 Silk, J., *Astrophys J* , **193**, 525 (1974)
28 Fall, S M., *Mon Not R. astr. Soc* , **172**, 23p (1975).
29 Peebles, P. J. E , *Astrophys. J* , **205**, 318 (1976)

Fossil hominids from the Laetolil Beds

M. D. Leakey, R. L. Hay, G. H. Curtis, R. E. Drake & M. K. Jackes

Olduvai Gorge, PO Box 30239, Nairobi, Kenya

T. D. White

Department of Anthropology, University of Michigan, Ann Arbor, Michigan 48104

Remains of 13 early hominids have been found in the Laetolil Beds in northern Tanzania, 30 miles south of Olduvai Gorge. Potassium–argon dating of the fossiliferous deposits gives an upper limit averaging 3.59 Myr and a lower limit of 3.77 Myr. An extensive mammalian fauna is associated. The fossils occur in the upper 30 m of ash-fall and aeolian tuffs whose total measured thickness is 130 m.

THE fossil-bearing deposits referred to variously as the Laetolil Beds, Garusi or Vogel River Series lie in the southern Serengeti Plains, in northern Tanzania, 20–30 miles from the camp site at Olduvai Gorge.

Fossils have been collected from the area on several occasions, the largest collection being made by L. Kohl-Larsen in 1938–39, who also found a small fragment of hominid maxilla which was named *Meganthropus africanus* by Weinert[1]. L. S. B. Leakey and M.D.L. visited the area in 1935 and in 1959, while a day trip was made in 1964 in company with R. L. H. The faunal material recovered on these occasions was all collected before the advent of isotopic dating and the age of the fossils remained uncertain until potassium–argon dating was carried out on samples of biotite obtained during the 1975 field season. In 1974, however, lava flows which unconformably overlie the Laetolil Beds had been dated by G. H. C. at 2.4 Myr.

We now report evidence that fossiliferous deposits of several different ages exist in the Laetolil area and that specimens found on the surface are not necessarily derived from the same beds. There are, however, noticeable variations in the colour and physical condition of the surface fossils which provide indications of their origin.

Discrepancies in the fauna were noted by Dietrich[2] and Maglio[3] who both postulated faunal assemblages of two different ages. In view of this, it was proposed for a time that the name Laetolil should be abandoned in favour of the more generalised term Vogel River Series, based on the colloquial German name for the Garusi river, which abounds in bird life. As the early fossiliferous deposits here referred to as the Laetolil Beds are not confined to the Garusi valley, this change of name seems unnecessary. Furthermore, the name Laetolil embraces a larger area, because it is the anglicised version of the Masai name (laetoli) for *Haemanthus*, a red lily that is abundant in the locality The Laetolil Beds, *sensu stricto*, form a discrete unit, distinguishable from later deposits, and M.D.L. considers that the original name proposed by Kent

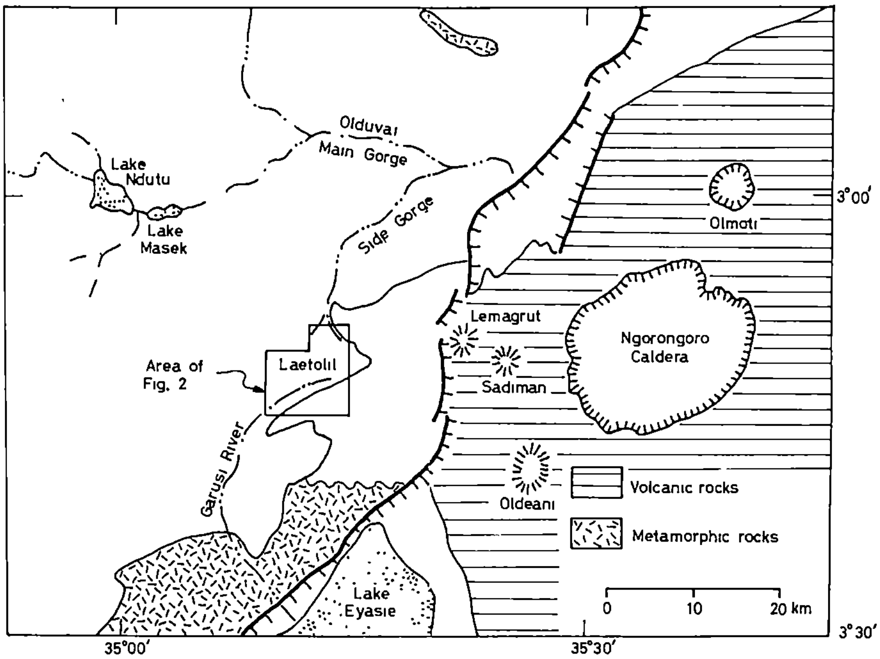

Fig. 1 Map of the southern Serengeti and volcanic highlands.

in 1941[4] should be retained for this part of the sequence.

The relationship of the Laetolil to the Olduvai Beds had been under discussion for some years, but in 1969 R. L. H. noted that they underlay bed I at the Kelogi inselberg in the Side Gorge and established that they antedated the Olduvai sequence. This has been further confirmed when tuffs correlatable with bed I as well as an earlier, fossil-bearing series of tuffs were found to lie unconformably on the Laetolil Beds.

Interest in the area was renewed in 1974 after the discovery by George Dove of fossil equid and bovid teeth in the bed of the Gagjingero river, which drains into Lake Masek at the head of Olduvai Gorge. These fossils were found to be eroding from relatively recent deposits, probably the beds named Ngaloba by Kent[4]. Exposures of the Laetolil Beds, not hitherto seen by M.D.L., were found to the east of the Gagjingero river, at the headwaters of the Garusi river and of the Olduvai Side Gorge (referred to as Marambu by Kohl-Larsen[5]). Several fossils, including a hominid premolar, were found at these localities and subsequent visits yielded further hominid remains.

The possibility of establishing the age of the hominid fossils from the Laetolil Beds by radiometric dating and of clarifying the discrepancies in the faunal material led to a 2-month field season during July and August 1975. Samples from the fossiliferous horizons, collected by R. L. H., have now been dated. On the basis of these results the hominid remains and associated fauna can be bracketed in time between 3.59 and 3.77 Myr.

No trace of stone tools or even of utilised bone or stone was observed in the material from the Laetolil Beds, although handaxes and other artefacts occur in conglomerates which are present in certain areas and which are unconformable to the Laetolil Beds.

Stratigraphy of Laetolil area

The bulk of the faunal remains and all of the hominid remains were found within an area of about 30 km² at the northern margin of the Eyasie plateau and in the divide between the Olduvai and Eyasie drainage systems (Fig. 1).

Kent studied this area as a member of L. S B. Leakey's 1934–35 expedition, and his short paper is the only published description of the stratigraphy. He recognised three main subdivisions of the stratigraphic sequence, which overlies the metamorphic complex of Precambrian age. The lower unit he named the Laetolil Beds and the upper the Ngaloba Beds The middle unit consists of olivine-rich lava flows and agglomerate, which are much closer in age to the Laetolil Beds than to the Ngaloba Beds. Kent briefly noted the local occurrence of tuffs younger than the lavas and older than the Ngaloba Beds. He described the Laetolil Beds as subaerially deposited tuffs, and he gave 30 m as an aggregate thickness in the vicinity of Laetolil. The Ngaloba Beds he described as tuffaceous clays, and he gave a thickness of about 5 m at the type locality. Pickering mapped this area as part of a 1:125,000 quarter degree sheet[6] and extended the known occurrence of the Laetolil Beds. He also recognised that at least some of the tuffs are of nephelinite composition.

This picture was modified considerably by stratigraphic work in 1974 and 1975. The Laetolil Beds proved to be far thicker and more extensive than previously recognised. The thickest section, 130 m, was measured in a valley in the northern part of the area (geological localities *A* to *C*, Fig. 2). The base is not exposed and the full thickness of the Laetolil Beds here is unknown. Sections 100–120 m thick and representing only part of the Laetolil Beds were measured about 10 km south-east of Laetolil. The Laetolil Beds are 15–20 m thick at a distance of 25–30 km to the south-west and 10–15 m thick at Lakes Masek and Ndutu, 30 km to the north-west. The Laetolil Beds are tuffaceous sediments, dominantly of nephelinite composition.

The lavas and agglomerates noted by Kent overlie an irregular surface deeply eroded into the Laetolil Beds. The lavas were erupted from numerous small vents to the south, south-west and west of Lemagrut volcano. Although designated as nephelinite by Kent, the flows proved to be vogesite, a highly mafic lava with interstitial alkali feldspar and phlogopitic biotite. The lavas have reversed polarity as determined by field measurements (personal communication from A. Cox). A sample of lava from geological locality *D* (Fig. 2) gave K–Ar dates of 2.38±0.5 Myr and 2.43±0.7 Myr (Table 1).

The 130-m section of the Laetolil Beds (Fig. 3) is divisible into an upper half consisting largely of wind-worked, or aeolian, tuff[7] and a lower half consisting of interbedded ash-fall and aeolian tuff with minor conglomerate and breccia. Tephra in the lower half are nephelinite, whereas nephelinite and melilitite are subequal in the upper half. Between these two divisions is a distinctive biotite-bearing coarse lithic-crystal tuff 60 cm thick. Hominid remains and nearly all of the other vertebrate remains are confined to the uppermost 30 m of aeolian tuffs beneath a widespread pale yellow vitric tuff 8 m thick (tuff *d* of Fig. 3). Several other marker tuffs, between 1 m and 30 cm thick, can be used for correlating within the fossiliferous 30-m thickness of sediments. The three prominent marker tuffs, designated *a*, *b*, and *c* (Fig. 3, column 2), can be recognised

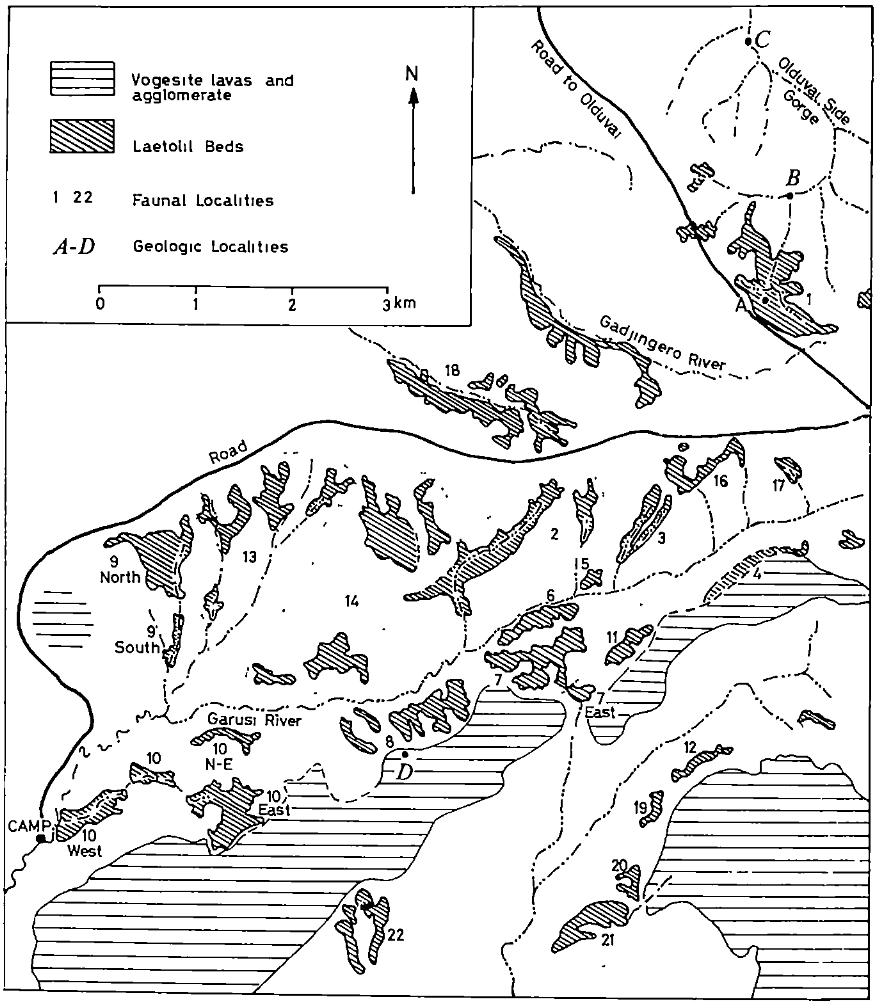

Fig. 2 Map of the Laetolil area showing the fossil beds.

throughout the area shown in Fig. 2. Widespread horizons of ijolite and lava (mostly nephelinite) xenoliths are at several levels in the fossiliferous part of the section and assist in correlating. Biotite is common in some of the ijolite.

Additional fossiliferous deposits, of mineralogical affinity to the Laetolil Beds and 10–15 m thick, lie between tuff *d* and the bed I (?) tuffs at several places. They are locally separated from tuff *d* and the underlying aeolian tuffs of the Laetolil Beds by an erosional surface with a relief of 8 m. These sediments comprise water-worked tuffs, aeolian tuffs, clay-pellet aggregate of aeolian origin and limestone. The tephra are of phonolite and nephelinite composition. It is not yet clear whether or not these sediments should be regarded as part of the Laetolil Beds.

Beds I and II are represented by sedimentary deposits that lie stratigraphically between the lava and the Ngaloba Beds. The bed II deposits locally contain fossils and artefacts.

Sadiman volcano, about 15 km east of the fossiliferous exposures, seems to have been the eruptive source of the Laetolil Beds. The one K–Ar date, of 3.73 Myr, obtained from Sadiman lava, fits with the K–Ar dates on the Laetolil Beds presented here. This date was published previously as K–Ar 2238 (ref. 8), where it was incorrectly assigned to Ngorongoro because of a mistake in listing the sample numbers.

Potassium–argon dating

The vogesite lava is composed of approximately 85–90% olivine and augite. The remainder is principally anorthoclase in the groundmass together with a very small amount of phlogopitic biotite. These two minerals proved too fine-grained and sparse for effective separation, and whole-rock samples were used for dating.

Table 1 K–Ar dates from the Laetolil area

Sample	KA no.	Dated material	Sample weight (g)	% K	mol g^{-1} ^{40}Ar radiation $\times 10^{-11}$	% ^{40}Ar atmosphere	Age yr (Myr)	Remarks
Vogesite lava,	2835	Whole rock	10.06588	1.013	0 419	74 0	2.38±.05	Unconformably over-
Location *D*	2837R	Whole rock	11.27408	1.013	0.427	84.4	2.43±.08	lying Laetolil Beds
	2929	Whole rock	1.98629	6.96±.03	4.118	77 5	3.41±.08	Treated with dilute
Tuff *c*,								HCl
location *A*	2977	Whole rock	2.544	6.98±.04	4.462	78.5	3.68±.09	Treated with warm
	2979	Whole rock	1.94298	6.95±.04	4.454	79.1	3.69±.10	dilute acetic acid
Xenolithic horizon,	2930	Whole rock	3 07730	7.58±.02	4.771	50.8	3.62± 09	Treated with dilute
location *A*	2930R	Whole rock	1.83909	7.58±.02	4.733	39.7	3.59±.05	HCl
Ash-fall tuff,	2932	Whole rock	1.05978	6.00± 1	3.996	75.0	3.82±.16	Crushed, hand picked,
location *B*	2938	Whole rock	1.42092	6.49±.04	4.182	78.8	3.71±.12	treated with dilute HCl

$^{40}K/K = 1.18 \times 10^{-4}$; $^{40}K_{\lambda} = 5.480 \times 10^{-10}\ yr^{-1}$; $^{40}K_{\lambda\beta} = 4.905 \times 4.905 \times 10^{-10}\ yr^{-1}$; $^{40}K_{\lambda\varepsilon} = 0.575 \times 10^{-10}\ yr^{-1}$.

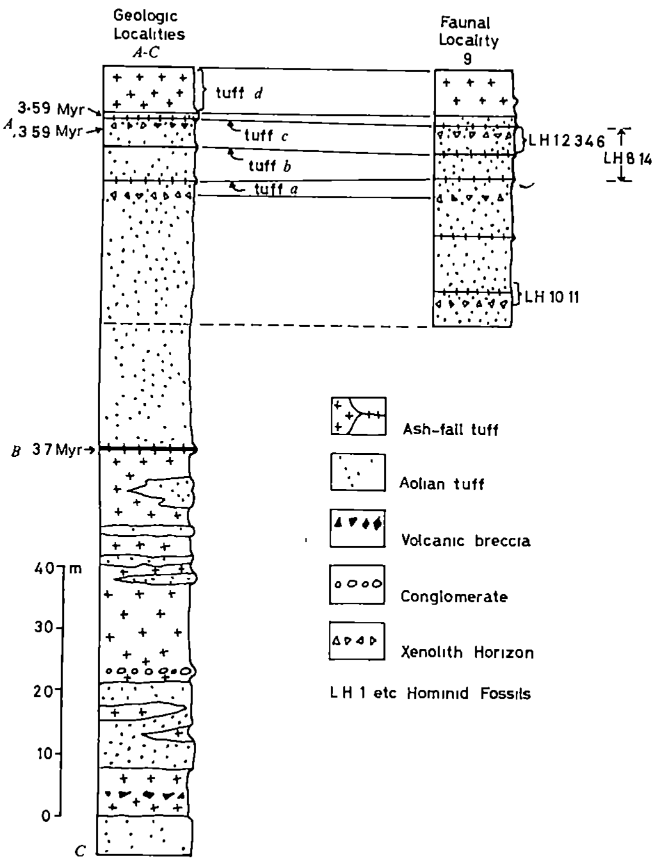

Fig. 3 Stratigraphic column of the Laetolil Beds showing the positions of the dated tuffs and hominid fossils.

In addition to the vogesite lava unconformably overlying the Laetolil Beds, three of the tuffaceous layers within the Laetolil Beds have been dated by the conventional, total degassing K–Ar method (Table 1), and one of these tuffaceous layers has also been dated by the ^{40}Ar/^{39}Ar method, using incremental heating.

Tuff *c* is the uppermost of the dated horizons, lying near the top of the fossiliferous deposits. It is a widespread crystal-lithic air-fall tuff cemented with calcite and generally 10–15 cm thick. Abundant biotite crystals 1–2 cm in diameter occur in the upper part of the tuff, which is composed of nepheline and milelitite. The dated crystals were hand-picked from two outcrops of the tuff at locality *A* (Figs 2 and 3). The cementing calcite adhering to and interleaving the biotite books was removed by treatment with dilute HCl for a few minutes on one sample and with warm dilute acetic acid on two other samples. This treatment was found to have negligible deleterious effects on biotite standard samples. The three dates obtained for tuff *c* (3.41±.08 Myr, 3.68±.09 Myr, and 3.69±.10 Myr) have about equal precision so were averaged to give a date of 3.59 Myr.

Two conventional K–Ar dates and one ^{40}Ar/^{39}Ar were obtained from a single biotite crystal from a xenolithic horizon at locality *A* (Figs 2 and 3) approximately 1–2 m below the youngest tuff dated (tuff *c*). This horizon lies within the upper part of the fossiliferous beds and is distinguished by its ejecta of ijolite xenoliths together with nephelinite lava xenoliths. Although the biotite occurs in some of the ijolite clasts, a large single free crystal picked from the tuff was used for dating. The good agreement between the two conventional K–Ar dates for this sample (3.62±0.09 Myr and 3.59±0.05 Myr) and the ^{40}Ar/^{39}Ar date which yielded an isochron age of 3.55 Myr (Fig. 4) indicates that initial excess ^{40}Ar is not a problem with this sample, and that these dates give an average age for this horizon of 3.59 Myr.

Two dates were obtained from a biotite-bearing crystal-lithic tuff 60 cm thick lying approximately 50 m below tuff *c* near the middle of the thickest section of the Laetolil Beds at location *B* (Fig. 2). The tuff is of nephelinite composition, containing abundant augite and altered nepheline and 2–3% of biotite, some crystals of which are as much as 1 cm in diameter. Calcite cements the crystals and fragments together. Biotite was separated by crushing, screening and hand picking and was cleaned of calcite with dilute HCl. Two dates, 3.82±0.16 Myr and 3.71±0.12 Myr, average 3.77 and give a lower limit to the age of the hominid remains (which occur below but close to the dated xenolithic horizon higher in the section) in the 30 m section at locality *A* (Fig. 2) whose base projects approximately 20 m above this tuff at locality *B* (Fig. 3).

Fauna

The fossiliferous deposits in the Laetolil area have been subdivided, for purposes of collecting, into 26 localities. These subdivisions are based on existing topographic features such as grassy ridges, lines of trees, stream channels and so on. This has provided a means of dividing the fossiliferous area into units of restricted size, but does not relate to the former topography.

Eighteen of these localities are in the Garusi valley, one in the valley at the head of the Olduvai Side Gorge, one in the Gadjingero valley, five in a valley to the south of the Garusi river and one in an isolated position to the west (Fig 2).

Identifiable fossils noted on the exposures were either collected and registered or listed on the sites. Specimens from the Laetolil Beds were distinctively cream coloured or white and sometimes chalky in texture, but the surface material also included brown, grey or black specimens, often rolled. These have been excluded from the material under review, together with fossils which have adhering matrix clearly dissimilar from the tuffs of the Laetolil Beds. Among these are all remains of *Hippopotamus*, *Equus*, *Theropithecus*, *Phacochoerus* and *Tragelaphus*, formerly included in the Laetolil fauna, with the exception of *Hippopotamus*.

The fossil material from the Laetolil Beds is dispersed and fragmentary and it is not possible to assess the number of individuals represented. In this article, 'numbers of fossils' refer to individual bones and teeth, except in the case of clear association, confined almost entirely to remains of *Serengetilagus* and *Pedetes*, some of which were associated and even articulated.

Table 2 shows the mean percentage frequency of the more common vertebrate groups at several of the richer localities. A total of 6,288 fossil specimens was identified from the localities considered here.

Reptiles are represented by snake vertebrae at three localities and by tortoises at all localities. The latter have an average frequency of 2.2% and include several giant specimens. Avian remains occur widely and at several localities birds' eggs were completely preserved. There is one example of a shattered clutch of at least eight eggs, rather smaller in size than eggs of domestic fowl. Primates were found at 15 localities, and in one area they constitute 3.8% of the fauna. Both cercopithecines and colobines are present (M. G. Leakey, personal communication).

Fig. 4 ^{40}Ar/^{39}Ar incremental heating of biotite from xenolithic horizon, locality *C*. Isochron age, 3.55 Myr; [^{40}Ar/^{39}Ar]$_0$ = 294; ^{10}Ar/^{39}Ar = 0.35318; J = 0.005204.

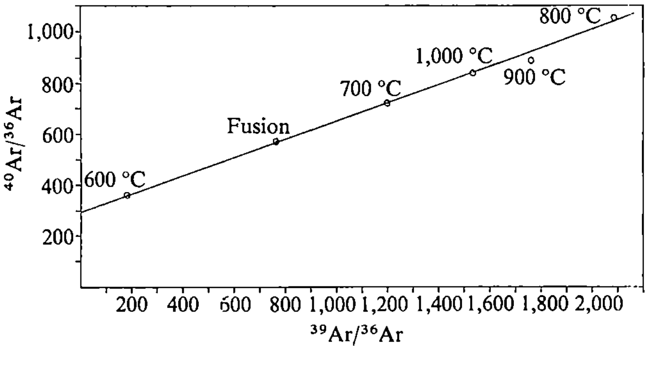

Rodents are fairly well represented, although not abundant. Of the specimens identified by J.J. Jaeger, the most common are *Pedetes*, *Saccostomus* and *Hystrix*. The carnivore fauna is characterised by a high percentage of viverrids, constituting 32% of all the carnivore specimens. Large carnivores are represented by hyaenids, of which there are several genera, by felids and a machairodont.

Proboscidea include *Deinotherium* and *Loxodonta sp.* (M. Beden, personal communication). There is no evidence that the equid material (other than that derived from later deposits) includes any genus except *Hipparion*. The suids consist only of two genera, *Potamachoerus* and *Notochoerus* (J. Harris, personal communication). The presence of *Ancylotherium* and *Orycteropus*, noted in previous collections, is confirmed and the existence of two rhinocerotids has been established by the discovery of skulls of both *Ceratotherium* and *Diceros*, although only the former was listed previously.

Among the giraffids, *Sivatherium* and a small form of giraffe are equally common. *Giraffe jumae* is also present but is much less well represented. The bovid fauna is chiefly characterised by the very high percentage of *Madoqua* (dikdik). In 18 localities dikdik range from 1.5 to 37.7% of all bovid specimens, with a mean percentage of 15.1%.

Table 2 Mean percentage frequency of bones of more common vertebrate groups

Group	Mean percentage	Range	Nos of localities
Bovidae	43.0	29.5–57.9	18
Lagomorpha	14.4	5.6–24.0	18
Giraffidae	11.2	6.8–23.2	18
Rhinocerotidae	9.7	5.7–17.3	18
Equidae	4.4	1.7–7.1	18
Suidae	3.6	1.0–7.1	18
Proboscidea	3.4	1.0–5.1	18
Rodentia	3.3	0.9–7.2	17
Carnivora	3.1	0.8–8.2	17

The 1975 field season, although mainly confined to surface collection, has established that previous collecting had sampled faunas of several time periods. It is now possible to exclude some genera from the published lists of fauna from the Laetolil Beds[2,9], such as *Theropithecus*, *Tragelaphus*, *Equus* and *Phacochoerus*.

Fossil hominids

Thirteen new fossil hominid specimens were recovered from the Laetolil site during 1974 and 1975. The remains include a maxilla, mandibles and teeth. This sample displays a complex of characters seemingly demonstrative of phylogenetic affinity to the genus *Homo*, but also features some primitive traits concordant with its great age.

The hominid specimens are listed in Table 3. Provisional stratigraphic correlation and dating have placed the hominid remains as shown in Fig. 3. With the exception of Laetolil hominids (LH) 7 and 8, all specimens retain the matrix characteristic of the Laetolil Beds from which they have been weathered or excavated. There is no reason to doubt that all the specimens derive from the Laetolil Beds as reported.

The Laetolil hominid sample consists of teeth and mandibles. Important features of these specimens are described here, followed by a brief preliminary discussion regarding the phylogenetic status of the fossils.

Remains of deciduous and permanent dentitions have been recovered. The dentitions consist of two maxillary and four mandibular partial tooth rows. Compared with the rest of the East African Pliocene/early Pleistocene hominid sample, the Laetolil anterior teeth are large and the postcanine teeth of small to moderate size.

Deciduous dentition

Canines (LH 2, 3) Single upper and lower deciduous canines are known. The lower is a slightly projecting, sharp conical tooth in its damaged state. It is smaller but its overall morphology is similar to its permanent counterpart.

First molars (LH 2, 3) The upper first deciduous molar displays spatial dominance of the protocone and a well-marked mesiobuccal accessory cusp defined by a strong anterior fovea. The lower first deciduous molar is molarised, with four or five main cusps depending on hypoconulid expression. There is a spatially dominant protoconid with a large flat buccal face, a lingually facing anterior fovea, and an inferiorly projecting mesiobuccal enamel line. Vertical dominance of the protoconid and metaconid is marked in lateral view.

Second molars (LH 2, 3, 6) Upper and lower deciduous second molars take the basic form of the analogous permanent first molars but are smaller in overall size. The dM$_2$ of LH 2 is the only lower molar in the Laetolil sample bearing any indication of a tuberculum sextum.

Table 3 Hominid remains recovered in 1974–75

Laetolil hominid (LH)	Locality	Specimen consists of	Discovered by
1	1	RP^4 fragment	M. Muoka
2	3*[1]	Immature mandibular corpus with deciduous and permanent teeth	M. Muluila
3 (a–t)	7*	Isolated deciduous and permanent teeth, upper and lower	M. Muoka
4	7	Adult mandibular corpus with dentition	M. Muluila
5	8	Adult maxillary row: I^2 to M^1	M Muluila
6 (a–e)	7*†	Isolated deciduous and permanent teeth, upper	M. Muoka
7	5	RM^1 or ^{2} fragment	M. Muoka
8	11	RM^2, RM^3	E Kandindi
10	10W	Fragment left mandibular corpus with broken roots	E. Kandindi
11	10W	LM^1 or ^{2}	E. Kandindi
12	5	LM^2 or ^{3} fragment	E. Kandindi
13	8	Fragment right mandibular corpus with broken roots	M. Jackes
14	19	Isolated permanent teeth, lower	E. Kandindi

LH 9 was not valid

**In situ.*

†LH 3 and 6 associated in mixed state.

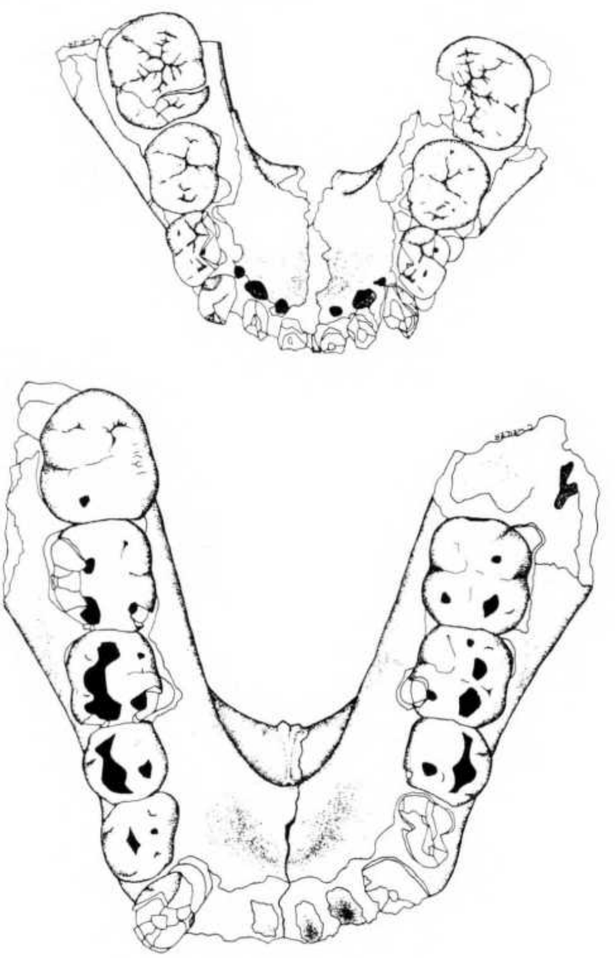

Fig. 5 Occlusal views of juvenile and adult mandibles (LH 2 and 4).

Permanent dentition

Incisors (LH 2, 3, 5, 6, 14) The single upper central incisor is very large and bears pronounced lingual relief. The upper lateral incisors are smaller, with variable lingual relief. The lower incisors are narrow and very tall, with minimal relief.

Canines (LH 2, 3, 4, 5, 6, 14) The incompletely-developed upper canine LH 3 is large, stout and pointed, bearing pronounced lingual relief. LH 6 is slightly smaller, with less lingual relief and a tall, pointed crown. LH 5 bears an elongate dentine exposure on its distal occlusal edge but does not project beyond the occlusal row in its worn state. The lower canines are similar to the uppers in their great size, height and lingual relief.

Premolars (LH 1, 2, 3, 4, 5, 6, 14) The upper premolars tend to be buccolingually elongate and bicuspid, with the lingual cusp placed mesially and an indented mesial crown face. The two lower third premolars each have a dominant buccal cusp with mesial and distal occlusal ridges, and a weak lingual cusp placed mesial of the major crown axis. The long axis of the oval crown crosses the dental arcade contour from mesiobuccal to distolingual, donating a 'skewed' occlusal profile to the tooth. The lower fourth premolars are fairly square in shape with major buccal and lingual cusps and moderate talonids.

Molars (LH 2, 3, 4, 5, 6, 7, 8, 11, 12, 14) The upper molars are of moderate size, their relative proportions unknown. They show a basic four-cusp pattern with spatial dominance of the protocone and typical expression of a pit-like Carabelli feature. The lower molars display progressive size increase from first to third in LH4. They have a fairly square occlusal outline with hypoconulid apressed anteriorly between hypoconid and entoconid and no trace of a tuberculum sextum. The Y-5 pattern of primary fissuration is constant.

Mandibles

Juvenile mandible (LH 2) This specimen (Figs 5 and 6) is incompletely fused at the midline, and the developing crowns of the permanent canines and premolars are exposed in the broken corpus. The first molars have just reached the occlusal plane. Only the posterior aspect of the symphysis shows fairly intact contours, with a concave post-incisive planum and incipient superior transverse torus. The genioglossal fossa is obscured by midline breakage. Associated distortion has artificially increased the bimolar distances.

Adult mandible (LH 4) The adult mandibular corpus is well preserved, with the rami missing (Figs 5 and 7). The dental arcade is essentially undistorted, and presents fairly straight sides which converge anteriorly. The anterior dentition has suffered *post mortem* damage and loss, except for the right lateral incisor which seems to have been lost in life. Largely resorptive alveolar pathology has obliterated its alveolus and has affected the adjacent teeth. There is development of wide interproximal facets for the canine teeth but no C/P$_3$ contact facet. This combines with observation of extensive wear on the buccal P$_3$ face to suggest that C/P$_3$ interlock has prevented mesial drift from eliminating the C/P$_3$ diastema. Judging from the preserved posterior incisor alveoli, these teeth were set in an evenly rounded arcade, projecting moderately anterior to the bicanine axis. The internal mandibular contour is a very narrow

Fig. 6 Juvenile mandible from the Laetolil Beds (LH 2). *a*, Occlusal view; except for the first molars all the teeth are deciduous. *b*, Front view showing the central incisors, canine and P$_3$ in the bone.

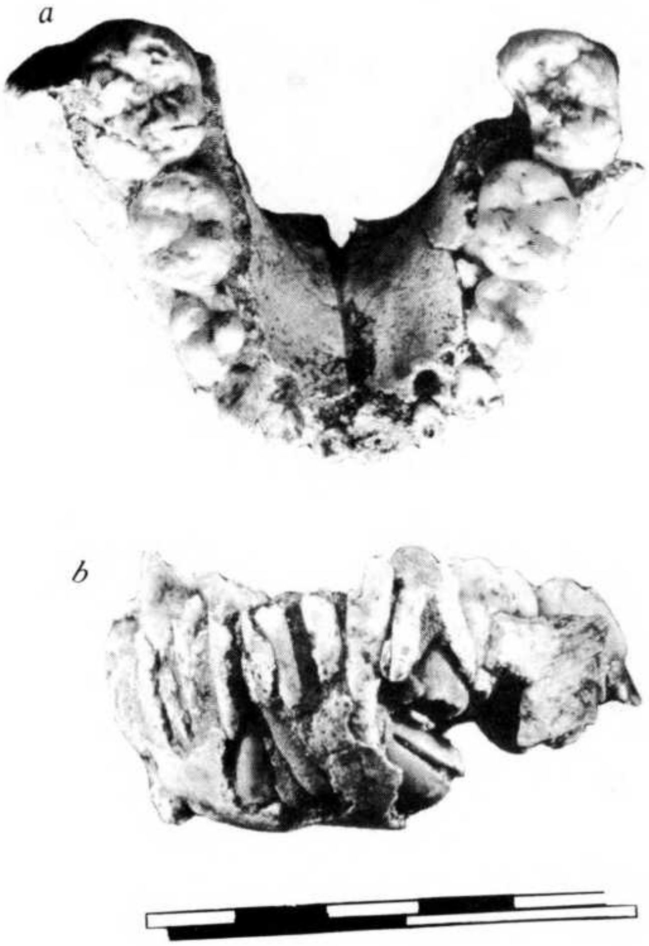

parabola in contrast to the wider basal contour which displays great lateral eversion posteriorly. There are weak to moderate superior and inferior transverse tori, the latter bearing strong mental spines.

The anterior root of the ramus is broken at its origin, lateral to M_2. Occlusal and basal margins diverge strongly anteriorly, resulting in a deep symphysis. The symphysis is angled sharply posteriorly and the anterior symphyseal contour is rounded and bulbous. The lateral aspects of the corpus have very flat posterior portions and distinctive hollowing in the areas above the mental foramina at the P_3 to P_4 position. The corpus is tall and fairly narrow, especially in its anterior portion.

Implications of the specimens

The Laetolil fossil hominid sample, including the original Garusi maxillary fragment[5], seems to be representative of only one phylogenetic entity or lineage. The variations observed in the material seem to be primarily size-based and stem from individual and sexual factors.

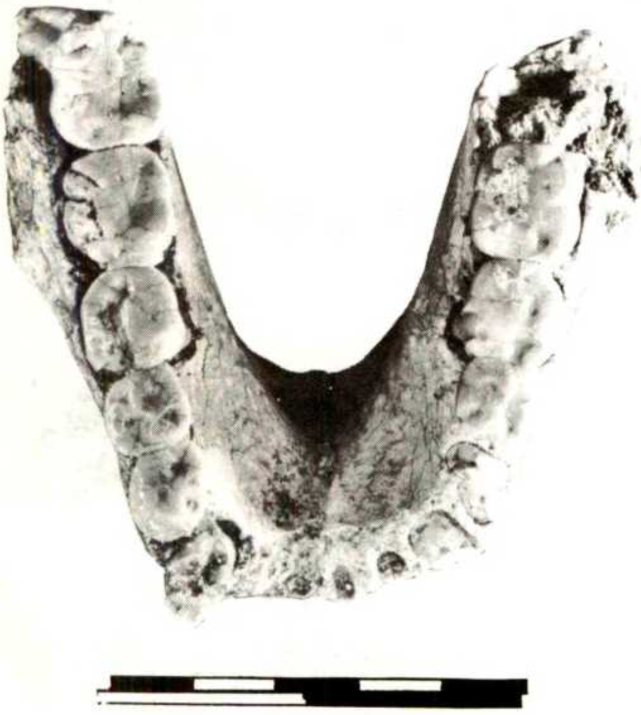

Fig. 7 Adult mandible from the Laetolil Beds (LH 2), occlusal view.

The deciduous teeth, particularly the lower deciduous first molars, display remarkable similarity to hominid specimens from South Africa (Taung; STS 24)[10] as well as to individuals tentatively assigned to *Homo* in East Africa (KNM ER 820, 1507)[11,12]. They depart strongly from the pattern of molarisation displayed in the South African "robust" specimens (TM 1601; SK 61, 64)[10] as well as from East African specimens generally assigned to the same hominid lineage (KNM ER 1477)[13].

The Laetolil permanent canines and incisors are relatively and absolutely large and bear a great deal of lingual relief. They ally themselves similarly to earlier hominid specimens such as STS 3, 50, 51, 52; MLD 11; OH 7, 16; KNM ER 803, 1590 (refs 10, 15, 18–21), as well as to the younger African and Asian specimens usually assigned to *Homo erectus*. These features set the Laetolil specimens apart from the sample including SK 23, 48, 876 and so on; Peninj; KNM CH 1; OH 5, 38; KNM ER 729, 1171 (refs 10, 15, 18–21). The Laetolil permanent premolars show none of the molarisation seen in the latter specimens and bear particularly strong resemblances to South and East African material (STS 51, 52, 55; OH 7, 16, 24; KNM ER 808, 992 (refs 10–12, 14).

The Laetolil permanent molars are consistent in aligning with the South African "gracile" australopithecus and the East African *Homo* material in both size and morphology. The molars do not display the increased size, extra cusps or bulging, expanded, "puffy" development of the individual cusps seen in high frequency among South and East African "robust" forms (SK 6, 13, 48, 52; TM 1517; Peninj; KNM CH 1; KNM ER 729, 801, 802) (refs 10, 17–20). The adult mandible has resemblances to certain East African specimens such as KNM ER 1802, with similar corpus section and basal eversion.

The Laetolil fossil hominids have several features possibly consistent with their radiometric age. These traits include the large crown size and lingual morphology of the permanent canines; the morphology and wear of the C/P_3 complex; the buccolingually elongate upper premolars; the overall square occlusal aspect of the lower permanent molars; the low symphyseal angle; the bulbous anterior symphysis; the relatively straight posterior tooth rows; the low placement of the mental foramina, and the distinctive lateral corpus contours including small, superiorly placed extramolar sulci.

Preliminary assessment indicates strong resemblance between the Laetolil hominids and later radiometrically-dated specimens assigned to the genus *Homo* in East Africa. Such assessment suggests placement of the Laetolil specimens among the earliest firmly dated members of this genus. It should come as no surprise that the earlier members of the genus *Homo* display an increasing frequency of features generally interpreted as "primitive" or "pongid like", which indicate derivation from as yet largely hypothetical ancestors.

Much of the recently discovered comparable fossil hominid material from the Hadar region of Ethiopia shows strong similarity to the Laetolil specimens[23], and further collection combined with detailed comparative analysis of material from both localities is essential for the further understanding of human origins. The Laetolil collection adds to the developing phylogenetic perspective of the early Hominidae and emphasises the need for taxonomic schemes reflective of and consistent with the evolutionary processes involved in the origin and radiation of this family.

We thank the following for facilities, financial support, permission to examine originals and for discussion: the United Republic of Tanzania, the trustees of the National Museums of Kenya, the NSF Graduate Fellowship Program, the Scott Turner Fund, the Rackham Dissertation Fund, the National Geographic Society, G. Brent Dalrymple, C. K. Brain, T. Gray, D. C. Johanson, K. Kimeu, P. Leakey, R. E. F. Leakey, P. V. Tobias, E. Vrba, A. Walker, C. Weiler and B. Wood.

Received March 30; accepted May 26, 1976.

[1] Weinert, H., *Z. Morph. Anthrop.*, **42**, 138–148 (1950).
[2] Dietrich, W. O., *Palaeontographica*, **94A**, 43–133 (1942).
[3] Maglio, V. J., *Breviora*, 336 (1969).
[4] Kent, P. E., *Geol. Mag., Lond.*, **78**, 173–184 (1941).
[5] Kohl-Larsen, L., *Auf des Spuren des Vormenschen*, **2**, 379–381 (1943).
[6] Pickering, R., *Endulen, Quarter degree sheet 52* (Geological Survey in Tanzania, 1964).
[7] Hay, R. L., *Bull. geol. Soc. Am.*, 1281–1286 (1963).
[8] Hay, R. L., *Geology of the Olduvai Gorge* (University of California Press, 1976).
[9] Hopwood, A. T., in *Olduvai Gorge* (edit. by Leakey, L. S. B.), (Cambridge University Press, 1951).
[10] Robinson, J. T., *Transvaal Museum Mem.*, **9**, 1 (1956).
[11] Leakey, R. E. F., and Wood, B. A., *Am. J. phys. Anthrop.*, **39**, 355 (1973).
[12] Leakey, R. E. F., and Wood, B. A., *Am J. phys. Anthrop.*, **39**, 355 (1974).
[13] Leakey, R. E. F., *Nature*, **242**, 170 (1972).
[14] Leakey, L. S. B., *Nature*, **188**, 1050 (1960).
[15] Leakey, L. S. B., and Leakey, M. D., *Nature*, **202**, 3 (1964).
[16] Day, M. H., and Leakey, R. E. F., *Am. J. phys. Anthrop.*, **41**, 367 (1974).
[17] Leakey, R. E. F., *Nature*, **248**, 653 (1974).
[18] Carney, J., Hill, A., Miller, J., and Walker, A., *Nature*, **230**, 509 (1971).
[19] Leakey, R. E. F., Mungai, J. M., and Walker, A. C., *Am. J. phys. Anthrop.*, **36**, 235 (1972).
[20] Leakey, R. E. F., and Walker, A. C., *Am. J. phys. Anthrop.*, **39**, 205 (1973).
[21] Tobias, P. V., *Olduvai Gorge*, **2** (Cambridge University Press, 1967).
[22] Leakey, M. D., Clarke, R. J., and Leakey, L. S. B., *Nature*, **232**, 308 (1971).
[23] Johanson, D. C., and Taieb, M., *Nature*, **260**, 293–297 (1976).

Non-genetic individuality: chance in the single cell

John L. Spudich & D. E. Koshland, Jr

Department of Biochemistry, University of California, Berkeley, California 94720

The individuality of bacterial cells grown in homogeneous conditions was demonstrated by showing characteristic behavioural differences which persist over their lifespans. Poissonian fluctuation of small numbers of generator molecules can explain this individuality and may apply to such processes as differentiation and asynchrony of cultures.

BIOLOGICAL systems are constantly confronted with chance occurrences in their environmental conditions and internal processes. An elaborate biological apparatus has evolved to utilise chance in genetics for the survival of the species. Some feedback mechanisms, on the other hand, are designed to insulate the individual against chance fluctuations of environmental conditions. How much influence has chance in internal cellular processes in determining the metabolic state and behaviour of the single cell? More specifically, if cells containing identical chromosomes could be grown in environmentally homogeneous conditions, how similar would they be in their biochemical characteristics?

Uniform growth conditions can be obtained with agitated suspension cultures, since the spatial inhomogeneities which inevitably develop in stationary surface growth (for example, tissue culture plates or agar surfaces) are continuously randomised in swirled liquid culture. The problem of apparently non-genetic variation of cells in such a homogeneous environment has arisen in studies of several phenomena. For example, bacteriophage burst sizes[1], cell division times[2], bacterial flagellar phases[3,4] and β-galactosidase concentrations[5-7] all show variation difficult to attribute to environmental inhomogeneities or genetic causes. The question of individuality is difficult to pursue in these cases because one needs measures of characteristics of individual cells which can be ascertained essentially instantaneously and which do not perturb the cell's biochemical state. With such instantaneous measures an individual cell can be compared with itself at various stages of its life cycle and with other individual cells in an isogenic population. Such measures became available in our studies on chemotaxis and enabled us to approach the question of individuality in bacteria as an illustration.

The chemotactic migration of bacteria can be studied quantitatively. In the absence of chemotactic stimuli a bacterium shows brief periods of swimming in an approximately straight line (smooth swimming), interrupted by a rapid irregular motion, which reorients its swimming direction (tumbling). Tumbling is suppressed when the bacterium swims in a favourable direction in a chemical gradient and this regulation of tumbling frequency results in net migration up gradients of attractants and down gradients of repellents[8-10]. The modulation of tumbling frequency is caused by temporal changes in attractant or repellent concentration which are analysed by the sensing system and transmitted to the flagella[8,11]. For example, if the concentration of an attractant in the bacterial environment is suddenly increased, this temporal gradient transiently suppresses tumbling in the bacteria. Although the details of the temporal gradient sensing mechanism are unknown, control of tumbling can be rationalised as caused by changes in the levels of a tumble regulator[8,12]. The concentration of this tumble regulator is thus a key property of the cell since it provides an important survival mechanism for the bacterium. Its properties can be measured quantitatively in two ways: (1) in the sensitivity to stimuli as measured by recovery from temporal gradients[12,13] and (2) in the tumbling frequency when there is no gradient[9,12] as an indicator of the steady-state level of tumble regulator. These two properties were studied for individual bacteria as a test for non-genetic variability.

Sensitivity to gradients of attractant

Our first study of individual bacteria involved subjecting a bacterial clone of a tumbly mutant strain to a temporal gradient of serine, using the sudden mixing methods described earlier[8,13]. The transient smooth swimming in response to a temporal gradient stimulus is especially easy to quantify with tumbly mutants. The individual bacteria were kept in focus by rough tracking through a movable microscope stage which keeps the

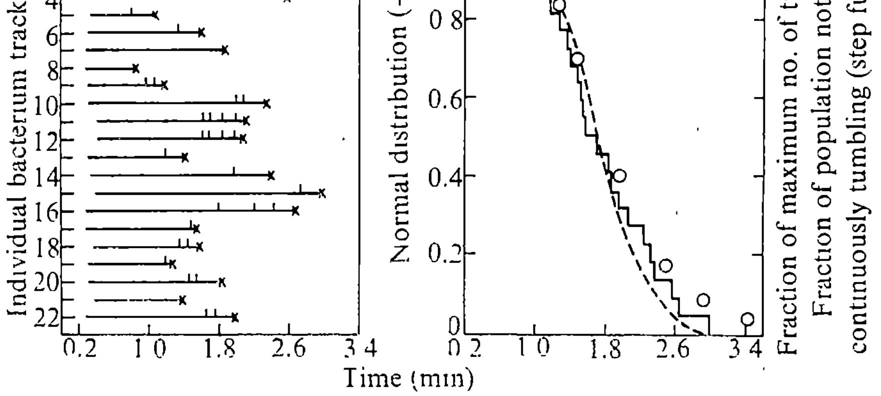

Fig. 1 Tumbly mutant recovery individuality. All bacteria were grown in homogeneous conditions as described previously[13]. In *a* the length of each line represents the time interval over which an individual bacterium was tracked. For each of the 22 lines the temporal gradient stimulus 0→0.5 mM L-serine was delivered to ST171 at time 0 (as previously described[13]) and the bacterium nearest the centre was followed until it tumbled continuously for 30 s. Times at which the bacterium briefly tumbles are are represented as ⊥, and the time at which it began to continuously tumble is represented as ×. From the data in (*a*) the fraction of the bacteria not yet continuously tumbling was plotted against time to yield the step function in (*b*). O, Tumble frequency assay[13] results for ST171 subjected to the same stimulus; – – –, a cumulative normal distribution with the same mean and variance as the data obtained from tracking.

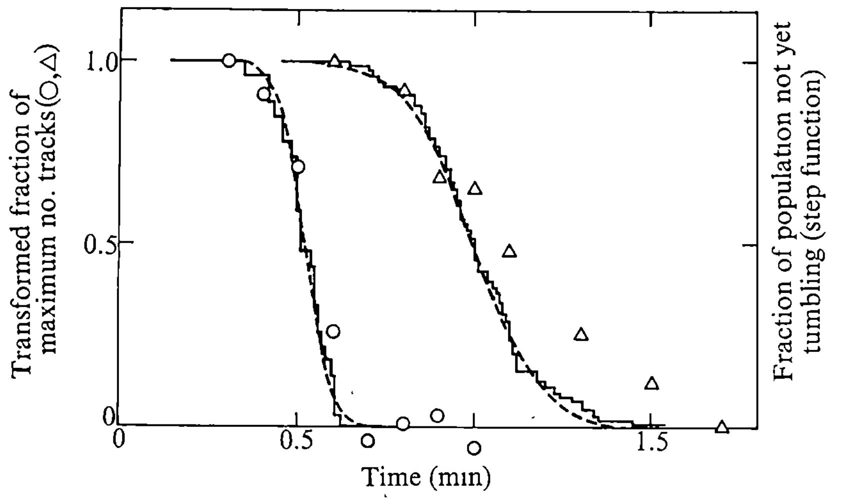

Fig. 2 Wild-type recovery individuality. Points are tumble frequency assay[13] results transformed by equation (1) (see text) for ST1 subjected at time 0 to the temporal gradient stimuli 0→0.01 mM (○) l-aspartate and 0→1.0 mM l-aspartate (△). Step functions are cumulative times to the first tumble after stimulation for these two same stimuli derived from tracking as described in Fig. 1. The dotted lines are cumulative normal distributions with the same means and variances as the two sets of tracking data.

bacterium in the centre of the field. A videotape recording could be played back in slow motion to describe in detail the behaviour over a long period. The results for 22 individuals of a constantly tumbling mutant subjected to a serine stimulus are shown in Fig. 1*a*. There is great variability in the time that individual bacteria take to return to their prestimulus tumbling pattern. Data of the same type (Fig. 2) were obtained for a wild-type strain which also swims smoothly immediately after stimulation and returns to intermittent tumbling (its normal non-gradient state). If data from tracking are plotted on the same graph as a recovery curve for a population subjected to the same stimulus in the tumble frequency assay[13], the curves are superimposable (Fig. 1*b*).

The results of Fig. 1*b* mean that the form of the recovery of a population from a stimulus is caused by the variability of the individuals in the population. In fact, if we define $F(t)$ as the fraction of a population which has recovered at time t after delivery of a stimulus and $S(t)$ as the probability of producing a smooth swimming track, equation (1) describes the behaviour of the bacteria. S_∞ is zero for the constantly tumbling mutant and has a finite value, greater than zero, for wild-type bacteria.

$$1-F(t)=\frac{S(t)-S_\infty}{1-S_\infty} \qquad (1)$$

The bacteria used in these experiments were at most 30 generations away from a single cell parent. An extremely high spontaneous mutation rate would have to be postulated to explain our data in terms of genetic variation, as the following calculation shows. Where m is the probability of occurrence of any mutation affecting chemotaxis per generation, after 30 generations the probability of a bacterium not containing a mutation is $(1-m)^{30}$. Therefore for at least 50% of the bacteria to have acquired one or more mutations affecting chemotaxis,

$$(1-m)^{30}<0.5$$

or

$$m>2.3\times10^{-2}$$

There are only about 10 genes specifically involved in *Salmonella* chemotaxis[14], but even the liberal estimate that a mutation in any one of 100 loci could alter chemotactic behaviour requires that the mutation rate per locus must be greater than 2×10^{-4}, which is at least 10^3 times higher than usual spontaneous mutation rates. Therefore we conclude that (1) there is a large non-genetic individual variability in the response of both tumbling mutants and wild-type bacteria to stimuli and (2) the results of the tumble frequency assay are a direct measurement of this variability.

Individuality and phase of cell cycle

The experiments described above establish that the cell types present do not show identical behaviour, but do not distinguish between the alternatives: (1) that the individuality is created by one or more random events in the history of the bacterium or (2) the cell has no intrinsic individuality but its properties vary according to its position in the cell division cycle. In the latter case the asynchrony of the culture would give the appearance of individuality where it does not in fact exist. To distinguish between these alternatives, the response of the bacteria were compared as a function of cell length. Cell length is known to be correlated with position in the division cycle[15] and bacterial lengths are clearly visible in the measurements from the tumble frequency assay. The lengths of smooth swimming tumbly mutant bacteria following stimuli at a time at which 95% of the bacteria were smooth swimming were compared with the same values when less than 10% of the bacteria were still smooth swimming. The former gives values for the overall population and the latter for the longest responding 10% of the bacteria. The distributions of the bacterial lengths are shown in Table 1. There is no significant shift in the distribution of the lengths as recovery proceeds and therefore the first alternative must be correct.

Repeated stimulation of a bacterium

If the different responses of isogenic bacteria are not related to the phase of the cell cycle, it can then be asked whether they (1) respond differently because of chance events during or

Table 1 Independence of recovery times and position in the cell division cycle

Body length (μm)	Fraction of population of body length indicated with > 95% smooth swimming	Fraction of population of body length indicated with < 10% smooth swimming
< 1.33	0.00	0.00
1.33–2.00	0.05	0.05
2.00–2.67	0.24	0.21
2.67–3.33	0.32	0.33
3.33–4.00	0.26	0.28
4.00–4.67	0.09	0.10
4.67–5.33	0.04	0.03
> 5.33	0.00	0.00

The lengths of ST171 bacterial bodies were measured on projected films from the tumble frequency assay[13]. 186 individual bacterial lengths were measured from photographs at times for which less than 5% of the bacteria had recovered from the serine stimuli to define the distribution designated >95% smooth swimming. 212 individual bacterial lengths were measured after more than 90% had recovered to establish the distribution in the last column.

Table 2 Response times (s) of individual bacteria on repetitive stimulation in growth conditions

Bacterium	*A*	*B*	*C*	*D*	*E*
Stimulus time (min)					
15	237	224	190	165	136
30	254	164	126	176	134
60	>300	265	191	136	145
75	>300	248	217	144	143
90	>300	253	172	152	148*
Average clockwise (smooth) response (s)	>278	231±18	179±15	155±7	141±3

Bacteria of strain SL3625, a leaky *fla AIII* mutant which produces small numbers of flagella, were tethered with flagella antibody to a coverslip by a modification of the procedure of Silverman and Simon[16]. Bacteria were grown as described[13] except 200 μM *p*-hydroxybenzoic acid (*p*HBA) was added to the growth medium to improve motility (unpublished results of J. Bar-tana, B. Howlett and D.E.K.). The coverslip with attached bacteria was used to cover an open temporal gradient observation cell of the type described by Macnab and Koshland[8]. The observation cell was previously filled with the wash medium to allow a liquid seal to form immediately the coverslip was put in place (time 0 min). The behaviour of bacteria in one microscopic field at ×500 magnification was recorded on videotape as follows. Cells were washed extensively (5 min at 12.7 chamber volumes per min) with the growth medium (without *p*HBA); at the times indicated the output line to the observation cell was switched to a line containing this same medium +10 mM α-methylaspartate and a 15-s pulse of 12.7 chamber volumes of attractant was delivered. The resulting immediate long clockwise rotation interval of an individual bacterium was measured as its "clockwise response". After 5 min, the line was switched back to medium not containing the attractant, and a 1-min pulse of 12.7 chamber volumes per minute delivered. Each bacterium in the field which was rotating for all stimuli was analysed by repetitive playback of the videotape. The doubling time of SL3625 in this medium is 112 min. Mean responses are reported ± 1 s.e.m.

*Bacterium *E* divided 20 s after the delivery of the stimulus at 90 min.

immediately preceding the time of the measurements, that is they are long responders at one time but short responders later, or (2) whether an individual bacterium is committed for an extended period to a certain type of response, that is some bacteria are short responders throughout their lifespan. To test the response of an individual bacterium over its cell division cycle, individual bacteria were tethered to the surface of microscope coverslips by antibodies to individual flagella, as described before[16]. Using this tethering technique, Berg and Tedesco[17] have shown that individual bacteria can be examined over extended periods and that tethered cells differ in their chemotactic behaviour. The tethering method permits attractant to be delivered and washed out at various intervals which are minutes or even hours apart and the response of the same individual bacterium recorded over the entire time span using videotape. Larsen *et al.*[18] established that counterclockwise rotation and clockwise rotation of a tethered cell (observed along the axis from the flagellum to the body) are equivalent to the tumbling and smooth swimming, respectively, of a free swimming cell.

Table 2 shows the results of repetitive stimulation of five tethered bacteria in the same microscopic field with the attractant α-methylaspartate. The attractant was delivered five times and removed completely between stimuli. The delivery of large stimuli of attractant suppressed counterclockwise (tumbling mode) rotation in each bacterium and caused a uniform clockwise (smooth swimming mode) rotation for several minutes with eventual recovery to intermittent clockwise and anticlockwise rotation. All bacteria were observed to increase to nearly double their mass during the measurements, yet the data show that their individual sensitivities to the stimulus were maintained. The same experiment was performed with six bacteria in a non-growth medium and these bacteria also maintained their tendencies to be either long or short responders to α-methylaspartate[19]. Thus, whether growing or not, individuals retain characteristically different sensitivity to stimuli for extended periods and the cells are not continuously randomising with respect to their chemotactic behaviour.

Relationship of unstimulated to stimulus-induced behaviour

If the bacteria differ in their characteristic recovery times, are they also different in some other feature of their sensory system? The unstimulated behaviour of tethered cells consists of alternating clockwise and anticlockwise rotation intervals with each of the two rotation modes terminated by Poissonian (random) processes[17]. The patterns of individual cells showed that the mean clockwise and counterclockwise intervals were not identical for all bacteria. In view of the randomness in lengths of clockwise and counterclockwise intervals for any individual bacterium, the theoretical standard error of the mean was calculated to compare with the empirical s.e.m. obtained from actual measurement of the clockwise and counterclockwise intervals (Table 3). The good agreement between theoretical and empirical values is assurance that the amount of data collected to determine the intervals is sufficient.

On comparison of these spontaneous rotation intervals with the response to stimuli (Table 3) an excellent correlation was observed. The size of the clockwise response to an α-methylaspartate stimulus for an individual bacterium depends nearly linearly on its mean clockwise (smooth swimming mode) interval in non-stimulus conditions as shown in Fig. 3. The size of the anticlockwise interval (tumbly mode) does not seem to influence the stimulus behaviour.

To check this in another way, 82 free swimming cells were examined both for the time to the first tumble after temporal gradient stimulation with aspartate and for the mean time between tumbles for 1 min after the first tumble. Although this measurement is less precise than measurements with tethered cells (because a particular individual can be observed for only one stimulation and for only a short time after the stimulus), we found a correlation coefficient of 0.5 between the average length of a run and the recovery time.

These data provide a correlation between the steady-state tumbling pattern of individual bacteria and their sensitivity and recovery from stimuli. The steady-state pattern of tumbling,

Table 3 Unstimulated behaviour and smooth responses of individual bacteria

Bacterium	*F*	*G*	*H*	*I*	*J*
No. of intervals	154	84	186	134	82
Mean clockwise (smooth rotation mode) length (s)	2.45	1.93	1.40	1.54	2.97
Measured s.e.m.	0.28	0.26	0.16	0.19	0.54
Calculated s.e.m.	0.28	0.30	0.15	0.19	0.46
Mean anticlockwise (tumbly rotation mode) length (s)	0.88	1.69	0.80	1.63	0.70
Measured s.e.m.	0.12	0.25	0.08	0.22	0.16
Calculated s.e.m.	0.10	0.26	0.08	0.20	0.11
Mean clockwise (smooth) response (s):	211±10	152±6	120±8	123±6	247±7

The experiment was performed by a procedure identical to that of Table 2 except: (1) instead of growth medium cells were washed with Vogel Bonner salts + 10^{-5}M EDTA; (2) attractant (10 mM α-methyl aspartate) was prepared in Vogel Bonner salts + 10^{-5}M EDTA; (3) after the initial wash of 5 min of 12.7 chamber volumes per min, a continuous flow rate of 1.6 chamber volumes per min was maintained throughout the experiment; (4) at 5 min intervals the input line was switched between attractant and buffer solutions to give a total of six repetitive stimuli. About 2 min of video recordings of the bacteria in periods immediately preceding delivery of attractant were examined in slow motion (sevenfold) replays. Keyboard inputs to a Data Span 500 paper tape punch with timing circuitry[28] were punched when the bacterium being analysed reversed rotation direction for at least 1/4 of a full turn. The paper tape containing the reversal information and the automatically entered times of keyboard entries was processed by computer. The calculated s.e.m. was determined with the assumptions that (1) the measured mean is the true mean and (2) both clockwise and anticlockwise intervals are distributed exponentially[17]. Clockwise responses are reported as the mean ± 1 s.e.m.

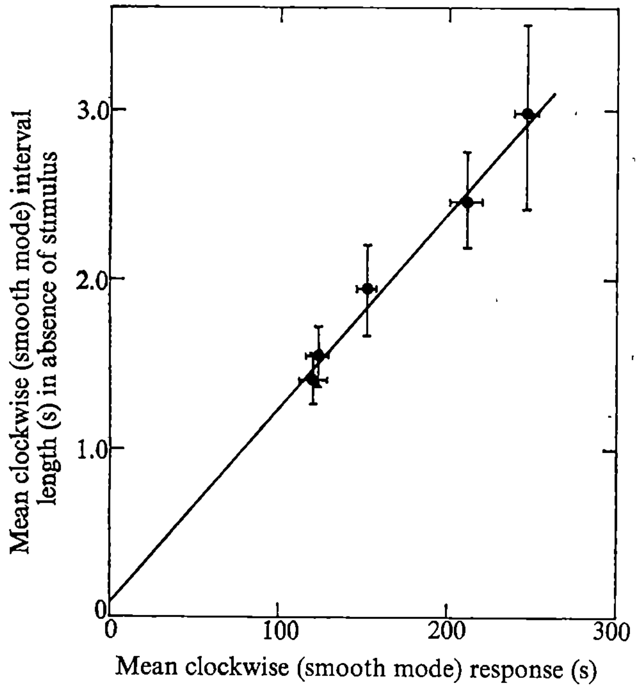

Fig. 3 Unstimulated clockwise (smooth mode) rotation related to stimulus induced clockwise (smooth mode) rotation. The prestimulus clockwise (CW) mean interval length and the mean CW response were taken from Table 3. Error bars represent ± one standard error of the mean. The line is a least squares fit to the data.

therefore, is also a feature of the bacterial individuality and is retained throughout the generation time of the bacterium.

Implications of individuality

Study of individual bacteria in various ways has established that a bacterial culture which is genetically homogeneous and grown in homogeneous nutrient conditions nevertheless produces characteristically different individuals. These individuals retain their properties throughout their life cycle, showing that the individuality is not a momentary effect of random chance bombardments by a fluctuating environment. Moreover, the individuality is not a function of position in the cell division cycle.

How could such individuality be produced? A bacterium is a small cell. In the process of division and replication of the cellular components there may well be certain molecules which are present in such low amounts that they are subject to Poissonian variation. In general, the standard deviation of a Poisson distribution is the square root of n, where n is the mean number of events. If there are 10^4 molecules of a particular type, the s.d. would be 100 molecules, giving a 1% deviation. If, on the other hand, only 100 molecules are produced, a 10% s.d. would arise. In many cellular processes less than 100 molecules participate (for example, there are only 10–20 molecules of *lac* repressor per cell[20] and enzyme cofactor concentrations are extremely low[21]). In other processes there may be more total molecules but their ultimate number may have been determined by a small number of generating molecules (for example, there are only 6–14 *trp* mRNA molecules per bacterial cell, and each mRNA molecule is translated an average of 20 times[22]). Probabilistic fluctuations in small numbers of molecules have been discussed as possible causes of bacteriophage burst size variation by Delbrück[1] and bacterial β-galactosidase concentration variation by several investigators[5–7].

In the case of chemotaxis, it has been postulated that the tumble regulator is produced and destroyed according to scheme 2, implying that some enzymes or structural molecules control the velocities of the steps represented by v_f and v_d. If a small number of mRNA molecules code for the enzyme which, for example, controls the step v_d, Poissonian fluctuation in the mRNA concentration would generate quite different total numbers of molecules of this enzyme in different individuals. If this affects not only the steady-state tumbling pattern, but also the rate of recovery from a stimulus[12], both properties would be different from individual to individual over the lifespan of the cells. Conversely, if a particular cellular component were produced in a much larger number of copies

$$W \xrightarrow{v_f} X \xrightarrow{v_d} Y \qquad (2)$$

where X = tumble regulator over a much longer interval, Poissonian variation would be relatively small and one would not expect much variation in this property from cell to cell. The number of copies of an individual cellular component, at some crucial period in the life of the cell, would therefore determine whether or not that component would contribute to the non-genetic variability of the population.

The existence of such variability leads one to ask whether it has some advantage to the organism or whether it is a disadvantage which must be surmounted in the development of the species. Although there may be no significant selective pressure against non-genetic variability, one can certainly make an argument that non-genetic variability aids in the survival of a population subjected to widely varying conditions during its lifetime. If the bacterium has a single or monolithic reaction to a particular chemical gradient, it might migrate as a colony into a toxic situation or fail as a colony to be sufficiently sensitive to an essential new nutrient. If there were individual bacterial variation in a genetically homogeneous population, a few fractions of the bacteria might either be supersensitive or insensitive. These bacteria would normally not survive as effectively as the bulk of the more average optimised population. They would then have lower survival probabilities in most circumstances, an unimportant loss if the main body of the colony survived. If, on the other hand, the toxic and lethal situations described above arose, a small fraction, on the wings of the probability distribution, might constitute the only bacteria to survive and would then reproduce the species for future generations. Genetic variation would not accomplish the same purpose, since selection in a rare toxic situation would produce a mutant poorly adapted to the more common conditions of the environment. The population, however, was selected over evolutionary time for survival in all of the widely varying conditions of the environment. Thus non-genetic variability would be a preferred mechanism for accommodation to random fluctuations in the environment and genetic variability the preferred mechanism for accommodation to long lasting environmental changes. Induction and repression of enzyme synthesis reflect intermediate accommodations to fluctuations of a lengthy but impermanent type.

It would be intriguing if certain properties were found to be insulated against chance by the large number of copies in the cell at all crucial stages and other properties deliberately to originate in a small number of starting molecules, to create non-genetic diversity. An interesting example may arise in the differentiation of individual *Dictyostelium* amoebae into multicellular fruiting bodies. This development depends on the existence of a small number of early cyclic AMP-emitting founder cells which are believed to be genetically identical to the other cells in the population which are not early emitters[23]. The difference between a founder cell and other cells in the culture seems to be the result of molecular accidents in the cell's individual history and this could be explained by a Poissonian distribution of properties deriving from small numbers of a cellular component as discussed here. Possibly over evolutionary time, larger cells and larger individuals were selected for decreased non-genetic variability; for example, identical human twins are morphologically much more similar than twin bacteria, and in higher species the genetic variability carries the main load of ensuring the survival of the species. Poissonian variation at early stages in differentiation may be an advantage for the species even though ultimately chance is eliminated because of large numbers of cells developed in the individual.

Poissonian variation may be the reason for the rapid asynchronisation of synchronised prokaryotic[24] and eukaryotic[25] cell cultures. If one or more steps leading to growth and cell division are controlled by a small number of molecules, then a Poissonian distribution should exist and cell cycles would quickly get out of phase. In fact there is evidence for individuality in bacterial division times[2] of the type we observe in chemotactic behaviour. Also in eukaryotic cells synchrony is not maintained even in populations selected for genetic homogeneity[25]. To explain this, Smith and Martin[26] have proposed that growth of cultured cells is dependent on a random event occurring with a probability which is constant for all individual cells in postulated "indeterminate" phase in G_1 (the "A-state"). As evidence for this hypothesis they present generation time distributions which are exponential over most of their range. A chance external event could explain the probabilistic transition out of the A-state, if the Smith and Martin model is correct. Alternatively, as suggested here, the number of generating molecules for an enzyme required for passage through G_1 could be so small that Poissonian fluctuations result in a broad distribution of concentrations of this enzyme among the cells. Such a non-genetic individuality would be consistent with rapid asynchronisation, correlation of sibling generation times[2,27,28] (if the enzyme half life is longer than one generation time), and the exponential character of the distributions of Smith and Martin. If Poissonian variation determines rates of passage through G_1, or any stage in the cell cycle, cell synchrony over extended periods will be difficult to attain. If our explanation is correct, a possible approach to obtaining a synchronous cell line would be genetic manipulation, for example by episomes, to increase significantly the concentrations of the rate limiting enzymes.

Biological systems therefore can produce individual non-genetic diversity through a few generating molecules which determine a property at some key stages of development or can ensure against such chance diversity by increasing the number of generating molecules to a size which eliminates significant internal variation.

This work was supported by a grant and a training grant from NIMS. We acknowledge suggestions from Drs A. Pardee, B. Stocker, G. Stent, J. Gerhart and C. Matessi.

Received April 5; accepted June 11, 1976.

[1] Delbruck, M, *J Bact.*, **50**, 131–135 (1945).
[2] Powell, E O., *J. gen. Microbiol*, **18**, 382–417 (1958).
[3] Stocker, B. A. D., *J. Hyg., Camb.*, **47**, 398–413 (1949).
[4] Lederberg, J., and Iino, T., *Genetics*, **41**, 743–757 (1956).
[5] Novick, A, and Weiner, M., *Proc. natn. Acad. Sci. U S.A*, **43**, 553–566 (1957)
[6] Maloney, P. C, and Rotman, B, *J molec. Biol*, **73**, 77–91 (1973)
[7] Benzer, S., *Biochim biophys. Acta.*, **11**, 383–395 (1953).
[8] Macnab, R. M, and Koshland, D E, Jr, *Proc. natn. Acad. Sci. U S A*, **69**, 2509–2512 (1972)
[9] Berg, H C., and Brown, D. A., *Nature*, **239**, 500–504 (1972).
[10] Tsang, N, Macnab, R. M, and Koshland, D E, Jr, *Science*, **181**, 60–63 (1973)
[11] Brown, D A., and Berg, H. O., *Proc natn Acad Sci. U.S.A.*, **71**, 1388–1392 (1974)
[12] Aswad, D, and Koshland, D E., Jr, *J. Bact*, **118**, 640–645 (1974).
[13] Spudich, J L., and Koshland, D. E., Jr, *Proc natn. Acad Sci U S A.*, **72**, 710–713 (1975).
[14] Koshland, D E., Jr, Warrick, H., Taylor, B., and Spudich, J. L., *Cold Spring Harbor Symp.* (in the press).
[15] Schaechter, M, Williamson, J. P., Hood, J R, Jr, and Koch, A. L., *J. gen. Microbiol.*, **29**, 421–434 (1962).
[16] Silverman, M R, and Simon, M. I., *Nature*, **249**, 73–74 (1974)
[17] Berg, H. C., and Tedesco, P. M., *Proc. natn. Acad Sci U.S.A*, **72**, 3235–3239 (1975).
[18] Larsen, S. H., Reader, R. W, Kont, E N, Tso, W. W, and Adler, J., *Nature*, **249**, 74–77 (1974).
[19] Spudich, J L., thesis, Univ California, Berkeley (1976)
[20] Gilbert, W., and Muller-Hill, B., *Proc. natn. Acad Sci U S.A*, **58**, 2415–2421 (1967).
[21] Wilson, A., *J. gen. Microbiol.*, **28**, 283–303 (1962).
[22] Baker, R., and Yanofsky, C., *Cold Spring Harbor Symp. Quant. Biol.*, **35**, 467–470 (1970).
[23] Loomis, W. F, *Dictyostelium discoideum, a Developmental System* (Academic, New York, 1975)
[24] Maaløe, O., in *The Bacteria*, **4**, *A Treatise on Structure and Function* (edit. by Gunsalus, E. C., and Stanier, R. Y.) (Academic, New York, 1962)
[25] Peterson, D F, and Anderson, E C, *Nature*, **203**, 642–643 (1964)
[26] Smith, J A., and Martin, L., *Proc. natn Acad. Sci. U.S.A*, **70**, 1263–1267 (1973)
[27] Hughes, W. H., *J. gen Microbiol.*, **12**, 265–268 (1955)
[28] Minor, P D., and Smith, J. A., *Nature*, **248**, 241–243 (1974).
[29] Macnab, R. M, and Koshland, D. E., Jr, *J. Mechanochem Cell Motil*, **2**, 141–148 (1973)

letters to nature

Observations of X-ray and γ bursts

We report on some bursts of hard X rays seen in March 1976 by the Ariel-V scintillation telescope (ST). The timescale of a few seconds, the correlation with low energy events seen by a proportional counter on the same satellite (ref. 1 and S. J. Bell-Burnell, private communication) and a photon energy > 50 keV, are factors which suggest a connection in origin between the gamma bursts of Klebesadel *et al.*[2] and the X-ray events noticed by Grindlay *et al.*[3]. A delayed arrival at high energies seems to be an important feature of our observations.

The Ariel-V scintillation telescope (area 8 cm^2, 11° effective FWHM field of view) observed in a direction centred on RA 17 h 27 min, dec. $-33.5°$ (1950) during March 8–11 with a broad energy channel extending from 50 to 190 keV. Counts from 0.5-s intervals were stored sequentially in sets (bins) of 16 locations which were scanned four times before proceeding to the next set. Each bin thus contained the superposition of 4 time profiles, 8 s long. An identical data mode was used for the 2–7-keV collimated proportional counter (CPC) of ref. 1. Burst sources MXB 1730–335, MXB1728−34, MXB1743−293 and MXB1742−297 were in the field of view of the ST but only the first two could be seen by the CPC. MXB1730−335 is the repetitive burster with small events as close as 7 s apart, while the others give at the most ~5 bursts d^{-1} (ref. 4).

Four very important proportional counter bursts were selected corresponding to those times when the ST data was expected to be free of all spurious events (events A, C, E, F Table 1), two of which (E, F) are plotted in Fig. 1, together with data from the ST. Absolute time is known to ±30 s and this is shown at the beginning of each 32-s bin. In two cases the CPC data showed a pulse at least 8 s long; the double peaks probably arise from two successive scans. In at least 3 cases, the ST increase appeared delayed with respect to the CPC data. Because of the superposition of scans the delay cannot be determined uniquely. Table 1 lists the limits within which the delays lie, the significance in s. d. (σ) of the ST events, the pulse durations and the total energy in erg cm^{-2} assuming all high energy photons were at 50 keV.

In the case of events A and F, the larger of the two figures for minimum delay is more likely; the smaller figure results from taking smaller, secondary peaks in the CPC data as the associated events. Note the tendency for the high energy channel to carry at least as much energy as the low energy channel. Suggestions have been made for 1.39- and 1.36-h periodicities in the intervals between some bursts from this region (ref. 1 and Carpenter *et al.*, to be published). Only event A fits such a scheme (with a 1.36-h period).

To relate our work to searches for γ bursts, a scan of all the suitable March 8–11 data was made to pick out statistically

Table 1 Data from scintillation telescope and collimated proportional counter on Ariel V

Event	Time at start of bin (day in 1976 March)	2–7-keV channel Width (s)	2–7-keV channel erg cm^{-2}	50–190-keV channel Width (s)	50–190-keV channel erg cm^{-2}	Significance (σ)	Delay (s) Min	Delay (s) Max
A	8.7765	8–32	2×10^{-7}	2.5	2.4×10^{-7}	3.7	11.5 or 1.5	59.5
B	8.9544	4	2.3×10^{-8}	3.5	4.1×10^{-7}	5.4	2.5	26.5
C	9.1656	8–32	1.8×10^{-7}	3.0	2.2×10^{-7}	3.3	0	28.0
D	9.4869	3	2.5×10^{-8}	6.5	4.3×10^{-7}	6	3.5	27.5
E	10.9419	4.5	5.2×10^{-8}	2.5	2.7×10^{-7}	5	3–4	34.3
F	11.0819	3.2	1.4×10^{-7}	1.6	2.9×10^{-7}	6.5	7.2 or 3.8	37.2

significant increases in 32-s intervals. Five such events were identified, corresponding to a rate of one every two hours with a significance such that the total chance probability of getting such increases in the data set was 10^{-6}. Two were events previously selected (A, F) and a further two, B and D, are added to Table 1 (B is also shown in Fig. 1) with correlated CPC data where any increase can only be in the 3–4σ region. To compare with previous γ-burst measurements we assume the typical burst spectrum of ref. 5, integrate all the energy > 25 keV and correct the rate for the telescope solid angle by assuming (*a*) the sources are isotropic and (*b*) the sources are distributed according to the density of mean galactic matter. These two rates are shown in Fig. 2, along with Vela, Imp-7 and the balloon data of Bewick *et al.*[6]. The balloon search only included the galactic disk between longitudes 70°–230° within its field of view. It is clear that at some times at least, 'X-ray' bursts, which could equally well be classified as small 'γ bursts' in the 10^{-7}–10^{-6} erg cm^{-2} energy range, are far more likely to be seen from the certain regions in the galactic disk than from elsewhere, a conclusion already suggested by Bewick *et al.*[6] We have insufficient data at present, however, to compare the results with the prediction of a globular cluster origin (compare with ref. 3). Although we cannot measure the energy spectrum with Ariel V, one notes that Grindlay *et al.*[3] found an exponential fit to their data with kT hardening from 5–20 keV. Thus it is possible to regard γ bursts as being particularly 'hot' X-ray bursts. Since, however, Lewin *et al.* saw no apparent hardening with time of bursts from MXB1730-335, it is clear that there is more than one source mechanism, or variant of the mechanism, at work. Also our events may not arise from this repetitive burster.

Fig. 1 Time profiles of three events showing scintillation telescope (ST) (top) data (50–190 keV) and collimated proportional counter (CPC) (bottom) data (2–7 keV) plotted on same timescale.

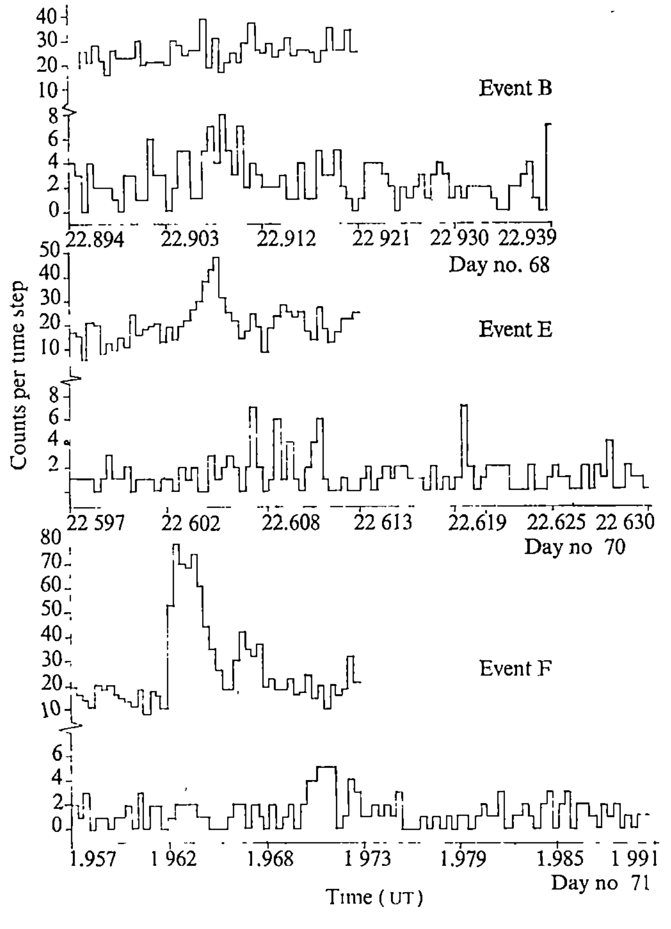

The importance of the spectral hardening with time has already been discussed by Grindlay *et al.*[3] who saw kT increase to 20 keV, but we have shown that at late times and for some events, the energy can reside almost entirely in > 7-keV photons. Their suggested mechanism, involving Inverse Compton acceleration of an initial low energy pulse, requires an optical depth > 1 and is unlikely to fit the acceleration (by a factor > 10) required by our observations, which consequently greatly increases the optical depth necessary. Let us instead think in terms of variants of a mechanism in which gravitational energy is transformed by a shock to an optically thick plasma emitting by a thermal process. Suppose at first that the shock is travelling between a companion star and a compact object, mass M, by near free fall in the gravitational field in a comparatively rarified medium, from an initial position $R_{9,0}$ (units of 10^9 cm). Individual particles behind the strong shock can reach a thermal energy $E \leqslant (1/4)^2\frac{1}{2}m_pU^2$ if the relative downstream velocity is randomised, for shock velocity U in the rest frame, position R_9, away from the compact object

Then

$$E = \frac{8.7\times10^3}{R_9}\left[\frac{M}{M_\odot}\right]\text{(eV)} \qquad (1)$$

and

$$t = 1.3\,(R_{9,0}{}^{3/2} - R_9{}^{3/2})\left[\frac{M}{M_\odot}\right]^{-\frac{1}{2}}\text{(s)} \qquad (2)$$

is the time travel between $R_{9,0}$ and R_9. If the object is a neutron star with magnetopause $\sim$ 0.2 R_9, it is possible by free fall to get temperatures $\sim$ 50 keV outside the magnetosphere. Equation (2) yields, however, a minimum delay between attaining 7 keV and 50 keV of $1.7(M/M_\odot)$ s, while the delay between 2 keV and 7 keV is $9.9(M/M_\odot)$ s. Thus it is difficult to explain observations where the low and high energy pulses are of comparable width unless a dramatic slowing of the shock by accreting material can be invoked. Increased energy in the higher channel does follow naturally from this mechanism, however.

Another possibility is to suppose that penetration of the magnetosphere by a large mass of transferring material occurs by some convection process (see ref. 4). Then this is followed by gravitational fall on to the neutron star atmosphere where the shock occurs to thermalise the energy. One must further suppose that deeper penetration at later times connects the material to different atmospheric conditions where the energy gets shared among fewer particles and hence a higher temperature results. Any short term periodicity (tens of seconds) can perhaps be related to the magnetosphere spin while long term periodicities

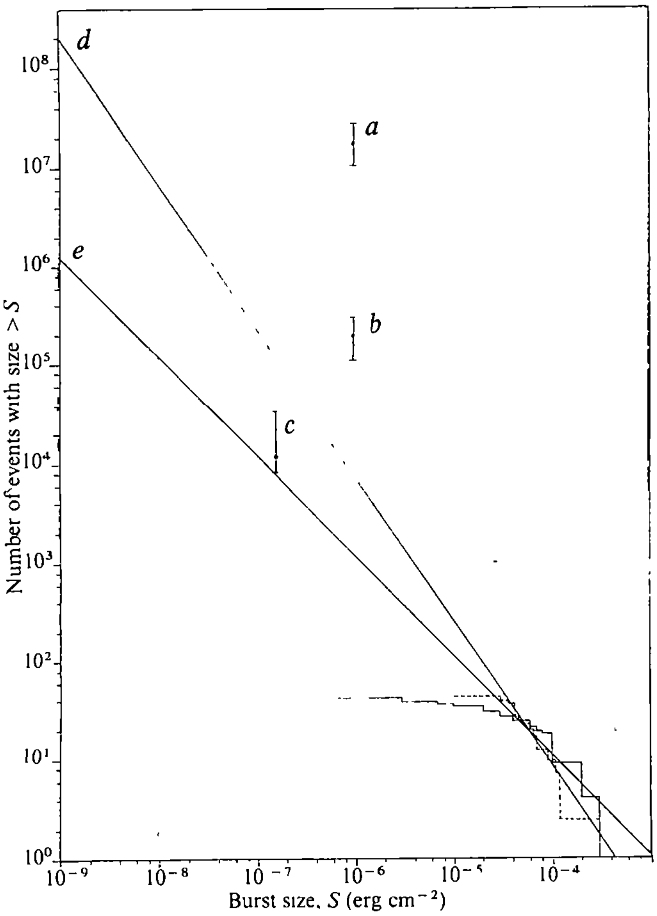

Fig. 2 Burst occurrence rates derived from our experimental results, for two source distributions; *a*, isotropic and *b*, galactic. Also illustrated for reference are the Vela (——) and Imp-7 (----) size spectra. *c*, From Imperial College balloon data. The two straight lines are extrapolations of the Vela/Imp-7 data assuming either *d*, $I^{-3/2}$ law or *e*, I^{-1} law. All rates have been normalised to Vela observation period July 3, 1969–December 23, 1973.

(~ hours) could depend on the orbital period of the companion ~ 4×10^{10} cm away.

We thank Dr S. J. Bell-Burnell for supplying advance information from the CPC experiment and the CPC data in Fig. 1. We acknowledge the Ariel-V Control Centre, Appleton Laboratory, for orbital operations and data distribution. J.S.M. acknowledges receipt of an SRC studentship.

J. J. QUENBY
M. J. COE
A. R. ENGEL
J. S. MILLS

Cosmic Rays and Space Physics Group,
The Blackett Laboratory,
Imperial College,
London SW7 2BZ, UK

Received April 15; accepted June 28, 1976

1 Mason, K O, Bell-Burnell, S J, and White, N. E, *Nature*, 262, 473–474 (1976)
2 Klebesadel, R W., Strong, I B., and Olson, R. A., *Astrophys J. Lett*, 182, L85 (1973)
3 Grindlay, J, *et al*, *Astrophys J Lett* (in the press).
4 Lewin, W H G., *et al*, *Astrophys J Lett.* (in the press)
5 Cline, T L, and Desai, U D, *Astrophys J Lett*, 196, 643 (1975)
6 Bewick, A, Coe, M J, Mills, J. S, and Quenby, J J, *Nature*, 258, 686 (1975).

Positions and evidence for a steady component for X-ray burst sources

DURING observations of the galactic centre region with the Ariel V RMC experiment we have observed X-ray flux from two sources within the error boxes for the burst sources MXB 1730−335 and MXB 1728−34. The observations were made in RMC mode and represent integrations over periods of about one satellite orbit (100 min). This is distinct from the time mode used for the observations described in a companian paper (to be published) in which the time resolution is 32 s but with which no spatial resolution is possible.

The two sources were each observed at various times during the period 1976, 28 February to 8 March. The positions of these sources are

(1) $\alpha_{1950} = 17$ h 30 min 14 s $\delta_{1950} = -33° 21'$
(2) $\alpha_{1950} = 17$ h 28 min 29 s $\delta_{1950} = -33° 48'$

each with an error circle radius of 2′. Position (1) lies wholly within the original error box[1] for the burst source MXB 1730−335 and overlaps the improved error circle given by Hearn[2] (Fig. 1). MXB 1730−335 is known to produce a rapid succession of bursts with an integrated intensity[3] of 1.7×10^{-9} erg cm^{-2} s^{-1} (1.5–20 keV). Lewin *et al.* place an upper limit of twice this level on any non-burst activity from the source[3]. The intensity of the source which we observe corresponds to an energy of ~3×10^{-9} erg cm^{-2} s^{-1} over the range 1.5–20 keV, although this represents an extrapolation from the 2.9–7.6 keV range in which our observations were made. Thus the observed intensity is consistent with the reported burst activity, probably together with a steady non-burst component of about one half of the level of the upper limit found by Lewin *et al.* Thus the position quoted above almost certainly represents an improved determination of the position of MXB1730−335. We note that the star cluster observed by Liller[4] lies close to the centre of our error circle.

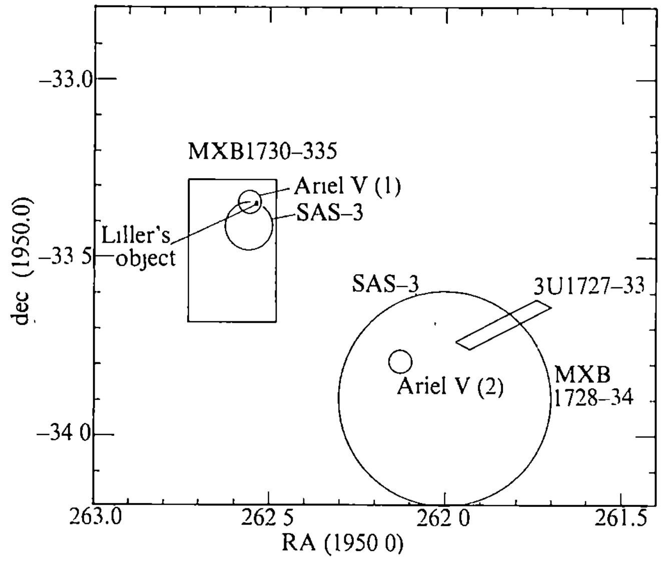

Fig. 1 90 per cent confidence error circles for the two sources reported here shown relative to the SAS-3 burst sources. The error circles should be shown as ellipses extended by 15% in the E–W direction.

The position of source (2) lies within the 18′ radius error circle of MXB1728−34 (unpublished). Only four bursts have been reported from this source, with a probable time between bursts of ~5 h. Each burst lasted only for a few seconds and the mean integrated flux associated with the bursts is at least two orders of magnitude lower than in MXB1730−335. The intensity of source (2) integrated over one orbit was typically similar to that of source (1) although it was rather more variable. Thus there is no question of the observed flux being the integral of bursts of the type which have been reported for this source. If the source (2) represents flux from MXB1728−34 then it must be due to a non-burst background emission.

We note that the position of source (2) lies close to the error box of the Uhuru source 3U1727−33. There is evidence for a source at position (2) in data collected in February–March, 1975, but we have found no evidence for flux from within the error box of 3U1727−33. Thus it is likely that 3U1727−33 lies outside its error box at position (2).

If 3U1727−33 and MXB1728−34 and our source (2) prove to be the same object then it will provide a useful clue to the nature of burst sources as 3U1727−33 has been shown to exhibit a periodicity indicating a 'slow rotator' type of source[5].

We acknowledge the financial support of the SRC.

G. F. Carpenter
G. K. Skinner
A. M. Wilson
A. P. Willmore

Department of Space Research,
University of Birmingham,
PO Box 363, Birmingham B15 2TT, UK

Received April 13; accepted May 26, 1976.

[1] Lewin, W H. G., *IAU Circ.*, No. 2922 (1976)
[2] Hearn, D., *IAU Circ.*, No 2925 (1976).
[3] Lewin, W. H. G., *et al Astrophy J. Lett* (in the press)
[4] Liller, W. *IAU Circ*, Nos. 2929, 2936 (1976).
[5] White, N. E., Mason, K. O., Sanford, P. W., Chevalier, C. and Ilovaisky, S. A, *IAU Circ.*, No. 2920 (1976).

Observations of X-ray bursts from the vicinity of 3U1727−33

Ariel V experiment C observed the region of sky near 3U1727−33 between March 8 and 10, 1976 and again between March 24 and 25. The experiment[1] consists of a multiwire collimated proportional counter with a field of view of 3.5° FWHM. The experiment is, however, offset from the spin axis of the satellite by 1.75°, so the effective field of view per spin cycle (4–5 s) is a Gaussian-like curve of 5.0° FWHM centred on the spin axis. The field of view during the present observations included the positions of 3U1727−33 (ref. 2), MX1716−30 (ref. 3) and two recently discovered burst sources, MXB1730−335 and MXB1728−34 (ref. 4).

Table 1 Data accumulated by experiment C on the Ariel V satellite

Time of burst (March 1976) (d)	Intensity ($\times 10^{-8}$ erg cm^{-2})	Time resolution (s)	Notes
(1) 8.7764	20.0	32	
(2) 8.8910	5.2	32	Probably two pulses but maybe one.
8.8914	14.0	32	
(3) 9.1655	18.0	32	
(4) 10.3487	13.6	20	One long pulse or two close together.
(5) 10.6251	4.0	0.5	
(6) 10.9420	5.2	20	
(7) 11.0820	14.4	20	
(8) 24.7959	8.0	20	
(9) 24.8462	6.4	20	
(10) 24.8513	4.4	20	
(11) 24.8539	18.0	20	
(12) 24.9885	12.4	20	
(13) 25.2432	6.4	0.5	
(14) 25.2494	11.2	0.5	
(15) 25.3097	16.4	0.5	
(16) 25.3170	18.8	0.5	
(17) 25.3774	8.8	0.5	

Bursts listed above with 0.5-s time resolution are included because they are sufficiently strong to have exceeded the threshold set for detection with a 32 or 20 s accumulation interval. Numbers 15 and 16 can be seen in the lowest panel of Fig 1.

Observations were made with a time resolution of 32 s, 20 s and 0.5 s in the 2–7 keV energy band. The mean counting rate from all the sources in the field of view, plus background, was ~ 12 counts s^{-1} (the detector records ~ 100 counts s^{-1} from the Crab Nebula in the same energy band).

The X-ray bursts seen by the ANS (ref. 5) and SAS-3 (refs. 4, 6) satellites generally last for of the order of a few

Fig. 1 Four orbits of experiment C data accumulated in 1-s intervals. The time of the beginning of each data record is given in days from the beginning of March 1976. The abscissae are graduated in 1-min intervals. The flux is plotted as experiment C 2–7 keV counts s^{-1} with no aspect correction. On the same scale the Crab Nebula would register 100 counts s^{-1} when aligned with the satellite spin axis. The field of view is occulted by the Earth towards the end of the records marked MAR 10.62 and MAR 10.69.

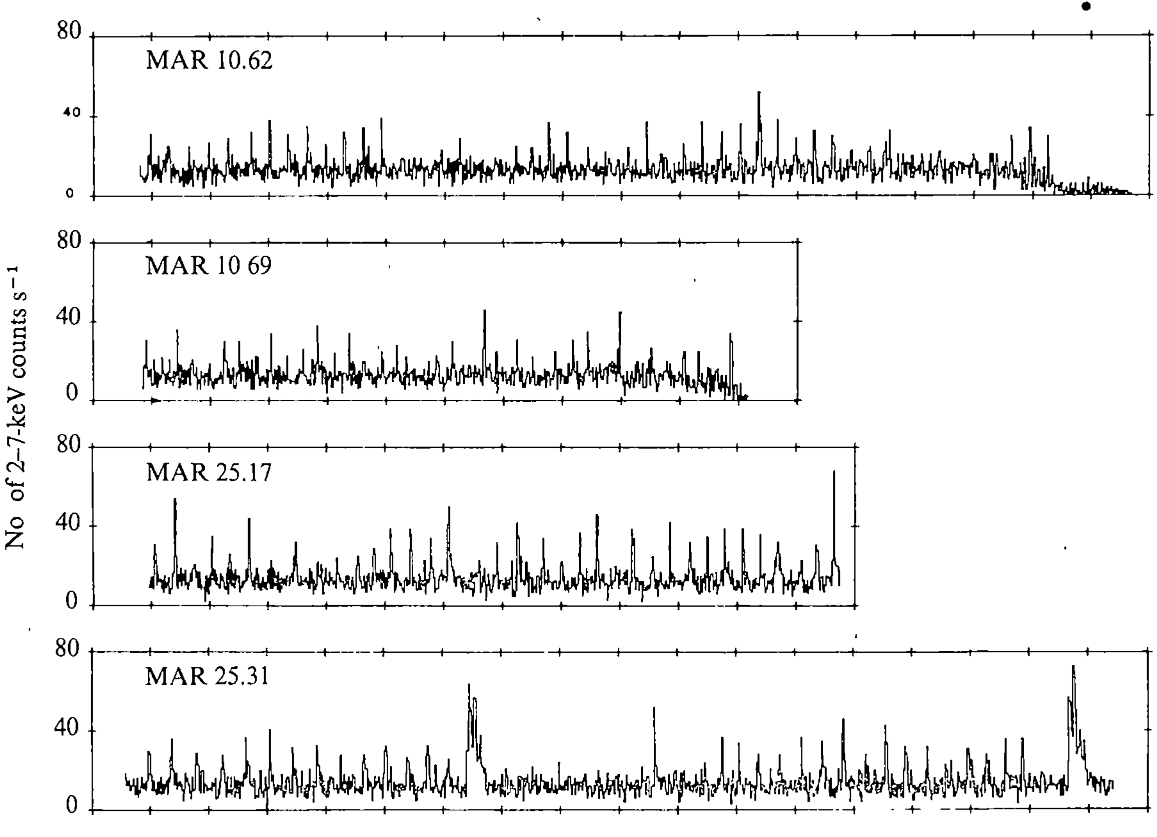

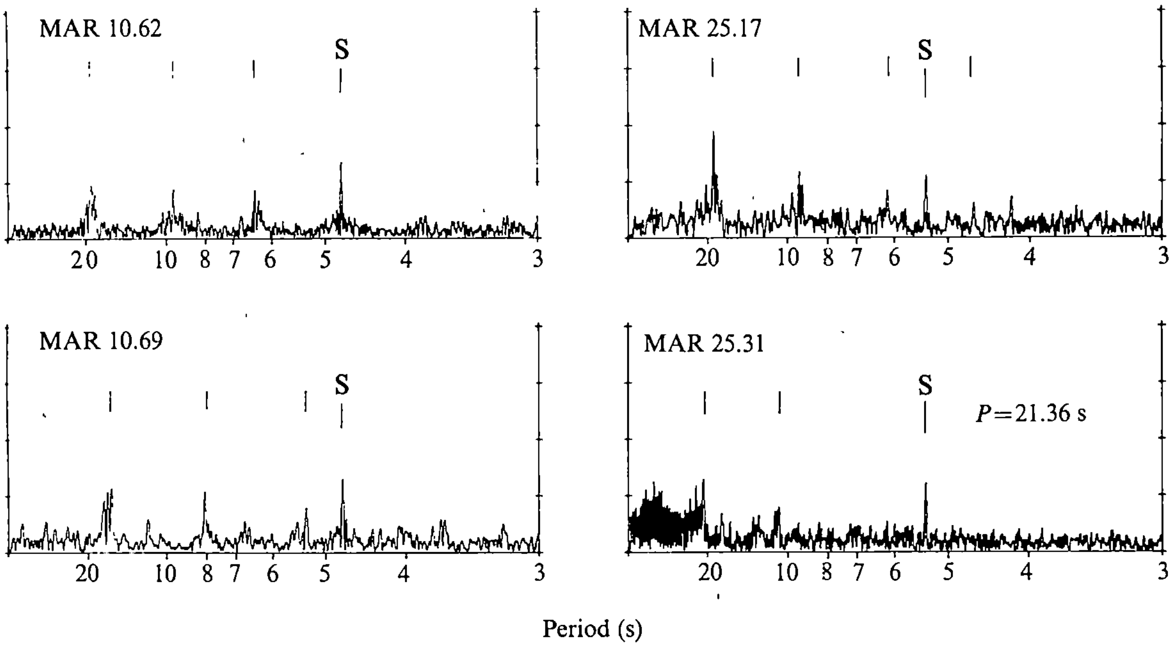

Fig. 2 Power spectra of the data shown in Fig. 1. Peaks near 20 s, plus their harmonics, are marked with vertical bars. The peak caused by the spin modulation is marked by a vertical bar with the symbol 'S' above

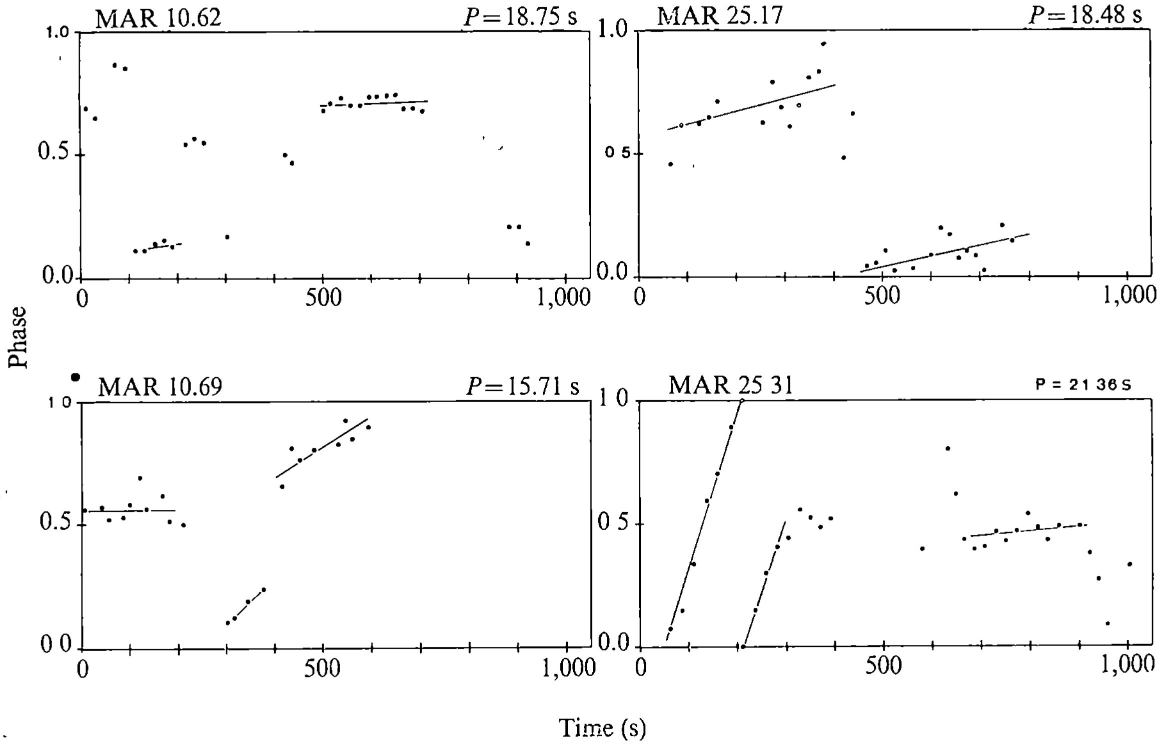

Fig. 3 The phase of bursts with respect to the folding period, P, is plotted against their arrival times (see text) Well defined burst trains are marked with straight lines.

seconds only, shorter than the 20 and 32 s accumulation intervals. The Ariel V data taken at these time resolutions can therefore only distinguish relatively intense or long lasting bursts. A threshold of 8 counts s^{-1} above the mean count rate was set as a criterion for identifying accumulation intervals containing such bursts. During a total of 17 h actual observing time, 17 of these events were recorded The strength of each burst and the start time of the accumulation interval in which it was seen are listed in Table 1. Carpenter *et al.*[7] have found a series of bursts originating from within the 17 ° FWHM field of view of experiment A which recur every 1.39 h. Using their epoch and period (G. K. Skinner, personal communication) we have computed the expected arrival times of bursts in the sequence for the experiment C observing intervals. None of the events listed in Table 1 coincides with the times predicted by the sequence, whereas we should have observed 11 of these. The nearest, event 12 in Table 1, occurred 5 min later than the time predicted by the experiment A data, well outside the jitter observed by Carpenter *et al.*[7]. We note, however, that the first five events recorded by experiment C, which span an interval of 1.9 d, can be fitted by a period of 1.35 h with a jitter of ±5%. One other event in the sequence should have been seen during the above interval and was not. Experiment A cannot collect data when experiment C is in a high time resolution mode, because of limits on spacecraft data storage, so two interpretations of the observations are possible: either the periodic bursting source seen by Carpenter *et al.*[7] changed its mode of behaviour during the experiment C observing periods or, more likely, the source lies outside the field of view of experiment C.

Examples of the data taken by experiment C at a time resolution of 0.5 s are shown in Fig. 1, accumulated in 1-s bins. The data show many significant bursts (> 3 s.d.) superimposed on the d.c. level of ~ 12 counts s^{-1} Most of the bursts last only a few seconds, but some persist for up to ~ 20 s. The longer lasting bursts show clear evidence for spin modulation (period 4–5 s) indicating that they originate from a source which is offset from the spin axis of the satellite (RA 17 h 28 min, dec. −33.5°). The depth (~ 25% peak to mean) and phase of the modulation are consistent with the position of MXB1730−335 (refs 3,7). On the other hand, the d.c. count rate shows no evidence of spin modulation and must originate primarily from a source close to the spin axis, probably 3U1727−33. The level of burst activity clearly diminishes following the longest bursts (for example the data beginning on March 25.31). This behaviour is reminiscent of the correlation between the size of bursts and their separation reported by Lewin[4]. It also suggests that both large and small bursts originate from the same source.

The spacing between many of the bursts in Fig. 1 is similar. This is confirmed by the power spectrum of each of the four data sets. These are shown in Fig. 2. In each case there is a well defined peak at a frequency corresponding to a period ~ 15–20 s, with further peaks at the harmonics of this frequency. Note, however, that the primary peaks come at a different frequency in each of the four data sets. A peak is also seen at the spin period of the satellite and is marked by the symbol 'S'. This corresponds to the spin modulation noted earlier.

To further investigate this behaviour we have folded the arrival times of the bursts on a period close to that given by the power spectra in Fig. 2. We then plot the phase of the burst against its arrival time as shown in Fig. 3. On these diagrams, bursts which recur at the folding period lie on a horizontal line. Bursts which recur at a period slightly different from the folding period will lie on diagonal lines. It is evident that the bursts observed come in groups within which the separation of pulses remains approximately constant, the typical r.m.s. jitter being ~ 5%. Transitions from one group to another, at a different phase and/or period, occur on a time scale short compared with the length of pulse trains.

In summary, therefore, we have observed, probably from MXB1730−335, sequences of periodic bursts which maintain their phase and period for several cycles and then may change abruptly in either phase or period. Longer lasting bursts (of the order of the separation of small bursts) are followed by relatively quiescent intervals. The abrupt changes in phase and period suggest that the burst trains are not produced by a rigid dynamical system such as a rotating star or orbiting stars; rather that they represent a characteristic oscillation period in the X-ray production mechanism or orbital motion in some non-rigid system such as an accretion disk. With regard to the latter possibility, and in view of the suggested identification of MXB1730−335 with a globular cluster[8,9] we note that a time scale of ~ 20 s is the inner orbital period of a ~ $10^5 M_\odot$ black hole ($t \simeq 0.1 M_{\mathrm{BH}}/10^3 M_\odot$(s)).

K.O.M. and N.E.W. acknowledge the financial support of the SRC.

K. O MASON

Mullard Space Science Laboratory,
University College, London and
Mullard and Radio Astronomy Observatory,
University of Cambridge, UK

S. J. BELL-BURNELL
N. E. WHITE

Mullard Space Science Laboratory,
University College, London

Received April 15, accepted June 28, 1976

[1] Sanford, P. W , and Ives, J. C., *Proc. R Soc* , A (in the press)
[2] Giacconi, R , *et al.*, *Astrophys J Suppl* , 27, 37 (1974)
[3] Markert T. H., *et al* , *IAU Circ* , No. 2765 (1975)
[4] Lewin, W H. G., *IAU Circ.*, No 2922 (1976)
[5] Grindlay, J., and Heise, J., *IAU Circ.*, No. 2879 (1975).
[6] Clark, G W , *IAU Circ* , No 2907 (1976).
[7] Carpenter, G F , Skinner, G. K , Wilson, A. M , and Willmore, A P , *Nature*, 262, 473–474 (1976)
[8] Liller, W , *IAU Circ* , No 2929 (1976)
[9] Liller, W., *IAU Circ* , No. 2936 (1976)

The radio tail galaxies in Abell 1314

THE study of radio tail objects is important to our understanding of extragalactic radio sources because the tail morphology allows inference of the temporal evolution of ejected radio components. Furthermore, with increased understanding of these objects, it may be possible to use radio tails as probes of extragalactic space in clusters of galaxies. All published models of radio tails require some form of streamlining resulting from the relative motion of the parent galaxy and the medium producing the tail shape. Therefore, to constrain the relevant dynamical quantities, we have obtained radial velocity measurements for 18 galaxies in the vicinity of A1314, including the two radio tail objects, IC708 and IC711.

The data were obtained with the Cassegrain spectrograph and RCA 33063 image tube camera mounted on the Steward Observatory 90″ telescope. The dispersion used was ~240 Å mm^{-1}, which allowed redshift measurements using the H and K lines of calcium, as well as, in some cases, the 3,727 Å and 5,007 Å lines in emission. The results of these measurements, using the one-dimensional Grant Measuring Engine at the Kitt Peak National Observatory, are listed in Table 1.

Assuming all galaxies observed are cluster members except number 3 and number 19, we derive a mean cluster velocity of 10,160 km s^{-1} and, assuming $H_0 = 50\ \mathrm{km\ s^{-1}\ Mpc^{-1}}$, a distance of 200 Mpc.

The radial velocity dispersion of the cluster, σ, is 708 km s^{-1} and the total dispersion, σ_{T}, is 1,226 km s^{-1}.

Both radio tail galaxies, IC708 and IC711, have radial velocities fairly near the cluster mean

$$(\langle v\rangle - v_{\mathrm{r}})_{\mathrm{IC708}} \simeq 1/3\ \sigma$$

$$(\langle v\rangle - v_{\mathrm{r}})_{\mathrm{IC711}} \simeq 1/2\ \sigma$$

and, considering their proximity to the cluster centre, we therefore conclude that both galaxies are cluster members.

Confirmation of the cluster membership of IC711 strongly implies that *in situ* acceleration must be important in its radio components, as suggested by Vallee and Wilson[1]. A model predicting such acceleration was suggested by Pacholczyk and Scott[2]. Using the radial velocity data we may place strict constraints on the amount of acceleration necessary in IC711 and IC708, and, therefore, test the available radio tail models.

Table 1 Spectrographic measurements (see text)

Galaxy	α (1950) (h	min	s)	δ (1950) (°	′	″)	Heliocentric velocity (km s^{-1})
1	11	29	26	+49	17	10	9,363
2	11	29	51	+49	23	08	10,097
3	11	30	46	+49	30	54	318
4 IC708	11	31	16	+49	20	17	9,613
5 IC709	11	31	31	+49	19	09	9,549
6 IC711	11	32	03	+49	13	57	9,724
7 IC712	11	32	06	+49	21	14	10,054
8	11	33	01	+50	00	52	9,727
9	11	33	22	+49	43	38	9,467
10	11	33	49	+49	24	29	11,223
11	11	33	54	+49	20	23	9,641
12	11	32	59	+49	04	49	11,179
13	11	33	04	+49	25	39	9,870
14	11	32	47	+49	23	00	11,307
15	11	33	01	+49	26	34	10,454
16	11	29	26	+49	16	13	9,863
17	11	30	06	+49	22	34	11,251
18	11	30	34	+49	33	38	3,180

Assuming that the space velocity of IC711 relative to the cluster medium is σ_T, the angle between the velocity vector of this galaxy and our line of sight is 70°. In this case the radio tail is ~ 900 kpc long. Using these values for the galaxy velocity and tail length with Vallee and Wilson's estimate of the magnetic field ($H = 4\times10^{-6}$ gauss) we may estimate the importance of *in situ* acceleration for this radio tail.

From the equations for energy loss due to inverse Compton and synchrotron emission[3] we calculate the e-folding decay time, t, for the energy of particles in the tail. Dividing the tail's length by the estimated velocity of the galaxies with respect to the centre of the cluster gives T, the length of time that particles emit detectable energy[4]. Then the ratio $N = T/t$ is a measure of the effect of *in situ* particle acceleration in the radio tail. For IC711 we find $N \simeq 20$, a typical value from the Pacholczyk and Scott[2] theory. For IC708 a similar calculation yields $N \simeq 4$.

From our spectroscopic study of galaxies in Abell 1314 we conclude that both reported radio tail galaxies are cluster members, and that *in situ* acceleration (with a magnitude consistent with Pacholczyk and Scott's[2] model) is an important effect in their radio components.

GARY D. COLEMAN

Steward Observatory,
University of Arizona,
Tucson, Arizona

PAUL HINTZEN
JOHN S. SCOTT

Kitt Peak National Observatory,
Tucson, Arizona

MASSIMO TARENGHI

Lab. Fis. Cosmica e Technologie Rel.,
C.N.R., Milano, Italy

Received June 7, accepted June 22, 1976

[1] Vallee, J. P and Wilson. A. S *Nature*, 259, 451 (1976)
[2] Pacholczyk, A G and Scott J. S., *Astrophys. J.*, 203, 313 (1976)
[3] Pacholczyk, A G , *Radio Astrophysics* (Freeman, San Francisco, 1970).
[4] Tarenghi, M , and Scott, J. S , *Astrophys J Lett* (in the press).

White dwarfs, the Galaxy and Dirac's cosmology

AN apparent absence, or deficiency, of white dwarfs fainter than $\sim 10^{-4} L_\odot$ has been noticed for a long time[1]. Often attributed to incomplete statistics for the coolest, faintest objects[2,3], this deficiency has nevertheless not been removed even after the most persistent spectroscopic surveys by Greenstein[4,5] (see also Liebert[6]). Moreover, Jones's[7] analysis of reduced proper motions for the very faint proper-motion stars observed by Eggen and by Luyten tends only to confirm the deficiency. If real, the lack of very faint white dwarfs may have its origin in a rapid drop of the internal heat content of the white dwarf as a result of ion crystallisation and of envelope convection when the star becomes sufficiently cool (see Greenstein[4] and Van Horn[8] and references therein). But perhaps it will eventually prove to be difficult, as Lamb and Van Horn[9] have already found, to increase the cooling rate by a sufficiently large amount to account for all the deficiency. Another explanation is proposed here on the basis of Dirac's[10–12] cosmological hypothesis that the gravitational constant, G, varies with the elapsed time since the beginning of the expansion of the Universe as t^{-1} and the number of particles in the Universe increases as t^2 (if the measurements are made in atomic units). For a white dwarf, the Chandrasekhar mass limit is a collection of fundamental constants proportional to $G^{-3/2}$, and therefore increases with time as $t^{3/2}$. In the 'additive' version of Dirac's theory, the actual mass, M, of a relatively small object like a star remains essentially unchanged by the creation of new matter in the Universe, and so a white dwarf becomes 'more stable' as time goes on. But, in the 'multiplicative' version of his theory, M increases as t^2 and may eventually exceed the Chandrasekhar limit. If so, gravitational collapse of the white dwarf into an invisible black hole or neutron star will quickly ensue. Since some possible empirical support has already been adduced for the multiplicative theory, although not for the additive theory[13–17], it is interesting to determine whether the multiplicative theory may also have something to do with the apparent deficiency of faint white dwarfs and whether there are any possible consequences for galactic evolution.

First it is necessary to evaluate what would be the luminosity of a white dwarf (assumed to be in hydrostatic equilibrium) if the formal change of internal energy and gravitational potential energy of the star arising from the creation of new matter is available as free energy partly to raise the heat content of the star and partly to be radiated away at the surface, and is the sole source of visible luminosity. The changes of G and M are assumed to be given by

$$G(t) = G_0[t/t_0]^{-1} \tag{1}$$

and

$$M(t) = M_0[t/t_0]^2 \tag{2}$$

where the subscript 0 refers to the present epoch. Although these expressions give an undesirable zero mass and infinite G at $t = 0$, they are only needed at comparatively large fractions of t_0, at which times they may serve as suitable approximations for the present purpose (Van Flandern's[16] observed value for the residual secular acceleration of the Moon, interpreted as being carried by a decrease of G, is consistent with equation (1) for $t_0 = 12\times10^9$ yr). The mass–radius relationship[18] relevant to most of the appropriate range of white-dwarf masses is approximately

$$\left[\frac{G}{G_0}\right]^2 \frac{R}{R_0} \simeq \left[\frac{M}{M_0}\right]^{-1} \tag{3}$$

The luminosity follows from evaluating the rate of change of total (internal plus potential) energy

$$L = \frac{d}{dt}\left[\beta \frac{GM^2}{R}\right] \tag{4}$$

where β extends from 3/7 to 0, for masses ranging from very low values to values close to the Chandrasekhar limit, respectively; β may, however, be held constant here. The result is, at the present epoch

$$L = 3\beta GM^2/Rt_0 \tag{5}$$

For a typical white dwarf with $M = 0.8\,M_\odot$, $R = 10^{-2} R_\odot$, and $\beta = 0.4$, and for an approximate age for the Universe of $t_0 = 12\times10^9$ yr (refs 16, 19), the expected luminosity is $L = 0.2\,L_\odot$. (An analogous derivation for main-sequence stars shows that the 'extra' luminosity is insignificant, except for the faintest main-sequence stars; in general, it will be negligible for any star whose Helmholtz–Kelvin time, GM^2/RL, is short compared with t_0.)

Since so high a white-dwarf luminosity is in serious conflict with observations[2], it may be concluded either that Dirac's theory is untenable, or that the radiation (and 'heating') is of an unknown type, or that the process of creation of new matter requires a corresponding supply of energy. For lack of a better alternative, I shall simply assume that the 'extra' energy somehow goes into work done creating the new matter and that the ordinary rates of stellar energy generation should be used to determine stellar temperatures and luminosities. Therefore, at least in its macroscopic effect, the process of creation is assumed to be a collective phenomenon involving the whole mass of the star; but this may be an unavoidable requirement of the multiplicative theory anyway, since Dirac[12] has already pointed out that, in the case of the Earth, new atoms may have to form at the surfaces, rather than in the interiors, of rock crystals. In the case of gaseous stars, I shall follow Dirac in assuming that new atoms emerge with the same basic properties, that is, species, state, and general location, as the existing atoms.

To proceed further, simple physical assumptions about the structure and luminosity source of white dwarfs will be adopted here: (1) Chandrasekhar's[18] classic mass limit of $1.44 M_\odot$ for a white dwarf at the present epoch; (2) Mestel's[20] simplified cooling theory of white dwarfs, as presented by Schwarzschild[21]; and (3) an average mass of $0.8 M_\odot$ for young (recently formed) white dwarfs. How this average mass has varied in the past is not easy to determine, but a good assumption is that it has been proportional to $G^{-3/2}$, since most critical stellar masses in astrophysics, such as the approximate upper and lower mass limits of ordinary stars[22,23], have this proportionality.

Schwarzschild's[21] standard relationship between the luminosity, L, of a white dwarf and its isothermal core temperature, T, is

$$L = KGMT^{3.5} \tag{6}$$

where K is a constant depending on the chemical composition of the radiative envelope. The luminosity of the white dwarf is supposed to be supplied solely by thermal cooling of the non-degenerate ions; the basic equation of thermal equilibrium is given by

$$\frac{\mathrm{d}L(r)}{\mathrm{d}M(r)} = -\frac{\mathrm{d}}{\mathrm{d}t}\left[\frac{3}{2}\mathscr{R}T\right] \tag{7}$$

whose correct integrated form is

$$L = -\frac{\mathrm{d}}{\mathrm{d}t}\left[\frac{3}{2}\mathscr{R}T\right]M \tag{8}$$

Solution of equations (1), (2), (6) and (8) for the core temperature can be simplified by assuming that the initial temperature is 'infinitely' hotter than the present temperature Then the time, t_f, at which the white dwarf actually formed is found to be given by

$$t_f/t_0 = \exp(-t_{cl}/t_0) \tag{9}$$

where

$$t_{cl} = \left[\frac{3}{2}\mathscr{R}T\right]/(2.5\,L) \tag{10}$$

and all quantities in parentheses are evaluated at the present epoch. Note that t_{cl} is simply the classical cooling time that would apply if G and M remained constant in time. For the brighter luminosities characteristic of most of the observed white dwarfs, the revised cooling times are not much different from the classical cooling times and therefore do not destroy the approximate agreement with observations already achieved[2].

The most recent period at which a white dwarf with mass typical of its epoch could have formed to reach the Chandrasekhar mass limit at the present epoch follows from $0.8(t_f/t_0)^{3/2} = 1.44(t_f/t_0)^2$ and is $t_f = 0.31 t_0$. Substitution of this result into equation (9) yields $t_{cl} = 1.2 t_0$, which may be directly entered into Schwarzschild's[21] Table 27.1 for the classical cooling times of white dwarfs as a function of their luminosities, if his cooling times are multiplied by a factor 1.3 to correspond to a mass of $1.44\ M_\odot$ and by another factor 0.3 to convert from a predominantly helium core composition to a more probable carbon core composition. With $t_0 = 12 \times 10^9$ yr, a value of $L = 2 \times 10^{-5} L_\odot$ is found for the present luminosity of an 'average' white dwarf that has cooled for $t_0 - t_f = 8 \times 10^9$ yr. Older white dwarfs would long ago have faded into invisibility through gravitational collapse. (Some older white dwarfs of smaller-than-average initial mass would still be visible, of course) Most younger white dwarfs would not yet have collapsed. It is interesting to note that most of the old white dwarfs with high space velocities[1,24] have large photometrically implied masses. Could some of these objects be on the verge of gravitational collapse? Accurate measurements of the surface gravities of the oldest white dwarfs will be necessary to determine whether these stars are, on the average, heavier than the brighter objects. Noticeable differences are expected to occur only for $L < 10^{-3} L_\odot$.

Allowance for a probable initial spectrum of white-dwarf masses, for the uncertainty of the adopted chemical composition, for known corrections to the classical white-dwarf mass limit, for various inadequacies of the white-dwarf cooling theory used here, and for the uncertainty of the adopted age of the Universe leads only to a general order of magnitude of 10^{-5} to $10^{-4} L_\odot$ as the predicted cutoff luminosity for most white dwarfs. This prediction seems to be in as good agreement with the available observations as could be expected.

The earliest generation of stars in the Galaxy probably formed within one galactic rotation period after the onset of collapse of the protogalaxy[25]. At the present time, this period in the outer galactic regions near the Sun is 2×10^8 yr, but, in Dirac's theory, it must be scaled down as t, since the rotational velocity stays at the same fraction of the speed of light while the radius of the Galaxy changes as t. The first white dwarfs could have originated about one main-sequence lifetime (which also scales as t—see below) after that era. Since the collapse of the protogalaxy could have begun as late as $0.25 t_0$ (ref. 19) the foregoing stellar formation time scales are seen to be relatively short in comparison, and the first-generation white dwarfs can therefore be expected to be, at the present time, invisible black holes or neutron stars with typical masses of $> 1.6\ M_\odot$. Consequently, simple counts of observed stars in the solar neighbourhood will, if uncorrected for cosmological effects, lead to errors in the extrapolated numbers and masses of dead stars formed since the collapse of the protogalaxy. (The present discussion will ignore the probably small contribution to the mass of the Galaxy from black holes and neutron stars that have formed as direct end-products of normal stellar evolution.)

At first sight, it may seem that a gross underestimate must have been made in the standard extrapolation for dead stars[21]. That this is not so can be seen upon the following reflection. Consider the average properties of typical bright main-sequence stars that give rise to white dwarfs. Their average main-sequence lifetime, t_{MS}, at any epoch t may be regarded as short compared to t (since it is known to be short at the present epoch and it will be shown that t_{MS}/t remains approximately constant in time). Then their birthrate follows simply as $\mathrm{d}N_{MS}/\mathrm{d}t = N_{MS}/t_{MS}$, where N_{MS} is the number of such stars present in the Galaxy at time t. The next task is to evaluate $t_{MS} = qEM/L$ by noting that q, the mass fraction of hydrogen eventually consumed in the star[26], and E, the energy released per gram of material, are independent of t, while the average mass, M, of these bright main-sequence stars at the time of their formation (like all critical stellar masses) probably varies as $G^{-3/2} \propto t^{3/2}$ and their luminosity, L, scales as $G^4 M^3$ (electron-scattering opacity) or as $G^7 M^5$ (Kramers opacity). In either case $L \propto t^{1/2}$. Certainly the evolutionary change in L/M can be neglected, both because $t_{MS} \ll t$ and because this change will in any case be small ($G \propto t^{-1}$, $M \propto t^2$, and hence $L/M \simeq$ constant). It then follows that $t_{MS} \propto t$. Next, the crude assumption is made that the ratio of the total mass in the form of bright main-sequence stars to that of interstellar gas in the Galaxy remains approximately constant after the collapse of the protogalaxy (anticipating the final result that the permanent loss of gas now tied up in dead stars is small). It then follows that $N_{MS} \propto t^{1/2}$, since the mass of the average bright star when it forms varies with the epoch as $t^{3/2}$ whereas the total mass of interstellar gas in the Galaxy increases as t^2. The birthrate of bright stars becomes $\mathrm{d}N_{MS}/\mathrm{d}t \propto t^{-1/2}$.

The deathrate of these stars may be assumed to be equal to their birthrate, so that the rate of addition of mass in the form of new white dwarfs to the Galaxy is $0.8 M_\odot (t/t_0)^{3/2}$ times

$(\mathrm{d}N_{\mathrm{MS}}/\mathrm{d}t)_0(t/t_0)^{-1/2}$. The rate of growth of the masses of dead stars that have already formed follows from equation (2) as $2M_{\mathrm{dead}}(t)/t$. The sum of these two terms yields the total rate

$$\frac{\mathrm{d}M_{\mathrm{dead}}(t)}{\mathrm{d}t} = \frac{2M_{\mathrm{dead}}(t)}{t} + 0.8M_\odot\left[\frac{\mathrm{d}N_{\mathrm{MS}}}{\mathrm{d}t}\right]_0\frac{t}{t_0} \tag{11}$$

By setting $M_{\mathrm{dead}}(t) = 0$ at $t = t_i$ (corresponding to the end of the collapse of the protogalaxy) and by noting that the quantity

$$M_{\mathrm{dead}}{}^* = 0.8M_\odot(\mathrm{d}N_{\mathrm{MS}}/\mathrm{d}t)_0 t_0 \tag{12}$$

is the result of the standard extrapolation for dead stars, the solution of equation (11) is

$$M_{\mathrm{dead}}(t) = M_{\mathrm{dead}}{}^*[t/t_0]^2\ln(t/t_i) \tag{13}$$

At the present time, $M_{\mathrm{dead}} = M_{\mathrm{dead}}{}^* \ln(t_0/t_i)$. Dead stars that formed at any time earlier than $t_f = 0.31t_0$ will now, however, be invisible objects rather than white dwarfs. If the total mass of dead stars at time t_f is multiplied by $(t_0/t_f)^2$, it follows that the present total mass of collapsed objects alone is $M_{\mathrm{collapsed}} = M_{\mathrm{dead}} \ln(t_f/t_i)$. Further, the present total mass of white dwarfs alone is found to be $M_{\mathrm{WD}} = M_{\mathrm{dead}}{}^* \ln(t_0/t_f)$, which is not significantly different from $M_{\mathrm{dead}}{}^*$!

With reasonable choices for the collapse epoch, say $t_i/t_0 = 0.25-0.01$, the sought-for result is finally obtained: $M_{\mathrm{dead}}/M_{\mathrm{dead}}{}^* = 2$–5 and $M_{\mathrm{collapsed}}/M_{\mathrm{WD}} = 0.2$–3. These are modest values. Therefore, in the framework of Dirac's multiplicative theory, there is no special mechanism to produce the vast numbers of black holes or other dead stars that are sometimes suggested to compose the 'missing matter' in the solar neighbourhood and in the galactic halo.

The predicted paucity of stars during the past history of the Galaxy arises from the smaller galactic mass then, and implies that the Milky Way must have been considerably dimmer than it is at present. Most of the luminosity may be assumed to have come then (as now) from the few brightest stars. Assuming that these stars form with masses in proportion to $G^{-3/2}$ leads, as above, to $L \propto t^{1/2}$ and $N_{\mathrm{brightest}} \propto t^{1/2}$, so that the total luminosity of the Galaxy, $N_{\mathrm{brightest}}\, L$, is found to rise as t (but its colour probably changes relatively little with time). Thus, at the end of the original collapse phase of the Galaxy, after the initial metals abundance had been produced and supermassive stars were no longer being formed, the Milky Way would have been only 0.01–0.25 times as bright as it is today *ceteris paribus*. It could have been even fainter if the upper end of the allowable range of stellar masses were underpopulated when the galactic mass was small (an effect observed today in external galaxies of small mass). But, if the mass of the Galaxy had not been varying along with G, the Milky Way would have been brighter in proportion to t^{-1} in the past than it is today. Observations of distant spiral galaxies may eventually be able to discriminate between these various evolutionary models.

I thank V. Canuto and C.-w. Chin for discussions.

R. Stothers

Institute for Space Studies,
Goddard Space Flight Center, NASA,
2880 Broadway, New York, New York 10025

Received January 13, accepted June 5, 1976

[1] Eggen, O. J., and Greenstein, J L., *Astrophys. J.*, 141, 83 (1965).
[2] Weidemann, V , *Z. Astrophys* , 67, 286 (1967).
[3] Hintzen, P., and Strittmatter, P. A , *Astrophys. J. Lett.*, 193, L111 (1974)
[4] Greenstein, J. L., *Comm. Astrophys. Space Phys* , 1, 62 (1969)
[5] Greenstein, J L , in *White Dwarfs* (edit by Luyten, W. J.), 46 (Reidel, Dordrecht, 1971).
[6] Liebert, J., *Astrophys. J. Lett.*, 200, L95 (1975)
[7] Jones, E. M., *Astrophys. J* , 177, 245 (1970)
[8] Van Horn, H M., in *White Dwarfs* (edit. by Luyten, W J), 97 (Reidel, Dordrecht, 1971)
[9] Lamb, D. Q., and Van Horn, H. M., *Astrophys. J.*, 200, 306 (1975)
[10] Dirac, P A. M., *Nature*, 139, 323 (1937)
[11] Dirac, P. A. M., *Proc R. Soc.*, A165, 199 (1938)
[12] Dirac, P. A. M., *Proc. R. Soc*, A338, 439 (1974).
[13] Teller, E , *Phys Rev.*, 73, 801 (1948)
[14] Pochoda, P., and Schwarzschild, M., *Astrophys J* , 139, 587 (1964).
[15] Gamow, G., *Proc. natn Acad Sci U.S.A.*, 57, 187 (1967)
[16] Van Flandern, T. C., *Mon. Not. R. astr. Soc* , 170, 333 (1975).
[17] Chin, C.-w., and Stothers, R., *Nature*, 254, 206 (1975).
[18] Chandrasekhar, S., *An Introduction to the Study of Stellar Structure* (University of Chicago Press, Chicago, 1939)
[19] Sandage, A , *Q. Jl R astr. Soc.*, 13, 282 (1972).
[20] Mestel, L., *Mon. Not R astr Soc.* 112, 583 (1952)
[21] Schwarzschild, M , *Structure and Evolution of the Stars* (Princeton University Press, Princeton, 1958).
[22] Chandrasekhar, S., *Nature*, 139, 757 (1937).
[23] Salpeter, E E , in *Perspectives in Modern Physics* (edit. by Marshak, R.), 463 (Interscience, New York, 1966).
[24] Eggen, O J , *Observatory*, 79, 135 (1959).
[25] Eggen, O. J., Lynden-Bell, D., and Sandage, A R , *Astrophys. J.*, 136, 748 (1962)
[26] Schonberg, M., and Chandrasekhar, S., *Astrophys J.*, 96, 161 (1942)

Extraction of metals from basalt by humic acids

In many studies, the activity of humic acid in weathering and other geological processes has been considered negligible. Only simple, low molecular weight organic acids are usually considered effective in mineral degradation[1]. Those acids, however, frequently constitute only a minor fraction of the soil organic matter, particularly in semi-arid and arid areas. In Israel, fulvic acid/humic acid ratios in the organic matter of major soil types range, with one exception, from 1.5 to 6 (ref. 2). Humic acids are also well represented in the organic matter of many sediments[3,4]. The effect of these high molecular weight compounds on mineral decomposition and metal dissolution is therefore of great interest in the earth sciences. The results presented here suggest that humic acids also may have a significant role in rock solubilisation and weathering, because of their capacity to extract considerable amounts of metals, particularly copper and zinc, from basalt rock.

Though the part played by fulvic acids and other low molecular weight organic acids in weathering has been widely documented, the action of humic acids in these processes has been examined in only a few cases. Schalscha *et al.*[5] extracted considerable amounts of Fe from minerals treated with humic acids. The solubilisation of major elements from alumosilicates has been shown to be considerably speeded up by treatments with humic acids or organic acid components of humic acid[6–8].

Baker[9] has reported on the strong solvent activity of humic acid from a podzolic soil in Tasmania, towards a number of minerals and metals. In his studies, separate mineral species were exposed to the action of humic acids. Here the effect of humic acids on basalt rock has been examined with the purpose of evaluating their role in the supply of soluble metals to soils.

Figure 1 shows that after a rapid initial rise, the dissolution rate of nearly all elements decreases rapidly. The dissolution capacity of the three humic acids is fairly similar. Ca, Mg, Co and Ni came to near equilibrium after 6–12 h, Al and Zn after 36 h. Fe, Mn, Cr and, to a lesser extent, Cu continue to be dissolved, though at a slow rate, after 108 h. Fe was the most extracted metal, followed by Al, Ca and Mg (Table 1). The transition metals were extracted in trace amounts. Relative to their contents in the basalt, Cu was the most extracted metal, followed by Zn. Next came Co, Cr and Mn, then Ni. Less than 0.5% of Fe, Al, Mg and Ca were extracted by the humic acids. Arranged according to the relative amounts extracted, the following sequence is obtained: Cu > Zn > Mn > Cr > Co > Ni > Al > Fe > Mg > Ca. The large amounts of metals extracted by the humic acids indicate the significant role these organic compounds may have in weathering and soil formation. An even more important aspect of that capacity is the role humic acids may play making micronutrients available (particularly copper and zinc) to plants growing on basalt-derived soils.

The capacity of humic acids to dissolve metals has been given as up to 682 mg g^{-1} (ref. 4). Thus, the total amounts

Table 1 Extraction of alkaline earths and metals from 1 g basalt after 108 h treatment with three humic acids

	Basalt (mg)	Humic acid 1 µg	Humic acid 1 %	Humic acid 2 µg	Humic acid 2 %	Humic acid 3 µg	Humic acid 3 %
Al	63.7	387	0.61	402	0.63	366	0.57
Fe	110.1	550	0.50	491	0.44	499	0.45
Ca	71.4	297	0.42	265	0.37	281	0.39
Mg	34.7	175	0.50	169	0.49	153	0.44
Co	41×10^{-3}	1.1	2.7	1.3	3.2	1.9	4.6
Cr	221×10^{-3}	7.9	3.6	7.6	3.4	7.2	3.3
Cu	59×10^{-3}	7.7	13.1	6.5	11.0	6.4	10.9
Mn	141×10^{-2}	48	3.4	53	3.8	47	3.3
Ni	211×10^{-3}	2.3	1.1	2.2	1.0	3.4	1.6
Zn	118×10^{-3}	5.5	4.7	6.8	5.8	6.7	5.7

dissolved in this experiment—10–15 mg g^{-1} humic acid—are far below the dissolving capacity of the acid. Incongruent dissolution of components from various alumosilicates by organic acids has been shown by Huang and Keller[7]. From most of the minerals, alkalis were removed preferentially so that the mineral surfaces remained enriched in Si–Al relative to the inner core. Further dissolution proceeds probably by diffusion through the residual envelope and is consequently slowed down considerably, or stopped altogether, as is the case with Ca and Mg in the experiment reported here. Fe and Mn, and to a lesser extent some of the other transition metals, particularly Cr, remain in basalt partly in the free oxide minerals magnetite and ilmenite, from which they continue to be dissolved, though at a slow rate.

Fig. 1 Extraction of alkaline earths and metals from basalt shaken for up to 108 h with humic acid. The humic acids were extracted from three Mediterranean soils: protogrumosol derived from basalt, under *Eucalyptus rostrata*; Mediterranean Brown Forest Soil derived from hard chalk, under annual grasses; and Rendzina, derived from soft chalk, under *Pinus halepensis*. Extraction, isolation and purification of the humic acids were similar to the methods described by Khan[10]. Alkaline olivine basalt, chemical composition given in Table 1, was pulverised in a Fritsch agate ball mill and then sieved through a 200 mesh Spex nylon sieve. The humic acid was redissolved in a NaCl solution to give a 0.1% w/v humic acid in 0.01 M NaCl final solution, and adjusted to pH 6.5 One gram of rock powder was shaken for 3, 6, 12, 36 and 108 h with the humic acid solutions at 25 °C, and the soluble elements were determined by atomic absorption. Controls of rock shaken with 0.01 M NaCl alone were run separately. Also determined was the metal content of the humic acids alone.

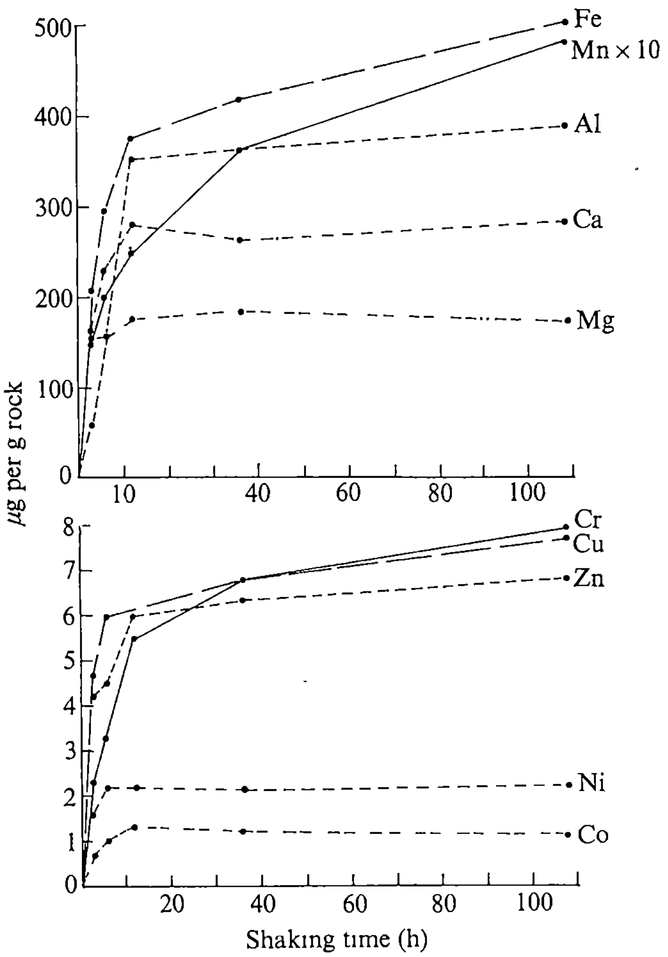

Incongruent dissolution is probably also related to the relative affinity of the cations for the ligands of the humic acid. Though the relative stabilities of metal–fulvic acid complexes have been studied extensively, only fragmentary data are available on metals–humic acids complexes. Courpron[11] has given stability constants of log $K = 7.00$ and log $K = 2.87$ for complexes of soil-derived humic acid with Cu and Zn, respectively. The following order of complex stability at pH 7 for soil humic acids and metals has been established by Verloo and Cottenie[12]: Zn > Cu > Pb > Fe > Mn. If the coagulation capacity of metals for humic acid is an indicator of their affinity for humic acid, the following series obtains[4]: Al > Fe > Cu > Co > Ni. The effectiveness of added metals in coagulating humic acids derived from soils follows the order[10]: Al > Fe > Cu > Zn > Ni > Co; and a similar sequence obtains in the order of magnitude of the pH drop of humic acids on addition of metallic cations. The relatively strong extraction of Cu and, to a lesser degree, of Zn from the basalt may therefore be explained by the strong affinity of those metals for humic acid.

Fe and Al were less extracted than may have been anticipated from their relative affinities for humic acid; it is very likely that the nature of the solid phase also influences the rate of dissolution. Complexes which may be theoretically possible on the basis of strictly chemical considerations may in fact not form because of geometric hindrance or bond strength[5]. Thus, in strongly complexing organic acids, the dissolution of Al progresses differently in labradorite and augite: in labradorite Al is retained, whereas in augite it is removed, though less readily than other cations[7].

Differences in the degrees of decomposition of minerals by organic acids have been explained by Ginzburg *et al.*[6] as consequent upon different relative stabilities. The relatively low extraction of iron is probably related to the relatively high Gibbs energies of formation of magnetite and ilmenite (two important host minerals of Fe in basalt) compared with the much lower formation energies of the alumosilicates, olivine, pyroxene, in which most of the transition metals are contained.

A. SINGER
J. NAVROT

Department of Soil and Water Science,
Faculty of Agriculture,
Hebrew University of Jerusalem,
Rehovot, Israel

Received March 31, accepted June 26, 1976.

[1] Krauskopf, K. B., *Introduction to Geochemistry* (McGraw-Hill, New York, 1967)
[2] Schallinger, K., thesis, Hebrew Univ., Jerusalem (1971)
[3] Rashid, M. A., *Soil Sci.*, 111, 298–306 (1971)
[4] Rashid, M. A., and Leonard, J. D., *Chem. Geol.*, 11, 89–97 (1973)

[5] Schalscha, E B, Appelt, H, and Schatz, A, *Geochim cosmochim. Acta*, **31**, 587–596 (1967)
[6] Ginzburg, I I, Yashina, R S, Matveeva, L. A, Belyatskii, V. V, and Nuzhdelovskaya, T S, in *Chemistry of the Earth's Crust* (edit by Vinogradov, A. P.), 304–320 (Israel Program for Scientific Translation, Jerusalem, 1966)
[7] Huang, W. H, and Keller, W D, *Am. Miner*, **55**, 2076–2094 (1970).
[8] Ponomareva, V. V., and Ragim-Zade, A I, *Pochvovedeniye*, **3**, 26–36 (1969); English translation in *Sov Soil Sci*, **00**, 157–166 (1969).
[9] Baker, W. E., *Geochim cosmochim. Acta*, **37**, 269–281 (1973)
[10] Khan, S. V., *Proc Am Soil Sci Soc*, **33**, 851–854 (1969).
[11] Courpron, C., *Annls agron.*, **18**, 623–638 (1967)
[12] Verloo, M., and Cottenie, A, *Pedologie*, **22**, 174–184 (1972).

Climatic information from $^{18}O/^{16}O$ ratios of cellulose in tree rings

THE high precision of dendrochronology makes possible the construction of short (~ 9,000 yr), detailed records of past climates. This paper explores the possibility of using the oxygen isotopic composition of cellulose from tree rings as a 'thermometer' to measure past temperatures. Using meteorological data from Edmonton we have shown that temperatures can be measured with a precision of ~ ±0.15 °C when averaged over a 5-yr period.

To investigate the variation of the ^{18}O-content of cellulose with temperature, we have studied a white spruce (*Picea glauca*) which grew in Edmonton, Alberta from 1882 to 1969. Detailed climate records for this location have been kept since 1880. Samples were taken from a 5-cm thick transverse section of the trunk cut ~ 1.5 m above ground. A 1-cm wide slice was cut from the section, divided into 5-yr groups of rings and the α-cellulose from each group extracted by standard chemical procedures[1]. After washing and drying in a vacuum oven (50 °C for 5 d), the cellulose was burnt in an evacuated nickel reaction vessel at 1,100 °C for 60 min. The water–gas reaction occurs producing a mixture of CO, CO_2 and H_2 The hydrogen produced diffuses through the walls of the reaction vessel forcing the reaction to completion. (This technique was developed at the California Institute of Technology by P.T and S. Epstein). The CO was converted to CO_2 and C in a high voltage discharge produced between platinum electrodes. Yields of CO_2 were normally 98–100% of the theoretical predictions. All samples were run as consecutive replicates and no significant memory effects were observed.

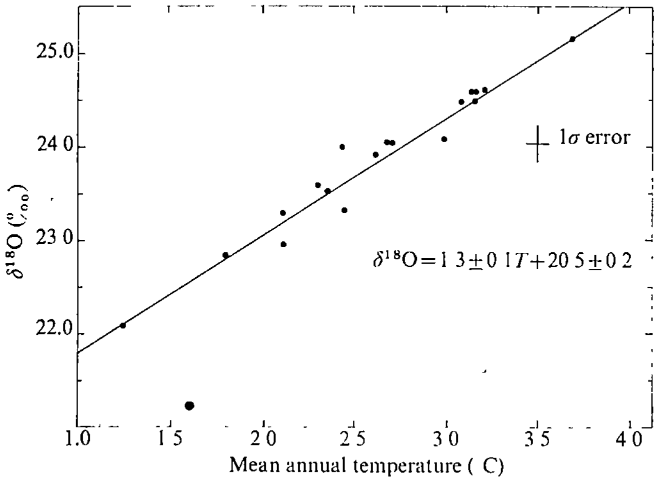

Fig. 1 The variation of $\delta^{18}O$ (SMOW) with September to August mean annual temperature for 5-yr periods. The equation of the line was obtained by a least-squares fit to the data points.

The isotopic composition of the CO_2 was measured using a 12" radius, double collecting isotope ratio mass spectrometer. Results are expressed as a δ value $^0/_{00}$ with respect to standard mean ocean water (SMOW)[2] ($\delta^{18}O_x = [(^{18}O/^{16}O)_x/(^{18}O/^{16}O)_{SMOW} - 1] \times 1{,}000\ ^0/_{00}$). The precision of the replicate analyses was generally better than ±0.20 $^0/_{00}$.

The results show a good correlation between the $^{18}O/^{16}O$ ratio and mean annual temperature calculated on the assumption that growth in any given year stops in September (Figs 1 and 2).

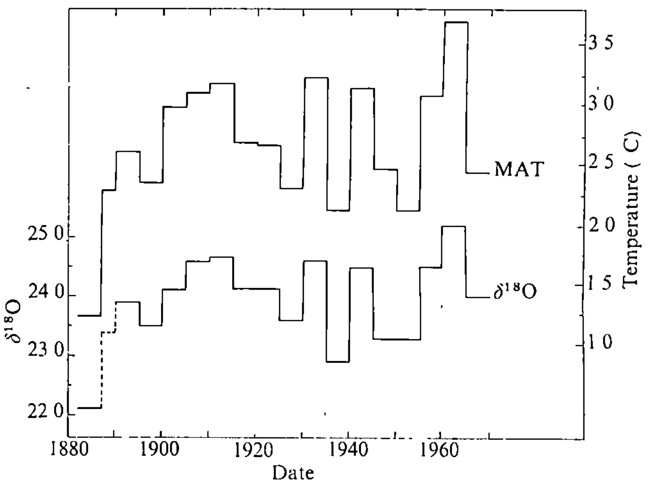

Fig. 2 A comparison between the mean annual temperature (MAT) curve obtained from the meteorological data and that obtained from $^{18}O/^{16}O$ ratios of cellulose. (The broken part of the isotope curve is calculated for some out-of-sequence rings that were not analysed.)

The $\delta^{18}O$ values range from 22.1 $^0/_{00}$ (1.23 °C) to 25.2 $^0/_{00}$ (3.64 °C). The temperature coefficient is 1.3 ± 0 1 $^0/_{00}$ per °C in reasonable agreement with the value of 2.2 ± 1.0 $^0/_{00}$ per °C obtained for algae[3]. The precision of the $^{18}O/^{16}O$ measurements corresponds to an uncertainty of ±0.15 °C in mean annual temperature.

The choice of growing period over which the temperatures are averaged is somewhat arbitrary but the September to August and January to December 5-yr means differ on average by only 0.1 °C. Table 1 shows the correlation between $\delta^{18}O$ and mean temperatures calculated for different growth periods. It is apparent that the best correlation occurs with mean annual temperatures for September to August. The correlation with mean summer temperatures is poor.

There are two possible explanations for this. First, in addition to the temperature effect on the fractionation factor, there is also variation in the isotopic composition of the source water being used to produce cellulose. This is also climate dependent[4]. Ruben[5] has shown that oxygen transpired during photosynthesis is derived only from water. It thus seems fair to assume that the cellulose oxygen is derived from CO_2. It is possible, however, that isotope exchange can occur between CO_2 and H_2O before photosynthesis occurs so that the isotopic composition of the CO_2 will reflect that of the source water ($\alpha_{CO_2-H_2O} = 1.0407$ at 25 °C (ref. 6)). Thus it is possible that winter precipitation stored as soil water after melting may have a significant role in the production of cellulose during the growing season. The results shown here suggest that the contribution from variation in source water is relatively small, however, since the temperature dependence of the fractionation factor is approximately four times as large as the observed variation in the Edmonton area (0.3$^0/_{00}$ per °C, calculated from data in the International Atomic Energy–World Meteorological

Table 1 Correlation between $\delta^{18}O$ and mean temperatures calculated for different growth periods

Temperature (5-yr mean)	Correlation coefficient $\delta^{18}O$ against temperature
Mean summer (May, June, July, August)	0.24
Mean winter (1) (January, February, March)	0.82
Mean winter (2) (December, January, February, March)	0.86
Mean annual (1) (January–December)	0.94
Mean annual (2) (September of previous year to August of final year)	0.97

Organization survey 1969, 1970, 1971 (ref. 7)). Second, it has been shown that net photosynthesis and growth in coniferous trees depends markedly on the production of stored foods (sugars from photosynthesis) during the winter[8], so that winter temperatures may have a direct bearing on the isotopic composition of the cellulose produced the following year.

It is apparent that much work remains to be done to understand fully the isotopic processes involved in the production of cellulose. The empirical results presented here, however, show that the temperature dependence of the isotopic fractionation can be measured and that the climate record in the cellulose is not destroyed by subsequent exchange over a period of up to 90 yr. Measurements of D/H ratios of cellulose are under way in this laboratory to provide an independent cross check with the oxygen data.

We thank the meteorological office of Edmonton for providing temperature records and Dr K. D. Hage for help with the acquisition of tree samples. We would also like to acknowledge the assistance of Professor S. Epstein in the early stages of the project. We thank the NRC of Canada for support.

JOHN GRAY
PETER THOMPSON

Department of Physics,
University of Alberta,
Edmonton, Alberta T6G 2E1,
Canada

Received April 12, accepted June 9, 1976.

[1] Green, J. W., in *Methods in Carbohydrate Chemistry*, 3 (edit by Whistler, R L.) (Academic, London, 1963)
[2] Craig, H., *Science*, 133, 1833–1834 (1961).
[3] Libby, L. M., and Pandolfi, L. J., *Coll. int. CNRS*, 219, 295–298 (1973).
[4] Dansgaard, W., *Tellus*, 16, 436–468 (1964).
[5] Ruben, S., Randall, M., Kamen, M., and Hyde, J L., *J. Am chem Soc.*, 63, 877–879 (1941).
[6] O'Neil, J R, and Epstein, S, *J geophys Res.*, 71, 4955–4961 (1966)
[7] International Atomic Energy Agency· *Environmental Isotope Data No 1*, Tech. Rep Series 96, IAEA, Vienna (1969); *Environmental Isotope Data No. 2*, Tech Rep. Series 117, IAEA, Vienna (1970); *Environmental Isotope Data No. 3*, Tech. Rep Series 129, IAEA, Vienna (1971).
[8] Fritts, H. C., *Scient Am*, 227, 92–100 (1972).

Geometry of river meanders

THERE are many factors affecting the geometry of rivers. Width, depth, slope, flow velocity and plan shape are all influenced by discharge, sediment load, sediment types, and valley slope through the operation of the continuity, flow resistance, bed load, bank competence and meander equations. If each of these equations could be determined accurately then their simultaneous solution would define the three-dimensional geometry of alluvial channels[1,2]. Although the equations cannot be specified accurately the basic mechanical principles underlying most of the relevant processes are understood. The one exception is the process responsible for plan geometry. Indeed, many theories have been presented to explain the development and maintenance of these patterns, with varying degrees of success. I show here that meander arc length may be a unique function of channel width.

Yalin[3] has proposed that the occurrence of meanders could be attributed to the law governing the spatial correlation among perturbations in turbulent flow. He demonstrated that the behaviour of the largest macroturbulent eddies would be systematically affected by a permanent discontinuity, and that this would result in the same and reverse kind of disturbance occurring alternately at equal length intervals along the direction of flow. On the basis of his theoretical analysis the wavelength of meanders, λ, in fully developed turbulent flow was related to the width of the channel, w, through

$$\lambda = 2\pi w$$

If turbulence were not fully developed, he has argued, the wavelength would be dependent on the Reynolds number and the relative roughness of the section. For width/median bed material grain size values greater or equal to a thousand, he has argued that

$$\lambda = 20w$$

Leopold and Wolman's[4] field data plot within these limits, which seems to substantiate Yalin's hypothesis. But as turbulent flow is normally fully developed at bankfull stage—the channel-forming discharge—the coefficient in Leopold and Wolman's best-fit relationship of

$$\lambda = 10.9w^{1.01} \text{ feet}$$

seems rather high.

This discrepancy between theory and practice could be explained by the fact that the repeating distance between discontinuities should be measured along the channel and not as a straight line distance. To check this hypothesis I have compared data from the rivers Wye and Tweed with Leopold and Wolman's data.

First, their equations linking wavelength with channel width and radius of curvature, r, were solved to obtain the relationship between radius of curvature and width

$$r = 2.37w^{1.03} \text{ feet}$$

As the exponent of this equation was not significantly different from unity, a linear relationship was assumed and the slope adjusted accordingly

$$r = 2.40w \text{ feet or m}$$

Most of the data for the Wye and Tweed plot above this line (Fig. 1) immediately indicating that Leopold and Wolman's curve is not a general one. This scatter was rationalised when information on meander arc angle, θ, measured between inflexion points was included. Leopold and Wolman's curve seems to relate to well developed meanders (150°) because points further above the line have progressively smaller arc angles. On the assumption that the arc angle for their curve is 150°, the relationship between arc length, z, measured between inflexion points, and channel width can be obtained

$$\begin{aligned} z &= 6.28w \text{ m} \\ &= 2\pi w \end{aligned}$$

If this is a general relationship for all channels it would explain the plotting positions of the Wye and Tweed data on the graph of radius of curvature against channel width. Substituting z for w allows a family of curves to be constructed for different arc angles (Fig. 1). Field data corroborate this substitution,

Table 1 Relationships between wavelength, radius of curvature and bankfull channel width for various arc angles*

Arc angle ($\theta°$)	Value of k in $r = kw$	Value of m in $\lambda = mr$	Value of n in $\lambda = nw$
270	1.33	2.83	3.77
225	1.60	3.70	5.91
180	2.00	4.00	8.00
150	2.40	3.86	9.27
135	2.67	3.70	9.85
120	3.00	3.46	10.39
90	4.00	2.83	11.31
60	6.00	2.00	12.00
45	8.00	1.53	12.25
30	12.00	1.04	12.42
15	24.00	0.52	12.53
10	36.00	0.35	12.55
5	72.00	0.17	12.56
1	360.00	0.04	12.57

*$k = 360/\theta$; $m = 4\sin(\theta/2)$; $n = (1{,}440/\theta)\sin(\theta/2)$.

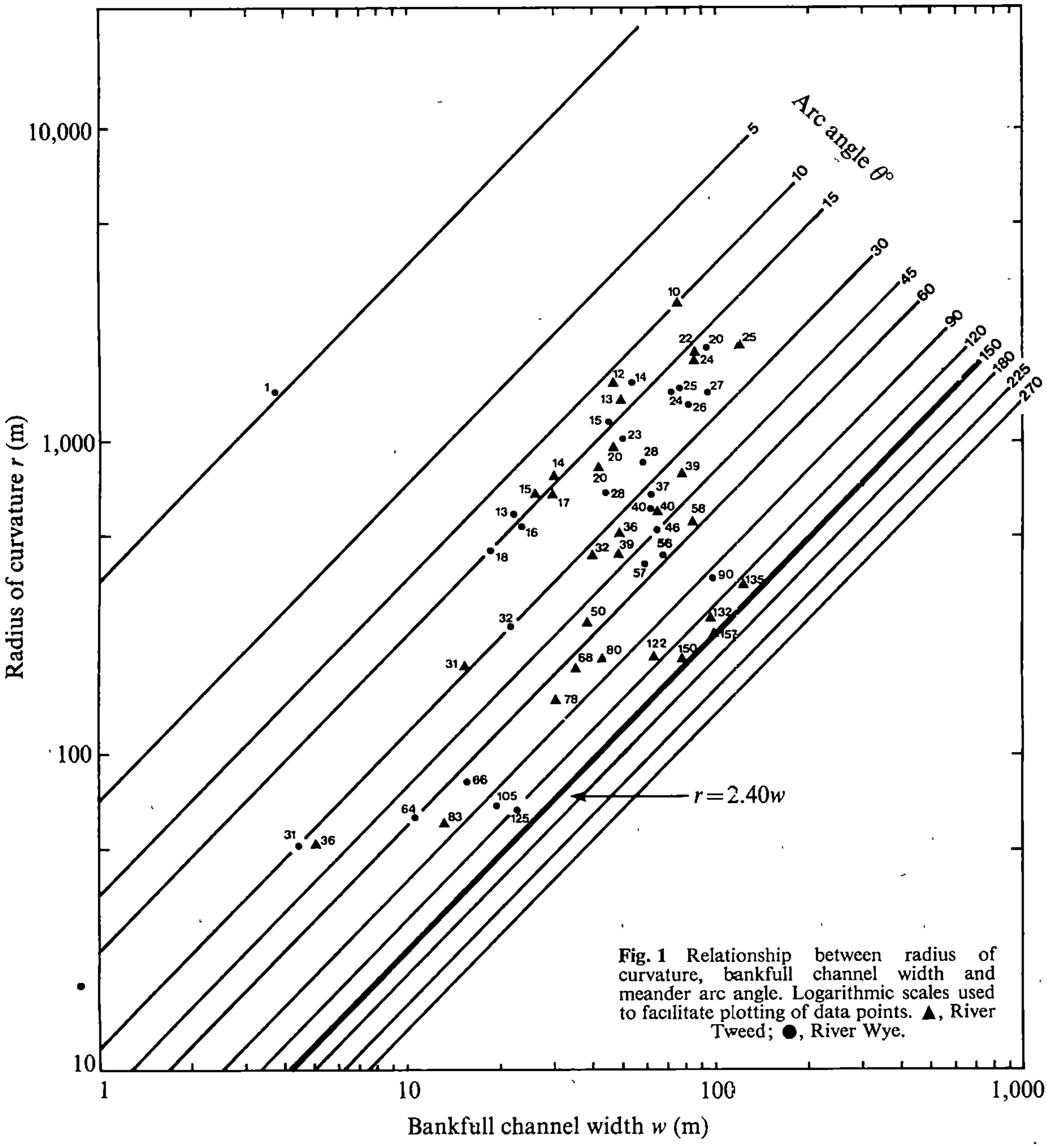

Fig. 1 Relationship between radius of curvature, bankfull channel width and meander arc angle. Logarithmic scales used to facilitate plotting of data points. ▲, River Tweed; ●, River Wye.

so the relationship between meander arc length and channel width seems to be general. Other research workers have noted that the spacing of riffles in straight and meandering channels is between five and seven channel widths[5] and that skew shoals in flumes have been found to be 6.5 channel widths apart[6].

This analysis indicates that the repeating distance measured down channel is $4\pi w$ which contrasts with Yalin's value for wavelength of $2\pi w$. Given that it would be more appropriate to use channel distance rather than plan distance in the calculation of repeating length, Yalin's model underestimates the repeating length by a factor of two.

How can this be explained? Closer inspection of Yalin's model indicates that he calculated repeating lengths by assuming that the largest macroturbulent eddy was equivalent to the width of the channel. Physically, this eddy must be interpreted as a helicoidal flow cell, and, as it systematically changes polarity, it influences the local pattern of accelerations and retardations. Approaching a pool (meander apex) the strength of the secondary circulation increases to a maximum with surface flows directed towards the eroding bank. Immediately downstream the polarity of the cell is reversed and the process repeated (Fig. 2*a*).

This pattern of secondary flows is probably incorrect, however. At high flow stages two cells, exhibiting surface flow convergences, have been identified at the pool (meander apex); whereas at the riffle (inflexion point) two cells, with surface flow divergence, have been observed[7] (Fig. 2*b*). On the assumption that the average size of this macroturbulent eddy is half the channel width, recalculation gives a repeating length of $4\pi w$.

As theory and practice indicate a general relationship between meander arc length and channel width it is possible to define the relationships between wavelength, radius of curvature and channel width for different arc angles (Table 1). This explains why empirical equations are specific to a given set of data unless meander arc angle is invariant.

Although this model helps to explain the regularity of channel patterns it does not successfully explain the initiation of meanders. A local increase in bank roughness is required to produce the asymmetry of flow but it does not explain how this can be achieved in homogeneous material. This approach merits further research however, particularly on the generation and effect of secondary flows on natural channels.

Even though it is not possible at present to explain meander mechanism, it is necessary to define the plan geometry of river channels for design purposes. Sinuosity, defined as the ratio of channel length to valley length or valley slope to channel slope, is probably the best measure because it is related to

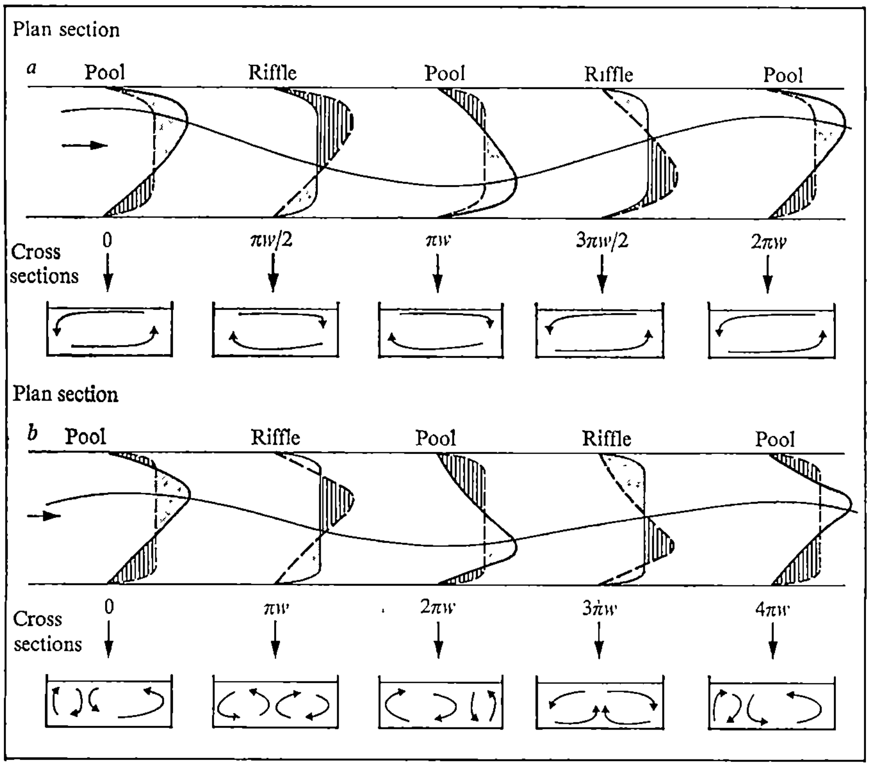

Fig. 2 Size of macroturbulent eddies in natural channels. *a*, Single secondary cell (after Yalin[3]); *b*, twin secondary cells (after Hey and Thorne[7]); —, surface velocity profile at section; - - - surface velocity profile at neighbouring upstream section; stippling, accelerated surface flow; vertical lines, retarded surface flow.

meander processes. Any change in channel slope, through erosion or deposition, to a value defined by the bed load transport equation will result in a new plan form because valley slope can be considered invariant for channel design purposes. Unfortunately, for a given value of sinuosity an almost infinite number of patterns are possible (Fig. 3). If the meander geometry is to be specified accurately then it will be necessary to determine the size of each meander arc. As arc length is a unique function of channel width, which in turn is defined by the bank competence equations, a determinate solution is possible.

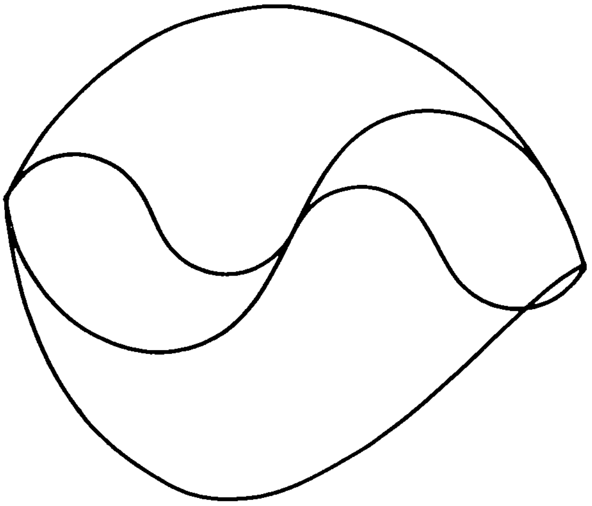

Fig. 3 Multivalued plan geometry for a given sinuosity (1.5 in case illustrated).

R. D. HEY

School of Environmental Sciences,
University of East Anglia,
Norwich NR4 7TJ, UK

Received April 20, accepted June 14, 1976.

[1] Kennedy, J. F., *et al.*, *Proc. Am Soc civ Engrs*, 97, 101–141 (1971)
[2] Hey, R D , *UK geol. Soc. Misc. Pap* 3, 42–56 (1974)
[3] Yalin, M. S , *Mechanics of Sediment Transport* (Pergamon, Oxford, 1972).
[4] Leopold, L. B , and Wolman, M. G., *Bull geol Soc Am.*, 71, 769–793 (1960).
[5] Leopold, L. B., Wolman, M G and Miller, J. P , *Fluvial Processes in Geomorphology* (Freeman, London, 1964)
[6] Shen, H. W , and Komura, S., *Proc. Am.Soc. civ. Engrs*, 94, 997–1015 (1968)
[7] Hey, R D., and Thorne, C. R., *Area*, 7, 191–195 (1975).

New hominid from Lake Ndutu, Tanzania

THIS report describes the stratigraphical and archaeological position of an hominid skull discovered in Pleistocene deposits around Lake Ndutu, on the Serengeti Plains (3°00′S; 35°00′E). The skull itself is described elsewhere[1]. Lake Ndutu, together with the adjacent Lake Masek, is geomorphologically a continuation of the Olduvai Pleistocene deposits. The names of both lakes have been used to designate the upper parts of the Olduvai Sequence—the Ndutu and Masek Beds (formerly bed V and bed IVB, respectively); both are soda lakes.

Lake Ndutu is the smaller of the two (Lake Masek had enough water during the dry season of 1974—September–November—to support a resident population of hippopotami), and shows very marked fluctuations in water level between the wet and dry seasons. During the wet season the whole lake shore is under water, whereas during the dry season the water recedes mostly southwards and eastwards to expose the larger part of the western and northern shores of the lake The exposed western flats are littered with lithic and faunal materials

The site was first visited during September 1972, when a one-week preliminary survey was undertaken. This work included random surface collections in seven areas, each 2 m in radius, and the excavation of 2 m×2 m trial trench with the objective of elucidating the stratigraphy of the site. During September and October 1973, the Tanzanian Department of Antiquities undertook the initial excavation of the site. These excavations, apart from exposing occupational floors with *in situ* lithic and faunal materials, also exposed a hominid skull[1].

The Ndutu deposits comprise a claystone member which can be subdivided into a greenish sandy clay unit, 15–45 cm thick, underlain by about 60 cm of sand-free, green clay with chert nodules in the lowest levels (R. Hay, California

Univ., Berkeley, private communication). The sandy clay unit can be further subdivided into sandy clay and silty clay subunits. To the north, along the shore, a hard, reworked tuff, 10–12 cm thick, overlies the claystone. The occupational floor containing the skull rested on the silty clay subunit, and below it, resting on sand-free, green clay, were *in situ* lithic and faunal materials of what has been tentatively designated the second occupational floor.

The surface of the western margin flats are littered with lithic and faunal material but one problem concerns its provenance Although the water level fluctuates at present it is not at all clear whether a similar situation obtained during the period when early man used either the lake or its vicinity as camping and hunting grounds. Did early man camp at the site seasonally during lacustrine recessions, or did he camp in the area when the lake was either nonexistent or had dried up during such climatic oscillations as are known to have occurred elsewhere in the Pleistocene epoch? Or has the lithic and faunal material been brought into the area from elsewhere?

During the excavations it was found that there is a noticeable discomformity between the sand-free, green clay unit, and the overlying greenish, sandy-clay unit. Several small channels were cut into the green clay, in some cases to a depth of approximately 30 cm. Lithic and faunal materials were found at the bottom of the channels. It is, therefore, possible that early man camped or hunted at the lake shore when there was a minor climatic change which either resulted in the lake temporarily drying up or the level of the lake receding. This hypothesis is supported by the fact that it is only the sandy clay unit which is fossiliferous and contains implements Although some of the artefacts are rolled it is nonetheless possible that both the lithic and faunal materials are archaeologically *in situ*; the rolling could be a consequence of the constant seasonal movements of lake currents.

During September and October 1973, an area of approximately 140 m² was excavated. The excavated deposits were situated in an area containing considerable amounts of surface lithic and faunal material. An area of approximately 80 m² included a high density of *in situ* lithic and faunal materials. It was in this area that the first and second occupational floors were exposed.

The *in situ* lithic materials are characterised by a very low percentage of finished tools. In the first floor, among the 270 plotted lithic and faunal materials only 20 are definitive tools (about 7.7%) Among the tools, spheroids and hammerstones predominate. There are six flakes in all, three of which are regular—two triangular and one rectangular. The remaining three are irregular. The cores are amorphous. Quartz and quartzite are the predominant raw material. The loose finds from within the sandy clay subunit overlying the first floor confirms this analysis They include five cores, four regular flakes (one with retouched edges), three irregular flakes, one core scraper, two quartz pebbles probably used as hammerstones, and twenty-two waste flakes.

The tools represented in this collection are rather nondescript and of an indeterminate industry. Although hand axes and cleavers occur in the surface material, they are few, and even among the surface collections spheroids seem to be the predominant tool type, with cores also well represented The absence of hand axes and cleavers among the *in situ* artefacts raises the question of the type of industry represented. The type of hominid represented by the skull is generally thought to be associated with the Acheulean industrial complex. The tentative date of the site as well as the mineralogical contents of the deposits also place the site within the chronological boundaries of the Acheulean industrial complex in the Olduvai Gorge and other sites in Tanzania and eastern Africa Two possible hypotheses can be used to explain the absence of the tool types widely found in the Acheulean industrial complex. Either the assemblage belongs to a different cultural and technological continuum and belongs to an industry post-dating, or contemporaneous with, later phases of the Acheulean industrial complex, or it belongs to the Acheulean, and the area excavated is only an indication of activity patterning. The latter hypothesis seems to be the most likely, and is supported by the fact that hand axes and cleavers, though few, are represented in the surface materials; moreover, excavation of a small trench on the site revealed an *in situ* hand axe (M. D. Leakey and R. Hay, private communication). The presence of a very high percentage of faunal materials in the collection—about 94 out of the 270 plotted *in situ* materials of the first floor are splinters and sizeable bone pieces including horns and antlers—seems to suggest that the area was probably a butchering site, though the presence of a hominid skull among the collection in such a context would be rather enigmatic.

The tuff overlying the claystone probably represents the Norkilili Member of the Masek Beds of Olduvai, though the possibility that it represents the lower unit of the Ndutu Beds cannot be ruled out (R. Hay, private communication). One preliminary chronometric date has been obtained from bone found in the first occupational floor, and preliminary racemisation measurements suggest a general age of ~500,000–600,000 yr (J. L. Bada, private communication). A sample of bone from the Masek Beds of Olduvai has given similar results.

I thank Mr F. T. Masao, the Curator of the National Museum, who participated in the 1972 preliminary survey, and the staff of the Department of Antiquities, who assisted in the excavations. I also thank M. D. Leakey for help, advice and encouragement.

A. A. MTURI

Director of Antiquities,
Antiquities Division,
PO Box 2280,
Dar es Salaam,
Tanzania

Received April 13; accepted June 14, 1976.

[1] Clark, R J., *Nature*, 262, 485–487 (1976).

New cranium of *Homo erectus* from Lake Ndutu, Tanzania

I DESCRIBE here the humanoid cranium recovered by Mturi[1] during excavations at Lake Ndutu in northern Tanzania. A fuller description will be published elsewhere.

The cranium is remarkable in that it seems to form an evolutionary link between *Homo erectus pekinensis* and *Homo sapiens*, having features in common with both. It cannot, however, be classified as *Homo sapiens*, and in spite of its strong resemblance to *H.e. pekinensis* its more advanced characteristics and its occurrence in Africa rather than Asia may eventually warrant the creation of a new subspecies of *H erectus* to accommodate it. This will be determined following full comparative studies.

The specimen is similar to *H.e. pekinensis* in the following features·

- The form and contour of the occipital, which has a markedly thickened nuchal torus.
- The form of the mastoid region.
- The almost vertical forehead.
- The inferred supraorbital torus.
- The great thickness of the vault.
- The outline, as seen in norma verticalis.

The cranium differs from *H.e. pekinensis* and is similar to *H. sapiens* in the following features:

SCIENCE COLLEGE

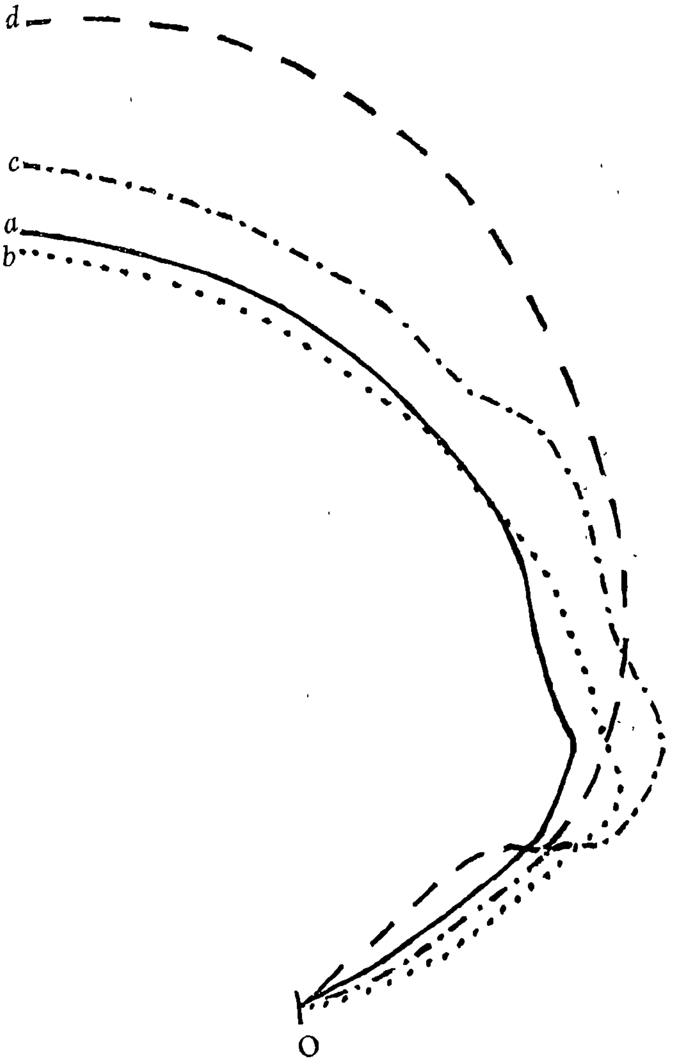

Fig. 1 Mid-sagittal craniograms of the occipital region: *a*, Ndutu cranium; *b*, *H.e. pekinensis* (Skull III from locus L); *c*, Ngandong (Solo), Skull V; *d*, Australian aborigine; O, opisthion. Adapted from Weidenreich[2].

- The presence in the adult of pronounced parietal bosses.
- The more vertical sides of the vault as viewed in norma occipitalis.
- The presence of an ossified styloid process.
- The apparent absence of a sagittal torus.
- The supramastoid crest does not extend over the external acoustic meatus.

The Ndutu cranium is housed at the National Museum of Tanzania in Dar es Salaam. The specimen includes the virtually complete occipital and left temporal; the right temporal lacks the glenoid fossa, parts of both parietals and part of the right side of the frontal, parts of the sphenoid, and the fragmentary central region of the face which is attached to a fragment of the left maxilla. In addition, there are isolated right tympanic plates and both isolated petrous temporals.

Before reconstruction the parts of the cranium were very much broken and separated, but were retained in their approximate anatomical position by a matrix of sand and clay which was impregnated with a hardener (Bedacryl) before the cranium was removed from the site. Much of the parietals had suffered badly from cracking and fragmentation, and also from a displacement of inner and outer tables. In parts the inner table only was present and in others only the outer table in the form of a thin shell with the diploë missing. In other places the inner and outer tables had been pushed apart from the diploë, and the spaces between were filled by the sandy matrix, thus giving an artificial, exaggerated thickness to the vault.

The occipital is nearly complete, lacking only the left occipital condyle and some small areas near the foramen magnum. The foramen magnum measures 37.5 mm in anteroposterior length and 28.7 mm in breadth. The apex of the occipital is represented by a sutural bone. There is also a sutural bone to the right of this along the lambdoid suture. On each side there are two small sutural bones at asterion, but one of those on the right had fallen out and was not recovered during the excavation.

There is a well developed nuchal torus as in *H.e. pekinensis*, giving the bone a markedly angulated lateral contour (Fig. 1). The bone is fairly thick, particularly at asterion.

The left of the temporals is the more complete. Its mastoid process is small and of a triangular horizontal cross section. The posterior part of the mastoid is flattened and lies in the nuchal plane. The mastoid is thus similar to that of *H.e. pekinensis*, and is particularly similar to that of Olduvai hominids 9 and 12. There is a well defined mastoid notch which is divided along its length by a central ridge.

An ossified styloid process is present and can be seen particularly well under cover of the isolated right tympanic plate.

The lower margin of the external acoustic meatus preserved on the left is thick and elongated in a downward direction.

A supramastoid crest can be seen, but it does not extend over the external acoustic meatus as in *H.e. pekinensis*.

The left glenoid fossa is deep, relatively small and short anteroposteriorly. The articular tubercle lacks its lateral margin.

The bone at asterion is very thick as is the case in *H. erectus pekinensis*.

The right parietal is missing large areas around its centre and anteromedially, but it has contact laterally at the coronal suture with a frontal fragment. The conformation of the bone around the centre of the parietal indicates that it had a pronounced parietal boss. The parietal thickness at a point anterior to the boss is 11.5 mm. This is well within the upper range of parietal thickness given by Weidenreich[2] for *H.e. pekinensis*, and much thicker than the range he quotes for *H. sapiens*.

The left parietal is represented mainly by the posteromedial portion externally and the posterolateral portion internally. The anterior part is missing but an anterolateral fragment adjoins the squamous part of the temporal. The left parietal is in articulation with the occipital and left temporal at asterion.

The temporal line is seen only very faintly on the right parietal and, from the contour of the surface of the parietals near the sagittal suture, there was apparently no sagittal torus, such as occurs in *H.e. pekinensis*.

The preserved right frontal fragment is 8.6 mm thick and thus well within the range of 7.0–13 mm given by Weidenreich[2] for *H.e. pekinensis*, and is at the same time greater than the maximum of 6.3 mm he quotes for *H. sapiens*.

The anterolateral corner of this frontal fragment curves forward and outward, indicating that there must have been a supra orbital torus in order for that fragment to meet with the glabellar fragment attached to the face. The glabella together with the face, could not be placed further back because it is restricted by other anatomical features such as the cribriform plate of the ethmoid bone, and by the necessity for room for the anterior fibres of the temporalis muscle. In reconstruction, allowance was made for only the smallest supraorbital torus permitted by the preserved anatomy, but it is possible that a larger torus could have been present.

The frontal bone rises in a high curve of the forehead as in *H.e. pekinensis* but unlike the frontals of *H. erectus erectus*, the Ngandong crania or the Broken Hill cranium.

The middle portion of the face is preserved, including much of the nasal aperture, the upper part of the left nasal bone, the lower medial parts of the orbital rims together with the lacrimal grooves, and much of the superior part of the right orbital plate. The crista galli is present and is attached to the cribriform plate behind the nasal bones.

On the right, the medial part of the face is preserved as far down as the infraorbital foramen, and on the left there is continuous bone contact from the nasal bone to the palate. The

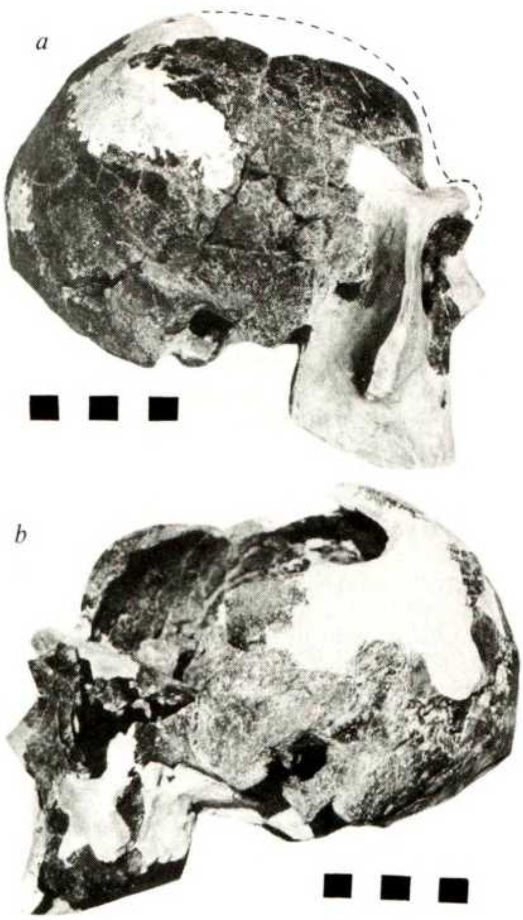

Fig. 2 *a*, Right norma lateralis of the Ndutu cranium; *b*, left norma lateralis of the Ndutu cranium.

conformation of the bone around the nasal aperture, and the angle between the nasal bones indicate that the nose was very prominent.

The left portion of the palate contains fragments of the roots of the canine, P^3, P^4 and M^1 and the mesiobuccal socket of M^2. This palatal fragment reaches almost to the midline of the cranium.

Areas of the cranium were reconstructed with plaster of paris both to strengthen the parietal region, where either inner or outer tables only were preserved, and to attach the face to the rest of the cranium. This reconstruction was minimal and preliminary. The reconstruction suggests that slight adjustments can be made to the position of the face, but this will not affect the conclusion that a supraorbital torus must have been present originally. The size and shape of the maxilla remain unknown as it is extremely fragmentary. The top of the cranium has been left open in order that the internal anatomy can be seen.

The cranium (Fig. 2) has some similarities to Olduvai hominid 12 in the thickness of the vault and the shape of the mastoid, but it is much larger. It differs from the Ngandong and Omo II crania in its outline as seen in norma verticalis. The former have a more rectangular outline whereas the Ndutu cranium and *H.e. pekinensis* have a pear-shaped outline. It differs from Ngandong and Omo II also in possessing a more vertical forehead, though it is similar to Ngandong in the morphology of the temporal. The mastoid of the Ndutu cranium differs from that of Omo II. It differs from the Broken Hill cranium in its temporal and frontal and in being much smaller. It differs from Swanscombe and Steinheim in its occipital curvature and in that the mastoid of Steinheim is sapient in form. It differs also from Skhul V in its occipital and mastoid. It bears little comparison with *H.e. erectus* except in vault thickness and in its outline seen in norma verticalis. The mastoid region is similar to that of Olduvai hominid 9, but otherwise, apart from thickness of the vault, there is little resemblance.

It would have been of interest to compare the Ndutu cranium with that of the Eyassi I cranium[3] but unfortunately the original disappeared in Berlin in 1945 according to Weinert[3], and available casts are too poor to allow comparison. Published descriptions and photographs are also not of any great help because the cranium was reconstructed from fragments, and it is difficult to ascertain what is reliable. In spite of all of these deficiencies, the Eyassi cranium does seem to have been rather similar to the Ndutu cranium. It was found not far away from Lake Ndutu in a similar deposit on the shore of the saline Lake Eyassi. It had also undergone separation of inner and outer tables of the vault bones, probably as a result of alternating crystallisation and solution of the salt within the diploë. A few broken handaxes and an early water-rolled fauna also occurred at the site, but Leakey[4,5] considered the cranium to be contemporary with an unrolled modern type of fauna, and with levalloisian artefacts that were also to be found on the surface. The possibility should not, however, be dismissed that the Eyassi cranium could have been contemporary with the hand axes and the rolled fauna. This is supported by the fact that, although Leakey[4] has described the skull as unrolled, Weinert[3] has claimed that the edges broken in antiquity were rounded and rarely fitted together.

The Eyassi II occipital fragment, which is preserved in the National Museum in Dar es Salaam has some similarity to that of the Ndutu cranium.

Finally, it is of interest to note that Dr Peter Andrews subjected the Ndutu cranium to a form of multivariate analysis described by Andrews and Williams[6]. He found that the cranium grouped with *H.e. pekinensis*, thus confirming by measurement the conclusion reached through observation.

I thank the Government of Tanzania and their Director of Antiquities, Amini Mturi, for giving me the privilege of cleaning, reconstructing and studying the Ndutu skull. I also thank Richard and Mary Leakey for providing facilities for the work, the L.S.B. Leakey Foundation for financing my study visit to Nairobi, and Professor P. V. Tobias for making the visit possible.

R. J. CLARK

Department of Anatomy,
Medical School,
Johannesburg,
South Africa

Received April 13; accepted June 14, 1976.

[1] Mturi, A. A., *Nature*, **262**, 484–485 (1976).
[2] Weidenreich, F., *Palaeont. sin.*, **127**, 163 (1943).
[3] Weinert, H., *Z. Morph. Anthrop.*, **38**, 252–308 (1940).
[4] Leakey, L. S. B., *Nature*, **138**, 1082–1084 (1936).
[5] Leakey, L. S. B., *Jl E. Africa nat. Hist. Soc.*, **19**, 40 (1946).
[6] Andrews, P., and Williams, D. B., *Am. J. phys. Anthrop.*, **39**, 291–303 (1973).

Antennal receptor response to sex pheromone mimics in the American cockroach

THE essential oils D-bornyl acetate, α- and β-santalol and several plant sesquiterpene hydrocarbons have been shown to induce sexual excitement in male American cockroaches[1], and thus seem to mimic the cockroach sex pheromone. Tahara *et al.*[2] have identified one of the active sesquiterpene hydrocarbon species obtained from Compositae plants as germacrene D. The contrast in structures of these various active compounds poses a serious problem as to the specificity of the sex pheromone receptor. To resolve this we have undertaken an electrophysiological study of the antennal receptors of both male and female cockroaches. The electroantennogram (EAG) responses of both sexes were examined during exposure to the compounds in question. Theoretically the sex specific receptors of the male antennae should respond singularly to natural sex-pheromone (and stereochemical mimics) whereas the female antennae should be unresponsive other than to general irritants and/or to food odours. In fact, the EAG response to the female sex attractant has been obtained in males but not in females[3,4].

EAGs were recorded from excised antennae of the adult American cockroach, *Periplaneta americana*. A tungsten electrode, whose tip has been electrolytically sharpened to about 1 μm with resistance of less than 1 MΩ, was inserted into the distal end of the antennae. The electrode was connected to the input probe of a unity gain d.c. pre-amplifier. A wider stainless steel electrode was placed in the scape of the antenna in a ground position. Germacrene D was isolated from the leaves of *Solidago juncea* Ait. by a combination of column chromatography over Florisil and silver nitrate coated Florisil. The spectral data are as follows: ultraviolet (hexane): 222(ε6590) and 257 nm (ε5020); infrared (film): 3,080, 1,670, 1,635, 1,610, 1,390, 1,375, 1,190, 987, 980 and 890 cm^{-1}; nuclear magnetic resonance (CCl_4): 0.84(3H, d., $J=6$ Hz), 0.90(3H, d., $J=6$ Hz), 1.53(3H, s.), 4.70 and 4.73(2H), 5.19(1H, q., $J=6$ and 10 Hz), and 5.72 p.p.m.(1H, d., $J=15$ Hz). A test chemical dissolved in acetone was completely absorbed on filter paper with the solvent evaporating at room temperature. The filter paper was placed on a vinyl tubing holder, which had been set in a 2-ml syringe. After 2 ml of air had been drawn into the syringe, the syringe plunger was quickly depressed to mix the odour into an airstream. The air taken from the ambient air supply, filtered through glass wool and distilled water, and passed continually at 60 ml min^{-1} through 5-mm diameter glass tubing. As a control the same procedure was carried out without a test compound.

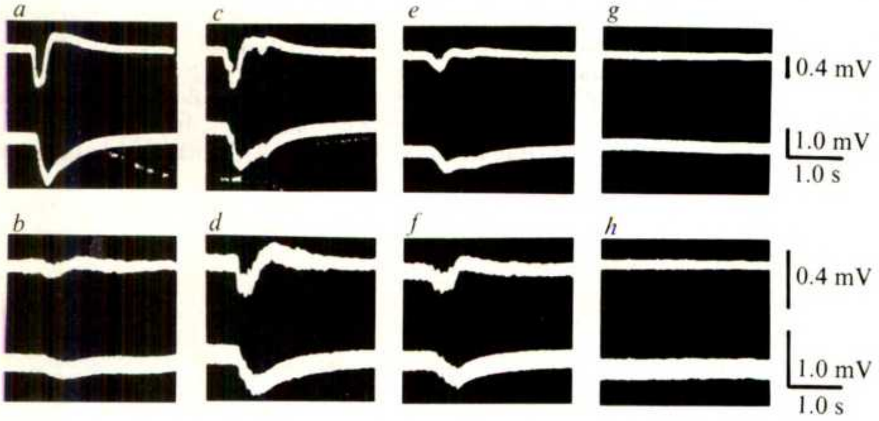

Fig. 1 EAGs recorded from a *Periplaneta americana* adult male (*a*, *c*, *e* and *g*) and female (*b*, *d*, *f* and *h*) in response to germacrene D (0.1 mg in *a* and 3 mg in *b*), D-bornyl acetate (3 mg in *c* and *d*) and L-bornyl acetate (3 mg in *e* and *f*). Controls (air without odour) are shown in *g* and *h*. In each record upper and lower traces show a.c. and d.c. recording, respectively. Note different calibrations in records of male and female antennae.

Adult male antennae showed strong EAG responses to germacrene D (Fig. 1*a*). In the female antennae, however, it caused very small negative potentials, even at much higher concentrations (Fig. 1*b*). The effect of increasing concentration of germacrene D was examined in male antennae. The amplitude of the responses increased in approximate proportion to the logarithm of the intensity of stimulus tested (Fig. 2). The threshold concentration was found to lie between 1 and 5 μg. The response approached a plateau at a concentration of 100 μg or slightly higher. In comparison with EAGs obtained to DL-bornyl acetate[4] the threshold concentration of germacrene D required to elicit the EAG response was much lower, being of the order of one-hundredth. The result of a single experiment to compare the threshold concentration of germacrene D and D-bornyl acetate showed that 5 μg of the former gave a detectable potential change, whereas 50 μg of the latter did not bring about any EAG response. Although strong EAG responses of male and female antennae to DL-bornyl acetate were obtained in agreement with earlier findings[4], we examined the effect of pure D- and L-bornyl acetate in the present work. The male antennal responses to D- and L-bornyl acetate (Fig. 1*c* and *e*) were found to be stronger than those of the female (Fig. 1*d* and *f*). Furthermore, both male and female antennae gave stronger EAG responses to D-bornyl acetate than to L-bornyl acetate. Another essential oil, santalol, was found to give very small EAG responses in both sexes.

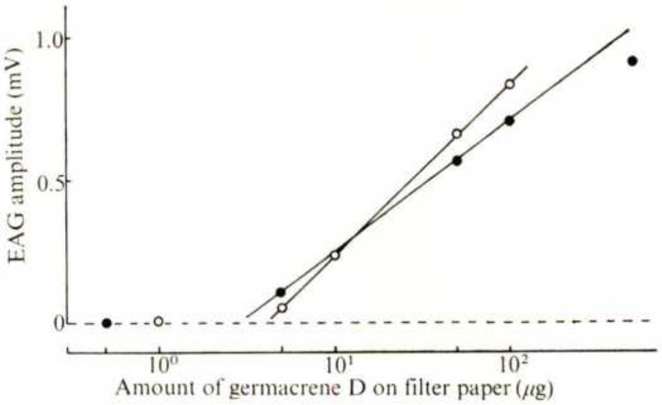

Fig. 2 Amplitude of the EAG responses of two male antennae (○, ●) as a function of the amount of germacrene D (μg) on a logarithmic scale.

It has already been shown that strong EAG responses to the female sex pheromone were obtained from the antennae of male adults but not from females[3,4]. On the other hand, bornyl acetate, which induced significant sexual excitement in the male[1], was found to give strong EAG responses with both male and female antennae. Although adult females show no change in overt behaviour when exposed to bornyl acetate, they show distinct sensitivity to bornyl acetate in EAG analysis. The response of female antennae to bornyl acetate may be due to the presence of generalised antennal receptors since it is unlikely that bornyl acetate has any natural role in female sexuality. Furthermore, in the present work it was confirmed that only the male antennae responded strongly to germacrene D, while the antennae of both sexes are stimulated by D- and L-bornyl acetate. We were unable to obtain other than minimal EAG responses from either sex with santalol.

Ritter *et al.*[5] have proposed two sesquiterpenoids for the American cockroach sex pheromone, and have suggested the germacrane skelton for one of these on the basis of spectral data. We also suggest that germacrene D is closely related to the natural sex pheromone of the cockroach since it induces strong sexual excitement[1,2], and shows a sex specific EAG response.

Cadinol, a sesquiterpenoid biogenetically related to germacrene D, has been isolated from a plant and shown to be a stimulant for both male and female cockroaches[6]. This compound together with germacrene D indicates the importance of sesquiterpenoids in the chemical communication of cockroaches. Lundgren and Bergström[7] also reported the identification of a cadinol (tentatively identified as δ-cadinol) as a constituent of a *Lepidoptera* wing scent complex, important to courtship behaviour. Thus, cadinol may be significant for other insects.

We thank Fritzsche Dodge and Olcott Inc. for analytically pure samples of D- and L-bornyl acetate, and Givaudan Inc. for α- and β-santalol. We also acknowledge technical assistance from Miss K. Tsuzuki and Miss N. Sekijima.

HIROSHI WASHIO
Mitsubishi-Kasei Institute of Life Sciences,
Machida, Tokyo, Japan 194

CHIKAO NISHINO
WILLIAM S. BOWERS
New York State Agricultural Experiment Station,
Cornell University,
Geneva, New York 14456

Received March 15, accepted June 8, 1976

[1] Bowers, W. S., and Bodenstein, W. G., *Nature*, **232**, 295–261 (1971).
[2] Tahara, S , Yoshida, M , Mizutani, J , Kitamura, C , and Takahashi, S., *Agric. biol. Chem* , 39, 1517–1518 (1975)
[3] Boeckh, J , Sass, H , and Wharton, D R A., *Science*, **168**, 589 (1970).
[4] Washio, H , and Nishino, C., *J Insect Physiol* , **22**, 735–741 (1976).
[5] Ritter, F J , and Persoons, C. J , *Netherlands J. Zool* , **25**, 261–275 (1975).
[6] Nishino, C , and Tsuzuki, K., *Botyu-Kagaku*, 40, 62–67 (1975).
[7] Lundgren, L., and Bergstrom, G., *J chem. Ecol* , **1**, 399–412 (1975).

Ecdysone and oocyte morphogenesis in *Bombyx mori*

ECDYSONE, one of the principal hormones of insects, controls the periodic shedding and rebuilding of the cuticle during larval development. (We use "ecdysone" to designate all ecdysoids (in the sense of P. Karlson in ref. 5), or, for the radioimmunoassay, all radioimmunoassay-active ecdysteroid compounds.) It also promotes changes in gene activity observed at the initiation of metamorphosis[1] and influences morphogenetic development of the imaginal disks in pupae Some reports also indicate that ecdysone is found in adult insects[2–4]. Recent work on *Drosophila* (M.L.D.-R., M. H. Hirn and M. A. Delaage, unpublished), *Tenebrio* (P. P. Delbecque, M. H. Hirn and M.L.D.-R , unpublished), *Locusta*[5] and termites[6] has shown that a significant level of ecdysone is generally found in adult insects of both sexes and that high titres of ecdysone can be found in ovarian tissues. In *Locusta*, the ecdysone titre of the ovary increases during each cycle of oocyte maturation[7], suggesting stimulation by ecdysone, in agreement with observations on *Aedes aegypti*[8]. This reveals an unexpected aspect of the action of ecdysone. Using a radioimmunoassay to study ecdysone action in *Bombyx mori*, we have found that not only is ecdysone present in the *B. mori* ovary during egg production, but that the oocyte itself contains a high concentration of ecdysone. Moreover, this concentration changes during successive phases of oocyte morphogenesis.

In *Bombyx*, oogenesis in a well defined sequence[9] during pupal development, and is terminated when the insect ecloses. Pupae were used 6, 9 and 15 d after larval–pupal ecdysis (at 22 °C). They were quickly dissected in Ringer solution For each experiment we removed one ovariole from the right ovary; it was cleaned of adipose tissue fragments and then transferred to a small vial containing a few millilitres of Ringer solution. Oocytes were extracted from the ovarian tube by microdissection. They were collected one after the other, from the bottom to the top of the tube, rank 1 indicating the lowest and therefore the first extracted. Generally, five adjacent oocytes, that is, less than 4 mg wet weight, were sampled for each ecdysone assay. The length and width of the central oocyte of each assay were determined using a micrometer These measures enabled a good estimate of oocyte volume[10]. The samples were then frozen in liquid nitrogen and lyophilised. Dissection and sample collection did not take longer than 20 min. In these conditions, there was no noticeable loss of ecdysone during collection of oocytes as verified by replicate dissections at various intervals of time. Ecdysone titre was determined in oocytes sampled from the bottom, middle and top of the ovariole. More detailed sampling was carried out on an ovariole from a 13-d-old pupa, to measure precisely the ecdysone gradient along the ovarian tube.

Ecdysone was determined quantitatively by radioimmunoassay, as before[11]. Lyophilised samples were homogenised in 200 μl 1 N $HClO_4$ by brief sonication. The precipitated protein and the insoluble fraction were removed by centrifugation at 15,000*g* for 5 min. A sample of 150 μl supernatant was neutralised with 15 μl 6 M K_2CO_3 and the resulting salts were removed by further centrifugation. A sample of 100 μl of the second supernatant was used for radioimmunoassay, after suitable dilution in 0.1 M citrate buffer, *p*H 6.2. Results are expressed as pg β-ecdysone equivalent.

Table 1 Ecdysone content (radioimmunoassay activity) of oocytes in *B. mori* pupae*

Pupal (d)	β-ecdysone†	Position of oocytes in the ovarian tube Bottom	Middle	Top	Total ovariole content (pg β-ecdysone)
6	1	1,300	40	ND	21,000
	2	1,870	400	ND	
	3	1.21×0.98	0.60×0.52		
9	1	3,490	2,920	30	123,000
	2	2,810	3,780	460	
	3	1.46×1.21	1.24×1.04	0.53×0.43	
15	1	660	1,170	450	134,000
	2	420	690	1,340	
	3	1.61×1.27	1.62×1.33	0.97×0.75	

*Radioimmunoassay activity is expressed as pg β-ecdysone equivalent.

†1, β-ecdysone equivalent content (pg per oocyte); 2, β-ecdysone equivalent concentration (pg μl^{-1}); 3, oocyte dimensions: length × width (mm).

ND, Not done because of small size of oocytes.

Oocytes were collected from the bottom, middle and top of the ovarian tube, in pupae aged 6, 9 and 15 d. Maturation of oocytes begins at the bottom of the ovariole and progresses to the top. To calculate concentration, oocyte volume was estimated by a geometric model[10].

Table 1 shows that maturing oocytes contain ecdysone at high concentrations (the highest value observed was 3,780 pg μl^{-1}, or 8×10^{-6} M). On day 6, the concentration of the hormone was 1,870 pg μl^{-1} in the lowest oocytes, which had just started to mature; whereas there was little or no ecdysone in higher oocytes Later (day 9) the morphogenetic activity in the ovariole had progressed upwards. The ecdysone titre was now at a maximum in the middle part; it had also increased in the top part of the tube, to 460 pg μl^{-1}. On day 9, the bottom oocytes had stopped growing; they contained more ecdysone than previously but less than did middle oocytes of the same ovariole. Finally, on day 15, maturing oocytes were the highest oocytes in the ovariole. They had the highest titre of ecdysone (1,340 pg μl^{-1}), whereas in those at the bottom of the ovariole, where ovulation had finished, the concentration had declined to 420 pg μl^{-1}. Table 1 also suggests that oocyte maturation leads to an increase in the ecdysone content of the entire ovariole.

Detailed ecdysone assays, on day 13, in oocytes of rank 1 to rank 70 confirm these results (Table 2) The concentration was relatively low in oocytes at the bottom and gradually increased towards the top of the ovariole; it peaked in oocyte 66, in good agreement with the data in Table 1.

Our work demonstrates that maturing oocytes of *B. mori* contain ecdysone, and that ecdysone concentration changes considerably during oocyte morphogenesis. The hormone

Table 2 Ecdysone (radioimmunoassay activity) gradient in one ovariole of a *B mori* pupa of 13 d

Oocyte rank*	1	16	26	46	56	66	71
Ecdysone content†	830	1,200	1,470	1,770	1,880	2,720	2,250

*Oocytes are numbered from the bottom to the top of the ovariole.
†pg β-ecdysone equivalent per oocyte.

appears at the beginning of maturation and increases during the growth phase, reaching a very high value (close to 10^{-5} M). It then decreases at the end of the process. This lowering of ecdysone concentration is noteworthy; it cannot be attributed to a dilution effect due to oocyte growth, since Table 1 shows that the ecdysone pool in the ovariole continues to increase up to 15 d This implies a gradient of hormone concentration along the ovariole, showing a maximum which moves from the bottom to the top of the ovariole as oocyte maturation progresses upward. The ecdysone titre peaks at the end of the ellipsoidal phase of oocyte morphogenesis, when the oocyte is about 1 mm wide and starts flattening to take on its final shape[9,12].

A few reports have discussed possible roles of ecdysone in ovarian development. In mosquitoes ecdysone controls vitellogenesis[13]; more precisely, it directly activates synthesis of vitellogenin[8]. In the ovary of *Tenebrio molitor,* ecdysone stimulates *in vitro* cell divisions and oocyte growth, and influences follicle organisation[14]. Our report of ecdysone in the oocyte itself raises new questions. We propose that ecdysone behaves as a metabolic symbol, that is, a specific intracellular effector molecule which accumulates when the cell is exposed to a certain environment[15]. Perhaps it has a double role—as suggested by Laverdure's[14] work *in vitro*—stimulating oocyte growth and influencing oocyte morphogenesis. The ecdysone variation we observed in the ovarian tube could reflect the organisational action mentioned by Laverdure[14]. It could also be one element of the longitudinal energy gradient proposed by Legay[12] By our hypothesis, ecdysone action on oocytes is connected to its known effects on the morphogenesis of imaginal disks *in vitro,* in *Galleria*[16] and in *Drosophila*[17].

We were intrigued by the lowering of ecdysone level during the last phase of oocyte development. Further observations indicate that the concentration of the hormone increases again in newly laid eggs of *B. mori* (M.H.H., M. Coulon and M.L.D.-R., unpublished). This shows that ecdysone does not simply accumulate in the cell as a passive component, and that specific pathways exist for ecdysone elimination from oocytes.

We thank Michel Delaage and Richard Grantham for help with the manuscript

JEAN-MARIE LEGAY
BERNARD CALVEZ

Departement de Biologie générale et appliquée,
Université Cl Bernard,
43 Boulevard du 11 Novembre 1918,
69621 Villeurbanne, France

MICHEL HIRN
MAX L DE REGGI

Centre de Biologie moléculaire CNRS,
31 Chemin Joseph Aiguier,
13009 Marseille, France

Received March 8, accepted June 8, 1976.

[1] Ashburner, M , and Richards, G., in *Proc. R ent. Soc Symp. Insect Dev , 1975* (edit. by Lawrence, P A) (Blackwell, Oxford, in the press)
[2] Shaaya, E., and Karlson, P., *Devl Biol.*, 11, 424–432 (1965)
[3] Wyatt, G R., in *Biochemical Actions of Hormones*, 2 (edit by Litwack, G), 385–490 (Academic, New York and London, 1972)
[4] Borst, D W , Bollenbacher, W E , O'Connor, J D., King, D S., and Fristrom, J , *Devl Biol* , 39, 308–316 (1974)
[5] Hoffman, J A., *et al* , in *Colloque int CNRS Invert. Endocr.*, Lille 1975 (in the press).
[6] Bordereau, C , Hirn, M , Delbecque, J. P , and De Reggi, M L , *C.r hebd Séanc Acad Sci Paris*, **282**, 885–888 (1976)
[7] Lagueux, M , Hirn, M H , De Reggi, M. L , and Hoffmann, J , *C r hebd Séanc. Acad. Sci Paris*, **282**, 1187–1190 (1976)
[8] Hagedorn, H. H , *et al., Proc natn. Acad Sci U S.A.*, **72**, 3255–3259 (1975).
[9] Legay, J. M., *Ann Embryol. Morph.*, **7**, 277–282 (1974)
[10] Legay, J. M , and Pernet, R., *Acta biotheoret* , **20**, 18–28 (1971).
[11] De Reggi, M. L., Hirn, M H , and Delaage, M. A., *Biochem biophys. Res. Commun.*, **66**, 1307–1315 (1975).
[12] Legay, J. M , *J. Embryol. exp Morph* (in the press)
[13] Fallon, A. M., Hagedorn, H H , Wyatt, G. R., and Laufer, H., *J. Insect Physiol* , **20**, 1815–1823 (1974).
[14] Laverdure, A. M , *C.r. hebd Séanc. Acad Sci Paris*, **281**, 1745–1748 (1975).
[15] Tomkins, G. M , *Science*, **189**, 760–763 (1975).
[16] Oberlander, H., *J. Insect Physiol* , **15**, 1803–1806 (1969).
[17] Mandaron, P., *Devl Biol.*, **31**, 101–113 (1973)

Covering response in sea urchins

THE tendency of many species of sea urchins to pick up particles and debris with their spines and tube feet, and to move and then hold the particles on their aboral surface is well known. Functional bases (decreasing the susceptibility to water or wave action, desiccation, light, or predation; supplying nutrients through skin digestion and absorption) have been ascribed to this "covering reaction"[1–13].

In contrast to these 'functional' explanations for the covering response of sea urchins, Dambach and Hentschel[14] concluded that the phenomenon is simply reflexive: mechanical, chemical or photic stimuli produce increased tube feet and spine activity involved in locomotion, or in a generally higher activity level, resulting in the covering of the individual. The suggestion that reflexes are involved has been made before[1,2], but Dambach and Hentschel are the first to provide experimental data to support it. The functional explanations of weight and protection from light involve stimuli (mechanical and photic) which lead to increased activity of the tube feet and spines[2,6]. Support for Dambach and Hentschel's proposal also comes from the previously unreported observation that there is a reversal of the covering response by *Lytechinus variegatus* when it is inverted; thus, material held on the aboral surface is quickly moved orally by inverted animals.

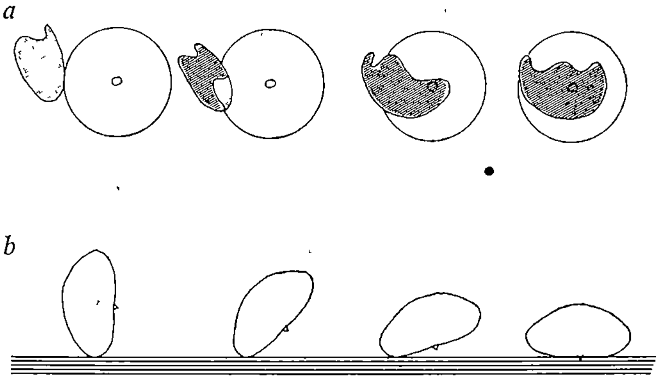

Fig. 1 *a*, Diagrammatic representation of the reversal of the covering response in *Lytechinus variegatus.* A shell, originally on the aboral surface of the animal, has been moved to the ambitus and is subsequently moved to the oral surface. (Drawn from a photographic series). *b*, Diagrammatic representation of the righting response in *Lytechinus variegatus.* The urchin has righted itself to the vertical position where the ambitus is in contact with the substratum. Subsequent positions of the animal in righting correspond to the positions involved in the reversal of the covering response indicated directly above.

Twenty individuals, which were well covered by shell and pebbles on the aboral surface, were collected. The animals were hand held in the inverted position below the surface of seawater in a large container. In each case, the material held by the sea urchin on the aboral surface was moved orally (Fig. 1*a*). This reversal of the covering response seems to be a reflex, particularly when compared with the well known righting response of sea urchins—the tendency of inverted animals to right themselves if physically possible. The activity of the tube feet and spines in the movement of particles in the reversal phenomenon cannot be distinguished from their activity in the righting response; the movement of a particle over the surface of the animal in reversal is identical to that of the animal's surface over the substratum in righting (Fig. 1*b*). A reflexive basis for the reversal of the covering reaction supports the suggestion of a reflexive basis for the covering reaction itself. The functional consequences of covering as proposed by other workers could still be valid, but would not be the casual explanations of the phenomenon.

This work was done at the Galeta Marine Laboratory of the Tropical Research Station of the Smithsonian Institution. I thank Dr G. Hendler for his assistance.

JOHN M. LAWRENCE

Department of Biology,
The University of South Florida,
Tampa, Florida 33620

Received April 1, accepted May 25, 1976.

[1] Gamble, J C , in *Symp Underwater Assoc Malta*, 1965 (edit by Lythgoe, J. N., and Woods, J D), 47–50 (1966).
[2] Dix, T. G., *N Z Jl mar. Freshwat Res* , **24**, 187–194 (1970)
[3] Lees, D. C., and Carter, G A , *Ecology*, **53**, 1127–1133 (1972)
[4] Lewis, J B , *Can J Zool* , **36**, 607–621 (1958).
[5] Sharp, D T , and Gray, I. E., *Ecology*, **43**, 309–313 (1962)
[6] Millott, N , *J exp. Biol.*, **33**, 508–523 (1956)
[7] Glynn, P , *Mar Biol* , **1**, 226–243 (1968)
[8] Orton, J. H , *J mar biol Ass U K* , **16**, 289–296 (1929)
[9] Dayton, P K , Robilliard, G A , and Paine, R T , in *Antarctic Ecology*, **1** (edit by Holgate, M W), 244–258 (Academic, New York, 1968)
[10] Pequignat, E., *Nature*, **210**, 397–399 (1966)
[11] Pequignat, E , and Tiffon, Y , *C. hebd Seanc Acad Sci. Paris*, **264D**, 3014–3015 (1967)
[12] Pequignat, E., *Mar. Biol* , **12**, 28–41 (1972)
[13] Yanagisawa, Y , *Publ Seto mar. Biol Lab* , **19**, 431–435 (1972).
[14] Dambach, M., and Hentschel, G , *Mar Biol* , **6**, 135–141 (1970)

Testing the neutral mutation hypothesis by distribution of single locus heterozygosity

ONE of the most controversial issues in population genetics at present is whether the widespread protein variation in natural populations is maintained by some form of balancing selection[1–3] or merely represents the drifting polymorphism of neutral or nearly neutral mutations[4–6]. By the neutral mutation hypothesis the level of genetic variability in an equilibrium population is determined by mutation rate, v, and effective population size, N_e. If we use the infinite allele model, in which new mutations are assumed to be always different from the pre-existing alleles in the population, the average heterozygosity per locus is given by

$$H = M/(1+M) \qquad (1)$$

where $M = 4N_e v$ (ref. 7).

Whether the observed heterozygosity agrees with the above theoretical value or not is, in practice, however, very difficult to examine, since the exact values of N_e and v in a population are hardly obtainable. Recently, it was shown[8,9] that the variance of single locus heterozygosities is given by

$$V(h) = \frac{2M}{(1+M)^2(2+M)(3+M)} \qquad (2)$$

From this the neutral mutation hypothesis can be tested without knowing the values of N_e and v separately. By estimating M from the observed value of average heterozygosity, we can compute the theoretical variance by using equation (2) and then compare it with the observed variance[10] Preliminary results of the application of this method to a number of organisms have suggested that the agreement between the theoretical and observed variances is rather good[11,12], but the amount of data used was too small to make any general conclusion. We have accumulated all published data which are amenable to such a test. In this report we show that the observed variances of heterozygosity in most organisms so far studied can be reasonably explained by the neutral mutation hypothesis. The pattern of the distribution of heterozygosity also agrees with that expected from this hypothesis.

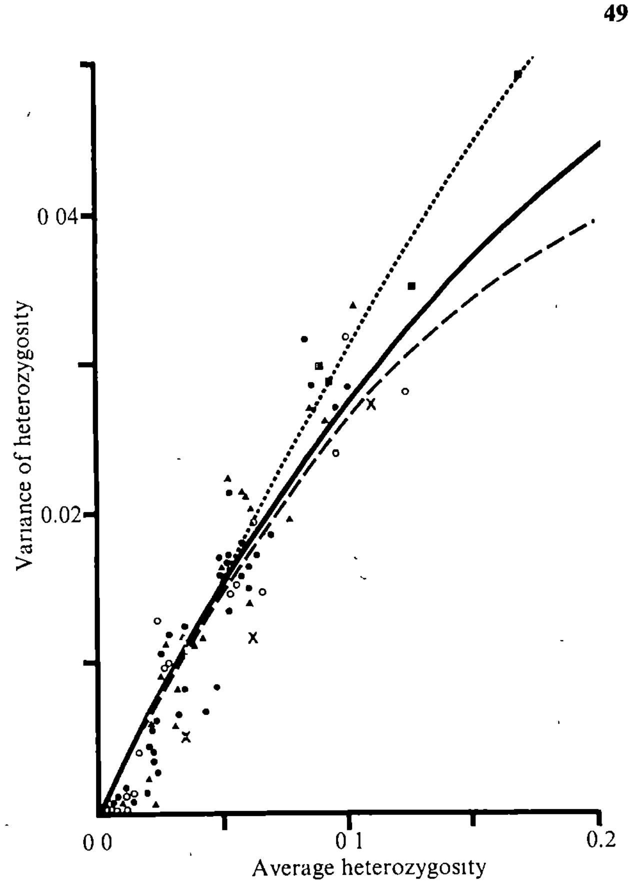

Fig. 1 Relationship between the mean and variance of heterozygosity for vertebrate species: ●, mammals (33 species); ×, birds (2 species, 1 subspecies); ○, fish (18 species, 1 subspecies); ▲, lizards (21 species); ■, amphibians (3 species, 1 subspecies). The solid and dashed lines are the theoretical relationships obtained from the infinite allele and stepwise mutation models, respectively. The dotted line is the theoretical relationship for the infinite allele model with varying mutation rate

Surveying 52 publications, we collected gene frequency data obtained by electrophoresis for 123 species and 8 subspecies, in which 15 or more loci were examined for at least 30 genomes. It is known that for estimating average heterozygosity a large number of loci should be used, whereas the sample size per locus can be rather small[10]. For each of the species and subspecies used, the mean, $\hat{H}$, and variance, $\hat{V}(h)$, of single locus heterozygosity was computed with a correction for sampling variance[10]. When a species or subspecies comprised a number of subpopulations, the average values of $\hat{H}$ and $\hat{V}(h)$ for these were used. The relationship between $\hat{H}$ and $\hat{V}(h)$ was compared with the theoretical one (solid lines in Figs 1 and 2) obtained from equations (1) and (2) It can be argued that the stepwise mutation model[13] is more appropriate for electrophoretic data than the infinite allele model. Therefore, we have also computed the theoretical curve for this model (broken line) using Ohta and Kimura's formula[13] for H and Moran's formula[14] for $V(h)$. Actually, as Figs 1 and 2 show, there is not much difference between the two models unless H is very large. Since there seems to be a significant difference in average heterozygosity between vertebrates and invertebrates[15], the two groups have been considered separately (Figs 1 and 2).

It is clear that the observed variances for vertebrates are generally in good agreement with the theoretical values, in spite of the fact that the number of loci used is relatively small and data on diverse organisms are included. A close examination of Fig. 1, however, indicates that when $\hat{H}$ is smaller than 0.05

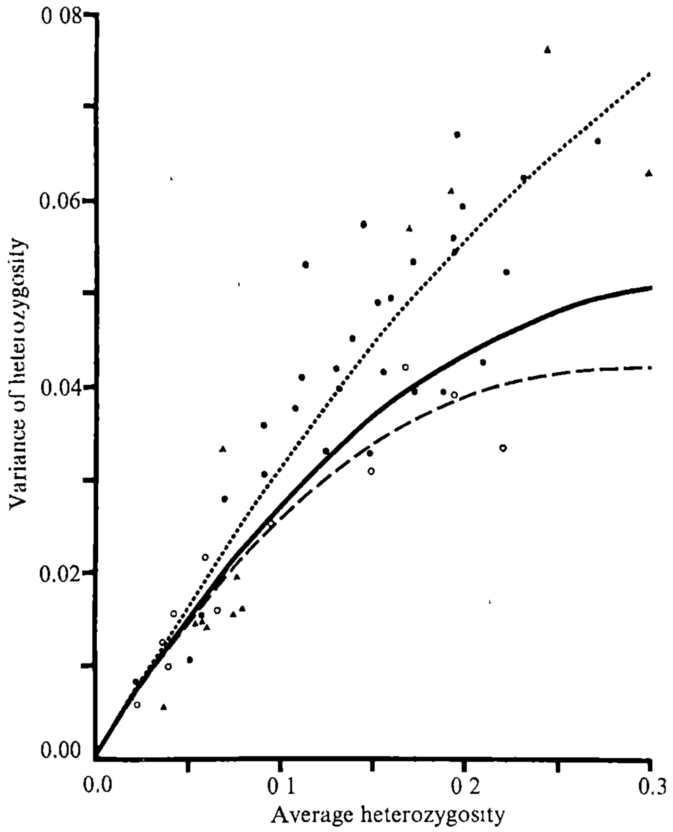

Fig. 2 Relationship between the mean and variance of heterozygosity for invertebrate species: ●, *Drosophila* (24 species, 5 subspecies); ▲, other insects (12 species); ○, other invertebrates (10 species). The solid and dashed lines are the theoretical relationships obtained from the infinite allele and stepwise mutation models, respectively. The dotted line is the theoretical relationship for the infinite allele model with varying mutation rate.

the observed variance tends to be smaller than the theoretical curve, whereas for $\hat{H} > 0.1$ it tends to be larger. The agreement between the theoretical and observed variances in invertebrates is also generally good, though the tendency for the observed variance to deviate upward is pronounced because of higher heterozygosities in this group of organisms.

The tendency for the observed variance to deviate upward for large $\hat{H}$ does not contradict the neutral mutation hypothesis and is expected to occur for the following reason. The formula for $V(h)$ is based on the assumption of identical mutation rates for all loci in both theoretical models used here. In practice, this assumption is surely incorrect, and when mutation rate varies among loci, the variance of heterozygosity is expected to inflate. To get an idea about the amount of inflation, we computed the expected variance of heterozygosity from the assumption that mutation rate varies among loci according to the gamma distribution with the coefficient of variation equal to one. The gamma distribution with this value of coefficient of variation was suggested by the examination of the rates of amino acid substitution for 19 polypeptides in evolution (Nei, Chakraborty and Fuerst, unpublished). From the assumption of neutral mutations the rate of amino acid substitution per polypeptide is equal to the mutation rate per locus, neglecting synonymous mutations[4]. At any rate, the results obtained are given by the dotted lines in Figs 1 and 2. It is clear that the agreement between the theoretical and observed variances is now very good.

The tendency for the observed variance to deviate downward for a small value of $\hat{H}$ is apparently caused by the relatively small number of loci studied (about 20) in this group of organisms. When the theoretical value of H is relatively small, the distribution of single locus heterozygosity, h, is extremely skewed towards the class of $h = 0$ (Fig. 3). Thus, whenever the sample estimate of H is small, the observed value of $V(h)$ tends to be smaller than its expected value. Our computer simulation has shown that the difference between the observed and theoretical variances for $\hat{H} \leqslant 0.05$ is of the order of magnitude that is expected to occur when the number of loci is about 20. The details of this study will be published elsewhere. Thus, the data presented in Figs 1 and 2 are consistent with the neutral mutation hypothesis.

In Fig. 3 the frequency distributions of single locus heterozygosity for three species groups in which a large number of loci have been studied are presented together with one theoretical distribution obtained by computer simulation[16]. This theoretical distribution is based on 2,000 replicate evaluations of h with the expected heterozygosity of 0.09, which is close to the observed average heterozygosities for the three species groups. All empirical distributions are L-shaped and very similar to the theoretical one. In both empirical and theoretical distributions there is a little peak around $h = 0.5$. Existence of this peak has been theoretically predicted[8,17]. In addition to those in Fig. 3, we examined the distribution of heterozygosity for all other species. The pattern of the distribution was essentially the same as that expected from the neutral mutation hypothesis for most species.

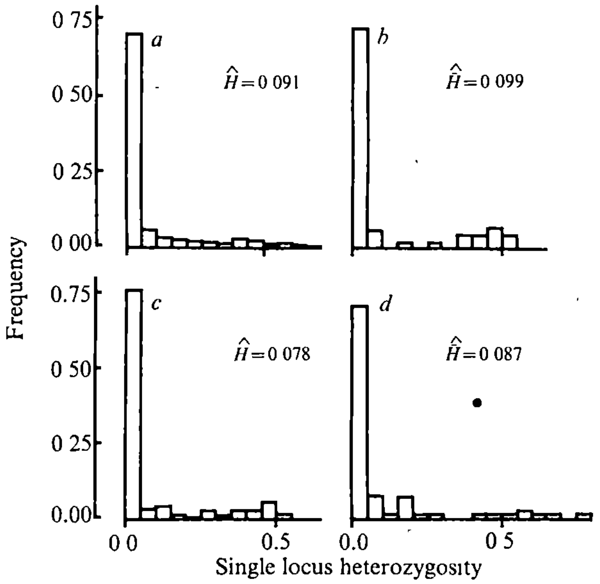

Fig. 3 Distributions of single locus heterozygosities for *b*, man (Caucasian)[11]; *c*, the house mouse[20,21] (*Mus musculus*) and *d*, the *Drosophila mulleri* species group[22]. The theoretical distribution (*a*) was obtained by computer simulation with the infinite allele model. $\hat{H}$ stands for the average heterozygosity. The distribution for the stepwise mutation model is almost identical with that for the infinite allele model when $\hat{H} = 0.09$.

We are aware that our observations about the variation and distribution of heterozygosity can be explained by some elaborate combination of different types of selection. Such an explanation is, however, strained, since we then have to assume that selection is adjusted so as to have a good agreement between the observed and theoretical variances in diverse organisms. It seems to us that the simplest and most natural explanation is the neutral mutation hypothesis. Note that this hypothesis does not exclude the existence of a small proportion of overdominant or selectively advantageous mutations. Furthermore, our analysis will not exclude the possible importance of slightly deleterious mutations[18,19], of which the contribution to heterozygosity is relatively small.

We thank Yoshio Tateno for some numerical computations involved in this study. We are also grateful to Professor P. A.

P. Moran for his unpublished formula. This work was supported by grants from the NIH.

MASATOSHI NEI
PAUL A. FUERST
RANAJIT CHAKRABORTY

Center for Demographic and Population Genetics,
The University of Texas at Houston,
1100 Holcombe Boulevard, Room 1109,
Houston, Texas 77030

Received January 21; accepted June 9, 1976.

[1] Sved, J. A , Reed, T. E., and Bodmer, W. F., *Genetics*, **55**, 469–481 (1967).
[2] King, J. L., *Genetics*, **55**, 483–492 (1967)
[3] Milkman, R. D., *Genetics*, **55**, 493–495 (1967).
[4] Kimura, M., *Nature*, **217**, 624–626 (1968).
[5] King, J. L., and Jukes, T. H., *Science*, **164**, 788–798 (1969).
[6] Kimura, M., and Ohta, T., *Nature*, **229**, 467–469 (1971).
[7] Kimura, M., and Crow, J. F., *Genetics*, **49**, 725–738 (1964).
[8] Stewart, F., *Theor. Populat. Biol.* (in the press)
[9] Li, W.-H., and Nei, M , *Genet. Res* , **25**, 229–248 (1975).
[10] Nei, M., and Roychoudhury, A. K., *Genetics*, **76**, 379–390 (1974).
[11] Nei, M., and Roychoudhury, A. K , *Am J. hum Genet.*, **26**, 421–443 (1974)
[12] Nei, M., *Molecular Population Genetics and Evolution* (North-Holland, Amsterdam, 1975).
[13] Ohta, T., and Kimura, M., *Genet. Res.*, **22**, 201–204 (1973)
[14] Moran, P. A. P., *Theor. Populat. Biol.* (in the press).
[15] Selander, R. K., and Kaufman, D. W., *Proc. natn Acad. Sci. U.S.A.*, **70**, 1875–1877 (1973).
[16] Nei, M , and Tateno, Y., *Proc. natn Acad. Sci U.S.A.*, **72**, 2758–2760 (1975).
[17] Ewens, W. J., and Gillespie, J H., *Theor. Populat. Biol* , **6**, 35–57 (1974).
[18] Ohta, T., *Proc. natn Acad Sci. U.S A* , **72**, 3194–3196 (1975).
[19] Latter, B. D. H., *Nature*, **257**, 590–592 (1975).
[20] Selander, R. K , Hunt, W. G , and Yang, S. Y , *Evolution*, **23**, 379–390 (1969).
[21] Selander, R. K., and Yang, S. Y., *Genetics*, **63**, 653–667 (1969).
[22] Zouros, E., *Evolution*, **27**, 601–621 (1973)

Y chromosome visibility in quinacrine-stained human spermatozoa

THE fluorescent dye, quinacrine, binds strongly to the Y chromosome and only to a lesser extent to the other chromosomes in human metaphase cell preparations[1]. A bright fluorescent spot (F body), which is presumed to be the Y chromosome, is clearly visible in stained interphase cells from various tissues from the human male[2-5] and in mature spermatozoa[6,7]. Spermatozoa bearing one F body (about 45% of the total) are taken to be Y spermatozoa, and the staining method is now being used widely to detect physical differences, for example, in DNA content and head size[7,8] and motility[9] between X and Y spermatozoa, and for testing the efficiency of procedures designed to separate them[10-13]. Spermatozoa bearing two F bodies (about 1.3% of the total) have been interpreted as YY spermatozoa[7,8], and the relatively high number of such spermatozoa has led to speculation concerning the seemingly high non-disjunction rates during spermatogenesis[8,14,15]. We here examine the factors which affect Y chromosome visibility in sperm heads, and conclude that the F body count depends critically on observer performance, that the presence of YY spermatozoa cannot be demonstrated decisively using the quinacrine stain, and that measured physical differences between spermatozoa with and without an F body may partly reflect a dependence of the Y chromosome detection efficiency on the size of the sperm head.

When a brightly fluorescent chromosome inside a nucleus is examined under the ultraviolet microscope it appears as a bright spot against a less bright background which is produced by fluorescence from the other nuclear contents and from any unbound dye which may be present. The chromosome is detected by the observer provided that the spot intensity is more than 1 or 2% above that of the background[16], the condition for detection then being

$$(I_0 \exp(-k\bar{x})-I_B)/I_B \gtrsim 0.01\text{–}0.02 \qquad (1)$$

where $\bar{x}$ is the mean depth (weighted and averaged over all directions which lie within the acceptance cone of the objective lens) at which the chromosome is buried in the head, I_0 is the intensity of the spot which would be produced if the chromosome were located at $\bar{x} = 0$, I_B is the background intensity and k is an optical attenuation coefficient.

Almost 50% of spermatozoa are expected to carry a Y chromosome, and since only about 45% exhibit an F body it seems that about a tenth of all Y chromosomes are not detected by the staining procedure. There are two possible explanations. The first is that stain uptake among Y chromosomes from cells of any one individual may be very variable, the missing chromosomes being those which absorb so little stain as to be indiscernible above the background fluorescence. The second is that the optical attenuation coefficient is sufficiently great that chromosomes lying deep in the head are not detected[6]. This coefficient has two components. The refractive index of the DNA within the head is high (probably about 1.5 (ref. 17)) compared with that of the aqueous mounting medium (1.33) which surrounds and permeates the sperm head. If the fluorescent Y chromosome is located at the bottom of a uniform sphere of refractive index 1.5 immersed in a medium of refractive index 1.33, the average refractive deviation of light leaving the chromosome and passing through the sphere is found using Snell's law to be about 15°, sufficient to reduce the intensity of a chromosome of diameter 500 nm to about 25% of its undiminished value. If the other chromosomes each refract the light from the Y chromosome in this way the total deviation will be considerably greater than 15° across the optically inhomogeneous sperm head. In addition, the dimensions of the chromosomes are comparable with the wavelength of the fluorescent light, and diffractive scattering will occur within the sperm head, increasing background fluorescence at the expense of spot intensity. Optical attenuation may therefore be the dominant mechanism, and some support for this hypothesis is afforded by the observation that about 70% of F bodies appear at or very near the region where the background fluorescence becomes less dense[15]. We have estimated the intensities of F bodies by comparing microscope images of quinacrine-stained spermatozoa with matching images projected on to a screen in the same conditions (green light; dark-adapted vision) and measuring the screen intensities with a photometer. F body intensities varied from about 10% (the brightest) to about 1% (that is, the detection threshold) above background. Assuming that the brightest spots correspond to Y chromosomes at $\bar{x} = 0$ and that the Y chromosome is randomly distributed within the head, then $k \sim 50$ mm^{-1} would give the observed proportion of spermatozoa carrying an F body.

Other chromosomes, although fluorescing less brightly than the Y chromosome, may nevertheless be detected if they are located near the surface of the sperm head. If P_y is the probability of detecting a Y chromosome in a Y spermatozoon, and P_c is the probability of detecting any other chromosome (or other artefact such as adhering bacteria or vacuoles within the head[15]) then, assuming that X and Y spermatozoa occur in equal numbers (and, initially, that no YY spermatozoa are present) the percentages of spermatozoa exhibiting one and two F bodies, P_1 and P_2, are given by

$$P_1 = 50P_y(1-P_c)+100(1-\tfrac{1}{2}P_y)P_c$$

and

$$P_2 = 50P_y\mathrm{P}_c+100(P_c)^2 \ .$$

Solving for $P_1 = 45\%$ and $P_2 = 1.3\%$ yields $P_y \sim 0.89$ and $P_c \sim 0.0275$, this being the only solution for which both P_y and P_c lie within the range 0–1. These figures may be compared with those from buccal mucosa cells and lymphocytes where cells of known karyotype are examined[2,3]. A fluorescent spot indistinguishable from a normal Y body[2] occurs in about 5.5% of cells from 46,XX females who carry no Y chromosome, and cells from 46,XY males, carrying one Y chromosome, have one F body in about 67% of cases[2,3]. Thus $P_y \sim 0.65$ and $P_c \sim 0.055$, and the Y chromosome is clearly more difficult to detect in these cells than in spermatozoa.

Several conclusions may be drawn from this analysis. First, if the artefact rate (P_c) in spermatozoa is comparable with that in somatic cells it is clearly unnecessary to invoke the presence of any YY spermatozoa to account for those which exhibit two F bodies. It therefore seems that no estimate of the non-disjunction rate for the Y chromosome can be obtained from staining data, and similar considerations probably apply to estimates obtained using differential stains which are specific for other chromosomes[8]. If YY spermatozoa are not present in appreciable numbers then about 90% of Y spermatozoa are detected by the technique, and of those with one F body about 97% are Y spermatozoa, the rest being X spermatozoa with another fluorescing chromosome or other artefact. These figures for the efficiency may be optimistic, however, since it is assumed that the criterion for detecting an F body is the same whether one or two are present in the cell, and it seems likely that spermatozoa are only classified as bearing two F bodies when both are reasonably bright[15].

Second, equation (1) shows that the counting rate depends critically on observer performance. An observer who decreases his threshold from, say, 2% (distinct spots) to 1% (where any slight local brightening of the background is taken to be an F body) will, on the basis of the present model, increase his F body count from 40 to 50% (with only 40% of the increase coming from newly detected Y chromosomes); and the increase will be even greater if other chromosomes become visible at the new threshold level.

Finally, the present theory suggests that Y chromosome visibility depends on sperm head size, and on the basis of a constant optical attenuation coefficient of 50 mm^{-1} we estimate that P_y will increase from 0.8 to 1.0 with decreasing head size over the range of naturally occurring head volumes[18], together with a corresponding variation in P_c. This may account for the higher detection efficiency in spermatozoa compared with that in the larger somatic cell nuclei. Larger Y spermatozoa will therefore tend to be categorised as X spermatozoa, although the effect could be reduced (or even reversed) if for some reason the background fluorescence of the head itself decreased with increasing head size. Unexpectedly large differences in head area between spermatozoa with and without an F body[8] may therefore reflect variations in chromosome visibility with head size, and need not necessarily imply the occurrence of haploid gene expression in spermatozoa.

We thank the MRC for support.

A. M. Roberts
H. Goodall

Department of Physics,
Guy's Hospital Medical School,
London SE1 9RT, UK

Received April 5; accepted June 8, 1976.

[1] Caspersson, T., Zech, L., and Johansson, C., *Expl Cell. Res.*, **60**, 315–319 (1970).
[2] Robinson, J. A., *Ann Hum Genet. Lond.*, **35**, 61–65 (1971).
[3] Polani, P. E., and Mutton, D. E., *Br. med. J.*, **1**, 138–142 (1971).
[4] Pearson, P. L., Bobrow, M., and Vosa, C. G., *Nature*, **226**, 78–80 (1970)
[5] Pearson, P. L., and Bobrow, M , *J Reprod Fert.*, **22**, 177–179 (1970).
[6] Barlow, P., and Vosa, C. G , *Nature*, **226**, 961–962 (1970).
[7] Sumner, A. T., Robinson, J. A , and Evans, H. J., *Nature new Biol* , **229**, 231–233 (1971).
[8] Pearson, P. L., Geraedts, J. P. M , and Pawlowitzki, I H., *Les Accidents Chromosomiques de la Reproduction* (edit. by Boue, A., and Thibault, C.), 219–229 (INSERM, Paris, 1973).
[9] Rohde, W , Portsmann, T., and Dorner, G., *J. Reprod. Fert* , **33**, 167–169 (1973).
[10] Ericsson, R J., Langevin, C. N , and Nishino, M., *Nature*, **246**, 421–424 (1973).
[11] Evans, J. M , Douglas, T. A , and Renton, J. P., *Nature*, **253**, 353–354 (1975).
[12] Ross, A., Robinson, J. A., and Evans, H. J., *Nature*, **253**, 354–355 (1975).
[13] Rohde, W., Porstmann, T., Prehn, S., and Dorner, G., *J. Reprod. Fert*, **42**, 587–591 (1975)
[14] Pawlowitzki, I. H., and Pearson, P. L., *Humangenetik*, **16**, 119–122 (1972).
[15] Evans, H. J., *Proc. Int. Symp. Genet. Spermatozoon*, 144–159 (University of Edinburgh, 1971).
[16] Davson, H., *The Physiology of the Eye* (Churchill Livingstone, London, 1972).
[17] Duijn, C., van, Jr, *Jl. R. Microsc. Soc.*, **77**, 12–27 (1958).
[18] Iversen, S., *J. Reprod. Fert.*, **9**, 197–202 (1965).

Absence of axonemal arms in nasal mucosa cilia in Kartagener's syndrome

A TOTAL lack of axonemal arms in the spermatozoa of infertile men has been described[1–3] and those results included those from four men, three of whom had situs inversus of the thoracic organs while the fourth was a brother to one of the others. The total absence of axonemal arms (dynein arms) was deemed to be responsible for the complete immobility of their sperm tails. Kartagener's syndrome[4] exhibits the following symptoms: chronic sinusitis, bronchiectasis and situs inversus Sperm flagella and cilia have similar ultrastructure in principle, so it was thought possible that the respiratory tract symptoms in patients with Kartagener's syndrome might be caused, by a lack of dynein arms in the cilia. We have thus investigated the cilia of Kartagener patients at the substructural level.

The patient examined was a 25-yr-old woman, who had had daily airway symptoms from birth consisting of a cough and mucopurulent secretion from the lower, as well as from the upper, respiratory tract. She underwent surgical treatment for sinusitis, nasal polyposis and bronchiectasis. Her hearing was also impaired by chronic secretory otitis media. X-ray examination demonstrated dextrocardia. Rhinoscopy revealed small nasal polyps, but patent nasal airways. Nasal mucociliary transport function was examined on three separate occasions using the saccharine-dye method[5]. After cocaine anaesthesia, a mucosal biopsy was taken from the inferior turbinate. An additional biopsy from a polyp was taken without anaesthesia. The tissue was immediately fixed in collidine-buffered glutaraldehyde and after a short buffer rinse, postfixed in osmium tetroxide with the same buffer. After dehydration in graded concentrations of ethanol and propylene oxide the tissue was embedded in Epon. Sections stained with uranyl acetate and lead citrate were examined in a Philips 301 electron microscope. The technique was identical to that used for the examination of immobile human spermatozoa[1,2].

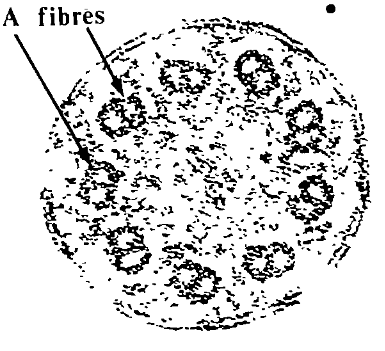

Fig. 1 Cross section of a cilium showing derangement of the axonemal matrix, but normally placed outer doublets. There is no consistent structure comparable with dynein arms on the A fibres. In this section the two central tubules are not recognisable, but in other sections they seem to be normal.

After intranasal application of the saccharine-dye particle, the patient was observed for at least 2 h, during which she did not notice any sweet taste in the mouth and no dye was observed in the throat. The normal mucociliar transport time in the nose is 10–30 min (ref. 5). Electron microscopy showed that the cilia had a uniform appearance and transverse sections revealed identical pathological findings. The microtubules were normal in position and appearance, but a common abnormal feature was an apparently total lack of dynein arms on the outer microtubules. The picture was obscured to a certain extent by complete disorganisation of the axonemal matrix (Fig. 1), so that only occasional remnants of the central sheath and spokes could be recognised. Many cross sections of cilia were examined and all showed the same abnormal features. One single cilium had structures similar to dynein arms, but whether or not these represented remnants of the C-tubule of the centriole could not be determined. All cross sections of centrioles seemed to be normal.

There is significant experimental evidence that dynein arms are essential for ciliary and flagellar motility, possibly by containing, or consisting of, protein with contractile properties (for review, see ref. 6). Spermatozoal motility is apparently not possible where there is a total lack of axonemal arms[1-3]. Our results suggest that these structures are also necessary for ciliary motility in the airways, as experiments have shown total absence of bronchial mucociliary transport in patients with Kartagener's syndrome[7]. Chronic infection, various pharmacological treatments and the preparatory procedures might, however, obscure the original basic defects and further studies, including more control measures, are needed.

If the present results and those described previously in human spermatozoa indicate the inability of such patients to produce dynein arms the same changes should be found in cilia from other sources, such as endometrium and uterine tubal mucosa. Such studies, including all the control measures mentioned above, are in progress in this laboratory. The patient described here has a long standing primary infertility of unknown origin.

Although Kartagener's syndrome simulates an immunodeficiency, immunological investigations have failed to disclose any factors of primary importance[8]. An hereditary disability to form dynein arms and the consequent lack of any mucociliary function could, however, explain the symptoms in these patients, and also why they are localised to ciliated organs.

We thank Dr Ib Andersen for supply of the saccharine-dye particles. H.P. was supported by Statens Laegevidenskabelige Forskningsraad, Denmark, and Den Laegevidenskabelige Forskningsfond for Storkøbenhavn, Faerøerne og Groenland, Copenhagen.

HENNING PEDERSEN
NIELS MYGIND

University of Copenhagen,
Department of Obstetrics and Gynaecology,
Otopathological Laboratory,
Rigshospitalet, Copenhagen, Denmark

Received May 21; accepted June 25, 1976

[1] Pedersen, H , *Dan. med Bull* , **21**, 1–36 (1974)
[2] Pedersen, H., and Rebbe, H., *Biol Reprod.*, **12**, 541–544 (1975).
[3] Afzelius, B A , Eliasson, R , Johnsen, Ö, and Lindholmer, C., *J Cell Biol.*, **66**, 225–232 (1975)
[4] Kartagener, M , *Beitr. Klin. Tuberk.*, **83**, 489–501 (1933)
[5] Andersen, I , Camner, P , Jensen, P. L , Philipson, K., and Proctor, D. F., *Archs Environ Hlth*, **29**, 290–293 (1974)
[6] Pedersen, H., *J. Ultrastruct. Res.*, **33**, 451–462 (1970)
[7] Camner, P., Mossberg, B , and Afzelius, B A., *Am Rev. Resp. Dis.*, **112**, 807–809 (1975)
[8] Holmes, L. B., Blennerhassett, J. B , and Austen, K F , *Am J med. Sci.*, **255**, 13–28 (1968).

Separation of suppressor and killer T cells by surface phenotype

AMONG thymus-derived (T) lymphocytes of the mouse, several functionally distinct subsets may be identified (for review, see ref. 1). Early studies have shown synergy in graft-*versus*-host reactions of different populations of lymphoid cells[2], and *in vitro* studies have demonstrated interactions between cells from anti-lymphocyte serum-treated mice (T_1 cells) and adult thymectomised mice (T_2 cells)[3]. A similar synergy has been observed in the generation of T helper and T suppressor cells *in vitro*[4]. Clearer definition of the subsets of T cells interacting in the induction of immune responses has come from the use of alloantisera recognising differentiation antigens on T cells. In particular, the use of antisera to the Ly series of antigens[5] has enabled the separation of amplifying (MLR) cells from killer cells[6]. Similarly in the humoral response helper T cells can be distinguished from suppressor T cells[7]. In this report, we show that killer and suppressor T cells, both generated *in vitro* and carrying the Ly-2 and 3 antigens can also be separated using antisera to surface antigenic markers. We also present data suggesting that suppressor cells of similar phenotype may have an important function *in vivo* in the immune response.

Soluble protein antigen-specific suppressor cells and alloimmune killer cells were both generated in Marbrook culture flasks, as described previously[8,9]. Keyhole limpet haemocyanin (KLH)-specific suppressor cells were assayed in a second culture by their ability to abrogate the effect of KLH-primed helper cells[8,10]. Killer cells were assayed in a 4-h ^{51}Cr release test on P815 mastocytoma cells[11].

Anti-Ly antisera were prepared and tested as described previously[7,12]. Anti-Ia^k was prepared by repeated intraperitoneal immunisation of A.TH mice with A.TL spleen cells[13], and used unabsorbed. Rabbit serum absorbed with mouse spleen cells was the source of complement.

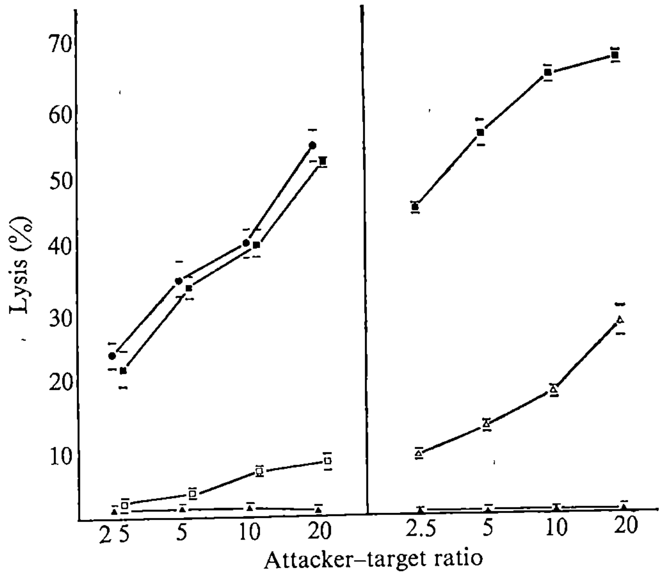

Fig. 1 Effect of anti-Ly, anti-Ia^k and anti-Thy-1 antisera and complement on alloimmune killer T cells. CBA killer cells were induced in Marbrook culture flasks by stimulation of spleen cells with 1,500 R irradiated BALB/c spleen cells[9]. Aliquots of 2×10^6 viable cells from the cultures were treated with 0.2 ml antiserum (at a concentration giving maximal lysis[7]) washed and treated with 0.2 ml absorbed rabbit complement at 1:10 dilution. After treatment cells were washed and resuspended to a fixed volume, giving a viable cell concentration in medium or complement-treated aliquots, of 2×10^6 cells ml^{-1}. Aliquots (0.1 ml) of treated cell suspensions were added to wells of round bottom microtitre plates (Linbro), containing 0.1 ml of a suspension of ^{51}Cr-labelled P815 mastocytoma cells at 10^5 cells ml^{-1}. After brief centrifugation at 150*g* (approximately 1 min) the plates were incubated for 4 h in a moist atmosphere of 10% CO_2 in air After a further centrifugation (300*g* for 1 min), 0.1 ml supernatant was collected from each well for γ counting. Low controls were incubated in medium (HEPES buffered Dulbecco's Eagles medium) alone and 100% ^{51}Cr release was taken as counts released by 5% Brij. ●, Anti-Ia^k; □, anti-Ly-2.1+3.2; ▲, anti-Thy-1.2; △, anti-Ly-1 1; ■, complement alone. Sera in absence of complement had no effect (data not shown). Four experiments with anti-Ly-1 1 and five with anti-Ia^k have been carried out using three batches of antiserum. All points are mean of triplicate cultures; bars represent standard error; % lysis calculated by the formula:
(c.p.m. killer cells – c.p.m. medium alone)/(c.p.m. detergent) × 100

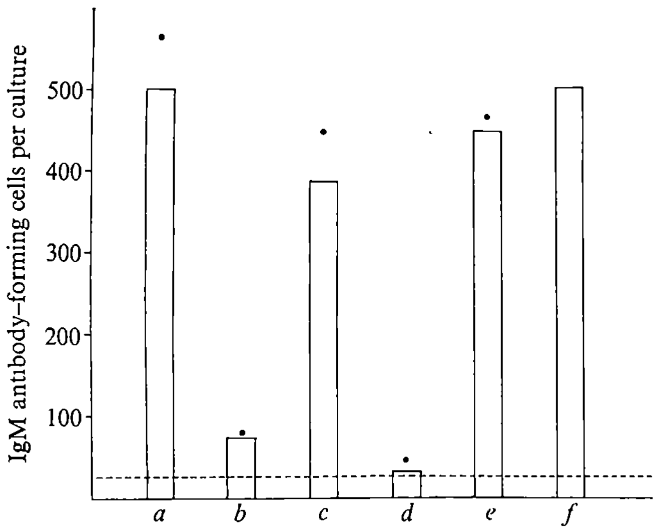

Fig. 2 Effect of anti-Ia^k and anti-Ly-3.2 sera and complement on specific suppressor cells generated *in vitro* from CBA spleen cells. Helper cells were induced as described previously[10]. In brief, spleen cells were cultured in Marbrook flasks with 0.1 µg KLH (a gift of Dr M. B. Rittenberg, Portland, Oregon) for 4 d in Eagle's MEM containing 5% foetal calf serum. Helper cells were assayed, in a second Marbrook culture, by their ability to cooperate with trinitrophenol (TNP)-reactive B cells present in normal CBA spleen in the presence of TNP–KLH. Anti-DNP or -TNP antibody-forming cells were assayed using hapten-conjugated anti-sheep red blood cell (SRBC) Fab′ fragments coupled to SRBC, using the Cunningham plaque assay. Suppressor cells were induced by culturing in similar conditions but with 100 µg KLH. Suppressors were assayed by their capacity to inhibit the helper effect of 3×10^5 helper cells. Tests for the specificity of the suppressor effect were as described previously[8]. Suppressor cells were treated with anti-Ia at 1:10 dilution or anti-Ly-3.2 at 1:20, washed and treated with absorbed rabbit complement at 1:10. After treatment cells were counted in Trypan blue and 10^4–10^5 viable cells assayed for suppressor activity. In absorption experiments sera were absorbed for 30 min at room temperature with an equal volume of packed spleen and thymus cells of appropriate mouse strain (A.TL or A.TH) and diluted to 1:10 for use. Dotted line, Number of plaques produced in presence of antigen but absence of helper cells. Dots above bars, s.e. *a*, Helper cells; *b*, helper cells+suppressor cells; *c*, complement+anti-Ia; *d*, complement+anti-Ia (absorbed using A.TL); *e*, complement+anti-Ia (absorbed using A.TH); *f*, complement +anti-Ly 3.2.

Figure 1 presents the results of two typical experiments on CBA (H–2^k, Thy-1.2, Ly-1.1, 2.1, 3.2) killer cells. In both experiments anti-Thy-1.2 completely abolished cytotoxicity, whereas anti-Ia^k had no effect. Anti-Ly-1.1 and the mixture of anti-Ly-2.1+3.2 both substantially reduce killer cell activity. In similar experiments anti-2.1 and anti-3.2 reduced but never abolished cytotoxicity, the effect of an individual serum being less than the mixture. In contrast to these results, Fig. 2 shows the effects of some of the same antisera on suppressor activity. Anti-Ia abolished suppressor activity, whereas anti-Ly-1.1 had no effect up to $1/10^7$. We have previously shown that anti-Ly-2.1 alone completely abrogates suppressor activity[7]; Fig. 2 shows that the same is true for anti-Ly-3.2.

That the effect of the anti-Ia antiserum was due to activity against antigenic determinants coded by the *I* region, was confirmed by the results of absorption experiments (Fig. 2). The anti-CBA suppressor activity could be removed by absorption with A.TL lymphocytes, which have the same H–2^k *I* region as CBA, but not by A.TH cells which are H–2^s. Note that the serum was also able to abolish the suppressor activity of C57BL/10 cells (data not shown) which share with CBA only a single known *I* region specificity[14].

Table 1 presents an *in vivo* correlate of the *in vitro* data. KLH-primed T cells, which are able to cooperate with B cells *in vivo* to give an anti-hapten response, gave a greatly increased response after treatment with anti-Ia and complement, indicating that the treatment had removed a population of suppressor cells bearing the Ia determinant.

We conclude that the antigenic phenotype of CBA killer T cells is Ly-1$^+$,2$^+$,3$^+$,Ia$^-$, whereas suppressor cells are Ly-1$^-$,2$^+$,3$^+$,Ia$^+$. The Ly phenotype for killer cells differs from that found in C57BL mice (Ly-1.2, 2.2, 3.2) in which killer cells are Ly-1$^-$,2$^+$,3$^+$ (refs 6 and 16), but agrees with the finding that in the C57BL Ly-1.1 congenic mouse, killer cells seem to be Ly-1$^+$,2$^+$,3$^+$ (ref. 16). In the same study, anti-Ly-2.1 alone had little effect on killer cells. Our data do not distinguish between the possibility that some CBA killer cells bear either 2.1 or 3.2, or alternatively that all killer cells bear low concentrations of both antigens, but it seems likely that there is heterogeneity among killer cells.

Table 2 Ly phenotype of T cell subsets

Function	Ly phenotype	Reference
Helper	1$^+$	7, 21
Suppressor	2$^+$ 3$^+$	7, 22, 23
Killer in Ly-1.1 mice	1$^+$ 2$^+$ 3$^+$	6, 16
in Ly-1.2 mice	2$^+$ 3$^+$	6, 16

It is also clear that although anti-Ly sera are useful markers for T cell subsets, antisera to the two alleles of each locus do not always have the same effect. The reason for this discrepancy is not yet clear but may reside in undetected residual genetic heterogeneity in the Ly congenic stocks or in the differences in titre of the various sera (discussed in ref. 16). Table 2 summarises current information on the Ly phenotype of T cell subsets.

Our findings confirm a previous report that suppressor

Table 1 Reduction of suppressor cell activity by treatment with anti-Ia serum and complement

DNP-primed cells	KLH-primed helper cells	Treatment	Antigen	Anti-DNP response (PFC/spleen)
10×10^6	Nil	Nil	50 µg DNP KLH	3,660±660
10×10^6	2×10^6	Nil	50 µg DNP KLH	9,240±686
10×10^6	2×10^6	C′ alone	50 µg DNP KLH	9,720±362
10×10^6	2×10^6	Anti-Ia+C′	50 µg DNP KLH	26,340±2,882
10×10^6	2×10^6	Anti-Thy-1.2+C′	50 µg DNP KLH	3,480±595

CBA mice (70–200-d old) were used. Mice were primed to dinitrophenol (DNP) by intraperitoneal immunisation, 6 weeks before use, with 100 µg alum-precipitated DNP–chicken γ globulin KLH helper cells were prepared by two intraperitoneal immunisations with 100 µg KLH absorbed to Bentonite at weekly intervals and subsequently boosted with 100 µg soluble KLH. Five days after the last injection a spleen cell suspension was prepared and passed over nylon wool columns to remove B cells[15]. Effluent cells were treated with anti-Ia^k or anti-Thy-1.2, followed by complement C′. Treated cells were mixed with DNP-primed cells and injected into 750 R irradiated CBA hosts These were boosted intraperitoneally 1 d later with 50 µg DNP–KLH. Seven days later the spleens were removed and assayed for IgG DNP plaque-forming cells.

cells bear Ia determinants[17], and provide new information that killer cells are Ia negative. The finding of Ia on suppressor cells is particularly interesting in view of recent data showing that specific suppressor factor isolated from T cells, carried similar antigens[18]. Although some workers have failed to detect Ia antigens on T cells[19], others have reported that both thymocytes and peripheral T cells carry these antigens[20]. Our data using functional assays for T cells show that at least suppressor T cells carry antigen(s) coded in the *I* region of the *H-2* complex. It is not clear whether exactly the same Ia antigen(s) was detected on B and T cells.

We thank Dr U. Hammerling (Memorial Sloan Kettering Cancer Center, New York) for anti-Ly and anti-Ia sera, and Dr H. O. McDevitt for anti-Ia.

P. C. L. BEVERLEY
J. WOODY
M. DUNKLEY
M. FELDMANN

Tumour Immunology Unit,
Department of Zoology,
University College London,
Gower Street, London WC1E 6BT, UK

I. MCKENZIE

Department of Medicine,
Austin Hospital,
Victoria, Australia

Received May 10; accepted July 6, 1976.

1 Beverley, P. C. L., in *T and B Lymphocytes in Immune Recognition* (edit. by Loor, F., and Roelants, G.) (Wiley, Chichester, UK, in the press).
2 Cantor, H., and Asofsky, R., *J. exp. Med.*, **131**, 235–246 (1970).
3 Simpson, E., and Cantor, H., *Eur. J. Immun.*, **1**, 337–343 (1975).
4 Feldmann, M., Erb, P., Kontiainen, S., and Dunkley, M., in *Membrane Receptors of Lymphocytes* (edit. by Seligmann, M., Preud'homme, J. L., and Kourilsky, F. M.), 305–310 (North-Holland, Amsterdam, 1975).
5 Boyse, E. A., Myazawa, M., Aoki, T., and Old, L. J., *Proc. R. Soc.*, **B170**, 175–193 (1968).
6 Cantor, H., and Boyse, E. A., *J. exp. Med.*, **141**, 1389–1399 (1975).
7 Feldmann, M., Beverley, P. C. L., Dunkley, M., and Kontiainen, S., *Nature*, **258**, 614–616 (1975).
8 Kontiainen, S., and Feldmann, M., *Eur. J. Immun.* (in the press).
9 Wagner, H., and Feldmann, M., *Cell. Immun.*, **4**, 39–50 (1972).
10 Kontiainen, S., and Feldmann, M., *Nature new Biol.*, **245**, 285–286 (1973).
11 Simpson, E., Gordon, R., Taylor, M., Mertin, J., and Chandler, P., *Eur. J. Immun.*, **5**, 451–455 (1975).
12 Scheid, M., Boyse, E. A., Carswell, E. A., and Old, L. J., *J. exp. Med.*, **135**, 938–955 (1972).
13 Hammerling, G. J., Deak, B. D., Mauve, D., Hammerling, U., and McDevitt, H. O., *Immunogenetics*, **1**, 68–81 (1974).
14 Klein, J., in *Biology of the Mouse Histocompatibility Complex*, 451 (Springer, Berlin, 1975).
15 Julius, M. H., Simpson, E., and Herzenberg, L. A., *Eur. J. Immun.*, **3**, 645–649 (1975).
16 Shiku, H., *et al.*, *J. exp. Med.*, **141**, 227–241 (1975).
17 Hammerling, G. J., Black, S. J., Segal, S., and Eichmann, K., *Proc. Tenth Leukocyte Culture Conf.* (edit. by Eijvoogel, V. P., Roos, D. and Zeiljmaker, W. P.), 367–378 (Academic, New York and London, 1976).
18 Tada, T., Taniguchi, M., and Takemori, T., *Transplant. Rev.*, **26**, 106–129 (1975).
19 Sachs, D. H., and Cone, J. L., *J. exp. Med.*, **138**, 1289–1304 (1973).
20 Frelinger, J. A., Niederhuber, J. E., David, C. S., and Shreffler, D. C., *J. exp. Med.*, **140**, 1273–1284 (1974).
21 Cantor, H., and Boyse, E. A., *J. exp. Med.*, **141**, 1376–1389 (1975).
22 Cantor, H., Shen, F. W., and Boyse, E. A., *J. exp. Med.*, **143**, 1391–1401 (1976).
23 Vadas, M. A., *et al.*, *J. exp. Med.* (in the press).

Plasma membrane glycoprotein which mediates adhesion of fibroblasts to collagen

DEFECTS in cell behaviour associated with malignancy may be causally related to alterations in the plasma membrane of the cell on transformation[1]. Much interest has focused on a protein found on the surface of normal but not transformed cells [2–7]. This protein, designated SF (ref. 5), LETS (ref. 8), band 1 (ref. 9), Ll (ref. 3) or CSP (ref. 10), is a glycoprotein[7,9,11] with a molecular weight of 210,000–250,000 (refs 7, 8 and 12). It is present in the serum[12] and is sensitive to removal from the surface of normal fibroblasts by low levels of trypsin[2,3,9]. Several biological properties of this protein have been described. Normal fibroblasts arrested in mitosis lack this protein[8,9]. As normal cells approach confluency, there is a quantitative increase in the amount of this protein present on the cell surface[8,9], whereas confluent normal cells, stimulated by the addition of serum, have lowered levels[8]. In conflict with these results, implying a growth regulatory function, is the finding that stimulation of growth-arrested normal cells by thrombin leads to thymidine incorporation without a concomitant decrease in the levels of this protein[13]. We now present evidence which points to a functional role for the protein as a mediator of the adhesion of fibroblasts to collagen. The protein is probably identical to a serum factor previously reported to be necessary for the attachment of SV40-transformed 3T3 fibroblasts to collagen-coated dishes[14]. Based on this functional role, we propose the name cell adhesion factor (CAF) for this protein.

Table 1 Attachment of PyBHK cells to collagen in the presence of added factors

Protein addition	Concentration of added protein	% PyBHK cells attached to collagen
None	—	8
Serum (%)	1	50
	10	90
	50	96
CAF (μg ml^{-1})	0.5	3 (0–6)
	1	4 (2–7)
	5	9 (7–12)
	10	12 (10–15)
	20	29 (25–32)
	30	71 (65–77)
	40	90 (86–93)
	80	96 (94–97)
PyBHK extract (μg ml^{-1})	100	5

Assessment of cell binding to collagen-coated dishes in the presence or absence of CAF was carried out essentially as described by Klebe[14]. Plastic Petri dishes (60-mm diameter) were evenly covered with 1.5 ml 0.25% collagen (acid soluble, Type IV, Sigma) in 0.2% acetic acid plus 0.002% phenol red. Dishes were placed in plastic containers, containing open dishes filled with NH_4OH and the containers were sealed for 10 min to allow for gelation of the collagen. The dishes were air-dried overnight, washed with 8 M urea for 20 min then three times for 5 min with H_2O, and allowed to air-dry. The treatment with urea decreased attachment of cells in the absence of added protein and increased the effectiveness of CAF-mediated attachment. Coated dishes were incubated with either 0.5 ml medium, calf serum, or CAF at various concentrations for 1 h at 37 °C. All solutions contained 200 μg ml^{-1} BSA. During this incubation, cells were removed from monolayers with 0.25% trypsin–EDTA (Gibco), washed twice with medium containing 200 μg ml^{-1} BSA, and counted in a Coulter counter. Incubated dishes then received 10^6 cells in 4.5 ml E4-BSA. After incubation for 1.5 h, unattached cells were removed by decanting the medium and washing gently once with fresh medium. Attached cells were removed by treatment with trypsin–EDTA and cells counted in a Coulter counter. The percentage of cells attached to the collagen was calculated as the number of attached cells/total number of attached cells plus the number of unattached cells. Usually 80–90% of plated cells were recovered. The average of five determinations and the range of values are given. Protein was determined by the method of Lowry *et al.*[19].

The BHK 21/C13 hamster cells and a derivative transformed by polyoma virus (PyBHK) were obtained from stocks at the Imperial Cancer Research Fund, London, and were maintained in Dulbecco's modification of Eagle's medium (E4) containing 10% calf serum (Gibco) in a 5% CO_2 incubator at 37 °C. The BHK cells possess high

Table 2 Ca^{2+} and Mg^{2+} dependence of cell attachment to collagen in the presence of CAF

Cell	CAF (μg ml^{-1})	Ca^{2+}/Mg^{2+}*	% Cells attached†
PyBHK	—	—	5
PyBHK	100	—	9
PyBHK	—	+	8
PyBHK	100	+	93

*Assayed in PBS (Gibco) in the presence or absence of CAF or in PBS containing Ca^{2+} and Mg^{2+} (Gibco) with or without CAF as described in Table 1 and ref. 14.

†Average of two determinations.

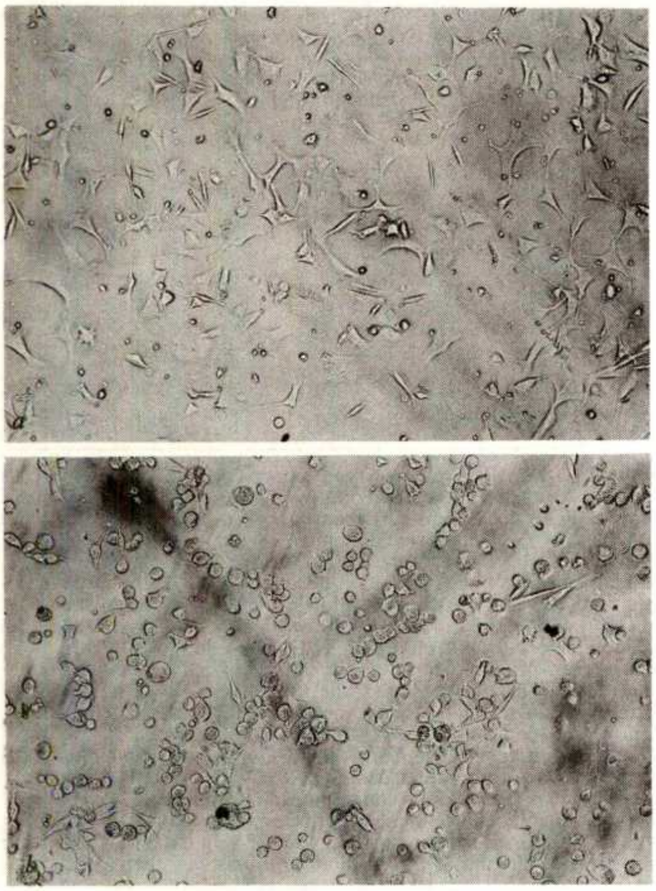

Fig. 1 Attachment of PyBHK cells to collagen-coated dishes under the influence of CAF (magnification × 65). Cells were incubated 1.5 h at 37 °C with 80 µg ml^{-1} CAF (*a*) and media containing 200 µg ml^{-1} BSA (*b*).

levels of CAF, whereas the PyBHK cells lack detectable amounts[9].

CAF was purified from BHK cells as described previously[15]. Polyacrylamide gel analysis demonstrated that the major purified protein co-migrated with the lactoperoxidase iodinated CAF obtained after surface labelling of BHK cells[9]. Immediately before use in the attachment assay, purified CAF was solubilised in medium containing 200 μg ml^{-1} BSA.

BHK-extracted CAF was effective in mediating the attachment of cells to collagen-coated dishes. The results shown in Table 1 clearly indicated a dose-dependent attachment to collagen in the presence of CAF. In agreement with others[14], no attachment was seen in medium containing only 200 μg ml^{-1} BSA. In optimal conditions, 96% of recovered cells had attached to the dishes. Table 1 shows that half-maximal attachment occurred at approximately 25 μg ml^{-1} CAF. Extracts of PyBHK at 100 μg ml^{-1} failed to enhance attachment of cells to the collagen.

The photographs of cells in Fig. 1*a* demonstrate that cells in the presence of CAF were flat and extended, morphologically identical to cells in the presence of serum. In contrast, cells plated on to collagen in medium containing 200 μg ml^{-1} BSA retained a rounded, refractile appearance (Fig. 1*b*). At concentrations of CAF which permitted half-maximal attachment of cells, a mixture of flat and rounded cells was apparent.

Attachment of cells to collagen in the presence of CAF was dependent on physiological concentrations of divalent ions, PyBHK cells failing to attach to collagen substrates in phosphate buffered saline (PBS) unless Ca^{2+} and Mg^{2+} were also present (Table 2).

When BHK cells, which contain high levels of CAF (ref. 9), were removed from confluent monolayers with trypsin–EDTA at levels of trypsin which completely remove surface CAF (ref. 9) their reattachment to collagen was also mediated by CAF with results paralleling those given for PyBHK (data not shown).

The demonstration[16] that CAF purified from chick embryo fibroblasts agglutinates formalinised erythrocytes and that agglutination could be inhibited by substances containing free amino groups, prompted our assessment of their inhibitory properties during adhesion of cells to collagen. Inhibition was determined at two stages of CAF-mediated cell-adhesion: during CAF binding to collagen and during interaction of cells with CAF–collagen complexes. The results demonstrate that when 0.1 M L-lysine was present during the first but not the second incubation, cell attachment proceeded unimpeded, but with L-lysine present during only the second incubation, the flat, extended morphology of attached cells was completely inhibited, and the cells retained a rounded morphology. They did seem, however, to be more firmly associated with collagen than they were in the presence of E4–BSA alone, as judged microscopically by shaking the dish and observing that in E4–BSA the cells floated freely, whereas in the presence of serum plus inhibitor, the cells were not freely floating but loosely associated with the collagen. Quantification of the extent of this association was difficult because the cells were readily dislodged by gentle washing.

Table 3 Inhibition of serum- or CAF-mediated adhesion of PyBHK cells to collagen

First incubation	Second incubation	Morphology
10% Serum	Media	Flat, extended
CAF	Media	Flat, extended
10% Serum + 0.1 M L-lysine	Media	Flat, extended
CAF + 0.1 M L-lysine	Media	Flat, extended
10% Serum	Media + 0.1 M L-lysine	Rounded
CAF	Media + 0.1 M L-lysine	Rounded
10% Serum + 0.1 M D-galactose	Media	Flat, extended
CAF + 0.1 M D-galactose	Media	Flat, extended
10% Serum	Media + 0.1 M D-galactose	Flat, extended
CAF	Media + 0.1 M D-galactose	Flat, extended

Final concentration of CAF 100 µg ml^{-1}. The following inhibitors also prevented adhesion of cells to collagen when added during the second incubation: D-mannosamine (0.1 M), L-arginine (0.1 M), D-glucosamine (0.1 M) and D-galactosamine (0.1 M). The following compounds failed to inhibit cell adhesion when present at either incubation: D-glucose (0.1 M), glycine (0.1 M), and α-methyl-D-mannoside (0.1 M). Substances were tested for inhibition of cell attachment to collagen in the presence of 10% calf serum or purified CAF as follows: collagen-coated 30-mm dishes were incubated 1 h at 37 °C with 0.5 ml medium with or without 0.1 M concentration of the test substances. All inhibitors were dissolved in PBS and adjusted to *p*H 7.4 before use. Dishes were then washed twice with E4–BSA (20 °C) and 1 ml E4–BSA was added containing 5×10^5 PyBHK cells with or without the test substance. After an additional 1.5 h at 37 °C, dishes were inspected microscopically to ascertain cell morphology and adhesion.

Inhibition of adhesion by L-lysine could not be attributed to cytotoxicity. When cells were exposed to 0.1 M L-lysine, washed twice with E4–BSA and plated on to collagen preincubated with serum, the cells attached and flattened. Thus, cell viability was unaffected by the inhibitor.

As an additional control, D-galactose, which was negative in agglutinating erythrocytes[16], was assayed for its ability to inhibit cell adhesion. It failed to inhibit cell attachment at either incubation step (Table 3).

Similar experiments employing CAF extracted from BHK cells (Table 3) showed that the pattern of inhibition with the purified protein was identical to that obtained in experiments with serum plus inhibitor.

It has been demonstrated[17] that transformed cells which lack surface CAF are capable of synthesising this protein and secreting it into the medium. Therefore, conditioned medium from normal and transformed cells were assayed for active CAF. The results (Table 4) demonstrate that factor secreted from either BHK or PyBHK cells was capable of mediating the adhesion of cells to collagen. L-lysine, an inhibitor of serum and CAF-mediated attachment during the second incubation step, also prevented adhesion in the presence of conditioned medium.

It seems that CAF, extracted from normal cells by urea, is active in promoting attachment of cells to collagen. The attachment is dependent on dose, with 50% attachment occurring at 25 μg ml^{-1} CAF (Table 1). Using the method of urea extraction with chick embryo fibroblasts, Yamada *et al.*[16] have extracted CAF in greater than 95% purity. With BHK cells, however, purity was never greater than approximately 60% as judged by electrophoresis in polyacrylamide gel, so that 25 μg ml^{-1} represents an overestimate of CAF added.

Table 4 Promotion of adhesion of cells to collagen by conditioned medium (CM)

Source of conditioned medium	First incubation	Second incubation	Morphology
BHK	CM	Medium	Flat, extended
BHK	CM+0.1 M L-lysine	Medium	Flat, extended
BHK	CM	Medium+0.1 M L-lysine	Rounded
PyBHK	CM	Medium	Flat, extended
PyBHK	CM+0.1 M L-lysine	Medium	Flat, extended
PyBHK	CM	Medium+0.1 M L-lysine	Rounded

Confluent monolayers of BHK and PyBHK cells on 6-cm dishes were washed three times with E4, replenished with 2 ml serum-free E4 and incubated for 24 h. The conditioned medium was removed, spun at 2,000 r.p.m. for 2 min in siliconised test tubes to pellet contaminating cells, dialysed for 48 h against distilled water, lyophilised in siliconised flasks and dissolved in E4–BSA immediately before use. Assays for cell adhesion in conditioned medium were identical to those described previously.

That a minor component of the BHK–urea extract was not responsible for promotion of adhesion is supported by the fact that: urea extracts of PyBHK cells which lack CAF failed to promote attachment; CAF and adhesion activity are both non-dialysable; and inhibition of adhesion by specific compounds exactly parallels results obtained by Yamada *et al.*[16] with pure CAF to inhibit the agglutination of erythrocytes. Production of an antibody specific for CFA, followed by inhibition experiments, would allow a direct demonstration of the role for CAF in cell attachment and spreading.

Specific inhibitors are effective in preventing firm cell adhesion and spreading when added during the second incubation (Table 3). As judged microscopically during gentle shaking of the dish, however, cells in the presence of CAF plus inhibitors were weakly adherent to the collagen when compared with cells plated solely in E4–BSA. In the presence of inhibitors, the cells retained a rounded morphology and failed to flatten and extend. It is unclear whether CAF is involved in both attachment and spreading, of which only the spreading is inhibited by the amino-containing substances; or whether another factor present in serum, urea extracts, and conditioned medium is responsible for attachment and CAF for cell spreading.

It has been demonstrated[17] that CAF is secreted by SV40-transformed human fibroblast lines although these cells do not retain membrane-bound CAF. It is also known that CAF is turned over from the surface of normal fibroblasts[9]. We have demonstrated (Table 4) that CAF released into the medium from normal or transformed cells is active in promoting attachment of cells. Therefore, CAF produced by transformed cells is a biologically functional molecule and might be absent from the plasma membrane of transformed cells because of some other defect of the transformed cell plasma membrane.

CAF is a normal constituent of serum[12], and Klebe[14] has shown that a serum factor necessary for the adhesion of cells to collagen has a molecular weight greater than 200,000, binds to DEAE, and requires physiological concentrations of Ca^{2+} and Mg^{2+} to express its function. CAF also has a molecular weight greater than 200,000 (refs 7, 8 and 12), binds to DEAE (unpublished observations) and requires Ca^{2+} and Mg^{2+} to promote adhesion (Table 2). In addition, we have found (Table 3) that whether the source of adhesion factor was serum or BHK extracts, the pattern of inhibition of adhesion by various substances was identical. Since in all these properties the serum factor corresponds to CAF it seems possible that they are identical. The activity of the serum factor was, however, resistant to 10 μg ml^{-1} trypsin[14], whereas CAF was susceptible to lower concentrations[16]. Therefore, additional work is needed to clarify the relationship between these factors.

Several types of transformed sarcoma-producing cell lines contain detectable levels of CAF (ref. 18) as determined by lactoperoxidase-catalysed iodination. Because PyBHK cells produce biologically active CAF (Table 4), it is likely that the CAF retained by some of the sarcoma-producing lines will also prove to be biologically active. Collagen is the natural substratum for fibroblasts *in vivo* and since CAF mediates the adhesion of these cells to collagen, it would be of great interest to correlate the presence or absence of CAF on transformed cells with tumour metastasis *in vivo*.

As mentioned, purified CAF can agglutinate formalinised sheep erythrocytes[16]. We believe the designation CAF to be broad enough to encompass the functions of both agglutination and adhesion.

I thank Mrs Beatrice Pyatt and Ms Marlene Chavis for assistance. Supported by a grant from the USPHS.

EDWARD PEARLSTEIN

Irvington House Institute and
Department of Pathology,
New York University Medical Center,
550 First Avenue,
New York, New York 10016

Received April 26; accepted June 9, 1976.

[1] Abercrombie, M., and Ambrose, E. J., *Cancer Res.*, **22**, 525–548 (1962).
[2] Hynes, R. O., *Proc. natn. Acad. Sci. U.S.A.*, **70**, 3170–3174 (1973).
[3] Hogg, N. M., *Proc. natn. Acad. Sci., U.S.A.*, **71**, 489–492 (1974).
[4] Gahmberg, C. G., Kiehn, D., and Hakomori, S., *Nature*, **248**, 413–415 (1974).
[5] Vaheri, A., and Ruoslahti, E., *Int. J. Cancer*, **13**, 579–586 (1974).

[6] Wickus, G. G., Branton, P. E., and Robbins, P. W., in *Control of Proliferation in Animal Cells* (edit. by Clarkson, B., and Baserga, R.), 541–545 (Cold Spring Harbor New York, 1974).
[7] Stone, K. R., Smith, R. E., and Joklik, W. K., *Virology*, **58**, 86–100 (1974).
[8] Hynes, R. O., and Bye, J. M., *Cell*, **3**, 113–120 (1974).
[9] Pearlstein, E., and Waterfield, M. D., *Biochim. biophys. Acta*, **362**, 1–12 (1974).
[10] Yamada, K. M., and Weston, J. A., *Cell*, **5**, 75–81 (1975).
[11] Hynes, R. O., and Humphryes, K. C., *J. Cell Biol.*, **62**, 438–448 (1974).
[12] Kuusela, P., Ruoslahti, E., and Vaheri, A., *Biochim. biophys. Acta*, **379**, 295 (1975).
[13] Teng, N. N. H., and Chen, L. B., *Proc. natn. Acad. Sci. U.S.A.*, **72**, 413–417 (1975).
[14] Klebe, R. J., *Nature*, **250**, 248–251 (1974).
[15] Yamada, K. M., and Weston, J. A., *Proc. natn. Acad. Sci. U.S.A.*, **71**, 3492–3496 (1974).
[16] Yamada, K. M., Yamada, S. S., and Pastan, I., *Proc. natn. Acad. Sci. U.S.A.*, **72**, 3158–3162 (1975).
[17] Vaheri, A., and Ruoslahti, E., *J. exp. Med.*, **142**, 530–535 (1975).
[18] Pearlstein, E., Hynes, R. O., Franks, L. M., and Hemmings, V. J., *Cancer Res.*, **36**, 1475–1480 (1976).
[19] Lowry, O. H., Rosebrough, N. J., Farr, A. L., and Randall, R. J., *J. biol. Chem.*, **193**, 265–275 (1951).

Temporary intestinal hypoxia induced by degradable microspheres

IN all mammalian cells and tissues studied, the adequate presence of molecular oxygen during irradiation enhances the effects of ionising radiations of low linear energy transfer (LET), such as X rays, γ rays or electrons, by a factor of 2 or 3, compared with the effects seen after irradiation in poor oxygenation conditions[1,2]. In radiotherapy, this oxygen enhancement ratio (OER) is assumed to be generally effective in all healthy tissues, whereas in poorly oxygenated tumour cells the partial radioprotection through hypoxia is believed to be efficient to an extent that the probability of tumour sterilisation may be affected critically[3,4]. It has been suggested that the relative concentration of oxygen in healthy and tumour tissues could be changed to improve the relative probability of curing the disease and of reducing clinical complications caused by radiation damage of healthy tissues. To this end, the introduction of 'high LET' radiations for which the oxygen effect is of little importance, is presently being attempted[5]. Attempts are also being made to increase the oxygen tension in poorly oxygenated areas by treatment of patients with hyperbaric oxygen during irradiation[6]. In experiments in our laboratories, we have tried various means of changing the oxygen concentrations in tissues to be irradiated by chemical removal of oxygen[7] or by mechanical obstruction of the blood flow (K.E.A., J.O.F., C. Clintenberg, B.L., B.R. and S.Ö., unpublished). We are now investigating, in experiments on pigs, the possibility of attaining temporary local hypoxia in intestinal segments by obstructing the blood flow at the level of the arterioles by intra-arterial injection of cross-linked starch microspheres, 43 μm in diameter, that are degraded by the amylase activity of the serum[8]. With a proper choice of the degree of cross linking and of particle concentration, a hypoxic period of about 5 min duration, followed by rapid normalisation, was achieved.

Three female pigs of native breed (15–20 kg) were used under Nembutal anaesthesia. A high midline abdominal laparotomy was carried out and the base of the superior mesenteric artery was freed and catheterised using an Argyle No. 5 baby feeding tube. The catheter was fixed at the base of the mesenteric artery by a purse string suture and brought, for access, through the left abdominal wall and subcutaneously to the left groin, a loop being left in the abdominal cavity. The abdominal incision was closed and a loop of the small intestine was made available for inspection and measurement through a second incision through the right flank. Oxygen tension was measured with a modified Clark platinum electrode[9] put in direct contact with the mucous membrane of the jejunum through a small incision in the intestinal wall.

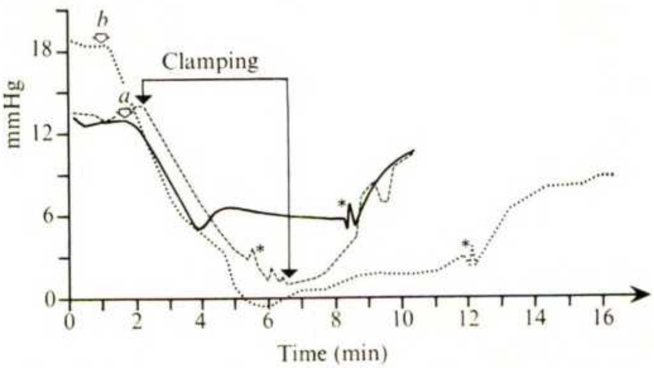

Fig. 1 Transient reduction in oxygen pressure on the jejunal mucous membrane after injection of 6×10^6 (*a*) or 30×10^6 (*b*) starch particles in the superior mesenteric artery of pigs. For comparison, the record seen after temporary mechanical 'clamping' of the vessel is also shown. *, Peristalsis.

Treatment, aimed at removal of oxygen from the intestinal segment under study, was carried out by injection of 6×10^6 (*a*) or 30×10^6 (*b*) microspheres suspended in 8 or 40 ml Ringer's solution for periods of 6 to 15 s, respectively. Alternatively, for comparison, the blood flow in the superior mesenteric artery was obstructed using a mechanical clamp.

Typical results are shown in Fig. 1. Curves *a* and *b* represent the records of the oxygen pressure during the experiments. Qualitatively, the curves are similar, showing a rapid decrease in the oxygen pressure to low values that persist for a period of 4–7 min. At the end of this phase of hypoxia a sudden peristaltic activity was apparent, initiating the phase of restoration in which the oxygen pressure rapidly returned to normal within 2–4 min (this phenomenon is also reflected in the diagram). The greater number of particles was more efficient in reducing the oxygen pressure in the intestinal mucous membrane to near zero. With the exception that restoration took place more rapidly, clamping led to similar behaviour of the recorded curves. When the oxygen pressure dropped below about 6 mmHg the intestinal segment became clearly pale. The measured and visually observed changes were well correlated in time and quite reproducible.

The results show that the intra-arterial injection of degradable starch microspheres, as described, can be used to bring about temporary intestinal hypoxia. By proper choice of the amount and concentration of particles in the injected suspension, the period of hypoxia can be programmed so as to enable experimental radiotherapy to be carried out in hypoxic conditions, seemingly without risk of damage caused by ischaemia.

The technique suggested is now subject to detailed experimental investigation in combination with irradiation. Its application to clinical radiotherapy is also being considered.

The experiments were supported by the Swedish Cancer Society.

K. E. ARFORS

Department of Experimental Medicine,
Pharmacia AB,
Uppsala, Sweden

J. O. FORSBERG
B. LARSSON

Department of Physical Biology,
The Gustaf Werner Institute,
University of Uppsala, Sweden

D. H. LEWIS
B. ROSENGREN
S. ÖDMAN

Department of Radiotherapy
and Clinical Research Center,
University of Linköping, Sweden

Received May 3; accepted June 2, 1976.

[1] Read, J., and Thoday, J. M., *Nature*, **160**, 608 (1947).
[2] Gray, L. J., Conger, A. D., Ebert, M., Hornsey, S., and Scott, O. C. A., *Br. J. Radiol.*, **26**, 638 (1953).

[3] Deschner, E. C., and Gray, L. H., *Radiat. Res.*, **11**, 115 (1959).
[4] Fowler, J. F., in *Current Topics in Radiation Research*, **II** (edit. by Ebert, M., and Howard, A.), 305 (North-Holland, Amsterdam, 1966).
[5] Barendsen, G. W., in *Current Topics in Radiation Research*, **IV** (edit. by Ebert, M., and Howard, A.), 295 (North-Holland, Amsterdam, 1968).
[6] van der Brenk, H. A. S., in *Current Topics in Radiation Research*, **V** (edit. by Ebert, M., and Howard, A.), 198 (North-Holland, Amsterdam, 1969).
[7] Larsson, B., and Sténson, S., *Nature*, **205**, 364 (1965).
[8] Arfors, E., *et al.* (in the press).
[8] Lindberg, B., Carlin, G., and Arfors, K. E., *AB Pharmacia, Uppsala*, Report File L302.
[9] Rink, R., and Kessler, M., in *Oxygen Transport to Tissue* (edit. by Bruly, D. F., and Bicher, H. I.), 469 (Plenum, New York, 1973).

Metabolic adaptation to pregnancy shown by increased biosynthesis of insulin in islets of Langerhans isolated from pregnant rats

MANY reports have indicated that insulin secretion is increased in pregnant women[1,2] although blood sugar levels may be unchanged, indicating an increased demand for insulin in human pregnancy. Similar findings have been reported for the effects of pregnancy on insulin secretion in pregnant rats[3,4] which begin to respond with a significantly increased insulin secretion at a lower glucose level than those found in the normal female[5]. In addition, the secretory response is considerably greater in islets of Langerhans from pregnant than in normal rats, indicating an overall increased sensitisation of the islets from pregnant rats to the effects of glucose[5]. Glucose has a major role in the metabolism of the mammalian β cell, in that at physiological concentrations it is capable of stimulating both insulin secretion and biosynthesis[6,7]. It is possible that increased insulin biosynthesis is necessary to support the increased secretory response to glucose in pregnancy, if the content of β cell insulin is to be maintained. We have therefore investigated whether the alterations in insulin secretion observed *in vivo* during pregnancy are paralleled by an enhanced insulin biosynthesis in isolated islets from pregnant rats, after exposure to increasing concentrations of glucose.

Islets of Langerhans were isolated by the method of Howell and Taylor[8], from age-matched normal female and 19-d pregnant rats. Groups of 15–20 islets were incubated in 0.5 ml bicarbonate-buffered medium *p*H 7.4[9], previously gassed with a mixture of 95% O_2 and 5% CO_2. The medium was supplemented with 1 mg ml^{-1} bovine albumin and contained various concentrations of glucose, as indicated in Fig. 1, together with 20 μCi ml^{-1} L-(4,5)-^{3}H-leucine of initial specific radioactivity 40 Ci $mmol^{-1}$. The tubes were then incubated with gentle shaking for 3 h at 37 °C. After incubation, the islets were rinsed twice in phosphate-buffered 0.9% saline, *p*H 7.4 (PBS), containing 1 mg ml^{-1} non-labelled L-leucine, and subsequently sonicated for 10 s in 150 λ μl of PBS. After a tenfold dilution, samples of the sonicate were taken for determination of protein content[10] using a crystalline bovine albumin standard. The synthesis of proinsulin and insulin in the pancreatic islets was estimated by determining the incorporation of labelled leucine into material reacting with insulin antibody (which also cross reacts with the precursor). The labelled insulin and proinsulin were separated from the rest of the islet proteins by incubation of a sample of the diluted islet sonicate with an excess of guinea pig anti-insulin serum (AIS) coupled to cyanogen bromide-activated Sepharose 4B (AIS–Sepharose)[11]. Normal guinea pig serum (NGPS) coupled to activated Sepharose (NGPS–Sepharose) served as a control for nonspecific binding of labelled proteins to the Sepharose beads. The nonspecific adsorption of proteins to the NGPS–Sepharose was examined after treatment of the beads with 2 M acetic acid. It was found that a small peak of radioactivity was eluted with the void volume on Sephadex G–50 gel chromatography, but there was virtually nothing present in the insulin or proinsulin regions. Normally the radioactivity bound to the AIS–Sepharose beads exceeded the nonspecific adsorption on NGPS–Sepharose by a factor of 2–5 in low (2 mM) and high (20 mM) glucose concentrations, respectively.

The biosynthetic response of the isolated islets to increasing glucose concentrations is shown in Fig. 1. Proinsulin–insulin biosynthesis was significantly greater ($P<0.01$) in islets from pregnant compared with non-pregnant rats, at all the glucose concentrations studied. Green and Taylor[5] have shown that there are increases in protein, DNA and insulin content of islets at day 19 of pregnancy, findings

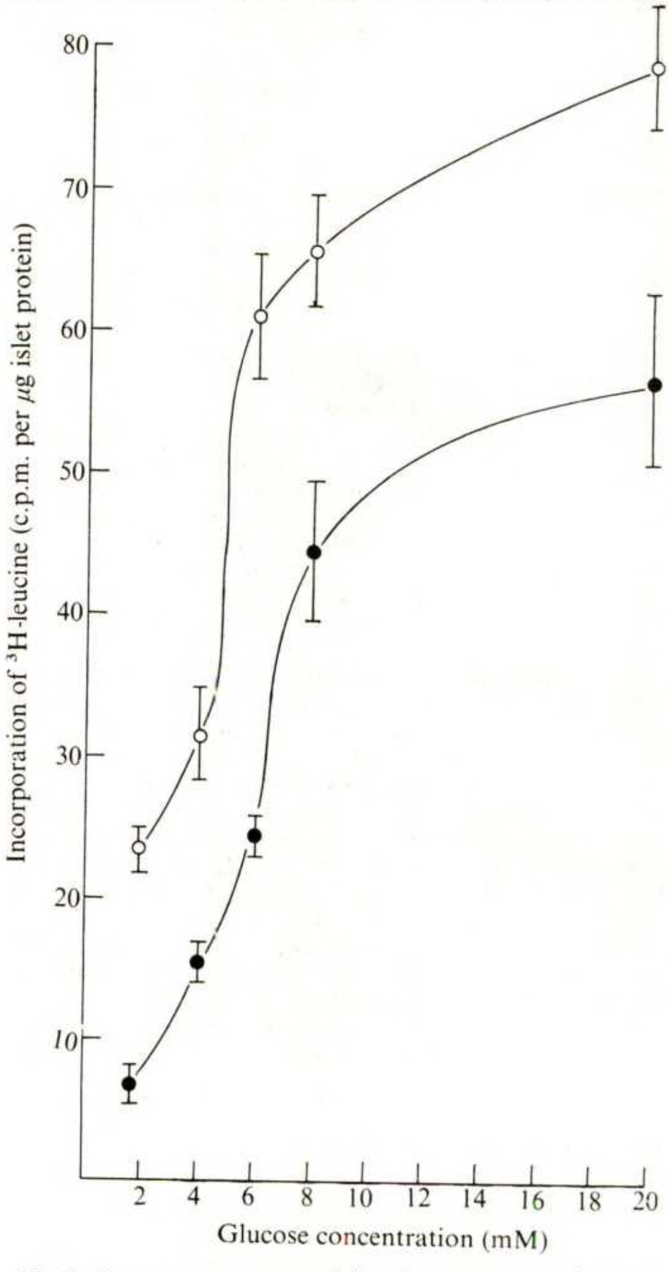

Fig. 1 Dose–response curve relating glucose concentration to the incorporation of L-4,5-^{3}H-leucine into AIS–Sepharose-bound proinsulin–insulin in islets from normal (●) and 19-d pregnant rats (○). Each point represents a mean of at least eight observations, with ±s.e.m. shown as vertical bars. Groups of 15–20 islets were incubated, washed and sonicated as described in the text; 20-μl samples of the diluted sonicates were then mixed with 1 ml PBS, supplemented with 2 mg ml^{-1} bovine albumin, and containing either 20 mg AIS–Sepharose or the same weight of NGPS–Sepharose according to the method of Berne[11]. The immune binding reaction was carried out in polythene tubes rotated end-over-end (20 r.p.m.) for 90 min at room temperature. The Sepharose beads were then washed six times with PBS and solubilised overnight in 0.8 ml Soluene 350 tissue solubiliser. Radioactivity was measured in a Beckman liquid scintillation counter after addition of 3 ml toluene-based scintillator.

confirmed by our islet protein estimations. Expressing incorporation per μg islet protein, however, we were able to nullify any differences in size and content of the isolated islets, thus enabling direct comparison of the biosynthetic response to glucose in islets from pregnant and non-pregnant rats. A sigmoidal curve is known to characterise the relationship between poinsulin–insulin biosynthesis and glucose concentration in normal islets[12]. The threshold value for the stimulant action of glucose, however, is lower in islets from pregnant rats, and in addition the rate of change of insulin biosynthesis is considerably greater than in normal islets (Fig. 1). Similar findings have been reported in the rat for the effects of pregnancy on the insulin secretory response of the islets of Langerhans[3–5]. On further examination of the sensitivity of the islets from pregnant rats to a glucose stimulus it is apparent that proinsulin–insulin biosynthesis has a lower threshold in terms of glucose stimulation than that for insulin release. Insulin biosynthesis is therefore more sensitive to glucose than is insulin release, and this will prevent the insulin stores of the β cells from becoming depleted at low glucose concentrations. This may be particularly important during pregnancy where blood sugar levels in fasted pregnant rats are significantly lower than those in fasted normal rats[5], such depressed glucose levels perhaps being associated with the increased plasma insulin levels reported in fasted rats during pregnancy[3].

The reasons for the heightened sensitivity of islets to glucose during pregnancy are at present uncertain. It has been suggested that there may be a possible involvement of increased adenylate cyclase activity or increased cyclic AMP concentrations in β cells, in controlling the altered secretory response[13]. Studies on the actions of theophylline and cyclic AMP at various glucose concentrations on biosynthesis of insulin compared with insulin secretion, prompted the suggestion by Schatz *et al.*[14], that the adenylate cyclase system besides regulating insulin secretion is involved in insulin biosynthesis. Other workers have postulated an increased sensitivity of a membrane receptor as a possible reason for changes in the sensitisation of islets to the effect of glucose[15], and changes of this type could also be operating during pregnancy. Whatever the mechanism by which it occurs, it is of great interest that at least three indices of islet activity are simultaneously increased in pregnancy. These are insulin release, insulin biosynthesis and islet glucose oxidation[16].

Further work is now in progress to elucidate more exactly the biochemical mechanisms by which the islets of Langerhans adapt to pregnancy.

We thank the British Diabetic Association for support. A.J.B. is an MRC research scholar.

A. J. BONE
K. W. TAYLOR*

Biochemistry Group,
University of Sussex,
Falmer, Brighton,
Sussex BN1 9QG, UK

Received May 10; accepted July 6, 1976.

*Present address: Department of Biochemistry, University of Sydney, New South Wales 2006, Australia.

[1] Spellacy, W. N., and Goetz, F. C., *New Engl. J. Med.*, **268**, 988–991 (1963).
[2] Trayner, I. M., Welborn, T. A., Rubenstein, A. H., and Russell-Fraser, T. R., *J. Endocr.*, **37**, 443–453 (1967).
[3] Costrini, N. V., and Kalkhoff, R. K., *J. clin. Invest.*, **50**, 992–999 (1971).
[4] Malaisse, W. J., Malaisse-Lagae, F., Picard, C., and Flament-Durand, J., *Endocrinology*, **84**, 41–44 (1969).
[5] Green, I. C., and Taylor, K. W., *J. Endocr.*, **54**, 317–325 (1972).
[6] Clark, J. L., and Steiner, D. F., *Proc. natn Acad. Sci. U.S.A.*, **62**, 278–285 (1969).
[7] Parry, D. G., and Taylor, K. W., *Biochem. J.*, **110**, 2c (1966).
[8] Howell, S. L., and Taylor, K. W., *Biochim. biophys. Acta*, **130**, 519–521 (1966).
[9] Gey, G. O., and Gey, M. K., *Am. J. Cancer*, **27**, 45–76 (1936).
[10] Lowry, O. H., Rosebrough, N. J., Farr, A. L., and Randall, R. J., *J. biol. Chem.*, **193**, 265–275 (1951).
[11] Berne, C., *Endocrinology*, **97**, 1241–1247 (1975).
[12] Pipeleers, D. G., Marichal, M., and Malaisse, W. J., *Endocrinology*, **93**, 1001–1011 (1973).
[13] Green, I. C., Howell, S. L., Montague, W., and Taylor, K. W., *Biochem. J.*, **134**, 481–487 (1973).
[14] Schatz, H., Maier, V., Hinz, M., Nierle, C., and Pfeiffer, E. F., *Diabetes*, **22**, 433–441 (1973).
[15] Matschinsky, F. M., *et al.*, *J. biol. Chem.*, **246**, 1007–1011 (1971).
[16] Green, I. C., and Taylor, K. W., *Diabetologia*, **11**, 344–5 (1975).

Electrophysiological evidence for coupling between β cells of pancreatic islets

IT has been shown that the β cells of pancreatic islets exhibit electrical activity when stimulated with insulin releasing agents[1–3]. There is evidence that this activity is directly correlated with the insulin release and that it has an important role in the secretory process[2,4,5]. More recently it was documented that β cells within an islet are connected by gap junctions[6,7] which are considered as low resistance pathways (ref. 8 and refs therein). The question therefore arises whether the electrical activity can spread electrotonically from one cell to another within an islet. To further elucidate this question the electrical activity from two different cells was measured by simultaneous impalement with two microelectrodes.

The experiments were done on microdissected islets of the mouse pancreas as described previously[2]. The islets were continuously perifused in a small Plexiglas chamber (volume ~1 ml) with a Krebs–Henseleit solution gassed with 95% O_2 and 5% CO_2. The temperature was kept constant at 37 °C. The basal medium had the following composition (mM): glucose 2.8, NaCl 103, KCl 4.7, $CaCl_2$ 2.56, $MgCl_2$ 1.13, $NaHCO_3$ 25, NaH_2PO_4 1.15, sodium pyruvate 4.9, sodium fumarate 2.7, sodium glutamate 4.9. When the glucose concentration was increased to 11.1 or 16.6 mM, NaCl was reduced by an appropriate amount to maintain the osmolarity.

The membrane potential was measured with microelectrodes filled with 2 M potassium citrate. Because the β cells are small (diameter ~10 μm) simultaneous recording from two cells was difficult and high resistance electrodes (tip resistance >200 MΩ) were necessary to obtain stable and long lasting impalements. The electrodes were mounted on two independent micromanipulators and impaled at an angle of approximately 10°. The distance between their tips was about 50 μm before impalement. Since the β cells in mouse islets are surrounded by a layer of α cells[9] they are invisible. Therefore, they could only be identified by their characteristic electrical activity in high glucose concentrations. Membrane potentials were recorded on a double beam oscilloscope (Tektronix 565) and a double trace chart writer (W+W 1200).

The glucose-induced electrical activity is characterised by a regular burst pattern[2,5]. It consists of periodic oscillations of the membrane potential (slow waves) between a depolarised state with superimposed fast spike activity, and a polarised, silent state (Fig. 1). The burst activity appears only in glucose concentrations which also stimulate insulin release[2]. The duration of the slow waves is strongly glucose dependent; it increases as the glucose concentration is raised[2,10]. The amplitude and the duration of the superimposed spikes are unaffected by a change of the glucose concentration.

When the electrical activity was simultaneously recorded from two cells within the same islet the slow waves were highly synchronised in 6 out of 7 double impalements; only in one case were the slow waves asynchronous. The synchronisation is demonstrated in Fig. 1. It is obvious that there was a strict temporal relationship between the depolarising as well as the repolarising phases of the slow waves in the two records. This relationship was unaltered also when during the regular burst pattern a slow wave with a shorter duration was interposed (Fig. 1*b*). The

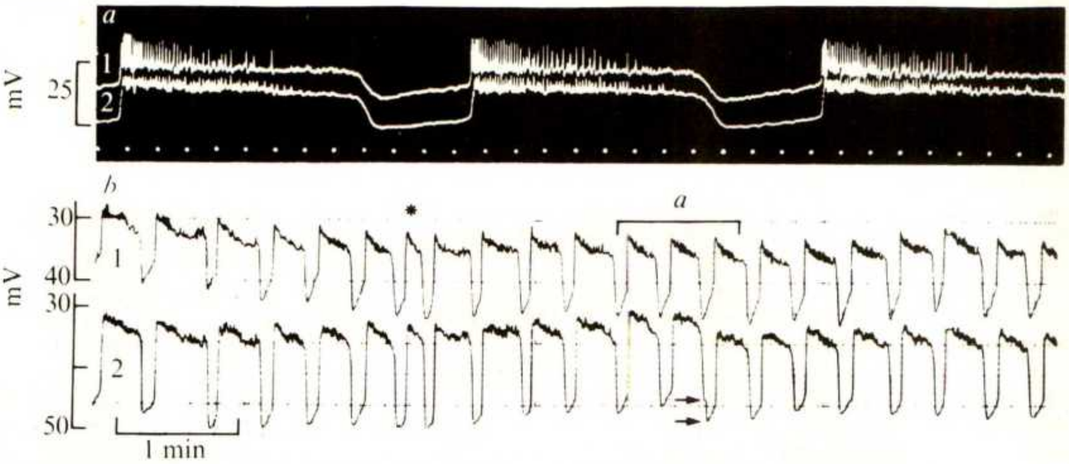

Fig. 1 Simultaneously recorded burst activity of two β cells perifused with 16.6 mM glucose. *a*, Oscilloscope record of the three bursts marked by the bar in record *b*. Distance between two subsequent points corresponds to 2 s. *b*, Train of bursts recorded with a chart writer. Trace 1 and 2 in *a* correspond to trace 1 and 2 in *b*, respectively. At the two arrows in *b* the offset was changed by about 3 mV. The asterisk in *b* denotes bursts with a short duration interposed between longer bursts. Note that the full amplitude of the spikes is not recorded in the chart recordings because of the inertia of the recording system.

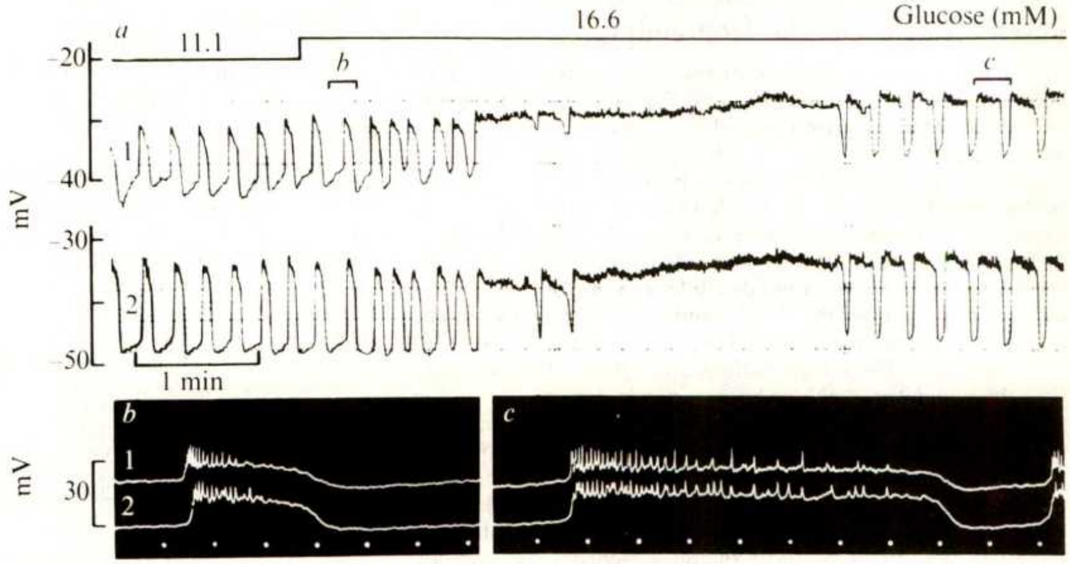

Fig. 2 Effect of changing the glucose concentration on the simultaneously recorded burst activity of two β cells. *a*, Continuous ink recording showing the time course of burst activity before and after changing the glucose concentration from 11.1 to 16.6 mM. *b* and *c*, Oscilloscope records taken at the times marked by bars in *a*. Time interval between two subsequent points in *b* corresponds to 2 s.

differences in the membrane potential values of the two cells shown in Fig. 1 are likely to be due to differences of the recording conditions and not to different properties of the impaled cells. As shown in Fig. 2, the synchronisation was also maintained when the external glucose concentration was changed, although the pattern of activity was markedly altered. It is unlikely that the synchronised activity was recorded from the same cell because the microelectrode tips were separated by distances which were several times the diameter of the β cell. This conclusion is supported by the observations shown in the oscilloscope records of Figs 1*a*, 2*b* and *c*; these records reveal that in contrast to the slow waves the superimposed spike activity was not identical at the two recording sites. From Fig. 3, which shows the spike activity on a faster time base, it becomes obvious that the spikes were well synchronised during the initial part of the burst (left half of Fig. 3) while later on, when the frequency decreased, the synchronisation was less pronounced. Thus, the spikes in the upper record of Fig. 3 appeared with an increasing delay compared with those in the lower trace (see spikes 20 to 30). Moreover, single spikes in one record were sometimes not accompanied by a corresponding spike in the other record (for example spike 30). Furthermore, if corresponding spikes were present in the two records the ratio of their amplitudes varied considerably; for instance spike 22 was larger in the lower than in the upper record, whereas for spike 29 the reverse was true.

The results show that the electrical activity is synchronised in a high percentage of β cells which are located closely together within an islet. This synchronisation concerns mainly the slow waves whereas the fast spike activity seems to be synchronised only partially. It has been established that the β cells are connected by gap junctions[6,7]; therefore it is probable that the synchronisation is due to electrical coupling. Although the ionic mechanisms producing the electrical activity in β cells so far are poorly understood it has been suggested that particularly the glucose-induced slow waves are an important link in triggering and regulating insulin release in the individual cell[2,5,10,11].

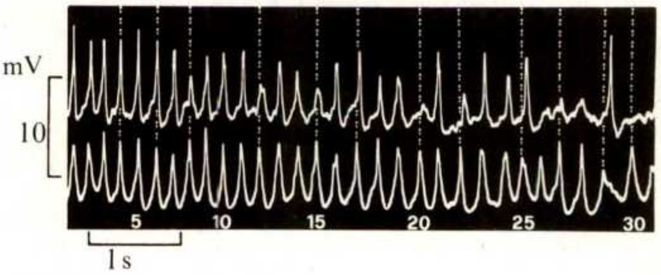

Fig. 3 Simultaneous oscilloscope records of spike activity of two β cells during the plateau phase of a slow wave. To allow comparison of the temporal relationship between spikes in the two records, the spikes have been numbered and dotted lines have been traced. Glucose concentration 16.6 mM.

Since many of these cells seem to be coupled electrically, it is possible that the slow wave originates in one cell and stimulates the coupled cells by electrotonic spread. From this point of view it is conceivable that within an islet the glucose molecule stimulates only a limited number of 'pacemaker cells' which then induce electrically the burst activity and insulin release in the coupled cells. The 'pacemaker cells' may be located in close vicinity to the blood capillaries and, therefore, be the first to come into contact with the glucose.

I thank Professor H. Schmidt for helpful comments on the manuscript. This work was supported by the Deutsche Forschungsgemeinschaft.

H. P. MEISSNER

Department of Physiology,
University of Saarland,
6650 Homburg/Saar, FRG

Received April 8; accepted May 6, 1976.

[1] Dean, P. M., and Matthews, E. K., *Nature*, **219**, 389–390 (1968).
[2] Meissner, H. P., and Schmelz, H., *Pflügers Arch.*, **351**, 195–206 (1974).
[3] Pace, C. S., and Price, S., *Endocrinology*, **94**, 142–147 (1974).
[4] Dean, P. M., Matthews, E. K., and Sakamoto, Y., *J. Physiol., Lond.*, **246**, 459–478 (1975).
[5] Meissner, H. P., and Atwater, I. J., *Horm. Metab. Res.*, **8**, 11–16 (1976).
[6] Orci, L., Unger, R. H., and Renold, A. E., *Experientia*, **29**, 1015–1018 (1973).
[7] Berger, W., Dahl, G., and Meissner, H. P., *Cytobiologie*, **12**, 119–139 (1975).
[8] Gilula, N. F., *Cell Communication* (edit. by Cox, R. P.) (Wiley, New York, 1974).
[9] Patent, G. J., and Alfert, M., *Acta anat.*, **66**, 504–519 (1967).
[10] Meissner, H. P., *J. Physiol., Paris* (in the press).
[11] Atwater, I., and Meissner, H. P., *J. Physiol., Lond.*, **247**, 56–58P (1975).

Decrease of Na^+ conductance during desensitisation of the frog endplate

THE membrane depolarisation of the frog endplate caused by acetylcholine (ACh), either released from the nerve terminals or applied externally, decreases when such applications of ACh are persisted or repeated[1,2]. This phenomenon, known as 'densitisation' or 'inactivation' of the receptor to ACh, was first analysed by Katz and Thesleff[1] and was suggested to be caused by a change in the receptor molecule from an effective to a refractory state. Subsequent investigations revealed that the rate of this desensitisation depends both on the extracellular concentration of Ca^{2+} ($([Ca^{2+}]_0)$)[3-5] and on membrane potential[6]; being speeded up by increasing $[Ca^{2+}]_0$ or hyperpolarisation of the membrane. These observations and others, demonstrating that the endplate membrane became permeable to Ca^{2+} during the action of ACh (ref. 7), led to the hypothesis that desensitisation was brought about by transmembrane movement of Ca^{2+} and the combination of the ions with anionic sites on the inner surface of the endplate membrane[4,5]. The question then arises of whether desensitisation is caused by molecular changes in the ACh receptor or by those of the subsequent step directly controlling the ionic conductance of the endplate membrane. This subsequent step may involve a macromolecule which has been termed "ion channel" or "ion conductance modulator"[8]. In an attempt to answer this question, we measured changes in the equilibrium potential of the endplate membrane during desensitisation, using a voltage-clamp technique[9,10].

Sciatic nerve–sartorius muscle preparations were isolated from frogs (*Rana nigromaculata*). Conventional intracellular recording techniques and a voltage clamp circuit were as used previously[11]. Ionic composition of Ringer's solution was as follows (mM): NaCl, 115; KCl, 2.0; $CaCl_2$, 1.8; NaH_2PO_4, 0.7; Na_2HPO_4, 1.3. Experiments were carried out at room temperature (20–22 °C). Electrodes for iontophoresis of ACh (2 M) had tip resistances of 100–140 MΩ and a braking current of a few nA was applied constantly.

Endplate currents (ACh-induced current) were evoked by iontophoretic applications of ACh at a rate of 0.2 Hz and at different levels of membrane potential. Thus, the endplate conductance ($G_{\rm epc}$) and its equilibrium potential ($E_{\rm epc}$) before desensitisation occurred were obtained (Fig. 2*a*). The endplate membrane was then desensitised by generating a series of ACh-induced currents at a relatively high rate (20 Hz), as demonstrated by Magazanik and Vyskocil[12] and as shown in Fig. 1. During repeated applications, the amplitude of ACh-induced currents decreased and after 20 s became 25% of the initial level. When the desensitisation had developed sufficiently, the level of membrane potential was changed from the holding potential of −50 mV up to −105 mV. Accordingly (Fig. 2*a*) changes in $G_{\rm epc}$ and $E_{\rm epc}$ during desensitisation can be compared with those before desensitisation occurred. There was a marked shift of the $E_{\rm epc}$ to a more negative value (the mean shift; -25.4 ± 5.6 mV (s.e.), $n = 9$) during desensitisation, accompanied by a decrease in the $G_{\rm epc}$ ($37.3 \pm 2.9\%$ of the control value, $n = 9$). It is unlikely that the lines, shown in Fig. 2*a*, relating the amplitude of the ACh-induced current to membrane potential before and during desensitisation will converge to the same membrane potential. In fact, in some cells, there was complete disappearance of ACh-induced currents at −50 mV during desensitisation, whereas the $E_{\rm epc}$ obtained by extrapolation before the development of densitisation was −10 mV. These results indicate that a decrease in the Na^+ conductance ($G_{\rm Na}$) of the endplate membrane would occur in these conditions.

Before this conclusion is accepted, however, the possibility should be considered that the shift in $E_{\rm epc}$ during desensitisation might be caused by a change in the equilibrium potential for Na^+ ($E_{\rm Na}$) because of an influx of Na^+ during repeated activation of the endplate membrane. To test this possibility, the $E_{\rm epc}$ was measured during repetitive generation of ACh-induced currents in low $[Ca^{2+}]_0$, where the rate of desensitisation was very slow. In this situation, if the shift of the $E_{\rm epc}$ during repetitive applications of ACh is a result of a change in the $E_{\rm Na}$, there would be a similar, or even a greater change, in the $E_{\rm epc}$ than that at normal $[Ca^{2+}]_0$, since the decrease in the amplitude of ACh-induced currents during repeated activations is smaller at low $[Ca^{2+}]_0$ (Fig. 2*b*). Even after the generation of 400 ACh-induced currents, there was only a small change in $E_{\rm epc}$ during applications of ACh at 0.45 mM $[Ca^{2+}]_0$, eliminating the possibility that the negative shift of $E_{\rm epc}$ during desensitisation seen at 1.8 mM $[Ca^{2+}]_0$ was the result of accumulation of Na^+ in the intracellular space. The change in the $E_{\rm epc}$ therefore seems to be caused by the reduction of $G_{\rm Na}$

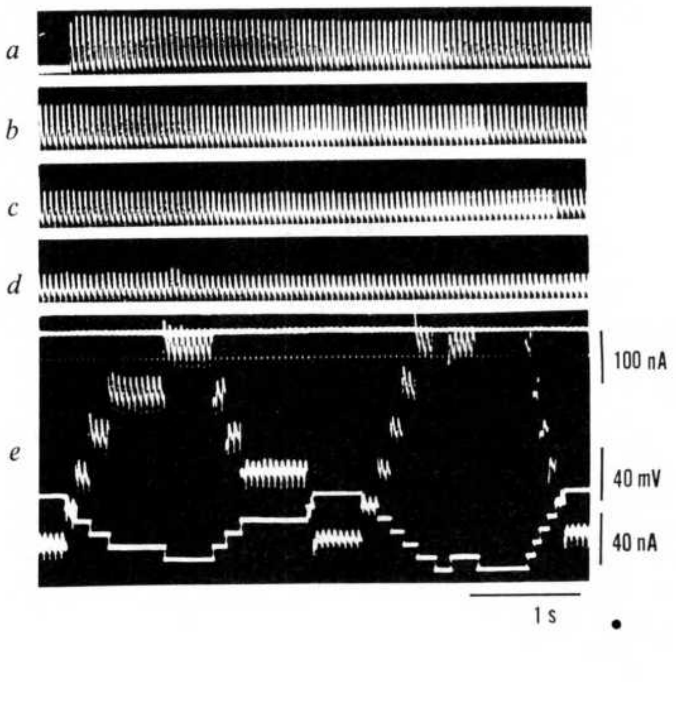

Fig. 1 ACh-induced currents evoked by repetitive applications of iontophoretic pulses (1 ms, 50 nA) at a rate of 20 Hz. Membrane potential was changed after ACh application for about 20 s, when sufficient desensitisation had occurred. *a–d*, ACh-induced currents; *e*, upper, middle (seen at the right- or left-hand margins) and lower (seen at the right- or left-hand margins) traces are the current for iontophoresis of ACh, membrane potential and ACh-induced current, respectively.

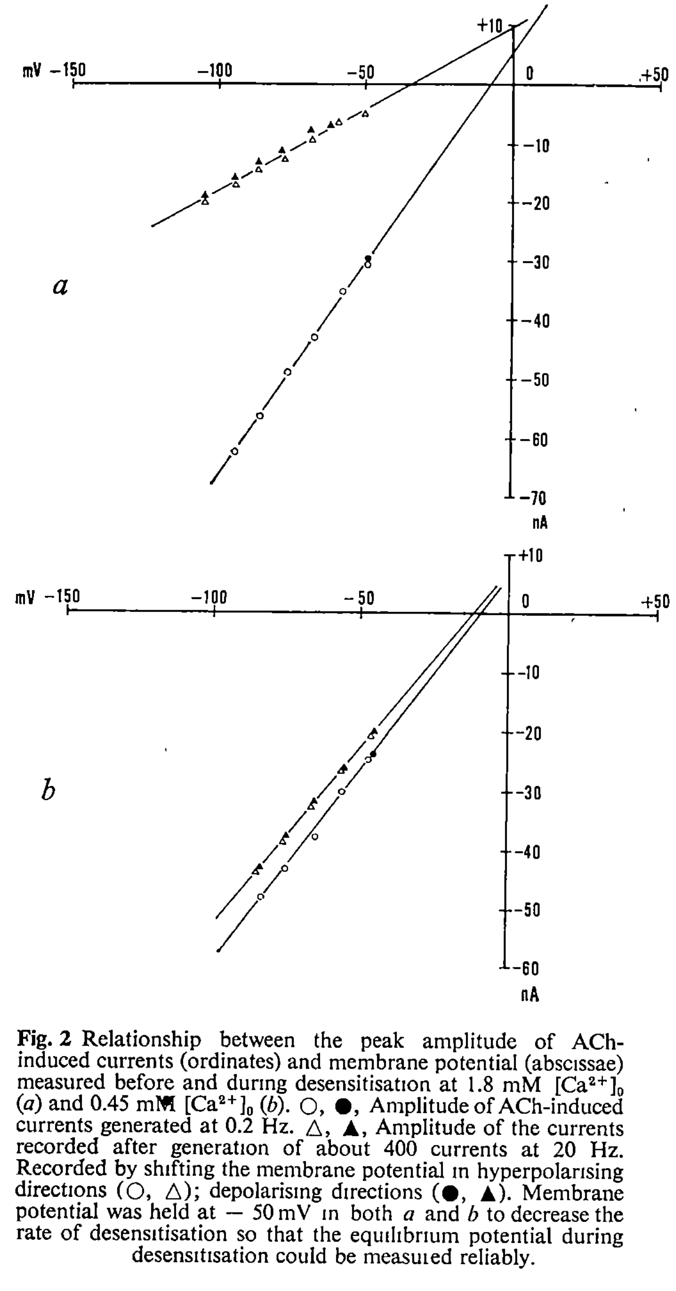

Fig. 2 Relationship between the peak amplitude of ACh-induced currents (ordinates) and membrane potential (abscissae) measured before and during desensitisation at 1.8 mM $[Ca^{2+}]_o$ (*a*) and 0.45 mM $[Ca^{2+}]_o$ (*b*). ○, ●, Amplitude of ACh-induced currents generated at 0.2 Hz. △, ▲, Amplitude of the currents recorded after generation of about 400 currents at 20 Hz. Recorded by shifting the membrane potential in hyperpolarising directions (○, △); depolarising directions (●, ▲). Membrane potential was held at − 50 mV in both *a* and *b* to decrease the rate of desensitisation so that the equilibrium potential during desensitisation could be measured reliably.

of the endplate membrane. This finding points directly to the idea that the site responsible for desensitisation is the ion channel directly controlling the conductance of the endplate membrane[6].

We also studied effects of high $[Ca^{2+}]_o$ on the ACh-induced currents which were evoked at a low rate (0.2 Hz) of ACh application, when there was no observable desensitisation. When $[Ca^{2+}]_o$ was increased from 1 8 mM to 7.2 mM, the amplitude of ACh-induced currents gradually decreased and reached a steady level. In these circumstances, there was a decrease in G_{epc} (71±6%, $n = 7$) and a negative shift of E_{epc} (−10.3±1.0 mV, $n = 7$), indicating a decrease in G_{Na}. These observations are in agreement with the original findings of Takeuchi[7]. In view of similar decreases in the G_{Na}, we suggest that two different effects of high $[Ca^{2+}]_o$—namely an increase in the rate of desensitisation and a decrease in the endplate conductance—are caused by a common mechanism, which may be explained as follows. It was proposed[4,5], that a major factor controlling the speed of desensitisation is a rise in intracellular Ca^{2+} concentration ($[Ca^{2+}]_i$) produced by activation of Ca^{2+} conductance. If this is the case, our present experimental findings indicate that an increase in $[Ca^{2+}]_i$ eventually decreases G_{Na} of the endplate membrane. When $[Ca^{2+}]_o$ is increased, $[Ca^{2+}]_i$ is also expected to rise, even at a low rate of ACh application. This leads to a similar decrease in the G_{Na}. It may thus be possible that desensitisation is caused by the acceleration of the mechanism which causes a decrease in G_{Na} of the endplate membrane by intracellular Ca^{2+}.

K. KUBA
K. KOKETSU

Department of Physiology,
Kurume University School of Medicine,
Kurume 830, Japan

Received April 5; accepted June 1, 1976.

[1] Katz, B , and Thesleff, S., *J. Physiol., Lond.*, **138**, 63–80 (1957).
[2] Thesleff, S., *Acta Physiol. scand.*, 34, 218–231 (1955).
[3] Manthey, A. A., *J. gen Physiol* , 49, 963–976 (1966).
[4] Manthey, A. A., *J gen. Physiol.*, 56, 407–419 (1970).
[5] Nastuk, W. L., and Parsons, R L., *J. gen. Physiol* , 56, 218–249 (1970).
[6] Magazanik, L. G , and Vyskocil, F., *J. Physiol., Lond.*, 210, 507–518 (1970).
[7] Takeuchi, N., *J Physiol , Lond.*, 167, 141–155 (1963).
[8] Kuba, K., Albuquerque, E. X., and Barnard, E. A., *Science*, **181**, 853–856 (1973).
[9] Oomura, Y., and Tomita, T , in *Electrical Activity of Single Cells* (edit. by Katsuki, Y.), 181–205 (Igaku Shoin, Tokyo, 1960).
[10] Takeuchi, A., and Takeuchi, N , *J Neurophysiol* , 22, 395–411 (1959).
[11] Kuba, K , Chikazawa, K., and Koketsu, K., *Jap. J. Physiol* , 26, 159–175 (1976).
[12] Magazanik, L. G , and Vyskocil, F., *J. Physiol., Lond* , 249, 285–300 (1975).

Elevated levels of enkephalin in morphine-dependent rats

NUMEROUS theories propose mechanisms regulating opiate dependence. Hughes[1,2] elegantly identified a morphine-like factor "enkephalin" which mimics effects of morphine on nerve plexus in smooth muscle in a fashion that can be antagonised by opiate antagonists, while a compound with the same properties has been identified in brain extracts by competition for opiate receptor binding[3–6]. Enkephalin activity has a regional and subcellular distribution similar to that of the opiate receptor[7,8] and was first shown to be a mixture of two peptides H-Tyr–Gly–Gly–Phe–Met–OH and H-Tyr–Gly–Gly–Phe–Leu–OH by Hughes *et al.*[9] with a preponderance of the methionine peptide in pig brain[9]. Independently, we identified the same two peptides in bovine brain but with four times more of the leucine than of the methionine peptide[10,11]. Brain enkephalin differs from substances in pituitary gland and hypothalamic extracts which mimic morphine[12,13].

Kosterlitz and Hughes proposed that reduced enkephalin release might explain tolerance and physical dependence to opiates[14]. Here we report enhanced enkephalin levels in brains of morphine-dependent rats, supporting the view that changes in enkephalin release account for symptoms of tolerance and physical dependence.

Enkephalin was extracted[4,6] from brains of Sprague–Dawley rats (150-175 g weight) by homogenising the brain in ten volumes of 0.32 M sucrose in a glass tube with a Teflon homogeniser. The homogenate was centrifuged at 100,000*g* for 1 h, the pellet resuspended in two volumes of 10 mM Tris-HCl buffer (*p*H 7 7 at 25 °C) and incubated in a boiling water bath for 15 min, centrifuged at 100,000*g* for 1 h and the clear supernatant lyophilised. To separate endogenous enkephalin from the administered opiates, all the lyophilised brain extracts were purified on Biogel-P_2 columns. Samples were suspended in 0 1 M ammonium-acetate buffer (*p*H 7.4) and run through Biogel P_2 columns (26×1.1 cm, 200-400 mesh) prepared in the same buffer. Fractions of 0 6 ml were collected, lyophilised, suspended in 50 mM Tris-HCl buffer (*p*H 7.7 at 25 °C) and assayed in triplicate in the opiate binding assay[4–6]. When ^3H-morphine was mixed with enkephalin, less than 1% of added ^3H-morphine emerged in the enkephalin containing fractions. The opiate binding assay was performed in 200 µl of 0 05 M Tris-HCl buffer containing membranes from Sprague–Dawley rat brains and 0 12 pmol ^3H-naloxone (5 mCi/0.04 mg). Specific opiate binding is defined as the difference

Table 1 Enkephalin activity and opiate content in morphine-dependent, withdrawn and acutely injected rats

	Enkephalin activity (Units per g wet weight)	Opiate content (ng morphine equivalents per g wet weight)
Control	3.38±0.32 (8)	
Acute morphine†, 30 min	3.42±0.43 (8)	87.5±16.2
Acute morphine, 1 h	4.20±0.51 (8)	154.4±24.0
Acute morphine, 2 h	4.05±0.37 (8)	65.4±13.3
Acute morphine, 4 h	3.78±0.40 (6)	18.3± 5.4
One day morphine pellet‡	3.65±0.44 (5)	27.7± 3.6
Five day morphine pellet§	5.96±0.72* (10)	64.1± 7.1
Five day morphine pellet plus naloxone injection (1.0 mg kg^{-1}) ‖	3.26±0.51 (8)	96.5±14.1
Naloxone injection (1.0 mg kg^{-1})¶	2.84±0.47 (5)	31.0± 4.0

For determination of enkephalin activity and opiate content, rats were decapitated and brains minus cerebella were homogenised as described in the text. Enkephalin activity was separated from opiates (morphine or naloxone) by Biogel-P_2 chromatography (see text and Fig. 1) and assayed in an opiate binding assay[4,6]. Each treatment was performed in 5–10 rats (indicated in parentheses) and enkephalin activity content quantified as described in the text. Data are means± s.e.m. with the number of rats in parentheses. For methionine and leucine enkephalins, 1 unit represents 1.25 pmol and 6.0 pmol respectively[10,11]. Thus control rat brain would contain 4.2 pmol g^{-1} or 20.3 pmol g^{-1} levels of enkephalin if it were exclusively methionine or leucine enkephalin respectively.

All samples were processed by Biogel-P_2 chromatography with assay of 50 fractions for each sample. There was no overlap between enkephalin values of 5-d pelleted rats and control rats or 5-d pelleted animals treated with naloxone.

*Significantly higher than values for control rats and morphine-dependent rats treated with naloxone, $P < 0.005$.

†Morphine sulphate (15 mg kg^{-1}) was injected intraperitoneally and animals decapitated for enkephalin extraction 30 min–4 h after injection.

‡Morphine pellets (75 mg) were inoculated subcutaneously 24 h before enkephalin extraction.

§One morphine pellet (75 mg) was inoculated. After 2 d two more morphine pellets (75 mg each) were inoculated together. Rats were decapitated and their brains extracted 5 d after inoculation of the first pellet.

‖Rats were treated as in § except that naloxone (1.0 mg kg^{-1} intraperitoneally) was injected 1 h before decapitation and brain extraction.

¶Naive animals were injected intraperitoneally with naloxone (1.0 mg kg^{-1} intraperitoneally) and the brains extracted 1 h later as in ‖.

in binding in the presence of 1 μM levallorphan from that in its absence. Enkephalin activity was quantified using a standard curve elaborated with different enkephalin concentrations. One unit of enkephalin is defined as that amount of enkephalin which yields 50% occupancy, determined according to Colquhoun[15] assuming classical binding interactions. The amount of opiate in the brain extracts that was run through Biogel-P_2 columns was also determined in the opiate binding assay and quantified by comparison with morphine. Synthetic methionine- and leucine-enkephalins emerged from these columns in the same fractions as enkephalin extracted from rat brain[10,11]. Chromatography on AG-1 columns also showed the same elution pattern for synthetic enkephalins and enkephalin activity extracted from rat brain Recovery of added methionine- and leucine-enkephalins (80-90%) was the same for control and morphine pelleted rats.

One hour after a single injection of morphine (15 mg kg^{-1} intraperitoneally) enkephalin levels increase about 25%, which attains statistical significance in some experiments (Table 1). No augmentation is detected 30 min after morphine injection and the levels of enkephalin then decline.

To evaluate the influence of tolerance and physical dependence, rats were implanted with slow-release morphine pellets and their brains assayed for enkephalin and morphine content 1 and 5 d later (Table 1; Fig. 1). At 1 d, enkephalin levels are no different from those of control animals, though brain levels of morphine at this time are only 15% of those obtained 1 h after an acute injection of morphine, consistent with the reported slow release of morphine from such pellets in rats[16,17]. Five days after initial pellet implantation and 3 d after the second pellets, when tolerance and physical dependence are maximal[16,17], enkephalin levels are increased 75% over control values; 1 h after precipitating abstinence in animals by naloxone treatment (1.0 mg kg^{-1} intraperitoneally), enkephalin levels have returned again to control values. In naive rats the same dose of naloxone produces no alteration in enkephalin levels.

Changes in enkephalin activity are not simply related to presence in the brain of the opiate administered to the animals, because naloxone injection reduces enkephalin levels in 5-d morphine pelleted rats, while it increases the opiate content of the brain (Fig. 1; Table 1). Moreover, after a single injection of morphine, enkephalin levels are substantially lower than after 5 d of morphine pellets, yet with the acute injection of morphine, the total opiate content of the brain is two- to threefold higher than after pellet implantation.

Do the elevated levels of enkephalin in morphine pelleted rats represent the same substance as that detected in control animals? One unique characteristic of enkephalin activity is its enhancement by manganese but not by calcium ions and its depression by sodium but not potassium ions[4,6]. As previously reported for crude and purified enkephalin preparations, in control rats as well as in morphine pelleted animals and rats treated with both morphine pellets and naloxone, ionic influences on enkephalin activity are essentially the same. Thus in all three cases, 15 mM and 100 mM sodium reduce enkephalin activity about 60 and

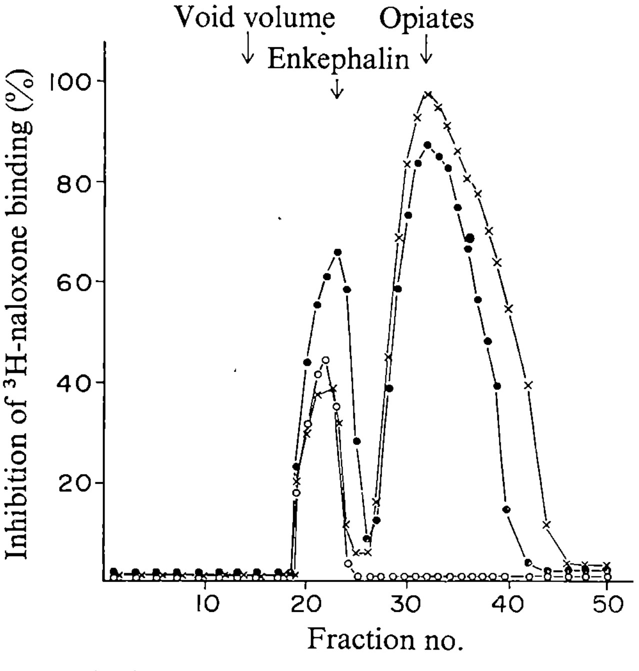

Fig. 1 Biogel-P_2 chromatography of enkephalin activity from control, morphine-dependent and morphine-dependent, naloxone-injected rats. Morphine dependence was elicited by implanting one morphine pellet (75 mg) for 2 d and then two other pellets (75 mg each) together for another 3 d before brain extraction. Abstinence was precipitated by intraperitoneal injection of 1.0 mg kg^{-1} naloxone to rats 5 d after morphine pellet implantation, and the brains were extracted 1 h after naloxone injection. Each treatment was performed with 5–8 animals. Enkephalin was extracted, run through Biogel-P_2 column and assayed in the opiate receptor binding assay as described in the text. The same Biogel-P_2 assay was calibrated with ^{3}H-morphine, synthetic methionine-enkephalin and non-radioactive insulin (molecular weight, 6,000). The negligible overlap of enkephalin and opiate profiles and their comparable magnitude ensures that enkephalin activity determinations are not affected to a great extent by opiate content of brain. ○, control; ●, morphine dependent; ×, morphine dependent+naloxone.

70% respectively, while the same concentrations of potassium have no effect. By contrast, 1 mM manganese increases enkephalin activity about 50–70% in all three groups of animals, although the same concentration of calcium has no appreciable influence. Elevated enkephalin levels in morphine-dependent rats remain apparent regardless of ionic manipulations.

How might these changes in enkephalin activity relate to opiate dependence? The jumping, wet shakes and diarrhoea associated with morphine abstinence are observable in our animals 5 min after naloxone injection, peak at about 15 min and subside by 60 min, as reported by others[16]. Coincident with the reduction in abstinence symptoms 1 h after naloxone administration, sensitivity to the analgesic effects of morphine returns almost to control levels[17], when enkephalin levels have also declined to control values. Thus the changes in enkephalin activity after chronic treatment with morphine and induction of abstinence correlate with behavioural changes associated with tolerance and physical dependence.

Brain levels of dopamine and acetylcholine reflect changes in the firing rate of cholinergic and dopaminergic neurones[18,19]. Cessation of firing is accompanied by an elevation of the levels of these transmitters. If enkephalin is a neurotransmitter or neuromodulator of analogous neuronal systems, elevations in enkephalin activity might reflect a slowing in the firing rate of "enkephalinergic" neurones. Conceivably large doses of morphine substitute for the physiological effects of enkephalin and, by a "feedback" message, cause the enkephalinergic neurones to reduce their activity as proposed by Kosterlitz and Hughes[14]. Such a mechanism could account for the behavioural manifestations of opiate tolerance and physical dependence. With acute morphine administration, opiate receptors are exposed both to morphine and enkephalin. With chronic morphine administration, enkephalin release slows or ceases, and opiate receptors, now exposed only to morphine, appear "tolerant". On abrupt cessation of opiate administration or with antagonist treatment, receptors are deprived both of the opiate and of enkephalin, resulting in "abstinence". As the firing rate of enkephalin neurones returns to normal, elevated levels of enkephalin decline to control values, and the organism is again normally responsive to opiates. Possibly, the "feedback" message to the enkephalin neurones is mediated by changes in cyclic nucleotides in postsynaptic cells containing opiate receptors[20].

This work was supported by a grant from the USPHS, an Eleanor Roosevelt fellowship to R.S. and Research Scientist Development Award from the NIMH to S.H.S. We thank Adele Snowman for inspired technical assistance.

RABI SIMANTOV
SOLOMON H. SNYDER

*Departments of Pharmacology and Experimental Therapeutics and Psychiatry and Behavioral Sciences,
Johns Hopkins University School of Medicine,
Baltimore, Maryland 21205*

Received March 1; accepted June 16, 1976.

[1] Hughes, J., *Brain Res.*, **88**, 295–308 (1975).
[2] Hughes, J , Smith, T., Morgan, B , and Fothergill, L., *Life Sci* , **16**, 1753–1758 (1975).
[3] Terenius, L , *Acta Pharmac. Tox.*, 35, 55 (1974).
[4] Pasternak, G. W., Goodman, R., and Snyder, S. H , *Life Sci* , **16**, 1765–1769 (1975)
[5] Terenius, L., and Whalstrom, A , *Life Sci* , **16**, 1759–1764 (1975).
[6] Pasternak, G. W., Simantov, R and Snyder, S. H., *Molec Pharmac.* (in the press)
[7] Simantov, R , Kuhar, M J , Pasternak, G W , and Snyder, S. H , *Brain Res* , **106**, 189–197 (1976)
[8] Simantov, R , Snowman, A M , and Snyder, S. H., *Brain Res* (in the press).
[9] Hughes, J., *et al.*, *Nature*, **258**, 577–579 (1975).
[10] Simantov, R , and Snyder, S H., *Life Sci.*, **18**, 781–788 (1976).
[11] Simantov, R., and Snyder, S H., *Proc natn Acad Sci U.S A.*, (in the press)
[12] Cox, B M , Opheim, K E , Teschemacher, H , and Goldstein, A , *Life Sci.*, **16**, 1777-1782 (1975).
[13] Guillemin, R., Ling, N., and Burgus, R., *C. r. hebd. Séanc. Acad Sci. Paris*, **282**, 783–785 (1976)
[14] Kosterlitz, H. W., and Hughes, H , *Life Sci.*, **17**, 91–96 (1975).
[15] Colquhoun, D., in *Drug Receptors* (edit. by Rang, H. P.), 149–182 (University Park Press, London, 1973).
[16] Cicero, T. J., and Meyer, E R., *J. Pharmac. exp. Ther.*, **184**, 404–408 (1973).
[17] Wei, E., *Psychopharmacologia*, **28**, 35–44 (1973).
[18] Roth, R. H., Walters, J. T., and Aghajanian, G. K., in *Frontiers of Catecholamine Research* (edit. by Usdin, E , and Snyder, S. H.), 567–574 (Pergamon, Oxford, 1973).
[19] Rommelspacher, H., and Kuhar, M. J., *Brain Res.*, **81**, 243–251 (1974).
[20] Sharma, S. K., Klee, W A., and Nirenberg, M., *Proc. natn. Acad. Sci. U.S.A.*, **72**, 3092–3096 (1975).

Prolactin suppresses release of luteinising hormone during lactation in the monkey

STUDIES with rats have shown that during lactation there is an inhibition of luteinising hormone (LH)-dependent physiological events, such as implantation[1], and a return to oestrus cyclicity[2]. This inhibition has been shown to occur only during the intense suckling phase and it has been correlated with the high levels of prolactin present in the circulation at this time. Although exogenous prolactin could substitute for the effects of intense suckling, it could do so only under the permissive influence of minimal suckling stimulus. We have shown that there is, in these conditions, a lowering of LH levels, and that this is due to interference by prolactin with the pituitary responsiveness to LH-releasing hormone (LHRH) (K. Muralidhar, R. M. and N. R. M., unpublished). Using the lactating monkey, we have now demonstrated a similar inhibitory effect of prolactin on pituitary responsiveness to LHRH, suggesting a mechanism by which amenorrhoeic conditions are maintained during lactation.

Four female bonnet monkeys (*Macaca radiata*), in the second month of lactation, were caged individually with their babies and maintained in standard laboratory conditions[3]. Synthetic LHRH (100 µg AY-24, 031-4, given by Dr F. Labrie) in 1 ml 0.9% NaCl was administered through the femoral vein. LHRH was first injected while the mother was suckling her baby and blood was withdrawn by venepuncture 10, 20 and 40 min later. The baby was then separated from the mother for 24 h, at the end of which period a second injection of 100 µg LHRH was given, followed by blood sampling at the intervals indicated above. After a rest of 2–3 weeks the same monkeys were used for the prolactin inhibition experiment. The experimental protocol was identical to that described above, except for the intramuscular injection of 5 mg ovine prolactin (NIH-P-S5)

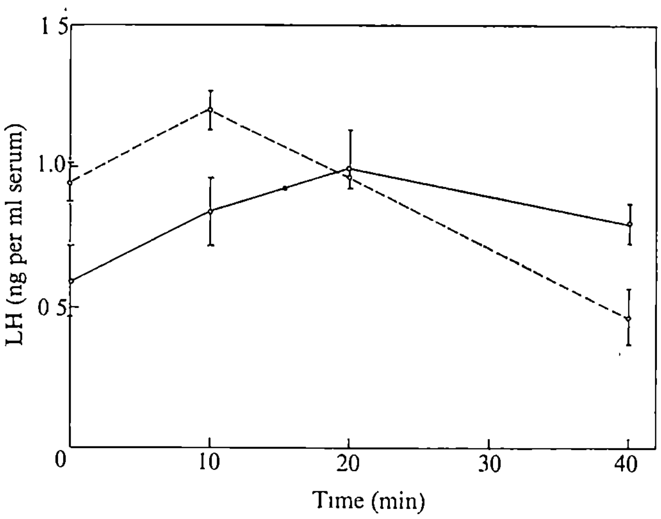

Fig. 1 Effect of suckling on pituitary response to LHRH. Four monkeys in the second month of lactation were used. LH was measured in duplicate in 0.1-ml samples by the double-antibody radioimmunoassay, using human LH (given by Dr C. H. Li), for iodination and standard and human chorionic gonadotrophin-β antiserum (NIAMDD, NIH) as a source of antibody. This assay accurately measured LH in the range of 0.1–5 ng. —, Suckling; — —, non-suckling.

in 0.5 ml 0.9% NaCl 1 h before administration of LHRH. In all experiments a control blood sample was taken 30 min before injection of either prolactin or LHRH. Serum LH was estimated by the double-antibody radioimmunoassay at 37 °C as described previously[4–6] (details in Fig. 1).

Administration of LHRH resulted in an increase in serum of LH within 10 min, in both the suckling group and those from which the suckling stimulus was withdrawn for 24 h (Fig. 1). Whereas this increase in LH levels was maintained until 40 min in the suckling group ($P < 0.02$ between control and 40-min sample), LH reached control values in the non-suckling group by 20 min ($P > 0.5$ between control and 20-min sample). The basal level of LH was significantly increased after withdrawal of the suckling stimulus for 24 h (from 0.6±0.12 ng ml^{-1} to 0.95±0.07 ng ml^{-1}, $P < 0.001$).

Administration of 5 mg prolactin 1 h before injection of LHRH resulted in a suppression of LH release into the circulation only in the group in which the suckling stimulus was present (Fig. 2*a*). This suppression of LH continued until 40 min after injection of LHRH. At any given time interval tested, LH levels in the prolactin-treated suckling group were significantly lower than in the corresponding controls. In contrast, withdrawal of the neurogenic stimulus of suckling for 24 h resulted in an inability of prolactin to block LH release (Fig. 2*b*). Although a comparison between the lactating and the non-lactating groups provided a means of assessing the influence of suckling/endogenous prolactin on LHRH responsiveness, the model in which exogenous prolactin was used, although it is a heterologous species, clearly shows that prolactin *per se* influences pituitary responsiveness to LHRH during lactation.

Ovarian quiescence during lactation has attracted the attention of several investigators. Our study with subhuman primates demonstrates that during lactation the monkey, similar to the rat, has a decreased responsiveness to LHRH. Although the ability of LHRH to release LH from the pituitary is reduced if suckling is present, the effect is further accentuated by a single injection of prolactin. Based on our results with the rat, it can be presumed that in the monkey also the inhibitory effect of prolactin on pituitary responsiveness is direct, and not mediated by ovarian or adrenal progesterone. The mechanism and duration of this inhibition is under investigation.

Fig. 2 Effect of prolactin on pituitary response to LHRH during lactation in the presence (*a*) and absence of suckling stimulus (*b*). *P* values were calculated for values at any given time between the treated and untreated groups. All values > 0.05 were considered to be not significant. —, No prolactin; - - , plus prolactin.

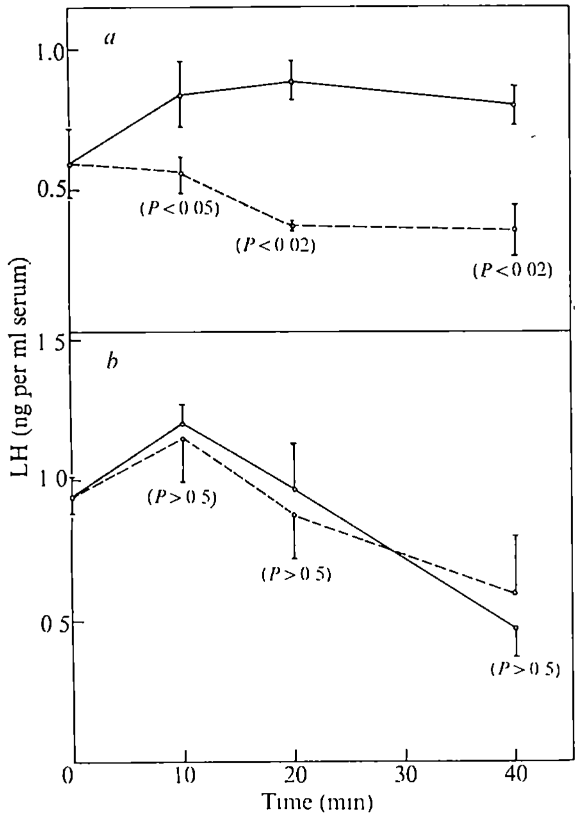

Although others have shown with rats that continued application of the suckling stimulus by litter replacement[7,8] or injection of prolactin[9] can prolong lactation considerably, we have observed that a single injection of prolactin can extend the anoestrus period significantly[2]. Recent studies in humans have shown that thyrotropin-releasing hormone (TRH) extends the lactational amenorrhoeic period[10]. Whether continued use of TRH would, in addition to releasing prolactin by continuously releasing thyroid-stimulating hormone (TSH), have an adverse effect on thyroid metabolism is a point to be considered. The present study, by demonstrating the possible mechanisms whereby gonadoptrophin release is suppressed during lactation, suggests the use of human prolactin to extend the amenorrhoeic condition in lactating women.

The monkey is known to be less responsive to LHRH than the human and the rat[11]. Consequently, the increase (28–66%) in LH levels observed after administration of LHRH and the maintenance of the response for 20–40 min suggests that we observed a true increase in LH. It has been suggested that there is no apparent difference in the levels of follicle-stimulating hormone and LH between lactating and non-lactating humans[12]. With the radioimmunoassay techniques available it may be difficult to pick out differences in the levels of these hormones, particularly when looking for a suppression over the tonic levels. Our study with the monkey, as well as our earlier work with the rat, has shown that withdrawal of the suckling stimulus results in an increase in LH levels over the basal value. Similarly, the use of LHRH has enabled us to show the presence of a clear difference in LH levels of lactating and non-lactating animals.

This study, however, does not exclude the effect of suckling/prolactin directly on the ovarian responsiveness to exogenous gonadotrophins. McNatty *et al.*[13], using *in vitro* cultures of human granulosa cells, have suggested that prolactin could have an influence on the end-organ responsiveness to exogenous gonadotrophins.

This work was supported by the Indian Council of Medical Research, New Delhi. R. M. is a senior research fellow of the Council of Scientific and Industrial Research.

RHODA MANECKJEE
B. R. SRINATH
N. R. MOUDGAL

Endocrinology Laboratory,
Department of Biochemistry,
Indian Institute of Science,
Bangalore 560012, India

Received April 23, accepted June 16, 1976.

[1] Maneckjee, R , and Moudgal, N R., *J. Reprod. Fert* , 43, 33–40 (1975).
[2] Maneckjee, R , and Moudgal, N R , *J. Reprod Fert.*, 44, 313–315 (1975).
[3] Prahalada, S , Mukku, V., Rao, A J., and Moudgal, N. R., *Contraception*, 12, 137–147 (1975).
[4] Moudgal, N. R., Moyle, W. R., and Greep, R. O., *J. biol. Chem* , 246, 4983–4986 (1971)
[5] Moudgal, N. R., and Raj, H G M., in *Methods of Hormone Radioimmunoassay* 57–85 (Academic, New York, 1974)
[6] Muralidhar, K., and Moudgal, N. R., *Biochem J.* (in the press)
[7] Bruce, H M., *Proc R Soc Lond* , B149, 421–423 (1958).
[8] Nicoll, C S , and Meites, J , *Proc Soc exp Biol. Med.*, 101, 81–82 (1959)
[9] Meites, J , and Nicoll, C. S , *Endocrinology*, 65, 572–579 (1959)
[10] Jewelewicz, R *et al*, *J clin. Endocr Metab.*, 39, 387 (1974).
[11] Krey, L. C , *et al* , in *Hypothalamic-Hypophysiotropic Hormones* 39–47 (Excerpta Medica, Amsterdam, 1973).
[12] Beling, C. G., *et al.*, *Acta Endocr. Suppl.* 155, 40 (1971).
[13] McNatty, K. P., Sawers, R S , and McNeilly, A S., *Nature*, 250, 653–655 (1974).

Bacteria necessary to produce experimental autoimmune myasthenia gravis in acetylcholine receptor-immunised rabbits?

WE have[1-3] described previously a paralytic disease observed in rabbits immunised with small doses, in Freund's complete adjuvant, of nicotinic cholinergic receptor protein (nAChR) isolated from the electric organ of *Torpedo marmorata* Decremental muscle response after nerve stimulation and positive effects of anticholinesterase administration, decrease in miniature endplate potential amplitude and increased curare sensitivity were similar to findings in patients suffering from myasthenia gravis. Nicotinic AChR antibody titres above 2–3 mg ml^{-1} have been found, the observed muscle decrement increasing with increasing antibody titre. Occasionally, variations in electromyographic activity were observed, suggesting denervation Morphological analysis[3,4] showed severe destruction of postsynaptic motor endplate areas and reduction of toxin-binding sites, followed by changes at the presynaptic side. A second stage of the disease was characterised by high sensitivity to nAChR injections and by the presence of motor endplates lacking secondary postsynaptic foldings. Our work and that of others (for review see ref 5) suggests that an immune response to nAChR seems to be involved in the aetiology of experimental autoimmune myasthenia gravis (EAM) just as is suggested for human myasthenia gravis. The role of a humoral and/or cellular immune response and that of the thymus are under discussion[5,6]. The decremental response to repetitive nerve stimulation may be caused directly and/or indirectly by nAChR antibodies, whereas defects in electromyographic activity such as high frequency discharges and fibrillation action potentials which we have observed may have been caused by other, accompanying mechanisms. This report deals with the role of bacteria in EAM and with the relationship of the antibody titre to the electrophysiological findings.

A sterile-filtered receptor solution produced a low antibody titre, and no decremental response on repetitive stimulation or response to Tensilon was observed. The nAChR used previously[1-3] in immunisation which always resulted in animals with EAM was obtained after solubilisation with phosphate buffer containing 1% Triton X-100 and purification by affinity and ion-exchange chromatography. Sodium azide (0.02%) was added to the purified receptor to prevent further growth of bacteria. About 30 rabbits were immunised with such preparations, all of which showed typical symptoms of EAM.

We have introduced a sterile filtration step (Millipore filters, pore size 0.22 μm) after Triton X-100 solubilisation to reduce bacteria present from 4,000–12,000 to 30 ml^{-1}. The receptor obtained had chemical and physical properties similar to those of material obtained previously, except for a considerably lower antigenicity, as expressed in obtained antibody titre in otherwise identical conditions. Rabbits immunised with a 'sterile' receptor show greater variability in the onset time for the disease, but the clinical picture observed is close to those animals observed previously. The electrophysiological investigations revealed only a very small decrement, about 5–10%, which could not be responsible for the severe visible symptoms in the examined rabbits. An analysis of the receptor antibody titres (rocket immunoelectrophoresis) showed that these are rather low, below 1.2 mg ml^{-1}. A return to receptor purification without sterile filtration resulted in rabbits with high antibody titres and greater decrement. Results from ten rabbits are summarised in Table 1.

Table 1 Relationship between nAChR antibody titre and decremental muscle response after repetitive stimulation of peroneal nerve

Rabbit no	Antibody titre (mg ml^{-1})	Decrement (%)
1	2.9	56
2	4.9	25
3	6.7	62
4	3.0	37
5	3.4	40
6	0.7	5
7	1.2	8
8	0.7	6
9	0.7	6
10	0.5	7

Antibody titres and decrement in rabbits immunised with a non-sterile (1–5) and a sterile (6–10) receptor preparation.

We conclude that so called 'EAM rabbits' may suffer from at least two different kinds of defects one at the neuromuscular junction, which may be of the kind observed in myasthenia gravis (this defect seems to be clearly correlated with the titre of circulating antibody to nAChR); and one, responsible for the severe symptoms visible in rabbits immunised with receptor isolated after sterile filtration, which seems to involve denervation rather than neuromuscular deficiency, revealed in the electromyographic investigation as high frequency discharges and fibrillation action potentials'. These effects were observed also at low nAChR antibody titres.

We have found therefore that besides 'myasthenic symptoms' EAM rabbits seem to have another type of weakness, not correlated with high antibody titre. We may be dealing with a potentiation of nAChR antigenicity, but a specific effect of a bacteria—for example, due to binding to and/or transformation of nAChR—may well be the explanation. It is also possible that the filtration step removes non-bacterial material—for example, aggregated proteins. We have, however, not noticed a lower receptor yield in our final preparations.

EDITH HEILBRONN
CHRISTER MATTSSON

Section of Biochemistry,
National Defence Research Institute,
S-172 04 Sundbyberg 4, Sweden

ERIC STÅLBERG

Department of Clinical Neurophysiology,
Academic Hospital,
S-750 14 Uppsala, Sweden

Received April 9; accepted June 29, 1976.

[1] Heilbronn, E , and Mattsson, C , *J Neurochem.*, 22, 315 (1974)
[2] Heilbronn, E , Mattsson, C., Stålberg, E , and Hilton-Brown, P , *J neur Sci*, 24, 59 (1975).
[3] Heilbronn, E., *et al*, *Ann N.Y Acad Sci*, 274, 337 (1976)
[4] Thornell, L -E., Sjostrom, M , Mattsson, C , and Heilbronn, E , *J neur Sci* (in the press)
[5] Heilbronn, E , in *Motor Innervation of Muscle* (edit by Thesleff, S) (Academic, New York and London, in the press)
[6] Lennon, V A., Lindstrom, J D , and Seybold, M E., *Ann N Y Acad Sci*, 274 (1976)

Cyclic AMP and cyclic GMP may play opposing roles in influencing force of contraction in mammalian myocardium

CYCLIC AMP and cyclic GMP have been suggested to play opposing regulatory roles in several biological systems[1]. Supporting evidence for the yin yang hypothesis of opposing biological regulation has been obtained in sympathetic ganglia[2,3] and pyramidal neurones in the rat cerebral cortex[4]. In the mammalian heart, the role of cyclic AMP in mediating the positive inotropic response to catecholamines was advanced by the observation that the inotropic effect was preceded by an increase

SCIENCE COLLEGE

in cyclic AMP levels[5]. On the other hand, the levels of cyclic GMP were found to be increased after cholinergic stimulation[6]. In frog, oscillations of cyclic AMP[7] and cyclic changes in the levels of cyclic AMP and cyclic GMP[8] during the cardiac cycle have been reported. The importance of cyclic AMP for the inotropic effects of catecholamines was confirmed by the observation that the dibutyryl derivative of cyclic AMP exerted a positive inotropic effect in cat papillary muscles[9] and in the isolated perfused hearts from rabbits, rats and guinea pigs[10]. I now report a direct negative inotropic effect of 8-Br-cyclic GMP on force of contraction (F_c) in rat auricles and papillary muscles from cats.

Rats and cats were anaesthetised with ether and either auricles or papillary muscles were dissected from the heart and mounted in a muscle chamber for recording mechanical activity as described previously[11]. Left auricles were driven electrically at 2 Hz and cat papillary muscles at 0.2 Hz. Drugs (all cyclic nucleotides from Boehringer/Mannheim) were freshly dissolved in distilled water and 0.1 ml was injected into the muscle chamber containing 5 ml of Tyrode solution (composition in mM: NaCl, 136.9; KCl, 5.4; $MgCl_2$, 1.05; $CaCl_2$, 1.8; NaH_2PO_4, 0.42; $NaHCO_3$, 11.9; glucose, 5.5) which was gassed with 95% CO_2–5% O_2 and heated to 35 °C.

Figure 1 shows the influence of 8-Br-cyclic GMP on F_c in electrically driven left auricles and on frequency of spontaneously beating right auricles isolated from rat hearts. 8-Br-cyclic GMP exerted a concentration-dependent negative inotropic effect; when the preparation was washed three times in drug-free solution, the negative inotropic effect was partially reversible, but F_c did not return fully to its previous control value within 60 min. The frequency of spontaneously beating right auricles was not significantly affected by 8-Br-cyclic GMP within the whole concentration range. Control experiments showed that the negative inotropic effect of 8-Br-cyclic GMP was not influenced when the preparations were pretreated with 5×10^{-6} M atropine sulphate. 10^{-3} M cyclic GMP (not substituted) or 10^{-3} M NaBr did not affect F_c. Figure 2 shows the influence of 8-Br-cyclic GMP on F_c in a cat papillary muscle (mean±s.e. of four experiments: decrease of F_c to 67.7±3.7% of control values). The negative inotropic effect of 8-Br-cyclic GMP was fully reversible within 60 min when the preparation was washed three times in drug-free solution. For comparison, the effects of 8-Br-cyclic AMP were also studied. In papillary muscles from cats, 8-Br-cyclic AMP did not affect F_c; however, after pretreatment with the strong phosphodiesterase inhibitor papaverine (2×10^{-5} M) a positive inotropic effect was observed (Fig. 3; mean±s.e. of six experiments: increase of F_c to 180±22.1% of control values before addition of 8-Br-cyclic AMP).

In atrial tissue, studies with cyclic AMP and its derivatives are complicated by the fact that the breakdown products of cyclic AMP or cyclic AMP itself—if applied from outside the cell—have a strong negative inotropic effect in auricles[12]. In rat left auricles, 8-Br-cyclic AMP caused a sharp decline of F_c that was followed by a second component of a slowly developing increase in F_c (Fig. 4). This second component seems to correspond to the positive inotropic effect seen in cat papillary muscles (Fig. 3), since it was augmented after pretreatment with 2×10^{-5} M papaverine.

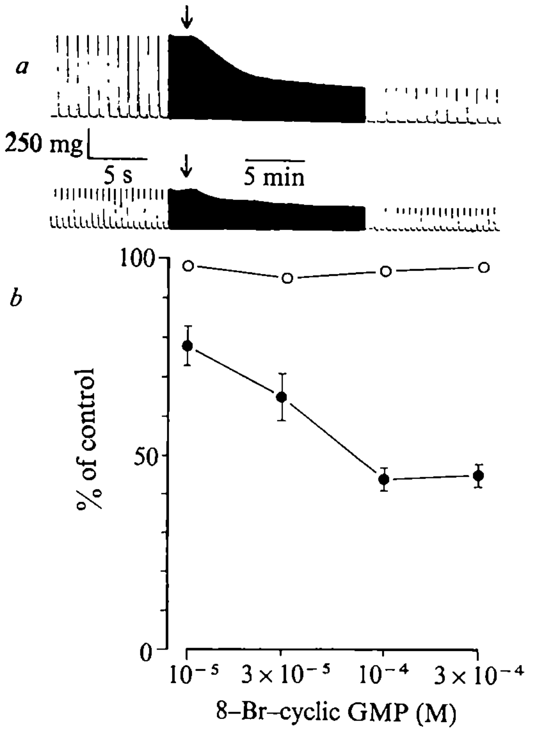

Fig. 1 Effect of 8-Br-cyclic GMP on force of contraction (F_c) and frequency in isolated auricles from rat hearts. F_c was determined in electrically driven left auricles, frequency in spontaneously beating right auricles. *a*, Original traces of a left (upper) and a right (lower) auricle in response to 3×10^{-4} M 8-Br-cyclic GMP. Addition of drug is indicated by the arrows. *b*, Concentration-response relationships. Each concentration was tested in individual preparations. Symbols represent means±s.e. of 8–16 preparations Values of s.e. for the frequency of contraction are smaller than the size of the symbols used and are therefore omitted. ○, Frequency; ●, F_c.

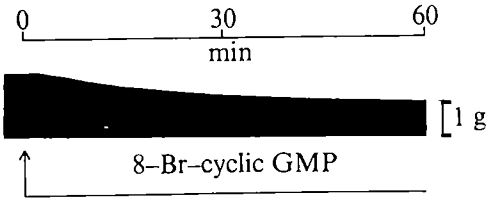

Fig. 2 Effect of 3×10^{-4} M 8-Br-cyclic GMP on F_c in a cat papillary muscle.

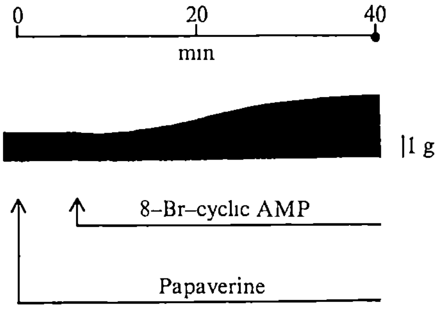

Fig. 3 Effect of 3×10^{-4} M 8-Br-cyclic AMP in a papillary muscle from a reserpinised cat (Serpasil, Ciba, 5 mg kg^{-1}, 18 h before the experiment) in the presence of 2×10^{-5} M papaverine Both papaverine and 8-Br-cyclic AMP alone did not affect F_c but only if given in combination. The same positive inotropic effect was obtained when 8-Br-cyclic AMP was added first and then papaverine. Papaverine itself (2×10^{-5} M) exerts a slight positive inotropic effect in papillary muscles from non-reserpinised cats that is accompanied by an increase in the slow inward current as measured by the voltage clamp technique (H.N., to be published). The positive inotropic effect disappears after pretreat- papaverine has a negative inotropic effect; this corresponds to the findings of Schneider *et al.*[14] who reported a depression of Ca-dependent action potentials in the guinea pig heart with 4×10^{-4} M papaverine. Papaverine (2×10^{-5} M) was given in preference to other drugs because it strongly inhibits the phosphodiesterase activity in the heart but does not affect F_c in cat papillary muscles provided that any adrenergic influences are excluded. Cats were reserpinised to exclude catecholamine effects due to either papaverine or 8-Br-cyclic AMP. This is an appropriate and widely used method to exclude any interference by noradrenaline which may be eventually released by the use of some drugs. The possibility that 8-Br-cyclic AMP releases noradrenaline is not excluded; papaverine, indeed, is able to release endogenously stored catecholamines[15].

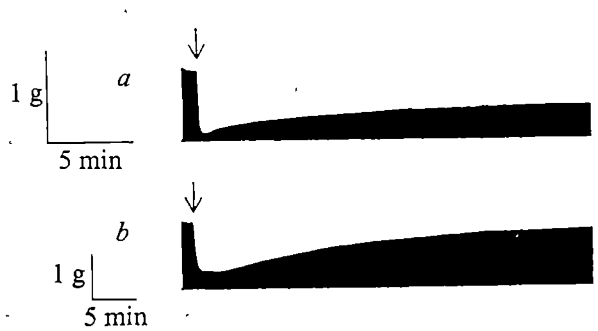

Fig. 4 Effect of 3×10^{-4} M 8-Br-cyclic AMP without (*a*) and in the presence of 2×10^{-5} M papaverine (*b*) in the same preparation (rat left auricle). Papaverine alone had a positive inotropic effect: control F_c in (*b*) before addition of 8-Br-cyclic AMP, indicated by the arrows, was about twice as big as in (*a*). The initial negative inotropic effect of 8-Br-cyclic AMP in rat atrial muscle most probably resulted from 8-Br-cyclic AMP *per se*, if applied from outside the cell, since 10^{-3} M 8-Br-5′ AMP (Schwarz/Mann)—the non-cyclic breakdown product of 8-Br-cyclic AMP—did not produce either the negative or the positive inotropic effect.

These findings indicate a positive inotropic action of 8-Br-cyclic AMP and the sum of results therefore suggests an opposite influence of cyclic GMP and cyclic AMP on F_c in atrial as well as in ventricular myocardium. In contrast to the negative inotropic action of 8-Br-cyclic GMP in rat auricles, the pacemaker activity was virtually unaffected by the drug. This points to a difference in the action of acetylcholine on rat atrial muscle. Voltage clamp experiments have shown that the negative inotropic effect of acetylcholine in mammalian atrial muscle can be explained by an increase in potassium conductance at lower doses and, additionally, by a decrease in calcium conductance at higher doses[13]. It remains open whether similar conductance changes are brought about by the action of cyclic GMP and can be related to the corresponding changes in force of contraction.

I thank Dr Wollenberger for suggesting use of the 8-Br-derivative of cyclic GMP and Mrs Gibson for technical help. This research was supported by a grant from the Deutsche Forschungsgemeinschaft.

HERMANN NAWRATH

Department of Pharmacology,
University of Mainz,
6500 Mainz, FRG

Received February 26; accepted June 11, 1976.

[1] Goldberg, N. D., Haddox, M. K., Hartle. D. K., and Hadden, J W , *Proc Fifth Int. Congr. Pharmac.* (edit by Maxwell, R A., and Acheson, G H.), 146–149 (Karger, Basel, 1973).
[2] McAfee, D A., and Greengard, P., *Science*, **178**, 310–312 (1972).
[3] Kebabian, J. W., Steiner, A. L , and Greengard, P , *J Pharmac. exp Ther.*, **193**, 474–488 (1975).
[4] Stone, T. W., Taylor, D. A., and Bloom, F E., *Science*, **187**, 845–847 (1975).
[5] Cheung, W Y., and Williamson, J. R., *Nature*, **207**, 979–981 (1965).
[6] George, W. J., Polson, J. B., O'Toole, A. G., and Goldberg, N D., *Proc. natn. Acad. Sci. U.S.A.*, **66**, 398–403 (1970).
[7] Brooker, G., *Science*, **182**, 933–934 (1973).
[8] Wollenberger, A., *et al.*, *Biochem. biophys. Res. Commun* , **55**, 446–452 (1973)
[9] Skelton, C. L., Levey, G. S., and Epstein, S. E., *Circulation Res.*, **26**, 35–43 (1970).
[10] Kukovetz, W. R., and Poch, G., *Naunyn-Schmiedebergs Arch. Pharmak.*, **266**, 236–254 (1970).
[11] Meinertz, T., Nawrath, H., and Scholz, H.. *Pflugers Arch. ges. Physiol.*, **333**, 197–212 (1972).
[12] Meinertz, T., Nawrath, H , and Scholz, H , *Naunyn-Schmiedeberg's Arch. Pharmac.*, **278**, 165–178 (1973).
[13] TenEick, R. E., Nawrath, H., McDonald, T. F., and Trautwein, W., *Pflugers Arch. ges. Physiol.*, **361**, 207–213 (1976).
[14] Schneider, J. A., Brooker, G., and Sperelakis, N., *J. molec. cell Cardiol.*, **7**, 867–876 (1975).
[15] Cubeddu, L. X., Barnes, E., and Weiner, N., *J. Pharmac. exp Ther.*, **191**, 444–457 (1974).

Opposing effects of cyclic AMP and cyclic GMP on protein phosphorylation in tubulin preparations

CYCLIC AMP and cyclic GMP have been postulated to be in certain cases, antagonistic intracellular messengers of many hormones and neurotransmitters acting at the cell membrane[1]. At least part of their antagonism may be the result of their ability to affect, in opposite directions, specific protein kinases and phosphates which work on common substrates (enzymes, structural proteins). Cyclic AMP and cyclic GMP have been found to activate, and the former also to inhibit, specific protein kinases[2–5]; cyclic AMP can activate or inhibit[5–8] specific protein phosphates, and both cyclic nucleotide-sensitive protein kinases and protein phosphates have been isolated forming a complex with their substrate[5]. Some of these effects of cyclic nucleotides, however, have been found to depend on the type and concentration (not necessarily physiological) of the ion used in the assay[5] and no direct evidence exists to show that one of the cyclic nucleotides opposes the effects of the other on protein phosphorylation. We report here that physiological concentrations (10^{-7} M–10^{-9} M) of cyclic GMP oppose the cyclic AMP (10^{-6} M) dependent phosphorylation of a soluble, perhaps tubulin-related brain protein, possibly by activation of a phosphoprotein phosphatase.

The enzyme preparation we used is the eluate of the second of two sequential isodeacetylcolchicine-deacetylcolchicine (I-DAC) affinity columns used[9] to purify tubulin from 100,000*g* rat brain supernatants (see legend to Table 1). Previous studies have shown that tubulin purified by these and other methods, contains endogenous protein

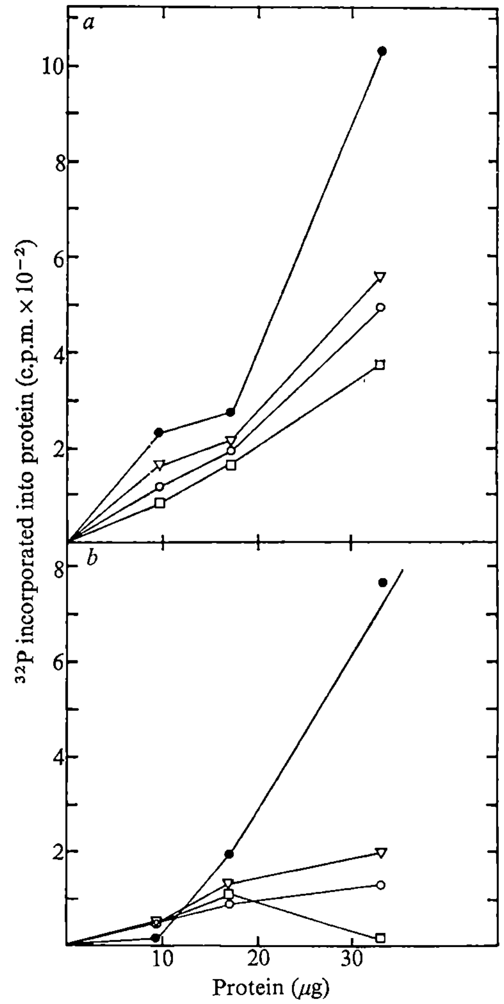

Fig. 1 Effect of cyclic GMP on endogenous protein phosphorylation as a function of the concentration of protein. Data presented correspond to the same experiment: *a*, whole protein kinase; *b*, cyclic AMP-stimulated protein kinase Preparation of the kinase and its assay (5 min, 37 °C) were as described in Tables 1 and 2. The following additions were made to the assay mixture: (●) 2.5×10^{-6} M cyclic AMP, (△) 2.5×10^{-6} M cyclic AMP plus 2.5×10^{-7} M cyclic GMP, (□) 2.5×10^{-6} M cyclic AMP plus 2.5×10^{-8} M cyclic GMP, (○) 2.5×10^{-6} M cyclic AMP plus 2.5×10^{-9} M cyclic GMP.

kinase activity[10-13] which specifically phosphorylates high molecular weight proteins closely associated with tubulin[9,14]. Furthermore, essentially all of the kinase activity in such preparations (including that observed in the absence of added cyclic AMP) is fundamentally cyclic AMP dependent since total suppression of activity occurs[9] on addition of a specific muscle protein kinase modulator[15].

Phosphorylation of endogenous protein in the various colchicine–Agarose eluate fractions is strongly opposed by very low, physiological concentrations of cyclic GMP (Table 1, fractions 3, 4 and 5). Although such inhibition is most marked when exogenous cyclic AMP is added, significant inhibition occurs reproducibly even in the absence of added cyclic AMP. The inhibition occurs at physiological *p*H (7.5) and temperature (37 °C), whether Mg^{2+} (5 mM), Mn^{2+} (5 mM), or both are used and the optimal concentrations of cyclic GMP vary between 10^{-7} and 10^{-9} M. Although there is some experimental variability, the data from many experiments indicate that cyclic GMP concentrations above or below 10^{-8} M are usually less effective (Tables 1 and 2*A*).

The inhibitory effect of cyclic GMP and the relative effectiveness of varying concentrations of this nucleotide are maintained over a relatively wide range of protein concentration in each individual experiment, although the total phosphorylation varies from preparation to preparation (for example, we have observed endogenous phosphorylation–dephosphorylation in preparations containing as little as 1 μg of protein per assay) (Fig. 1).

During the early stages of the kinase assay (for example, 1 min) the inhibitory effect of cyclic GMP is usually not apparent (Table 2*A*) As incubation progresses (from 5 to 10 min), with the concomitant increase in the quantity of

Table 1 Cyclic GMP inhibition of protein kinase activity in various fractions of a rat brain tubulin preparation

Addition	^{32}P incorporated into protein (c.p.m.) Column effluent (fraction number) 1	2	3	4	5	6
None	0	0	0	120	450	480
2.5×10^{-6} M cyclic AMP	0	50	2,580	1,850	830	290
2.5×10^{-6} M cyclic AMP+2.5×10^{-7} M cyclic GMP	220	100	60	260	590	380
2.5×10^{-6} M cyclic AMP+2.5×10^{-8} M cyclic GMP	250	320	0	80	0	410
2.5×10^{-6} M cyclic AMP+2.5×10^{-9} M cyclic GMP	180	0	0	160	370	400

Cyclic GMP inhibition of protein kinase activity in various fractions of a rat brain tubulin preparation chromatographed on a I-DAC–Agarose affinity column. Rat brains (10 g) were homogenised in 10 ml of 10 mM sodium phosphate, *p*H 7.65, containing 5 mM $MgCl_2$ and 1 mM GTP (buffer A). The 100,000*g* (1 h, 4 °C) supernatant of the homogenate was applied (4–10 °C) on a 2 ml I-DAC–Agarose column[9] (containing 160 nmol of bound ligand) equilibrated with buffer A. The column was washed thoroughly (50 ml) with buffer A before the protein was eluted with the same buffer containing 0 1 M NaCl (4 °C). The eluate was desalted on a 40-ml Sephadex G-25 (coarse grade) column equilibrated with buffer A. The protein was then reapplied to the same I-DAC column after washing with 7 M guanidine-HCl followed by equilibration with buffer A. The 0.1 M NaCl eluate of this column was collected in sequential 0 7-ml fractions, each of which was tested for protein kinase activity using the endogenous protein present in the sample as substrate. The enzymatic assay mixture contained, in a total final volume of 200 μl, 50 μmol potassium phosphate, *p*H 7.5, 5 μmol $MnCl_2$, 2 nmol of unlabelled ATP, 2×10^6 c.p.m. of γ-^{32}P-ATP and 50 μl of sample (column eluent) which contained 5 mM $MgCl_2$, 1 mM GTP and 0.1 M NaCl. The samples were incubated for 5 min at 37 °C and the reaction was stopped by the addition of 3 ml of ice-cold 20% trichloroacetic acid plus 300 μg of serum albumin per 200 μl of assay mixture. The values have been corrected for blanks (880 c p.m.), which were determined by adding the radioactivity after stopping the reaction. The ^{32}P incorporated into protein was determined (liquid scintillation) in the second 20% trichloroacetic-acid precipitate after dissolving in 0.5 ml of 1 M NaOH. Values are averages of duplicate replications.

Table 2 Effect of length of incubation on the cyclic GMP inhibition of cyclic AMP-stimulated protein kinase activity of tubulin preparations

Cyclic nucleotide added	^{32}P (c.p.m.) incorporated into protein Incubation time (min) 1	2	5
Experiment *A*			
None	130	220	540
2.5×10^{-6} M cyclic AMP	380	1,000	2,570
2.5×10^{-6} M cyclic AMP+2.5×10^{-6} M cyclic GMP	240	640	1,640
2.5×10^{-6} M cyclic AMP+2.5×10^{-7} M cyclic GMP	570	430	1,410
2.5×10^{-6} M cyclic AMP+2.5×10^{-8} M cyclic GMP	430	780	180
2.5×10^{-6} M cyclic AMP+2.5×10^{-9} M cyclic GMP	360	660	400
2.5×10^{-6} M cyclic AMP+2.5×10^{-10} M cyclic GMP	310	570	740
2.5×10^{-6} M cyclic AMP+2.5×10^{-11} M cyclic GMP	470	740	500
	5	10	15
Experiment *B*			
None	1,180	800	160
2.5×10^{-6} M cyclic AMP	2,260	910	340
2.5×10^{-6} M cyclic AMP+2.5×10^{-7} M cyclic GMP	710	1,020	20
2.5×10^{-6} M cyclic AMP+2.5×10^{-8} M cyclic GMP	1,240	0	0
2.5×10^{-6} M cyclic AMP+2.5×10^{-9} M cyclic GMP	440	550	50

Effect of length of incubation on the cyclic GMP inhibition of cyclic AMP-stimulated protein kinase activity of tubulin preparations. The two independent experiments shown were carried out with protein purified on two sequential I-DAC affinity columns, as described in Table 1. The eluent samples of the second column were pooled before assay. Kinase activity was determined as described in Table 1, using the endogenous protein as the substrate (15 μg). Results essentially similar to those described here have been obtained in at least 20 separate experiments. The data have been corrected for blanks (490 c.p.m. in *A*, 1,100 c.p.m. in *B*).

phosphorylated protein, the effect of cyclic GMP becomes apparent. With progressively longer periods of incubation, however, the effects of cyclic GMP become less obvious, or are obscured by the obvious dephosphorylation which occurs spontaneously in all conditions (Table 2*B*). The kinetic data are most consistent with a cyclic GMP-induced acceleration of a protein dephosphorylation reaction. Addition of adenosine thiotriphosphate (as a carrier) together with γ-^{32}P-ATP decreases greatly the rate of spontaneous dephosphorylation, consistent with the presence of protein phosphatases[16].

Although the kinase activity in the tubulin preparation can effectively phosphorylate exogenously added proteins such as histone (lysine enriched, f1), such phosphorylation is not opposed by cyclic GMP (Table 3). On the other hand, phosphorylation of aged (24 h, −20 °C) colchicine–Agarose eluates (I-DAC), which also occurs readily in the absence of cyclic AMP, is clearly inhibited by cyclic GMP in the absence, but not presence, of cyclic AMP. This suggests that the cyclic GMP-enhanced dephosphorylation may be restricted to certain specific sites of natural protein substrates. These latter sites are probably not the only ones available for phosphorylation in the aged natural substrate when the protein kinase activity is fully expressed (that is, in the presence of cyclic AMP).

Table 3 Effect of cyclic GMP on the phosphorylation of endogenous and exogenous substrates by the eluate of I-DAC–Agarose affinity columns

Cyclic nucleotide additions	^{32}P (c.p.m.) incorporated into protein Fresh I-DAC protein	 Aged I-DAC protein	 Histone*
None	700	4,070	3,210
5×10^{-6} M cyclic AMP	3,770	4,580	5,120
5×10^{-7} M cyclic GMP	780	2,920	3,980
5×10^{-8} M cyclic GMP	600	1,900	5,560
5×10^{-9} M cyclic GMP	580	3,820	6,320
5×10^{-6} M cyclic AMP+5×10^{-7} M cyclic GMP	1,270	3,850	5,490
5×10^{-6} M cyclic AMP+5×10^{-8} M cyclic GMP	2,000	4,390	7,620
5×10^{-6} M cyclic AMP+5×10^{-9} M cyclic GMP	1,120	4,110	6,810

Effect of cyclic GMP on the phosphorylation of endogenous and exogenous substrates by the eluate of I-DAC–Agarose affinity columns. The kinase preparation described in Table 2 was incubated for 5 min (37 °C) with no other addition (fresh I-DAC protein), with an aged, desalted eluent fraction (10 µg of protein) which had been stored at −20 °C for 24 h (aged I-DAC protein) or with 10 µg of histone. Assay conditions were as described in Table 1.

*Histone type V (Sigma), lysine-rich subgroup f1.

The effects of cyclic GMP cannot be explained on the basis of competition or direct antagonism of a cyclic AMP effect since they can occur even in the absence of cyclic AMP, they clearly follow an initial phosphorylation reaction, the inhibition is much less effective at the highest concentrations of cyclic GMP tested, and direct binding studies using ^{3}H-labelled cyclic AMP (10^{-8} M) show no competition of binding with cyclic GMP concentrations varying from 10^{-7} M to 10^{-9} M. With regard to nucleotide specificity, it is important that the cyclic GMP (10^{-7}–10^{-9} M) effect on protein phosphorylation is observed in reaction mixtures containing much higher concentrations of cyclic AMP (10^{-6} M), ATP (10^{-6} M) and GTP (10^{-4} M). In certain types of experiments it has been observed consistently that prolonged incubation of the kinase assay mixture results in a slow cyclic GMP-stimulated phosphorylation, suggesting the possible additional existence in this system of a specific cyclic GMP-dependent kinase which can complicate observations of the specific phosphatase effect described here (Table 3). For this reason, careful attention to the time course of the assay at a given protein concentration is critical for the demonstration of the cyclic GMP-enhanced dephosphorylation reaction.

These studies suggest the existence of a highly specific, cyclic GMP-sensitive phosphoprotein phosphatase which acts on specific sites of natural substrates which are themselves phosphorylated by a cyclic AMP-dependent protein kinase. We will not speculate further on the possible mechanism of this cyclic GMP effect. These observations, together with earlier studies demonstrating that the kinase activity of the tubulin preparation used here is completely cyclic AMP dependent[9], and that the proteins phosphorylated (*in vivo* as well as *in vitro*) are specific high molecular weight proteins closely associated with the 36S tubulin molecule[9,14], may be pertinent to understanding the regulation of the structure and function of tubulin and microtubules The specific cyclic GMP effect described here may also have broader significance with respect to the biochemical actions of this cyclic nucleotide. The low levels of protein phosphatase activity in preparations of tubulin obtained by two cycles of polymerisation–depolymerisation may reflect a weak association of the protein phosphatase with tubulin, or may be uniquely related to the specific method of purification. The fact, however, that certain colchicine derivatives, such as that used in the affinity adsorbent used here, inhibit bacterial and animal non-protein alkaline phosphatases as well as vegetable non-protein acid phosphatases[17] opens the possibility that the I-DAC affinity column may also retain protein phosphatases physiologically unrelated with tubulin or functionally related proteins.

This work was supported by grants from the NIH, the American Cancer Society and the Kroc Foundation. I.V.S. was a recipient of a postdoctoral fellowship from the Program of Cultural Cooperation Spain–USA, and P.C of a USPHS research career development award.

I. V. SANDOVAL
P. CUATRECASAS

Department of Pharmacology and Experimental Therapeutics,
and Department of Medicine,
Johns Hopkins School of Medicine,
Baltimore, Maryland 21205 and
The Wellcome Research Laboratories,*
Research Triangle Park, North Carolina 27709

Received February 25; accepted June 8, 1976

*Address for reprint requests

1 Goldberg, N. D., *et al.*, *Adv. Cyclic Nucleotide Res.*, 5, 307–330 (1974)
2 Krebs, E. G , *Curr. Top. cell Regul.*, 5, 99–133 (1972).
3 Kuo, J. F., *Proc. natn. Acad. Sci. U S A* , 71, 4037–4041 (1974)
4 Casnellie, J. E., and Greengard, P., *Proc. natn. Acad Sci. U.S.A.*, 71, 1891–1895 (1974).
5 Ueda, T., Rudolph, S. A., and Greengard, P , *Archs. Biochem. Biophys* , 170, 492–503 (1975).
6 DeLorenzo, R. J., and Greengard, P., *Proc. natn Acad Sci U S.A.*, 70, 1831–1835 (1973).
7 Maeno, H., Ueda, T., and Greengard, P , *J Cyclic Nucleotide Res.*, 1, 37–48 (1975).

8 Huang, F. L., and Glinsman, W. H., *Proc. natn. Acad. Sci. U.S.A.*, **72**, 3004–3008, (1975).
9 Sandoval, I., and Cuatrecasas, P., *Biochemistry* (in the press)
10 Goodman, D. B., Rasmussen, H., Di Bella, F., and Guthrow, C. E., Jr, *Proc. natn. Acad. Sci. U.S.A.*, **67**, 652–659 (1970).
11 Soifer, D., *J. Neurochem.*, **24**, 21–33 (1975)
12 Eipper, B. A., *J. biol. Chem.*, **249**, 1398–1406 (1974)
13 Shigekawa, B. L., and Olsen, R. W., *Biochem. biophys. Res. Commun.*, **63**, 455–462 (1975).
14 Sloboda, R. D., Rudolph, S. A., Rosenbaum, J. L., and Greengard, P., *Proc. natn. Acad. Sci. U.S.A.*, **72**, 177–181 (1975).
15 Walsh, D. A., *et al.*, *J. biol. Chem.*, **246**, 1977–1985 (1971).
16 Gratecos, D., and Fischer, E. H., *Biochem. biophys. Res. Commun.*, **58**, 960–967 (1974).
17 Siebert, G., Schonharting, M., Monika, O., and Surjana, S., *Hoppe-Seyler's Z. physiol. Chem.*, **356**, 855–860 (1975).

Structural properties of rat serum proteins which correlate with their degradative rates *in vivo*

SERUM proteins[1,2] like intracellular proteins[3–7], are continually being degraded and replaced at characteristic rates. Although there is appreciable evidence that structural alterations can influence the half lives of serum proteins[8–11], the features of serum proteins which normally influence their degradative rates are unknown. The present experiments were undertaken to learn more about the factors influencing the degradation of serum proteins and to explore any possible relationship of this process to the catabolism of intracellular proteins.

There is now strong evidence that the degradative rates of intracellular proteins are determined to a large extent by their conformations[5,6]. For example, in both animal and bacterial cells, the catabolic rates of different proteins correlate with their relative sensitivities *in vitro* to purified endoproteases[5–7] and to lysosomal extracts[12–14]. In addition two structural features of normal proteins have been shown to correlate with their half lives in a wide variety of organisms and tissues: (1) proteins with large subunits tend to be degraded more rapidly on the average than those with small subunits[5–7,15], and (2) proteins with acidic isoelectric points tend to be degraded more rapidly than proteins with neutral or basic isoelectric points[16].

Analogous studies of the possible relationship between the degradative rates of serum proteins and these structural properties have not been reported. We now present evidence that the catabolism of serum protein shows two of the characteristics previously reported for degradation of intracellular proteins: (1) the rates of catabolism of rat serum proteins *in vivo* correlate with their relative sensitivity *in vitro* to a wide variety of endoproteases, and (2) the more acidic serum proteins turn over *in vivo* more rapidly than neutral or basic ones. In contrast to findings with intracellular proteins, no relationship was found between the molecular weights of serum proteins and their half lives *in vivo*

To test whether half lives of serum proteins are related to their sensitivity to proteolytic attack, we used the double-isotope approach of Arias *et al.*[17] to differentiate serum proteins which turn over rapidly from those which turn over slowly *in vivo*. This same technique was used previously to establish a correlation between degradative rates and protease sensitivity for intracellular proteins[7]. ^{14}C-leucine was administered to a rat 4 d before an injection of ^{3}H-leucine, and the animal was killed 4–12 h after the second injection. The ^{14}C remaining in protein after 4 d is primarily contained in the more stable proteins, while the ^{3}H is found preferentially in proteins that turn over rapidly[5,17,18].

We then compared the susceptibility to various proteases of proteins having shorter *in vivo* half lives (enriched for ^{3}H) and those that are more stable (enriched for ^{14}C). As shown in Fig. 1, serum proteins rapidly degraded *in vivo* were more susceptible to digestion at *p*H 7.2 by Pronase (*a,f*), trypsin (*b*) and chymotrypsin (*c*) and at *p*H 4.0 by the acidic proteases, pepsin (*d*) and lysosomal cathepsins from rat liver (*e*). Similar results were obtained with three separate preparations of double-labelled proteins from rat serum. These findings are analogous to those obtained earlier with intracellular proteins[5–7,12–14], although the serum proteins on the average appeared much less susceptible to trypsin and chymotrypsin than were liver proteins (J.F.D. and A.L.G., unpublished).

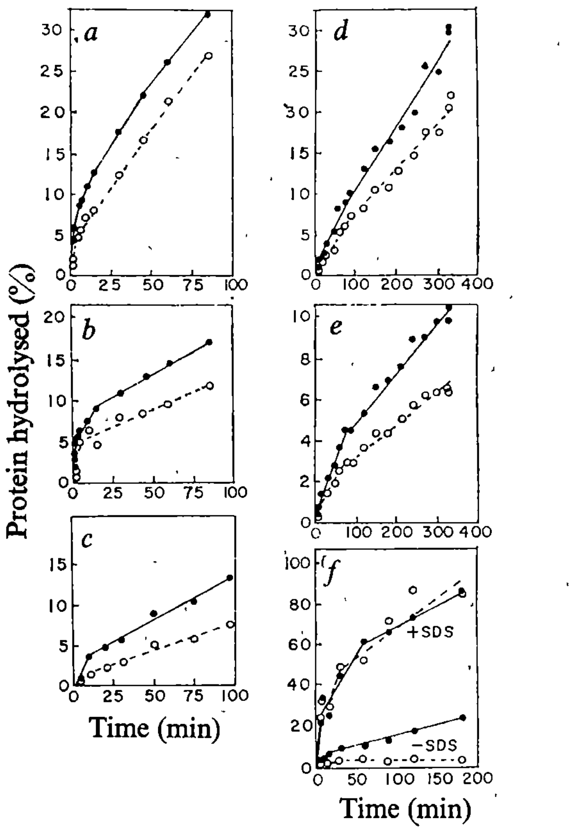

Fig. 1 Comparison of the susceptibility of stable and rapidly turning-over serum proteins to proteolytic enzymes To label these fractions preferentially, 100 µCi of ^{14}C-leucine was administered intraperitoneally to a male rat (125 g) Four days later, the same animal was injected with 500 µCi of ^{3}H-leucine and killed 4 or 12 h thereafter. Consequently, the ^{14}C is found primarily in proteins with relatively long half lives (○) while ^{3}H-proteins (●) are enriched for more labile polypeptides. To prepare the serum, the rats were anaesthetised with ether, blood (about 5 ml) was collected from the aorta into a heparinised tube, and cells were separated by centrifugation at 100*g* for 10 min. The clear supernatant containing the serum proteins was dialysed against phosphate-buffered saline (*p*H 7.2, ref. 7) (for experiments *a–c* and *f*) or 100 mM citrate buffer (*p*H 4.0) (for experiments *d* and *e*) to remove free amino acids. The procedure for incubation with proteases, and the sources for all materials have been reported previously[7]. Each incubation mixture contained approximately 5 mg of serum protein with a specific activity of about 70,000 d.p.m. ^{3}H and 5,000 d.p.m. ^{14}C per mg. Enzymes were added at the following concentrations: *a*, Pronase, 100 µg ml^{-1}; *b*, trypsin, 100 µg ml^{-1}; *c*, chymotrypsin, 1 mg ml^{-1}; *d*, pepsin, 50 µg ml^{-1}; *e*, crude lysosomal fraction (prepared as described in (31)), 10 mg ml^{-1}; *f*, Pronase, 50 µg ml^{-1}. Conformations of serum proteins were disrupted in (*f*) by addition of 1% SDS and 50 mM dithiothreitol (final concentration) and boiling for 5 min. (Pronase is at least partially active in SDS.) Protein hydrolysis is expressed as radioactivity (d.p.m.) initially in protein that is converted to a trichloroacetic-acid soluble form.

These results indicated that the rates of catabolism of serum proteins are related to their inherent susceptibility to proteolytic attack, which is presumably a function of the proteins' native conformations. In fact, the susceptibility of both rapidly and slowly turning-over proteins to digestion by Pronase increased markedly when the native conformations of the proteins were destroyed by boiling in sodium dodecyl sulphate (SDS). Following such treatment, the correlation between degradative rates *in vivo* and susceptibility to Pronase was abolished (Fig. 1*f*).

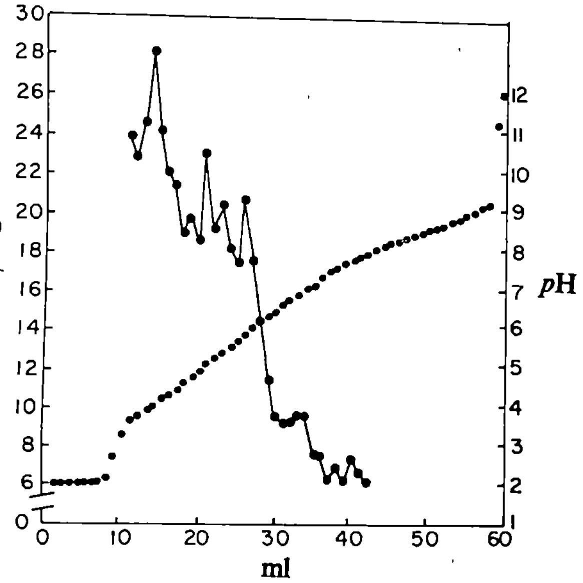

Fig. 2 Comparison of degradative rates of rat serum proteins with different isoelectric points. Double-labelled serum proteins were prepared as described in Fig. 1 and separated by isoelectric focusing as reported previously[16]. A high $^{3}H/^{14}C$ ratio indicates more rapid turnover of the fraction[17]. Radioactivity in each fraction was determined as described previously. Ratios are not plotted for fractions containing less than 200 d.p.m. for each isotope. The variation in $^{3}H/^{14}C$ ratios inherent in these experimental protocols has been reported previously[16]. Fractions from isoelectric focusing contained between 0 and 10,000 d.p.m. of ^{3}H and 0 and 500 d.p.m. of ^{14}C. The correlation between $^{3}H/^{14}C$ and *p*H is highly significant ($r = -0.957$, $P < 0.01$). *p*H, ●●●; $^{3}H/^{14}C$, ●—●.

We used the same labelling procedures to compare the degradative rates *in vivo* of serum components differing in their isoelectric points. For any protein, the amount of isotope remaining after 4 d (^{14}C) relative to the amount of isotope initially incorporated (^{3}H) reflects its rate of degradation. Thus, proteins that are synthesised and degraded rapidly will have high $^{3}H/^{14}C$ ratios, as has been discussed critically elsewhere[5,7,17,18]. The double-labelled serum proteins were then separated according to their isoelectric points by isoelectric focusing[16].

The more acidic proteins consistently had higher $^{3}H/^{14}C$ ratios ($r=0.957$, $P<0.01$). Thus on the average they are degraded more rapidly than the less acidic ones. Qualitatively similar results were obtained with three separate preparations of double-labelled proteins from rats and with two preparations from mice. Thus, a similar correlation between degradative rates and isoelectric points holds for serum proteins (Fig. 2) as for intracellular proteins, even though serum was found to contain much fewer basic proteins than most mammalian tissues (J. F. D. and A.L.G., unpublished observations).

Many earlier studies have demonstrated a correlation between degradative rates of intracellular proteins and their subunit molecular weight as determined by SDS–acrylamide gel electrophoresis[5-7,15]. But when double-labelled serum proteins were separated by SDS gel electrophoresis, no relationship was found between subunit molecular weight and degradative rates (Fig. 3). These findings differ from those obtained with all mammalian tissues tested. These negative results are complicated by the fact that most serum proteins are glycoproteins which have been shown to migrate more slowly than expected in SDS gels primarily because of a decrease in detergent binding[19,20]. Since glycoproteins should behave less anomalously during Sephadex gel filtration in the absence of SDS, we have also fractionated serum proteins according to their multimeric size by Sephadex chromatography. For intracellular proteins multimer molecular weights also correlate with half lives[1], since larger multimers tend to be composed of larger subunits[15]. On gel filtration of the serum proteins, however, no relationship was found between molecular weight and degradative rate (Fig. 4).

Thus degradative rates of serum proteins, unlike those of intracellular proteins, do not correlate with their molecular weights (Fig. 3 and 4). Larger intracellular polypeptides have been shown in general to be more sensitive to proteases *in vitro* than smaller ones, and this relationship has been suggested to be the basis for the observed correlation between molecular weight and *in vivo* degradative rates[7]. It is possible that large and small serum components do not differ in susceptibility to proteases. On the other hand, physiological processes are known that can cause the selective loss of small polypeptides from serum and may therefore obscure any general relationship that may exist between protein size and degradative rates. For instance, smaller proteins are lost especially rapidly from the circulation due to ultrafiltration in the renal glomeruli as well as in other capillary beds[22]. In addition, specific degradative mechanisms appear responsible for the rapid catabolism of small peptide hormones[7]. Thus the reasons and significance of this lack of a size correlation for serum proteins are unclear.

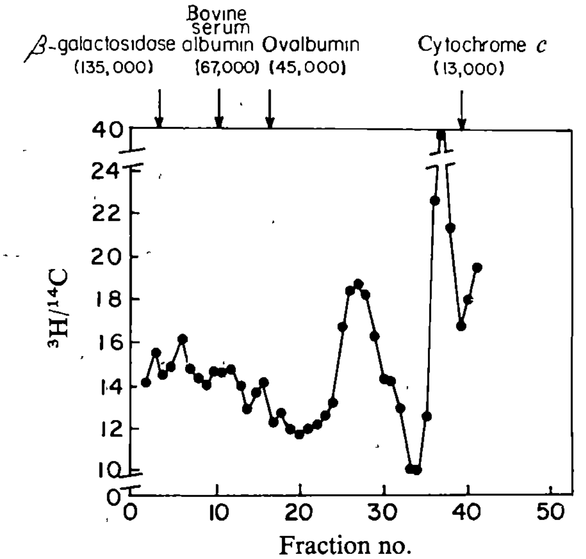

Fig. 3 Relative degradative rates of rat serum polypeptides of different molecular weights. Double-labelled serum proteins were prepared as described in Fig. 1 and separated by SDS–acrylamide gel electrophoresis. A high $^{3}H/^{14}C$ ratio indicates more rapid turnover of the fraction. The electrophoresis was performed in large diameter gels, which were sliced and counted as described earlier[7]. Electrophoretic fractions contained between 0 and 14,000 d.p.m. ^{3}H and 0 and 1,200 d.p.m. ^{14}C. Ratios are not plotted for fractions containing less than 100 d.p.m. of each isotope. The variation in $^{3}H/^{14}C$ ratios inherent in these methods has been reported previously[7].

A variety of studies have indicated that the pathway of catabolism of serum proteins involves pinocytosis and subsequent appearance of the proteins in lysosomes[8,9]. Pinocytosis has been generally assumed to be the rate-limiting step in the degradation of serum proteins. This conclusion is based primarily on studies of the fate of injected enzymes[23,24] or specific labelled serum proteins[8,25-27]. The present findings on the turnover of native serum proteins in normal conditions suggest alternative possibilities. Since the degradative rates of serum proteins *in vivo* correlate with their relative susceptibility to a variety of proteases (Fig. 1), the rate-limiting step in the catabolism of most serum proteins may be an initial proteolytic cleavage within the circulation followed by pinocytosis of the partially degraded protein. A rate-limiting proteolytic cleavage also

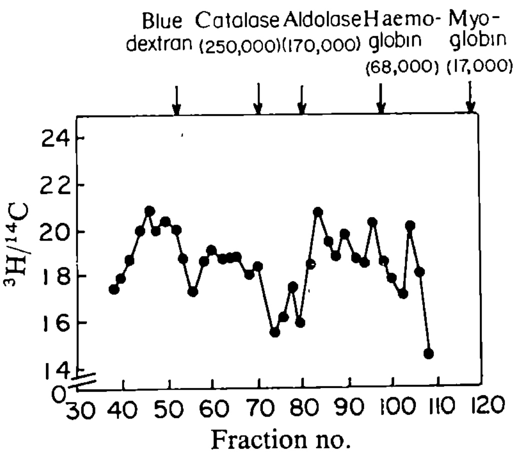

Fig. 4 Comparison of the degradative rates of serum proteins of different multimer size in the absence of SDS. Double-labelled serum proteins were prepared as in Fig. 1 and separated by Sephadex G-150. The protein fractionation and counting of radioactivity was carried out as reported earlier[7,16]. Chromatographic fractions contained between 0 and 50,000 d.p.m. ^{3}H and 0 and 2,000 d.p.m. ^{14}C. Ratios are not plotted for fractions containing less than 100 d.p.m. of each isotope.

might possibly occur within the secondary lysosome. According to this hypothesis, proteins that are relatively resistant to lysosomal proteases, might then be released and re-enter the circulation[27-29].

Alternatively, if pinocytosis of serum proteins is actually the rate-limiting step in their degradation, the structural features of the serum proteins which determine their rates of pinocytosis must correlate with their protease sensitivity (Fig. 1) and their isoelectric points (Fig. 2). For example, proteins that are more sensitive to proteases or more acidic may tend to denature more easily[5,6], and denaturation can promote pinocytosis[9,30]. Whatever the mechanism underlying the correlations with charge and proteolytic susceptibility, the fact that they apply to both intracellular and extracellular proteins suggests that degradation of these two types of proteins involves similar principles and may even share common mechanisms.

This work was supported by grants from the NINDS and the Muscular Dystrophy Associations of America. J.F.D. was a postdoctoral fellow of the MDA and A.L.G. holds a Research Career Development Award from the NINDS.

J. FRED DICE*
ALFRED L. GOLDBERG

Department of Physiology,
Harvard Medical School,
Boston, Massachusetts 02115

Received March 19; accepted June 8, 1976

* Present address Thimann Laboratories, Division of Natural Sciences, University of California, Santa Cruz, California 95064

1 Schreier, K , and Porath, U , in *Physiology and Pathophysiology of Plasma Protein Metabolism* (edit by Koblet, H , *et al*), 122–134 (Grune and Stratton, New York, 1966).
2 McFarland, A S (ed), *Protein Turnover Ciba Foundation Symposium* 9 (North Holland, Amsterdam, 1973)
3 Schimke, R T , *Mammalian Protein Metabolism*, 4 (edit by Munro, H N), 178–228 (1970)
4 Rechcigl, M , in *Enzyme Synthesis and Degradation in Mammalian Systems* (edit. by Rechcigl, M), 237–311 (University Park Press, Baltimore, 1971)
5 Goldberg, A L , and Dice, J F , *A Rev Biochem* , 43, 835–869 (1974)
6 Goldberg, A L , and St John, A , *A Rev Biochem* , 45 (in the press)
7 Dice, J F , Dehlinger, P J , and Schimke, R T , *J biol Chem* , 248, 4220–4228 (1973)
8 Mego, J L , and McQueen, J D , *Biochim biophys. Acta*, 100, 136–143 (1965).
9 Kirsch, R E , Frith, L O and Saunders, S J , *Biochim biophys Acta*, 279, 87–91 (1972)
10 Morell, A G , Gregoriadis, G , and Scheinberg, I H , *J biol Chem* , 246, 1461–1467 (1971)
11 Ashwell, G , and Morell, A G , *Adv Enzymol* , 41, 99–128 (1974)
12 Segal, H L , Winkler, J R , and Miyagi, M P , *J biol Chem* , 249, 6364–6365 (1974)
13 Dean, R T , *Eur J Biochem* , 58, 9–14 (1975).
14 Bohley, P , Langner, J , Ansorge, S , Miehe, M , Miehe, C , and Hanson, H , *Acta biol med Ger* , 28, 321–328 (1972)
15 Dice, J F , and Goldberg, A L , *Archs biochem Biophys.*, 170, 213–219 (1975).
16 Dice, J F , and Goldberg, A L , *Proc natn Acad Sci U S A* , 72, 3893–3897 (1975)
17 Arias, I M , Doyle, D , and Schimke, R T , *J biol Chem* , 244, 3303–3315 (1969).
18 Poole, B , *J biol. Chem* , 246, 6587–6591 (1971)
19 Bretscher, M S , *Nature new Biol* , 231, 229–232 (1971)
20 Segrest, J. P , Jackson, R L., Andrews, E P., and Marchesi, V T , *Biochem biophys Res. Commun* , 44, 390–395 (1971)
21 Dehlinger, P J., and Schimke, R T , *Biochem biophys Res Commun* , 40, 1473–1480 (1970)
22 Pappenheimer, J F , *Phys. Rev.*, 33, 387–423 (1953)
23 Davidson, S. J , *J Cell Biol* , 59, 213–222 (1973)
24 Creemers, J , and Jacques, P. J , *Expl Cell Res* , 67, 188–203 (1971).
25 Williams, K. E , Lloyd, J B., Davies, M , and Beck, F , *Biochem J* , 125, 303–308 (1971)
26 Williams, K E., Kidston, E M , Beck, F., and Lloyd, J B , *J Cell Biol* , 64, 123–134 (1975)
27 Gordon, A H., and Jacques, P J , in *Labelled Proteins in Tracer Studies* (edit by Donato, L , Milhaud, G , and Sirchis, J), 127–133 (Euratom, 1966).
28 Jacques, P J , in *Pathologic Aspects of Cellular Membranes* (edit by Trump, B. J , and Arstila, A) (Academic, New York, 1974)
29 Wild, A F , in *Biology and Pathology*, 3 (edit by Dingle, J T), 169–215 (North Holland, Amsterdam, 1973)
30 Buys, C. H C. M., Elferink, M. G L., Bouma, J M. W., Guber, M , and Nieuwenhuis, P., *J. Reticuloendothel Soc* , 14, 209–223 (1973)
31 Penn, N W , *Biochim biophys Acta*, 37, 55–61 (1960)

Accessibility of DNA in condensed chromatin to nuclease digestion

RECENT evidence indicates that a large portion of the DNA of higher organisms is organised in compact nucleoprotein structures. Initial studies on nuclease digestion of chromatin showed that about half the nuclear DNA is present in the form of small resistant chromatin fragments[1-3]. Subsequent studies have shown that the sites of nuclease digestion are regularly spaced, and that, at the limit of digestion, the majority of the DNA that remains is in the form of relatively homogeneous small fragments, which vary from about 120 to 200 nucleotide pairs in length[4-7]. This concept of small repeating resistant structures in chromatin is further supported by electron microscope studies on chromatin fibres spread from hypotonically treated nuclei[8] and from isolated chromatin[9]

Here we examine whether two types of 'condensed' chromatin—mitotic chromosomes and the fraction of interphase chromatin that contains satellite DNA—have the same subunit structure as 'non-condensed' chromatin. The experiments were performed on cells of *Dipodomys ordii* (kangaroo rat) because (1) mitotic cells can be shaken off monolayer cultures selectively to yield pure mitotic cell preparations and (2) this species contains 52% of its DNA in the form of satellite components[10] which are associated with a dense interphase chromatin fraction[11].

The kinetics of staphylococcal nuclease digestion of DNA in interphase nuclei or mitotic chromosomes to acid-soluble material are essentially identical At an enzyme concentration of 30 units ml^{-1} there is a rapid phase of digestion such that 65% of the DNA remains acid insoluble after 15 min, followed by a slower linear digestion until 50% remains acid insoluble after 1 h. Accessibility of DNA to the enzyme is similar in both chromatin states.

Another test for similarity in the sub-structure of interphase nuclei and mitotic chromosomes is to observe the size distribution of DNA fragments generated at various times during nuclease digestion of the chromatin Cells were uniformly labelled with ^{3}H-thymidine for two cell generations. ^{3}H-labelled chromosomes and ^{3}H-labelled interphase nuclei were prepared from these cultures and separately mixed with unlabelled interphase nuclei in the ratio of 1 : 10 in DNA amount. DNA extracted from partial nuclease digests was analysed on 1.5% Agarose gels which were photographed after staining with ethidium bromide The gels were subsequently processed for fluorography, and the sizes of unlabelled DNA fragments detected by ethidium bromide staining were compared with the sizes of ^{3}H-labelled DNA fragments detected by fluorography (Fig 1).

At all stages of nuclease digestion of the chromatin mixtures we could detect no differences in the size of the DNA fragments from single or multiple subunits derived from unlabelled interphase chromatin (Fig. 1*a* and *c*), ^{3}H-labelled interphase chromatin (Fig 1*b*), or mitotic

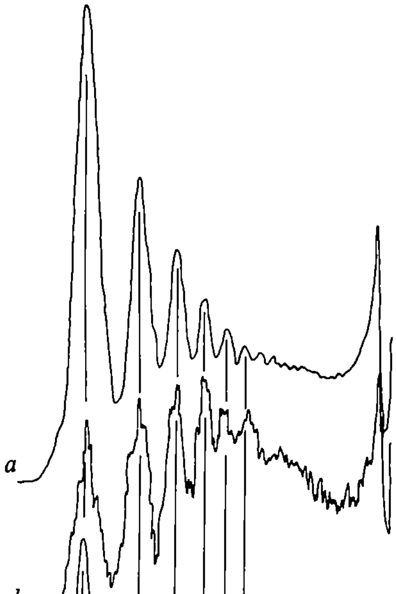

Fig. 1 Agarose gel and fluorogram analysis of DNA from interphase and mitotic chromatin digested with staphylococcal nuclease. Mitotic and interphase cells of *D. ordii*, labelled for 60 h with 0.2 µCi ^{3}H-thymidine (54 Ci mM^{-1}, Amersham) in F-12 medium lacking unlabelled thymidine, were collected separately as described elsewhere[13]. Equal quantities of each ^{3}H-labelled sample were mixed with 10 times the number of unlabelled cells. The nuclei and chromosomes were prepared by one of a number of methods[3,14,15], and resuspended in 20 mM Tris, 1 mM CaCl$_2$, 1 mM MgCl$_2$, *p*H 7.5 at a concentration equivalent to 200 µg total DNA ml^{-1}. Staphylococcal nuclease was added at 30 units ml^{-1}. At various intervals after the start of digestion, samples were removed and digestion stopped by addition of 2 ml 50 mM sodium phosphate buffer, *p*H 6.8, containing 5 mM EDTA. Sodium dodecylsarcosinate and NaCl were added to final concentrations of 0.5% and 1 M respectively, and the lysate was extracted twice with water-saturated phenol. DNA was precipitated by the addition of two volumes of absolute ethanol followed by storage overnight at −20 °C. DNA precipitates were collected by centrifugation, redissolved in 10 mM Tris, 10 mM EDTA, *p*H 8.0, and electrophoresed in 1.5% Agarose slab gels (18 cm × 18 cm × 5 mm) for 16 h at 10 mA at room temperature The electrophoresis buffer was 40 mM Tris, 20 mM sodium acetate, 1 mM EDTA, *p*H 8 2. Gels were stained with 0.5 µg ml^{-1} ethidium bromide dissolved in electrophoresis buffer, and the fluorescence photographed under light at 254 nm. Photographed gels were processed for fluorography essentially as described by Bonner and Laskey[16] except that ethoxyethanol was used as the solvent in place of dimethyl sulphoxide. Fluorograms were exposed on presensitised Kodak RP-Royal Xomat film at −75 °C and developed in Kodak D-19 developer. Photographic negatives of the stained gels and the fluorograms were scanned in a Joyce Loebl densitometer. The tracings shown are both of chromatin digested for 15 min (20% of the DNA rendered acid soluble). *a*, Ethidium bromide fluoroscence distribution; unlabelled plus ^{3}H-labelled interphase chromatin; *b*, distribution of ^{3}H-labelled DNA fragments from interphase chromatin; *c*, ethidium bromide fluorescence distribution; unlabelled interphase chromatin plus ^{3}H-labelled mitotic chromatin; *d*, distribution of ^{3}H-labelled DNA fragments from mitotic chromatin The size of the DNA fragments (in base pairs) is indicated at the bottom of the figure. These values were obtained by comparison with DNA fragments produced by *Eco*RII restriction enzyme digestion of mouse satellite DNA[17] and *Hin*dIII restriction enzyme digestion of SV40 DNA[18].

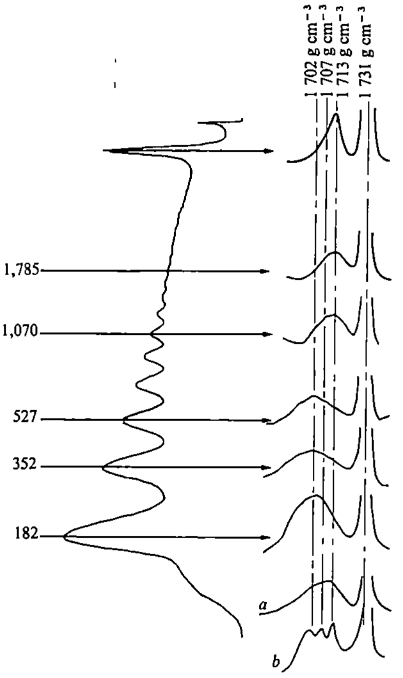

Fig. 2 Caesium chloride neutral density gradient analysis of DNA of different fragment sizes following partial digestion of nuclei by nuclease. Nuclei were isolated and digested with staphylococcal nuclease and then several slab gels were run as described in Fig. 1. The individual DNA bands were cut out, and the DNA was recovered by crushing the gel through a 24-gauge hypodermic needle and centrifuging the crushed gel at 200,000*g* for 30 min. The supernatant was removed, solid caesium chloride added to a density of 1.70 g cm^{-3} and ethidium bromide extracted with *n*-propanol. After removal of ethidium bromide, the density was adjusted to 1.710 g cm^{-3} and *Micrococcus lysodeikticus* DNA was added as a density marker. Centrifugation was at 44,700 r.p.m. at 25 °C for 24 – 48 h in the 6-place analytical rotor in an MSE Centriscan. Left, Densitometer tracing of a photographic negative of DNA from a partial digest separated on 1.5% Agarose gel as described in Fig. 1. Right, Neutral caesium chloride banding profiles of DNA isolated from the various regions of the gel as indicated. The buoyant density profiles of *a*, total DNA after partial digestion and *b*, total undigested DNA, are shown at the bottom The size of the DNA fragments (in base pairs, see Fig. 1) is indicated on the left.

chromatin (Fig. 1*d*). The distribution of the majority of nuclease-sensitive sites is thus the same in both mitotic and interphase chromatin.

We have measured the relative rates of digestion of the fractions containing satellite and non-satellite DNA in interphase chromatin. The satellite DNA component is less rapidly digested by nuclease than chromatin containing non-satellite DNA. We have shown this by measuring the amounts of satellite DNAs present in DNA fragments of different size at various stages of digestion of interphase chromatin. The DNA fragments were recovered from Agarose gels and analysed by analytical caesium chloride density centrifugation or thermal denaturation in 0.1 × SSC. The three satellite DNAs of *D. ordii* band on the heavy side of the main band DNA. HS-α and HS-β satellite DNAs have a density of 1.713 g cm^{-3} and MS satellite DNA has a density of 1.707 g cm^{-3} (ref. 12). The HS-β satellite has a G+C content of 66%, and can be distinguished clearly as a separate component in a thermal melting profile. Buoyant density analysis has the advantage that it can identify all three major satellite components, but the disadvantage of giving poor resolution at the molecular sizes of the smaller DNA fragments. Thermal denaturation, on the other hand, can reliably distinguish HS-β satellite DNA component in large and small DNA fragments, but can only detect about 20% of the total satellite DNA.

Buoyant density analysis of DNA of different fragment sizes from partially digested chromatin (Fig. 2) shows that the DNA remaining as high molecular weight structures—larger than six times the single subunit size—is almost entirely satellite DNA. DNA fragments of single subunit size, or low multiples thereof, have broad banding profiles, but with a peak density characteristic of main band DNA. The enrichment of satellite DNA in high molecular weight DNA fragments is unambiguous, but the depletion of satellite DNA in low molecular weight pieces is less convincing, owing to the diffuse banding profiles.

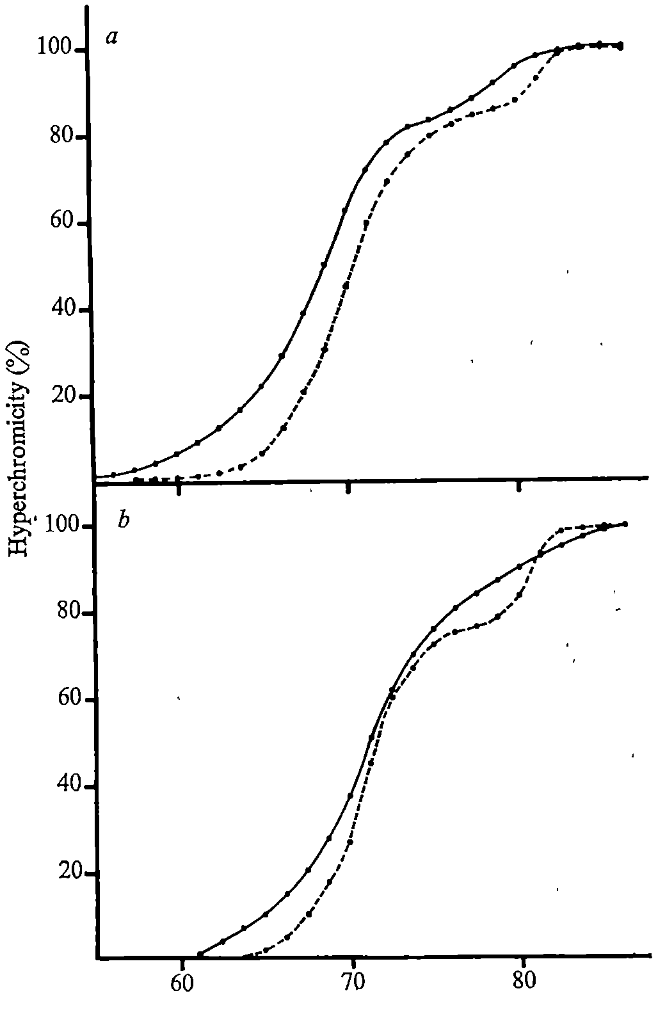

Fig. 3 Thermal denaturation profiles of *a*, total undigested DNA (— — —) and single subunit sized DNA after complete nuclease digestion (———). *b*, Single subunit sized DNA (———) from partially digested (20% acid soluble) chromatin and high molecular weight DNA (— — —) fragments of partially digested (20% acid soluble) chromatin. Total undigested DNA was isolated from nuclei by the method of Marmur[19] with slight modifications. DNA fragments from digested chromatin were recovered from the supernatants of crushed gels (see Fig. 1) by adding NaCl to a final concentration of 1 M, extracting twice with 2 volumes of water-saturated phenol, and precipitating the DNA by addition of 2 volumes of ethanol followed by storage overnight at −20 °C. The precipitates were collected by centrifugation, dissolved in 1/100 × SSC and dialysed exhaustively against 1/10 SSC. All samples were thermally denatured in 1/10 SSC in a Unicam SP800 spectrophotometer. (SSC is 0.15 M sodium chloride, 0.015 M sodium citrate.)

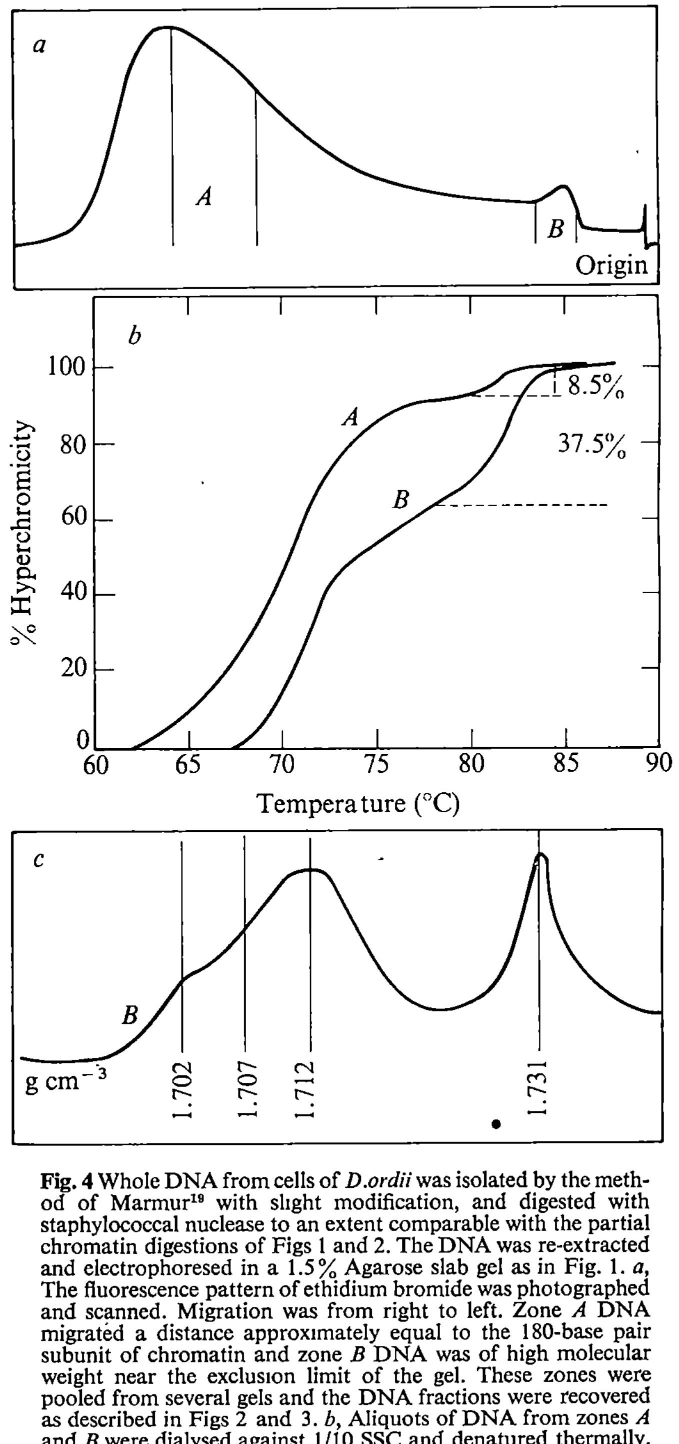

Fig. 4 Whole DNA from cells of *D.ordii* was isolated by the method of Marmur[19] with slight modification, and digested with staphylococcal nuclease to an extent comparable with the partial chromatin digestions of Figs 1 and 2. The DNA was re-extracted and electrophoresed in a 1.5% Agarose slab gel as in Fig. 1. *a*, The fluorescence pattern of ethidium bromide was photographed and scanned. Migration was from right to left. Zone *A* DNA migrated a distance approximately equal to the 180-base pair subunit of chromatin and zone *B* DNA was of high molecular weight near the exclusion limit of the gel. These zones were pooled from several gels and the DNA fractions were recovered as described in Figs 2 and 3. *b*, Aliquots of DNA from zones *A* and *B* were dialysed against 1/10 SSC and denatured thermally. *c*, DNA of high molecular weight from zone *B* was centrifuged to equilibrium in neutral CsCl as described in Fig. 2.

This ambiguity is overcome by thermal denaturation. When chromatin was digested for 1 h (as in Fig. 1) the 50% of DNA that remained acid insoluble was entirely at the size of single subunits. The melting profile of this DNA was similar to that of total undigested DNA (Fig. 3*a*). Although the T_m of the single subunit-sized DNA is lower because of its decreased molecular weight[20], the second transition (HS-β satellite DNA) is about 15% of the total hyperchromicity in both samples. Thus, at this stage of digestion to single subunit size, the distribution of satellite and non-satellite DNAs is the same as in undigested chromatin. In a partial digest of chromatin, however, (Fig. 3*b*) DNA of single subunit size is considerably depleted HS-β DNA, whereas DNA remaining at high molecular weight is enriched in HS-β to a degree consistent with the sample containing only the total satellite mixture

We are grateful to a reviewer for the suggestion that the apparent resistance of satellite DNA-containing chromatin during brief digestion could be due to the known preference of the nuclease for AT-rich DNA[21]. As a result, free DNA isolated from cells of *D. ordii* was digested to various extents in the same conditions as for chromatin digestion. Similar to the partial chromatin digestion (Fig. 3), most of the DNA fragments formed a broad band in 1 5% Agarose gel, the size of the single subunit of chromatin and smaller, whereas a small amount of DNA was almost excluded from the gel (Fig. 4*a*). Zones at approximately 180-base pair size and of high molecular weight were extracted and the recovered DNA fractions were centrifuged in a CsCl gradient and melted. The density gradient pattern of the high molecular weight DNA (Fig. 4*c*) corresponded with the 1,070-base pair pattern of Fig. 2, thus showing enrichment in satellites and depletion of main band DNA. Thermal denaturation (Fig 4*b*) revealed that the second transition (representing HS-β satellite) was smaller than that of whole DNA for the low molecular weight fraction and very much larger for the high molecular weight fraction.

The results with partial digestion of free DNA are very similar to those of chromatin. The apparent resistance of chromatin containing satellite DNA to nuclease digestion may be due to the base preference of the enzyme rather than to a difference between extended and condensed chromatin in accessibility of DNA to the enzyme Other factors may, however, be involved since only HS-β satellite is substantially richer in GC content than main band DNA, yet all three satellites seem to behave similarly towards nuclease digestion. This question is receiving further study.

From our results it can be concluded that, firstly, the structures of extended and condensed chromatin in the forms of mitotic chromosomes or satellite DNA-containing interphase chromatin do not differ significantly in respect to accessibility to digestion by staphylococcal nuclease and secondly, the size and distribution of nuclease-resistant chromatin subunits are similar in extended and condensed chromatin. These findings support models of chromatin structure which place the DNA moiety in an exposed position outside the subunits[22–25]. A condensed state of chromatin does not arise therefore from greater coverage by proteins in a manner that obstructs the access of nuclease to the DNA.

This work was supported in part by the MRC and by a contract with the US ERDA. We thank Mr Norman Davidson for graphic artwork.

C. J. Bostock
S. Christie

Medical Research Council,
Clinical and Population Cytogenetics Unit,
Western General Hospital,
Edinburgh EH4 2XU, UK

F. T. Hatch

Lawrence Livermore Laboratory,
University of California,
Livermore, California 94550

Received December 2, 1975; accepted June 8, 1976.

[1] Clark, R. J., and Felsenfeld, G., *Nature new Biol.*, **229**, 101–106 (1971).
[2] Rill, R , and Van Holde, K. E., *J. biol Chem.*, **248**, 1080–1083 (1973).
[3] Hewish, D. R , and Burgoyne, L. A., *Biochem biophys. Res Commun.*, **52**, 504–510 (1973).
[4] Oosterhof, D. K., Hozier, J. C., and Rill, R. L , *Proc natn. Acad Sci U S.A.*, **72**, 633–637 (1975).
[5] Noll, M., *Nature*, **251**, 249–251 (1974).
[6] Lohr, D., and Van Holde, K E., *Science*, **186**, 165–166 (1975).
[7] Shaw, B. R., Corden, J. L., Sahasrabuddhe, C. G., and Van Holde, K. E., *Biochem. biophys. Res. Commun.*, **61**, 1193–1198 (1974).
[8] Olins, A. L , and Olins, D. E., *Science*, **183**, 330–332 (1974).
[9] Oudet, P , Gross-Bellard, A , and Chambon, P , *Cell*, **4**, 282–290 (1975).
[10] Mazrimas, J. A., and Hatch, F. T., *Nature new Biol* , **240**, 102–105 (1972).
[11] Mazrimas, J. A , and Hatch, F. T., *Exp. Cell. Res.*, **63**, 462–466 (1970).
[12] Hatch, F T , and Mazrimas, J. A , *Nucleic Acids Res.*, **1**, 559–575 (1974).
[13] Bostock, C J , and Christie, S., *Chromosoma*, **48**, 73–87 (1974).
[14] Wray, W., in *Methods in Cell Biology*, 6 (edit. by Prescott, D. M.), 283–306 and 307–315 (Academic, New York and London, 1973).
[15] Maio, J. J., and Schildkraut, C. L., *J molec. Biol* , **24**, 29–39 (1967).
[16] Bonner, W. M., and Laskey, R A., *Eur. J. Biochem.*, **46**, 83–88 (1974).
[17] Southern, E M., *J. molec. Biol* , **94**, 51–69 (1975).
[18] Nathans, D., and Smith, H. O., *A. Rev. Biochem.*, **44**, 273–293 (1975).
[19] Marmur, J. J., *J molec. Biol.*, **3**, 208–218 (1961).
[20] Crothers, D. M , Kallenbach, N R., and Zimm, B. H., *J. molec. Biol.*, **11**, 802–820 (1965).
[21] Wingert, L., and Von Hippel, P. H., *Biochim. Biophys. Acta*, **157**, 114–126 (1968).
[22] Van Holde, K. E., Sahasrabuddhe, C. G., and Shaw, B. R., *Nucleic Acids Res* , **1**, 1579–1586 (1974).
[23] Baldwin, J. P., Boseley, P. G., and Bradbury, E M., *Nature*, **253**, 245–249 (1975).
[24] Hyde, J. E., and Walker, I. O., *Nucleic Acid Res.*, **2**, 405–421 (1975).
[25] Gilmour, S., *New Scient* , **14**, February, 390–392 (1975)

Amphipathic enzyme–polymer conjugates

IMMOBILISATION of enzymes on solid supports to give reusable and stabilised catalysts has been studied extensively[1] but the concept of chemically modifying a water-soluble enzyme to enable its activity to be utilised in the form of a water-immiscible liquid phase has received little attention. Potential advantages of liquid-phase immobilisation include ease of continuous operation, freedom from the effects of solid particle breakdown and the possibility of enhanced activity against water-insoluble liquid substrates. Although the effects of detergent–protein association on protein extractability into *iso*-octane have been studied[2] and considerable effort has been expended on the liquid membrane entrapment concept[3,4], another possible type of liquid-phase immobilised enzyme system seems to have been neglected. The latter comprises droplets of a water-immiscible liquid bearing a surface layer of modified enzyme. We have found that some enzymes may be converted into surface-active amphipathic conjugates by covalent coupling to certain types of polymeric detergents (polysoaps) and that the resulting conjugates may bind sufficiently strongly to dispersed water-immiscible liquids to give an enzymatically active emulsion that can be handled as a quasi-liquid phase. The amphipathic enzyme conjugates are analogous to certain membrane-bound proteins such as cytochrome b_5, which have been shown to comprise a hydrophilic protein core anchored to a lipid bilayer by a hydrophobic polypeptide tail[5,6].

A particularly simple and convenient route to conjugates of proteins with random copolymer amphipaths is shown in Fig. 1.

A linear hydrophilic polymer such as the non-cross-linked types of ethylene–maleic anhydride copolymers previously used for enzyme immobilisation[7,8] or the maleic anhydride–vinyl methyl ether copolymer Gantrez AN[9] can be modified with hydrophobic nucleophiles (for example, RNH_2) by partial substitution of the anhydride functions. The remaining anhydride units may then be used to couple the polymer to a protein.

The modification reaction is conveniently carried out in *NN*-dimethylformamide in the presence of an organic base and the reaction mixture can be added directly to a solution of the enzyme with homogenisation. Alternatively, the modified polymer can be hydrolysed and the protein coupled to it using established carboxyl group activation techniques such as conversion to the acid azide[10] and the use of water-soluble carbodiimides[11] or Woodward's reagent K (ref. 12). These general methods enable control of net hydrophobicity, degree of enzyme substitution and, since cross linking by the protein can be minimal, of conjugate molecular weight. There is scope for introduction of spacer groups, different enzymes on the same polymer and other refinements.

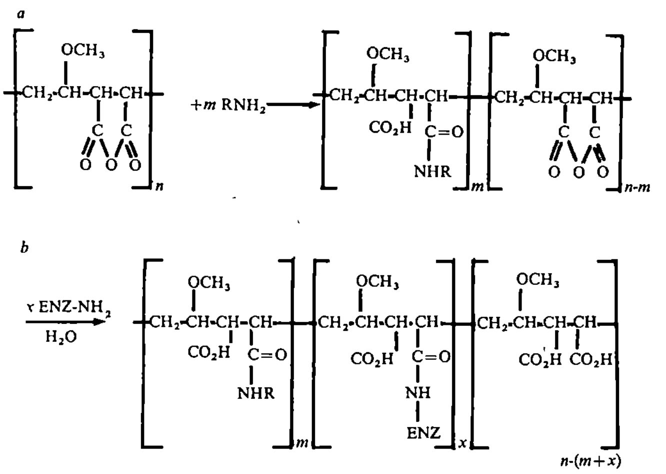

Fig. 1 Route to conjugates of proteins with a random copolymer amphipath.

Using the technique described, penicillin acylase and other enzymes have been conjugated with good recovery of enzyme activity. For example: a polymer solution prepared from Gantrez AN119 (0.5 g) and *n*-octadecylamine (0.28 g) in *NN*-dimethylformamide (2 5 ml) and pyridine (0.1 ml) was homogenised with *Escherichia coli* penicillin acylase (175 mg partially purified enzyme) in water (30 ml). After reaction at 4 °C overnight, sodium chloride (5.8 g) was added to precipitate the amphipathic solute, and the polymer conjugate isolated by centrifugation at 25,000*g* at 0 °C for 1 h A gel (4 0 g wet weight) of high specific activity resulted, and recovery of enzyme activity was 70%. Table 1 lists further conjugates of the same type. The physical form of these preparations varies from highly aggregated solids that sediment rapidly to materials that are soluble in low ionic strength aqueous media according to the extent of substitution by hydrophobic groups in the polymer or protein in the final conjugate. Some conjugate preparations may be fractionated by salt precipitation into materials of varying net hydrophobicity. Enzyme lability does not usually increase on conjugation, indicating that linkage to a polymeric detergent does not necessarily destabilise the catalytically active conformation of a protein.

Homogenisation of such conjugates with buffer and liquids such as *n*-decane, *n*-decanol and glycerol trioleate results in emulsions which can readily be separated by flotation or gentle centrifugation into an aqueous phase and a droplet phase with which the enzyme activity is associated. For example. homogenisation of the penicillin acylase conjugate described in the text above, with *n*-decanol in a wet gel–solvent weight ratio of 1 : 5 resulted in 90% of the enzyme activity being associated with the droplet phase on separation. The unconjugated enzyme does not bind significantly to solvent droplets formed using the Gantrez-based polysoaps. Some of the enzymatically active emulsions are quite stable: the droplet phase described above retained more than 40% of the initial enzyme activity after ten flotation–reuse cycles (batch cleavage of 5% w/v benzylpenicillin) Binding of the conjugates to dispersed phospholipid–cholesterol mixtures and whole cells has been observed. Photomicrography of solvent dispersions produced with penicillin acylase and other conjugates shows that solid gel particles are not visible at the droplet surfaces; and it is likely that the conjugate is distributed largely as a monolayer If bifunctional spacer groups or enzyme coupling agents such as glutaraldehyde are used in the preparation of conjugates, the resulting cross-linked gels form visible aggregates which, when dispersed with a solvent, adhere to the surface of the droplets Such a three-phase sludge can, nevertheless, be handled as a discrete enzymatically active layer.

Table 1 Amphipathic enzyme conjugates*

Enzyme	Hydrophobic group $CH_3(CH_2)_yNH-$	*m*/*n*†	Method of coupling polymer to protein	% Recovered enzyme activity
E. coli penicillin acylase	$y = 11$	0.33	Direct reaction with anhydride polymer¶	80
E. coli penicillin acylase	17	0.33	Conversion to half hydrazide polymer and activation to polymer azide‖	32
Bovine trypsin	9	0.30	Direct reaction with anhydride polymer**	24
Bovine trypsin	17	0.33§	Carbodiimide activation of hydrolysed polymer carboxyl groups††	~ 5

*Based on Gantrez AN119-substituted polymers. *m* and *n* refer to Fig. 1.

†Stoichiometry in polymer modification reaction, $n \simeq 1{,}500$.

‡Based on activity in original coupling mixture.

§$n \simeq 5{,}000$.

¶Ether-precipitated polymer (0.25 g) dissolved in *NN*-dimethylformamide (1 ml), homogenised with acylase (100 mg) in 0.1 M sodium phosphate, *p*H 7.0 (14 ml), reacted for 16 h at 4 °C, and conjugate gel isolated by precipitation with ammonium sulphate (70% saturation).

‖Hydrazide polymer prepared from anhydride polymer (21 μmol) and hydrazine hydrate (0.2 mol) in *NN*-dimethylformamide (50 ml). Polymer isolated by precipitation from 1.4 M aqueous NaCl (500 ml). Wet polymer (5 g) activated with $NaNO_2$ (0.5 g) in 2 N HCl (50 ml) and reacted with acylase (55 mg) in water (100 ml). Gel isolated by centrifugation.

**Polymer reaction mixture from Gantrez AN119 (1.0 g), *n*-decylamine (0.3 g) in *NN*-dimethylformamide (6 ml) added to trypsin (0.3 g) in 0.1 M sodium phosphate, *p*H 7.0 (60 ml). Titrated with 2 N NaOH until base uptake complete and gel isolated by successive precipitations with 1 M NaCl and 70% saturated ammonium sulphate.

††Hydrolysed polymer gel (15 g wet weight) reacted with 1-cyclohexyl-3-(2-morpholinoethyl)-carbodiimide metho-*p*-toluenesulphonate (0.5 g) in 0.1 M sodium phosphate, *p*H 4.7 (25 ml) for 5 min at room temperature; then treated with bovine trypsin (75 mg) at *p*H 5.9 and room temperature for 3 h. Conjugate gel isolated by centrifugation.

The amphipathic conjugation technique is a novel method of modifying proteins and has a large number of possible applications. In the field of biotechnology it provides a means of immobilising enzymes on solvent droplets, or, in the case of water-soluble conjugates, effecting the extraction of enzyme activity from an aqueous phase. It could also be used for locating well-characterised enzymes on natural or model biological membranes. Further details of the techniques, for which patents are pending, will be presented elsewhere.

I thank Dr J. Green for discussions and Mr I. Dodd for assistance.

RICHARD A. G. SMITH

Beecham Pharmaceuticals Research Division,
Walton Oaks, Dorking Road,
Tadworth, Surrey KT20 7NT,UK

Received April 12; accepted June 9, 1976.

[1] Zaborsky, O., *Immobilised Enzymes* (Chemical Rubber Co., Cleveland, Ohio, 1973).
[2] Yonath, J., Burstein, N., and Blauer, G., *Biochem. biophys. Res. Commun.*, 54, 507–511 (1973)
[3] May, S. W., and Li, N. N., *Biochem. biophys. Res. Commun.*, 47, 1179–1185 (1972).
[4] May, S. W., and Li, N. N., in *Enzyme Engineering*, 2 (edit by Pye, E. K., and Wingard, L. B., Jr), (Plenum, New York and London, 1974).
[5] Spatz, L., and Strittmatter, P., *Proc. natn. Acad. Sci. U.S.A.*, 68, 1042–1046 (1971). Spatz, L., and Strittmatter, P., *J. biol. Chem.*, 248, 793–799 (1973).
[6] Segrest, J. P., Kahane, I., Jackson, R. L., and Marchesi, V. T., *Arch. Biochem. Biophys.*, 155, 167–183 (1973).
[7] Levin, Y., Pecht, M., Goldstein, L., and Katchalski, E., *Biochemistry*, 3, 1905–1913 (1964).
[8] Goldstein, L., Levin, Y., and Katchalski, E., *Biochemistry*, 3, 1913–1919 (1964).
[9] Zingaro, R. A., and Uziel, M., *Biochim. biophys. Acta*, 213, 371–379 (1970).
[10] Erlanger, B. G., Isambert, M. F., and Michelson, A M , *Biochem. biophys. Res. Commun.*, 40, 70–76 (1970).
[11] Mosbach, K., *Acta chem Scand.*, 24, 2084–2902 (1970).
[12] Patel, R P., Lopiekes, D. V , Brown, S. P., and Price, S., *Biopolymers*, 5, 577–582 (1967).

●

reviews

Nutrition and the developing brain

John Dobbing

Malnutrition and Brain Development. By Myron Winick. Pp xv+169. (Oxford University· Oxford and New York, April 1976.) £5.

Nutrition and the Developing Nervous System By Philip R. Dodge, Arthur L. Prensky and Ralph D. Feigin. Pp. xvi+538. (Mosby: Saint Louis; Kimpton: London, January 1976.) £27.25.

THE suspicion is very strong that malnutrition during fetal and early neonatal life may lead to an irrecoverable diminution of intellect: and since the majority of the pregnant mothers and children in the world are underfed, this adds up to an assault on one of man's most distinguishing features by environmental circumstances which are theoretically within his control. The problem is proving it.

Human achievement is difficult to measure in any significant terms. Human growth from babyhood to adulthood is very slow, and nothing short of a longitudinal prospective study over many years is going to be satisfactory in communities where a reliable retrospective history of fetal and baby life is always especially difficult. Environmental contributions to the shaping of personal development (which are of course so numerous and so powerful compared with any genetic contribution) are nevertheless very difficult to enumerate and evaluate separately, especially as they are interacting as well as additive.

One mechanism amongst many by which early malnutrition may reduce eventual performance, may be by way of permanent alterations to the structure and some of the metabolic biochemistry of the physical brain, and we are now beginning to understand a great deal about this; Unfortunately the less well nourished members of any infant community who will probably suffer from this physical neuropathology are usually the most impoverished in every other facet of their environment, both physical and 'emotional'; and so it is exceedingly difficult to know whether the newly discovered growth pathology of the brain matters, and if so how (relatively) much?

Both these books are predominantly about the physical effects of nutrition on the developing brain, and as such inevitably only consider that one aspect of the huge problem in any detail. Dodge's book is a compendious and suitably critical account for the serious student and is likely to have few competitors for a good time to come.

If Winick's much smaller book had been simplified in the sense of being a reliable introduction for the less professionally interested it could have been very useful for a wider readership. Unfortunately it is not. I think Winick confuses the main issues of vulnerable periods in developing brain and the relative importance of fetal and postnatal brain growth, to the point of being potentially misleading to nutritionist and politician alike; and in spite of its attractive appearance I am worried by it.

Dodge, painstakingly and with abundant references, reasons his way through a morass of much incompletely collected and questionably argued literature with remarkable astuteness; although he and his colleagues have occasionally tended to catalogue the information rather than evaluate it.

Both books in their way cover the elements of normal brain growth; and since the brain is an organ of the body like any other, both have paid attention to the very relevant effects of nutrition on somatic growth.

Dodge, as a clinical paediatric neurologist, adds some valuable shorter sections on minerals, vitamins and diseases of amino acid metabolism with implications for the brain. Neither book seems to have heard of our own finding that the period of vulnerability of the human brain is almost certainly predominantly postnatal, an important fact for practical social and political policy; or perhaps they do not agree At all events they might have said so. Dodge discusses the rest of our work in Manchester very fully and appreciatively, but I do not think my very strong preference for his version over Winick's is entirely due to that. □

John Dobbing is Professor of Child Growth and Development in the Department of Child Health of the University of Manchester, UK.

Aspects of polymeric carbons

Polymeric Carbons· Carbon Fibre, Glass and Char. By G. M. Jenkins and K. Kawamura. Pp. vi+178. (Cambridge University: Cambridge and London, May 1976.) £8.50.

THE decomposition of resins at temperatures up to 2,500 °C gives rise to graphite in the form of small and highly distorted crystals. As every Materials Scientist knows such distortions can confer strength well above that of more perfect graphite; the resultant materials are very useful but very difficult to characterise. Vitreous carbon is used for crucibles and in some biomedical applications where high strength, chemical inertness or high temperature resistance are needed; whereas carbon fibres are used in a wide range of composites.

This book covers the production, properties and structure of these polymeric carbons and puts them in the context of other forms of carbon. The style is easy to read and the treatment is mainly factual, the emphasis being on what happens rather than why. The 200 references cover the scientific and patent literature up to 1973. A lot of attention is given to the author's own work on pyrolysed phenolic resins, which lends the book coherence.

As a text it has its limitations; there is not enough theoretical explanation and the treatment of chemistry is sloppy. For instance, the statement that "Commercial PAN is atactic and so contains two-dimensional order only" is simplistic, considering the importance of the resultant carbon structure on properties. It is also regrettable that there is no discussion of surface structure and properties when these are so important in practice.

In spite of this, for people in research or development using polymeric carbons, this monograph will be a good introduction and guide to the literature. Here, it fills a real lack.

Paul Calvert

Paul Calvert is a lecturer in polymer science in the School of Molecular Sciences at the University of Sussex, UK.

Beauty of original experiments

Landmark Experiments in Twentieth Century Physics. By George L. Trigg. Pp. x+303. (Crane Russak: New York; Edward Arnold: London, February 1976.) £11.50.

It is a sad fact, but unfortunately a true one, that most physicists' knowledge of the fundamental papers of their subject can only be described as fragmentary, even if one is feeling charitable. How many of us have in fact read the paper by Michelson and Morley, or the verification using α-particle scattering of the Rutherford nuclear atom by Geiger and Marsden, or nearer at hand the papers on the de Broglie wavelength of the electron by Davisson and Germer or G. P. Thomson.

We all know of the existence of these experiments and what they prove but our knowledge is second-hand, acquired from the writings of others. It is perhaps not as bad as reading Shakespeare through the eyes of another person, since aesthetic appreciation doesn't enter. If as sometimes happens for a colloquium or lecture course however, we have to examine a bit of fundamental experimentation in detail it is surprising how much rationalisation and perhaps even falsification enters the conventional picture

This is not deliberate misrepresentation, but it is just that the removal of an awkward corner or fact here and there facilitates understanding and is thus tacitly accepted. For example, one often finds the Michelson–Morley experiment discussed in terms of the time of arrival of pulses of light going down the separate paths. No doubt if the experiment were done this way the result would still be as given and the consequences would be identical; but it is a pity to depart from complete accuracy.

The whole situation stems from the expansion in physics over the past few decades, the need to keep university courses to a sensible length, and the reluctance of physicists to split their subject into more manageable parts. Tiresome examiners at the end of the three undergraduate years demand that we show some powers as practising physicists able to marshal our equations and solve our problems. They are not so concerned as a rule with the way the subject has developed to its present state. Schrödinger's equation, or operators in quantum mechanics, or matrix algebra take precedence over Davisson and Germer, and de Broglie. In this of course they are right, but something important is being lost

This is true also of books, in which as a particular subject matures so the formal structure grows and the experimental details recede. The present book, however, is of a different kind and attempts to redress the balance. The author takes a list of important twentieth-century experiments, first puts them briefly in their context, and then goes on to describe what was really done in great detail. To do this he uses long sections taken from the original papers which he joins and makes coherent by a minimum of connecting explanation. He thus maintains the authentic flavour of the subject at the time of the experiment, and much of the work is described in the original author's phraseology.

The list of experiments discussed is reasonably well chosen. It begins with the discovery of the wave nature of X-rays using diffraction from crystals, of isotopes, of the concept of atomic number and of superconductivity During this early period of the century many other possible subjects could of course be chosen but the ones used are not at all unreasonable. It may be that if the book is successful the author might return to this early era and write a second volume on some of the experiments he has omitted.

After this early period, and in fact, coming within the reviewer's memory, the list becomes more restricted and progressively less open to variation. From the early 1930s to the present day the complete list of topics covers the fluid properties of liquid helium below the λ point, the use of molecular beams for the determination of magnetic moments, the Lamb-Retherford effect, the anomalous g factor for the electron, the transistor, the non-conservation of parity for weak interactions, the Mössbauer effect, the experimental verification of the existence of the neutrino, the maser and laser, tunneling and superconductivity, the Ω^- meson and the microwave demonstration of the 3K intergalactic radiation temperature.

In spite of its intrinsic interest the book is not easy to read. The subjects cover quite a good cross section of contemporary physics and the use of extracts from the original papers sets a level of difficulty which cannot be entirely overcome by the explanatory connecting parts. This, however, cannot be helped. A student of scientific history or of scientific logic or of experimental technique or anyone just interested in how things really happened could not do better than begin with this book. The reader will get in a few hours an insight which has obviously taken the author a long time and much labour to achieve, and will be left with a feeling that at least some experiments in physics have a beauty which is more akin to art than science. **R. Latham**

Dr Latham is a reader in the Department of Physics at Imperial College, University of London, UK.

Nucleon–nucleon forces

The Nucleon–Nucleon Interaction By G. E. Brown and A. D. Jackson. Pp. viii+242. (North-Holland. Amsterdam and Oxford; American Elsevier: New York, 1976.) n p.

When students start research on a particular topic in theoretical physics their first problem is to learn all the essentials of previous work in a finite time. This nearly impossible task is helped by providing them with courses of lectures in which early developments are outlined and more recent work is spelled out in sufficient detail for the student to proceed immediately to the frontiers of the subject equipped to make further progress. G. E. Brown and A. D. Jackson have given such courses in Copenhagen which form the basis of their book The first four chapters give a simple outline of the well-established theory of nucleon interactions at low energies. In chapters 5 and 6 the reader is introduced to techniques in scattering theory, the use of relativistic equations and form factors; a description is also included of a more specialised technique, the eikonalisation of soft vector bosons, which is used by the Copenhagen group to provide convergence.

The final four chapters (half the book) are devoted to a detailed and explicit account of the steps required to derive realistic internucleon potentials and their relativistic corrections from one- and two-boson exchanges. The intimate interweaving of the various pion–nucleon and nucleon–nucleon amplitudes is explicitly demonstrated and a clear picture emerges of the physical principles underlying the calculations. This book will be essential reading and remain a basic reference for all those working on nucleon–nucleon forces, as well as being an introduction to the subject for the uninitiated.

Leonardo Castillejo

Leonardo Castillejo is Professor of Physics and head of the theoretical elementary particle physics group in the Department of Physics and Astronomy at University College, London, UK

Living history of science

Pioneers in Neuroendocrinology. (Perspectives in Neuroendocrine Research, Vol. 1.) Edited by Joseph Meites, Bernard T. Donovan and Samuel M. McCann. Pp. viii+327. (Plenum: New York and London, 1975.) $27.

THE majority of the scientists that have ever lived are alive at the present time. Thus it is possible for followers of the ever-growing subject of the History of Science to actually discourse with the people who made this history: they have the opportunity to examine at first hand the politics, philosophy, and circumstances that resulted in the scientific progress that has been made.

The subject of Neuroendocrinology—the study of the effects of the nervous system on the release of hormones, as well as the study of the effects of hormones on the nervous system—is a particularly young discipline, having only evolved since the period between the two world wars. Thus Joe Meites, Bernard Donovan and 'Don' McCann (themselves pioneers in this field) have been able to seize successfully the opportunity to call on 21 neuroendocrine pioneers "to write a personal, and even idiosyncratic, account" of the background behind the major contributions that each felt he or she had made to this subject. The editors have indeed extracted idiosyncratic accounts from their authors, and each chapter can very much be considered to reflect the character of the respective contributor. Whereas some authors, therefore, have used their publications as mileposts in the passage of time, others have given only a very technical and clinical survey of their research careers, without reference to other events occurring at the time, either in the scientific world, or in the world at large (such reference, if included, being of the greatest value and interest to the historian and to the lay-reader).

There are three chapters that I should particularly like to single out—those by the late Hans Heller, by Dora Jacobsohn, and by Dorothy Price—in that not only do they excel in the good qualities described above, but they also reflect the charm and humility of their respective authors.

It is regrettable that in the present volume two of the chapters are of a similar nature to the respective chapters in a comparable volume, *The Neurosciences: Paths of Discovery* (MIT Press, Boston). This book has, however, already met sufficient acclaim in America that the editors are presently commissioning writers for a second volume. That there should be so many pioneers available, and willing, to write presumably indicates that each and every scientist is a pioneer in his or her own way: the willingness, as pointed out by M. C. Shelesnyak, derives, at least in part, from the scientist "seeking self-satisfaction and nurturing (his) ego".

Although I would recommend that anyone involved in endocrine or physiological research should read this book, since they will do so with interest, I feel that the price is such that few will be able to afford to buy it. I fear, too, that this book is not sufficiently 'applied' for most science libraries to purchase, unless, that is, they have a shelf principally intended for reference by after-dinner speakers.

Barend ter Haar

Barend ter Haar is a Senior Scientific officer (MRC) attached to the ARC Institute of Animal Physiology, Babraham, Cambridge, UK.

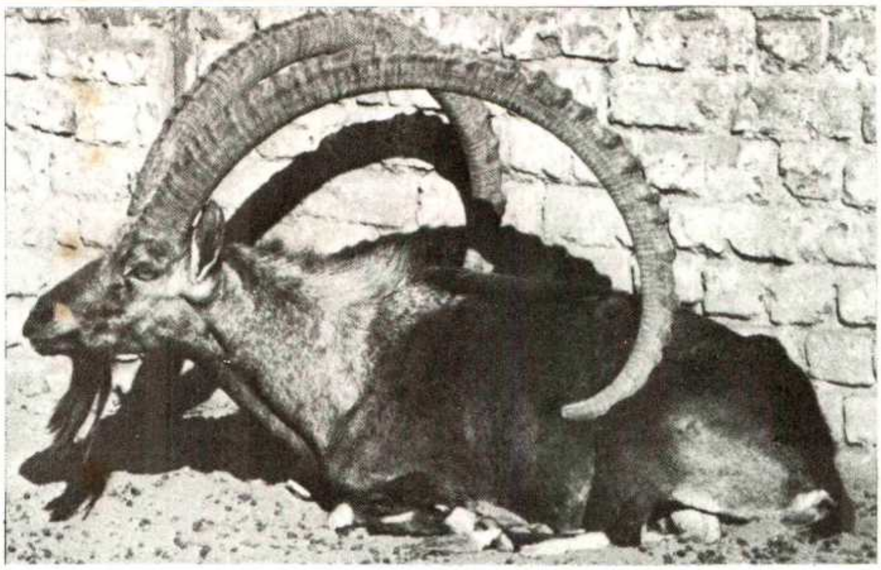

Hunting Nubian ibex (*Capra nubiana*) in the Red Sea Hills of the Sudan. Nubian ibex have long, slender, knotted horns, gracefully curved. Among males, 42-inch trophies are not uncommon, and the new world record (*shown above*) measures 54.5 inches. Taken from *African Hunter*. By James Mellon. Pp. xx+522. (Cassell: London, June, 1976.) £15.00.

Climate and man

Climate and the Environment: The Atmospheric Impact on Man. (Environmental Studies.) By John F. Griffiths. Pp. vii+148. (Elek: London, May 1976.) £2.95.

INTENDED for "students of geography and environmental studies at undergraduate and pre-university level" this book is a useful quick guide to the relationship between the workings of the atmosphere and the activities of man, without anything like the in-depth treatment of M. I. Budyko's classic work *Climate and Life* (Academic: New York and London, 1974; for review, see *Nature*, **251**, 362). The comparison is a natural one, since Griffiths approaches his subject through the energy budget–heat balance approach, drawing to some extent on the work of the Voeikov Geophysical Observatory, where Budyko was until recently Director. He also draws on the work of many other climatologists, as is usual in a book of this kind, but with comprehensive references to the original sources at the end of each chapter—a rarer, but welcome, practice for a text at this level.

There are many clear and useful illustrations, again culled from a variety of published works, and the text is well suited to the intended readership, with some of the mathematical details contained in appendices, again conveniently at the end of the appropriate chapters. The success of the author in reaching his planned market does, however, limit the usefulness of the book to anyone with a more advanced knowledge of the physical sciences who might have become interested in the subject through the continuing debate about the impact of climatic change on man, and the impact of man on climatic change. In the specified teaching context this book is likely to prove invaluable and is strongly recommended; at the next step up the academic ladder, however, Budyko's book remains the essential introduction to the subject. **John Gribbin**

John Gribbin is a Visiting Fellow in the Science Policy Research Unit at the University of Sussex, UK.

obituary

Alexander Naumovich Frumkin the father of modern electrochemistry died in Tūla (200 km from Moscow) after a heart attack on May 27, 1976.

He was born in 1895 in Kishinev, capital of Moldavia (now the Moldavian Soviet Socialist Republic), and attended the St Paul's Real School in Odessa, 150 km from his birthplace. On leaving school in 1912, he studied in Strasbourg and Bern but returned to graduate in the physico-mathematical faculty of the Novorussian University at Odessa, and become a staff member there. During this period he laid the foundations of the electrochemical studies which formed the mainstream of his work. His thesis, published in 1919 (he never in fact received a doctorate, as such distinctions were abolished in the early days of revolutionary Russia) besides giving a masterly survey of the current views on these problems, contained several notable original contributions (among which, many of the major themes of Frumkin's later work may be seen to have their origin): a careful experimental test of the basic equations of electrocapillarity, the identity of the point of zero charge determined by several methods, how Gibbs' equation may be used to derive surface excesses from electrocapillary curves, the nature of the potential-dependence of the adsorption isotherm, the lack of a simple relation between the double-layer capacity and the bulk dielectric constant, and finally the origin of the e.m.f. of a galvanic cell (one of the basic problems of electrochemistry).

In 1922 he moved to the Karpov Institute of Physical Chemistry in Moscow, formed to investigate the fundamental physico-chemical basis of industrial processes. Here he extended his interests to the gas–liquid interface, to the adsorption of electrolytes on activated charcoal and platinum black and to the problems of wetting and contact angles. He made pioneer measurements of the Volta potentials of solutions and showed how they depended on molecular orientation at the surface. His outstanding research was recognised by his election to the Academy of Sciences of the USSR.

His work in the decade after 1930 was even more important for electrochemistry. His first achievement was the marriage of surface chemistry and electrode reactions, in a paper which brilliantly used some earlier polarographic studies to give a rational theory of the salt effect on electrode reactions. The second major success was the first reliable direct measurement of the double-layer capacity and the demonstration of the catastrophic effect of minute traces of impurities. This led to the first reproducible measurements of hydrogen overvoltage through the use of adequate purification by adsorption (on platinum black) and by electrolysis. Similar careful studies of the charging curves of the platinum electrode were used to study the adsorption properties of this complex system for hydrogen and oxygen as well as electrolytes, and culminated in the proposal of the logarithmic adsorption isotherm as well as in the first use of the alternating current method for the measurement of the rate of electrode reactions. He later showed how this method may also be used for studying rates of adsorption.

During the second world war Frumkin was Director of the Colloido-Electrochemical Institute and, after the war, became for a time Director of the Institute of Physical Chemistry before, in 1958, a new Institute of Electrochemistry was formed with him as its Director, a post he held until his death. His own work broadened and extended in all directions in collaboration with the eminent coworkers he had attracted. This work was characterised by the intimate collaboration of experimentalists and theoreticians (notably V. G. Levich) which led to such developments as the rotating disc and ring-disc electrodes, the laws of photo-electric emission into solutions and the detailed understanding of the structure of electrified interfaces. His own interest in the last few years centred on the development and testing of the thermodynamic theory of interfaces across which charge may be freely transferred.

His encyclopaedic knowledge of all parts of electro- and surface-chemistry earned the admiration of everyone who knew him and his achievements were recognised by many honours (including the title of Hero of Socialist Labour, on his 70th birthday). He was also a man of broad general culture. He spoke English, French and German fluently and had a passionate interest in literature and the visual arts—he would travel far under difficult conditions to see an early church with fine frescoes. His other passion was mountaineering; naturally his activities were more restricted in recent years, yet as late as last September he organised a car trip from Alma Ata as high as possible into the Tien Shan range, and was delighted to find that he suffered no ill effects. **Roger Parsons**

announcements

Appointments

Dr R. C. Smith as professor of Physical Electronics at the University of Southampton.

Drs J. B. Harborne and **D. M. Moore** as Professors of Botany at the University of Reading.

Professor Sir John Dacie has been nominated President-elect of the Royal Society of Medicine.

M. Hubert Curien has been appointed president of the Centre National d'Etudes Spatiales (CNES).

Meetings

August 2–6, **Cell Wall Biochemistry Related to Specificity in Host–Plant Pathogen Interactions,** Tromsø, Norway (Jan Raa, University of Tromsø, Tromsø, Norway).

August 17–19, **Water Relations in Membrane Transport in Plants and Animals,** Philadelphia (American Physiological Society, c/o Dr Robert E. Forster, A-201 Richards Building G4, University of Pennsylvania, Philadelphia 19174).

August 23–27, **Congress of the International Primatological Society,** Cambridge (Dr D. J. Chivers, c/o Laundry Farm, Barton, Road, Cambridge, UK).

September 7–9, **Arboricultural Conference,** Worplesdon, Guildford (P. H. Bridgeman, c/o Merrist Wood Agricultural College, Worplesdon, Guildford, Surrey GU3 3PE, UK).

•

nature

August 12, 1976

Aftermath of the Mark VA

THE tale of the Jodrell Bank Mark VA radiotelescope that was never built is a gloomy one from any point of view. The Fifth Report from the Commons Committee of Public Accounts (HMSO; £3.45) takes a look at it.

Original plans were for the Science Research Council (SRC) to construct a 400-foot steerable dish (the Mark V); the council sought approval from the Department of Education and Science (DES) in 1970 on the basis of an estimate of £6.2 million (January 1970). A revision of the cost to £8 million caused the SRC to propose a smaller telescope—the Mark VA, with a 375-foot aperture, which they hoped could be built within the £6.2 million figure. A detailed design was to be prepared by the consulting engineers Husband and Company (a firm well experienced in radiotelescopes), covering drawings, bills of quantities and an invitation to tender for construction. The United Kingdom Atomic Energy Authority (UKAEA) would act as project managers, and it was estimated that £245,000 would be needed in consultants' fees. A large fraction of this figure was tied to the final tender price for construction.

Treasury approval for the design stage was given in June 1971. Ten months later the consultants were given the go-ahead to complete the design, if possible, within twelve months. They were told to alert the UKAEA if it seemed that the construction would cost more than was originally planned (due allowance had been made for inflation). Within six months they reported that the limit had been reached. After that, however, they were under no obligation to report costs further, and indeed had declined to have any further reporting written into their contract. The SRC's explanation for this was that "the consulting engineer . . . was designing the telescope to make it as cheap to build as he could. He was still finding out how it could be built cheaply, and it was more important for him to do that than to keep estimating what the cost was".

The inevitable happened. In October 1973 the consultants finished; tenders received in March 1974, reflecting the great uncertainties then prevailing in the construction industry, were around the £14 million mark. The total cost was put at £16 to £17 million. (It had been estimated just before by the UKAEA that the £6.2 million—at 1970 prices—which was the original total cost would have inflated to £10.7 million by January 1974.) Faced with a 50% growth in real terms in costs, and having to live with negligible overall growth, the SRC abandoned the telescope in June 1974, having learnt that total costs had risen even more in the interim to £22 million.

But this left one matter outstanding—the consultants' fee. As it was related to the tender price, it now amounted to the sum of almost £600,000, although on this the consultants eventually offered a rebate of £30,000. Even so, the amount they received was rather more than double what they must have expected on starting—a tidy windfall even when inflation had taken its toll. The SRC, which had not been informed itself of price escalation, had in its turn not been able in 1973 to keep the DES and the Treasury alerted to rising real costs, and had to seek special Treasury authority for the total design bill of £660,000.

It is fairly easy now to look back and see what went wrong. People were unused to dealing with inflationary conditions, and so didn't exercise such stringent controls as they would now. Even so, the telescope might have come through unscathed were it not for the situation which developed nationally during precisely the months that potential contractors were preparing their tenders. As it is the SRC gets a mild rap over the knuckles for letting matters drift, and rightly so, although the report has a rather optimistic view of the willingness of the scientific community to drop major projects when costs escalate. But what about the method by which the consultants were paid?

It must be made clear that the issue here is in no sense one of indulging in any gold-plating. The figures mentioned and the evidence of the SRC and the DES all fit in with the appalling way in which construction costs escalated. Be that as it may, the taxpayer ended up paying the consultants an "uncovenanted benefit", in the words of the committee, totally unrelated to the cost of the project. What is more, the SRC, having decided not to go ahead, would have to pay an additional fee if it chose to think again, as the plans are the copyright of the consultants. The SRC did at the very outset enquire about retaining the drawings, but was told that this would roughly double the fees.

All of this is legal and common practice. Fees are related to tender price, and copyright stays with the designer. But it does seem to the outsider to be open to charges of being inequitable, and it can lead to cynicism. The Public Accounts Committee calls for further consideration to be given to the way consultancy agreements work in the public sector. We hope someone is doing just that. □

Energy from warm rocks

Ron Oxburgh examines the prospects for geothermal energy in Britain, where a new research programme is to begin

IN the first few years of this century, an electrical generator with an output of several kilowatts was installed at Lardarello in northern Italy, to be driven by the steam which emanated naturally from the ground. It was the first modern attempt to harness the natural heat of the Earth to man's purposes. Relatively little further progress was made until the 1930s, but since then the use of geothermal energy has increased considerably, until today about 1100 MW are generated by this means in seven countries. Most of these installations pre-dated the rapid rise in fossil fuel prices of the past few years, and even then were competitive with conventional means of power generation. Today their situation is still more favourable.

Fifty or more countries are now involved in geothermal exploration. The number was recently increased by one with the decision announced by the UK Department of Energy to spend £840,000 on the geothermal exploration of Britain over the next three years. That decision was made largely on the basis of Energy Paper No. 9 (*Geothermal energy: the case for research in the United Kingdom*), a special report prepared by the Energy Technology Support Unit at Harwell, in which Dr John Garnish, the author, argues cogently for a cautiously optimistic approach to the prospects of geothermal energy in the UK.

Heat by convection

Heat is continuously generated within the Earth by the radioactive decay of unstable isotopes (mainly of U,Th and K) and is lost from the surface at an average rate of about 1.5 μcal cm^{-2} s^{-1} (63 mW m^{-2}). At depths greater than about 80 km heat transfer within the Earth is mainly by convection, but above that mainly by conduction; rocks are relatively poor conductors of heat and within this outer zone the conductive thermal gradient ranges from less than 10 °C km^{-1} to about 60 °C km^{-1}. This is true over more than 95% of the Earth's surface, within the interiors of the great tectonic plates.

Along the margins of the plates, however, and very occasionally within them, heat may locally be transferred to the surface or to within a few kilometres of it by convection. The convective medium in these cases is magma, or molten rock, at temperatures between 800 °C and 1100 °C. The magma commonly interacts with ground water circulating in the pores of the near surface rocks to give rise to geysers, hot springs or fumaroles. Drilling to 1,000 m or so in such areas may provide flows of water or steam at between 200 °C and 300 °C which, in favourable circumstances, can be used to drive turbines and generate electricity. All the major producers of geothermal electricity—Italy, the Western USA, New Zealand, Japan and Mexico (1,030 MW together)—exploit situations of this kind, and are all situated in the tectonically unstable earthquake and eruption-prone margins of plates.

Rocks at comparable temperatures may be found beneath other parts of the Earth's surface, such as the UK, where subsurface temperatures are governed largely by conduction, but they are much deeper. At the depth limit of present drilling experience (~9 km for a cost of £2–3 million), temperatures in such areas rarely exceed 300 °C. Furthermore, it is not sufficient to reach hot rock; if the heat is to be used it must be extracted by means of circulating fluids, and for this process to be effective the fluid must be able to permeate the hot medium thoroughly through pores and fissures. With increasing depth, however, the weight of the overlying rock tends to close pores and fissures and reduce the permeability to a very low value.

For these reasons, in most places the hot rocks which everywhere underlie us are at present both too expensive to reach and too impermeable to exploit, and are rather unlikely to provide the large quantities of water suitable for the economic generation of electricity by conventional technology (temperatures in excess of 200 °C are required).

Alternative applications

If, however, we consider alternative applications of geothermal energy, the position is quite different. There is a wide range of uses for water above 65 °C when it is used directly in a heat exchanger rather than to generate electricity. Taking 100 °C as a convenient reference value, rocks at this temperature may be reached virtually anywhere in the world by drilling holes well within the depth range of present technology. Whether these "warm rocks" constitute an exploitable natural resource depends upon the drilling costs of reaching them, their permeability structure, and the availability of a local demand for the low grade heat they can supply.

The economic considerations are now more finely balanced. As a very rough indication: given both suitable reservoir conditions at depth, and a suitable local market for the hot water, warm rock geothermal energy is at present competitive with fossil fuels if temperatures of 100 °C can be reached at 3 km or less. If, however, the cost of fossil fuels rises faster than drilling costs, this depth will be increased and the position of geothermal resources relatively improved.

Viewed in this way, the evaluation of UK geothermal resources becomes a problem of identifying those areas with slightly higher than average geothermal gradient and of understanding the subsurface distribution of permeability sufficiently well to distinguish those which are capable of successful exploitation. This latter problem is not a simple one, but is tractable by combining the expertise of the oil industry in understanding and controlling the flow of fluids underground with experience of hydrogeologists of rock permeabilities and natural underground circulations of water in the UK.

The problem of identifying regions of sufficiently high temperature is less easy. In the UK these are unlikely to be so pronounced that they give rise to significant perturbations of the surface magnetic field or the electrical conductivity structure of the crust, and there is little alternative to some kind of direct measurement of temperatures. Broadly, two approaches are possible. Deep holes may be drilled and temperatures measured at the proposed depth of exploitation. This is undoubtedly the safest method of exploration, but it is impossibly expensive unless the hole has been drilled for some other purpose which meets most of the costs.

The other approach is to make very precise measurements in shallow holes and use these as a basis for extrapolation to greater depth. The difficulty here is that near surface temperatures may be influenced by climatic changes (ice age effects may still be recognised hundreds of metres below the surface), the circulation of ground water, topographic irregularities of the surface and even erosional processes; for these reasons measurements are made in holes more than 200 m deep and preferably more than twice that depth, and are then corrected for the effects of the various perturbing factors. The heat flux, q, is given by $q = k\beta$ where k is the mean thermal conductivity of the rock, and β the mean thermal gradient, over a particular depth interval. The heat flow value determined in this way may then be used to predict the temperature at some greater depth with an accuracy which depends largely upon how well the thermal conductivity of the rocks down to that depth is known. Heat flow measurements of this kind must form the main basis of any exploration programme.

Although a relatively large number of underground temperatures have been measured in the UK, there have been relatively few reliable heat flow measurements—about 25. Although many of the temperature measurements were sufficiently accurate for the purposes for which they were made (ventilation in mines, for example), they do do not form a reliable basis for extrapolation to significantly greater depths. Similarly the temperature logs obtained by oil companies, by measurement in holes when drilling is complete, are subject to very large errors because the temperatures around the hole have been seriously perturbed by the drilling process itself; the circulation of cold drilling fluid from the surface to the bottom of the hole may change the rock temperature by some tens of degrees and it is months or years before the rock returns to its initial temperature.

Information inadequate

Energy Paper No. 9 synthesises the observational information at present available from a variety of sources and concludes that although there are some parts of the country where it is very likely that geothermal energy would be competitive with fossil fuels, the temperature information at present available is inadequate to make any overall assessment of the country's geothermal resources. Detailed cost analyses are presented to support the main recommendation that the possible benefits to the national energy budget justify the initiation of a national programme of geothermal exploration. Although the report itself makes an excellent case for such a programme, perhaps the most telling argument is that in France today there are several district heating schemes operating competitively on low grade geothermal energy, and that a number more are planned or are under constructon; these schemes have been established in situations which can be matched closely in the geology, and probably in thermal structure, by the Mesozoic sedimentary basins of this country.

It should perhaps be emphasised that although heat is continuously generated within the Earth, in most situations geothermal energy must be regarded as a depletable resource, and its exploitation as heat mining; the rate of convective removal of heat from the rocks of a hot source area is orders of magnitude faster than the heat can be replaced by conduction from below. In most cases geothermal fields are exploited at a rate designed to exhaust them in about twenty years. In a minority of situations (active volcanic regions, for example), the transport of heat to the surface by magma may match or exceed its extraction rate and the resource is not depletable, at any rate not significantly so. Questions now arise of just how and when possible geothermal resources should be exploited, and how large a contribution they might be expected to make to the national energy budget.

The answer to the first of these questions to some extent depends upon the answer to the second. If legitimate geological expectations were satisfied and suitable markets for the available energy were found, it would not be unreasonable to think of geothermal energy providing 1% or even 2% of the country's energy for 20 years. The greatest uncertainty must, however, be the availability of the market. The energy is available in the form of hot water in the temperature range 65–100 °C, temperatures which at present are generally considered too low for the efficient generation of electricity, and so the heat must be extracted from the water directly.

Furthermore, if additional heat losses by conduction are to be avoided, the hot water should ideally be used within a few miles, but certainly a few tens of miles, of the well head. There are various uses for low grade heat of this kind—domestic and industrial space heating, greenhouse heating, soil warming, fish farming and animal husbandry, various industrial fermentations, the drying of a range of organic materials and so on. It has also been shown to be economically viable to use geothermal energy for pre-heating of water, which may then be heated further by electricity, for a wider range of applications.

Policy decisions required

The problem therefore of exploiting "warm rock" geothermal resources is not purely scientific or technological. It involves either a happy geographical coincidence, by which suitable consumers who are willing to change to a geothermal supply are situated in or near a geothermal source area, or the deliberate encouragement of suitable industrial development in the geothermal areas and the use of district heating schemes in any new housing developments in the area. These clearly require major decisions of public policy. Attractive features of such developments would be the fact that warm-rock geothermal energy is virtually pollution-free—rejected warm water which has been used is reinjected into the ground for re-circulation. The surface plant is small and inconspicuous by comparison with any conventional power station.

The time scale of possible exploitation of UK geothermal resources now becomes clearer. It is reasonable to expect that the programme planned for the next three years will give reconnaissance information for much of the country. If the prospects appear reasonable at that level it would be appropriate to undertake a more intensive study of areas of particular interest. This second stage would require extensive shallow drilling (about 500 m) and some deep drilling, and could take five years; the rate of progress would be constrained by both the availability of drilling capacity and the time taken for drilling—although there is great variation, a 4 km hole could

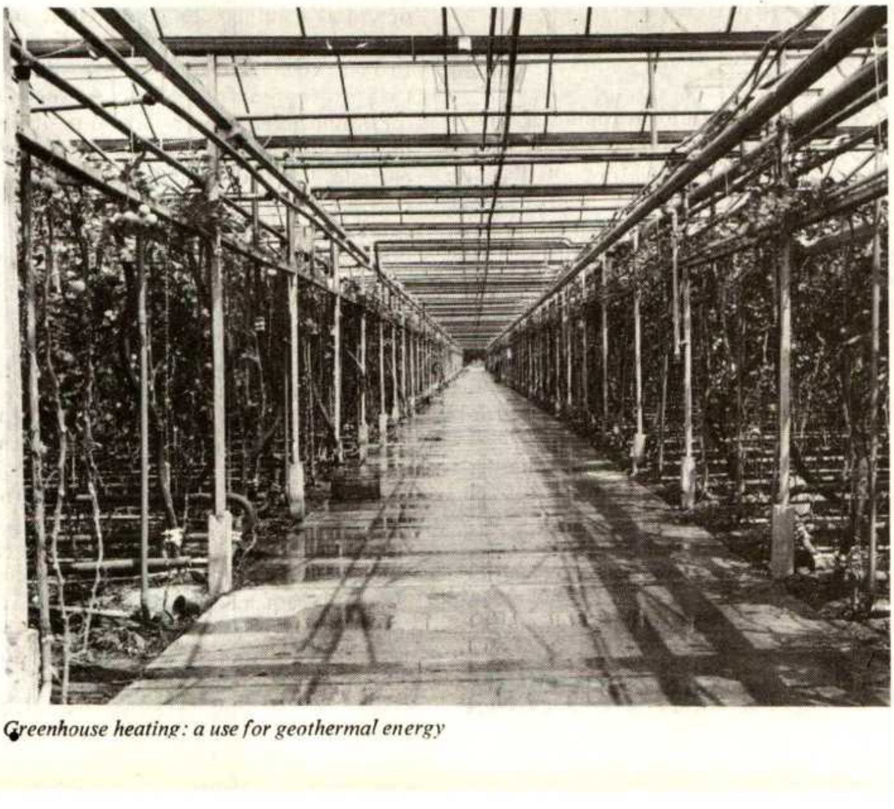

Photo: *The Grower*

Greenhouse heating: a use for geothermal energy take nearly 12 months to drill. It might then be possible to make an informed decision on whether to attempt commercial exploitation of the country's geothermal resources in the latter part of the 1980s.

If a positive decision were taken at that stage a third phase of development could begin with drilling of production holes, the planning of distribution systems and the stimulation of the potential market. The use of geothermal energy on any significant scale could not be expected before the turn of the century. This timetable is probably about the fastest which is practicable, and if desirable it could easily be lengthened; it would, however, mean that geothermal power became available about the time that production from the North Sea oil and gas fields began to drop significantly, and Britain changed from being a net exporter of oil to an importer once more.

Any consideration of the geothermal prospects of the UK, however, goes beyond the question of the heat which may be extracted from warm rocks of the upper crust. Experiments have been going on for some years at the Los Alamos Scientific Laboratory in the United States with a view to generating fractures artificially to permit water circulation both through rocks which are naturally impermeable, and through those which are so deeply buried in the crust that natural pores and fissures have normally closed. If these experiments were successful, it could become feasible to use such "hot rocks" to heat circulating water sufficiently for the generation of electricity.

The economic viability of such a scheme would be much enhanced by improvements in deep drilling methods; at present drilling costs roughly double for every 2 km increase in hole depth. Such a development would increase the available geothermal resource by more than a factor of 10 and free it from the geographical constraints which limit the use of warm water. The national long term geothermal strategy should, therefore, be seriously re-appraised if the Los Alamos experiments are promising. But no one should pretend that geothermal energy will solve the UK's energy problem; a small and possibly highly profitable resource, on the other hand, probably does exist—it is also a resource for the exploitation of which there are no large savings of scale, so that piecemeal development to satisfy local requirements is possible.

No complacency

It is probably fair to say that in the present world economic climate a country cannot afford not to investigate its geothermal resources further. It might be asked whether it is proposed to carry out the UK's geothermal exploration sufficiently rapidly; at present there is neither the drilling capacity nor sufficient trained manpower to mount an extensive crash programme, but even if there were it would not necessarily be more effective than a phased and progressively increasing effort over the next 10 years. The essential point is that no one be lured into a false sense of energy complacency during the next two decades of oil abundance, to the detriment of the development of other resources on which everyone will later depend.

A few may wish to ponder the point that many of the UK's large power stations reject hot water at temperatures which are regarded as suitable for geothermal exploitation in other parts of the world, and perhaps to question the wisdom of today continuing to charge a government authority with the limited mandate of generating electricity at the lowest possible price. And for those to whose lot it falls from time to time to defend the role of "pure science" in straitened economic circumstances, it is worth pointing out that the study of terrestrial heat flow which was until two years ago one of the most esoteric, albeit fascinating, branches of geophysics, has overnight become directly "relevant" and applied. Had not the Natural Environment Research Council (NERC) supported two university groups in this fields for a number of years, the UK would have completely lacked the technical expertise with which to implement fully its present geothermal programme. ☐

Adjust, amend and heal

The face of big science is changing constantly. **Wil Lepkowski** reports from Berkeley, California, on the way a famous laboratory has tried to adapt

OSCAR WILDE was once heard to say of an old acquaintance, "There goes a man with a promising past." One might be tempted to direct the same comments at the Lawrence Berkeley Laboratory of Berkeley, California, where eight men have won Nobel Prizes for work in high energy physics, nuclear physics, nuclear chemistry, and photosynthesis. All winners, save the famed, forceful Ernest Orlando Lawrence, still live and form a solid command of senior directors who continue to chart the fortunes of the facility.

It is clear that the time of grand high drama in research is over at the old Lawrence Radiation Laboratory. For one thing, its support now comes from the Energy Research and Development Administration (ERDA), whose mission is much more broad and ambitious than that of its predecessor, the Atomic Energy Commission (AEC). For another, the research budget for the things the Rad Lab always did best no longer arises at the rate it once did. And for a third, ERDA's new mission is not only much broader that the AEC's but is focusing its formula on industrial commercialisation of energy research and development, chiefly big scale systems.

Physics remains the most potent resource of the Lawrence Berkeley Laboratory (LBL). But the Laboratory is no longer the mecca for the brightest young minds seeking achievement through that once unique Rad Lab combination of men and machines. The men might still be around (and the use of the word "men" is deliberate, for the Laboratory is distinctly male dominated), but the machines are not. High energy physics is no longer done on site. The famed Bevatron is used now for cancer research and treatment and for nuclear physics. Officials say a new and exciting era could come into being through the Positron–Electron Project with Stanford University. In that project Stanford's Linear Accelerator would inject electrons and positrons into a new storage ring and the two particles would collide to produce energy patterns of unprecedentedly fine detail. But critics note that the new machine will not be at Berkeley but at Stanford. Laboratory officials may say it doesn't matter, but it really does. The place to be will be Stanford.

Sinking sensation

One thus hears oddments of commentary in the labs, and on the bus that shuttles researchers between the University of California campus and the Laboratory, that LBL is "sinking". The precise reasons are hard to track down because the Laboratory is no longer laying people off and the research budget is rising—from the current $47 million to around $60 million by the end of the next fiscal year. The sinking sensation is easily

•

Research for this article was supported by the Center for Science in the Public Interest.

explained on psychological grounds—anxiety over a vanishing pride and autonomy. Fundamental physics is no longer choice at LBL. Money in that field—once LBL's pride—is hard to come by. "The motto at this place once was, 'why use lead when gold will do,' " comments one researcher. LBL has had to become austere since 1970 and still is searching for a guiding star.

In 1970 the Atomic Energy Commission was still in existence. But its basic research budget was beginning to drop and LBL, along with AEC's seven other national laboratories, was forced to cut projects and personnel. The Laboratory formed an environmental division which with some success sought funds from agencies other than AEC. Still, the mood continued downward. As the concern over energy rose, the environment division became the energy and environment (E and E) department. By 1974, ERDA was created and with it an injection of energy research dollars. E and E will attain a budget of nearly $17 million by next year.

E and E's acting director Robert Budnitz, a physicist, literally bubbles with optimism over the future of at least his division. Programmes include geothermal power, solar energy, fusion, and energy conservation, and the enthusiasm a visitor unerringly sees comes from scientists who like their work and know that someone who funds it appreciates it.

But LBL must still live with the fact that it is no longer the centre for intellect and excitement in basic science. ERDA, in fact, defines it as a general purpose laboratory uniquely linked to a great university. The hope is that LBL will utilise university scholars in law, economics and the social sciences to integrate energy research and technology with their application. One always wonders about the effectiveness of this kind of activity under an agency whose theme is big systems. The work may be funded but will it make a difference? And even more fundamentally, will it be any good anyway? Yet, such work is supremely important in an era of rising terrorism and nuclear proliferation.

A style that suits?

An issue that is not being tackled directly as yet is whether the management style of LBL is really suitable for the kind of work that needs doing for the development of energy research. LBL created what Alvin Weinberg has called Big Science—the need to expend large sums of money on big machines to carry out research on the smallest particles of matter. The Lawrence Laboratory owes most of its Nobel Prizes to that style of research emphasising machines, teams, and discipline. But was the work really scientifically creative? Or was it creative engineering in the service of science?

The Lawrence Berkeley Laboratory, California

One critic, physicist Robert Yaes of Memorial University, St. John's Newfoundland, thinks LBL's science has been over-rated. He said the Berkeley group was more interested in building larger and larger machines rather than with "doing experiments with the ones they had." One of the most significant discoveries in nuclear physics, nuclear fission, he says, was made by Hahn, Strassman, Meitner, and Frisch in Europe, "even though the Lawrence group had the world's most intense neutron beam." Similarly, the first nuclear disintegrations were made by Cockroft and Walton with an electrostatic generator that produced protons of only several hundred KeV.

"In short", he says after citing other examples, "even though the Berkeley group possessed beams of energy and intensity available nowhere else in the world, the most significant discoveries were still being made by the 'string and sealing wax' people in Europe".

There is growing debate over whether large scale technology is in society's best interests, with its tendency toward more and more control by a technical elite, towards the necessity of producing elaborate security structures around it, and toward increasing social fragility out of the possibility of breakdown. It may be that at least one highly sophisticated laboratory would serve ERDA well by emphasising the "string and sealing wax" approach to energy research and development through a focus on small systems. At the very least ERDA might put aside one laboratory to question prevailing philosophy and probe the basics of energy systems. At the moment it has no such place—a place that preserves and nourishes first principles.

ERDA taking a view

ERDA is studying the future role of the national laboratories in light of its mission to commercialise energy technology. It is asking practical questions about how one goes about linking their research and development functions with industrial development and demonstration. In the case of LBL, it is serious about integrating research at the University of California, which is contract manager of the Laboratory, with research at LBL.

But ERDA is also undecided about its overall research management strategy. It talks of regional programmes and projects and speaks of using the national laboratories somehow in the regionalisation of energy research. At the same time it says many laboratories, especially Berkeley, have a broad spectrum of capability in many fields. And all the while, ERDA policies are subject to political whims, since their Associate directors are all politically appointed. It is little wonder LBL officials are confused and worried. It is a centre with a rich tradition in research, and once bursting with pri and confidence. Now it searches for prevailing philosophy against a b drop of an agency that cannot yet exactly how it plans to steer its ship.

•

Pure Che [illegible] try Library
[illegible] COLLEGE

USA

Coping with variability

Wil Lepkowski reports on the response of US agriculture to climatic change, the subject of a recent report

THE one sure thing about the weather—and the climate—is that it will change. Therefore farmers, who depend on the weather, must be nimble. That is the essence of a report issued last month by the Washington-based Institute of Ecology under support from the Kettering Foundation of Dayton, Ohio. The report says climatoligists may not agree for some time over whether the climate is warming or cooling. But what they can agree on is that it will fluctuate. The strange point the report makes is that North American agriculture may be unprepared for the normal fluctuations in climate.

Why? It may have grown complacent over the good run of weather experienced during the 1950s and 1960s, when agriculture boomed. As a result, the technology of fertilisation, pest control, and plant genetics may have softened crop resistance to fluctuation with the result that agriculture may have made itself vulnerable to trouble.

The panel, which had only six months to study the issue, makes three major recommendations: that weather scientists step up research on the processes and mechanisms of climatic change, that scientists develop research leading to improved strategies for food production under climatic stress, and that governments expand agricultural information networks to inform farmers more quickly of conditions affecting their crops.

The saga of the American farmer is that of a crusty realist always prepared for climatological vagaries. But this report emphasises agriculture's soft underbelly — that behind the legend lies bureaucratic complacency. It says with world population continuing to expand by 200,000 souls a day, and virtually all arable land under cultivation, agriculture is at the brink. It must be more watchful of its assumptions, more anticipatory of trouble. And the bureaucracy isn't.

The study, which was chaired by Professor James E. Newman, a Purdue University bioclimatologist, is ecology's first major try at tackling the agricultural policy issue. Its range was limited to Canadian wheat and American wheat, sorghum, corn, and soybeans, and it traced the production record of these crops under various degrees of climatological stress during the past 40 years. Its tone is that of a gentle warning rather than a vigorous call to action. One senses that farmers gathered for gossip at the general store would nod tired agreement but that the boardrooms of agribusiness corporations would pay only passing heed.

There is an undercurrent of concern over the vulnerability of technological agriculture, especially in view of its dependence on fossil fuel technology. And climate remains a concern. Four big studies are continuing in the US and each bears watching:

- "Study of Changing Climate Patterns and their Effect on Agricultural and Renewable Resource Productivity", by the National Academy of Sciences.
- "Living with Climatic Change", co-sponsored by the American Meteorological Society, the Canadian Meteorological Society, the Geophysical Institute of the National Autonomous University of Mexico, and the Science Council of Canada.
- The Large Crop Inventory experiment, by the National Aeronautics and Space Administration, US Department of Agriculture, and National Oceanographic and Atmospheric Administration.
- "Impact of Climate Change on the Character and Quality of Human Life", by the Aspen Institute for Humanistic Studies. ☐

BRITAIN

Genetic manipulation: report due

For many of Britain's molecular biologists, a long wait is almost over. Eleanor Lawrence reports

THE long-awaited report of the Williams Working Party on the Practice of Genetic Manipulation is "being printed and will be published shortly", according to Mr Fred Mulley, the UK Secretary of State for Education and Science, in a written reply to a Parliamentary question last week.

Mr Mulley was giving few details away on the code of practice itself, except that it will in the first instance be a voluntary one, with the possible introduction of specific statutory controls later in the light of experience. It will set out principles for categorising experiments and recommend various levels of safety precautions necessary for particular categories of experiment. But he shed a little light on the intended role of the proposed central advisory group. From this it looks as though scientists will have to wait until the advisory group is set up before their long-deferred experiments can begin.

The provision of a central advisory service for laboratories wishing to carry out genetic engineering was originally recommended by the Ashby Working Party which reported in January 1975. The experiments involve the transfer of alien genes to the common gut bacterium *Escherichia coli* by splicing the foreign genes onto a plasmid or bacteriophage vector.

One consequence of this might be that *Escherichia coli* with unusual and possibly harmful properties conferred on it by the transplanted genes might escape from the laboratory and infect the population at large. One of the fears when these experiments were first proposed was that they would be carried out in laboratories with little previous experince of the microbiological techniques developed to contain potentially dangerous organisms.

The Williams Working Party has endorsed the idea of a central advisory service but apparently sees it as a watchdog as well as adviser. According to Mr Mulley's statement the Working Party has recommended that any laboratory contemplating experiments likely to come under the code should be required to notify the central advisory service before beginning work. This recommendation can be implemented through regulations which can be drawn up under the present Health and Safety at Work Act.

These recommendations will in some respects provide the proposed British scheme with an advantage over the recently-published American guidelines, which only strictly apply to work funded by the National Institutes of Health; in Britain, all laboratories, whether university, government or industrial, will be covered.

The Working Party report is expected within the month, and Mr. Mulley intends to appoint the members of the central advisory group as quickly as possible and make immediate arrangements for it to get to work. The Health and Safety Commission will also soon be circulating for comment its proposals for regulations requiring notification of proposed experiments. ☐

UK ENERGY

• The UK Energy Secretary, Mr Anthony Wedgwood Benn, rarely out of the news these days, has been asked to delay his autumn decision on the 1,300 MW demonstration fast breeder reactor, CFR-1, pending the forthcoming report from the House of Commons Select Committee on Science and Technology on alternative energy sources. The request came last week from Mr Arthur Palmer, the Committee's Chairman, and in response Mr Benn has indicated that he does not at the moment want to wait beyond the end of October.

This tight autumn schedule is not new, but Mr Benn's implication that he may not wait is. What is more, the UK Atomic Energy Authority (UKAEA) this time round is believed to be seeking clearance only for a firm timetable and site selection, and is prepared to wait as long as two years for a final decision on whether to build the fast breeder. As for the Select Committee, which is considering the likely future role of the reactor in Britain for the purposes of its report, it is understood to be more disposed towards the reactor than against it at present.

The UKAEA's drive to keep progress on the fast breeder ticking over smoothly is meanwhile slipping into a higher gear following Treasury approval of a £10.5 millions contract for three steam generators. The generators, expected to be ready for the 250 MW prototype fast breeder at Dounreay in Scotland by 1979, are exactly similar in design and size to those planned, in greater number, for CFR-1. The design in use at the moment is unlikely to prove entirely satisfactory for commercial operation, and represents little more than an interim stage of development.

Also making progress, it seems, is the Central Electricity Generating Board's (CEGB) attempt to negotiate a share in the 1,200MW Superphénix project on the Rhône. Discussions have been proceeding for some months, but details have remained secret. Now it is reported that the French–German–Italian consortium involved has offered the CEGB a 10% interest for an initial stake of £60 millions.

• Why has Mr Benn appointed Mr Francis Tombs, head of the South of Scotland Electricity Board, as successor to Sir Peter Menzies, Chairman of the UK Electricity Council, when he retires in March 1977? Insofar as it is a matter of alternatives, the simple answer is that Tombs is only 52, whereas his counterpart at the CEGB and his obvious competitor, Sir Arthur Hawkins, is himself close to retirement at 64.

But, like most problems facing the Energy Minister, this is not being seen as a simple matter of alternatives. In his present position, for instance, Tombs heads the only electricity board in the country which both generates and markets electricity. So, one argument runs, the government could be preparing to implement the Plowden Report's call for closer integration of both aspects of the business throughout Britain.

More controversially, there is the suggestion that Tombs' support for the Steam Generating Heavy Water Reactor (SGHWR), now under review by the Department of Energy (DEN), won him his new position—that he would be able to keep the SGHWR programme firmly on course. Equally, though, with Tombs placed where he may have to compromise with individual generating boards, the project might more easily slip quietly away

Not so, says the Department of Energy, chary of every hypothesis. Then why has Tombs been appointed so far in advance? Once bitten, twice shy, says the DEN, adding that it burned its fingers over the delay in the recent reappointment of Sir Derek Ezra as head of the UK National Coal Board.

• The SGHWR receives a mention in the report released last week of the Public Accounts Committee (PAC), the committee of MPs which oversees government spending. In the interests of "effective financial and technical control", it says, the financial responsibilities of the various parties involved "should be clearly defined as soon as possible". Every inducement to efficiency and economy should be incorporated in the contractual arrangements, and the absence of a fully costed design should not delay agreement in principle on these matters. The committee was told that the total cost of the SGHWR programme would be about £100 million.

The committee also made some comments on British Nuclear Fuels Ltd (BNFL). BNFL had in the previous week published its annual report showing an increase in both profits and export earnings; Alex Eadie, junior minister at the Department of Energy, had at the same time revealed in a Commons answer that the government had agreed a massive £715 million investment programme for the next ten years.

BNFL (profits last year: £11.9 million) has paid no dividends for the past four years; this, says the PAC, is equivalent to the Exchequer providing interest-free advances of capital, and the no-dividend policy should be re-examined if the company is to operate on a normal commercial basis. There should also be close control of BNFL's investment programme; expenditure should be approved only if there are good prospects of an adequate return.

The main feature of BNFL's investment programme is the expenditure of £300 million enlarging the capacity of its uranium enrichment facility at Capenhurst in Cheshire. The plant, based on the gas centrifuge process, involves BNFL working in association with West Germany and Holland as partners in Urenco, which last year won sizeable enrichment orders. Another £130 million focuses chiefly on the conversion of uranium oxide to uranium hexafluoride for enrichment, for which BNFL also won orders last year; £245 million is going on extensions and improvements to the facilities at Windscale used for reprocessing nuclear fuel; and £40 million is being devoted to developing the process for the vitrification of waste.

According to Mr Eadie, the saving to the balance of payments through Magnox fuel reprocessing for domestic customers is "at least £200 million", and the revenue from reprocessing carried out at Windscale for overseas customers has so far been "about £12 million".

• A British Government reply made recently to the 42 recommendations on energy conservation from the Select Committee on Science and Technology last year latches on to some of the committee's ideas but parries the criticisms about weakness in central direction on conservation by saying that there are "limits on how active a part government can play without getting into a situation where it is taking consumers' decisions for them". That said, the government has gone some of the way to meeting the committee's call for a full-time task force of Ministers and others, and has also announced more help for small companies, an extension of the energy-saving loan scheme for companies, the provision of better information on energy-saving, and an extra £1 million for the "Save It" campaign (described by the Select Committee as a "feeble" exercise). If these moves are more than marginally effective they will need to be factored in to the ongoing debate on Britain's future requirements of nuclear power.

IN BRIEF

More nuclear deals

There's no relief in sight for those campaigning for greater restraint in the burgeoning international trade in nuclear technology. At the end of last week the delayed Franco–South African deal for the construction of two pressurised water reactors finally went through when Escom and the French consortium headed by Framatome signed contracts in South Africa. Only a couple of days earlier France's Foreign Trade Minister initialled an agreement in Seoul under which Framatome will build two similar reactors for South Korea.

France's sale of a small reprocessing plant to South Korea was stalled earlier this year following US pressure. Now similar pressure has been brought to bear over an almost identical deal between France and Pakistan. At the weekend Dr Henry Kissinger told President Bhutto that Pakistan risked losing US military and economic aid if it went ahead. Bhutto reportedly insisted that Pakistan be treated in the same way as Iran, which apparently wishes to reprocess nuclear waste from its reactors locally rather than outside the area Israel and Egypt, on the other hand, with which the US has now initialled agreements on the sale of reactors, have agreed to let any reprocessing be done outside the Middle East.

In the US, meanwhile, the State Department has conceded that American materials may have been involved in India's nuclear explosion in 1974.

Biblis problems

A senior executive of Kraftwerk Union (KWU) announced this week that the huge nuclear power plant at Biblis, West Germany, would be technically capable of returning to service by the end of the week, although clearance from the relevant authorities would still take some time.

The twin pressurised water reactors were closed for a routine inspection three months ago. In a joint statement last week, the operators, RWE, and builders, KWU, disclosed that "incipient cracking" had been found in the cooling water reservoirs of both reactors, and that steel bolts which had sheared off in the main cooling circuit of the commercially operating 'A' block reactor had been carried close to the nuclear core. The shutdown was originally scheduled to last eight weeks. The Biblis installation is the model for the four reactors to be built by KWU in Brazil and Iran, and officials are stressing that the breakdowns are not a cause for alarm One estimate which has been made of the cost to the operators is $50 million.

Mountain streets

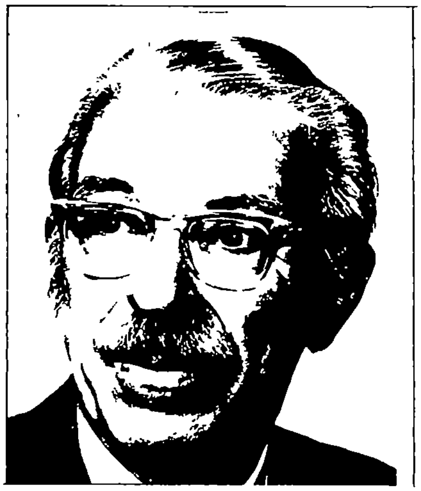

THOMAS H. JUKES

JULY is the prime time for the High Country in the southern Sierra Nevada of California. This was so in 1976 more than usual, because of the severe drought that had prematurely melted the big snowbanks. It was in July 1935 that I had first tasted their icy waters, as addictive as the most insidious of narcotics. And so, for the 39th summer, in a series broken only by war years, I set forth to regions above timberline, knapsack on back. What new changes would I find that had been wrought by technology and human beings?

Within the mountains of California, Yosemite, Kings Canyon and Sequoia National Parks are known for small areas that can be reached by road, but beyond these are hundreds of square miles that are reserved for what has been called "the aristocracy of the physically fit." Even this elite group dwindles as one heads away from the trails. It is curious that, even in the mountains, human beings tend to collect in herds. I still have no difficulty in finding big lakes, above 11,000 feet, where I am alone with peaks, trout and jet planes.

Thirty years ago, many beauty spots of the High Country were defiled by monumental piles of cans and bottles. Most of these have been patiently removed by volunteer labour. The volunteers, helped by officials, have also removed wrecked planes, piece by piece. Travel by horses and mules has been greatly reduced by high costs, and has been mostly replaced by the use of ingenious lightweight backpacking equipment and dried food.

The US Government, as may be expected, increasingly regulates travel in the wilderness. The official and praiseworthy concept is that "man as a temporary visitor, should leave no permanent imprint." One has to file the equivalent of a "flight plan" before being permitted to take off. Simultaneously, nine pages of "suggestions" and rules are thrust into one's hand Enforcement of these is often by female rangers who are the spiritual granddaughters of members of the Women's Christian Temperance Union. One of these rangers is spoken of with admiration by her colleagues as having recently written twenty "traffic tickets" for offences committed by feckless hikers on the eastern slopes of Mount Whitney.

Years ago, the "organic waste problem" in mountain travel was officially given only a casual reference We were archly advised to "do like the cat; dig a hole and bury it " Today the instructions for "sanitation and waste disposal" occupy seven column inches. The dimensions of the pertinent hole are now specified as 5 to 6 inches deep and 8 to 10 inches across. I notice that the indigenous cats (*Felis couguar*) apparently do not read, and do not dig holes, preferring to leave evidence of their passage in the open as a defiant challenge to territorial intruders.

On July 15, I lay for twelve hours in a small plastic tube tent, at 10,800 feet, as a magnificent electric storm crashed incessantly in the darkness and, at midnight, a huge rain-loosened rock avalanche roared down a nearby granite cliff Next day, in the bright sunlight, I caught golden trout. A few nights later, a Pacific Fisher (*Martes pennanti*) stealthily and silently made off with a string of golden trout that I had hung above my head in a pine tree while I slept in the open, well above the altitudes where bears live. My vexation was tinged with admiration when I got up at dawn to find the loss. I headed for the lake to replace the theft, and then walked for nineteen miles, through the rocky streets of the mountains, back to the road-head

news and views

Chromatin superstructure

from H. G. Davies

PROGRESS in understanding the structure of chromatin and eukaryotic chromosomes continues apace. Early electron micrographs by Ris and others had shown that the long fibres obtained from chromosomes were either thin, about 10 nm, or thick, about 25 nm, depending on the presence or absence of chelating agents Hitherto, however, it has not been clear how the two fibres are related. The past few years have seen the emergence of evidence that chromatin has a subunit structure; nuclease digestion of chromatin yields pieces of DNA which are multiples of about 200 base pairs, histones occur as oligomers, and electron micrographs of suitably lysed nuclei show linear arrays of interconnected roughly spherical particles about 10 nm diameter called beads, ν-bodies, or nucleosomes. Kornberg has put forward a model for the 10 nm fibre—a flexible chain of repeating structural units, like "beads on a string" (*Science*, **184**, 868; 1974), each bead containing two each of the four major histones.

Finch and Klug (*Proc. natn. Acad. Sci. U.S.A.*, **73**, 1897; 1976) now provide evidence to show that thin fibres about 40 repeat-units long, obtained from rat liver nuclei by brief nuclease digestion, can undergo helical folding to form a solenoidal structure about 30 to 50 nm wide. The evidence for helices is based first on electron micrographs which show more-or-less clear striations, separation about 12–15 nm crossing the thick fibre, and second, on new X-ray diffraction data and a reinterpretation of the earlier patterns obtained by Wilkins and collaborators, and Luzzati and Nicolaieff, showing maxima 11.0, 5.5, 3.7, 2.7 and 2.2 nm The key experiment is a comparison of the X-ray spectra of thin and thick fibres and the results are different from those obtained previously, due, presumably, to improved methods of preparing chromatin. Sperling and Tardieu (*FEBS Lett*, **64**, 89, 1976) find that the scattering from thin fibres in the region of spacings 40 to 3 nm fits the theoretical curve for a continuous density rod with no peaks at 11 and 5.5 nm. The 11 nm and other reflections appear, however, under conditions where solenoidal structures can be seen in electron micrographs. Hence Finch and Klug now propose that the reflections at about 11 nm and higher orders arise from the spacings between the turns of solenoids of low pitch angle and not from an interbead spacing of 10–11 nm along the thin fibre as had been universally, and quite reasonably, assumed, and indeed used by Kornberg to support his model. The new explanation of the spectra is similar to that originally proposed by Pardon and Wilkins (*J. molec. Biol.*, **68**, 115; 1972) except that they thought in terms of supercoiling DNA, rather than the continuous 10 nm fibre The data appear to confirm a suspicion held by many that the repeating unit in the thin fibre only becomes visible as ν-bodies or nucleosomes under special conditions. Those electron microscopists who, for one reason or another, did not see the thin fibres as beaded, but continuous, a result confirmed by Finch and Klug, will be unable to resist a smile at this latest turn of events.

Another key observation is that by Carpenter *et al.* (*Nucleic Acids Res.*, **3**, 1739; 1976) on neutron diffraction from oriented fibres of chromatin. The meridionally oriented reflection at about 10 nm, is now seen to be split, forming a cross pattern with semi-meridional angle of 8° to 9°. This is a sure sign to the cognoscenti that it originates from a helix. They propose as a model a coil of nucleosomes of pitch 10 nm and an outer diameter about 30 nm, dimensions corresponding to about six nucleosomes per turn of the helix. Of course, such a splitting of this meridional reflection could also be expected in the solenoidal model formed from a continuous 10 nm thread.

On the basis of electron microscopy of sections, we have described thread-like units within condensed interphase chromosomes, or chromatin bodies. These "superunit threads" about 28.0 nm diameter, are clearly recognisable because they tend to line up into layers at the surfaces of nuclei, and can also form monolayers, width independent of species, plant and animal Davies and Haynes (*J. Cell Sci*, **21**, 315; 1976) now report that nucleoli are attached to the nuclear envelope by a monolayer of these superunits. We have suggested that the superunit thread is formed from some type of helical arrangement of a subunit thread—"close-packed beads-on-a-string". This would account for the earlier observation that the unit appears tubular. Finch and Klug comment that their solenoidal model being of similar geometry can be equated with superunit threads found within nuclei.

Much clearly remains to be learned about the detailed molecular structure of these proposed helically arranged repeating units, how they are further folded up in mitotic chromosomes and how they unfold in those parts of interphase nuclei where RNA transcription occurs Also the way the DNA molecule is folded around the repeating unit is not clear, but results on sections suggest the repeating unit is asymmetric with more DNA on an inward pointing face. The spiralling of mitotic chromosomes and the helical nature of the DNA molecule have long been known and the above results will come as no surprise to those who believed that there were orders of coiling in between. The point is that speculation is now being replaced by fact □

A hundred years ago

IN the *Bulletin International* of August 3, M. de Tastes relates some interesting particulars of a waterspout (*trombe*) which was observed near Tours, on May 25 1876. It first appeared as a mass of whitish vapour against a background of dark-coloured clouds, which gradually assumed the form of an inverted cone pointing to the ground, and terminating in a long sinuous band A whitish sinuous column soon appeared suddenly between it and the ground, and rapidly enlarged upwards, the whole phenomenon soon assuming the appearance of two cones united at their summits. The lower cone, at first lightish-coloured and in a certain degree transparent, gradually assumed a darker shade, which was propagated from the base towards the summit.

from *Nature*, **14**, August 10, 320, 321; 1876.

Anaesthetic mechanisms

from C. D. Richards

ANAESTHETICS affect every variety of living system, from microorganisms to mammals; they are very nonspecific drugs which depress a whole battery of cell functions including cell motility, cell division, photosynthesis, oxidative metabolism and electrical excitability. Their mode of action poses one of the fundamental problems in biology. Their clinical value rests solely on their ability (at low concentrations) to impair certain higher nervous functions such as consciousness and memory without disrupting the function of the heart and respiratory system.

Four key observations suggest that anaesthesia is the result of some physical interaction of the anaesthetic with certain constituents of the cell rather than a specific chemical reaction. First, the effects of anaesthetics are freely and rapidly reversible; second, the potency of an anaesthetic is directly related to its lipid solubility; third, anaesthetic properties are shown by a wide variety of chemically unrelated substances; and fourth, the effects of anaesthetics can be reversed by high pressures.

The critical volume hypothesis first discussed by Mullins more than 20 years ago (*Chem. Rev.*, **54**, 289, 1954) seems to be the most successful of the various hypotheses proposed to explain the action of anaesthetics. In its simplest form it proposes that anaesthesia (narcosis) occurs whenever a critical fraction of anaesthetic has been achieved in the membranes of the cell; this critical volume is held to be dependent on the species under study but independent of the nature of the anaesthetic.

In its original form the critical volume hypothesis added little to the well established Meyer–Overton concept of a role for lipid solubility in the mechanism of anaesthetic action, but recent investigations of the reversal of anaesthesia by pressure by Miller *et al.* (*Nature*, **231**, 368; 1971; *Molec. Pharmac.*, **9**, 131; 1973) have led to a more satisfying model. They propose that anaesthetic dissolves in some hydrophobic region of the cell—presumably lipid—causing that region to expand, thereby impairing some vital function From the amount of pressure required to reverse the effects of various doses of anaesthetic they calculated that during general anaesthesia the hydrophobic region should expand by about 0.4% (v/v). This prediction has subsequently been verified by Seeman and Roth (*Biochim. biophys. Acta*, **255**, 171; 1972) for erythrocyte membranes.

This still leaves four important questions. How is the membrane expansion brought about? How does the membrane expansion lead to impaired membrane function? Which of the many functions of the membrane are impaired by anaesthetics? Does anaesthesia result from the impairment of one or several specific functions?

Membrane effects

Metcalfe *et al* (*Mol Pharmac*, **4**, 87; 1968) found that benzyl alcohol which can act as an anaesthetic increased the fluidity of biological membranes This observation was later extended by Trudell *et al.* (*Biochim. biophys. Acta*, **291**, 328; 1973) to include clinically important anaesthetics, such as halothane. It was subsequently proposed that anaesthetics cause membrane expansion by increasing the disorder of the fatty acid chains of the phospholipids of the membrane bilayer. During general anaesthesia, anaesthetics occupy only 0.2% (v/v) of the membrane whereas membrane expansion is of the order of 0.4% Seeman has shown, however, that artificial phospholipid bilayers only expand by 0 2% and so he proposed that changes in the conformation of the membrane proteins are the cause of the large expansion of natural membranes (*Experientia*, **30**, 759; 1974). Furthermore, in a recent paper Boggs *et al* (*Molec. Pharmac.*, **12**, 127; 1976) have shown that concentrations of anaesthetic sufficient to cause general anaesthesia or which block the conduction of impulses along a nerve ("local anaesthesia") have little or no effect on the fluidity of artificial membranes Although such observations cast doubt on the view that anaesthetics impair membrane function through a generalised perturbation of the structure of the lipid membrane they are consistent with the view that the interface between lipid and protein may be the site of anaesthetic action.

There is now evidence to suggest that at least some membrane-bound proteins require the presence of a layer of tightly bound lipid to stabilise them in their active form. This has been shown for cytochrome oxidase (Jost *et al.*, *Proc. natn. Acad. Sci. U S A.*, **70**, 480; 1973) and for the calcium transport protein of the sarcoplasmic reticulum (Warren *et al*, *Nature*, **255**, 684; 1975). By studying the effects of temperature on the calcium transport protein reconstituted in defined lipid mixtures, Warren *et al* (*Biochemistry*, **13**, 5501; 1974) showed that the enzymatic activity of the complex decreased as the lipid became more crystalline This suggests that the activity of this protein is governed by the fluidity of the lipid in which it is embedded In the light of this data, Lee (page 545, this issue of *Nature*) has proposed that the sodium channel in nerve membranes may be surrounded by a ring of rigid lipid molecules that serves to keep it open. He suggests that anaesthetics block nerve impulse conduction by fluidising this boundary lipid so causing the sodium channel to collapse inwards. One consequence of the model is that a nerve blocked by an anaesthetic should have its conduction restored when the temperature is lowered, and this has indeed been shown for the action of ethanol on squid axon (Spyropoulos, *J. gen. Physiol.*, **40**, 849; 1957).

Specific interactions

It is not difficult to envisage other membrane proteins such as receptors being similarly surrounded by boundary lipid which serves to keep the protein poised in an optimal conformation. The fact that some anaesthetics affect one function rather than another could then be explained by relatively specific interactions either with the boundary lipid or with the individual protein. Certain volatile anaesthetics have been shown to inhibit the bacterial enzyme luciferase apparently by competing for the substrate binding site (White, in *Molecular Mechanisms in General Anaesthesia*, Ch 13, Churchill–Livingstone, London, 1974; Middleton and Smith, *Proc. R Soc. Lond.*, **B193**, 173; 1976)

Moreover, specific interactions of this sort could account for the antagonism of the depressant effects of the steroid anaesthetic alphaxalone by the non-anaesthetic steroid Δ16 alphaxalone observed in isolated preparations of mammalian brain tissue (Richards and Hesketh, *Nature*, **256**, 179; 1975). Nonetheless, such ideas must remain speculative until it becomes possible to isolate receptors and reconstitute them in artificial membranes of defined composition With the recent developments in understanding the rôle of lipid-protein interactions in membrane biochemistry, the next period of anaesthetic research should be an exciting one. ☐

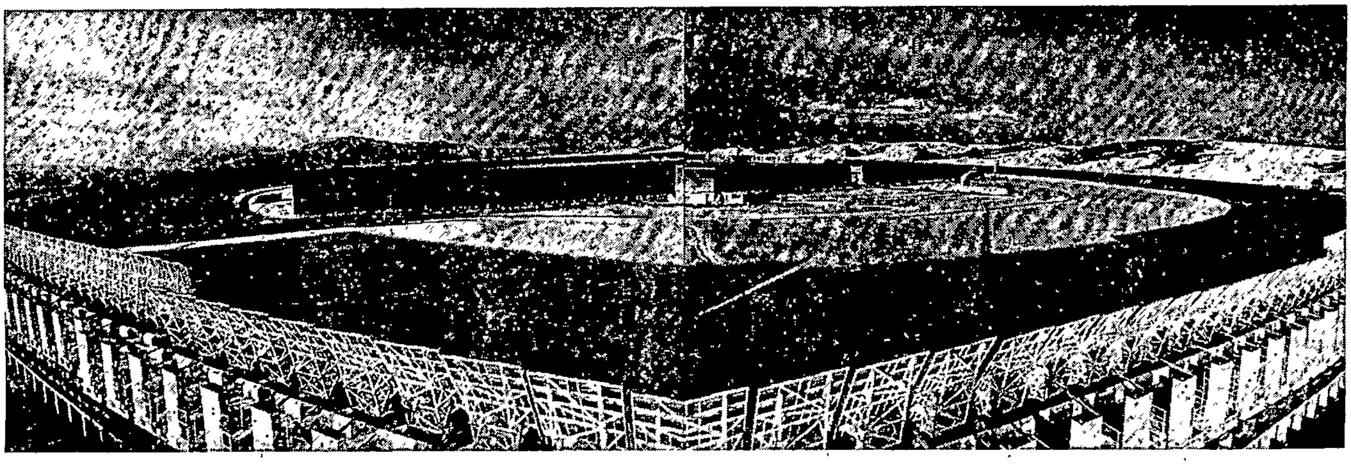

New giant Soviet radiotelescope

from Boris Belitzky

THE RATAN-600 radiotelescope, under construction at Zelenchuk in the North Caucasus since 1968, is now completed and fully operational. RATAN-600 is an acronym derived from the Russian for "radio-astronomical telescope of the Academy of Sciences" and a figure approximating the 576-m diameter of the telescope. Zelenchuk is also the home of the world's biggest optical telescope, the fully-operational 240-inch BTA reflector. Together with a large neutrino detector, under construction nearby, this unique array of instruments comes under the general umbrella of the Special Astrophysics Observatory founded there by the Soviet Academy.

Unlike Britain's Mark I instrument at Jodrell Bank or the slightly bigger West German instrument in the Efflesberg mountains, RATAN is not a 'steerable' dish, but embodies the variable profile concept.

Despite its size—its geometric area equals 10,000 square metres—the new radio telescope has been designed to operate in the short-wave spectrum down to 8 mm (Cornell University's Arecibo instrument, by way of comparison, stops short at 10 cm). As for RATAN's upper limit, this was selected to take in both the 18-cm hydroxyl wavelength and the 21-cm neutral hydrogen wavelength.

It is at the less well explored, shorter end of this spectrum, however, that the designers (a Pulkovo team under Dr Y. N. Pariisky and Dr N. L Kaidanovsky, with support from Moscow University) expect it to yield the most valuable results, and RATAN's record sensitivity and resolving power are, accordingly, in that region. Its aerial comprises a circular reflector, a flat reflector, and several feeds. The circular reflector is a variable profile aerial consisting of 895 cells mounted on a circular foundation and capable of tilting, rotating and moving radially. The flat reflector, mounted in the southern part of the circle, consists of 124 cells that can only be tilted.

The principal mode of operation requires pointing the telescope's axis at a source and observing its passage through the aerial pattern Observations of sources near the horizon involve approximately a quarter of all the reflecting cells and can be conducted according to four independent programmes simultaneously. At angles of 30 to 80° about a third of the cells are operational and three independent programmes can be pursued simultaneously. Finally, zenithal observations involve the entire circular reflector, and the telescope has a pencil-beam pattern equivalent to that of a continuous-surface reflector 576 m in diameter.

Each cell is fitted with pickups, which control all its movements and adjust it to the exact position required. Feed movement takes place along 12 radial tracks spaced azimuthally at 30° intervals. A turntable in the centre of the circular reflector serves to shunt a feed from one radial track to another Apart from the variable profile mode, the flat reflector makes it possible to use the telescope as a parabolic cylinder according to the Kraus system In this case the telescope has a constant knife-edge pattern, and the time needed for sky surveys is substantially reduced. By combining the circular and flat reflectors in the southern sector it is possible to use the telescope in certain other operational modes, such as tracking a source. This mode of operation is, of course, a particular asset whereever maximum sensitivity is required.

RATAN was begun in 1968, and the first part of the project—the northern sector of the circular reflector—became operational in 1974. Some significant astrophysical results were obtained during the running-in period These included the discovery of a solar "radio granulation"—a fine structure of the Sun's radio emission in the centimetre range, which appears to coincide with its chromospheric net. The radio astronomers at Zelenchuk have been able to observe the radio emission of the solar corona at large angular distances from the Sun and to observe quasars through the corona.

Simultaneous observations of radio sources on several frequencies have yielded their instantaneous spectra and permitted the sources to be separated into components. One of the most interesting findings concerning the structure of radio sources has been the discovery of a bar linking the components of such well-known double sources as Cygnus A There have also been measurements of the Einstein effect—beam deflection in the Sun's gravitational field.

Now that the telescope is fully operational, the programme of research is being expanded. Inside the Solar System it is proposed to study physical conditions on the surfaces of the planets, their satellites, and the minor planets. Solar studies, which command growing interest among Soviet astronomers, will include investigations of the brightness distribution in the active regions of the Sun to determine the structure of magnetic fields and condensations in the lower corona and the upper chromosphere, and also the structure of the chromosphere and the transition zone.

Further afield there are to be radio observations of the Galaxy and of the Solar System neighbourhood, of the Galactic nucleus, of the fine structure and kinematics of gaseous and planetary nebulae, and of pulsars and the nearest stars.

Extragalactic studies, which in Pariisky's view are the most interesting application for RATAN, will be conducted mainly in the decimetre range. Naturally, there is particular interest in studying quasars and radio galaxies with anomalously intense radio emissions in the hope of learning more about the nature of these objects and the sources of their energy. There are also to be studies of the fine structure of many radio galaxies, with particular reference to their brightness distribution spectrum and magnetic field structure. According to Dr Lev Gindilis, who has been concerned with planning the RATAN sky surveying activities, these are to be conducted on a systematic basis and at the highest frequencies possible. This is prompted by the paucity of information in this range and the hope of observing quasars at the initial stage of their evolution. Gindilis considers RATAN to be an optimal instrument for surveys in the entire range from 4 mm to 20 cm, in which there is a minimum of natural interference for observing cosmic sources. RATAN sky surveying work will also take in account the wishes of radio astronomers interested in the problem of communication with extraterrestrial intelligence (CETI).

Ultimately the RATAN control complex is to be linked to the main radioastronomical centres of the Soviet Union, with the result that the potential of this giant instrument will be used more effectively. RATAN-600 is also seen by Soviet radio telescope designers as a stepping stone towards far more powerful facilities. ☐

Aspects of plasmid behaviour

from J. R. Saunders

A NATO Advanced Study Institute on the Biology of Bacterial Plasmids was held at Kavouri, Nr Athens from July 5–16, 1976.

INTEREST in the biology of bacterial plasmids has been stimulated both by their use as cloning vehicles for genetic engineering and by the increasing knowledge that a multitude of important bacterial properties are plasmid specified. The role of R plasmids in mediating antibiotic resistance in clinically important bacteria is well known. Bacterial pathogenicity for plants can, however, also be encoded by plasmids. N. Van Larebeke (University of Ghent) showed that the ability of *Agrobacterium tumifaciens* to cause "crown gall" tumours in wounded plant tissues is determined by tumour-inducing (Ti) plasmids Furthermore tumorigenic ability can be transmitted to other Agrobacteria either by transformation or by conjugation mediated by the R plasmid RP4. M. Holsters from the same group demonstrated that Ti plasmids allow host bacteria to synthesise and utilise either nopaline or octopine. It is interesting that tumours produced by *A. tumifaciens* contain, (depending on the strain) either of these unusual amino acids, suggesting that certain plasmid genes may be expressed in tumour cells.

P. Williams (University of Wales, Bangor) hailed the 'degradative' plasmids of *Pseudomonas*, unlike most plasmids, as being totally beneficial to the biosphere as a whole. The ability of some *Pseudomonas* species to degrade and utilise many natural and synthetic organic substrates is due in part to the existence of plasmids determining the enzymes of specific catabolic pathways The manipulation of these plasmids could therefore be used to construct bacterial strains capable of 'mopping-up' oil spillages and industrial wastes.

The translocation of resistance genes continues to generate interest. S N. Cohen (Stanford University) stated that Transposon A (TnA) encoding resistance to ampicillin comprises part of the larger transposon TnS which specifies resistance to ampicillin, streptomycin and sulphonamides and that TnA may provide the driving force for the translocation of the larger unit. Evidence for interactions between transposons was also presented by M. H. Richmond (University of Bristol) He reported that the presence of TnA on a plasmid reduces the frequency of transposition of a second copy of TnA to it by a factor of 10,000 in recombination-deficient (*rec*$^-$) cells. On the other hand, in *rec*$^+$ cells the presence of a resident copy of TnA merely reduces the frequency of accretion of a second copy by 90%. In the latter case however the incoming copy of TnA apparently replaces the resident TnA probably by reciprocal recombination rather than transposition The results therefore suggest that one transposon in some way interferes with the *rec*-independent translocation of like elements. The as yet unpublished work of several laboratories on the genetic structure and nature of proteins required for transposition may help to elucidate these phenomena.

J. Davies (University of Wisconsin) and R. Hermann (University of Heidelberg) advocated the use of λ and fd phages respectively as host molecules for studying transposons. Phages possess the distinct advantage in that generally their genetical and physical properties, for example the location of promoters and partial known base sequences, are better characterised than those of plasmids. The ability to synthesise antibiotic-modifying enzymes *in vitro*, described by G. Hogenauer (Sandoz, Vienna) should also help our understanding of the structure and operation of resistance genes.

A major problem in genetic engineering is the expression of eukaryotic genes in prokaryotes (see *News and Views*, **262**, 256, 1976). D. H Gelfand (University of California, San Francisco) described the construction of plasmids carrying inserted *Xenopus laevis* 28S rDNA "downstream" of the operator–promoter region and part of the β-galactosidase gene of the lactose operon. Induction of the *lac* operon in cells carrying such plasmids causes increased production of RNA complementary to rDNA Furthermore, some derivatives with inserted genes produce β-galactosidase with reduced enzymic activity but increased molecular weight The production of polypeptides fused to this enzyme suggests that it may be possible to 'translate' some foreign genes in bacteria.

Potential vectors for natural spread of genes between bacterial genera are plasmids of the P incompatibility group (Datta *et al.*, *J. Bact*, **108**, 1244; 1971). P group plasmids are characterised by an extraordinary ability to transfer themselves to a wide range of Gram negative bacteria. They are thus attractive research tools for studying intergeneric gene transfer (see, for example, *News and Views*, **260**, 191; 1976) and for the promotion of chromosomal gene transfer in species which lack their own sex factors. They could in addition contribute to the spread of resistance genes by crossing species barriers and depositing transposons in new hosts V. Stanisich (University of Bristol) has also found that genes of plasmids normally restricted to *Pseudomonas aeruginosa* can be transferred to and expresed in *E. coli* by a technique essentially involving the formation of genetic hybrids with P group plasmids.

What then confers on these plasmids their unusual capacity for intergeneric transfer? One possibility is that their conjugation mechanism and specificity of attachment of P group sex pili is unaffected by the nature of recipient cells D. R. Helinski (University of California, San Diego) pointed out that P group plasmids not only exhibit a paucity of cut sites for many restriction endonucleases, but also that their replication machinery may be more complex and hence less dependent on host chromosome function than other plasmids. This could endow them both with some immunity against the battery of restriction enzymes likely to be encountered in intergeneric transfer and with the ability to replicate in a wide range of cellular environments. Accordingly the ability of P group plasmids to cross interspecies barriers in bacteria could well make them mediators of 'natural' genetic engineering. ☐

Iliopoulos wins his bet

from F. E. Close

The 18th International Conference on High Energy Physics was held in Tbilisi, USSR on July 15-21, 1976

It was the moment of truth for J. Iliopoulos. In his talk at the 17th International Conference on High Energy Physics held in London in 1974 (*Nature*, **250**, 186, 1974) he had declared "I am prepared to bet a whole case of wine that the next conference in this series will be dominated by the discovery of charmed particles". Anyone who accepted the wager should now be preparing shipment because the 18th International Conference, which has just taken place in Tbilisi, USSR, was indeed dominated by that very discovery—the latest in a series of dramatic developments that have revolutionised particle physics in the past two years.

Readers will recall the dramatic breakthrough that occurred in November 1974 when workers at Stanford Linear Accelerator Center, California, and at Brookhaven National Laboratory in New York independently and simultaneously announced the discovery of a heavy metastable meson (called J or ψ) (see *Nature*, **252**, 438, and **254**, 387; 1975) In the decade preceding this discovery all known mesons and baryons that were discovered had fitted in nicely with the idea of Gell-Man and Zweig (*Phys. Lett.*, **8**, 118; 1964) that there should exist quarks coming in three types or "flavours" distinguished by quantum numbers such as isospin or strangeness and that the mesons and baryons were bound states of these quarks The high mass and remarkable stability of the J/ψ suggested that this meson might be a bound state of a fourth flavour of quark ("charmed quark") and its antiquark In the jargon this state had "hidden charm" and theoreticians expected that there should be a spectroscopy of similar states which has become known as the "charmonium spectroscopy" by analogy with the spectroscopy of positronium Several heavy metastable states have been discovered since November 1974 and the latest information on their properties was discussed at Tbilisi The spectrum that is emerging is in excellent agreement with that expected for charmonium though the precise values of the masses are in some cases not quite what had been theoretically predicted.

The idea that there might be a charmed quark had been suggested by many people as long ago as 1964. Theoretical interest in this idea took on new significance when Glashow, Iliopoulos and Maiani noticed (*Phys. Rev* , **D2**, 1285; 1970) that a charmed quark could provide a mechanism (the GIM mechanism) for overcoming a stumbling block that had arisen in attempts to unify theoretically weak and electromagnetic interactions. Their theory required that there should exist mesons made from a charmed quark and its antiquark and that the lightest of these mesons should have a mass around 3 GeV/c^2 (about three times as heavy as the proton). The J/ψ and the other heavy metastable states certainly fit in with this idea and are even in the predicted mass region.

The second consequence of their theory is that there should exist mesons made from a charmed quark and one of the old faithful uncharmed quarks. After the discovery of the J/ψ it was predicted that the lightest of these states ("charmed mesons") should exist with a mass of about 2 GeV/c^2. Furthermore it was predicted that strange particles (such as the K meson) should be an important feature of the decay products of these charmed meson states.

In May of this year came a strong suggestion that such a state had been found in a study of the debris produced in the annihilation of electrons with their antimatter (positrons) at SPEAR in Stanford, California. An electrically neutral metastable particle was observed with a mass of 1.86 GeV/c^2 (compare the predicted 2 GeV/c^2!) decaying into K and π and sometimes into K and three pions. A study of the energy and momentum balance suggested that in the electron–positron annihilation a state with mass of 2.02 GeV/c^2 was being produced in conjunction with the 1.86 GeV/c^2 state, although the decay modes of this second particle have not yet been isolated. These two states were reported on at Tbilisi and the popular feeling was that they are charmed mesons where the quark and antiquark, from which they are composed, have coupled their spins to give a total angular momentum of 0 or 1 respectively (like π and ρ mesons). The observations of the strange meson, K, in the decay products is as anticipated for a charmed meson.

Only two weeks before the conference physicists at SPEAR working in collaboration with colleagues from the Lawrence Radiation Laboratory at the University of California, Berkeley, discovered the electrically charged partners of these mesons. The masses of these states are identical to or perhaps marginally heavier than their neutral counterparts. The charged state at 1.86 GeV/c^2 was seen decaying into a K and two pions. The important discovery, which is crucial to the charm interpretation, is that the positively charmed meson (D$^+$) is predicted to decay to K and two pions with electrical charges distributed as in

$$D^+ \rightarrow K^-\pi^+\pi^+$$

but should not decay by the mode

$$D^+ \not\rightarrow K^+\pi^+\pi^-$$

This is precisely what is observed in the data presented at Tbilisi.

Other phenomena that are probably due to charmed particle production were reported from several laboratories around the word. Of most immediate comparison with the SPEAR results are the experiments involving electron–positron annihilation at the Hamburg facility (DORIS) B. Wiik (Hamburg) reported that when electrons and positrons annihilate at DORIS with a total energy of just over 4 GeV (the same energy region in which SPEAR saw the simultaneous production of the 1.86 and 2.02 GeV/c^2 mesons) an electron was observed in the debris more frequently than expected from previously known sources It was reported last year (see *News and Views*, **257**, 535; 1975) that anomalous production of electrons and muons were seen in this energy range by Perl's group at SPEAR where it was argued that these were the decay products of a heavy lepton. Several features of the DORIS results suggest that at Hamburg, on the contrary, one is seeing electrons produced in the decays of charmed mesons (probably the same mesons that were seen decaying into K and pions at SPEAR). Furthermore, in two independent experiments at DORIS, it has been found that these electrons tend to be produced in conjunction with K mesons. The nature of these events is therefore consistent with pair production of charmed mesons (D,D*) followed by their "semileptonic" decay

$$e^+e^- \rightarrow D(1.86) + D^*(2.02)$$
$$\hookrightarrow e + K + \text{pions} + \text{neutrino}$$

the ubiquitous K meson is as expected in charm theories.

While it seems fairly certain that these leptons are coming from the weak decay of long lived particles, the precise relation of this signal with the anomalous lepton signal observed by Perl's group at SPEAR is unclear and generated much discussion. While the majority opinion still appeared to be that the Perl group's leptons are coming from a heavy lepton source several people were unhappy with this interpretation.

Now that the first charmed particles have apparently been found, the status of the heavy lepton has taken on a particularly pivotal position in the theoretical development of high energy physics as was emphasised in the talk given by A. de Rujula (Harvard University). As noted above, the priorities of the charmed mesons appear to be in line with those expected by Gashow, Iiopoulos and Maiani if charm is the way to overcome the stumbling block in the weak and electromagnetic unified theories. The discovery of charm with, apparently, these very properties lends indirect support to these theories. Other tests of these ideas were presented at Tbilisi. What seems astonishing is the amount of evidence that has accumulated in the last two years increasingly suggesting that the GIM mechanism allied with the original unification idea of Weinberg (*Phys. Rev Lett*, **19**, 1264; 1967) and Salam (in *Elementary particle physics,* edit. by Svartholm, N , 367, Stockholm, 1968) could be, if not the whole story, at least a first qualitative approximation to the correct theory. Almost all of the data on weak interactions reported at the conference agree with the Weinberg–Salam theory with four flavours of quark. There was some discussion as to whether a fifth and sixth flavour of quark may be necessary to describe data (on the theoretical front, confirmation of Perl's heavy lepton would lead people to prefer six flavours of quark—hence its "pivotal position") There does not yet appear to be any widely accepted need for extra complexity however.

The weak neutral currents (where neutrinos scatter from a target without any transfer of electrical charge taking place), reported on in London in 1974 have been studied in detail. Several groups reported evidence that parity is violated in these interactions, moreover the nature of this violation appears to be in accord with the Weinberg–Salam theory. Beautiful evidence for parity violation in atomic physics was also reported, again in line with the Weinberg–Salam theory.

The consensus of opinion was that it is rapidly becoming accepted that weak and electromagnetic interactions are indeed probably unified and that the "gauge field theories" are underlying not only weak-electromagnetic but perhaps also strong interactions (the new jargon here being quantum chromodynamics, or QCD, analogous to quantum electrodynamics). One consequence of such theories is that the scaling phenomenon seen previously in deep inelastic scattering of leptons on hadron targets should be violated in a systematic way at the very high energy experiments now taking place at the Fermi National Accelerator Laboratory near Chicago. Experimental data were presented by T. Quirk (University of Oxford) which showed a pattern of scaling violation consistent with the predictions of such theories.

One possibility raised by QCD theories is that quark confinement inside hadrons may be a natural consequence There was discussion among theorists of this possibility but as yet no clear idea has emerged. Some thoughts on how to proceed were presented by K. Wilson (Cornell University), and one contribution that excited much interest was that of A. Migdal of the Soviet Union who reported his calculations of meson spectroscopy in QCD with some phenomenological success

When in the future we look back on the two years leading up to this conference, they will surely be seen to rank with the most significant periods of advance in our understanding of subatomic behaviour. A very clear direction for investigation has emerged. With SPEAR having already been perhaps the most productive machine in particle physics history, and DORIS still in its infancy, these electron–positron annihilation machines promise yet more to come. There was also excitement at the great successes in building the new super proton synchrotron at CERN which promises to be ready for experimental research within a few months. East and West at Tbilisi were united in their belief that the next few years in high energy physics may reveal further significant advances that will rank alongside those just made in the past few weeks. I think Iliopoulos would not bet against that. ☐

Britain in European space

from David W. Hughes

A one day meeting to discuss the future scientific projects to be undertaken by the European Space Agency was held at the Royal Society, London on July 23, 1976 under the sponsorship of the Science Research Council.

DURING the current year ESA will spend £270 million, £200 million of which goes on the space applications programme (which includes Spacelab, communications satellites and the development of Ariane, a three-stage rocket which will make Europe independent of American launch facilities) and £26 million on the science programme. Great Britain contributes about one sixth of this (£6.5 m). The science programme budget is mainly spent on scientific satellites, a typical satellite being funded for five years, the expenditure maximising between the second and third year and totalling in all about £20 million (on average one satellite is launched each year). At present COS-B, GEOS, IUE, ISEE-B and EXOSAT are in orbit or about to be launched. COS-B was launched in August, 1975 and is measuring high energy gamma rays. 1977 is the planned launch year for GEOS which will study particle fluxes and electric and magnetic fields in the outer magnetosphere, IUE, which is an ultraviolet observatory in a geosynchronous orbit (so the satellite is always above the same place as Earth), and ISEE-B which will look at wave–particle interactions in conjunction with the NASA satellite ISEE-A. It is planned to launch EXOSAT in 1980 to study X-ray sources using lunar occultation techniques These satellites account for a considerable amount of the projected budget but obviously the amount of uncommitted funds will increase as each satellite comes to fruition, so that in 1978 and beyond there is a considerable amount of money to spend.

Scientific projects in ESA go through a series of stages. First comes the mission definition study in which a group of scientists and space technologists discuss the feasibility of the project in general terms. Then follows a more detailed and searching Phase A study, a Phase B study, construction and launch. Needless to say there is a pyramid structure to this series, the twelve or so mission definition studies per year leading to about three phase A studies and one probable launch.

The main purpose of the London meeting was to canvass the opinions of British space scientists as to what the next main mission should be, what should be flown on the second test launching of the Ariane rocket and which phase A studies should be instigated in 1976/77. With these opinions in mind the Science Research Council will then brief the British delegation for the October meeting of the Science Program Committee of ESA. The fact that the British voice only makes up 17% of the votes makes the discussion rather academic but democracy being what it is a firm decision by Britain's 17% could sway the day.

Four major missions were discussed, the Space Telescope clearly winning the day and being regarded as an instrument of outstanding and paramount importance. It is hoped that the telescope will appear in NASA's 1978 budget although it has already slipped considerably in time and in size, the main mirror now being 2.4 m in aperture. From its 500–600 km high orbit it will be able to detect objects 100 times fainter that those detectable from the Earth's surface (it will be able to pick up 29th magnitude stars) and will have an angular resolution better than 0.1 arc s, some 10 times better than attainable from the ground. Coupled with this diffraction-limited performance is the fact that being free from atmospheric absorption it will have a spectral range of 912 Å to 1 mm. Within our Galaxy it will study the early and late stages of stellar evolution, the position and proper motion of stars, the dust distribution and hydrogen concentration and also our Solar System. Extragalactic work will include investigations of the structure, scale and evolution of the Universe, the structure and content of galaxies and also quasars. It is obviously a project that no astronomical nation wants to be left out of. NASA and the US Congress look to ESA to contribute more than 10% of the cost in return for an equal percentage of the observing time and an involvement in directing the project. This 10% of the cost would be spent in Europe, designing, developing and constructing some of the instrumentation and the technology (for example the faint object camera and the solar arrays). This cooperation would of course mop up a considerable amount of ESA's science budget for a few years and, while recognising the great importance of the project, some of the scientists present at the meeting pointed out that science *per se* would not suffer if we did not participate, the Americans probably going on by themselves, whereas spending the money on specifically European ideas might open up new horizons in different fields.

The second mission considered was again a cooperation wth NASA and involved two spacecraft launched simultaneously towards Jupiter from a space shuttle, and then guided in such a way that one would be deflected by Jupiter towards the north pole of the Sun, the other passing over the south pole. ESA would supply one spacecraft and NASA would use a Pioneer type spacecraft for the other. This "out of ecliptic" mission would provide a new insight into interplanetary and solar physics and the science of the Jovian magnetosphere, mainly by taking the observer away from the plane of the planetary orbits where the large majority of observations have been made to date. The two satellites would obtain a stereoscopic view of the Sun and help to test the fundamental symmetry of the Solar System. The basic experiments would consist of a magnetometer, a plasma probe, a solar particle telescope, a cosmic ray telescope, a receiver for studying radio propagation, a coronagraph and a XUV heliograph The 85° inclination of the orbits to the ecliptic will enable the development of equatorial structures on the Sun to be followed continuously through several solar rotations.

Three other projects are to be studied further. LIRTS, a 2–3 metre classical, uncooled Cassegrain infrared telescope on Spacelab would provide high sensitivity photometry with high spatial resolution enabling many astronomical objects to be studied through the measurement of atomic and molecular lines in the far infrared. EXPOS again uses Spacelab to fly a set of instruments to study the spectra of cosmic X-ray sources and to detect polarised X-ray emission. The payload comprises a number of large area Bragg spectrometers each selected to study particular features in the 0.5 to 10 keV range. Spatial resolution of about 1 arc min and energy resolution of 10 to 20% at 1 keV is obtained by using an X-ray grating with a large area Walter I grazing incidence mirror. The third project concerned magnetospheric experiments from Spacelab and drew the fascinating picture of a series of tethered subsatellites around Spacelab, like dogs on leads, making multipoint plasma measurements. All these projects have the advantage to the UK that they support research fields in which British scientists are very active and proficient.

The afternoon session of the meeting discussed last year's batch of mission studies and chose the ones that the British scientists would like to go forward for a phase A (feasibility) study. These projects stretched the

Aphids, ants and pheromones

from our Insect Physiology Correspondent

It was shown by J. S. Edwards many years ago that the secretion from the cornicles of aphids consists of oily droplets, now known to be a mixture of triglycerides, in aqueous suspension. On release in contact with a solid surface this secretion quickly crystallises to form a hard waxy plaque. It thus provides a mechanical protection against small predators and parasites.

In recent years the cornicles have been found to liberate also alarm pheromones, which are secreted in response to predators and parasites. Bowers *et al.* (*Science*, **177**, 1121; 1972), isolated and identified *trans-β-*farnesene (TBF) as the alarm pheromone in several aphid species; this secretion seems also to repel other aphids encroaching on occupied feeding sites. As with the alarm pheromones of many insects, TBF is interspecific: it is present in all species examined in the subfamily Aphidinae, and all of them (with the exception of the turnip aphid *Hisdaphis*) show alarm activity to pure synthetic TBF. But other unidentified alarm pheromones are present in addition to TBF and these different blends of pheromone probably account for the different responses in different aphid species. Thus the turnip aphid which fails to react to TBF, secretes this pheromone in its cornicle fluid, and it reacts to the secretions of other aphid species.

Nault, Montgomery and Bowers (*Science*, **192**, 1349; 1976) have now studied the response to these pheromones in the ants which herd certain aphid species. These myrmecophilous aphids enjoying, as they do, protection by their ants from predators, are much less responsive to the alarm pheromones than non-myrmecophilous species. They may walk away on exposure to the alarm pheromone, but they do not drop off the feeding site. At the same time, and not surprisingly, the ants themselves respond to aphid alarm pheromones In experimental trials it appeared that the ants were prepared to stroke with their antennae any aphid species they were offered; but the different aphid species vary widely in the readiness with which they excrete droplets of honeydew for their ant keepers Some species will not respond at all. The Macrosiphini were caused to disperse by the ants' stroking: this provoked a predatory response by the ants, and the aphids were carried off to the nest and presumably eaten.

The acceptance of the attentions of ants replaces response to alarm pheromones· the myrmecophilous aphids rely on their ants for protection. Indeed, artificial liberation of TBF leads to attack by the ants, not on the aphids but on any suspected predators by which they appear to be attacked. The threshold of response to the pheromone by the ant is, indeed, even lower than the threshold in the aphids themselves.

imagination much more than the morning's batch as now people were looking towards the space research of the late 1980s.

Space astrometry had an instant appeal, bringing space science and technology to bear on one of the fundamental tasks of astronomy, the observation of the positions of stars and planets as a function of time. The increase in accuracy from ground-based observations has been very limited in the last half-century and no breakthroughs seem to be around the corner. Space astrometry would give positions to between 0.001 and 0.003 arc s (0.04 arc s is the present best for ground-based work); proper motions (the star's velocity perpendicular to the line of sight) could be measured to about ± 0.002 arc s yr^{-1} after 3 years of observation, such accuracy requiring 50 years at present; parallax (stellar distance) of stars of 11th magnitude, as opposed to 7.5 magnitude at present could be measured to $\pm$ 0.001$-$0.004 arc s (in contrast to $\pm$ 0.013 arc s from the ground). This increased accuracy has enormous astrophysical significance—improving the definition of the cosmic distance scale, calibrating Cepheid variables, increasing the accuracy of stellar luminosity and cluster age estimations being only a few examples to which it might be applied.

The Solar Probe also caused much discussion. Using a Jupiter gravity assist this can get to within 10 solar radii of the Sun's surface. The mission definition scientists decided that the problems of thermal control and telemetry coverage within the corona could be overcome. Scientific objectives are the measurement of the solar gravitational field (J_2), the testing of Einstein's theory of general relativity and the measurement of the rate of change of Newton's constant of gravitation. Also a whole series of experiments dealing with particles and fields in the expanding corona would be flown. A Climatology satellite, to obtain measurements of the Earth's radiation budget and especially a value of the solar constant to $\pm$ 0 1% (as opposed to $\pm$ 1.5% at present) was widely welcomed as was a more unusual Dumb-bell Mission Here two satellites launched into a near polar Earth orbit are deployed so that they are 10 to 20 km apart but tethered together by a long wire Measurement of the tension variations in the tether gives the gravity field anomalies in the Earth's upper crust. The tether would also be used to measure induced electric fields and the two satellites would be used for active and passive magnetospheric experiments Finally, an ultraviolet and X-ray satellite (10–1000 Å) with two Baez telescopes and a spectrograph on board was considered. A year's observation with this satellite would provide a 5 arc min resolution map of the whole sky plus detailed spectra of new sources.

Although one could not help getting the feeling that Britain was a small fish in the ESA pool (which is itself small in comparison to NASA and the USSR's Space Agency) whenever brains combine, new ideas are forthcoming and Britain and Europe can still provide ideas even if they cannot compete in finance and firepower.

Phase changes at 650 km

from Peter J. Smith

It has often been assumed that the Earth's 650-km seismic discontinuity, which involves a large increase in bulk modulus as well as seismic velocity, is largely the result of a phase change in the olivine component of the mantle. Anderson (*Science,* **157,** 1165; 1967), for example, attributed this discontinuity to the disproportionation of spinel to a structure with the properties of mixed oxides—a phase involving the simple oxides, a Sr_2PbO_4 structure or perovskite plus periclase, all of which have similar densities. But as Anderson himself now admits (*Geophys. Res. Lett.,* **3,** 347; 1976), there are problems with this interpretation which suggest that the discontinuity in question may have little to do with transformations in olivine after all.

For example, although the disproportionation of spinel to oxides involves a large increase in density, it also involves an increase in coordination, increasing the average silicon-oxygen separation and reducing the repulsive forces between ions. The increase in bulk modulus is therefore much reduced (and may even be converted into a decrease) compared with that expected from a transformation with no associated change in coordination—a point previously made by Liebermann and Ringwood (*J. geophys Res.,* **78,** 6926; 1973) In fact, the elastic moduli of spinels and mixed oxides are similar. On this basis, disproportionation as envisaged would be expected to produce a decrease, rather than an increase, in seismic velocity.

Because this is clearly unsatisfactory, Anderson now suggests that the 650-km discontinuity is primarily the result of phase changes in the pyroxene and garnet components of the mantle rather than in the olivine. The basic premise upon which this proposition rests (and detailed evidence for which is promised in a later report) is that the bulk moduli of silicate and oxide solid solutions are almost independent of iron content. In particular, as Mg^{2+} is replaced by Fe^{2+} in systems such as pyroxenes, olivines and garnets, the density increases in accordance with the Birch formula but the bulk modulus increases or decreases only slightly. The bulk modulus cannot therefore be used to make deductions about the composition of the mantle It is, on the other hand, a good indicator of crystal structure, its magnitude's increasing from pyroxene to α-olivine to β-spinel to garnet to γ-spinel to oxides in pyroxene proportions to perovskite.

With this in mind, Anderson has attempted to extrapolate the bulk moduli (K) and densities (ρ) of the various regions of the mantle to a pressure of 1 bar and a temperature of 20 °C and has compared the resulting K-ρ points with the K-ρ curves for the appropriate crystal structures. He thus deduces that between depths of 200 and 400 km (Region I) the mantle is predominantly olivine and pyroxene with subordinate garnet, the pyroxene to garnet ratio being 7 · 2 to satisfy the bulk modulus. Region II, between 400 and 500 km, is close to β-spinel and is consistent with olivine-pyroxene-garnet with a higher proportion of garnet than Region I. Anderson concludes that Region II comprises olivine in the β phase, pyroxene and pyroxene–garnet solid solution with garnet structure.

By contrast, Region III, which lies between 500 and 650 km, is closer to garnet. Its most likely composition is $(\beta+\gamma)$-olivine and pyroxene–garnet solid solution, all the pyroxene now having entered the garnet structure. However, because of uncertainties in the data upon which the K-ρ curves are based, Region III could be entirely β-spinel and garnet. The properties of Region IV (650–800 km) are consistent with this layer's being either mixed oxides or γ-spinel plus stishovite (SiO_2). And finally, Region V, below 800 km, could be either mixed oxides with more stishovite than Region IV or perovskite plus MgO.

In the light of these phase changes Anderson thus proposes that it is the pyroxene–garnet component, transforming from the garnet structure to the mixed oxides or perovskite structure, which is chiefly responsible for the 650-km discontinuity. Unfortunately the thermodynamic data currently available are insuficient to enable the reaction boundary between the mantle pyroxene-garnet solid solution and mixed oxides to be calculated However, calculations made assuming this complex garnet to behave as almandine–pyrope garnet imply that the transition is sharp (perhaps less than 12 km thick on the basis of admittedly inadequate data and questionable assumptions), a property required by some of the seismic data ●

articles

Small-angle scattering experiments on biological materials using synchrotron radiation

J. Bordas & I. H. Munro
Daresbury Laboratory, Daresbury, Warrington WA4 4AD, Cheshire, UK

A. M. Glazer
Wolfson Unit for the Study of Phase Transitions in Dielectrics, Cavendish Laboratory, Madingley Road, Cambridge CB3 0HE, UK

This article describes an alternative approach to small-angle scattering experiments on biological specimens. The method makes use of the unique properties of synchrotron radiation and provides very fast data acquisition with good resolution. Preliminary experiments on rat-tail tendon are described.

UNDERSTANDING the mechanism by which a biological sample responds to a perturbation is a subject of continuing interest and an obvious way of dealing with the problem is to study structural changes by X-ray diffraction. The lattice periodicity in biological specimens is usually larger than that commonly encountered in non-biological crystals and may be as great as 1,000 Å or more. A conventional X-ray tube is normally used to produce characteristic X-ray lines with wavelengths between 0.6 Å and 2.0 Å, and so the first-order diffraction peak will be produced at a small angle to the direction of the incident X-ray beam. As a consequence, the experimenter uses a long camera to achieve reasonable separation of the diffraction pattern from the main beam. Because of the rapid fall-off in intensity with distance from the source, photographic recording of the intensities requires long exposure times, but, in practice, a compromise between spatial resolution and exposure time has to be made. If focusing techniques are used, the exposure times can be shortened but at the expense of complexity in instrument design. Even so, the intensities are still recorded over a long interval.

If one could achieve more rapid data acquisition, then it would be possible to carry out low-angle X-ray diffraction studies of biological material during some temporal process, for instance, muscle contraction. With the technique described here it is possible to record the pattern rapidly and with high resolution using simple apparatus, thus making a dynamic experiment of this type feasible. To do this, we make use of the unusual properties of synchrotron radiation.

Synchrotron radiation has four important characteristics: high intensity, low beam divergence, a high degree of linear polarisation and, probably most important, a smoothly varying white radiation profile[1].

At present, work is in progress to study the applications of this rather special radiation to X-ray diffraction problems. Preliminary work has already been carried out in the field of X-ray topography[2–4] and in powder diffraction (J. B. and A. M. G., unpublished).

Synchrotron radiation

In the synchrotron NINA, at the Science Research Council's Daresbury Laboratory, electrons are accelerated up to 5 GeV and emit electromagnetic radiation which extends as a continuum from the infrared to the hard X-ray region (about 0.1 Å). The radiation is 100% linearly polarised in the electron orbital plane. The emitted X-ray beam is well collimated, with the photons confined to a cone of half angle between 10^{-3} and 10^{-4} rad. When NINA is operating at 5 GeV with a circulating current of 20 mA, approximately 10^9 photons s^{-1} are predicted at 1 Å within a band width of 0.1% for the apertures used in the experiment (J. H. Poole, private communication). This high flux is particularly valuable for small-angle scattering experiments. Focusing X-ray diffraction cameras have already been constructed and used with synchrotron radiation at DESY (Hamburg), NINA (Daresbury) and SPEAR (Stanford). These cameras use vertically focusing mirrors and curved monochromatising crystals to collect as many photons as possible and, at the same time, to provide small, high contrast diffraction spots on a position-sensitive detector or on a photographic plate.

Here we present an alternative approach to the measurement of X-ray diffraction patterns, which we believe makes good use of the unique characteristics of synchrotron radiation and which does not require any optical components. Furthermore, it allows the very fast collection of data already mentioned. To illustrate the method we have used rat-tail collagen because it combines a large fundamental lattice spacing (670 Å) with well defined, sharp reflections.

Extending energy—dispersive techniques

Our approach to the measurement of X-ray scattering at small angles is conceptually very simple and is an extension of the recent use of energy-dispersive techniques with white radiation from conventional X-ray sources[5–8].

The Bragg equation for X-ray diffraction is usually expressed by

$$2d\sin\theta = n\lambda \qquad (1)$$

From this it is clear that for a particular spacing, d, and a single X-ray wavelength, λ, the orders $n = 1, 2 \ldots$, will appear at the angles 2θ which fulfil equation (1).

If, however, a parallel beam of white (polychromatic) radiation falls on an oriented sample, then for a particular spacing and for a selected scattering angle there will be a number of discrete wavelengths, λ/n, which will satisfy equation (1).

In other words, in place of a conventional X-ray scattering experiment in which the sample is illuminated with monochromatic radiation and the spatial distribution of the scattered radiation is measured, one measures a photon energy spectrum giving all the wavelengths diffracted at a preselected angle.

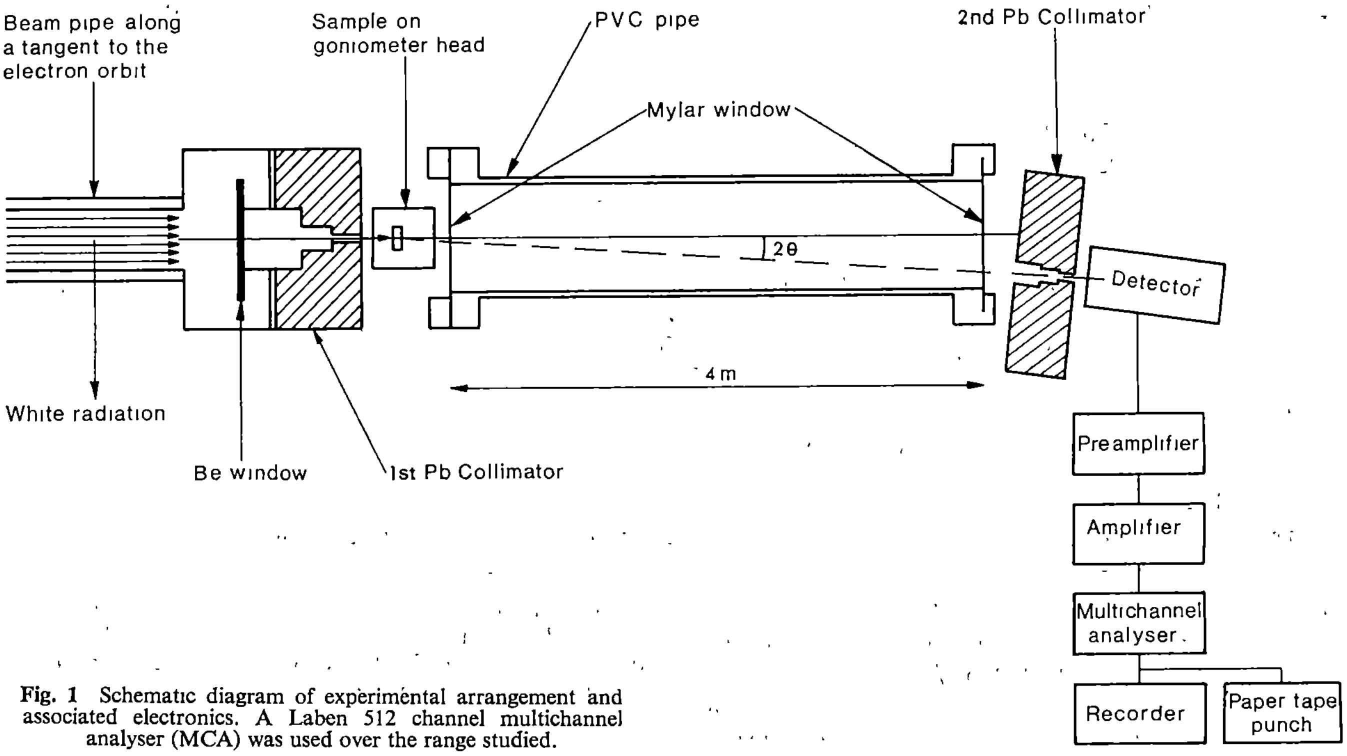

Fig. 1 Schematic diagram of experimental arrangement and associated electronics. A Laben 512 channel multichannel analyser (MCA) was used over the range studied.

We can write the energy, E, in the form

$$E\,(\text{keV}) = \frac{12.4}{\lambda\,(\text{Å})} = \frac{12.4n}{2d\sin\theta} \qquad (2)$$

Thus, taking θ to be constant we have a strict proportionality between E and n/d. In the normal diffraction experiment, λ is held constant and then sinθ is proportional to n/d. Thus, a plot of intensity against energy is similar, qualitatively at least, to the conventional plot against θ. There is a 1:1 spatial correspondence between peaks observed in the two plots for small θ.

The precision of this method relies on the performance of an energy-resolving solid state detector which is commercially available with an energy resolution at best of about 150 eV at 12 keV (information supplied by AERE Harwell and Ortec Ltd). With conventional X-ray sources this technique is handicapped by the complicated X-ray profile comprising white and characteristic wavelengths, as well as the inherent lack of collimation. This means that the measurement of intensities is difficult and, furthermore, in a small-angle scattering experiment high collimation is vital. Most of the uses of energy-dispersive techniques so far have been of a relatively qualitative nature and confined to large scattering angles. In our experiments, a lithium-drifted silicon solid state detector (supplied by AERE Harwell) was used to give a combined resolution for the detector and amplifier system of about 230 eV FWHM, at 12 keV. The time constant of the overall system (25 μs) could be reduced at the cost of decreasing the energy resolution. The experiments were run at maximum count rates of 1.6×10^4 c.p.s. with a collection efficiency of better than 95%.

Experimental arrangement

A schematic drawing of the apparatus is shown in Fig. 1. White X radiation from circulating electrons in NINA passed down an evacuated pipe, 47 m long, before traversing a 0.016-inch (0.041-cm) beryllium window into air at the end of the pipe. A lead X-ray collimator shaped to minimise any scattered radiation at the detector (mainly from fluorescence of the collimators) was placed in air immediately after the beryllium window. The sample was supported on a goniometer head and could be rotated within the beam to provide equatorial and meridional reflections at the detector. The collimator aperture was adjusted to suit the size of the specimens and was of diameter 1.0 mm or 0.5 mm. The specimens used were less than 0.25 mm in diameter and 1 mm long.

Immediately behind the sample, a 4-m-long evacuated plastic tube with Mylar end windows was used to eliminate any effects of air scatter or of absorption between the sample and the detector. The angular acceptance of the detector was accurately defined by a second lead collimator placed directly in front of the solid state detector. The main, undiffracted beam was absorbed in a lead beam stop. The scattering angle (2θ) was defined by measuring the distance between the main beam and the detector collimator aperture using X-ray sensitive paper to locate the undiffracted radiation. The entire apparatus was aligned simply and rapidly using a small, portable He/Ne laser. The beryllium windows on the beam pipe and detector restricted the lowest energies available to less than about 3 keV (~ 4 Å). Because of the relatively low counting efficiency of the detector and the source cutoff at high energies, the highest energies accessible were about 40 keV (~ 0.3 Å). The synchrotron was running at 4.6 GeV and approximately 10 mA.

The samples of rat-tail tendon were kept wet during the experiment and were usually stretched, although they were not kept under tension. Orientation of the samples to yield equatorial and meridional reflections was defined by reference to the line joining the centre of the detector collimator aperture to the centre point of the undiffracted beam.

From equation (1)

$$\Delta\theta = \tan\theta(\Delta\lambda/\lambda) = -\tan\theta\frac{\Delta E}{E} \qquad (3)$$

and therefore for the particular resolution $\Delta E/E$ of the solid state detector used, the correct angular acceptance Δθ (that is, the appropriate diameter for both collimators) for a particular angle θ was easily calculated. A typical detector collimator would be ~ 0.5 mm in diameter with a separation of aperture from the main beam of from 10 to 50 mm. To calibrate the energy at a particular channel of the multi-channel analyser we used calibrated X-ray fluorescence lines obtained from commercially available sources. The calibration energies (wavelengths) were those of Cu, Mo, Ag, Rb, Ba and Tb.

Handling the data

In Fig. 2. we plot the raw data from the multi-channel analyser (MCA) display obtained from the meridional diffraction of wet rat-tail tendon. The detector collimator angle (2θ) was set at 3.14 mrad in order to ensure that the first-order diffraction peak fell within the range transmitted by the beryllium window. In the example shown, the prominent first-order peak was already well resolved after only 1 s of data accumulation. A qualitative view of the full spectrum could be obtained within a few seconds but to obtain good statistics data were collected for 200 s. In this experiment, the collimator apertures at the detector and at the sample were chosen to be 1.0 mm and 0.5 mm, respectively. This, combined with the sample size, gave a geometrical resolution comparable with that of the detector. The observed peak widths were twice that expected for the detector resolution and are almost certainly due to the finite size of the aperture collimators. Although the rate of data accumulation could be significantly increased by enlarging the collimator apertures (for a large sample), these experiments are normally limited by count-rate saturation at the detector output.

To make quantitative estimates of the structure factor for each reflection, it is necessary to correct the data in Fig. 2 for the NINA intensity profile, the efficiency of the detector and any other instrumental factors. The first two quantities are, in principle, calculable, but the uncertainty in the remaining correction factors makes it essential to calculate the effect of all of the factors taken together (the total instrument function). Normally, this would be done by using the detector to measure the intensity spectrum of the main beam; but, unfortunately, the detector saturates at a count rate of 10^4 photons s^{-1}, much less than that of a synchrotron source.

There is, however, a neater and simpler method which can be used. The intensity of the background in Fig. 2 arises from incoherent scattering by random atoms, mainly in the air traversed by the X-ray beam, and is given by

$$I = \text{constant} \times (\sum_j f_j)^2 \tag{4}$$

where f_j is the scattering factor for the jth atom. Although it is possible to eliminate this background scatter almost completely, it is better to allow some of this scatter to occur, because it can be used to normalise the diffraction peak intensities. To do this, we note that the value of $\sin\theta/\lambda$ used is extremely small ($\lesssim 7.5\times10^{-3}$ Å^{-1}) and corresponds to the flat part of the atomic scattering factor curve (flat to within 1–2% over the range of $\sin\theta/\lambda$ used). Thus, the background intensity, which is a measure of

$$(\sum_j f_j)^2$$

is also a direct representation of the total instrument function. It is then simple to correct for this function by dividing each data point by the background, taking care to extrapolate the background under the diffraction peaks, and then subtracting the number 1.

In Fig. 3 we show the background (total instrument function) on an enlarged scale It is clear that it rises to a maximum near 7 keV. The resulting normalised intensities of the first- to fifth-order peaks of our sample of rat-tail collagen are shown in Fig. 4. To extend the measurements to higher order peaks, the detector collimator angle (2θ) can be reset to a different angle five times larger than before. This has the effect of shifting fifth-order to the same energy at which first-order diffraction appeared previously. Therefore, if identical synchrotron running conditions are maintained, an angular increase (in 2θ) of five times yields the fifth- to the twenty-fifth-order diffraction peaks in place of first- to fifth-order peaks.

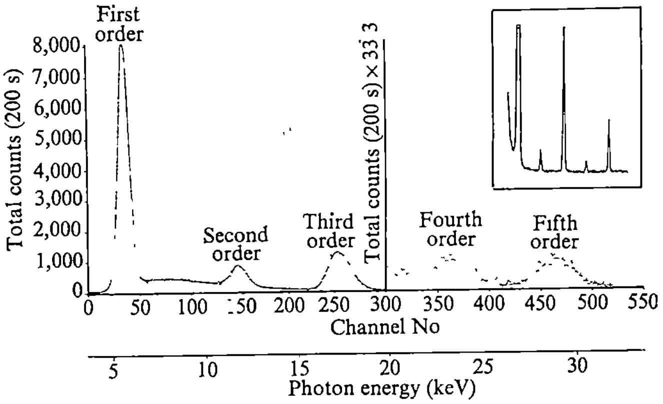

Fig. 2 Raw intensity data from the meridional plane of a wet and stretched rat-tail tendon. Total measuring time, 200 s. Note the low noise level and clean separation of diffracted peaks. Inset, meridional profile obtained with a conventional rotating-anode generator and focusing camera with intensities collected on a photographic film and subsequently densitometered (J C. Haselgrove, private communication). The sample was approximately 6×0.5×0.5 mm, camera length 0.65 m, generator at 40 kV, and 60-mA Cu target. Exposure time 30 min.

The relative intensities of the diffracted peaks given in Fig. 3 agree qualitatively with existing published results[9] for wet rat-tail tendon.

An example of a profile taken with a conventional rotating-anode X-ray source and a focusing camera is shown in the inset in Fig. 2 and is typical of what can be obtained with conventional sources (J. C. Haselgrove, private communication). The two measured profiles are closely similar: the important difference is in the exposure times and sample size used. The exposure time of the focusing method could be shortened but at a cost of resolution. We note also that in the energy-dispersive experiment all lines are very cleanly resolved with negligible noise. Moreover, the conventional experiment often requires sample preparation involving the mounting and alignment of many collagen strands to achieve sufficiently high intensities. This difficulty is not encountered in our experiment.

Table 1 shows the integrated intensities after the above corrections have been applied. Before we can compare these results with published values, however, it is necessary to take into account the special nature of the energy-dispersive technique. It can be shown[10] that with a white radiation source the integrated diffracted intensity, measured by an energy dispersive system, is a function of λ^2. Moreover, for small absorption, it depends inversely on the absorption coefficient μ.

Fig. 3 Background intensity profile (total instrument function). ———, Interpolations under diffraction peaks.

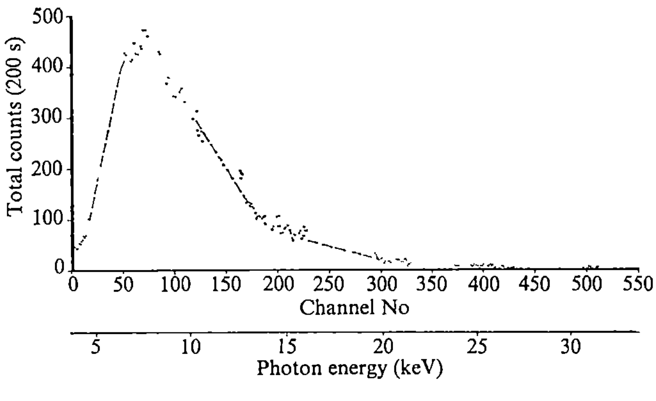

Since to a first approximation $\mu \simeq \lambda^3$, the scattered intensity is given by

$$I = \text{constant} \times \frac{|F|^2}{2\lambda \sin^2\theta} \sim \frac{E|F|^2}{2 \sin^2\theta} \qquad (5)$$

where E is the energy of the diffracted beam and F is the structure factor. The second column in Table 1 lists the intensities after correcting for this variation. The next two columns list published results[9] for wet and dry samples and the final column gives our results scaled to the third-order intensity of wet rat-tail collagen.

We find that the intensity of the first-order peak lies well below that measured by Tomlin and Worthington[9]. This probably arises from a combination of effects. In particular, the position of this peak is directly over that region of the background which is changing fastest (Fig. 3), and therefore in dividing by the small background values the resulting estimate of the integrated intensity is subject to a large uncertainty. In addition, this reflection corresponds to a longer X-ray wavelength (2.11 Å) than the other peaks, and, because the scattering efficiency depends on λ^2, it can be severely affected by extinction. Moreover, the higher absorption at this wavelength will mean that the inverse relationship between I and μ is no longer sufficiently good. One way of getting round these difficulties would be to remeasure the intensity of this peak accurately at a smaller angle. The two measurements thus obtained would allow the absorption effects to be precisely determined. Moreover, if the second angle is chosen to be a third of the present angle, the first-order peak will appear at three times the present energy where absorption becomes less serious.

The intensities of the remaining peaks agree very closely with those measured by Tomlin and Worthington for wet rat-tail collagen. The slightly high value for the second peak may be due to drying of the specimen. In fact, it was observed that the relative intensities of the diffraction peaks changed considerably as a result of drying out of the specimen in agreement with the results of Tomlin and Worthington. Also, in at least one of the muscle samples used, severe radiation damage (a brown spot on the sample) was observed after irradiation for about 20 min. The rapid rate of collection of data means, however, that radiation damage is minimised. The reasonably good agreement between our results for rat-tail collagen and the published intensities suggests that radiation damage is not serious with a collagen sample for the exposure times used. Experiments with muscle showed that exposures of up to 120 s were feasible with NINA at 5 GeV, 10 mA before any change in the pattern was observed.

Table 1 Integrated intensities after application of corrections

n	Integrated intensity (I)	I/E	Tomlin and Worthington Wet	Tomlin and Worthington Dry	Scaled I/E
1	396.1	67.36	1,000	1,000	190
2	52.6	4.47	8	188	13
3	695.9	39.45	111	132	111
4	71.4	3.04	8	49	9
5	307.9	10.47	33	43	30

Fig. 4 Normalised energy-dispersive pattern from Fig. 2. The basic periodicity is 670 Å.

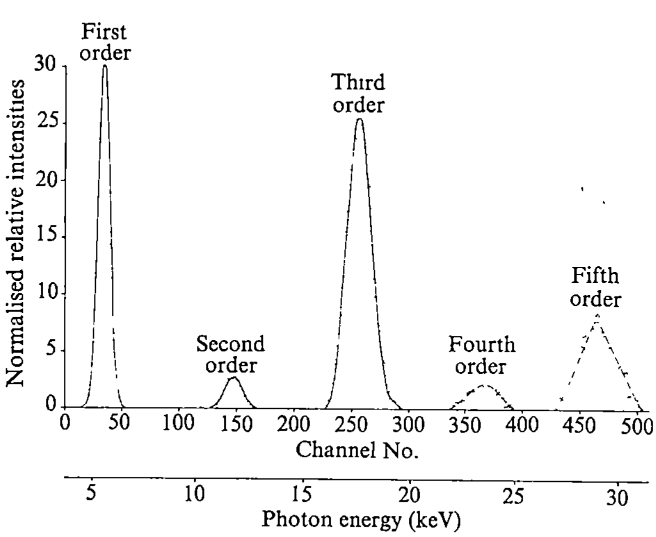

Outlook

We have shown that with relatively simple equipment at a synchrotron, it is possible to obtain small-angle scattering patterns from biological specimens which are of extremely high quality and almost noise free. The technique has many advantages over other methods, namely, the high speed of data acquisition, the potential precision of relative intensity measurements, the low level of background radiation and high resolution for material with large spacings.

Data can be collected at very high rates using the collimated white radiation from a synchrotron source, and the data acquisition rate is restricted solely by the relatively slow response time of the solid state detector and its associated amplifier. When this limitation is overcome, there could be a further increase in data acquisition rates by several orders of magnitude. Even with presently available electronics we have been able to achieve a four- or fivefold increase in the speed of data collection, simply by using appropriate balanced filters to select a small range of X-ray energies, so that the counter is not saturated by unwanted photons. This allows a larger sample with a larger area of irradiation, and thus more diffracted photons within the energy range selected. Although only one or two reflections can be examined at a time, the advantages of the high speed of collection may compensate for this When the dedicated storage-ring facility becomes available at the Daresbury Laboratory the X-ray intensities produced will be about 100 times greater than from the existing synchrotron. The storage ring will provide a considerably more stable intensity source, but if full use is to be made of its high intensity output faster energy-dispersive counting devices are needed.

Lattice periodicities of from a few tens of Å to around 1,000 Å can be investigated simply by reducing the detector viewing angle from 10^{-2} rad to a few mrad A new experimental arrangement under construction at Daresbury will permit the detector to scan through an angular range of 1 to 20 mrad. This could, in principle, permit the observation of up to the 80th order ($\sim$ 8 Å) in materials such as rat-tail tendon. Peak-stripping computational techniques together with a high resolution detector should permit peak energy positions to be determined to an accuracy of at least 0.1%. This will offer valuable and complete structure determinations when combined with a two-axis rotation of the sample in the incident beam. Dynamic X-ray diffraction studies should now become feasible if the sample is perturbed periodically and the experiment carried out in the same way as in modulation spectroscopy. For example, an electrical stimulus applied to the sample periodically, with measurements made in and out of phase, would enable a derivative signal to be built up yielding important and new time-dependent structural information on biological specimens.

We thank Professor Zvi Kalman for drawing our attention to energy-dispersive methods and to Drs A. R. Faruqui and D. Hukins for samples and discussions. We are particularly grateful to Dr J. C. Haselgrove for advice and permission to publish measurements made with a conventional source.

We wish, also, to thank the Science Research Council and the staff of the Daresbury Laboratory for their cooperation.

●

Financial support by the Wolfson Foundation is acknowledged (A.M.G.).

Received December 9, 1975; accepted June 26, 1976.

1 Codling, K., *Rep. Progr Phys*, 36, 541–624 (1973)
2 Tuomi, T., Naukkarinen, K., and Rabe, P, *Phys stat sol. A.*, 25, 93–106 (1974).
3 Hart, M, *J. appl Crystallogr*, 8, 436–444 (1975).
4 Bordas, J., Glazer, A. M., and Hauser, H., *Phil. Mag*, 32, 471–489 (1975)
5 Sparks, C. J, and Gedcke, D. A., *Adv X-ray Analysis*, 15, 240–253 (1971)
6 Fukamachi, T., Hosoya, S, and Terasaki, O, *J appl. Crystallogr*, 6, 117–122 (1973).
7 Chwaszczewska, J., Szarras, S, Szmid, Z., and Szymczak, M, *Phys stat. sol. A*, 4, 619–626 (1971).
8 Buras, B., Olsen, J. S., Gerward, L, Selsmark, B, and Andersen, A L, *Acta crystallogr*, A31, 327–333 (1975)
9 Tomlin, S G, and Worthington, C. R, *Proc R Soc*. A235, 189–201 (1956)
10 Zachariasen, W H., *Theory of X-ray Diffraction in Crystals* (Wiley, London, 1945)

Model for action of local anaesthetics

A. G. Lee

Department of Physiology and Biochemistry, University of Southampton, Southampton SO9 3TU, UK

Sodium channels in nerve membranes are postulated to be surrounded by lipid molecules in the gel (or crystalline) phase. Addition of local anaesthetics triggers a change in the surrounding lipids to the fluid, liquid crystalline phase, allowing the sodium channel to close with resulting local anaesthesia. The experimental evidence for this model is discussed.

DIRECT study of sodium channels in nerve membranes is made exceedingly difficult by their sparsity: it has been estimated that in $1\ \mu m^2$ of nerve membrane there are between 2 and 500 sodium channels, depending on the animal[1], compared with about 3×10^6 lipid molecules. Information about the molecular nature of the sodium channel has therefore had to be inferred indirectly, largely from electrophysiological studies. In particular, it has been postulated that the sodium channel contains a narrow slit 3×5Å surrounded by a ring of oxygen atoms, the slit being both the pathway for ion flow and the selectivity filter which determines which ions can flow[2,3]. I suggest here that the effects of local anaesthetics can be used to probe the lipid environment of the sodium channel.

The block of nervous conduction by local anaesthetics follows largely from a reduction in the sodium conductance[4], although there are also changes in the time course of the channel gating[5]. The mechanism of this block of sodium conductance has not yet been explained satisfactorily. Since a wide variety of different compounds can act as local anaesthetics, including neutral and both negatively and positively charged molecules, it is not clear whether there is a single mechanism for local anaesthesia, or whether each class of anaesthetic acts in a different way Staiman and Seeman[6], however, have shown that effects of anaesthetic mixtures are close to being additive, suggesting a single mode of action.

There are several theories for the action of local anaesthetics. One suggests specific receptors for local anaesthetics in the nerve membrane, and was proposed largely to explain the action of tertiary amine anaesthetics such as procaine, which are most potent in the charged, protonated form and which act only on the inside surface of the nerve membrane[4] But the receptor (probably the sodium channel itself) would have to be surprisingly unselective, since a very wide range of amines act as anaesthetics, their only obvious similarity being both a lipophilic region and a hydrophilic region[7]. In contrast, very minor changes in the structure of tetrodotoxin, which is known specifically to bind to the outside surface of the sodium channel, cause complete loss of activity[8]. Further, different sites of action would have to be postulated for the action of neutral and negatively charged anaesthetics. A second proposal is that effects of local anaesthetics on the membrane surface charge are important[4], and although this could account for the action of the positively charged amines, it fails to account for the action of neutral or negatively charged molecules.

The third, and perhaps most popular theory, is the membrane expansion theory. This proposes that anaesthetics increase the fluidity of membrane lipids and expand the membrane[9]. Although anaesthetics have indeed been shown to cause an expansion of erythrocyte membranes[10], it is not clear how an expansion of the nerve membrane would lead to a block of sodium conductance. Further, the theory would predict that an increase in pressure would reverse local anaesthesia, and whereas this is observed for ethanol[11], for some other anaesthetics, increasing pressure enhances nerve block[12]. Also, local anaesthetics at nerve blocking concentrations would be expected to have little effect on the fluidity of the bulk of the membrane lipids. Thus it has been estimated that the "microviscosity" at the centre of a bilayer of dimyristoyl phosphatidylcholine in the liquid–crystalline state is about equal to that in *n*-decane, and that the viscosity near the glycerol head group of the lipid is only approximately 15 times greater[13,14] Since rates of rotation about C–C bonds in short-chain alkanes and alcohols[15] are similar to those at the centre of the bilayer, addition of these alkanes and alcohols would be expected to have only relatively slight effects on membrane viscosity, and yet they are local anaesthetics[9]. Indeed, using a spin-label method, Boggs *et al.* have shown that anaesthetics do not affect order parameters in bilayers of egg lecithin at anaesthetic concentration[16].

The last model for local anaesthetic action is the protein perturbation model, in which interaction between anaesthetics and the sodium channel causes conformational changes resulting in a block of conductance[12] On such a model it is again surprising that neutral and both positively and negatively charged molecules should act as anaesthetics, especially since the tertiary amines can act in the neutral form, although being more effective when positively charged The observed competition between Ca^{2+} and the amine anaesthetics is also hard to account for[17], as is the "cutoff" effect (in a homologous series of compounds, anaesthetic potency increases with increasing chain length up to a particular compound, beyond which they cease to be anaesthetics[9]) binding of long chain alcohols to bovine serum albumin simply increases with increasing chain length[18].

A new hypothesis is now presented for the action of local anaesthetics, based on a particular model for the sodium channel.

Annular transition model

The basic postulate of the new model is that the sodium channel is surrounded by an annulus of lipid, which is in the crystalline, or gel, state. If the sodium channel has the

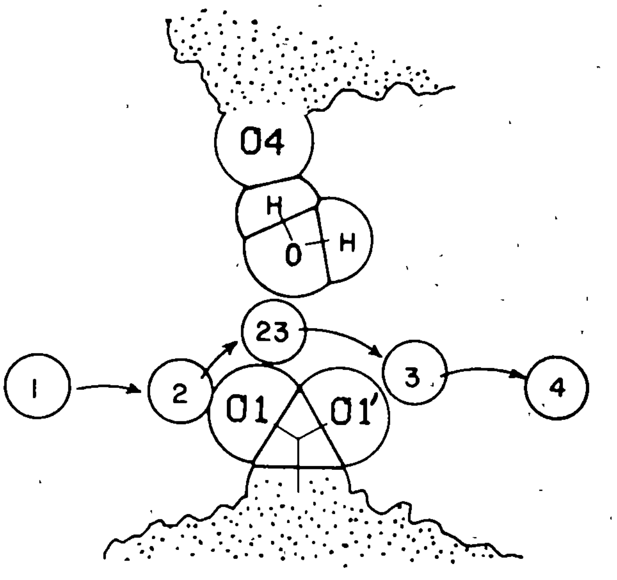

Fig. 1 Model for the sodium channel, with a sodium ion moving through the slit from position 1 to 4 (from Hille, ref. 3).

structure suggested by Hille[3], then it is the rigidity of the surrounding lipid microenvironment that keeps the sodium channel open. Addition of anaesthetics triggers a change in the surrounding lipid from the crystalline, gel state to a fluid, liquid-crystalline state. When the surrounding lipid is in a fluid state, the sodium channel is free to relax into its most stable state, with a consequent closing of the oxygen-lined slit which provides the ion channel through the membrane. Figure 1 shows the picture of the sodium channel presented by Hille[3], and it can be seen that relaxation of the protein would decrease the distance between the oxygens lining the slit, perhaps allowing hydrogen bonding between the water molecule postulated to be bound in the slit and one of the oxygens O_1 or O_1^1 of the carboxyl group.

Although the bulk lipids of the biological membrane seem to be free to diffuse within the plane of the membrane[13], there is strong evidence for relatively long-lived interactions between lipids and at least some membrane proteins. Persistent lipid–protein interactions giving rise to a lipid annulus have been proposed for cytochrome oxidase[19], rhodopsin[20] and the calcium transport protein[21,22]. The model for the sodium channel is, however, unusual in requiring the surrounding lipid to be in the gel phase to allow for activity. For the calcium pump, for example, it has been shown that the enzyme is only active when the surrounding lipid is in the fluid, liquid-crystalline state[23]. This presumably arises because in the energy-requiring pumping process, conformational changes occur which are inhibited by rigid, gel phase lipid In contrast to these relatively slow pumping processes[13], the rate of passage of Na$^+$ ions through the open sodium channel is so fast that any change in conformation during ion passage seems unlikely[24]. Two other membrane proteins have been established to operate within a rigid lipid matrix, bacteriorhodopsin in the purple membrane of *Halobacterium halobium*[25] and the microsomal cytochrome P-450 (ref. 26).

Experimental evidence

The fact that anaesthetics do trigger a change in state for lipids from a gel to a liquid-crystalline state has been established in several recent papers. Alcohols up to *n*-octanol have been shown to lower the phase transition temperatures of phosphatidylcholines and phosphatidylethanolamines[27,28]. The effects are linear with respect to concentration, and the concentrations required to produce a 5 °C drop in transition temperature are comparable with those required to block nervous conduction[9]. More interestingly, however, it has been found that whereas *n*-decanol lowers the phase transition temperature of dipalmitoyl-phosphatidylcholine (42 °C in the absence of alcohol), it raises that of dimyristoyl-phosphatidylcholine (24 °C in the absence of alcohol). Dodecanol raises the phase transition temperatures of both dimyristoyl- and dipalmitoyl-phosphatidylcholines[28]. This then is sufficient to explain the "cutoff" effect observed with the alcohols. *n*-nonanol is a local anaesthetic[9], and it has been reported that dodecanol is less effective than undecanol in suppression of swimming in tadpoles and that tridecanol has no effect[29]. Similarly, it has been found that the *n*-alkanes up to *n*-octane are anaesthetics, whereas decane is not.

The anaesthetic amines such as procaine and dibucaine also lower the phase transition temperatures of phosphatidylcholines and phosphatidylethanolamines[30,31]. Now, however, effects are nonlinear with respect to concentration, because of the buildup of charge on the liposomes caused by the binding of the positively charged anaesthetics. This can be overcome by the introduction of negatively charged lipid, which considerably increases the effect of the anaesthetic. When the added negatively charged compound is myristic acid, the effect of the negative charges is masked completely by addition of about 0.5 mM Ca^{2+} or Mg^{2+} (ref. 31). When the negative charge is due to phosphatidylserine, however, there is a differential effect between Ca^{2+} and Mg^{2+}: the effect of the negative charge is removed by about 0.6 mM Ca^{2+} or about 5 mM Mg^{2+} (ref 30). Differences between the effects of Ca^{2+} and Mg^{2+} on aqueous dispersions of phosphatidylserine have also been found in other studies. Thus the increase in temperature of the phase transition caused by addition of 0.5 mM Ca^{2+} is equal to that caused by 5 mM Mg^{2+}, and whereas Ca^{2+} causes a segregation of phosphatidylserine in mixed bilayers of phosphatidylserine and phosphatidylcholine, Mg^{2+} does not[32,33]. Furthermore, Hille *et al.* found that Mg^{2+} applied to the outside surface of myelinated nerve fibres had less effect than Ca^{2+} on the voltage dependence of peak sodium permeability, consistent with a weaker binding[34]. These observations are important because they provide, at least in part, a possible explanation for the fact that the amine anaesthetics are most active when applied to the inside surface of the nerve[4]. Negatively charged lipid has been postulated to be close to the sodium channel in nerve, with the highest concentration on the outside surface. But the Ca^{2+} and Mg^{2+} concentrations of the external medium are about 2 mM and 10 mM, respectively, whereas the Ca^{2+} concentration inside the nerve has been estimated to be micromolar or less[35] and the Mg^{2+} concentration is about 3 mM (ref. 36). Thus positively charged anaesthetics will partition most strongly into the inner membrane close to the negatively charged lipid Similar effects apply to the interactions of chlorpromazine and propranolol (my unpublished observations)

Barbiturates also lower the phase transition temperatures of phosphatidylcholines and phosphatidylethanolamines[31]. Because of the buildup of negative charge, they are most effective in the uncharged form at lower *p*Hs. It has been found that barbiturates are more effective local anaesthetics at low *p*H, and anaesthetic concentrations are comparable with those required to produce significant changes in lipid phase transition temperature[31,37]. There seems to be no significant interaction with the negatively charged dipalmitoyl-phosphatidylserine[31]. Connor *et al.*[38] have reported that anaesthetic steroids such as alphaxalone also lower lipid phase transition temperatures.

There are several other experimentally testable consequences of the model First, if anaesthesia results as a consequence of a lipid transition from the gel to the liquid-crystalline state, then a decrease in temperature should restore the lipid to the gel state and consequently reverse

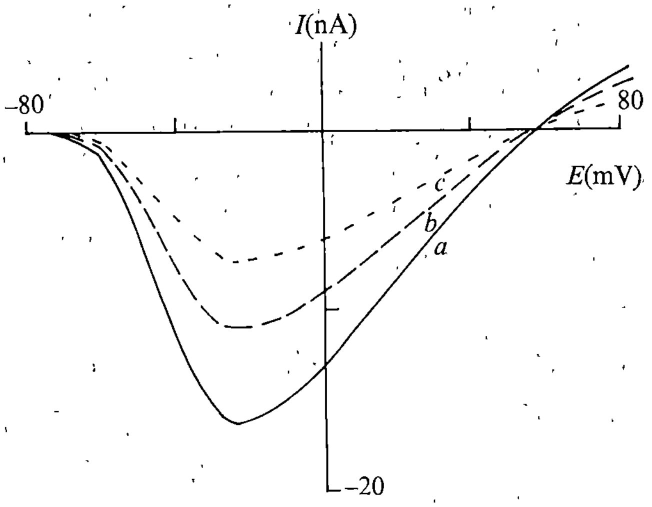

Fig. 2 Peak current (I)–voltage (E) relations as a function of the height of the selectivity barrier. Internal Na^+, 11.2 mM; external Na^+, 116 mM; T, 5 °C; curve a, barrier height G23 = 5 kcalorie mol^{-1}; curve b, G23 = 5.26 kcalorie mol^{-1}; curve c, G23 = 5.53 kcalorie mol^{-1}.

anaesthesia. Only one experiment of this kind seems to have been reported· Spyropoulos did indeed find that the anaesthetic effect of ethanol on squid axon at 22 °C was reversed completely by lowering the temperature to 4 °C (ref. 11) (in the absence of a lipid phase transition, the partition coefficient for small hydrophobic molecules between lipid and aqueous phases changes only slightly in this temperature range[39]). A second consequence is that the sodium conductance of nerve should be little affected by a decrease in temperature from the acclimatisation temperature of the animal (until a temperature is reached at which the gating mechanisms are affected), whereas an increase in temperature should lead to loss of conductance. Unfortunately, the appropriate experiments do not seem to have been performed. Moore[40], however, has observed that the sodium conductance of squid axon is a linear function of temperature within the range 5–25 °C with a temperature coefficient only slightly higher than that for electrolyte conductance in water: this contrasts with the very sharp drop in the activity of membrane-bound proteins such as the Na^+-K^+-ATPase with decreasing temperature. Interpretation of the effects of temperature on nervous conduction are likely to be complex, because of changes in rate constants and conductances for both the sodium and the potassium channels. Nevertheless, with frog nerve the spike amplitude increases slightly on cooling from 25 °C to 8 °C, even though spin-label studies have shown a considerable decrease in fluidity for the bulk lipids within the same temperature range[41,42]. In contrast, increasing temperature produces a reversible conduction block, the temperature of block depending on the animal[43,44]. Thus the available evidence certainly does not contradict the hypothesis of a rigid microenvironment for the sodium channel. Even if more detailed data were available on the effects of temperature on sodium conductance, their interpretation would likely be difficult because of the hysteresis effects expected in such a system. In fact Inoue *et al* [45] have found marked hysteresis in the effects of temperature on the membrane potential of squid axon internally perfused with NaF and bathed in $\mathrm{CaCl_2}$ and NaCl.

Increased pressure is predicted to have two distinct, and contradictory, effects. First, it has been found that increased pressure increases the temperature of a lipid phase transition, simply because a lipid in the liquid-crystalline state occupies a larger volume than one in the gel state[46]. Initially, therefore, an increase in pressure would be expected to inhibit the effect of an anaesthetic. Once the anaesthetic has caused the lipid to transform from the incompressible gel state to the compressible liquid-crystalline state, however, an increase in pressure would be expected to increase the relaxation of the protein (since a relaxed protein with a partially closed sodium channel occupies a smaller volume than that with a fully open channel) and so enhance the effect of the anaesthetic. Both inhibition and enhancement have been observed experimentally[11,12].

Simulation of anaesthetic effects

Although relaxation of the sodium channel caused by anaesthetics could cause blocking of the passage of sodium ions at any point along the length of the channel, the most likely point of blockage in Hille's model[3] is in the narrowest region of the channel, referred to as the selectivity filter. The size and molecular nature of this filter was chosen so that passage of Na^+ through the filter should be favoured over any other ions, whether larger or smaller than Na^+. Hille[3] has presented a four-barrier model for the sodium channel, with the largest of the barriers corresponding to this selectivity filter. It is interesting therefore to see how well the effects of local anaesthetics can be simulated by this four-barrier model, assuming that the relaxation of the protein affects only the height of the barrier constituting the selectivity filter. The following results were obtained using the equations for the one-ion pore model as presented by Hille, and the parameters for the energy profile found by Hille to give the best fit to the ion-selectivity of the sodium channel of frog myelinated nerve. Figure 2 shows the effect of varying the peak height of the selectivity filter (G23 in Hille's notation) on the peak current–voltage relations. The effect clearly is to reduce the sodium current, with no effect on the reversal potential or on the position of maximum sodium current. This is what is observed for the action of neutral anaesthetics such as ethanol[47], although charged anaesthetics sometimes cause shifts along the voltage axis.

As Fig. 3 shows, effects of increasing barrier height on

Fig. 3 Effect of external sodium ion concentration on peak sodium current as a function of barrier height G23 (kcalorie mol^{-1}), with internal 11.2 mM Na^+, 5 °C. The data are normalised to 100 for peak current with external 116 mM Na^+ and G23 = 5 kcalorie mol^{-1}. External Na^+ concentration: 1, 14.5 mM; 2, 58 mM; 3, 166 mM; 4, 200 mM.

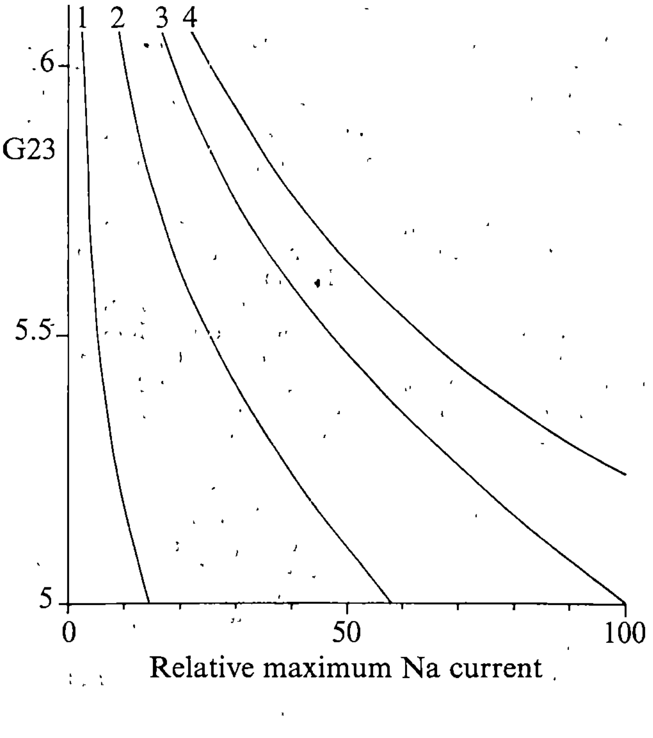

peak sodium current gradually decrease Thus the expected dose–response curve would be hyperbolic. The anaesthetic would have no effect until its concentration was sufficiently high to trigger a lipid phase transition for some of the lipid surrounding the sodium channel. This would make possible a partial relaxation of the channel, with an increase in the height of the energy barrier of the selectivity filter, and a corresponding large effect on sodium conductance. Increasing anaesthetic concentration would increase the proportion of surrounding lipid in the liquid-crystalline state and further increase the height of the energy barrier, but with a gradually lessening effect on sodium conductance. Although no detailed comparison is possible, published dose–response curves have this general form[48,49]. The data for Fig. 3 also show that the effect of changing the barrier height is more marked at high external sodium concentration than at low, although complete block of the sodium current occurs first at lower sodium concentrations. This latter observation has been confirmed experimentally by Condouris[50].

Received May 6, accepted July 6, 1976.

[1] Levinson, S R , and Meves, H., *Phil. Trans. R Soc.*, **B270**, 349–352 (1975).
[2] Hille, B., *J. gen Physiol.*, **59**, 637–658 (1972)
[3] Hille, B., *J. gen. Physiol* , **66**, 535–560 (1975)
[4] Ritchie, J. M., *Br. J Anaesth* , **47**, 191–198 (1975).
[5] Keynes, R. D , and Rojas, E , *J Physiol., Lond.*, **239**, 393–434 (1974)
[6] Staiman, A. L., and Seeman, P , *Can J. Physiol Pharmac.*, **53**, 513–524 (1975)
[7] Weidling, S , and Tegner, C , in *Progress in Medicinal Chemistry*, 3 (edit by Ellis, G. P., and West, G. B.), 332–398 (Butterworths, London, 1963)
[8] Deguchi, T , *Jap J Pharmac* , **17**, 267–278 (1967).
[9] Seeman, P , *Pharmac. Rev.*, **24**, 583–655 (1972)
[10] Seeman, P , *Experientia*, 30, 759–760 (1974).
[11] Spyropoulos, C. S , *J. gen Physiol* , 40, 849–856 (1957).
[12] Boggs, J M., Roth, S. M , Young, T , Wong, E , and Hsia, J C., *Molec. Pharmac.*, **12**, 136–143 (1976).
[13] Lee, A. G., *Prog. Biophys molec. Biol* , **29**, 3–56 (1975).
[14] Lee, A G., Birdsall, N. J. M , Metcalfe, J C , Warren, G. B., and Roberts, G. C. K., *Proc. R. Soc.*, **B193**, 253–274 (1976).
[15] Levine, Y K , *et al.*, *J. chem. Phys* , 60, 2890–2899 (1974).
[16] Boggs, J. M., Young, T., and Hsia, J C , *Molec Pharmac* , **12**, 127–135 (1976).
[17] Blaustein, M. P , and Goldman, D E., *J. gen. Physiol* , **49**, 1043–1063 (1966).
[18] Ray, A , Reynolds, J A , Polet, H , and Steinhardt, J , *Biochemistry*, **5**, 2606–2616 (1966).
[19] Jost, P. C., Griffiths, O. H , Capaldi, R. A., and Vanderkoi, G , *Proc natn. Acad Sci U S A* , **70**, 480–484 (1973)
[20] Hong, K., and Hubbell, W. L , *Proc natn Acad. Sci U S A.*, **69**, 2617–2621 (1972).
[21] Robinson, J. D , Birdsall, N J. M., Lee, A. G., and Metcalfe, J. C., *Biochemistry*, **11**, 2903–2909 (1972)
[22] Warren, G. B , Houslay, M D., Metcalfe, J C., and Birdsall, N J M., *Nature*, **255**, 684–687 (1975).
[23] Warren, G. B., Toon, P A , Birdsall, N. J M , Lee, A G., and Metcalfe, J. C., *Proc. natn. Acad Sci U.S.A* , **71**, 622–626 (1974).
[24] Keynes, R D , *Nature*, **239**, 29–32 (1972).
[25] Blaurock, A. E., and Stoeckenius, W , *Nature new Biol* , **233**, 152–156 (1971).
[26] Stier, A , and Sackmann, E., *Biochim. biophys Acta*, **311**, 400–408 (1973).
[27] Hill, M. W , *Biochim. biophys. Acta*, **356**, 117–124 (1974)
[28] Lee, A G , *Biochemistry* (in the press)
[29] Brink, F., and Posternak, J M., *J cell comp. Physiol.*, **32**, 211–233 (1948).
[30] Papahadjopoulos, D., Jacobson, K., Poste, G , and Shepherd, G , *Biochim. biophys Acta*, **394**, 504–519 (1975).
[31] Lee, A G., *Biochim. biophys Acta* (in the press).
[32] Jacobson, K , and Papahadjopoulos, D , *Biochemistry*, **14**, 152–161 (1975).
[33] Ito, T , Ohnishi, S-i, Ishinago, M., and Kito, M , *Biochemistry*, **14**, 3064–3069 (1975).
[34] Hille, B., Woodhull, A. M , and Shapiro, B. I , *Phil Trans R. Soc.*, **B270**, 301–318 (1975).
[35] Baker, P. F , *Prog Biophys molec. Biol* , **24**, 177–223 (1972)
[36] Brinley, F J., and Scarpa, A , *FEBS Lett* , **50**, 82–85 (1975)
[37] Frazier, D. T , Murayama, K., Abbott, N. J , and Narahashi, T., *Eur J Pharmac.*, **32**, 102–107 (1975).
[38] Connor, P , Mangat, B S , and Rao, L. S., *J. Pharm. Pharmac.*, **26**, 120P (1974).
[39] Lee, A. G , Birdsall, N. J. M , Metcalfe, J. C , Toon, P. A., and Warren, G. B., *Biochemistry*, 13, 3699–3705 (1974).
[40] Moore, J W., *Fedn Proc* , **17**, 113 (1958).
[41] Schoepfle, G. M., and Erlanger, J., *Am J. Physiol.*, **134**, 694–704 (1941)
[42] Schummer, U , Hegner, D , Schnepel, G H., and Wellhoner, H. H , *Biochim. biophys Acta*, **394**, 93–101 (1975)
[43] Davis, F. A., and Jacobson, S., *J Neurol Neurosurg Psychiat.*, **34**, 551–561 (1971).
[44] Hodgkin, A L , and Katz, B , *J Physiol , Lond* , **109**, 240–249 (1949)
[45] Inoue, I , Kobatake, Y , and Tasaki, I., *Biochim. biophys. Acta*, **307**, 471–477 (1973)
[46] Trudell, J. R., Payan, D. G , Chin, J H., and Cohen, E. N., *Biochim. biophys. Acta*, **373**, 141–144 (1974)
[47] Moore, J W , Ulbricht, W , and Takata, M , *J. gen Physiol* , **48**, 279–295 (1964).
[48] Wu, C H , and Narahashi, T , *J. pharm Pharmac.*, **184**, 155–162 (1973).
[49] Schauf, C. L., Davis, F A., and Kesler, R. L., *J. pharm Pharmac.*, **193**, 669–675 (1975).
[50] Condouris, G. A , *J pharm. Pharmac* , **131**, 243–249 (1961).

Dietary practices and growth responses as predictors of longevity

M. H. Ross & E. Lustbader

The Institute for Cancer Research, The Fox Chase Cancer Center, Philadelphia, Pennsylvania 19111

G. Bras

Pathologic Institute, Faculty of Medicine, University of Utrecht, Utrecht, The Netherlands

The longevity of rats permitted freedom of dietary choice can be predicted accurately solely on the basis of their dietary behaviour and growth responses early in life.

CHRONIC underfeeding of a complete diet is the only means known for increasing the length of life of homoeothermic laboratory animals beyond the limits characteristic for the species[1–8]. At the other extreme, chronic overfeeding, or other dietary excesses or imbalances, curtails lifespan[2–5,9,10]. For animals allowed freedom of dietary choice, a mode of feeding that approximates natural conditions, longevity correlates highly with both the amount and type of diet an animal elects to consume before mid-life[11]. Dietary practices during early life are particularly important. The quantity and composition of the diet determines in large part the progression of body weight changes throughout life. Growth rate and other body weight-related expressions should therefore also correlate with longevity[1,2,8,12–16]. We show here that there are, in fact, several parameters involving body weight that correlate more closely with lifespan than any of the dietary variables.

The dietary practices, body weight changes and duration of life of rats fed on a self-selection basis differ from individual to individual. In assessing the extent to which an animal's lifespan is directly linked with its dietary and growth behaviour, we began the analyses at a stage similar to that used by others working with fixed dietary regimens. Each lifespan-related trait was thus considered separately, but the variety and interdependence among these traits require a more complex treatment to understand their synergistic effects. Here, therefore, we have stressed the multiple variable approach for forecasting lifespan. We show that regardless of the proximate cause of death, there are combinations of specific conditions early in life which allow accurate prediction of an individual's lifespan.

Dietary and growth traits

Individually housed male Charles River COBS-CD rats were offered daily, throughout postweaning life, three complete purified isocaloric diets[17] in separate containers. The diets differed only in their protein and carbohydrate content. To ensure that each of the 121 rats in this study had sufficient freedom to exhibit its individual preference, the proportions of the protein and carbohydrate components of the diets

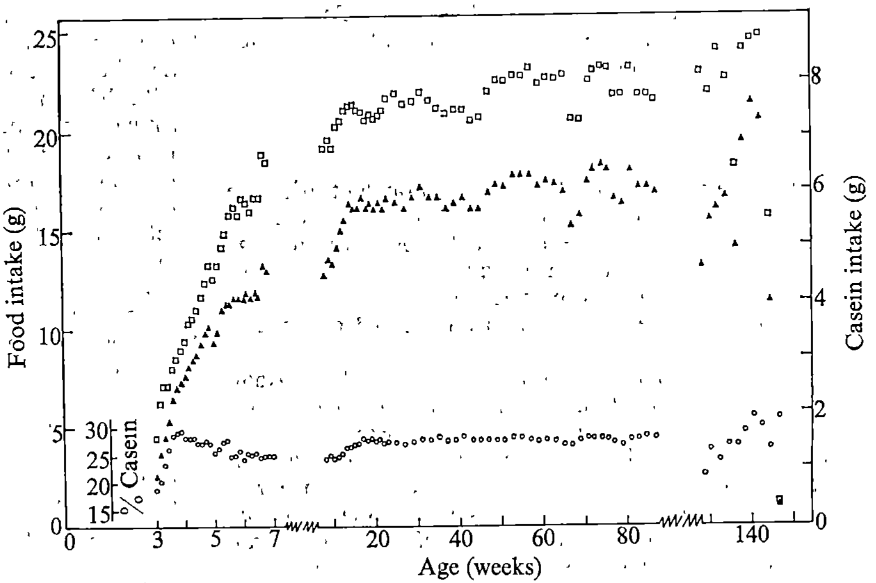

Fig. 1 Average food and protein intake of rats fed on a self-selection basis throughout life. □, Mean daily food intake; ▲, mean daily protein (casein) intake; ○, proportion of protein in the composite diet selected by the rats.

were set at 10 and 70.5%, 22 and 58.5%, and 51 and 29.5%. Vitamin-free casein, sucrose and corn oil (13.5%) were the sources of protein, carbohydrate and fat, respectively. The adequacy of the mineral (6%), vitamin and trace element content has been demonstrated earlier with conventionally fed animals[17–19]. The dietary history during gestation and suckling and the critical maintenance of constant environmental conditions have been described[17].

The absolute and relative intake of the diets differed; consequently, each rat selected a diet differing in quantity and composition In general, after an initial rapid increase in food intake (Fig. 1), the daily amount consumed remained relatively constant for a prolonged period. This phase persisted, for most of the rats, for as least 30 weeks.

The protein–carbohydrate content of the composite diet selected by some rats changed with age. A change in preference, if it occurred, was generally to diets of lower protein content and was detectable by the end of week 2 or 3 of feeding. At approximately 8 weeks of age, this trend reversed so that the diets subsequently chosen contained progressively higher percentages of protein. Beyond 4 months of age, the average protein content of the diet selected by some of these rats generally exceeded that preferred by rats whose preference had more or less stabilised within the first month. For the entire population, however, the average proportion of protein remained uniform throughout the greater part of life (Fig. 1).

The rats were weighed weekly, when they were also examined for gross signs of disease. No therapeutic measures were undertaken except for shortening excessively long incisors. The presence, type and severity of disease were based on histopathological assessment. These results have previously been reported[20].

The average changes in body weight with age are shown in Fig. 2. No two rats had identical rates of growth and durations of the growth period. The differences among the rats were further accentuated when body weight and changes in body weight were related to gross efficiency of food utilisation[18] and the quantity of food, or of protein, consumed relative to body weight.

The heavier the rat, the more food it tended to eat but, relative to body weight, the less food it consumed. The latter is explained by the fact that the heavier rats were generally more efficient than lighter, slower growing rats in

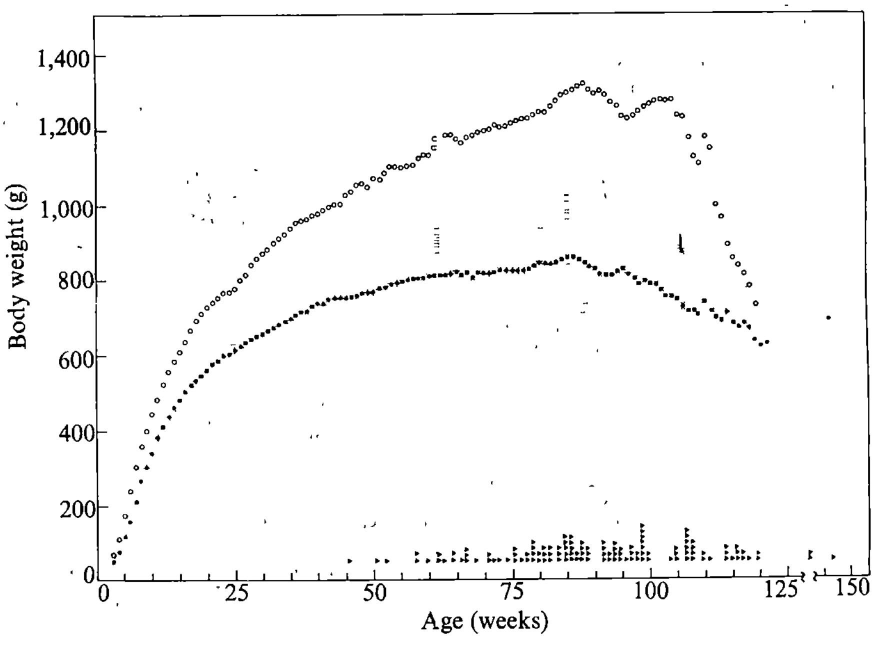

Fig. 2 Growth pattern of rats fed on a self-selection basis throughout life. ●, Mean body weight (shaded area represents 1 s.d. above and one below the mean); ○, heaviest weight attained by any individual; ▶, age at death of a rat. Irregularities in weight curves due to weight loss that generally precedes death.

converting what they consumed into body mass. The heavier rats thus tended to gain more weight than would be expected on the basis of food intake alone.

Correlation of individual variables with lifespan

The mean lifespan (632±125 d), population half life, age when most deaths occurred, and life expectancy[21] were in close agreement. The frequency distribution curve for age at death was nearly symmetrical and the age-specific mortality rates increased in a near-exponential manner. The age at death of the shortest lived rat was 314 d and the longest was 1,026 d (Fig. 2).

The correlation data are summarised in Table 1. Additional details on the relationships among lifespan and dietary practices have been presented elsewhere[12]. For most variables, significant associations were found relatively early in life and in all cases, before mid-life. In addition to differences in age when a correlation was first detected, the duration, direction and magnitude also differed. In general, the body weight variables correlated more closely with lifespan than did the dietary variables. The highest simple correlation values were obtained when lifespan was related to the number of days needed by the rat to reach a preassigned weight (Table 1). Of all the variables examined, only the maximum body weight attained during maturity did not correlate significantly with lifespan.

Combinatorial effects of diet and weight-related variables on lifespan

The simple correlation values presented in Table 1 represent only associations between pairs of variables; they do not imply causality. Furthermore, the interdependence among the parameters (Table 2) precludes ascribing to an isolated factor a direct connection to length of life. The correlation may be indirect, in that a variable might be closely associated with another factor that is directly related to lifespan. Since each variable has a unique period when it correlates with lifespan, there are added difficulties in interpreting simple correlation data. It is necessary, therefore, to determine how a number of variables interact and this can be best accomplished by construction of a model. If the mathematical model is accurate, it shows a dependence relationship and thereby allows the estimation of lifespan. Since countless factors can affect length of life, however, it would not be realistic to expect that the lifespan estimated from a mathematical model, based on a limited number of variables, would exactly match the observed lifespan. Deviations of the estimated lifespan from those observed represent errors; the smaller the error, the better a model explains the longevity data. Since on a simple correlation basis, nearly all the variables relate significantly with lifespan, model building was used to reveal the combination of factors that best explain the lifespan data. We applied the methods of Furnival and Wilson[22] to our problem and their usefulness lies in the fact that they minimise the total squared error[23]. When the best combination was identified, the relative importance of each variable was then determined by the least squares method[23] and expressed in terms of a multiple regression equation. In no case was a model acceptable unless the contribution of each factor was statistically significant ($P<0.05$). To compare models, the proportion of variance explained (R^2) was useful, in that it describes the extent to which the errors have been minimised.

The differences in length of life among the animals were best explained by a model that incorporated seven factors (see equation *a* in Table 3; the correlation matrix is given in Table 2). Four of these variables characterised the growth pattern and the remaining three defined the preference for protein and the efficiency with which the amount of food consumed is utilised for growth. Deletion of any one of

Table 1 Summary of simple lifespan correlation with dietary and body weight-related variables

Variable	Significant association (age and body weight limits) (d)	(g)	Maximum correlation coefficient* (r)	(P)
Food intake†(g)	49–372		−0.40	< 0.00001
Non-protein calorie intake†	49–309		−0.39	< 0.0001
Carbohydrate intake†(g)	49–299		−0.36	< 0.0001
Protein intake†(g)	43–49		0.18	< 0.05
Protein content of diet‡(%)	200–499		−0.27	< 0.01
	43–49		0.18	< 0.05
Body weight‡(g)	300–499		−0.21	< 0.05
	63–406		−0.43	< 0.00001
Weight gain‖(g)	49–294		−0.44	< 0.000001
Relative growth rates ‖ ¶	49–147		−0.28	< 0.01
Maximum body weight attained (g)	—	—	−0.07	< NS
Age to attain specified weight§(d)		300–600	0.46	< 0.000001
Age-independent body weight acquisition time**(d)				
for 100-g increments		200–300 to 500–600	0.48	< 0.000001
for body-weight doubling		200–400 to 300–600	0.49	< 0.0000001
Food intake per kg body weight††(g)	148–294		0.23	< 0.01
Protein intake per kg body weight‡(g)	43–49		0.22	< 0.05
Gain in weight, g per total food intake(g)	49–196		−0.29	< 0.001

*n = 120 or 121.
†Average daily intake for successive weekly intervals.
‡Computed for successive weekly intervals.
‖Computed for successive 7-week intervals.
¶Instantaneous relative growth rate (K)

$$= \frac{\log_e \text{weight}_2 - \log_e \text{weight}_1}{t_2 - t_1};\ t_2 - t_1 = \text{age in weeks}$$

§Computed for successive 100-g intervals.
**Age at weight$_2$−age weight$_1$.
††Value for each period represents the mean of a series of 7 successive weekly values:

$$\Sigma\left(\frac{\text{average daily intake for 1 week}}{\text{body weight at end of week}}\right)\Big/7$$

Table 2 Relationships between diet, body weight and lifespan

	Correlation matrix (r)*										
	Body weight† 119 d	Body weight† 133 d	Time to double weight‡	Age to attain specified weight‖	Daily food intake¶	Feed efficiency§	Protein intake**	Protein content of diet††	Protein intake per kg body weight¶¶	Length of life
Body weight at 119 d	1.000									
Body weight at 133 d	0.987	1.000								
Time to double weight‡	−0.755	−0.759	1.000							
Age to attain specified weight‖	−0 782	−0.777	0.992	1.000						
Daily food intake¶	0.751	0.790	−0.493	−0.485	1.000					
Feed efficiency§	0.438	0.466	−0.614	−0.558	0.211	1.000				
Protein intake**	0.300	0.269	−0.195	−0.255	0.150	−0.146	1.000			
Protein content of diet††	0.204	0.182	−0.167	−0.213	0.059	−0.006	0.924	1.000		
Protein intake per kg body weight¶¶	0.096	0.086	−0.120	−0.143	0.063	−0.018	0.900	0.922	1.000	
Length of life	−0.460	−0.455	0.481	0.455	−0.428	−0.331	0.226	0.216	0.255	1.000

*Level of significance (P) of correlation coefficient values (r); r values 0.18, not significant; r values 0.18–0.22, 0.23–0.28, 0.29–0.33, 0.34–0.39, . . . , correspond to $P < 0.05$, < 0.01, < 0.001, < 0.0001, . . . , respectively. One rat did not attain 500 g and protein intake data for the 43–49 -d period was not available for another because of excess spillage of food; correlation matrix and multiple regression analysis therefore based on $n = 119$.

†Body weight at 119 d, mean = 522 g (range: 298–665); at 133 d, mean = 549 g (range: 312–708).

‡Time (d) to double initial body weight of 250 g; mean = 64.2 (range: 33–399).

‖Age of animal (d) when it reached 500 g body weight; mean = 119 (range: 83–494).

¶Average daily food intake (g) between 14 and 21 weeks of age; mean = 21.0 (range: 15.5–25.7).

§ $\frac{\text{Body weight at 98 d} - \text{body weight at 49 d}}{\text{Total food intake (g) for same period}}$; mean = 0.26 (range: 0.13–0.31)

**Average daily protein intake (g) between 43 and 49 d of age; mean = 4.2 (range: 1.4–9.6).

††Average daily protein content of composite diet (%) selected between 43 and 49 d of age; mean = 24.4 (range: 10.1–49.2).

¶¶Average daily intake (g) between 43 and 49 d per kg body weight at 49 d; mean = 19.6 (range: 9–40).

these variables, or the substitution of any parameter with data representing other age or time periods, or weight changes, led to a less informative multiple regression equation. The addition of other variables to the model or logarithmic transformations of the data did not improve the fit either.

The seven variables acting in concert, accounted for 46% of the variance in the length of life (Table 3). In contrast, on the basis of simple correlation analysis, no single variable explained more than 24% of the variance. The data given in Table 3 show that the changes in body weight occurring long before the growth pattern had been completed accounted for the greater proportion of the explained variance in the duration of life.

The predictive capability of the multiple regression equation was evaluated by comparing the estimated length of life with the actual length of life. This form of analysis also served to identify major sources of error in the predictions. The average absolute error of 12% from the actual number of days lived indicated that, at the very least, a rat's lifespan can be predicted as being of short, intermediate or long duration.

An additional series of analyses were made to determine to what extent the elimination of several of the shortest lived rats would improve the model for the others. Only those rats that lived longer than 425 d, representing 95% of the population, were used to derive the 'conditional' regression equation *b* (Table 3). The small changes in the coefficient values from *a* to *b* resulted in estimated lifespans that more closely approximated actual lifespans. The increase from 46 to 52% in the proportion of variance explained was greater than would have been obtained by the application of equation *a* to the same animals.

These observations suggested that as the number of animals in the population decreased because of attrition, a prospective, step-wise redefining of the best association between the independent variables and lifespan for the survivors would increase the accuracy of lifespan estimate. This was confirmed as indicated by the conditional multiple regression equations *c* to *f* (Table 3).

The most precise estimate of lifespan was obtained for rats that survived more than 700 d (equation *f*), where the average absolute error was less than 4% and, moreover, only four variables were needed. With the exception of this subset of animals, the progressive reduction in the absolute error with the other conditional regression equations was not due to an increase in the degree to which the specific combination of variables correlated with lifespan. Rather, the apparent increase in accuracy was the result of reductions in the number of cases of extreme over- and underestimates. These adjustments, however, were not as critical as changes in the type and relative importance of the variables comprising the series of conditional regression equations. Thus, the information required to estimate lifespan of all the rats was not identical to that needed for a segment of the population The contribution of dietary preference and food efficiency data became progressively less important as the number of short and intermediate lived animals included in a cohort decreased Body weight-related variables, however, took on greater importance (Table 3). Thus, those animals that choose and efficiently utilise early in life a low-protein but otherwise adequate diet, and that complete the greater part of their growth by the time they are approximately 100 d old, will probably be the shortest lived members of the population At the other extreme, rats that grow slowly, particularly between 50 and 150 d of age. will more likely have extended lifespans.

In view of the lifespan-dependent changes in the number and type of variables, a single all inclusive equation cannot be expected to describe adequately the length of life of all the rats At best it represents a compromise. The underestimation of lifespan for long lived rats obtained when equation *a* was used, was partly the result of having included dietary variables. At the other extreme, the overestimation for the short lived rats probably resulted from inclusion of body weight variables. A retrospective analysis confined to the shortest lived rats (25% of the population) confirmed that the weight of the rat *per se* was not needed to estimat lifespan. The protein intake was replaced by the amou of carbohydrate consumed, but the age to reach 500 g

Table 3 Estimation of individual lifespan as determined from growth and dietary practices early in life (conditional multiple regression analysis)

				Coefficients of linear regression equation for estimating lifespan*							
	Fraction of population (%)	Range in lifespan (d)	Cohort size (no.)	Body weight 119 d (g)	Body weight 133 d (g)	Age at 500 g (d)	Body weight doubling time† (d)	Gross food efficiency†	Protein intake† (g)	Protein fraction of diet† (%)	Protein intake per kg body weight† (g)
(*a*)‡	100	317–1,026	119	−3.54	2.13	−7.51	9.41	1,634	59.90	−6.24	
(*b*)	95	425–1,026	113	−3.69	2.24	−7.84	9.71	1,820	56.76	−6.62	
(*c*)	85	500–1,026	101	−3.54	2.30	−6.36	8.00	1,389	51.96	−6.19	
(*d*)	70	575–1,026	83	−2.54	1.69	−5.27	6.66	747	14.26		
(*e*)	50	620–1,026	60	−2.75	2.28	−4.72	5.92				2.58
(*f*)	25	700–1,026	30	−3.87	3.54	−4.64	5.73				

			Statistical summary					
			Estimated compared with actual lifespan		Fraction of variance explained by			
	Fraction of population (%)	Correlation coefficient (r)	Mean standard deviation (d)	Absolute average error (%)	Weight + dietary factors (R^2)∥	Weight factors only (R_w^2)¶	Dietary factors only (R_d^2)	Contribution of weight factors to lifespan (%)§
(*a*)‡	100	0.680	±95	12.1	0.462	0.340	0.159	74
(*b*)	95	0.722	±81	10.2	0.521	0.400	0.152	77
(*c*)	85	0.711	±73	8.8	0.506	0.392	0.170	77
(*d*)	70	0.688	±68	7.5	0.473	0.405	0.169	86
(*e*)	50	0.691	±60	6.2	0.477	0.427	0.023	90
(*f*)	25	0.815	±43	3.8	0.665	0.665		100

*Coefficients for the linear regression equation of the form: Estimated lifespan $= -c_1$ (body weight at 119 d)$+c_2$(body weight at 133 d) $-c_3$(age at 500 g)$+c_4$(body weight doubling time)$+c_5$(gross food efficiency)$+c_6$(protein intake)$-c_7$(protein fraction of diet)$+c_8$(protein intake per kg body weight). Blank entry implies that the variable is not necessary in the equation.

Intercept coefficient±s.d. for equations *a*, *b*, *c*, *d*, *e* and *f*: 1,085±227, 1,113±196, 1,065±185, 1,026±187, 1,027±207 and 1,031±214, respectively.

†See footnotes of Table 2 for source of data and range of the values.

‡Equation designation.

∥All F values significant at $P<0.0001$.

¶R^2, coefficient of determination (proportion of variance explained).

§$(R_w^2/R^2)100$.

the time to double a body weight of 250 g were still significant lifespan predictors.

The sequential redefinition of the best combination of variables, therefore, afforded the only available means of improving the lifespan forecast over that obtained with a single mathematical model. The weighted, overall mean standard deviation from the actual lifespan determined by the step-wise application of the appropriate regression equation to each of the rats within a cohort, was ± 69 d This corresponded to an absolute error of 8% and the proportion of the variance explained approached 50%.

Comparison of fixed and self-selection regimens

In experimental studies using fixed diets, the changes in life expectancy and the frequency of age-related diseases attributable to chronic severe under-nutrition and excessive over-nutrition have stressed the influence of the quantity of food consumed[1–10]. Deviations in life expectancy and disease frequency that may occur among animals maintained on fixed diets differing in composition have also been interpreted to result in part from changes in appetite and therefore in intake of food or calories[7] These changes may accentuate or obscure the effects of a dietary component. With self-selection feeding, food intake data *per se* are not necessary to forecast duration of life. Useful information is however obtained from data which describe the composition of the diet, the efficiency with which it is used for growth purposes, and the manner in which age-dependent and age-independent changes in body weight occur The omission of caloric intake as an important factor which influences the rate of ageing should not be considered to be at variance with earlier conclusions Rather, it indicates that the interactions among lifespan-related factors provide other combinations of variables that are more revealing of future events. Some of these variables may be influenced by food intake. The absolute changes in body weights and time required to attain a specific weight act as substitute information for food intake. Body weight, which as an isolated variable correlated even more closely with lifespan than food intake, is also unnecessary, since these data are also incorporated in the absolute body weight changes and the time required to attain a specific weight.

A fixed diet high in protein and low in carbohydrate, when maintained throughout life, is associated with a higher life expectancy compared with that obtained with diets containing relatively lower levels of protein[17,24–26] With self-selection feeding, the proportion of protein in the diet early in life also correlates directly with lifespan, but later, the opposite condition prevails[11]. Only the protein–carbohydrate ratio of the diet selected early in life seems to be relevant in the context of the other variables. In the multiple regression equations *a*–*c*, however, the coefficient values for this variable are negative This does not indicate that a lower proportion of protein in the diet implies a longer lifespan Instead the negative value serves to moderate the effects on lifespan contributed by the absolute amount of protein consumed Thus, apart from the influence of the other variables, the magnitude of the life-shortening effect resulting from a low protein intake early in life is accentuated or minimised depending on the relative amount of protein in the diet selected. Analogous feedback systems are evident among the two pairs of variables in equation *a* that describe growth In both cases, one member of a pair exerts an influence opposite, but not of equal force, to that supplied by the other. ●

Since dietary intervention has been shown to modify longevity, regimens designed to conform with the dietary practices of long lived rats, may be effective in increasing lifespan The extent to which this type of dietary manipulation would be successful depends on the interactions among the specificity in dietary requirements of the individual, the stage of life when the new regimen is begun and the genetically determined growth potential. These interactions provide at least part of the explanation as to why there is such a high degree of variation in lifespan among animals maintained on a single fixed dietary regimen in identical environmental conditions.

Implications of long-lasting effects of early dietary and growth behaviour

The fact that 50% of the total variance in lifespan has been explained on the basis of early life dietary and dietary-related parameters, assigns to diet a major determinant function. No two rats are identical in their dietary preferences and growth characteristics; yet the long term interactions can be calculated with sufficient accuracy as to allow a close prediction of the duration of life of individual animals

All the weight-related data needed in the mathematical model can be obtained for nearly all the rats before 150 d of age. The dietary data can be obtained before they reach 100 d. The quantity of protein consumed and the protein–carbohydrate ratio of the diet selected during days 43–49 are most critical, since substitution of data obtained later greatly reduces the accuracy of the lifespan forecast.

The temporal specificity implies that the self-determined dietary habits and body weight changes during the mature phase have little bearing on lifespan This assumes that the same mode of feeding is kept throughout postweaning life and that essential constituents needed for life are always available. Additional persuasive evidence of the importance of the early dietary environment comes from fixed diet studies[10,18,24,27–31]. Certain forms of nutritional intervention limited to early life modify life expectancy and disease risk, whereas dietary intervention later in life may not result in the same degree or type of response We cannot, however, extend this proposal to include the role of dietary fat[26,28,32,33] and of the micronutrient[3,34,35] components, since their relative importance and age relationships were not investigated. Nevertheless, the temporal specificity demonstrated here raises the question whether, through a physiological imprinting mechanism, the variables serve as determinants or signals of an existing underlying programme of events to take place later in life The data obtained through short term self-selection studies indicating that dietary preference of young animals may have a genetic basis[36–39], supports the latter possibility Conversely, the compensatory changes in dietary preference associated with a variety of conditions that alter metabolism[40–46] supports the determinant view.

Throughout the greater part of life, the rats were vigorous, clean and free from symptoms of disease. At death, however, a pathological process could be assigned in nearly every case as a contributory or proximate "cause of death"[20] Tumours of different tissue origin occurring in many sites and other age-related affections of the lung, heart, kidney, and prostate were particularly prominent among the rats in this study The ability to make a long range lifespan forecast is therefore all the more remarkable, in that it incorporates differences in the age of onset and the rate of progression of one or more of the debilitating, fatal diseases It is difficult not to conclude that the individual specificity in early life conditions that govern lifespan are interwoven with those that regulate the susceptibility to several age-related diseases.

The models developed for rats maintained in an unvarying laboratory environment are not directly applicable to other mammals and probably not even for the same stock of rats living in natural conditions, experiencing many environmental forces. The feeding methods and analytical procedures are applicable, however, to other animals to determine whether the processes that regulate lifespan and disease susceptibility have common denominators and if so, to develop a model that is not restricted to one species The self-selection method of feeding also allows determination of the extent to which normal physiological or environmentally caused perturbations in appetite and growth at different ages modify length of life and disease risk. At the very least, our observation on the consequences of dietary habits and growth responses early in life have immediate relevance to questions concerned with the appraisal of nutritional adequacy, the relationship between diet and some diseases of age, and the mechanism of the ageing process.

Acknowledgements

We thank M Cahalan and L. Sweeny for their help in collecting and organising the data and M Schleifer for preparing and executing the computer programs. We are grateful to Amstar Corp., Best Foods, a division of CPC International, Hoffman–LaRoche Inc., Lederle Laboratories, Merck Institute for Therapeutic Research and Mead Johnson Co for donating some of the ingredients used in the diets. Supported in part by USPHS grants from the NIH and grants from the American Cancer Society, the Stichting Koningin Wilhelmina Fonds, and an appropriation from the Commonwealth of Pennsylvania.

Received January 19, accepted June 22, 1976.

1 McCay, C. M., Maynard, L. A., Sperling, G., and Barnes, L L , *J. Nutr* , **18,** 1–13 (1939)
2 Saxton, J. A., *Biol Symp.*, **11,** 177–196 (1945)
3 Silberberg, M., and Silberberg, R , *Physiol Rev* , **35,** 347–362 (1955).
4 Lane, P W , and Dickie, M. M , *J. Nutr* , **64,** 549–554 (1958).
5 Ross, M H , *Fedn Proc.*, **18,** 1190–1207 (1959).
6 Berg, B N., and Simms, H. S , *J. Nutr.*, **71,** 255–263 (1960).
7 Ross, M H., *J. Nutr* , **75,** 197–210 (1961).
8 Ross, M H., in *Current Concepts of Nutrition, Nutrition and Aging*, ch 3 (edit. by Winnick, M), 43–57 (John Wiley, New York, in the press)
9 Marks, H. H , *Bull N.Y. Acad. Med* , **36,** 296–312 (1960).
10 Stuchlikova, E , Juricova-Horakova, M., and Deyl, Z , *Expl Geront.*, **10,** 141–144 (1975)
11 Ross, M H., and Bras, G., *Science*, **190,** 165–167 (1975).
12 Robertson, T B , and Ray, L. A , *J biol. Chem* , **42,** 71–107 (1920)
13 Brody, S , in *Bioenergetics and Growth*, ch. 18 (Reinhold, New York, and Waverly, Baltimore, 1945).
14 Lansing, A. I , *J Geront.*, **2,** 327–338 (1947).
15 Everitt, A. V , and Webb, C., *J. Geront* , **12,** 128–134 (1957)
16 Evans, E , and Miller, D S., *Proc. nutr Soc* , **27,** 121–128 (1968).
17 Ross, M. H , and Bras, G., *J Nutr* , **103,** 944–963 (1973)
18 Ross, M H., and Bras, G., *J. natn Cancer Inst.*, **47,** 1095–1113 (1971).
19 Ross, M H , *Am. J clin. Nutr.*, **25,** 834–838 (1972).
20 Ross, M H , and Bras, G , *Nature*, **250,** 263–265 (1974)
21 Dublin, L I., Lotka, A. J , and Spiegelman, M., *Length of Life*, revised ed. (Ronald Press, New York, 1946).
22 Furnival, G. M , and Wilson, R. W., *Technometrics*, **16,** 499–511 (1974).
23 Daniel, C , and Wood, F. S , *Fitting Equations to Data* (Wiley-Interscience, New York, 1971).
24 McCay, C. M , Maynard, L. A., Sperling, G., and Osgood, H S , *J. Nutr* , **21,** 45–60 (1941)
25 Miller, D S , and Payne, P. R., *Expl Geront* , **3,** 231–234 (1968)
26 Fernandes, G , Yunis, E. J , Smith, J , and Good, R. A , *Proc. Soc. exp. Biol. Med* , **139,** 1189–1196 (1972)
27 Ross, M H., *Proc 7th Int. Congr. Nutr.*, **5,** 35–38 (Verlag Friedr Vieweg and Sohn GmbH , Hamburg, 1966).
28 Silberberg, R , and Silberberg, M., *Can J. Biochem. Physiol.*, **33,** 167–173 (1955).
29 Hartroft, W S , and Best, C. H , *Br. med. J.*, **1,** 423–436 (1949).
30 Wilson, R. B , and Newberne, P M , *Archs Path.*, **96,** 372–390 (1973)
31 Dahl, L. K., Heine, M , Leitl, G , and Tassinari, L., *Proc. Soc exp Biol. Med* , **133,** 1405–1408 (1970).
32 French, C E., Ingram, R H., Uram, J. A., Barron, G. P., and Swift, R W., *J Nutr.*, **51,** 329–340 (1953).
33 Silberberg, M , and Silberberg, R , *Am. J. Physiol.*, **177,** 23–26 (1954).
34 Pelton, R B , and Williams, R J , *Proc. Soc exp Biol Med* , **99,** 632–633 (1958)
35 Campbell, H. L., Pearson, C. S , and Sherman, H. C., *J. Nutr* , **26,** 323–325 (1943).
36 Mayer, J , Dickie, M. M., Bates, M. W., and Vitale, J. J , *Science*, **113,** 745–746 (1951).
37 Mayer, J., Bates, M. W , and Dickie, M M., *Science*, **113,** 746–747 (1951).
38 Valenstein, E. S , Kakolewski, J W , and Cox, V. C , *Science*, **156,** 942–943 (1967)
39 Thiel, A , Schemmel, R., Mickelsen, O., Johnson, J. T., and Gill, J. L , *Nutr. Rep Int* , **5,** 101–110 (1972)
40 Richter, C P , in *The Psychology of Curt Richter, Part II* (edit. by Blass, E. M.), 194–226 (York, Baltimore, 1976).
41 Griffiths, W. J , Jr, *Ann N.Y Acad. Sci.*, **67,** 1–10 (1956)
42 Jacobs, H L , *J comp Physiol Psych* , **51,** 304–310 (1958)
43 Donhoffer, S., *Triangle*, **4,** 233–239 (1960)
44 Appledorf, H , and Tannenbaum, S. R , *J. Nutr.*, **92,** 267–273 (1967).
45 Harper, A E , in *Handbook of Physiology*, ch 29 (edit by Code, C F , and Heidel, W), 399–410 (American Physiological Society, Washington, 1967).
46 McConnell, S. D., and Henkin, R. I., *Proc. Soc. exp. Biol Med.*, **143,** 185–188 (1973)
47 Peng, Y , Meliza, L. L., Vavich, M. G., and Kemmerer, A. R., *J. Nutr.*, **105,** 1395–1404 (1975).

gag Gene of mammalian type-C RNA tumour viruses

Mariano Barbacid, John R. Stephenson & Stuart A. Aaronson
Laboratory of RNA Tumor Viruses, National Cancer Institute, Bethesda, Maryland 20014

The translation product of the gag *gene of mammalian type-C RNA viruses is a 65,000–68,000 molecular weight precursor polypeptide (Pr65) whose cleavage leads to the formation of four virion proteins, p30, p15, p12 and p10. An immunological approach has been used to establish the arrangement of the sequences coding for these proteins within the viral genome as (5′) p15–p12–p30–p10 (3′).*

TYPE-C RNA viruses have been implicated as causative agents of leukaemias and sarcomas in many vertebrates. A genetic approach to the understanding of type-C virus-coded functions may be useful in determining the mechanisms of replication and transformation by these agents. It is well established that translational products of the viral genome include a reverse transcriptase, envelope glycoprotein, and several lower molecular weight proteins[1], some of which are known to be synthesised as part of a precursor polypeptide[2–7]. The regions of the viral genome coding for these functions have been termed *pol, env,* and *gag* genes, respectively[8]. Another gene, designated *src* (ref. 9), has been identified in transforming type-C viruses of avian and mammalian origin. Evidence obtained by the isolation of conditional and non-conditional mutants of sarcoma viruses indicates that the translation product(s) of the *src* gene are involved in cell transformation (for review, see refs 10–12). Whether type-C viruses, which do not transform fibroblasts in culture but induce lymphoid tumours *in vivo,* contain genes analogous to *src* responsible for lymphoid cell transformation is not yet known.

Among approaches used in attempts to sequence the type-C viral genome, the oligonucleotide fingerprint method has been useful in mapping regions near the poly(A)-containing 3′ end of the genome. Analysis of deletion mutants of avian sarcoma viruses by this method has led to mapping of the *env* and *src* genes[9,13]. Information concerning the composition and partial sequence of the avian *gag* gene has been obtained by techniques involving immunoprecipitation of pulse-labelled polypeptides synthesised by pactamycin-treated cells[14]. There is as yet no evidence concerning the genetic sequence of mammalian type-C viruses. There are, however, reports in which immunoprecipitation techniques have been used to detect a variety of intermediate precursor polypeptides involved in the synthesis of mature virion components[6,15].

A different approach to the definition of the composition and sequence of type-C virus-coded genes takes advantage of highly sensitive and specific competition radioimmunoassays for detection and identification of the known structural components of various mammalian type-C viruses. By such procedures, it has recently been shown that one class of temperature-sensitive mutants of Rauscher-murine leukaemia virus (MuLV) is restricted at the non-permissive temperature in cleavage of a precursor polypeptide[4]. We report here an analysis of the size and composition of this viral precursor polypeptide and of its partial cleavage-products. Analogous studies have been performed with cells infected with several naturally-occurring mammalian transforming type-C viruses, that express different numbers of type-C viral structural proteins[16–18]. The present studies make it possible to establish tentatively the components of the *gag* gene of mammalian type-C viruses, as well as to determine its genetic sequence.

Proteins coded by *gag* gene

Table 1 summarises some of the biochemical and immunological properties of type-C viral proteins for which competition immunoassays were performed. These proteins include gp70 (refs 19, 20), p30 (ref. 22), p15 (ref 23), p12 (refs 17), and p10 (ref. 24). Each has been demonstrated to be immunologically distinct from the others and to retain its antigenic characteristics when the virus is grown in cells of different species, indicating that each represents a mature translational product of the viral genome. In the first series of experiments, the distribution of these viral proteins was examined in extracts of NIH/3T3 mouse cells infected at the permissive (31 °C) or non-permissive (39 °C) temperature with *ts25,* a Rauscher-MuLV mutant defective in precursor polypeptide cleavage[4]. Post-microsomal cell extracts were subjected to Agarose gel filtration under denaturing conditions (6 M GuHCl). As shown in Fig. 1*A*, the antigenic reactivities of viral proteins in extracts of cells infected at 31 °C, eluted at molecular weight regions corresponding to those of each of the respective mature proteins isolated from intact virions.

When the same cells were infected at 39 °C instead, antigenic reactivities corresponding to all four proteins, p30,

Table 1 Biochemical and immunological characteristics of type-C viral structural proteins*

Viral protein†	Molecular weight ($\times 10^{-3}$) (6 M GuHCl)	Phosphocellulose elution (*p*H 6.5)	Primary antigenic determinants	Other characteristics
gp70	69–71‡	0.1–0.2 M KCl	Type, group, interspecies	Envelope glycoprotein; involved in neutralisation
p30	28–31	0.3–0.4 M KCl	Group, interspecies	Major internal antigen
p15	15–17	0.4–0.5 M KCl	Type, group, interspecies	High tendency to aggregate
p12	11–12	Not bound	Type, group	Phosphoprotein
p10	8–10	0.6–0.8 M KCl	Group, interspecies	Found in ribonucleoprotein complexes

*The data presented in this Table have been summarised from refs 1, 41–43.
†Designated according to convention[40].
‡Determined by sodium dodecylsulphate–polyacrylamide gel electrophoresis.

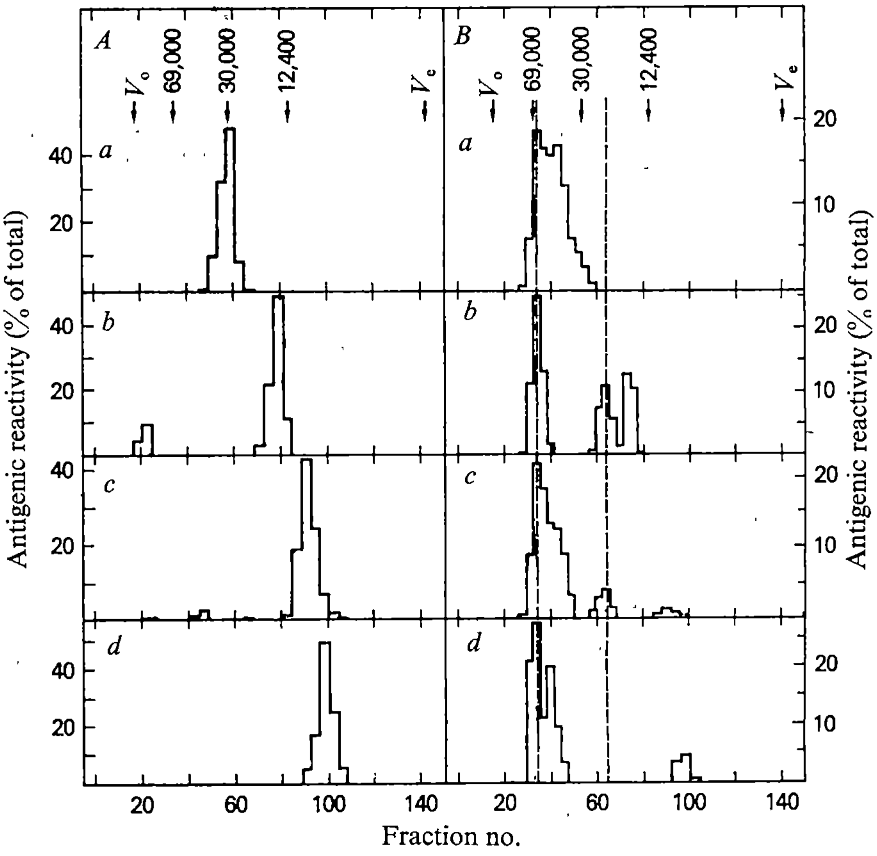

Fig. 1 Molecular sizing chromatography of Rauscher-MuLV, *ts*25 mutant, grown in NIH/3T3 mouse cells at: *A*, the permissive temperature (31 °C), and, *B*, the restrictive temperature (39 °C). Twenty milligrams of the post-microsomal fraction of *ts*25-infected NIH/3T3 cells were lyophilised and resuspended in a 50 mM Tris-HCl *p*H 8.0 buffer containing 8 M guanidine-HCl (GuHCl), 1 mM EDTA and 20 mM of freshly prepared dithiothreitol. After 30 min incubation at 37 °C, the sample was applied to an A-5 Agarose (100–200 mesh, BioRad) 1.5 × 90 cm column equilibrated with a 6 M GuHCl solution containing 20 mM dithiothreitol, adjusted to a final *p*H of 6.5 units. The sample was chromatographed at room temperature at a flow rate of 1.6 ml h^{-1} with a head pressure of 15 cm. Fractions (0.5 ml) were collected, and exhaustively dialysed at 4 °C for 36 h against a 10 mM Tris-HCl *p*H 7.8 buffer containing 100 mM NaCl, 0.5 mM EDTA and 0.1 % Triton X-100. Samples were tested at twofold serial dilutions in homologous competition radioimmunoassays for Rauscher-MuLV: *a*, p30; *b*, p15; *c*, p12; and *d*, p10 proteins, as described in Table 2. Results are expressed as the percentage of total antigenic reactivity. Molecular weight standards, chromatographed along with the sample, included ^{125}I-labelled bovine serum albumin (69,000), ^{125}I-labelled Rauscher p30 (30,000), cytochrome *c* (12,400) and ^{125}iodine (125). The vertical dotted lines indicate the chromatographic positions of Pr65 and Pr25 precursor polypeptides.

p15, p12, and p10, migrated as a 65,000–68,000 molecular weight precursor polypeptide termed Pr65 (Fig. 1*B*). No reactivity corresponding to any of these proteins was detectable at any higher molecular weight, indicating that if Pr65 is initially synthesised as a precursor polypeptide with a molecular weight greater than 65,000, it must be efficiently cleaved. The size of Pr65 would seem to account for not more than the entire translational information of the four viral proteins coded for by the *gag* gene of Rauscher-MuLV.

The results in Fig. 1*B* also indicate the existence of polypeptides containing p30, p15, p12 and p10 antigenic determinants, and possessing molecular weights less than 65,000. These results suggest that even at the restrictive temperature some precursor cleavage takes place in cultures infected with *ts*25 mutant. It was reasoned that systematic analysis of such intermediate cleavage products should provide information concerning the virus maturation process. More importantly, this approach might also provide evidence needed for mapping of individual proteins within the viral genome. For example, the detection of a 23,000–26,000 molecular weight polypeptide containing p15 and p12 antigenic determinants (Fig. 1*Bb* and *c*), suggested that these proteins were located at adjacent positions within the Pr65 precursor polypeptide. Further, antigenic reactivities of p30, p12 and p10 but not of p15 were found in polypeptides eluting in the 40,000 to 60,000 molecular weight region of the guanidine HCl column. In combination with findings of relatively higher levels of mature p15 compared with the other viral proteins, the above data suggested that p15 might be located at a terminal position in the *gag* gene translational product.

Use of mammalian sarcoma virus-transformed cells in sequencing type-C viral genes

Mammalian sarcoma viruses are defective in functions needed for their replication as infectious viruses (for review, see ref. 12). Helper functions including the viral envelope and reverse transcriptase are conferred by a type-C helper leukaemia virus, invariably present in sarcoma virus stocks. Molecular hybridisation studies have indicated that mammalian sarcoma viruses do contain some helper virus genetic sequences[25,26]. In fact, several sarcoma viruses express specific helper viral proteins immunologically detectable in transformed cells[16,18]. That these properties are genetically stable[18,27,28] provides independent evidence of the association of helper viral sequences with these transforming viral genomes. The viruses analysed here included the S$^+$L$^-$ (ref. 16) variant of Moloney-murine sarcoma virus (MSV), a natural sarcoma virus isolate from the BALB/c mouse[29], designated BALB-MSV, and a sarcoma virus isolated from the woolly monkey[30], designated woolly monkey sarcoma virus (WSV). Another virus, the Abelson-murine leukaemia virus (Abelson-MuLV), which induces lymphomas rather than sarcomas[31], was also examined Like the S$^+$L$^-$ Moloney-MSV, this virus transforms fibroblasts in culture and is defective for replication[32] The origins and designations of cell lines transformed by each virus are summarised in Table 2.

The specific antigenic determinants of viral proteins expressed by S$^+$L$^-$ Moloney-MSV and Abelson-MuLV-transformed cells were found to be those of Moloney-MuLV by analysis in radioimmunoassays for type-specific antigenic determinants of p12 and p15 viral proteins, while BALB-MSV transformants expressed antigens specific for a mouse cell tropic helper leukaemia virus indistinguishable from AKR-MuLV by these techniques (data not shown). WSV-transformants contained antigens specific for the woolly monkey helper virus[18]. Thus, each transformed cell line and its appropriate uninfected parental line were compared for reactivity in immunoassays for proteins of the specific helper virus in question (Table 2). Uninfected human and rat cells showed no detectable reactivity in any of the assays used (<10 ng of viral antigen per mg cellular protein) Mouse cells that are known to express antigens of their endogenous viruses[33–35] were, however, cross

Table 2 Patterns of type-C viral antigen expression in cells infected with different mammalian transforming viruses

Transforming virus	Transformed cells			Levels of viral protein* (ng of antigen per mg cell extract)				
	Species	Designation	Reference	gp70	p30	p15	p12	p10
NP Moloney-MSV	Mouse	M-NIH	27	<20	<10	<10	<10	<40
	Rat	M-NRK	27	<10	<10	<10	<10	<10
$\mathrm{S^+L^-}$ Moloney-MSV	Mouse	D56	16	80†	700	1,700	1,300	<40
	Rat	$\mathrm{S^+L^-}$-NRK	27	<10	800	1,500	1,300	<10
	Human	HuACl$_1$	44	NT‡	2,000	4,500	3,900	<10
	Rat	$\mathrm{S^+L^-}$-NRK infected with Moloney-MuLV		3,300	7,600	4,100	3,700	3,400
Abelson leukaemia virus	Mouse	ANN-1	32	<20	<10	1,900	1,100	<40
BALB-MSV	Rat	MAI-3206	Unpublished	<10	<10	600	400	<10
Woolly monkey sarcoma virus	Rat	WSV Cl 9	18	<10	<10	NT	<10	<10
	Rat	WSV Cl 11	18	<10	100	NT	100	100
	Rat	WSV Cl 9 infected with woolly monkey helper virus		6,100	5,100	NT	3,400	3,700

Viral structural proteins of Rauscher-, Moloney- and AKR-MuLV as well as from the woolly monkey helper virus isolate were purified to apparent homogeneity by a combination of ion exchange and molecular sizing chromatographic techniques as described[20,24]. These included the gp70, p30, p12 and p10 viral proteins of all the four viruses as well as the p15 protein of Rauscher- and Moloney-MuLV. High specific activity ^{125}I-labelling of these proteins was achieved by the chloramine T method[45]. After three cycles of freezing and thawing cells were sonicated for 1 min (Biosonic II sonic oscillator) in a 10 mM Tris-HCl *p*H 7.8 buffer containing 100 mM NaCl, 0.5 mM EDTA and 0.5% Triton X-100, and centrifuged for 2 h at 100,000*g*. The final supernatant was divided into aliquots and stored at −70 °C. These post-microsomal fractions were tested at twofold serial dilutions in the appropriate competition radioimmunoassays for their ability to displace the ^{125}I-labelled viral antigen for binding limiting amounts of goat antiserum raised against homologous virus purified on sucrose gradients. Antiserum and unlabelled competing antigen were incubated at 37 °C for 1 h in a 0.15 ml reaction mixture containing 10 mM Tris-HCl *p*H 7.8, 10 mM EDTA, 0.4% Triton X-100, 1% bovine serum albumin, 0.1% normal goat serum and 10 mM NaCl (p30, p12 assays) or 300 mM NaCl (gp70, p15 and p10 sasays). Around 10,000 c.p.m. of ^{125}I-labelled antigen contained in 0.05 ml of the same buffer were added and incubation continued for 3 h at 37 °C and a further 18 h at 4 °C. Following the addition of 0.025 ml of undiluted swine anti-goat immunoglobulin G to each tube to precipitate the antigen–antibody complexes, reaction mixtures were incubated for 1 h at 37 °C and 3 h at 4 °C. Finally, 1 ml of cold 10 mM Tris-HCl *p*H 7.8 buffer containing 100 mM NaCl and 0.1% Triton X-100 was added to each tube, samples were centrifuged (2,500 r p m for 15 min), supernatants were aspirated, and the radioactivity in the precipitates measured in a Searle gamma counter Model 1285. The results were calculated on the basis of the displacement of the complete competition curve for the unknown relative to that achieved with the corresponding purified viral antigen. Protein concentrations were determined according to Lowry *et al.*[46] using bovine serum albumin as standard.

*Moloney sarcoma- and Abelson leukaemia virus-transformed cells were tested in homologous immunoassays for Moloney-MuLV proteins. MAI 3206 was assayed in the AKR-MuLV homologous assays except for p15, where anti-AKR-MuLV: ^{125}I-Rauscher p15 was utilised. Finally, woolly monkey sarcoma virus-transformed cells were tested in immunoassays for woolly monkey helper virus proteins. Controls for the specificity of each immunoassay included homologous assays for the analogous protein of at least one immunologically distinct type-C virus as well as for the p30s of avian myeloblastosis and RD114 viruses

†Slightly raised levels of gp70 were observed only in $\mathrm{S^+L^-}$ Moloney-MSV-transformed mouse cells. This gp70 was, however, found to contain type-specific antigenic determinants of an endogenous mouse type-C virus[47] (data not shown). These findings together with the lack of detectable gp70 in $\mathrm{S^+L^-}$ NRK rat cells indicate that this gp70 is not coded for by the $\mathrm{S^+L^-}$ Moloney-MSV genome.

‡N.T., Not tested.

reactive at low levels (<50 ng of viral antigen per mg cellular protein) in assays for Moloney-MuLV gp70 and p10 proteins. Therefore, these were subtracted from values obtained with each virus-transformed mouse cell line. As a positive control, virus-transformed cells productively infected with the appropriate helper virus produced high levels of each of the five viral antigens tested.

As shown in Table 2, none of the transformants analysed produced significant amounts of the envelope glycoprotein. gp70. In the analysis of *gag* gene products, several different patterns of expression were observed. For example, cells transformed by the non-producer (NP) variant of Moloney-MSV and by one genetically stable variant of WSV (WSV Cl 9), demonstrated no antigen expression above the levels observed in uninfected parental cells. In contrast, mouse, rat or human cells transformed by the $\mathrm{S^+L^-}$ variant of Moloney-MSV expressed high levels of three Moloney-MuLV proteins, p30, p15 and p12. The production of the same antigens in cells of different species strongly indicates that they are coded by the virus. The fact that p10 was the only missing protein among the Moloney-MuLV *gag* gene products expressed by $\mathrm{S^+L^-}$ Moloney-MSV-transformed cells suggested that this low molecular weight protein might be located at the carboxy-terminal end of the *gag* gene precursor polypeptide.

BALB-MSV and Abelson-MuLV transformants demonstrated high levels of p15 and p12 viral proteins in the absence of p30 or p10, indicating that p30 is the viral protein in closest proximity to p10 These results do not establish the positions of p15 and p12 viral proteins with respect to each other. The presence of *ts*25 Rauscher-MuLV-infected cells of a 23,000–26,000 molecular weight intermediate cleavage product containing both antigens, along with the results presented in Table 2, suggests, however, that p15 and p12 occupy adjacent positions at the amino-terminal region of the *gag* gene translational product.

Transformants of one WSV variant (WSV Cl 11) expressed readily detectable levels of p10 in addition to p30 and p12 woolly monkey helper virus proteins. The unavailability of a radioimmunoassay for woolly monkey viral p15 made it difficult to establish directly the presence of this antigen. The cells were, however, found to express a 65,000–68,000 molecular weight polypeptide containing p30, p12 and p10 and another of 23,000–26,000 molecular weight, possessing p12 but not p30 or p10 (data not shown). Their sizes are evidence that these polypeptides are analogous to those found in Rauscher-MuLV-infected cells and, therefore that p15 is present in both polypeptides. Thus, the WSV Cl 11 transforming virus seems to contain sequences accounting for the entire helper viral *gag* gene.

p15 is the amino-terminal protein of the *gag* gene translational product

In an attempt to determine the relative position of p15 and p12 within the *gag* gene Pr65 product, the molecular size distribution of individual viral antigens was examined in cell extracts of certain of the mouse virus-transformed cell lines described above. The results presented in Figs 2–4 demonstrate the existence of high molecular weight precursor polypeptides as well as several intermediate cleavage products containing *gag* gene-coded structural proteins. Each transformant exhibited a 23,000–

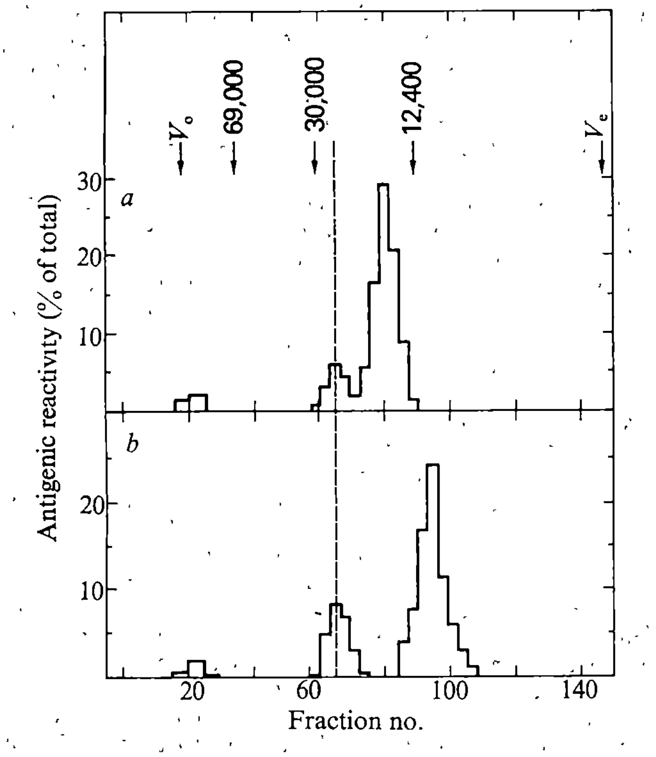

Fig. 2 Molecular sizing chromatographic analysis of helper leukaemia virus-specific antigens expressed in BALB-MSV-transformed rat cells. Twenty-five milligrams of a post-microsomal fraction were submitted to gel filtration chromatography under denaturing conditions as described in the legend to Fig. 1. Dialysed fractions were tested at twofold serial dilutions in the following competition radioimmunoassays: *a*, anti-AKR-MuLV ^{125}I-Rauscher-MuLV p15 assay; and *b*, anti-AKR-MuLV: ^{125}I-AKR-MuLV p12 assay. Results are expressed as percentages of total antigenic reactivity. Molecular weight standards are those described in the legend to Fig. 1. The vertical dotted line represents the chromatographic position of the Pr25 precursor polypeptide.

26,000 molecular weight precursor polypeptide (Pr25) containing p15 and p12 viral proteins analogous to the intermediate cleavage product of the Rauscher-MuLV *ts*25 mutant (Fig. 1*B b* and *c*) The identification of this polypeptide as a precursor to p15 and p12 was particularly obvious in BALB-MSV (Fig. 2) and Abelson-MuLV (data not shown) transformed cells that lacked either p30 or p10. These findings indicate that sequences coding for p15 and p12 occupy adjacent positions within the viral genome.

Analysis of S$^+$L$^-$ Moloney-MSV-transformed mouse cells revealed the presence of additional intermediate cleavage products involved in the synthesis of viral antigens (Fig. 3). These included a 58,000–62,000 molecular weight precursor polypeptide (Pr60) containing p30, p15, and p12 but not p10 and a 43,000–47,000 molecular weight precursor polypeptide (Pr45) containing p30 and p12 antigens in the absence of p15 or p10. The finding that Pr60 lacks only p10 provides further evidence that this low molecular weight protein occupies the carboxy-terminal position in the complete *gag* gene-coded precursor polypeptide. Moreover, the detection of a precursor containing p30 and p12 (Pr 45), but lacking p15, argues for the adjacent location of p30 and p12 within the *gag* gene product. As shown in Fig. 4, the results obtained with S$^+$L$^-$ Moloney-MSV-transformed human cells provide additional evidence supporting this possibility. Cell extracts of this transformant contained proportionally less Pr60 but demonstrated considerably increased amounts of the Pr45 intermediate cleavage product containing p30 and p12, but not p15.

The identification of the intermediate cleavage products, Pr25 and Pr45, led to the establishment of two pairs of adjacent proteins, p15–p12 and p12–p30, respectively. These findings imply that p12 is located between p15 and p30. Moreover, since p30 is missing in BALB-MSV- and Abelson-MuLV-transformed cells that express p15 and p12, the location of p15 must be at the amino terminal end of the *gag* gene translational product.

Sequence and tentative mapping of the *gag* gene

The present evidence utilising a Rauscher-MuLV *ts* mutant blocked in precursor polypeptide cleavage indicates that the *gag* gene translational product (Pr65) contains the major internal protein, p30, as well as the low molecular weight proteins, p15, p12, and p10 (Fig. 1). Moreover, analysis of the expression of helper virus-coded proteins in cells infected with replication-defective transforming viruses revealed that p10 is the carboxy-terminal protein of the *gag* gene-coded precursor polypeptide, and that p30 is adjacent to it (Table 2). Analysis of intermediate cleavage products of the Pr60 polypeptide provided information necessary for the relative positioning of p15 and p12 (Figs 3 and 4). These results led to the following sequence of the *gag* gene product: NH_2–p15–p12–p30–p10–COOH. Since the viral RNA genome is the positive strand[36], the genetic information contained in the *gag* gene would then be arranged in an identical manner from the 5′ to 3′ end of the RNA molecule. A summary of these findings is presented in Fig. 5.

The sequence of the mammalian type-C viral *gag* gene was deduced from analysis of a conditional lethal mutant of mouse leukaemia virus defective in precursor polypeptide

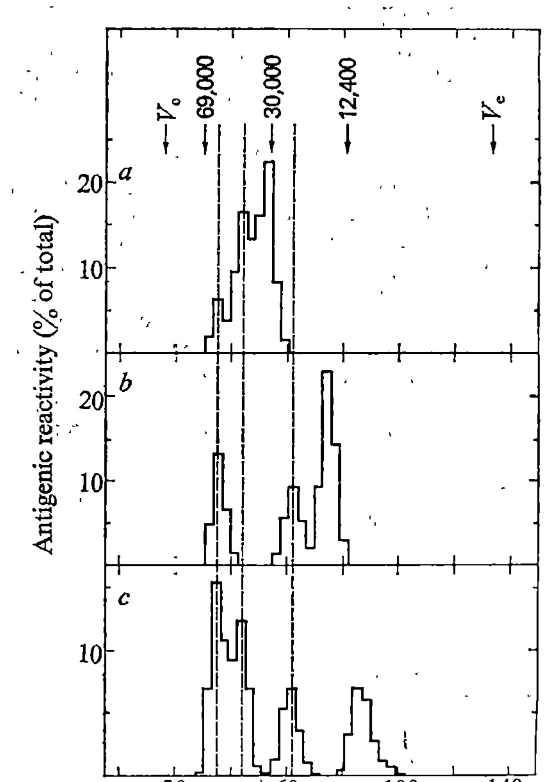

Fig. 3 Molecular sizing chromatographic analysis of helper leukaemia virus-specific antigens expressed in S$^+$L$^-$ Moloney-MSV transformed mouse cells. Twenty mg of a post-microsomal fraction were submitted to gel filtration chromatography under denaturing conditions as described in the legend to Fig. 1. Samples were tested in homologous competition radioimmunoassays for Moloney-MuLV: *a*, p30; *b*, p15; *c*, p12; proteins as described in Table 2. Results are expressed as the percentage of total antigenic reactivity. Molecular weight standards are those described in Fig. 1. The vertical dotted line indicates the elution positions of Pr60, Pr45, and Pr25 *gag* gene-coded precursor polypeptides.

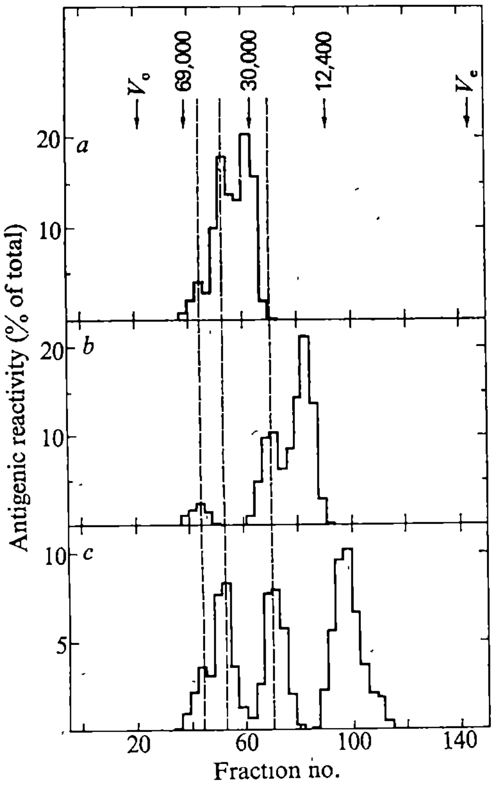

Fig. 4 Molecular sizing chromatographic analysis of S^+L^- Moloney-MSV-transformed human cells. The analysis of Moloney-MuLV helper antigens was performed as indicated in Fig. 3. Vertical dotted lines represent the elution positions of Pr60, Pr45 and Pr25 *gag* gene-coded precursor polypeptides.

cleavage and several independent isolates of replication-defective transforming viruses. These viruses contain stably-associated genetic information of their respective helper leukaemia viruses. Specific patterns of expression of *gag* gene helper viral proteins were demonstrated in cells infected with these transforming viruses. In each case, the size of the highest molecular weight precursor polypeptide corresponded to that expected for a helper leukaemia viral precursor containing only those *gag* gene translational products. Furthermore, the intermediate cleavage products detected in cells infected with each transforming virus were analogous to those detected in cells infected with the conditional lethal mutant of MuLV. The final cleavage products were also identical in sizes and immunological properties to the mature viral proteins of the helper leukaemia virus. These findings all argue against any drastic rearrangement of *gag* gene sequences in sarcoma as opposed to helper leukaemia viruses.

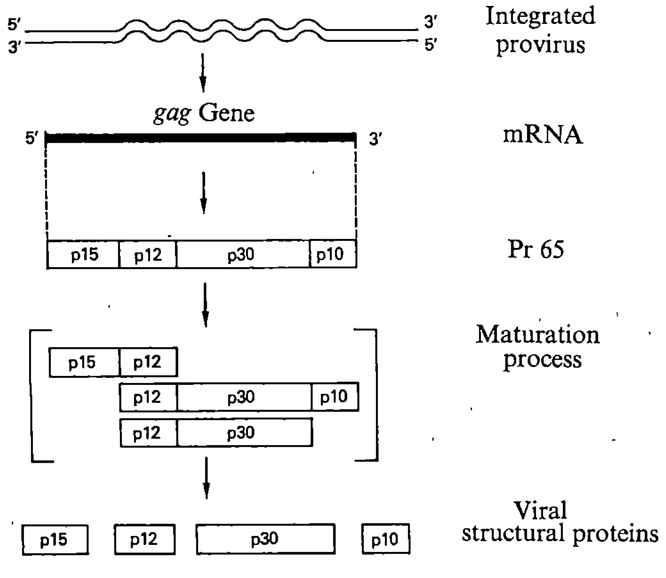

Fig. 5 The sequence and maturation process of the *gag* gene translational product of mammalian type-C RNA viruses.

Our studies of several independent isolates of transforming viruses were consistent with only one possible ordering of *gag* gene sequences on the basis of the above reasoning. Thus, if this gene order were to result from some alteration of the *gag* gene normally present in the helper leukaemia virus, this alteration must be highly specific The ability of different genetic variants of the same transforming virus to transform cells does not seem to be affected by whether they express particular *gag* gene products[18,27]. Thus, the possibility of a specific genetic rearrangement of *gag* gene sequences having any functional significance in the transforming virus seems highly unlikely. Instead, the evidence strongly argues that the *gag* gene sequence as deduced from studies of defective mammalian transforming viruses represents the *gag* gene sequence of the helper leukaemia virus.

With avian type-C viruses, a different experimental approach has led to the following partial sequence of the avian *gag* gene 76,000 molecular weight translational product: NH_2–p19–(p12–p27)–p15–COOH (ref. 14). The position of p12 with respect to p27 is not resolved. Moreover, another low molecular weight protein, p10 (ref. 37) has not been identified within this precursor. Mapping studies of *gag* gene may make it possible to assign similar functions to viral proteins of avian and mammalian type-C viruses on the basis of their positions within their respective viral RNA genomes.

Genetic mapping of *env* and *src* genes at the 3′ end of the avian sarcoma viral genome[9,15] leaves only the *gag* and *pol* genes among the known viral genes that may exist at the 5′ end of the genome. The present evidence does not make it possible to assign the position of the *gag* gene within the mammalian type-C viral RNA molecule. When helper leukaemia viral translational products were detected in the virus transformed cells studied here, however, they invariably included *gag* gene products in the absence of detectable glycoprotein (Table 2). Moreover, one cell line tested, a S^+L^- Moloney MSV transformant of human origin, has been shown to lack detectable viral reverse transcriptase as well[48]. These findings, together with recent reports concerning *in vitro* synthesis of *gag* gene products directed by 35S viral RNA[3,7] indicate that an initiation codon must exist at (or close to) the 5′ end of the *gag* gene. Thus, if the viral genome were to contain a single protein synthesis initiation site, the above information would be sufficient to map the *gag* gene at the 5′ end of the viral genome Reports concerning the size of the viral mRNA[38,39] as well as its translational products[6], taken together would argue for a single initiation site. This possibility remains speculative, however, and awaits further experimental verification.

We thank Janet A. Steel for technical assistance. This research was supported in part by a contract from the Virus Cancer Program of the National Cancer Institute. M.B. is a visiting fellow at the NIH, on leave from the Instituto de Bioquimica de Macromoleculas, Madrid, Spain.

Received April 14; accepted June 15, 1976.

[1] *Cold Spring Harb Symp. quant Biol.*, 39, part 2 (1975)
[2] Vogt, V. M , and Eisenman, R., *Proc. natn. Acad. Sci U.S A.*, 70, 1734–1738 (1973)
[3] Der Helm, K V., and Duesberg, P. H., *Proc natn. Acad Sci U S.A.*, 72, 614–618 (1975).
[4] Stephenson, J. R., Tronick, S. R., and Aaronson, S. A., *Cell*, 6, 543–548 (1975)
[5] Oskarson, M. K , *et al* , *Proc. natn. Acad Sci U S.A* , 72, 2380–2384 (1975).
[6] Arcement, L J., Karshin, W L , Naso, R B , Jamjoom, G , and Arlinghaus, R B., *Virology*, 69, 763–774 (1976)
[7] Salden, M., Asselbergs, F., and Bloemendal, H , *Nature*, 259, 696–699 (1976).
[8] Baltimore, D., *Cold Spring Harb. Symp quant. Biol* , 39, 1187–1200 (1975).
[9] Wang, L. H , Duesberg, P H., Kawai, S , and Hanafusa, H , *Proc. natn. Acad Sci. U S.A* , 73, 447–451 (1976)
[10] Hanafusa, H., in *Cancer A Comprehensive Treatise.* (edit by Becker, F F.), 2, 49–90 (Plenum, New York, 1975).

[11] Vogt, P. K., in *Comprehensive Virology*, (edit by Fraenkel-Conrat, H., and Wagner, R. R.) (Plenum, New York, in the press).

[12] Aaronson, S. A., and Stephenson, J R., *Biochim. biophys Acta Rev Cancer* (in the press).

[13] Joho, R. H., Billeter, M. A., and Weissman, C., *Proc. natn Acad. Sci U S.A.*, **72**, 4772–4776 (1975).

[14] Vogt, V. M , Eisenman, R., and Diggelmann, H., *J molec Biol* , **96**, 471–493 (1975).

[15] Zaane, D. V., Gielkens, A L J., Dekker-Michielsen, M. J. A., and Bloemers, H. P. J., *Virology*, **67**, 544–552 (1975).

[16] Bassin, R. H., Tuttle, N., and Fischinger, P J., *Int J. Cancer*, **6**, 95–107 (1970).

[17] Tronick, S. R , Stephenson, J R., and Aaronson, S A., *Virology*, **54**, 199–206 (1973).

[18] Aaronson, S. A., Stephenson, J. R , Hino, S , and Tronick, S R , *J. Virol* , **16**, 1117–1123 (1975).

[19] Strand, M., and August, J. T , *J biol Chem.*, **248**, 5627–5633 (1973)

[20] Hino, S., Stephenson, J R., and Aaronson, S. A , *J Immun.*, **115**, 922–927 (1975).

[21] Oroszlan, S., Huebner, R. J., and Gilden, R. V , *Proc. natn. Acad Sci. U.S A* , **68**, 901–904 (1971).

[22] Parks, W. P., and Scolnick, E M , *Proc. natn Acad Sci. U S A* , **69**, 1766–1770 (1972)

[23] Strand, M., Wilsnack, R , and August, J T , *J Virol* , **14**, 1575–1583 (1974).

[24] Barbacid, M., Stephenson, J R , and Aaronson, S A , *J. Biol Chem.* **251**, 4859–4866 (1976)

[25] Scolnick, E. M , *et al* , *Proc. natn. Acad Sci U.S A* , **72**, 4650–4654 (1975).

[26] Frankel, A E., Neubauer, R. L., and Fischinger, P. J., *J. Virol* , **18**, 481–490 (1976).

[27] Aaronson, S. A., Bassin, R H , and Weaver, C , *J. Virol* , **9**, 701–704 (1972).

[28] Peebles, P. T , Gerwin, B. J , and Scolnick, E M , *Virology*, **70**, 313–323 (1976).

[29] Peters, R. L , Rabstein, L. S., Vanvleck, R., Kelloff, G J , and Heubner, R J., *J. natn Cancer Inst.*, **53**, 1725–1129 (1974)

[30] Wolfe, L G., Smith, R K., and Deinhardt, F , *J natn. Cancer Inst.*, **48**, 1905–1908 (1972).

[31] Abelson, H. T., and Rabstein, L. D., *Cancer Res* , **30**, 2213–2222 (1970)

[32] Scher, C. D., and Siegler, R , *Nature*, **253**, 729–731 (1975).

[33] Huebner, R. J., *et al* , *Proc. natn. Acad Sci. U S.A.*, **67**, 366–376 (1970).

[34] Parks, W. P , Livingston, D M., Todaro, G J., Benveniste, R E and Scolnick, E. M., *J. exp. Med.*, **137**, 622–635 (1973)

[35] Stephenson, J. R., Tronick, S. R , Reynolds, R. K., and Aaronson, S. A., *J. exp. Med* , **139**, 427–438 (1974)

[36] Temin, H. M., *Adv Cancer Res.*, **19**, 48–105 (1974).

[37] Fleissner, E., *J Virol* , **8**, 778–785 (1971).

[38] Fan, H., and Baltimore, D., *J. molec. Biol.*, **80**, 93–117 (1973).

[39] Tsuchida, N., and Green, M , *Virology*, **59**, 258–265 (1974).

[40] August, J. T., Bolognesi, D P., Fleissner, E., Gilden, R V. and Nowinski, R. C , *Virology*, **60**, 595–601 (1974).

[41] Lilly, F , and Steeves, R., *Biochim biophys. Acta Rev. Cancer*, **355**, 105–118 (1974).

[42] Bolognesi, D P., Huper, G., Green, R. W , and Graf. T., *Biochim biophys. Acta Rev. Cancer*, **355**, 220–235 (1974)

[43] Stephenson, J R , Barbacid, M., Tronick, S R., Hino, S and Aaronson, S. A., in *Cancer Research Cell Biology, Molecular Biology and Tumor Virology* (edit by Gallo, R) (CRC Press, Cleveland, in the press).

[44] Peebles, P T , Fischinger, P. J , Bassin, R H., and Papageorge, A G , *Nature new Biol* , **242**, 98–101 (1973)

[45] Greenwood, F. C., Hunter, W. M., and Glover, J. S , *Biochem. J.*, **89**, 114–123 (1963)

[46] Lowry, O K., Rosebrough, N. J., Farr, A. L., and Randall, R J., *J. biol. Chem* , **193**, 265–275 (1951)

[47] Hino, S , Stephenson, J. R., and Aaronson, S A., *J. Virol.*, **18**, 933–941 (1976).

[48] Peebles, P. T., Gerwin, B. I., Papageorge, A. G., and Smith, S. G., *Virology*, **67**, 344-355 (1975).

---

letters to nature

Solar neutrinos and solar accretion of interstellar matter

McCrea[1] has recalled the suggestions[2,3] that the gravitational energy released by material accreted by the Sun from interstellar clouds could trigger the onset of terrestrial Ice Ages. The purpose of this communication is to point out that if the Hoyle–Lyttleton mass accretion rate applies, this accretion is sufficient to enhance the surface heavy element abundances of the Sun and other solar-type stars. The enhancement may be sufficient to allow the construction of consistent solar models with an interior heavy element abundance significantly lower than the observed surface abundance. This condition lowers the predicted solar neutrino flux[4]. Joss[5] has suggested that a similar enhancement of surface abundances might occur by accretion of planetesimals left over after formation of the Solar System. Both mechanisms may occur, thereby increasing the effect.

In the simple accretion model of Hoyle and Lyttleton[3] a body of mass M accretes matter at a rate

$$\dot{M} = 2.4\times 10^{22}(M/M_{\odot})^{2} n(\mathrm{H}_2) V^{-3}\,\mathrm{g\ yr}^{-1} \qquad (1)$$

where $n(\mathrm{H}_2)$ is the equivalent number of hydrogen molecules cm^{-3} and V is the velocity relative to the cloud in $\mathrm{km\ s}^{-1}$.

If the clouds with internal densities of $n_c(\mathrm{H}_2)$ are distributed randomly with N_c clouds pc^{-3}, and if they may be characterised by spheres of radius, R_c pc, then the fraction of the volume of the galactic disk occupied by cloud material will be $f_c = N_c(4\pi/3)R_c^{3}$. For the age, A, of the Sun, the fraction of time spent inside such clouds will be f_c, and consequently the total mass accreted will be

$$\delta M \simeq \langle \dot{M} f_c\rangle A = 8.2\times 10^{-2} M_{\odot}\langle f_c n_c(\mathrm{H}_2) V^{-3}\rangle \qquad (2)$$

The product $f_c n_c(\mathrm{H}_2)$ is the density of H_2 which would result from smoothing out clouds into a uniform density disk. It is important to note that to compute δM one should include only those clouds for which the internal cloud densities are large enough to choke off the solar wind flow and allow material to accrete on to the stellar surface. As pointed out below, this is approximately $n_c(\mathrm{H}_2) = 10^{4}\ \mathrm{cm}^{-3}$. From Gordon and Burton[6] we adopt the smoothed out density at 10 kpc from the galactic centre of $\langle n(\mathrm{H}_2)\rangle = f_c n_c(\mathrm{H}_2) = 0.5\ \mathrm{cm}^{-3}$. This figure is based on H_2 deduced from CO molecular lines, which require $n_c(\mathrm{H}_2) \gtrsim 10^{4}\ \mathrm{cm}^{-3}$, and consequently it includes the type of clouds which will cause accretion. Consequently, we obtain

$$\delta M \simeq 4\times 10^{-2} M_{\odot}\langle V^{-3}\rangle \qquad (3)$$

Interstellar H I clouds have a turbulent velocity dispersion of $\sim 6.4\ \mathrm{km\ s}^{-1}$ (ref. 7), the mean gas velocity changes by several $\mathrm{km\ s}^{-1}$ during the full cycle of a galactic spiral density wave[8], and the velocity of the Sun oscillates $\sim 20\ \mathrm{km\ s}^{-1}$ around its mean motion about the galactic centre. Thus one expects the relative velocity of the Sun and interstellar clouds to vary over the range 0–$\sim 30\ \mathrm{km\ s}^{-1}$. For any reasonable distribution function of cloud velocities $\langle V^{-3}\rangle$ diverges; consequently the figure to use in equation (3) is dominated by rare, low velocity encounters.

To illustrate this sensitivity, consider the 37 clouds studied by Hobbs[9]. The velocity dispersion of the clouds relative to the Sun was $\langle V^{2}\rangle^{1/2} = 15.7\ \mathrm{km\ s}^{-1}$ (note that this figure includes the systematic motions as well as what would be called turbulent motions about the mean cloud motions observed towards each star). In contrast, the quantity appropriate for use in equation (3) is $\langle V^{-3}\rangle^{-1/3} = 3.1\ \mathrm{km\ s}^{-1}$. To emphasise the sensitivity to rare encounters of low relative velocity, if the one cloud towards ε Aur with velocity $1\ \mathrm{km\ s}^{-1}$ is dropped from the mean, then $\langle V^{-3}\rangle^{-1/3} = 5.4\ \mathrm{km\ s}^{-1}$.

It is not clear whether this sample of clouds is broad enough to determine the appropriate figure to use in equation (3), especially since these clouds are not the same type of objects which have densities of $n_c(\mathrm{H}_2) \gtrsim 10^{4}\ \mathrm{cm}^{-3}$. Nevertheless, we expect that the appropriate mean velocity is likely to be in the range 2–5 $\mathrm{km\ s}^{-1}$ and this gives

$$\delta M \simeq 5\times 10^{-3}\ \text{to}\ 3\times 10^{-4} M_{\odot} \qquad (4)$$

A crucial question which must be answered by future research is whether or not accretion on to the solar surface will actually occur. One of the most obvious obstacles is the outward flowing solar wind. A simple computation may be done by setting the dynamic pressure of the solar wind flow equal to the dynamic pressure of the dense interstellar gas[10]. It is easy to show that for interstellar cloud densities of $n(\mathrm{H}_2) \simeq 10^{2}\ \mathrm{cm}^{-3}$ the solar wind terminates at ~ 1 AU. For larger densities the heliosphere is compressed further and for densities of a few $10^3\ \mathrm{cm}^{-3}$ the termination is within a few solar radii of the Sun. To decide what occurs for higher densities requires knowledge of the mechanisms which affect the solar wind within its critical sonic point at a few solar radii. It appears that the outward flow can be reversed to an inward flow for cloud densities which characterise the dense H_2 clouds used for the estimate in equation (5).

If the accreted mass contains a heavy element abundance by mass $Z_g(t)$ and it has been continually mixed into a surface convection zone of mass ΔM, then the surface abundance of heavy elements will be

$$Z_S(t) = e^{-y(t)}\left[Z_0 + \int_{t_0}^{t} e^{y(t')} Z_g(t') \frac{\dot{M}\,\mathrm{d}t'}{\Delta M}\right] \qquad (5)$$

where Z_0 is the heavy element abundance of the star at its time of formation t_0, and

$$y(t) = \int_{t_0}^{t} \frac{\dot{M}\,\mathrm{d}t'}{\Delta M}$$

The presently observed solar Z_S is $\sim 1.5 \times 10^{-2}$. The heavy element abundance of the interstellar gas at the present time, T, deduced from young stars and H II regions is about the same. If the heavy element abundance in the gas has increased with time and therefore $Z_g(t) > Z_0$, then equation (5) is satisfied providing $y(T) \gtrsim 1$. Standard solar models give surface convection zones with $\Delta M \simeq 10^{-2} M_\odot$. This together with the predicted range for δM given in equation (4) seems to indicate $y(T)$ somewhat <1. Ulrich (personal communication) has, however, shown that ΔM is even smaller if the interior abundance Z_0 is smaller than the surface abundance Z_S. Therefore for sufficiently low values of Z_0 it seems that equation (5) will be satisfied.

The initial solar value Z_0 is difficult to estimate. It is most likely substantially greater than zero. Simple models for the evolution of the Galaxy (for example ref. 11) suggest that 4.5×10^9 yr ago the interstellar gas may have had a value of Z at least as great as $\frac{1}{2}$–$\frac{2}{3}$ the present value Z_g. If these values for Z_0 reduce ΔM to approximately the size of δM, then the solar neutrino counting rate is reduced by a factor of $\sim (Z_0/Z_S)^{1\ 1}$ (ref. 12) to 2 6–3.6 SNU.

Although the precise magnitude of the effect is still uncertain, it seems probable that some enhancement of the solar surface heavy element abundance must occur. Hence, it appears that this mechanism could significantly reduce the discrepancy between the observations and predictions of solar models.

This work was supported in part by the NSF.

MICHAEL J. NEWMAN
Kellogg Radiation Laboratory 106-38,
California Institute of Technology,
Pasadena, California 91125

RAYMOND J. TALBOT, JR
Department of Space Physics and Astronomy,
Rice University,
Houston, Texas 77001

Received January 29, accepted June 28, 1976

[1] McCrea, W H , *Nature*, 255, 607–609 (1975)
[2] Shapley, H , *J Geol* , 29, 502–504 (1921)
[3] Hoyle, F , and Lyttleton, R A , *Proc Camb phil Soc math phys Sci* , 35, 405–415 (1939)
[4] Bahcall, J N , Huebner, W F , Magee, N H , Jr, Mertz, A L , and Ulrich, R K , *Astrophys J* , **184**, 1–4 (1973).
[5] Joss, P C , *Astrophys J* , 191, 771–774 (1974)
[6] Gordon, M A., and Burton, W B , *Astrophys. J* (in the press).
[7] Falgarone, E , and Lequeux, J , *Astro Astrophys* , 25, 253–260 (1973)
[8] Shu, F. H , *et al* , *Astrophys J* , 173, 557–592 (1972)
[9] Hobbs, L M., *Astrophys. J* , 191, 395–399 (1974)
[10] Talbot, R J., Jr, Butler, D M , and Newman, M J., *Nature*, **262**, 561–563 (1976)
[11] Talbot, R J., Jr, and Arnett, W D , *Astrophys J* , **186**, 51–67 (1973).
[12] Bahcall, J N , Bahcall, N A , and Ulrich, R K , *Astrophys J.*, **156**, 559–568 (1969).

Solar neutrinos and galactic contamination of the Sun

ONLY recently-published observations permit a useful estimate of the total accretion of interstellar matter (ISM) by the Sun since it became a main sequence star. Using measurements from the OAO-2 satellite, Jenkins and Savage[1] conclude that " . . . possibly the most secure estimate of the amount of hydrogen within 1 kpc of the Sun is . . . an overall density n_H (total) = 1.5 atoms cm^{-3} (in the form of protons, atoms and molecules)". Using this number we suggest here a possible explanation of the low observed solar neutrino rate.

Taking hydrogen to be 70% by mass gives for the density of ISM in units of the atomic mass of hydrogen

$$n \simeq 2\ \mathrm{cm}^{-3} \qquad (1)$$

If the Sun of mass 2×10^{33} g traverses ISM of density n at speed V km s^{-1} the mass $m(L)$ accreted in travelling L pc is

$$m(L) = 1\ 2 \times 10^{28} L n V^{-4}\ \mathrm{g} \qquad (2)$$

and the total mass $m(T)$ accreted in time $1T$ (in units of 10^{10} yr) is

$$m(T) = 1.2 \times 10^{32} T \langle n \rangle \langle V^{-3} \rangle\ \mathrm{g} \qquad (3)$$

assuming n, V to be uncorrelated[2,3]. Now a region of radius 1 kpc around the Sun seems to be quite typical along the path of the Sun in present conditions in the Galaxy. Also the amount of ISM was presumably somewhat greater in the past. So from equation (1) we infer that it is not an overestimate to use in equation (3)

$$\langle n \rangle \simeq 2 \qquad (4)$$

If the Sun is in a cloud of ISM the relative speed V is usually taken to be in the range 5–25 km s^{-1}. In equation (3) smaller values are weighted more strongly, so we take

$$\langle V^{-3} \rangle \simeq 10^{-3} \qquad (5)$$

According to standard estimates, the Sun reached the main sequence about 5×10^9 yr ago. The total mass $m(T = 0.5)$ accreted since then is estimated from equations (3), (4) and (5) as

$$m \simeq 10^{29}\ \mathrm{g} \qquad (6)$$

This is an underestimate because it takes no account of the densest parts of the ISM that produce so much obscuration that no stars can be seen through them. Indeed, if the Sun traverses even a single 'very dense' cloud it can accrete between 10^{29} and 10^{31} g, as follows from equation (2) using appropriate values of L, n, V. The Sun must have had a good chance of accreting some such amount each of the $\sim$ 50 times it has crossed a dust-lane associated with a spiral arm of the Galaxy. From all this we may safely take m to be in the range

$$10^{29} < m < 10^{30}\ \mathrm{g} \qquad (7)$$

and we should not exclude still higher values.

On current models, the Sun has an outer convective zone that, along with a region of convective overshooting immediately beneath it comprising altogether a mass M_{conv}, is itself kept mixed but undergoes no mixing with material from the interior. Quoting R. K. Ulrich, Joss[4] gives for two models

$$Z_0 \lesssim 0.002 \quad M_{\text{conv}} \simeq 10^{29}\ \text{g} \qquad (8)$$

$$Z_0 \simeq 0.02 \quad M_{\text{conv}} \simeq 5\times10^{31}\ \text{g} \qquad (9)$$

Z_0 is the initial heavy-element abundance by mass, here assumed to have the same value throughout a model.

Amongst general conclusions from the literature[5] on the chemical composition of the stars are: (a) Clouds from which stars are being formed at the present time have Z-values on average 1.5–2 times higher than those from which stars were formed when the Sun was born. (b) There is an intrinsic spread in the Z_0-values of stars born about any particular time; this is seen especially in the work of Clegg and Bell[6] who find, for stars younger than the Sun, a sixfold range of Z_0. At present IMS has $\langle Z \rangle \simeq 0.02$. Allowing a factor 2 on account of (a) and 2 either way on account of (b) would give a range

$$0.005 \lesssim Z_0 \lesssim 0.02$$

for the Sun at birth, and would not exaggerate the possible range.

These bounds for Z_0 give two possible interpretations of the fact that the observed spectrum of the Sun gives $Z \simeq 0.02$:

(A) $Z_0 \simeq 0.005$. Here M_{conv} is near the low value in model (8) and this can be exceeded by $\dot{m}$ in condition (7). In that case the convective zone is composed of accreted matter for which $Z \simeq 0.02$.

(B) $Z_0 \simeq 0.02$. Here M_{conv} having the high value in model (9) is unlikely to be significantly affected by accretion, and accretion of ISM having $Z \simeq 0.02$ would not in any case affect the composition.

Case (B) is the usual standard uniform model. But from the present standpoint, apart from accretion, a uniform model with $Z_0 \simeq 0.005$ is about as likely as one with $Z_0 \simeq 0.02$; accretion would, however, cause (A) to show the same spectrum as (B). There could be intermediate cases, but we are concerned to demonstrate the plausibility of quite widely different cases.

Bahcall *et al.*[7] predict for uniform solar models

$$Z_0 = 0.002,\ \text{neutrino detection rate} \simeq 1.4\ \text{SNU} \qquad (10)$$

$$Z_0 = 0.02,\ \text{neutrino detection rate} \simeq 5.6\ \text{SNU} \qquad (11)$$

A roughly linear dependence of detection rate upon Z_0 near $Z_0 = 0.015$ inferred earlier[8] would have required it to go from 5.6 to 1.4 SNU if Z_0 goes from $Z_0 = 0.02$ to $Z_0 = 0.005$. In view of result (10) this may not be quite correct, but it shows the predicted rate to be not much above 1.4 SNU if $Z_0 = 0.05$, that is, for case (A). The result (11) predicts 5.6 SNU in case (B).

As their most up-to-date determination, R. Davis, Jr, and J. C. Evans (private communication) find 1.5 SNU as the 1σ upper bound on the solar neutrino detection rate (see also ref. 9). We suggest as the simplest explanation of this low value the possibility that the Sun actually has a low heavy-element content, except in its convection zone which has been enriched by accretion.

The phenomenon of a considerable difference between surface and interior Z-values because of accretion is likely only for stars not much different from the Sun. Population II stars will have space velocities that are too high for significant accretion to occur. Stars of smaller mass would have deeper convective zones, while stars of much greater mass would generate H II regions tending to inhibit accretion, and would not be old enough for significant changes in Z to develop in the ISM from the time of formation. Therefore our suggestion would not require any changes in composition (Z) for the ISM from that normally assumed, either for the present period or when the population II stars were being formed.

In a highly suggestive paper, Joss[4] has considered the possible enhancement of the heavy-element abundances in stellar surfaces by the accretion of chemically fractionated matter in the form of comets and planetesimals. It follows fairly conclusively from his discussion, however, that such material in the required quantity is not available in the case of the Sun. Our suggestion differs from his in a simple way, but it is the crucial one that we appeal only to ISM known to exist in the amount needed.

Amongst possible objections is, for instance, any reason for the inapplicability of the simple theory of accretion; in particular the solar wind might combat accretion, though this seems unlikely to be important since heavy accretion would occur mainly in relatively short intense bursts. Anyhow, little is known about the cause of the solar wind or its time dependence. Again there is the question as to whether the mere addition of material of relatively high Z-value might automatically increase the extent of the convective zone, thereby rendering our process self-defeating. There are also known problems regarding particular abundances (lithium in the Sun, planetary compositions, to name but two) that are still unresolved in any theory. On the other hand, were the neutrino observations accepted as demanding a low Z-value inside the Sun, this would clarify these other problems.

This research has been supported in part by the NRC of Canada. W. H. M. thanks the Head of the Department of Geophysics and Astronomy, UBC, for hospitality.

J. R. AUMAN
W. H. MCCREA

Department of Geophysics and Astronomy,
University of British Columbia,
Vancouver, Canada

Received March 16, accepted July 9, 1976

[1] Jenkins, E. B., and Savage, B. D., *Astrophys. J.*, **187**, 243–255 (1974).
[2] Hoyle, F., and Lyttleton, R. A., *Proc. Camb. phil. Soc. math. phys. Sci.*, **35**, 405–415 (1939).
[3] Lyttleton, R. A., *The Comets and their Origin*, ch. III (Cambridge University Press, London, 1953).
[4] Joss, P. C., *Astrophys. J.*, **191**, 771–774 (1974).
[5] Trimble, V., *Rev. mod. Phys.*, **47**, 877–976 (1975).
[6] Clegg, R. E. S., and Bell, R. A., *Mon. Not. R. astr. Soc.*, **163**, 13–28 (1973).
[7] Bahcall, J. N., Huebner, W. F., Magee, N. H., Mertz, A. L., and Ulrich, R. K., *Astrophys. J.*, **184**, 1–4 (1973).
[8] Bahcall, J. N., Bahcall, N. A., and Ulrich, R. K., *Astrophys. J.*, **156**, 559–568 (1969).
[9] Bahcall, J. N., and Davis, R., Jr, *Science*, **191**, 264–267 (1976).

Climatic effects during passage of the Solar System through interstellar clouds

IT seems likely that the Solar System passes through regions where there are a large number of dense interstellar clouds as the compression zone of the galactic spiral density wave passes the Sun. When this occurs, several processes may cause significant changes in the climate of the Earth and other planets. We discuss here the influences of compression of the solar wind cavity, accretion by the Sun, and particulate input into the Earth's atmosphere. The first two may produce radiation hazards for life in addition to causing climate stress.

Shapely[1] and Hoyle and Lyttleton[2] have discussed the idea that gravitational energy released by the accretion of interstellar material to the Sun at a rate $\dot{M}$ would enhance the solar luminosity. The Hoyle–Lyttleton mechanism gives an enhancement of $\delta L \approx \dot{M}\ (GM_\odot/R_\odot) \propto n(\text{H}_2)/V^3$, where $n(\text{H}_2)$ is the equivalent number of hydrogen molecules per cm^3 and V is the velocity of the Sun with respect to the interstellar medium. In contrast to the small accretion rates predicted from earlier data, McCrea[3] has pointed out that there exist very dense interstellar clouds with $n(\text{H}_2)$ values as large as 10^6–$10^7\ \text{cm}^{-3}$, which may produce $\delta L \approx 10^{-2}(n(\text{H}_2)/10^6\ \text{cm}^{-3})L_\odot$ using $V = 20\ \text{km s}^{-1}$. Simple arguments about terrestrial heat balance suggest that luminosity enhancements of 1% or greater will produce significant variations in climate.

The spiral pattern in the Galaxy sweeps by the Sun at intervals of about 10^8 yr, and the sharp compression behind a shock front is believed to initiate the collapse of some interstellar clouds and to induce star formation; see, for example, Shu *et al.*[4]. The width of the compression zone corresponds to an interval of about 10^6 yr. McCrea has estimated that within each compression zone the Sun would encounter several dense clouds, and that the traversal of each would last about 5×10^4 yr (McCrea also considered how these varied times may relate to observed time scales for ice ages).

Observational data are sparse, but it seems that most lines of sight from the Sun encounter cloud complexes of CO molecules[5,6] with emission line strengths implying $n(\mathrm{H}_2)\gtrsim10^3\ \mathrm{cm}^{-3}$. Observed clouds probably have lifetimes of about 10^6 yr, so Earth is unlikely to pass through any of those. If the pattern is continuously maintained by cloud compression in the spiral shock, however, then approximately the same number of clouds can be expected in the compression zone when it passes the Sun. This reinforces McCrea's suggestion[3] that the Sun will regularly encounter dense clouds, but the number of such clouds and the probability of encountering very dense clouds with $n(\mathrm{H}_2)\gtrsim10^5\ \mathrm{cm}^{-3}$ is still uncertain. It seems, however, that encounters with clouds of $n(\mathrm{H}_2)\gtrsim10^3\ \mathrm{cm}^{-3}$ are almost inevitable. We have analyses (unpublished) suggesting that during its lifetime the Solar System has passed through at least 45 clouds with $n(\mathrm{H}_2)\gtrsim10^2\ \mathrm{cm}^{-3}$ and at least five clouds with $n(\mathrm{H}_2)\gtrsim10^3\ \mathrm{cm}^{-3}$.

Dennison and Mansfield[7] have discussed some of the observational difficulties of McCrea's suggestion that each individual glaciation is caused by passage through a separate cloud (there is apparently no trace of the cloud which would have caused the last glaciation). Those arguments, however, do not vitiate the general idea that passage through interstellar clouds may influence climate.

When the Solar System moves through a cloud, the dynamic ram pressure will balance the outward flowing solar wind at a stand-off distance R_s on the upstream side. Under most circumstances of interest V will be much greater than the sonic speed of the interstellar gas, so the flow will be supersonic on both sides of R_s, the two flows being separated by a relatively thin subsonic region. The position of R_s may be estimated by balancing the dynamic pressures of the two opposing flows. The solar wind dynamic pressure is approximately $p_E = m_H n_E (R_E/R)^2 V_E^2$, where m_H is the mass of the hydrogen atom, $n_E\simeq7\ \mathrm{cm}^{-3}$ is the average density currently at $R_E = 1$ AU, and $V_E\simeq400\ \mathrm{km\ s}^{-1}$ is the velocity at 1 AU. The dynamic pressure of the interstellar gas after falling into R is approximately given by

$$p_G = 2m_H n(\mathrm{H}_2)\left(V^2+\frac{2GM_\odot}{R}\right) \qquad (1)$$

If R is greater than the 'accretion radius' $r_c=GM_\odot/V^2$, then $n(\mathrm{H}_2)$ remains approximately equal to its value at large distances from the Sun, and therefore $p_G\simeq$ constant. If $R<r_c$, however, the inflowing gas density increases roughly proportionally to $R^{-3/2}$, and $p_G\propto R^{-5/2}$. With that behaviour the stand-off radius is approximately

$$R_s\simeq750\,n(\mathrm{H}_2)^{-1/2}V^{-1}\ \mathrm{AU} \qquad (2)$$

for small $n(\mathrm{H}_2)$, where V is expressed in $\mathrm{km\ s}^{-1}$. If $n(\mathrm{H}_2)$ is greater than a critical value of approximately $0.4V^2\ \mathrm{cm}^{-3}$ pressure balance is no longer possible and the interstellar gas overwhelms the solar wind. When that occurs $R_s\simeq1.2\times10^3V^{-2}$ AU. That is altered only slightly if non-fluid behaviour resulting from the large mean free path of the neutral gas is considered.

As a typical case we here adopt $V = 20\ \mathrm{km\ s}^{-1}$ for the velocity of the Sun relative to clouds. For that value of V the critical values of $n(\mathrm{H}_2)$ and R_s are about $160\ \mathrm{cm}^{-3}$ and 3.0 AU. In this analysis the conditions on the downstream side are not clearly discernible; nevertheless it is clear that for clouds of $n(\mathrm{H}_2)>10^2\ \mathrm{cm}^{-3}$ the Earth will be outside the solar wind cavity for at least part of the year. Furthermore, the flow becomes an accretion flow which may produce a significant alteration of the chemical abundances at the solar surface and, by implication, surface abundances of other stars as well (R.J.T. and M.J.N., unpublished).

Observational evidence suggests that there is some mechanism producing a relationship between solar wind flow and climate[8–11]. One proposed mechanism is that contemporary solar wind modulation of galactic cosmic rays influences climate[12–14]. Consequently, the fact that the Earth would be outside the solar wind cavity for all or part of the year may have an effect on terrestrial climate. Outside the heliosphere the Earth will presumably be exposed to the full galactic cosmic ray flux; furthermore, there may be an enhanced flux in those environments because of the supernova deaths of massive stars which spend their entire lives in the vicinity of the dense interstellar clouds from which they form. Ruderman[15] has discussed the consequences of nearby supernovae explosions for atmospheric ozone and terrestrial life.

One discussion about the relationship between solar wind and weather has focused on the passage of the Earth through sector boundaries of the interplanetary magnetic field[8]. If those magnetic field discontinuities are important, then discontinuities encountered as the Earth moves in and out of the heliosphere should also be important.

McCrea's discussion of the accretion luminosity δL considered only its magnitude. Its spectrum will be largely determined by the temperature of the gas after the bow shock at R_s or the accretion shock at the solar surface. The temperature will reach at least 40,000 K, which is the value the gas would attain by converting the energy of $20\ \mathrm{km\ s}^{-1}$ bulk relative motion into thermal energy. The spectral character of this radiation will be quite different from the normal solar spectrum, for it will be mostly ultraviolet and X-ray radiation.

During quiet solar periods, solar radiation contains about $1.5\times10^{-6}L_\odot$ on the short wavelength side of Lyman α (ref. 16); this portion governs the thermosphere of the Earth. Therefore, $\delta L\approx10^{-6}L_\odot$ will produce changes of order unity both in the properties of the Earth's atmosphere above about 150 km and in the ionsopheric regions of all planets. Solar radiation contains about $1.5\times10^{-2}L_\odot$ between 2,100 and 3,100 Å (ref. 16), the wavelength region influencing the stratosphere.

The suspected relationships between observed, contemporary solar activity and climatic change[12,13,17] suggest that relatively small variations in solar ultraviolet radiation input may have perceptible influences on climate. If a variation of 1% in radiative input to the stratosphere has a significant effect, then an accretion producing $\delta L\simeq10^{-4}L_\odot$ in ultraviolet and X rays may have a large impact on terrestrial conditions, even though the change in the total heat balance is negligible. Thus, moderately dense interstellar clouds with $n(\mathrm{H}_2)\approx10^3\ \mathrm{cm}^{-3}$ may have significant effects. The $\delta L\approx10^{-2}L_\odot$ relationship discussed by McCrea[3] would have a devastating effect on the Earth's upper atmosphere and perhaps cause ultraviolet fluxes hazardous to life[15].

Dense interstellar clouds are well known because of the optical obstruction caused by dust grains about 0.2 μm in radius. Silicate and ice particles will survive solar radiation at distances from the Sun of a few $R_\odot$ and about 2 AU, respectively (see, for example, refs 18 and 19). Using 1% for the mass in grains per unit mass of H_2, we estimate that once in a cloud the Earth will sweep up an average of about $6\times10^6\,n(\mathrm{H}_2)\ \mathrm{g\ yr}^{-1}$ of dust.

Our computations of the dynamics of infalling dust show that it will reach terminal velocity by the time it falls to about 90 km altitude, and that negligible ablation occurs. The residence time above the tropopause is at least 1 yr. This implies a dust loading of the terrestrial atmosphere of about 6×10^6 tonnes when the Solar System is in a cloud with $n(\mathrm{H}_2)\approx10^5\ \mathrm{cm}^{-3}$.

This is about the level produced by volcanic activity, believed by some investigators[20] to produce perceptible climatic changes through alteration of atmospheric transparency and albedo. This dust may also provide nucleation sites and thereby influence precipitation. Both processes suggest that the accretion of interstellar dust by the Earth will lead to global cooling and glaciation. The frequency of passage through such dense clouds is probably very low, so that the significance of this effect is difficult to evaluate.

We estimate that during the lifetime of the Solar System the mass of dust grains (mostly silicon, magnesium, and oxygen) accreted by the Earth should have been about 10^{16}–10^{18} g. Is there any evidence for their presence? These grains may contain freshly created, short-lived radioactive nuclei produced by supernova nucleosynthesis processes, and they may reveal themselves by exhibiting abundances appreciably greater than would be expected if the species had been decaying in isolation since the origin of the Solar System. Clayton[21] has suggested that this may have already been observed in the detection of naturally occurring ^{244}Pu. Lindsay and Srnka[22] have evidence for the accretion of interstellar dust by the Moon.

The processes proposed here have very complex implications for global weather patterns. We cannot at this time evaluate which, if any, will unquestionably affect the Earth's climate; however, astronomical influences upon climate seem to be far more complex and significant than considered previously. Begelman and Rees[23] have also considered some of the ideas discussed here.

This work was supported in part by the National Science Foundation.

RAYMOND J. TALBOT, JR
DIXON M. BUTLER

Department of Space Physics and Astronomy,
Rice University,
Houston, Texas 77001

MICHAEL J. NEWMAN

Kellogg Radiation Laboratory 108-38,
California Institute of Technology,
Pasadena, California 91125

Received April 5; accepted June 26, 1976

[1] Shapeley, H , *J Geol* , **29**, 502–504 (1921).
[2] Hoyle, F., and Lyttleton, R. A., *Proc. Camb phil Soc. math phys. Sci.*, **35**, 405–415 (1939).
[3] McCrea, W. H , *Nature*, **225**, 607–609 (1975).
[4] Shu, F H., Milione, V , Gebel, W , Yuan, C , Goldsmith, D. W., and Roberts, W. W., *Astrophys. J* , **173**, 557–592 (1972)
[5] Scoville, N. Z , and Solomon, P. M., *Astrophys J Lett* , **199**, L105–L109 (1975).
[6] Burton, W. B., Gordon, M A , Bania, T M , and Lockman, F. J , *Astrophys. J* , **202**, 30–49 (1975)
[7] Dennison, B , and Mansfield, V. N., *Nature*, **261**, 32–34 (1976).
[8] Wilcox, J. M., Scherrer, P. H., Svalgaard, L , Roberts, W O , Olson, R H , and Jenne, R L., *J. atmos. Sci.*, **31**, 581–588 (1974)
[9] Wilcox, J. M , *J atmos. terr. Phys* , **37**, 237–256 (1975).
[10] Wilcox, J M., *Science*, **192**, 745–748 (1976)
[11] Roberts, W O , and Olson, R. H , *Rev. Geophys Space Phys* , **11**, 731–741 (1973)
[12] Roberts, W O , in *Proceedings of Symposium of Possible Relationships between Solar Activity and Meteorological Phenomena* (edit by Bandeen, W R , and Maran, S. P), (NASA preprint X-901-74-156, Goddard Space Flight Center, Greenbelt, Maryland, 1974)
[13] Kellogg, W W., *ibid.*
[14] Ruderman, M J , and Chamberlain, J W., *Planet Space Sci* , **8**, 247–268 (1975)
[15] Ruderman, M J , *Science*, **184**, 1079–1081 (1974)
[16] Smith, E v P., and Gottlieb, D M., *Space Sci. Rev* , **16**, 771–802 (1974)
[17] Heath, D F., and Wilcox, J. M , in *Proceedings of Symposium of Possible Relationships between Solar Activity and Meteorological Phenomena* (edit. by Bandeen, W R , and Maran, S P), (NASA preprint X-901-74-156, Goddard Space Flight Center, Greenbelt, Maryland, 1974).
[18] Lamey, Ph L., *Astr. Astrophys* , **33**, 191–194 (1974)
[19] Lamey, Ph. L , *Astr. Astrophys* , **35**, 197–207 (1974)
[20] Bryson, R A , *Science*, **184**, 753–760 (1974).
[21] Clayton, D D , *Astrophys J* , **199**, 765–769 (1975).
[22] Lindsay, J F , and Srnka, L. J , *Nature*, **257**, 776–777 (1975)
[23] Begelman, M C , and Rees, M J , *Nature*, **261**, 298–299 (1976).

Hard X-ray observations of Circinus X-1 during an outburst

WHILE the Ariel V satellite was observing in the Circinus–Norma region an outburst was detected from Cir X-1 on 1976 February 15 by the rotation modulation collimator (RMC) experiment[1]. One day before the outburst began the Imperial College hard X-ray scintillation telescope (ST) experiment (8° FWHM, 26 keV–1.2 MeV) completed a 4-d observation of this source and a strong signal was detected. For the following eight days, 1976 February 14–22, the source remained within the field of view, though at low sensitivity. Consequently only upper limits were obtained for the hard flux during the outburst and only a limited measure of the spectrum immediately afterwards. We have combined our results with the RMC results from reference 1 to obtain an overall view of the spectral behaviour of Cir X-1 during this outburst. We suggest that the large scale low energy X-ray outbursts of the 'super-variable' Cir X-1 may be interpreted as corresponding to the periodic removal of a dense screening gas to expose a relatively stable source with a power law spectrum.

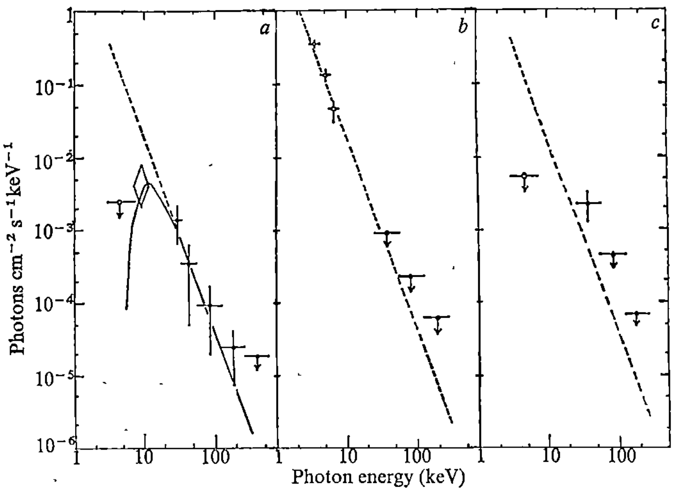

Fig. 1 Observed spectra of Cir X-1 before (*a*, February 10.5–14.5), during (*b*, February 16.5–19.5) and after (*c*, February 19.5–22.5) the outburst of 1976 February. ○, RMC results[1]; ◇, OSO-7 quiet-state result[2]; ●, our ST results.

For the period before the outburst the best fit to our data (see Fig. 1*a*) is found to be the power law

$$\frac{dN}{dE} = 14.6\, E^{-2.7} \text{ photons cm}^{-2}\text{ s}^{-1}\text{ keV}^{-1}$$

Baity *et al.*[2] summarise OSO-7, balloon and rocket results at various times with the law

$$\frac{dN}{dE} = 4.8\, E^{-2.6} \text{ photons cm}^{-2}\text{ s}^{-1}\text{ keV}^{-1}$$

although they have evidence for some spectral hardening as the overall intensity diminishes. Also this data shows intensity variations by a factor of >5 at energies below 10 keV. The power law given by Baity *et al.* also fits our data well. These authors provide a plot of the (7–11) keV flux at various times over the period 1971–1973 and note a relatively steady flux between outbursts of $(2\text{–}8)\times 10^{-3}$ photons cm^{-2} s^{-1} keV^{-1}. We therefore have included this data point in Fig. 1*a*.

During the outburst the soft X-ray flux increased by at least two orders of magnitude but there is no indication of any comparable increase in the flux of hard X-rays (Fig. 1*b*). Our experimental points for the period following the outburst, although less precise, indicate that the spectrum has not greatly changed (Fig. 1*c*). The ST results in Fig. 1*a* and the balloon data of Guo *et al.*[3] from an earlier epoch do not fit a single temperature thermal spectrum. Wilson and Carpenter[1] suggest an absorption column density of 10^{22} atoms cm^{-2} to explain their low energy data during the outburst. Margon *et al.*[4] during a previous outburst find a sharp spectral cutoff, approximately consistent with this value.

Recently Kaluzienski *et al.*[5] have reported that this source has a 16.5-d period with a phase consistent with the time of this outburst, though we note that an earlier event reported by Buff *et al.*[6] does not fall on this period.

We interpret the totality of the data by assuming that there is an intrinsic power law source extending to $\lesssim 1$ keV and that varying amounts of cold gas change the cutoff from 2 keV to 12 keV thereby producing the outburst. A 12-keV cutoff requires a column density of 2.5×10^{24} atoms cm^{-2} of 'typical' interstellar matter and the resulting spectrum is shown as a solid line in Fig. 1*a*. One could imagine a compact object source immersed for most of the time in a dense, cold stellar wind or other 'cloud' of cold material which periodically thins to allow out the soft radiation. An eccentric orbit binary pair is an obvious model for the source.

Our results do not exclude the possibility that the absorbing cloud of gas could radiate by the blackbody mechanism with $kT \lesssim 7$ keV and the emerging spectrum at times of low intensity could be a superposition of this thermal radiation and intrinsic source spectra. The cold cloud is, however, more plausible because to prevent violation of the Eddington limit the hot cloud would have to be no larger than a neutron star. Cir X-1 may thus provide an extreme example of a source where large variations in the amount of surrounding material dramatically changes the spectral shape up to 10 keV or more.

We acknowledge the help of Terence Wyatt in much of the data analysis and the Appleton Laboratory for satellite operations.

M. J. Coe
A. R. Engel
J. J. Quenby

Space Physics Group,
Blackett Laboratory,
Imperial College,
London SW7 2BZ, UK

Received May 13; accepted June 24, 1976.

[1] Wilson, A. M., and Carpenter, G. F., *Nature* (in the press).
[2] Baity, W. A., Ulmer, M P., and Peterson, L. E , *Astrophys. J.*, 198, 447 (1975).
[3] Guo, D. D., Webber, W. R., and Damle, S. V , *Proc. Int. Cosmic Ray Conf.*, 5, 3044 (1973).
[4] Margon, B., Lampton, M., Bowyer, S., and Cruddace, R., *Astrophys. J. Lett.*, 169, L23 (1971).
[5] Kaluziensky, L. J., Holt, S. S., Boldt, E. A., and Serlomitsos, P. J , *IAU Circ.*, No. 2939 (1976).
[6] Buff, J., Bradt, H., and Laufer, D., *Bull. Am. phys. Soc.*, 21, 543 (1976).

New H_2O maser near NGC7538

A NEW, strong, water vapour maser has appeared at the position of a very compact radio and infrared source near the H II region NGC7538. The radio source is NGC7538-B (infrared source IRS-1), the most intense of a group of three compact H II regions[1–4] at a distance of ~ 3 kpc from the Earth. The continuum source is optically thick below 20 GHz (ref. 5), and thus has one of the highest emission measures yet observed in a compact H II region. At 10 μm, it has one of the strongest silicate absorption features known[6], and this source and the KL nebula in Orion are the only sources in the Galaxy which show formaldehyde in emission at 4.8 GHz (ref. 7). The area has been searched many times during the past 5 yr without the detection of this particular H_2O maser. Its sudden appearance may be related to the dynamics of the high-density shell surrounding the compact ionised region.

The observations were made on May 1 and 2, 1976, with the Effelsberg 100-m telescope, which at 22 GHz has a half-power beamwidth (HPBW) of $40'' \times 43''$ and, in the zenith, beam and aperture efficiencies of 35% and 15%, respectively, of the entire 100-m surface. The primary calibration source, NGC7027, had a zenith antenna temperature of 2.1 K and an assumed flux density of 5.9 Jy. The telescope pointing was determined relative to 3C84, 3C273, NRAO530 and 3C454.3, to an accuracy of $\pm 3''$. The mixer receiver had a system temperature of 1,000 K, single sideband, and was followed by a 384-channel autocorrelation spectrometer. With typical spectral resolution of 32 kHz (0.43 km s^{-1}) and integration time of 3 min, the root mean square (r.m.s.) noise was 0.6 K. The rest frequency of the H_2O transition was assumed to be 22.23507985 GHz, and the atmospheric extinction to be 15% in the zenith. All of the observations were made at night, in clear weather.

An area slightly larger than that shown in Fig. 1 was mapped with a grid of 36 points, separated by 20″. Table 1 summarises the properties of the H_2O sources found in this map, and the inset in Fig. 1 shows their spectra. The southern H_2O source has been under observation since 1972 (refs 8–12), and it coincides with a 1,665-MHz OH maser[13] for which no corresponding radio continuum or infrared source has yet been found. The newly discovered H_2O source coincides in position with the more northern OH source[13–15] and with the very compact radio and infrared source. Although some previous workers using larger beamwidths than ours have listed the position of the northern OH source for their observations, it seems clear from the radial velocities that they were actually observing the southern H_2O maser. Two groups[11,12] report limits of 3 Jy for any H_2O emission from the northern position. We conclude that the northern H_2O source has only recently appeared, or that it has reappeared after a long, quiet period.

The main component of this new H_2O source has a radial velocity of -60.8 ± 0.2 km s^{-1} and a width to half-power of 0.6 km s^{-1}. Like many other H_2O sources, it has weaker components at other velocities. On our map, these components coincide in position to within $\pm 5''$ with the main feature at -60.8 km s^{-1}. Similarly, all of the velocity features in the spectrum of the southern H_2O source come from the same, southern position. Nowhere in the map could we find, to a limit of 6 Jy, the components at -112 km s^{-1} reported by Cato *et al.*[11].

The sudden appearance of the northern H_2O source may be related to other unusual properties of the compact H II region. A schematic model of the source (Fig. 2) is as follows.

(1) The exciting star is probably of spectral type O6, since both the far infrared spectrum[16] and the near infrared measurements[6] correspond to a luminosity of $3 \times 10^5 L_\odot$. In contrast, the luminosity of the new H_2O maser is $< 10^{-4} L_\odot$.

(2) Surrounding the exciting star is a compact H II region with an angular size of ~ 1″. Its unusually high turnover frequency of 15–20 GHz (ref. 5) means that it is one of the most compact H II regions known, with an emission measure $> 10^8$ cm^{-6} pc, and an electron density $> 10^5$ cm^{-3}. At 15 GHz (ref. 5), the H II region is 100 times weaker (0.5 Jy) than would be expected from its infrared luminosity. This may be evidence for a high density of dust within the H II region, which absorbs most of the ionising photons. An alternative explanation is that the exciting star has not yet reached the main sequence.

Table 1 Parameters of the H_2O masers near NGC7538

Source	Position (1950)			Radial velocity (line *a*) and line flux density (*b*)							
New H_2O maser	23 h 11 min 36.6	± 0.4 s	*a*	−89.4,	−84.4,	−70.7,	−60.8	(± 0.2)	(km s^{-1})		
	61° 11′ 49	± 3″	*b*	13,	14,	10,	204	(± 4)	(Jy)		
Previously known H_2O maser	23 h 11 min 36.4	± 0.4 s	*a*	−61.3,	−58.6,	−56.1,	−54.1,	−53.1,	−46.6	(± 0.2)	(km s^{-1})
	61° 10′ 28	± 3″	*b*	133,	48,	12,	124,	41,	24	(± 4)	(Jy)

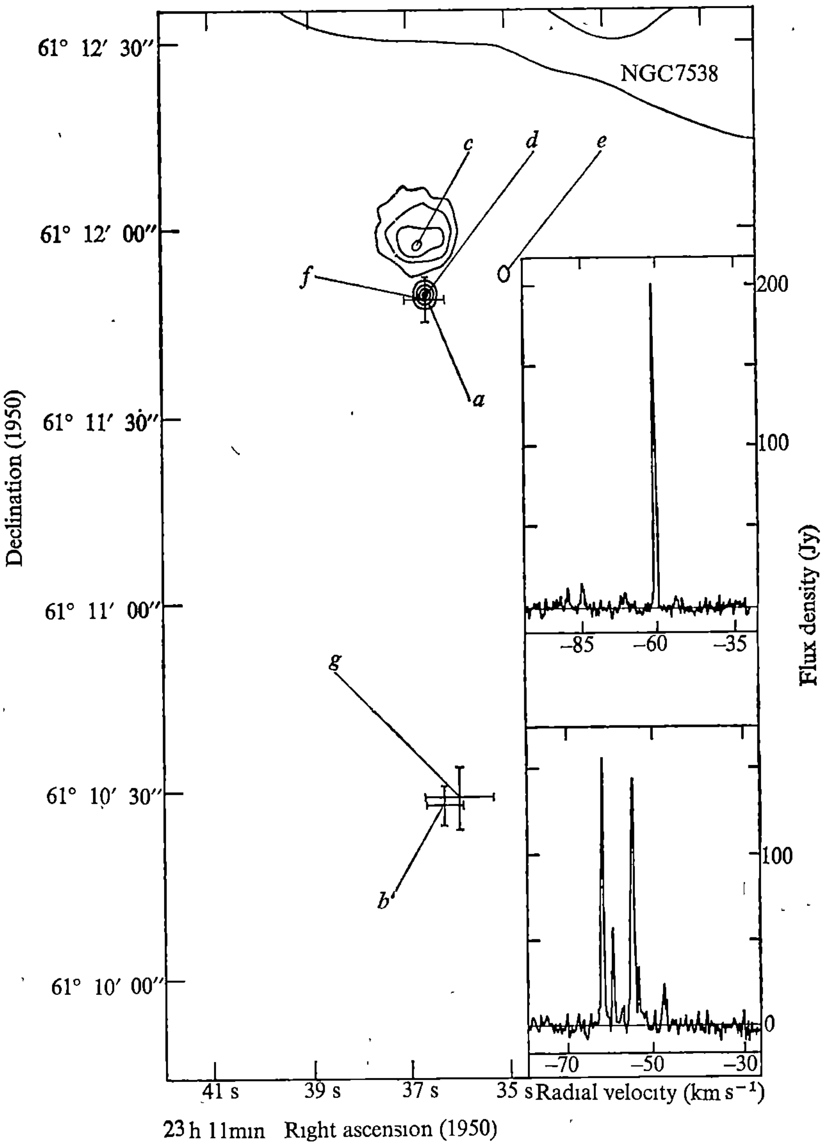

Fig. 1 Location of H_2O and OH masers and continuum sources in the vicinity of NGC7538: *a*, New H_2O source; *b*, previously known H_2O source; *c*, infrared source (IRS) 2; *d*, IRS 1; *e*, IRS 3; *f*, OH 1665/1720 MHz; *g*, OH 1665 MHz. The positions and error bars for the northern H_2O and OH sources are the same. Radio contours are taken from Martin[1]. Inset: Spectra of the northern (upper profile) and southern (lower profile) H_2O masers, obtained with a resolution of 0.43 km s^{-1}.

(3) Around the ionised region is a dense shell of dust and neutral gas of angular size < 10″. The visual extinction through this shell is mag 90, and the silicate absorption at 10 μm is one of the strongest known[6]. From the silicate absorption, Willner[6] has derived a hydrogen column density of 1.3×10^{23} cm^{-2}, which with his size limit of 10″ for the dust shell, implies a number density $n_{H_2} > 2\times10^5$ cm^{-3}. This density is high enough to destroy the anomalous refrigeration of formaldehyde, and to explain why H_2CO is seen in emission from this source at 4.8 GHz (ref. 7). The agreement of density estimates from the silicate absorption, the H_2CO emission, and the radio continuum emission indicates that the compact H II region is ionisation bounded.

Fig. 2 Schematic model of the radio source NGC7538-B (= infrared source IRS 1). *a*, Compact H II region, $n_e > 10^5$ cm^{-3}; *b*, shell of dust and neutral gas, $n_{H_2} > 10^5$ cm^{-3}; *c*, ~3 kpc to Earth; d_1, θ < 10″, diameter < 0.1 pc; d_2, θ = 1″, diameter = 10^{-2} pc; *e*, zone of silicate absorption at 10 μm (visual extinction mag 90); *f*, transition zone between ionisation and shock fronts (location of H_2O masers); *g*, O6 star, $L = 3\times10^5 L_\odot$.

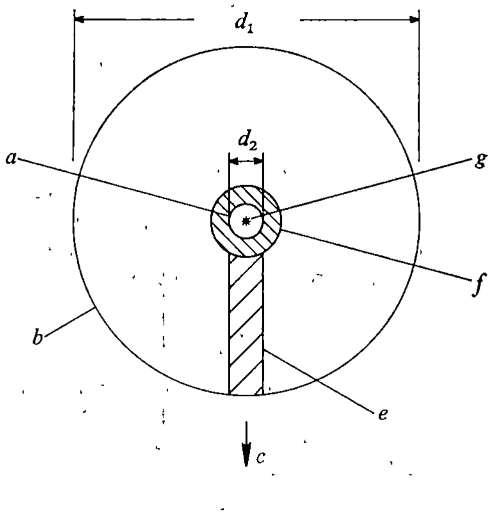

According to current ideas[17,18] the ionisation front of the compact H II region is moving into the neutral material at a velocity of ~ 10 km s^{-1}. The radius of the ionisation front is now 5×10^{-3} pc, and the age of the source is ⩽ 10^3 yr. Ahead of the ionisation front, by perhaps 1″ on the sky, is a shock front, moving through the surrounding, dense, neutral matter. The H_2O maser features may arise in the heated region which has a kinetic temperature of 500–1,000 K between the ionisation front and the shock front. The velocity range of 30 km s^{-1} observed in the new H_2O source may correspond roughly to the difference between the radial velocities of the shock front and the exciting star. The H_2CO emission at 4.8 GHz and the OH masers at 1,665 and 1,720 MHz would come from somewhat cooler regions in the dense, neutral shell.

A fair amount of radio continuum, radio line and infrared data are now available for this source. Its geometry seems to be relatively simple, with a single exciting star surrounded by a compact H II region and a dense shell of dust. The object may therefore be a useful prototype for the study of newly formed O stars and H_2O masers in general.

R. GENZEL
D. DOWNES

Max-Planck-Institut für Radioastronomie,
Auf dem Hügel 69,
53 Bonn, FRG

Received May 21; accepted June 26, 1976.

[1] Martin, A. H. M., *Mon. Not. R. astr. Soc.*, 163, 141 (1973).
[2] Wink, J. E., Altenhoff, W. J., and Webster, W. J., *Astr. Astrophys.*, 38, 109 (1975).
[3] Israel, F. P., Habing, H. J , and de Jong, T., *Astr Astrophys.*, 27, 143 (1973).
[4] Wynn-Williams, C. G., Becklin, E. E., and Neugebauer, G., *Astrophys J.*, 187, 473 (1974).
[5] Harris, S., and Scott, P. F., *Mon. Not. R. astr. Soc.*, 175, 371 (1976).
[6] Willner, S. P., *Astrophys. J.* (in the press).
[7] Downes, D., and Wilson, T. L., *Astrophys. J. Lett* , 191, L77 (1974).
[8] Johnston, K. J., Sloanaker, R. M., and Bologna, J. M., *Astrophys. J* , 182, 67 (1973).
[9] Baudry, A., and Welch, W. J., *Astr. Astrophys.*, 31, 471 (1974).
[10] Yngvesson, K. S., Cardiasmenos, A. G., Shanley, J F , Rydbeck, O. E. H., and Elldér, J., *Astrophys. J.*, 195, 91 (1975).
[11] Cato, B. T., *et al.*, *Onsala Res. Rep. No. 123*, Gothenburg (1975).
[12] Lo, K. Y., Burke, B. F., and Haschick, A. D., *Astrophys. J.*, 202, 81 (1975)
[13] Wynn-Williams, C. G., Werner, M. W., and Wilson, W. J., *Astrophys. J.*, 187, 41 (1974).
[14] Downes, D., *Astrophys. Lett.*, 5, 53 (1970).
[15] Hardebeck, E G., *Astrophys. J.*, 170, 281 (1971).
[16] Harper, D. A., in *H II Regions and Related Topics* (edit. by Wilson, T. L., and Downes, D.), 343 (Springer, Berlin, 1975).
[17] Strelnitskii, V. S., and Sunyaev, R. A., *Astr. Zh.*, 49, 704 (1972), *Sov. Astr.*, 16, 579 (1973).
[18] Burdjuzha, V. V., Ruzmaikina, T. V., and Varshalovich, D. A., in *H II Regions and Related Topics* (edit. by Wilson, T. L , and Downes, D.), 195 (Springer, Berlin, 1975).

The identity of lunar hydrolysable carbon

LUNAR soils treated with deuterated acid release a variety of deuterocarbon gases including CD_4, C_2D_6, C_2D_4, C_2D_2 and C_3 species[1-3]. We now suggest that the principal hydrolysable carbon phase in lunar samples is carbon in solid solution in body-centred cubic iron (α-Fe). The yield of deuterocarbons (excluding C_2D_2) from a lunar soil is probably a quantitative estimate of this carbon.

The iron–carbon–oxygen system provides a useful basis for the evaluation of the iron phases in lunar samples although this does not mean that iron in lunar soil is necessarily formed by equilibrium gas phase reduction. We have examined synthetic alloys of carbon in α-Fe, together with some samples of cementite (Fe_3C), prepared by reduction of pure Fe_2O_3 in mixtures of CO and CO_2 at selected temperatures and 1 atm total pressure. The gases released by treatment with 38% DCl in D_2O were analysed by gas chromatography[1]. The conditions of sample preparation, together with X-ray diffraction (XRD) data and the yields of deuterocarbons, are listed in Table 1

The yields of deuterocarbons were low from samples which have been shown by XRD to contain cementite (A3, A5, 8224) and also from sample A1 which, according to the phase diagram, should contain this material. The majority of samples, indicated by XRD to be α-Fe, release considerable quantities of deuterocarbons (up to 0.6% by weight is hydrolysable carbon) the largest amounts being evolved from specimens prepared in conditions of high carbon solubility. An α-Fe (8225) prepared in non-carburising gases (H_2–CO_2 mixtures) had only a minimal amount of reactive carbon.

Our results were unexpected for two reasons. first, we obtained α-Fe samples in conditions which, according to the Fe–C–O phase diagram[4,5], should produce the γ phase; and second, the quantity of carbon present in the α-Fe is greater (up to 0.6 weight %) than the published solubility limit (0.02 weight %) of carbon in α-iron[4,6]. Our starting materials were of much higher purity than those used to establish the phase diagram, and prepared samples were quenched[7] after synthesis, which may allow solubility limits to be exceeded.

From the results, we conclude that iron carbides are unlikely to be the hydrolysable carbon phase in lunar soils. Carbon in solid solution in iron, probably associated with α-Fe, is a more likely candidate. All deuterocarbon gases liberated from lunar soils, with the exception of C_2D_2, can be accounted for by carbon in solid solution in iron phases. None of the synthetic samples released C_2D_2. In the investigation of lunar soils this species presumably results from hydrolysis of groups I and II metal acetylides which are the only carbides shown to release acetylene[8,9]. Since the suggestion[3] that the hydrolysable carbon phase in lunar soil might be the meteoritic carbide, cohenite $(FeNi)_3C$, the iron–carbon phase which is the precursor of the deuterocarbons has been referred to as carbide, "carbide", carbide-like or material reacting as carbide. On the basis of the present results, the use of the term carbide should be discontinued, as iron carbide seems to be essentially inert to acid attack[10]. The only fragments of true carbide to be identified in lunar fines are those recognised by microscopy[11]. As only 1–2% of the carbon in samples of meteoritic cohenite could be converted to deuterocarbons by DCl, it has been suggested that almost all the total carbon present in lunar soils might be associated with iron[12]. If the deuterocarbons released from lunar soil are considered as a quantitative yield of C in α-Fe, then only 15–25% of the total carbon is connected with free metal. The bulk of lunar carbon is presumably implanted solar wind atoms which exist in the silicate matrix of soil grains in an as yet unidentified chemical state.

There is considerable evidence that finely divided submicron-sized iron, which is ubiquitous in lunar soils[13,14] is the α phase. Opaque inclusions $\sim$ 150 Å in diameter in glassy agglutinates, give a diffraction pattern consistent with α-Fe (ref. 15). Ferromagnetic resonance data[16] imply that α-Fe has a low nickel content. The Curie points determined for iron in lunar soils[17,18] ($\sim$ 770 °C) are greater than those for γ-iron and cohenite, which are less than 600 °C and 215 °C respectively[19]. The ratios of C_1 to C_2 deuterocarbons obtained by the Berkeley group[8,20] from lunar soils are similar to the values listed for C in α-Fe in Table 1.

Using data for carbon as CD_4 from 15 lunar soils[1] and values obtained by ferromagnetic resonance spectroscopy[13,21] for the abundance of finely divided metal in aliquots of the same samples, the concentration of carbon in the α-iron in lunar material can be calculated as 0.27–0.77% by weight. The calculated values are in excess of the solid solubility limits of C in α-Fe but are similar to the values obtained for our synthetic α-Fe samples.

The processes of formation of lunar metal and/or the incorporation of carbon evidently allow the normally accepted solid solubility limits to be exceeded. Perhaps iron grains $\sim$ 150 Å in diameter contain insufficient crystal boundaries and defects to promote the crystallisation of carbide. As already stated, it is unlikely that iron in lunar soils was formed in equilibrium conditions. We have tried to reduce silicate glasses of lunar composition in conditions similar to those used for the preparation of α-Fe samples. In all cases, the amounts of CD_4 released from reduced glasses were very small: $<$ 0.05% of the glass had been reduced to Fe metal, even though reaction times of up to 24 h were used. The presence of silicate is known to require more strongly reducing conditions for iron formation[22]. The subsolidus reduction process suggested[17] as the origin of iron in lunar soil may, in fact, be appropriate only to major impacts which produced highly metamorphosed breccias containing coarse grained iron and very little hydrolysable carbon[23].

Of the mechanisms which have been suggested for the formation of metallic iron in the lunar regolith, only preferential sputtering by the solar wind has been shown to be both theoretically feasible[24] and practically possible[25].

Table 1 Deuterocarbons released by DCl dissolution of synthetic iron–carbon phases

Sample	Temp. (° C)	Preparation CO in reducing gas* (%)	Deuterocarbon yield µg C per g CD_4	C_2D_4	C_2D_6	Total	$CD_4/C_2D_4+C_2D_6$	XRD
A1	700	80	346	NM	NM	346	—	No peaks
A3	800	90	ND	ND	ND	ND	—	Fe_3C
A4	900	90	4,891	493	1,071	6,455	3.13	α
A5	900	96	1,088	NM	NM	1,088	—	α+Fe_3C
8222†	800	79	2,488	527	1,230	4,245	1.42	α
8224	800	100	ND	ND	ND	ND	—	Fe_3C
8225	800	0§	49	ND	6	55	8.36	α
8226	800	86	1,433	285	729	2,447	1.41	α
8227	800	84	3,976	149	1,002	5,127	3.45	α
8228	900	86	313	41	164	528	1.53	α
8229	900	90	1,621	733	984	3,338	0.94	α
8231	930	90	1,196	463	722	2,381	1.01	α
8232	900	80	908	186	437	1,531	1.46	α
8233	800	72	947	149	310	1,406	2.06	α
8234	700	70	2,327	530	1,368	4,225	1.23	α
8235	900	73	113	152	53	318	0.55	α

* Balance due to CO_2, total pressure 1 atm.
† Average of four analyses.
§ Non-carburising reactions conditions 1:1 mixture of H_2 and CO_2.
NM, Not measured; ND, not detected.

Carbon could form solid solutions in surface layers of α-iron produced by sputtering in one or more of the following ways: (1) direct implantation of solar wind carbon into metal—this process is capable of producing solid solutions of carbon in α-iron in excess of solubility limits[26]; (2) under the influence of sputtering, the particle surface will be eroded and iron at the surface will gradually reach carbon previously implanted by the solar wind[27]; (3) thermal events associated with agglutination could induce migration of solar wind carbon from implantation sites to the surface iron[27], and micrometeorite impacts may release carbon species which carburise metal on the surfaces of adjacent grains[10]. All of these suggested processes for carbon could be applicable to the accumulation of chemically bound nitrogen in lunar samples[28]. The increased solubility of nitrogen in iron[6] would account for the greater retentivity of nitrogen[28,29].

We thank the SRC for support and for fellowships to C.T.P. and A.J.T.J. Work in Edinburgh (G.M.B.) was supported by the NERC. B.D.B. thanks Macquarie University for leave of absence. We are also grateful to Dr A. K. Galwey, Queen's University Belfast, for samples of cementite and Hägg carbide, which were used in preliminary investigations.

A. J. T. Jull
G. Eglinton
C. T. Pillinger

Organic Geochemistry Unit,
School of Chemistry,
University of Bristol,
Bristol BS8 1TS, UK

G. M. Biggar

Grant Institute of Geology,
University of Edinburgh,
Edinburgh EH9 3JW, UK

B. D. Batts

Department of Chemistry,
Macquarie University,
North Ryde, NSW, Australia

Received May 4; accepted July 7, 1976.

[1] Pillinger, C. T , *et al* , *Geochim. cosmochim. Acta*, *suppl.* 5, 2, 1949–1961 (1974), and references cited therein.
[2] Holland, P. T , Simoneit, B. R , Wszolek, P. C., and Burlingame, A. L., *Geochim. cosmochim. Acta, suppl.* 3, 2 (edit. by Heymann, D.), 2131–2147 (1972).
[3] Chang, S., *et al* , *Geochim cosmochim. Acta*, *suppl* 1, 2 (edit by Levinson, A. A), 1857–1869 (1970).
[4] Benz, M. G., and Elliot, J. F., *Trans. Met. Soc. AIME*, 221, 323–331 (1961).
[5] Elliot, J. F., Glieser, M , and Ramakrishna, V., *Thermo Chemistry for Steel Making*, 2 (Addison-Wesley, New York, 1963).
[6] Hume-Rothery, W., *The Structures of Alloys of Iron—an Elementary Introduction* (Pergamon, London, 1966)
[7] Biggar, G. M., *Min. Mag.*, 39, 580–586 (1974).
[8] Wszolek, P. C., Simoneit, B. R , and Burlingame, A. L , *Geochim. cosmochim. Acta*, *suppl.* 4, 2, 1693–1706 (1973).
[9] Evered, S., thesis, Univ. Bristol (1963).
[10] Jull, A J. T., *et al.*, *Lunar Sci.*, VI, 457–459 (1975).
[11] Frondel, C., Klein, C., Ito, J., and Drake, J. C., *Geochim. cosmochim. Acta, suppl* 1, 1, 445–474 (1970).
[12] Cadogan, P H., *et al.*, *Geochim. cosmochim. Acta*, *suppl.* 4, 2, 1493–1508 (1973).
[13] Grant, R. W , Housley, R. M , and Paton, N. E., *Geochim. cosmochim. Acta, suppl.* 4, 3, 2737–2749 (1973).
[14] Cisowski, C S., Fuller, M., Rose, M. F , and Wasilewski, P. J., *Geochim. cosmochim. Acta*, *suppl.* 4, 3, 3003–3017 (1973).
[15] Pillinger, C. T., Davis, P. R., Gardiner, L. R., Naziri, H., and Champness, P. E , *Geochim cosmochim. Acta*, *suppl.* 6, 2, 2343–2352 (1975).
[16] Tsay, F. D., Manatt, S. I , Live, D. H., and Chan, S. I., *Geochim. cosmochim. Acta*, *suppl* 4, 3, 2751–2761 (1973).
[17] Pearce, G. W., Gose, W. A , and Strangway, D. W., *Geochim. cosmochim Acta, suppl.* 4, 3, 3045–3076 (1973).
[18] Runcorn, S K., *et al.*, *Geochim. cosmochim. Acta*, *suppl.* 1, 3, 2369–2387 (1970).
[19] Brecher, A., thesis, Univ. California, San Diego (1972).
[20] Wszolek, P. C., and Burlingame, A. L , *Geochim. cosmochim. Acta*, *suppl.* 4, 2, 1681–1692 (1973).
[21] Housley, R. M., Cirlin, E. H., Paton, N. E , and Goldberg, I. B., *Geochim. cosmochim. Acta*, *suppl* 5, 3, 2623–2642 (1974).
[22] Darken, L. S., *J Am. chem. Soc.*, 70, 2046–2053 (1948).
[23] Eglinton, G., *et al.*, *Geochim. cosmochim. Acta*, *suppl.* 5, 2, 1159–1180 (1974).
[24] Pillinger, C. T., Gardiner, L. R., Jull, A J T., and Woodcock, M. R., *Lunar Sci.* VII, 706–708 (1976).
[25] Yin, L. I., Tsang, T , and Adler, I., *Geochim. cosmochim Acta*, *suppl* 6, 3, 3277–3284 (1975).
[26] Feldman, L. C., Kaufmann, E. N , Poate, J. M., and Augustiniak, J., *Proc. Third Int. Conf. Ion Implantation in Semiconductors and Other Materials*, 491–502 (Plenum, Oxford, 1973).
[27] Pillinger, C. T., Jull, A J T., Eglinton, G., and Epstein, S., *Lunar Sci.*, VII, 703–705 (1976).
[28] Muller, O., *Geochim. cosmochim. Acta*, *suppl.* 4, 2, 1625–1634 (1973).
[29] DesMarais, D. J., Hayes, J. M., and Meinschein, W. G., *Geochim. cosmochim. Acta*, *suppl.* 5, 2, 1811–1822 (1974).

Implications of metal dispersion from submarine hydrothermal systems for mineral exploration on mid-ocean ridges and in island arcs

METAL enrichments in sediments on open ocean mid-ocean ridge segments and in island arcs have been known for some time[1–4], but, to date, no deposits have been found which are rich in copper, zinc and other heavy metal sulphides to a degree comparable to those in the Red Sea. The fact that concentrated brines were thought to have played an essential role in the formation of the Red Sea metalliferous sediments may have inhibited the search for similar deposits elsewhere, because brines of the Red Sea type are unlikely to occur in the open ocean. The discovery at Matupi Harbour, New Britain, however, that high salinity is not a prerequisite for metal enrichment in hydrothermal solutions[5], indicates that any area of submarine volcanic activity has a potential for high grade metalliferous sediment formation given suitable depositional conditions. In this report the dispersion of metals from submarine hydrothermal sources

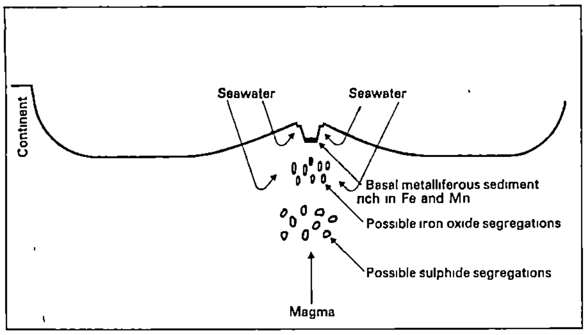
Continent
Seawater
Seawater
Basal metalliferous sediment rich in Fe and Mn
Possible iron oxide segregations
Possible sulphide segregations
Magma

Fig. 1 Hypothetical vertical sequence of precipitates on mixing of ascending metal-bearing hydrothermal solution with seawater beneath mid-ocean ridge crests in the open ocean. This sequence occurs horizontally on the sea floor around hydrothermal centres in restricted environments like the Atlantis II Deep in the Red Sea and in shallow water volcanic areas, indicating that the nature of the environment of deposition controls the initiation of the depositional process.

is discussed, and its usefulness in developing guidelines for undersea mineral exploration in volcanic areas is considered.

Metalliferous sediments on mid-ocean ridges and in island arcs are thought to form largely as a result of hydrothermal leaching of the oceanic crust by circulating seawater, which in turn becomes both acid and reduced[6,7]. Precipitation of the metals so derived gives rise to deposits which are characteristically rich in iron oxides and sometimes in a variety of other metals such as manganese, copper, zinc and lead; and occasionally, as in the Red Sea, include metal sulphides of localised distribution and very variable composition. It is the latter which are of potential economic value.

Evidence that mid-ocean ridge sediments vary in composition over short distances in the open ocean, and thus may locally be of high grade has been obtained on the Mid-Atlantic Ridge at 45°N (ref. 8). The chemical variations, particularly in the relative dispersion of iron and manganese, were thought to be related partly to the proximity of the samples analysed to submarine hydrothermal sources of the metals and partly to their selective precipitation on mixing with seawater. Unfortunately, the implications of these variations, in terms of geochemical exploration, for metalliferous sediments could not be evaluated because the location of the presumed hydrothermal outlets on the sea floor were not known. More recently, the selective dispersion and precipitation of iron and manganese from a known hydrothermal source has been noted in the FAMOUS area on the Mid-Atlantic Ridge (X. Le Pichon, personal communication), and hydrothermal manganese deposits have been found on the Mid-Atlantic Ridge at 26°N (ref. 9). Nevertheless, there has been no systematic study published to date of metal dispersion from a submarine hydrothermal source in the deep ocean. Fortunately, however, the likely nature of deep-sea hydrothermal metal dispersion can be deduced from studies of submarine hydrothermal systems in the Red Sea and off Santorini. On this basis a model has been constructed which attempts both to predict the most favourable environments for high grade metalliferous sediment formation on the ocean floor and to aid in the location of the sediments.

Metalliferous sediments of hydrothermal origin have been studied in both the Red Sea, and off the volcano of Santorini in the Cyclades Volcanic Arc in the eastern Mediterranean Sea. In each case there is a dispersion halo of metals around the hydrothermal source, showing, among other things, the selective dispersion of manganese from iron[10,11] (Fig. 1). A similar sequence has been observed around hydrothermal springs debouching into Matupi Harbour, New Britain[12]. These variations probably reflect the well known separation of manganese from iron with changing *p*H and *E*h (ref. 13). Poorly oxidised or reduced acid hydrothermal solutions precipitate the metals selectively on mixing with more alkaline oxidising seawater. Metals other than manganese and iron also exhibit a fractional precipitation in submarine hydrothermal systems. In the Atlantis II Deep of the Red Sea, for example, the first formed precipitates on discharge of the hydrothermal solutions are heavy metal sulphides which occupy a restricted area of the Deep adjacent to the hydrothermal vents[14]. Similarly, sulphides occur underneath the sediments rich in iron oxides near the hydrothermal vents in the caldera of Santorini[15], and immediately adjacent to fumaroles off the Island of Vulcano in the Eolian Archipelago, Western Mediterranean[16]. It seems, therefore, that a model for the complete sequence of precipitates on mixing of hydrothermal solutions with seawater would include the fractional dispersion and precipitation of metal sulphides, followed by iron silicates and/or iron oxides, and finally manganese oxides.

This complete sequence of precipitates has not been reported to date on mid-ocean ridges in the open ocean. The iron- and manganese-rich metalliferous sediments characteristic of such ridges, however, are compositionally similar to the widely dispersed iron and manganese oxides around the Atlantis II Deep where the complete sequence is observed. This suggests that the former may be the equivalent of the sediment in the outer zone of the Atlantis II dispersion halo. If this is so, the sulphide deposits which the model predicts should be present in association with the iron and manganese oxides may occur either in restricted locations near to the hydrothermal vents or within the oceanic crust below the oxide deposits. The general physicochemical nature of seawater over mid-ocean ridge crests in the open ocean would favour the latter alternative in most cases. Oxidising seawater can be expected to penetrate fractures and fissures in the upper part of the oceanic crust leading to mixing with ascending hydrothermal solutions and the precipitation of metal sulphides before the solutions reach the surface (Fig. 1). Disseminated sulphides within rocks of the oceanic crust have been reported by several authors[17–19]. Special conditions leading to a reducing environment at elevated temperature, such as occur in the Atlantis II Deep of the Red Sea, would be required to delay sulphide precipitation until the hydrothermal solutions debouch on to the sea floor.

If sulphides are largely precipitated from submarine hydrothermal solutions within the oceanic crust, where else on the sea floor other than in the Red Sea and in small restricted embayments around volcanic islands might they be expected to form? One obvious locale is within the deep fracture zones which cut mid-ocean ridges in all the oceans and which often expose the oceanic crust to considerable depths. Deep hydrothermal circulation under these fracture zones coupled with the possibility of locally reducing conditions in narrow deep basins, could lead to the precipitation of heavy-metal sulphides. Bonatti *et al.*[20] have explained high heat flow in some fracture zones on the basis of sub-seafloor hydrothermal circulation, and have reported the occurrence of pyrite concretions of supposed hydrothermal origin in the Romanche Fracture Zone, Equatorial Atlantic. In addition, Scott *et al.*[21] have reported the occurrence of manganese deposits of probable hydrothermal origin in the Atlantis II Fracture Zone in the North Atlantic. An additional likely locale for heavy metal sulphide precipitation is in the basins associated with island arcs. These can be both volcanically active[22] and sufficiently topographically diverse to possibly lead to a locally restricted circulation and reducing conditions favourable for sulphide deposition. Ancient marginal seas associated with island arcs are thought to have been the environment of formation of some massive sulphide deposits now exposed on land[23]. Iron- and manganese-rich sediments similar to those on mid-ocean ridges have been found in association with the island arc system in the south-western Pacific Ocean[24], and submarine sulphide deposits may also be present.

It is evident from the above that mid-ocean ridge fracture zones and island arcs warrant more attention in the search for ocean floor metalliferous sediments. The dispersion model discussed here may additionally be of use in locating such deposits. The dispersion halo of manganese around the Atlantis II Deep deposit is up to 20 km in diameter even though the sulphide deposit itself is much smaller[25]. Thus in designing a grid sampling program to locate heavy metal sulphides on the ocean floor, one could look initially for manganese dispersion haloes on a wide-spaced sampling pattern, and, if located, design a smaller grid to search the vicinity for heavy metal sulphides. Tests of the model as an exploration tool are currently being conducted around the TAG hydrothermal field on the Mid-Atlantic Ridge at 26°N, and in a fracture zone transecting the East Pacific Rise at 9°S.

This work was supported by the NERC.

D. S. CRONAN

AGRG, Department of Geology,
Imperial College, London SW7, UK

Received May 26; accepted July 5, 1976.

[1] Bostrom, K., and Peterson, M. N. A., *Econ. Geol.*, **61**, 1258 (1966).
[2] Bostrom, K., Peterson, M. N. A., Joensuu, O., and Fisher, D. E., *J. geophys. Res.*, **74**, 3261 (1969).
[3] Bertine, K., *Geochim. cosmochim. Acta*, **38**, 629 (1974).
[4] Cronan, D. S., in *The Sea*, **5** (edit. by Goldberg, E. D.), 491 (Wiley, New York, 1974).
[5] Ferguson, J., and Lambert, J. B., *Econ. Geol.*, **67**, 25 (1972).
[6] Corliss, J. B., *J. geophys. Res.*, **76**, 8128 (1971).
[7] Spooner, E., and Fyfe, W., *Contrib. Miner. Petrol.*, **42**, 287 (1973).
[8] Cronan, D. S., *Can. J. earth Sci.*, **9**, 319 (1972).
[9] Scott, R. B., Rona, P. A., McGregor, B. A., and Scott, M. R., *Nature*, **251**, 301 (1974).
[10] Bignell, R., Cronan, D. S., and Tooms, J. S., *Trans. Inst. Min. Metal.* (in the press).
[11] Smith, P. A., and Cronan, D. S., *Oceanology International Conference*, Brighton, 111 (BPS Exhibitions, London, 1975).
[12] Ferguson, J., and Lambert, J. B., *Econ. Geol.*, **67** (1972).
[13] Krauskopf, K., *Geochim. cosmochim. Acta*, **12**, 61 (1957).
[14] Backer, H., and Richter, H., *Geol. Rdsch.*, **62**, 697 (1973).
[15] Butuzova, G., *Dokl. Acad. Nauk. SSSR*, **168**, 1400 (1966).
[16] Honnorez, J., Honnorez-Guerstein, B., Valette, J., and Wauschkuhn, A., in *Ores in Sediments* (edit. by Amstutz, G., and Bernard, A.), 139 (Springer, Berlin, 1972).
[17] Baturin, G. N., in *The History of the World Ocean* (edit. by Zenkevitch, L. A.), 259 (Nauka, Moscow, 1971).
[18] Dmitriyev, L. V., Barsukov, V. L., and Udintsev, G. B., *Geochemistry*, **8**, 935 (1970).
[19] Bonatti, E., Honnorez-Guerstein, B., and Honnorez, J., *Econ. Geol.* (in the press).
[20] Bonatti, E., Honnorez-Guerstein, M., Honnorez, J., and Stern, C., *Earth planet. Sci. Lett.* (in the press).
[21] Scott, R., Rona, P. A., Butler, L. W., Nalwalk, A. J., and Scott, M. R., *Nature*, **239**, 77 (1972).
[22] Weissel, J. K., and Watts, A. B., *Earth planet. Sci. Lett.*, **28**, 121 (1975).
[23] Taylor, G., *Trans. Inst. Min. Metal.*, **83**, 120 (1974).
[24] Bertine, K., *Geochim. cosmochim. Acta*, **38**, 629 (1974).
[25] Bignell, R., Cronan, D. S., and Tooms, J. S., *Trans. Inst. Min. Metal.* (in the press).

Observation of the interference of neutrons reflected from thin films

DURING measurements of the reflection of neutrons from metallic thin films, we have observed an optical interference phenomenon analogous to the interference of light reflected from plane parallel plates; the experimental arrangement is the neutron analogue of the Lummer–Gehrcke interferometer[1].

A simple application of Snell's Law[2] predicts the essential features of the effect, which is illustrated in Fig. 1. We recall that neutrons of wavelength λ incident at glancing angles θ_1, on a material characterised by a mean coherent scattering length b and with a density of scattering centres N, undergo total reflection when $\theta_1 < Re\,(\theta_c)$ where the critical glancing angle θ_c is given by[3]

$$\theta_c = \lambda\,(Nb/\pi)^{\frac{1}{2}} \tag{1}$$

The refractive index n_2 of the film material may be written as

$$n_2 = 1 - \theta_c^2/2 \tag{2}$$

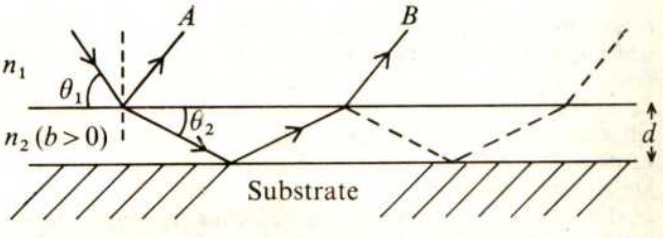

Fig. 1 Reflection of neutrons from a plane parallel plate. n_1 and n_2 are the refractive indices in air and in the thin film respectively. (Note that for neutrons $\theta_2 < \theta_1$, in contrast to the case for light.) Angles are greatly exaggerated for clarity.

Since b may be positive or negative, n_2 may be larger or smaller than 1. From classical optics[1], the path difference for beams A and B can be shown to be

$$\Delta = 2d(\theta_1^2 - \theta_c^2)^{\frac{1}{2}} \tag{3}$$

As there is no phase change for the reflection of neutrons, the condition for constructive interference is given by

$$\Delta = m\lambda \qquad (\text{where } m = 0, 1, 2 \ldots) \tag{4}$$

For positive values of b, $m = 0$ corresponds to the limit for total reflection, and interference fringes will only be observed when $\theta_1 > \theta_c$; for negative values of b, interference is possible at all glancing angles. From equations (3) and (4) we see that at a given angle of reflection θ_1, intensity maxima will occur when

$$\lambda = \frac{2d}{m}(\theta_1^2 - \theta_c^2)^{\frac{1}{2}} \tag{5}$$

This analysis determines only the relation between θ_1 and λ at the intensity maxima, and is unaffected by multiple reflection effects.

Interference fringes were observed by reflecting a narrow (1-mm wide), well collimated (divergence $= 1.5 \times 10^{-4}$ rad) neutron beam from thin metallic films evaporated on to plane glass substrates. The film materials used (Be and a magnetised $Co_{0.5}Fe_{0.5}$ alloy) have critical glancing angles greater than that of glass, thus ensuring that substrate reflections do not contribute to the interference peaks. At angles of incidence $\theta_1 > \theta_c$ interference fringes will be observed at wavelengths which satisfy equation (5). For the magnetised material

Fig. 2 Interference fringes measured for neutron reflection from a magnetised $Co_{0.5}\,Fe_{0.5}$ thin film. The wavelength spectrum of the incident beam is shown dashed (not to scale) for comparison. λ^* is the critical wavelength (equation (1)) above which all neutrons are totally reflected at this incident angle ($\theta_1 = 1.5 \times 10^{-2}$ rad). △ represents the wavelength resolution.

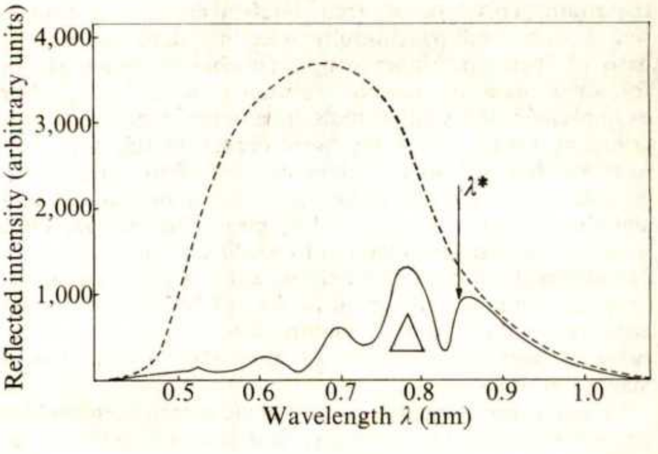

b (equation (1)) is replaced by $(b+p)$ and $(b-p)$ for the two neutron spin states in the incident beam, where p is a magnetic scattering length, and where $|b| \simeq |p|$ it is only for the $(+)$ neutron spin state that n_2 differs significantly from unity. This situation exists for the magnetised alloy we used, therefore the neutrons detected in the interference peaks for this thin film are also spin polarised.

The experiment consisted of reflecting a polychromatic incident beam (mean wavelength $\lambda_0 = 0.7$ nm) at a fixed angle θ_1, and analysing the wavelength spectrum of the reflected beam by the neutron time of flight method. The measurements were carried out on the IN11 instrument at the High Flux Reactor, Institut Laue–Langevin, Grenoble; the angular resolution $\delta\theta/\theta_1$ was 1% and the wavelength resolution $\delta\lambda/\lambda_0$ was 5%.

Figure 2 shows the time of flight data observed for a magnetised $Co_{0.5}Fe_{0.5}$ film of thickness 100 ± 15 nm (as measured by a quartz crystal thickness monitor) at $\theta_1 = 1.5 \times 10^{-2}$ rad. Fitting equation (5) to the measured fringe positions gave a 'best-fit' thickness $d = 88 \pm 5$ nm, in agreement with the thickness measured during the evaporation of the film.

The wavelength spectrum of the incident beam (see Fig. 2) limited our observation to four orders of interference. For the beam divergence used, and assuming that the film thickness is completely uniform, the Heisenberg Uncertainty Principle requires the neutron coherence length in this example to be at least 70 nm; it should therefore be possible to observe interference fringes to much higher orders than are reported here.

J. B. HAYTER

Institut Laue-Langevin,
Grenoble, France

J. PENFOLD
W. G. WILLIAMS

Neutron Beam Research Unit,
Rutherford Laboratory,
Chilton, Didcot OX11 0QX, UK

Received March 29; accepted May 4, 1976.

[1] Born, M., and Wolf, E., in *Principles of Optics*, ch. VII (Pergamon Press, Oxford, 1970).
[2] Just, W., Schneider, C. S., Ciszewski, R., and Shull, C. G., *Phys. Rev. B*, **7**, 4142–4145 (1973).
[3] Gurevich, I. I., and Tarasov, L. W., in *Low-Energy Neutron Physics*, ch. 1.2, (North-Holland, Amsterdam, 1968).

Optical methods to select diamonds of very high lattice perfection

WE describe here recent developments which permit the selection of diamonds very free from strain by purely optical inspection. Figure 1*a* shows the edge of a diamond slab which chipped while being polished, and Fig. 1*b* the same slab viewed between crossed polars[1]. The birefringent pattern indicates a region of strain centred near the crack, and a dark area where the chip has come away relieving the strain. This type of strain birefringence is, of course, well known, and by carefully selecting diamonds on the basis of their birefringence it is possible to obtain stones for tools with a superior resistance to chipping. For example, the six similar tools in a wear experiment described by Casey and Wilks[2] were chosen in this way, and wore steadily without any chipping. Bell, Wilks and Wilks[3] have described how the resistance of a diamond to cracking and chipping may be estimated by measuring the load on a small diamond sphere required to produce a ring crack on a flat diamond surface. In these experiments, measurements on a diamond slab chosen to be free of birefringence gave consistent values of the fracture load which were about twice as high as those on another slab which showed marked birefringence.

Minimal birefringence is an obvious requirement for strain free stones, but a more critical selection can be made by inspecting the natural octahedron surfaces of a diamond using phase contrast or Nomarski interference techniques. This method had its genesis in an observation[4] of a good quality gem octahedron which exhibited a small group of very shallow pyramidal depressions, or trigons, situated somewhat away from the centre of each face. The fact that the three lines joining the centres of opposite groups of trigons met approximately in the same internal region of the diamond, suggested the presence of an inclusion, from which dislocations spread out to the surface, where they gave rise to the trigon etch features. This interpretation was subsequently confirmed by Frank and Lang[5] using X-ray topography. The presence of trigons on a natural face is thus a further indication of internal strain, and subsequent experiments by Wilks and Wilks[6] showed a marked correlation between the density of trigons and the degree of birefringence. A third indication of lattice imperfection is that carefully polished cube faces of diamond containing impurities deposited on octahedral planes during growth often exhibit rectangular markings or traces where these planes of impurities intersect the surface[7]. In fact, we have never observed any such traces on diamonds selected to have minimum birefringence and freedom from trigons[6].

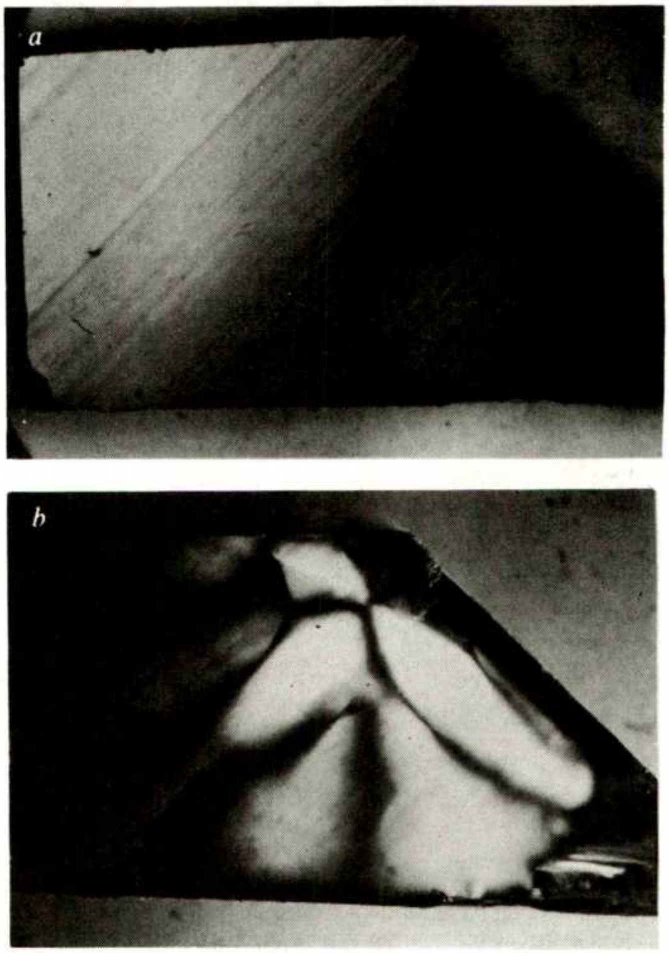

Fig. 1 The polished face of a slab of diamond viewed *a* in incident light, *b* between crossed polars (×36).

Perhaps the most refined selection of strain free diamonds yet made is our recent selection of diamonds for targets for the production of polarised photons in the 5-GeV electron synchrotron NINA of the SRC Daresbury Laboratory, as described by Jackson[8]. To produce polarised photons, the diamond must be oriented so that the synchrotron beam makes an angle of ~ 2×10^{-3} rad with a set of lattice planes in the diamond, with an accuracy of better than 10^{-4} rad. It follows that any local misorientations of the diamond lattice must be small compared with 2×10^{-3} rad, but natural diamonds frequently show lattice curvature of this order. The first stone selected by our optical inspection had a curvature as indicated by an X-ray rocking curve analysis of $<5\times10^{-5}$ rad, and was the first diamond to give a satisfactory beam of polarised photons at Daresbury[8]. Subsequently two more diamonds selected in the same way have met the same stringent requirement of producing a satisfactory beam of photons. Of course, to obtain such a degree of perfection it is necessary to use high quality optics and to make the selection from a large sample of diamonds.

I thank De Beers Industrial Diamond Division for their support, and Mr W. F. Cotty for discussions.

E. M. WILKS

Clarendon Laboratory,
Oxford, UK

Received May 26, accepted July 2, 1976.

[1] Wilks, J., *Ind Diam. Rev.*, 382 (1973).
[2] Casey, M., and Wilks, J., *Diam Res.* 11 (1972), *Int. J. Mach Tool Des Res.*, 16, 13 (1976).
[3] Bell, J. G., Wilks, E. M., and Wilks, J., *Ind. Diam. Rev*, 135 (1975)
[4] Frank, F. C., Puttick, K. E., and Wilks, E M., *Phil. Mag.*, 3, 1262 (1958).
[5] Frank, F C., and Lang, A. R., *Phil. Mag.*, 4, 383 (1959).
[6] Wilks, E M., and Wilks, J., *Ind. Diam. Rev.*, 238 (1971)
[7] Wilks, E. M., *Diam. Res.*, 7 (1969).
[8] Jackson, A., *Nucl. Instrumen. Meth.*, 129, 73 (1975).

Ordered states in systems of macroscopic particles

ONE of the most striking observations of systems consisting of macroscopic particles (~ 1 μm in diameter) dispersed in a uniform background, is that in certain circumstances the particles can form themselves into an ordered or solid-like array. The importance and significance of these structures to a wide range of materials, including virus suspensions, soils, lacquers and latices, was recently discussed quite extensively by Efromov[1]. In recent years this has also been the subject of considerable experimentation on well characterised polystyrene latices[2–4]. We have developed a theoretical model for a stable colloidal dispersion[5] in which this disorder–order transition in a system of macroscopic particles is treated as the analogue of the fluid–solid transition in molecular materials. This theoretical approach shows that this ordering is a consequence of the repulsive forces between the particles. We show the more detailed features of the structure of the disordered and ordered phases of systems of colloidal or macroscopic particles.

Briefly, the model replaces an infinite system of interacting particles by a small (32 or 108 particles) periodic system. The interaction[6], consisting of a combination of van der Waals' attraction and double layer repulsion, is assumed to operate between all possible pairs of particles in the system. The properties of the system, such as excess pressures, internal energies and radial distribution functions, are then obtained by Monte Carlo averaging over the likely configurations of the particles. The results obtained are very similar to the measured properties of aqueous polystyrene colloids[5,7]; thus the model is at least qualitatively correct.

One significant advantage of the Monte Carlo model, over perhaps more expedient but less exact approaches[7], is that it enables one to obtain much finer details of the structure of a system than can be obtained experimentally. For example, one cannot only calculate the experimentally accessible radial distribution function, but also the higher order distribution functions[8,9] and, even more interestingly, typical configurations can be displayed with the Monte Carlo model[10].

We have chosen a colloidal system consisting of spherical particles of diameter 595 nm with a surface potential of 60 mV, dispersed in an aqueous electrolyte (relative permittivity of 80) at room temperature[5]. The results of the Monte Carlo model at electrolyte concentrations of 0.5 mol m^{-3} and 0.05 mol m^{-3} will be discussed.

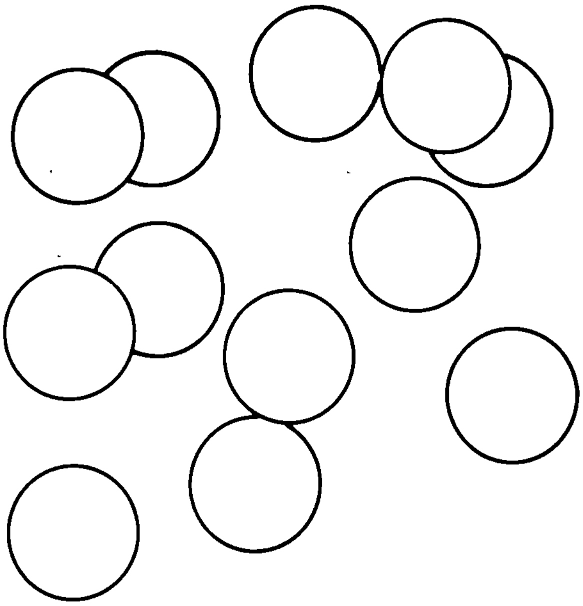

Fig. 1 Two-dimensional projection of a typical Monte Carlo (MC) configuration for a volume fraction φ = 25% and concentration of monovalent 1:1 background electrolyte $n = 0.5$ mol m^{-3}.

For the higher electrolyte concentration the particles form an ordered array (face-centred cubic (fcc)) for percentage volume fractions, φ, in excess of 43%. This may be seen from the radial distribution functions, $g(r)$, calculated for the respective volume fractions at this electrolyte concentration[5]. To demonstrate what this gross structure indicator, $g(r)$, is showing, we display typical particle configurations for φ=25% and φ=50% in Figs 1 and 2, respectively. (In these diagrams we have drawn only those particles whose centres lie in a slice of thickness approximately equal to one particle diameter.) As may be seen, the system of particles at the higher volume fraction is indeed ordered and nearly conforms to a perfect fcc structure

Fig. 2 Two-dimensional projection of a typical MC configuration for φ = 50% and $n = 0.5$ mol m^{-3}.

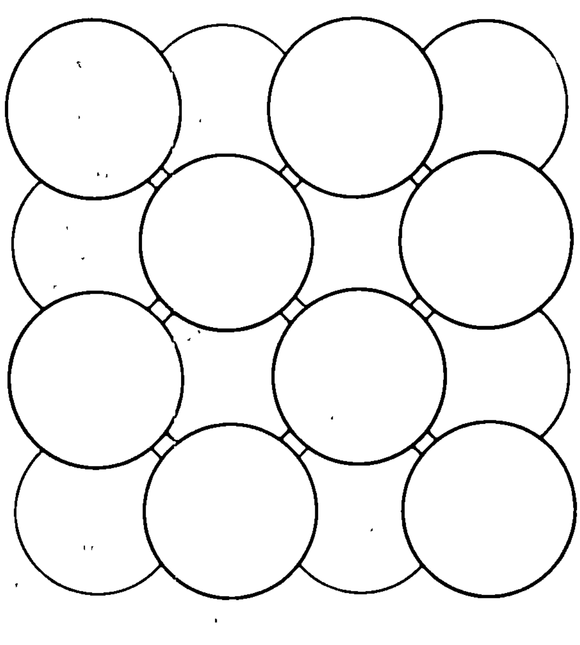

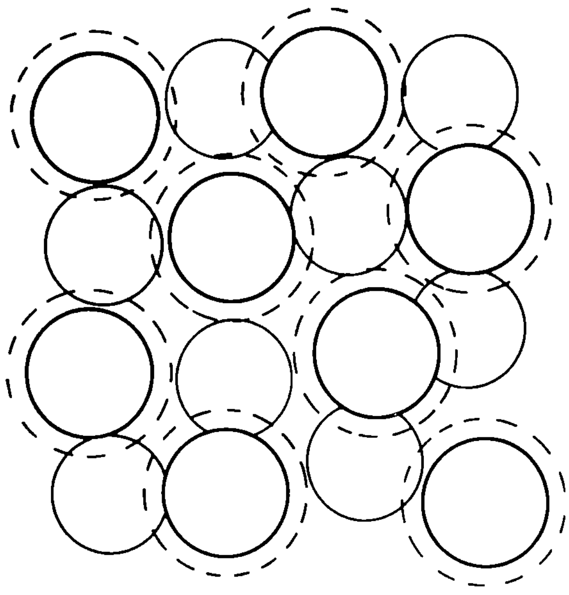

Fig. 3 Two-dimensional projection of a typical MC configuration for $\varphi = 25\%$ and $n = 0.05$ mol m^{-3}. The dashed circles represent the effective particles.

with a particle surface to surface separation as one would expect in a microscopic crystal. On the other hand, no such ordering is evident for the system of particles at the lower volume fraction.

At the lower electrolyte concentration (0.05 mol m^{-3}) the particles change to an ordered state at $\sim \varphi=25\%$. Figure 3 shows the distribution of particles for this case for $\varphi=25\%$. Again, an almost regular fcc arrangement is indicated but now with a particle surface to surface separation of $\sim$ 280 nm. As one lowers the background electrolyte concentration the particles order themselves at progressively lower volume fractions.

The reason for this behaviour is that the bare particle diameter is not a good indicator of the real size of the particle. Rather, the effective size of the particle is that of the particle plus the effective thickness of the attached double layer, the latter being a measure of the range of the repulsive potential acting between the particles. In terms of this effective diameter the properties of the system, including the disorder–order transition, can be very simply accounted for by means of a hard sphere model[11]. Some simple criteria exist for calculating the effective hard sphere diameter and Fig. 3 shows the effective particles superposed on the real particles. The effective volume fraction of the system is $\sim$ 50% with the mean surface to surface separation of the effective particles $\sim$ 25 nm (see Fig. 2).

One final point to be made is that the exact lattice type observed for the ordered phase will depend strongly on the interparticle potential, particularly on its range.

In conclusion, it is hoped that this short article has demonstrated the power of machine methods to explore and display the structure of physical systems in general, and that it will be used more in the future to help visualise and understand the fascinating properties of colloidal dispersions, in particular.

WILLIAM VAN MEGEN
IAN SNOOK

Department of Applied Physics,
Royal Melbourne Institute of Technology,
Melbourne, Victoria, Australia

Received May 18, accepted June 30, 1976.

[1] Efromov, I F., in *Surface and Colloid Science* (edit. by Matijevic, E.), **8** (Wiley-Interscience, New York, 1976).
[2] Brown, J. C., Pusey, P. N., Goodwin, J W., and Ottewill, R. H., *J. Phys. A*, **8**, 664–682 (1975).
[3] Hachisu, S., Kobayashi, Y., and Kose, A., *J. Colloid Interface Sci.*, **42**, 342–348 (1975).
[4] Hiltner, P. A., and Krieger, I. M., *J. Phys. Chem.*, **73**, 2386–2389 (1969).
[5] van Megen, W., and Snook, I., *J. Colloid Interface Sci.*, **53**, 172–177 (1975); *J chem. Soc. (Faraday Trans.)*, **72**, 216–223 (1976)
[6] Kruyt, H R., (ed), *Colloid Science*, **I** (Elsevier, Amsterdam, 1952).
[7] van Megen, W., and Snook, I., *J. Colloid Interface Sci* (in the press).
[8] Raveche, H. J., Mountain, R. D., and Streett, W. B., *J. chem. Phys*, **61**, 1970–1984 (1974).
[9] Woodcock, L V., *Proc. R Soc.*, **A328**, 83–95 (1972).
[10] Woodcock, L. V., *Nature*, **232**, 63–64 (1971).
[11] van Megen, W., and Snook, I, *Chem. Phys. Lett.*, **35**, 399–402 (1975)

Polymer effects on microjet impact and cavitation erosion

THERE is a growing interest in using high molecular weight polymers as additives in various fluid-engineering systems. These activities are mainly stimulated by the anomalous drag reducing characteristics some high polymers exhibit in turbulent flows[1]. Early experiments also showed that polymeric additives suppress flow-generated cavitations[2,3]. An interesting question may therefore be raised as to the effects of high molecular weight polymers on cavitation erosion. We report here attempts made to examine such effects on static vibration-generated cavitation and flow cavitation.

It is generally accepted that in cavitation erosion the main damage results from the collapse of single cavitation bubbles near the solid surface. In such a collapse an inward moving microjet is always formed against the solid surface[4] and the damaging effect of the microjet with velocity as high as 130 m s^{-1} impinging on the surface[5] has been confirmed[6]. It was proposed earlier[7] that polymer viscoelastic effect might introduce very high stresses by stretching the fluid, and consequently the formation of the microjet might be retarded. It was not, however, realised until recently that the development of such high stresses requires substantial flow time[8]. In the case of a microjet, although the jet velocity increases rapidly to apply a strong stretching to polymer molecules, the flow time involved is only $\sim 10^{-6}$ s, considerably shorter than polymer relaxation times ($\sim 10^{-3}$ s). Therefore one may have to expect that any polymer effect on microjet formation and thus cavitation erosion would be minimal.

Recently, Ashworth and Proctor[9] reported the results of standard vibratory tests in solutions of a hydrolysed polyacrylamide, where the cavitation erosion rate is increased. They also showed that the viscous effect was not responsible for the increased damage because, in a water–glycerol mixture, the cavitation damage was actually decreased greatly. While no indication of the possible mechanism was given, the result of increased damage was considered to be analogous to that of enhanced jet-cutting in polymer solutions[10]. Some remarks will now be offered with regard to this proposed analogy.

First, the high speed liquid jets for jet-cutting operations have very high Reynolds numbers and are therefore turbulent. In these applications fluid momentum is converted into stagnation pressure to erode away the solid material. The effect of polymer in this case is mainly to introduce improved local stability to prevent small scale jet breakup. The result is that the turbulent jet possesses less violent appearance, higher velocity and longer throw[11]. In the case of cavitation microjet, however, because of their extremely short lifetime and small physical size, instability-type disturbances would not have enough time to grow so the laminar flow prevails. The damage caused by the microjets is perhaps of an impact nature, characterised by the water-hammer pressure, estimated[5] to be as high as 600 atm. This most impressive stress is sufficient to crack the solid to initiate subsequent material removal, and is in direct contrast to the gradual 'chew-away' actions in turbulent jet-cutting. This consideration is further shown by the liquid viscous effects. In the case of jet-cutting, Semerchan[12] demonstrated that a systematic increase in viscosity causes the jet forces to increase accordingly. But in the more viscous glycerol–water mixture cavitation erosion rate was lower as compared with the water

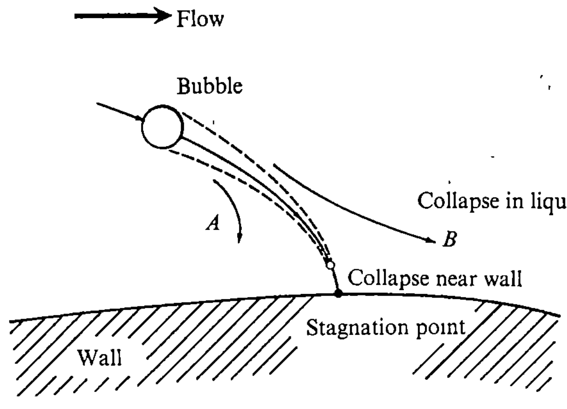

Fig. 1 Schematic representation of collapsing travelling bubbles approaching a stagnation point.

case[9]. This clearly suggested that the nature of the microjet is different from that of the turbulent jets for jet-cutting and the erosive activity of microjets is less intensive in a more viscous environment.

The explanation for the observed increase in cavitation erosion rate in polymer solution may still have its origin in polymer viscoelasticity. A deformational process in polymer solutions may be characterised by the relative scale between the duration of the deformation process and the polymer relaxation time. If the deformation time is sufficiently long, the polymer molecules adjust readily to the new deformed state. But if the duration of the deformation is much shorter than the polymer relaxation time, not enough time is allowed for the polymer molecules to adjust themselves and the material can only respond in a 'solid-like' elastic fashion. Since in the case of cavitation microjet the time scale is only $\sim 10^{-6}$ s and much shorter than polymer relaxation time ($\sim 10^{-3}$ s), it is expected that the polymer jet impinges on the wall with more solid-type impact than the water case. This additional impact stress may be briefly developed.

Consider a simple viscoelastic model for rapid deformation[13] where the total stress τ is

$$\tau = -pI + GB^{(1)}\Delta t + 2K[B^{(1)}\Delta t]^2 + \frac{G}{2}B^{(2)}\Delta t^2 + \ldots$$

where $B^{(n)}$ are deformation tensors defined as

$$B_{ij}^{(1)} = \frac{\partial v_i}{\partial x_j} + \frac{\partial v_j}{\partial x_i}$$

$$B_{ij}^{(n+1)} = \frac{\mathrm{D}B_{ij}^{(n)}}{\mathrm{D}t} - B_{mj}^{(n)}\frac{\partial v_i}{\partial x_m} - B_{im}^{(n)}\frac{\partial v_j}{\partial x_m}$$

G and K are the material moduli, and Δt represents the very short duration of deformation. For an axial motion with velocities

$$v = (\gamma x_1, -\frac{\gamma}{2}x_2, -\frac{\gamma}{2}x_3)$$

it can be readily shown that

$$\tau_{11} = -p + 2G\gamma\Delta t + (8K - 2G)\gamma^2\Delta t^2$$

For extremely small Δt ($\sim 10^{-6}$ for the interest here) as compared with polymer relaxation time ($\sim 10^{-3}$), we may approximate

$$\tau_{11} = -p + G\gamma\Delta t$$

A modified Bernoulli equation may be written as

$$\frac{1}{2}\rho U^2 - \tau_{11} = \frac{1}{2}\rho U^2 + p - 2G\gamma\Delta t = p_\infty$$

where p_∞ is the pressure in a quiescent reference state of uniformity. Compared with the Newtonian case

$$\frac{1}{2}\rho U^2 + p_{\mathrm{N}} = p_\infty$$

one observes that the difference represents an additional impact stress (or pressure)

$$\Delta p = p - p_{\mathrm{N}} = 2G\gamma\Delta t$$

This term, which may be responsible for the increased cavitation erosion effect in polymer solution, is proportional to the elasticity of the liquid represented by an elastic modulus G, which normally scales with polymer concentration c and molecular weight like $c[\eta]$ if $[\eta]$ is the polymer intrinsic viscosity. This is in agreement with the observed result that the cavitation erosion rate is slightly higher in 1,000 p.p.m. solution than in 100 p.p.m. solution[9].

Finally, while the results of Ashworth and Procter were obtained in a static vibratory-test system, it is noted that the cavitation fields occurred in most actual engineering applications are involved in a flow system. It is known[6] that only one out of 10^4–10^{10} cavitation bubbles that are swept into a stagnant flow region seems to collapse adjacent to a solid surface and actually produces a damage pit (Fig. 1). Therefore the effect of flow behaviour is extremely important to this highly selective collapse process in causing damage. The suppression of flow-generated cavitation has been attributed primarily to higher viscoelastic stresses built up near the nose of a blunt body[2]. Similarly, it may be expected that a proper application of the polymer additives may introduce higher stresses in the stagnation region which would lead to the following consequences. First, for a bubble travelling along the stagnation line, a higher external pressure would cause the bubble to collapse faster, and the chance for the cavity to be carried towards the surface is less. Second, for bubbles travelling along paths close to the stagnation line, higher stresses in the stagnation zone cause them to be repelled away from this region to take either path A or B shown in Fig. 1. A cavity that takes path A would be somewhat against the flow and quickly collapse in the liquid, causing practically no surface damage. On the other hand, a cavity following path B would be swept away downstream so that it would never come close enough to the surface to cause damage. Consequently, a reduction in flow-cavitation erosion may be expected. Experiments studying polymer effects on cavitation collapse and erosion in a flow system would be of some interest, and efforts along this line are now under way at this laboratory.

R. Y. TING

US Naval Research Laboratory,
Washington, DC 20375

Received April 26; accepted July 7, 1976.

[1] Gadd, G E., *Encyclopaedia of Polymer Science and Technology*, 15, 224 (Interscience, New York, 1971)
[2] Ellis, A. T., Waugh, J. G., and Ting, R. Y., *A S.M.E. J. basic Engng*, 92, 459 (1970).
[3] Hoyt, J W., *Proc. 16th Am. Towing Tank Conf., Sao Paulo, Brazil*, 1, 7 (1971).
[4] Benjamin, T. B , and Ellis, A. T., *Phil. Trans. R. Soc.*, A260, 211 (1966).
[5] Plesset, M. S., and Chapman, R. B., *J. Fluid Mech.*, 47, 283 (1971).
[6] Kling, C L., and Hammitt, F. G , *A S M.E. J. basic Engng*, 94, 825 (1972).
[7] Ting, R Y., *US natn. Bur Standards, Spec Publ* , 394, 100 (1974)
[8] Ting, R Y., and Hunston, D. L., *J. appl. Polym. Sci.* (in the press).
[9] Ashworth, V., and Proctor, R P. M , *Nature*, 258, 64 (1975).
[10] Kudin, A. M , *et al., Nature phys Sci.*, 245, 95 (1973).
[11] Hoyt, J. W., Taylor, J. J , and Runge, C. D., *J. Fluid Mech.*, 63, 635 (1974).
[12] Semerchan, A. A., *Soviet Phys.*, 3, 1894 (1958).
[13] Metzner, A. B., *Trans. Soc. Rheol.*, 12, 57 (1968).

Leaf cultivar influences composition and ripening of apples

POMOLOGICAL literature contains two reports of the influence of grafted scions on the size, colour and ripening season of apples borne on the stock portions of topworked trees[1,2]. The experiment reported here, initiated as part of of a larger study of apple ripening control mechanisms, confirms those reports.

Buds from a Lodi apple tree were grafted into branches of several Golden Delicious apple trees. When the Lodi scions bore fruit, half the scion branches were defoliated in early July, one month before the normal Lodi ripening season. Thereafter, these Lodi fruits received synthates translocated from Golden Delicious leaves. In late July, gas-sampling tubes (8 mm in diameter × 40 mm) were secured with grafting wax to the intact calyx ends of these Lodi fruits; the open end of each tube was fitted with a serum cap. Similar tubes were also secured to Lodi fruits borne on the other scion branches which still had Lodi leaves attached. The atmosphere inside the gas-sampling tubes equilibrated with apple internal atmospheres. A 1-cc syringe was used on alternate days to withdraw gas samples from the tubes and ethylene present in the samples was determined as described previously[3]. The ethylene analyses indicated the Lodi apples fed with synthates translocated from Golden Delicious leaves ripened slightly earlier than Lodi apples fed with synthates translocated from their own leaves.

In the second season, half of the Lodi-fruited branches were girdled in early July to prevent translocation of synthates from Golden Delicious leaves. On the same date, all the leaves were removed from the remainder of the fruited Lodi limbs. Lodi fruits on defoliated limbs received synthates translocated from Golden Delicious leaves. To ensure comparable accumulation of Golden Delicious leaf synthates in Lodi apples on the defoliated scions, bark girdles were located a few side branches below the Lodi graft unions. A similar procedure was followed in mid-September for limbs bearing Golden Delicious fruits.

Fig. 1 Ripening of *a*, Lodi and *b*, Golden Delicious apples borne on limbs fed with synthates from Golden Delicious (×) or from Lodi (○) leaves. In each of the four treatments there was a total of 16 fruits on 6–10 trees.

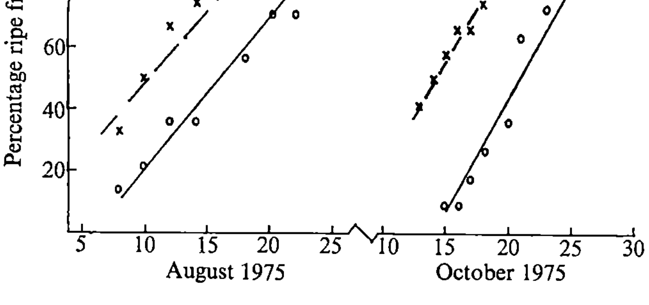

Lodi fruits were judged to be ripe when the ethylene in the gas-sample tubes reached 10 p.p.m. or higher; or when, in a few cases, the fruits abscised or split open. Golden Delicious fruits, which ripen with lower levels of ethylene, were judged to be ripe when ethylene in the gas-sample tubes was 4.5 p.p.m. or higher. The data (Fig. 1) indicate that Lodi and Golden Delicious apples fed with synthates translocated from Golden Delicious leaves ripened 5–7 d earlier than comparable apples fed with synthates translocated from Lodi leaves. Although the source of the synthates influenced the time of fruit ripening, the source of the synthates did not seem to influence the level of ethylene in the apples once they began to ripen on the tree.

During the Golden Delicious ripening season, red stripes appeared on fruits fed with Lodi leaves. An analysis of skin composition indicated that, in comparison with similar fruit fed with Golden Delicious leaves, fruit fed with Lodi leaves contained higher levels of anthocyanin and flavonols, but similar levels of soluble carbohydrates, starch and flavolans (Table 1).

Table 1 Skin composition of Golden Delicious apples from girdled limbs fed with synthates from Golden Delicious or Lodi leaves

Leaves	Soluble carbohydrate (mg cm^{-2}) (4)	Starch (mg cm^{-2}) (4)	Anthocyanin (nmol cm^{-2}) (5)	Flavonols (nmol cm^{-2}) (6)	Flavolans as monomers (μmol cm^{-2}) (5)
Golden Delicious	3.0	0.69	0.84	47.9	0.95
Lodi	2.9	0.75	4.09	101.0	0.90

Reference numbers in parentheses.

In summary, our analytical study verified orchard observations made in 1880 and 1927 that the cultivar of apple leaves may influence the composition and the time of ripening of apple fruits.

G. D. BLANPIED
L. L. CREASY
V. A. BLAK
L. W. LEWIS

Department of Pomology,
Cornell University,
Ithaca, New York 14850

Received March 8, accepted June 29, 1976.

1 Heinicke, A. J., *Proc Am Soc. hort. Sci* , 24, 143–146 (1927).
2 Trowbridge, G. W , *Ohio State hort. Soc* , 14, 93 (1880)
3 Edgerton, L J , and Blanpied, G. D., *Nature*, 219, 1064–1065 (1968)
4 Creasy, L L , *Phytochemistry*, 7, 1743–1749 (1968).
5 Creasy, L. L., *Proc Am Soc. hort. Sci.*, 93, 712 (1968).
6 Creasy, L. L., *Phytochemistry*, 10, 2705–2711 (1971)

Watering converts a CAM plant to daytime CO_2 uptake

THREE different photosynthetic options have been identified in plants[1,2]: (1) most plants have the reductive pentose phosphate or C_3 pathway, where CO_2 is incorporated into ribulose-1,5-diphosphate (RuDP) to yield two molecules of 3-phosphoglyceric acid, a three-carbon compound; (2) the C_4 mode, where the first photosynthetic products are four-carbon dicarboxylic acids like oxaloacetate and malate formed following CO_2 incorporation into phosphoenolpyruvate (PEP); and (3) crassulacean acid metabolism (CAM), found in many succulent plants growing in arid regions. In the last, stomatal opening and net CO_2 uptake occur at night, CO_2 being incorporated by way of PEP carboxylase into organic acids. The tissue acidity decreases as the organic acids are decarboxylated during the day, when the internally released CO_2 is prevented from leaving by the closed stomata. The water vapour concentration difference between the tissue and ambient air is less at night, and thus the night-time stomatal opening of CAM plants leads to overall water conservation. For example, the water lost per CO_2 fixed averages about sixfold higher for C_4 plants and tenfold higher for C_3 ones than for CAM plants in natural conditions[2]. The net daily CO_2 uptake by CAM plants is less than for C_3 or C_4 plants, so CAM plants tend to be relatively slow growing.

We investigated the results of giving CAM plants an adequate water supply, thereby obviating the need for water conservation and show that this leads to their conversion to daytime CO_2 uptake. We used *Agave deserti* Engelm. (Agavaceae) plants, which are common in the sandy soils of the Colorado, Mojave and Sonoran deserts[3], and experimented on plants maintained in a glasshouse so that the watering regime could be controlled. Gas exchange was measured with a Siemens null-point closed-circuit flow system[4,5] with a Cambridge Systems EG&G 880 dew-point hygrometer for measuring water vapour concentrations and a Beckman 315A infrared gas analyser for CO_2 concentrations. At about weekly intervals, the distal end of an attached leaf representing about 100 cm² of surface area was sealed into the leaf chamber and maintained under natural illumination for a determination of gas exchange over 24 h. The resistance for water vapour diffusion from a leaf (R_{wv}) equals the concentration of water vapour within a leaf (assumed to be the saturation value at the leaf surface temperature) minus the water vapour concentration in the leaf chamber, divided by the measured rate of water vapour loss per unit leaf area. To measure leaf acidity[6,7] approximately 4 g of leaf tissue were removed with a cork borer, ground in 100 ml of distilled water, boiled for 5 min, and then filtered. Two 40-ml aliquots were titrated to an endpoint of *p*H 6.4 using 0.011 N NaOH. For determination of PEP and RuDP carboxylase activities, each gram of freshly removed leaf tissue was ground in 5 ml of 0.2 M HEPES buffer (*p*H 8.0), 1 mM Na-EDTA, 1 mM dithiothreitol, and 40 mg ml^{-1} polyvinyl pyrrolidone; enzyme activities were assayed by following the conversion of $KH^{14}CO_3$ into stable products[8]. Soil water potential (Ψ_{soil}) was measured daily with a Wescor HR 33 dew-point microvoltmeter and PT 51-05 soil thermocouple psychrometers.

Four plants were potted in the field when no natural stomatal opening was occurring ($\Psi_{soil} < -90$ bar, where 1 bar = 10^5 Pa). Ψ_{soil} was then raised to -0.1 ± 0.1 bar, which induced night-time stomatal opening After two weeks in a wet soil, CAM-type stomatal movements (Fig. 1*a*), a night-time CO_2 influx (Fig. 1*b*), and diurnal variations in the tissue acid level (Fig. 1*c*) were clearly evident. After four more weeks with a wet soil, the stomata remained open in the morning; the net CO_2 influx was 0.24 nmol cm^{-2} s^{-1} at 0900 and did not cease until 1130. After a total of 12 weeks with a Ψ_{soil} maintained at -0.1 ± 0.1 bar by daily watering, the night-time stomatal opening was replaced by a daytime opening, characteristic of C_3 and C_4 plants (Fig. 1*a*). Net CO_2 uptake (97% of the daily total) now occurred during illumination (Fig. 1*b*) and there was little diurnal change in tissue acidity (Fig. 1*c*). Allowing the soil to dry for 3 weeks caused the plants to revert to a more-or-less normal CAM mode with night-time stomatal opening and daytime closing.

When the plants were exhibiting photosynthesis primarily during the daylight hours and there was an apparent lack of the circadian fluctuation of organic acids, some form of either the C_3 or C_4 photosynthetic pathway was presumably being followed. The vascular tissue of *A. deserti* seemed to have a bundle sheath containing chloroplasts, but the cells were not as conspicuous as for most C_4 plants. Measurements of PEP carboxylase and RuDP carboxylase indicated a ratio of the activities similar to that observed for C_4 and CAM plants[1]. For samples taken at 1200 from a plant exhibiting daytime stomatal opening, the PEP carboxylase activity was 1.01 μmol CO_2 fixed per g wet weight per min compared with 0.080 for RuDP carboxylase. In the CAM mode (at 0000) there was also high PEP carboxylase activity relative to the RuDP carboxylase activity (0.80 as against 0.078 μmol per g wet weight per min). Whether the CO_2 assimilation in the light involves primarily PEP or RuDP carboxylase remains to be determined. The CO_2 compensation value measured at 1200 during daytime CO_2 uptake for plants at 17 °C in saturating light conditions and 21% O_2 was relatively high (an average of 88 μl l^{-1} for three experiments). This is not characteristic of C_4 plants (CO_2 compensation point generally less than 10 μl l^{-1} (ref. 9)), but is similar to CO_2 compensation points for C_3 plants.

The maximum R_{wv} for *A. deserti* was twofold greater in the CAM mode (~300 s cm^{-1}, Fig. 1*a*) than for the daytime CO_2 uptake, indicating a tighter closing of the stomata when water conservation is more critical. The daytime stomatal opening did not produce a much greater maximum rate of photosynthesis than the CAM night-time opening (0.63 compared with 0.57 nmol cm^{-2} s^{-1}, Fig. 1*b*). These maximum rates are two- to sixfold lower than those for conventional C_3 and C_4 plants[2], primarily because of the rather high resistance for the gas phase part of the pathway for *A. deserti* (minimum R_{wv} of about

Fig. 1 Conversion from crassulacean acid metabolism (CAM, △) to daytime CO_2 uptake (○) after watering *Agave deserti*. Gas exchange data were obtained in identical conditions using attached leaves 2 weeks (CAM) and 12 weeks after raising Ψ_{soil} from < −90 bar to −0.1 bar. Acidity was determined for leaves on a companion plant showing the same stomatal movements. Air in the leaf chamber was maintained at 17.0±0.4 °C and 5.0±0.1 μg H_2O cm^{-3}. Illumination was provided by natural sunlight (supplemented with a xenon arc lamp during brief cloudy periods) and controlled using neutral density screens so that it was representative for a cloudless winter day (for example, January 1, 1976). Illumination had a maximum of 80 klx at 1200 with values of 10 klx at 0730 and 1645, as determined using a Spectra FC 200-TV-B meter. Data are expressed on the basis of total area (both sides) for these succulent leaves.

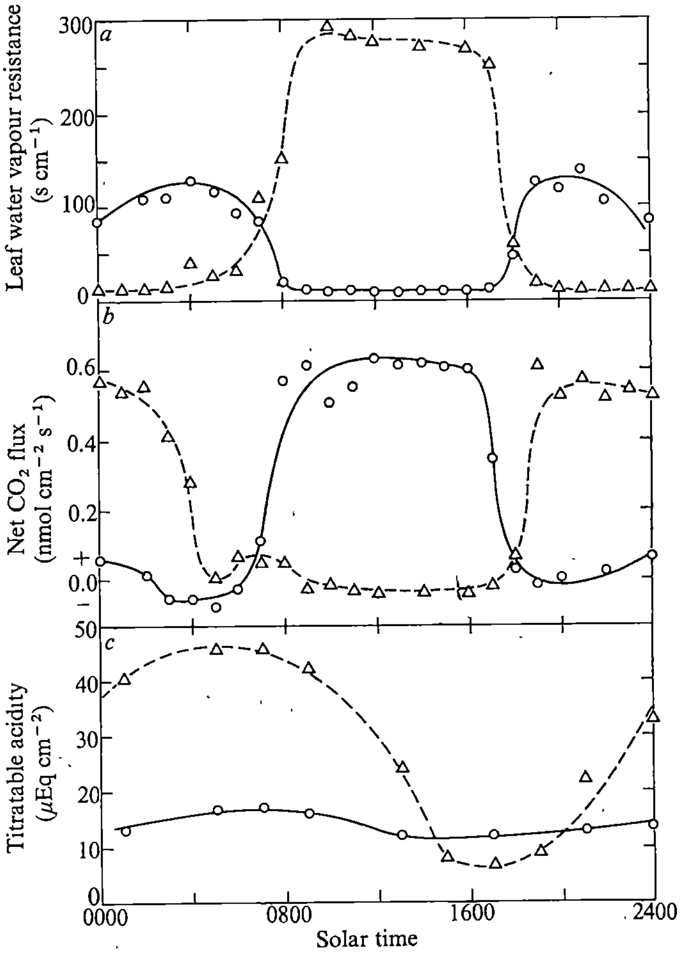

7 s cm^{-1} for both modes). This succulent arid-region plant would thus still grow relatively slowly if switched to the daytime mode of photosynthesis. For the CAM mode, the net CO_2 fixation was 18.3 μmol cm^{-2} for 24 h (Fig. 1*b*), whereas it was 21.0 μmol cm^{-2} for daytime CO_2 uptake. These values of net daily photosynthesis were obtained in conditions of wintertime illumination. The relative advantage of predominantly daytime photosynthesis would be greater for the longer days (a longer period for daytime CO_2 uptake) and shorter nights (less time for the CAM night-time CO_2 influx) that would occur at other times of the year. The time course of the increase in titratable acidity closely followed the net accumulation of CO_2 in the leaf during the night-time period in the CAM mode and 2 μEq of acidity were produced per μmol CO_2 taken up as expected (Fig. 1*b* and *c*).

When water is readily available, strictly adhering to the water-conserving CAM mode may no longer be beneficial to a CAM plant. At least some supplemental daytime stomatal opening and CO_2 uptake would become advantageous. Indeed, many CAM plants show a net CO_2 uptake during the day when not under water stress; such daytime CO_2 uptake increased as water became more available for *Bryophyllum daigremontianum*[10], *Agave americana*[11], and *Dudleya farinosa*[12]. The shift to daytime photosynthesis was only partial, however, as in all cases the night-time stomatal opening and net CO_2 influx characteristic of CAM plants still occurred. In different experiments, Osmond *et al.*[13] showed that subjecting *Kalanchoe daigremontiana* to 9 weeks of drought caused the carbon isotope discrimination ratio to shift from a value close to that for C_3 plants towards that expected if all CO_2 uptake took place at night in a CAM mode. For *A. deserti*, it seems that watering can cause an essentially complete switch from CAM to daytime photosynthesis (Fig. 1). Such switching did not lead to greater net daily photosynthesis for winter days, but greater photosynthetic productivity would be predicted for the longer daylight periods occurring at other times of the year. Thus, the ability to shift modes of photosynthesis when water is not a limiting factor could be a distinct advantage to this plant.

This research was supported by the ERDA.

TERRY L. HARTSOCK
PARK S. NOBEL

Division of Environmental Biology,
Laboratory of Nuclear Medicine and Radiation Biology,
University of California,
Los Angeles, California 90024

Received April 23; accepted June 15, 1976.

[1] Black, C. C., *A. Rev. Pl. Physiol.*, 24, 253–286 (1973).
[2] Szarek, S. R , and Ting, I P., in *Environmental and Biological Control of Photosynthesis* (edit. by Marcelle, R.), 289–297 (W. Junk, The Hague, 1975).
[3] Munz, P. A., *A Flora of Southern California*, 864 (University of California Press, Berkeley, 1974).
[4] Koller, D., *U S. Atomic Energy Commission Report TID-4500* (*UCLA 12-797*), 1–28 (1970).
[5] Mork, H. M , Farmer, R. W., and Flygare, K A , *Soil Sci* , 114, 61–68 (1972).
[6] Neales, T. F , *Aust. J. biol. Sci.*, 26, 705–714 (1973).
[7] Szarek, S. R., and Ting, I. P., *Pl Physiol* , *Baltimore*, 54, 76–81 (1974).
[8] Wallace, A., Hale, V. Q., Kleinkopf, G. E , and Huffaker, R C., *Ecology*, 52 1093–1095 (1971).
[9] Downton, W. J. S., and Tregunna, E. B., *Can. J. Bot.*, 46, 207–215 (1968).
[10] Kluge, M , and Fisher, K., *Planta*, 77, 212–223 (1967).
[11] Neales, T. F., Patterson, A. A., and Hartney, V. J., *Nature*, 219, 469–472 (1968).
[12] Bartholomew, B., *Photosynthetica*, 7, 114–120 (1973).
[13] Osmond, C. B., *et al.*, *Nature*, 246, 41–42 (1973).

Memory phases in *Drosophila*

MEMORY in many organisms can be disrupted by anaesthesia or electroconvulsive shock applied shortly after training. Later, if left undisturbed, the memory becomes immune to these agents. This suggests that learned information is stored by the brain in more than one form[1–4]. A population of *Drosophila melanogaster* can be trained to avoid an odorant by presenting the odour in combination with electric shock. When tested later without shock, the flies avoid this odorant specifically (ref. 5 and unpublished results of Y.D.). By anaesthetising the flies briefly with cold at various times between training and testing, we have found two memory components in *Drosophila*.

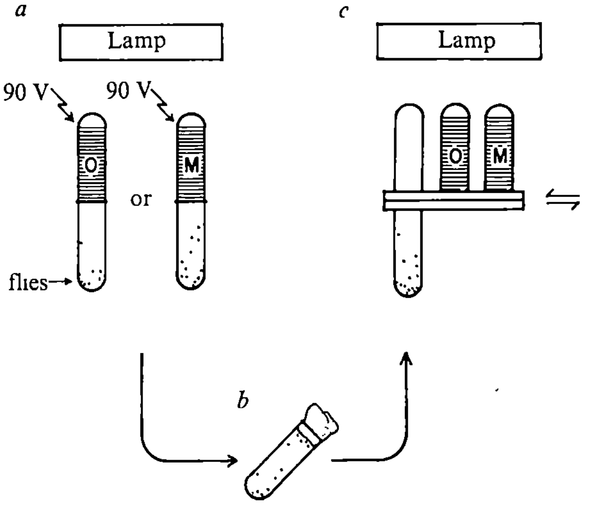

Fig. 1 Procedure for measuring memory retention. *a*, Training: a population of 30–50 flies was trained in two horizontal plastic tubes, joined open end to open end (in a behavioural countercurrent device[5]). The light attracted the flies from a start tube, containing 1 μl of a chemical odorant (either 3-octanol (O) or 4-methyl-cyclohexanol (M)) spread on an electrified grid (60 Hz, 90 V a.c.)[5]. After 60 s, the flies were shaken back into the start tube and another run was begun. This cycle was repeated ten times. By the tenth training cycle fewer than 20% of flies entered the grid tube. *b*, Waiting: flies were left undisturbed in dim illumination at room temperature (22 °C), in a perforated plastic tube closed with a polyurethane foam plug. *c*, Testing: the sliding countercurrent apparatus[5] allowed the start tube, with flies, to be shifted opposite any of several illuminated tubes. Selective odour avoidance of the flies was measured by testing them alternately with two (non-electrified) grids, one spread with O, the other with M. In each test, the flies were shifted opposite a tube containing the grid and odorant and given 15 s to run, after which the flies remaining in the start tube were counted. Before each test, flies were allowed to run to a perforated rest tube for 45 s. The order of odorants was reversed in half the experiments.

D. melanogaster of the Canton-special wild-type strain were used. Culture methods, experimental conditions, chemical odorants and the apparatus for training and testing were as described before[5], except that, to enhance memory retention, we used a more intensive training procedure consisting of ten consecutive exposures to one odorant coupled with shock (Fig. 1*a*). Between training and testing, flies were left undisturbed in ventilated plastic tubes (Fig. 1*b*). They were tested, as before[5], by allowing them to run sequentially into two new grid tubes (non-electrified), each containing one of the odorants above (Fig. 1*c*). The index of learning used was the fraction of the population which avoided the odorant associated with shock during their training, minus the fraction which avoided the novel (control) odorant. Each experiment was run in reciprocal halves; two groups of flies, each trained to avoid one of the odorants, were both tested in the same apparatus to compensate for asymmetries in the apparatus or in the flies' intrinsic reaction to the odorants. The learning index, Λ, for a complete experiment was the average of the indices for the two halves. Learning indices are reported as mean ± s.e. of mean for four experiments. With the training procedure described above, selective avoidance was present immediately after training, $\Lambda = 0.25 \pm 0.02$, and remained high; when tested 45 min after training $\Lambda = 0.34 \pm 0.06$.

Brief cooling induces rapid and reversible anaesthesia in *Drosophila*. Flies to be treated were transferred to a glass test tube (18 × 150 mm), shaken to the bottom, and the tube was placed in a bath of moving water at 4 °C. Within 15 s the flies stopped climbing, fell over and became immobile. After a further 60 s they were transferred back to perforated plastic tubes at room temperature (22 °C). Two minutes later they began to walk, and locomotion appeared normal by 7 min.

We tried to disrupt the flies' memory by applying this cold treatment at various times before and after training, and in each case measured their retention 45 min after training (Fig. 2). Flies anaesthetised before training (at −10 or −5 min) perform as well as untreated flies, indicating that the cooling *per se* does not interfere with subsequent neural function, sensory perception or capacity to learn and remember. Flies anaesthetised 0 or 5 min after training, on the other hand, showed almost no selective avoidance when tested at 45 min. Apparently cold-induced anaesthesia can disrupt recently acquired memory in *Drosophila*. From 10 to 30 min after training, the memory became progressively more resistant to anaesthesia. This time-dependent increase suggests the onset of a second memory phase. The following experiments examine alternatives to this interpretation.

Populations of flies were trained as above, immediately anaesthetised, maintained at room temperature and tested at 5, 15, 30, 45 or 60 min. In all cases they showed little retention, with values of Λ less than 0.10. This indicates that in *Drosophila* cold-induced anaesthesia after training either eradicates learned information or permanently interferes with its normal expression. The amnestic effect of cold anaesthesia is not an artefact of the time chosen for testing.

Memory-disruption experiments are complicated by the possibility that the disruptive agent, applied shortly after training, itself acts as a reinforcement, causing gratuitous learning which cancels the effect of previous training[6]. In our case, the learning task is aversive, and anaesthesia decreases avoidance of the shock-associated odorant. Therefore, the anaesthesia cannot act as a negative reinforcement. Positive reinforcement effects were excluded by a separate control: populations of flies were cold-anaesthetised in the presence of either 3-octanol or 4-methylcyclohexanol, at the concentrations used above. When tested later they showed the same slight aversion to both odorants as did naive control flies.

Time-dependent sensitivity of memory to cold anaesthesia has also been demonstrated using the original paradigm of Quinn *et al.*[5], which contains an internal control of sensitisation. Flies were trained by alternate exposure to two odorants, one of which was associated with shock. Testing was as above. Cold anaesthesia disrupted memory if applied 5 min after training (Λ = 0.05±0.04), but not if applied at 30 min (Λ = 0.18±0.04) (unpublished results of Y.D.).

Fig. 2 Effect of cold anaesthesia on memory. Populations of 30–50 flies were trained and tested 45 min later as described in Fig. 1. Populations were anaesthetised at the times shown, by cooling them for 60 s at 4 °C. (The decreased learning performance of flies anaesthetised at 40 min may be due to incomplete recovery by testing time.) The abscissa shows time between training and cold anaesthesia. Negative times indicate anaesthetisation before training; positive values indicate anaesthetisation between training and testing. The point shown after testing (hollow circle) represents unanaesthetised control flies. The ordinate shows Λ, the selective avoidance due to learning.

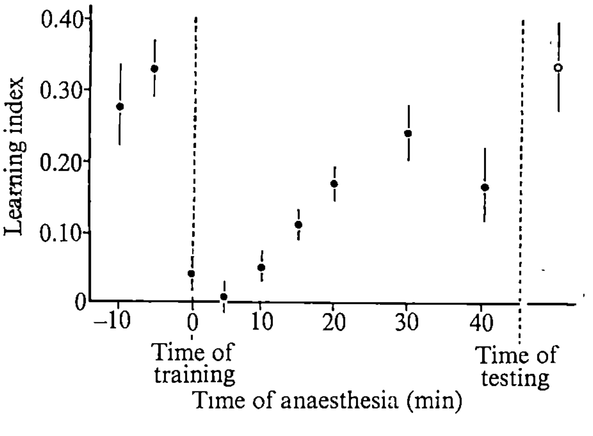

The extent to which the mechanisms underlying memory storage are shared among species is unknown. Nevertheless, analogous techniques can be used to resolve memory phases in creatures ranging from dipterans to primates. Among the insects, multiple memory components have been shown in cockroaches by use of lesions[7], and in honey bees by use of anaesthesia and electroconvulsive shock[8]. The demonstration of two forms of memory in *Drosophila* may be useful because of the suitability of this organism for behaviour-genetic analyses[9]. At present, work on memory phases is limited to phenomenology, and fundamental questions remain unanswered. Short and long term memory storage could proceed by different physiological processes, or the second phase could represent merely a saturation or intensification of the first. Information may proceed serially through short term to consolidated memory, or the two forms may have parallel inputs. These questions could be studied if mutations affecting different memory components were obtained. In this respect, it is interesting that a single-gene mutant deficient in learning has been isolated recently[10].

We thank many friends for help with the manuscript, especially Seymour Benzer, Yuh Nung Jan and Donald Ready. This work was supported by grants from the NSF to W.G.Q. and Seymour Benzer. Y.D. is a fellow of EMBO.

WILLIAM G. QUINN

Department of Biology,
Princeton University,
Princeton, New Jersey 08540

YADIN DUDAI

Division of Biology,
California Institute of Technology,
Pasadena, California 91125

Received April 30; accepted June 22, 1976.

1 McGaugh, J. L , *Science*, **153**, 1351–1358 (1966).
2 Agranoff, B. W., in *Neurosciences Study Program* (edit by Quarton, G. C., Melnechuk, T O , and Schmitt, F O.), 756–764 (Rockefeller University Press, New York, 1967).
3 Barondes, S. H , in *Neurosciences Second Study Program* (edit. by Schmitt, F. O), 272–278 (Rockefeller University Press, New York, 1970).
4 McGaugh, J L , Zornetzer, S. F., and Gold, P. E , *Q Rev. Biophys* , **5**, 163–186 (1972)
5 Quinn, W. G., Harris, W A , and Benzer, S., *Proc natn. Acad. Sci U.S.A.*, **71**, 708–712 (1975).
6 Madsen, M. C , and McGaugh, J. L , *J comp. physiol Psychol.*, **54**, 522–527 (1961)
7 Chen, W Y , Aranda, L. C., and Luco, J. V., *Anim. Behav.*, **18**, 725–732 (1970).
8 Menzel, R , Erber, J T , and Masuhr, T., in *Experimental Analysis of Insect Behaviour* (edit. by Barton Browne, L.), 195–217 (Springer, Berlin, 1975).
9 Benzer, S., *Scient. Am.*, **226**, 24–37 (1973).
10 Dudai, Y., Jan, Y N , Byers, D., Quinn, W G , and Benzer, S , *Proc. natn. Acad Sci U.S.A.*, **73**, 1684–1688 (1976).

Maintenance of fluid volume in the starfish water vascular system

LOCOMOTION in the starfish *Asterias forbesi* involves many tube feet, each functioning independently as a hydrostatic skeleton; the circular muscles of the ampulla acting antagonistically to the longitudinal muscles of the tube foot itself through the constant volume of fluid contained in the ampulla–foot unit[1]. The fluid for each tube foot comes from the water vascular system to which each foot is connected through its own lateral canal. The water vascular system in *Asterias* consists of three interconnecting series of canals: (1) radial canals running the length of each arm; (2) a circular canal running around the gut at the base of the arms, and (3) the stone canal which runs from the radial canal up to the aboral ("dorsal") surface, terminating in the madreporite. The madreporite, an orange disk, is porous and associated with several sets of cilia. For some time it has been presumed, and is still presented or indicated in some textbooks, that the fluid contained within the starfish water vascular system is pumped by ciliary activity through the madreporite into the canal system, although it has been pointed out that no experimental evidence supports this assumption[2]. Ionically, the fluid within the water vascular system is nearly identical to the external seawater with the exception of internal K^+, which is present in a concentration up to 60% higher than that of the seawater[3,4]. On the basis of this difference, it was suggested that K^+ accumulation by the water vascular system is responsible for water uptake by this system, either by creating a slight osmotic gradient within the tube feet or by direct movement of water with hydrated K^+ ions, as opposed to direct uptake of seawater through the madreporite[5]. We have investigated the generation of the fluid in the water vascular system more thoroughly by determining the osmotic and ionic characteristics of the fluid within the tube feet and the ionic transport characteristics of the isolated tube foot epithelium.

We used *A. forbesi* collected in Jamestown, Rhode Island and maintained for up to 1 week before use in tanks of artificial seawater at 7 °C. Fluid from the water vascular system was obtained from an intact starfish by placing it on its aboral surface and tying off individual tube feet close to their base with silk thread. The foot was then isolated from the animal, washed quickly in distilled water, blotted dry and cut open. The released fluid was taken up into a micropipette. Na^+ and K^+ concentrations in the tube foot fluid were determined by flame photometry, and Cl^- was measured by a modified microelectrometric titration technique[6], and the total osmolality of the fluid was obtained with a Clifton nanolitre osmometer. These determinations are summarised in Table 1. The Na^+ concentration of the tube foot fluid was identical to that of the external medium, while internal Cl^- was slightly but significantly higher than environmental Cl^-. In agreement with earlier measurements on other echinoderms[3,4], the K^+ concentration of the tube foot fluid from *A. forbesi* was considerably higher than that of the external seawater. In addition, the tube foot fluid was distinctly hyperosmotic to the surrounding seawater, by up to 22 mosM. The perivisceral (coelomic) fluid was osmotically and ionically (Na^+, K^+ and Cl^- ion concentrations) identical with the external seawater.

To investigate whether or not the tube foot epithelium itself is in part responsible for K^+ secretion, individual tube feet were cut off at the base, filled with fresh seawater and tied off with silk thread. Thus initially identical ion concentrations were present on both sides of the isolated tube foot epithelium. The tube foot–sac preparation was allowed to equilibrate in aerated seawater for 90 min. Analysis then showed that, as in the intact tube foot, the K^+ concentration of the fluid in the isolated tube foot was higher than that of the surrounding medium. The internal K^+ concentration was 16.8 mM, while that in the external seawater was 9.5 mM. The secretion of K^+ by the isolated tube foot epithelium could be inhibited by addition of CN^- (1×10^{-4} M) to the external medium. The isolated tube foot could also be set up as a tubular system and perfused[7]; in this manner unidirectional K^+ fluxes, using ^{42}K (New England Nuclear), could be measured. Unidirectional K^+ influx was 4.2×10^{-9} mol cm^{-2} min^{-1} and unidirectional K^+ efflux was 3.4×10^{-9} mol cm^{-2} min^{-1}.

Table 1 Osmotic and ionic characteristics of fluid from intact starfish tube feet and of surrounding seawater

Ion concentration (mmol kg^{-1})	Seawater	Tube feet fluid
Na^+	469±2.9 (17)	471.4±2.6 (17)
K^+	9.5±0.8 (21)	17.3±1.8 (21)
Cl^-	543.3±2.6 (19)	551.7±3.1 (19)
Total osmolality mosmol l^{-1}	1,095±3.3 (25)	1,117±3.8 (25)

Figures are mean±s.e.m., with number of determinations in parentheses.

Connection of the tube feet with the outside medium through the canals of the water vascular system and the madreporite was investigated by equilibrating intact starfish for 24 h in seawater with ^{14}C-polyethylene glycol (New England Nuclear); molecular weight 4,000. Samples of fluid were then removed from the tube feet as before and counted in a liquid scintillation counter. Negligible amounts of label were found inside the tube feet, indicating that no direct connection exists between the fluid in the tube feet and the outside medium across the madreporite, an observation consistent with studies performed with dyes[5].

None of these observations supports the assumption that the fluid in the tube feet of the starfish is simply seawater pumped into the water vascular system through the madreporite by the action of cilia. The fluid in the tube feet, as well as that in the connecting water vascular system, is higher in K^+ and Cl^-, and is hyperosmotic with respect to the external seawater. This hyperosmotic condition is probably brought about by the active secretion of K^+, with Cl^- following passively, across the tube foot epithelium. Other epithelial structures in addition to the tube foot epithelium itself in the starfish may contribute to total K^+ secretion into the water vascular system, for example, the ampulla epithelium. The generation of a slightly hyperosmotic condition in the tube foot lumen by solute secretion would create a driving force for water across the tube foot epithelium into the tube foot lumen. This water provides the fluid through which the circular muscles of the ampulla and the longitudinal muscles of the foot are antagonised. In addition, water uptake in this fashion could make up for water losses through ultrafiltration across contracted tube feet and through damaged tube feet.

The lack of any direct connection of the madreporite with the more distal portions of the water vascular system in the starfish does not rule out any exchange whatsoever between different parts of the water vascular system and the external seawater through the madreporite. The water vascular system in some echinoderms is probably connected entirely to the outside environment through the madreporite. Water movements which do occur through the madreporite in asteroids may serve either a sensory role or could serve to equalise pressure differentials[8] between the water vascular system and the outside environment.

ROBERT D. PRUSCH
FREDERICK WHORISKEY

Division of Biological and Medical Sciences,
Brown University,
Providence, Rhode Island 02912

Received April 19; accepted June 22, 1976.

[1] Smith, J. E., *Q. Jl Microsc Sci*, 88, 1.14 (1947)
[2] Hyman, L H., *The Invertebrates Echinodermata*, 4 (McGraw-Hill, New York, 1955)
[3] Robertson, J. D., *J. exp. Biol.*, 26, 182–200 (1949)
[4] Binyon, J , *J. mar. Biol. Ass. U K*, 42, 49–64 (1962).
[5] Binyon, J., *J. mar Biol. Ass. U.K.*, 44, 577–588 (1964).
[6] Ramsay, J. A., Brown, R. H. J., and Croghan, P. C , *J exp. Biol.*, 32, 822–82 (1955)
[7] Prusch, R. D., and Benos, D. J., *J. Insect Physiol.*, 22, 629–632 (1976).
[8] Fechter, H., *Z. Vergl. Physiol*, 51, 227–257 (1965).

Evolution of responses to relative homozygosity

ACCORDING to the theory of kin selection first elaborated by Hamilton[1,2], all individual behaviour is selected to maximise the increment to inclusive fitness $\Delta W_i + \Sigma \Delta W_j r_{ij}$, where ΔW_i is the effect of an act on the fitness of the actor, ΔW_j is the effect of the same act on the fitness of a conspecific, and r_{ij} is the coefficient of relationship between the actor and the conspecific. Acts that lower an individual's direct fitness can thus be favoured by natural selection if, by conferring benefits on relatives of the actor, they cause a positive increment to the actor's inclusive fitness[3,4]. Since the average r_{ij} between an individual and the targets of its behaviour varies because of fluctuations in local population structure, an individual is most likely to secure a positive increment if its behaviour is conditioned on as accurate an estimate as possible of the particular local distribution of r_{ij}. I describe here a mechanism by which this estimate could be improved on the basis of information derived from the relative homozygosity of the individual's own genotype, in species with certain kinds of life histories.

A geographically viscous, sexually reproducing population is locally inbred, reflecting the fact that the parents of a typical individual are more highly related to each other than are two adults taken from the population at large[5]. Since relative homozygosity correlates with the extent of inbreeding, an individual that is homozygous at an unusually high proportion of its population's polymorphic loci is almost certain to be one whose ancestors for several preceding generations were closely related. In a viscous population, neighbouring individuals tend to share largely overlapping sets of ancestors. Thus given any mating system, characteristic pattern of dispersal, and level of genetic polymorphism, an individual more (or less) homozygous than its population's recent average expects a larger (or smaller) than average coefficient of relationship to conspecific near neighbours[6]. In many species these neighbours are likely to be its principal ecological competitors.

Particular developmental and behavioural responses to homozygosity could be favoured by natural selection, if the relationship between individual fitness and some limiting resource can be described by an increasing function that becomes concave downwards above a level of use commonly reached by members of the population. The summed fitness of two individuals who divide a given resource may then exceed the fitness either of them would attain by taking all of that resource. Given sufficiently high r_{ij} and a sufficiently large shareable resource, each individual is selected to take less than all of that resource and so attain less than the direct fitness it might. An unusually homozygous individual may, on average, increase its inclusive fitness by being relatively small and reproductively efficient. A very heterozygous conspecific may be selected to exhibit greater competitiveness over the shareable limiting resource because its inclusive fitness is less likely to be increased by any benefits (positive ΔW_j) it bestows on neighbours.

The logic of this argument has been tested in a series of numerical experiments. The model species is monoecious, semelparous and synchronously breeding. Each site on a 24×24 stepping-stone array accommodates, at most, one individual, who may be more or less 'competitive'. This phenotypic variance in competitiveness has two selective effects. First, the risk of juvenile mortality is a positive linear function of the competitiveness (and the number) of an individual's immediate neighbours. Second, more competitive individuals draw resources from less competitive neighbours, and fertility is an increasing sigmoid function of resource accrued. Competitiveness is controlled by two alleles at each of four independently assorting loci. One allele at each locus is dominant for maximum competitiveness; the other is recessive for reduced competitiveness. Phenotypic effects of the four loci are multiplicative. Symmetrical binomial probabilities govern the dispersal of male gametes and of zygotes, which experience average migrations of slightly more than one step and slightly less than one step, respectively.

Each experiment simulated one hundred generations of selection and reproduction. The recessive allele was strongly favoured at rates of self-fertilisation ranging between zero and 0.975. Gene frequencies changed very little during corresponding control runs in which all genotypes produced the same intermediate level of competitiveness. Individual fertility in experimental runs was observed to correlate positively with competitiveness. Thus, the success of the allele that responded to homozygosity by lowering the competitiveness of its phenotype could have been due only to benefits it conferred on replica copies occurring in neighbours.

Predictions derived from this model have been tested on published hybridisation experiments from a number of species. Embryos *in utero* stand in competition for a bounded set of resources. Relatively homozygous embryos, with high coefficients of relationship to each other, should compete less strongly than relatively heterozygous embryos. Not only should they be smaller than the heterozygotes, they should also be less variable at birth if competition tends to increase the variance of resource accrual. Where crosses are made between completely inbred lines there exists among F_1 littermates no genotypic variance to which their phenotypic variance might be attributed. Taketomi and Matsuo reported a large and well controlled hybridisation experiment with mice[7], where the coefficient of variation of weight at 10 d of age was significantly larger for F_1 hybrid than for inbred litters ($P < 0.01$). This difference is unlikely to have been caused by some special incompatibility between inbred females and their hybrid embryos, because backcross litters on inbred females were less variable than backcross litters on F_1 females ($P < 0.01$).

For another series of hybridisation studies on mice, there is a strong and significant positive correlation between the hybrid litters' heterosis for birth weight and their 'heterosis' for variability[8]. This supports the assumption that intrauterine competition for resources tends to increase the variance of birth weight.

Barley is a predominantly self-fertilising species with very low rates of pollen and seed dispersal. In several hybrid populations synthesised from parents of diverse origin, yields per unit area and average homozygosities both increased during early generations[9,10], although barley is strongly heterotic for individual yield[11]. Available evidence does not permit an unequivocal rejection of the possibility that selection produced late generation plants that were as large as early generation plants and even higher yielding. But since late generation plants were very homozygous, it seems likely that they were also smaller and individually less fit than their more heterozygous ancestors. Their greater yields per unit area are then assumed to reflect higher densities and greater efficiency in the utilisation of resources such as light. The response of individual yield to plant spacing in barley is smoothly asymptotic[12], so selection in a viscous population would seem to favour a response to homozygosity like that modelled in the numerical experiments.

In these barley populations, however, the seeds used to initiate each generation were a large and thoroughly randomised sample produced the previous generation. Therefore differentiated neighbourhoods could not actually develop. Close relatives would seldom have received the benefits dispensed by uncompetitive individuals. In such unusually heterogeneous and chaotically arrayed populations, selection should favour those homozygous genotypes that lead to relatively unreduced competitiveness. Electrophoretic surveys on one of these populations revealed an apparent narrowing of the difference between single-locus homozygous and heterozygous fitnesses within the first twenty-eight generations[13], in spite of a marked increase of gametic phase disequilibrium[10]. During the same series of generations, highly significant increases in the rate of outcrossing also occurred[14]. Both of these changes can be interpreted as evolutionary responses to a situation in which direct fitness and inclusive fitness have become nearly synonymous.

The accuracy of an estimate of average genetic relationship to near neighbours that is derived from homozygosity must depend on the number of loci entering into the estimate, and on the independence with which those loci assort. Traits whose expression depends heavily on the amount of fitness-limiting resources accrued are thus expected to show low additive genetic variance, relatively high non-additive genetic variance and strong heterosis, and this pattern is widely observed[15,16]. Much of the inbreeding depression seen in normally outbred species must result from the expresion of truly deleterious recessive alleles. But such alleles should be relatively rare in species that inbreed to any considerable extent; particularly in such species, the loss of direct fitness that accompanies inbreeding may result in part from mechanisms favoured by natural selection.

Published observations seem to satisfy many predictions derived from the hypothesis, but plausible alternative explanations can be advanced for most and none constitutes a clear critical test. An important and largely unexamined general implication of the model is that particular features of the mating and genetic systems of species to which it applies, should seem designed to facilitate the proposed responses to relative homozygosity.

For many helpful criticisms I thank F. Benford, S. Blaffer Hrdy, J. Coyne, I. DeVore, R. Lande, N. A. Nicolson, O. T. Solbrig, E. O. Wilson, and especially M. A. Etter and R. L. Trivers. This work was supported in part by a USPHS training grant from the NIGMS.

JON SEGER

The Biological Laboratories,
Harvard University,
Cambridge, Massachusetts 02138

Received April 20; accepted June 29, 1976.

[1] Hamilton, W. D., *Am. Nat.*, **97**, 354–356 (1963).
[2] Hamilton, W. D., *J. theor. Biol.*, **7**, 1–52 (1964).
[3] Hamilton, W. D., *A. Rev. Ecol. Syst.*, **3**, 193–232 (1972).
[4] Trivers, R. L., and Hare, H., *Science*, **191**, 249–263 (1976).
[5] Wright, S., *Genetics*, **28**, 114–138 (1943).
[6] Wright, S., *Am. Nat.*, **56**, 330–338 (1922).
[7] Taketomi, M., and Matsuo, T., *Agric. Bull. Saga Univ.*, **6**, 1–12 (1957).
[8] Poiley, S. M., *Lab. Anim. Sci.*, **22**, 759–779 (1972).
[9] Suneson, C. A., *Agron. J.*, **48**, 188–191 (1956).
[10] Allard, R. W., and Kahler, A. L., *Proc. 6th Berk. Symp. math. Stat. Prob.*, **5**, 237–254 (1972).
[11] Sakai, K.-I., and Gotoh, K., *J. Hered.*, **46**, 139–143 (1955).
[12] Sakai, K.-I., in *The Genetics of Colonizing Species* (edit. by Baker, H. G., and Stebbins, G. L.), 215–239 (Academic, New York and London, 1965).
[13] Allard, R. W., Kahler, A. L., and Weir, B. S., *Genetics*, **72**, 489–503 (1972).
[14] Kahler, A. L., Clegg, M. T., and Allard, R. W., *Proc. natn. Acad. Sci. U.S.A.*, **72**, 943–946 (1975).
[15] Falconer, D. S., *Introduction to Quantitative Genetics* (Ronald, New York, 1960).
[16] Leng, E. R., *Crop Sci.*, **3**, 187–190 (1963).

Non-random inactivation of X chromosome in the rat yolk sac

THE Lyon hypothesis postulates that the mammalian female is a natural mosaic for clones of cells with either the maternally derived X chromosome (X^m) or the paternally derived one (X^p) which is randomly inactivated early in development[1,2]. We have presented evidence for the dominance of the inactive X^p in extraembryonic regions of 7.5- and 8.5-d mouse embryos heterozygous for Cattanach's translocation[3] in which the two X chromosomes could be readily identified[4]. Though we presumed that this might not be an exceptional phenomenon restricted to mice bearing this X-autosome translocation, this has been difficult to confirm because of the lack of a system suitable for experiments. Here we report further cytological evidence that the inactive X is predominantly paternal in the yolk sac of the laboratory rat.

We used X^t-X^{st} dimorphism in the laboratory rat[5]; the X chromosome is telocentric (X^t) in F344 and ACI strains, whereas it is subtelocentric (X^{st}) in the WKA strain bred at our laboratory (I. Hayata, unpublished). X^tX^{st} heterozygotes were obtained from the cross ACI(X^tX^t) × WKA($X^{st}Y$) and WKA($X^{st}X^{st}$) × F344(X^tY). The X chromosome transmitted from the father is X^{st} in the former cross, whereas it is X^t in the latter. Embryos were recovered from the decidual swelling at 10.5 d gestation when the yolk sac had enveloped the amnion, and the allantois had fused with the chorion. Mosaic composition was studied only in the embryo proper, and in the yolk sac, by means of a technique essentially similar to the one described elsewhere[6,7].

Distinction between X^{st} and X^t was unequivocal and an asynchronously replicating X was identified as the palest red element in the great majority of metaphase spreads with banded chromosomes (Fig. 1). It should be mentioned, however, that the short arm of the isocyclic X^{st} failed to show up in occasional black and white photographs. Cytogenetic examination was carried out in 8 and 7 embryos from the cross $X^{st}X^{st} \times X^tY$ and $X^tX^t \times X^{st}Y$, respectively. In the former 8 embryos the percentage of cells with the X^p allocyclic ranged from 82.1% to 97.8% with an average of 94.7% in the yolk sac, whereas it ranged from 46.7% to 71.4% with an average of 55.3% in the embryo proper. The difference between the two was highly significant ($P < 0.001$). The results were similar in the latter 7 embryos; the average for the yolk sac, although slightly lower

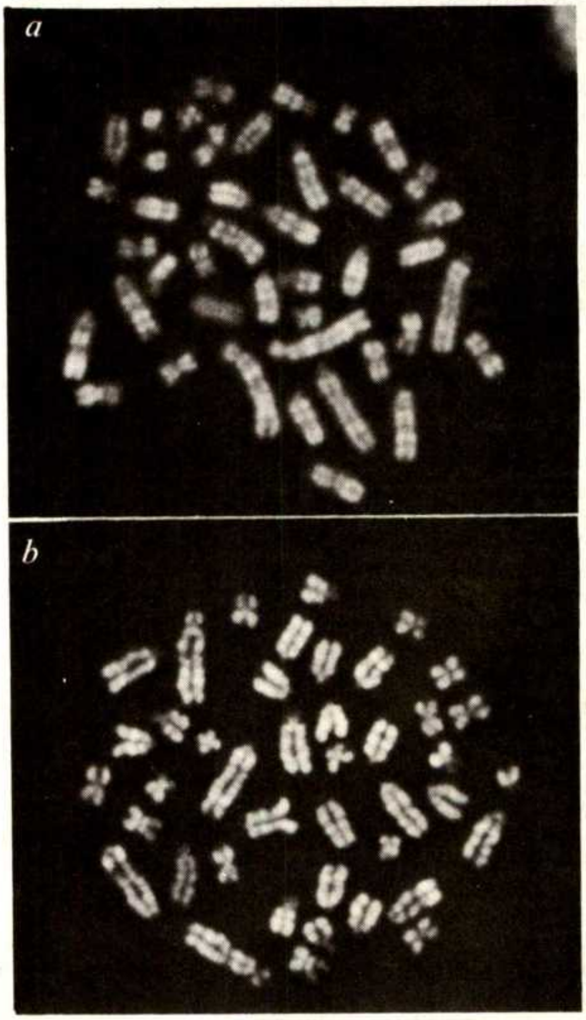

Fig. 1 BUdR–AO differential staining of the allocyclic X chromosome in cells of a 10.5-d-old X^tX^{st} embryo from the cross $X^tX^t \times X^{st}Y$. The allocyclic X which fluoresced faintly is maternal (X^t) in *a*, whereas it is paternal (X^{st}) in *b*. Embryos were taken out of the uterine cavity, incubated at 37 °C for 10 h in Eagle's medium supplemented with foetal calf serum (20%) and bromodeoxyuridine (100 μg ml^{-1}). Colcemid (1 μg ml^{-1}) was added 1 h before collection. Air-dried slides were prepared according to a modified method of Wroblewska and Dyban[6] as described by Takagi and Oshimura[7], and stained with acridine orange (0.5 mg ml^{-1}) in 0.15 M Sörensen's phosphate buffer (*p*H 7.0).

Table 1 Parental influence on X-inactivation mosaic composition in 10.5-d-old female rat embryos

Embryo	Area examined	No. of cells examined	No. of cells with allocyclic X^p (%)
(1) $X^{st}X^{st} \times X^{t}Y$			
1	Y	46	45 (97.8)
	E	67	42 (62.7)
2	Y	169	155 (91.7)
	E	152	97 (63.8)
3	Y	67	55 (82.1)
	E	135	63 (46.7)
4	Y	152	148 (97.3)
	E	84	53 (63.1)
5	Y	242	233 (96.3)
	E	173	86 (49.7)
6	Y	302	288 (95.4)
	E	136	67 (49.3)
7	Y	82	79 (96.3)
	E	35	25 (71.4)
8	Y	53	51 (96.2)
	E	26	14 (53.8)
Total	Y	1,113	1,054 (94.7)
	E	808	447 (55.3)
(2) $X^{t}X^{t} \times X^{st}Y$			
1	Y	162	146 (90.1)
	E	103	71 (68.9)
2	Y	165	145 (87.9)
	E	275	162 (58.9)
3	Y	93	84 (90.3)
	E	124	55 (44.4)
4	Y	201	182 (90.5)
	E	179	95 (53.1)
5	Y	219	199 (90.9)
	E	124	69 (55.6)
6	Y	121	109 (90.1)
	E	107	63 (58.9)
7	Y	160	154 (96.3)
	E	140	83 (59.3)
Total	Y	1,121	1,019 (90.9)
	E	1,052	598 (56.8)

Y, Yolk sac; E, embryonic body.

Table 2 Comparison of average percentages and standard deviations of cells with an allocyclic X^p in the yolk sac and embryo proper

Cross type	Yolk sac	Embryo proper
$X^{st}X^{st} \times X^{t}Y$	94.1* ± 4.9	57.5 ± 8.3
$X^{t}X^{t} \times X^{st}Y$	90.9* ± 2.4†	57.0 ± 6.9
Combined	92.6* ± 4.2†	57.3 ± 7.3

*$P < 0.001$.
†$P < 0.05$ (compared with the embryo proper).

compared with that in the former embryos, was not statistically significant ($0.1 < P < 0.2$). It seemed that there was more variation in mosaic composition among embryos themselves than yolk sacs, as indicated by a significantly higher standard deviation ($P < 0.05$). It should also be mentioned that there was no correlation in the proportions of the two cell types between these structures within an embryo ($r = 0.33$, $0.2 < P < 0.3$). Thus the present study substantiated the previous observation made in the mouse heterozygous for Cattanach's translocation. Another aspect in common with the mouse embryo was a slight excess of cells with the X^p inactive in the embryo proper. But the source of departure from the equal representation expected on random basis is not known.

We have already discussed elsewhere[3] possible ways to bring about the extreme mosaicism and its potential significance. A salient feature may be mentioned in connection with the recent findings. There are at least three possible ways of explaining the apparently preferential inactivation of the paternal X chromosome: (1) reactivation of the inactive X^m with simultaneous inactivation of the active X^p; (2) selective growth of cells with the X^m active after random inactivation; (3) preferential inactivation of the X^p. Takagi (in preparation), by means of a double labelling method with ^{3}H-thymidine and 5-bromodeoxyuridine, could exclude the first possibility in mouse embryos. Which of the remaining two is more likely? Isozyme activities of glucose-6-phosphate dehydrogenase in various organs from mules[8] strongly suggest *in vivo* selection for cells with the horse X active in certain organs. Extra-embryonic regions in mouse and rat might also be under strict selective pressure which favours the cell having the X^m active. Our recent observation (N.W. and N.T., unpublished) in 3.5-d mouse embryos, on the contrary, suggests that the initial event may not be random, in that the X^p was allocyclic in more than 90% of informative metaphases. Resolution of this problem will require fuller cytological studies of embryos in early development.

The result reported here implies that the overwhelming excess of the X^p inactive in the yolk sac and probably in some other extraembryonic tissues may hold at least in the family *Muridae*. Further studies will disclose whether it is an evolutionary specialisation in a small group of species, or a widespread phenomenon among eutherian mammals. In either case, it seems highly unlikely that the specific pattern of inactivation has been retained without any advantage. Cells having the active X^m may somehow be advantageous for the interaction between mother and embryo after implantation. We may assume that the majority of primordial germ cells, arising in the yolk sac, would possibly have the active X^m. If this is the case, it is tempting to consider the extreme mosaic composition in the yolk sac as a mechanism controlling X chromosome activity in female germ cells.

This study was supported in part by grants from the Ministry of Education, Science and Culture, and the Ministry of Health and Welfare of Japan.

NORIO WAKE
NOBUO TAKAGI
MOTOMICHI SASAKI

Chromosome Research Unit,
Faculty of Science,
Hokkaido University,
North 8, West 5,
Sapporo 060, Japan

Received May 24; accepted June 25, 1976.

[1] Lyon, M. F., *Biol. Rev.*, **47**, 1–35 (1972).
[2] Lyon, M. F., *Proc. R. Soc.*, **B187**, 243–268 (1974).
[3] Takagi, N., and Sasaki, M., *Nature*, **256**, 640–642 (1975).
[4] Ohno, S., and Cattanach, B. M., *Cytogenetics*, **1**, 129–140 (1962).
[5] Hungerford, D. A., and Newell, P. C., *J. Morph.*, **113**, 275–285 (1963).
[6] Wroblewska, J., and Dyban, A. P., *Stain Technol.*, **44**, 147–150 (1969).
[7] Takagi, N., and Oshimura, M., *Expl Cell Res.*, **78**, 127–135 (1973).
[8] Hook, E. B., and Brustman, L. D., *Nature*, **232**, 349–350 (1971).

Parallel distribution of sister chromatid exchanges and chromosome aberrations

THE role of chromatid exchange in the origin of chromosome aberrations has been a subject of research since the chromatid exchange hypothesis of chromosome aberrations was proposed[1]. Which of the breakage-reunion hypothesis[2] and the exchange hypothesis better explains the origin of chromosome aberrations is still disputed[3,4]. The part played by DNA repair in aberration and exchange formation has been identified[5,6], and there is much evidence for non-random distribution of chromosome aberrations, especially in the heterochromatic regions[7,8]. We have shown previously by autoradiography, that sister chromatid exchanges (SCEs) induced by 7,12-dimethylbenz(*a*)anthracene (DMBA) are frequently associated with aberrations[8]. Newly introduced 5-bromodeoxyuridine(BUdR)–33258 Hoechst methods for SCEs[9,10] have made it possible to reanalyse these problems in more detail and with considerable accuracy. The results presented here indicate that two different hydrocarbon carcinogens, DMBA and 7,8,12-trimethylbenz(*a*)-

anthracene (TMBA), induce aberrations localised in the same chromosomal regions of the rat bone marrow cells and that the targets for chromosome aberrations and for SCE are identical; in other words, both phenomena are related.

Two of the largest chromosomes (Nos 1 and 2) of the rat have extremely vulnerable regions to DMBA, especially when the carcinogen is administered shortly before cell collection, probably because of late DNA replication in these regions[8]. These vulnerable sites were therefore used to study the relationship between chromosome aberration and SCE. Male Long–Evans rats (30 d old) were used and were injected intravenously with a lipid emulsion of DMBA or TMBA (Upjohn) at 50 mg per kg body weight, 6 h before killing. Colchicine (0.3 mg) was administered intraperitoneally 1 h before killing and chromosome specimens were prepared from femur bone marrow by the standard air-drying method and stained with Giemsa. Chromosome aberrations observed consisted of gaps and breaks. Gaps were defined by a clear achromatic lesion with continuity, and breaks by displacement of the distal segment. Both ends of a break, or a gap from the centromere projected on the chromosome axis, were measured as accurately as possible in photographic prints and expressed by the percentage in the length of these chromosome arms. Distribution curves were plotted of the relative location of 100 breaks and gaps along both chromosomes. For SCE, an *in vitro* system was used, because *in vivo* BUdR-labelling of rat bone marrow cells was unsuccessful. The bone marrow cells from femur were suspended in 5 ml of thymidine-free F-12 medium containing 15% foetal calf serum and $2\ \mu g\ ml^{-1}$ of BUdR and were cultured for 26 h, or two rounds of the cell cycle[8]. DMBA or TMBA (5×10^{-4} mM) was dissolved in 0.1 ml of dimethylsulphoxide, and $0.2\ \mu g\ ml^{-1}$ of colchicine were added to the medium 6 and 2 h respectively before collecting the cells. Chromosome specimens were prepared and differential staining of sister chromatids was carried out using the modified 33258 Hoechst–Giemsa method[11]. One hundred SCEs in the long arms of both chromosomes were located in photographic prints by measuring the relative distance from the centromere. The distribution curves of SCEs were made by plotting the relative site of each exchange along the chromosome axis divided into 20 segments.

Fig. 1 Distribution of DMBA-induced chromosome aberrations (*a*) and sister chromatid exchanges (*b*) along the long arms of No. 1 and No. 2 chromosomes. The graphs are a combination of results from several samples. Numbers on the abscissa represent percentage distance from the centromere; 0, centromere; 100, telomere. The ordinate indicates the frequency per 100 aberrations in each chromosome. Six hours after DMBA (50 mg kg^{-1}, intravenously), 23.4% of metaphase bone marrow cells had aberrations. The mean number of aberrations per cell was 0.27; 13.7% were in No. 1; 17.9% in No. 2; and 68.4% in the remaining chromosomes. Of the aberrations 14% were breaks as defined by chromatid displacement and the rest were gaps. On the other hand, 289 SCEs were found in 26 metaphases (11.5 per cell) 6 h after addition of DMBA (5×10^{-4} mM) *in vitro*; 9.7% were in No. 1; 11.7% in No. 2; and 78.5% in the remaining chromosomes.

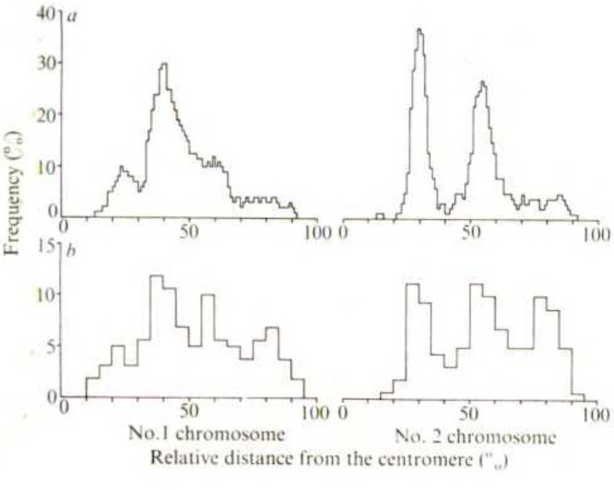

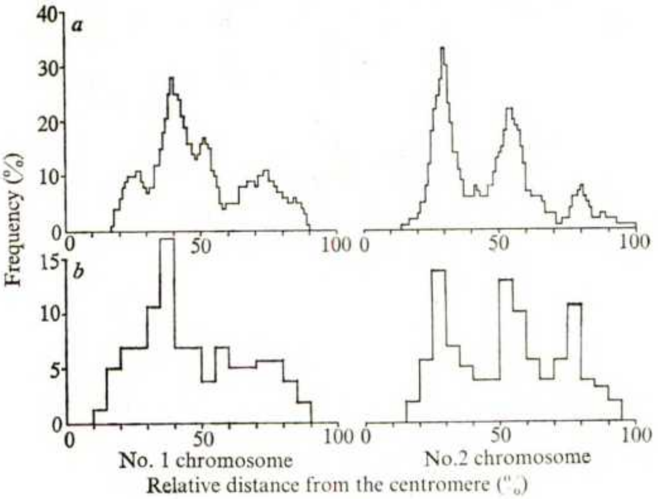

Fig. 2 Distribution of TMBA-induced aberrations (*a*) and sister chromatid exchanges (*b*) along the long arms of No. 1 and No. 2 chromosomes. At 6 h, 17.7% of metaphase bone marrow cells revealed aberrations. The mean aberration per cell was 0.20; 18.6% were in No. 1; 22.9% in No. 2; and 58.6% in the remaining chromosomes. Of the aberrations 14.5% were breaks and the rest were gaps. 253 sister chromatid exchanges were found in 26 metaphase cells (9.7 per cell) 6 h after addition of TMBA (5×10^{-4} mM) *in vitro*; 10.2% were in No. 1; 9.0% in No. 2; and 76.7% in the remaining chromosomes.

The DMBA- and TMBA-induced breaks and gaps were shown to distribute along the chromosomes non-randomly and reproducibly (Figs 1 and 2). The No. 1 chromosome had a susceptible site 40% of the distance along the long arm. In the No. 2 chromosome, there were three target sites for breaks and gaps; they were about 30, 55, and 80% along the chromosome from the centromere, although the last peak was not evident in the animals referred to in Fig. 1 treated with DMBA. SCEs were, however, also distributed non-randomly. The distribution curves of exchanges in No. 1 chromosome were similar to those for aberrations. There were also three susceptible regions for exchanges in the No. 2 chromosome. They coincided completely with the target sites for aberrations although the third susceptible region was far more susceptible to exchanges than to aberrations. Some SCEs were associated with aberrations (Fig. 3).

These results indicate that aberrations and SCEs are correlated. From this correlation, it is possible that aberrations represent incomplete SCEs that were not repaired.

Fig. 3 Sister chromatid exchanges in the susceptible regions of No. 1 chromosome (*a*) and No. 2 chromosome (*b*, *c* and *d*). *b* and *d*, Exchanges are incomplete, but are associated with a gap.

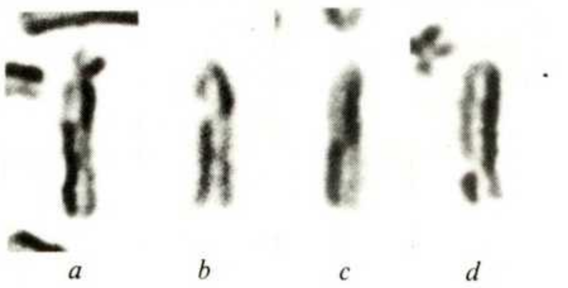

Whether SCEs comprise 25% of the total chromosome lesions as expected from Revell's hypothesis[1] is unknown from the present studies. Because late DNA replication in and the late vulnerability of these susceptible regions to DMBA have been suggested[8], it is possible that DNA replication is important in the induction and non-random distribution of these changes, although the part played by other factors such as repetitious DNA, intranuclear distribution of carcinogens, and chromosome association in the interphase nuclei[7] cannot be excluded. These non-random actions of chemical carcinogens need further studies in relation to carcinogenesis, because they parallel carcinogenicity of the chemicals[5,12] and the chemical carcinogens with a completely different chemical structure such as 4-nitroquinoline-1-oxide and *N*-nitroso-*N*-butylurea also induce the same genetic effects (unpublished data).

We thank the Ministry of Education, Science, and Culture, Ministry of Health and Welfare, and Princess Takamatsu Cancer Research Foundation for financial support. TMBA and DMBA were gifts from Professor C. Huggins, University of Chicago.

NORIFUMI UEDA
HIROSHI UENAKA
TOMOTOSHI AKEMATSU
TAKETOSHI SUGIYAMA

Department of Pathology,
Kobe University School of Medicine,
Ikuta-ku, Kobe, Japan 650

Received April 26, accepted June 25, 1976.

[1] Revell, S H., in *Proc. Radiobiol. Symp, Liège, 1954* (edit by Bacq, Z. M., and Alexander, P.), 243–253 (Butterworths, London, 1955).
[2] Sax, K., *Genetics*, 23, 494–516 (1938)
[3] Heddle, J A., Whissel, D., and Bodycote, D. J., *Nature*, 221, 159–160 (1969).
[4] Commings, D E., in *Chromosomes and Cancer* (edit. by German, J.), 95–133 (John Wiley, New York, London, Sydney, and Toronto, 1974)
[5] Perry, P., and Evans, H. J., *Nature*, 258, 121–125 (1975).
[6] Latt, S. A., *Proc. natn. Acad Sci U.S.A.*, 71, 3162–3166 (1974).
[7] Natarajan, A T, and Ahnstrom, G., in *Modern Aspects of Cytogenetics Constitutive Heterochromatin in Man* (edit. by Pfeiffer, R. A.), 215–223 (F. K. Schattauer Verlag, Stuttgart and New York, 1973).
[8] Sugiyama, T., *J. natn. Cancer Inst.*, 47, 1267–1275 (1971).
[9] Latt, S. A., *Proc. natn. Acad. Sci U.S.A.*, 70, 3396–3399 (1973).
[10] Perry, P.. and Wolff, S, *Nature*, 251, 156–158 (1974).
[11] Goto, K., Akematsu, T., Shamazu, H., and Sugiyama, T., *Chromosoma*, 53, 223–230 (1975).
[12] Sugiyama, T., *Gann*, 64, 637–639 (1973).

Communication through fimbriae during conjugation in a fungus

LONG fine hairs, termed fimbriae[1] or pili[2], have been observed in many bacteria and in fungi[3–5]. Bacterial sex pili transfer chromosomal and plasmid DNA during conjugation[6]. This paper describes evidence that the fimbriae of the smut fungus *Ustilago violacea* also transfer sex-specific molecules between the two conjugants.

The cells of this fungus may mate while they are touching (contact mating) or at distances of up to 20 μm on water agar (distant mating)[5,7]. During distant mating a tube grows from the a_2 mating type to the other cell (a_1 mating type; Fig. 1). Fimbriae up to 15 μm long are found on both mating types and are therefore long enough to account for distant mating, if it is assumed that the fimbriae of the two mating cells may attach end-on. The evidence that such fimbrial contacts between cells are formed and that they are essential for conjugation is as follows:

The behaviour of the cells, as observed under the light microscope, provides very strong evidence for the existence of an invisible connecting fibre at distances of more than 5 μm apart. Such cells floated together in water suspensions, rotating in unison and maintaining a constant maximum distance apart. The axis of rotation indicated that the cells were connected by a fibre that was laterally flexible but torsionally rigid, and was attached to the cell surface at a discrete site. They therefore rotated very similarly to two balloons fixed together with thin wire. The connection was fragile and could be broken by pressure on the cover slip. When water suspensions of cells were made carefully, such attached cells were found in mating cultures, but not in pure cultures or in mixed cultures of opposite mating type kept in conditions unsuitable for mating. Fimbriae are the only structures on the cell wall which could act as these invisible fibres.

The conjugation tube in cells mating at a distance seemed to grow along the line of the fimbrial connection. On nine occasions to date cells were observed similar to those in Fig. 1*a*, in which one mating partner produced a conjugation peg that had grown part way towards the other cell. The cells remained connected by an invisible thread and in every case their rotation as a pair clearly showed that the invisible fibre connected the tip of the conjugation tube to the other cell. The distance covered by the fibre varied

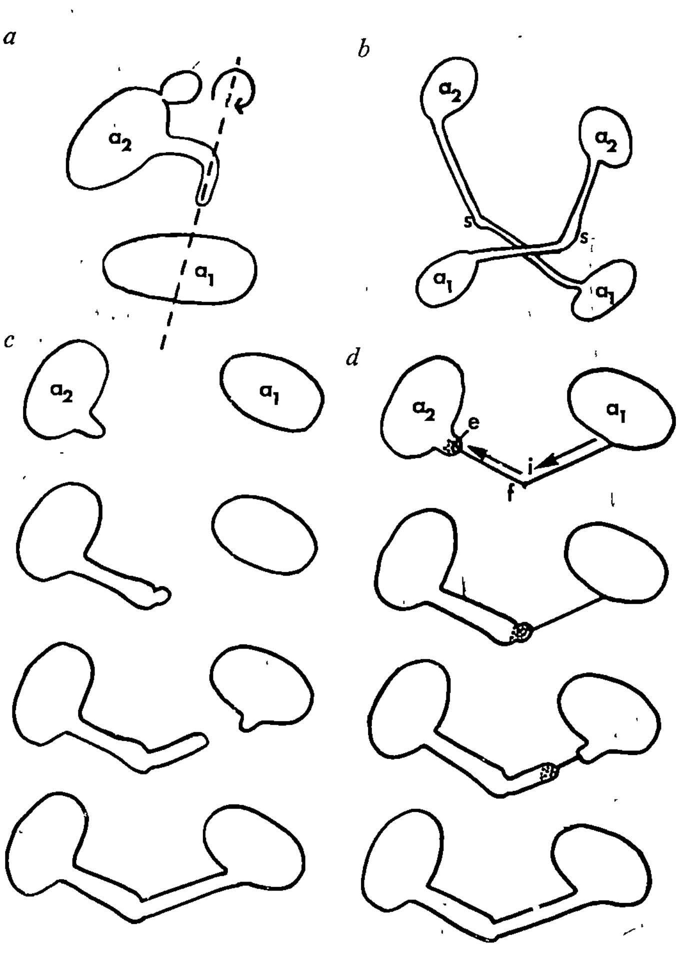

Fig. 1 *a*, Pair of mating cells attached by an 'invisible' fibre as observed under the light microscope in a water suspension. Dotted line represents axis of rotation of the pair of cells. *b*, Route taken by conjugation tubes from a pair of a_2 cells to two a_1 cells. Note that the tubes do not necessarily contact the nearest partner, and that they may swell before changing direction. *c*, Pair of cells during distant mating, showing the development of the conjugation tube from the a_2 cell, the swelling at the point where the direction changes and the growth of a small peg on the a_1 cell opposite the tube. *d*, Interpretation of the stages in *c*. The cells are considered to be connected by end-to-end joining of fimbriae *f*, from each partner. An inducer (i) is transported along this fimbrial connection from the a_1 cell to the a_2 cell. The inducer stimulates local production of wall-softening enzyme (e), at the a_2 terminus of the fimbrium, causing development of a peg. Further transport of inducer along the fimbriae results in continued growth of the tube along this path. As the growing tube nears the other cell transport of enzyme or of an inducer from a_2 may occur in a reverse direction causing some tube development on the a_1 cell.

from 1 to 5 μm; probably longer fimbrial connections tend to break in water suspension.

During distant mating the tube frequently did not grow directly across to the other cell but curved or turned at a sharp angle. Frequently the tip of the tube swelled before resuming growth in a new direction (Fig. 1*b–d*). The tube sometimes passed by a nearby cell of opposite mating type to reach one further away (Fig. 1*b*). The nearer cell later mated with another cell. These observations are difficult to explain if chemical diffusion is the cause of tube growth, but are readily explained if the tube follows the line of a previously established fimbrial connection.

Observations of several closely related species of *Ustilago* have established that only fimbriated strains can conjugate. Thus Kniep[9] showed that strains of *U. scabiosae*, *U cardui*, *U. vinosa*, *U. utriculosae* and *U. violacea* will conjugate with each other. Modern strains of these species that have become afimbriate have also lost the ability to conjugate, whereas strains that still produce fimbriae have full mating activity.

In an earlier report[5] it was shown that fimbriation and conjugation both have the same maximum temperature[2,5], the same response to temperature shifts, the same response to enzyme treatments, and are both blocked before translation by high temperatures. The cells still grow in conditions which limit both conjugation and fimbriation.

Electron microscopy of thin section and freeze-etched preparations demonstrated that fibres of similar appearance to fimbriae connect cells that are very close together[5,7,8]. These fibres were also found on the ends of the conjugation tubes[5,7]. Unfortunately, the fragility of the connection in distantly mating cells has so far frustrated attempts to demonstrate it by shadow casting.

Although these results establish that fimbriae are essential for conjugation, their exact function is not yet known. It is possible that there are both common fimbriae and sex fimbriae as in bacteria, since one or two fimbriae may differ from the others in having a terminal knob[5], just as frequently occurs with the sex pili of bacteria[6], and since only one or two conjugation tubes are produced per haploid cell, although there are hundreds of fimbriae on most cells.

The growth of the conjugation tube along the line of the fimbrial connection suggests that this fibre may be used to provide chemical communication between the cells[5]. It is suggested that 'inducer' molecules are transmitted along the fimbrial connection mainly from the a_1 cell to the a_2 cell, and that these molecules stimulate production of a wall-softening enzyme locally near the a_2 terminus of the fimbrial connection. This would cause bulging of the cell wall at the fimbrial terminus and initiate development of the conjugation tube. Further transmission of inducer together with continued growth in the a_2 cell would cause the tube to grow at its tip along the line of the fimbrium. If the connection between the two fimbriae is a poor one, inducer may accumulate at the junction resulting in swelling of the tip of the conjugation tube before growth along the fimbrium is resumed. The tendency of the a_1 cell to produce a conjugation peg as the conjugation tube approaches (Fig. 1*c* and *d*) may be due to movement of the enzyme itself along the fimbrium, or to the slow transport of inducer molecules from a_2 to a_1.

The inducer is perhaps most likely to be an enzyme subunit or coeffector, but it could also be a regulatory protein, messenger RNA or perhaps even DNA. The ability of fimbriae to transmit such large molecules was doubted for a while but has received strong support from recent work with bacteria[6], including the decisive experiments of Ou and Anderson[10] who showed that *E. coli* cells could complete conjugation and undergo recombination while remaining separated by distances of up to 3 μm and connected only by an 'invisible' thread. The similarity between the ultrastructural features of conjugation in bacteria and in *Ustilago* is very striking in view of the differences in nuclear organisation. It remains to be seen to what extent this similarity extends to the biochemical, genetical and regulatory levels.

Alan W. Day

Department of Plant Sciences,
University of Western Ontario,
London, Ontario, Canada

Received May 3; accepted May 28, 1976.

[1] Duguid, J A., and Wilkinson, R., *11th Symp. Soc. gen. Microbiol*, 69–99 (1961).
[2] Brinton, C. C., *Trans. N.Y. Acad. Sci.*, Ser. II, 27, 1003–1054 (1965).
[3] Poon, N. H., and Day, A. W., *Nature*, 250, 648–649 (1974)
[4] Poon, N H., and Day, A W., *Can. J Microbiol.*, 21, 537–546 (1975).
[5] Day, A W., and Poon, N. H., *Can. J. Microbiol.*, 21, 547–557 (1975).
[6] Ottow, J. C. G, *A. Rev Microbiol.*, 29, 80–108 (1975).
[7] Poon, N H., and Day, A. W., *Can J Microbiol.*, 20, 187–191 (1974)
[8] Cummins, J. E., and Day, A W., in *Cell Cycle Controls* (edit by Cameron, I, Padilla, G, and Zimmerman, A.), 181–200 (Academic, New York, 1974)
[9] Kniep, H., *Z. Bot.*, 11, 275–284 (1919).
[10] Ou, J T., and Anderson, T. F., *J. Bact.*, 102, 648–654 (1970).

Induction of "natural killer" cells by BCG

THE past decade has witnessed numerous attempts to suppress tumour growth by the administration of immune stimulants. Notable successes have been achieved, particularly following the intralesional injection of Bacille Calmette-Guérin (BCG) which has been observed to cause the regression of local tumour nodules in both experimental animals[1,2] and man[3–5]. Although there is some controversy as to the mode of action of BCG, it has become widely accepted that its anti-tumour effects are principally mediated through host macrophages, "activated" by the immunostimulant[6–8]. Observations we have recently made in studies of the peritoneal exudates of BCG-infected mice suggest an alternative possibility: that tumour destruction is caused by a non-macrophage population of cytotoxic cells which is induced by BCG immunisation.

Young adult (6–8 weeks) C57BL/6 mice were immunised intraperitoneally with 10^7 viable BCG organisms (Pasteur Strain, Trudeau Institute, New York). Peritoneal exudates were harvested at frequent intervals thereafter and the lytic activity of washed cells assessed against a variety of ^{51}Cr-labelled target cells using a 4-h microcytotoxicity assay[9]. Exudates from unimmunised animals were not cytotoxic under these assay conditions. In contrast, peritoneal cells obtained 2–15 d after

Table 1 Lytic activity of murine peritoneal exudates

Treatment used to induce exudate	% Specific cytolysis P815-X2*	EL-4 (G-)†
BCG	21	15
Thioglycollate	0	2.9
Proteose peptone	0	2.2
None (normal PEC)	0	0.5

*A methylcholanthrene-induced mastocytoma of DBA/2 origin, maintained in ascites form.

†A methylcholanthrene-induced thymoma of C57BL/6 origin, maintained in ascites form.

Young adult C57BL/6 mice were immunised intraperitoneally with 10^7 viable BCG organisms (Pasteur strain, Trudeau Institute, New York), with 2 ml 3% (w/v) thioglycollate medium or with 1.5 ml 10% (w/v) proteose peptone. Peritoneal exudates were collected 3 d later and lytic activity of 1.5×10^6 cells assayed against 10^4 ^{51}Cr targets. A 4-h microcytotoxicity assay was performed in RPMI 1640 containing 10% foetal calf serum. Specific cytolysis was calculated relative to target cells in the absence of any effector cells. The standard deviation of quadruplicate cultures was ±2% of the mean We have also observed extensive lysis of Chang (human liver cell line) cells by BCG exudates and, to a much reduced extent, by exudates induced by thioglycollate and proteose peptone (data not shown).

Table 2 Characteristics of the peritoneal exudate killer cell

Expt	Treatment of effector cells	% Specific cytolysis
(1)	None	18
	Adherent to tissue culture dish	7.7
	Non-adherent	37
(2)	None	15
	Carbonyl iron	25
(3)	None	22
	C	17
	Anti-θ+C	17
(4)	None	17
	C	17
	Anti-Fab+C	19

Peritoneal exudates were collected from C57BL/6 mice 3–6 d after immunisation with 10^7 viable BCG organisms. The following fractionation procedures were performed in attempts to identify the cytotoxic cell. (1) Exudates were centrifuged (300*g*, 3 min) on to a tissue culture dish (Falcon Plastics) and were then incubated for 40 min at 37 °C. Non-adherent cells were decanted, adherent cells removed with 5 mm EDTA in ice-cold Ca^{2+}-free HEPES buffer. (2) Carbonyl iron depletion was carried out by method of Lundgren[14]. (3) The anti-θ serum used was an AKR anti-C3H thymus previously described[15]. Normal rabbit serum was used as the source of complement (C). (4) A rabbit anti-mouse Fab serum was a gift from Dr Keith James, University of Edinburgh. Rabbit serum was again used as a complement source. The cytolytic activity of the fractionated populations was in each case assessed in a 4-h assay using 5×10^5 effector cells and 10^4 ^{51}Cr-labelled P815 target cells.

immunisation invariably caused target cell destruction. While there was considerable animal to animal variation in the amount of cytotoxicity exhibited, peak lytic activity was observed in exudate populations harvested 4–8 d after immunisation. The decline in reactivity was gradual, and some lytic activity was noted in populations harvested up to 3 weeks after BCG administration.

Several features of the lysis observed deserve comment: (1) the amount of lysis occurring in a 4-h period was directly proportional to the number of exudate cells added to the cultures (range used: 2×10^5–2×10^6 exudate cells per 10^4 target cells); (2) lysis, over a 3-h incubation period, was a linear function of time; and (3) C57BL/6-derived peritoneal exudates were capable of lysing syngeneic EL-4 thymoma targets as well as allogeneic P815 mastocytoma targets. Data from a typical experiment are shown in Table 1. The lytic effect noted was not confined to the C57BL/6 mouse; similar cytolysis has been observed with BCG induced exudates in the DBA/2 mouse. Interestingly, while thioglycollate and proteose peptone induced more copious, macrophage-rich, peritoneal exudates than did BCG, such cell populations were only minimally lytic (Table 1).

Attempts were made to characterise the nature of the cytotoxic cell present in BCG-induced exudates. The cytotoxic cell did not adhere to tissue culture plates (Table 2) nor was it phagocytic. Depletion of phagocytes by treatment of 2×10^7 peritoneal exudate cells with 200 mg carbonyl iron for 40 min at 37 °C, followed by application of magnetic field, removed 60% of the total cells. There was a concomitant increase in the lytic activity of the residual population (Table 2). It thus seems extremely unlikely that the cytotoxic cell in the exudates is a macrophage.

The lytic activity of BCG-induced peritoneal exudates was not affected by treatment with an AKR-antiserum directed against θ-alloantigen in the presence of a source of rabbit complement (Table 2). Identical treatment removed 91% of the T cell-mediated cytotoxic activity of spleen populations obtained from C57BL/6 mice immunised with P815 (DBA/2) alloantigen (data not shown). We conclude therefore that the killer cell in BCG exudates is not a thymus-derived lymphocyte.

Cells bearing surface immunoglobulin were quantitated by the use of a flouresceinated goat IgG with anti-mouse Fab activity. Treatment of exudates with a rabbit antiserum to the Fab portion of mouse IgG in the presence of rabbit complement diminished the number of flourescent cells from 12% to 2.4%. This treatment was without effect on the lytic activity of the exudates (Table 2). We conclude that the killer cell lacks surface immunoglobulin.

Soluble immune complexes were without effect on cytolysis by BCG-induced exudate cells under conditions which readily inhibited antibody-dependent K cell-mediated cytolysis (Table 3). This suggests that the BCG exudate cytolytic cell is not dependent on an Fc receptor for its activity. Furthermore, although K cells are notably trypsin resistant[10], cytolysis by BCG exudates was inhibited by trypsinisation of the effector cells before the assay (Table 3).

The effector cell present in BCG-induced peritoneal exudates therefore lacks: (1) the adherent and phagocytic characteristics of macrophages, (2) the surface characteristics of both T and B lymphocytes, and (3) the Fc-dependency and trypsin resistance of the K cell. By these criteria the cell is comparable to the "natural killer" cell described by Herberman *et al.*[11,12] and by Kiessling *et al.*[10,13].

To further this comparison, we investigated whether the exudate cell possessed an additional feature which has been reported to be peculiar to the natural cytotoxic cell: namely, a marked lability at 37 °C in culture[11].

Peritoneal exudate cells harvested 5 d after BCG infection were cultured at 37 °C at a concentration of 5×10^6 cells ml^{-1} in RPMI 1640 containing 10% foetal calf serum. After incubation for varying periods of time at 37 °C, the cells were held at 4 °C until a total time of 4 h had elapsed. At this time ^{51}Cr-labelled P815 cells were added, the cultures transferred to an incubator at 37 °C and the lysis of target cells evaluated 4 h later. As can be seen from Table 4, the lytic activity of exudate cells was extremely labile, a 50% reduction in lytic activity being observed within 7 h (3 h incubation + 4 h assay) at 37 °C. In contrast, T cell-mediated cytotoxic activity of alloimmune

Table 3 Inhibition of cytotoxicity by immune complexes or trypsinisation of effector cells

Effector cells	Target cells	Immune complex inhibition Antibody control	Complex	Inhibition (%)	Trypsin sensitivity Control	Trypsin	Inhibition (%)
Alloimmune spleen	P815	16	17	0	8.7	0.2	98
Normal spleen	Antibody coated CRBCs	14	3.6	74	4.5	5.0	0
BCG exudate	P815	20	23	0	23	12	48

Alloimmune spleen cells were obtained by culturing normal C57BL/6 mouse spleen cells with DBA/2 stimulating cells for 4 d in the condition described by Cerottini *et al.*[16]. Normal spleen cells were from C57BL/6 mice, and peritoneal exudate cells were obtained from the same strain 4 d following BCG inoculation. Both alloimmune spleen and BCG-induced peritoneal exudates were assayed against 10^4 ^{51}Cr-P815 target cells, the former at a 5:1, and the latter at a 50:1 effector–target cell ratio. Antibody-dependent cytolytic (K cell) activity was measured by culturing 10^6 normal spleen cells with 5×10^4 ^{51}Cr-labelled chicken erythrocytes (CRBCs) which had been coated with a 10^4 dilution of a mouse anti-CRBC serum. Soluble immune complexes were prepared by incubating a rabbit anti-DNP antiserum (40 μg ml^{-1}) with DNP-BSA (4 μg ml^{-1}) for 1 h at 37 °C. A 0.05-ml volume of this mixture was then added to 0.1 ml of effector cells and incubated 30 min at 37 °C, followed by addition of target cells in an 0.05-ml volume. Trypsin treatment of effector cells was carried out for 45 min at 37 °C using a cell concentration of 2×10^7 cells ml^{-1}, and either 0.25% trypsin (Sigma) or medium alone. Cells were washed and adjusted for viable cell recovery before assay. All cultures were in the presence of target cells for 4 h at 37 °C.

spleen (or peritoneal exudate cells) did not fall during identical culture conditions (Table 4 and unpublished observations).

In summary we have observed a cytotoxic cell population in the peritoneal exudates of mice 2–15 d after infection with viable BCG organisms. The cell population lacks those characteristics that are associated with B and T lymphocytes, macrophages and K cells. The BCG exudate cytotoxic cell shows a marked lability to temperature that the directly cytotoxic T cell does not. Additionally, in agreement with Kiessling *et al.*[10], it shows a susceptibility to trypsin treatment similar to the cytotoxic T cell, but in contrast to cytotoxic K cells. The exudate killer cell we describe here thus seems similar, if not identical, to the natural cytotoxic cell previously described[10–13].

It is interesting to note therefore that Herberman's studies[11] have shown that the mouse strain used here (C57BL/6), and specifically its peritoneal exudate, has a very low incidence of natural cytotoxic cells. This is presumably reflected in an inability to detect lytic activity in our assay system using normal exudate populations. It is not yet clear which of several alternatives is responsible for the vastly augmented activity seen in exudates after BCG administration. The principal possibilities seem to be: (1) that BCG induces a cytotoxic population *ab initio*; (2) that BCG causes the expansion of a population of cytotoxic cells which is initially present at an incidence below detection; (3) that BCG recruits into the peritoneal cavity cells which normally reside in other compartments or (4) that BCG "activates" an exudate cell population, rendering it cytotoxic.

Table 4 Lability of the cytotoxic cell

Cell	Time (h) 37 °C	Time (h) 4 °C	Specific cytolysis (%)	Inhibition (%)
BCG peritoneal exudate	0	4	27	0
	1	3	30	0
	2	2	21	21
	3	1	13	52
	4	0	6.4	76
Alloimmune spleen	0	4	68	0
	1	3	67	2
	2	2	69	0
	3	1	74	0
	4	0	78	0

Peritoneal exudates were harvested 5 d after immunisation of 6-week-old C57BL/6 mice with 10^7 viable BCG organisms. Alloimmunised spleens were obtained from C57BL/6 mice 10 d after immunisation with 3×10^7 P815 cells. Effector cells were incubated alone at 37 °C for various periods of time and then placed in an ice water bath at 4 °C until a total time of 4 h had elapsed. At this time 5×10^5 effector cells were incubated for 4 h at 37 °C with 10^4 ^{51}Cr-P815 cells and the degree of target cell destruction evaluated. Inhibition following culture at 37 °C was calculated relative to the activity of effector cells stored continuously at 4°C.

Further investigations will clearly be needed to define the nature of the inductive process, to delineate the lineage of the cytolytic cell, and to see whether other bacterial products with anti-tumour reactivity (for example *C. parvum;* MER) also produce cytotoxic cells. It may not be coincidental that of the three agents we have used to induce peritoneal exudates only BCG substantially augments natural cytotoxicity and only BCG shows anti-tumour activity *in vivo*.

The induction of cytotoxic cells following BCG administration suggests to us that this population might be at least partially responsible for the tumour regression associated with BCG therapy. Furthermore, these observations imply that measurement of the natural cytotoxic cell population might prove to be a useful adjunct to studies aimed at optimising therapy with bacterial adjuvants.

We thank Drs Keith James and John Cebra for their gifts of rabbit anti-Fab serum and the flouresceinated Ig reagents.

This work was supported by a grant from the NIAID and by a grant from the Jane Coffin Childs Memorial Fund for Medical Research. C. S. H. is the recipient of a research career development award from the NIAID.

SETH A. WOLFE
DANIEL E. TRACEY
CHRISTOPHER S. HENNEY

Departments of Biology, Medicine and Microbiology,
Johns Hopkins University and
O'Neill Memorial Research Laboratories,
Good Samaritan Hospital,
Baltimore, Maryland 21239

Received May 27; accepted June 22, 1976.

1 Zbar, B., Bernstein, I. D., Bartlett, G. L., Hanna, M. G., Jr, and Rapp, H. J. *J natn Cancer Inst.*, **49**, 119–130 (1972).
2 Baldwin, R., and Pimm, M., *Br. J Cancer*, **28**, 281–287 (1972).
3 Morton, D L., *Seminars in Oncology*, **1**, 297–310 (1974)
4 Laucius, J F, Bodurtha, A. J., Mastrangelo, M J, and Creech, R. H, *J. Reticuloendothel Soc.*, **16**, 347–373 (1974).
5 Bast, R. C, Jr, Zbar, B., Borsos, T., and Rapp, H J., *New Engl. J. Med.*, **290**, 1413–1420, 1458–1469 (1974)
6 Alexander, P, *Natn. Cancer Inst. Mongraph*, **39**, 127–133 (1973)
7 Hibbs, J. B., Jr, *Science*, **180**, 868–870 (1973).
8 Germain, R N., Williams, R. M, and Benacerraf, B, *J natn Cancer Inst.*, **54**, 709–720 (1975).
9 Thorn, R. M, Palmer, J C., and Manson, L A, *J. Immun Meth.*, **4**, 301–315 (1974).
10 Kiessling, R., *et al.*, *J. exp. Med.*, **143**, 772–780 (1976)
11 Herberman, R. Nunn, M., and Lavrin, D., *Int. J. Cancer*, **16**, 216–229 (1975)
12 Herberman, R, Nunn, M., Holden, H., and Lavrin, P, *Int. J Cancer*, **16**, 230–239 (1975)
13 Kiessling, R., Klein E, Pross, H., and Wigzell, H., *Eur J. Immun*, **5**, 117–121 (1975).
14 Lundgren, G., Zukosi, C. F., and Moller, G., *Clin exp. Immun.*, **3**, 817–836 (1968).
15 Kamat, R, and Henney, C. S., *J. Immun.*, **115**, 1592–1598 (1975)
16 Cerottini, J.-C, Engers, H., MacDonald, H, and Brunner, K T., *J. exp Med.* **140**, 703–717 (1974).

Spleen cells from *Schistosoma mansoni*-infected mice produce diffusible stimulator of eosinophilopoiesis *in vivo*

WE have previously demonstrated that a diffusible stimulator of eosinophilopoiesis is produced in mice after secondary injection with tetanus toxoid (TT)[1]. Lymphoid cells from TT-primed animals are capable of producing a diffusible eosinophilopoietic stimulator in non-primed hosts on intraperitoneal TT injection[2]. To establish that this is not a unique phenomenon, limited to this antigen, but rather that it is characteristic of antigen-induced eosinophilias and associated eosinophilopoietic responses, we have studied eosinophilopoiesis in a parasite-induced eosinophilia.

Mice with experimental schistosomiasis exhibit marked peripheral eosinophilia[3], also observed in patients with this infection[4]. Spleen cells (SC) from *Schistosoma mansoni*-infected mice were tested for their ability to produce a diffusible stimulator of eosinophilopoiesis in response to an injection of a soluble schistosomal egg antigenic (SEA) preparation[5].

Prospective SC donors were injected intraperitoneally with 125 *S. mansoni* cercariae 8–12 weeks before use; control SC donors were untreated. Peripheral eosinophil levels in infected mice remained at normal levels (<5%) until between weeks 7 and 8 after infection. They then increased to 7–14%, at which level they remained until the last animal was killed at week 12. Liver and lung sections from infected mice contained large eosinophil-containing granulomas surrounding schistosoma ova.

The quadrachamber diffusion assembly[2] was used to culture normal C57BL/6Ja bone marrow cells transfilter *in vivo* from SC from *S. mansoni*-infected, or normal, non-infected, isogeneic mice Chamber assemblies were implanted in the peritoneal cavities of non-infected C57BL/6Ja or B6D2F$_1$ (C57BL/6Ja×DBA/2) mice. One hour after implantation, host mice received an injection of 25 μg protein SEA intraperitoneally. Six days after implantation, chambers were recovered and assayed for total and differential cell counts (see Fig. 1).

After killing and assaying, significantly greater total and

Table 1 Quadrachamber diffusion assembly bone marrow cellularity 6 d after intraperitoneal implantation in normal C57BL/6Ja mice*

Spleen cell source‡	Chamber marrow cellularity† Total cells	% Granulocytes (non-eosinophil)	% Eosinophils	Granulocytes (non-eosinophil) ($\times 10^{-6}$)	Eosinophils ($\times 10^{-6}$)	% Eosinophils Granulocytes
Uninfected mice (13)§	0.77±0.08	40.88±1.91	2.95±0.36	0.324±0.040	0.022±0.004	6.5±0.6
S. mansoni-infected mice (13)	0.65±0.07	35.70±2.33	7.01±0.59	0.232±0.029	0.042±0.004	17.0±1.6
P value¶	NS	NS	<0.001	NS	<0.005	<0.001

* Data are summarised from two independent experiments.
† Mean±s.e.m.
‡ 10^7 cells from the source indicated. All host mice received 25 μg protein-soluble (SEA) preparation intraperitoneally within 1 h after implant.
§ Number of chamber assemblies assayed.
¶ Test for significance determined by independent *t* test on data from paired chambers only.
NS, Not significant ($P > 0.1$).

percentage eosinophil granulocyte counts were present in bone marrow populations transfilter from infected SC compared with those transfilter from non-infected SC (Table 1). Total eosinophils were 0.042×10^6 compared with 0.022×10^6 in controls ($P<0.005$), representing a percentage eosinophil granulocytes of 7.01 and 2.95, respectively ($P<0.001$). The difference in eosinophil levels was not attributable to differences in total cell counts, percentage granulocytes or total granulocytes, as no significant differences were seen in these parameters for the two bone marrow cell populations Expression of eosinophils as a percentage of total granulocytes (%E/TG) gives a further indication that increases in eosinophil levels did not correlate with total granulocyte changes. In these studies, the %E/TG was 17.0% transfilter from infected SC compared with 6 5% across from non-infected SC, confirming the specificity of the stimulus for eosinophils.

These results indicate that spleen cells from schistosoma-infected mice are capable of producing a diffusible substance stimulatory for eosinophilopoiesis and are consistent with previous[2] experiments that demonstrated the production of a diffusible eosinophilopoietic factor by TT-primed lymphoid cells on secondary challenge.

Fig. 1 Quadrachamber diffusion assembly assay. SC donors received either 125 *S. mansoni* cercariae intraperitoneally or no treatment 8–12 weeks before quadrachamber diffusion assembly implantation. Chamber assemblies composed of two diffusion chamber doublets with 0.22 Millipore filters on both sides, and between upper and lower chambers, enable diffusion within doublets, and with the peritoneal fluid, but not directly between doublets. Upper chambers received 10^7 spleen cells from either the normal or schistosome-infected donors in 0.1 ml suspending fluid (6 parts M199 : 2 parts buffer : 1 part plasma-EDTA). Lower chambers received 10^6 normal bone marrow cells in 0.1 ml suspending fluid. Chamber assemblies were implanted intraperitoneally in C57BL/6Ja or B6D2F$_1$ mice. Within 1 h after implantation, host mice received an intraperitoneal injection of 25 μg SEA in 0 2 ml saline. Six days later chambers were recovered, shaken in 0 5% protease in 5% Ficoll in PBS, and individual bone marrow chamber contents were assayed for total and differential cell counts.

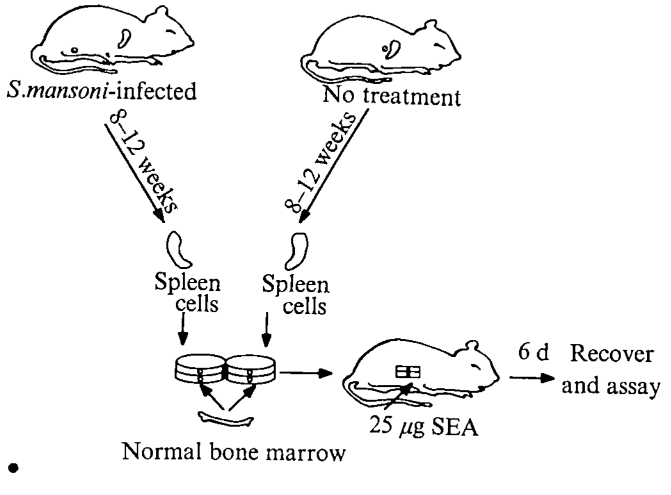

Increased peripheral eosinophil levels are seen in experimental animals and man during the course of *S. mansoni* infection. It has been shown that eosinophil granulocytes are prime components in the immune response to schistosoma eggs[6], and *in vitro* studies indicate that they may additionally be involved in immune-dependent destruction of schistosomula. It is therefore not surprising that an eosinophilopoietic factor would be produced in schistosomiasis.

Functional lymphoid cells are necessary for eosinophil response to antigens in which this has been tested[8,9]. The lymphoid cells evidently produce the stimulator of eosinophilopoiesis *in vivo* as a part of their response to antigens which elicit eosinophilia and medullary eosinophilopoiesis, as in the case of TT and schistosomiasis. Murine or human lymphoid cells from schistosoma-infected individuals produce a lymphokine-termed eosinophil stimulation promotor (ESP) on exposure to SEA *in vitro*[10,11]. ESP causes increased eosinophil migration in the *in vitro* assay conditions. Whether the eosinophilopoiesis stimulating factor is identical or distinct from ESP needs to be determined.

Further understanding of the processes regulating eosinophil production may assist our understanding of the reaction to parasitic infection, and the mechanisms of granulopoiesis.

We thank A. Nasrallah, R. Reszka, and B. Styles, and the Museum of Zoology, University of Michigan for assistance. Materials used in this study were provided by the US–Japan Cooperative Medical Science Program, NIAID.

ALAN M. MILLER

Department of Physiology,
State University of New York at Buffalo,
Roswell Park Division,
Buffalo, New York 14263

DANIEL G. COLLEY

Department of Microbiology,
Vanderbilt University and
the Veterans Administration Hospital,
Nashville, Tennessee 37232

MICHAEL P. MCGARRY

Department of Biological Resources,
Roswell Park Memorial Institute,
New York State Department of Health,
666 Elm Street,
Buffalo, New York 14263

Received March 31; accepted June 1, 1976.

[1] McGarry, M P , and Miller, A. M., *Expl Hemat.*, **2**, 372–379 (1974).
[2] Miller, A. M , and McGarry, M. P , *Blood* (in the press).
[3] Colley, D. G , *J Lab. clin. Med* , **81**, 871–876 (1974).
[4] Diaz-Rivera, R. S., *et al.*, *Am. J. Med.*, **21**, 918–943 (1956).
[5] Boros, D L , and Warren, K. S., *J exp. Med* , **132**, 488–507 (1970)
[6] Mahmoud, A A F., Warren, K. S., and Graham, R. C , Jr, *J exp Med* , **142**, 560–574 (1975)
[7] Butterworth, A E , *et al.*, *Nature*, **256**, 727–729 (1975)
[8] McGarry, M. P., Speirs, R. S , Jenkins, V. K., and Trentin, J. J., *J. exp Med.*, **134**, 801–814 (1971).
[9] Basten, A , and Beeson, P. B., *J. exp. Med* , **131**, 1288–1305 (1970).
[10] Colley, D G., *J. Immun.*, **110**, 1419–1423 (1973)
[11] Kazura, J. W , Mahmoud, A A. F., Karb, K. S., and Warren, K. S , *J. Infect. Dis* , **132**, 702–706 (1975)

Novel approach to the treatment of hydatid disease

HYDATID disease is a cyclozoonotic infection of man and certain other mammals which results from the cystic intermediate stage of the cestodes *Echinococcus granulosus* and *E. multilocularis*. The growth of these two species of parasites is basically similar except that the latter undergoes tumour-like metastatic dissemination. The present knowledge about immunity to this disease is incomplete; however, recent reports from this laboratory[1-3] have defined certain basic aspects of the immune response to secondary echinococcosis. These studies have demonstrated the rapid *in vitro* lysis of protoscoleces by the complement proteins when these are activated by surface immunoglobulins acquired *in vivo* by the larvae within the cysts. We also have evidence (unpublished data) that host serum proteins, including IgG and IgM immunoglobulins, are found within the cyst tissues of *E. multilocularis*, as previously demonstrated in *E. granulosus*[4]; Rau and Tanner[3] have demonstrated that heat-inactivated serum from infected hosts is cytotoxic to the protoscolices of *E. multilocularis in vitro*. Based on these results, we now hypothesise that anti-*Echinococcus* antibodies in the serum of infected animals can "recognise" antigenic sites on the parasite but are unable to reach these sites in sufficient quantities under the natural conditions of the infection; given the opportunity of contact, these cytotoxic antibodies would subject the parasites to the deleterious effects of the immune response. We now present results which show that cysts of *E. granulosus* are killed when the fluid within these cysts is replaced with the fresh serum of infected animals and suggest this immunotherapy as a novel treatment of hydatid disease. Similar replacement of the fluid of *E. multilocularis* cysts also successfully killed the treated cysts; but the cyst mass continued to grow by surface budding.

In a series of experiments, sterile and fertile free peritoneal cysts of *E. granulosus* from infected A/J mice were transplanted into the peritoneal cavities of normal cotton rats (*Sigmondon hispidus*). Sixty days later, laparotomy was performed and the cysts treated as described in Table 1.

When the fluid was replaced with fresh serum from infected hosts (group 3), the cysts showed signs of regression by day 30 and became opaque, compared with the healthy transparent cysts in the controls (groups 1 and 2). From day 60–150, the laminated membrane of the treated cysts thickened, fluid was lost and the germinal membrane collapsed; the protoscolices within these cysts were degenerated and dead and failed to produce an infection when inoculated into susceptible animals.

Various hypotheses have been proposed to account for the survival of parasites in immunologically competent hosts[5-11]. The data presented in this report confirm our working hypothesis and also offer a practical approach to the biological/medical treatment of *E. granulosus* cysts. Thus, in spite of the claim that hydatid cysts induce an insufficient adverse host response[12], our results indicate that circulating anti-*Echinococcus* antibodies can kill these cysts if they contact the inner surface of the germinal membrane in sufficient quantities. These results raise the possibility that the cyst membrane is either impermeable to cytotoxic antibodies and thus selectively permeable to macromolecules, or that these antibodies pass into the cysts in quantities too small to destroy the parasite. Since macromolecules of host origin have been demonstrated in hydatid cysts[4,13,14], we conclude that the latter mechanism is operative in hydatid infections and would explain the long persistence of hydatid cysts in the immunologically hostile environment of the host. Furthermore, a breakdown in the mechanisms controlling permeability of the membrane and the consequent leakage of cytotoxic antibodies into the cysts could account for dead hydatid cysts found sometimes in infected animals.

Table 1 Effect of the replacement of hydatid fluid by serum on the growth of *Echinococcus granulosus* cysts in cotton rats

Group	No. of animals	Treatment	No. of viable cysts / Total no. of cysts
1	6	None	6/6
2	6	Normal cotton rat serum	6/6
3	6	Infected cotton rat serum	0/6

Adult cotton rats were each surgically transplanted with one cyst (1–3 cm in diameter) of *E. granulosus*. Two months later laparotomy was performed and the following treatments carried out: Group 1: no treatment; groups 2 and 3: the cysts were punctured with a 22 gauge needle and the fluid was aspirated and replaced by an equal volume of 20% ice-cold fresh serum (in Medium 199) from normal or heavily infected cotton rats (>30 g cyst mass), respectively. The needle, an empty syringe and a syringe containing the diluted serum were fitted on to a 3-way valve (Pharmaseal) and used in the above procedure. Cyst growth and survival was determined every 30 d on laparotomy in alternate animals. The experiment was terminated on day 150 after treatment when the viability of the cysts was determined both macroscopically at necropsy as well as by an increase in cyst size and/or by the eventual formation of protoscolices in the sterile cysts after subsequent transplantation into susceptible animals

Although surgery is the commonest treatment for hydatid disease[15,16], it is often unsuccessful since spillage of cystic contents, particularly protoscolices, during surgical resection can result in anaphylactic shock and secondary hydatidosis. Furthermore, surgery is impractical when the cysts are embedded in vital organs, such as heart and brain, or when resection of the parasite also necessitates the excision of tissues that are vital to the host. Our findings suggest the possibility that a hydatid infection with *E. granulosus* can be treated and the parasite killed by replacing the fluid within the cysts with fresh serum from the infected host. Since the need for surgical resection would no longer be necessary, spillage of protoscolices and hydatid fluid is minimised and the host need not be subjected to ethanol, formalin or hypertonic saline which are currently used to kill the parasite before resection. Protoscolices that might escape as a result of this treatment would have been lysed by the complement proteins in the injected fresh serum. This new approach provides, for the first time, a practical immunotherapeutic method to treat and kill surgically non-resectable *E. granulosus* cysts.

This research was supported by grants from the Research Programs Directorate, DNHW, and from the Medical Research Council to C.E.T. Research at the Institute of Parasitology is supported by the National Research Council of Canada.

AMIN I. KASSIS
CHARLES E. TANNER

Institute of Parasitology,
McGill University,
Macdonald College Post Office,
Province of Quebec,
Canada HOA 1CO

Received April 12; accepted June 26, 1976

1. Kassis, A I., and Tanner, C. E., *Int J. Parasit* , 6, 25–35 (1976).
2. Kassis, A I., Goh, S. L., and Tanner, C. E., *Int J. Parasit.*, 6, 199–211 (1976).
3. Rau, M. E , and Tanner, C. E., *Int. J Parasit.*, 6, 195–198 (1976)
4. Varela-Diaz, V M , and Coltorti, E A., *J. Parasit* , 59, 484–488 (1973)
5. Capron, A , Biguet, J., Vernes, A , and Afchain, D., *Path. Biol.*, 16, 121–138 (1968)
6. Damian, R. T , *Am. Nat.*, 98, 129–149 (1964).
7. Dineen, J. K , *Nature*, 197, 471–472 (1963).
8. Rickard, M. D., *Z. Parasit* , 44, 203–209 (1974)
9. Smithers, S R , and Terry, R. J., *Adv. Parasit* , 7, 41–93 (1969).
10. Sprent, J. F. A , in *The Evolution of Living Organisms* (edit by Leeper, G. W.), 149–165 (University Press, Melbourne, 1962).
11. Varela-Diaz, V. M , Gemmell, M. A., and Williams, J. F., *Expl Parasit.*, 32, 96–101 (1973).
12. Varela-Diaz, V. M., Williams, J. F., Coltorti, E A., and Williams, C S F., *J Parasit.*, 60, 608–612 (1974)

●

[13] Chordi, A., and Kagan, I. G., *J. Parasit.*, **51**, 63–71 (1965).
[14] Coltorti, E. A., and Varela-Diaz, V. M., *J. Parasit.*, **58**, 753–756 (1972).
[15] Noble, E. R., and Noble, G. A., in *Parasitology: the Biology of Animal Parasites*, 3rd ed., 244–249 (Lea and Febiger, Philadelphia, 1971).
[16] Marcial-Rojas, R. A., in *Pathology of Protozoal and Helminthic Diseases*, 635–657 (Robert E. Krieger, Huntington, New York, 1975).

Identification of breast cancer transcortin and its inhibitory role in cell-mediated immunity

THE successful development and maintenance of a neoplastic malignancy is generally accepted to result from a temporary or lasting suppression of cell-mediated immune mechanisms. Many studies illustrate that whereas lymphocytes of a cancer patient are functionally sound, their participation in cell-mediated immune responses to an antigenic neoplasm is abrogated by factors present in the plasma[1]. Among such factors identified are certain plasma proteins whose concentrations are markedly higher in the plasma of the cancer patient[2]. We have shown that the content of transcortin, the cortisol-binding protein of human plasma, is higher in patients with demonstrable cancer[3], and since transcortin inhibits the response of human lymphocytes to phytohaemagglutinin[4], a test generally accepted as demonstrative of active cell-mediated potential, we have attempted to study the relationship of such elevated levels of plasma transcortin to breast cancer.

The question of whether serum obtained from freshly diagnosed breast cancer cases inhibits the response of normal human lymphocytes to the presence of phytohaemagglutinin is answered by the data presented in Table 1. The inhibition of the incorporation of ^{3}H-thymidine into DNA promoted by such sera remains even after exhaustive dialysis, and therefore the responsible factor must be a species whose molecular weight is in excess of 10,000. In addition, we have tested the suppressive property of these sera on the incorporation of DNA precursors by lymphocytes of the RPM I-1788 cell line, and a similar inhibition was also found with all such sera tested. We also note that transcortin inhibits the incorporation of thymidine by either normal or RPM I-1788 lymphocytes.

Since breast cancer sera have been shown previously to contain two to three times as much transcortin as those of the corresponding normal females (our unpublished work), and since transcortin also inhibits the synthesis of DNA by human lymphocytes[4], we investigated the relationship of increased levels of transcortin to the existence of the breast tumour; of primary concern was the question of the source of the increase in plasma transcortin. Previously, we used a transcortin-specific antibody tagged with fluorescence, which we applied to frozen sections of tissues. This permitted the *in situ* identification of intracellular transcortin in human liver[5] and lymphocytes[6] as well as in the syncytiotrophoblastic cells of the human placenta[4]. In the case of both the liver and the placenta, this molecule seems to be synthesised within the tissues studied and subsequently released to the immediate circulatory supply of the representative tissues. On the basis of the placental transcortin study, we reasoned that breast tissue might also demonstrate the *in situ* presence of a species recognisable by the fluorescein-labelled transcortin-specific antibody.

Table 1 Effect of breast cancer sera and transcortin on the incorporation of ^{3}H-thymidine by normal lymphocytes stimulated with PHA, and by RPM I-1788 lymphocytes

	N	Mean c.p.m. ± s.d.	% Difference
(1)* Normal lymphocytes stimulated with PHA			
Normal sera	5	6,680 ± 180	—
Breast cancer sera	10	4,290 ± 165	−36%
Transcortin	5	3,460 ± 51	−48%
(2)† RPM I-1788 lymphocytes			
Normal sera	5	2,065 ± 82	—
Breast cancer sera	10	842 ± 38	−60%
Transcortin	5	1,386 ± 18	−33%

*5 × 10^5 Normal human lymphocytes were incubated in 2 ml of medium containing PHA with 0.2 ml of sera from normal or breast cancer patients, or with 50 mg of purified human transcortin[4]. At the end of 72 h incubation, 2 μCi of ^{3}H-thymidine was added to each culture and incubation was continued for an additional 2 h.

†5 × 10^5 RPM I-1788 lymphocytes were incubated in 2 ml of media with normal or breast cancer sera, or transcortin as above.

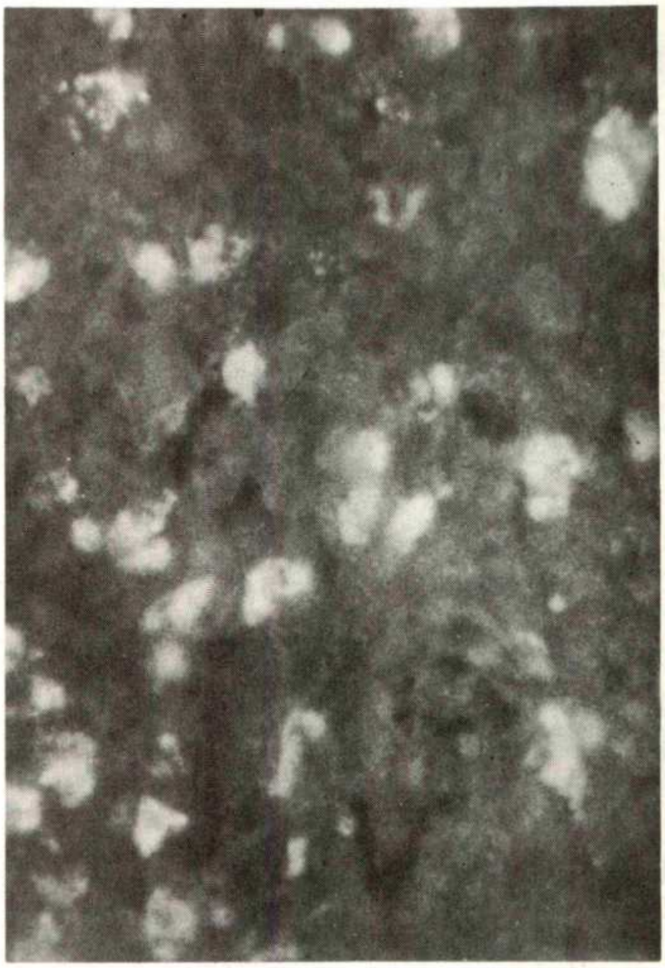

Fig. 1 Fresh biopsy breast tissues frozen rapidly and sectioned at a thickness of 4 μm. The sections were air dried and fixed in ice-cold acetone, and stored at −20 °C. Fluorescein-labelled transcortin antibody was applied as previously described[4].

Figure 1 illustrates that transcortin is present within the sectioned cells of the human breast cancer tissue. No transcortin has been detected by this technique in normal breast tissue. We have also studied other breast diseases in this way and have noted that transcortin almost exclusively occurs in malignancies of the breast. Table 2 shows that whereas 52 normal breast tissues gave negative results, almost 95% of all breast cancers examined contained transcortin. It is interesting to note that the condition of gynocomastia in the male, a benign tumour influenced by

Table 2 Fluorescent localisation of transcortin in breast lesions

	No. of cases	% Positive
Normal breast	52	0
Duct cell carcinoma	18	94
Lobular carcinoma	1	0
Fibroadenoma	12	8
Fibrocystic disease	16	13
Gynaecomastia	1	100

excessive oestrogen levels, is also positive for transcortin.

In an effort to define the functional role of breast cancer transcortin, we have tested the possibility that cytosols of breast cancer tissues could, as transcortin and breast cancer sera, limit the response of lymphocytes to PHA stimulation. Table 3 illustrates that only breast cancer cytosol exhibits appreciable inhibitory qualities in the incorporation of thymidine into the DNA of either normal or RPM I-1788 lymphocytes. The inhibitory factor is non-dialysable, and furthermore the inhibition can be obviated if cytosols are stripped of transcortin by previous incubation with the transcortin-specific antibody.

In summary, our studies indicate quite strongly that breast cancer tissue contains a transcortin-like species capable of limiting the response of human lymphocytes to PHA. Since oestrogens are known to induce breast cancer in both females[7] and males[8], and since oestrogen also induces the biosynthesis of transcortin in liver[9], the observation that the oestrogen-induced gynocomastic lesion also contains transcortin lends support to the hypothesis that oestrogen promotes the successful development and maintenance of a breast cancer by inducing the synthesis of transcortin within the abnormal cells. It is the release of this transcortin and its subsequent role in inhibiting the responses of T cells to the antigenic neoplasm which we believe to result in the successful maintenance of the breast cancer.

Table 3 Effect of normal and breast tumour cytosol on the incorporation of ^{3}H-thymidine by PHA-stimulated human lymphocytes and RPM I-1788 lymphocytes

	No. of separate experiments	Average difference from controls (%)
(1) Normal lymphocytes stimulated with PHA		
Normal breast cytosol	11	−11 (±6)
Dialysed	1	−2
Tumour breast cytosol	11	−62 (±12)
Dialysed	2	−58
Transcortin	6	−50 (±2)
Dialysed	2	−48
(2) RPM I-1788 lymphocytes		
Control cultures	8	—
Cancer breast cytosols	6	−80
(3) Preincubation of breast cytosols with transcortin-specific antibody		
Normal breast cytosol		−10
Tumour breast cytosol		−8
Transcortin		−11

Breast tissues were obtained surgically, homogenised in 0.010 M Tris-phosphate *p*H 7.4, the lipid layer removed and cytosols prepared by centrifugation for 3 h at 105,000*g*. Protein concentrations were adjusted to 10 mg ml^{-1}. All cytosols prepared were used on that same day for all the above experiments. 0.2 ml of breast cytosols were added to cultures containing normal lymphocytes and PHA, or RPM I-1788 lymphocytes. Incubations were for 72 h at 37 °C. At the end of this period, 2 μCi of ^{3}H-thymidine was added. Breast cytosols for some experiments were dialysed against 3 l of buffer for 24 h at 4 °C. In other experiments, breast cytosols were incubated with transcortin-specific antibody for 24 h at 4 °C. The antibody–antigen complexes were removed by centrifugation.

We thank Bennie Denson and Daniel Pina for technical assistance, Gloria Daniti for the preparation of the manuscript and Allan Brown for the preparation of the figure.

LEONARD AMARAL
SEYMOUR WERTHAMER

Department of Pathology and Clinical Laboratories,
The Methodist Hospital,
Brooklyn, New York 11215 and
Department of Pathology,
State University of New York Downstate Medical Center,
Brooklyn, New York 11203

Received May 11; accepted June 22, 1976.

[1] Hanna, N., Kalderron, R., and Nelken, D., *Immunology*, **29**, 433–443 (1975).
[2] Ovadia, H., Hanna, N., and Nelken, D., *Eur. J. Cancer*, **11**, 413–417 (1975).
[3] Amaral, L., and Werthamer, S., *Ann. Clin. Lab. Sci.*, **4**, 435–440 (1974).
[4] Werthamer, S., Govindaraj, S., and Amaral, L., *J. clin. Invest.*, **57**, 1000–1008 (1976).
[5] Amaral, L., Lin, K. B., Samuels, A. J., and Werthamer, S., *Biochim. biophys. Acta*, **362**, 332–345 (1974).
[6] Werthamer, S., Samuels, A. J., and Amaral, L., *J. biol. Chem.*, **248**, 6398–6407 (1973).
[7] Shellabarger, C. J., Stone J. P., and Holtzman, S., *Cancer Res.*, **36**, 1019–1022 (1976).
[8] Strong, L. C., and Williams, W. L., *Cancer Res.*, **1**, 886–891 (1941).
[9] Guidollet, J., and Louisot, P., *Acta Endocr.*, **62**, 468–476 (1969).

Cyclic nucleotide-dependent phosphorylation of intestinal epithelium proteins

THE function of cyclic AMP as an important regulator of ion and fluid transport in the small intestine has been well documented[1]. The non-dividing maturating crypt cells and the differentiated villous cells are the main sources of cyclic AMP-mediated secretion of water and electrolytes during experimental cholera in rats and guinea pigs[2,3]. It has been proposed that cyclic AMP, analogous to its possible mode of action in kidney[4] and toad bladder[5] epithelial cells, controls ion movements across the apical membrane of the intestinal epithelial cell (enterocyte) by changing the state of phosphorylation of some protein(s) in the intestinal brush border[6]. Studies have shown, however, that adenylate cyclase[2,7], the high affinity form of particulate cyclic AMP phosphodiesterase (unpublished observation) and receptor bound cyclic AMP (ref. 8) are localised predominantly in the basal–lateral membranes of the villous cell. In contrast, the luminal membrane is enriched in components of the cyclic GMP system, such as guanylate cyclase[9,10], cyclic GMP phosphodiesterase (unpublished observation) and receptor-bound cyclic GMP (ref. 8). The polarisation of both systems in the enterocyte would be more consistent with a model in which cyclic GMP, rather than cyclic AMP, is involved in the regulation of ion transport across the brush border, whereas cyclic AMP action might be confined to the contraluminal membrane. To test this hypothesis further, we have studied the subcellular distribution of specific substrate proteins for cyclic nucleotide-dependent protein kinases in isolated villous cells from rat small intestine.

Brush borders, microsomal fractions (enriched in basal–lateral membrane markers, compare ref. 11) and a 100,000*g* supernatant fraction (containing the cytosolic proteins) from villous cells were prepared as described previously[2,9,12]. Subcellular fractions were incubated with γ-^{32}P-ATP in the presence of Mg^{2+}, the proteins were separated by sodium dodecyl sulphate (SDS)–polyacrylamide gel electrophoresis and stained with Coomassie blue. Subsequently, the gels were dried and processed for autoradiography.

Protein staining patterns of brush-border preparations (Fig. 1) were characterised by a high content of an actin-like protein (molecular weight ~ 46,000) identified earlier by Tilney and Mooseker in microvillous cores from chicken intestine[13]. Incubation in the absence of cyclic nucleotides revealed a number of ^{32}P-labelled proteins, most of them not coinciding with major protein staining bands. Low concentrations of cyclic GMP (0.05–1.0 μM) or high concentrations of cyclic AMP (1.0–10 μM) caused an additional phosphorylation of a single brush-border protein (hereafter called protein B) with an apparent molecular weight of 86,000. The radioactivity of this band most probably reflects labelled phosphate esterified to serine or threonine residues of the protein because: no radioactive band could be detected using α-^{32}P-ATP; lipid extraction, treatment with hydroxylamine, cold or hot trichloroacetic acid or cold sodium hydroxide before electrophoresis did not influence the extent of labelling; and treatment with 0.4 M NaOH at 37 °C for 15 h removed the label almost completely (results

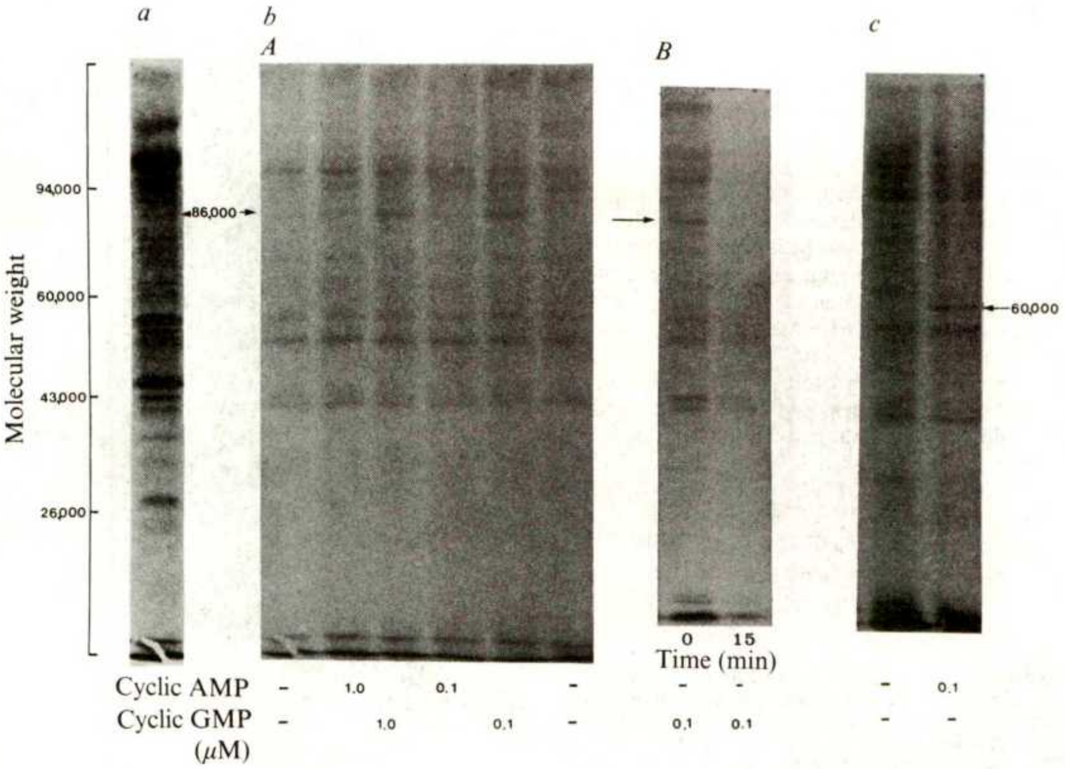

Fig. 1 *a*, Protein staining. *b* and *c*, Autoradiographs: Effects of cyclic GMP and cyclic AMP on endogenous phosphorylation of brush borders isolated from rat enterocytes. Intestinal brush borders (100–150 μg of protein) without (*b*) or with (*c*) cytosolic proteins (60 μg) were preincubated for 3 min at 30 °C in a volume of 50 μl containing 40 mM histidine buffer, 50 mM manitol, 10 mM Tris-HCl, 5 mM sodium-β-glycerophosphate (to diminish degradation of ATP by alkaline phosphatase), 5 mM theophylline, 10 mM $MgCl_2$ and cyclic nucleotide concentrations as indicated (final *p*H 6.8). Phosphorylation (*A* and *c*) started by addition of 2 μCi γ-^{32}P-ATP (final concentration 20 μM) and terminated after 10 s with 25 μl of a solution containing 60 mM Tris-HCl, 2 mM ATP, 3% SDS and 30% glycerol (*p*H 7.4). To stop the reaction the mixture was heated immediately in a boiling water bath, cooled and provided with 0.5% β-mercaptoethanol. 40 μl aliquots were loaded on 10% acrylamide–0.1% SDS slab gels (thickness 1 mm) with a 3% acrylamide stacking gel and run in the discontinuous buffer system of Laemmli[13] using a Slabophor apparatus (Pleuger, Wijnegem, Belgium). Electrophoresis was carried out for 6–8 h at 30 mA. For the procedures of gel staining, drying and autoradiography we refer to Ueda *et al.*[14]. In the dephosphorylation experiments (*B*) brush borders were labelled first for 2 min at 0 °C as described above, followed by rapid sedimentation in an Eppendorf 3200 centrifuge (30 s, 10,000 r.p.m.). The pellet was suspended in 50 μl of fresh medium prewarmed at 30 °C containing 10 mM $MgCl_2$, 5 mM ATP and 50 mM Tris-HCl (*p*H 7.0). After 5–15 min of incubation at 30 °C, dephosphorylation was terminated as described above. Molecular weight determinations were carried out according to Weber and Osborn[15] using phosphorylase *a*, catalase, ovalbumin and chymotrypsinogen as markers.

not shown). The phosphoprotein B caused one of the major peaks in optical density tracings of brush-border autoradiographs but corresponded with only a minor band in the protein staining pattern (Fig. 1). Densitometric analysis also showed that incorporation of label into protein B proceeded linearly with time for 10 s at 30 °C or 30 s at 0 °C. Incorporation was much lower in the presence of 10 mM Mn^{2+} or Ca^{2+} and was nearly absent in the presence of Zn^{2+} (5 mM) or γ-^{32}P-GTP instead of ATP (data not shown). The apparent K_a value for its phosphorylation by cyclic GMP (0.06 μM) was about 30-fold less than for cyclic AMP (2 μM; Fig. 2). The endogenous dephosphorylation of protein B was a relatively slow process. At 30 °C, half of the ^{32}P label was removed after 5 min whereas 20% of the initial label was left after 15 min (Fig. 1). Dephosphorylation rates did not change by addition of cytosolic proteins or cyclic nucleotides. The different turnover rates of the phosphoproteins on the autoradiograph (Fig. 1) suggest that the intrinsic phosphatase(s) in the brush border possess a certain degree of specificity towards their substrates.

A cyclic GMP-dependent phosphorylation could not be detected in villous cell fractions other than brush borders. Presumably, protein B is an integral and specific component of the microvillous membrane. Its phosphorylation was still manifest in brush-border preparations purified according to Hopfer *et al.*[17] with a relatively low content of core material (result not shown).

In spite of a wide variation in experimental conditions we were unable to show any specific effect of cyclic AMP on protein phosphorylation in isolated brush borders. If a cytosolic fraction was included in the system as a possible source of cyclic AMP-dependent protein kinase, a specific cyclic AMP-dependent phosphorylation of a 60,000 molecular weight protein was decided (Fig. 1*c*), but a similar radioactive peak of equal intensity appeared if the same amount of cytosolic protein was incubated alone (Fig. 3*c*). The corresponding apparent K_a for cyclic AMP was 0.04 μM (Fig. 2). A protein with similar properties was also found in microsomal membranes (Fig. 3*b*). This protein is probably identical to the so-called 'steroid and cyclic AMP regulated phosphoprotein'. (SCARP) detected by Greengard's group in cytosolic and membranous fractions from a large number of other rat tissues[18,19]: its molecular weight is comparable to that of SCARP (49,000–54,000); it is seen as the highest labelled band on autoradiographs of cytosolic fractions (Fig. 3); replacement of Mg^{2+} by Zn^{2+} 5 mM or Ca^{2+} 2 mM led to inhibition instead of stimulation of the phosphorylation rate by cyclic AMP, both in cytosolic and microsomal preparation (data not shown); and cyclic GMP up to 10 μM was entirely ineffective and was also unable to modify the cyclic AMP response (Figs 2 and 3). The only unusual property of the microsomal substrate protein was the strong stimulation of its phosphorylation by cyclic AMP in the presence of Mg^{2+}. In particulate fractions from most other tissues (synaptic membranes excepted[14]), cyclic AMP was hardly effective in this condition or even displayed an inhibitory action (toad bladder[5]).

The present discovery of cyclic GMP-dependent phosphorylation of a specific microvillous protein provides a possible mechanism by which cyclic GMP might change the properties of transport systems exclusively at the luminal membrane of the villous cell. Phosphorylation of protein B might exert a direct effect on the ion transport properties of the membrane or, alternatively, might work rather indirectly by changing the contractility of the microvillous core. The latter mechanism could then be quite analogous to the action of cyclic GMP on smooth muscle contractility, most probably also mediated by changes in the phosphorylation state of specific membrane-bound substrate proteins for cyclic GMP-dependent protein kinases[20].

Since high concentrations of cyclic AMP are able to promote the phosphorylation of protein B as efficiently as cyclic GMP (Fig. 2) it may be proposed that brush border phosphorylation could also be changed by cyclic AMP in pathological conditions characterised by high levels of this nucleotide (cholera) or during *in vitro* incubations with high concentrations (10^{-3}–10^{-2} M) of exogenously added cyclic AMP, dibutyryl cyclic AMP or theophylline[21,22]. Cyclic GMP levels might also be augmented in these conditions as a consequence of inhibitory or competitive effects on cyclic GMP phosphodiesterases (unpublished and refs 23–25). In contrast, phosphorylation of the SCARP-like protein—most probably absent in the brush border but enriched in microsomal preparations—could then be involved in cyclic AMP-dependent changes of ion transport across the basal–lateral plasma membrane. Direct measurements of the degree of phosphorylation of protein B and the SCARP-like protein in intact epithelium in different hormonal conditions and absorption or secretion states will be necessary to further substantiate this model.

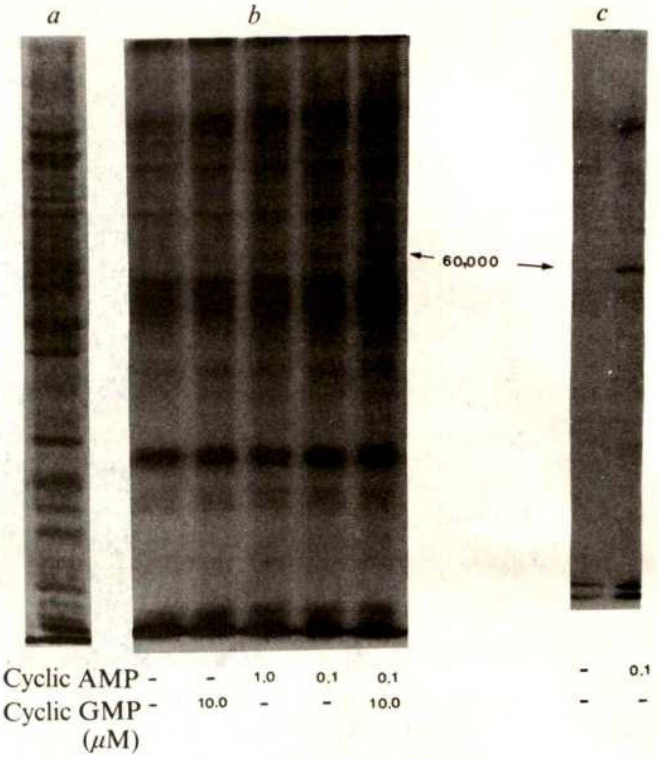
a
b
c
← 60,000 →
Cyclic AMP - | - | 1.0 | 0.1 | 0.1 | - | 0.1
Cyclic GMP - | 10.0 | - | - | 10.0 | - | -
(μM)

Fig. 3 Effects of cyclic AMP and cyclic GMP on the endogenous phosphorylation of microsomal (*a* and *b*) and cytosolic fractions (*c*) from isolated rat intestinal villous cells. Microsomes (200–250 μg protein) or soluble fractions (containing 60–100 μg protein) were phosphorylated for 15 s at 30 °C as described in Fig. 1. *a*, Protein staining; *b* and *c*, autoradiographs.

Fig. 2 Incorporation of ^{32}P label in endogenous substrate proteins as a function of cyclic nucleotide concentrations. *a*, Protein B (brush border); *b*, SCARP-like protein (cytosol). For experimental conditions, see Fig. 1. ■, Cyclic AMP; ▲, cyclic GMP. Absorbance of the 86,000 and 60,000 molecular weight bands on the autoradiographs were measured by scanning with a Vitatron Densitometer TLD 100 and peak areas were taken to be proportional to the amount of ^{32}P incorporated into each band.

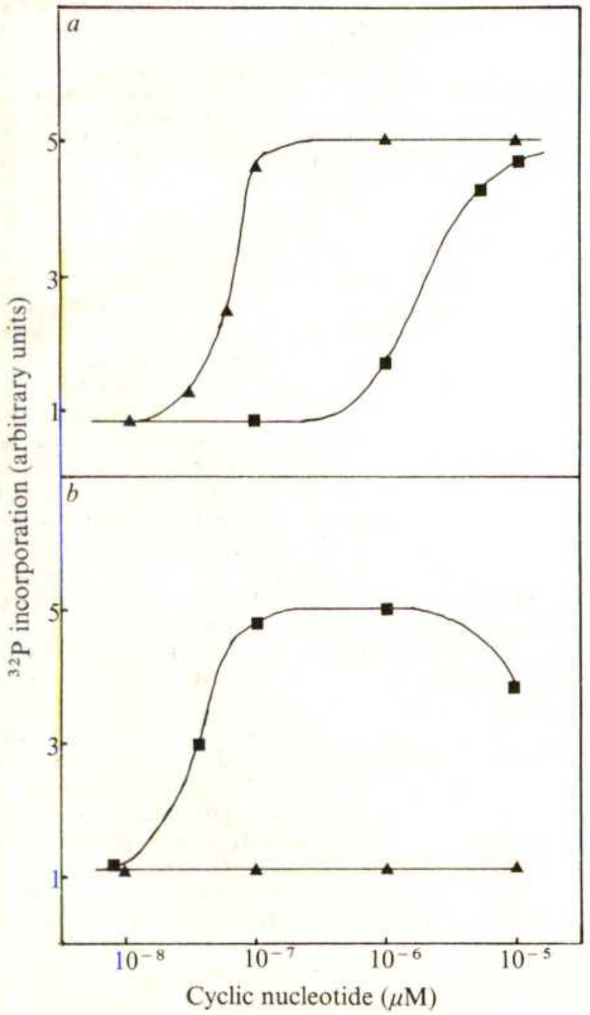

HUGO R. DE JONGE

Department of Biochemistry I,
Erasmus University Rotterdam,
PO Box 1738,
Rotterdam, The Netherlands

Received May 6; accepted June 1, 1976.

[1] Kimberg, D. V., *Gastroenterology*, **67**, 1023–1064 (1974).
[2] de Jonge, H. R., *Biochim. biophys. Acta*, **381**, 128–143 (1975).
[3] de Jonge, H. R., thesis, Univ. Rotterdam (1975).
[4] Schwartz, I. L., Shlatz, L. J., Kinne-Saffran, E., and Kinne, R., *Proc. natn. Acad. Sci. U.S.A.*, **71**, 2595–2599 (1974).
[5] Walton, K. G., DeLorenzo, R. J., Curran, P. F., and Greengard, P. J., *J. gen. Physiol.*, **65**, 153–177 (1975).
[6] Lucid, S. W., and Cox, A. C., *Biochem. biophys. Res. Commun.*, **49**, 1183–1186 (1972).
[7] Parkinson, D. K., Ebel, H., DiBona, D. R., and Sharp, G. W. G., *J. clin. Invest.*, **51**, 2292–2298 (1972).
[8] Ong, S., Whitley, T. H., Stowe, N. W., and Steiner, A. L., *Proc. natn. Acad. Sci. U.S.A.*, **72**, 2022–2026 (1975).
[9] de Jonge, H. R., *FEBS Lett.*, **53**, 237–242 (1975).
[10] Kimura, H., and Murad, F., *Life Sci.*, **17**, 837–844 (1975).
[11] de Jonge, H. R., *FEBS Lett.*, **55**, 143–152 (1975).
[12] Hülsmann, W. C., van den Berg, J. W. O., and de Jonge, H. R., in *Methods in Enzymology*, **32** (edit. by Fleischer, S., and Packer, L.), 665–673 (Academic, New York, 1974).
[13] Laemmli, U. K., *Nature*, **227**, 680–685 (1970).
[14] Ueda, T., Maeno, H., and Greengard, P., *J. biol. Chem.*, **248**, 8295–8305 (1973).
[15] Weber, K., and Osborn, H., *J. biol. Chem.*, **244**, 4406–4412 (1969).
[16] Tilney, L. G., and Mooseker, M., *Proc. natn. Acad. Sci. U.S.A.*, **68**, 2611–2615 (1971).
[17] Hopfer, U., Nelson, K., Perrotto, J., and Isselbacher, K. J., *J. biol. Chem.*, **248**, 25–32 (1973).
[18] Liu, A. Y. C., and Greengard, P., *Proc. natn. Acad. Sci. U.S.A.*, **73**, 568–572 (1976).
[19] Malkinson, A. M., *et al.*, *Metabolism*, **24**, 331–343 (1975).
[20] Casnellie, J. E., and Greengard, P., *Proc. natn. Acad. Sci. U.S.A.*, **71**, 1891–1895 (1974).

●

[21] Nellans, H. N., Frizzel, R. A., and Schultz, S. G., *Am. J. Physiol.*, **226**, 1131–1141 (1974).

[22] Frizzel, R. A., Nellans, H. N., Rose, R. C., Markscheid-Kaspi, L., and Schultz, S. G., *Am. J. Physiol.*, **224**, 328–337 (1973).

[23] Ishikawa, E., Ishikawa, S., Davis, J. W., and Sutherland, E. W., *J. biol. Chem.*, **244**, 6371–6376 (1969).

[24] Haymovits, A., and Scheek, G. A., *Proc. natn. Acad. Sci. U.S.A.*, **73**, 156–160 (1976).

[25] Kiefer, H. C., Atlas, R., Moldan, D., and Kantor, H. S., *Biochem. biophys. Res. Commun.*, **66**, 1017–1023 (1975).

In vitro inhibition of cyclic AMP phosphodiesterase by cortisol

HORMONAL effects on cyclic nucleotide phosphodiesterase activity are assumed to play an important role in the regulation of intracellular cyclic nucleotide concentrations[1]. The respective hormones vary widely with respect to function and structure, and comprise polypeptides, biogenic amines, and steroids including the glucocorticoids[2–4]. In no case, however, has the mechanism of hormonal action on cyclic AMP phosphodiesterase clearly been established. It is not known whether the enzyme itself is the primary point of attack by the hormone or whether the observed changes in enzyme activity (for review, see ref. 1) are side-effects of hormonal action, since no conclusive *in vitro* studies have been undertaken so far.

In the course of experiments designed to elucidate the possible function of the adrenal glucocorticoids as stimulators of the cyclic AMP-mediated human chorionic gonadotropin (hCG) sensitivity of the postnatal Leydig cell in the rat[5], we have tested the influence of cortisol on cyclic AMP phosphodiesterase activity in crude testis homogenates. For comparison, we have examined the effect of cortisol on the activity of the commercially available enzyme purified from beef heart.

Fig. 1 Inhibition of cyclic AMP phosphodiesterase from rat testicular tissue. Dixon plot of the reciprocal of reaction velocity against cortisol concentration. Each point represents the mean of duplicate determinations. Cyclic AMP concentrations in the assay were 0.120 (●), 0.058 (■), and 0.036 (▲) mM. Pooled testes from 20-d-old SIV 50 rats were homogenised with a motor-driven glass pestle in 10.9% sucrose 1:10 (w/v). The homogenate was sonicated with a Branson B12 sonifier at setting 1 for 30 s. All steps were carried out in an ice bath. The homogenate was adjusted to *p*H 6.0 with 1 M acetic acid[6], and a clear supernatant was obtained by centrifugation at 20,000*g* at 4 °C for 20 min.

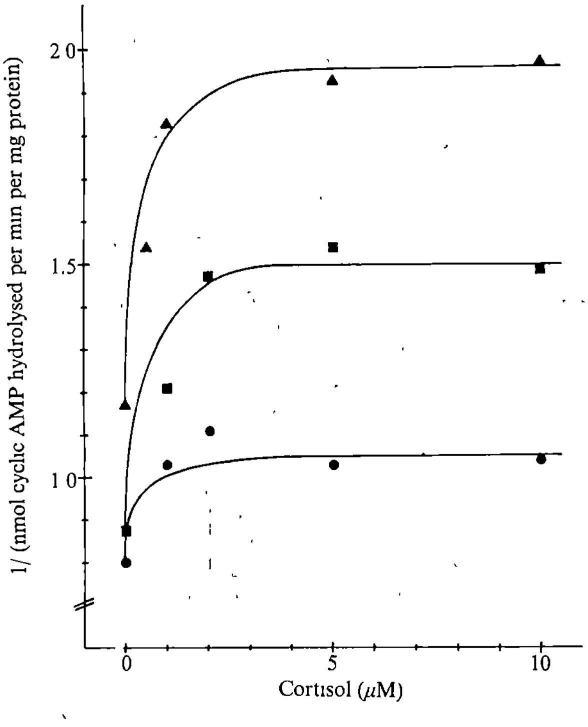

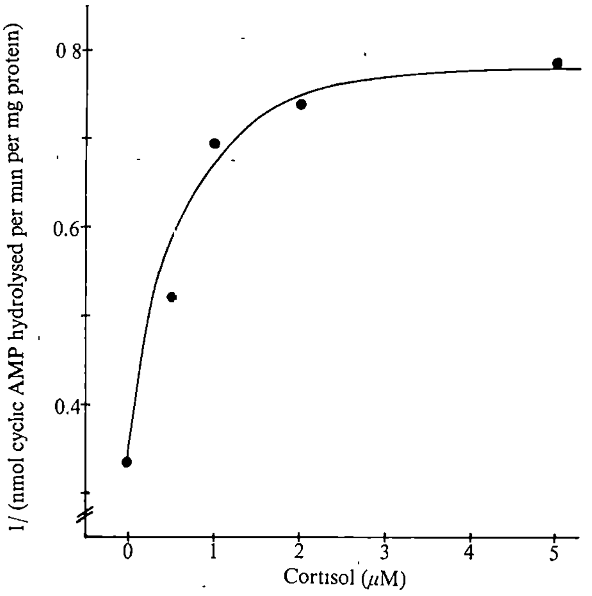

Fig. 2 Inhibition of cyclic AMP phosphodiesterase from beef heart. Dixon plot of the reciprocal of reaction velocity against cortisol concentration. Each point represents the mean of duplicate determinations. Cyclic AMP concentration in the assay was 0.0124 mM. The substrate was solved in 66 mM Tris-HCl buffer, *p*H 8.5, containing 1 mM $MgCl_2$.

Cyclic AMP phosphodiesterase was assayed as described by Rutten *et al.*[7]. The incubation medium contained 66 mM Tris-HCl, *p*H 8.5, 1 mM $MgCl_2$, 0.5 μM ^3H cyclic AMP (Amersham Buchler, specific activity 27 Ci $mmol^{-1}$), varying concentrations of unlabelled cyclic AMP (Boehringer, Mannheim, Germany), and 25 μl diluted tissue homogenate supernatant or enzyme solution in a final volume of 140 μl. Homogenate supernatant and enzyme concentrations were adjusted to a total substrate conversion not exceeding 10% of the initial concentrations. After 20 min incubation at 37 °C (the reaction was at least 2 h linear) the reaction was stopped by placing the tubes into boiling water for 2 min; 8 mU 5′ nucleotidase (Sigma) were added, the mixture was centrifuged (10 min at 10,000 *g*) and 100 μl of the supernatant were applied to a column (20×6 mm) filled with DOWEX 200–400 mesh (Serva). The column was eluted with 10 ml 0.1 M $NaHCO_3$, the eluate mixed with 10 ml scintillation fluor (Szintigel; Roth, Karlsruhe, Germany) and counted in a Tri-Carb scintillation counter. Inhibition experiments were carried out with homogenate supernatants as well as with enzyme solutions preincubated with 0.5–10 μM cortisol (Merck, Darmstadt, Germany) at 37 °C for 20 min. The ethanol, in which cortisol had been dissolved, was evaporated before addition of the enzyme solutions, since the presence of ethanol heavily interfered with the phosphodiesterase assay. The phosphodiesterase assay mixture was adjusted to the corresponding concentrations of cortisol. Controls, containing no cortisol, were preincubated and assayed in parallel.

The results of our experiments demonstrate that both testicular and beef heart cyclic AMP phosphodiesterase can be inhibited by cortisol at low concentrations. In Figs 1 and 2 the reciprocals of the reaction velocities are plotted against cortisol concentration[8]. The curves obtained can be easily interpreted as a partially competitive type of inhibition. This type of inhibition occurs when an intermediate complex of enzyme–substrate–inhibitor is formed, which then breaks down at the same rate as the enzyme–substrate complex, the inhibition therefore being purely an effect on affinity (Fig. 3). Assuming that product formation is rate-limiting and the enzyme, enzyme–substrate, enzyme–inhibitor, enzyme–inhibitor–substrate are rapidly equili-

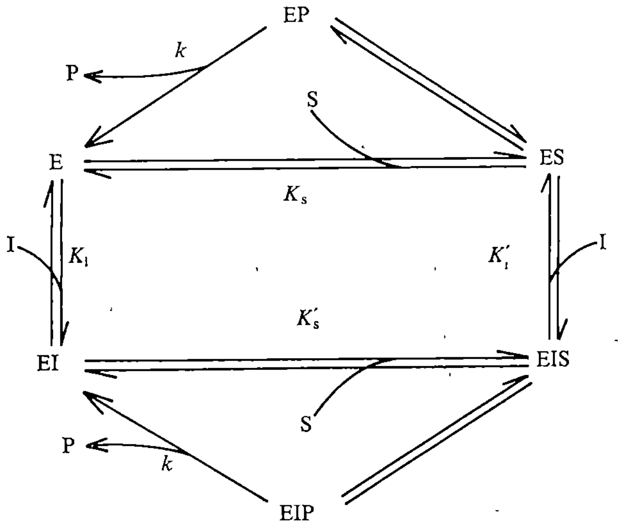

Fig. 3 Reaction scheme: partially competitive inhibition. E, Enzyme; EP, enzyme–product; EI, enzyme–inhibitor; EIP, enzyme–inhibitor–product; P, product; S, substrate; ES, enzyme–substrate; I, inhibitor.

brating, the 'rapid equilibrium treatment' easily leads to the rate equation[9]

$$v = \frac{V}{1+\dfrac{K_m(1+i/K_i)}{s(1+(i/K_i)(K_m/K'_s))}}$$

The plateau of the resulting curve is attained when all the enzyme is combined with inhibitor, and the degree of inhibition can increase no further.

Electrophoretic investigations of testis homogenates from 20-d-old rats revealed a single enzyme species possessing cyclic AMP phosphodiesterase activity. This enzyme exhibited true Michaelis–Menten behaviour in the range of substrate concentrations tested (0.6 mM–4.5 μM). Before the inhibition constants could be calculated, K_m and V had to be determined. We found the specific activity to be 1.5 mU per mg protein and the Michaelis constant to be 0.018 mM. Our results are largely consistent with the data reported by other workers[10]. The K_m and the specific activity of the commercially available phosphodiesterase purified from beef heart were 0.13 mM and 37 mU per mg protein, respectively. The range of substrate concentrations tested was 0.36 mM–2.9 μM.

K_i and K'_s were calculated by fitting a curve to the experimentally determined values of Figs 1 and 2 in an iterative procedure making use of an appropriate computer program. Subsequently the equilibrium constant K'_i was determined according to the equation

$$K_i/K'_i = K_s/K'_s$$

Values of K_m, K'_s, K_i and K'_i for the enzymes from rat testis and beef heart are summarised in Table 1.

Thus, high K_m cyclic AMP phosphodiesterases from two different sources, regardless of purity, seem to be inhibited by the same mechanism at low concentrations of cortisol. We have recently shown that low K_m cyclic AMP phosphodiesterase present in the testicular tissue of the 10-d-old rat can be inhibited by cortisol in a manner indicative of the partially competitive type of inhibition (W. E., M. F., J. Frowein and J. S., unpublished). It is tempting, therefore, to speculate that many of the so-called 'permissive effects' produced by glucocorticoids on cyclic AMP-mediated processes[11,12] reflect in fact a direct interaction of these hormones with cyclic AMP phosphodiesterase[8].

Table 1 Equilibrium constants for enzymes from rat testis and beef heart

	K_m (mM)	K'_s (mM)	K_i (μM)	K'_i (μM)
Rat testis	0.018	0.075	0.05	0.21
Beef heart	0.13	0.37	0.15	0.43

This work was supported by the Deutsche Forschungsgemeinschaft.

J. SCHMIDTKE
Th. WIENKER
M. FLÜGEL
W. ENGEL

Institut für Humangenetik und Anthropologie
der Universität, 78 Freiburg,
Albertstrasse 11, West Germany

Received February 9; accepted June 28, 1976.

[1] Amer, M S., and Kreighbaum, W. E., *J. Pharm. Sci*, 64, 1–37 (1975).
[2] Senft, G , Schultz, G , Munske, K., and Hoffmann, M , *Diabetologia*, 4, 330–335 (1968).
[3] Manganiello, V., and Vaughan, M., *J clin. Invest.*, 51, 2763–2767 (1972).
[4] Manganiello, V., and Vaughan, M , *J. biol. Chem* , 248, 7164–7170 (1973).
[5] Engel, W., and Frowein, J., *Nature*, 251, 146–148 (1974).
[6] Thompson, W. J., and Appleman, M M., *Biochemistry*, 10, 311–316 (1971).
[7] Rutten, W. J., Schoot, B. M., and De Pont, J. J. H. H. M , *Biochim biophys. Acta*, 315, 378–383 (1973).
[8] Dixon, M., *Biochem. J.*, 55, 161–170 (1953).
[9] Dixon, M , and Webb, E. C., *Enzymes*, 320 (Longmans, London, 1967).
[10] Monn, E , Desautel, M., and Christiansen, R. O., *Endocrinology*, 91, 716–720 (1972).
[11] Jost, J. P., and Rickenberg, H. V., *A. Rev Biochem.*, 40, 741–774 (1971).
[12] Gospodarowicz, D , *Nature*, 249, 123–127 (1974).

(−)-Propranolol inhibits the behavioural responses of rats to increased 5-hydroxytryptamine in the central nervous system

THERE are now several reports of the beneficial effect of large doses of (±)-propranolol in the treatment of various psychoses, particularly schizophrenia[1–3]. These reports prompted us to investigate whether propranolol had any effect on the behavioural syndrome produced in rats by increasing the functional activity of 5-hydroxytryptamine (5-HT) or dopamine (DA) in the central nervous system. Our results indicate that large doses of (−)-propranolol but not (+)-propranolol inhibit the behavioural responses resulting from increased functional activity of central 5-HT but not DA.

To investigate the action of propranolol on brain 5-HT function we used a behavioural model[4] reviewed elsewhere[5]. This involves the injection of tranylcypromine and L-tryptophan and measurement of the hyperactivity that results from the increased synthesis of 5-HT and its "spillover" into functional activity.

Rats were given (±)-propranolol (40 mg kg^{-1}) by intraperitoneal injection or saline and 45 min later given tranylcypromine followed by L-tryptophan (details in legend to Fig. 1). All aspects of the hyperactivity syndrome were almost totally inhibited by (±)-propranolol pretreatment (Table 1).

No evidence was found for alteration of the steady-state concentration of whole brain 5-HT, 45 min after (±)-propranolol (40 mg kg^{-1}). Both the rate of 5-HT synthesis and the rate of accumulation of 5-HT following administration of tranylcypromine and L-tryptophan were also unaltered by the single injection of (±)-propranolol. This demonstrated that propranolol was not exerting its effect on the hyperactivity syndrome by altering 5-HT biosynthetic mechanisms and suggested that the drug was in some way altering postsynaptic responses to 5-HT receptor stimulation.

This was examined indirectly by injection of the suggested 5-HT agonist 5-methoxy *N,N*-dimethyltryptamine (5-MeODMT). This compound produces a hyperactivity syndrome qualitatively identical to that seen when tranylcypromine and L-tryptophan are given but with a different time course and it has been suggested that this compound stimulates central 5-HT receptors[6].

Pretreatment of rats with (±)-propranolol (40 mg kg^{-1}) 45 min before tranylcypromine (20 mg kg^{-1}), with 5-MeODMT (2 mg kg^{-1}) given 30 min later resulted in almost complete abolition of the hyperactivity response. A similar reduction in the hyperactivity was seen in rats pretreated with (±)-propranolol (40 mg kg^{-1}) following subsequent administration of tranylcypromine and 5-methoxytryptamine, another suggested 5-HT agonist[7,8]. These results indicated therefore that propranolol inhibits the behavioural changes produced by central 5-HT stimulation and that it probably does so by means of a postsynaptic 5-HT receptor mechanism or through an effect on neuronal structures connected to these receptors.

The hyperactivity once established could be considerably reduced within 5 min by injection of (±)-propranolol (40 mg kg^{-1}) (Fig. 1). Furthermore, no inhibition was observed when (±)-propranolol (40 mg kg^{-1}) was given 3 h before the tranylcypromine administration. Since the half life of propranolol is about 40 min (ref. 9) these results suggested that the effect of propranolol was due to the parent compound rather than a metabolite. This view was strengthened by the observation that pretreatment of the rats with the drug metabolising enzyme inhibitor SKF525A, while not altering the hyperactivity seen when tranylcypromine and tryptophan were given, did make (±)-propranolol effective in inhibiting the hyperactivity at a dose (20 mg kg^{-1}) which is normally almost ineffective (Table 1).

The effect of the two isomers was next examined to determine whether both forms of the drug were equally active in inhibiting the 5-HT induced hyperactivity response. Injection of (−)-propranolol (20 mg kg^{-1}) 45 min before the tranylcypromine administration abolished the hyperactivity following subsequent tryptophan injection as effectively as when (±)-propranolol (40 mg kg^{-1}) had been given (Fig. 1 and Table 1) and the hyperactivity was inhibited by (−)-propranolol in a dose dependent manner (Fig. 1) Injection of (+)-propranolol (20 mg kg^{-1}) however was without effect on the hyperactivity (Fig. 1) suggesting that it is only the (−)-form of the drug in the racemate that is inhibiting the 5-HT induced behavioural changes.

To find out if propranolol had any effect on brain dopaminergic function we examined whether propranolol administration altered the locomotor activity produced by administration to rats of tranylcypromine and L-dopa since this activity seems to be almost solely the result of stimulation of dopaminergic systems in the brain[10]. Administration of (±)-propranolol (40 mg kg^{-1}) or (+) or (−)-propanolol (20 mg kg^{-1}) 45 min before the tranylcypromine did not alter the locomotor activity seen after subsequent L-dopa administration (Fig. 2). This indicated that propranolol has no inhibitory action on DA neurotransmission, a conclusion strengthened by two further observations. First (−)-propanolol (20 mg kg^{-1}) did not inhibit the rotation produced by amphetamine (5 mg kg^{-1}) in unilateral nigrostriatal lesioned rats and it is believed that turning produced in these animals by amphetamine is the result of dopaminergic stimulation[11,12]. Furthermore, propranolol is ineffective in inhibiting striatal dopamine sensitive adenylate cyclase[13], a finding confirmed in our current studies. It was also found that (±)-propranolol (40 mg kg^{-1}) had no effect on brain DA or noradrenaline concentration 45 min later.

The effect of other β-adrenergic receptor blocking drugs was also investigated. Propranolol is a β_1 and β_2 receptor blocking agent, and being lipid soluble enters the brain. The structurally related drug pronethalol (40 mg kg^{-1}) was almost ineffective in inhibiting the 5-HT mediated response, as was butoxamine (40 mg kg^{-1}) a lipid soluble β_2 antagonist (Table 1). Practolol (40 mg kg^{-1}) a β_2 receptor blocking agent that does not enter the brain in significant quantity[14] did not inhibit hyperactivity (Table 1). Thus propranolol

Fig. 1 Effect of (+)- and (−)-propranolol on the hyperactivity produced by administration of tranylcypromine and L-tryptophan. Groups of 3 rats (male Sprague–Dawley, 160–200 g, Anglia Laboratory Animals, Huntingdon) were injected with either saline (■), (−)-propranolol, 20 mg kg^{-1} (●), 15 mg kg^{-1} (○), 10 mg kg^{-1} (△) or (+)-propranolol, 20 mg kg^{-1} (▲). After 45 min all groups were injected with tranylcypromine (20 mg kg^{-1}) and L-tryptophan (L-Trp; 50 mg kg^{-1}) 30 min later. Fig. 1 shows subsequent changes in activity in each group using LKB Animex activity meters (sensitivity and tuning: 30 µA). The behavioural changes observed and method of measurement were exactly as described previously[4]. The effect of administration of (±)-propranolol (40 mg kg^{-1}) to rats already displaying hyperactivity is also shown (□), the drug being administered at the arrow.

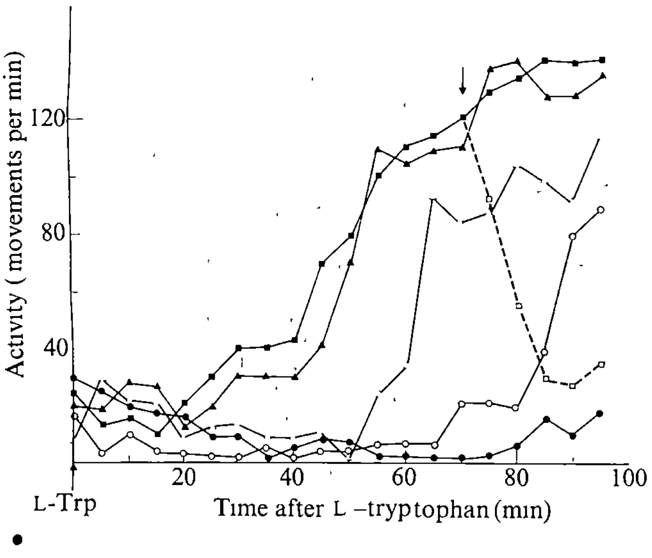

Table 1 Effect of (±)-propanolol pretreatment on hyperactivity induced by tranylcypromine and L-tryptophan

Injected	Total movements during 90 min following L-tryptophan (50 mg kg^{-1})
Saline	5,316± 598 (8)
(±)-Propranolol (40 mg kg^{-1})	886± 284 (3)*
(−)-Propranolol (20 mg kg^{-1})	1,041± 357 (3)*
(+)-Propranolol (20 mg kg^{-1})	4,558± 319 (3)
(±)-Propranolol (20 mg kg^{-1})	4,090± 759 (4)
(±)-Propranolol (20 mg kg^{-1}) +SKF 525A (2×10 mg kg^{-1})	1,740± 180 (3)‡
Pronethalol (40 mg kg^{-1})	3,631± 475 (4)†
Practolol (40 mg kg^{-1})	4,728± 920 (4)
Butoxamine (40 mg kg^{-1})	5,355±1,031 (3)
	Total movements during 60 min following L-dopa (50 mg kg^{-1})
Saline	3,140± 180 (3)
(−)-Propranolol (20 mg kg^{-1})	3,305± 110 (3)

Rats were injected with propranolol, pronethalol, practolol or butoxamine 45 min before tranylcypromine and activity measured following subsequent L-tryptophan or L-dopa administration as described in caption to Fig. 1. All drugs were dissolved in 0.9% saline except practolol which was suspended in 0.9% saline containing 1% carboxymethylcellulose and all these drugs were injected intraperitoneally. In the SKF 525A experiment rats were injected subcutaneously with SKF 525A (10 mg kg^{-1}) 30 min before and 30 min after the propranolol administration, tranylcypromine being given 45 min after propranolol as before. Results expressed as mean±s.e.m. with number of observations in brackets.

*Different from saline $P < 0.01$.

†Different from saline $P < 0.05$.

‡Different from (±)-propranolol (20 mg kg^{-1}) $P < 0.01$.

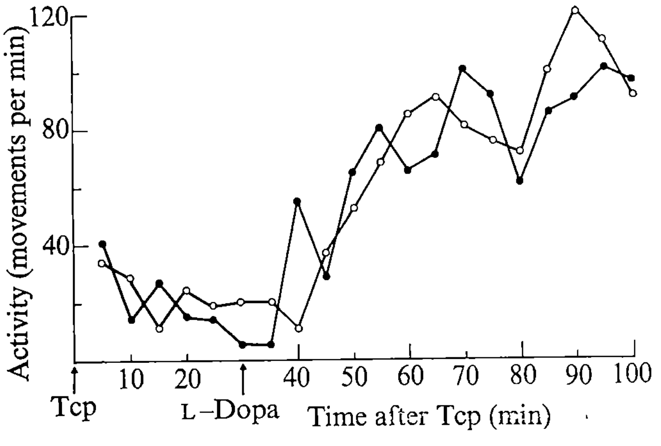

Fig. 2 Effect of (−)-propranolol on the locomotor activity produced by administration of tranylcypromine (Tcp) and L-dopa. Groups of 3 rats were injected with either saline (●) or (−)-propranolol, 20 mg kg^{-1} (○). After 45 min both groups were injected with tranylcypromine (20 mg kg^{-1}) with L-dopa (50 mg kg^{-1}) 30 min later. The figure shows subsequent changes in activity. The behavioural changes observed were as described previously[10].

was the only one of the β-adrenergic blocking drugs tested to inhibit 5-HT induced hyperactivity. Furthermore, this action cannot be ascribed to any tranquillising action of propranolol, since previous studies in rats have shown both isomers to be equipotent in this respect[15,16]

The results therefore all suggest that propranolol inhibits central 5-HT function, a finding that is analagous to the recent observation that (−)-propranolol (but not the (+)-isomer) blocks neurotransmission produced by 5-HT in the cat cervical ganglion[17].

If our conclusions are correct that propranolol inhibits central 5-HT neurotransmission and if future studies confirm its efficacy in the treatment of schizophrenia then there are several important implications.

Much interest has been focused on the dopamine receptor blocking action of neuroleptics as their mode of action, as anti-psychotic drugs[18,19] and indeed this has led to suggestions that increased activity of dopamine pathways may be involved in the aetiology of schizophrenia. If propranolol inhibits the central effects of 5-HT but not dopamine and if it is effective by this mechanism in schizophrenia then indirectly this points to an involvement of 5-HT as well as, or instead of, dopamine in this condition. Indeed, if 5-HT mechanisms were involved at a higher organisational level than dopaminergic mechanisms then the action of current neuroleptics could still be explained by their action on dopaminergic mechanisms. In rats inhibition of dopaminergic function either by use of neuroleptic drugs[6,20] or the decrease of brain dopamine concentration[21] blocks the behavioural responses to increasing 5-HT functional activity in the brain. Thus it seems that blocking dopaminergic activity can result in inhibition of certain aspects of central 5-HT function.

The demonstrated effect of propranolol on central 5-HT function, raises the question as to whether this is the mode of its action as an anti-schizophrenic drug and, if so, the role of 5-HT in schizophrenia.

We thank Ann F. C. Tordoff for technical assistance, Dr D. T. Greenwood of ICI Pharmaceuticals for propranolol and discussions and Burroughs Wellcome for butoxamine.

A. R. GREEN
D. G. GRAHAME-SMITH

MRC Unit and University Department of Clinical Pharmacology,
Radcliffe Infirmary,
Oxford OX2 6HE, UK

Received April 30; accepted June 16, 1976.

[1] Atsmon, A., Blum, I., Wijsenbeek, H., Maoz, B., Steiner, M., and Ziegelman, G., *Psychiat. Neurol. Neurochir*, 74, 251–258 (1971)
[2] Atsmon, A., Blum, I., Steiner, M., and Wijsenbeek, H., *Psychopharmacologia*, 27, 249–254 (1972)
[3] Yorkston, N. J., Zaki, S. A., Malik, M. K. U., Morrison, R. C., and Havard, C. W. H., *Br. med. J.*, 4, 633–635 (1974).
[4] Grahame-Smith, D. G., *J Neurochem*, 18, 1053–1066 (1971)
[5] Green, A. R., and Grahame-Smith, D. G., *Nature*, 260, 487–491 (1976).
[6] Grahame-Smith, D. G., *Br. J. Pharmac.*, 43, 856–864 (1971).
[7] Bradley, P. B., and Briggs, I., *Br. J. Pharmac.*, 50, 345–354 (1974).
[8] Green, A. R., Hughes, J. P., and Tordoff, A. F. C., *Neuropharmacology*, 14, 601–606 (1974).
[9] Shand, D. G., Rango, R. E., and Evans, G. H., *Pharmacology*, 8, 344–352 (1972).
[10] Green, A. R., and Kelly, P. H., *Br. J. Pharmac*, 57, 141–147 (1976).
[11] Ungerstedt, U., *Acta physiol. scand.*, 83, Suppl. 367, 49–68 (1971)
[12] Kelly, P. H., *Brain Res.*, 100, 507–522 (1975).
[13] Clement-Cormier, Y. L., Kebabian, J. W., Petzold, G. L., and Greengard, P., *Proc. natn. Acad. Sci. U.S.A.*, 71, 1113–1117 (1974).
[14] Scales, B., & Cosgrove, N. B., *J Pharmac. exp. Ther*, 175, 338–347 (1970).
[15] Bainbridge, J. G., and Greenwood, D. T., *Neuropharmacology*, 10, 453–458 (1971).
[16] Weinstock, M., and Speiser, Z., *Psychopharmacologia*, 30, 241–250 (1973).
[17] Weinstock, M., and Schechter, Y., *Eur. J. Pharmac*, 32, 293–301 (1975)
[18] Miller, R. J., Horn, A. S., and Iversen, L. L., *Molec. Pharmac.*, 10, 759–766 (1974).
[19] Iversen, L. L., *Science*, 188, 1084–1089 (1975).
[20] Heal, D. J., Green, A. R., Boullin, D. J., and Grahame-Smith, D. G., *Psychopharmacologia* (in the press)
[21] Green, A. R., and Grahame-Smith, D. G., *Neuropharmacology*, 13, 949–959 (1974)

Decreased uptake of 5-hydroxytryptamine in blood platelets from depressed patients

THE search for biological aberrations in affective disorders has been intensified within the last few years[1]. Special attention has been given to the changes in the metabolites of 5-hydroxytryptamine (5-HT) and of catecholamines in the cerebrospinal fluid[2]. In this laboratory[3] as well as in several others[4,5] the blood platelet has been used as an easily obtainable model of 5-HT neurones. Studies on the storage, metabolism and uptake of 5-HT in various neurological and mental illnesses have been largely negative[1,6,7] except in Down's syndrome[8–10]. Neither in schizophrenia[6] nor in affective illness[7] have any changes been found. By using low substrate concentrations and measuring the initial uptake rate, both the uptake kinetics in platelets and the inhibitory potencies of antidepressant drugs were recently shown to correlate well with those found in synaptosomes[11]. It was therefore of considerable interest to examine the kinetics of 5-HT uptake anew, in the platelets of certain psychiatric patients, notably those with manic-depressive illness. This report indicates that in the platelets of depressed patients the uptake of 5-HT is clearly decreased.

The patients studied were newly hospitalised with a diagnosis of depression. None of them had used tricyclic antidepressants or any other drugs known to interfere with the amine transport mechanisms for at least two days before the study commenced and some of them had never used antidepressants. Nor were any differences observed between patients who had recently ingested drugs and those who had not. The controls were healthy laboratory personnel, and the sample was taken at the same time as that of the patient. Platelets from one patient and one control were usually examined simultaneously.

The experiments were performed essentially as described previously[11]. Blood platelets were isolated and incubated in Krebs–Henseleit bicarbonate buffer with tritiated 5-HT. The accumulation of radioactive 5-HT to platelets in 5 min was determined. After subtracting the portion taken up by non-active processes, the data were subjected to kinetic analysis[12].

A very clear and highly significant difference was found in the 5-HT uptake by platelets from patients as compared to those from the controls (Fig. 1). The initial uptake by the platelets of depressed patients was about half as active as that of the controls. This is also reflected in the V_{max} of the process (Fig. 2) On the other hand, no difference was noted in the K_m. This suggests that there are less of the hypothetical transport molecules or "amine carriers"[13,14] in the cell membranes, or that some of them are

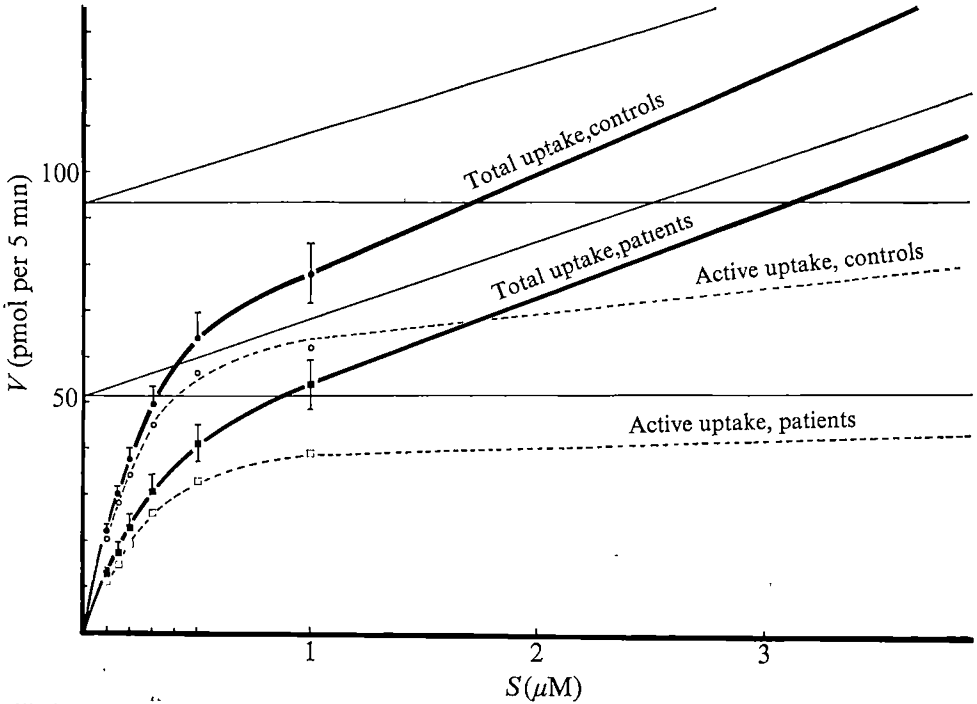

Fig. 1 Uptake of 5-HT by blood platelets of patients with depression (■) and controls (●) when the 5-HT concentration was varied from 10^{-7} to 10^{-4} M. The continuous thick lines show the total accumulation which continued linear to 10^{-4} M (thin lines indicate extrapolation from the highest concentrations). The dotted lines show the active uptake after subtraction of the linear part[11]. Before the incubation, the platelet-rich plasma was diluted with autologous platelet-free plasma to contain 200,000 platelets·mm^{-3}. An aliquot (100 μl) of diluted plasma (containing 0.15% EDTA) was added to 3.9 ml of prewarmed (37 °C) Krebs–Henseleit bicarbonate buffer (*p*H 7.4), containing 10^{-8}M ^{3}H-5-HT (5.66 Ci mmol^{-1}) and a necessary amount of cold 5-HT to make up total 5-HT concentrations of 10^{-7} to 10^{-4} M. After 5 min of incubation in a metabolic shaker, the platelets were separated by filtration (cellulose nitrate filters, pore size 0.2 μm) and washed with 10 ml of ice-cold saline. The radioactivity accumulated to the filters was assayed by liquid scintillation. Means±s.e.m. of duplicate experiments on 10 patients and 10 controls.

Fig. 2 Double-reciprocal plots of 5-HT uptake by platelets from controls (●), from untreated patients (■) and from patients treated for 4 weeks with imipramine or amoxepine (▲). The plots were calculated by the method of least squares. The kinetic data were: controls V_{max} 92 pmol per 2×10^7 platelets per 5 min, K_m 0.40 μM; untreated patients V_{max} 49 pmol per 2×10^7 platelets per 5 min, K_m 0.41 μM; treated patients V_{max} 59 pmol per 2×10^7 platelets per 5 min, K_m 0.75 μM. Conditions as in Fig. 1.

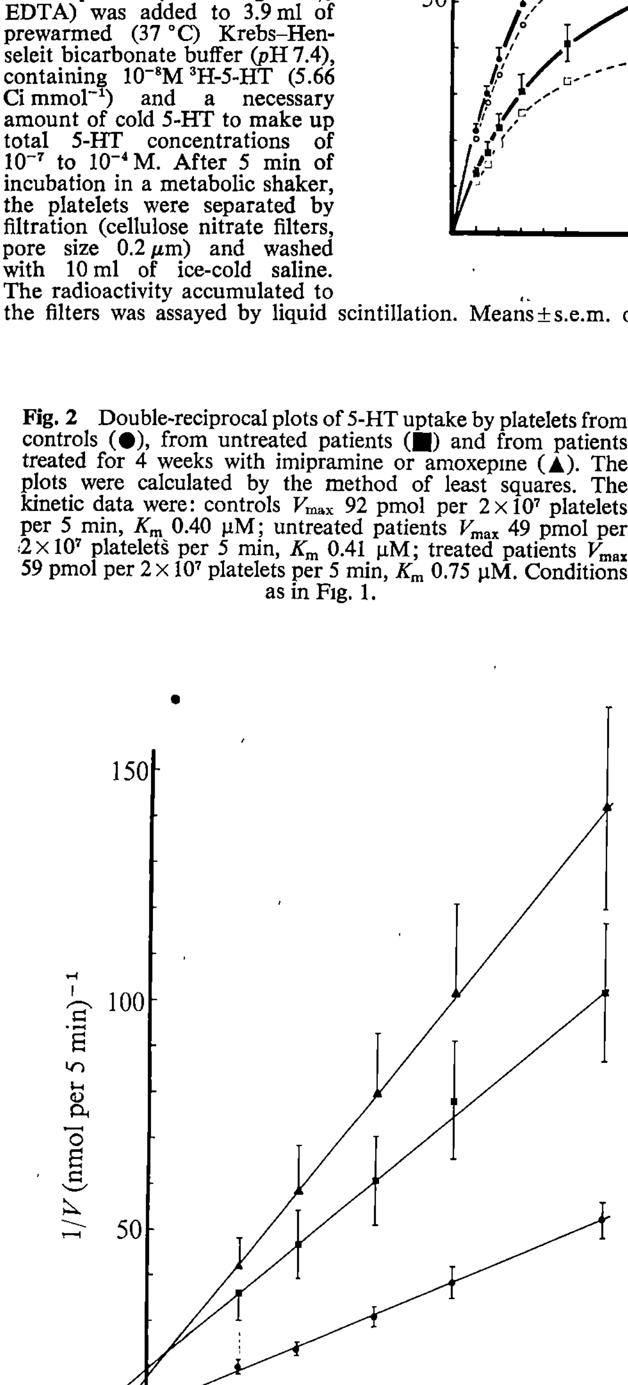

in an inactive state. Those which remain, however, are in a fully functional state as indicated by the unchanged K_m. The change is quite contrary to that seen in platelets or in brain synaptosomes after exposing them to tricyclic drugs[11]: they increase the K_m but the V_{max} remains the same, that is, the affinity to the transport is decreased, but the number of hypothetical carrier molecules remains the same. Also in the present study the V_{max} remained the same, but the K_m increased, when imipramine 10^{-8} M was added to the incubation medium. The same change was caused by imipramine both in the patients and in the controls. The different mode of kinetics rules out the possibility that the decrease in 5-HT uptake would be due to some tricyclic drug in the plasma and in the platelets of these patients.

After 4 weeks' treatment with antidepressants (either imipramine or amoxepine) a change in uptake characteristics was observed. The V_{max} had moved towards the control. At the same time, however, an increase in the K_m, apparently due to the antidepressant, was noted (Fig. 2). Patients under chronic lithium treatment, but at present without depressive symptoms, did not differ from the controls (J.T., E.T., Ahlfors and Levä, to be published).

We feel that these findings are most exciting and might be investigated along two lines: first, to find out whether it is feasible to use these aberrations as a basis for laboratory tests for certain subtypes of depression, and second, what these changes imply about the functioning of tryptaminergic neurones in the brain. If a similar change could be demonstrated in the neurones, the most crucial question would be whether this decrease in the 5-HT uptake is a constitutional change typical of the individual and common to both platelets and neurones, which seem to have the same or very similar mechanism to take up 5-HT[5,11]. On the other hand, the change could also be secondary and, possibly, compensatory to depression. In that case a question is how the change is transmitted to platelets. Perhaps hormonal or some other chemical regulatory mechanism might then be considered. Either way, these results may add a new dimension to the biological parameters in affective illness.

We thank Dr U. Ahlfors, Professor T. Pihkanen, and Mrs Sirkku Tuomikoski for help in obtaining the patient samples, Dr Leena Tuomisto for many consultations, and Mrs Anneli v. Behr for technical aid.

JOUKO TUOMISTO
ERKKI TUKIAINEN

Medical Research Council,
Academy of Finland, and
Department of Pharmacology,
University of Helsinki,
Siltavuorenpenger 10,
SF-00170 Helsinki, Finland

Received March 29; accepted June 16, 1976

[1] Schildkraut, J J., *A. Rev. Pharmac* , 13, 427–454 (1973)
[2] Symposium (several authors), in *Proceedings of the Sixth International Congress of Pharmacology*, 3, (edit. by Tuomisto, J., and Paasonen, M. K , volume editor Airaksinen, M.), 243–332 (Pergamon, Oxford 1976)
[3] Paasonen, M. K., in *Proceedings of the Fifth International Congress of Pharmacology*, 4, (edit by Acheson, G H., volume eds. Bloom, F. E , and Acheson, G. H.), 327–342 (Karger, Basel, 1973)
[4] Pletscher, A., *Br J. Pharmac.*, 32, 1–16 (1968).
[5] Sneddon, J. M , *Progress in Neurobiology*, 1, part 2,1 51–158 (Pergamon Oxford, 1973).
[6] Lucas, A. R., Warner, K., and Gottlieb, J. S., *Biol. Psychiat.* 3, 123–128 (1971)
[7] Shaw, D. M., MacSweeney, D. A , Woolcock, N., and Bevan-Jones, A B , *J. Neurol. Neurosurg. Psychiat.*, 34, 224–225 (1971)
[8] Boullin, D. J., and O'Brien, R A , *J. Physiol , Lond.*, 212, 287–297 (1971).
[9] Airaksinen, E. M., *J ment Defic. Res* , 15, 244–256 (1971).
[10] Lott, I. T., Chase, T. N., and Murphy, D. L , *Pediat. Res.*, 6, 730–735 (1972).
[11] Tuomisto, J., *J. pharm Pharmac.*, 26, 92–100 (1974)
[12] Lineweaver, H., and Burk, H , *J. Am chem. Soc.*, 56, 658–666 (1934)
[13] Lingjaerde, O. Jr, *FEBS Lett.*, 3, 103–106 (1969).
[14] Sneddon, J M., *Br J Pharmac* , 37, 680–688 (1969)

Reduction of quantum contents of synaptic potentials after postsynaptic axotomy

THE loss of synaptic transmission in the chick ciliary ganglion that is observed after the postganglionic section of the ciliary nerves is accompanied by both a decrease in acetylcholine (ACh) sensitivity of the axotomised cells and a change in the transmitter release characteristics of the presynaptic terminals[1,2]. Evidence for the presynaptic change included a decrease in the mean quantum content *m* of the excitatory postsynaptic potentials (e.p.s.p.s) and a greater susceptibility to fatigue during repetitive stimulation. The reduction in quantum content after axotomy was inferred from an increase in the coefficient of variation of the e.p.s p. amplitude distribution in the depressed state. In the experiments reported here it was possible to measure miniature synaptic potentials (m.e.p.p.s) in axotomised preparations so that more accurate estimates of the mean quantum content of e.p.s.p.s could be made .

Experiments were done on 3- and 4-d-old chickens. Axotomy of the ciliary nerves was performed within a few hours after hatching. Surgical and experimental procedures have been described before[1,3]. To ensure that transmission failure in axotomised preparations was not caused by disuse of the ganglionic synapses, in some chickens only the eyelids were sutured together and the animals were kept and fed in the dark for 4–5 d. No impairment of transmission was observed in ganglia taken from these control animals.

The *m* of the e.p.s.p.s was estimated by dividing their mean amplitude ($\bar{v}$) by the mean quantal size ($\bar{v}_1$). Mean e.p.s.p. amplitudes were determined from 5–15 measurements, taken at 10-s intervals to avoid synaptic depression. In the axotomised cells action potential initiation by the e.p.s.p.s could be blocked by hyperpolarising the cell (Fig. 1*a*). In some normal cells with large e.p.s.p.s it was not possible to pass sufficient hyperpolarising current to achieve such block. In such cases the e.p.s.p. amplitude was estimated from the inflexion at the onset of the action potential (Fig. 1*b*, arrow) or, if no such inflexion was present, from the residual synaptic depolarisation after the action potential (Fig. 1*c*, arrow). The latter two measurements represent underestimates of the true e.p.s.p. amplitudes. Quantal sizes were determined in two ways. In most experiments spontaneous release of quanta could be induced by stimulating the preganglionic nerve at 30–50 Hz for 30 s. The modal amplitude of the spontaneous m.e.p.s.p.s was taken as the quantal size. In some of the axotomised cells single quantal responses to nerve stimulation were obtained by perfusing the preparation with saline solution containing $\frac{1}{3}$ normal Ca^{2+} and 6×normal Mg^{2+}. Measurements of quantal size were corrected to correspond to the hyperpolarised level of membrane potential at which the e.p.s.p.s were measured; that is, *m* was determined from the relation: $\bar{v}_{hyp}/\bar{v}_{1hyp}$, where $\bar{v}_{1hyp}=\bar{v}_1(E_{hyp}-15)/(E_r-15)$. E_{hyp} is the membrane potential at which the e.p.s.p. was measured and E_r the resting membrane potential. The equation assumes the reversal potential for the e.p.s.p. is at −15 mV (refs 2 and 3). Input resistances (*R*) were determined routinely in all cells. The conductance (Δg) produced by a single quantum of ACh was calculated from the relation: $\Delta g=\bar{v}_1/R(E_r-15)^4$.

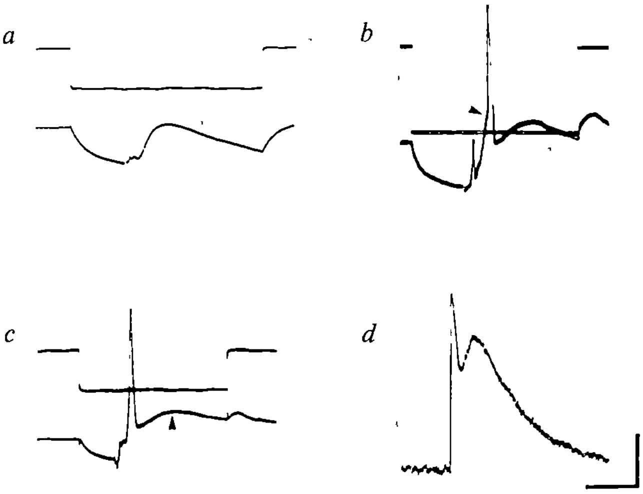

Fig. 1 Examples of e.p.s.p.s (used for calculation of mean quantum contents) from axotomised (*a* and *d*) and control cells (*b* and *c*). Amplitudes were corrected for nonlinear summation[9], neglecting the influence of membrane capacitance. The resulting overestimation of the mean quantum contents, *m*, were, at least partially, balanced by the underestimated measurements of e.p.s.p. amplitudes, when the generation of action potentials could not be blocked. Occasionally, e.p.s.p.s in such cells were large enough to initiate two action potentials. Calibration: 40 mV (*a*, *b* and *c*), 4 mV (*d*); 10 ms.

Table 1 summarises the mean quantal contents of e.p.s.p.s in which the signal-to-noise ratio was high enough for the average quantal amplitude of the m.e.p.s.p.s to be estimated with an accuracy of ±10%. The mean quantum contents of e.p.s.p.s recorded from axotomised cells were significantly lower than in control cells. The actual difference might be somewhat greater than indicated in Table 1 because of the underestimate of control e.p.s.p. amplitudes already mentioned in connection with Fig. 1*b* and *c*. The results summarised in Table 1 therefore confirm the observations obtained previously by more indirect measurements[1].

It could be argued that the lower quantum contents measured after axotomy were due to partial detachment of the presynaptic terminal from the postsynaptic cell so that the number of release sites apposed to the postsynaptic receptors was reduced. Detachment of presynaptic terminals after postsynaptic axo-

Table 1 Comparison of *m* of e.p.s.p. and of Δg produced by one quantum in control and axotomised cells

	$m\pm$s.d.	$\Delta g\pm$s.d. ($\times 10^{-10}$ mho)	*N*
Control	82.4±34.0	4.32±3.41	12
Axotomised	40.6±21.7	2.51±1.11	10
P (*t*-test)	<0.01	>0.1	

N, number of experiments.
For unknown reasons, *m* in control cells is significantly higher and Δg lower than found by Martin and Pilar[5].

tomy has indeed been found to be the major reason for loss of synaptic transmission in several preparations[6,7]. In the ciliary ganglion of chickens, synapses are electrically coupled[3] and detachment would be expected to reduce the coupling between presynaptic terminals and ganglion cells. The fact that the average amplitude of the coupling potentials was reduced after axotomy (6.6 mV compared with 18.3 mV in the control group) and that the percentage of cell profiles lacking synaptic contacts was increased[1], may therefore suggest partial detachment. As reported previously, however, the faster rate of fatigue of chemical transmission at synapses in axotomised preparations[1] cannot be explained on this basis. Moreover, in several axotomised cells, e.p.s.p.s smaller than ever observed in control cells were preceded by a coupling potential of normal amplitude (Fig. 1*d*). These findings suggest that the effects of axotomy on the parameters of synaptic transmission can occur before significant detachment. Similar observations have been made on axotomised cat spinal motoneurones[8].

Table 1 also indicates that the unit conductance change, Δg, produced in the postsynaptic membrane by the interaction with one quantum of transmitter substance, was lower in axotomised than in control cells. The difference in Δg, however, is not statistically significant. In fact, two out of three of the axotomised cells had values of Δg larger than the smallest Δg observed in the control cells. This suggests that a decrease in transmitter release can occur before, or in the absence of, a reduction in postsynaptic ACh sensitivity. The lack of significant reduction in Δg is in contrast to the reduced sensitivity of the axotomised cells to iontophoretically applied ACh[2].

In the present experiments described here, however, the axotomised cells were selected for particularly high miniature potential amplitudes. Many of the cells impaled, particularly those with small e.p.s.p. amplitudes, could not be used for calculations of *m* because m.e.p.s.p.s were absent or too small to be measured accurately. Such cells had resting potentials and input resistances similar to those of cells listed in Table 1 and therefore would have been expected to produce measurable m.e.p.s.p.s if the underlying unit conductances had been the same. The disparity between the reduced sensitivity to exogenous ACh and lack of a marked reduction in Δg can also be explained in another way, namely by supposing that single receptor sites are lost after axotomy one at a time, together with the release sites apposed to them. This would lead to a decrease in overall ACh sensitivity with no reduction in the quantal conductance change, Δg, at the remaining sites. The reduction in quantum content would then be due, at least in part, to loss of release sites. Alternatively, postsynaptic receptor sites might disappear without accompanying loss of corresponding presynaptic release sites. Quantal release in such regions would then be ineffective and there would be an apparent reduction in *m*. In this case the increased susceptibility of the e.p.s.p. to fatigue during repetitive stimulation[1] would be the only electrophysiologically identifiable presynaptic consequence of postsynaptic axotomy. At present it is not possible to decide between these mechanisms.

I thank Dr A. R. Martin for advice. This work was supported by grants from the USPHS and the Holderbank–Stiftung (Switzerland).

H. R. BRENNER

Department of Physiology,
University of Colorado Medical Center,
Denver, Colorado 80220

Received April 23; accepted June 15, 1976.

[1] Brenner, H. R., and Johnson, E. W , *J. Physiol , Lond* (in the press).
[2] Brenner, H. R., and Martin, A. R., *J Physiol , Lond* (in the press).
[3] Martin, A. R., and Pilar, G , *J Physiol , Lond* , 168, 443–463 (1963).
[4] Katz, B , and Thesleff, S., *J. Physiol., Lond* , 137, 267–278 (1957).
[5] Martin, A. R., and Pilar, G , *J. Physiol , Lond.*, 175, 1–16 (1964)
[6] Matthews, M. R., and Nelson, V , *J Physiol , Lond* , 245, 91–135 (1975).
[7] Purves, D., *J. Physiol., Lond.*, 252, 423–463 (1975).
[8] Mendell, L. M., Munson, J. B., and Scott, J. G., *J Physiol., Lond* , 255, 67–79 (1976)
[9] Martin, A. R., *J. Physiol., Lond.*, **130**, 114–122 (1955).

Re-examination of avian cochlear potentials

THE aim of this study is to provide a basic description of the cochlear receptor potentials, the cochlear microphonic (CM) and the summating potential (SP) of the bird. Although several workers have examined these avian potentials in limited aspects, a comprehensive survey of their frequency and intensity behaviour is long overdue. Moreover, a re-examination of the avian potentials has seemed necessary because the potentials are reported to differ vastly from the mammalian CM and SP and one is left with the baffling implication that the middle and/or inner ears of these classes operate with a degree of dissimilarity exceeding what might reasonably be expected on the basis of structural difference. For example, the avian CM sensitivity function has been reported[1] to be flatter than the middle ear transfer function in a comparable species[2] thus implicating an unknown sort of cochlear element in the frequency response of the avian system. Second, the slopes of avian CM input–output functions have been reported as considerably less than unity and thus less steep than in the mammal[1,3–7] leaving unanswered the question of whether the mechanics of the middle ear or basilar membrane, or peculiarities of the receptor cells *per se*, enforce the nonlinear intensity response in the bird. Third, if, as reported, the avian summating potential is appropriately described as a unitary negative response, manifest only at frequencies above 600 Hz (refs 4, 7–10), one can hardly reconcile this with the observation that the SP exists as both a positive and negative response in the mammal, and certainly occurs at even the lowest audible frequencies[11,12] in that class. While each of the above differences implies a fundamental dichotomy between the avian and mammalian cochleae, such differences were not found in the present study. We did however use a new intracochlear electrode configuration in the elucidation of the parametric behaviour of the CM and SP in the pigeon. Fine tungsten electrodes, flame-sealed in capillary tubing, were placed in the basal scala vestibuli (SV) and the scala tympani (ST) proper. This electrode configuration made differential recordings possible and avoided electroanatomical effects, believed to be inherent in previous recessus tympani or round window recordings in the bird. The following differentially measured avian functions are discussed: the 1-μV r.m.s. CM isopotential curve, CM isovelocity curves (relative to a constant footplate velocity of 10^{-6} mm s^{-1}), CM input–output functions, CM "degree of nonlinearity" functions and SP isovelocity functions. Our results show that these functions do not differ significantly from their mammalian counterparts.

Racing pigeons (*Columba livia*), generally less than three

Fig. 1 Illustration of electrode locations used in obtaining intracochlear differential recordings in a pigeon preparation. SV, scala vestibuli; ST, scal tympani.

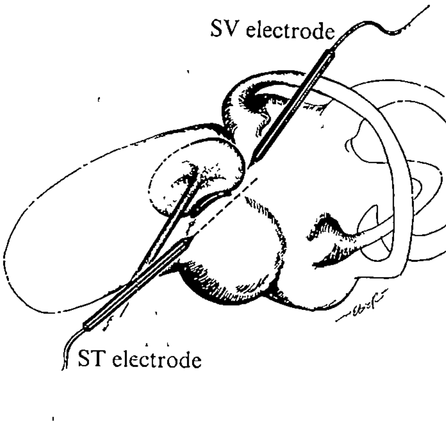

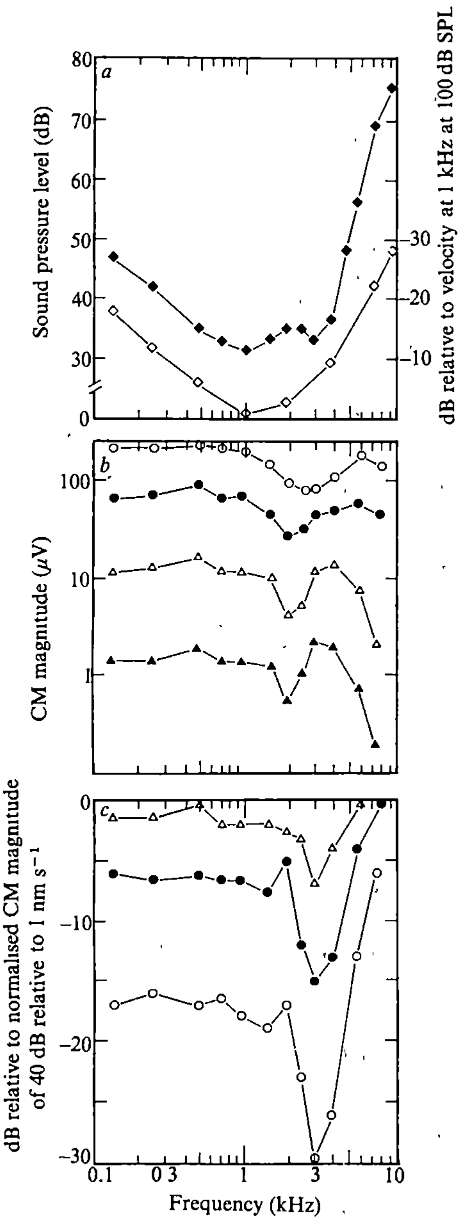

Fig. 2 *a*, Median, differentially recorded, 1-μV r.m.s. CM isopotential curve from seven pigeons (left ordinate, ◆). For comparison (right ordinate, ◇) is shown an inverted representation (see text) of an average middle ear transfer function measured by the Mössbauer technique in five Barbary doves[2]. *b*, Differential CM isovelocity functions from one pigeon. The parameter is footplate velocity in dB relative to 1 nm s^{-1}. *c*, "Degree of CM nonlinearity" exhibited by the pigeon shown in *b*. The deviations of the 60, 80 and 100 dB isovelocity curves from their projected values, assuming a simple linear operation, are expressed in dB (see text). The parameter is footplate velocity in dB relative to 1 nm s^{-1}, ○, 100 dB; ●, 80 dB; △, 60 dB; ▲, 40 dB.

months old, were used. The birds were sedated with 20 mg kg^{-1} pentobarbital 15 min before anaesthetisation with 64 mg kg^{-1} ketamine. Supplemental half-doses of ketamine were administered every 90 min thereafter. A tracheostomy was performed and the pigeons were respirated throughout surgery and the data collection period. The animals were maintained at 107 °F with a feedback-controlled heating pad. The surgical approach used was a dorsolateral one described by Wever and Bray[1]. Figure 1 shows the electrode locations used. The wire of the SV electrode could be cut quite short since that scala is shallow in the bird[13,14]. By contrast the wire of the ST electrode had to traverse the recessus tympani before the tip could be appropriately positioned for differential recordings. It was therefore necessary to fuse a 1.5–2.0-mm glass insulating shoulder along the wire of that electrode. To assess whether damage occurred during the placement of this long electrode tip into the rather inaccessible scala tympani, the sensitivity of the CM and the magnitude of whole nerve action potential, both recorded from the SV electrode, were compared before and after the ST electrode was placed.

In Fig. 2*a*, a median, differentially measured 1-μV CM isopotential curve (that is, sound pressure levels (SPL) required to produce 1-μV r.m.s. CM) for 7 pigeons is presented in conjunction with a reciprocal form of an average middle ear transfer function measured in five Barbary doves[2]. The inversion of that middle ear function was achieved by expressing footplate velocity measurements[2] in dB relative to the maximum velocity obtained at a constant SPL (that is velocity at 1,000 Hz). In Fig. 2*a*, it should be noted that the contours of the inverted middle ear transfer function and the CM isopotential function are well matched below 4,000 Hz. This agreement corresponds well with other studies in suggesting that the CM sensitivity in a normal cochlea is proportional to the footplate velocity[15,18] up to a cutoff frequency that depends on electrode location. Moreover, the correspondence suggests that the influence of the middle ear on cochlear response could be minimised by referencing input levels to a constant footplate velocity. This has been shown to be the case in studies of mammalian cochlear function[18]. Consequently, in the parametric measurements being reported, the SPL at the eardrum was adjusted from frequency to frequency on the basis of the middle ear transfer function of the Barbary dove to produce an approximately constant footplate velocity across frequency. To this end a velocity of 10^{-6} mm s^{-1} (1 nm s^{-1}) was arbitrary called 0 dB in the present study and corresponds approximately to a 20 dB SPL signal at 1,000 Hz.

Figure 2*b* shows differentially measured CM isovelocity functions (that is, CM magnitude measured at constant footplate velocity) at 20-dB intervals in one pigeon. As expected using a constant footplate velocity, the functions are quite flat below the best frequency of the electrode pair. The notch seen at 2 kHz could be a consequence of the irregularity of the middle ear response (not manifested in the average transfer function) or a cochlear effect. Similar notches below the best frequency are also seen in guinea pig CM functions[17]. At the 40 dB level, the 3,000-Hz en-

Fig. 3 Differential SP isovelocity functions from one pigeon. Using averaged responses, measurements were made 25 ms after stimulus onset. The parameter is footplate velocity level expressed in dB relative to 1 nm s^{-1}. Symbols as for Fig. 2.

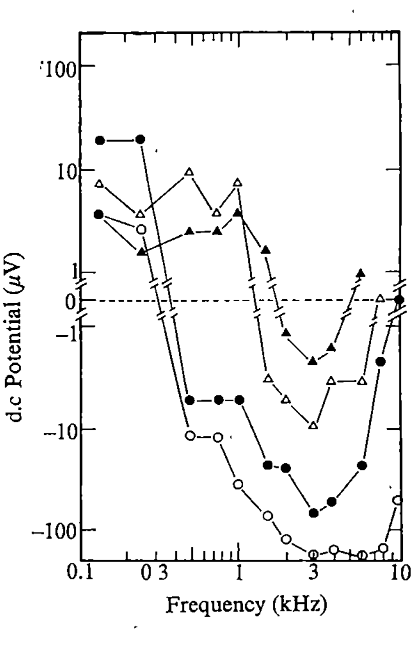

hancement indicated this to be the best frequency of the differential electrode location used in this, and most (see Fig. 2*a*) pigeons. Were input output functions to be derived at low frequencies from the data shown in Fig. 2*b*; they would have an initial slope of 1.0 in double logarithmic coordinates. This indicates that the avian middle ear, the basilar membrane, and the contributing receptor cells have an operating range characterised by simple linearity over at least some portion of their dynamic range.

Figure 2*c* was derived from the data contained in Fig. 2*b*. In the construction of Fig. 2*c*, the response magnitude of the curves in 2*b* was normalised by shifting each curve vertically by an amount equivalent to the expected linear increase in the CM (commensurate with the increase in input level). The "degree of nonlinearity"[18] functions shown in Fig 2*c* were then derived by converting to dB the deviations of each normalised curve from the 40-dB isovelocity output. In Fig. 2*c*, it is seen that a region of pronounced nonlinearity develops around the best frequency. As the input level increases, the region of nonlinearity spreads to increasingly lower frequencies. The coincidence of the best frequency and the frequency of earliest and most pronounced nonlinearity is noteworthy inasmuch as CM nonlinearities are most prominent $\frac{1}{3}$ to $\frac{1}{2}$ octave above the best frequency in the guinea pig[18]. Nonlinearities at frequencies below the region of early nonlinearity, although clearly present, do not seem to be frequency-dependent in their severity. This is suggestive that two mechanisms produce CM nonlinearities; one mechanism being simply dependent on input level and one being also influenced by frequency.

The frequency response pattern of the differential component (SV–ST potential difference) of the summating potential is shown in Fig. 3. The earliest (40 dB level) and most pronounced negative component occurs at the best frequency (3,000 Hz) of the electrode pair. Similar to the summating potential in the mammal, the negative response band spreads to increasingly lower frequencies as the input level is increased. It is apparent, contrary to earlier reports, that there is a positive SP component at lower frequencies in the pigeon.

One may conclude that the salient properties of both receptor potential components (CM and SP) are very similar in representative avian and mammalian cochleas. It is likely that the differences shown between the results of the present and earlier work on avian receptor potentials are accountable by the generally excellent physiological condition of our animals, the lack of prolonged or excessive sound exposure in the present work, and by the electroanatomical differences between the present differential electrode location and the previously used round window or recessus tympani sites.

The only significant discrepancy found between avian and mammalian receptor potentials is that the CM nonlinearities and the most pronounced negative differential SP component (itself a nonlinear phenomenon) occur at the best frequency in the pigeon, whereas these nonlinearities occur above the best frequency in the guinea pig[18]. In both classes the occurrence of these nonlinearities seems to correspond to the relative frequency at which noise-induced hearing loss occurs. In the parakeet, such losses occur at the centre frequency of the eliciting noise[19], while in the mammal, they appear at about $\frac{1}{2}$ octave above the centre frequency. A possible explanation, one suggested by Saunders and Dooling[19], relates to the observation that travelling wave envelopes are sharper in the bird than in the mammal.

MARTHA PIERSON*
PETER DALLOS

Auditory Physiology Laboratory (Audiology),
Francis Searle Building,
Northwestern University,
Evanston, Illinois 60201

Received December 16, 1975; accepted June 22, 1976.

*Present address: Armed Forces Radiobiology Research Institute, National Naval Medical Center, Bethesda, Maryland 20014.

[1] Wever, E G., and Bray, C. W , *J. comp. Psychol* , 22, 353–363 (1960).
[2] Saunders, J. D., and Johnstone, B. M., *Acta Oto-lar* , 73, 353–361 (1972).
[3] Heise, G., and Rosenblith, W. A., *J. comp Psychol* , 45, 401–412 (1952).
[4] Schwartzkopff, J., in *Ciba Found Symp.: Hearing Mechanisms in Vertebrates* (edit. by de Reuck, A. V. S , and Knight, J), 41–59 (Churchill, London, 1968).
[5] Schwartzkopff, J., in *Basic Mechanisms in Hearing* (edit. by Møller, A.), 423–452 (Academic, New York, 1973)
[6] Schwartzkopff, J , in *Avian Biology* (edit. by Farner, D. S., King, J R , and Parkes, K. C.), 417–477 (Academic, New York, 1973)
[7] Necker, R., *Naturwissenschaften*, 56, 143–144 (1969).
[8] Stopp, P E., and Whitfield, I. C., *J Physiol., Lond.*, 175, 45–46 (1964).
[9] Necker, R., *Verh. Dtsch. Zool Ges* , 64, 178–182 (1970).
[10] Necker, R., *Z. Vergl Physiol.*, 69, 367–425 (1970).
[11] Davis, H., Deatherage, B.. Rosenblut, B., Fernández, C., and Smith, C., *Laryngoscope*, 68, 596–627 (1958).
[12] Dallos, P., Schoeny, Z. G., and Cheatham, M. A , *Acta Oto-lar.* (Suppl 305), 44 (1972).
[13] Takasaka, T., and Smith, C. A., *J. Ultrastruct. Res.*, 35, 20–65 (1971).
[14] Smith, C. A , and Takasaka, T , in *Contributions to Sensory Physiology*, 5 (edit. by Neff, W. D.), 129–179 (Academic, New York, 1972)
[15] von Békésy, G , *Experiments in Hearing*, 745 (McGraw-Hill, New York, 1960)
[16] Weiss, T. F., Peake, W. T., and Sohmer, H , *J. Acoust. Soc. Am.*, 50, 587–601 (1971).
[17] Dallos, P., in *Basic Mechanisms of Hearing* (edit. by Møller, A.), 335–376 (Academic, New York, 1973).
[18] Dallos, P., Cheatham, M. A , and Ferraro, J., *J. Acoust. Soc. Am.*, 55, 597–605 (1974).
[19] Saunders, J. D., and Dooling, R., *Proc. natn. Acad. Sci. U S A.*, 71, 1962–1965 (1974).

Rod–cone mechanism underlying the Purkinje shift

TABLES have been published[1] of averaged brightness matches made by 16 observers who had compared 11 spectral lights (from 410 to 710 nm) with the CIE standard radiator in a 15° field set at various levels in the mesopic range. The scotopic and photopic luminances (S,P) of each light were calculated by multiplying the spectral radiant power for the match by the corresponding values of the CIE V' and $\bar{y}_{10}$ functions, with appropriate weighting factors. $\bar{y}_{10}$ was used because of the large field. The spectral data can readily be converted to the usual CIE system, and in fact the choice is immaterial in the following argument. As the matches were mesopic, neither S nor P alone can represent the luminance, and the Tables were used later[2] to define this quantity as a function of (S,P). Arithmetic manipulation of the data now suggests a simple rod–cone mechanism responsible for the sensation of brightness.

The first aim of my study was to refer the matches to an ideal light which would stimulate the cones preferentially. A deep red would fulfil this, as even at absolute threshold, redness is still visible[3], indicating a considerable cone response compared with the rod response. The S value for 680 nm is only 1/70 of the P value (P_{680}), and this wavelength was selected as the reference. Light at 710 nm would also be suitable, but the data were deficient at higher levels.

For shorter wavelengths, the ratio S/P gradually increases to a limit of about 10/1 at 440 nm. To compare the various values of (S,P) with the reference, the P value of each light was subtracted from P_{680} and this showed that the difference, ΔP, depended only on S (Fig. 1).

Although derived from experiments done at seven levels spanning an enormous luminance range, most of the points lie on a straight line with a slope of about 0.5. The obvious conclusion is that

$$\Delta P \simeq \sqrt{(M^*S)} \qquad (1)$$

where M^* is some constant with the dimensions of luminance. Thus a light with scotopic and photopic luminances, S and P respectively, is equivalent in brightness to a red light at 680 nm of photopic luminance P_{680}, where

$$P_{680} \simeq P + \sqrt{(M^*S)} \qquad (2)$$

Some points stray far from the line, especially those for long wavelengths. Here ΔP is the difference between similar quantities and is thus bound to fluctuate widely. But a more subtle explanation is required, because the points for 590 nm, 620 nm and 650 nm generally lie below the basic line of the graph (Fig. 1).

The points at variance can be brought into line, *ad hoc*, by reducing their S values, and to do this the CIE $V'\lambda$ curve from which S is calculated must also be reduced at long wavelengths. (Without some correction, equation (2) is bound to fail at 680 nm because the S contribution, although small, is finite.) More measurements are needed for an accurate estimation of the required factor, but inspection suggests a value of about 0.5 at 620 nm, dropping to about 0.25 beyond 680 nm. The equation could then be made to sum to a similar total for all lights of a given equivalent luminance, even for reds deeper than 680 nm, and it could be postulated to represent that combination of rod and cone responses which initiates the sensation of brightness, without reference to a standard.

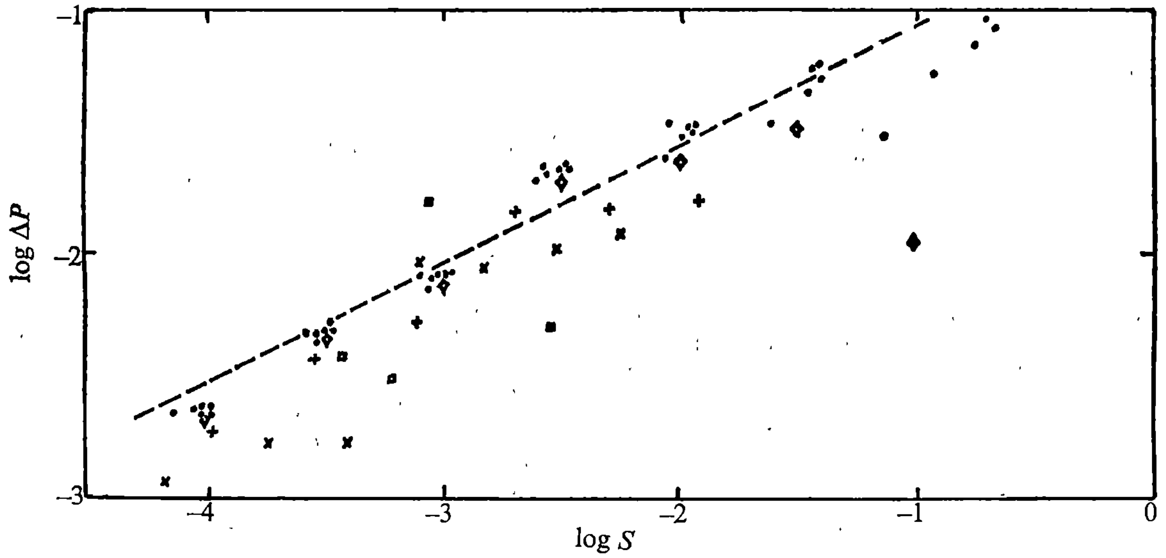

Fig. 1 Plot of ΔP against S on log scales. The quantities $\Delta P, S$ are in cd m^{-2}. +, 590 nm; ×, 620 nm; ▣, 650 nm; ●, 410–560 nm; ◇, standard radiator; — — — —, equation (2) with $M^* = 0.08$ cd m^{-2}.

The suggested modification to $V'\lambda$ is consistent with the initial assumption that, even at threshold, red lights still stimulate cone vision. The likely extrapolation of the graph in Fig. 1 is also intriguing in this respect, because if it continued at a slope of less than unity until it reached the threshold, which lies only one log unit below the lowest point, this would mean that the Purkinje shift is never completed.

For generality, the scheme must include non-monochromatic lights, which have been shown to behave photometrically like monochromatic lights with the same (S,P) coordinates[1,4]. The special case of the standard radiator (a black body at 2,043 K) can be derived from the Tables because its luminance L_v is by definition identical to its S and P values, and can be subtracted from P_{680} to yield ΔP, which is then plotted against L_v ($\equiv S$).

The resultant points (Fig. 1, ◇), follow the general trend through the mesopic range, except that the point at the highest level falls well below the graph. This apparently high discrepancy represents about 25% of P and is caused by additivity failure at high levels[1,4]. The problem is not directly relevant here, where the rod–cone mechanism, and not the cone–cone systems, is being analysed. It may be concluded that equation (2) is valid to a good approximation for a variety of lights throughout the mesopic range.

This general relationship invokes several considerations. It suggests first, a simple mechanism underlying the Purkinje shift. As there are no cross-product terms, neither inhibition of the rods by the cones at high levels, nor inhibition of the cones by the rods at low levels, needs to be postulated. The systems are independent, the rate of increase of the rod contribution diminishing progressively the higher the level. For this effect, a power function with an exponent less than unity is required, not necessarily exactly 0.5. Whether this represents any particular physiological feature in the retina or subsequent neural pathway is problematical, but at least one could search for a 'square-rooting' synapse involving the rod output.

Second, the formula suggests a simple mesopic photometer. This would require two photocells calibrated to the photopic and scotopic curves respectively, the scotopic signal being processed by a square-root circuit before addition to the photopic signal. Lights with the same luminance would therefore generate the same combined output in accordance with equation (2).

Third, intractable mesopic calculations are rendered relatively straightforward. The ideal reference stimulus may be used as a dummy, to convert to any other reference light. For example, for the CIE standard radiator, $S \equiv P \equiv L_v$ by definition. Thus for a light with components (S,P) the simultaneous equations are

$$P_{680} = P + \sqrt{(M^* S)} \qquad (3)$$

$$P_{680} = L_v + \sqrt{(M^* L_v)} \qquad (4)$$

By elimination of P_{680}, L_v emerges as a quadratic solution in terms of S, P and M^*.

M^* is related to a parameter M, dependent on field size[2]. A value of 0.06 cd m^{-2} has been suggested for a 15° field; a somewhat higher figure of about 0.08 cd m^{-2} is needed to fit the data in Fig. 1, if the discrepant long wavelength points are ignored.

By an extension of this mathematical analysis 'mesopic spectral visibility curves' can be produced. Although these are somewhat misleading[4], since they cannot be used to calculate luminances from spectral power distributions, they are commonly used to display the results of spectral brightness matches. Observer D's results from Kinney's classic set[5], measured in a 2° field at a peripheral angle of 10°, are shown in Fig. 2, together with examples of curves calculated using equation (2). The agreement is close, except that the smooth theoretical curves do not reproduce the bumps ascribed by Kinney to cone activity.

Evidently, much information about brightness matching in

Fig. 2 Comparison of Kinney's mesopic visibility curves for subject D with curves calculated from equation (2). The radiant power for a match is plotted in nW m^{-2} on an inverted log scale against the wavelength (λ) in nm.

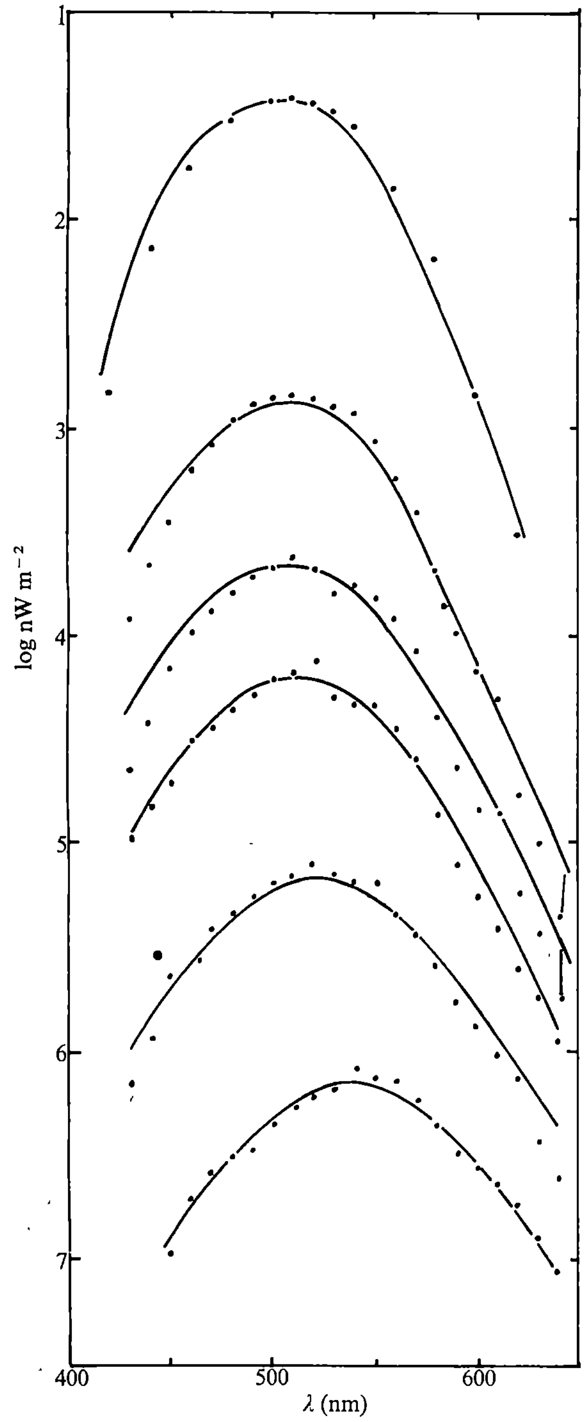

the mesopic range can be derived from equation (2). Even its inadequacies suggest plausible modifications to the CIE $V'\lambda$ curve, in order to represent the rod response to long wavelength light more accurately. I suggest therefore, that it expresses some fundamental rod–cone mechanism mediating the sensation of brightness.

I thank Dr Kinney for providing the data used in Fig. 2.

D. A. PALMER

Visual Science Department,
Institute of Ophthalmology,
Judd Street,
London WC1H 9QS, UK

Received April 14; accepted July 2, 1976.

1 Palmer, D. A., *Vision Res.*, 7, 619–628 (1967).
2 Palmer, D. A., *J. opt. Soc. Am.*, 58, 1296–1299 (1968).
3 Le Grand, Y., *Light, Colour and Vision*, 259 (Chapman and Hall, London, 1968).
4 Palmer, D. A., *Nature*, 209, 276–281 (1966).
5 Kinney, J. A. S., *J. opt. Soc. Am.*, 48, 185–190 (1958).

Effects of enkephalin and morphine on Renshaw cells in feline spinal cord

IT has been suggested that enkephalin is the endogenous ligand for the opiate receptor[1-3]. This substance is unevenly distributed throughout the brain[3,4] and occurs as two pentapeptides—met- and leu-enkephalin[5]. These substances have been shown to possess analgesic activity when injected intracerebroventricularly into rodents[6,7] and to depress the firing rate of single neurones in the brainstem of cats[8] and rats[9]. In the present experiments the effects of synthetic met-enkephalin have been compared with those of morphine on Renshaw cells in the feline spinal cord using the microelectrophoretic technique. This cholinoceptive interneurone is particularly suitable for such a comparison since it possesses stereospecific opiate receptor sites[10,11]. The results obtained show that both met-enkephalin and morphine directly excite Renshaw cells and that these actions are antagonised by naloxone.

Experiments were carried out on four cats anaesthetised with pentobarbitone sodium (35 mg kg^{-1} intraperitoneally initially). Blood pressure and temperature were monitored continuously. The spinal cord was exposed by lumber laminectomy and the central ends of S_1 and L_7 ventral roots were stimulated to identify Renshaw cells. Extracellular recordings were obtained with the centre barrel (4 M NaCl) of seven barrel microelectrodes (tip diameter 6 μm). The outer barrels contained aqueous solutions of the drugs to be ejected electrophoretically; these were: morphine sulphate (0.05 M), naloxone hydrochloride (0.1 M), L-glutamate sodium (0.5 M), acetylcholine chloride (0.5 M), glycine (0.5 M, *p*H 3) and met-enkephalin (0.018 M, *p*H 4). Action potentials were recorded and displayed using conventional techniques.

The effects of electrophoretic ejections of met-enkephalin were compared with those of morphine on 14 Renshaw cells. Met-enkephalin (50–80 nA for 15–40 s) ejected as a cation, directly excited eight neurones. The onset of and recovery from the excitatory action of met-enkephalin was rapid (3–8 s) and similar to that observed with morphine (50–100 nA), which directly excited eleven neurones including the eight excited by met-enkephalin (Fig. 1*a*). Desensitisation to the excitatory effects of met-enkephalin were not observed on repeated ejection of this substance. Compared with morphine, met-enkephalin was approximately equipotent as an excitant on the basis of equieffective ejecting currents (Fig. 1*a*).

The specific opiate antagonist, naloxone, has previously been shown to antagonise the excitatory effects of morphine and acetylcholine but not those of excitatory amino acids on Renshaw cells[10-13]. This effect of naloxone was also demonstrated in the present experiment (five tests on three cells). In addition, Figure 1*a* shows that naloxone (30 nA for 3–4 min) reversibly antagonised the excitatory effects of met-enkephalin. Similar effects were obtained in six tests on four more Renshaw cells.

Neither met-enkephalin nor morphine directly depressed the firing rate of any of the neurones studied in this investigation. When met-enkephalin (40–80 nA) was ejected for prolonged periods (2 min or more) however, the sensitivity of neurones to acetylcholine was decreased. This effect of met-enkephalin was observed on each of eight neurones, four of which were directly excited by a previous brief ejection of met-enkephalin. In contrast, prolonged ejections of morphine (25–40 nA) enhanced the excitatory effects of acetylcholine (five cells) and L-glutamate (two cells) in agreement with previous findings[10]. The reduction in acetylcholine sensitivity seemed to be a selective action of met-enkephalin in so far as the excitatory effects of morphine and L-glutamate were either unaffected (three neurones) or only slightly reduced (two neurones). Furthermore, the sensitivity of neurones to both morphine and amino acids recovered immediately on terminating the ejection of met-enkephalin, whereas recovery of the acetylcholine sensitivity was often prolonged, requiring up to 5 min or more. The effects of met-enkephalin on the acetylcholine- and morphine-induced excitation is illustrated in Fig. 1*b*.

Met-enkephalin (40–100 nA) had no obvious effect on the depressant action of glycine in tests on five neurones whereas morphine (25–40 nA) reversibly reduced this action of glycine in tests on the same neurones. This action of morphine reported previously is not antagonised by naloxone[12,13].

In the present study it was significant that the only effect of met-enkephalin in common with that of morphine was an ability to excite Renshaw cells, an action which was also antagonised by naloxone. The excitatory action of morphine has previously been shown to be stereospecific at this site[11,12]. The present experiments therefore provide direct evidence that met-enkephalin acts on a central opiate receptor and supports the notion that enkephalin is the endogenous ligand for the stereospecific opiate receptor[1].

The enhancement of the excitatory responses to acetylcholine and amino acids excitants by morphine has been considered to be related to the excitatory properties of morphine on cholinoceptive neurones[12]. The apparent selective reduction in neuronal sensitivity to acetylcholine produced by met-enkephalin was therefore unexpected, since this substance also directly excited cholinoceptive neurones. The reasons for these different actions of met-enkephalin and morphine are not known. Note, however, that the active opiate levorphanol also causes a prolonged reduction in acetylcholine sensitivity of Renshaw cells[12].

Thus the present experiments indicate that enkephalin has complex actions on a central cholinoceptive neurone, including a specific opiate type effect. Preliminary results obtained on non-cholinoceptive interneurones suggest that the effects of met-enkephalin described here are confined to cholinoceptive neurones. More extensive experiments are necessary, however, to verify this point and to establish a possible physiological role for endogenous enkephalin.

Fig. 1 Ratemeter record. *a*, Excitatory effects of acetylcholine (ACh, 1 nA); met-enkephalin (ME, 50 nA) and morphine (M, 50 nA), and antagonism of these effects by naloxone (NX, 30 nA). *b*, Effects of a prolonged ejection of met-enkephalin on the excitatory responses induced by morphine (40 nA) and acetylcholine (6 nA). Both records are from the same Renshaw cell.

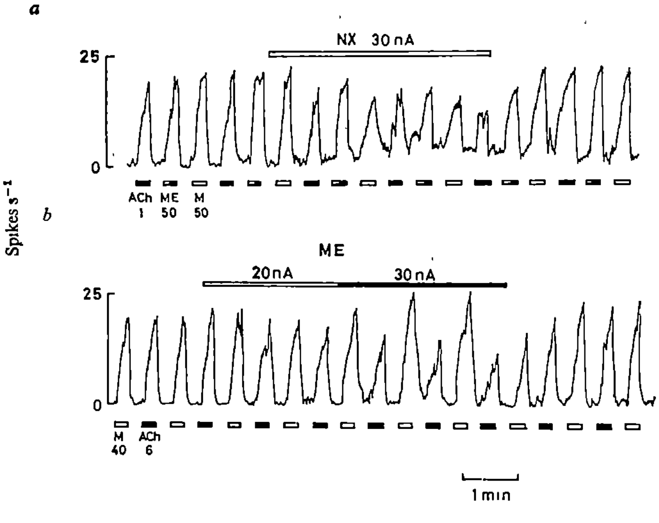

This work was supported by an MRC programme grant to Professor D. W. Straughan. We thank Dr B. A. Morgan (Reckitt and Colman Ltd, Hull) for gifts of met-enkephalin, and Endo Laboratories Inc., New York, for naloxone hydrochloride.

J. DAVIES
A. DRAY

Department of Pharmacology,
The School of Pharmacy,
29–39 Brunswick Square,
London WC1N 1AX, UK

Received May 14; accepted July 6, 1976.

1 Kosterlitz, H. W., and Hughes, J , *Life Sci.*, 17, 91–96 (1975).
2 Terenius, L., and Wahlstrom, A., *Acta physiol. scand.*, 94, 74–81 (1975).
3 Pasternak, G. W., Goodman, R., and Snyder, S H., *Life Sci.*, 16, 1765–1769 (1975).
4 Hughes, J., *Brain Res.*, 88, 295–308 (1975).
5 Hughes, J., *et al.*, *Nature*, 258, 577–579 (1975).
6 Belluzzi, J. D., *et al.*, *Nature*, 260, 625–626 (1976).
7 Buscher, H. H., *et al.*, *Nature*, 261, 423–425 (1976).
8 Gent, J. P , and Wolstencroft, J. H , *Nature*, 261, 426–427 (1976).
9 Bradley, P. B., Briggs, I , Gayton, R. J., and Lambert, L. A., *Nature*, 261, 425–426 (1976).
10 Davies, J., and Duggan, A. W., *Nature*, 250, 70–71 (1974).
11 Davies, J , *Brain Res.* (in the press)
12 Duggan, A. W , Davies, J , and Hall, J. G., *J. Pharmac. exp. Ther.*, 196, 107–120 (1976).
13 Curtis, D. R., and Duggan, A W., *Agents Actions*, 1, 14–19 (1969).

Depression of nociceptive and other neurones in the brain by iontophoretically applied met-enkephalin

IT has been suggested that enkephalin might act as a neurotransmitter or neuromodulator in the mammalian brain[1], and recent experiments[2,3] have shown that microiontophoretic application of enkephalin will depress brainstem neurones in both rat and cat. We have confirmed these observations on neurones in other regions of the rat brain and have extended the study to an investigation of the action of iontophoretic met-enkephalin on neurones activated by painful stimuli.

Experiments were carried out on adult male rats anaesthetised with 1% halothane in O_2 and prepared for single neurone recording from the cerebral cortex and thalamus (12 rats) or dorsal medulla (4 rats). Conventional techniques were used for single neurone recording and the iontophoretic application of drugs[4]. Five-barrelled micropipettes (tip-size about 6 μm) were used in most experiments with the outer barrels filled with solutions of L-glutamate (0.2 M, *p*H 8), GABA (0.2 M, *p*H 3.5), glycine (0.2 M, *p*H 3.5) and met-enkephalin (5 mg ml^{-1}, that is, about 8 mM in either 200 mM NaCl or in water; no adjustment of *p*H). In 7 of the 12 experiments some microelectrodes were double-barrelled and the only drug tested was met-enkephalin. NaCl 4 M was used in the recording barrel of all electrodes.

In a preliminary survey, in the cerebral cortex, thalamus and dorsal medulla, met-enkephalin applied with positive (0–400 nA), but not negative current, was found to inhibit 59 out of 88 neurones considered to be adequately tested. On 4 of the 88 neurones the action of enkephalin seemed to be excitatory. Appropriate controls to exclude current artefacts were carried out. The action of short applications (< 60 s) of met-enkephalin was uniformly rapid in onset and offset, typically taking less than 10 s to develop and this is similar to the time course of GABA's action in our experimental conditions, although extended application of enkephalin had effects which persisted for several minutes (Fig. 1). Desensitisation to the depressant actions of met-enkephalin was not observed when repeated short applications at intervals of 90–120 s were made to many neurones, sometimes over a period of 1 h or more. This is in contrast

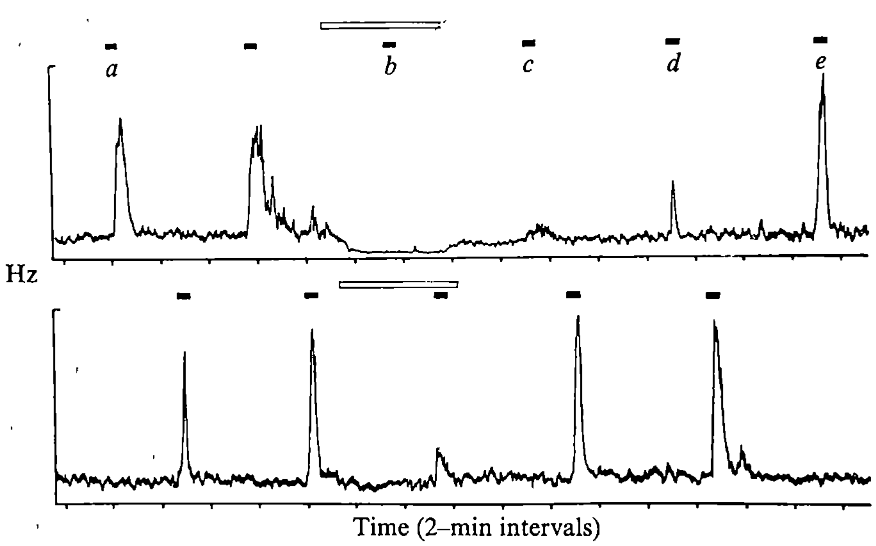

Fig. 1 Analogue ratemeter record of spontaneous firing of a nociceptive neurone (located at a depth of 4,430 μm below the cortical surface) in the rat thalamus. Lower section continuous with upper section. Short horizontal filled bars above record indicate immersion of rat's tail in water at 50 °C for 30 s; this treatment resulted in a brisk discharge of the neurone. For the duration of the first open bar over the record met-enkephalin was applied to the neurone with a current of 100 nA; this completely depressed the spontaneous firing and abolished the response to tail warming. The response to hot water was substantially recovered 16 min after removing the met-enkephalin. The second open bar above the record indicates removal of a 10 nA negative retaining current from the met-enkephalin barrel; although this had no detectable effect on the spontaneous firing rate, it markedly reduced the response to tail warming. The response was fully recovered within 5 min. The firing of this neurone was also depressed by GABA at 50 nA and the response to tail warming was partially blocked by GABA at 10 nA (not shown). *a–e*, Photographic records from the same experiment shown in Fig. 2.

to the action of morphine, in which case desensitisation has been reported after iontophoretic application to central neurones[5,6], but is consistent with the lack of desensitisation to the effects of enkephalin on peripheral tissues[1].

Met-enkephalin has also been tested on thalamic neurones thought to be excited by noxious stimuli[7,8]. The position of the micropipette in the thalamus at the stereotaxic coordinates AP+3, L3, H 4 to 7 (ref. 9) was confirmed both histologically and by recording field potentials[10,11] evoked by electrical stimulation of the limbs and tail. In the present study neurones excited by either a strong tail pinch with a thermometer clamp or immersion of the tail in hot (50 °C) water were considered to be nociceptive in nature. Such nociceptive neurones were very sensitive to met-enkephalin, and this observation is supported by the reduction in the evoked excitation shown in the latter part of Fig. 1 produced simply by removing the 10-nA retaining current from the met-enkephalin-containing barrel of the pipette. The photographic traces in Fig. 2 show that high currents (50–100 nA) of met-enkephalin completely abolished both the background spontaneous activity of this neurone and its response to noxious stimulation. This reduction in the response to noxious stimulation persisted for at least 12 min after the end of the met-enkephalin application (Figs 1 and 2). On seven other nociceptive neurones similar responses to met-enkephalin were obtained.

On eight unidentified neurones tested the depressant action of enkephalin was antagonised by intravenous naloxone (80–320 μg) on only two. This finding in the central nervous system is consistent with the results of experiments on isolated peripheral tissues[3], in which it was discovered that the depressant action of enkephalin was less sensitive to reversal by naloxone than was the similar action of morphine.

The implications of the observations reported here can only be fully explored by further experiments, but it is evident that met-enkephalin will depress many neurones in the mammalian brain and, most interestingly, those located in the thalamus and which are excited by noxious inputs. The observations of Hughes[12] and others[13] that enke-

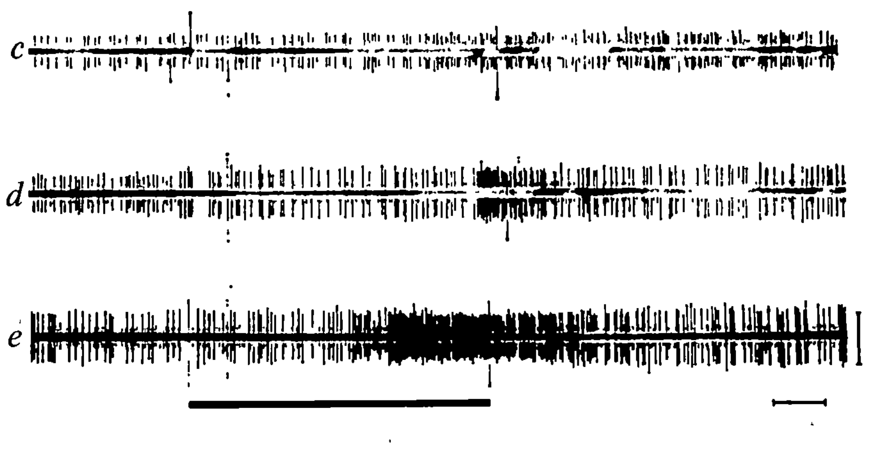

Fig. 2 Continuous photographic records of the firing of the same nociceptive neurone illustrated in Fig. 1. *a–e*, Similarly marked ratemeter traces in Fig. 1. Each vertical deflection on the filmed record represents a burst of 4 or 5 action potentials, the larger deflections visible on some records (for example, *b*) are artefacts caused by touching the animal to apply a heat stimulus. The solid black bar beneath the records indicates the 30-s period over which the animal's tail was immersed in hot (50 °C) water. This produced a sharp increase in firing shown by the increase in density of record *a*. Before record *b*, met-enkephalin was applied at a current of 100 nA and completely abolished the spontaneous firing of the neurone and its response to tail warming. Before record *c*, this met-enkephalin application was terminated; although spontaneous firing had returned, the response to tail warming was still virtually absent. Records *d* and *e* illustrate the gradual recovery of the response to tail warming over the next 12 min. Horizontal bar, 5 s; vertical bar, 0.4 mV.

phalin is found in many areas of the brain not yet implicated in the organism's responses to pain, suggests that this substance may be an important inhibitory transmitter candidate at both nociceptive and other sites.

We thank the MRC for financial support, and Dr Morgan (Reckitt & Colman) for met-enkephalin. C.M.P. is an MRC Scholar.

R. G. HILL
C. M. PEPPER
J. F. MITCHELL

Department of Pharmacology,
University of Bristol Medical School,
University Walk, Bristol BS8 1TD, UK

Received March 16; accepted June 29, 1976.

[1] Kosterlitz, H. W., and Hughes, J., *Life Sci.*, **17**, 91–96 (1975).
[2] Bradley, P. B., Briggs, I., Gayton, R. J., and Lambert, L. A , *Nature*, **261**, 425–426 (1976).
[3] Gent, J. L , and Wolstencroft, J H , *Nature*, **261**, 426–427 (1976)
[4] Hill, R. G., and Simmonds, M A., *Br J. Pharmac.*, **48**, 1–11 (1973).
[5] Bradley, P. B., and Dray, A., *Br. J. Pharmac.*, **50**, 47–55 (1974).
[6] Satoh, M., Zieglgänsberger, W., Fries, W., and Herz, A , *Brain Res.*, **82**, 378–382 (1974)
[7] Poggio, G. F., and Mountcastle, V B., *Johns Hopkins Hosp. Bull.*, **106**, 266–316 (1960).
[8] Hellon, R. F., and Mitchell, D., *J. Physiol., Lond.*, **250**, 29–30P (1975).
[9] Fifkova, E., and Marsala, J., in *Electrophysiological Methods in Biological Research* (edit. by Bures, J., Petran, M., and Zachar, J.), 653–731 (Academic, New York, 1967).
[10] Emmers, R , *J. comp. Neur.*, **124**, 215–228 (1965)
[11] Davidson, N., *J. comp Neur.*, **124**, 377–390 (1965).
[12] Hughes, J., *Brain Res.*, **88**, 295–308 (1975).
[13] Simantov, R., Kuhar, M. J., Pasternak, G. W., and Snyder, S. H., *Brain Res.*, **106**, 189–197 (1976).

Changes in amino acid sensitivity during polypeptide 'desensitisation'

CURRENT interest in polypeptides as neurotransmitter substances in the central nervous system (CNS) has been focused on their ability to depolarise motoneurones[1] and to excite single cells in various parts of the brain[2–6]. An additional feature of their actions on nervous tissue, however, is the development of 'tachyphylaxis' or 'desensitisation' to their effects during repeated administration. This phenomenon has been reported with two structurally related undecapeptides in particular, substance P and eledoisin, both in spinal cord[7] and in brain[3–5]. We report here that in the substantia nigra additional changes in amino acid sensitivity occur during such a period of desensitisation to eledoisin.

Albino rats (220–270 g), anaesthetised with urethane 1.4 g kg^{-1}, were used during this study. Multibarrelled glass micropipettes (tip diameter 6 μm) were used to record action potentials extracellularly and to administer substances by electrophoresis on to spontaneously firing neurones in the substantia nigra. Micropipettes were filled immediately before use by a glass-fibre method or by centrifugation. The recording barrel contained 3 M sodium chloride and another containing 1 M sodium chloride was used to balance the net current at the electrode tip to zero or to test for electrophoretic current effects. Other barrels contained eledoisin dihydrochloride (Calbiochem) 24 mM, *p*H 4.5; sodium glutamate 0.2 M, *p*H 7.2; GABA 0.2 M, *p*H 3.5; glycine 0.2 M, *p*H 3.5; taurine 0.2 M, *p*H 4.0; and acetylcholine chloride 0.5 M *p*H 4.5.

Action potentials were recorded and displayed using conventional techniques. Substantia nigra neurones were identified histologically after pontamine-blue dye ejection or by their response after stimulation of the ipsilateral caudate nucleus[8].

Short lasting application (30–60 s) of eledoisin ejected as a cation (50–100 nA; mean 77.3 nA) excited the majority of substantia nigra neurones tested (50 out of 55 cells). One neurone was depressed. The time course of these effects was similar to that described previously[5]. When brief applications of eledoisin were repeated at short intervals the excitatory response became progressively smaller until it could no longer be distinguished from the spontaneous activity. A progressive reduction in the excitation also occurred when a single administration of eledoisin with rather less current (25–75 nA; mean 45.6 nA) was prolonged for 3.5–17 min.

Prolonged applications of eledoisin also reversibly reduced the inhibitory responses to GABA (11 out of 20 cells), glycine (5 out of 13 cells) and taurine (9 out of 20 cells). Such effects, however, were not always observed on the same neurones, since glycine or GABA responses could be depressed without changes in taurine sensitivity occurring (Fig. 1); or taurine responses were depressed without any significant changes in GABA sensitivity. In only 4 of the 13 cells tested with all three inhibitory amino acids, were the responses to each compound entirely unaffected. In addition the excitatory effects of glutamate could be reversibly reduced (10 out of 11 cells), although on one occasion glutamate excitation was potentiated. Acetylcholine excitation was also reduced (2 out of 2 cells), although relatively fewer neurones were tested. These interactions during prolonged applications of eledoisin were not usually accompanied by changes in background firing rate; neither

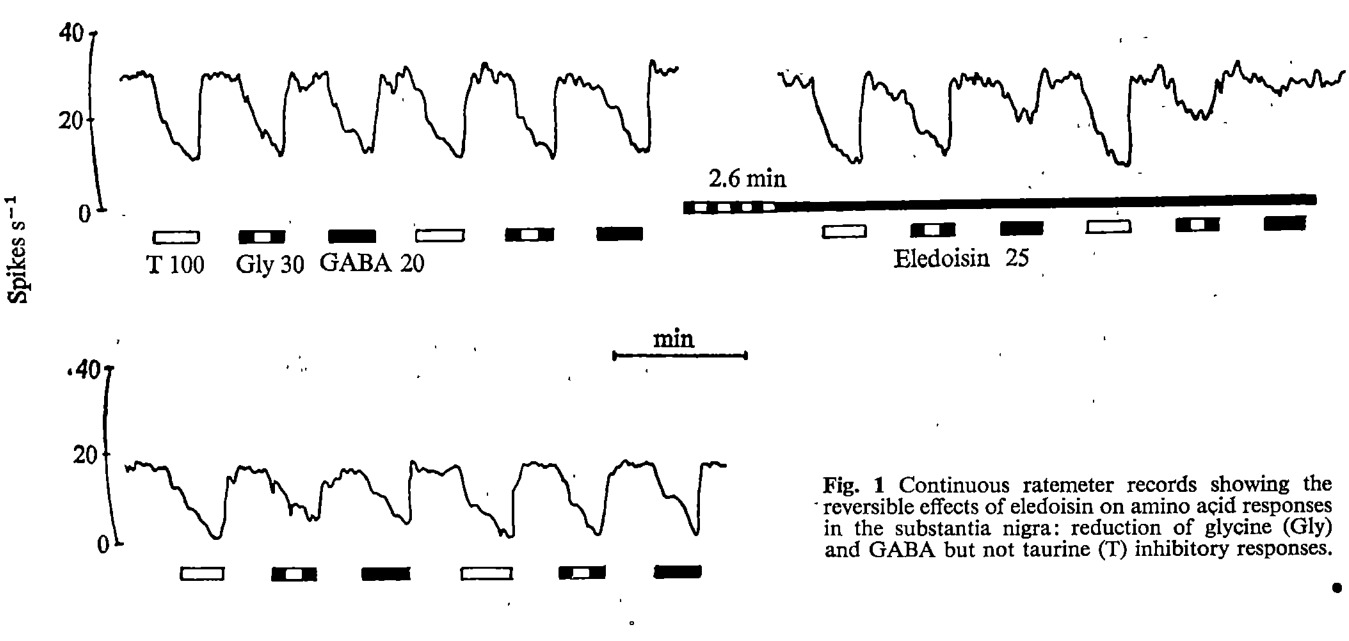

Fig. 1 Continuous ratemeter records showing the reversible effects of eledoisin on amino acid responses in the substantia nigra: reduction of glycine (Gly) and GABA but not taurine (T) inhibitory responses.

were there any alterations in neuronal spike size, although occasionally this was slightly decreased.

Recovery of the responses to amino acids, after termination of eledoisin administration sometimes occurred within about 5 min, but more commonly was considerably prolonged (up to 25.6 min). After recovery of neuronal sensitivity to these agonists, however, a repeated administration of eledoisin produced the same pattern of interactions as observed previously. This suggested that on individual cells the observed interactions were reproducible and could indeed be selective.

Our results, in agreement with previous observations[8], show that substantia nigra neurones are more sensitive to exogenously administered GABA than glycine and are more sensitive to glutamate than acetylcholine. Taurine, which occurs in significant amount in the substantia nigra[9], also exhibits significant inhibitory actions, although it is less potent than either GABA or glycine. In addition the undecapeptide eledoisin excited most substantia nigra neurones, confirming our previous observations[5]. Moreover, repeated or prolonged administration of eledoisin produced desensitisation. During such a period of desensitisation the sensitivity of neurones to exogenously applied GABA, glycine, taurine, glutamate or acetylcholine was reduced. Overall, eledoisin reduced neuronal sensitivity to inhibitory compounds less consistently than to excitatory ones. It is not clear why selectivity to one or more neuronally active substance could be observed on some neurones but not others. Note, however, that a reduction in the sensitivity of central neurones to exogenously administered glutamate or acetylcholine occurs after administration of the naturally occurring and structurally related undecapeptide, substance P (ref. 4).

Attention has been drawn to the potent excitant actions of polypeptides in the spinal cord[1] and in other areas of the brain[2–4,6] but it is possible that such effects may be an artefact resulting from the exogenous administration of non-physiological concentrations of these substances. Many active polypeptides including eledoisin and substance P have a common C-terminal amino acid sequence[1]. This property may be related to their depolarising properties as well as to the production of desensitisation and the modification of endogenous neurotransmission.

Although little is known concerning the precise mechanism of action or physiological role of polypeptides in the CNS their excitation of single neurones may be related to a neurotransmitter function. The modification of neuronal sensitivity to other putative neurotransmitters, however, suggests a more complex function which requires further elucidation.

This work was supported by an MRC programme grant to Professor D. W. Straughan.

J. Davies
A. Dray

Department of Pharmacology,
The School of Pharmacy,
University of London,
29–39 Brunswick Square,
London WC1N 1AX, UK

Received May 14; accepted July 6, 1976.

[1] Otsuka, M., Konishi, S., and Takahashi, T., *Fedn Proc.*, 34, 1922–1928 (1975).
[2] Krnjevic, K., and Morris, M. E., *Can. J. Physiol. Pharmac.*, 52, 736–744 (1974).
[3] Phillis, J. W., and Limacher, J. J., *Brain Res.*, 69, 158–163 (1974).
[4] Henry, J. L., Krnjevic, K., and Morris, M. E., *Can J. Physiol. Pharmac.*, 53, 423–432 (1975).
[5] Davies, J , and Dray, A., *Brain Res.*, 107, 623–627 (1976).
[6] Walker, R. J., Kemp, J. A., Yajima, H., Kitagawa, K., and Woodruff, G. N., *Experientia*, 32, 214–215 (1976).
[7] Evans, R. H., Francis, A. A., and Watkins, J. C., *Br. J. Pharmac.* (in the press).
[8] Dray, A., Gonye, T. J., and Oakley, N. R., *J. Physiol., Lond.* (in the press).
[9] Dray, A., and Straughan, D. W., *J. Pharm. Pharmac., Suppl.*, 28, 400–405 (1976).

Hypothermia and intolerance to cold induced by intracisternal administration of the hypothalamic peptide neurotensin

Neurotensin is a tridecapeptide (pGlu–Leu–Tyr–Glu–Asn–Lys–Pro–Arg–Arg–Pro–Tyr–Ile–Leu–COOH)[1] isolated from bovine hypothalami[2]. Using a sensitive and specific radioimmunoassay, Carraway and Leeman have demonstrated immunoreactive neurotensin in hypothalamic extracts of rat, mouse, rabbit and human tissue[3]. Intravenous (i.v.) administration of neurotensin to rats has been reported to cause hypotension (minimum effective dose 100 pmol kg^{-1} = 0.167 μg kg^{-1}), cyanosis (minimum effective dose 1 nmol kg^{-1} = 1.67 μg kg^{-1})[2], and hyperglycaemia (minimum effective dose 200 pmol kg^{-1} = 0.33 μg kg^{-1})[4]. These effects are not prevented by adrenalectomy or hypophysectomy. The hypotensive effects are not altered by α- or β-adrenergic blockers. Neurotensin also stimulates the contraction of guinea pig ileum while relaxing rat duodenum *in vitro*. Neurotensin is as potent as bradykinin in its effects on guinea pig ileum and rat duodenum and thus is classified as a kinin[2]. It increases plasma gonadotropin levels in ovariectomised, oestrogen–progesterone-treated rats after intravenous injection (minimum effective dose 5 nmol kg^{-1} = 8.4 μg kg^{-1})[5]. Intravenous administration of a dose of 3 μg kg^{-1} to rats produces hypoinsulinaemia, hyperglycaemia and hyperglucagonaemia[6].

Intracisternally (i.c.) administered thyrotropin-releasing hormone (TRH, effective dose 10 μg) and TRH analogues antagonise the depressant and hypothermic properties of various barbiturates[7–9] and ethanol[10]. Neurotensin, administered i.c. but not peripherally, potentiates markedly the sedative effects of pentobarbital in the mouse[11]. To understand this apparent synergistic interaction with pentobarbital further, we have

Fig. 1 Effect of i.c. neurotensin on the core temperature of mice subjected to a cold environment (4 °C). Data are expressed as °C±s.e.m. Experimental values were compared with those of controls by Student's *t*-test (two-tailed). Small open circles, 0.1 μg of neurotensin ($n = 11$); small closed squares, Saline ($n = 22$); closed circles, 0.030 μg of neurotensin ($n = 11$); closed triangles, 1 μg of neurotensin ($n = 121$); small open squares, 0.3 μg of neurotensin ($n = 6$); large open circles, 3 μg of neurotensin ($n = 6$); large closed squares, 10 μg of neurotensin ($n = 6$); open triangles, 30 μg of neurotensin ($n = 6$). †$P < 0.001$; ††$P < 0.01$; †††$P < 0.05$.

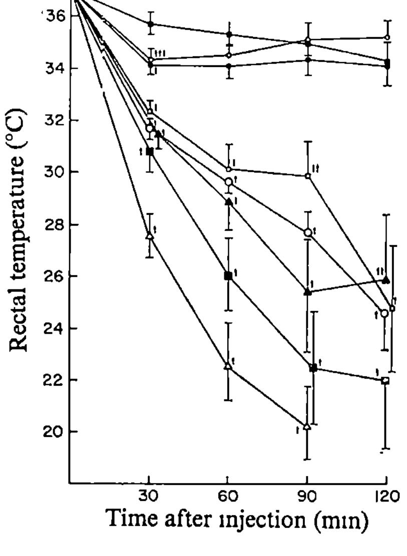

Table 1 Effect of intracisternal neurotensin on temperature regulation at 25 °C in the mouse

Substance	Rectal temperature (°C)±s.e.m.				
	0 min	30 min	60 min	90 min	120 min
Saline ($n = 7$)	37.6±0.184	38.1±0.134	37.9±0.315	37.7±0.358	37.6±0.280
Neurotensin 10 μg ($n = 7$)	37.8±0.275	34.8±0.253*	35.3±0.155*	35.8±0.193†	35.6±0.420
Neurotensin 30 μg ($n = 7$)	37.7±0.180	34.5±0.421*	34.7±0.506*	34.9±0.641†	35.7±0.476†

*$P < 0.001$ by t test.
†$P < 0.01$ by t test.

investigated the effects of centrally administered neurotensin on thermoregulation.

Adult male Swiss–Webster mice (24–25 g) were anaesthetised lightly with ether and injected i.c. with neurotensin (0.03–30 μg in 10 μl of vehicle) or 10 μl of vehicle (0.9% NaCl solution). Recovery from anaesthesia required about 1 min. Mice were then placed in individual plastic cages without bedding in a room maintained at 4 °C or room temperature (25 °C). Rectal temperatures were assessed at 30-min intervals with a thermistor probe. TRH, luteinising hormone-releasing hormone (LHRH), melanocyte-stimulating hormone-release-inhibiting hormone (MIF I), substance P and somatotropin release-inhibiting hormone (SRIF) were also tested at 4 °C by intracisternal injection in doses equimolar to 30 μg of neurotensin. Neurotensin was also injected i.v. at 10, 30 and 100 μg kg^{-1}. Those doses were substantially greater than those reported to cause peripheral vascular changes and were administered to assess the possibility that such changes contribute to cold-induced hypothermia. Differences in rectal temperatures between control and experimental groups were analysed for statistical significance by Student's t-test (two-tailed).

Table 2 Effect of i.c. hypothalamic peptides on cold-induced (4 °C) hypothermia in the mouse

Substance*	Rectal temperature (°C)±s.e.m.				
	0 min	30 min	60 min	90 min	120 min
Saline ($n = 12$)	37.2±0.390	36.4±0.476	36.0±0.540	35.4±0.550	35.3±0.546
TRH ($n = 6$)	37.1±0.177	34.4±0.929	34.2±0.947	34.3±0.757	33.7±1.22
LHRH ($n = 6$)	37.9±0.196	35.2±0.508	34.8±0.734	34.0±1.12	33.3±1.40
MIF I ($n = 6$)	37.4±0.095	36.2±0.522	35.4±0.876	35.2±1.19	34.3±1.55
Substance P ($n = 6$)	37.6±0.236	36.8±0.395	36.2±0.585	35.2±0.843	34.0±1.57
SRIF ($n = 6$)	37.4±0.293	36.0±0.777	36.2±0.650	34.6±0.852	33.6±1.44

*Doses equimolar to 30 μg of neurotensin in 10 μl of vehicle (0.9% NaCl).

Neurotensin given i.c. to mice in a cold environment markedly accentuated the decline in core temperature over 120 min (Fig. 1). This effect was dose related; the minimum dose showing an effect at 30 min was 0.03 μg. The i.c. administration of 10 and 30 μg of neurotensin also caused a significant decrease in core temperature at 25 °C (Table 1). The intracisternal delivery of TRH, LHRH, MIF, substance P and SRIF failed to produce any significant changes in rectal temperature from the control values at 4 °C during the 2-h period of observation (Table 2). In contrast to the action of neurotensin after intracisternal delivery no significant effect on cold tolerance was observed after intravenous administration of neurotensin (Table 3).

TRH is the only peptide previously reported to affect thermoregulation. Intracerebroventricular and intravenous administration of TRH has been reported to induce hyperthermia in rabbits[12], while others have shown that intracerebroventricular TRH induces hypothermia in cats[13]. Both the hypothermia at 25 °C and the considerable changes in cold tolerance at 4 °C observed after the i.c. administration of neurotensin suggest that it is involved in central thermoregulatory processes. This is also suggested by its only reported endogenous location, the hypothalamus, long implicated in control of temperature. It is premature to hypothesise a mechanism or locus of action of neurotensin in cold tolerance. The fact that central administration of this peptide has marked effects on both maintenance of body temperature and the duration of pentobarbital-induced sedation[11] indicates that it can affect the central nervous system directly. This is supported by lack of action of this peptide in both these situations after peripheral administration. The failure to find activity in these tests after peripheral administration of substantially greater amounts than are active centrally suggests the site of action of neurotensin lies within the blood–brain barrier. But the possibility that neurotensin i.c. exerts its effects by acting directly on cerebral vasculature or on central mechanisms that control peripheral vasomotor changes cannot be excluded. It is interesting that substance P, an unadecapeptide that also induces hypotension after intravenous administration[14,15], has no effect on thermoregulation in a cold environment after central administration. In a similar manner, SRIF, a tetradecapeptide, failed to affect cold tolerance significantly. These findings suggest specificity of the neurotensin effect we have described.

In our experiments with mice, we found that even i.v. neurotensin at 100 μg kg^{-1} failed to induce cold intolerance. On the other hand, Carraway and Leeman found in the rat that less than 2 μg kg^{-1} given intravenously produces cyanosis and hypotension[2]. We did not measure possible blood pressure changes in our mice, but constant observation revealed no cyanosis. Species differences may account for this discrepancy.

Table 3 Effect of intravenous neurotensin on cold-induced (4 °C) hypothermia in the mouse

Substance	Rectal temperature (°C)±s.e.m.				
	0 min	30 min	60 min	90 min	120 min
Saline ($n = 16$)	38.6±0.172	37.1±0.191	36.8±0.242	36.4±0.358	35.8±0.522
Neurotensin 10 μg kg^{-1} ($n = 8$)	37.8±0.213	37.0±0.245	36.8±0.281	36.7±0.313	36.3±0.384
Neurotensin 30 μg kg^{-1} ($n = 8$)	39.0±0.152	37.3±0.243	37.1±0.543	36.0±1.22	35.4±1.14
Neurotensin 100 μg kg^{-1} ($n = 8$)	38.8±0.137	37.4±0.195	37.3±0.177	36.8±0.205	36.5±0.288

Species differences may also explain the null effect of TRH in our study, which contrasts with its reported effects on thermoregulation in rabbit[12] and cat[13].

In the light of the evidence presented here, neurotensin can apparently be included in the growing list of peptides which seem directly to influence central nervous system function[16].

This work was supported in part by grants from the US PHS. We thank Abbott Laboratories for TRH and MIF I and Wyeth Incorporated for SRIF. Other compounds were purchased from Beckman Instrument Company.

GARTH BISSETTE
CHARLES B. NEMEROFF
PETER T. LOOSEN
ARTHUR J. PRANGE, JR
MORRIS A. LIPTON

Departments of Anatomy, Psychiatry, Biochemistry
and the Neurobiology Program,
Biological Sciences Research Center,
University of North Carolina School of Medicine,
Chapel Hill, North Carolina 27514

Received April 28; accepted June 29, 1976.

[1] Carraway, R. E., and Leeman, S. E., *J. biol. Chem.*, **250**, 1907–1911 (1975).
[2] Carraway, R. E., and Leeman, S. E., *J. biol. Chem.*, **248**, 6854–6861 (1973).
[3] Carraway, R. E., and Leeman, S. E., *Fedn Proc.*, **33**, 548 (1974).
[4] Carraway, R. E., and Leeman, S. E., *Fedn Proc.*, **32**, 211 (1973).
[5] Makino, T., Carraway, R., Leeman, S., and Greep, R. O., *Soc. Study Repro.*, Abstr. No. 26 (1973).
[6] Brown, M., and Vale, W., *Endocrinology*, **98**, 819–822 (1976).
[7] Prange, A. J., Jr, *et al.*, *Life Sci.*, **14**, 447–455 (1974).
[8] Prange, A. J., Jr, *et al.*, *Life Sci.*, **16**, 1907–1914 (1975).
[9] Breese, G. R., *et al.*, *J. Pharmac. exp. Ther.*, **193**, 11–22 (1975).
[10] Breese, G. R., *et al.*, *Life Sci.*, **14**, 1053–1063 (1974).
[11] Nemeroff, C. B., Bissette, G., Prange, A. J., Jr, Loosen, P. T., and Lipton, M. A., *Proceedings Endocrine Society Annual Meeting*, 312 (1976).
[12] Horita, A., and Carino, M. J., *Psychopharm. Commun.*, **1**, 403–414 (1975).
[13] Metcalf, G., *Nature*, **252**, 310–311 (1974).
[14] von Euler, U. S., and Gaddem, J. H., *J. Physiol., Lond.*, **72**, 74–87 (1931).
[15] Leeman, S. E., and Mroz, E. A., *Life Sci.*, **15**, 2033–2044 (1974).
[16] Prange, A. J., Jr, Nemeroff, C. B., Lipton, M. A., Breese, G. R., and Wilson, I. C., in *Handbook of Psychopharmacology* (edit. by Iversen, L. L., Iversen, S. D., and Snyder, S. H.) (Plenum, New York, 1976).

Pancreatic gastrin in foetal and neonatal rats

IT has been suggested[1,2] that pancreatic gastrin is stored in islet A_1 (or D) cells. There are, however, conspicuous histological and histochemical differences between antral gastrin cells and A_1 cells, indicating the storage of different peptide molecules in these two types of cell[3,4]. Furthermore, pancreatic tumours producing gastrin are composed of cells that have no features in common with A_1 cells but often resemble antral gastrin cells[5,6]. We have now tested a large number of gastrin antisera, most of which were specific for the C-terminal, bioactive, sequence of gastrin-17, on both unfixed and formaldehyde-fixed tissue, and found that all antisera reacted with antral gastrin cells but not with A_1 cells. Also, radioimmunoassayable pancreatic gastrin occurs at levels far below those expected if the A_1 cells stored gastrin[7]. We conclude that if gastrin-like peptides occur in the pancreatic A_1 cells they must be devoid of the bioactive, C-terminal sequence. While studying the ontogeny of the rat gastrin cell we have, however, found, at a certain stage of development, true gastrin cells in the pancreas.

In the pancreas, gastrin-immunoreactive cells were observed at day 18 of foetal life (the earliest stage studied). The cells occurred both in islets and scattered among exocrine cells (Fig. 1*a*). The gastrin cell number increased up to day 4 after birth, when it slowly began to decrease. A few pancreatic gastrin cells were seen in 12- to 20-d-old rats but at this stage they were usually restricted to the ductal epithelium. In rats older than 20 d gastrin cells were never observed in the pancreas (except for occasional cells in the epithelium of large excretory ducts). During all stages the gastrin cells seemed uniformly distributed between the tail and the duodenal lobe.

In the duodenum of adult rats gastrin cells were scarce[11]. The duodenum of rat foetuses contained, however, a fair population that could be detected at a foetal age of 18 d. Like the pancreatic gastrin cells, these cells increased in number until a few days after birth when their number (per unit area) started to decrease. In the antral mucosa, gastrin cells could be detected only after birth[11]. Cells, with an ultrastructure indistinguishable from that of the presumed gastrin cells (G cells) of rat antral mucosa, were detected in antral and duodenal mucosa and in pancreas of neonatal rats (4-d-old) (Fig. 1*b*). The distribution pattern and number of G cells was in good agreement with that of the gastrin-immunoreactive cells. Cells with an ultrastructure reminiscent of G cells have previously been detected in cultures of neonatal rat pancreas[12,13]. Such cells were not found in

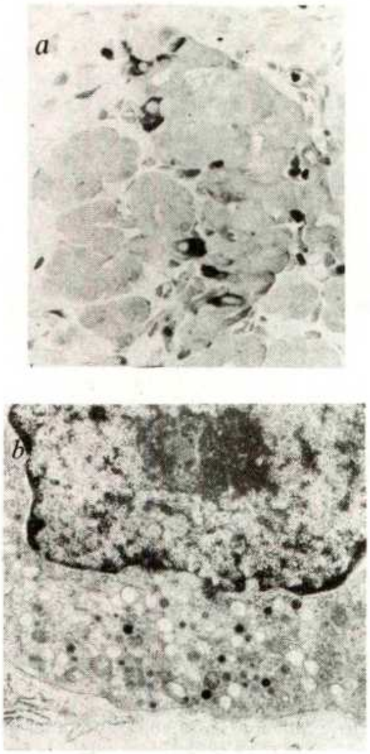

Fig. 1 *a*, Pancreas from 19-d-old rat foetus, showing an islet containing several peripheral gastrin cells (immunoperoxidase staining; ×217). *b*, Pancreas from 4-d-old rat, showing a typical G cell (glutaraldehyde-fixed, osmicated specimen; ×7,800). Foetal rats were removed at 18, 20 and 21 d of gestation, and newborn and young rats taken 1–30 d after birth. Adult male and female rats (200–300 g) were also used. After diethyl ether anaesthesia the antropyloric region, the duodenum and the duodenal lobe (that is, the portion of the pancreas that is adjacent to the duodenum) and the tail of the pancreas were dissected out. The specimens were freeze-dried and fixed with formaldehyde vapour. Paraffin sections were subjected to an indirect immunohistochemical method for demonstrating gastrin immunoreactivity[3]. Gastrin antisera numbers 2604, 2609, 2720 and 4562 (ref. 8) were used at dilutions 1:20, 1:40, 1:80 and 1:640, respectively. As a specificity control, these antisera were inactivated by the addition of synthetic human gastrin I (100 μg per ml diluted serum). Thus inactivated antisera failed to produce immunohistochemical staining. Samples for radioimmunoassay were taken from the same locations in 4- and 20-d-old and adult rats and extracted for 25 min in boiling redistilled water. The extracts were stored in the deep freeze until analysis. Each extract was analysed in triplicate at six different dilutions. Dilution curves for all extracts were identical with the standard curve. Gastrin was measured with antiserum 2604–8 (ref. 8). This antiserum is specific for the bioactive, C-terminal sequence of gastrin-17 and binds components I, II and III with equimolar potency[9]. It reacts very poorly with cholecystokinin, the molar ratio between ID_{50} of synthetic human gastrin-17 and highly purified porcine cholecystokinin being <0.006. Monoiodinated gastrin-17 was used as tracer[10] and synthetic human gastrin-17 as standard.

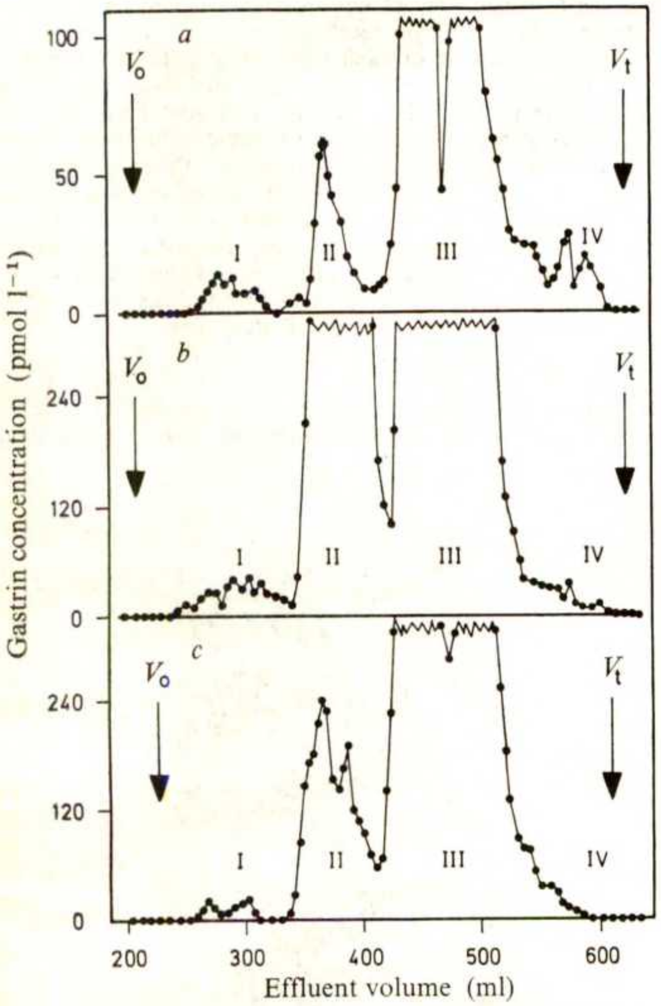

Fig. 2 Elution diagrams of gastrin components from extracts of *a*, pancreas (3.2 μEq synthetic human gastrin-17 per g wet weight tissue); *b*, duodenum (10.5 μEq synthetic human gastrin-17 per g wet weight tissue); and *c*, antrum (18.4 μEq synthetic human gastrin-17 per g wet weight mucosa). Pancreas and duodenum were from 4-d-old rats, antral mucosa from adult rats. The tissues were frozen and then boiled for 25 min in redistilled water, homogenised and centrifuged. The supernatants were applied to Sephadex G-50 superfine columns (25 × 2,000 mm) and eluted with 0.25 mol l^{-1} NH_4HCO_3 at 4 °C in 3.0 ml fractions at a flow rate of 15.0 ml h^{-1}. The columns were calibrated with albumin (void volume V_0), $^{22}NaCl$ (total volume V_t), highly purified human gastrin-34 (component II), gastrin-17 (component III), and gastrin-14 (component IV) donated by Professor R. A. Gregory and Dr Hilda Tracy (Liverpool). Roman numbers I–IV indicate elution volumes of components I–IV from calibration studies.

the pancreas or duodenum of adult rats. As gastrin cells are rare in the duodenum of the adult rat[11], however, they may therefore have escaped attention in the electron microscope.

Gastrin immunoreactivity was observed to a considerable extent in the duodenum (10.5 μEq synthetic human gastrin-17 per g wet weight tissue) and pancreas (3.2 $\mu g\, g^{-1}$) of 4-d-old rats. The level of antral gastrin at this age was considerably lower (0.9 $\mu g\, g^{-1}$). For comparison, the concentration of antral gastrin in the adult rat was 18.4 $\mu g\, g^{-1}$. In the pancreas of 20-d-old rats no gastrin could be detected.

Gel-permeation chromatography revealed that gastrin immunoreactivity from the pancreas (and antrum) of 4-d-old rats eluted in the same pattern as gastrin from antral mucosa of adult rats (Fig. 2). In the duodenal extracts (4-d-old rats) the proportion of component II (gastrin-34) was greater (Fig. 2) than in the antral and pancreatic extracts.

We refer to the immunoreactive pancreatic cells as gastrin cells because: like antral and duodenal gastrin cells they can be demonstrated in sections from formaldehyde-fixed, paraffin-embedded specimens; they can be demonstrated using a variety of gastrin antisera, of which most are directed against the bioactive C-terminal portion of gastrin-17 (ref. 9); in extracts of foetal and newborn rat pancreas significant quantities of gastrin have been demonstrated by radioimmunoassay; the extracted gastrin eluted by gel-permeation chromatography in a pattern indistinguishable from that of antral gastrin.

Little is known about the ontogeny of gastrin cells. Using a bioassay procedure Zelenkova and Gregor[14] observed that in the rat antral gastrin appears first after weaning. We have reported previously[11] that antral gastrin as revealed by immunohistochemistry and radioimmunoassay, appears far earlier. Also, in rabbit[15] and man[3] gastrin cells have been shown to occur prenatally. In the 18-d-old rat foetus, gastrin cells were found in the duodenum and in the pancreas but not in the antrum. Thus, gastrin cells do not seem to appear first in antral mucosa but instead make their debut in the duodenum and in the pancreas. The role of this early gastrin is unknown, but it may exert trophic actions on the pancreas and/or the gastrointestinal tract[16].

This work was supported by the Swedish and Danish MRC and the Landsforeningen for kraeftens bekaempelse.

L.-I. LARSSON
J. F. REHFELD
F. SUNDLER
R. HÅKANSON

Institute of Medical Biochemistry,
University of Aarhus, Aarhus
Departments of Histology and Pharmacology,
University of Lund,
Lund, Sweden, and
Department of Clinical Chemistry,
Bispebjerg Hospital,
Copenhagen, Denmark

Received April 26; accepted June 24, 1976.

[1] Lomsky, R., Langr, F., and Vortel, V., *Nature*, **223**, 618–619 (1969).
[2] Greider, M. H., and McGuigan, J. E., *Diabetes*, **20**, 389–396 (1971).
[3] Larsson, L.-I., Håkanson, R., Sjöberg, N.-O., and Sundler, F., *Gastroenterology*, **68**, 1152–1159 (1975).
[4] Rufener, C., Dubois, M. P., Malaisse-Lagae, F., and Orci, L., *Diabetologia*, **11**, 321–324 (1975).
[5] Creutzfeldt, W., Creutzfeldt, C., and Perings, E., in *Non-Insulin Producing Tumours of the Pancreas* (edit. by Demling, L., and Otterjann, R.), 86–89 (Thieme, Stuttgart, 1969).
[6] Larsson, L.-I., *et al., Am. J. Path.*, **79**, 271–279 (1975).
[7] Creutzfeldt, W., Creutzfeldt, C., and Arnold, R., *Rendic. Gastroent.*, **7**, 93–109 (1975).
[8] Rehfeld, J. F., Stadil, F., and Rubin ,B., *Scand. J. clin. Lab. Invest.*, **30**, 221–232 (1972).
[9] Rehfeld, J. F., Stadil, F., Malmström, J., and Miyata, M., in *Gastrointestinal Hormones* (edit. by Thompson, J. C.), 43–58 (Univ. Texas, Austin and London, 1975).
[10] Stadil, F., and Rehfeld, J. F., *Scand. J. clin. Lab. Invest.*, **30**, 361–368 (1972).
[11] Larsson, L.-I., Håkanson, R., Rehfeld, J. F., Stadil, F., and Sundler, F., *Cell Tissue Res.*, **149**, 275–281 (1974).
[12] Pictet, R., and Rutter, W. J., in *Handbook of Physiology*, Section 7, **I** (edit. by Steiner, D. R., and Freinkel, N.), 25–66 (Waverly, Baltimore, 1972).
[13] Orci, L., *et al., J. ultrastruct. Res.*, **43**, 270–297 (1973).
[14] Zelenkova, J., and Gregor, O., *Scand. J. Gastroent.*, **6**, 653–656 (1971).
[15] Larsson, L.-I., Rehfeld, J. F., Sundler, F., Håkanson, R., and Stadil, F., *Cell. Tissue Res.*, **149**, 329–332 (1974).
[16] Johnson, L. R., *Gastroenterology.*, **70**, 278–288 (1976).

Kinetics of reaction in calcium-activated skinned muscle fibres

A PROCEDURE reducing the diffusion-limited equilibration time of the Ca^{2+} concentration within skinned muscle fibres[1] activated from outside has been used to investigate the kinetics and the stoichiometry of Ca^{2+} in the process of tension development in frog skeletal muscle. The diffusion problems are minimised by activating (or relaxing) the myofibrillar preparation in a solution with a very high Ca^{2+}-buffering capacity compared to that of the fibre as a whole[2,3] (solution in the interfilament space, sarcoplasmic reticulum, myofibrillar proteins); by using only thin fibres; and by using an efficient *p*H buffer (TES: *N*-Tris (hydroxymethyl) methyl-2-aminoethanesulphonic acid) and a

Table 1 Apparent binding constants of the ligands used in the bathing solutions

Ligand	Cation	Average apparent binding constant (M^{-1})	Experimental conditions	Observations
ATP	Mg^{2+}	5,800±400	Measured at *p*H 7.10	Very good agreement with the calculated[3] apparent binding constant based on the "absolute" values reported by Taqui and Martell[28] and Phillips *et al.*[29], for the same temperature values and ionic strength.
EGTA (molecular weight 380.4)	Ca^{2+}	$(5\pm0.5)\times10^6$	Measured at *p*H 5.7–5 8, presence of TES 0–250 mM, extrapolation[30] to *p*H 7.10	The measured apparent binding constant at room temperature was ~ 20% higher and is in good agreement with the calculated[30] value based on the results of Schwarzenbach[7] obtained at room temperature and in the presence of 0.1 M K^+.
	Mg^{2+}	25±5	Measured at *p*H 7.10	The measured value at room temperature was 46±6 M^{-1} and is in very good agreement with the calculated value based on the result of Schwarzenbach[7] (see above).
HDTA (molecular weight 348.4)	Mg^{2+}	8±1.5	Measured at *p*H 7.10	Agreement with Anderegg[13].
	Ca^{2+}	6.5±1		
TES	Mg^{2+}	≃ 1	Measured at *p*H 7.10	Agreement with Good *et al.*[31].
	Ca^{2+}	≃ 1		
Creatine phosphate (CP)	Mg^{2+}	12±1.5	Measured at *p*H 5.0–5.10, extrapolated to *p*H 7.10	Considering that at *p*H 7.10 the creatine phosphate is divalently charged, the apparent binding constant is in agreement with the value reported by Smith and Alberty[32] for room temperature and 0.1 M ionic strength.

The determinations were made with a *p*H metric method at $[K^+] = 130$ mM, $[Na^+] = 40$ mM, temperature 1±0.5 °C.

high ATP concentration in conjunction with a powerful ATP regenerative system (creatine phosphate (CP) and creatine kinase (CK)). Great care has been taken in preparing bathing solutions with similar concentrations of monovalent metallic cations (~150 mM), protons (*p*H 7.1)[4] and $[Mg^{2+}]$ (~1 mM) (refs 5 and 6) to those *in vivo.* For this purpose, the apparent binding constants of the various ligands for Ca^{2+} and Mg^{2+} have been measured by a *p*H metric method (Table 1).

A first important observation is shown in Fig. 2*g*, where a myofibrillar preparation was activated in a solution with a high Ca^{2+}-buffering capacity around *p*Ca 3 (using NTA:nitrilotriacetate)[7,8] after being equilibrated in 0.1 mM EGTA (ethanedioxy*bis*(ethylamine)tetraacetate). Although the fibre is activated from outside[9] force develops rapidly, with a time constant similar to that observed *in vivo* during a tetanus[10,11]. This record can only be used for qualitative interpretations since here diffusion still remains a problem.

In the other experiments (Figs 1 and 2*a–f*), the Ca^{2+}-buffering capacity of the interfilament space has been lowered by incubating the myofibrillar preparation in 0.15 mM EGTA and by adding 10 mM caffeine to all bathing solutions[12]. Subsequently, the preparations were activated in 50 mM EGTA+CaEGTA. To maintain other ionic species constant during the tension response, HDTA (hexamethylenediamine-*NNN′N′*-tetraacetate)[13] was used. The loading of the skinned fibre preparation with the Ca^{2+}-sensitive photoprotein aequorin[14] has indicated that for the conditions in Fig. 2*a–f*, the myofibrillar Ca^{2+} concentration will practically equilibrate within 150 ms of the change of solutions (unpublished).

The results presented in Figs 1 and 2*a–f* were obtained from the same preparation in order to reduce their scatter. These results are typical of more than 20 experiments. For the kinetic analysis it is important to note that for the experimental conditions described in the legends, the absolute steady-state level for a given $[Ca^{2+}]$ has a much more pronounced tendency to change[15–17] (dropping by 3–8% from one contracture to the next) than the time course of the tension development, which remains essentially the same even after 7 activation–relaxation cycles (see Fig. 2 and legend). The relative steady-state isometric tension levels, unlike the absolute force values associated with different $[Ca^{2+}]$ are not affected by repetitive contractures and this relationship is illustrated in Fig. 1. A fourfold increase in $[Ca^{2+}]$ (from *p*Ca 6.5 to 5.88) corresponds to an increase of the relative tension from about 9 to 92%. Since the minimum number of calcium ions involved in the process of tension activation is suggested by the smallest integer *n* which satisfies the

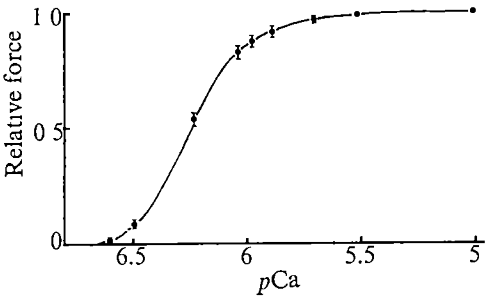

Fig. 1 Dependence of the relative steady-state isometric tension response on $[Ca^{2+}]$ expressed as *p*Ca ($-\log[Ca^{2+}]$) in skinned fibres from the iliofibularis muscle of *Rana esculenta.* The experimental values (●) have been obtained on the same preparation, from 25 cycles of contraction (some of which are shown in Fig. 2), to reduce the scatter indicated by the vertical bars. The relative force values have been corrected for the drop in tension due to multiple activation–relaxation cycles (see Fig. 2 and text). The continuous solid line represents the theoretical prediction from equations (1)–(3) for the constants mentioned in the text. The isometric tension has been measured with an RCA force transducer The recording system had a sensitivity of 0.3 mV μN^{-1}, a resonant frequency of 150 Hz and a compliance of 1.4 cm N^{-1}. The bathing solutions (volume 3 ml) have been changed using a method similar to that of Hellam and Podolsky[2,3,16]. All but the incubating solution were covered to avoid volume changes. The solutions contained substances of reagent grade (mM): $[Ca\text{-}EGTA^{2-}] + [EGTA^{2-}]$, 50; $[Na_2\text{-}CP]$, 10; $[Na_2\text{-}ATP]$, 8; [Caffeine], 10; [TES], 140 Creatine kinase 10 U ml^{-1}. The *p*H was adjusted to 7.10±0.01 with KOH at 1 °C so that the final value for $[K^+]$ was 137.5±2 mM. The concentration of the added $MgCl_2$ varied slightly (within 1 mM) in order to maintain a free Mg concentration of 1 mM in each solution, based on the apparent affinity constants shown in Table 1. To improve the accuracy of the relative and absolute $[Ca^{2+}]$ determinations in the bathing solutions, the free EGTA concentration has been always retitrated in each solution after the experiments[27], and care has been taken to maintain the *p*H in all solutions within 0.01 units. Temperature: 2 ± 0.5 °C.

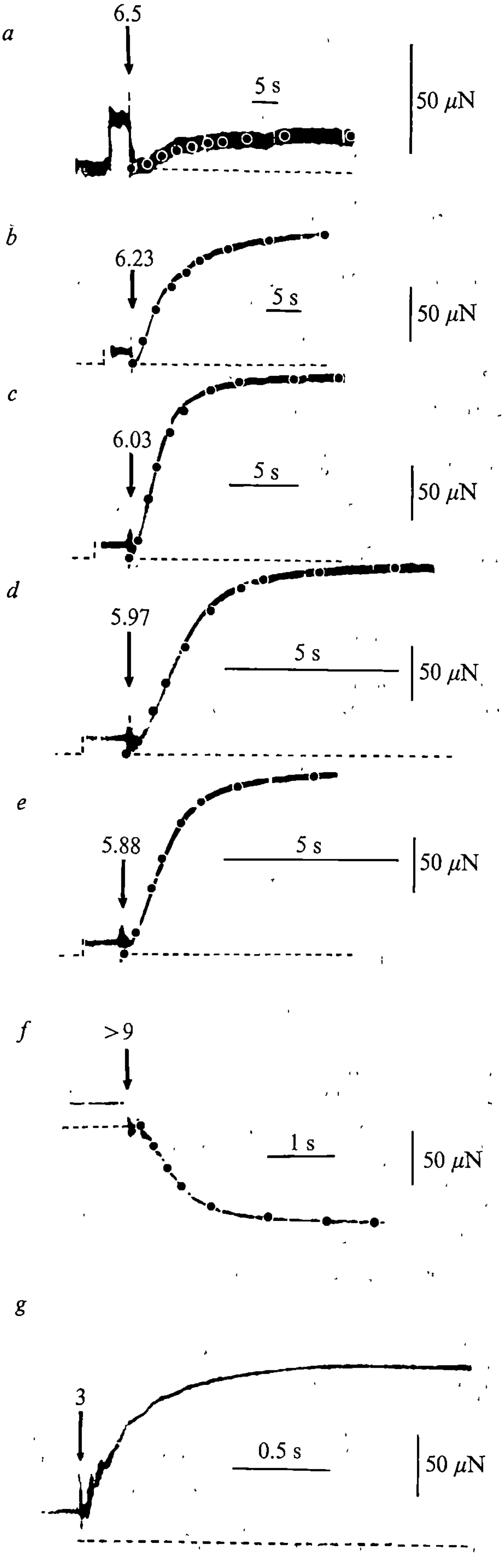

Fig. 2 *a–e* Time course of the 2nd, 4th, 5th, 6th and 7th isometric tension responses in the same frog myofibrillar bundle as for Fig. 1, when activated in EGTA containing solutions (for composition see legend Fig. 1). Diameter 50 μm, length 1.2 mm; sarcomere length close to its value *in situ*, 2.3–2.5 μm. The *p*Ca values of the activating solutions are shown above the arrows which indicate the moment of immersing the preparation in the contracting solution. Before each contracture, the preparation has been equilibrated for at least 4 min in a relaxing solution which had the same free cationic composition as the activating solution with the exception of $[Ca^{2+}]$. The relaxing solution contained 50 mM $HDTA^{2-}$ and 0.15 mM free $EGTA^{2-}$ in order to balance the activating solutions which contained 50 mM $Ca\text{-}EGTA^{2-} + EGTA^{2-}$. The contamination level of calcium was about 10 μM, due mainly to TES, caffeine and HDTA, so that the *p*Ca value in the myofibrillar preparation before the activating step was around 8. The artefact which appears in front of the arrows is due to the movement of the myofibrillar bundle through the solution–air–solution interface. The temperature of the solutions and of the air around the preparation has been maintained to 2 ± 0.5 °C throughout the experiment. During the first several high contraction cycles, the maximum tension had a tendency to drop by about 6% per cycle. After the 12th cycle, the steady-state values dropped less. The rate of tension development for a given *p*Ca was more stable, decreasing for example only by 8% between the 5th and the 12th cycle of contraction, but maintaining very accurately the same shape. *f*, Time course of the relaxation (20th cycle) of the preparation in a solution containing 50 mM free $EGTA^{2-}$ ($pCa > 9$) after being contracted for 3 min in a similar solution as the relaxing one (see above), but in which $EGTA^{2-}$ was replaced by $HDTA^{2-}$ (see text). This contracting solution contained 10 μM unbuffered Ca in addition to the contamination level of about 10 μM. *g*, Time course of the tension development in a frog myofibrillar bundle (diameter 45 μm, length 1.5 mm, sarcomere length about 2.3–2.5 μm) at 4 °C, when activated in a solution containing (mM): NTA, 30; TES, 100 (*p*H 7.10±0.01 with KOH); $CaCl_2$, 27.15; $MgCl_2$, 6.3; K^+, about 115; Na_2-ATP, 6. In this solution the level for both $[Ca^{2+}]$ and $[Mg^{2+}]$ should be close to 1 mM (refs 7, 8). The preparation had been previously equilibrated for 5 minutes in a relaxing solution containing (mM): TES, 100 (*p*H 7.10±0.01 with KOH); KCl, 86; Na_2-ATP, 6; $MgCl_2$, 6.12; EGTA, 0.1, in which the free Mg concentration should also be about 1 mM. The dashed lines represent the level of the isometric tension in the solution before the activating (*a–e* and *g*) or the relaxing (*f*) step. The solid dots (●) superposed on the experimental records *a–f* are the predicted values for the relative tension development from the kinetic scheme presented in the text.

inequality $R^n \geq 100$ (R being the ratio between the free calcium concentration corresponding to the relative tension of 91% and that corresponding to 9% relative tension)[18], it follows that in order to explain the experimental results plotted in Fig. 1, where $n = 4$, one has to assume at least 4 Ca^{2+} per 'functional unit'.

Figure 2*a–e* is a set of experimental tension records obtained as a result of a rapid increase of $[Ca^{2+}]$ in the myofibrillar bundle by the procedure described. First, up to $[Ca^{2+}] \simeq 1.2$ μM tension develops much slower than the expected time for $[Ca^{2+}]$ equilibration within the preparation (< 150 ms, see above) and this provides a good resolution for the kinetic analysis. The fact that the relatively slow development of tension here is not due to a simple physical process such as diffusion is supported by the large variation of the apparent rate of relative tension development for different experimental conditions. Second, all the tension transients in Fig. 2*a–e* are S-shaped, that is, the maximum rate of tension development is reached a significant time after the moment of activation. This observation suggests that at least two relatively slowly equilibrating steps are involved in the chain of reactions leading to the development of tension[3,19,20]; otherwise the curves would rise exponentially in time. A third important observation to be made is that the rate of tension development as indicated by the inverse value of the time required to reach 50% of the steady-state level, rises faster than the increase in the free calcium concentration over the *p*Ca range shown in Fig. 2*a–e*. For an increase of 4 times in Ca^{2+} (from *p*Ca 6.5 to 5.88) the half time for the tension development decreases sevenfold. This alone suggests that at least one of the slowly equilibrating steps of reaction must involve at least 2

Ca^{2+} apparently, while the other involves at least 1. This third observation taken together with the fact that the relative tension increases over the same *p*Ca range 6.5–5.88 such as to require at least 4 Ca^{2+} (see above) suggests that more than 4 Ca^{2+} must be involved per functional unit to produce tension. Finally, the relaxation in a 50 mM free EGTA solution (*p*Ca > 9) of the same myofibrillar preparation, which has been previously equilibrated in a solution containing about 20 µM unbuffered Ca (Fig. 2*f*), can be approximated with an exponential having a rate constant of $-1.75\ s^{-1}$, a value similar to that obtained by Huxley and Simmons[11] *in vivo*. The time course of the relaxation is considerably faster than the time course of the activation at *p*Ca 6.5–5.88, and this implies that an additional Ca^{2+} must be involved in a faster step of reaction, following the rate-limiting steps for activation. In addition, Fig. 2*g* suggests that, taken separately, the reaction steps which follow those in which Ca^{2+} is directly involved for the activation of tension should be considerably faster than the relatively slowly equilibrating steps strongly controlled by Ca^{2+} at *p*Ca > 5.5.

A detailed quantitative analysis of the results such as those presented in Figs 1 and 2, based on the assumption of reversible calcium reactions and on the suggestion that the isometric tension response in these fibres is directly correlated with the interaction between the myofilaments[10,11], has ruled out reaction schemes involving less than 6 Ca^{2+} per functional unit. The simplest scheme of reaction to explain the results for *p*Ca > 5.5, which can also be connected with recent biochemical data is one in which the isometric tension response, *P*, is proportional to the concentration of a product $Ca_4A{-}MCa_2$, resulting from two independent reaction schemes, each one involving one slowly equilibrating step of reaction

$$A \underset{\text{rapid}}{\underset{k_{-1}}{\overset{k_1[\mathrm{Ca}]}{\rightleftharpoons}}} \mathrm{Ca}A \underset{\text{rapid}}{\underset{k_{-2}}{\overset{k_2[\mathrm{Ca}]}{\rightleftharpoons}}} \mathrm{Ca_2}A \underset{\text{rapid}}{\underset{k_{-3}}{\overset{k_3[\mathrm{Ca}]}{\rightleftharpoons}}} \mathrm{Ca_3}A \underset{\text{slow}}{\underset{k_{-4}}{\overset{k_4[\mathrm{Ca}]}{\rightleftharpoons}}} \mathrm{Ca_4}A \tag{1}$$

$$M \underset{\text{slow}}{\underset{k_{-5}}{\overset{k_5[\mathrm{Ca}]}{\rightleftharpoons}}} \mathrm{Ca}M \underset{\text{rapid}}{\underset{k_{-6}}{\overset{k_6[\mathrm{Ca}]}{\rightleftharpoons}}} \mathrm{Ca_2}M \tag{2}$$

and

$$P \propto [\mathrm{Ca_4}A{-}M\mathrm{Ca_2}] \propto [\mathrm{Ca_4}A]\cdot[\mathrm{Ca_2}M] \tag{3}$$

where $A-M$ is the tension functional unit containing the two types of Ca^{2+} reacting sites. The value of k_{-6} has been chosen such as to correspond to the rate constant of the relaxation, that is $1.75\ s^{-1}$, and the value for k_{-4}, suggested by the slowest rate of rise for tension (Fig. 2*a*), was chosen as $0.06\ s^{-1}$. The values for the other parameters used for explaining the experimental results in Figs 1 and 2 are: $k_{-1}, k_{-2}, k_{-3} \gg 15\ s^{-1}$; $100K_1 < K_2$; $10^4K_3 < K_4$; $K_1K_2 = 7\times10^{11}\ M^{-2}$; $K_3K_4 = 2.02\times10^{13}\ M^{-2}$ ($K_i = k_i/k_{-i}$ for $i = 1,2,3,4$); $k_5 = 9.44\times10^5\ M^{-1}s^{-1}$; $k_{-5} = 8.75\ s^{-1}$; $k_6 = 3.2\times10^8\ M^{-1}\ s^{-1}$. The predictions of this kinetic scheme have been superposed over the experimental results in Figs 1 and 2*a–f*. One can see that the agreement between theory and experiment is good.

Recent experiments suggest that the skeletal muscle in vertebrates might have a Ca^{2+} control mechanism of contraction linked with both myosin and actin filaments[21–24]. There is also evidence that the actin control could involve 4 Ca^{2+} per troponin[25,26]. The kinetic scheme presented here based solely on experiments using skinned frog muscle fibres in which $[Ca^{2+}]$ has been rapidly changed can be attractively connected with this new biochemical evidence, and suggests in addition that the myosin control in frog might involve two Ca^{2+} per functional unit.

I thank Professor H. Ch. Lüttgau for continuous interest and support, Professor Sir Andrew Huxley for his stimulating comments on the manuscript, Dr P. C. Caldwell for his constant encouragement and Dr C. C. Ashley for providing the aequorin. This work was supported by the Deutsche Forschungsgemeinschaft.

D. G. MOISESCU

Ruhr University,
Department of Cell Physiology,
D4630 Bochum, Postfach 2148, FRG

Received March 1, accepted June 29, 1976.

[1] Natori, R., *Jikeikai med J.*, **1**, 119–126 (1954).
[2] Ashley, C. C , and Moisescu, D. G , *J Physiol., Lond* , **233**, 8–9P (1973).
[3] Moisescu, D G., thesis, Univ. Bristol (1974)
[4] Caldwell, P. C , *J. Physiol., Lond.*, **142**, 22–62 (1958)
[5] Endo, M., *Proc. Japan Acad.*, **51**, 479–484 (1975).
[6] Ashley, C. C., and Ellory, J. C , *J. Physiol , Lond* , **226**, 653–674 (1972).
[7] Sillén, L. G., and Martell, A. E , *Stability Constants of Metal-ion Complexes* (The Chemical Society, Special Publication No 17, London, 1964)
[8] Sillén, L. G., and Martell, A E., *Stability Constants of Metal-ion Complexes* Supplement 1 (The Chemical Society, Special Publication No. 25, London, 1970).
[9] Hill, A V , *Proc. R. Soc.*, **B136**, 399–420 (1949).
[10] Huxley, A F , and Simmons, R. M., *Nature*, **233**, 533–538 (1971).
[11] Huxley, A F., and Simmons, R. M., *Cold Spring Harb. Symp. quant. Biol.*, **37**, 660–680 (1972).
[12] Endo, M., Tanaka, M., and Ogawa, Y , *Nature*, **288**, 34–36 (1970).
[13] Anderegg, G., *Helv Chim. Acta*, **47**, 1801–1814 (1964)
[14] Ashley, C C., Moisescu, D G., and Rose, R. M , *J. Physiol., Lond.*, **241**, 104–106P (1974).
[15] Julian, F. J , *J Physiol., Lond* , **218**, 117–146 (1971).
[16] Hellam, D. C., and Podolsky, R J , *J Physiol , Lond.*, **200**, 807–819 (1969)
[17] Endo, M., *Nature new Biol* , **237**, 211–213 (1972)
[18] Moisescu, D G., Ashley, C. C , and Campbell, A. K., *Biochim. biophys. Acta*, **396**, 133–140 (1975)
[19] Ashley, C. C , and Moisescu, D G , *Nature new Biol.*, **237**, 208–211 (1972).
[20] Rodiguin, N. M , and Rodiguina, E N., *Consecutive Chemical Reactions*, 42–46 (Van Nostrand, Princeton, 1964).
[21] Lehman, W., and Szent-Gyorgyi, A. G , *J gen. Physiol.*, **66**, 1–30 (1975).
[22] Hazelgrove, J C., *Cold Spring Harb. Symp quant Biol* , **37**, 341–352 (1972)
[23] Werber, M M., Gaffin, S L., and Oplatka, A., *J. Mechanochem. Cell Motility*, **1**, 91–96 (1972).
[24] Morimoto, K , and Harrington, W. F., *J. molec. Biol* , **83**, 83–97 (1974)
[25] Bremel, R. D , and Weber, A , *Nature new Biol.*, **238**, 97–101 (1972).
[26] Potter, J D., and Gergely, J., *J. biol Chem* , **250**, 4628–4633 (1975)
[27] Moisescu, D. G , and Pusch, H , *Pflugers Arch* , **355**, R-122 (1975).
[28] Taqui Khan, M. M , and Martell, A. E., *J Am. chem. Soc.*, **88**, 668–671 (1966)
[29] Phillips, R. C., George, P., and Rutman, R. J., *J. Am. chem. Soc.*, **88**, 2631–2640 (1966)
[30] Porzehl, H , Caldwell, P. C., and Ruegg, J. C., *Biochim. biophys. Acta*, **79**, 581–591 (1964)
[31] Good, N E , *et al* , *Biochemistry*, **5**, 467–477 (1966)
[32] Smith, R M , and Alberty, R. A , *J. Am. chem. Soc.*, **78**, 2376–2380 (1956)

X-ray titration of binding of β,γ-imido-ATP to myosin in insect flight muscle

WE have attempted to establish a correlation between the binding of an ATP analogue, β,γ-imido-ATP (hereafter termed imido-ATP), and a structural change induced in muscle in the presence of this analogue. Imido-ATP binds tightly at the enzymatic site of myosin, but is not hydrolysed there[1]. When applied to glycerol-extracted muscle, it binds to the myosin *in situ* without causing the muscle to relax—that is, a ternary actin–myosin–nucleotide complex is formed[2]. Muscle fibres in this condition have the same mechanical stiffness as in rigor, but their zero tension point is displaced to a slightly greater muscle length, and both X-ray diffraction and electron microscopy indicate that the conformation of the attached myosin has altered, as if the head was rotated relative to the actin[2–5].

Unfortunately both structural signs can be faulted, the electron microscopy because of the possibility of fixation or postfixation changes[6], and the X-ray diffraction because of the long time which was used to obtain the required exposures[2,4]. We have tried to overcome these objections by observing diffraction changes within a short time after the nucleotide was added, and checking their relevance to the nucleotide binding by their relationship to the concentration used—that is, to obtain an X-ray titration of the nucleotide binding. For this purpose, the most powerful source of X rays available was used. The experiments were carried out at the EMBL synchrotron radiation facility at the DESY synchrotron, Hamburg[7,8], on glycerol-extracted dorsal longitudinal flight muscle from *Lethocerus cordofanus* dissected into bundles of 25 to 40 fibres. These were mounted on a mechanical apparatus in which their stiffness and tension could be monitored[2], and immersed in a neutral, calcium-free buffer at low ionic strength at 13–15 °C (20 mM imidazole, 10 mM NaN_3, 4 mM EGTA, 10 mM $MgCl_2$, pH 6.9, as described previously[4]). An intense monochromatic X-ray beam of wavelength 1.5 Å was passed through the sample and the resultant small angle diffraction pattern from the hexagonal lattice of myosin and actin filaments was recorded at 80-cm specimen–counter distance using a position-sensitive gas detector with a resolution of approximately 0.2 mm full width at half maximum (FWHM) (ref. 9).

The two strongest diffraction peaks on the equator deriving from the basic 530 Å lattice periodicity and designated $10\bar{1}0$ and $20\bar{2}0$ were readily recorded in conveniently short times. By slight displacement of the beamstop, it was possible to observe one $10\bar{1}0$ and both $20\bar{2}0$ diffraction peaks clearly (Fig. 1*a*). The entrance slit of the detector was opened wide (2 mm) so that the entire width of the equatorial peaks were received; the efficacy of this was checked by comparison of the counting scans with densitometer traces from films of the same specimens. Data were usually collected in 300 s, representing $0.5–1.0\times10^4$ counts per channel at the peak of each reflection. The intensity of each of the three peaks was estimated from the product of its peak height above background and half-height width. The $20\bar{2}0/10\bar{1}0$ intensity ratio R was calculated from the mean value of the two outer peaks, $R = (20\bar{2}0_{\mathrm{L}}+20\bar{2}0_{\mathrm{R}})/2\times(10\bar{1}0)_{\mathrm{R}}$.

In rigor (that is, in the absence of nucleotide) R was slightly greater than unity (mean ±s.e. 1.26±0.03; $n = 27$), which agrees with previous estimates[10]. On addition of sufficient imido-ATP to ensure binding to myosin[2], the ratio fell by approximately one-third of its value (Table 1). The widths of the peaks did not alter significantly. Two-thirds of the change in R occurred before the mid-time of the first measurement (3–6 min after addition of the nucleotide), the remaining change occurring gradually over the ensuing 20 min. On removal of the nucleotide, the change was partially reversed (mean recovery 60±10%; $n = 10$); again, approximately two-thirds of the reversal occurred 5–7 min after the start of removal and the rest over the following 30 min. Sequential increases of nucleotide concentration at 10-min intervals produced a graded increase in R. The data fitted a hyperbolic binding curve (Fig. 1*b*) with a dissociation constant (Table 1) similar to that obtained by direct binding measurements[2]. On removal of the nucleotide after the 2-h immersion necessary to obtain this curve, the ratio reverted towards the rigor value, as in the shorter immersions.

Fig. 1 *a*, Trace of output from position-sensitive detector aligned along the equator of the diffraction pattern from insect flight muscle in rigor. The $10\bar{1}0$ peak on the left-hand side of the diagram is elevated by the background and interrupted by the beamstop; it was not used for calculation. *b*, Change in R on addition of β,γ-imido-ATP in a single experiment. The continuous line is the best fitting hyperbola ($K_d = 65\pm6$ μM, $\Delta R_{max} = 0.31\pm0.01$) (ref 18).

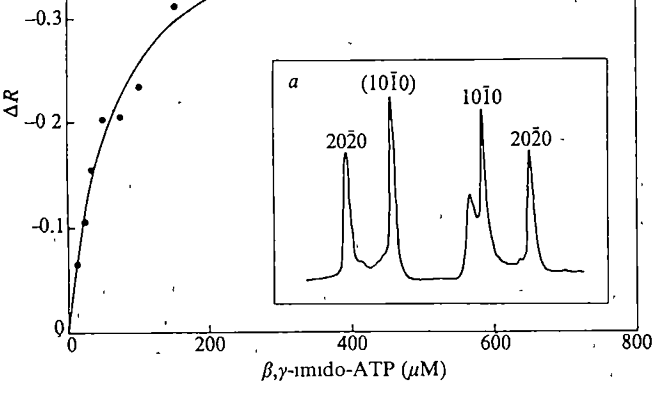

Table 1 Changes in R on adding various ligands to insect flight muscle

Ligand	ΔR
β,γ-imido-ATP	
500–1,700 μM	−0.34±0.05 (10)
Limiting value*	−0.41±0.03 (46); $K_d = 90\pm19$ μM
ADP 200–400 μM†	−0.01±0.01 (7)
Pyrophosphate	
600–1,200 μM	−0.17±0.03 (4)
Limiting value†	−0.25±0.04 (16); $K_d = 450\pm120$ μM
ATP 15 mM	−0.59±0.07 (5)

Mean ±s.e. cited; number of experiments in brackets. ΔR was calculated from the change in peak heights of the two reflections on adding the ligand.

* Calculated by hyperbolic fitting to the measurements at different ligand concentrations[18]. 10 mM Mg^{2+} present in all solutions except ATP, where 15 mM Mg^{2+} was added; pH 6.9, ionic strength=0.1, 14°C.

† 50–100 μM diadenosyl pentaphosphate was also added to these solutions to block adenylate kinase activity[20].

The effect of other ligands was also studied. ADP, in a concentration well above its known dissociation constant[11], had no significant effect on R (Table 1). Pyrophosphate reduced R by a smaller amount than imido-ATP at comparable concentrations. Its effect was graded over the range available, which was limited by the solubility of Mg-pyrophosphate. Application of a hyperbolic fit indicated that the full effect of binding pyrophosphate was probably greater than that observed, but still less than that for imido-ATP (Table 1). On removal of pyrophosphate the ratio reverted to or beyond its initial value (mean recovery 125±25%; $n = 4$).

In all these cases the 5-Hz stiffness (that is, muscle stiffness measured by the change in tension resulting from a small amplitude 5-Hz sinusoidal length oscillation) of the muscle remained high (approximately 20 mg per fibre % extension) in the presence of nucleotide, as expected from previous results[2]. On addition of ATP the muscle relaxed; the 5-Hz stiffness fell by a factor of four and could not be restored by extension. The ratio R fell by approximately half its value (Table 1) in agreement with previous observations[10]; the widths of the peaks did not alter. The effect was reversed by removal of the nucleotide (mean recovery 87±3%; $n = 3$).

During the course of each of these experiments, which lasted 3–15 h, the filament lattice spacing gradually decreased by approximately 5% (mean initial value 533±5 Å; $n = 5$; final value 510±4 Å; $n = 5$). Addition of any of the unhydrolysed ligands had little or no effect on the spacing.

These results show that within a short time of the binding of imido-ATP to myosin, a structural change occurs in the muscle, the magnitude of which is directly proportional to the amount of nucleotide bound. They do not show the nature of the change, since according to model studies either rotation of the attached myosin, redistribution of the locus of attachment along the actin filament or detachment of a proportion of the myosin from the actin would all cause such a change (refs 10 and 12, and K. C. Holmes, J. B. L. and R. T. T., unpublished). We believe that the third possibility is excluded by the retention of the muscle's stiffness and the high intensities of the actin-based layer lines in the presence of imido-ATP[2–4]. It is not possible to differentiate the other two possibilities. Whichever structural change is responsible, it certainly occurs quickly; the main objection to the X-ray diffraction evidence has been removed.

It is probable that the change in R produced by pyrophosphate has the same molecular origin, since electron microscopy[13] shows elements of the same changes occurring in the muscle. The observed concentration dependence agrees with that deduced from mechanical observations[14]. The failure of ADP to shift the ratio indicates that this nucleotide causes relatively little redistribution or rotation of the myosin; the outer layer lines of the X-ray diffraction pattern are also little altered by this ligand[15].

These results are also relevant to vertebrate skeletal muscle, since Lymn has shown that imido-ATP produces a large shift in the $11\bar{2}0/10\bar{1}0$ ratio in glycerol-extracted rabbit psoas fibres[16]. As imido-ATP does not reduce the 5-Hz stiffness of these fibres at a given tension[2], it is probable that this change is also due to a redistribution or rotation of attached myosin, rather than its release from the actin. If so, this invalidates the assumption that a change in R can be used to predict the proportion of myosin attached to actin[17,19].

In conclusion, we now have evidence that ligands which attach to the enzymatic site of myosin do alter either its position relative to the actin or the location of the actin to which it tends to attach. The effect is both rapid and specific, and may well be relevant to the state of the myosin during its contractile cycle.

R. S. GOODY
J. BARRINGTON LEIGH
H. G. MANNHERZ

MPI für Medizinische Forschung,
Abteilung Biophysik
Jahnstresse 29,
6900 Heidelberg, West Germany

R. T. TREGEAR

University of Oxford
Department of Zoology,
South Parks Road, Oxford, UK

G. ROSENBAUM

EMBL, Postfach 10.2209,
6900 Heidelberg, West Germany

Received May 17; accepted June 28, 1976.

1 Yount, R. G., Ojala, D, and Babcock, D., *Biochemistry*, 10, 2490–2496 (1971)
2 Marston, S. B., Rodger, C D, and Tregear, R. T, *J. molec Biol.*, 104, 263–276 (1976).
3 Barrington Leigh, J., *et al.*, *Cold Spring Harb Symp. quant. Biol*, 37, 443–447 (1972)
4 Goody, R. S, Holmes, K C., Mannherz, H G., Barrington Leigh, J, and Rosenbaum, G., *Biophys J*, 15, 687–705 (1975).
5 Beinbreck, G., Kuhn H. J., Herzig, J. W, and Ruegg, J. C., *Cytobiologie*, 12, 385–396 (1976).
6 Reedy, M. K., *Am Zool*, 7, 465–481 (1967).
7 Barrington Leigh, J., and Rosenbaum, G., *A. Rev. Biophys. Bioengng*, 5, 239–270 (1976).
8 Barrington Leigh, J, and Rosenbaum, G, *J appl Crystallogr.*, 7, 117–121 (1974).
9 Gabriel, A., and Dupont, Y., *Rev Sci Instrum*, 43, 1600–1602 (1972)
10 Miller, A., and Tregear, R. T., *J. molec Biol.*, 70, 85–104 (1972).
11 Marston, S. B, *Biochim. biophys Acta*, 305, 397–412 (1973).
12 Holmes, K. C., *et al.*, in *Molecular Basis of Motility* (edit. by Heilmeyer, L. M. G., Ruegg, J. C. and Wieland, Th), 26–41 (Springer, Heidelberg, 1976).
13 Beinbrech, G., Kuhn, H J., and Ruegg, J. C., *Experientia*, 28, 513–515 (1972)
14 White, D. C. S., *J Physiol., Lond*, 208, 583–605 (1970)
15 Rodger, C. D., and Tregear, R. T, *J molec Biol*, 86, 495–497 (1974).
16 Lymn, R. W., *J molec Biol*, 99, 567–582 (1975).
17 Haselgrove, J. C, and Huxley, H. E, *J molec. Biol.*, 77, 549–568 (1973).
18 Wilkinson, G N, *Biochem. J*, 80, 324–332 (1961).
19 Armitage, P. M., Tregear, R. T, and Miller, A., *J. molec. Biol.*, 92, 39–53 (1975).
20 Feldhaus, P., Frohlich, T., Goody, R. S., Isakov, M., and Schirmer, R. H.. *Eur. J. Biochem.*, 57, 197–204 (1975).

Phosphorylation of troponin I and the inotropic effect of adrenaline in the perfused rabbit heart

THE regulation of contractile activity in cardiac muscle by changes in the intracellular Ca^{2+} concentration involves the regulatory protein system, consisting of tropomyosin and the troponin complex that is located in the I filament. Although the regulatory protein system of cardiac muscle is essentially similar in function to that of skeletal muscle, the components differ in the two tissues. Cardiac tropomyosin consists principally of α subunits, whereas the skeletal protein is composed of α and β subunits[1]. Troponin I, troponin C and troponin T are all specific for cardiac muscle in that they have different chemical and immunochemical properties from the corresponding skeletal muscle proteins[2–4]. In addition, cardiac troponin I and cardiac troponin C have been shown to have different amino acid sequences from their skeletal muscle counterparts[3,5].

Although rabbit cardiac troponin I shows considerable sequence homology with troponin I from fast skeletal muscle, it has an additional 26 residues at the N terminus[3]. The rapid phosphorylation of a serine at position 20 in this extra N-terminal part of the cardiac troponin I molecule is mainly responsible for the fact that the phosphorylation catalysed by cardiac cyclic AMP-dependent protein kinase is about 30 times faster with cardiac troponin I than with fast skeletal troponin I (ref. 4). When isolated immediately after death by stunning, a phosphate content of 2–3 mol mol^{-1} has been reported for cardiac troponin I, compared with 0.5–1.0 mol mol^{-1} for skeletal muscle troponin I (ref. 4). These differences suggest that the phosphorylation of troponin I may have a special significance for the regulation of the contractile activity of cardiac muscle. Further evidence for such a role indicates that there is a correlation between the contractile force developed on adrenaline application and the extent of phosphorylation of troponin I in the perfused rat heart[6].

We describe here investigations extending our studies on the enzymic phosphorylation of isolated rabbit cardiac troponin I to the perfused heart. We have attempted to relate the effects of adrenaline on the contractile activity of the perfused rabbit heart to the phosphorylation of specific sites on the troponin I.

The total phosphate content of rabbit cardiac troponin I varied with the conditions in which the heart was removed. Troponin I was immediately isolated by affinity chromatography[7] and, before analysis, was washed four times with 7.5% (w/v) cold trichloroacetic acid to remove non-covalently bound phosphate. Values of 2.1 ± 0.4 mol P per mol were obtained when hearts were removed immediately after death by stunning. If hearts were made anoxic by clamping the aorta for 30 s just before removal from the animal, similar or slightly higher values were obtained. If the rabbits were anaesthetised with pentobarbital, and troponin I subsequently isolated from hearts removed after freezing *in situ* in Wollenberger clamps chilled with liquid nitrogen, a value of 1.5 ± 0.2 mol P per mol troponin I was obtained.

Hearts removed rapidly from stunned rabbits, as described[8] for rats, were cooled for 15–20 s in ice-cold saline and perfused by the Langendorff procedure at 37 °C with modified Krebs–Henseleit buffer[9] in an apparatus fitted with a recirculation chamber similar to that described by Morgan *et al*[10]. Force and rate were recorded on a polygraph using a force transducer attached to a stainless steel hook in the apex of the heart At various times, the ventricles (about 4 g tissue) were cut rapidly from the heart and homogenised immediately in 30 ml of 9 M urea, 75 mM Tris-HCl, pH 8.0, 1 mM $CaCl_2$, 15 mM β-mercaptoethanol and the troponin I isolated by affinity chromatography[7]. During the 2–5 min initial equilibration period, cardiac troponin I contained 2.5 ± 0.4 mol P per mol. After 10–15 min perfusion, the phosphate content of troponin I fell to 1.5–1.6 mol P per mol and remained nearly constant for at least 100 min, during which heart rate and force also remained virtually unchanged.

Addition of 0.1–4.0 μM adrenaline to the perfusion media after an initial equilibration period of 15 min caused a rapid and dose-dependent increase in the force developed by the myocardium. Hearts were removed rapidly from the apparatus at the moment of peak force development, homogenised and troponin I isolated. Total phosphate content increased in parallel with increasing force, reaching a maximum of about 3 mol P per mol troponin I at 2 μM adrenaline, when the maximum contractile response was obtained (Fig. 1).

If troponin I was isolated 5–10 min after the maximum inotropic response when the contractile force had returned

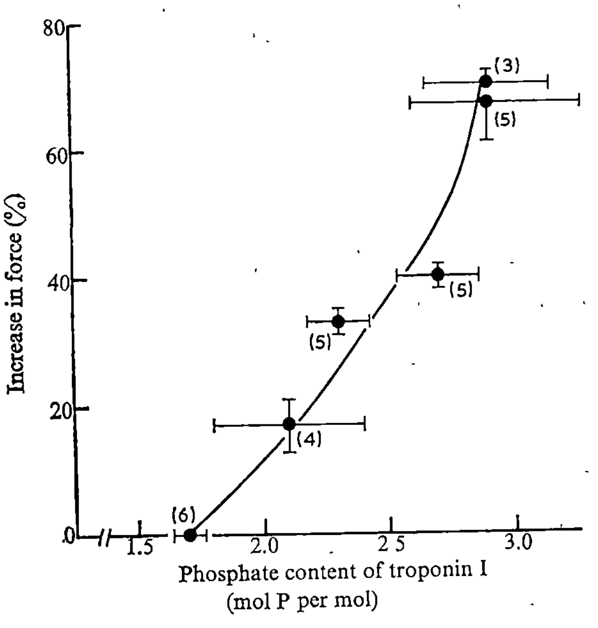

Fig. 1 Relationship between the phosphate content of troponin I and the increase in force developed in the perfused rabbit heart. Force changes were induced by adding 0.3–4.0 μM adrenaline to modified Krebs–Henseleit buffer (118 mM NaCl, 4.7 mM KCl, 2.5 mM $CaCl_2$, 1.2 mM $MgSO_4$, 0.2 mM KH_2PO_4, 0.5 mM Na_2 EDTA, 25 mM $NaHCO_3$ and 5 mM glucose) equilibrated with 95% O_2:5% CO_2 at 37 °C, *p*H 7.4. Hearts were first perfused for a 15-min equilibration period with normal buffer and then switched to buffer containing adrenaline. At the peak of the force change, the hearts were homogenised rapidly in buffered 9 M urea and troponin I isolated as described in the text. Phosphate content was calculated from total phosphate and nitrogen contents measured in duplicate samples of trichloroacetic acid-washed troponin I as described previously[15], using a molecular weight of 22,500 and a nitrogen content of 16% for cardiac troponin I. Figures in parentheses indicate number of hearts analysed.

to a value similar to that before adrenaline application, the total P content was similar to that obtained after equilibration but before addition of adrenaline. In the presence of β-adrenergic blockers such as propranolol, the inotropic response to adrenaline was inhibited and no significant rise in the phosphate content of troponin I occurred.

In a parallel series of experiments, the troponin I isolated after perfusion was washed repeatedly with cold 7.5% trichloroacetic acid to remove non-covalently bound phosphate and digested with cyanogen bromide. In control hearts perfused for 20 min, 90–95% of the total covalently bound phosphate was present in the N-terminal cyanogen bromide peptide of cardiac troponin I that contains residues 1–48 (ref. 3).

After 15–20 min perfusion with Krebs–Henseleit–bicarbonate medium containing phosphate labelled with ^{32}P, the N-terminal cyanogen bromide peptide became radioactively labelled. Of the ^{32}P recovered from a tryptic digest of this N-terminal peptide 80–90% was bound to serine 20, indicating that in the perfused beating heart there was rapid exchange between the pool of intracellular phosphate compounds and the phosphate on serine 20. If the troponin I was isolated at the peak of the inotropic response to adrenaline, the total incorporation of ^{32}P increased. The distribution of radioisotope in the peptides present in the cyanogen bromide digest of this troponin I indicated that 90–95% of the total ^{32}P incorporated was associated with the region of the cardiac troponin I molecule represented by residues 1–48.

These results suggest that at least three phosphorylation sites are significant for the function of cardiac troponin I in the rabbit. One of these, serine 20, is readily phosphorylated by cyclic AMP-dependent protein kinase. This site is usually phosphorylated in the perfused heart and readily exchanges with the intracellular phosphate pool. The precise location in the region consisting of residues 1–48, of the other two sites that must be phosphorylated when the total phosphate content rises to 3 mol mol^{-1}, is not clear. The sequence studies of Grand *et al.*[3], have shown that there are serines at positions 4, 20, 32, 37 and 39 and threonines at positions 26 and 46. Of these, serine 37 might be expected to be a site for phosphorylation by phosphorylase kinase by analogy with the action of this enzyme on troponin I from fast skeletal muscle of the rabbit[11,12]. As yet we have no information as to whether phosphorylation of serine 37 is involved in the inotropic response.

The results indicate, however, that the increase in the phosphate content of troponin I from about 2 mol mol^{-1} to 3 mol mol^{-1} is closely associated with the increase in contractile force obtained in cardiac muscle treated with adrenaline.

In troponin I from fast skeletal muscle, the N-terminal region is somehow involved with interaction with troponin C (ref. 13). Judging from the sequence data of Grand *et al.*[3], and the inhibition of the phosphorylase kinase-catalysed phosphorylation of cardiac troponin I by troponin C (ref. 4), a similar interaction probably occurs in the cardiac system. The introduction of negative charges by phosphorylation in the N-terminal region of the molecule, which contains an excess of positively charged amino acids, would be expected to alter the strength of the interaction with the negatively charged troponin C and thereby possibly change the affinity of troponin C for Ca^{2+}.

Preliminary investigations in this laboratory on natural and desensitised actomyosin indicate that after phosphorylation of cardiac troponin I by cyclic AMP-dependent protein kinase, the Ca^{2+} concentration required for 50% activation of the ATPase is increased, that is, the system is less sensitive to Ca^{2+} concentration (H. A. Cole and S.V.P., unpublished). This finding does not confirm those of Rubio *et al.*[14], who reported an increase in Ca^{2+} sensitivity of the ATPase of cardiac natural actomyosin on phosphorylation of troponin I.

Although our results do not permit us to say whether there is a direct casual relationship between the phosphorylation of troponin I and the inotropic effect of adrenaline, the events are undoubtedly closely associated in time. In view of the results of the enzymic studies, we suggest that one function of phosphorylation of troponin I is to act as a negative feedback system. Thus by reducing the sensitivity of the actomyosin ATPase to Ca^{2+}, it smoothes out the contractile response to the rise in intracellular Ca^{2+} which results from the action of adrenaline on the myocardium. A detailed account of this work will be published elsewhere in due course.

This work was supported in part by research grants from the MRC and the British Heart Foundation and carried out during the tenure by R.J.S. of a British American Research Fellowship of the American Heart Association and the British Heart Foundation.

R. J. SOLARO
A. J. G. MOIR
S. V. PERRY

*Department of Biochemistry,
University of Birmingham,
Birmingham B15 2TT, UK*

Received May 25, accepted June 25, 1976

1 Cummins, P., and Perry, S. V , *Biochem. J.*, 141, 43–49 (1974).
2 Hirabayashi, T., and Perry, S V., *Biochim biophys Acta*, 351, 273–389 (1973).
3 Grand, R J A , Wilkinson, J. M , and Mole, L. E , *Biochem J* (in the press).
4 Cole, H. A., and Perry, S V , *Biochem J.*, 149, 525–533 (1975).
5 van Eerd, J. P., and Takahashi. K , *Biochemistry*, 15, 1171–1180 (1976).
6 England, P., *FEBS Lett.*, 50, 57–60 (1975)
7 Syska, H , Perry, S V , and Trayer, I. P , *FEBS Lett* , 40, 253–257 (1974).
8 Neely, J R., Leibermeister, H., Battersby, E. J , and Morgan, H. E., *Am. J. Physiol.*, 212, 804–814 (1967).

[9] Krebs, H. A , and Henseleit, K., *Z. physiol. Chem.*, 210, 33–66 (1932).
[10] Morgan, H E., Henderson, M. J , Regen, D. M., and Park, C. R., *J. biol Chem.*, 236, 253–261 (1961)
[11] Moir, A. J. G., Wilkinson, J. M., and Perry, S. V., *FEBS Lett* , 42, 253–256 (1974)
[12] Huang, T S , Bylund, D. B , Stull, J. T , and Krebs, E. G., *FEBS Lett.*, 42, 249–252 (1974)
[13] Syska, H , Wilkinson, J. M , Grand, R. J A., and Perry, S V , *Biochem. J* , 153, 375–387 (1976)
[14] Rubio, R., Bailey, C., and Villar-Palasi, C., *J. Cyclic Nucleotide Res.*, 1, 143–150 (1975).
[15] Perry, S. V., and Cole, H. A , *Biochem J* , **141**, 733–743 (1974)

Increase in human skeletal muscle lactate produced by fenfluramine

OUR recent hypothesis[1] that "anorectic agents" such as fenfluramine and mazindol owe at least part of their anti-obesity properties to a peripheral action on glucose metabolism by causing an increase in glucose uptake into skeletal muscle and a subsequent "wasting of calories" has been criticised[2] on the grounds that there is no information on the fate of the glucose so taken up, nor convincing evidence for an increase in metabolic rate with these drugs. We have now studied the effect of fenfluramine on lactate production in isolated human skeletal muscle, our previous work having shown no increase in glycogen levels[3] nor in carbon dioxide production[4]. An increase in lactate production would indicate metabolism of the glucose entering the cell under the influence of fenfluramine.

Human skeletal muscle was obtained at surgery for total hip joint replacement. The preparation and incubation of the tissue (in Krebs–bicarbonate buffer with added bovine serum albumin 2 mg ml^{-1} and glucose 16.67×10^{-3} M) was carried out using the method of Kirby, Leighton and Turner[5]. Muscle strips, wet weight 80–140 mg, were prepared from each sample and incubated in 2 ml of media containing (1) 100 μU ml^{-1} insulin, (2) 100 μU ml^{-1} insulin plus 100 ng ml^{-1} fenfluramine (previously shown to cause a maximal increase in glucose uptake[6]), (3) 100 μU ml^{-1} insulin plus 100 ng ml^{-1} amphetamine (amphetamine has no significant effect on glucose uptake into isolated muscle[3]). For each muscle sample two strips were prepared and used for control lactate determinations; they were not incubated Flasks were flushed with a mixture of 95% oxygen and 5% carbon dioxide for 10 s before incubation at 37 °C for 90 min. The lactate content of the muscle and the residual media were then determined.

The method for measurement of muscle and residual media lactate was based on that for blood lactate using NAD/LDH enzymes[7] and the Boehringer Mannheim Biochemica Test Combination for lactate. Muscle strips were removed from the media and homogenised for 5 min at 25,000 r.p.m. with a blade homogeniser in 2 ml of 0.6 M perchloric acid. The homogenate was centrifuged for 10 min at 3,000 r.p.m. and 0.2 ml of the supernatant used for the lactate determination. One millilitre of the residual medium was added to 1 ml of 0.6 M perchloric acid and centrifuged as before, 0.2 ml of the supernatant being used for the subsequent analysis, with the Biochemica Test Combination. A lactate standard (0.5 mM) was included as a blank. Preliminary work had demonstrated a linear relationship between absorbance at 340 nm and lactate concentration over the range 0–1.0 mM. Good reproducibility was obtained with the method, the mean of six muscle lactate determinations in strips from the same sample being 6.91 ± 0 21 mmol per kg wet weight of muscle.

Table 1 Lactate formed by isolated human skeletal muscle incubated with insulin, fenfluramine or amphetamine

Insulin*	Fenfluramine plus insulin: change compared with insulin alone*	Amphetamine plus insulin. change compared with insulin alone*
13.85	+1.04	−0.10
14.11	−2.09	+1.82
9.79	+2.33	+0.84
9.12	+0.23	−3.00
10.97	+0.10	−0.53
8.78	+1.67	+2.07
7.68	+1.07	−1:67
8.58	+1.53	−1.57
7.48	+2.53	−0.08
8.79	+1.07	−0.70
Means ± s.e m.	+0.95 ± 0.42	−0.29 ± 0.50
t	2 26	0.58
Significance	$P = 0.05$	NS

All values are means of two incubations
*mmol lactate per kg wet weight skeletal muscle per 90 min; 100 μU ml^{-1} insulin, 100 ng ml^{-1} fenfluramine and 100 ng ml^{-1} amphetamine.

The results (Table 1) demonstrate that fenfluramine produced an increase in muscle lactate concentrations. Amphetamine, which has no effect on glucose uptake, has no significant effect on lactate concentration. Further studies are needed to determine in more detail the metabolic fate of the glucose taken up under the influence of fenfluramine, but these results are further evidence for a peripheral metabolic mechanism in its anti-obesity activity.

M. J. K. is a recipient of the Williams fellowship for scientific and medical research, awarded by London University.

MARILYN J. KIRBY
P. TURNER

Department of Clinical Pharmacology,
St Bartholomew's Hospital Medical College,
London EC1A 7BE, UK

Received May 19; accepted June 8, 1976.

[1] Kirby, M. J., and Turner, P , *Lancet*, i, 566–567 (1976).
[2] Garrow, J S., *Lancet*, i, 691–692 (1976).
[3] Kirby, M J , and Turner, P , in *Recent Advances in Obesity Research* 1 (edit. by Howard, A), 378–380 (Newman Publishing Ltd, London, 1975)
[4] Kirby, M. J., thesis, London Univ (1975).
[5] Kirby, M J , Leighton, M , and Turner, P , *Br J clin. Pharmac.*, 3, 299–304 (1976)
[6] Kirby, M J., *Br J clin. Pharmac.*, 1, 511–512 (1974).
[7] Hohorst, H J., in Bergmeyer, H. U , *Methods of Enzymatic Analysis*, first edn., 622 (Verlag Chemie, Weinheim, 1962).

Ribosome slowed by mutation to streptomycin resistance

ALTHOUGH the basic mechanisms of protein synthesis are now rather well understood, particularly in *Escherichia coli*, it is less clear how the high accuracy of this process is achieved. (The error rate in protein synthesis in *E. coli* seems to be about one in 10^4 amino acid misincorporations (Edelman and Gallant, unpublished results, and our own unpublished data)). A major site determining accuracy in protein synthesis is the ribosome, and in addition to the ribosome-mediated effects on accuracy (*in vivo* and *in vitro*) of various metal ions, aminoglycoside antibiotics and organic solvents, there are ribosomal mutations which increase or decrease accuracy[2]. Certain mutations of the 30S ribosomal protein S12 conferring streptomycin resistance (the *strA* locus) enhance accuracy[3–5], whereas certain mutations in the S4 protein (the *ram* locus) are known to decrease accuracy[6]. The *strA* mutations are restrictive (reducing) in their effect on both missense and nonsense suppression *in vivo* and on miscoding *in vitro*[3], the *ram* mutation, on the other hand, has the opposite effect in both cases[6]. It is possible that it is the kinetics of polypeptide synthesis at the ribosome that determines accuracy and that the kinetics in turn are affected by the *strA* and *ram* mutations. Because the same transfer RNA (tRNA) discrimination kinetics that may determine accuracy may also contribute to the elongation speed, we have investigated the effect of mutation to streptomycin resistance on the speed of polypeptide elongation.

A simple kinetic model for discrimination of charged tRNA at the ribosome, like that described by Ninio[7], may be constructed. Such models imply directly that the more accurate a given ribosome, the slower is the transpeptidation reaction, and therefore the longer is the time required to synthesise a polypeptide of given length. In such a model one can attribute the specificity of message-directed polypeptide synthesis to the energy differences between binding of the complementary and non-complementary amino-acyl-tRNAs to the message codon and the amino-acyl site on the ribosome. Although we do not know what part of the elongation cycle time is required for transpeptidation, we expect that a mutation to streptomycin resistance, and therefore to a more accurate ribosome, should cause an increase in this time and thus a slowdown in elongation. We investigated this hypothesis by examining an otherwise isogenic set of independent spontaneous mutants, resistant to high levels of streptomycin, and have found that they do translate message at a slower rate.

Translation speed was determined by measuring the time required for the first newly synthesised β-galactosidase molecules to appear after induction of the lactose operon. This induction lag was measured in exponentially growing cultures by sampling every 5 (or 10) s into chloramphenicol to stop protein synthesis and assaying each of these samples for β-gal activity to generate an induction curve. The time between induction and the appearance of the first newly synthesised enzyme was determined to an accuracy of ±3 s. For the wild type, streptomycin-sensitive strain (IH79), the lag time we measured agrees with the results of Lacroute and Stent[9] and Kepes[10]. Although we are interested here in the relative differences in the measured lag times and not necessarily the absolute chain elongation times, the results of their experiments[9,10] indicate that the chain elongation time is at least 90% of the lag time (see also our unpublished work).

Fig. 1 Measurement of lag time to first completed β-galactosidase molecule (β-gal). Cultures of a lac permease negative (derivative of W1485) K12 strain, IH79(Str^S), and a spontaneous mutant derivative to streptomycin (200 µg ml^{-1}) resistance, IH82, were grown in glycerol minimal medium at 37 °C to a well-established exponential phase and then induced at $t=0$ by adding isopropyl-β-D-thiogalactopyranoside to a concentration of 1.0 mM. The cultures were sampled every 5 s by taking 0.5 ml into test tubes containing 0.5 ml of a solution (1.0 mg ml^{-1}) of chloramphenicol in distilled water These samples were then assayed for β-galactoxidase activity. Cell lysis was accomplished with chloroform and β-gal activity measured by hydrolysis of orthonitrophenol-β-D-galactopyranoside at 37 °C (ref. 8). The data are reported here in terms of the uninduced level of β-gal. From the observed point to point variation in the measured basal level (points before 80 s, for example) and by repeating the experiment several times we determined the inherent error in specifying the intercept and estimate that the time lag was measured to an accuracy of ±3 s. △, IH32, streptomycin resistant; ○, IH79, streptomycin-sensitive.

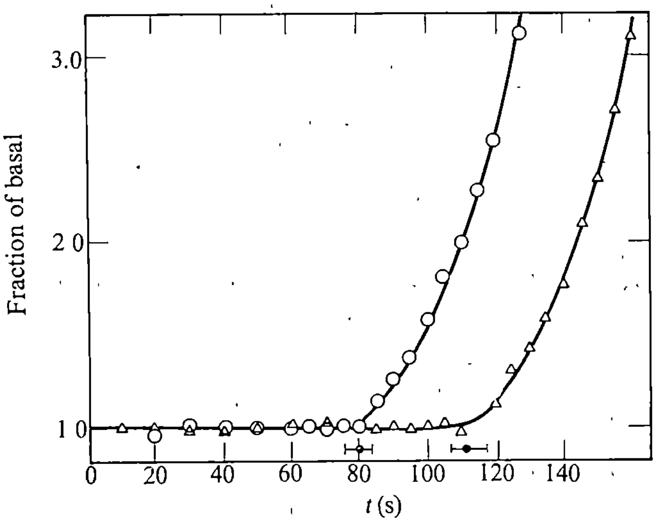

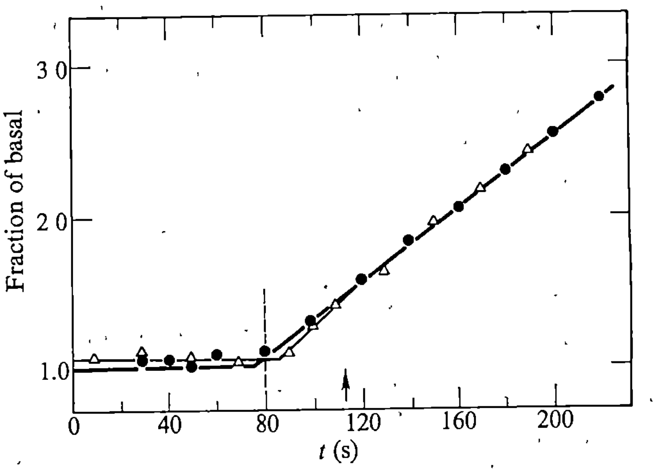

Fig. 2 Induction curves for IH79 and IH82 with actinomycin D. The conditions and sampling procedures for the chloramphenicol experiments were as described in the legend to Fig. 1. The cultures for the actinomycin experiments were treated by resuspension at 37 °C in EDTA–Tris buffer[13] (1 mM EDTA, 0.12 Tris, 1 mM Na$_2$PO$_4$, 0.5% glycerol at pH 7.6) for 2 min. The EDTA-treated culture was then diluted 10:1 into prewarmed medium. The induction was begun 5 min after dilution. The sampling scheme was as in the chloramphenicol experiments except that the samples were held at 37 °C for 30 min after sampling to permit all free message to be completely translated. △, Strain IH82 (Str^R); ○, IH79 (Str^S). The intercepts are not significantly different from each other or the chloramphenicol measured intercepts for IH79 (Fig 1) (into 0.5 ml of actinomycin D 20 µg ml^{-1}). - - -, Lag time for IH79; arrow, lag time for IH82 (Fig. 1).

We isolated a set of streptomycin-resistant mutants (to 200 µg ml^{-1} of streptomycin) which were produced spontaneously from independent cultures. This strain set is therefore, with high confidence, isogenic for all loci but the *strA* locus. Identical procedures for measuring the induction lag revealed a significant increase in the lag time for the streptomycin-resistant derivatives of IH79 over the parent strain (see Fig. 1 in which data for the parent and one such derivative are presented). The independence of the *strA* mutations in this set, the negligible probability of double mutation and the well characterised nature of the *strA* locus as the structural gene for the 30S ribosomal protein S12 and the only mutational locus for the high level streptomycine resistance[11], strongly suggest that the change in speed of protein synthesis is caused by a change in the ribosome speed during translation, rather than by a change in transcription rate.

This conclusion can be tested further by measuring the lag time for the completion of the first messenger RNA (mRNA) transcript of the gene. We have measured this time by using the DNA-binding drug actinomycin-D to stop transcription in a set of samples taken in a time series identical to that described above[12]. The time lag observed by this method (see legend to Fig. 2) is the time required for the passage of the RNA polymerase molecule down the full length of the *z* gene, the time for completion of the initial mRNA. The results (shown in Fig. 2) revealed no significant difference between sensitive and resistant strains and support our presumption that the mutation to streptomycin resistance affects the elongation speed and leaves the transcription speed essentially unchanged.

There is evidence that translation speed and transcription speed are coupled[14] by some yet unknown mechanism. Judging from the results of Gupta and Schlessinger[14] we would expect, however, to see a significant shift in transcription speed only for translation speeds much less than we observe in IH82.

These experiments show clearly that ribosome speed in *E. coli* is not a fixed parameter inherent to the protein synthetic apparatus, but a variable determined by the kinetics of translation and ultimately by the structure of the ribosome. (After this work was completed another, possibly related, phenomenon was reported in which increased levels of streptomycin in streptomycin-dependent strains apparently cause a proportional increase in the speed of translation[14]) We have observed a shift from about 14.7 amino acids per s in the wild type (*Str*^{s}) to about 10.5 amino acids per s in some ribosomal mutants (based on a β-galactosidase length of approximately 1,173 amino acids[15]). Furthermore, the correlations between speed and ribosomal accuracy which are expected from simple kinetic models are in agreement with the observations that mutation to streptomycin resistance but not to spectinomycin resistance (data not shown), which does not affect ribosomal accuracy, increases accuracy and decreases ribosome speed. The nature of the delayed induction curve seen in the streptomycin-resistant strains suggests that the delay is caused by a change in elongation speed and not in the ribosomal initiation rate: a decreased initiation frequency would cause a decreased rate of β-gal synthesis, not just a delay in an otherwise unchanged induction curve as we observe. A more direct separation of the two effects will, however, be necessary before this question can be settled completely.

Further experiments, designed to investigate the accuracy–speed connection suggested by this work, have been carried out on previously characterised *strA* alleles and on a characterised *ram* allele. This work (to be reported elsewhere) indicates that the *ram* allele reverses the effect of mutation to *Str* resistance, and that *strA* alleles may be ordered by their ribosome speeds. Further biochemical and genetic investigations of the kinetics of translation may lead to a fundamental understanding of the molecular processes underlying the discriminatory functions central to the information transfer which occurs at the ribosome during protein synthesis.

This work was carried out under the auspices of the USERDA.

David J. Galas
Elbert W. Branscomb

Biomedical Division,
Lawrence Livermore Laboratory,
University of California,
PO Box 808,
Livermore, California 94550

Received May 3; accepted June 15, 1976

[1] Loftfield, R. B, *Biochem J*, 89, 82–92 (1963)
[2] Gorini, L, and Davies, J., *Curr Top Microbiol Immun*, 44, 100–122 (1968).
[3] Gorini, L., and Kataja, E, *Proc. natn Acad Sci U.S.A.*, 51, 487 (1964)
[4] Gorini, L., *Cold Spring Harb Symp. quant Biol.*, 31, 101–111 (1969)
[5] Gorini, L, *Nature new Biol*, 234, 261–264 (1972)
[6] Rosset, R, and Gorini, L, *J molec Biol*, 39, 95–112 (1969)
[7] Ninio, J., *J. molec Biol*, 84, 297–313 (1974)
[8] Kepes, A., and Bequin, S, *Biochim biophys. Acta*, 123, 546–560 (1966)
[9] Lacroute, F, and Stent, G. S., *J. molec Biol.*, 35, 165–173 (1968)
[10] Kepes, A, *Biochim biophys Acta* 76, 293–309 (1963).
[11] Ozaki, M, Mizushima, S, Nomura, M., *Nature*, 222, 333–339 (1969).
[12] Leive, L, *Biochem biophys Res. Commun*, 20, 321–327 (1965)
[13] Perlman, R, and Pastan, I., *Biochem. biophys. Res. Commun.*, 30, 656–664 (1968)
[14] Gupta, R., and Schlessinger, D, *J Bact*, 125, 84–93 (1976).
[15] Zabin, I, and Fowler, A V, in *The Lactose Operon* (edit by Beckwith, J R, and Zipser, D) (Cold Spring Harbor Laboratory, New York, 1970)

Regulation of ribosomal RNA methylation in a temperature-sensitive mutant of BHK cells

CONSERVATION of methylated sequences of mammalian ribosomal precursor RNA (pre-rRNA) into mature cytoplasmic ribosomes suggests an essential structural or regulatory function for these modified bases[1–3], although the role of post-transcriptional methylation is not clear At the non-permissive temperature (39 °C), *ts 422E*, a temperature-sensitive mutant of BHK 21/13 cells[4–6], is deficient in 28S rRNA maturation and assembly of 60S ribosomal subunits, although transcription of 45S pre-rRNA and cytoplasmic appearance of 18S rRNA and 40S subunits remains unimpaired[3]. To examine the relationship between RNA methylation and the processing of ribosomes, we have studied this mutant and find it contains methyl-deficient pre-rRNA. Our results show an expanded pool of nuclear 45S pre-rRNA molecules in the mutant at 39 °C, suggesting an inhibition of its processing to 32S RNA. In addition, 45S and 32S precursor molecules in *ts 422E* are substantially undermethylated relative to the pre-rRNAs of wild-type BHK cells at 39 °C but identical at the permissive temperature (33 °C). The residual amount of mature

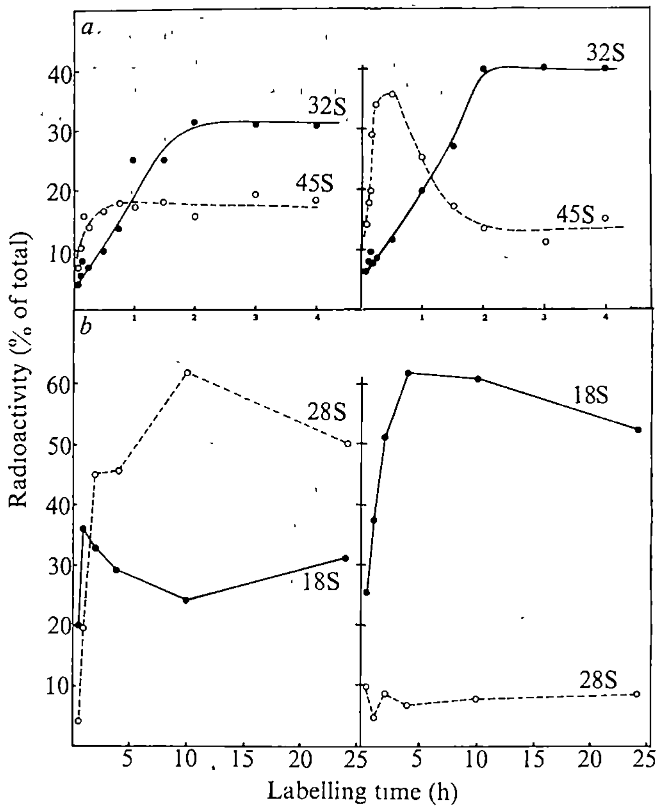

Fig. 1 Accumulation of nuclear (*a*) and cytoplasmic (*b*) ribosomal RNA in *ts 442E* and BHK cells. Monolayer cultures of wild-type BHK (left panels) and *ts 422E* cells (right panels) were shifted from 33 to 39 °C, and after 12 h were labelled with 25 µCi ml^{-1} 5,6-^{3}H-uridine (37.6 Ci mmol^{-1}) in Dulbecco–Vogt Modified Eagle's Medium (DME) supplemented with 3 µM uridine plus 10% calf serum. Collected cells were lysed in 2% citric acid, 0.5% Triton X-100 (Rohm and Haas, Philadelphia) and nuclei were deposited and washed twice with the same buffer by centrifugation at 800*g* for 2 min Nuclear pellets suspended in 10 mM Tris-HCl (*p*H 9.0), 0.2 M NaCl, 10 mM EDTA, 0.5% SDS (NETS buffer) were extruded through a 22 gauge needle to shear DNA then alternately extracted at room temperature with phenol: chloroform. isoamyl alcohol (50:50:1) and chloroform · isoamylalcohol (24:1) until the interfacial layer was clear of denatured protein[18] Post-mitochondrial supernatants prepared from cells lysed as described previously[19] by centrifugation at 10,000 r.p.m. for 10 min in the Sorvall SS-34 rotor, were adjusted to 70 mM $MgCl_2$ for 45 min at 0 °C to precipitate cytoplasmic ribonucleoproteins (RNP)[20]. Ribosomes pelleted by centrifugation at 10,000 r.p m for 10 min were dissolved in NETS buffer, deproteinised, and RNA was precipitated with 2 vol. 95% ethanol. Nuclear RNA samples dissolved in 200 µl NETS buffer were centrifuged in 4 ml linear 15–30% sucrose density gradients in NETS buffer at 23 °C for 90 min at 56,000 r p.m. in a Beckman SW56 rotor. Cytoplasmic RNA dissolved in 1 ml NETS buffer were centrifuged in 36 ml SDS-containing 15–30% sucrose density gradients at 23 °C for 17 h at 23,000 r.p.m in a Beckman SW27 rotor. Radioactivity in 45S, 32S, 28S, 18S RNA were expressed as a percentage of the total acid-insoluble radioactivity in the gradient, including the pellets. In these analyses, 32S and 36S pre-rRNAs were combined since the distribution of these RNA molecules can vary in *ts 422E* cells[21].

28S rRNA that appears in *ts 422E* cytoplasm at 39 °C is markedly methyl deficient.

In a precursor–product relationship, a reduced rate of conversion of intermediate species results in an increased proportion of precursor. If both wild-type and mutant cells are grown at 39 °C, inhibition of 45S processing in *ts 422E* should result in apparent nuclear accumulation of precursor molecules in the temperature-sensitive variants. This prediction was tested in the experiment shown in Fig. 1 where both cell types were labelled with ^{3}H-uridine at the non-permissive temperature and the kinetics of accumulation of nuclear pre-rRNA and cytoplasmic rRNA were followed.

The cells were labelled in growth medium supplemented with unlabelled uridine to ensure that the specific activity of the UTP pool would be constant throughout the period of incorporation (unpublished data). In BHK cells, 45S and 32S pre-rRNAs and 28S and 18S rRNAs exhibited accumulation patterns consistent with their known precursor–product relationship[7,8] (Fig. 1). Accumulation of 45S pre-rRNA in the mutant was, however, aberrant. During the first 30 min of labelling, the content of nuclear 45S RNA in *ts 422E* was 30–35% of the total labelled RNA compared with a maximum of only 15–20% in BHK cells in similar conditions (Fig. 1). As stable nuclear and nucleolar RNAs accumulated, the fraction of radioactivity in 45S pre-rRNA decreased until by 2–3 h the relative amount of pre-rRNA was the same in the mutant and wild-type cells. The kinetics of mature cytoplasmic 18S and 28S rRNA accumulation in the mutant showed, as before[5], a marked inhibition of new 28S rRNA appearance at 39 °C. The early increase in nuclear 45S pre-rRNA content in the mutant indicated an expansion of the nucleolar pool of 45S pre-rRNA, suggesting that the transcript was deficient in some essential aspect.

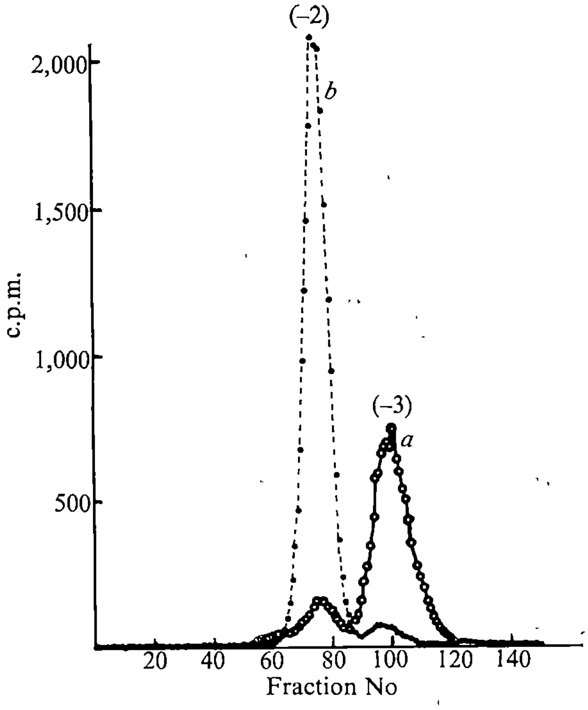

Fig. 2 Separation of mononucleotides and dinucleotides by DEAE–Sephadex chromatography. BHK cells were labelled for 3.5 h with (*a*) 20 μCi ml^{-1} L-methyl-^{3}H-methionine (6.3 Ci mmol^{-1}) and (*b*) 0.1 μCi ml^{-1} ^{14}C-uridine (57 mCi mmol^{-1}) in DME containing 20 μM methionine, 4 μM uridine, 20 mM sodium formate, and 20 μM guanosine to suppress non-methyl purine ring labelling[12] beginning 16 h after shift up to 39 °C. Ribosomal RNA prepared from $MgCl_2$-precipitated cytoplasmic RNP was sedimented at 23 °C in a 36 ml SDS-containing 15–30% sucrose gradient for 17 h at 23,000 r.p.m in an SW27 rotor. 18S rRNA was precipitated from the gradient with 2 vol 95% ethanol, dissolved in 2 ml 0.3 N KOH, and hydrolysed for 18 h at 37 °C. The alkaline hydrolysate was neutralised with ice-cold 0.3 N perchloric acid, chilled at 0 °C for 10 min, and centrifuged at 5,000 r.p.m. for 5 min to remove precipitated potassium perchlorate. The neutralised sample was applied to a column of DEAE–Sephadex (19 × 1.2 cm; A-25, Pharmacia Fine Chemicals, Piscataway, New Jersey), washed into the column with 25 ml 20 mM Tris-HCl (*p*H 7.4), 7 M urea, 0.1 M NaCl, and eluted with a linear 100 ml gradient of 0.1–0.4 M NaCl in 20 mM Tris-HCl (*p*H 7.4), and 7 M urea[10,22]. After completion of the gradient, the column was washed with 40 ml 0.4 M NaCl, 20 mM Tris-HCl (*p*H 7.4), and 7 M urea. Fractions were assayed for radioactivity by counting in a gel of 2.0 ml H_2O plus 10 ml scintillation fluid containing 2 parts xylene, 1 part Triton X-100 and 8 g Omnifluor (New England Nuclear, Boston, Massachusetts) per litre.

Because methylation of 45S pre-rRNA is an apparent requirement for completion of ribosome maturation[1,9], we compared the extent of 45S methylation in the wild-type and mutant cells. Ninety-five per cent of methylations found in HeLa cell 45S pre-rRNA are modifications of the 2′-OH ribose moiety of the nucleoside[1]. Since this modification protects the phosphodiester linkage between the 3′-hydroxyl of that nucleotide and the 5′-hydroxyl of the neighbouring nucleotide from alkaline hydrolysis, separation of mononucleotides from dinucleotides on anion exchange columns[10] after alkaline hydrolysis provides an estimate of rRNA methylation (Fig. 2). As shown in Fig. 2, approximately 96% of the uridine incorporated into 18S rRNA is found in the mononucleotide fraction, but methyl label is preferentially incorporated into the dinucleotides. This pattern demonstrates the general labelling characteristics of ^{3}H-uridine and the relative specificity of methyl-^{3}H-methionine for incorporation into 2′-hydroxyl ribose residues.

The relative methylation of pre-rRNA in BHK and *ts 422E* cell lines was examined initially by pulse labelling at 39 °C with methyl-^{3}H-methionine and ^{14}C-uridine (Table 1). The ratio of ^{3}H-methyl/^{14}C-uridine radioactivity was used as an index of the extent of methylation. By this criterion, 45S pre-rRNA from the mutant is approximately 50% undermethylated, and the 32S RNA has only a third of the methyl content of wild-type 32S RNA at the non-permissive temperature. Since 28S rRNA in mammalian cells is derived from the 32S molecule[11,12], undermethylation of 28S sequences would result in 32S RNA exhibiting a lower degree of methylation than complete 45S molecules which also contain properly methylated 18S RNA sequences (Table 1).

The apparent undermethylation observed in *ts 422E* at 39 °C could also be explained by decreased uptake of methionine relative to uridine. Therefore, we estimated ribose methylation of precursor and mature ribosomal RNA in BHK and *ts 422E* cells by measuring radioactivity in alkali-resistant dinucleotides of uridine-labelled cells. Although this approach measured only 2′-*O*-methylribose in or adjacent to uridine and/or cytidine, difficulties resulting from possible pool and transport differences were eliminated. The extent of undermethylation would seem less by

Table 1 Relative extents of methylation at 39 °C in BHK and *ts 422E* pre-rRNA

RNA	Radioactivity (c.p.m.) ^{3}H-methyl	^{14}C-uridine	^{3}H-methyl/ ^{14}C-uridine
BHK 45S	2,230	8,034	0.28
422E 45S	3,407	21,689	0.16
BHK 32S	5,115	28,611	0.18
422E 32S	5,717	98,716	0.06

BHK and *ts 422E* cells were labelled 45 min with 25 μCi ml^{-1} L-methyl-^{3}H-methionine and 0.1 μCi ml^{-1} ^{14}C-uridine as in Fig. 2, beginning 18 h after shifting to 39 °C. Nucleoli prepared as described by Penman[23] were deproteinised (Fig. 1) and nucleolar RNA was centrifuged in 36 ml linear 15–30% sucrose density gradients in NETS at 20,000 r.p.m. for 16 h at 23 °C in an SW27 rotor. Aliquots (50 μl) of gradient fractions were assayed for acid-insoluble radioactivity. Nominal 45S RNA and 32S RNA peak fractions were precipitated with ethanol, and chromatographed on DEAE–Sephadex after alkaline hydrolysis as in Fig. 2. Values represent total combined radioactivity in the mononucleotide and dinucleotide peaks. ●

Table 2 Estimation of 2′-*O*-methyl ribose in uridine-labelled ribosomal pre-rRNA

	Radioactivity					
	Mononucleotides (−2) (c.p.m. × 10^{-4})		Dinucleotides (−3) (c.p.m. × 10^{-3})		Total radioactivity in dinucleotides (%)	
	33 °C	39 °C	33 °C	39 °C	33 °C	39 °C
Experiment 1						
BHK 45S	–	60.0	–	8.3	–	1.36
422E 45S	–	53.3	–	4.8	–	0.89
Experiment 2						
BHK 45S + 32S	75.6	105.1	18.1	24.7	2.33	2.34
422E 45S + 32S	252.8	57.9	56.9	11.9	2.20	1.75
BHK 28S	82.1	70.7	23.1	19.5	2.73	2.69
422E 28S	112.0	7.7	31.3	1.0	2.55	1.32
BHK 18S	67.6	25.5	25.3	11.9	3.60	4.47
422E 18S	115.1	38.2	57.0	17.1	4.70	4.30

In experiment 1, BHK and *ts 422E* cells were pulse labelled in DME with 100 μCi ml^{-1} ^{3}H-uridine beginning 22 h after shift-up to 39 °C. 45S pre-rRNA prepared by sucrose density gradient sedimentation of nucleolar RNA was hydrolysed with 0.3 N KOH at 37 °C and chromatographed on DEAE–Sephadex (Table 1). In experiment 2, wild-type and mutant cells were labelled 3.5 h with 5 μCi ml^{-1} ^{14}C-uridine at 33 °C. 45S and 32S nucleolar RNA was prepared and analysed as described above. $MgCl_2$-precipitated cytoplasmic RNP was deproteinised and RNA was sedimented in sucrose density gradients as in Fig. 1, and the major fractions under the separated 28S and 18S rRNA peaks were pooled and precipitated with 2 vol 95% ethanol. Contaminating poly(A)-containing mRNA was removed by oligo(dT)-cellulose chromatography[25]. Purified rRNAs hydrolysed with KOH were chromatographed on DEAE–Sephadex. Details of experiment 3 are the same as for experiment 2, except that wild-type and mutant cells were labelled beginning 19 h after shift-up to 39 °C. Three replicate samples of uridine-labelled HeLa cell rRNA were hydrolysed and chromatographed on DEAE–Sephadex to test the reproducibility of the technique. For these replicates the mean fraction of ^{3}H-uridine in the dinucleotide region was 2.83% with a standard deviation of 0.096 or 3.4% of the mean value.

this assay, because these experiments only scored for uridine label in dinucleotides against mononucleotides.

The results of DEAE–Sephadex chromatography of alkali-hydrolysed RNA from cells labelled for 30 min or 3.5 h with uridine (Table 2) confirmed the previously observed undermethylation of *ts 422E* nucleolar and 28S cytoplasmic rRNA. With the exception of 18S rRNA which yielded less reproducible values than other species of RNA, the differences between mutant and wild-type cells seen at the permissive temperature can be attributed to variation in the method (see legend to Table 2), but the differences observed at 39 °C must reflect the conditional lethal phenotype. The similarity of RNA methylation in the wild-type cells at 33 and 39 °C is a further indication of the accuracy of this analysis (Table 2).

Methylation of rRNA is of two types: 2′-*O*-ribose modification and methylation of specific sites in the purine and pyrimidine rings. In HeLa cells, 80–90% of methyl derivatives in rRNA are modifications of the 2-OH-ribose moiety[1,13,14]. The experiments presented above clearly show deficient methylation of 2′-*O*-ribose moieties in 28S rRNA and its precursors in *ts 422E* cells grown and labelled at 39 °C. Since phosphodiester bonds adjacent to base methyl derivatives may also be resistant to alkaline hydrolysis[15], however, the observed differences may not be due exclusively to alterations in 2′-*O*-methylation.

Physical studies have shown that methylation of ribose residues can alter the conformation of single-stranded RNA molecules[16] Although the details of eukaryotic ribosome maturation are not known, it is likely that processing of 28S rRNA requires the sequential association of specific proteins and 32S RNA to give rise to the nucleolar 55S pre-ribosomal particles. Inadequate methylation of the 28S segment could alter the conformation of the ribosomal precursors, preventing the normal association of processing enzymes and thus inhibiting the appearance of 28S RNA in the cytoplasm. Assuming 18S RNA sequences at the 5′ end of the transcript[17] are properly methylated, and that methylation and transcription are closely coupled, it is possible that the distal portions of the transcript containing 28S sequences are inhibited from being adequately modified. Alternatively, a precursor-associated protein may be the primary target of the temperature-sensitive lesion, placing the transcript in a conformation within the precursor particle that is unfavourable for completion of adequate methylation.

After submission of this paper, Toniolo and Basilico reported increased accumulation of nucleolar pre-rRNA in *ts 422E* at 39 °C compared with wild-type cells, but these authors did not detect differences in extent of pre-rRNA methylation[25]. Our assay for rRNA methylation may have been more specific, however, since we labelled with methionine in conditions which suppressed non-methyl purine ring labelling (see legend to Fig. 2).

This work was supported by grants from the NIH. A.K. is a recipient of a Cancer Research Scholar Award from the American Cancer Society, Massachusetts Division; A.J.O. is a Research Fellow of the Medical Foundation Inc., Boston, Massachusetts. The wild-type and mutant cell lines were generously supplied by Dr C. Basilico. We thank Ms R. Huffman and D. Frederick for valuable assistance and Dr R. A. Malt for encouragement and extensive use of his facilities.

ANDRE J. OUELLETTE
EVERETT BANDMAN
AJIT KUMAR

Cell Biology Unit,
Shriners Burns Institute,
51 Blossom Street,
Boston, Massachusetts 02114

Received March 29, accepted June 8, 1976.

[1] Maden, B E. H., and Salim, M , *J. molec Biol.*, **88**, 133–164 (1974)
[2] Maden, B. E. H., in *Progr. Biophys. molec. Biol*, **22** (edit. by Butler, J A. V., and Noble, D), 127–177 (Pergamon, Oxford and New York, 1971).
[3] Warner, J R , in *Ribosomes* (edit. by Nomura, M., Tissieres, A , and Lengyel, P.), 461–488 (Cold Spring Harbor Laboratory, 1974).
[4] Meiss, H. K., and Basilico, C , *Nature new Biol.*, 239, 66–68 (1972)
[5] Toniolo, D , Meiss, H. K., and Basilico, C., *Proc. natn. Acad Sci. U.S A.*, **70**, 1273–1277 (1973).
[6] Darnell, J. E., *Bact Rev.*, **32**, 262–290 (1968).
[7] Penman, S., Smith, I , and Holtzman, E., *Science*, **154**, 786–789 (1966).
[8] Greenberg, H., and Penman, S., *J molec. Biol.*, **21**, 527–535 (1966).
[9] Vaughan. M. H., Jr, Soeiro. R., Warner, J. R., and Darnell, J. E , Jr, *Proc. natn. Acad. Sci. U S.A.*, **58**, 1527–1534 (1967).
[10] Tener, G. M , in *Methods in Enzymology*, **12** (edit. by Grossman, L., and Moldave, K), 398–404 (Academic, New York and London, 1967).
[11] Weinberg, R. A., and Penman, S , *J. molec. Biol.*, **47**, 169–178 (1970).
[12] Maden, B. E. H., Salim, M., and Summers, D. F., *Nature new biol* , **237**, 5–9 (1972).
[13] Brown, G. M., and Attardi, G , *Biochem biophys. Res Commun.*, 20, 298–302 (1965).
[14] Wagner, E K., Penman, S , and Ingram, V M., *J. molec Biol* , **29**, 371–387 (1967).
[15] Nichols, J L., and Lane, B. G., *Biochim. biophys. Acta*, **119**, 649–651 (1966).
[16] Rottman, F., Friderici, K , Comstock, P , and Khan, K , *Biochemistry*, **13**, 2762–2771 (1974).
[17] Liau, M C., and Hurlbert, R. B , *J. molec. Biol.*, **98**, 321–332 (1975).
[18] Perry, R P., LaTorre, J , Kelley, D. E., and Greenberg, J R., *Biochim. biophys. Acta*, **262**, 220–226 (1972).
[19] Kumar, A., Bandman, E., and Melvin, W. T , *Nature*, **259**, 692–694 (1976).
[20] Warner, J. R., *J molec Biol* , **19**, 383–398 (1966).
[21] Winocov, I , *J. molec. Biol.*, **100**, 141–155 (1976).
[22] Ouellette, A. J., Frederick, D., and Malt, R A , *Biochemistry*, **14**, 4361–4367 (1975).
[23] Penman, S., *J. molec. Biol* , **12**, 117–129 (1966)
[24] Aviv, H., and Leder, P., *Proc. natn. Acad. Sci U.S.A.*, **69**, 1408–1412 (1972).
[25] Toniolo, D., and Basilico, C., *Biochim. biophys. Acta*, **425**, 409–418 (1976).

Restriction of template capacity of rat liver chromatin by a non-histone peptide from calf thymus

We have reported[1] the isolation of a thymic peptide which strongly inhibits DNA-directed RNA polymerase *in vitro*. We have shown that transcription is controlled at the level of initiation. The active factor was isolated from aqueous ultrafiltered thymus extracts, purified by chromatography, first on DEAE–cellulose and then on Dowex 50 WX2, and characterised as a peptide of low molecular weight (<5,000). Its biological activity cannot be attributed to the presence of a nuclease or of a histone fragment. The inhibition of RNA synthesis is due to an ionic interaction between the peptide and DNA. The physicochemical and thermodynamic properties of this interaction are described elsewhere[2]. We report here the effect(s) of the thymic peptide on transcription of rat liver chromatin With some obvious limitations[3], the *in vitro* chromatin transcription system is closer to the *in vivo* state than the purified DNA. Our experiments were prompted by our previous results, which demonstrated that the thymic extract modifies the physicochemical state of DNA and the interactions between DNA and nuclear proteins in the liver of old rats[4,5].

The purified thymic fraction, designated fraction 1_6 (see legend to Fig. 1), strongly inhibited chromatin transcription by *Escherichia coli* RNA polymerase (Fig 1). This effect was proportional to the concentration of factor up to 70% inhibition. Contrary to our data on inhibition of DNA transcription[1], even when doses of the factor larger than shown in Fig. 1 were added, chromatin transcription was never completely stopped, indicating that the thymic factor affected only part of the RNA synthetic pathways. Since the thymic factor acts on initiation of transcription rather than on elongation[1], it is possible that the peptide cannot inhibit chromatin transcription by endogenous RNA polymerases, which are probably linked to the chromatin itself. We therefore tested for chromatin-directed RNA synthesis *in vitro* without added *E. coli* polymerase, in both the presence and absence of the thymic extract. Figure 2*a* shows that, in the absence of exogenous RNA polymerase, chromatin transcription constituted only 10–15% of total transcription observed in the presence of exogenous RNA polymerase from *E. coli* In these conditions the thymic factor was ineffective. These data support the hypothesis that the thymic factor exerts its activity on initiation.

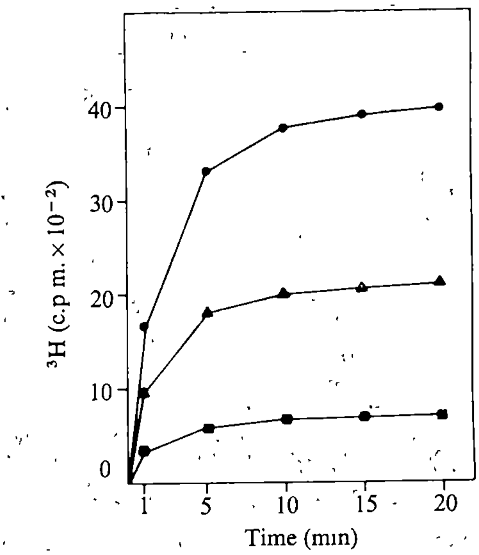

Fig. 1 Time course of RNA synthesis directed by rat liver chromatin: incorporation of ^{3}H-CMP. 0 75 ml of the complete incubation mixture for RNA synthesis contained: 30 μmol Tris buffer (*p*H 7.5), 3 μmol $MgCl_2$, 0.75 μmol $MnCl_2$, 9 μmol β-mercaptoethanol, 0.3 μmol each of ATP, GTP, CTP and UTP, 2 nmol ^{3}H-CTP (22 Ci, nmol^{-1}, Radiochemical Centre, Amersham), 4 U RNA polymerase from *E. coli* and 10 μg chromatin DNA. 0.1 or 0.2 ml of the purified thymic fraction corresponding respectively to 4 μg and 8 μg protein was added to the incubation mixture; in the controls the extract was replaced by 0.1–0.2 ml saline. Incubation for RNA synthesis was carried out in 10-ml Erlenmeyer flasks at 37 °C, 75 shakes per min. Determinations of the radioactivity incorporated into the acid-insoluble fraction of RNA, the preparation of the thymus extracts and the purification of the active factor, designated fraction 1_6, were carried out as before[1]. Fraction 1_6 consisted of peptide(s) of low molecular weight: thin layer high voltage electrophoresis showed four ninhydrin-positive bands. As far as the affinity binding between DNA and thymus factor is concerned, evidence presented elsewhere[2] indicates that when DNA at 1 mg ml^{-1} is incubated with a fraction 1_6 (100 μg ml^{-1}), about 20 μg protein binds to DNA. This is taken as evidence that fraction 1_6 is mostly composed of active thymic factor. Total chromatin was extracted from livers of 12-month-old Sprague–Dawley rats according to the modified method of Bostock and Prescott[12]: nuclei were not broken by sonication but by homogenisation twice in Potter Helvehyem after rapid freezing and thawing. We modified Bostock and Prescott's method to obtain the chromatin in the most native state possible. The RNA polymerase from *E coli* was purified as described before[13]. The data in the experiments described are the average of experiments made in duplicate, the values of which have never shown variations above 10%. ●, Control; ▲, fraction 1_6:5 μg protein per ml (final concentration); ■, 10 μg protein per ml (final concentration).

Table 1 Template capacity of calf thymus DNA and of rat liver heterochromatin and euchromatin

Reaction mixture		^{3}H-CMP incorporation (c.p.m. mean ± s.e.m.) Control	Thymus factor added	% Inhibition
Calf thymus DNA	+ *E. coli* RNA polymerase	22,015±810	1,601±245	93
Calf thymus DNA	+ calf thymus RNA polymerase	20,242±640	1,721±315	91
Rat liver heterochromatin	+ *E. coli* RNA polymerase	2,570±180	960±105	63
Rat liver euchromatin	+ *E. coli* RNA polymerase	4,015±215	1,120±148	72
Rat liver heterochromatin	+ calf thymus RNA polymerase	1,137±110	653±80	42
Rat liver euchromatin	+ calf thymus RNA polymerase	1,701±98	855±60	49
Rat liver heterochromatin	+ rat liver RNA polymerase	1,580±124	615±132	61
Rat liver euchromatin	+ rat liver RNA polymerase	2,424±170	715±97	70

Incorporation of ^{3}H-CMP by means of RNA polymerase from *E. coli*, calf thymus or rat liver, in both the presence and absence of the thymic factor (final concentration 10 μg protein per ml), after 30 min of incubation. The preparation of thymus extract, the incubation mixture and other conditions for RNA synthesis were as in the legend to Fig. 1. RNA polymerase from *E. coli* was purified as described by Hurwitz[13] and the RNA polymerases II from calf thymus and rat liver as described by Stein and Hausen[14]. The extraction of the chromatin from rat liver and the fractionation of the total chromatin in heterochromatin and euchromatin were carried out according to the modified method (see legend to Fig. 1) of Bostock and Prescott[12] In some experiments the fractionation of the total chromatin in heterochromatin and euchromatin was carried out by means of gel filtration on BioGel A-50 (BioRad) as described by Janowski *et al.*[15]. The determinations of the buoyant density and of the DNA, RNA and protein contents of hetero- and euchromatin were effected by means of the determination of the refraction index[16] and of diphenylamine, orcinol and Lowry reactions respectively:

	Buoyant density	DNA	RNA	Protein
Heterochromatin	1.711	1	0.160	2.071
Euchromatin	1.699	1	0.175	1.714

To confirm this hypothesis, chromatin was preincubated for 1 min in the presence of *E. coli* RNA polymerase and UTP, GTP and ATP nucleotides. At time zero the reaction mixture was made 0.4 M in ammonium sulphate, the thymic fraction or saline was added and the propagation reaction was started by adding CTP and ^{3}H-CTP. During preincubation polymerase binds to chromatin and initiates transcription, but propagation is blocked by the absence of CTP: when CTP is added propagation proceeds, but the presence of high concentrations of ammonium sulphate precludes further initiation or reinitiation[6,7]. Figure 2*b* shows that in these conditions the thymic factor did not affect RNA synthesis and therefore inhibited the initiation reaction of transcription. Later we investigated the action of the thymic factor on transcription in different states of chromatin condensation: that is heterochromatin and euchromatin, the characteristics of which are given in the legend to Table 1. The transcription of heterochromatin and euchromatin, in both the absence and presence of thymic factor, was tested by adding various RNA polymerases: different specificities of chromatin transcription by RNA polymerase from prokaryotic or eukaryotic cells have been reported[8,9]. RNA polymerases from *E. coli* and RNA polymerases II from rat liver and calf thymus were used. Table 1 shows that the thymic peptide inhibited transcription of heterochromatin and euchromatin by polymerases from both prokaryotic and eukaryotic cells, regardless of the organ of origin of eukaryotic polymerases.

The data presented here provide evidence for our hypothesis that the thymic peptide is responsible for regulation at the level of transcription. The addition of the factor restricts the distribution of available sites for the initiation of transcription on the chromatin. These observations suggest that the factor regulates transcriptional capacity, which may be related to cell differentiation. This is supported by our finding that the thymic factor was not extracted from differentiated tissues such as kidney, whereas it was particularly abundant in bull spermatozoa (unpublished results). The inhibition of chromatin transcription by this factor extracted from spermatozoa may explain our previous data[10] showing that extracts of spermatozoa inhibit differentiation of seminiferous tubule cells of testicles from young rabbits.

The data presented here are in good agreement with the demonstration[11] that chromatin from several mammalian species contains non-histone protein fractions including specific negative regulatory factors ionically linked to DNA.

Fig. 2 Time course of RNA synthesis directed by rat liver chromatin: incorporation of ^{3}H-CMP. *a*, In the absence of exogenous *E. coli* RNA polymerase in the incubation mixture. Other ingredients for RNA synthesis were as given in the legend to Fig. 1. ●, Control; ■, thymic fraction 1_6 (final concentration 10 μg protein per ml). *b*, The chromatin was preincubated for 1 min in the presence of *E. coli* RNA polymerase and ATP, GTP and UTP. At time zero the reaction mixture was made 0.4 M in ammonium sulphate, thymic factor or saline was added and the propagation reaction was started by adding CTP and ^{3}H-CTP. Incubation mixture and other conditions for RNA synthesis were as given in the legend to Fig. 1. ●, Control; ■, fraction 1_6 (final concentration 10 μg protein per ml).

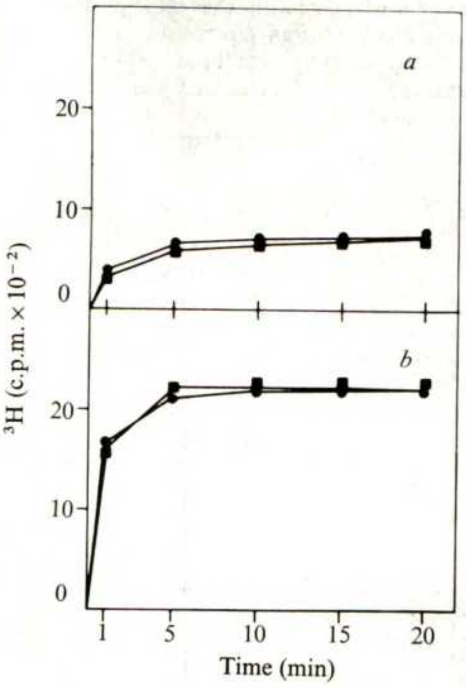

G. L. GIANFRANCESCHI
D. AMICI
L. GUGLIELMI

Institute of General Physiology,
University of Camerino, Italy

Received February 26; accepted June 25, 1976.

1 Gianfranceschi, G. L., Amici, D., and Guglielmi, L., *Biochim. biophys. Acta*, **414**, 9–19 (1975).
2 Gianfranceschi, G. L., Amici, D., and Guglielmi, L., *Molec. Biol. Reps.* (in the press).
3 Honjo, T., and Reeder, R. H., *Biochemistry*, **13**, 1896–1899 (1974).
4 Amici, D., Gianfranceschi, G. L., Marsili, G., and Michetti, L., *Experientia*, **30**, 633–635 (1974).
5 Gianfranceschi, G. L., Amici, D., and Guglielmi, L., *Experientia*, **30**, 1049–1050 (1974).
6 Cedar, H., and Fenselfeld, G., *J. molec. Biol.*, **77**, 237–254 (1973).
7 Simpson, R. T., *Proc. natn. Acad. Sci. U.S.A.*, **71**, 2740–2743 (1974).
8 Keshgegian, A. A., Garibian, G. S., and Furth, J. J., *Biochemistry*, **12**, 4337–4342 (1973).
9 Henner, D., Kelley, R. I., and Furth, J. J., *Biochemistry*, **14**, 4764–4771 (1975).
10 Gianfranceschi, G. L., Magaudda, G., Amici, D., and Piantanelli, L., *Endokrinologie*, **63**, 176–180 (1974).
11 Paul, J., and Gilmour, R. S., in *The Structure and Function of Chromatin*, Ciba Found. Symp. No. 28, 181–192 (Elsevier–Excerpta Medica–North-Holland, Amsterdam, 1975).
12 Bostock, C. J., and Prescott, D. M., *J. molec. Biol.*, **60**, 151–162 (1971).
13 Hurwitz, J., *Meth. Enzymol.*, **6**, 23–27 (1963).
14 Stein, H., and Hausen, P., *Eur. J. Biochem.*, **14**, 270–277 (1970).
15 Janowski, M., Nasser, D. S., and McCarthy, B. J., *Acta Endocr.*, **71**, Suppl. 168, 112–125 (1972).
16 Yasmineh, W. G., and Yunis, J. J., *Biochem. biophys. Res. Commun.*, **35**, 779–782 (1969).

Independence of plasmid incompatibility and replication control functions in *Staphylococcus aureus*

THERE are two basic requirements for the stable maintenance of an autonomous plasmid replicon, namely replication at a constant rate with respect to the cell division cycle and distribution of replicas to daughter cells.

The precise nature of the genetic functions involved in satisfying these two requirements has yet to be ascertained; but it is probable that in general, both plasmid-linked and host chromosome-linked genetic determinants are involved. Of the former there are two well defined functional classes: (1) genes involved directly in replication[1–3] and its control, including the origin, and (2) genes involved in the determination of plasmid incompatibility specificity[4–6]. No genes known to affect distribution of plasmid replicas have been identified.

Incompatibility, the inability of closely related plasmids to be stably co-maintained[7], has been found for the penicillinase plasmids of *S. aureus* to be determined by a genetic locus, *inc*, that has not been separable by recombination from *repA*, a gene encoding a diffusible product required for autonomous replication[1,4]. Together, these two genetic functions plus the origin define a local region of the plasmid that is both necessary and sufficient for autonomy, the *mcr* region[4]. Similar localisation of autonomy functions has been observed for plasmids of enteric organisms[8].

Because the replication of a plasmid entering a cell carrying another with which it is incompatible is temporarily or, possibly in some cases permanently, inhibited[9–11], it has been

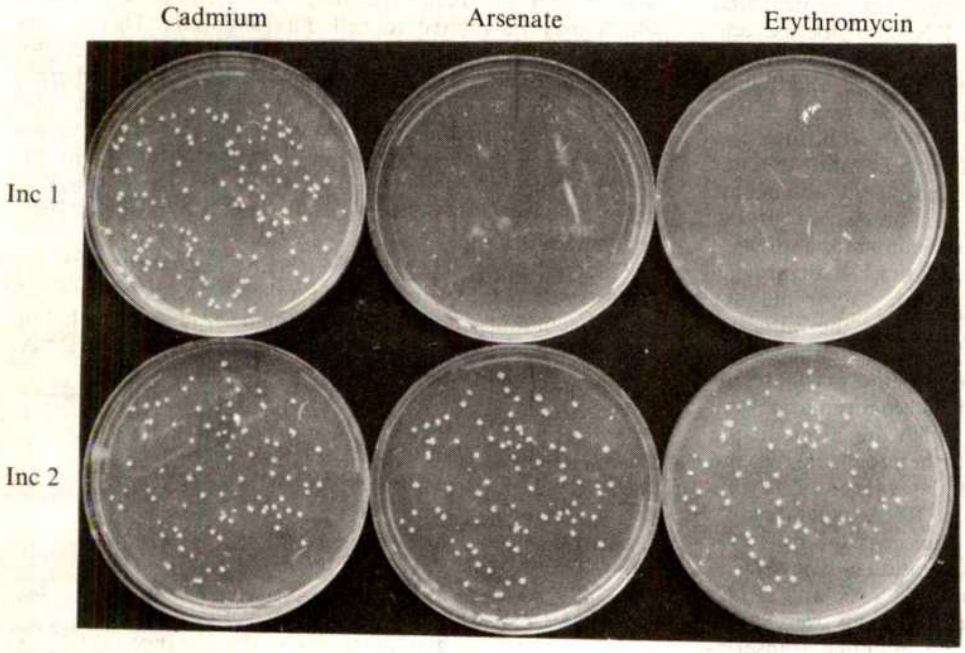

Fig. 1 Incompatibility between integrated and autonomous plasmids. Cultures of RN2428 (upper part of photograph) and RN2429 were diluted and plated on non-selective medium and incubated at 43 °C. The resulting colonies were replica-plated to three different selective media: GL-cadmium agar (selective for the integrated plasmid, pRN3091); GL-arsenate; and GL-erythromycin (selective for the autonomous plasmid, pRN3025 and pRN4031). The replicas were photographed after 18 h of incubation at 32 °C.

assumed that the incompatibility determinant is involved in replication control, for example, it may encode a specific repressor of replication[12].

In this report we present evidence suggesting that in the *S. aureus* system, the plasmid *inc* and *repA* determinants are genetically as well as functionally distinct and that the *inc* locus is not involved in replication or its control but instead may be involved in the distribution of replicas.

Two different chromosomally integrated derivatives of an incompatibility type 1 (Inc1) *S. aureus* penicillinase plasmid, pI258, were studied. One of these, pRN3150, is incompatibility-defective, yet expresses the *repA* function[1]; the other, pRN3091, is *repA*$^-$ (thermosensitive for replication) yet expresses incompatibility at the restrictive as well as at the permissive temperature. Strains carrying the *repA*$^+$ *inc*$^-$ pRN3150 were able to maintain stably and complement for replication seven different superinfecting *repA*$^-$ Inc1 plasmids[1]. But a recombinant derivative, pRN3151, in which the *repA36* allele had been substituted for the *repA*$^+$, was unable to complement for replication any of the seven *rep*$^-$ mutants (unpublished data); thus, there is evidence for only one plasmid-linked *rep* cistron.

The converse test, namely whether a *repA*$^-$ mutant can express incompatibility or not was also performed with an integrated plasmid (in this case the Rep$^-$(Ts) pRN3091[13]) since there is no simple way to test an *autonomous* Rep$^-$(Ts) plasmid for the expression of incompatibility at the restrictive temperature. Transductional superinfection of strain RN1979 (carrying the integrated pRN3091) with plasmids pRN3025 (Inc1) and pRN4031 (Inc2) was accomplished by selection for erythromycin resistance[14]. Eight transductants from each cross were examined and the following results were obtained: as expected, the Inc2 plasmid, pRN4031, was always maintained stably without selection. The Inc1 plasmid, pRN3025, could also be maintained but only by continued selection for erythromycin or arsenate resistance. Organisms grown on arsenate-containing medium, selective for the donor plasmid, were diluted and plated on non-selective medium (GL agar[8]) and allowed to form colonies at 32 °C and at 43 °C (the restrictive temperature for the Rep$^-$(Ts) mutation). These were then replicated separately to plates containing cadmium, arsenate, or erythromycin. As shown in Fig. 1, colonies of RN2428 (RN1979 superinfected with the *inc1* plasmid, pRN3025) lost arsenate and erythromycin resistance during growth at 43 °C on non-selective medium, whereas colonies of

Table 1 Staphylococcal strains and plasmids*

a Plasmids

Plasmid number	Genotype	Derivation
pI258	$bla^+ asa^+ asi^+ ermB^+ inc1^+ mer^+ rep^+ cadA^+ bis^+ lea^+$	Naturally-occurring
pII147	$bla^+ asa^+ inc2^+ rep^+ mer^+ cadB^+ bis^+ lea^+ cadA^+$	Naturally-occurring
pRN3025	pI258 *bla-401 cadA52* $ermB^+$	Mutation of pI258
pRN3032	pI258 *bla-401 cadA52 mer-14 repA36*	Mutation of pI258
pRN3091	pI258 *blaI443 asa-33 ermB20 repA18*	Mutation of pI258
pRN3150	pI258 *blaI443 asa-33 ermB18* $inc1^-$ $repA^+$	Integration of pI258 mutant
pRN3151	pI258 *blaI443 asa-33 ermB18* $inc1^-$ *repA36*	Recombinant pRN3150 × pRN3032
pRN4031	pII147[$inc2^+ cadB^+ bis^+ lea^+$]:pI258[*bla-401* $asa^+ asi^+ ermB^+$]mer^+ *cadA11*	Recombinant pII147 × pI258

b Strains†

Strain number	Plasmids contained	Reference
RN325	pRN4031	
RN557	pRN3025	
RN1500	Ω42[pRN3150]	ref. 1
RN1974	Ω42[pRN3151]	This report
RN1979	Ω50[pRN3091]	ref. 13
RN2428	Ω50[pRN3091];pRN3025	This report
RN2429	Ω50[pRN3091];pRN4031	This report

* Gene abbreviations and other nomenclature are as recommended by Novick *et al.*[7].
† The host bacterium is strain 8325–4, except for RN1974 in which the host is strain 147 (ref. 14).

RN2429 did not. Similar results were obtained for colonies of these two strains grown at 32 °C. These results are interpreted as the expression of incompatibility by the intergrated *repA*$^-$ plasmid at both permissive and restrictive temperatures, demonstrating the independence of the *inc* and *repA* determinants.

To verify the inference that loss of arsenate and erythromycin resistance is an indication of loss of the entire plasmid, thirty colonies of strain RN2428 that had been grown on non-selective medium were scored by disk sensitivity tests and by the PNCB stain for penicillinase activity[14]. There were scorable allelic differences at four plasmid loci —*bla, asa, cad*, and *erm*; on subculture, twenty-eight of the colonies showed the same resistance pattern as the resident plasmid and a penicillinase stain pattern indicative of homozygosity for the integrated *bla* locus. Two colonies showed stable patterns suggestive of recombination between the integrated and autonomous plasmids.

Although it seemed likely on the basis of the foregoing results that the superinfecting penicillinase plasmid could replicate in the autonomous state, it seemed important to attempt to demonstrate this replication directly and to assess it quantitatively. Accordingly, a dye-buoyant density gradient analysis of plasmid replication was done[1], and the results shown in Fig. 2 were obtained. Incorporation of thymidine into circular duplex plasmid DNA by the incompatible heterozygote, RN2428 (Fig. 2*a*) was nearly as extensive as that by the compatible heterozygote RN2429 (Fig. 2*b*), by comparison with strains carrying the autonomous plasmid alone in each case. As this result could have been due to the presence of unsuspected recombinants, the cultures were tested at the end of the labelling period for the proportion of organisms that would still lose the superinfecting plasmid during incubation on non-selective media. Accordingly, a replica-plating test similar to that shown in Fig. 1 was performed and showed that approximately 80% of the oragnisms in the RN2428 culture were still arsenate-resistant and that at least 95% of these lost resistance on incubation on non-selective medium. On the other hand, 95% of the organisms in the RN2429 culture were arsenate-resistant and of these, less than 1% lost arsenate resistance during incubation on non-selective medium.

It is possible that the somewhat reduced incorporation into plasmid DNA in strain RN2428 (see Fig. 2*a*) was due to a reduction in the number of autonomous copies of the plasmid, normally 8 to 12 per cell[15], in that strain. Experiments are in progress to test this possibility.

We conclude from these experiments that the known plasmid loci affecting incompatibility and replication seem to be genetically separate and functionally distinct in *S. aureus* and that in this system, the expression of incompatibility does not involve inhibition of replication.

Consistent with this conclusion is the fact that it is generally possible, both in *S. aureus* and in *E. coli*, to construct strains carrying pairs of incompatible autonomous plasmids. In such heterozygotes, which can be maintained only by double selection, the two incompatible plasmids replicate side-by-side, and segregate at a measurable, constant rate on nonselective media[9,16,17]. We should like to propose, therefore, a model in which incompatibility between autonomous plasmids is an automatic consequence of the partition process. This model would apply to plasmids with random partition as well as to those with equipartition. Our primary formulation is, however, for the latter since equipartition is evidently a property of staphylococcal plasmids[1].

(1) Copies of a given plasmid are partitioned at cell division by transient attachment to a "partition structure" (the membrane?—compare Jacob *et al.*[2]).

(2) The partition and replication control mechanisms are incompatibility-type specific; that is, they cannot distinguish among plasmids belonging to the same incompatibility set (but they can distinguish among members of different sets).

(3) Plasmids belonging to the same incompatibility set are randomised between cell divisions so that there is a high probability that gross disproportion will develop among them during cell division.

(4) Any disproportion generated during division is likely to be maintained by replication during the next interdivision period; such disproportions will then be amplified during subsequent divisions until subclones containing only one of the pair are generated.

Note that the behaviour of homogenic incompatible plasmids illuminates a feature of equipartition that would otherwise remain obscure, namely randomisation of the plasmid copy pool. The crux of the model is that disproportions generated by this randomisation cannot be corrected because their existence cannot be recognised. The model makes a number of predictions that are readily testable: (1) the segregation behaviour of homogenic

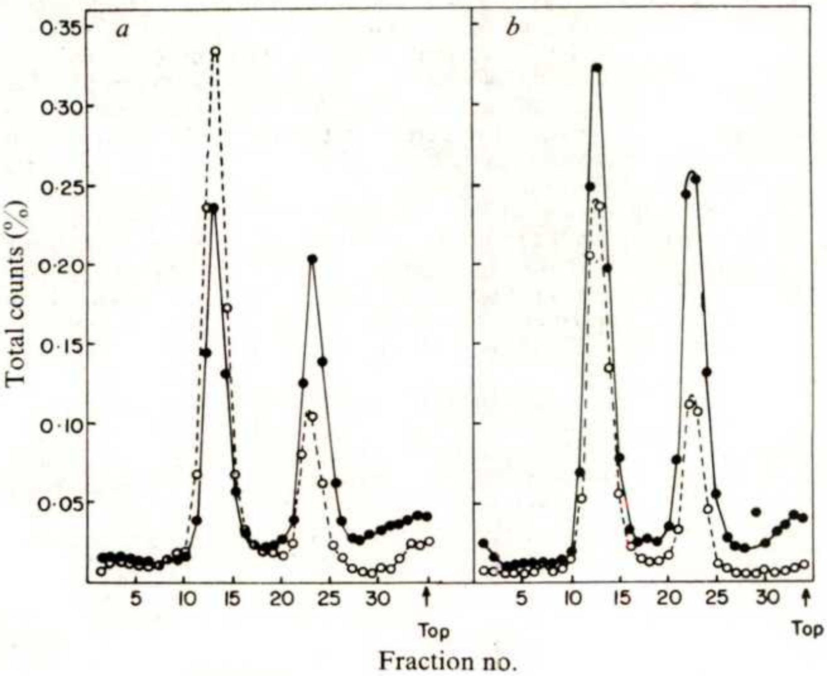

Fig. 2 Replication of incompatible plasmids. *a*. A cleared lysate[19] of a ^{3}H-labelled RN2428 culture mixed with a ^{14}C-labelled RN557 culture was centrifuged to equliibrium in an ethidium bromide–caesium chloride gradient which was fractionated and counted by standard procedures. Counts were mormalised to total incorporatio into the respective cultures. *b*. Dye-buoyant density gradient pattern for lysate of a mixture of a ^{3}H-labelled RN2429 cultures and ^{14}C-labelled RN325. For both, dashed curve, ^{14}C; solid curve, ^{3}H. Density increases from right to left.

incompatible plasmid heterozygotes is solely a function of copy numbers and can be predicted by simple combinatorial analysis; (2) the incompatibility locus is a recognition site for partition and so does not encode a protein—thus it may be regarded as a prokaryotic centromere analogue; (3) a (membrane) protein exists that recognises and binds to this site—such a protein could either be plasmid- or host-coded; (4) the incompatibility locus is not essential for autonomous replication; (5) plasmids with absent or defective *inc* loci will be partitioned randomly in the absence of other plasmids; (6) paradoxically, Inc$^-$ plasmids will not be compatible with Inc$^+$ plasmids of the same original class.

It should be pointed out that this model as stated deals with the hereditary consequences of only one of several possible combinations of replication and partition specificities. For example, it is implict in prediction 6 (above) that equipartition is not a prerequisite for incompatibility; so long as the replication system cannot distinguish between plasmids, the inevitable disproportions arising during cell division will not be correctable and the result will be segregation. In such cases, the incompatibility locus will not be a centromere analogue but rather will correspond to the determinant(s) of replicon recognition specificity.

It should also be mentioned that there are two known situations in which the presence of one plasmid evidently inhibits the replication of another with which it is incompatible. These two situations are (1) delayed replication of an entering plasmid[9,11] and (2) inhibition by a cointegrate replicon of the replication of an autonomous plasmid incompatible with the subsidiary component of the cointegrate. Two examples of the latter are, Hfr strains superinfected by F plasmids[10] and a colE1-pSC101 cointegrate superinfected by pSC101[17]). All of these situations may be manifestations of a copy number control mechanism. In case (1) above, the resident plasmid is present at its full complement of copies and so an entering one is disadvantaged for that reason. Eventually, however, the entering plasmid is able to establish and replicate. In case (2) involving cointegrates, if the number of copies of the subsidiary replicon (for example, integrated F or pSC101) is maintained automatically at a level equal to or greater than its normal autonomous multiplicity, one would expect replication of autonomous copies of the corresponding plasmid to be inhibited and the establishment of that plasmid to be prevented.

The above considerations suggest that as many as three different kinds of genetic mechanism, each operative under a particular set of conditions, may be mainfested as plasmid incompatibility. These are (1) a recognition site for equipartition, (2) a recognition site for replication specificity, and (3) a copy number control mechanism.

The basis of the expression of incompatibility by the integrated *S. aureus* plasmid described here is not intuitively obvious from these considerations. It is unlikely that copy control is involved, since the autonomous plasmid (when alone) is normally present at 8–12 copies per cell[15] and the integrated one at 2–4[18]. Presumably, therefore, the integrated plasmid somehow causes random partition of the autonomous one and prevents correction of the deficiencies in the copy number of the latter that consequently arise during division. Experimental analysis of this possibility is in progress.

This work was supported by USPHS grants awarded to R.P.N. from the National Institute of General Medical Sciences. M.S. was supported by a training grant from the NIGMS administered by the Department of Microbiology of the New York University School of Medicine. The authors would like to acknowledge helpful discussions with Robert Pritchard, Kurt Nordstrom, Werner Maas and Leonard Mindich, and the secretarial assistance of Annabel Howard.

RICHARD P. NOVICK
MARJORIE SCHWESINGER

Department of Plasmid Biology,
The Public Health Research Institute,
of the City of New York, Inc.,
New York, New York 10016

Received April 22; accepted June 29, 1976.

[1] Novick, R., Wyman, L., Bouanchaud, D., and Murphy, E., in *Microbiology 1974* (edit. by Schlessinger, D.), 115–129 (American Society for Microbiology, Washington, DC, 1975).
[2] Jacob, F., Brenner, S., and Cuzin, F., *Cold Spring Harb. Symp. quant. Biol.*, **28**, 329–348 (1963).
[3] Kingsbury, D. T., and Helinski, D. R., *Genetics*, **74**, 1–16 (1973).
[4] Novick, R. P., *Fedn Proc.*, **26**, 29–38 (1967).
[5] Novick, R. P., *Bact. Rev.*, **33**, 210–263 (1969).
[6] DeVries, J. K., Pfister, A., Haenni, C., Palchaudhuri, S., and Maas, W., in *Microbiology 1974* (edit. by Schlessinger, D.), 166–170 (American Society for Microbiology, Washington DC, 1975).
[7] Novick, R. P., Clowes, R. C., Cohen, S. N., Curtiss R., III, Datta, N., and Falkow, S., *Bact. Rev.*, **40**, 168–189 (1976).
[8] Timmis, K., Cabello, F., and Cohen, S. N., *Proc. natn. Acad. Sci. U.S.A.*, **72**, 2242–2246 (1975).
[9] Novick, R. P., and Brodsky, R., *J. molec. Biol.*, **68**, 285–302 (1972).
[10] Dubnau, E., and Maas, W. K., *J. Bact.*, **95**, 531–539 (1968).
[11] Hershfield, V., LeBlanc, D. J., and Falkow, S., *J. Bact.*, **115**, 1208–1211 (1973).
[12] Pritchard, R. H., Barth, P. T., and Collins, J., *Symp. Soc. gen. Microbiol.*, **19**, 263–297 (1969).
[13] Schwesinger, M. D., and Novick, R. P., *J. Bact.*, **123**, 724–738 (1975).
[14] Novick, R. P., and Richmond, M. H., *J. Bact.*, **90**, 467–480 (1965).
[15] Rush, M., Novick, R., and DeLap, R., *J. Bact.*, **124**, 1417–1423 (1975).
[16] Uhlin, B. E., and Nordström, K., *J. Bact.*, **124**, 641–649 (1975).
[17] Cabello, F., Timmis, K., and Cohen, S. N., *Nature*, **259**, 285–290 (1976).
[18] Novick, R., Zouzias, D., and Rush, M., *J. Bact.*, **124**, 1424–1428 (1975).
[19] Clewell, D. B., and Helinski, D. R., *Proc. natn. Acad. Sci. U.S.A.*, **62**, 1159–1166 (1969).

Low angle X-ray diffraction patterns of squid retina

THE structure of photoreceptor membranes in the rod outer segments of vertebrates has been studied using X-ray diffraction[1–3], and electron density profiles of the disk membrane at a resolution of 14 Å have been obtained[4]. The ultrastructure of invertebrate rhabdomeric visual cells have been studied using electron microscopy[5] and birefringence[6], but not X-ray methods. We report here low angle X-ray diffraction patterns recorded from squid retina after fixation in glutaraldehyde.

In the squid the rhabdomere structures of the retinula cells[7] are contained within the distal segments[8] (by analogy with the retinal rod outer segments of vertebrates). Electron micrographs[7,8] of the distal segments of squid show an array of microvilli and show that the long axes of the microvilli are perpendicular to the light direction. A single microvillus[7,8] is shown as a thin hollow cylinder about 1–2 µm long and about 700–1,000 Å in diameter. The microvilli appear to be in regular hexagonal arrays. A three-dimensional reconstruction of the squid distal segment[7] shows that the adjacent hexagonal arrays of different retinula cells are approximately perpendicular to each other. The squid retina is well suited to X-ray study because the volume fraction of the microvilli in the squid retina is large when compared with other invertebrates. The distal segments are rather long, about 300 µm, and the distal segments of squid[7] like those of octopus[9] are closely packed together.

Fresh squids were obtained at Marine Biological Laboratory, Woods Hole. After dissection the squid eyes were immediately fixed in 6% glutaraldehyde in Tris buffer (*p*H 7.0) and stored in a refrigerator at about 4 °C. In the X-ray experiment a 1-mm strip was cut from the fixed eye and mounted in a specimen chamber. The X-ray procedures for recording diffraction from squid retina were very similar to those used in obtaining X-ray patterns from vertebrate retina[1–3]. Low angle X-ray diffraction patterns were taken with the X-ray beam incident parallel to the retina surface, and incident perpendicular to the light direction and to the long axis of each distal segment. Exposure times varied from 1 h to 1 d using an Elliott rotating anode microfocus X-ray generator and an optically focusing X-ray camera[10].

Initially, slit collimation was used to explore whether low angle X-ray diffraction could be recorded from our X-ray specimens of squid retina. A series of diffraction orders from a lamellar repeating distance of $d = 620 \pm 10$ Å along the light

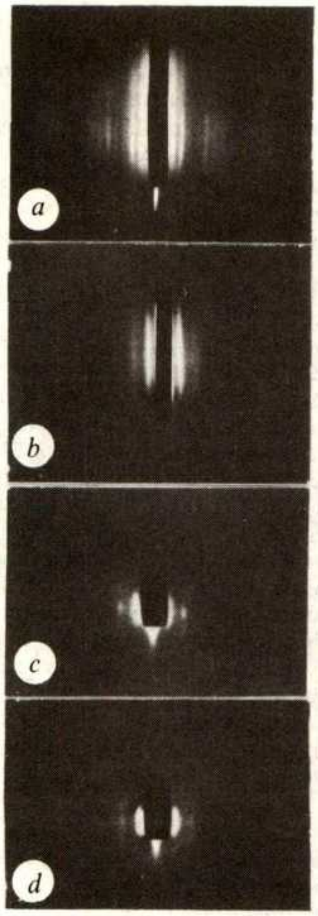

Fig. 1 *a*, Low angle X-ray diffraction pattern of squid retina after fixation in glutaraldehyde. The X-ray pattern was obtained using slit collimation and a specimen-to-film distance of 9 cm. Orders $h = 2$ to 8 of $d = 620$ Å and a diffuse reflection centred at $d \sim 48$ Å are visible. Scattering close to the beam stop obscures the first order of diffraction. *b*, Low angle X-ray diffraction pattern of squid retina after fixation in glutaraldehyde. The X-ray pattern was obtained using slit collimation and a specimen-to-film distance of 20 cm. The first two orders of $d = 620$ Å are visible. The first order has a strong intensity, whereas the second is comparatively weak. *c*, Low angle X-ray diffraction pattern of squid retina after fixation in glutaraldehyde. The X-ray pattern was obtained using pinhole collimation and a specimen-to-film distance of 15 cm. The (01) and (10) reflections on the first layer line are off-meridional but appear to overlap as they have strong intensity. Three reflections are seen on the second layer line. The (11) reflection is on the meridian, whereas the (02) and (20) reflections are off-meridional. *d*, Low angle X-ray diffraction pattern of squid retina after fixation in glutaraldehyde. The X-ray pattern was obtained using pinhole collimation and a specimen-to-film distance of 15 cm. Less X-ray exposure was used to obtain this pattern. The (01) and (10) reflections on the first layer line are resolved as off-meridional reflections. The three reflections on the second layer line are also visible but faint.

direction, was recorded. Generally, the first three orders of diffraction were discrete, whereas the higher orders merged together. When moderate exposure times were used the X-ray pattern extended out to a resolution of about 20 Å. Occasionally, the first eight discrete orders could be seen. A low angle X-ray diffraction pattern, showing discrete orders $h = 2$ to 8 of a lamellar repeating distance of $d = 620$ Å and a diffuse reflection centred at $d \sim 48$ Å, is reproduced in Fig. 1*a*. The first order of diffraction $h = 1$ is not resolved in Fig. 1*a* because of scattering close to the beam stop. In an X-ray experiment using less exposure time and an increased specimen-to-film distance of 20 cm the first two diffraction orders $h = 1$ and 2 of $d = 620$ Å were recorded. This pattern is reproduced in Fig. 1*b*.

Unfortunately, the interpretation of the low angle X-ray patterns obtained using slit collimation is not straightforward. The first step in interpreting the lamellar diffraction is to identify the orientation of the two-dimensional arrays relative to the light direction. The orientation of the arrays of microvilli is not easily obtained from a study of electron micrographs[7,8]; and, so far, the orientation has not been established by electron microscopy. The recording of discrete orders of a lamellar repeat distance in the slit-collimated X-ray patterns indicates that the microvilli arrays have the same lattice dimensions and that they have the same orientation relative to the light direction. Thus it is important to verify whether the lattice is hexagonal, to establish the lattice dimensions and to determine the orientation of the microvilli arrays relative to the light direction.

The orientation of the two-dimensional arrays of microvilli has been determined by recording low angle X-ray diffraction patterns using pinhole collimation. The pinhole-collimated X-ray patterns require longer exposure times because of the weaker main beam and because of having to use a specimen-to-film distance of 15 cm to resolve diffraction orders along the layer lines. So far, only the first few diffraction orders have been recorded. Typical low angle X-ray diffraction patterns of squid retina are shown in Fig. 1*c* and *d*. The angle between the off-meridional reflections in our pinhole-collimated X-ray patterns is close to 60°; and therefore it is assumed that the microvilli lattice is hexagonal. Note that the angle appears to be slightly less than 60° (it is about 55° in Fig. 1*c* and *d*), indicating that our X-ray specimens contain a microvilli lattice which is slightly compressed along the (1,1) direction. This slight compression probably arises as a result of sectioning and mounting the retina strip in the specimen chamber. The pinhole patterns do not reproduce well, but the off-meridional reflections (01) and (10) on the first layer line and the (11) meridional reflection and the weaker off-meridional reflections (02) and (20) on the second layer line can be seen in Fig. 1*c*. The off-meridional reflections (12) and (21) on the third layer line can be seen in the original negatives. In Fig. 1*c* the off-meridional reflections (01) and (10) are overexposed and tend to overlap in the reproduction. The pinhole pattern shown in Fig. 1*d* has less X-ray exposure and the (01) and (10) off-meridional reflections on the first layer are seen as discrete reflections. A drawing of the pinhole-collimated X-ray patterns

Fig. 2 A drawing of the two-dimensional microvilli lattice as shown by the pinhole collimated X-ray diffraction patterns. The light direction is along the meridian. The a^* and b^* axes of the hexagonal reciprocal lattice is indicated and the (11) direction is along the meridian. The reflections (01), (10), (11), (02), (20), (12) and (21) on the first three layer lines have been seen in a number of negatives. The reflections (13), (22) and (31) on the fourth layer line have not been recorded but are included for illustrative purposes. Note that this figure is rotated 90° relative to Fig. 1 so that the beam stop is along the equator.

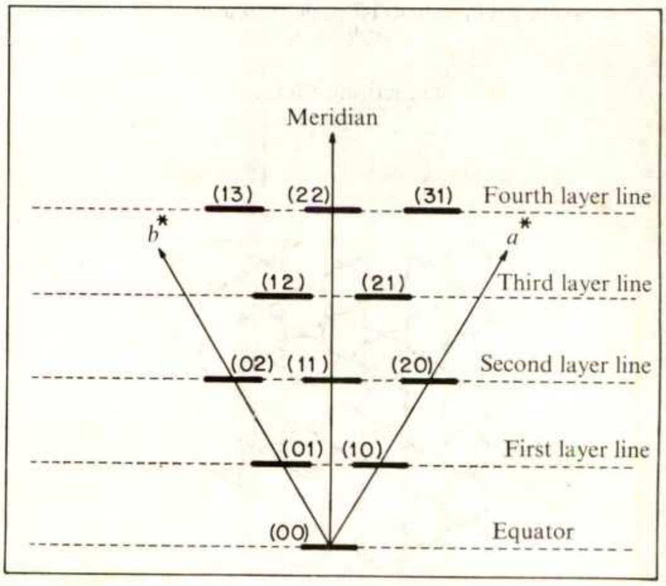

is shown in Fig. 2. Note that Fig. 2 is rotated 90° relative to Fig. 1 so that the beam stop is along the equator. The two-dimensional array is hexagonal with $a = 620$ Å and the light direction is coincident with the (11) direction of the two-dimensional arrays. The orientation of the two-dimensional array of microvilli relative to the light direction is shown in Fig. 3.

It is known from electron microscopy[7,8] that the adjacent microvilli arrays of different retinula cells are approximately perpendicular to each other but it is not known to what extent this kind of packing is followed throughout the whole retina. If the X-ray specimen of squid retina contained only two orientations (which are perpendicular to each other) then the recording of the off-meridional reflections would be sensitive to the direction of the incident X-ray beam. But no such sensitivity has been recorded. The pinhole-collimated X-ray patterns indicate that the (11) direction is a rotation axis. Thus, although adjacent arrays may be perpendicular to each other[7,8], this kind of packing is not maintained over the whole retina.

A model for a single microvillus is a long thin cylinder where the wall is made up of a single membrane of width m. It is assumed that $m \sim 75$ Å—that is, the microvillus membrane has the same thickness as the disk membrane[1–4]—and that the outer surfaces of the cylinders are separated by a fluid layer about 5 Å wide. The single membrane is centred at a distance r from the axis of the cylinder and $r = 1/2\ (620-m-5)$ Å, that is, $r = 270$ Å. The Fourier transform of the membrane with respect to its centre is denoted by $M(R)$ where R is the reciprocal space coordinate. The Fourier transform of the two-dimensional array of microvilli is denoted by $T(R)$; and using X-ray diffraction theory appropriate to concentric membrane layers[11], $T(R)$ can be written

$$T(R) \sim 2\pi r J_0(2\pi r R) M(R) \Phi(R)$$

where J_0 is the zero-order Bessel function and Φ is the interference function for the two-dimensional array.

A test of the correctness of the above model can be made by comparing the calculated and observed intensities for the (10), (11) and (20) reflections. In the squid retina the two-dimensional arrays of microvilli are effectively rotated about the (11) direction. To refer intensities to an unrotated array the following corrections are made. The off-meridional reflections (01),(10) and (12),(21) are increased four to five times, while the off-meridional reflections (02),(20) and (13),(31) are increased eight to ten times. The X-ray intensities for the first three reflections of the unrotated array have the following variation: $I(10) \gg I(20) > I(11)$. To calculate intensities from our model it is necessary to first estimate values of $M(R)$, the Fourier transform of the microvillus membrane. For the first two or three reflections which correspond to very small angles of diffraction, $M(R)$, can be approximated[11] by a membrane of constant density so that $M(R)$ is proportional to $(1/R)\sin(\pi m R)$ and where $m \sim 75$ Å. The $J_0(2\pi r R)$ variation is sensitive to the choice of r and we use $r = 270$ Å. By combining the $M(R)$ and $J_0(2\pi r R)$ variations, our model provides an intensity variation for the first three reflections, which is the same as recorded experimentally. Thus, the observed intensities of the first few reflections in the pinhole-collimated X-ray patterns are in agreement with the microvillus membrane having a thickness of about 75 Å and with the concentric membrane having a radius of about 270 Å.

Fig. 3 A drawing of a section through the two-dimensional hexagonal array of microvilli. The section contains the light direction and is perpendicular to the long axes of the microvilli cylinders.

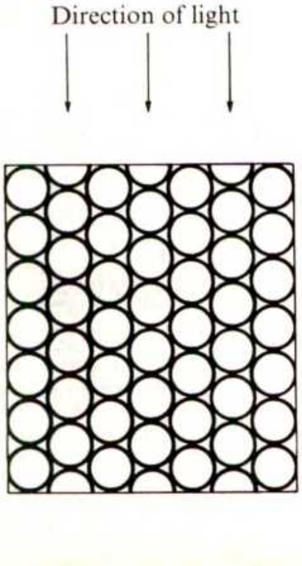

In summary, it has been possible to record X-ray diffraction from the photoreceptor structures of squid retina. So far, these X-ray patterns refer to fixed eyes. X-ray analysis of the pinhole-collimated patterns has provided information on the dimensions of the microvilli and on the molecular organisation of the microvilli in the distal segments of squid retina. Information on the internal structure of the microvillus membrane has not been obtained but this information may be forthcoming in future work provided that more reflections can be recorded in pinhole-collimated X-ray patterns.

This work was supported by the USPHS. C.M.F. was supported by a research fellowship from the USPHS.

C. R. WORTHINGTON
S. K. WANG
C. M. FOLZER

Departments of Biological Sciences and Physics,
Carnegie-Mellon University,
Pittsburgh, Pennsylvania 15213

Received March 8; accepted June 9, 1976.

[1] Gras, W. J., and Worthington, C. R., *Proc. natn. Acad. Sci. U.S.A.*, **63**, 233–238 (1969).
[2] Blaurock, A. E., and Wilkins, M. H. F., *Nature*, **223**, 906–909 (1969).
[3] Corless, J. M., *Nature*, **237**, 229–231 (1972).
[4] Worthington, C. R., *A. Rev. Biophys. Bioengng*, **3**, 53–80 (1974).
[5] Eakin, R. M., in *Handbook of Sensory Physiology*, **VII/1**, *Photochemistry of Vision*, 625–684 (Springer, Berlin, 1972).
[6] Moody, M. F., *Biol. Rev. Camb. phil. Soc.*, **39**, 43–86 (1964).
[7] Zonana, H. V., *Johns Hopkins Hosp. Bull.*, **109**, 185–205 (1961).
[8] Cohen, A. I., *J. comp. Neurol.*, **147**, 351–378 (1973).
[9] Yamamoto, T., Tasaki, K., Sugawara, Y., and Tonosaki, M. D., *J. Cell Biol.*, **25**, 345–359 (1965).
[10] Elliott, G. F., and Worthington, C. R., *J. Ultrastruct. Res.*, **9**, 166–170 (1963).
[11] Worthington, C. R., in *Biophysics and Physiology of Excitable Membranes*, 1–46 (Van Nostrand-Reinhold, New Jersey, 1971).

Corrigendum

In the article "Intact 3′ end of 16S rRNA is not required for specific mRNA binding" by J. V. Ravetch and K. S. Jakes (*Nature*, **262**, 150; 1976) the sentence at the beginning of paragraph 4 should read "The colicin-treated ribosomes used in the experiment shown in Fig. 1 were lowered in their ability to carry out f2 RNA-directed protein synthesis by 75%" and not as printed.

Errata

IN the article "Constraints on the nature of the ancient lunar magnetic field" by J. N. Goswami (*Nature*, **261**, 675; 1976) two lines were omitted from the end of page 676. The sentence 'One of these . . . Fe–FeS . . . ' should continue ' . . . melt a few hundred kilometres below the lunar surface, initiating such local fields[13] on the Moon, is yet to be verified.'

The title of the article by M. S. N. Carpenter and L. Civetta (*Nature*, **262**, 276; 1976) should read "Hercynian high pressure/low temperature metamorphism in the Ile de Groix Blueschists" and not as printed.

matters arising

Ionic clustering and collagen specificity

PIEZ and Torchia[1] agreed with us[2] that pairs of unlike charged residues in the collagen amino acid sequence are important for the assembly of molecules into fibrils. The described their use of three-dimensional molecular models to examine specific interactions and in doing so criticised our earlier one-dimensional treatment, in particular the dipole formalism used.

One-dimensional analyses of the collagen sequence proved fruitful in earlier work, when it was found that two-thirds of the charged amino acid residues behaved as if they were arranged in pairs of unlike charge[3,4]. We simplified our calculations by treating these 100 paired charges as 50 dipoles; an approach commonly used as, for example, in the treatment of dielectric materials.

Contrary to the belief of Piez and Torchia, our aim was not to suggest a detailed interaction scheme of the type shown in their Fig. 1*a;* we were only suggesting an important role for the paired charges in specifying an inter-into fibrils. They described their use of molecular 1 D stagger. It is difficult to extrapolate this result to determine details of the arrangement of interacting charged residues in three dimensions. Nevertheless paired, unlike unpaired, charges are distributed in the collagen sequence in a manner which is intimately associated with the D stagger[5]. An understanding of this specificity in three dimensions, whether or not the concept of charge clustering is invoked, must await the outcome of a full three-dimensional analysis.

BARBARA BRODSKY DOYLE
Department of Biochemistry,
Rutgers Medical School,
Piscataway, New Jersey 08854

DAVID W. L. HUKINS
Department of Medical Biophysics,
University of Manchester,
Manchester M13 9PT, UK

DAVID J. S. HULMES
ANDREW MILLER
EMBL Outstation,
LMA, CENG, 38041 Grenoble, Cedex,
France

CHRISTOPHER J. RATTEW
Department of Biophysics,
University of London King's College,
London WC2B 5RL, UK

JOHN WOODHEAD-GALLOWAY
Medical Research Council,
20 Park Crescent,
London W1N 4AL, UK

[1] Piez, K. A., and Torchia, D., *Nature*, **258**, 87 (1975).
[2] Doyle, B. B., *et al.*, *Biochem. biophys. Res. Commun.*, **60**, 858–864 (1974).
[3] Hulmes, D. J. S., Miller, A., Parry, D. A. D., Piez, K. A., and Woodhead-Galloway, J., *J. molec. Biol.*, **79**, 137–148 (1973).
[4] Doyle, B. B., Hukins, D. W. L., Hulmes, D. J. S., Miller, A., and Woodhead-Galloway, J., *J. molec. Biol.*, **91**, 79–99 (1975).
[5] Hulmes, D. J. S., thesis, Univ. Oxford (1975).

PIEZ AND TORCHIA REPLY—We are pleased to read the statement of Doyle *et al.*[1] that we[2] inferred more from their dipole treatment[3] than they meant us to. We would point out, however, that our Fig. 1*a* is essentially identical to their Fig. 1*b*. In any case, we seem to be agreed that charge groupings (pairs or clusters) are associated with molecular packing of collagen and that a three-dimensional analysis is needed to sort out exactly how they are associated.

A recent rereading of the early literature has reminded us that charge clustering is not a new idea. It was originally proposed by Hodge and Schmitt[4] from electron microscopic studies of positively stained native collagen fibrils and SLS segments. We are, however, now able to treat the question at a much higher degree of resolution.

National Institute of Dental Research,
Bethesda, Maryland 20014

[1] Doyle, B. B., *et al.*, *Nature*, **262**, 629 (1976).
[2] Piez, K. A., and Torchia, D. A., *Nature*, **258**, 87 (1975).
[3] Doyle, B. B., *et al.*, *Biochem. biophys. Res. Commun.*, **60**, 858–864 (1974).
[4] Hodge, A. J., and Schmitt, F. O., *Proc. natn. Acad. Sci. U.S.A.*, **46**, 186–197 (1960).

Retinal sensitivity to short wavelength light

THE recent article[1] on potential hazards due to exposure of the primate retina to visible radiation of short wavelengths contains a number of conclusions which are open to argument.

The lesions are believed to be mediated essentially by (unspecified) photochemical mechanisms. The reciprocity law is not, however, obeyed in the data shown in Table 1, although both human rods and human cones[2] obey it in the timespan used by the authors. The contribution of thermal effects is minimised even though the action spectrum bears a striking similarity to the absorption spectrum of melanin[3].

The protection afforded by the crystalline lens is emphasised in so far as the retina is concerned, although the vitreous may be at risk in aphakic eyes[4,5].

The morphology of the lesion is virtually ignored, even though it has been successfully studied elsewhere[6].

The authors write that a threshold lesion occurs when one views the Sun for not less than 100 s. In our view it should not be implied that a shorter period is safe in their experimental conditions.

J. MARSHALL
R. A. WEALE

Institute of Ophthalmology,
Judd Street,
London WC1H 9QS, UK

[1] Ham, W. T., Mueller, H. A., and Sliney, D. H., *Nature*, **260**, 153 (1976).
[2] Weale, R. A., *Vision Res.*, **1**, 354 (1962); *Optica Acta*, **6**, 158 (1959).
[3] Hunold, W., and Malessa, P., *Ophthal. Res.*, **6**, 355 (1974).
[4] Weale, R. A., *Br. J. Ophthalmol.*, **55**, 853 (1970).
[5] Weale, R. A., in *The Human Lens in Relation to Cataract* (edit. by Pirie, A.), (Elsevier, North Holland, Amsterdam, 1973).
[6] Marshall, J., Hamilton, A. M. and Bird, A. C., *Experientia*, **30**, 1335 (1974).

HAM REPLIES—According to our best judgment, there are at least three types of radiation damage to the retina in the spectral range, near infrared to near ultraviolet (1,400–400 nm). These are: sonic transient or shock damage from picosecond to nanosecond pulses[1–3], thermal damage (independent to a first approximation of wavelength) from microsecond to second pulses[4,5], and photochemical damage from long term exposure (>1 s) to the shorter wavelengths in the visible spectrum (approximately 500–400 nm)[6]. There is no sharp transition between these three types of retinal damage, either from the standpoint of wavelength or exposure time. We believe that Marshall's report[8] of retinal damage belongs in the general category of thermal damage as outlined here.

In response to the specific comments of Marshall and Weale[7] we offer the following: (1) Not even thermal lesions obey a reciprocity law[4]. There is no particular reason to believe that long term photic damage should obey a reciprocity relation and, as we pointed out in the paper[8], we do not know the relationship of rods and cones to the observed funduscopic pathology. (2) Thermal effects are minimised only for long term exposure to the shorter wavelengths in the visible spectrum where maximum temperatures in the retina do not exceed a few °C above ambient. The absorption spectrum of melanin would be expected to correspond to the action spectrum for thermal damage. Our action spectrum includes both thermal and photochemical damage and its relationship to the melanin absorption spectrum is suspect but should not be overlooked. (3) The hazard to the retina rather than the vitreous for aphakic eyes is emphasised because the vitreous does not absorb radiation appreciably between 300 and 1,400 nm (ref. 9). (4) The morphology of the lesion is not ignored but undetermined to date. Extensive efforts are under way, using both light and electron microscopy, to determine the nature of the lesion. The subtleties of these lesions bear no relationship to those reported by Marshall *et al.*[5]. Calculations show that the minimal irradiance on the retina in their experiments was greater by a factor of 10^3 than those we reported[8]. In other words, Marshall *et al.*, were dealing with a totally different phenomenon, thermal injury, whereas we were seeking to characterise a long term photic damage mechanism or mechanisms in the retina.

Department of Biophysics,
Medical College of Virginia

---

[1] Cleary, S. F., and Hamrick, P. E., *J. Acoust. Soc. Am.*, **46**, 1037–1044 (1969).
[2] Ham, W. T., Jr, Mueller, H. A., and Goldman, A. I., *Science*, **185**, 362–363 (1974).
[3] Goldman, A. I., Ham, W. T., Jr, and Mueller, H. A., *Expl Eye Res.*, **21**, 457–469 (1975).
[4] Ham, W. T., Jr, *et al.*, *Trans. N.Y. Acad. Sci. Ser. II*, **28**, 517–526 (1966).
[5] Marshall, J., Hamilton, A. M., and Bird, A. C., *Experientia*, **30**, 1335 (1974).
[6] Ham, W. T., Jr, Mueller, H. A., and Sliney, D. H., *Nature*, **260**, 153–155 (1976).
[7] Marshall, J., and Weale, R. A., *Nature*, **262**, 629 (1976).
[8] Ham, W. T., Mueller, H. A., and Sliney, D. H., *Nature*, **260**, 153 (1976).
[9] Boettner, E. A., and Wolter, J. R., *Invest. Ophthalmol.*, **1**, 776–783 (1962).

Exudate-eating and tree-gouging in marmosets

KINZEY *et al.*[1] discuss an unusual sap-eating behaviour in the pygmy marmoset (*Cebuella pygmaea*) of upper Amazonian South America. We have observed similar exudate-eating behaviour patterns in southern Brazilian marmosets of the genus *Callithrix* and and would like to discuss briefly their significance.

Like *Cebuella*, *Callithrix* spp. are "short tusked"[2]: in other words, they have an unusual lower anterior dentition in which the canines are short and the incisors long and roughly equal in length to the canines. The other two callitrichid genera, *Leontopithecus* and *Saguinus*, are "long tusked", with normal, long lower canines and short lower incisors. In *Callithrix* and *Cebuella*, the "short tusked" lower anterior dentition is apparently used as a gouge or scraper to perforate the bark and the superficial layer of the cambium of certain trees. When attacked in this manner, the trees exude gums and sap which are important food sources for the marmosets.

Free-living *Callithrix jacchus* have been observed gouging several species of trees (*Anacardium occidentale*, Anacardiaceae; *Tapirira guianensis*, Anacardiaceae; *Terminalia catappa*, Combretaceae) in the Brazilian states of Alagoas and Rio de Janeiro. Favourite trees are sometimes riddled with holes on all surfaces. Captive *Callithrix* (including *C. flaviceps*, *C. geoffroyi*, *C. jacchus* and *C. penicillata*) gouge holes in fresh branches and also in the dry wooden fixtures of their cages (Fig. 1). In addition to feeding on exudates that flow from holes in the fresh branches, captive (and probably also wild) *Callithrix* use the holes in both dry and fresh wood as foci for marking behaviour. High-ranking males and females frequently urinate in them and genital-rub in their vicinity. The gouging process in *Callithrix* is usually accomplished by anchoring the upper incisors on the substratum and scraping with the lower anterior teeth (Fig 1). In both *Cebuella* and *Callithrix*, wear patterns on the occlusal surface of the upper incisors indicate that they are used to hone the tips of the lower incisors (personal communication from R. D. Martin). Depending on their hardness, exudates are either licked up or collected with teeth. In contrast to *Cebuella* and *Callithrix*, the "long-tusked" *Leontopithecus* and *Saguinus* have never been observed gouging holes in wood, although they occasionally chew on strips of bark and feed on already-exuded gums if they happen to come across them.

Fig. 1 Captive *Callithrix geoffroyi* gouging hole in dry branch in its cage. Note the positions of the upper and lower teeth.

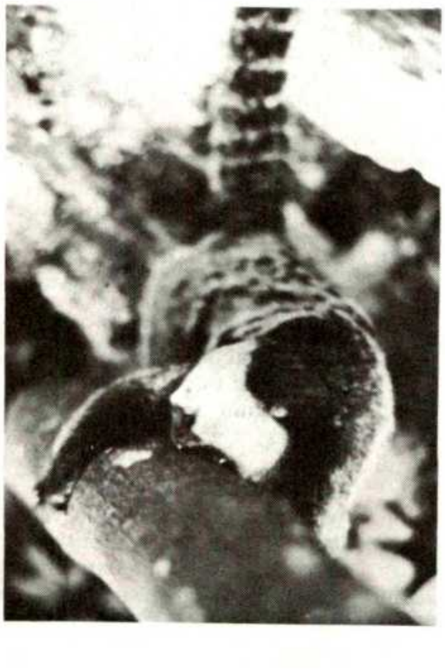

An analysis of the gum of *Anacardium occidentale* gives an indication of the food value of exudates. The gum of this species is 84% carbohydrate and contains several minerals, including iron, aluminum, calcium, silicon, potassium and traces of magnesium and sodium[3]. These substances therefore provide small primates like *Callithrix* and *Cebuella* with a high energy food source not used to any great extent by larger primates and other potential competitors, and helps them to, at least in part, avoid competition for fruit, the major high energy food source for many tropical mammals and birds.

Sporadic exudate-eating from sites where insect infestation or mechanical damage has caused it to flow is a fairly common pattern in primates. The same can be said for occasional use of the teeth to pry, gouge, strip or break bark from trees. In addition, certain prosimians (for example, *Euoticus elegantulus*, *Microcebus murinus* and *Galago senegalensis*) use their specialised "tooth combs" or "tooth scrapers", formed by the lower anterior dentitions, as scoops to collect gums from areas where they have already exuded (personal communication from R. D. Martin). But, the regular use of tree gouging specifically to elicit exudate flow has so far been found only in *Callithrix*, *Cebuella* and the Madagascan fork-marked dwarf lemur *Phaner-furcifer*[5] and seems to be rare not only among primates but among vertebrates in general.

ADELMAR F. COIMBRA-FILHO

Department of Environmental
Conservation, FEEMA,
Rio de Janeiro, Brazil

RUSSELL A. MITTERMEIER

Department of Anthropology and
Museum of Comparative Zoology,
Harvard University,
Cambridge, Massachusetts 02138

---

[1] Kinzey, W. G., Rosenberger, A. L., Ramirez, M., *Nature*, **255**, 327–328 (1975).
[2] Napier, J. R., and Napier, P. H., *Handbook of Living Primates* (Academic, New York, 1967).
[3] Machado, A., and Leite, O. C., *Bol. Inst. Quim. Agric.*, **50**, 7–15 (1957).
[4] Coimbra-Filho, A. F., and Mittermeier, R. A., in *Conf. Biology and Conservation of the Callitrichidae*, Front Royal, Virginia (in the press).
[5] Petter, J. J., *et al.*, *La Terre et la Vie*, **118** (3), 287–327 (1971).

●

nature

August 19, 1976

Shadowy threshold

THE ridiculous consequences of the threshold nuclear test-ban treaty, pressed on an unwilling world in 1974 and scheduled to take effect in April 1976, begin to make themselves known. The treaty is a strictly bilateral affair between the United States and the Soviet Union and the two parties have agreed to restrain weapons to yields not exceeding 150 kilotons. A related treaty covered peaceful nuclear explosions. Although formal ratification is still awaited, both parties have been honouring the treaty for some months.

In 1974 there was vigorous criticism of almost all aspects of the treaty in many parts of the world: a bilateral treaty was too coy; the threshold was too high for any sensible arms control purposes; the complications of geology made accurate seismic monitoring of the threshold difficult. On the last count, the period of nearly two years between proposal and enforcement was put forward by the treaty's proponents as a time when data exchange would allow accurate calibrations of test sites to be made. Certainly there was a mild flurry of activity as scientists moved between capitals clutching seismograms. But on July 4, in the case of one of the first tests to be fired by the Soviet Union since the April deadline, there was a sufficient element of doubt in American official quarters to push the whole concept of the treaty right back into the public arena. The arguments have since continued.

No official American estimate of the yield has been forthcoming but the figures first being passed around were 100 to 200 kilotons; a later figure to be mentioned was "exactly 150 kilotons". In the midst of all this an unpublished understanding between the two powers was wheeled out, to the effect that "technical uncertainties . . . may result in slight unintended breaches . . . one or two such per year would not be considered a violation of the treaty". In other words, since yields can be predetermined to within a few per cent knowing the conformation of the device, at least one party to the treaty—probably the Soviet Union—intended to test right up to the threshold. Some arms control measure.

There has been much justifiable tut-tutting over these loose edges to the treaty in the past week, but little about the calculations which have helped provoke it. Yet there is a vast amount of seismic data in the public domain and this explosion will have been excellently recorded all over the world. United States government estimates take into account we know not what, but it is open to anyone else to make his or her own reasonable estimate. There are published papers giving clear recipes for how to convert a seismic signal to explosive yield, with the help of some modest knowledge of Soviet geology. And when we do the sums we can't see how the yield can be much more than 100 kilotons.

The cause of the discrepancy is an old problem. It is easiest to measure the yield seismically by observation of the so-called body waves generated by the explosion. These have the larger signal-to-noise ratio and are measured routinely. The so-called surface waves from blasts, on the other hand, are smaller and need a little more time for their analysis. But at the sort of yields we are talking about there begin to be discrepancies between yields from the same explosion measured routinely by the two techniques—and there are good theoretical grounds for favouring the surface-wave method.

In the past, the body-wave method has been known seriously to overestimate the yield. This has led to the publication of information about the yields of Soviet tests, placing them in the multi-megaton region when the yield has probably been barely a megaton. Admittedly all estimates of seismic yield are accurate only to perhaps 20%. But now we see an old problem emerging to befuddle the issue of the threshold treaty, which is made to look silly right from the word go. One wonders whether the two years could not have been more profitably spent in avoiding such a hassle. □

Toxic cloud over Seveso

The fall-out from last month's explosion in Italy involves more than dust, as **Alastair Hay** points out

ON JULY 10, an explosion at a chemical factory in the North Italian town of Seveso released a cloud of vapour which contaminated the surrounding area. The vapour, a chemical cocktail consisting primarily of trichlorophenol (TCP), also contained an extremely toxic by-product, TCDD (2,3,7,8 - tetrachlorodibenzopara - dioxin), a virulent poison.

It happened six and a half hours after the plant, belonging to Givaudan ICMESA, a subsidiary of Hoffman-La Roche, had closed down for the weekend. There was a "runaway reaction" in the reactor producing trichlorophenol. The pressure increased as the reaction became exothermic, and reached the critical limit, blowing the safety valve and thus discharging the reactor contents. The valve, situated outside the plant, discharged the hot vapour directly into the atmosphere. When the solvents evaporated, trichlorophenol crystals and 2 kg of TCDD, in the form of dust, were precipitated south of the factory over an area inhabited by some two thousand people.

Local police were informed of the explosion on the day that it occurred; the following day the mayor of Seveso was told; and on Monday, July 12, ICMESA notified the local authorities of areas bordering on Seveso. A statement was issued by these local officials, warning against the consumption of fruit and other crops from the area surrounding the factory. On July 15, the first animal deaths were reported. The first reports of children suffering from skin rashes came a day later. By July 22, when over thirty people were reported to be showing symptoms of burns and poisoning, local authorities were still insisting that there was no cause for panic. No general evacuation had been planned.

Not until two weeks after the explosion was TCDD first identified, by a provincial diagnostic centre. The identity of the dioxin was confirmed by Givaudan three days later, on July 26. Local officials had meanwhile been alerted to the seriousness of the situation by the ICMESA management, and on Tuesday, July 27, fully 2½ weeks after the explosion, evacuation began, at first only of children. Since then the known area of serious contamination has grown severalfold, and by the middle of last week over 800 people had been evacuated from this zone. Another 1,300 children had been evacuated, as a precautionary measure, from the area outside that of immediate contamination.

Delayed action

Only after it had been established that TCDD had also been released in the vapour cloud did the authorities realise the need for urgent action. Up to this point, the information supplied to them by the ICMESA management had implied that the worst component of the vapour was trichlorophenol. This undoubtedly led the local authorities to believe that the situation, although serious, did not warrant a general exodus from the contaminated area.

It is this delay which has given cause for concern, particularly in view of the known toxicity of the dioxins. Experimental evidence is available of the effects of TCDD on a range of animals, and is to be found in the US National Academy of Sciences (NAS) document *Effects of Herbicides in South Vietnam*. A single dose of this dioxin is lethal in guinea pigs at a concentration of $0.6\,\mu g\,kg^{-1}$. In male rats the lethal dose is $22\,\mu g\,kg^{-1}$; in rabbits $115\,\mu g\,kg^{-1}$; and in humans, it has been calculated to be less than $5\,mg\,kg^{-1}$. This means that the toxicity of TCDD can be compared to that of strychnine.

Clinical signs of TCDD poisoning include atrophy of the kidney; necrotic changes of the liver; ulceration of the stomach; haemorrhages in the gastrointestinal tract and other organs; and atrophy of the thymus and other lymphoid organs and tissues. The latter changes are those most commonly observed.

Teratogenicity of TCDD has been demonstrated in mice, although evidence of teratogenic effects in other animals is more equivocal. According to Neubert *et al.* (*Environ. Health Perspectives*, Exp. Issue No. 5, 67–80; 1973), when TCDD was given to mice daily on days 6 to 15 of pregnancy, at least 50% of the progeny exhibited kidney anomalies at concentrations of $1\text{–}3\,\mu g\,kg^{-1}$; death occurred at concentrations of $7\,\mu g\,kg^{-1}$.

Reports from Seveso confirm that 500 people are being treated for poisoning. Many are showing symptoms of kidney and liver malfunction. Others from the area affected by TCDD fall-out have chloracne, a persistent and disfiguring form of acne associated with contact with chlorinated compounds. If treated, the acne may clear up in six months. There is evidence, however, of a worker in a chemical factory producing chlorophenols who is still disfigured 15 years after exposure to the chemicals.

AP

Not the first time

As the painful assessment begins of the effects of the dioxin contamination, evidence has accrued almost daily of chemical explosions involving trichlororophenol production which have already occurred and which were similar to the one at the ICMESA plant.

The first accident occurred in 1953 at the Ludwigshafen works of the Badische Anilin und Soda Fabrik AG (BASF) in Germany. Fifty-five workers were exposed to dioxin, all of whom developed chloracne. Twenty-one developed symptoms of systemic poisoning, including damage to the liver, kidney and spleen; the heart, respiratory tract, eyes and nervous system were also affected. Five years after the accident, a worker engaged on repair work on the site developed symptoms of dioxin poisoning; nine months after the appearance of the first symptoms, this worker died from an inflammation of the pancreas. Following medical advice, BASF later stopped production of trichlorophenol.

In 1963, at the Philips Duphar complex in Amsterdam, an explosion released between 30 and 200 g of dioxin into the factory hall. Fifty people were affected, at least ten of whom are still suffering from skin complaints. Four workers died within two years of the accident, but there is no proven connection between their deaths and dioxin poisoning. After an unsuccessful attempt to remove dioxin from the factory walls, the firm closed down the trichlorophenol plant for ten years. When information on dioxin contamination had been reviewed, the only course of action open to the company was to dismantle the plant brick by brick working from the inside outwards. The rubble, embedded in concrete, was eventually dumped into the Atlantic.

At the Coalite and Chemical Products plant at Bolsover, Derbyshire (UK), seventy-nine men developed chloracne following an explosion at the trichlorophenol plant in 1968. Since the Seveso accident, this firm and the West German firm of Bayer of Leberkusen have both temporarily ceased production and are reviewing their manufacturing procedures.

The most disturbing reports relating to dioxin poisoning, however, are undoubtedly those from Vietnam. Increasing criticism of the American use of herbicides in the war in Indochina resulted in the National Academy of Sciences conducting a thorough investigation. The report of their findings, published in 1974, has been criticised over its interpretation of the data concerning deaths and birth defects in communities sprayed with herbicides. In an introduction to the report, Dr Philip Handler, the NAS President, claimed that no definite connection existed to confirm findings of herbicide-induced birth defects or deaths.

The NAS report itself does, however, contain considerable information about the effects of herbicides and the contaminant TCDD on humans, animals and vegetation in Vietnam. One anthropologist who submitted evidence to the NAS study, Dr Gerald Hickey of the South-East Asia Programme of Cornell University, has reported evidence of deaths from among the children of the Montagnard peoples of South Vietnam, deaths directly related to herbicide spraying. The first-hand interviews he conducted with Montagnard villagers revealed the additional evidence that other children had shown symptoms such as skin rashes, diarrhoea and abdominal pains.

Hickey was cautious in attributing these effects directly to TCDD; the evidence is more circumstantial. During the Vietnam war, the Americans repeatedly sprayed these mountainous areas of South Vietnam, inhabited by the Montagnard people, with the herbicide "Agent Orange", a 50 : 50 mixture of the n-butyl esters of 2,4-D (2,4-dichlorophenoxyacetic acid) and 2, 4, 5-T (2,4,5-trichlorophenoxyacetic acid). The dioxin TCDD is a contaminant present in 2,4,5-T at levels variously estimated at between 0.07 and 50 p.p.m.

Although the NAS report claimed that no evidence is available to substantiate herbicide-induced birth defects in humans, the Italian authorities are currently paying serious attention to the advice of a Vietnamese doctor. Professor Ton That Tung of the Viet Duc Hospital in Hanoi insists (in *Vietnamese Studies*, **29**, 53–81; 1971) that such evidence is available.

Unanswered questions

Certainly the assembled evidence points to some unanswered questions. Because previously recorded accidents at other trichlorophenol-producing plants had released TCDD, the chance existed that the same would be true in any accident at Seveso, and the authoritites might have expected to have been informed accordingly. But even in the unlikely event that the ICMESA management was unaware of the historical evidence pointing to this danger, simple theoretical knowledge of the factors favouring TCDD production should have alerted them to the possibility of dioxin contamination. Moreover, the plant's safety valve was situated outside the plant, allowing a discharge of vapour directly into the atmosphere. This served to protect the plant itself from the vapour, but did so at the cost of serious contamination of the surrounding countryside.

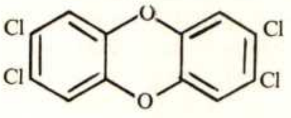

TCDD

(2,3,7,8-tetrachlorodibenzopara-dioxin)

TCDD is produced as a by-product during the alkaline hydrolysis of tetrachlorobenzene with methanolic sodium hydroxide to form 2,4,5-trichlorophenol **(1)**.

Trichlorophenol is both the industrial precursor of 2,4,5-T (2,4,5-trichlorophenoxyacetic acid), a herbicide normally used in esterified form as the butyl ester **(2)**, and an intermediate product in the manufacture of hexachlorophene, an antibacterial agent added to soaps, shampoos, deodorants and toothpastes.

The hydrolysis of tetrachlorobenzene is carried out at high temperatures and under pressure. This reaction, if not very carefully controlled, is favourable to the formation of TCDD, the most common chlorodibenzoparadioxin present in 2,4,5-T. Other toxic polychlorodibenzoparadioxins are also produced in the manufacture of chlorinated phenols.

Theoretically, at least 75 different chlorodibenzoparadioxins can be predicted having one to eight chlorine atoms attached to the two benzene rings. At least ten have been synthesised, and one or two more have been found in food, animal feeds and 2,4,5-T.

Hexachlorophene is prepared by the condensation of two molecules of 2,4,5-trichlorophenol with formaldehyde in the presence of concentrated sulphuric acid **(3)**. The preparation procedure has been improved, and the Givaudan Corporation hold the US patents Nos. 2,435,593 (1948) and 2,812,365 (1957).

Properties of TCDD

Like other chlorodioxins, TCDD is stable to heat, acids and alkali; a temperature of 800 °C is required for thermal decomposition. TCDD is virtually insoluble in water (0.0002 p.p.m.), only slightly soluble in fats (44 p.p.m. in lard oil), more soluble in hydrocarbons (570 p.p.m. in benzene), and at its most soluble in chlorinated organic solvents (1400 p.p.m. in ortho-dichlorobenzene).

Uptake of TCDD occurs slowly in plants (oats and soybeans). No accumulation above external concentration occurs, however, and plants grow to maturity (A. R. Isensee and G. E. Jones, *Agric. Food Chem.*, **19**, 1210–1214; 1971).

TCDD is almost immobile in soil. Even in very porous soil it remains close to the point of application (P. C. Kearney *et al.*, *Environ. Health Perspectives*, Exp. Issue No. 5, 273–278; 1973).

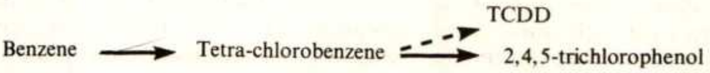

(1)

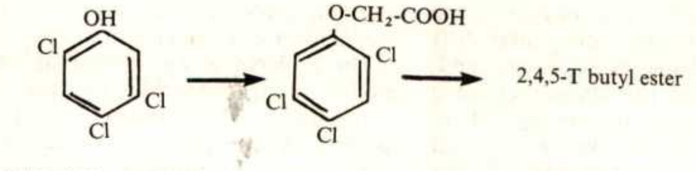

(2)

2,4,5-trichlorophenol 2,4,5-T

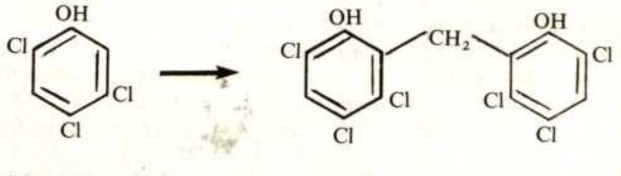

(3)

2,4,5- trichlorophenol hexachlorophene

The question of decontamination is now presenting Givaudan, Roche and the Italian government with serious problems. An Italian government commission recommended removal of topsoil to a depth of 10 cm in an area of 280 acres, the dismantling of all buildings in the Seveso area and the total disruption of all wildlife. These recommendations may take up to three years to implement. The sheer volume of soil to be processed and the number of buildings involved will create enormous technical problems of disposal. Great care will have to be taken to avoid further contamination by TCDD when material is removed from Seveso.

The British firm of Cremer and Warner have been retained by Givaudan to help in the task of decontamination. Cremer and Warner are chemical engineers specialising in the environmental safety aspects of industrial pollution. Data already accumulated indicate that the intensity of contamination does not conform to any uniform pattern, and the feeling is that it would be premature to implement the Italian commission's proposals, at least until potential alternatives are considered.

But no one doubts that a satisfactory policy for accident prevention and control can possibly be formulated if vital information is withheld from those whom it may affect most directly. In Seveso, the local mayors did make attempts to find out what was actually being produced at the ICMESA plant. But that was four years ago. Only last year did Givaudan finally provide some information. No mention was made of the dioxin risk, and therefore no safety measures were suggested. Even now there is conflicting information about the processes for which the ICMESA works were designed. One senior Roche executive has said the plant was producing trichlorophenol for the manufacture of the herbicide 2,4,5-T; another spokesman claimed that the plant was making trichlorophenol for the manufacture of hexachlorophene at another site.

Few unaffected

Few people have been uninvolved by the actions of the Roche subsidiary. Scientists and engineers at the Seveso plant failed to predict the extent of dioxin contamination and its spread over the countryside. Workers at the factory demanded to know of any dangers involved. Management did not inform them until two weeks after the explosion. Local residents knew nothing of the real hazards of the contamination. The medical profession, lacking an antidote, must give only symptomatic treatment. Pregnant women, agonising over the teratogenic effects of TCDD, must decide with little firm guidance from the Church whether to undergo abortions. Ecologists cannot predict the long term effects of dioxin contamination. The authorities know that the decontamination proposals themselves are at best a mixture of policies adopted at previous accidents, leavened with a good deal of hope.

The suggestions being made now involve at the very least the implementation of strict codes of practice, to be adopted between industrial concerns and the local authorities to which they bear a great measure of responsibility. Such codes would include detailed procedures to be followed in the event of an accident. As for the withholding of information, few are accepting the obvious convenience this represents for manufacturers as a satisfactory explanation. Many are saying that with all the facts more freely available, it may, for example, be decided that the risks involved in producing trichlorophenol outweigh the necessity of a 2,4,5-T weedkiller—or a TCP mouthwash. Only the inquest now to come will reveal whether some sort of political solution is needed to ensure that the necessary information is available and to prevent a recurrence of this kind of disaster. □

Europe's ageing research staffs

Mike Duckenfield reports from Stockholm on the problem of an "unhealthy" age profile among researchers and teachers

WITH one or two exceptions, notably Finland where spending is to be increased from 1% to 1.7% of the GNP during the next five years, research budgets in most Western European countries are having a struggle to keep pace with rising costs. Not only is government spending being cut back or slowed down, but what funds there are available are being affected by an incremental drift of salaries as young staff get older and, as in Britain and the USA, increasing unionisation. Even in Norway, where unemployment is well below 2% and economic growth at a steady 7%, the prospects for those wanting research jobs are very slim.

Graduate unemployment is a problem in itself, but there is also another side to the coin: the likely prospect of universities and research institutes in most nations losing a generation of teachers and researchers during the next 15 years due to the lack of job opportunities. The problem, in short, is that the universities are now moving into the shadow of the massive expansion of higher education which took place in the 1960s. Due to this boom the average age of teachers and researchers is now very low, retirements are relatively few and future openings for new blood and ideas drastically diminished. According to academics in several countries, promotion, mobility and possibly even creativity are all likely to suffer.

The problem of an "unhealthy" age profile among researchers and teachers is beginning to be studied in nations ranging from France to Norway. Due to large scale recruitment in the middle and late 1960s, too large a proportion of staff are now only at the beginning of their careers. A recent Federal German survey shows that while 45.9% of professors and senior lecturers in 1966 were over 50 years old and only 22.3% under 40, corresponding figures for 1972 were 28% and 30.5.%. In addition, while other teaching staff under 35 accounted for 17.4% of the total in 1966, six years later the figure was 27.3%.

In Britain, too, the average age of university teachers has fallen significantly; now 63% of academic staff are under 40, 26% are under 30 and 13% over 50. In Norway 18.8% of staff are over 50 compared with 43.7% under 35, while a survey of French research workers in the Centre National de la Recherche Scientifique showed the average age of those engaged in mathematics was 28 years and 7 months and those in physics and chemistry 34 years and 5 months. In Sweden as many as two-thirds of researchers in some branches of social science are under 35.

With comparatively young staff holding most of the senior positions, future promotion prospects are well below normal. A report prepared for the Council of Europe by Gert Elstermann, academic director of the University of the Saarlands, says that the annual replacement demand for teachers in Federal German universities and colleges up to 1990 will remain much the same as it is at present in law and the social sciences. For other subjects it will stay unchanged until the mid-1980s. Similarly, in Norway prospects for the next 15 years suggest annual recruitment levels below those of any year since the early 1960s. In

•

1972 there were 270 new jobs, this year only about 30 are expected.

Elstermann calculates that while an assistant lecturer in Germany had more than a 70% chance of being appointed as an established university teacher—in many cases as full professors—in the 1960s, in the 1976–85 period these chances will fall to only 15% before rising slowly to 23% in 1990 and 30% in the year 2000. Writing in last year's annual Norwegian research review, Hans Skoie, deputy director of Norway's Science and Humanities Research Council's Institute for Studies in Research and Higher Education, commented: "There is a definite danger that universities and research establishments may develop into communities of senior citizens leaving membership of future classes of graduates with miniscule chances of getting research jobs."

He fears that potential scientists will be discouraged from going on to higher studies and many of the best talents lost. This in turn would lead to less research being performed through thesis work, thereby deteriorating the chances of senior staff to carry out their own projects. The trend against further studies has been evident for several years in neighbouring Sweden. In 1968, 37% of graduates went on to further studies. By 1971 this had fallen to 22.5% and last year it was down to only 14%. The Swedes are especially worried about their failure to attract students in mathematics and the natural sciences.

Another fear is that as the present research population gets collectively older fewer will be likely to change jobs—a trend reinforced by the tight employment market. This lack of mobility could then affect contacts between the universities, research institutes and commercial laboratories, and a Council of Europe report presented recently to a meeting of the organisation's committee for higher education and research concludes that the overall result could be stagnation and a possible decline in research creativity.

Attempts to overcome the age imbalance problem vary widely. In France priority is being given to the recruitment of contractual staff as against creating new tenured positions which would have the status and security of those of civil servants. In Federal Germany the remedy advocated has been a strict adherence to temporary contracts, with nearly all staff below professorial level being untenured, the idea being to maintain a steady flow of young academics through the universities. However, long term solutions of this kind are almost certain to be opposed by the trade unions.

Other suggestions include encouraging older researchers to apply for senior administrative posts, introducing productivity or merit increments instead of those based on seniority or simply age, making the retirement age more flexible, offering increased opportunities for leave of absence, more academic exchange programmes and, perhaps rather optimistically, simply filling staff vacancies as soon as they occur. □

CHEMICAL WEAPONS

Disarmament by phases

At the Conference of the Committee on Disarmament (CCD) in Geneva, Britain last week tabled a draft convention on the prohibition and destruction of chemical weapons to complement the 1925 protocol banning their use in war. Chris Sherwell reports

THE search for a convention to cover unconventional weapons continues. The latest initiative has come from Britain in the sphere of chemical weapons, and, as the UK representative explained to the 720th plenary meeting of the CCD, combines new ideas and constructive and realistic elements from previous drafts into a draft treaty which is being presented as a focus for negotiation.

The 17-Article draft, which the CCD's 30 member states will study before their spring session in February next year, has several features. The emphasis on "confidence building" is one. Under Article II signatories would each establish or nominate a national verification agency; in declaring whether or not they were in possession of chemical weapons and producing figures they would, it is hoped, be generating the confidence without which the main provisions of the treaty would not come into effect.

Article III is also aimed at confidence building. It amounts to a moratorium on production of the chemical weapons specified in a protocol still to be negotiated for Article I, by which signatories would have undertaken "never, in any circumstances, to develop, produce, or otherwise acquire, or use" chemical weapons or munitions or their delivery systems.

Another feature is the draft's three-stage implementation. After the first phase, in which signatories would stop production of chemical weapons and would provide information, the main provisions of the treaty would come into operation. The third stage, marked by Article VII, provides for the phased destruction or conversion to peaceful use of chemical weapons and the destruction of stockpiles. The exact programme is left for negotiation, but a Consultative Committee would arrange for the vital aspects of verification, inspection and exchange of information. Article IX offers a framework, which could also be amplified in a protocol.

Britain does not have any specific time scale in mind for the conclusion of a chemical warfare treaty, and with the summer session of the CCD about to end, is looking only for preliminary reactions. She has shown some eye for timing, however. Eastern bloc countries put up a draft convention in March 1972, as did Japan in April 1974; non-aligned countries had suggested a series of guidelines the previous year. In 1974 Canada suggested the phased destruction of all CW agents. This received the crucial support of the USA in April this year which, in the absence of the promised US–USSR initiative, made this the appropriate time for consolidation.

The time was also right because of technological improvements in monitoring techniques and because the experience of the International Atomic Energy Agency over nuclear safeguards showed that monitoring and protection of military and commercial secrets were not mutually exclusive. The US–USSR agreement earlier this year concerning on-site inspection of "peaceful" nuclear explosions is also regarded as an important breakthrough.

Whether Britain thinks member states now really believe that chemical weapons are unnecessary or that there is no need for stockpiles is another matter; the purpose of the latest proposal, however, is not seen as being to establish which countries are thinking along these lines by discovering their reactions to the draft. A readiness to move forward is apparently perceived, although it is acknowledged that the USSR might choose to describe any concessions it makes over verification in terms of "peaceful collaboration", rather than admit the change. □

COMECON

• The 30th meeting of Comecon in Berlin last month, held to assess the first joint five-year plan and discuss future integration, considered the prospect of integration over a fifteen to twenty year period in certain major sectors, including nuclear power. According to the joint communique of the meeting, there has been a "rapid growth" in the use of nuclear power during the past five years; the present capacity of nuclear power stations in the Comecon countries amounts to 7.5×10^6 MW, with an expected increase by 1980 to 30×10^6 MW, and Mr Kosygin in his address stressed the great importance of the "acceleration of the construction of nuclear power stations".

There have, however, been reports of the breakdown of Interatomenergo, the supranational Comecon body responsible for the construction of nuclear power stations, particularly since, shortly before the meeting, the Hungarian Deputy Premier Istvan Huszar strongly criticised the establishment of such supranational bodies whose policies may well run counter to those of individual members. In fact there seems to be no direct evidence that Interatomenergo (founded in December 1974) has broken down, although power supplies are, indeed, a pressing problem to Comecon.

About half, perhaps more, of the Comecon countries' electricity could be nuclear by 2000, but the short term solution cannot be a nuclear one: immediate plans for the exchange of power resources, which should in turn allow the reserve capacities of individual countries to be reduced, will for the moment be based largely on thermal power stations. Thermal power stations at present contribute some 87% to the total generating capacity of Comecon, and even with the planned nuclear expansion of the next five years, when nuclear power capacity will increase from 2.5% to 8% of the total, the role of the coal- and lignite-powered thermal stations will remain significant.

It seems doubtful that the Comecon countries will be able to fulfil all their long term plans without outside (that is, western) help, however, at least insofar as these plans depend on the development of more advanced reactors, such as the fast breeder, by the USSR. For the moment, though, the focus is on pressurised water reactors of the Voronezh type, which the USSR has developed commercially and can supply to its Comecon partners, including Cuba. And few in the West's nuclear industries doubt the benefits conferred by Comecon's unquantified but adequate uranium resources and by an equally unquantified but certainly unorganised anti-nuclear lobby.

• An agreement between the Comecon countries (including Mongolia and Cuba) on further cooperation in space exploration was signed in Moscow last month. According to Academician Anatolii Aleksandrov, President of the Academy of Sciences of the USSR, the agreement envisages cooperation in launching spacecraft, designing equipment, geological and meteorological surveying, joint technological research and the exchange of scientific data.

Such joint research has, of course, been taking place for some seven years now, under the Interkosmos programme. The latest two satellies in this series, Interkosmos 15 and 16, were launched on June 19 and July 27 respectively, and mark a new development in the programme—the monitoring of data from the satellites by member countries other than the USSR. Suitable receiver stations have already been built in Hungary, the GDR and Czechoslovakia, with Cuba and Bulgaria scheduled to join the monitoring network in the near future. The new Interkosmos satellites carry a special unified telemetry system developed jointly by Hungary, the GDR, Poland, Czechoslovakia and the USSR.

This stress on greater participation by the non-Soviet members of Comecon inevitably invites debate about the further development of the programme. Already there seems to be a trend for countries to specialise in individual fields of the programme. The data on solar radiation being gathered in the current experiments is being processed by a Polish team in Torun, although it is also being assessed in Moscow by the Lebedev Physics Institute, which acts as coordinator. The GDR and Czechoslovakia appear to be especially concerned with the development of sophisticated electronic and optical equipment.

Such devolution and specialisation, if carried through, could well provide a new impetus to a programme in which, to date, one or two non-Soviet experiments at a time have been included in a still largely Soviet project.

The growing participation of member countries in the back-up research for manned space flights is another new feature of Comecon space research. The recent joint "Biosputnik" programme, according to a statement from Professor Stanislaw Baranski, Chairman of the Commission on Biology and Space Medicine of the Polish Academy of Sciences, has shown that three weeks in conditions of weightlessness "posed no danger" to the locomotor system or to muscle and bone tissue, but that the adrenal gland functions "revealed changes typical of stress". Similarly, the Hungarian Joliot-Curie Radiation Biology Institute has developed a model which absorbs various types of radiation in the same way as does the human organism. Although other, more conventional applications of this model are possible, notably in monitoring laboratory and industrial radiation hazards, its application to space research is especially emphasised.

This participation in space biology by the non-Soviet members of Comecon, which will continue with another "Biosputnik" project next year, raises the question of possible participation by Comecon crew members in Soviet space flights. Soviet space planning is greatly influenced by the concepts of Tsiolkovskii, who envisaged a large permanent orbiting space station as a *sine qua non* for any exploration deeper into space, and among the crew of several hundreds which he postulated for such a station, room for a token number of participants from Comecon member countries could presumably be found. The Soviet Academician Boris Petrov, Chairman of the Interkosmos Council, discussing the new Comecon space agreement, has meanwhile said that the Soviet Academy of Sciences is to hold talks in the near future with NASA about further cooperation in manned spaceflight.

Vera Rich

IN BRIEF

Immunisation clearance

A major hurdle to President Ford's $130 million nationwide programme of immunisation against swine 'flu has been removed with the successful passage through Congress of legislation providing for individual claims for damages as a result of inoculations to be filed against the government. Mr Ford last week signed the bill introducing Federal liability following threats of withdrawal from vaccine manufacturers themselves unable to arrange cover with private insurance companies. Under the new law injured parties would sue the government which could in turn sue programme officials accused of negligence or malpractice.

Marine conservation moves

Good news and bad for marine conservationists. The bad news came last week when Britain, having lodged an objection with the North East Atlantic Fisheries Commission against continued overfishing of herring in international waters, itself decided to exceed the commission's recently-set catch quotas. Britain had earlier called for a complete ban on North Sea herring fishing, and only the Norwegian Prime Minister has asked his country's fishermen not to exceed existing catch limits when the exclusive economic zone extends to 200 miles.

The good news arrived with agreement between Brazil, Japan, South Africa and the USSR on catch figures for minke and sei whales in southern oceans over the next year. The new shares are based on reduced overall quotas set by the International Whaling Commission during its recent annual meeting in London.

Animal experiment proposals

A memorandum from a Parliamentary committee urging tighter controls over laboratory experiments with animals is now before the UK Home Secretary, Mr Roy Jenkins. The memorandum calls for new legislation more appropriate to modern experimental requirements, a more stringent system of licensing, and an increase in the number of government inspectors. It also urges an enlargement and greater powers for the Home Office Advisory Committee on Animal Experiments, which has met only 7 times in 10 years. The memorandum marks the launching of Animal Welfare Year and coincides with the centenary of the still current Cruelty to Animals Act. Last year saw a 3.3% drop in the number of experiments with living animals in Britain to just over 5.3 million.

Censor judgment

KENNETH MELLANBY

Progress in science depends on the communication of the results of research between scientists. There are those who think that the usual channels—the learned journals—do this inefficiently, and who propose novel techniques, but in practice the old methods continue. However, journals can only do their job if scientists submit papers describing their work, and if editors select good papers and reject bad ones.

This selection means that some sort of censorship operates, however much we may dislike the idea. Papers are refused because they are badly presented, or because their scientific content is considered unsatisfactory. Unfortunately many scientists cannot write clearly, and some ignore the instructions about presentation given by the journals to which they submit their work. Editors consider themselves justified in refusing badly written papers, but if the work described is good, they should try to encourage the author to resubmit an acceptable draft. Unfortunately few editors have the time to rewrite a manuscript, and therefore the results of some good work may be lost.

Fortunately for editors, in many university departments or research institutes the writings of junior workers are vetted by their senior colleagues, and this may ensure a proper standard of presentation and content. Generally this system works well, but occasionally the publication of valuable results is unnecessarily delayed by what amounts to internal censorship. There are those who are so obsessed by the bogy of premature publication that they always advise, or even insist on, delay. At the same time many scientists find writing up their work to be tedious and difficult, and again they delay publication. Research workers who accept public money and then delay or do not publish their results could be considered guilty of fraud to the scientific community.

To judge the scientific merit of papers offered to them, editors usually rely on expert referees. Most referees take their duties responsibly, and make satisfactory assessments. Unfortunately some referees are prejudiced and recommend rejection of results contrary to their preconceptions; editors must be on their guard against this type of censorship. Even with the greatest care, however, mistakes are made, as it may be hard to distinguish originality from idiocy. Outstanding scientists whose work is rejected may console themselves with the knowledge that, if it is good, recognition will not long be delayed. Unfortunately many of the unrecognised geniuses who complain that their work remains unpublished have little of worth to contribute to science.

The most controversial issue is the use of censorship on moral or ethical grounds. Most scientists consider that certain types of cruel animal experiments should be forbidden, and some journals have a policy of refusing to print articles describing such work. Papers describing what are considered to be unethical medical practices are also refused by a number of editors. At first sight this type of censorship seems to be justified, but has an editor the right to assume this "holier than thou" attitude? If the work is of scientific importance, or is likely to advance medicine substantially, has he a right to suppress it in this way?

If a research worker has done something which is illegal, or which contravenes the conditions of a vivisection licence, he should perhaps be warned of the possible consequences of the publicising of such acts. Editors may need to take legal advice regarding their possible liability for publishing such results. But scientific merit must surely remain the criterion by which scientific research and publication is judged. Unethical practices should be prevented, but not by censorship.

correspondence

Scientists in Argentina

SIR,—My intention in writing this letter is to present another point of view regarding the position of scientists in Argentina. The letter written by 70 Italian scientists (July 22, page 253) has indeed surprised me.

I can remember that a law identical to the one which the Italian scientists referred to (Ley de Prescindibilidad) was passed two years ago by the constitutional government of Argentina. Under that law the Peronist government "released from duty", for "reasons of service" with no further justification, thousands of public workers from both scientific and non-scientific institutions. It is funny that at that time this group of Italian scientists did not air complaints. In this previous instance the Minister of Education of the Peronist government established very clearly a policy inspired by the criterion "who is not occidental and Christian is subversive". He repeated this criterion in several public talks, and again at that time no complaints from this group of Italian scientists were heard.

If scientists are interested in the advancement of science and not in politics then they should be impartial in judging the internal political situations that affect a scientist's work, especially in South America where these problems very frequently arise.

Subversion in Argentina could be found in every department and institution of the government. Subversives are not only those who plant bombs; they are also those who support the "guerrilla" in different ways, those who steal public money and those who use power to their own benefit. Argentina is now fighting for its survival against these groups and fortunately it is winning. Of course there may be some unjustified cases in which an innocent person is "released from duty", but many more innocent people lost their lives in bombings and terrorist acts.

I am completely sure that among the 550 scientists (according to the Italian scientists' letter) who lost their jobs there might be a few innocent victims. These mistakes are unavoidable; but there are also many more who have used their public jobs for political activism. I know personally a number of scientists who in many years have not published a single paper describing their research. Apparently there was no research which suited their personal interest; only politics. During these many years the taxpayers paid their salaries.

It is not true that leftist people are being pursued in Argentina. Terrorists and guilty people, disregarding their political preferences, are being pursued. Numerous rightist members of the last government are now in jail because of mismanagement of public funds and robbery.

Because of the economic disaster produced by the previous government scientific institutions had to cancel their subscriptions to practically all scientific publications. Since I am temporarily in the USA continuing my research, I am perhaps one of the few Argentinian scientists who can read *Nature* and other publications in my field of interest. My colleagues in Argentina are not so lucky.

It is very difficult for Italian scientists to imagine the real situation in my country in all aspects (not only science) over the past four years. For that reason I understand that it must be difficult for them to state an impartial opinion taking into account all the facts. Certainly it was an incorrect evaluation by these 70 Italian scientists that led them to write their uncritical letter to *Nature.*

HUGO LEVATO

Kitt Peak National Observatory,
Tucson, Arizona

Alternative refrigerants

SIR,—F. A. Cotton (Correspondence, March 25, page 280) attributes to us the suggestion that, "if we do not choose to give up refrigerators, we may have to continue tolerating atmospheric pollution by chlorofluorocarbons, even if we ban aerosol cans". In fact, we made no such suggestion, as any reader can verify (Correspondence, March 4, page 8). Our letter dealt with facts only, and we suggested that any decision to ban R-12 take those facts into account.

Cotton states that "refrigerators . . . normally release their refrigerant gas only when junked". Actually, the reverse is usually true; refrigerators are junked once their moving parts are so worn that they can no longer retain the refrigerant for a reasonable length of time For this reason alone, Cotton's suggestions for laws promoting the recovery of refrigerant from refrigerators would not solve the problem of chlorofluorocarbon refrigerant release to the atmosphere.

W. J. Megaw (Correspondence, May 6, page 261) says a short release time of two years for a refrigerant is partly due to freeze drying applications and partly due to head and tail collisions of automobiles containing air conditioning systems. A Bureau of Domestic Commerce study (*Economic Significance of Fluorocarbons,* December 1975) does not identify freeze drying as a significant source of fluorocarbon emission. The one- to two-year replacement time for automobile refrigerants is again due to leakage; automobile air conditioners are of necessity light weight and are subjected to vibrations and temperature extremes of the automobile engine. Automobile air conditioners use R-12 exclusively.

The BDC study attributes R-22 as being 30% of the total refrigerant used, not 50% as Megaw states. R-22 is used primarily in building air conditioning where low temperature is not required. Commercial and home refrigerators and freezers use R-12 almost exclusively. R-12 and R-22 are not interchangeable in existing refrigeration equipment, valued at $100,000 million, because they have quite different physical properties. Total replacement of R-12 and R-22 would require redesigning many refrigeration systems. These refrigeration systems will necessarily be more expensive since they must operate at higher pressures. Difficulties posed by compressors burning out have thus far prevented the use of R-22 in refrigerators and freezers This design problem is a consequence of the high heat of compression, low density and high specific heat of R-22.

Model calculations by Sze and others indicate that an additional two years of fluorocarbon production will lead to 0 1% additional ozone reduction. This assumes an infinite troposphere lifetime for R-11 and R-12, that is, a maximum reduction in the ozone. We believe that an immediate ban on refrigerant or aerosol propellent uses of R-11 and R-12 would be unwise in view of present uncertainties in the theory. The two-year moratorium requested by industry to continue research programmes that began over a year ago, and which have already been fruitful, is very reasonable.

THOMAS J LECK
JOHN W. BIRKS

School of Chemical Sciences,
University of Illinois, Urbana

news and views

Assumed dipolar geomagnetic field

from Peter J. Smith

WHEN Johnson *et al.* (*Terr. Magn. atmos. Elect.*, **53**, 349, 1948) carried out their early palaeomagnetic work on recent Pacific sediments and the Holocene glacial clays of New England, they clearly saw their studies as just part of a much grander design. In respect of the wider aim their point was that "in order to determine the origin and nature of the Earth's magnetic field and to test the various hypotheses which have been advanced to explain the field, it is desirable to determine the history of this field throughout geologic time and to investigate more carefully its spatial variations, both inside and outside the Earth's surface".

As it turns out, it has been possible to make progress on the origin of the geomagnetic field largely without invoking the geological time dimension, and to this limited extent Johnson and his colleagues were mistaken. The self-exciting dynamo, the only viable field source known, may be regarded as an explanation of the present and recent fields without necessarily accepting that the details of any dynamo model applicable to today's field were valid throughout the Earth's history. Since the dynamo was discovered, detailed models have, of course, been extended to the geological time scale by the incorporation of field reversals and field intensity fluctuations, and for this and other reasons it is implicit in most modern models that the geomagnetic field has always been predominantly dipolar But there is nothing in the dynamo principle as such that would preclude higher order fields in the past; and to the extent that more than the principle is applied to past ages, the dipolar nature of the field could be said to appear as an assumption.

It also appears as an assumption in most studies involving palaeomagnetic directions. Until the 1950s, palaeomagnetists generally felt that sufficient measurements would make it possible to define the morphology of the geomagnetic field throughout much of the Earth's life, subject only to the availability of enough rocks with sufficiently stable magnetisations. But ironically they were to be thwarted in this by their greatest achievement, the quantitative proof of continental drift. Once it became clear that continents had moved, it became equally evident that no simple test for dipolarity based on a stationary frame of reference could exist beyond very strict limits. It would be impossible to separate easily the effects of definitely moving rocks from those of possibly changing field shapes.

So the dipole assumption now appears in two different situations, making it just as desirable to determine the history of the geomagnetic field as it was in the time of Johnson *et al.* But how can the dipole hypothesis be put to the test? As far as very recent times are concerned there is no problem, for movement of the reference frame resulting from drifting continents has been small and changes in palaeomagnetic pole positions on that account have been within the errors of measurement. Thus more than a decade ago, Irving (*Paleomagnetism and Its Application to Geological and Geophysical Problems*, Wiley, New York, 1964) showed that the eleven then-available poles covering approximately the past 7,000 yr were grouped around the present geographic pole, and McElhinny (*Palaeomagnetism and Plate Tectonics*, Cambridge University Press, 1973) has shown that British archaeomagnetic poles taken at 100-yr intervals from AD 1900–1000 and AD 300–100 were distributed likewise. Both results suggest that during the past few thousand years at least the geomagnetic field has been dipolar and that on average the dipole lay along the rotational axis.

In practice, this test may also be successfully extended somewhat further back in time. According to McElhinny, for example, 67 poles covering the past 5 Myr are clearly grouped around the geographic pole with a mean pole at 88.8°N, 131.9°E. Opdyke and Henry (*Earth planet. Sci. Lett.*, **6**, 139; 1969) showed that palaeomagnetic inclinations from 52 deep sea sediment cores less than 3 Myr old were in close agreement with those to be expected from an axial geocentric dipole. And Tarling (*Principles and Applications of Palaeomagnetism*, Chapman and Hall, London, 1971) has even shown that poles from igneous rocks up to 20 Myr old are grouped around the geographic pole, albeit with a greater scatter than for shorter, more recent periods.

Wilson and Ade-Hall (in *Palaeogeophysics*, Academic, New York, 1970), on the other hand, found a tendency for Quaternary and Upper Tertiary poles from individual regions to lie on their respective far sides of the geographic pole. On the face of it, this would seem to call in question the average axial nature of the dipole, although Wilson (*Geophys. J.*, **19**, 417; 1970) attributed the phenomenon to deviations from geocentricity; the axial dipole is apparently shifted northward with respect to the Earth's centre. In any event, the effect is small enough to be regarded as a second approximation. In no case is the basic dipolarity of the field in question; on the contrary, the dipole assumption is strengthened.

Beyond the Upper Tertiary, however, interference from continental movements causes difficulty. Over the longer geological period, poles of similar age from different regions of a single rigid landmass seem to be consistent with an average axial dipole, the variation of the dispersion of palaeomagnetic directions with palaeolatitude is usually comparable with that to be expected from the present dipolar field, and palaeolatitudes calculated on the axial dipole hypothesis are broadly consistent with latitude-dependent palaeoclimatic indicators. But none of these can be regarded as a rigorous test of dipolarity; the best that can probably be said is that there is little evidence actually to refute the dipole. The new test for dipolarity and its application to the Phanerozoic, reported by Evans on page 676 of this issue of *Nature*, is thus very welcome, although other tests may still be required before the persistence of the dipole can be said to be scientifically certain. ☐

Predator or prey?

Peter D. Moore

It is not unreasonable to suppose that a predator normally reduces the numbers of its prey, but there are certain exceptions to this general principle. One example emerged from the experiments of Porter (*Nature*, **244**, 179; 1973) on the grazing of zooplankton upon planktonic algae. In a small mesotrophic lake in Connecticut she enclosed water samples in 0.5 m^3 polythene bags and artificially enriched the population of zooplanktonic grazers within some of these. After four days Porter sampled the various bags and determined whether each of the phytoplanktonic taxa represented had decreased or increased in density.

Flagellates, nanoplankton and diatoms were suppressed by raised grazing pressures; desmids, dinoflagellates and chrysophytes were unaffected but, rather surprisingly, the larger green algae increased in density under more intense grazing. The unaffected groups were rarely found in the guts of the grazers; they were probably selectively avoided. The greens, particularly those species with a gelatinous sheath around their cells, were found to be viable after passing through the guts of grazing zooplankton. Porter suggested that the fragmentation of larger colonies of gelatinous greens in *Daphnia* guts could enhance population growth rates. She also considered it possible that the gelatinous sheaths could protect the cells against digestive enzymes and yet allow the cells to take up inorganic ions and small molecules even within the animal's gut.

Porter has now put these ideas to the test (*Science*, **192**, 1332; 1976) in a series of experiments involving radioactive tracers. The colonial alga *Sphaerocystis schroeteri*, which has a mucilage sheath, was fed to the grazing crustacean *Daphnia magna*, together with the desmid *Ankistrodesmus falcatus* (no mucilage sheath) which had been supplied with $NaH^{14}CO_3$ and $K_2H^{33}PO_4$. Subsequent sectioning and autoradiography of the *Daphnia* gut showed that both ^{33}P and ^{14}C had been taken up by *Sphaerocystis* from the broken cells of *Ankistrodesmus*. ^{14}C uptake was enhanced by light, suggesting that its uptake was autotrophic. Thus nutrient supply, as well as the physical dissociation of algal colonies, may contribute to the observed enhancement in population growth rate. Porter has now been able to quantify the enhancement, for in a controlled experiment, the population of algae which had passed through a *Daphnia* gut had grown by 63% in 24 h. Ungrazed populations were unchanged in the same period.

Porter points out that the mucilaginous green phytoplanktonic taxa like *Sphaerocystis* have summer rather than spring blooms. At this time free nutrients in the water are depleted and the guts of grazers provide a locally enriched microhabitat. Porter refers to the relationship as one of 'nascent symbiosis' between acquatic plants and grazing animals. But it is certainly not a mutualistic one. It is a refreshing example of an evolutionary confidence trick whereby the hunter is exploited by its supposed prey.

How closely should continents fit together?

A recent article by Hallam (*News and Views*, **262**, 94; 1976) in which my paper on global expansion and continental displacement during the Mesozoic and Cenozoic (*Phil. Trans. R. Soc.*, **A281**, 223; 1976) is reviewed, contains certain factual errors which need to be corrected. Less important is his initial statement that I have argued post-Pangaea continental displacement to be a consequence of global expansion since the early Jurassic. This is not entirely correct, and the importance of the role of convection in the asthenosphere in the production of the Earth's oceanic crust is implicit throughout the paper. The continental geological information, oceanic-floor spreading patterns and the distribution of present and former subduction zones during the last 180 Ma indicate global expansion at the rate envisaged in my paper. These data do not support the concept of an Earth of constant modern dimensions, as progressive subtraction of isochronous oceanic crustal area on such a model readily shows.

Hallam cites three examples of areas of continental crust which occur in the magnetic quiet zones, and which might affect the fit of the continents together to reform Pangaea such as that given in my maps. The paper by Jansa and Wade (*Geol. Surv. Canada Pap.*, **74–(30)2**, 51; 1975) to which he refers actually describes the submerged continental shelf off Newfoundland including Flemish Cap. It is indeed continental crust and is shown as such on my maps. The adjacent Atlantic oceanic crust with its typical seismic and magnetic characteristics is well described by Grant (*Geol Surv. Canada Pap.*, **74–30(2)**, 217; 1975) in the same volume. The magnetic quiet zone east of the Vöring Escarpment described by Talwani and Eldholm (*Bull. geol. Soc. Am.*, **83**, 3575; 1972) is also included in my maps as continental crust; the area to the west of it shows simatic crustal characteristics. The paper by Burollet and Byramjee (*Notes Mém. Comp. Fr. Pétroles*, **11**, 71; 1974) does not provide definitive evidence that widespread crustal areas off the continental shelf of Africa consists of downfaulted continental crust. The evidence available does indicate that east of the margin of the east African continental shelf, a thick sequence of sediments occurs probably extending back into the mid-Mesozoic as in the case of the eastern region of the Wharton Basin adjacent to the Australian continental shelf. The continental shelf off Tanzania shown on my maps has a sequence of sediments extending back into the Palaeozoic (Kent and Perry (*Sedimentary Basins of the African Coasts* (Edit. by Blant, G.) **2**, 113; 1973) and Kent and Tarling (*Nature*, **261**, 304; 1976)). The examples given by Hallam, therefore, cannot be considered as convincing evidence against the major geometric problems considered in my paper, and indeed, the mounting geological evidence against the triangular Tethys Ocean required by constant dimensions reconstructions cannot be ignored (and this specific problem is recognised by Burollet and Byramjee (*op. cit*)).

Hallam refers to the controversy about the original position of Madagascar in the Gondwanaland reconstructions. There is evidence that Madagascar reached its northern position relative to the eastern African margin in the early Mesozoic, having moved northward during the Palaeozoic in response to pre-Pangaea crustal movements. The evidence put forward by Flores (*Trans. geol. Soc. S. Afr.*, **73**, 1; 1970) for a position of Madagascar adjacent to South East Africa and Rhodesia—Mozambique during the deposition of the lower Karroo should be given careful consideration by workers interested in this area.

H. G. Owen

How approximate are the laws of plate tectonics?

HALLAM (*News and Views*, **262**, 94; 1976) has commented on a paper by Owen (*Phil. Trans. R. Soc.*, **A281**, 223; 1976) who put forward a case for very substantial recent expansion of the Earth. Both writers discussing this problem (and certainly the history of *G* is still a very open question, (Lewis, *Nature*, **261**, 302; 1976)) appear to base their arguments on what Hallam terms a fundamental tenet of plate tectonics, "that the amount of crust created at ocean ridges must equal the amount subducted elsewhere". This is in fact, a law of constancy of mass of both oceanic and continental crust. The purpose of this comment is to point out that such a basic tenet cannot hold exactly for a body like the Earth which is mixing as it cools. A major problem of our science today is to find out just how approximate such laws really are. It also seems that if continents are to fit like pieces of a puzzle, there must also be laws of constancy of area and shape. Again, this cannot be exact for we know that the processes which lead to separation change thickness.

While at present we certainly cannot exactly quantify major earth-shell interactions, certain facts must be considered and I would here draw attention to a few examples:

(1) The rate of delivery of potassium to the oceans by solution processes alone is about 7×10^{13} g yr^{-1}. If such a value was typical throughout Earth history, then a mass of potassium equivalent to all that present in the continents would be delivered to the oceans in about 5×10^9 yr. If we add the particulate contribution then the rate of removal of continents is much faster. As stated by Gilluly, Waters and Woodford (*Principles of Geology*, Freeman, 1975) "were the present rate of erosion for the United States maintained without further uplift or isostatic rebound, the country would be reduced to sea level in about 14 m.y."

(2) According to Sibley and Vogel (*Science*, **192**, 551; 1976) "pelagic sediments, in contrast to other sediments, are not usually recycled; most are subducted and therefore act as a geochemical sink". Assuming some truth to this statement, then, as the rate of formation of pelagic sediments with about 3% potassium is about 1 km^3 yr^{-1}, again this would subduct all continental potassium in 5×10^9 yr. The formation of such sediments involves the oceanic mixing process and a potassium atom from the Mississippi may well be subducted at the Chile–Peru trench.

(3) Low K basalt comes up and higher K spilite is subducted (Keen, *Geosci. Can.*, **2**, 36; 1975). The surface layers of the ocean floor crust appear to average about 1% potassium. While there are many uncertainties (Fyfe, *Geosci. Can.*, **3**, 82; 1976) potassium removal by way of spilite subduction seems in the same order of magnitude as that supplied to the oceans by solution.

(4) Low quartz andesites debris (graywacke) may well be subducted at appropriate sites by way of the reactions graywacke-glaucophane schist-quartz-phlogopite eclogite. We know little of this process except that we do know that graywackes are dragged to depths of at least 30 km to form glaucophane schists.

In summary, there is good evidence that the continents cycle through the oceans and back to the mantle at a rate that could change crustal balance. In the spreading process, leading edges (the Andes for example) thicken and trailing edges must suffer massive erosion, even by solution. During the motions there need be no perfect conservation of mass or shape of continental crust.

Finally, it should be noted that the present configuration of the Earth would not be stable for a cooler, mixed, body. In such an Earth, the hydrosphere would hydrate the mantle, and "continental" elements like K, Na, SiO_2, would form stable compounds like phlogopite and pyroxene in the mantle. Our crust and hydrosphere, even if subducted (Fyfe, *loc. cit.*) tend to be thrown back by thermal processes.

But if the Earth is cooling, there must be increased mantle fixation of crustal components because the Earth is mixing. If we allow that the combined influences of all the above mentioned processes, subduct the continental mass about each billion years, then we could lose 20% in 200 Myr. Perhaps the interesting fact is that the steady-state approximation of plate tectonic theory is rather good.

W. S. FYFE

Reply

HALLAM REPLIES: I AM pleased that my *News and Views* article should have provoked Fyfe into writing his interesting letter giving geochemical reasons why the 'basic tenet' that crust created equals crust destroyed cannot be exactly true. It is indeed apparent that continental crustal thickness must change when separation takes place; the remarkable fact is that computer-based 'jigsaw fits' are for the most part so accurate to a first approximation. I feel no need to make further comments but Owen's letter calls for a brief reply.

My purpose was less to review Owen's paper than to use it as an excuse to discuss some awkward anomalies in continental fits which have not been adequately acknowledged or discussed by Earth scientists. I cited the Jansa and Wade, and Talwani and Eldholm, papers as examples of detailed recent work undermining the reliability of the geometric 500 fathom fit, with the implication that the same geological situation very probably holds for similar continental margins elsewhere in the world. The African margins are a good example, and absolutely crucial to reconstructions of Pangaea and to Owen's expanding Earth hypothesis. Yet Owen makes no allowance whatever for a broad zone of attenuated and subsided crust around this continent (see, for instance, his figure 11). The Burollet and Byramjee paper does not, admittedly, provide "definitive evidence", because it is in effect a broad-ranging review, and most of the critical data is based on unpublished work by oil companies. The paper does in fact contain substantial data for the region off Angola which cannot be lightly dismissed. Furthermore, Jansa and Wade spell out very clearly, with good evidence, that the north-west African continental margin is virtually a mirror image of that off eastern Canada and the United States. As for Madagascar, it is not very helpful to cite once again the much discussed paper by Flores. His purely geological arguments for a southerly position of that island can be countered by other geological arguments for a more northerly fit. The point is that the arguments based on geological comparisons with mainland Africa have proved indecisive, and that is why the palaeomagnetic results of McElhinny and Embleton are so important.

In conclusion, I repeat that I find Owen's paper a stimulating one which deserves to be widely read, even though I am sceptical about his interpretation. If it serves to point up critical areas for further analysis it will have served a very useful purpose whatever one thinks of the conclusions.

A HALLAM

Irreproducible results

from Robert M. May

CONSIDER the following game, played with the combinatorial theorist's mythical urn containing black and white balls. Initially the urn contains only two balls, one black and one white. Choose one ball at random from the urn, note its colour, and then replace it plus a new ball of the same colour as the chosen ball. The game thus proceeds, each round consisting of the random selection of one ball from the urn and replacement of this ball together with a new ball of the same colour. After N such rounds, the urn will contain a total of $N+2$ balls.

After many rounds, the urn will contain a large number of balls. What fraction of the balls will be white? The reader is invited to pause here, and to make a determined effort to guess the answer.

The answer is that for large N the proportion of white balls will tend to converge to some limiting value, p say: but this limiting value p is equally likely to take any value between 0 and 1. That is, when I play this game my plot of the proportion of white balls in the urn as a function of the number of rounds (or, equivalently, time) will exhibit some initial wiggles, but will eventually settle to a steady flat line corresponding to, say $p=0.391..$. When you play the game you see similar initial fluctuations, which damp out as the total number of balls gets large, and your experiment will similarly settle to some steady but different value of, say, $p=0.893..$, and so on. Each run of this experiment will yield to the experimenter an illusion of determinism, as his results settle to a steady limiting value; this value is, however, a random variable, differing from one experiment to the next, and determined largely by the statistical vagaries of the first few turns.

In short, this simple game provides an example where an underlying stochastic process gives results which appear deterministic (at least to the person who witnesses but one run). It is, in a sense, the mirror image of the phenomenon I recently reviewed (*Nature*, **261**, 459–467; 1976) whereby simple deterministic processes can produce results which appear indistinguishable from random fluctuations.

The above game has been known to mathematicians for some time, and has been discussed in relation to the spread of infection (Eggenberger and Polya, *Zeit. angew. Math. Mech.*, **3**, 279–289; 1923) and to stochastic population growth (Blackwell and Kendall, *J. appl. Prob.*, **1**, 284–296; 1964), but the basic messages have tended to become buried under mathematical encrustations. Cohen (*BioScience*, **26**, 391–394; 1976), in a paper exuberantly entitled "Irreproducible Results and the Breeding of Pigs (or Nondegenerate Limit Random Variables in Biology)", has disinterred the phenomenon, and suggested that it may have widespread relevance in population biology.

Geneticists such as Robertson (*Proc. R. Soc. Lond.*, **B153**, 234–249; 1960) and Hill (*Biometrics*, **30**, 363–366; 1974) have realised that this urn-and-ball game captures some of the essential features of plant and animal breeding programmes, and that replicate lines from the same initial population can be very different in the limit they reach. Cohen suggests that similar "nondegenerate limits" may arise in many ecological contexts. For example, differences in successional sequences and in climax states in apparently similar habitats may not be due to causal differences between habtitats, but may arise as variations in an ensemble of habitats (ultimately dependent on the statistical accidents of early colonisation). Differences in "species composition on apparently similar islands may result from the operation of identical forces which produce regularity only in an ensemble of islands. Differences in the sizes of prides of lions or in the social organisation of troops of Japanese macaques may reflect the inherently but lawfully variable outcome of identical underlying forces, rather than deterministic ecological differences". Most of these suggestions have been made previously by other people, but not in so precise a form.

Turning to behaviour, Cohen suggests that it is "possible that some of the significant differences among mother–child interactions, which are obvious by the time a child reaches five years of age, are due neither to inherent differences among individuals nor to environmental differences, but to sequentially dependent random forces applying equally to all mother–infant pairs".

Cohen concludes on a metaphysical note. If we had been born in another universe which had started from exactly the same initial conditions as our present one and which had been subject to the same dynamics, would we necessarily infer the same laws of nature as we infer for this universe? The urn-and-ball game holds the suggestion that our present Universe may be an irreproducible result. □

Bibliography of plant genetic resources

DURING the replacement of traditional crops by new varieties a great deal of the potential genetic variation present in the old varieties and their wild relatives has been lost. Over the past two decades however, interest in the conservation and use of the plant genetic resources that remain has been rapidly growing. The literature on the subject has naturally grown with it, and the first extensive bibliography of work in plant genetic resources has just been produced. It has been compiled by J. G. Hawkes, J. T. Williams and Jean Hanson of the University of Birmingham and as well as covering the literature devoted specifically to crop genetic resources, there is also extensive coverage of crop origins, variation and evolution, along with appropriate references in ecology, genetics, practical agriculture, phytopathology, and entomology.

The bibliography is produced by the International Board for Plant Genetic Resources and can be obtained from FAO, Rome.

Human trypanosomiasis today

from F. E. G. Cox

TRYPANOSOMIASIS has received a considerable amount of attention recently (see *Nature*, **249**, 677; 1974; **262**, 85; 1976 and the *Pan American Health Organisation Symposium on New Approaches to American Trypanosomiasis*, 1975) and the latest number of the *Transactions of the Royal Society of Tropical Medicine and Hygiene* (**70** part 2, 1976) contains a refreshingly summarised statement of the current status of this group of diseases under the title "Trypanosomiasis Today". Missing are the results of biochemical, ultrastructural and immunological studies that have made this field so attractive to many scientists over the past few years and instead there is basic information emphasising the need for sustained effort to be applied in the field and in the pharmaceutical laboratory.

In Africa, human trypanosomiasis, or sleeping sickness, is still widespread in the tsetse fly-infested areas where it exists in the form of unstable "controlled endemicity" (de Raadt, *Trans. R. Soc. trop. Med. Hyg.*, **70**, 114; 1976) Even in West Africa where the disease is under control in many places the number of new cases is increasing by about 10 per 100,000 people and there were 2,511 recorded new cases in Africa in 1974. This is a vast improvement on the 1970 figures of 9,140 but trypanosomiasis is still prevalent and the problem of "controlled endemicity" is that the movements of individuals and populations and any decrease in control measures are likely to bring about epidemics.

It is true that without control measures the situation would be worse than it is now and some of the success is due to the introduction of the drug pentamidine in 1949. No new drugs have been developed for field use for 20 years, however, (Williamson, *op. cit.*, 117). Pentamidine is only useful during the early stages of the disease and resistance to it has been recorded. The commercial production of other useful drugs is very restricted.

The immunological control of sleeping sickness is unlikely because humans seem to be unable to mount a good immune response to natural infections and because the parasites are capable of antigenic variation (Gray, *op. cit.*, 119) so control of the tsetse fly remains the best hope for eradicating this disease. The objective of insecticide control has been to eradicate the genus *Glossina* from a particular area and ground spraying has been quite successful, for example, in Nigeria, 27,500 km^2 of riverine area have been cleared of *G. morsitans* but in its natural habitat, the savannah, this species may present a different problem (Jordan, *op. cit.*, 128). The application of insecticides from the air is a relatively recent innovation and although the results are promising it is too early to evaluate this success. Without doubt insecticides will have to be used for some time to come while the possibilities of genetic and biological control are being investigated. Jordan points out that the tsetse flies are acting as conservation agents maintaining the *status quo* in Africa. Advances in trypanosomiasis control, tsetse fly eradication and land development will have to be carried out side by side if anyone is to benefit from such schemes.

Human trypanosomiasis in South America is called Chagas' disease and 35 million people are afflicted. Control of this disease is a major problem because man shares it with 100 species of wild mammals and up to 100 species of bugs that might transmit it (Minter, *op. cit.*, 124). Vector control, either by traditional insecticides or new methods, provides no immediate hope (Lumsden, *op. cit.*, 121) nor does chemotherapy. Only eight effective substances have been developed in 66 years (Gutteridge, *op. cit.*, 123) and of these only three are undergoing extensive tests. Lampit (5-nitrofuran) may soon be generally available but it is not completely effective and may have severe side effects. Possibly immunisation may be useful in the future because the parasite that causes Chagas' disease does not undergo antigenic variation (Lumsden, *op. cit.*). Immunisation is only a remote possibility, however, but with only three companies testing compounds against Chagas' disease and with insecticides such as DDT becoming scarce and expensive the immediate prospects of eradicating the disease do not look good. The increasing scarcity and expensiveness of insecticides is also a problem in attempts to eradicate sleeping sickness in Africa. □

Spiral galaxies at Cambridge

from Vincent Icke

> About 35 astronomers interested in the structure of spiral galaxies discussed their findings and frustrations during a study week at the Institute of Astronomy, Cambridge.

SPIRAL galaxies are common, as Donald Lynden-Bell (Institute of Astronomy, Cambridge) pointed out in his introductory talk; considering the extremely slow evolution of galaxies, this implies that spiral structure in one form or another is almost as old as the Universe. To be explained are, among other things: why spirals occur in disk galaxies only; why spiral galaxies always contain interstellar gas; why any one form of spiral occurs, and why some spirals have bar-shaped inner parts. Recalling that it seems to be very difficult to stabilise a disk of stars against a bar-like gravitational instability, Lynden-Bell proposed that such a bar does, in fact, develop, and subsequently generates a spiral-shaped shock wave in the interstellar gas. After this introduction, contributions along six main routes followed.

The problem of the linear stability analysis of a differentially rotating disk of self-gravitating point particles (stars), has been haunting theorists especially after Lindblad's pathfinding attempts to explain galactic spirals as a normal mode of oscillation. Alar Toomre (Massachusetts Institute of Technology) described the analysis of a disk wherein all stars have the same mean orbital velocity. In such a disk, the random velocities of the stars as expressed in their distribution function (a solution of the Vlasov equation) assume a manageable analytic form. With his coworker Zang, Toomre discovered that v=constant disks are, surprisingly enough, stable with respect to two-armed instabilities, but, an even greater surprise, strongly unstable with respect to one-armed spiral perturbations! Quite the opposite has been found for disks where the rotation curve goes to zero in the centre, as is observed in spiral galaxies. In an impressive piece of analysis, Agris Kalnajs (Mt Stromlo and Siding Spring Observatories) concluded that this inner region of solid-body rotation (where velocity is proportional to radius) is largely responsible for the instability. The usual procedure to avoid instabilities is to reduce the effective mass of the stars, by, for example, surrounding the disk with a massive halo. Kalnajs showed that it is sufficient to introduce a 'nuclear bulge', that is, a small halo near the galactic centre where the rotation curve follows the solid-body line. A decrease of a factor of 4–5 in the growth rate of the instabilities was readily obtained in this way. Introduction of a bulge or halo effectively means the assumption of a vertical dimension in the disk, and Douglas Heggie (Royal Observatory, Edinburgh) showed that this may lead to resonant interaction between horizontal and vertical stellar motions. Approximating the stellar orbits as a three-dimensional Lissajous figure, he calculated that 1–4% of all stars may participate in resonances that bring them as far as half the disk radius out of the plane.

Linear instabilities attempt to grow indefinitely, but are ultimately stopped by non-linear effects. The analysis of these entails an awesome amount of mathematical physics, and has therefore barely begun. Elly Dekker (Sterrewacht te Leiden) described her application of quasi-linear techniques borrowed from plasma physics to the evolution of the particle distribution function in a stellar disk. Assuming that the potential can be split in a large, slowly varying, and a small, rapidly varying part, Dekker derived a diffusion equation for the evolution of the mean particle distribution. If the perturbation is stationary in a corotating frame, the diffusion coefficients depend on the contributions from the resonant stars only. She also demonstrated that the distribution function evolves so as to increase the coarse-grained entropy associated with it.

Bar-shaped distributions of stars are dynamically even more complex than disks. Some equilibrium models have been derived, and Scott Tremaine (California Institute of Technology) analysed the particular family that is obtained by squashing a homogeneous tri-axial ellipsoid along its rotation axis to zero thickness. He found that these bars are unstable if they are nearly circular or rotating very rapidly. The remaining configurations are stable, at least up to third-order harmonic deformation. Apparently, rather elongated bars can survive when rotating slowly.

Increasing computational power has facilitated numerical studies of gravitating *N*-body systems. The main problem remains the simultaneous modelling of the long and the short range forces. Special techniques are needed to approximate both close encounters and global structure in such a way as to preserve the collisionless behaviour of the system. Robert Berman (University of Reading) gave a progress report on a potential-solving technique developed by Hockney and Brownrigg for a fully three-dimensional 25,000-body system. Studies of disk-halo models with halo potentials more realistic than those hitherto used, showed that the disk can be stabilised against bar formation if the halo is only marginally more massive than the disk. Also, if bars did develop, they often showed structure in their interior, in the form of nested rings or a smaller bar.

The considerable mathematical difficulties arising in the attempt to solve the Vlasov equation naturally lead to a search for shortcuts, preferably by assuming that the system can be described as a gas or similar continuum. An especially successful dodge was employed by Jim Bardeen (University of Seattle) to determine the unstable modes of a gaseous disk. He expanded the potential to first order in the disk thickness, and wrote the resulting equations in terms of Legendre polynomials. This enabled him to reduce the stability problem to a matrix eigenvalue equation. Truncating the matrix to 96×96, a set of growing modes emerged with some interesting properties. An increase in gas pressure decreased the number of growing modes, but did not reduce their growth rates very much. The potential of the modes was not a simple multiple of their surface density, unlike the WKBJ modes studied by others. Most significantly, the modes appeared to be superpositions of short-wave partial modes travelling inwards and outwards. The flow of gas induced in the plane of a bar-like potential depression was studied by Karl-Juhan Donner (Institute of Astronomy), who followed up Lynden-Bell's earlier suggestion, and by Takuya Matsuda (University College, Cardiff), who in collaboration with Sorensen and Fujimoto employed a 50×30 point fluid-in-cell method to obtain a numerical simulation of the gas flow in a barred spiral galaxy. Matsuda showed that standing shocks develop roughly parallel to the bar, through which gas is deflected so strongly that it rapidly assembles in the galaxy's nucleus. A second pair of shocks, detached from the first set, occurred near the region where the Keplerian velocity in the galactic plane equals the rotation velocity of the bar. The behaviour of motions out of the galactic plane, induced by shocks in the disk, was calculated by Alastair Nelson (University College, Cardiff), who found that the perturbations propagated almost vertically upwards, reaching considerable amplitudes in the tenuous regions at 300 pc height.

The last word, obviously, was for the observers, who produced something like a fascinating cold shower. Renzo Sancisi (Sterrekundig Laboratorium 'Kapteyn', Groningen) produced new radio maps obtained with the Westerbork synthesis radio telescope of NGC5383, the best maps of a barred spiral obtained to date. Gas was found concentrated near the ends of the bar and especially in the nucleus. Also, a low-brightness disk extending over a diameter of fully three disk lengths was observed, which made it possible to determine the rotation curve in this region. It appears that the central parts (out to half the length of the bar) rotate like a solid body. Thereafter the rotation speed stays almost constant. The bar was also seen in 1,415 MHz continuum, and deep plates taken by Van der Kruit and Bosma show that the optical extent of the galaxy is about as large as the neutral hydrogen disk. Evidence that even nicely-looking galaxies like M81 can be involved in spectacular events was produced by Leonid Weliachew (Observatoire de Paris, Meudon) and by Geoffrey Cottrell (Mullard Radio Astronomy Observatory, Cambridge) who described observations of the region around M81, M82 and NGC3077. These are surrounded by a huge hydrogen halo, in which the velocities of the gas clouds link up nicely with those of the galaxies. Cottrell presented a computer model of a tidal encounter between M81 and NGC3077, which properly reproduced the radio appearance of the latter. Presumably the hydrogen halo consists of debris left over from an encounter between M81 and M82. Finally, it was demonstrated that many spiral galaxies are not flat at all, perhaps necessitating some drastic rethinking of extant models. Darrell Emerson summarised an observational programme of the MRAO on M33 and M31, both members of the Local Group of galaxies. The plane of M33 was known to be warped, and the new observations conclusively showed the enormous extent of these distortions, with warps rearing above the plane to heights almost equal to the galaxy's radius. In M31, the Andromeda Nebula, smaller warps were discovered at the edge of the observable radio disk (about 30 kpc radius). Then Sancisi proceeded to show that possibly all spiral galaxies are warped: four members of a nearby, but otherwise random, sample of five spirals seen almost edge-on showed up to 20% warping of their planes. Two of these have no nearby companions, so that if the warps are due to tidal distortion during an encounter between two galaxies, the distorted galaxy must maintain a rather crisp warp during 4–5 galactic years at least. This baffling finding left the participants in the discussion appropriately wondering how much progress, exactly, has been made in understanding spiral structure. □

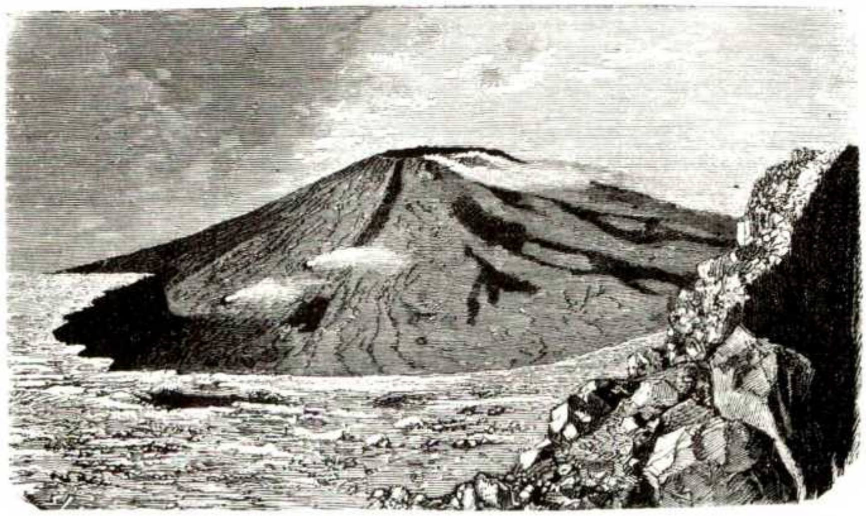

A hundred years ago

The Inclosure and Cone of the present Crater: The Volcano of Réunion. from *Nature*, **14**, August 17, 335; 1876.

articles

Dynamo model of double radio sources

R. V. E. Lovelace

Department of Applied Physics and Laboratory of Plasma Studies, Cornell University, Ithaca, New York 14853

A model of radio sources is proposed in which the magnetised accretion disk of a massive black hole acts as an electric dynamo producing two oppositely-directed beams of ultra-relativistic particles.

WE give here a brief development of a model of double radio sources with the conducting, magnetised accretion disk of a massive black hole acting as an electric dynamo. The electric field created by the rotating disk results in the steady generation of two oppositely-directed, collimated, tenuous beams of ultra-relativistic protons. The output power in the beams is $\sim 10^{44}$ erg s^{-1} and the proton energies are $\lesssim 10^{19}$ eV for a poloidal magnetic field of the disk of 10^3 gauss and a black-hole mass of $10^8 M_\odot$. The beams propagate parallel to the angular momentum vector of the disk. The energy transported by the proton beams is gradually degraded because instabilities lead to the sharing of the beam energy with the ambient plasma. It seems possible that the two-stream interaction can convert the energy of a tenuous proton beam into a relatively dense, collimated beam of relativistic electrons. Energy carried by the electron beams is released as synchrotron radiation in the radio components.

Fig. 1 Schematic drawing of the electric dynamo formed by a conducting magnetised accretion disk. The radio wave emitting regions are discussed in the text.

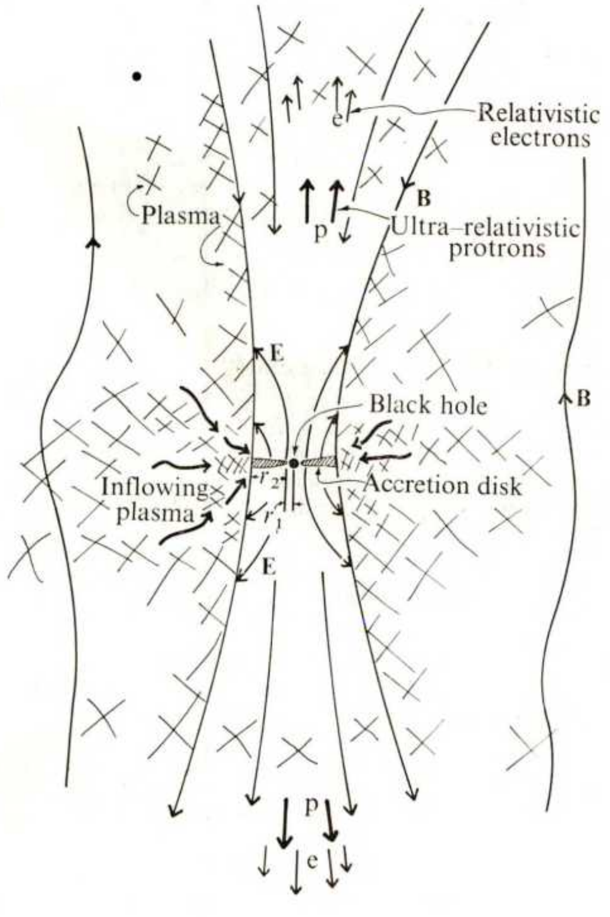

With this model it seems possible (1) to have a large, steady supply of energy to widely separated small radio components, (2) to obtain alignment and symmetry of the two radio components, and (3) to have a correlation between the axis of the radio components and the direction of the angular momentum of the parent galaxy. The model includes some of the features of the 'twin exhaust' model[1], the spinar or oblique-rotator models[2-5], the magneto-hydrodynamic models[6,7] and the axisymmetric pulsar model[8]. The isotropic production of low energy ($\sim 10^{12}$ eV) cosmic rays from the accretion disk of a massive black hole has been discussed previously[9,10].

Model

Consider the possibility[9,10] that a black hole of mass M_h ($\sim 10^8 M_\odot$) has formed in the centre of a galaxy (or in the nucleus of a quasar) and that the black hole is surrounded by a massive, flat accretion disk (see Fig. 1). Gaseous material accreted on to the disk is supplied from the mass loss of stars, possibly increased by disruptive collisions between stars and/or the close approach of stars to the black hole[11]. It is evident that the angular momentum vector of the disk will have a direct correlation with the angular momentum vector of the parent galaxy. If the mass of the disk is sufficiently large, $M_d \gg M_\odot$ (but $M_d \ll M_h$), then the angular momentum of the disk may have a fixed direction in space for long periods, greater than the lifetime of a radio source. For $M_d \gg M_\odot$, the disk angular momentum corresponds to an average of the angular momenta of a large number of stars.

The magnetic field

Ionised matter moving into the accretion disk will carry with it a weak ambient magnetic field. The gradual inward radial motion of matter in the disk will amplify the field, tending to establish $B_z(r) \propto \sigma(r)$, where σ is the surface density of the disk, r is the radial distance from the black hole, and the z axis is normal to the plane of the disk. We consider that B_z at some particular epoch has a single polarity throughout the inner part of the disk. Because of differential rotation of the disk, the poloidal field (B_r, 0, B_z) is expected to be axisymmetric. It is, however, possible that the poloidal field is augmented by non-axisymmetric turbulent fluid motions[12] in the disk. Reconnection of the poloidal field lines occurs in the region $r < r_1, |z| < r_1$ (where r_1 is the inner radius of the disk) so that there is no build up of flux through the surface $r < r_1$, $z = 0$. (For the moment, consider that the space above and below the disk is a vacuum. Thus, although there may be a toroidal field (B_φ) embedded in the disk[9,10], $B_\varphi = 0$ in the space above and below the disk.)

The electric field

The material of the disk may be assumed highly conducting so that an observer in a non-rotating (inertial) reference frame sees a strong radial electric field, $E_r(r) = -[u_\varphi(r)/c]B_z(r)$, on the top and bottom surfaces of the disk, where $u_\varphi = (GM_h/r)^{\frac{1}{2}}$ is the Keplerian velocity, assumed much larger than u_r. Thus the potential difference across the disk is

$$V_{12} = -\frac{1}{c}\int_{r_1}^{r_2} \mathrm{d}r u_\varphi(r) B_z(r) \tag{1}$$

where $r^1 = 6GM_h/c^2 \simeq 10^{14}$ cm $(M_h/10^8 M_\odot)$ is the inner radius of the disk, and $r_2 \gg r_1$ is the effective outer radius where material enters the disk. If we assume $u_r(r) = \varepsilon u_\varphi(r)$, with $\varepsilon =$ a constant, $\ll 1$, then $\sigma \propto r^{-\frac{1}{2}}$. Because $B_z(r) \propto \sigma(r)$, we find

$$V_{12} \simeq -\surd(6) B_*(GM_h/c^2)\ln(r_2/r_1) \tag{2a}$$

where $B_* = \max(B_z) = B_z(r_1)$. In practical units

$$V_{12} \sim 10^{19}\left(\frac{B_*}{10^3\ \text{gauss}}\right)\left(\frac{M_h}{10^8 M_\odot}\right)\ln\left(\frac{r_2}{r_1}\right)\text{V} \tag{2b}$$

Observe that V_{12} is proportional to r_1, which is well defined, but depends only weakly on r_2.

Magnetic flux and time scales

The magnetic flux through the disk is

$$\Phi \sim 4\times 10^{31}\left(\frac{B_*}{10^3\ \text{gauss}}\right)\left(\frac{M_h}{10^8 M_\odot}\right)^2\left(\frac{r_2}{r_1}\right)^{3/2}\text{gauss cm}^2 \tag{3}$$

For $B_* = 10^3$ gauss, $M_h = 10^8 M_\odot$, and $r_2/r_1 = 10$, this flux ($\sim 10^{33}$ gauss cm^2) corresponds to an ordered field of 10^{-6} gauss spread over a region of $\sim$ 10 pc. A characteristic time scale for rapid dynamical variations of the disk is the orbital period at $r = r_1$, $T_d \simeq 5\times 10^4 (M_h/10^8 M_\odot)$ s. At the other extreme, the time scale for significant changes in the large scale magnetic field structure, once it is established, is $T_B = \mathscr{L}/R$, where $\mathscr{L}$ is the inductance and R the resistance of the configuration. We estimate that T_B is at least as long as the lifetime of the disk because of the large size and high conductivity of the disk.

Resulting particle acceleration

Consider the particle acceleration resulting from the disk potential. In the space outside the cylinder $r > r_2$, there is assumed to be plasma, possibly in turbulent motion, but not in rapid rotation. The electrical potential of this plasma may be taken to be zero. The region $r < r_2$ above and below the disk is for the moment assumed a vacuum. We consider in the present study only the case where B_z is anti-parallel to the angular momentum vector of the disk. Thus the potential on the disk surfaces, $V(r, \pm 0)$, produces a vacuum field in the space above and below the disk. That is, $\nabla^2 V = 0$, with $V(r, \pm 0)$ specified, with $V(r_2, z) = 0$, and with $V(r, |z| \gg r_2) = 0$. The potential $V(r, z)$ implies an electric field which tends to accelerate protons (and other ions) in the $+\mathbf{z}$ ($-\mathbf{z}$) direction out of the top (bottom) surface of the disk. The electric field, E, is $\sim (u_\varphi/c)Bz \lesssim 10^5$ V cm^{-1} for $B_* = 10^3$ gauss and $M_h = 10^8 M_\odot$. The electric force on a proton exceeds the gravitational attraction of the black hole by a large factor, $\sim 10^{12}$. The electric field is, however, small compared with the poloidal magnetic field, $E^2/B_z^2 \sim u_\varphi^2/c^2 \ll 1$.

The self-consistent, space-charge-limited flow of protons off the disk surface follows from general dimensional considerations (ref. 13 and E. Ott, T. Antonsen, and R. Lovelace, unpublished) in that the particle motion is extremely relativistic. If I denotes the total current of protons in, say, the $+\mathbf{z}$ direction, then

$$I = \kappa c V_{12} \tag{4a}$$

where κ is a dimensional factor which depends on the geometry through $V(r, \pm 0)$. We may assume that κ is not greatly different from unity (ref. 13 and E. Ott, T. Antonsen and R. Lovelace, unpublished). An estimate analogous to equation (4a) occurs in the axisymmetric pulsar model[8]. Using equation (2b), we rewrite equation (4a) as

$$I \sim 3\times 10^{17}\kappa\left(\frac{B_*}{10^3\ \text{gauss}}\right)\left(\frac{M_h}{10^8 M_\odot}\right)\ln\left(\frac{r_2}{r_1}\right)\text{A} \tag{4b}$$

Charge neutrality of the disk is maintained by a non-relativistic electron current in the region $r > r_2$. For $r < r_2$ and $|z| > 0$, there is a positive space–charge density J_z/c, where $J_z(r)$ is the beam current density.

The output power in the two beams is, from equations (2b) and (4b)

$$L_R \simeq 2IV_{12} \sim 10^{44}\kappa\left(\frac{B_*}{10^3\ \text{gauss}}\right)^2\left(\frac{M_h}{10^8 M_\odot}\right)^2\left[\ln\left(\frac{r_2}{r_1}\right)\right]^2 \text{erg s}^{-1} \tag{5}$$

The power in the beams derives from the infall of matter into the gravitational potential of the black hole. There is a corresponding flow of angular momentum[8] out of the disk carried by the poloidal-magnetic field and self-electric field of the beam and the beam protons. The beam emission may, however, represent only a small dynamical influence on the disk if $L_R \ll L_{\text{tot}}$, where L_{tot} is the total luminosity of the disk. In particular, an irregular magnetic field embedded in the disk may be dynamically important[9,10,14]. For comparison, the Eddington limit on the electromagnetic emissions of the disk is $L_E \sim 10^{46}(M_h/10^8 M_\odot)$ erg s^{-1}.

Evidence in support of equations (4) and (5) comes from many laboratory experiments which have demonstrated the production of high-current electron beams[15,16] ($I_e \sim 10^5$ A) and ion beams (P. Dreike, C. Eichenberger, S. Humphries, and R. Sudan, Cornell University Laboratory of Plasma Studies Report **172** (1975)) ($I_p \sim 10^4$ A) in this type of field configuration[15-18] ($E^2/B_z^2 < 1$) at low voltages ($V_{12} \lesssim 10^6$ V) with electric fields $E \lesssim 10^6$ V cm^{-1}. The observed beam particle energies are $\sim$ eV$_{12}$.

Beam energy/magnetic energy

An important dimensionless parameter for the dynamics of the beams is the ratio, denoted β, of the kinetic energy density of the beam to the energy density of the magnetic field. We first estimate $\beta = \beta_0$ near the disk, $|z| \lesssim r_2$. Note that we have a limit on the proton Lorentz factors γ from equation (2b)

$$\gamma \leqslant \gamma_0 \sim 10^{10}\left(\frac{B_*}{10^3\ \text{gauss}}\right)\left(\frac{M_h}{10^8 M_\odot}\right)\ln\left(\frac{r_2}{r_1}\right) \tag{6}$$

The spectrum of γ values as a function of r is expected to be relatively flat for $\gamma < \gamma_0$. An estimate of the beam density, n_B, follows from equation (4b)

$$n_B \sim 2\times 10^{-3}\kappa\left(\frac{r_1}{r_2}\right)^2\ln\left(\frac{r_2}{r_1}\right)\left(\frac{B_*}{10^3\ \text{gauss}}\right)\left(\frac{10^8 M_\odot}{M_h}\right)\text{cm}^{-3} \tag{7}$$

The total number of protons emitted per second is thus $\sim 4\times 10^{36}$ for $n_B = 2\times 10^{-5}$ cm^{-3}, $r_1 = 10^{14}$ cm, and $r_2/r_1 = 10$.

From equations (6) and (7), we find

$$\beta_0 = 8\pi \frac{n_B \gamma_0 m_p c^2}{B_z{}^2} \sim 0.7\kappa \left[\frac{r_1}{r_2} \ln\left(\frac{r_2}{r_1}\right)\right]^2 \qquad (8)$$

where m_p is the proton rest mass. Evidently, we have $\beta_0 \ll 1$ if $r_2 \gg r_1$. That $\beta_0 \ll 1$, is a result of the fact that $u_\varphi{}^2/c^2 \ll 1$ over most of the surface area of the disk. Thus for the proton acceleration and streaming in the vicinity of the disk, the magnetic field B_z is very strong. To a good approximation the protons follow the magnetic field lines and the configuration is force-free. (Values of β small compared with unity are known to be favourable to the magnetohydrodynamic stability of beams electrically neutralised by plasma[20].)

In the vicinity of the disk there is a small toroidal self-field B_φ from the proton beams. We estimate that

$$\frac{B_\varphi}{B_z} \simeq \frac{2I}{cr_2 B_z} \sim (\beta_0 \kappa)^{1/2}$$

is small compared with unity if $\beta_0 \ll 1$. This toroidal magnetic field counteracts the radial space-charge repulsion of the beam and thus tends to collimate the beam.

Divergence of beam

For distances $|z| \gg r_2$ above and below the disk, the proton beams diverge. The outer beam radius is approximated as $a(z) = r_2 (1 + |z|/H)$, where H is the scale height for the divergence. We assume that processes involved in the initial outward propagation of the beams give $H \gg r_2$. Because the beam particles start off following the field lines, $B_z(z) \propto [a(z)]^{-2}$. The β factor of the beam is proportional to a^2, and, therefore, we have $\beta \simeq 1$ at a distance $|z| \simeq z_* \equiv H(\beta_0)^{-\frac{1}{2}} \gg H \gg r_2$, where β_0 is given in equation (8). For distances $|z| \gg z_*$, where $\beta \gg 1$, the beam divergence comes from the ballistic motion of the protons (in the absence of instabilities). The usual adiabatic energy losses, involved, for example, in the expansion of a cloud of particles, do not occur for a particle beam in ballistic motion.

Radiation effects

In the initial outward propagation of the beam there may be significant curvature radiation. If ρ denotes the instantaneous radius of curvature of a proton trajectory, then the typical energy of the curvature photon is

$$\left(\frac{3}{2}\right)\gamma^3\left(\frac{\hbar c}{\rho}\right) \sim 3\times 10^{10}\left(\frac{\gamma}{10^{10}}\right)^3\left(\frac{10^{15}\text{cm}}{\rho}\right)\text{eV}$$

The rate at which a proton emits energy is

$$\frac{\mathrm{d}\gamma}{\mathrm{d}z} = \frac{2r_e}{3}\left(\frac{m_e}{m_p}\right)\frac{\gamma^4}{\rho^2}$$

where r_e is the classical electron radius, and m_e is the electron rest mass. Thus the path length for a proton to lose half its initial energy ($\gamma m_p c^2$) is

$$l_{\text{cur}} \sim 2 \times 10^{16}\left(\frac{10^{10}}{\gamma}\right)^3\left(\frac{\bar{\rho}}{10^{15}\text{ cm}}\right)^2 \text{cm}$$

where $\bar{\rho}$ is an average of the radius of curvature. In the initial stages of formation of a source we may have $l_{\text{cur}} \lesssim \bar{\rho} \simeq r_2$ if $B_* M_h \gtrsim 10^{11}$ gauss $M_\odot$. One effect of the curvature photons may be that of expelling matter and thus straightening the magnetic field in two conical regions of small solid angle defined by the velocity distribution of the protons at $|z| < r_2$. The effect is, however, inefficient because the production and scattering cross sections for the curvature photons interacting with electrons and protons are small ($\lesssim 2 \times 10^{-26}$ cm^2). The curvature photon production of electron–positron pairs off the magnetic field[21] is negligible.

The beam protons may interact with low energy photons[22] emitted by the accretion disk[9,10] and surrounding plasma to give pions and electron–positron pairs. The proton energy threshold for pion production is

$$\sim 10^{17}(1-\cos\Theta)^{-1}\left(\frac{1\text{ eV}}{\mathscr{E}}\right)\text{eV}$$

where Θ is the angle between the proton and photon momenta, and $\mathscr{E}$ is the average photon energy. The threshold for e^-/e^+ production is a factor 1/135 smaller. We estimate that the proton energy loss is small if

$$L_{\text{ph}} < 10^{46}\left(\frac{\mathscr{E}}{1\text{ eV}}\right)\left(\frac{R}{10^{17}\text{ cm}}\right)\text{erg s}^{-1}$$

where L_{ph} is the photon luminosity, and R is the effective radius of the photon-emitting region.

Counter flow instability

For distances $|z|$ larger than a certain value z_{neut} (discussed below), the proton beams become both charge and current neutralised by plasma in the beam channels. In the outward propagation of a beam, plasma enters the beam front, and, furthermore, plasma may leak radially into the beam channel because of instabilities (particularly for $|z| > z_*$, where $\beta > 1$). Thus the presence of free electrons on magnetic field lines connecting with the accretion disk presents the possibility of electrons counter-flowing and partially 'shorting-out' the proton accelerating potential. This shorting would result in an ohmic dissipation (and radiation) of a fraction ($\sim 1/2$) of the power $2IV_{12}$ in a small region of size $\lesssim r_2$ centred on the black hole with the remaining fraction of the power in the two proton beams. There is, however, a definite asymmetry between the proton acceleration and the counter acceleration of electrons.

Consider the two-stream interaction: let n_p denote the density of cold electrons (speeds $\ll c$) within the beam channel at some distance z. Then the dispersion relation for electrostatic waves with frequency ω and wavevector $\mathbf{k}$ is

$$0 = 1 - \frac{\omega_p{}^2}{\omega^2} - \frac{\omega_B{}^2 \psi^2}{(\omega - kv_B \cos\psi)^2} \qquad (9)$$

where $\mathbf{k}$ is at an angle ψ to the beam velocity $\mathbf{v}_B$, with $\gamma^{-1} \ll \psi \ll 1$, and where $\omega_p = (4\pi e^2 n_p/m_e)^{\frac{1}{2}}$, $\omega_B = (4\pi e^2 n_B/\gamma m_p)^{\frac{1}{2}}$, $k = |\mathbf{k}|$, and $v_B = |\mathbf{v}_B| = c(1 - 1/2\gamma^2)$ is the local proton speed. It is evident from equation (9) that the proton beam may be considered weak in the limit where $n_p \gg (m_e/\gamma m_p) n_B \psi^2$. In this limit a simple form of the two-stream instability occurs[23]. The frequency of the unstable wave is written as $\omega = \omega_p + \delta$, with $|\delta| \ll \omega_p$, and $k = \omega_p (v_B \cos\psi)^{-1}$ so that

$$\text{Im}(\delta) = \frac{\sqrt{3}}{2}\left(\frac{\omega_B{}^2 \omega_p}{2}\right)^{1/3} (\psi)^{2/3}$$

or

$$\text{Im}(\delta) \sim 3 \times 10^{-5}\left(\frac{10^{10}}{\gamma}\right)^{1/3}\left(\frac{pc}{a}\right)^{2/3}\left(\frac{n_p}{10^{-3}\text{ cm}^{-3}}\right)^{1/6} \psi^{2/3}\,\text{s}^{-1} \qquad (10)$$

where we have taken

$$n_B = 10^{-12}\left(\frac{pc}{a(z)}\right)^2 \text{cm}^{-3}$$

with $a(z)$ the beam radius. The characteristic wavelength of the unstable wave is

$$\lambda \simeq \frac{2\pi c}{\omega_p} \sim 10^8\,\mathrm{cm}\left(\frac{10^{-3}\,\mathrm{cm}^{-3}}{n_p}\right)^{1/2}$$

The phase velocity of the unstable wave

$$v_\varphi = c\left[1-\frac{\psi^2}{2}-\tfrac{1}{2}\left(\frac{\omega_B{}^2\psi^2}{2\omega_p{}^2}\right)^{1/3}\right] < v_B \tag{11}$$

is quite close to the speed of light. As an illustration of equation (10), for $a = 10^{-2}$ pc ($=3\times10^{16}$ cm), $\gamma = 10^{10}$ and $n_p = 10^{-3}$ cm^{-3}, an e-folding of a wave with $\psi = 10^{-3}$ occurs over a distance of $\sim 10^{-3}$ pc ($=3\times10^{15}$ cm). Thus an unstable wave may grow considerably before it convects out of the beam channel.

Because of the two-stream instability, plasma waves of finite but small amplitude are expected to coexist with the plasma in the beam channel[24,25]. One important effect of the waves is to produce an anomalous electrical resistivity (which does not depend on binary collisions). This resistivity acts to prevent electrons from partially shorting the proton accelerating potential. A self-consistent, non-linear theory of the interaction would determine the neutralisation length z_{neut}. It is of course possible that the nonlinear theory would allow only a quasi-periodic acceleration[21] of protons with a time scale $\sim z_{\mathrm{neut}}/c$.

Linear instability of the proton beams may also involve the circularly polarised Alfvén and/or cyclotron plasma waves propagating parallel to the magnetic field. The interaction of streaming cosmic rays with Alfvén waves has been studied[26,27], but apparently only under conditions where the cosmic rays are nearly isotropic.

For distances $|z| > z_{\mathrm{neut}}$, the magnetic field is the 'stretched-out' poloidal field of the accretion disk, and is nearly parallel to the local proton velocity. For example, if the magnetic flux through the disk is 10^{33} gauss cm^2 (from equation (3)) then

$$B_z \sim 10^{-4}\left[\frac{pc}{a(z)}\right]^2 \text{gauss} \tag{12}$$

where $a(z)$ is the beam radius. The proton gyro-radii implied by equation (12) are $\simeq 10^2\,pc\,\sin(\theta)\,(\gamma/10^{10})(a/pc)^2$, where $\theta \ll 1$ is the pitch angle.

The electron beams

It is possible that the energy loss per unit distance of the proton beam is determined by the two-stream interaction. A small fraction of the cold electrons in the beam channel get trapped and untrapped in the unstable plasma waves and are thereby accelerated to relativistic energies[24,25]. At the same time the proton spectrum is shifted to lower energies. A nonlinear theory is required to predict the energy spectra of the electrons and protons. It is, however, relevant that equation (11) implies that an electron trapped with the phase velocity of an unstable plasma wave has a Lorentz factor

$$\gamma_w = \Gamma(\psi^{2/3}+\Gamma^2\psi^2)^{-1/2}$$

$$\Gamma \equiv 2^{1/6}\left(\frac{\omega_p}{\omega_B}\right)^{1/3} \sim 5\times10^3\left(\frac{n_p}{10^{-3}\,\mathrm{cm}^{-3}}\right)^{1/6}\left(\frac{\gamma}{10^{10}}\right)^{1/6}\left(\frac{a}{pc}\right)^{1/3} \tag{13}$$

where we have taken $n_B = 10^{-12}(pc/a)^2$ cm. The energetic electrons are collimated with the proton beams, having small pitch angles and small synchrotron losses. An upper limit on the range of electron Lorentz factors may however occur because the pitch angles are not negligibly small. For small pitch angles the synchrotron radiation is collimated with the proton beams.

The radio components

The collimated propagation of the oppositely travelling beams of electrons terminates in two regions of size a_R at $z = \pm z_R$, which are the radio components. In these regions the magnetic field of the beam channel connects with a non-uniform irregular field. Thus relativistic electrons arriving at $\pm z_R$ rapidly lose their energy by incoherent synchrotron emission. The collimated propagation of protons with gyro-radii $\gg a_R$ continues beyond z_R, and these protons may continue to accelerate cold electrons by the two-stream interaction. The observed values of z_R extend from <1 pc to ~ 1 Mpc. Consider first the small sources with, say, $z_R < 10^2$ pc. The magnetic field is that carried by the beam (equation (12)). The momentum of the beam electrons corresponds to a pressure $\lesssim P_R \equiv (L_R/\pi c)\,[a(z)]^{-2}$, where L_R is given by equation (5). The electron pressure compresses the external medium and gives rise to shock wave structures[28,1] at $z = \pm z_R$. These structures may move with relativistic velocities in the $\pm z$ directions if $P_R > n_{\mathrm{ext}}\, m_p\, c^2$, or $L_R > 10^{42}\,(a/pc)^2\,(n_{\mathrm{ext}}/10^{-3}\,\mathrm{cm}^{-3})$ erg s^{-1}, where n_{ext} is the ambient density of the external medium. For the extended sources with $z_R > 10^2$ pc, the location of the shock structures (and associated radio emitting regions) is determined by the pressure balance conditions[28,1] $P_R \gtrsim n_{\mathrm{ext}} m_p U_z{}^2$, where U_z ($<c$) is the velocity of the structures in the $\pm z$ directions into the external medium. For the large sources, the magnetic field carried by the beam is exceedingly weak. Amplification of the field may, however, occur by field line stretching at the expense of the energy of the turbulent motions of the plasma and relativistic electrons. Subsequent to the formation of an extended double source, a second pair of oppositely travelling shock wave structures may be generated, for example, by an instability involving the accretion disk. The secondary shock structures will be aligned with the disk angular momentum and thus approximately aligned with the extended double.

The high energy protons which reach the large radio components escape into extragalactic space without appreciable synchrotron losses if the magnetic field strengths are $<10^{-3}$ gauss. It appears possible that the accumulation over time of the high energy protons lost from nearby ($\lesssim 300$ Mpc) dynamo sources has produced the high-energy end (10^{16}–10^{20} eV) of the observed cosmic ray spectrum.

An analytic solution to the electrodynamics of a magnetised accretion disk has recently come to our attention[29].

We thank Drs M. J. Rees, E. N. Parker, P. A. G. Scheuer, E. E. Salpeter, K. Greisen, and R. D. Blandford for discussions and comments. We also thank Drs L. Woltjer and G. Setti for hospitality at the 1975 Urbino Summer Institute on Physics of Radio Sources where this work was developed. This research was supported by the NSF.

Received March 10; accepted June 1, 1976.

[1] Blandford, R. D., and Rees, M. J., *Mon. Not. R. astr. Soc.*, **169**, 395–415 (1974).
[2] Morrison, P., *Astrophys. J. Lett.*, **157**, L73–76 (1969).
[3] Cavaliere, A., Pacini, F., and Setti, G., *Astrophys. Lett.*, **4**, 103–105 (1969).
[4] Woltjer, L. J., *Semaine d'Etude, Les Noyeaux des Galaxies*, 477 (Pontificial Academicae Scientiarum, Paris, 1971).
[5] Ozernoy, L. M., and Usov, V. V., *Astr. Space Sci.*, **25**, 149–194 (1973).
[6] Piddington, J. H., *Cosmic Electrodynamics*, 261–262 (Wiley, New York, 1969); *Mon. Not. R. astr. Soc.*, **148**, 131–147 (1970).
[7] Sturrock, P. A., and Barnes, L., *Astrophys. J.*, **176**, 31–45 (1972).
[8] Goldreich, P., and Julian, W. J., *Astrophys. J.*, **157**, 869–880 (1969).
[9] Lynden-Bell, D., *Nature*, **223**, 690–694 (1969).
[10] Lynden-Bell, D., and Rees, M. J., *Mon. Not. R. astr. Soc.*, **152**, 461–475 (1971).
[11] Hills, J. G., *Nature*, **254**, 295–298 (1975).
[12] Bisnovaty-Kogan, G. S., and Vainstein, S. I., *Astrophys. Lett.*, **8**, 151–152 (1971).
[13] Nation, J., *J. Plasma Phys.*, **13**, 361–366 (1975).
[14] Eardley, D. M., and Lightman, A. P., *Astrophys. J.*, **200**, 187–203 (1975).
[15] Friedman, M., and Ury, M., *Rev. Sci. Instrum.*, **41**, 1334–1335 (1970).
[16] Friedman, M., *Rev. Sci. Instrum.*, **42**, 1255–1256 (1971).
[17] Lovelace, R. V., and Ott, E., *Phys. Fluids*, **17**, 1263–1268 (1974); *Appl. Phys. Lett.*, **27**, 378–380 (1975).
[18] Sudan, R. N., and Lovelace, R. V., *Phys. Rev. Lett.*, **31**, 1174–1177 (1973).
[19] Orzechowski, T. J., and Bekefi, G., *Phys. Fluids.*, **19**, 43–51 (1976).
[20] Lovelace, R. V., *Phys. Fluids*, **19**, 723–737 (1976).
[21] Ruderman, M. A., and Sutherland, P. G., *Astrophys. J.*, **196**, 51–72 (1975).
[22] Greisen, K., *Phys. Rev. Lett.*, **16**, 748-750 (1966).
[23] Ferch, R. L., and Sudan, R. N., *Plasma Phys.*, **17**, 905–915 (1975).
[24] Thode, L. E., and Sudan, R. N., *Phys. Fluids*, **18**, 1552–1563 (1975).
[25] Thode, L. E., thesis, Cornell Univ. (1974).
[26] Wentzel, D. G., *Astrophys. J.*, **156**, 303–314 (1969).
[27] Kulsrud, R. M., and Pearce, W. P., *Astrophys. J.*, **156**, 445–469 (1969).
[28] De Young, D., and Axford, W. I., *Nature*, **216**, 129–131 (1967).
[29] Blandford, R. D., *Mon. Not. R. astr. Soc.* (in the press).

Actual and anticipated petrographic effects of carbonate undersaturation in shallow seawater

E. T. Alexandersson

Section for Sedimentology, Palaeontological Institute, S-751 22 Uppsala, Sweden

In the near future, atmospheric carbon dioxide from the combustion of fossil fuels may cause the surface layers of the ocean to become generally undersaturated with calcium carbonate. The hypothetic sedimentary effects of such an event are here discussed in the light of studies in the Skagerrak Bay, North Sea. In this area, nearshore sediments in the depth range 0–40 m are affected by present-day carbonate dissolution. Not surprisingly, evidence of inorganic carbonate precipitation is absent. Stages in the dissolution process are microscopic etch patterns on calcareous grains, partially dissolved grains, and finally structural breakdown and complete dissolution of skeletal elements. Mineral phases affected are calcite, aragonite, and a spectrum of magnesian calcites. Dissolution is quantitatively unimportant in living calcareous organisms, but preservation of shells and skeletons as fossils is much impeded. A future change towards similar conditions in all the world's shelf seas would certainly mean an end to the typical warm-sea carbonate sedimentation as it is known today on the Bahama Banks and in other supersaturated regions.

IT is a serious possibility that the industrial production of atmospheric carbon dioxide will cause the surface layers of the sea to become generally undersaturated with calcium carbonate—perhaps within no more than 30 yr (refs 1–6). If indeed this prospect is true—the hypothesis has its opponents[7]—it will have radical consequences for carbonate sedimentation in the world's shelf seas which are now mainly supersaturated. I attempt to show here that the diagenetic processes affecting carbonate sediments in undersaturated waters are in striking contrast to what is known from warm, carbonate-supersaturated regions. Should carbonate diagenesis of the undersaturation model indeed become universal in the world's shallow seas by the turn of the century, the event would certainly mean an end to the typical warm-sea carbonate sedimentation as we know it today. Carbonate sedimentation in cold, high-latitude seas would become still more restricted. A change of this nature would leave an extensive mark of lasting geological significance in the shelf sediments, well worthy of its own footnote in the history of man's influence on the natural environment.

I can take no stand for or against the probability of a future carbonate undersaturation in the surface layers of the sea. Others are conducting that debate[1–7]. My intention is to point out some of the effects such an event might have on existing carbonate sediments and related organisms in shallow waters—if ever it does occur.

My story is based on factual observations in the present-day sea. Contrary to common belief, areas with carbonate-undersaturated shallow marine waters actually exist at the present time, and they seem to be the result of natural—as contrasted to man-made—environmental conditions. Such is the case, for example, in the Skagerrak Bay in the North Sea, where the petrographic effects of carbonate undersaturation are very prominent in nearshore sediments in the depth interval 0–40 m (refs 8–10).

Knowledge in this particular field of marine carbonate sedimentation is still fragmentary, and this account can touch only on two basic aspects of the problem: first, the evidence of marine carbonate undersaturation, and second, the most obvious effects of carbonate dissolution in nearshore sediments and related organisms.

Petrographic saturometry

No one really knows the precise level of carbonate saturation in the sea, and estimates vary considerably, both of the undersaturation in the deep sea[11–13], and of the supersaturation in surface waters[14–16]. The disagreement on this point need not concern us here, however, since undersaturation in natural sedimentary environments can be diagnosed by a direct petrographic approach. The most explicit evidence of marine carbonate undersaturation is obviously the condition that carbonate sediments dissolve. During the Challenger expedition—which ended on May 24 exactly 100 yr ago—the realisation that foraminiferal ooze dissolves at depth meant the original discovery of marine carbonate undersaturation (ref. 17). Today, dissolution can be petrographically diagnosed in exceedingly small samples, even in individual sediment grains, by means of scanning electron microscopy (SEM), and one is motivated to speak of petrographic saturometry. The method is sensitive only to such levels of undersaturation that actually lead to dissolution, and hence is well suited for field studies of carbonate diagenesis. The primary diagnostic criteria are microscopic etch patterns which develop on the surfaces of sediment grains as soon as these are affected by dissolution[8]. Each kind of calcareous grain—a mollusc shell, a barnacle plate, an echinoid stereome—has its own distinctive etch pattern which is related to the mineralogy and structure of the grain fabric (Fig. 1). The SEM analyses allow identification of separate mineral species in the grains, and the degree of undersaturation thus can be related to the solubility of the various minerals, and even to different phases of the same mineral[8–10].

Petrographic saturometry in natural sediments has its limitations, however. Most important here is that etch patterns may either reflect uninterrupted dissolution in continual undersaturation, or they may be cumulative records of several dissolution events, representing occasional drops of the saturation level in an otherwise saturated, or even supersaturated, environment.

In the Skagerrak—as in other high-latitude shelf seas—seasonal fluctuations in carbonate saturation seem very likely. Three factors contribute to lower saturation levels

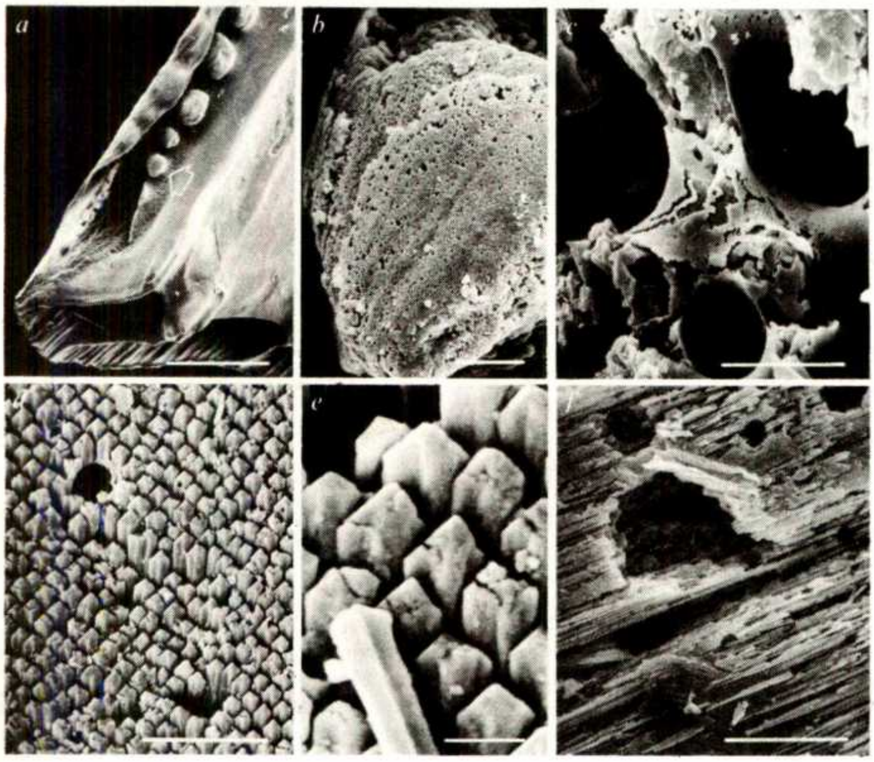

Fig. 1 Dissolution features in carbonate sediments from the Skagerrak: SEM micrographs, scale bars 10 µm, except for (*a*) 250 µm, and (*e*) 2 µm. *a*, Plate of dead barnacle collected *in situ* on rock face at 4-m depth. The entire shell was weak and crumbly. Arrow points to hinge tooth shown in detail. *b*, Corroded appearance of the calcite fabric in barnacle hinge tooth. *c*, Echinoderm fragment of magnesian calcite, grain size fraction 125–250 µm, water depth 12 m. Echinoderm fragments behave as single calcite crystals in the petrographic light microscope, but reveal an intricate core-and-rind structure during natural dissolution. *d*, Etch pattern exposing the tips of prismatic calcite fibres in *Mytilus* fragment. Grain size fraction 250–500 µm, water depth 12 m. *e*, Tips of etched *Mytilus* fibres. *f*, Transverse fracture through cross-lamellar aragonite in bivalve shell, showing partial dissolution of the fabric. The holes are corroded borings after endolithic organisms. Grain size 4 mm, water depth 6 m.

during the winters: first, photosynthesis is at its minimum so organic uptake of CO_2 is small; second, water temperatures are low so solubility of CO_2 is high and third, large amounts of CO_2 are released in the water through the decay of the summer crop of organisms.

Carbonate diagenesis in the Skagerrak

Even a cursory examination of the processes in the Skagerrak will show the fundamental differences between the carbonate-supersaturation diagenetic model so well known from warm shallow seas (refs 18, 19), and the undersaturation model in these cooler waters. The effects of a universal change to carbonate-undersaturated conditions may then be more properly assessed.

In the depth interval studied (0–40 m), the carbonates derive mainly from macroscopic benthic organisms, such as, bivalves, gastropods, barnacles, echinoderms and calcareous algae. Benthic foraminifers are of local importance. The most common single constituent is the blue mussel *Mytilus edulis* whose shell fragments give many sands a bluish tinge.

The sediments studied are nearshore sands of varying carbonate content, from a few % by weight in terrigenous sands, to > 90% by weight in skeletal sands. The grain size ranges from several cm in complete shells, to a few μm in the most comminuted material, with the median value commonly in the 200–800-μm interval.

From a mineralogical point of view, the carbonate fraction consists of aragonite, calcite, and a spectrum of magnesian calcites (Fig. 2). The proportions of mineral species in the sediments depend on the composition of the local carbonate-producing population, but calcite is nearly always dominant.

The effects of carbonate dissolution in the sediments can be seen with a simple binocular microscope: calcareous grains have a frosted, sometimes even chalky appearance, and many grains are weak and crumbly. The frosted texture is caused by surface etch patterns, whereas the chalky and powdery state originates from partial dissolution of the grain fabric.

In the Skagerrak, etch patterns occur on all kinds of calcareous grains, and it is clear that the environment is undersaturated with respect to all carbonate phases present: calcite, aragonite, and magnesian calcites[8–10]. In principle, the solubility of the carbonates varies according to the following pattern: most soluble among the sediment constituents are magnesian calcites with $\gtrsim$ 15 mol % $MgCO_3$ in solid solution; next come aragonite and the intermediate magnesian calcites, whereas pure calcite is the least soluble[20–22]. It is, however, a complicating factor that biogenic carbonate grains are intricate constructions of organic matrices and mineral substance, with the mineral part organised in various submicroscopic units of calcification. Within a single grain, the skeletal units may vary considerably in solubility because of variations in mineralogy and composition[23–25].

The heterogeneous nature of the skeletal grains determines their dissolution behaviour. Minor spatial variations in solubility in the particle fabrics control the etch topography which develops as soon as dissolution begins (Fig. 1). On continued exposure, deeper parts of the grains are gradually affected and the intragranular fabrics are partially dissolved. The process produces the familiar chalky appearance of many skeletal grains[8]. An instructive example is the cross-lamellar arogonite fabric in mollusc shells: some lamellae are selectively dissolved out of the shells while other lamellae remain as a residual chalky fabric (Fig. 1*f*).

This mechanism suggests that the rate of dissolution is slow so that the ambient undersaturation is not fully compensated by dissolution at the grain surface but exists as an undersaturation gradient some distance into the grain. The depth of the zone thus affected by intragranular dissolution is several hundred μm, and skeletal grains of medium sand size and finer may be affected by dissolution right through the particle fabric.

An interesting aspect of the degradation of skeletal carbonates in the Skagerrak is the decomposition of intraskeletal organic substances. The decomposition contributes heavily to the structural breakdown of skeletal grains, and the process is particularly evident in mollusc shells. In these, decomposition affects, for example, the organic sheets between layers of aragonite nacre and the sheaths around the calcite fibres in *Mytilus* shells. The aragonite nacre peels off in thin flakes, whereas the prismatic calcite disaggregates to free fibres, and both components last on their own for some time. Aragonite flakes and *Mytilus* fibres are the dominating constituents in a subordinate 'lime mud' fraction which is the final stage before complete dissolution (Fig. 3). A similar disaggregation of mollusc shells or other animal carbonates is not known from warm, carbonate-supersaturated waters, but why this is so is not understood—particularly not in the light of the abundant evidence of disaggregation of calcareous plant tissue. Recent studies indicate that the disaggregation of calcareous algae is the main producer of lime muds in warm shallow environments[26].

The Skagerrak sediments differ from warm-sea carbonate sands, not only by having a specific set of dissolution features which are unknown in carbonate-supersaturated areas, but also by lacking the various signs of precipitation which accompany supersaturation. The relationship between supersaturation and precipitation in seawater is in itself a complex problem[22,27], and it seems that the ordinary carbonate supersaturation in warm surface waters leaves a rather erratic petrographic record in the sediments[10,18,19]. Sand constituents commonly attributed to precipitation are ooids, grapestones, cemented pellets, and cements in micrite envelopes and hollow grains[18,19,28,29]. As might be expected, such constituents do not occur in the Skagerrak carbonates.

The only carbonate cements observed are all small amounts of internal aragonite and Mg-calcite cement, formed within coralline algal nodules and crusts through the calcifying processes of the red algae[30]. This biogenic cement is totally dependent on the algal life processes, and after death of the algae both skeletons and cement are attacked by dissolution.

The picture emerging from the petrographic studies of carbonate diagenesis in the Skagerrak is very consistent. It shows the absence of carbonate precipitation related to ambient supersaturation, and instead the presence of carbonate dissolution because of ambient undersaturation.

Fig. 2 X-ray powder diffractograms of various size fractions in a calcareous sand taken with Ni-filtered Cu-radiation. The black peaks at 26 and 27 are aragonite, the broad peak at 29–30 is calcite with the Mg-calcite area hatched. Relative amounts of the minerals can be calculated from peak areas (ref. 19). The relative amounts of Mg-calcite and aragonite increase with decreasing grain size, indicating a more rapid structural breakdown of these constituents.

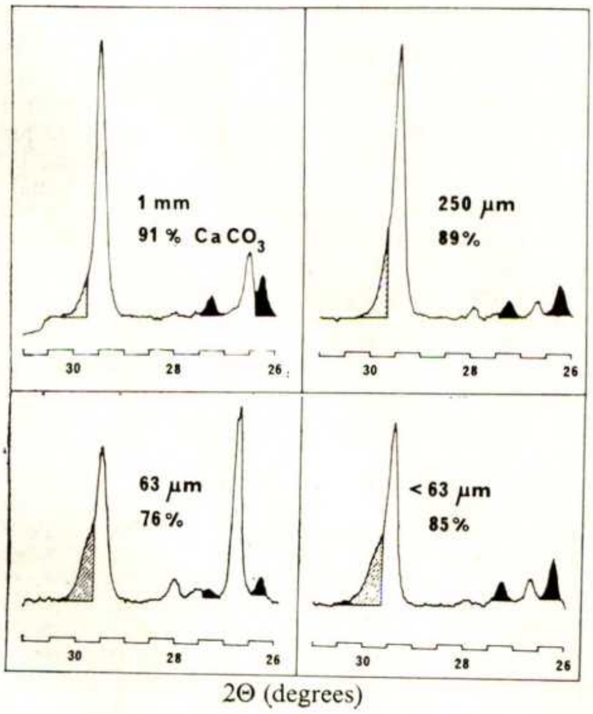

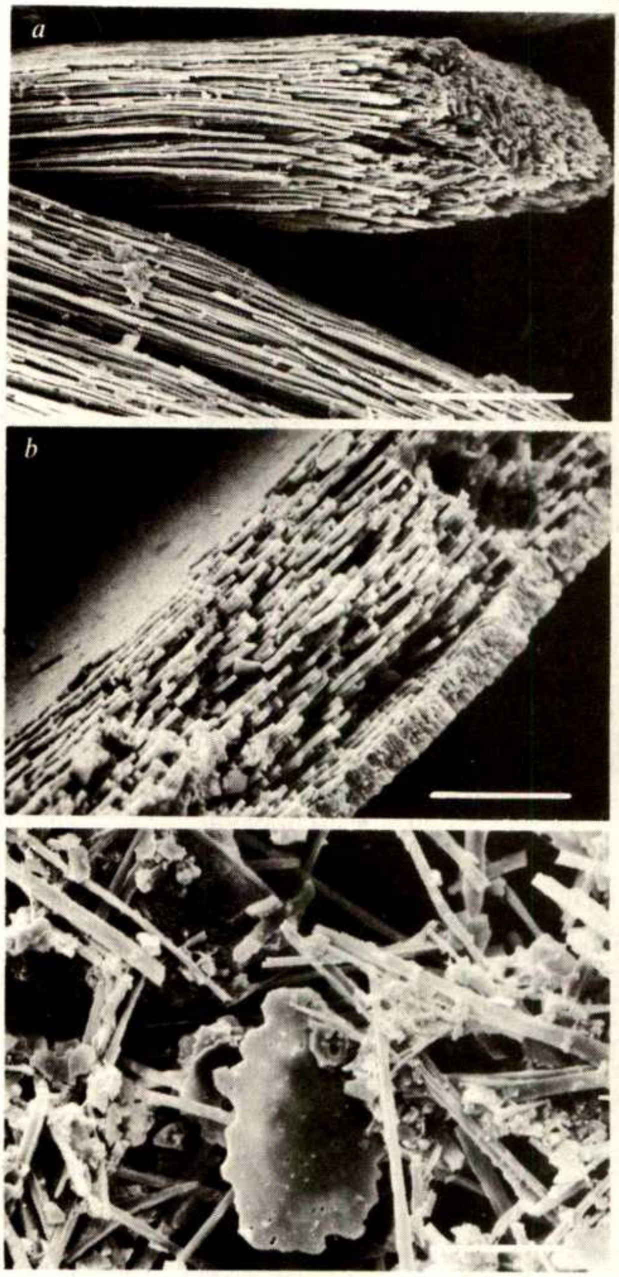

Fig. 3 Structural breakdown of skeletal carbonates in the Skagerrak: SEM micrographs, scale bars in (*a*) 50 µm, in (*b, c*) 20 µm. *a*, *Mytilus* fragments in their natural state. The calcite part of the shells is reduced to bundles of weakly coherent elastic fibres which easily disaggregate to free fibres. Grain size fraction 125–250 µm, water depth 12 m. *b*, Transverse fracture through bivalve shell with layers of peeling aragonite nacre. Grain size 1 mm, water depth 6 m. *c*, Molluscan aragonite flakes and *Mytilus* fibres in a 'lime mud' fraction of skeletal debris. Grain size fraction < 63 µm, water depth 15 m.

Is the dissolution really caused by ambient carbonate undersaturation in the seawater? Considering the various processes of organic decay that must occur in the sediments —especially when the summer crop of organisms dies off in response to the harsh winter conditions—is it not more likely that dissolution is an interstitial process at some depth in the sediments? This question was studied by monitoring the breakdown of calcareous epibionts on submarine rock surfaces away from the sediments, collecting skeletal material during SCUBA dives every fourth month. The results show that dead epibionts, such as coralline algal crusts, barnacle cups, and serpulid tubes, are attacked by dissolution while still in growth positions on naked rock-faces. The barnacle plate in Fig. 1 is an example of this. To a diver, accustomed to cuts and scratches from barnacles on rocky shores, it was a surprise sometimes to find as much as one third of a barnacle colony as friable cups which could be crushed with the tip of a finger.

The impression is that isolated calcareous organisms, freely exposed to circulating seawater on stones and rocks, are more rapidly destroyed than organisms and carbonate grains within calcareous sands. Dead calcareous epibionts disappear from their growth sites in a year or two, partly because of decomposition of the binding organic substances, and partly because of carbonate dissolution. For example, *Mytilus* shells fall off and go into the sediments because of organic decomposition, as do barnacle cups with the exception of the basal plates. Barnacle basal plates, crustose coralline algae, and serpulid worm tubes are firmly cemented to the rocks and provide good examples of dissolution *in situ*. It is worth noting that calcareous crusts do not accumulate on rock surfaces in the area, even if growth of encrusters is vigorous—a marked contrast to the conditions in many warm, supersaturated seas.

In living organisms, susceptibility to carbonate dissolution varies widely among different groups. The decisive factor is the degree of organic protection of the mineral phase, and this depends on the structural organisation of the organism. In living crustose coralline algae, echinoderms, and benthic foraminifers, the skeletons are fully protected by living substance and there is no dissolution. As previously mentioned, crustose coralline algae actually control the microenvironment in their crusts to the extent that intraskeletal carbonate cement may form in spite of the ambient undersaturation[30]. More exposed to dissolution are the shells of bivalves, gastropods, and barnacles, and etch patterns have been observed, for example, on the apical ends of shells of living gastropods. Quantitatively, however, the dissolution is insignificant in these large animals, and their life processes are unaffected. The conditions may be different for microscopic organisms suspended in seawater—for example coccolithic algae—but calcareous plankton has not yet been studied from this point of view.

As constituents of calcareous sands, skeletal fragments obviously may last for a very long time. In areas of net accumulation of sediments, the grains are buried by sedimentation and are then out of reach of the marine carbonate dissolution which does not proceed far beneath the sediment–seawater interface. The destiny of an individual calcareous sediment grain depends on a complex set of processes, involving organic carbonate production, physical sedimentation processess, wave and current action, bioturbation, bioerosion, and the degree of ambient carbonate saturation. How to define a meaningful 'rate of dissolution' in these conditions, and how to calculate such a parameter, are problems which remain to be solved.

Concluding remarks

As mentioned earlier, knowledge of carbonate undersaturation in shallow seawater is still fragmentary, and the story from the Skagerrak must be left with several holes in it. Perhaps the most annoying question is: why is carbonate undersaturation in shallow seawater so little understood from a chemical point of view? To my knowledge, the consensus among chemists is that the surface layers of the sea are supersaturated throughout, although there are discussions as to the degree[6,14–16]. Part of the answer may lie in a sampling problem. Few, if any, saturation data represent the nearshore conditions in the Skagerrak, let's say in the dark and cold at four o'clock on a January morning, when the sublittoral environment is absolutely devoid of photosynthesis, but has considerable respiration and bacterial decay. Should carbonate undersaturation occur in these conditions, however, it would be faithfully recorded as dissolution features in the sediments, clearly diagnostic in petrographic analysis.

In the absence of chemical data, it cannot be determined whether carbonate undersaturation in the Skagerrak is general and permanent, or if it is limited in space and time —for example, to the bottom waters in winter. Even if we assume that undersaturation here is limited, it does not, however, invalidate the main hypothesis of this paper—namely, that a future change to general carbonate undersaturation in the ocean's surface layers would cause radical changes in carbonate sedimentation in the shelf seas. Rather on the contrary: if an extensive dissolution record like the one in the Skagerrak can be produced by fairly limited carbonate undersaturation, how severe must be the effects of a universal change.

As far as it goes, the record in the Skagerrak sediments is entirely consistent. First, there is no petrographic evidence of ambient carbonate supersaturation, as known from warm shallow seas. Second, all carbonate phases present—calcite, aragonite, and magnesian calcites—are attacked by dissolution and gradually lost from the sediments. The petrographic record of the dissolution process consists of etch patterns and partially dissolved grains. The structural breakdown of skeletal carbonates is much promoted by decomposition of intraskeletal organic substances.

A change towards similar conditions in all the world's shelf seas would mean a radical change of the present pattern of carbonate sedimentation. The changes cannot be calculated in detail, especially the net effects of dissolution. From a petrographic point of view, an early and fundamental effect would be the termination of shallow marine carbonate precipitation. This would mean an end to largely inorganic processes such as growth of ooids, and formation of cements in grapestones, micrite envelopes, pellets, hollow grains and other sand constituents: probably also to interparticle cementation in submarine sands and beachrock. The pattern of preservation of calcareous shells and skeletons would certainly change, with effects on the accumulation of fossil assemblages in the sediments.

Sedimentary changes of this nature would stand out most drastically in present areas of high carbonate supersaturation. They would mean an end to—or rather an interruption of—the typical warm-sea carbonate sedimentation as we know it from, for example, the Bahama Banks and the Persian Gulf. In geological terms, a man-made carbonate undersaturation would probably be a brief event, but it would be irrevocably recorded in the sediments and thus take its place in the general geological record with its amazing permanence. Every geologist who has studied, for example, the details of an Ordovician limestone will probably share my conviction that sedimentary changes, however subtle, in carbonate sediments have the potential to last for hundreds of millions of years. An event of man-made carbonate undersaturation in the shallow seas might indeed produce one of the most universal and permanent records of human activity ever formed on Earth.

In a shorter perspective, it is reassuring that the evidence from the Skagerrak of today indicates that carbonate undersaturation in shelf seas does not necessarily mean serious problems for the marine environment and its inhabitants.

This study was supported by grants from Magnus Bergvalls Stiftelse, and from the Swedish Natural Science Research Council. I thank Mrs Dagmar Engström and Mr Gustav Andersson for patient and competent technical assistance, and Drs Marianne Pedersén and Anna Tolstoy for help in the field.

Received April 5; accepted July 1, 1976.

[1] Broecker, W. S., Li, Y-H., and Peng, T-H., *Impingement of Man on the Oceans* (edit. by Hood, D. W.), ch. 11 (Wiley, New York, 1971).
[2] Holland, H. D., *Geochim. cosmochim. Acta*, **36**, 637 (.972).
[3] Fairhall, A. W., *Nature*, **245**, 20 (1973).

4 Zimen, K. E., and Altenhein, F. K., *Naturwissenschaften*, 4, 198 (1973).
5 Fairhall, A. W., and Erickson, J. L., *Nature*, 254, 273 (1975).
6 Moller, P., and Parekh, P. P., *Sci. total Environ.*, 4, 177 (1975).
7 Whitfield, M., *Nature*, 247, 523 (1974); *ibid.*, 254, 274 (1975).
8 Alexandersson, E. T., *Bull. geol. Instn Univ. Uppsala*, 3, 201 (1972).
9 Alexandersson, E. T., *Science*, 189, 47 (1975).
10 Alexandersson, E. T., *Society of Economic Paleontologists and Mineralogists, 50th Anniversary Special Publication* (edit. by Fairbridge, R. W.), ch. 29 (SEPM, Tulsa, Oklahoma, in the press).
11 Pytkowicz, R. M., *Limnol. Oceanogr.*, 10, 220 (1965).
12 Li, Y-H., Takahashi, T., and Broecker, W. S., *J. geophys. Res.*, 74, 5507 (1969).
13 Edmond, J. M., *Deep-Sea Res.*, 21, 455 (1974).
14 Broecker, W. S., and Takahashi, T., *J. geophys. Res.*, 71, 1575 (1966).
15 Möller, P., and Parekh, P. P., *Marine Chemistry*, 3, 63 (1975).
16 Lees, A., *Marine Geology*, 19, 159 (1975).
17 Murray, J., and Renard, A. F., *Deep-sea Deposits. Report on the Scientific Results of the Voyage of H.M.S. Challenger During the Years 1873–76* (H.M. Stationery Office, 1891).
18 Bathurst, R. G. C., *Developments in Sedimentology*, 12 (Elsevier, Amsterdam, 1971); *A. Rev. Earth planet. Sci.*, 2, 257 (1974).
19 Milliman, J. D., *Recent Sedimentary Carbonates, part 1, Marine Carbonates* (Springer, New York, 1974).
20 Chave, K. E., Deffeyes, K. S., Weyl, P. K., Garrels, R. M., and Thompson, M. E., *Science*, 137, 33 (1962).
21 Chave, K. E., and Schmalz, R. F., *Geochim. cosmochim. Acta*, 30, 1037 (1966).
22 Weyl, P. K., *Stud. trop. Oceanogr. Miami*, 5, 178 (1967)
23 Schroeder, J. H., Dwornik, E. J., and Papike, J. J., *Bull. geol. Soc. Am.*, 80, 1613 (1969).
24 Milliman, J. D., Gastner, M., and Muller, J., *Bull. geol. Soc. Am.*, 82, 573 (1971)
25 Mutvei, H., *Calcified Tissue Res.* (in the press).
26 Neumann, A. C., and Land, L. S., *J. sedim. Petrol.*, 45, 763 (1975).
27 Alexandersson, E. T., *J. sedim. Petrol.*, 42, 441 (1972).
28 Glover, E. D., and Pray, L. C., *The Johns Hopkins University Studies in Geology* (edit. by Bricker, O. P., 19), 80 (Johns Hopkins University Press, 1971).
29 Boyer, B. W., *J. sedim. Petrol.*, 42, 205 (1972).
30 Alexandersson, E. T., *J. sedim. Petrol.*, 44, 7 (1974).

Cellular basis for the T wave of the electrocardiogram

I. Cohen, W. Giles & D. Noble

University Laboratory of Physiology, South Parks Road, Oxford, UK

Differences in action potential duration in different regions of the mammalian ventricle are not systematically present when quiescent tissue is first stimulated, but develop rapidly during repetitive activity. The effects of ouabain and temperature suggest the involvement of the Na$^+$–K$^+$ exchange pump.

THE electrocardiogram (ECG) has proved to be a remarkably useful tool in the diagnosis and management of many types of malfunction or disease of the heart. But after nearly a century of use and refinement, and in spite of recent advances in cellular cardiac electrophysiology, certain features of the ECG are not well understood. One example is the T wave of the mammalian ECG. It is empirically described as arising from differences in action potential duration in different anatomical regions of the ventricle. Most attempts[•] to account for the T wave have utilised indirect measurements of the sequence of repolarisation in ventricular tissue. For example, detailed studies of the relative refractory period in several anatomical locations in both ventricles and on the intraventricular septum have been reported[1]. And Spach and Barr[2] have used arrays of chronically implanted electrodes simultaneously to record potential distributions in the intact dog heart during excitation and repolarisation. We have used conventional microelectrode techniques to record action potentials in isolated preparations from sheep ventricle. The results show unexpected, activity-dependent changes in action potential duration which may provide further understanding of the mechanism of the T wave.

The T wave of the mammalian ECG is synchronous with the repolarisation phase of the ventricular action potential, and is therefore thought to represent the net extracellular field produced by the spreading of the repolarisation wave throughout the ventricular myocardium. But it is somewhat surprising that the T wave is found to be positive in the same ECG leads as the R wave of the QRS complex, since this complex corresponds to depolarisation of the ventricular myocardium.

Extracellular recordings of the potentials produced by the conduction of nerve impulses produce a diphasic wave, so that, if the leads are arranged such that depolarisation corresponds to a positive extracellular wave, repolarisation is represented by a negative extracellular wave. This result is necessary if depolarisation and repolarisation propagate in the same direction.

The apparent paradox in the directionality of the T wave is usually explained by postulating that the depolarisation and repolarisiation waves in at least some parts of the ventricle travel in opposite directions, so that regions that are excited latest repolarise earliest. This explanation requires that the duration of the action potential should be greater at the point of entry of the wave (in the endocardial muscle of the septum) than at later points in the conduction pathway (for example, in the epicardial surface of the apex). Early work using extracellular electrodes provided strong evidence for this conclusion (for discussion and references see ref. 3). More recently, recordings made with intracellular microelectrodes have shown that, during normal repetitive activity, the action potential at the epicardial surface of the ventricle is shorter than that at the endocardial surface[4].

An important possible function for such a difference is that the longer action potential at early points in the conduction pathway may prevent re-excitation and re-entry. It is therefore important to attempt to determine the cellular basis for this difference. The experiments we describe here show two important results. First, the duration differences responsible for the normal T wave develop as a consequence of repetitive activity; they are not present in the first action potential of a previously quiescent ventricle. Second, the effects of repetitive activity are strongly influenced by cardiac glycosides and by temperature.

Small pieces of tissue (2–4 mm square and 1 mm thick) were dissected from two regions of sheep left ventricles—the upper part (base) of the interventricular septum and the epicardial surface of the apex. The former is endocardial and the latter is epicardial. Some theories of the T wave regard the difference in action potential duration as being primarily between endocardial and epicardial surfaces. The alternative view is that a base/apex gradient exists. The two views are not, of course, mutually exclusive. Our choice of regions allows the correlate of either kind of gradient to be detected in action potential recordings. For simplicity we refer to the two regions as 'base' and 'apex', respectively.

After a suitable period for recovery (20–30 min) action potentials from each region were recorded using conventional 3-M KCl microelectrodes. All measurements of action potential duration were made from heat-sensitive pen recordings at the point of 80% repolarisation. In contrast to recordings made on the whole heart, it is possible to remain impaled in small pieces of tissue for prolonged periods. Moreover, since the preparations are quiescent until

•

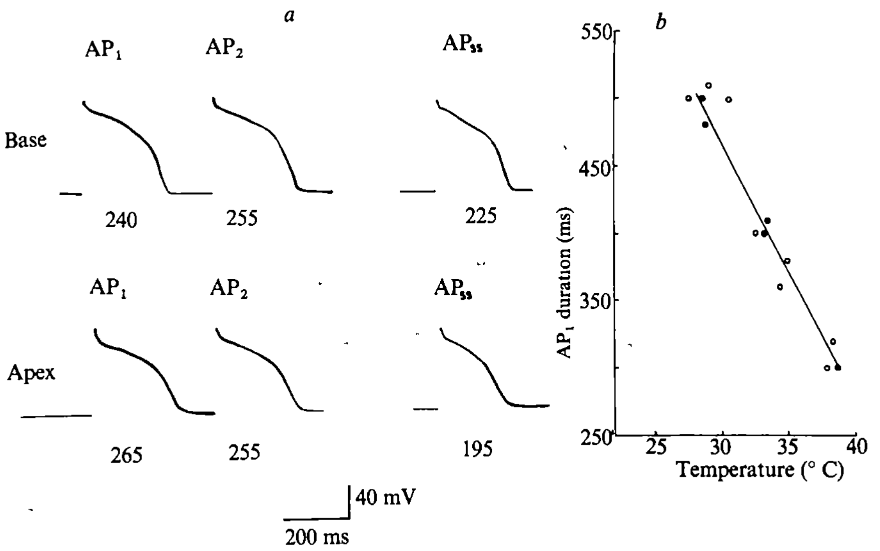

Fig. 1 *a*, Records obtained during trains of action potentials produced in base (endocardial) and apex (epicardial) preparations from sheep ventricle. Stimuli were applied at 150 per s after a 30–60-s quiescent period The time to 80% repolarisation is shown in ms below each action potential. AP_1 is the first action potential in each train, AP_2 the second and AP_{SS} is taken when there are no further changes (usually 10–20 action potentials) There is a considerable difference in the effect of activity in the two regions. At the base AP_2 lengthens and AP_{SS} is only 15 ms shorter than AP_1. At the apex AP_2 shortens and AP_{SS} is 70 ms shorter than AP_1. These particular records show a 25-ms difference between AP_1 in the two regions. This difference is in the wrong direction for explaining the normal T wave and was not found to be significant (see *b*). *b*, Duration of AP_1 as a function of temperature. There is no systematic difference between AP_1 durations at the base (●) and apex (○). Similar results were found in other experiments (although the precise functional dependence of duration on temperature was not always linear).

stimulated it is also possible to determine whether any differences that occur in the action potentials are dependent on the presence of repetitive activity.

First action potential

This question was answered by studying trains of action potentials following a short (30–60 s) period of rest. We found that there were no systematic differences between the first action potentials in the base and apex regions Moreover, this similarity between the two regions occurred at all the temperatures investigated. Figure 1*b* shows a plot of the first action potential durations obtained from the base (filled circles) and apex (open circles) between 28 and 38 °C. There is a scatter of up to about 20 ms in the durations but it is clear that the durations are not systematically different. They can be fitted by the same relationship as a function of temperature. This result was also obtained in other experiments provided that adequate time was allowed for recovery and that the results were compared from pieces of tissue taken from the same heart.

These experiments strongly suggest that there are no substantial differences between the basic ionic conductance mechanisms that control the plateau and repolarisation phases in the two regions. If such differences exist we should have to suppose both that differences in the individual conductance mechanisms are balanced to produce identical durations and that this balance is preserved for the whole temperature range. This seems very unlikely in view of the fact that the net current flow during the plateau is approximately 1% of the magnitude of the individual inward and outward currents involved[5].

Repetitive activity and second action potential

Although there are no systematic differences between the first action potential durations, it is clear from Fig. 1*a* that the effect of activity is strikingly different in the two regions. At the base we invariably found that the second action potential duration (AP_2) is substantially longer than the first (AP_1) and that the steady-state action potential (AP_{ss}) is either similar to or only slightly shorter than the first. In the case illustrated, AP_{ss} is 225 ms compared with 240 ms for AP_1. In contrast, at the apex we generally found a substantial shortening so that AP_{ss} is much shorter than AP_1. This effect is particularly striking in Fig. 1*a* since the duration of AP_1 at the apex (265 ms) is longer than at the base (240 ms). Such a difference would result in a negative T wave, as would also be the case when the durations are identical Nevertheless, in the apex AP_{ss} is 70 ms shorter than AP_1 and becomes 30 ms shorter than AP_{ss} at the base. Such a difference would lead to the positive T wave observed during normal repetitive activity. We shall discuss the results for AP_2 and AP_{ss} separately.

Twin pulse studies on sheep Purkinje fibres usually show that the second action potential shortens as the interstimulus interval is reduced. This shortening is primarily caused by residual activation of i_{x1}, the outward current which speeds repolarisation[6]. But lengthening of the second action potential has also occasionally been observed in Purkinje fibres[7]. Such experiments have shown that 10^{-6} M ouabain reduces or eliminates the increase in duration of AP_2.

Fig. 2 *a*, Records obtained during paired pulse stimulation at various intervals (indicated in ms). *b*, Duration ratios (AP_2/AP_1) as a function of interstimulus intervals from experiment illustrated in (*a*). The solid curves were drawn by eye. Note that the ratio is less than 1 at the apex (○) and substantially greater than 1 at the base (●).

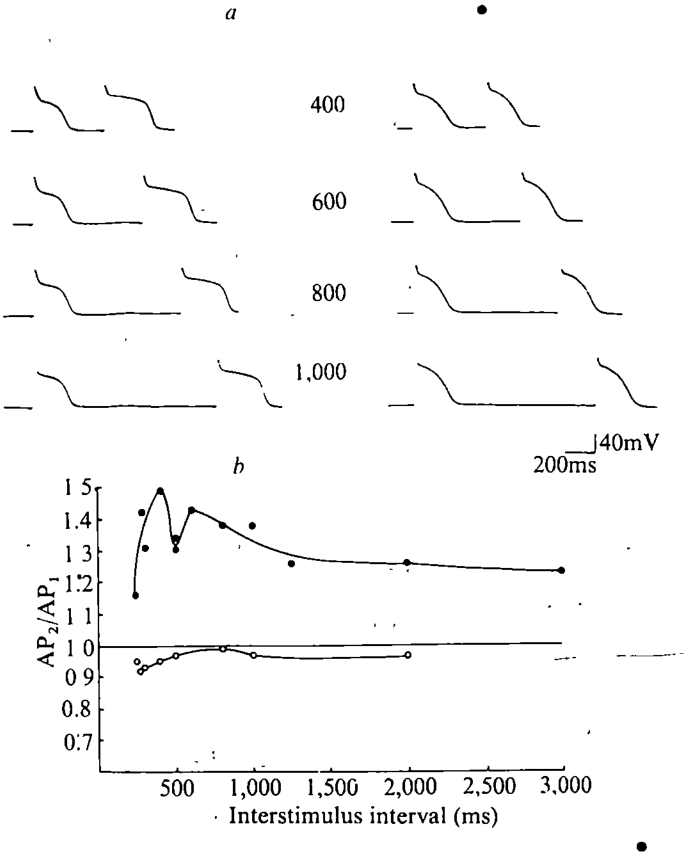

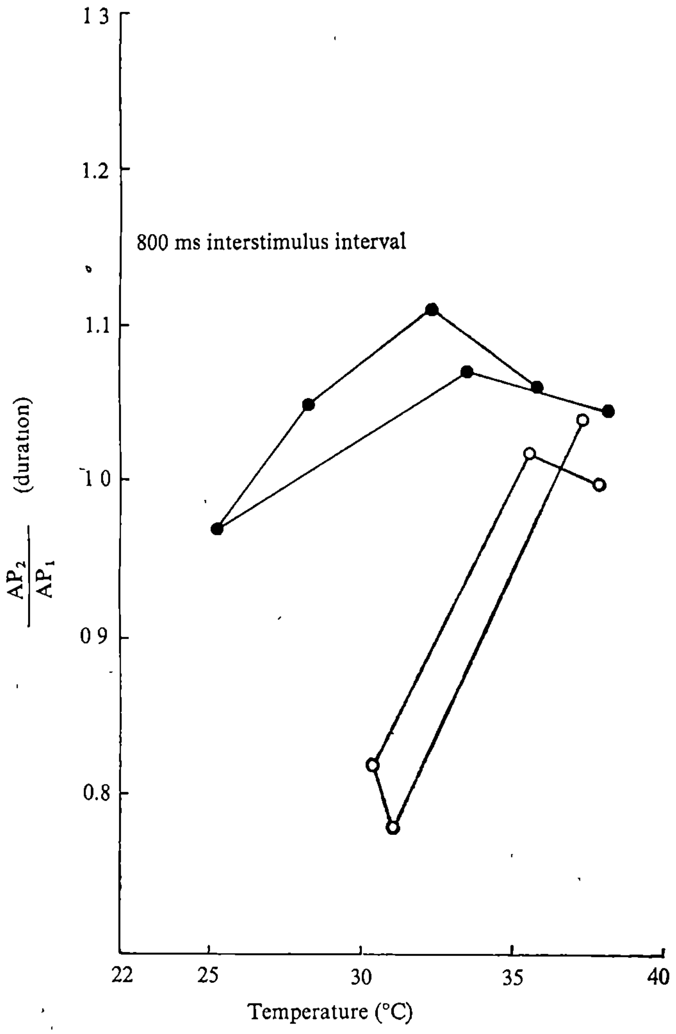

Fig. 3 Influence of temperature on the AP_2/AP_1 duration ratios at the base (●) and apex (○) at an interstimulus interval of 800 ms. Cooling has a larger influence on the apex than on the base. The effects are completely reversible in both regions.

We have studied the duration of AP_2 after application of paired stimuli at various interstimulus intervals to the base and apex regions of the ventricle. As before, a 30–60-s rest period followed each pair of stimuli. As shown in Fig. 2*a*, AP_2 at the base was substantially longer than AP_1, whereas the opposite result was obtained at the apex. Figure 2*b* shows plots of the AP_2/AP_1 ratio as a function of interstimulus interval. At all intervals, the ratio is much smaller at the apex than at the base. This result was obtained in all healthy preparations. It was important, however, to allow adequate time (about 1 h) for recovery after dissection. During recovery in apex preparations, while the resting potential was low and the first action potential was relatively short, a striking prolongation of AP_2 could be obtained. Such preparations conformed to the pattern of response shown in Fig. 2 after they reached their normal resting potential and AP_1 became normal in duration.

To test whether the prolongation of AP_2 at the base is attributable to the activity of the Na^+–K^+ exchange pump, we used two methods of blocking pump activity—cooling and application of ouabain. Figure 3 shows the results of cooling at an interstimulus interval of 800 ms. In both regions the AP_2/AP_1 duration ratio becomes smaller at low temperatures but the effect was always found to be more dramatic at the apex than at the base. At 38 °C the AP_2/AP_1 ratio is slightly larger than 1.0 in the apex but falls to about 0.8 when the tissue is cooled to 30 °C. By contrast, in the base, the ratio is still larger than 1.0 at that temperature and cooling to 25 °C was required to reduce the ratio significantly. These effects were totally reversible when the preparations were rewarmed.

Figure 4 shows the results of experiments on the effects of various concentrations of ouabain. In both regions, the AP_2/AP_1 ratio is significantly reduced by ouabain at concentrations that are thought to reduce the activity of the pump significantly. Unlike cooling, these effects were not reversible. This result is not surprising in view of the well known difficulty in reversing the inhibitory action of ouabain on the Na–K exchange pump.

Steady-state action potential

It is clear from the results described so far that very marked differences between the base and apex regions may develop

Fig. 4 The effects of ouabain on AP_2/AP_1 (○) and AP_{ss}/AP_1 (●) duration ratios. The stimulus frequency is 240 per s at the base and 150 per s at the apex. Further explanation in text.

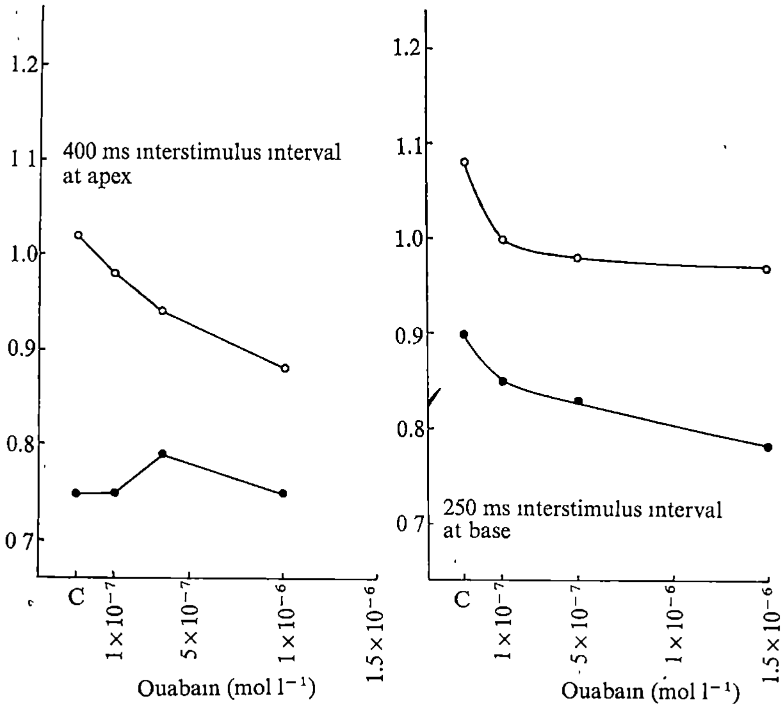

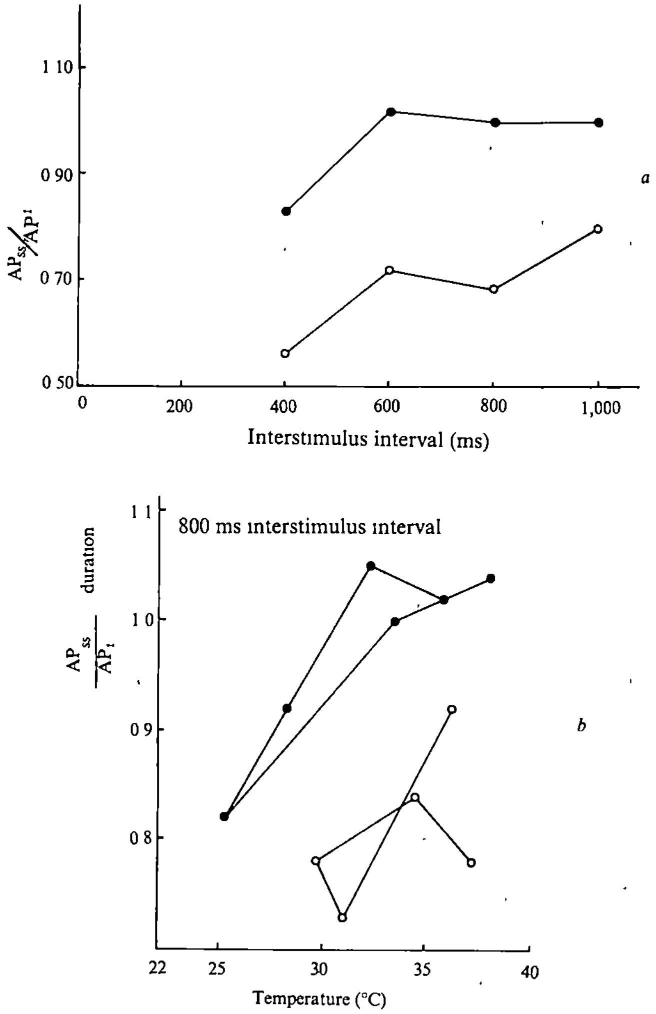

Fig. 5 *a*, AP_{ss}/AP_1 duration ratios at base (●, 38.6 °C) and apex (○, 38.0 °C) as a function of interstimulus interval. The precise influence of changes in frequency on AP_{ss} in the two regions varies somewhat between experiments but, as in this experiment, a significant difference between the two areas is found over the whole frequency range investigated. *b*, Influence of temperature on the AP_{ss}/AP_1 duration ratios in the base (●) and apex (○). These results can be compared with those for the AP_2/AP_1 ratios shown in Fig. 3. The same general phenomenon is observed, that is the apex ratio is reduced to lower levels than the base ratio by cooling. In this particular experiment, the effects were perfectly reversible at the base but not at the apex. Reversible effects on AP_{ss} were obtained in the apex in other experiments.

as a consequence of only one action potential. The difference between the durations of AP_2 in the two regions would produce a positive T wave. It is important, however, to remember that the normal T wave is determined by the steady-state action potential characteristics of maintained repetitive firing. It is therefore essential to study the durations of AP_{ss} in each region of the ventricle.

Figure 1*a* shows that AP_{ss} is longer at the base than at the apex. Figure 5*a* shows that this difference persists for a wide range of frequencies. The filled circles show the AP_{ss}/AP_1 ratio at the base as a function of interstimulus interval. The results for the apex are shown by the open circles. Although in both cases there is a tendency for the ratio to decrease at high frequencies, the difference is always substantial. This result suggests that changes in frequency *per se* should not influence the polarity of the T wave.

Figure 5*b* shows the influence of cooling on the AP_{ss}/AP_1 duration ratios. As with the results for AP_2, cooling decreases the ratio although a higher ratio is always maintained at the base than at the apex.

The influence of ouabain on the AP_{ss}/AP_1 duration ratios is shown as filled symbols in Fig. 4. The results are more difficult to interpret than those from the cooling experiments. Thus the marked shortening of the action potentials (including AP_1) produced by inhibitory doses of ouabain may give a fairly constant AP_{ss}/AP_1 duration ratio even when both AP_{ss} and AP_1 are substantially shortened. This applies to the apex results. In the case of the base, there is a decrease in the AP_{ss}/AP_1 duration ratio. This means that the AP_{ss}/AP_1 duration ratios become more similar in the presence of ouabain. If this effect is sufficiently large it could lead to a reduction or to inversion of the T wave.

Implications of the results

Several important conclusions can be drawn from our results. (1) Since the first action potentials from the base and apex are very similar in duration it is likely that the ionic currents involved are the same in the two regions. (2) It therefore follows that the differences in duration that occur during normal beating, and that are responsible for determining the polarity of the T wave, develop as a consequence of activity. The onset of this effect must be very rapid since large differences in duration are evident in the second action potential in a train. The second action potential is always longer than the first at the base. It is sometimes longer at the apex but the AP_2/AP_1 duration ratio is always greater at the base than at the apex. (3) In both base and apex regions subsequent action potentials in a train become shorter but the difference in duration between the two areas is always maintained. At normal temperatures the base AP_{ss}/AP_1 duration ratio is near unity. At the apex it is always significantly less than 1. (4) Because the prolongation of AP_2 is reduced or abolished by cooling and by inhibitory doses of ouabain it is possible that the effects are attributable to the response of the Na–K exchange pump to repetitive activity. This response, or its consequences, must be significantly different in the two regions.

Can we offer any explanation for an increase in action potential duration after increased activity of the Na–K pump? At first sight this may seem to be opposite to the expected effect since activation of outward electrogenic pumping would by itself speed repolarisation. This suggests that the effect may arise as a secondary consequence of ionic concentration changes rather than as a direct result of increased pumping. During activity, the cells will gain Na ions and lose K ions. During a single action potential the concentration changes involved will be small unless the movements occur into very restricted spaces. Narrow extracellular spaces do exist in cardiac muscle[8–10], and rapid changes in extracellular K^+ concentration may occur in them[11,12]. In particular, $[K^+]$ in the space will increase during activity. It is possible therefore that this increase in $[K^+]$ is responsible for activating the Na–K exchange pump.

It remains, however, to explain how this might prolong the action potential. If $[K^+]$ remains elevated, the action potential will shorten as a consequence of the well known effect of $[K^+]_0$ on plateau duration[13]. To obtain prolongation we would have to suppose that the pump can transiently reduce the $[K^+]$ in the small extracellular spaces or clefts to levels below normal. The action potential would then be prolonged[14].

This interpretation of our results is clearly very tentative. We have no direct evidence that cleft $[K^+]$ is reduced below normal after the first action potential. Moreover, it may be very difficult to test the idea directly as even K^+-sensitive microelectrodes are not likely to detect the $[K^+]$ level in very narrow cleft spaces. They are more likely to monitor the $[K^+]$ level in the larger extracellular spaces in the preparation.

An alternative view is to postulate that the prolongation of AP_2 is attributable to an increased inward (for example, calcium) current, which is partly (base) or completely (apex) masked by the shortening effect produced by potassium accumulation. This hypothesis leaves the mechanism of the prolongation unexplained but the difference between the base and apex regions would still be attributable to differences in the capacity of the sodium pump to respond to activity.

Whatever ionic mechanisms form the basis of the effects we have observed, our results do enable us to explain various observations on the T wave. The occurrence of myocardial ischaemia or infarction leads to inversion of the T wave, as does treatment with cardiac glycosides. We can explain these effects as a result of inhibition of the Na–K exchange pump. It is also conceivable that inversion occurs as a consequence of increasing the pump's capacity to respond so that the behaviour of the apex is made to approach that of the base, rather than the opposite. Thus, warming may allow the apex to show prolongation of the action potential during activity (Fig. 3) and so in this manner become similar to the base. This phenomenon could form the basis of T-wave inversion during fever. This possibility also serves to emphasise that it may be misleading to regard T-wave inversions as having a common cause. Any manoeuvre that leads to a decrease in the difference in AP duration will reduce or invert the T wave. This may be produced either by inhibiting the property of the basal (endocardial) region that allows unexpectedly long action potentials to occur or by stimulating the apex (epicardial) areas to respond to activity in a manner resembling that of the base.

Our results also lead to the expectation that the T-wave should be reduced or inverted after a period of quiescence. This has been observed in whole hearts of frog and tortoise after a short period of quiescence produced by vagal stimulation.

We acknowledge the support of the MRC, the Canadian MRC and the Muscular Dystrophy Association of America.

Received February 23; accepted June 25, 1976.

[1] Burgess, M. J., Green, L. S , Millar, K., Wyatt, R , and Abildskov, J. A., *Am Heart J.*, 84, 660–669 (1972).
[2] Spach, M. S., and Barr, R. C., *Circulation Res* , 37, 243–257 (1975)
[3] Mines, G. R., *J Physiol* , *Lond.*, 46, 188–235 (1913).
[4] Solbery, L E., Singer, D H., Ten Eick, R. E., and Duffin, E. G., *Circulation Res.*, 30, 783–797 (1974).
[5] Noble, D., and Tsien, R. W , in *Electrical Phenomena in the Heart* (edit. by de Mello, W. F.), 133–161 (Academic, New York, 1972)
[6] Hauswirth, O., Noble, D., and Tsien, R. W., *J. Physiol., Lond* , 222, 27–51 (1972).
[7] Cohen, I., Daut, J., and Noble, D., *J. Physiol., Lond.* (in the press).
[8] Mobley, B. A., and Page, E , *J. Physiol., Lond.*, 220, 547–563 (1972).
[9] Page, S., and Niedergerke, R., *J. cell. Sci.*, 11, 179–203 (1972)
[10] Hellam, D. C , and Studt, J W., *J. Physiol., Lond.*, 243, 637–660 (1974).
[11] Noble, S. J., *J Physiol., Lond.* (in the press).
[12] Cohen, I., Daut, J., and Noble, D., *J. Physiol., Lond.* (in the press).
[13] Weidmann, S , *J. Physiol., Lond.*, 132, 157–163 (1956).
[14] Noble, D., *J. cell. comp. Physiol* , 66, Suppl. 2, 127–136 (1965).

Intracellular *p*H and activation of sea urchin eggs after fertilisation

James D. Johnson & David Epel

Marine Biology Research Division, Scripps Institution of Oceanography, University of California, San Diego, La Jolla, California 92093

Miles Paul

Department of Biology, University of Victoria, Victoria, British Columbia, Canada V8W 2Y2

The intracellular pH of the sea urchin embryo increases 0.3 pH units between 1 and 4 min after fertilisation. The increase in pH is required for initiating development. The increase results from an exchange of extracellular Na$^+$ for intracellular H$^+$.

ACTIVATION of sea urchin eggs after fertilisation can be separated experimentally into two phases[1]. The first, which occurs in the first 60 s after insemination and includes the exocytosis of 1-μm granules in the cell cortex, seems to be initiated by an increase in intracellular free calcium[2–4]. The second, which begins 5 min after insemination and includes increased protein synthesis, commencement of DNA synthesis and other biosynthetic events, seems to result from a nonspecific and pervasive event[5]. The first phase is not a prerequisite for the second, since incubation of eggs in mM concentrations of ammonia[5,6] or treatments altering the egg surface[7,8] will start biosynthesis in the absence of the cortical granule exocytosis. This second phase of activation has been shown[9] to have an obligatory sodium requirement only during the first 5–10 min after insemination at 15 °C. If eggs are transferred to sodium-free seawater between 1 and 5 min after fertilisation, there is no activation of development; however, if sodium (>2.5 mM) is added, development resumes[9,10].

Here we present evidence that ammonia and sodium are agents in an efflux of H$^+$ ions (the 'fertilisation acid') that occurs after fertilisation. This acid represents H$^+$ ions and not a weak organic acid[11], and the result of this efflux is increased intracellular *p*H. Our data indicate that in normal fertilisation, the hydrogen efflux is mediated through a sodium–hydrogen facilitated transport system in which a transient period of sodium influx is coupled to a period of hydrogen efflux. The latter can also be induced directly by ammonia or other organic amines, in the absence of extracellular sodium. It is this hydrogen efflux, with the resultant change in intracellular *p*H, and not the sodium influx, that is the prerequisite for metabolic activation.

We suggest that the suppression of metabolism of the unfertilised egg is a result of maintaining a low intracellular *p*H and that the rapid efflux of hydrogen ions after fertilisation by way of the sodium-coupled exchange raises the intracellular *p*H. This change allows the increased metabolism referred to as egg activation.

Sodium–proton exchange

We followed acid release by measuring the extracellular *p*H of a stirred 5% suspension of *Strongylocentrotus purpuratus* eggs (17 °C), using a Corning Model 12 expanded scale *p*H meter with recorder. After acid efflux was complete, the solution has titrated back to the original *p*H with standardised sodium hydroxide to determine the amount of acid released. We used two different experimental systems for studying H$^+$ release. In the first, normal eggs were suspended in seawater and fertilised by addition of sperm or artificially activated by addition of various amines. The second system, which we refer to as 'choline-arrested eggs', is similar to that described by Chambers for demonstrating the sodium requirement for egg activation[9,10].

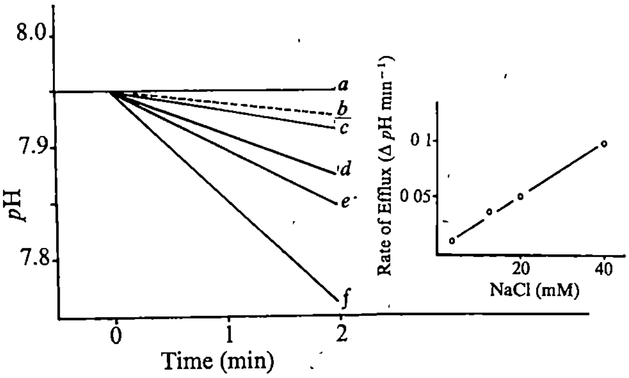

Fig. 1 Acid efflux from eggs as a function of sodium concentration (17 °C). A 2% suspension of eggs was fertilised in seawater, resuspended after 60 s in sodium-free seawater and washed twice. Sodium or lithium chloride was added, at zero time to these 'choline-arrested eggs' at the following concentrations and the initial (0–2 min) acid release measured with a Corning expanded scale *p*H meter and attached chart recorder *a*, 0.1 mM Na; *b*, 100 mM Li; *c*, 3 mM Na; *d*, 10 mM Na; *e*, 20 mM Na; *f*, 40 mM Na. Inset is the slope (rate of efflux against time) plotted against sodium chloride concentration. The relationship between *p*H and H^+ ion concentration is approximately linear over these small *p*H ranges.

Eggs were fertilised in normal seawater and then washed and resuspended in sodium-free seawater (choline substituted) 1 min after fertilisation. We then sedimented the eggs rapidly 50 s after insemination in a hand centrifuge, resuspended them in sodium-free seawater at 70 s, and then sedimented and resuspended then again in sodium-free seawater. These eggs have thus undergone a complete cortical exocytosis.

The release of protons by choline-arrested eggs can be linked directly to sodium. Varying amounts of sodium were added to choline-arrested eggs and the rates of H^+ efflux measured. The rate of H^+ efflux is linearly dependent on Na^+ concentration (Fig. 1). Although lithium replaces sodium[9,10], it is at least 50 times less effective in mediating the efflux.

To test further the nature of the sodium requirement for hydrogen ion efflux, the effects of the diuretic drug amiloride (3,5-diamino-6-chloropyrazinoyl-guanidine) were determined. This compound inhibits passive sodium transport across toad bladder membranes and has no effect on Na^+–K^+ ATPase pump[12]. Eggs were fertilised and after 1 min were transferred to the Na^+-free choline-substituted seawater. When sodium (40 mM) was added in the absence of amiloride, acid efflux was induced (Fig. 2) and the eggs were activated, as evidenced by subsequent cell division. When 40 mM NaCl was added to choline-arrested eggs in the presence of amiloride (1×10^{-4} M), no acid efflux was observed (Fig. 2); these eggs were not activated and did not divide.

Previous work in our laboratory using eggs activated by ionophore A23187 suggested that about 25% of the H^+ release is independent of sodium[13]. If this part of acid release occurs early (that is, during the first 60 s after insemination), we would not observe this Na^+-independent acid release with choline arrested eggs. We tested this possibility by fertilising eggs in the presence of 1×10^{-4} M amiloride. There was an initial phase of acid release beginning at 30 s and ending at 60 s, equivalent to 20% of the total acid; 80% of the efflux was prevented (Fig. 3). An early phase of acid efflux (30–60 s after fertilisation) thus accounts for 20% of the total hydrogen release and is independent of Na^+ and insensitive to amiloride. The second phase requires sodium and is sensitive to amiloride.

We had previously found that the various amines which activate metabolism also induce acid release (our unpublished results). The induction of acid release by ammonia (10 mM NH_4Cl, *p*H 8) is depicted in Fig. 2. The efflux is insensitive to amiloride. Similar results were obtained with procaine (10 mM, *p*H 8).

To test whether Na^+ ions are transported across the plasma membrane in exchange for H^+ ions, ^{22}Na influx and H^+ efflux were measured during the first 20 min of development. To measure ^{22}Na uptake, a 1% suspension of eggs was incubated in low-sodium seawater (choline substituted) containing 25 mM sodium and 0.75 μCi ml^{-1} of ^{22}Na. Uptake was measured for 15 min, the eggs were then fertilised and changes in sodium influx (see legend to Fig. 4) determined at 1-min intervals. ^{22}Na accumulation was first detectable 1 min after fertilisation, continued for 6 min and then levelled off (Fig. 4). The same time course is seen for acid efflux in choline-substituted seawater containing 25 mM sodium. $^{22}Na^+$ accumulation occurs only during this interval. Its termination does not result from an equilibration of internal and external ^{22}Na; when isotope was added 10 min after fertilisation in the same conditions there was minimal isotope uptake (100 c.p.m. as opposed to 5,000).

The H^+ efflux in 25 mM Na^+-seawater was measured in a separate experiment. A 1% suspension (5 ml) was fertilised and after 10 min the eggs were centrifuged and the supernatant was back-titrated to the original *p*H with standardised NaOH. The Na^+-dependent portion of the hydrogen efflux (that is, 80% of the total efflux) for 1 ml of a 1% suspension of eggs in seawater *p*H 8.0 was 4.80×10^{-8} mol and the calculated sodium influx was 4.76×10^{-8} mol. This sodium influx is in agreement with that reported by Chambers[14] and the data indicate a 1 : 1 exchange of sodium for hydrogen in these conditions.

Amiloride (1×10^{-4} M) rapidly blocked ^{22}Na uptake. When added to eggs 50 s after fertilisation, there was no ^{22}Na accumulation (Fig. 4). The 1 : 1 stoichiometry and inhibition of both acid efflux and Na^+ influx by amiloride indicates a passive, coupled facilitated transport system with the efflux of each H^+ ion coupled to the influx of a Na^+ ion.

At constant sodium concentration (0.46 M in seawater) the Na^+–H^+ exchange is dependent on external H^+ ion concentration. Confirming earlier results[11], we found that the rate and extent of acid efflux was directly related to the extracellular *p*H. Total efflux was approximately 10 μmol per ml packed cells when fertilisation was at *p*H 9 and 6 μmol ml^{-1} at *p*H 8. Below an external *p*H of 6.5 there was no detectable acid efflux and also no activation of development.

Fig. 2 Effect of amiloride on sodium-induced acid efflux from choline-arrested eggs (17 °C). A 5% suspension of choline-arrested eggs was prepared as described in the legend to Fig. 1. The *p*H of the suspension was then recorded following addition at zero time of 40 mM NaCl—— (*b*), 10 mM NH_4Cl - - - (*c*), or 40 mM NaCl with 1×10^{-4} M amiloride present - - - - - (*a*). Amiloride had no effect on acid release induced by the ammonia addition.

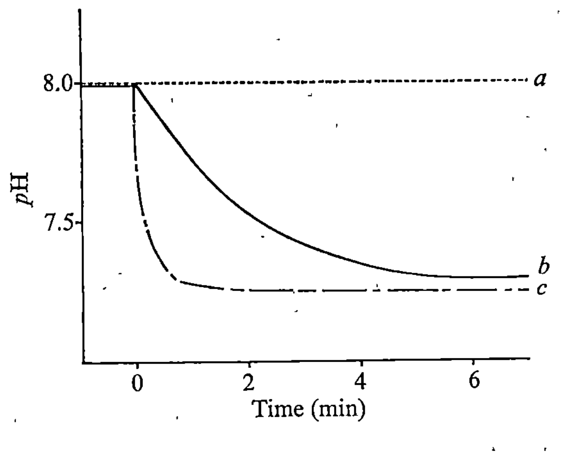

*p*H of cytoplasm

The observed acid efflux is quite large and should be reflected by an increased intracellular *p*H. (If the egg cytoplasm were unbuffered, addition of 6 μmol of H^+ to 1 ml of cell water at neutral *p*H would decrease the *p*H to 2.2.) An estimate of any total cytoplasmic *p*H changes was made by homogenising eggs before and after insemination and measuring the *p*H of the homogenate. A 5-ml sample of a 5% suspension of eggs was washed once in unbuffered (bicarbonate free) artificial seawater, resuspended in 5 ml of 0.5 M KCl and then disrupted with 10 strokes in a Dounce homogeniser. The *p*H was then measured immediately on the expanded scale *p*H meter with constant stirring. At an external *p*H of 8.0, the *p*H of unfertilised egg homogenates (13 separate batches of eggs) was 6.48 (±0.01) and in homogenates prepared from embryos 10 min after fertilisation (9 separate batches of eggs) was 6.76 (±0.02), a change in *p*H of 0.28.

Most of this *p*H shift can be attributed to the efflux of hydrogen ions already present in the egg, as indicated by titration experiments in which an amount of base equivalent to the released acid (0.37 μmol per 5 ml of a 5% egg suspension) was added back to homogenates of unfertilised eggs (5% egg suspension homogenised in 0.5 M KCl). The *p*H of this homogenate rose from 6.54 to 6.73, which is identical to the *p*H change seen after fertilisation. The bulk of the buffering capacity of egg homogenates is probably in small molecules, and not in heat-labile proteins. The buffering capacity of an egg homogenate that is boiled is in the 10,000*g* supernatant fluid.

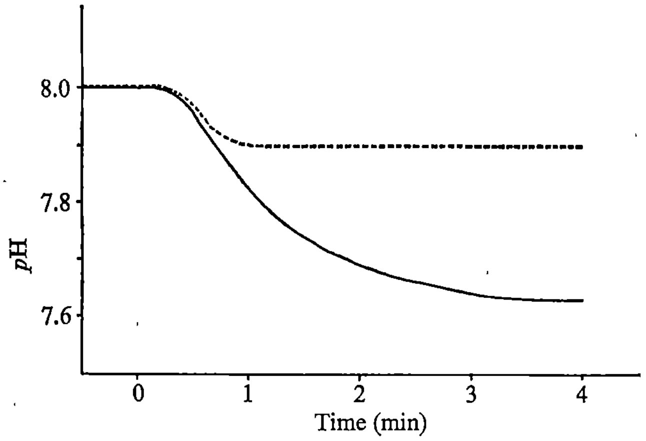

Fig. 3 Acid efflux following fertilisation of eggs in amiloride (17 °C). Eggs (2% suspension) were suspended in choline-substituted seawater containing 50 mM sodium chloride with or without 1×10^{-4} M amiloride. The eggs were then fertilised with sperm at zero time and acid release determined as described (see Fig. 1 legend). The low sodium seawater was used since amiloride is insoluble at higher sodium concentrations. Curves as in Fig. 2.

The *p*H of homogenates of fertilised eggs prepared at various times after fertilisation is shown in Fig. 5. There was an initial decrease in *p*H between 30 and 60 s, possibly related to the Na^+-insensitive phase of acid release. Then, at 1 min and continuing until 4 min, the *p*H increased to 6.74 and remained unchanged thereafter. The kinetics correspond extremely well with the time course of H^+ release in seawater.

Implications for development

As already mentioned, it has been shown previously that activation of development requires Na^+ in the extracellular environment for a 5–10 min interval after fertilisation[9,10]. Our results indicate that this Na^+ requirement for initiating development can be attributed to its effect in raising the cytoplasmic *p*H. First, the Na^+ uptake is transitory and is linked stoichiometrically to the H^+ efflux. Second, we find that activation is prevented by the concentrations of amiloride (1×10^{-4} M) which prevent Na^+ influx and H^+ efflux. This inhibition occurs only during the first 5 min after fertilisation, again corresponding to the period of Na^+ influx and H^+ efflux. Thereafter, amiloride has no effect on development (at least through first cleavage), indicating that its effects are specific to the period of Na^+ influx and not some nonspecific or toxic side effect. Third,

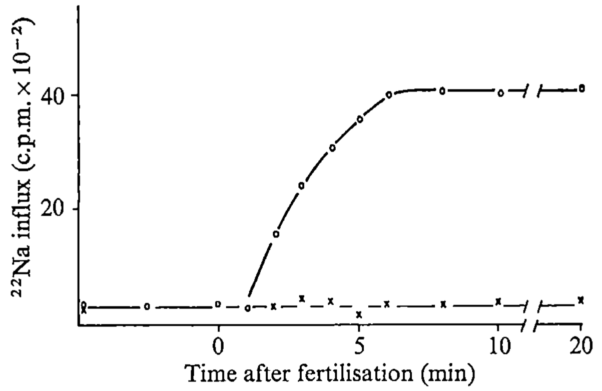

Fig. 4 ^{22}Na influx after fertilisation (17 °C). A 1% suspension of eggs was suspended in 20 ml of choline-substituted seawater containing 25 mM sodium chloride. The low sodium seawater was used because of low amiloride solubility and to increase the specific activity of the sodium isotope. ^{22}Na (15 μCi) was added 15 min before fertilisation and 2-ml samples were taken at the times indicated. These samples were added to 8 ml ice-cold seawater, quickly washed once in cold seawater, centrifuged, and 1 ml of NCS tissue solubiliser (Amersham/Searle) added to the pelleted eggs. The eggs were allowed to dissolve in NCS, transferred to a toluene-based scintillation cocktail, and then radioactivity measured in a Beckman LS-230 scintillation counter. Zero time indicates addition of sperm. ^{22}Na influx in the absence of amiloride (○) and in the presence of 10^{-4} M amiloride (×).

Fig. 5 *p*H of egg homogenates at various times after fertilisation. A 5% suspension of eggs was lightly treated with trypsin to prevent elevation of the fertilisation membrane and generation of the perivitelline space[20]. This was necessary to eliminate the contribution of seawater in this space to the *p*H of the homogenate. Samples (5 ml) of the trypsin-treated eggs were inseminated (17 °C) and at the times indicated, the eggs were washed once in bicarbonate-free artificial seawater, centrifuged and suspended in 5 ml of 0.5 M KCl. This fertilised egg suspension was homogenised with ten strokes of a Dounce homogeniser and the *p*H was determined immediately on a Corning expanded scale *p*H meter.

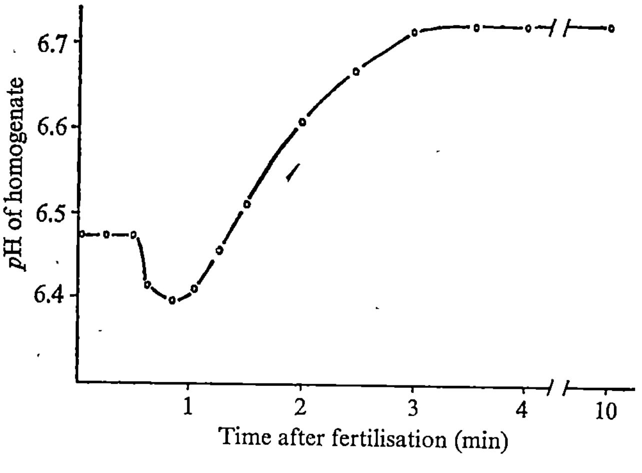

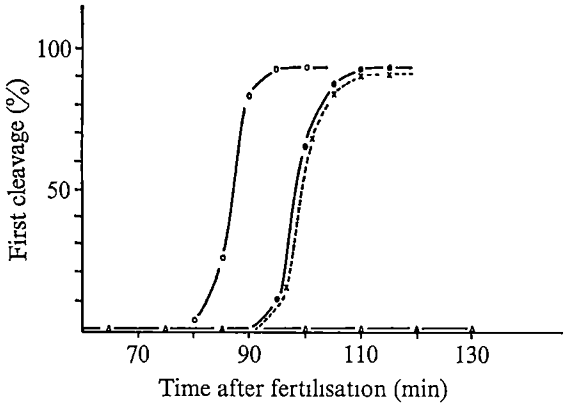

Fig. 6 Capacity of ammonia to substitute for sodium in initiating development. A 1% suspension of eggs was fertilised in seawater and, at 1 min after fertilisation, washed twice in choline-substituted seawater. Aliquots (5 ml) of these choline-arrested eggs were then immediately transferred to 50 ml of seawater (○), sodium-free choline substituted seawater (△), choline-substituted seawater containing 50 mM sodium (●), or choline-substituted seawater containing 5 mM NH_4Cl (×). The embryos were incubated at 17 °C and, beginning at 65 min, 2-ml samples were taken every 5 min and fixed in 5% formalin. The percentage of fully cleaved cells was then determined at each time point.

activation can be prevented by lowering the extracellular *p*H below 6.5, which prevents acid efflux. As with the amiloride effect, this is seen only during the first few minutes after insemination; embryos develop at least through first cleavage if placed at *p*H 6.0 after the first 10 min of development.

The fourth and most important observation stems from our finding that ammonia will initiate H^+ efflux in the absence of external sodium (Fig. 2). We found that these concentrations of ammonia can initiate the development of choline-arrested eggs, again in the absence of sodium. The capacity of ammonia to substitute for sodium is shown in the following experiment. Eggs were fertilised and transferred at 1 min to choline-substituted seawater containing either 50 mM sodium or 5 mM ammonia. Control eggs in regular seawater cleave at about 85 min (Fig. 6), whereas eggs transferred to Na^+-free seawater at 1 min do not cleave (pronuclei do not swell or fuse and no cytasters form). If eggs are transferred to choline seawater with either sodium or ammonia present, however, cleavage occurs—albeit slightly later than the control eggs (the 10-min delay probably results from the presence of choline).

The developmental behaviour of inseminated eggs is identical when either ammonia or Na^+ is present, demonstrating that the important factor in initiating development is not the presence of sodium *per se*. That it is the cytoplasmic *p*H change that is critical is suggested by the aforementioned induction of H^+ efflux by ammonia and also by the other amines which activate metabolism (1 mM nicotine and 5–10 mM procaine). This H^+ efflux induced by amines is accompanied by a parallel increase in the *p*H of cell homogenates. These findings, together with the lack of inhibition of amine-induced H^+ efflux by amiloride, indicate that the amines bypass the normal mechanism of coupling H^+ efflux to Na^+ influx. Moreno and Diamond have noted that simple amines can interact with Na^+ channels in frog bladder[15]. In eggs, they may be inducing one component only (H^+ efflux) of the vectorial exchange or substituting directly for sodium. Certainly the amines are not increasing cell *p*H through their action as weak bases. The *p*H change seen in homogenates prepared from ammonia or procaine-activated eggs can be accounted for completely by the induced efflux of H^+ ions (determined by back-titration of homogenates).

The mechanism of initiating the Na^+–H^+ transport system that begins 60 s after fertilisation is unknown. Alteration of the egg surface by physical, chemical and enzymatic treatments[7,8] activates metabolism and we have previously implicated a surface glycoprotein in egg activation[8]. This protein is released from the egg surface between 45 s and 120 s after insemination. The close temporal correlation between release of this protein and the beginning of the Na^+-sensitive H^+ efflux is consistent with the possibility that this protein acts as an inhibitor of the exchange. If so, the observed suppression of metabolism of partially activated eggs by concentrated solutions of this protein[8] could result from its rebinding to the cell surface and preventing Na–H^+ exchange, with a resultant lowering of cell *p*H. Alternatively, the cell surface proteins may be an additional but separate factor controlling egg activation.

These data should be considered in light of the metabolic transitions that occur at fertilisation. The egg is in a state of metabolic inhibition and is rapidly transformed into a metabolically active cell with striking increases in diverse enzymatic and structural processes. Ca^{2+} is involved in the initial phase[2–4]. The second phase, which can be directly activated by amines and which includes increased biosynthesis, seems to result from a nonspecific pervasive change in the cytoplasmic environment. Our data suggest that this pervasive change may be the increase in cytoplasmic *p*H. Although this change can be initiated independently of the Ca^{2+} phase by the various amines, the amine activation is an incomplete regimen in that a functional mitotic apparatus does not form and cleavage does not occur. All observed changes, Ca^{2+}, *p*H, and perhaps loss of cell surface protein, seem to be prerequisites for complete development.

Do similar regulatory mechanisms occur in other eggs and other kinds of cells? Calcium regulation of cellular processes is widespread, and the calcium ionophores which activate eggs[17] can also activate various metabolic processes in somatic cells (see, for example, ref. 16). Proton efflux associated with cell activation has so far been described only in sea urchin and *Urechis* eggs[18]; in these eggs it is one of the earliest post-fertilisation changes. Extracellular *p*H can alter cell activity[19], but to our knowledge, intracellular *p*H has not been seriously considered as an on–off metabolic regulator of other kinds of cells. It is intriguing to speculate that the transition of cells from actively dividing to a resting or G_0 state or from the G_0 to the actively dividing state may be mediated through changes in intracellular *p*H.

Supported by grants from the NSF, the NIH and the NRC of Canada We thank Elizabeth Baker for technical assistance and E. W. Byrd, Jr, D. Fanestil, A. B. Hastings, J. Miller and G. Somero for critical discussion, and N. Cross, D. Fox, T. Humphreys, K. Nealson, M. Somero and N. K. Wessells for criticisms of this manuscript.

Received March 29; accepted June 8, 1976.

1 Epel, D., *Am. Zool.*, **15**, 507–522 (1975)
2 Steinhardt, R. A., and Epel, D., *Proc. natn Acad. Sci. U.S.A.*, **71**, 1915–1919 (1974)
3 Vacquier, V. D., *Devl Biol.*, **43**, 62–74 (1974).
4 Chambers, E. L., Pressman, B., and Rose, B., *Biochem. biophys. Res. Commun.*, **60**, 126–132 (1974)
5 Epel, D., Steinhardt, R , Humphreys, T., and Mazia, D., *Devl Biol.*, **40**, 245–255 (1974).
6 Steinhardt, R. A., and Mazia, D., *Nature*, **241**, 400–401 (1973).
7 Mazia, D., Schatten, G., and Steinhardt, R. A., *Proc natn. Acad. Sci. U.S.A.*, **72**, 4469–4473 (1975).
8 Johnson, J. D., and Epel, D., *Proc. natn. Acad. Sci U.S A.*, **72**, 4474–4478 (1975).
9 Chambers, E. L., *J. Cell Biol*, **67**, 60a (1975).
10 Chambers, E L , and Dinnich, R. A., *J. gen. Physiol.*, **66**, 66a (1975).
11 Mehl, J. W , and Swann, M. M., *Expl Cell Res.*, **22**, 233–245 (1961).
12 Bentley, P. J., *J. Physiol , Lond.*, **195**, 317–330 (1968)
13 Paul, M , and Epel, D., *Expl Cell Res.*, **94**, 1–6 (1975)
14 Chambers, E L., *The Physiologist*, **15**, 103 (1972).
15 Moreno, J. H., and Diamond, J M., *J. Memb. Biol*, **21**, 197–259 (1975)
16 Maino, V. C., Green, N. M , and Crumpton, M. J., *Nature*, **251**, 324–325 (1974).
17 Steinhardt, R. A., Epel, D., Carroll, E. J., and Yanagamachi, R , *Nature*, **252**, 41–43 (1974).
18 Paul, M., *Devl Biol.*, **43**, 299–312 (1975).
19 Rubin, H., *J. Cell Biol.*, **51**, 686–701 (1971).
20 Epel, D., *Expl Cell Res*, **61**, 69–70 (1970).

λ repressor regulates the switch between P_R and P_{rm} promoters

Alfred Walz, Vincenzo Pirrotta & Kurt Ineichen

Biozentrum der Universität Basel, Klingelbergstrasse 70, CH-4056 Basel, Switzerland

The DNA region containing the O_R operator, P_R and P_{rm} promoters and their transcription initiations is sequenced. By binding to O_R, repressor turns off P_R, turns on P_{rm} and at higher concentrations turns off P_{rm}, regulating its own synthesis. P_{rm} mRNA is unique in beginning immediately with the initiation of translation, without a preceding leader sequence.

THE right hand operator–promoter region of phage λ is a complex regulatory structure containing the sites of action of at least three proteins which interact with specific DNA sequences: the λ repressor, RNA polymerase and the *tof* or *cro* gene product. The operator itself is a multiple structure containing at least three repressor binding sites[1,2]. The strongest of these sites overlaps partially with the site to which RNA polymerase binds and from which it initiates rightward transcription of the *tof* gene[3]. Because of this overlap, repressor binding prevents polymerase binding and therefore blocks transcription.

An additional promoter is located in the vicinity of O_R. This is the P_{rm} promoter, active in the transcription of *c*I, the repressor gene, in the lysogenic state. *In vivo*, the activity of this promoter is dependent on the earlier presence of repressor bound to O_R[4]. We have previously presented[3] arguments for the location of P_{rm} within the O_R sequence and predicted that, at high concentrations, repressor should block P_{rm} and therefore turn off its own synthesis, thus acting both as a positive and as a negative autoregulator.

More recently, a mutation in P_{rm} has been localised in the O_R sequence[5,6] and the autoregulation of repressor synthesis has been demonstrated *in vitro* using as template DNA fragments produced by restriction enzymes.

In this article we report the sequence of the DNA region bounded by the *Hin*dII cut in O_R and the *Alu*I cut 85 base pairs to the left of it (Fig. 1). This region contains the repressor binding sites O_R2 and O_R3 and the beginning of the *c*I gene. We have used this DNA fragment for direct DNA sequencing using the method of Gilbert *et al.*[7]. In the presence of limited amounts of repressor this fragment or the *Hae*III 790 fragment from the same region are also good templates for P_{rm} transcription. We have sequenced the beginning of the mRNA species stimulated by repressor and we have located it in the DNA sequence. We find that, as predicted by our model, P_{rm} transcription initiates a few nucleotides to the left of O_R3. The message begins with AUG and is followed immediately by the codons specifying the amino acid sequence of the amino terminal of the λ repressor protein[8].

Sequence of the O_R-P_{rm}-*c*I DNA

The restriction endonuclease *Alu*I produces a DNA fragment from the O_R region of λ DNA, which is about 185 base pairs long and contains in the middle the *Hin*dII cleavage site which separates the operator primary site O_R1 from the rest of the operator. The *Alu* 185 fragment can therefore be terminally labelled with polynucleotide kinase, cleaved with *Hin*dII and the desired fragment, now labelled only at one 5′ end, separated by gel electrophoresis. The shorter fragment, 85 base pairs long, contains the secondary repressor binding sites O_R2 and O_R3 and must contain also the beginning of the *c*I gene. We have subjected this fragment, now labelled only at the *Alu* 5′ terminal, to the chemical sequencing method of Gilbert *et al.*[7]. Partial methylation with dimethyl sulphate renders the A and G residues sensitive to depurination and chain scission by β elimination. The products are analysed by gel electrophoresis. Strong bands correspond to cleavage at G residues and the weak bands to cleavage at A residues, since the former are methylated six times more rapidly than the latter. Hydrazinolysis in aqueous medium, followed by piperidine-catalysed β elimination, leads to cleavage at C and T residues. An increased specificity of cleavage is obtained by performing the hydrazinolysis in the presence of high ionic strength which leads to preferential reaction at C residues. The sequence is obtained by identifying successive bands present in the purine specific reactions or in

Fig. 1 Restriction endonuclease cleavage sites in the vicinity of O_R. Distances are shown in base pairs. The approximate location of the three repressor binding sites O_R1, O_R2 and O_R3 and of the two promoters P_R and P_{rm} are indicated. The dotted lines represent transcription of the *c*I gene and of the *cro* or *tof* gene.

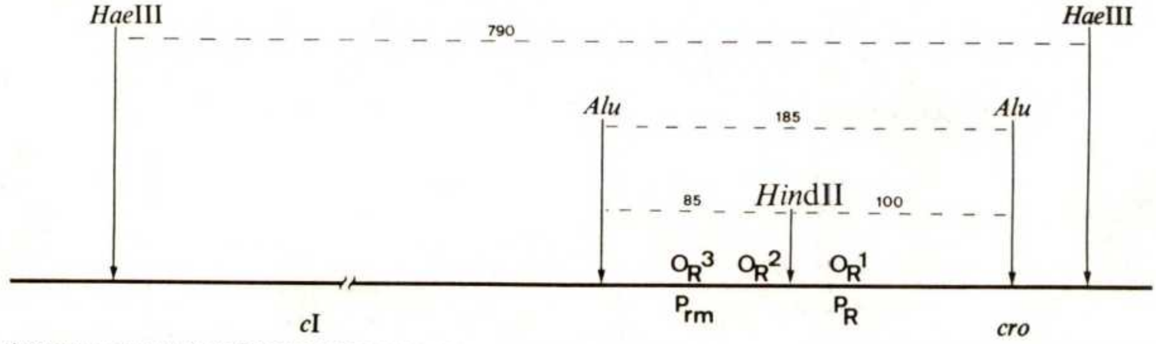

the pyrimidine specific reactions. Figure 2 shows that the 3′ terminal sequence, though difficult to decipher, corresponds to the previously known sequence of the O_R2 and O_R3 repressor binding sites. The sequence towards the 5′ end according to the model should contain the P_{rm} promoter sequence and the initial part of the *c*I gene.

Repressor stimulated transcription

To identify the initiation of the P_{rm} mRNA in the sequence obtained above, we used the *Hae*III 790 or the *Alu* 185 restriction fragments as templates for transcription. In the absence of repressor we expect P_R transcription to be dominant. In the *Hae* 790 fragment this should yield a transcription product about 100 bases long. In the *Alu* 185 this product should be about 65 bases long. The P_{rm} transcript from *Hae* 790 should be much longer than the P_R transcript, while if the *Alu* 185 is used as template we expect the P_{rm} transcript to be a maximum of 45 bases long. Furthermore, increasing amounts of repressor in the transcription reaction should block P_R transcription, but stimulate P_{rm} transcription. Figure 3 shows that these expectations are borne out. Using the *Alu* 185 as template, a strong band about 65 bases long is produced in the absence of repressor and disappears at low repressor concentrations. This must be the P_R product. One band, about 35 bases long, is missing in the absence of repressor, appears at low repressor doses and disappears at higher doses. This must be the P_{rm} product. As observed in other systems, glycerol facilitates transcription[9]. We find that at low glycerol concentrations, transcription from P_{rm} is much less efficient even in the presence of suitable amounts of repressor.

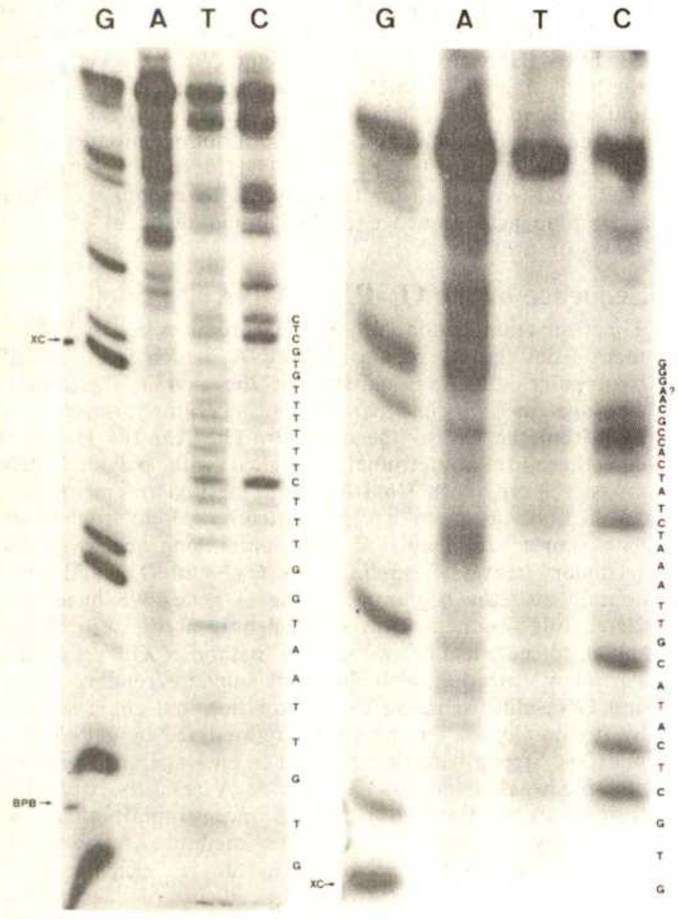
G A T C
G A T C
XC
BPB
XC
C T C G T G T T T T T T C T T T G G T A A T T G T G
G G G A ? A C G C C A C T A T C T A A T T G C A T A C T C G T G

Fig. 2 DNA sequence of the *Alu-Hin*dII fragment. Purified *Alu* 185 fragments were treated with 2 μg bacterial alkaline phosphatase for 1 h at 37 °C. After 4 phenol extractions, followed by 4 ether extractions, 1 nmol γ-^{32}P-ATP (400–800 mCi μmol^{-1}) and 5–10 units of polynucleotide kinase were added and the reaction mixture was incubated at 37 °C for 1 h. The labelled fragments were cleaved with *Hin*dII and the products, now labelled at only one 5′ end, were purified by gel electrophoresis on 0.7% Agarose–3% acrylamide gels in 0.09 Tris-borate (*p*H 8.2). The desired band was extracted from the gel and treated with dimethylsulphate (purine specific cleavage) or with hydrazine either low salt (T specific cleavage) or in 1 M KCl (C specific cleavage), according to the method of Gilbert *et al.*[7] and of Gilbert and Maxam (personal communication). Preferential cleavage at *A* is obtained by depurinating the methylated DNA at acid rather than alkaline *p*H. The products were analysed on a 40 cm gel containing 20% acrylamide, 7 M urea and 0.05 M Tris-borate (*p*H 8.2). Electrophoresis proceeded at 600 V for about 14 h. One glass plate was removed, the gel was wrapped in plastic film and autoradiographed at −20 °C (left). To obtain better resolution in the upper part of the gel, the glass plate could be replaced and electrophoresis could be continued with little loss in the definition of the bands (to the right, shown at slightly greater magnification). BPB and XC indicate the positions of the marker dyes which comigrate with fragments 10 and 29 bases long, respectively.

Sequence of the P_{rm} mRNA

To verify that the transcription product stimulated by repressor originates from the P_{rm} region and from the correct strand, we eluted the material from the gel and determined its sequence. Figure 4 shows an RNase T_1 fingerprint obtained by electrophoresis on cellulose acetate (*p*H 3.5), followed by chromatography on a PEI thin layer Analysis of the spots with pancreatic RNase permitted us to determine their sequence. The 5′ triphosphate end, which is barely visible at the lower left corner of the fingerprint, is pppAUG. A rapid inspection of the T1 oligonucleotide sequences shows that they are in fact complementary to part of the DNA sequence obtained from the *Alu* fragment. The distinctive $CACA_nG$ sequence corresponds to the CT_6GTG in the DNA sequence. The initial pppAUG corresponds to the CAT as shown in Fig. 5. No other ATG occurs in the $\mathscr{L}$ strand in this vicinity. We conclude that the repressor stimulated transcription originates from a unique site, copies the left strand and initiates with AUG.

Initiation of translation

The amino acid sequence near the NH_2 terminal of the λ repressor protein has been determined recently[8].

The initial 11 amino acids of this sequence fit perfectly with the DNA sequence that we have established and with the sequence of the P_{rm} mRNA. Unlike other known prokaryotic mRNAs, the P_{rm} message initiates immediately with a f-Met codon which is followed by the amino acid sequence of the protein. If the P_{rm} mRNA *in vivo* initiates at the same site as *in vitro*, it contains no leader sequence and thus no provision for a sequence complementary to 16S ribosomal RNA[10,11]

Structure of the O_R operator

The sequence upstream of O_R3 shows first of all that there is nothing recognisable as a fourth repressor binding site. The characteristic sequence TATCACCG which constitutes the most strongly conserved feature of the repressor recognition sites[1,12] is missing or is drastically altered. The fourth repressor tetramer which was observed to bind at very high repressor concentrations[13], was probably due to a relatively nonspecific interaction stabilised by protein interaction with the preceding repressor tetramer. There are then only three functional repressor binding sites in O_R. Recent experiments indicate that this is also the case for O_L (V. P., unpublished). In O_R, the primary site and O_R2 contain sequence elements necessary for the recognition of the P_R promoter by RNA polymerase. Occupation of these sites by the repressor therefore leads to repression of P_R transcription. In consequence these two sites are the targets of mutations which result in constitutive expression of the *tof* gene[1]. Smith *et al.*[5], using deletions which enter O_R from the left, find that

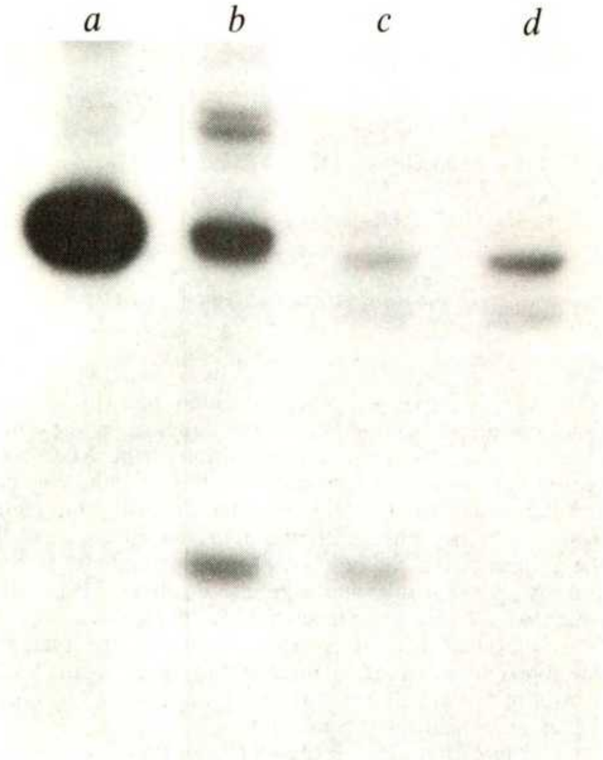

Fig. 3 Turn-on and turn-off of P_{rm} transcription. 1 pmol of *Alu* 185 fragment was incubated at 20 °C for 10 min with (*a*) no repressor, (*b*) 0.5 µl, (*c*) 2 µl and (*d*) 10 µl of λ repressor in 50 µl containing 20 mM Tris (*p*H 7.9), 0.1 mM EDTA, 0.1 mM dithiothreitol, 8 mM $MgCl_2$, 40 mM KCl and 15% glycerol. RNA polymerase (2 µg or 1.7 U) and ATP (200 µM final concentration) were added and incubation was continued for 10 min at 37 °C. 1 µl of 2 mg ml^{-1} heparin was then added, followed 2 min later by GTP and UTP at a final concentration 10 µM and α-^{32}P CTP (100 mCi μmol^{-1}) at 2 µM. The reaction was stopped after 10 min at 37 °C by a phenol extraction and ethanol precipitation. The material was analysed on a 12% acrylamide gel containing 7 M urea and 90 mM Tris-borate (*p*H 8.2). The strong band in (*a*) is the P_R transcript while the band that appears in (*b*) and (*c*) is presumed to be the P_{rm} transcript. The weak band, of roughly the same size as the P_R transcript, which seems to be stimulated by repressor, was also sequenced and found to be due to contaminating traces of a different *Alu* fragment.

the first two sites, but not O_R3, are required for effective repression.

P_{rm} promoter

In an earlier article[3] we have pointed out a remarkable degree of symmetry centred around the middle of O_R2. This symmetry is absent in O_L because of the different disposition of the repressor binding sites. As a consequence of this symmetry, O_R contains another sequence similar to that of P_R but with orientation opposite to it. This, we proposed, was the P_{rm} promoter. This conclusion was supported by the finding that a mutation in P_{rm} is located between O_R2 and O_R3 (refs 5, 6).

The symmetry results in substantial sequence homology between the P_R and the P_{rm} region, but it is not perfect. If the P_R and P_{rm} sequences are aligned as in Fig. 6, good agreement is obtained only if half of the sequence is displaced by one base. Therefore, assuming that the P_R sequence is representative of a good promoter, some adjustment needs to be made in order for P_{rm} to resemble it. This probably accounts for the finding that in the absence of repressor, P_{rm} is inactive. By binding to O_R1, the repressor in some way facilitates the recognition of P_{rm} by the RNA polymerase. We do not yet know the mechanism of this facilitation.

A possible interpretation is suggested by the observation that RNA polymerase is unable to bind to the *Hin*dII fragment containing O_R1 (ref. 14) even though the site at which it forms the initiation complex is entirely to the right of the *Hin*dII cleavage site (Fig. 7). We conclude that the polymerase must interact with the region of O_R2 in order to bind to the P_R promoter. The symmetric arrangement of P_R and P_{rm} suggests that the same region is required for binding to P_{rm}. This region would then be a non-directional recognition site from which RNA polymerase could move in either direction to form the initiation complex at P_R or P_{rm}. Repressor might activate P_{rm} simply by blocking the stronger promoter P_R and removing a competitive binding site for polymerase. Alternatively the repressor might change the conformation of the DNA in the vicinity of O_R2–O_R3, making it possible for the polymerase to recognise P_{rm}.

We do not know yet what particular sequence features at what positions are required for RNA polymerase binding. The substantial variety in the promoter sequences determined so far, suggests that the polymerase can accommodate a wide range of sequences. The fact that single base changes can inactivate promoter sites indicates, however, that in a given sequence, certain nucleotides play a key role. For example, the *sex* 1 mutation in P_L affects a

Fig. 4 RNase T_1 fingerprint of P_{rm} transcription initiation. In this case the template used was the *Hae* 790 fragment. In the transcription reaction the ATP concentration was 200 µM. The other 3 nucleotide triphosphates were labelled and at 1.7 µM. A partial transcription product about 45 bases long was eluted from the gel as described previously[2], digested with RNase T1 and fractionated in the first dimension by electrophoresis on cellulose acetate (*p*H 3.5). This was followed by chromatography in the second dimension on a PEI cellulose thin layer with 2 M pyridine formate (*p*H 3.5) and 7 M urea. The spots were analysed by digestion with pancreatic RNase and electrophoresis on DEAE cellulose paper (*p*H 3.5).

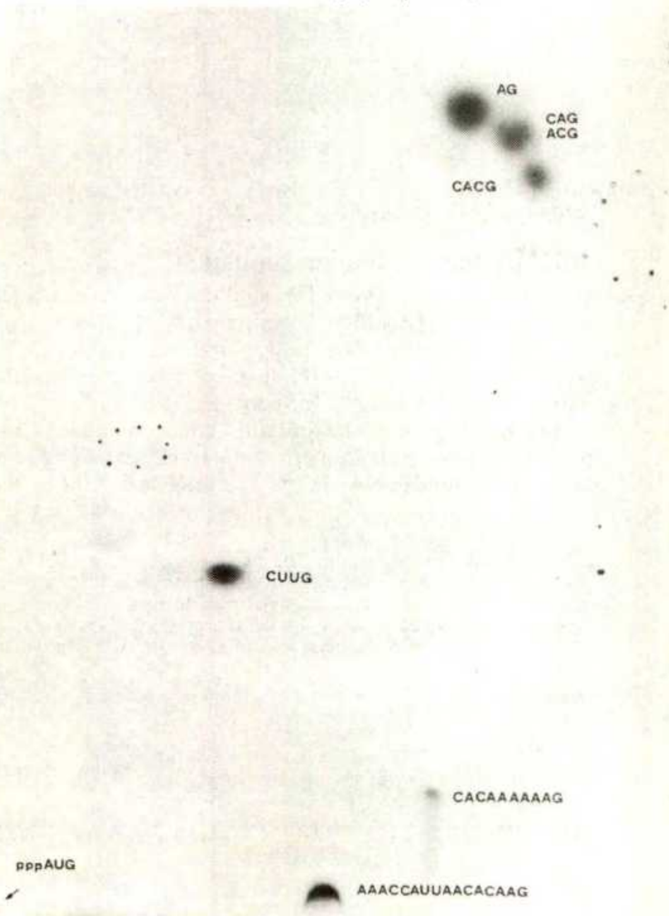

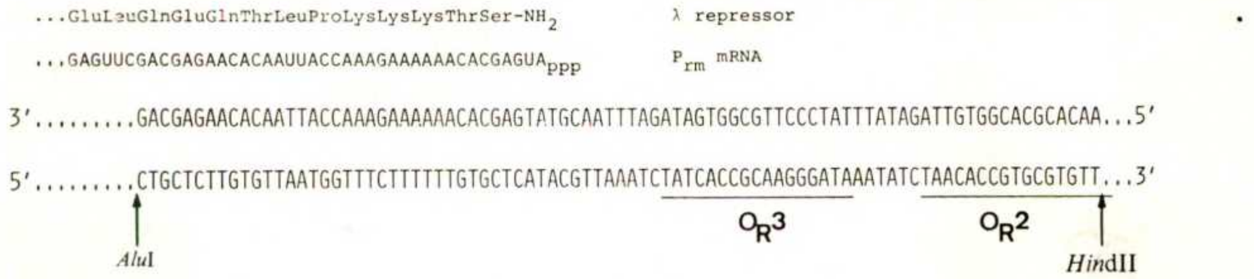
...GluLeuGlnGluGlnThrLeuProLysLysLysThrSer-NH2
λ repressor
...GAGUUCGACGAGAACACAAUUACCAAAGAAAAAACACGAGUAppp
Prm mRNA
3'........GACGAGAACACAATTACCAAAGAAAAAACACGAGTATGCAATTTAGATAGTGGCGTTCCCTATTTATAGATTGTGGCACGCACAA...5'
5'........CTGCTCTTGTGTTAATGGTTTCTTTTTTGTGCTCATACGTTAAATCTATCACCGCAAGGGATAAATATCTAACACCGTGCGTGTT...3'
OR3
OR2
AluI
HindII

Fig. 5 Sequence of the *Alu–Hin*dII fragment. The arrows indicate the cleavage sites of the two restriction enzymes. The sequence of the $\mathrm{P_{rm}}$ mRNA and the corresponding amino acid sequence of the λ repressor are also shown[8].

GC pair in the position shown in Fig. 6[1]. The corresponding position in $\mathrm{P_{rm}}$ is also of crucial importance. This is the site where Meyer *et al.*[6] place the $\mathrm{P_{rm}}$ 116 mutation and it is also the site where the $\mathrm{P_{rm}}$ sequence goes out of register with that of $\mathrm{P_R}$. Significantly, the effects of the *sex* 1 mutation can be compensated by the presence of glycerol in an *in vitro* transcription reaction[9]. This suggests that both in the *sex* 1 mutation and in the normal $\mathrm{P_{rm}}$, the limiting step is the opening of the strands by the polymerase to form the so-called "open" complex (for review see refs 15 and 16).

Another possible recognition element is the heptanucleotide which can be discerned, with certain variations, in all RNA polymerase binding sites, 6–7 nucleotides upstream of the transcription initiation site[17]. This heptanucleotide, whose canonical form is TATpupuTpu, is present in $\mathrm{P_R}$ as GATAATG. In $\mathrm{P_{rm}}$ it is further changed to GATAGAT.

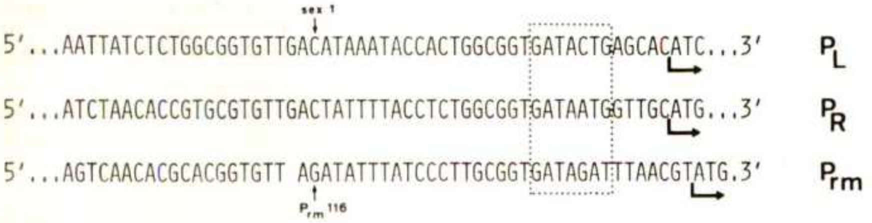
sex 1
5'...AATTATCTCTGGCGGTGTTGACATAAATACCACTGGCGGTGATACTGAGCACATC...3'
PL
5'...ATCTAACACCGTGCGTGTTGACTATTTTACCTCTGGCGGTGATAATGGTTGCATG...3'
PR
5'...AGTCAACACGCACGGTGTT AGATATTTATCCCTTGCGGTGATAGATTTAACGTATG.3'
Prm
Prm 116

Fig. 6 Comparison of promoter sequences. The λ $\mathrm{P_L}$, $\mathrm{P_R}$ and $\mathrm{P_{rm}}$ sequences are aligned to emphasise their homology. The arrows indicate the initiation of transcription. Maximum homology is obtained if part of the $\mathrm{P_{rm}}$ sequence is displaced by one base. The sites of the *sex* 1 and of the $\mathrm{P_{rm}}$ 116 promoter mutations[6] are indicated. The dotted line encloses the heptanucleotide generally found in RNA polymerase binding sites[17].

$\mathrm{P_{rm}}$ mRNA has no leader sequence

All prokaryotic mRNAs so far studied contain a stretch of variable length preceding the initiator AUG codon. This stretch has been called the leader and is thought to be important in directing the binding of ribosomes to the translation initiation site[10]. In contrast, the $\mathrm{P_{rm}}$ mRNA begins immediately with the initiator codon and lacks the polypurine tract which is thought to interact with the 3′ end of the 16S ribosomal RNA. If the $\mathrm{P_{rm}}$ mRNA begins at the same site *in vivo*, we must conclude that in this case, ribosome interaction with the initiation site on the mRNA is entirely dependent on the recognition of the AUG codon. We do not know the significance of this finding. We speculate, however, that the lack of other stabilising interactions would make the binding of ribosomes less efficient and limit the utilisation of the mRNA. Moreover, attack at the 5′ end by *exo*V would immediately inactivate $\mathrm{P_{rm}}$ mRNA which would then be expected to have an unusually short functional half life. It is remarkable that the phage has developed such elaborate mechanisms both at the level of transcription and of translation to limit the expression of the *c*I gene in the lysogenic state.

Upon infection of a sensitive cell, on the other hand, the *c*I gene is transcribed from a different promoter, the so-called $\mathrm{P_{re}}$ promoter, located to the right of the *tof* gene[4]. Transcription originating from this promoter has potentially a leader region several hundred nucleotides long which contains the anti-sense sequence of the *tof* gene and includes the $\mathrm{O_R}$ sequence. This region, as far as we know, is not translated. In this case, the sequence preceding the initiator codon AUG contains all the features of a typical ribosomal binding site. There is in fact a GGTGAT in the operator sequence which is complementary to the AUCACC close to the 3′ end of the ribosomal 16S RNA. The sequence contains a UUU which is also found in several other ribosomal binding sites [11,18] and, finally, three terminator codons in

Fig. 7 The $\mathrm{P_{rm}}$-$\mathrm{O_R}$-$\mathrm{P_R}$ region. The two promoters are shown symmetrically disposed and overlapping the two ends of the operator. In $\mathrm{P_R}$, RNA polymerase forms the tight binding and initiation complex at the site indicated, partially overlapping $\mathrm{O_R1}$. A presumed corresponding site for $\mathrm{P_{rm}}$ is shown by a dashed line. The initiation of transcription is indicated by arrows. The entire structure is symmetrically arranged around the centre of $\mathrm{O_R2}$. This is the region where the RNA polymerase might form the initial recognition complex. Repressor bound to $\mathrm{O_R1}$ would then steer the polymerase to the $\mathrm{P_{rm}}$ binding and initiation site.

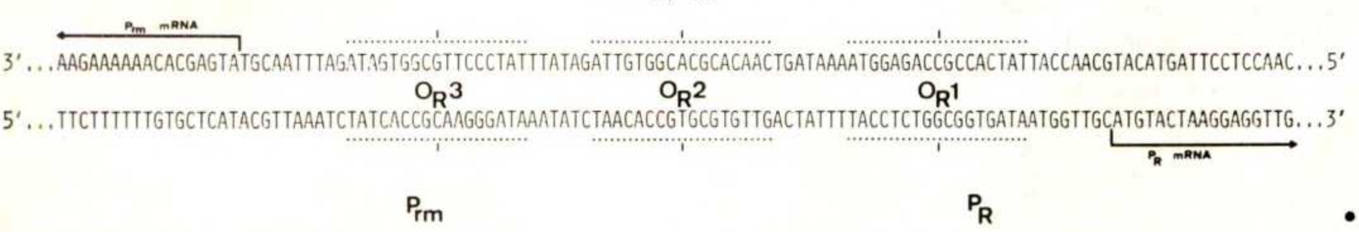
recognition site for RNA polymerase ?
RNA polymerase binding site
Prm mRNA
3'...AAGAAAAAACACGAGTATGCAATTTAGATAGTGGCGTTCCCTATTTATAGATTGTGGCACGCACAACTGATAAAATGGAGACCGCCACTATTACCAACGTACATGATTCCTCCAAC...5'
OR3
OR2
OR1
5'...TTCTTTTTTGTGCTCATACGTTAAATCTATCACCGCAAGGGATAAATATCTAACACCGTGCGTGTTGACTATTTTACCTCTGGCGGTGATAATGGTTGCATGTACTAAGGAGGTTG...3'
PR mRNA
Prm
PR

phase precede the initiator AUG codon.

To conclude, we note that *tof* mRNA, like the $\mathrm{P_{rm}}$ mRNA, also begins with an AUG This similarity may not be entirely fortuitous. It is in keeping with the above-mentioned symmetry of the entire $\mathrm{O_R}$ region and with the fact that *tof* product, like the *c*I product, acts as a repressor, albeit a weak one. Its sites of action, like those of the *c*I repressor, are $\mathrm{O_L}$ where it performs the eponymous function of turning off the *N* operon, and $\mathrm{O_R}$, where it turns off transcription of $\mathrm{P_{rm}}$ and of $\mathrm{P_R}$ and hence its own transcription[19]. In short, the *tof* product may formally be considered a mini version of the *c*I repressor. In the *tof* mRNA, however, the initial AUG is not the start of translation because it is followed two triplets later by a UAA codon in phase.

We thank T Bickle and P. Schedl for discussions and criticism. This work was supported in part by a grant from the Swiss National Foundation for Scientific Research.

Received May 6; accepted June 16, 1976.

1 Maniatis, T., Ptashne, M., Backman, K , Kleid, D., Flashman, S , Jeffrey, A , and Maurer, R., *Cell*, 5, 109–113 (1975)

2 Pirrotta, V., *Nature*, **254**, 114–117 (1975).

3 Walz, A , and Pirrotta, V , *Nature*, **254**, 118–121 (1975)

4 Reichardt, L , and Kaiser, A D , *Proc. natn Acad Sci U S A.*, **68**, 2185–2189 (1971)

5 Smith, G , Eisen, H , Reichardt, L., and Hedgpeth, J., *Proc. natn Acad. Sci U S.A.*, **73**, 712–716 (1976)

6 Meyer, B., Kleid, D , and Ptashne, M., *Proc natn. Acad Sci. U S.A* , **72**, 4785–4789 (1975).

7 Gilbert, W , Maxam, A., and Mirzabekov, A , in *Control of Ribosome Synthesis* (edit by Kjelgaard, N , and Maaløe, O) (Munksgaard, Copenhagen, in the press).

8 Beyreuther, K., and Gronenborn, B., *Molec. gen. Genet.* (in the press).

9 Nakanishi, S , Adhya, A , Gottesman, M , and Pastan, I , *J. biol Chem.*, **249**, 4050–4056 (1974)

10 Shine, J , and Dalgarno, L , *Proc. natn Acad. Sci. U.S A* , **71**, 1342–1346 (1974)

11 Steitz, J , and Jakes, K , *Proc natn Acad. Sci U S A* , **72**, 4734–4738 (1975)

12 Pirrotta, V , in *Curr Top. Microbiol Immun* , **74**, 21–54 (1976)

13 Brack, C., and Pirrotta, V , *J molec. Biol* , **96**, 139–152 (1975).

14 Walz, A , thesis, Univ Basel (1976)

15 Chamberlin, M , *A Rev Biochem* , **43**, 721–775 (1974).

16 Travers, A , *Cell*, **3**, 97–104 (1974)

17 Pribnow, D , *Proc natn Acad Sci. U S.A.*, **72**, 784–788 (1975).

18 Pieczenik, G., Model, P , and Robertson, H , *J molec. Biol.*, **90**, 191–214 (1974).

19 Reichardt, L., *J. molec Biol* , **93**, 267–288 and 289–309 (1975)

---

letters to nature

The second highly polarised radio outburst in Cygnus X-3

We detected a second outburst with a high degree of linear polarisation from Cyg X-3 in August 1975, following the alert by Kawajiri[1] The first such outburst was observed in May 1974 (refs 2 and 3) Here we report observations of both polarised outbursts as well as of an unpolarised outburst in January 1975. At 8 GHz the observed polarisation position angle was the same for both polarised outbursts. The Faraday rotation measure associated with the source is much larger than previously reported[2] We suggest that the orientation of the magnetic field in the source and the rotation measure are both stable with time In addition, we find that the highly polarised outbursts decay significantly more slowly than the unpolarised outbursts

All measurements were made with the University of Michigan 85-foot paraboloid operating at frequencies of 8 and 14.5 GHz. The equipment and on-off observing techniques used at 8 GHz have been described previously[4–6]. Similar equipment and techniques were used at 14.5 GHz. All the observations were made with linear polarimeters except for those made at 8 GHz on May 26 and June 2, 1974 and on August 27–28, 1975, which were obtained with a single-horn circular polarimeter. Observations of Cyg X-3 were alternated with observations of the standard sources Cyg A or DR21 to determine the flux density calibration. Daily averages of the data for the polarised outbursts are presented in Table 1 The total flux density measurements have been corrected for confusion effects by the addition of 0.071 Jy at 14.5 GHz and the subtraction of either 0.73 or 0.49 Jy at 8 GHz for observations made with the linear or circular polarimeters respectively. The standard errors include the statistical noise and the uncertainties in the antenna gain and telescope pointing

The total and polarised flux densities for August and September 1975 are displayed in Fig 1. Only the decay phase of the outburst was observed Observations[7] at 5 GHz indicate that the maximum flux density occurred on August 22 or 23, 2 or 3 d before our measurements began From August 26 to September 3, the decay of the total flux density at 8 GHz was exponential with time. The line through the 8-GHz data points is a least squares fit to the data from August 26–27 to September 1–2 and represents an e-folding time of 86±1 h The 14.5-GHz data are consistent with the same exponential decay rate The spectral index from 14.5 to 8 GHz during the exponential decay remained at $\alpha = -0.65 \pm 0.06$ where $\alpha = (\Delta \log S_\nu / \Delta \log \nu)$. The same spectral index appears to fit the data at 5 GHz (ref. 7) which indicates that the source was transparent above 5 GHz from August 24 to September 5. After September 3 the rapid exponential decay ceased and the total flux density slowly and irregularly declined until September 20. By September 10 the flux density seems to have been nearly the same from 5 GHz to 14.5 GHz, coresponding to a spectral index $\alpha \sim 0$.

Table 1 Flux density and linear polarisation variations with time

Date	(UT)	S_ν(Jy)	P(%)	Position angle (degrees)
		8.0 GHz		
1974				
May	26.5	4.18±0.35	9.7±0.8	80±2
June	2.4	1.70±0.35	7.0±1.8	87±7
1975				
August	25.3	7.34±0.12	5.8±0.5	75±2
	26.3	6.32±0.14	7.6±0.7	80±2
	27.1	5.48±0.08	8.4±0.5	80±2
	28.1	4.25±0.18	8.4±0.5	86±2
	29.0	3.21±0.09	11.6±1.6	83±4
September	2.1	1.04±0.03	12.5±2.7	87±6
	3.0	0.90±0.06	17.1±5.1	97±7
	5.2	0.46±0.04	8.6±9.5	
	8.1	0.54±0.04	19.8±7.0	83±7
	10.1	0.36±0.08	23.4±14.8	84±16
	11.0	0.47±0.06	18.4±14.6	88±14
	17.1	0.27±0.05	25.6±18.5	143±18
		14.5 GHz		
1975				
August	27.2	3.69±0.25	12.6±2.1	146±5
	28.2	2.65±0.13	17.4±2.5	154±4
	29.3	2.04±0.16	17.7±4.9	145±7
September	3.1	0.64±0.07	27.9±14.9	151±19
	9.1	0.58±0.10	22.2±15.3	2±23
	12.0	0.33±0.11	15.3±28.8	

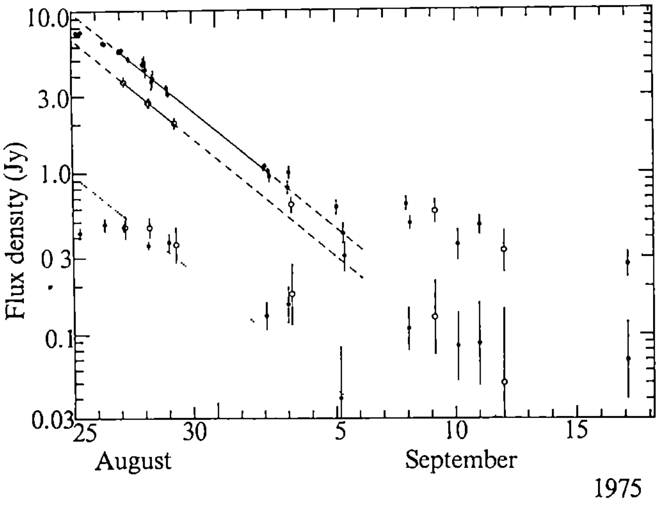

Fig. 1 Semilog plot of total and polarised flux density against universal time at 8.0 (●) and 14.5 (○) GHz for Cyg X-3. The total flux density measurements in the upper portion of the plot are 40-min averages of the data. The polarised flux density measurements in the lower portion are daily averages. The two lines through the total flux density measurements are fits to an exponential decay with time for the data where the lines are solid. The dotted line through the polarised flux density measurements represents a constant 10% degree of linear polarisation for the exponential decay of the total flux density at 8 GHz.

It has been noted that the decay of the first September 1972 outburst evolved from an exponential to a power-law time dependence with the exponential phase lasting longer at higher frequencies[8]. The same phenomenon may have occurred during this outburst. The irregular flux variations and the apparent change in the spectral index indicate, however, that renewed injection or acceleration of particles may have obscured the decay of the outburst after September 3. Hence, fits to the data extending after September 3, such as the one made at 5 GHz (ref. 7) may not give a true indication of the decay process.

No circular polarisation was detected in either polarised outburst. A 2σ upper limit of 0.5% for the degree of circular polarisation was obtained on August 27–28, 1975. Our measured degree of circular polarisation of 0.4±0.4% for the May 1974 outburst agrees with the upper limit of 0.5% obtained by Seaquist *et al.*[2].

During the August 1975 outburst the degree of linear polarisation increased to > 10% at both frequencies, as illustrated in Fig. 1. The level of polarisation at 8 GHz is comparable to that observed by us and by Seaquist *et al.*[2] during the May 1974 outburst. Although the total flux density was already decreasing when we started observing on August 25, 1975, the polarised flux density did not begin to decrease until August 27. The increase in the degree of polarisation with time, and the fact that the degree of polarisation was significantly higher at the higher frequency (14.5 GHz) are both similar to the pattern observed during the May 1974 outburst[2,3].

Fig. 2 Linear polarisation position angle against universal time at 8.0 (●) and 14.5 (○) GHz. The points represent daily averages of the data.

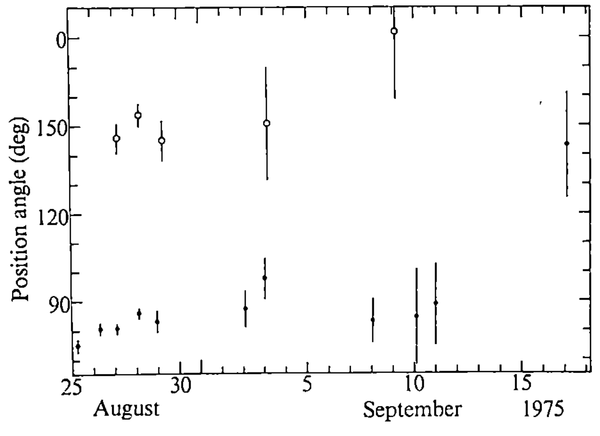

The position angles of the linear polarisation for the August 1975 outburst are shown in Fig. 2. The average position angle observed at 8 GHz from August 25 to September 3 of 81.1±1.0° is the same within uncertainties as the value of 80.5±2.2° observed by us for the May 1974 outburst The position angle may have changed at 8 GHz by ~ 10° during the 1975 outburst. The average position angle observed at 14.5 GHz was 150±3°. If the difference in position angle is caused by Faraday rotation, the rotation measure must be at least −1,265±56 rad m^{-2}. This value is more than twelve times that derived from data at the frequencies 2.7 and 8.1 GHz (ref. 2). Observations at 4.2 GHz for the May 1974 outburst[3] also indicate that the original determination of the rotation measure was too small because of the $n\pi$ ambiguity in the amount of rotation at 2.7 GHz. The excellent agreement of the observed position angles for the two polarised outbursts strongly suggests that the rotation measure and intrinsic position angle were the same for both outbursts. If the position angles of the two outbursts were completely independent, the probability that the difference would be not more than 0.6° is 0.7%. The probability that the difference would be not more than the quadratically summed error of 2.4° is 2.7%. We have fitted the observed position angles from both outbursts together and find that a rotation measure of −1,233±10 rad m^{-2} is consistent with all the data. The intrinsic position angle of the linear polarisation was 0±3°.

The stability of the 8-GHz polarisation position angle during the outbursts and between the first outburst and the second indicates that most of the Faraday rotation must occur in a region which is unaffected by the evolution of the outbursts. It is extremely unlikely that the rotation measure within the expanding emitting region would be the same for two separate bursts or that the internal rotation measure would not change as the emitting region expanded. The region producing the observed Faraday rotation could be either the long path through the Galaxy between Cyg X-3 and the Earth or a volume around Cyg X-3 in which material has accumulated from previous activity in the source. The sign of the rotation measure is the same as that observed for other sources in the Cygnus direction through the Galaxy, although the magnitude is much larger[9,10]. If the distance to Cyg X-3 is taken as 11 kpc (refs 11 and 12), the observed rotation measure could be produced by an average longitudinal component of the magnetic field of 10^{-6} gauss and an average electron density of 0.14 cm^{-3}. These are reasonable values, especially since the source is located on the far side of the Cyg X complex of H II regions.

The similar degrees of polarisation and the agreement between the polarisation position angles for the two outbursts suggest that the structure of the magnetic field in Cyg X-3 was the same for both outbursts The periodicity observed in the radio[6,8], infrared[13] and X-ray[14] emissions indicates that Cyg X-3 is a rotating or revolving system with a period of 4.8 h. The absence of large changes in the polarisation position angle data indicates that the magnetic field in the emitting region is oriented near a direction parallel or perpendicular to the angular momentum axis of the object.

Since the intrinsic position angle of the linear polarisation produced in an optically thin source is perpendicular to the transverse projection of the magnetic field, the axis of

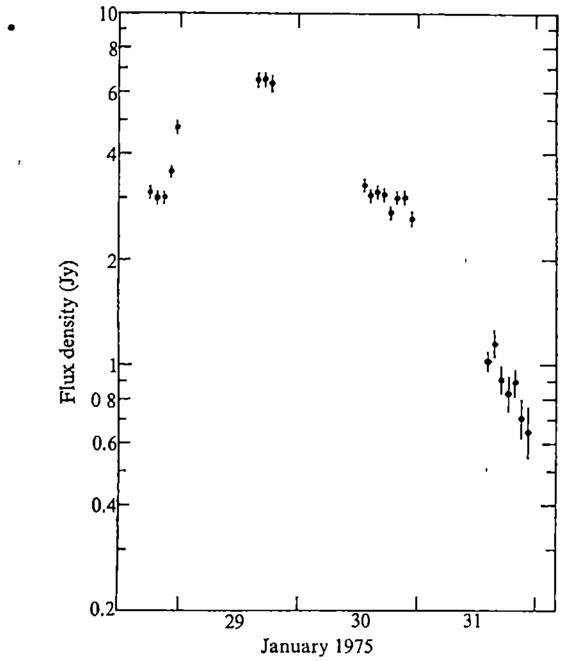

Fig. 3 Semilog plot of total flux density against UT at 8.0 GHz for Cyg X-3. The points represent 40-min averages of the data.

rotation or revolution of the system should be near a position angle of 0° or 90°. Any model for the radio emission from this source, especially those involving expansion where the particles control the magnetic field[15,16], must explain the observed stability of the field structure.

Observations at 8 GHz of an unpolarised outburst in Cyg X-3 during January 1975 are shown in Fig. 3. The average degree of linear polarisation from our 23 measurements was 1.3±0.5% at a position angle of 66±12°. The characteristic time for the decay of the total flux density was ~27 h which is similar to the decay times found for the other unpolarised outbursts[5,17]. It is noteworthy that the two highly linearly polarised outbursts have decayed significantly more slowly than all the other observed outbursts, of which four are known to have been unpolarised[2,6,18,19].

If there is a correlation between the decay rate and the existence of linear polarisation, it is an important feature which must be explained by any model for the radio outbursts in Cyg X-3. For instance, there is a natural correlation between the decay rate and the amount of linear polarisation if the absence of polarisation in the unpolarised events is caused by Faraday depolarisation and the energy losses of the radiating particles arise from thermal bremsstrahlung. This energy loss mechanism has been suggested to explain the exponential nature of the decay[5]. The difference in the amount of thermal matter required for polarised and unpolarised outbursts is much larger, however, than the difference required to explain the different decay rates. On the other hand, it is not obvious why a correlation between the decay rate and the state of polarisation would exist for expanding source models in which the energy losses are due to adiabatic expansion[15] or to both adiabatic expansion and synchroton radiation[16] Source models for Cyg X-3 must account for the smaller degree of polarisation at lower frequencies during the polarised outbursts. For example, the ratio of the degree of polarisation at 8 GHz to that at 14.5 GHz was 0.54±0.06. It has been suggested that this depolarisation effect arises from Faraday depolarisation[2]. This explanation is, however, hard to reconcile with the stability of the polarisation position angle observed at 8 GHz.

We thank F. T. Haddock, T. V Seling, G E. Latimer and K. G. Holmes for making these observations possible. This research was supported by grants from the NSF.

John E. Ledden
Philip E. Hodge
Hugh D. Aller

Radio Astronomy Observatory,
The University of Michigan,
Ann Arbor, Michigan 48109

Received June 8; accepted June 22, 1976.

[1] Kawajiri, N., *IAU Circ.*, No. 2819 (1975).
[2] Seaquist, E. R., *et al*, *Nature*, 251, 394–396 (1974).
[3] Kawano, N., and Kawajiri, N, *Publs astr. Soc. Japan*, 27, 191–193 (1975).
[4] Aller, H. D., *Astrophys. J.*, 161, 1–18 (1970)
[5] Aller, H. D., and Dent, W. A., *Nature phys. Sci.*, 239, 121–123 (1972).
[6] Aller, H. D, and Hodge, P. E., *Nature phys. Sci.*, 245, 40–41 (1973).
[7] McEllin, M., *Mon. Not. R. astr. Soc.*, 175, 5P–8P (1976).
[8] Hjellming, R. M., Brown, R. L., and Blankenship, L. C., *Astrophys. J Lett.*, 194, L13–L18 (1974).
[9] Manchester, R N., *Astrophys. J.*, 188, 637–644 (1974)
[10] Vallée, J. P., and Kronberg, P P., *Astr. Astrophys.*, 43, 233–242 (1975).
[11] Chu, K. W., and Bieging, J. H, *Astrophys. J. Lett.*, 179, L21–L23 (1973).
[12] Lauqué, R, Lequeux, J., and Nguyen-Quang Rieu, *Nature phys. Sci.*, 241, 94–95 (1973)
[13] Becklin, E. E., *et al.*, *Nature*, 245, 302–304 (1973).
[14] Parsignault, D. R., *et al.*, *Nature phys Sci.*, 239, 123–125 (1972).
[15] Peterson, F. W., *Nature*, 242, 173–177 (1973).
[16] Marscher, A. P., and Brown, R. L., *Astrophys. J*, 200, 719–726 (1975).
[17] McEllin, M., *Mon Not. R. astr. Soc.*, 170, 1P–6P (1975).
[18] Aller, H. D., *Nature phys. Sci.*, 239, 128 (1972).
[19] Dent, W. A., *Nature phys. Sci.*, 239, 127 (1972).

Competition of neutrino and gravitational radiation in neutron star formation

We look here into the possibility that neutrino radiation (rather than gravitational radiation) may be the dominant way by which non-radial pulsations are damped out in a collapsing star. If true, such a result implies that estimates and hopes to detect gravity waves from supernovae explosions may have been overly optimistic.

It has been known for some time that neutron stars and black holes are probably the collapsed central remnants of a supernova explosion. These objects presumably originate from the collapse of the cores of sufficiently massive ($M \gtrsim 7M_\odot$) stars[1], following the cessation of thermonuclear burning. Although at the present no completely consistent detailed theory exists showing exactly how the collapse of the core and the subsequent supernova explosion take place, there does exist a general model[2] for the final stages of stellar evolution and supernovae explosions. According to this, the electrons of a sufficiently massive stellar core, due to the high density and temperature, get absorbed by the protons, through $p+e^- \rightarrow n+v$. At the same time, huge numbers of neutrinos, resulting from this and other thermal processes (pair annihilation, plasma decay, bremsstrahlung) (refs 3 and 4) are emitted, taking away most of the gravitational energy of the collapse. These neutrinos possibly drive the ejection of the overlying stellar mantle, while the neutron-rich core further collapses to a condensed remnant.

The leftover remnant is of very high density (10^{14}–10^{15} g cm^{-3}) and its radius will eventually be only a few times its Schwarzschild radius. This implies that general relativistic effects may be important in situations involving neutron stars. In particular, the possibility of gravitational radiation emission from non-radially pulsating neutron stars has been extensively examined and it has been shown that gravitational waves can carry away the pulsational energy, thus damping out the star's oscillations. (Such non-radial pulsations presumably might occur during the collapse and formation of the neutron star.) Some workers have estimated[5] that the energy emitted in gravitational radiation in such an event would be sufficient to trigger existing or future gravitational radiation detectors. Consequently one might expect detectable gravitational wave pulses to be associated with supernovae explosions from the non-radial pulsations of the newly formed neutron stars.

As previously discussed, however, the dominant mechanism by which energy is carried away from the collapsing core is by neutrinos rather than gravitational radiation, the latter coming into play only at the very late stages of the collapse. This implies that neutrino radiation might also contribute to the decay of the non-radial oscillations of the collapsing core and the newly formed neutron star, possibly damping out these oscillations much faster than gravitational radiation.

To give a more quantitative answer to this question, the effects of neutrino radiation on the non-radial oscillations of such objects have been examined (D. Kazanas and D. N. Schramm, unpublished). The oscillations are assumed small enough so that the linear approximation in the perturbation is sufficient. The equilibrium configuration is assumed to be static (the velocity of the fluid $\bar{u} = 0$ when in equilibrium) and homogeneous ($\nabla\rho_0 = 0$). (The subscript zero denotes unperturbed quantities.) Its mass was taken to be $0.75M_\odot$ (to avoid an overestimate of the central temperatures) and it was assumed to obey an ideal gas law (not unreasonable for such a hot neutron gas). Together with the density, these completely specify the equilibrium configuration (the radius, and temperature and pressure distributions). Table 1 gives the radii and central temperatures for such a configuration for four different density regimes. (Of course, the figures for the highest density are only formal, because the equation of state then differs significantly from that of an ideal gas.) Assuming also an $\exp(i\sigma t)$ time dependence for all perturbed quantities, one can estimate a damping time scale from the neutrino radiation. This will be, approximately, the total kinetic energy of the perturbation, E_{tot}, divided by the rate at which energy is lost by neutrino radiation, dE_ν/dt. This neutrino damping time scale is, as shown elsewhere (D. Kazanas and D. N. Schramm, unpublished), given by

Table 1 Variation of central temperature and radius with density for a neutron star

ρ(g cm^{-3})	T(10^9 K)	R(km)
10^{12}	84	70.7
10^{13}	181	32.8
10^{14}	389	15.2
10^{15}	839	7.0

$$\frac{1}{\tau} = \frac{dE_\nu/dt}{E_{tot}} = \frac{1}{2}\frac{(\Gamma-1)\int\delta L(\delta\rho/\rho_0)_a dV}{(\sigma_a{}^2/2)\int(\delta r)_a{}^2\rho_0 dV}$$

where the integrals extend over the volume of the configuration and where Γ is the adiabatic index, δL the perturbation of the neutrino luminosity in erg s^{-1} cm^{-3}, and the subscript a denotes that the quantities have to be evaluated for the corresponding adiabatic solution (with $L = 0$). The expression for the quantities $(\delta r)_a$ and $(\delta\rho/\rho_0)_a$ and values for σ_a can be found in the literature[6].

One can now evaluate the damping times with δL corresponding to a particular neutrino production mechanism. Using only the dominant thermal neutrino production process, which for the densities and temperatures involved, appears to be pair annihilation, one can obtain upper limit estimates of the damping times due to neutrino radiation. The results for the four different density regimes are shown in Table 2.

It is interesting to compare these to the corresponding damping times due to gravitational radiation. A variational calculation[7] gives $t = 10$ s for $\rho = 10^{14}$ g cm^{-3} and $t = 0.4$ s for $\rho = 10^{15}$ g cm^{-3}. For lower densities gravitational radiation is essentially absent and thus $\tau_G \gg \tau_\nu$.

Table 2 Density dependence of neutrino-damping time

ρ(g cm^{-3})	σ_a(s^{-1})	τ(s)
10^{12}	1,531	0.7
10^{13}	4,842	5×10^{-2}
10^{14}	15,310	10^{-3}
10^{15}	48,416	2×10^{-6}

The implication of the above result is easy to see. It seems that neutrino radiation, by more rapid damping of the non-radial oscillations of a newly formed neutron star in a supernova explosion, would hinder gravitational radiation, thus reducing the possibility of its detection.

We would like to acknowledge discussion with W. D. Arnett, K. Hainebach, J. Lattimer, M. Murphy and in particular with D. L. Tubbs on this problem. This work was supported in part by the NSF and NASA.

DEMOSTHENES KAZANAS
DAVID N. SCHRAMM

Enrico Fermi Institute,
The University of Chicago,
Chicago, Illinois 60637

Received May 26, accepted July 2, 1976

1 Schramm, D N , and Arnett, W. D., *Mercury*, 4, 16 (1975).
2 Schramm, D. N., and Arnett, W. D , *Astrophys. J.*, 198, 629 (1975).
3 Baudet, G., Petrosian, V , and Salpeter, E., *Astrophys. J* , 150, 979 (1967)
4 Dicus, D. A., Kolb, E. W., Schramm, D N , and Tubbs, D. L., *Astrophys J* (in the press).
5 Misner, C. W., Thorne, K S , and Wheeler, J A., *Gravitation*, (Freeman, San Francisco, 1973)
6 Ledoux, P., and Walraven, T., *Variable Stars*, Handbuch der Physik, Astrophysics II (1958).
7 Detweiler, S. L., *Astrophys. J* , 197, 203 (1975)

Detection of interstellar HN^{13}C

INTERSTELLAR hydrogen isocyanide (HNC) was first tentatively identified[1] on the basis of a calculated frequency for the $J=1\rightarrow0$ transition of the most abundant isotopic species H^{14}N^{12}C. The observed interstellar line was quite strong and widespread in the galaxy. A more definitive identification of the observed U90.7 emission line (90,663.6 MHz)[2] by searching for other isotopes was not possible because of the large uncertainties in the calculated molecular structure of HNC, and the corresponding large uncertainties in the calculated transition frequencies for H^{14}N^{13}C and H^{15}N^{12}C. Hydrogen isocyanide is very short lived in terrestrial laboratory conditions, and therefore it has proven difficult to measure the rotational spectrum directly. The $J=0\rightarrow1$ transition has, however, been recently measured independently by three groups[3-5] and the frequency of the major isotope is in excellent agreement with that of U90.7. The laboratory spectroscopy has also

Fig. 1 HN^{12}C (*a*) and HN^{13}C (×10) (*b*) in W51. Note the HN^{12}C line is broader: resolution = 1 MHz (≃3.3 km s^{-1}).

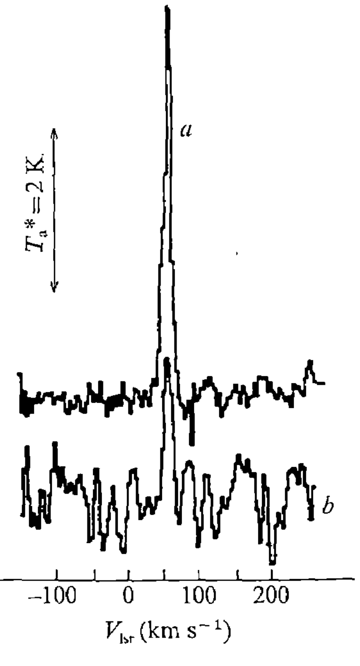

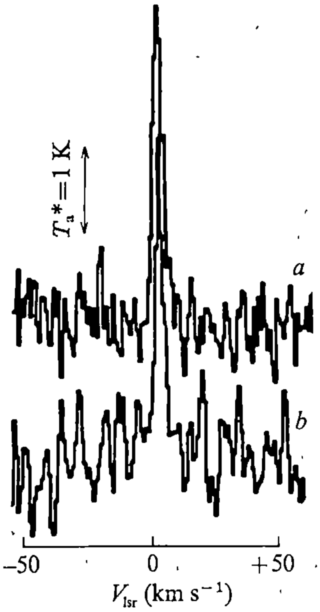

Fig. 2 HN^{12}C (*a*) and HN^{13}C (×10) (*b*) in DR21 (HCN peak). Note HN^{12}C line is significantly broader: resolution = 250 kHz (≃0.83 km s^{-1}).

Fig. 3 HN^{12}C (*a*) and HN^{13}C (*b*) in Sag B2. Note gross difference in line profiles, both to same scale. Resolution = 1 MHz (≃3.3 km s^{-1}).

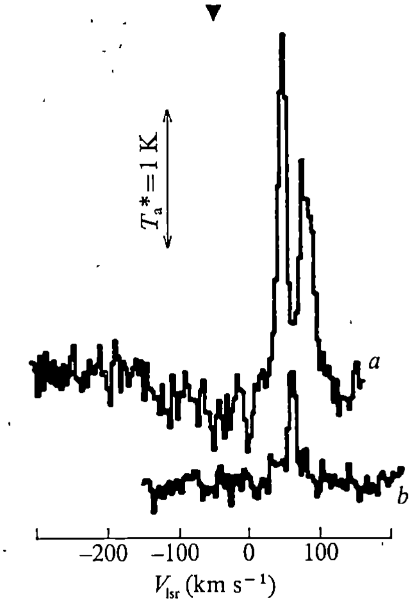

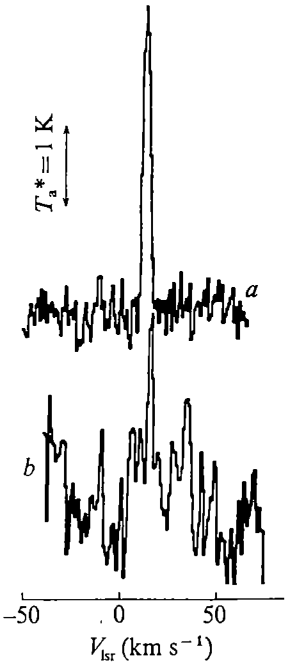

Fig. 4 HN^{12}C (*a*) and possibly HN^{13}C (×10) (*b*) in NGC2264. Resolution = 250 kHz (≃0.83 km s^{-1}).

yielded the ^{13}C isotope transition frequency[4]. Immediately following this measurement, we searched for and detected the HN^{13}C $J=1\rightarrow0$ rotational spectral line at 87,090.6 MHz in the galactic molecular source W51 (Fig. 1) on the NRAO 11-m telescope in March, 1976. Because of calibration problems with our receiver, we simultaneously observed the ^{12}C isotope so that relative abundance determinations might ultimately be made from our data. Appropriately, W51 was the source in which Snyder and Buhl first detected the $J=1\rightarrow0$ transition of HN^{12}C. In addition, the HN^{13}C line was detected in DR21, Sag B2, and possibly also NGC2264 and IRC+10°216 (Figs 2–5). All of these sources also showed the HN^{12}C emission line. In addition, we detected HN^{12}C in W3 (Fig. 6), but were unable to detect the ^{13}C isotope there due to equipment failure. These results are summarised in Table 1.

We attempted to refine the HN^{13}C rest frequency in the narrow line source DR21. Assuming that HN^{13}C occurs at the common velocity of −3 km s^{-1} for this source position, our observations indicate a rest frequency of 87,090.71 (0.25) MHz. This compares favourably with our laboratory data and those of Creswell *et al.*[5]. Snyder and Hollis's[6] rest frequency for HN^{12}C of 90,663.37 MHz indicates, however, a velocity of −5.25 km s^{-1}. This would necessitate a rest frequency of 87,091.36 MHz for HN^{13}C which is further from the laboratory data than one would like. Thus our data indicate the HN^{13}C frequency to be slightly higher in frequency than our laboratory measurement. This is also more consistent with our data in W51 and Sag B2 (taken with lower resolution).

Table 1 Results of observations

Source name	RA (1950.0)	dec. (1950.0)	T_a* HN^{12}C (K)	T_a* HN^{13}C (K)
	(h min s)			
W51	19 21 23	+14° 24′ 30″	4.8	0.18
DR21	20 37 10	42° 09′ 00″	3.3	0.39
Sag B2	17 44 11	−28° 22′ 30″	2.8 (complex)	0.95
NGC2264	6 38 28	9° 32′ 06″	4.1	(0.27 ?)
IRC+10°216	9 45 15	13° 30′ 40″	0.6	(0.11 ?)

T_a* is antenna temperature divided by the beam efficiency corrected to outside the Earth's atmosphere.

Our Sag B2 spectra (Fig. 3) are very interesting. The HN^{12}C spectrum displays a double peaked structure with a profound dip in the middle. A similar double structure has also been observed in N_2H^+ (ref. 7) and the $J=2$–1 transition of ^{12}C^{32}S (ref. 8) (we observed the $J=2$–1 of ^{13}C^{32}S to be a single broad feature centred on roughly 60 km s^{-1}). HN^{13}C, however, displays a very narrow feature almost exactly centred on the HN^{12}C dip, with a weak broad base underneath. The most straightforward interpretation of these data is that the HN^{12}C is optically thick and self absorbed while the HN^{13}C is not. The position of the narrow HN^{13}C peak is consistent with this interpretation, as is the broad base. The very narrow HN^{13}C feature is,

Fig. 5 HN^{12}C (*a*) and possibly HN^{13}C (*b*) in IRC+10°216. Note scales are unrelated. Resolution = 1 MHz (≃3.3 km s^{-1}).

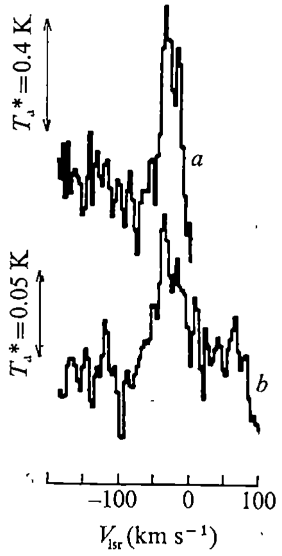

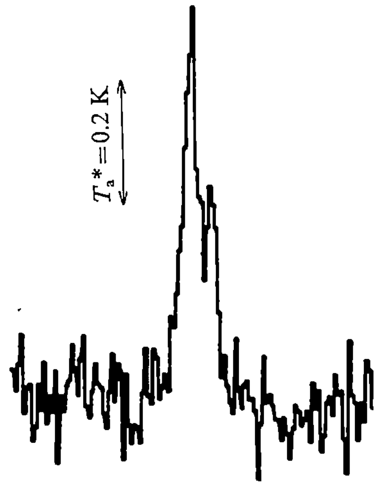

Fig. 6 HN^{12}C in W3. No data were obtained on HN^{13}C due to equipment problems. Resolution = 250 kHz ($\simeq$0.83 km s^{-1}).

however, intriguing and we cannot help but be impressed with the possibility that the HN^{12}C and HN^{13}C are not spatially coexistent. Perhaps both conditions occur to some extent. One interpretation of the extremely narrow HN^{13}C feature is that it results from a localised region considerably enhanced in ^{13}C. This problem is certainly worthy of further study. Similar effects in the isotopes of HCN have previously been observed by R. A. Linke (private communication) and are currently under study by him (and coworkers).

We thank the staff of the NRAO at Tucson, and especially Dewey Ross and Jack Cochran. We also thank the University of Kentucky Graduate School and the Australia Research Grants Committee for support. NRAO is operated by Associated Universities Inc. under contract with the NSF.

R. D. BROWN
P. D. GODFREY
J. W. V. STOREY

Department of Chemistry,
Monash University,
Clayton, Victoria, 3168, Australia

F. O. CLARK

Department of Physics and Astronomy,
University of Kentucky,
Lexington, Kentucky 40506

Received March 15; accepted May 26, 1976.

1 Snyder, L. E., and Buhl, D , *Ann. N. Y Acad Sci.*, 194, 17 (1972).
2 Zuckerman, B., Morris, M , Palmer, P , and Turner, B. E , *Astrophys. J. Lett.*, 173, L125 (1972).
3 Saykally, R. J., Szanto, T. G., Anderson, T. G., and Woods, R. C., *Astrophys. J. Lett.*, 204, L143 (1976).
4 Blackman, G. L., Brown, R. D., Godfrey, P. D., and Gunn, H. I., *Nature* (in the press).
5 Creswell, R. A , Pearson, E. F., Winnewisser, M., and Winnewisser, G., *Z. Naturforsch.*, 31a, 221 (1976).
6 Snyder, L. E., and Hollis, J. M., *Astrophys. J. Lett.*, 204, L139 (1976).
7 Turner, B. E., *Astrophys. J. Lett* , 193, L83 (1974).
8 Turner, B. E., Zuckerman, B., Palmer, P., and Morris, M., *Astrophys. J.*, 186, 123 (1973).

The second *Z*-propagation window

ELLIS[1,2] investigated the condition in the ionosphere under which an upgoing ordinary radio wave is converted, through a coupling process, into an upgoing extraordinary wave in the *Z* mode. (Propagation in the *Z* mode requires the presence of both an ionised gas and a magnetic field; hence such waves cannot be received in free space.) This occurs for a wave incident on the ionosphere from below with its wave normal close to a critical direction in the magnetic meridian plane. This direction is such that when the wave reaches the level where $X = 1$, which is normally a complete reflector for the ordinary wave, its wave-normal direction has become close to the magnetic field line direction. The symbols X and Y are as usually defined in magnetoionic theory (see Ratcliffe[3]). The level $X = 1$ becomes semi-transparent for a cone of angles centred on the critical direction. This cone is called the 'Ellis window'. The *Z*-mode waves are reflected at a higher level where $X = 1+Y$. Here I wish to draw attention to a window which is relevant to the escape of *Z*-mode radiation produced naturally in the topside ionosphere.

It is well known from satellite observations that radio noise is produced by charged particles streaming through the magnetosphere and ionosphere (see Mosier *et al.*[4] and references therein). One frequency range in which particularly intense noise is observed is that lying between the plasma frequency f_p and the upper hybrid resonance (UHR) $f_{UHR} = (f_p^2+f_g^2)^{\frac{1}{2}}$ where f_g is the gyro-frequency; all frequencies refer to conditions local to the spacecraft. This is the frequency range where *Z*-mode radiation can attain very low phase velocities allowing interaction between waves and particles, and it is generally accepted that the intense noise is in the *Z* mode. Normally the noise cannot escape very far from the source region since it is reflected from the level where $X = 1+Y$ and absorbed at the level where $X = (1-Y^2)/(1-Y^2\cos^2\theta)$ where θ is the wave-normal direction. If, however, the waves propagate past the level $X = 1$, which lies between the above two levels, with their wave-normal directions close to the magnetic field direction then the coupling process between *Z* mode and ordinary mode considered by Ellis becomes operative. If, in addition, $Y > 1$ at the level $X = 1$ then another propagation window appears involving coupling between *Z*-mode and whistler-mode waves, the latter being free to propagate to the ground.

The condition that $Y > 1$ at $X = 1$ is probably met at geomagnetic latitudes $\gtrsim 70°$ for altitudes $\gtrsim 3{,}000$ km, as is apparent from Fig. 1 which is based on our present limited knowledge of the plasma-density in this region[5]. The frequencies which could be coupled are seen to be ~20 kHz–800 kHz.

It is significant that auroral hiss, which is broadband noise observed on the ground and on satellites in the geomagnetic

Fig. 1 Polar ionospheric model showing the expected radial variation of the plasma frequency f_p, the gyro frequency f_g, and the UHR frequency f_{UHR}. The region between f_p and f_{UHR} is where UHR noise from charged particle fluxes is expected. Whistler-mode noise appearing as a consequence of propagation through the second *Z*-mode window is shown shaded below the f_p curve.

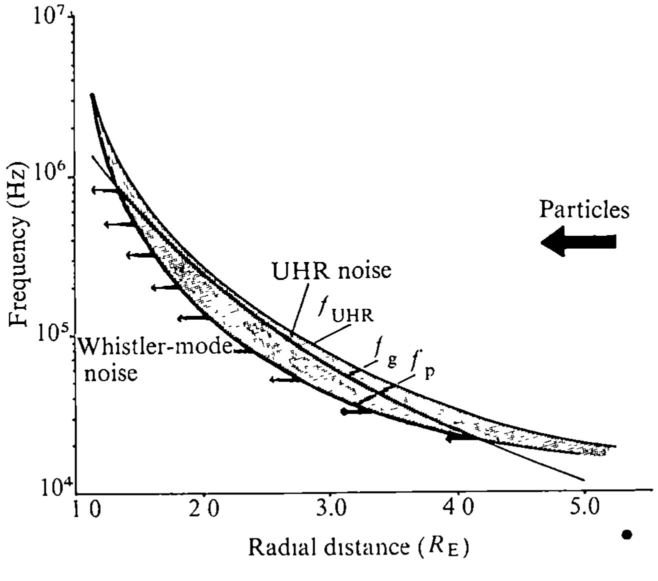

latitude range 70°–80°, covers a rather similar frequency range[6]. Therefore in any computation of hiss intensities it is important to consider the possible contribution from radiation which has passed through the second Z-propagation window mentioned here.

It is clear that the process is reversible, in that upgoing whistler waves with wave normals lying within a cone centred on a certain critical direction, can be coupled to Z radiation at $X = 1$ in the topside ionosphere. The Z radiation so produced will be absorbed at the level $X = (1-Y^2)/(1-Y^2\cos^2\theta)$ where the wave energy is transferred into heat resulting in an increase in the temperature of the local plasma. Thus it may be possible to consider this process as a means of modifying the topside ionosphere by using a high power, low frequency transmitter at high latitudes.

DYFRIG JONES

Space Science Department,
European Space Agency,
Noordwijk, The Netherlands

Received May 7; accepted June 28, 1976.

[1] Ellis, G. R A., *J atmos. terr. Phys.*, 8, 243 (1956).
[2] Ellis, G R. A., *Nature*, 193, 862 (1962)
[3] Ratcliffe, J. A., *Magnetoionic Theory* (Cambridge, 1959)
[4] Mosier, R. M , Kaiser, M. L , and Brown, L. W , *J. geophys Res* , 78, 1673 (1973).
[5] Gurnett, D A., *J. geophys Res* , 79, 4227 (1974).
[6] Jorgensen, T. S , *J geophys. Res* , 73, 1055 (1968).

Is the Earth expanding?

THERE have been many determinations of the acceleration of the Moon's mean longitude, mostly based on observations of occultations since 1680 and on records of ancient eclipses[1–9]. All these results have been expressed in Ephemeris Time, based on the annual apparent motion of the Sun about the Earth. Since 1955 Atomic Time came into use based on the period of oscillation of the caesium atom which is, by definition, constant. A new analysis of lunar occultations observed from 1955 to 1974 using Atomic Time, by Van Flandern (unpublished) gives a value for the acceleration of the Moon's mean longitude differing from other determinations which used the Ephemeris Time scale. His new results differ from earlier work[10]. The data reveal a difference between Ephemeris Time and Atomic Time of 25 s a century. Van Flandern suggests that the most probable explanation is a decrease in the gravitational constant, G, by 8 parts in 10^{11} per yr. Such a decrease would mean that the Earth is expanding somewhat and there is some geological evidence supporting this. We tried to check this conclusion using a method for determining the lengthening of the day verified by Wells[11] in which the number of tiny lines of ridges on well preserved epitheca of corals in their annual growth increments are counted. We found no evidence for any expansion of the Earth in the past 5×10^8 yr.

More extensive results have been published by Panella *et al.*[12] giving the number of days in the year for different geological periods. Their oldest corals are from the Cambrian, 520 Myr ago. The Table of Panella *et al.* giving the number of days, T_E, in the sidereal year has been extended by us to derive the length of the day, D, in hours and the angular rotational velocity, Ω, of the Earth. By plotting the time dependence of Ω (Fig. 1) and by assuming a linear decrease, which seems fully justified, we find a value of the time derivative

$$\dot{\Omega} = (-6.88\pm0.05)\times10^{-22}\ \text{rad s}^{-2}$$

From this it follows that

$$\dot{\Omega}/\Omega = -(29.91\pm0.05)\times10^{-11}\ \text{yr}^{-1}$$

is in excellent agreement with ref. 9.

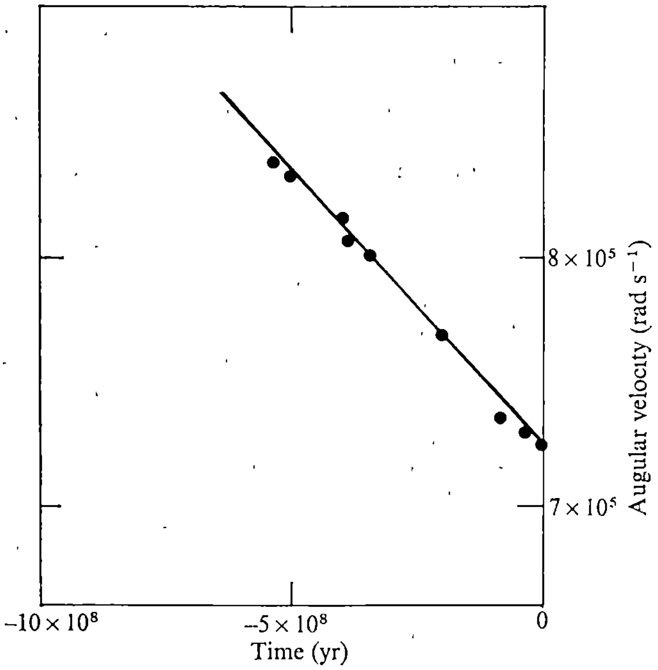

Fig. 1 The rotational velocity of the Earth derived from fossil corals during the past 540 Myr.

The total angular momentum of the Earth–Moon system is given by

$$P = C\Omega + mvr + c\omega$$

where m is the mass of the Moon, v is the linear velocity of the Moon in its orbit, r is the distance of the Moon, ω is the angular velocity of rotation of the Moon, and c is the moment of inertia of the Moon. As both $c \ll C$ and $\omega \ll \Omega$ we can ignore $c\omega$ so that

$$P \simeq P_E + P_M$$

where $P_E = C\Omega$ and $P_M = mvr = m(GMr)^{1/2}$ where M is the mass of the Earth.

As a closed system cannot lose angular momentum, the Moon must gain the angular momentum lost by the spinning Earth. If

Fig. 2 The decrease of the angular momentum of the Earth calculated by counting growth ridges in fossil corals.

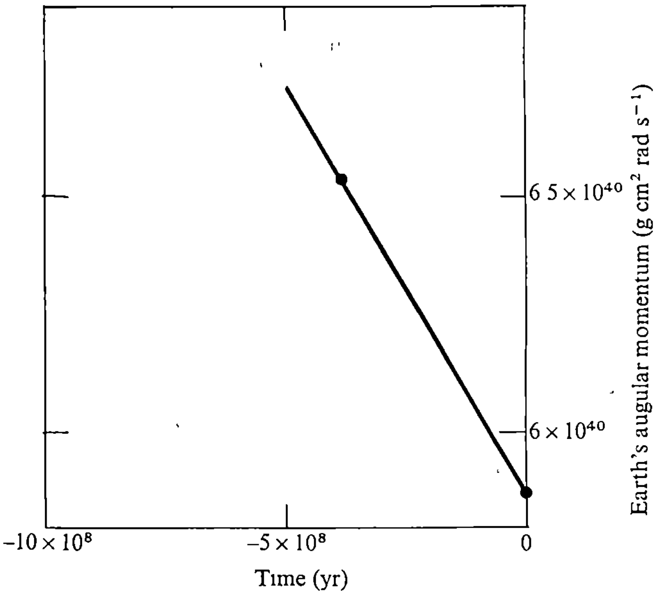

we define the present angular momentum of the Earth as $P_E = 1$, the present value for the Moon is $P_M = 4.964$, and $P = 5.964$. Therefore

$$P_E = 5.964 - 4.964(r/r_0)^{1/2} \qquad (1)$$

where r_0 is the present distance of the Moon and we ignore the small variation of G.

Scrutton[13] has studied other bands between the yearly expansions found on some fossil corals and he suggested that they might reflect monthly fluctuations in growth influenced by variations in the light of the Moon. Each band contained 30.6 d and the corals investigated lived ~ 380 Myr ago in the Middle Devonian. From his 30.6 d we can calculate the length of the synodic month in hours for that time by using the length of the day, D, found in ref. 12. By using the number of days in the year we can then calculate the length of the sidereal month in the Middle Devonian and with the third law of Kepler we can easily derive from it the lunar distance r at that time.

The value of P_E in the Middle Devonian can now be found by substituting the value of r in equation (1), and from its value 6.53×10^{40} g cm^2 rad s^{-1}, plotted in Fig. 2, we derive

$$P_E = -1.76 \times 10^{40} \text{ per } 10^9 \text{ yr}$$

and

$$P_E/P_E = (-30 \pm 3) \times 10^{-11} \text{ per yr}$$

As $P_E \simeq 0.4MR^2\Omega$, where R is the radius of the Earth, we may write

$$\frac{\dot{P}_E}{P_E} = 2\frac{R}{R} + \frac{\dot{\Omega}}{\Omega}$$

The value of $\dot{\Omega}/\Omega$ derived from Fig. 1 is practically the same as the value of $\dot{P}_E/P_E$ found from Fig. 2. The conclusion seems inevitable that

$$\dot{R}/R \approx 0$$

so that the Earth has not expanded much during the past 5×10^8 yr.

An expansion of the Earth has already been pointed out by Holmes[14] and by Wesson[15] in a discussion of continental drift and seafloor spreading. If G is decreasing, the Earth should expand because of the decreased weight of the surface layers. This idea has been developed by Van Flandern (unpublished) in his discussion of the decrease of G. It would be very desirable that more extended counts on growth lines be made for fossil corals of different geological periods to check the points in Fig. 2.

J. VAN DIGGELEN

The Astronomical Institute,
University of Utrecht,
The Netherlands

Received May 10, accepted May 28, 1976

1 de Sitter, W., *Bull. Astr. Insts. Neth.*, **4**, 21 (1927).
2 Spencer Jones, H., *Mon. Not. R. astr. Soc.*, **99**, 541 (1939).
3 Clemence, G. M., *Astr. J.*, **53**, 169 (1948)
4 Morrison, L., *The Moon*, **5**, 253 (1972).
5 Murray, C. A., *Mon. Not. R. astr. Soc.*, **117**, 478 (1957)
6 Newton, R. R., *J. geophys. Res.*, **73**, 3765 (1968).
7 Oesterwinter, C., and Cohen, C. J., *Celest. Mech.*, **5**, 317 (1972).
8 Curott, D. R., *Astron. J.*, **71**, 264 (1966).
9 Muller, P. M., and Stephenson, F. R., in *Growth Rhythms and History of the Earth's Rotation* (edit by Rosenberg, G. D., and Runcorn, S. K.), (John Wiley and Sons, London, 1974)
10 Morrison, L., *Nature*, **241**, 519 (1973)
11 Wells, J. W., *Nature*, **197**, 948 (1963)
12 Panella, G., MacClintock, G., and Thompson, J., *Science*, **162**, 792 (1968)
13 Scrutton, C. T., *Palaeontology*, **7**, 552 (1964).
14 Holmes, A., *Principles of Physical Geology*, 2nd rev. ed., 34 (Nelson, London, 1964).
15 Wesson, P., *Q. Jl R. astr. Soc.*, **14**, 9 (1973).

Test of the dipolar nature of the geomagnetic field throughout Phanerozoic time

THE morphology of the geomagnetic field throughout the Earth's history is of interest first, in a general way, to geomagnetists in terms of long term implications concerning the Earth's core, its thermal regime and the motions in it, and, second, in a very particular way, to palaeomagnetists since the geocentric dipole model is universally used in mapping observed field directions into palaeomagnetic poles. Runcorn[1,2] has given strong reasons for supposing the mean geomagnetic field to be symmetrical about the Earth's spin axis. He has also argued[3], on the basis of early palaeomagnetic data, that a dipolar field coupled with continental motion is preferable to higher order axial multipole fields. Here I discuss an observational test, based on the much larger body of palaeomagnetic data now available, to discriminate between a dipole field and those of higher order multipoles.

Attention is restricted to the angle of inclination, I, since absolute reference meridians are not available in palaeomagnetic studies. Suppose a large number of instantaneous measurements of $|I|$ are made at randomly distributed geographical sites. For any given geomagnetic field a definite frequency distribution of $|I|$ exists, and can be obtained by simply estimating the relative surface areas of the globe corresponding to any chosen set of $|I|$ classes. For instance, a dipole field is horizontal at the equator and has $|I| = 10°$ at latitude 5.1°, whereas the field is vertical at the spin axis and has $|I| = 80°$ at latitude 70.6°. The surface areas of these two zones imply that if sampling is sufficient and geographically random we expect the $0 \leq |I| \leq 10°$ band to constitute 8.8% of the results and the $80° \leq |I| \leq 90°$ band to constitute only 5.7%. Figure 1 shows the dependence of inclination, $|I|$, on latitude, λ for the first four multipoles (dipole, quadrupole and so on) obtained from the relationship

$$\tan Il = -(1+l)Pl/(\partial Pl/\partial\theta) \qquad (1)$$

where Pl is the Legendre polynomial of degree l, and θ is the colatitude ($\theta = 90 - \lambda$). In Fig. 2 the corresponding frequency distributions of $|I|$ are given. The most notable features are the markedly low value in the range 80°–90° and the high peak in the range 60°–70° for the dipole curve.

Before comparing the palaeomagnetic data with the theoretical curves it is essential to enquire if they do, in fact, represent a random geographical sampling. Referred to the present latitude/longitude grid they clearly do not, because of uneven distribution of land and the existence of areas of relatively intense scientific effort. Throughout the past 500–600 Myr, however, considerable polar wander and/or continental drift has taken place[4,5] and we proceed on the assumption that these have been sufficient to render the palaeomagnetic sampling random in a palaeogeographical sense.

Values of $|I|$ have been compiled from the list of Hicken *et al.*[6], who feel that it is "approximately complete up to 1971". To minimise the effects of spatially and/or temporally concentrated sampling, unit weight has been given to each $10° \times 10°$ latitude/longitude square for each geological period from Cambrian to Tertiary inclusive (~ 600 to 2 Myr BP). Thus if, for example, N results are available from a certain latitude/longitude square for a particular geological period, each $|I|$ datum has been given a weight of $1/N$. Use of the geological periods is convenient and can be justified on the grounds that apparent polar wander takes place at about 0.2° Myr^{-1} and that the periods represent about 50 (±20) Myr, which implies typical within-period movement of about 10°. This is comparable with typical palaeomagnetic errors, and thus implies that a finer subdivision would be of little value.

Data from the Quaternary and the Precambrian were not included. The large body of data from the Quaternary would

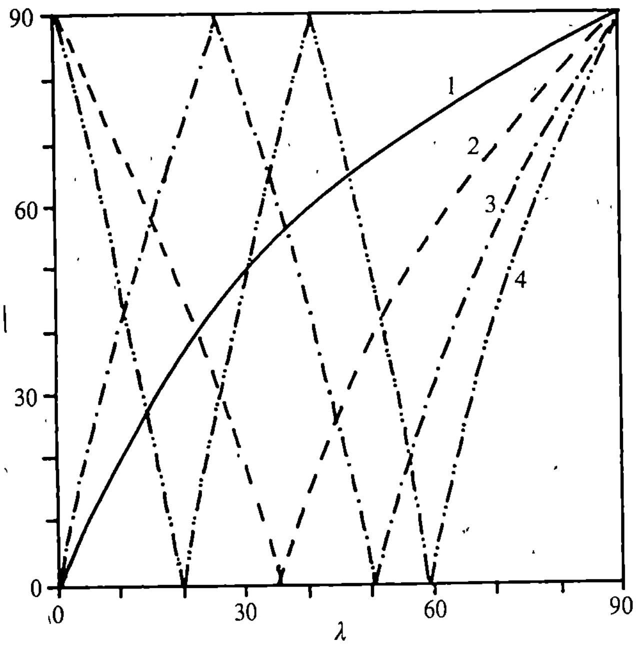

Fig. 1 Variation of angle of inclination, |*I*|, with latitude λ, for axial multipole fields. The numbers by the curves refer to the degree of the appropriate Legendre polynomial (1 = dipole; 2 = quadrupole and so on, see equation 1).

Fig. 2 Frequency polygons showing the distribution of |*I*| for axial multipole fields. The curves, and the numbers by them, correspond to the curves of Fig. 1. +, Observations.

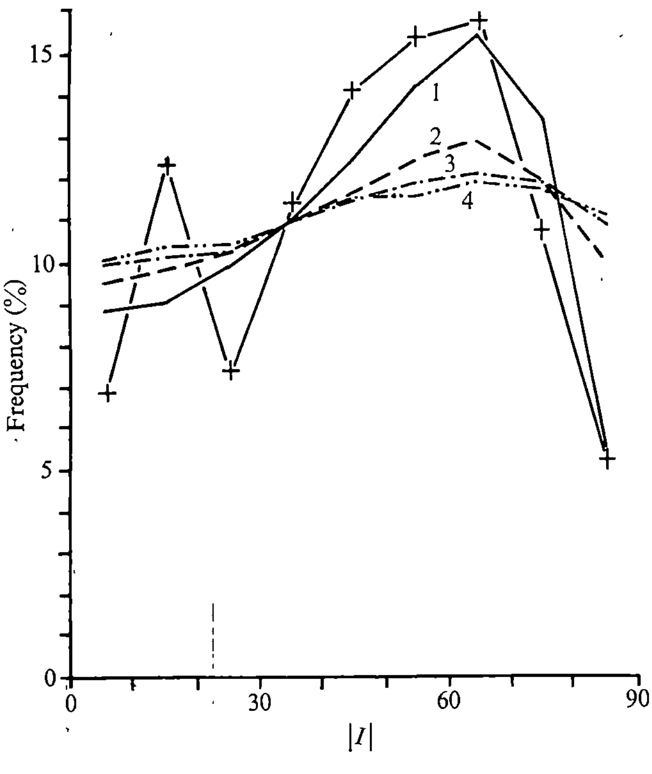

give undue weight to the past 2 Myr that it represents and, in any case, several authors[7,8] have convincingly demonstrated the essentially dipolar nature of the field for this time interval. In the case of the Precambrian, the time involved is very long (~ 2×10^9 yr) but the data density is generally too low and is highly variable, and furthermore the assignment of accurate ages is often not feasible. For the time interval Cambrian to Tertiary the list of Hicken *et al.* yields a total of 1,271 inclination values, but the weighting procedure adopted reduces this to 430. The distribution of |*I*| is shown in Fig. 2, which indicates that the fit to the dipole curve is very reasonable, and is certainly favoured over the higher order multipoles. The main discrepancy, at low inclinations, probably reflects sampling inadequacies rather than any real feature since the total observations in the range 0–30° is 26.8% which agrees closely with the expected value of 27.7%. Another factor adding noise preferentially to a dipole model at low inclinations could be the enhanced effects of secular variations at low latitudes[9].

A χ^2 test can be used to compare the observations with the predicted distributions and yields $\chi^2 = 13.49$ for the dipole case. With eight degrees of freedom the critical value of χ^2 is 15.51 ($P = 0.05$) which indicates that we cannot assert that the two distributions differ. For $l \geq 2$ the same test strongly indicates that the observed distributions differ significantly from the expectations, χ^2 having values 27.98, 34.57, and 37.15 for $l = 2$, 3, and 4, respectively. Since palaeomagnetic errors are generally of the same magnitude as the class widths used here, it is perhaps worth while to calculate χ^2 for a coarser subdivision. Using three classes (0–30°, 30°–60°, and 60°–90°) yields $\chi^2 = 2.37$, 6.61, 8.88, and 9.98 for $l = 1$, 2, 3, and 4 respectively, compared with the critical value of 5.99 (two degrees of freedom, $P = 0.05$). Again, no difference can be claimed for the dipole case.

I conclude that the frequency distribution of palaeomagnetic inclination angles implies that the geomagnetic field has been essentially dipolar throughout Phanerozoic time.

I thank Dr M. C. Frazer for discussion and collaboration during the initial stages of this work, Mrs W. I. Gough for assistance, and Dr D. I. Gough for reading the manuscript. Financial support was received from the National Research Council of Canada.

M. E. Evans

Institute of Earth and Planetary Physics,
University of Alberta,
Edmonton, Alberta, Canada

Received April 19, accepted May 12, 1976.

[1] Runcorn, S. K., *Trans. Am. geophys Un.*, **35**, 49–63 (1954).
[2] Runcorn, S. K., *Ann. Geophys.*, **15**, 87–92 (1959).
[3] Runcorn, S. K., *J atmos. terr. Phys.*, **14**, 167–174 (1959).
[4] Irving, E., *Paleomagnetism and its Application to Geological and Geophysical Problems* (Wiley, New York, 1964).
[5] Goldreich, P., and Toomre, A., *J. geophys. Res.*, **74**, 2555–2567 (1969).
[6] Hicken, A., Irving, E., Law, L. K., and Hastie, J., *Publ. Earth Phys. Br., Energy, Mines Resour. Ottawa, Can.*, **45**, 1–135 (1972)
[7] Opdyke, N. D., and Henry, K. W., *Earth planet. Sci Lett.*, **6**, 139–151 (1969).
[8] Wilson, R. L., and McElhinny, M. W., *Geophys. J. R astr. Soc*, **39**, 570–586 (1974).
[9] Brock, A., *Geophys. J. R. astr. Soc.*, **24**, 303–317 (1971).

Frequency of foreshocks

In February 1975, the Chinese Seismological Bureau successfully predicted a magnitude 7.3 earthquake near Haicheng, Liaoning Province. From their reports, it is obvious that many methods such as radon count, abnormal animal behaviour, seismic velocity, and tilt and telluric current anomalies were considered in making the long term prediction[1]. The short term prediction, however, was based primarily on foreshock activity[2,3]. That foreshocks were important in the prediction raises the question of how common they are. We here analyse the frequency of foreshocks before shallow earthquakes with magnitudes greater than 7. Our findings show that 44% of all large shallow events in the world from 1950 to 1973 had foreshocks large enough to be teleseismically recorded, and that 21% of the large earthquakes that occurred in China between 1900 and 1949 had foreshocks large enough to be noted in local records.

We used two catalogues to cover the different periods of time. We searched the catalogue of Chinese earthquakes[4] for the period 1900–49 for events preceding and near each earthquake with $M > 7.0$. Since the smallest magnitudes listed are about 4.5, and since they are listed only for the more recent portion of this period, the catalogue does not include many

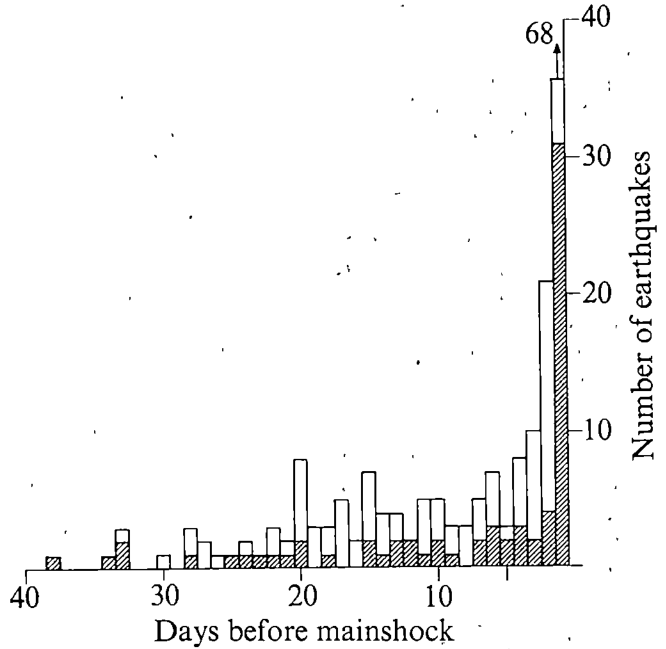

Fig. 1 Foreshock activity as a function of time before main shocks. For each day before main shocks the total number of foreshocks and the number of days before which the foreshock closest in time to the main shock (hatched area) occurred are shown.

small events that would have been recorded and located with present-day instrumentation. For the period 1950–73, we searched a catalogue of world events compiled by the National Oceanic and Atmospheric Administration (NOAA) for foreshocks before all events in the world with $M > 7.0$ (1950–64)[5], and (1965–1973)[6]. The NOAA list includes all events located with teleseismic recordings by US Government agencies (Coast and Geodetic Survey, NOAA and Geological Survey) and by the Bureau Central International de Seismologique. Therefore, only events with $M \gtrsim 4$ are included. The list is complete only for events with $M \gtrsim 5$ (refs 7 and 8) for more recent years. For some periods of time and some epicentral areas the location capability was particularly low, and no relatively large foreshocks or aftershocks were located. As we were interested in how many major earthquakes were preceded by foreshocks, we decided not to include events with two or less aftershocks listed in this catalogue. Thus, of the 246 events between 1950 and 1973 with $M > 7.0$, we used only 163. In fact, of 83 events with two or less aftershocks, 7 were preceded by at least one teleseismically located foreshock.

Because the source dimensions of earthquakes with $M > 7$ are of the order of 100 km, and, because of expected inaccuracies in epicentral determinations, only events located within 100 km of the main shocks were considered to be foreshocks, even though aftershocks often occurred at greater distances from them. To be classified as a foreshock an earthquake also had to occur within 40 d of the main event. By that criterion, however, 31 of the 72 cases of foreshock activity actually occurred within 24 h of the main shocks and 58 were within two weeks (Fig. 1).

Figures 2 and 3 show the geographical distribution of the main shocks studied, and also show which had teleseismically located foreshocks. Seventy-two of 163 major earthquakes between 1950 and 1973, or 44%, had at least one foreshock in the NOAA list. Of the earlier earthquakes in China, 10 of 48, or 21%, had foreshocks. The lower value for China probably reflects a less complete record for the period 1900–49 than for more recently. In fact, Immamura[9] noted in 1937 that "big earthquakes" are preceded by foreshocks only 20% of the time, but anticipated that this percentage would increase as better instrumentation was installed.

It seems that even 44% is too low an estimate. Many earthquakes that had no foreshocks in the NOAA list (and thus not included in the 44%) are, in fact, known to have been preceded by foreshocks. For instance, Richter[10] mentioned that a foreshock occurred within 24 h of both the 1952 Kern County, California, and the 1954 Fairview Park, Nevada, earthquakes. There were 35 earthquakes in the two days before the March 1966 earthquake in the Republic of the Congo[11], a week of foreshock activity preceding the 1965 earthquake in the Ceram Sea[6], and 10 foreshocks within 24 h of the August 1, 1968 Luzon earthquake[12]. Evidently, none of these foreshocks was

Fig. 2 Map showing earthquakes with $M \geq 7.8$ (circles) and $7.0 \geq M < 7.8$ (triangles) during 1950–1973, exclusive of China, for which 3 or more aftershocks were located. Events for which at least one foreshock (closed symbols) was located and no foreshocks (open symbols) were located are shown. ×, Events with less than 2 teleseismically located aftershocks, but with foreshocks.

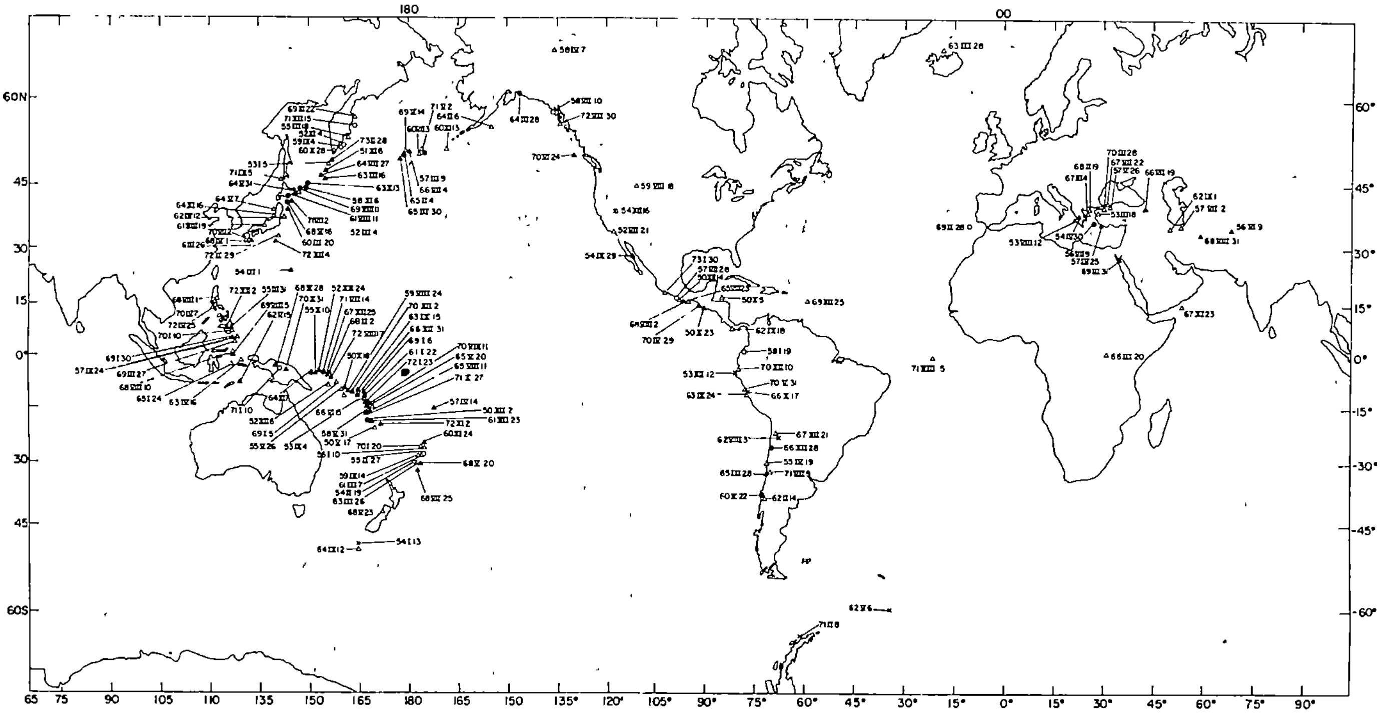

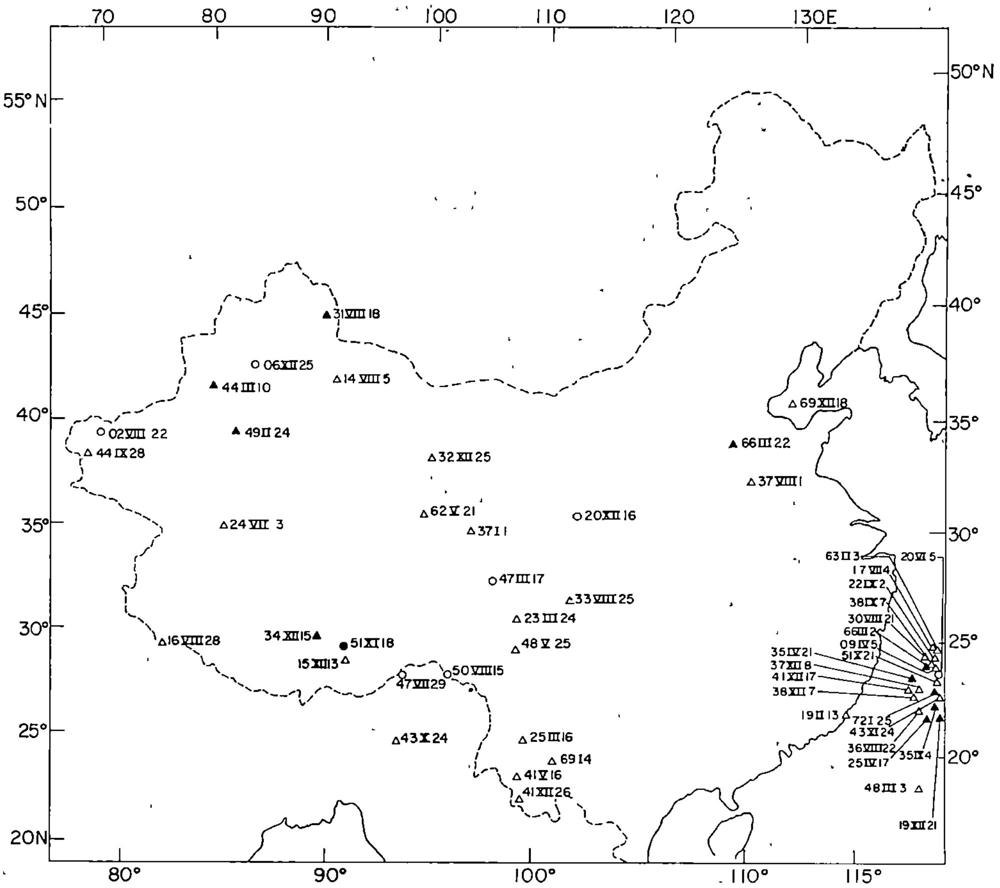

Fig. 3 Map of earthquakes in China. Symbols as in Fig. 2.

located teleseismically. Although foreshocks were the basis of the prediction of the 1975 Haicheng earthquake, none was teleseismically located by the US Geological Survey. We searched for field reports of the major events between 1950 and 1973, and found documentation of foreshocks in eight cases, for which no teleseismically located foreshocks were listed.

We sought possible correlations between the incidence of foreshocks and the magnitude or the tectonic setting of the earthquake, but no definite pattern emerged. Thirteen of the twenty-five great earthquakes ($M \geq 7.8$) had foreshocks, giving an incidence rate greater than 50%, but there are not enough data to make this conclusive.

That 44% of the earthquakes with $M \geq 7.0$ and at least three teleseismically located aftershocks were preceded by at least 1 teleseismically located foreshock suggests that foreshocks are a common occurrence. The Chinese have shown that they can be used to predict major earthquakes. The large number of locally recorded foreshocks preceding the 1965 Ceram Sea, 1966 Republic of Zaire, and 1968 Luzon earthquakes could have provided a data base comparable to that of Haicheng, and with adequate instrumentaion may have opened the door to prediction. That is not to say that all earthquakes can be predicted by foreshock activity, as there do not yet seem to be definitive methods for discriminating foreshock activity from background seismicity. Not all earthquakes, in fact, seem to be preceded by foreshocks. The February 9, 1971, San Fernando earthquake ($M = 6.6$) is an example[13]. Moreover, it is not obvious that the magnitude of an impending earthquake could be predicted by foreshocks alone.

Nevertheless, with the growing evidence of short term premonitory slip before major earthquakes[9,14–18], the frequent occurrence of foreshocks may indicate that premonitory fault slip or accelerated deformation in the focal area is a ubiquitous phenomenon preceding all major earthquakes. Indeed, the rapid increase of seismic activity before major earthquakes (Fig. 1) is similar to that of microfracturing observed in the laboratory[19]. Foreshock activity could well be the cause of many of the reports of anomalous animal behaviour. Together with aseismic deformation it could also be responsible for ground tilt, telluric current, magnetic field and well water level changes in the few days preceding major earthquakes. Thus it seems possible that all short term (and perhaps long term[18]) premonitory phenomena are a consequence of either seismic or aseismic slip before major earthquakes.

We thank W. F. Brace and F. Press for interest and encouragement. This research was supported by an Alfred P. Sloan fellowship and by the National Science Foundation.

LUCILE JONES
PETER MOLNAR

Department of Earth and Planetary Sciences,
Massachusetts Institute of Technology,
Cambridge, Massachusetts 02139

Received June 14; accepted June 23, 1976.

[1] Anon., *Paper distributed at Intergovernmental Conference on Mitigation of Earthquake Risk, UNESCO, Paris, February 10–19* (1976).
[2] Li, Teh-run, *Earthq Frontiers*, 2, 8–9 (1975).
[3] Adams, R. D., *Bull N.Z. natn. Soc. Earthq. Engng* (in the press)
[4] Zhong Guo Di Zhen Mu Lu, *Chronological Tables of Earthquake Data of China*, 1653 (Academica Sinica, Pekin, 1970).
[5] Duda, S., *Tectonophysics*, 2, 409 (1965).
[6] *United States Earthquakes*. 1965–1973 (US Govt Printing Office, Washington, DC, 1967–1975)
[7] Evernden, J F , *Bull Am. seism Soc* , 60, 393 (1970).
[8] Evernden, J. F , *Bull. Am. seism Soc.*, 61, 241 (1971)
[9] Immamura, A., *Theoretical and Applied Seismology*, 55–57 (Maruzan, Tokyo, 1937).
[10] Richter, C. F., *Elementary Sesimology* (Frerman, New York, 1958).
[11] Lahr, J , and Pomeroy, P. W., *Bull Am seism. Soc.*, 60, 1245 (1970).
[12] Su, S. S , *Bull. Am seism Soc.*, 59, 459 (1969).
[13] Allen, C R., *et al.*, *Prof. Pap. US geol. Surv.*, 733, 17 (1971).
[14] Thatcher, W R., *Science*, 184, 1283 (1974).
[15] Thatcher, W. R., *J. geophys Res.*, 80, 4862 (1975)
[16] Kanamori, H., and Cipar, J., *Phys. Earth planet Interiors*, 9, 128 (1974)
[17] Kanamori, H., and Anderson, D. L., *J. geophys. Res.*, 80, 1075 (1975)
[18] Johnston, M. J. S., and Morgenstern, C. E., *Science*, 186, 1031 (1974).
[19] Scholz, C. H., *J. geophys. Res.*, 73, 1417 (1968).

Semiconductor liquid junction solar cells based on anodic sulphide films

ALTHOUGH good performance has been achieved with established solid state junction solar cells, their cost remains well above that required for large scale terrestrial applications. New concepts[1,2] for photovoltaic energy conversion have been introduced which involve the junction between a semiconductor and an electrolyte. These schemes may lead to new possibilities of considerably reduced materials and fabrication costs, providing that many technical problems could be solved. We report here metal–semiconductor–liquid electrolyte junctions in which an n-type sulphide semiconductor is anodically formed *in situ* on its metal and, under photoexcitation, drives a sulphide–polysulphide redox couple when connected to a suitable cathode. The original contribution in this area was made by Gerischer[2] who demonstrated that the cell (single crystal *n*-CdS/$Fe(CN)_6^{4-}$, $Fe(CN)_6^{3-}/SnO_2$) has an initial conversion efficiency > 5% (ref. 3) for sunlight to electric power, in spite of the 2.4-eV band gap of CdS, which implies that wavelengths > 550 nm (the greater part of the incident solar photons) are ineffective.

In the Gerischer cell, photoexcitation of an n-CdS single crystal causes the transfer of holes to the reduced form of the redox couple and forms the anode of the solar battery. The circuit is completed through the transparent cathode of doped SnO_2 at which $Fe(CN)_6^{3-}$ is reduced. As Gerischer has pointed out, the major problem in such a cell is that the reaction.

$$CdS+2h^+ \rightarrow Cd^{2+}+S \qquad (1)$$

competes with the desired hole injection

$$Fe(CN)_6^{-4}+h^+ \xrightarrow[CdS]{} Fe(CN)_6^{-3} \qquad (2)$$

and leads to rapid surface degradation. Such corrosion problems are inherent in most semiconductors with the exception of wide band gap materials such as n-TiO_2 used by Fujishima and Honda[1] for the photo-assisted oxidation of water.

Experience with CdS in this laboratory and elsewhere[4] has shown that the problem of poor stability can be reduced, at the expense of lowering the driving potential and thus the conversion efficiency, by using an aqueous Na_2S–Na_2S_x redox couple. The overall anode reaction

$$xS^{2-}+2(x-1)h^+ \longrightarrow S_x^{2-} \qquad (3)$$

competes more efficiently than reaction (2) with the corrosion path (1) because it proceeds at an electrode potential that is more negative by ~ 0.6 V. Additionally, any low level formation of sulphur can be prevented from covering the electrode by the dissolution reaction

$$S+S^{2-} \longrightarrow S_2^{2-} \qquad (4)$$

We show that polycrystalline CdS, anodically formed in the presence of Na_2S, can replace single crystal CdS in solar cells. The preparation of such cells is simple and inexpensive. Other metals may be used to produce sulphide semiconductors with responses into the infrared which overlap better with the spectrum of sunlight.

Electrodes were made from materials of ⩾ 99.99% purity using 10-mm sheet or cast rods of cadmium and bismuth cast from melted shot. The electrodes were defined by potting in epoxy resin. The current–voltage curves shown were obtained with rotating electrode disk configuration of active areas 0.429 cm² and 0.183 cm² for Cd and Bi, respectively. Counter-electrodes were either platinum or spectroscopic grade carbon rods. Spectra were obtained on stationary electrodes in vertical potted configurations. Potentials were measured against a standard calomel electrode (SCE).

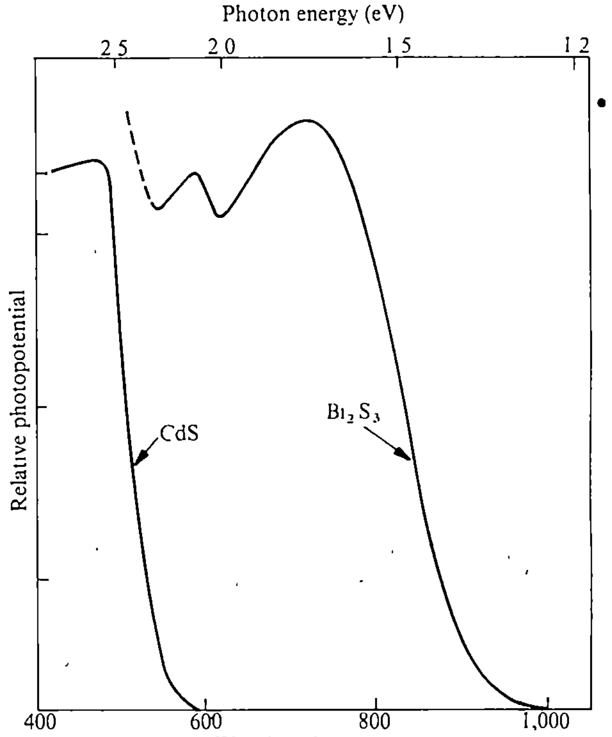

Fig. 1 Photoresponse spectra of the Cd/CdS electrode in 1F Na_2S and the Bi/Bi_2S_3 electrode in 1F Na_2S–0.05F S.

Cells with Pyrex windows at the side (vertical specimens) or the bottom (rotating disk electrodes) were used for appropriate illumination of the sample. For present purposes no attempt was made to optimise the design or electrode placement for power efficiency.

Solutions were prepared from reagent Na_2S and flowers of sulphur and were filtered before use. Spectra of the yellow polysulphide solution were obtained on a Cary 14 spectrometer.

For photoresponse spectra, electrodes were illuminated by 400-Hz chopped, monochromatic radiation obtained with a 650-W tungsten (iodine) lamp and a 1-m Spex Czerny–Turner grating monochromator. The electrochemical response was processed with a lock-in amplifier referred to the chopper frequency. A Corning 2-58 filter, which cuts off wavelengths < 6,300 Å, was used to prevent harmonic response at the higher wavelengths. The photoresponse spectra were corrected for

Fig. 2 Current–voltage characteristics of the non-illuminated and illuminated cells (*a*) Cd/CdS/Na_2S–Na_2S_x/C and (*b*) Bi/Bi_2S_3/Na_2S–Na_2S_x/C with electrolyte concentrations 1F Na_2S and 0.05F S.

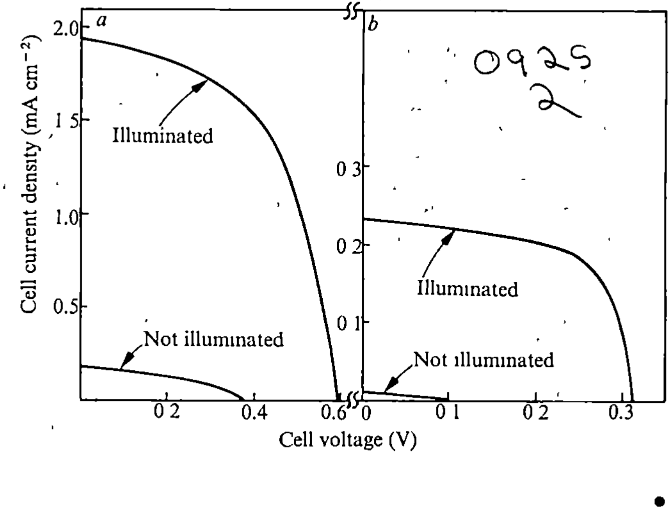

0925
2

monochromator throughput, light source spectrum, and solution absorbance.

The cells were activated by anodising the metal (Cd or Bi) in the Na_2S_x electrolytic solution. Anodisation could be accomplished both galvanostatically and potentiostatically. Following anodisation, the electrodes develop an opaque layer of the sulphide which, as expected, is yellowish in the case of CdS and black in the case of Bi_2S_3.

The electrochemical control circuitry used a conventional operational amplifier galvanostat–potentiostat. Photovoltaic cell operation was simulated by applying constant or linearly scanned currents in the spontaneous direction (Cd or Bi sulphides anodic) and then measuring the cell voltage (counter-electrode positive) and/or the potential of the photoelectrode against SCE which separated out any appreciable polarisation from the counterelectrode reaction. Photo-response spectra were obtained by chopping the incident beam and using as synchronously chopped output either (a) the potential relative to the counterelectrode or the SCE at open circuit or constant load current or (b) the current output when the photoelectrode was operated potentiostatically. The spectral response was found to be independent of the mode of operation or load.

The two cells considered in this work are

$$Cd/CdS/Na_2S\text{–}Na_2S_x\,(aq)/C$$

and

$$Bi/Bi_2S_3/Na_2S\text{–}Na_2S_x(aq)/C$$

The anode reaction of these cells is shown in equation (3). The cathode reaction is

$$S_x^{2-}+2(x-1)e^- \rightarrow xS^{2-} \qquad (5)$$

As noted from the sum of equations (3) and (5), there is no net chemical change in the functioning cells.

Figure 1 shows the photoresponse spectra of the n-CdS and n-Bi_2S_3 surfaces formed by anodisation in 1F Na_2S and 1F Na_2S–0.05F S respectively. As expected from the 2.4-eV band gap of CdS (ref. 5), the response of the electrode starts declining at 480 nm and becomes negligible at 580 nm. The band gap of Bi_2S_3 is ~ 1.3–1.4 eV (refs 6, 7) and the photoresponse is observed even at 900 nm, as expected. This response overlaps a substantial part of the solar spectrum after atmospheric filtering[8].

The current–voltage curves of Cd or Bi disk electrodes paired with a carbon rod cathode in very low level light and with illumination are shown in Fig. 2. The curves of both CdS and Bi_2S_3 are reasonably close to being rectangular, indicating no dominating internal resistance losses. The changes in cell voltage and the changes in the Cd or Bi potentials measured against the reference electrode (SCE) are nearly identical, and the latter are not shown. Overpotentials attributable to the carbon cathode appear to be negligible with the large cathode/anode area ratio of these cells.

The open circuit voltage of the $Cd/CdS/Na_2S\text{–}Na_2S_x/C$ solar cell under illumination is 0.59 V (see Fig. 2) or about half that reported by Gerischer[2] for the CdS (single crystal)/Fe (CN)-$_6{}^{3-,4-}$/SnO_2 system. This difference results from the higher Fermi level (redox potential) of the Gerischer solution. Sacrifice of part of the working potential leads to a cell which does not deteriorate by oxidation of surface sulphide to sulphur during operation.

It is apparent that the technique can easily be extended to other sulphides or anodic films. Considerable work remains to be done to establish whether efficiency and long term stability can be brought to levels that would make such cells practical for terrestrial solar energy conversion.

A helpful discussion with E. A. Chandross is gratefully acknowledged.

BARRY MILLER
ADAM HELLER

Bell Laboratories,
Murray Hill, New Jersey 07974

Received May 24, accepted July 2, 1976

[1] Fujishima, A., and Honda, K , *Nature*, 238, 37–38 (1972).
[2] Gerischer, H., *J electroanalyt. Chem.*, 58, 263–274 (1975)
[3] Gerischer, H , and Gobrecht, J , *Ber. Bunsenges phys Chem.*, 80, 327–333 (1976).
[4] Ellis, A B., Kaiser, S. W , and Wrighton, M W , *J. Am. Chem., Soc.* 98, 1635–1637 (1976).
[5] Balkanski, M., and Waldron, R D , *Phys. Rev.*, 112, 123–135 (1958).
[6] Black, J F., Conwell, E M , Seigle, L., and Spencer, C. W., *J. Phys. Chem. Solids*, 2, 240–251 (1957).
[7] Gildart, L., Kline, J. M., and Mattox, D. M., *J Phys. Chem Solids*, 18, 286–289 (1961)
[8] Archer, M D , *J appl Electrochem.*, 5, 17–38 (1975)

Opto-acoustic spectroscopy of products of continuous photolysis of nitromethane

THE photolysis of nitromethane has been carried out with both continuous (see ref. 1) and flash sources (see ref. 2), but for continuous photolysis no concurrent spectroscopy has been reported. This is in general true of most photolysis experiments, since the steady-state concentration of intermediates produced by continuous sources is usually insufficient to record spectra without depending on some matrix isolation procedure. We report here on gas phase continuous wave photolysis experiments using opto-acoustic detection of the energy absorbed by intermediates from a continuous wave (CW) tunable dye laser[3]. This allowed the detection of intermediate concentrations of ~ 10^{13} mol cm^{-3}. Opto-acoustic detection was discovered by Bell[4] nearly a century ago, but was recently revived as a means of monitoring low concentrations of pollutant molecules[5,6]. In our experiments the intermediates act as the 'pollutant' molecules to be detected.

The reaction vessel was a 5-cm long block of stainless steel through which a channel 0.5 cm × 1.0 cm had been cut. This channel was connected to a sidearm containing a sensitive microphone and to a small reservoir containing the sample. Two quartz windows sealed the ends of the channel. The unchopped and unfiltered output from a 250-W medium pressure Hg lamp was focused down to pass through the channel from one end. Tunable CW dye laser radiation, chopped at ~ 1.4 kHz, passed through the cell in the opposite direction. If the incoming chopped radiation is absorbed by a constituent in the cell that part of the absorbed energy degraded to heat will, in a constant volume enclosure, set up a modulated pressure wave at 1.4 kHz detected by the microphone.

Previous experiments[2] on pure nitromethane yielded evidence of nitroxyl and formaldehyde production together with OH and CN radicals. Neither nitrogen dioxide nor nitrosomethane were detected in these conditions, whereas they had been detected in the presence of excess nitrogen. Since the primary process is most probably

$$CH_3NO_2 \rightarrow CH_3+NO_2 \qquad (1)$$

NO_2 at least should be formed in the photolysis of pure CH_3NO_2, and indeed was detected by electron paramagnetic resonance (EPR) measurements[7].

Figure 1*a* shows the opto-acoustic spectrum between 580 and 610 nm obtained from a sample of pure nitromethane at a temperature of 50 °C (pressure ~ 90 mmHg) under continuous photolysis. It was confirmed that, before photolysis commenced, no signal in this wavelength region existed. The spectrum of Fig. 1*a* thus corresponds to a species created by the photolysis. Figure 1*b* shows the spectrum obtained on buffering the nitromethane with 275 mmHg of argon and Fig. 1*c* using 275 mmHg

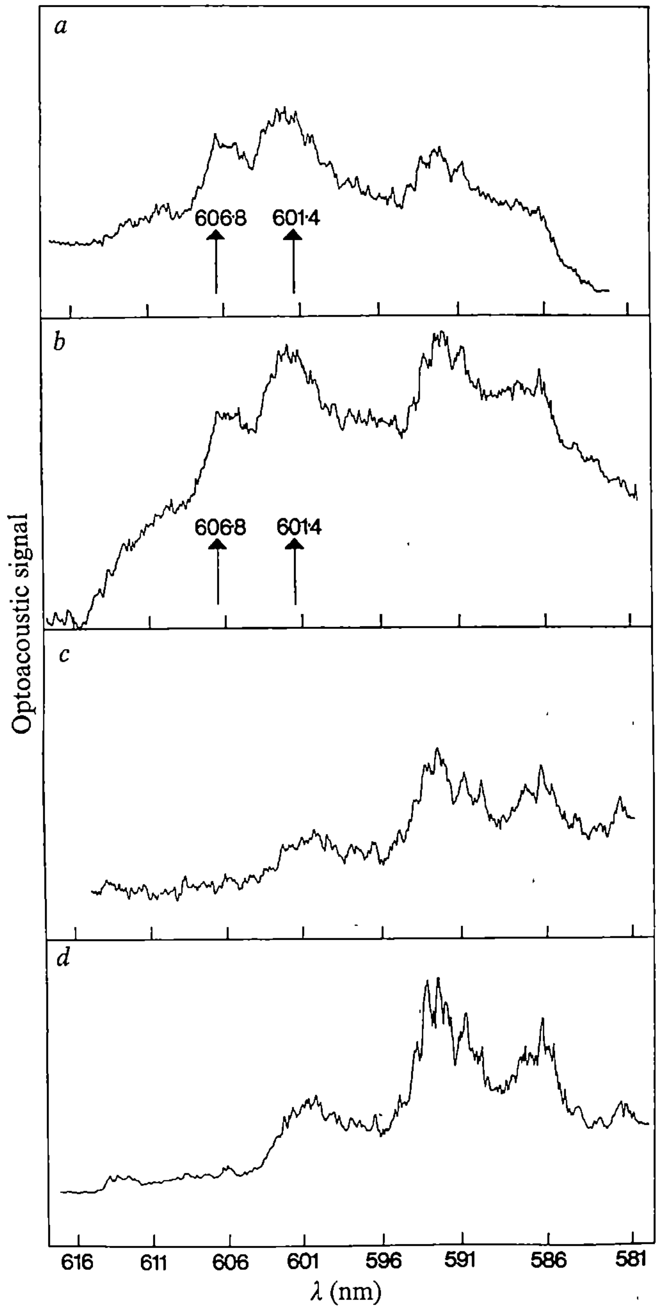

Fig. 1 Opto-acoustic spectra of CH_3NO_2 during continuous photolysis: *a*, pure CH_3NO_2; *b*, CH_3NO_2 in 275 mmHg argon; *c*, CH_3NO_2 in 275 mmHg oxygen; *d*, Opto-acoustic spectrum of 3×10^{-4} mmHg NO_2 in 300 mmHg N_2. (The spectra are uncorrected for the smooth variation in dye laser power output over its tuning range.)

of oxygen as a buffer. For comparison we show the spectrum of NO_2 taken in the same cell (but without the photolysis lamp) at ~ 3×10^{-4} mmHg in 300 mmHg of N_2. It is evident from a comparison of the spectral features ~ 586 and 590 nm that we are recording the presence of NO_2 at levels ~ 10^{-4} mmHg during the photolysis of nitromethane. The additional features at 607 and 610 nm disappear when oxygen is used as a buffer (Fig. 1*c*) leaving the pure NO_2 spectrum. The spectrum towards longer wavelengths of this second product is shown in Fig. 2, again from the photolysis of CH_3NO_2 in argon at 50 °C. From the positions of the band centres by comparison with those given by Dixon and Kroto[8] we can identify this product as nitrosomethane. It was confirmed in a separate experiment that NO_2 absorption in this region and at the concentrations inferred from Fig. 1*c* was not contributing >10% to the observed signal. In addition, its spectrum is markedly different to that of the nitrosomethane. We conclude that the spectrum of Fig. 2 is that of CH_3NO and that the features on the long wavelength end of the NO_2 spectrum of Fig. 1*a* and *b* come from the tail of CH_3NO absorption.

The build up of both CH_3NO and NO_2 on initial exposure took the same time of ~ 10 s. Similarly, the decay, a non-exponential with a fast initial fall changing gradually to give a long tail lasting ~ 20 min, was the same for both products. This decay behaviour was very different when O_2 was used as a buffer. In this case the NO_2 signal initially increased by ~ 20% and then followed a slower decay of up to ~ 30 min.

These results are consistent with the following set of secondary reactions following the primary split 1.

$$CH_3+NO_2 \rightarrow CH_3O+NO \quad (2)$$
$$CH_3+NO \rightarrow CH_3NO \quad (3)$$
$$NO_2 \xrightarrow{h\nu} NO+O \quad (4)$$
$$CH_3+NO_2 \rightarrow CH_3NO_2 \quad (5)$$
$$CH_3NO+NO_2 \rightarrow CH_3NO_2+NO \quad (6)$$
$$CH_3O+NO_2 \rightarrow CH_3ONO_2 \quad (7)$$

It is clear that in our relatively cool photolysis conditions and low intermediate concentrations (2) and (4) produce enough NO to yield measurable quantities of CH_3NO, whereas in the flash photolysis of Napier and Norrish[2] added amounts of NO were required before CH_3NO was detected. The alternative reaction[2]

$$CH_3O+NO \rightarrow HNO+CH_2O \quad (8)$$

is presumably less efficient than reaction (3). (We did not observe nitroxyl formation but, since its spectrum[9] would be partially obscured by nitrosomethane, we do not rule out its formation.)

Reaction (6) (ref. 10) accounts for the identical bimolecular decay nature of NO_2 and CH_3NO although at some stage reaction (7) and the formation of nitrosomethane dimers become important[2]. The change in decay behaviour of the NO_2 in the

Fig. 2 Opto-acoustic spectrum (620–650 nm) of CH_3NO_2 in 275 mmHg of argon during continuous photolysis. Arrows mark the positions of band centres assigned to nitrosomethane (from Dixon and Kroto[8]).

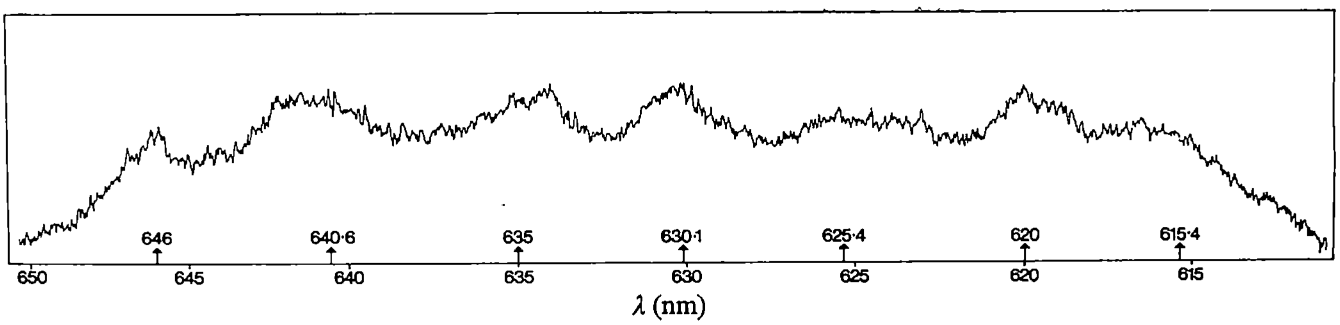

O_2 mixtures, that is, without CH_3NO formed, is strong evidence for the influence of reaction (6). With O_2, CH_3NO formation is quenched, presumably by

$$2CH_3+O_2 \rightarrow 2CH_3O \qquad (9)$$

or similar processes, and

$$CH_3NO+O_2 \rightarrow CH_3ONO_2 \qquad (10)$$

and the decay of NO_2 governed solely by reaction (7). The rise in the NO_2 signal on removing the photolysing source probably arises from recombination of excess NO with oxygen.

We are indebted to Dr J. Pfab for helpful discussions. This research was supported by the SRC.

M. J. Colles
A. M. Angus
E. E. Marinero

Department of Physics,
Heriot-Watt University,
Edinburgh, UK

Received May 21; accepted July 7, 1976.

1. Honda, K., *et al.*, *Bull. chem. Soc. Japan*, **45**, 3534 (1972).
2. Napier, I. M., and Norrish, R. G. W., *Proc. R. Soc.*, **299**, 317 (1967).
3. Marinero, E. E., Angus, A. M., and Colles, M. J., *Opt. Commun.*, **14**, 223 (1975).
4. Bell, A. G., *Phil. Mag.*, **11**, 510 (1881).
5. Angus, A. M., Marinero, E. E., and Colles, M. J., *Opt. Commun.*, **14**, 226 (1975).
6. Kreuzer, L. B., *J. appl. Phys.*, **42**, 2934 (1971).
7. Bielski, B. H., and Timmons, R. B., *J. phys. chem.*, **68**, 342 (1964).
8. Dixon, R. N., and Kroto, H. W., *Proc. R. Soc.*, **283**, 423 (1965).
9. Dalby, F. W., *Can. J. Phys.*, **36**, 1336 (1958).
10. Phillips, L., and Shaw, R., *10th Symp. Combustion, Connbridge*, 453 (1964).

New light on the skull anatomy and systematic position of *Oviraptor*

Oviraptor philoceratops Osborn, 1924—a plunderer allegedly fond of ceratopsian eggs—is an Upper Cretaceous vertebrate assigned to the theropod dinosaurs[1]. The holotype, comprising a compressed skull with mandibles, several cervical vertebrae, fragmentary shoulder girdle and forelimbs, was found in the Djadokhta Formation (?Santonian), Gobi Desert, Mongolia. For many years this was the only specimen known and its poor preservation showed only that *Oviraptor* was a toothless bipedal animal, with a lightly built skull, unusually short and deep. The lack of teeth and the structure of the manus were the main arguments for assigning it to the family Ornithomimidae[1,2].

In 1970 and 1971 the Polish–Mongolian palaeontological expeditions to Mongolia found two skulls (Fig. 1) of *Oviraptor* sp. with a few postcranial fragments in the Khermeen Tsav Formation (?Middle Campanian) as well as a fragmentary skull in the Nemegt Formation (?Upper Campanian—? Lower Maastrichtian), all in the Gobi Desert[3]. This material is housed in the Zaklad Paleozoologii (ZPAL) in Warsaw and I am now studying it. Five skeletons with skulls of *Oviraptor* sp. were found in 1972 by the Soviet–Mongolian palaeontological expeditions in the Khermeen Tsav formation[4]. This latter material is being studied by Dr R. Barsbold (Institute of Geological Sciences, Ulan Bator). All the specimens found recently belong to a new species. As the material being investigated by Barsbold is more complete than that at my disposal, I leave him to name and diagnose the new species, referring here to the forms housed in Warsaw as *Oviraptor* sp.

In the light of this new material the systematic assignment of *Oviraptor* may be questioned. The structure of the palate (Fig. 1*e*, *f*) is completely different from the palate of all other known dinosaurs. Its most striking feature is the form of the pterygoids. They are massive bars, with their lateral portions turned strongly ventrad. The ectopterygoids, which in all other dinosaurs are directed transversely, joining the pterygoids with the jugal arches, lie parasagittaly in *Oviraptor* and join the ptergoids with the maxillae, medial to the anterior roots of the jugal arches. Such a pterygoid–ectopterygoid structure is highly convergent with the dicynodont reptiles. The same may be said of the anterior palatal region formed of the premaxillae and maxillae, which bears a pair of ridges along its medial portion. Each maxilla in *Oviraptor* sp. produces a 'tooth' posteriorly, which is directed ventrally (Fig. 1*a*, *b*) and lies very close to its fellow. These 'teeth' are buttressed posteriorly by the thickened vomer. They do not bear any trace of wear and were therefore evidently covered in by a horny or soft tissue. The position of the palatine bones in *Oviraptor* is also different from that in other dinosaurs. The medial wings of the palatines border the choanae posteriorly, but laterally they form the ventral links between the maxillae and the ectopterygoids in a manner never seen in other dinosaurs.

Another unusual feature in a dinosaur is the very strong pneumatisation of the skull bones, especially those of the roof and snout. The nasals, in addition to being pneumatised as a whole, each bear a large air chamber connected with the external nare.

The endocranial cavity is well exposed on the two skulls I have studied, and is unusually large for a dinosaur, relative to the size of the skull. The approximate length of the cavity of the skull ZPAL No. Mg-I/95, measured from the foramen magnum to the dorsal border of the exit of the optic nerve, is 40 mm; its height (at the level of the optic nerve) is 17 mm; and its maximal width (just in front of the optic nerve) is 27 mm. The length of the skull is only 98 mm. The rapid broadening of the endocranial cast in front of the optic lobes is very striking, and corresponds to the position of the cerebral hemispheres, its total width almost double that of the diencephalon. The olfactory tracts must have been very short, as judged from the preserved portion of the endocranial cavity and from the close position of the external nares. Such a structure in the olfactory part of the brain seems to be non-dinosaurian and even non-reptilian (pterosaurs excluded).

The structure of the mandible of *Oviraptor* is also very different from that of other dinosaurs, and it was investigated in detail using the new material housed in Warsaw. The *Oviraptor* mandible (Fig. 1*g*, *h*) is basically similar to those described as *Caenagnathus collinsi* Sternberg, 1940 (ref. 5) and *C. sternbergi* Cracraft, 1971 (ref. 6) and assigned to the birds. The mandibles of *Caenagnathus* and *Oviraptor* have a similar shape, the same relationships between the bones and an identical articular region, consisting of a low ridge directed anteroposteriorly. They differ mainly in their proportions. Cracraft[6] noticed that the jaw of *Caenagnathus* is structurally convergent with that of the dicynodonts; and this is in perfect agreement with my study of the skull of *Oviraptor*. *Oviraptor* and *Caenagnathus* should thus be assigned to the same family, Caenagnathidae Sternberg[5].

Should the Caenagnathidae, however, be considered as birds? It is hardly possible that they are birds, taking into account the fact that known forelimbs of *O. philoceratops* do not show any distinct avian adaptations. In fact, the manus structure of this animal, with its three clawed digits subequal in length, conforms to that of the ornithomimids. The generally saurischian and theropod postcranial skeleton (confirmed by the Soviet–Mongolian expeditions; R. Barsbold, personal communication) may be evidence that, in spite of all the differences mentioned here, the Caenagnathidae should be regarded as theropod dinosaurs. Their skull structure is so peculiar, however, that long independent evolution of the group must be presumed. The caenagnathids may represent a Cretaceous continuation of the same dinosaur lineage that gave rise to the birds[7]. This could

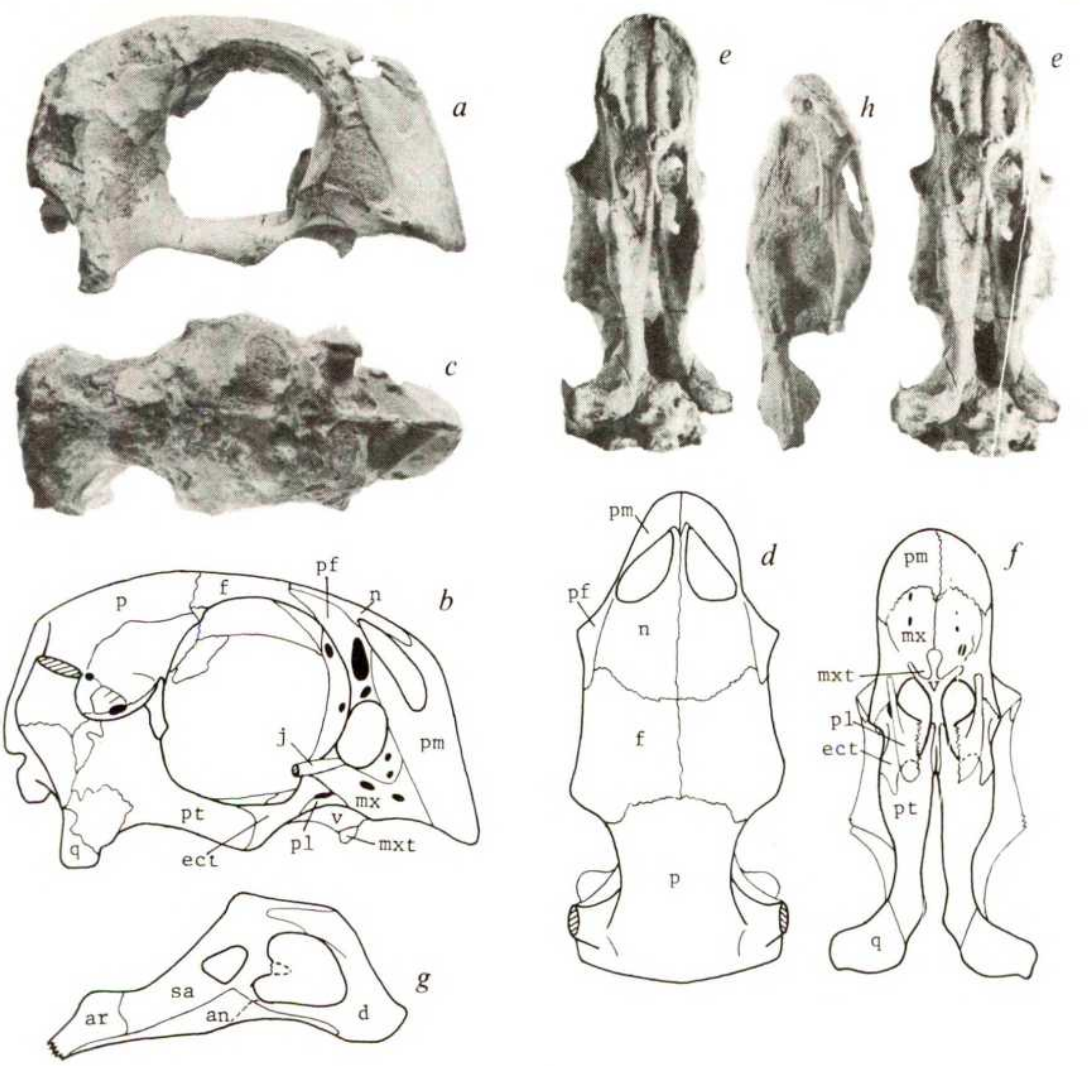

Fig. 1 *Oviraptor* sp. ZPAL No. MgD-I/95 skull lacking temporal and jugal arches: *a*, *b*, lateral view; *c*, *d*, top view; *e*, stereophotograph, palatal view; *f*, palatal view; *g*, mandible of the same specimen, lateral view; *h*, ventral view (approx. ×0.59). an, Angular; ar, articular; d, dentary; ect, ectopterygoid; f, frontal; j, jugal; mx, maxilla; mxt, maxillary 'tooth'; n, nasal; p, parietal; pf, prefrontal; pl, palatine; pm, premaxilla; pt, pterygoid; q, quadrate; sa, surangular; v, vomer.

explain the presence of some para-avian characters in the caenagnathid skull, such as the separation of the pterygopalatine complex from the jugal arch, the pneumatisation of the skull, the possible enlargement of the brain with the simultaneous shortening of the olfactory tracts and some structural characteristics of the mandibles. For these reasons it is not possible to assign the Caenagnathidae to any of the known theropod infraorders. A new suprafamilial taxon will have to be established as soon as the new material of *Oviraptor* has been described.

HALSZKA OSMOLSKA

Polska Akademia Nauk,
Zaklad Paleozoologii,
02-089 Warszawa,
al. Zwirki i Wigury 93, Poland

Received May 3; accepted June 25, 1976.

[1] Osborn, H. F., *Am. Mus. Novit.*, **144**, 1–12 (1924).
[2] Romer, A. S., *Osteology of Reptiles* (University of Chicago Press, Chicago, 1956).
[3] Kielan-Jaworowska, Z., and Barsbold, R., *Palaeont. pol.*, **27**, 5–13 (1972).
[4] Kramarenko, N. N., *Trudy Sovm. Sov.-Mong. Pal. Exped.*, **1**, 5–18 (1974).
[5] Sternberg, R. M., *J. Paleont.*, **14**, 81–85 (1940).
[6] Cracraft, J., *J. Paleont.*, **45**, 805–809 (1971).
[7] Ostrom, J. H., *Nature*, **242**, 136 (1973); *Biol. J. Linn. Soc.*, **8**, 91–182 (1976).

Hallucial tarsometatarsal joint in an Oligocene anthropoid *Aegyptopithecus zeuxis*

SINCE the grasping hallux is such a significant characteristic of the order Primates, its evolutionary history is of some importance to palaeoprimatologists. Although the origin and development of the grasping hallux in primates is usually hailed as a major "evolutionary event", very little factual data from the palaeontological record can be brought to bear in documenting this feature throughout primate evolution[1]. Two fossil primates in which an hallucial metatarsal is known are *Notharctus* (an Eocene prosimian) and *Dryopithecus africanus* (a Miocene hominoid); hence the specimen discussed here is the earliest document of hallucial morphology in the anthropoids[2,3].

The earliest known postcranial remains of fossil anthropoids are from the Oligocene Jebel el Qatrani Formation of the Fayum badlands, Egypt. Most of the primate skeletal remains have been referred to the parapithecid *Apidium phiomense*; one ulna has been referred to *Aegyptopithecus zeuxis*[4,5]. Included among the various mammalian postcranial remains is an hallucial metatarsal of an anthropoid primate which was discovered by E. L. Simons at Yale

Quarry I in the Upper Fossil Wood zone. This is the quarry that has yielded mandibular and/or maxillary dental remains of several primate genera—*Parapithecus, Apidium, Aeolopithecus* and *Aegyptopithecus*[6]. Of these fossil primates, only *Aegyptopithecus* could have had a hallax as large as that suggested by the fossil hallucial metatarsal. For this reason the specimen is here referred to *Aegyptopithecus zeuxis.*

The specimen (YPM 25806) consists of the proximal two-thirds of a right hallucial metatarsal (Fig. 1). The bone is perfectly preserved except for a small sliver missing from its medial side. The proximal articular surface for the medial cuneiform is complete and undistorted. Its overall size suggests an animal whose body weight might be approximated by *Ateles belzebuth* (Fig. 2).

fig 1

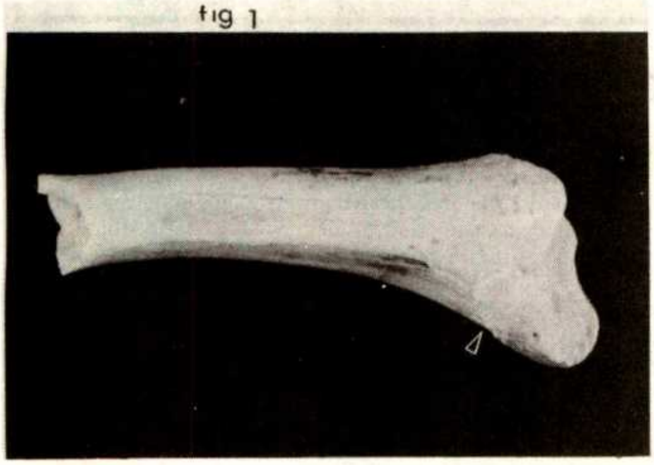

Fig. 1 Medial view of right hallucial metatarsal of *Aegyptopithecus zeuxis* (YPM 25806). Note prehallucial facet (arrow).

Much information concerning the morphology of the primitive anthropoid hallucial tarsometatarsal point can be gathered through examination of the proximal articular surface of the hallucial metatarsal of *Aegyptopithecus zeuxis.* Of particular interest is a well defined, raised oval facet on the medioplantar aspect at the base of the metatarsal. This undoubtedly reflects the fact that a large prehallux bone participated in the hallucial tarsometatarsal joint. Thus, this joint consisted of three bones in primitive anthropoids, the first metatarsal, medial cuneiform and prehallux. This condition is unlike that of any extant Old World monkey or great ape; it is seen in most platyrrhines and hylobatids[7]. On the lateral plantar aspect of the metatarsal base is a large, blunt, bony projection for the insertion of M. peroneus longus tendon. This muscle, an everter of the tarsus and an adductor of the hallux, was obviously large in this primitive, arboreal fossil ape. In contrast, *Simopithecus,* a large, terrestrially adapted Pleistocene monkey, had a rather small peroneus longus muscle. This is evidenced by the relatively small peroneal tubercle and the small facet for the peroneus longus sesamoid on the cuboid[8]. The Fayum metatarsal also has a rather pronounced longitudinal curvature, indicative of strong flexor tendons[9].

fig 2

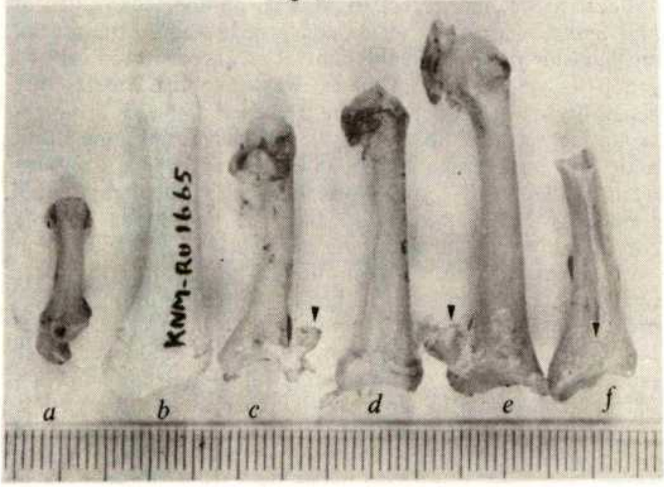

Fig. 2 Comparison of hallucial metatarsals of several primates. *a, Galago crassicaudatus; b, Dryopithecus africanus; c, Cebus nigrivittatus; d, Hylobates hooloch; e, Ateles belzebuth; f,* YPM 25806. Note the attached prehallux in *Cebus* and *Ateles* and prehallucial facet on YPM 25806 (arrows).

The shape of the joint surface itself, for articulation with the medial cuneiform, is essentially a concave ovoid with a nearly vertical axis around which abduction–adduction took place (Fig. 3). The ovoid widens in a plantar direction, thus producing an effect where the plantar surface of the metatarsal rotates around a greater arc than the dorsal surface. Because any point which traverses an arc along an ovoid surface will undergo conjunct rotation, this morphology is advantageous in any joint where opposition is desirable[10]. Thus, as the metatarsal moves over the articular surface of the medial cuneiform it undergoes conjunct rotation and comes more into opposition with the lateral four digits. The prehallux would have completed the joint surface at the medioplantar border. The dorsal and lateral margins of the metatarsal base show rugosities for tarsometatarsal ligaments. During adduction of the hallux, the plantar surface of the bone would have been oriented towards the lateral digits as in opposition. This is due to the morphology of the joint surface itself (see above) and to the fact that the shaft of the metatarsal shows a high degree of torsion in this direction. This torsion is evidenced by the fact that the greatest diameter of the shaft in cross section is nearly parallel to the vertical axis of the hallucial base.

fig 3

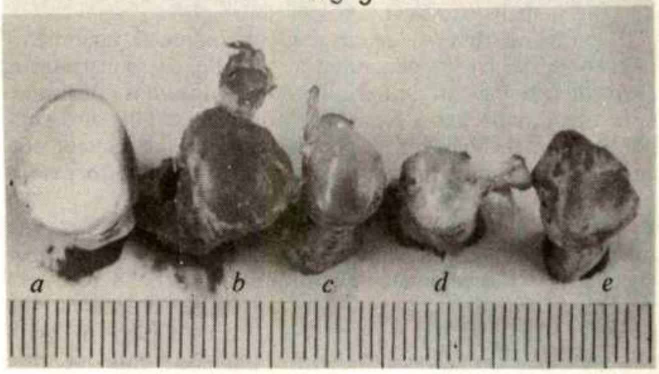

Fig. 3 View of proximal articular surface of hallucial metatarsals. *a, Dryopithecus africanus; b, Ateles belzebuth; c, Hylobates hoolock; d, Cebus nigrivattatus; e,* YPM 25806.

Lewis has described the hallucial tarsometatarsal joint in anthropoids, and his predictions concerning the morphology of the hallucial tarsometatarsal joint in primitive anthropoids can be verified by the fossil evidence presented here[7]. He has shown that in primitive mammals (for example, *Didelphis*) an hallucial prolongation of the flexor tibialis muscle (the homologue of the M. flexor digitorum longus in the human) contains the prehallux. When the prehallux occurs in primates it forms an integral part of the hallucial tarsometatarsal joint and is invariably associated with the dual insertion of tibialis anterior into it and the medial cuneiform. The prehallux, judging from the shape of its articular facet on the hallucial metatarsal of *A. zeuxis,* had a sellar-shaped articular surface and formed part of a true synovial joint, as do most sesamoid bones in the body. Sellar-shaped surfaces are characteristic of joints which have opposition as a habitual movement[10]. The prehallux, or a cartilagenous remnant, is characteristic of

Ceboidea but not Ceropithecoidea. Among Hominoidea, it is seen in Hylobatidae but not Pongidae[7].

It is perhaps interesting that a vestigial prehallux is occasionally found in modern man[11-13]. The so-called "os paracuneiforme" was first described clinically in 1902 (ref. 14). Although surgeons were unsure of what this small accessory bone really represented, evidence now suggests that it is the vestige of the primitive anthropoid prehallux (my unpublished results). The "os paracuneiforme", like the prehallux, articulates with the medial cuneiform and is protected by an overlying bursa; as in anthropoids, the bone is partly incorporated in the substance of the tibialis anterior tendon. It is still unclear whether or not this is a true accessory bone or a sesamoid[15]. Alternatively, it might represent one of the unfused multiple ossification centres in the epiphysis of the metatarsal[16]. It seems most likely, however, that it is a sesamoid formed by pressure in the tendon of tibialis anterior as it passes over the medial cuneiform; indeed, such bones sometimes occur late in life in this position[17]. Experimental evidence on the patella, the largest sesamoid in the body, suggests that both phylogenetic and ontogenetic factors are responsible for the formation of sesamoid bones. For example, development of the patella has followed transplantation of limb bud fragments from chick embryos to the chorioallantoic membrane of other host embryos[18]. Conversely, patellar cartilage and bone which has been removed from young dogs will regenerate from young connective tissue cells which had not been destined as specific formers of bone if the tendon of the quadriceps femoris is sutured to the patellar ligament and the joint is exercised[19].

The finding that *A. zeuxis* had an hallucial tarsometatarsal joint which incorporated a prehallux demonstrates a clear morphological similarity between this most primitive anthropoid and extant New World primates. This also supports recent evidence that the postcranial skeleton of the earliest anthropoids in general was more similar to extant platyrrhines than to catarrhines[4,20].

The morphological similarities between the Oligocene primates of the Fayum and extant platyrrhines have led to speculations regarding an African origin for the New World primates through rafting across the South Atlantic in the early Tertiary. Such a voyage seems hard to reconcile with the geophysical evidence suggesting that the South Atlantic was 3,000 km wide by Oligocene times[21]. Others have suggested that some primate family with a holarctic distribution in the Eocene (Adapidae?) might have given rise to both New and Old World anthropoids by the early Oligocene[22]. One point is becoming increasingly clear however—platyrrhines are the best models for depicting the earliest stages of anthropoid postcranial and locomotor evolution. Lewis' contention that the earliest anthropoids must have possessed an hallucial tarsometatarsal joint including a prehallux is undoubtedly correct. It is interesting that *Dryopithecus africanus*, a putative descendant of *A. zeuxis*, also apparently had a prehallux incorporated into its hallucial tarsometatarsal joint[7]. Thus there is nothing in the anatomy of the hallucial tarsometatarsal joint which would preclude *Aegyptopithecus* from being broadly ancestral to later dryopithecines and hylobatids.

I thank Professor E. L. Simons for permission to study fossils collected by his expeditions to the Fayum and Professors C. Jolly and M. Schon for comments on the manuscript.

GLENN C. CONROY

Department of Cell Biology,
New York University Medical Center and
Department of Anthropology,
New York University,
New York, New York 10016

Received May 6; accepted June 29, 1976.

[1] Le Gros Clark, W., *Antecedents of Man* (Edinburgh University Press, Edinburgh, 1959).
[2] Gregory, W., *Mem. Am. Mus. Nat. Hist.*, **3**, 49–243 (1920).
[3] Napier, J., and Davis, P., *Foss. Mamm. Afr.*, **16** (1959).
[4] Conroy, G., *Contrib. Primat.*, **8**, 1–134 (1976).
[5] Fleagle, J., Simons, E., and Conroy, G., *Science*, **189**, 135–137 (1975).
[6] Simons, E., *Primate Evolution* (Macmillan, New York, 1972).
[7] Lewis, O., *Am. J. Phys. Anthrop.*, **37**, 13–34 (1972).
[8] Jolly, C., *Bull. Br. Mus. Nat. Hist. (Geol.)*, **22**, 1–123 (1972).
[9] Preuschoft, H., *Symp. fifth Int. Primat. Soc.*, 345–359 (1974).
[10] MacConaill, M., *J. Bone Jt Surg.*, **35B**, 290–297 (1953).
[11] Morrison, A., *J. Bone Jt Surg.*, **35B**, 254–255 (1953).
[12] Zimmer, E., *Acta Radiol.*, **34**, 102–114 (1950).
[13] O'Rahilly, R., *J. Bone Jt Surg.*, **35A**, 626–642 (1953).
[14] Dwight, T., *Anatomischer Anzieger*, **20**, 465–472 (1902).
[15] Haines, R., *Biol. Rev.*, **17**, 267–291 (1942).
[16] Roche, A., and Sutherland, S., *J. Bone Jt Surg.*, **41B**, 375–383 (1959).
[17] Warwick, R., and Williams, P., *Gray's Anatomy* (Saunders, Philadelphia, 1973).
[18] Murray, P., *Proc. Linn. Soc. New South Wales*, **51**, 187 (1926).
[19] Carey, E., Zeit, W., and McGrath, B., *Am. J. Anat.*, **40**, 127–158 (1927).
[20] Schon, M., and Ziemer, L., *Folia Primat.*, **20**, 1–11 (1973).
[21] Maxwell, A., *et al.*, *Science*, **168**, 1047–1059 (1970).
[22] Gingerich, P., *Contrib. Mus. Paleo., Univ. Michigan*, **24**, 163–170 (1975).

Control of intragroup aggression by male pigtail monkeys *(Macaca nemestrina)*

CERCOPITHECINE primates (*Macaca, Papio,* and *Cercocebus* spp.) typically live in cohesive groups containing many more adult females than adult males. Strong status hierarchies often exist within established groups, and one male in each group usually exerts an especially powerful influence on the behaviour of other group members. This individual commonly places himself between the group and any potential external threat and frequently interferes in intragroup aggressive encounters by attacking or threatening to attack one of the participants in the altercation[1]. An animal displaying this pattern of behaviour has been referred to as a "control animal" or as fulfilling a "control role"[2].

While the existence of such a control role has been generally accepted, most descriptions of this behaviour have not measured the magnitude of the influence of male presence on the inhibition of violence among females. Cessation of aggression contiguous with attacks or threats by males has provided the bulk of evidence for control role behaviour. In one experimental study, however, removal of the control male from a group of pigtail macaques (*M. nemestrina*) resulted in increased aggression among other group members and his reinstatement in the group reduced aggression to preseparation level[3]. The removal and reinstatement of other group members did not influence intragroup aggression. Unfortunately that experiment used only one group of monkeys under one set of housing conditions, a situation hardly sufficient to establish the generality of the phenomenon.

Because we had access to a large number of groups of *M. nemestrina* and were concerned about the social mechanisms involved in the control of aggression in captive groups of non-human primates, we felt obliged to test the generality of the effect of mere presence of males on intragroup aggression. Six groups, each containing one adult male and an average of 8.5 adult females and 1.1 infants were studied. Each group was housed in identical spatial conditions (2.2×3.1×2.8 m), but the conditions differed considerably from those of the previously cited experiment. Each group was tested according to a sequence of three phases (each 20 min long): a pretest with all group members present to establish basal aggression rates; an experimental test immediately following removal of the male from each group; and a post-test immediately following reintroduction of the male into the group. An experienced observer recorded absolute frequencies of agonistic interactions of group members, noting the sex of the perpetrator and recipient of each act. The following activities were recorded: contact aggression (grab, push, hit, and bite); non-contact aggression (chase, open-mouth "threat", and "bark" vocalisation); and submission (grimace, "screech" vocalisation, and crouch).

973)
..ates, 9, 319–322 (1968).
..win, J , J biol Psychol., 17, 17–20 (1975).
Inim Ethol (in the press)
1 , Martenson, J , and Erwin, J , Am. J phys

---

eproductive correlates ova emissions by baboons

species of rodents, the social and reproductive f a host individual has been shown to affect its ...y to intestinal parasites and the maturation rate of sites once established[1,2]. The relationship between nd reproductive condition of host individuals and aspects of parasite development and transmission, in-ding ova emissions, has not previously been examined for y non-human primate species. Information on parasite ova emissions by non-human primates is important for understanding the life-cycle of the parasites and for understanding the spread of parasites both within and between social groups and to individuals of other species, including humans and domestic stock[3].

In 1974, as part of an ongoing longitudinal study of free-living yellow baboons (*Papio cynocephalus*) in the Amboseli National Park, Kenya, we collected 100 faecal samples from the 29 adult and subadult members of a single well studied group[4]. Intestinal parasite ova were recovered from these samples by zinc sulphate flotation[5] and number of ova per g of faeces was analysed in relation to dominance rank and reproductive condition of host. Egg recovery and counting was done "blind"; samples were identified only by a sequence number and not by name or other information concerning the host. Two nematode genera, *Trichuris* and *Trichostrongylus* accounted for 89% ($N = 2{,}119$) of all parasite ova recovered in the samples. The distribution of number of ova per g of faeces for all samples combined was positively skewed and roughly Poisson in shape; thus, significance testing was carried out with the variance ratio[6].

Figure 1 shows that among adult and subadult males, high ranking individuals had higher egg emissions than did more subordinate individuals. All differences in mean egg counts between adjacent dominance rank classes were statistically significant ($P < 0.01$ for all comparisons); the Spearman rank correlation coefficient between mean egg count and dominance rank in adult and subadult males was 0.67 ($P < 0.05$). Subadult males generally had lower egg counts than did older, fully adult males, and ranks 13–16 were occupied exclusively by subadults. But, examination of the mean egg counts for ranks 1–12 alone, which eliminated the age-related low egg counts of subadults, still showed a strong correlation between mean egg output and dominance rank in adult males ($r_s = 0.56$, $P < 0.05$). Since adult male baboons change rank frequently[4], Fig. 1 is based only on samples collected when adult males were stable, or consistent, in their dominance relationships. Egg output by adult males during periods of inconsistency was usually lower than egg output before the period of inconsistency, but only a small number of such samples were obtained.

The mean egg count for adult females, 26.58 ova per g, was significantly higher than the mean egg count for adult males during periods of rank stability, 20.69 ova per g ($F_{max} = 1.28$, d.f. = 2,552, 1,490, $P < 0.01$), and this difference was even greater when subadult males and adult males inconsistent in their dominance relationships were included in the comparison. Parasite ova emissions among adult females, however, were not correlated with dominance rank ($r_s = 0.02$, $P > 0.05$), although middle ranking females did have significantly higher egg counts than did low ranking females ($F_{max} = 1.24$, d.f. = 1,054, 714, $P < 0.01$) (Fig. 1).

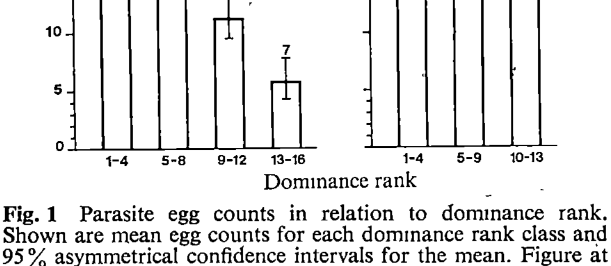

Fig. 1 Parasite egg counts in relation to dominance rank. Shown are mean egg counts for each dominance rank class and 95% asymmetrical confidence intervals for the mean. Figure at top of each bar gives number of samples on which mean is based. For adult males, analysis included only samples collected during periods of rank stability. Subadult males are the same age as young adult females.

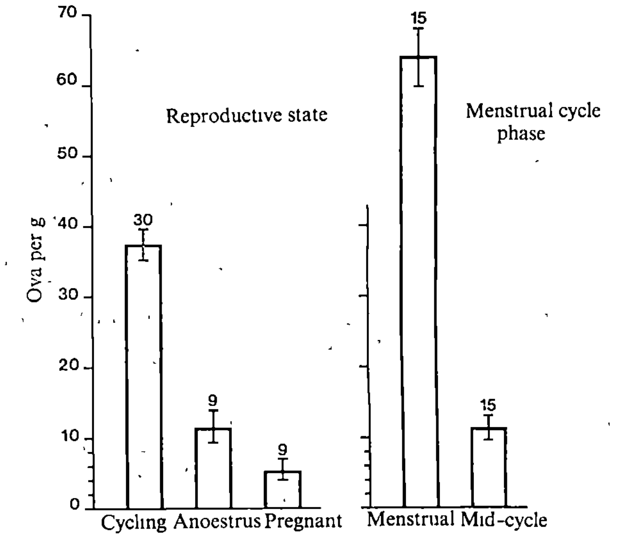

Fig. 2 Parasite egg emissions in relation to female reproductive state and menstrual cycle phase. Conventions as in Fig. 1.

Adult female baboons rarely change dominance rank, but changes in their reproductive state or menstrual cycle phase occur frequently[4]. Sexually cycling females had significantly higher egg emissions than did anoestrous (lactating or otherwise non-cycling) females ($F_{max} = 3.26$, d.f. = 2,250, 206, $P < 0.01$); anoestrous females in turn had significantly higher egg emissions than did pregnant females ($F_{max} = 2.14$, d.f. = 206, 96, $P < 0.01$) (Fig. 2). Among sexually cycling females, mean egg counts were significantly higher during the one week immediately before and the one week immediately after the onset of menstruation compared with the remaining 3 weeks mid-cycle that include oestrus and ovulation ($F_{max} = 5.65$, d.f. = 1,912, 338, $P < 0.01$) (Fig. 2).

One simple but plausible explanation for the observed pattern of parasite ova emissions is that individuals differ in ingestion rate of infective and non-infective ova or in other aspects of food intake, gut passage time or faecal output. Alternatively, high ranking adult males and sexually cycling females may provide a generally more favourable internal environment for egg production by parasites than do individuals of other social and reproductive classes. Of course, the above correlations might also reflect actual differences in the burden of adult worms harboured by individuals of each social and reproductive class. Although unlikely, it is also possible that parasite ova emissions affect social and reproductive condition, for example, dominance rank, rather than the other way around as presumed by the above alternatives. Regardless of their precise explanation, the relationships described in this note, if substantiated by more extensive studies, will be of interest and importance to many scientists concerned with primates, parasites or public health.

Support of this research by the NSF, research clearance from the government of Kenya and the cooperation and advice of S. K. Fisk are gratefully acknowledged. This note benefited from critical readings by M. J. Homzie and D. G. Mook.

GLENN HAUSFATER

Departments of Psychology and Biology,
University of Virginia, Charlottesville, Virginia 22901

D. F. WATSON

Department of Veterinary Science,
Virginia Polytechnic Institute and State University,
Blacksburg, Virginia 24061

Received April 21, accepted June 22, 1976.

[1] Jackson, L. A, and Farmer, J. N, *Ecology*, 51, 672–679 (1970)
[2] Mankau, S. K., *Can J Zool*, 50, 597–602 (1972).
[3] Pitchford, R J, *et al*, *J. S Afr Vet Ass*, 44, 405–420 (1973).
[4] Hausfater, G, *Dominance and Reproduction in Baboons* (Papio cynocephalus) *A Quantitative Analysis* (Karger, Basel, 1975).
[5] Markell, E K, and Voge, M, *Medical Parasitology*, 3rd ed (W. B Saunders, Philadelphia, 1971)
[6] Cox, D. R, and Lewis, P. A W., *The Statistical Analysis of Series of Events* (Methuen, London, 1966).

Inhibition of *Leishmania donovani* transformation by hamster spleen homogenates and active human lymphocytes

HAEMOFLAGELLATES are protozoan parasites responsible for many important diseases of man and domestic animals[1]. *Leishmania donovani*, the cause of visceral leishmaniasis or kala azar, is a widespread human parasitic haemoflagellate. Its life cycle involves man (and other mammals) and an insect vector (sandflies) with a different stage in each of the two host types. Transformation from one stage to the next includes morphological antigenic, physiological, and infectivity changes[2–5].

Transformation in these organisms is a fundamental developmental transition whose regulation is incompletely understood. In this report we present evidence that transformation from the mammalian (amastigote) stage of *L donovani* to the insect and/or culture (promastigote) stage is inhibited by host hamster spleen homogenates and by a soluble factor(s) synthesised by activated human lymphocytes In the absence of this factor transformation proceeds in an orderly series of steps (Fig. 1).

Synchrony of transformation by a population of amastigotes is rather poor; transformation to the promastigotes begins after 18 h with all cells capable of developmental transition (~ 60–80% of the cells undergo transformation) completing cytodifferentiation by about 60 h (Fig. 2). Transforming amastigotes do not incorporate ^{14}C-thymidine[6] into DNA; however, promastigotes readily incorporate this substrate into DNA (~ 70% of recoverable ^{14}C from labelled thymidine is found in DNA). This suggested that *de novo* DNA synthesis does not occur in transforming amastigotes.

We then incubated freshly isolated amastigotes in glucose-free Locke's solution (*p*H 7.7) for 8 h at 27 °C before transfer to transformation medium (HO–MEM)[7] to deplete possible contaminant compounds carried over during isolation that might inhibit cytodifferentiation. The cells transformed more synchronously and the times required for initiation and completion of transformation were markedly reduced (Fig. 2). Even shorter initiation and completion times for developmental transition of amastigote populations were found when cells were preincubated in glucose-free Locke's solution for 8 h at 34 °C before transfer to HO–MEM (Fig. 2).

To determine if a host factor(s) carried as a contaminant with amastigotes during their isolation delayed transformation, 2.5 ml of the first wash from infected spleen homogenates (see legend to Fig. 1) was added to 2.5 ml of

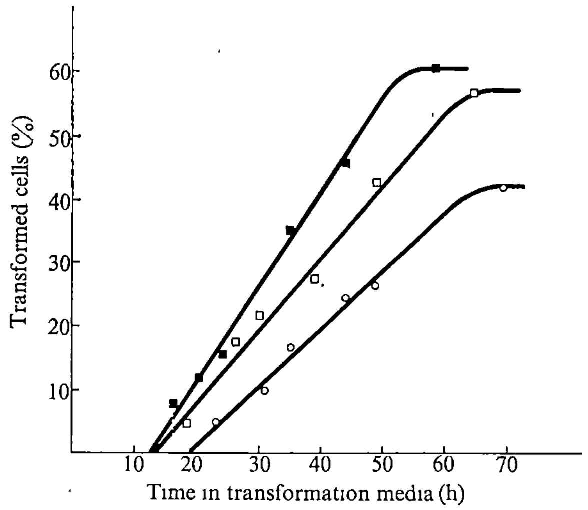

Fig. 2 Transformation of *L. donovani* amastigotes to promastigotes: influence of preincubation in glucose-free Locke's solution on the times of initiation and completion of transformation by a population of washed amastigotes. ○, Control amastigotes transferred to transforming medium (incubated at 27 °C) immediately after isolation from hamster spleen; □, amastigotes preincubated for 8 h at 27 °C before transfer to transformation medium; ■, amastigotes preincubated for 8 h at 34 °C before transfer to incubation medium. Amastigotes (~ 10^8 cells) were incubated in 25-ml Erlenmeyer flasks containing 5 ml HO-MEM (containing glucose). Samples were removed from flasks at various times and the percentage of transformed cells (stage *d* in Fig. 1) determined by microscopic observation. In all experiments the final samples were tested for bacterial contamination; the data from contaminated flasks were discarded.

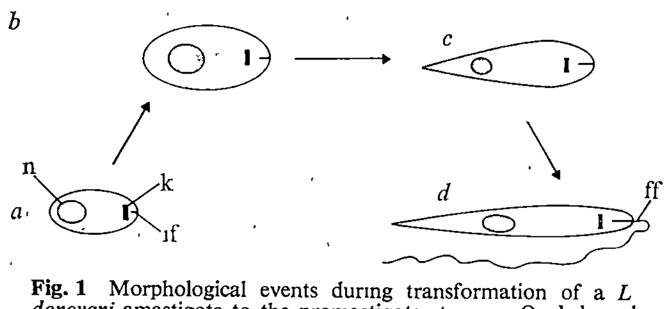

Fig. 1 Morphological events during transformation of a *L donovani* amastigote to the promastigote stage. *a*, Oval-shaped amastigote with nucleus (n), kinetoplast (k) and internal flagellum (if), 0–8 h; *b*, tenfold enlargement of the oval stage, ~ 8–16 h; *c*, elongation of the enlarged parasite, ~ 16–18 h; *d*, formation of free flagellum (ff) and further elongation to complete cytodifferentiation, ~ 18–20 h. Amastigotes were obtained as follows: male hamsters were killed with ether about 2 months after intraperitoneal inoculation with freshly isolated amastigotes (Malakal area Sudan strain, 1S) and the spleen excised in sterile conditions. The spleen was homogenised in 10 ml Tris (0.2 M)–sucrose (0.25 M) buffer, *p*H 7.8, with a Ten Broeck glass homogeniser. Homogenates were centrifuged at 150*g* for 10 min and the pellet discarded; the supernatant was centrifuged at 1,000*g* for 20 min and the resultant supernatant (first wash) discarded. The pellet was resuspended in 10 ml Tris–sucrose buffer and this procedure repeated two more times. After resuspending the final pellet (washed amastigotes) in a small amount of Tris–sucrose buffer, amastigotes were counted and 10^8 cell aliquots incubated in HO–MEM[7] medium at 27 °C. Isolation procedures were carried out in the cold to retard spontaneous transformation, and sterile techniques were used to prevent bacterial contamination. The cell depicted was preincubated in glucose-free Locke's solution (see Fig. 2). About 10% of the preincubated cells started to transform after 8 h in transforming medium. Although stage *a* lasts longer for non-preincubated cells, the duration of time spent in the other stages is the same as that for preincubated cells.

Table 1 Secretion of factors inhibiting *L. donovani* amastigote to promastigote transformation by cell culture systems*

Cell line tested	Effect of cell culture† on transformation	Effect of conditioned† medium on transformation
Triatoma infestans embryo cells BTC-32	—‡	
Mouse sarcoma 338	—	
Mouse lymphocyte sarcoma 815	Inhibited 3–5 d (8)§‖	Delayed 12–20 h (8)
Mouse fibroblast L cells	—	
Mouse glial tumour C6	—	
Mouse transformed fibroblast THC-1	—	
Bovine embryonic trachea EBTR	—	
Dog kidney (epithelium) with mycoplasma mdck	Inhibited 5 d (3)¶‖	Delayed 24–48 h (3)
Monkey fibroblasts TC7	—	
HeLa	—	
Primary human lymphocytes (from adenoid and tonsil)	Inhibited 3–5 d (5)¶‖	Delayed 12–20 h (5)
Phytohaemagglutinin-activated primary human lymphocytes	Inhibited at least 5 d (5)¶‖	Delayed 24–48 h (5)

*10^8 washed amastigotes in each flask, incubation temperature 27 °C, transformation determined as in Fig. 2.

†Control amastigotes incubated in absence of cells in same media used to grow tissue cells: RPMI 1640 (GIBCO) or Hanks' MEM (GIBCO).

‡—, No effect on transformation.

§Culture medium RPMI 1640.

¶Culture medium MEM.

Number of experiments in parentheses.

‖Amastigotes inhibited for 3 d or more were washed and transferred to fresh media lacking culture cells to ensure that they were viable and still capable of transformation.

2×HO–MEM before incubation with washed Locke's solution preincubated amastigotes. Addition of the first wash delayed initial transformation times by 12–24 h (four experiments) compared with control cells incubated in 2.5 ml Tris–sucrose buffer and 2.5 ml 2×HO–MEM. Similar results were found when the first wash from uninfected spleen homogenates was tested. Supernatants obtained after the first wash had no effect on amastigote transformation.

Analysis of hamster spleen transformation-blocking activity is difficult because the spleen is small (1–3 g in infected hamsters) and the concentration of the factor(s) responsible for inhibition is low; 1 : 1 dilution of the first wash before adding it to test media resulted in total loss of activity. We decided to find a model system capable of 'mimicking' hamster spleen tranformation-blocking activity and which produced sufficient amounts of factor(s) to analyse inhibition of transformation. Since many developmental processes are mediated by mammalian growth and activating factors (for example, nerve growth factor, epithelial growth factor and lymphocyte-activating factor)[8,9], we therefore tested a number of cell culture systems for their ability to secrete high concentrations of factors capable of inhibiting *L. donovani* amastigote cytodifferentiation.

Conditioned media from four mammalian cell culture lines were able to delay initiation of transformation for at least 12 h· mouse lymphocyte sarcoma cell line 815, phytohaemagglutinin-activated primary human lymphocytes[10], unactivated primary human lymphocytes and mdck, a dog kidney cell line infected by an unidentified mycoplasma (Table 1). Activated primary human lymphocytes and mdck both produced high levels of blocking factors. Further experiments were carried out with only the activated lymphocyte system because it was more active and was better defined than mdck in that it was not infected by mycoplasma. Collection of a large volume of media conditioned by the lymphocytes is relatively simple[10]; this is another advantage with the lymphocyte system.

Incubation of washed amastigotes in medium conditioned by activated lymphocytes delayed the start of developmental transition by 24–48 h (Table 1). Amastigotes incubated with lymphocyte cultures were inhibited from transforming for at least 5 d. When these amastigotes were washed and transferred to fresh media free of lymphocytes cytodifferentiation proceeded normally.

Conditioned medium from activated lymphocyte cultures was separated by ultrafiltration into fractions containing molecules of decreasing molecular weight; these fractions were assayed for transformation-inhibiting activity (Table 2). Activity was localised in fraction IIIc (molecular weight <500); addition of fraction IIIc to amastigotes in HO–

Table 2 Transformation-inhibiting activity in water-soluble fractions secreted by phytohaemagglutinin-activated primary human lymphocytes*

Test material† (molecular weight)	Effect on transformation‡
Fraction I (>30,000)	—
Fraction II (5,000–30,000)	—
Fraction III (<5,000)	Delayed 48–72 h (5)§
Fraction IIIa (1,000–5,000)	—
Fraction IIIb (<1,000)	Delayed ≈48 h (3)
Fraction IIIb′ (500–1,000)	—
Fraction IIIc (<500)	Delayed ≈48 h (3)

*Details of primary human lymphocyte preparation, cell culture and collection of conditioned media have been published[10]. Lymphocytes were cultured in MEM supplemented with essential amino acids, glutamine, sodium pyruvate and with 10% foetal calf serum. Cells were activated by addition of 20 μg ml^{-1} phytohaemagglutinin (PHA-P, Difco) and incubated for 5–7 d. Cultures were centrifuged at 300*g* for 5 min to pellet the lymphocytes, and the supernatant saved. Supernatant could be stored frozen or separated into different fractions and then stored frozen.

†Supernatants separated by ultrafiltration into fractions with solutes of different approximate molecular weight. Filtration with an Amicon PM30 resulted in a concentrated fraction of molecular weight >30,000 (fraction I) and a filtrate containing solutes of molecular weight <30,000. The filtrate was further concentrated with an Amicon PM10; the concentrate contained solutes of about 5,000–30,000 molecular weight (fraction II). The material passing through with solutes of molecular weight <5,000 (fraction III) was concentrated using an Amicon UM2; this concentrate is defined as fraction IIIa (solutes of about 1,000–5,000 molecular weight). The material going through the UM2 is defined as fraction IIIb (solutes of molecular weight <1,000). Fraction IIIb was concentrated with an Amicon UM05; the concentrate is defined as fraction IIIb′ (solutes of molecular weight 500–1,000) and filtrate is fraction IIIc (<500 molecular weight).

‡Amastigotes (10^8 cells) incubated in 5.0 ml HO–MEM containing test fraction; concentrated HO–MEM was added to concentrated test fraction in the proper proportions for a final concentration of 1× HO–MEM and 1× test fraction. Transformation was determined as in Fig. 2. Cells were not permanently affected by inhibitory fractions; after delay of transformation the number of amastigotes completing cytodifferentiation was similar to that of controls. Control amastigotes were incubated in 5.0 ml HO–MEM. In all experiments the final samples were tested for bacterial contamination and the data from contaminated flasks discarded.

§Number of experiments in parentheses.

MEM delayed initiation of cytodifferentiation by ~ 48 h. The solutes in fraction IIIc are present in fractions III (molecular weight <5,000) and IIIb (molecular weight <1,000); as would be expected, the latter two fractions show transformation-blocking activity. The lower activity found in fractions IIIb and IIIc may be due to inefficient passage of filtrate through the Amicon UM2 filter membrane. This fraction is relatively stable; it is not inactivated by boiling for 30 min and can be stored at 4 °C for 5 d or at −17 °C for at least several months with little loss of activity.

Transforming amastigote populations can be blocked at any time before the process is complete. Addition of fraction IIIc to amastigotes after 9 h incubation in HO–MEM delayed initiation of cytodifferentiation by about 9 h. Addition of the fraction after 27 h incubation, a time when a few of the cells have already transformed, delayed further transformation for about 15 h. These are unusual results because in most developmental systems there is a point when cells are irreversibly committed to change independent of the initial factor(s) causing that change.

Addition of fraction IIIc or of the first wash from hamster spleen homogenates had no effect on promastigote cultures in HO–MEM. The cells maintained their normal morphology and continued to divide.

The above results present the first evidence for the presence of mammalian regulatory compounds affecting haemoflagellate transformation. There are factors produced by activated human lymphocytes and in hamster spleen homogenates that inhibit transformation of *L. donovani* amastigotes to the promastigote stage. The *in vitro* studies by Lamy[11] with macrophage and Sticker sarcoma cell cultures demonstrating that *L. donovani* amastigotes may occasionally transform into promastigotes while still inside the host cells, can be explained by the possible absence of 'blocking' factors in his cultures.

It remains to be confirmed whether one or more inhibitory factors is present in the lymphocyte secretions and to determine if blocking factors from hamster spleen and cell lines 815 and mdck are similar to those produced by lymphocytes.

We thank Ms B Flory for assistance. This study was supported by the USPHS (S.M.K.) and the Janggen–Poehn Stiftung, St Gallen, Switzerland (R.B.).

RETO BRUN

Swiss Tropical Institute,
Basel, Switzerland

RANDY L BERENS

Medical Microbiology,
Barnes Hospital,
St Louis, Missouri

STUART M. KRASSNER

Developmental and Cell Biology,
University of California,
Irvine, California 92717

Received January 22; accepted June 22, 1976.

[1] Hoare, C. A., *Trypanosomes of Mammals*, 60–80 (Blackwell Scientific, Oxford, 1972).
[2] Simpson, L., *J. Protozool.*, 15, 210–207 (1968).
[3] Honiberg, B M , in *Chemical Zoology*, 1 (edit by Florkin, M. and Scheen, B. T.), 711–759 (Academic, New York and London, 1967)
[4] Bowman, I B R , Srivistava, H. K., and Flynn, I. W , in *Comparative Biochemistry of Parasites* (edit by Van Den Bossche, H), 329–342 (Academic, New York and London, 1972)
[5] von Brand, T., *Biochemistry of Parasites*. 368–425 (Academic, New York and London, 1973)
[6] Stevens, L A , *J Parasitol.*, 56 (II), 330 (1970)
[7] Berens, R . Brun, R , and Krassner, S. M.. *J. Parasitol.* (in the press)
[8] Rutter, W. M , Pictet, R. L , and Morris, P W., *A Rev Biochem* , 42, 601–646 (1973).
[9] Pastan I. H., Johnson, G S., and Anderson, W B., *A Rev Biochem* , 44, 491–522 (1975)
[10] Kolb, W. P., Williams, T. W , and Granger, G A , in *In Vitro Methods in Cell-Mediated Immunity* (edit by Bloom, B and Glade, P.), 333–342 (Academic, New York and London, 1971).
[11] Lamy, L. H., *Protistologica*, 6, 457–466 (1970).

Generation of cytotoxic lymphocytes *in vitro* against autologous human leukaemia cells

NORMAL lymphocytes cultured with allogeneic cells in one-way mixed leukocyte culture (MLC) respond proliferatively to the "lymphocyte-defined" (LD) antigens and subsequently cytotoxic cells are generated against the target antigens on the stimulating cells[1]. In contrast, when responding lymphocytes are cultured with stimulating lymphocytes that differ with respect to target antigens but not LD antigens, proliferative and cytotoxic responses are not easily generated; the addition of a second stimulating cell differing from the responding cell with respect to LD antigens in a 'three-cell' experiment allows the generation of cytotoxic lymphocytes directed against target antigens[1–4]. Consistent with results of others[5–9], we have detected low but significant MLC responses after culturing remission lymphocytes with irradiated autologous leukaemia cells; however, cytotoxic lymphocytes were not generated. Using the 'three-cell' approach, where remission lymphocytes, irradiated leukaemia cells and irradiated allogeneic stimulating cells were cocultured, we have generated lymphocytes specifically cytotoxic for autologous human leukaemia cells.

Peripheral blood was obtained at the time of diagnosis from C.T., a 40-yr-old woman with acute myelomonocytic leukaemia (AMML). The peripheral white blood cell count at this time was 200,000 per mm^3, consisting of 52% blast cells. The blood was diluted with medium 199 and layered on a Ficoll–Hypaque gradient[10]; the resulting cells at the interface consisted of 74% blast cells. These cells were washed and control-frozen in RPMI 1640 with 25 mM HEPES buffer and 20% heat-inactivated normal human serum and stored in liquid nitrogen. Eight and twelve weeks after diagnosis, after several courses of intensive chemotherapy, peripheral blood and bone marrow aspirates were obtained. At these times, no leukaemic cells were present in the peripheral blood. Lymphocytes were separated from peripheral blood by Ficoll–Hypaque sedimentation and suspended in culture medium consisting of RPMI 1640 with 25 mM HEPES buffer and 20% heat-inactivated normal human serum. Specimens of bone marrow aspirate obtained at these times were purified in the same way. Approximately 5% of the marrow cells collected from the interface of the gradient were blast cells.

Cultures were set up in 50-ml Falcon flasks, each containing 5×10^6 responding lymphocytes (either the patient's remission lymphocytes or lymphocytes from normal individuals) and $5–10 \times 10^6$ stimulating cells rendered incapable of DNA synthesis by exposure to 2,500 R X irradiation. Stimulating cells were either irradiated leukaemia cells, allogeneic lymphocytes, a mixture of leukaemia cells and allogeneic lymphocytes or a mixture of bone marrow cells and allogeneic lymphocytes. Cultures were incubated at 30 °C in a humidified 5% CO_2 incubator and were fed with 5 ml of culture medium on days 2 and 5. Target cells, to be used on day 7 in the cell-mediated ^{51}Cr release assay (CML) were prepared by culturing either $5–15 \times 10^6$ normal lymphocytes or bone marrow cells in flasks that were fed on days 2 and 5. The leukaemic cells were thawed on the day of the CML assay, incubated for 2 h at 37 °C before labelling with 250 µCi ^{51}Cr ($Na_2\,^{51}CrO_4$,New England Nuclear). Effector cells generated in flasks were collected on day 7 and the CML assay was performed as described in the legend of Table 1*a* and *b*.

In our first experiment shown in Table 1*a*, C.T. remission lymphocytes cultured with autologous leukaemia (L_x) cells alone were not cytotoxic for that patient's leukaemia cells—less ^{51}Cr was released in the presence of CL_x effector cells than was released spontaneously. In contrast, lymphocytes that had been cultured with a mixture of autologous leukaemia cells (L_x) and allogeneic lymphocytes (A_x) were cytotoxic for the patient's

Table 1 *In vitro* generation of lymphocytes specifically cytotoxic for autologous AMML cells

	Responding lymphocytes	Stimulating cells	Effector–target-cell ratio	% Specific ^{51}Cr release ±s.d.			
				Leukaemic cells	Remission marrow cells	Normal lymphocytes from A	Normal lymphocytes from B
(*a*)	C (patient's lymphocytes)	L_x (patient's leukaemia cells) + A_x (normal allogeneic lymphocytes)	40:1	17.8±6.5	3.5±1.4	44.0±4.1	1.8±2.3
	C	L_x	40:1	0.0	0.0		
	C	A_x	40:1	2.9±1.1	0.45±1.6	60.7±10.1	2.2±2.2
	B (normal individual)	L_x	20:1	17.5±12.0	14.7±2.0	−0.7±3.4	−0.4±2.8
	B	A_x	20:1			27.7±2.3	−0.2±3.4
(*b*)				Leukaemic cells	Normal lymphocytes from D	Normal lymphocytes from E	
	C (patient's lymphocytes)	L_x (patient's leukaemia cells) + D_x (normal allogeneic lymphocytes)	20:1	25.0±6.9	30.3±1.7	7.2±3.6	
	C	M_x (remission marrow) + D_x	20:1	22.0±8.9	39.7±3.5		
	C	C_x (patient's remission lymphocytes)	20:1	0.0	0.0	0.0	
	D (normal individual)	L_x	20:1	36.8±6.5	−2.4±4.1		

In both experiments *a* and *b*, lymphocytes were collected 7 d after stimulation, resuspended at 1×10^6–2×10^6 cells ml^{-1} and 0.2 ml effector cells were mixed with 1×10^4 ^{51}Cr-labelled target cells in wells of round-bottom Linbro plates. Supernatants were collected after 6 h (Exp. *a*) or 8 h (Exp. *b*) incubation at 37 °C and % specific ^{51}Cr release was calculated according to the following formula: $[(E-SR)/(M-SR)]\times100$, where E is experimental release, SR is spontaneous release of ^{51}Cr from normal target cells in the presence of medium alone, and M is maximal release of ^{51}Cr from target cells after adding detergent (0.4% Cetrimide). Specific ^{51}Cr release from leukaemic cells and bone marrow cells was calculated from the following formula: $[(E-C)/(M-C)]\times100$, where E is experimental release, C is release of ^{51}Cr from target cells by CL_x or CC_x effector cells and M is maximal release.

leukaemia cells: 17.8% specific ^{51}Cr released observed by 6 h. These same effector cells that were cytotoxic for autologous leukaemia cells and A target cells did not lyse unrelated normal lymphocytes from B and caused only 3.5% ^{51}Cr release from autologous bone marrow cells containing 5% blast cells. It should be noted, however, that these remission bone marrow cells and leukaemia cells were nearly equally sensitive to lysis by allogeneic normal lymphocytes (B) that had been cultured with the patient's leukaemic (L_x) cells Remission lymphocytes that had been cultured with allogeneic (A_x) cells were highly cytotoxic for A target cells (60.7% specific ^{51}Cr release) but caused only 2.9% ^{51}Cr release from autologous labelled leukaemic cells. This indicates that lysis of autologous leukaemia cells by remission lymphocytes that had been cultured with a mixture of A_xL_x stimulating cells was not due to cross reacting target antigens expressed on leukaemia cells and allogeneic (A) lymphocytes. Furthermore, the presence of leukaemic stimulating cells in the mixed culture was necessary for the generation of an anti-leukaemic cytotoxic response.

Remission lymphocytes were obtained 1 month later and it was again possible to generate cytotoxic lymphocytes directed against autologous leukaemia cells (Table 1*b*). Remission lymphocytes cultured with leukaemic cells and allogeneic (D_x) cells caused 25% ^{51}Cr release from leukaemic cells after an 8-h CML assay at the ratio of 20 effector cells per target cell and 30% ^{51}Cr release from allogeneic D target cells. Nearly the same amount of ^{51}Cr (22%) was released from leukaemic cells by lymphocytes that were cultured with bone marrow and allogeneic cells. A probable explanation for this finding is that the number of blast cells carrying target antigens in the stimulating marrow population was sufficient to induce a cytotoxic lymphocyte response. In the experiment shown in Table 1*a*, however, lymphocytes that had been cultured with leukaemic and allogeneic cells caused only 3.5% ^{51}Cr release from labelled marrow cells, for only a minor proportion (5%) of the ^{51}Cr-labelled target cells were blasts, many of which may not have been leukaemic.

The results presented here demonstrate the presence of target antigens on AMML cells against which a cytotoxic autologous lymphocyte response was generated when a strong proliferation-inducing signal (in this case, allogeneic stimulating cells) was provided that presumably stimulates the proliferating helper T cells[1]. The relationship between the target antigens we have detected on AMML cells by cell-mediated cytotoxicity and antigens detected serologically on AMML cells[11] is unknown. We have not had access to cells of other patients with AMML; however, consistent with the results we have reported here, we found that in a patient with acute lymphocytic leukaemia, the development of cytotoxic response aimed at the patient's leukaemia cells was again dependent on the providing of a helper stimulus in a three-cell protocol. Similar experiments with five patients in remission from acute myelogenous leukaemia (AML) have not as yet resulted in generation of cytotoxic lymphocytes directed against autologous leukaemic cells. In some of these cases, the AML cells did not generate cytotoxic activity even in allogeneic responder lymphocytes. The explanation for the lack of finding of cytotoxicity in cases where allogeneic lymphocytes did respond cytotoxically to target antigens on leukaemic cells is not clear.

Consistent with our studies are the independently derived findings of Sondel *et al.* (personal communication) showing that adding a helper stimulus enhances anti-leukaemia cell-mediated cytotoxicity by lymphocytes from siblings HLA identical with the leukaemia patient. The 'three-cell' type approach used in these experiments may thus provide a means for generating cytotoxic lymphocytes directed against other autologous or HLA identical leukaemia or tumour cells that express target antigens but cannot induce a strong lymphocyte proliferative response.

This work was supported by grants from the NIH and the National Foundation–March of Dimes.

JOYCE M. ZARLING
PETER C. RAICH
MARK MCKEOUGH
FRITZ H. BACH

Immunobiology Research Center,
Departments of Medical Genetics, Surgery and Medicine,
University of Wisconsin,
Madison, Wisconsin 53706

Received April 20, accepted July 2, 1976.

[1] Bach, F H , Bach, M. L., and Sondel, P. M., *Nature*, **259**, 273–281 (1976).
[2] Eijsvoogel, V P., *et al* , *Transplant Proc* , **5**, 1675–1678 (1973)
[3] Schendel, D J , Alter, B J , and Bach, F H , *Transplant. Proc.*, **5**, 1651–1655 (1973)
[4] Bach, M L , and Bach, F H , *Transplant Proc* , **5**, 1755–1757 (1973)
[5] Bach, M L., Bach, F H , and Joo, P., *Science*, **166**, 1520–1522 (1969)
[6] Fridman, W. H , and Kourilsky, F M , *Nature*, **224**, 227–278 (1969)
[7] Leventhal, B. G , Halterman, R H , Rosenberg, E B , and Herberman, R B , *Cancer Res.*, **32**, 1820–1825 (1972)
[8] Gutterman, J V , *et al* , *Cancer Res.*, **32**, 2524–2529 (1972)
[9] Fefer, A , Mickelson, E , and Thomas, E D , *Clin exp Immun* , **23**, 214–218 (1976)
[10] Boyum, A , *Scand J clin Lab Invest.*, **21**, suppl 97, 77–89 (1968).
[11] Metzgar, R S , Mohanakumar, T , and Bolognesi, D P., *J exp. Med* , **143**, 47–63 (1976)

Sensitivity of H–2-less target cells and role of H–2 in T-cell-mediated cytolysis

THERE is no definitive teleological interpretation of the involvement of H–2 determinants in the recognition by mouse cytolytic T cells of various non-H–2 antigens[1,2]. While it is generally believed that T-cell immunity against non-H–2 structures (determined, for example, by infectious agents) may benefit from the known special reactivity of T cells against non-self H–2, other interpretations have been proposed, such as the possibility that H–2 is necessary for cytolysis at a postrecognition stage as the "weak point" of the target-cell surface[3]. A prediction of this hypothesis is that target cells devoid of H–2 should be resistant to T-cell-mediated cytolysis. We have tested this prediction using male germinal cells, embryonal carcinoma and virus-transformed testicular cells as targets, in the presence of the lectin concanavalin A (con A). Con A binding apparently by-passes[4] the normal recognition system, so that lack of recognition of H–2 on H–2-less target cells would not be a limiting factor for cytolysis. We found that H–2-less embryonal carcinoma cell lines, including one with barely detectable levels of F9 antigen, were sensitive to lysis, strongly suggesting that at a postrecognition stage H–2 is not required for T-cell-mediated cytolysis.

Mouse male germinal cells, in practice testicular cells, acquire serologically detectable surface H–2 as late as 12 d of age[5,6]. We wondered whether acquisition of H–2 would be accompanied by a change from resistance to sensitivity to lysis. We found, however, that even testicular cells from several-month-old mice were relatively resistant to lysis, in the presence or absence of con A (Table 1). Further findings (not shown) were: first, ^{51}Cr could be released from testicular cells in the presence of rabbit anti-mouse serum and complement; second, con A induced agglutination of testicular cells at the concentration used in these experiments; third, various ratios of cytolytic to testicular cells and various concentrations of con A did not yield different results. These experiments showed at least that the presence of serologically detectable H–2 was not sufficient to ensure sensitivity to lysis, thus underlining the existence of other, unknown target cell requirements for lysis.

To investigate whether H–2 was necessary for lysis, we then used as targets F9 embryonal carcinoma cells of H–2*b* genotype but devoid of serologically detectable membrane H–2 (ref. 7). Table 2, experiments 1–3, shows, first, that F9 cells were not lysed by anti-*b* cytolytic cells in the absence of con A, and second, that a significant degree of lysis occurred in the presence of con A. This dual pattern was observed in each of eight experiments, not only with *d* anti-*b* and *b* anti-*d*, but also with *k* anti-*b* and *b* anti-*k* cytolytic cells (not shown). Lysis in the presence of con A showed that F9 cells are sensitive to lysis (which incidentally strengthens the conclusions drawn from interesting negative results obtained with TNP-coated F9 cells[8]). That no lysis should occur in the absence of con A therefore strongly suggests that specific anti-H–2 cytolytic cells do not recognise H–2 determinants at the surface of F9 cells. Thus, F9 cells are sensitive to lysis in the presence of con A, in spite of the absence of any H–2 determinant detectable either by specific antisera[7] or by specific cytolytic cells.

Table 1 Lack of demonstrable T-cell-mediated cytolysis of mouse testicular cells

Experiment	Target cells*	Cytolytic cells			
		k anti-*d*		*d* anti-*k*	
	Con A†:	−	+	−	+
(1)	P815	51	49	2	29
	Test. CBA 3w	−1	1	−3	1
(2)	P815	32	31	0	16
	Test. CBA 3w	0	0	1	−2
	Test. CBA 5w	−1	0	−2	1
(3)	P815	37	41	1	42
	Test. CBA 5w	−5	2	1	4
(4)	Blasts BALB/c	28	28	1	22
	Blasts C3H	1	16	29	31
	Test. BALB/c 6w	7	6	−1	5
	Test. C3H 6w	0	2	1	4
(5)	Blasts BALB/c	24	5	−3	18
	Blasts C3H	−2	9	30	20
	Test. BALB/c 4m	−5	−4	−3	4
	Test. CBA 7m	−1	−3	−2	6

C3H anti-BALB/c (*k* anti-*d*) and BALB/c anti-C3H (*d* anti-*k*) sensitised cytolytic cells were prepared and tested in a ^{51}Cr-release assay as described previously[18], at an effector–target cell ratio of 20:1 in these experiments. Cytotoxicity is expressed as percentage ^{51}Cr release averaged from triplicate wells, minus spontaneous release by target cells alone. In this type of assay, an experimental difference of 5% or more is statistically significant ($P = 0.05$).

*Target cells (prelabelled with ^{51}Cr, 10^4 per V-shaped well of microplates) were P815 mastocytoma cells (H–2*d*), either CBA and C3H (H–2*k*) or BALB/c (H–2*d*) mechanically dispersed testicular cells from mice aged 3 weeks to 7 months, and con A-induced blasts (obtained through 2–4-d incubation of normal spleen cells in the presence of con A (2.5 μg ml^{-1}) then labelled with ^{51}Cr and incubated for two consecutive periods of 15 min with 0.1 M α-methylmannose). Spontaneous release was 9–15 for P815, 20–41 for testicular cells and 14–35 for con A blasts.

†Con A at a final concentration of 10 μg ml^{-1} consistently induced in the presence of sensitised cells nonspecific cytolysis of most target cells tested except testicular cells. It sometimes induced a decrease of specific cytolysis, especially marked here in experiment 5.

F9 cells, however, bear the F9 embryonic antigen[9] and in view of the claimed homology[10] between H–2 and F9 one can argue that the F9 antigen can serve as a substitute for H–2 in lysis. This led us to use strain PCC3/A/1/D-G1, derived from the primitive embryonal carcinoma cell line PCC3/A/1 (ref. 11). PCC3/A/1/D-G1 cells bear neither H–2 nor F9 antigens detectable with antisera and complement and have at least 100 times less F9 antigen than F9 cells in adsorption experiments and only about 1–2% positive cells in an anti-F9 antigen immunofluorescence assay[11]. Table 2, experiments 4–6, and Table 3 show that cytolysis of PCC3/A/1/D-G1 cells followed a pattern similar to that of F9 cells.

Con A-dependent lysis of H–2-less target cells was T-cell-mediated, since it was significantly decreased by anti-Thy 1 serum in the presence of complement, in a specific brain-adsorbable manner (Table 3). Using H–2-bearing target cells, it was found, first, that con A-dependent nonspecific lysis is probably mediated by T cells also capable of mediating specific lysis[4,12–14], and second, that the same drugs inhibit with similar dose–response curves the lethal hit stage of specific cytolysis[15] and con A-dependent nonspecific lysis (P.G., unpublished results). It therefore seems reasonable to assume that both types of T-cell-mediated lysis differ only at the recognition stage and

Table 2 Sensitivity to T-cell-mediated cytolysis of embryonal carcinoma and virus-transformed testicular cell lines

Experiment	Target cells*	Serotype†		Cytolytic Cells‡							
				b anti-*d*				*d* anti-*b*			
		H–2	F9	Con A: −		+		−		+	
				20:1§	5:1	20:1	5:1	20:1	5:1	20:1	5:1
1	EL_4	*b*	−	3	2	29	24	29	14	27	21
	F9	−	+	0	1	13	3	−1	−1	10	12
2	EL_4	*b*	−	8	2	23	18	38	19	38	25
	P815	*d*	−	40	14	44	17	2	1	39	16
	F9	−	+	0	2	13	14	0	0	25	17
3	EL_4	*b*	−	7	2	28	35	51	38	49	42
	P815	*d*	−	45	19	48	25	5	2	44	32
	F9	−	+	−2	−2	6	8	1	−1	20	18
	TSV	*b*	+	3	0	4	4	11	6	20	12
4	EL_4	*b*	−	−1	0	17	12	24	13	26	16
	PCC3/A/1/D–G1	−	−	−3	−1	14	7	2	0	16	13
5	EL_4	*b*	−	0	−2	30	36	44	25	46	35
	P815	*d*	−	46	32	58	42	8	2	44	34
	PCC3/A/1/D–G1	−	−	−2	−3	27	20	3	1	26	20
	TSV	*b*	+	1	0	16	12	13	5	17	11
6	EL_4	*b*	−	−1	−3	38	28	38	22	41	27
	P815	*d*	−	38	17	44	23	2	1	37	24
	PCC3/A/1/D–G1	−	−	−2	0	18	11	2	0	19	11
	TSV	*b*	+	0	−1	11	4	9	5	12	4

*Target cells were: EL_4 (C57Bl/6 lymphoma) and P815–X2 (DBA/2 mastocytoma) cultivated *in vitro* in standard conditions; F9 (strain 129 embryonal carcinoma) grown in 15% foetal calf serum in gelatinised flasks, used for experiments within 2 months of subculture; PCC3/A/1/D–G1 (derived *in vitro* from mouse strain 129 embryonal carcinoma cell line PCC3/A/1) grown in 15% foetal calf serum, also used within 2 months of subculture; TSV (SV40-transformed mouse strain 129 testicular cells). Spontaneous release was 11–20, 8–10, 15–31 and 13–30, respectively. The embryonal carcinoma cells were especially sensitive to careless handling.

†Serotypes after refs 7, 9, 11 and unpublished results.

‡Cytolytic cells were C57Bl/6 anti-BALB/c (*b* anti-*d*) and BALB/c anti-C57Bl/6 (*d* anti-*b*). The latter were usually superior to the former in terms of number of cells recovered after sensitisation, percentage of blasts and efficiency of lysis of all types of target cells in the presence of con A.

§Ratio of cytolytic to target cells.

follow the same mechanism after recognition. If this assumption is not correct, then our conclusions below about the sensitivity of H–2-less target cells would still be valid for some cytolytic T cells, but not necessarily for the specifically cytolytic ones.

In this series of experiments, we also tested as targets TSV cells derived from SV40-transformed mouse testicular cells and expressing both H–2*b* and F9 antigen (F.K., unpublished). These cells were lysed to a moderate but significant extent by specific anti-*b* cells with and without con A and by anti-*d* cells in the presence of con A (Table 2). The availability as T-cell-sensitive targets of $H\text{–}2^+$ $F9^+$ virus-transformed and of $H\text{–}2^-$ $F9^+$ carcinoma cells seems of great potential interest. A study of the induction and expression of anti-F9 antigen autoimmunity as a function of the presence of H–2 may help eventually to reveal not only a genetic[16] and ontogenic[10], but also an immunological relationship between H–2 and F9. It is clear from the results reported here that the presence of F9 determinants does not prevent recognition by T cells of H–2 determinants at the target cell surface.

The nature of the primary target cell lesion caused by cytolytic T cells is unknown. Molecular channels can be inserted into the target cell membrane, as in the "doughnut" model proposed by Mayer for complement-mediated lysis[17]. It may also be that 'target molecules' on the target cell membrane have a role, for example as substrates for effector cell membrane enzymes. If this is so, this report shows that neither H–2 nor very probably F9 are the exclusive target molecules, or are exclusively associated with target molecules, since lysis can proceed in their apparent absence. This strongly suggests there is no strict requirement for H–2 at a postrecognition stage, which would account for the H–2 restriction of T-cell-mediated cytolysis.

We thank Mrs L. Andrean for technical assistance, Dr P. Lake for anti-Thy 1 antiserum and the MRC, INSERM, CNRS and Délégation Générale á la Recherche Scientifique et Technique for support.

PIERRE GOLSTEIN

Tumour Immunology Unit,
Department of Zoology,
University College London,
Gower Street, London WC1E 6BT, UK

FRANCOISE KELLY
PHILIP AVNER
GABRIEL GACHELIN

Laboratoire de Génétique Cellulaire,
Institut Pasteur,
25 rue du Dr Roux, 75015 Paris, France

Table 3 Effect of anti-Thy 1 serum on cells mediating con A-dependent lysis of embryonal carcinoma cells

Target cells*	Con A	Cytolytic cells†	*k* (Thy 1–1) anti-*b*			*k* (Thy 1–2) anti-*b*				
		Anti-Thy 1–2‡	none	absorbed on Thy 1–1 brain		none	absorbed on Thy 1–1 brain		absorbed on Thy 1–2 brain	
		Complement	−	−	+	−	−	+	−	+
EL_4	−		30	28	31	26	21	−2	21	22
	+		34	33	33	27	25	−2	25	24
PCC3/A/1/D–G1	−		4	−3	2	1	−1	2	−4	0
	+		25	32	25	21	27	6	19	20

*Target cells were EL_4 lymphoma and PCC3/A/1/D–G1 embryonal carcinoma cells. Spontaneous release was 13 and 30, respectively. Cytolysis was tested in the presence or absence of con A, at a ratio of 20 effector cells (adjusted before treatment with antiserum) to one target cell.

†Cytolytic cells were either AKR (*k*, Thy 1–1) or C3H (*k*, Thy 1–2) sensitised against C57Bl/6 cells (*b*)

‡Thy 1–1 anti-Thy 1–2 (AKR anti-CBA) antiserum was absorbed either on Thy 1–1 or on Thy 1–2 brain cells. Samples of 0.2 ml were then added to 0 1 ml of medium containing 2×10^6 cytolytic cells, for 30 min at 4 °C. After two washes, the cells were resuspended in 0.5 ml of a 1:10 dilution of complement (guinea pig serum adsorbed on mouse spleen cells) and incubated for 30 min at 37 °C. The cells were again washed twice, resuspended in medium and tested for residual cytolytic activity.

Received May 27; accepted July 2, 1976.

[1] Shearer, G. M., *Eur. J Immun.*, 4, 527–533 (1974)
[2] Zinkernagel, R. M., and Doherty, P C , *Nature*, 248, 701–702 (1974).
[3] Forman, J . *J. exp. Med.*, 142, 403–418 (1975).
[4] Forman, J., and Moller, G , *J exp. Med* , 138, 672–685 (1973).
[5] Vojtiskova, M., and Pokorna, Z , *Folia Biol* , 18, 1–9 (1972).
[6] Fellous, M , Erikson, R , Dubois, P., and Gachelin, G., *Folia Biol.* (in the press)
[7] Artzt, K., and Jacob, F., *Transplantation*, 17, 633–634 (1974)
[8] Forman, J , and Vitetta, E S., *Proc natn. Acad. Sci. U.SA*, 72, 3661–3665 (1975)
[9] Artzt, K., *et al.*, *Proc natn. Acad Sci U S.A.*, 70, 2988–2992 (1973)
[10] Artzt, K., and Bennett, D., *Nature*, 256, 545–547 (1975)
[11] Nicolas, J. F., Avner, P., Gaillard, J., Jacob, H , and Jacob, F., *Cancer Res.* (in the press)
[12] Bevan, M. J., and Cohn, M., *J Immun.*, 114, 559–565 (1975).
[13] Bonavida, B., and Bradley, T. P., *Transplantation*, 21, 94–102 (1976)
[14] Rollinghoff, M , Pfizenmeier, K , Trostmann, H., and Wagner, H., *Eur. J. Immun.*, 5, 560–564 (1975).
[15] Golstein, P., and Smith, E. T , *Contemp. Topics Immunobiol* , 7 (in the press).
[16] Hammerberg, C , and Klein, J , *Nature*, 258, 296–299 (1975)
[17] Mayer, M. M , *Proc natn Acad Sci. U S A.*, 69, 2954–2958 (1972).
[18] Golstein, P., *Nature*, 252, 81–83 (1974)

Immune destruction of virus-infected cells early in the infectious cycle

TARGET cells acutely infected with herpes simplex virus (HSV) can be destroyed by human blood mononuclear cells (MC) in the presence of IgG antibody to HSV[1–3], a process termed antibody-dependent cellular cytotoxicity (ADCC). The major effector cell which mediates this reaction is a K cell; it possesses surface Fc receptors which permit attachment to IgG antibody-sensitised target cells[4–6], although the way in which the lethal hit is delivered is poorly understood. For an immune cytolytic mechanism to be maximally effective in limiting the spread of virus in a host, it should be able to destroy the infected cell at an early stage in the viral maturation cycle, before infectious viral progeny can be produced. This requirement seems to be of particular importance for viruses such as HSV, which can avoid exposure to the neutralising antibody in extracellular fluid by spreading from cell to cell across intercellular bridges[7,8]. In this report, we demonstrate that the ADCC mechanism can recognise viral surface antigens as early as 2 h after cells are infected with HSV and can produce target cell death by 3 h after infection (PI), well in advance of the first appearance of both viral progeny and the susceptibility of infected cells to lysis by antibody and complement (AbC).

MC and HSV antibody added to HSV-infected target cells 2 h after infection uniformly led to substantial cytotoxicity but did not injure uninfected target cells (Table 1). Target cell damage induced by ADCC was somewhat decreased at each successive sampling period. This diminished cytotoxicity might be explained by the fact that the MC, prepared at the beginning of each experiment, may have lost some of their cytotoxic activity while standing at room temperature before use. In contrast to ADCC, AbC did not cause significant target cell damage until at least 8 h after infection, and cytotoxicity equivalent in magnitude to that of ADCC was not seen until 24 h PI. In separate experiments, we found that the amount of ADCC-mediated damage of cells 2 h after infection was related directly to the input of infectious virus. In a representative experiment, cytotoxicity was 43.9% when a relatively high multiplicity of infection (MOI) (15 PFU per cell) was used, 15.7% at a moderate MOI (1 PFU per cell), and only 2.3% at a low MOI (0.1 PFU per cell).

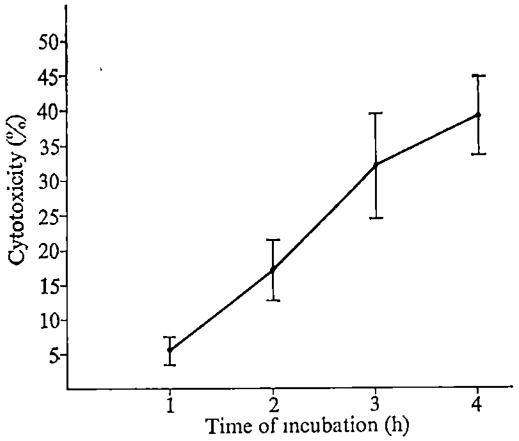

Fig. 1 Kinetics of killing of HSV-infected target cells 2 h PI by antibody-dependent cellular cytotoxicity. The curve represents the mean of four experiments. The vertical bars indicate 1 s.e.m.

Because the ADCC assay uses an incubation period of 4 h, during which the density of viral surface antigen would be expected to increase, the cells used as targets 2 h after infection may have been lysed at any time between 2 and 6 h after infection. To determine when lysis actually began, we measured the release of ^{51}Cr from target cells 2 h after infection at hourly intervals during the standard 4-h incubation period. The results (Fig. 1) indicate that a small but significant cytotoxic effect occurred as early as 1 h after the start of incubation, although most of the cell damage occurred during the ensuing 3 h. These findings indicate that some target cells are lysed as early as 3 h after infection starts.

To determine how early after infection HSV-infected cells could be recognised as foreign by the ADCC process, we

Table 1 Lysis of HSV-infected cells at various times by antibody-dependent cellular cytotoxicity and by antibody and complement

Time after infection (h)	Cytotoxicity (%) Expt 1 ADCC	Expt 1 AbC	Expt 2 ADCC	Expt 2 AbC	Expt 3 ADCC	Expt 3 AbC	Expt 4 ADCC	Expt 4 AbC	Expt 5 ADCC
2	36.4	0.0	28.4	0.0	43.9	0.0	49.5	0.2	56.3
4	32.7	0.0	23.7	3.5	NT	NT	NT	NT	57.6
8	27.0	3.9	20.5	6.1	NT	NT	NT	NT	51.6
24	19.6	18.0	21.0	20.1	NT	NT	NT	NT	30.9
Uninfected	0.0	0.0	0.0	0.0	NT	NT	NT	NT	0.0

NT, not tested. ^{51}Cr-labelled Chang liver cells (CL) in suspensions were exposed to the VR3 strain of type 1 HSV at a multiplicity of infection (MOI) of 15 plaque forming units (PFU) per cell for 1 h at 37 °C. The CL were then washed and adjusted to 6–10 × 10^5 ml^{-1} in Eagle's minimum essential medium (MEM) with 2% inactivated foetal calf serum (FCS). The cell suspension was incubated at 37 °C in a humid air–5% CO_2 atmosphere. The time of transfer to the incubator was designated zero hour PI. At various times PI, portions of the cell suspension were frozen at −70 °C for determination of infectious virus titres. The remaining cells were chilled in an ice–water bath, washed by centrifugation at 4 °C, and then adjusted to 5 × 10^4 ml^{-1} in MEM with 10% FCS for assessment of their susceptibility to lysis by ADCC and lysis by AbC. ADCC and AbC were assayed as before[3], except that the incubation period (4 h) for ADCC was shorter. The effector cells for ADCC were Ficoll–Hypaque separated MC from the venous blood of normal subjects. The effector cell–target cell ratio was 50:1. Fresh guinea pig serum at a final dilution of 1:10 was the source of complement (C) in the AbC assay. The antibody source was a pool of heat-inactivated human serum from ten HSV seropositive donors; it had a lymphocyte-dependent antibody titre of 30,000 and a complement-dependent cytolytic antibody titre of 800 against type 1 HSV-infected CL[3]. Heat-inactivated pooled serum from six seronegative donors served as a control. The serum pools were used at final dilutions of 1:100 for ADCC and 1:10 for AbC, which have been shown to produce optimal lysis[3]. Cytotoxicity due to ADCC was defined as the percentage ^{51}Cr released from target cells in the presence of MC and antibody-positive serum (PS) minus the percentage ^{51}Cr released from target cells in the presence of MC and antibody-negative serum (NS). PS alone was without effect. Cytotoxicity due to AbC was defined as $[(W-X)-(Y-Z)]$, where the symbols represent the percentage ^{51}Cr release from cells treated with PS and C (W), with PS and heat-inactivated C (X), with NS and C (Y), and with NS and inactivated C (Z). Background release for infected CL was 4–10% during 4 h except for cells 24 h PI, whose release was as high as 20%. Background release for uninfected cells was 10–15%. All values are the means of triplicate determinations. Significant cytotoxicity was defined as calculated values of at least 5% (ref. 3).

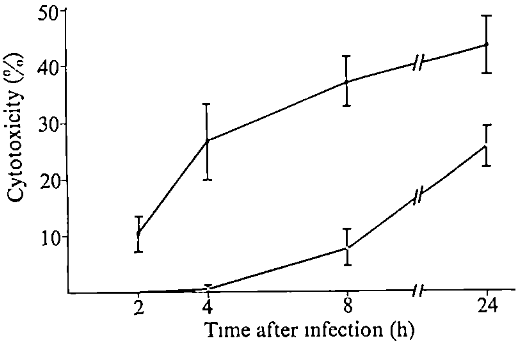

Fig. 2 Recognition of viral antigens on HSV-infected cells at various times after infection by antibody-dependent cellular cytotoxicity (●) and by antibody and complement (○). The curves represent the mean of five experiments in which lysis by ADCC was measured and the mean of three experiments in which lysis by antibody and complement was also measured.

incubated 10^6 CL at various times after infection with 1 ml of a 1:10 dilution of either HSV antibody-positive or HSV antibody-negative serum for 15 min at room temperature. The cells were then chilled in an ice–water bath, and excess unbound antibody was removed by washing them three times at 4 °C with MEM containing 2% foetal calf serum. We confirmed the absence of free lymphocyte-dependent antibody (LDA) by testing the supernates of the final cell washing for LDA activity against HSV-infected CL[2]. Thus, any cytotoxicity shown by these cells after subsequent exposure to MC or complement indicates recognition of viral antigens which were present at the time antibody was added rather than later during the test period. As Fig. 2 shows, ADCC recognised infected cells as antigenically foreign as early as 2 h after infection, whereas AbC, as before, was inactive until 8 h after infection. Presensitisation of target cells followed by removal of free antibody resulted in less ADCC at 2 h after infection than was observed when antibody and MC were added together (as in Table 1). This may be due to two factors. First, when unbound antibody is removed, the free antibody is not available to recognise infected cells that develop a density of viral surface antigen sufficient to support ADCC later than 2 h after infection but before the end of the 4-h test period. Second, the sparseness of viral surface antigens 2 h after infection may not permit firm attachment of antibody to the cell surface so that bound antibody may dissociate during cell washing.

To confirm that the ADCC mechanism recognises and destroys HSV-infected cells before infectious viral progeny appears, we determined the amount of infectious virus in the CL cultures at various times after infection by plaque titration. The results (Table 2) are typical of four experiments and show that infectious viral progeny were not detected until 8–12 h after infection. On the other hand, viral surface antigen, as measured by direct immunofluorescence, was first noted at 4 h after infection and reached a plateau at 8 h after infection (Table 2). Twenty-five to fifty per cent of the infected, but none of the uninfected cells, also showed a very faint, randomly distributed granular fluorescence within several minutes after exposure to HSV. This fluorescence persisted unchanged until at least 2 h after infection. We interpreted this as indicating the presence on the cell surface of virus which had adhered but not penetrated. Using the binding of radioiodinated antibody to detect viral surface antigen, other investigators have made a similar observation with cells exposed to HSV at a relatively high MOI (ref. 9). Perhaps, by coating the cell surface with antigenic material, this adherent non-penetrating virus may contribute to the early killing of infected cells by ADCC. The quantitative contribution of this phenomenon to ADCC activity is probably small, however, since cytotoxicity seems to be directly related to the *de novo* synthesis of viral antigen by the infected cell (Fig. 2) as indicated by the increase in ADCC with increasing time after infection.

Table 2 Infectious virus titre and membrane fluorescence at various times after infection

Times PI (h)	Virus titre (PFU ml^{-1})	Membrane fluorescence (% positive)
0	2.3×10^6	0
2	1.4×10^6	0
4	1.2×10^6	9
6	9.0×10^5	NT
8	1.3×10^6	84
12	6.7×10^6	NT
24	5.0×10^7	95

For determination of total virus at various times PI, cell suspensions (7×10^5 per ml) were frozen and thawed three times, and 0.1-ml samples were plated on to CL monolayers for 1 h at 37 °C. The monolayers were incubated for 5 d at 37 °C in a CO_2 incubator under a semi-solid overlay of 0.7% Agarose before staining with crystal violet and counting of plaques. Surface membrane fluorescence at various times PI was assessed by incubating 3-5×10^5 cells with 0.1 ml of a 1:15 dilution of a fluorescein-conjugated rabbit anti-HSV serum (supplied by A.J. Nahmias, Emory University) for 15 min at 37 °C. The cells were washed three times in ice-cold normal saline. At least 200 cells per preparation were then examined for surface fluorescence under ortho-illumination in a Zeiss fluorescence microscope. Cells with partial or complete rims of fluorescence were counted as positive.

In summary, ADCC can recognise cells infected with type 1 HSV as early as 2 h after infection and produces detectable cell lysis by 3 h after infection. This is well in advance of the appearance of the first mature viral progeny at 8 h PI or later. Consistent with previous studies using HSV-infected cells[10], susceptibility to lysis by antibody and complement is not apparent earlier than 8 h PI. Although we have not directly shown that ADCC inhibits viral replication *in vitro*, our observations suggest that this is a likely consequence of cellular injury at such an early stage in the viral maturation cycle. Because ADCC requires only modest amounts of antibody to operate efficiently[11], it should be particularly important in host defence by helping to limit viral spread during the acute phase of a primary infection when specific viral antibody is just beginning to be produced.

S. L. Shore
T. L. Cromeans
T. J. Romano

Center for Disease Control,
Atlanta, Georgia 30333

[1] Shore, S. L., Nahmias, A J., Starr, S. E., Wood, P. A., and McFarlin, D E, *Nature*, 251, 350–352 (1974)
[2] Rager-Zisman, B., and Bloom, B., *Nature*, 251, 542–543 (1974)
[3] Shore, S. L., Black, C. M., Melewicz, F. M, Wood, P. A., and Nahmias, A. J., *J. Immun.*, 116, 194–201 (1976).
[4] Larsson, A., and Perlmann, P., *Int. Archs Allergy*, 43, 80–88 (1972).
[5] Shore, S. L., Melewicz, F M., Milgrom, H., and Nahmias, A J, in *The Reticuloendothelial System in Health and Disease* (edit by Reichard, S M., Escobar, M. R., and Friedman, H.), (Plenum, New York, in the press)
[6] Romano, T. J., and Shore, S. L., *Fedn Proc*, 35, 474 (1976).
[7] Hoggan, D. B, Roizman, B., and Roane, P R, *Am. J Hyg*, 73, 114–122 (1961).
[8] Christian, R T., and Ludovici, P. P., *Proc Soc. exp. Biol. Med*, 138, 1109–1115 (1971).
[9] Rosenthal, J., Hayashi, K., and Notkins, A. L., *J gen. Virol*, 18, 195–199 (1973).
[10] Lodmell, D L., Niwa, A., Hayashi, K., and Notkins, A. L., *J. exp. Med.*, 137, 706–720 (1973).
[11] Perlmann, P., Perlmann, H., and Wigzell, H., *Transplant. Rev.*, 13, 91–114 (1972).

Increased ornithine decarboxylase activity in murine sarcoma virus infected cells

POLYAMINE biosynthesis is one of the earliest events occurring during cellular proliferation[1,2], and the rate at which it proceeds[3] is limited by ornithine decarboxylase (ODC), an enzyme which catalyses the formation of putrescine from ornithine. ODC levels are low, but stable, in resting cells, and a large increase in activity occurs rapidly after the onset of growth[4,5]. Elevated ODC levels occur in certain tumour cells, including hepatoma, neuroblastoma and SV40-

transformed cells[3-7]. Fast growing hepatomas have higher enzyme levels than slow growing ones[6]. During Rous sarcoma virus (RSV) transformation, elevation of ODC levels precedes morphological change[8].

Here we describe the marked elevation of ODC levels which occurs in murine sarcoma virus (MSV)-infected cells. The continuous, contact inhibited, non-tumorigenic cell line BALB/3T3 (ref. 9) was used for these studies because it has a short doubling time and is readily transformed by MSV. Gz-MSV (ref. 10), which consists of a transforming virus and a non-transforming strain of murine leukaemia virus (MuLV), was grown in BALB/3T3 cells. The MuLV acts as a 'helper' virus, enabling the defective MSV to complete its replication cycle. Cells transformed by MSV in the absence of 'helper' virus contain the sarcoma genome, but do not release infectious virus (non-producer cells)[11]. Rauscher leukaemia virus[12] (RLV), a non-transforming strain of MuLV, was obtained from the supernatant fluids of chronically infected BALB/c cells. BALB/3T3 cells, clone A31, and KA31, Kirsten MSV virus-transformed non-producer A31 cells, were obtained from Dr Stuart Aaronson.

Table 1 Properties of cell lines

Cell line	Population doubling time (h)	Colony forming efficiency (%) Liquid medium	Colony forming efficiency (%) Soft Agarose	Virus production (% infectious centres) MSV	Virus production (% infectious centres) MuLV
B/3T3	23	51.5	<0.01	<0.1	<0.1
RLV infected (MOI* 3:1)	23	48.5	<0.01	<0.1	75.0
MSV infected (MOI 1:1)	43	10.5	0.8	46.5	100
KA31	16	48.0	28.0	<0.1	<0.1

Cells were seeded at a density of 5×10^3 cm^{-2} in growth medium (Dulbecco's modification of Eagle's minimal medium, supplemented with 10% foetal bovine serum and antibiotics). Virus infections were performed in suspension (1 h, 37 °C) before seeding. Total and Trypan blue resistant cell counts were performed 1, 3, 4, 5 and 7 d after seeding. Cells were collected 7 d after seeding and tested for colony forming efficiency in liquid (growth) medium and soft Agarose (0.4%). Virus production was measured 7 d after infection by infections centre assays. Indicator cells were seeded (1×10^5 cells per 60-mm dish) 24 h before addition of test cells, and foci of morphologically altered cells enumerated 5 d later[12,13]. BALB/3T3 cells were the indicator for MSV production and the S+H− cell line A1-2 for MuLV production.

*MOI, multiplicity of infection.

The properties of the cell lines used are presented in Table 1. RLV infection of BALB/3T3 cells did not alter the growth rate or colony forming efficiency (CFE) in liquid medium The RLV infected cells remained contact inhibited, and were unable to grow in soft Agarose. KA31 non-producer cells were morphologically transformed, had a short doubling time, and formed colonies when suspended in soft Agarose. MSV infected B/3T3 cells released MSV and MuLV, and were morphologically transformed but their CFE in soft Agarose was low. Their population doubling time was greatly increased and their CFE in liquid medium decreased. Trypan blue uptake studies revealed only a modest increase in the number of non-viable cells (from < 2% in the control cells to up to 8% in the MSV infected cells). The reason for the increased doubling time after acute MSV infection is not understood, but it also occurs in cat cells acutely transformed by the feline leukaemia virus pseudotype of MSV (ref. 14). Apparently many of the cells acutely infected with MSV retain the ability to exclude Trypan blue, but fail to divide, perhaps due to cytogenetic alterations (chromosome breaks and pulverisation) induced by MSV (P. Fischinger, personal communication).

ODC levels of BALB/3T3 cells were growth dependent (Fig. 1). Maximum levels, reached during exponential growth, occurred four days after seeding. The decrease in cell growth that preceded saturation density was accompanied by a rapid drop in ODC activity, and basal levels were reached at saturation density. RLV infection had no effect on ODC levels. Transformed KA31 cells had a maximum ODC level approximately twice that of BALB/3T3 cells. Acute MSV infection, at both high and low multiplicities, resulted in a rise of 6–26-fold in maximum ODC activity. The rise commenced at the onset of morphological transformation, and maximum levels coincided with mass transformation of the culture. ODC activity remained elevated during the remainder of the 7-d observation period. When MSV infected cells were trypsinised and reseeded at seven-day intervals (Fig. 2), maximum ODC levels during subsequent passages were about twice as much as uninfected control cells.

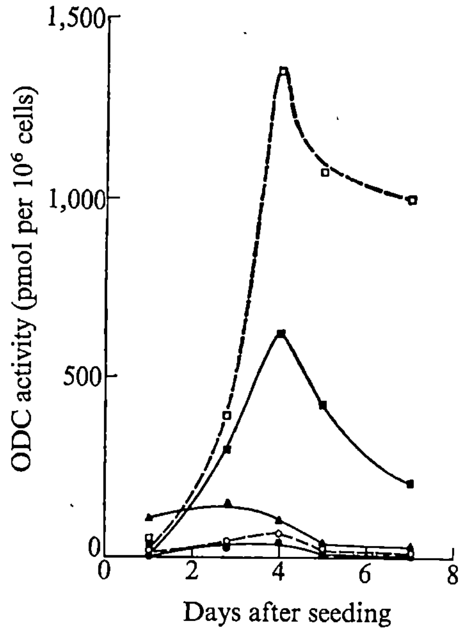

Fig. 1 ODC activities of cell lines. See Table 1. Cell lines were virus infected at the multiplicities (MOI) indicated immediately before seeding. Cells were seeded in 100-mm plastic plates (Falcon) at densities of 5×10^3 cm^{-2}. At 1, 3, 4, 5 and 7 d after seeding, replicate plates of each line were rinsed twice with saline and frozen (−20 °C), until assayed. For ODC assays, cells were gently scraped into 1 ml buffer (50 μM EDTA, 25 μM pyridoxal phosphate, 2.5 mM dithiothreitol in 25 mM Tris-HCl, *p*H 7.1), freeze–thawed three times, and centrifuged (4,500*g* for 10 min). Supernatant fluids (0.25 ml) were incubated with 50 μl 1-^{14}C-ornithine (0.2 μCi, 6.25 nmol) in plastic tubes equipped with a rubber stopper supporting a polyethylene centre well. After incubation (37 °C, 45 min), 0.2 ml hydroxide of hyamine was injected into each centre well. After a further incubation of 15 min, 0.2 ml 6% perchloric acid was added to stop the reaction. Tubes were agitated for 15 min to release bound CO_2, the centre wells were then removed and their radioactivities determined. The experiments were performed five times. Results of a representative experiment are demonstrated. ●, BALB/3T3 control; ○, RLV infected (MOI 3:1); ■, MSV infected (MOI 0.1:1); □, MSV infected (MOI 1:1); ▲, KA 31.

Our data demonstrate that a marked rise in ODC activity occurs in cells acutely infected with MSV. This rise is due to the transforming virus component of the MSV complex, as infection with non-transforming MuLV has no effect. The rise in MSV infected cells is not due to an increased rate of cellular division, since most acutely infected cells fail to divide. Rapidly dividing, chronically transformed cells (both virus producing and non-producing) have maximum ODC levels approximately double that of non-transformed parent cells.

The increased ODC levels of virus transformed and other malignant cells may be related to the higher polyamine content of tumour cells and to the increased excretion of polyamines in the urine of cancer patients[15].

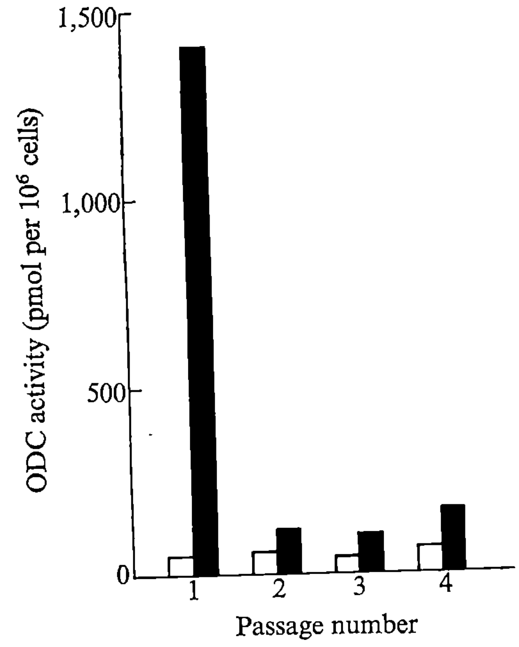

Fig. 2 Maximal ODC levels of MSV BALB/3T3 cells. See Table 1 and Fig 1. Cells were infected at a MOI of 0.1:1 immediately before seeding at a density of 5×10^3 cm^{-2}. Control and infected cells were trypsinised at 7-d intervals and reseeded at the same density. Cells were collected 4 d after seeding for ODC determinations. Open columns, control cells; solid columns, MSV infected cells.

We thank Drs George J. Todaro and John D. Minna for advice and encouragement, and Mrs Theresa Gregorio for technical assistance.

ADI F. GAZDAR
HAROLD B. STULL

Veterans Administration Hospital,
Washington, DC 20422

LARY J. KILTON

National Cancer Institute,
Bethesda, Maryland 20014

URIEL BACHRACH

Hebrew University-Hadassah Medical School,
Jerusalem, Israel

Received May 13, accepted June 29, 1976.

[1] Cohen, S S., *Introduction to the Polyamines* (Prentice Hall, New Jersey, 1971).
[2] Bachrach, U., *Function of Naturally Occurring Polyamines* (Academic, New York, 1973).
[3] Russell, D , and Snyder, S. H., *Proc. natn. Acad. Sci U S A* , 60, 1420–1427 (1968).
[4] Lembach, K J , *Biochim. biophys. Acta*, 354, 88–100 (1974)
[5] Hogan, B L., *Biochem. biophys. Res. Commun* , 45, 301–307 (1971)
[6] Williams-Ashman, H. G , Coppoc, L , and Weber, G , *Cancer Res.*, 32, 1924–1932 (1972)
[7] Bachrach, U., *Proc. natn. Acad Sci U S.A* , 72, 3087–3091 (1975)
[8] Don, S., and Bachrach, U , *Cancer Res* (in the press).
[9] Aaronson, S A., and Todaro, G. J., *Science*, 68, 1024–1027 (1968)
[10] Gazdar, A. F , Sarma, P. S., and Bassin, R. H , *Int J. Cancer*, 9, 234–241 (1972)
[11] Aaronson, S. A , and Rowe, W. P , *Virology*, 42, 9–14 (1970)
[12] Rauscher, F. J., *J natn Cancer Inst* , 29, 515–542 (1962)
[13] Gazdar, A F., Russell, E. K., and Minna, J. D , *Proc. Soc. exp Biol. Med.*, **148**, 688–692 (1975).
[14] Fischinger, P. J , and Haapala, D K , *J. gen Virol.*, 13, 203–214 (1971)
[15] Bachrach, U , and Ben-Joseph, M , *Polyamines in Normal and Neoplastic Growth* (edit. by Russell, D. H), 15–26 (Raven, New York, 1973).

Single ionic channels induced in lipid bilayers by polyene antibiotics amphotericin B and nystatine

AMPHOTERICIN B and nystatine increase the permeability of lipid membranes to ions, water and non-electrolytes[1,2]. Cholesterol (or some other sterols) is a necessary membrane component for the antibiotics to be effective[1,3]. Permeability to water and non-electrolytes increases linearly with ion permeability[2]. The molecules of the size of glucose and larger are essentially impermeant. It is concluded[2,4] that amphotericin B and nystatine form aqueous pores with an effective radius of approximately 4 Å in thin lipid membranes. The changes in membrane conductance connected with the formation of a single pore have, however, not yet been observed. In this paper the properties of individual conductance channels induced in black lipid membranes by amphotericin B and nystatine are described briefly.

Black lipid membranes were formed across a 0.5-mm diameter hole in a 1-ml Teflon cup from *n*-hexane solutions of brain lipids (20 mg ml^{-1}) purified from neutral lipids by acetone extraction. A certain amount of recrystallised cholesterol (usually 1 mg ml^{-1}) was added to the membrane-forming solution. The membrane currents were measured with the Keithley-301 electrometer. The water-soluble sodium salt of amphotericin B or stock solution of nystatine in dimethylsulphoxide (10^{-3} M) were added at equal concentrations to both aqueous solutions buffered with 10 mM potassium phosphate. All the measurements were carried out at *p*H 6.0 and 22–23 °C. The specific conductance of black lipid membranes in the 2 M KCl solution in the absence of antibiotics was about 2×10^{-9} mho cm^{-2}.

When amphotericin B was added at a concentration of $2\text{–}3\times10^{-8}$ M to both electrolyte solutions discrete current jumps can be observed on the membranes formed from the heptane–lipid solution with a phospholipid–cholesterol weight ratio of 20:1 (Fig. 1).

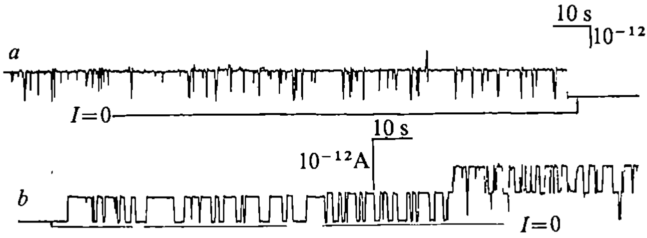

Fig. 1 Fluctuations in membrane current in the presence of 3×10^{-8} M amphotericin B and 2M KCl (*a*), and 1×10^{-7} M amphotericin B and 2 M KNO_3 (*b*). Membrane potential 200 mV. Arrows show current through an unmodified membrane. Phospholipid–cholesterol ratio, 20:1.

The probability of the appearance of these conductance jumps (about 6 pmho in 2 M KCl with a membrane potential of 200 mV) depended markedly on the cholesterol content of the membrane-forming solution. With the cholesterol-depleted lipids the membrane conductance did not increase even if amphotericin B at a concentration of 5×10^{-7} M was added symmetrically to the aqueous solutions. At a phospholipid–cholesterol ratio of 100:1, the current jumps could be observed at 10^{-7} M amphotericin B, whereas at a ratio of 2:1, only a $1\text{–}2\times10^{-9}$ M concentration of the antibiotic was required. The size of the jumps did not depend on the cholesterol concentration. Being added only to one side of the membrane with a 20:1 ratio of phospholipid–cholesterol, amphotericin B did not increase the membrane conductance even at a concentration of 4×10^{-5} M. In all the experiments described below the phospholipid–cholesterol ratio was 20:1.

The stepwise conductance changes observed seem to be the result of the formation of single ionic channels, each having only two states: one open and one closed. After being formed, the channel exhibits many transitions between the two states. All the transitions shown in Fig. 1*a* can be related to the same channel because there are no double or other multiple levels characteristic of simultaneous operation of several independent channels. The distribution functions of dwell times for both the open and closed states of an individual channel are single exponentials. The average dwell time in each state does not depend on the membrane potential.

The dependence of a single-channel conductance on KCl

Table 1 Variation in amphotericin B channel parameters with KCl concentration

	KCl (M)				
	0.5	1.0	1.5	2.5	3.5
g (mho × 10^{12})	2.0±0.4	3.75±0.5	5.5±0.5	6.9±0.5	8 4±0.8
Amph. (M × 10^8)	10	6.5	5	3	2
τ_o(s)	1.9±0.2	—	2.5±0 6	—	4.3±0.5
τ_c(s)	0.14±0.01	—	0.12±0.02	—	0 13±0.02

g, A single-channel conductance measured with membrane potential 200 mV.

Amph., Amphotericin B concentration necessary to obtain a stationary record (about 10 min) in a few channels.

τ_o, Average dwell time of a channel in the open state.

τ_c, In the closed state.

concentration (Table 1) shows saturation. The voltage–current characteristic of a single channel and a multichannel membrane are shown in Fig. 2. The channel conductance increased slightly with membrane potential. In asymmetrical conditions (1 and 3 M KCl), the values of the zero current potentials were the same for the single channel (17±2.0 mV) and for the multichannel membranes (18.5±0.5 mV), within the limits of experimental errors. Transport numbers for the channel (T_{Cl} = 0.85 and T_K = 0.15) were similar to those found previously for the multichannel membranes in the experiments with low salt concentration[1]. Thus, non-ideal anionic permeability of a membrane in the presence of amphotericin B is not the result of simultaneous operation of two types of channels—cationic and anionic—but it is an intrinsic property of each individual channel.

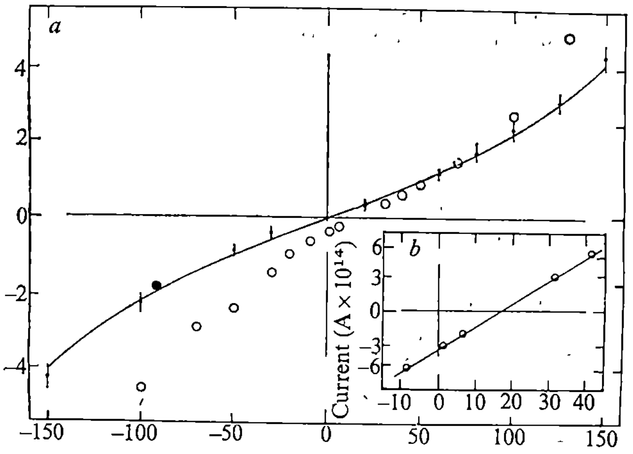

Fig. 2 Current–voltage characteristics of the membrane in the presence of amphotericin B; *a*, points characteristic of a single-channel membrane in a symmetrical solution: 1 M KCl and 6 × 10^{-8} M amphotericin B; curve, characteristic of the membrane with approximately 200 channels, in a symmetrical solution: 1 M KCl and 2 × 10^{-7} M amphotericin B. The current scale for the curve was chosen to fit the point at +100 mV. ○, Characteristic of a single-channel membrane separating solutions of 1 M KCl and 3 M KCl; 3 × 10^{-8} M amphotericin B in both solutions. The sign of the potential is given for the 3 M KCl solution *b*, Region of characteristic of a single-channel membrane in asymmetrical conditions near the point of zero current potential.

The main feature of amphotericin B channels is the dependence of their formation and properties on the type and concentration of salt. Single channels could be observed in solutions of high concentrations of such salts as KCl, KBr, KF, KNO_3, CsCl, CsBr, CsF, $CsNO_3$, $RbNO_3$, $CaCl_2$. As a rule these channels have only two states. The jumps of intermediate values, however, were rarely observed, as can be seen in Fig. 3. Table 1 demonstrates that the amphotericin B concentration necessary to obtain a few channels was influenced by salt concentration. Formation of the channels depended on the type of cation as well as anion. If the membrane was formed in solutions of electrolyte with a large cation (2 M acetylcholine chloride) or a large anion size (2 M potassium propionate), the membrane conductance did not increase even at an amphotericin B concentration of 10^{-6} M. In NaCl solutions single channels were observed only at a rather low salt concentration (up to 2 M). In a solution of 2 M NaCl the channel conductance was about 3 pmho. In solutions of higher NaCl or NH_4Cl concentrations (3–4 M), there are only random changes of conductance with irregular jumps of no more than 0.2 pmho.

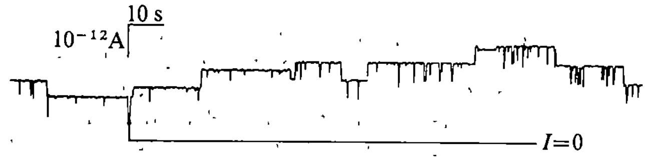

Fig. 3 Current against time record: 5 M CsCl and 2 × 10^{-8}M amphotericin B. Membrane potential 100 mV.

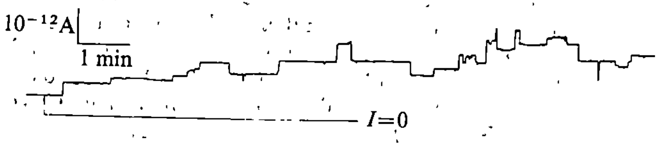

Fig. 4 Current against time record: 3 M KCl and 10^{-7} M nystatine. Membrane potential 200 mV.

One more interesting property of amphotericin B channels is the salt dependence of their gates. Figure 1 shows that the dwell time of the channel in both states at a given voltage were different in KCl and KNO_3 solutions of the same concentration. Moreover the average time which the channel spends in the open state (τ_O) depends on salt concentration, as can be seen in Table 1.

Another polyene antibiotic, nystatine, also induced discrete changes of lipid membrane conductance. In contrast to amphotericin B channels, the presence of smaller jumps and somewhat longer dwell times for the open channels were characteristic of the nystatine channels (Fig. 4).

We thank Dr E. D. Etingov for amphotericin B and nystatine, and Dr A. Ya. Silberstein for discussions.

L. N. ERMISHKIN
Kh. M. KASUMOV
V. M. POTZELUYEV

Institute of Biological Physics,
USSR Academy of Sciences,
Pushchino, Moscow Region
Institute of Physics,
Azerb. SSR Academy of Sciences,
Baku, USSR

Received April 12; accepted May 26, 1976

[1] Andreoli, T E., and Monahan, M., *J. gen Physiol.*, 52, 300–325 (1968).
[2] Holz, A., and Finkelstein, A., *J gen. Physiol*, 56, 125–145 (1970).
[3] Kasumov, Kh M, and Liberman, E. A., *Biofizika*, 17, 1024–1031 (1972).
[4] Dennis, V. W., Stead, N. W., and Andreoli, T. E, *J. gen. Physiol.*, 55, 375–400 (1970)

Release of novel prostaglandins and thromboxanes after immunological challenge of guinea pig lung

THE ability of lung tissue from various species to synthesise and release parent prostaglandins (PGs) has been well established[1,2] and metabolic conversions of PGs occur rapidly after very efficient uptake from the circulation[3,4]. Using an isolated perfusion system to allow uptake of the PG precursor, arachidonic acid

(1-^{14}C labelled), the sensitised guinea pig lungs released a number of radiolabelled substances following challenge with specific antigen[5]. Our attempts to characterise these substances and prepare sufficient material for biological testing have revealed at least two compounds which have not been previously described and others not previously seen in this release system.

Guinea pigs were sensitised to ovalbumin (100 mg intraperitoneally and subcutaneously) and after 3 weeks were killed and their lungs perfused with Tyrode solution[6]. The sensitised lungs were challenged during perfusion with ovalbumin (5 mg), the perfusate collected for 10 min after challenge and stored at 4 °C under nitrogen. A control group of guinea pigs was also perfused without challenge. The compounds of interest in the perfusate were transferred into organic solvent by adsorbing them on to XAD-2 resin (Rohm and Haas) and eluting with methanol. The concentrated methanol extract was then applied on to a silicic acid column and the various substances removed by stepwise elution with increasing concentration of methanol (0–10%) in chloroform. The eluates were concentrated by vacuum distillation and derivatised for gas liquid chromatography and mass spectrometric analysis (GLC–MS).

The following known PGs and related compounds were identified by GLC–MS following their isolation from sensitised challenged guinea pig lungs; (1) 12-hydroxy-5,8,10-heptadecatrienoic acid (HHT)[7], (2) the hemiacetal of 8-(1-hydroxy-3-oxopropyl)-9,12-dihydroxy-5,10-heptadecadienoic acid (PHD: thromboxane B$_2$)[7,8], (3) PGE$_2$, (4) 15-oxo-PGE$_2$, (5) 15-oxo-13,14-dihydro-PGE$_2$, (6) PGF$_{2\alpha}$, (7) 15-oxo-PGF$_{2\alpha}$, (8) 15-oxo-13,14-dihydro-PGF$_{2\alpha}$. In addition, two new related compounds were characterised, namely 6-oxo-PGF$_{1\alpha}$ (compound 1) and 7-{2, 4-dihydroxy-6-(3-oxo-1-octanyl)-tetrahydropyran-5-yl}-*cis*-5-heptenoic acid (compound 2). No identifiable levels of these compounds were noted in the control extracts.

The mass spectrum and the source of the major fragments of compound 1 as its methyl ester, methoxime, trimethylsilyl derivative is shown in Fig. 1. Ions at *m/e* 173 and *m/e* 199 support the presence of a 15-hydroxy group and a 13,14-double bond[9]. The ion at *m/e* 217 is typical of the F-prostaglandin ring system[9]. The ion at *m/e* 187 is formed by a McLafferty rearrangement (not possible for a methoxime substituent at C7) with the hydrogen at C9 and confirms the structure of the α chain. Additional evidence for the location of the oxo group at C6 is provided by the ion at *m/e* 115.

The structures of the ions at *m/e* 115 and *m/e* 187 are supported by the appearance of ions at *m/e* 118 and *m/e* 190 in the spectrum of the corresponding trideuteromethyl ester of compound 1*A*. Significantly, this spectrum lacks ions at *m/e* 104 and 176, thereby excluding location of the oxo group in compound 1 at C5. The corresponding benzyl-oxime of compound 1*A* also exhibits the ion at *m/e* 115 but in this case the McLafferty rearrangement ion appears at *m/e* 263. Finally, the spectrum of compound 1 after methylation, borohydride reduction of the oxo group, followed by silylation, exhibits an intense ion at *m/e* 217. The intensity of this ion reduces by approximately 50% in the corresponding sodium borodeuteride product, and appearance of an ion at *m/e* 218 is noted. This ion at *m/e* 218 is consistent with the incorporation of one deuterium atom at C6 and subsequent cleavage in the derivative at the C7, C6 bond, alpha to the newly incorporated trimethylsilyl group. These facts are all consistent with the structure of compound 1 being 6-oxo-PGF$_{1\alpha}$.

The mass spectrum of compound 2 as its methylester, methoxime, trimethylsilyl derivative, is shown in Fig. 2 with its major fragments. The ion at *m/e* 174 is typical of the aldehydic unit of the thromboxane system[7] (this appears at *m/e* 183 in the spectrum of the *d*-9 trimethylsilyl derivative). The absence of an

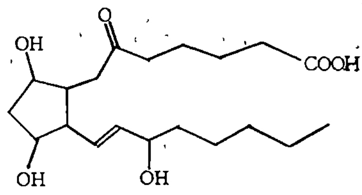

1

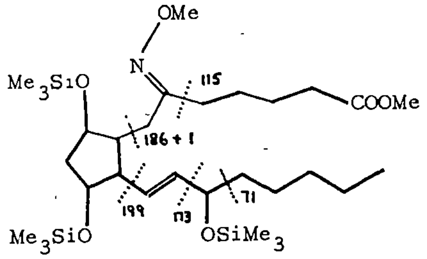

1*A*

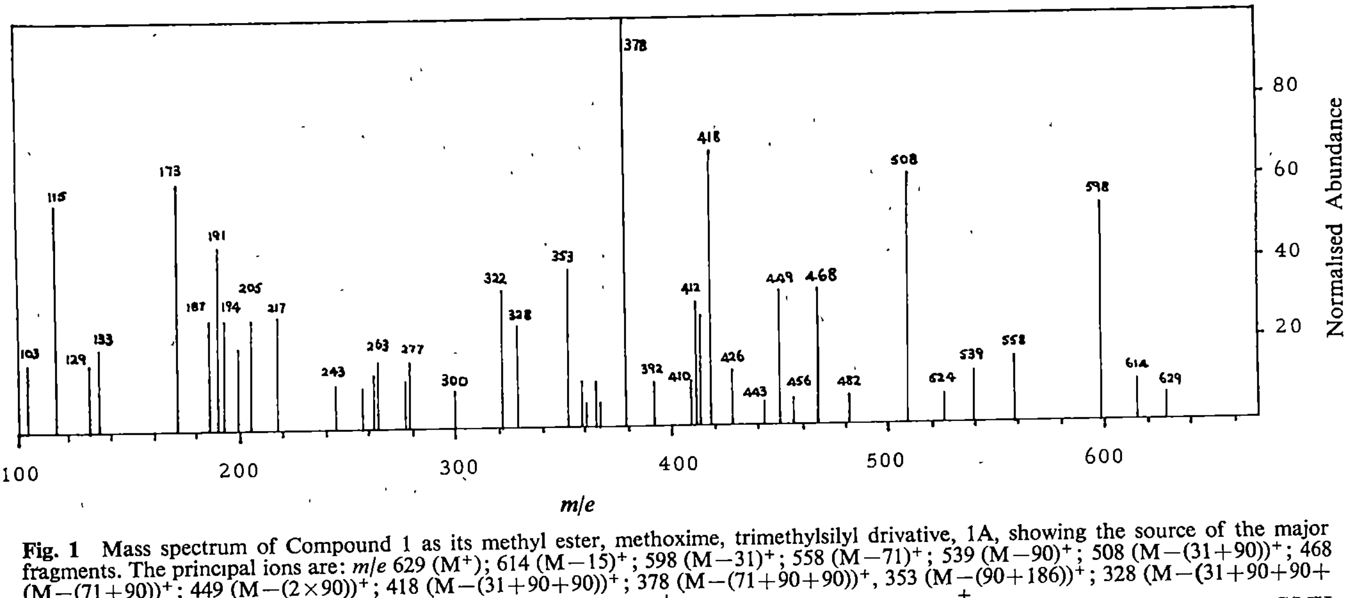

Fig. 1 Mass spectrum of Compound 1 as its methyl ester, methoxime, trimethylsilyl drivative, 1A, showing the source of the major fragments. The principal ions are: *m/e* 629 (M$^+$); 614 (M−15)$^+$; 598 (M−31)$^+$; 558 (M−71)$^+$; 539 (M−90)$^+$; 508 (M−(31+90))$^+$; 468 (M−(71+90))$^+$; 449 (M−(2×90))$^+$; 418 (M−(31+90+90))$^+$; 378 (M−(71+90+90))$^+$, 353 (M−(90+186))$^+$; 328 (M−(31+90+90+90))$^+$; 217 ($Me_3Si\overset{+}{O}=CH-CH-OSiMe_3$); 199 ($CH=CH-CH(\overset{+}{O}SiMe_3)C_5H_{11}$); 191 ($Me_3Si\overset{+}{O}=CH-OSiMe_3$); 187 ($(CH_2=C(NH OMe)(CH_2)_4COOMe)^+$); 173 ($Me_3Si\overset{+}{O}=CHC_5H_{11}$); 115 ($((CH_2)_4COOMe)^+$).

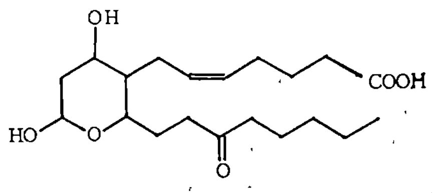

2

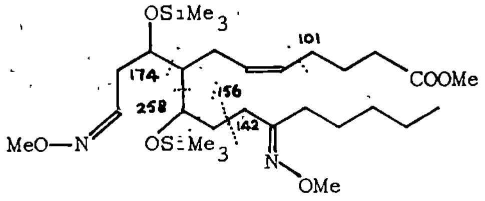

2A

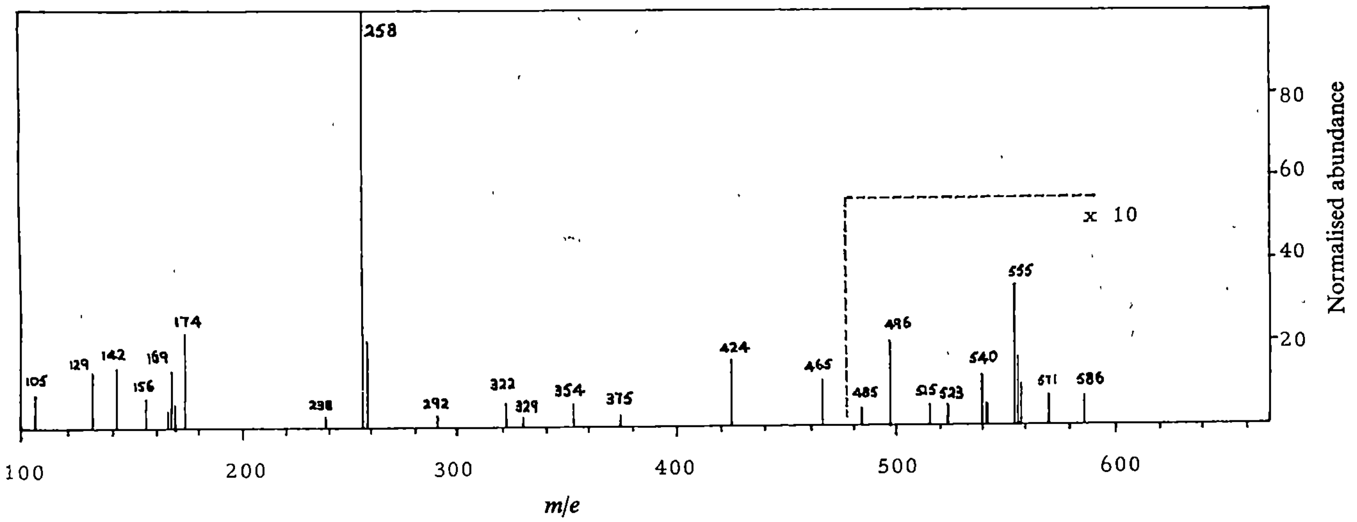

Fig. 2 Mass spectrum of compound 2 as its methyl ester, methoxime, trimethylsilyl derivative 2*A*, showing the source of the major fragments. The principal ions are: *m/e* 586 (M^+); 555 $(M-31)^+$: 496 $(M-90)^+$; 485 $(M-101)^+$; 465 $(M-(31+90))^+$; 424 $(M-(90+72))^+$; 375 $(M-(31+90+90))^+$; 354 $(M-(31+90))^+$; 329 $(M-(101+156))^+$; 322 $(M-(90+174))^+$; 258 $(Me_3Si\overset{+}{O}=CH(CH_2)_2C(=NOMe)C_5H_{11}$, 174 $(HC(=NOMe)CH_2CH=\overset{+}{O}SiMe_3)$; 156 $((CH_2)_2C(=NOMe)C_5H_{11})^+$; 142 $(CH_2C(=NOMe)\ C_5H_{11})^+$; and $(Me_3Si\overset{+}{O}=CH\text{–}CH_2CN)$.

ion at *m/e* 173 suggests modification of the lower chain from that of thromboxane B_2. Losses of 156 and 142 and ions at these masses (all noted for the *d*-9 trimethylsilyl derivative) indicate a saturated β chain containing an oxo substituent. The base peak at *m/e* 258 (267 in the *d*-9 trimethylsilyl derivative) is equivalent to that at *m/e* 301 in the corresponding thromboxane B_2 derivative[7]. The structure of the top chain is supported by the loss of the 101 fragment (104 in the corresponding trideuteromethylester of 2*A*). These facts accord with compound 2 having a structure equivalent to that of an oxo-dihydro derivative of thromboxane B_2.

Table 1 Chromatographic characteristics and relative amounts of compounds isolated after immunological challenge of guinea pig lung

Compound	Fraction no.*	C-value†	Approximate % of total‡
15-oxo PGE_2	3	24.4§	Trace
15-oxo-13,14-dihydro PGE_2	3	24.3§	Trace
15-oxo-13,14-dihydro $PGF_{2\alpha}$	3	24.4	3
PGE_2	3,4	24.5§	1
Compound 2	4,5	25.3	42
15-oxo-$PGF_{2\alpha}$	4	24.5	6
Thromboxane B_2	6,7,8	25.1	30
$PGF_{2\alpha}$	7	24.0	0.6
Compound 1	7,8	25.5	11
Other unidentified substances with PG-like mass spectral characteristics	—	—	6

*% MeOH in $CHCl_3$ on silicic acid, each fraction being 20 ml total volume.

†Retention time relative to fatty acid esters on 1.2% SE 30 at 230 °C for methylated, methoximated, silylated compounds. Compound 1 is not resolved into doublet except as benzyl-oxime derivative.

‡Calculation based on 3 groups of pooled perfusates each derived from 200 guinea pigs. There was less than 10% variation in the percentages quoted from each group. GLC analysis indicated that the total PG and thromboxane content is 1.3–1.8 µg per guinea pig.

§Major geometric isomer.

Table 1 lists the relative amounts of the PGs and thromboxanes observed, along with their chromatographic elution characteristics.

Very little PGE_2 or $PGF_{2\alpha}$ were detected, although there was a significant amount of 15-oxo-$PGF_{2\alpha}$ and 15-oxo-13,14-dihydro-$PGF_{2\alpha}$. A high proportion of the content occurred as compound 2, perhaps indicating a significant formation of thromboxane B_2. Hamberg[10] described the release of thromboxane B_2 after challenge in a chopped lung system and our data would suggest that *in vivo*, thromboxane B_2 may be metabolised rapidly within the cells after its synthesis and in the lung system, at least, may not exert its full pharmacological action.

The biological activities of compounds 1 and 2 have been compared with those of $PGF_{2\alpha}$ and thromboxane B_2 on a variety of smooth muscle preparations *in vitro*. Compound 2 had no detectable activity, whilst thromboxane B_2 had minimal and variable activity only on respiratory smooth muscle (1/100–1/1000 that of $PGF_{2\alpha}$).

Compound 1, however, had considerable biological activity, being 1/3 as active as $PGF_{2\alpha}$ on respiratory smooth muscle and having 1/5 to 1/100 the activity on a variety of intestinal smooth muscle preparations. Compound 1 occurs as approximately 11% of the total PGs released on challenge ($PGF_{2\alpha}$ 0.6%) and probably accounts for a significant proportion of the PG spasmogenic activity.

Only three of the compounds listed in Table 1 have significant spasmogenic activity: $PGF_{2\alpha}$, 15-oxo-$PGF_{2\alpha}$ (ref. 11) and 6-oxo-$PGF_{1\alpha}$ and the activity of the last two seems to be reasonably selective for respiratory smooth muscle. It would seem, therefore, that the identification of this novel PG (compound 1) is of considerable relevance to the immunological reaction in guinea pigs and may relate to the symptomology of human asthma.

Although there is no evidence in the present study for metabolic conversion of thromboxane B_2 to compound 2, by inference from the metabolism of the parent PGs, it seems likely that this is its probable mode of formation. The activity of the enzymes responsible for these metabolic reactions in asthmatic individuals could, therefore, be of considerable importance in an analysis of the role of PGs and thromboxanes in asthma.

W. Dawson
J. R. Boot

Pharmacological Research

A. F. Cockerill
D. N. B. Mallen
D. J. Osborne

Physical Organic Research,
Lilly Research Centre Limited,
Erl Wood Manor,
Windlesham,
Surrey GU20 6PH, UK

Received January 20, accepted June 11, 1976.

1 Anggard, E., *Biochem. Pharmac.*, **14**, 1507–1516 (1965).
2 Piper, P. J., and Vane, J. R., *Ann. N.Y Acad. Sci.*, **180**, 363–385 (1971).
3 Anggard, E., and Samuelsson, B., *Nobel Symposium 2, Prostaglandins* (edit. by Bergstrom, S , and Samuelsson, B.), 97–105 (Almquist and Wiksell, Stockholm, 1967).
4 Ferreira, S H., and Vane, J R., *Nature*, **216**, 868–873 (1967)
5 Dawson, W., and Tomlinson, R., *Br. J. Pharmac.*, **52**, 107–108P (1974).
6 Brocklehurst, W E., *J Physiol., Lond.*, **151**, 416–435 (1960).
7 Hamberg, M., and Samuelsson, B , *Proc natn. Acad. Sci U.S.A.*, **71**, 3400–3404 (1974).
8 Hamberg, M., Svensson, J , and Samuelsson, B., *Proc. natn Acad Sci. U.S.A.*, **75**, 2994–2998 (1975).
9 Crain, P. F , Desiderio, D. M., and McCloskey, J. A., *Meth. Enzym.*, **45**, 359–377 (1975).
10 Hamberg, M., and Samuelsson, B., *Biochem. biophys. Res. Commun.*, **61**, 942–949 (1974).
11 Dawson, W., Lewis, R. L., McMahon, R. E., and Sweatman, W. J. F , *Nature*, **250**, 331–332 (1974).

ABO blood group determinants with branched cores

Although the biochemical basis of ABO and Lewis blood types in man has on the whole been elucidated[1], more detailed information is needed about the carbohydrate structures of the A and B subgroups[2]. But investigation has been limited by the complexity of the sugar chains of these antigens[3]. Information can, however, be obtained from the study of human milk oligosaccharides, which are synthesised by a series of glycosyl transferases which mediate the formation of glycoproteins, especially those of blood group substances[1]. Our studies have shown that, contrary to the composite structures of ABO and Lewis blood group determinants described by Lloyd and Kabat[3] (Fig. 1), the H determinant is located only on the type 1 carbohydrate chain (Galβ1→GlcNAc....) of the branched sugar grouping.

Lacto-*N*-hexaose, a branched oligosaccharide with the same structure as the distal portion of the backbone carbohydrate chain of blood group substances, and its fucosyl derivatives have been found in human milk[4,5]. We have isolated three of them which have the Fucα1→2Gal grouping and elucidated their structures (Fig. 2). Details of structural studies will be published elsewhere.

Fig. 1 Composite structure of the blood group determinants proposed by Lloyd *et al.*[3].

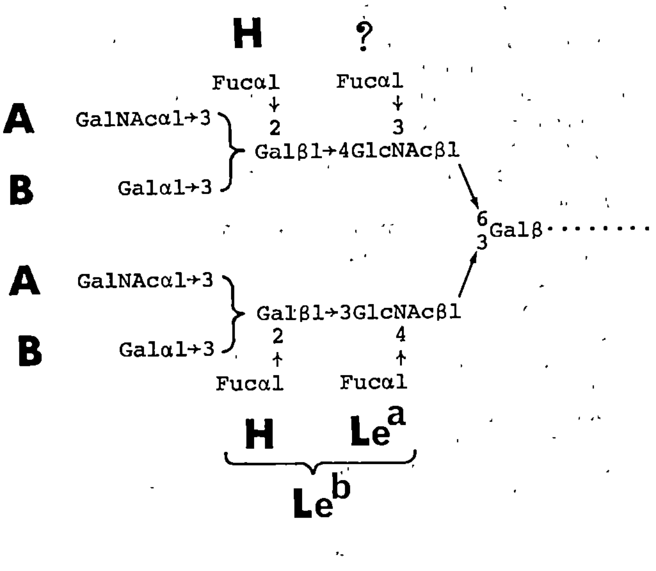

A survey of these structures suggested that the Fucα1→2Gal grouping is limited on the type 1 chain of the branched portion of the backbone, in contrast to the widely accepted idea that the grouping occurs both on type 1 and type 2 chains of the branched core[6]. To verify this concept, the possible occurrence of even a minor isomeric component that has the Fucα1→2Gal grouping on the type 2 chain had to be eliminated. An *N*-acetylgalactosaminyl transferase (A enzyme) found in the milk of women with blood type A transfers *N*-acetylgalactosamine from UDP-GalNAc to the C3 position of the galactose residue of both Fucα1→2Galβ1→3GlcNAc.... and Fucα1→2Galβ1→4GlcNAc.... groupings[7,8]. With UDP-*N*-^{14}C-acetylgalactosamine as a donor, this enzyme can be used to detect specifically the H determinants with type 1 and type 2 chain backbone[9].

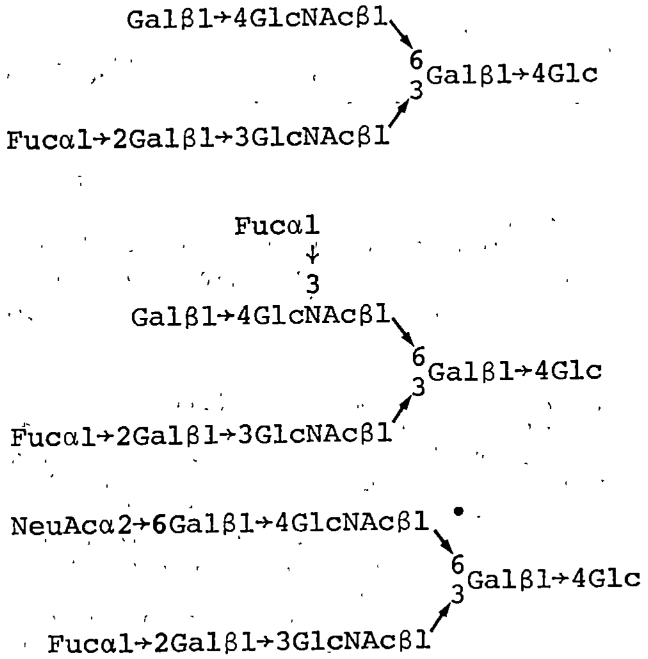

Fig. 2 Structures of three lacto-*N*-hexaose derivatives with blood group H determinant.

An endo-β-galactosidase, purified in our laboratory from *Diplococcus pneumoniae*, hydrolyses the blood group A determinant of type 2 chain but not of type 1 chain[10]. A combination of these two enzymes thus provides a sensitive method to discriminate type 1 and type 2 H determinants in heterosaccharide chains as indicated in Fig. 3.

N-2, a mixture of monofucosyllacto-*N*-hexaoses, and N-3, a mixture of difucosyllacto-*N*-hexaoses, were isolated from milk of four secretor individuals as before[11]. Each oligosaccharide was incubated with UDP-*N*-^{14}C-acetylgalactosamine and A enzyme[12], and the products were analysed by paper chromatography. A radioactive octaose was detected in all the incubation mixtures of N-2 fractions and a nonaose in all the mixtures of N-3 fractions (Table 1). When the N-2 and N-3 fractions were incubated with 20 μg of *Bacillus fulminans* α-L-fucosidase[13], which cleaves only the Fucα1→2Gal linkage, no radioactive products were detected. We conclude that the *N*-acetylgalactosamine incorporated into oligosaccharides was catalysed by the A enzyme.

The radioactive octaose and nonaose were eluted from the paper chromatogram, incubated with endo-β-galactosidase, and the release of GalN-^{14} C-Acα1→3Gal2←1αFuc was determined

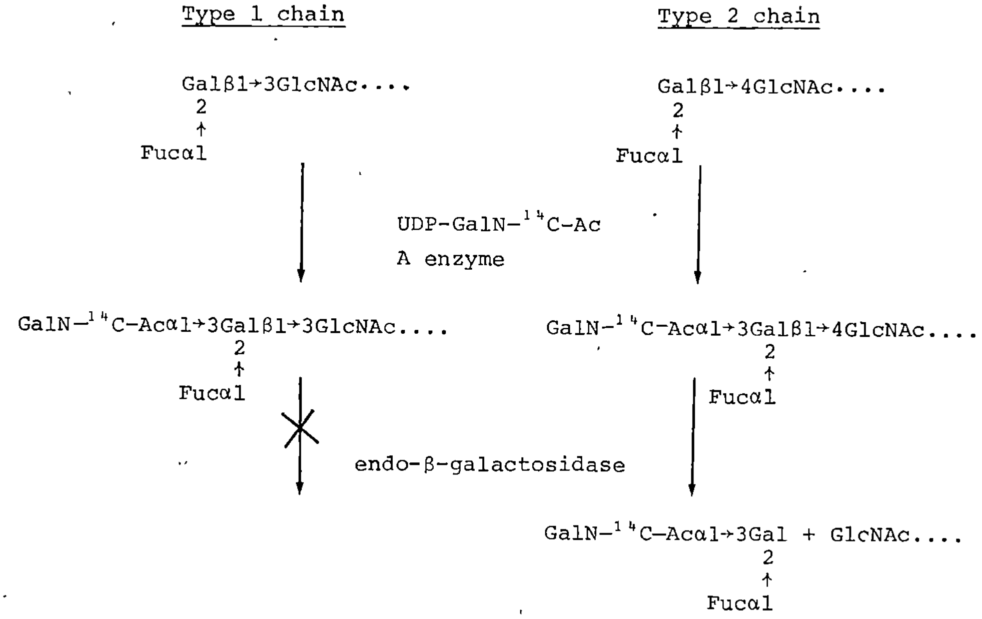

Fig. 3 Enzymatic discrimination of type 1 and type 2 H determinants

as described in the legend of Table 1. No radioactive trisaccharide was observed. Lacto-*N*-fucopentaose I and Fucα1→2Galβ1→4GlcNAcβ1→3hexene-1,2,5,6-tetrol as standards of type 1 and type 2 H determinants, respectively, were treated in the same way. Similar levels of *N*-acetylgalactosamine were incorporated into both oligosaccharides by incubation with A enzyme and UDP-*N*-^{14}C-acetylgalactosamine (Table 1). The activity incorporated into Fucα1→2Galβ1→4GlcNAcβ1→3-hexene-1,2,5,6-tetrol was recovered completely as GalNAcα1→3Gal2←1αFuc by the subsequent endo-β-galactosidase digestion, while that of lacto-*N*-fucopentaose I remained unhydrolysed (Table 1). These results confirm that the Fucα1→2Gal groupings of N-2 and N-3 fractions are located only on the type 1 chain of lacto-*N*-hexaose. The limited location of the Fucα1→2Gal grouping may be the reflection of the specificity of the *H* gene-associated α-2-L-fucosyltransferase. This enzyme adds α-fucosyl residues at the C-2 position of the non-reducing terminal galactose units of both type 1 and type 2 groupings when these are present on unbranched sugar chains[14,15]. This enzyme, however, may not be able to add a fucosyl residue at the Galβ1→4GlcNAc grouping of the branched core.

Table 1 Incorporation of *N*-^{14}C-acetylgalactosamine into oligosaccharides catalysed by A enzyme and their degradation by endo-β-galactosidase

Olgosaccharides	Gal*N*-^{14}C-Ac incorporated (c.p.m. $\times 10^{-3}$)	Counts released as trisaccharide (c.p.m. $\times 10^{-3}$)
N-2 fraction		
1	2 1	0
2	1.9	0
3	0.8	0
4	0.9	0
N-3 fraction		
1	4.8	0
2	2.9	0
3	3.2	0
4	1.8	0
Lacto-*N*-fucopentaose I	7.4	0
Fucα1→2Galβ1→4GlcNAc β1→3 hexene-1, 2, 5, 6-tetrol	6.8	6.7

A sample (50 µg) of each sugar was mixed with 300 U of purified A enzyme, 20 nmol (0 1 µCi) of UDP-*N*-^{14}C-acetylgalactosamine and 50 µl of 0.05 M Tris-HCl buffer, *p*H 7.5, containing 0.02 M $MnCl_2$. The A enzyme was obtained from the milk of an A_1 individual. After addition of a drop of toluene, the mixtures were incubated at 37 °C for 42 h. The reaction mixtures were then passed through a small column (0.5×4 cm) containing a mixed bed of BioRad AG-3 (OH^-) and BioRad AG-50 (H^+), and washed with five bed volumes of distilled water. Eluate and washings were combined, spotted on Whatman No. 3MM paper as a 3-cm band and subjected to descending paper chromatography using ethylacetate-pyridine-acetic acid-water (5:5:1:3) as a solvent for 14 d Radioautoscanning revealed a single radioactive octasaccharide and a single radioactive nonasaccharide in the incubation mixtures of N-2 and N-3 fractions, respectively. Radioactive GalNAcα1→3Gal(2←1αFuc)β1→3GlcNAcβ1→3Galβ1→4Glc and GalNAcα→3Gal(2←1αFuc)β1→4GlcNAcβ1→3-hexene-1, 2, 5, 6-tetrol were detected as the sole reaction products in the incubation mixtures of lacto-*N*-fucopentaose I and Fucα1→2Galβ1→4GlcNAcβ1→3-hexene-tetrol, respectively. These radioactive oligosaccharides were recovered from the paper chromatograms by elution with water, and the radioactivities were determined by a Packard Tri-Carb liquid scintillation spectrophotometer, after mixing aliquots of each sample with scintillation cocktail. The remaining samples were incubated with 1.0 mU of purified endo-β-galactosidase for 24 h. The incubation mixtures were spotted on Whatman No. 3MM paper, and subjected to descending paper chromatography using ethylacetate-pyridine-water (12:5:4) as a solvent for 20 h. The areas corresponding to authentic GalNAcα1→3Gal2←1αFuc (ref. 9) were cut out from the chromatogram, placed in scintillation vials, and the radioactivities were determined after incubating the paper pieces with 1 ml of water and adding 7 ml of scintillation fluid.

The Galβ1→4GlcNAcβ1→6Gal . . . . grouping has been shown to be one of the I blood group determinants[16,17]. Absence of the H blood group determinant on this grouping means that the ABO blood group system does not interfere with the phenotypic expression of the *I* gene, and that the I antigen may be able to coexist with A, B or H antigen on the same branched heterosaccharide core.

KATSUKO YAMASHITA
YOKO TACHIBANA
SEIICHI TAKASAKI
AKIRA KOBATA

Received March 12, accepted May 7, 1976

[1] Ginsburg, V ; Kobata, A , Hickey, C , and Sawicka, T , *Glycoproteins of Blood Cells and Plasma* (edit. by Jamieson, G A , and Greenwalt, T. J), 114–126 (Lippincott, Philadelphia, 1971)
[2] Race, R R , and Sanger, R., *Blood Groups in Man*, 5th ed , 9–86 (Blackwell, Oxford, 1968)
[3] Lloyd, K. O , Kabat, E A , and Licerio, E , *Biochemistry*, 7, 2976–2990 (1968)
[4] Kobata, A , and Ginsburg, V., *J biol Chem* , **247**, 1525–1529 (1972)
[5] Kobata, A , and Ginsburg, V , *Archs Biochem Biophys* , **150**, 273–281 (1972)
[6] Watkins, W M , *Glycoproteins* (edit. by Gottschalk, A), 830–891 (Elsevier, Amsterdam, 1972).
[7] Kobata, A , Grollman, E. F , and Ginsburg, V , *Archs Biochem Biophys* , **124**, 609–702 (1968)
[8] Hearn, V M., Smith, Z G., and Watkins, W M., *Biochem. J* , **109**, 315–317 (1968)
[9] Takasaki, S , and Kobata, A, *J. biol. Chem.* **251**, 3610–3615 (1976)
[10] Takasaki, S , and Kobata, A , *J. biol. Chem* **251**, 3603–3609 (1976).
[11] Kobata, A., *Methods in Enzymology* (edit by Ginsburg, V), **28**, 511–514 (1972).
[12] Kobata, A and Ginsburg, V , *J biol Chem* , **245**, 1484–1490 (1970)
[13] Kochibe, N., *J Biochem.*, **74**, 1141–1149 (1973)
[14] Shen, L , Grollman, E. F , and Ginsburg, V., *Proc natn Acad Sci. U.S A.*, **59**, 224–230 (1968).
[15] Chester, M. A., and Watkins, W M , *Biochem biophys. Res. Commun.*, **34**, 835–842 (1969).
[16] Feizi, T., Kabat, E. A., Vicari, G., Anderson, B , and Marsh, W. L , *J. Immun.*, **106**, 1578–1592 (1971).
[17] Zopf, D. A., and Ginsburg, V., *Archs Biochem. Biophys.*, **167**, 345–350 (1975)

Lead competitively inhibits calcium-dependent synaptic transmission in the bullfrog sympathetic ganglion

Many polyvalent cations have been used in studies of synaptic transmission either as tools for gaining a better understanding of synaptic processes or, in their own right, as potentially toxic substances[1–7]. Inorganic lead although long known to have neurotoxic effects, has not been studied extensively at the synaptic level until recently. Kostial and Vouk[8] found that lead blocked transmission in the perfused superior cervical ganglion of the cat *in vitro* by reducing the amount of acetylcholine released from presynaptic nerve terminals without affecting the response of ganglion cells to applied acetylcholine. The addition of excess calcium to the perfusion solution restored acetylcholine output and relieved the lead block. Manalis and Cooper[9], working with the frog sciatic nerve–sartorius muscle preparation *in vitro*, showed that lead depresses phasic transmitter release evoked by nerve stimulation and increases spontaneous release as evidenced by an increase in frequency of miniature endplate potentials. Lead had only a weak, curare-like effect on the postsynaptic response to applied acetylcholine. In this paper we show, using electrophysiological techniques, that $PbCl_2$ blocks synaptic transmission presynaptically by competitive inhibition of calcium. In support of this data, we further show, using ^{45}Ca, that lead in fact does reduce the uptake of calcium by preganglionic nerve terminals.

In all experiments the 9th or 10th sympathetic ganglion was removed from the bullfrog (*Rana catesbeiana*) along with several cm of preganglionic trunk and postganglionic ramus and connecting spinal nerve. After removal of the connective tissue sheath, the ganglion was placed in a sucrose gap chamber similar to that described by Koketsu and Yamamoto[10]. This chamber allowed for the selective perfusion of the ganglion with normal or modified Ringer's solutions. Supramaximal stimuli were applied at a rate of 1 s^{-1}. Control ganglionic compound action potential was measured after 30 min of stabilisation in normal Ringer. Then the ganglion was perfused for 30 min with Ringer's solution containing lowered calcium, added lead, or both. Control and experimental periods were alternated in this way for the duration of an experiment.

Data for 4 concentrations of lead at several calcium concentrations are presented in Fig. 1. Figure 1*a* shows that the log of ganglionic response amplitude is a positive linear function of the log of calcium concentration between 0.2 and 1.0 mM. Lead shifts the response to the right with no appreciable change in slope. The slopes of the log–log curves are similar to those obtained for cobalt and magnesium at the neuromuscular junction[1,11]. The same data replotted on modified Lineweaver–Burk coordinates as described by Dodge and Rahamiandmoff[11] are shown in Fig. 1*b*. These curves intercept with the ordinate at the same point, indicating a competitive antagonism of calcium by lead. The potency of lead as a synaptic blocking agent is great when compared with magnesium, cobalt, and manganese, all of which have been shown to interfere with synaptic transmission at the frog neuromuscular junction through a competitive antagonism of calcium. Cobalt and manganese are 20 times[1,2] and lead is 1,000 times[9] more potent than Mg at the frog neuromuscular junction. Our data reported here are in general agreement since lead is at least 200 times more effective than magnesium in blocking ganglionic transmission[3].

Several other parameters were examined to ascertain whether the sole effect of lead at these concentrations was through an antagonism of the action of calcium at presynaptic nerve terminals. Axon conduction amplitude and velocity in the preganglionic nerve trunk were measured before and after exposure to lead in a concentration which completely blocked ganglionic transmission. No changes were seen. Presynaptic spike amplitude was measured by the method of Dunant[12]. Again, lead had no appreciable effect. Ganglionic response to bath-applied acetylcholine as described by Koketsu and Yamamoto[10] was used as a test of postsynaptic receptor function. Only a 5% decrease in response was observed at levels of lead which completely block synaptic transmission.

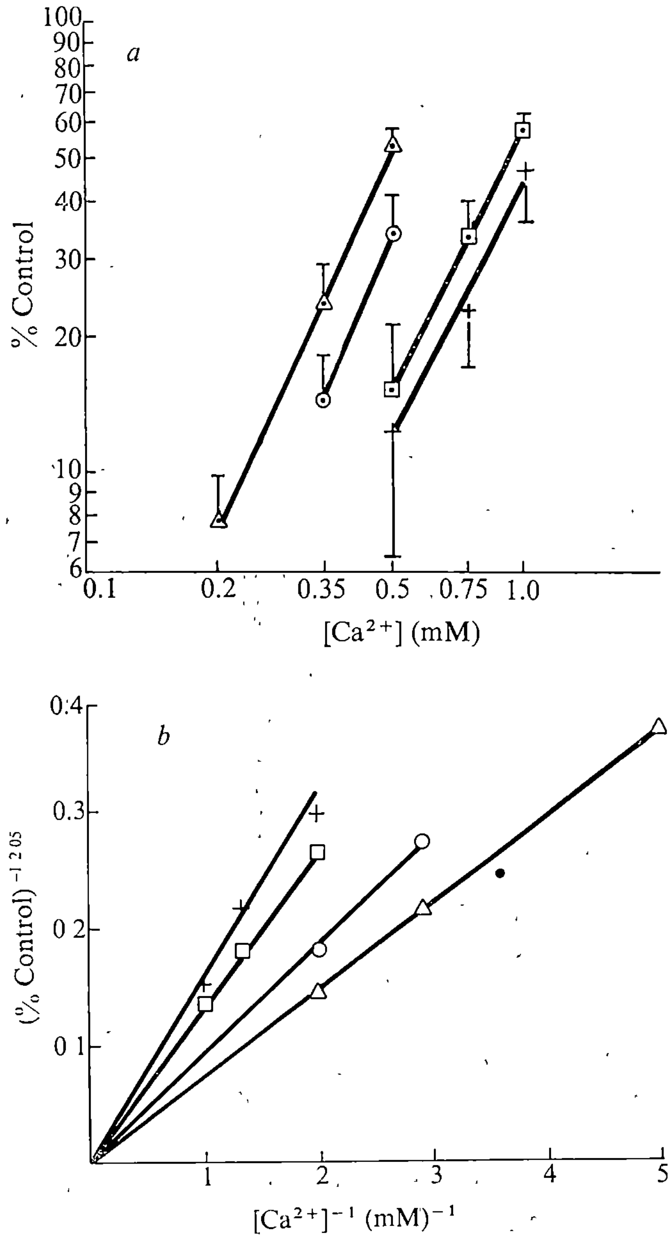

Fig. 1 *a*, A log–log plot of postganglionic response amplitude against Ca^{2+} concentration for 0, 5, 10, and 20 μM Pb^{2+}. The average slope of the lines is 2.05. Each point is the average of at least 5 determinations. The standard error of the mean is shown with each point. *b*, The same data plotted on modified Lineweaver–Burk coordinates. Control Ringer contained 111 mM NaCl, 2.5 mM KCl, 2.0 mM CaCl and 4 mM Tris buffer. All straight lines were determined by least-squares regression. Concentration of Pb^{2+} in modified Ringer's solution: △, 0 μM; ○, 5 μM; □, 10 μM; +, 20 μM.

From the data presented above we infer that lead competitively inhibits calcium-mediated transmitter release from presynaptic nerve terminals. Additional support of this conclusion was obtained in a series of experiments in which the effects of lead on the uptake of ^{45}Ca by presynaptic nerve terminals were examined. The method of Blaustein was used with several minor modifications[13]. ^{45}Ca was added to a bath containing a pair of ganglia. One member of the pair was stimulated supramaximally for 20 min at a rate of 6 stimuli s^{-1}. After rinsing, weighing, and digestion, the amount of ^{45}Ca taken into the ganglia was measured by conventional scintillation counting.

Figure 2 shows that stimulation of the preganglionic nerve resulted in a threefold increase in ^{45}Ca uptake. Antidromically stimulated ganglia took up no more ^{45}Ca than unstimulated ganglia indicating that the activity of ganglion cells and postganglionic axons did not contribute to the ^{45}Ca uptake. Furthermore, ganglia blocked by (+)-tubocurarine took up quantities of ^{45}Ca comparable to the uptake of unblocked preparations suggesting that postsynaptic receptor activity was not contributory. The ^{45}Ca uptake of stimulated lead-blocked ganglia was however, reduced to 9% of control, indicating that lead strongly blocks the uptake of calcium normally associated with the arrival of action potentials at the presynaptic nerve terminals. This is in agreement with the data and the conclusion derived from the electrophysiological studies. In addition, lead reduced the ^{45}Ca uptake of unstimulated ganglia to 16% of unstimulated control indicating an effect of lead on calcium exchange which is not related to the presence of an action potential.

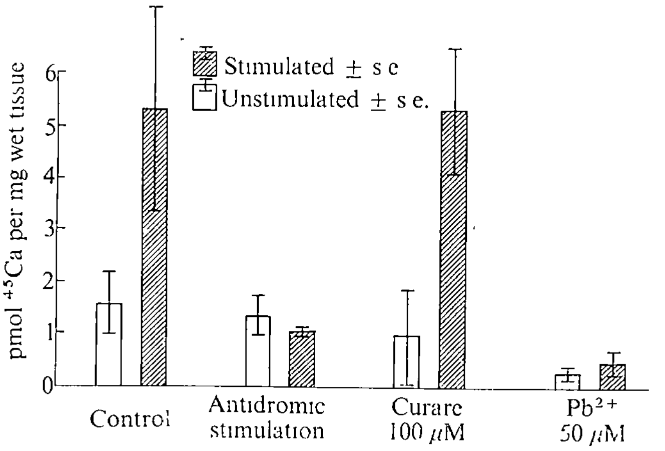

Fig. 2 The amount of ^{45}Ca taken up by ganglia under the following conditions: *a*, unstimulated ganglia and ganglia activated by preganglionic nerve stimulation, both in normal Ringer's solution; *b*, unstimulated ganglia and ganglia activated by stimulation of the postsynaptic nerve, both in normal Ringer's solution; *c*, unstimulated ganglia and preganglionically stimulated ganglia in Ringer's solution containing 100 mM (+)-tubocurarine; *d*, unstimulated and preganglionically-stimulated ganglia in Ringer's solution containing 50 μM Pb^{2+}. 50 μM Pb^{2+} blocks 100% of the postganglionic response. Modification of Blaustein's method was as follows: 5 μCi of ^{45}Ca in 50 μl HOH were added to a bath containing 2.5 ml of Ringer's solution. After stimulation, the pre- and postganglionic nerves were removed and the ganglia blotted on filter paper. Wet weights were then taken. Digestion was done in 0 5 ml of 10% tetramethyl ammonium hydroxide heated to 90 °C for 20 min. 5 ml of Bray's solution were then added for conventional scintillation counting.

From these experiments we conclude that lead blocks synaptic transmission in the sympathetic ganglion by competitive antagonism of spike-evoked entry of calcium into presynaptic nerve terminals and a subsequent reduction of transmitter release. It is not possible to say whether such a mechanism contributes significantly to the central or peripheral nervous system dysfunction seen in acute or chronic lead poisoning. Carroll *et al*[14] have, however, shown that K-induced release of acetylcholine from brain slices of mice exposed to lead during developent is reduced and is also dependent on the presence of calcium in the medium. Since the presently accepted upper limits of normal, "safe", blood lead levels of human children and adults are 2 μM and 4 μM respectively[15], it may well be that the mechanism described here is a factor in chronic lead poisoning.

This work was supported by grants from the Environmental Protection Agency and the NIH.

THOMAS E. KOBER
GARY P. COOPER

Department of Environmental Health,
University of Cincinnati Medical Center,
3223 Eden Avenue,
Cincinnati, Ohio 45267

Received April 28; accepted June 29, 1976.

[1] Weakly, J. N , *J. Physiol., Lond.*, **234**, 597–612 (1973)
[2] Meiri, U , and Rahamimoff, R., *Science*, **176**, 308–309 (1972).
[3] Guerrero, S , and Riker, W K., *J Pharmac exp. Ther.*, **186**, 152–159 (1973)
[4] Manalis, R S., and Cooper, G P., *Nature*, **257**, 690–691 (1975)
[5] Kostial, K., and Landeka, M , *Experientia*, **31**, 834–835 (1975).
[6] DeBassio, W A , Schnitzler, R. M., and Parsons, R L., *J. Neurobiol* , **2**, 263–278 (1971).
[7] Del Castillo, J., and Engback, L , *J. Physiol., Lond.*, **124**, 370–384 (1954).
[8] Kostial, K., and Vouk, V. B., *Br J. Pharmac* , 12, 219–222 (1957)
[9] Manalis, R S , and Cooper, G. P., *Nature*, **243**, 354–356 (1973)
[10] Koketsu, K., and Yamamoto, K., *Br. J. Pharmac* , **50**, 69–77 (1974)
[11] Dodge, F. A., and Rahamimoff, R , *J. Physiol , Lond.*, **193**, 419–432 (1967)
[12] Dunant, Y , and Dolivo, M., *Brain Res* , 10, 268–270 (1968).
[13] Blaustein, M. P , *Science*, **172**, 391–393 (1971).
[14] Carroll, P. T , Silbergeld, E K , and Goldberg, A M., *Neurosci Abstr* , 1, 250 (1975).
[15] Goyer, R. A , and Mahaffey, K R , *Environ. Hlth Perspect* , **2**, 73–80 (1972)

Type of sensory nerve fibre sprouting to form a neuroma

WHEN a peripheral nerve is cut across, the axons in the central end send out sprouts. If these sprouts fail to reach the distal part of the cut nerve they form a tangled mass called a neuroma[1]. Neuromas which occur in man after amputation or after failure of regeneration of a damaged nerve are always tender on pressure and are sometimes the source of ongoing pain[2]. When experimental neuromas are stimulated, it is known that a delayed volley of nerve impulses arrives at the central nervous system[3] and it was assumed that the delay was occurring in the fine sprouts. Now that we have examined single fibres originating from a neuroma, we find that this conclusion was wrong and that there is a much more surprising explanation: only the small diameter, slowly conducting axons within the peripheral nerve seem to send sprouts into the neuroma and the delay in arrival of the afferent volley is primarily due to the fact that it runs only in slowly conducting fibres. This selective outgrowth of small fibres may be of considerable practical interest. These fibres include those which normally carry signals from injured tissue. In the normal situation, however, injury detection signals are accompanied by impulses in large diameter nerve fibres which decrease the central effect of the injury signals. The neuroma, as a pure culture of small fibres, may generate pain producing impulses[3] where the pain has an intensity and peculiarly unpleasant quality due to the absence of the normal modulating impulses[4] in the larger fibres which have failed to regenerate.

The experiments were carried out on 70 adult male albino rats, Sabra strain, weighing more than 300 g at the time of nerve section. Under ether anaesthesia, the sciatic nerve of one leg was transected and the central stump was drawn by a strand of epineurium into a polythene tube so that the nerve fitted snugly without compression. The end of the tube was usually capped with bone wax. Some nerves were studied in an acute preparation immediately after cutting, and others were studied 1 d to 6 months after section. For this examination the animals were anaesthetised with urethane or Nembutal, paralysed with Flaxedil, and had the lumbo-sacral spinal cord exposed. To record compound action potentials, a low lumbar dorsal rootlet originating in the neuroma was cut centrally and placed on a pair of Ag–AgCl recording hooks. For single units, fine filaments, about 20 μm in diameter and 1–2 mm long were stripped from the end of the root, placed on a single hook, and recordings made with reference to a nearby indifferent electrode. The sciatic nerve was exposed and the neuroma freed from its tube.

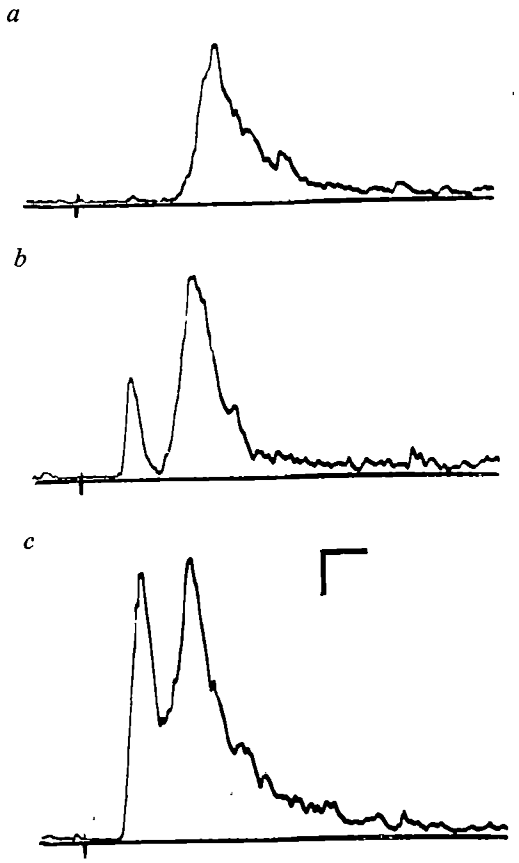

Fig. 1 Compound action potentials recorded on an L5 dorsal root following stimulation of a sciatic nerve neuroma (*a*), a point on the proximal edge of the neuroma (*b*), and a region of relatively intact sciatic nerve (*c*). Recordings were made 52 d after the sciatic nerve had been cut. The neuroma was 4 mm long. Stimulus points for *a*, *b* and *c* were 2.5, 7.5 and 12.5 mm central to the distal end of the neuroma. A cathodal square wave pulse (2.0 mA, 0.05 ms) was delivered at the point indicated in each sweep. The calibration marks are 1 ms and 200 μV negative upwards. The results show that only a slowly conducting wave was produced from the neuroma while a bimodal compound action potential was evoked by stimulation only slightly proximally on the nerve.

The exposed surface of the neuroma and nerve was then stimulated at selected points by silver hook or mono- or bipolar fine tungsten electrodes delivering square wave pulses of 0.01–0.5 ms duration from a constant current source.

By one week after the nerve had been cut, an obvious swelling appeared on the end. When this was stimulated at a current adequate to stimulate intact nerve, no response was recorded. If the stimulus was increased, a compound action potential appeared on the root after an unusually long delay. An example is shown in Fig. 1*a* where the nerve was examined 52 d after section and the stimulus applied midway along the 4-mm neuroma. Using the same intensity of stimulus, compound action potentials were also evoked by stimulation at points 5.0 mm (Fig. 1*b*) and 10.0 mm (Fig. 1*c*) proximally along the nerve. It will be seen that the compound action potential evoked from 10.0 mm proximal to the neuroma has two peaks and arrives in 0.8 ms. The wave evoked from the neuroma itself, only 10 mm distally, however, takes an extra 1.4 ms to arrive. Similar results were seen in all nerves tested from a few days to 6 months after section. The extent of the delay depended on the survival time with delays increasing for about 3 weeks. Thereafter, little further slowing occurred. The question of whether this delay is due entirely to slowing of spike conduction within the neuroma or to the possibility that only slowly conducting parent fibres penetrate the neuroma was only settled with certainty by single unit studies.

Single fibres originating from the neuromas were examined by recording from fine dorsal root filaments and by stimulating at two locations, one (S_1) on the intact nerve, usually about 20 mm from the neuroma, and one (S_2) on the neuroma itself (Fig. 2, top). The two stimulus locations allowed the single unit nature of the spike to be defined by the collision technique. First a unit driven from the neuroma was identified and its latency measured and conduction velocity (S_2 velocity) calculated. Then a shock was applied to the proximal stimulating electrode (S_1) 0.5–10 ms before the neuroma stimulus, and its intensity raised gradually. Suddenly the spike originating in the neuroma vanishes and is replaced by an earlier identical spike. The proximal stimulus has generated an orthodromic spike which is recorded and an antidromic spike which has collided with the spike originating from the neuroma, abolishing it (Fig. 2). The latency of the spike from the S_1 stimulus can now be measured and the conduction velocity of the fibre from the S_1 position to the recording electrode (S_1 velocity) calculated. This technique allowed single myelinated and unmyelinated afferents to be identified and

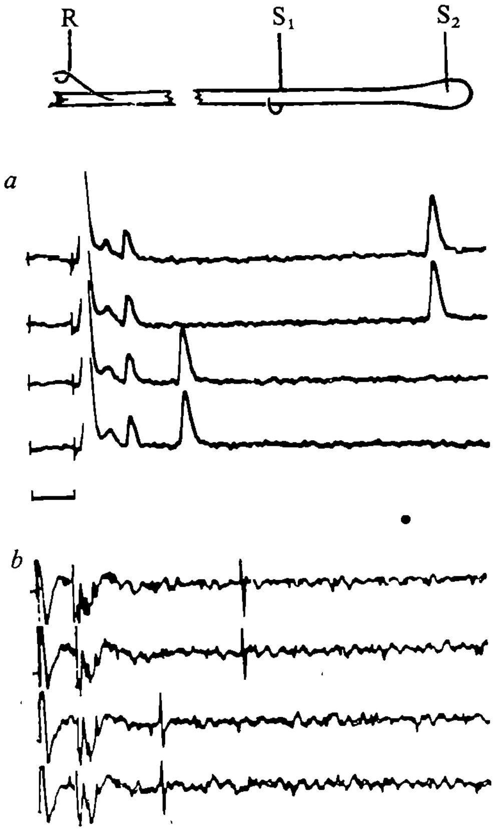

Fig. 2 Single units identified by the collision technique. The recording and stimulation arrangement is shown in the diagram at top. *a*, Top sweep, S_1 stimulus is delivered at the beginning of the sweep and evokes a volley of spikes (compound action potential) on the dorsal root filament from 1–2 ms after the stimulus. The S_2 stimulus is given 1 ms after the S_1 stimulus and it evokes a single spike with a latency of 7.9 ms seen on the right of the sweep. The stimulus current on S_1 is increased in the second sweep but is still below threshold for the single unit. In the third and fourth sweeps, the strength of the S_1 stimulus has reached the unit's threshold and a spike now appears 3.3 ms after the S_1 stimulus. This spike has the same height and slope as the one evoked by the S_2 stimulus in the sweeps above. When the spike is produced by the S_1 stimulus it collides with the spike produced distally in the neuroma (S_2) so that the spike produced from S_2 cannot travel to the recording root. This proves that the action potential from the two stimulus points occupied the same fibre. The overall conduction velocity from S_1 was 24.8 m s^{-1} and from S_2 was 11.9 m s^{-1}. *b*, Using the same procedure as in *a*, a single unit with a lower conduction velocity was identified. Here the S_1–S_2 time difference was 10 ms and the overall conduction velocity was 2.2 m s^{-1} from the S_1 stimulus point and 2.2 m s^{-1} from the S_2 point. The time mark is 1 ms for *a* and 10 ms for *b*.

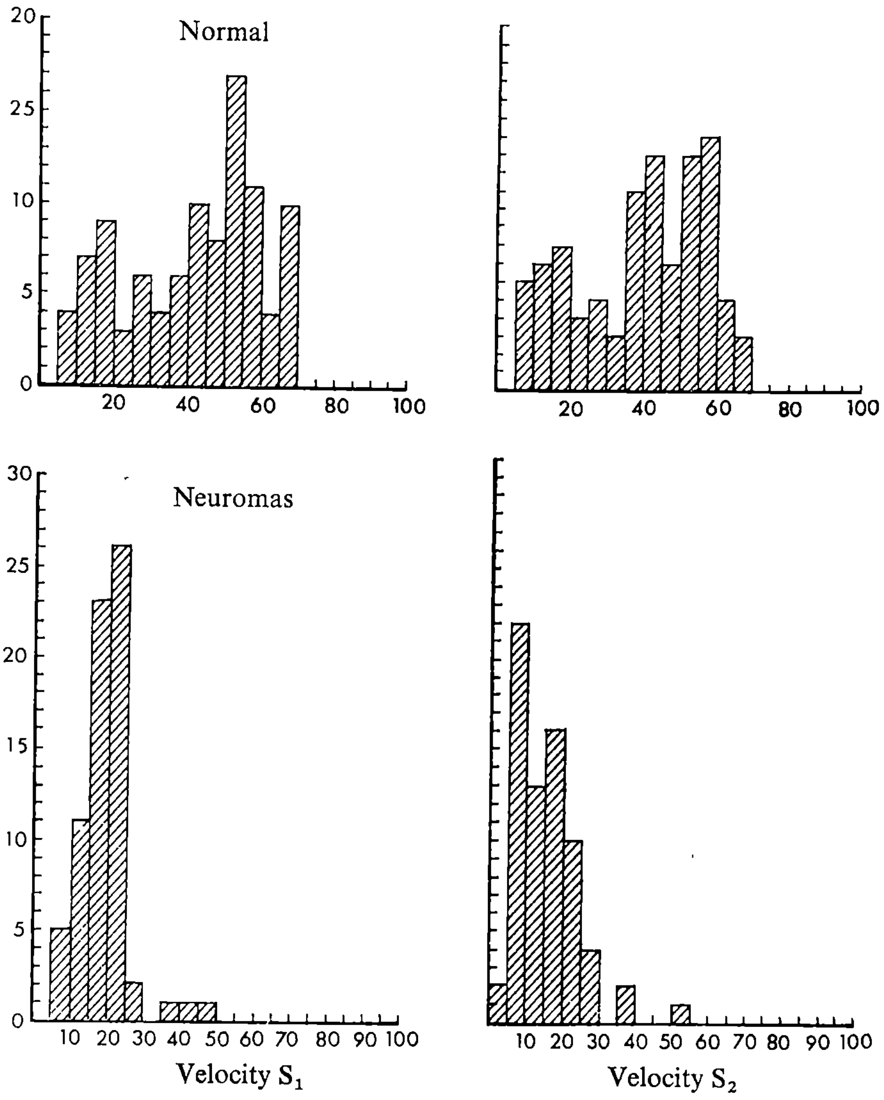

Fig. 3 Histogram of conduction velocities of 99 successively encountered single fibres in normal nerves and of 70 originating from neuromas of 50–84 d standing. The recording and stimulus situation is shown in the diagram in Fig. 2. For normal fibres, the sciatic nerve was intact and the stimulus points were at the standard positions used in the neuroma animals. The conduction velocity of each single fibre was calculated, using the collision method, both for the S_1 stimulus position on proximal nerve and for the S_2 position at the neuroma. It will be seen that virtually all impulses elicited by electrical stimulation of the neuroma run in fibres which have a low conduction velocity in the proximal nerve. Only sprouts of slowly conducting fibres appear to contribute to the neuroma. The velocities from S_2 are slower than those from S_1 because there has been a slowing of the impulses in the fine sprouts within the neuroma.

allowed the calculation of conduction velocities both for the parent fibre alone and its extension into the neuroma.

In a series of unoperated rats, and rats with sciatic neuromas, this was done for every unit encountered from the S_2 stimulus position that was sufficiently well isolated to allow for unequivocal determination of its velocity also from the S_1 position. The histogram of S_2 conduction velocities in normal nerves (Fig. 3, upper right) shows a distribution ranging from 5 m s^{-1} up to 80 m s^{-1} with the expected bimodal distribution. The histogram for S_1 velocities of these same fibres is very similar (Fig. 3, upper left) since normal fibres have relatively uniform velocities along most of their course. The histogram of conduction velocities from the neuroma shows, however, that almost all the units sampled from neuromas had slow overall velocities (Fig. 3, lower right) and furthermore their parent fibres in the intact part of the nerve were also slow (Fig. 3, lower left). In addition to the small myelinated fibres whose sprouts make up the neuroma, a number of unmyelinated parent fibres were observed which extended into the neuroma. These fibres, which may have a role in pain along with the small myelinated fibres, will not be discussed further here. They were not included in the histograms because they were specifically sought and not randomly encountered as was the rest of the sample.

Most of the fibres from neuromas had overall (S_2) conduction velocities somewhat slower than the velocities of their parent fibres (Figs 2*a* and 3, bottom). This difference undoubtedly represents a slowing of the impulses in the tangled fine sprouts within the neuroma. In a few fibres one S_2 response latency was observed when near-threshold stimulating currents were used, but when the current was increased the unit's response latency suddenly jumped to a smaller value. Apparently, the stimulus had now become suprathreshold at a slightly more proximal position on the sprout. For each spike initiation point within the neuroma, however, the parent fibre velocity measured at S_1 was identical. It has been reported that there is a slight shrinkage of myelinated fibres proximal to a nerve section[5], a phenomenon reflected in the slight slowing of the fast component of the compound action potential elicited from positions proximal to neuromas as compared with an intact nerve. This change however, is quite inadequate to explain the marked low velocity of the parent fibres of neuroma sprouts.

These data indicate that electrical stimulation of neuromas formed on the transected sciatic nerve activates slowly conducting myelinated (A-delta) but not more rapidly conducting myelinated fibres. This presumably means that only small fibres sprout to form a neuroma. Alternatively, it may be that large fibres also emit sprouts but that orthodromic conduction along them is blocked, perhaps because the fine sprout is unable sufficiently to depolarise the large parent axon[6].

M.D. is a post-doctoral fellow of the Foundations' Fund for Research in Psychiatry. This work was supported by a grant from the Thyssen Foundation. We acknowledge the valuable contributions of Ms D. Schonfeld.

M. DEVOR
P. D. WALL

Neurobiology Unit, Russian Compound,
Hebrew University, Jerusalem, Israel, and
Department of Anatomy,
University College,
London WC1, UK

Received April 14; accepted June 29, 1976.

[1] Cajal, S. R., *Degeneration and Regeneration in the Nervous System* (Oxford University Press, London, 1928).
[2] Sunderland, S., *Nerves and Nerve Injuries* (William and Wilkins, Baltimore, 1968).
[3] Wall, P. D., and Gutnick, M., *Nature*, **248**, 740–743 (1974)
[4] Melzack, R., and Wall, P. D., *Science*, **150**, 971–979 (1965).
[5] Aitken, J. T., and Thomas, P. K., *J. Anat.*, **96**, 121–129 (1962)
[6] Parnas, I., Hochstein, S., and Parnas, H., *J. Neurophysiol* (in the press).

Swimming in the sea anemone *Stomphia coccinea* triggered by a slow conduction system

THERE has been great interest in the sea anemone *Stomphia coccinea* since its remarkable swimming response to the starfish *Dermasterias imbricata* was first discovered[1]. On contact with *Dermasterias*, this anemone rapidly detaches from the substrate and undergoes a series of swimming movements involving flexions of the column. The starfish *Hippasteria spinosa*[2] and a nudibranch, *Aeolidia papillosa*[3] also evoke swimming. Previous attempts to analyse this response physiologically were based on indirect observations of swimming induced by electrical stimulation. There were difficulties in explaining the coordination of the swimming response in terms of a single nerve net and it has been suggested that the swimming response is controlled by a separate system[4]. The electrical activity from sea anemones can be measured and correlated with various behaviour patterns[5,6]. Use of these techniques with *S coccinea* has shown that a slow conduction system, quite distinct from the familiar through-conducting nerve net[7] always becomes active when *Dermasterias* contacts *Stomphia*. This activity, it seems, triggers the entire swimming sequence.

Polythene suction electrodes were used for both recording and electrical stimulation, as described elsewhere[8]. An electrode was attached to the tentacles of the anemone for recording purposes and the animal was harnessed (Fig. 1*a*) by pinning a sector of the oral disk of a completely intact anemone to a rigidly fixed platform of Sylgard resin. This ensured that those tentacles within the sector would be fixed in space, thereby reducing the possibility of the electrode being thrown off during swimming movement. This procedure does not unduly affect the swimming response.

A single shock (5 ms duration, 10 V intensity) delivered through a stimulating electrode attached to a tentacle evokes a response (Fig. 1*b*), detected by a recording electrode on an adjacent tentacle. Similar pulses have been recorded from other sea anemones[6,9] and seem to originate from three separate conduction systems: the through-conducting nerve net (conduction velocity up to 120 cm s^{-1}) and two slowly conducting systems, the SS1 (conduction velocity 3–14 cm s^{-1}) and SS2 (conduction velocity ~4 cm s^{-1}). The properties of these systems have been described elsewhere[6]. Activity occurring within any one system may be distinguished from that occurring in the others by comparing the conduction velocities, thresholds of excitation and characteristic waveforms of the recorded pulses (see Fig. 1*b*).

The complete swimming sequence can be triggered by bringing *Dermasterias* into contact with a single tentacle of *S. coccinea*. Previous accounts[1,2] have described the stages in this behaviour pattern as follows: (1) an "alerting" response of the entire tentacular crown on contact with the starfish; (2) temporary contraction of the upper region of the column often shielding the tentacles from view and breaking the tentacle–starfish contact; (3) extension of the column because of a gradual constriction of the mid-column region; (4) re-emergence of the tentacular crown, relaxation of the upper column region and expansion of the entire oral disk; (5) constriction of the pedal disk margin, detachment of the pedal disk from the substrate and formation of a cone-shaped projection from its centre, (6) alternating ipsilateral and contralateral flexions of the column wall constituting the swimming movements of the animal. The entire sequence, stages (1)–(6) may take ~ 5–15 s, and the swimming flexions continue, with lengthening pauses between bursts, for up to 5 min.

The electrical activity recorded from a single tentacle of the anemone at the beginning of this response is shown in Fig. 1*c*. In this instance, the starfish was placed against the tip of a single tentacle, 4.5 cm from the recording site, for 1.5 s. The evoked electrical activity was a series of pulses identified by their waveforms as originating in the SS1. There was no accompanying activity associated with the through-conducting nerve net or SS2 This was not because the recording equipment could not detect ongoing activity in these systems, since a test shock applied during the response evokes characteristic pulses in all three systems. The behavioural responses accompanying this electrical activity included stages (1)–(5); but no electrical activity has yet been recorded, either from the SS1 or any other identifiable system, during the swimming flexions (stage (6)).

The SS1 can be electrically stimulated alone by placing a stimulating electrode on an ectodermal flap cut into the column and applying shocks at an intensity above SS1 threshold[6]. With the exception of the temporary, upper-column contraction (stage (2)), the entire swimming response can be triggered by stimulating the SS1 within the appropriate frequency range; about 1 shock every 250 ms to 1 shock every 4 s. At greater frequencies, the SS1 becomes refractory and does not conduct. At lower frequencies, the

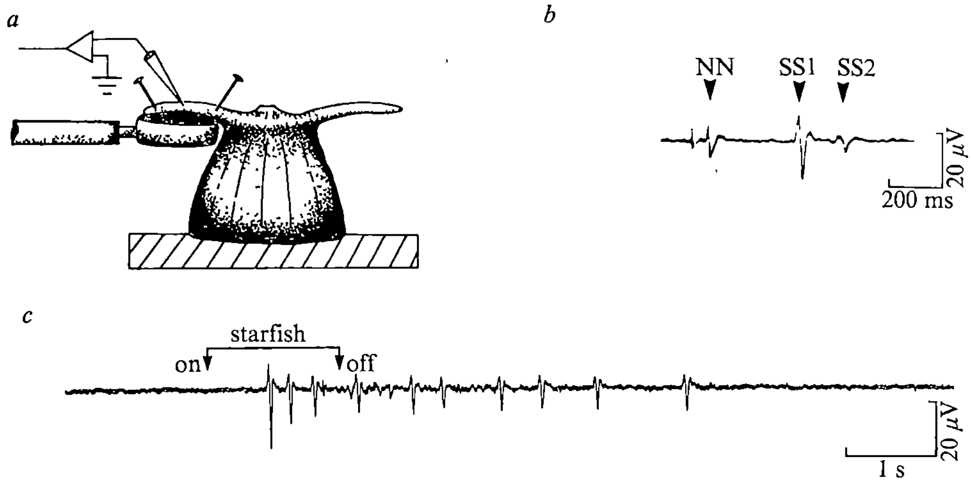

Fig. 1 *a*, *Stomphia coccinea* tethered to an immobile platform for recording purposes. A suction electrode is attached to a tentacle pinned to the platform and the pedal disk has affixed itself firmly to the substrate *b*, Electrical activity recorded from a tentacle in response to a single shock to an adjacent tentacle. The first pulse denotes the stimulus artefact. The recorded pulses are associated with three separate conducting systems: the through-conduction nerve net (NN) and two slowly conducting systems, SS1 and SS2. *c*, Electrical activity recorded from a tentacle during the initial stages of the swimming response. The starfish *Dermasterias imbricata* was brought into contact with another tentacle to initiate the response (on) and removed 1.5 s later (off). This evokes repetitive firing in the SS1.

swimming response cannot be triggered. A minimum of about 4 shocks (at a frequency of 1 shock every 250 ms) is usually required to elicit the response but more shocks were often required if the anemone had not swum within about the preceding 10 h. This indicates that the internal state of the animal may exert an influence over the activation threshold of the swimming response[10].

The through-conducting nerve net and SS2 do not seem to be involved in triggering the swimming response. Electrical stimulation of the intact column above SS1 threshold excites both the nerve net and the SS1, but in this case the swimming response may be triggered with a slight modification: the anemone sometimes contracts or 'twitches' as the shocks are applied. If the stimulus intensity is above threshold for the nerve net but below that for the SS1 so that the nerve net alone is stimulated, the anemone will contract but swimming behaviour is not triggered. This confirms and explains earlier results with electrical stimuli applied to the intact column[4] where the threshold for swimming was shown to be higher than that for contraction. The failure of electrical stimulation of the SS1 to cause the initial contraction of the column (stage (2)) that occurs in the response to *Dermasterias* is, nevertheless, puzzling. This stage in the response may be caused by mechanoreceptors[10] activating a system whose electrical activity cannot be detected by the techniques used here.

The SS1 pulses seem to constitute a sensory response to the unidentified active chemical found in *Dermasterias*[11]. This sensory response operates over a much faster time scale than comparable activity previously encountered in sea anemones. In Fig. 1*c* a total of 10 pulses occurs over a period of 4.8 s (mean inter-pulse interval (i.p.i.)=533 ms). In the response of the anemone *Calliactis parasitica* to *Buccinum* shells, the SS1 fires at a mean i.p.i. of approximately 7 s (ref. 12), and in the prefeeding response of the anemone *Tealia felina*, the same system fires at a mean i.p.i. of approximately 25 s (ref 13). Anti-facilitation of pulse amplitude occurs in addition to a process of sensory adaptation (Fig. 1*c*) phenomena also encountered in *Tealia*[13].

The SS1 coordinates pedal disk detachment in *Calliactis*[12] and it probably has a similar function in *Stomphia*, operating the entire process at a much faster rate. The observation that continuous activity of the SS1, SS2 or through-conducting nerve net is not necessary to maintain the swimming flexions suggests that the SS1 may feed into and trigger a 'swimming programme' which is maintained and coordinated by a localised motor system, perhaps the network of large multipolar nerve cells found in the column[14]. So far, however, it has not been possible to record electrical activity from this network during swimming.

These results extend the direct evidence for the view that the behaviour of sea anemones is not controlled by a single nerve net. Swimming in *Stomphia*, like the transfer of *Calliactis* to shells[12] and other complex behaviour patterns, involves interactions between different conduction systems. These findings should allow a reappraisal of current ideas about the control of behaviour and the organisation of the nervous system in these so called 'simple' animals. Species of *Stomphia*, which display a variety of specific, stereotyped and repeatable behaviour patterns, should be prime subjects in further investigations to the end.

This work was carried out at the Friday Harbor Laboratories of the University of Washington. Thanks are due to the Director, Dr Dennis Willows, for the provision of space and facilities and to Dr D. M. Ross for advice and criticism. The financial assistance of the NRC of Canada and the University of Alberta is acknowledged.

I. D. Lawn

Bamfield Marine Station,
Bamfield, British Columbia VOR 1B0, Canada

Received March 19; accepted June 29, 1976.

[1] Yentsch, C. S., and Pierce, D. C., *Science*, **122**, 1231–1233 (1955).
[2] Sund, P. N., *Q. Jl microsc. Sci.*, **99**, 401–420 (1958).
[3] Robson, E. A., *J. exp. Biol.*, **38**, 685–694 (1961).
[4] Ross, D. M., and Sutton, L., *J. exp. Biol.*, **41**, 735–749 (1964).
[5] Josephson, R. K., *J. exp. Biol.*, **45**, 305–319 (1966)
[6] McFarlane, I. D., *J. exp. Biol.*, **51**, 377–385 (1969)
[7] Pantin, C. F. A., *J. exp. Biol.*, **12**, 139–155 (1935).
[8] Lawn, I. D., and McFarlane, I. D., *J. exp. Biol.* **64**, 419–429 (1976)
[9] McFarlane, I D., and Lawn, I. D., *J. exp Biol.*, **57**, 633–649 (1972)
[10] Wilson, D. M., *J. exp. Biol*, **36**, 526–532 (1959).
[11] Ward, J. A., *J. exp. Zool.*, **158**, 357–364 (1965).
[12] McFarlane, I. D., *J. exp. Biol*, **51**, 387–396 (1969).
[13] Lawn, I. D., *J exp. Biol.*, **63**, 525–536 (1975).
[14] Robson, F A., *Q. Jl microsc. Sci.*, **104**, 535–549 (1963).

Polarised light-sensitive interneurones in a swimming crab

THIS report shows that there are polarisation-sensitive interneurones in the crab visual system, contrary to recent speculations[1]. It also shows that polarised light information in crabs is elaborately processed.

Naturally-occurring light polarisers include water surfaces, particles suspended in air and water[2], and many larger objects, especially of biological origin (unpublished observations). Five uses of this diversity of environmental polarised light by animals have been put forward. Animals such as bees[3,4] may infer the position of the sun for navigation although the sun itself is obscured. Polarised light patterns may enable aquatic animals to detect an 'artificial horizon'. For animals flying above water surfaces this may result from the fact that reflected light is horizontally polarised[5]. In the underwater case light is polarised by reflection from suspended particles; here the area of greatest brightness is always horizontally polarised[6]. The water skater *Gerris* may use polarisation sensitivity (PS) to screen out the predominantly single plane of reflected light from water surfaces, enabling a better view into the water[7]. PS may enable extra discriminations about visual contrast through a system analogous to colour vision. This approach has been suggested for human divers[8], but has not until now been proposed as a physiological mechanism. Finally, PS in photoreceptors has been shown to enhance quantum capture and thus absolute sensitivity to light[9].

In spite of this wealth of possibility, evidence of the interneuronal processing which must underlie the behaviours listed above has been presented in only one, anomalous, case: PS interneurones have been reported in the goldfish[2]; the anomaly is that goldfish receptors exhibit no PS.

I looked for PS interneurones in the optic lobes of the eye of a swimming crab, *Scylla serrata*, an animal which has known PS in the receptors (ref. 10 and unpublished observations) (Fig. 1*a* and *b*). I used a broad field stimulator not reported before in polarised light vision research, which in some ways simulated the light environment found underwater. This paper presents evidence of PS interneurones in *Scylla*: the result does not agree with the recent suggestion that the neural wiring pattern of the crustacean eye cancels out the PS information present in the receptors, producing only a polarisation-independent system[1].

In the experiments reported here, single spots were projected from behind on to a paper diffusing screen 30 cm from the rigidly cemented left eye of a legless but otherwise intact crab. The screen measured 16×9 cm, and on it spots from 2 to 30° diameter subtended at the eye could be displayed. All stimuli were plane polarised by a 60-cm diameter rotatable disk of polaroid positioned between the screen and the eye. A 360° potentiometer mounted coaxially with the disk enabled its position, and its rate and direction of rotation, to be recorded.

In the experiments, two essential precautions were taken. The problem of spurious reflections dependent on the light source had already been recognised[11]. These were avoided

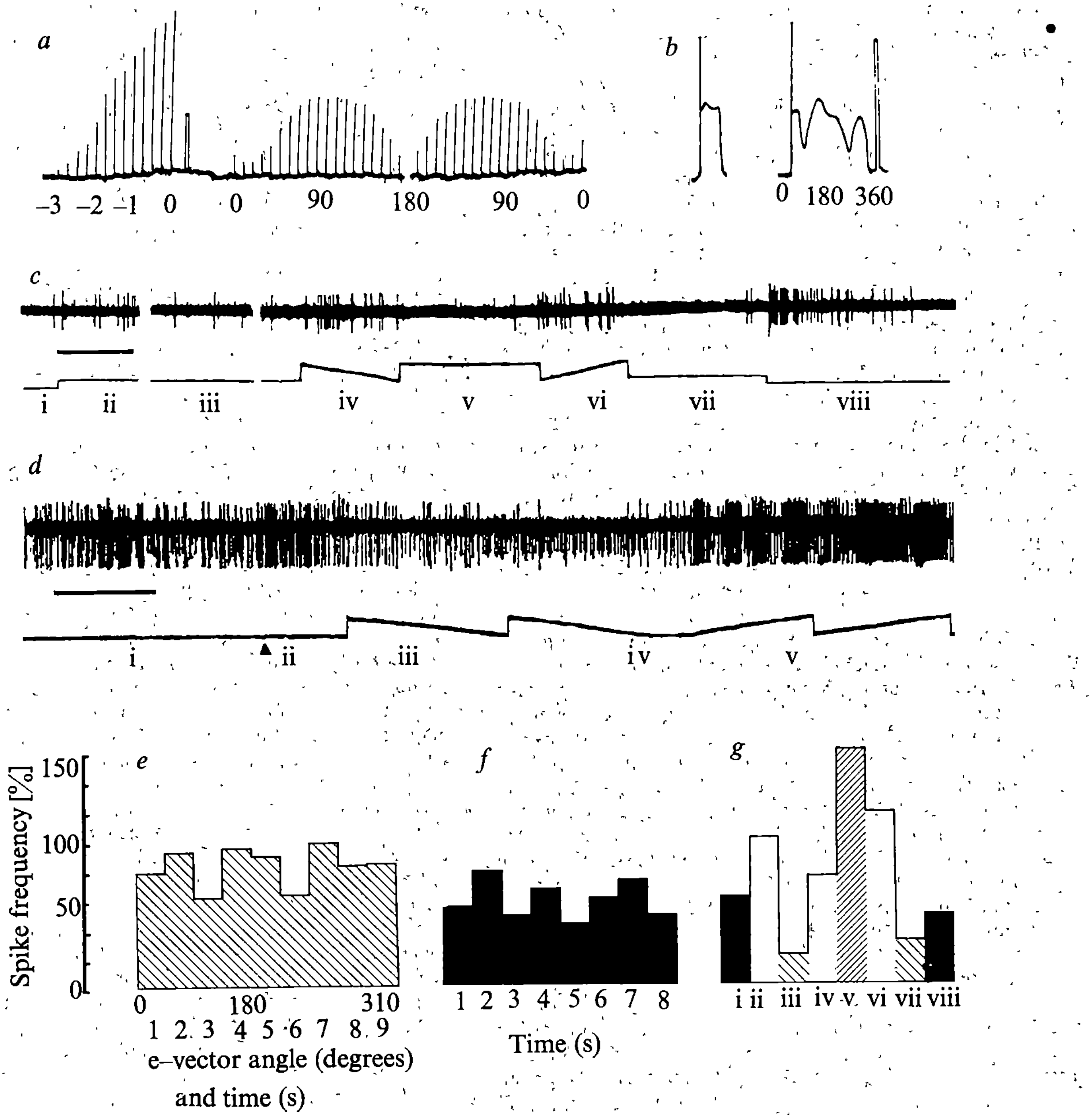

Fig. 1 *a*, Photoreceptor responses to increasingly intense flashes of light over 3 log units of intensity, and then photoreceptor responses to flashes of polarised light with the e vector moved first clockwise and then anticlockwise in 10° steps, one 40-ms flash every 5 s. Calibration 20 mV. The difference in response at maximum and minimum is equivalent to 1 log unit of intensity and thus the cell has a polarisation sensitivity of 10. *b*, Photoreceptor responses to continuous polarised light, e vector stationary and vertical, and then to continuous polarised light, e vector rotated through 360°. *c*, Interneurone I. The stimulus channel shows: i, dark discharge; ii, light-on (polaroid static and vertical); iii, response after 30 s of this unchanged stimulus; iv, polaroid rotation clockwise 360°; v, polaroid left, stationary and vertical; vi, polaroid rotation anticlockwise; vii, polaroid stationary and vertical; viii, light-off. Time mark 5 s. Note that the response is independent of stimulus direction, and that light-off has the strongest effect. *d*, Interneurone II. The stimulus channel shows: i, dark discharge; ii, dim light-on (▲) with polaroid static and vertical; iii, polaroid rotation clockwise; iv, polaroid static and vertical; v, polaroid rotation anticlockwise. Time mark 5 s. Note directional selectivity of response, and that polaroid rotation has a stronger effect than light on. *e*–*g*, Interneurone II. Data showing absence of stationary, presence of rotational PS. *e*, Response of a unit to a stimulus similar to that given the receptor cells in continuous light but 45° steps. There is no significant stationary PS as the response range is not significantly different from a similar period of dark discharge (*f*). *g*, Distinct response of three class II units to the rotational stimulus sequence (i–viii) listed above.

by placing a black screen with a small (3×2 mm) window close (2 mm) to the eye. The screen acted as a light baffle and ensured that the crab saw only the light spot and not, for example, its reflection from the floor of the preparation holder. Second, the fact that the stimulating variable really was polarised light and not intensity was checked. Measurements with a Hewlett Packard 8334A radiant flux meter showed only 0.57% intensity variation during an e-vector rotation of 360°.

Units were recorded extracellularly from the external medulla by conventional glass microelectrode techniques. Examples of two classes of unit are presented here. Both classes have very broad receptive fields, responding to test spots applied anywhere over the whole eye. For both units the experimental protocol was similar.

Unit 1 (20 cells recorded) responds to polaroid rotation, but is insensitive to the direction of rotation. In a typical trial (Fig. 1*c*, i–viii), a class I unit showed a small increase in discharge to light-on (e vector stationary and vertical). The cell was allowed to adapt to a low frequency of discharge (iii) and 30 s after light-on, polaroid rotation at a rate of about 50° s^{-1} was commenced (iv). This led to a fivefold increase in discharge rate. The opposite direction of rotation (vi) showed the same effect, and that it was independent of the orientation or direction of rotation of the **e** vector. Stopping rotation led to cessation, then a gradual return of activity.

Figure 1*d* and *e* show the responses of a class II unit which responds to both rotation *and* direction of rotation of **e** vector (6 cells recorded). Here, illuminating the spot with the **e** vector stationary and vertical, led to a doubling of discharge rate (ii). Rotating the polaroid clockwise at about 50° s^{-1} (iii) led to a progressive decrease in rate to a fifth of that induced by light-on. In complete contrast, an anticlockwise rotation (v) led to a progressive and sevenfold increase on the previous clockwise rate.

In discussing these results a point first arises as to categories of polarised light stimulus. When a polarising filter is rotated between a light source and the crab eye, the intracellular response of a retinula cell varies with the angular position of the filter (Fig. 1*a*). The commonly used definition of receptor PS has always been derived from responses to flashes of light, each being through a different stationary e-vector angle. I term this stimulus a stationary stimulus. It contrasts with the stimulus used in the interneurone experiments reported here, which I term a rotational stimulus.

The receptors of the crab eye are modulated by both stationary and rotational polarised stimuli (Fig. 1*a* and *b*). Because they respond to both, receptors by themselves cannot distinguish betwen stationary and rotational stimuli. It is clear that the interneurones demonstrated here are more specialised elements in a polarisation detection system. Both are more highly tuned to **e**-vector rotation than the receptors; furthermore, unit II is more highly tuned to rotation than unit I.

Although there are no data on the static PS of unit I, its response to rotation is quite different from that of a receptor. It has a flat response to rotation, whereas the receptor response is modulated (Fig. 1*b*).

In turn, unit II is more highly organised than unit I. First, in terms of the weighting given to intensity change relative to **e**-vector change: in unit I, the greatest response modulation was caused by light-off; in unit II, the greatest modulation was caused by **e**-vector change. Second, and most important, only unit II responds with directional selectivity.

These results demonstrate the existence of polarised light information in the crab central nervous system. The crab may use this information in three of the five ways mentioned in the introduction.

The first of these is contrast enhancement. The units reported here have been shown to respond to changes both in light intensity and in rate of **e**-vector rotation. It may be, however, that the general response is to moving patterns composed of variations in intensity and of polarisation. If this is the case visual contrast in the system could be enhanced in the following way. It is possible to imagine a grey moving object invisible against an equally grey background. If, however, the light coming from the object were different from the background in amount and **e**-vector angle of polarised light—a situation common in the ocean—the above PS system would detect a contrast difference. In this way the otherwise invisible object would become visible.

Second, orientation : in servo systems it is advantageous that rate of change detectors feed back to the output. If information from the units reported here were fed back to the motor system, *Scylla* could swim so as to minimise output from the PS interneurones and therefore move at a fixed angle relative to the polarised background. Such a system would minimise rolling and would act as a visual stabilisation system. Note, however, that units of class I and II alone would not enable a crab to orientate to one particular angle as opposed to another. This is because neither unit measures stationary **e**-vector angle. For this, a channel carrying positional information is required. This could be from the gravity detection system—in crabs, the statocysts—or from as yet undiscovered interneurones with stationary PS. Bodies of water are often turbid to the extent that swimming animals can see neither bottom nor solar position. In these very conditions, however, the polarised artificial horizon would be easily visible to an animal with the polarisation-sensitive system I have outlined. Such a system would enable animals to orientate visually in otherwise featureless water.

Finally, the underwater polarised pattern, while maintaining its horizontal component, moves with the Sun's movement during a day. If PS interneurones were allied with an internal clock, the system, as in the bee, could be used for navigation.

I thank Dr Y. Tsukahara and Dr S. Laughlin for useful discussions.

L. M. W. LEGGETT

Department of Neurobiology,
Research School of Biological Sciences,
Australian National University,
Canberra, ACT 2600, Australia

Received April 5; accepted May 28, 1976.

[1] Meyer-Rochow, V. B., *Nature*, **254**, 522–523 (1975).
[2] Waterman, T. H., in *Photoreceptor Optics* (edit. by Snyder, A. W., and Menzel, R.), 339–371 (Springer, Berlin, 1975).
[3] Frisch, K. v., *The Dance Language and Orientation of Bees* (Belknap, Cambridge, 1967).
[4] Helversen, O. v., and Edrich, W., *J. comp. Physiol.*, **94**, 33–48 (1974).
[5] Laughlin, S. B., *Austr. J. biol. Sci.* (in the press).
[6] Waterman, T. H., *Science*, **120**, 927–932 (1954).
[7] Schneider, L., and Langer, H., *Z. Zellforsch.*, **99**, 538–559 (1969).
[8] Lythgoe, J. N., in *Underwater Science*, 103–139 (Oxford University Press, London, 1971).
[9] Laughlin, S. B., Menzel, R., and Snyder, A. W., in *Photoreceptor Optics* (edit. by Snyder, A. W., and Menzel, R.), 237–262 (Springer, Berlin, 1975).
[10] Shaw, S. R., *Nature*, **211**, 92–93 (1966).
[11] Waterman, T. H., Wiersma, C. A. G., and Bush, B. M. H., *J. cell comp. Physiol.*, **63**, 135–155 (1964).

Aerial gas exchange in Australian arid-zone crab, *Parathelphusa transversa* Von Martens

Parathelphusa transversa is a brachyuran crab of the family Potamonidae and is found over much of inland Australia, including arid areas[1]. Permanent water sources, such as water holes, rivers and dams are avoided and during prolonged dry periods the animals lead a fossorial existence, their air-filled burrows being found in the clay soils of dry swamps and water courses. After heavy rain or flooding they emerge from their burrows to forage in the surface water, leading an amphibious existence. Their mode of life requires the capacity for gas exchange in both air and water and this is associated with structural adaptations of the branchial chamber to form a lung. We describe here the animal's unusual and hitherto undescribed mechanism of tidal ventilation of the lung.

Several other families of the Decapoda include terrestrial and semi-terrestrial representatives[2]. Most attention has been paid to those crabs which evolved from intertidal forms so that it is of interest to examine the parallel adaptations to air breathing which have occurred in this crab of freshwater origin.

The branchial chambers which are enclosed by lateral extensions of the carapace (the branchiostegites) are much expanded compared with aquatic forms (Fig. 1). There are seven pair of gills (a smaller number than in most aquatic crabs). These are reduced in size and only occupy a small proportion of the total volume of the branchial chambers. The remaining epibranchial spaces are normally air-filled, when the crab has access to air.

The branchiostegite is highly vascularised as in other terrestrial crabs (Figs 1–3). Blood channels between the inner and outer integument of the branchiostegites are separated by a system of connective tissue partitions, which

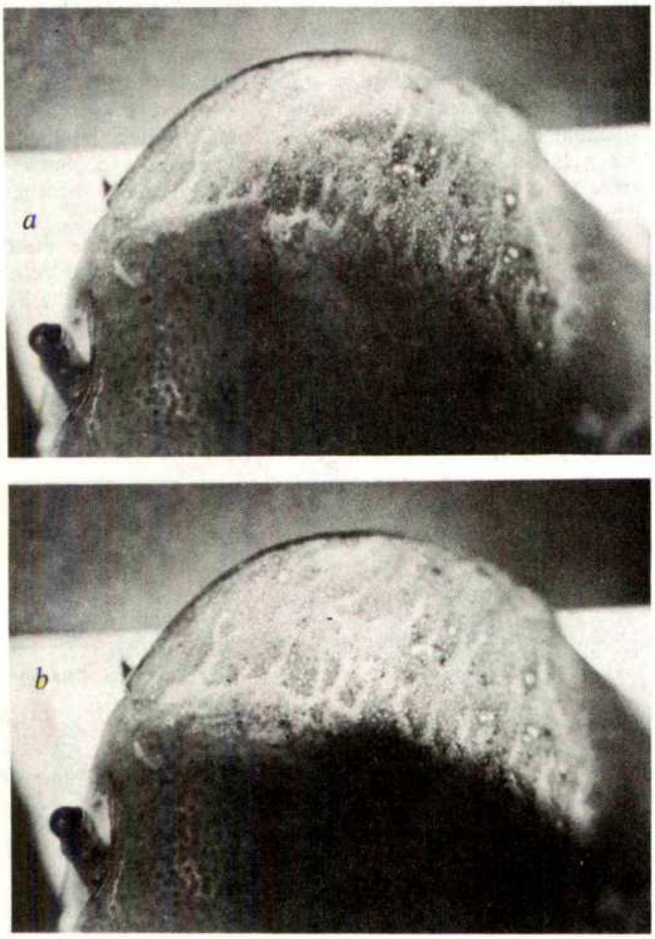

Fig. 1 *P. transversa* supported in air and illuminated strongly from the ventral side. Markings on carapace above branchial chamber delineate the major blood channels. *a*, Near-maximal expiration. Note the shadow of the thoracic wall penetrating into the branchial chamber. *b*, Maximal inspiration; thoracic wall has retracted out of the branchial chamber.

fulfil the dual role of directing blood flow and acting as a suspensory system for the inner integument. Support for this delicate membrane is presumably also provided by the hydrostatic pressure of the haemolymph.

Although the inner surface of the branchiostegite is smooth and lacks the surface amplification described in the Ocypodidae[2] and Coenobitidae[3] it is well adapted for air–blood gas exchange. The inner cuticle (Fig. 3) is extremely thin (about 0.2 μm). For comparison, the cuticle covering the gill leaflets and filaments in this and other crustaceans is generally about 1–3 μm thick (refs 4 and 5, and unpublished observations). The cuticle here seems to be represented only by a thin epicuticle[6]. There are no lamellae of helicoidally oriented chitin–protein microfibrils as seen in the exocuticle and endocuticle of the gills and other regions (ref. 6 and unpublished observations).

Fig. 2 0.5-μm epoxy section of dorsal region of branchiostegite stained with methylene blue. Extensive blood channels are partitioned by connective tissue. The thin epidermal lining of the inner cuticle (lower area) is unresolvable at this magnification (×168).

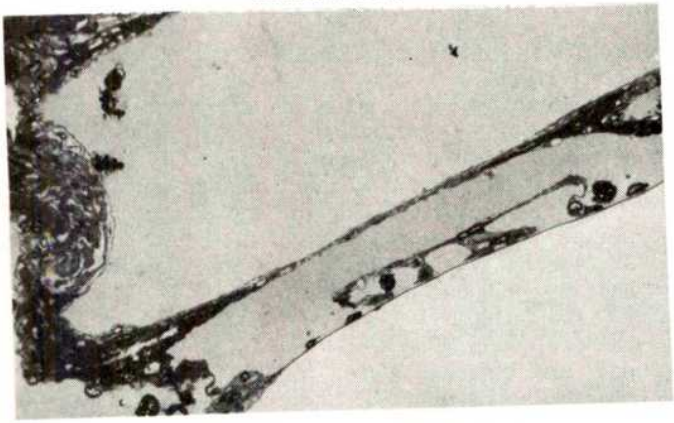

The blood–air diffusion path is further minimised by extreme attenuation of the epidermal cells underlying the inner cuticle. Except in the sparsely distributed perinuclear regions of the cells the cuticle is separated from the blood by a cellular layer only 20–100 nm thick, of which about 15 nm is represented by the apical and basal plasma membranes. The apical plasma membrane is applied directly to the cuticle. A thin (about 40 nm) basal lamina covers the haemolymph surface of the cells. Thus the total blood–gas distance is about 0.2 μm over most of the surface of the lung. This is of the same order of magnitude as the blood–gas distance in the lungs of the most active vertebrates and considerably less than in some[7].

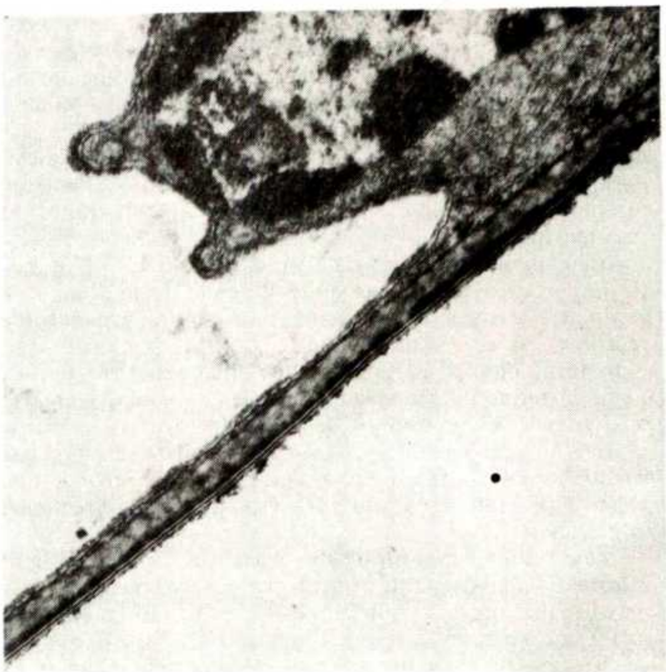

Fig. 3 Electron micrograph of inner cuticle of branchiostegite showing very attenuated extensions of the epidermal cell over the blood side of the cuticle. Formaldehyde–glutaraldehyde fixation with post-osmication (×10,500).

The mechanism of ventilation when breathing air has been examined. Surprisingly the scaphognathites, which are important in producing respiratory water currents in the aquatic mode and which are involved in aerial ventilation in other crabs[2,3,8], are not involved. Expiration is brought about by expansion of the membranous thoracic wall and roof of the branchial chamber (dorsal region of the thoracic epimera and pleura) into the epibranchial chamber (Fig. 1*a*). Inspiration is achieved by the retraction of the membrane to assume its normal concave form (Fig. 1*b*). Inspiration in one epibranchial chamber is accompanied by simultaneous expiration in the other. These movements may be observed by shining an intense light (with heat filter) through the animal from the ventral surface and observing the shadows of the thoracic wall on the carapace. This movement involves a slow lateral oscillation of the thoracic viscera (dark areas in Fig. 1*a* and *b* are probably mainly the digestive gland).

Direct observation reveals that the scaphognathites do not beat during aerial ventilation, the prebranchial apertures above the mouth remaining open. By placing detergent films over these so-called 'exhalent apertures', it was established that ventilation was tidal, both inspiration and expiration occurring through these apertures. The Milne-Edwards apertures at the base of the chelipeds are not involved in aerial respiration. In another freshwater crab, *Trichodactylus petropolitanus* (Trichodactylidae) the scaphognathites cease beating in air, although it was considered that air entered the branchial chamber by diffusion during aerial respiration in this animal[9].

In resting *Parathelphusa* the ventilatory movements are sporadic but after exercise become regular in frequency and depth, reaching a maximum rate of 20 cycles min^{-1} (each cycle represents one inspiration and expiration for each lung). During maximal ventilation the thoracic wall moves almost completely across the epibranchial chambers. It is estimated that at least 70–80% of the air in the lung is exchanged in each ventilatory cycle.

The oxygen extraction efficiency of the lung of *Parathelphusa* has not yet been measured. Ventilation of the gas exchange surface seems, however, to be more efficient than in *Birgus* or gecarcinids, where diffusion distances between the branchial tufts or gills are relatively long[4].

The muscular basis of ventilation is not yet known. It is possible that muscles homologous to the 'dorso–ventral muscles' described by Pearson[10] in *Cancer* are involved. These muscles run from the roof of the branchial chamber to the carapace. Contraction of these could effect inspiration while expiration in the contralateral branchial chamber would be simultaneously effected by hydraulic displacement of the haemolymph and viscera.

No similar ventilatory movements have been described in other crabs, although in *Birgus* carapace movements contribute in a minor way to air flow through the lungs[3]. Unlike a vertebrate, a crab's total volume is essentially fixed by its rigid exoskeleton. In this light the simultaneous inspiration and expiration in opposite chambers could be seen as a neat solution to the problem of lung ventilation.

P. GREENAWAY

School of Zoology,
University of New South Wales,
PO Box 1, Kensington,
New South Wales 2033, Australia

H. H. TAYLOR

Department of Zoology,
University of Canterbury,
Christchurch 1, New Zealand

Received May 26; accepted June 25, 1976.

1 Bishop, J. A., *Aust. J. mar. Freshwat Res.*, 14, 218–38 (1963).
2 Bliss, D. A., *Am. Zool.*, 8, 355–92 (1968).
3 Cameron, J N., and Mecklenburg, T. A., *Resp. Physiol.*, 19, 245–61 (1973)
4 Copeland, D. E., *Am Zool.*, 8, 417–32 (1968).
5 Strangeways-Dixon, J., and Smith, D. S., *Tissue Cell*, 2, 611–24 (1970)
6 Green, J. P., and Neff, M. R., *Tissue Cell*, 4, 137–71 (1972).
7 Weibel, E. R., in *Handbook of Physiology*, Section 3, 1, 285–307 (American Physiological Society, Washington).
8 Cameron, J. N., *Comp. Biochem Physiol*, 52A, 128–34 (1975).
9 Valente, D, *Sao Paulo Univ. Faculdade de filosofia ciencias e letres, Zoologia* 13, 259–316 (1948).
10 Pearson, J, Cancer, *Liverpool Mar. Biol., Comm Mem*, XVI (Williams and Nordgate, London, 1908).

Calcium couples flagellar reversal to photostimulation in *Chlamydomonas reinhardtii*

SEVERAL recent findings[1–3] suggest that the intracellular concentration of free calcium, $[Ca]_i$, has an important role in the regulation of ciliary and flagellar beating. For example, *Paramecium* extracted with Triton X-100 and reactivated with Mg^{2+} and ATP swim backwards when the Ca^{2+} concentration of the test medium, $[Ca]_o$, is raised above 10^{-6} M (ref. 1). Similarly, extracted cells of the typanosomid *Crithidia* show a reversal in wave propagation that is controlled by Ca ions. In studies on the intact flagellar apparatus isolated from a wall-less mutant of *Chlamydomonas reinhardtii*, the flagella have been shown to reverse direction of the effective stroke when external $[Ca]_o$ is raised above 10^{-6} M (ref. 3). Electrophysiological evidence indicates that, in *Paramecium*, reversal of ciliary beating is caused by Ca which enters the cell when the Ca permeability of the membrane is increased[4,5]. We have investigated whether Ca is involved in the phototactic response and more specifically whether this Ca influx is regulated by the cell membrane. Electrophysiological recording was impractical because of the small size of these cells (< 10 μm), and so the approach was to photograph the light-induced motor responses of cells swimming in solutions containing different concentrations of Ca or Ca-blocking agents. The results demonstrate that the reversed beating response of the flagella depends on Ca. Inhibition of the response by Ca-blocking agents supports the view that reversed beating response of the flagella is coupled to photostimulation by an influx of Ca ions.

Wall-less mutants of *C. reinhardtii* strain CW92 were grown axenically in liquid medium[6] at 25 °C with constant shaking under a 14-h light, 10-h dark cycle. Light was provided by Cool-white and Gro-lux fluorescent illumination at an intensity of 2.6 W m^{-2}. Response variability was minimal when cells were used between hours 67 and 77 after inoculation and between hours 3 and 6 of the light cycle.

Cells were centrifuged and resuspended twice in the experimental solution and were kept in the dark before transfer to a microscope slide. They were then examined by phase illumination under red light (Corning glass 2-62 sharp-cut filter, 600-750 nm) and left undisturbed while exposed continuously to the red light for 60–75 min before stimulation. Red illumination did not produce any overt behavioural response in these cells. The stimulus, a substitution of white light for the red light, was achieved by electromechanically replacing the red filter by a neutral density filter for approximately 280 ms. The red light had an energy before entering the microscope optics of ~ 80 W m^{-2} and the white stimulus light plus neutral density filter ~ 70 W m^{-2}. The temperature at the microscope stage was 20±1 °C. A fresh sample of cells was used for each experiment and each group of cells was stimulated only once.

The control solution contained 2 mM EGTA (ethylene glycol-*bis*-(β-aminoethylether)-*N*,*N*′-tetraacetic acid), 3 mM $CaCl_2$, 1 mM KCl, 0.1 mM $MgCl_2$, and 5 mM HEPES (*N*-2-hydroxyethylpiperazine-*N*′-2-ethanesulphonic acid) at *p*H 7.1. Experimental solutions were identical except for the concentration of Ca or the addition of test substances as described below. $CaCl_2$ was added to the fixed concentration of EGTA in amounts yielding the desired concentration of free Ca for $[Ca]_o$ between 10^{-8} and 10^{-5} M (ref. 7). At higher concentrations the free Ca was regarded as the total Ca concentration minus the EGTA concentration.

Analysis of cell and flagellar motion was carried out at 1,000× image magnification on Kodak 2496RAR film exposed in a LOCAM 16-mm camera at 200 frames per s. Frame-by-frame analysis of the recorded sequence was made on a Vanguard motion analyser, and representative flagellar configurations were traced by hand, and reproduced schematically in Fig. 1*a*. Backward swimming velocity is defined as the distance covered by the cell during an episode of backward swimming divided by the time elapsed during reversed locomotion. Forward swimming velocity was calculated from the distance covered by the cell in 150 ms. In those instances where forward locomotion was determined during a light stimulus the period of measurement began 20 ms after stimulus onset.

During forward swimming under red light the flagellar motion resembled a breaststroke[8,9] (Fig. 1*A*, bottom left, *a*). The power stroke consisted of the simultaneous movement of both flagella in a rather straight sweep bending only near the base. This stroke propelled the cell forward with the base of the flagella leading. The recovery stroke consisted of a wave propagating along the flagella from base to tip, which pushed the cell backwards slightly. A complete cycle of beating lasted about 20 ms. The time required for one complete cycle was determined to ±10 ms by measuring the time required for 5 beats to ± 10 ms.

Photostimulation in the control solution always produced a constant modification of flagellar movement and hence swimming behaviour (Fig. 1). The cell continued to swim forward for about one cycle (that is, 20 ms) after the onset of the stimulus and then stopped for about 20 ms. The power stroke then reversed (reversal in *b*, Fig. 1*A*), increased in frequency and caused the cell to back up. This reversed swimming was only seen in response to the photostimulation. Backward swimming continued for 200 ms after the stimulus. After 550±100 ms from the initiation of backward swimming the cell eventually slowed to a stop and for about 200 ms wobbled around its transverse axis (*c*, Fig. 1*A*). The cell moved about 14 μm in the reverse direction before resuming forward movement.

Changes in $[Ca]_0$ did not significantly affect forward swimming in the unstimulated cell (Fig. 1*B*) but markedly modified the light-induced responses (Fig. 1*A*, b_1–b_3). In the range of

Fig. 1 Dependence of *Chlamydomonas* photoresponse on $[Ca]_0$. *A*, Bottom, normal sequence (*a*, *b*, *c* and *d*) of flagellar behaviour and cell movement before, during and after a 300-ms light stimulus in control (that is 10^{-3} M Ca) solution. Durations of backward swimming and wobble are about 550 and 200 ms respectively. Reversal and termination of backward swimming latencies are 20 and 200 ms respectively. The response during light is shown on a larger scale in the expanded portion of the stippled area. Backward locomotion was progressively inhibited (b_1, b_2, b_3) by reduced $[Ca]_0$. *B*, Prestimulus velocity (μm s^{-1}) plotted against pCa_0. Bars give s.e.m. There was no significant difference in forward swimming velocity at $[Ca]_0$ between 10^{-8} and 10^{-2} M. *C*, Rate of swimming during photostimulation plotted against *p*Ca as percentage of prestimulus control swimming rate. Control swimming rates for both forward and backward locomotion represent rates measured at 10^{-3} M $[Ca]_0$. Backward locomotion was normalised to the forward control swimming rate. Bars give s.e.m. Backward locomotion is plotted above, and forward locomotion below the dashed line. Control swimming rate was restored after cells were transferred from a 10^{-8} M Ca solution to the control solution, 10^{-3} M.

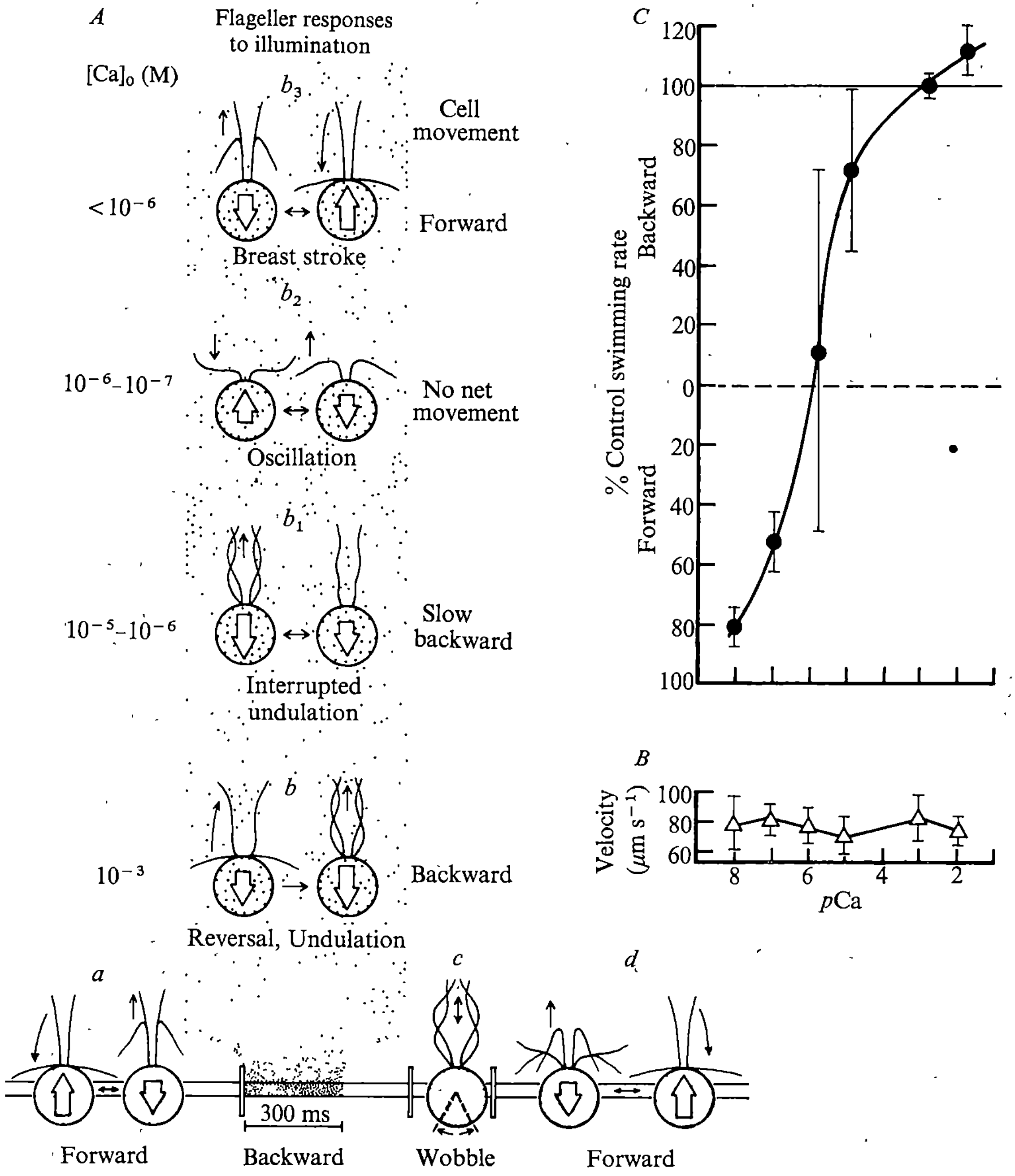

10^{-5} to 10^{-6} M Ca there appeared interrupted undulations of the flagella (b_1, Fig. 1*A*). In addition, the velocity of reversed swimming became progressively slowed. At 10^{-6} M Ca the flagella of about 10% of the cells exhibited an oscillation in the focus plane which produced no net cell movemet (b_2, Fig. 1*A*). At concentrations less than 10^{-6} M Ca no reversed beating was observed in response to the stimulus (b_3, Fig. 1*A*) but there was a significant slowing of forward motion.

The rate of swimming in response to photostimulation is plotted against *p*Ca in Fig. 1*C*. The highest rate of backward swimming recorded was in 10^{-2} M Ca solution. At 10^{-6} M some cells swam backwards slowly while others swam forward. At less than Ca 10^{-6} M backward swimming could not be evoked with photostimulation; swimming continued in the forward direction during photostimulation with the highest observed rate at the lowest Ca concentration, 10^{-8} M. The effects of reduced Ca concentration on the response to photostimulation were reversed completely when cells were returned to the control solution.

The velocity of light-induced backward swimming was measured in the presence of agents known to block Ca influx in excitable membranes. Addition of 10^{-2} M Ba or 10^{-2} M Mg to the control solution resulted in a reduced velocity of backward swimming (Fig. 2). The effect was fully reversible. In addition, the organic Ca-blocking compound D-600 (α-isopropyl-α-α-[(*N*-methyl-*N*-homoveratryl)-γ-aminopropyl]-3,4,5-trimethoxyphenylacetonitrile)[10] inhibited backward swimming at 10^{-4} M or greater (Fig. 2). In contrast to Ba and Mg, however, the inhibition caused by this drug was irreversible. Procaine, a local anaesthetic which reversibly blocks membrane excitability[11] and is reported to be a competitor of Ca in the lobster axon[12], was found to block reversibly backward swimming at 10^{-2} M or greater (Fig. 2).

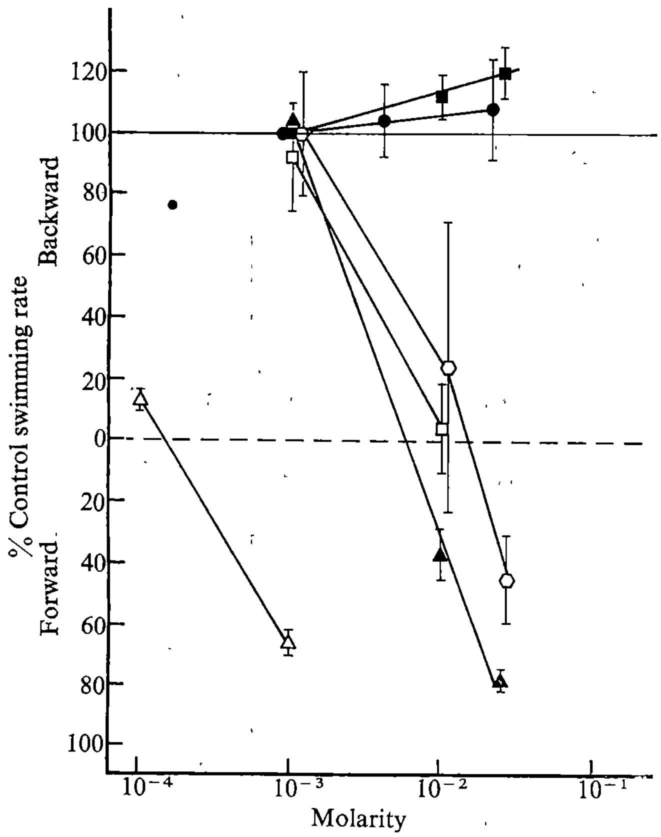

Fig. 2 Effect of several agents on backward swimming velocity in the presence of 10^{-3} M Ca. Percentage of swimming rate in control solution is plotted against concentration of each agent. Bars give s.e.m. Procaine concentrations were maintained at a constant 20 mosM with pentaerythritol. Ba, Mg and procaine inhibition was fully reversed by return to control solution. ●, Pentaerythritol; ▲, procaine; △, D-600; □, Ba^{2+}; ■, Ca^{2+}; hexagon, Mg^{2+}.

Lanthanum, Ni, Co and Mn ions, which generally block Ca currents in other membranes[13], have no effect on backward swimming at concentrations up to 1, 5, 50 and 80 mM respectively. At higher concentrations these cations were toxic. These agents also fail to block in *Paramecium* the Ca influx which mediates ciliary reversal[4,5,14,15].

The results presented here indicate that photostimulated flagellar reversal depends on extracellular Ca. The inhibition of the response by certain Ca-blocking agents such as D-600, procaine, Ba, and Mg, which are known to block Ca influx in other systems, suggests that photostimulation normally results in an influx of Ca through the cell membrane, producing a transient increase in $[Ca]_i$. The induction of reversed beating by Ca in the isolated basal body–flagellar apparatus[3] of *Chlamydomonas* supports this conclusion. Thus it seems that Ca^{2+} acts as the agent that couples flagellar responses to photostimulation in flagellate. This is reminiscent of the role of calcium in coupling ciliary reversal to membrane stimulation in the ciliated protozoa.

We thank Dr J. S. Hyams for providing the wall-less mutants of *C. reinhardtii* and Dr P. O'Lague for helpful discussion and critical reading of the manuscript. This work was supported by the NSF and USPHS.

JEFFREY A. SCHMIDT
ROGER ECKERT

Department of Biology,
University of California,
Los Angeles, California 90024

Received April 30; accepted June 26, 1976.

[1] Naitoh, Y., and Kaneko, H., *Science*, **176**, 524–532 (1972).
[2] Holwill, M. E., and McGregor, J. L., *Nature*, **255**, 157–158 (1975).
[3] Hyams, J. S., and Borisy, G. G., *J. Cell Biol.*, **67**, 186 (1975).
[4] Eckert, R., *Science*, **176**, 478–481 (1972).
[5] Eckert, R., Naitoh, Y., and Machemer, H., *Symp. Soc. exp. Biol.*, **30** (edit. by Duncan, C.), (Academic, London, 1976).
[6] Sueoka, N., *Proc. natn. Acad. Sci. U.S.A.*, **46**, 83–91 (1960).
[7] Portzehl, H., Caldwell, P. C., and Ruegg, J. C., *Biochim. biophys. Acta*, **79**, 581–591 (1964).
[8] Ringo, D. L., *J. Cell Biol.*, **33**, 543–571 (1967).
[9] Ulehla, V., *Biol. Zbl.*, **31**, 696–701 (1911).
[10] Fleckenstein, A., Tritthart, H., Fleckenstein, B., Herbst, A., and Grun, G., *Pflugers Arch. ges. Physiol.*, **307**, 25 (1969).
[11] Seeman, P., *Pharmac. Rev.*, **14**, 583–655 (1972).
[12] Blaustein, M. P., and Goldman, D. E., *J. gen. Physiol.*, **49**, 1043–1063 (1966).
[13] Hagiwara, S. in *Membranes*, **3** (edit. by Eisenman, G.), 359–378 (Dekker, New York, 1975).
[14] Naitoh, Y., Eckert, R., and Friedman, K., *J. exp. Biol.*, **56**, 667–681 (1972).
[15] Friedman, K., and Eckert, R., *Comp. Biochem. Physiol.*, **45A**, 101-114 (1973).

Bioconversion of light energy into chemical energy through reduction with water of nitrate to ammonia

PHOTOSYNTHESIS is first and foremost a process for converting the radiant energy of sunlight into physiological chemical energy, that is, reducing power and high energy phosphate bonds[1]. Since, for historical and quantitative reasons, however, photosynthesis in a broad sense is commonly identified with the reduction of carbon dioxide to carbohydrate, the fact is often overlooked that photosynthetic organisms manufacture their most representative biomolecules—proteins and nucleic acids—not only from carbon dioxide, but also from other oxidised inorganic nutrients, especially nitrate, that, more or less directly, has to be reduced to ammonia by water before being incorporated into amino acids[2,3]. It was first thought[4] that the reduction of nitrate in green cells was a process far removed from the light reactions of photosynthesis and that carbohydrates were the *in vivo* source of reducing power for nitrate reduction, but it now seems that, at least in blue-green algae[5-7], the photosynthetic reduction of nitrate is even more direct than that of carbon dioxide, since it does not depend on adenosine triphosphate (ATP) and reduced nicotinamide adenine dinucleotide phosphate (NADPH), but only on reduced

Table 1 Photoreduction of nitrate to nitrite and ammonia coupled to oxygen evolution by particles of *Anacystis nidulans*

System	Nitrite formed (μmol)	Ammonia formed (μmol)	Oxygen evolved (μmol)
Complete	0.9	2.0	4.1
−Fd	0.7	1.6	3.5
$-NO_3^-$	0	0	0
+CMU	0	0.2	−0.4
Dark	0	0.2	−0.5

The complete system included in a final volume of 3 ml: 150 μmol Tricine–KOH buffer, *p*H 8.0; 30 μmol $MgCl_2$; 20 μmol KNO_3; 40 nmol *A. nidulans* ferredoxin (Fd); *A. nidulans* particles containing 0.63 mg chlorophyll. Where indicated, 0.3 μmol of 3-(*p*-chlorophenyl)-1-1-dimethylurea (CMU) was added. The reaction was carried out in air at 30 °C in Warburg vessels illuminated from below (20,000 lx) or kept in the dark. Reaction time 90 min. Other analytical methods as previously described[6]. Particles were prepared as follows: cells grown on nitrate in the light, as described previously[6], were collected in the exponential phase of growth, washed with 50 mM Tricine–KOH buffer, *p*H 8.0, 0.5 M sucrose, 10 mM $MgCl_2$, resuspended in the same buffer and broken with a precooled French press at 16,000–18,000 pound inch^{-2}. After digestion of the broken material with DNase and RNase for 10 min at 2 °C, the suspension was centrifuged at 3,000*g* for 10 min, the pellet discarded, and the supernatant centrifuged again at 40,000*g* for 20 min. The resulting sediment was washed once with the buffer, collected after centrifugation at 40,000*g* for 30 min, and finally resuspended in the buffer, to be used as a preparation of particles.

ferredoxin, the first electron acceptor from photosystem I. Also the enzymes for the reduction of nitrate to ammonia are retained tightly bound by the pigment-containing particles from these prokaryotes.

We report here the preparation of active and stable particles from the blue-green alga *Anacystis nidulans*, which, in the light and in aerobic conditions, can use water as the electron donor for the steady reduction of nitrate to nitrite and ammonia without the requirement of any exogenous enzyme system (Table 1).

During the past 15 yr, the assimilatory nitrate-reducing system, its regulation and its relation to photosynthesis have been studied, using a great variety of organisms[3,8,9]. Our results, as well as those from other groups[10], have firmly established that the nitrate-reducing enzyme system consists of only two metalloproteins—nitrate reductase and nitrite reductase—which catalyse in series the reduction of nitrate to nitrite and ammonia, through an unexpectedly short sequence of reactions

$$NO_3^- \xrightarrow{2e} NO_2^- \xrightarrow{6e} NH_4^+$$

Both enzymes are ferredoxin-dependent in the photosynthetic prokaryotes, but only nitrite reductase has such a dependence in the photosynthetic eukaryotes, a group which includes algae and higher plants. Nitrate reductase from eukaryotes is an NAD(P)H-dependent enzyme complex.

We have previously obtained isolated pigment-containing particles from *A. nidulans* that could carry out the ferredoxin-dependent photosynthetic reduction of nitrate and nitrite with the couple ascorbate–dichlorophenol indophenol as an artificial electron donor for photosystem I. The coupling of the process with the photolysis of water remained, however, an unsolved problem. There is also at the present time a direct interest in the photolysis of water by photosynthetic systems for fuel production, especially hydrogen gas, but these systems require auxiliary enzymes from other sources, and the removal of even traces of molecular oxygen is an absolute requisite[11]. Biological photofixation of nitrogen is also an anaerobic process but with high ATP requirements and its coupling with water photolysis will be even more difficult to accomplish (compare ref. 12).

In the system described here the electrons derived from the photolysis of water at photosystem II are transported to photosystem I and used for the stepwise reduction of nitrate to ammonia by the ferredoxin-dependent nitrate-reducing system, oxygen being evolved in stoichiometric amounts, according to the equations

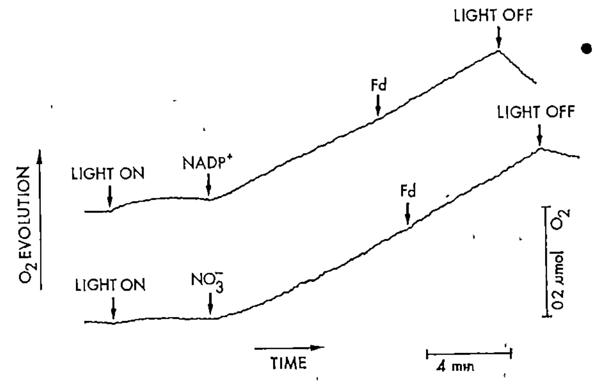

Fig. 1 Time course of oxygen evolution by *Anacystis nidulans* particles with either $NADP^+$ or NO_3^- as 'natural' Hill reagents. The reaction was carried out at 30 °C in the chamber of an oxygen electrode, either in the light (40,000 lx) or in the dark as indicated. Other experimental conditions were the same as in Table 1, except that a particulate preparation equivalent to 0.31 mg chlorophyll was used and that 4 μmol of $NADP^+$ were added as indicated in the corresponding system.

$$\begin{array}{r}
NO_3^- + H_2O \rightarrow NO_2^- + \tfrac{1}{2}O_2 + H_2O \\
NO_2^- + 3H_2O + 2H^+ \rightarrow NH_4^+ + \tfrac{3}{2}O_2 + 2H_2O \\
\hline
NO_3^- + 4H_2O + 2H^+ \rightarrow NH_4^+ + 2O_2 + 3H_2O
\end{array}$$

It can be seen in the table that the reaction depended on nitrate, was slightly stimulated by ferredoxin, and did not proceed in the dark or when an inhibitor of the photolysis of water was added. In the conditions of the experiment, the activity of the system was linear for at least 90 min. The small O_2 uptake in the presence of the inhibitor or in the dark might be related to the presence of an endogenous reducing material in the preparation.

Gerhardt and Trebst[13] have reported the ferredoxin-dependent non-cyclic photophosphorylation coupled to $NADP^+$ reduction and oxygen evolution by *A. nidulans* preparations obtained by vacuum drying. $NADP^+$ photoreduction by ferredoxin-NADP reductase and nitrate photoreduction by the ferredoxin-nitrate-reducing system are thus similar reactions. As Fig. 1 shows, our *A. nidulans* particles exhibited the same photosynthetic activities with either $NADP^+$ or nitrate as 'natural' Hill reagents[14]. Particles stored for 1 d at 2 °C remained fully active with respect to its nitrate-dependent, oxygen-evolving capacity, except for the ferredoxin requirement, that stimulated activity twofold after several hours and threefold after 24 h. Cell-free preparations from another blue-green alga—the N_2-fixer *Nostoc muscorum*—behave in a similar way (unpublished work from this laboratory).

Fig. 2 Diagrammatic representation of the ferredoxin-dependent photosynthetic reduction of nitrate to ammonia with water as the electron donor by blue-green algae particles. Fd, Ferredoxin.

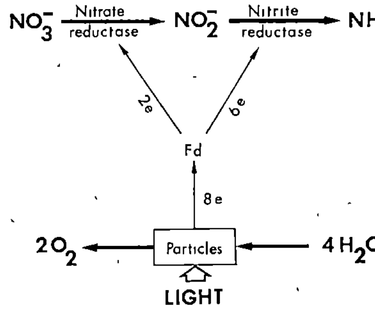

In summary, subcellular preparations of blue-green algae can utilise the photochemically-generated reducing power coming from water for the direct reduction of nitrate to ammonia. The process can be considered as one of the most simple and relevant examples of photosynthesis. According to present knowledge, the ferredoxin-dependent photosynthetic reduction of nitrate and nitrite is shown in Fig. 2. Since 16 quanta of light are required to transfer 8 electrons from water to completely reduce one nitrate, the efficiency of the process (disregarding coupled photophosphorylation) is about 13%. Besides its biochemical and chemical interest, ammonia is an excellent fuel and can also be regarded as a portable source of hydrogen[15].

This research was supported by grants from Philips Research Laboratories and the NSF.

P. CANDAU
C. MANZANO
M. LOSADA

Departamento de Bioquimica,
Facultad de Ciencias, CSIC,
Universidad de Sevilla, Spain

Received June 1; accepted June 11, 1976.

[1] Arnon, D. I., *Proc. natn. Acad. Sci. U.S.A.*, 68, 2883–2892 (1971).
[2] Whatley, F. R., and Losada, M., in *Photophysiology*, 1 (edit. by Giese, A. C.), 111–154 (Academic, London and New York, 1964).
[3] Losada, M., in *Reflections on Biochemistry* (edit. by Kornberg, A., Horecker, B. L., and Oró, J.) (Pergamon, Oxford, in the press).
[4] Warburg, O., *A. Rev. Biochem.*, 33, 1–14 (1964).
[5] Hattori, A., and Uesugi, I., in *Comparative Biochemistry and Biophysics of Photosynthesis* (edit. by Shibata, K., Takamiya, A., Jagendorf, A. T., and Fuller, R. C.), 201–205 (University of Tokyo Press, Tokyo, 1968).
[6] Guerrero, M. G., Manzano, C., and Losada, M., *Pl. Sci. Lett.*, 3, 273–278 (1974).
[7] Manzano, C., Candau, P., Gomez-Moreno, C., Relimpio, A. M., and Losada, M., *Molec. cell. Biochem.*, 10, 161–169 (1976).
[8] Losada, M., in *Metabolic Interconversion of Enzymes 1973* (edit. by Fischer, E. H., Krebs, E. G., Neurath, H., and Stadtman, E. R.), 257–270 (Springer, Berlin, 1974).
[9] Losada, M., *J. molec. Catal.*, 1, 245–263 (1976).
[10] Hewitt, E. J., *A. Rev. Pl. Physiol.*, 26, 73–100 (1975).
[11] Rao, K. K., Rosa, L., and Hall, D. O., *Biochem. biophys. Res. Commun.*, 68, 21–28 (1976).
[12] Fogg, G. E., Stewart, W. D. P., Fay, P., and Walsby, A. E., *The Blue-Green Algae* (Academic, London, 1973).
[13] Gerhardt, B., and Trebst, A., *Z. Naturforsch.*, 20b, 879–885 (1965).
[14] Hill, R., in *Essays in Biochemistry*, 1 (edit. by Campbell, P. N., and Greville, G. D.), 121–151 (Academic, New York, 1965).
[15] Jones, K., *The Chemistry of Nitrogen* (Pergamon, Oxford, 1975).

Cell differentiation without morphogenesis in *Dictyostelium discoideum*

To understand pattern formation in an organism one needs to know what factors control the differentiation of each cell type and what elements are responsible for the spatial arrangement of these cell types. In the cellular slime mould *Dictyostelium discoideum*, the problem is relatively simple since the mature fruiting body consists of two basic cell types—stalk cells and spores. The stalk cells of the mature fruiting body are derived from the anterior cells of the multicellular masses formed by aggregation, whereas the spores are derived from the posterior cells[1]. Cells that are plated at a density too low for aggregation, or are allowed to aggregate under water do not normally differentiate into stalk or spore cells. In many of our experiments we have made use of the fact that cells plated on agar at any density fail to undergo development beyond the stage of aggregation if they are covered by a thin layer of Cellophane. In this paper we present observations on cell differentiation which derive from the original report of Bonner[2] of stalk-cell induction by cyclic AMP in isolated cells. We have found that stalk-cell induction by cyclic AMP is markedly dependent on cell density, and present evidence for the involvement of a low molecular weight diffusible factor in this process. We also describe the isolation of a mutant which gives rise to spore cells under cellophane.

Bonner[2] reported that a proportion of amoebae of strain NC4 developed into large vacuolated stalk-like cells when plated on agar containing 1 mM cyclic AMP at cell densities that were too low to allow aggregation in controls without cyclic AMP. This observation was extended by Chia[3] who showed that when cells of P4 (a 'stalky' mutant of strain NC4) were plated at high density on a Cellophane support over a reservoir of 1 mM cyclic AMP, they collected into mounds in which all the cells differentiated into stalk cells. Cells of the parent strain NC4 collected into similar mounds, but only a proportion of them differentiated into stalk cells. In conditions similar to those of Bonner[2] (described in Fig. 1) we found that strains NC4, NC4/P4 and NC4/Ax-2 differentiate at a relatively low frequency, whereas strain V-12 M2 formed almost 100% stalk cells. Thus when cells were spread at a denstiy of 10^5 cells cm^{-2} on agar containing 5 mM cyclic AMP, the stalk-cell induction frequencies in strains V-12 M2, NC4, P4 and Ax-2 were 93, 4, 10 and 2%, respectively. At a density of 10^4 cells cm^{-2} and on 1 mM cyclic AMP, V-12 M2 produced 24% stalk cells, whereas the other three strains did not produce any. No stalk cells were observed in controls in the absence of cyclic AMP at 10^4 cells cm^{-2} or in controls at 10^5 cells cm^{-2} where the cells were overlain with Cellophane to prevent fruiting.

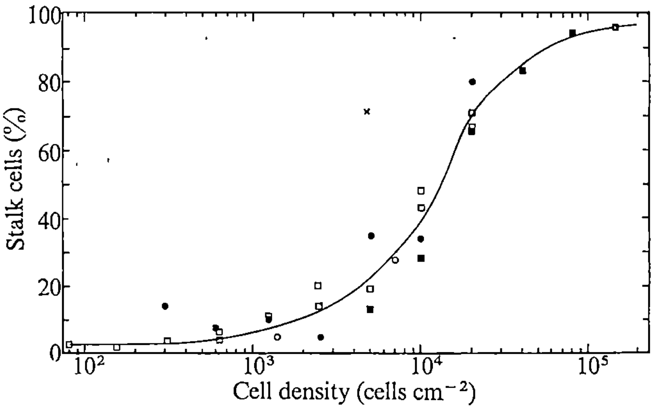

Fig. 1 Effect of cell density on stalk-cell induction by cyclic AMP. Cells were grown for 18–24 h with *K. aerogenes* on SM agar at 22 °C. They were collected and washed three times in 1% Bonner's salts and then spread at various cell densities on non-nutrient stalk-cell agar plates with or without cyclic AMP. The stalk-cell plates contained 1% Difco Bacto agar in 1% Bonner's salts, 100 μg ml^{-1} streptomycin sulphate, 25 μg ml^{-1} Calcofluor White 'New M2R' (Cyanamid, UK) with or without cyclic AMP; a total volume of 2.0 ml in a 5-cm plastic Petri dish. The plates were incubated in moist, dark conditions for 2–3 d and then examined by phase and fluorescence microscopy. Independent experiments are shown by different symbols. Cyclic AMP concentration was 1 mM in all experiments except one at the highest cell densities (■) when it was increased to 5 mM to prevent fruiting and ensure efficient-stalk cell induction. All control plates had less than one stalk-cell in 200 cells examined.

We have examined stalk-cell induction in strain V-12 M2 over a range of cell densities from 80 to 10^5 cells cm^{-2} (a density at which aggregation occurs on the control plates but not on those containing 1–5 mM cyclic AMP). The results are shown in Fig. 1. At cell densities greater than 4×10^4 cells cm^{-2}, almost all of the initially vegetative amoebae were transformed in 2–3 d into stalk-like cells, as judged by their morphology under phase-contrast and in electron micrographs, as well as by their staining with the cellulose-specific indicator calcofluor[4]. The frequency of stalk-cell induction decreased quite rapidly as cell density was reduced, reaching a basal level of approximately 3% below 500 cells cm^{-2}. At high cell densities, a considerable proportion of the initially separate cells were present in small clumps after 2–3 d incubation and this proportion declined as cell density was lowered.

At cell densities between 5×10^3 and 2×10^4 cells cm^{-2}, 70–100% of the cells in small clumps became stalk cells, whereas only 30% of the single cells on the same plates were induced. This latter figure is in turn much higher than the value of 3% observed at very low density (Fig. 1). It therefore seems that cyclic AMP can induce differentiation of isolated amoebae

Table 1 Enhancement of stalk-cell differentiation in isolated cells by a diffusible factor from cells differentiating at high density

Tester cell density (no. of determinations)	% Stalk-cell differentiation			
	Tester cells alone		Tester cells plus high density helper cells	
	Control	Cyclic AMP	Control	Cyclic AMP
10^3 cells cm^{-2} (3)	1.3	4.3	0	80.0
2×10^3 cells cm^{-2} (2)	0	1.3	0	39.6
5×10^3 cells cm^{-2} (1)	0	4.5	0	79.6

Cells were prepared and spread on 1% agar containing 1% Bonner's salts with or without 5 mM cyclic AMP as described in Fig. 1. The first layer of cells was overlaid with Cellophane and, where appropriate, a second layer of cells. In some experiments buffer (5 mM MES, *p*H 6.0) was included in the agar to exclude the possibility of a *p*H artefact. This buffer has no effect on the induction process. After 2–3 d, a coverslip was placed on the upper layer of cells and the dishes examined by phase contrast microscopy. Stalk cells were identified by their vacuolated morphology, the remaining cells appearing amoeboid. Induction in the high density population was essentially 100% in all cases. Cellophane 325P (British Cellophane) was prepared by boiling in 1 mM EDTA for 15 min followed by extensive washing in distilled water. It was impermeable to Dextran blue 2000 (molecular weight 2×10^6) and to inulin (molecular weight ~ 5,000).

into stalk cells, but that the efficiency of conversion is greatly enhanced by some kind of cell interaction.

The density dependence of stalk-cell induction and the enhanced conversion of single cells at high density could be interpreted in terms of a diffusible inducer or of a process of contact-dependent induction. To distinguish between these possibilities, we asked whether cells undergoing stalk cell differentiation at high density could enhance the frequency of stalk-cell formation in a low density population separated from them by a Cellophane membrane. Similar tests of synergism have been used by other workers[5,6]. The results are shown in Table 1. The low density populations alone had an induction frequency of 0–5%, whereas the same cells plated over a dense layer of 'helper' cells gave a frequency of 40–80%. In similar experiments we have found that V-12 M2 'helper' cells also increase the efficiency of stalk-cell induction in strain NC4 and its derivatives. These results suggest that cells undergoing stalk-cell differentiation at high density secrete a dialysable factor which is capable of enhancing cyclic AMP-induced differentiation in isolated cells. It is still possible that actual cell contact is required for the synthesis of this factor by the 'helper' cells.

We have isolated a number of developmentally defective mutants of V–12 M2 after nitrosoguanidine or ethylmethanesulphonate mutagenesis and have screened them for stalk-cell inducibility by cyclic AMP. Only two out of seven totally aggregation-defective mutants were inducible. On the other hand, 14 out of 15 mutants which aggregated but either failed to develop further, or gave aberrant or delayed fruits, were inducible by cyclic AMP. This result suggests that certain events involved in the attainment of aggregation competence are essential for stalk-cell induction.

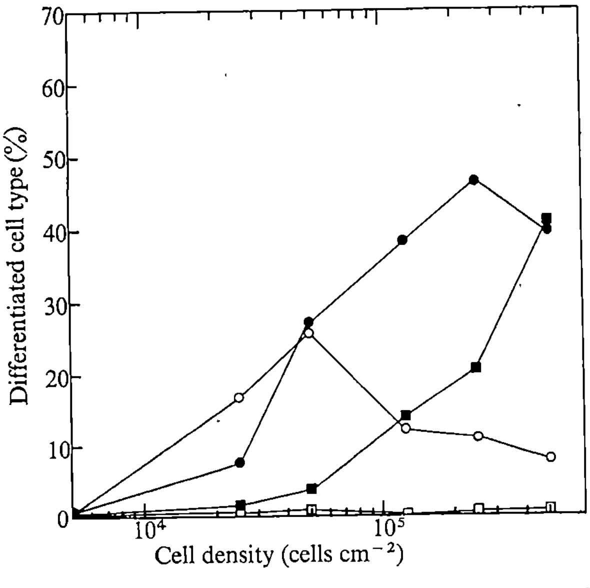

Fig. 2 Formation of stalk and spore cells by mutant *sci-1* under Cellophane. *Sci-1* cells were collected from growth plates in KK_2 buffer (16.5 mM KH_2PO_4, 3.8 mM K_2HPO_4, 2 mM $MgSO_4$, *p*H ~ 6.2) with 60 mM KCl added and pelleted at 200*g* for 5 min. After three further washes in KK_2 and one in 1% Bonner's salts solution, the cells were spread at the stated densities on 2 ml 1.5% agar (Oxoid L28) containing 1% Bonner's salts, 250 μg ml^{-1} streptomycin with or without 5 mM cyclic AMP, in a 5-cm diameter Petri dish. Cellophane was then placed over the cells and after 2–4 d incubation at 22 °C, stalk and spore cells were scored microscopically. At least 200 cells were scored on each plate and the results given are the average of five separate experiments. Two of these experiments were carried out on the original isolate of the mutant and three on clone 5 derived from it. ■, Spore+cyclic AMP; ●, stalk+cyclic AMP; □, spore, no cyclic AMP; ○, stalk, no cyclic AMP.

Table 2 Enhancement of differentiation of *sci-1* at low density by high density wild-type or *sci-1* cells

Cell density and genotype		% Differentiated cell type observed			
Above Cellophane	Below Cellophane	Above Cellophane		Below Cellophane	
		Stalk	Spore	Stalk	Spore
5×10^3 cm^{-2} mutant	None	4.3	0.4	—	—
5×10^3 cm^{-2} mutant	2.5×10^5 cm^{-2} mutant	43.3	8.1	39.5	12.6
5×10^3 cm^{-2} mutant	2.5×10^5 cm^{-2} wild type	27.0	8.9	79.3	0

Cells of the mutant (*sci-1*, clone 5) and wild type were collected as described in Fig. 2. Cells of either type were plated at high density directly on to agar (2 ml 1.5% agar containing 1% Bonner's salt solution, 5 mM cyclic AMP, 250 μg ml^{-1} streptomycin in a 5-cm diameter dish). Cellophane (325P) was placed on top and a low density of *sci-1* cells spread on it. In control plates the high density cells were omitted. After 2–4 d at 22 °C a coverslip was placed on the upper layer of cells and the cells scored above and below the Cellophane. Results are means of three experiments.

Because stalk cells are non-viable[7] and our induction procedure is efficient, we have been able to use the cyclic AMP induction procedure to enrich for resistant mutants in a mutagen-treated population. These experiments were carried out using an acriflavine-resistant mutant of V-12 M2 which gives reasonably compact plaques when plated with *Klebsiella aerogenes* on medium containing acriflavine. The majority of the non-inducible mutants isolated by this procedure show aberrant development, most being aggregation defective. During the screening of colonies surviving the selection procedure, we encountered one unusual mutant (*sci-1*) in which cyclic AMP induced the formation of spores—identified by their morphology and survival after exposure to heat[8] or detergent (R. R. Kay, unpublished and ref.9). Figure 2 shows the pattern of differentiation of cells of *sci-1* at various densities under Cellophane in the presence and absence of cyclic AMP. In the presence of cyclic AMP the mutant formed both stalk cells and spores. The formation of both was density dependent; however, stalk-cell differentiation was relatively more efficient at low density and was reduced at high density. In the absence of cyclic AMP, few spores were produced at any density, whereas the frequency of stalk-cell differentiation reached a maximum at 5×10^4 cells cm^{-2} and then declined. The mutant cells incubated at low density in the presence of 5 mM cyclic AMP could be induced to differentiate into both stalk and spore cells by a high density of either *sci-1* or wild-type V-12 M2 cells (Table 2).

In normal developmental conditions the mutant produces pyramidal fruits, sometimes with a bulbous tip, composed of jumbled patches of stalk and spore cells. Similarities between the fruit of *sci-1* and the mutant *Fr17* previously isolated by Sonnenborn *et al.*[10,11] prompted us to examine the behaviour of *Fr17* under Cellophane. Vegetative cells of *Fr17* at low density (5×10^3 cells cm^{-2}) placed under Cellophane produced less than 1% stalk or spore cells, with or without cyclic AMP. At high cell densities (5×10^5 cells cm^{-2}), however, it produced 60–70% spores and 1–10% stalk cells in the presence or absence of cyclic AMP.

We are at present attempting to purify the putative factor(s) that enhances stalk-cell induction by cyclic AMP. The factor seems to be stable since cell-free medium collected after stalk-cell induction in dense cells increases the yield of stalk cells in low density populations. Knowledge of the identity of the factor(s) should be helpful in elucidating its role (if any) in normal development, and will also enable us to test whether the same factor is implicated in the density-dependent differentiation of stalk cells and spores in mutants *sci-1* and *Fr17*. In any event the use of a Cellophane overlay to examine cell differentiation in the absence of normal morphogenesis should facilitate further analysis of the interplay of elements responsible for pattern formation in *D. discoideum*.

We thank Eileen Stanford and Jennifer Trent for assistance.

C. D. TOWN
J. D. GROSS
R. R. KAY

Imperial Cancer Research Fund,
Mill Hill Laboratories,
London NW7 1AD, UK

Received May 18; accepted June 1, 1976.

[1] Raper, K. B., J., *Elisha Mitchell Scientific Soc.*, **56**, 241–282 (1940).
[2] Bonner, J. T., *Proc. natn. Acad. Sci. U.S.A.*, **65**, 110–113 (1970).
[3] Chia, W. K., *Devl Biol.*, **44**, 239–252 (1975).
[4] Harrington, B. J., and Raper, K. B., *Appl. Microbiol.*, **16**, 106–113 (1968).
[5] Sussman, M., and Lee, F., *Proc. natn. Acad. Sci. U.S.A.*, **41**, 70–78 (1955).
[6] Darmon, M., Brachet, P., and Pereira da Silva, L. H., *Proc. natn. Acad. Sci. U.S.A.*, **72**, 3163–3166 (1975).
[7] Wittingham, W. F., and Raper, K. B., *Proc. natn. Acad. Sci. U.S.A.*, **46**, 642–649 (1960).
[8] Cotter, D. A., and Raper, K. B., *Proc. natn. Acad. Sci. U.S.A.*, **56**, 880–887 (1966).
[9] Ennis, H. L., and Sussman, M., *J. Bact.*, **124**, 62–64 (1975).
[10] Sonnenborn, D. R., White, G. J., and Sussman, M., *Devl Biol.*, **7**, 79–93 (1963).
[11] Brackenbury, R., and Sussman, M., *Cell.*, **4**, 347–351 (1975).

Somatic hybridisation of *Penicillium roquefortii with P. chrysogenum* after protoplast fusion

FUSION of fungal protoplasts after treatment with polyethylene glycol (PEG) has been described as a new technique for intraspecific heterokaryon formation at high frequency[1-3]. We now report the formation of interspecific somatic hybrids between *Penicillium roquefortii* and *P. chrysogenum* by PEG-induced fusion of their protoplasts.

Stable auxotrophic mutants of *P. roquefortii* (University of Nottingham Collection) and *P. chrysogenum* Wis. 49-2105 were obtained after treatment with *N*-methyl-*N'*-nitro-*N*-nitrosoguanidine[4]. Symbols designating the requirements of the mutant strains and the mutant spore colour are as follows: *met/cys/glu/val* (methionine or cysteine or glutamine or valine); *met* (methionine); *trp* (tryptophan); *lys* (lysine); *arg* (arginine); *leu* (leucine); *lys pro/arg* (lysine and proline or lysine and arginine); *leu met/cys* (leucine and methionine or leucine and cysteine); *whi* (white spore colour); *ylo* (yellow spore colour). Strains were maintained and allowed to sporulate on a complete medium (CM)[5]. Mycelium for protoplast formation was grown in a production medium (PM), consisting of inorganic minimal medium (MM)[5] supplemented with 0.2% Difco yeast extract and the requirements of the auxotrophs. Protoplasts were produced as described previously[5] and fusion was carried out as for intraspecific protoplast fusion[1,3]. Suitable dilutions were plated on to hypertonic MM to select fused protoplasts of nutritionally complementary strains. Surviving protoplasts were counted on hypertonic PM.

After PEG treatment of a mixture of complementing *P. roquefortii* and *P. chrysogenum* protoplasts, small prototrophic colonies developed on MM. No growth was observed on MM when protoplasts of the two strains were mixed without PEG or when they were treated separately with PEG and then mixed. Spores could not be fused and did not germinate on MM in any of the conditions tried. These results indicated that the prototrophic colonies arose from balanced fused protoplasts of *P. roquefortii* and *P. chrysogenum* and that they were not the result of back mutation or cross feeding between unfused protoplasts. Fusion frequency was 0.03–3.4% (Table 1). These yields were similar to those obtained for PEG-induced intraspecific protoplast fusion[1,3]. Pure lines of interspecific hybrids were established by repeated cloning of single protoplasts produced from mycelium grown in MM shake cultures inoculated with prototrophic mycelial fragments. After plating on MM, single protoplasts reverted to prototrophic colonies and this procedure could be repeated indefinitely.

The colonies of the interspecific hybrids were morphologically different from the parental strains and they could be classified into three main types (Fig. 1). On MM, type 1 colonies were slowly growing with limited hyphal branching and failed to sporulate. On CM, on PM or on MM supplemented with the requirements of either one of the parental strains, they grew faster and produced parental auxotrophic *P. roquefortii* spores. *P. chrysogenum* spores, however, were never observed. Type 1 colonies predominated in the first culture after fusion treatment and when protoplasts were prepared from 6-d-old MM cultures of type 1 mycelial fragments. On the other hand, when type 1 mycelium was incubated for 10–12 d, more protoplasts developed into type 2 colonies, consisting of a loosely meshed network of broadly spreading hyphae. Like type 1 colonies, they did not sporulate on MM, and they produced only *P. roquefortii* auxotrophic spores on CM or PM. Protoplasts from type 2 mycelium reverted to type 2 colonies, irrespective of the age

Table 1 Percentage of fusion between protoplasts of *P. roquefortii* and *P. chrysogenum* complementing auxotrophs

P. roquefortii auxotrophs*	*P. chrysogenum* auxotrophs*				
	lys pro/arg whi	*leu met/cys ylo*	*lys*	*leu*	*arg*
met/cys/glu/val	1.60	1.25	2.00	0.80	0.60
met	0.45	0.30	NT	NT	NT
trp	0.31	0.03	0.24	3.40	0.18

NT, Not tested.

Protoplasts, produced by treatment (27 °C, 4 h) of 20-h-old mycelium with *Oxyporus* cellulase (5 mg ml^{-1}) and Strepzyme 12,705 (10 mg ml^{-1}) in 0.8 M $MgSO_4$ (for *P. roquefortii*) or 0.6 M NaCl (for *P. chrysogenum*) were separated from mycelial debris by filtration through a sintered glass filter (porosity 1). Fusion was achieved by mixing washed protoplasts (10^5 of each auxotroph), treating them (30 °C, 10 min) with 1 ml of 30% (w/v) PEG molecular weight 6,000 in 0.01 M $CaCl_2$ and 0.05 M glycine adjusted to *p*H 8.0 with NaOH, and eliminating PEG by three washes in 0.8 M NaCl. Protoplasts were plated on to MM and PM to determine percentage of fusion.

*About 10% of the protoplasts regenerated on PM after fusion treatment[3].

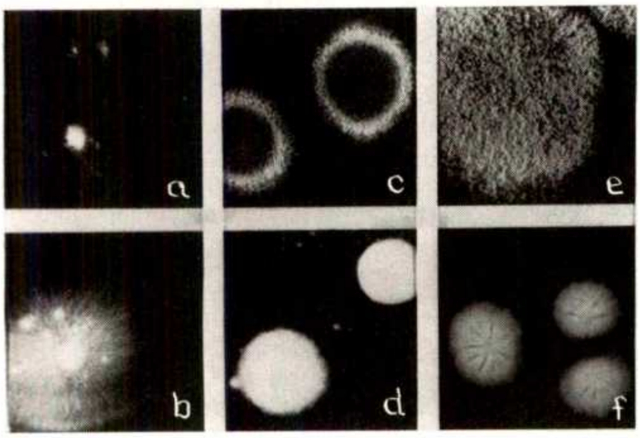

Fig. 1 Different types of colonies after reversion of protoplasts of *P. roquefortii met/cys/glu/val*, *P. chrysogenum lys pro/arg whi* and their interspecific somatic hybrids. *a*, Type 1 colonies on MM; *b*, type 2 colonies on MM; *c*, sporulating type 1 colonies on MM supplemented with methionine; *d*, type 3 colonies sporulating on MM; *e*, parental *P. roquefortii met/cys/glu/val* on MM supplemented with methionine; *f*, parental *P. chrysogenum lys pro/arg whi* on MM supplemented with lysine and proline.

of the mycelium. Colonies with compact mycelium and conidiophores branched similarly to *P. chrysogenum* were designated type 3. They appeared, usually less than 0.1% of the total, among type 1 and type 2 colonies after reversion of protoplasts from type 1 or type 2 mycelium. Type 3 colonies sporulated even on MM and released greenish-white prototrophic spores with a larger diameter than those of the parental strains (Table 2). Single spore isolates and protoplasts again developed into type 3 colonies. Occasionally, the latter colonies showed sectors of *P. roquefortii* spores.

The ability of type 1 and type 2 mycelia to release parental *P. roquefortii* spores showed that *P. roquefortii* nuclei were present in the interspecific mycelium. On the other hand, the prototrophy as well as the ability of type 1 and type 2 mycelium to revert to *P. chrysogenum*-like type 3 colonies indicated that at least part of the *P. chrysogenum* genome was present. Further evidence for this was obtained from studies of penicillin production by the interspecific progeny (Table 2). When grown in a rich fermentation medium[6] or in the medium of Jarvis and Johnson[7] (JJ), mycelium of all colony types produced antibiotic substances, which were inhibitory to *Sarcina lutea* ATCC 9341 and to a penicillin-sensitive *Staphylococcus aureus* ATCC 6558•P, but not to a penicillin-resistant *Staphylococcus*. The antibiotic activity disappeared on treatment with penicillinase. Paper chromatography[8] and gas–liquid chromatography[9] showed that the antibiotics were a mixture of benzyl penicillin, *n*-amyl penicillin and 2-pentenyl penicillin. When grown in a suitable medium[6], the parental *P. chrysogenum lys pro/arg whi* produced a similar mixture of penicillins. But growth of this strain, either alone or cocultivated with *P. roquefortii*, was completely inhibited by the ammonium lactate and ammonium acetate in JJ medium. In contrast, the interspecific hybrids and *P. roquefortii* grew well in JJ medium, but neither the *P. roquefortii* culture filtrates nor mycelial extracts contained any antibiotic substance when assayed against *S. lutea* or *St. aureus*. Thus it seems unlikely that the penicillins in the cultures of the interspecific mycelium were produced by segregated parental *P. chrysogenum*. Moreover, the latter was never re-isolated.

Although conclusive evidence is lacking, several observations indicated that mycelium from type 1 and type 2 colonies was heterokaryotic, whereas type 3 mycelium might be diploid. Type 1 and type 2 colonies were prototrophic and produced penicillins, but released parental *P. roquefortii* spores. Moreover, growth and sporulation were stimulated by addition of the amino acids required by either of the parental strains (Table 2), indicating that the nuclei of both complementing strains were still present. Type 3 colonies produced penicillins and formed prototrophic spores with a larger diameter. Furthermore, they sometimes showed sectors of haploid *P. roquefortii* segregants. Those characteristics obviously suggest diploidy. It is, however, still unclear why only *P. roquefortii* and not *P. chrysogenum* could be re-isolated. *P. roquefortii* might be dominant over *P. chrysogenum* for certain alleles and could have repressed the formation of *P. chrysogenum* spores. On the other hand, it cannot be excluded that *P. chrysogenum* should have lost chromosomal material. Loss of chromosomes is a common phenomenon after somatic fusion of mammalian cells[10,11].

The present studies demonstrate that somatic hybrids of related species of *Penicillium* can be produced by PEG-induced fusion of their protoplasts. Whether it will be possible to obtain viable hybrids of less related species is under investigation.

We thank P. Adriaens and B. Meesschaert for chromatographic determination, Dr J. F. Peberdy for discussion and

Table 2 Properties of *P. roquefortii met/cys/glu/val*; *P. chrysogenum lys pro/arg whi* and their interspecific somatic hybrids

	P. roquefortii met/cys/glu/val	*P. chrysogenum lys pro/arg whi*	Interspecific heterokaryon of *met/cys/glu/val* + *lys pro/arg whi* (type 1 colonies)	Supposed diploid of *met/cys/glu/val* + *lys pro/arg whi*
Spores				
Colour	Bright green	White	Dark green*	Greenish-white
Size (μm)	3.35 ± 0.50	3.67 ± 0.62	3.44 ± 0.44*	4.96 ± 0.31
Auxotrophy	Methionine or cysteine or glutamine or valine	Lysine and proline or lysine and arginine	Methionine or cysteine or glutamine or valine	Prototrophic
Colony morphology				
Type	Loose	Very compact	Intermediate compact	Very compact
Diameter (mm) after 8 d (27 °C) in:				
MM	No growth	No growth	3.78 ± 0.86	7.70 ± 1.70
MM, supplemented with methionine	8.0	No growth	5.31 ± 0.86	7.60 ± 1.0
MM, supplemented with lysine and proline —or lysine and arginine	No growth	9.0	5.96 ± 1.71	7.50 ± 1.4
MM, supplemented with leucine and alanine	No growth	No growth	4.24 ± 1.40	NT
Penicillin production (as μg benzyl penicillin per ml) in:				
Rich fermentation medium	0	32.0	1.8	± 0.1†
JJ	0	No growth	0.30	± 0.1†

*On MM, supplemented with methionine or with lysine and proline; no spores were formed on unsupplemented MM.
†Penicillins were partly inactivated by alkalinisation of the medium.

Emy Storms for technical assistance. J.A. is aspirant of the Belgian Nationaal Fonds voor Wetenschappelijk Onderzoek.

J. Anne
H. Eyssen
P. De Somer

Rega Institute for Medical Research,
University of Leuven,
Minderbroedersstraat 10,
B-3000 Leuven, Belgium

Received April 30; accepted July 6, 1976.

[1] Anné, J., and Peberdy, J. F., *Archs Microbiol.*, **105**, 201–205 (1975).
[2] Ferenczy, L., Kevei, F., and Szegedi, M., *Experientia*, **31**, 1028–1029 (1975).
[3] Anné, J., and Peberdy, J. F., *J. gen. Microbiol.*, **92**, 413–417 (1976).
[4] Adelberg, E. A., Mandell, M., and Chen, C. C., *Biochem. biophys. Res. Commun.*, **18**, 788–795 (1965).
[5] Anné, J., Eyssen, H., and De Somer, P., *Archs Microbiol.*, **98**, 159–166 (1974).
[6] Fawcett, P. A., Usher, J. J., and Abraham, E. P., *Biochem. J.*, **151**, 741–746 (1975).
[7] Jarvis, F. G., and Johnson, M. J., *J. Am. chem. Soc.*, **69**, 3010–3017 (1947).
[8] Vanderhaeghe, H., Parmentier, G., and Evrard, E., *Nature*, **200**, 891 (1963).
[9] Evrard, E., Claesen, M., and Vanderhaeghe, H., *Nature*, **201**, 1124–1125 (1964).
[10] Harris, H., *Cell Fusion* (Harvard University Press, Cambridge, 1970).
[11] Ruddle, F. H., *Adv. hum. Genet.*, **3**, 173–235 (1972).

Molecular imaging of dislocations in 16 chlorocopper phthalocyanine

DISLOCATIONS in molecular crystals are well known, but have been studied on the microscale chiefly with a view to establishing their role in phase changes[1] or topotactic transformations[2]. Here, the positions of individual molecules can be identified, and, in so far as 16 chlorocopper phthalocyanine is a typical molecular crystal, the results are important for concepts of dislocations and intercrystalline boundaries in such crystals.

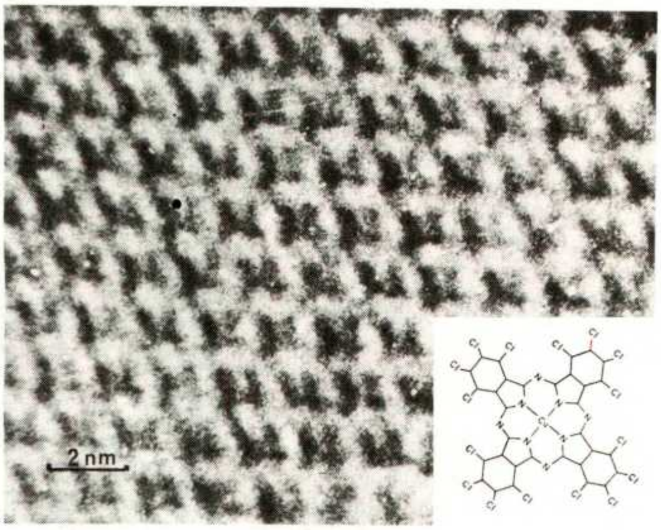

Fig. 1 Perfect crystal of 16 chlorocopper phthalocyanine lying on (001) face.

Figure 1 shows an area of a perfect crystal and illustrates some facets of the electron microscopy used for imaging. First, the crystalline film was prepared epitaxially on KCl at 200 °C at a maximum thickness < 20 nm. The film was then supported on a dimpled micromesh specimen grid—dimpled to provide a varied orientation of the specimen film, rather than using a tilting stage, with its commensurately poorer resolution. The film was lying on the (001) face and as Fig. 2 shows, the specimen had to be tilted, so that the columns of molecules are parallel to the electron beam[3]. This material, like all molecular crystals, is very sensitive to electron radiation damage, so exposure to the electron beam must be minimised. Ilford Industrial G X-ray film was used to record the image, with a very short exposure time.

With this specimen thickness and for this material in this orientation, dynamical imaging effects should be absent and computed images[4,5], allowing for instabilities of lens constants and for partial coherence, showed that 80 nm was the optimum defocus position. Also, for this size of molecule rapid oscillations of the phase contrast transfer functions do not occur within 20 nm of the optimum defocus position, so there should not be significant contrast change within the thickness of the film. In the light of present knowledge of electron optical imaging, therefore, we believe that the images represent the structure of the specimen.

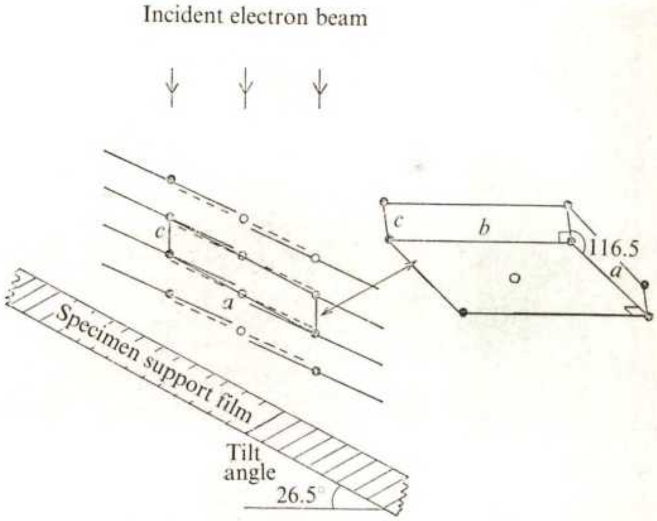

Fig. 2 Projection of molecular stacking along *b* axis showing required specimen tilt for molecular imaging, and geometry of unit cell. (Space group $C2/c$) ●, Copper atom at corners; ○, copper atom at face centre.

Many dislocations were observed, but since the crystallite size was small (< 2,000 nm^2) the internal dislocation density was small and was not statistically significant compared with the extent of grain boundaries. Dislocations of all types were present and examples of each will be discussed.

Figure 3 shows a dislocation A–B which, at first sight, suggests a tilt or twin system, but since the contrast on either side of A–B is similar, the vertical orientation of the columns of molecules on either side must be similar; a screw dislocation of vector $\frac{b}{2}\langle 110\rangle$ would explain the image. There is a contrast change at B that could be ascribed tentatively to the interaction of this screw dislocation with the strain field of a mainly edge

Fig. 3 Imperfect region of crystal showing line dislocations and boundaries.

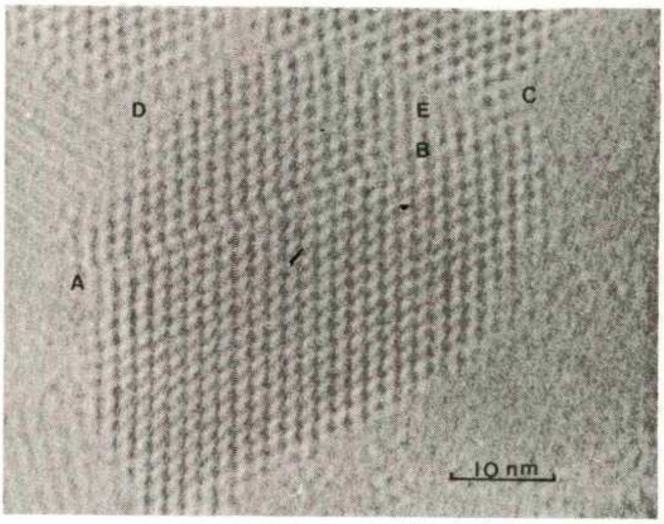

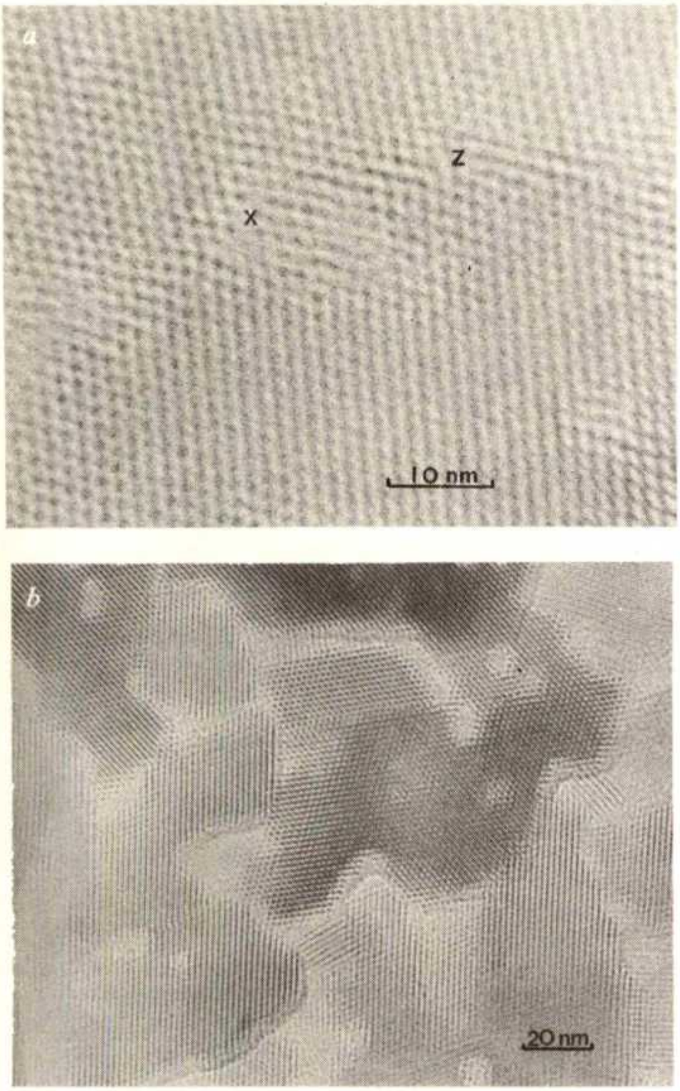

Fig. 4 *a*, Imperfect region of crystal showing column vacancies and other dislocations. *b*, Crystal boundaries showing distortion of peripheral molecular stacking, to reduce the boundary strain energy.

dislocation situated at C, but the presence of the boundary, DE, prevents more accurate identification. DE may be described as a grain boundary in spite of the close geometric relationship across the boundary which is a feature of these crystals.

Figure 4*a* shows a region of distortion with an apparent vacancy at X. This corresponds to the absence of a column of molecules, since even half a column would still have significant contrast in spite of its different defocus position. To the right of the vacancy, there is some tilting of the crystal as shown by the absence of images of discrete molecular columns, but a clear boundary between the two regions of the crystal cannot be determined. Individual dislocations—for example, in region Z—can be distinguished, but they are notable for both their small cores and small strain fields, although the dislocations may be affected by the presence of the boundary. Similar accommodation of distortion is also shown for the grain boundaries in Fig. 4*b*.

It is this lack of definition of boundaries and high distortion that is unexpected in these micrographs. We had anticipated that crystallites would be isolated entities, and that there would be a well defined strain field around each dislocation and internal boundary. In fact, neither is evident; the grain boundaries are not clearly defined, and there has been considerable molecular mobility at boundaries to reduce strain. The accommodation of considerable distortion in these crystals therefore suggests that molecular orientation is not sharply defined in these molecules and their effective radii can vary considerably. This is important for the concept of minimum-energy boundaries and implies that polycrystalline aggregates have a more intimate relationship than has hitherto been thought.

We are grateful to the SRC for provision of equipment, and also a maintenance grant (to Y.M.).

Y. Murata
T. Baird
J. R. Fryer

Chemistry Department,
University of Glasgow,
Glasgow G12 8QQ, UK

Received May 20; accepted June 11, 1976.

[1] Fryer, J. R., and Tedstone, D. R., *Proc. Int. Crystallogr. Conf.* (Australian Academy of Science, Melbourne, 1974).
[2] Jones, W., Thomas, J. M., Williams, J. O., and Hobbs, L. W., *J. Chem. Soc. Farad. II*, **71**, 138, 1975.
[3] Uyeda, N., Kobayashi, T., Suito, E., Harada, Y., and Watanabe, M., *Proc. 7th Int. Congress Electron Microscopy Grenoble*, **1**, 23 (Societe Francaise de Microscopie Electronique, Paris, 1970).
[4] Erickson, H. P., and Klug, A., *Phil. Trans. R. Soc.*, **B261**, 105, (1971).
[5] Uyeda, N., and Ishizuka, K., *J. Electron Microsc.*, **23**, 79, (1974).

Models for the bacterial iron-transport chelate enterochelin

MICROBIAL iron-transport compounds, or siderochromes are of two general structural types, the phenolates and the hydroxamates[1,2]. X-ray studies of several of the latter, for example, ferrichrome A (ref. 3), ferrioxamine E (ref. 4) and mycobactin P (ref. 5), establish the anion of hydroxamic acid ($-N(O^-)CO-$) as the dominant metal-binding moiety, with discrete, neutral $[FeO_6]$ (refs 3 and 4) or $[FeO_5N]$ (ref. 5) units being involved. No similar structural data are at present available, however, for any member of the phenolate class and there is some ambiguity about the metal-binding sites. This is demonstrated for the most widely studied member of the group, enterochelin (or enterobactin), in Fig. 1. Both modes of attachment have parallels in the well known colour reactions of iron(III) with phenols, polyphenols and catechols and in the strong coordination of deprotonated amide nitrogen in simple peptide complexes of the transition elements[7]. Furthermore, molecular models (Drieding or CPK) of iron (III) enterochelin can readily be constructed with either bonding combination. Here we report our studies of two catechol (1,2-dihydroxybenzene) complexes containing the coordination type given by Fig. 1*a* and compare some of their properties with those of iron(III)-enterochelin (part of this work was presented in ref. 8).

Following Selles[9], two complexes were crystallised from ethanol or ethanol–water mixtures containing ferric acetate, catechol and piperidine. Conditions of low base yielded deep purple crystals, whereas excess piperidine resulted in burgundy-red crystals. X-ray data for both compounds were recorded with graphite-monochromated CuKα radiation ($\bar{\lambda} = 1.5418$ Å), using a Picker-FACS I four-circle diffractometer and a θ–2θ scan technique.

Crystals of the purple racemic piperidinium μ-acetato-di-μ-1,2-benzenediolato-*bis*-1,2-benzenediolatoferrate(III), $(C_5H_{12}N)_3[(CH_3COO)\{Fe(C_6H_4O_2)_2\}_2]$ are tetragonal, space group $P\bar{4}$, with $a = b = 27.593(3)$, $c = 12.234(2)$ Å, $Z = 8$, $D_m = 1.23$, $D_c = 1.227$ g cm^{-3}. The crystals showed a rapid decrease in reflection intensity with increasing scattering angle and only 2,467 unique reflections of some 16,000 collected had intensities greater than $3\sigma(I)$. The structure was solved by Patterson and Fourier techniques, and refined by large-block least-squares methods, giving $R = 0.092$. At the present stage of refinement, hydrogen atoms have not been included in the scattering model and although the correctness of the structure is not in doubt, the precision of the final result will be limited by the unfavourable data–parameter ratio and by the apparent disordering of one piperidinium cation. Two crystallographically distinct dimeric units of similar structure are present in the asymmetric unit together with piperidinium cations. As Fig. 2*a* shows, the two $[FeO_6]$ octahedra share a common edge using oxygens of two catechol dianions and adjacent apical coordination sites are bridged by an acetate ion. Each octahedron contains one bidentate catechol moiety which is not involved in bridging the metal atoms. The Fe–O bond lengths are in the range 1.94–2.08 Å, the O–Fe–O chelate ring angles are in the range 82.5–85.1°, with no apparent distinction between terminal and bridging chelates at the present stage of refinement, and the mean Fe–Fe distance is 3.15 Å for the two discrete dimer units. With the acetate considered to occupy the apical positions, the interplanar angle for the two basal planes is 150°. One piperidinium cation forms two intramolecular hydrogen bonds, whereas the other two cations bridge neighbouring $\bar{4}$-related anions. The overall structure can be described as rosettes of associated cations and anions, each containing four dimeric units arranged about the crystallographic $\bar{4}$ centres.

The burgundy-red crystals of the high base form have the composition $(C_5H_{12}N)_3[Fe(C_6H_4O_2)_3]\cdot H_2O$ and belong to the monoclinic space group $C2/c$ with $a = 22.887(4)$, $b = 11.747(1)$, $c = 23.999(3)$ Å, $\beta = 118.19(1)°$, $Z = 8$, $D_m = 1.29$, $D_c = 1.282$ g cm^{-3}; 6,320 X-ray reflections were collected of which 3,422 had $I > 3\sigma(I)$. The coordinates of all non-hydrogen atoms were determined using the direct phasing programme MULTAN[10] followed by several cycles of structure factor/difference Fourier calculations. Hydrogen atoms were positioned by calculation (O–$\underline{H}$ not included) and anisotropic refinement by full matrix least-squares methods resulted in a conventional R value of 0.054. The structure contains the expected 'propeller' of three bidentate catechol dianions, providing the octahedral coordination geometry $[FeO_6]^{3-}$ (Fig. 2*b*). Fe–O bond lengths vary between 1.991 and 2.036(8) Å, with a mean value of 2.020 Å. The O–Fe–O angles of the five-membered chelate rings, 81.1, 82.3 and 80.2(3)°, and the mean twist angle about the threefold axis, 46.4° (60° for a regular octahedron, 0° for a trigonal prism), reflect significant distortions from regular octahedral geometry. In the analogous potassium salt recently reported[11] the mean Fe–O bond length is 2.015(6) and the mean values of the O–Fe–O and twist angles are 81.26(7) and 44.7°, respectively. Considerably less distortion is found in the *tris*-catechol complexes of Cr(III) (83.56, 50.5°) (ref. 11), As(V) (88.2, 55.2°) (ref. 12) and P(V) (91.4, 54.9°) (ref. 13).

A comparison of the spectroscopic and magnetic properties given in Table 1 suggests that the monomeric, but not the dimeric, iron(III)–catechol complex is an appropriate model for the coordination geometry in iron(III)-enterochelin. Furthermore, these data suggest a similar electronic environment for the monomer and iron(III)-enterochelin. The ESR and Mössbauer data for the monomer are generally consistent with those reported for other iron-transport compounds but there are some differences in detail. Thus at 4.2 K in small applied fields (~2 koersted) the Mössbauer spectrum of the solid monomer does not display the degree of fine structure exhibited by that of methanol solutions of iron(III)-enterochelin[14]. The hyperfine field is also somewhat smaller in the monomer. Oosterhuis has recently given a detailed analysis of the ESR and Mössbauer spectra of iron transport compounds in terms of a rhombically distorted electronic model[15]. The crystal structure of the monomer certainly exhibits small variations in bond lengths and bond angles about the metal and in the pattern of hydrogen bonding to the phenolic oxygen atoms. The ESR spectrum for the dimer is complex showing transitions ranging from about $g = 5$ to 1, and the Mössbauer and magnetic susceptibility data are similar to those observed[16] for other exchange-coupled iron(III) dimers which normally have J values of the order of 10 cm^{-1} (ref. 6). Also all three complexes liberate three equivalents of Na$^+$ ion from Sephadex C-25 cation exchange resin from which they can be eluted with unchanged visible spectra. This apparent robustness in solution and in the solid state[17] together with the physical properties given in Table 1 strongly suggest a monomeric *tris*-catecholate coordination environment (Fig. 1*a*) for iron(III)-enterochelin.

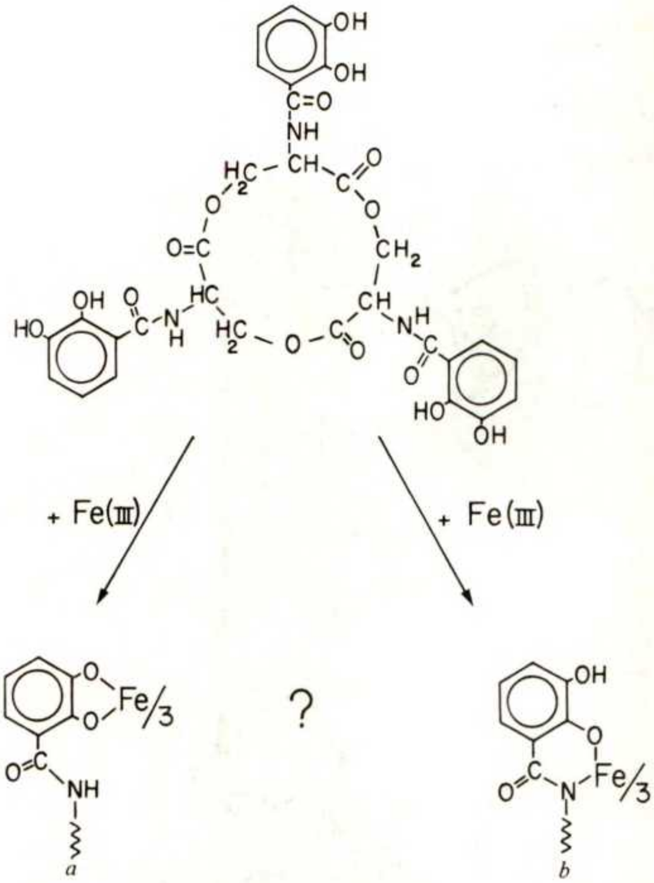

Fig. 1 Structure of enterochelin, the cyclic triester of 2,3-dihydroxy-*N*-benzoyl-1-serine[6], and two possible coordination geometries with iron(III). Coordination by way of the six catechol oxygens leads to a $[FeO_6]^{3-}$ unit containing three five-membered chelate rings (*a*), whereas coordination of a phenolate oxygen and a deprotonated amide nitrogen of each serine residue gives rise to a $[FeO_3N_3]^{3-}$ environment and six-membered chelate rings (*b*). Although the $[FeO_6]^{3-}$ coordination type has been proposed by several workers[1,6], it should be pointed out that all known phenolate siderochromes contain amide linkages to amino acids or amino acid fragments[1].

Table 1 Spectroscopic and magnetic properties of iron(III)-enterochelin and iron(III)-catechol complexes

	$[\text{Fe(III)-enterochelin}]^{-3}$	$[\text{Fe(catechol)}]^{3-}$	$[(\text{acetato})\{\text{Fe(catechol)}_2\}_2]^{3-}$
λ_{max}(nm) (ε/Fe)	496(5,600) (ref. 6)	496(4,700)	570(3,400)
ESR (*g* values)*	4.3 (ref. 6)	4.3	Complex (see text)*
Mössbauer (hyperfine† coupling constant, koersted per unit spin)	222 (ref. 15)	201	~0
Magnetic susceptibility‡	$S = {}^5/_2$	$S = {}^5/_2$§	$S_1 = S_2 = {}^5/_2$§ $J \approx 10$ cm^{-1}

* Data collected on frozen aqueous solutions at temperatures close to 77 K.
† Data collected at 4.2 K (ref. 16). The hyperfine field was resolved in an applied field of 52 koersted parallel to the γ-ray direction.
‡ Data collected from 300–4.2 K as described elsewhere[17].
§ P. D. W. Boyd and R. L. Martin, unpublished data.

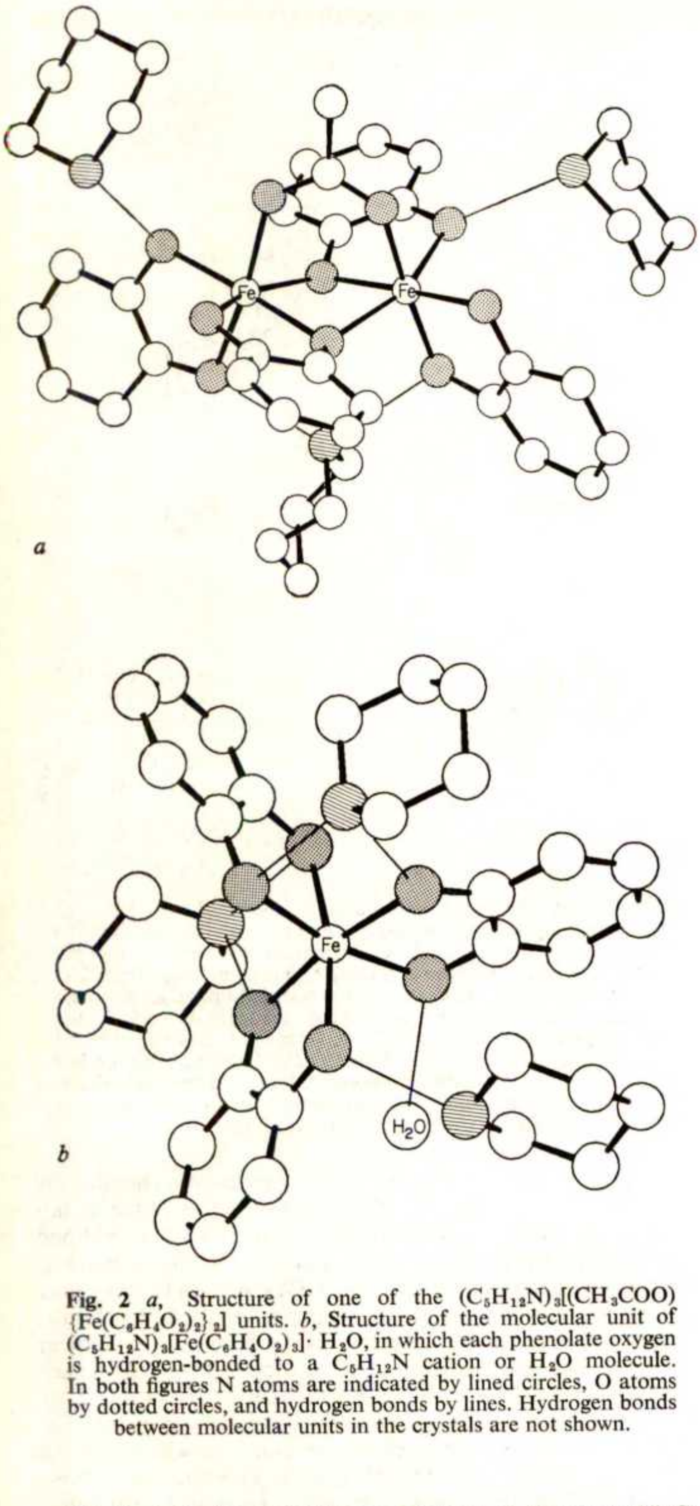

Fig. 2 *a*, Structure of one of the $(C_5H_{12}N)_3[(CH_3COO)\{Fe(C_6H_4O_2)_2\}_2]$ units. *b*, Structure of the molecular unit of $(C_5H_{12}N)_3[Fe(C_6H_4O_2)_3]\cdot H_2O$, in which each phenolate oxygen is hydrogen-bonded to a $C_5H_{12}N$ cation or H_2O molecule. In both figures N atoms are indicated by lined circles, O atoms by dotted circles, and hydrogen bonds by lines. Hydrogen bonds between molecular units in the crystals are not shown.

We thank Professor F. Gibson and Drs I. G. Young and I. G. O'Brien for assistance in preparing enterochelin and for other helpful advice. Iron(III)-enterochelin has been isolated from aqueous solution as the Ph_4As^+ or Ph_3MeP^+ salts. These compounds are very soluble in $CHCl_3$, CH_2Cl_2 and acetone, and may be readily converted to other salts by titration with the appropriate perchlorate salt (T. Rauchfuss, unpublished).

Bryan F. Anderson
David A. Buckingham
Glen B. Robertson
John Webb

Research School of Chemistry,
Australian National University,
PO Box 4, Canberra ACT,
Australia 2600

Keith S. Murray

Department of Chemistry

Paul E. Clark •

Department of Physics,
Monash University,
Clayton, Victoria,
Australia 3168

Received May 6; accepted June 10, 1976.

[1] Neilands, J. B., in *Inorganic Biochemistry*, **1** (edit. by Eichhorn, G. L.), 167–202 (Elsevier, Amsterdam, 1973).
[2] Rosenberg, H., and Young, I. G., in *Microbial Iron Metabolism. A Comprehensive Treatise* (edit. by Neilands, J. B.), 67–82 (Academic, New York, 1974).
[3] Zalkin, A., Forrester, J. D., and Templeton, D. H., *J. Am. chem. Soc.*, **88**, 1810–1814 (1966).
[4] van der Helm, D., and Poling, M., *J. Am. chem. Soc.*, **98**, 82–86 (1976).
[5] Hough, E., and Rogers, D., *Biochem. biophys. Res. Commun.*, **57**, 73–77 (1974).
[6] O'Brien, I. G., and Gibson, F., *Biochim. biophys. Acta*, **215**, 393–402 (1970).
[7] Freeman, H. C., in *Inorganic Biochemistry*, **1** (edit. by Eichhorn, G. L.), 121–166 (Elsevier, Amsterdam, 1973).
[8] *6th Royal Australian Chemical Institute C.O.M.O. Conference, Adelaide, May 1975*, Abstract ME3.
[9] Sellès, E., *Anales de Quim.*, **27**, 569–586 (1927).
[10] Main, P., Woolfson, M. M., and Germain, G., *MULTAN. A Computer Programme for Automatic solution of Crystal Structures* (University of York, York, 1971).
[11] Raymond, K. N., Isied, S. S., Brown, L. D., Fronczek, F. R., and Nibert, J. H., *J. Am. chem. Soc.*, **98**, 1767–1774 (1976).
[12] Kobayashi, A., Ito, T., Morumo, F., and Saito, Y., *Acta crystallogr.*, **B28**, 3446–3451 (1972).
[13] Allcock, H. R., and Bissell, E. C., *J. Am. chem. Soc.*, **95**, 3154–3157 (1973).
[14] Spartalian, K., Oosterhuis, W. T., and Neilands, J. B., *J. chem. Phys.*, **62**, 3538–3543 (1975).
[15] Oosterhuis, W. T., *Structure Bonding*, **20**, 59–100 (1974).
[16] Buckley, A. N., Rumbold, B. A., Wilson, G. V. H., and Murray, K. S., *J. chem. Soc. A.*, 2298–2302 (1970).
[17] Mackey, D. J., Evans, S. V., and Martin, R. L., *J. chem. Soc., Dalton* (in the press).

Erratum

In the article "Effect of phloridzin and phloroglucinol on apple shoots" by O. P. Jones (*Nature*, **262**, 392; 1976) Figs 1 and 2 have been transposed. The legends are correct as they stand. In Table 1 the column headed 'Medium' should read

1−IAA
1−IAA+PZ

1
1+PZ

1
1+PZ

1
1+PG

and not as printed.

Nature Index and Binders

The **Index** for 1975 is now available, price £2.25. Copies of the 1974 index are still on sale, price £3.00. **Binders** for the journal are also available at £7.00 for four (a year of *Nature* fits into four binders).
Postage is included in the above prices. Orders should be sent, accompanied by remittance to Macmillan Journals Ltd, Brunel Road, Basingstoke, Hampshire, England.

matters arising

B-emission stars and X-ray sources

In 1975, an hypothesis of the binary nature of B-emission (Be) stars was proposed[1,2]. Referring partly to this and to the observed association of some X-ray transients with Be stars, Maraschi *et al.*[3] suggested that the classical Be stars, as the optical counterparts of the X-ray transients, could be responsible for the X-ray bursts of these objects. We present here some arguments against this interpretation.

Be stars are essentially normal, rapidly-rotating B stars situated (on average) about one magnitude above the main sequence in the Hertzsprung–Russell diagram. They are enclosed by an extended envelope producing emission (and sometimes also sharp absorption) lines in their spectra. The envelope lines usually exhibit several kinds of variability (for review see refs 1, 2): (1) long term profile and velocity variations, including sometimes even complete disappearance and reappearance of the envelope lines within 1–10 yr; (2) periodic velocity and profile variations with typical periods of 10–100 d; (3) rapid profile variations taking place within several hours or minutes. The main idea of the binary hypothesis of the Be phenomenon is that the Be envelope is formed as an accretion disk enclosing the mass-gaining components of certain mass-exchanging systems and that the high rate of rotation of Be stars is induced by infalling matter. Periodic velocity and profile variations are interpreted as reflecting the orbital motion while the long term changes are understood as consequences of varying rate of mass transfer between components (similar to the Algol binaries). This view is supported by observational data. In every known case, the basic properties of the Be stars recognised as binaries agree well with the theoretical predictions.

Maraschi *et al.*[3] suggested that the X-ray transients represent some later evolutionary stage of the Be binaries after mass exchange. In other words, they implicitly assume that the Be envelope once formed is a long lived phenomenon lasting even after the original mass-losing component has evolved to a compact object. They then interpret the X-ray bursts as a consequence of occasional infalls of matter from the Be on to the compact component controlled by some (unspecified) rotational instability of the Be envelope. There is no observational evidence to support this view. The long term variations of Be stars seem to indicate that the envelopes can dissipate rather quickly without the presence of a continuing supply of matter. Also, practically all known Be binaries exhibit clear signs of continuing mass transfer towards the Be component.

A more serious objection exists, however. It is important to realise that two groups of Be binaries are observed. In many cases, it is indeed the mass-gaining star enclosed by an envelope which dominates in the spectrum. Such a system can then appear as a 'single' Be star (ζ Tau, 4 Her or 88 Her can serve as examples). In other cases, however, it is the mass-losing star, which is the brighter of the two. But even then, some emission lines originating in the envelope around the (now invisible) mass-gaining star (or, alternatively, around the whole system) can be observed. If, at the same time, the mass-losing star is of a B type, such an object is often also classified as a Be star. This is the case of Be binaries HD 187399 (ref. 4) and HD 173219 (ref. 5), which are listed in all catalogues of Be stars. HD 72754, β Lyr, W Cru and probably X Per itself belong to the same category. This classification of Be binaries is convincingly documented by observations. Radical velocities of the hydrogen emission lines of all these objects invariably indicate that in any known case the emitting envelope does not enclose the mass-losing star—in clear contradiction to the expectations of the model of Maraschi *et al.*[3]. The Be stars assumed in that model do not seem to be identical to the Be stars normally observed and only by measuring the emission and absorption velocities of the X-ray transients can the existence of the objects postulated by Maraschi *et al.* be confirmed.

Petr Harmanec
Astronomical Institute of the Czechoslovak Academy of Sciences, 251 65 Ondrejov, Czechoslovakia

[1] Kriź, S., and Harmanec, P., *Bull. astr. Inst. Czech.*, 26, 65 (1975).
[2] Harmanec, P., and Kriź, S., *IAU Symp.*, 70 (1975).
[3] Maraschi, L., Treves, A., and van den Heuvel, E. P. J., *Nature*, 259, 292 (1976).
[4] Hutchings, J. B., and Redman, R. O., *Mon. Not. R. astr. Soc.*, 163, 209 (1973).
[5] Hutchings, J. B., and Redman, R. O., *Mon. Not. R. astr. Soc.*, 163, 219 (1973).

Environmental effects on alcohol selection by mice

Randall and Lester[1] attempted, by transplanting fertilised ova to mothers of a different strain, to estimate the relative contribution of heredity and environment to alcohol selection by mice. Their experiment was designed to allow the following comparisons of alcohol consumption to be made:

(1) *a*, Offspring resulting from the transfer of C57BL/6 strain ova to DBA/2 mothers were compared with *b*, offspring from C57 ova transferred to C57 mothers (control transplants) and with *c*, naturally bred (untreated control) C57 mice;

(2) *a*, Offspring resulting from DBA ova transferred to C57 mothers were compared with *b*, control transplant DBAs and with *c*, untreated control DBA mice.

The absence of a difference between groups *b* and *c* would imply that the transplantation procedure did not affect offspring and then a difference between groups *a* and *b* would imply that the maternal environment affects alcohol consumption of offspring. This pattern of findings is what they report: DBAs transferred to C57s and C57s transferred to DBAs showed increased alcohol consumption, findings which Randall and Lester conclude "uphold the hereditary basis of alcohol selection in C57BL mice, but show the avoidance of alcohol drinking by DBA mice to be amenable to environmental alteration".

Even if there were no questions about the findings themselves, there is no reason to regard an increase in consumption by one strain as less indicative of an environmental effect than the increase in consumption of the other. Both strains showed a similar effect.

It seems possible, however, that the composition of the *b* groups was not as represented. Randall and Lester state that experimental pups were identified by differences in eye pigment at birth. This method is liable to produce errors in identification, since both strains have pigmented eyes. Even if it was successful in the case of between strain (experimental) transfers it is difficult to see how it could have been used at all in the case of control transfers. The natural progeny of a C57 female mated to a C57 male will be indistinguishable from C57 transplants she has received (and, *mutatis mutandis*, the same problem arises with DBAs). It seems likely, then, that groups 1*b* and 2*b* consisted of both control transplants and natural offspring. Given the small yield of transplants (three or fewer per litter), it is also likely that a majority of pups identified as control transplants were instead natural offspring, equivalent, except for the surgical stress to the mother, to the untreated controls.

Uncertainty about the composition of the control transplant groups precludes any conclusion about the effects of maternal environment: the increased alcohol consumption of the between-strain transplants could equally well be due to the transplant procedure in general or the surgical stress it entails. In this latter case, *b* groups (stressed) should have differed from *c* groups (unstressed), which they did not. The stress to the mother is, however, confounded with the transplantation procedure (affecting the ova?) in the *b* groups; if the two events oppose each other in their effects, the offspring might not differ from naturally bred ones.

Unfortunately, the confounding of variables does not permit any definite conclusion.

J. M. Joffe
Joel Najman
Nancy Nettleton

Department of Psychology,
University of Vermont,
Burlington, Vermont 05401

[1] Randall, C. L., and Lester, D., *Nature*, **255**, 147–148 (1975).

Randall and Lester reply—We agree with some of the arguments presented by Joffe, Najman and Nettleton[1], but we take issue with others. The difference in eye pigment between newborn C57BL and DBA pups is obvious at birth: C57BL pups have dark black eyes and DBA pups have lightly pigmented eyes. While differences in coat colour become evident within a few days and could be used, eye pigment allows immediate identification and the early and accurate culling of the litter.

In control transfers (C57BL–C57BL and DBA–DBA), the pups are, obviously, indistinguishable. We could have used mates of the opposite strain to ensure identification of the transferred ova, but this approach has its own inherent problems; we could also have mated females to infertile males of the same strain, but this was not a preferable method: the female is only pseudopregnant, no control uterine horn is provided and the transferred offspring are not intermixed with natural offspring. We thus considered other controls; without prior knowledge of the outcome, we chose the method described in our paper. We do not deny the validity of the arguments against this approach: the possibility certainly exists that natural, rather than experimental offspring, were examined. These other control procedures can, of course, also be used to determine whether transplantation *per se* exerts no effect; should the results not agree, the issue would remain unresolved because of the differences in methods and the introduction of other confounding variables.

Preimplanted mouse embryos are resistant even to the most severe types of chemical and drug intervention, at least in regard to morphological development in a foster mother's uterus[2]. Runner[2] suggests that nucleic information is not integrated until implantation occurs. Rather than attributing the increase in ethanol intake to the transplantation procedure *per se*—because surgery is performed at least 2 d before implantation—it is more likely that the outcome is a result of critical mother–foetal interactions. This issue is unresolved, however, since we do not know whether biochemical changes associated with implantation and pregnancy are similar in natural and transplanted offspring.

Maternal surgical stress does not explain the increase in alcohol intake of transferred young, unless we assume that transplanted ova are differentially sensitive to subtle changes in the maternal milieu or to subsequent postnatal events. In unpublished pilot work, we found anaesthesia alone did not alter phenotypic alcohol intake. Further, natural offspring tested concurrently with transferred pups did not demonstrate an atypical strain effect. For the sake of brevity and because we regarded the data as superfluous, these data were not in our report; obviously, in retrospect, they should have been included.

We can hardly argue that the alcohol consumption of C57BL and DBA mice is not subject to environmental alteration because we have produced such alterations[3]. The issue raised here is, however, the contribution of genetic and maternal variables to the strain extremes, since differences in intake are evident at weaning. We argue that if alcohol selection were determined by maternal rather than by genetic inputs, we should observe selections resembling the phenotypic norm of the foster mother. We noted no such effects in either strain: although alcohol choice increased in DBA mice transferred to C57BL mothers, the offspring never demonstrated C57BL-like high selection of alcohol.

Our report cannot be read to exclude the importance of environmental variables in determining behaviour, although it assuredly emphasises that maternal behaviour is not as important a determinant of alcohol intake as is genetic constitution.

Rutgers University, New Jersey 08903

[1] Joffe, J. M., Najman, J., and Nettleton, N., *Nature*, **262**, 725–726 (1976).
[2] Runner, M. N., in *Teratology: Principles and Techniques*, (edit. by Wilson, J. G., and Warkany, J.), (University of Chicago Press, Chicago, 1965).
[3] Randall, C. L., and Lester, D., *Science*, **189**, 149–151 (1975).

Molecular structure of NAD

Viswamitra[1] has speculated on the structure of free NAD which he then extrapolates to the NAD conformation when bound to enzymes. Unfortunately, he has neglected to take into account the extensive results which have been obtained during the past five years on the conformation of NAD when bound to lactate dehydrogenase[2], malate dehydrogenase[3], liver alcohol dehydrogenase[4] and glyceraldehyde-3-phosphate dehydrogenase[5]. Suffice it to say here that his speculations are inconsistent with facts and that the only 'fact' he does quote concerning the fit of his proposed NAD model to the low resolution difference map of Adams *et al.*[6] is incorrect.

Michael G. Rossmann

Department of Biological Sciences,
Purdue University,
West Lafayette, Indiana 47907

[1] Viswamitra, M. A., *Nature*, **258**, 540–542 (1975).
[2] Holbrook, J. J., Liljas, A., Steindel, S. J., and Rossmann, M. G., *The Enzymes*, XI (edit. by Boyer, P.), 191–292 (Academic, London, 1975).
[3] Banaszak, L. J., and Bradshaw, R. A., *The Enzymes*, XI (edit. by Boyer, P.), 369–396 (Academic, London, 1975).
[4] Brändén, C. I., Jörnvall, H., Eklund, H., and Furugren, B., *The Enzymes*, XI (edit. by Boyer, P.), 104–190 (Academic, London, 1975).
[5] Buehner, M., Ford, G. C., Moras, D., Olsen, K. W., and Rossmann, M. G., *J. molec. Biol.*, **90**, 25–49 (1975).
[6] Adams, M. J., McPherson, A., Jr, Rossmann, M. G., Schevitz, R. W., and Wonacott, A. J., *J. molec. Biol.*, **51**, 31–38 (1970).

Viswamitra replies—The model proposed for NAD[1] was essentially for a free molecule. The reference to the work of Adams *et al.*[2] was to point out that NAD conformations with the adenine and nicotinamide bases far apart had been considered earlier. Although the statement about the possible compatibility of the model with the low resolution electron density maps of Adams *et al.* was unfortunate, it was only made as it was felt that electron density maps at 5-Å resolution, could admit, in general, a certain flexibility where the derivation of the shape of a small substrate molecule is concerned. It is also difficult to rule out conformational states of coenzyme molecules other than those derived from structural studies of bound enzymes as inconsistent with facts. The molecular structures found for ADP in the crystal structure of its rubidium[3] and *tris* salts (M.A.V., Z. Shakked and O. Kennard, to be published) are different from those deduced for the coenzyme from structural studies of bound enzymes[4].

University of Cambridge

[1] Viswamitra, M. A., *Nature*, **258**, 540–542 (1975).
[2] Adams, M. J., McPherson, A., Jr, Rossmann, M. G., Schevitz, R. N., and Wonacott, A. J., *J. molec. Biol.*, **51**, 31–38 (1970).
[3] Viswamitra, M. A., Hosur, M. V., Shakked, Z., and Kennard, O., *Nature*, **262**, 234–236 (1976).
[4] Chandrasekhar, K., McPherson, A. Jr., Adams, M. J., and Rossmann, M. G., *J. molec. Biol.*, **76**, 503–517 (1973).

reviews

Genuine passion for research

E. H. S. Burhop

Frederic Joliot-Curie : A Biography. By Maurice Goldsmith. Pp.260. (Lawrence and Wishart : London, June 1976.) £6.

Courtesy Association Joliot-Curie

At a memorial meeting for Rutherford (November, 1947). Left to right: Desmond Bernal, Joliot-Curie, and Lady Rutherford

To the genuine scientific research worker there is no greater satisfaction than that of discovery. Frederic Joliot-Curie was just such a man with a genuine passion for research. In addition he was an unusually fine and talented craftsman, skilled with his hands and appreciative of beauty in technique no less than in art. He was married to Irene, daughter of Pierre and Marie Curie, born and bred to the laboratory and the exacting standards of scientific integrity and hard work, as well as the vision that characterised the work of her famous parents. There are three great highlights in the scientific work of the Joliot-Curies.

In 1931 they observed that a penetrating radiation emitted when beryllium was bombarded by α particles was capable of ejecting energetic protons from a thin layer of paraffin wax. They erroneously interpreted the penetrating radiation as due to 50 MeV nuclear γ rays but this was an unlikely explanation; and Chadwick, as soon as he heard of the work of the Joliots repeated it and established conclusively that the radiation consisted of neutrons, for which Rutherford had been searching for 13 years. For this Chadwick received the Nobel prize.

In 1934 they discovered the new phenomenon of artificial radioactivity, showing that light elements bombarded with α particles could be made radioactive, emitting positrons with characteristic half-life. For this discovery they shared a Nobel prize in 1935, just 32 years after a similar joint award to Irene's parents.

In 1939 Joliot and his colleagues studying the newly discovered process of nuclear fission after the capture of a neutron by uranium, showed that more than two neutrons were emitted in the subsequent fission, thus establishing the possibility of initiating a nuclear chain reaction and, incidentally, although they did not realise it at the time, of the breeder reactor.

Frederic and Irene Joliot-Curie could no doubt have derived the greatest satisfaction and sense of fulfilment from continuing to work together in their laboratory for their whole lives. But they shared in their family backgrounds the finest traditions of French radicalism. They were conscious of the power of science and technology to provide the material basis on which a transformation of society could be effected. The reality they saw was of a society in which science was underused or misused, with poverty, unemployment, inequality, threatened internally and externally by fascism. War came and with it humiliation for their country.

Can a scientist remain tied to his laboratory, indifferent to what is going on about him in such circumstances? Or if he can, should he? The life of Frederic Joliot-Curie epitomises the problem of the social responsibility of the scientist. It is a tribute to Maurice Goldsmith that in this short and brilliantly written biography he not only captures the excitement and drama of the scientific discoveries to which the Joliot-Curies contributed in such ample measure. He also brings out the significance of the decisions Joliot had to make and the deeper meaning of his life.

Joliot-Curie had, no doubt, what the answer to the above rhetorical question should be. He would have accepted the viewpoint of Paul Langevin, his teacher and friend: "I must devote myself to these political activities. It is true that I could be doing my science, but the science I could do will be done by others, and this task comes to me because it is not being done by others".

Joliot's sense of social concern led him along a hard and stony path, to great misfortune, and possibly to premature death for his wife and himself. He became Head of the World Peace Council. The great Stockholm Peace Appeal against nuclear weapons, signed by 500 million people throughout the world was his brainchild. This built up such a worldwide public reaction against nuclear weapons that it made the idea of a pre-emptive nuclear strike, for which some 'hawks' were clamouring, unthinkable. He became President of the World Federation of Scientific Workers which had been set up under the influence of scientists like Joliot, Langevin and Bernal to try to ensure effective planning, policy making, peaceful application of science, and proper training and conditions of work for scientists. Joliot first raised with Bertrand Russell the possibility of the organisation of a world conference of scientists against nuclear weapons which eventually led to the Pugwash Conferences. The first contacts of the reviewer with both Joliot and Russell were connected with this initiative.

In the post-war period, alongside activities of this kind, Joliot was deeply involved in questions of French science and nuclear energy policy. Soon after the liberation of France he was given the task of reformulating science research policy. He reorganised the National Fund for Scientific Research (CNRS), laying a basis for French scientific research that persists today. On the setting up in October 1945 of the French Commissariat for Atomic Energy, Joliot was appointed its High Commissioner and in this capacity was responsible for planning the highly successful first decade of the French peaceful nuclear energy program.

But Joliot's increasing commitment to the struggle against nuclear weapons led to a virulent campaign against him in the French press and increasing pressure on the French Government to dismiss him. Eventually in 1950 his one time friend and colleague in the Resistance, Prime Minister Georges Bidault, delivered the *coup de grace*.

Joliot was a sensitive man and his dismissal and the abusive and deeply wounding insinuations that accompanied it saddened his last years. Certainly Irene, to whom he was devoted, and possibly he himself, suffered from the effects of radiation. He died in 1958, surviving Irene for two years.

This is a significant book and successfully portrays the warmth, greatness and vision of its subject. Some parts read as excitingly as a detective novel, as when it describes how Joliot's foresight and initiative led to his arranging for France to acquire the whole Norwegian stock (~ 180 litres) of heavy water to prevent its falling into German hands; and then arranging for its transfer to Britain, just ahead of the Nazi invasion of France. This was a signal contribution to the Allied cause for which he received scant recognition when he was refused permission to enter Britain in 1950 to attend the Sheffield Congress of the Partisans of Peace. Again there is the account of his courageous work in the French resistance, especially in the preparations for the Paris rising of 1944, for which his laboratory organised the supply of munitions.

But the key question that will be raised by the book and one that still confronts us today is the way in which the scientist must reconcile his duty to his profession of scientific research worker with his responsibility to society as a whole. Joliot had to make this decision under circumstances of very great difficulty and there will certainly be differences of view concerning the correctness of his choice. If, however, the 500 million signatures of the Stockholm Peace Appeal helped significantly to prevent the further use of nuclear weapons then surely one must conclude Joliot's choice was the correct one. ☐

Professor E. H. S. Burhop, FRS, is Professor of Physics at University College, London, UK. He was associated with F. Joliot-Curie in the World Federation of Scientific Workers and eventually succeeded him and C. F. Powell as President.

Marine mussels

Marine Mussels: Their Ecology and Physiology. (International Biological Programme 10.) Edited by B. L. Bayne. Pp. xviii+506. (Cambridge University: Cambridge and London, June 1976.) £22.

THIS excellent volume is strongly recommended for purchase by universities, polytechnics, museums, and marine biological research stations, on a worldwide basis. It will be an indispensible tool for professional biologists who are concerned with biology of bivalve molluscs, or productivity of coastal waters, and who can afford the price. It will form a stimulating basis for university courses in marine biology.

The editor and authors are to be commended for their lucid, narrative style, for every chapter makes interesting reading. The authors' authority lies in their own contributions to the literature. They comprise: Sir Maurice Yonge (The 'mussel' form and habit); R. Seed (Ecology); D. Roberts (Mussels and pollution); B. L. Bayne (The biology of mussel larvae); B. L. Bayne, R. J. Thompson and J. Widdows (Physiology I, II, Physiological integrations); P. A. Gabbott (Energy metabolism); J. S. Levinton and R. K. Koehn (Population genetics of mussels); J. Mason (Cultivation).

Mussels have a global distribution in coastal waters and estuaries, and provide a major part of the world crop of bivalve shellfish; and they are important components of their ecosystems. The book deals with the whole range of biology of mussels—how their physiological attributes equip them for their environments and the variables with which they contend. We are informed on the biology of mussel larvae, their food preferences, primary settlement, and subsequent movement to beds of adult mussels. Growth rates at different tidal levels, predators, and parasites, are considered in turn.

Physiology of nutrition, and respiration, and the functioning of the vascular and excretory systems are studied in depth. Physiological features are related to the ecological setting—for example, the ability of mussels to acclimate their filtration rate and oxygen consumption (but not heart beat) to short-term fluctuations in temperature and ration.

Seasonal changes in biological composition of mussel flesh, food reserves, metabolic pathways, and control mechanisms are considered, the last with reference to compensation for environmental change. Population genetics, with reference to isoenzymes, reveals variation on a geographic scale, and also on a small scale within an estuary or tidal flat.

Consideration is given to pollutants, and to purification before marketing; care must be taken against paralytic shellfish poisoning arising from unusual blooms of *Gonyaulax* or *Gymnodinium*. The book ends with a review of mussel cultivation in Western European seas.

The book is illustrated by 142 text figures which are commendably clear; most of these are graphs and line diagrams, but there are also some good photographs. The reference list, which must contain about 1,500 entries, will be a valuable tool in itself. There is a good index.

Typographical errors are rare. The Reviewer regrets the general misuse of the word 'visualisation' by chromatographers, and the increasing mistreatment of 'data' as a singular noun; and he is disappointed to find both these usages here. What, incidentally, is 'vagile' (p 358)—it is not in the reviewer's copy of the Shorter Oxford English Dictionary. **R. D. Purchon**

R. D. Purchon is Professor of Zoology in the University of London, Head of the Department of Zoology at Chelsea College, and presently the Chairman of the Biological Sciences Group of Departments at Chelsea College, London, UK.

Primitive sensory systems

Primitive Sensory and Communication Systems: The Taxes and Tropisms of Micro-Organisms and Cells. Edited by M. J. Carlile. Pp. vii+258. (Academic: London, New York and San Francisco, January 1976.) £8.50; $21.

THERE has been a renewed interest and considerable progress in the study of cell orientation, and this compact book shows some of the new results and the new excitement. If I had any criticism, it would be one of omission rather than what the book contains.

It starts off with a clear and systematic introductory essay by M. J. Carlile. The effects of light on orientation are treated in an organised fashion by W. Nultsch. Julius Adler provides a short, lucid review of his own beautiful work; I am only sorry he did not go into further detail, especially on the work of Berg, Koshland and others; but there are a number of other good recent reviews on this subject published elsewhere. T. M. Konijn provides the best review I have seen anywhere of all the work on cellular slime mold chemotaxis, and I feel equally enthusiastic about G. W. Gooday's review of chemotaxis (and tropisms) in the algae and fungi.

Finally, P. C. Wilkinson provides a brief review of the work on leukocyte chemotaxis which is succinct and clear, as one would have expected if one has read his fine book on the same subject. He stresses the point that macromolecules seem to be important leukocyte attractants, which contrasts with the role of small molecules as attractants in the earlier chapters.

Besides more on bacterial chemotaxis, I would have liked to see a review of all the work on pollen tubes; it would have fitted in well. I also missed a concluding chapter which might have attempted to bring together some of the photo- and chemo-orientation ideas, as well as some of the common and contrasting details in the different chapters. But perhaps these complaints are merely an indication that I found myself stimulated (and oriented!) by the book.

J. T. Bonner

J. T. Bonner is Professor of Biology at the University of Princeton, New Jersey.

Radiation and matter

The Dynamics of Spectroscopic Transitions: Illustrated by Magnetic Resonance and Laser Effects. (Wiley-Intersciences Monographs in Chemical Physics.) By James D. Macomber. Pp. xxiv+332. (Wiley-Interscience: New York and London, February 1976.) $23; £11.50.

THIS book is concerned with the mechanisms by which radiation can interact with matter and, in particular, with the processes involved when electromagnetic radiation stimulates a transition from one quantised energy level to another. The author points out that discussions of the physical principles involved are often omitted in books on spectroscopy and has directed this book at advanced undergraduates, graduates and research spectroscopists. The first three chapters outline the essential quantum theory and theory of electromagnetic radiation that is required. Chapters 4 and 5 give the theory of the interaction of radiation with matter, and in chapter 6 the theory is ilustrated with reference to magnetic resonance; in this area the physical principles are particularly easily understood. In the last two chapters the theory is generalised to other systems and to two-level systems.

The subject inevitably requires mathematical treatment, and this is set out very clearly in the book. At the same time the author is at pains to give, wherever possible, physical explanations of the processes involved. These are often of great value in thinking about spectroscopic experiments, and many spectroscopists would find much to fascinate and enlighten them.

I was a little surprised to find in the historical introduction no mention of Purcell, Torrey and Pound as discoverers of magnetic resonance in bulk matter at the same time as Bloch and his colleagues. There are one or two minor and obvious errors (for example in Fig. 4.3), but these do not significantly mar a clear and lucid account of an important aspect of spectroscopy.

R. E. Richards

Dr Richards is Warden of Merton College, Oxford, and Chairman of the Oxford Enzyme Group working in the Department of Biochemistry at the University of Oxford, UK.

Trace elements

Trace Element Analysis. By V. Valkovic. Pp. x+229. (Taylor and Francis: London, November 1975.) £7.

Trace Element Analysis is a unique book as far as its content can be judged in relation to its title. There are many books which treat techniques of trace analysis in monographic form or are devoted to a wide range of physicochemical techniques but which in general say little about the reasons or rationale for doing such work. This slender attractive volume does set out to describe *some* techniques, but concentrates to an unusual degree on setting the scene and giving the background to the philosophy and fundamental reasons for the importance of analysing for trace elements under particular sets of circumstances. This part of the book is extremely well done and the author is to be congratulated on his grasp of such a wide field of knowledge and his ability to write in such an interesting way. This part of the text (128 pages) occupies the first six chapters: elements in nature; trace elements in the environment; environmental pollution; trace elements in biology and medicine; general aspects of trace analysis.

The remaining 67 pages are devoted to chapters on activation analysis, X-ray emission spectroscopy, optical methods and mass spectrometry. Here the book is not quite so satisfactory in that the treatment is more restricted and a good deal less detailed and rather less critical in its assessment than other books which are available. It is, for example, disappointing to find no mention of work on electroanalytical techniques of trace analysis and scant attention given to the preconcentration techniques that are so important to trace analysis in all its guises. Some of the descriptions of atomic spectroscopic techniques are also rather outdated and oversimplified.

The strength and the excellence of this book lies, however, in the first six chapters which are unusually good and make it a worthwhile text for all who are concerned with the broader aspects of trace element analysis.

T. S. West

Professor West is Director of the Macaulay Institute for Soil Research, Craigiebuckler, Aberdeen, UK.

obituary

Georgii Samsonovich Dzotsenidze, the eminent Soviet geologist died on May 5, 1976, aged 66.

Dzotsenidze was born in 1910, in the Georgian town of Kutaisi. He was educated at Tbilisi University, graduating in 1929, and from then on his academic career was closely connected with the University, rising from the position of laboratory assistant in the Department of Mineralogy and Petrology, to become a lecturer, Dean of the Faculty of Geology and Geography, and finally, in 1958, Rector of the University. His research was concerned mainly with the geology of Georgia; in 1933–34 he led the geological survey team of the Georgian Geological Board. His more than 120 publications include *Premiocine extrusive vulcanism of Georgia*, *Question of the genesis of barytic deposits in Georgia*, *Analcite level in the coal–bearing formation of the Kutaisi–Gelat region*, and *Petrology of the Bath Deposits of Okribri*. He was elected a full member of the Georgian Academy of Sciences, having served for four years as acting Academic Secretary of the Academy. In the same year (1955), he became a Vice-President of the Georgian Academy of Sciences. In 1968 he became a full member of the Academy of Sciences of the USSR.

Dzotsenidze combined his academic career with considerable political activity. He served as a Deputy of the Supreme Soviets of the Georgian SSR and the USSR several times, and was a member of the Central Revision Commission of the CPSU and of the Central Committee of the Communist Party of Georgia.

For his academic and political activities Dzotsenidze received a number of high Soviet honours, including the Order of Lenin (three times), the order of the October Revolution, the Order of the Red Banner of Labour, a Stalin (now State) prize, and numerous medals.

announcements

The **1976/77 Moscow Seminars on Collective Phenomena** will take place on Sundays at 1200 starting on September 12, at Ulitsa Veshnyakovskaya, Dom 4, Korpus 2, Appartment 5, Moscow. Letters, reprints and preprints may be sent to **Professor M. Ya. Azbel'** at the above address, but all correspondence must be registered and insured. All visiting scientists are very welcome to attend the seminars unannounced.

The programme is:

September 12, 1976: Dr Yu. Mniukh on **Polymorphic Transitions in Crystals.**

September 19, 1976: Professor Yu. Orlov on **Wave-logic and its Applications to Wave-Mechanics.**

September 26, 1976: Dr A. May on **Cybernetic Ideas and Empirical Sociology.**

October 3, 1976: Corresponding Member B. Levich on **The Semi-empirical Theory of Turbulence.**

October 10, 1976: Professor M. Ya. Azbel' on **Decoding DNA.**

October 17, 1976: Dr I. Andryukin on **The Theory of Exactness of Mechanical Treatment.**

October 24, 1976: Dr E. Trifonov on **Genetic Engineering.**

October 31, 1976: Dr G. Rosenstein on **Models of Mental Distress.**

November 7, 1976: Dr V. Brailovsky, on **Deducing Relationships from Experimental Data.**

November 14, 1976: Professor N. Salanski on **Physics of Magnetic Films.**

November 21, 1976: Dr Yu. Kalenov on **Hydrodynamic Lasers.**

November 28, 1976: Dr V. Lazaris, on **The Creativity of Ben Galevi.**

December 5, 1976: Professor Ya. Alpert on **Wave-Phenomena in Cosmic Plasmas.**

December 12, 1976: Dr A. Kaplan on **Dynamics of Quantum Systems in a Non-linear Resonance Field.**

December 19, 1976: Professor N. Meyman on **Spectral Properties of the Schrödinger Equation in a Periodic Field.**

December 26, 1976: Professor B. Fain on **An Experimental Investigation of Psychological Pecularities.**

January 2, 1977: Dr I. Brailovskaya on **Supersonic Viscous Flow Around a Body.**

January 9, 1977: Dr I. Gildengorn on **The Influence of Oxidation on Thermoelectric Properties of Alloys.**

January 16, 1977: Dr M. Shepelev and Dr V. Dubrovskaya on **The Order of Reaction in Vulcanisation of Rubber.**

January 23, 1977: Professor A. Tzinober on **Hydrodynamics of Liquid Metals in a Magnetic Field.**

January 30, 1977: Professor N. Salansky on **Yoga and Judaism.**

February 6, 1977: Corresponding Member B. Levich on **Electrocapillary Phenomena.**

February 13, 1977: Professor M. Ya. Azbel' on **Entropy and Phase Transitions.**

February 20, 1977: Dr A. Schuster on **An Optical Problem in Combination Theory.**

February 27, 1977: Dr G. Shapiro on **Hormonal Regulation of Vital Functions.**

March 6, 1977: Dr L. Regelson on **Interaction of Weak Fields with Biological Structures.**

March 13, 1977: Professor N. Meyman on **Dispersion Relations and the Flow Increase Principle.**

March 20, 1977: Dr V. Retz on **Determination of the Electronic Density Function of Protein.**

March 27, 1977: Dr L. Vilenskaya on **Possible Interpretation of some Psychological Phenomena.**

April 3, 1977: Professor M. Kovner on **Earth's Radiative Belts and their Origin.**

April 10, 1977: Dr A. Kaplan on **Non-linear Fresnel Reflection.**

April 17, 1977: Professor S. Alber on **Asymptotic Methods in the Theory of Eigenvalues.**

April 24, 1977: Dr E. Tzifonev on **Evaluation of Nucleotide Sequences (Experimental).**

May 1, 1977: Professor B. Fain on **Non-radiative Transitions in Condensed Matter.**

May 8, 1977: Corresponding Member B. Levich on **Surface Turbulence in a Liquid.**

May 15, 1977: Dr G. Volk on **Viscosimetric Determination of Molecular Weights.**

May 22, 1977: Dr A. Dolgopolsky on **The Hebrew Language and Alphabet: The History of Languages.**

May 29, 1977: Professor M. Ya. Azbel' on **New Statistics of Quasiparticles.**

June 5, 1977: Dr A. Malitzky on **The Planning of an Experiment.**

June 12, 1977: Dr E. Tzifonev on **The Spatial Structure of RNA.**

To get to Professor Azbel's apartment: Take the Metro to Zhdanovskaya (end of line in Eastern suburbs), then the No 64 Trolleybus North along Ulitsa Veshnyakovskaya until the road forks (about 6 stops).

nature

August 26, 1976

Which way now for journals?

Barnaby Rich said in 1613 that: "One of the diseases of this age is the multiplicity of books; they doth so overcharge the world that it is not able to digest the abundance of idle matter that is every day hatched and brought forth into the world". He would undoubtedly have used similar words in 1976 to articulate the concern that most practising scientists express from time to time about the proliferation of journals and the number of papers published, but perhaps he would also have come up with some practical suggestions about how the problem should be solved in the light of diminishing library budgets. It is really only when a university library, say, cuts out by mistake what a substantial number of people regard as a vital journal that there is any significant outcry.

Interestingly, though, only about 55% of the expenditure of a typical university library on journals (in the UK at least) is devoted to 'essential' titles. The remainder are 'desirable' or 'marginal', spending on these categories being 40% and 5% of the total, respectively. If the coming academic year proves to be another tough one financially, marginal titles are likely to become a thing of the past, and the list of desirable ones will be on the chopping block, So if things don't get any better for libraries, what is to be done?

First of all, one might wish for an unwritten rule that the creation of a new journal had to be a true reflection of the appearance of a new subject grouping or synthesis of subjects, and not merely a rather meaningless subdivision of an old subject. (No marks out of 10 for *Slide Rules in Laryngology*, for example.) And on this basis, why not aim to have two journals shut down for every one started? (True, this would imply the publication of fewer papers, but that would be no bad thing in the light of claims that more than 90% of papers written eventually get published somewhere.) The plain facts of the matter, however, are that of about 35,000 journals in existence at present, only 1,300 disappear each year whereas a full 2,000 are added.

Second, as the pious hopes of the previous paragraph can at best be only partly realised, what can be done to existing journals to reduce their bulk and their cost? The bulk is particularly important both because it determines how much the reader has to read, and because postage is now such an important element (some 15% of the cost of a subscription to *Nature* in the UK, for example).

One of the ultimate solutions is to publish a journal solely in microform—probably microfiche, a single piece of photographic sheet film some 10 × 15 centimetres containing reduced images of 100-odd journal pages. There are no paper or machining charges and minimum postal costs—but the spectre of user resistance rears it head. How can we browse in a library that uses uninviting gadgetry like a microfiche reader, they ask. It seems that nobody is ready yet for a complete revolution like that, however, and maybe they never will be. Microform for archival use, yes; for current use, probably no.

So what are journal publishers (which include many learned societies, large and small, as well as commercial concerns) to do? The most accurate indicators of current thinking are the experimental publishing projects being carried out by the Chemical Society in the UK and the American Chemical Society in the United States. These cautious steps forward involve what are called 'synopsis journals', in which the author writes a synopsis of perhaps 1,000 words, which is printed conventionally and backed up by more detailed information, on microfiche for example, to which the reader can have access if he requires.

As the microfiche part of such a journal can make use of directly photographed typewritten pages while the synopsis part can still be printed in a way that makes it look no different to a comparable publication, the average reader, who likes his journal to look 'right' and to be printed on good old-fashioned paper, can be tempted to move in the right direction without sacrificing any of the things he holds dear. The librarian, for his part, would hope to see the changes reflected in the subscription price.

The browsing reader can still browse in the time-honoured way, with the added advantage of not having so much to read or skim through. Those who need to consult the back-up information will only have to suffer microform in pursuit of the small number of papers that directly interest them and ought not to find its use an excessive chore in these circumstances. In fact, if one believes the tales that most papers are only read in detail by one or two people, it could turn out that librarians in a synopsis era would find relatively little call on their microfiche facilities for this purpose. Which raises the whole question of whether all that detail actually needs to be published at all. Could it not equally well be submitted for scrutiny by the referee and then made available by the author to those who care to request it?

Tennessee valley energy

The Tennessee Valley Authority represents an American historical landmark. **Colin Norman** reports

WHEN the Tennessee Valley Authority (TVA) was established in 1933, at the height of the great depression, it rapidly became one of the more controversial instruments of President Franklin D. Roosevelt's famed New Deal. Designed, in Roosevelt's words, for the reclamation of land and of human beings, the creation of TVA was a unique federal attempt to attack the grinding poverty of an entire region by developing and conserving its natural resources.

Like much of the New Deal, the experiment was controversial because it went against the capitalist grain for the federal government to play such a strong role in economic and social enterprises. To many conservatives, it smacked of socialism. Now, 43 years later, TVA is still controversial, though for different reasons.

In 1933, the Tennessee Valley was an economic and environmental disaster area. Most of the region's people were at the bottom of the pile, living in desperate poverty. The land, which had been worked to death, was fast being eroded and turned into a barren waste. The hillsides, which once boasted the largest hardwood forests in North America, were denuded. And the 1,000-mile Tennessee River would frequently burst its banks, flooding vast areas; in many places, shoals and shallows also made it impossible to navigate. Then along came TVA's armies of engineers, scientists and agriculturalists to dam up the rivers, reforest the hillsides and reclaim the land. By most measures, they have been spectacularly successful.

Although family income in the region is still a little below the national average, it is no longer an economically depressed area. It has a productive agricultural system and industries have been attracted into the area by cheap electricity rates. And the Tennessee River has been tamed by numerous dams, so that it is navigable and it no longer rampages through the fields and towns each spring. The stark before-and-after contrast in the valley in fact gradually made true believers of all but the most diehard conservatives.

Consequently, TVA is now held in the highest regard by many of the people who live in the seven-state area which it serves, a fact painfully discovered by Senator Barry Goldwater in 1964 and by Ronald Reagan a few months ago. Both hinted that, if elected President, they may consider selling TVA off to private industry to get rid of this socialist monstrosity. They paid dearly at the polls as a result, losing important elections in Tennessee.

Highly charged issues

TVA is controversial now because it is facing many highly charged issues endemic to an industrial society, such as energy planning, strip mining, air pollution, and public participation in governmental decision-making. The sheer scale of TVA's operations ensures that the way it tackles those issues often has national implications.

A description of TVA's activities reads like a list of superlatives. It is the largest energy supplier in the United States, providing electricity to a region the size of Great Britain. It is the single largest user of coal in the nation, consuming more than 40 million tons a year in its power plants. It has more nuclear power plants under construction than any other electric utility. The 33 major dams which have been constructed on the Tennessee River and its tributaries harness lakes whose combined shorelines are longer than those of the Great Lakes. And it is the region's largest employer, providing 31,000 jobs.

Even the criticisms being levelled at TVA are impressive in their scope. During Senate testimony on TVA last year, for example, one critic suggested that "the Tennessee Valley Authority is a part of the problem in Appalachia, not a part of the solution", while another stated that TVA "began as an experiment in democracy but has turned into an example of how our government can practise colonialism on its own people".

TVA is really two separate operations. One, financed entirely by federal appropriations of more than $100 million a year, is responsible for running a vast range of programmes, including agricultural assistance, fertilizer research and development, and the management of parks, dams and recreational facilities. The other, more controversial, side of TVA's activities is its role as supplier of electricity to the region. It is a self-supporting, $1,000 million-a-year operation, financed by revenues and by the sale of bonds for capital projects.

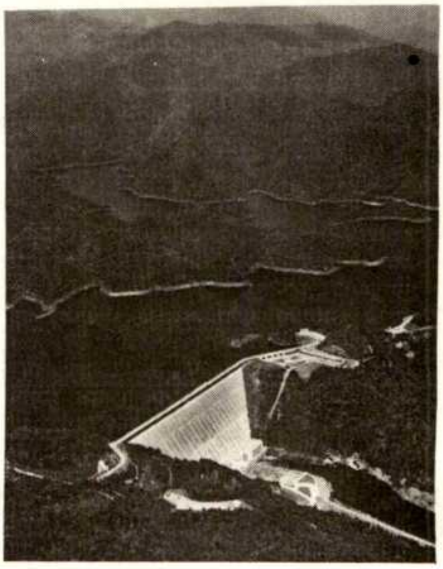

Fontana dam, the TVA's highest

Problems, controversies

The problems and controversies encountered by TVA's energy operations are similar to those being faced by other electric utility companies, but TVA's unique structure gives it some advantages in tackling them. For one thing, the agency's Congressional charter requires that it be run as a nonprofit enterprise, which means that it doesn't have to pay dividends to stockholders. It is also fortunately situated right next door to the Appalachian coal fields, and its numerous dams provide a secure source of cheap electricity. For those reasons, TVA's electricity is the cheapest in the country, selling at about 60% of the national average.

At present, about 20% of TVA's power comes from hydroelectric sources, and the rest comes from coal-fired power stations. A few years ago, however, the agency decided that all its future energy growth would come from nuclear power plants, and it embarked on a massive nuclear construction programme. By the mid-1980s, TVA expects to have 17 nuclear reactors in operation at seven different sites, adding up to a staggering 20,000 MW. It would be the largest user of nuclear power in the country. Clearly, TVA's espousal of the atom, at a time when many other electric utilities are deferring or cancelling their nuclear orders, has enormous impact on the United States nuclear power programme.

Why does a utility which is sitting on top of a vast coal field decide to go nuclear? TVA has already dammed up most of the rivers in the region so that there is virtually no scope for expanding its hydroelectric generating capacity. "The choice is between coal and nuclear", says TVA General Manager Lynn Seeber, "and we believe that nuclear will be cheaper and environmentally more acceptable". The agency's critics disagree, however, pointing out that TVA's brief experience so far with nuclear power has been disastrous—it owns and operates the Browns Ferry plant which caught fire last year—and the critics also argue that the cost estimates will prove to be grossly inaccurate.

Be that as it may, environmental factors clearly played a key role in TVA's decision to opt for nuclear power instead of expanding its coal-fired generating capacity. In short, federal pollution control regulations are becoming more and more expensive to meet, particularly since TVA recently lost a major court battle with the Environmental Protection Agency (EPA).

Regulation problems

The pollution control regulations which are causing TVA most of its problems are embodied in the 1970 Clean Air Act, a bill which sets air quality standards and a timetable for meeting them. In some places, the Act is a little fuzzy in its definitions, and there has been a royal battle on several fronts over compliance with the standards. TVA decided early on that it could meet the regulations by a combination of tall smokestacks on its power plants, and continuous meteorological monitoring to ensure that the pollutants are not blown back to the ground in large concentrations.

It developed a sophisticated forecasting and monitoring system which would automatically give orders to curtail, or shut down entirely, individual power plants when meteorological conditions prevent proper dispersal of the stack gases. TVA has recently computerised the entire operation.

EPA interpreted the Clean Air Act differently, however, insisting that it requires stack gases, such as sulphur dioxide, to be removed entirely. Simply spewing them into the atmosphere through tall stacks will cause problems downwind, when the SO_2 is washed out of the atmosphere as so-called acid rain, EPA argued. As usual in such matters, the dispute ended up in the courts and the outcome was closely watched by environmentalists and by industry since it represented a crucial test of EPA's strategies.

TVA lost the battle earlier this year. According to TVA officials, it will cost about $250 million a year to install and operate the required pollution control equipment on several power plants. By contrast, TVA's proposed meteorological approach would have cost about $20 million a year.

And there have been other problems with TVA's heavy use of coal. For one thing, coal prices have escalated from about $10 to $30 per ton in the past three years. And for another, most of TVA's coal comes from strip mines, which are causing considerable environmental destruction and bitter resentment in some areas of Appalachia.

Although TVA officials take deserved pride in the fact that all their contracts with coal suppliers contain a clause requiring that strip mined lands be restored and revegetated, it's clear from testimony before a Senate committee last year that those requirements haven't always been met. "We can show anyone who would like to tour our area that TVA has never strictly enforced their regulations against certain operators", says J. W. Bradley, President of a group called Save Our Cumberland Mountains. Bradley went on to describe how "with every turn of the dozer's track and every bite taken by a large shovel, dragline, or front end loader, and by every blast of dynamite, we are furnished with more and more polluted water, fractured rock, loss of land and vegetation." Clearly, whatever requirements are imposed, TVA has been responsible for supporting a vast amount of strip mining, a practice which some regard as being unacceptably destructive.

Nuclear future

Those are some of the factors which have led TVA to seek a nuclear future, but it has found that it has in some respects traded one type of problem for another. So far, TVA has completed two of three units at the Browns Ferry nuclear plant, and four more units—at the Sequoyah Nuclear Plant and the Watts Bar Nuclear plant—are expected before 1980. All have experienced cost overruns, and the fire last year at Browns Ferry was a considerable setback. Started by an electrician checking for air leaks with a candle, the fire knocked out several safety systems, came close to causing a nuclear accident (how close is a matter of debate), and has so far shut down the plant for about 16 months. According to Seeber, the fire has cost TVA about $100 million in repairs and lost time.

TVA is, however, fortunate in one respect. There is little grass roots opposition to nuclear power in the region, and there have been few delays caused by anti-nuclear groups forcing public hearings and challenging power plant plans in court. In part, the lack of opposition can be explained by the fact that the area has always been associated with nuclear power through the Oak Ridge National Laboratory, which provided the plutonium and enriched uranium for the Manhattan Project and which is still a major nuclear facility.

Whatever the problems, TVA has so far shown no sign of backing off from its commitment to nuclear power. In fact, it has taken two steps to enhance its nuclear future. It is now investing heavily in uranium exploration in the Western states, with a view to securing uranium supplies. And it is a major partner in the liquid metal fast breeder reactor programme, providing some money and other support for the demonstration plant to be built at Oak Ridge.

TVA domination

Aside from the controversies over TVA's energy planning, there's one broad factor which seems to bother some people living in the Tennessee Valley. TVA's operations are so extensive that it literally dominates much of the economic life of the region, and there seems to have developed a feeling that it has become a faceless bureaucracy unresponsive to local needs. The chief problem is that TVA

Watts Bar nuclear plant

is a federal agency under the control, not of local legislative bodies, but of the US Congress 500 miles away.

Until very recently, TVA has been held in such affection by most residents of the Tennessee Valley—particularly those with long memories—that the remoteness of the control over the agency has been no problem. But recent sharp increases in TVA's electricity rates in response to escalating coal prices have caused some alienation and frustration because there's no local body to which complaints can be addressed. The frustration was voiced on several occasions during last year's Senate hearings on TVA, the most provocative comment being the reference to colonialism, but few suggestions for improving the situation were voiced.

Nevertheless, to most of the people in the region, TVA remains an instrument for economic progress. Certainly, few would deny that it has more than lived up to Roosevelt's hopes that it would reclaim the Tennessee Valley's land and people. ☐

US SPACE

Biological business boom

Sandy Grimwade reports from Washington on the progress of the Viking 1 experiments on Mars

AFTER more than five weeks of practically faultless operation the Viking 1 Mars lander continues to send a wealth of geological, meteorological, biological, chemical and visual information back to Earth. The only instrument which has failed to function correctly is a set of miniature seismometers which remains locked in the safe landing position, despite efforts to free it. The other teams of scientists have, however, been kept busy by the sheer volume of information being supplied to them.

Some of the most puzzling and to the general public most fascinating data have come from the three biology experiments and the related molecular analysis of the Martian soil. Although control and duplicate experiments—the *sine qua non* of all biological investigation—have not yet been done, speculation is rife as to the meaning of the results so far. The scientists involved are understandably cautious about delivering a yes–no answer to the question of life on Mars, when only a small portion of their programme is complete. The results so far are certainly not what would be expected if Earth-type organisms were present, nor are they explicable in terms of "simple" non-biological chemistry.

In the labelled release (LR) experiment, a mixture of ^{14}C-labelled nutrients in a small amount of water was added to a soil sample and incubated at about 15 °C, which is 35–135 °C warmer than the Martian surface temperature. The totally unexpected result showed a massive and rapid release of radioactivity into the gas phase—presumably as carbon monoxide or dioxide. The radioactive counts released reached 4,500 in 10 hours, levelling off after 48 hours at about 8,500. A second dose of radioactive nutrients caused an initial burst followed by a drop in the released radioactivity, after which the graph almost flattened out for the remaining four days of the experiment.

That "almost" is the tantalising part, because careful statistical analysis revealed a possible trend of very slow accelerating release of radioactivity. Unfortunately, the exigencies of operating one's laboratory by remote control across 200 million miles required the experiment to be stopped for performance of a control test with heat-sterilised soil. A later repetition of the experiment is planned with an incubation time of weeks or months rather than days. The results certainly do not look like anything one would expect from an Earth sample in the same situation. A chemical explanation involving oxidation of the labelled nutrients is at present the most popular explanation for the initial burst of activity.

The possibility that the Martian soil contains active oxidising agents was strengthened by the result from the gas exchange (GE) experiment. In this experiment the soil sample is either humidified or wetted with a concentrated "chicken soup" of amino acids, salts, vitamins and other nutrients, and the atmosphere is periodically monitored for changes in the concentration of gases by gas chromatography. The initial humidifying of the soil sample produced a remarkable release of oxygen which levelled off after several hours and remained stable for days. Wetting of the soil caused a rapid drop in the atmospheric CO_2, probably due to the formation of bicarbonate in the alkaline solution, and a slower drop in the oxygen, which is speculated to be due to oxidation of ascorbic acid which is present in the nutrients. At present, CO_2 is slowly being released into the atmosphere and the experiment is intended to continue for some time to see if any further changes occur. As the instrument is capable of detecting very small changes in hydrogen, methane, nitrogen and other gases, a wide range of possible biological activities could be detected.

The results of the GE and LR experiments are open to several more or less imaginative interpretations, and attempts are at present being made to duplicate the results in several Earth laboratories using simple catalysts and oxidising agents. The third experiment, the pyrolytic release experiment (PR), although perhaps the most complex technologically, is also the least equivocal when it comes to interpretation of the results. It is designed to detect the fixation of labelled carbon monoxide and dioxide in organic compounds. A sample of soil is incubated in a Martian atmosphere with added water vapour and irradiated with a simulated sunlight xenon lamp. After five days the sample is heated to 625 °C to pyrolyse organic compounds which are trapped as vapours, and to drive off unreacted CO and CO_2. This unreacted gas is passed through a radioactivity detector and forms the first "non-biological" peak. The organic vapour trap is then heated to 700 °C to release and oxidise

Photo: NASA

Martian dune field

the remaining organic compounds which form the second, "biological" peak.

With a sterile sample a peak ratio of about 500 to 1 would be expected. The result from the Martian soil was about 75 to 1 due to the high "biological" peak. This is several times more active than non-sterilised soils from the dry valleys of Antarctica. The result from the control experiment with heat-sterilised soil is crucial in this instance, a high peak ratio indicating the possibility that biological rather than chemical processes capable of fixing atmospheric carbon monoxide or dioxide in the presence of light are taking place in the soil. If life exists on Mars, this is what might be expected in the soil surface which is strongly illuminated and bathed in an atmosphere of about 95% carbon dioxide. The biologists would be even more encouraged if organic compounds were detected in the Martian soil.

Unfortunately, the initial run of the organic chemistry analysis was less than satisfactory due to the temperamental soil sampling boom which apparently failed to deliver a full load of soil to the gas chromatograph-mass spectrometer. No organic compounds were detected. A full soil load has now been obtained and a further analysis is being carried out. If organic compounds are not detected this would be a blow, though not a fatal one, to the concept of life on Mars, and would render interpretation of the three biology experiments more difficult. □

USSR SPACE

Forward with the programme

Vera Rich reports on the latest Soviet space missions

> "Soviet science considers the creation of orbital space stations with interchangeable crews as the main highway of mankind into space. They can form 'cosmodromes in space', launch pads for flights to other planets. Large-scale scientific laboratories will arise for the investigation of space technology and biology, medicine and geophysics, astronomy and astrophysics."

So said Mr Brezhnev in a recent statement. The idea was by no means new; it is a fundamental tenet of all Tsiolkovskii's work that such a station would and must precede manned exploration of the moon and planets. There are, indeed, some indications that Soviet space planners have at times been prepared to consider the alternative of manned exploration direct from earth—the argument that a lunokhod-carrying automatic spacecraft could carry out its survey work at "half the cost" of a manned mission, for example, suggests that the latter possibility had at least reached the costing stage. Now, the flight of the unmanned Luna 24 has repeated the task of Luna 16 by obtaining and returning with a sample of moon-rock, though from a depth of two metres and from *Mare crisium*, from which no samples had yet been obtained. Presumably present space plans still do not envisage cosmonauts venturing beyond earth orbit.

Whatever the overall timetable of the Soviet Union's space plan, though, many of the experiments now being conducted by the 7-week-old Salyut 5 mission suggest that the concept of a permanently manned space station is still well to the fore. These latter experiments fall into three main groups: geophysical and astrophysical observations, technological experiments and biological experiments. Of the technological experiments, some are directly concerned with processes and techniques which would be required in the construction of a space station—notably the study of the behaviour of gases in liquids in space and, of some importance, a soldering experiment. Unlike the welding experiments of an earlier mission, the soldering, which uses a highly exothermal chemical reaction to produce the necessary heat, is aimed less at testing the cosmonaut's dexterity than at investigating the process itself. The welded metal specimens are to be returned to earth for further investigation of their structure.

The emphasis has clearly shifted to the properties of materials treated under conditions of weightlessness. Other experiments include the growing of crystals (also to be returned to earth), and the cooling of molten metals—bismuth, lead, tin and cadmium—to determine surface tension. These experiments will, of course, provide data of considerable theoretical significance: crystals grown under weightlessness, for example, should be free of convection-induced defects, and should, it is hoped, provide valuable comparative data for crystallographers and geologists. It is significant, however, that all these experiments are described in the official announcements as "technological", suggesting that their practical importance should not be minimised.

The medical problems of prolonged spaceflight are also receiving considerable attention. Apart from such obvious parameters as muscle tone, cardiovascular and respiratory performance, and loss of body weight—measured on the special "massometer"—the medical programme includes special monitoring of the cosmonauts in a "vertical" position (however that is to be interpreted), tests on reaction time in performing complex operations and manual control (real or simulated) of the spacecraft (the simulated control presumably relates to possible emergencies), and even possible variations in taste.

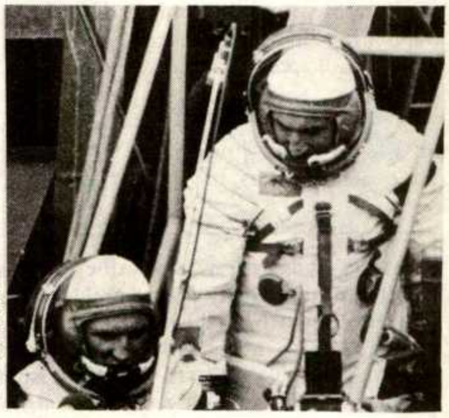
Photo: Novosti

Before blast-off for Salyut 5

Press comment on the medical programme suggests a growing concern over the psychological effects of prolonged spaceflight. These would arise from a lack of external stimuli, the restriction of living space and general monotony—an aspect of spaceflight which will assume ever greater importance in future missions when the length of flight and the crew size increases. Aboard Salyut 5 are such simple prophylactics as recorded music (from folk to classical) and a varying make-up of the ration-packs.

Commenting on the radiation safety system used aboard the Salyut craft, Ludvig Palmbakh of the USSR Institute of General Genetics stated that the protective measures used are "well adapted" for work near Earth, since, if solar radiation rises to danger level, the crew can be quickly evacuated and brought back. For deep-space missions, however, "more active" means of protection would probably be required, possibly involving the deflection of high-energy particles by electromagnetic fields. The design of such systems entails considerable technical difficulty, so the fullest possible information is required both on the nature of the radiation and the actual hazard involved. The cytological and genetic experiments, using drosophila and hawksbeard, carried by Salyut 5, should provide further data on these hazards. □

IN BRIEF

Seabed hearings

The dispute between Greece and Turkey over the Aegean seabed is due to receive a hearing at the International Court of Justice at The Hague this week. Greece is seeking to prevent the Turkish oceanographic research ship *Sismik I* from continuing its oil exploration, and wants a ruling on the limits of the continental shelf. In New York at the latest round of the Law of the Sea Conference, meanwhile, Dr Kissinger is reportedly threatening unilateral action by the US over exploitation of deep-sea minerals, on the regulation of which the conference has been deadlocked.

Pesticide dumping

In what Federal prosecutors in the US have described as the largest environmental case ever brought, the Allied Chemical Corporation last week pleaded *nolo contendere* on 940 counts connected with the dumping of the pesticide Kepone in the James River. Fish in the river and in Lower Chesapeake Bay (where an Allied Chemical barge containing 250,000 tons of sulphuric acid capsized last week) were found to contain Kepone. The corporation could now face fines of about $13 million.

Coal gasification 'option'

On the basis of a report it published last week, the UK National Coal Board (NCB) has decided not to resume, at least for the moment, applied research into underground coal gasification—the direct extraction of gases from coal seams burnt underground. The NCB identifies underground gasification as a realistic energy option, however, and will continue monitoring international research efforts until costs—now put at 7–24 pence a therm—can be reduced to something nearer those associated with conventional mining techniques.

Cooperation in an international pilot scheme costing £10–15 millions could, the NCB feels, become worthwhile within five years or so. Outstanding problems of underground gasification include the poor quality of the gases produced, the lack of control over supplies, and the danger of seepage to the surface or into mineshafts and groundwater. During the 1950s Britain was among the pioneers of underground gasification research, which is now led by Belgium, Canada, the USA and West Germany. The Soviet Union operates a small-scale commercial facility.

Wildcat story

THOMAS H. JUKES

YEARS ago, as a young father, I was often asked by my infant children for a bedtime story. On one such occasion, I gave a partially true account of a camping trip to a lonely spot where I was suddenly confronted, at dusk, by a ferocious animal, yellow-eyed and snarling. It was a wildcat! At this point in the narrative, the children screamed and hid beneath the covers. Soon they were sleeping soundly. Next evening, I asked what they wanted to hear in the way of a soporific monologue. The answer, to my surprise, was: *The Wildcat Story*. It was a best-seller for weeks. People love tales that make their flesh creep.

As time went by, I recognised many versions of the wildcat story in scientific writings. Whether or not these are true, their common property is that they are entrancing because they are "scary". One of the most fascinating is the recombinant DNA story. My grandchildren are too ecologically sophisticated to be terrified by wildcats. Perhaps I can startle them with an imaginary account of meeting up with a genetically-engineered *E. coli* cell.

According to a recent news report, many inhabitants of Cambridge, Massachusetts, are greatly worried by the possibility that "hot" *E. coli* cultures might escape into the sewers, nowadays called "the environment". Carelessness in the laboratories of Harvard University and the Massachusetts Institute of Techonology was named as a cause that might lead to this disaster, which could be accentuated by the decrepitude of the facilities at Harvard. It was said that George Wald has explained the danger to the Mayor of Cambridge, Massachusetts, Mr Vellucci, who has been an advocate of converting Harvard Yard into a parking lot. The mayor was apparently a ready listener, this being a rare case of a progressive public official giving ear to erudite eloquence. Perhaps, with the Mayor's attention diverted by colon bacilli, Harvard Yard may be saved.

The incident is somehow typical of a shift in attitudes towards scientific discoveries. Once we were eager to try new things, and none would say us nay. Today, dangers are recognised even before they have been shown to exist. If penicillin had been discovered in the 1970s instead of the 1930s, it would probably have been kept out of the hospitals after preliminary tests had shown it to be potentially allergenic, and the testers had been sued for medical malpractice.

Somehow I have a feeling that anything *E. coli* could do to us has already been done during the millions of years that this organism has lived in countless numbers within the intestinal tracts of vertebrates. It has a set of genes that code for transfer RNA molecules. But these molecules have different base sequences from those in human tRNAs, although both sets of tRNAs function similarly. The differences indicate that the sets have evolved separately for hundreds of millions of years. Why has there been no mixing? Are all the transformations phenotypic? Would the new, human-tailored bugs take over the sewers? Or would they stand about as much chance as a hothouse orchid in a patch of good healthy ragweeds?

If Mr Vellucci prevails, we are not likely to find out. I would be a bit peeved if I were a young bacteriologist, being held back by the old guard who have made it to the top. However, many young scientists seem quite satisfied to join, or even to excel, the elderly prophets of doom.

Now that Viking has landed, we can brace ourselves for an airing of the greatest of all wildcat stories. It seems that a capsule of unsterilized Martian soil came back to Earth, swarming with weird organisms that gobbled up atmospheric nitrogen. The first news we heard was that millions of people were dying east of the Urals. . . .

news and views

Concentration factors and radiological protection

from Pamela M. Bryant

THE behaviour of plutonium in the environment is of topical interest especially in view of proposals in several countries of the world to embark on power programmes involving the use of fast breeder reactors. Knowledge is currently expanding as a result of studies on plutonium present in the environment from nuclear weapons tests and disposal of wastes from nuclear fuel reprocessing plants From a knowledge of the levels of plutonium activity in relevant environmental materials it is possible to estimate the associated radiation exposure of humans. When that knowledge is sufficiently broad to quantify the behaviour of plutonium in inter-related environmental materials, it is possible to predict the approximate level of radiation exposure of humans corresponding to the postulated additions of plutonium to the environment.

In a paper in this issue of *Nature* (page 745) reporting the results of measurements of plutonium concentrations in the water of Kwajalein lagoon in the Marshall Islands, Noshkin *et al.* examine published data on plutonium concentrations in water and fish from nearby and distant locations. This examination leads the authors to conclude that all the available data on plutonium in fish are seemingly inconsistent and that, if the available Enewetak and Kwajalein data are correct, the availability to all fish and invertebrates of plutonium, from whatever source, depends more upon the type of environment than on plutonium levels in that environment. They state that such a conclusion would greatly affect future plans for discharging low activity transuranic wastes to the marine environment. They also say that it would force them to concede that the concept of a plutonium concentration factor for fish (the ratio of the concentration of plutonium in fish to its concentration in the surrounding water) is meaningless.

In a preliminary report on levels of plutonium isotopes and ^{241}Am in various tissues in plaice from the north-eastern Irish Sea, Pentreath and Lovett (this issue of *Nature*, page 814) include data on discharges of these nuclides from the nuclear fuel reprocessing plant at Windscale, Cumbria. Plaice is a fish of commercial importance in the area; it is monitored regularly, as part of the established control procedure of the Ministry of Agriculture, Fisheries and Food (MAFF), primarily to ensure the radiological safety of the discharges in public health terms. Pentreath and Lovett comment that in view of the fluctuating discharges a steady-state burden will not exist for fish caught close to the pipeline; thus, an accurate estimate of the concentration factor between fish and seawater cannot be made. The concentration factor would, in any case, depend on the location of the seawater sample and the movement of the local population of plaice.

Yet another complication in the estimation of concentration factors is evident from recent reports which suggest a preferential biological availability of ^{238}Pu over ^{239,240}Pu in terrestrial and aquatic organisms. The reports were noted with interest by Beasley and Fowler (page 813 of this issue of *Nature*) in a paper describing plutonium isotope ratios in polychaete worms. These authors found that these deposit-feeding marine worms, living in sediments contaminated with plutonium isotopes from a variety of sources, did not preferentially accumulate ^{238}Pu over ^{239,240}Pu. They conclude that until the reasons for the disparities become clear general statements regarding preferential biological availability of ^{238}Pu over ^{239,240}Pu should be viewed cautiously

The limitations of values for concentration factors between water or sediments and marine organisms are well recognised by persons using them for prediction purposes in the field or radiological protection and carrying out research programmes connected with control procedures for waste discharges

A basic policy applied to the control of radioactive discharges to the marine environment from nuclear establishments in the United Kingdom is that the government departments responsible authorise discharges at levels below those which correspond by calculation to the dose limits for the general public recommended by the International Commission on Radiological Protection (ICRP) The authorised limits are set on the basis of the need to do what is reasonably practicable, having regard to cost, convenience and the national importance of the subject, to reduce doses far below the ICRP dose limits. The environmental consequences of such discharges of radioactivity are also borne in mind, although it is generally found that the public health considerations are more limiting than considerations relating to environmental resources.

The first stage in determining discharge levels corresponding to ICRP dose limits, for example when a new discharge is being considered, involves modelling of the environmental pathways likely to be of greatest importance. Such modelling seeks to estimate the long-term average level of radiation exposure, under steady-state conditions, corresponding to the postulated disposal practice. Where an element of doubt exists, pessimistic values of concentration factors are used. In the early stage of an operation, discharge of no more than a small fraction of the level indicated by this modelling is permitted; at this stage research additional to control monitoring is undertaken to check the predicted relationships.

In the particular case of plutonium discharges from Windscale, monitoring is carried out by the MAFF Fisheries Radiobiological Laboratory of materials which include the important elements of human food chains such as fish, shellfish and the edible seaweed *Porphyra umbilicalis*; as well as seawater and sediment whose role as a "sink" for plutonium introduced into the sea is well recognised. The object of this study is to answer some of the questions posed by the introduction of a long-lived radionuclide into the marine environment. The expected results of this study include improved understanding of the concentration factors between environmental materials in the region and their limitations. Control of public health, however, is exercised by the direct measurement of radioactivity in those environmental materials responsible for human exposure; in the case of actinides discharged from Windscale the most important measurements concern plutonium and americium in the edible fraction of Irish Sea plaice taken from the sea area most liable to contamination. It is difficult to understand, therefore, why the uncertainty as to the validity of the concept of concentration factors for fish expressed by Noshkin *et al.* should lead to their conclusion that future plans for discharging low activity transuranic wastes to the marine environment would be affected.

Enkephalin: the latest instalment

from Leslie Iversen and Raymond Dingledine

> The 5th International Narcotic Research Conference was held in Aberdeen on July 19–22, 1976. The full proceedings of the meeting will be published by North-Holland in September under the title *Opiates and Endogenous Opioid Peptides.*

THE central effects of morphine and opiate-like drugs have been known for thousands of years, but only in the past five years has real progress been made in understanding the actions of these drugs on the brain, or the significance of the existence of specific opiate receptors in normal brain function. The first catalytic breakthrough was the discovery by Pert and Snyder[1] of a simple, sensitive assay for brain opiate receptors. Equally exciting was the report by Hughes *et al.* last December[2] of the identification of two naturally occurring pentapeptides in brain—the enkephalins—whose properties mimic those of morphine, and this was the focus of attention at the recent meeting in Aberdeen.

Although the identification of the enkephalins has since been confirmed[3], it has also become apparent that there are several other, larger, naturally-occurring peptides that share similar pharmacological properties. Most of these peptides, now known generically as the "endorphins", derive from the 91-amino acid pituitary peptide β-lipotropin. Thus several groups have now reported that a pituitary peptide corresponding to the C-terminal portion of β-lipotropin (residues 61–91, known as C-fragment of lipotropin or β-endorphin) has morphine-like properties in various test systems[4–6]. Similar properties are exhibited by other naturally occurring fragments of β-lipotropin, for example the C'-fragment (residues 61–87, also known as γ-endorphin) and α-endorphin (residues 61–76)[7]. Met-enkephalin (Tyr-Gly-Gly-Phe-Met) consists of residues 61–65 of β-lipotropin, and all of the above peptides share this common sequence at their N-terminal region. However, Leu-enkephalin (Tyr-Gly-Gly-Phe-Leu) does not seem to be derived from β-lipotropin, and there may be yet more morphine-like peptides still to be characterised. A. Goldstein (Stanford University) reported at the meeting that it seems unlikely that the β-lipotropin derived peptides can account for all of the opioid material extractable from pituitaries, and A. Wahlström (University of Uppsala) reported on an opioid peptide from human cerebrospinal fluid that appears to be chemically different from all known fragments of β-lipotropin. In addition, C. Pert (National Institute of Mental Health) reported that normal human blood contains a low molecular weight opioid, named "anodynin", which is not an enkephalin[8]. The anodynin content of rat blood was abolished after hypophysectomy, strongly suggesting pituitary origin.

All this is, to say the least, a little confusing. Are the pentapeptides in brain really the naturally occurring morphine-like substances? Should one perhaps regard the pituitary peptides and brain enkephalins as belonging to completely different functional systems; or could the enkephalins merely represent breakdown products of the larger peptides? If so, it would be a unique situation among peptide hormones for their precursor molecules to exhibit strong physiological activity, since the larger endorphins seem to be more potent than the enkephalins in most test systems. The enkephalins are, however, rapidly destroyed by peptidases in brain and other tissues[9], and the metabolic stability of the larger endorphins may account for their dramatic and prolonged pharmacological actions. In support of this A. Pert (National Institute of Mental Health) reported that the simple chemical derivative D-Ala^2-Met-enkephalinamide, which has half the affinity for the opiate receptor of Met-enkephalin but is resistant to enzymatic degradation, produced powerful long-lasting analgesia in rats when injected into the brain. Other synthetic analogues of the enkephalins that are metabolically stable were reported by D. Smyth (National Institute for Medical Research, Mill Hill), and they seem likely to become useful research tools.

A disappointing finding for interested clinicians was that prolonged treatment with the endorphins seems to induce tolerance and dependence, just like other opiates. The clearest evidence for this came from E. Wei (University of California), who reported that following the chronic infusion of very small amounts of β-endorphin or Met-enkephalin into the brain (using an ingenious implanted osmotic mini-pump), rats exhibited typical withdrawal signs when challenged with naloxone (see also ref. 10).

Further progress in identifying central sites for the analgesic effect of opiates was provided by H. Takagi (Kyoto University), who reported that microinjection of morphine into the nucleus reticularis gigantocellularis resulted in naloxone-sensitive analgesia and mimicked the inhibitory effect of systemic morphine administration on spinal lamina V cells. H. Akil (Stanford University) demonstrated that endorphin levels in rat brain rise during a stress-induced analgesic state, and postulated that environmental situations that activate the endogenous pain-inhibitory system[11] may involve the opioid peptides. Of potential importance also is the recent finding by Simantov and Snyder[12] that enkephalin levels are increased in the brains of morphine-tolerant rats.

Many speakers described the close similarity between the actions of morphine and the endorphins in brain and peripheral targets. Thus the endorphins produce a naloxone-sensitive analgesia when injected into the brain (see also refs 13 and 14), have characteristic morphine-like actions on the guinea pig myenteric plexus and mouse vas deferens preparations, and display other behavioural opiate-like effects such as catatonia in rats and locomotor activity in mice. In addition, all the endorphins displayed a respectable affinity for binding to opiate receptors, but here some curious anomalies were described. N. Birdsall (National Institute for Medical Research) showed that the displacement by morphine or Met-enkephalin of a radiolabelled opiate agonist followed different kinetics from their displacement of labelled antagonists (see also refs 15 and 16). Met-enkephalin was less effective in competing for binding sites for labelled naloxone than in competing for its own binding sites in brain, and morphine was much less potent in competing for labelled enkephalin binding sites than in displacing ^{3}H-opiates. These differences might be explained by multiple receptor conformations[17], but H. Kosterlitz (University of Aberdeen) proposed the existence of a family of opiate receptors, on the basis of the binding anomalies and variations in rank order of potency for a series of opiates when tested in different peripheral assays.

In terms of cellular responses it was clear that the enkephalins closely mimic morphine. Thus, B. Hamprecht (Max-Planck-Institut für Biochemie, Martinsried) found that very low concentrations of enkephalin stimulate cyclic GMP formation in cultures of neuroblastoma × glioma cells, and W. Klee (National Institute of Mental Health) that enkephalins inhibit basal and prostaglandin-stimulated cyclic AMP formation in the same cells (see also refs 18 and 19). K. Minneman (University of Cambridge) reported a similar stimulation of cyclic GMP formation by morphine and the enkephalins in slices of rat striatum, although high concentrations of the peptides were needed because of their metabolic instability[20]. Several groups have studied the responses of single neurones in different brain regions to iontophoretically applied enkephalin, and in general these peptides mimic the inhibitory actions of morphine[21–24], although specific excitatory actions have been observed on Renshaw cells[25]. Intracellular records from spinal interneurones and motoneurones by W. Zieglgansberger (Max-Planck-Institut für Psychiatrie, Munich) suggested that the inhibitory effect of morphine and enkephalin may be due to blockade of ionic conductance at chemically excitable Na$^+$ channels, an hypothesis similar to that of Snyder's group[17]. Intracellular recordings from morphine-sensitive neurones in the myenteric plexus by R. North (Loyola University) however, showed that at this peripheral site opiates may hyperpolarise cells by causing an increase in membrane conductance.

Several other new pieces of information relevant to understanding the possible physiological function of the endorphins were presented. R Simantov (Johns Hopkins University) and J. Hughes (University of Aberdeen) found that the regional distribution of enkephalin in brain is similar to that of the opiate receptor itself: with high levels, for example, in corpus striatum and hypothalamus and negligible amounts in the cerebellum. Hughes also described a calcium-sensitive release of enkephalin-like material from brain synaptosome preparations in response to depolarising concentrations of potassium. Progress in discovering possible "endorphinergic" synapses will be aided by two other technical developments: the autoradiographic mapping of the anatomical distribution of opiate receptors (reported on by M. Kuhar, Johns Hopkins University), and the mapping of possible endorphin-containing neuronal pathways in the brain by immunohistochemistry. The latter method has recently been successfully applied by T. Hokfelt and reported at the Collegium Internationale Psychopharmacologium meeting in Quebec last month. Further instalments of this bulletin may be expected before long!

[1] Pert, C. B., and Snyder, S. H., *Science*, **179**, 1011 (1973).
[2] Hughes, J , *et al* , *Nature*, **258**, 577 (1975).
[3] Simantov, R., and Snyder, S. H., *Life Sci* , **18**, 781 (1976).
[4] Bradbury, A. F , Smyth, D. G , Snell, C R , Birdsall, N J. M., and Hulme, E. C , *Nature*, **260**, 793 (1976).
[5] Li, C H , and Chung, D., *Proc. natn. Acad. Sci., U.S.A* , **73**, 1145 (1976).
[6] Cox, B M , Goldstein, A , and Li, C H , *Proc. natn. Acad. Sci , U S.A.*, **73**, 1821 (1976).
[7] Guillemin, R., Ling, N , and Burgus, R , *C. r. hébd. Séanc Acad Sci Paris*, **282**, 783 (1976).
[8] Pert, C. B., Pert, A , and Tallman, J. F , *Proc. natn. Acad. Sci., U.S.A* , **73**, 2226 (1976).
[9] Hambrook, J. M , Morgan, B A., Rance, M J , and Smith, C. F. C , *Nature*, **262**, 782 (1976)
[10] Waterfield, A. A., Hughes, J , and Kosterlitz, H. W., *Nature*, **260**, 624 (1976).
[11] Akil, H , Mayer, D. J , and Liebeskind, J. C., *Science*, **191**, 961 (1976).
[12] Simantov, R., and Snyder, S. H , *Nature*, **262**, 505 (1976).
[13] Belluzzi, J. D , *et al.*, *Nature*, **260**, 625 (1976)
[14] Buscher, H H , Hill, R C , Romer, D , Cardinaux, F., Closse, A., Hauser, D., and Pless, J , *Nature*, **261**, 423 (1976).
[15] Pert, C B , and Snyder, S. H , *Molec Pharmac.*, **10**, 868 (1974).
[16] Simon, E , Hiller, J. M., Groth, J , and Edelman, I., *J. Pharmac exp. Ther* , **192**, 531 (1975)
[17] Snyder, S. H., *Nature*, **257**, 185 (1975).
[18] Iversen, L L., *Nature*, **256**, 8 (1975)
[19] Brandt, M., *et al* , *Nature*, **262**, 311 (1976).
[20] Minneman, K. P , and Iversen, L. L , *Nature*, **262**, 313 (1976)
[21] Duggan, A W., Davies, J., and Hall, J G , *J. Pharmac. exp. Ther* , **196**, 107 (1976).
[22] Bradley, P B , Briggs, I , Gayton, R. J., and Lambert, L. A , *Nature*, **261**, 425 (1976).
[23] Gent, J. P., and Wolstencroft, J. H., *Nature*, **261**, 426 (1976)
[24] Hill, R. G., Pepper, C. M., and Mitchell, J. F., *Nature*, **262**, 604 (1976)
[25] Davies, J , and Dray, A., *Nature*, **262**, 603 (1976).

Farmington: an Apollo meteorite

from David W. Hughes

FARMINGTON Township, Washington County, Kansas, is famous, at least to meteoritisists, as the place where an L5 chondrite fell to ground in June, 1890. The meteorite itself is famous because it has a uniquely short cosmic-ray exposure (or "radiation") age, having left its parent body a mere 25,000 years ago. This latter fact is most significant because it means that the orbit the meteorite had as it intersected the Earth was its original orbit, the one it obtained immediately after release from its parent body. This orbit therefore gives a direct clue to its place of origin.

Meteorite ages are obtained by looking at the accumulated spallation products and nuclear tracks produced in the body of the meteorite due to the penetration of galactic cosmic rays. This irradiation usually begins as soon as the meteorite is ejected from its parent body, so the radiation age equals the transit time between that body and Earth. On average this is 10^7 years. Now every time a meteorite passes close to a planet its orbit changes, and a pass as far away as 10 planetary radii will alter the direction of motion of the meteorite by a few degrees. Opik (*Adv. Astron. Astrophys.*, **4**, 301; 1966) calculated that this happens about every 5×10^5 yr so Farmington, which had had a separate existence in the Solar System for a twentieth of this time, was most probably on its pristine, unaltered orbit. This would differ slightly from the orbit of the parent body because of the random velocity given to Farmington on ejection but as this velocity is generally less than a few hundred metres per second the change is only marginal. So with Farmington (and Farmington alone, as other meteorites have been in the Solar System much longer and have greatly altered orbits) there is a real chance of finding out exactly where it came from. To do this its orbit has to be calculated and Boris Levin and Alla Simonenko (Academy of Sciences of the USSR, Moscow) and Edward Anders (University of Chicago) have done just this in a recent paper in *Icarus* (**28**, 307; 1976).

They enlisted the help of the Kansas and Nebraska Historical Societies who diligently went through 280 different newspapers from 91 counties published around June, 1890, looking for reports of the fall. Thousands of people over a 300×300 km area saw the bolide and 144 news items appeared in the press. There were many vivid descriptions: "a bright meteor passed swiftly to the north-west and burst into glittering fragments high in the air"; "it was a ball of fire as large as a table. It had a trail like a comet and it wobbled like a kite"; "its path could be discerned by the smoke that followed it". To some it sounded like the firing of a cannon, to others it had a "long rumbling rolling noise like thunder". Close to the impact point the ground shook just as in an earthquake. The most startled person was a Mr J. H. January who was "breaking the prairie sod" when the 85 kg meteorite fell almost vertically some 150 m in front of him and made a hole with nearly vertical sides.

None of these descriptions of the Farmington bolide contains any quantitative data on the azimuths and angular heights of the beginning and end points of the fireball. But near the point of fall anyone seeing the meteorite would be looking along the trajectory and the fireball would appear to be stationary and in the direction of the apparent radiant. Just such an effect was observed from Washington, Kansas, 7.1 km south of Farmington where the meteorite was also seen to be just below the Sun. The explosion and extinction happened after the passage over Washington, at an end height of about 10 km. The zig-zag course reported by some people near Washington was due to a physiological effect. The eye can only follow a moving object if its angular velocity is less than 30° s^{-1}. At greater velocities the eye pursues the object in jumps (the so-called saccadial movement). As this jumping was seen, the object must have been moving at about 5 km s^{-1} or somewhat slower.

Combining all the observations, Levin, Simonenko and Anders conclude that the apparent radiant was 20° west of south at an azimuth of 60°, giving Farmington a very steep trajectory through the atmosphere. The beginning and end heights were very similar to the Příbram and Lost City meteorites (98, 87 km and 13, 17 km respectively), the only other two meteorites to have known orbits (these being obtained from photographs taken from networks of cameras). The pre-atmospheric velocity must have been in the range 11.3 to 22 km s^{-1}. The lower bound is the Earth's escape velocity, the upper one being due to the fact that meteors moving faster than 22 km s^{-1} suffer complete ablative destruction. Using velocities in this range and the apparent radiant position obtained from the eyewitness reports the authors calculate a set of pre-collision orbits for the meteorite. They find that the meteorite struck the Earth at the ascending node of its orbit ($\Omega=275°$) and that the orbit had a small semi-major axis (between 1 and 1.3 a.u.) and a low inclination (5 to 10°). The eccentricity was around 0.21 and the argument of perihelion between 240 and 270°. The aphelion was at 3.0 a.u., in the densest part of the asteroid belt, and the perihelion could not have been less than 0.4 a.u. (interestingly chemical analysis showed that ^{3}He and ^{4}He had not been lost by the meteorite during its lifetime supporting the argument against a small perihelion). Fortunately all these results are insensitive to errors in the apparent radiant.

The facts point towards Farmington being a fragment from the collision between an Apollo asteroid and some other meteorite or asteroid. The Apollos are a short lifetime (10^7–10^8 yr) group of asteroids which have Earth-crossing orbits. They are thought by some to be too rare to provide all the stony meteorites. If they do, then the undiscovered Apollos should exceed the known Apollos by one or two orders of magnitude.

Of the 11 known Earth-crossing asteroids with encounter velocities below 22 km s^{-1}, Hermes, 1862 Apollo and 1865 Cerberus have orbits which fall within the error limits of the Farmington orbital elements, however none can be singled out definitely as the parent body. The uranium–helium age of Farmington is 5.5×10^8 yr (Heymann, *Icarus*, **6**, 189; 1967) indicating that it was reheated extensively, as were all L chondrites, in the collision that broke up the parent body. This collision must have involved an unusually large projectile which deposited more energy per unit mass than a typical cratering event. The remnants of the body could comprise a highly fragmented Hirayama or Flora family with a steep mass distribution.

So amidst a plethora of theories concerning asteroidal origin Farmington's place of birth seems to be known and was most probably an Apollo asteroid, this fact coming to us by courtesy of the careful scrutinising of the 1890 files of such worthy papers as the *Atchison Patriot*, the Omaha *Daily Bee* and the Wymore *Weekly Wymorian*.

EMBO ribosome workshop

from Richard Brimacombe

The fifth EMBO workshop on ribosomes took place in Brussels from August 2–6, 1976 under the organisation of Dr Alex Bollen of the Université Libre de Bruxelles.

THE ever-increasing complexity of ribosomology was reflected in the large number of participants (about 150), but the meeting was also characterised by a notable change of emphasis in the range of topics discussed, which was largely a result of the increasing contribution of chemical and physicochemical studies to the subject, at least in the case of prokaryotes. Progress over the past two years was summarised in the opening lecture by the organiser of the previous EMBO meeting (C. G. Kurland, Uppsala University), who laid particular stress on the developments in physical chemistry, which has become not only concerned with the structural aspects of the ribosome problem, but is also beginning to be concerned with the question of the specificity of the translation process in terms of kinetics.

One of the physicochemical methods now being used successfully to investigate ribosome structure is neutron scattering; results obtained with this technique were presented by P. Moore (Yale University), who, by making reconstituted ribosomes containing two deuterated proteins, has been able to estimate the distances between centres of mass of a number of pairs of proteins within the *E coli* 30S subunit The technique also indicates that many proteins are far from spherical in shape. Neutron scattering gives information about the overall shape and size of the subunits, and has been used in addition to probe the distribution of RNA and protein within the subunits; it seems that the central cores of the subunits are rich in RNA, particularly in the case of the 50S, whereas the surface regions are richer in protein (M. Koch, University of Louvain).

The neutron data are not yet sufficiently advanced to be compared in detail with the data from another very topical technique—the direct electron-microscopic demonstration of protein-specific antibodies bound to the ribosome surface. This method has produced two models of the *E. coli* ribosomal subunits, one of which was presented by G. Stöffler (Berlin) and the other by J. Lake (University of California, Los Angeles). Both protagonists arrived armed with an impressive array of hideously-coloured plastic ribosomal sculpture, and there was some lively discussion of the differences between the two models, which rather tended to obscure the fact that despite these differences there is substantial agreement, with regard both to the overall shapes of the subunits and to the details of the protein arrangement. In particular, there can now be no doubt that many proteins have very irregular and elongated shapes within the ribosome.

Physical chemistry is now being applied to the kinetics of the translation process. Ten years ago the question of codon–anticodon recognition did not seem to be a problem, but now it is by no means simple when considered in detail (J. Ninio, Paris; H. Grosjean, Brussels). The crux of the matter seems to be the degree of "stickiness" of the interaction between a codon and a potential anticodon; the correct anticodon will have a longer sticking time, and thus more chance of leading to amino acid incorporation, than an incorrect anticodon. The ribosome therefore needs to have time to make up its mind what to incorporate, an idea supported by some results from A. Spirin (Poustchino), who showed that stimulation of the rate of the translocation process by addition of

Mercury's magnetic field

THE origin of Mercury's magnetic field has recently become a subject of considerable research interest. Still debatable is whether the dipolar field (less than a thousandth of that on Earth) comes from a currently active dynamo or is a relic of earlier fields (or, of course, is some combination of these). We wish to take up some of Peter Smith's points in an earlier *News and Views* article (*Nature*, **260**, 578; 1976) on this subject.

If the field observed comes from remanent magnetisation only, the first question that has to be decided is down to what depth this magnetisation exists. Mercury's core, if not generating a magnetic field, would probably still be above the Curie point (Solomon, *Icarus* (in the press)), so it is reasonable to think only of a shell of material with modest magnetic susceptibility. Goldstein (*Nature*, **258**, 175; 1975) showed that a dipole moment results, in general, in such a shell after it has been magnetised in the field of an internal, now extinct, dipole. Stephenson, in a quantitative analysis of the problem (*Earth planet. Sci. Lett.*, **28**, 454; 1976) obtained an ancient surface polar field of less than 10 Oe only if the volume percentage of iron in rocks of a 243 km-thick mantle were 5%—more than a hundred times the typical value in lunar basalts. No support for such an anomalously high iron content comes from the Mariner 10 photometric observations (Hapke, *et al.*, *J. geophys. Res.*, **80**, 2431; 1975). Srnka has recently carried out a similar, though more detailed calculation (*EØS*, **57**, 271; 1975), from which he concludes that an ancient surface field of about 16 Oe was required along with a volume percentage of iron of about 3.0%. We currently believe that on the basis of this work, the remanent magnetisation hypothesis for the field is not a likely one.

We admit that these calculations could be significantly modified; Solomon, for instance has pointed out that if the segregation of metals from silicates is incomplete in the mantle and crust of Mercury, the resulting increased thermal conductivity could lead to a thicker shell below the Curie temperature, somewhat reducing the required magnitude of the ancient magnetising field. Furthermore, if the iron content were as high as Stephenson assumes, then ferromagnetic effects might dominate.

There are, on the other hand, additional difficulties for remanent magnetisation models; among them is the observation of Murray *et al.* (*J. geophys. Res*, **80**, 2508; 1975) and others, that craters such as the Caloris basin must have modified the planetary structure to depths greater than 100–200 km, approximately the thickness of the shell in which remanent magnetisation would be acquired. Cratering could thus severely disrupt any extant magnetisation pattern (Wasilewski, *Moon*, **9**, 335; 1974).

The other major alternative is a currently active dynamo for which a necessary but not sufficient requirement is a molten core—what evidence do we have for this? Solomon and others have pointed out that cosmochemical models not including a substantial heat source predict core solidification within about 1 billion years after infall. That would result in a contraction of Mercury's radius of some 18 km (Solomon, *op cit.*), which is not observed—indirect evidence that a molten core may exist. Proposals for heat sources include the retention of some U and Th in the core after differentiation; the presence of about 156 p.p.b. ^{40}K; presence of elements such as S in the core, which would lower the solidus temperature; and models which distribute the gravitational heating over more of the planet's history.

Finally, there is the remote possibility that the field of Mercury is due to remanent magnetism from an external source field. Sharpe and Strangway (*Geophys. Res. Lett.*, **3**, 285; 1976) propose a cool model in which a 100 km shell of a few per cent iron cools rapidly below 800 °C in a field of some 10 Oe. In their calculation, they suggest that if Mercury accreted cold (at about 300 K; as opposed to 1,200 K which is usually used as the base temperature) the present-day field could result from fossil remanent magnetisation retained in the inner half of the planet.

Peale, in this week's *Nature* (page 765), proposes an experiment which would contribute to a solution of the origin question. The dynamical behaviour of Mercury will be slightly affected by the existence of a liquid core; measurements of the amplitude of libration in longitude, the obliquity to the ecliptic and two functions of moments of inertia should suffice. None of these measurements would be easy—the last two would require tracking of artificial satellites, the first two would require the establishment of some form of astronomical observatory on Mercury.

The origin of Mercury's magnetic field will probably not be resolved without additional visits to the planet.

M. L. GOLDSTEIN
N. F. NESS
P. J. WASILEWSKI

GTP caused a concomitant increase in miscoding rate.

Another novel feature of this meeting was the devotion of a whole day to the question of ribosomal genetics. Large numbers of new mutant ribosomal proteins were described, which should prove useful in both genetic and functional studies, and some very impressive work on the ordering of individual genes within the *E. coli* chromosome was reported by S. Jaskunas and L. Lindahl (University of Wisconsin) Transducing phages carrying segments of bacterial DNA were isolated and the genes these contained could be identified using a DNA-dependent cell-free protein-synthesising system. The arrangement of the genes within the DNA segments was analysed with the help of restriction enzymes, and genes for rRNA, several factors, and many ribosomal proteins have at least been partially ordered in this manner.

Activity in these new areas meant that less time than usual was available for discussion of the more traditional aspects of ribosomal research. Little was heard in Brussels on the primary structures of ribosomal proteins and RNA, in order to avoid repetition of the extensive reports in this field which had been presented at the International Congress in Hamburg during the previous week. A number of delegates described protein–protein cross-linking, RNA–protein cross-linking and affinity labelling results, and here the picture of the *E coli* ribosome is becoming more and more complex. This is an obvious consequence of the irregularity of the protein shapes; as long as it was possible to think of the ribosome as a neat array of ping-pong balls, it was sufficient to identify which proteins were involved in a cross-link or affinity label experiment. Now that the ribosome has become a plate of spaghetti, researchers will be forced to push the analysis one stage further and identify the amino acid residues within the proteins which are involved in the reaction in order to be able to interpret the results fully, and this is not an easy task. For the same reason, the functional investigation of the *E. coli* ribosome has become more complex; more and more proteins are becoming implicated in each individual ribosomal function, and active participation of the rRNA is also now being frequently invoked, although here there is a notable lack of hard evidence. Nevertheless, various promising experimental approaches were reported, which should in due course converge on a clearer understanding of ribosomal function.

Finally, the eukaryotes had a short session to end the meeting. This session did not really do justice to the large amount of work now being done on the eukaryotic ribosome, which, roughly speaking, has reached the stage at which the *E. coli* work stood four years ago, in that (for example) ribosomal proteins are being isolated and characterised. Perhaps for this reason, the eukaryotic research seemed deceptively simple and straightforward at the moment, although the present state of the *E coli* ribosome can leave nobody with any illusions as to what lies ahead in the eukaryotic field. □

Familial dysautonomia

from Felicia Axelrod, Thomas W. Mittag and J. P. Green

The Familial Dysautonomia Foundation sponsored a conference on familial dysautonomia and related diseases at New York University Medical Center on May 14, 1976.

FAMILIAL dysautonomia is a rare autosomal recessive disorder characterised by specific dysfunctions in the autonomic nervous system and the sensory nervous system. Prominent manifestations include postural hypotension; excessive sweating; diminished perception of pain, temperature, hypoxia, and taste—the last associated with an absence of fungiform papillae in the tongue. The corneal reflex is absent and the deep tendon reflex diminished. After intradermal injection of histamine, the axon flare, one of Lewis's triple responses, does not occur. The patients can cry but there are no overflow tears because the lacrimal glands function poorly. Methacholine restores the tendon reflex and the histamine response and stimulates the lacrimal gland, but conscientious symptomatic and supportive therapy is the only means to prolong life.

An unusual characteristic of the disease is that some organs show supersensitivity to sympathomimetic and parasympathetic agents, as though denervated. A diminished number of unmyelinated nerve fibres as reported by A. A. Aguayo (McGill University) can account for some of these signs and symptoms. Similarly, J. Pearson (New York University) reported that dorsal root ganglia and sympathetic ganglia show a reduced number of normal neurones and the sympathetic ganglia contain a large number of cells resembling undeveloped neuroblasts. Additional evidence of peripheral nerve defects was presented by N. Grover-Johnson (New York University) who showed that blood vessels have a diminished number of autonomic nerve ending in these patients. By contrast the parasympathetic ganglia (ciliary and submaxillary) appear normal under the microscope (Pearson) even though it has long been known that in dysautonomic patients parasympathetically innervated structures such as the iris and lacrimal gland are supersensitive to parasympathomimetic drugs. E. Krikun and A. A Smith (New York Medical College) presented evidence that an isozyme of choline acetyltransferase was deficient in the basal ganglia of a patient dying of the disease, suggesting a basis for the parasympathetic defect. The apparent developmental arrest of unmyelinated axons and certain sympathetic neurones in familial dysautonomia led to investigations into a possible defect in nerve growth factor or other trophic factors. F. B. Axelrod (New York University) reported that nerve growth factor activity in the serum of these patients was within the normal range when measured by bioassay (the ability to stimulate growth of chick ganglion cell dendrites). Yet a recent report (Rogers *et al., Pediatric Res.,* **9,** 384; 1975 (Abstr. 764)) showed greater than normal concentration of the β-subunit of nerve growth factor in dysautonomic serum, measured by radioimmunoassay, but normal activity by bioassay. It was suggested (T. W. Mittag, Mount Sinai School of Medicine) that one possible explanation of this paradox is that patients have, in addition to the normal nerve growth factor, an abnormal nerve growth factor inactive in the chick bioassay but detectable by radioimmunoassay, which interferes with the action of normal nerve growth factor on human cells. There was general agreement that continuing studies of trophic factors that regulate the growth and development of autonomic and sensory nerves could be fruitful, perhaps leading to treatment and to prenatal diagnosis.

Although the disease is almost exclusively restricted to Ashkenazi Jews (in whom its frequency is 1 in 10,000) it was reported that some of the same signs and symptoms are present in other diseases such as idiopathic orthostatic hypotension (I. B. Black, Cornell University Medical College and A. Rubenstein, Mount Sinai School of Medicine) and diabetes mellitus (N. Grover-Johnson). The New York University group also reported that 75% of dysautonomics showed pathological changes in the renal glomeruli.

An understanding of the cause of familial dysautonomia will provide increased understanding of the development of the autonomic and sensory nervous systems. And, in turn, progress towards understanding the molecular basis of familial dysautonomia could come from investigations of other diseases manifesting autonomic dysfunction such as idiopathic orthostatic hypotension and diabetes mellitus.

A hundred years ago

IN connection with the general introduction of the now celebrated Liberian coffee plants into most of the coffee-producing countries, as noticed by Dr. Hooker in his recently issued report on Kew Gardens, we may draw attention to what our consul says on the decrease of the production of coffee in Cayenne The kind there cultivated is the Mocha, which at one time was an important staple of the colony, the country being especially adapted for its cultivation. This valuable product of Cayenne, although temporarily abandoned, is not lost to the world; the trees continue to thrive in a wild state, and may be reclaimed hereafter There are thousands of coffee trees interspersed in the forests of the inhabitable part of the colony which have been abandoned for years. They attain a height of about fifteen or sixteen feet, with a circumference, a few feet from the ground, of thirty inches; they are rich in foliage, but do not bloom. The coffee tree also appears to be safe from the ravages of insects, whereas many other trees suffer vitally from this evil.

THE proposal to submerge a portion of North Africa by means of a canal from the Gulf of Gabes, letting the water of the Mediterranean westwards over the lake region of Djerid, seems from the facts detailed by MM Roudaire and Dupuis to be not only a practicable, but also likely to turn out a remunerative undertaking. Owing to the comparatively small area it is proposed to submerge, the meteorological changes which the submersion would occasion can only be slight, strictly local, and altogether beneficial in their general tendency—differing absolutely in all these respects from the meteorological changes which would result from the submersion of the western portion of the Sahara, proposed some time ago. From this latter project it would follow, owing to the great extent of the water surface which would thus overspread the Western Sahara, and its proximity to the Atlantic, that the present disposition of the lines of atmospheric pressure would be seriously altered, a result necessarily attended with changes in the prevailing winds and and currents of the North Atlantic, seriously affecting international interests in a manner which our present knowledge does not enable us in any way accurately to predict.

from *Nature,* **14,** August 24, 361; 1976.

articles

The distribution of stars around a massive black hole

Stuart L. Shapiro & Alan P. Lightman
Centre for Radiophysics and Space Research, Cornell University, Ithaca, New York 14853

The stellar density distribution around a massive black hole at the centre of a spherical star cluster is determined from a simple scaling argument. The distribution is obtained by examining the net diffusion timescales associated with star and energy transport in a spherical, N*-body system in dynamic equilibrium. The same analysis is also used to determine the stellar density profile in the halo of a star cluster. The approximate distribution obtained here for a relaxed,* N*-body system with (or without) a central, massive black hole agrees qualitatively with the results of detailed numerical calculations.*

THE suggestion[1,2] that accretion on to a massive black hole ($M \sim 10^3 M_\odot$) might be responsible for the X-ray emission observed from globular clusters has stimulated new interest in the dynamical consequences of a collapsed object at the centre of an N-body system. Some confusion has arisen, however, concerning the resulting steady-state, stellar distribution near the black hole. In his pioneering analysis[3,4], Peebles used a simple scaling argument to suggest that the stellar density varied as

$$n(r) \sim n_a(r/r_a)^{-9/4}$$

in the region $r_t < r < r_a$. Here n_a is the central density of the isothermal cluster core,

$$r_a \sim GM/\langle v^2 \rangle$$

is the 'capture' radius within which core stars with velocity dispersion $\langle v^2 \rangle$ are bound to the black hole of mass M, and $r_t \ll r_a$ is the radius at which stars tidally disrupted by the black hole. All stars are assumed to have the same mass, m, with $m \ll M \ll M_c$, where M_c is the total cluster mass. Recently, more detailed calculations (J. Bahcall and R. Wolf, unpublished; A. P. L. and S. L. S., unpublished) have indicated that the appropriate density law near the black hole is more aptly described by the relation

$$n(r) \sim n_a(r/r_a)^{-7/4}$$

where the magnitude of the exponent decreases slowly with decreasing r because of the consumption of low angular momentum stars (A. P. L. and S. L. S., unpublished; J. Frank and M. J. Rees, unpublished).

Here we use a simple scaling argument to obtain the approximate density law $n(r) \propto r^{-7/4}$ and provide a simple explanation for the discrepancy between our derivation and the original argument suggested by Peebles. In particular, we emphasise the distinction and general inequality between the net energy diffusion timescale and the net particle diffusion timescale in an N-body system in dynamic equilibrium. We use the same analysis to determine the density distribution in the cluster halo surrounding the isothermal core. (The halo solution applies whether or not the cluster contains a black hole.) Thus, by careful delineation and the appropriate use of the two different timescales mentioned above, we obtain, in a few lines, the approximate stellar density distribution throughout a relaxed, spherical, N-body system containing a central black hole. As becomes evident, the analysis applies equally to any sufficiently massive compact object (for example, a supermassive star) at the centre of a star cluster.

Diffusion timescales in N-body systems in dynamic equilibrium

As a conservative, N-body system of identical point stars (mass m) approaches equilibrium stochastically through mutual gravitational encounters, stellar velocities change, and thus both energy and angular momentum are exchanged, on a relaxation timescale

$$t_R \sim \langle v^2 \rangle^{3/2}/(G^2 m^2 n).$$

If the entire stellar system were confined in a spherical container with perfectly reflecting walls, the system would achieve thermal equilibrium with no net flow of stars or energy out of the system. (Here we assume that the container radius is sufficiently small that the ratio of the central density to the density at the wall < 709. In this case the equilibrium is stable, and runaway evolution through the 'gravothermal instability' will not occur (see refs 5, 6).) If, however, the system is not confined by rigid walls and if, in addition, there exists a star 'sink' at its centre (for example, a black hole), significant departures from thermal equilibrium will exist near the centre and in the outer halo of the stellar system. The steady-state behaviour of the cluster in these distinct, non-thermal regions will be one of dynamic equilibrium, characterised by a constant net flux of stars and energy out of the two regions. As energy is continually exchanged between stars, a given group of stars occupying the radial zone between r and $2r$ in a non-thermal region will be scattered out of the zone in a time t_R. The timescale associated with the net diffusion of stars (or energy) across a sphere at r may, however, be considerably longer, since stars (and energy) from neighbouring radial zones are scattered into the zone between r and $2r$ in roughly the same timescale, t_R. Clearly, no physical quantity can be transported from one zone to the next on a net rate exceeding $\sim t_R^{-1}$. Only by examining the boundary layers of a given non-thermal region can one determine the net flux of stars and energy into the region. In general, the net energy and net particle diffusion timescales will not be equal and only the minimum of the two will equal t_R in any region in dynamic equilibrium.

Let the net star and net energy diffusion timescales at radius r in the cluster be denoted by $t_S(r)$ and $t_U(r)$, respectively. For a steady state, both the net star flux S and net energy flux U are constant and independent of radius. If $n(r)$ is the stellar density and $E(r)$ is the mean energy (per unit mass) at r, then the number of stars between r and $2r$ is $\sim nr^3$ and in the steady state we may write

$$S \sim \frac{n(r)r^3}{t_S(r)} = \text{constant} \qquad (1a)$$

$$U \sim \frac{n(r)r^3E(r)}{t_U(r)} = \text{constant} \qquad (1b)$$

In thermal equilibrium the constants on the right-hand sides of equation (1) are zero. In dynamic equilibrium, they are generally non-zero and equation (1) gives

$$t_U(r) \propto t_S(r)E(r) \qquad (2)$$

demonstrating the simple but important result that stars and energy do not, in general, diffuse on the same timescale in systems in dynamic equilibrium. The proportionality constant in equation (2) is obtained by analysis of the boundary conditions of the region of interest, as will be illustrated below. The resulting steady-state star distribution will always be valid whenever the local value of τ_R ($\sim 10^8$–10^9 yr in the cores of typical globular clusters) is much less than the timescale for the dynamic evolution of the cluster ($\sim 100\ \tau_R$ for evaporation (see below) and $\sim 10^{11}$ yr for a $10^3 M_\odot$ black hole to swallow its own mass of stars in a globular cluster (A.P.L. and S.L.S., unpublished; J. Frank and M. J. Rees, unpublished)).

Density distribution in a spherical cluster containing a central black hole

Equations (1a, b) and (2) may be used to determine the density distribution in a spherical cluster containing a massive black hole. The cluster may be conveniently divided into four distinct regions.

Region I: central cusp; $r_t < r < r_a$

This innermost region consists of negative energy stars bound to the central black hole. In steady state, the consumption of stars at r_t is balanced by a net inward flux of stars originating from the isothermal core at $r \gtrsim r_a$. Since bound stars of negative energy are removed at r_t, there exists a net outward flux of energy from this region, thereby allowing distant stars to move closer to the black hole to replenish the depleted star distribution. In this region $E(r) \sim -GM/r$, so from equation (2)

$$t_U \propto t_S r^{-1}$$

The absence of outgoing stars at r_t implies that the net diffusion time for stars to move from $2r_t$ to r_t equals the timescale for their (negative) energy to decrease by a factor of two. Thus $t_U(r_t) \sim t_S(r_t)$, and from equation (2)

$$t_U(r) \sim (r_t/r)t_S(r) \qquad (3)$$

For $r > r_t$, t_U is clearly the minimum timescale and can be equated to the relaxation timescale, $t_U \sim t_R \sim \langle v^2\rangle^{3/2}/(G^2m^2n)$. For bound stars near the black hole $\langle v^2\rangle \sim GM/r$, so equation (1b) yields

$$n(r) \propto r^{-7/4} \qquad (4)$$

The above result has been obtained previously (J. Bahcall and R. Wolf, unpublished; A. P. L. and S. L. S., unpublished) by detailed analysis of the steady-state diffusion of stars toward a central black hole. Peebles obtained equation (1a) and assumed the relation $t_S \sim t_R$, thereby overlooking the distinction between t_U and t_S and the fact that nearly equal ingoing and outgoing star fluxes at r result in a reduced net inward flux. His resulting solution

$$n(r) \propto r^{-9/4}$$

thus requires $t_U(r) < t_R(r)$, which forces stars at small radii $r' \ll r$ (and so small $t_R' \ll t_R$) to move towards r and results in a net outward star flux in violation of the boundary conditions. In region III of the globular cluster, t_S is the minimum diffusion timescale, rather than t_U, and there t_S can be equated to t_R legitimately.

Region II: isothermal core; $r_a < r < r_c$

In this region, which contains most of the cluster mass, thermal equilibrium prevails with a Maxwellian velocity distribution law and an isothermal density distribution law. To lowest order $S \sim U \sim 0$. In each relaxation time t_R (r_a), only those few high velocity stars on the tail of the distribution with velocities exceeding the escape velocity

$$\langle v_{esc}{}^2\rangle^{1/2} = 2\langle v^2\rangle^{1/2}$$

(roughly 1% of the total number) evaporate[7,8] from the core and populate the halo. The outer radius of the core r_c is determined by equating the local relaxation time $t_R(r_c)$ to the mean evaporation timescale, $\sim 100t_R(r_a)$; stars with $r > r_c$ cannot thermalise sufficiently rapidly to maintain thermal equilibrium in the presence of escaping stars. Since

$$t_R(r) \propto n^{-1}$$

in the isothermal core, we have

$$n(r_c)/n_a \sim 10^{-2}$$

or

$$r_c \sim 10/(12\pi G n_a m/\langle v^2\rangle)^{1/2}$$

where we use the standard isothermal profile in the region $r_a < r < r_c$. Detailed numerical calculations[9] confirm this qualitative picture.

Region III: halo; $r_c < r < r_{\varepsilon_2}$

The cluster halo is populated by high energy, bound stars ejected from the isothermal core. Halo stars move in highly eccentric orbits and, in each orbital period, penetrate the dense core where they suffer repeated, small angle gravitational encounters. Since all halo stars move with nearly the same velocity during their periastron passage through the core, they all experience roughly the same r.m.s. energy boost, ε_2, each period, independent of their energy E. Consequently, ε_2 is given by the (random walk) relation

$$\varepsilon_2 \sim \left(\frac{t_d}{t_R}\right)^{1/2} E = \text{constant} \qquad (5)$$

where

$$t_d \sim 2\pi G M_c/(2|E|)^{3/2}$$

is the ($\sim$ Keplerian) orbital period of a halo star of energy $E \sim -GM_c/r$. Equation (5) implies that

$$t_R(r) \propto r^{-1/2}.$$

In steady state, a constant net flux of stars moves outwards in the halo, providing a constant escape rate of positive energy stars ejected from the outermost halo or 'fringe' beyond $r \gtrsim r_{\varepsilon_2}$. At $r_{\varepsilon_2} \sim GM/\varepsilon_2$, stars can acquire positive energy in just one additional passage through the core. Since at r_{ε_2} there are no ingoing stars, we have, in analogy to the discussion for

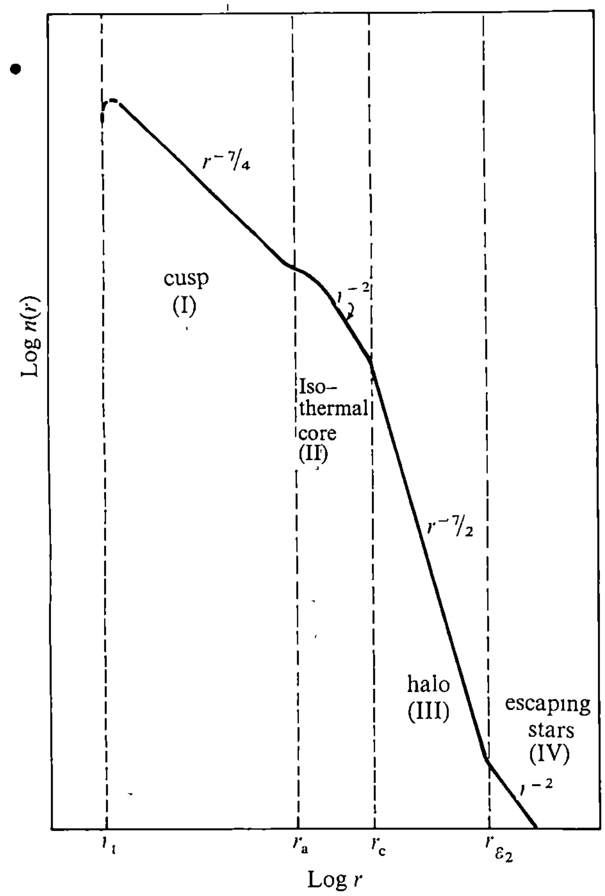

Fig. 1 The stellar density $n(r)$ as a function of radius r in a spherical cluster containing a massive, central black hole (see text for discussion of the different regions).

region I, $t_U(r_{\varepsilon_2}) \sim t_S(r_{\varepsilon_2})$. Equation (2) then implies

$$t_U(r) \sim (r_{\varepsilon_2}/r)t_S(r) \qquad (6)$$

In the halo, $r_c < r < r_{\varepsilon_2}$, t_S is now the minimum timescale; and so $t_S(r) \sim t_R(r)$. This disparity in diffusion timescales merely reflects the fact that energy is nearly conserved in a cluster experiencing stellar evaporation. Substituting

$$t_S(r) \sim t_R \sim r^{-1/2}$$

into equation (1a) yields the halo density distribution law

$$n(r) \propto r^{-7/2} \qquad (7)$$

Region IV: escaping stars; $r_{\varepsilon_2} < r < \infty$

In this non-thermal region, unbound, non-interacting stars with energy $E \sim \varepsilon_2$ move radially outwards to infinity with constant velocity

$$v_\infty \sim (\varepsilon_2)^{1/2}$$

A steady state requires $S \sim nv_\infty r^2 =$ constant, hence

$$n(r) \propto r^{-2} \qquad (8)$$

Similarly, $U \sim S\varepsilon_2 \sim$ constant. The above results derived for regions II–IV pertain with or without a central black hole, provided $M \ll M_c$. Detailed numerical calculations of the outer regions of a spherical cluster confirm[10] equations (7) and (8).

The entire run of the stellar density in a spherical cluster containing a central black hole is illustrated schematically in Fig. 1. For a $10^3 M_\odot$ black hole at the centre of the globular cluster NGC7078 (M15), where[11] $\langle v_\parallel^2\rangle^{1/2} \sim 10$ km s^{-1}, $n(r_a) \sim 5\times10^4$ pc^{-3} and $m \sim M_\odot$, the critical radii separating the different regions are (approximately) $r_t \sim 3\times10^{-7}$ pc, $r_a \sim 3\times10^{-2}$ pc, $r_c \sim 3$ pc, and $r_{\varepsilon_2} \sim 10^3$ pc. Since r_{ε_2} is larger than the tidal radius of the cluster in the galactic field, the stellar distribution in the outer halo will be modified as the energy required for escape falls below zero. By observing the stellar density distribution in the core of globular clusters with a large telescope, black holes with masses $> 10^3 M_\odot$ may be detected (J. Bahcall and R. Wolf, unpublished).

We thank E. E. Salpeter for several useful discussions, and the NSF for support.

Received March 25, accepted July 7, 1976.

[1] Bahcall, J., and Ostriker, J. P., *Nature*, **256**, 23 (1975).
[2] Silk, J., and Arons, J., *Astrophys. J. Lett.*, **200**, L131 (1975).
[3] Peebles, P. J. E., *Astrophys. J.*, **178**, 371 (1972).
[4] Peebles, P. J. E., *Gen. Rel. Grav.*, **3**, 63 (1972).
[5] Antonov, V. A., *Bull Leningrad State Univ.* (*Ser. Math. Mech. Astr.*), **7**, 135 (1962).
[6] Lynden-Bell, D., and Wood, R., *Mon Not. R. astr. Soc.*, **138**, 495 (1968).
[7] Chandrasekhar, S., *Principles of Stellar Dynamics* (University of Chicago Press, Chicago, 1942).
[8] Spitzer, L., *Astrophys. J.*, **127**, 544 (1958).
[9] Spitzer, L., and Hart, M. H., *Astrophys. J.*, **166**, 483 (1971).
[10] Spitzer, L., and Shapiro, S. L., *Astrophys. J.*, **173**, 529 (1972).
[11] Peterson, C. J., and King, I. R., *Astrophys. J.*, **80**, 427 (1975).

Plutonium levels in Kwajalein Lagoon

V. E. Noshkin, R. J. Eagle & K. M. Wong

Biomedical and Environmental Research Division, Lawrence Livermore Laboratory, University of California, Livermore, California 94550

Reported plutonium levels in fish from both Kwajalein and Enewetak lagoons, suggest that Kwajalein Lagoon contains significantly more plutonium in its environment than would be expected from worldwide fallout levels alone, although quantities of plutonium greater than fallout concentrations have not been detected in the lagoon water. If there is no reason to reject the published fish data, then individuals on Kwajalein Atoll who supplement their diet with foods from the local marine environment may have plutonium body burdens similar to the low levels predicted for individuals on similar diets at Enewetak Atoll.

KWAJALEIN ATOLL (9°N 167°40′E) is located in the western (Ralik) chain of the Marshall Islands. In the same island chain and some 300 miles to the north-west is Enewetak Atoll (11°20′N 162°20′E), one of the United States nuclear testing sites during the 1940s and 1950s. It has been reported[1] that no immediate debris from the nuclear tests at Enewetak and Bikini (another Pacific test site) was deposited at Kwajalein. Measurements during 1972 and 1973 between 5 and 15°N, over a wide range of longitudes, indicated concentrations of between 0.22 and 0.44 pCi m^{-3} for ^{239,240}Pu in Pacific surface water[2,3]. The mean ^{239,240}Pu concentration in the surface waters of Kwajalein and other Pacific atoll lagoons located in this latitude band, therefore, would be expected to be similar to the surface oceanic level (0.34±0.11 pCi m^{-3}).

Table 1 Lognormal median concentrations of ^{239,240}Pu in fish tissues (pCi g^{-1} dry weight) collected at Enewetak and Kwajalein atolls*

	Enewetak Atoll (all samples)			Kwajalein Atoll			Enewetak Island	
			Kwajalein Island		Meck Island			
All fish species								
Bone	0.038	(24)	0.086	(3)				
Muscle	0.013	(123)	0.023	(11)	0.01	(6)	0.53	(3)
Gut	0.45	(6)	0.051	(3)			0.42	(2)
Surgeonfish								
Muscle	0.028	(28)	0.02	(3)			0.96	(1)
Gut	0.019	(26)	0.03	(2)			0.43	(1)
Mullet								
Muscle	0.014	(25)						
Gut	0.75	(19)						
Goatfish								
Muscle	0.008	(21)						
Gut	0.093	(18)						
All other fish								
Bone	0.038	(24)	0.086	(3)				
Muscle	0.009	(49)	0.024	(8)	0.01	(6)	0.40	(2)
Gut	0.25	(44)	0.14	(1)			0.41	(1)

*See refs 1 and 5.

†Values in parentheses are numbers of samples analysed. Average muscle and gut values in pCi g^{-1} dry weight can be converted to average pCi g^{-1} wet weight by dividing by 3.5.

This is not true of Enewetak Lagoon. In late 1972, the average measured concentration of ^{239,240}Pu in the lagoon surface water[3] was 39 pCi m^{-3}, approximately 100 times the level predicted from worldwide fallout. Clearly, some components of the atoll contaminated by fallout debris during the tests are contributing substantial amounts of ^{239,240}Pu to the lagoon water masses. The difference in ^{239,240}Pu concentrations between the two lagoons is a direct reflection of the activity levels in the environments of the two atolls. It also follows that if plutonium uptake in living organisms is expressed in terms of a concentration factor (the concentration of plutonium in the tissue of the marine organism divided by its concentration on an equivalent weight basis in the surrounding water), invertebrates, fish, or other marine organisms can be useful as indicator species of the level of environmental contamination.

Schell and Watters[4] have given ^{239,240}Pu concentrations in various organs of selected marine organisms collected at Enewetak and Kwajalein atolls. They concluded, however, that the plutonium and americium concentrations in the convict surgeon fish from Enewetak Atoll, for example, are not significantly higher than those measured at the control station, Kwajalein Atoll. The mantle and muscle tissues of a clam (*Tridacna* sp.) collected in the south-eastern region of Enewetak Atoll were, moreover, found to contain only one-sixth as much plutonium as those of a *Tridacna* sp. collected at Kwajalein Atoll[4]. On the other hand, the viscera and kidney of the same Enewetak Atoll clam had higher concentrations than those of the Kwajalein Atoll specimen.

In an assessment of the possible plutonium dose to man from food and other environmental pathways, Wilson *et al.*[5] compiled, in the form of lognormal median concentrations, all the plutonium survey data collected at Enewetak Atoll during 1972 and 1973 (ref. 1). The concentration values for all the fish muscle samples taken are reproduced here in Table 1, together with similar lognormal mean concentrations compiled from the same survey[1] data for fish bone and gut from Enewetak Atoll and muscle, bone, and gut concentrations, also from the same survey data[1], for fish collected off three islands of Kwajalein Atoll (W. R. Robison, private communication). Wilson *et al.*[5] found no significant differences in mean plutonium concentrations among four fish groups, which included, among others, planktonic and detritus feeders, grazing herbivores, bottom-feeding carnivores, and pelagic carnivores. Accordingly, they based their predictions of exposures to plutonium from ingestion of marine foods on the mean concentration of plutonium in the muscles of all the fish taken from the lagoon of Enewetak Atoll. Significantly, however, the ^{239,240}Pu in the lagoon water ranged from 1 to 96 pCi m^{-3} at the fish sampling sites[1].

Radionuclide concentration independent of environment?

The data of Schell and Watters[4], together with those of Table 1, show that average levels of ^{239,240}Pu in fish bone, muscle, and gut from Enewetak Atoll are similar to, or even lower than, those of the fish indigenous to the control station, Kwajalein Lagoon. There are several possible important conclusions that can be derived from these data. The first is that fish collected for consumption by man will contain, on average, essentially the same concentrations of plutonium radionuclides regardless of the source or level of plutonium in the local environment. Obviously, such a conclusion would greatly affect future plans for releasing low-level transuranics to the marine environment. Furthermore, it would force us to concede that the concept of a plutonium concentration factor for fish is meaningless. Also, it conflicts with a large body of plutonium concentration data for Atlantic fish species that derive their plutonium body burdens from worldwide fallout levels in the Atlantic Ocean. For example, for a number of Atlantic species, including bottom feeders, water-column feeders, and large predators[6-8], a lognormal median of all available bone concentration data is only 1×10^{-4} pCi g^{-1} (wet or dry), 900 times less than that for the bones of the Kwajalein fish (Table 1). A similar large discrepancy remains when the concentrations in the muscle of the Atlantic and Kwajalein fish are all normalised to an equivalent weight basis (wet or dry).

Plutonium levels in the Atlantic waters (where some of the fish were caught) range only between 0.2 and 1.1 pCi m^{-3}, according to Bowen *et al.*[8]. Calculating a concentration factor from the data for Atlantic fish and water and using a value of 0.4 pCi m^{-3} as the assumed mean plutonium level from fallout in the Kwajalein Lagoon, provides values of between 0.2 and 1.0 10^{-4} pCi g^{-1} for the bone of fish for this lagoon. These values are orders of magnitude lower than the lognormal median concentrations in Table 1. This discrepancy cannot be accounted for by any possible differences related to trophic levels or feeding habits. A similar calculation also yields large discrepancies between predicted and measured concentrations for fish muscle.

Excess plutonium at Kwajalein

An alternative explanation to account for these discrepancies would be that Kwajalein Lagoon contains significantly more plutonium in its environment than would be expected from worldwide fallout levels alone. To test this possibility, 55 l unfiltered water samples were collected during May and June of 1975 from the locations shown in Fig. 1. During June, two samples were also collected outside the Atoll in the north equatorial surface waters, to provide information on the plutonium levels in the open ocean in this region. Unfortunately, our schedule did not allow time to collect fish on Kwajalein Atoll.

The water samples were analysed for ^{239,240}Pu and ^{137}Cs using the methods described in refs 9 and 10. Our analytical results are shown in Table 2. Although the lagoon was not sampled in great detail, the data are sufficient to show that the average ^{239,240}Pu concentration in Kwajalein Lagoon (0.45 ± 0.21 pCi m^{-3}) is nearly the same as the mean for the surface water of the ocean in the area, and that it agrees reasonably well with the levels previously predicted from worldwide fallout.

At the time the Kwajalein water samples were being processed we were also participating in an intercomparison exercise with Woods Hole Oceanographic Institution to determine ^{239,240}Pu levels in replicate surface-water samples from one location in the North Atlantic. The mean value for eight samples from Woods Hole (V. T. Bowen, unpublished) was 0.63 ± 0.16 pCi m^{-3}, whereas ours for 10 samples was 0.70 ± 0.30 pCi m^{-3}. This analytical agreement (as well as that in other national and international intercomparisons that we have completed) lends a measure of confidence to our data. In addition, these comparative data show that, as expected from worldwide depositional data[11], average plutonium levels are somewhat lower in Kwajalein Lagoon than in North Atlantic surface waters. The average ^{239,240}Pu/^{137}Cs ratio of 0.0032 for Kwajalein Lagoon is also in good agreement to the average value for open ocean, in contrast to the ratio of 0.07–0.12 in the Bikini and Enewetak lagoons[3]. This illustrates that both the ^{239,240}Pu and the ^{137}Cs content of the lagoon are derived from worldwide fallout.

We are still without an obvious explanation for the discrepancy in the fish-tissue data; that is, why should the Kwajalein fish, in a region of the equatorial Pacific contaminated only by worldwide fallout, have significantly higher body burdens of plutonium than fish in the North Atlantic which is also contaminated only with worldwide fallout? Furthermore, why do the Kwajalein Atoll fish have the same or even higher body burdens than the fish at Enewetak Atoll, where higher levels of plutonium are found in the lagoon? And why were the concentrations in Enewetak Lagoon fish not correlated with those in the specific local environment where they were sampled, or with feeding habit or trophic level? A cursory search of the literature surprisingly revealed only one other relevant fallout report—the plutonium level in the body of a single marine fish in fallout-contaminated waters of the Pacific[12]. The plutonium concentration in this sample and the computed concentration factor are closer to those from the North Atlantic fish than to those from Kwajalein. On the other hand, plutonium levels in tissues from catfish from Trombay[13], in plaice from the vicinity of Windscale[14], and in several species from areas of Thule[15] are higher than those in the tissues of the North Atlantic fish, and close in value to those from Kwajalein and Enewetak. But as the last three sets of data are from areas known to have local plutonium contamination from reprocessing plants (and one nuclear accident), they support our argument that levels of plutonium in fish reflect local environmental levels.

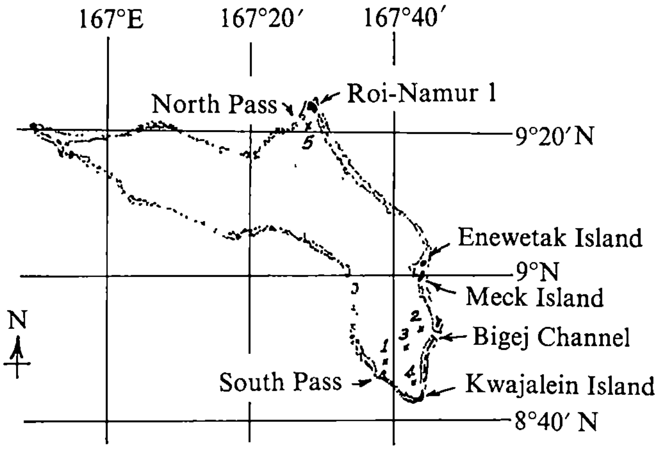

Fig. 1 Locations of sampling sites (see Table 2).

To sum up, it appears that available plutonium data from fish tissues are inconsistent. If we accept the available Enewetak and Kwajalein Atoll data as correct, then we can only conclude that the availability to all fish and invertebrates of plutonium from fallout, or for that matter from any local source, depends more on the type of environment than on the plutonium levels in that environment. The data could also suggest that coral atolls may have specific biogeochemical processes that regulate the availability of plutonium regardless of levels in the environment or in food. On the other hand, if we assume that concentrations in fish and invertebrates are proportional to those in the environment, then we can only conclude that many of the atoll fish data from the laboratories involved in analytical programmes[1,4] are in error. Since there is no other evidence at this time to refute the analytical results from the atolls, we can only urge caution in applying concentration factors measured in one marine area to predict approximate plutonium levels in fish from other marine areas. In addition, it seems, on the basis of the published data[1,4] and the summary assembled in Table 1, that individuals on Kwajalein Atoll who supplement their diet with foods from the local marine environment may have plutonium body burdens similar to the low levels predicted[5] for individuals at Enewetak on similar diets.

Table 2 Concentrations of ^{239,240}Pu and ^{137}Cs (pCi m^{-3}) in seawater in Kwajalein Lagoon and two locations in north equatorial waters

Station*	Depth (m)	Collection date	^{239,240}Pu	^{137}Cs	^{239,240}Pu/^{137}Cs
1	Surface	5/10/75	0.33 (20)†	137 (3)	0.0024 (20)
1	44	5/10/75	0.87 (13)	144 (5)	0.0060 (14)
2	Surface	5/08/75	0.29 (27)	131 (5)	0.0022 (27)
3	Surface	5/08/75	0.26 (24)	127 (3)	0.0020 (24)
3	47	5/08/75	0.33 (25)	129 (3)	0.0026 (25)
4	Surface	5/08/75	0.54 (16)	129 (4)	0.0041 (16)
5	Surface	6/14/75	0.52 (18)	132 (4)	0.0039 (18)
10°26′N 166°31′E	Surface	6/15/75	0.36 (32)	132 (3)	0.0027 (32)
11°16′N 165°45′E	Surface	6/15/75	0.53 (23)	143 (4)	0.0037 (23)

*Kwajalein stations are shown in Fig. 1.
†Values in parentheses are the 1σ counting errors expressed as percentages of the listed values.

This work was performed under the auspices of the US Energy Research and Development Administration.

Received April 14, accepted June 26, 1976.

[1] *Enewetak Radiological Survey, Nevada Operations Office, Las Vegas, Nevada, Rep NVO-140*, I-III (1973).
[2] Miyake, Y., and Sugimura, Y., in *Int Symp. on Transuranium Nuclides in the Environment, 1975* (Int Atomic Energy Agency, Vienna, in the press)
[3] Noshkin, V. E., Wong, K. M., Eagle, R. J., and Gatrousis, C., *Lawrence Livermore Laboratory Rep*, UCRL-51612 (1974)
[4] Schell, W. R, and Watters, R. L, *Hlth Phys.*, 29, 589–597 (1975)
[5] Wilson, D. W., Ng, Y C., and Robison, W L., *Hlth Phys.*, 29, 599–611 (1975)
[6] Noshkin, V. E., *Hlth Phys*, 22, 537–549 (1972).
[7] Bowen, V. T., Livingston, H. D, and Burke, J. C., in *Int Symp. on Transuranium Nuclides in the Environment, 1975* (Int. Atomic Energy Agency, Vienna, in the press).
[8] Livingston, H. D., and Bowen, V T., in *Symp. Interaction between Water and Living Matter, 1975* (publisher, in the press)
[9] Wong, K. M., *Analytica chim. Acta*, 56, 355–364 (1971).
[10] Marsh, K M, Wong, K. M, Holladay, G., Noshkin, V. E., and Buddemeier, R, *Lawrence Livermore Laboratory Rep.*, UCRL-51913 (1), (1975)
[11] Hardy, E P, Krey, P. W, and Volchok, H L, *Nature*, 241, 444–445 (1973).
[12] Pillai, K C., Smith, R C, and Folson, T. R, *Nature*, 203, 568–571 (1964).
[13] Pillai, K. C., and Mathen, C., in *Int. Symp Transuranium Nuclides in the Environment, 1975* (Int Atomic Energy Agency, Vienna, in the press).
[14] Hetherington, J. A, Jefferies, D. F, Mitchell, N. T., Pentreath, R. J., and Woodhead, D. S., in *Int. Symp Transuranium Nuclides in the Environment, 1975* (Int Atomic Energy Agency, Vienna, in the press)
[15] Aarkrog, A, *Hlth Phys.*, 20, 31–47 (1971)

Identification of phage SP01 proteins coded by regulatory genes *33* and *34*

Thomas D. Fox*

Biological Laboratories, Harvard University, Cambridge, Massachusetts 02138

Bacillus subtilis *phage SP01 induces polypeptides of 24,000 and 13,500 daltons that are bound to a form of RNA polymerase that directs phage "late" transcription* in vitro. *These proteins are the products of SP01 genes* 34 *and* 33, *regulatory cistrons that control "late" gene expression* in vivo.

GENE expression during the lytic cycle of *Bacillus subtilis* phage SP01 is controlled in a temporally defined sequence[1]. Phage "early" genes are transcribed almost immediately after infection and this RNA synthesis is directed by the sigma subunit of the host RNA polymerase. Next, phage "middle" genes are turned on at 4–5 min into the lytic cycle; this transcription is activated by the protein product of SP01 regulatory gene *28* (refs 2 and 3). Gene *28* is now known to code for a phage-induced protein that binds to *B. subtilis* RNA polymerase[4] and that apparently directs specific transcription *in vitro* in the absence of sigma factor[5–8]. A host protein, δ, has been described that improves the accuracy of middle-gene transcription by the phage-modified RNA polymerase.

Activation of SP01 "late" genes between 8 and 14 min into the lytic cycle seems to require a further modification of RNA polymerase. Pero *et al.*[6] have shown that a form of the *B. subtilis* transcriptase containing phage-induced subunits of 24,000 (termed V) and 13,500 (termed VI) daltons preferentially copies 'late' genes *in vitro*. The work reported here establishes that these phage-induced subunits are coded by SP01 genes *34* and *33*, regulatory cistrons that control late gene expression *in vivo*[2,3]. An accompanying article[9] demonstrates that the purified protein products of genes *33* and *34* and host delta factor act synergistically to direct the synthesis of late RNA by core RNA polymerase.

Induction of polypeptides V and VI by mutants

As an initial step in investigating the possible relationship of phage-induced polypeptides VI and V, to genes *33* and *34*, the synthesis of these proteins in bacteria infected with wild-type SP01 was examined. Cells of a non-suppressing (su^-) strain of *B. substilis* were infected with wild-type phage and pulse labelled with ^{35}S-methionine at an intermediate time in the lytic cycle. RNA polymerase was isolated from an extract of the infected cells by gel filtration and phosphocellulose chromatography. The enzyme was radiochemically highly purified at this stage of purification and contained essentially only host subunits of RNA polymerase and previously identified phage-induced proteins that copurify with polymerase[10]. Phosphocellulose-purified polymerase was then analysed by the two-dimensional gel electrophoresis procedure of O'Farrell[11]; radioactive enzyme was denatured in urea and subjected to isoelectric focusing in the first dimension and sodium dodecyl sulphate (SDS) slab gel electrophoresis in the second dimension. Figure 1*a* is an autoradiogram of a region of the two-dimensional gel that contained a 26,000-dalton polypeptide termed IV (the product of gene *28*)[4], polypeptide V (24,000) and polypeptide VI (13,500). The approximate isoelectric points of proteins IV, V and VI were 5.4, 7.3 and 7.4 respectively. The identification of these proteins was confirmed by a mixing experiment in which the radioactive phosphocellulose-purified polymerase was coelectrophoresed in two dimensions with unlabelled phage-modified enzymes from a previous study[5].

High resolution two-dimensional gel analysis also made possible the identification of polypeptides V and VI in crude extracts of SP01-infected bacteria. Radioactive protein extracted from bacteria infected with wild-type phage was subjected to two-dimensional electrophoresis. Figure 1*b* is an autoradiogram of a region of the gel corresponding to that of Fig. 1*a* and containing polypeptides IV, V, and VI. Since the relative position of spots varied somewhat from gel to gel, it was necessary to identify the phage-induced subunits of RNA polymerase by means of a mixing experiment (not shown) in which radioactive enzyme of Fig. 1*a* was coelectrophoresed with the crude extract of Fig. 1*b* (and with extracts of mutant-infected bacteria described below) Polypeptides V and VI were well resolved from other radioactive proteins and are designated with arrows. Polypeptide IV on the other hand, was partially occluded by another intensely labelled protein and is not designated in the figure.

To examine the effect of a mutation in gene *34* on the synthesis of the phage-induced subunits of polymerase, the su^- bacteria were infected with the nonsense mutant *sus*F4 (refs 2 and 3) and radioactively labelled at an intermediate time in the lytic cycle. Two-dimensional analysis revealed that polypeptide V was specifically lacking in both phosphocellulose-purified polymerase (Fig. 1*c*) and unfractionated extract (Fig. 1*d*) from the mutant-infected cells. This finding is consistent with the possibility that subunit

---

*Present Address: Biozentrum der Universität Basel, Klingelbergstrasse 70, CH-4056 Basel, Switzerland

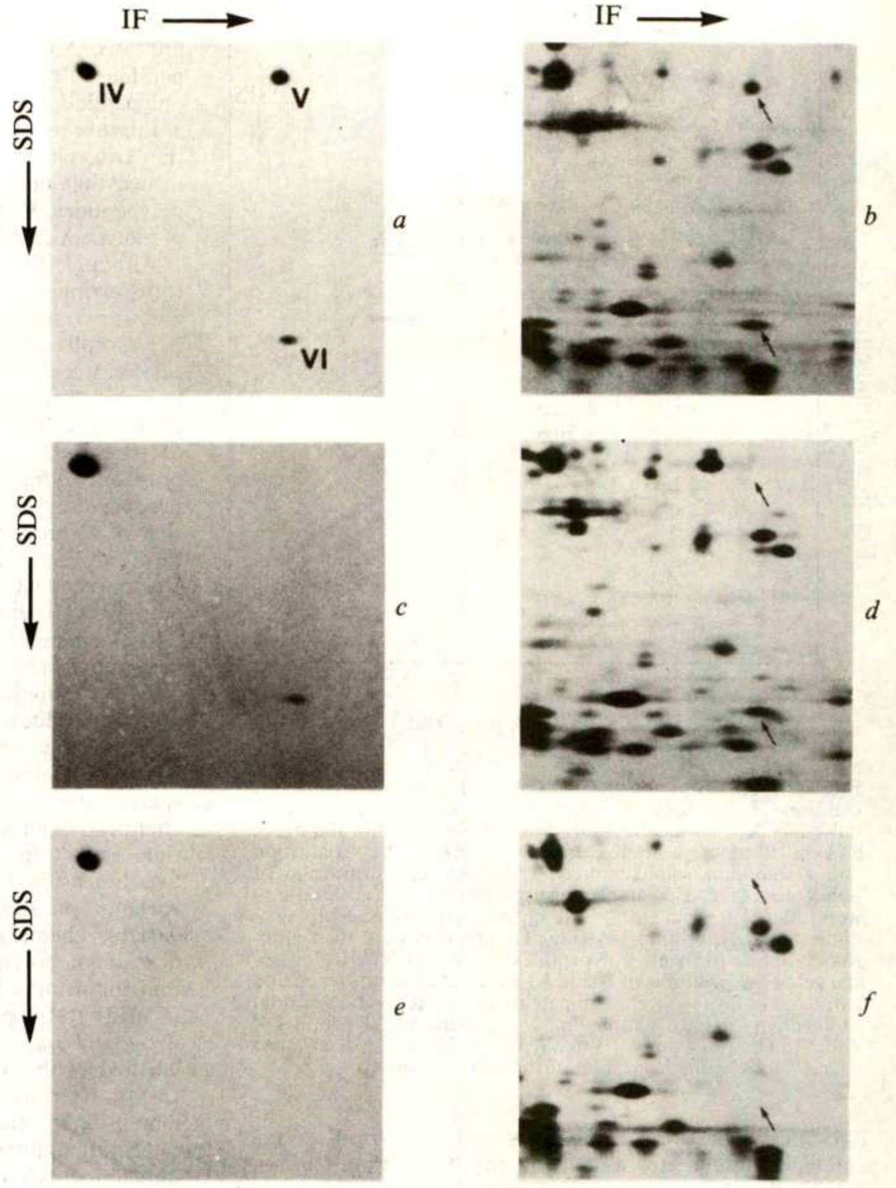

Fig. 1 Two-dimensional electrophoresis of subunits IV, V and VI in RNA polymerase and in crude extracts from non-suppressing bacteria infected with wild-type and mutant phage. The *su*⁻ strain was a methionine prototrophic derivative of *B. subtilis* Mu8u5u6 (ade⁻, leu⁻, met⁻)[12] and was obtained from A. L. Sonenshein. Cells were grown at 37 °C in a modification of 121A medium[13] containing leucine (50 μg ml^{-1}) and adenine (100 μg ml^{-1}). Cultures of the bacteria (150 ml) were labelled by the addition of 2 mCi of ^{35}S-methinoine (high specific activity; prepared as described before[14]) 10–14 min after infection with the mutant (obtained from S. Okubo) and wild-type phage indicated below (multiplicity of infection 5). RNA polymerase (*a*, *c* and *e*) was purified from 0.3 g of infected cells as described before[4], concentrated by trichloroacetic acid precipitation[10] and dissolved in "lysis buffer" (ref. 11, modified to contain 2% ampholines (LKB) *p*H range 3–10). Crude extracts (*b*, *d* and *f*) were prepared from 6 mg of infected cells as follows. Infected cells were suspended in 0.2 ml of buffer containing 0.01 M Tris-HCl (*p*H 7.9), 0.01 M EDTA and lysozyme (300 μg ml^{-1}), incubated for 1 h at 0 °C and then disrupted by brief sonication. Next, $MgCl_2$ (to 0.02 M), RNase and DNase (to 50 μg ml^{-1}) were added. After low speed centrifugation, the resulting supernatant fluids were incubated at 0 °C for 1 h and then added at room temperature to 0.43 ml of the modified "lysis buffer" containing an additional 235 mg of urea. Samples of RNA polymerase (~10^5 c.p.m.) and of crude extract (~2.3×10^6 c.p.m.) in the "lysis buffer" were then subjected to isoelectric focusing as described by O'Farrell[11] but with the following modifications. The gels contained 5.4% polyacrylamide[4] and 1.9% ampholines (LKB) comprised of 1.5% *p*H range 3–10, 0.2% *p*H range 9–11, 0.1% *p*H range 5–7 and 0.1% *p*H range 4–6. The lower electrode (cathode) solution contained 0.4% ethylenediamine. The isoelectric focusing gels were then subjected to electrophoresis in a second dimension through discontinuous SDS slab gels as described[4]. (It should be noted that the separation of subunits IV and V in discontinuous SDS gels is strongly dependent on the commercial brand of SDS (J. Pero, J. Nelson and T.D.F., unpublished results and ref. 15) and that the separation achieved here using a crystalline form of SDS from BioRad is less than was previously obtained using SDS in powdered form from BioRad (refs 5 and 6) and less than can be obtained using SDS from Pierce Chemical Co. (unpublished results).) Each picture is an autoradiogram[16] (100 h exposure) of a region of the two-dimensional gels to which subunits IV, V and VI migrate. The following samples were subjected to electrophoresis: *a*, RNA polymerase from bacteria infected with wild-type SP01; *b*, crude extract of bacteria infected with wild-type SP01; *c*, RNA polymerase from bacteria infected with the mutant *sus*F4; *d*, crude extract of bacteria infected with the mutant *sus*F4; *e*, RNA polymerase from bacteria infected with the mutant *sus*F14; *f*, crude extract of bacteria infected with the mutant *sus*F14. The IF (isoelectric focusing) arrows point in the direction of increasing *p*H; the SDS arrows point in the direction of decreasing molecular weight. The arrows in the autoradiograms of crude extracts indicate the positions of subunits V and VI.

V is the product of gene *34*.

Figure 1*e* and *f* shows the effect of a nonsense mutation in gene *33*, *sus*F14 (refs 2 and 3), on the induction of the phage-induced subunits. Surprisingly, *su*⁻ bacteria infected with the gene *33*⁻ mutant failed to synthesise detectable quantities of both polypeptides VI and V (although in experiments comparable with Fig. 1*f* faint traces of a protein in the position of V were observed). This finding is consistent with an assignment of subunit VI as the product of gene *33* if, as discussed below, the *sus*F14 mutation in gene *33* somehow interferes with the synthesis of polypeptide V, the putative product of gene *34*.

Although mutations in either gene *33* or gene *34* alone interfere with the global transcription of late genes[2,3], close inspection of Fig. 1 reveals certain protein species whose synthesis is blocked uniquely in either the gene *33*⁻ or the gene *34*⁻ mutants. While this has yet to be investigated, the kinds of arguments used to explain the pleiotropic effect of *sus*F14 on the synthesis of polypeptide V (see below) could be applied here.

The ability to detect polypeptides V and VI in crude extracts by means of two-dimensional gel analysis made it possible to determine whether the synthesis of these proteins is induced at a middle time in the phage lytic cycle, as would be expected for regulatory proteins that control late gene expression. Bacteria were infected with wild-type SP01 and then pulse labelled at various times after infection. Crude extracts of the infected cells were then subjected to two-dimensional gel electrophoresis. Figure 2 indicates the proportion of total radioactivity that was incorporated into proteins V and VI during each pulse-labelling period. These results indicate that the synthesis of polypeptides V and VI was turned on synchronously at a middle time in the lytic cycle, after the appearance of polypeptide IV, the product of the early gene *28*, but before the onset of late protein synthesis (not shown).

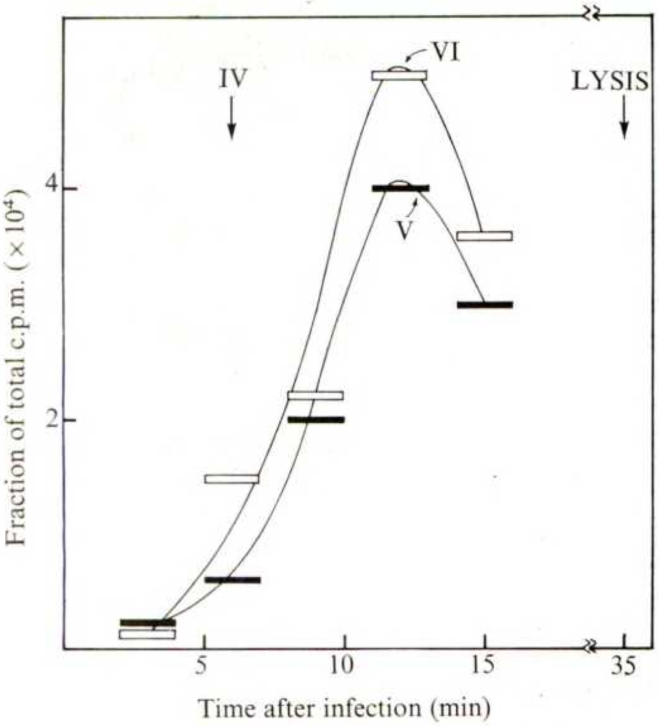

Fig. 2 Time course for the induction of subunits V and VI. Cultures of *su*$^-$ bacteria were infected with wild-type SP01, pulse labelled during the 2-min intervals indicated in the figure and chilled quickly. Crude extracts were prepared by sonication and ammonium sulphate precipitation as for purification of polymerase (Fig. 1). Samples of each extract ($\sim 8 \times 10^6$ c.p.m.) were diluted tenfold into "lysis buffer" and subjected to two-dimensional electrophoresis (Fig. 1). The gels were then autoradiographed to locate polypeptides IV, V and VI. Regions of the gel in the positions of V and VI were cut out, moistened and extracted in Protosol. The ordinate indicates the fraction of total radioactivity in each sample that was present in polypeptides V and VI. The peak time of subunit IV synthesis was determined by visual inspection of the autoradiograms.

(Two-dimensional electrophoresis did not resolve polypeptide IV sufficiently well to quantitate its time course of appearance. But the synthesis of this regulatory protein could be followed by visual inspection of the autoradiograms, and the arrow in Fig. 2 indicates the peak time of subunit IV synthesis.) The findings of Fig. 2 agree with a study[10] that compared the time of appearance of polypeptides IV and V in association with RNA polymerase at different times in the lytic cycle.

Gene *34* codes for subunit V

To test directly whether subunit V is the protein product of gene *34*, the gene *34*$^-$ nonsense mutant *sus*F4 was grown in two different suppressor (*su*$^+$) strains of *B. subtilis* that carried the nonsense suppressors *sup-1*[17,18] and *sup-3*[19,20] in isogenic backgrounds. The *sup-1* and *sup-3* suppressors are thought to insert different amino acids[12] and a recent study in this laboratory[4] indicated that the amino acid inserted by *sup-3* is more basic (or less acidic) than the residue inserted by *sup-1*. Thus, if subunit V is the product of gene *34*, then polypeptide V generated by suppression of *sus*F4 with *sup-3* ought to be slightly more basic than the corresponding protein generated by suppression with *sup-1*. This strategy was previously used to assign subunit IV as the product of gene *28* (ref. 4).

To test the prediction that suppression would generate altered forms of polypeptide V, radioactively labelled RNA polymerase was separately purified by phosphocellulose chromatography from *sus*F4-infected bacteria carrying either *sup-1* or *sup-3*. The phosphocellulose-purified enzymes were then subjected to two-dimensional gel electrophoresis. A comparison of Fig. 3*a* and *b* suggests that polypeptide V from *sup-3* bacteria was slightly more basic than polypeptide V from the *sup-1* bacteria. Electrophoresis of a mixture of the phosphocellulose-purified enzymes from the two phage-infected suppressor-strains (Fig. 3*c*) confirmed that nonsense suppression had generated variants of polypeptides V but had not affected the isoelectric points of polypeptides IV and VI.

Although the two supressor strains were constructed by transferring (by means of genetic transformation) the *sup-1* and *sup-3* suppressors into the same genetic background, it was still conceivable that the altered forms of polypeptide V were caused by some unknown difference between the suppressor strains other than the nonsense suppressors themselves. Therefore, to examine whether the generation of variants of polypeptide V was related directly to suppression of the *sus*F4 mutation, the isoelectric point of V produced by *sus*F4 in *sup-3* bacteria was compared with that of V produced by a spontaneous revertant of *sus*F4 in the same *sup-3* strain. Figure 3*d* and *e* shows that subunit V induced by the revertant was less basic than the corresponding polypeptide induced by the nonsense mutant. (Subunit V induced by the revertant in *sup-3* bacteria was indistinguishable from the corresponding protein generated by suppression of *sus*F4 in *sup-1* bacteria or the protein produced by wild-type SP01 in *su*$^-$ bacteria.)

A possible complication in analysis of the isoelectric points of proteins is that charge changes in a single protein species can arise artefactually *in vitro* as a result of chemical modification, and cause the appearance of "multiple spots" in the isoelectric focusing dimension of the two-dimensional gels[11]. To eliminate the possibility that the variants of subunit V had actually been produced by variable chemical modification *in vitro*, either during purification of polymerase or during two-dimensional analysis, the following 'double-label' mixing experiment was performed. RNA polymerase was purified from a mixture of *sup-1* and *sup-3*-carrying bacteria that had been separately labelled with ^{3}H-methionine and ^{35}S-methionine, respectively, after infection with the mutant *sus*F4. After two-dimensional electrophoresis, the distribution of each radioisotope in the isoelectric focusing dimension was determined for subunits IV, V and VI. While the distribution of both radioisotopes was identical for polypeptides IV and VI (Fig. 4*a* and *c*), the ^{35}S radioactivity in subunit V from the *sup-3* bacteria was in a more basic position than the ^{3}H radioactivity from the *sup-1* strain (Fig. 4*b*). The reverse "double-label" mixing experiment (not shown), with ^{35}S-labelled *sup-1* bacteria and ^{3}H-labelled *sup-3* bacteria, confirmed that the form of subunit V induced by *sus*F4 in *sup-3* cells was more basic than that induced by the mutant in the *sup-1* strain.

Gene *33* codes for subunit VI

If subunit VI is the product of gene *33*, then suppression of the gene *33*$^-$ nonsense mutation, *sus*F14, should generate altered forms of polypeptide VI without affecting the isoelectric point of subunits IV and V. The experiment shown in Fig. 3 confirms this prediction; *sus*F14 growing in *sup-3* bacteria produced a more basic form of VI (Fig. 3*g*) than that produced by *sus*F14 in *sup-1* bacteria (Fig. 3*f* and *h*) or that produced by a spontaneous revertant of *sus*F14 in *sup-3* bacteria (Fig. 3*i* and *j*) (or that produced by wild-type phage in *su*$^-$ bacteria).

Close examination of Fig. 3*i* and *j* reveals a faint spot of radioactivity on the acidic side of VI; this is probably attributable to charge heterogeneity introduced *in vitro* as referred to above. The "double-label" mixing experiment of Fig. 4 (as well as a corresponding experiment with the radioactive isotopes reversed) eliminates the possibility,

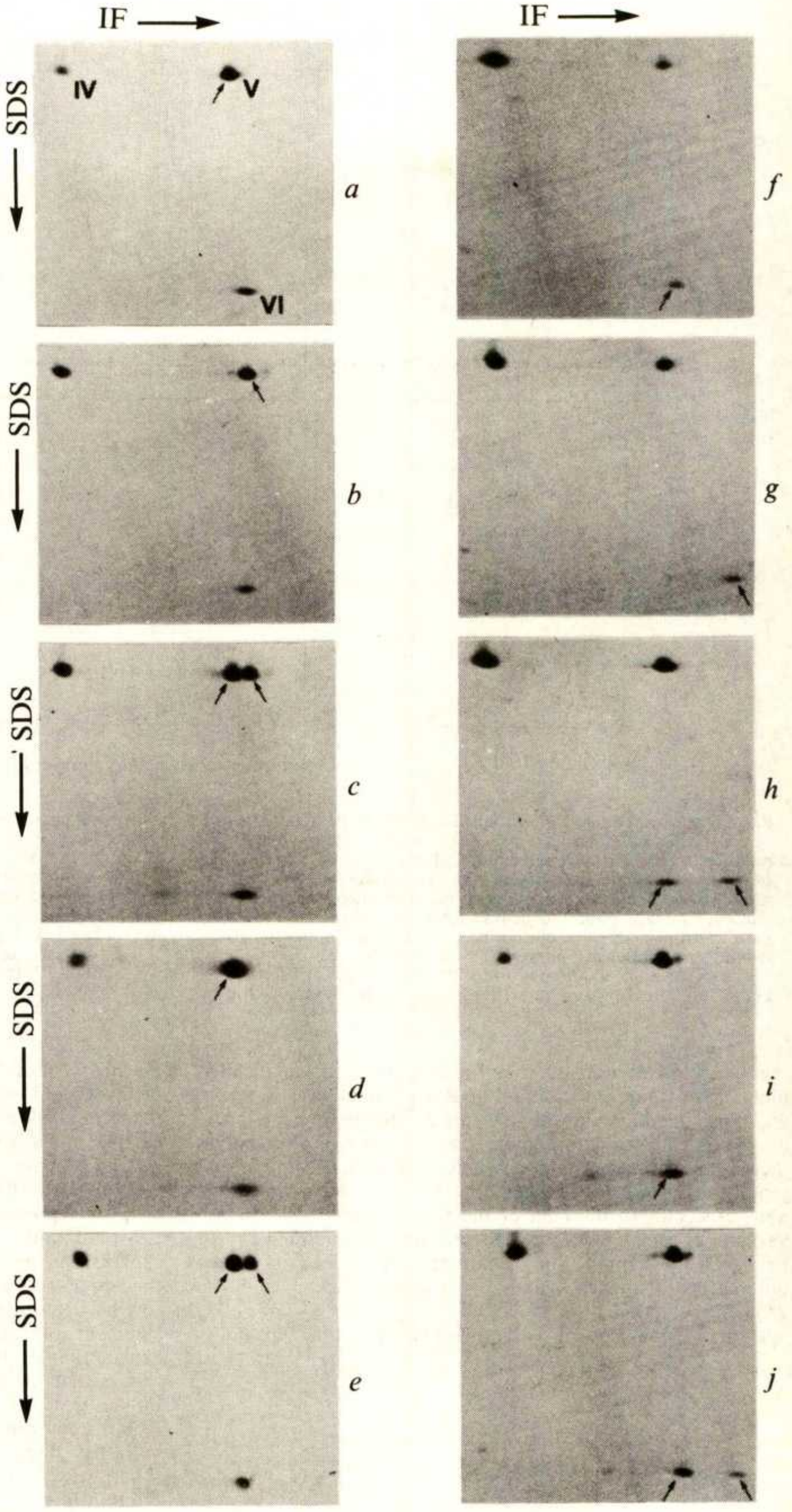

Fig. 3 Two-dimensional electrophoresis of RNA polymerase from *sup-1* and *sup-3* bacteria infected with SP01 nonsense mutants. Strains of *B. subtilis* carrying the nonsense suppressors *sup-1* and *sup-3* in isogenic backgrounds were constructed by transformation[21] of the su^- strain Mu8u5u6 (Fig. 1) with DNA from the *sup-1* strain HA-101-B (ref. 15) and the *sup-3* strain su^+3 (ref. 17). Suppressor-carrying transformants were isolated by selecting simultaneously for adenine and methionine prototrophy; the *purB6* and *metB5* mutations in Mu8u5u6 are suppressable markers[12,19]. Purification and two-dimensional electrophoresis of RNA polymerase from phage-infected cells were as described in the legend to Fig. 1 except that the bacterial growth medium did not contain adenine. The autoradiograms are from electrophoreses of the following enzymes: *a*, RNA polymerase from *sup-1* bacteria infected with the mutant *sus*F4 (gene *34*$^-$); *b*, RNA polymerase from *sup-3* bacteria infected with the mutant *sus*F4 (gene *34*$^-$); *c*, a mixture of the enzymes from the experiments of *a* and *b*; *d*, RNA polymerase from *sup-3* bacteria infected with a spontaneous revertant of the mutant *sus*F4 (isolated by plating mutant phage on su^- bacteria); *e*, a mixture of the enzymes from the experiment of *b* and *d*; *f*, RNA polymerase from *sup-1* bacteria infected with the mutant *sus*F14 (gene *33*$^-$); *g*, RNA polymerase from *sup-3* bacteria infected with the mutant *sus*F14 (gene *33*$^-$); *h*, a mixture of the enzymes from the experiments of *f* and *g*; *i*, RNA polymerase from *sup-3* bacteria infected with a spontaneous revertant of the mutant *sus*F14 (isolated by plating mutant phage on su^- bacteria); *j*, a mixture of the enzymes from the experiments of *g* and *i*.

however, that the difference in charge of the *sup-1* and *sup-3*-generated variants of polypeptide VI could have been caused completely by variable chemical modification introduced *in vitro*. Figure 4 also confirms that suppression of the gene *33*$^-$ nonsense mutant had specifically affected the isoelectric point of VI (Fig. 4*f*) without affecting subunits IV (Fig. 4*d*) or V (Fig. 4*e*).

Scheme for regulation

The finding that altered forms of polypeptides V and VI can be generated independently by suppression of nonsense mutations in SP01 genes *34* and *33* strongly suggests that these phage-induced subunits of RNA polymerase are coded by the regulatory cistrons that control late gene expression. A complicated alternative interpretation is that the SP01

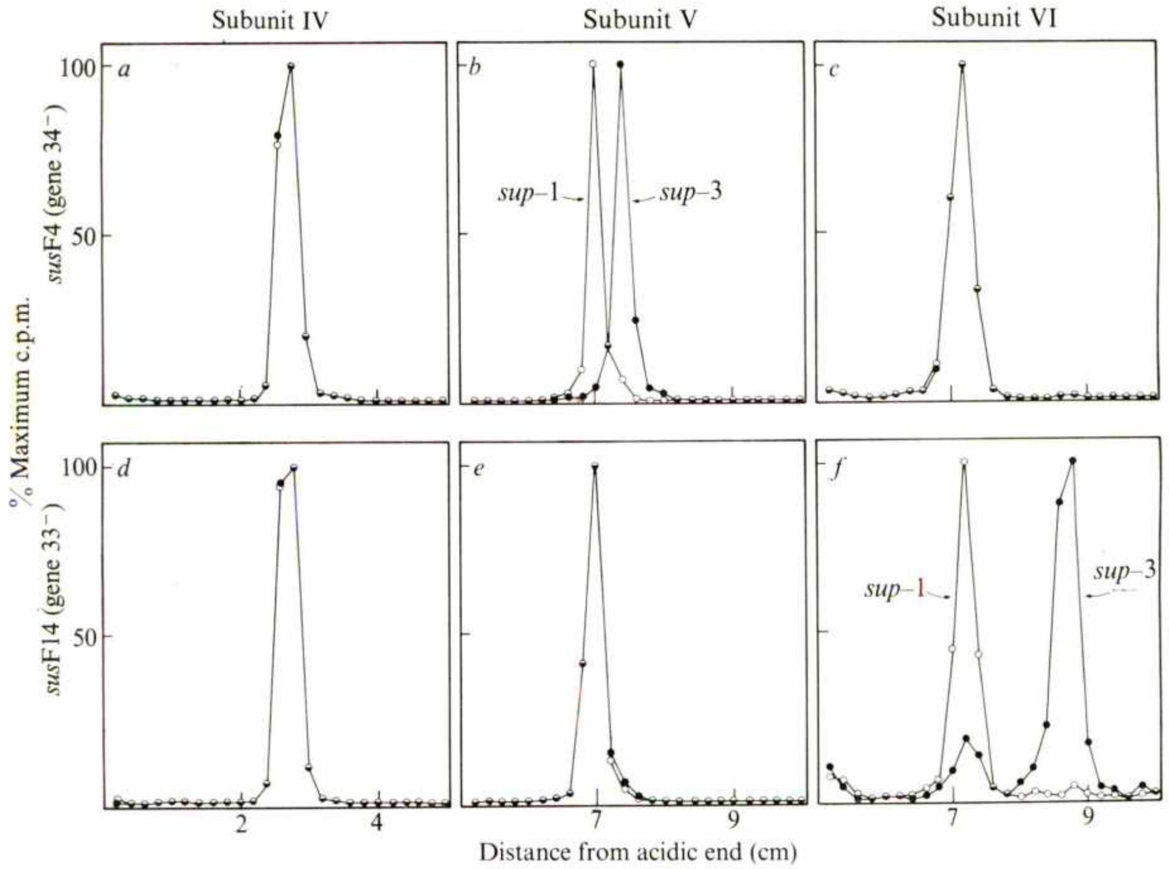

Fig. 4 Isoelectric focusing of subunits IV, V and VI from mixtures of *sup-1* and *sup-3* bacteria separately labelled with different radioisotopes after phage-infection. Cultures of *sup-1* and *sup-3* bacteria were labelled separately with ^{3}H-methionine (Schwarz/ Mann) and ^{35}S-methionine respectively, after infection with the nonsense mutant indicated below. RNA polymerase was then purified from a mixture of the infected cells and subjected to two-dimensional electrophoresis as described in the legend to Fig. 1. After autoradiography to locate the position of subunits IV, V and VI, strips were cut from the gels along the isoelectric focusing dimension at the positions of IV, V and VI in the SDS dimension. Each strip was then cut into 2-mm slices and the amount of ^{3}H (○) and ^{35}S (●) in each slice was measured in a scintillation counter after moistening and extracting the slices in Protosol. *a–f* show the distribution of each radioisotope along the IF dimension in *a*, subunit IV from *sus*F4 infected cells; *b*, subunit V from *sus*F4-infected cells; *c*, subunit VI from *sus*F4-infected cells; *d*, subunit IV from *sus*F14-infected cells; *e*, subunit V from *sus*F14-infected cells; *f*, subunit VI from *sus*F14-infected cells.

regulatory genes actually code for enzymes that chemically modify SP01-induced subunits of RNA polymerase *in vivo*, and that modifications by the *sup-3*-suppressed gene products somehow generate more basic (or less acidic) polymerase subunits than modifications by the *sup-1* suppressed gene products. This interpretation, however, seems improbable, especially in the light of the fact that isoelectric point variants of three different proteins can be generated independently by suppression of nonsense mutations in three different SP01 genes (genes *33* and *34*, Figs 3 and 4; gene *28*, ref. 4).

If these gene-product assignments are correct, why does the *sus*F14 mutation in gene *33* prevent the normal synthesis of the gene *34* protein (Fig. 1)? Since genes *33* and *34* are tightly linked on the genetic map of SP01 (ref. 3), one possible explanation is that the regulatory cistrons that control late transcription are located in the same operon and that the *sus*F14 nonsense mutation exerts a "polar" effect on the expression of gene *34*. But since the *sus*F4 and *sus*F14 mutants complement each other (albeit weakly)[3], this explanation demands that the *sus*F14 mutant actually synthesises a small amount of the gene *34* protein (smaller than can be detected in Fig. 1) and that this small quantity is sufficient to promote late gene expression. Another possible explanation of the pleiotropic effect of the *sus*F14 mutation is that the expression of gene *34* is controlled directly by the gene *33* protein. This possibility is not necessarily inconsistent with the time course experiment of Fig. 2, or with the finding that the genes *33* and *34* proteins act synergistically to alter the global pattern of SP01 transcription *in vitro*[9].

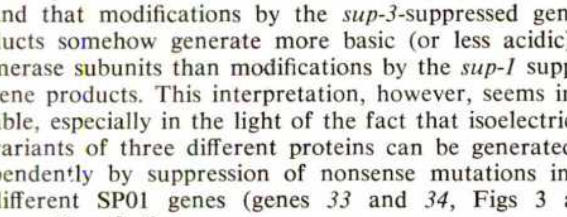

Fig. 5 Proposed model for the temporal control of phage SP01 gene expression. The figure illustrates schematically the three major categories of SP01 gene transcription; the figure is not intended to represent the actual physical arrangement of early, middle and late genes on the phage genome or the number and arrangement of promoter sites. The cross-hatched ellipses represent the host subunits of RNA polymerase other than sigma factor.

In conjunction with the previous finding that regulatory gene *28* codes for a phage-induced subunit of RNA polymerase[4], the further gene-product assignments reported here suggest the following scheme for the temporal control of phage SP01 gene expression (Fig. 5). Immediately on infection, host sigma factor directs the transcription of phage early genes. Next, at an intermediate time in the lytic cycle the gene *28* protein (itself the product of an early gene) turns on the expression of middle genes by binding to the host polymerase in the place of sigma factor. Finally, the gene *33* and *34* proteins (the products of middle genes) bind to the host transcriptase and activate late gene expression. This scheme is undoubtedly an oversimplification since it does not account for the turn off of subclasses of the early and middle genes at different times in the lytic cycle (see ref. 1). In analogy with the model of Fig. 5, the coliphage T4 regulatory genes that control late gene expression code for proteins that bind to the host RNA polymerase[22-24].

I thank J. Pero and R. Losick for helpful discussions, A. L. Sonenshein for assistance with genetic transformations and R. Losick for help with the manuscript. This work was supported by a grant from the NSF.

Received April 26; accepted July 7, 1976.

[1] Gage, L. P., and Geiduschek, E. P., *J. molec. Biol.*, **57**, 279–300 (1971).
[2] Fujita, D. J., Ohlsson-Wilhelm, B. M., and Geiduschek, E. P., *J. molec. Biol.*, **57**, 301–317 (1971).
[3] Okubo, S., Yanagida, T., Fujita, D. J., and Ohlsson-Wilhelm, B. M., *Biken J.*, **15**, 81–97 (1972).
[4] Fox, T. D., Losick, R., and Pero, J., *J. molec. Biol.*, **101**, 427–433 (1976).
[5] Pero, J., Nelson, J., and Fox, T. D., *Proc. natn. Acad. Sci. U.S.A.*, **72**, 1589–1593 (1975).
[6] Pero, J., Tjian, R., Nelson, J., and Losick, R., *Nature*, **257**, 248–251 (1975).
[7] Duffy, J. J., and Geiduschek, E. P., *J. biol. Chem.*, **250**, 4530–4541 (1975).
[8] Duffy, J. J., Petrusek, R. L., and Geiduschek, E. P., *Proc. natn. Acad. Sci. U.S.A.*, **72**, 2366–2370 (1975).
[9] Tjian, R., and Pero, J., *Nature*, 753–757 (1976).
[10] Fox, T. D., and Pero, J., *Proc. natn. Acad. Sci. U.S.A.*, **71**, 2761–2765 (1974).
[11] O'Farrell, P. H., *J. biol. Chem.*, **250**, 4007–4021 (1975).
[12] Tevethia, J. J., Baptist, J. N., and Mandel, M., *J. Bact.*, **119**, 961–975 (1974).
[13] Sonenshein, A. L., and Roscoe, D. H., *Virology*, **39**, 265–276 (1969).
[14] Crawford, L. V., and Gesteland, R. F., *J. molec. Biol.*, **74**, 627–634 (1973).
[15] Swaney, J. B., Vande Woude, G. F., and Bachrach, H. L., *Analyt. Biochem.*, **58**, 337–346 (1974).
[16] Linn, T. G., and Losick, R., *Cell*, **8**, 103–114 (1976).
[17] Okubo, S., and Yanagida, T., *J. Bact.*, **95**, 1187–1188 (1968).
[18] Shub, D. A., *J. Bact.*, **122**, 788–790 (1975).
[19] Georgopoulos, C. P., *J. Bact.*, **97**, 1397–1402 (1969).
[20] Camacho, A., Moreno, F., Carrascosa, J. L., Vinuela, E., and Salas, M., *Eur. J. Biochem.*, **47**, 199–205 (1974).
[21] Sonenshein, A. L., Cami, B., Brevet, J., and Cote, R., *J. Bact.*, **120**, 253–265 (1974).
[22] Stevens, A., *Proc. natn. Acad. Sci. U.S.A.*, **69**, 603–607 (1972).
[23] Horvitz, H. R., *Nature new Biol.*, **244**, 137–140 (1973).
[24] Ratner, D., *J. molec. Biol.*, **89**, 803–807 (1974).

Bacteriophage SP01 regulatory proteins directing late gene transcription *in vitro*

Robert Tjian & Janice Pero

Biological Laboratories, Harvard University, Cambridge, Massachusetts 02138

Expression of the temporally defined "late" genes of Bacillus subtilis *phage SP01 requires the protein products of regulatory genes* 33 *and* 34. *These proteins have now been isolated in pure form. Together with a host factor delta, they act synergistically to direct "late" gene transcription* in vitro *by core RNA polymerase.*

THE temporal programme of gene expression by *Bacillus subtilis* phage SP01 is controlled by phage-coded regulatory proteins that interact with the bacterial RNA polymerase (for a review see ref. 1). Phage middle-gene transcription is activated at 4–5 min into the lytic cycle by the SP01 gene *28* product[2,3], a regulatory protein that binds to *B. subtilis* RNA polymerase[4,5]. Enzyme containing the gene *28* protein asymmetrically transcribes phage middle genes *in vitro*[6-9]. Phage late-gene transcription is turned on 8–12 min after infection and this RNA synthesis seems to require the products of two SP01 regulatory genes called *33* and *34* (refs 2 and 3). As Fox shows in an accompanying article[10], genes *33* and *34* code for phage-induced subunits of the bacterial RNA polymerase, and Pero *et al.*[7] have shown that enzyme containing these phage-coded polypeptides preferentially synthesises late RNA *in vitro*. Pero *et al.*[6,7] have also identified a *B. subtilis* protein called δ that is associated with RNA polymerase from both uninfected and infected bacteria, and that markedly enhances the specificity of transcription by the phage-modified forms of RNA polymerase that copy middle and late genes *in vitro*.

To determine whether the subunits of RNA polymerase coded by genes *33* and *34* are directly responsible for the synthesis of late RNA *in vitro*, we have isolated these phage gene products in pure form free of the host subunits of RNA polymerase. By a reconstitution experiment we have shown that the gene *33* protein, the gene *34* protein and host δ protein act cooperatively to activate late gene transcription by core RNA polymerase.

Isolation of phage regulatory proteins

Highly purified RNA polymerase containing the protein products of genes *33* and *34* (formerly called subunits VI and V, respectively[6,7]) was isolated from phage SP01-infected cells of *B. subtilis* collected late in the lytic cycle (see legend to Fig. 1). The phage regulatory proteins were dissociated from core enzyme by denaturation in 6 M urea. To separate the proteins from the host subunits of polymerase, the denatured enzyme complex was applied to a phosphocellulose column equilibrated with buffer containing 6 M urea, and eluted with a linear gradient of KCl. The phage regulatory proteins were located by subjecting alternate fractions from the gradient elution to sodium dodecyl sulphate (SDS) polyacrylamide slab gel electrophoresis (Fig. 1*a*). Next, fractions 15–19 and 31–33 containing the phage regulatory proteins and some contaminating host polymerase subunits were subjected to gel filtration on Sephadex G-100 as a final purification step. SDS slab gel analysis showed that gel filtration had separated the proteins from each other and from the subunits of core polymerase (Fig. 1*b*). It is interesting that the phage proteins which have molecular weights of 24,000 and 13,500 (ref. 6), respectively, eluted from the Sephadex column at positions corresponding to ovalbumin (molecular weight 43,000) and to chymotrypsinogen (25,700). This could indicate either that the regulatory proteins have an unusual shape or that they form dimers in 6 M urea.

Purified gene *33* and gene *34* proteins were obtained by pooling fractions 40 to 46, and fractions 32 to 34, respectively, from the gel filtration column. Figure 2 shows that each pooled fraction apparently contained only a single highly purified polypeptide (Fig. 2*b* and *c*), corresponding in size to the regulatory proteins in phage-modified RNA polymerase (Fig. 2*a*). As further evidence for the identification of the purified regulatory proteins, a mixing experiment showed that the purified phage proteins of Fig. 2 comigrated during SDS gel electrophoresis with the radioactively-labelled protein

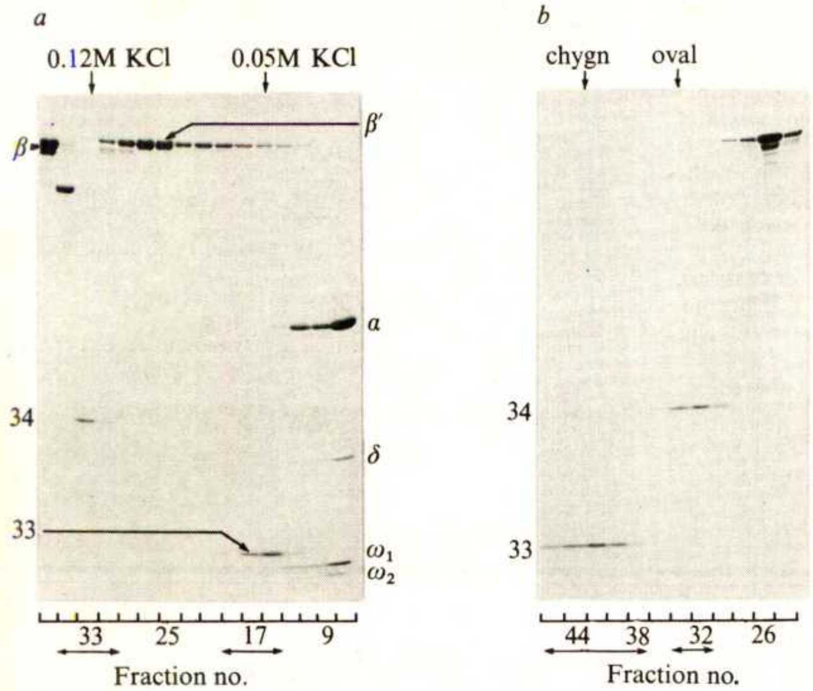

Fig. 1 Purification of the protein products of genes *33* and *34* by phosphocellulose chromatography and gel filtration in denaturing conditions. *B. subtilis* was infected with SP01 at a multiplicity of infection of 5 and collected 22 min after infection. RNA polymerase was purified from 80 g of infected cells through DEAE–Sephadex chromatography as described previously[11] except that the 2 M NaCl extraction during the phase partitioning step was omitted. One sixth of the DEAE–Sephadex-purified enzyme (5 mg), containing the subunits of core RNA polymerase[8] (β′, β, α, ω_1 and ω_2), δ protein, and the polypeptide products of genes *33* and *34*, was denatured by dialysis against buffer D (6 M urea, 0.05 M Tris, *p*H 8.0, 0.1 mM EDTA, 0.4 mM DTT and 0.05 M KCl). *a*, Denatured enzyme was then applied to a phospho-cellulose column (2 cm × 8 cm) equilibrated with buffer D and eluted with a linear gradient of 0.05–0.33 M KCl in buffer D. Fractions (3 ml) were collected and samples (25 µl) from every other fraction were subjected to electrophoresis on 25-cm-long slab gel containing SDS in a Tris–glycine buffer and a linear gradient of 7–15% acrylamide[12]. *b*, Fractions 15–19 and 31–33 containing the protein products of genes *33* and *34* were pooled, concentrated against Ficoll (Sigma) to a final volume of 1.5 ml, dialysed against buffer D for 2 h at 4 °C and then applied to a Sephadex G-100 column (0.9 cm × 100 cm) equilibrated with buffer D. Fractions (1 ml) were collected and samples (50 µl) from every other fraction were subjected to SDS slab gel electrophoresis. To renature the phage-coded proteins, gene *34* protein (in the pooled fractions 32–34) and gene *33* protein (in the pooled fractions 40–46) were mixed separately with core RNA polymerase (300 µg) from uninfected cells, concentrated threefold against Ficoll and then dialysed against the renaturation buffer (0.05 M Tris, *p*H 8.0, 0.1 mM EDTA, 25% glycerol, 8 mM DTT and 0.3 M KCl) for 3–6 h at 4 °C (ref. 13). The added core RNA polymerase which was inactivated on mixing with the regulatory proteins in buffer D did not regain significant activity (less than 0.2%) during renaturation. Thus the renatured regulatory protein fractions contained inactive core enzyme. The renatured regulatory proteins were stored at −20 °C until used in the reconstitution experiments. We were guided in the isolation and renaturation of the SP01-coded regulatory proteins by a discussion of the reconstitution of *E. coli* RNA polymerase by Zillig *et al.*[13].

products of genes *33* and *34* described in Fig. 1*a* of the accompanying article[10] (date not shown).

Finally, the two proteins which had been purified in the presence of 6 M urea were renatured in the presence of core RNA polymerase from uninfected cells (see legend to Fig. 1 for experimental details). In the conditions we used the presence of core enzyme was essential for recovery of the phage regulatory proteins in active form.

Strand selectivity of transcription

As a test of whether the renatured phage regulatory proteins would direct specific RNA synthesis, we asked whether these phage-coded polypeptides would cause selective transcription from the heavy (H) strand of native SP01 DNA, the strand from which late RNA is copied *in vivo*[6,14]. Figure 3*b* shows that in the presence of both phage proteins and host δ protein, purified core enzyme preferentially transcribed strand H of SP01 DNA (an H/L hybridisation ratio of 5.3). For comparison, core enzyme containing only added δ protein exhibited only a small preference for strand H (an H/L ratio of 1.9, Fig. 3*f*) while the original phage-modified polymerase plus added δ exhibited a strong preference for H strand DNA (an H/L

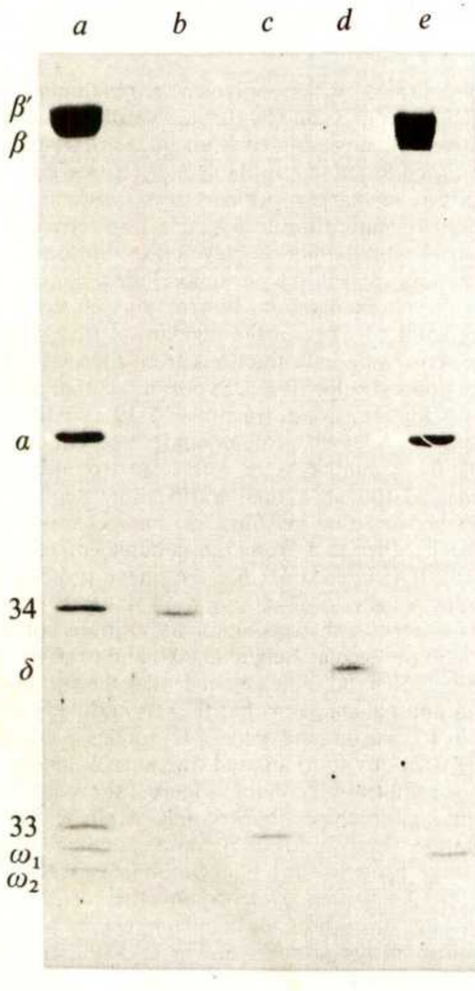

Fig. 2 SDS–polyacrylamide slab gel electrophoresis of RNA polymerase subunits from uninfected and SP01-infected *B. subtilis*. RNA polymerase containing the protein products of genes *33* and *34* was purified as described previously (enzyme C in ref. 6). Purification of the regulatory protein products of genes *33* and *34* is described in the legend to Fig. 1. Delta was isolated from uninfected cells as previously described[7] except that a DEAE–Sephadex column was used instead of a poly(C)–cellulose column to separate the δ subunit of RNA polymerase from the σ subunit; δ eluted at 0.5 M KCl while σ eluted at 0.25 M KCl. Purification of core RNA polymerase from uninfected cells has been described previously[11]. The purified proteins were subjected to electrophoresis as described in the legend to Fig. 1. *a*, RNA polymerase containing the protein products of genes *33* and *34*; *b*, gene *34* protein (fractions 32–34 from Fig. 1*b*); *c*, gene *33* protein (fractions 40–46 from Fig. 1*b*); *d*, δ protein; *e*, core RNA polymerase.

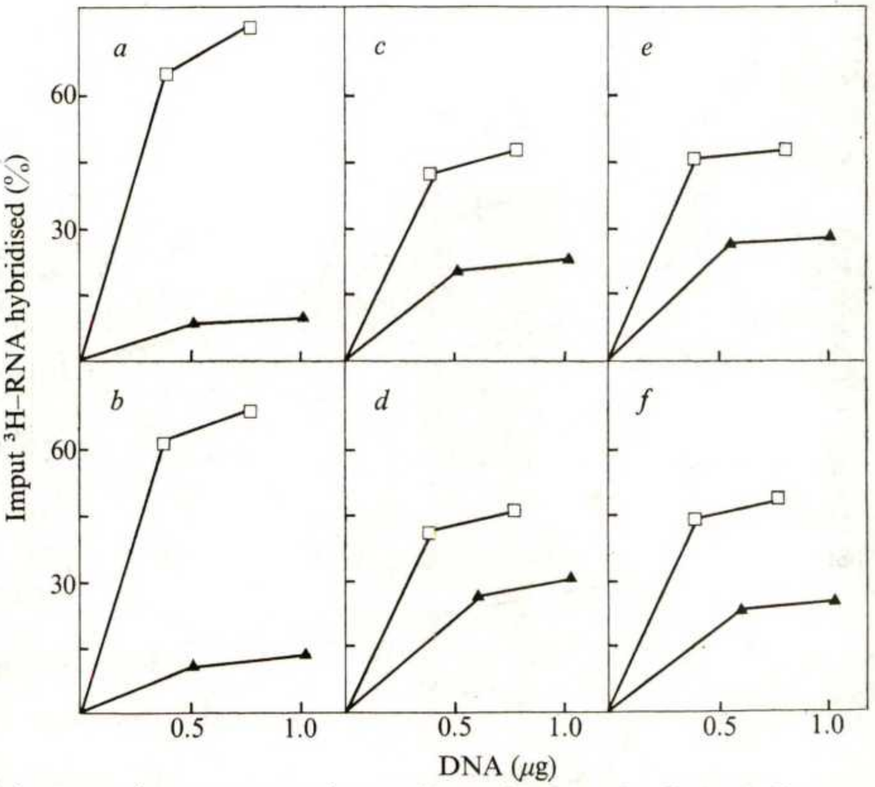

Fig. 3 Effect of phage regulatory proteins and host protein on strand selective transcription. Core RNA polymerase (13 μg) from uninfected cells (Fig. 2*e*) was mixed with the indicated combination of the following: 1.1 μg of renatured gene *33* protein, 1.5 μg of renatured gene *34* protein, 2.0 μg of δ protein, or mock renaturation reaction mixture to which no regulatory protein had been added. ^{3}H-RNA was synthesised *in vitro* as described previously[6] except that the reaction mixtures (0.5 ml) contained 0.025 M KCl, 0.9 mg anti-sigma gamma globulin[15] and were incubated at 32 °C for 30 min. (The anti-sigma gamma globulin was necessary to inactivate traces of σ that contaminated the core RNA polymerase and that severely interfered with the transcriptional specificity of the reconstituted enzymes.) Hybridisation of RNA and preparation of DNA strands were as described previously[6]. Hybridisation reactions contained the indicated amounts of H strand (□) and L strand (▲) SP01 DNA and the following ^{3}H-RNAs (representing about 5% of the product of the *in vitro* RNA synthesis reactions) in 125 μl of 2×SSC. *a*, RNA synthesised by RNA polymerase (6.0 μg) containing the protein products of genes *33* and *34* together with host δ purified as described in the legend to Fig. 1 (input 8,960 c.p.m.; background 490 c.p.m.). *b*, RNA synthesised by core polymerase+renatured gene *33* protein+renatured gene *34* protein+δ protein (input 9,180 c.p.m.; background 250 c.p.m.). *c*, RNA synthesised by core polymerase+renatured gene *33* protein+δ protein (input 10,510 c.p.m.; background 250 c.p.m.). *d*, RNA synthesised by core polymerase+renatured gene *34* protein+δ protein (input 7,250 c.p.m.; background 130 c.p.m.). *e*, RNA synthesised by core polymerase+renatured gene *33* protein+renatured gene *34* protein (input 15,830 c.p.m.; background 340 c.p.m.). *f*, RNA synthesised by core polymerase+δ protein+mock renaturation reaction mixture (input 7,010 c.p.m.; background 200 c.p.m.).

ratio of 8.4, Fig. 3*a*). Specific RNA synthesis by the reconstituted enzyme required both the protein products of genes *33* and *34*, for the strand selectivity of transcription in the absence of either regulatory protein (H/L ratio of 2.0 and 1.8, Fig. 3*c* and *d*) was not measurably higher than in the absence of both regulatory gene products (H/L = 1.9, Fig. 3*f*). Also, as expected from our previous findings[7], specific transcription by reconstituted enzyme required host δ protein in addition to the phage regulatory proteins; the strand selectivity of transcription by reconstituted enzyme lacking added δ (an H/L ratio of 1.9, Fig. 3*e*) was only slightly higher than that for core enzyme alone (an H/L of 1.3, ref. 6 and data not shown). Thus, the reconstitution of enzyme directing strand selective transcription required the addition of both regulatory proteins and host δ factor to core polymerase.

As an independent test of the asymmetry of transcription we measured the formation of RNA·RNA duplexes between labelled RNA synthesised *in vitro* and unlabelled early, middle and late RNAs isolated from phage-infected cells. The percentage of ^{3}H-RNA that annealed to the *in vivo* synthesised messenger RNAs was taken as a measure of the proportion of *in vitro* generated RNA representing anti-messenger sequences. As expected, a large percentage of the RNA synthesised by core RNA polymerase contained anti-mRNA sequences (line 1, Table 1). Similarly, RNA synthesised by partially reconstituted enzyme containing core polymerase and host δ but lacking the products of either gene *34* (line 2, Table 1) or gene *33* (line 3, Table 1) contained high levels of anti-mRNA. Likewise, if both phage gene products were included but host δ factor was omitted, a large proportion of the *in vitro* synthesised RNA contained anti-messenger sequences (line 4, Table 1). In contrast, very little anti-mRNA was generated by the fully reconstituted enzyme containing both phage-coded regulatory proteins and host δ factor (line 5, Table 1). For comparison, core polymerase plus host σ factor also synthesised low levels of anti-messenger (line 6, Table 1). Thus, the genes *33* and *34* proteins and host δ protein act cooperatively to catalyse asymmetric transcription of native SP01 DNA.

Synthesis of late RNA

Hybridisation–competition experiments indicated that core enzyme that had been reconstituted with the protein products of genes *33* and *34* and host δ factor preferentially synthesised

Table 1 Anti-mRNA synthesised *in vitro*

Enzyme	% ^{3}H-RNA forming duplexes with *in vivo* RNAs Early RNA	 Middle RNA	 Late RNA
Core polymerase	32	33	44
Core polymerase+δ+ gene *33* protein	31	30	40
Core polymerase+δ+ gene *34* protein	32	31	43
Core polymerase+ gene *33* protein+ gene *34* protein	41	34	34
Core polymerase+δ+ gene *33* protein+ gene *34* protein	12	9	13
Core polymerase+σ	6	7	15

RNA synthesis *in vitro* was as described in the legend to Fig. 3 except that no anti-sigma gamma globulin was included in the experiment of line 6. Early RNA was isolated from bacteria treated with chloramphenicol (150 μg ml^{-1}) before infection; middle RNA was isolated from bacteria collected 25 min after infection by a mutant phage (*sus*F4) blocked in the synthesis of late RNA[2]; and late RNA was isolated from cells collected 25 min after infection by wild-type SP01. Unlabelled RNA was prepared as previously described[7]. The RNA·RNA annealing reactions contained about 10 ng of ^{3}H-RNA (800 c.p.m. ng^{-1}) synthesisied *in vitro* by the indicated enzyme and about 0.15 mg of the indicated unlabelled RNA in a total volume of 150 μl of 2×SSC. The reactions were incubated at 70 °C for 3 h, chilled and incubated with RNase A (20 μg) and RNase T1 (20 U) in 1 ml of 2×SSC for 1 h at 35 °C. RNase resistant material was precipitated with 5% trichloroacetic acid.

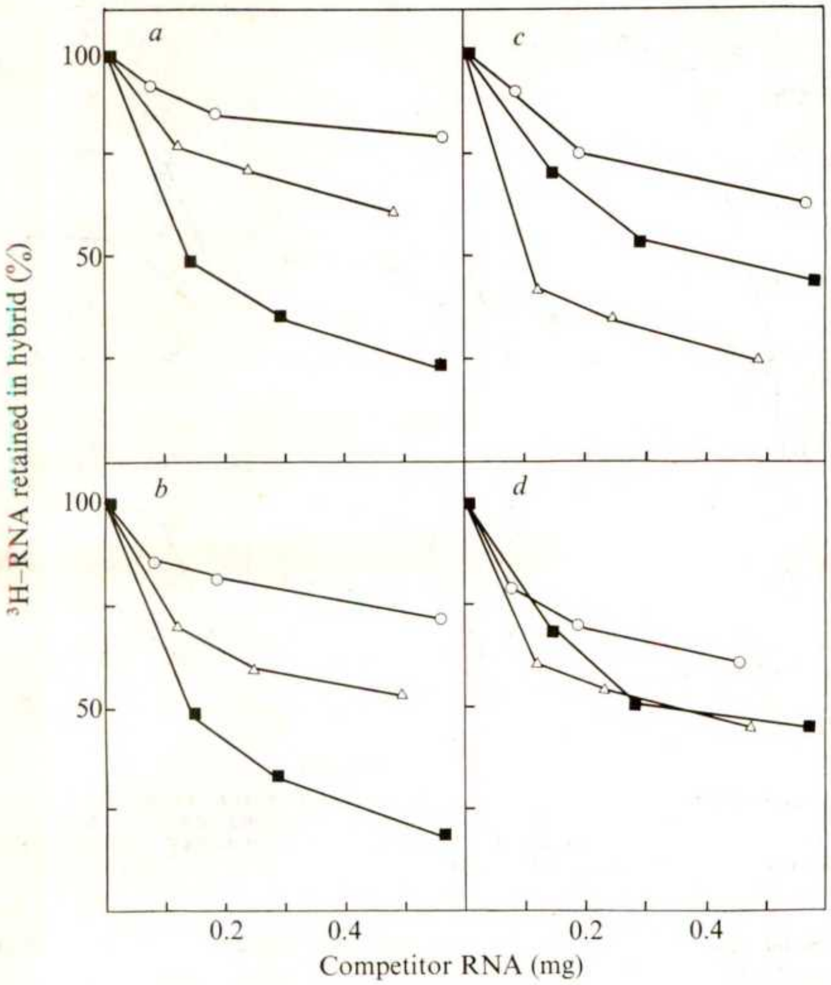

Fig. 4 Hybridisation competition of *in vitro* synthesised ^{3}H-RNAs. RNA was synthesised and hybridisations were performed as described in the legend to Fig. 3 except that the hybridisation reaction was incubated for 3 h at 68 °C. Hybridisation reactions contained 2.5 μg of denatured SP01 DNA, the indicated amounts of unlabelled early (○), middle (△) or late (■) competitor RNAs prepared as described in the legend to Table 1, and the following, *in vitro* synthesised ^{3}H-RNA (representing about 5% of the product in the reactions listed below) in a total volume of 200 μl of 2×SSC. *a*, RNA synthesised by RNA polymerase (6.0 μg) containing the protein products of genes *33* and *34* together with host δ; 50% of the input RNA (8,440 c.p.m.) hybridised in the absence of competitor. *b*, RNA synthesised by core polymerase (13 μg)+renatured gene *33* protein (1.0 μg)+renatured gene *34* protein (1.5 μg)+δ protein (2.0 μg); 51% of the input RNA (9,570) hybridised in the absence of competitor. *c*, RNA synthesised by RNA polymerase (10 μg) containing the gene *28* protein (enzyme B of ref. 7)+δ protein (1.2 μg); 50% of the input RNA (9,600 c.p.m.) hybridised in the absence of competitor. *d*, RNA synthesised by core polymerase (13 μg)+δ (2.0 μg)+mock renaturation reaction mixture; 52% of the input RNA (7,150 c.p.m.) hybridised in the absence of competitor. For each hybridisation a background of less than 7% of the input radioactivity was subtracted.

late RNA sequences. ^{3}H-RNA synthesised *in vitro* by reconstituted enzyme was annealed to denatured SP01 DNA in the presence of unlabelled competitor RNAs containing predominantly early, middle or late classes of RNA. To be sure that the middle RNA did not contain late sequences, this competitor was isolated from bacteria that had been infected with a mutant blocked in late gene expression (see legend to Table 1). (Similar competition results, however, were obtained with competitor RNA isolated at a middle time after infection with wild-type SP01 (unpublished results and ref. 7).) Figure 4*b* shows that the hybridisation of RNA synthesised *in vitro* by the reconstituted enzyme was more effectively inhibited by the late RNA competitor than by the middle or early RNA competitors. This pattern of competition was similar to that obtained for the hybridisation of RNA synthesised by the original phage-modified polymerase containing the protein products of genes *33* and *34* together with δ protein (Fig. 4*a*). In contrast, the hybridisation of RNA synthesised *in vitro* by polymerase containing the gene *28* protein plus δ factor was more effectively inhibited by middle RNA competitor than by late or early RNA competitors (Fig. 4*c*). As a control, the hybridisation of the symmetrical RNA generated by core polymerase plus δ was not preferentially inhibited by the late RNA competitor (Fig. 4*d*). Also, analogous hybridisation experiments indicated that partially reconstituted enzymes lacking either the gene *33* product, the gene *34* product or δ protein did not preferentially generate late RNA sequences. Thus, like the strand selectivity of transcription, the preferential transcription of SP01 late genes *in vitro* required the combined effects of both phage-coded regulatory proteins and host δ factor.

Gene products control transcription

Our reconstitution experiments establish that the products of genes *33* and *34* are directly responsible for promoting the asymmetrical transcription of phage SP01 late genes *in vitro*. Since the protein products of genes *33* and *34* were isolated in pure form, we further conclude that these two regulatory proteins are apparently the only SP01-coded proteins required for the synthesis of late RNA *in vitro*. We have not, however, determined whether these two proteins are sufficient to direct the transcription of all SP01 late genes or only a subset of phage late sequences. As expected from an earlier study[7], the reconstitution experiments also show that the specific transcription of phage late genes required host protein δ but not the σ subunit of RNA polymerase.

The synergistic effect of the protein products of genes *33* and *34* on late gene transcription *in vitro* is in apparent agreement with earlier genetic studies indicating that a mutation in either gene *33* or gene *34* alone is sufficient to block late RNA synthesis *in vivo*[2,3]. The genetic experiments do not, however, necessarily predict that both regulatory proteins are simultaneously required for the expression of late genes *in vivo*. For example, as discussed by Fox[10], it is possible, though unlikely, that the gene *33* protein serves only to activate regulatory gene *34* and that the gene *34* protein alone is sufficient to direct late RNA synthesis *in vivo*. The *in vitro* requirement for both regulatory proteins for asymmetric transcription of late genes casts doubt on such a model.

It is likely that the SP01 gene *28* protein also interacts with *B. subtilis* RNA polymerase to activate middle-gene expression. Fox *et al.*[4] have shown that gene *28* codes for a phage-induced subunit of polymerase, and Pero *et al.*[6,7] and Duffy and Geiduschek[8] have shown that RNA polymerase containing the gene *28* product asymmetrically transcribes phage middle genes *in vitro*. In further support for the idea that a phage-coded protein confers specificity for middle genes on RNA polymerase, Duffy *et al.*[16] have partially purified a fraction from crude extracts of SP01-infected cells that causes preferential synthesis of middle RNA by core enzyme. This fraction contained a phage-induced protein similar in size to the gene *28* product that was able to bind to core RNA polymerase from uninfected cells. Petrusek *et al.*[17] have attempted to isolate this transcriptional determinant by denaturing in urea an RNA polymerase fraction containing several phage-induced proteins, including polypeptides that apparently correspond to the products of genes *28*, *33* and *34*. Unfortunately, in both cases the protein presumed to direct middle-gene transcription was only one component of a partially purified fraction containing several proteins and it was not excluded that another polypeptide had been responsible for conferring transcriptional specificity on the core enzyme. Indeed, a new protein species has been identified that is apparently distinct from the product of gene *28* and that promotes asymmetric transcription of phage middle genes *in vitro*[18]. Proof that the gene *28* protein itself directly influences the transcriptional specificity of RNA polymerase therefore awaits the isolation of this phage-coded regulatory protein in pure form.

In summary, our findings establish that two phage-coded subunits of RNA polymerase are directly responsible for promoting specific gene transcription. How do the protein products of genes *33* and *34* work? As they influence transcription in the absence of the host σ factor, we suppose that they cause RNA polymerase to initiate transcription at specific promoter sites for phage late genes. A test of this idea now requires the isolation of fragments of SP01 DNA specifying individual late gene transcripts.

We thank Jane Nelson for preparing the DNA strands and competitor RNAs, R. Losick, T. Fox and W. Gilbert for helpful discussions, and R. Losick for help with the manuscript. This work was supported by a grant to J.P. and R. Losick from the NSF. R.T. is a junior fellow of the Harvard Society of Fellows.

Received April 26; accepted July 7, 1976.

[1] Losick, R., and Pero, J., in *RNA polymerase* (edit. by Losick, R., and Chamberlin, M.), 227–246 (Cold Spring Harbor Laboratory, New York, 1976).

[2] Fujita, D. J., Ohlsson-Wilhelm, B. M., and Geiduschek, E. P., *J. molec. Biol.*, **57**, 301–317 (1971).

[3] Okubo, S., Yanagida, T., Fujita, D. J., and Ohlsson-Wilhelm, B. M., *Biken J.*, **15**, 81–97 (1972).

[4] Fox, T. D., Losick, R., and Pero, J., *J. molec. Biol.*, **101**, 427–433 (1976).

[5] Fox, T. D., and Pero, J., *Proc. natn. Acad. Sci. U.S.A.*, **71**, 2761–2765 (1974).

[6] Pero, J., Nelson, J., and Fox, T. D., *Proc. natn. Acad. Sci. U.S.A.*, **72**, 1589–1593 (1975).

[7] Pero, J., Tjian, R., Nelson, J., and Losick, R., *Nature*, **257**, 248–251 (1975).

[8] Duffy, J. J., and Geiduschek, E. P., *J. biol. Chem.*, **250**, 4530–4541 (1975).

[9] Whiteley, H. R., Spiegelman, G. B., Lawrie, J. M., and Hiatt, W. R., in *RNA polymerase* (edit. by Losick, R., and Chamberlin, M.), 587–600 (Cold Spring Harbor Laboratory, New York, 1976).

[10] Fox, T. D., *Nature*, 748–753 (1976).

[11] Shorenstein, R., and Losick, R., *J. biol. Chem.*, **248**, 6163–6169 (1973).

[12] Studier, F. W., *J. molec. Biol.*, **79**, 237–248 (1973).

[13] Zilling, W., Palm, P., and Heil, A., in *RNA polymerase* (edit. by Losick, R., and Chamberlin, M.), 101–126 (Cold Spring Harbor Laboratory, New York, 1976).

[14] Gage, L. P., and Geiduschek, E. P., *J. molec. Biol.*, **57**, 279–300 (1971).

[15] Tjian, R., Stinchcomb, D., and Losick, R., *J. biol. Chem.*, **250**, 8824–8828 (1975).

[16] Duffy, J. J., Petrusek, R. L., and Geiduschek, E. P., *Proc. natn. Acad. Sci. U.S.A.*, **72**, 2366–2370 (1975).

[17] Petrusek, R. L., Duffy, J. J., and Geiduschek, E. P., in *RNA polymerase* (edit. by Losick, R., and Chamberlin, M.), 567–586 (Cold Spring Harbor Laboratory, New York, 1976).

[18] Tjian, R., Pero, J., Losick, R., and Fox, T. D., in *Molecular Mechanisms in the Control of Gene Expression* (edit. by Nierlich, D. P., Rutter, W. J., and Fox, C. F.), (Academic, New York, in the press).

Nonsense suppressors of *Saccharomyces cerevisiae* can be generated by mutation of the tyrosine tRNA anticodon

Peter W. Piper*† **& Marilyn Wasserstein**
Department of Molecular Biology

Frode Engbaek, Keld Kaltoft & Julio E. Celis
Department of Biostructural Chemistry

Jesper Zeuthen
Department of Human Genetics, University of Aarhus, 8000 Aarhus, Denmark

Susan Liebman & Fred Sherman
Department of Radiation Biology and Biophysics, University of Rochester School of Medicine and Dentistry, Rochester, New York 14642

The yeast amber suppressor, SUP5-***a***, *was previously shown to cause the insertion of tyrosine at the sites of UAG nonsense codons. Nucleotide sequencing established that this* SUP5-***a*** *suppressor specifies a mutant tyrosine transfer RNA (tRNA) which has the anticodon CΨA instead of the normal GΨA, an alteration identical to that found in the tyrosine-inserting amber suppressor from* Escherichia coli.

THE three codons UAG (amber), UAA (ochre) and UGA (opal) serve as signals for polypeptide chain termination during messenger RNA translation in various prokaryotic and eukaryotic organisms[1–9]. When one of these codons arises internally in a structural gene as a result of mutation, the gene product is an incomplete polypeptide. Such nonsense mutations can be reverted by an unlinked suppressor mutation, which alters one of the components required for protein synthesis and facilitates the formation of a completed polypeptide through the insertion of an amino acid at the position of the nonsense codon. The most extensively studied suppressors arise by mutation of the structural genes for tRNA although other suppressors can arise by mutation of genes controlling tRNA modification enzymes or ribosomal proteins (for review see refs 10–12). Sequencing of suppressor tRNAs has shown that the base changes giving rise to the suppressor function can occur at the anticodon[13–16] and in other regions of the tRNA structure[17].

The eukaryotic yeast *Saccharomyces cerevisiae* can form nonsense suppressors similar to those of *E. coli* (for review see ref. 18). Several of these nonsense suppressors have been characterised by their action on *iso*-1-cytochrome *c* mutants which contain defined ochre (UAA) and amber (UAG) mutations[19,20]. In contrast to any of the *E. coli* suppressors, a major class of suppressors from yeast acts specifically on UAA and not UAG codons. Whereas bacterial ochre suppressors recognise both UAA and UAG codons, suppressors acting specifically on only UAG codons are found in both *E. coli* and yeast. The amino acids inserted by the yeast suppressors have been determined from protein analysis of *iso*-1-cytochrome *c* in suppressed mutants. So far tyrosine, serine and leucine-inserting suppressors have been identified (refs 21–25, 45). Studies of translation *in vitro* of mRNA containing nonsense codons have shown that the suppressor activities of at least some of the yeast suppressors are due to altered tRNAs[26,27]. Such yeast suppressor tRNAs may have a potential application in methods for the selection and biochemical characterisation[28,46] of nonsense mutants of mammalian cells and their viruses. But although the *in vitro* studies showed that suppression is mediated by tRNAs, the results did not indicate whether the suppressor mutations caused alterations in either the nucleotide sequences of tRNAs or the enzymes that modify them. Also the tRNA giving rise to a suppressor cannot always be identified from the amino acid inserted at the nonsense codon. This is true in the case of the recessive-lethal glutamine and trytophan-inserting Su 7 suppressor of *E. coli*, which is derived from trytophan tRNA by a single base substitution in the anticodon[16,29,30] as well as for the glutamine-mischarging mutants derived from *E. coli*, Su$^{+}_{3}$ tRNA$^{\text{Tyr}}$ (ref. 34).

---

*To whom reprint requests should be addressed.

†Present address: Imperial Cancer Research Fund Laboratories, Lincolns Inn Fields, London WC2 3PX, UK.

We present here direct evidence that at least one yeast suppressor arose by the mutational alteration of the nucleotide sequence of a tRNA, and we report the nucleotide change in this suppressor tRNA. The suppressor examined in this study, *SUP5*-**a**, is typical of one of the eight distinct suppressors (*SUP2*-**a**, *SUP3*-**a**, *SUP4*-**a**, *SUP5*-**a**, *SUP6*-**a**, *SUP7*-**a**, *SUP8*-**a** and *SUP11*-**a**) that cause insertion of tyrosine at UAG sites[22,24]. In addition, a parallel series of allelic suppressors, *SUP2*-**o**, *SUP3*-**o**, and so on, causes the insertion of tyrosine at UAA sites[21]. Nucleotide sequencing established that *SUP5*-**a** determines a mutant form of tyrosine tRNA which has the anticodon CΨA instead of the normal GΨA. This altered anticodon was observed whether the amber suppressor arose from the wild-type gene or from the UAA suppressor *SUP5*-**o.** With our techniques we were unable to reveal the tRNA alteration associated with the *SUP5*-**o** suppressor. We were also unable to detect altered tRNA when the *SUP5*-**a** suppressor mutated to the less efficient *SUP5*-**a**→**a**^{1} suppressor[32].

Minor tRNA$^{\text{Tyr}}$ with altered anticodon in amber-suppressing strains

Only one tyrosine tRNA is found in *S. cerevisiae* and its nucleotide sequence is known[33]. If the tyrosine-inserting suppressors of this organism are the products of single-base substitutions of tRNA$^{\text{Tyr}}$ genes, such a suppressor tyrosine tRNA would be expected to copurify with the bulk of the tyrosine tRNA. Eight loci can mutate to these suppressors. Therefore when one of them mutates, the product of the mutated gene should be a minor component of the total tRNA$^{\text{Tyr}}$. This can be investigated by sequencing tRNA$^{\text{Tyr}}$ associated with strains possessing these suppressors, provided this species can be isolated to a high degree of purity. We have found that the two-dimensional electrophoretic separation of tRNAs on polyacrylamide gel[37] can be used routinely to isolate small amounts of extremely pure ^{32}P-tRNA$^{\text{Tyr}}$ from yeast cultures (Fig. 1). The relative positioning of different tRNAs on the gels was sufficiently reproducible for the tRNA$^{\text{Tyr}}$ spot (arrowed in Fig. 1) to be identified from the spot pattern, once it had initially been characterised on the basis of its fingerprint. The sequence analyses described here were carried out on the purified total tRNA$^{\text{Tyr}}$ of the strains listed in Table 1.

S. cerevisiae strain L-133, with the highly efficient tyrosine-inserting amber suppressor *SUP5*-**a**[24,32], was examined for the presence of an altered tRNA$^{\text{Tyr}}$. As a control, tRNA$^{\text{Tyr}}$ was also

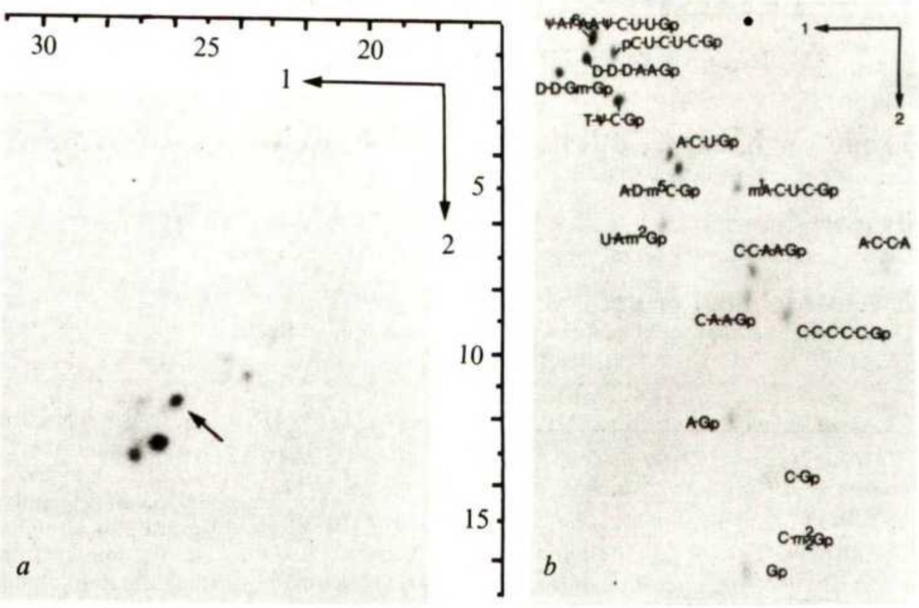

Fig. 1 Purification of tyrosine tRNA from yeast. Cultures (50 ml) were grown at 30 °C in nutrient low phosphate medium[34] containing 6 mCi of carrier-free ^{32}P-orthophosphate. Immediately before collection of each culture, a few cells were plated so that the proportion retaining the original suppressor at the time of collection could be determined subsequently by measuring suppression of auxotropic and *iso*-1-cytochrome *c* nonsense mutants. Levels of *iso*-1-cytochrome *c* were used to distinguish between amber suppressors with different efficiencies of suppression. This was necessary because of the instability of suppressors and their tendency to mutate to less efficient forms[32]. Only cultures in which more than 90% of the cells retained the phenotype of the original suppressor were retained for the analyses. After the rest of the cells had been collected by centrifugation, RNA was extracted from the cell pellets[34], precipitated with ethanol and lyophilised. RNA samples were then dissolved in small volumes of 0.35 M NaCl, 0.01 M MgCl$_2$, 0.01 M sodium acetate, *p*H 5.0, and applied to 1 cm × 8 cm columns of benzoylated DEAE–cellulose previously equilibrated with the same buffer. tRNA was eluted in two consecutive steps, by applying to the columns first: 0.85 M NaCl, 0.01 M MgCl$_2$, 0.01 M sodium acetate, *p*H 5.0; and later: 1.0 M NaCl, 0.01 M MgCl$_2$, 20% ethanol, 0.01 M sodium acetate, *p*H 5.0. The tRNA fraction eluted by the ethanol-containing buffer was concentrated by ethanol precipitation, lyophilised and redissolved in 0.035 ml of gel sample buffer (60% sucrose, 4 M urea, 0.1 M sodium acetate, *p*H 5.0, 1% xylene cyanol FF). It was then separated by two-dimensional gel electrophoresis[35]. tRNA spots were located by autoradiography of the wet gels, extracted[34] and individual tRNA species were identified from their fingerprints. *a*, Autoradiogram of a two-dimensional gel. The scales indicate the distances of migration (cm) in the first dimension (1) 10% gel and second dimension (2) 20% gel. The tRNA$^{\text{Tyr}}$ spot is indicated by an arrow. *b*, Fingerprint of a ribonuclease T$_1$ digest of tRNA$^{\text{Tyr}}$. The RNA sample was purified on a two-dimensional gel, and individual oligonucleotides on the fingerprint are identified by their sequences. The first (1) and second (2) dimensions of electrophoretic separation[38] are indicated.

Table 1 Yeast strains

Strain no.	Abbreviated genotype	Derived from:	Suppresses	Suppressor inserts	Efficiency	Anticodon of tyrosine tRNA product of *SUP5* locus
SL210-3A	*sup*$^+$	—	None	—	—	GΨA
L-133	*SUP5*-**a**	*sup*$^+$	UAG	Tyrosine	high	GΨA→CΨA
SL171-2C	*SUP5*-**o**	*sup*$^+$	UAA	Tyrosine	high	GΨA→?
L-58	*SUP5*-**o**→**a**	*SUP5*-**o**	UAG	Not determined	high	?→CΨA
L-133a	*SUP5*-**a**→**a′**	*SUP5*-**a**	UAG	Not determined	low	Unknown

examined for the non-suppressing *sup*$^+$ strain (SL210–3A) from which the *SUP5*-**a** mutant had been derived. No difference between the total tRNA$^{\mathrm{Tyr}}$ of these two strains could be discerned when T$_1$ or pancreatic ribonuclease digests were fingerprinted in two dimensions, using electrophoresis on cellulose acetate at *p*H 3.5 in the first dimension and on DEAE paper in 7% formic acid[36] in the second dimension, as in Fig 1*b*. If, however, T$_1$ ribonuclease digests were separated by homochromatography[36] in the second dimension, so as to effect better separation of the large oligonucleotides, a distinct difference in the fingerprints was apparent. Figure 2*a* shows a fingerprint of *sup*$^+$ tRNA$^{\mathrm{Tyr}}$ digested with T$_1$ ribonuclease, and Fig. 2*b* and *c* shows the corresponding fingerprints of total rRNA$^{\mathrm{Tyr}}$ from two different *SUP5*-**a** cultures. A large oligonucleotide (marked C in Fig. 2*b* and *c*) is present in the T$_1$ ribonuclease digest of the *SUP5*-**a** tRNA$^{\mathrm{Tyr}}$ but is absent from the corresponding digest of the *sup*$^+$ tRNA$^{\mathrm{Tyr}}$. Since this fragment is not one of the normal digestion products of yeast tRNA$^{\mathrm{Tyr}}$, its nucleotide sequence was determined. It was degraded by pancreatic ribonuclease (Fig. 3) to give Ai^{6}AAΨp, ACp, Gp, Cp, Ψp, and Up. Also, after reacting the U, G and Ψ residues with carbodiimide reagent and analysing the products of subsequent pancreatic ribonuclease digestion[36], it was possible to show that this fragment contained the sequences (C)UC and (C)UUG (results not shown). Partial digestion with ribonuclease U$_2$ gave a series of fragments shown separated in Fig. 3, which were identified from their base compositions. The data obtained were only consistent with the nucleotide sequence: ACUCΨAi^{6}AAΨCUUGp. Figure 4 shows that this oligonucleotide is derived from a tRNA$^{\mathrm{Tyr}}$ with anticodon CΨA. The species with such an anticodon would be expected to function as a UAG suppressor. Minor nucleotide analyses carried out in conjunction with the sequence analysis of fragment C showed that the second anticodon base of the suppressor tyrosine tRNA is pseudouridine, as in the wild-type tRNA$^{\mathrm{Tyr}}$. The weak intensity of the mutant anticodon spot C (Fig. 2*b* and *c*) indicates that only 5–8% of the total tRNA$^{\mathrm{Tyr}}$ from the *SUP5*-**a** strain existed in the form of this amber suppressor species, a level that is consistent with this species being the product of one of the eight genes for tyrosine tRNA. A UAG-specific suppressor can therefore be generated in both *E. coli*[13] and yeast by mutation of the first base of the tyrosine tRNA anticodon.

The tRNA$^{\mathrm{Tyr}}$ from other amber suppressor alleles of *SUP5* was also examined. The *SUP5*-**o**→**a** allele was obtained[24] by mutation of the *SUP5*-**o** UAA suppressor, in contrast to the *SUP5*-**a** allele which was obtained directly from the *sup*$^+$ wild type. But *SUP5*-**o**→**a** and *SUP5*-**a** are phenotypically indistinguishable and the sequence analyses of their tRNA$^{\mathrm{Tyr}}$ (Figs 2*e* and 3*c* and *f*) indicate that they are identical.

Since we have shown that these suppressors arise by mutation of the tyrosine tRNA anticodon, it is possible to study the structure and function of this species, as has been done with *E. coli* and bacteriophage tRNA suppressors. It has been shown that second base changes in the yeast amber suppressor tRNA$^{\mathrm{Tyr}}$ result in the suppressor functioning at a lower efficiency[32]. We have analysed one of these suppressors, *SUP5*-**a**→**a**^{1} in strain L-133a which arose by an intragenic mutation of *SUP5*-**a** in L-133. In the fingerprint of tRNA$^{\mathrm{Tyr}}$ from *SUP5* **a**→**a′** (Fig. 2*f*), the anticodon fragment of the amber suppressor tRNA$^{\mathrm{Tyr}}$ was either absent or present at an undetectable level. It is possible that the second site mutation of the *SUP5*-**a**→**a′** locus causes a reduced synthesis of suppressor tRNA, in much the same way as certain mutations of the *su*$_3^+$ tRNA$^{\mathrm{Tyr}}$ gene of *E. coli* impair tRNA maturation[37].

Lack of identification of UAA-specific suppressor

Unlike bacterial ochre suppressors which recognise both UAA and UAG codons, yeast UAA suppressors act only on UAA

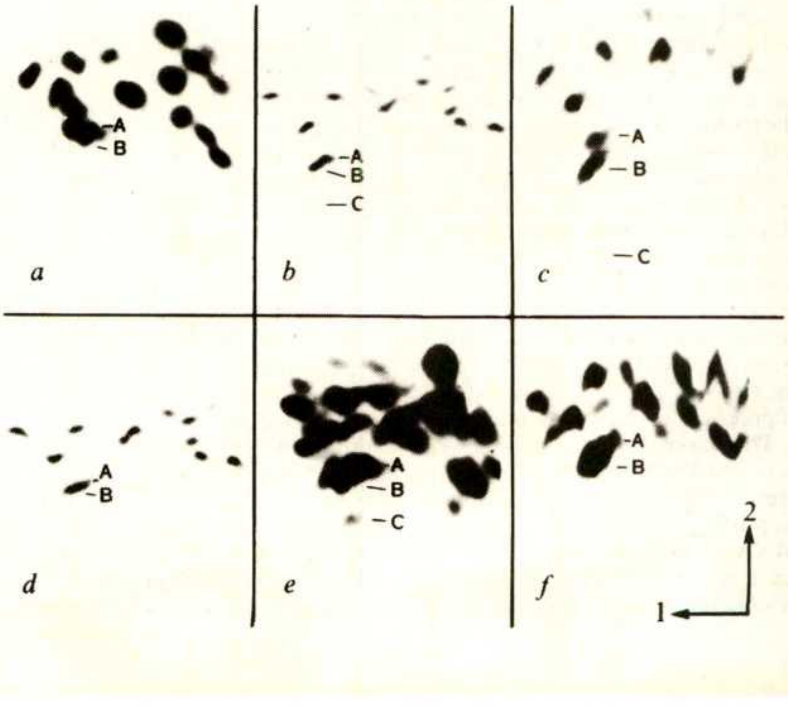

Fig. 2 T$_1$ ribonuclease digests of tyrosine tRNA isolated from: *a*, *SUP*$^+$ (SL210-3A); *b* and *c*, two different cultures of *SUP5*-**a** (L-133); *d*, *SUP5*-**o** (SL171-2C); *e*, *SUP5*-**o**→**a** (L-58), and *f*, *SUP5*-**a**→**a′** (L-133a). Oligonucleotide separation was by electrophoresis on cellulose acetate in the first dimension (1) and ascending chromatography on DEAE–cellulose thin layers in the second dimension (2) using a 3% dialysed homomixture[38]. A and B identify respectively the oligonucleotides pCUCUGp and ΨAi^{6}AAΨCUUGp. C, ACUCΨAi^{6}AAΨCUUGp, is the anticodon fragment of the amber suppressor tRNA$^{\mathrm{Tyr}}$, present only in fingerprints (*b*), (*c*) and (*e*). Other differences between the fingerprints are due to differences in the resolving power of homomixtures and fluctuations in the extent to which T$_1$ ribonuclease has cleaved the fragment Cm$^2_2$GCAAGp into Cm$^2_2$G>p and CAAGp.

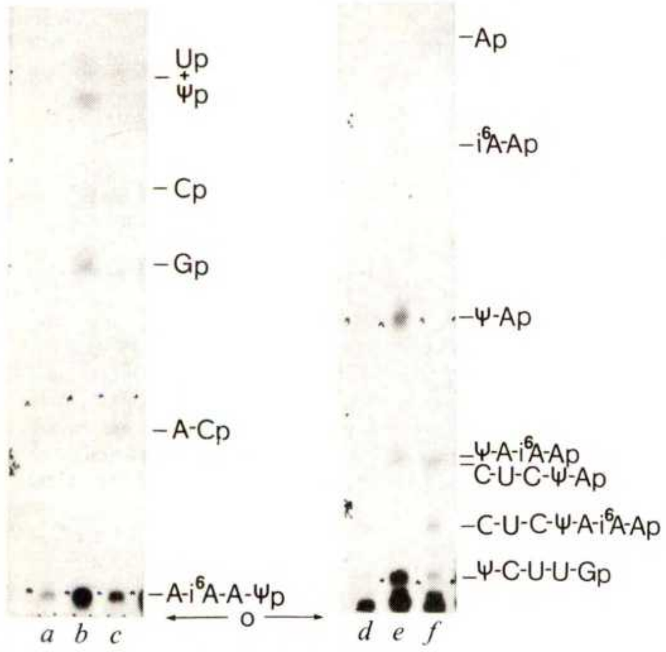

Fig. 3 Pancreatic and U$_2$ ribonuclease digests of the anticodon oligonucleotides of the UAG suppressor tRNA$^{\mathrm{Tyr}}$. *a* and *c*, Pancreatic ribonuclease digests of ACUCΨAi^{6}AAΨCUUGp, the anticodon loop fragments of the amber suppressor tRNA$^{\mathrm{Tyr}}$, derived, respectively, from strains *SUP5*-**a** and *SUP5*-**o**→**a**. *b*, Marker digest of ΨAi^{6}AAΨCUUGp. Separation was by electrophoresis, 1 kV for 3 h, on DEAE paper at *p*H 3.5. *d* and *f*, U$_2$ ribonuclease digests of the anticodon loop fragment of amber suppressor tRNA$^{\mathrm{Tyr}}$ derived from *SUP5*-**a** and *SUP5*-**o**→**a**, respectively. *e*, Marker U$_2$ digest, of ΨAi^{6}AAΨCUUGp. Digestion was with 0.05 ml of U$_2$ ribonuclease (0.1 U ml^{-1}), 0.05 M sodium acetate, *p*H 4.5, for 4 h at 37 °C, and separation was by electrophoresis, 1 kV for 6 h on DEAE paper in 7% formic acid.

and not on UAG codons. The only *E. coli* ochre suppressor which has been sequenced is the tRNAoc$^{\mathrm{Tyr}}$. This species has the anticodon U*UA[14,38] and should therefore decode both UAA and UAC to UAG according to the 'wobble' theory of codon-anticodon recognition[39]. A mutant suppressor glutamine tRNA of phage T$_4$, with NUA anticodon, also recognises both UAA and UAG[15,40]. There have been two proposals to explain how an ochre suppressor tRNA$^{\mathrm{Tyr}}$ of yeast might be able to decode UAA but not UAG. According to the first hypothesis[41], the anticodon is presumed to be IΨA (topaz) obtained by mutation of the anticodon to AUA, followed by enzymatic modification, thus giving a tRNA which should translate UAA in addition to the two normal tyrosine codons. The second hypothesis[21] is that the mutant tRNA$^{\mathrm{Tyr}}$ has the anticodon SΨA (sepia) where S is 2-thio-5-carboxymethyluridine methyl ester. This modified nucleoside has been identified as the first anticodon base in tRNA$_3^{\mathrm{Glu}}$ (ref. 42) and tRNA$_2^{\mathrm{Lys}}$ (refs 43, 44) from yeast. In this position it pairs preferentially with adenosine rather than guanosine in the third position of a codon. A third possibility might be that a weak recognition of UAA by tRNA$^{\mathrm{Tyr}}$ is enhanced by a base change outside the anticodon. This is known to be the case for UGA recognition by a suppressor tRNA$^{\mathrm{Trp}}$ of *E. coli*[17]. An anticodon change, however, is much more probable in view of the demonstration that tyrosine-inserting ochre suppressors of yeast can mutate to allelic amber suppressors.

To explore these possibilities, we fingerprinted tRNA$^{\mathrm{Tyr}}$ from strain SL171-2C which carries a tyrosine-inserting ochre suppressor, *SUP5*-**o**, that is allelic to the amber suppressor *SUP5*-**a**. According to the second hypothesis, the UAA suppressing tRNA$^{\mathrm{Tyr}}$ should yield the fragment ACUSΨAi^{6}AAΨCUUGp on digestion with T$_1$ ribonuclease. This oligonucleotide differs in only one base from the anticodon fragment of the *SUP5*-**a** tRNA$^{\mathrm{Tyr}}$. Assuming the unstable S nucleoside does not produce anomalous behaviour, such an oligonucleotide should occupy almost the same position on the fingerprints as the amber suppressor anticodon at spot C. In the fingerprint of the *SUP5*-**o** tRNA$^{\mathrm{Tyr}}$ (Fig. 2*d*) no spot could be seen in this position. If, however, the ochre suppressor has an IΨA anticodon, then the sole difference between a T$_1$ ribonuclease digest of this species and that of normal tRNA$^{\mathrm{Tyr}}$ will be the presence of ACUIp in place of ACUGp (Fig. 1*b*), since the enzyme cleaves polynucleotides after both G and I. Because of technical difficulties in identifying a small amount of a ^{32}P-labelled minor nucleotide from a very small fraction of the *SUP5*-**o** tRNA$^{\mathrm{Tyr}}$, we did not pursue this analysis further.

Interpretation

Nucleotide sequencing established that the yeast amber suppressor *SUP5*-**a** determines a mutant form of tRNA$^{\mathrm{Tyr}}$ which has the anticodon CΨA instead of the normal GΨA. This mutationally altered anticodon is consistent with amber suppressibility according to the wobble hypothesis and it corresponds to the anticodon of a tRNA$^{\mathrm{Tyr}}$ amber suppressor of *E. coli*. Although we were unable to detect the nucleotide changes of tRNA$^{\mathrm{Tyr}}$ associated with the UAA suppressor *SUP5*-**o**, the amber suppressor anticodon was clearly absent. The nature of the anticodon in the *SUP5*-**a** tRNA$^{\mathrm{Tyr}}$ could be inferred from the observation that the tRNA$^{\mathrm{Tyr}}$ corresponding to the amber suppressor *SUP5*-**o**→**a**, which was derived by a single-step mutation from *SUP5*-**o**, seemed to have an identical sequence to *SUP5*-**o** tRNA$^{\mathrm{Tyr}}$ which was derived by a single-step mutation from the wild-type gene. Assuming that the mutations occurred by single-base changes, the simplest interpretation of these results is that the UAA suppressor is a

Fig. 4 Primary structure of yeast tRNA$^{\mathrm{Tyr}}$ (ref. 35) showing the anticodon base substitution present in the amber suppressor tRNA$^{\mathrm{Tyr}}$ species.

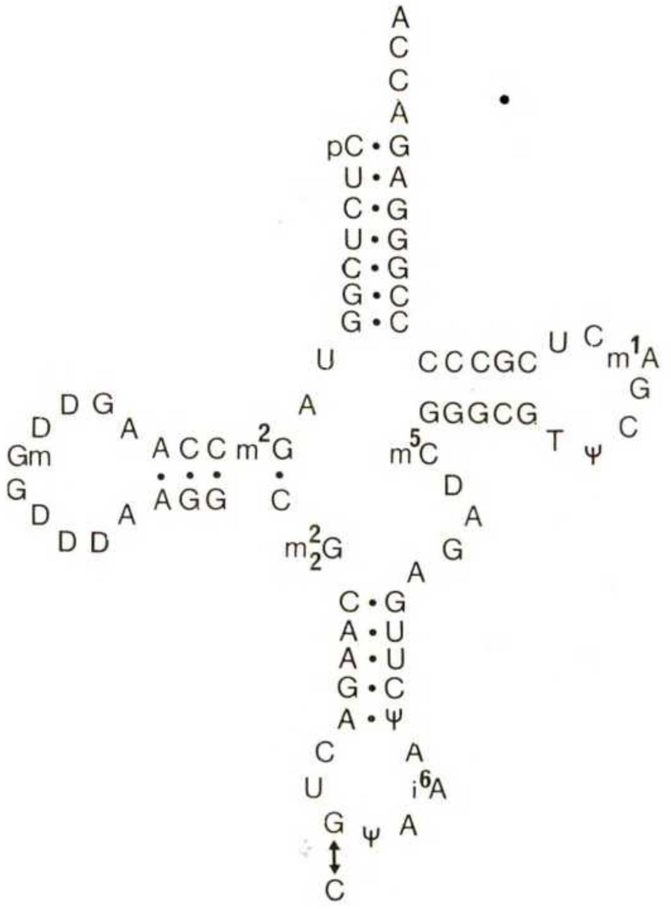

tRNA^{Tyr} having an alteration of the first base in the anticodon, although the base in question has not been identified.

This work was supported in part by grants from Landforeningen til Kraeftens Bekaempelse, the Danish Research Council, NIH the American Cancer Society and ERDA. P.W.P was supported by an EMBO fellowship and M.W. by a Danish Government scholarship.

Received May 31; accepted June 29, 1976.

[1] Nichols, J. L., *Nature*, **225**, 147–151 (1970).

[2] Min Jou, W., Haegeman, G., Ysebaert, M., and Fiers, W., *Nature*, **237**, 82–88 (1972).

[3] Contreras, R., Ysebaert, M., Min Jou, W., and Fiers, W., *Nature new Biol.*, **241**, 99–101 (1973).

[4] Horiuchi, K., Webster, R. E., and Matsuhashi, S., *Virology*, **45**, 429–439 (1972).

[5] Moore, C. H., Farron, F., Bohnert, D., and Weissman, C., *Nature new Biol.*, **234**, 204–206 (1971).

[6] Weiner, A. M., and Weber, K., *Nature new Biol.*, **234**, 206–209 (1971).

[7] Lu, P., and Rich, A., *J. molec. Biol.*, **58**, 513–531 (1971).

[8] Kaplan, S., *Molec. gen. Genet.*, **120**, 191–200 (1973).

[9] Roth, J. R., *A. Rev. Genet.*, **8**, 319–346 (1974).

[10] Garen, A., *Science*, **160**, 149–159 (1968).

[11] Gorini, L., *A. Rev. Genet.*, **4**, 107–134 (1970).

[12] Hartman, P. E., and Roth, J. R., *Adv. in Genet.*, **17**, 1–105 (1973).

[13] Goodman, H. M., Abelson, J., Landy, A., Brenner, S., and Smith, J. D., *Nature*, **217**, 1019–1024 (1968).

[14] Altman, S., Brenner, S., and Smith, J. D., *J. molec. Biol.*, **56**, 195–197 (1971).

[15] Seidman, J. G., Comer, M. M., and McClain, W. H., *J. molec. Biol.*, **90**, 677–689 (1974).

[16] Yaniv, M., Folk, W. R., Berg, P., and Soll, L., *J. molec. Biol.*, **86**, 245–260 (1974).

[17] Hirsh, D., *J. molec. Biol.*, **58**, 439–458 (1971).

[18] Hawthorne, D. C., and Leopold, U., *Curr. Top. Microbiol. Immun.*, **64**, 1–47 (1974).

[19] Stewart, J. W., and Sherman, F., *J. molec. Biol.*, **68**, 429–443 (1972).

[20] Stewart, J. W., and Sherman, F., *J. molec. Biol.*, **78**, 169–184 (1973).

[21] Gilmore, R. A., Stewart, J. W., and Sherman, F., *J. molec. Biol.*, **61**, 157–173 (1971).

[22] Sherman, F., Liebman, S. W., Stewart, J. W., and Jackson, M., *J. molec. Biol.*, **78**, 157–168 (1973).

[23] Liebman, S. W., Stewart, J. W., and Sherman, F., *J. molec. Biol.*, **94**, 595–610 (1975).

[24] Liebman, S. W., Sherman, F., and Stewart, J. W., *Genetics*, **82**, 251–272 (1976).

[25] Brandriss, M. C., Stewart, J. W., Sherman, F., and Botstein, D., *J. molec. Biol.*, **102**, 467–476 (1976).

[26] Capecchi, M. R., Hughes, S. H., and Wahl, G. M., *Cell*, **6**, 269–277 (1975).

[27] Gesteland, R. F., *et al.*, *Cell*, **7**, 381–390 (1976).

[28] Secher, D. S., Gesteland, R. F., and Milstein, C., *Biochem. Soc. Trans.*, **3**, 873–875 (1975).

[29] Soll, L., *J. molec. Biol.*, **86**, 233–243 (1974).

[30] Celis, J. E., Coulondre, C., and Miller, J. H., *J. molec. Biol.*, (in the press).

[31] Celis, J. E., Hooper, M. L., and Smith, J. D., *Nature new Biol.*, **244**, 261–264 (1973).

[32] Liebman, S. W., and Sherman, F., *Genetics*, **82**, 233–249 (1976).

[33] Madison, J. T., Everett, G. A., and Kung, H. K., *Cold Spring Harb. Symp. quant. Biol.*, **31**, 409–416 (1966).

[34] Rubin, G. M., *Eur. J. Biochem.* **41**, 197–202 (1974).

[35] Fradin, A., Gruhl, H., and Feldmann, H., *FEBS Lett.*, **50**, 185–189 (1975).

[36] Barrell, B. G., in *Proc. Nucleic Acid Res.*, **2** (edit. by Cantoni, G. L., and Davies, D. R.), 751–779 (Harper and Row, New York, 1971).

[37] Anderson, K. W., and Smith, J. D., *J. molec. Biol.*, **69**, 349–356 (1972).

[38] Altman, S., *Nucleic Acids Res.*, **3**, 441–448 (1976).

[39] Crick, F. H. C., *J. molec. Biol.*, **19**, 548–555 (1966).

[40] Comer, M. M., Guthrie, C., and McClain, W. H., *J. molec. Biol.*, **90**, 665–676 (1974).

[41] Bock, R. M., *J. theoret. Biol.*, **16**, 438–439 (1967).

[42] Yoshida, M., Takeishi, K., and Ukita, T., *Biochim. biophys. Acta*, **228**, 153–166 (1971).

[43] Madison, J. T., Boguslawski, S. J., and Teetor, G. H., *Science*, **176**, 687–689 (1972).

[44] Sen, G. C., and Ghosh, H. P., *Nucleic Acids Res.*, **3**, 523–353 (1976).

[45] Liebman, S.W., Stewart, J. W., Parker. J. H., and Sherman, F., *J. molec. Biol.* (in the press).

[46] Kaltoft, K., Engbaek, F., Piper, P. W., Zeuthen, J., and Celis, J. E., *Proc. natn. Acad. Sci. U.S.A.* (in the press).

Systematic approach to the correction of intonation in wind instruments

Richard A. Smith

Boosey and Hawkes Ltd, Edgware, Middlesex, UK and Department of Physics, Southampton University

Geoffrey J. Daniell

Department of Physics, Southampton University, Southampton SO9 5NH, UK

The effect of perturbations in the bore diameter on the intonation of wind instruments is investigated. From measurements of the bore and the amplitude of the standing waves, a modified bore shape is calculated to give any desired correction in intonation.

MUSICAL instruments have evolved over the centuries very much by trial and error. In spite of scientific investigation, many undetermined factors critically affect the performance of instruments, and empirical methods of design are still necessary. Some features, however, are easily amenable to quantitative treatment, and we present here the results of some calculations and experiments on improving the intonation and tone colour of the trumpet.

All brass instruments have acoustical and mechanical inadequacies for which most players automatically compensate[1]. To the average listener an instrument may sound perfectly in tune but this largely results from the competence of the player who may be able to 'lip' a note by ± 1 semitone, usually at the expense of tone colour. Similarly, the intonation of inexperienced players tends to be more affected by the deficiencies of their instruments.

The frequency of a note produced by a trumpet is determined by a complex interaction between the vibrating air column in the instrument and the player's lips. It is also affected by acoustical feedback to the player's ears, and differences of more than 10 cents (1 cent = 0.01 tempered semitone) occur when different players use the same instrument. The frequency is, however, always very close to a resonance frequency of the air column in the trumpet.

The necessity of first eliminating the contribution of the individual player to the intonation has been recognised by several workers[2–7], but no satisfactory method of artificial excitation has yet been described. We have used a modification of the method originally described by Webster[3] to measure the resonance frequencies of the air column in the trumpet. The apparatus (Fig. 1) operates over the frequency range C_2 (65 Hz) to B_7 (3,951 Hz) (C_4 = middle C) and includes an automatic locking device for the location and tracking of resonance peaks. It gives a digital display and printed record of the amplitude and intonation of each resonance (in cents) relative to the equitempered scale.

It was found that the frequency of each resonance of an instrument corresponded closely with the mean of the frequencies produced for this note by a number of players, so that observations with this apparatus can therefore be used for the basis of quantitative measurement of the intonation of the instrument.

Resonances and tone colour

The resonance frequencies are principally determined by the shape of the bore of the trumpet, and evolution has produced a bore shape with resonances fairly close to the appropriate notes of the equitempered scale. Unfortunately intonation is not the only consideration in fixing the resonances as the following example shows.

Figure 2 shows the first 10 resonances of the tube with their corresponding equitempered frequencies. When the trumpet is

Pure Cbc [illegible] Library
[illegible] COLLEGE

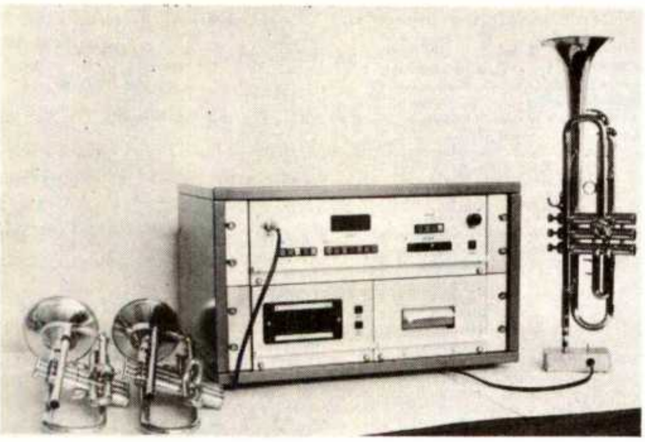

Fig. 1 The apparatus designed to locate automatically and track the resonances of a wind instrument. Digital displays indicate the intonation and amplitude of the resonances.

sounding a steady note, D_5 (587.33 Hz), the frequency of the second harmonic of this fundamental is 1,174.7 Hz, and this strongly excites the resonance at 1,174.7 Hz. This resonance is also near the fourth harmonic (at 1,165.4 Hz) of the fundamental $B\flat_3$ (233.08 Hz). But because this harmonic misses the resonance peak by 14 cents, its strength is not so strongly reinforced, and this has a significant effect on the tone colour of $B\flat_3$.

In practice, the harmonics of any note fall near but not exactly on the resonances of the tube, and are, to varying degrees, reinforced by resonance. The resonances strongly affect the tone colour of notes, and hence the choice of a set of resonances is inevitably a compromise between their intonation when used as fundamentals, and their reinforcement of the harmonics of other notes. We are not concerned here with this compromise, but we show how the design of the bore shape can be modified to move selected resonance frequencies by small amounts to desired values.

Perturbations in the bore

It has been known for many years that small changes in the bore cross section near a node or antinode of the standing wave will change the resonance frequency. A decrease in area at a pressure antinode produces an increase in that frequency, and an increase in area gives a frequency decrease. At a pressure node the effects of changing the area are reversed. We have used perturbation theory to calculate the change in a given bore shape necessary to produce prescribed changes in each of the resonance frequencies.

The pressure oscillations $P_n(x)$, at frequency f_n in a standing wave in the air column in a horn, of cross section $S(x)$, at a distance x from one end, are described by the approximate wave equation[8]

$$\frac{\mathrm{d}}{\mathrm{d}x}\left[S(x)\frac{\mathrm{d}P_n}{\mathrm{d}x}\right]+\frac{4\pi^2 f_n^{\,2}}{c^2}S(x)P_n(x)=0 \tag{1}$$

where c is the velocity of sound. The boundary conditions at the mouthpiece and open end are assumed to be

$$P(x)=\beta\frac{\mathrm{d}P}{\mathrm{d}x}\bigg|_{x=0,L}$$

where the constant β may be different at the two ends of the instrument but the values are assumed to be independent of the mode of oscillation. This is a standard Sturm–Liouville equation and the solutions form a complete orthonormal set[9].

If the cross section $S(x)$ is perturbed by a small change $\delta S(x)$ and $s(x)=\delta S(x)/S(x)$ the first-order change in the resonance frequencies can be shown to be

$$\frac{\delta f_n}{f_n}=\int_0^L s(x)G_n(x)\mathrm{d}x \tag{2}$$

where

$$G_n(x)=\frac{1}{2}S(x)\left\{\frac{c^2}{4\pi^2 f_n^{\,2}}\left[\frac{\mathrm{d}P_n}{\mathrm{d}x}\right]^2-P_n^{\,2}(x)\right\} \tag{3}$$

In deriving this, it is necessary to take δS zero at both ends of the instrument so that the boundary conditions are not changed. The values of $P_n(x)$ used above are taken to be normalised so that

$$\int_0^L S(x)P_n^{\,2}(x)\mathrm{d}x=1 \tag{4}$$

This implies that the dimensions of P are $L^{-3/2}$, and not those of pressure. An alternative expression for $G_n(x)$ can be derived using equation (1)

$$G_n(x)=\frac{c^2}{16\pi^2 f_n^{\,2}}\frac{\mathrm{d}}{\mathrm{d}x}\left[S(x)\frac{\mathrm{d}}{\mathrm{d}x}P_n^{\,2}(x)\right] \tag{5}$$

We wish to prescribe δf_n and calculate $\delta S(x)$. It is clear that the solution is not unique and we shall seek the 'smoothest' change in the bore that produces the required frequency shifts. It may be inconvenient to make changes over the whole instrument, because of the valves and tuning slides, and we shall restrict them to the section $x=0$ to $x=l$. To avoid discontinuities in the bore we need $\delta S(0)=0$ and $\delta S(l)=0$.

Fig. 2 The first 10 resonances of a trumpet with their associated equitempered frequencies. *Not normally used.

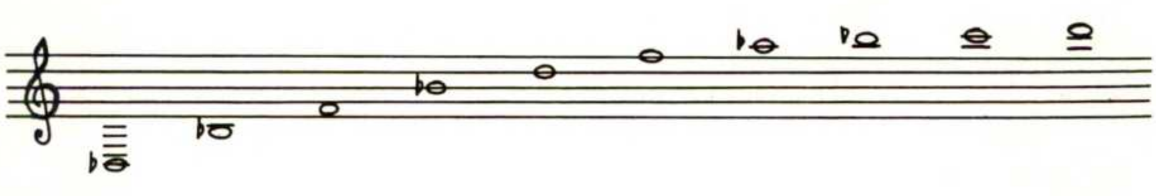

Resonance	1*	2	3	4	5	6	7*	8	9	10
Note	$B\flat_2$	$B\flat_3$	F_4	$B\flat_4$	D_5	F_5	$A\flat_5$	$B\flat_5$	C_6	D_6
Frequency (Hz)	116.54	233.08	349.23	466.16	587.33	698.46	830.61	932.33	1,046.5	1,174.7

A suitable measure of smoothness is the mean square derivative

$$\int_0^l S(x)[s'(x)]^2\mathrm{d}x$$

and we minimise this, subject to the constraints that $s(x)$ produces the required frequency shifts using Lagrange's method of undetermined multipliers, that is we minimise

$$\int_0^l S(x)[s'(x)]^2\mathrm{d}x-\sum_{m=1}^{N}\lambda_m\left[\frac{\delta f_m}{f_m}-\int_0^l s(x)G_m(x)\mathrm{d}x\right]$$

The Euler equation for this problem is

$$\frac{\mathrm{d}}{\mathrm{d}x}[S(x)2s'(x)]=\sum_{m=1}^{N}\lambda_m G_m(x)$$

$$=\frac{c^2}{16\pi^2 f_m^2}\sum_{m=1}^{N}\lambda_m\frac{\mathrm{d}}{\mathrm{d}x}\left[S(x)\frac{\mathrm{d}}{\mathrm{d}x}P_m^2(x)\right]$$

Integrating twice gives

$$s(x)=\sum_{m=1}^{N}\mu_m P_m^2(x)+A\int_0^x\frac{\mathrm{d}\xi}{S(\xi)}+B \qquad (6)$$

A and B are arbitrary constants of integration and they can be chosen to make $\delta S(0)=0$ and $\delta S(l)=0$, and μ_m is a multiple of λ_m.

Substituting this into (2) gives N linear equations which, together with the conditions on δS, determine the $N+2$ constants μ_m, A, B. Equation (6) then gives the required change in bore.

Fig. 3 The physical shape of a trumpet (not to scale) with $P_n(x)$ and $G_n(x)$ for selected modes.

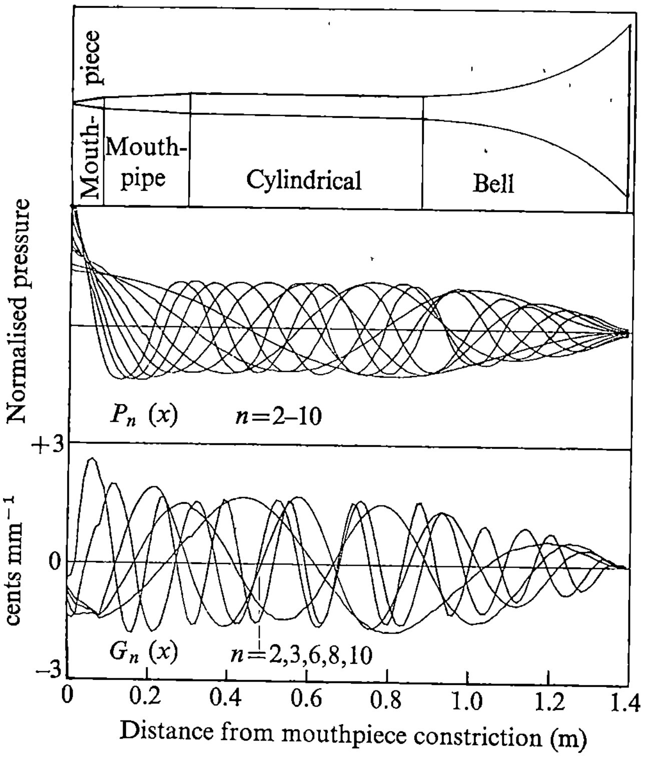

The reader may wonder why we have used the 'smoothest' perturbation rather than the 'smallest' one. If we define

$$\varepsilon=\int_0^l[s(x)]^2\mathrm{d}x$$

and find the function $s(x)$ that minimises this and produces the required frequency shifts we get

$$s(x)=\sum_m\mu_m G_m(x) \qquad (7)$$

This cannot, however, be used as a solution to our problem as it does not ensure that $\delta S(0)=0$ and $\delta S(l)=0$.

The eigenfunctions for the standing waves

To perform the calculations of the previous section the functions $P_n(x)$ are required. Although it is possible, in principle, to calculate these given the cross-sectional area of the trumpet, it is undoubtedly easier to observe them.

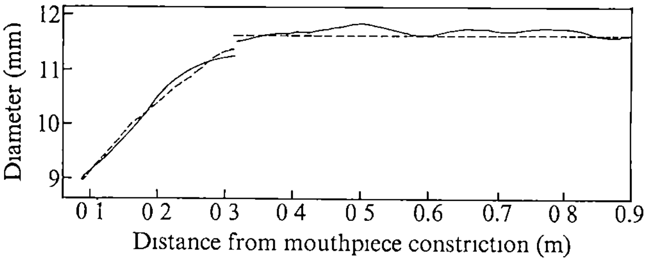

Fig. 4 The bore shape of a trumpet (conical and cylindrical portions) before and after perturbation. ——, Perturbed bore; — —, original bore.

In a standing wave, when damping is very small, the oscillations have the same phase at all points between adjacent nodes, and the phase changes by π across each node. The result is not exact if damping is included, but as we have neglected damping, even in equation (1), there is no advantage in observing the phase of the pressure oscillations, and we assume the phase is 0 or π. The function $P_n(x)$ is therefore given by the observed pressure amplitude between alternate pairs of nodes and minus the observed pressure in the gaps.

The derivative $\mathrm{d}P_n/\mathrm{d}x$ is also required. Because of the well known dangers of numerical differentiation we obtain this by integrating equation (1) giving

$$\frac{\mathrm{d}P_n(x)}{\mathrm{d}x}=-\frac{4\pi^2 f_n^2}{c^2 S(x)}\int_0^x S(\xi)P_n(\xi)\mathrm{d}\xi+\frac{C}{S(x)}$$

The value of the constant of integration C is found by integrating again, thus introducing another constant, and finding both constants by satisfying the equations at two particular values of x.

Varying the length of pipe over which the perturbation is made

An interesting result can be derived about the mean square perturbation, which can be evaluated using equation (7). This can be differentiated with respect to l, bearing in mind that the numbers μ depend on l. The derivatives of μ can be eliminated by differentiating equation (2) and we get the remarkable result

$$\frac{\partial\varepsilon}{\partial l}=-[s(l)]^2 \qquad (8)$$

It follows that $\partial\varepsilon/\partial l$ is never positive, and the mean square value of the perturbation required always decreases as we spread the perturbation over longer lengths of the tube.

Asymptotic results

The high eigenvalues of a Sturm–Liouville equation have simple asymptotic distributions[9]. When n is large, $f_n \sim nc/2L$ and

$$P_n(x) \sim \left(\frac{2}{LS(x)}\right)^{1/2} \cos\left[\left(n-\frac{1}{2}\right)\frac{\pi x}{L}+\theta_n\right]$$

in which θ_n depends on the boundary conditions. A musical instrument like the trumpet has evolved into a shape such that the frequencies of the resonances are almost uniformly spaced. In other words, the formula $f_n \sim nc/2L$, which can be proved for large n, is in fact almost exact for all n. This suggests that the associated asymptotic eigenfunctions, $P_n(x)$, might be good approximations for all n. This would avoid the difficult measurement of $P_n(x)$. If the boundary conditions in the trumpet are approximately

$$P_n(L) = 0 \text{ and} \left[\frac{\mathrm{d}P_n}{\mathrm{d}x}\right]\Bigg|_{x=0} = 0$$

we can show that

$$G_n(x) \sim -\frac{1}{L}\cos\left(\frac{(2n-1)\pi x}{L}\right)$$

The integrals involved in the calculations can now be evaluated analytically.

We have tested the usefulness of this by prescribing some values for δf_n, calculating the bore shape required using the asymptotic expression for $G_n(x)$ and then calculating the exact frequency shifts (equation 2) that this bore shape would produce, using the correct observed value of $G_n(x)$. The changes produced are found to be in the right direction, but the magnitude of error is large. The asymptotic results can, however, be usefully employed if (a) a rapid approximate answer is required: the measurement of $P_n(x)$ is time consuming, or (b) if a very high harmonic needs adjustment, where the observations of the resonance are impossible.

Verification of the theory

The trumpet was driven by the automatic tuner described in the first section and the sound pressure was measured in two ways; using probe tubes inserted radially through holes in the bore at each centimetre of the instrument's length and using a long flexible probe drawn through the instrument. There was little variation between the results of either method and they are shown with the computed functions $G_n(x)$ in Fig. 3.

An earlier section has indicated the difficulties involved in deciding upon the optimum intonation of an instrument. To verify our ideas, however, these arbitrary changes were chosen: for the fifth and tenth order resonance, a change of +5 cents for the sixth order resonance a change of −5 cents, and all other resonances to be unaltered. Similarly, the perturbed length was arbitrarily restricted to the first 0.9 m of the instrument. This bore provides the 'open' notes of the instrument and additional tubing is inserted by valves to produce a chromatic scale. Consequently the effect of our perturbation is likely to be less accurate as more tubing is added; the perturbation method could be applied to this valve tubing for further correction to notes using valve tubes. Equation (8) implies that because of the relatively short length of the valve tubing, only small intonation corrections could be made in this way without unacceptably large diameter changes.

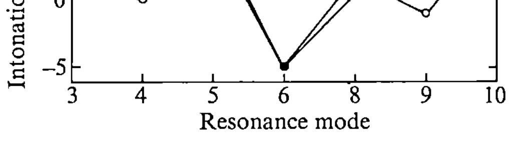

Fig. 5 Relative intonation of seven resonance modes. ●, Required change in intonation; ○, change obtained by perturbation.

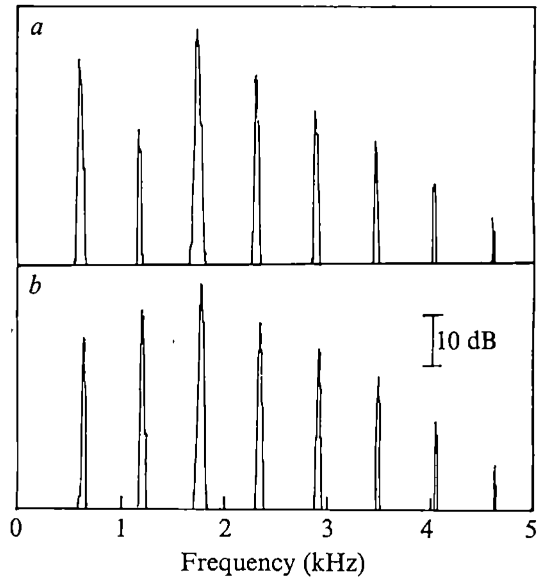

Fig. 6 The spectra of note D_5 (587.33 Hz) blown by a professional musician. (*a*) before, and (*b*) after perturbation. Both notes were played *mezzo forte* in an anechoic chamber with the michrophone at 1 m along the axis of the instrument.

A graph of the new bore shape (Fig. 4) indicates a maximum change in diameter of < 0.2 mm. This may be compared with a maximum of 0.14 mm for the smallest mean square perturbation mentioned earlier.

The new shape was reproduced with glass reinforced plastic and its resonances measured using the automatic tuner. There is close correspondence between the required and measured intonation (Fig. 5); the small errors mainly arise from the difficulty in producing a new bore to an accuracy of better than 0.02 mm.

It can be appreciated from the qualitative effects of diameter changes at nodes and antinodes that some prescribed frequency shifts may require conflicting diameter changes. The result in these cases is that very large increases and decreases in diameter are required over short distances. These would be unacceptable for a musical instrument and would also render our first-order perturbation theory invalid. Our optimisation procedure makes sure that large changes in diameter are not used unnecessarily.

For comparison another calculation has been made which assumes a non-optimum bore shape given by a superposition of sine waves. The maximum diameter change required here was 3 mm.

Curing a faulty trumpet

Although the foregoing theory is not ideally suited to the complete acoustical design of a new instrument, the best application of this work is with the improvement of the individual notes of prototype or production instruments. One such instrument was found to have a weak second harmonic when playing D_5 (587.33 Hz) (Fig. 6*a*). As already mentioned, this harmonic uses the tenth resonance for reinforcement; and this was found to be flat with respect to the fifth. The tenth resonance is not normally played as a fundamental and hence can be altered to improve the tone colour. Using our new technique we were able to raise this tenth resonance by ten cents to give the improved response (Fig. 6*b*).

This work was supported in part by the SRC and Boosey & Hawkes Ltd. We thank Dr D. M. A. Mercer for encouragement and also acknowledge the assistance of Mr W. Tompkins and the trumpet player, Michael Laird.

Received May 13; accepted July 21, 1976

[1] Smith, R. A., thesis, Univ Southampton (1974).
[2] Martin, D. W., thesis, Univ. Illinois (1941).
[3] Webster, J. C , *J acoust. Soc. Am* , 19, 902–906 (1947).
[4] Igarashi, J , and Koyasu, M., *J. acoust. Soc. Am.*, 25, 122–128 (1953)
[5] Hunt, F. V., *J acoust Scc. Am.*, 10, 216–227 (1939).
[6] Backus, J., and Hundley, T. C , *J. acoust Soc. Am* , 49, 509–519 (1970).
[7] Benade, A. H., and Jansson, E. V., *Technical Report* (Speech Transmission Laboratory, Royal Institute of Technology, Stockholm, 1973).
[8] Morse, P. M., *Vibration and Sound*, 2nd ed , 269 (McGraw-Hill, New York, 1948).
[9] Morse, P. M., and Feshbach, H , *Methods of Theoretical Physics*, par. 6 3 (McGraw-Hill, New York, 1953).

letters to nature

Does Mercury have a molten core?

THE discovery of an intrinsic magnetic field for the planet Mercury by Mariner 10 (ref. 1) and its preferred source in an internal dynamo[2] imply the existence of a conducting molten core. We propose here a feasible, non-seismic observational experiment to determine the existence and extent of such a molten core, which would be vital for calculations of Mercurian thermal histories and dynamo field generation.

Siegfried and Solomon[3] have calculated two thermal histories for Mercury leading to a differentiated and an undifferentiated planet respectively. In the latter models, of course, Mercury would have no core. Even in the differentiated model a once molten core tends to solidify as the planet cools. Whether or not a given differentiated model leads to a molten core persisting to the present depends critically on assumptions about initial conditions (the time of core formation), the time varying distribution of radioactive elements within the planet, thermal conductivities and the extent and efficiency of convective heat transport. Even with all the radioactive elements being removed from an initially differentiated molten core, Fricker *et al.*[4] have shown that a liquid outer core 500-km thick may still persist if one accounts for a thermal barrier at a liquid iron–solid silicate core–mantle boundary. The thermal barrier results from the higher melting point and lower thermal conductivity of the silicates—the liquid iron core temperature rises above the melting curve near the core–mantle boundary thereby decreasing the core temperature gradient. If the solid mantle is allowed to convect, however, it must contain a density of heat sources comparable to the Earth's mantle-wide average if the core is to remain molten[5].

Since we cannot be certain about the convective heat transport or the distribution of heat sources, theoretical predictions about the nature of the Mercurian core are not conclusive. There is thus a severe need for the experimental determination of some of the key internal parameters or, more directly, for an experiment which would determine unambiguously the extent of any fluid core. The latter would motivate considerable research into the generation of planetary magnetic fields and would place bounds on the internal parameters related to the thermal history—whether or not the core was found to be molten. Fortunately, the effects of a liquid core on the dynamics of Mercury's rotation affords a technically feasible, albeit expensive means of determining unambiguously the nature of Mercury's core[6].

There are two necessary conditions for this scheme to work. First, a liquid core must not follow the mantle's forced librations (88-d period) in longitude, which arise from the periodic solar torque on its asymmetric mass. Second, the core must follow the mantle on the time scale of the 250,000-yr precession. We shall assume these two conditions are satisfied to develop the method and subsequently establish bounds on the core viscosity for which they are satisfied.

The amplitude of the physical librations in longitude with the period of a Mercury year is[7]

$$\varphi_0 = \frac{3}{2}\left(\frac{B-A}{C_m}\right)\left(1-11e^2+\frac{959}{48}e^4+\ldots\right)\simeq\frac{B-A}{C_m} \qquad (1)$$

where $A<B<C$ are principal moments of inertia of the entire planet, e is the orbital eccentricity and C_m is the moment of inertia of the mantle alone. The physical libration is thus larger than it would have been if the core were solid. (The core is assumed axially symmetric, so it does not contribute to $B-A$.) The tides carry Mercury to a configuration which is a generalisation of Cassini's laws for the Moon[8], where the spin axis, orbit normal and normal to the invariable plane remain coplanar as the first two vectors precess around the last with a 250,000-yr period. In this 'Cassini state', the following relation is satisfied[8,9]

$$K_1(\theta)\left(\frac{C-A}{C}\right)+K_2(\theta)\left(\frac{B-A}{C}\right) = K_3(\theta) \qquad (2)$$

where K_1, K_2, K_3 are constants involving the orbital eccentricity, inclination and mean motion and the planetary spin angular velocity and explicitly the obliquity θ. In equation (2), $K_2 \ll K_1$ and can sometimes be neglected as it has been in the classical determination of $(C-A)/C$ for the Moon[9]. Note that C and not C_m is appropriate here, because of our assumption that any liquid core is able to keep up with the mantle precession. Also, θ and φ_0 are measurable quantities.

The second degree gravitational harmonics are related to the moment of inertia differences by

$$J_2 = \frac{C-A}{MR^2} - \frac{1}{2}\frac{(B-A)}{MR^2} \qquad (3)$$

$$C_{22} = \frac{B-A}{4MR_2}$$

where M and R are the planetary mass and radius respectively. Equations (3) can be solved for $(B-A)/MR^2$ and $(C-A)/MR^2$ in terms of J_2 and C_{22}, where the latter two quantities can be determined by tracking one or more artificial satellites. Substitution of the solutions of equations (3) into equation (2) yields a numerical value for C/MR^2 since the K are known once the obliquity θ is determined. This number, already determined for the Moon by the same procedure[10], is a measure of the density distribution in the planet. ($C/MR^2 \simeq 0.33$ for the Earth, $\simeq 0.40$ for the Moon, $\simeq 0.40$ for an homogeneous sphere.)

Finally, measurement of the amplitude of the physical libration φ_0 yields $(B-A)/C_m$ from which three known factors yield

$$\left(\frac{C_m}{B-A}\right)\left(\frac{B-A}{MR^2}\right)\left(\frac{MR^2}{C}\right) = \frac{C_m}{C} \leq 1 \quad (4)$$

A value for C_m/C of 1 would indicate the core to be firmly coupled to the mantle and hence most probably solid. If the entire core or the outer part is fluid, $C_m/C \simeq 0.5$ for the large core size ($R_c \simeq 0.75R$) in current models of the interior[5].

How good are the assumptions that a fluid core will not follow the short period physical librations but will follow the long period precession? The appropriate time scale to compare with the 88-d and 250,000-yr periods is the 'spin up' or 'spin down' time for the core fluid (rotating at a slightly different angular velocity) to approach the perturbed angular velocity of the mantle[11].

$$\tau = R_c/(\nu\dot{\psi})^{\frac{1}{2}} \quad (5)$$

where R_c is the core radius, ν is the kinematic viscosity and $\dot{\psi}$ is the spin angular velocity of the planet. If $\tau > 88$ d the core will not follow the mantle libration, whereas if $\tau < 250{,}000$ yr, the core will follow the mantle precession. These bounds on τ lead to the bounds on ν of

$$8\times10^{-4} < \nu < 2\times10^{9}\ \mathrm{cm^2\ s^{-1}} \quad (6)$$

where both necessary conditions for the determination of C_m/C are satisfied if ν is within these bounds. This is almost certainly true since the range in equation (6) includes the complete range estimated for the Earth's core of 5×10^{-3}–10^7 cm² s⁻¹ (ref. 12).

The numbers φ_0, θ, J_2 and C_{22} must be determined to find C_m/C and hence the extent of the Mercurian liquid core. The first two are O(20″–40″) and O($\lesssim 1°$) (ref. 9, and B. A. Smith, personal communication) respectively and will almost certainly require rather sophisticated instrumentation on the surface of the planet. The latter two can be obtained from precise tracking of artificial satellites. The design of instrumentation to measure the small angles φ and θ which is within the weight limitations and which will survive the possibly hard landing of any spacecraft sent to Mercury's surface is a severe challenge. The large scientific return which could, however, be realised from such surface instrumentation means that the attempt at the design should be made.

S. J. PEALE

Department of Physics,
University of California,
Santa Barbara, California 93106

Received March 4, accepted July 7, 1976

[1] Ness, N. F., Behannon, K. W , Lepping, R. P., Whang, Y. C., and Schatten, K. H., *Science*, **185**, 151–160 (1974).
[2] Ness, N. F., Behannon, K. W., Lepping, R. P , and Whang, Y. C., *J. geophys. Res* , **80**, 2708–2716 (1975).
[3] Siegfried, R. W., II, and Solomon, S. C., *Icarus*, 23, 192–205 (1974).
[4] Fricker, P. E., Reynolds, R. T., Summers, A. L., and Cassen, P. M., *Nature*, **259**, 293–294 (1976).
[5] Cassen, P. M., Young, R. E , Schubert, G., and Reynolds, R. T., *Icarus* (in the press).
[6] Peale, S. J., *Icarus* (in the press).
[7] Peale, S. J , *Icarus*, **17**, 168–173 (1972).
[8] Peale, S. J., *Astr. J.*, **79**, 722–744 (1974).
[9] Peale, S. J., *Astr. J.*, **74**, 483–489 (1969).
[10] Kaula, W. M., *EOS, Trans. Am. geophys. Un.*, 56, 309–316 (1975).
[11] Greenspan, H. P., and Howard, L. N., *J. Fluid Mech.*, 17, 385–404 (1963).
[12] Jeffreys, H., *The Earth*, 254 (Cambridge University Press, 1959).

Structure of the extended solar magnetic field and the sunspot cycle variation in cosmic ray intensity

THE interplanetary magnetic field within several astronomical units of the Sun appears to have one polarity in most of the hemisphere north of the solar equatorial plane and the opposite polarity in most of the hemisphere south of the equatorial plane[1–7]. The two hemispheres are separated by a curved current sheet that typically crosses the solar equatorial plane in either two or four places, thus dividing the equatorial region into either two or four sectors. Near sunspot minimum, at 1 AU the curved current sheet has a spread in latitude of typically ± 15°, so that the sector boundary (the current sheet separating the two hemispheres of opposed field polarity) is almost parallel to the solar equatorial plane. In the photosphere, on the other hand, the sector boundary makes an angle of ~ 90° with the equatorial plane[8]. At $1.5R_\odot$, in 1972 and 1973, the angle between the sector boundary and the equatorial plane was ~ 45° (ref. 9), and at 3–$10R_\odot$ the angle between boundary and plane was ~25° (ref. 10). A schematic diagram of this structure for the case of four sectors is shown in Fig. 1. We here propose that a connection exists between the extent of these magnetic fields and the observed variations in cosmic ray intensity at the Earth.

In the photosphere, near sunspot minimum, the sector magnetic fields cover a range in latitude of typically ±40° (ref. 8), while at 1 AU the comparable range in latitude has been compressed to perhaps ±15°. How is this compression in latitude accomplished? A typical magnitude of the sector magnetic fields in the photosphere is 0.5 gauss (P. H. Scherrer and T. L. Duvall, personal communication). This is a measure of the large scale field that will dominate in the region a few $R_\odot$ above the photosphere, where the smaller scale but much stronger fields associated with active regions do not reach. In the polar regions of the Sun the large scale unidirected photospheric field has a typical magnitude of perhaps 5 gauss (R. Howard, personal communication). Thus, at 1 or $2R_\odot$

Fig. 1 Schematic showing the warped current sheet in the inner Solar System (inside 6 AU). This current sheet divides the interplanetary magnetic field in the heliosphere into two regions with oppositely directed field lines. In one region the field polarity is away from the Sun (at present this region is north of the solar equator), in the other region the field polarity is toward the Sun. The situation is shown for a four-sector structure, that is, as the current sheet is rotated past a stationary observer in the course of a solar rotation, the observer will see four changes of magnetic polarity, suggesting that the interplanetary magnetic field is divided into four sectors of alternating polarity. Where the current sheet lies above the solar equatorial plane it is shown by full lines, while dashed lines indicate that the current sheet is below the equatorial plane. The extent in latitude of the current sheet was assumed to be ±15°. The Sun at the centre is not shown to scale.

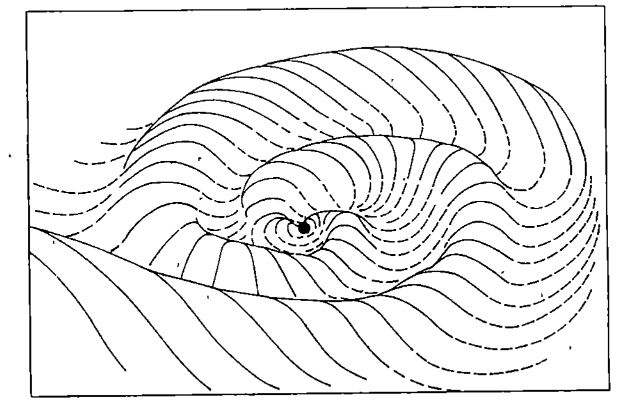

above the photosphere, and above the region of influence of active regions, the magnetic pressure associated with the solar polar regions is two orders of magnitude larger than the magnetic pressure associated with the equatorial sector structure. This will compress the equatorial sector field structure into a narrow range of latitudes. This effect can be clearly seen in the sketch in Fig. 2 made from an eclipse photograph taken at solar minimum in 1954 (ref. 11).

During an interval near sunspot maximum, when the solar polar field polarities are reversing, the magnitude of the polar fields may be considerably less, and the resulting compression of the equatorial field structure also much less. The sector structure fields may then occupy a much larger fraction of the heliosphere. Since the sector structure fields reverse polarity typically four times or two times per solar rotation, a galactic cosmic ray headed towards the Sun may encounter considerably more magnetic scattering from the complex sector structure field than from the unidirectional field that fills most of each solar hemisphere near sunspot minimum. This geometrical effect may be the principal cause of the 11-yr modulation of cosmic-ray intensity observed at the Earth, since the solar-wind velocity[12] and the magnitude of the interplanetary field[13] observed near the Earth have not changed very much during the present sunspot cycle.

The fraction of the heliosphere occupied by sector-structure fields as a function of time through an average sunspot cycle can be estimated in the following way. Because the current sheet shown in Fig. 1 is warped with respect to the solar equatorial plane, during the half year when the earth is north of the equatorial plane an interplanetary sector with the same polarity as the northern solar polar region is observed to be wider than it would be if observed when the Earth is in the equatorial plane of the Sun. For example, assume that there are two sectors per solar rotation and that the extent in heliographic latitude of the sector structure near the Earth is ±20°. When the Earth is at a latitude near 7°N (near September 7), the sector whose polarity is the same as the northern polar region will be observed to last 16.5 d, as compared with the 13.5 d it would last if observed when the Earth is near the solar equatorial plane. For comparison, if the extent in heliographic latitude of the sector structure near the Earth is ±45°, then the sector with the same polarity as the northern polar region will have a length of 14.6 d when observed near the Earth at 7°N. We see that if we measure the magnitude of this Rosenberg–Coleman effect[14,15] through a sunspot cycle we can estimate the extent in heliographic latitude of the sector structure.

We have used an harmonic analysis to compute the average amplitude of the Rosenberg–Coleman effect as a function of years from the time of sunspot minimum for the four sunspot cycles whose minima were near 1934, 1944, 1954 and 1965. Interplanetary field polarities inferred from polar geomagnetic variations[16] were used, and the resulting amplitude of the Rosenberg–Coleman effect was multiplied by 1.43 to correct for the ~85% accuracy[17,18] of the inferred interplanetary field polarities.

Figure 3 shows the resulting value for the extent in heliographic latitude of the sector structure through an average sunspot cycle. Three-year running means were used to reduce the scatter. Year 0 is the average of the sunspot minimum years 1934, 1944, 1954 and 1965. The effect of uncertainties in the computation of the magnitude of the Rosenberg–Coleman effect will usually be to decrease the amplitude of the effect and, therefore, the latitude values shown in Fig. 3 should be considered upper limits. We may expect considerable variation from the average effect shown in Fig. 3, and in particular for intervals of several months near sunspot minimum the current sheet may occupy only a few degrees of latitude.

As a first approximation, we assume that galactic cosmic rays have relatively difficult access to the inner Solar System in the portion of the heliosphere occupied by the changing fields of the sector structure, and relatively easy access through the portions of the heliosphere occupied by the extended uniform solar polar fields. This assumption is consistent with the observational evidence now available. A final evaluation must await *in situ* observations with out-of-ecliptic spacecraft. It is also observed[8] that high speed solar wind streams are contained within sectors. Kinks and irregularities in the interplanetary magnetic field that can scatter cosmic rays are produced as the fast plasma in a high speed stream overtakes slower plasma. The solar-wind plasma coming from higher solar latitudes may have a more uniform (albeit larger) velocity than the solar wind plasma from lower solar latitudes, and thus be not as effective in producing scattering of cosmic rays.

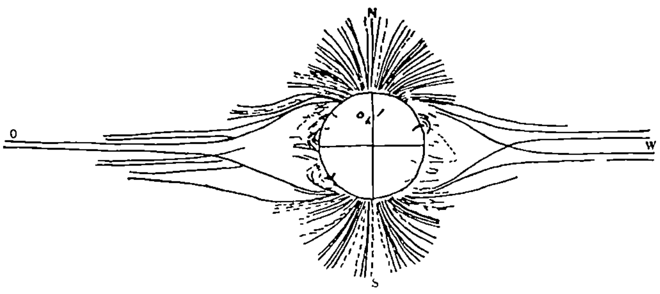

Fig. 2 The structure of a sunspot minimum solar corona drawn from eclipse photographs[11] (June 30, 1954) obtained in Kozeletsk.

In Fig. 4 we show the solid angle of the heliosphere occupied by the extended solar polar fields through an average sunspot cycle, where the latitude angles shown in Fig. 3 are used to compute the solid angles shown in Fig. 4. Also shown in Fig. 4 are the monthly averages of the absolute intensity of primary cosmic rays of rigidity > 0.5 GV observed near Murmansk and at Mirny from 1958 to 1973 (ref. 19). The total flux of such galactic cosmic rays in the interstellar medium in the vicinity of the earth is estimated to be 4,000 $m^{-2} s^{-1} sr^{-1}$ (ref. 19). Therefore, in Fig. 4 we have set the total solid angle 4π of the heliosphere as equivalent to a flux of 4,000 $m^{-2} s^{-1} sr^{-1}$, and the zero of the solid angle scale corresponds to zero flux. This corresponds to the assumption that galactic cosmic rays have easy access to the inner Solar System through the solid angle of the heliosphere occupied by the extended solar polar fields, and difficult access through the solid angle occupied by the sector structure fields.

In Fig. 4 we see that the average sunspot cycle variation of the solid angle of the extended solar polar fields is rather similar to the observed variation of the flux of primary cosmic rays of rigidity > 0.5 GV between 1961 and 1969. We should not

Fig. 3 Computed variation of the average extent in heliographic latitude of the extended solar sector magnetic fields. Year 0 is the average of the sunspot minimum years 1934, 1944, 1954 and 1965. The value 20° on the ordinate means that the extended sector fields are in the interval 20°N to 20°S.

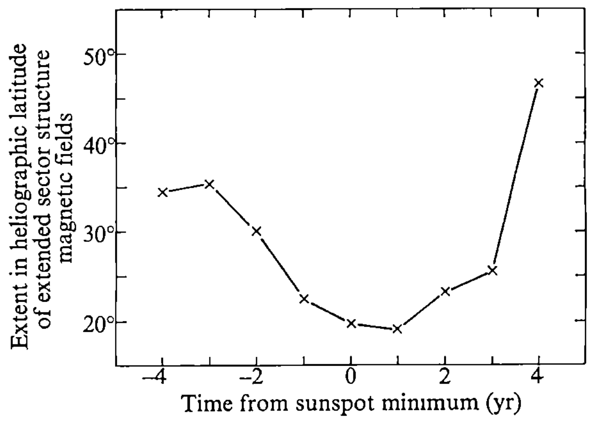

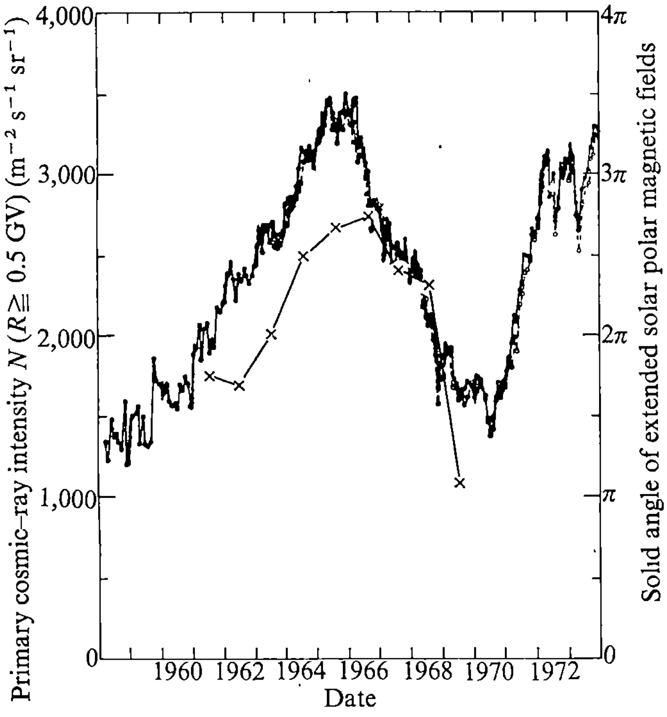

Fig. 4 Galactic cosmic-ray intensities with rigidity 0.5 GV observed near Murmask (●) and at Mirny (○) from 1958 to 1973 (ref. 19). Also shown is the computed average solid angle (×) of the heliosphere occupied by the extended solar polar magnetic fields.

expect a detailed agreement between the computed variation of solid angle averaged over four sunspot cycles and the observed cosmic-ray flux around a single sunspot minimum. The similarity of the two curves in Fig. 4 suggests that there may be some validity to the considerations advanced in this paper. The detailed computation of the diffusion lengths of cosmic rays related to these considerations is beyond the scope of this paper.

We thank the NASA–Skylab Workshop on Coronal Holes for discussions. This work was supported in part by the Office of Naval Research, by NASA, by the Atmospheric Sciences Section of the NSF and by the Max C. Fleischmann Foundation.

Leif Svalgaard
John M. Wilcox

Institute for Plasma Research,
Stanford University,
Stanford, California 94305

Received March 22, accepted July 5, 1976

[1] Schatten, K , *Solar Wind* (edit by Sonnett, C P , Coleman, P J , and Wilcox, J. M.), 65–92 (Scientific and Technical Office, NASA, 1972)
[2] Schultz, M , *Astrophys Space Sci* , **24**, 371–383 (1973).
[3] Sawyer, C , *Geophys. Res. Lett.*, **1**, 295–297 (1974).
[4] Alfven, H., *Proc. Nobel Symposium on the Physics of Hot Plasma in the Magnetosphere* (Kiruna, Sweden, 1975)
[5] Levy, E H , *Proc. 14th int Cosmic Ray Conf , 15–29 August 1975*, 4, 1215–1220 (Max-Planck-Institut fur Extraterrestrische Physik, Munchen, FRG, 1975).
[6] Svalgaard, L , Wilcox, J. M , Scherrer, P H , and Howard, R., *Sol Phys* , **45**, 83–91 (1975)
[7] Saito, T , *Sci Rep Tohoku Univ . Geophys* , 23, 37–54 (1975)
[8] Wilcox, J. M , *Space Sci. Rev* , **8**, 258–328 (1968)
[9] Hansen, S , Sawyer, C , and Hansen, R T , *Geophys Res Lett* , **1**, 13–15 (1974).
[10] Howard, R. A , and Koomen, M. J , *Sol Phys* , 37, 469–475 (1974)
[11] Vsekhsvjatsky, S K , *The Solar Corona, Proc int astr Un Symp , 16, Cloudcroft, New Mexico, 28–30 August 1961* (edit by Evans, J W.) 271–280 (Academic, New York, 1963)
[12] Diodato, L , Moreno, G , Signorini, C , and Ogilvie, K. W , *J geophys. Res.*, **79**, 5095–5108 (1974).
[13] Barouch, E , and King, J. H., *Proc. 14th int Cosmic Ray Conf , 15–29 August 1975*, 3, 1036–1041 (Max-Planck-Institut fur Extraterrestrische Physik, Munchen, FRG, 1975)
[14] Rosenberg, R L , and Coleman, P J , Jr, *J geophys Res* , 74, 5611–5622 (1969)
[15] Wilcox, J M., and Scherrer, P H , *J. geophys Res* , 77, 5385–5388 (1972)
[16] Svalgaard, L , *J. geophys Res* , 77, 4027–4034 (1972)
[17] Russell, C. T , and Rosenberg, R L , *Sol Phys* , 37, 251–256 (1974)
[18] Wilcox, J M., Svalgaard, L , and Hedgecock, P C , *J geophys. Res* , 80, 3685–3688 (1975).
[19] Vernov, S O., Charakhchyan, A N , Stozhkov, Ju I , and Charakhchyan, T N , *Proc 14th int Cosmic Ray Conf , 15–29 August 1975*, 3, 1015–1024 (Max-Planck-Institut fur Extraterrestrische Physik, Munchen, FRG, 1975)

Glass-rich basaltic sand and gravel within the oceanic crust at 22°N

During Leg 46 of the Deep Sea Drilling Project (January 29–March 10, 1976), the second leg of the International Phase of Oceanic Drilling, the Glomar Challenger drilled into 255 m of basaltic basement at hole 396B, 160-km east of the Mid-Atlantic Ridge valley at 22°59.14′N, 43°30.90′W. The hole was drilled into crust with a magnetic anomaly age of ~ 10 Myr. This site is located in a N–S trending sediment pond which measures ~ 4 km × 10 km and is concordant with local topographic trends. There are 150 m of sediment at the drill site; however, the basement slopes regionally to the east and sediment thickness is probably > 250 m along the fault-bounded (?) eastern margin (G. M. Purdy, unpublished, and report of work by the Soviet research vessel Akademik Kurchatov). The bottom 90 m of this hole contained basaltic sand and gravel. This material is not believed to be a drilling artefact, but caused by *in situ* spalling or brecciation of basaltic pillow rinds.

On a number of other occasions, for example, on Legs 34 and 45, there was some indication, principally the sticking or jamming of the drill bit within young basement, that clastic zones had been encountered. At hole 396B a zone of rapid penetration was followed by an interval of difficult drilling and frequent sticking of the bit which eventually led to termination of drilling. In the lower part of the hole, the core catcher assembly was modified to catch fine clastic material and in cores 30 and 33, the core barrel contained 82 and 90 cm respectively, of basaltic gravel and sand. The recovery rate immediately above these two intervals was < 1% and on the basis of this and other shipboard data, in particular results from a unique downhole logging programme, we believe that the clastic zone was first encountered at 310 m sub-bottom and was apparently continuous down to at least 405.5 m where the hole was abandoned.

Stratigraphic units within 396B were determined on the basis of macroscopic and microscopic lithologies, magnetic properties, chemical composition, alteration features and density of recovered samples. In addition, we have been able to correlate these units with downhole logging records which include sonic velocity, natural γ-ray intensity, porosity, density and electrical conductivity. Figure 1 summarises the general lithologies, magnetic inclination, chemical stratigraphy (typified by TiO_2 concentrations) and dual induction lateral (conductivity) log. All indicators show a marked change in character below the 310-m depth where samples of the clastic material were first recovered.

The gravel and sand from cores 30 and 33 are largely in the coarse sand to fine gravel size range (0.5–3.0 mm) and are moderately sorted. The sorting, however, may be the result of preferential loss of fine grained material during core recovery. The fragments are generally non-vesicular and consist of angular chips of glass and variolitic, cryptocrystalline and intersertal basalt. Olivine and plagioclase occur as phenocrysts in the clasts and as crystal fragments. A small number of pieces of calcite-cemented basaltic microbreccia, a few chips with calcite spherules and clasts with cross-cutting calcite veins were found. In general, the glass appears quite fresh, palagonite rims are uncommon and few palagonite fragments were found.

Two small fragments (5–10 cm) of bedded hyaloclastite were also recovered in core 30. One of these samples is a moderately indurated fine to coarse grained hyaloclastite sandstone with graded bedding and evidence for scouring. Both rocks offer clear evidence for some sort of current action and the redistribution of dominantly sand-sized fragments of sideromelane and fine grained basalt.

The last 90 m, which we have called the clastic zone, is divided into four units: an upper clastic breccia, an upper basaltic gravel, a plagioclase phyric pillow basalt (breccia ?) and a lower gravel unit. The two gravel units seem to have been derived locally. Crystalline fragments in the upper gravel are

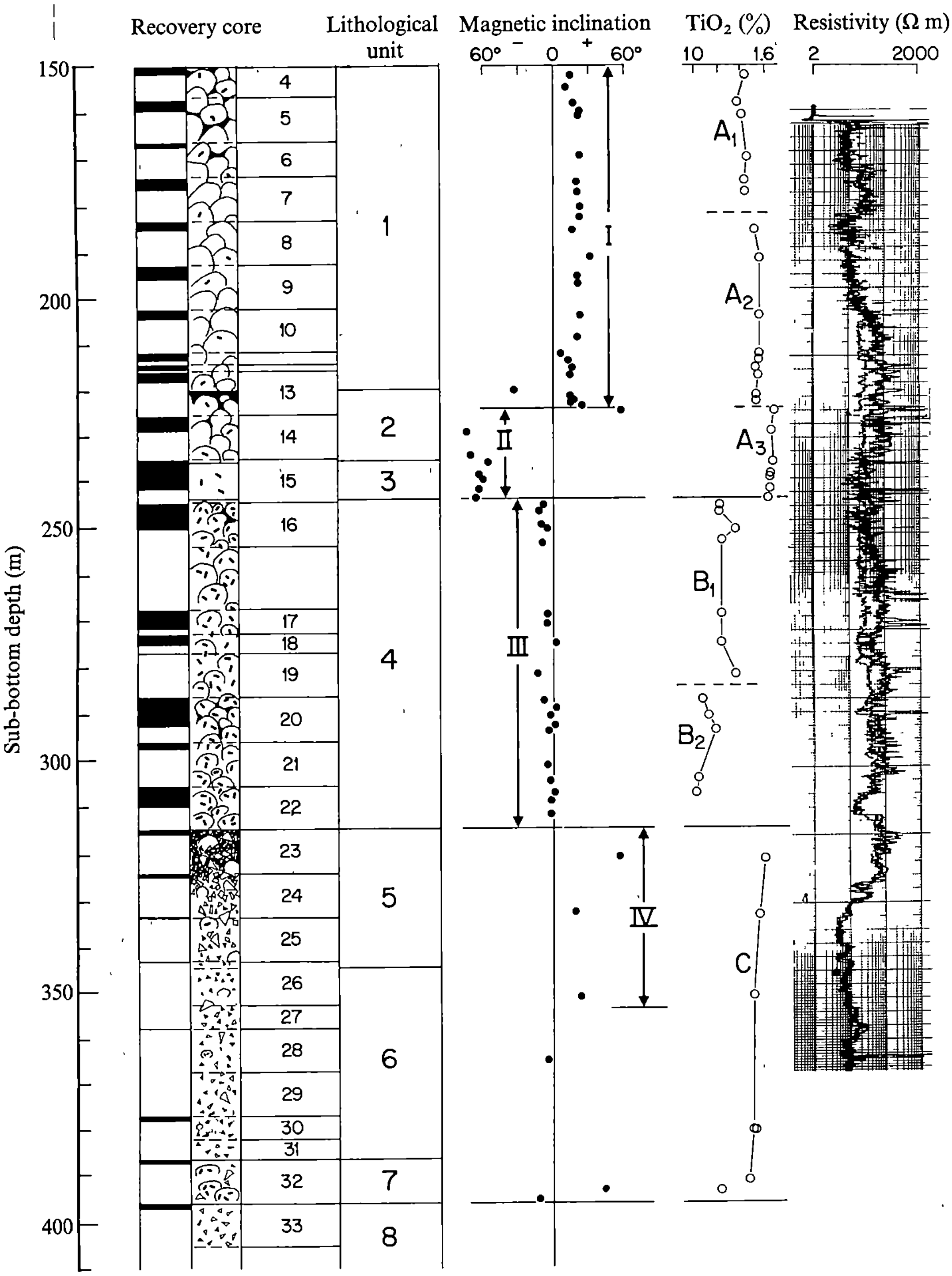

Fig. 1 Variations of lithological units, magnetic inclination, TiO_2, and electrical resistivity log as a function of depth below the sea floor for hole 396B.

dominantly olivine–plagioclase phyric with proportions of olivine to plagioclase (ol.–plag. = 0.55) similar to the basalt in the overlying breccia unit, but unlike the basalt cored previously above the clastic zone. The lower gravel unit, on the other hand, contains predominantly plagioclase phyric crystalline fragments (ol.–plag. = 0.13) similar to the intervening plagioclase phyric pillow basalt (breccia?).

Four major processes may be invoked to explain the fragmentation of the basalt:

(1) Fragmentation during eruption and cooling: this may involve several interrelated processes peculiar to submarine lava flows. (a) Glassy fragments could form by granulation due to thermal shock resulting from quenching of lava by seawater. (b) Spalling and crumbling of pillow rinds as a result of continued or multiple flow of basaltic lava causing inflation of a pre-existing pillow crust. (c) Brecciation from the oversteepening of pillow mounds causing them to tumble or slump. Mechanical shock from earthquakes or other tectonic processes may facilitate in this type of break-up.

(2) Tectonic brecciation after consolidation. Faulting and fissuring within the median valley, and on the flanks and away from the ridge is ubiquitous.

(3) Erosion, transport and deposition including the formation of talus slopes associated with fault scarps. Erosion would probably be largely restricted to reworking of material previously broken by processes 1 and 2.

(4) Shaving or reaming out of the hole by the drill bit during re-entry or fragmentation by drilling.

Origin 4 is unlikely: no re-entry was made immediately before coring the fragmented debris; the penetration rates were exceptionally high; lithified sandstone fragments were found with the loose gravel and sand; the lithic clasts do not seem to have been derived from higher in the bore hole and the data from the downhole logs strongly suggests that the clastic material represents a distinct lithological unit. The abundance of fragments of basaltic glass in the clastic material indicates that much or all of it is derived from basaltic pillows; however, as the majority of the fragments are partly crystallised (origin 1(a)), spallation of glass rinds on quenching, would seem to be ruled out as a major source for the clastic material. The calcite fragments, spherulites, clasts with cross-cutting calcite veins and calcite cemented basaltic microbreccia fragments demonstrate that some of the gravel and sand must be late clastic debris from previously altered flows. On the basis of available data, however, it is impossible to make a clear choice between origins 1(b), 1(c), 2 and 3 as the predominant source of the gravel sand and other clastic debris in the clastic zone.

Although deposits of coarse talus have been well known for many years from photographs of the sea floor we believe that this is the first time that a deposit of relatively fine grained clastic material has been recovered from beneath the sea floor, and it represents a hitherto unknown element among these rocks. We have provided evidence that it comprises the greater part of the lower 90 m of the core, but may extend deeper. Since this material cannot be strongly magnetised and cannot contribute to the lineated magnetic anomalies of this region, it probably does not make up a significant portion of the basement.

We wish to thank Captain Lloyd E. Dill and his ship's crew, Cotton Guess, Drilling Superintendent, and his drilling crew, Robert Knapp, Operations Manager, G. Bode and the DSDP technicians and Dalhousie University, CNEXO, Schlumberger Well Services for supplying major equipment and services. The International Programme of Ocean Drilling is funded by the governments of England, France, Germany, Japan, the United States and the USSR through the NSF and managed by the Scripps Institution of Oceanography.

SCIENTIFIC PARTY DEEP SEA DRILLING PROJECT, LEG 46*

Received May 17, accepted July 8, 1976

*Henry Dick, James Heirtzler, Woods Hole Oceanographic Institution, Woods Hole, Massachusetts, Leonid Dmitriev, Academy of Sciences of the USSR, Michael Dungan, NASA–Lyndon B Johnson Space Center, Houston, Texas; Al Erickson, Department of Geology, University of Georgia, Athens, Georgia, Floyd N Hodges, State University of New York at Stony Brook, Department of Earth and Space Sciences, Stony Brook, New York; Jose Honnorez, Rosenstiel School of Marine and Atmospheric Science, University of Miami, Miami, Florida, James Kirkpatrick, DSDP, Scripps Institution of Oceanography, University of California, La Jolla, California; Drummond Matthews, Department of Geodesy and Geophysics, Cambridge University, Cambridge, UK, Daniel Ohnenstetter, Laboratoire de Petrologie, Nancy, France, Nikolai Peterson, Ludwig-Maximilians-Universitat Munchen, Munchen, Theresienstr, FRG, Hiroaki Sato, Department of Earth Sciences, Kanazawa University, Ishikawa, Japan, Hans Schmincke, Institut fur Mineralogie, Bochum, FRG.

The post-spinel phase of forsterite

THE nature of the post-spinel phase of forsterite (the olivine structure of Mg_2SiO_4) and its importance to our understanding of the mineralogy, petrology and seismological discontinuities in the transition zone and the lower mantle of the Earth has attracted much recent attention[1,2]. Kumazawa *et al.*[1] reported that the post-spinel phase of forsterite recovered from 3.3×10^{10} Pa and 1,000 °C was a component oxide mixture of stishovite (SiO_2) plus periclase (MgO). In their studies of Mg_2SiO_4–Fe_2SiO_4 solid solutions at pressures up to 2.5×10^{10} Pa, Ming and Bassett[2] agreed with the conclusions of Kumazawa *et al.* Consequently, the oxide mixture seems to be widely accepted as the post-spinel phase of forsterite[3]. In this paper, however, I present results that disagree with this.

I have previously found that forsterite transforms into an assemblage of perovskite ($MgSiO_2$) plus periclase (MgO) when subjected to pressures $> 3.0\times 10^{10}$ Pa and $\sim$ 1,000 °C (ref. 4). Since the zero pressure density for the perovskite + periclase assemblage is 1.9% greater than that of the mixed oxides, I have designated this assemblage as the post-oxide phase of forsterite and have postulated that the Earth's lower mantle comprises mainly the perovskite phase of $MgSiO_3$ (ref. 5).

Until my work on the detailed high pressure phase transformations in $MgSiO_3$ (ref. 6), I had not doubted the interpretation of the post-spinel phase for Mg_2SiO_4 as representing mixed oxides. A schematic isothermal phase diagram for the system MgO–SiO_2 at 1,000 °C is shown in Fig. 1. If Mg_2SiO_4 were to disproportionate into its component oxide mixture at certain pressure and temperature conditions, so also should $MgSiO_3$. The latter, in fact, has been reported by Ming and Bassett[7] who have found that $MgSiO_3$ disproportionates into its component oxides, stishovite plus periclase, at a pressure of $\sim 2.5\times 10^{10}$ Pa. In my recent study of the high pressure phases of $MgSiO_3$ between 1.5×10^{10}–3.0×10^{10} Pa loading pressure[6], however, I have found that the sequence of phase transformations in $MgSiO_3$ with increasing pressure is as follows

$$\begin{array}{ccccccccc} 2MgSiO_3 & \rightarrow & Mg_2SiO_4 & + & SiO_2 & \rightarrow & Mg_2SiO_4 & + & SiO_2 \\ \text{clinoenstatite} & & \beta\text{ phase} & & \text{stishovite} & & \text{spinel} & & \text{stishovite} \end{array}$$

$$\begin{array}{cccc} \rightarrow & 2MgSiO_3 & \rightarrow & 2MgSiO_3 \\ & \text{ilmenite} & & \text{perovskite} \end{array}$$

If there were a stability field for the mixed oxides, it would have intervened between the ilmenite and the perovskite phases.

The ilmenite phase of $MgSiO_3$ transforms directly into the perovskite phase with increasing pressure. This behaviour is consistent with phase transformations observed in all the available ilmenite analogues, $CdTiO_3$ (ref. 8), $CdSnO_3$ (ref. 8), $MnVO_3$ (ref. 9), (Fe,Mg)TiO_3 (ref. 10), $MnGeO_3$ (ref. 11), and $MgGeO_3$ (L.L., unpublished). With the exception of $ZnSiO_3$, for which only a very small stability field of mixed oxides has been reported[12], the ilmenite phase of all the above-mentioned compounds has been found to transform directly into the

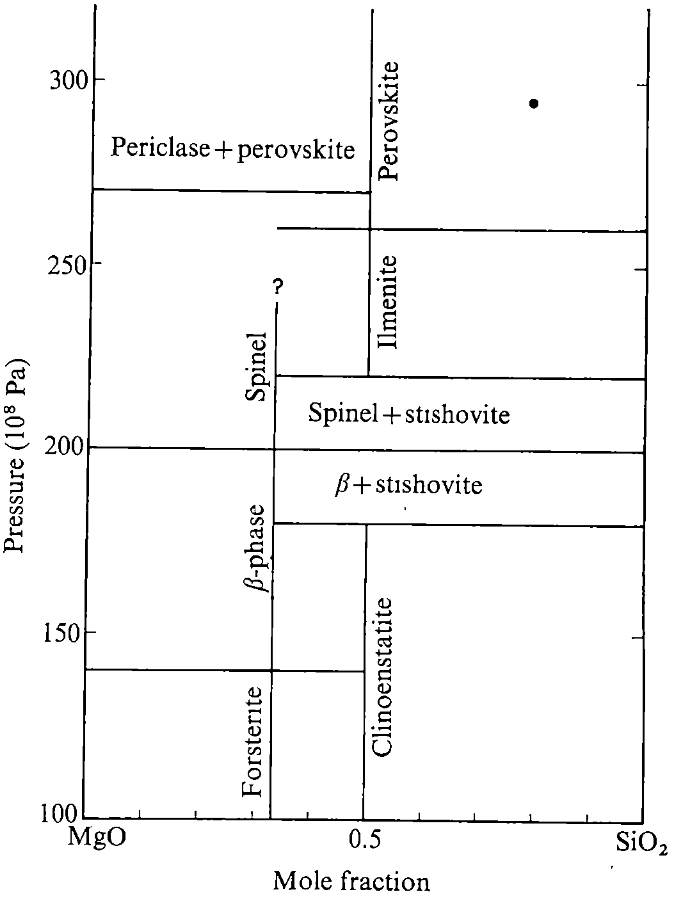
Fig. 1 Schematic isothermal phase diagram for the system MgO–SiO_2 at 1,000 °C.

Table 1 X-ray diffraction data (room temperature and 10^5 Pa pressure) for forsterite quenched from a loading pressure of $\sim 2.2 \times 10^{10}$ Pa and temperature of ~ 1,000 °C (CoKα)

Observed*		Forsterite†			Spinel‡			Perovskite§			Periclase†			Stishovite¶		
d(Å)	I/I_{100}	*d*(Å)	I/I_{100}	*hkl*	*d*(Å)	I/I_{100}	*hkl*	*d*(Å)	I/I_{100}	*hkl*	*d*(Å)	I/I_{100}	*hkl*	*d*(Å)	I/I_{100}	*hkl*
5.12	10	5.11	26	020												
3.90	25	3.88	69	021												
3.74	20	3.73	25	101												
3.51	10	3.50	10	111												
3.45	25							3.45	60	002						
3.09	15							3.08	15	111						
3.00	20	3.00	17	121												
	—													2.955	100	110
2.863	35				2.855	23	220									
2.774	25	2.768	53	130												
2.520	25	2.513	73	131												
2.445	100*b* }	2.458	100	112	2.435	100	311	2.471 2.435	20 100	020 112	2.431	10	111			
2.396	15							2.395	20	200						
2.333	10				2.331	5	222									
2.263	20	2.268	59	122												
	—													2.247	25	101
2.199	5							2.196	5	120						
2.161	20	2.161	15	211												
2.110	50										2.106	100	200			
2.081	10							2.085	30	013						
2.059	15							2.057	25	211						
2.025	40				2 019	50	400									
1.970	10							1.967	10	202				1.979	40	111
1.915	15							1.911	25	113						
1.884	5	1.878	5	150												
	—													1.869	20	210
1.856	15							1.853	15	122						
1.830	5							1.828	5	212						
1.752	30	1.748	60	222												
1.723	40 }							1.724 1.720	 80	004 220						
1.688	5							1.683	10	023						
1.671	5	1.670	13	241				1.669	10	221						
1.652	10				1.649	9	422									
1.575	5	1.572	10	043												
1.558	35				1.554	25	333									
1.541	5							1.539	15	222						
	—													1.530	60	211
1.521	15							1.520	20	131						
1.493	30	1.497	27	004												
1.484	5							1.484	5	311						
	—													1.478	25	220
1.430	45				1.428	63	440									
1.418	10							1.420	40	132						
1.403	10							1.399	10	204						
1.392	25	1.394	9	233				1.390	45	312						
1.352	5	1.351	17	322												
	—													1.332	9	002
	—													1.322	4	310
1.317	5	1.316	9	134												
1.232	15				1.232	10	533							1 234	35	301
1.218	25							1.216	15	041	1.216	12	222	1.215	10	112
1.195	5							1.197	5	140						
	—													1.184	3	311
1.167	10	1.166	2	—	1 166	6	444	1.164	10	410						
1.155	<5	1.155	1	352				1.158	5	323				1.159	7	320
1.092	5	1 099	1	412				1.098	15	240						
1.077	10				1.079	5	642	1.078	10	420						
1.051	20				1.051	12	553				1.053	5	400			
1.035	<5	1.036	3	334												
1.021	<5	1.020	3	0,10,0												
1.009	10				1.009	7	800									
6 extremely weak lines																
0.9417	10										0.9419	17	420			

* With the exception of film shrinkage, no other corrections to the data have been made. Values for I/I_{100} were estimated visually. *b*, Broad line.

† From ASTM Card Catalogue (4-0768 and 4-0769) for forsterite and (4-0829) for periclase.

‡ From ref. 15.

§ From ref. 4.

¶ From ref. 16.

perovskite phase without the intervention of any other phases.

The fact that the ilmenite phase of $MgSiO_3$ transforms directly into the perovskite phase limits the post-spinel phase for Mg_2SiO_4 to the following possibilities: (1) a single denser phase of Mg_2SiO_4; (2) a mixture of ilmenite ($MgSiO_3$) plus periclase (MgO); (3) a mixture of perovskite ($MgSiO_3$) plus periclase; or (4) any combination of them (see Fig. 1). The second possibility has been previously postulated[12].

I have made 12 experimental runs on forsterite in the loading pressure region between 1.5×10^{10} and 3.2×10^{10} Pa and temperatures ~ 900–1,200 °C. The starting material is a synthetic forsterite (Mg_2SiO_4) powder (Tem-pres Research Inc.). The fine polycrystalline sample was mixed intimately with a small amount of powdered graphite, which serves to absorb laser radiation and to heat the sample under compression. The sample was then compressed in a diamond anvil press fitted with a lever and spring assembly and heated by the continuous YAG laser while the sample was maintained at pressure. The

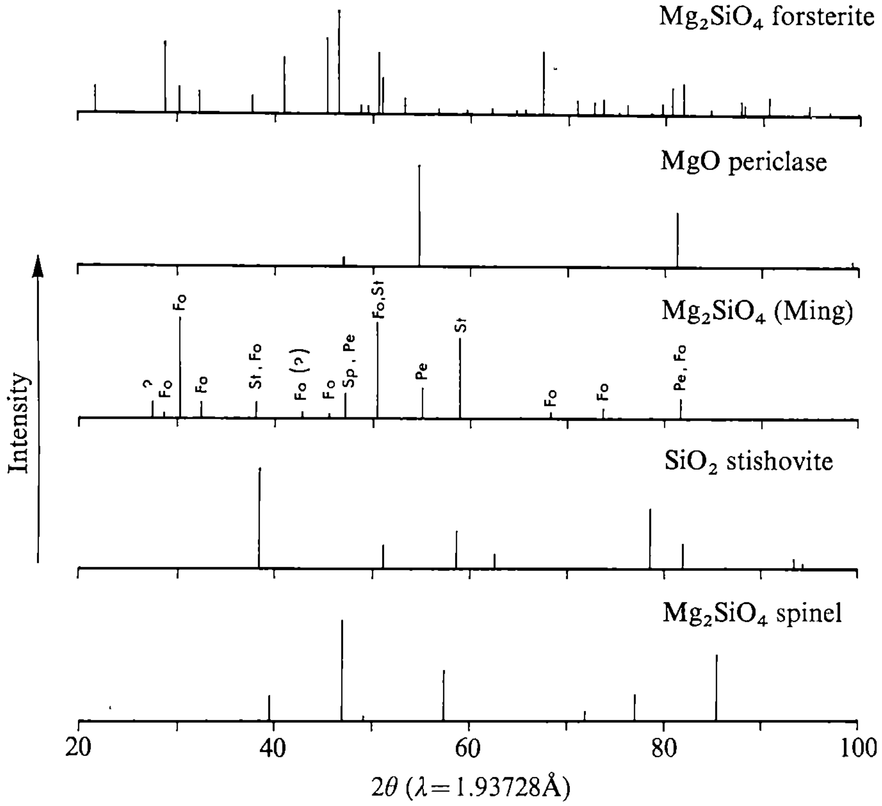

Fig. 2 X-ray diffraction data for forsterite quenched from ~2 5×10^{10} Pa and 1,400 °C (the temperature is highly uncertain) from ref. 14 in comparison with other relevant patterns. Fo, Forsterite; St, stishovite; Pe, periclase.

loading pressures of the sample at the central portion of the anvil were estimated from the length of the spring, and are probably accurate to ±10%. Sample temperatures were estimated to be ~ 1,000 °C with large uncertainty. After quenching and release of pressure, samples were transferred to a modified 57.3-mm Debye–Scherrer camera for X-ray diffraction study. Details of the procedure have been described elsewhere[13].

In the pressure region between 1.7×10^{10} and 2.5×10^{10} Pa (inclusive), nine runs were made at 10^9-Pa intervals; additional runs have been made at 1.5, 2.8 and 3.2×10^{10} Pa. The spinel phase of Mg_2SiO_4 seems to transform directly into a mixture of perovskite ($MgSiO_3$) plus periclase (MgO) at ~ 2×10^{10} Pa. The results obtained at pressures $> 2\times10^{10}$ Pa showed a steady increase of the yield of the perovskite + periclase assemblage with increasing pressure (Table 1). No stishovite, that is, no component oxide mixture, has been identified in the entire pressure region between 1.5×10^{10} and 3.2×10^{10} Pa in this study. These results are in accordance with those of my previous studies on $MgSiO_3$ (ref. 6), but contrast markedly with those reported in refs 1 and 2.

Ming and Bassett[2] did not report the detailed experimental results for Mg_2SiO_4 in their paper, but these data can be found in Table 10 of ref. 14 and have been reproduced graphically here in Fig. 2, together with all the other related phases. In the pattern obtained by Ming, there are only three lines which were attributed to stishovite, but their relative intensities contrast greatly with those for the pattern of stishovite shown in Fig. 2. It is also very surprising that the second intense line of stishovite at 2θ = 78.5° was not observed in Ming's pattern.

Kumazawa et al.[1] reported that forsterite disproportionated into a mixture of stishovite plus periclase on the basis of a single run at 3.3×10^{10} Pa and 1,000 °C for 30 min. (Their pressure should be revised to ~ 2.2×10^{10} Pa and temperature should be much higher (Kumazawa, personal communication).) In none of the present experiments at loading pressures between 1.5×10^{10} and 3.2×10^{10} Pa did I observe the mixed oxide phase assemblage. It is unlikely that the differences in the experimental conditions of pressure and temperature can explain this apparent discrepancy between my results and theirs.

Further support for the present results on the post-spinel phase of Mg_2SiO_4 is provided by studies of the post-spinel phases for 12 silicate and germanate compounds with the olivine stoichiometry in this laboratory. At pressures $> 2.5\times10^{10}$ Pa, only Mg_2SiO_4 Mg_2GeO_4 and Mn_2GeO_4 have been found to transform into the perovskite + rocksalt assemblage. The remainder transform into their component oxides with the rutile and rocksalt structures. The oxide mixture phase assemblage was not found as an intermediate phase between the spinel phase (or the β phase, which is a distorted spinel phase) and the perovskite + rocksalt assemblage in any of the above three compounds.

The associated increase in zero pressure density from the spinel phase of Mg_2SiO_4 to the mixture of perovskite ($MgSiO_3$) plus periclase (MgO) was calculated to be 10.7%. This spinel–post-spinel reaction is characterised by an increase in coordination number of oxygen for Si^{4+} from 4 to 6 and for half of the Mg^{2+} from 6 to 8.

I am grateful to A. E. Ringwood and R. C. Liebermann for comments.

LIN-GUN LIU

Research School of Earth Sciences,
Australian National University,
Canberra, ACT Australia

Received June 4; accepted July 7, 1976

1 Kumazawa, M, Sawamoto, H., Ohtani, E., and Masaki, K, *Nature*, **247**, 356–358 (1974).
2 Ming, L, and Bassett, W. A, *Science*, **187**, 66–68 (1975).
3 Hammond, A L, *Science*, **190**, 967–968 (1975).
4 Liu, L, *Geophys Res. Lett.*, **2**, 417–419 (1975).
5 Liu, L., *Nature*, **258**, 510–512 (1975).
6 Liu, L., *Earth planet Sci Lett.*, **31**, 200–208 (1976).
7 Ming, L, and Bassett, W. A, *Earth planet. Sci. Lett*, **27**, 85–89 (1975).
8 Liebertz, J, and Rooymans, C J W., *Phys Chem Neue Folge*, **44**, 242–249 (1965).
9 Syono, Y, Akimoto, S, and Endoh, Y, *J Phys Chem Solids*, **32**, 243–249 (1971).
10 Liu, L, *Phys Earth planet. Int*, **10**, 167–176 (1975).
11 Liu, L, *Earth planet Sci. Lett* (in the press).
12 Ito, E, and Matsui, Y., *Phys Earth planet Int.*, **9**, 344–352, (1974).
13 Liu, L., *Earth planet. Sci Lett*, **24**, 357–362 (1975).
14 Ming, L., thesis, Univ Rochester (1974).
15 Ito, E, Matsui, Y, Suito, K., and Kawai, N., *Phys. Earth planet. Int.*, **8**, 342–344 (1974)
16 Chao, E. C. T., Fahey, J. J., Littler, J, and Milton, D J, *J. geophys. Res.*, **67**, 419–421 (1962).

Liquid nitrogen enhancement of partially annealed fission tracks in glass

THE number density of fission tracks in solids is reduced if the sample is heated before chemical etching, and the effect of annealing must be accounted for before an age date can be assigned to the sample[1–3]. The extent of the annealing can be observed by a measurement of the reduction in the track parameters (diameter and/or length) and subsequent comparison to unannealed tracks. Correct ages can be obtained by careful calibration studies of track density reduction against track diameter or length reduction at different annealing temperatures and times[4,5]. For crystalline minerals, however, these correction techniques are not generally valid[6]. In this study, glass samples were partially annealed and then immersed in liquid nitrogen for various periods and we show that the properties of the glass and/or the track parameters can be altered so as to observe tracks that would normally be erased by annealing.

An NBS glass standard (SRM-962) with latent fission tracks was cut in half with a diamond cutting wheel. The exterior surfaces were ground and polished with 12.5-μm and 0.3-μm alumina powder such that at least 30 μm was removed from the surface. The halves were etched simultaneously in 16% HF at room temperature for 75 s and rinsed in warm running water for several minutes. Etched tracks were observed and counted with a Leitz microscope at overall magnifications of 800 and 1,600. The ×800 magnification was used to increase the counting statistics and the ×1,600 was used to identify the fission tracks properly[7]. Track length and width measurements were made at ×1,600 with an eyepiece reticule.

Fig. 1 Track density ratios as a function of liquid nitrogen immersion time. t/t', Track density after immersion/track density at zero immersion time. ● Values found for unannealed sample; ■ values for partially annealed sample.

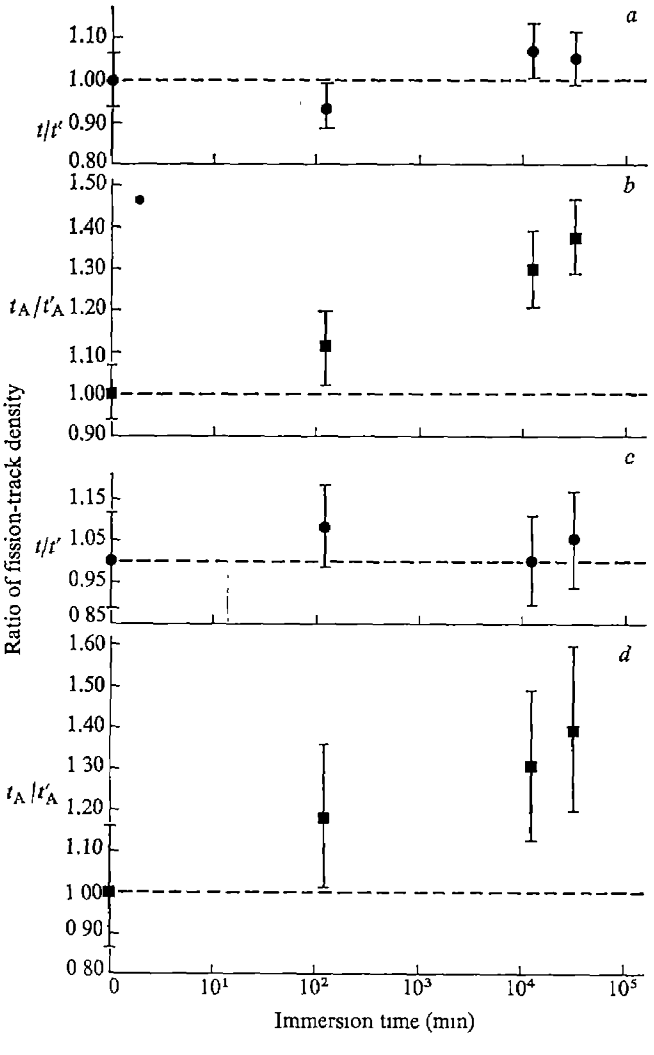

One of the samples was partially annealed at 230 °C for 1 h. Both halves were ground, polished and etched together as described previously. The track density of the partially annealed sample was found to be half that of the unannealed sample. The length and width of the partially annealed tracks were found to be similarly reduced.

Both samples were then immersed in liquid nitrogen for varying periods At the conclusion of each immersion the samples were polished, etched and counted in the manner described above. The results of the track density measurements against liquid nitrogen immersion time are given in Fig. 1. To compensate for possible variations in etch conditions the ratios of track densities were determined by normalising with the track density having zero immersion time. Figure 1*a* and *c* shows the track ratios against immersion time for the unannealed sample at magnifications of 800 and 1,600 respectively. The ratio remains essentially constant about a value of one. Figure 1*b* and *d* shows the partially annealed track density increasing with immersion time for magnifications of 800 and 1,600 respectively. A gain of ~ 40% was achieved after 760 h of immersion in liquid nitrogen.

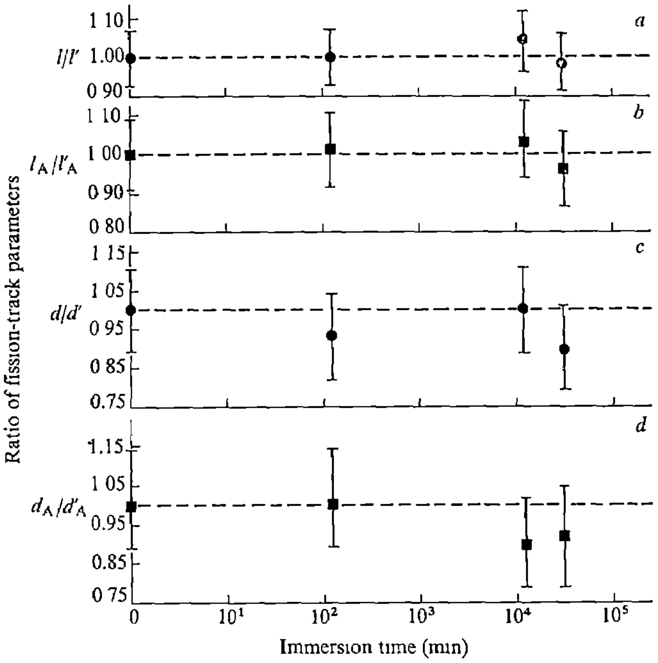

Fig. 2 Track parameter characteristics as a function of immersion time. l/l', Length of track after immersion/length of track at zero immersion time; d/d', diameter of track after immersion/diameter of track at zero immersion time. ●, Unannealed sample; ■, partially annealed sample.

To ascertain whether the track parameters were changing with immersion time, the length and diameter of the tracks were measured after each etching at a magnification of 1,600. Figure 2 shows the ratio of length and diameter for the unannealed (2*a*, *c*) and the partially annealed (2*b*, *d*) samples. For each ratio, the measured quantity with zero immersion time was used to normalise the graphs. The size of the tracks was not noticeably affected by immersion in liquid nitrogen (Fig. 2).

It was thought that thermal shock (room temperature →liquid nitrogen temperature → room temperature) along

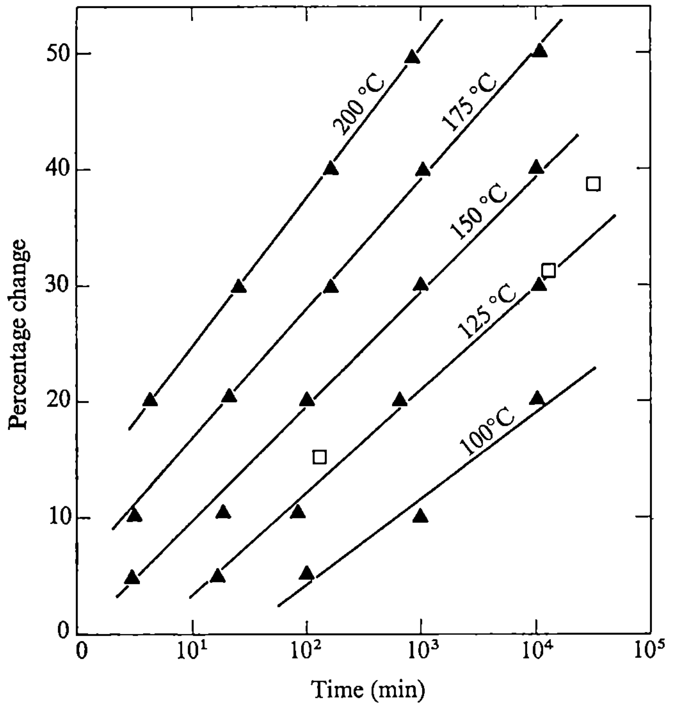

Fig. 3 Percentage change in track density against time for NBS glass standards. □, Percentage track enhancement found in the present study; (——) connecting the points (▲) indicate the percentage track reduction at different annealing temperatures (reported in ref. 8).

the latent track was the cause of the track enhancement. It was found, however, that repeated (four times) immersion of the samples in the liquid nitrogen (for 2 h) did not lead to an increase in the track density.

A recent study[8] of the thermal stability of fission tracks in NBS glass standards reported a track density decrease with increasing annealing time and temperature. The percentage track reduction at different annealing temperatures and times from that investigation are replotted in Fig. 3, together with the average gain (×800 and ×1,600 magnifications) against immersion time obtained in the present study. The slopes of the annealing plots and liquid nitrogen immersion plot seem to be compatible. This suggests that the mechanism which erases the track damage through annealing may be partially reversed when the temperature of the sample is significantly lowered for a sufficient length of time. Further work is under way (at different immersion temperatures and partial annealing conditions) to test whether or not the process of enhancement is a reversal of the annealing process. Similar enhancement effects using liquid nitrogen have been found for α-particle tracks in polycarbonate detectors and those results will be published.

Although the mechanism of track reduction with temperature rise (annealing) is not clearly understood[7], track enhancement by cooling may provide a new avenue of research into this problem In addition, this method has possible application in dating geological samples partially annealed by post-emplacement thermal events.

L. J. Pilione

Department of Physics, Altoona Campus,
Pennsylvania State University,
Altoona, Pennsylvania 16603

D. P. Gold

Department of Geosciences,
Pennsylvania State University,
University Park, Pennsylvania 16802

Received May 12, accepted July 12, 1976.

[1] Fleischer, R. L., *et al*, *Science*, **143**, 349–351 (1964).
[2] Fleischer, R. L., *et al.*, *J. geophys. Res.*, **70**, 1497 (1965).
[3] Naeser, C W., *Bull. geol. Soc. Am.*, **78**, 1523 (1967).
[4] Mehta, P. P., and Rama, *Earth planet Sci. Lett.*, **7**, 82–86 (1969)
[5] Wagner, G. A., and Storzer, D., *Eclog. geol. Helv.*, **63/1**, 335–344 (1970).
[6] Naeser, C. W., and Fleischer, R. L., *Geophys Res. Lett.*, **2**, 67–70 (1975).
[7] Fleischer, R. L., *et al.*, *Nuclear Tracks in Solids* (University of California Press, 1975).
[8] Reimer, G. M , Wagner, G. A., and Carpenter, B. S , *Radiat Effects*, **15**, 273–274 (1972).

Direct measurement of long range forces between two mica surfaces in aqueous KNO$_3$ solutions

We have constructed an apparatus for measuring the forces between two surfaces immersed in a liquid directly as a function of separation, and report initial results for the forces between two crossed cylindrical sheets of molecularly smooth muscovite mica in aqueous solutions of KNO$_3$.

The apparatus is shown schematically in Fig. 1. It is similar to earlier models used for measuring the van der Waals' forces between two freshly cleaved mica sheets in air *in vacuo*[1,2]. The present apparatus has been refined to allow for the measurement of the very different types of forces in the conditions that occur in liquids. Multiple beam interferometry is used for measuring the shape of the surfaces and their separation to within 0.1 nm (ref. 3). The separation between the two surfaces is controlled by a three-stage mechanism: an upper micro-driven rod (to $\sim$1 µm), lower micrometer-driven rod (to $\sim$ 1 nm) and a piezoelectric crystal (to < 0.1 nm). The lower rod operates by a differential spring mechanism· the double cantilever spring is about a thousand times stiffer than the helical spring so that a 1-µm movement of the motor-driven lower rod is reduced to a 1-nm movement between the two mica surfaces. All parts of the apparatus are made of 316 stainless steel, Teflon, Delrin and glass. Extreme precautions were taken to purify the water and potassium nitrate, and a high degree of surface cleanliness was maintained in the equipment. The apparatus is suspended by springs to isolate it partially from extraneous vibrations. Some residual vibrations of the surface (a few Å) was found to be an asset, in that it indicated that the surfaces were truly separated and not in contact through a dust particle or a mica flake In view of the repulsive forces measured, this precaution was essential, since a minute particle between the surfaces far from the region of closest approach could go undetected and lead to a spurious repulsion being measured.

In the present set-up the glass disk supporting the lower mica sheet was suspended at the end of a cantilever spring of stiffness $\sim 10^2$ N m^{-1}. The forces were measured by applying a sudden voltage to the piezoelectric crystal, which causes it to expand or contract by a known amount, say 10 nm. The resulting change in the separation between the two surfaces is then measured optically and any difference in the two values, when multiplied by the stiffness of the single cantilever spring, gives the force difference, whether attractive or repulsive, between the initial and final separations. In this way, forces may be measured at any separation down to contact.

Figure 2 shows some of these results for mica in KNO$_3$ solutions at 20 °C, pH$\sim$6. The repulsive forces were all found to be exponential, with a decay length close to the Debye length. Below a certain separation, however, the repulsion increased more rapidly. The onset of this enhanced repulsion occurred very roughly at about half a Debye length separation. The magnitude of the repulsive forces was found to be different for the different mica samples used. In 0.1 M and 1 M solutions the onset of repulsion was preceded by an attractive region for those samples in which the repulsion was weak, thereby indicating the existence of a secondary minimum at these concentrations. It

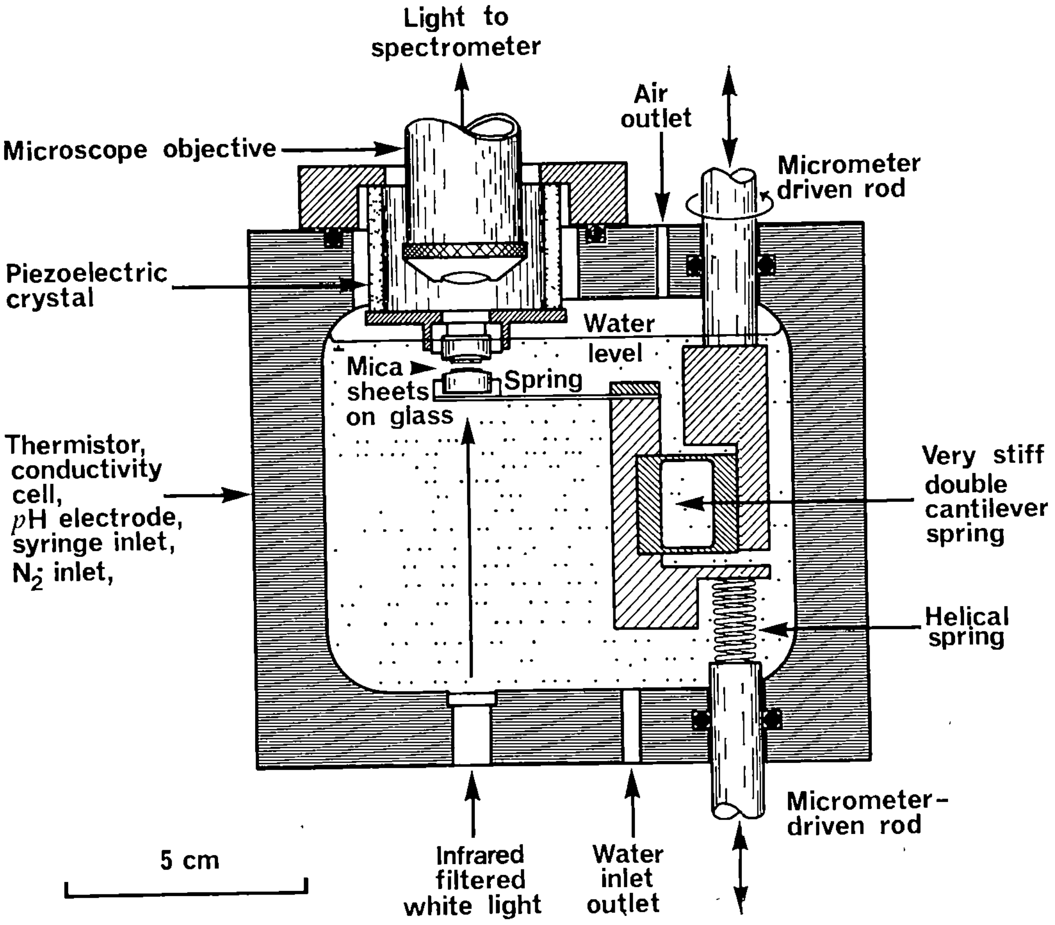

Fig. 1 Schematic drawing of apparatus to measure long range forces between two crossed cylindrical sheets of mica (of thickness ~ 1 μm and radius of curvature ~ 1 cm) immersed in liquid. By use of white light and multiple beam interferometry the separation between the two mica surfaces may be measured to ~ 0.1 nm. The separation between the two mica surfaces may be controlled by use of two micrometer-driven rods and a piezoelectric crystal to better than 0.1 nm.

was also observed that the repulsion was irreversibly reduced after the surfaces had been brought very close together (<4 nm), reminiscent of qualitatively similar observations on aqueous dispersions of sodium montmorillonite sheets in NaCl solutions[4,5]. At larger separations, however, the results were reversible and reproducible and clearly exhibit all the essential features of a DLVO-type interaction involving repulsive double layer forces and attractive van der Waals' forces[6,7]. In particular, we note that even in 0.1 M KNO_3 the decay length of the exponential repulsive region is equal to the Debye length (~1 nm) indicating that the Poisson–Boltzmann equation, at least for KNO_3, seems to remain valid even at this high concentration. The observation that at separations smaller than the Debye length the repulsive forces increased even more rapidly is qualitatively consistent with theoretical predictions of double-layer forces based on the nonlinear Poisson–Boltzmann equation[8]. The magnitude of the attractive forces in the region of the secondary minimum is of the order to be expected from the general theory of van der Waals' forces.

It is difficult to say without more detailed analysis, whether at very small separations, <1 nm, there is also a primary minimum, since at these separations the mica sheets have deformed appreciably under the influence of the strong forces. Tearing of mica was, however, often observed on separation after very close approach, thus indirectly pointing to the existence of strong adhesion at or near contact. The lack of a clear-cut turnover in the force into a primary minimum is consistent with previous measurements on the interactions between other silicate sheets[4,5], as well as the observation that silica dispersions are sometimes stable at very high electrolyte concentrations and undergo reversible coagulation[9].

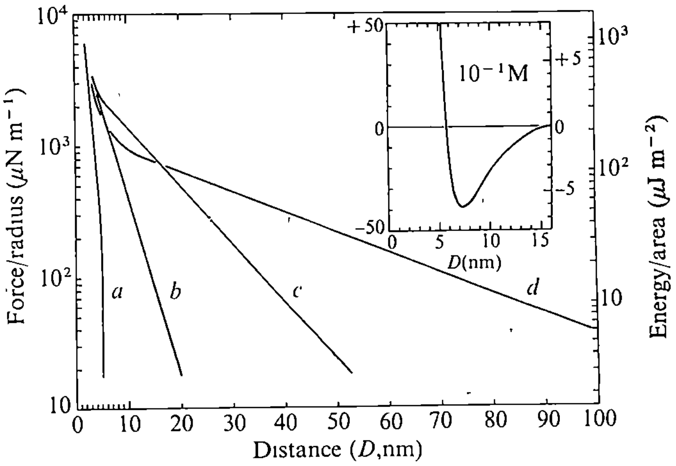

Fig. 2 Experimental results of direct measurement of force as a function of separation between two crossed mica cylinders of radius R in various KNO_3 solutions. The right-hand ordinate gives the interaction energy per unit area for two parallel plates, calculated according to the 'Derjaguin approximation'[7]. The ordinate of the inset is linear. The magnitude of the repulsive forces was found to be different for different mica samples. The results shown here are for those samples in which the repulsion was relatively weak and where a secondary minimum was clearly observed. The scatter in the experimental points is ~ 10 μN m⁻¹ for the force/radius. *a*, 10^{-1} M; *b*, 10^{-2} M; *c*, 10^{-3} M; *d*, 10^{-4} M.

We thank Dr T. W. Healey, Professors R. J. Hunter and B W. Ninham for helpful discussions, Mr P. East for machining, and Mr J Gascoigne for technical assistance.

J. N. ISRAELACHVILI
G. E. ADAMS

Research School of Physical Sciences,
Institute of Advanced Studies,
The Australian National University,
Canberra, ACT 2600, Australia

Received June 23; accepted July 9, 1976.

[1] Tabor, D , and Winterton, R H S., *Proc. R. Soc* , A312, 435–450 (1969).
[2] Israelachvili, J. N , and Tabor, D , *Nature*, 236, 106 (1972), *Proc. R. Soc.*, A331, 19–38 (1972).
[3] Israelachvili, J N., *Nature*, 229, 85–86 (1971); *J. Colloid Interface Sci.*, 44, 259–271 (1973).
[4] Barclay, L. M , and Ottewill, R. H., *Spec. Discuss. Faraday Soc.*, 1, 138–147 (1970).
[5] Callaghan, I C., and Ottewill, R. H., *Faraday Discuss. Chem. Soc.*, 57, 110–118 (1974)
[6] Derjaguin, B. V., and Landau, L , *Acta phys.-chim. URSS*, 14, 633–662 (1941)
[7] Verwey, E. J. W., and Overbeek, J. Th G , *Theory of the Stability of Lyophobic Colloids* (Elsevier, Amsterdam, 1948).
[8] Ninham, B W., and Parsegian, V A., *J. theor Biol.*, 31, 405–428 (1971).
[9] Napper, D H , and Hunter, R. J , in *Surface Chemistry and Colloids* (edit by Kerker, M), 241–306 (Butterworths, London, 1972).

Axial, magnetron, cyclotron and spin-cyclotron-beat frequencies measured on single electron almost at rest in free space (geonium)

THE monoelectron oscillator[1] consists of a ~ 1-meV electron contained in a weak electric quadrupole field plus strong axial magnetic field (the Penning trap) on which the axial oscillation is continuously observable. It may profitably be looked on as an ultraheavy metastable pseudoatom, 'geonium' (through the trap and the magnet, the electron is bound to the Earth ultimately). The energy levels are given by[2]

$$h^{-1}E_{\mathrm{mnkq}} = m\nu_{s}+(n+\tfrac{1}{2})\nu_{c}+(k+\tfrac{1}{2})\nu_{z}-(q+\tfrac{1}{2})\nu_{m}$$

$$m = \pm\tfrac{1}{2};\, n = 0,1,2,3\ldots ;\; k = 0,1,2,3\ldots ;\; q = 0,1,2,3\ldots$$

with $\nu_c = eH/2\pi mc$, $2\nu_c\nu_m - 2\nu_m{}^2 = \nu_z{}^2$. We report here the measurement of the axial, magnetron, cyclotron, and spin-cyclotron-beat frequencies ν_z, ν_m, $\nu_c-\nu_m$ and $\nu_s-\nu_c+\nu_m$ using this apparatus, held at 4 K. A new axial-frequency-shift technique using a 30-gauss deep magnetic bottle superimposed on the 18-kgauss field supplied by a superconducting magnet was used for the last two frequencies. The road to this advance was paved by two developments, namely the anharmonicity compensated trap[3] yielding an axial line width of 10^{-7} and the "entropy reduction by motional sideband excitation" (ref. 4) method. The latter allows the centring of an electron liberated in the trap to close tolerance guaranteeing the constancy of ν_z.

Fig. 1 First spin flip seen in the monoelectron oscillator (geonium). Because of the random fluctuations in the thermally excited cyclotron motion, the axial frequency shift $\delta\nu_z$ associated with the magnetic bottle shows a corresponding unsymmetric fluctuation always staying above a fixed floor for a given spin direction. This floor, however, suddenly changes by 2 5 Hz when the spin is flipped, which occurs occasionally near resonance, $\nu_z-\nu_d \simeq 2$ *k*Hz. No auxiliary drive was used. Three superimposed traces are seen, only the heavy one showing the spin flip.

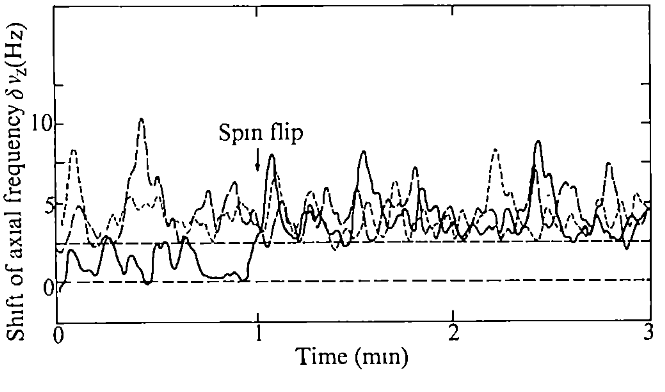

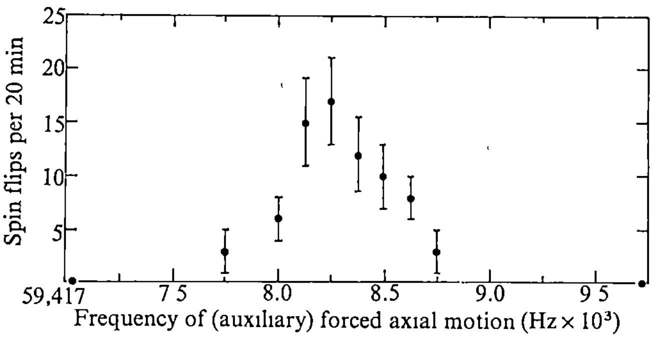

Fig. 2 Resonance at the spin-cyclotron-beat frequency ν_d in geonium. The auxiliary axial drive amplitude has been adjusted thus, that spin flips occur no faster than 1 min^{-1}, and can be conveniently counted in 20-min periods, during which the auxiliary drive frequency is kept constant. Data from a later run are shown.

Essentially as proposed by us[5-7], the resonance at $\nu_d = \nu_s - \nu_c + \nu_m$ was observed by making the electron see an effective, adjustable (< 10 μgauss) rotating magnetic field at ν_s, the spin frequency, occurring as the sum of an (auxiliary) forced axial motion frequency ν_d = 59.415890 MHz and $\nu_c - \nu_m \simeq 51206.11$ MHz, the frequency of the thermal cyclotron motion through the inhomogeneous static field of the magnetic bottle. Spin flips, thereby induced at a rate of 1 min^{-1}, were detected by continuously monitoring the bottle-related shift $\delta\nu_z \simeq (m+n+\tfrac{1}{2})$ 2.5 Hz of the axial resonant frequency ν_z = 59.4101 MHz and focusing on the minimum values, 2.5 and 0 Hz, corresponding to $n = 0$, $m = \pm\tfrac{1}{2}$, which occur as the electron jumps frequently between the cyclotron levels, *n*, and rarely between the spin levels, *m* (Fig. 1).

The minimum ν_d linewidth of ~500 Hz realised so far (see Fig. 2), arises primarily from the continuous ν_z monitoring. Pulsed operation promises a 100-fold sharper line. With the measured ν_m = 34.464 kHz, our preliminary value of $a \equiv (\nu_s - \nu_c)/\nu_c$ is 0.001159655(5). This agrees with the theoretical value[6] for $(g-2)/2$ quoted with an error ten times smaller. The empirical dimensionless ratio *a* can contain information only on the structure of the electron. Just as in an atom the experimental *g*-factor provides an important check on the 'purity' of an actual stationary state when expanded after states of an approximate Hamiltonian, thus *a* is a measure of the contribution to the actual electron wave function by other elementary particles which, together with the Dirac electron, may all be considered as stationary states of the same approximate Hamiltonian describing the spectrum of matter–energy. As a consequence, useful bounds are put on weak interaction models[9].

D. Wineland and P. Schwingberg have made important contributions to the work. Critical comments on the experiment by D. G. Boulware, L. S. Brown, P. Franken, O. Haxel, E. M. Henley, W. E. Lamb, Jr, R. Peierls, E. M. Purcell, E. Teller, L. Wilets, and R. W. Williams are acknowledged by H. D. We thank the NSF for support.

R. VAN DYCK, JR
P. EKSTROM
H. DEHMELT

Department of Physics,
University of Washington,
Seattle, Washington 98195

Received June 1, accepted July 2, 1976.

[1] Wineland, D., Ekstrom, P , and Dehmelt, H., *Phys Rev Lett* , 31, 1279 (1973).
[2] Sokolov, A A , and Pavlenko, Yu. G , *Opt. Spectrosc* , 22, 1 (1967).
[3] Van Dyck, R , Jr, Wineland, D , Ekstrom, P., and Dehmelt, H , *Appl. Phys Lett* , 28, 446 (1976).
[4] Dehmelt, H., *Nature*, 262, 777–778 (1976)
[5] Dehmelt, H., and Ekstrom, P., *Bull Am. phys. Soc* , 18, 727 (1973).
[6] Dehmelt, H , Ekstrom, P , Wineland, D., and Van Dyck, R., Jr, *Bull. Am. phys. Soc* , 19, 572 (1974).

[7] Dehmelt, H , *Adv atom. molec. Phys.*, 3, 53–72 (1967); *ibid* , 5, 109–154 (1969).
[8] Barbieri, R., and Remiddi, E., in *Atomic Masses and Fundamental Constants*, 5, 520 (Plenum, New York and London, 1976).
[9] Primack, J. R., in *Proc. XVIth Int. Conf. High Energy Physics* (Chicago, 1972).

Entropy reduction by motional sideband excitation

EVERYONE is intuitively familiar with the second law of thermodynamics: the disorder in any closed system can only increase with time. A familiar example is the spreading of a scent through a room. It is also well known that the spreading greatly accelerates when exterior agents are at work, for example, a stirrer. The reverse task of 'bottling up' the diffused scent back in the flask from which it expanded is much more difficult. So if one had somehow succeeded in collecting a cloud of particles in a vacuum at the bottom of a suitable potential well, as would be desirable in removing Doppler shifts in coherent spectroscopy or even in nuclear fusion machines, there will be all sorts of effects at work to spread the particles out again. The principle of entropy reduction by motional sideband excitation[1] could be effective in re-collecting the spread out cloud at the bottom of the well.

As a specific example, consider an atom emitting optical radiation at ν_1 while vibrating in a translational mode at a radiofrequency ν_v in a parabolic well. Because of the Doppler effect, the optical radiation will then be frequency modulated at the radiofrequency ν_v. This implies that its spectrum will consist of a carrier at ν_1 and symmetric sidebands spaced at the radiofrequency ν_v. Inversely, if the vibrating atom is irradiated at one of the spectral optical components, say at the one at $\nu_1 - \nu_v$, it will be optically excited and will in turn radiate symmetrically at all the frequencies ν_1, $\nu_1 \pm \nu_v$, $\nu_1 \pm 2\nu_v$ . . . . So, while absorbing quanta of energy $h(\nu_1 - \nu_v)$ it will radiate quanta of average energy $h\nu_1$, that is, larger by $h\nu_v$. This incremental energy can only come from the translational vibrational motion in the well, which is thereby reduced, bringing the atom closer to the centre of the well and possibly completely freezing out the quantised vibration. The principle is equally effective if the sidebands are created by amplitude modulation caused by motion through an inhomogeneous alternating field. The latter effect has, in fact, recently been demonstrated on a single electron confined in a Penning trap in ultra high vacuum. In such an axially symmetric trap, the electron is axially contained by an electric parabolic well while the corresponding radial potential hill is effectively overcompensated by an axial magnetic field. The guiding centre of the small diameter cyclotron orbit carries out a circular magnetron motion at $\nu_m \simeq \nu_z^2/2\nu_c \simeq 80$ kHz for an axial frequency $\nu_z \simeq 60$ MHz and a cyclotron frequency $\nu_c \simeq 20$ GHz. When the moving electron is now subjected to an axial r.f. field at ν_{zd} varying along the magnetron orbit, the electron will see spectral components at ν_{zd}, $\nu_{zd} \pm \nu_m$, $\nu_{zd} \pm 2\nu_m$. If one now chooses $\nu_{zd} = \nu_z + \nu_m$ the damped axial oscillation at ν_z will be excited. Hereby the energy excess $h\nu_m$ per absorbed $h\nu_{zd}$-quantum will be used to move the electron up the radial electric potential hill until it reaches the axis. This effect and also the inverse one, namely rapid increase of the magnetron motion radius for excitation at $\nu_{zd} = \nu_z - \nu_m$, has recently been demonstrated by Van Dyck *et al.*[2]. Monitoring the radial coordinate, r, of the electron was made possible by the presence of a small anharmonic term in the electric trapping potential which made ν_z a weak function of r.

HANS G. DEHMELT

Department of Physics,
University of Washington,
Seattle, Washington 98195

Received June 1; accepted July 2 1976.

[1] Wineland, D., and Dehmelt, H., *Bull. Am. Phys. Soc.*, 20, 637 (1975), *Int. J. Mass Spectrosc. Ion Phys.*, 16, 338 (1975) (Erratum).
[2] Van Dyck, R., Ekstrom, P., and Dehmelt, H , *Nature*, 262, 776–777 (1976).

The low frequency dielectric constant of supercooled water

THE extension of computer dynamical calculations of water structure[1] to temperatures < 0 °C has encouraged speculation that the supercooled liquid might exhibit ferroelectricity. The discovery that, by use of surfactants such as sorbitan stearates, water can be emulsified[2] in hydrocarbon solvents and then readily supercooled, opens up extensive new fields of experimentation. We have measured at 1,652 Hz the real part of the low frequency permittivity of 0.5% and 1% water emulsions down to −36 °C and thence calculated the real part of the dielectric constant of liquid water, which is essentially static in this range of frequency and temperature. The values, shown graphically in Fig. 1, lie on a smooth curve and compare with data for polycrystalline ice[3]; no ferroelectric transitions are observed.

Emulsions of deionised water were made in *n*-hexane using as emulsifier polyoxyethylene sorbitan tristearate (Tweens 65, from Honeywell-Atlas, Ltd); these were cooled and measurements made in a temperature-controlled refrigerator. The mean diameter of the water spheres was found by microscopy to be ~ 40 μm, but the spread is an order of magnitude in each direction. The Wayne-Kerr D121 permittivity cell and General Radio GR1621 precision measurements system were used. At each volume concentration, including 0% water with emulsifier present, three measurement runs were taken at 2 °C intervals, and the mean value of the mixture permittivity ε_m taken.

According to the Maxwell–Lewin dielectric mixture formula[4] for a volume fraction, ν, of spheres of substance 1 (water) in a matrix of substance 2 (*n*-hexane)

$$\frac{\varepsilon_m - \varepsilon_2}{3\varepsilon_2} = \nu \left[\frac{\varepsilon_1 - \varepsilon_2}{2\varepsilon_2 + \varepsilon_1} \right]$$

Since in the temperature range 0–20 °C the low frequency permittivity of water ε_1 is known accurately[5], the formula can be fitted to the best value of ν, taking for ε_2 the present 0% data. The value of ν is found to be within 0.7% of the volumetrically-determined value over the 0–20 °C range; there are a number of errors and effects contributing to this apparent volume defect, including the molar volume of the surfactant molecules. Assuming the value of ν calculated thus to be independent of temperature, ε_1 can be calculated from the data at temperatures ⩽ 0 °C. The consistency between the 1%

Fig. 1 The temperature dependence of the real part of the dielectric constant of water. ○, 1% volume fraction emulsion; ●, 0.5% emulsion.

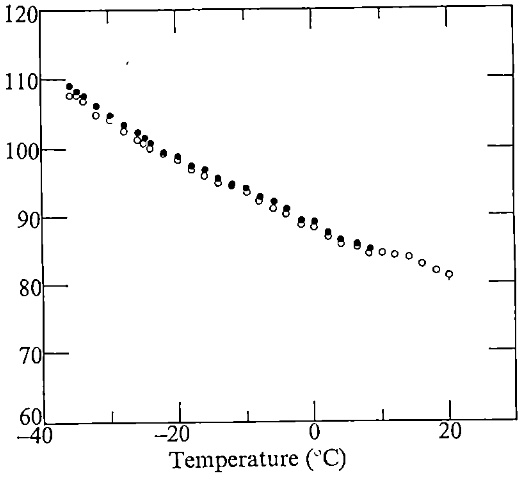

Table 1 Best values for temperature dependence of the permittivity of water

T(°C)	ε (water)
−35	107.7
−30	104.2
−25	100.8
−20	98.3
−15	95.6
−10	93.4
−5	90.9

and 0.5% data in Fig. 1 is such that ± 2% confidence limits might be placed on the mean of the two sets. The neglect of the temperature variation of ν from thermal expansion gives rise to a positive error of 0.2% at −35 °C, with correspondingly smaller errors at higher temperatures. Neglecting these errors, the best values are given in Table 1. They fall well outside the polynomial fit to the data that has been made at temperatures ⩾ 0 °C (ref. 5), a feature of supercooling which has been noted in other polar liquids[6].

There is apparently very little Maxwell–Wagner effect arising from conduction processes. A detailed study of the dielectric relaxation processes in the supercooled state is planned.

J. B. HASTED
M. SHAHIDI

Birkbeck College,
University of London,
London, UK

Received June 10; accepted July 15, 1976.

1 Stillinger, F. H , and Rahman, A , *J chem. Phys* , 57, 1281 (1972).
2 MacKenzie, A. P., *Non-equilibrium Freezing Behaviour of Aqueous Systems* (Royal Soc. Mt. on Water Structure and Transport in Biology, 1975).
3 Auty, R.P., and Cole, R.H , *J chem Phys.*, 20, 1309 (1952)
4 Lewin, L., *J Instn. elect Engrs.*, 94, 65 (1947).
5 Malmberg, C. G., and Maryott, A. A , *J Res natn. Bur. Stand.*, 56, 1 (1956).
6 Dodd, C., and Roberts, G. N , *Proc. phys. Soc.*, 62, 814 (1950).

Conformation of Met^5-enkephalin determined by high field PMR spectroscopy

THE discovery by Hughes *et al.*[1] that peptides (the enkephalins) could be the endogenous agonists of opiates in brain represents a challenge to medical chemistry both in its fundamental aspects and for the possible development of new therapeutic approaches. To understand how non-peptidic substances belonging to various chemical classes can mimic the action of the pentapeptide enkephalins it is first necessary to determine the spatial arrangement of the latter. We have thus synthesised large quantities of Met^5-enkephalin (H–Tyr–Gly–Gly–Phe–Met–OH) and determined its preferential conformation in solution using high field proton magnetic resonance (PMR) spectroscopy at variable temperatures, coupling constants in relation with Karplus–Bystrov curves[2] and conformational energy steric maps[3].

The most characteristic features of this conformation, which could account for some of the physicochemical and biological properties of the molecule seem to be: (1) a highly folded structure; (2) a precise homology between morphine and Met^5-enkephalin as regards their respective functional groups (the phenol ring corresponding to the Tyr residue and the tertiary amine corresponding to the terminal ammonium function of the peptide); and (3) a relative freedom of the N-terminal peptide Tyr–Gly.

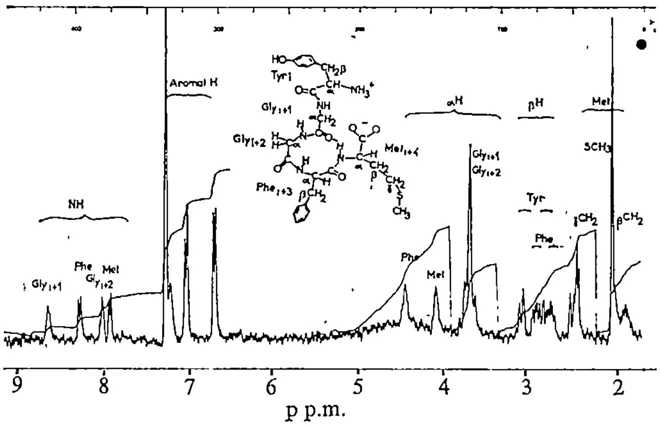

Fig. 1 300-MHz spectrum of Met^5-enkephalin (5×10^{-1} M) in DMSOd$_6$. Probe temperature, 17 °C. TMS as internal reference.

Met^5-enkephalin was prepared by liquid phase synthesis (unpublished). Its 300-MHz PMR spectrum was recorded in DMSOd$_6$ in which it dissolves readily (Fig. 1). All the $^3J_{NH-CH\alpha}$ and $^3J_{CH\alpha-CH\beta}$ have been measured experimentally and the most probable values of torsional angles φ and ψ were determined from the Karplus–Bystrov curves and conformational energy steric maps, respectively. The chemical shift variation of the Met NH proton, as a function of temperature, is somewhat lower than that of the other NH protons of the molecule, suggesting that this proton is involved in a hydrogen bond or is in a buried position. Only minor changes in coupling constants were observed with temperature variation, indicating that in the present conditions, the conformation is well defined, and corresponds to a relatively deep energy well. The conformational behaviour of Met^5-enkephalin in aqueous medium also parallels very closely that found in DMSO (our unpublished results). On the basis of these results, we propose the conformation reported in Fig. 2 with a β_I turn[4] involving the sequence Gly–Gly–Phe–Met and a hydrogen bond between the NH of the Met$_{i+4}$ and the CO of the Gly$_{i+1}$ following the Tyr residue. In this conformation, the two aromatic residues (Tyr and Phe) are pseudoequatorial and the side chain of Met is pseudoaxial to the mean plane of the peptide backbone.

Interestingly, in this structure, the three hydrophobic chains (Tyr, Phe, Met) are situated at the periphery of the pseudocycle of the β_I turn and the NH$_3^+$ and the COO$^-$ terminal groups exhibit a spatial proximity (end-to-tail interaction). These

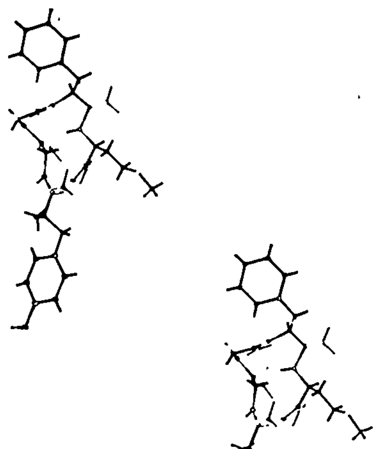

Fig. 2 Representation of the characteristic parts of opiates (left) and opiate-like peptides (right) exhibiting structural homology.

features probably account for the marked hydrophobic properties of Met^5-enkephalin (water solubility < 0.7%), which suggest that the peptide could cross lipid-containing membranes with relative ease, including the so-called 'blood–brain barrier', a property which might be of considerable therapeutic interest.

The conformation of Met^5-enkephalin deduced experimentally from its spectra in solution is different from the hypothetical conformation recently proposed[6] and characterised by a β turn involving a hydrogen bond between the CO of the Tyr residue and the NH of the Phe residue. Nevertheless, the preferential conformation of Met^5-enkephalin that we propose also shows all the steric requirements found in morphine for a stereospecific interaction with the receptor. In the N-terminal part of the molecule, the distance between the OH phenolic group and the ammonium function are the same, namely 6.8 Å, in morphine and in the proposed conformation of Met^5-enkephalin (Fig. 3). Moreover, the spatial orientation of the ammonium groups in respect to the phenol rings is similar in both compounds.

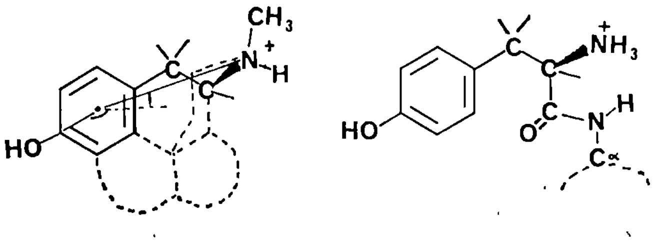

Fig. 3 Stereoscopic view of enkephalin along the mean plane of β_I turn with $\psi_i=0°$ (to allow for end-to-tail association), and $\varphi_{i+4}=-160°$ (avoiding steric strain for the side chain of methionine). Carbonyl peptide functions are visualised by bend bonds, C–N bonds are recognised by their change in colour (black–grey). The head (Tyr) is at bottom right, the tail (Met) at top right. The methionine side chain is pointing towards the observer (axial character); that of Phe has a pseudo-equatorial character. The aromatic rings are almost coplanar to the β_I turn. Typically, NH_{i+4} is the only peptide NH proton pointing inwards.

The structural analogies between Met^5-enkephalin and opiates suppose the existence of the opiates in the protonated form at physiological *p*H. Any modification of the N-terminal Tyr leading to a non-protonated form at this position should therefore inhibit biological activity. This assumption seems to be substantiated by the observation that substitution of the N-terminal function of the Tyr residue in opiate-like peptides leads to a loss of affinity for the receptor[6].

In addition, it should be stressed that the β_I turn gives a large degree of freedom to the Tyr–Gly moiety towards the rest of the molecule and this could be of importance in understanding the activity of other peptides with opiate-like activity. The primary attachment of Met^5-enkephalin to the receptor could conceivably involve the Tyr–Gly moiety and the relative freedom of this moiety would allow the secondary attachment of the hydrophobic part of the molecule. It can be assumed that similar features (presence of an N-terminal Tyr–Gly moiety in a state of relative freedom) could account for the common affinity of many peptides like the two enkephalins, lipotropin C and the synthetic compounds of Goldstein *et al.*[6]. The relative differences in affinity between these compounds would depend essentially on the secondary interactions (for example, hydrophobic, hydrogen bond). The decreased affinity in Leu^5-enkephalin compared with Met^5-enkephalin[1] could thus be attributed to the loss of a hydrogen bond involving the sulphur atom of the Met residue.

It is hoped that these features of enkephalins will facilitate synthesis of opiate-like peptides of high potency and appropriate pharmacological properties, particularly in connection with the search for a non-addictive analgesic[7].

This work was supported by the CNRS, the University Rene Descartes and the University of Gent. We thank Professor J. C. Schwartz, Unité de Neurobiologie, INSERM, Paris, for discussions and Dr J. M. Lecomte for assistance.

B. P. ROQUES
C. GARBAY-JAUREGUIBERRY
R. OBERLIN

ERA No. 613 (CNRS),
Departement de Chimie,
Ecole Polytechnique,
17, rue Descartes,
75230 Paris Cedex 05, France

M. ANTEUNIS
A. K. LALA

Laboratory for NMR Spectroscopy,
University of Gent,
Krigslaan 271, Gent B-9000, Belgium

Received April 30, accepted June 26, 1976.

[1] Hughes, J., *et al.*, *Nature*, 258, 577–579 (1975).
[2] Cung, M. T , Marraud, M , and Neel, J , *Macromolecules*, 7, 606–613 (1974).
[3] Goodman, M , Verdini, A. S., Choi, N S , and Masuda, Y., in *Topics in Stereochemistry*, 5 (edit. by Eliel, E. L , and Allinger, N L.), 69-166 (Wiley-Interscience, New York, 1970).
[4] Lewis, P. N., Momany, F. A., and Scheraga, H. A., *Biochim biophys. Acta*, 303, 211–229 (1973).
[5] Bradbury, A. F , Smyth, D. G., and Snell, C R., *Nature*, 260, 165–166 (1976).
[6] Goldstein, A , Goldstein, J. S., and Cox, B. M , *Life Sci.*, 17, 1643–1654 (1975).
[7] Iversen, L , *Nature*, 258, 567–568 (1975).

Proton magnetic resonance studies of conformation and flexibility of enkephalin peptides

ENKEPHALIN, an endogenous pentapeptide which has the analgesic properties of morphine[1], has recently been isolated, purified and characterised both chemically and pharmacologically[2,3]. The fact that enkephalin and the opiates interact with the same receptor raises the possibility that the similarity in their function might be based on common structural features[4,5]. Particular attention has been paid to the geometric relationship between the aromatic ring of the tyrosine residue and the terminal amino group of enkephalin compared with the known geometry of similar functional groups in morphine. The relative spatial disposition of the phenylalanine and tyrosine aromatic side chains is also of special interest because of the possible resemblance of enkephalin to oripavine[4,5]. So far, however, no experimental determination of conformational parameters has appeared. Here we report proton magnetic resonance (PMR) studies of Met^5-enkephalin which indicate that the methionine amino proton is involved in a hydrogen bond, most probably within a Gly–Gly–Phe–Met type I β turn, but not with a turn involving Tyr–Gly–Gly–Phe as proposed previously[6]. Although our data exclude a γ turn, they do not rigorously exclude other conformations, especially if these have small statistical weights.

Assignments of the 270-MHz PMR spectrum made by double resonance and difference double resonance are shown in Fig. 1. The only possible ambiguity in assignment, distinguishing Gly_2 and Gly_3, was removed by titration from $^2H_6$-DMSO into ^2H_2O, the assignments in ^2H_2O having been previously made by *p*H titration. The chemical shifts and scalar coupling constants obtained by spectral analysis are shown in Table 1. The side-chain rotamer populations derived from these are also listed.

It has been demonstrated[7,8] that very small temperature dependencies such as observed here for Met (Fig. 2) are strong evidence for a hydrogen bond involving that amide proton. The coupling constants ($^3J_{NH-CH}$) in Table 1 enable us to rule

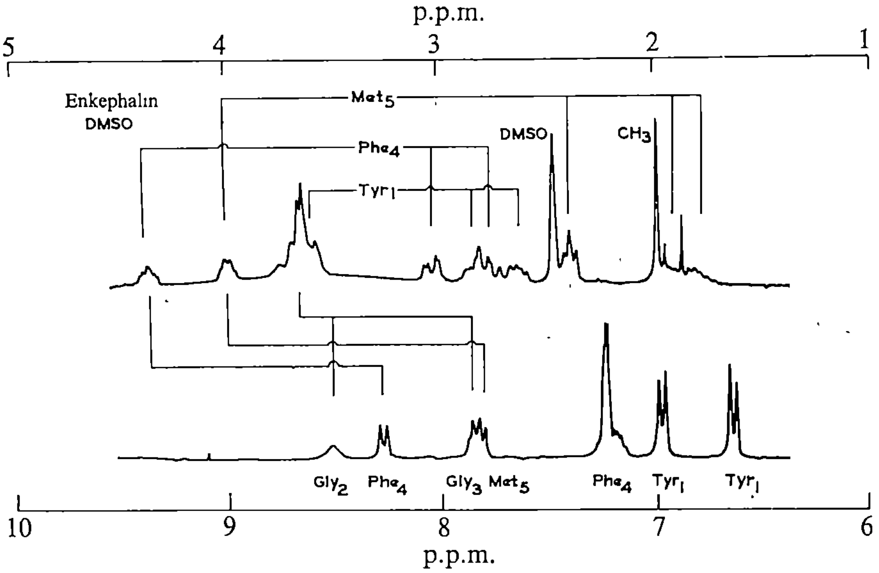

Fig. 1 PMR spectrum of Met^5-enkephalin in $^2H_6$-DMSO. The Tyr$_1$-OH and NH$_3$ signals are not present and the Gly$_2$-NH is broadened. Scale is p.p.m. from HMS.

out the possibility that the hydrogen bond is involved in a γ turn[9] and are instead indicative of a type I β turn. A type II β turn would not be in such good agreement with the observed coupling constants as a type I β turn but cannot be rigorously excluded by these data. Further studies of the Gly$_2$ and Gly$_3$ residues are needed since accidental degeneracy of the C_α protons has so far prevented an analysis of the NH–CH$_2$ spin system of Gly$_3$, and since the two $^3J_{NH-CH}$ values for Gly$_2$ are not available from the spectrum because of line broadening. A similar line broadening has been observed in oxytocins[10].

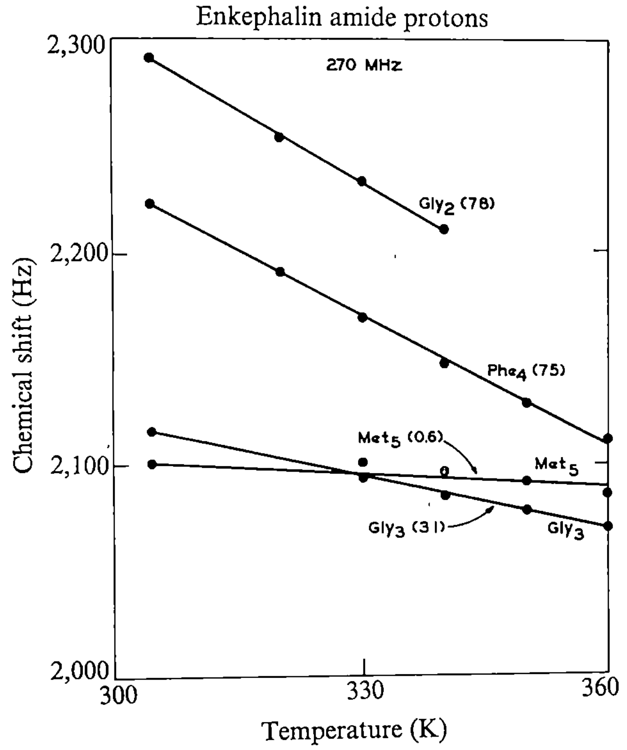

Fig. 2 Effect of temperature on the amide proton chemical shifts. The slopes (p p.10^9 per °C) are given in parentheses.

The analysis of the side-chain rotamer population[11] (Table 1) shows that the Met, Phe, and Tyr side chains favour one of the two possible *trans–gauche* rotamers[12], but for each of these residues all three rotamers have significant populations. Two conclusions can be drawn from this fact. First, there are $3^3 = 27$ possible forms of enkephalin which differ in the orientation of at least one of these three side chains. Second, for each of these three amino acids the Boltzmann energy differences (ΔE) between the various rotamer states must all be $\sim RT$. Consequently, we conclude that there may not be a simple direct relationship between the rotamer preferences observed here and the side-chain conformation on the receptor. Note, however, that a *trans–gauche* isomer of tyrosine (Table 1) is required to give a tyrosyl geometry resembling morphine.

Clearly, the more stable a conformational feature is, the more likely it is to be preserved in the substrate–receptor complex. Since β turns are often stabilised to the extent of several kcalories, the β turn which we are suggesting for the solution conformation of enkephalin may be an important feature in the interaction of enkephalin with its receptor. There are two pieces of indirect evidence which support this. First, a model of enkephalin in a type I β turn involving the Met–Phe–Gly–Gly residues shows a distinct topological resemblance to oripavine in the relative disposition of the tyrosyl and phenyl rings. The importance of the conformation of the β turn and Phe is clearly shown by the fact that the replacement of L-Phe by D-Phe in Met^5-enkephalin results in a peptide which is inactive (Garsky *et al.*, unpublished). Although a β turn of the residues Tyr–Gly–Gly–Phe (ref. 6) also resembles oripavine, the chemical shift data in Fig. 2 show no evidence for a hydrogen bond between the amino proton of Phe and the carbonyl group of tyrosine[6]. Second, the side-chain rotamer populations of Phe exhibit the normal tendency toward $a = b = c = 1/3$ as temperature is increased (Fig. 3). This behaviour is indicative of a situation in which there is only one degree of rotational freedom (that is, the rotation about the C_α–C_β bond in this case) which has Boltzmann energy differences $\Delta E \sim RT$ and is the behaviour we find in other peptides with rigid ($\Delta E > RT$ backbone structures. In contrast, non-rigid backbones ($\Delta E \sim RT$) would be expected to add considerable complexity to the temperature dependence of side-chain rotamer populations. As Fig. 3 shows, both the Met and Tyr side-chain rotamer populations show a less conventional temperature dependence than Phe and this may indicate greater flexibility for the φ, ψ angles of Met and Tyr than for the corresponding angles involved in the β turn.

Our data are consistent with a backbone conformation of enkephalin having a type I β turn with a hydrogen bond between the amide proton of Met$_5$ and Gly$_2$ (Fig. 4). Correlation of this conformation and that of morphine with their respective biological functions is not simple. The predominant *trans–gauche* geometry of the Tyr$_1$ residue certainly correlates

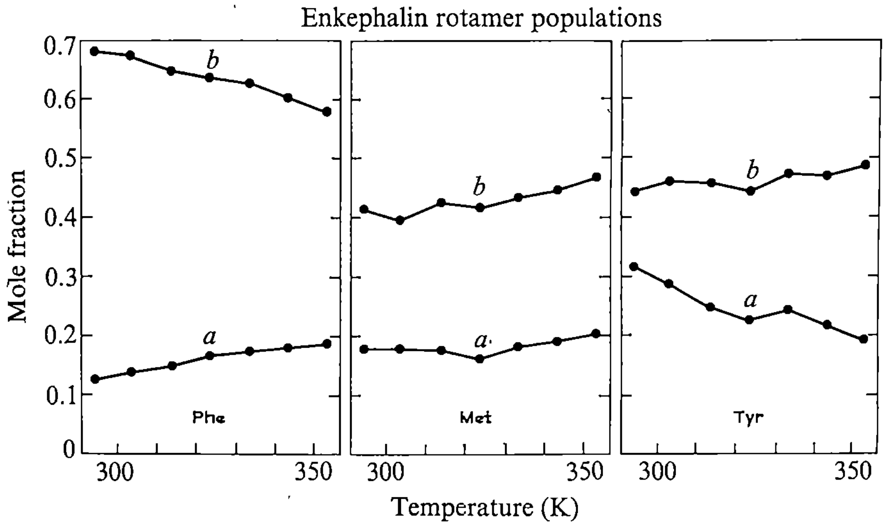

Fig. 3 Effect of temperature on the rotamer populations of Met^5-enkephalin (calculated by the method of Pachler[11]). The third rotamer population can be obtained from the graphs, since $a+b+c = 1$.

Table 1 PMR parameters for enkephalin in $^2H_6$-DMSO (2 mg per 0.5 ml) at 25 °C

	Tyr_1	Gly_2	Gly_3	Phe_4	Met_5
Chemical shift*					
δ CαH	3.61	3.67	3.74	4.35	3.96
δ CβH	2.85	—	—	3.04	1.92
δ CβH	2.67	—	—	2.78	1.79
Coupling constant†					
^3J α β1	6.2	—	—	4.0	4.5
^3J α β2	7.5	—	—	10.1	7.3
^2J α ββ	−13.7	—	—	−13.9	−13.3
$^3J_{NH-CH}$	—	—	—	8.3	7.2
Rotamer populations‡					
g^+g^-	0.33	—	—	0.13	0.17
tg^+	0.44	—	—	0.68	0.43
tg^-	0.23	—	—	0.19	0.40
Temperature dependence of amide shifts δ	—	−7.8	−3.1	−7.5	−0.6

* Units = p.p.m. from hexamethyldisilane (HMS).

† Hz at 270 MHz.

‡ Statistical weights of rotamers calculated according to Pachler[11] parameters. This method does not unequivocally distinguish the tg^+ from tg^- rotamers.

§ Units = p.p.10^9 per °C.

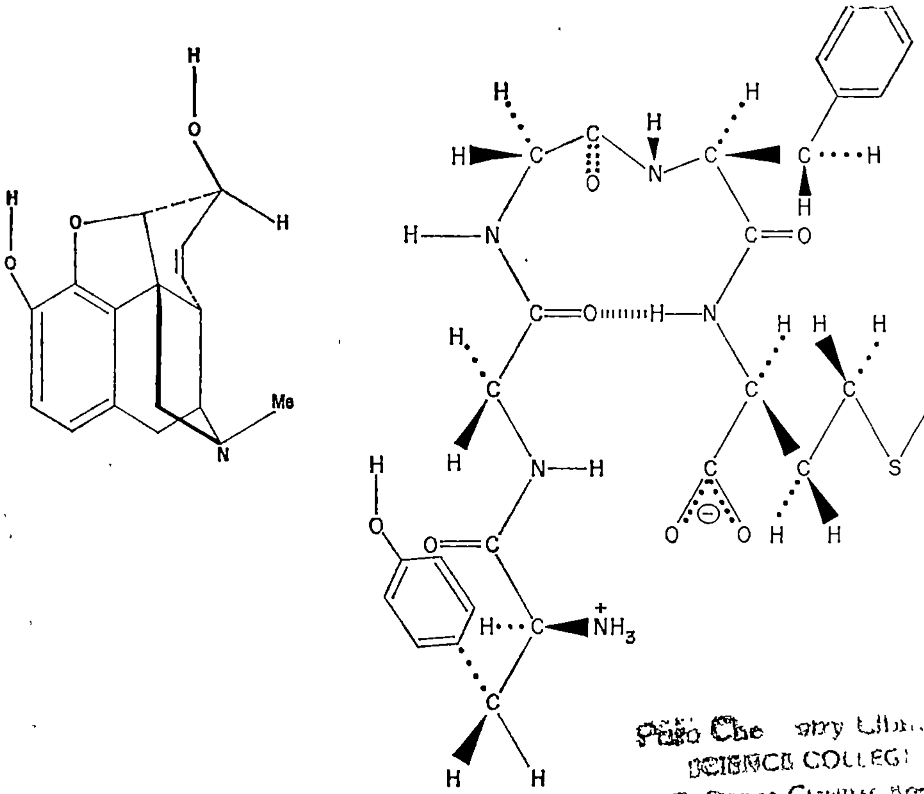

Fig. 4 Diagramatic representation of one conformation of Met^5-enkephalin. Note the β turn, the proximity of the NH_3 and CO_2 groups, the conformation of the Tyr_1 residue, and the L-Phe in the β turn.

Pure Chemistry Library
SCIENCE COLLEGE
92, Upper Circular Road

with the known steric requirements of morphine[4,13], but there is not yet a simple explanation of the requirement for a type I β turn (except that L-Phe and not D-Phe is active) or that there can exist 27 rapidly interconverting enkephalin forms. The time scale for this rearrangement will be approximately 10^{-10}–10^{-11} s, which is faster than the residence time of the hormone–receptor complex. Consequently, all 27 enkephalin forms may bind initially to the receptor which then selects the appropriate form in accordance with the induced-fit theory of hormone action[14].

In H_2O solution, both Gly_2 and Gly_3 $NH–CH_2$ spin systems are degenerate as $^2H_6$-DMSO and the Phe_4 and Met_5 have $^3J_{NH-CH}$ values close (1 Hz) to the value in $^2H_6$-DMSO. The interpretation of these data is that the enkephalin conformations and internal motions are qualitatively similar in both solvents. Leu^5-enkephalin has basically the same conformation as Met^5-enkephalin in $^2H_6$-DMSO.

This research was supported by the Colleges of Agriculture and Life Sciences of the University of Wisconsin–Madison, and by the NIH and the NSF. C. R. J. was supported by an Enzymology Postdoctoral Training Grant.

CLAUDE R. JONES
WILLIAM A. GIBBONS

Department of Biochemistry,
University of Wisconsin–Madison,
Madison, Wisconsin 53706

VICTOR GARSKY

Wyeth Research Laboratories,
PO Box 8299, Philadelphia 1,
Pennsylvania 19104

Received May 28, accepted July 18, 1976.

1 Belluzi, J. D., *et al.*, *Nature*, **260**, 625–626 (1976).
2 Hughes, J., *et al.*, *Nature*, **258**, 577–579 (1975).
3 Waterfield, A. A., Hughes, J., and Kosterlitz, H. W., *Nature*, **260**, 624–625 (1976)
4 Horn, A. S., and Rodgers, J. R., *Nature*, **260**, 795–797 (1976).
5 Bradbury, A. F., Smyth, D. G., Snell, C. R., Birdsall, N. J. M., and Hulme, E. C., *Nature*, **260**, 793–795 (1976).
6 Bradbury, A. F., Smyth, D. G., and Snell, C. R., *Nature*, **260**, 165–166 (1976)
7 Kopple, K. D., Ohnishi, M., and Go, A., *J. Am. chem Soc.*, **91**, 4264–4272 (1969)
8 Ohnishi, M., and Urry, D. W., *Biochem biophys. Res. Commun.*, **36**, 194–202 (1969).
9 Nemethy, G., and Printz, M. P., *Macromolecules*, **5**, 755–758 (1972).
10 Glickson, J. D., Urry, D. W., Havran, R. T., and Walter, R., *Proc. natn. Acad. Sci. U.S.A.*, **69**, 2136–2140 (1972)
11 Pachler, K. G. R., *Spectrochim. Acta*, **20**, 581 (1964).
12 Wyssbrod, H. R., and Gibbons, W. A., *Survey of Progress in Chemistry*, **6**, (edit. by Scott, A. I.), 209–325 (Academic, New York and London 1973).
13 Goldstein, A., Aronow, L., and Kalman, S. M., *Principles of Drug Action*, 50–60 (Harper and Row, New York, 1969).
14 Wessels, P. L., Feeney, J., Gregory, H., and Gormley, J. J., *J. chem. Soc. Perkin*, II, 1691–1698 (1973)

Mode of deactivation of the enkephalins by rat and human plasma and rat brain homogenates

SEVERAL groups of workers have recently demonstrated the existence of naturally-occurring peptides which show agonist activity at the opiate receptor[1-4], and Hughes *et al.*[5] have shown that the opiate activity isolated by them is due to a mixture of two peptides H-Tyr-Gly-Gly-Phe-Met-OH and H-Tyr-Gly-Gly-Phe-Leu-OH termed methionine-enkephalin and leucine-enkephalin respectively.

The agonist activity of these two peptides was established using *in vitro* techniques and early work[2] demonstrated that the enkephalins were subject to rapid deactivation when exposed to tissue homogenates and purified enzyme preparations such as carboxypeptidase-A and leucine aminopeptidase. In view of these results, it was perhaps not surprising to find that *in vivo*, even after central administration, the antinociceptive actions of the peptides are, at best, transient (refs 6 and 7 and G. Metcalf, personal communication). Using the depressant effects of the enkephalins on the electrically-evoked contractions of the mouse vas deferens as a bioassay, the half-life of both peptides in rat plasma was shown to be very short (Table 1). In this study we attempted to identify the mode of deactivation of the peptides in rat plasma and brain homogenates, which we believe could be responsible for the limited *in vivo* activity of the enkephalins.

^{3}H-Gly^3-Met^5-enkephalin was synthesised from ^{3}H-glycine using solutions methods[15] 3,5-^{3}H-Tyr-Leu^5-enkephalin was synthesised from the unlabelled pentapeptide by the Radiochemical Centre, Amersham.

Met^5-enkephalin, Leu^5-enkephalin, H-Tyr-Gly-Gly-Phe-OH, H-Gly-Gly-Phe-Met-OH, and H-Gly-Gly-Phe-Leu-OH were synthesised by standard methods[15]. Thin-layer chromatography was carried out on silica plates (Keiselgel F_{254}, Merck Ag) using the following solvent systems: (1) chloroform–methanol–acetic acid–water, 45:30:6:9 (2) *n*-butanol–pyridine–acetic acid–water, 60:20:6:24 (3) *n*-butanol–ethyl acetate–acetic acid–water, 1:2:1:1 (4) chloroform–methanol–acetic acid, 18:2:1. Distribution of radioactivity on the plates was determined using a zonal scraping technique. Column chromatography was carried out on DEAE–Sephadex in the acetate form with 1% pyridine, 0.04% acetic acid as eluting solvent. Peptides were hydrolysed in 6 M hydrochloric acid in sealed tubes (108 °C; 20 h) before analysis using a Jeol 6 AH automatic amino acid analyser.

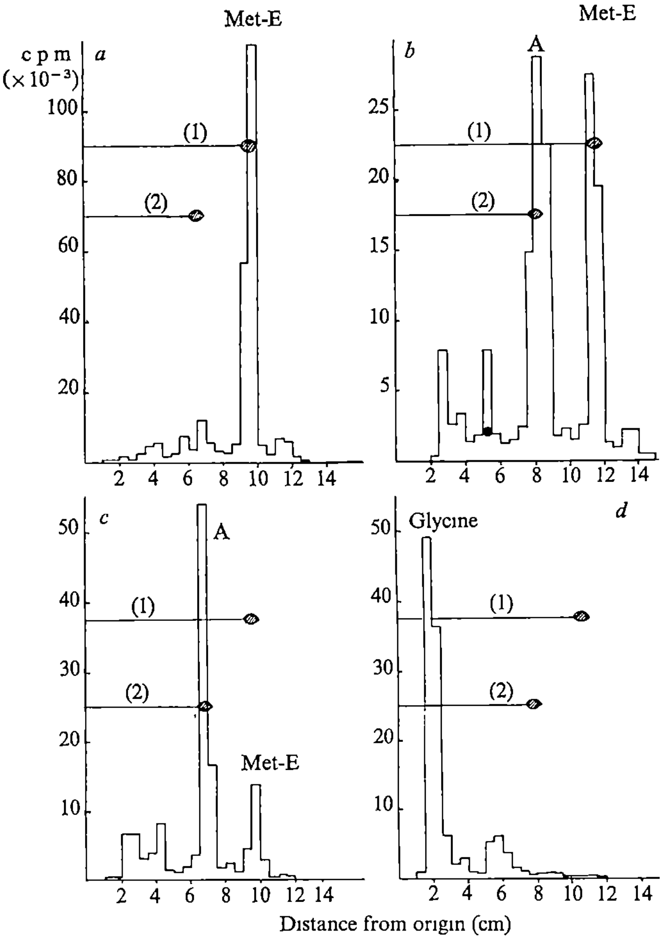

Fig. 1 Breakdown pattern of ^{3}H-Gly^3-Met^5-enkephalin (0.3 × 10^{-6} M) at 37 °C by rat plasma (20% v/v) in 50 mM Tris-HCl buffer (*p*H 7.4). *a*, 0 min; *b*, 5 min; *c*, 10 min; *d*, 30 min. Samples (0.2 ml) were taken periodically, added to methanol (0.1 ml) and stored in ice. The supernatants were applied to silica plates and eluted with solvent system 1. Authentic standards were visualised with ninhydrin, the plates divided into bands (0.5 cm) and the silica scraped into scintillation vials. Water (2.0 ml) and an aliquot (5 ml) of a solution of butyl-PBD (7.5 g) in toluene (666 ml) and Triton X-100 (333 ml) were added and the vials shaken to form a stiff gel. Radioactivity was determined using a Packard 2450 scintillation spectrometer. The histograms represent the distribution of radioactivity (c.p.m.) on the plates with reference to the R_f values of authentic standards: 1, Met^5-enkephalin; 2, H-Gly-Gly-Phe-Met-OH.

Initial studies were carried out at 37 °C with ^{3}H-Gly^3– Met^5-enkephalin (0.3×10^{-6} M) in an incubation mixture consisting of rat plasma (20% v/v) in 50 mM Tris–HCl (*p*H 7.4). These showed a breakdown pattern for the pentapeptide which is represented by the histograms in Fig. 1. At this concentration, the disappearance of Met^5-enkephalin was rapid, which is consistent with the rapid deactivation of the peptide in rat plasma. Continuation of the incubation resulted in the recovery of essentially all radioactivity as ^{3}H-glycine, indicating complete degradation of the peptide under these conditions. The main product (A), which was somewhat more stable than the parent pentapeptide, appeared to be chromatographically similar to the tetrapeptide H-Gly–Gly–Phe–Met–OH (all possible Gly^3-containing peptides were used as chromatographic standards). Product A was isolated from a larger scale incubation by chromatography on DEAE–Sephadex and purified by preparative thin layer chromatography on silica plates. After acid hydrolysis, the amino acid composition was determined and found to be compatible with the structure H–Gly–Gly–Phe–Met–OH (glycine 1.83, phenylalanine 1.17, methionine 0.85); no tyrosine was detected. The metabolite proved to be chromatographically identical to the synthetic tetrapeptide on silica plates using the solvent systems above. On the basis of this evidence, the primary step in the breakdown of Met^5-enkephalin in rat plasma is assigned as cleavage of the Tyr–Gly amide bond. As the tetrapeptide H–Gly–Gly–Phe–Met–OH shows very little activity using the mouse vas deferens assay procedure (Table 1), this cleavage is consistent with the deactivation of Met^5-enkephalin in rat plasma.

Table 1 The depressant effects of the enkephalins and degradation products on the electrically induced contractions of the mouse vas deferens

Structure	Relative activity* mouse vas deferens	$t_{\frac{1}{2}}$(rat plasma)‡ (min)
H–Tyr–Gly–Gly–Phe–Met–OH	100	2.0
H–Tyr–Gly–Gly–Phe–Leu–OH	170	2.5
H–Gly–Gly–Phe–Met–OH	0.1	–
H–Gly–Gly–Phe–Leu–OH	0.1	–

*Determined by the method of Henderson *et al.*[8].

‡Rat plasma containing the test compound (100 μg ml^{-1}) was incubated at 37 °C. Samples (0.1 ml) were taken periodically and added to 0.01M hydrochloric acid (0.1 ml). Each sample was diluted (×10) with Krebs solution and aliquots (0.1–0.3 ml) of the resulting solution injected into an organ bath (4 ml) containing the vas deferens. The depression in twitch height obtained with each sample was compared to a dose–response curve constructed for authentic methionine-enkephalin and the half life of biological activity determined.

Experiments carried out using human plasma showed that an essentially identical pattern of breakdown was taking place, though the rate of cleavage seemed to be somewhat slower.

Incubation of ^{3}H-Tyr–Leu^5-enkephalin with rat and human plasma in similar conditions resulted in the formation of a single radiolabelled product which was stable to further incubation. The R_f value of this product corresponded closely with that of tyrosine in the above thin-layer chromatographic systems, and when the product was applied to an amino acid analyser the radioactivity was eluted concurrently with authentic tyrosine. At no time was any radioactive product present which had chromatographic properties similar to any of the possible tyrosine-containing degradation products, authentic samples of which were used as chromatographic standards. This is consistent with ^{3}H-tyrosine being the primary labelled product of the degradation of ^{3}H-Tyr-Leu^5-enkephalin. Thus it seems that Leu^5-enkephalin is degraded in rat and human plasma in an identical way to Met^5-enkephalin, that is, by cleavage of the Tyr–Gly amide bond.

Breakdown of the enkephalins takes place very rapidly in the presence of rat brain homogenates: ^{3}H-Tyr–Leu^5-enkephalin (10^{-7} M) was completely destroyed within 1 min at 37 °C in a homogenate of whole rat brain containing approximately 3 mg protein ml^{-1}. The mode of deactivation seemed to be identical to that observed in plasma for both enkephalins. The subcellular localisation of the enzyme(s) responsible for the cleavage of the Tyr–Gly bond is under investigation.

The observation that the enkephalins are subject to rapid deactivation mediated by cleavage of the Tyr–Gly bond in both plasma and brain is compatible with the observed properties of the peptides *in vivo*[6,7]. It has been reported that the addition of bacitracin (a polypeptide antibiotic which has been shown to be a potent glucagon inactivation inhibitor[10]) enhances enkephalin-mediated effects on cyclic GMP accumulation in slices of rat neostriatum[9]. This enhancement may well be due to inhibition of peptidase activity by the antibiotic. It is interesting to note that, despite the lability of the peptides in brain homogenates, several groups of workers have been able to demonstrate the affinity of the enkephalins or related peptides for the opiate receptor in brain[3,4,11,12].

The important observation[7,12] that porcine β-lipotropin C-fragment (a 31-residue peptide isolated from pig pituitary which has the Met^5-enkephalin sequence at its N terminus[13]) shows potent and long lasting morphine-like effects in the cat is surprising in view of its structural relationship to the enkephalins. It is possible, however, that the tertiary structure of the longer peptide is such that the labile Tyr–Gly bond is protected from the metabolising enzyme, thus conferring greater stability on the molecule *in vivo*.

In conclusion, the deactivation of the enkephalins in rat and human plasma and in rat whole brain homogenate has been shown to take place through cleavage of the Tyr–Gly amide bond. The localisation, nature and specificity of the enzyme system responsible for the cleavage is unknown but its precise role and mode of action may be expected to have a major effect on the pharmacology and biochemistry of the enkephalins and related compounds.

Since this paper was submitted, further evidence that cleavage of the Tyr–Gly amide bond is the initial deactivation step of the enkephalins *in vivo* has been provided by structure–activity studies on enkephalin analogues. In particular D-Ala^2-Met^5-enkephalin is extremely resistant to plasma enzymes. This superactive analogue (5×Met^5-enkephalin potency in the mouse vas deferens assay) has a $t_{\frac{1}{2}}$ of at least 20× Met^5-enkephalin in rat plasma indicating the importance of the Tyr–Gly region of the molecule to the substrate specificity of the degrading enzyme(s). Similar results have been reported by other workers[14].

We wish to thank Dr J. D. Bower, Mrs C. Calverley, Mr P. Coffin, Mr R. Pape, Mr J. D. Robinson and Mr A. Wilson for their technical assistance.

JEAN M. HAMBROOK
BARRY A. MORGAN
MICHAEL J. RANCE
COLIN F. C. SMITH

Pharmaceutical Division,
Reckitt and Colman,
Dansom Lane,
Hull HU8 7DS, UK

Received June 7; accepted July 15, 1976

[1] Terenius, L , and Wahlstrom, A., *Acta pharmac tox* , 35, 55 (1974).
[2] Hughes, J , *Brain Res.*, 88, 295–308 (1975)
[3] Pasternak, G. W , Goodman, R , and Snyder, S H , *Life Sci.*, 16, 1765–1769 (1975).
[4] Teschemacher, H , Opheim, K. E., Cox, B. M., and Goldstein, A., *Life Sci* , 16, 1771–1775 (1975).
[5] Hughes, J., Smith, T. W., Kosterlitz, H W . Fothergill, L. A , Morgan, B. A , and Morris, H. R , *Nature*, 258, 577–579 (1975).
[6] Belluzzi, J D , Grant, N , Garsky, V., Sarantakis, D., Wise, C. D , and Stein, L., *Nature*, 260, 625–626 (1976).
[7] Feldberg, W., and Smyth, D G., *J Physiol Lond.* (in the press)
[8] Henderson, G., Hughes, J., and Kosterlitz, H , *Br J. Pharmac* , 46, 764–766 (1972).
[9] Minneman, K P., and Iversen, L. L., *Nature* (in the press)
[10] Desbuquois, B , Krug, F., and Cuatrecasas, P , *Biochim biophys Acta*, 343, 101–120 (1974)
[11] Terenius, L , and Wahlstrom, A , *Life Sci* , 16, 1759–1764 (1975)
[12] Bradbury, A F , Smyth, D. G., Snell, C. R., Birdsall, N. J. M., and Hulme, E C., *Nature*, 260, 793–795 (1976)
[13] Bradbury, A F , Smyth, D G , and Snell, C. R , in *Peptides, Chemistry Structure and Biology, Proc IV American Symp* (edit by Meienhofer, J), 61–75 (Ann Arbor Science Inc., Ann Arbor, 1975).
[14] Pert, C., *Proc. Narcotics Club, Aberdeen*, 1976 (in the press).
[15] Bower, J. D , Guest, K P., and Morgan, B. A., *J. Chem. Soc. Perkin Trans* , I (in the press).

Substance P and analgesia

SUBSTANCE P (SP)[1] has long been known to have marked effects on the central nervous system (CNS). Lembeck[2] suggested that SP might be a transmitter of primary sensory impulses, an hypothesis supported by subsequent investigators[3,4]. Early work on SP was carried out using natural material, which unless highly purified, is known to be contaminated with bradykin or some other kinin-like material[5]. As bradykinin also has marked effects on the CNS, experiments carried out using impure SP may be misleading. This may account for some of the conflicting observations that exist regarding the action of SP on sensory transmission, and may also explain its interaction with opioids. Whereas impure SP has been shown to antagonise morphine[6], synthetic SP was found to substitute effectively for morphine in mice chronically treated with morphine[7]. SP does not act like morphine in the field-stimulated guinea pig ileum[8] and does not combine with morphine receptors[9]. Furthermore, SP has been reported to be the most potent algogenic substance known on the human blister base[10]. Recent reports on the characterisation and activity of enkephalin[11,12] suggested that enkephalin may be acting as an analogue of SP. We have therefore examined SP for morphine-like activity.

This hypothesis was tested initially by examination of the effects of intracerebral injection[13] of SP and morphine into 30-g male Swiss Webster mice. Response of the animals to heat stimuli was tested using a hot plate analgesiometer[14]. Each mouse's reaction time (RT; s) was determined before administration of any drug and again at 30-min intervals after drug injection. Naloxone and morphine were administered in physiological saline; SP was administered in physiological saline containing 0.01 N acetic acid, to prevent adsorption of SP to glass. When used, naloxone was injected intraperitoneally immediately before intracerebral injection of other drugs. Vehicle controls were carried out. The pre-drug RT was subtracted from each of the RTs observed after treatment, and these differences in RT are reported in Table 1.

SP and morphine each caused an increase in RT, indicating analgesia; and the analgesic action of each was prevented by naloxone Mice which received SP seemed to be quiet compared with normal mice. They would cease movement, seeming to sleep, often in an abnormal posture. These animals were readily aroused, and seemed to be alert, however, while being handled and while on the analgesiometer. These behavioural effects of SP were similar to those described previously[15].

Table 1 Analgesic action of intracerebrally administered SP and morphine sulphate (MS)

Treatment	Increase in RT at: 30 min	60 min	90 min
SP (7)	3.0±0.83	5.23±0.72	8.23±1.09
SP vehicle (7)	−0.11±1.57	1.43±1.28	2.03±1.53
MS (7)	8 03±1.75	4.86±1.46	2.49±0.61
Saline (7)	−1.14±0 51	−0 41±1.16	0.63±0 6
SP+naloxone i.p. (7)	−0.54±0.23	1.11±0.48	2.97±0.52
SP+SP vehicle i.p. (7)	3.6±1.32	4.77±1.85	7.23±1.44
MS+naloxone i.p (5)	0.0±0.93	1.84±1.15	4 52±1.92
MS+saline i.p. (5)	8.69±4.50	7.32±3.97*	5.80±2.76*
Naloxone i.p.+SP vehicle i.c. (7)	−0.74±1.06*	−0.31±0.67*	
Saline i.p.+SP vehicle (7)	−0.23±0.84*	−0.31±0.88*	
Chronic MS i.p.+SP (7)	0.37±0.92	−0.26±0.72	1 51±0.66
Chronic MS i.p.+MS (5)	−0.92±1.41	1.72±1 39	0.32±1.48
Chronic saline i.p.+ SP (5)	3.77±1.70	7.50±2.11	7.90±1.83

Injections were in 0.04 ml intracerebrally (i.c.) and 0.1 ml intraperitoneally (i.p.). Doses (per mouse): SP 2 ng; MS 0 4 μg; naloxone 60 ng (i.p.). All increases in RT were statistically significant with respect to the corresponding controls using Student's *t* test ($P<0\ 05$) except those marked with an asterisk.

Number of animals per group is given in parentheses. All drug injections were made at 1030.

Table 2 Analgesic action of intraperitoneally administered SP

Time of testing (min)	Increase in RT (s) Group 1	Group 2	Group 3
30	7.04±1.91	7 6±2.69	0.3±1.48
60	6.56±2.4	11.44±3.49	2.08±1.48
90	8.36±3.2	10.96±1.33	1.12±1.41
120	6.24±1.4	8.2±3.18	3.0±0.86
150	3.84±2.12	4.08±1 26	2.32±1.20

Each group contained 5 mice, each weighing 30 g. Injections (0.1 ml intraperitoneally) were: group 1, SP 5 ng per mouse; group 2, SP 1 μg per mouse, group 3, SP vehicle alone. For other details of testing, see text and Table 1. Increased RTs of animals in groups 1 and 2 were all significant compared with group 3 ($P<0.05$) except at 150 min.

To determine whether animals made tolerant to morphine also showed cross tolerance to the analgesic action of SP, animals were given morphine chronically before testing. On the first day of this experiment the RT of each mouse was tested on the analgesiometer before drug or placebo administration. Mice were then divided into three groups. Groups 1 and 2 received three injections of morphine intraperitoneally (0.25 mg per mouse per injection) on day 1, three injections on day 2 (0.5 mg) and three injections on day 3 (1 0 mg). On day 4 mice of group 1 were given SP intracerebrally and the mice of group 2 were given morphine intracerebrally. Animals of group 3 were given saline injections on days 1, 2, and 3, and received SP on day 4. The last part of Table 1 shows that mice treated chronically with morphine did not show any analgesic reaction to morphine or SP, whereas mice given chronic saline responded normally to SP.

Since SP has been reported to cross the blood–brain barrier[7], it was also tested for analgesic action after peripheral administration. The experimental protocol was similar to that of the initial experiment described above, except that SP was administered by intraperitoneal injection Table 2 shows that SP caused significant analgesia in mice at dose levels of 5 ng or 1 μg per mouse At all times except 150 min, the changes in RT of animals in groups 1 and 2 were statistically significant compared with vehicle controls (group 3). The changes in RT at 150 min were not statistically significant, probably because of the small number of animals used and the fact that the analgesia was wearing off at that time.

In view of these results, the reported algogenic action of SP on the human blister base was re-examined using synthetic SP Blisters were raised on the volar surface of human forearms by application of Cantharone (0.7% canthardin in collodion). After 20 h the blister top was removed and the fibrin layer removed from the base. Substances to be tested were dissolved in buffered physiological saline and applied to the blister base[10]. Synthetic SP was not algogenic at concentrations up to 1 mg ml^{-1}, whereas acetylcholine and bradykinin were potent algogens. Algogenicity of acetylcholine and bradykinin was not antagonised by SP or Leu^5-enkephalin. The previously-reported[10] algogenicity of SP on the blister base may have been attributable to kinin contamination, since the SP used was isolated material. The failure of SP to produce analgesia on the blister base suggests that its site of action is central, as is that of morphine. The interaction we observed between SP, morphine and naloxone also supports this postulate.

We have found SP to be a potent analgesic in mice. This action of SP *in vivo* is in sharp contrast to the reported failure of SP to act like morphine on the field-stimulated guinea pig ileum[8] or in binding to morphine receptors[9]. Since SP is a powerful stimulant for contraction of the ileum, it is possible that this latter activity may have obscured any morphine-like inhibition of contraction. With respect to receptor binding, it is possible that more than one type of morphine receptor exists in CNS tissue and that the one tested by Terenius[9] may not combine with SP. The SP receptor may possibly be degraded during the isolation procedure. It is possible that the analgesic action of SP may be mediated through the release of other substances. Another possibility is that the analgesia after administration of SP is not attributable to the intact molecule, but a metabolite of it. The slow onset and prolonged duration of action of SP compared with morphine may lend support to this hypothesis. Arguing against this possibility is the observation of Otsuka *et al.*[4], who found that shorter C-terminal fragments of SP, which retain relatively high myotropic potency, had little depolarising activity in frog spinal motoneurones.

It has been reported that enkephalin, which comprises residues 61–65 of β lipotropin, has only very transient and probably insignificant analgesic action *in vivo*[16], whereas the much larger C-fragment (residues 61–91 of β lipotropin) is an active, potent, *in vivo* analgesic[17]; these data were obtained by intracerebral injection of the peptides. Our finding of the potent analgesic action of SP after peripheral administration suggests that the development of a small peptide as a practical analgesic drug may be possible. The intraperitoneal route of administration should minimise any undesirable hypotensive effects of SP, and its already prolonged analgesic action may be further prolonged by depot forms of administration.

JOHN M. STEWART
CARL J. GETTO
KENNETH NELDNER
E. BASIL REEVE

University of Colorado School of Medicine,
Denver, Colorado 80220

WILLIAM A. KRIVOY

National Institute for Drug Addiction,
Lexington, Kentucky 40511

EMERY ZIMMERMANN

UCLA School of Medicine,
Los Angeles, California 90024

Received June 14; accepted July 6, 1976.

[1] Leeman, S. E., and Mroz, E. A., *Life Sci.*, **15**, 2933–2044 (1974).
[2] Lembeck, F., *Naunyn-Schmiedebergs Arch. exp. Path. Pharmak.* 213 (1953).
[3] Krivoy, W. A., Lane, M., and Kroeger, D., *Ann. N.Y. Acad. Sci.*, **104**, 312–325 (1963).
[4] Otsuka, M., Konishi, S., and Takahashi, T., *Fedn Proc.*, **34**, 1922–1928 (1975).
[5] Stewart, J. M., *Pharmacologist*, **12**, 265 (1970).
[6] Zetler, G., *Arch. exp. Path. Pharmak.*, **228**, 513–538 (1956).
[7] Stern, P., Catovic, S., and Stern, M., *Arch. int. Pharmacodyn. Ther.*, **202**, 259–262 (1973).
[8] Cox, B. M., Opheim, K. E., Teschmacher, H., and Goldstein, A., *Life Sci.*, **16**, 1777–1782 (1975).
[9] Terenius, L., *J. Pharm. Pharmac.*, **27**, 450–453 (1975).
[10] Armstrong ,D., in *Bradykinin, Kallidin and Kallikrein, Handbuch Exp. Pharm.*, **25** (edit. by Erdos, E. G.), 434–481 (Springer, Heidelberg, 1970).
[11] Hughes, J., Smith, T., Morgan, B., and Fothergill, L., *Life Sci.*, **16**, 1753–1758 (1975).
[12] Hughes, J., *et al.*, *Nature*, **258**, 577–579 (1975).
[13] Haley, T. J., and McCormick, W. G., *Br. J. Pharmac.*, **12**, 12–15 (1957).
[14] Eddy, N. B., and Leimbach, D., *J. Pharmac. exp. Ther.*, **107**, 385–393 (1953).
[15] Euler, U. S. von, and Pernow, B., *Acta physiol. scand.*, **36**, 265–275 (1956).
[16] Belluzzi, J. D., *et al.*, *Nature*, **260**, 625–626 (1976).
[17] Bradbury, A. F., *et al.*, *Nature*, **260**, 793–795 (1976).

Colchicine inhibits mitogenesis in C1300 neuroblastoma cells that have been arrested in G_0

CELLS in G_1 or G_0 usually progress through the cell cycle and stop in metaphase when colchicine is added to the growth medium[1–6]. I have observed, however, using two different experimental techniques, that mouse C1300 neuroblastoma cells reversibly arrested in G_0 by serum limitation[7] are unable to re-enter the cell cycle in the presence of colchicine.

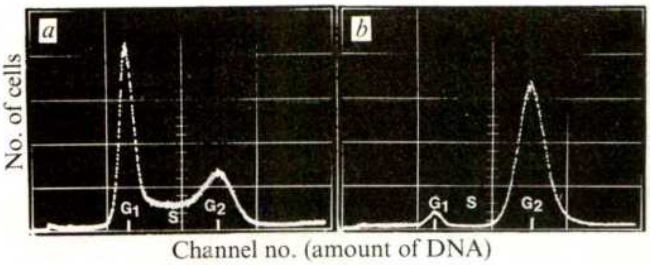

Fig. 1 Effect of colchicine on exponentially growing C1300 neuroblastoma cells. FMF analysis (*a*) before colchicine and (*b*) 40 h after addition of 1 μg ml^{-1} colchicine to the growth medium. C1300 cells were treated as described by Crissman and Tobey[11] to obtain a monodisperse suspension. Cells were stained with mithramycin and passed through a Los Alamos design microfluorometer[10] equipped with an argon laser excited at 457 nm. The fluorescent light flash from each cell, which is proportional to the cell's DNA content, was converted to an electrical pulse by a photomultiplier and stored in a multichannel pulse-height analyser. The data were also displayed on an oscilloscope as shown above.

Colchicine inhibited by about 85% the incorporation of ^{3}H-thymidine into DNA from 21 to 28 h after the arrested C1300 cells were returned to complete growth medium (Table 1). This could mean that C1300 cells do not leave G_0, or progress more slowly through the cell cycle, or do not take up thymidine[8]. A second technique, flow microfluorometric (FMF) analysis[9–11], which can determine the distribution in the cell cycle of a cell population by measuring the DNA content of individual cells, was used to distinguish among these possibilities. FMF analysis showed that after 44 h in growth medium plus colchicine about 85% of the original cell number is still in G_0 (Table 1). Colchicine therefore prevents C1300 cells from leaving G_0. The effect of colchicine additions at 10, 17, and 20 h after the cells were returned to DEM+10% calf serum (Table 2) suggests that the block involves the latter part of G_0 but not S phase. Colchicine inhibits mitogenesis in C1300 cells in G_0 but not

Table 1 Inhibition by colchicine of re-entry of C1300 neuroblastoma cells from G_0 into the cell cycle

Colchicine (μg ml^{-1})	% Inhibition of TCA-precipitable ^{3}H-thymidine counts*	%Inhibition of release from G_0 as determined by FMF analysis†
1	88	85
0.5	86	82
0.10	87	82

*C1300 cells, which were arrested in G_0 by serum limitation[7], were plated in Dulbecco's modified Eagle's medium (DEM)+10% calf serum at 2.5 × 10^5 cells per 60-mm Petri dish (Falcon). Colchicine was added about 30 min later. Cultures were pulsed with 5 μCi ^{3}H-thymidine in 0.10 ml 1.5 × 10^{-4}M non-radioactive thymidine from 21 to 28 h after plating. Cells were collected on glass-fibre filter papers, washed twice with Tris-saline buffer, twice with 10% TCA and once with 95% ethanol. The filter papers were counted in a scintillation fluid containing 4.2% Liquifluor in a liquid scintillation counter. Each sample point was done in duplicate. The variation between points was less than 10%. These results are from one of several experiments, all of which showed this effect. The sample without colchicine added had 70,000 c.p.m.

Cells were monitored for their ability to maintain a healthy clumped morphology in the suspension culture and to exclude Trypan blue. At all colchicine concentrations, for the first 30 h of the experiment, the cells grew in healthy clumps in suspension and over 90% excluded Trypan blue. By 48 h, however cultures with 1 μg ml^{-1} colchicine had smaller clumps and only 75% of the population excluded Trypan blue. The cells appeared to deteriorate after 45 to 50 h at this colchicine concentration. At the lower colchicine concentrations, the cells appeared clumped and at least 85% excluded Trypan blue after 48 h.

†FMF analysis in parallel cultures to the first part of the experiment was carried out as described previously[7,9–11] using the mithramycin staining procedure[11]. FMF experiments carried out parallel with other ^{3}H-thymidine incorporation experiments gave similar results.

Table 2 Interval of sensitivity to colchicine additions to cell cultures after arrested C1300 cells were returned to complete growth medium

Time of colchicine addition* (h)	% Inhibition of TCA-precipitable ^{3}H-thymidine counts†
1	88
10	79
17	31
20	15

*Results for colchicine concentration of 1 μg ml^{-1}. Similar results were observed at colchicine concentrations of 0.5 and 0.1 μg ml^{-1}.

†TCA-precipitable ^{3}H-thymidine incorporation was measured 21 to 28 h after the arrested cells were returned to DEM+10% calf serum. Assay was carried out as described in Table 1 and ref. 7. In addition, FMF analysis was carried out on parallel cultures 48 h after the cells were returned to DEM+10% calf serum.

in G_1, since only 5% of an exponentially-growing cell population is in G_1 (Fig. 1) 40 h after addition of 1 μg ml^{-1} colchicine to the growth medium. Vinblastine sulphate (1 μg ml^{-1}) also inhibits the re-entry into the cell cycle of C1300 cells arrested in G_0.

The mechanisms of growth regulation in normal and transformed cells are still being elucidated[6,7,12,13]. The cell membrane is thought to have a central role in controlling cell growth, in part by mediating the effects of serum factors that signal a cell to proliferate early in G_1 or G_0 (refs 14–17). This concept and the evidence that colchicine and other microtubule-disrupting drugs can affect the topographical distribution of receptors in the cell membrane[18–23] could explain my results. Colchicine may be altering the topographical distribution of receptor(s) for serum factor(s) required by the arrested C1300 cells to re-enter the cell cycle.

The results presented in Table 2 show that C1300 cells can receive a 'stop' signal late in G_0, some considerable time after the initial 'go' signal is received from serum factors[17]. This suggests that the mechanism of mitogenesis depends on specific receptor configuration(s) in late G_0 as well as in early G_1 or G_0 (refs 15–17).

Combinations of drugs that include a microtubule-disrupting agent are more effective than single drugs in treating tumours[24,25]. The results presented here suggest that this may be due, in part, to the effect the microtubule disrupting agent has on cells in G_0. The development of selective approaches to alter the mobility of receptors on the plasma membrane may prove useful in controlling malignant cell growth.

Gunther *et al.*[26] have shown that colchicine inhibits mitogenesis in lymphocytes. Also, colchicine inhibits mitogenesis in mouse 3T3 cells and dog MDCK kidney cells that have been reversibly arrested in G_0 (M. Baker, unpublished).

I thank Drs H. Friedman, R. W. Holley, J. Lockwood, G. Sato, J. Schneider, S. Varon, and the Human Biochemical Genetics Program, USPHS, for facilities and/or supplies. During part of this study, I was supported by a Senior Dernham Fellowship from the California Division of the American Cancer Society. I also thank Dr R. W. Holley for additional financial support (USPHS grant from the NCI) and encouragement; G. Baker, P. Schwalbe, and M. F. Weissberg for financial assistance; and Nathan Belcher, Pfizer Inc., for mithramycin.

MICHAEL E. BAKER*

The Salk Institute,
PO Box 1809,
San Diego, California 92112, and
Department of Biology,
University of California, San Diego,
La Jolla, California 92093

Received April 5; accepted July 6, 1976.

*Address for correspondence: Department of Medicine, M-013, University of California, San Diego.

1 Taylor, E. W., *J. Cell Biol.*, **25**, 145–160 (1965).
2 Olmsted, J. B., and Borisy, G. G., *A. Rev. Biochem.*, **42**, 507–540 (1973).
3 Wilson, L., Bamburg, J. R., Mizel, S. B., Grisham, L. M., and Creswell, K. M., *Fedn Proc.*, **33**, 158–166 (1974).
4 Wilson, L., and Bryan, J., *Adv. Cell molec. Biol.*, **3**, 21–72 (1974).
5 Temin, H. M., *J. Cell Physiol.*, **78**, 161–179 (1971).
6 Pardee, A. B., *Proc. natn. Acad. Sci. U.S.A.*, **71**, 1286–1290 (1974).
7 Baker, M. E., *Biochem. biophys. Res. Commun.*, **68**, 1059–1065 (1976).
8 Mizel, S. B., and Wilson, L., *Biochemistry*, **11**, 2573–2578 (1972).
9 Tobey, R. A., Crissman, H. A., and Kraemer, P. M., *J. Cell Biol.*, **54**, 638–645 (1972).
10 Van Dilla, M. A., Trujillo, T. T., Mullaney, P. F., and Coulter, J. R., *Science*, **163**, 1213–1214 (1969).
11 Crissman, H. A., and Tobey, R. A., *Science*, **184**, 1297–1298 (1974).
12 Dulbecco, R., *Science*, **166**, 962–968 (1969).
13 Holley, R. W., and Kiermam, J., *Proc. natn. Acad. Sci. U.S.A.*, **60**, 300–304 (1968).
14 Fox, T., Sheppard, J., and Burger, M. N., *Proc. natn. Acad. Sci. U.S.A.*, **68**, 244–247 (1971).
15 Pardee, A., *In Vitro*, 7., 95–104 (1971).
16 Holley, R. W., *Proc. natn. Acad. Sci. U.S.A.*, **69**, 2840–2841 (1972).
17 Mannino, R. J., and Burger, M. M., *Nature*, **256**, 19–22 (1975).
18 Singer, S. J., and Nicolson, G. L., *Science*, **175**, 720–731 (1972).
19 Nicolson, G. L., *Nature new Biol.*, **233**, 244–246 (1971).
20 Nicolson, G. L., in *Control of Proliferation in Animal Cells*, (edit. by Clarkson, B., and Baserga, R.), 251–270 (Cold Spring Harbor Laboratory, New York, 1974).
21 Edelman, G. M., *ibid.*, 357–378.
22 Yin, H. H., Ukena, T. E., and Berlin, R. D., *Science*, **178**, 867–868 (1972).
23 Edelman, G. M., Yahara, I., and Wang, J. L., *Proc. natn. Acad. Sci. U.S.A.*, **70**, 1442–1446 (1973).
24 Livingston, R. B., and Carter, S. K., *Single Agents in Cancer Chemotherapy* (Plenum, New York, 1970).
25 Arenson, E. B., Hutter, J. J. Jr., Restuccia, R. D., and Holton, C. P., *J. Am. med. Ass.*, **235**, 727–729.
26 Gunther, G. R., Wang, J. L., and Edelman, G. M., *Expl Cell Res.*, **98**, 15–22 (1976).

Inhibitory action of glutamic acid on cerebellar interneurones

GLUTAMIC acid strongly excites almost all central neurones examined, and it has been considered to be a main excitatory transmitter in the mammalian brain[1,2]. Although some neurones in the olfactory bulb have been inhibited by glutamic acid[3], this has been explained by the assumption that glutamate primarily activated γ-aminobutyrate (GABA)-releasing inhibitory interneurones, which in turn inhibited the neurones in question[1]. In the experiments reported here, glutamate inhibited neurones in the granular layer of the cerebellum: this action does not seem to be mediated by inhibitory interneurones.

Thin sections of guinea pig cerebellum (80–120 μm thick) were prepared from the uvula and nodulus perpendicular to the long axis of the folium as before[4]. They were incubated in glucose–saline medium saturated with 95% O_2 and 5% CO_2 at 37 °C for more than 40 min, and transferred one by one into an observation chamber under a microscope[5]. Single cell discharges were recorded extracellularly from neurones in the granular layer with glass microelectrodes of tip diameter 2–4 μm.

About half the neurones encountered in the granular layer were excited by glutamate (GE cells) and others were inhibited (GI cells) (Fig. 1). When glutamate was administered electrophoretically to a point about 30 μm from the tip of the recording pipette, the discharge rate of a GE cell started to increase within 1 s (Fig. 1*b*). The rate of firing of a GI cell, on the other hand, gradually decreased and then stopped (Fig. 1*a*, 1). Firing resumed after the electrophoretic current was turned off. An increase in electrophoretic current shortened the latency of inhibition (Fig 1*a*, 2). In some GI cells, contact of a pipette containing glutamate with the section near the recording site induced suppression of the firing even if a retaining current of 25 nA was passed continuously through the pipette (Fig. 2*a*, 1). This was probably due to a background leakage of glutamate which was reported to occur occasionally in spite of the retaining current[5]. In these cells, reduction of the retaining current caused stronger inhibition, and reversal of the current further increased the inhibition. Therefore, the inhibition observed during administration of glutamate cannot be explained by the electrotonic effect of current flow. This conclusion is strengthened by the observation that the neurones identified as the GI cells by electrophoretic administration of glutamate were also inhibited consistently when the sections were perfused with medium containing 0.1–0.3 mM glutamate.

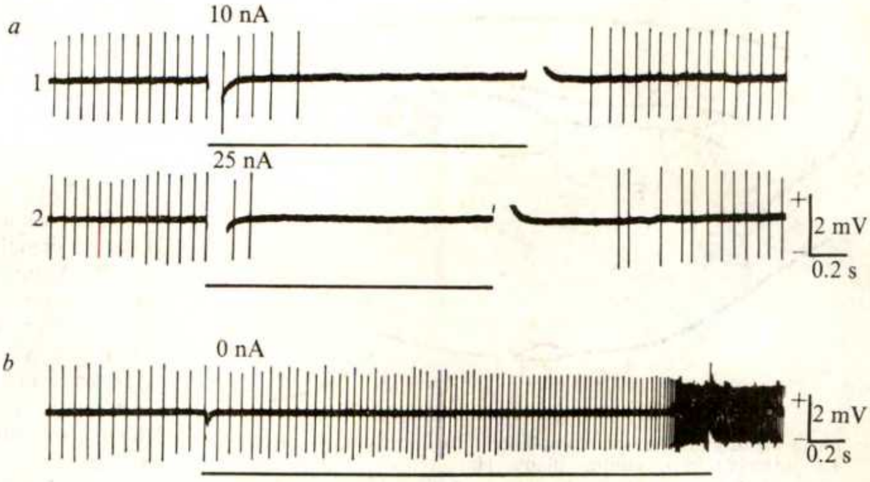

Fig. 1 Responses of cerebellar interneurones to glutamic acid administered to nearby points. *a*, Recorded from a GI cell. Electrophoretic currents were administered during the periods indicated by the solid lines beneath the records. Intensities of the currents are shown above the records. *b*, Recorded from a GE cell. Solid line: the retaining current of 25 nA was turned off.

The firing of the GI cells was suppressed not only by glutamate but also by GABA. In the experiment illustrated in Fig. 2, the extension of the area in which GABA administration effectively suppressed the firing of a GI cell (GABA-sensitive area) was compared with the extension of the glutamate-sensitive area defined similarly. If GABA inhibits a GI cell directly and glutamate works through mediation of inhibitory interneurones, it would be expected that the extension of the GABA-sensitive area would not coincide with that of the glutamate-sensitive area. In all six GI cells studied, however, both areas almost agreed with each other (Fig. 2). Inhibition by glutamate was not blocked by strychnine (0.5 mg l^{-1}) or pictrotoxin (50 mg l^{-1}), the latter being found to block the action of GABA. Although inhibition by GABA was blocked in the medium in which Cl^- was substituted by propionate ions, inhibition by glutamate was not affected in Cl-free medium. Thus inhibition by glutamate is not mediated by GABA-releasing neurones. Moreover, inhibition by glutamate was maintained in the medium containing 16 mM Mg^{2+}, in which synaptic transmission in brain slices was reported to be completely blocked[6]. This result excludes the possibility that interneurones intervene in the inhibition by glutamate.

In the cerebellar sections used in these experiments, individual neurones in the granular layer were not distinctly visible under a microscope. Therefore, the GI cells have not been identified morphologically. At least some of the GI as well as GE cells, however, seem to be large Golgi cells, because action potentials exceeding 5 mV in amplitude were sometimes recorded from the GE and GI cells with electrodes of relatively large tips. When an electric shock was applied to the white matter, the GI cells were inhibited and the GE cells were activated. This suggests that the distinction between the GE and GI cells is not only of pharmacological but also of physiological significance.

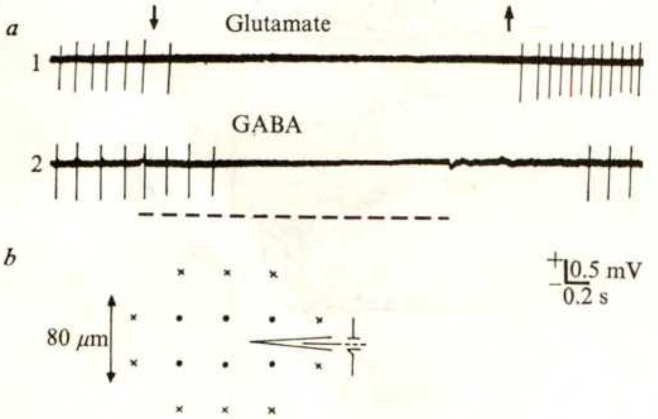

Fig. 2 Suppression of firing of a GI cell by glutamic acid and GABA. *a*: 1, the tip of a pipette filled with 1 M sodium L-glutamate, *p*H 8.2, touched a point indicated by dots in (*b*) approximately at the time marked by an arrow pointing downwards. The approximate time at which the pipette was removed is marked by an arrow pointing upwards. The retaining current of 25 nA was passed continuously through the pipette. 2, GABA was administered to the same point with an electrophoretic current of 25 nA during the period indicated by a broken line. *b*, Glutamate and GABA inhibited the cell when administered to the points indicated by dots but had no effect when administered to the points indicated by crosses.

CHOSABURO YAMAMOTO
HIROYUKI YAMASHITA
TADASHI CHUJO

Department of Physiology,
University of Kanazawa Medical School,
Kanazawa, Ishikawa-ken, Japan

Received June 1; accepted July 6, 1976.

[1] Curtis, D. R., and Johnston, G. A. R., *Ergebn. Physiol.*, **69**, 97–188 (1974).
[2] Krnjević, K., *Physiol. Rev.*, **54**, 418–540 (1974).
[3] Von Baumgarten, R., Bloom, F. E., Oliver, A. P., and Salmoiraghi, G. C., *Pflügers Arch. ges. Physiol.*, **277**, 125–140 (1963).
[4] Yamamoto, C., *Jap. J. Physiol.*, **24**, 177–188 (1974).
[5] Chujo, T., Yamada, Y., and Yamamoto, C., *Expl Brain Res.*, **23**, 293–300 (1975).
[6] Richards, C. D., and Sercombe, R., *J. Physiol., Lond.*, **211**, 571–584 (1970).

Growth of transplanted monoaminergic neurones into the adult hippocampus along the perforant path

CENTRAL and peripheral monoaminergic neurones have been found to survive transplantation to certain sites in the adult rat brain[1]. The neurones grow extensively in their new location and the newly formed axons extend through the surrounding scar tissue into the host brain. We now report experiments in which transplants of adrenergic, dopaminergic or indolaminergic neurones were transplanted to a cavity in the retrosplenial cortex to give them the opportunity to grow along the lesioned temporoammonic perforant path into the partly denervated hippocampal formation. The results demonstrate a remarkable ability of the regenerating axons to establish reproducible and characteristic terminal patterns in large areas of the hippocampus.

As described previously[1], transplantation involved the placement of pieces of embryonic brainstem—containing major noradrenaline (NA), dopamine (DA), or indolamine (IA) cell groups—or a piece of a mature sympathetic ganglion in a resection cavity in the occipital pole[1], in contact with or in proximity to the dorsal hippocampus (Fig. 1). The operation involved a major portion of the perforant path fibres innervating the dorsal part of the hippocampal complex[2–5]. Four types of material were transplanted: (1) a half to a third of the superior cervical

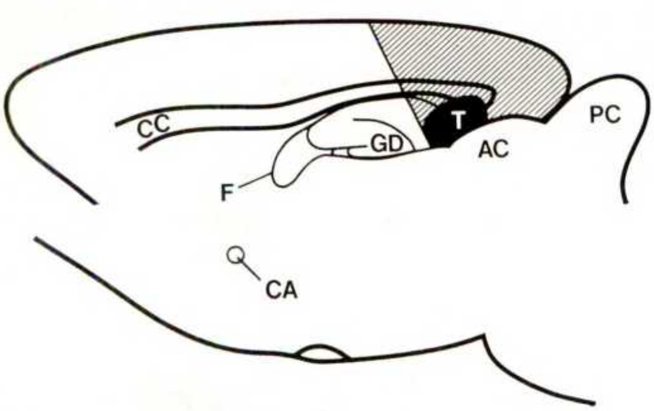

Fig. 1 Position of the neural implants in the hippocampal region, as illustrated in a sagittal plane. Hatched area denotes the extent of the resection cavity. The transplant (T) was placed, under visual control, on to the richly vascularised pia covering the underlying colliculi. The lesion involved part of the entorhinal, retrosplenial and occipital cortex, and the dorsal part of the subicular complex. All animals were subjected to complete intracranial sympathectomy before or at the time of transplantation. AC, Anterior colliculus; CA, anterior commissure; CC, corpus callosum; F, hippocampal fimbria; GD, dentate gyrus; PC, posterior colliculus.

ganglion taken from the adult recipient rat (autologous transplantation); (2) the ventromedial mesencephalon taken from embryos, containing primarily DA neurones; (3) the locus coeruleus region of the pons, taken from embryos, containing primarily NA neurones; (4) the pontine raphe region, taken from embryos, containing primarily IA neurones. These pieces of central nervous system (CNS) were dissected from embryos with a crown–rump length of 15–25 mm, essentially as described by Olson and Seiger[8], and they were transplanted homologously into adult rats (Sprague–Dawley; 180–200 g body weight).

The animals were killed 1–6 months later. To remove the normal monoaminergic innervations of the hippocampal formation, about half the recipients were given an intraventricular injection of either 6-hydroxydopamine (6-OHDA; 250 μg) or 5,7-dihydroxytryptamine (5,7-DHT; 150 μg) 2–6 d before transplantation. Brains were processed for fluorescence histochemistry according to the Falck–Hillarp formaldehyde method (for technical details, see ref. 7). Animals bearing IA transplants were treated with the monoamine oxidase inhibitor nialamide (300 mg $\mathrm{kg^{-1}}$) 3–5 h before killing, to facilitate visualisation of fibres containing 5-hydroxytryptamine (5-HT).

There were up to about 200 surviving, fluorescent neurones in the peripheral NA transplants, and up to about 500 in the central NA, DA and IA transplants (see ref. 1 for further details of fluorescence microscopical features of the transplants). Of the 18 ganglionic transplants studied, all survived except one, and 26 of the 33 CNS transplants survived. Abundant fibre outgrowth was demonstrable from all four types of transplant. In 19 out of the 26 surviving CNS transplants and in 16 of 17 surviving ganglionic transplants the outgrowing fibres grew into the hippocampal formation, above all the dentate gyrus. The transplantation lesion involved the dorsal presubiculum and subiculum, and a minor adjoining portion of CA 1. In some cases there was also a minor lesion in the dentate gyrus (Fig. 2*a* and *b*). Consequently, the outgrowing nerve fibres grew towards a largely intact dentate gyrus and towards the cut surface of CA 1, as shown semischematically in Fig. 2. There was an obvious preferential orientation of the newly formed fibres towards the dentate gyrus; this was most clearly demonstrated when the transplant was placed some distance from the dentate, as in Fig. 2*a* and *c*. In such cases the fibres had grown through the surrounding scar tissue for up to

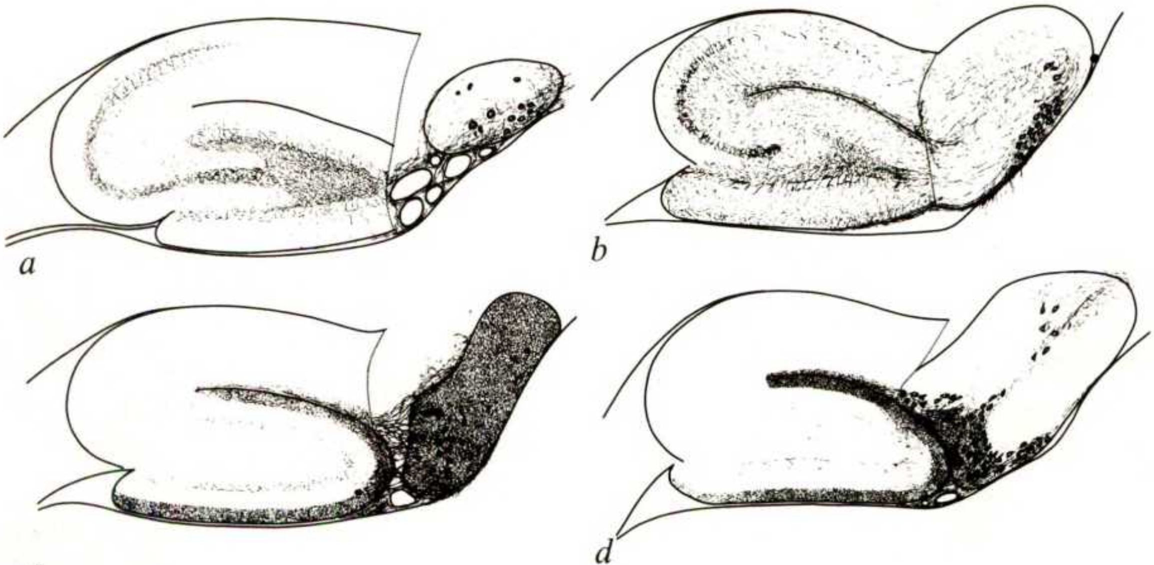

Fig. 2 *a–d*, Semischematic drawings, in the sagittal plane, of the fibre outgrowth from four types of neural transplants towards the hippocampus (compare Fig. 1). *a*, Superior cervical ganglion, 6 months survival. The recipient rat was given 250 μg 6-OHDA, intraventricularly, 2 d before transplantation. The transplant, which underwent considerable atrophy, contained about 90 ganglionic nerve cells with a fairly normal and healthy fluorescence microscopical appearance. This animal had also a minor lesion of the fimbria, which probably caused some increase in the fibre ingrowth. *b*, NA transplant taken from an embryo with a crown-rump length of 25 mm, 3 months survival. The normal adrenergic and indolaminergic innervations of the hippocampus had been removed with an intraventricular injection of 150 μg of 5,7-DHT, 6 d before transplantation. The transplant, which retained approximately its original size, contained about 450 surviving catecholamine-containing neurones confined to two major cell clusters. *c*, IA transplant taken from an embryo with a crown-rump length of 15 mm, 3 months survival. The transplant was filled with a dense pattern of newly formed IA fibres. Because they obscured many of the surviving IA cell bodies it was not possible to assess their number. *d*, DA transplant from an embryo with a crown-rump length of 20 mm, 6 weeks survival. The normal hippocampal adrenergic and indolaminergic innervations had been removed by a 5,7-DHT injection 3 d before transplantation. The transplant, which probably had increased somewhat in size, contained several hundred surviving fluorescent catecholamine neurones, intermingled with a dense plexus of locally ramifying DA fibres.

1–1.5 mm in rostral, lateral and ventrolateral directions to reach the adjacent dorsal part of the hippocampus and the dentate gyrus. In those specimens where the fibres had failed to reach the hippocampus the transplant had either been displaced more than 1–1.5 mm away from the dentate gyrus, or (in the case of CNS tissue) the surviving monoamine neurones were separated from the dentate by 1 mm or more of transplanted tissue devoid of monoamine neurones.

The fibres grew into the dentate gyrus either along the shortest course straight into the dentate, or along the hippocampal fissure into the dentate gyrus and the hippocampal CA 1 and CA 3 regions. In some cases the fibres also passed for some distance along the pia of the ventral surface of the dentate gyrus before entering the underlying tissue. Although the amount of fibres that grew into the hippocampal formation from the transplant varied from specimen to specimen, their patterning was remarkably reproducible and showed distinct and consistent differences among the several types of grafted neurones.

The peripheral NA neurones had formed a dense varicose terminal pattern in the hilar region as illustrated in Fig. 2*a* for a specimen taken 6 months after transplantation. Only a few fibres had passed through the granular layer into the basal part of the molecular layer. The outer part of the molecular layer was consistently devoid of fibres. Growth into the hippocampus proper was much more sparse. The fibres appeared to reach the CA 3 region from the dentate gyrus, and in most specimens fibres occurred only in the part of CA 3 close to the dentate. In the 6-month specimen (Fig. 2*a*) the ganglionic fibres had grown through CA 3 into part of the CA 1 region. The patterning of the ganglionic fibres was remarkably similar to that of the normal adrenergic nerve supply (Fig. 3*a*, compare refs 8 and 9). These fibres were identified as coming from the transplant by observations with recipients in which the normal adrenergic innervation of the hippocampal formation had been removed by pretreatment with 6-OHDA. The completeness of the denervation was checked in the contralateral hippocampus.

The growth of fibres from the transplanted central NA neurones was studied in rats pretreated with 5,7-DHT. This removed both the normal NA and 5-HT innervations of the hippocampal complex, and the denervation persisted for at least 6 months (Fig. 3*b*). Within 1–3 months of transplantation the dorsal part of the dentate gyrus and, in some specimens, the hippocampal CA 3 and CA 1 regions received a new fluorescent fibre supply that could be traced back to the NA transplant (Fig. 2*b*). In the dentate gyrus these fibres had—like the normal adrenergic innervation—their densest distribution in the hilar region. From here fibres could be traced through the granular layer into the molecular layer where irregularly running fibres were found throughout its width (Fig. 3*c*). In some specimens, such as the one in Fig. 2*b*, the ingrowing fibres tended to aggregate in the outer part of the molecular layer. The fibres reached CA 3 and CA 1 either from the hilus or along the hippocampal fissure. The magnitude of ingrowth into these areas varied considerably. In the richest specimens (Fig. 2*b*) the new fibre supply covered approximately the dorsal two-thirds of the hippocampus. There was a marked difference between the CA 3, which demonstrated a fairly rich fibre supply in all layers, and the CA 1, where the ingrowing fibres were only sparse and scattered.

The distribution of fibres growing from the central IA transplants (observed in both non-pretreated and in 5,7-DHT-pretreated recipients) was different from that of the central and peripheral NA fibres. The IA transplants formed a layer of densely packed varicose fibres in the outer half of the molecular layer in the dentate gyrus (Figs 2*c* and 3*d*). Occasionally, fibres were seen to have grown along the hippocampal fissure to form a similar fibre band in part of the stratum lacunosum-moleculare in CA 1 (Fig. 2*c*). The position of these fibre bands seems to conform to the normal distribution of the terminals of the perforant path fibres[4,5,10]. The fibre supply to the lower half of the molecular layer and the granular layer was much more sparse. This was the case also in the hilar region where usually the densest 5-HT innervation is found (compare ref. 11). The IA fibres were not seen to extend into CA 3.

The fibres from the central DA transplants had a characteristic delicate and fine varicose appearance (similar to that of normal central DA terminals) and they were thus well distinguishable from the normal NA innervation also seen in the non-pretreated animals. Like the IA fibres, the outgrowing DA fibres formed a dense, fine varicose fibre band in the outer half of the molecular layer in the dentate gyrus. Figure 2*d* illustrates a case with an unusually large number of surviving DA neurones, where the ingrowing fibres had covered the entire dorsal dentate. Moreover, a dense band of DA fibres had been formed also in the stratum lacunosum-moleculare of CA 1. The inner part of the dentate molecular layer occasionally had a dense supply in the portion closest to the transplant. Otherwise, only few fibres were observed in the inner part of the molecular

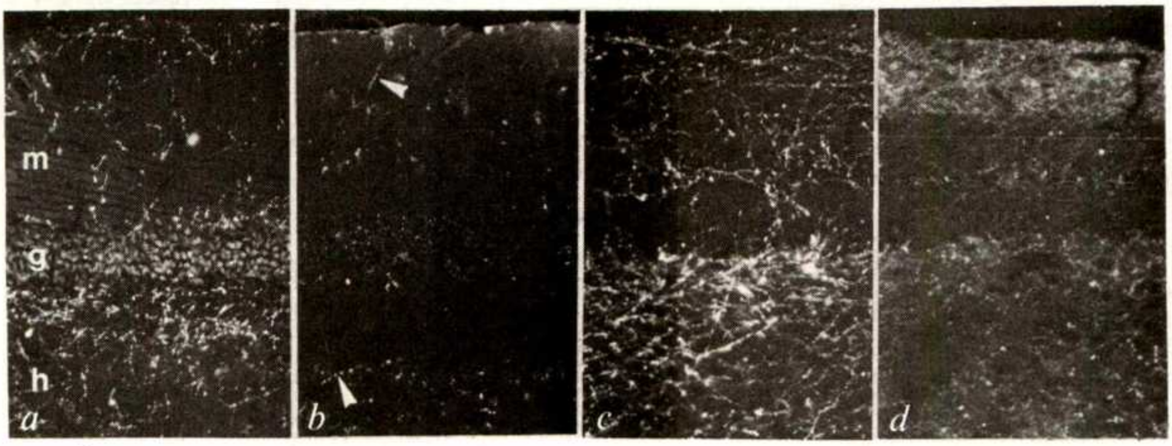

Fig. 3 Detail of the dorsal part of the dentate gyrus showing: *a*, normal adrenergic innervation in a control rat; *b*, adrenergically denervated dentate gyrus in a rat treated with 150 µg of 5,7-DHT (taken from the contralateral, control side of the transplanted rat shown in (*c*)). Only some single, scattered terminals remain (arrows). *c*, Patterning of adrenergic fibres originating from a NA transplant, 3 months survival (the dentate was adrenergically denervated before transplantation, as shown in (*b*). *d*, Patterning of indolaminergic fibres originating from an IA transplant, 3 months survival. m, Molecular layer; g, granular layer; h, hilus. Compare Fig. 2. (× 90)

layer and in the hilus, and none was found in the hippocampus proper.

The transplanted central and peripheral neurones were allowed to grow towards a hippocampus that had been partially deafferented through a lesion in the perforant path system and by removal of the monoaminergic brainstem afferents. From the transplant, located in the resection cavity in the retrosplenial cortex, the growth of the new fibres was directed along a course roughly corresponding to that of the lesioned perforant path fibres (compare refs 2–5). Entering the hippocampus through presubiculum and subiculum, the perforant path fibres are known to run through and along the hippocampal fissure to terminate heavily in the outer part of the molecular layer in the dentate gyrus. In interpreting our data, it seems that the outgrowing fibres of all different monoamine neurone types will find their way into the dentate gyrus along the degenerated perforant path, and that two of them, the IA and DA neurones, will distribute their fibres in a manner strongly resembling that of the perforant path fibres. The central and peripheral NA fibres, on the other hand, pattern themselves differently, the most heavy termination being in the hilar region, just as the normal adrenergic innervation. This growth process can be viewed as an attempt at a heterologous reinnervation of the dentate gyrus by regeneration of peripheral adrenergic neurones or by outgrowth of developing central neurones. Contrary to the traditional view that the scar tissue and the composition of the CNS tissue prevent axonal outgrowth in the adult mammalian brain[12–14], the axons of the transplanted neurones grew without any apparent obstacle up to at least 1 mm through the developing scar tissue, through the pial covering in the hippocampal fissure, and penetrated deeply into the dentate gyrus and the hippocampus. Here the newly formed fibres extended for distances of up to 3–4 mm from the transplant.

The most intriguing feature of this process is that different types of fibres, although growing along the same route, form distinctly different and highly consistent patterns in the hippocampal formation. This strongly suggests that directional and organising forces—not unlike those demonstrated in lower vertebrates[15–17]—are operating also in the brains of adult mammals. And in view of the fact that such biochemically closely related neurones as the DA and NA neurone types pattern themselves entirely differently, it seems that these mechanisms have a high degree of precision and selectivity. Nothing is known so far about the ultrastructural mode of termination of the outgrowing fibres. But on the basis of their light microscopic distribution it seems possible that the transplanted IA and DA neurones (and to some minor degree perhaps also the central NA neurones) had grown to fill the terminal space vacated by the lesion of the non-monoaminergic perforant path, and that the adrenergic neurones had regenerated a fairly normal innervation pattern. This is in line with the idea that mechanisms adequate for the re-establishment of severed fibre connections are present in the mammalian brain, but that these mechanisms are not entirely specific for the appropriate neurone type.

This work was supported by grants from the Swedish MRC, Trygg-Hansas fond för personskadeforskning and the Åke Wiberg and Gross foundations.

ANDERS BJÖRKLUND
ULF STENEVI
NIELS-AAGE SVENDGAARD

Departments of Histology,
Ophthalmology and Neurosurgery,
University of Lund, Lund, Sweden

Received May 10; accepted July 6, 1976.

1 Stenevi, U., Björklund, A., and Svendgaard, N.-Aa., *Brain Res.* (in the press).
2 Cajal, S. R., *Histologie du Système Nerveux de l'Homme et des Vertébrés*, 2, 733–761 (Maloine, Paris, 1911).
3 Lorente de No, R., *J. Psychol.*, 46, 113–177 (1934).
4 Blackstad, T. W., *Acta Anat.*, 35, 202–214 (1958).
5 Hjort-Simonsen, A., and Jeune, B., *J. comp. Neurol.*, 144, 215–232 (1972).
6 Olson, L., and Seiger, Å., *Z. Zellforsch.*, 195, 175–194 (1972).
7 Björklund, A., Falck, B., and Owman, C., in *Methods of Investigative and Diagnostic Endocrinology, 1, The Thyroid and Biogenic Amines* (edit. by Rall, J. E., and Kopin, I. J.), 318 (North-Holland, Amsterdam, 1972).
8 Blackstad, T. W., Fuxe, K., and Hökfelt, T., *Z. Zellforsch.*, 78, 463–473 (1967).
9 Swanson, L. W., and Hartman, B. K., *J. comp. Neurol.*, 163, 467–506 (1975).
10 Raisman, G., Cowan, W. M., and Powell, T. P. S., *Brain*, 88, 963–996 (1965).
11 Moore, R. Y., and Halaris, E., *Brain Res.* (in the press).
12 Windle, W. F., Clemente, C. D., and Chambers, W. W., *J. comp. Neurol.*, 96, 359–370 (1952).
13 Chambers, W. W., in *Regeneration in the Central Nervous System* (edit. by Windle, W. W.), 135–146 (Thomas, Springfield, Illinois, 1955).
14 Clark, W. E. L., *J. Anat.*, 77, 251–259 (1943).
15 Attardi, D. G., and Sperry, R. W., *Expl Neurol.*, 7, 46–64 (1963).
16 DeLong, R. G., and Coulombre, A. J., *Devl Biol.*, 16, 513–534 (1968).
17 Gaze, R. M., *The Formation of Nerve Connections* (Academic, London and New York, 1970).

Progesterone may act at hypothalamus and pituitary by way of enhancement of oestrogen retention

PROGESTERONE injection given 24 h or more before ovulation inhibits the ovulatory cycle[1–5]. There is evidence that progesterone can act directly on the hypothalamus[6–9] to block ovulation and on the pituitary to reduce pituitary sensitivity to luteinising releasing hormone[10,11]. Steroid-sensitive target tissues including hypothalamus[12,13] and pituitary[14–16] contain

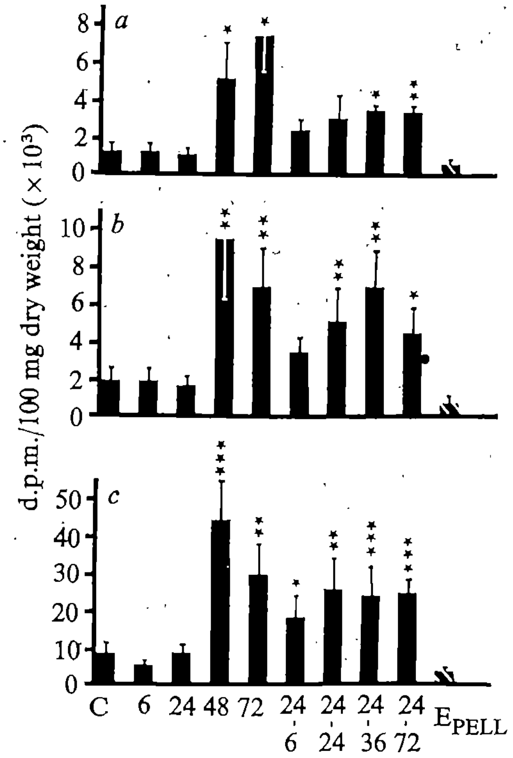

Fig. 1 Adult Sprague–Dawley rats, ovariectomised 14 d previously, received an intraperitoneal injection of 2 μCi per 100 g body weight of 2,4,6,7-^{3}H-oestrodiol (100 Ci mM^{-1}) in 0.9% NaCl. Previously the animals ($n = 10$) received a 50-mg subcutaneous pellet of progesterone for 6, 24, 48 or 72 h. Other groups had the progesterone pellet removed after 24 h and ^{3}H-oestradiol injected 6, 24, 36 or 72 h later. Saturation of the specific retention system was achieved by subcutaneous implacement of an oestradiol pellet for 72 h (E_{pell}). Two hours after ^{3}H-oestradiol injections, the animals were killed, perfused with saline and the tissues removed as described previously for hypothalamus[19]. Tissues were dried at 60 °C, weighed and then rehydrated in Tris–EDTA. After grinding in all-glass homogenisers extraction was carried out twice with 5 ml ethyl acetate. Combined extracts from a single tissue were dried in scintillation vials. The scintillation cocktail was 0.4% POP and 0.03% POPOP in toluene. Thin lines indicate s.e.m. Student's t test was used in the statistical analysis: $^*P = 0.05$; $^{**}P = 0.01$; $^{***}P = 0.001$. *a*, Preoptic–anterior hypothalamus; *b*, arcuate–median eminence; *c*, pituitary. E_{pell}, non-saturable oestrogen retention.

a specific oestrogen retention mechanism of limited capacity. Oestrogen-regulated events can be demonstrated only in the presence of a functional retention (receptor) system for oestrogen. In contrast, no specific progesterone retention system has yet been demonstrated for hypothalamus or pituitary. Does progesterone interact with these target tissues in a novel manner? This seems unlikely since other steroids which have been studied—for example, adrenal corticoids[17] and androgens[18]—have been found to bind to specific receptors in their target tissues. We therefore tested an alternate possibility that progesterone action on hypothalamus and pituitary might result in modification of the oestrogen receptor system. We tested ^{3}H-oestradiol retention by hypothalamus and pituitary after *in vivo* treatment with progesterone (subcutaneous pellet; release rate=1.5–3 mg d^{-1}) of various durations from hours to days. *In vitro* ^{3}H-oestradiol-specific retention by oestradiol–receptor complexes transferred to the nuclear fraction of these tissues was also compared for animals receiving previous *in vivo* progesterone treatment compared with ovariectomised animals not receiving progesterone treatment.

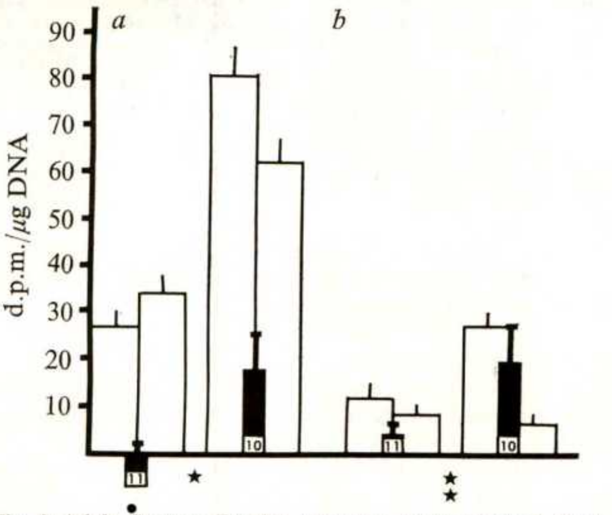

Fig. 2 Adult Sprague–Dawley rats were ovariectomised 14 d before the experiment. Half the animals (right-hand sets of columns) received a 50-mg subcutaneous pellet of progesterone on day 11. The animals were killed by exsanguination. Left-hand sets, controls. After homogenisation of the tissue (0.32 M sucrose, 3 mM $MgCl_2$, 3 mM K_2MP04, 14 mM 2 mercaptoethanol, *p*H = 6.5) one half of each homogenate was incubated at 30 °C for 1 h in 1.0×10^{-8} M 2,4,6,7-^{3}H-oestradiol. The other half was incubated in the same concentration of ^{3}H-oestradiol plus 1.0×10^{-8} M unlabelled oestradiol plus 1.0×10^{-5} M diethylstilboestral. Nuclear purification followed the methods of Løvtrup–Rein and McEwen[20] with slight modification. The nuclear fractions were extracted twice with ethyl acetate and twice with ethanol–diethyl ether (50:50) at 50 °C. Extracts were dried in scintillation vials and counted using 0.4% POP and 0.03% POPOP in toluene. DNA was extracted from the nuclear fraction and measured by the method of Kissane and Robins[21]. *a*, Hypothalamus; *b*, pituitary.

Our *in vivo* studies (Fig. 1) show that in the continued presence of progesterone a significant increase in ^{3}H-oestradiol retention has occurred by 48 h and is still expressed at 72 h. The magnitude of this increase was pituitary> arcuate–median eminence > preoptic–anterior hypothalamus. When the animals are exposed to progesterone for 24 h, no change in ^{3}H-oestradiol was observed if the progesterone source was removed at that time; a significant increase in ^{3}H-oestradiol retention was found for pituitary at 30 h, at 48 h in the arcuate–median eminence region, and at 60 h in the preoptic–anterior hypothalamic region. Thus, in the continued presence of the progesterone source, all tissues showed a response at 48 h. When the response was measured after removal of the progesterone source, however, the pituitary showed the shortest response interval (30 h). These data on *in vivo* total tissue retention are supported by the demonstration that the specific *in vitro* oestrogen retention by the nuclear fraction was significantly enhanced when ovariectomised animals were pretreated with progesterone for 72 h (Fig. 2).

Our study shows that progesterone treatment *in vivo* significantly modified oestradiol retention, studied *in vivo* for whole tissue and *in vitro* for the nuclear fraction from hypothalamus and pituitary of female rats. This supports the concept of progesterone acting both at the neural level[6–9] and pituitary[10,11] level in regulation of the ovulatory cycle. Exposure of the pituitary and the neural tissues to progesterone for 48 h resulted in an increase in specific oestradiol retention. This increase could be observed for at least 72 h after the end of 24 h progesterone treatment. The change in oestradiol retention observed after 24 h of progesterone treatment correlates with the time required for progesterone to inhibit events of the ovulatory cycle.

At present, no nuclear progesterone receptor has been demonstrated for the hypothalamus or the pituitary. Through some mechanism requiring progesterone and at least 24 h, however, the amount of oestradiol receptor found in the nuclear fraction is increased. The possibilities of whether the biological effect of progesterone on the ovulatory cycle is mediated by an increase in oestradiol receptors in these tissues, or whether the increase in oestradiol receptors is caused by a progesterone-mediated block of a later step in the oestradiol–receptor–genome interaction is under investigation.

This work was supported by the USNSF and was carried out with the facilities of the Whitehall Foundation. We thank Mrs Ginger Wang and Mrs Kay Chien for assistance.

LAWRENCE A. REUTER
ROBERT D. LISK

Department of Biology,
Princeton University,
Princeton, New Jersey 08540

Received February 3; accepted June 8, 1976.

[1] Everett, J. W., *Endocrinology*, **34**, 136 (1944).
[2] Zeilmaker, G. H., *Acta Endocr. (Kbh.)*, **51**, 461 (1966).
[3] Reuter, L. A., Ciaccio, L. A., and Lisk, R. D., *Endocrinology*, **86**, 1287 (1970).
[4] Caligario, L., Astrada, J. J., and Taleisnik, S., *Endocrinology*, **89**, 331 (1971).
[5] Brown-Grant, K., and Naftolin, F., *J. Endocr.*, **53**, 37 (1972).
[6] Kanematsu, S., and Sawyer, C. H., *Endocrinology*, **76**, 691 (1965).
[7] Smith, E. R., Weick, R. F., and Davidson, J. M., *Endocrinology*, **85**, 1129 (1969).
[8] Malvin, P. V., and Ruiz-Diaz, R., *J. Anim. Sci.*, **32**, 919 (1971).
[9] Reuter, L. A., and Lisk, R. D., *Neuroendocrinology*, **12**, 17 (1973).
[10] Arimura, A., and Schally, A. V., *Endocrinology*, **87**, 653 (1970).
[11] Hilliard, J., Schally, A. V., and Sawyer, C. H., *Endocrinology*, **88**, 730 (1971).
[12] Kahwanago, I., Heinrichs, W. L., and Herrmann, W. L., *Nature*, **223**, 313 (1969).
[13] Kato, J., *Acta endocr. (Kbh.)*, **72**, 663 (1973).
[14] Notides, A. C., *Endocrinology*, **87**, 987 (1970).
[15] Kato, J., Atsumi, Y., and Muramatsu, M., *J. Biochem.*, **67**, 871 (1970).
[16] Friend, J. P., and Leavitt, W. W., *Acta endocr. (Kbh.)*, **69**, 230 (1972).
[17] DeKloet, R., Wallach, G., and McEwen, B. S., *Endocrinology*, **96**, 598 (1975).
[18] Sar, M., and Stumpf, W. E., *Experientia*, **28**, 1364 (1972).
[19] McGuire, J. L., and Lisk, R. D., *Neuroendocrinology*, **4**, 289 (1969).
[20] Løvtrup-Rein, H., and McEwen, B. S., *J. Cell Biol.*, **30**, 405 (1966).
[21] Kissane, J. M., and Robins, E., *J. biol. Chem.*, **233**, 184 (1958).

Combination of insulin chains on an anti-insulin antibody–Sepharose column

WHEN the mixture of products obtained by combining insulin A and B chains in solution (for a review, see ref. 1) was chromatographed on an anti-insulin antibody–Sepharose column[2] no clear separation was achieved[3]. From the low biological activity (24.1%) of the material with the same antibody affinity as natural insulin (10.9% of the total bound products) it was concluded[3] that resynthesised insulin with authentic structure constituted only a small portion of this fraction. Combination of insulin chains in solution has always involved a number of steps[4,5] and has produced a mixture of products from which pure active insulin could be isolated by gel filtration and ion-exchange chromatography[6]. Linking the chains using the procedure described in this report, however, has given only one combination product that, according to various criteria, was identical with insulin and could be separated from unreacted A and B chains in one step.

That the B chain of insulin cross reacts with anti-insulin antibodies, whereas the A chain does not[7], formed the basis for our new method of resynthesising insulin from the two chains. This method also involved the participation of antibodies (Fig. 1). During resynthesis of insulin from the isolated chains, a major product formed is a polymer consisting mainly of disulphide-linked B chain molecules[8]. Thus, active insulin can be obtained in good yield only if the polymerisation of the B chain is prevented. We assumed that S-sulphonate B chain, when bound to Sepharose-coupled anti-insulin antibodies, could no longer polymerise on reaction with reduced A chain if the distance between the B-chain molecules on the solid matrix was too large for inter-B chain disulphide bridges to form. Furthermore, antibody-bound S-sulphonate B chain was presumably fixed in a conformation identical or nearly identical to that of the B chain in the insulin molecule. This would to a great extent assist the 'parallel alignment' of reduced A chain and the closing of the right disulphide bonds to give active insulin.

Anti-insulin antibodies were prepared by injecting each of six guinea pigs with a suspension of 1.2 mg pig insulin in a mixture of 0.1 M Na_2HPO_4 (0.7 ml, *p*H 7.21) and Freund's complete adjuvant (0.3 ml). Sera were obtained by heart puncture 30 d after immunisation, and assayed using the immunodiffusion test[9] against pig insulin. The IgG fraction of strong sera was isolated using the procedure of Levy and Sober[10]. The concentration of purified antibodies was 6.4 mg ml^{-1}. To 22 ml of this solution 5 g freshly BrCN-activated Sepharose 4B was added, and the antibodies were coupled to the solid support by the method of Axen *et al.*[11]. After careful washing, an aliquot of the antibody–Sepharose gel was subjected to acid hydrolysis (6 N HCl, 105–110 °C, 24 h) followed by amino acid analysis. This showed that 0.054 µmol IgG was bound per g of Sepharose. Since there are two antigen-binding sites per antibody molecule the maximum capacity of the antibody–Sepharose for insulin or insulin B chain was 0.108 µmol g^{-1}.

S-sulphonate chains were prepared from natural insulin and separated on Dowex 50 as described previously[8]. B chain-bi-S-sulphonate ($B(S\text{–}SO_3^-)_2$; 7.65 mg; 2.125 µmol) was added to 5 g antibody–Sepharose in 0.01 M Tris-HCl, *p*H 8.3 (total volume 10 ml). The mixture was stirred for 3–4 h and then filtered. The gel containing 0.076 µmol antibody-bound B chain was washed thoroughly with the same buffer. From the combined filtrates, unbound $B(S\text{–}SO_3^-)_2$ was recovered. Tetrathiol A chain was prepared from $A(S\text{–}SO_3^-)_4$ by reduction with mercaptoethanol (100-fold molar excess per $S\text{–}SO_3^-$ group) in 5 M urea, *p*H 5. After 16 h a 15-fold amount of acetone containing 1.4% (v/v) 1 N HCl was added to precipitate the reduced A chain. The precipitate was centrifuged

Fig. 1 Combination of insulin chains on Sepharose-coupled anti-insulin antibodies. AIA, anti-insulin antibody; $A(SH)_4$, tetrathiol A chain; $(S\text{–}S)A(S\text{–}S)_2B$, combination product with one intrachain and two interchain disulphide bonds.

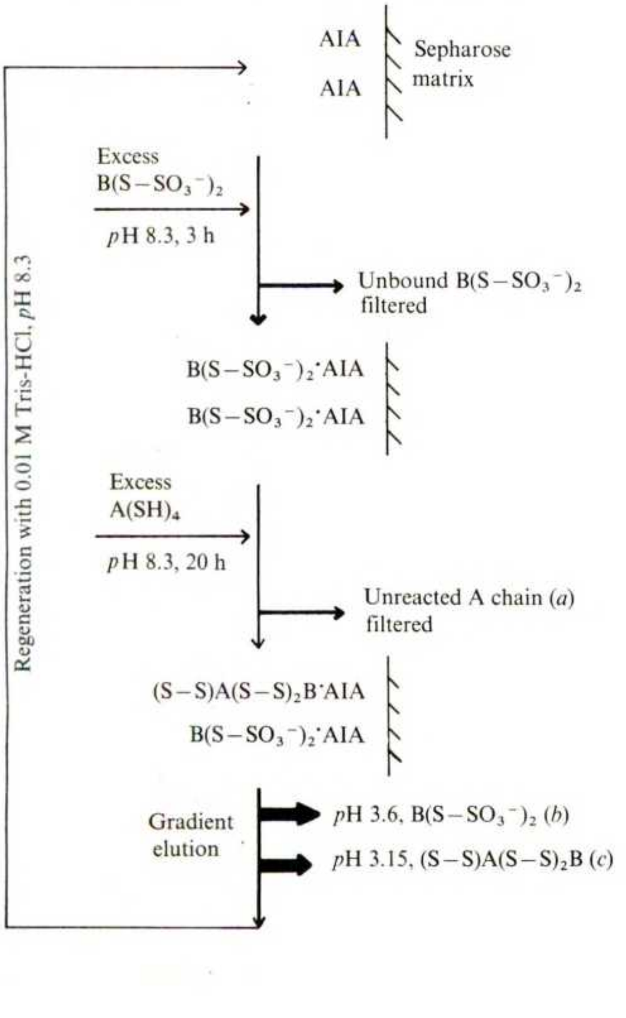

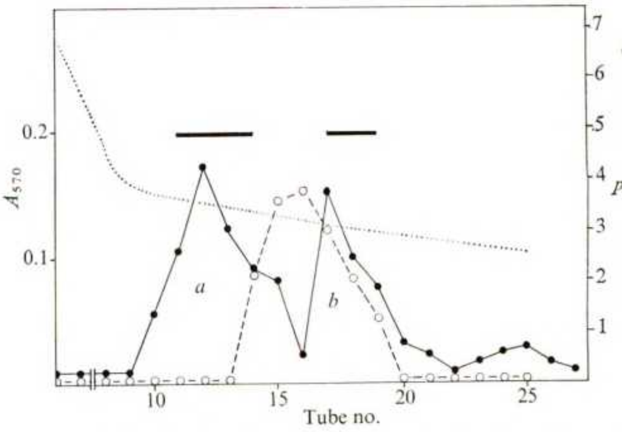

Fig. 2 Gradient elution of natural insulin (○) and recombination products (●) from anti-insulin antibody–Sepharose column (3.2 × 1.3 cm). Solvents used were 0.01 M Tris-HCl (*p*H 8.3, 40 ml) and 1 M acetic acid (*p*H 2.6, 40 ml)[2] (volume per tube approximately 1.5 ml). From each tube a 0.5-ml aliquot was removed for alkaline hydrolysis[13] followed by the ninhydrin reaction. Extinctions were read at 570 nm. By comparison with standard curves the protein content of tubes 11–14 (*a*, $B(S\text{–}SO_3^-)_2$) was found to be 0.159 mg or 44.2 nmol, that of tubes 17–19 (*b*, insulin) was 0.102 mg or 17.8 nmol. The total amount of B chain bound by the antibody–Sepharose column was 0.076 µmol compared with the maximum capacity of 0.540 µmol. The antibody–Sepharose column was used repeatedly. All elution patterns were identical to that shown above. In later runs $B(S\text{–}SO_3^-)_2$ and insulin could therefore be localised by measuring the *p*H value of each fraction of the eluate.

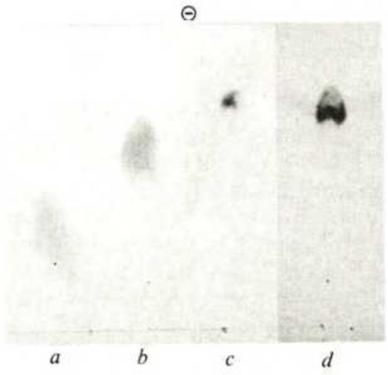

Fig. 3 Electrophoresis of recombination products and natural insulin on cellulose-coated thin-layer plates (20 × 20 cm) in 1.2 M formic acid and 2 M urea, *p*H 2.2, at 600 V for 50 min. The plates were sprayed with Pauly reagent. *a*, A chain-bi-disulphide; *b*, unreacted $B(S\text{–}SO_3^-)_2$; *c*, resynthesised insulin; *d*, natural insulin.

off and dried *in vacuo*. Its sulphydryl content, determined using the Ellman reagent[12], was found to vary between 3.6 and 3.8 mol per mol reduced A chain. Reduced A chain (4.06 mg, 1.735 μmol) was dissolved in 0.01 M Tris-HCl, *p*H 8.3, the solution added to the $B(S\text{–}SO_3^-)_2$– antibody–Sepharose complex (volume of recombination mixture 12–13 ml) and stirred gently. After approximately 20 h no more sulphydryl groups were detected. The gel was filtered and washed carefully. Electrophoresis (Fig. 3*a*) showed that the only product present in the filtrate was A chain which had not reacted with the antibody-bound B chain but had been oxidised to give the bidisulphide derivative.

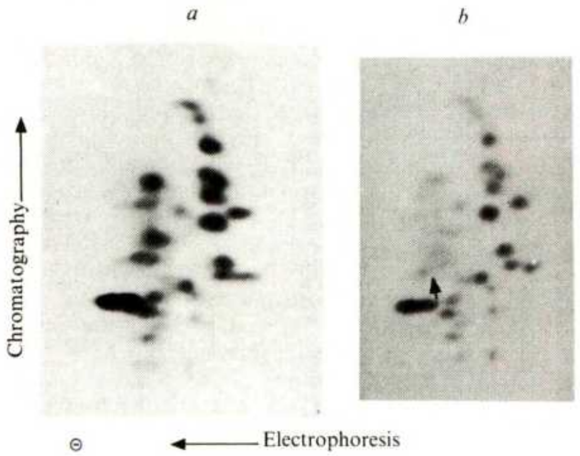

Fig. 4 Peptide maps of peptic digests of natural insulin (*a*, 0.12 mg) and recombined insulin (*b*, 0.03 mg)[14]. The digestion mixtures were applied on cellulose-coated thin-layer plates (20 × 20 cm) and were resolved by electrophoresis at 600 V for 75 min. in 12% acetic acid (v/v), adjusted to *p*H 1.9 with formic acid; and by thin-layer chromatography in 1-butanol–acetic acid–pyridine–water (30:6:20:24). The plates were sprayed with ninhydrin solution. The arrow in *b* marks the two weak spots that were not observed on the peptide map of pepsin-treated natural insulin.

The gel was then placed in a column (3.2 × 1.3 cm) and the products which were linked non-covalently to the antibody–Sepharose complex were eluted by a *p*H gradient (8.3–2.6), (Fig. 2). The first peak (absorption maximum at *p*H 3.6) contained unreacted $B(S\text{–}SO_3^-)_2$ as shown by amino acid analysis and electrophoresis (Fig. 3*b*). The absorption maximum of the second peak was at *p*H 3.15 and was close to that of amorphous natural insulin (Fig. 2). The material of peak *b* was desalted on Biogel P-2 in 0.05 M NH_4HCO_3 (yield, 0.018 μmol or 23.7% based on the amount of bound B chain) and then submitted to electrophoresis (Fig. 3*c*), peptic digestion followed by peptide mapping (Fig. 4), and amino acid analysis of an acid hydrolysate. Electrophoretic mobility (Fig. 3), peptide map (Fig. 4) and amino acid composition of product *c* agreed well with those of natural insulin.

Amino acid ratios were as follows (values reported for pig insulin[15] are in parentheses): Asp 2.7 (3); Thr 1.9 (2); Ser 3.2 (3); Glu 7.0 (7); Pro 1.0 (1); Gly 3.8 (4); Ala 2.8 (2); Cys 5.7 (6); Val 3.6 (4); Ile 1.6 (2); Leu 6.0 (6); Tyr 3.7 (4); Phe 3.0 (3); His 2.1 (2); Lys 1.0 (1); Arg 0.9 (1). In the fat cell assay[16,17] the product of peak *a* was inactive whereas the product of peak *b* (Fig. 2) had an insulin activity of 67%. The effective yield of authentic recombined material was thus 15.9% based on the amount of bound B chain.

Antigenic properties, electrophoretic mobility, and amino acid composition of recombination product and natural insulin were in good agreement. The peptide map of the recombined material showed two additional spots (Fig. 4*b*, arrow) but was otherwise indistinguishable from that of natural insulin, indicating that very few, if any, wrong disulphide bridges had formed during the coupling of A and B chains on the antibody–Sepharose matrix. The additional spots on the peptide map and the fact that the recombination product was not fully active may have been caused by the presence of a small amount of antibody eluted from the affinity column as insulin–antibody complex.

The chain combination method described here offers several advantages. Reconstituted insulin which was almost identical to natural insulin was obtained in one step without further purification. Unreacted A and B chains were isolated separately and could be easily reintroduced into the combination reaction. Finally, the antibody–Sepharose column could be used repeatedly. The possibility of using an anti-B chain-antibody–Sepharose matrix has not yet been studied.

This work was supported by the Deutsche Forschungsgemeinschaft. We thank Farbwerke Hoechst AG, Frankfurt (Main), for insulin; Drs K. Rajewsky and K. Eichmann for discussions; and Drs B. Hansen and J. H. Nielsen (Steno Memorial Hospital, Gentofte, Denmark) for carrying out the biological assays.

MECHTHILD KLOTZ
BERND GUTTE

Institut für Genetik der Universität Köln,
5 Köln-Lindenthal,
Weyertal 121, Germany

Received December 22, 1975; accepted June 24, 1976.

[1] Lübke, K., and Klostermeyer, H., *Adv. Enzym. rel. Areas molec. Biol.*, **33**, 445–525 (1970).
[2] Akanuma, Y., Kuzuya, T., Hayashi, M., Ide, T., and Kuzuya, N., *Biochem. biophys. Res. Commun.*, **38**, 947–953 (1970).
[3] Klotz, M., Diplomarbeit, Univ. Köln (1974).
[4] Brandenburg, D., Schermutzki, W., and Zahn, H., *Hoppe-Seyler's Z. physiol. Chem.*, **354**, 1521–1524 (1973).
[5] Geiger, R., and Obermeier, R., *Biochem. biophys. Res. Commun.*, **55**, 60–66 (1973).
[6] Rüegg, U. T., and Gattner, H.-G., *Hoppe-Seyler's Z. physiol. Chem.*, **356**, 1527–1533 (1975).
[7] Yagi, Y., Maier, P., and Pressman, D., *Science*, **147**, 617–619 (1965).
[8] Gutte, B., thesis, Technische Hochschule Aachen (1967).
[9] Ouchterlony, O., *Prog. Allergy*, **5**, 1–78 (1958).
[10] Levy, H. B., and Sober, H. A., *Proc. Soc. exp. Biol. Med.*, **103**, 250–252 (1960).
[11] Axen, R., Porath, J., and Ernback, S., *Nature*, **214**, 1302–1304 (1967).
[12] Ellman, G. L., *Archs Biochem. Biophys.*, **82**, 70–77 (1959).
[13] Fruchter, R. G., and Crestfield, A. M., *J. biol. Chem.*, **240**, 3868–3874 (1965).
[14] Du, Y.-c., Zhang, Y.-s., Lu, Z.-x., and Tsou, C.-l., *Scientia Sinica*, **10**, 84–104 (1961).
[15] Brown, H., Sanger, F., and Kitai, R., *Biochem. J.*, **60**, 556–565 (1955).
[16] Rodbell, M., *J. biol. Chem.*, **239**, 375–380 (1964).
[17] Gliemann, J., *Diabetologia*, **3**, 382–388 (1967).

Increase of glucagon receptors in hyperthyroidism

THYROID hormones influence the lipolytic response of rat adipocytes to adrenaline, glucagon, ACTH and TSH[1,2]. Krishna, Hynie and Brodie[3] provided evidence that hyperthyroidism is followed by an increase in the noradrenaline-sensitive adenylate cyclase without any change in phosphodiesterase activity. Subsequent investigations have shown that adenylate cyclase activity measured as fluoride stimulated activity is unchanged in hyperthyroidism[4] and confirmed that phosphodiesterase activity is normal[4,5]. Since the amount of hormone-sensitive lipase does not appear to be increased in hyperthyroidism[3] these studies indicate an action of thyroid hormones either on the hormone receptors for lipolytic hormones or on the transmission of the hormonal message from the receptors to adenylate cyclase. This prompted the present study in which we found that hyperthyroidism was associated with an increased binding of glucagon to fat cells as well as increased glucagon stimulated production of cyclic AMP and glycerol.

Male Wistar rats (120–175 g) were rendered hyperthyroid by daily subcutaneous injections of 20 μg triiodothyronine (T3) (Glaxo) for 8 d. Paired litter mates received in the same period injections of the vehicle for T3. Epididymal

Pure Che[illegible]stry Library

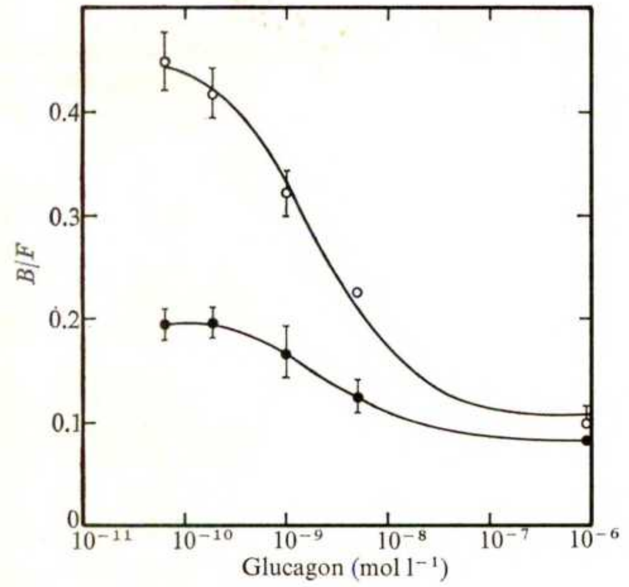

Fig. 1 Binding of glucagon to fat cells from a T3-treated (○) and a control (●) rat. Fat cells (10 µl ml^{-1}) were incubated at 37 °C in a Krebs–Ringer buffer with 25 mM HEPES (*p*H 7.4) and 1% of human serum albumin (Behringwerke) with ^{125}I-labelled glucagon or 0.18 nM ^{125}I-labelled glucagon plus unlabelled glucagon to give the indicated concentrations. After 30 min of incubation 6 aliquots of the cell suspension were transferred to microtubes containing approximately 100 µl of silicone oil and the cells were separated from the medium by centrifugation through the oil in a Beckman Model 152 Microfuge at 2,500*g* for 1 min. After cutting through the oil layer the cells and aliquots of the medium were counted for ^{125}I-activity. The ordinate is expressed as ^{125}I-activity per cells divided by ^{125}I-activity per l medium. Bars represent s.d., $n = 6$.

and perirenal fat pads were then removed and suspensions of isolated fat cells prepared[6].

Binding of glucagon to the isolated fat cells was measured at equilibrium by the displacement of ^{125}I-labelled glucagon (NOVO, Copenhagen, Denmark) by unlabelled glucagon. Cells were separated from medium by centrifugation through a silicone oil and counted for radioactivity in a gamma counter with a background of 3 c.p.m. and an efficiency of 35% (ref. 7). The number of glucagon receptors were calculated from a computerised fit of the experimental data[7], since the binding of glucagon to the receptor can be described as a reversible binding between the glucagon molecule and a single class of receptors[8].

Figure 1 shows binding curves for glucagon to fat cells from a hyperthyroid and a control rat. The binding of glucagon was measured in seven consecutive, paired experiments. The mean number of glucagon receptors on fat cells from control animals were 260±161 (s.d.) pmol per l cells, $1.8\times10^4 \pm 1.5\times10^4$ per cell and 1.6±1.1 per µm^2 cell surface; the corresponding values for fat cells from T3 treated rats were 658±331 pmol/l cells ($P<0.01$ by a paired two-tailed Student's *t* test), $2.8\times10^4 \pm 1.6\times10^4$ per cell ($P<0.05$) and 3.5±1.8 per µm^2 cell surface ($P<0.01$). Calculated as percentage of control values, the hyperthyroid fat cells possessed 227±101% (s.d.) glucagon receptors per l cells ($P<0.01$), 233±116% per cell ($P<0.05$) and 255±100% per µm^2 cell surface ($P<0.01$). Variations in cell size could not account for the differences between the two groups since mean cell diameter was virtually the same in some experiments. The dissociation constant (K_d) for the binding of glucagon was nearly identical for the two groups investigated (mean value 2.0 nM for controls and 2.2 nM for T3 treated). The degradation of glucagon measured as the ^{125}I-activity in a trichloroacetic acid supernatant was not changed by treatment with T3.

The glucagon stimulated production of cyclic AMP and glycerol was measured in order to study if the increased binding was reflected in the physiological response to the hormone. Figure 2 shows the correlation between the amount of glucagon receptor per l cells and the amount of cyclic AMP measured in the presence of 10^{-6} M glucagon. There is a highly significant correlation between these two parameters ($r=0.877$, $P<0.001$). Figure 3 shows the correlation between the amount of glucagon receptors and the production of glycerol in the presence of 10^{-6} M glucagon ($r=0.838$, $P<0.001$).

These results suggest that the increased glucagon stimulated production of cyclic AMP and glycerol in hyperthyroid fat cells is a consequence of an increased binding of hormone. The increased biological response to other lipolytic hormones might be explained by a similar increase in the number of receptors. To investigate whether T3 could also exert an effect on the binding of non-lipolytic hormones, we studied the specific binding of insulin, measured at a concentration of 0.7 nM insulin, in the same experiments where binding of glucagon was determined. The amount of specifically bound insulin was correlated to the amount of glucagon receptors ($r=0.816$, $P<0.001$). This increase in binding of insulin concomitant with the increase in glucagon receptors occurred without changes in the unspecifically bound insulin, and without changes in the K_d for insulin in three experiments where this was determined.

As intravenous injection of glucagon is followed by a supranormal rise in plasma cyclic AMP in patients with hyperthyroidism[9,10] and adrenaline causes supranormal urinary excretion of cyclic AMP in these patients[11], it seems reasonable to suppose that the observed effect is not confined to the glucagon and insulin receptors of fat cells from experimentally hyperthyroid rats.

Rosenqvist[12] demonstrated that the catecholamine receptors of fat cells from hypothyroid patients changes from

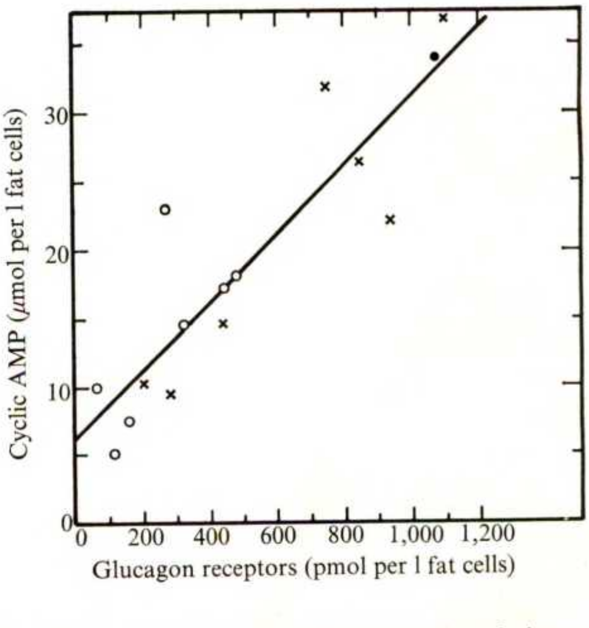

Fig. 2 Relationship between the calculated number of glucagon receptors and the glucagon stimulated cyclic AMP production. Fat cells from T3-treated (×) or control (○) rats were incubated at 37 °C in a Krebs–Ringer buffer with 25 mM of HEPES (*p*H 7.4), 1% human serum albumin, and 2.5 mM of theophylline in the presence of 10^{-6} M glucagon. After 330 s the incubation was stopped by addition of an equal volume of boiling EDTA (20 mM) and the mixture was boiled for another period of 330 s. Cyclic AMP was determined by a competitive protein binding assay[15]. The number of glucagon receptors was calculated from binding curves as shown in Fig. 1. The correlation coefficient between the two parameters is 0.877, $P<0.001$.

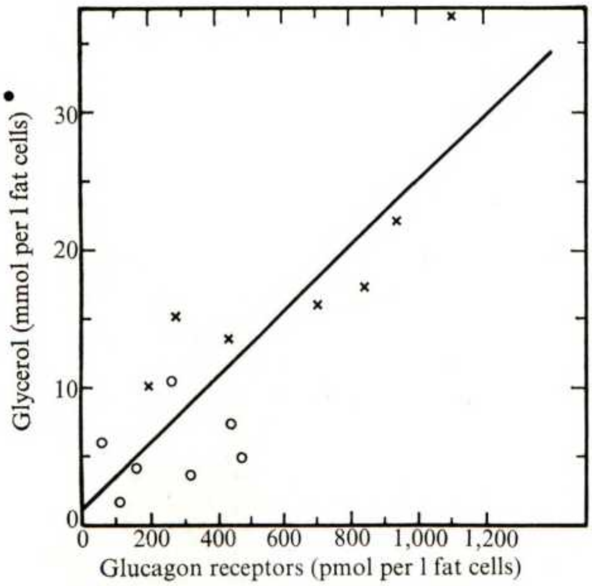

Fig. 3 Relationship between the calculated number of glucagon receptors and the glucagon stimulated production of glycerol. Fat cells from T3-treated (×) or control (○) rats were incubated for 60 min. at 37 °C in a Krebs–Ringer buffer containing 25 mM HEPES (*p*H 7.4), 2% of human serum albumin and 10^{-6} M glucagon. The incubation was stopped by addition of double volumes of 87 mM $ZnSO_4$ and 83 mM $Ba(OH)_2$. Glycerol was determined by a double enzymatic fluorometric assay[16]. The number of glucagon receptors was calculated from binding curves as shown in Fig. 1. The correlation coefficient between the two parameters is 0.838, $P < 0.001$.

predominantly β adrenergic to α adrenergic characteristics, and similar findings have been reported in the hearts of hypothyroid rats[13]. These results and the present study suggest that thyroid hormones are important regulators of the properties of hormone receptors located to the plasma membrane. Other examples of hormonal regulation of hormone receptors has been discussed by Tata[14].

This investigation was supported by a grant from the NOVO foundation.

S. NISTRUP MADSEN

Medical Department F,
Gentofte Hospital,
DK 2900, Copenhagen

O. SONNE

Institute of Medical Physiology C,
University of Copenhagen,
DK 2200, Copenhagen,
Denmark

Received April 22; accepted June 16, 1976.

[1] Goodman, H. M., and Bray, G. A., *Am. J. Physiol.*, **210**, 1053–1058 (1966).
[2] Vaughan, M., *J. clin. Invest.*, **46**, 1482–1491 (1967).
[3] Krishna, G., Hynie, S., and Brodie, B. B., *Proc. natn. Acad. Sci. U.S.A.*, **59**, 884–889 (1968).
[4] Challoner, D. R., and Allan, D. O., *Metabolism*, **19**, 480–487 (1970).
[5] Caldwell, A., and Fain, J. N., *Endocrinology*, **89**, 1195–1204 (1971).
[6] Gliemann, J., *Diabetologia*, **3**, 382–388 (1967).
[7] Gammeltoft, S., and Gliemann, J., *Biochim. biophys. Acta*, **320**, 16–32 (1973).
[8] Sonne, O., Gliemann, J., and Gammeltoft, S., *Acta Endocr. Copenh., Suppl.* **177**, 274 (1973).
[9] Elkeles, R. S., Lazarus, J. H., Siddle, K., and Campbell, A. K., *Clin. Sci. molec. Med.*, **48**, 27–31 (1975).
[10] Madsen, S., Nistrup, Badawi, I., and Christensen, S. E., *Acta Endocr. Copenh., Suppl.* **199**, 333 (1975).
[11] Guttler, R. B., Shaw, J. S., Otis, C. L., and Nicoloff, J. T., *J. clin. Endocrinol. Metab.*, **41**, 707–711 (1975).
[12] Rosenqvist, U., *Acta Med. scand.*, **192**, 353–359 (1972).
[13] Kunos, G., Vermes-Kunos, I., and Nickerson, M., *Nature*, **250**, 779–781 (1974).
[14] Tata, J. R., *Nature*, **257**, 740–741 (1975).
[15] Madsen, S., Nistrup, Badawi, I., and Skovsted, L., *Acta Endocr. Copenh.*, **81**, 208–214 (1976).
[16] Laurell, S., and Tibbling, G., *Clin. chim. Acta*. **13**, 317–322 (1966).

Simultaneous detection of two cell populations by two-colour fluorescence and application to the recognition of B-cell determinants

CELL separation techniques, the possibility of recognising different markers by immunofluorescence and functional tests, have subdivided cells once thought to be a homogeneous group into different subclasses. This development has been most prominent for the so-called mononuclear cells. A difficulty inherent in the classification of such subclasses (of, for example, mononuclear cells) is that it is often almost impossible to determine precisely what percentage of the cells belongs to a certain subclass, and whether the sum of the subclasses is equal to, lower than or even higher than 100% of the total of the cells analysed. A typical recent example was the identification of the "null" or K cell[1,2]. Such analysis is greatly facilitated if we analyse a cell suspension stained with two or more different fluorescent dyes visible at the same time. This is feasible.

With the use of a monochromatic 50-W light source (HBO 50 W/a.c.) an LP455 and SP490 excitation filter combination, an FT510 dichroic mirror and LP520 barrier filter, the green fluorescence of isothiocyanate and the red fluorescence of rhodamine or ethidium bromide become visible simultaneously.

We have exploited these techniques to develop a rapid, simple and sensitive method of recognising polymorphism of B-cell determinants. Interest in these B-cell determinants (which are called Ia determinants in the mouse) is growing rapidly. They may be directly involved in T–B cell interaction in the immune response[3,4], code for disease predisposition[5] and the MLC-stimulating determinants[6] and determine allograft survival[7]. Most information on the genetics and possible biological importance of these B-cell determinants has been collected in the mouse[8], but information in man[6] and the rhesus monkey[9] is rapidly growing. Although B-cell determinants were identified virtually at the same time in the mouse and in man[10–13], the study of these antigens in man was hindered by the lack of sera and, especially, appropriate techniques to detect them. For routine work in man only peripheral blood lymphocytes can be used and here the proportion of B cells can be as low as 5–10%. Although the original enriching process by T-cell rosetting with SRBC and Ficoll–Isopaque gradient centrifugation[14] has been improved by the addition of papain or dextran (ref. 15 and W. Bodmer, personal communication), it remains (especially if the starting material contains a low percentage of B cells) a cumbersome, time-consuming and not fully predictable procedure. For this reason, a modifica-

Table 1 A comparison of the long B-cell complement-dependent cytotoxicity test[14] and the two-colour B-cell test

		Long B-cell cytotoxicity		
		Positive	Negative	Total
Two-colour B cell	Positive	58	10	68
	Negative	9	103	112
		67	113	180
			χ_1^2 (Yates) = 104.8 $P = < 0.000001$	

These data illustrate the excellent agreement between the two techniques and provide also information on the reproducibility of B-cell typing. The discrepancies were mainly caused by 2 of the 15 sera tested and were partly due to anti non-B cell cytotoxicity which cannot be recognised in the long B-cell complement-dependent cytotoxicity test.

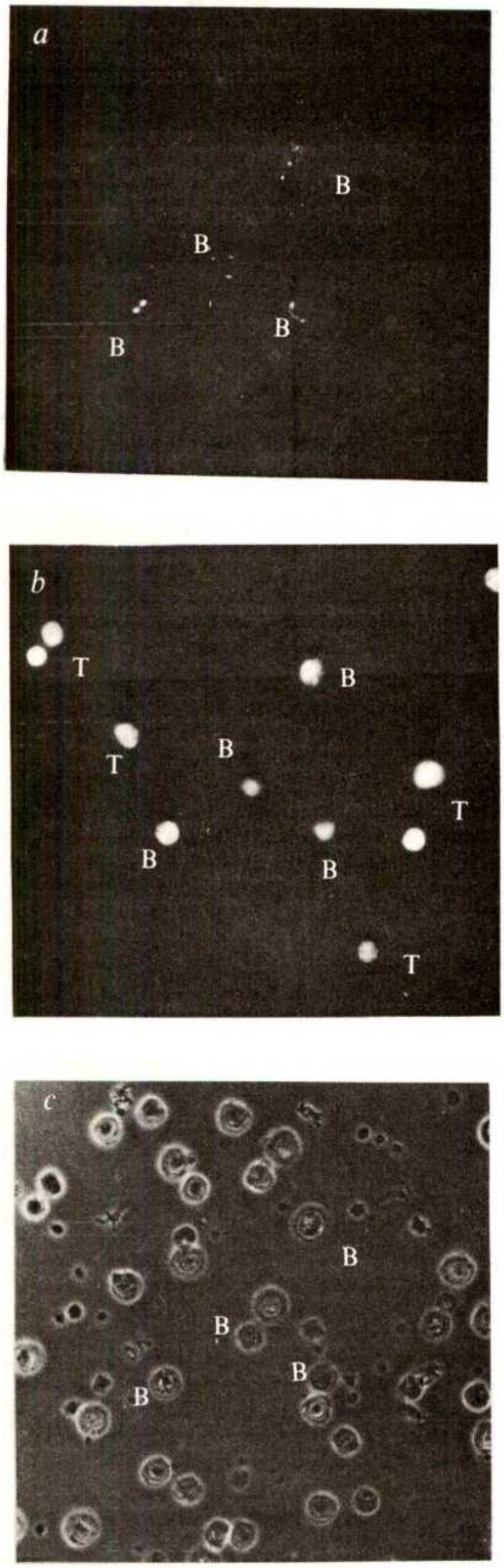

Fig. 1 Picture been taken of the green fluorescence of the immunoglobulins separately (*a*), from the red fluorescence of the nucleus (*b*). Note that also some non-B cells (presumably T cells) have been killed. The green and red fluorescence are depicted separately so that they can be seen in black and white only. When the test is read they are visible at the same time. *c*, The cells visible in phase contrast; many more cells were present than are visible in fluorescence.

tion lacking many of the drawbacks of the previously published method using two-colour fluorescence is described here.

In short, mononuclear cells were isolated from peripheral blood, the B cells were stained by fluorescein-conjugated anti-immunoglobulin and these so identified B cells (together with the unlabelled T and K cells) were incubated with anti-B-cell antibody and complement. Killed cells were stained by the addition of ethidium bromide. The exact procedure was as follows: 4 ml of heparinised blood was diluted twice in phosphate-buffered physiological saline (PBS) and 4 ml of this suspension was carefully layered on Böyum type Ficoll–Isopaque gradient[16]. The tubes were spun for 15 min at 1,000*g* and the mononuclear cells were collected from the interphase, washed 3 times in phosphate-buffered saline containing 1% bovin serum albumin (PBS–BSA 1%). Cells (4×10^6–6×10^6) suspended in 0.5 ml PBS+BSA 1% were incubated with 2 drops (0.05 ml) of goat anti-human immunoglobulin diluted 1 : 3 (Behringwerke AG, Marburg/Lahn, Germany) for 5 min at 37 °C. After three washings with PBS–BSA 1% the cells were adjusted to 8,000 mm^3. A sample (0.5 μl) of platelet-absorbed anti-B-cell serum was incubated in a Möller-Coates A/S tray (Moss, Norway) under paraffin oil with 0.5 μl of mononuclear cell suspension (4,000 cells) for 60 min at 20 °C. After that 2.5 μl fresh rabbit serum was added to provide an excess of complement factors and incubated for 2 h at room temperature. Finally, 0.5 μl of a 1 : 70 dilution of a stock solution (100 $\mu\text{g ml}^{-1}$) of ethidium bromide (Sigma) dissolved in EDTA 5% in saline was added. After putting a coverglass on the tray the reading was done on an inverted Leitz or Zeiss microscope with an epi-illuminator. Figure 1*a* shows a picture of the green fluorescence of the immunoglobulins, Fig. 1*b* the red fluorescence of the killed cells and Fig. 1*c* the corresponding phase-contrast picture. Note that also some non-B cells (presumably T cells) were killed.

The two-colour B-cell cytotoxicity technique was compared with the results obtained with the long B-cell cytotoxicity technique previously described. Excellent agreement was found between the two techniques (Table 1).

The red fluorescence of ethidium bromide can be strongly enhanced by switching the filterset in the two-wavelength vertical illuminator to green excitation (Table 2), which can be done with the new Leitz and Zeiss type of two-wavelength illuminators after Ploem quite easily[17]. It is thus possible to use about 4–8 times lower concentration of ethidium bromide than described above for blue excitation only. By using these lower ethidium bromide concentrations and the two-wavelength excitation method with subsequent excitation with blue followed by green light, it is also possible to make black and white micrographs for documentation. With green excitation of the same cell the red fluorescence of the (dead) nucleus is recorded. This two-wavelength procedure is also promising for future automation of this method since it provides sequential images which can be counted more easily.

As Fig. 1 shows, an advantage of the two-colour method is that it not only indicates whether a part of the mononuclear cells from peripheral blood is killed, but also whether there are B cells or also non-B cells killed. As a matter of fact, in our first trials with the new technique, two sera were identified which were thought to contain only anti-B-cell antibodies but could be shown to contain what looked like antibodies recognising a T-cell polymorphism as well. The method seems to be reliable and reproducible. Using the two-colour fluorescence method it was thus possible to facilitate greatly the recognition of the polymorphism of B-cell determinants. The advantage of this new method compared with the long B-cell complement-dependent lymphocyte toxicity technique is that it takes about 6 h (inclusive of reading) against 12 h for the

Table 2 Filter combinations for fluorescence microscopy of mononuclear cells stained with FITC conjugate and ethidium bromide

Combination	Excitation wavelength (nm)	Excitation filters	Barrier filter	Colour and strength of fluorescence	
1	Blue	$\text{LP}^{\times}455\text{–SP}^{+}490$	LP520	FITC green:	+++
				Ethidium bromide (higher concentration) red:	+++
2	Blue	LP455–SP490	LP520–SP560	FITC green:	+++
				Ethidium bromide (lower concentration) greenish:	±
3	Green	LP515–SP560	LP590	FITC:	±
				Ethidium bromide (lower concentration) red:	++++

$\text{LP}^{\times}$: long-wave pass filter; SP^{+}: short-wave pass interference filter (SP = German KP).

old method; and that one can be certain that if a fraction of the cells are killed, these cells are indeed B cells.

The point of more general importance is, however, that this approach makes possible the direct identification of two (or three) cell subclasses in one preparation. It is expected that this will improve the accuracy of the determination of the fraction of the different subclasses in cells only recently thought to be homogeneous.

This work was in part supported by the NIH, the Dutch Organization for Health Research (TNO), the Dutch Foundation for Medical Research (FUNGO) which is subsidised by the Dutch Organization for the Advancement of Pure Research (ZWO), and the J. A. Cohen Institute for Radiopathology and Radiation Protection (IRS).

Note added in proof: After completion of this letter it was pointed out to us that two-colour fluorescence has been described previously[18,19]. We compared our approach with that previously described and found that only our filter combination and protocol makes it possible to detect the B-cell antigens satisfactorily, because resolution was significantly better.

J. J. van Rood
A. van Leeuwen

Department of Immunohaematology,
University Hospital Leiden,

J. S. Ploem

Department of Histochemistry and Cytochemistry,
University of Leiden,
Leiden, The Netherlands

Received June 7; accepted July 2, 1976.

[1] Perlmann, P., Holm, G., and Stejskal, V., *Transplant. Proc.*, **5**, 127–131 (1973).
[2] Greenberg, A. H., Shen, L., and Roitt, I. M., *Clin. exp. Immun.*, **15**, 251–259 (1973).
[3] Munro, A. J., and Taussig, M. J., *Nature*, **256**, 103–106 (1975).
[4] Katz, D. H., and Benacerraf, B., in *The Role of Products of the Histocompatibility Gene Complex in Immune Response* (edit. by Katz, D. H., and Benacerraf, B.), 355–389 (Academic, New York, 1976).
[5] Keuning, J. J., Peña, A. S., van Leeuwen, A., van Hooff, J. P., and van Rood, J. J., *Lancet*, **i**, 506–508 (1976).
[6] van Rood, J. J., van Leeuwen, A., Parlevliet, J., Termijtelen, A., and Keuning, J. J., in *Histocompatibility Testing 1975* (edit. by Kissmeyer-Nielsen, F.), 629–636 (Munksgaard, Copenhagen, 1975).
[7] van Rood, J. J., *et al.*, *Transplant. Proc.*, **7**, 25–30 (1975).
[8] Shreffler, D. C., Meo, T., and David, C. S., in *The Role of Products of the Histocompatibility Gene Complex in Immune Response* (edit. by Katz, D. H., and Benacerraf, B.), 3–29 (Academic, New York, 1976).
[9] Roger, J. H., van Vreeswijk, W., Dorf, M. E., and Balner, H., *Tissue Antigens* (in the press).
[10] David, C. S., Shreffler, D. C., and Frelinger, J. A., *Proc. natn. Acad. Sci. U.S.A.*, **70**, 2509–2514 (1973).
[11] Hauptfeld, V., Klein, K., and Klein, J., *Science*, **181**, 167–169 (1973).
[12] Sachs, D. H., and Cone, J. L., *J. exp. Med.*, **138**, 1289–1304 (1973).
[13] van Leeuwen, A., Schuit, H. R. E., and van Rood, J. J., *Transplant. Proc.*, **5**, 1539–1542 (1973).
[14] van Rood, J. J., van Leeuwen, A., Keuning, J. J., and Blussé van Oud Alblas, A., *Tissue Antigens*, **5**, 73–79 (1975).
[15] Thompson, J. S., Blaschke, J. W., Severson, C. D., Ferrone, S., and Walford, R. L., in *Proceedings of The First HLA Workshop of The Americas* (edit. by Duquesnoy, R. J., and Fuller, T. C.), 215–222 (US Department of Health, Education and Welfare, Public Health Service, Publication No. (NIH) 76–1064, 1975).
[16] Böyum, A., *Scand. J. clin. Invest.*, **21**, suppl. 97 (1968).
[17] Ploem, J. S., *Ann. N. Y. Acad. Sci.*, **254**, 4–20 (1975).
[18] Takasugi, M., *Transplantation*, **12**, 148–151 (1971).
[19] Martel, J. L., Jaramillo, S., Allen, F. H., Jr, and Rubinstein, P., *Vox Sang.*, **27**, 13–20 (1974).

Helper T cells recognise antigen and macrophage surface components simultaneously

Although the T-cell antigen receptor has been shown to be as highly specific for antigen as the immunoglobulin receptor of B cells, considerable evidence suggests that genes other than those which code for immunoglobulins are involved in the recognition of antigen by T cells. Research in this area has centred on the role of gene products of the major histocompatibility complex (MHC), in particular of the I region of the H–2 complex of mice, in the antigen-specific receptor of T cells[1–3]. Other evidence has suggested that the specificity of T cells is determined by the simultaneous recognition of antigen and MHC cell-surface components. The best evidence for this comes from experiments with mice in which T-cell cytotoxic effectors specifically raised to the H–Y (ref. 4) or other minor histocompatibility antigens[5], viral antigens[6] or the hapten trinitrophenol (TNP)[7] were shown to recognise simultaneously both the antigen and the products of the *D* or *K* locus of H–2 expressed on the target cells. Investigations of the role of MHC gene products in the antigen-mediated interaction of T cells with B cells or macrophages (MΦ) can be interpreted similarly[1,8–15]. We present here evidence that in the mouse, helper T cells primed with the antigen, keyhole limpet haemocyanin (KLH), bound to the surface of MΦ, simultaneously recognise KLH and genetically controlled surface components of the MΦ. The rationale for our approch was as follows. In F_1 animals whose parents differ at loci controlling surface components (for example, H–2, Mls), if T cells could be primed with antigen bound to MΦ from one or the other parent, they should then cooperate preferentially with parental B cells and MΦ of the type used for priming.

To test these predictions we took advantage of the nonspecific association between protein antigens and the MΦ surface[12]. As described in the legend to Fig. 1, BDF$_1$ (C57B/6×DBA/2), C57BL/6, and DBA/2 mice were injected intraperitoneally with KLH. Peritoneal cells (PC), rich in MΦ were collected and used to prime three groups of BDF$_1$ mice. T cells isolated from these mice were tested for their ability to cooperate with BDF$_1$ or C57BL/6 B cells and MΦ in the response to TNP–KLH. All three groups of F_1 T cells were able to cooperate effectively with BDF$_1$ B-cells and MΦ (Fig. 1*a*). But as predicted, when tested with C57BL/6 cells and MΦ (Fig. 1*b*), F_1 T cells primed with KLH bound to C57BL/6 PC were the most efficient helpers, those primed with DBA/2 PC were the least effective and those with BDF$_1$ PC were intermediate.

Several control experiments have been carried out to eliminate alternative explanations for the results in Fig. 1. For example, it was possible that parental T cells contaminating the PC preparations were stimulated in the F_1 recipients and responsible for the subsequent properties of the primed helper cells. This

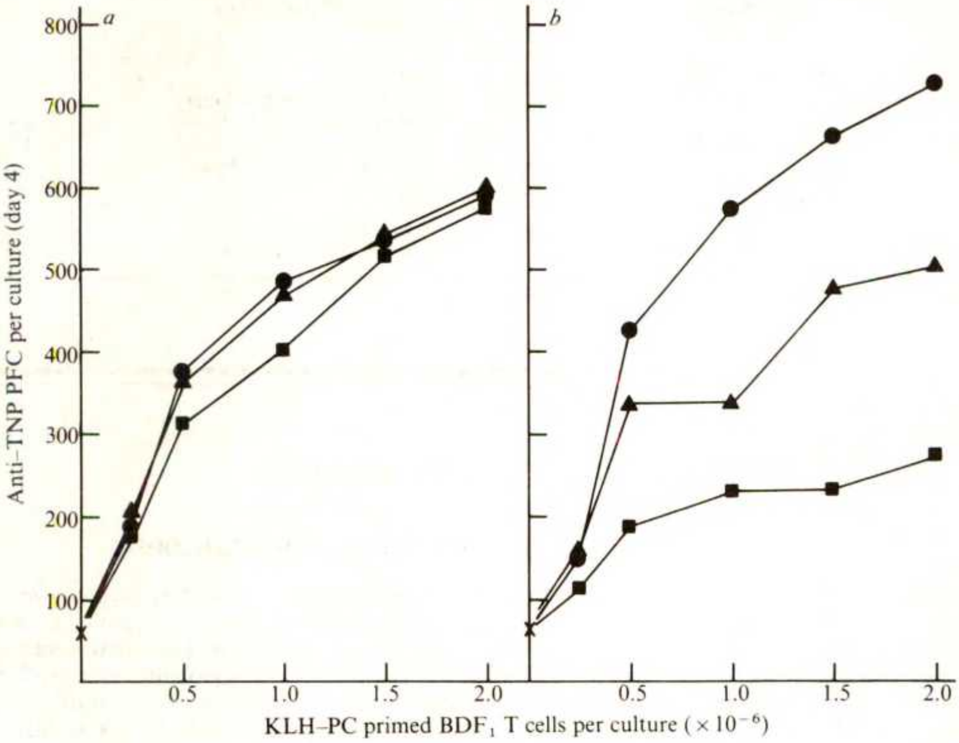

Fig. 1 Restriction of F$_1$ helper T cells in their ability to cooperate with parental B cells and MΦ. Groups of three BDF$_1$, C57BL/6 and DBA/2 mice (Jackson Laboratory) were injected intraperitoneally with 100 µg of KLH (Calbiochem) in 0.3 ml of balanced salt solution (BSS). After 4 h PC were collected by rinsing the peritoneal cavity with 4 ml of BSS containing 5% foetal bovine serum (FBS). The average yield was 3×10^6–4×10^6 PC per mouse. Pooled suspensions of each type of PC were washed twice with 5% FCS in BSS then resuspended to 5×10^6 cells per ml in BSS. Groups of three BDF$_1$ mice were injected with each type of PC (1.5×10^6 intraperitoneally and 1.5×10^6 intravenously). After 7 d a pooled spleen cell suspension was prepared from each group and depleted of B cells and MΦ on nylon wool columns[16]. The resulting T-cell preparations were titrated for KLH-specific helper activity as below. ▲, BDF$_1$, ●, C57BL/6 and ■, DBA/2 PC-primed BDF$_1$ T-cells. For B cells, BDF$_1$ and C57BL/6 mice were primed with 1.0 µg of TNP–LPS[17]. After 7 d spleen cell suspensions were prepared and treated with anti-T-cell serum and complement as described before[18] to deplete T cells but leave macrophages and hapten–primed B cells unaffected. Various combinations of the T-cell and B-cell preparations were tested in the the *in vitro* response to TNP–KLH. Cultures (0.5 ml) contained 4×10^6 B cells and macrophages, various numbers of BDF$_1$ T cells and TNP–KLH (0.05 µg ml^{-1}). After 4 d three identical cultures were pooled and assayed for anti-TNP plaque-forming cells (PFC). Both the culture methods and PFC assay have been described previously[18,19]. The responses (PFC per culture) are shown compared with the number of T cells added to the cultures. *a*, BDF$_1$ B cells and MΦ; *b*, C57BL/6 B cells andMΦ. For each titration the response of the B cells and MΦ cultured alone (×) is also shown. These figures represent the average responses obtained in six experiments with similar results.

possibility was eliminated by demonstrating that results identical to those in Fig. 1 were obtained even after pretreatment of the KLH–pulsed PC with anti-T-cell serum and complement before priming of F$_1$ animals (data not shown). In a second control experiment (Fig. 2) we tested whether, rather than a selective priming of helper T cells in the F$_1$, our results indicated a selective priming of specific suppressor cells. BDF$_1$ T cells which had been primed with KLH bound to either C57BL/6 or DBA/2 PC were prepared. The helper activities of these T cells and a 1:1 mixture of the two were assayed on C57BL/6 B cells and MΦ. As above, T cells primed with C57BL/6 PC were more efficient than those primed with DBA/2 PC. If the helpers primed with DBA/2 PC were ineffective because of the presence of suppressive activity specific for C57BL/6 cells, then the observed activity of the 1:1 mixture should be less than the calculated average of the responses obtained with the two helper preparations alone. In fact there was no difference between the calculated and observed responses, eliminating a role for a suppressive mechanism in this phenomenon.

We have begun experiments formally to identify the genes expressed in the parental cells that are responsible for imposing this restriction of F$_1$ helper T cells. For example, BDF$_1$ mice

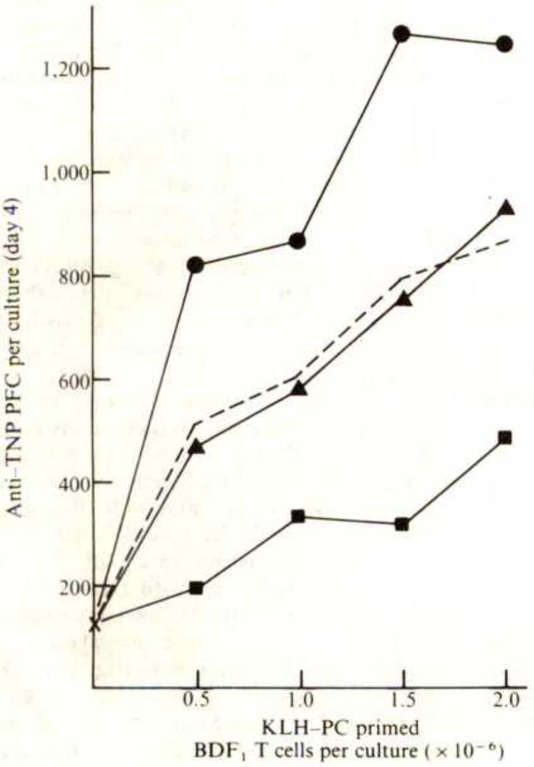

Fig. 2 Suppression is not the mechanism of restriction of F$_1$ T cells. BDF$_1$ T cells primed with KLH bound to either C57BL/6 (●) or DBA/2 (■) PC were prepared as in Fig. 1. Both T-cell preparations and a 1:1 mixture of the two (▲) were titrated on C57BL/6 B cells and MΦ. The calculated average of the responses seen with each T-cell preparation alone is also shown (- - - -). The response of B cells and MΦ cultured alone is shown (×).

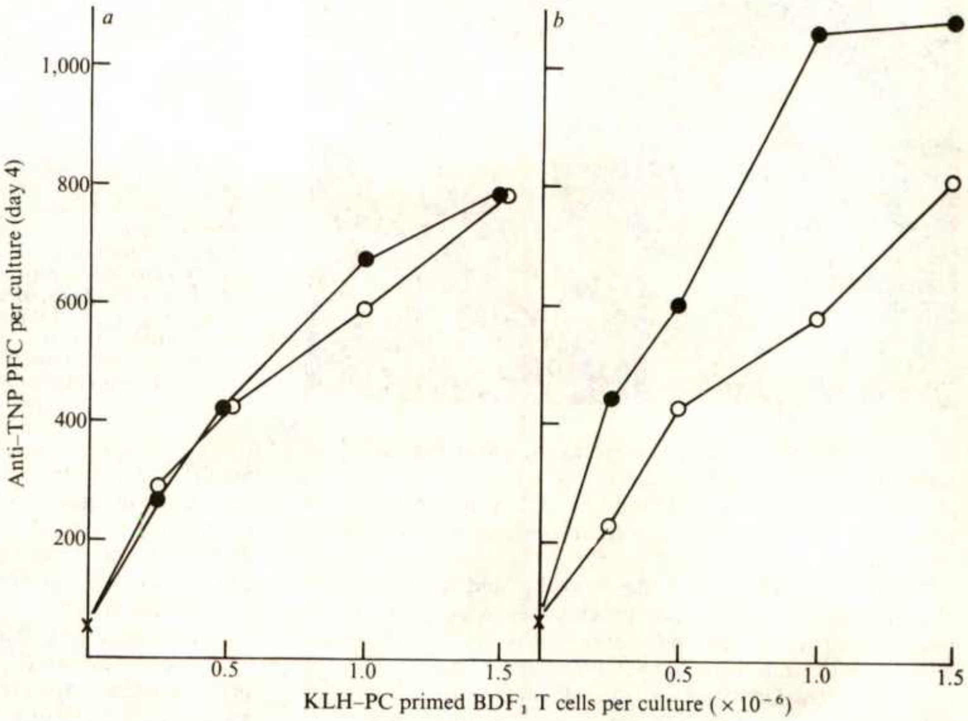

Fig. 3 Involvement of H–2-linked genes in restriction of F$_1$ T cells. BDF$_1$ T cells primed with KLH bound to either C57BL/10 (●) or B10.D2 (○) PC were prepared as in Fig. 1. These T cells were titrated on either BDF$_1$ (*a*) or C57BL/10 (*b*) B cells and MΦ as in Fig. 1. In each figure the response of B cells and MΦ cultured alone is shown (×). The figures represent the average responses seen in three similar experiments.

were primed with KLH bound to C57BL/10 (H–2^b) PC or to B10.D2 (H–2^d) PC. The resulting primed helper T cells were titrated for their ability to cooperate with either BDF$_1$ or C57BL/10 B cells and MΦ. The results (Fig. 3) indicate that although both F$_1$ T-cell preparations were equally effective when tested on BDF$_1$ B cells and MΦ, those primed with C57BL/10 PC were more effective with C57BL/10 B cells and MΦ than those primed with B10.D2 PC. Since these two strains are genetically identical except at the MHC, these results suggest a role for H–2-linked genes in the phenomenon. It is interesting that the differences in helper activity seen in Figs 1 and 2, where the priming PC differed at multiple genetic loci were greater than seen in Fig. 3 where the differences were confined to H–2-linked genes. These results may indicate that genes outside the MHC also contribute to the phenomenon.

Several previous studies of the role of histocompatibility gene products on antigen-mediated interactions between T cells and B cells or macrophages have suggested that such interactions require MHC identity between the cooperating cells[1,8,12]. Other studies[1,9–11,13,15] and the results presented here enable us to make an alternative interpretation of these findings. They suggest that T cells acquire the restricted ability to cooperate with B cells or macrophages of a particular MHC type, not as a result of some inherent genetic mechanism controlling interactions, but perhaps simply through the selection of relevant clones during the initial contact of T-cell precursors with an antigen in association with the surface components of the MΦ.

We thank Lee Harwell and George Berry for technical assistance. This work was supported by grants from the USPHS and the American Cancer Society.

JOHN W. KAPPLER
PHILIPPA C. MARRACK

Department of Microbiology,
School of Medicine and Dentistry,
University of Rochester,
Rochester, New York 14642

Received May 28; accepted July 6, 1976.

[1] *The Role of Products of the Histocompatibility Gene Complex in Immune Responses* (edit. by Katz, D. H., and Benacerraf, B.), (Academic, New York, 1976); Benacerraf, B., and Katz, D. H., *Adv. Cancer Res.*, **21**, 121–173 (1975).
[2] Hämmerling, G. J., and McDevitt, H. O., *J. Immun.*, **112**, 1734–1740 (1974); *J. exp. Med.*, **140**, 1180–1188 (1974).
[3] Munro, A. J., and Taussig, M. J., *Nature*, **256**, 103–106 (1975); Taussig, M. J., Munro, A. J., Campbell, R., David, C. S., and Staines, N. A., *J. exp. Med.*, **142**, 694–700 (1975).
[4] Gordon, R. D., Simpson, E., and Samelson, L. E., *J. exp. Med.*, **142**, 1108–1120 (1975).
[5] Bevan, M. J., *J. exp. Med.*, **142**, 1349–1364 (1975).
[6] Zinkernagel, R. M., and Doherty, P. C., *J. exp. Med.*, **141**, 1427–1436 (1975).
[7] Shearer, G. M., Rehn, T. G., and Garbarino, C. A., *J. exp. Med.*, **141**, 1348–1364 (1975).
[8] Katz, D. H., Graves, M., Dorf, M. E., Dinuzio, H., and Benacerraf, B., *J. exp. Med.*, **141**, 263–268 (1975); Katz, D. H., Hanaoka, T., Dorf, M. E., and Benacerraf, B., *J. exp., Med* **138**, 734–739 (1973).
[9] Bechtol, K. B., Freed, J. H., Herzenberg, L. A., and McDevitt, H. O., *J. exp. Med.*, **140**, 1660–1675 (1974).
[10] Von Boehmer, H., Hardson, L., and Sprent, J., *J. exp. Med.*, **142**, 989–997 (1975).
[11] Heber-Katz, E., and Wilson, D. B., *J. exp. Med.*, **142**, 914–935 (1975).
[12] Rosenthal, A. S., and Shevach, E. M., *J. exp. Med.*, **138**, 1194–1212 (1973); Shevach, E. M., and Rosenthal, A. S., *J. exp. Med.*, **138**, 1213–1229, (1973).
[13] Erb, P., and Feldmann, M., *J. exp. Med.*, **142**, 460–472 (1975); *Eur. J. Immun.*, **5**, 759–766 (1975).
[14] Miller, J. F. A. P., Vadas, M. A., Whitelaw, A., and Gamble, J., *Proc. natn. Acad. Sci. U.S.A.*, **72**, 5095–5098 (1975).
[15] Waldmann, H., Pope, H., and Munro, A. J., *Nature*, **258**, 728–730 (1975).
[16] Greaves, M. F., and Brown, G. J., *J. Immun.*, **112**, 420–423 (1974).
[17] Jacobs, D., and Morrison, D. J., *J. Immun.*, **114**, 360–364 (1975).
[18] Kappler, J. W., and Marrack (Hunter), P. C., *Cell. Immun.*, **18**, 9–20 (1975).
[19] Mishell, R. I., and Dutton, R. W., *J. exp. Med.*, **126**, 423–442 (1967); Kettman, J. R., and Dutton, R. W., *Proc. natn. Acad. Sci. U.S.A.*, **68**, 699–703 (1971).

Distribution of β_2 microglobulin and HLA in chorionic villi of human placentae

ANALOGIES are often made between transplantation and placental immunology. The role of histocompatibility antigens is of undisputed importance in transplantation immunology but it is not clear whether such antigens are important in pregnancy. Indeed, it is not known whether trophoblasts manifest histocompatibility antigens. If HLA antigens are relevant in pregnancy, it is of central importance to know if trophoblasts have these antigens. This is a difficult problem because human anti-HLA sera often contain other antibodies, and heterologous anti-HLA sera often lack precise HLA specificity[1]. But HLA has been shown to be invariably associated with β_2-microglobulin[2], and here we present data in support of the concept that human trophoblasts contain neither β_2 microglobulin nor

Pure Che stry Librar
SCIENCE COLLEGE

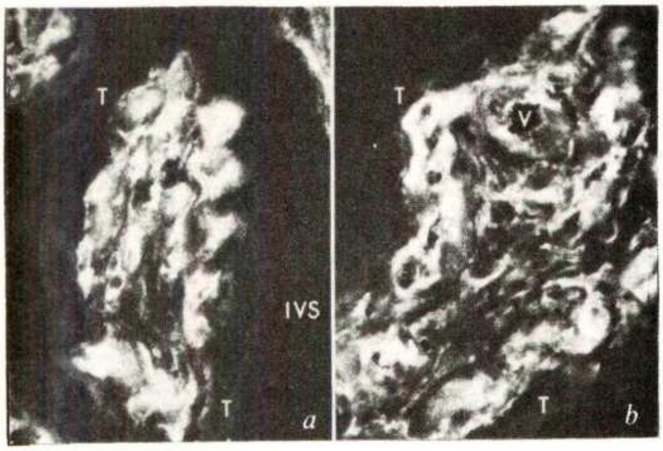

Fig. 1 Immunohistology of full term human placentae with antisera to: *a*, β_2 microglobulin, and *b*, HLA-2. Note negative trophoblasts (T) and positive staining of cells in mesenchymal stroma as well as vessel (V) endothelium. Thin (4-μm) sections were cut on a cryostat, air dried, and studied by indirect immunofluorescence[23] using an IgG fraction of rabbit antiserum to human β_2 microglobulin (Dakopatts A/S, Denmark) and rabbit anti-HLA sera from Dr A. Sanderson. Anti-HLA sera were prepared to HLA-1, HLA-2, HLA-7 and HLA-12 that were isolated by gel filtration, DEAE–cellulose chromatography and polyacrylamide gel electrophoresis. After absorption of these antisera with human erythrocytes, they were specific at low titre when tested for cytotoxicity with rabbit complement against human peripheral lymphocytes. Fluorescein isothiocyanate (FITC)-labelled sheep anti-rabbit Ig serum was obtained from Wellcome Reagents, Beckenham, Kent. Optimum dilutions of antisera (1:75) and conjugate (1:60) were determined by serial titrations[24] that gave minimum nonspecific staining and maximum specificity. Further details are given in the legend of Fig. 3. (Photographed at original magnification of ×400.)

HLA. Also, treatment with several enzymes has failed to reveal these antigens. In addition, we have not been able to identify either β_2 microglobulin or HLA on trophoblasts from 6-week or 13-week placentae or on placental tissues maintained *in vitro* for 5 d.

Thirty-two full term, one 6-week, and one 13-week placentae were studied. All pregnancies were normal and uncomplicated, all neonates were healthy, and all placentae were grossly and microscopically normal. Small pieces of tissue obtained from the central cotyledon within 15 min of delivery were either snap frozen or washed for 16 h at 4 °C with gentle rotation in minimum essential medium supplemented with glutamine, bicarbonate, 10% foetal calf serum (FCS) and antibiotics[3], and then snap frozen. *In vitro* cultures were prepared from tissues aseptically dissected from a 36-week placenta obtained by Caesarian section. Small pieces of tissue were placed on stainless steel grids supported in organ culture dishes (Bio-Cult Laboratories) containing 0.5 ml of medium RPMI supplemented with L-glutamine and 15% FCS (Bio-Cult) and incubated in 5% CO_2 in air. The medium was replaced daily, and the FCS concentration was reduced to 5% after the first day. Cultures were snap frozen after 1, 2 and 5 d in culture.

Tissues that were snap frozen either immediately or after washing overnight in growth medium consistently gave a characteristic pattern of staining for β_2 microglobulin by immunofluorescence. Trophoblasts and trophoblastic basement membranes (TBM) were unstained, and all other cells of the chorionic villus were positive (Fig. 1*a*). Using the antibody–peroxidase technique for light and

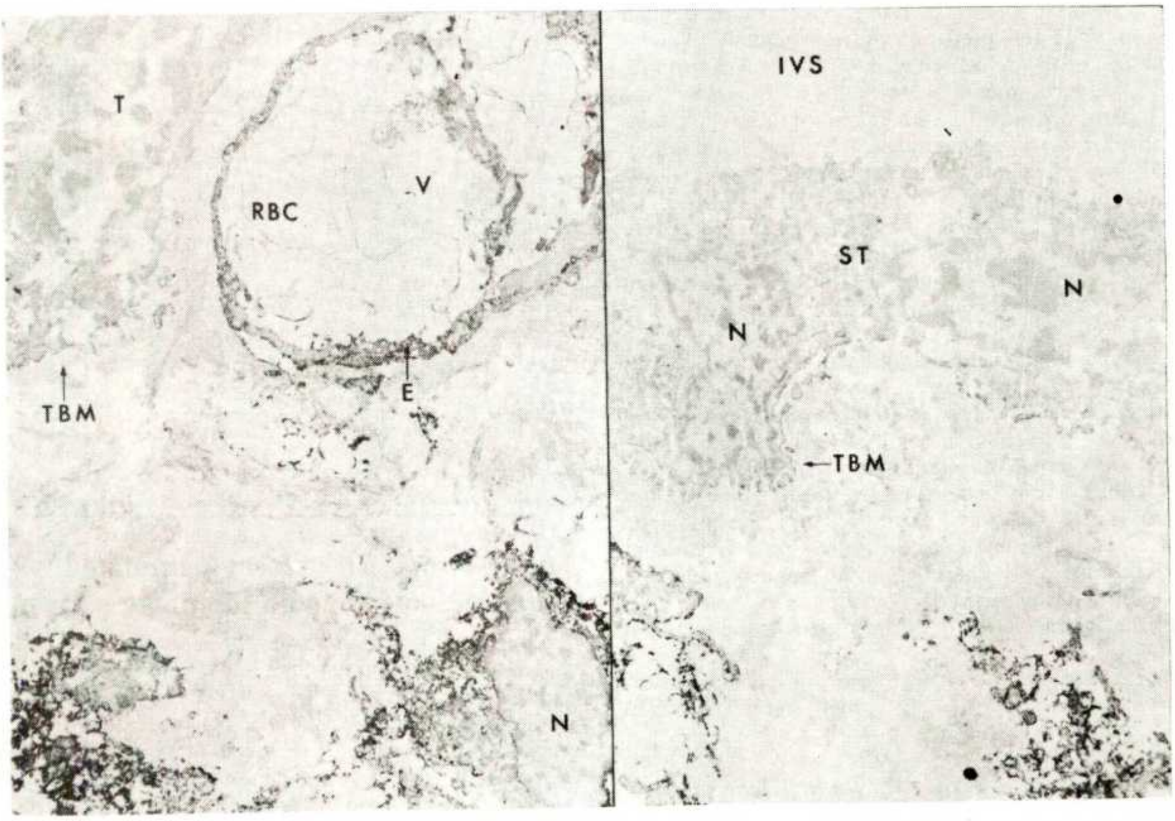

Fig. 2 Immunohistology of full term human placentae with antisera to β_2 microglobulin, achieved using the antibody–peroxidase technique by indirect staining for electron microscopy[4]. An AEI-EM-6B electron microscope was used. IVS, Intervillous space; RBC, red blood cell within vessel (V) in villous stroma; E, vascular endothelium; TBM, trophoblastic basement membrane; N, nuclei of trophoblasts; ST, syncitiotrophoblast. As it is not always possible accurately to differentiate between cytotrophoblasts and syncitiotrophoblasts by immunofluorescence, we restricted morphological definitions of trophoblasts to ultrastructural criteria[25]. Note negative trophoblasts and TBM, and positive cells and endothelium in villous stroma. Placentae were fixed for 30 min at 4 °C in 1% paraformaldehyde in 0.1 M PO_2, *p*H 7.4, containing 7.5% sucrose, and washed overnight in 13% sucrose and 0.1 M PO_4. (Original magnification ×3,000.)

Table 1 Effect of enzyme treatment on β_2-microglobulin staining

Treatment	Dose *	Time of incubation	Temp. (°C)		Immunofluorescence	
				Trophoblasts	Endothelium	Stroma cells
Neuraminidase (*Clostridium perfringens*)	3.6	1 h	20	−	++	++
	9.0	2 h	20	−	+	+
	9.0	3 h	20	−	+	+
Neuraminidase (*Vibrio cholerae*)	500	3 h	20	−	++	++
Collagenase (Sigma)	920	1 h	20	−	++	++
Hyaluronidase (Sigma)	920	1 h	20	−	++	++
	2,300	1 h	20	−	−	++
	4,600	1 h	37	−	−	−
Hyaluronidase (Fisons)	1,500	1 h	20	−	−	++
Trypsin (Sigma)	67	30 min	20	−	++	++
	67	1 h	20	−	+	+
PBS	—	2 h	20	−	+	+
	—	18 h	20	−	−	+

Collagenase was dissolved in 0.5 M Tris buffer, *p*H 7.5, containing 0.05 M Ca^{2+}, hyaluronidase in phosphate-buffered saline (PBS), *p*H 7.2 and trypsin in PBS, *p*H 7.4. Neuraminidase from *Cl. perfringens* was dissolved in PBS, and neuraminidase from *V. cholerae* (Koch-Light) was in 0.05 M acetate buffer, *p*H 5.5 containing 1% NaCl and 1% $CaCl_2$.

*Enzyme units ml^{-1}.

electron microscopy[4], it was possible positively to identify cells staining within villi, and confirm the absence of staining of trophoblasts, TBM and stromal connective tissues (Fig. 2). Tissues from 6-week and 13-week placentae as well as sections from a 36-week placenta that had been cultured *in vitro* for 5 d gave no trophoblast or TBM staining for β_2 microglobulin, but all cells on the foetal side of TBM in these tissues were positive (Fig. 3*a* and *c*). Treatment of cryostat sections of the above tissues with neuraminidase, hyaluronidase, collagenase or trypsin also failed to reveal β_2 microglobulin on trophoblasts or TBM by immunofluoroescence (Table 1), although exposure to large amounts of hyaluronidase and prolonged washing in phosphate-buffered saline diminished staining reactions of stromal and endothelial cells in some experiments (Table 1).

Several rabbit anti-HLA sera gave a pattern of staining by immunofluorescence identical to that obtained using anti-β_2-microglobulin serum. No positive staining of either trophoblasts or TBM was obtained with any of the anti-HLA sera, but cells in the villous stroma of all placentae being studied were stained with all these antisera (Figs 1*b* and 3*b*). The presence of HLA on endothelial cells of placental vessels is consistent with the report[5] of HLA on endothelial cells of the umbilical cord. Furthermore, our failure to identify HLA on trophoblasts is compatible with the observation[6] that human trophoblasts in cryostat sections do not bind concanavalin A. It is interesting that HLA is a glycoprotein that can be partially characterised by its ability to bind to concanavalin A-linked columns[7].

Whether or not trophoblasts manifest histocompatibility antigens is controversial. For example, Currie *et al.*[8] have shown that neuraminidase-treated A$_2$G ectoplacental cone cells injected into CBA mice cause the recipients subsequently to reject donor homografts in an accelerated fashion. Simmons *et al.*[9], however, using a similar experimental model were unable to confirm this, and our results also do not support the concept of masked histocompatibility antigens being present on human trophoblasts (Table 1). Loke *et al.*[10], using mixed cell agglutination reported that HLA antigens were present on trophoblasts, and Lawler *et al.*[11] favour an interpretation of HLA antigens on trophoblasts to explain their results of raised anti-HLA activity of paternal specificity in the sera of women with persistent trophoblastic disease after a first pregnancy with a hydatidiform mole. Perhaps mole tissues do contain HLA, but our experience with a large number of normal placentae suggests that HLA is absent from trophoblasts. The absence of HLA from trophoblasts is consistent with the results of Seigler and Metzgar[12] who used agglutination and antibody absorption techniques. Faulk *et al.*[13] have also reported that eluates prepared from exhaustively washed human placentae contain IgG that inhibits mixed leukocyte culture reactions without demonstrating HLA specificity, again suggesting an absence of HLA antigens from trophoblasts.

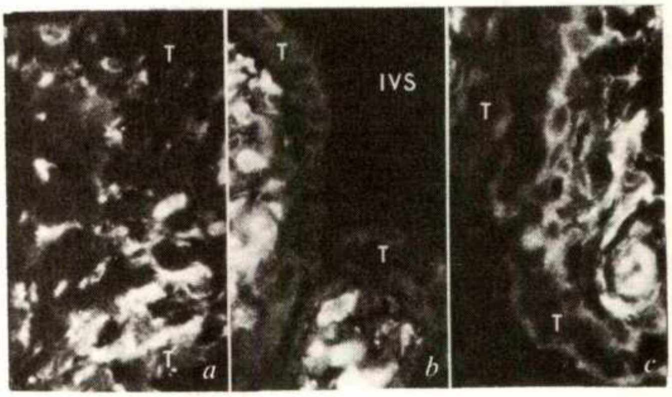

Fig. 3 Immunohistology of: *a*, 6-week placenta; *b*, 13-week placenta; *c*, 5-d culture of term placenta studied with antisera to: *a*, β_2 microglobulin; *b*, HLA-7; *c*, $\beta_2$microglobulin. Specificity and nonspecific-staining controls were done using immunoelectrophoresis, membrane immunofluorescence[3] with human leukocytes and red blood cells, and tissue immunofluorescence[23] using human spleen and rat kidney, liver, muscle and stomach as substrates. The anti-β_2-microglobulin serum gave one line in immunoelectrophoresis against concentrated urine from an oligouric patient with renal amyloid and was negative against five control urines of equivalent concentration. The anti-β_2 microglobulin and the anti-HLA sera gave bright membrane fluorescence at 1:30 dilution with human leukocytes but failed to stain human red cells. These antisera also stained leukocytes in human spleen but did not stain any of the rat tissues. Normal rabbit, sheep, and human sera were used as controls in all experiments. Sera were absorbed for 30 min at 18 °C before use by gentle rotation with an equal volume of washed, packed, sheep erythrocytes, and staining reactions were done according to standard methods[23,24]. Tissues prepared for immunofluorescence were examined by transmitted light using a Reichert Zetopan microscope fitted with a quartz–iodide light source, a Tiyoda wide-field dark-ground condenser incorporating a toric lens, and a FITC-3 Balzer interference primary filter and a Wratten 12 barrier filter. Photographs of transmitted fluorescence were made using Agfa-Gevaert CT18 (ASA 50) 35-mm film. Tissues were also examined by incident light using a Zeiss Photomicroscope 11 fitted with a Ploem epi-illuminator and an HBO 200 high-pressure mercury-vapour burner light source. Photographs of incident light were made using Gaf 500 (ASA 500) high speed 35-mm film. IVS signifies intervillous space, and correspondingly black areas on other photographs are also IVS. (Photographed at original magnification of ×400.)

Heyner[14], using direct immunofluorescence has reported H–2 antigens on cells of 6.5-d embryo cells but not on trophoblasts, and Searle *et al.*[15], using cytotoxicity reactions and a tailskin homograft model, found no evidence for histocompatibility antigens on trophoblasts, but did find H–2 antigens on cells of the embryonic sac. Billington[16] and Gardner *et al.*[17] have also questioned the presence of histocompatibility antigens on mouse trophoblasts, and Searle *et al.*[18], using the antibody–peroxidase technique for electron microscopy, have shown H–2 antigens on blastocysts which are lost from the trophectoderm at the time of implantation.

Experimental models that necessitate the physical separation of trophoblasts from other placental cells may contaminate trophoblast preparations with cells of the villous stroma that bear histocompatibility antigens. Similar technical considerations could account for the diversity of opinion regarding the presence of HLA or H–2 on trophoblasts. The geometrical relationship of trophoblasts to TBM and stroma is retained on cryostat sections studied by immunofluorescence, and using this approach we have been able to show a type of antigenic segregation in the distribution of β_2-microglobulin and HLA within chorionic villi. It is also important to know, however, whether or not histocompatibility antigens are present on the cell membranes of trophoblasts. This could technically be done by membrane fluorescence[3], using trophoblasts from *in vitro* cultures, but the possibility of contaminating trophoblast preparations with other villous cells still exists. What is needed is a membrane marker for human trophoblasts, and preliminary studies suggest that this might be transferrin[19].

These observations of the absence of histocompatibility antigens on trophoblasts suggest that analogies between transplantation and placental immunology are not entirely correct. There is no apparent mechanism to explain why trophoblasts lack β_2-microglobulin and HLA when these antigens are present on cells within mesenchymal stroma of the same organ. Genetic studies have shown, however, that the absence of β_2-microglobulin and HLA is not unique to trophoblasts. The B-cell-derived human Daudi lymphoblastoid line lacks both these proteins, but retains the capacity to express products of immune response-associated genes[20]. Goodfellow *et al.*[21] have shown that the gene responsible for β_2 microglobulin is not in the HLA region but is on chromosome 15, and Heyningen *et al.*[22] have reported that the genes responsible for mannose–phosphate isomerase and pyruvate kinase are also located on chromosome 15. We are studying the ability of human trophoblasts to manifest these enzymes. If the absence of β_2 microglobulin and HLA is associated with the specific capacity of human trophoblasts to avoid maternal recognition, then an understanding of the mechanism will perhaps be useful as an approach to biomedical and pharmacological studies of the more general problem of escape from immunological surveillance.

We thank Dr A. Sanderson for anti-HLA sera and information about their preparation and specificity; Dr Nancy Smith for 6-week and 13-week placentae; Drs Peter Johnson and Peter Page-Thomas for useful discussions; Mr Jack Dorling for assistance with antibody–peroxidase experiments; Mr Robin Faulk for technical assistance, and the WHO and the MRC for support.

W. PAGE FAULK*
ANNE TEMPLE

MRC Rheumatism Unit,
Canadian Red Cross Memorial Hospital,
Taplow, Maidenhead,
Berkshire SL6 0HN, UK

Received April 9; accepted July 13, 1976.

*Present address: Deparment of Basic and Clinical Immunology and Microbiology, Medical University of South Carolina, Charleston, South Carolina 29401.

1 Robb, R. J., Humphreys, R. E., Strominger, J. L., Fuller, T. C., and Mann, D. L., *Transplantation*, 19, 445–447 (1975).
2 Nilsson, K., Evrin, P. E., and Welsh, K. I., *Transplant. Rev.*, 21, 53–84 (1974).
3 Faulk, W. P., Conochie, L. B., Temple, A., and Papamichail, M., *Nature*, 254, 123–125 (1975).
4 Webb, J., and Dorling, J., *J. Immun. Meth.*, 2, 145–157 (1972).
5 Gibofsky, A., Jaffe, E. A., Fotino, M., and Becker, C. G., *J. Immun.*, 115, 730–733 (1975).
6 Johnson, P. M., and Faulk, W. P., *Clin. exp. Immun.* (in the press).
7 Billing, R. J., and Terasaki, P. I., *J. Immun.*, 112, 1124–1130 (1974).
8 Currie, G. A., Doorninck, W. van, and Bagshawe, K. D., *Nature*, 219, 191–192 (1968).
9 Simmons, R. L., Lipschultz, M. L., Rios, A., and Ray, P. K., *Nature*, 231, 111–112 (1971).
10 Loke, Y. W., Joysey, V. C., and Borland, R., *Nature*, 232, 403–405 (1971).
11 Lawler, S. D., Klouda, P. T., and Bagshawe, K. D., *Am. J. Obstet. Gynec.*, 120, 857–861 (1974).
12 Seigler, H. F., and Metzgar, R. S., *Transplantation*, 9, 478–486 (1970).
13 Faulk, W. P., Jeannet, M., Creighton, W. D., and Carbonara, A., *J. clin. Invest.*, 54, 1011–1019 (1974).
14 Heyner, S., *Transplantation*, 16, 675–677 (1973).
15 Searle, R. F., Jenkinson, E. J., and Johnson, M. H., *Nature*, 255, 719–720 (1975).
16 Billington, W. D., in *Immunology of Reproduction* (edit by. Bratanov, K., Edwards, R. G., Vulchanor, V. H., Dikov, V., and Somlev, B.), 475–479 (Bulgarian Academy of Sciences Press, 1973).
17 Gardner, R. L., Johnson, M. H., and Edwards, R. G., in *Immunology of Reproduction* (edit. by Bratanov, K., *et al.*), 480–486 (Bulgarian Academy of Sciences Press, 1973).
18 Searle, R. F., Sellens, M. H., Elson, J., Jenkinson, E. J., and Billington, W. D., *J. exp. Med.*, 143, 348–359 (1976).
19 Faulk, W. P., and Johnson, P. M., *Clin. exp. Immun.*, (in the press).
20 Jones, E. A., Goodfellow, P. N., Bodmer, J. G., and Bodmer, W. F., *Nature*, 254, 650–651 (1975).
21 Goodfellow, P. N., *et al.*, *Nature*, 254, 267–269 (1975).
22 Heyningen, V. van, *et al.*, *Ann. Human Genet.*, 38, 395–403 (1974).
23 Faulk, W. P., and Hijmans, W., *Prog. Allergy*, 16, 9–39 (1972).
24 McCormick, J. N., Faulk, W. P., Fox, H., and Fudenberg, H. H., *J. exp. Med.*, 133, 1–18 (1971).
25 Boyd, J. D., and Hamilton, W. J., *The Human Placenta*, 140–174 (Heffer, Cambridge, 1970).

Human milk samples from different ethnic groups contain RNase that inhibits, and plasma membrane that stimulates, reverse transcription

WE have compared human milk samples from American, Hindu and Parsi donors with a view to determining the relative amounts of reverse transcriptase inhibitors[1–5] present in them. Our intention was to find out whether samples from any specific ethnic group are advantageous for the study of type B virus-like particles in milk[2,6–8] and for purification of virus-associated enzymes. We also hoped that when sufficient data become available, such studies would be interesting from an epidemiological point of view, to test whether the inhibitors provide protection from mammary cancer. We have confirmed the presence of RNase in milk samples, and have observed variations in the level of RNase in samples from different ethnic groups. Careful examination has also revealed the presence of a protein factor, associated with plasma membranes in milk samples, that stimulates RNA-directed DNA synthesis (RDDS) *in vitro* in oncornaviruses.

To determine the effect of RNase-like inhibitors in different milk plasmas, each was examined for RNase content as judged by its ability to degrade ^{14}C-labelled yeast RNA (Table 1). The percentages shown against each group are averages of 15 independent experiments. Each sample tested for RNase activity was also tested for possible inhibitory activity in RDDS (see legend to Table 1). The mean values obtained are listed in Table 1 against the different ethnic groups. Although the mean values differ, the standard deviations are large and so it is difficult to place too much emphasis on the differences at this stage. With a view to minimising deviations arising from various factors involved in the enzyme assays, a more direct quantification was attempted.

Figure 1*a*, *b* and *c* shows the results on the basis of quantitative correlation for individual samples. In each graph all experimental points derive from a single set of experiments. The RNase-resistant counts for the individual samples are plotted on the abcissa, and the corresponding ^{3}H-TTP counts incorporated in the reverse transcriptase reaction using AMV pelleted through the milk samples are plotted directly on the ordinate. In a single set of experiments the same reaction mixture, with identical specific activity of ^{3}H-TTP, was used

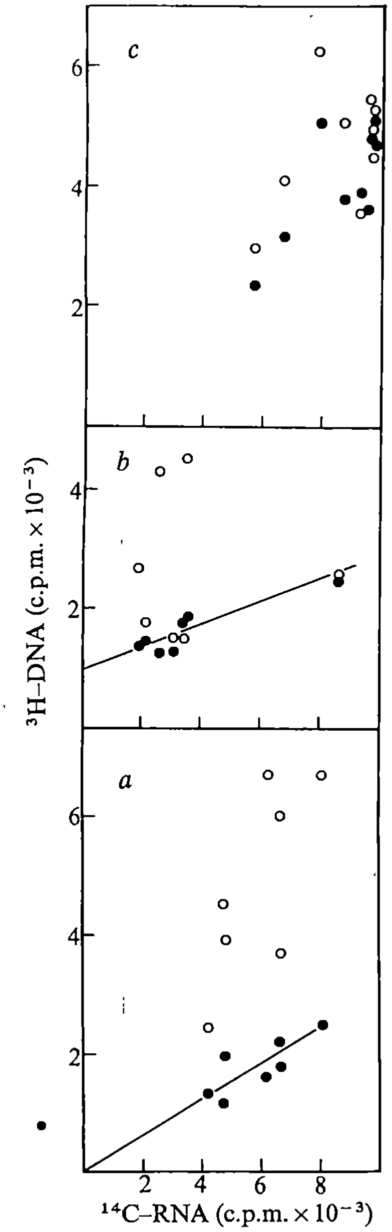

Fig. 1 Direct correlation of RNase content in milk samples and ^{3}H-TTP incorporation in reverse transcriptase reaction using AMV pelleted through the milk samples. Data from a single set of experiments from the different ethnic groups are presented. Milk plasma (2 ml) from each sample was halved. One half was used for incubation with ^{14}C-labelled yeast RNA, and the other for mixing with AMV (see legend to Table 1 and text). The AMV recovered after pelleting was halved, one half was used for primary reaction using endogenous template, and the other for the reaction with synthetic template. RNase-resistant counts are plotted on the abcissa and the ^{3}H-TTP incorporation in the parallel reverse transcriptase reactions plotted on the ordinate (see text). ●, Primary reactions; ○, reactions on synthetic template. *a*, American samples; *b*, Hindu samples; and *c*, Parsi samples. Specific activity of ^{3}H-TTP in primary reactions: 2,500 c.p.m. pmol^{-1}; 800 c.p.m. pmol^{-1} with synthetic template.

and the numbers obtained for ^{3}H-TTP incorporation were used directly to test possible correlation with the RNase-resistant counts. This provided a more direct comparison than plotting percentage RNase-resistance against percentage incorporation of label.

For samples from American and Hindu donors there was a direct correlation between RNase-resistant RNA counts in the milk plasma and DNA synthesis in primary reactions. This was not so for poly(dT) synthesis with poly(dT)·poly(rA) as template: which is understandable as the susceptibility to RNase of a single-stranded viral RNA template would be expected to be different from that of a synthetic hybrid template. Figure 1*c* shows that for the Parsi samples most points are grouped together towards the extreme right hand region of the curve. Very few points reach even towards the central region. Together with the data in Table 1 for the mean RNase level, these observations indicate a lower level of RNase in Parsi samples.

Although most milk samples contained inhibitors of reverse transcriptase, 40% of the Parsi samples did not inhibit RDDS. And in three out of 15 samples (Table 1) there was enhanced DNA synthesis compared with the control. Figure 2*a* shows the kinetics of an AMV reaction in which enhancement was observed. Samples belonging to this group have been tested repeatedly and the observation has been validated both for AMV and murine mammary tumour virus. Similar behaviour was observed for two of the 15 American samples, and later in several more Parsi samples (unpublished results). The stimulation observed in all these cases was RNase sensitive.

In a variation of this experiment the milk pellet prepared without AMV was taken up in 0.01 M Tris (*p*H 8.3), and then mixed with AMV instead of pelleting AMV through milk plasma. This had no effect on the observed results. If the milk pellets alone from these samples were tested for reverse transcriptase, there was no detectable reaction which could

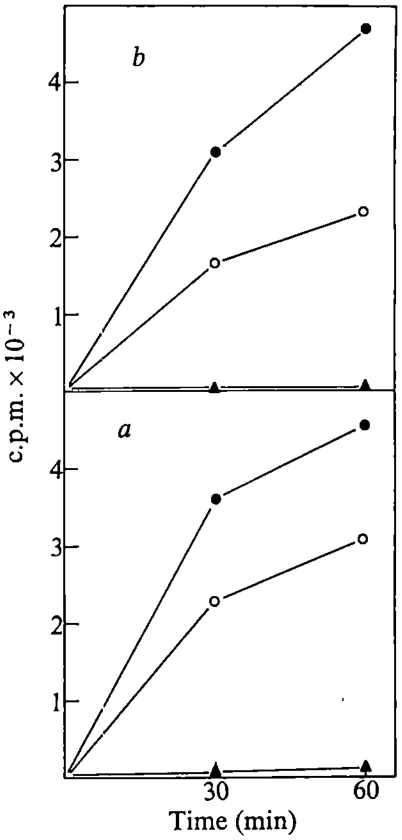

Fig. 2 Kinetics of stimulation of AMV primary reactions by plasma membrane factor from milk pellet (*a*, see text) and from milk fat suspension (*b*). ▲, Control reaction without AMV, but milk pellet alone (*a*) or fat suspension (*b*). ○, AMV primary reaction without any added milk component. ●, AMV primary reaction with milk pellet (*a*) corresponding to 60 μg of total protein, and with fat globule suspension (*b*) corresponding to 200 μg of fat with 10 μg of membrane-associated proteins as determined by Lowry method. In either case the milk factor was added to AMV before incubation with Nonidet P-40. The stock fat globule preparation was made by suspending freshly separated fat from milk plasma in 0.01 M Tris, *p*H 8.3, at 37 °C at a concentration of 20 mg ml^{-1}, and mixing thoroughly in a vortex mixer before pipetting out the required amount.

Table 1 Inhibition of RDDS by human milk plasma

Ethnic group	mg fat per ml	% RNase-resistant counts*	% DNA synthesis in AMV pelleted through milk plasma† Primary	Synthetic template
American	9.9±2.5	57.2±23.8	78.7±17.1	87.2±15.9
Hindu	17.7±7.8	62.1±14.3	63.3±18.5	76.1±14.3
Parsi	22.2±2.8	81.3±19.6	89.9±10.3	95.1±11.2

Hindu and Parsi milk samples were collected from maternity homes in Bombay and the samples were cooled immediately in ice, and later stored in liquid N_2. American samples were from the Michigan Cancer Foundation. The milk plasma was separated and the viral pellet prepared by the method of McCormick *et al.*[5]. The fat layer separated from a known amount of milk sample was extracted twice with a mixture of chloroform–methanol (2:1), the pooled extract was filtered and the fitrate was evaporated to dryness at 80 °C under a jet of dry nitrogen. The amount of dry residue left was determined by direct weighing and the content of fat in milk (mg ml^{-1}) was calculated. The relative amount of RNase in the samples was determined by incubating known amounts of ^{14}C-labelled yeast RNA (~8,000 c.p.m.) in 1 ml of the plasma for 30 min at 0 °C and determining the trichloroacetic acid (TCA)-precipitable counts after incubation. The percentage acid precipitable counts after incubation was determined for 15 samples each from the different ethnic groups and the mean values were calculated with standard deviations. Incubation of yeast RNA in control experiments at 0 or at 37 °C made no appreciable difference to the degradation of the RNA, and so we chose 0 °C as the temperature of incubation. Reverse transcriptase reactions were carried out as described before[8,14]. To determine the inhibition of AMV reaction by milk plasma, AMV (corresponding to 50 μg of viral protein) was mixed with 1 ml of milk plasma and kept at 0 °C for 30 min. This was layered over 4 ml of 20% glycerol in TNE (0.01 M Tris, *p*H 7.2, 0.1 M NaCl and 0.002 M EDTA) and the virus was pelleted by centrifugation at 234,000*g* for 30 min in a Beckman 50.1 rotor. The residue was taken up in 0.01 M Tris, *p*H 8.3, and used for reverse transcriptase reactions. ^{3}H-TTP incorporation from an equal amount of AMV (without milk plasma) pelleted through 20% glycerol was used to determine percentage DNA synthesis. The numbers reported are mean values from 15 determinations for each ethnic group. The specific activity of ^{3}H-TTP used was 2,500 c.p.m. p mol^{-1} for primary reactions, and 800 c.p.m. $pmol^{-1}$ for reactions with synthetic template.

* % Acid precipitable ^{14}C-RNA counts after incubation for 30 min at 0 °C.

† % ^{3}H-TTP incorporation in reverse transcriptase reactions using AMV pelleted through milk plasma compared with AMV pelleted through TNE.

account for the stimulation of AMV RDDS by an equivalent amount of pellet (Fig. 2*a*). Thus it is unlikely that the stimulation results from milk viral RNA-dependent DNA synthesis. We also examined the possibility that the enhanced synthesis was due to the protection of the AMV reverse transcriptase from proteolytic enzymes, as a consequence of the presence of additional proteins in the milk pellets. In control reactions in which an equivalent amount of either bovine serum albumin or casein was added in place of milk pellets there was no increase in the incorporation of ^{3}H-TTP.

In a separate experiment, a sample of milk pellet treated with Nonidet P-40, that stimulated AMV, was equilibrated with DEAE–cellulose for 30 min at 4 °C. The slurry was poured on to a column (0.7×3 cm), washed with buffer (0.01 M Tris' *p*H 8.3, 2 mM dithiothreitol (DTT) and 10% glycerol) containing 0.05 M NaCl, and eluted with the same buffer containing 0.4 M NaCl. RDDS stimulatory activity was present in the eluate. No activity remained either in the 0.05 M NaCl wash or in the loading solution draining out of the column after equilibration with DEAE–cellulose.

Table 2 Membrane marker enzymes in human milk samples

Marker enzyme	Specific activity of enzyme per mg protein Casein pellet	Ultracentrifuge pellet from milk plasma	Fat fraction
Alkaline phosphatase	0.326 μmol	0.283 μmol	0 107 μmol
Acid phosphatase	0.360 μmol	0.200 μmol	0.890 μmol
Xanthine oxidase	236 U	194 U	178 U

Membrane marker enzymes (selected from those listed in ref. 11) were assayed from different fractions of the milk samples. The casein pellet was obtained by centrifuging the milk sample at 5,000 r.p.m. in a Sorvall HB4 rotor for 20 min. The fat fraction is obtained by removing the top layer of fat, and the milk plasma pellet was obtained by layering the intermediate layer of milk plasma on 20% glycerol (see legend to Table 1) and isolating the pellet obtained by centrifugation at 234,000*g* for 30 min in a Beckman 50.1 rotor. To enrich the membranes, these fractions were suspended separately and uniformly in TM buffer (0.05 M Tris, *p*H 7.4, and 0 005 M $MgCl_2$) containing 20% sucrose. The fat suspension was treated differently. Skimmed fat (1 ml) was suspended in 5 ml of TM buffer and homogenised in a Potter–Elvehjem homogeniser (30 strokes). This was centrifuged at 10,000 r p.m. in an HB4 rotor for 10 min and the pellet was collected. The fat layer remaining at the top was collected, rehomogenised and pelleted in the same way twice more. The pellets were pooled and suspended in TM buffer containing 20% sucrose. The different suspensions in TM containing 20% sucrose were layered over a discontinuous sucrose gradient (TM) with 60% sucrose in the bottom overlain with 50, 40, 35 and 30% sucrose solutions. The samples were centrifuged at 1,380*g* in an HB4 rotor for 15 min. The band between 35 and 40% sucrose was collected. The membrane was isolated by repelleting after dilution with TM. This was dissolved in appropriate buffers for different enzyme assays. Alkaline phosphatase was assayed as described by Malamy and Horecker[15], acid phosphatase as described by Hollander[16] and xanthine oxidase by the method of Roussos[17]. Incubation was for 1 h at 37 °C.

We have made similar observations with the fat components. Reports have implicated lipid-associated inhibitor(s) present on milk particle isolates[1,4,9], but no systematic investigation of any such inhibitors has been reported. We observed variations in fat contents of milk samples from different ethnic groups (Table 1), and the freshly separated fat portions were tested for the presence of inhibitors. With samples for which the milk pellets showed strong inhibition of AMV reverse transcriptase, the addition of the corresponding fat suspension also showed inhibition. With samples that showed no inhibition, addition of the fat suspension had no inhibitory effect on ^{3}H-TTP incorporation in AMV reactions. There was, on the contrary, increased incorporation of ^{3}H-TTP in about 30% of such samples. This was clearly noticeable in the Parsi samples. Furthermore, samples showing enhanced DNA synthesis with milk pellets in AMV RDDS invariably stimulated the AMV reaction with the fat components as well (Fig. 2*b*).

We have observed stimulation of DNA synthesis[10] in the AMV reverse transcriptase reaction by plasma membrane preparations from chicken embryonic cells. To test the possibility that the stimulation in AMV reactions caused by milk plasma pellets, as well as fat globules, results from the presence of membranes in the preparations, these fractions were analysed carefully. Electron micrographs indicated the presence of small but definite amounts of membranes present in the plasma pellet preparations in the conditions[5-7] in which these pellets are made for detecting RDDS. In addition, both the pellets and fat fractions were layered on discontinuous sucrose gradients to enrich the membrane preparations which were assayed for marker enzymes (Table 2): the same preparations in turn stimulated AMV RDDS. Even when a milk pellet or fat fraction was not stimulatory at first, once the membranes were purified they were stimulatory There is evidence that the fat globules are covered by a double layer membrane which is very similar in composition to plasma membrane[11-13], suggesting that the stimulation from the milk pellet and from the fat component results from the same membrane-bound factor. This factor, like that isolated from chicken embryos[10], is not dialysable and yet is inactivated by heat. Experiments to enrich the stimulatory factor as well as to characterise the stimulated DNA product are in progress.

We thank Professor J. Beard for AMV.

M. R. DAS
L. C. PADHY

Tata Institute of Fundamental Research,
Bombay-5, India

RAJEN KOSHY
SATYAVATI M. SIRSAT

Cancer Research Institute, Parel,
Bombay-12, India

MARVIN A. RICH

Michigan Cancer Foundation,
Michigan 48201

Received April 2, accepted July 7, 1976.

1 Sarkar, N. H, Charney, J, Dion, A S, and Moore, D H., *Cancer Res.*, 33, 626–629 (1973)
2 Schlom, J, Spiegelman, S, and Moore, D H., *Science*, 175, 542–544 (1972).
3 Feldman, S, Schlom, J, and Spiegelman, S, *Proc natn Acad Sci U.S.A.*, 70, 1976–1980 (1973)
4 Schlom, J, Spiegelman, S., and Moore, D H., *J natn. Cancer Inst*, 48, 1197–1203 (1972).
5 McCormick, J J., Larson, L J., and Rich, M. A, *Nature*, 251, 737–740 (1974).
6 Moore, D H, *et al*, *Nature*, 229 611–614 (1971).
7 Schlom, J, Spiegelman, S, and Moore, D. H., *Nature*, 231, 97–100 (1971).
8 Das, M. R., Vaidya, A B., Sirsat, S. M, and Moore, D. H., *J. natn Cancer Inst.*, 48, 1191–1195 (1972).
9 Fieldsteel, A H., *Cancer Res*, 34, 712–715 (1974)
10 Padhy, L C, Kar, S K, Rao, K K, and Das, M R, *Nature*, 805–807 (1976).
11 Patton, S., and Keenan, T W., *Biochim biophys Acta*, 415, 273–309 (1975)
12 Keenan, T. W, Moore, D J, Olson, D E, Yunghans, W N., and Patton, S., *J Cell Biol*, 44, 80–93 (1970).
13 Keenan, T W., and Huang, C. M., *J. Dairy Sci*, 55, 1586–1596 (1972)
14 Das, M. R, Sadasivan, E, Koshy, R, Vaidya, A B., and Sirsat, S M, *Nature new Biol*, 239, 92–95 (1972)
15 Malamy, M, and Horecker, B. L., in *Methods in Enzymology*, 9 (edit by Wood, W. A.), 639–642 (Academic, New York, 1966).
16 Hollander, V. P, in *The Enzymes*, 4 (edit by Boyer, P. D), 449–496 (Academic, New York, 1971).
17 Roussos, G G., in *Methods in Enzymology*, 12A (edit. by Grossman, L., and Moldave, K), 5–16 (Academic, New York, 1967)

Role of plasma membranes in stimulation of RNA-directed DNA synthesis

THERE has been considerable speculation about the small size of DNA transcripts (less than 10S) obtained by reverse transcription *in vitro* of 60–70S RNA from oncornaviruses[1–4]. On the basis of evidence suggesting that at least part of the virus-specific DNA synthesis could be taking place at the plasma membrane[5,6], we have examined the role of membrane-bound factors on RNA-directed DNA synthesis (RDDS). We report here the existence of a protein factor, associated with plasma membrane preparations from chick embryonic cells, that stimulates RDDS in avian myeloblastosis virus (AMV). The stimulated synthesis is sensitive to RNase, and the product DNA is 33–35S in alkaline sucrose gradients.

The effect of added plasma membrane on AMV incubated with Nonidet P-40 is shown in Table 1. The properties of the purified membrane preparations are shown in Table 2. There was a marked increase in ^{3}H-TTP incorporation in the primary reaction with AMV endogenous template. Similarly, there was increased incorporation of ^{3}H-dGTP when the synthetic template oligo(dG)·poly(rC) was used. In the absence of AMV there was no DNA synthesis with membrane preparation alone, or in conjunction with oligo(dG)·poly(rC). This rules out the possibility that any DNA-polymerising enzymes were present in the membrane and contributed to the increased synthesis.

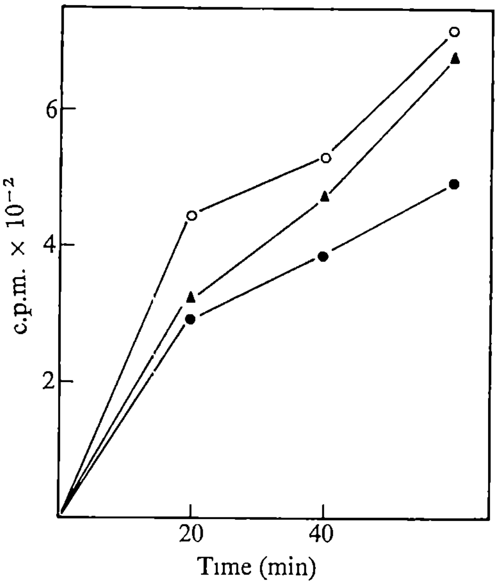

Fig. 2 Solubilisation of stimulation factor. Plasma membrane preparation containing 1 mg of proteins per ml was made 0.4% with respect to Nonidet P-40 and 0.1 M with respect to DTT. The mixture was incubated in ice for 30 min and was centrifuged in a Sorvall HB4 rotor at 7,500 r.p.m. for 10 min. The supernatant was removed and the pellet was resuspended in 0.01 M Tris, *p*H 8.3. After determining the protein concentrations in the supernatant and the pellet suspension, equivalent amounts of protein were added to AMV reverse transcriptase incubation mixtures (see legend to Table 1). From reaction mixtures containing 100 μg of membrane protein per ml, 30-μl samples were withdrawn at different times and the acid-precipitable radioactivity determined. ○, Supernatant; ▲, whole; ●, pellet.

Figure 1 shows the dependence of stimulation on the concentration of the membrane preparation in the reaction mixture. We found that in our experimental conditions the optimum concentration corresponded to 100 μg of membrane proteins per ml of reaction mixture. It was similar when a synthetic template was used. The reason for this is unknown. It is likely that there is a stimulatory activity and an inhibitory factor present in the unfractionated membrane proteins. Even after the stimulatory activity

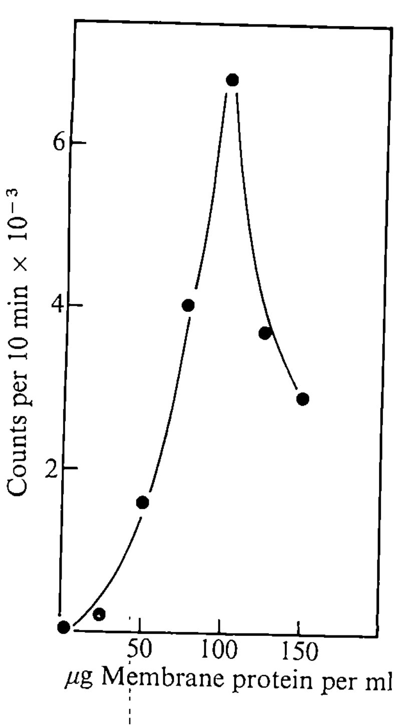

Fig. 1 Stimulation of RNA-directed DNA synthesis by AMV in presence of increasing amounts of plasma membrane. The results of primary reactions with endogenous RNA template are shown. Reactions were carried out in conditions described in the legend to Table 1. Incorporation of ^{3}H-TTP into TCA-precipitable radioactivity in 45-min reactions was determined, as were excess counts above control (reaction with no membrane protein present) and are plotted against different membrane concentrations.

Table 1 Stimulation of AMV reverse transcription by plasma membrane preparations

Reaction	c.p.m. of ^{3}H-TTP incorporated in 40 min
Primary reaction	
AMV control reaction	3,200
AMV+plasma membrane (120 µg protein per ml)	6,024
Membrane without AMV (120 µg protein per ml)	36
Reaction using oligo(dG)·poly(rC)	
AMV control reaction	6,172
AMV+plasma membrane (120 µg protein per ml)	21,399
Membrane without AMV (120 µg protein per ml)	81

Plasma membrane was prepared from 7–9-d-old chicken embryos as described in the legend to Table 2. The amount of total protein present in each preparation was determined by the Lowry procedure and purity was checked by marker enzymes (Table 2). The standard reverse transcriptase assay mixture contained, 5×10^{-2} M Tris, pH 8.3, 4×10^{-2} M NaCl, 8×10^{-3} M $MgCl_2$, 2×10^{-3} M dATP, dCTP and dGTP, and ^{3}H-TTP at 1,500 c.p.m. pmol^{-1} for the primary reactions. The mixture for the synthetic template reactions contained oligo(dG)$_{12-18}$·poly(rC) at a concentration of 10^3 µg ml^{-1}. Of the triphosphates these mixtures contained only cold dCTP (2×10^{-3} M) and ^{3}H-dGTP (500 c.p.m. pmol^{-1}). The membrane preparations (1 mg ml^{-1}) were made 0.4% with respect to Nonidet P-40 and 0.1 M with respect to dithiothreitol (DTT) and incubated separately at 0 °C for 30 min. Required amounts of this preparation were added to the standard reverse transcriptase assay mixtures before incubation at 37 °C. The primary reactions were in the presence of actinomycin D (50 µg ml^{-1}). The reactions described above were done using 50 µg of AMV preincubated for 10 min at 0 °C with 0.4% Nonidet P-40 and 0.1 M DTT. The total reaction volume was 100 µl. Samples of 30 µl were withdrawn after 0 min, 20 min and 40 min of incubation and the trichloroacetic acid (TCA) preciptable radioactivity present in the different samples was determined.

reaches saturation, the inhibitory activity may be increasing as membrane concentration increases.

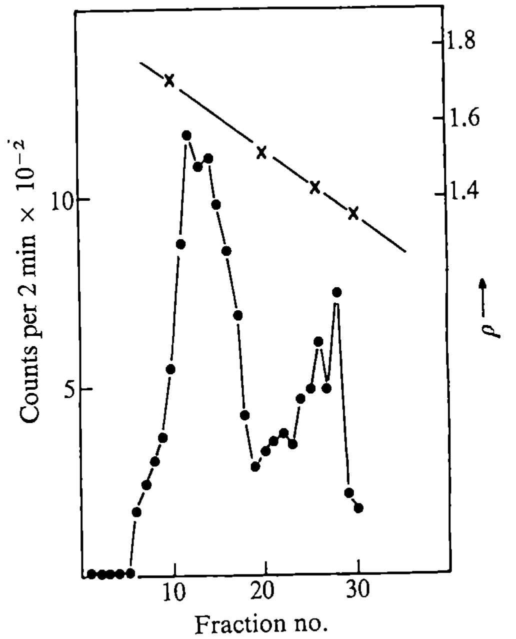

Fig. 4 Hybridisation of DNA product from a plasma membrane stimulated AMV primary reaction with high molecular weight AMV RNA. Purification of single-stranded DNA product and preparation of AMV high molecular weight RNA have been described before[16]. The incubation mixture for hybridisation contained, 50 µg of AMV RNA; 10,000 c.p.m. of purified ^{3}H-DNA; 0.45 M NaCl, and 0.002 M EDTA, pH 7.2 and 75 µl formamide in 150 µl. After incubation at 37 °C for 24 h, the solution was diluted with 2.35 ml of 5×10^{-2} M EDTA and 2.56 ml of saturated Cs_2SO_4. This solution had a refractive index of 1.375. It was centrifuged for 60 h at 20 °C using a Spinco SW50.1 rotor at 40,000 r.p.m. After centrifugation the contents were fractionated by bottom puncture of the Polyallomer centrifuge tube and the TCA-precipitable radioactivity in the fractions determined.

The stimulatory activity associated with the membrane preparations can be solubilised. When a preparation was centrifuged after incubation with Nonidet P-40 the activity was present in the supernatant. But, not all the activity was recovered (Fig. 2), some remained in the pellet fraction, although at a reduced level. In a different experiment, the membrane preparation from chick embryo cells, after treatment with Nonidet P-40, was centrifuged in a Sorvall HB 4 rotor at 7,500 r.p.m. for 10 min, and the supernatant was equilibrated with DEAE-cellulose for 30 min at 4 °C. The thick slurry was poured on to a column (0.7×2 cm), washed with buffer (0.01 M Tris, pH 8.3, 2 mM DTT, 10% glycerol) containing 0.05 M NaCl, and eluted with the same buffer containing 0.4 M NaCl. RDDS stimulatory activity was present in the eluate, and none remained in either the 0.05 M NaCl wash or the loading solution draining out of the column. The activity was destroyed by heating for 10 min at 100 °C and it was non-dialysable. These observations, together with the fact that stimulation was observed when a synthetic template was used with only two deoxynucleoside triphosphates in the reaction mixture, eliminate

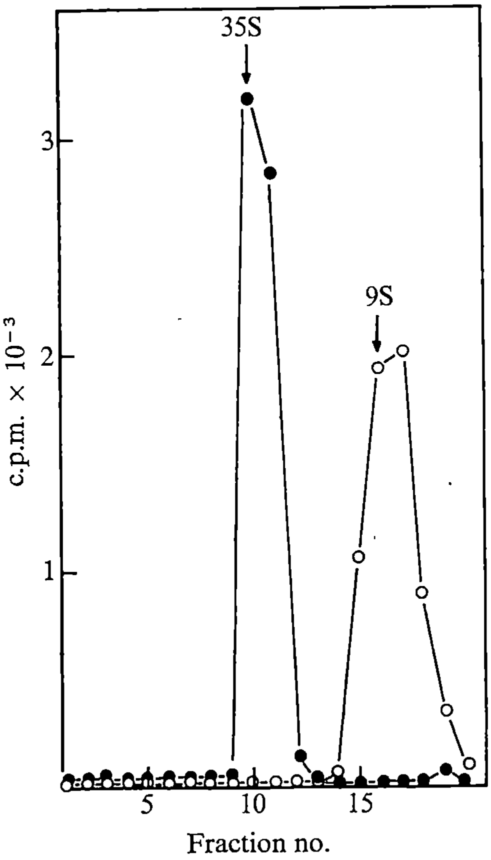

Fig. 3 Comparison of the size of DNA product of AMV reverse transcription in the presence and absence of plasma membrane preparations. The DNA products were made using reaction conditions described in the legend to Table 1. For size determination we have used reaction mixtures containing ^{3}H-TTP at 2,500 c.p.m. pmol^{-1}. After incubation for 60 min the reactions were stopped by the addition of sodium dodecyl sulphate to 1% and NaCl solution to 0.4%. The nucleic acid products were isolated by phenol extraction as described before[16]. The isolate was incubated with 0.3 M NaOH for 18 min at 37 °C and after cooling was layered on a 5–20% linear sucrose gradient (10^{-2} M Tris; 10^{-2} M EDTA; 0.7 M NaCl, and 0.3 M NaOH). Centrifugation was done in a Spinco SW50.1 rotor at 48,000 r.p.m. for 120 min. The gradients were fractionated and the TCA-precipitable radioactivity was determined. Purified DNA from phage PlKC, and *Haemophilus influenzae* phage (HPlC$_1$) were used as external markers in separate tubes, ●, DNA synthesised in the presence of plasma membrane (110 µg proteins per ml); ○, DNA synthesised in control reactions without added membrane proteins.

Table 2 Marker enzymes present in plasma membranes isolated from chick embryos

Enzyme	Specific activity per mg per h Homogenate*	Purified preparation	Enrichment factor
ADPase	1.02 μmol	2.31 μmol	2.3
5′-Nucleotidase	0.49 μmol	2.00 μmol	4.1
Na^+, K^+-ATPase	0.75 μmol	2.00 μmol	2.7
Alkaline phosphatase	0.16 μmol	1.40 μmol	8.8
CTPase	0.82 μmol	4.04 μmol	4.9
Succinate dehydrogenase	8.7 U†	2.1 U†	0.24

*Homogenate after filtration through cheesecloth (see below)

†Increase in A_{490} units; see ref. 15.

The membranes were made from 7–9-d-old chick embryos[8,9], which were dissected to remove internal organs, head and limbs. The tissue was minced, washed thoroughly with TM buffer (5×10^{-2} M Tris, *p*H 7.4 and 5×10^{-3} M $MgCl_2$) and homogenised by 30 gentle strokes in a Potter–Elvehjem homogeniser It was filtered through two layers of cheesecloth. It was centrifuged at 2,500 r.p.m. in a GSA rotor for 15 min and the pellet was resuspended in TM and placed on top of a discontinuous sucrose gradient in TM consisting of 60% sucrose in the bottom (4 ml) overlain with solutions containing 50% (4 ml), 40% (4 ml), 35% (10 ml), 30% (5 ml) and 20% (5 ml) of sucrose. The gradient was made in a cellulose nitrate tube for the Beckman SW27 rotor, but spun in an HB4 rotor at 1,380*g* for 15 min. The fraction that collected between 35% and 40% sucrose was withdrawn with a syringe and pelleted by centrifugation at 6,000*g* for 15 min after adjusting the sucrose concentration to 5%. This pellet was resuspended in TM and purified twice more by passage through the discontinuous gradient and isolation between 35% and 40% sucrose. The pellet obtained after the third discontinuous gradient was taken up in 30% sucrose in TM and placed over a different discontinuous gradient with 60% sucrose at the bottom (3 ml) overlain with solutions having 55% (3 ml), 50% (3 ml), 48% (6 ml), 45% (6 ml) 43% (4 ml), and 40% (4 ml) of sucrose and centrifuged at 90,000*g* for 90 min in an SW27 rotor. The membrane formed a band between 43% and 40% sucrose. This fraction was separated and the membrane pelleted by centrifugation at 6,000*g* for 15 min after adjusting the sucrose concentration to 5%. This was resuspended in the required buffers for the assay of marker enzymes. The amount of total proteins present in each preparation was determined by the Lowry procedure. ADPase and CTPase were assayed as described by Perdue and Sneider[10], Na^+, K^+-ATPase by the method of Post and Sen[11], 5′-Nucleotidase by the method of Morre[12], alkaline phosphate by the method of Malamy and Horecker[13], and succinate dehydrogenase by methods described by King[14] and Pennington[15].

the possibility that stimulation was due to a DNA or RNA contaminant in the membrane preparation.

The DNA product of the stimulated primary reactions was larger (33–35S in alkaline sucrose gradients (Fig. 3)). than the product synthesised in the absence of plasma membrane preparation. The distribution of size varied slightly from experiment to experiment· this could have resulted from variations in length of viral RNA template.

The hybridisability of the product was also examined. The results of hybridisation with 70S RNA from AMV are shown in Fig. 4. Most of the counts were present in the RNA and RNA–DNA hybrid density region The spilling over of the counts to the hybrid region when hybridisation was done with an excess of AMV RNA probably indicates the presence of full length DNA transcripts. Unlike small pieces of DNA hybridising to large RNA molecules, resulting in RNA–DNA hybrids with densities close to that of RNA, full length DNA or nearly full length DNA can form 1 : 1 RNA–DNA hybrids. This type of hybrid would band at a region with the mean density of DNA and RNA.

Based on these observations, we suggest that the stimulation of DNA synthesis is caused by a thermosensitive and non-dialysable factor associated with the membrane. But the method used to purify the membrane may also have purified some of the membraneous organelles of the cell, such as endoplasmic reticulum, for their density is very close to that of the outer plasma membrane. At present the mechanism of stimulation and chain elongation is not clearly understood. Experiments are in progress to determine whether the stimulation of the reaction is due to interaction of the factor with the template or reverse transcriptase. In this respect, the factor can be compared with the DNA binding proteins reported by Hung and Lee[7]. Rigorous characterisation (such as genomic complexity) of the longer DNA molecules synthesised in the presence of the membrane preparation is in progress. If the longer DNA molecule contains the same information as the viral RNA faithfully represented in the same proportion, such radioactive molecules will provide 'superior probes' in studies of viral gene expression in infected cells.

L. C. PADHY
S. K. KAR
K. K. RAO*
M. R. DAS

Tata Institute of Fundamental Research,
Bombay 400 005, India

Received April 2, accepted July 5, 1976.

*On deputation from Bhabha Atomic Research Centre, Trombay, Bombay 400 085.

1 Temin, H M., and Baltimore, D., *Adv Virus Res.*, 17, 129–186 (1972).
2 Mizutani, S , and Temin, H M., *Cold Spring Harb. Symp. quant. Biol*, 35, 847–849 (1970).
3 Gillespie, D , Saxinger, W C., and Gallo, R. C., *Prog. Nucleic Acids Res. Molec. Biol.*, 15, 1–108 (1975).
4 Junghuns, R. P , Duesberg, P. H , and Knight, C A., *Proc. natn. Acad. Sci. U.S.A* , 72, 4895–4899 (1975).
5 Hatanaka, M , Kakefuda, T., Gilden, R V., and Callan, E. A. O., *Proc natn. Acad. Sci U S.A.*, 68, 1844–1847 (1971).
6 Takano, T., and Hatanaka, M., *Proc natn. Acad Sci U.S A.*, 72, 343–347 (1975).
7 Hung, P P , and Lee, S G., *Nature*, 259. 499–502 (1976)
8 Emmelot, P , Bos, C. J , van Hoeven, R P., and van Blitterswijk, W J., in *Methods in Enzymology*, 31 (edit. by Fleischer, S., and Packer, L.), 75–90 (Academic, New York, 1974).
9 Warren, L., and Glick, M C , in *Fundamental Techniques in Virology* (edit. by Habel, K., and Salzman, N. P), 66–71 (Academic, New York, 1969)
10 Perdue, J. F , and Sneider, J., *Biochim. biophys Acta*, 196, 125–140 (1970).
11 Post, R L., and Sen, A. K , in *Methods in Enzymology*, 10 (edit. by Estabrook, R. W., and Pullman, M E.), 762–768 (Academic, New York, 1967)
12 Morre, D J , in *Methods in Enzymology*, 22 (edit by Jakoby, W. B.), 137–138 (Academic, New York, 1967).
13 Malamy, M , and Horecker, B. L , in *Methods in Enzymology*, 9 (edit by Wood, W A.), 639–642 (Academic, New York, 1966)
14 King, T. E., in *Methods in Enzymology*, 10 (edit. by Estabrook, R. W., and Pullman, M E), 322–331 (Academic, New York, 1967).
15 Pennington, R J., *Biochem J.*, 80, 649–654 (1961)
16 Das, M R., Sadasivan, E , Koshy, R., Vaidya, A. B , and Sirsat, S M , *Nature new Biol.*, 239, 92–95 (1972).

Ion effects on macromolecules in aqueous solution

APART from their nonspecific electrostatic interactions, ions can produce specific effects on the conformation and solubility of macromolecules in aqueous solution[1]. The relative effectiveness of anions and cations in altering macromolecular configurations is remarkably independent of the nature of the macromolecule and is generally referred to as the lyotropic or Hofmeister series. To explain the generality of the effects, the influence of the ions on the structure of the solvent has often been invoked, but as yet no theory has been able to link satisfactorily ion–water interactions with the effects of ions on macromolecules. We argue here that it is the effect of the ions on the empty volume of the solvent which underlies the Hofmeister series and we derive a simple thermodynamic equation which accounts for the effect of a salt on the transition temperature for a polymer chain aggregation process. To test the equation we have taken data from the literature relating to the cloud point of polyvinylmethylether (PVME; intermolecular aggregation); and to the thermal transition temperature of ribonuclease (intramolecular aggregation).

Aqueous solutions of PVME have a lower critical solution temperature or cloud point (T_c) at 34 °C—that is, above this temperature two immiscible phases are formed, one of which contains almost all the polymer in an aggregated form. On cooling the change is reversed but redissolution of the polymer is slow. Horne *et al.*[2] studied the effect of a number of salts on T_c and found that it could be either raised or lowered according

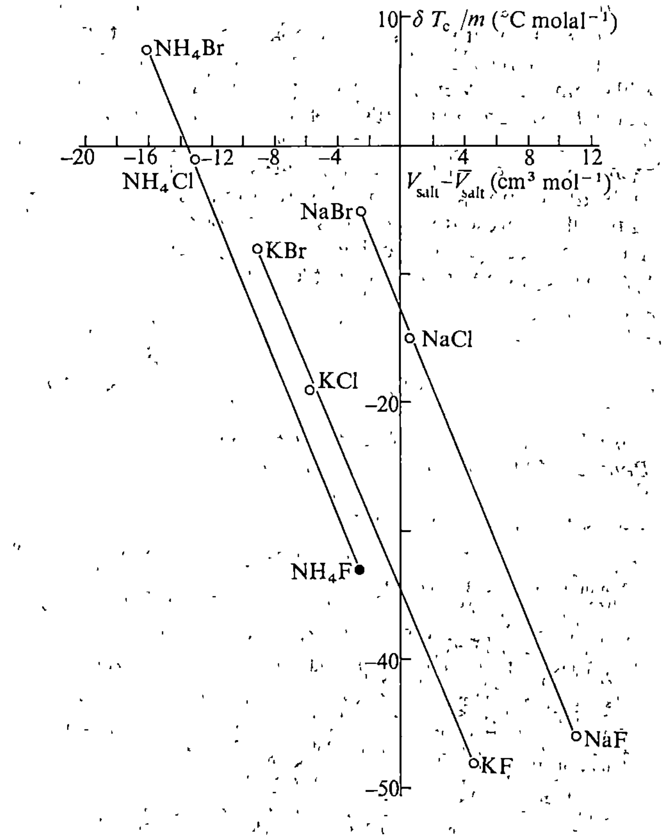

Fig. 1 Salt effects on T_c of a 2.5 weight % aqueous solution of PVME. ○, Ref. 2; ●, present work.

to the particular salt added and that often the change was approximately linear with salt concentration. Similarly, it has been shown that the temperature (T_m) of the midpoint of a cooperative transition involving the unfolding of the native ribonuclease molecule can be shifted up or down, often approximately linearly by increasing concentrations of neutral salts[3,4]. In both cases the rank order of molar effectiveness follows the Hofmeister series.

At either T_c or T_m we can write an equilibrium: dissolved polymer segments ⇆ aggregated polymer segments. The transfer from the dissolved to the aggregated state in water at a pressure P will involve changes in the partial molal internal energy ($\bar{U}$), volume ($\bar{V}$) and entropy ($\bar{S}$) of the polymer segments, which will be related to the transition temperatures by

$$T_{c,m} = (\Delta\bar{U} + P\Delta\bar{V})/\Delta\bar{S} \qquad (1)$$

For a salt solution in which $\Delta\bar{S}$ remains unaffected, the change in the transition temperature will be given by

$$\delta T_{c,m} = (\delta\Delta\bar{U} + P\delta\Delta\bar{V})/\Delta\bar{S} \qquad (2)$$

We shall neglect the temperature dependence of the partial molal quantities over the range $T_{c,m}$ to $T_{c,m}+\delta T_{c,m}$ and assume that $\delta T_{c,m}$ is solely determined by the salt effect. To calculate $\delta\Delta\bar{V}$ we consider the empty volume which exists in the solvent and which is defined by: observed volume − van der Waals' volume of the molecules[5]. Because of its hydrogen-bonded structure, water is exceptional in having a very large empty volume (about 46%), and Bernal and Fowler[6] pointed out that the main contribution to the volume change associated with the solution of ions arises from the collapse of this structure. If the polymer can utilise the voids in the solvent, we can write

$$-\delta\Delta\bar{V} = V_e(\text{water}) - V_e(\text{soln}) \qquad (3)$$

where V_e(water) is the empty volume existing in the volume of water containing 1 mole of transferring segments and V_e(soln) is the corresponding volume in the salt solution. By considering the transfer of a mole of segments from 1 kg water to 1 kg water + m moles of salt at a given temperature an expression for $\delta\Delta\bar{V}$ in terms of salt concentration can easily be obtained since

$$V = V_e(\text{water}) + 55.5\, V_{H_2O} \qquad (4)$$

$$m\bar{V}_{salt} + 55.5\,\bar{V}_{water} = m\,V_{salt} + V_e(\text{soln}) + 55.5\,V_{H_2O} \qquad (5)$$

where V is the observed volume of water, V_{H_2O} and V_{salt} are molar van der Waals' volumes, and $\bar{V}_{salt}$ and $\bar{V}_{water}$ are partial molal volumes. Subtracting (5) from (4) gives

$$V_e(\text{water}) - V_e(\text{soln}) = m(V_{salt} - \bar{V}_{salt}) + (V - 55.5\,\bar{V}_{water}) \qquad (6)$$

In dilute solutions $V \simeq 55.5\,\bar{V}_{water}$, so that

$$-\delta\Delta\bar{V} = m(V_{salt} - \bar{V}_{salt}) \qquad (7)$$

Any change in $\Delta\bar{U}$ brought about by the presence of ions is likely to be due to weak binding of ions to sites on the dissolved segments, and if a Langmuir-type isotherm[7] is followed we can expect $\delta\Delta\bar{U}$ to be a linear function of m, so that finally we obtain

$$\frac{\delta T_{c,m}}{m} = \frac{(\delta\Delta\bar{U} - P(V_{salt} - \bar{V}_{salt}))}{\Delta\bar{S}} \qquad (8)$$

Figure 1 shows a plot of $\delta T_c/m$ against $V_{salt} - \bar{V}_{salt}$ for the effect of sodium, potassium and ammonium halides on the PVME T_c. With the exception of NH$_4$Br, these salts have approximately constant values of $\delta T_c/m$ up to 1 M concentration. In the case of NH$_4$Br an initial slope was estimated from the curved T_c against salt concentration graph in ref. 2. V_{salt} values were calculated from Pauling ionic radii[8] and

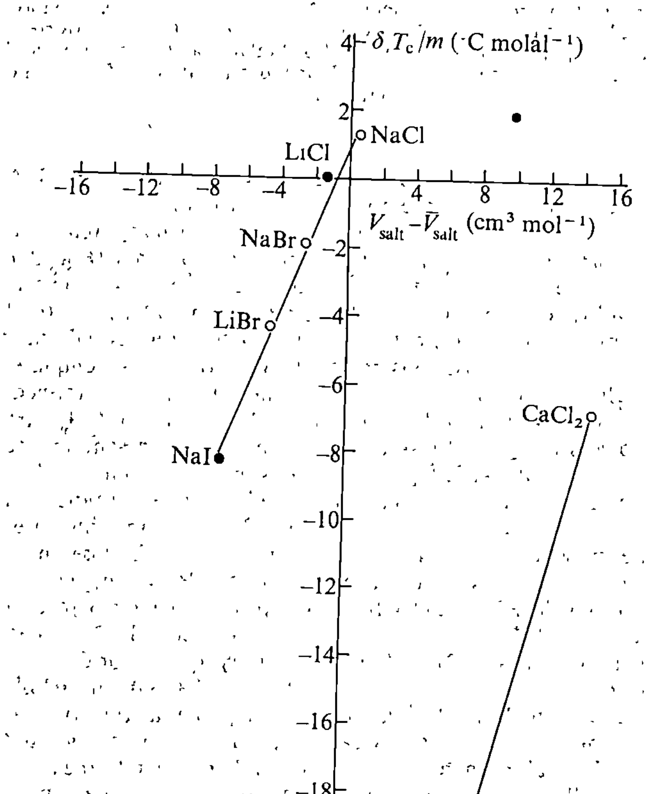

Fig. 2 Salt effects on the thermal denaturation of ribonuclease in aqueous solution. ○, Ref. 3; ●, ref. 4.

$\bar{V}_{\text{salt}}$ values at infinite dilution and 25 °C were taken from a compilation by Millero[9]. The resulting points fall on three parallel lines, one line for each series of anions with a common cation. This justifies the assumption of constant $\Delta\bar{S}$ and implies that $\delta\Delta\bar{V}$ is dictated by both the cation and anion of a particular salt but that $\delta\Delta\bar{U}$ only depends on the cation. The different intercepts on the $\delta T_c/m$ axis may be interpreted in terms of a greater tendency to ion binding in the order $NH_4^+ < K^+ < Na^+$.

Figure 2 shows a similar plot for the effect of seven salts on the ribonuclease transition. A similar picture is obtained except that the lines have positive slopes because the aggregation process is favoured at low temperatures. Lithium and sodium salts give almost the same positive intercept on the $\delta T_m/m$ axis, whereas the calcium salts have a large negative intercept. Bearing in mind that $\Delta\bar{S}$ is now negative, this can be understood on the basis of a relative binding strength for sites on the protein in the order Na^+, $Li^+ < H_2O < Ca^{2+}$. If this interpretation is correct and if this type of plot proves to be general for other ions and macromolecules, the above approach could provide a useful method for separating solvent effects from ion-binding effects. If the interpretation is incorrect, then the interesting empirical observation of common cation lines requires explanation.

M. J. HEY
J. M. CLOUGH
D. J. TAYLOR

Department of Chemistry,
The University,
Nottingham NG7 2RD, UK

Received May 13; accepted July 7, 1976.

[1] von Hippel, P. H., and Schleich, T., in *Structure and Stability of Biological Macromolecules* (edit. by Timasheff, S. N., and Fasman, G. D.), ch. 6, 417–574 (Dekker, New York, 1969).
[2] Horne, R. A., Almeida, J. P., Day, A. F., and Yu, N-T., *J. Colloid Interface Sci.*, **35**, 77–84 (1971).
[3] von Hippel, P. H., and Wong, K. Y., *J. biol. Chem.*, **240**, 3909–3923 (1965).
[4] Schrier, E. E., and Schrier, E. B., *J. phys. Chem.*, **71**, 1851–1860 (1967).
[5] Bondi, A., *J. phys. Chem.*, **58**, 929–939 (1954).
[6] Bernal, J. D., and Fowler, R. H., *J. chem. Phys.*, **1**, 515–548 (1933).
[7] Tanford, C., in *Physical Chemistry of Macromolecules*, ch. 8, 526–586 (Wiley, New York, 1961).
[8] Cotton, F. A., and Wilkinson, G., in *Advanced Inorganic Chemistry*, third ed. ch. 2, 52 (Interscience, New York, 1972).
[9] Millero, F. J., *Chem. Rev.*, **71**, 147–176 (1971).

Structural order in chromatophore membranes of *Rhodospirillum rubrum*

STRUCTURAL studies of the purple membranes of *Halobacterium halobium*[1–4] have raised the question of whether the in-plane structural order is an exceptional feature of very limited biomembranes or whether it is somewhat more common. We have found that the structural order exists in the chromatophores of *Rhodospirillum rubrum* and *Rhodopseudomonas spheroides* and the outer membranes of *Salmonella typhimurium*, although extension of the order is limited compared with purple membranes. The present paper reports our results concerning the chromatophores of *R. rubrum*.

Chromatophores were prepared from the carotenoid-deficient blue-green mutant (*G-9*) of *R. rubrum* by grinding cells with aluminum oxide[5], a mild treatment used to isolate chromatophores. Oda and Horio[6] have reported that the chromatophores are vesicles with a diameter of 400–800 Å. Our electron microscopic observations have supported their results. According to Kakuno *et al.*[7], the chromatophore membrane consists mainly of proteins and lipids, the weight ratios of protein, phospholipid, bacteriochlorophyll and ubiquinones being 1.00 : 0.24 : 0.04 : 0.03. Major protein components are those which have been termed structural proteins by Kakuno *et al.*[7], and have the molecular weights of 13,000 and 27,000, respectively. The population of the former is about twice the latter (T. Kakuno and T. Horio, personal communication).

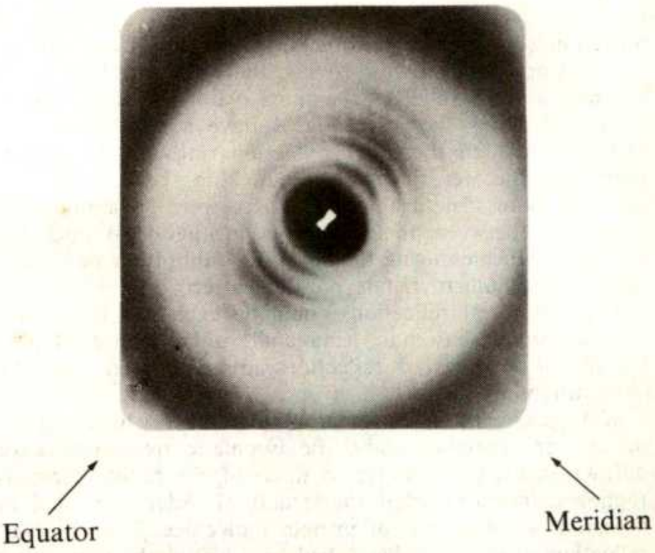

Fig. 1 X-ray diffraction pattern for a dried specimen of chromatophores obtained by grinding cells with aluminium oxide. Specimen-to-film distance 69.3 mm. Exposure time 44 h. See text for equator and meridian.

Pellets of chromatophores were prepared by centrifugation (for example, at 100,000*g* for 1 h). Two kinds of specimens were used for X-ray studies: wet pellets which were a dispersion of chromatophores in the solution of 0.1 M Tris-HCl buffer (*p*H 8.0); and dried specimens which were prepared by placing the wet pellets on a freshly cleaved mica surface, maintained at about 5 °C in a refrigerator for more than 2 d. Strips were then cut off from the dried matter. Each specimen was sealed in a thin-walled glass capillary and its temperature maintained at 4 °C for X-ray exposure. A Rigaku rotating-anode microfocus generator (RU-3HM) was used with a copper target, of which the effective focal spot was 100×100 μm^2. The camera used was of the Elliott point-focusing type[8] with a set of double-sector apertures. X-ray diffraction patterns were recorded on Fuji medical X-ray film KX.

All the wet specimens gave diffraction patterns consisting of a series of distinct diffraction rings in the region of the spacing d of $6\ \text{Å} < d < 22\ \text{Å}$ and a sharp ring at $d = 4.16$ Å, indicating crystalline packing of hydrocarbon chains in the membranes. All the dried specimens gave diffraction patterns as shown in Fig. 1, when the incident beam was parallel to the plane attached to the mica plate. We have termed the direction parallel to this plane equator and the

Table 1 Observed and calculated spacings *d* for equatorial reflections

h, *k*	*d* calc (Å)	*d* obs (Å)
0, 1	36.9	—
1, 1	21.3	—
0, 2	18.4	17.9
1, 2	13.9	14.1
0, 3	12.3	12.4
2, 2	10.6	10.5
1, 3	10.2	—
0, 4	9.2	9.4
2, 3	8.5	8.4
1, 4	8.1	—
0, 5	7.4	7.4

Period of 42.6 Å was used for calculations.
h, *k*, Miller indices.

perpendicular direction meridian. In Fig. 1 the 4.16Å reflection (clearly seen on the original film) came out as an equatorial reflection, proving that the membranes lie approximately parallel to the mica plate. The inner equatorial reflections shown in Fig. 1 have a one-to-one correspondence with the inner reflection rings on the photographs of the wet specimens, indicating the existence of some in-plane structural order. There were no appreciable differences between their spacings in the dried and wet specimens. In measuring the spacings, calibration was made using the sodium myristate powder pattern.

The equatorial reflections could be explained by assuming a two-dimensional hexagonal unit cell $a=42.6$Å. Calculated spacings of reflections are compared with the observations in Table 1.

Wet specimens of chromatophores from which ubiquinones were removed using the isooctane treatment[9] gave diffraction patterns similar to those of the native chromatophores, indicating that the structural order is related to a regular arrangement of protein molecules. The observed reflections listed in Table 1 had broader widths than those of the purple membranes of *H. halobium* measured with the same camera, implying that the structural order extends only in a limited area of the chromatophore. On the assumption that the protein molecules form small two-dimensional crystalline clusters, the observed line width gave the diameter of the cluster as being about 120Å, roughly three times the lattice constant *a*, on the basis of Scherrer's formula.

Dried specimens gave several meridional reflections as seen in Fig. 1. Six meridional reflections were observed for the native chromatophores and eight for the ubiquinone-deficient chromatophores. In the latter case the eight were indexed approximately by assuming a lamellar stacking of membranes with a period of 155 Å, with reasonable accuracy up to the fourth-order reflection; such an indexing was not successful for the native chromatophores. In addition to these, there was an off-meridional reflection with a spacing of 37 Å in both cases. The lamellar reflections and the period of 155 Å suggest that the chromatophores are flattened in the dried specimens, since a thickness for the membrane of 155 Å/2=76 Å is plausible.

Similar diffraction patterns indicating structural orders have been found in the chromatophores of *Rps. spheroides* and the outer membrane of *S. typhimurium*. A dried specimen of the former also exhibited lamellar reflections as in the case of *R. rubrum*. Further investigations are in progress.

We thank Professor T. Horio for discussions; and Mr G. Soe and Miss K. Sakata for preparation of chromatophores.

TATZUO UEKI
MIKIO KATAOKA
TOSHIO MITSUI

Department of Biophysical Engineering,
Faculty of Engineering Science,
Osaka University,
Toyonaka, Osaka 560, Japan

Received June 22; accepted July 7, 1976.

[1] Blaurock, A. E., and Stoeckenius, W., *Nature new Biol.*, **233**, 152–155 (1971).
[2] Henderson, R., *J. molec. Biol.*, **93**, 123–138 (1975).
[3] Blaurock, A. E., *J. molec. Biol.*, **93**, 139–158 (1975).
[4] Unwin, P. N. T., and Henderson, R., *J. molec. Biol.*, **94**, 425–440 (1975).
[5] Horio, T., Nishikawa, K., Katsumata, M., and Yamashita, J., *Biochim. biophys. Acta*, **94**, 371–382 (1965).
[6] Oda, T., and Horio, T., *Expl Cell Res.*, **34**, 414–416 (1964).
[7] Kakuno, T., Bartsch, R. G., Nishikawa, K., and Horio, T., *J. Biochem.*, **70**, 79–94 (1971).
[8] Elliott, A., *J. Sci. Instrum.*, **42**, 312–316 (1965).
[9] Okayama, S., Yamamoto, N., Nishikawa, K., and Horio, T., *J. biol. Chem.*, **243**, 2995–2999 (1968).

Bacterial utilisation of organic matter in the deep sea

DISSOLVED organic carbon (DOC) in the deep sea is, after sedimentary humus, the largest reservoir of organic carbon in the hydrosphere. It is utilised primarily by heterotrophic bacteria, which over a long period, in steady-state conditions consume dissolved O_2 from the seawater and produce an equivalent amount of CO_2 by respiration. Knowledge of the rates of O_2 consumption (Table 1) and CO_2 production is useful for quantifying the mixing and circulation of deep-sea water through variations in its O_2 or natural radiocarbon content[1,2]. The aim of the work reported here was to determine the growth rate of a heterotrophic, low nutrient bacterium isolated from seawater collected at a depth of 2,000 m in the north-central Pacific Ocean (25°03′N, 154°53′W), and to equate this growth rate with O_2 consumption and utilisation of DOC.

We have determined the doubling time in batch culture for this low nutrient bacterium (referred to as 169 and able to grow well in unenriched seawater) in deep-sea water at 5, 13 and 20 °C and under 200 atmospheres of hydrostatic pressure (equivalent to a depth of 2,000 m). The doubling time was 260 h when normalised to the *in situ* temperature of 2 °C using the Arrhenius plot. This growth rate results in a maximum rate of O_2 consumption of 1.4 ml m^{-3} yr^{-1}, and is discussed in terms of the flux of organic and inorganic carbon between various carbon reservoirs in the deep sea.

The equation for determining bacterial respiration in steady-state conditions was

$$R\,(\mathrm{ml\,O_2\,m^{-3}\,yr^{-1}}) = \frac{1.6\times 10^{10} A(100-E)}{D},$$

$$(1\ \mathrm{ml\,O_2\,m^{-3}\,yr^{-1}}) = 0.44\ \mathrm{mg\,C\,m^{-3}\,yr^{-1}}$$

where R is respiration, A is biomass of synthesised microbial cell carbon (g), E is percentage of carbon assimilated, $100-E$ is percentage of carbon respired, and D is doubling time of microbial cells (h). The factor 1.6×10^{10} takes into account the normalisation of doubling times of hours to years, and conversion of g carbon to ml of O_2. A was calculated using the following expression

$$A = 10^{-13} NV$$

where N represents numbers of bacteria per l, V is volume of each bacterium (μm³), and 10^{-13} is the weight of one bacterium of volume 1 μm³ expressed as g of carbon. Each bacterium is assumed to be 80% water and 10% carbon. In our calculations, bacterial volumes were determined from many enumerations of bacteria in deep-sea samples, either by direct microscopy or with the scanning electron microscope (SEM). SEM observations were made on cells fixed *in situ*. We used cell volumes calculated for cocci (0.2 and 0.5 μm diameter) and rods (0.2×0.5 and 0.5×1.0 μm). Numbers of bacteria per l in the central Pacific Ocean deep water were obtained from two sources[4,7], and from our own observations. These values ranged from 10^6 to 10^7 l^{-1}.

The percentage of carbon assimilated (E) in the above equation is difficult to estimate for deep-sea bacteria *in situ*. Most terrestrial heterotrophic bacteria studied in the laboratory in enriched conditions show 10–20% efficiency. Sorokin[4] found that 40% and Jannasch[3] 95% of acetate added to seawater (100 and 2,000 mg l^{-1}, respectively) was assimilated by deep-sea bacterial populations.

To calculate R, we used combinations of the above cell volumes, and assumed that the carbon cycle in the deep sea, including bacteria, is in a steady state (otherwise, there would

Table 1 Utilisation of organic carbon in the deep sea

Method	Depth (km)	Location	DOC and/or POC utilisation (mg C m^{-3} yr^{-1})*
Calculated from a vertical diffusion[1] advection model	1–4	Central Pacific	About 1.8 (4.1)
Calculated from a vertical diffusion[2] advection model	1–4	South Pacific	About 0.67 (1.5)
In situ incubation with ^{14}C-labelled[3] substrates	5	North-east Atlantic	2–13 (4.6–29.6)
In situ incubation with ^{14}C-labelled[4] substrates	4	Western Pacific	11.2–33.6 (25.6–76.7)
O_2 uptake by electron transport[5] system	1–6	Eastern tropical Pacific	About 0.70 (1.6)
Adenosine triphosphate[6] content of cells	1–4	North-east Pacific	About 0.44 (1)
This report	2	North-central Pacific	0.04–0.61 (0.09–1.4)

Calculated and experimental values are given. Equivalent O_2 consumption rates are based on 1.0 ml O_2 consumed = 0.44 mg C utilised, assuming a C/N ratio by atoms of 10 in deep-sea DOC and POC.
*In parentheses: O_2 consumption (ml O_2 m^{-3} yr^{-1}).

be a net increase in biomass); we therefore assumed 100% of DOC to be respired; that is $E = 0$. The range of values for R obtained from these combinations was 0.09–1.4 ml O_2 m^{-3} yr^{-1} (0.04–0.61 mg C m^{-3} yr^{-1}). But from what seems to be the most reasonable assumptions for N and V (3.8×10^6 l^{-1} and 0.26 μm^3 respectively), a value of 1.4 ml O_2 m^{-3} yr^{-1} (0.61 mg C m^{-3} yr^{-1}) for R is the most realistic and represents the upper limit of R. In this calculation we treated all bacteria in the deep sea as growing in a manner similar to that of low nutrient bacteria. This is probably not true; some bacteria may be less, and some more active, than bacterium 169.

Previous *in situ* measurements of bacterial uptake of DOC[3,4] were based on high concentrations of added substrate and so may not be relevant to measurements of the actual activities of deep-sea bacteria. Because little is known of the chemical composition of the DOC in deep water, the estimates for utilisation of DOC we have obtained using the natural substrate are more appropriate for calculating organic carbon fluxes and rates of utilisation of O_2 in the deep sea than rates derived from experimental work with added substrates. The particular fraction of the DOC which is utilised by low nutrient bacteria may be organic material of a more labile nature than the 'old', refractory DOC constituting the bulk of the organic matter, but we cannot judge which fraction is utilised.

This determination of organic carbon utilisation, 0.61 mg C m^{-3} yr^{-1} (1.4 ml O_2 m^{-3} yr^{-1} consumed), may be used in a qualitative way to estimate the organic carbon balance at 2,000 m in the north-central Pacific. If we assume a steady state, ($-dDOC/dt = -dPOC/dt = -dO_2/dt = +dCO_2/dt = 0$), and concentrations of DOC (unpublished results from cruise Cato-1, Institute of Marine Resources, University of California, San Diego, June–July, 1972), POC, particulate organic carbon[8] and O_2 (ref. 9) of 450 mg m^{-3}, 3 mg m^{-3} and 1.7 l m^{-3}, respectively, then the residence time of DOC, POC and O_2 would be 738, 4.9, and 1,214 yr, respectively. This calculated DOC residence time of 738 yr is three to five times lower than the value of 2,600–3,500 yr determined by natural radiocarbon measurements of the DOC at 2,000 m in the north-east Pacific[10,11]. This suggests that R is less than 1.4 ml O_2 m^{-3} yr^{-1} and that the rate of utilisation of DOC is > 0.1 and < 0.5 mg C m^{-3} yr^{-1}. The POC would be utilised in ~ 5 yr if the entire microbial population is using POC and not DOC as a substrate. This is unlikely for two reasons: first, the percentage of attached, non-filterable bacteria compared with the free-living population is 25% or less[7], and second, the consumption of POC by bacteria during the estimated mean time of 2 yr it takes the POC to sink from 500 to 2,000 m (ref. 11) would be 1.22 mg C m^{-3} ($2R$). Such a rate of utilisation would require a gradient (decreasing concentration) of POC from 500 to 2,000 m. This is not observed in the north-central Pacific from 500 m to the bottom, where the concentration of POC is essentially invariant[8]. It thus seems that DOC is the main source of energy for the low nutrient, heterotrophic bacteria in the deep water of the north-central Pacific, and that the rate of utilisation of organic carbon or consumption of O_2 we have measured is of the same magnitude, and probably less, than earlier experimental estimates of a more indirect nature given in Table 1. Indeed, if the rates of O_2 consumption were much greater than 0.6 ml O_2 m^{-3} yr^{-1}, vast areas of the deep sea would be anoxic.

Finally, the results reported here support the validity of using vertical-diffusion, vertical-advection models[1,2] for calculating such non-conservative properties such as O_2 consumption and carbon utilisation in the deep sea.

We thank Ms S. L. Shimp for technical assistance. This work was supported by the ERDA.

P. M. Williams
A. F. Carlucci

Institute of Marine Resources,
University of California, San Diego,
La Jolla, California 92093

Received April 27; accepted July 14, 1976.

1 Munk, W. H., *Deep-Sea Res.*, **13**, 707–730 (1966).
2 Craig, H., *J. geophys. Res.*, **76**, 5078–5086 (1971).
3 Jannasch, H. W., Eimhjellen, K., Wirsen, C. O., and Farmanfarmaian, A., *Science*, **171**, 672–675 (1971).
4 Sorokin, Y. I., in *Proc. twentieth Nobel Symp.* (edit by Dryssen, D., and Tagner, D.), (Wiley–Interscience, New York and London, 1972).
5 Packard, T. T., Healy, M. L., and Richards, F. Q., *Limnol. Oceanogr.*, **16**, 60–70 (1971).
6 Holm-Hansen, O., and Paerl, H. W., *Mem. Ist. Ital. Idrobiol.*, **29**, Suppl., 149–168 (1972).
7 Taga, N., and Matsuda, O., in *Effect of the Ocean Environment on Microbial Activities* (edit. by Colwell, R., and Morita, R.), (University Park Press, Baltimore, London and Tokyo, 1974).
8 Gordon, D. C., *Deep-Sea Res.*, **18**, 1127–2234 (1971).
9 *Prelim. Data Rep. Geochemical Ocean Sections Study, Pacific Expedition, Leg I, Station 206, August–September, 1973* (Scripps Inst. Oceanogr., San Diego, 1974).
10 Williams, P. M., Oeschger, H., and Kinney, P. J., *Nature*, **224**, 256–258 (1969).
11 Arhelger, M. E., Kinney, P. J., Linick, T. W., and Williams, P. M., *Research on the Marine Food Chain*, AEC Progress Report, 363–389 (University of California, San Diego, 1974).

Circadian rhythm of anaerobiosis in a polychaete annelid

ALTHOUGH intertidal organisms which cannot breathe air must be regularly subjected to tidal conditions in which they must respire anaerobically, there are no known cases in which these or other animals reduce environmental conditions to the point at which they must respire anaerobically. Indeed such reduction of microhabitat conditions would not be expected because of the relative inefficiency of known anaerobic energy-generating pathways. This report describes a rhythm of alternating aerobic and anaerobic metabolism in the polychaete *Nereis virens*. The rhythm is circadian under low intensity constant illumination.

Burrows of *N. virens* are ventilated with undulatory movements of the body which serve to draw well-oxygenated water and food into the burrow. I have conducted long term monitoring of the ventilation rhythms of animals adapted to 10.0-ml synthetic burrows[1]. Individuals have been maintained in synthetic burrows in the laboratory for periods of up to 20 months. Ventilation activity was measured with a directly heated thermistor flowmeter inserted through the wall of the synthetic worm burrow and separated from the animal by a nylon screen[1].

Twelve individuals were tested in continual light (LL 12 : 12), eight individuals were tested in a light–dark regime of 12 h light and 12 h dark (LD 12 : 12), and six individuals were tested in continual darkness (DD 12 :12). A total of 325 d of continuous recording was obtained for the 26 animals tested. Both incadescent and fluorescent light sources were used, and light intensity was maintained at approximately 3,000 lx at the burrow. Before experimentation, all animals (5.0–6.0 g) were maintained on a daily cycle of 14 h light and 10 h darkness at 10±2 °C for 5–70 d. At the start of an experiment individuals in burrows were transferred to a 15-l tank (10 °C) which received a continuous flow of aerated seawater. The thermistor was inserted through the wall of the worm burrow near either end. Vibration and noise from activity in the laboratory were minimised. Several animals were tested in closed as well as open-system conditions to prevent possible influence of chemical time-cues from entering the seawater system.

Ventilation for each hour of each day was measured in relative volume units by determining the areas under the curves of the continuous activity records. Period lengths of ventilation rhythms were estimated using the periodogram procedure of Enright[2] which is particularly appropriate for serially correlated time series data. The experimental amplitudes for a series of computer-generated assumed period lengths are compared; the measure of amplitude is the standard deviation of the hourly means of activity (area under the activity records). The plot of amplitude estimates against the assumed period length is a periodogram, and the period value with a large amplitude represents the most likely correct period length for the observed function. All ventilation rhythms were analysed for likely period lengths from 3 to 33 h in 0.1-h increments.

Burrow $p\text{O}_2$ was monitored continuously with a 1.0-mm polarograph (IBC) during long term ventilation recordings. Burrow *p*H was monitored continuously with a combination microelectrode (Bolab) inserted through the wall. Levels of lactate in burrow water and tissue were determined enzymatically according to the appearance of NADH at 340 nm (ref. 3). In separate experiments groups of six worms were placed in 10-ml sealed burrows and sampled for either tissue lactate or burrow water lactate after a chosen period of forced burrow closure. Respiratory rates were determined separately for 22 individuals placed in air-saturated seawater (10 °C), after various periods of forced closure in 10-ml synthetic burrows.

While I have observed short term (3–20 min) cycling of ventilation and rest periods similar to those observed for other polychaetes[4–9], I have also observed longer rest periods (>1 h) superimposed on the short term irregular pattern. These long rest periods (up to 9 h) create anaerobic burrow conditions and appear in recordings only after 2–4 d. In conditions of constant illumination, the ventilation activity shows a circadian periodicity (Fig. 1*a* and *b*). While one of 12 animals tested in LL was aperiodic, the average observed period length was 21.3±s.d. 0.65 h and the average duration of rest periods >1 h was 3.85±2.4 h. While all animals tested in LD and DD were aperiodic (Fig. 1*c*–*f*),

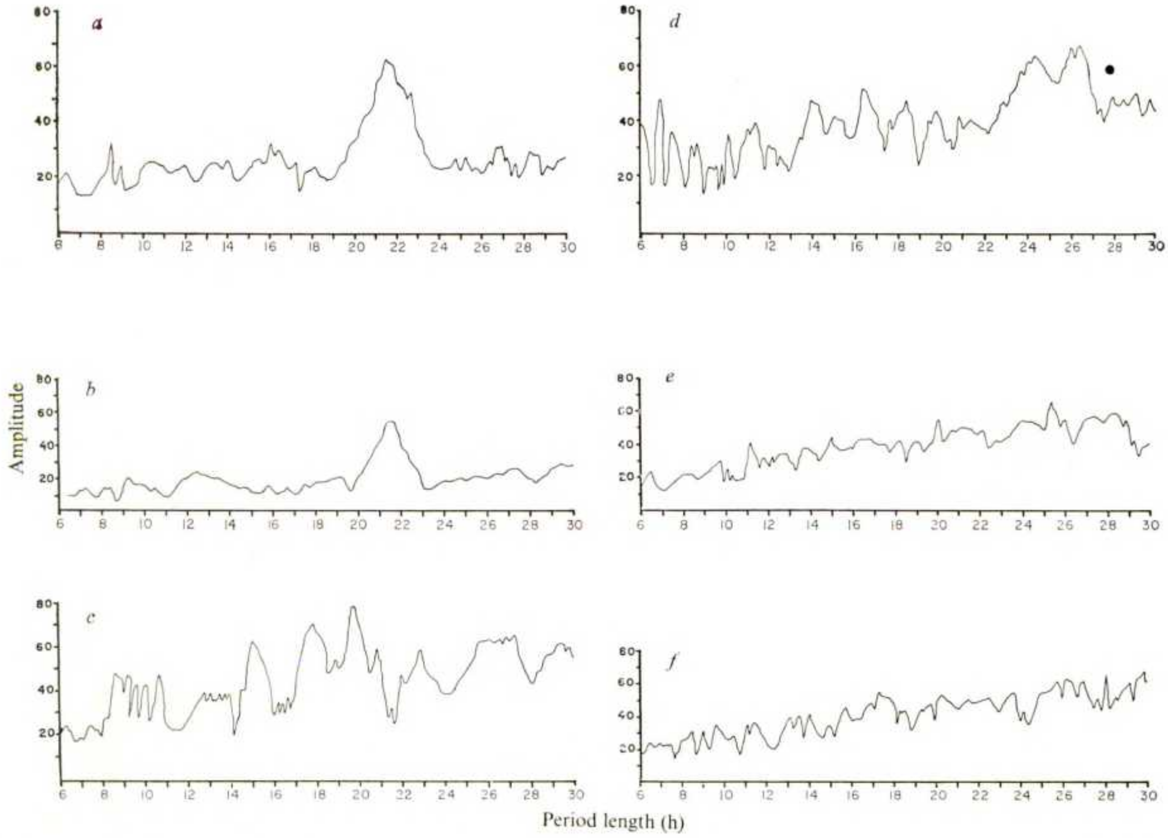

Fig. 1 Typical periodograms of burrow ventilation. *a*, *b*, Periodic anaerobiosis under constant illumination; *c*, *d*, aperiodic activity under light–dark cycle; *e*, *f*, aperiodic activity in constant darkness.

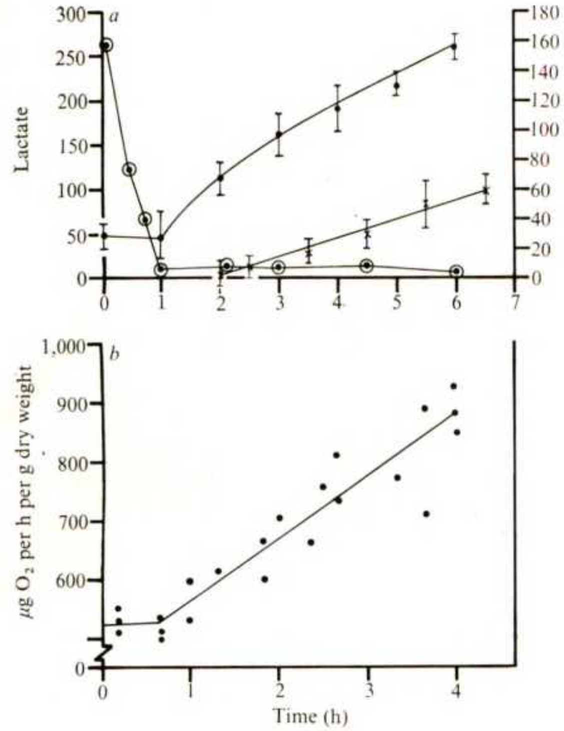

Fig. 2 *a*, Tissue lactate (●, μg per g wet tissue ± s.e., $n = 6$), burrow lactate (×, μg per ml burrow water ± s.e., $n = 6$), and pO_2 (circle and dot) as a function of length of rest period ($n = 8$). *b*, Maximum oxygen consumption following various lengths of rest periods ($n = 22$). Tissue lactate, burrow lactate and respiratory debt were determined for groups of six animals placed in sealed 10-ml burrows (10 °C) for predetermined times, since it was impractical to obtain tissue or water samples during the rest periods observed in the ventilation studies. The *p*H records obtained from burrows during spontaneous rest periods of the ventilation studies agree closely with those obtained at the end of the forced-closure experiments.

long rest periods were nevertheless observed in both of the latter conditions. The average lengths of rest periods >1 h in the LD and DD groups were 3.39 ± 1.45 and 3.13 ± 2.0 h, respectively. The frequencies of occurrence of rest periods >1 h varied for animals tested in LL, LD and DD and were 1.15 ± 0.21, 0.60 ± 0.14 and 0.52 ± 0.10 per d, respectively. Furthermore, the DD group spent an average of 71% of each day involved in ventilation activity while the LL and LD groups averaged 21 and 35%, respectively.

Measurements of oxygen consumption, lactate and *p*H within the polychaete burrow indicate that during rest periods, the worms respire anaerobically, accumulate small amounts of lactic acid and later pay an oxygen debt.

At a burrow oxygen tension of 5–10 mmHg (10 °C), detectable aerobic respiration ceased and presumably there was a switch to anaerobic pathways. Lactate appeared in the sealed burrow after a 2-h rest period and reached 92 $\mu g\,ml^{-1}$ after 6.5 h (Fig. 2*a*). Increased tissue lactate levels were evident after about 1 h, which is approximately the time required to reduce the burrow pO_2 to 5–10 mmHg, and reached approximately 260 μg per g wet tissue after 6 h. When a rest period ended and the burrow was again ventilated, the oxygen debt was repaid in part, as indicated by increased respiratory rates (Fig. 2*b*), which were directly related to the length of the period of forced closure.

Continuous monitoring of burrow *p*H during ventilation studies showed that burrow acidity was a function of the length of the rest period, with *p*H on one occasion reaching a low value of 5.97 after 8.2 h of rest. Organic acids other than carbonic and lactic must account for such observed depressions in *p*H because, in theory, *p*H could be reduced only from 8.1 to about 7.0 by animal respiration.

In summary, *N. virens* seems to cease burrow ventilation for periods of up to 9 h during which respiration continues anaerobically and the worms accumulate lactic and other organic acids. It is doubtful that the vascular haemoglobin serves an oxygen storage function during extended tidal exposure[5].

Newell[10] has suggested that temperature-independent resting metabolism (O_2 consumption) is associated more often with animals found intertidally than with those found subtidally, although two polychaete species have resting metabolic rates that are temperature dependent[11]. The observation of a spontaneous creation of anaerobic burrow conditions is important since normal rest metabolism of many invertebrates may include a significant non-oxidative component involving accumulation of lactate or other partially oxidised products of the Embden–Meyerhoff pathway. Any function of the observed periods of anaerobiosis, as well as the role of low intensity illumination in synchronising the anaerobic periods is as yet unknown.

It is interesting that the bivalve *Arctica islandica* has been shown to burrow aperiodically into sediments and respire anaerobically[12].

I thank A. H. Price, II and S. Kraul for review of the manuscript. This work was supported in part by NOAA Office of Sea Grant.

DANA M. SCOTT

Department of Oceanography,
University of Maine,
Walpole, Maine 04573

Received May 4; accepted July 6, 1976.

[1] Scott, D. M., *et al.*, *Comp. Biochem. Physiol.*, **53A**, 65 (1976).
[2] Enright, J. T., in *Circadian Clocks* (edit. by Aschoff, J.), 31 (North Holland, Amsterdam, 1965).
[3] Hohorst, H. J., in *Methods of Enzymatic Analysis*, **2** (edit. by Bergmeyer, H. U.), 1425 (1970).
[4] Lindroth, A., *Zool. Bidr, Uppsala*, **17**, 367 (1938).
[5] Economides, A. P., and Wells, R. M. G., *Comp. Biochem. Physiol.*, **51**, 219 (1975).
[6] Mangum, C. P., *Comp. Biochem. Physiol.*, **11**, 239 (1964).
[7] Mangum, C. P., *et al.*, *Mar. Biol.*, **2**, 128 (1968).
[8] Mangum, C. P., and Miyamoto, D. M., *Mar. Biol.*, **7**, 7 (1970).
[9] Dales, R. P., *et al.*, *J. mar. Biol. Ass. U.K.*, **50**, 365 (1970).
[10] Newell, R. C., *Biology of Intertidal Animals*, 404 (American Elsevier, New York, 1970).
[11] Mangum, C. P., and Sassaman, C., *Comp. Biochem. Physiol.*, **30**, 111 (1969).
[12] Taylor, A. C., *J. mar. Biol. Ass. U.K.*, **56**, 95 (1976).

Plutonium isotope ratios in polychaete worms

WE have noted with interest recent reports which suggest a preferential biological availability of ^{238}Pu over $^{239+240}$Pu in terrestrial and aquatic organisms[1–4]. Although kinetic isotope effects do occur in biological systems for low mass number elements (H, C, N), such effects are generally discounted as the mass number of the element increases. Thus, differential biological availability of isotopes of high mass number elements, such as plutonium, would normally be attributed to differences in the chemical or physical forms of the isotopes or to the different weights of isotope available to organisms as a result of large differences in their specific activities. These arguments have indeed been used to explain differential plutonium isotope behaviour in animals in controlled laboratory conditions[5–7]. It is not certain, however, that the same arguments can be used to explain anomalies of plutonium isotope behaviour in organisms contaminated by nuclear test debris or by wastes from nuclear fuel reprocessing plants. Plutonium activity levels, while easily measurable, do not approach those generally used in laboratory studies. In addition, geochemical weathering could conceivably alter any original differences in physical or chemical form of the plutonium. We report here the results of experiments which show that deposit-feeding marine worms living in sediments contaminated with plutonium isotopes in different ways do not preferentially accumulate ^{238}Pu over $^{239+240}$Pu. This is particularly significant in that the worms held in sediments contaminated in the natural environment may have been exposed to different chemical and physical forms of plutonium isotopes.

Table 1 Plutonium isotope ratios in polychaete worms and sediment

Sediment sample	Mean ^{238}Pu/$^{239+240}$Pu ratios	
	Worms	Sediment
Mediterranean	0.0076 ± 0.0030 (4)	0.0082 ± 0.0006 (5)
Bravo Crater	0.10 ± 0.02 (4)	0.082 ± 0.004 (5)
Windscale	0.25 ± 0.04 (3)	0.231 ± 0.004 (4)

Errors associated with the ratios are propagated at the 2σ confidence interval. Numbers in parentheses indicate number of samples used in calculating mean ratio.

We exposed polychaete worms (*Nereis diversicolor*) to laboratory-labelled sediment, sediment collected from a former weapons test site and sediment contaminated by wastes from a nuclear fuel reprocessing plant, in an attempt to observe any preferential uptake of ^{238}Pu over $^{239+240}$Pu. To prepare our laboratory-labelled sediment, we added 91 nCi of $^{239+240}$Pu (containing trace amounts of ^{238}Pu) in either the +4 or +6 oxidation state to 1 l of Millipore-filtered (0.45 µm) Mediterranean seawater with constant stirring. Some 200 ml of Mediterranean sediment was then introduced into the seawater and the slurry was allowed to mix for 2 d. After settling, the seawater was decanted and several fresh seawater washes were performed to remove any plutonium not bound to the sediments. A portion of a core sample (23–49 cm deep) collected from Bravo Crater at Bikini atoll and several hundred grams of surface sediment collected from the Irish Sea near the Windscale fuels reprocessing plant on the Cumbrian coast were equilibrated for several days with filtered Mediterranean seawater in a manner identical to that of our laboratory-labelled sediment. Aliquots of all sediment samples had easily measurable quantities of ^{238}Pu and $^{239+240}$Pu ($\sim 2\times10^4\times$ higher than fallout levels in coastal ocean sediments for the lowest activity sample) and homogeneity was good. Since the Bravo Crater sediment was contaminated as the result of testing a large thermonuclear device (1954) we tested the homogeneity of plutonium isotopes further by leaching an aliquot of the sample with a dilute solution of EDTA at *p*H 3 and determined the ^{238}Pu/$^{239+240}$Pu ratio in portions of the leachate with time. No differences in isotope ratios were observed, suggesting that both small and large particles of the sediment were homogeneous with respect to both isotopes.

Worms introduced into the sediments were allowed to accumulate plutonium for between 5 and 40 d. At prescribed times during this interval, 5 to 31 individuals were removed from the sediments, rinsed several times in clean seawater and placed in uncontaminated Mediterranean sediments for 24 h, where they were allowed to void their gut contents by ingesting sediment. Finally, all sediment was removed from the organisms by placing them on a mat of wet algae for a further 24 h. Radiochemical analyses of both worms and sediment were accomplished by standard techniques[9] designed to ensure the radiochemical purity of the separated plutonium. Isotope ratios were determined by α-spectrometric techniques.

Table 1 sets out the results of the isotope ratios observed in the worms and the sediments to which they were exposed. Since no significant differences in isotope ratios were observed in worms killed at different times (5, 9, 15, 25, 40 d), we have averaged all results for each sediment type. The somewhat unsatisfyingly large error terms associated with the Mediterranean and Bikini worm samples result from the extremely low levels of plutonium ultimately taken up by these organisms[9] and the low initial ^{238}Pu/$^{239+240}$Pu ratio in the sediments. Counting times for many samples approached 10 d.

Our results indicate that at least for the polychaete worms studied, no preferential uptake of ^{238}Pu over $^{239+240}$Pu occurs whether the sediment is labelled with known chemical forms of plutonium or whether the sediments contain plutonium from aged nuclear test debris or plutonium from fuel reprocessing wastes. This is in contrast to the near twofold magnification of ^{238}Pu over $^{239+240}$Pu observed between plants and organisms with respect to sediment in a freshwater ecosystem contaminated by nuclear fuel processing wastes[4] and the near 20-fold magnification observed between rodent tissue and soil in a terrestrial landscape contaminated by fallout[2]. Although the reasons for these disparities await clarification, general statements regarding preferential bioavailability of ^{238}Pu over $^{239+240}$Pu after its introduction into different ecosystems should be viewed cautiously. It is moreover worth emphasising that naturally occurring α-emitting radionuclides can follow plutonium in any radiochemical separation scheme, and unless scrupulous attention is paid to the radiochemical purity of the plutonium isolation technique, erroneous values for ^{238}Pu can result[8]. Clearly, such considerations become important for environmental samples where plutonium activity levels are low.

We thank N. Mitchell and F. Lowman for samples and V. T. Bowen for suggesting the EDTA leach experiment. The International Laboratory of Marine Radioactivity operates under a tripartite agreement between the International Atomic Energy Agency, the Government of the Principality of Monaco and the Oceanographic Institute at Monaco. Support for this work is gratefully acknowledged.

THOMAS M. BEASLEY
SCOTT W. FOWLER

International Laboratory of Marine Radioactivity,
Musée Océanographique,
Principality of Monaco

Received May 4; accepted July 7, 1976.

[1] Volchok, H. L., *et al.*, in *Assessing Potential Ocean Pollutants*, 27–63 (National Academy of Sciences, Washington DC, 1975).
[2] Hakonson, T. E., and Johnson, L. J., LA-UR-73-1291, 1–6 (Los Alamos Scientific Laboratory, 1973).
[3] Emery, R. M., Klopher, D. C., and Weimer, W. C., BNWL-1867, UC-48, 1–76 (Battelle Pacific North-west Laboratory, 1974).
[4] Emery, R. M., and Garland, T. R., BNWL-1879, UC-48, 1–26 (Battelle Pacific North-west Laboratory, 1974).
[5] Thompson, R. C., in *Plutonium Handbook: A Guide to the Technology* (edit. by Wick, O. J.), 785–829 (Gordon and Breach, New York, 1967).
[6] Mahlum, D. D., and Sikov, M. R., *Hlth Phys.*, **17**, 346–347 (1969).
[7] Bair, W. J., Willard, D. H., Nelson, I. C., and Case, A. C., *Hlth Phys.*, **27**, 392–396 (1974).
[8] Noshkin, V. E., Bowen, V. T., Wong, K. M., and Burke, J. C., in *Proc. third natn. Symp. Radioecol*, CONF-710501-P2, 681–688 (1971).
[9] Beasley, T. M., and Fowler, S. W., in *Acct int. Lab. mar. Radoiact. Tech. Rep., Monaco* (in the press).

Occurrence of plutonium and americium in plaice from the north-eastern Irish Sea

SMALL amounts of transuranic nuclides are discharged routinely into the north-eastern Irish Sea from the nuclear fuel element reprocessing plant at Windscale, Cumbria. Regular monitoring of the marine environment, as part of the established control procedure is made by the Ministry of Agriculture, Fisheries and Food[1,2], primarily to ensure the radiological safety of the discharges in public health terms. Data on the partitioning of plutonium and americium between seawater, suspended material and sediment have already been published[2,3] and the purpose of this communication is to present a preliminary report of these radionuclides in the plaice (*Pleuronectes platessa*). This is a demersal fish of commercial importance in the area and the critical material for discharges of transuranic nuclides. There are few published data on the concentrations of plutonium in marine fish[4] and no data for americium have been reported.

During 1975 four catches of plaice were made approximately 5 km south of the pipeline. Thirty fish—principally group III, 25–30 cm long—were selected from each catch and their dissected organs were bulked and ashed. Analysis for the plutonium isotopes was based on the method of Wong[5] except that concentration was obtained initially by coprecipitation on calcium oxalate and subsequently on neodymium hydroxide. Separation of americium from plutonium, and purification of the latter, was effected by anion exchange from a hydrochloric acid medium. The americium was separated from lanthanides by anion exchange at 80 °C using ammonium thiocyanate. Both

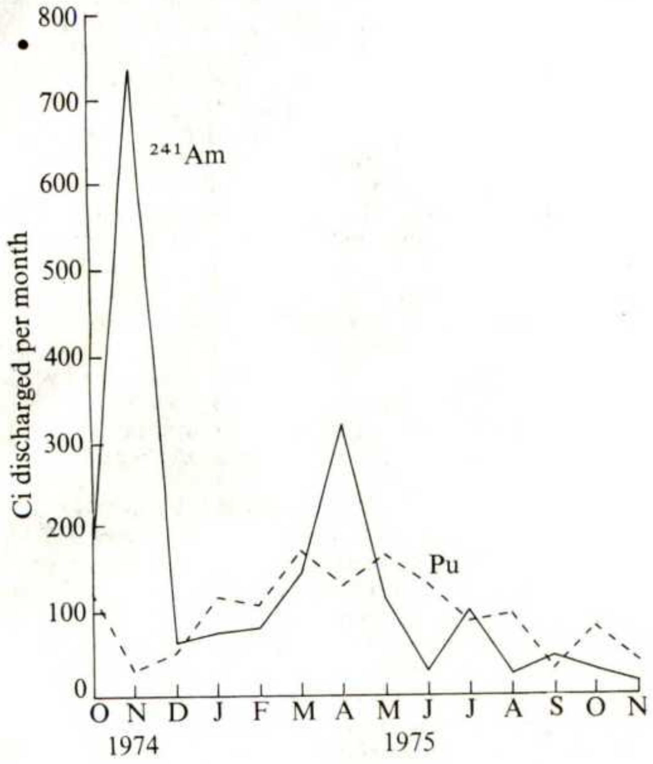

Fig. 1 Monthly discharges of ^{238}Pu, ^{239}Pu, ^{240}Pu and ^{241}Am from Windscale for the period October 1974–November 1975 (from returns made by British Nuclear Fuels Ltd).

plutonium and americium were electrodeposited from a slightly acid ammonium sulphate medium on to stainless steel disks. Radionuclide content was measured by α spectrometry using a 128-channel pulse height analyser and a silicon surface barrier detector (100 mm^2) to ensure adequate separation of the isotopes from the yield tracers ^{236}Pu and ^{243}Am. Chemical recoveries were > 70%. The results, ±2σ counting error, are given in Tables 1 and 2•

The highest concentration of plutonium in the internal organs of the fish collected in February was in the kidneys. Concentrations in the kidneys of fish caught later in the year, however, were exceeded by those in the gut. Plaice feed little during the winter and most of those caught in February were void of gut contents. The other three samples all contained various food species, consisting largely of *Amphiura filiformis*, which was particularly dominant in the sample collected in May, and several lamellibranchs including *Ensis ensis*, *Abra alba*, *Cultellus pellucidus* and *Nucula turgida*. Less frequent were *Nephthys*, *Pectinaria* and *Aphrodite*. The predominance of these species suggests that the fish had been feeding in an area of muddy sand, and not inshore of the pipeline[6]. It is interesting that although during the summer the food intake was greatly increased, and the discharges of plutonium were somewhat higher during the early summer (Fig. 1), neither the concentration of plutonium in the liver, nor that in the muscle, increased significantly. The concentrations in the gut wall, although higher in the samples taken after February, were about two orders of magnitude lower than the gut contents. Concentration by the gill was highest in the samples collected in May and August, although external contamination may have been variable in spite of their being well rinsed in clean water during dissection.

Table 2 ^{241}Am in organs of the plaice

Organ	Date of sample collection February 18, 1975	May 13, 1975	August 12, 1975	November 11, 1975
Kidney	440±50	103±15	65±5	120±14
Liver	590±120	186±29	35±6	54±6
Gut	160±20	89±14	114±22	122±17
Gut contents	930±600	6,600±540	4,940±270	7,390±36
Gill	210±60	128±23	310±40	89±7
Skin	20±8	15±2	6.2±2.8	11±0.9
Bone	110±50	33±9	28±6	2.1±0.5
Muscle	2.3±0.5	1.4±0.2	0.9±0.2	0.3±0.08

Results are expressed in fCi per g wet weight.

The concentrations of ^{241}Am in the internal organs were all generally higher than those of plutonium, the ratios being somewhat higher than those of the gut contents for May, August and November. The ^{241}Am data are also interesting in that the concentrations in kidney, liver, muscle and bone decreased markedly from February to August and may well have been influenced by the relatively large release during November 1974 (Fig. 1). It is not certain, however, that the fish sampled during the year have been taken from the same population.

Sufficient material was obtained from the fish in November to analyse gonad tissue. The bulked testis sample contained 0.64±0.3 fCi per g wet weight $^{239+240}$Pu and < 0.5 fCi per g wet weight ^{241}Am. In contrast, the ovaries contained 1.5±0.5 fCi per g wet weight $^{239+240}$Pu and 9.3±3.2 fCi per g wet weight ^{241}Am.

In view of the fluctuating discharges (Fig. 1) it is evident that a steady-state body burden will not exist for fish caught close to the pipeline. An accurate estimation of a concentration factor over seawater therefore cannot be made, and would in any case depend on the location of the seawater sample and the movements of the local population of plaice. Seawater samples were taken from the area fished during July 1975 and contained ≈1 pCi l^{-1} of $^{239+240}$Pu and ≈0.2 pCi l^{-1} of ^{241}Am in the filtrate (< 0.22 μm) (personal communication from D. F. Jefferies). Thus the approximate concentration factors over seawater (filtrate) for the samples of muscle collected in August are of the order of < 1 for $^{238+239}$Pu and ≈5 for ^{241}Am. The data obtained also emphasise the very low levels of plutonium and americium in the edible fraction of Irish Sea plaice taken from the area most liable to contamination; the concentrations measured in fish muscle are equivalent to less than 0.01% of

Table 1 Plutonium in organs of the plaice

Organ	Date of sample collection February 18, 1975 $^{239+240}$Pu	$^{239+240}$Pu/^{238}Pu	May 13, 1975 $^{239+240}$Pu	$^{239+240}$Pu/^{238}Pu	August 12, 1975 $^{239+240}$Pu	$^{239+240}$Pu/^{238}Pu	November 11, 1975 $^{239+240}$Pu	$^{239+240}$Pu/^{238}Pu
Kidney	88±32	7.0	18±6	4.9	20±4	3.2	44±5	3.9
Liver	29±9	3.9	9.1±2.8	7.5	5.3±0.9	4.5	18±3	3.9
Gut	15±5	3.9	35±7	5.4	72±4	4.4	66±4	4.4
Gut contents	540±30	4.8	3,570±250	4.0	2,710±180	4.5	5,010±200	4.3
Gill	13±4	—	450±39	4.1	770±50	3.8	38±8	1.6
Skin	3.2±1.5	4.2	4.2±1.5	4.1	4.3±0.6	4.0	2.9±0.4	3.4
Bone	14±5	3.6	2.9±1.1	6.1	2.8±0.9	1.5	0.65±0.07	4.6
Muscle	0.16±0.04	—	0.34±0.05	3.1	0.47±0.07	4.8	0.17±0.03	2.3

• Results are expressed in fCi per g wet weight.

the derived working limit, as defined by the International Commission on Radiological Protection[7,8], based on calculations using a dose limit to the public of 3 rem per yr and a maximum rate of consumption of 300 g of fish per d.

Part of the work was supported by contract with the European Atomic Energy Community.

R. J. PENTREATH
M. B. LOVETT

MAFF Fisheries Radiobiological Laboratory,
Hamilton Dock,
Lowestoft, Suffolk, NR32 1DA, UK

Received May 7; accepted July 6, 1976.

[1] Mitchell, N. T., *Technical Rep.*, FRL 10, 40 (Ministry of Agriculture, Fisheries and Food, London, 1975).
[2] Hetherington, J. A., Jefferies, D. F., Mitchell, N. T., Pentreath, R. J., and Woodhead, D. S., *Transuranium Nuclides in the Environment*, IAEA-SM **199**, 139–154 (International Atomic Energy Agency, Vienna, 1976).
[3] Hetherington, J. A., in *Radioisotopes in the Aquatic Environment; Models and Mechanisms* (Ann Arbor, in the press).
[4] Cherry, R. D., and Shannon, L. V., *Atomic Energy Rev.*, **12**, 3–45 (1974).
[5] Wong, K. M., *Analyt. chim. Acta*, **56**, 355–364 (1971).
[6] Pentreath, R. J., and Jefferies, D. F., *J. mar. Biol. Ass. U.K.*, **51**, 963–976 (1971).
[7] *International Commission on Radiological Protection Publication* No. 9 (Pergamon, Oxford, 1966).
[8] Preston, A., in *Environmental Aspects of Nuclear Power Stations*, IAEA-SM, 146, 147–157 (International Atomic Energy Agency, Vienna, 1971).

Presence of a buried mammalian carcass indicated by fungal fruiting bodies

Hebeloma vinosophyllum Hongo is a terrestrial agaric originally found in broad-leaved and conifer forests but not described as having any special ecological requirements[1]. It now seems that this species often fruits where a dead mammal has been buried.

On August 24, 1968 I found a group of luxurious fruiting bodies of this species in a stand of *Castanopsis cuspidata* at Iwakura, Kyoto. The fruiting bodies appeared to be well nourished and covered an area of about 1,500 cm². The surface of the ground did not seem to have been disturbed. This fungus had been found to fruit well only when the ground in forests has been dressed with urea or a similar material which releases ammonia on decomposition[2]. The presence of fruiting bodies in an untreated area suggested that there might have been a source of nitrogen in the soil. At a depth of less than 10 cm I found the remains of a dog carcass, which consisted of bones and decayed skin, and the soil around the carcass contained abundant white mycelia.

Fig. 1 *a*, Fruiting body of *H. vinosophyllum* on the superficially normal ground. *b*, Fruiting body together with cat bones taken from soil under that fruiting body.

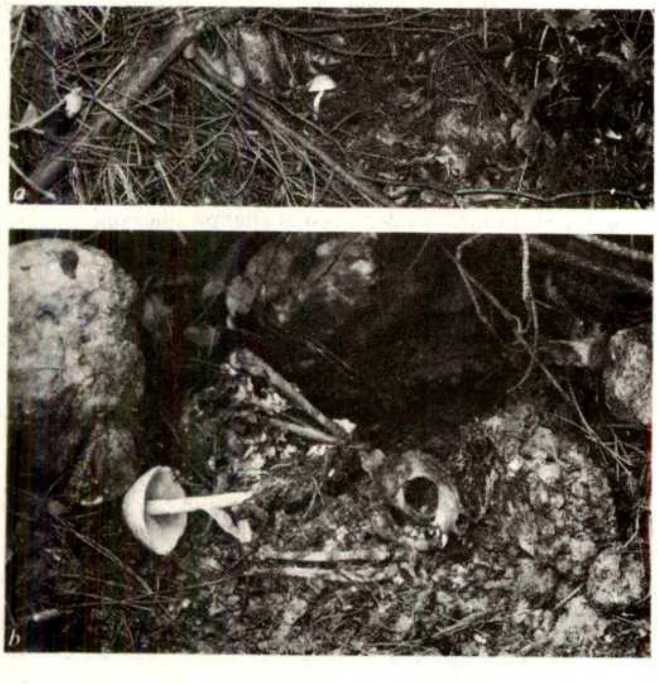

On October 8, 1975 a single well developed fruiting body of the same species was found in a stand of *Pinus densiflora* at Yoshida-yama near the Kyoto University campus. As before, the ground appeared to be superficially normal but some pieces of cat bone were found in the top 20 cm of soil. The soil and bones were replaced and on October 30 another fruiting body appeared (Fig. 1*a*). The bones were removed from the soil and are shown in Fig. 1*b*. On this occasion denatured fatty tissue was found and there was a smell of decaying animal matter. As before, no flesh remained and the soil was whitish with mycelia. In May to June 1976, several fruiting bodies appeared again on the same spot.

These facts do not exclude the possibility that this species colonises normal (untreated) soils. It is often very difficult, however, to determine whether or not a soil is really normal, since human urine and faeces, which also yield this fungus, leave nothing after decomposition. It is well known that entomogenous fungi or caterpillar fungi occur directly on the bodies of some invertebrates but there are no reports of indirect (soil-mediated) occurrences of agarics on mammals. The present finding may lead to speculation that a victim of homicide buried in soil could be located using the fruiting bodies of this or some other fungi, assuming the burial was shallow. (In forensic medicine, 'filamentous fungi' or 'fungal hyphae' are known to occur sometimes directly on human corpses or in graves[3].) After urea or ammonia application this species appears after 3–8 months and continues to fruit over a period of 1–2 yr, forming part of a succession, all the members of which respond to this treatment, and are called ammonia fungi[2]. It is not known whether this species could be used to determine how long a corpse has been buried.

The closely related species *Hebeloma sarcophyllum* Peck (=*H. porphyrosporum* R. Maire) is found in Europe, North Africa and North America[4]. It would be interesting to know if this species has similar ecological requirements.

I thank Dr R. F. O. Kemp, University of Edinburgh, for reading the manuscript.

NAOHIKO SAGARA

Biological Laboratory,
Yoshida College,
Kyoto University,
Kyoto 606, Japan

Received June 24; accepted July 7, 1976.

[1] Hongo, T., *J. Jap. Bot.*, **40**, 311–318 (1965).
[2] Sagara, N., *Contr. biol. Lab. Kyoto Univ.*, **24**, 205–276 (1975).
[3] Mueller, B., *Gerichtliche Medizin* (Springer, Berlin, Göttingen and Heidelberg, 1953).
[4] Kühner, R., and Romagnesi, H., *Flore analytique des champignons supérieurs* (Masson, Paris, 1953).

Appetitive learning, patterned alternation, and extinction in 10-d-old rats with non-lactating suckling as reward

HUGHLINGS-JACKSON[1] has expressed the view that, during ontogenesis, neural centres responsible for inhibition develop more slowly than centres responsible for excitation. Since then, the working hypothesis has been that the later-developing, phylogenetically 'higher' neural centres act to regulate (inhibit?) the excitation of the 'lower' centres. There has been some behavioural and physiological support for this position. In altricial mammalian species the hippocampus and neocortex become functionally mature relatively late in development[2], and the hippocampus, in particular, has been implicated in the expression of behavioural inhibition[3-5] Preweanling rats, during weeks 3 and 4 of life, seem to lack maturity for tasks requiring suppression of responding; for example, they are deficient in passive avoidance[6] learning and in habituating to novel stimuli[7,8] Their performance in excitatory tasks, such as active avoidance[9] and approach for food[10], seems to be less deficient. These task-specific deficits resemble those shown in hippocampally lesioned adult animals[11]. Campbell *et al.* have noted the correspondence between later-developing inhibitory centres in the rat and the decline in spontaneous activity occurring during ontogenesis[12], and have demonstrated that psychopharmacological agents[13] and brain lesions[14] specific to inhibitory systems are ineffective in increasing behavioural arousal early in development. In our laboratory, experiments on instrumental appetitive learning in preweanling rats have involved the use of dry food pellets as reinforcers in pups as young as 17 to 20 d of age. In animals as young as this, we have demonstrated acquisition, extinction, immediate persistence, and long term persistence using procedures that are similar to those for adult rats[15-17]. We now report two experiments demonstrating behavioural plasticity in the 10-d-old rat, involving acquisition and subsequent extinction of an approach response where reward is the opportunity to suck briefly from an anaesthetised mother rat.

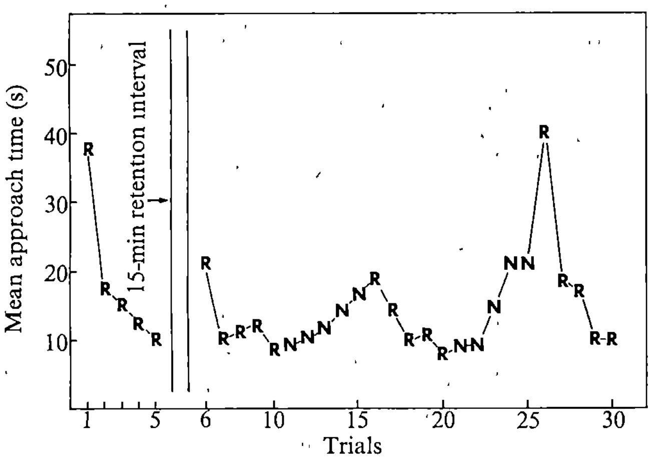

Fig. 1 Mean approach time for animals in experiment 1.

Our first experiment established that infant rats will quickly learn to approach when the reward is an opportunity to attach to a nipple of an anaesthetised mother rat for a brief interval, and that this learned tendency to approach can be successively weakened and strengthened by making the mother inaccessible and accessible on alternating blocks of trials. Our second experiment provided data from acquisition and extinction for two groups of subjects which differed in their schedule of reward in acquisition. The general procedure in both experiments, including deprivation treatment, was as follows: On the morning of day 10 pups from litters culled to 8 at birth were separated from their mother 8 h before training by being placed in a Plexiglas chamber partially filled with pine shavings. Temperature in the chamber was maintained at 37 °C (the average temperature in an undisturbed nest) using thermostatically controlled commercial heating pads placed under the Plexiglas floor. Experimental training was conducted in a clear Plexiglas alley (32 cm long and 8 cm wide) also maintained at 37 °C. Approximately 20 min before the first trial, the mother received intraperitoneally a 2 ml kg^{-1} injection of EquiThesin, a general anaesthetic producing a surgical level of anaesthesia and blocking milk release.

Preliminary training in both experiments consisted of placing each pup separately against the mother and allowing it to attach to a nipple for 15 s. At the end of this interval the pup was gently detached from the nipple, carried by hand to the opposite end of the alley, and placed facing away from the mother. On reward (R) trials the mother was positioned on her side at the end of the alley and the pup was permitted to attach to a nipple for 15 s On non-reward (N) trials the mother was removed from the alley and the pup was picked up when it reached the end of the alley. Time to the nearest 0 01 s for the pup to reach the end of the alley on each trial was recorded. In experiment 1 ($n=5$) preliminary training was followed by 5 massed (3-s intertrial interval) R trials, a 15-min retention interval during which the pup was returned to the deprivation chamber, and 25 massed trials in which R and N trials alternated (ALT) in blocks of 5 trials, starting and terminating with 5 R trials. In experiment 2 the initial 5 R trials and the retention interval were not included and two groups ($n=6$ each) were formed a 5-trial ALT group (as in the last 25 trials of experiment 1), and a group designated continuous reward (CR). Group CR was rewarded on every trial in the acquisition phase by access to a nipple for 15 s. A 10-trial extinction phase began, without signal, immediately after the last acquisition trial. Pups meeting an extinction criterion of 100 s on any trial were terminated and assigned a nominal latency of 100 for all remaining trials.

The results of experiment 1 are shown in Fig. 1. Approach time decreased sytematically over the first 5 R trials ($P<0.05$). After the retention interval, 'savings' was reflected in the first 5 R trials of the ALT phase, the block and block-by-trials interaction effects were both significant ($P<0.05$). This was the first clear evidence of which we were aware of systematic acquisition of an instrumental appetitive response and savings in reacquistion in rat pups as young as 10 d of age. There is also a systematic influence on approach times of alternating blocks of R and N trials across the 25 trials after the retention interval approach times decrease and increase, respectively, in the R and N blocks ($P<0.01$).

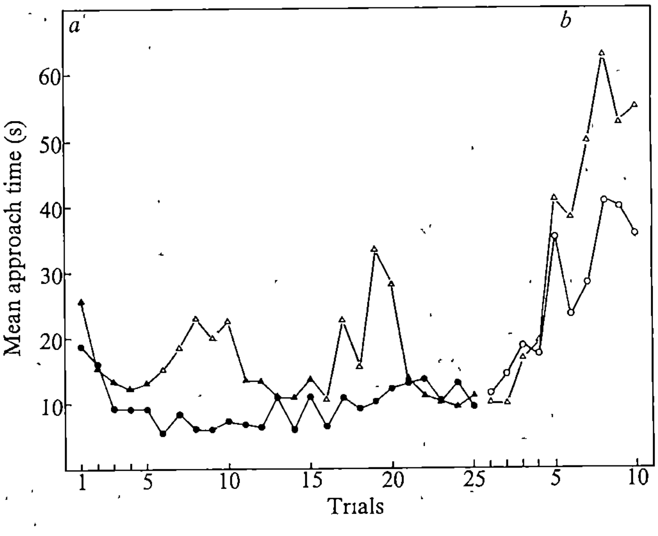

Fig. 2 Mean approach latencies in acquisition (*a*) and extinction (*b*) for the two groups in experiment 2. △, ▲, ALT; ●, ○, CR; ▲, ●, R; △, ○, N.

Figure 2 depicts mean approach latencies in acquisition and extinction for the two groups in experiment 2. Acquisition performance of the ALT group again reflected a behavioural sensitivity to 5-trial blocks of R and N trials. No such patterning was apparent in the CR group, where there was systematic reduction in approach time characteristic of learning across acquisition trials. Both groups showed clear extinction of approach behaviour with successive non-rewards ($P<0.01$). The tendency for the ALT group to extinguish at a faster rate than CR may reflect an extension of the successive 'extinctions' in acquisition.

These results implicate contact with the mother and/or sucking on a dry nipple as sufficient reinforcing events to establish and maintain approach behaviour in 10-d-old rats. Puerperal females under a general anaesthetic, within the range of dosages we used, do not demonstrate normal patterns of milk release from the nipple, and rarely release milk when stimulated by the sucking of a single pup[18]. We have not observed the characteristic milk-ingestion reflex in the pup while it was attached to a nipple of an anaesthetised mother, and we did not find an increase in body weight between pretraining and the end of training. It is therefore unlikely that the pups obtained milk during the brief nursing episodes. If the pups did not receive milk, some other feature(s) of the contact–suckling episodes must have served as the reinforcing stimulus. But to attribute reinforcing properties to contact–suckling we must rule out any distance cues—for example, odour and visual—as factors that strengthen and weaken the approach response. Visual cues are ruled out because the eyes of 10-d-old rats are not yet open, but the extent to which rats of this age can use odour cues is not clear. In the presence of a maternal odour, spontaneous activity in 10-d-old rats is reduced[19]. Rats as young as 12 d of age, but not younger, prefer shavings from home cages to clean wood shavings, presumably on the basis of odour[20]. On the other hand, 10-d-old pups given a choice between their own mother and a nulliparous female show virtually no tendency to approach either one; and the lactating female does not begin to emit the maternal pheromone until about 14 d *post partum,* which is the age at which the young are first responsive to the pheromone[21]. In our own data, there is nothing to suggest that odour cues are the basis for differential responding on R and N trials. Odour cues cannot account for the extinction differences between the two groups found in experiment 2 because both groups were run in identical conditions in this phase. These extinction differences may reflect an associative factor which develops differentially in the two groups in acquisition. As a final check on the involvement of odour cues in our experiments, we have replicated the basic finding of experiment 1 (ALT condition) using a procedure in which the anaesthetised mother is present on all trials at the end of the alley. The mother rat is behind a barrier which is raised on R trials after the pup reaches the goal box, but not on N trials. This procedure rules out the possibility that distance cues emanating from the mother on R but not on N trials control the patterned responding in the ALT group.

These results suggest that the development of forebrain structures in the rat during weeks 3 and 4 of life may not be essential for at least certain kinds of learned response suppression. In our experiments appetitive extinction, suppression of approach in the absence of the mother, reflects an 'inhibitory' effect in rats at 10 d of age; in experiments using electric shock, suppression of approach responses in rats shows up much later in development. Although the concept of inhibition has been applied in a variety of contexts, it has always lacked precise definition in psychology[22], and psychologists, physiologists and biochemists explain a number of disparate phenomena with the term 'inhibition'. Our results demonstrate that the infant rat can learn to anticipate the absence of a previously present appetitive event at an age before recognised inhibitory neural centres are said to be operating.

This work was supported by the NSF.

ABRAM AMSEL
DAVID R. BURDETTE
RICHARD LETZ

Department of Psychology,
University of Texas at Austin,
Austin, Texas 78712

Received April 26, accepted July 6, 1976.

[1] Hughlings-Jackson, J , *Brain,* 9, 1–23 (1886).
[2] Altman, J., and Das, G. D , *J. comp. Neurol* , 124, 319–336 (1965).
[3] Altman, J , Brunner, R. L., and Bayer, S A , *Behav. Biol* , 8, 557–596 (1973).
[4] Douglas, R J., *Psych. Bull* , 67, 416–442 (1967)
[5] Kimble, D. P., *Psych Bull.*, 70, 285–295 (1968).
[6] Riccio, D. C., Rohrbaugh, M , and Hodges, L A , *Devl Psychobiol.*, 1, 108–111 (1968).
[7] Feigley, D A., Parsons, P. A , Hamilton, L. W , and Spear, N. E , *J comp. Physiol. Psych* , 79, 443–452 (1972)
[8] Bronstein, P. M , Neiman, H., Wolkoff, F D , and Levine, M. J , *Anim. Learn. Behav* , 2, 92–96 (1974)
[9] Kirby, R. H , *J comp. Physiol. Psych* , 56, 158–162 (1963).
[10] Campbell, B A., Jaynes, J. R , and Misanin, J , *J. comp Physiol. Psych* , 66, 467 (1968).
[11] McCleary, R. A , in *Progress in Physiological Psychology* (edit by Stellar, E , and Sprague, J M) (Academic, New York, 1966)
[12] Campbell, B A , Lytle, L. D., and Fibiger, H. C , *Science,* 166, 637–638 (1969).
[13] Mabry, P. D , and Campbell, B. A., *J comp. Physiol Psych.*, 86, 193–201 (1974).
[14] Moorcroft, W H., *Brain Res* , 35, 513–522 (1971).
[15] Chen, J S., and Amsel, A., *J comp. Physiol Psych* , 89, 238–245 (1975).
[16] Burdette, D R., Brake, S. C., Chen, J S., and Amsel, A., *Anim. Learn. Behav* , 4, 131–138 (1976).
[17] Amsel, A., and Chen, J. S., *J. comp. Physiol Psych.* (in the press)
[18] Lincoln, D W , Hill, A , and Wakerley, J B , *J. Endocr* , 57, 459–476 (1973).
[19] Schapiro, S , and Salas, M , *Physiol Behav.*, 5, 815–817 (1970)
[20] Gregory, E. H., and Pfaff, D W., *Physiol Behav* , 6, 573–576 (1971).
[21] Leon, M., and Moltz, H , *Physiol. Behav* , 8, 683–686 (1972)
[22] Amsel, A , in *Inhibition and Learning* (edit by Boakes, R. A., and Halliday, M S.) (Academic, London, 1972).

Models and statistics for species diversity

INTEREST in the pattern of species abundances in a population takes two forms. On the one hand a study of the full distribution of the relative abundances of species may be sought to give insight into the internal mechanisms of the community; in other cases one or more summary statistics which suitably characterise the population may be required to investigate effects of evolutionary or environmental change. The first approach has led

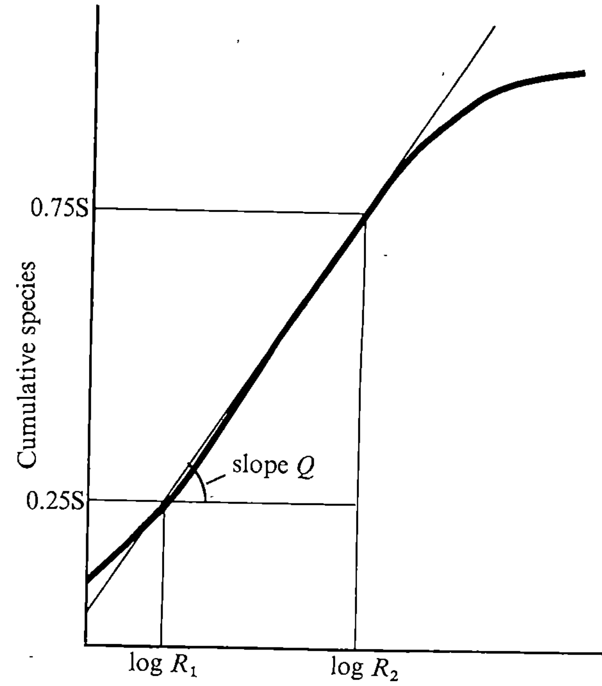

Fig. 1 Evaluation of quantile statistic, Q, from cumulative species abundance curve.

Table 1 Analysis of variance of diversity statistics for 7 replicate samples of moth catches from light traps at 14 sites in the Rothamsted Insect Survey

Source of variation	d.f.	Variance mean square			
		Simpson	H	Q	α
Between sites	13	0.00174	0.977	832.4	1037.5
Within sites	78	0.00014	0.018	6.4	6.4
Between to within sites variance ratio		12.1	54.0	130.5	163.1

Ability of the statistics to discriminate between sites is indicated by the size of the variance ratio, between to within sites.

α, Diversity parameter of the log-series.

to much argument over the appropriate mathematical form for the distribution of abundances, often in the belief that the acceptance of a particular mathematical model will tell us something about the causal biological mechanism. In our opinion, however, the primary purpose of fitting a mathematical model is to smooth the data and enable efficient estimation of population statistics from the parameters of the model; for this we would choose the simplest model which adequately describes the data. Further, there are clear advantages in fitting a single model to describe a series of sets of data—even if this model does not give the best fit to each one—rather than fitting several different models, as has often been suggested, particularly in the literature on succession.

The use of a single diversity statistic to summarise the full distribution of the relative abundances of species has obvious appeal, in spite of recent criticism of many statistics in common use. Here again we would make no pretence at functional modelling but suggest that species diversity is most usefully regarded as a descriptive statistic for multispecies populations of the same type as, say, population density. Like average density, it is best represented by a statistic that does not overemphasise the commonest or the rarest species, particularly as species frequency distributions are usually very long tailed. We have strongly criticised[1] the two diversity statistics in common use, the information statistic (H) and Simpson's index, because of their sensitivity to the few commonest species, the numbers of which we have found to fluctuate erratically from year to year, rather than to those more stable species with medium abundance.

An alternative diversity index which does not suffer from these disadvantages is based on the slope of the cumulative species curve in the mid-range of abundances (Fig. 1). Mathematically we define

$$Q = S/2 \log(R_2/R_1)$$

where S is the total number of species in the sample and R_1 and R_2 are the lower and upper quartiles of the species abundance distribution (see ref. 2, p. 226). Clearly, Q is much less sensitive to the commonest species in the sample, than H or Simpson's index, and we have found that it shows smaller relative variability between years and discriminates better between different sites (Table 1).

Fitting a model to the data enables the diversity statistics to be

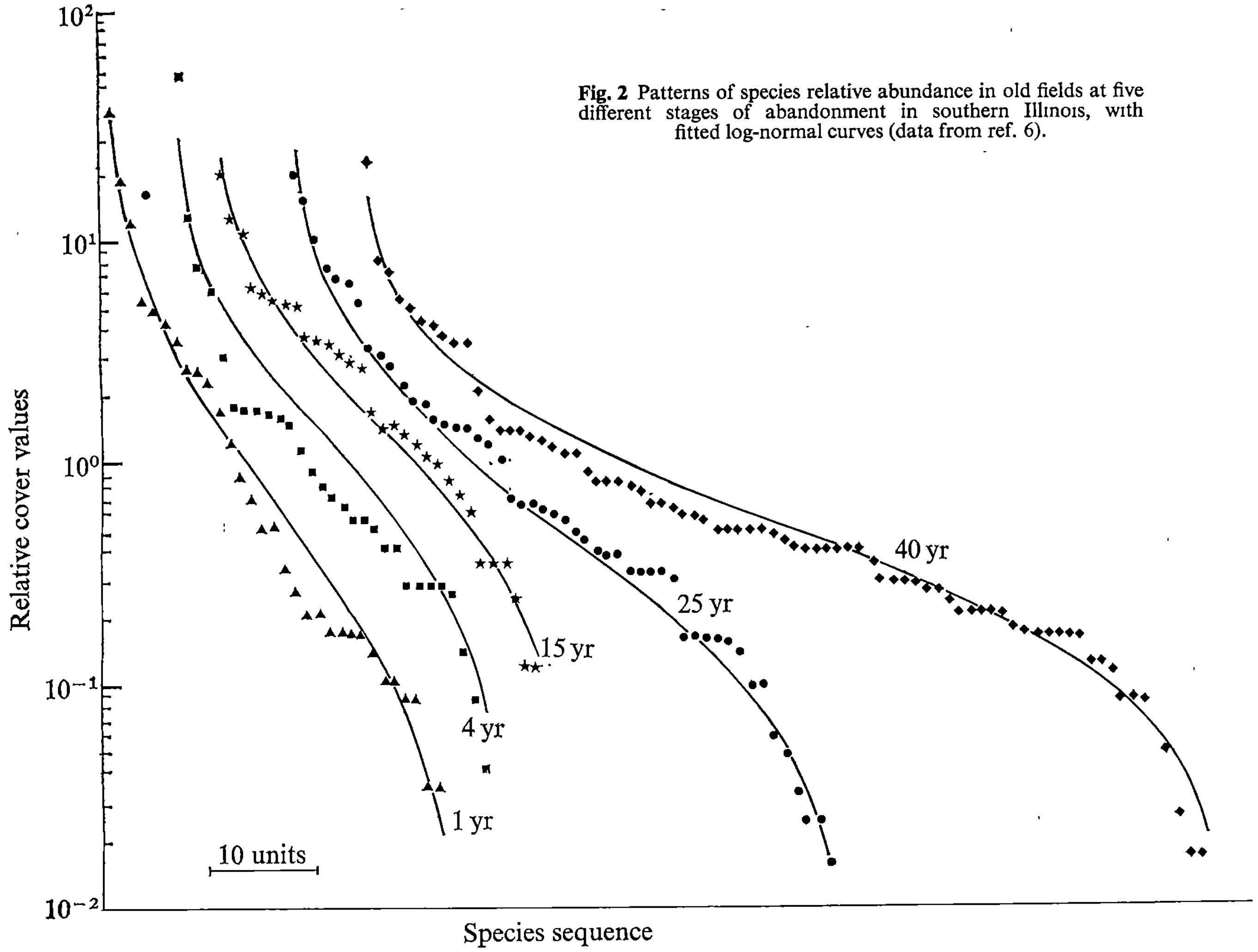

Fig. 2 Patterns of species relative abundance in old fields at five different stages of abandonment in southern Illinois, with fitted log-normal curves (data from ref. 6).

Table 2 Diatom samples showing replicate variability of the mid-range statistic Q evaluated directly from the data and from the parameters of the log-series and log-normal models (data from ref. 4)

	Replicate								Mean	Variance
	1	2	3	4	5	6	7	8		
Empirical Q	20.9	17.9	26.4	22.4	20.1	19.2	19.8	23.7	21.3	7.54
Log-series α	19.2	18.3	20.4	19.9	20.5	19.7	18.2	19.9	19.5	0.77
Log-normal cS^*/σ	21.9	20.7	24.3	21.4	23.8	22.7	21.2	23.1	22.4	1.67

estimated much more efficiently than by direct evaluation from the relative frequencies. The mid-range statistic Q is particularly simply represented in terms of the parameters of both the log-series and log-normal models; for the log-series $Q = \alpha$, Fisher *et al.*'s index of diversity[3], whereas for the log-normal $Q = cS^*/\sigma$, where S^* is the hypothetical number of species in the population, σ is the standard deviation of logged abundances, and c depends on the proportion of species present in the sample. When all species are present, $S^* = S$ and $Q = 0.371S/\sigma$. Fitting a model enables all the information in the data to be utilised in estimating Q, this should result in smaller variation between replicates. This is shown in Patrick's diatom samples[4] (Table 2) for which Q has been estimated directly from the data and from the parameters of the fitted log-series and log-normal models, for each of the eight replicates. The mean values of Q are similar for all three methods but the advantage of fitting a model is shown in the resulting smaller replicate variability; this will enable better discrimination between sites (Table 1). The choice of model is of secondary importance but the log-series parameter α shows somewhat smaller variability than the log-normal S^*/σ (Table 2), demonstrating the advantages of using the simpler model, even though the log-series is, for this series of data, nearly always a worse fit[5].

Table 3 Change of diversity with succession in abandoned fields in Southern Illinois (data from ref. 6)

Stage of succession (yr)	1	4	15	25	40
Information statistic, H	2.0	1.7	2.8	2.9	3.2
Mid-range statistic, Q	5.6	8.4	8.0	10.0	24.1
Number of species, S	31	29	30	50	77
Log-normal σ	1.9	1.5	1.3	1.7	1.4
$Q = 0.371S/\sigma$	6.2	7.1	8.4	10.7	20.6

The importance of choice of diversity statistic is also seen in data by Bazzaz[6] on the change of pattern with plant succession in old fields in Illinois (Fig. 2). In this instance, the pattern of ecological succession, as summarised by May[7], assumes that in the early stages of succession the Niche Pre-emption Model applies and the ranked abundances of the species may be expected to follow a geometric series. Later, a multiplicity of other factors affecting abundance come into play, and the distribution of species abundance moves closer to the log-normal form. Although this sequence of models may have theoretical appeal, on purely statistical grounds the use of two models seems unjustified, for the data seem to support just as well the use of the same, log-normal distributional model to fit each stage of succession (Fig. 2).

Bazzaz evaluates the information statistic, H, for fields at each stage of succession, and argues that after an initial drop, diversity increases rapidly from year 5 to 15 and then only slowly over the remaining years (Table 3). H seems to reflect the relative abundance of a small number of dominant species. The pattern suggested by the great majority of species is, however, very different, indicating a slow initial increase in diversity followed by more rapid increase in the later stages, changes reflected by the mid-range statistic Q. With one common distribution fitted to all the data we may use the parameters from the model to chart the increase in diversity, described, not by the number of species S, or evenness σ, taken individually but by their ratio S/σ (Table 3), which more closely reflects the visible trend.

R. A. KEMPTON

Department of Statistics,

L. R. TAYLOR

Department of Entomology,
Rothamsted Experimental Station,
Harpenden, Hertfordshire, UK

Received April 29, accepted June 17, 1976

[1] Taylor, L R , Kempton, R. A , and Woiwod, I P , *J. anim Ecol.*, **45**, 255–271 (1976).
[2] Whittaker, R H., *Taxon*, **21**, 213–251 (1972)
[3] Fisher, R. A , Corbet, A S , and Williams, C. B , *J anim Ecol* , **12**, 42–58 (1943).
[4] Patrick, R *Am. Nat* , 102, 173–183 (1968)
[5] Kempton, R. A , and Taylor, L R , *J. anim Ecol* , 43, 381–399 (1974).
[6] Bazzaz, F A , *Ecology*, 56, 485–488 (1975)
[7] May, R M , *Nature*, 258, 285–286 (1975)

Errata

In the article "Promotion and retardation of heat transfer by electric fields" by Y. Asakawa (*Nature*, **261**, 220; 1976) the last sentence to the legend to Fig. 2 should read . . . The cylinder was heated within an electric furnace, and cooling was 1.7 times faster (*b*) and 1.8 times slower (*c*) than in case *a*. and not as printed.

In the article "Age relationships along the Hermitage Bay–Dover Fault System, Newfoundland by J. Blenkinsop, P. F. Cucman and K. Bell (*Nature*, **262**, 377; 1976) the figure in the fourth line of the first paragraph should be 400 Myr and not 4 Myr as printed.

In the article by O. K. Wilby (*Nature*, **262**, 387; 1976) the title should read ". . . and the effects of antibiotics . . ." and not antibodies as printed.

Nature **Index and Binders**

The **Index** for 1975 is now available, price £2.25. Copies of the 1974 index are still on sale, price £3.00. **Binders** for the journal are also available at £7.00 for four (a year of *Nature* fits into four binders).
Postage is included in the above prices. Orders should be sent, accompanied by remittance to Macmillan Journals Ltd, Brunel Road, Basingstoke, Hampshire, England.

matters arising

Nuclear composition of cosmic rays

WHEN the phenomenological constant in the local source model of Rasmussen and Peters[1] is given a more physical basis, its large value cannot be easily understood.

I begin by deriving their equation (1). For each species i, the steady-state equation for the density η_i^b[cm^{-3} GeV^{-1}], of high energy particles coming from a background of uniformly distributed sources with strength S_i^b[cm^{-3} s^{-1} GeV^{-1}] and undergoing spallation is

$$\frac{d\eta_i^b}{dt} = 0 = -n\sigma_i c\eta_i^b + S_i^b + \sum_{j>i} n\omega_{ij} c\eta_j^b \qquad (1)$$

where n [cm^{-3}] is the mean density of hydrogen, c is the velocity of light, and the cross sections σ_i and ω_{ij} [cm^2] were defined by Rasmussen and Peters. To write equation (1) in terms of the total density, η_i, and total source strength, S_i, let L_i[s^{-1} GeV^{-1}] be the mean luminosity of the cosmic ray sources, then

$$\eta_i^b = \eta_i - \eta_i^l,\ S_i = NL_i/V_G \qquad (2)$$

$$S_i^b \sim (1-N^l/N)S_i \qquad (3)$$

$$\eta_i^l = \sum_\alpha \frac{L_i^\alpha f_\alpha}{4\pi c d_\alpha^2} = \left(\sum_\alpha \frac{L_i^\alpha f_\alpha}{4\pi c d_\alpha^2}\frac{V_G}{NL_i}\right)S_i = \frac{KS_i}{nc} \qquad (4)$$

where N is the total number of sources, V_G is the containment volume, L_i^α is the luminosity of and d_α the distance to the αth of the N^l local sources, and f_α is the enhancement from diffusion. Note that equation (4) pertains to stable nuclei and assumes negligible spallation. After substituting equations (2)–(4), equation (1) becomes

$$\frac{S_i}{n} = \frac{\sigma_i c\eta_i - \sum_{j>i} \omega_{ij}[c\eta_j - KS_j/n]}{1+\sigma_i K} \qquad (5)$$

(if $N^l/N \ll 1$). If $S_i/n \to S_i$ (the relative strength) and $\eta_i c \to F_i$, then equation (5) becomes equation (1) of Rasmussen and Peters.

Next, approximate the transport from a steady source by assuming isotropic, three-dimensional diffusion in an infinite medium (see ref. 2). Then the equilibrium value of the factor f_α is given by[3]

$$f_\alpha = (d_\alpha c/D) \qquad (6)$$

and, after an interval Δt, the root mean square distance, r_{rms}, for newly produced particles is

$$r_{rms} = (6D\Delta t)^{\frac{1}{2}} \qquad (7)$$

where $D(\equiv\lambda c/3)$ is the diffusion constant and λ is the scattering mean free path. If spallation is negligible, the random path $c\Delta t$ must be much smaller than a spallation mean free path for the heaviest element injected by a source. Thus equation (7) implies that the boundary of the local source region, R^l, is

$$R^l = (2\lambda\xi/n\sigma_U)^{\frac{1}{2}} = 180(\lambda/n)^{\frac{1}{2}}\text{ pc} \qquad (8)$$

where $\xi = 0.1$ permits up to 10% spallation, $\sigma_U(=2\text{ barn})$ is the spallation cross section for uranium, and where the units for λ and n are pc and cm^{-3}. Also, if all of the sources are distributed uniformly, the mean number of local sources is just

$$\langle N^l\rangle = \left(\frac{4}{3}\frac{\pi(R^l)^3}{V_G}\right)N \qquad (9)$$
$$= 7.2\times10^{-5}(\lambda/n)^{3/2}N$$

for $V_G = 10^{67}$ cm^3.

Rasmussen and Peters then found the source abundances of Li, Be, and B were minimised if $K = 0.02$ mbarn^{-1}. From equations (4), (6), and (9) this means

$$d_* = 0.90(N^l/\langle N^l\rangle)(\lambda/n)^{\frac{1}{2}}\text{ pc} \qquad (10)$$

where d_* is the equivalent distance to the local sources defined by

$$\frac{1}{4\pi d_*} = \frac{1}{N^l}\sum \frac{L_i^\alpha/L_i}{4\pi d_\alpha} \qquad (11)$$

Note that if the local sources were identical and spherically distributed, then equation (11) says $d_* = (2/3)R^l(L_i/L_i^\alpha)$. While if there is only one local source $d_* = d_\alpha(L_i/L_i^\alpha)$.

Equation (10) poses a severe problem for the local source model. If $N^l \approx \langle N^l\rangle$, $d_* \sim 1$ pc, which implies either the source(s) is extremely close or extremely luminous. If $N^l \sim 30\langle N^l\rangle$, then d_* becomes acceptable, but the total number of sources becomes uncomfortably small. Using equation (9), such a fluctuation yields 2,300 sources (5 local) but with a probability of 9.2×10^{-7} (according to Poisson statistics). These problems become even more severe if the enhancement factor, f_α is set to unity.

To summarise, the size of the phenomenological constant K seems inconsistent with a physical interpretation in terms of source properties and distances. The difficulties in understanding the small value of d_* arise because the model requires the local source(s) to contribute extremely large amounts of unspalled C and O to match the observed L/M ratio.

I thank C. McKee and R. Gordon for discussions. This work was supported by NASA.

LANCE W. WILSON

Department of Physics,
University of California,
Berkeley, California 94720

[1] Rasmussen, I. L., and Peters, B., *Nature*, 258, 412 (1975).
[2] Lingenfelter, R. E., *Nature*, 224, 1182 (1969).
[3] Ginzburg, V. L., and Syrovatskii, S. I., *The Origin of Cosmic Rays*, 301 (MacMillan, New York, 1964).

The cosmic X-ray background

MATTER–antimatter annihilation has had great appeal in astrophysical situations involving apparently overdrawn energy budgets. In spite of observational evidence that antimatter is no panacea[1], annihilation theories rise periodically, phoenix-like, in explanation of a wide class of astrophysical phenomena. In a recent letter, Carlqvist and Laurent[2] proposed that the X-ray background (1–100 keV) arises from Compton scattering of starlight photons by annihilation-produced, relativistic electrons and positrons. We show here that the Carlqvist–Laurent proposal is in conflict with γ-ray and neutrino observations. Were the X-ray background caused by annihilation produced electrons, the 100-MeV γ-ray flux would exceed that observed[3] by six to ten orders of magnitude, the muon-neutrino flux would exceed the observational upper limit[4] by one to five orders of magnitude and, a flux of 511 keV annihilation γ rays would be produced in excess of that observed[5] by up to eight orders of magnitude.

To produce the cosmic X-ray background, Carlqvist and Laurent[2] require the Universe to be filled with annihilation-produced electrons and positrons at a density $n_e \simeq 10^{-9}$ cm^{-3}. Since, in a typical annihilation, roughly one γ ray ($\sim$100 MeV) is produced for each electron[1], the γ-ray flux at Earth should be

$$F_\gamma \simeq cn_\gamma \simeq cn_e \simeq 30\,\mathrm{cm^{-2}\,s^{-1}} \tag{1}$$

This predicted flux exceeds that observed[3] by some six orders of magnitude. To avoid this embarrassment, Carlqvist and Laurent[2] suggest that the γ rays may be absorbed if annihilation were to occur in galactic nuclei instead of intergalactic space. Since the range of a 100-MeV photon exceeds the range of a 100-MeV electron (because of annihilation, the range of a 100-MeV positron is even shorter), it is impossible to absorb the γ rays without, first, stopping the electrons. Furthermore, since the electrons are tied to magnetic fields[2], they must pass through more material than the γ rays to escape from the annihilation volume. There is no way to bury the γ rays without also interring the electrons and positrons.

Although the previous discussion shows that the density of annihilation-produced electrons must be at least six orders of magnitude lower than that required by Carlqvist and Laurent[2] to produce the X-ray background, it is of interest to consider two other, independent constraints which support this conclusion.

As Steigman and Strittmatter[6] have shown, a typical annihilation yields two detectable μ neutrinos for every three electrons. Such annihilation-produced neutrinos are extremely difficult to detect and have been of only marginal value in constraining matter–antimatter theories[6]. The Carlqvist–Laurent proposal[2] is virtually unique in predicting a flux of μ neutrinos which exceed the upper limit to the observed flux[4] (F_{ν_μ} (obs) $\lesssim 3$ cm^{-2} s^{-1}).

$$F_{\nu_\mu} \sim cn_{\nu_\mu} \simeq 2/3\, cn_e \simeq 20\,\mathrm{cm^{-2}\,s^{-1}} \tag{2}$$

The neutrinos, of course, will not be absorbed in the annihilation region.

Finally, a relativistic positron in a medium of density n will annihilate in a time $t \simeq 10^{14}\ n^{-1}$ s, producing two 511-keV γ rays. The predicted flux of these annihilation γ rays is

$$F_{511} \simeq 10^5 n\ \mathrm{cm^{-2}\,s^{-1}} \tag{3}$$

For an average intergalactic density[7] ($n \simeq 10^{-7}$ cm^{-3}), the predicted flux exceeds that observed[5] (F_{511} (obs) $\lesssim 2\times10^{-3}$ cm^{-2} s^{-1}). In the Carlqvist–Laurent scheme[2], the situation is much worse, however. They require the annihilation to occur in quasars or galactic nuclei where the ambient density is very high. For example, for an average galactic density ($n \simeq 1$ cm^{-3}), the 511-keV flux would exceed that observed[5] by some eight orders of magnitude. Furthermore, every electron or positron which annihilates to produce a 511-keV γ ray was originally produced along with γ rays and neutrinos. Thus, the γ-ray flux would exceed that observed by some ten orders of magnitude and the μ-neutrino flux would exceed the observational upper limit by some five orders of magnitude! (The reason for the increase over our earlier estimates is that Carlqvist and Laurent[2] assumed that the electrons and positrons lived for $\sim 10^{10}$ yr; however, because of annihilation, their lifetimes are much shorter and, thus the original annihilation rate must be increased by the ratio of the age of the Universe to the lifetime of the electrons.)

Matters arising

Matters Arising is meant as a vehicle for comment and discussion about papers that appear in *Nature*. The originator of a Matters Arising contribution should initially send his manuscript to the author of the original paper and both parties should, wherever possible, agree on what is to be submitted. Neither contribution nor reply (if one is necessary) should be longer than 300 words and the briefest of replies, to the effect that a point is taken, should be considered.

It is clear that observational limits to the flux of annihilation products (γ rays and neutrinos) provide serious constraints to annihilation as an astrophysical energy source[1,6]. Since the recently proposed[2] annihilation explanation of the X-ray background is incompatible with these limits by many orders of magnitude, it is untenable.

GARY STEIGMAN

National Radio Astronomy Observatory,
Edgemont Road,
Charlottesville, Virginia 22901

[1] Steigman, G , *Nature*, **224**, 447 (1969); *Cargese Lect. in Phys.*, **6**, 505 (1973), *Proc. IAU Symp.*, **63**, 347 (1974); *A. Rev. Astr. Astrophys* (in the press).
[2] Carlqvist, P., and Laurent, B., *Nature*, **260**, 225 (1976).
[3] Fichtel, C. E., *et al.*, *Astrophys J*, **198**, 163 (1975).
[4] Wolfendale, A. W., and Young, E. C. M., *CERN Neutrino Mtg Proc.*, 95 (1969).
[5] Johnson, W. N., III, *et al.*, *Astrophys. J. Lett.*, **172**, L1 (1972).
[6] Steigman, G., and Strittmatter, P. A., *Astr. Astrophys.*, **11**, 279 (1971).
[7] Gott, J. R , III, *et al.*, *Astrophys. J.*, **194**, 543 (1974).

CARLQVIST AND LAURENT REPLY—In Steigman's[1] criticism of our paper[2] he raises three points, with which we shall deal in order. One of these points concerns the γ rays produced by collisions of annihilation electrons (positrons) with positrons (electrons) in intergalactic space. Steigman believes that two 511-keV γ rays are formed in each electron–positron annihilation. This is not correct. If one highly relativistic electron (positron) annihilates on a positron (electron) at rest, one very high energy photon is produced and one photon with an energy in the region $m_ec^2/2$ to $\sim m_ec^2$. Consequently no discrete γ line is formed but a continuous spectrum. Steigman further uses a value of 10^{-7} cm^{-3} as the average intergalactic particle density, which is rather the density of smeared out galactic material. The true intergalactic density is not known. It should be pointed out that there is no reason why electrons and positrons must penetrate galaxies, which may be shielded by their magnetic fields.

A second point that Steigman raises concerns the production of γ rays in connection with the proton–antiproton annihilation. His objection here is based on a homogeneous model and does not apply to the model used by us. If annihilation occurs as a result of collisions between matter and antimatter objects which are sufficiently dense, most of the γ rays from the annihilation will be absorbed by the objects themselves[3,4]. The annihilation electrons and positrons may, on the other hand, be temporarily confined by magnetic fields to regions with a much lower density than in the surroundings and then be released into intergalactic space. One cannot therefore state categorically, as Steigman does, that the γ rays cannot be absorbed without stopping the electrons and positrons.

Steigman's third point concerns μ neutrinos formed on annihilation. He has used our suggestion to estimate the flux, and finds that it exceeds the measured number by one order of magnitude. It should be stressed that this estimate is necessarily very uncertain for two reasons. First, we have calculated the electron density only to an order of magnitude; and secondly, it is questionable how much value one should attribute to the old experiments referred to.

Finally it should be pointed out that Steigman has implicitly assumed an homogeneous cosmological model. If, however, the metagalactic model[5-7] is adopted, neutrinos and γ rays created long ago would have escaped through the boundary of the system.

In itself it is legitimate to use specific models but Steigman uses specific models in an illegitimate way to draw general conclusions.

[1] Steigman, G., *Nature*, **262**, 821–822 (1976).
[2] Carlqvist, P., and Laurent, B., *Nature*, **260**, 225–226 (1976).
[3] Alfvén H., and Elvius, A., *Science*, **164**, 911–917 (1969)
[4] Elvius, A , *IAU Symp* , **44**, 306–310 (1972).
[5] Alfvén, H., and Klein, O., *Ark. Fys.*, **23**, 187–194 (1963)
[6] Klein, O , *Nature*, **211**, 1337–1341 (1966)
[7] Alfvén, H., *Phys. Today*, **24**, 28–33 (1971).

reviews

Games of chance and necessity

I. Prigogine

Das Spiel: Naturgesetze Steuern den Zufall. By Manfred Eigen and Ruthild Winkler. Pp. 404. (R. Piper: Munchen and Zurich, 1975.) DM38.

TODAY, we are very far from the ideals of classical science centred on stability and permanence. We now see that such qualifications apply only to very limited aspects. Wherever we look, we discover evolutionary trends leading to diversification and increasing complexity. The monograph by Eigen and Winkler provides us with an excellent introduction to this new, more dynamic, vision of the physical world.

Dr Eigen is one of the key figures in contemporary physical chemistry and molecular biology, but the present work goes far beyond the field to which Eigen has made important contributions. It spans an extraordinarily wide range from fundamental concepts in mathematics and theoretical physics such as game theory or symmetry, to problems of aesthetics and epistemology. It shows that a synthetic approach to both the scientific and cultural problems of our time is still possible.

Photo: R. Piper & Co. Verlag

Ruthild Winkler and Manfred Eigen

The central theme is self-organisation. How can complexity arise spontaneously? The approach taken by the authors is clearly indicated in their Preface: ". . . All happenings in our world are similar to a big game in which only the rules are fixed *a priori* . . . We consider the game to be the natural phenomenon which, with its dichotomy of chance and necessity, is the basis of all change" (translation by the reviewer). This starting point leads to the search for unity in nature "as revealed by relationships between structures" and for unity between nature and spirit "as revealed by the existence of languages both in molecular biology and in human communication". The central theme, Nature as a game, is analysed using many examples.

It is impossible to analyse in detail the content of this monograph, which is subdivided into four parts, covering the simplest situations which game theory and physics can analyse, and ranging to problems of ecology, linguistics and aesthetics (the chapter on music is specially informative and original).

The concept of game (or play) is taken as the basis of both the unity and the self-organisation of the physical world. This theme is a recurrent one in the German *Natur Philosophie* of the romantic period (*Histoire de la Philosophie,* **III**, Encyclopedie de la pléiade, Gallimard, 1974). According to this view, game (or play) is the very expression of the creativity of Nature. It is interesting to note the contrast between the intellectual atmosphere of Eigen and Winkler's book with that of Monod's classic *Chance and Necessity* (Editions du Seuil, 1970). Monod stresses the analogy between living beings and chemical machines, and this analogy is repeated several times. Monod is, in fact, following in this respect the mechanistic cartesian tradition so strong in French thought. It is not surprising that, starting from this view, he has great difficulties in incorporating adaptation and biological evolution in his theory. Life appears as a phenomenon existing *de facto* but not *de jure,* as its presence can only be understood in terms of extremely unlikely, even unique, events.

Eigen and Winkler avoid, from the beginning, such difficulties as games having both deterministic and stochastic aspects: the rules are given in a deterministic fashion, whereas the time sequence of events contains stochastic elements. Instead of opposing chance and necessity, Eigen and Winkler show how these two aspects may cooperate to produce the complexity and diversity we observe in Nature.

Obviously, in a book devoted to a synthetic view of Nature the problems are of such a wide range and depth that different opinions may be held. This is only one more positive aspect which must be credited to the authors.

For example, it is difficult to accept the postulate of Eigen and Winkler that long time processes may all be identified with games. Games are mathematically associated with semigroups, such as those involved in Markov processes. On the other hand, classical and quantum mechanics lead to dynamic groups, involving unitary transformation. The transition from dynamic groups to games contains all the difficulties of going from dynamics to the theory of probabilities. There is no reason to believe that the description of the motion of a harmonic oscillator will ever need new elements over and above those contained in dynamics. Inversely, there is no reason to believe that probabilistic laws such as those describing Mendel's laws will ever be reduced to deterministic schemes. We now begin to understand that a minimum amount of complexity will lead to the introduction of stochastic elements where long time scales are involved (J. Moser, *Stable and Random Motions in Dynamical Systems*, Princeton University Press, Princeton, 1974). It seems that no reduction of Nature to a single fundamental level (either law or game) is possible. We have to accept a more complex situation involving the continued interplay between multiple levels (such as the interplay between macroscopic and microscopic levels emphasised by Bohr and Rosenfeld).

Also, the distinction between rules and events as used by Eigen and Winkler seems to be somewhat too rigid. In particular, when dealing with problems involving human behaviour, we cannot really speak of *given* rules. The games are so highly non-linear that essentially the rules themselves become situation-dependent. A well-known example is that of traffic flow, in which the strategy of the drivers depends on the specific situation (I. Prigogine and R. Herman, *Kinetic Theory of Vehicular Traffic*, American Elsevier, New York, 1971).

An important feature of the book by Eigen and Winkler comes from the fact that it shows how to go beyond the classic paradigms of molecular biology. Molecular biology has essentially been aiming to identify and isolate the characteristic biomolecules. Because of the very success of molecular biology it becomes today possible to proceed in new directions, and to relate structure on the supermolecular level to the characteristic properties and interactions of these biomolecules. To do so we need as emphasised by Eigen and Winkler, both conservative and dissipative structures. Conservative structures arise mainly through short range interactions (valency and van der Waals' forces), whereas dissipative structures result from chemical kinetics and transport processes if suitable conditions are satisfied. An essential feature of dissipative structure is that they depend on the system as a whole, or alternatively that they are similar to long range forces that lead to coherent behaviour.

Interesting chapters are devoted to the laws of population dynamics and to Darwinian evolution theory. Again, many points deserve a more detailed discussion. Can Darwinian theory really reduce to a model of molecular kinetics involving competition, similar to that operating for macromolecules? It seems to me that the position of Eigen and Winkler is somewhat optimistic, since the molecular mechanism of genetic fluctuations on one side and the laws of ecology on the other are still far from being clarified.

Still, it is interesting to apply models to specific situations, as in Eigen's original work, to be able to attach a precise meaning to concepts such as the survival of the fittest.

There is a deep concern with human fate. To quote Eigen and Winkler: "Man is neither a mistake of Nature nor is Nature taking care automatically of his preservation. Mankind is participating in a big game the result of which is still open. Man has to develop his potentialities to assert his role as a player in order not to be reduced to a mere object of chance" (translation by the reviewer). ☐

Professor Prigogine is Professor of Physics at the Free University of Brussels, Belgium.

Lay guide to mircobiology

Invisible Allies: Microbes and Man's Future. By Bernard Dixon. Pp. 251. (Temple Smith: London, May 1976.) £4

IT was difficult for me, now approaching the end of a career in microbiology, to judge a book intended for lay-people. Too often 'nit picking' intervened. The opinion which follows is partly my own and partly that of friends and relations, all lay-people (except for an acquaintance with me). The title of the book underlies an admirable intention. That is, it seeks to dispel the attitude, still too common even in our new students, that sees microbiology in terms of medicine and thus all microbes as enemies. How disappointing, for instance, was the BBC Television series *Microbes and Man* in this respect: Dixon's book might well form the basis of a remedial programme. The treatment has less detailed biology than that out of the classic *Microbes by the Million* and is possibly less professional than John Postgate's *Microbes and Man* (obligatory for our first-year students). Dixon's book should be obligatory to all lay people with a spark of interest in their own relationship to the living world. After a brief, rather sketchy description of microbes, it goes on to describe their role in the biological production cycle, and their exploitation. Besides having value in their own right microbes now play an important role in experimental biology; this, and especially the advances in molecular biology, are well treated but some of the examples used in talking about evolution could have been more relevant. Microbial infection, so often seen as an all-or-none process, is placed in the perspective of ecology. Aspects of microbiology now causing alarm such as germ warfare and genetic engineering are briefly discussed. A general criticism was of the rather concentrated writing and the lack of good diagrams or other illustrations. These undoubtedly would have improved the book considerably and reduced the concentrated wordiness, provided time for reflective pauses and given some indication of the scale of industrial process.

If a good book is one that helps a change of mind then this is undoubtedly a good book. My copy will be to hand to press on those who wonder how I have spent my time and their taxes. **D. E. Hughes**

D. E. Hughes is Professor of Microbiology at University College, Cardiff, UK.

BOOKS
ON PURE
AND APPLIED SCIENCE

Books reviewed or mentioned in this journal are available from stock.

Catalogues on application.

Please state interests.

SCIENTIFIC LIBRARY
ANNUAL SUBSCRIPTION from £5.00
Reduced rates for multiple subscriptions
Available in U.K. only
Prospectus free on request

H. K. LEWIS & Co. Ltd.
LONDON: 136 GOWER STREET,
WC1E 6BS
Telephone: 01-387 4282

Circle No. 10 on Reader Enquiry Form.

Ultrastructural masterpiece

Ultrastructure and The Biology of Plant Cells Pp.312 (49 plates). £27.50. *Plant Cell Biology: An Ultrastructural Approach.* Pp.280. £2.75 paper. By Brian E. S. Gunning and Martin W. Steer. (Arnold: London, 1975.)

THERE is currently available a number of books dealing with the ultrastructure of plant cells, each of which provide a series of excellent electron micrographs. They are, however, often flawed by an indifferent text. The pair of books presented here are a welcome exception. The smaller student book is derived from the other (a reference tome), and they collectively represent a masterpiece. The authors have been wholly successful in the enormously difficult task of illustrating the dynamic nature of cell structure using the essentially static medium of electron microscope snapshots.

The major book, although hideously expensive, is beautifully produced; and the photographs, collected together at the end, are superb. There are 49 plates, almost all of which comprise multiple montages; and virtually every conceivable aspect of plant cell structure, from general features common to all cells, to specialised structures, such as cuticles, pollen grains and glands are represented The illustrated material is amply supported by an extensive and erudite text which deals with the subject at a very high level—not really suitable for students—but of great value to university teachers and research workers.

The book begins, as is almost obligatory with this topic, by describing in detail the various methods used to prepare, section and visualise plant material, giving due emphasis to the advantages and shortcomings of all the techniques. After a general chapter on cell structure with particular reference to membranes, the coverage subsequently works from the outside inwards—that is, cell wall and plasma membrane, vacuole and tonoplast, nucleus, endoplasmic reticulum, Golgi apparatus, mitochondria, plastids, microbodies and sphaerosomes, microtubules and microfilaments, and cell division. As may be expected from these authors, the chapter on plastids is particularly rewarding, with a masterly coverage of the structure of the granum and the prolamellar body. This chapter, however, is merely a prominent peak in a high mountain range. I was particularly impressed by the careful attention of the authors to comparative sizes of cell constituents. The book is finished off with a scholarly treatment of the cell as an integrated unit and a very comprehensive list of references.

The smaller book is in reality a reprint of the 49 plates of the larger book together with the figure legends and a minimum of extra text. As a book for students it is likely to be quite useful, although it could have been improved by the addition of a précis of the text from the larger book. It seems rather remarkable that the figures of the larger book can be put on sale for one-tenth of the price of the whole book, when we are always being told that half-tone reproduction is extremely expensive. Publishing houses clearly move in a mysterious way . . .

Apart from the price, the larger book is an excellent buy and lecturers might well consider using it as a basic text, recommending their students to use the cheaper version with the photographs. **Harry Smith**

Harry Smith is Professor of Plant Physiology in the Department of Physiology and Environmental Studies at the University of Nottingham, UK.

Optical multilayers

Optics of Thin Films. (An Optical Multilayer Theory.) By Zdenek Knittel. (Wiley Series in Pure and Applied Optics.) Pp. 548. (Wiley-Interscience: London and New York, February 1976.) £15; $33.

THE appearance of this volume is timely. Since the appearance of the first book on this subject, in 1955, considerable developments have occurred, and the optical multilayer has become a normal—and in some cases crucial—component in many optical systems. With the availability of computers, multilayer calculations have become straight-forward and great progress has been made in automatic design routines in which the computer is given the desired reflection–transmission curve and is asked to determine appropriate layer thicknesses. Dr Knittl's long experience in the optical industry has put him in a strong position to write with authority on the many developments of the past twenty years. Many of the methods described enable an insight to be obtained on the way in which multilayer properties are influenced by changes in particular layers. Such methods can assist in design problems without the need for mammoth number-crunching powers and can serve for many simple systems. A useful section is included on inhomogeneous layers which still remain to be fully exploited in the practical field.

The book will form a useful reference work for the multilayer designer. There are one or two unfortunate features which make for difficulties in reading. In the text, the boundaries between layers are envisaged as being in a vertical plane, so that waves are described as going towards right or left, whereas in figures the boundaries are shown as horizontal planes. Some graphs have no labels on the axes and in some cases too little information is given to understand readily the significance of graphs bearing several curves In one example, curves are given for an anti-reflecting system embedded in a medium of refractive index 1 2—a curious choice in view of the absence of any real material with this value of refractive index. These are, however, fairly minor points.

O. S. Heavens

O. S. Heavens is Professor of Physics at the University of York, UK.

SCIENCE EDITOR

THE MACMILLAN PRESS

As our rapid but controlled growth continues, we have decided to separate the pure science and medical lists. We are therefore seeking someone to take over and develop our established pure sciences programme.

The successful applicant will report to the Publisher for the Scientific, Technical & Medical Division, but will assume complete responsibility for both the undergraduate and postgraduate programmes in chemistry, physics, biochemistry, biological sciences, computer science, and applied mathematics.

Ability, enthusiasm, and potential are more important than either age or experience, although we will be looking for some publishing background.

The appointment is based in Basingstoke. The salary will be competitive and a company car will be provided. Applications (which will be treated in strictest confidence) to:

Sydney A Josephs
Publishing Director
The Macmillan Press
Houndmills
Basingstoke
Hampshire RG21 2XS

obituary

Harry Nyquist, widely known for his theoretical studies and practical inventions in the field of communications, died on April 4 at the age of 87 in Harlingen, Texas. Born in Nilsby, Sweden, on February 7, 1889, Nyquist was the son of Lars and Katarina Nykvist. He emigrated to Minnesota in 1907 and taught at the Southern Minnesota Normal School in Austin, Minnesota. Nyquist earned his BA, BS and MS degrees from the University of North Dakota, and in the summers worked at the National Bureau of Standards and the US Patent Office.

He joined the American Telephone and Telegraph Company in 1917, shortly after he had obtained his PhD in physics from Yale University, and moved to the Bell Telephone Laboratories in 1934.

From 1917 to 1921 he worked primarily on the development of the metallic telegraph system and methods of measuring telegraph distortion. From 1921 to 1935 he devoted considerable time investigating television techniques, and worked on projects aimed at extending and improving long-distance telephone circuits.

After 1935, Nyquist devoted most of his time to research work where he applied his broad knowledge and analytical ability to the most difficult of challenges in the field of communications development. For the two years before his retirement in 1954 he was Bell Laboratories' Assistant Director of Systems Studies.

Nyquist was awarded 138 patents during his 37 years with the Bell System. Many of his inventions and theories are widely accepted as fundamental to voice, picture and data transmission. His discovery of the conditions necessary to keep feedback circuits stable, the 'Nyquist Criterion', brought him widespread acclaim. It is used not only in the study of electronic devices, such as amplifiers, but even in the study of human regulating processes—for example, to describe the way in which a person steers a car.

He gave the first quantitative explanation of thermal noise, and through theoretical analysis determined the minimum band of frequencies required to transmit various kinds of communication signals. These studies laid the foundation for modern information theory and data transmission. In the television field, Nyquist invented a method of transmission used in broadcasting today, and also discovered a way to correct delay distortion of TV images.

Among the many honours Nyquist received were: the Mervin J. Kelly Award of the AIEE (1961), the National Academy of Engineering founders Medal (1969) and the Rufus Oldenburger Medal from the ASME (1975).

Harald Trap Friis, a pioneer in the development of radio communications and an initiator of microwave radio transmission and radio astronomy, died on June 15. He was 83 years old.

Friis was born in Naestved, Denmark, February 22, 1893. He attended the Royal Technical College in Copenhagen, where he received his Electrical Engineering degree in 1916 and his Doctorate in Science in 1938. From 1917 to 1918 he worked as Technical Advisor at the Royal Gun Factory in Copenhagen. In 1919, upon receipt of a Fellowship from the American-Scandinavian Foundation, he moved to the United States to study at Columbia University.

In 1920 Friis joined the Western Electric Company's research department, the predecessor organisation to Bell Laboratories, and in the twenties he designed the first commercial 'double-detection super-heterodyne broadcast radio receiver', the forerunner of present-day radios. In 1923, Friis spent several months in England devising receivers for a long-wave transatlantic telephone link. In the decade that followed he is credited with designing a receiver that automatically compensated for fading signals, an improved directional antenna, and methods for recording static and measuring fading shortwave signals.

His most famous achievement was, however, in the design of antennae. One designed by Friis together with Bell Labs colleague, Karl Jansky, was the first to detect 'star noise' in 1932—the birth of radio astronomy. The rhombic antenna designed by Friis and another colleague, Edmond Bruce, found worldwide use in shortwave radio telephony, and yet another of his antennae—the Multiple Unit Steerable Antenna—made it possible, Friis said, "to unravel the phenomena of shortwave transmissions". He was the coauthor of the book *Antennas: Theory and Practice* (1952).

In 1938 Friis moved from shortwaves to microwaves and created the horn-reflector antenna, now seen on tower tops all over the country. During this period Friis put together the basic elements of a microwave telephone system. A year after the end of the war, the first experimental microwave circuits based on Friis' designs were installed for domestic use and today, Bell System microwave radio facilities provide some 380 million miles of long distance telephone circuits.

Following his retirement, Friis spent 10 years as a research consultant to the Hewlett–Packard company in Palo Alto, California. He published an autobiography, *Seventy Five Years in an Exciting World* in 1971.

announcements

Meetings

September 9–10, **565th Meeting of the Biochemical Society,** Stirling (The Meetings Officer, The Biochemical Society, 7 Warwick Court, Holborn, London WC1R 5DP).

September 15–17, **Herbicides and Fungicides, Factors Affecting Their Activity,** Bangor, Wales (Dr S. Turner, Reckitt and Colman Pharmaceutical Division, Dansom Lane, Hull HU8 7DS.).

October 11–13, **Transportation and Communications,** Genoa (Segretaria Generale IIC, Villa Piaggio, Via Pertinace–16125 Genova, Italy).

October 22, **Human and Animal Endoparasites,** London (The Assistant Secretary, Society of Chemical Industry, 14 Belgrave Square, London SW1X 8PS).

November 15–26, **Weather Forecasting in Africa,** Dakar, Senegal (The Secretariat, WMO, Geneva, Switzerland).

November 19, **The Newer Applications of Pyrethroids,** London (The Assistant Secretary, Society of Chemical Industry, 14 Belgrave Square, London SW1X 8PS).

nature

Author Index for Volume 262

July–August 1976
Numbers 5563–5571
Pages 1–826

Author Index Volume 262

Aaronson S. A. *see under* Barbacid M , **262,** 554
Adams G. E. *see under* Israelachvili J N., **262,** 774
Adams R. N. *see under* Wightman R M , **262,** 145
Adinolfi M., Beck S. E., Haddad S. A. and Seller M. J. Permeability of blood-cerebrospinal fluid barrier during foetal and perinatal life — Reply, *matters arising,* **262,** 156
Akematsu T. *see under* Ueda N , **262,** 581
Albano J., Bhoola K. D. and Harvey R. F. Intracellular messenger role of cyclic GMP in exocrine pancreas, **262,** 404
Alexander M. *see under* Dean-Raymond D , **262,** 394
Alexandersson E. T. Actual and anticipated petrographic effects of carbonate undersaturation in shallow seawater, **262,** 653
Aller H. D. *see under* Ledden J E , **262,** 669
Allison A. C. Purine and pyrimidine metabolism, *news and views,* **262,** 7
Amaral L. and Werthamer S. Identification of breast cancer transcortin and its inhibitory role in cell-mediated immunity, **262,** 589
Amici D. *see under* Gianfranceschi G L , **262,** 622
Amsel A., Burdette D. R. and Letz R. Appetitive learning, patterned alternation, and extinction in 10-d-old rats with non-lactating suckling as reward, **262,** 816
Anderson B. F., Buckingham D. A., Robertson G. B., Webb J., Murray K. S. and Clark P. E. Models for the bacterial iron-transport chelate enterochelin, **262,** 722
Andrew R., Grant W. A., Grundy P. J., Williams J. S. and Chadderton L. T. Non-crystallinity of ion-irradiated metals, **262,** 380
Angus A. M. *see under* Colles M J , **262,** 681
Anné J., Eyssen H. and De Somer P. Somatic hybridisation of *Fenicillium roguefortii* with *P chrysogenum* after protoplast fusion, **262,** 719
Anteunis M. *see under* Roques B P , **262,** 778
Arfors K. E., Forsberg J. O., Larsson B., Lewis D. H. Rosengren B. and Odman S. Temporary intestinal hypoxia induced by degradable microspheres, **262,** 500
Arny D. C., Lindow S. E. and Upper C. D. Frost sensitivity of *Zea mays* increased by application of *Pseudomonas syringae,* **262,** 282
Arst H. N. Jr. Integrator gene in *Aspergillus nidulans,* **262,** 231
Asato A. *see under* DeGrip W J , **262,** 416
Ashton B. A. *see under* Triffitt J T , **262,** 226
Asimakopoulos D. N *see under* Caughey S J , **262,** 274
Atkins J. Expression of a eukaryotic gene in *Escherichia coli,* *news and views,* **262,** 256
Audigier Y., Virion A. and Schwartz J.-C. Stimulation of cerebral histamine H_2 receptors by clonidine, **262,** 307
Auman J. R. and McCrea W. H. Solar neutrinos and galactic contamination of the Sun, **262,** 560
Austen D. E. G. Factor VIII, *news and views,* **262,** 91
Avner P. *see under* Golstein P , **262,** 693
Axelrod F., Mittag T. W. and Green J. P. Familial dysautonomia, *news and views,* **262,** 742
Ayyash S. *see under* McComb W D , **262,** 47
Azzarone B., Pedulla D. and Romanzi C. A. Spontaneous transformation of human skin fibroblasts derived from neoplastic patients, **262,** 74
Baba M. *see under* Mitsuoka A , **262,** 77
Bach F. H. *see under* Zarling J M , **262,** 691
Bachrach U. *see under* Gazdar A F , **262,** 696
Bada J. L. *see under* Helfman P M , **262,** 279
Bahcall J. N. and Ostriker J. P. X-ray pulses from globular clusters, **262,** 37
Baird T. *see under* Murata Y , **262,** 721
Baker M. E. Colchicine inhibits mitogenesis in C1300 neuroblastoma cells that have been arrested in G, **262,** 785
Bandman E. *see under* Ouellette A J , **262,** 619
'Bandu M.-T. *see under* Stewart W E II, **262,** 300
Barbacid M., Stephenson J. R. and Aaronson S. A. *gag* Gene of mammalian type-C RNA tumour viruses, **262,** 554
Barnaby W. Down Georgia way, *news,* **262,** 250
Bartram C. R. *see under* Rudiger H W , **262,** 290
Batts B. D. *see under* Jull A J T , **262,** 566
Baulieu E.-E. *see under* Schorderet-Slatkine S , **262,** 289
Beasley T. M. and Fowler S. W. Plutonium isotope ratios in polychaete worms, **262,** 813
Beck S. E. *see under* Adinolfi M , **262,** 156
Beezley D. N. *see under* Sharman O K , **262,** 62
Belitzky B. New giant Soviet radiotelescope, *news and views,* **262,** 535
Bell K. *see under* Blenkinsop J , **262,** 377
Bell-Burnell S J. *see under* Mason K O , **262,** 474
Ben T. *see under* Yuspa S H , **262,** 402
Bencze G. *see under* Kiss I., **262,** 136
Ben-Menahem A. Dating of historical earthquakes by mud profiles of lake-bottom sediments, **262,** 200
Berendsen H. J. C. *see under* Robillard G T , **262,** 363
Berens R. L. *see under* Brun R , **262,** 689
Berman B. L. *see under* Browne J. C , **262,** 197
Bertaux J. L and Blamont J. E. Possible evidence for penetration of interstellar dust into the Solar System, **262,** 263
Beverley P. C. L., Woody J., Dunkley M., Feldmann M. and McKenzie I. Separation of suppressor and killer T cells by surface phenotype, **262,** 495
Bhoola K. D. *see under* Albano J , **262,** 404
Bigg D C. H. and Purvis S. R. Muscarinic argonists provide a new class of acaricide, **262,** 220
Biggar G. M. *see under* Jull A J T , **262,** 566
Billeter M. A. *see under* Cashion L M , **262,** 186
Bissette G., Nemeroff C. B., Loosen P. T., Prange A. J. Jr and Lipton M. A. Hypothermia and intolerance to cold induced by intracisternal administration of the hypothalamic peptide neurotensin, **262,** 607
Bjorklund A., Stenevi U., Svendgaard N.-A. Growth of transplanted monoaminergic neurones into the adult hippocampus along the perforant path, **262,** 787
Blackshaw S. and Warner A. Onset of acetylcholine sensitivity and endplate activity in developing myotome muscles of *Xenopus,* **262,** 217
Blackwood G. C. *see under* Johnson C B , **262,** 133
Blak V. A. *see under* Blanpied G D , **262,** 574
Blake C. C. F. Interpreting protein electron density maps, *news and views,* **262,** 172
Blamont J. E. *see under* Bertaux J L , **262,** 263
Blanpied G. D., Creasy L. L., Blak V. A. and Lewis L. W. Leaf cultivar influences composition and ripening of apples, **262,** 574
Blenkinsop J., Cucman P. F. and Bell K. Age relationships along the Hermitage Bay-Dover Fault system, Newfoundland, **262,** 377
Boccara M. *see under* Kelly F , **262,** 409
Boddy K. Activation analysis *in vivo,* **262,** 6
Boehme D. E., Vincent K. and Brown O. R. Oxygen and toxicity inhibition of amino acid biosynthesis, **262,** 418
Bolton P. H. and Kearns D. R. Quantification of secondary and tertiary structure base pairs in *E coli* tRNA$_1$(Val), *matters arising,* **262,** 423
Bone A. J. and Taylor K. W. Metabolic adaptation to pregnancy shown by increased biosynthesis of insulin in islets of Langerhans isolated from pregnant rats, **262,** 501
Bonnett R., Davies J. E. and Hursthouse M. B. Structure of bilirubin, **262,** 326
Boot J. R. *see under* Dawson W , **262,** 699
Bordas J., Munro I. H. and Glazer A. M. Small-angle scattering experiments on biological materials using synchrotron radiation, **262,** 541
Borek E. *see under* Sharma O K., **262,** 62
Bostock C. J., Christie S. and Hatch F. T. Accessibility of DNA in condensed chromatin to nuclease digestion, **262,** 516
Botnik L. E., Hannon E. C. and Hellman S. Limited proliferation of stem cells surviving alkylating agents, **262,** 68
Bowers W. S. *see under* Washio H., **262,** 487
Bowling D. J. F. Malate-switch hypothesis to explain the action of stomata, **262,** 393
Boyan G. S. *see under* Hill K G , **262,** 390
Bradshaw W. E. Geography of photoperiodic response in diapausing mosquito, **262,** 384
Brandt M., Gullis R. J., Fischer K., Buchen C., Hamprecht B., Moroder L. and Wunsch E. Enkephalin regulates the levels of cyclic nucleotides in neuroblastoma × glioma hybrid cells, **262,** 311
Branscomb E. W. *see under* Galas D J , **262,** 617
Bras G. *see under* Ross M H , **262,** 548
Bray J. R. Volcanic triggering of glaciation — Reply, *matters arising,* **262,** 330
Bray M. A. *see under* Gordon D , **262,** 401
Brenner H. R. Reduction of quantum contents of synaptic potentials after postsynaptic axotomy, **262,** 598
Brent L. and Kilshaw P. J. Anti-idiotypic antibodies a clinical future? *news and views,* **262,** 443
Bridle A. H., Davis M. M., Meloy D. A., Fomalont E. B., Strom R. G. and Willis A. G. Giant radio galaxy NGC315, **262,** 179
Briggs G. A. D. and Briscoe B. J. Effect of roughness on rubber friction when waves of detachment are present, **262,** 381
Brimacombe R. EMBO ribosome workshop, *news and views,* **262,** 740
Briscoe B. J. *see under* Briggs G A. D , **262,** 381
Brockes J. Muscle disease at Durango, *news and views,* **262,** 446
Broughton W. J., Wooi K. C. and Hoh C. H. Acetylene reduction by legume root nodule protoplasts, **262,** 208
Brown R. D., Godfrey P. D., Storey J. W. V. and Clark F. O. Detection of interstellar HN^{13}C, **262,** 672
Brown O. R. *see under* Boehme D E , **262,** 418
Browne J. C. and Berman B. L. Neutron-capture cross sections for ^{186}Os and ^{187}Os and the age of the Universe (Browne J C and Berman B. L) **262,** 197
Brun R., Berens R. L. and Krassner S. M. Inhibition of *leishmania donovani* transformation by hamster spleen homogenates and active human lymphocytes, **262,** 689
Brune J. N. *see under* Prothero W A , **262,** 121
Brutsaert D. L. *see under* Housmans Ph R , **262,** 56
Bryant P. Concentration factors and radiological protection, *news,* **262,** 737
Buchen C. *see under* Brandt M , **262,** 311
Buckingham D. A. *see under* Anderson B F , **262,** 722
Bunge R. *see under* Johnson M., **262,** 308
Burdette D. R. *see under* Amsel A , **262,** 816
Burleigh R. and Hewson A. Evidence for short term atmospheric ^{14}C variations about 4,000 yr BP, **262,** 128
Burrows M. and Siegler M. V. S. Transmission without spikes between locust interneurones and motoneurones, **262,** 222
Burton H. *see under* Johnson M , **262,** 308
Butler D. M. *see under* Talbot R J Jr , **262,** 561
Calvez B. *see under* Legay J -M , **262,** 489
Calvin M. *see under* Philp R P , **262,** 134
Campbell R. D., Josephson R. K., Schwab W. E. and Rushforth N. B. Excitability of nerve-free hydra, **262,** 388
Candau P., Manzano C. and Losada M. Bioconversion of light energy into chemical energy through reduction with water of nitrate to ammonia, **262,** 715
Carlisle T. R. *see under* Dawkins R., **262,** 131
Carlqvist P. and Laurent B. The cosmic X-ray background — Reply, *matters arising,* **262,** 821
Carlucci A. F. *see under* Williams P M , **262,** 810
Carpenter G. F., Skinner G. K., Wilson A. M. and Willmore A. P. Positions and evidence for a steady component for X-ray burst sources, **262,** 473
Carpenter M. S. N. and Civetta L. Hercynian high pressure/low temperature metamorphism in the Ile de Groix Blueschists, **262,** 276
Carter J. Expression of maternal and paternal antigens on trophoblast, **262,** 292
Carter J., Dean A. J., Manchada R. K. and Ramsden D. New limit on the size distribution of gamma-ray bursts, **262,** 370
Cashion L. M., Joho R. H., Planitz M. A., Billeter M. A. and Weissmann C. Initiation sites of Rous sarcoma virus RNA-directed DNA synthesis *in vitro,* **262,** 186
Casoli C. *see under* Pesce A , **262,** 412
Caughey S. J., Crease B. A., Asimakopoulos D. N. and Cole R. S. A comparison of acoustic Doppler vertical velocities with direct measurements in the atmospheric boundary layer, **262,** 274
Cavalier-Smith T. Long palindromes in eukaryotic DNA, *news and views,* **262,** 255
Celis J. E. *see under* Piper P W , **262,** 757
Chabre M. *see under* Saibil H , **262,** 266
Chadderton L. T. *see under* Andrew R , **262,** 380
Chakraborty R. *see under* Nei M , **262,** 491
Chapman R. W., Morris R. O. and Zaerr J. B. Occurrence of *trans*-ribosylzeatin in *Agrobacterium tumefaciens* tRNA, **262,** 153
Chase R. *see under* Honigman A , **262,** 112
Chivers R. C. Acoustic Bragg diffraction from human tissues, *matters arising,* **262,** 330
Cho H. J. Is the scrapie agent a virus, **262,** 411
Chow T. J. *see under* Goucher C L , **262,** 130
Christie S. *see under* Bostock C J , **262,** 516
Chujo T. *see under* Yamamoto C , **262,** 786
Chutná J. *see under* Hašek M , **262,** 295
Ciavarella N. *see under* Mannucci P M , **262,** 141
Civetta L. *see under* Carpenter M S N , **262,** 276
Claisse P. J. *see under* Roscoe J P , **262,** 314
Clark F. O. *see under* Brown R D , **262,** 672
Clark P. E. *see under* Anderson B F , **262,** 722
Clark R. J. New cranium of *Homo erectus* from Lake Ndutu, Tanzania, **262,** 485
Close F. E. Iliopoulos wins his bet, *news and views,* **262,** 537
Clough J. M. *see under* Hey M J , **262,** 807
Cockerill A. F. *see under* Dawson W , **262,** 699
Coe M. J *see under* Quenby J J , **262,** 471
Coe M. J., Engel A. R. and Quenby J. J. Hard X-ray observations of Circinus X-1 during an outburst, **262,** 563
Cohen I., Giles W. and Noble D. Cellular basis for the T wave of the electrocardiogram, **262,** 657
Coimbra-Filho A. F. and Mittermeier R. A. Exudate-eating and tree-gouging in marmosets, *matters arising,* **262,** 630
Colburn N. *see under* Yuspa S H , **262,** 402
Cole R. S. *see under* Caughey S J , **262,** 274
Coleman G. D., Hintzen P., Scott J. S. and Tarenghi M. The radio tail galaxies in Abell 1314, **262,** 476
Colles M. J., Angus A. M. and Marinero E. E. Opto-acoustic spectroscopy of products of continuous photolysis of nitromethane, **262,** 681
Colley D. G. *see under* Miller A M , **262,** 586
Colston M. J. and Hilson G. R. F. Growth of *Mycobacterium leprae* and *M marinum* in congenitally athymic (nude) mice, **262,** 399
Conroy G. C. Hallucial tarsometatarsal joint in an oligocene anthropoid *Aegyptopithecus zeuxis,* **262,** 684
Cooke B. A. *see under* Pye J P , **262,** 195
Cooke H. Repeated sequence specific to human males, **262,** 182
Cooper G. P. *see under* Kober T E , **262,** 704
Cowdin H. P. *see under* Jokiel P L , **262,** 212
Cox F. E. G. Human trypanosomiasis today, *news and views,* **262,** 646
Coxon D. T. *see under* Hargreaves J A , **262,** 318
Crease B. A. *see under* Caughey S J , **262,** 274
Creasy L. L. *see under* Blanpied G D , **262,** 574
Cromeans T. L. *see under* Shore S L , **262,** 695
Cronan D. S. Implications of metal dispersion from submarine hydrothermal systems for mineral exploration on mid-ocean ridges and in island arcs, **262,** 567
Cross H. E. Population studies and the Old Order Amish, **262,** 17
Crozier R. H. Counter-intuitive property of effective population size, **262,** 384
Cuatrecasas P. *see under* Sandoval I V , **262,** 511
Cueman P. F. *see under* Blenkinsop J , **262,** 377
Cull-Candy S. G., Donnellan J. F., James R. W. and Lunt G. G. 2-Amino-4-phosphonobutyric acid as a glutamate antagonist on locust muscle, **262,** 408
Curtis G. H. *see under* Leakey M D , **262,** 460
Curzon G. *see under* Hutson P H , **262,** 142
Dallos P. *see under* Pierson M , **262,** 599
Daniell G. J. *see under* Smith R A , **262,** 761
Das M. R. *see under* Padhy L C , **262,** 805
Das M. R., Padhy L. C., Koshy R., Sirsat S. M. and Rich M. A. Human milk samples from different ethnic groups contain RNase that inhibits, and plasma membrane that stimulates, reverse transcription, **262,** 802
Davidson A. and McGregor D. C. Palynomorphs indicating Permian rocks in Ethiopia, **262,** 371
Davies D. K. 'Space' charging of insulators, **262,** 277

Charges and vacuum flashover, **262,** 279
Davies H. G. Chromatin superstructure, *news and views,* **262,** 533
Davies J. and Dray A. Changes in amino acid sensitivity during polypeptide 'desensitisation', **262,** 606
Effects of enkephalin and morphine on Renshaw cells in feline spinal cord, **262,** 603
Davies J. E. *see under* Bonnett R , **262,** 326
Davies P. A. *see under* Sigurdsson J B , **262,** 386
Davis M. M. *see under* Bridle A H , **262,** 179
Dawkins R. and Carlisle T. R. Parental investment, mate desertion and a fallacy, **262,** 131
Dawson W., Boot J. R., Cockerill A. F., Mallen D. N. B. and Osborne D. J Release of novel prostaglandins and thromboxanes after immunological challenge of guinea pig lung, **262,** 699
Day A. W. Communication through fimbriae during conjugation in a fungus, **262,** 583
de Jonge H. R. Cyclic nucleotide-dependent phosphorylation of intestinal epithelium proteins, **262,** 590
De Reggi M. L. *see under* Legay J.-M , **262,** 489
De Somer P. *see under* Anné J , **262,** 719
Dean A. J. *see under* Carter J , **262,** 370
Dean-Raymond D. and Alexander M. Plant uptake and leaching of dimethylnitrosamine, **262,** 394
DeGrip W. J., Liu R. S. H., Ramamurthy V. and Asato A. Rhodopsin analogues from highly hindered 7-*cis* isomers of retinal, **262,** 416
Dehmelt H. *see under* Van Dyck R Jr, **262,** 776
Dehmelt H. G. Entropy reduction by motional sideband excitation, **262,** 777
Dev V. G. *see under* Tantravahi R , **262,** 63
Devor M. and Wall P. D. Type of sensory nerve fibre sprouting to form a neuroma, **262,** 705
Dice J. F. and Goldberg A. L. Structural properties of rat serum proteins which correlate with their degradative rates *in vivo,* **262,** 514
Dickson C. *see under* Shyamala G., **262,** 107
Dickson J. H., Jardine W. G and Price R. J. Three late-Devensian sites in West-central Scotland, **262,** 43
Dingledine R. *see under* Iversen L , **262,** 738
Dixon R. O. D. Hydrogenases and efficiency of nitrogen fixation in aerobes, *news and views,* **262,** 173
Donnellan J. F. *see under* Cull-Candy S G , **262,** 408
Donovan R. J., Kaufmann K. and Wolfrum J. Reactions of $O(2^1D_2)$ with chlorofluoromethanes and CCl_4, **262,** 204
Dorozynski A. The attack on tropical disease, *news,* **262,** 85
Dover S. D. Metals in proteins, *news and views,* **262,** 176
Downes D. *see under* Genzel R , **262,** 564
Doyle B. B., Hukins D. W. L., Hulmes D. J. S., Miller A., Rattew C. J. and Woodhead-Galloway J. Ionic clustering and collagen specificity, *matters arising,* **262,** 629
Drake R. E. *see under* Leakey M D , **262,** 460
Dray A. *see under* Davies J , **262,** 603
see under Davies J , **262,** 606
Dubey J. P. Reshedding of *Toxoplasma* oocysts by chronically infected cats, **262,** 213
Duckenfield M. Europe's ageing research staffs, *news,* **262,** 638
Dudai Y. *see under* Quinn W G , **262,** 576
Dunkley M. *see under* Beverley P C L , **262,** 495
Dziegielewska K. M. *see under* Saunders N R , **262,** 156
Dziewonski A. M. *see under* O'Connell R J , **262,** 259
Eagle R. J. *see under* Noshkin V E , **262,** 745
Eardley D. D. *see under* Gershon R K , **262,** 216
Eardley D. M. and Lightman A. P. Inverse Compton spectra and the spectrum of Cygnus X-1, **262,** 196
Eckert R. *see under* Schmidt J A , **262,** 713
Edmunds M. G. Do exploding stars leave tracks in the dust? *news and views,* **262,** 350
Eglinton G. *see under* Jull A J T , **262,** 566
Egyházi E. Initiation inhibition and reinitiation of the synthesis of heterogeneous nuclear RNA in living cells, **262,** 319
Ekers R. D., van der Hulst J. M. and Miley G. K. The 21-cm absorption line in NGC1275, **262,** 369
Ekstrom P. *see under* Van Dyck R Jr, **262,** 776
Ellis D. and Thomas R. C. Microelectrode measurement of the intracellular *p*H of mammalian heart cells, **262,** 224
Elsner R. F. and Lamb F. K. Accretion flows in the magnetospheres of Vela X-1, A0535+26 and Her X-1, **262,** 356
Elvis M. *see under* Pye J P , **262,** 195
Enaka K. *see under* Sakakibara K , **262,** 316
Engbaek F. *see under* Piper P W , **262,** 757
Engel A. R. *see under* Coe M J , **262,** 563
see under Quenby J J , **262,** 471
Engel W. *see under* Schmidtke J , **262,** 593
Epel D. *see under* Johnson J D , **262,** 661
Ermishkin L. N., Kasumov Kh. M. and Potzeluyev V. M. Single ionic channels induced in lipid bilayers by polyene antibiotics amphotericin B and nystatine, **262,** 698
Erwin J. *see under* Oswald M , **262,** 686
Etienne P., Young S. N. and Sourkes T. L. Inhibition by albumin of tryptophan uptake by rat brain, **262,** 144
Evans M. E. Test of the dipolar nature of the geomagnetic field throughout Phanerozoic time, **262,** 676
Eyssen H. *see under* Anne J , **262,** 719
Fall S. M. and Jones B. J. T. Isotropic cosmic expansion and the Rubin-Ford effect, **262,** 457
Faulk W. P. and Temple A. Distribution of B^2 microglobulin and HLA in chorionic villi of human placentae, **262,** 799
Feldmann M. *see under* Beverley P C L , **262,** 495
Fernandez H. L. and Inestrosa N. C. Role of axoplasmic transport in neurotrophic regulation of muscle end-plate acetylcholinesterase, **262,** 55
Fichtel C. E. *see under* Stecker F. W., **262,** 447
Fischer K. *see under* Brandt M., **262,** 311
Flugel M. *see under* Schmidtke J., [illegible], 593
Fodor A. *see under* Kiss I , **262,** 136
Folzer C. M. *see under* Worthington C. R., **262,** 626
Fomalont E. B. *see under* Bridle A H., **262,** 179
Forsberg J. O. *see under* Arfors K E , **262,** 500
Fowler S. W. *see under* Beasley T M , **262,** 813
Fox T. D. Identification of phage SP01 proteins coded by regulatory genes 33 and 34, **262,** 748
Francis P. W. Volcanic triggering of glaciation, *matters arising* **262,** 329
Franks F. and Skaer H. le B. Aqueous glasses as matrices in freeze-fracture electron microscopy, **262,** 323
Friedrich W. *see under* Pichler H , **262,** 373
Fristrom J. W. *see under* Kiss I , **262,** 136
Fryer J. R. *see under* Murata Y , **262,** 721
Fuerst P. A. *see under* Nei M , **262,** 491
Furcht L. T. *see under* Haddox M K , **262,** 146
Furukawa T., Sakuma S. and Plotkin S. A. Human cytomegalovirus infection of WI-38 cells stimulates mitochondrial DNA synthesis, **262,** 414
Fyfe W. S. How approximate are the laws of plate tectonics? *news and views,* **262,** 645
Gachelin G. *see under* Golstein P , **262,** 693
Galas D. J. and Branscomb E. W. Ribosome slowed by mutation to streptomycin resistance, **262,** 617
Gallo R. C. *see under* Wong-Staal F , **262,** 190
Garbay-Jaureguiberry C. *see under* Roques B P , **262,** 778
Garsky V. *see under* Jones C R , **262,** 779
Gaskell P. H. *see under* Krivanek O L , **262,** 454
Gazdar A. F., Stull H. B., Kilton L. J. and Bachrach U. Increased ornithine decarboxylase activity in murine sarcoma virus infected cells, **262,** 696
Gebauer U. *see under* Triffitt J T , **262,** 226
Gelin B. R. *see under* McCammon J A , **262,** 325
Gentry S. R. *see under* Haddox M K , **262,** 146
Genzel R. and Downes D. New H_2o maser near NGC7538, **262,** 564
Germeraad S. Genetic transformation in *Drosophila* by microinjection of DNA, **262,** 229
Gershon R. K., Eardley D. D. and Ptak W. Functional inactivation of suppressor T cells by heat-killed macrophages, **262,** 216
Getto C. J. *see under* Stewart J M , **262,** 784
Gianfranceschi G. L., Amici D. and Guglielmi L. Restriction of template capacity of rat liver chromatin by a non-histone peptide from calf thymus, **262,** 622
Gibb R. A. and Thomas M. D. Gravity signature of fossil plate boundaries in the Canadian Shield, **262,** 199
Gibbons W. A. *see under* Jones C R , **262,** 779
Giles W. *see under* Cohen I , **262,** 657
Gillespie D. *see under* Wong-Staal F , **262,** 190
Gillmor C. S. The history of the term 'ionosphere', *news and views,* **262,** 347
Glazer A. M. *see under* Bordas J , **262,** 541
Godfrey P. D. *see under* Brown R D , **262,** 672
Gold D. P. *see under* Pilione L J , **262,** 773
Goldberg A. L. *see under* Dice J F , **262,** 514
Goldberg N. D. *see under* Haddox M K , **262,** 146
Goldstein M. L., Ness N. F. and Wasilewski P. J. Mercury's magnetic field, *news and views,* **262,** 741
Golstein P., Kelly F., Avner P. and Gachelin G. Sensitivity of H-2-less target cells and role of H-2 in T-cell-mediated cytolysis, **262,** 693
Goodall H. *see under* Roberts A M , **262,** 493
Goody R. S., Leigh J. B., Mannherz H. G., Tregear R. T. and Rosembaum G. X-ray titration of binding of beta, gamma-imido-ATP to myosin in insect flight muscle, **262,** 613
Gordon D., Bray M. A. and Morley J. Control of lymphokine secretion by prostaglandins, **262,** 401
Goucher C. L., Teilhet J. H., Wilson K. R. and Chow T. J. Lead isotope studies of metal sources for ancient Nigerian 'bronzes', **262,** 130
Graham J. M. *see under* Knutton S , **262,** 52
Grahame-Smith D. G. *see under* Green A. R , **262,** 594
Grant W. A. *see under* Andrew R , **262,** 380
Gray J. and Thompson P. Climatic information from $^{18}O/^{16}O$ ratios of cellulose in tree rings, **262,** 481
Green A. R. and Grahame-Smith D. G. (—)-Propranolol inhibits the behavioural responses of rats to increased 5-hydroxytryptamine in the central nervous system, **262,** 594
Green J. P. *see under* Axelrod F , **262,** 742
Greenaway P. and Taylor H. H. Aerial gas exchanges in Australian arid-zone crab, *Parathelphusa transversa* Von Martens, **262,** 711
Gresser I. *see under* Stewart W E II, **262,** 300
Grewal M. S. *see under* Kochupillai N , **262,** 60
Gross J. D. *see under* Town C D , **262,** 717
Grundy P. J. *see under* Andrew R , **262,** 380
Guellaen G. *see under* Lacombe M -L , **262,** 70
Guglielmi L. *see under* Gianfranceschi G L , **262,** 622
Gullis R. J. *see under* Brandt M , **262,** 311
Gutte B. *see under* Klotz M , **262,** 791
Håkanson R. *see under* Larsson L -I , **262,** 609
Haddad S. A. *see under* Adinolfi M , **262,** 156
Haddox M. K., Furcht L. T., Gentry S. R., Moser M. E., Stephenson J. H. and Goldberg N. D. Periodate-induced increase in cyclic GMP in mouse and guinea pig splenic cells in association with mitogenesis, **262,** 146
Hallam A. How approximate are the laws of plate tectonics? — Reply, *news and views,* **262,** 645
How closely did the continents fit together? *news and views,* **262,** 94
Ham W. T. Retinal sensitivity to short wavelength light — Reply, *matters arising,* **262,** 629
Hambrook J. M., Morgan B. A., Rance M. J. and Smith C. F. C. Mode of deactivation of the enkephalins by rat and human plasma and rat brain homogenates, **262,** 782
Hamilton W. J. III and Seely M. K. Fog basking by the Namib Desert beetle, *Onymacris unguicularis,* **262,** 284
Hamlyn P. Borrowed polypeptides in Q Beta replicase, *news and views,* **262,** 257
Hammel H. T. *see under* Zachariassen K E , **262,** 285
Hamprecht B. *see under* Brandt M , **262,** 311
Hannon E. C. *see under* Botnik L E , **262,** 68
Hanoune J. *see under* Lacombe M -L , **262,** 70
Hansen C. T. *see under* Hzu C -K , **262,** 397
Harding J. M. Long term variations in western tropical Pacific cyclogenesis associated with the Southern Oscillation, **262,** 41
Hargreaves J. A., Mansfield J. W. and Coxon D. T. Identification of medicarpin as a phytoalexin in the broad bean plant (*Vicia faba* L) **262,** 318
Harmanec P. B-emission stars and X-rays sources, *matters arising,* **262,** 725
Harris J. W. K. and Isaac G. The Karari Industry Early Pleistocene archaeological evidence from the terrain east of Lake Turkana, Kenya, **262,** 102
Harrison P. R. Analysis of erythropoeisis at the molecular level, *review article,* **262,** 353
Hartsock T. L. and Nobel P. S. Watering converts a CAM plant to daytime CO_2 uptake, **262,** 574
Harvey R. F. *see under* Albano J , **262,** 404
Hašek M., Chutná J., Holáň V. and Sládeček M. Induction of transplantation tolerance using serum as antigen source, **262,** 295
Hasted J. B. and Shahidi M. The low frequency dielectric constant of supercooled water, **262,** 777
Hatch F. T. *see under* Bostock C J , **262,** 516
Hausfater G. and Watson D. F. Social and reproductive correlates of parasite ova emissions by baboons, **262,** 688
Hay A. Toxic cloud over Seveso, *news,* **262,** 636
Hay R. L. *see under Leakey M D ,* **262,** 460
Hayter J. B., Penfold J. and Williams W. G. Observation of the interference of neutrons reflected from thin films, **262,** 569
Heilbronn E., Mattsson C. and Stålberg E Bacteria necessary to produce experimental autoimmune myasthenia gravis in acetylcholine receptor-immunised rabbits? **262,** 509
Heirtzler J. Glass-rich basaltic sand and gravel within the oceanic crust at 22°N, **262,** 768
Helfman P. M. and Bada J. L. Aspartic acid racemisation in dentine as a measure of ageing, **262,** 279
Heller A. *see under* Miller B , **262,** 680
Hellman S. *see under* Botnik L E , **262,** 68
Henney C. S. *see under* Thorn R M , **262,** 75
see under Wolfe S A , **262,** 584
Hennings H. *see under* Yuspa S H , **262,** 402
Herbert J. *see under* Yates C A , **262,** 219
Hersey J. A. *see under* Yip C W , **262,** 202
Hershey H. V. and Werner D. Evidence for non-deoxynucleotide linkers in Ehrlich ascites tumour cell DNA, **262,** 148
Hesser J. E., Walborn N. R. and P. Ugarte P. Sigma Orionis E as a mass-transfer binary system, **262,** 116
Hewson A. *see under* Burleigh R , **262,** 128
Hey M. J., Clough J. M. and Taylor D. J. Ion effects on macromolecules in aqueous solution, **262,** 807
Hey R. D. Geometry of river meanders, **262,** 482
Hill C. R. *see under* Nicholas D., **262,** 330
Hill K. G. and Boyan G. S. Directional hearing in crickets, **262,** 390
Hill M., *see under* Kopecka H , **262,** 72
Hill R G., Pepper C M. and Mitchell J. F. Depression of nociceptive and other neurones in the brain by iontophoretically applied met-enkephalin, **262,** 604
Hillova J. *see under* Kopecka H , **262,** 72
Hilson G. R. F. *see under* Colston M J , **262,** 399
Hintzen P. *see under* Coleman G D , **262,** 476
Hirn M. *see under* Legay J -M , **262,** 489
Hodge P. E. *see under* Ledden J E , **262,** 669
Hodgson P. E. Fission of medium weight nuclei, *news and views,* **262,** 176
Quasi-superheavy nuclei, *news and views,* **262,** 445
Hoh C. H. *see under* Broughton W J , **262,** 208
Holaň V. *see under* Hašek M , **262,** 295
Honigman A., Hu S.-L., Chase R. and Szybalski W. 4S *oop* RNA is a leader sequence for the immunity-establishment transcription in coliphage lambda, **262,** 112
Horowitz N. H. *see under* Klein H P , **262,** 24
Horrell R. I. *see under* Redgrave P , **262,** 305
Hounam I. *see under* Slesser M , **262,** 244
Housmans Ph. R. and Brutsaert D. L. Three-step yielding of load-clamped mammalian cardiac muscle, **262,** 56
Howie A. *see under* Krivanek O L , **262,** 454
Hozur M. V. *see under* Viswamitra M A., **262,** 234
Hsu S. H. *see under* Hzu C -K., **262,** 397
Hu S.-L. *see under* Honigman A , **262,** 112
Hughes D. Farmington an Apollo meteorite, *news and views,* **262,** 739
Hughes D. W. Britain in European space, *news and views,* **262,**

538
Meteoroid swarms colliding with the Moon, *news and views*, **262,** 175
Hui S. W. Direct measurement of membrane motion and fluidity by electron microscopy, **262,** 303
Hukins D. W. L. *see under* Doyle B B , **262,** 629
Hulmes D. J. S. *see under* Doyle B B , **262,** 629
Hursthouse M. B. *see under* Bonnett R , **262,** 326
Hutson P. H., Knott P. J. and Curzon G. Control of brain tryptophan concentration in rats on a high fat diet, **262,** 142
Hzu C.-K., Hzu S. H., Whitney R. A. Jr and Hansen C. T. Immunopathology of schistosomiasis in athymic mice, **262,** 397
Icke V. Spiral galaxies at Cambridge, *news and views*, **262,** 647
Ineichen K. *see under* Walz A , **262,** 665
Inestrosa N. C. *see under* Fernandez H L., **262,** 55
Isaac G. *see under* Harris J W K., **262,** 102
Israelachvili J. N. and Adams G. E. Direct measurement of long range forces between two mica surfaces in aqueous KNO_3 solutions, **262,** 774
Iversen L. and Dingledine R. Enkephalin the latest instalment, *news and views*, **262,** 738
Iversen L. L. *see under* Minneman K P , **262,** 313
Jackes M. K. *see under* Leakey M D , **262,** 460
Jackson D. *see under* Knutton S , **262,** 52
Jacobson J. L. and Snowdon C. T. Increased lead ingestion in calcium-deficient monkeys, **262,** 51
Jakes K. S. *see under* Ravetch J V , **262,** 150
James R. W. *see under* Cull-Candy S G , **262,** 408
Jardine W. G. *see under* Dickson J H , **262,** 43
Joffe J. M., Najman J. and Nettleton N. Environmental effects on alcohol selection by mice, *matterss arising*, **262,** 725
Johnson C. B., Whittington W. J. and Blackwood G. C. Nitrate reductase as a possible predictive test of crop yield, **262,** 133
Johnson J. D., Epel D. and Paul M. Intracellular *p*H and activation of sea urchin eggs after fertilisation, **262,** 661
Johnson M., Ross D., Meyers M., Rees R., Bunge R., Wakshull E. and Burton H. Synaptic vesicle cytochemistry changes when cultured sympathetic neurones develop cholinergic interactions, **262,** 308
Joho R. H. *see under* Cashion L. M , **262,** 186
Jokiel P. L. and Cowdin H. P. Hydromechanical adaptation in the solitary free-living coral *Fungia scutaria*, **262,** 212
Jones B. J. T. *see under* Fall S M , **262,** 457
Jones C. R., Garsky V. and Gibbons W. A. Proton magnetic resonance studies of conformation and flexibility of enkephalin peptides, **262,** 779
Jones D. The second Z-propagation window, **262,** 674
Jones L. and Molnar P. Frequency of foreshocks, **262,** 677
Jones O. P. Effect of phloridzin and phloroglucinol on apple shoots, **262,** 392
Jones P. B. Orientation of pulsar magnetic dipole moments, **262,** 120
Josephson R. K. *see under* Campbell R D , **262,** 388
Jukes T. H. Mad about safrole, *news*, **262,** 252
Mountain streets, *news*, **262,** 532
Jull A. J. T., Eglinton G., Pillinger C. T., Biggar G. M. and Batts B. D. The identity of lunar hydrolysable carbon, **262,** 566
Kaltoft K. *see under* Piper P. W , **262,** 757
Kanamori H. Are earthquakes a major cause of the Chandler wobble? *news and views*, **262,** 254
Kappler J. W. and Marrack P. C. Helper T cells recognise antigen and macrophage surface components simultaneously, **262,** 797
Kar S. K. *see under* Padhy L C , **262,** 805
Karplus M. *see under* McCammon J A , **262,** 325
Kassis A. I. and Tanner C. E. Novel approach to the treatment of hydatid disease, **262,** 588
Kasumov Kh. M. *see under* Ermishkin L N , **262,** 698
Kataoka M. *see under* Ueki T , **262,** 809
Kaufmann K. see under Donovan R J , **262,** 204
Kay R. R. *see under* Town C D , **262,** 717
Kazanas D. and Schramm D. N. Competition of neutrino and gravitational radiation in neutron star formation, **262,** 671
Kearns D. R. *see under* Bolton P H , **262,** 423
Kelly F. *see under* Golstein P , **262,** 693
Kelly P. M. and Lamb H. H. Prediction of volcanic activity and climate, *news and views*, **262,** 5
Kelsey W. *see under* Yuspa S H , **262,** 402
Kemper B. Inactivation of parathyroid hormone mRNA by treatment with periodate and aniline, **262,** 321
Kempton R. A. and Taylor L. R. Models and statistics for species diversity, **262,** 818
Kennard O. *see under* Viswamitra M A , **262,** 234
Kilshaw P. J. *see under* Brent L , **262,** 443
Kilton L. J. *see under* Gazdar A F , **262,** 696
Kirby M. J. and Turner P. Increase in human skeletal muscle lactate produced by fenfluramine, **262,** 617
Kiss I., Bencze G., Fodor A., Szabad J. and Fristrom J. W. Prepupal larval mosaics in *Drosophila melanogaster*, **262,** 136
Klein H. P., Lederberg J., Rich A., Horowitz N. H., Oyama V. I. and Levin G. V. The Viking Mission search for life on Mars, **262,** 24
Klotz M. and Gutte B. Combination of insulin chains on an anti-insulin antibody—Sepharose column, **262,** 791
Knight E. Jr. Antiviral and cell growth inhibitory activities reside in the same glycoprotein of human fibroblasts interferon, **262,** 302
Knighting E. The weather a week ahead, *news*, **262,** 162
Knott P. J. *see under* Hutson P H , **262,** 142
Knutton S., Jackson D., Graham J. M., Micklem K. J. and Pasternak C. A. Microvilli and cell swelling, **262,** 52
Kobata A. *see under* Yamashita K , **262,** 702
Kochupillai N., Verma I. C., Grewal M. S. and Ramalingaswami V. Down's syndrome and related abnormalities in an area of high background radiation in coastal Kerala, **262,** 60
Kohl F. *see under* Rudiger H W , **262,** 290
Koketsu K. *see under* Kuba K , **262,** 504
Kopecka H., Hillova J. and Hill M. Effect of restriction endonucleases on infectivity of Rous sarcoma virus DNA, **262,** 72
Koppenol W. H. Reactions involving singlet oxygen and the superoxide anion, **262,** 418
Koshy R. *see under* Das M R , **262,** 802
Kosland D. E. Jr. *see under* Spudich J L , **262,** 467
Koutts J. *see under* Mannucci P M , **262,** 141
Krassner S. M. *see under* Brun R , **262,** 689
Krebs J. Aggression in sticklebacks, *news and views*, **262,** 352
Suspicious husbands, *news and views*, **262,** 177
Krishna Murthy B. V., Krishna Murthy K., Raghava Reddi C. and Vaidyanathan S. Frequency variation of equatorial ionospheric scintillations, **262,** 38
Krishna Murthy K. *see under* Krishna Murthy B V , **262,** 38
Krivanek O. L. Gaskell P. H. and Howie A. Seeing order in 'amorphous' materials, **262,** 454
Krivoy W. A. *see under* Stewart J M , **262,** 784
Kuba K. and Koketsu K. Decrease of Na+ conductance during desensitisation of the frog endplate, **262,** 504
Kumar A. *see under* Ouellette A J , **262,** 619
Lacombe M.-L., Rene E., Guellaen G. and Hanoune J. Transformation of the beta₂ adrenoreceptor in normal rat liver into a beta₁ type in Zajdela hepatoma, **262,** 70
Lake P. Antibody response induced *in vitro* to the cell-surface alloantigen Thy-1, **262,** 297
Lala A. K. *see under* Roques B P , **262,** 778
Lamb F. K. *see under* Elsner R F , **262,** 356
Lamb H. H. *see under* Kelly P M , **262,** 5
Larsson B. *see under* Arfors K E , **262,** 500
Larsson L.-I., Rehfeld J. F., Sundler F. and Håkanson R Pancreatic gastrin in foetal and neonatal rats, **262,** 609
Laurent B. *see under* Carlqvist P , **262,** 821
Lavergne J.-M. *see under* Mannucci P M , **262,** 141
Lawn I. D. Swimming in the sea anemone *Stomphia coccinea* triggered by a slow conduction system, **262,** 708
Lawrence J. M. Covering response in sea urchins, **262,** 490
Le Goff S. *see under* Stewart W E II, **262,** 300
Leakey M. D., Hay R. L., CurtisG. H., Drake R. E., Jackes M. K. and White T. D. Fossil hominids from the Laetolil Beds, **262,** 460
Ledden J. E., Hodge P. E. and Aller H. D. The second highly polarised radio outburst in Cygnus X-3, **262,** 669
Lederberg J. *see under* Klein H P , **262,** 24
Lee A. G. Model for action of local anaesthetics, **262,** 545
Legay J.-M., Calvez B., Hirn M. and De Reggi M. L. Ecdysone and oocyte morphogenesis in *Bombyx mori*, **262,** 489
Leggett L. M. W. Polarised light-sensitive interneurones in a swimming crab, **262,** 709
Leigh J. B. *see under* Goody R S , **262,** 613
Lepkowski Wil. Adjust, amend and heal, *news*, **262,** 528
Lester D. *see under* Randall C L , **262,** 726
Letz R. *see under* Amsel A , **262,** 816
Leventhal M. *see under* Rust B , **262,** 118
Levin G. V. *see under Klein H P* , **262,** 24
Lewis D. H. *see under* Arfors K E , **262,** 500
Lewis L. W. *see under* Blanpied G D , **262,** 574
Lichti U. *see under* Yuspa S H , **262,** 402
Liebman S. *see under* Piper P W , **262,** 757
Lightman A. P. *see under* Eardley D M , **262,** 196
see under Shapiro S L , **262,** 743
Lindow S. E *see under* Arny D C , **262,** 282
Lipton M. A. *see under* Bissette G , **262,** 607
Lisk R. D. *see under* Reuter L A , **262,** 790
Liu L.-G. The post-spinel phase of forsterite, **262,** 770
Liu R. S. H. *see under* DeGrip W J , **262,** 416
Lodish H. F. *see under* Rose J K., **262,** 32
Loosen P. T. *see under* Bissette G., **262,** 607
Lorenz V. Formation of Hercynian subplates, possible causes and consequences, **262,** 374
Losada M. *see under* Candau P , **262,** 715
Lovelace R. V. E. Dynamo model of double radio sources, **262,** 649
Lovett M. B. *see under* Pentreath R J , **262,** 814
Lowe P. and Worboys M. The ecology of ecology, *news*, **262,** 432
Lunt G. G. *see under* Cull-Candy S G , **262,** 408
Lustbader E. *see under* Ross M H , **262,** 548
Lyman G. H., Priesler H. D. and Papahadjopoulos D. Membrane action of DMSO and othe chemical inducers of Friend Leukaemic cell differentiation, **262,** 360
Madsen S. N. and Sonne O. Increase of glucagon receptors in hyperthyroidism, **262,** 793
Malinowska D. H. *see under* Saunders N R , **262,** 156
Mallen D. N. B. *see under* Dawson W , **262,** 699
Mallucci L. and Wells V. Determination of cell shape by a cell surface protein component, **262,** 138
Manchada R. K. *see under* Carter J , **262,** 370
Maneckjee R., Srinath B. R. and Moudgal N. R. Prolactin suppresses releases of luteinising hormone during lactation in the monkey, **262,** 507
Mangels W. *see under* Rudiger H W , **262,** 290
Mannherz H. G. *see under* Goody R S , **262,** 613
Mannucci P. M., Meyer D., Ruggeri Z. M., Koutts J., Ciavarella N. and Lavergne J.-M.) **262,** 141
Mansfield J. W. *see under* Hargreaves J A , **262,** 318
Manuel O. K. *see under* Sabu D D , **262,** 28
Manzano C. *see under* Candau P , **262,** 715
Marinero E. E. *see under* Colles M J , **262,** 681
Marrack P. C. *see under* Kappler J W , **262,** 797
Marshall J. and Weale R. A. Retinal sensitivity to short wavelength light, *matters arising*, **262,** 629
Maruyama K., Natori R. and Nonomura Y. New elastic protein from muscle, **262,** 58
Mason K. O., Bell-Burnell S. J. and White N. E. Observations of X-ray bursts from the vicinity of 3U1727—33, **262,** 474
Mattsson C. *see under* Heilbronn E , **262,** 509
Matus A. J. The cytonet protein, *news and views*, **262,** 176
Maudlin I. Inheritance of susceptibility to *Trypanosoma cruzi* infection in *Rhodnius prolixus*, **262,** 214
May R. M. Irreproducible results, *news and views*, **262,** 646
McCall S. L. *see under* Rust B , **262,** 118
McCammon J. A., Gelin B. R., Karplus M. and Wolynes P. G. The hinge-bending mode in lysozyme, **262,** 325
McComb W. D. and Ayyash S. Effect of drag-reducing polymers on pulsation noise of small air bubbles, **262,** 47
McCrea W. H. *see under* Auman J R , **262,** 560
McGarr A. Upper limit to earthquake size, **262,** 378
McGarry M. P. *see under* Miller A M., **262,** 586
McGregor D. C. *see under* Davidson A , **262,** 371
McKenzie I. *see under* Beverley P C L , **262,** 495
McKeough M. *see under* Zarling J M , **262,** 691
Meissner H. P. Electrophysiological evidence for coupling between beta cells of pancreatic islets, **262,** 502
Mellanby K. Censor judgment, *news*, **262,** 641
Forecasting error, *news*, **262,** 441
Nature conservation, *news*, **262,** 170
Meloy D. A. *see under* Bridle A H , **262,** 179
Meyer D. *see under* Mannucci P M , **262,** 141
Meyers M. *see under* Johnson M , **262,** 308
Micklem K. J. *see under* Knutton S , **262,** 52
Miley G. K. *see under* Ekers R D , **262,** 369
Miller A. *see under* Doyle B B , **262,** 629
Miller A. M., Colley D. G. and McGarry M. P. Spleen cells from *Schistosoma mansoni*-infected mice produce diffusible stimulator of eosinophilopoiesis *in vivo*, **262,** 586
Miller B. and Heller A. Semiconductor liquid junction solar cells based on anodic sulphide films, **262,** 680
Miller D. A. *see under* Tantravahi R., **262,** 63
Miller O. J. *see under* Tantravahi R , **262,** 63
Mills J. S. *see under* Quenby J J , **262,** 471
Minneman K. P. and Iversen L. L. Enkephalin and opiate narcotics increase cyclic GMP accumulation in slices of rat neostriatum, **262,** 313
Mitchell J. F. *see under* Hill R G., **262,** 604
Mitsui T. *see under* Ueki T , **262,** 809
Mitsuoka A., Baba M. and Morikawa S. Enhancement of delayed hypersensitivity by depletion of suppressor T cells with cyclophosphamide in mice, **262,** 77
Mittag T. W. *see under* Axelrod F , **262,** 742
Mittermeier R. A. *see under* Coimbra-Filho A F , **262,** 630
Møllgard K. *see under* Saunders N R , **262,** 156
Moir A. J. G. *see under* Solaro R J , **262,** 615
Moisescu D. G. Kinetics of reaction in calcium-activated skinned muscle fibres, **262,** 610
Molnar P. *see under* Jones L , **262,** 677
Moor R. M. *see under* Trounson A O , **262,** 329
Moorbath S. and Pankhurst R. J. Further rubidium-strontium age and isotope evidence for the nature of the late Archaean plutonic event in West Greenland, **262,** 124
Moore P. D. r, K and evolution, *news and views*, **262,** 351
Influence of grazing, *news and views*, **262,** 6
Predator or prey? *news and views*, **262,** 644
Morgan B. A. *see under* Hambrook J M , **262,** 782
Morgan D. C. and Smith H. Linear relationship between phytochrome photoequilibrium and growth in plants under simulated natural radiation, **262,** 210
Morikawa S., **262,** 77
Morley J. *see under* Gordon D , **262,** 401
Moroder L. *see under* Brandt M , **262,** 311
Morris R. O. *see under* Chapman R W , **262,** 153
Moser M. E. *see under* Haddox M K , **262,** 146
Moudgal N. R. *see under* Maneckjee R , **262,** 507
Mturi A. A. New hominid from Lake Ndutu, Tanzania, **262,** 484
Munro I. H. *see under* Bordas J , **262,** 541
Murata Y., Baird T. and Fryer J. R. Molecular imagining of dislocations in 16 chlorocopper phthalocyanine, **262,** 721
Murray K. S. *see under* Anderson B F , **262,** 722
Musgrove P. J. Energy analysis of wave-power and wind-power systems, **262,** 206
Mygind N. *see under* Pedersen H , **262,** 494
Naik M. S. *see under* Naik M S , **262,** 396
Naik M. S., Sardhambal K. V. and Prakash S. Non-enzymatic photochemical reduction in nitrate in rice seedlings, **262,** 396
Najman J. *see under* Joffe J M , **262,** 725
Natori R. *see under* Maruyama K , **262,** 58
Navrot J. *see under* Singer A , **262,** 479
Nawrath H. Cyclic AMP and cyclic GMP may play opposing roles in influencing force of contraction in mammalian myocardium, **262,** 509
Nei M., Fuerst P. A. and Chakraborty R. Testing the neutral

mutation hypothesis by distribution of single locus heterozygosity, **262,** 491
Ne[illegible]ner K. *see under* Stewart J M , **262,** 784
Nemeroff C. B. *see under* Bissette G , **262,** 607
Ness N. F. *see under* Goldstein M L , **262,** 741
Nettleton N. *see under* Joffe J M , **262** 725
Newell R. E and Weare B. C. Ocean temperatures and large-scale atmospheric variations, **262,** 40
ewman M. J. *see under* Talbot R J Jr , **262,** 561
ewman M. J. and Talbot R. J., Jr. Solar neutrinos and solar accretion of interstellar matter, **262,** 559
icholas D. and Hill C R. Acoustic Bragg diffraction from human tissues — Reply, *matters arising,* **262,** 330
ishino C. *see under* Washio H , **262,** 487
obel P. S. *see under* Hartsock T L , **262,** 574
oble D. *see under* Cohen I , **262,** 657
onomura Y. *see under* Maruyama K , **262,** 58
orman C. Exports time for a stand? *news,* **262,** 345
Genetic manipulation guidelines issued, *news,* **262,** 2
Tennessee valley energy, *news,* **262,** 732
oshkin V. E., Eagle R. J. and Wong K. M. Plutonium levels in Kwajalein lagoon, **262,** 745
ovick R P. and Schwesinger M. Independence of plasmid incompatibility and replication control functions in *Staphylococcus aureus,* **262,** 623
berlin R. *see under* Roques B P , **262,** 778
'Connell R. J. and Dziewonski A. M. Excitation of the Chandler wobble by large earthquakes, **262,** 259
dman S. *see under* Arfors K E , **262,** 500
sborne D. J. *see under* Dawson W , **262,** 699
smolska H. New light on the skull anatomy and systematic position of *Oviraptor,* **262,** 683
striker J. P. *see under* Bahcall J N , **262,** 37
swald M. and Erwin J. Control of intragroup aggression by male pigtail monkeys (*Macaca nemestrina*) **262,** 686
uellette A. J., Bandman E and Kumar A. Regulation of ribosomal RNA methylation in a temperature-sensitive mutant of BHK cells, **262,** 619
wen H. G. How closely should continents fit together? *news and views,* **262,** 644
wen J. J. T. Haemopoiesis discussed, *news and views,* **262,** 177
wen M. E. *see under* Triffitt J T , **262,** 226
xburgh R. Energy from warm rocks, *news,* **262,** 526
yama V. I. *see under* Klein H P , **262,** 24
Ugarte P. *see under* Hesser J E , **262,** 116
adhy L. C. *see under* Das M R , **262,** 802
almer D. A. Rod-cone mechanism underlying the Purkinje shift, **262,** 601
ankhurst R. J. *see under* Moorbath S , **262,** 124
apahadjopoulos D *see under* Lyman G H , **262,** 360
[illegible] E. *see under* Rudiger H W , **262,** 290
ak C. A. *see under* Knutton S , **262,** 52
on E. *see under* Yuspa S H , **262,** 402
Paul M. *see under* Johnson J D , **262,** 661
Peale S J. Does Mercury have a molten core? **262,** 765
Pearlstein E Plasma membrane glycoprotein which mediates adhesion of fibroblasts to collagen, **262,** 497
Pearse A. G. E. Peptides in brain and intestine, *news and views,* **262,** 92
Pederson H. and Mygind N. Absence of Axonemal arms in nasal mucosa cilia in Kartagener's syndrome, **262,** 494
Pedulla D. *see under* Azzarone B , **262,** 74
Penfold J. *see under* Hayter J B , **262,** 569
Pentreath R. J. and Lovett M B. Occurrence of plutonium and americium in plaice from the north-eastern Irish Sea, **262,** 814
Pepper C. M. *see under* Hill R G , **262,** 604
ro J. *see under* Tjian R , **262,** 753
ry S. V. *see under* Solaro R J , **262,** 615
utz M F Fundamental research in molecular biology relevance to medicine, *review article,* **262,** 449
ce A., Casoli C. and Schito G. C. Rifampicin-resistant RNA polymerase and NAD transferase activities in coliphage N4 virions, **262,** 412
ilp R. P. and Calvin M. Possible origin for insoluble organic (Kerogen) debris in sediments from insoluble cell-wall materials of algae and bacteria, **262,** 134
hler H. and Friedlich W. Radiocarbon dates of Santorini volcanics, **262,** 373
rson M. and Dallos P. Re-examination of avian cochlear potentials, **262,** 599
z K. A. and Torchia D. Ionic clustering and collagen specificity — Reply, *matters arising,* **262,** 629
ler G. M. *see under* Spelsberg T C **262,** 65
ione L J. and Gold D. P. Liquid nitrogen enhancement of partially annealed fission tracks in glass, **262,** 773
linger C. T. *see under* Jull A J T., **262,** 566
er A. FBR will it ever be stopped? *news,* **262,** 342
GHWR green to amber? *news,* **262,** 248
er P. W., Wasserstein M., Engbaek F., Kaltoft K., Celis J E., Zeuthen J., Liebman S. and Sherman F. Nonsense suppressors of *Saccharomyces cerevisiae* can be generated by mutation of the tyrosine tRNA anticodon, **262,** 757
rotta V. *see under* Walz A , **262,** 665
nitz M. A. *see under* Cashion L M , **262,** 186
em J. S *see under* van Rood J J , **262,** 795
tkin S. A *see under* Furukawa T , **262,** 414
sky P. M. *see under* Wightman R M , **262,** 145
ter J. W. *see under* Wethey D S , **262,** 281
eluyev V. M. *see under* Ermishkin L N , **262,** 698
lhy L. C., Kar S. K., Rao K. K. and Das M. R. Role of plasma membranes in stimulation of RNA-directed DNA synthesis, **262,** 805
Prange A. J. Jr. *see under* Bissette G , **262,** 607
Price R. J. *see under* Dickson J H , **262,** 43
Priesler H. D. *see under* Lyman G H , **262,** 360
Prothero W. A., Reid I., Reichle M. S. and Brune J. N. Ocean bottom seismic measurements on the East Pacific Rise and Rivera Fracture Zone, **262,** 121
Prusch R. D. and Whoriskey F. Maintenance of fluid volume in the starfish water vascular system, **262,** 577
Ptak W. *see under* Gershon R K , **262,** 216
Purvis S. R. *see under* Bigg D C H , **262,** 220
Pye J. P., Cooke B. A. and Elvis M. Identification of Abell Cluster 754 with the X-ray source 3U0901-09 by Ariel V, **262,** 195
Quenby J. J. *see under* Coe M J , **262,** 563
Quenby J. J., Coe M. J., Engel A. R. and Mills J. S. Observations of X-ray and gamma bursts, **262,** 471
Quinn J. G. *see under* Van Vleet E S , **262,** 126
Quinn W. G. and Dudai Y. Memory phases in *Drosophila,* **262,** 576
Raghava Reddi C. *see under* Krishna Murthy B V , **262,** 38
Raich P. C. *see under* Zarling J M , **262,** 691
Rajan S. S. S. Changes in net surface charge of hydrous alumina with phosphate adsorption, **262,** 45
Ramachandran V. S. Learning-like phenomena in stereopsis, **262,** 382
Ramalingaswami V. *see under* Kochupillai N , **262,** 60
Ramamurthy V. *see under* DeGrip W J , **262,** 416
Ramsden D. *see under* Carter J , **262,** 370
Rance M. J. *see under* Hambrook J M , **262,** 782
Randall C. L. and Lester D. Environmental effects on alcohol selection by mice — Reply, *matters arising,* **262,** 726
Rao K. K *see under* Padhy L C , **262,** 805
Rasool S. I. Future of space science, *news and views,* **262,** 95
Rattew C. J. *see under* Doyle B B , **262,** 629
Ravetch J. V. and Jakes K. S. Intact 3′ end of 16S rRNA is not required for specific mRNA binding, **262,** 150
Redgrave P. and Horrell R. I Potentiation of central reward by localised perfusion of acetylocholine and 5-hydroxytryptamine, **262,** 305
Rees R. *see under* Johnson M , **262,** 308
Reeve E. B *see under* Stewart J M , **262,** 784
Rehfeld J. F. *see under* Larsson L -I , **262,** 609
Reichle M. S. *see under* Prothero W A , **262,** 121
Reid B. R. Quantification of secondary and tertiary structure base pairs in *E coli* tRNA1(Val), Reply — *matters arising,* **262,** 424
Reid I. *see under* Prothero W A , **262,** 121
Reingold N. Reflections on 200 years of science in the USA, **262,** 9
Rene E. *see under* Lacombe M -L , **262,** 70
Reuter L. A. and Lisk R. D. Progesterone may act at hypothalamus and pituitary by way of enhancement of oestrogen retention, **262,** 790
Reynolds J. J. *see under* Triffitt J T , **262,** 226
Reynolds J. M. *see under* Saunders N R , **262,** 156
Reynolds M. L. *see under* Saunders N R , **262,** 156
Reyss J.-L. and Yokoyama Y. Aluminium-26 in a manganese nodule, **262,** 203
Rich A. *see under* Klein H P , **262,** 24
Rich M. A. *see under* Das M R , **262,** 802
Richards C. D. Anaesthetic mecnanisms, *news and views,* **262,** 534
Richards E. G. Irregular associations, *news and views,* **262,** 173
Riddle P. N. *see under* Robinson J H , **262,** 298
Roberts A. M. and Goodall H. Y chromosome visibility in quinacrine-stained human spermatozoa, **262,** 493
Robertson G. B. *see under* Anderson B F , **262,** 722
Robertson M. Artificial intelligence in education, *news,* **262,** 435
Robillard G. T., Tarr C. E., Vosman F. and Berendsen H. J. C. Similarity of the Crystal and solution structure of yeast tRNA(Phe), **262,** 363
Robinson J. H. *see under* Robinson J H , **262,** 298
Robinson J. H., Smith J. A., Totty N. F. and Riddle P. N. Transition probability and the hormonal and density-dependent regulation of cell proliferation, **262,** 298
Robson B. Protein folding experiments do proteins cheat? *news and views,* **262,** 447
Romano T. J. *see under* Shore S L , **262,** 695
Romanzi C. A. *see under* Azzarone B , **262,** 74
Roques B. P., Garbay-Jaureguiberry C., Oberlin R., Anteunis M and Lala A. K Conformation of Met-enkephalin determined by high field PMR spectroscopy, **262,** 778
Roscoe J. P. and Claisse P. J. A sequential *in vivo–in vitro* study of carcinogenesis induced in the rat brain by ethylnitrosourea, **262,** 314
Rose J. K. and Lodish H. F. Translation *in vitro* of vesicular stomatitis virus mRNA lacking 5′-terminal 7-methylguanosine, **262,** 32
Roseman S. *see under* Umbreit J , **262,** 67
Rosenbaum G. *see under* Goody R S , **262,** 613
Rosengren B. *see under* Arfors K E , **262,** 500
Ross D. *see under* Johnson M , **262,** 308
Ross M H , Lustbader E. and Bras G. Dietary practices and growth responses as predictors of longevity, **262,** 548
Rossmann M. G. Moleculat structure of NAD, *matters arising,* **262,** 726
Rowan-Robinson M. Quasars and the cosmological distance scale, *review article,* **262,** 97
Rudiger H W., Kohl F., Mangels W. and von Wichert P., Bartram C. R., Wohler W and Passarge E Benzpyrene indusces sister chromatid exchanges in cultured human lymphocytes, **262,** 290
Ruggeri Z. M. *see under* Mannucci P M , **262,** 141
Rushforth N. B. *see under* Campbell R D , **262,** 388
Rust B. W., Leventhal M. and McCall S. L. Evidence for a radioactive decay hypothesis for supernova luminosity, **261,** 118
Sabu D. D. and Manuel O. K. Xenon record of the early solar system, **262,** 28
Sadler P. J. Zinc in enzymes, *news and views,* **262,** 258
Sagara N. Presence of a buried mammalian carcass indicated by fungal fruiting bodies, **262,** 816
Saibil H., Chabre M. and Worcester D. Neutron diffraction studies of retinal rod outer segment membranes, **262,** 266
Saito M. *see under* Sakakibara K , **262,** 316
Sakakibara K., Saito M., Umeda M., Enaka K. and Tsukada Y. Native collagen formation by liver parenchymal cells in culture, **262,** 316
Sakuma S. *see under* Furukawa T , **262,** 414
Salaman D. F. *see under* Westley B R , **262,** 407
Sandoval I. V. and Cuatrecasas P. Opposing effects of cyclic AMP and cyclic GMP on protein phosphorylation in tubulin preparations, **262,** 511
Sardhambal K. V. *see under* Naik M S , **262,** 396
Sasaki M. *see under* Wake N , **262,** 580
Saunders J. R. Aspects of plasmid behaviour, *news and views,* **262,** 536
Saunders N. R., Dziegielewska K. M., Malinowska D. H., Reynolds M. L., Reynolds J. M. and Møllgard K. Permeability of blood-cerebrospinal fluid barrier during foetal and perinatal life, *matters arising,* **262,** 156
Schito G. C. *see under* Pesce A , **262,** 412
Schmidt J. A. and Eckert R. Calcium couples flagellar reversal to photostimulation in *Chlamydomonas reinhardtii,* **262,** 713
Schmidtke J., Wienker Th., Flugel M. and Engel W. *In vitro* inhibition of cyclic AMP phosphodiesterase by cortisol, **262,** 593
Schorderet M. *see under* Schorderet-Slatkine S , **262,** 289
Schorderet-Slatkine S., Schorderet M. and Baulieu E.-E. Initiation of meiotic maturation in *Xenopus laevis* oocytes by lanthanum, **262,** 289
Schramm D. N. *see under* Kazanas D , **262,** 671
Schwab W. E. *see under* Campbell R D , **262,** 388
Schwartz J.-C. *see under* Audigier Y , **262,** 307
Schwesinger M. *see under* Novick R P , **262,** 623
Scientific Party, Deep Sea Drilling Project, Leg 46. Glass-rich basaltic sand and gravel within the oceanic crust at 22QN, **262,** 768
Scott D. M. Circadian rhythm of anaerobiosis in a polychaete annelid, **262,** 811
Scott J. S. *see under* Coleman G D **262,** 476
Scott T. W. and Venugopalan M. Plasma treatment of coal, **262,** 48
Seely M. K. *see under* Hamilton W J III, **262,** 284
Seger J. Evolution of responses to relative homozygosity, **262,** 578
Seller M. J. *see under* Adinolfi M , **262,** 156
Seymour R. S. Dinosaurs, endothermy and blood pressure, **262,** 207
Shahidi M. *see under* Hasted J. B , **262,** 777
Shakked Z. *see under* Viswamitra M A , **262,** 234
Shapiro S. L. and Lightman A. P. The distribution of stars around a massive black hole, **262,** 743
Sharma O. K., Beezley D. N. and Borek E Modulation of the synthesis *in vitro* of a hormone-induced protein by transfer RNA, **262,** 62
Sherman F. *see under* Piper P W , **262,** 757
Sherwell C. JET will it ever get started? *news,* **262,** 338
Shore S. L., Cromeans T. L. and Romano T. J. Immune destruction of virus-infected cells early in the infectious cycle, **262,** 695
Shyamala G. and Dickson C. Relationship between receptor and mammary tumour virus production after stimulation by glucocorticoid, **262,** 107
Siegler M. V. S. *see under* Burrows M , **262,** 222
Sigurdsson J. B., Titman C. W. and Davies P. A. The dispersal of young post-larval bivalve molluscs by byssus threads, **262,** 386
Silver H. B. Deposit-forming by zinc dithiophosphates in base oils during oxidation, *matters arismg,* **262,** 329
Simantov R. and Snyder S. H Elevated levels of enkephalin in morphine-dependent rats, **262,** 505
Simons S. and Williams I. P. A plum-pudding model for interstellar grains, **262,** 273
Singer A. and Navrot J. Extraction of metals from basalt by humic acids, **262,** 479
Sirsat S. M. *see under* Das M R , **262,** 802
Skaer H. le B. *see under* Franks F , **262,** 323
Skinner G. K. *see under* G F Carpenter, **262,** 473
Sladeček M. *see under* Hašek M , **262,** 295
Slaga T. J. *see under* Yuspa S H , **262,** 402
Slesser M. and Hounam I. Solar energy breeders, *news,* **262,** 244
Smith C. F. C. *see under* Hambrook J M , **262,** 782
Smith H. *see under* Morgan D C , **262,** 210
Smith J. A. *see under* Robinson J H , **262,** 298
Smith L. A., Hill S. and Yates M. G. Inhibition by acetylene of conventional hydrogenase in nitrogen-fixing bacteria, **262,** 209
Smith P. J. Assumed dipolar geomagnetic field, *news and views,* **262,** 643
Chemistry does not define environment, *news and views,* **262,** 352
More rapidly growing manganese, *news and views,* **262,** 257

Phase changes at 650 km, *news and views*, **262,** 540
Smith R. A. and Daniell G. J. Systematic approach to the correction of intonation in wind instruments, **262,** 761
Smith R. A. G. Amphipathic enzyme-polymer conjugates, **262,** 519
Snook I. *see under* van Megen W , **262,** 571
Snowdon C. T. *see under* Jacobson J L , **262,** 51
Snyder S. H. *see under* Simantov R , **262,** 505
Sochacka J. H. M. and Woodruff R. C. Induction of male recombination in *drosophila melanogaster* by injection of extracts of flies showing male recombination, **262,** 287
Solaro R. J., Moir A. J. G. and Perry S. V. Phosphorylation of troponin I and the ionotropic effect of adrenaline in the perfused rabbit heart, **262,** 615
Soliman M. H. pH-dependent heterosis of heavy metal-tolerant hybrid of the monkey flower *Mimulus guttatus,* **262,** 49
Sonne O. *see under* Madsen S. N., **262,** 793
Sourkes T. L. *see under* Etienne P , **262,** 144
Spelsberg T. C., Webster R. A. and Pikler G. M. Chromosomal proteins regulate steroid binding to chromatin, **262,** 65
Spudich J. L. and Koshland D. E. Jr. Non-genetic individuality· chance in the single cell, **262,** 467
Spurgeon D. Council rift over report, *news,* **262,** 440
Modelling the world, again, *news,* **262,** 246
Towards a conserver society, *news,* **262,** 248
Srinath B. R. *see under* Maneckjee R , **262,** 507
Stålberg E. *see under* Heilbronn E , **262,** 509
Stecker F. W. and Fichtel C. E. NASA Goddard gamma-ray symposium, *news and views,* **262,** 447
Steigman G. The cosmic X-ray background, *matters arising,* **262,** 821
Stenevi U. *see under* Bjorklund A , **262,** 787
Stephenson J. H. *see under* Haddox M K , **262,** 146
Stephenson J. R. *see under* Barbacid M , **262,** 554
Stewart A. F. Scrotal asymmetry an appendix, *matters arising,* **262,** 155
Stewart J. M., Getto C. J., Neldner K., Reeve E. B., Krivoy W. A. and Zimmermann E. Substance P and analgesia, **262,** 784
Stewart W. E. II, Gresser I., Tovey M. G., Bandu M.-T. and Le Goff S. Identification of the cell multiplication inhibitory factors in interferon preparations as interferons, **262,** 300
Storey J. W. F. *see under* Brown R D , **262,** 672
Stothers R. White dwarfs, the Galaxy and Dirac's cosmology, **262,** 477
Strom R. G. *see under* Bridle A H , **262,** 179
Strope E. *see under* Wightman R M., **262,** 145
Sugiyama T. *see under* Ueda N , **262,** 581
Sundler F. *see under* Larsson L -I , **262,** 609
Svalgaard L. and Wilcox J. M. Structure of the extended solar magnetic field and the sunspot cycle variation in cosmic ray intensity, **262,** 766
Svendgaard N.-A. *see under* Bjorklund A , **262,** 787
Szabad J. *see under* Kiss I , **262,** 136
Szybalski W. *see under* Honigman A., **262,** 112
Tachibana Y. *see under* Yamashita K , **262,** 702
Takagi N. *see under* Wake N , **262,** 580
Takasaki S. *see under* Yamashita K , **262,** 702
Talbot R. J. Jr. *see under* Newman M J., **262,** 559
Talbot R. J. Jr. Butler D. M. and Newman M. J. Climatic effects during passage of the Solar System through interstellar clouds, **262,** 561
Tanner C. E. *see under* Kassis A I., **262,** 588
Tantravahi R., Dev V. G., Miller D. A. and Miller O. J. Human-mouse cell hybrid with human multiple Y chromosomes, **262,** 63
Tarenghi M. *see under* Coleman G. D , **262,** 476
Tarr C. E. *see under* Robillard G T , **262,** 363
Taylor D. J. *see under* Hey M J , **262,** 807
Taylor H. H. *see under* Greenaway P , **262,** 711
Taylor K. W. *see under* Bone A J , **262,** 501
Taylor L. R. *see under* Kempton R A , **262,** 818
Teilhet J. H. *see under* Goucher C L., **262,** 130
Temple A. *see under* Faulk W P., **262,** 799
Thackray A. Scientific networks in the age of the American Revolution, **262,** 20
Thomas M. D. *see under* Gibb R A , **262,** 199
Thomas R. C. *see under* Ellis D , **262,** 224
Ionic mechanism of the H+ pump in a snail neurone, **262,** 541
Thompson P. *see under* Gray J., **262,** 481
Thorn R. M. and Henney C. S. Enumeration of specific cytotoxic T cells, **262,** 75
Ting R. Y. Polymer effects on microjet impact and cavitation erosion, **262,** 572
Titman C. W. *see under* Sigurdsson J B , **262,** 386
Tjian R. and Pero J. Bacteriophage SP01 regulatory proteins directing late gene transcription *in vitro,* **262,** 753
Tomlinson P. B. Trees in the tropics, *news and views,* **262,** 96
Toner W. T. Associated production of charm, *news and views,* **262,** 444
Torchia D. *see under* Piez K. A , **262,** 629
Totty N. F. *see under* Robinson J H , **262,** 298
Tovey M. G. *see under* Stewart W E. II, **262,** 300
Town C. D., Gross J. D. and Kay R. R. Cell differentiation without morphogenesis in *Dictyostelium discoideum,* **262,** 717
Tracey D. E. *see under* Wolfe S A , **262,** 584
Tregear R. T. *see under* Goody R S , **262,** 613
Triffitt J. T., Gebauer U., Ashton B. A., Owen M. E. and Reynolds J. J. Origin of plasma α_2HS-glycoprotein and its accumulation in bone, **262,** 226
Trounson A., O., Willadsen S. M., Moor R. M. and Tucker E. M. Haemoglobin-type and superovulation in ewes, *matters arising,* **262,** 329
Tsukada Y. *see under* Sakakibara K , **262,** 316
Tucker E. M. *see under* Trounson A O , **262,** 329
Tukiainen E. *see under* Tuomisto J , **262,** 596
Tuomisto J. and Tukianinen E. Decreased uptake of 5-hydroxytryptamine in blood platelets from depressed patients, **262,** 596
Turner P. *see under* Kirby M J , **262,** 617
Ueda N., Uenaka H., Akematsu T. and Sugiyama T. Parallel distribution of sister chromatid exchanges and chromosome aberrations, **262,** 581
Ueki T., Kataoka M. and Mitsui T. Structural order in chromatophore membranes of *Rhodospirillum rubrum,* **262,** 809
Uenaka H. *see under* Ueda N , **262,** 581
Umbreit J. and Roseman S. Effect of maternal age on intercellular adhesion of embryonic chick liver cells, **262,** 67
Umeda M. *see under* Sakakibara K , **262,** 316
Upper C. D. *see under* Arny D C , **262,** 282
Vaidyanathan S. *see under* Krishna Murthy B V , **262,** 38
van der Hulst J. M. *see under* Ekers R D , **262,** 369
van Diggelen J. Is the Earth expanding? **262,** 675
Van Dyck R. Jr, Ekstrom P. and Dehmelt H. Axial, magnetron, cyclotron and spin-cyclotron-beat frequencies measured on single electron almost at rest in free space (geonium) **262,** 776
van Leeuwen A. *see under* van Rood J. J., **262,** 795
van Megen W. and Snook I. Ordered states in systems of macroscopic particles, **262,** 571
van Rood J. J., van Leeuwen A. and Ploem J. S. Simultaneous detection of two cell populations by two-colour fluorescence and application to the recognition of B-cell determinants, **262,** 795
Van Vleet E. S. and Quinn J. G. Chacterisation of monounsaturated fatty acids from an estuarine sediment, **262,** 126
Venugopalan M. *see under* Scott T. W , **262,** 48
Verma I. C. *see under* Kochupillai N , **262,** 60
Vincent K. *see under* Foehme D E , **262,** 418
Virion A. *see under* Audigier Y , **262,** 307
Virk P. S. Conformational effects in drag reduction by polymers, **262,** 46
Viswamitra M. A. Molecular structure of NAD, — Reply, *matters arising,* **262,** 726
Viswamitra M. A., Hozur M. V., Shakked Z. and Kennard O. X-ray study of the rubidium salt of ADP, **262,** 234
von Wichert P. *see under* Rudiger H W , **262,** 290
Voskan F. *see under* Robillard G T , **262,** 363
Wake N., Takagi N. and Sasaki M. Non-random inactivation of X chromosome in the rat yolk sac, **262,** 580
Wakshull E. *see under* Johnson M , **262,** 308
Walborn N. R. *see under* Hesser J E., **262,** 116
Walker J. Cathodoluminescence of dislocations, *news and views,* **262,** 94
Wall P. D. *see under* Devor M , **262,** 705
Walz A., Pirrotta V. and Ineichen K. Gamma repressor regulates the switch between PR and Prm promoters, **262,** 665
Wang S. K. *see under* Worthington C R , **262,** 626
Warner A. *see under* Blackshaw S , **262,** 217
Washio H., Nishino C. and Bowers W. S. Antennal receptor response to sex pheromone mimics in the American cockroach, **262,** 487
Wasilewski P. J. *see under* Goldstein M L , **262,** 741
Wasserstein M. *see under* Piper P W , **262,** 757
Watson D. F. *see under* Hausfater G , **262,** 688
Weale R. A. *see under* Marshall J., **262,** 629
Weare B. C. *see under* Newell R E , **262,** 40
Weart S. R. The rise of 'prostituted' physics, **262,** 13
Webb J. *see under* Anderson B F , **262,** 722
Webster R. A. *see under* Spelsberg T C , **262,** 65
Weissmann C. *see under* Cashion L M , **262,** 186
Wells V. *see under* Mallucci L , **262,** 138
Werthamer S. *see under* Amaral L , **262,** 589
Westley B. R. and Salaman D. F. Role of oestrogen receptor in androgen-induced sexual differentiation of the brain, **262,** 407
Wethey D. S. and Porter J. W. Sun and shade differences in productivity of reef corals, **262,** 281
White N. E. *see under* Mason K O , **262,** 474
White S. H. The lipid bilayer as a 'solvent' for small hydrophobic molecules, **262,** 421
White T. D. *see under* Leakey M D , **262,** 460
Whitney R. A. Jr. *see under* Hzu C -K , **262,** 397
Whittington W. J. *see under* Johnson C B , **262,** 133
Whoriskey F. *see under* Prusch R D , **262,** 577
Wienker Th. *see under* Schmidtke J , **262,** 593
Wightman R. M., Strope E., Plotsky P. M. and Adams R. N. Monitoring of transmitter metabolites by voltammetry in cerebrospinal fluid following neural pathway stimulation, **262,** 145
Wigzell H. *see under* Binz H , **262,** 294
Wilby O. K. Nematocyst discharge and the effects of antibodies on feeding in hydra, **262,** 387
Wilcox J. M. *see under* Svalgaard L , **262,** 766
Wilks E. M. Optical methods to select diamonds of very high lattic perfection, **262,** 570
Willadsen S. M. *see under* Trounson A O , **262,** 329
Williams J. S. *see under* Andrew R , **262,** 380
Williams P. M. and Carlucci A. F. Bacterial utilisation of organic matter in the deep sea, **262,** 810
Williams W. G. *see under* Hayter J B , **262,** 569
Willis A. G. *see under* Bridle A H , **262,** 179
Willmore A. P. *see under* Carpenter G F , **262,** 473
Wilson A. M. *see under* Carpenter G F., **262,** 473
Wilson K. R. *see under* Goucher C L , **262,** 130
Wohler W. *see under* Rudiger H W., **262,** 290
Wolfe S. A., Tracey D. E. and Henney C. S. Induction "natural killer" cells by BCG, **262,** 584
Wolfrum J. see under Donovan R. J , **262,** 204
Wolynes P. G. *see under* McCammon J A , **262,** 325
Wong K. M. *see under* Noshkin V E , **262,** 745
Wong-Staal F., Gillespie D. and Gallo R. C. Proviral sequences of baboon endogenous type C RNA virus in DN of human leukaemic tissues, **262,** 190
Woodhead-Galloway J. *see under* Doyle B B , **262,** 629
Wooding E. R. Ball lightning in Smethwick, **262,** 379
Woodruff R. C. *see under* Sochacka J H M., **262,** 287
Woody J. *see under* Beverley P C L , **262,** 495
Wooi K. C *see under* Broughton W J , **262,** 208
Worboys M. *see under* Lowe P , **262,** 432
Worcester D. *see under* Saibil H., **262,** 266
Worthington C. R., Wang S. K. and Folzer C. M. Low angl X-ray diffraction patterns of squid retina, **262,** 626
Wunsch E. *see under* Brandt M , **262,** 311
Yamamoto C., Yamashita H. and Chujo T. Inhibitory actio of glutamic acid in cerebellar interneurones, **262,** 786
Yamashita H. *see under* Yamamoto C , **262,** 786
Yamashita K., Tachibana Y., Takasaki S. aand Kobata A. ABO blood group determinants with branched cores **262,** 702
Yates C. A. and Herbert J. Differential circadian rhythms i pineal and hypothalamic 5-HT induced by artifici photoperiods or melatonin, **262,** 219
Yip C. W. and Hersey J. A. Ordered powder mixing, 26 202
Yokoyama Y. *see under* Reyss J -L , **262,** 203
Young S. N. *see under* Etienne P., **262,** 144
Yuspa S. H., Lichti U., Ben T., Patterson E., Hennings P Slaga T. J., Colburn N. and Kelsey W. Phorbol est stimulate DNA synthesis and ornithine decarboxyl activity in mouse epidermal cell cultures, **262,** 402
Zachariassen K. E. and Hammel H. T. Nucleating agents the haemolymph of insects tolerant to freezing, **262,** 2
Zaerr J. B. *see under* Chapman R W , **262,** 153
Zarling J. M., Raich P. C., McKeough M. and Bach F. Generation of cytotoxic lymphocytes *in vitro* agai autoolgous human leukaemia cells, **262,** 691
Zeuthen J. *see under* Piper P W , **262,** 757
Zimmermann E. *see under* Stewart J. M , **262,** 784
Znajek R. On being close to a black hole without falling i **262,** 270
Zouros E. Hybrid molecules and the superiority of th heterozygote, **262,** 227